2008 Annual Progress Report

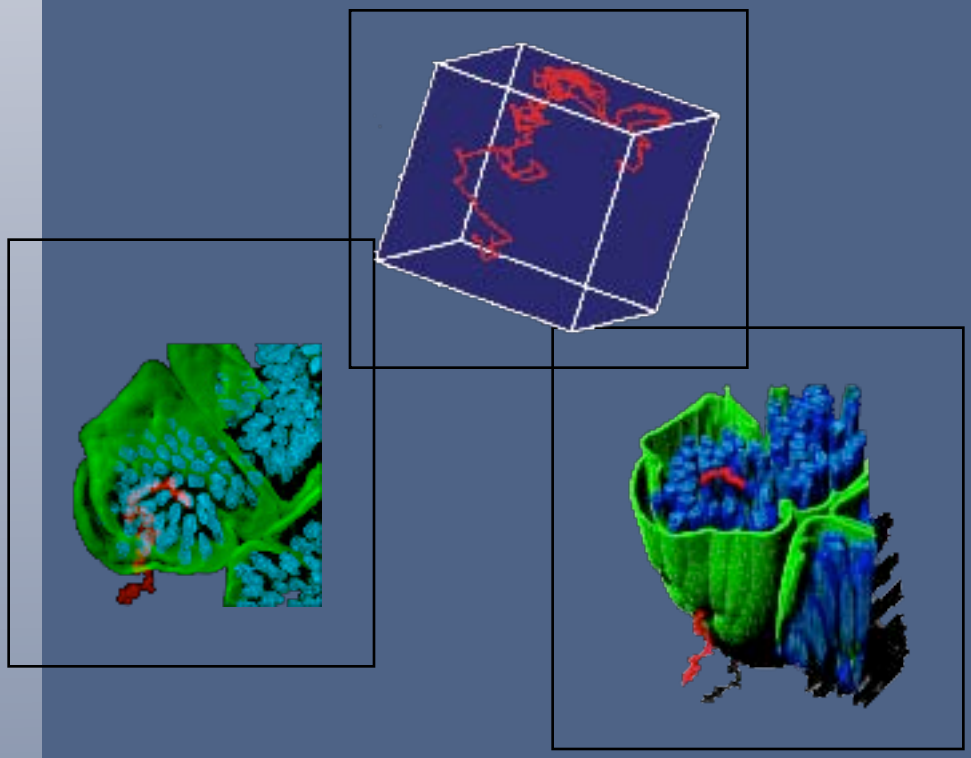

# Innovation for our nation

Los Alamos NATIONAL LABORATORY EST. 1943

Laboratory Directed Research & Development
at Los Alamos National Laboratory

## About the Cover

Los Alamos National Laboratory researchers have developed the 3-D tracking microscope, the only confocal microscope capable of following the motion of nanometer sized objects, such as quantum dots, organic florophores, and tagged single proteins, as they move through 3-dimensional space at rates faster than many intracellular transport processes. On the cover, the top image shows a 3D trajectory of an individual semiconductor quantum dot followed with the 3D tracking microscope. The image to the left is a single XY slice of a mouse intestine imaged via standard confocal microscopy. A number of XY slices taken at different Z locations in the sample were combined to form the 3D rendering shown in the image to the right.

The 3-D tracking microscope was developed by Jim Werner of the Laboratory's Center for Integrated Nanotechnology (CINT). Werner's work grew out of a single LDRD Exploratory Research project titled "Tracking Single Molecules in Three Dimensions." The project ended two years ago, but instrument development continued with funding from the National Nanotechnology Enterprise Development Center (NNEDC) and the National Institutes of Health (NIH). Werner received a 2008 R&D 100 Award for his work on the 3-D tracking microscope.

## Disclaimer

The Los Alamos National Laboratory strongly supports academic freedom and a researcher's right to publish; therefore, the Laboratory as an institution does not endorse the viewpoint of a publication or guarantee its technical correctness. With respect to documents available from this server, neither the United States Government nor the Los Alamos National Security, LLC., nor any of their employees, makes any warranty, express or implied, including the warranties of merchantability and fitness for a particular purpose, or assumes any legal liability or responsibility for the accuracy, completeness, or usefulness of any information, apparatus, product, or process disclosed, or represents that its use would not infringe privately owned rights. Reference herein to any specific commercial products, process, or service by trade name, trademark, manufacturer, or otherwise, does not necessarily constitute or imply its endorsement, recommendation, or favoring by the United States Government or the Los Alamos National Security, LLC. The views and opinions of authors expressed herein do not necessarily state or reflect those of the United States Government or the Los Alamos National Security, LLC., and shall not be used for advertising or product endorsement purposes. Unless otherwise indicated, this information has been authored by an employee or employees of the Los Alamos National Security, LLC. (LANS), operator of the Los Alamos National Laboratory under Contract No. DE-AC52-06NA25396 with the U.S. Department of Energy. The U.S. Government has rights to use, reproduce, and distribute this information. The public may copy and use this information without charge, provided that this Notice and any statement of authorship are reproduced on all copies. Neither the Government nor LANS makes any warranty, express or implied, or assumes any liability or responsibility for the use of this information.

Issued April 2008

LA-UR-09-01881

## Structure of this Report

In accordance with U.S. Department of Energy Order (DOE) 413.2B, the Laboratory Directed Research and Development (LDRD) annual report for fiscal year 2008 (FY08) provides summaries of each LDRD-funded project for the fiscal year, as well as full final reports on completed projects. The report is organized as follows:

Overview: An introduction to the LDRD Program at Los Alamos National Laboratory (LANL), the program's structure and strategic value, the LDRD portfolio management process, and highlights of outstanding accomplishments by LDRD researchers.

Success Stories: A selection of FY08 success stories that illustrate the innovative, ground-breaking research funded by the LDRD program. The one-page articles feature LDRD researchers who are at the forefront of their fields in science and technology.

Project Summaries: The project summaries are organized first by science and technology categories: Physics, Chemistry and Material Sciences, Environmental and Biological Sciences, Information Science and Technology, and Technology. Within each category, summaries are organized by LDRD component: Directed Research (DR) projects first, Exploratory Research (ER) second, and Postdoctoral Research and Development (PRD) projects last. Full final reports are included at the end of each section.

Projects are listed in numerical order according to their project identification number, which consists of three parts. The first is the fiscal year in which the project began; the second is a unique numerical identifier; and the third identifies the project component.

## Acknowledgements

**Technical Review**
William Priedhorsky, Robert Kraus Jr.

**Publication Editor and Designer**
Andrea Maestas

**Team Contributors**
Lennett Rendon
Stephen Schultz
Debbie Martinez
Ronnie Quintana

# Program Overview

# Innovation for our nation

*More than 90 LDRD researchers showcased their work at the ER Symposium and Poster Session in September 2008. LDRD Deputy Program Director Robert Kraus (right) visits a poster by Blas Uberuaga (left) and colleagues.*

**The vision of the LDRD program is to be the acknowledged cornerstone of NNSA's preeminence in national security science and technology.**

Established by Congress in 1991, the LDRD program is LANL's premier source of research and development support to address emerging mission needs. The LDRD program follows a strategic guidance derived from the missions of the U.S. Department of Energy, the National Nuclear Security Administration, and the Laboratory. The vision of the LDRD program is to be the acknowledged cornerstone of NNSA's preeminence in national-security science and technology. The goals for the program are to 1) Maintain the scientific and technical vitality of the NNSA Laboratories, 2) Enhance the laboratories' abilities to address future DOE/NNSA missions, 3) Foster creativity and stimulate exploration of forefront science and technology, 4) Serve as a proving ground for innovative concepts in research and development, 5) Support forward-thinking, potentially high-value research and development, and 6) Recruit and retain the best and brightest scientists and engineers.

In FY08, overall responsibility for the LDRD program at LANL rested with Michael Anastasio, Laboratory Director, and Terry Wallace, Principal Associate Director for Sciences, Technology and Engineering. Under their direction, William Priedhorsky, LDRD Program Director, and Robert Kraus Jr., LDRD Deputy Program Director managed the LDRD Program Office.

The LDRD program at LANL creates a free market for ideas that draws upon the bottom-up creativity of the Laboratory's best and brightest researchers. The combination of strategic guidance and free-market competition provides a continual stream of capabilities that strengthens LANL's capabilities in DOE's mission areas of Energy Security, Nuclear Security, Scientific Discovery and Innovation, and Environmental Responsibility.

## Program Structure

The LDRD program at LANL is organized into three program components with distinct institutional objectives: Directed Research (DR), flagship investments in mission solutions; Exploratory Research (ER), smaller projects that invest in people and skills; and Postdoctoral Research and Development (PRD), recruiting bright, qualified, early-career scientists and engineers.

The DR component makes long-range investments in multidisciplinary scientific projects in key competency or technology-development areas vital to LDRD's long-term ability to execute Laboratory missions. This component is directly tied to the strategic vision for the Laboratory, as articulated in the Science and Technology Grand Challenges. These challenges were set out in the Los Alamos National Security contract and refined in a Laboratory-wide workshop held in October 2006. In

*Pinaki Sengupta was one of 272 postdoctoral researchers funded by LDRD in FY08. Sengupta received a LANL Distinguished Performance Award for his contributions to quantum magnetism theory and received honorable mention for the 2008 Leon Heller Postdoctoral Publication Prize in Theoretical Physics*

**The LDRD program at LANL creates a free market for ideas that draws upon the bottom-up creativity of the Laboratory's best and brightest researchers.**

In FY09, the Laboratory will hold workshops and meetings to discuss the evolution of the Grand Challenges and their refinement for FY10, including a new Grand Challenge in engineering, "Intelligent Adaptive Engineered Systems."

The ER component consists of projects focused on a single discipline or capability. These projects primarily explore highly innovative ideas, often fundamental, in science and technology disciplines that underpin Laboratory programs. Exploratory Research projects focus on maintaining or developing competencies of the Laboratory staff in key strategic disciplines. The ER categories for FY08 were Nuclear Physics, Astrophysics and Cosmology; Materials Science; Earth, Environmental, and Space Physics; Chemistry and Chemical Sciences; Biological Sciences, Biosecurity, and Cognitive Sciences; High-Energy Density, Plasma, and Beam Physics; Atomic, Molecular and Quantum Physics; Engineering and Engineering Sciences; Energy Sciences, Technology and Engineering. Within these strategically defined categories, ER proposals are driven by staff initiative and selected with a strong emphasis on scientific innovation and creativity.

The PRD component of the program seeks to ensure the vitality of the Laboratory by recruiting early-career researchers. Through this component, the LDRD program funds postdoctoral fellows to work under the mentorship of PIs on highly innovative projects. The primary criterion for selection of LDRD-supported postdocs is the raw scientific and technical talent and performance of the candidate, with the exact specialty of the candidate a secondary factor.

## LANL' Science and Technology Grand Challenges (FY09)

***Challenges addressing science***

- Beyond the standard model
- Superconductivity and actinide science
- Complex systems
- Fundamental understanding of materials

***Challenges addressing mission***

- Carbon neutral fuel cycle
- Ubiquitous sensing
- Boost physics

***Overarching capability***

- Information science and technology

The key to managing science at Los Alamos lies in anticipating the mission's needs and ensuring the development of strategic capabilities. Today the nation faces an evolving set of threats to its environment and to its energy and information systems, threats that endanger national security. By investing in basic and discovery science and managing them properly, we can address those evolving threats and continue to fulfill our national-security mission.

- Terry Wallace

LANL Principal Associate Director for Science and Technology

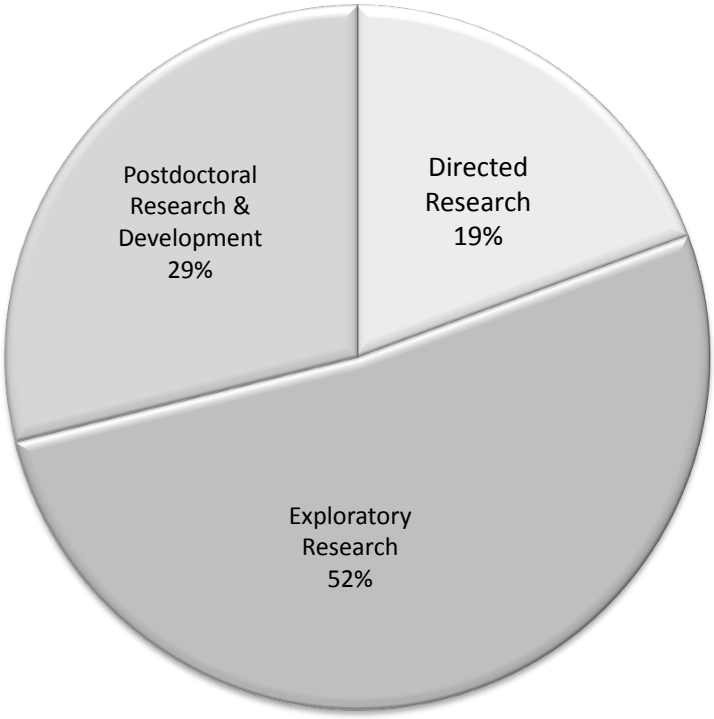


*Chart 1. Distribution of projects among the three components of the LDRD program in FY08. The total number of projects was 284.*

## The FY08 LDRD Portfolio

In FY08, the LDRD Program funded 284 projects with a total budget of $127 million. These projects were selected though a rigorous and highly competitive process, and were reviewed formally and informally throughout the fiscal year. The distribution of funding among the LDRD program components is shown in Chart 1.

### Directed Research

In FY08, the LDRD program funded 55 DR projects, which represented 60% of the program's research funds. DR projects can be funded up to $1M. The distribution of DR projects among the Grand Challenges is shown in Chart 2.

### Exploratory Research

Funded at the $175K to $300K level. The 147 ER projects funded in FY08 represented 33% of the programs research funds. The distribution of ER projects among the capability categories is shown in Chart 3.

### Postdoctoral Research and Development

A total of 82 PRD projects were funded though LDRD in FY08. Funded at $150K to $200K, this category represents 7% of the program's research funds.

# FY08 DR Portfolio

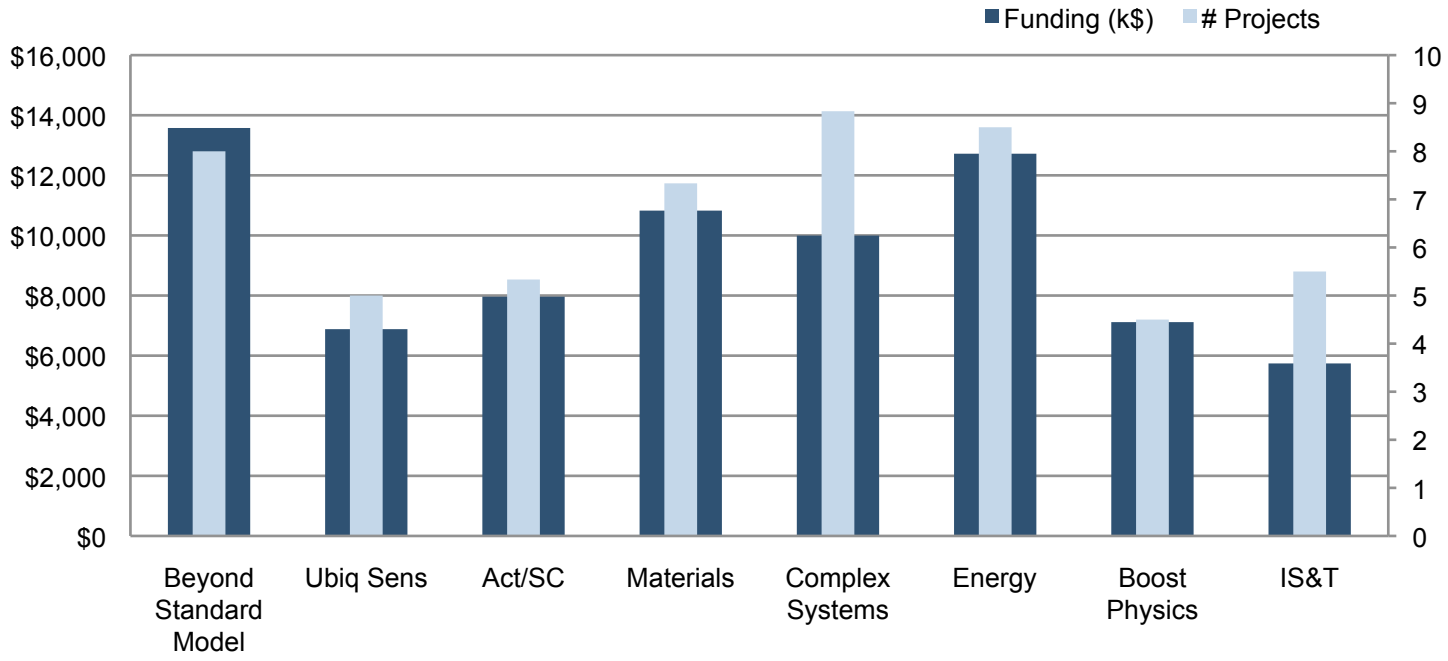


*Chart 2. Distribution of Directed Research (DR) projects among the Los Alamos Science and Technology Grand Challenges in FY08. There was a total of 55 DR projects.*

# FY08 ER Portfolio

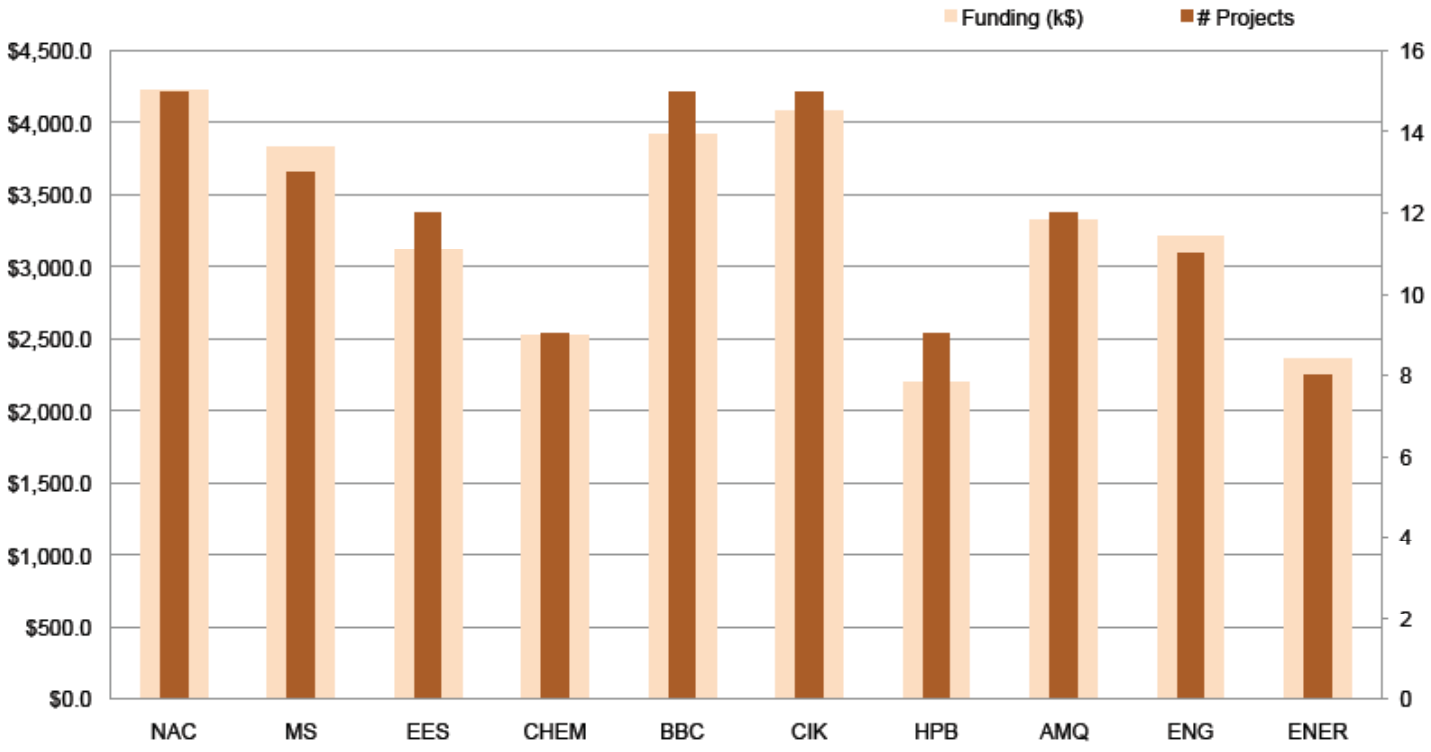


*Chart 3. Distribution of Exploratory Research (ER) projects among the ER Science and Technology Categories in FY08. There was a total of 147 ER projects.*

## "The Nation expects the Labs to provide a response to emerging national threats..."

Jamileh Soudah, NNSA LDRD Program Director

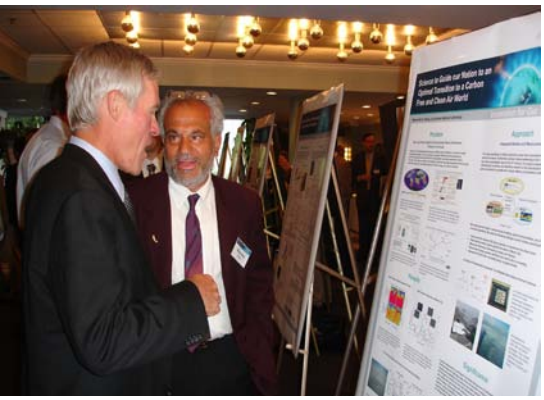

*Pictured above, LDRD researchers from LANL discuss their posters on Energy Security at the 2008 NNSA LDRD Symposium in Washington, DC.*

## Mission Relevance

The LDRD Program Office closely monitors all LDRD projects to ensure that they support the Laboratorys's national security missions. Principal investigators assess the roles of the projects in supporting the Laboratory's missions, and the LDRD Program Office reviews their assessments to determine the net fraction of LDRD investment that supports each DOE mission. Because LDRD is advanced research and development, at an early stage in the path from concept to application, it typically benefits more than one mission. The distribution of LDRD projects among DOE's national security missions is shown in Chart 4.

## Program Impacts

The LDRD program is a key resource for addressing the long-term science and technology goals of the Laboratory, as well as for enhancing the scientific capabilities of Laboratory staff. Though careful investment of LDRD resources, the Laboratory attracts programmatic resources, recruits and retains excellent scientists and engineers, and prepares to meet evolving national needs. The impacts of the LDRD program are particularly evident in the number of publications, patents, and disclosures resulting from LDRD-funded research; the number of postdoctoral candidates supported by the program; and the number of awards received by LDRD researchers.

### Publications

The LDRD program produces a large volume of high-quality scientific contributions relative to its portion of the Laboratory's budget (typically 6.5%, and not to exceed 8%). Through numerous publications, the LDRD program helps the Laboratory maintain a strong presence and scientific reputation in the broader scientific community. In FY08, LDRD researchers generated 307 peer-reviewed publications. This accounted for 17% of the Laboratory's publications. Of the Laboratory's top 100 cited publications, 35% resulted from LDRD-funded projects.

### Patents and Disclosures

A strong indication of the cutting-edge nature of the research funded by the LDRD program is the contribution the program makes to the intellectual property of the Laboratory. LDRD projects consistently generate at least one quarter of

# FY08 Mission Impact

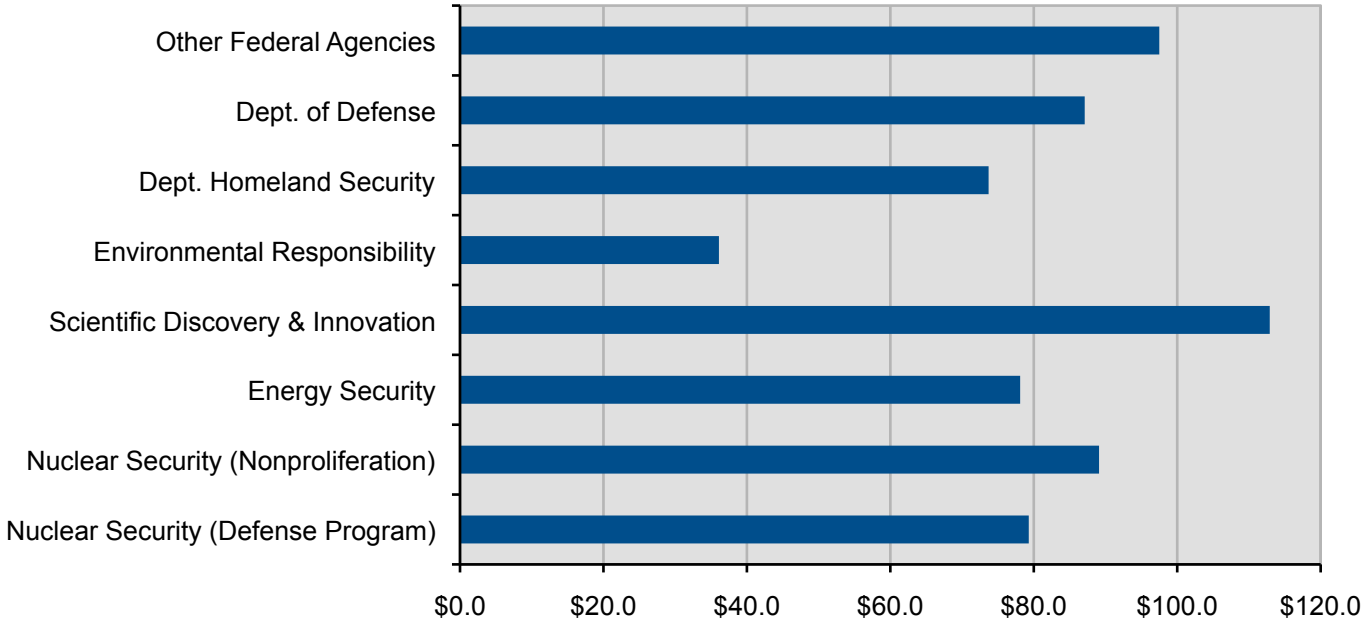


*Chart 4. Distribution of LDRD projects among DOE's national security missions in FY08. LDRD projects may support more than one mission, hence the total is more than 100% of the program's total research funds.*

the patents awarded to the Laboratory. In FY08, LDRD-supported research resulted in five patents, accounting for 26% of the Laboratory's patents, and 26 disclosures, which accounted for 29% of the Laboratory's disclosures.

### Postdoctoral Support

In an increasingly competitive job market, the Laboratory must foster an environment that attracts the best talent so that it may be applied to solving national security problems. The LDRD program remains an important vehicle for recruiting the best and brightest researchers to the LANL, where they become innovators and scientific leaders. In FY08, LDRD supported 272 postdocs (in-full or in-part), accounting for 57% of the Laboratory's postdocs. In FY08, the Laboratory converted 28 postdocs converted to full-time Technical Staff members; LDRD funded 64% of those conversions.

# Success Stories

# INNOVATION

Another success story from the NNSA Laboratory Directed Research and Development Program at Los Alamos National Laboratory

FOR OUR NATION

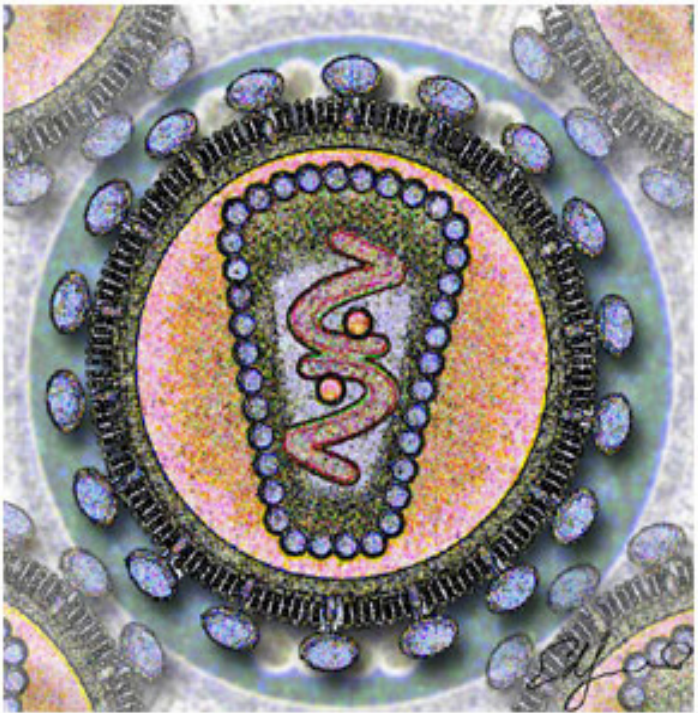

Stylized rendering of a cross-section of HIV.

## YOUR LDRD INVESTMENT

In a fight against a pandemic that has killed more than 25 million people, LDRD Principal Investigator Bette Korber and colleagues have designed three vaccines targeting HIV.

Korber's AIDS research has been funded in-part by LDRD since 2005. She currently leads a Directed Research project titled, "Understanding Drug Resistance and Co-inefctivity in HIV and TB Infections."

## Curing AIDS

Scientists are finding the cure to stop a virus that has killed more than 25 million people. Research at the Lab targeting the immune response to HIV and viral mutation might stop the pathogen that causes AIDS.

Although current Human Immunodeficiency Virus (HIV) treatment hinders the infection rate and delays death, there is no HIV vaccine or cure available for the Acquired Immune Deficiency Syndrome (AIDS).

LANL researcher Bette Korber and her team are solving challenging problems regarding HIV evolution and transmission and, importantly, how the human immune system reacts to the virus. Korber's team is designing three vaccines to target this rapidly mutating virus. Animal tests are underway, with promising results and human trials will begin soon. These vaccines might finally deal a lethal blow to the AIDS virus.

"HIV expands and contracts like an accordion," Korber, recipient of acclaimed awards, told an audience during a Los Alamos lecture. "The mystery is why we can't clear it with our immune response."

The HIV virus's mechanisms make it extraordinarily good at avoiding triggering an immune response, making it nearly impossible to fight the infection. Korber's team's vaccine model is based on a mixture of synthetic proteins that address the virus's evasive nature. Not only does the HIV-1 virus mutate quickly, increasing its drug resistance, but its evolution affects the virus's sequence. The virus is also protected by a cloak of sugar molecules that prevents antibodies from blocking the HIV proteins used to invade the cell.

In mid-October, nine hundred experts convened at the international AIDS vaccine conference in South Africa. Doubts were expressed about whether a vaccine is on the horizon. "Fundamentally we don't understand enough about the human immune system and we don't know how the immune system deals with HIV," said Lynn Morris, conference co-chair.

Korber's HIV immunity research might quickly turn the tides.

# INNOVATION

Another success story from the NNSA Laboratory Directed Research and Development Program at Los Alamos National Laboratory

FOR OUR NATION

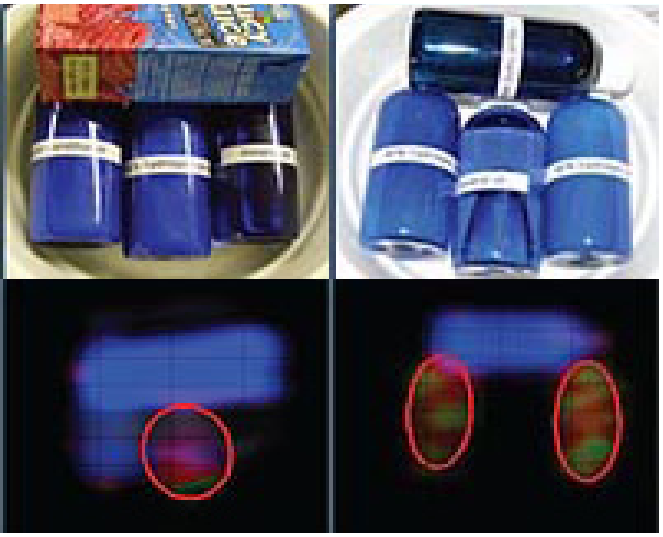

The screen of the MagViz unit displays each tray of liquid or gel items, with the target materials highlighted by color according to potential risk.

## YOUR LDRD INVESTMENT

Ultra-low-field MRI technology developed with funding from LDRD is now being used in MagViz – a revolutionary scanning machine that distinguishes potential-threat liquids from harmless shampoos and sodas screened at airport baggage checkpoints.

Originally developed for brain and medical imaging, the ULF-MRI technology is being applied to MagViz though a large grant from the U.S. Department of Homeland Security.

# MagViz Detects Liquid Explosives

The U.S. Department of Homeland Security is testing new airport baggage screening technology that differentiates between different types of liquids, gels, and lotions – everything you want to carry on the plane but no longer can. Currently, U.S. travellers must pack toothpaste tubes, shampoo bottles, and cosmetics following the "3-1-1 rule," with containers holding no more than three ounces of fluid sealed in a single one-quart, plastic zip-lock bag. New technology developed by Los Alamos researchers may make the plastic-bag component of travel a distant memory.

Based on research of ultra-low-field Magnetic Resonance Imaging (ULF-MRI), the new MagViz technology grew out of a project to make MRI images of the human brain at magnetic fields 100,000 times smaller than a typical hospital MRI machine. Screeners using the MagViz system will be able to differentiate and identify many materials that may be packaged together or separately. The physics that underlies how MRIs differentiate between the tissue types in the brain (i.e. white and gray matter) is the same as that used by MagViz to tell the difference between safe liquids and threat substances. This effort has successfully completed a proof of concept of an extremely sensitive screening technology that scans magnetic changes of individual materials at the molecular level.

The goal for the airport screening technology is reliable, high-throughput detection of liquids, in a form that is non-contact, non-invasive, requires no radiation, produces no residue, and uses the existing airport security portal. The long-range goal for MagViz is to develop the capability to screen carry-on bags without requiring the "3-1-1" bag system. While such a goal is several years in the future, a more near-term goal for MagViz is to screen materials in the presence of or through virtually any packaging, including leather, cardboard, wood, clothing, and even metallic containers.

# INNOVATION

Another success story from the NNSA Laboratory Directed Research and Development Program at Los Alamos National Laboratory

FOR OUR NATION

Detectors such as this infrasound array operated by LANL have helped detect meteors and missiles and have played a key role in helping scientists determine the frequency by which giant meteors enter Earth's atmosphere.

## YOUR LDRD INVESTMENT

Missiles and meteors are often silent; some are designed to be concealed, but LDRD Principal Investigator Douglas ReVelle perfected a method to detect these quiet dangers.

ReVelle's research on bolide infrasound was partly funded by an LDRD Exploratory Research project titled "Infrasound Signatures of Ballistic Missiles."

## Hear No Evil

Los Alamos National Laboratory (LANL) scientist Doug Revelle perfected a method to detect infrasonics—sound waves below the range of human hearing—produced by meteors, volcanoes and man-made explosions.

This program—the only one of its kind in the nation—operates six infrasonic-sensor arrays in western states. The arrays are routinely used to monitor White Sands Missile Range test explosions, NASA Space Shuttle launches and reentries, and geological changes.

ReVelle and his collaborators have documented the explosions of hundreds of bolides (meteors) in Earth's atmosphere, as well as other manmade explosions in the atmosphere. His team uses an array of sensitive microphones that were originally developed to listen for distant clandestine nuclear weapons tests.

The researchers also use radar, video cameras, seismic sensors and radio devices. Every month the scientists observe at least one meteor that can produce infrasound detectable at the ground—a flux at least 100 times higher than earlier observations had suggested.

"Infrasound can also be used to observe large man-made chemical and nuclear explosions," ReVelle says. "Although such explosions can be intentionally hidden from satellites, their 'sound effects' can still give them away."

The ultimate value of these detections is that they can be combined with satellite data to forecast threats.

When a meteor enters the atmosphere—or when a large explosion is detonated—it creates a sound or pressure wave that during its propagation eventually falls below the range of human hearing. This infrasonic wave travels through the atmosphere and can be detected by special pressure sensing microphones set up in an array at ground-level. By examining the arrival time of the sounds at different stations and the frequency of the infrasonic boom, researchers are able to precisely pinpoint the location of the explosive source and determine the amount of energy that created it.

# INNOVATION

Another success story from the NNSA Laboratory Directed Research and Development Program at Los Alamos National Laboratory

FOR OUR NATION

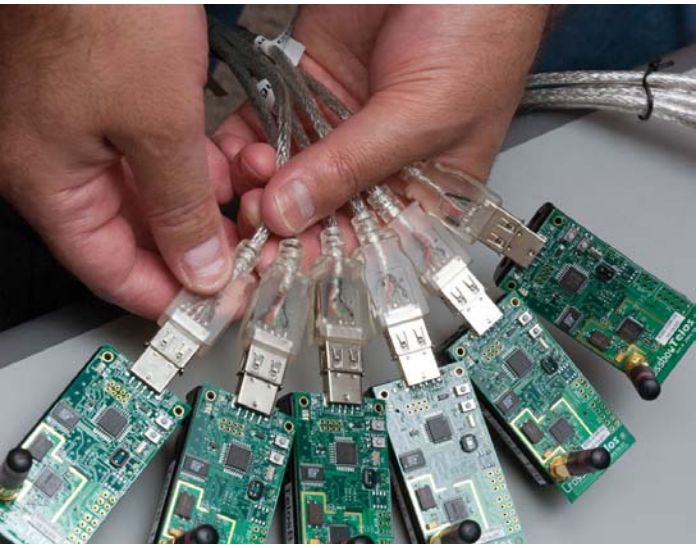

Like cell phones, wireless sensor networks depend on small, independently powered devices, often called motes, to communicate.

## YOUR LDRD INVESTMENT

LDRD Principal Investigator Sami Ayyorgun's self-organizing communication scheme drives the tiny "motes" of a wireless network to new heights of performance, increasing their versatility in defense, disaster, environmental, and industrial applications.

Ayyorgun's research is funded though an LDRD Postdoctoral Research and Development project titled "Self-Organizing Wireless Ad-Hoc and Sensor Networks with Functional Guarantees."

## Networks of the Future

The picture of a future with wireless sensor networks— webs of sensory devices that function without a central infrastructure— is coming into sharper focus through the work of Laboratory computer scientist Sami Ayyorgun.

Proponents of this new technology see a world with deployments to improve a wide range of operations. Engineers could wirelessly monitor miles of gas and oil pipelines stretching across arid land for ruptures, damage, and tampering. Rescue workers might detect signs of life under the rubble of a collapsed building after an earthquake, thanks to a network of sensors inside the structure. Armed forces could keep an eye on a combat zone or a vast international border via a sensor network that promptly could provide alerts of any intrusion or illicit trafficking.

"It's not easy to envision the impacts that sensor networks will make, both socially and economically," Ayyorgun said. "Like many other researchers, I think they are likely to rival the impact that the Internet has made in our life."

Ayyorgun has developed a new communication scheme that brings the reality of these and other applications a step closer. He has shown for the first time that concurrent gains in many measures of performance are possible, including connectivity; energy; delay, or time it takes for data to be transported; throughput, or the amount of data the system can handle at once; system longevity; coverage; and security.

In recognition of the multifaceted improvements Ayyorgun's research makes on state-of-the-art technology in this field, his recent paper, "Towards a Self-organizing Stochastic-Communications Paradigm for Wireless Ad-hoc/Sensor Networks," has been nominated for the Best-Paper Award from a pool of more than 250 manuscripts at the International Conference on Mobile Ad-hoc and Sensor Systems of the Institute of Electrical and Electronics Engineers.

# INNOVATION

Another success story from the NNSA Laboratory Directed Research and Development Program at Los Alamos National Laboratory

FOR OUR NATION

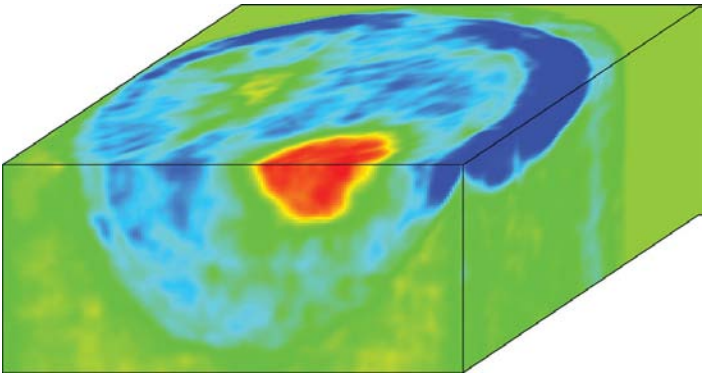

This view of a 3D ultrasound CT image was obtained, from a patient, using KCI's prototype device. It shows a cross section of the breast near the chest wall (top of image) and a vertical cross section through the remainder of the breast. A tumor (red) is visible near the chest wall.

## YOUR LDRD INVESTMENT

LDRD Principal Investigator Lianjie Huang and collaborators have developed a safer, more comforatable, inexpensive and accurate way to detect early-stage cancer by using sound waves that replace dangerous x-ray technology used for mammograms.

Huang's research is funded though an LDRD Exploratory Research project titled "Seeing Undetectable Cancers with Time-Reversed Ultrasound."

## Better Breast Cancer Detection

Women may eventually have access to safer, more-comfortable, and more-accurate breast cancer scans. Currently, the only routine breast-screening technology is mammography, which uses low-dose x-rays to scan through tissue and capture on film a two-dimensional (2D) projection of the breast.

Los Alamos scientist Lianjie Huang, in collaboration with researchers from Karmanos Cancer Institute (KCI), London's Imperial College, and Stanford University, has developed a better way, producing a three-dimensional (3D) image, using not x-rays, but sound waves.

The technique, called ultrasound computed tomography (ultrasound CT), uses a prototype scanning device built at KCI. A woman's breast is immersed in water and surrounded by a ring-shaped array of hundreds of ultrasound elements. Each element emits ultrasound waves and then receives waves that are scattered from the soft tissue. The array is moved incrementally down the entire breast, gathering data at each step.

A suite of newly developed computer algorithms converts the stepwise ultrasound data into a series of high-resolution, 2D images and then turns the series into a single 3D image. The technology actually obtains three kinds of images, corresponding to the speed, attenuation, and reflectivity of the waves. The wealth of information allows ultrasound CT to single out cancerous lesions more accurately than can today's mammography.

Ultrasound CT has the potential to detect cancer in its earliest stages. And since it is both safer (no ionizing radiation) and more comfortable (there is no need to compress tissue as there is in mammography), it should prove an attractive alternative for future breast cancer screening.

# INNOVATION

Another success story from the NNSA Laboratory Directed Research and Development Program at Los Alamos National Laboratory

FOR OUR NATION

Johnson examines the cracks and other defects buried within a translucent plastic box.

## YOUR LDRD INVESTMENT

LDRD Principal Investigator Paul Johnson and his team are finding ways to use time-reversed soundwaves to locate defects inside mechanical parts, as well as locate vibrational tremors within the earth. Tremors may prove to be the key to predicting when and where major earthquakes occur.

Johnson's research is funded through an LDRD Directed Research project titled "Image Reconstruction with Time-Reversal Mirrors."

## Retrovision

Retrace your steps. It's a good way to find lost items: your glasses, your keys . . . the TV remote. It can also be a good scientific way to find things. Just ask Paul Johnson.

The Los Alamos geophysicist heads a team that uses time reversal—a technique that relies on the ability of waves to retrace their steps to their source—to find defects inside mechanical parts or to locate the sources of earthquakes deep underground.

Time reversal is quite different from most techniques that use waves as locators. By comparison, time reversal is a no-brainer, as Johnson points out. The waves that leave a source, travel through a medium, and that arrive at any number of sensor locations are recorded during a specified time interval. A set of time-reversed signals is then created by "flipping" the recorded signals: the last wave recorded becomes the first wave in the time-reversed signal. These new signals are then "broadcast" back into the medium from the same positions where they were recorded. Some time after the broadcast starts, major portions of the time-reversed waves converge back at the source—as if one had filmed the circular waves produced when a pebble is dropped into a pond and then had run the film backwards.

If the source location is unknown, time reversal can usually find it. Moreover, if the recording captures the higher-frequency waves—those with short-enough wavelengths—time reversal can often reconstruct the source's physical extent and evolution in time with remarkable detail.

Time reversal achieves this great advantage over other wave-locator methods by using the information contained in all of the waves that reach a sensor during the recording interval, including waves of different types, waves that come directly from the source, and waves reflected from boundaries.

Johnson's team is finding lots more applications for this technique. The method is currently being developed as one of the many diagnostic techniques used to inspect weapons and could easily transfer to industry for examining machine parts.

# INNOVATION

Another success story from the NNSA Laboratory Directed Research and Development Program at Los Alamos National Laboratory

FOR OUR NATION

Cantaloupe seedlings with Take-Off (left) outstrip their same-age but untreated neighbors on the right.

## YOUR LDRD INVESTMENT

The global agricultural system is struggling to sustain growing populations. To meet this challenge, LDRD Principal Investigator Pat Unkefer and her team developed a revolutionary product that helps plants grow faster, mature earlier and leave fewer contaminants in the ground.

The success of "Take-Off" is rooted in several LDRD Directed and Exploratory Research projects - one as early as 1984.

## A Natural "Take-Off"

Growing more and better food crops has traditionally meant pouring on the nitrogen fertilizer, which is expensive to use and pollutes waterways through runoff. This is not a good situation, especially now when the world needs to add biofuel production to a global agricultural system that is struggling to feed rapidly growing populations. Can we cost effectively produce more food and biofuel and do so without further degrading the environment?

Pat Unkefer and her team in Bioscience Division say yes, and they've got a product that proves it.

Take-Off, licensed by Biagro Western, is a metabolite, an amino acid that coordinates aspects of a plant's metabolism. It increases both the amount of carbon dioxide that the plant converts to carbohydrates and the amount of nitrogen it draws from the soil. When Take-Off is sprayed on crops, they grow faster, mature earlier, and leave less nitrogen fertilizer in the ground to contaminate water supplies. Plants treated with Take-Off also use more of their nitrogen for growth instead of storing it in their tissues.

Unkefer and her team discovered the metabolite—2-oxoglutaramate—while studying plant metabolism. They learned they could stimulate growth, without the use of hormones, by increasing a plant's supply of this naturally occurring substance.

Synthesizing 2-oxoglutaramate proved prohibitively expensive, however, so the team identified a cheaper compound of similar structure (an analog) that replicates the metabolite's function. It is that analog that is now on the market as Take-Off. The analog is biosynthesized and biodegradable and is thus a very eco-friendly technology, certifiable even for organic farming.

Take-Off is now being used commercially on wheat, barley, and grapes and on the biodiesel crop canola. It is significantly increasing overall yields, and is being developed for additional crops as well. Farmers are also realizing greater profitability, thus increasing their own sustainability.

# INNOVATION

Another success story from the NNSA Laboratory Directed Research and Development Program at Los Alamos National Laboratory

FOR OUR NATION

Sanbonmatsu stands inside his ribosome simulation, the largest biomolecular-dynamics simulation to date.

## YOUR LDRD INVESTMENT

LDRD Principal Investigator Kevin Sanbonmatsu and collaborators developed the largest biological simulation ever. New medicines that save lives by combating drug-resistant bacteria are just one of the results.

Sanbonmatsu's research on ribosomes is funded though two LDRD Exploratory Research projects. A third project titled "Using Small Molecules to Control RNA Conformations" was awarded funding in Fiscal Year 2009.

## Nanotech Discovery Saves Lives

Nanoscience—the study of things of "little" importance, one might quip—led to the largest biological simulation ever, which helped Los Alamos scientists decode genetic information. The methodology paved the way for developing new antibiotics and modeling the entire protein synthesis process—a process crucial to saving lives.

The body comprises enumerable nanofactories called ribosomes that work overtime to keep us alive. In each of our trillions of cells, a million ribosomes create proteins—chains of amino acids—that are the basis of life. A quintillion protein factories rebuild our entire body every seven years.

Ribosome study is nothing new but, "only now we can use supercomputers to investigate, in atomic detail, how this very complex machine really works," says Los Alamos National Laboratory theoretical biologist Kevin Sanbonmatsu. "It has been the holy grail and now our team at Los Alamos is making it happen."

Sanbonmatsu and Theoretical Biology and Biophysics Group Leader Chang-Shung Tung created the first atomic-level computer model of a single ribosome.

Sanbonmatsu and his team hope their 3D simulations can solve conflicting interpretations about ribosomes. Secondly, this technology will provide information required to design new medicine to combat drug-resistant bacteria, such as the prevalent Staph (Staphylococcus aureus), which causes many diseases and fatal infections such as food poisoning.

Nanoscience enables improvements in medical diagnostics and drug delivery, bioscience, chemical sensing, military platforms, and nuclear defense systems and even helped Los Alamos National Laboratory (LANL) create a supreme superconductor. Sanbonmatsu's team is also preparing a new ribosomal simulation code for Roadrunner, LANL's world's most powerful computer.

# INNOVATION

Another success story from the NNSA Laboratory Directed Research and Development Program at Los Alamos National Laboratory

FOR OUR NATION

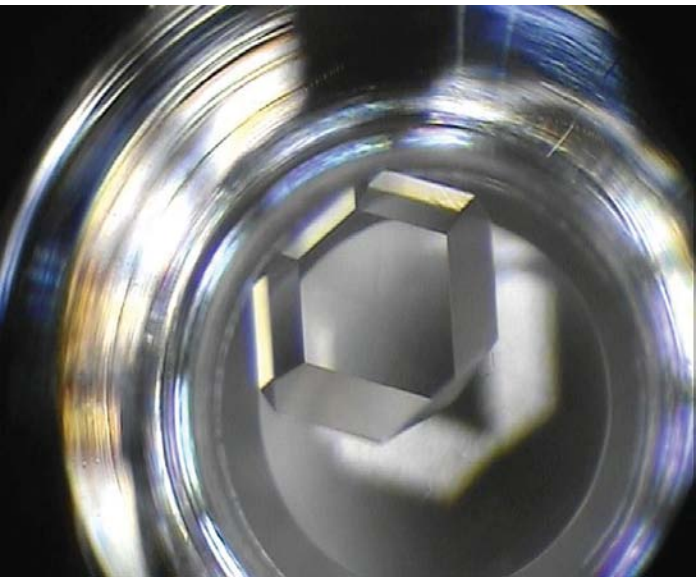

This crystal may help scientists produce more biofuel.

## A Sweet Reaction

Recent studies done at Los Alamos on an enzyme that turns one type of sugar into another have yielded some unexpected insights into the reaction.

The enzyme xylose isomerase (XI) can convert the sugar glucose into fructose and is used in manufacturing high-fructose corn syrup for food products. Similarly, XI can convert the sugar xylose into xylulose, which can be used in producing different kinds of biofuels. Understanding those conversion reactions in detail may aid efforts to make the enzyme work better and hence contribute to more-efficient production of fuel and food products.

Xylose has five carbon atoms and one oxygen atom bonded into a hexameric ring, with several hydrogens and hydrogen-oxygen pairs dressing the carbons. To convert from xylose to xylulose, the enzyme helps the ring to open and then helps move two hydrogen atoms from the second to the first carbon in the now-linear molecule.

Researchers used the Los Alamos Protein Crystallography Station (PCS) for their studies. They collected neutrons diffracted from a crystal of XI that had been soaked in a solution of xylose and that the enzyme had converted to xylulose. The neutron crystallographic data revealed the location and charge states (positive or negative charges) of atoms in the XI-xylulose complex. When the results were compared with the team's studies of XI alone, it became possible to see how the atoms had been rearranged during the reaction.

In particular, the researchers discovered that a water molecule held in the active site of XI loses a hydrogen, whereas the enzyme itself acquires one during the shuffling of atoms. The finding, which suggests the water may play some role in the conversion reaction, may help researchers differentiate among several possible reaction mechanisms.

Paul Langan, who built the PCS with Benno Schoenborn, led the Los Alamos team. The work was published as a Rapid Report in the journal *Biochemistry* (Vol. 47, p. 7595, 2008) and listed as a "Hot" article.

### YOUR LDRD INVESTMENT

LDRD Principal Investigator Paul Langan and colleagues are achieving a greater understanding of an important enzyme that may improve production of biofuels and food products.

Langan's research is largely funded by LDRD through a Directed Research project titled, "One-Step Biomass Conversion: Looking to Nature for Solutions to Energy Security."

# INNOVATION

Another success story from the NNSA Laboratory Directed Research and Development Program at Los Alamos National Laboratory

FOR OUR NATION

Tom Vestrand (left) and Przemek Wozniak, with the RAPTOR telescope that recorded the rebrightening event in 2006.

## YOUR LDRD INVESTMENT

Keeping our nation at the forefront of robotic, fast response astronomy, LDRD Principal Investigator Tom Vestrand and colleagues have constructed the RAPTOR - a robotic telescope array that patrols the night sky, detecting anomalies without human intervention.

Vestrand's work is funded though a Directed Research project titled, "Thinking Telescopes: Pursing a New Paradigm for Discovery in Observational Science."

## Thinking Telescope

On the night of February 6, 2006, Los Alamos astrophysicist Przemek Wozniak was awakened by a cell-phone call from RAPTOR, the small robotic optical telescope array on Fenton Hill, about 30 miles from Los Alamos in northern New Mexico's Jemez Mountains. RAPTOR had found something strange—a rapidly rising light signal coming from the position of a very short gamma-ray burst detected and located. These bursts announce the birth of stellar-size black holes and are the most powerful events since the Big Bang.

Following its own logic, RAPTOR recorded the light signal every 30 seconds and noted a doubling in brightness over four minutes—an afterglow that was rising rather than fading. Running real-time analysis software, RAPTOR decided to report the anomaly to a human.

"This was a first, an autonomous optical telescope finding an anomaly on its own with no human intervention," said Tom Verstrand. "If humans had been in the loop they would have said, as we did, 'Gamma-ray bursts don't act like that. Forget it.' And RAPTOR wouldn't have found anything."

RAPTOR's observation of that spectacular "rebrightening" hints that a gamma-ray burst can sometimes "turn itself on" a second time, emitting intense visible light but no gamma rays—an intriguing possibility.

For the RAPTOR team, the discovery had a broader significance. It was proof that RAPTOR has a mind of its own—truly a thinking telescope system.

The Los Alamos team is working to make RAPTOR a "discovery engine" for astronomy, scanning the entire night sky frequently, screening a hundred million visible objects and alerting us to something important. The same autonomous technology that detects eruptions at the edge of the universe can be used to detect objects orbiting the earth, and will contribute to the security of our space infrastructure.

# FY08 Project Directory

# Project Directory



## Chemistry & Material Sciences

### Directed Research


**40** **Strongly Correlated Electrons: Duality and Implications**
*Cristian Daniel Batista*

**44** **Novel Inclusion Compounds for Hydrogen Storage**
*Yusheng Zhao*

**47** **Correlations and Control of Properties of Metallic U and Pu**
*Jeremy Neil Mitchell*

**52** **Metamaterials for Threat Reduction Applications: Imaging, Signal Processing, and Cloaking**
*Antoinette Jane Taylor*

**55** **Coexistence of Magnetic and Superconducting Electrons in Strongly Correlated Matter**
*Joe David Thompson*

**60** **Physics of Helium Retention in Palladium/Tritum Systems**
*Douglas Joseph Safarik*

**64** **Quantum Control in Condensed Media for Studies of Direct Optical Initiation of Explosives**
*David Steven Moore*

**67** **Biomimetic Hydrogen Production by Photoinitiated Transition Metal Catalysis**
*Richard Brian Dyer*

**71** **Hot Spot Physics and Chemistry in Energetic Materials Initiation**
*Dana Mcgraw Dattelbaum*

**75** **Design, Synthesis, and Theory of Molecular Scintillators**
*Rico Emilio Del Sesto*

**78** **Ultrafast Nanoscale XUV Photoelectron Spectroscopy**
*George Rodriguez*

**80** **Advanced Fuel Forms with Microstructures Tailored to Naturally Induce Fission Product Separation During Service**
*Kurt Edward Sickafus*

**84** **Nanoscale Fluctuations in Multifunctional Materials**
*Alexander V Balatsky*

**89** **Structure and Bonding in Actinide Oxides**
*David Lewis Clark*

**96** **Dynamics of the Onset of Damage in Metals Under Shock Loading**
*Aaron Clyde Koskelo*

**103** **Advanced Actinide Separations in Alkaline Media for Spent Nuclear Fuel and Defense Materials Processing**
*Gordon Dennis Jarvinen*

**110** **Biological Effects of Molecularly Engineered Nanomaterials**
*Andrew Paul Shreve*

**115** **New Classes Of Materials For Gamma-Ray and Neutron Detection**
*Darryl Lyle George Smith*

**120** **Advancing the Chemistry Material Science and Theoretical Understanding of Actinides**
*Albert Migliori*


### Exploratory Research


**128** **Improved Length Scaling in Accelerated Molecular Dynamics Methods**
*Arthur Ford Voter*

**132** **Coulomb Mechanisms for Ion Damage in Insulators in the Electronic Stopping Regime**
*Cynthia Jane Reichhardt*

**134** **Synthesis of Nanowire Heterostructures for Strain-Controlled Bandgap Engineering**
*Samuel Thomas Picraux*

**137** **Synthetic Decoys for Biothreat Agents**
*Rashi S Iyer*

**140** **Magnetic Resonance Force Microscopy Studies of Ferromagnets on a Nanometer Scale**
*Roman Movshovich*

**143** **Controlling Oxidation-States in Actinide-Oxides through Crystal Lattice Pinning**
*Quanxi Jia*

**145** **Tunable Infra-Red Chromophores through N-Type Doping of Wide-Gap Semiconductor Nanocrystals**
*Sergei A Ivanov*

**148** **Non-Precious Metal Nanocomposites for Fuel Cell Catalysis**
*Piotr Zelenay*

**152** **Detection of Respiratory Infection by Scent**
*Jurgen G Schmidt*

**155** **Spins in Organic Semiconductors**
*Brian Keith Crone*

**157** **Strain-induced novel physical phenomena in epitaxial ferroic nanocomposites**
*Quanxi Jia*

**160** **Genetically Engineered Polymer Libraries**
*Jennifer Martinez*

**163** **Probing Unconventional Superconductivity in Heavy Fermion Thin Films**
*Vladimir Matias*

**166** **Photocatalytic Materials Based on Quantum Confined Semiconductor Nanocrystals**
*Milan Sykora*

**170** **Novel Materials for Gamma-Ray Detection based on Nano-Engineered Semiconductor Nanocrystals**
*Richard Daniel Schaller*

**172** **Parallel-Replica Dynamics Study of Tip-Surface and Tip-Tip Interactions in Atomic Force MicrosCopy and the Formation and Mechanical Properties of Metallic Nanowires**
*Arthur Ford Voter*

**176** **Hierarchical Assembly of Porous Materials: Obeying Bio-Inspired Allometric Scaling Laws**
*Michael Timothy Janicke*

**180** **Nanobiomaterials: Building New Nanoarchitectures Using Biomolecular Scaffolds**
*Jennifer Martinez*

**185** **Understanding the Process of Intercalation Using Stable Isotope Labeled Polyaromatic Hydrocarbons (PAHs) and Oligomeric DNA; the Quantitation of Weak Bonding in DNA.**
*Louis A Silks III*

**189** **Development of Redox Affinity Materials for the Separation of Carbon Nanotubes into Pure Chiral Fractions**
*Stephen K Doorn*

**195** **Nanocomposite Thin Films for Surface Assisted Mass Spectrometry**
*Andrew Martin Dattelbaum*

**200** **Use of Strain Engineering to Tune the Physical Properties of Nanoscale Metal-Oxide Films**
*Quanxi Jia*

**205** **Improved Molecular Catalysts for Water Splitting**
*Reginaldo Cesar Rocha*

**211** **Shedding Light on the Mechanical Unfolding of Individual Proteins**
*Peter Marvin Goodwin*

**215** **Nanoscale Textured Composite Energetic Materials**
*Steven Joseph Buelow*

**220** **Visualization Applied to Electronic Properties of Novel Superconductors**
*Alexander V Balatsky*

**225** **New High-Nitrogen Polydentate Ligands for Actinide Separations**
*David Lewis Clark*

**228** **Integrated Multiscale Simulation for Advanced Nuclear Fuel**
*Francis L Addessio*

## Postdoctoral Research & Development

**232** **Lifting the Quantum Critical Conundrum**
*Joe David Thompson*

**235** **Synthesis of Molecular Actinide Nitrides**
*David Lewis Clark*

**238** **Accelerated Molecular Dynamics at Complex Interfaces**
*Arthur Ford Voter*

**241** **A Chemical Route to Integrate Carbon Nanotubes into Microelectromechanical Systems**
*Quanxi Jia*

**243** **Flexible Plastic Electrodes for Cheap Solar Cells**
*Quanxi Jia*

**245** **Molecular Actinide Alkylidene Complexes**
*Jaqueline Kiplinger*

**248** **Superconductivity in Non-Centrosymmetric Materials**
*John Singleton*

**252** **Multifunctional Copper-Carbon Nanotube Nanocomposites**
*Amit Misra*

**255** **Multiscale Simulations for Cascade Overlap in Irradiated Materials**
*Arthur Ford Voter*

**258** **Ultrafast Non-equilibrium Physics of the Fractional Quantum Hall System**
*Antoinette Jane Taylor*

**260** **Time-Dependent Density Functional Theory for Ultrafast Optical Phenomena in Strongly Correlated Electron Materials**
*Jian-Xin Zhu*

**263** **Sensitization of Lanthanide Ion Fluorescence Using Nanocrystal Quantum Dots**
*Jennifer Ann Hollingsworth*

**266** **Chemically Synthesized Germanium Nanocrystals for Applications in Solar-Energy Conversion**
*Victor Ivanovich Klimov*

**268** **Molecular Level Investigation of Tunable Energetic Mixtures**
*David Steven Moore*

**270** **Synthesis, Chemistry and Theoretical Studies of 5f-Element Hydride Complexes**
*Jaqueline Kiplinger*

**273** **First-Principles-Based Equations of State Including Multi-Phase Chemical Equilibrium**
*Milton S Shaw*

**276** **Study of Hybrid Semiconductor/Molecular Systems for Photo-production of Hydrogen**
*Andrew Paul Shreve*

**278** **Structure-Property Relationship for Strained One Dimensional Ferroelectric Nanostructures**
*Quanxi Jia*

**280** **Synthesis and Characterization of Novel Metal-Organic Frameworks for Hydrogen Storage**
*Amr I Abdel-Fattah*

**282** **Semiconductor Nanowire Heterostructures**
*Samuel Thomas Picraux*

**284** **Size Effects in Nanoscale Ferroelectric Thin Films**
*Quanxi Jia*

**288** **Fundamental Oxygen Reduction Reaction Studies at High pH**
*Brian Pivovar*

**291** **Effects of Length Scale on the Fracture Behavior of Ultra High Strength Nano-composite Materials**
*Amit Misra*

**295** **Biological and Chemical Sensor Design Using Linearly-Scaled TD-DFT Methods**
*Anders Mauritz Niklasson*

**297** **Ultrafast Dynamics of Novel Magnetic Materials by Time Domain Spectroscopy**
*Antoinette Jane Taylor*

**302** **High P-T Synthesis of Superhard Carbon Nitride from Graphite-Like Precursors**
*Yusheng Zhao*

**304** **Studies of Sub-Micron Ferromagnetic Particles Using Magnetic Resonance Force Microscopy**
*Roman Movshovich*

**308** **Interface-Governed Behavior of Nano-Layered Metallic Composites**
*Richard Hoagland*

**311** **Ion Synthesis of Novel SiGe Structures**
*Michael Anthony Nastasi*

**315** **Searching for New Uranium Based Superconductors**
*Joe David Thompson*

**318** **Multiscale Modeling of Irradiation-induced Defect Processes in High-Cr Ferritic Steels**
*Srinivasan G Srivilliputhur*

**322** **High Efficiency Carbon Nanotube-$TiO_2$ Nanostructured Solar Cells**
*Quanxi Jia*

**325** **Theoretical Investigations of Plastic Deformation in Energetic Materials**
*Thomas Dan Sewell*

**330** **Structure and Function of Human Mineralised Tissue**
*John G Swadener*

**332** **Vibrational Features and Quantum Transport in Molecular Electronics**
*Sergei Tretiak*

**334** **Lanthanide Main-Group Element Multiple Bonds**
*Jaqueline Loetsch Kiplinger*

## Environmental & Biological Research

### Directed Research

**340** **High-Resolution Physically-Based Model of Semi-Arid River Basin Hydrology**
*Everett Springer*

**343** **Rapid Iterative Detection Using Smart Pathogen Signatures**
*John Martin Dunbar*

**346** **A Systematic Strategy for Gene Function Discovery**
*Clifford Jay Unkefer*

**348** **Host-Pathogen Interactions (Pathomics) in Avian Influenza**
*Ruy Miguel Ribeiro*

**352** **One-Step Biomass Conversion: Looking to Nature for Solutions to Energy Security**
*Paul Alfred Langan*

**354** **Flash before the Storm: Predicting Hurricane Intensification using LANL Lightning Data**
*Christopher Andrew Munn Jeffery*

**357** **Genomes to Behavior: Predicting Bacterial Response by Constrained Network Interpolation**
*John Martin Dunbar*

**360** **Complex Biological and Bio-Inspired Systems**
*Robert Everett Ecke*

**364** **Rational Vaccine Design: Theory and Experimental Validation**
*Bette Tina Marie Korber*

**374** **Pathogen Detection Based on Biomodulation**
*Basil Ian Swanson*

379 **Computational Methods for Protein Function Inference**
*Michael E Wall*

## Exploratory Research

384 **Functional Proteomics Studies of Bacillus Anthracis**
*Ryszard Michalczyk*

387 **Drug Binding and Catayltic Mechanism in DHFR**
*Paul Alfred Langan*

389 **Substrates for the Detection and Differentiation of Influenza Viridae**
*David Bryan Kimball*

391 **Magnetic Turbulence and Kinetic Dissipation in Solar Wind and Solar Corona Plasmas**
*Hui Li*

394 **Understanding a Killer: A Predictive Model of Tumor Development**
*Yi Jiang*

397 **An Experimental and Theoretical Framework for Reactive Micromixing**
*Amr I Abdel-Fattah*

400 **Subsurface Transport Parameter Estimation with Multiscale, Multiobjective Optimization**
*Andrew Victor Wolfsberg*

404 **Identifying High Risk Species Critical for the Emergence of Pandemic Influenza**
*Jeanne Marie Fair*

408 **The Effect of Acoustical Waves on Stick—Slip Behavior in Sheared Granular Media: Implications for Earthquake Recurrence and Triggering**
*Paul Allan Johnson*

411 **Developing a Remote Sensing of the Solar Surface**
*Joseph Eric Borovsky*

413 **A New Approach to Unravel Complex Microbial Community Processes**
*Cheryl Rae Kuske*

415 **Nonequilibrium Mechanics of Geomaterials**
*James Alan Tencate*

418 **Evolution and Function of Microbial Signatures**
*Murray Alvin Wolinsky*

421 **Coupling of Genetics and Metabolism and the Orgin of Life**
*Hans Joachim Ziock*

425 **New Frontiers in Viral Phylogenetics**
*Tanmoy Bhattacharya*

427 **Cellulosomes in Action: Peta-Scale Atomistic Bioenergy Simulations**
*Kevin Yosh Sanbonmatsu*

430 **Testing Embedded Model Assumptions of Stable Isotopic Dynamics with Continuous Sampling: Are Modelers' Assumptions of the Global Carbon Cycle Correct?**
*Nathan Gabriel Mcdowell*

433 **Nascent Protein Folding Inside the Tunnel of the Ribosome: Cotranslational Folding**
*Kevin Yosh Sanbonmatsu*

436 **Multigene Correlations and Their Implications for Cardiovascular Disease**
*Rajan Gupta*

440 **Quantifying the Role of the Cold Plasmasphere in the Loss of the Electron Radiation Belts**
*Joseph Eric Borovsky*

444 **Non-blinking and Robust Quantum-Dot Fluorophores for Applications in Biology**
*Jennifer Ann Hollingsworth*

449 **Acoustic Effects on Microscopic and Core-Scale Colloid Interactions and Porous Fluid Transport**
*Peter Morse Roberts*

454 **Complex Dynamical Climate Systems Analysis**
*Gerald Leroy Geernaert*

457 **Solid Earth Geoscience: Transient & Steady-State Earth Processes**
*Claudia Johnson Lewis*

**464** **A Strategy for Effective Antibiotic Delivery**
*Srinivas Iyer*

**467** **Trapping Rare Culture Mutations for Bioweapon Attribution and Forensics**
*John Martin Dunbar*

**473** **Experimentally Constraining Climate Forcing by Black Carbon Deposition on Snow**
*Manvendra Krishna Dubey*

**475** **Modeling Influenza Infection and the Early Immune Response**
*Alan S Perelson*

**479** **Ultra Deep Sequencing of HIV Acute Infection Sample to Determine Nature of Transmitted Virus and Understand Immune Escape**
*Bette Tina Marie Korber*

**482** **Climate Change Forecasts Using Ensemble Forecasting Games**
*Marian Anghel*

## Postdoctoral Research & Development

**486** **Creating a Mathematical Foundation for High-Dimensional Search and Optimization Algorithms to Solve Complex Nonlinear Models**
*Bruce Alan Robinson*

**491** **The Role of NS1 in Disrupting Imune Responses During Influenza Infection: A Modeling and Experimental Approach**
*Alan S Perelson*

**493** **Photodegradation of Leaf Litter in Water-Limited Ecosystems**
*Thomas A Rahn*

**495** **Pore-Scale Modeling of Multiphase Flow and Reaction in Charged Porous Media**
*Qinjun Kang*

**498** **Modeling Fast Basal Sliding of Ice Sheets for Climate and Sea Level Prediction**
*William Henry Lipscomb*

**501** **Modeling the Immune Response to Pathogens**
*Alan S Perelson*

**504** **Spectroscopic Studies and Photonic Applications of "Giant" Nanocrystal Quantum Dots**
*Victor Ivanovich Klimov*

**506** **Modeling Control of Viruses by Immune Responses**
*Alan S Perelson*

**508** **Multi-scale Analysis of Multi-physical Transport Processes of Electroosmosis in Porous Media**
*Qinjun Kang*

**511** **Fluvial Geomorphic Response to Permafrost Thawing: Implications for the Global Carbon Budget and Arctic Hydrology**
*Cathy Jean Wilson*

**513** **Determinaing the Mechanisms of Enzymes Xylose Isomerase and HIV Protease Using Neutron Crystallography**
*Paul Alfred Langan*

**516** **Exploring the Membrane Penetration Machinery of Bacterial Toxins**
*Jaroslaw Majewski*

**520** **Numerical Techniques of Rifting and Passive Margin Formation: The Role of Mantle Plumes**
*David Coblentz*

**527** **Measurements of Absorption and Scattering by Aerosols: How do they Offset Global Warming?**
*Manvendra Krishna Dubey*

**530** **Fluorescence Lifetime Spectroscopy by Flow Cytometry**
*James Paul Freyer*

# Information Science & Technology

## Directed Research

**538** **The Physics of Algorithms**
*Michael Chertkov*

**543** **Automated Change Detection in Remote Sensing Imagery**
*James Patrick Theiler*

**548** **Information Science and Technology: Metagenomics**
*Nicolas W Hengartner*

**551** **Statistical Physics of Networks, Information and Complex Systems**
*Robert Everett Ecke*

**555** **Information Science and Technology: Streaming Data**
*Sarah Ellen Michalak*

**558** **New Approach to Bayesian Inference Under Modeling Uncertainty**
*Nicolas W Hengartner*

**561** **Sharp characterization of minimizers (typically) involving interfaces in images**
*Pieter Johan Swart*

**563** **Instabilities Driven Turbulence and Mixing in Convergent Geometries**
*Daniel Livescu*

**566** **Moment-Based Interface Tracking for Multi-Material Flows**
*Rao Veerabhadra Garimella*

**569** **Hyperbolic Polynomials Approach to Approximate Counting and Lower/Upper Bounds in Combinatorics, Statistical Physics and Computational Geometry**
*Leonid Gurvits*

**572** **Excited States and Optical Response of Nanosized Molecules at Linear Scaling Numerical Cost**
*Sergei Tretiak*

**575** **Agent-Based Modeling and Simulation of Cellular Signaling Systems**
*William Scott Hlavacek*

**577** **Fast Approximation Algorithms for Systems of Linear Inequalities**
*Donald Rhea Hush*

**579** **Minimal Description of Complex Shapes with Applications to Experiments and Validationof Large-Scale Codes**
*Mark B Mineev*

**582** **Conconvex Compressed Sensing**
*Rick Chartrand*

**585** **Foundations for Practical Pattern Recognition Systems**
*Reid Buchanan Porter*

**588** **Multilevel Adaptive Sampling for Multiscale Inverse Problems**
*John David Moulton*

**591** **Adaptive Algorithms for Inverse Problems in Imaging**
*Brendt Egon Wohlberg*

**593** **Stochastic Transport on Networks: Efficient Modeling And Applications to Epidemiology**
*Ilya Mark Nemenman*

**597** **Critical and Crossover Behaviors at Jamming Transitions**
*Charles Reichhardt*

**599** **Time-reversible Born-Oppenheimer Molecular Dynamics**
*Anders Mauritz Niklasson*

## Exploratory Research

**602** **Implicit Adaptive Mesh Refinement: A Magnetohydrodynamics Application**
*Bobby Philip*

**607** **Automatic Video Analysis Integrating Depth, Shape, Texture and Color**
*Garrett Kenyon*

**611** **Automated Induction of Templates for Extracting Information from Text**
*Cornelia Maria Verspoor*

**615** **Monte Carlo Estimation of Eigenvalues of Ultradimensional Matrices and Continuous Operators**
*James E Gubernatis*

**620** **New Method for Complex Contingency Analysis**
*William Henry Press*

**625** **Energy Distributions in Granular Flows**
*Eli Ben-Naim*

**629** **A Faster Multipole Method**
*Michael S Warren*

**634** **Novel Physics Inspired Approach to Error-Correction**
*Michael Chertkov*

**638** **Simulation and Modeling of the Quantum Response**
*Anders Mauritz Niklasson*

**642** **Statistics for the Engineering and Physical Sciences**
*Christine Michaela Anderson-Cook*

**646** **Integrated Feature Vector for Human Pathogen Characterization**
*H Helen Cui*

## Postdoctoral Research & Development

**650** **Towards Human Level Artificial Intelligence: A Cortically Inspired Semantic Network Approach to Information Processing and Storage**
*Luis Bettencourt*

**653** **Finite State Projection for Accurate Solution of the Master Equation**
*Ilya Mark Nemenman*

**655** **Statistical Physics of Optimization**
*Michael Chertkov*

**658** **Self-Organizing Wireless Ad-Hoc and Sensor Networks with Functional Guarantees**
*Sami Ayyorgun*

# Physics

## Directed Research

**664** **Beyond the Neutrino Matrix**
*Andrew Hime*

**667** **Dark Energy and the Cosmic Web**
*Katrin Heitmann*

**671** **High-Current, High-Energy, Laser-Driven Ion Accelerators: An Enabling and Revolutionary Scientific Research Tool**
*Juan Carlos Fernandez*

**677** **Cold Atom Surface Imaging**
*Eddy Marcel Elvire Timmermans*

**681** **Multiscale Modeling of Strongly Interacting Systems**
*Robert Everett Ecke*

**688** **Development of a Magnetically Driven Target for Thermo-Nuclear Burn Studies (*U)**
*Robert Gregory Watt*

**691** **Prompt and Radiochemical NTS Diagnostics and New Measurements (U)**
*David J Vieira*

**693** **Global Monitoring of the Sky with Thinking Telescopes: Finding and Interrogating Cosmic Explosions**
*W Thomas Vestrand*

**696** **Carrier Multiplication in Nanoscale Semiconductors for High-Efficiency, Generation-III Photovoltaics**
*Victor Ivanovich Klimov*

**700** **Probing Physics Beyond the Standard Model through Neutron Beta Decay**
*Alexander Saunders*

**704** **Cosmic Explosions Probing the Extreme: X-Ray Bursts, Superbursts, and Giant Flares on Neutron Stars**
*Sanjay Reddy*

**708** **Novel Signatures of Beyond the Standard Model at the Large Hadron Collider**
*Rajan Gupta*

**711** **High-Precision Spectroscopic Search for Variation of the Fine-Structure Constant**
*Justin Roald Torgerson*

**714** **New Approaches to Quantum Computing and the Dynamics of Quantum Phase Transitions**
*Wojciech Hubert Zurek*

**720** **Heavy Quarks as a Probe of a New State of Matter**
*Patrick Lee Mcgaughey*

**726** **DREAM: A Dynamic Radiation Environment Assimilation Model to Understand Acceleration, Transport, and Losses in Natural and HANE-Produced Radiation Belts**
*Geoffrey D Reeves*

**733** **Mix Processes in Inertial Confinement Fusion**
*Anna Catherine Hayes-Sterbenz*

## Exploratory Research

**738** **Experimental Study of Driven Magnetic Relaxation in a Laboratory Plasma**
*Scott Chia Hsu*

**740** **Beta Decay of Polarized Radioactive Atoms in an Optical Tweezer**
*Xinxin Zhao*

**742** **Nano-Engineered Casimir Forces**
*Diego Alejandro Roberto Dalvit*

**745** **Understanding Dynamical Diversity of Extrasolar Planets**
*Hui Li*

**747** **Probing Correlated Electron Behavior via Direct Uranium-235 Nuclear Magnetic Resonance**
*Eric Dietzgen Bauer*

**750** **Cold Atom Quantum Liquid Mixtures**
*Eddy Marcel Elvire Timmermans*

**753** **Investigation of Energetic Ion Generation and Transport in Ultra-Intense Laser-Matter Interaction**
*Brian James Albright*

**757** **New States of Matter in Stars, Nuclei and Cold Atoms**
*Sanjay Reddy*

**760** **Ultra-Low Field Resonant Absorption Magnetic Resonance Imaging of Neural Activity**
*Petr Lvovich Volegov*

**764** **Unique Observations of Nature's Largest Explosions**
*W Thomas Vestrand*

**767** **Electron-Neutrino Correlation in Neutron Beta Decay**
*Wesley Scott Wilburn*

**769** **Experimental and Computational Studies of Magnetic Bubble Expansion as a Model for Extra-galactic Radio Lobes**
*Scott Chia Hsu*

**771** **Precision Cosmology and the Neutrino Sector**
*Salman Habib*

**773** **Finding the First Cosmic Explosions**
*Daniel Holz*

**777** **Materials and Device Optimization Towards Room Temperature Spin-Transport Through Single-Walled Carbon Nanotubes**
*Stephen K Doorn*

**780** **The First Precise Determination of Quark Energy Loss in Nuclei**
*Ivan Mateev Vitev*

**784** **Entanglement in Quantum Ground States**
*Matthew B Hastings*

**787** **CP-violating Moments of Atoms and Nuclei**
*Anna Catherine Hayes-Sterbenz*

**789** **Ultrafast Nanoplasmonics for Photonics and Quantum Control at the Nanoscale**
*Anatoly V Efimov*

**791** **Probing physics beyond the Standard Model with supernovae**
*Alexander Friedland*

**794** **Three-Dimensional Dynamics of Magnetic Reconnection in Space and Laboratory Plasmas**
*William Scott Daughton*

**797** **The Roadrunner Universe**
*Salman Habib*

**799** **Implicit Monte Carlo Calculations of Supernova Light-Curves**
*Aimee L Hungerford*

**801** **Instabilities Driven Reacting Compressible Turbulence**
*Daniel Livescu*

**803** **Saturation of Backward Stimulated Scattering of Laser In The Collisional Regime**
*Lin Yin*

**806** **Physics of Astrophysical Jets**
*Hui Li*

**810** **Chemical Thermoacoustics**
*Drew Adam Geller*

**813** **The S-Process in the Sm-Eu-Gd Region - A Probe for Stellar Mixing**
*Aaron Joseph Couture*

**820** **Role of Electrostatic Forces in Space and Astrophysics**
*Gian Luca Delzanno*

**827** **Detecting Spinons with the Wiedemann-Franz Law**
*Filip Ronning*

**831** **Amplification of Surface Plasmons by Stimulated Emission from Semiconductor Nanocrystals**
*Victor Ivanovich Klimov*

**836** **Exploring the Darkness: Cosmic Voids**
*Katrin Heitmann*

**841** **Quantum Nondemolition Detection of Photons**
*Michael David Di Rosa*

**846** **Manipulation and Control of Electron Spins in Semiconductors with Strain Engineering**
*Darryl Lyle George Smith*

**850** **Structure and Evolution in Cosmology and Astrophysics**
*Richard Ira Epstein*

**854** **Supersymmetry Breaking in Various Dimensions**
*Tanmoy Bhattacharya*

**858** **The Secret Life of Quasiparticles**
*Stuart Alan Trugman*

**862** **Steps Toward Practical Quantum Information Processing**
*Malcolm Geoffrey Boshier*

**866** **Trapped-ion Quantum Simulations of Condensed-Matter Systems for Understanding of Novel Materials**
*John Chiaverini*

## Postdoctoral Research & Development

**870** **Ultrafast Phenomena: Short-Pulse laser Interactions with Atoms and Molecules**
*Lee A Collins*

**873** **Gamma-Ray Bursts and Gravitational Waves from Compact Mergers**
*Christopher Lee Fryer*

**875** **Theoretical and Experimental Investigation of Relaxation Mechanisms in Ultra-low Field NMR for Magnetic Resonance Imaging**
*Michelle A Espy*

**878** **Noise in Biochemical Networks: Rigorous Analysis with Field-Theoretic Tools**
*Ilya Mark Nemenman*

**881** **Detecting the Highest Energy Gamma-Rays and Neutrinos to Determine the Origin of Cosmic Rays**
*Brenda L Dingus*

**883** **Anti-Neutrino Oscillation and Cross Section Measurements at MiniBooNE**
*Geoffrey Blount Mills*

**885** **Phase Transitions in Quantum Systems and Quantum Information**
*Wojciech Hubert Zurek*

**889** **Detecting Dark Matter with Cryogenic Liquids**
*Andrew Hime*

**891** **The Dynamics of Dark Energy**
*Katrin Heitmann*

**893** **Dynamics of Quantum First Order Phase Transitions**
*Dima V Mozyrsky*

**895** **Nonequilibrium Quantum Phase Transitions**
*Eli Ben-Naim*

**898** **Dissipation and Decoherence in Complex Many-Body Systems**
*Wojciech Hubert Zurek*

**900** **Strongly Coupled Fermion Systems: From Atomic Gases to Dark Matter**
*Sanjay Reddy*

**901** **Matter and Light**
*Katrin Heitmann*

**904** **High Energy Particles in Astrophysical Outflows**
*Christopher Lee Fryer*

**907** **The Neutrino Matrix and Beyond**
*Andrew Hime*

**910** **A Multiscale Approach to Modeling Continental Rift Tectonics**
*Carl Walter Gable*

**914** **Quantum Fluctuations of Event Horizons**
*Emil Mottola*

**916** **Three-dimensional Magnetic Reconnection Experiments**
*Thomas P Intrator*

**919** **Theoretical Studies of Cold Atom Fermi-liquids and Bose-Einstein Condensates on Chips**
*Eddy Timmermans*

**923** **Search for Temporal Variation of the Fine Structure Constant**
*Justin Roald Torgerson*

**928** **Quantum Fluctuations in Bose-Einstein Condensates**
*Eli Ben-Naim*

# Technology

## Directed Research

**934** **Image Reconstruction with Time-Reversal Mirrors**
*Paul Allan Johnson*

**937** **Construction and Use of Superluminal Emission Technology Demonstrators with Applications in Radar, Astrophysics, and Secure Communications**
*John Singleton*

**942** **Science-Based Prediction and Control of Complex Manufacturing Processes**
*Matthew Thomas Bement*

## Exploratory Research

**948** **Cerium-Doped Glass Scintillators**
*Markus Peter Hehlen*

**951** **Nano-Structured Foams for Hydrogen Storage**
*Erik Paul Luther*

**954** **Nano-Composite Scintillator for Neutron Capture Measurements**
*Ernst Ingo Esch*

**956** **From Novel Principles to Novel Device Structures for High-Efficiency Generation of Solar Electricity**
*Victor Ivanovich Klimov*

**959** **X, Gamma, Alpha : Ultra-High Resolution Spectroscopy**
*Michael W Rabin*

**962** **A Novel Approach to Manufacturing Ultra-Tall Carbon Nanotube Forests**
*Quanxi Jia*

**964** **Optical, Electronic, and Magnetic Doping of ENABLE Grown Semiconducting Films**
*Mark Arles Hoffbauer*

**967** **Terahertz Generation Harnessing the Two-Stream Instability**
*Kip A Bishofberger*

**969** **Nano-Fission-Material based Neutron Detectors**
*Ernst Ingo Esch*

**971** **Efficient Structures for Low-Energy Acceleration of Light Ions**
*Sergey S Kurennoy*

**975** **Compact Millimeter Wave Spectrometer Based on a Channel Drop Filter**
*Lawrence M Earley*

**978** **Novel High Performance Terahertz Metamaterial Photonic Devices**
*John F O'Hara*

**981** **Accuracy of Laser-Induced Breakdown Spectroscopy for Trace Detection**
*Roger Craig Wiens*

**984** **Development of an Engineering Model for Rubber Elasticity**
*David Edward Hanson*

**988** **MRI in Microtesla Magnetic Fields with Simultaneous MEG**
*Michelle A Espy*

**994** **Seeing Undetectable Cancers with Time-Reversed Ultrasound**
*Lianjie Huang*

**998** **Surface Enhanced Raman (SERS) Based Flow Cytometry Detection**
*Stephen K Doorn*

**1003** **Processing of Ultra-High Strength Electrical Conductors using a Novel Nano-Twinned Structure**
*Amit Misra*

**1007** **Stabilization of Hydrogen Clathrates: Engineering a Solution to Hydrogen Storage**
*Yusheng Zhao*

**1011** **Generation, Detection, and Manipulation of a Single Magnetic Spin**
*Scott A Crooker*

# Chemistry & Material Sciences

# Strongly Correlated Electrons: Duality and Implications

*Cristian Daniel Batista*

20060043DR

## Introduction

Actinide and Lanthanide elements are among the most complex materials from the point of view of their electronic structure. This complex behavior is one of the paradigms of modern condensed matter physics due to the diversity of quantum states of matter that emerge from it. The goal of the current project is to model heavy elements such as actinide and lanthanide based compounds in order to reconcile several experimental observations that seem to be contradictory. In particular, we are explaining the origin of the "dual nature" of *f*-electrons (electrons seem to be localized or itinerant depending on the experimental probe) and finding novel forms of "normal" states that are precursors of the unconventional superconductors. One of the high potentials of these new findings is the comprehensive understanding of different classes of seemingly unrelated materials through the identification of universal low-energy models. In this way, our results will have an important impact not only in *f*-electron materials, but also in other systems such as the high-temperature cuprate superconductors.

## Benefit to National Security Missions

Many DOE's materials-dependent mission needs depend critically on strong electronic correlations, whether it is the equation of state and metallurgy of actinides or control of quantum excitations for new sensor technologies. Understanding the consequences of electronic interactions ties to the Office of Science missions and can improve environmental quality.

## Progress

Building on discoveries during the preceding year for the dual nature of *f*-electrons in specific materials, we identified physical characteristics that signal this dual nature. With this information, we have found that many previously unexplained phenomena in strongly correlated *f*-electron systems can understood self-consistently as arising from electronic duality. Using this now much broader base of data, we have developed a simple phenomenology of duality. At 'high' temperatures, *f*-electrons are localized and interact weakly through the Kondo effect with conduction electrons, but below a material-dependent characteristic temperature T*, the localized electrons begin to become collectively entangled, through a long-ranged Rudermann-Kittel-Kasuya-Yosida (RKKY) magnetic interaction, with conduction electrons starting to assume a partially delocalized character. The scale T* is reflected in diverse spin- and charge-dependent physical properties, for example, optical conductivity, spin susceptibility, thermodynamic and electrical transport, and all these measurements give the same value of T* for a given material. Having identified T* and the Kondo temperature scale $T_K$ for these materials, we could determine from experiments the magnetic exchange parameter *J* that controls both the RKKY and Kondo scales and discovered the remarkably simple *material-independent* relationship $T^*=0.45J^2N(E_F)$ that collapses all of these strongly correlated 4*f*- and 5*f*-electron materials onto a universal phase diagram [1]. One of the most surprising aspects of this work is that the simple relationship involves only *J* and the density of electronic states $N(E_F)$ of the non-magnetic, uncorrelated counterpart compound, e.g., the La analog of strongly correlated Ce compounds or the Th analog of correlated U-based compounds. These discoveries will be highlighted in Discover magazine of one of the 100 most important scientific developments in 2008. Extending these insights to strongly correlated Pu-based compounds should be possible but will require experimental data that presently are unavailable.

This simple phenomenology is unable to predict the nature of ground states that could emerge from electronic duality. One of the consequences of duality is our discovery of a precursor state to unconventional superconductivity in $CeIrIn_5$ [2] .Detailed measurements of the Hall coefficient and magnetoresistivity of this compound have shown that the mobility of charge carriers assume a distinctly different nature below T* but above the superconducting transition temperature $T_c$ and that the magnetic field dependence of this precursor state scales with the magnetic field that destroys superconductivity. In many respects, the precursor state, defined

by the change in mobility, is similar to the much studied pseudogap state in the curprate high-temperature superconductors.

Work started last year on the development of a strongly correlated model of the actinides, its applications to Pu, and its comparison with experiment was completed and submitted for publication. For Pu, the principal finding was a blocking of the direct hopping between *f*-orbitals. This result reduced the model to one similar to the one used for the lanthanides, Ce, Sm, and Yb and likely provides the basis for explaining the observed similarities of some properties of Pu and these other materials. Our findings have been published recently in Physical Review Letters.

Other research focused on the other light actinides and consisted of developing a slave-boson-like mean-field approximation for the model and a computer program for its numerical solution. Completed are the programs to compute the required matrix elements. In progress is the development of the mean-field solver. The initial application will be the computation of the photoemission spectroscopy of U.

Quantum criticality has been invoked to explain non-fermi liquid behavior in strongly correlated electron systems. Anomalous magnetic susceptibility has been observed with neutron scattering in CeCu compounds doped with Au. This phenomenon cannot be explained with conventional theories, so a local quantum criticality scenario was proposed. Since the magnetization exhibits large anisotropy in $CeCu_{6-x}Au_x$, we started with a Kondo-Ising model for describing the competition between the local Kondo exchange coupling and the RKKY interaction. Within the extended dynamical mean-field theory, the Bose-Fermi Kondo impurity model was solved by a zero-temperature Numerical Renormalization Group method. We found that local quantum criticality is obtained for a two-dimensional spin-excitation dispersion and that the magnetic transition point is accompanied by a simultaneous breakdown of local Kondo energy scale. This new result answered a long-standing question about the order of the magnetic transition.

We also found that the Fermi surface topology can induce a Kondo stripe phase in heavy fermion compounds. When the 4*f* or 5*f* systems have weak but isotropic magnetism, the spin liquid scenario is an alternative to the antiferromagnetic or Neel state at zero temperature.

Within this scenario, the nature of resultant heavy Fermi liquid depends on the Fermi surface topology that results from hybridizing the conduction and *f*-electron bands. We investigated this problem within a Kondo-Anderson lattice model. In the limit of infinite on-site Hubbard interaction, we showed that a heavy Fermi liquid with a stripe-like pattern is more favorable when the Fermi surface topology meets certain criteria.

## Future Work

Strong electronic correlations that arise from competing interactions are responsible for the complexity and associated rich spectrum of ordered states and exotic quantum behavior observed in lanthanide and actinide materials (*f*-electron systems). Though minimal many-body models have been proposed that capture aspects of these strongly correlated effects, these models are far from complete and are unable to reproduce essential consequences of strong correlations on low-energy quantum behavior that are of so much worldwide interest. One of the most striking departures from current models is recently discovered experimental evidence that *f*-electrons can assume dual roles, by responding collectively to their environment to produce simultaneously localized and itinerant behavior. The duality imposed by strong electronic correlations offers a previously unrealized explanation for the multiplicity of connected length and time scales characteristic of correlated matter and its extreme sensitivity to small perturbations. The scientific opportunity, and our objective, is to create and exploit essential, new understanding demanded by these discoveries. Achieving our goal will provide the scientific underpinning for a predictive understanding of plutonium's solid state, stretch scientific capabilities crucial to world-class, mission-relevant materials science, and lay the foundation for emerging civilian and defense initiatives. By integrating acknowledged expertise in experiment, theory and computation and capitalizing on special Los Alamos capabilities for neutron scattering and research at high magnetic fields, this project fills a critical gap in the understanding of strongly correlated behaviors and their consequences. To achieve our goals, a closely coupled theoretical and experimental effort is underway to:

- Establish the generality of *f*-electron duality,
- Apply a necessarily broad suite of techniques required to reveal the physical conditions that determine *f*-duality, and
- Explore the consequences of duality for understanding exotic states that appear in correlated *f*-electron materials

## Conclusion

We expect to produce new understanding to answer questions based on previous discoveries in lanthanide and actinide compounds. This will provide the scientific underpinning for a predictive understanding of the plutonium solid state, stretch scientific capabilities crucial to world-class, mission-relevant materials science, and lay the foundation

for emerging civilian and defense initiatives. By integrating acknowledged expertise in experiment, theory and computation and capitalizing on Los Alamos capabilities for neutron scattering and research at high magnetic fields, we are filling a critical gap in the understanding of strongly correlated electronic behaviors and consequences.

## References


1. Yang, Y., H. O. Lee, Z. Fisk, J. D. Thompson, and D. Pines. Scaling the Kondo lattice. 2008. *Nature.* **454**: 611.
2. Nair, S., S. Wirth, M. Nicklas, J. L. Sarrao, J. D. Thompson, Z. Fisk, and F. Steglich. Precursor state to unconventional superconductivity in CeIrIn5. 2008. *Physical Review Letters.* **100**: 137003.


## Publications


P.Julien, J., J. -X. Zhu, and R. C. Albers. Coulomb correlation in presence of spin-orbit coupling: application to plutonium. *Phys. Rev. B .*

X.Zhu, J., A. K. McMahan, M. D. Jones, T. Durakiewicz, J. J. Joyce, J. M. Wills, and R. C. Albers. Spectral Properties of delta-Plutonium: Sensitivity to 5f Occupancy. 2007. *Physical Review B .* **76** (245118): 245118.

Albers, R. C., and J. -X. Zhu. Vacillating Valence. 2007. *Nature.* **446**: 504.

Batista, C. D.. Effective Hamiltonian for metallic Plutonium. To appear in *Journal of Nuclear Materials.*

Batista, C. D., J. E. Gubernatis, T. Durakiewicz, and J. J. Joyce. Strong coupling approach to actinide metals. 2008. *Physical Review Letters.* **101**: 016403.

Bauer, E. D., C. Wang, V. R. Fanneli, J. M. Lawrence, E. A. Goremychkin, N. R. de Souza, F. Ronning, J. D. Thompson, A. V. Silhanek, V. Vildosola, A. M. Lobos, A. A. Aligia, S. Bobev, and J. L. Sarrao. Simplifying strong electronic correlations in uranium: localized uranium heavy fermion UM2Zn20 (M=Co,Rh) compounds. 2008. *Physical Review B.* **78**: 115120.

Bauer, E. D., J. D. Thompson, J. L. Sarrao, and M. F. Hundley. Ferromagnetism and crystalline electric field effects in cubic UX2Zn20 (X=Co, Rh, Ir). 2007. *Journal of Magnetism and Magnetic Materials.* **310**: e449.

Capan, C., L. Balicas, T. P. Murphy, E. C. Palm, R. Movshovich, D. Hall, S. W. Tozer, M. F. Hundley, E. D. Bauer, J. D. Thompson, J. L. Sarrao, J. F. Di Tusa, and R. G. Goodrich. Evolution of the Fermi Surface and Electrical Transport Properties across the Metamagnetic Transition in CeIrIn5. *Submitted to Physical Review B.*

Durakiewicz, T., C. G. Olson, K. S. Graham, D. P. Moore, J. J. Joyce, and L. A. Morales. Localized and itinerant states in actinide materials. 2007. *Materials Research Society Symposium Proceedings.* **986**: 35.

Durakiewicz, T., J. J. Joyce, J. M. Wills, and C. D. Batista. Notes on the dual nature of 5*f*-electrons. 2006. *Journal of the Physical Society of Japan.* **75**: 39.

Goodrich, R. G., N. Harrison, and Z. Fisk. Fermi surface changes across the Neel phase boundary of NdB6. 2006. *Physical Review Letters.*

Gout, D., O. Gourdon, E. D. Bauer, F. Ronning, J. D. Thompson, and T. Proffen. An experimental and theoretical study of the variation of the 4f hybridization across La1-xCexIn3. 2008. *Inorganic Chemistry.* **47**: 2569.

Harrison, N., S. E. Sebastian, C. H. Mielke, A. Paris, M. J. Gordon, C. A. Swenson, D. G. Rickel, M. D. Pacheco, P. F. Ruminer, J. B. Schillig, J. R. Sims, A. H. Lacerda, M. -T. Suzuki, H. Harima, and T. Ebihara. Fermi Surface of CeIn3 above the Neel Critical Field. 2007. *Phys. Rev. Lett. .* **99**: 056401.

Heffner, R. H., D. E. MacLaughlin, J. E. Sonier, M. F. Hundley, and J. D. Thompson. Two-fluid model of heavy fermion formation and muon spin resonance Knight shift measurements in UBe13. 2007. *Journal of Magnetism and Magnetic Materials.* **310**: e6.

Joyce, J. J., J. Wills, T. Durakiewicz, M. T. Butterfield, E. Guziewicz, D. P. Moore, J. L. Sarrao, L. A. Morales, A. J. Arko, O. Eriksson, A. Delin, and P. H. Anderson. Dual nature of the 5f electons in plutonium materials. 2006. *Physica B.* **378-380**: 920.

Julien, J., J. Zhu, and R. C. Albers. Coulomb correlation in presence of spin-orbit coupling: application to plutonium. 2008. *Physical Review B.* **77**: 195123.

M.Chia, E. E., H. J. Lee, N. Hur, E. D. Bauer, T. Durakiewicz, R. D. Averitt, J. L. Sarrao, and A. J. Taylor. Quasiparticle relaxation across the spin gap on the itinerant antiferromagnet UNiGa5. 2006. *Physical Review B.* **74**: 140409.

M.Chia, E. E., J. -X. Zhu, D. Talbayev, R. D. Averitt, K. -H. Oh, I. -S. Jo, S. -I. Lee, and A. J. Taylor. Observation of competing order in a high-Tc superconductor with femtosecond optical pulses. 2007. *Phys. Rev. Lett. .* **99**: 147008.

Nair, S., S. Wirth, M. Nicklas, A. Glaudun, J. L. Sarrao, J. D. Thompson, and F. Steglich. A precursor state to superconductivity in CeIrIn5. 2008. *Physical Review Letters.* **100**: 137003.

Oh, Y. S., K. H. Kim, P. A. Sharma, N. Harrison, H. Amitsuka, and J. A. Mydosh. Interplay between Fermi Surface Topology and Ordering in URu2Si2 Revealed through Abrupt Hall Coefficient Changes in Strong Magnetic Fields. 2007. *Phys. Rev. Lett. .* **98**: 016401.

Ohishi, K., R. H. Heffner, G. D. Morris, E. D. Bauer, M. J. Graf, J. -X. Zhu, L. A. Morales, J. L. Sarrao, M. F. Fluss, D. E. MacLaughlin, L. Shu, W. Higemoto, and T. U. Ito. Muon spin rotation measurements of the superfluid density in fresh and aged superconducting PuCoGa5. 2007. *Phys. Rev. B .* **76**: 064504.

Park, W. K., H. Salzer, J. L. Sarrao, J. D. Thompson, L. D. Pham, Z. Fisk, J. Federick, P. C. Canfield, and L. H. Greene. Point-contact Andreev spectroscopy of heavy-fermion/superconductor junctions. 2008. *Physica B.* **403**: 818.

Park, W. K., J. L. Sarrao, J. D. Thompson, L. D. Pham, Z. Fisk, and H. L. Greene. Andreev reflection spectroscopy of the pure and Cd-doped heavy-fermin superconductor CeCoIn5: detecting order parameter symmetry and competing phases. 2008. *Physica B.* **403**: 731.

Park, W. K., J. L. Sarrao, J. D. Thompson, and L. H. Greene. Andreev reflection study of the heavy-fermon superconductor CeCoIn5: Detecting order parameter symmetry. 2008. *Physical Review Letters.* **100**: 177001.

Park, W. K., L. H. Greene, J. L. Sarrao, and J. D. Thompson. Andreev reflection spectroscopy of the heavy-fermion superconductor CeCoIn5 along different crystallographic directions. 2007. *Physica C.* **460-462**: 206.

Qi, Y., J. Zhu, S. Zhang, and C. S. Ting. Kondo resonance in the presence of spin polarized currents. 2008. *Physical Review B.* **78**: 045305.

Sabastian, S., N. Harrison, P. Sengupta, C. D. Batista, S. Francoual, E. Palm, T. Murphy, N. Marcano, H. A. Dabkowska, and B. D. Gaullin. Fractalization drives crystalline states in a frustrated spin system. To appear in *Proceedings of the National Academy of Sciences.*

Sebastian, S. E., N. Harrison, C. D. Batista, S. A. Trugman, V. Fanelli, M. Jaime, T. P. Murphy, E. C. Palm, H. Harima, and T. Ebihara. Heavy holes precursor to superconductivity in antiferromagnetic CeIn3. *Nature Physics.*

Sharma, P. A., N. Harrison, M. Jaime, Y. S. Oh, C. D. Batista, J. A. Mydosh, and H. Amitsuka. Phonon thermal transport of URu2Si2: Broken translational symmetry and strong-coupling of the Hidden Order to the lattice.. 2006. *Physical Review Letters.* **97** (15): 156401/1.

Yang, Y., H. O. Lee, Z. Fisk, J. D. Thompson, and D. Pines. Scaling the Kondo lattice. 2008. *Nature.* **454**: 611.

Zhu, J., I. Martin, and A. R. Bishop. Kondo stripes in an Anderson-Heisenberg model of heavy fermions. 2008. *Physical Review Letters.* **100**: 236403.

Zhu, J., S. Kirschner, R. Bula, and Q. Si. Zero-Temperature Magnetic Transition in an Easy-Axis Kondo Lattice Model. 2007. *Physical Review Letters.* **99**: 227204.

continuing project

# Novel Inclusion Compounds for Hydrogen Storage

*Yusheng Zhao*

20070008DR

## Introduction

Hydrogen storage is the top technological challenge for the future hydrogen economy, which requires revolutionary improvements and breakthroughs in science and technology. The recent discovery of hydrogen clathrate presents a new methodology for hydrogen storage using hydrate polyhedral cages to host substantial amounts of molecular hydrogen. Strong intermolecular interactions result in multiple hydrogen molecules occupying a single nanoscale clathrate cage, yielding an $H_2$ content of about 5 wt% at P = 100 MPa and T = 180 K. This content is higher than the current "state-of-the-art" for $H_2$ storage in metal hydrides. The local $H_2$ density within the polyhedral cage is even higher (>30%) than in solid/metallic hydrogen due to quantum intermolecular bonding. High energy content, fast kinetics, easy reversibility, and excellent recharge ability are the ultimate materials objectives for hydrogen storage.

We have been performing fundamental studies of hydrogen clustering in nano-scale cavities, guest-host intermolecular interactions, and framework stability. A crystal engineering approach is used to synthesize novel hydrogen inclusion compounds (e.g., clathrate hydrates { $H_2$- $H_2O$} and metal-organic frameworks: { $H_2$-MOFs}) with cage-/channel-topology and hydrogen-/intermolecular-bonding chosen to facilitate hydrogen storage. We address effective gas separation and encapsulation, $H_2$ storage capacity and phase stability, and controlled kinetics of formation and degassing. We apply shape-, size-, and bonding-selectivity rules to maximize capture efficiency. Our integrated experimental approaches of neutron diffraction, thermodynamics, kinetics, synthetic chemistry, and chemical engineering enable innovative molecular design, thermochemical control, and ultimately process scale-up. Theoretical modeling is used to guide the experiments relevant to gas separation and hydrogen storage applications

## Benefit to National Security Missions

We address vital research issues on energy, providing underpinning S&T to address materials science focusing on hydrogen storage. The project integrates approaches of molecular design, thermochemical control, and high-pressure neutron diffraction. Efficient separation and storage of gaseous phases are crucial bottlenecks in the future hydrogen economy of the Nation.

## Progress

To develop desired materials for hydrogen storage, we have synthesized several new metal-organic frameworks (MOFs) using hydrothermal/solvothermal methods. The new MOFs include:

- $[Zn_2(OH)(3,4\text{-PBC})_3]_n$ (3,4-HPBC = 3,4-pyridylbenzenecarboxylate acid)
- $[Zn(3,3\text{-PBC})_2.\ H_2O]n$ (3,3-HPBC = 3,3-pyridylbenzenecarboxylate acid)
- $[Cu(4\text{-TYMP})_2]_n$ (4-HTYMP = 4-(1h-1,2,4-triazol-1-ylmethyl) benzoic acid)
- $[Cd(4\text{-TYMP})2]_n$
- $[Y(BTC).4.3\ H_2O]_n$ (H3BTC = 1,3,5-benzenetricarboxylate acid) [1]
- $[Er(BTC).5\ H_2O]_n$
- Zn(II)-4-tetrazole-pyridine
- Cu(II)-4-tetrazole-benzonic acid framework
- $ZnNa(BTC)(DMF)(H_2O)_{0.5}$ (BTC = 1,3,5-benzenetricarboxylate) (Figure 1)
- $[Zn_4O(BTB)(H_2O)_2](H_2O)_{3.5}$ (BTB = benzene-1,3,5-tribenzoate) (Figure 2).

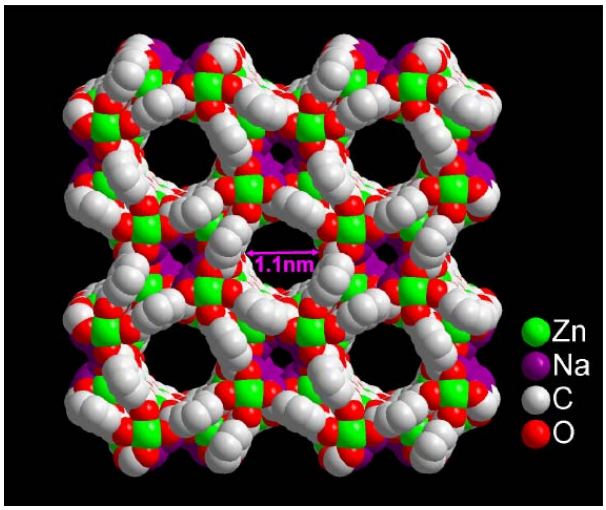


*Figure 1. Crystal structure of ZnNa(BTC)(DMF)($H_2O$)0.5 (BTC = 1,3,5-benzenetricarboxylate).*

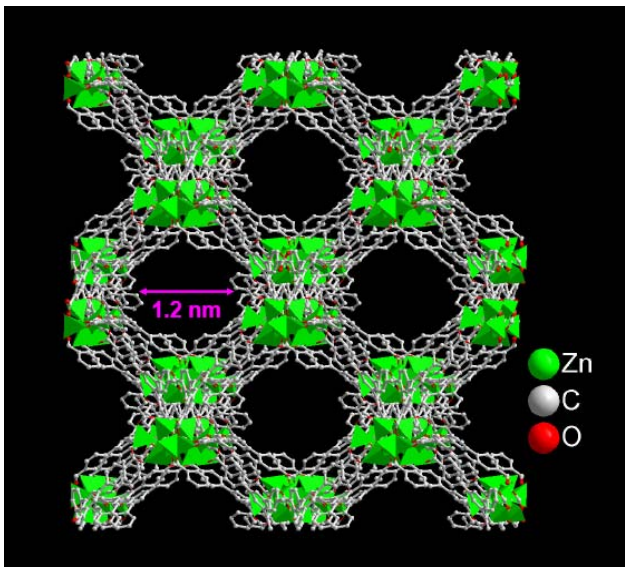


*Figure 2. Crystal structure of [$Zn_4O$(BTB)($H_2O$)2]($H_2O$)3.5 (BTB = benzene-1,3,5-tribenzoate).*

High-quality crystals of these compounds were grown, and their structures were solved with single-crystal X-ray diffraction. The samples were also characterized by IR spectrometry, thermogravimetry, powder X-ray diffraction and gas adsorption measurements. Moreover, we have developed a new type of porous materials, named "metal-organic aerogels", that have high surface areas (> 1000 $m^2$/g) and good solvent/chemical stability.

We performed neutron diffraction experiments of Prussian blue analogue $Cu_3[Co(CN)_6]_2$ and Y(BTC) at various $H_2$ gas loading, temperature and pressure conditions. Rietveld analysis of the diffraction data allowed determination of lattice parameters, atomic positions and atomic displacement parameters (especially for hydrogen). Our results reveal that hydrogen interacts with the "naked" metal cations (Cu) in $Cu_3[Co(CN)_6]_2$ but with the organic ligands (BTC) in Y(BTC) due to the steric effects of the framework channels/cavities. In addition, we have explored the methodology of using GC-MS to study gas separation capabilities of MOFs. This technique also has the advantages of determining their thermal stability and activation conditions and has proved very useful in MOF research.

To determine the kinetics of $H_2$ sorption/desorption process, we have conducted quartz crystal microbalance (QCM) measurements of $Cu_3[Co(CN)_6]_2$ as a function of particle size, film thickness and temperature. The $H_2$ uptake capacity of $Cu_3[Co(CN)_6]_2$ film with a thickness of a few micron can be as high as 4.6 wt% at ambient conditions. However, as the film thickness increases, the $H_2$ uptake decreases, suggesting that gas diffusion dominate its $H_2$ sorption/desorption process. In addition to hydrogen, we studied gas adsorption of He, $N_2$, and $CO_2$ in $Cu_3[Co(CN)_6]_2$. This compound shows strong interaction with $H_2$ and $CO_2$ and can thus be used for separation of $H_2$ and $CO_2$ from their $N_2$ mixtures. A parallel effort was devoted to studies of conducting polymers for hydrogen storage. In particular, we have studied interaction of polyaniline (PANi) with $H_2$ to form "quasi-chemical" bonding that has significant effects on its electrical conductivity. The hydrogen storage potential of PANi was explored via PANi morphology control and synthesis of MOF/PANi composites.

We focused our theoretical effort on the Cu Prussian Blue analogue system to understand hydrogen sorption properties. First-principles quantum chemical calculations have been performed on both cluster and periodic representations of the crystal structure. At the periodic level, it has been determined that currently available density functionals provided in plane wave codes are inadequate to correctly represent the weak interactions present involving hydrogen molecules interacting with both the isocyanide and metal centres. At the cluster level, wavefunction methods such as Hartree Fock with $MP_2$ corrections appear to account for the interactions correctly. We predict binding energies ranging from 4-8 $kJmol^{-1}$ at the free Cu(II) binding sites, which are considerably less than for molecular nitrogen and carbon dioxide at the same site. This result correlates well with our QCM measurements.

A new concept for electric field enhancement of gas adsorption was developed that includes design of highly polarizable centers within porous adsorbents. We have conducted an initial experimental demonstration of electric field modulated gas storage centered on $CO_2$ capture. We realized that the strong quadrupole found in $CO_2$ was a "handle" that, if properly exploited, could facilitate separation. A series of proof-of-concept experiments were performed in a small Metal-Insulator-Metal capacitor bank. Thin copper sheets were used as the capacitor plates while MOF-5 was used as the insulator material. Once loaded, the capacitor bank

was inserted into a pressure vessel equipped with electrical leads. The gas used was a mixture of $CO_2$, $O_2$, and $N_2$. These experiments showed that $CO_2$ was selectively pulled into MOF-5 upon application of an electrical potential. This system was found to be reversible; upon discharging the capacitor the $CO_2$ was released back into the gas phase. Quantification of $CO_2$ uptake showed that the $CO_2$ held within the energized capacitor cell was in fact enhanced over the concentration found in the absence of the electric field.

## Future Work

High-Pressure (Hydrostatic) Neutron Diffraction is a powerful tool for the study of crystal chemistry, formation kinetics, and structural phase transitions of hydrogen-bearing inclusion compounds, since neutrons directly probe hydrogen atoms. Substitution of deuterium for hydrogen sufficiently increases the contrast and efficiency of neutron diffraction. It also eliminates the incoherent scattering and enhances the signal-to-background ratio. We have developed a unique hydrostatic pressure cell with large sample volume (up to 10 $cm^3$) and precise control of pressure and temperature in a range of 1-1,000 MPa and 30-300 K.

Integration of Diffraction and Calorimetry provides a unique in-situ technique to better understand the complex crystallographic and thermodynamics associated with the formation and decomposition of inclusion compounds. It provides comprehensive insights of crystal structures and thermodynamic properties. Our new design of a hybrid pressure cell with large sample volume and insertion of thermocouples will permit simultaneous neutron diffraction and DSC and/or DTA measurements of the same sample under identical P-T conditions.

Chemical Manipulation of Molecular Structure takes on the challenge of synthesizing highly reversible inclusion compounds that can selectively store large quantities of gaseous phases and readily release it. Each of these materials, clathrates, cryptates, clathrasil, and MOFs, lend themselves to chemical and structural modification. The alteration of molecular building blocks can enforce chemical control over these materials, potentially altering the cavity shape, chemical functionality, and formation energetics. Carefully engineered alterations in cavity topology can allow multiple occupancies of hydrogen molecules.

Theoretical Modeling and Computational Simulation can improve thermodynamic (P-T-x) stability of inclusion compounds as hydrogen storage materials while maintaining storage capacity and fast kinetics in reversible cycling of capture/release will require subtle modifications of composition and structure. Computer simulations of such compounds can efficiently identify and test models of the pertinent molecular bonding mechanisms critical for hydrogen storage and transportation.

## Conclusion

Novel inclusion compounds for hydrogen storage must be workable over readily accessible temperatures and pressures, in order to be economically feasible. Within the R&D scope of the project, we expect to: 1) provide novel engineering materials that can potentially be used for hydrogen and byproduct gases separation and storage in energy application and environmental protection; 2) develop new unique experimental capabilities and innovative theoretical modeling methods for the Laboratory that may be applicable to tritium problems relevant to the national security; 3) strengthen Laboratory-industrial partnerships working on the next generation of energy technologies

## References

1. Luo, J., H. Xu, Y. Liu, Y. Zhao, L. L. Daemen, C. Brown, T. V. Timofeeva, S. Ma, and H. C. Zhou. Hydrogen adsorption in a highly stable porous rare-earth metal-organic framework: Sorption properties and neutron diffraction studies. 2008. *Journal of the American Chemical Society.* **130** (30): 9626.

## Publications

Luo, J., H. Xu, Y. Liu, Y. Zhao, L. L. Daemen, C. Brown, T. V. Timofeeva , S. Ma , and H. C. Zhou. Hydrogen adsorption in a highly stable porous rare-earth metal-organic framework: Sorption properties and neutron diffraction studies. 2008. *Journal of the American Chemical Society.* **130** (30): 9626.

Luo, J., Y. Zhao, H. Xu, T. L. Kinnibrugh, D. Yang, T. V. Timofeeva, L. L. Daemen, J. Zhang, W. Bao, J. D. Thompson, and R. P. Currier. A novel helical double-layered cobalt(II)-organic framework with tetranuclear [Co4( 3-OH)2] clusters linked by an unsymmetrical pyridylbenzoate ligand. 2007. *Inorganic Chemistry (Communication).* **46** (22): 9021.

Mao, W. L., C. A. Koh, and E. D. Sloan. Clathrate, hydrates under pressure. 2007. *Physics Today.* **60** (10): 42.

Zhao, Y., H. Xu, L. L. Daemen, K. Lokshin , K. T. Tait , W. L. Mao , J. Luo , R. P. Currier , and D. D. Hickmott . High-pressure/low-temperature neutron scattering of gas inclusion compounds: Progress and prospects. 2007. *Proceedings of the National Academy of Sciences.* **104**: 5727.

# Correlations and Control of Properties of Metallic U and Pu

*Jeremy Neil Mitchell*

20070013DR

## Introduction

Electronic correlation effects are recognized as the key physics that accounts for the many anomalous properties of uranium and plutonium metals, alloys, and compounds. This project takes advantage of recent advances in condensed matter theoretical and experimental techniques to make a fresh attempt to sort out and understand this physics. Because of the complexity of the actinides, it is necessary to address these problems from many directions. We are measuring transport properties, photoemission, specific heat, thermal expansion, elastic moduli, and microwave absorption, with varying magnetic field and temperature where appropriate. We are applying the most advanced theoretical physics tools to understand correlation effects and how they affect the properties of actinides. Uranium has weaker electronic correlations than Pu and working on both simultaneously, as well as understanding the difference between the two, provides important clues as to how correlations control the properties of these materials.

## Benefit to National Security Missions

This project is generating state-of-the-art data on Pu and U. Unique experiments are being performed and theoretical understanding of electron correlations are being developed. This project is providing LANL with solid footing to predict the effect of extreme perturbations on relevant nuclear weapons systems and their evolution over time.

## Progress

### Plutonium Compounds

We spent much of FY08 re-establishing our plutonium compound growth laboratories in Wing 5 of the CMR Building. This effort was necessitated by the closure of Wing 2 early in 2007. The materials we produced this year include dilute Pu Kondo single crystals of $Lu_{1-x}Pu_xInCu_4$ (x = 0.005-0.02), $Lu_{1-x}Pu_xCoGa_5$ (x = 0.005-0.02), $Th_{1-x}Pu_xIn_3$ (x = 0-0.01), and $Th_{1-x}Pu_xSn_3$ (x = 0- 0.02). Our electrical resistivity measurements show no evidence for the development of a characteristic (Kondo) energy scale for Pu in these systems.

We prepared single crystals of $PuGa_3$, $PuSb_2$, and $PuCoGa_5$ to investigate strong correlations by means of de Haas van Alphen (dHvA) and angle-resolved photoemission. Preliminary dHvA measurements on $Lu_{1-x}Pu_xCoGa_5$ (x = 0.005) reveal oscillations in a Pu-bearing compound for the first time ever. There is a small change in the Fermi surface in the Pu-doped compound compared to pure $LuCoGa_5$. We measured the effective mass of a few of the orbits, indicating that this is a powerful method for understanding correlation effects. Work is underway to map the Fermi surface more completely at higher fields.

We grew $PuPt_2Si_2$ and $PuNiSi_2$ to better understand the role of strong electronic correlations in new Pu systems. Magnetization measurements on $PuNiSi_2$ indicate that it has a complex magnetic structure involving ferromagnetism at $T_C$=70 K and subsequent antiferromagnetic transition at $T_N$=35 K (Figure 1). Finally, optical conductivity measurements on $PuCoGa_5$ will provide new information about 1) electron-phonon coupling, which is a necessary ingredient for a realistic model of the band structure, 2) a characteristic energy scale for the Pu magnetic moments, and 3) the nature of the superconducting state below 18.5 K.

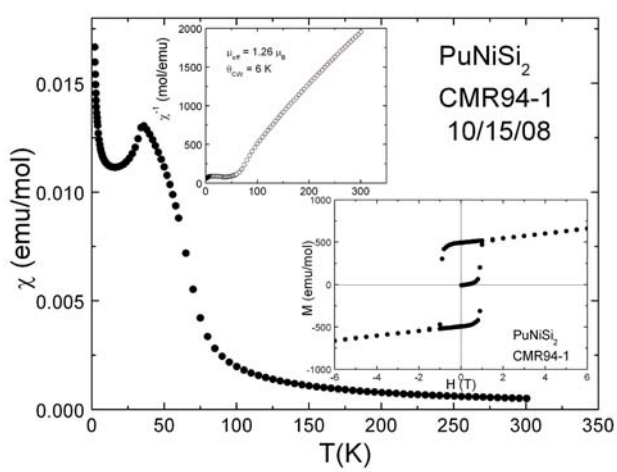


*Figure 1. Magnetic susceptibility measurements of $PuNiSi_2$. Note the antiferromagnetic transition at 35 K.*

**Uranium Compounds**

During the Wing 5 laboratory setup, our efforts focused on U and U compounds. Conductivity measurements on α-U to fields of 143 T and optical transmission studies were conducted with new apparatus to 185 T. These measurements led to the development of a new magnetic susceptibility capability that has been applied to actinide materials to 170 T.

We discovered a new family of $UM_2Zn_{20}$ (M=Co, Rh) in which the U atoms are weakly hybridized with a shell of Zn atoms and behave as local-moments embedded in a metallic host. Anderson model fits in the extreme Kondo (local) limit to the magnetic susceptibility, specific heat, and dynamic susceptibility data reveal that these materials have a characteristic energy scale (Kondo temperature) of order $T_K$=20 K. Thus, $UM_2Zn_{20}$ are model systems to investigate a particularly simple (localized) limit of the Anderson model that incorporates strong electronic correlations.

**Technique Development**

Our intensive technique developments are directed to measurements at the National High Magnetic Field Laboratory (NHMFL). Significant effort went into a quasi-optical GHz technique for measurement of the cyclotron resonance of metals for application to the single-turn magnet system. Electron paramagnetic resonance experiments and conductivity measurements were successfully demonstrated with the basic components to assess the time response feasibility of the technique.

We recently began measurements on $USb_2$ using the piezolever torque magnetometer and tunnel diode oscillator (TDO) contactless resistivity systems. Quantum oscillations were observed using both techniques, although the piezolever has superior resolution (Figure 2).

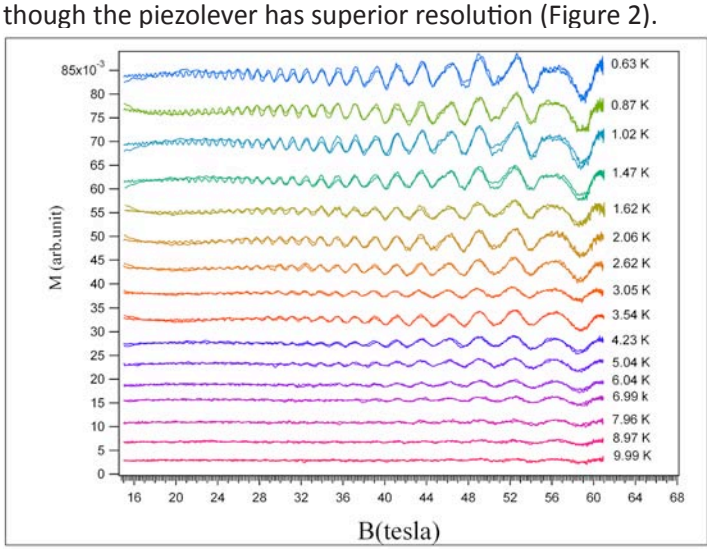


*Figure 2. Quantum oscillations in $USb_2$ as a function of temperature measured using the piezolever torque magnetometer.*

These results are an important step towards doing the first-ever measurements on Pu materials, which we will begin early in 2009.

**Theory**

Our theoretical studies continue to be extremely productive. We have derived an effective Hamiltonian for α and δ Pu, calculated the integrated photoemission spectrum for these phases (Figure 3), and calculated their specific heats [1, 2]. The latter two compare favorably to experiments conducted by co-investigators on this project.

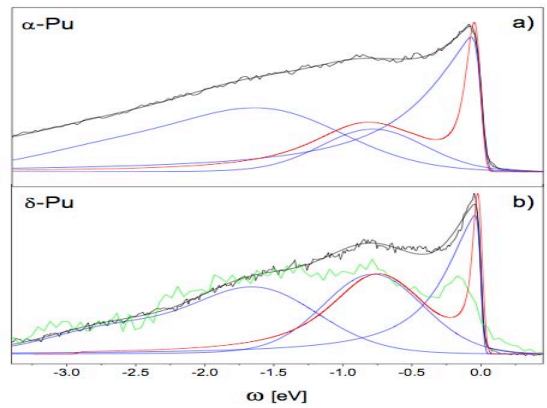


*Figure 3. Measured angle-integrated PES for alpha-Pu (a) and delta-Pu (b). Experimental data and fit are shown in black lines. The different peak components obtained from the fit are shown as blue lines, while the measured curve convoluted with the experimental conditions is shown in red. Panel (b) also shows the hv=115eV Fano resonance scan for delta-Pu as a green line.*

Our dynamical mean field theory (DMFT) work on the spectral properties of Pu [3] was a significant advance in the field in several respects: we did the calculations at the temperature at which δ-Pu is stable; we use a Quantum Monte Carlo solver, which is the only exact DMFT solver; we used a tight-binding fit that made the separation of the many-body and one-electron band-structure aspects very clean and transparent; and, we showed that it was extremely important to allow the *f*-electron occupancy to be treated as an adjustable parameter. We showed that the *f*-electron occupancy drastically changes the photoemission spectra, and hence the DMFT results cannot be trusted to give the correct physics without examining the dependence of the properties on the *f*-electron occupancy [3].

We applied LDA+U and GW approaches towards understanding how they modify the correlations in Pu. Within the LDA+U framework, the short bonds in α-Pu stabilize the electronic structure from correlation effects, whereas the longer bonds in δ-Pu are not as effective. The short bonds in α-Pu create an effective large kinetic energy term that inhibits volume expansion as the Hubbard U (correlation) is increased. In contrast, correlation effects (large U) quickly cause a large volume expansion in δ-Pu. This

explains one of the main physical characteristics that ties electronic structure and physical properties.

We performed the very first GW calculations on U and Pu. GW is the only rigorous first-principles method to include correlation physics beyond the band-structure level. We find significant band narrowing in U that is characteristic of strongly correlated materials [4]. Our Pu calculations show that besides the narrowing of individual bands, correlation effects also dramatically reduce crystal field effects, which cause the largest reduction in the effective density of states [5].

We carefully considered the effect of more realistic Coulomb correlations to provide a better treatment of intra-atomic Coulombic effects on more sophisticated many-body theories for Pu. We have shown that starting from a $jm_j$ basis rather than the usual $lm_l$ basis has significant advantages for Pu, since a simpler density-density approximation for the Coulomb terms are a good approximation compared to an exact treatment of these effects when strong spin-orbit coupling is present [6]. We submitted a paper to include spin-orbit properly for *f*-electron systems when using tight-binding theory [7].

We developed a new solver for the single impurity Anderson model that is based on recursion operator techniques [8]. This is an important since more accurate solvers are needed at zero and low temperatures for sophisticated DMFT calculations of Pu and other actinides. Finally, we published a new mechanism for the atomic pathways for the α´ to δ transformation in Pu based on symmetry considerations [9].

## Future Work

We made several strategic changes to our project that enhance our capabilities: 1) addition of photoemission spectroscopy, and angle-resolved photoemission (ARPES) in particular, to understand band hybridization and bonding; 2) focusing efforts on simpler 2D compounds such as $PuSb_2$ that are better suited for piezolever and TDO magnetometry; and 3), begun development of a δ-Pu single crystal synthesis technique that will allow us to measure single-crystal Pu properties. We will also:

- Install induction melter in Wing 5 to make Pu Kondo alloys
- Prepare $PuCoGa_5$, $PuSb_2$, and $Pu_2MIn_8$ (M=Co, Rh, Ir) for dHvA and angle-resolved photoemission
- Measure ARPES of $PuSb_2$ and $Pu_2RhGa_8$ for *f*-to-conduction band hybridization and bonding
- Measure angle-integrated temperature dependence of δ-Pu for electron-phonon coupling
- Calculate the Fermi surface for $USb_2$, $PuSb_2$, and $Pu_3Ga$ for integration with experiments
- Finish analyzing GW calculations for δ-Pu as a function of volume and extend these calculations for α-Pu
- Make new DMFT calculations on $Pu_3Ga$ to understand the role of Ga in stabilizing the fcc crystal structure as well as the strong correlations in Pu
- Improve the new recursion operator technique for the single-impurity Anderson-model solvers.

## Conclusion

We are collecting experimental data and developing theoretical models to elucidate how correlations quench the magnetism of U and Pu. This allows an explanation of how differences in the electronic correlations in U and Pu modify properties of these metals. Innovative cyclotron-band mass and Fermi surface measurements of U and Pu in ultra-high magnetic fields are starting to challenge our theories, enabling us to select the best. DMFT is the theoretical framework to integrate our experimental results. We will calculate effective mass, high-temperature atomic forces, and the Kondo properties, understanding how electronic correlation effects quench magnetism in pure Pu.

## References


1. Batista, C. D.. Effective Hamiltonian for metallic Pu. To appear in *Journal of Nuclear Materials.*
2. Batista, C. D., J. E. Gubernaitis, T. Durakiewicz, and J. Joyce. Strongly correlated approach to actinides. 2008. *Physical Review Letters.* **101** (1): 016403.
3. Zhu, J. X., A. K. McMahan, M. D. Jones, T. Durakiewicz, J. J. Joyce, J. M. Wills, and R. C. Albers. Spectral properties of delta-plutonium: sensitivity to 5f occupancy. 2008. *Physical Review B.* **76** (24): 245118.
4. Chantis, A. N., R. C. Albers, M. D. Jones, M. van Schilfgaarde, and T. Kotani. Many-body electronic structure of metallic alpha-uranium. 2007. *Physical Review B.* **78** (8): 081101.
5. Chantis, A. N., R. C. Albers, A. Savane, and N. E. Christensen. GW correlation effects on plutonium quasiparticle energies: changes in crystal field splitting. To appear in *Philosphical Magazine.*

6. Julien, J. P., J. X. Zhu, and R. C. Albers. Coulomb correlation in presence of spin-orbit coupling: application to plutonium. 2008. *Physical Review B.* **77** (19): 195123.

7. Jones, M. D., and R. C. Albers. Role of spin-orbit coupling in a tight-binding total energy method. *Physical Review B.*

8. Julien, J. P., and R. C. Albers. Extended recursion in operator space (EROS), a new impurity solver for the single impurity Anderson model. *Physical Review Letters.*

9. Lookman, T. A., A. Saxena, and R. C. Albers. Phonon mechanisms and transformation paths in Pu. 2008. *Physical Review Letters.* **100** (14): 145504.

## Publications

Albers, R. C., and J. X. Zhu. Vacillating valence. 2007. *Nature.* **446**: 504.

Batista, C. D.. Effective Hamiltonian for metallic Pu. To appear in *Journal of Nuclear Materials.*

Batista, C. D., J. E. Gubernatis, T. Durakiewicz, and J. Joyce. Strongly correlated approach to actinides. 2008. *Physical Review Letters.* **101** (1): 016403.

Bauer, E. D., J. N. Mitchell, D. S. Schwartz, J. D. Thompson, and J. L. Sarrao. From delta-Pu to PuCoGa5: Kondo effect investigations of strong electronic correlations in Pu. Presented at *American Physical Society March Meeting.* (Denver, CO, 5-9 March 2007).

Booth, C. H., E. D. Bauer, M. Daniel, R. E. Wilson, J. N. Mitchell, L. A. Morales, J. L. Sarrao, and P. G. Allen. Quanitfying structural damage from self-irradiation in a plutonium superconductor. 2007. *Physical Review B.* **76**: 064530.

Booth, C. H., M. Daniel, R. E. Wilson, E. D. Bauer, J. N. Mitchell, N. O. Moreno, L. A. Morales, J. L. Sarrao, and P. G. Allen. Self-irradiation damage and 5f localization in PuCoGa5. 2007. *Journal of Alloys and Compounds.* **444-445**: 119.

Bouchet, J., R. C. Albers, and G. Jomard. GGA and LDA+U calculations of Pu phases. 2007. *Journal of Alloys and Compounds.* **444**: 246.

Bouchet, J., and R. C. Albers. Elastic properties of the light actinides at high pressure. *Physical Review B.*

Chantis, A. N., R. C. Albers, A. Savane, and N. E. Christensen. GW correlation effects on plutonium quasiparticle energies: changes in crystal field splitting. To appear in *Philosophical Magazine.*

Chantis, A. N., R. C. Albers, M. D. Jones, M. van Schilfgaarde, and T. Kotani. Many-body electronic structure of metallic alpha-uranium. 2008. *Physical Review B.* **78** (8): 081101.

Cox, S., E. Rosten, R. D. McDonald, and J. Singleton. Comment on 'Pinning frequencies of the collective modes in alpha-uranium'. 2007. *Physical Review Letters.* **98**: 249701.

Hu, S. Y., M. E. Baskes, M. Stan, and J. N. Mitchell. Phase-field modeling of coring structure evolution in Pu-Ga alloys. 2007. *Acta Materialia.* **55**: 3641.

Hu, S. Y., M. L. Baskes, M. Stan, J. N. Mitchell, J. X. Zhang, and L. Q. Chen. Effect of elastic anisotropy and inhomogeneity on coring structure evolution in Pu-Ga alloys - phase field modeling. 2007. *Journal of Computer-Aided Materials Design.* **145**: 389.

Jones, M. D., and R. C. Albers. Role of spin-orbit coupling in a tight-binding total energy method. *Physical Review B.*

Julien, J. P., J. X. Zhu, and R. C. Albers. Coulomb correlation in presence of spin-orbit coupling: application to plutonium. 2008. *Physical Review B.* **77** (19): 195123.

Julien, J. P., R. C. Albers, and J. Bouchet. Effect of spin-orbit coupling on an ab initio Gutzwiller approach for Pu. 2007. *Journal of Alloys and Compounds.* **444-445**: 285.

Julien, J. P., and R. C. Albers. Extended recursion in operator space (EROS), a new impurity solver for the single impurity Anderson model. *Physical Review Letters.*

Lookman, T., A. Saxena, and R. C. Albers. Phonon mechanisms and transformation paths in Pu. 2008. *Physical Review Letters.* **100** (14): 145504.

M.Chia, E. E., J. X. Zhu, H. J. Lee, N. Hur, N. O. Moreno, R. D. Averitt, J. L. Sarrao, and A. J. Taylor. Time-resolved quasiparticle dynamics in the spin-density-wave state. *Physical Review Letters.*

Manley, M. E., A. Said, M. J. Fluss, M. Wall, J. C. Lashley, A. Alatas, and K. T. Moore. Phonon density of states of alpha- and delta-plutonium measured using inelastic x-ray scattering. *Physical Review B.*

Mielke, C. H.. Multi-megagauss single turn system for the study of plutonium. To appear in *Megagaus XI.* (London, UK, 8 - 14 September, 2006).

Mielke, C. H., and R. D. McDonald. Single turn multi-megagauss system at the NHMFL-Los Alamos to study plutonium. 2007. In *Megagauss Magnetic Fields and High Energy Liner Technology.* (Santa Fe, NM, USA, 4-8 November 2006). , p. 227. New York, NY: IEEE.

Migliori, A., C. Pantea, H. Ledbetter, I. Stroe, J. B. Betts, J. N. Mitchell, M. Ramos, F. Freibert, D. Dooley, S. Harrington, and C. H. Mielke. Alpha-plutonium's polycrystalline elastic moduli over its full temperature range. 2007. *Journal of the Accoustical Society of America.* **122** (4): 1994.

Migliori, A., I. Mihut, J. B. Betts, M. Ramos, C. Mielke, C. Pantea, and D. Miller. Temperature and time-dependence of the elastic moduli of Pu and Pu-Ga alloys. 2007. *Journal of Alloys and Compounds.* **444-445**: 133.

Mitchell, J. N., F. J. Freibert, M. E. Bange, and D. S. Schwartz. Unconventional delta-phase stabilization in Pu-Ga alloys. To appear in *Journal of Nuclear Materials.*

Ohishi, K., R. H. Heffner, G. D. Morris, E. D. Bauer, M. J. Graf, J. X. Zhu, L. A. Morales, J. L. Sarrao, M. J. Fluss, D. E. MacLaughlin, L. Shu, W. Higemoto, and T. U. Ito. Influence of self irradiation on the magnitude of superfluid density in PuCoGa5 probed by muon spin rotation. 2008. *Physica B.* **403** (5-9): 1013.

Rhyne, J. J., F. Trouw, A. J. Hurd, and J. N. Mitchell. Pu neutron scattering studies - magnetism and structure. To appear in *Journal of Nuclear Materials.*

Sarrao, J. L., and J. D. Thompson. Superconductivity in cerium- and plutonium-based 115 materials. 2007. *Journal of the Physical Society of Japan.* **76**: 051013.

Thompson, J. D.. Actinide superconductivity: PuCoGa5 and related materials. Invited presentation at *Materials Research Society Symposium Proceedings.* (Boston, Nov. 2006).

Thompson, J. D., N. J. Curro, T. Park, E. D. Bauer, and J. L. Sarrao. PuCoGa5 and related materials. 2007. *Journal of Alloys and Compounds.* **444-445**: 19.

Zhu, J. X.. Spectral properties of elemental plutonium. Presented at *International Conference on Strongly Correlated Electron Systems.* (Houston, 13-18 May, 2007).

Zhu, J. X., A. K. McMahan, M. D. Jones, T. Durakiewicz, J. J. Joyce, J. M. Wills, and R. C. Albers. Spectral properties of delta-plutonium: sensitivity to 5f occupancy. 2007. *Physical Review B.* **76** (24): 245118.

Zhu, J. X., A. K. McMahan, M. D. Jones, T. Durakiewicz, J. J. Joyce, J. M. Wills, and R. C. Albers. Spectral properties of elemental plutonium. Presented at *American Physical Society March Meeting.* (Denver, CO, 5-9 March 2007).

Zhu, J. X., A. K. McMahan, M. D. Jones, T. Durakiewicz, J. J. Joyce, J. M. Wills, and R. C. Albers. Theoretical studies of spectral properties of plutonium. 2008. In *Materials Research Society Symposium Proceedings.* (San Francisco, 25-28 March 2008). Vol. 1104, p. 59. Warrendale, PA: MRS.

# Metamaterials for Threat Reduction Applications: Imaging, Signal Processing, and Cloaking

*Antoinette Jane Taylor*

20070060DR

## Introduction

The field of metamaterials has blossomed with the realization that it is possible to create "artificial" electromagnetic composites that combine tailored magnetic and electric response. This has led to the demonstration of unique functional behavior such as a negative index of refraction, which is not attainable with naturally occurring materials. Such novel electromagnetic properties, coupled with the scalability of the metamaterial response from radio-frequency to near optical frequencies, have resulted in a flurry of research activity with a view towards both fundamental understanding and practical applications. In short, metamaterials provide a new scale-invariant design paradigm to create functional materials that revolutionize our ability to manipulate, control, and detect electromagnetic radiation. The grand challenge in metamaterials research is to fully exploit this potential to create new electromagnetic devices addressing threat reduction applications. Our objective is to advance the understanding of metamaterial properties with a view towards utilizing such structures to create functional electromagnetic structures and devices relevant to threat reduction applications at far-infrared frequencies. Specifically, we will design, fabricate, and characterize the following metamaterial devices for communication, detection, and electromagnetic cloaking applications at far-infrared frequencies. The ability to image objects at far-infrared frequencies, to covertly transmit data at high bit-rates at difficult to detect wavelengths, or to cloak an object from interrogating radiation is highly desirable goals with regards to threat reduction. Thus, such electromagnetic metamaterials devices offer considerable potential as transformational components of an overall system architecture designed to mitigate or detect a potential threat.

## Benefit to National Security Missions

This work will develop metamaterial devices to push the state of the art in terahertz communication and detection and lays the foundation for electromagnetic cloaking applications. As such, this work supports NNSA's mission of threat reduction by advancing the possibility of using THz radiation for, as one example, secure communication.

## Progress

We designed, fabricated, and characterized a series of planar THz metamaterials and their inverse structures termed complementary metamaterials. These planar THz metamaterials can serve as THz filters, transparent THz windows, find applications in FIR spectroscopy, astronomy, laser cavity output couplers, and form the base in developing more advanced functional THz devices and components. When planar THz metamaterials are fabricated on a high resistivity semiconductor substrate, their resonant response can be dynamically switched upon photoexcitation of substrate free charge carriers, which short-circuit the split gaps of the metamaterial elements and turn off the THz metamaterial resonance. In such a way, the metamaterial effective permittivity is switched between negative and positive values, and the THz transmission intensity is effectively modulated with very high modulation depth under relatively low photoexcitation fluence Although the switching on could be ultrafast (<1 ps), the switching off recovery time is relatively slow due to the long carrier lifetimes in crystalline semiconductors. We overcome this issue by the use of MBE grown ErAs/GaAs nanoisland superlattice substrates, where the carrier lifetimes can be designed to have desired values from sub-picosecond to tens of picoseconds. With a designed carrier lifetime of ~10 ps, we demonstrate a switching recovery time of ~20 ps using either an original or complementary metamaterial structures by optical-pump THz-probe measurements. In such a way we demonstrated high performance ultrafast dynamical THz metamaterial switches. In many applications it is desirable to have electrically switchable metamaterials. We demonstrated a unique design of hybrid THz metamaterial employing the Schottky diode structure. When the all-connected metal metamaterial elements are fabricated on a slightly doped semiconductor sub-

strate, a Schottky diode structure forms and the depletion regions can be actively controlled by applying a voltage bias between the metamaterial and substrate. This leads to a modified conductivity of the substrate particularly near the split gaps, thereby actively switching the metamaterial resonant response and the THz transmission. The results show a switching/modulation depth of 50% for the transmitted THz intensity, which is one order of magnitude improvement over the existing electrically driving terahertz switch/modulator based on quantum well structures, and importantly, operates at room temperatures.

For THz detection we are developing the use of bimaterial cantilever detectors where the absorption of electromagnetic radiation is enhanced through the incorporation of resonant metamaterials. This approach is based on metamaterials, which provide for the synthesis of design-specific electromagnetic resonances coupled with MEMS cantilever technology. Fabrication of strongly absorbing MM elements on a MEMS cantilever will lead to a deflection of the cantilever when terahertz (THz) radiation is incident. The principle of operation is that cantilevers are fabricated from two materials with different coefficients of thermal expansion (typically $Si_3N_4$ and Au). The absorption induced deflection can, in turn, be measured using optical readout. The possibility of incorporating MM into the detector is of crucial importance at THz frequencies where it is difficult to find highly absorbing materials at this wavelength range that, further, are compatible with MEMS processing. A crucial aspect of any thermally-based detection radiation detector is to have a low thermal mass to obtain the greatest possible temperature change for a given incident flux. Free standing cantilevers meet this requirement. A preliminary thermal analysis of these detectors suggests that it should be possible to achieve a noise equivalent temperature difference of ~10mK, a very competitive technology for the detection of THz radiation. To date, we have fabricated initial structures of free-standing metamaterials on bimaterial cantilevers. In the next stage of this work, we will fabricate single pixel samples, which are optimized for THz radiation detection. The deflection of the cantilever upon absorption of THz radiation will be measured using optical readout methods.

An issue that determines, in part, how well a metamaterial enhanced thermal detector works is how much of the incident radiation is absorbed. We have previously demonstrated that approximately 25% of the radiation incident on a single layer metamterial structure is absorbed and converted to heat. We have also been investigating more advanced two-layer structures to further enhance the absorption of terahertz radiation. Our design consists of a bilayer unit cell, which allows for maximization of the absorption through independent tuning of the electrical permittivity and magnetic permeability. Theoretical calculations suggest that near unity absorption can be obtained. The reflection and transmission were both measured and from this the absorption determined. An experimental absorptivity of 70% at 1.3 terahertz is demonstrated. In subsequent work, we plan on increasing the absorptivity through refinement of the fabrication process. Ultimately, our goal is to incorporate the two-layer metamaterial structure onto the bimaterial pixels to maximize sensor sensitivity.

One of the key steps to creating an electromagnetic cloak at THz frequencies is to fabricate a flexible THz metamaterial, one that can be wrapped into a circular or tubular shape without affecting performance. We have recently demonstrated fabrication and characterization of THz metamaterials based on flexible Kapton substrates. Kapton is a very flexible substrate but at the same time maintains enough transverse dimensional stability to ensure that the metallic SRRs fabricated on its surface do not “break up” thus destroying their electrical properties. In addition, we have demonstrated that these metamaterials can be stacked in multiple layers to create a quasi-bulk metamaterial, with important implications towards creating a real THz cloak.

## Future Work

Our objective is to advance the understanding of metamaterial properties with a view towards utilizing such structures to create functional electromagnetic structures and devices relevant to threat reduction applications at far-infrared frequencies. Specifically, we will design, fabricate, and characterize the following metamaterial devices:

1. Bolometric focal plane array: the pixels will be comprised of highly absorptive electric metamaterials optimized for far-infrared imaging and detection.

2. Active metamaterial switches: we will develop metamaterial modulators for high-bit-rate signal processing and covert communication.

3. Electromagnetic cloaking: recent theoretical research suggests the possibility of using electric and magnetic metamaterials to hide objects from electromagnetic radiation. We propose to theoretically and experimentally investigate the potential electromagnetic “cloaking” property of metamaterials.

The ability to image objects at far-infrared frequencies, to covertly transmit data at high bit-rates at difficult to detect wavelengths, or to cloak an object from interrogating radiation is highly desirable goals with regards to threat reduction. Thus, such electromagnetic MM devices offer considerable potential as transformational components of an overall system architecture designed to mitigate or detect a potential threat.

The scientific underpinnings of such devices derives from

the recent realization that it is possible to design and fabricate resonant sub-wavelength "particles". Importantly, particles can be designed to exhibit an electrically resonant or magnetically resonant response and, further, can be combined to achieve novel electromagnetic behavior (e.g. negative index). However, as we have recently demonstrated, SRRs also exhibit a pronounced (and functional) electric response. In short, we will create new MM particles that can subsequently be incorporated into our proposed devices to enhance their operational characteristics.

## Conclusion

This project will develop metamaterial devices to push frontiers in terahertz communication, detection, and electromagnetic cloaking applications. Four major results are anticipated during the course of this work:

1. Develop terahertz metamaterial switches wherein the switching is accomplished using optical or voltage control.
2. Develop enhanced detectors of THz radiation wherein metamaterials serve to more efficiently capture the incident radiation.
3. Develop theoretical and experimental tools to fabricate initial metamaterial cloaks to hide an object from interrogation by radiation.
4. Quite generally, advance the state of the art in metamaterials research paving the way for additional advances using this new material design paradigm.

## Publications


Azad, A. K., A. J. Taylor, E. Smirnova, and J. F. O'Hara. Characterization and analysis of terahertz metamaterials based on rectangular split-ring resonators. 2008. *Applied Physics Letters.* **92**: 011119.

Azad, A. K., H. T. Chen, A. J. Taylor, E. Akhadov, N. R. Weisse-Bernstein, and J. F. O'Hara. Flexible quasi-three-dimensional metamaterials. To appear in *Optics Letters.*

Chen, H. T., H. Lu, A. K. Azad, R. D. Averitt, A. C. Gossard, J. F. O'Hara, S. A. Trugman, and A. J. Taylor. Electronically switchable terahertz surface plasmon resonance. 2008. *Optics Express.* **16**: 7641.

Chen, H. T., J. F. O'Hara, A. J. Taylor, R. D. Averitt, C. Highstrete, M. Lee, and W. J. Padilla. Complementary planar, terahertz materials. 2007. *Optics Express.* **15**: 1084.

Chen, H. T., J. F. O'Hara, A. K. Azad, A. J. Taylor, R. D. Averitt, D. B. Shrekenhamer, and W. J. Padilla. Experimental demonstration of frequency agile terahertz metamaterials. 2008. *Nature Photonics.* **2**: 295.

Chen, H. T., W. J. Padilla, J. M. O. Zide, A. C. Gossard, A. J. Taylor,, and R. D. Averitt. All Solid-State Metamaterial Devices. 2006. *Nature.* **444**: 597.

Chen, H. T., W. J. Padilla, J. M. O. Zide, S. R. Bank, A. C. Gossard, A. J. Taylor, and R. D. Averitt. Ultrafast optical switching of terahertz metamaterials fabricated on ErAs/GaAs nanoisland superlattices. 2007. *Optics Letters.* **32**: 1620.

Landy, N. I., S. Sajuyigbe, J. J. Mock, D. R. Smith, and W. J. Padilla. Perfect Metamaterial Absorber. 2008. *Physical Review Letters.* **100**: 207402.

O'Hara, J. F., A. K. Azad, H. T. Chen, A. J. Taylor, and E. Smirnova. Effects of microstructure variations on macroscopic terahertz metafilm properties. 2007. *Active and Passive Electronic Components .* **2007**: 49691.

O'Hara, J. F., E. Smirnova, H. T. Chen, A. J. Taylor, R. D. Averitt, C. Highstrete, M. Lee, and W. J. Padilla. Properties of Planar electric metamaterials for novel terahertz applications. 2007. *Journal of Nanoelectronics and Optoelectronics .* **2**: 90.

O'Hara, J. F., R. Singh, I. Brener, E. Smirnova, J. Han, A. J. Taylor, and W. Zhang. Thin film sensing with planar metamaterials: sensitivity and limitations. 2008. *Optics Express.* **16**: 1786.

Padilla,, W. J., M. T. Aronsson, C. Highstrete, M. Lee, A. J. Taylor, and R. D. Averitt. Novel electrically resonant terahertz metamaterials: Theoretical and experimental investigations. 2007. *Physical Review B.* **75**: 041102R.

Singh, R., A. K. Abul, J. F. O'Hara, A. J. Taylor, and W. Zhang. Effect of metal permittivity on resonant properties of terahertz metamaterials. 2008. *Optics Letters.* **33**: 1506.

Singh, R., E. Smirnova, A. J. Taylor, J. F. O'Hara, and W. Zhang. Optically thin terahertz metamaterials. 2008. *Optics Express.* **16**: 6537.

Tao, H., N. I. Landy, C. Bingham, X. Zhang, R. D. Averitt, and W. J. Padilla. A metamaterial absorber for the terahertz regime: design, fabrication and characterization" . 2008. *Optics Express.* **16**: 7181.

# Coexistence of Magnetic and Superconducting Electrons in Strongly Correlated Matter

*Joe David Thompson*

20070064DR

## Introduction

There are many hundreds of materials that, at sufficiently low temperatures, become superconducting. The physics of their conventional superconductivity is very well understood theoretically, and this theory also predicts that the electrons participating in superconductivity cannot be magnetic, a conclusion supported by many experiments. Unexpected discoveries during the past two decades have shown, however, that some materials become superconducting only when magnetism is present or 'nearby' and when complex electron-electron correlations are very strong. These unconventional superconductors cannot be explained by any theory, yet they hold substantial promise for future energy-saving technologies. The problem posed by coexisting unconventional superconductivity and magnetism is Grand Challenge to US science, and its solution also will bring entirely new understanding to the physics of actinide materials, such as plutonium, whose complexity arises from strong electronic correlations. The goal of this project is to establish experimentally and theoretically how strong correlations allow the same electrons to create coexisting magnetism and unconventional superconductivity.

## Benefit to National Security Missions

This project supports DOE, Office of Science missions by enhancing our understanding of unconventional superconductivity, which is needed for future energy transmission and storage applications, and addresses the Laboratory's mission in superconductivity from 5*f* electrons.

## Progress

This year, substantial progress has been made theoretically and experimentally in revealing and understanding the coexistence of magnetic and superconducting electrons in strongly correlated matter. Experimentally, research has focused on a class of strongly correlated materials $CeMIn_5$ (where M=Rh, Co and Ir) that led to the discovery of the first Pu-based superconductor $PuCoGa_5$. Though superconductivity in $PuCoGa_5$ can be destroyed by a very high magnetic field, higher than any currently available, the critical field required to completely suppress superconductivity in its relative $CeCoIn_5$, though high, is accessible. Using neutron diffraction at extremes of very low temperatures and high magnetic fields, we have discovered that a magnetic field creates quantized units of magnetic flux with a very unusual distribution in the superconducting state of $CeCoIn_5$. This result, published in the journal Science [1], led us to suspect that the unusual distribution of flux could be due to magnetism. Indeed, further neutron measurements have shown that long range magnetic order is established in the low temperature, high field superconducting state of $CeCoIn_5$, and most significantly that magnetism exists only inside the superconducting state. This exciting result, also published in Science [2], confirms our earlier conclusion from NMR studies that superconductivity is, in fact, necessary for magnetic order, a totally new and unexpected phenomenon that derives from strong electronic correlations and that should be observed in related systems. We also have shown that this unusual state is highly sensitive to a small amount (a few hundred parts per million) of chemical disorder [3].

$CeRhIn_5$ offers an example where we can study coexisting magnetic order and superconductivity in the absence of an applied field, but applied pressure is necessary to access this coexistence. In a very productive collaboration, we have used the unique capability of field-angle dependent specific heat measurements under pressure to establish that pressure-induced superconductivity in $CeRhIn_5$ is unconventional when it coexists with antiferromagnetic order [4] and that the nature of that unconventional state is inconsistent with some theoretical predictions [5].

Besides field-induced coexistence of magnetism and superconductivity in $CeCoIn_5$, replacing a small number (~0.5 %) of In atoms by Cd or Hg also induces a phase of coexistence in the absence of a magnetic field. Us-

ing NMR, we have found that magnetism nucleates initially around the Cd 'impurity' and then spreads spatially to coexist uniformly and homogeneously throughout the sample's bulk [6]. Neutron diffraction on this material shows that the development of magnetic order is arrested abruptly as superconductivity sets in, providing very strong evidence that the same electrons are involved in producing both magnetic order and unconventional superconductivity. We are pursuing these discoveries aggressively using the full arsenal of techniques available to our collaborators and us.

One of those techniques is photoemission spectroscopy that has been used to reveal the role of strong correlations in modifying the microscopic electronic structure of the $CeMIn_5$ materials and a related but non-superconducting 5*f*-electron material $USb_2$. These studies show that fine details of the electronic structure in $USb_2$ are changed in the same way as they are in the high-temperature cuprate superconductors, and we have shown for the first time theoretically how this change develops from strong correlations.

More broadly, theory and modeling have revealed new perspectives on the origin and consequences of coexisting magnetic and superconducting electrons. At the level of phenomenology, we have developed Ginzburg-Landau models to capture the highly anomalous pressure and field responses of $CeRhIn_5$. These models account for the pressure-dependence of hybridization of d- and f-electrons and capture qualitative aspects of experimental observations. Related models have been constructed to incorporate interactions necessary for a field-induced magnetic phase in unconventional superconductors, such as $CeCoIn_5$. At a microscopic level, we have constructed a model that incorporates local spin correlations in a magnetically disordered system with strong electronic correlations and have shown that this model leads to novel inhomogeneous states that are characterized by non-harmonic charge modulation and spatially dependent interactions among correlated electrons. The existence of these 'Kondo stripes' opens the possibility of coexisting superconductivity or magnetism [7]. In parallel and complementing this work, we have studied a low-dimensional version of a Kondo-Lattice model in which the conduction band is correlated. In contrast to the conventional boson-mediated paring mechanism, we have discovered that the 1D version of the model contains a robust, non-conventional pairing mechanism due to a confining interaction between topological defects (solitons) attached to each carrier. For a long enough antiferromagnetic correlation length, this pairing mechanism leads to a ground state with dominant superconducting fluctuations (long-ranged superconductivity cannot be stabilized in 1D). These developments represent major steps toward understanding how magnetic and superconducting electrons might emerge and coexist from strong electron-electron correlations.

Though this project focuses on *f*-electron materials, the report this year of new *3d*-electron systems in which superconductivity developed in close proximity to magnetic order presented an opportunity to apply our expertise to understand these (possibly) complementary materials. In just three months, we discovered four new superconductors, $CaFe_2As_2$ (under pressure), $BaNi_2As_2$, $SrNi_2As_2$ and $SrNi_2P_2$. Our study of these single crystals and related systems by NMR and thermodynamic as well as electrical and thermal transport techniques has shown that magnetism of Fe could play a role in producing superconductivity, which it certainly does in the correlated f-electron compounds we study, but unlike the *f*-electron systems, magnetism also is coupled in some cases to structural transitions. Magnetism seems to play a secondary, if any, role in the Ni-containing materials, which more likely are conventional superconductors, and this is being tested by field-dependent thermal conductivity studies.

## Future Work

Theoretical and experimental research has established unambiguously that the same electrons in a metal cannot support simultaneously magnetic order and conventional superconductivity, but a clear separation between magnetic and superconducting electrons is not possible in all materials, such as the high-Tc cuprates and f-electron heavy-fermion compounds, whose complexity is dominated by strong electronic correlations. Understanding how electronic correlations allow the same electrons to participate simultaneously in creating both unconventional superconductivity and magnetic order is a significant scientific challenge and has unexplored consequences for anticipated new energy applications of these materials. Our scientific objective is to use superconductivity as an experimental diagnostic to develop a semi-microscopic theory that captures essential commonalities of cuprate and heavy-fermion superconductors, particularly how the same electrons simultaneously create magnetism and unconventional superconductivity. To achieve this goal, a closely integrated experimental and theoretical effort will delineate the feedback effects of magnetism on superconductivity and superconductivity on magnetism, establish the nature and role of intrinsic inhomogeneity in electronic degrees of freedom, and apply universal principles to predict and discover new strongly correlated electron superconductors

## Conclusion

The discovery nearly 20 years ago of high temperature superconductivity in complex copper oxide materials held great promise for revolutionizing electrical power transmission and storage. The promise of this discovery has not been realized fully, in part because we still do not understand how electrons interact strongly to produce unconventional superconductivity in these and related materials formed from f-electron elements. This project focuses on

providing basic understanding of the interacting electrons and how these electrons affect the utility of unconventional superconductors for energy applications.

## References


1. Bianchi, A., M. Kenzelmann, L. DeBeer-Schmitt, J. S. White, E. M. Forgan, J. Mesot, M. Zolliker, J. Kohlbrecher, R. Movshovich, E. D. Bauer, J. L. Sarrao, Z. Fisk, C. Petrovic, and M. R. Eskildsen. Superconducting vortices in CeCoIn5: toward the Pauli limiting field. 2008. *Science.* **319**: 177.

2. Kenzelmann, M., T. Strassle, C. Niedermayer, M. Sigrist, B. Padmanabhan, M. Zolliker, A. D. Bianchi, R. Movshovich, E. D. Bauer, J. L. Sarrao, and J. D. Thompson. Coupled superconducting and magnetic order in CeCoIn5. 2008. *Science.* **321**: 1652.

3. Tokiwa, Y., R. Movshovich, F. Ronning, E. D. Bauer, P. Papin, A. D. Bianchi, J. F. Rauscher, S. M. Kauzlarich, and Z. Fisk. Anisotropic effect of Cd and Hg doping on the Pauli limited superconductor CeCoIn5. 2008. *Physical Review Letters.* **101**: 037001.

4. Park, T., E. D. Bauer, and J. D. Thompson. Probing the nodal gap in the pressure-induced heavy-fermion superconductor CeRhIn5. 2008. *Physical Review Letters.* **101**: 177002.

5. Park, T., V. A. Sidorov, F. Ronning, J. X. Zhu, Y. Tokiwa, H. O. Lee, E. D. Bauer, R. Movshovich, J. L. Sarrao, and J. D. Thompson. Isotropic quantum scattering and unconventional superconductivity. To appear in *Nature.*

6. Urbano, R. R., B. L. Young, N. J. Curro, J. D. Thompson, L. Pham, and Z. Fisk. Antiferromagnetism and superconductivity in a hole-doped Kondo lattice. 2007. *Physical Review Letters.* **99**: 146402.

7. Zhu, J. X., I. Martin, and A. R. Bishop. Kondo stripes in an Anderson-Heisenberg model of heavy fermion systems. 2008. *Physical Review Letters.* **100**: 236403.


## Publications


Al-Hassanieh, K. A., C. D. Batista, P. Sengupta, and A. E. Feiguin. Topological confinement and superconductivity. *Physical Review Letters.*

Baek, S. H., N. J. Curro, T. Klimzcuk, E. D. Bauer, F. Ronning, and J. D. Thompson. First First order magnetic transition in single crystal BaFe2As2 detected by 75As NMR . *Physical Review Letters.*

Baek, S. H., T. Klimczuk, F. Ronning, E. D. Bauer, N. J. Curro, and J. D. Thompson. Evidence of an incommensurate spin-density wave instability in single crystal CaFe2As2 detected by 75As NMR. *Physical Review Letters.*

Bao, W., Y. Chen, K. Yamada, A. Savic, P. Russo, J. E. Lorenzo, and J. H. Chung. Fincher-Burke spin excitations and omega/T scaling in insualting La.195Sr.05CuO4. 2007. *Physical Review B (Rapid Commun.).* **76**: 247203.

Bauer, E. D., F. Ronning, B. L. Scott, and J. D. Thompson. Superconductivity in SrNi2As2 single crystals. To appear in *Physical Review B.*

Bauer, E. D., F. Ronning, S. Marquillon, L. D. Pham, J. D. Thompson, and Z. Fisk. Occurrence of magnetism in CeMIn5-xHgx (M=Rh, Ir). 2008. *Physica B.* **403**: 1135.

Bianchi, A. D., M. Kenzelmann, L. DeBeer-Schmitt, J. S. White, E. M. Forgan, J. Mesot, M. Zolliker, J. Kohlbrecher, R. Movshovich, E. D. Bauer, J. L. Sarrao, Z. Fisk, C. Petrovic, and M. R. Eskildsen. Superconducting vortices in CeCoIn5: toward the Pauli limiting field. 2008. *Science.* **319**: 177.

Bulaevskii, L. N., and E. M. Chudnovsky. Electromagnetic radiation from vortex flow in type-II superconductors. 2006. *Physical Review Letters.* **97**: 197002.

Durakiewicz, T., P. S. Riseborough, C. G. Olson, J. J. Joyce, E. D. Bauer, J. L. Sarrao, S. Elgazzar, P. M. Oppeneer, D. P. Moore, M. T. Butterfield, and K. S. Graham. Observation of a kink in the dispersion of f-electrons. 2008. *Europhysics Letters.* **84**: 37003.

Hruvska, M., and L. N. Bulaevskii. Effects of magnetic excitations on the I-V characteristics of magnetic superconductors. 2006. *Comptes Rendus Physique.* **7**: 42.

Kaneshita, E., I. Martin, and A. R. Bishop. Commensurate-incommensurate transition and coolective modes in the stripe phase of cuprates near 1/8 hole-doping. 2007. *Physical Review B.* **76**: 054507.

Kenzelmann, M., T. Strassle, C. Niedermayer, M. Sigrist, B. Padmanabhan, M. Zolliker, A. D. Bianchi, R. Movshovich, E. D. Bauer, J. L. Sarrao, and J. D. Thompson. Coupled superconducting and magnetic order in CeCoIn5. 2008. *Science.* **321**: 1652.

MendoncaFierreira, L., T. Park, V. A. Sidorov, M. Nicklas, E. M. Bittar, R. Lora-Serrano, E. N. Hering, S. M. Ramos, M. B. Fontes, E. Baggio-Saitovich, H. O. Lee, J. L. Sarrao, J. D. Thompson, and P. G. Pagliuso. Tuning the pressure-induced superconducting phase in doped CeRhIn5. 2008. *Physical Review Letters.* **101**: 0175005.

Nicklas, M., C. F. Miclea, J. L. Sarrao, J. D. Thompson, G. Sparn, and F. Steglich. Antiferromagnetic fluctuations and the Fulde-Ferrell-Larkin-Ovchinnikov state in CeCoIn5. 2007. *Journal of the Physical Society of Japan.* **76**: 128.

Nicklas, M., C. F. Miclea, J. L. Sarrao, J. D. Thompson, G. Sparn, and F. Steglich. Influence of antiferromagnetic fluctuations on the Fulde-Ferrell-Larkin-Ovchiinikov state in CeCoIn5. 2007. *Journal of Low Temperature Physics.* **146**: 669.

Nicklas, M., O. Stockert, T. Park, K. Habichy, L. D. Pham, J. D. Thompson, Z. Fisk, and F. Steglich. Magnetic structure of Cd-doped CeCoIn5. 2007. *Physical Review B.* **76**: 052401.

Park, T., E. D. Bauer, and J. D. Thompson. Probing the nodal gap in the pressure-induced heavy-fermion superconductor CeRhIn5. 2008. *Physical Review Letters.* **101**: 177002.

Park, T., J. L. Sarrao, and J. D. Thompson. New quantum state in the heavy fermion superconductor CeRhIn5. 2007. *Physica C.* **460-462**: 137.

Park, T., J. L. Sarrao, and J. D. Thompson. Upper critical field (Hc2) scaling near a quantum critical point in the heavy fermion compound CeRhIn5. 2007. *Journal of Magnetism and Magnetic Materials.* **310**: 712.

Park, T., M. J. Graf, L. Bulaevskii, J. L. Sarrao, and J. D. Thompson. Electronic duality instrongly correlated matter. 2008. *Proceedings of the National Academy of Science.* **105**: 6825.

Park, T., V. A. Sidorov, F. Ronning, J. X. Zhu, Y. Tokiwa, H. O. Lee, E. D. Bauer, R. Movshovich, J. L. Sarrao, and J. D. Thompson. Isotropic quantum scattering and unconventional superconductivity. To appear in *Nature.*

Ronning, F., N. Kurita, E. D. Bauer, B. L. Scott, T. Park, T. Klimczuk, R. Movshovich, and J. D. Thompson. First order transition and superconductivity in BaNi2As2 single crystals. 2008. *Journal of Physics: Condensed Matter .* **20**: 342203.

Ronning, F., T. Klimczuk, E. D. Bauer, H. Volz, and J. D. Thompson. Synthesis and properties of CaFe2As2 single crystals. 2008. *Journal of Physics: Condensed Matter.* **20**: 322201.

Tokiwa, Y., F. Ronning, J. D. Thompson, R. Movshovich, L. D. Pham, and Z. Fisk. Effect of Cd doping on superconductivity in CeCoIn5. 2008. *Physica B.* **403**: 879.

Tokiwa, Y., R. Movshovich, F. Ronning, E. D. Bauer, P. Papin, J. F. Rauscher, S. M. Kauzlarich, and Z. Fisk. Anistropic effect of Cd and Hg doping on the Pauli limmited superconductor CeCoIn5. 2008. *Physical Review Letters.* **101**: 037001.

Urbano, R. R., B. L. Young, N. J. Curro, J. D. Thompson, L. D. Pham, and Z. Fisk. Coexistence of antiferromagnetism and superconductivity in a hole doped Kondo lattice. 2008. *Physica B.* **403**: 1056.

Urbano, R. R., B. L. Young, N. J. Curro, J. D. Thompson, L. Pham, and Z. Fisk. Antiferromagnetism and superconductivity in a hole doped Kondo lattice. 2007. *Physical Review Letters.* **99**: 146402.

Voronstov, A. B., I. Vekhter, and M. J. Graf. Pauli-limited upper critical field in dirty d-wave superconductors. To appear in *Physical Review B-Rapid Communications.*

Vorontsov, Anton B., and Matthias J. Graf. Fermi-liquid effects in the Fulde-Ferrell-Larkin-Ovchinnikov state of two-dimensional d-wave superconductors. 2006. *Phys. Rev. B .* **74**: 172504.

Yang, X., P. S. Riseborough, T. Durakiewicz, C. G. Olson, J. J. Joyce, E. D. Bauer, J. L. Sarrao, D. P. Moore, K. S. Graham, S. Elgazzar, P. M. Oppener, E. Guziewicz, and M. T. Butterfield. Unusual quasiparticle renormalizations from angle resolved photoemissin on USb2. *Philosophical Magazine.*

Young, B. L., R. R. Urbano, N. J. Curro, J. D. Thompson, J. L. Sarrao, A. B. Voronstov, and M. Graf. Microscopic evidence for field-induced magnetism in CeCoIn5. 2007. *Physical Review Letters.* **98**: 036402.

Zhu, J. X., I. Martin, and A. R. Bishop. Kondo stripes in an Anderson-Heisenberg model of heavy fermion systems. 2008. *Physical Review Letters.* **100**: 236403.

continuing project

# Physics of Helium Retention in Palladium/Tritum Systems

*Douglas Joseph Safarik*

20070074DR

## Introduction

The goal of this LDRD project is to develop an atomic-level understanding of the "aging" of palladium tritide. "Aging" refers to the decreased capacity of the palladium host to store radioactive tritium gas, and to retain $^3$He generated by the decay of the tritium, with time.

Tritium (T), and its non-radioactive isotopes hydrogen (H) and deuterium (D), is easily incorporated into Pd, where it occupies interstitial sites of the type (½, 0, 0). In Pd-tritide, $^3$He atoms are continuously born by radioactive decay of tritium (half-life = 12.3 years). It is normally assumed that newly born $^3$He atoms reside in the same (½, 0, 0)-type position occupied by the parent tritium atom. Eventually, the $^3$He atoms coalesce into dimers, trimers, and higher-order aggregates. The physics of this coalescence process is not understood. When a $^3$He aggregate reaches a critical size, it transforms into a bubble, where the $^3$He atoms are not in registry with the Pd lattice. Over time, more $^3$He is incorporated into a bubble, causing it to grow. Ultimately, all the $^3$He contained in the bubbles is released, presumably by fracture in the Pd-tritide host. This completes the aging process.

In this project, we are integrating experiment, theory, and computer modeling to develop an atomic-level understanding of aging. Below we outline the studies undertaken and discuss our progress to-date.

## Benefit to National Security Missions

This project supports the NNSA mission in Nuclear Weapons by enhancing our understanding of the long-term retention of $^3$He in a metal tritide host.

## Progress

### Thermodynamics of Pd-(H, D, T) and Pd-T-$^3$He systems

The Pd-H and Pd-D systems have been extensively studied, but many of their thermodynamic properties are only partially known or poorly understood. Furthermore, the literature contains scarcely little thermodynamic data for the Pd-T system. It is therefore imperative to carefully characterize the thermodynamic properties of Pd-H isotope systems.

We have built two Sieverts' machines for measuring the equilibrium phase diagram of Pd-H isotope systems. One machine, located at MST-8, is being used to characterize PdH and Pd-D. The other machine, located at the WETF tritium facility, is being used to study Pd-T-$^3$He.

Figure 1 shows the pressure-composition equilibrium phase diagram for the absorption and desorption of D by Pd at various temperatures. The "plateaus" in these curves denote the two-phase equilibrium between the dilute Pd(D) solid solution (α phase) and the concentrated deuteride (β phase). Notice that the plateau pressures for absorption are higher than those for desorption, which is known as "hysteresis" [1]. From detailed analysis of these and similar data, we have discovered that the Pd-D(H) phase diagrams published previously [2] are likely not correct. Our work suggests that there are two equilibrium phase diagrams: one for coherent and one for incoherent coexistence of α and b phases. We have further shown that decomposition of single-phase Pd-D into α and β phases follows a Curie-Weiss law and can thus be treated analogously to a second-order phase transition. These are completely new ideas, and represent significant advances in our understanding of Pd-H systems. Two manuscripts about this work are currently in preparation.

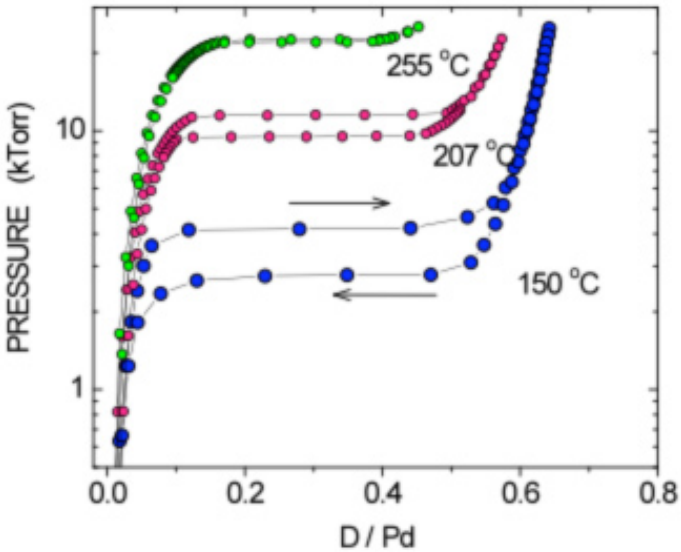


*Figure 1. Pressure-composition isotherms (at three different temperatures) for absorption and desorption of deuterium in Pd, measured in our Sieverts machine located at MST-8.*

The Sieverts' machine we built at WETF has undergone exhaustive testing, as required for certification for operation inside a nuclear facility. Preliminary data for the Pd-T system show high precision and good agreement with the literature. To date, however, we have measured fewer than 10 pressure-composition isotherms for the Pd-T system, mainly because WETF was non-operational for approximately 11 of the past 13 months. During the last year alone, the WETF facility was non-operational (no tritium delivered) during 11/1/07 to 3/15/08 and 6/1/08 to present. As a user of this LANL DOE facility, we feel that accomplishment of the scientific work is given a low priority.

**Ultrasonic studies of hydrogen short-range ordering in palladium-hydride**

In β-phase Pd-H(D,T), the hydrogen atoms are not randomly distributed on the octahedral interstitial sites of the Pd host. Indeed, ultrasonic [3] and neutron diffraction [4] measurements suggest the presence of short-range ordering (SRO) of the hydrogen atoms. This implies that there are regions within the Pd-tritide lattice that are devoid of tritium atoms, and hence $^3$He atoms cannot be born.

We studied the H-atom SRO by measuring the elastic constants of $PdH_x$ single crystals ($0.58 < x < 0.71$) between 1.4 and 300 K. Figure 2 shows the temperature dependence of the shear moduli C' and $C_{44}$ for $PdH_{0.59}$ during both fast cooling and slow warming. Notice that for C', we observe an anomaly at ≈50 K during warming, and a hysteresis between cooling and warming, whereas for $C_{44}$ we observe no anomaly or hysteresis. Based on these data, we proposed that the H-atom SRO becomes kinetically "frozen" as the Pd-H alloy is cooled to low temperatures, and then "thaws" as it is warmed. Furthermore, the presence of the hysteresis in C' but its absence in $C_{44}$ strongly suggest preferential crystallographic orientation of the SRO. Our data are inconsistent with a low-temperature thermodynamic phase transition, as is claimed in the literature. We have published two papers on these studies [5, 6].

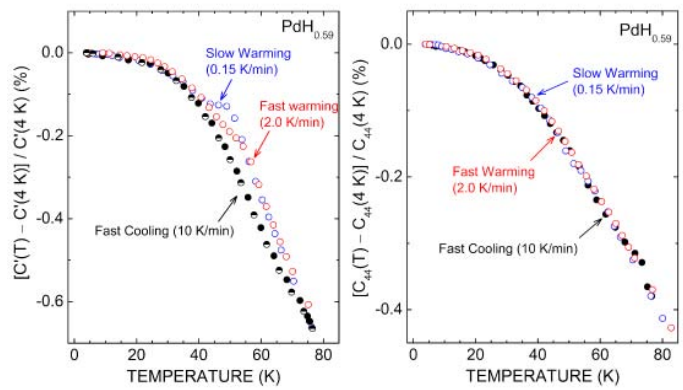


*Figure 2. Temperature dependence of shear moduli C' = ($C_{11}$ – $C_{12}$)/2 (left) and $C_{44}$ (right) for $PdH_{0.59}$, plotted as the relative change in the modulus measured with our Resonant Ultrasound Spectroscopy system at MST-8.*

**Atomistic simulations of the Pd-H system, and prediction of the phase diagram**

To provide an atomistic-level description for the behavior of $^3$He atoms in β-phase Pd-T-$^3$He, we must first model the atom-level behavior of the Pd-T(H) host (without He). Previous modeling efforts have little applicability to this problem because 1) calculations were done for He in pure metals, not hydrides, or 2) the atomic interactions were described by pair potentials, which does not account for many-body electronic effects present in a transition metal such as Pd. Indeed, all previous efforts to model even the binary Pd-H system have failed to reproduce its phase diagram.

We have developed modified-embedded-atom-method (MEAM) potentials that represent the Pd-Pd, Pd-H, and H-H interactions in Pd-H alloys in a more realistic manner. As input data for these potentials we used all the known physical and thermodynamic properties of pure Pd and Pd-H alloys. Using these MEAM potentials, we calculated the Pd-H phase diagram. Our calculated phase diagram is in good agreement with the measured one for the Pd-H system, far better than all previous modeling efforts. This is an important advance in our ability to perform atomistic simulations of transition-metal/hydrogen-isotope systems. A manuscript on this work is in preparation.

**Ion channeling studies of the position of $^3$He in Pd**

To understand aging, we must know where a newly born $^3$He atom resides within the Pd-tritide lattice. Because the recoil energy of the $^3$He atom is only a few electron volts, it is usually assumed that a newly born $^3$He atom resides in the same octahedral interstitial site occupied by the parent tritium atom. This assumption, however, has never been verified by experiment.

We have performed ion channeling/nuclear reaction analysis experiments on single crystals of $PdD_{0.02}$, using 750 keV $^3He^+$ ions. Our measurements confirmed that deuterium atoms indeed occupy the octahedral interstitial sites of the Pd lattice. Results for channeling along two different axes of the same $PdD_{0.02}$ crystal are shown in Figure 3. Here, the ordinate is the relative signal intensity, either from Rutherford backscattering of $^3He^+$ ions (for Pd), or from 14 MeV protons generated by the $^3He^+$ + D reaction (for D). The abscissa is the tilt angle between the incident beam and the axial channel (either <100> or <110>).

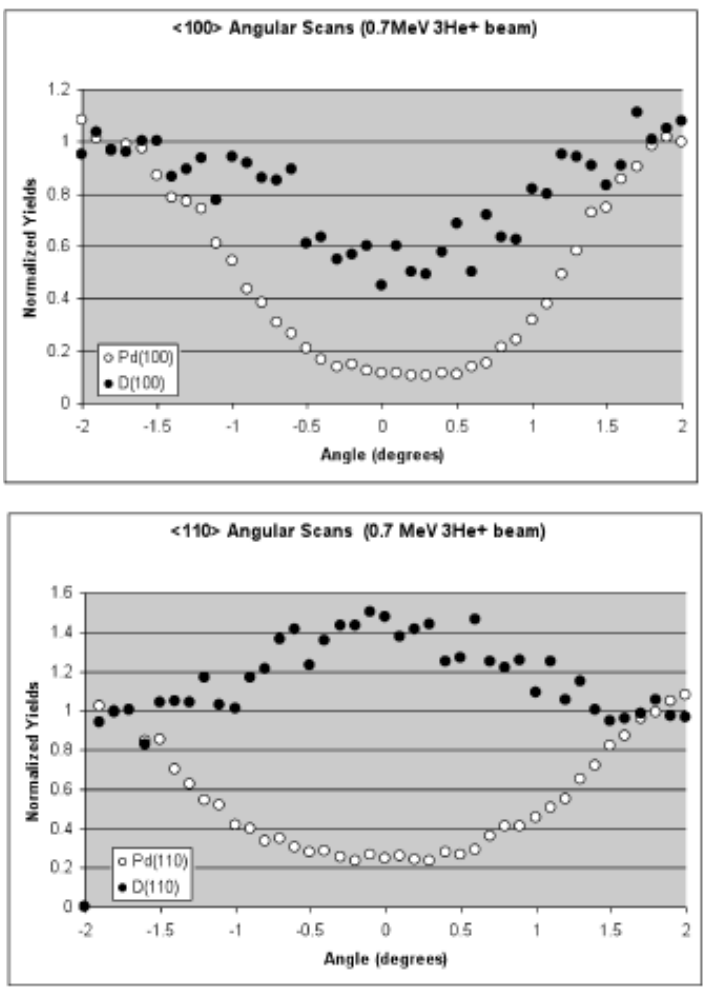


*Figure 3. Normalized yield (relative signal intensity) versus tilt angle for axial channeling along <100> and <110> directions of a PdD0.02 single crystal, measured at our MST Ion Beam facility (collaboration with Y. Wang).*

As shown in the figure, for both <100> and the <110> axial channeling the Pd signal shows a dip centered about zero. Moreover, the D signal shows a dip centered at zero for <100> channeling, but a broad peak for <110> channeling. These two results for D are possible on the same crystal only if the D atoms are located in octahedral interstitial sites [7].

**Set-up of liquid-helium cooled, tritium-capable Resonant Ultrasound Spectroscopy (RUS) system**

We have completed installation of a tritium-capable RUS apparatus, and received all necessary authorizations for its operation in the tritium facility. This apparatus will be used to measure the elastic constants of Pd-T and Pd-T-$^3$He single crystals to 1) study the kinetics and dynamics of $^3$He coalescence, 2) deduce the symmetry of $^3$He aggregates at various stages of coalescence, and 3) aid in development realistic MEAM interatomic potentials for Pd-T and Pd-T-$^3$He systems.

## Future Work

In the remaining eleven months of this project, we will focus on the following activities, listed in order of decreasing priority.

Measure pressure-composition isotherms for Pd-T and Pd-T-$^3$He systems.

Ion channeling/nuclear reaction analysis studies of the position of $^3$He in Pd-$^3$He.

Elastic constant measurements for Pd-T during aging at room and cryogenic temperatures.

Swelling measurements for Pd-T during aging (using a capacitance dilatometer).

Development of realistic MEAM interatomic potentials for Pd-T and Pd-T-$^3$He.

A significant problem is that the WETF tritium facility was non-operational for the majority of the first two years of this project. At present, the facility is again shut down, stopping all tritium work. Whenever the facility resumes operations, we will immediately resume activities 1-3 above.

This project has also been hindered by personnel loss. All but one of the key participants who started on this project are now gone. Ricardo Schwarz (Laboratory Fellow

and former PI), Mike Baskes (Laboratory Fellow), and José Archuleta (Tech-7) all participated in the Laboratory's Self-Selection Voluntary Separation Plan (SSP). Also, Co-PI and leader of the tritium facility work, Erica Baron, changed career paths and left the project only 8 months after its start. Baron and Archuleta have now been replaced, and Schwarz works 20% time as an unpaid Guest Scientist. Nonetheless, personnel loss has caused us to revise the project scope, as discussed at our mid-term review.

## References


1. Schwarz, R. B., and A. G. Khachaturyan. Thermodynamics of open two-phase systems with coherent interfaces: Application to metal–hydrogen systems. 2006. *Acta Materialia.* **54**: 313.

2. Manchester, F. D., A. San-Martin, and J. M. Pitre. Hydrogen-Palladium. 2000. In *Phase Diagrams of Binary Hydrogen Alloys.* Edited by Manchester, F. D.. First Edition, p. 158. Materials Park, OH: American Society of Metals.

3. Leisure, R. G., T. Kanashiro, P. C. Riedi, and D. K. Hsu. Hydrogen motion in single-crystal palladium hydride as studied ultrasonically. 1983. *Physical Review B.* **27**: 4872.

4. Blaschko, O., R. Klemencic, P. Weinzierl, O. J. Eder, and P. van Blanckenhagen. Structural Changes in PdDx in the Temperature Region of the 50K Anomaly. 1980. *Acta Crytallographica.* **A36**: 605.

5. Safarik, D. J., and R. B. Schwarz. The 50 K Anomaly in the Shear Modulus of β-PdH0.71. 2008. *Proceedings of TMS (The Minerals, Metals, and Materials Society) 2008 Annual Meeting: Materials Processing and Properties.* **1**: 601.

6. Safarik, D. J., and R. B. Schwarz. Ultrasonic Study of Short-Range Hydrogen Ordering in Pd-Hydride. 2008. *international Journal of Materials Research.* **99**: 535.

7. Carstanjen, H. D.. Interstitial Positions and Vibrational Amplitudes of Hydrogen in Metals Investigated by Fast Ion Channeliing. 1980. *Physica Status Solidi A.* **59**: 11.


## Publications


Safarik, D. J., and R. B. Schwarz. The 50 K Anomaly in the Shear Modulus of β-PdH0.71. 2008. *Proceedings of TMS (The Minerals, Metals, and Materials Society) 2008 Meeting: Materials Processing and Properties.* **1**: 601.

Safarik, D. J., and R. B. Schwarz. Ultrasonic Study of Short-Range Hydrogen Ordering in Pd-Hydride. 2008. *International Journal for Materials Reserach.* **99**: 535.

continuing project

# Quantum Control in Condensed Media for Studies of Direct Optical Initiation of Explosives

*David Steven Moore*

20070077DR

## Introduction

The current generation of exploding bridge wire (EBW) detonators has the inherent potential for accidental initiation via electrostatic discharge (ESD) events, which has driven the development of direct optical initiation (DOI) schemes. Current DOI are essentially an "optical" EBW. Recent advances in ultrafast laser technology are being extended in this project to achieve direct quantum controlled initiation (QCI) of explosives. In QCI, a laser pulse is temporally shaped to achieve initiation, an iterative process using adaptive genetic algorithms. The use of shaped laser pulses tailored specifically to each energetic material offers a new approach for efficient initiation at much lower energies than used in DOI. At these low laser energies, only the shaped pulse can achieve initiation, leading to safer, and perhaps encryptable, systems.

We have achieved coherent control of photoisomerization branching in our model system - stilbene. The laser source, ultrafast pulse shapers, control algorithms, and closed-loop optimization from those studies are being applied to carefully manufactured explosives samples. The feedback that indicates successful initiation is obtained using one of several spectroscopic or thermal diagnostics. Large-scale modeling is performed to guide experiments and gain insight into the fundamental reaction dynamics, with perhaps clues towards new potential detonator materials with strong quantum key links.

More fundamentally, experimental quantum control of molecular dynamics in condensed phases is an emerging field with widespread application in controlling and understanding mechanisms of chemical and physical reactions.

## Benefit to National Security Missions

The QCI approach may provide resilience not only against accidental initiation through the use of less sensitive explosives, but also against illicit initiation, by acting as a "quantum key". This which both nuclear weapons (NW) and threat reduction (TR) NNSA missions by improving the safety and security of the stockpile.

## Progress

We designed a simple scheme for efficient, global (coarse-grained) parameter space optimization for the stilbene ground and excited state potential energy surface (PES) dynamics. Our progress includes the means for efficient calculation of the ground and excited state PES and the inclusion of the shaped electric field into the quantum molecular dynamics simulations. We generated a program that can simulate the numerically exact quantum wavepacket dynamics for a single degree of freedom interacting with an electric field of arbitrary form. The electric field was also added to a more approximate quantum MD code that is capable of treating the dynamics of molecules with many degrees of freedom. The latter code was tested successfully against the numerically exact code for an ultra-short electric field pulse.

We calculated the reaction chemistry of high explosives (HMX and TATB) at high temperature and pressure, in preparation for modeling the control of high explosive (HE) reaction chemistry, with classical molecular dynamics using the ReaxFF reactive force field from Caltech. This produced significant headway in understanding the reaction kinetics of HMX decomposition and the difference in carbon condensation for the two explosives. We developed a first principles computational package for determining the anharmonic couplings between vibrational normal modes (phonons and vibrons) in molecular crystals and in particular in

energetic materials, including an efficient parallel code to handle the extended super cell geometry.

We developed a generalized time dependent variational approach for calculations of electronic spectra during transit near and through a conical intersection. The results will guide experiments by indicating the optimal spectroscopic probes. We determined some of the critical initiation diameters of HE of interest using a flexible test bed for initiation spot size testing. We utilized single crystal HE samples to understand basic HE material phenomena such as defect concentration, quasistatic compression, isothermal compression, isentropic compression, and THz spectroscopy. We utilized 2D-IR spectroscopy to measure vibrational dynamics in thin PETN polycrystalline films. The 2D-IR results include the homogeneous line width, inhomogeneous line width, dephasing times (from 1.8 to 3.5 ps) and intra-vibrational mode couplings.

We developed a state of the art optimal quantum control capability including pulse shaping, measurement of fitness or result, and closed-loop computer controlled optimization of the pulse shape to maximize or minimize the fitness. We developed this capability in the visible (800 nm) as well as UV (both 400 and 266 nm - the latter a world's first). Using this capability, we demonstrated control of the photoisomerization branching ratio in stilbene, enhancing or suppressing the cis and trans yields at will. We have begun producing the well-controlled HE samples needed to extend this optimal quantum control capability into the realm of HE initiation control. We constructed and tested pulse spectral broadening in a gas cell to allow greater control bandwidth, and have achieved more than a factor of four increase in control bandwidth. Greater bandwidth allows a larger choice of molecular vibronic features in the control space. We developed and optimized a spectrally resolved electronic transient absorption spectrometer that can measure small changes in spectra across the range 320-750 nm in a single laser shot.

We formulated a nanogold / PETN detonator powder and performed direct optical initiation experiments to demonstrate plasmonic resonance enhancement. The gold nanoparticle size was chosen to maximize coupling to the 1064 nm drive laser wavelength. DOI data is being analyzed.

Finally, we investigated the properties of the control pulse shape needed to achieve a quantum key. The idea of "quantum key" hinges on the assumptions that these pulse shapes are 1) relatively rare due to the complexity of the system, and 2) hard to obtain. Due to the complex nature of the chemical control landscape, we tend to think that both these assumptions are probably valid.

## Future Work

Explosives are very difficult to directly initiate using lasers; low-density pressings and large laser energies are required, if initiation can be achieved at all. A new approach that promises efficient initiation is coherent control using shaped laser pulses tailored specifically to each energetic material. A model system (photochemical branching in stilbene) was used to optimize laser sources and develop and test control algorithms. Those results are being extended to direct quantum-controlled initiation of explosives, which may not only lead to the most efficient pathway for initiation, it also naturally embodies a "quantum key" to enable the event. Large scale modeling is being performed to guide the control feedback experiments, and also to achieve inversion of the optimal control waveform into real molecular coordinate space on the potential energy surfaces, giving insight into the fundamental reaction dynamics and perhaps promoting a discovery path towards new potential (and better) detonator materials. We are continuing to address the tasks that were originally proposed for this project:

1. Use adaptive pulse shaping to control both the cis/trans isomerization ratio and cyclization quantum yield in stilbene solutions and solid mixtures, using UV/visible absorption as feedback. Perform accurate dynamics simulations on stilbene's well-characterized potential energy surfaces; compare to experiment (Complete).

2. Extend task 1 results to explosives.

- Manufacture several HE (e.g., PETN, HMX, RDX, HNS) single crystals and polycrystalline thin films; measure vibrational dephasing times (when not known).

- Perform control algorithm feedback experiments on thin single crystal HE samples using UV/visible absorption, Raman, and infrared absorption feedback (UV/visible absorption is the easiest experimentally).

- Extend subtask 2b to polycrystalline samples.

3. Compare molecular modeling to experimental results; use modeling to guide feedback experiments.

4. Develop theory and modeling necessary to invert the optimal control algorithm onto molecular coordinates.

5. Devise methods to transfer optimal pulse shapes to photonics engineered devices.

## Conclusion

The detonator is the weak safety link in explosive systems. Detonators can use environmentally hazardous materials (lead and mercury), or be accidentally set off by electrostatic discharge or illicit means. These drawbacks can be avoided using less sensitive materials, but with larger energy requirements. This project seeks to develop a new laser method to initiate detonation in low sensitivity energetic materials, increasing the safety of detonators. The technique uses adaptive pulse-shaping techniques to drive the desired chemical reaction. An additional layer of safety is achieved because the pulse shape is like a "key" in the detonation "lock."

## Publications


Cawkwell, M. J., K. J. Ramos, T. D. Sewell, and D. E. Hooks. Homogeneous dislocation nucleation and anomalous hardening in cyclotrimethylene trinitramine (RDX). To appear in *Physical Review B.*

Greenfield, M., S. D. McGrane, and D. S. Moore. Control of cis-stilbene photochemistry using shaped ultraviolet pulse. To appear in *Journal of Physical Chemistry A.*

Hooks, D. E., and K. J. Ramos. Measurement of the dynamic elastic limit in cyclotrimethylene trinitramine: Wave profiles from 1.0 GPa shocks including the effects of voids and cracks. *Propellants, Explosives and Pyrotechnics.*

Lee, H. J., J. Workman, J. S. Wark, R. D. Averitt, A. J. Taylor, J. Roberts, Q. McCulloch, D. E. Hof, N. Hur, S. W. Cheong, and D. J. Funk. Optically induced lattice dynamics probed with ultrafast x-ray diffraction. 2008. *Physical Review B.* **77**: 132301.

McGrane, S. D., M. Greenfield, and D. S. Moore. Construction and characterization of ultraviolet acousto-optic modulator based femtosecond pulse shapers. *Review of Scientific Instruments.*

Moore, D. S.. Optimal coherent control of sensitivity and selectivity in spectrochemical analysis. To appear in *Analytical and Bioanalytical Chemistry.*

Piryatinski, A., S. Tretiak, and V. Chernyak. Dynamical variational approach to non-adiabatic electronic structure. 2008. *Chemical Physics.* **347**: 25.

Quenneville, J., T. C. Germann, A. P. Thompson, and E. M. Kober. Molecular dynamics studies of thermal induced chemistry in TATB. 2007. In *Shock Compression of Condensed Matter 2007.* (Kailua-Kona, 24-29 June 2007). Vol. 955, p. 451. Melville, NY: AIP.

Stevens, L. L., D. E. Hooks, and D. M. Dattelbaum. Hydrostatic Compression Curve for Triamino-trinitrobenzene (TATB) Determined to 14.0 GPa with Powder X-ray Diffraction. 2008. *Propellants, Explosives and Pyrotechnics.* **33** (4): 286.

Stevens, L. L., D. M. Dattelbaum, and D. E. Hooks. The high-pressure phase behavior and compressibility of 2,4,6-trinitrotoluene (TNT). 2008. *Applied Physics Letters.* **93**: 081912.

Velizhanin, K. A., S. Kilina, T. D. Sewell, and A. Piryatinski. First-principles calculations of vibrational normal modes in polyatomic materials with translational symmetry: application to PETN molecular crystal. 2008. *Journal of Physical Chemistry B.* **112**: 13252.

Velizhanin, K. A., T. D. Sewell, and A. Piryatinski. First-principles calculations of anharmonic normal mode couplings and energy transfer in polyatomic materials: application to PETN molecular crystal. *Journal of Physical Chemistry B.*

Yellampalle, B., E. E. M. Chia, K. Kim, A. J. Taylor, and R. Averitt. Three pulse envelope approach for ultrashort pulse characterization in a pump-probe experiment. 2008. *Applied Physics Letters.* **92**: 061111.

Yellampalle, B., K. Y. Kim, and A. J. Taylor. Amplitude ambiguities in second harmonic generation frequency resolved optical gating. 2007. *Optics Letters.* **32**: 3558.

# Biomimetic Hydrogen Production by Photoinitiated Transition Metal Catalysis

*Richard Brian Dyer*

20070096DR

## Introduction

The overall objective of this LDRD-DR project is to develop a new approach to the production of hydrogen from renewable sources, water, and solar energy. Photosynthetic water oxidation is catalyzed by the oxygen evolving complex (OEC) of photosystem II. Hydrogenases from various microorganisms catalyze the production of hydrogen from protons and electrons at extraordinarily high rates (up to $10^4$ turnovers/sec) using nonprecious metals (principally iron). Despite decades of effort, scientists have not yet come close to mimicking these natural systems. Two major scientific barriers persist: developing efficient (molecular) catalysts for water oxidation and hydrogen production, and coupling these reactions to a photochemical energy source. Our approach is to use natural systems to guide the design of synthetic inorganic catalysts and their assembly for photochemical water splitting, to produce hydrogen and oxygen. Our approach follows the lead of biology, to develop functional modules that can be individually optimized and assembled to create a complete system. Our specific aims are: 1) to develop hydrogen and oxygen catalyst modules inspired and informed by analogous biological systems; 2) to couple these catalysts to photochemical modules that will provide the energy to drive the reactions; 3) to integrate each of these modules into a system capable of splitting water using solar energy.

## Benefit to National Security Missions

This project supports the DOE mission in Energy and Renewable Energy by providing the scientific foundation for the development of efficient photochemical production of hydrogen from water and solar energy. Deployable energy sources are also critical to the Department of Defense and other deployed national security assets.

## Progress

### Photochemical Water Oxidation

We have developed a family of molecularly bridged dyads from terpyridine/bipyridine complexes of ruthenium that combine a sensitizing unit for photoexcitation by visible light and a catalytic unit with capability for multi-electron/multi-proton reactivity. The preparation of such dyads was based on a synthetic methodology involving coupling of the two units (chromophore and catalyst) via metal-catalyzed reactions using various linkers. The bimetallic dyads and corresponding monometallic components were structurally and electronically characterized by spectroscopic techniques and electrochemistry, including spectroelectrochemical approaches for the study of all redox states in situ (e.g. $Ru^{II}/Ru^{III}/Ru^{IV}$). The chemically relevant metal-to-ligand charge-transfer states of the photoexcited chromophore-catalyst dyads were investigated using time-resolved fluorescence and transient absorption spectroscopies. Also essential to the photophysical studies were the analytical comparisons between the absorption/emission properties of the dyad systems and their building blocks. Among our key accomplishments this year was the successful demonstration that, under simulated sunlight and in the presence of sacrificial electron acceptors, the chromophore-catalyst assemblies can 1) undergo activation by photoinitiated stepwise electron transfer and charge separation, and 2) perform photocatalytic oxidation of organics (such as the 2-electron/2-proton conversion of isopropyl alcohol into acetone) with several tens of turnovers, as probed by NMR spectroscopy and gas chromatography/mass spectrometry. We also initiated kinetic and mechanistic studies of water oxidation with $O_2$ evolution for monometallic catalysts and will then focus on incorporating and optimizing such units in new dyads with capability for the 4-electron/4-proton photooxidation of water. As a strategy to promote efficient, intramolecular electron transfer upon photoexcitation, we also designed a triad assembly containing an electron acceptor (methyl viologen) covalently attached to the photosensitizing unit. Following our initial efforts on the characterization of homogeneous photocatalysis in

solution, we are preparing dyad assemblies functionalized with suitable anchoring groups for attachment onto metal-oxide semiconductor surfaces (especially $TiO_2$) to drive heterogeneous water-oxidation photocatalysis in a scheme integrated with the $H_2$ module.

**Hydrogen Catalyst development**

We have continued to make progress on the synthesis and characterization of divalent, mononuclear iron complexes as hydrogen catalysts. A series of aromatic N-S ligands including pyridine 2-thiol, 2- and 8-mercaptoquinoline have been investigated for their ability to stabilize (and aid in crystallization) suitable Fe(II) synthons. Preliminary results indicate these moieties can indeed be isolated as shown in Figure 1. Current efforts are focused on preparing singly ligated versions of these compounds, because double chloride ion abstraction from the (dcpe)$FeCl_2$ precursor (using only 1 eqiv of N-SH) seems to compete with mono-substitution to yield the desired (dcpe)FeCl(N-S) species. Addition of a (sterically encumbered) $\pi$-accepting ligand directly to the (dcpe)$FeCl_2$ precursor and then reaction with one equivalent of pyridine 2-thiol, 2- or 8-mercaptoquinoline leads to the desired mono-chloride product that is currently being investigated for its ability to form coordinate H/$H_2$ fragments. Current efforts are also focused on a series of $(py)_2FeCl_2$ derived targets as $(py)_4FeCl_2$ is a readily available synthon, as are a series of alkyl/chloride derived adducts derived from this molecule.

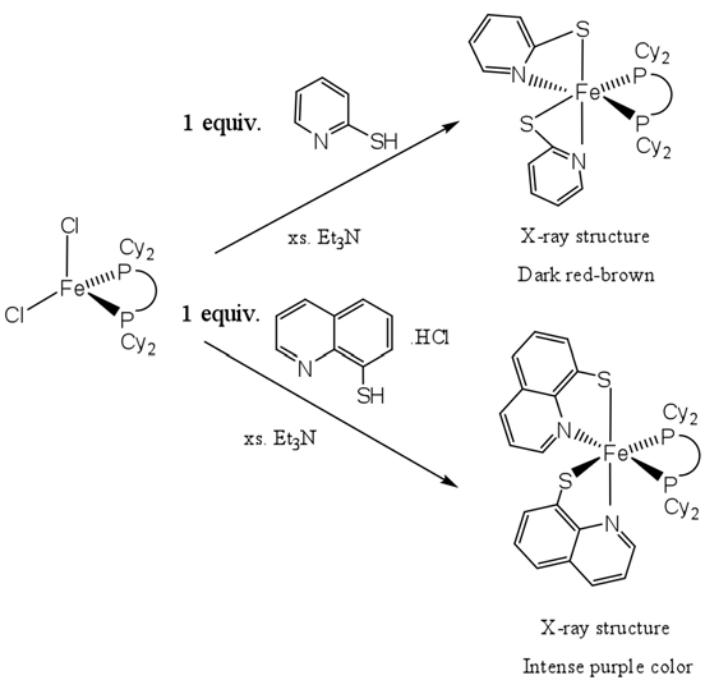


*Figure 1. Synthetic scheme for preparation of Fe(II) hydrogen production catalysts*

Our second approach to hydrogen production involves the development of catalysts based on Pd-Trost chemistry. Upon addition of acid ($(CF_3SO_3)_2NH$) or formic acid) to the Pd-Trost catalyst, we observe the formation of $H_2$ and the $Pd^0Trost^*$ species reverts to $Pd^{II}Trost^*$. Conversely, $H_2$ can also be liberated by first, addition of acid to $PdTrost^*$ to form the fully protonated $Pd^{II}Trost^*(H)_2^{2+}$ then reduction by $(Cp^*_2Co)$. We have been able to observe pertinent intermediates along both pathways via NMR spectroscopy.

Catalyst development has been guided by theory and computation, using high level Density Functional Theory (DFT). For example, a close interaction between theory and experiment has helped to elucidate the mechanism of $H_2$ formation in the Pd-Trost catalyst. Much of our effort to date has been on generating optimized geometries for the intermediate species based on different Pd oxidation states and $H^+$ binding sites. Using a simplified model shown in Figure 2a, we are able to show that the structure remains fairly intact upon reduction or addition of two $H^+$ atoms to the $Pd^{II}$ species. However, more interesting chemistry occurs upon protonation of the doubly reduced species and we believe that one of the intermediate products is a $Pd^0$ 14-electron species shown in Figure 2b with a Pd-H distance of 2.627 Å. We are currently analyzing the energetic landscape of these species to determine a thermodynamically and kinetically favorable route to $H_2$ formation.

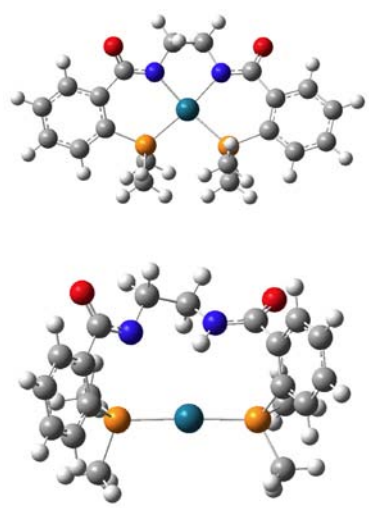

*Figure 2. (a) Simplified model used in DFT calculations of the Pd-Trost catalyst; (b) Optimized geometry of [Pd-TrostH]-*

A second fruitful contribution of theory is our work on calculating redox potentials of Fe(II) systems. First, we accurately predicted the redox potentials of a series of bimetallic $Fe^IFe^I$ complexes based on the hydrogenase metalloenzyme. More recently, we have extended our research to other transition metal complexes, which contain varying oxidation states and charges, to benchmark our methods to redox couples that are not necessarily reversible on

the electrochemical time scale. A natural starting point to probe the abilities of DFT to provide accurate redox potentials was an analysis of ferrocene. To date, many other researchers calculate redox potentials using DFT methods and they reference their results to a standard electrode, such as the standard hydrogen electrode (SHE). However, using ferrocene as an example, we have shown that calculating solvation free energies alone is not an appropriate quantity when referencing results to SHE.

**Photochemistry Module**

Work on the photochemistry module has focused on the use of nanocrystalline semiconductor materials to accomplish light harvesting and initial charge separation. Specifically we have investigated the use of $WO_3$ nanocrystalline thin films for solar water splitting. We developed a sol gel method for constructing thin films of nanocrystalline $WO_3$ that could be incorporated into a tandem cell for solar water splitting. This tandem cell was used to successfully demonstrate the proof of principle of our water splitting scheme. We plan to add both $H_2$ production and water oxidation catalysts (developed as described above) to this scheme that we expect to greatly increase the overall efficiency of the process.

## Future Work

Our general approach to the complex problem of a catalytic water splitting cycle is to subdivide the problem into tractable pieces. The key elements of our approach are synthetic "modules" involving molecular chemistry that for the most part can be conceptualized and developed independently of one another. Thus, we will develop a photochemistry module, an $H_2$ production module and an $O_2$ production module. Their individual chemistry will be established, and then they will be assembled pairwise (using covalent attachments or nanostructures) to test photochemical behavior. The focus is on molecular catalysis of $H_2$ and $O_2$ production, which sets our approach apart from existing photochemical water splitting schemes based on solid-state materials. This is an important distinction because the major deficiencies of existing approaches are their lack of efficiency and durability. These shortcomings are a direct consequence of the difficulty in carrying out the multi-step electron transfer and coupled proton transfer reactions. The bond making steps are critical, and in uncatalyzed systems, incompletely oxidized oxygen intermediates are produced. Thus, it is crucial for the catalyst design to minimize the production of incompletely oxidized, reactive oxygen species.

## Conclusion

One of the primary lessons from biology about efficient water splitting is the use of functional modules (proteins that perform light harvesting, water oxidation, electron transfer and $H_2$ production) that are independently produced, assembled and optimized to perform the overall catalytic cycle. We expect to mimic this approach to develop synthetic molecular catalysts coupled to light harvesting and photochemical modules to produce an efficient system capable of hydrogen production from water and solar energy.

## Publications

Baker, R. T., R. B. Dyer, J. C. Gordon, G. J. Kubas, T. Li, B. L. Scott, and A. D. Sutton. Biomimetic hydrogenase models: synthesis, structure and properties of iron(II) complexes containing thioamine, diphosphine, and carbonyl/isocyanide ligands. *Journal of the American Chemical Society.*

Beck, D., J. Brewer, J. Lee, D. McGraw, B. A.. DeGraff, and J. N. Demas. Localizing molecular probes: Inclusion of Re(I) complexes in -cyclodextrin. 2007. *Coordination Chemistry Reviews.* **251** (3-4): 546.

Dattelbaum, D. M., J. B. Butler, J. R. Schoonover, M. W. George, and T. J. Meyer. Application of Transient Infrared and Near-infrared Spectroscopy to Excited States in Transition Metal Complexes. 2007. *Coordination Chemistry Reviews.* **251**: 492.

Demadis, K. D., D. M. Dattelbaum, J. D. Paul, J. Conception, T. J. Meyer, and P. S. White. Vibrational Mapping of Molecular and Electronic Structures in [Os(pp)3]n+ (pp = 2,2'-bipyridine, 1,10-phenanthroline, n = 2+, 3+). 2007. *Inorganica Chimica Acta .* **360** (3): 1143.

Dyer, R. B., and W. H. Woodruff. Vibrational Spectroscopy. 2007. In *Applications of physical methods to inorganic and bioinorganic chemistry.* Edited by Scott, R. A., and C. M. Lukehart. , p. 489. Chichester, UK: John Wiley & Sons.

Fleming, C. N., D. M. Dattelbaum, D. W. Thompson, A. Y. Ershov, and T. J. Meyer. Excited State Intervalence Transfer in a Rigid Polymeric Film. 2007. *Journal of the American Chemical Society.* **129** (31): 9622.

Hornstein, B. J., D. M. Dattelbaum, J. R. Schoonover, and T. J. Meyer. The Reactivity of a Bound Ru(VI)-oxo complex:

Oxidation of Benzyl Alcohol. 2007. *Inorganic Chemistry.* **46** (20): 8139.

Jude, H., F. N. Rein, P. S. White, D. M. Dattelbaum, and R. C. Rocha. Synthesis, structure, and electronic properties of a dimer of Ru(bpy)2 doubly bridged by methoxide and pyrazolate. 2008. *Inorganic Chemistry.* **47**: 7695.

Jude, H., F. N. Rein, W. Chen, B. L. Scott, E. R. Batista, D. M. Dattelbaum, and R. C. Rocha. Pyrazole and pyrazolyl complexes of cis-bis(2,2'-bipyridine)ruthenium(II/III): synthesis, structural and electronic characterization, acid-base chemistry and proton-coupled redox properties. *Inorganic Chemistry.*

Kubas, G. J.. Breaking The H2 Marriage And Reuniting the Couple. 2006. *Science.* **314**: 1096.

Kubas, G. J.. Metal-Dihydrogen Complexes. Prototypes for The Coordination Chemistry of Saturated Molecules. 2007. *Proceedings of the National Academy of Sciences USA.* **104**: 6901.

Kubas, G. J.. Fundamentals of H2 Binding and Reactivity on Transition Metals Underlying Hydrogenase Function and H2 Production and Storage. 2007. *Chemistry Reviews.* **107**: 4152.

Kubas, G. J.. Dihydrogen and Other Sigma Bond Complexes. 2006. In *Comprehensive Organometallic Chemistry III.* Edited by Crabtree, R. H., and D. M. P. Mingos. Vol. 1, p. 671. Oxford: Elsevier.

Roy, L. E., E. R. Batista, and P. J. Hay. Theoretical studies of reduction potentials of mono-iron complex models of hydrogenases. 2008. *Inorganic Chemistry.* **47**: 9228.

Roy, L. E., P. J. Hay, and R. L. Martin. Revised Basis Sets for Transition Metal Atoms Using the LANL Effective Core Potentials. 2008. *Journal of Chemical Theory and Computation.* **4**: 1029.

# Hot Spot Physics and Chemistry in Energetic Materials Initiation

*Dana Mcgraw Dattelbaum*

20080015DR

## Introduction

In most instances of practical relevance, and especially for *accident scenarios* and *non-ideal formulations*, initiation of energetic materials results from a physical concentration of "hot spots." Hot-spots are localized regions of high temperature and pressure within which thermal chemistry occurs on a rapid time scale. They can originate from dynamic pore collapse, plastic shear band formation, friction along closed cracks, or reflections from other interfaces. A complex interplay among numerous physical and chemical factors, spanning several length and time scales, determines whether one or several hot-spots will quench or ignite. Currently, our understanding of hot-spot physics is mostly phenomenological – this research will fill in critical and significant gaps in our knowledge relating to the initiation and sensitization of explosives, facilitating the development of predictive models for hot-spot creation and growth that in turn will form the basis for a new generation of predictive reactive flow models for energetic materials.

An understanding of hot spot phenomena will be obtained by studying prototypical energetic materials – nitromethane, trinitrotoluene (TNT), RDX, and ammonium nitrate – seeded with defect sources that are well controlled and tractable. These scientific investigations will substantially improve our understanding regarding several fundamental yet longstanding questions regarding hot spot physics and chemistry, including:

How are hot spots formed and what functional characteristics influence their behavior for a specified material, thermodynamic state, or dynamic load?

What combinations of parameters define the boundaries that separate chemical detonation criticality from extinction or deflagration?

What is the influence of specific parameters on initiation mechanism, sensitivity, chemical reaction zone length, and detonation propagation in geometrically interesting situations?

Experiments and simulations conducted over multiple spatial scales will be used to glean unprecedented information relating to the dynamics of hot spots. This fundamental understanding will allow us to develop physically based mesoscale models for thermal and convective evolution within and among hot spots, including temperature-dependent chemistry, thermal transport, and mechanics. In doing so, the project will significantly advance us toward a robust, rapid-response predictive capability for multi-agency National security needs.

## Benefit to National Security Missions

The ultimate goal of the work is a fundamental understanding of hot spots that will translate into the ability to design explosives with improved reproducibility, performance, and surety, as well as provide a credibly predictive set of tools for simulating explosives behavior. The research described supports our principal mission in stockpile stewardship, and will potentially have a major impact to the Laboratory's emerging roles in threat reduction and homeland security, as well as DOE-DoD collaborative programs.

## Progress

### Preparation and Characterization of Energetic Materials with Hot Spot Features

We have prepared gelled nitromethane using guar gum at 1.5-2.0 wt%, and selected 1.75 wt% for gelling nitromethane containing 6 wt% solid silica beads of discrete diameters: ~ 2-4, 40, and 100 microns. To characterize inter-bead (hot spot) spacing and settling times, a sub-micron x-ray tomographic method has been developed for collecting time lapse images of

1-4 and 40 micron silica beads in guar gum/NM solutions. Optical and scanning electron microscopy methods have been used to characterize bead diameters and agglomeration in gelled solutions. A new gelling agent, high molecular weight polyethylene oxide, has been tested and will be applied to preparation of gels for laser- and gas gun-driven shock wave experiments. Glass microballoons, with and without W coatings, have also been selected and will be sorted as a second type of hot spot to be interrogated [1]. To prepare controlled hot spot arrays in explosive crystals, we have assembled a femtosecond laser micromachining apparatus and used it to successfully machine void features into HMX, PETN, and RDX. The relevant parameters that allow for successful machining of controlled defects internally without cracking the crystals have been obtained. Figure 1 shows examples of laser-drilled voids.

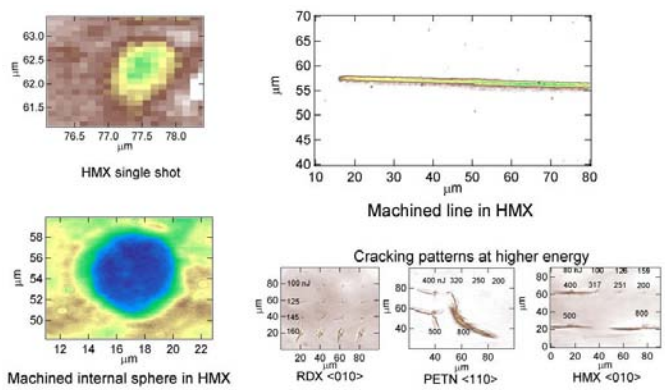


*Figure 1. Laser-drilled voids in explosive crystals produced by femtosecond-laser micromachining.*

### Shock Wave Initiation Behavior

Laser-driven shock wave experiments (HERCULES facility, ≤50 GPa for 250 ps), diagnosed with interferometric dynamic ellipsometry, were proofed on the non-reactive liquid cyclohexane [6] in a thin layer target, deriving multiple Hugoniot loci from a single laser shot. The results showed good agreement with explosively-driven measurements by Marsh. We then applied laser shock generation and dynamic ellipsometry on liquid nitromethane samples to compare to gas gun results. Unexpected features occur in the dynamic ellipsometry above an threshold energy. Samples of seeded nitromethane (nitromethane with 100, 450, or 1000 nm silica beads at the surface) have been prepared by spin coating and characterized with atomic force and optical microscopy. Laser shock experiments on seeded and chemically sensitized (with DETA) nitromethane have begun. A femtosecond stimulated Raman spectroscopy (FSRS) diagnostic is being implemented to measure temperature in laser-shocked energetic liquids, and provide experimental information on deflagration (burn) front velocities under shock conditions.

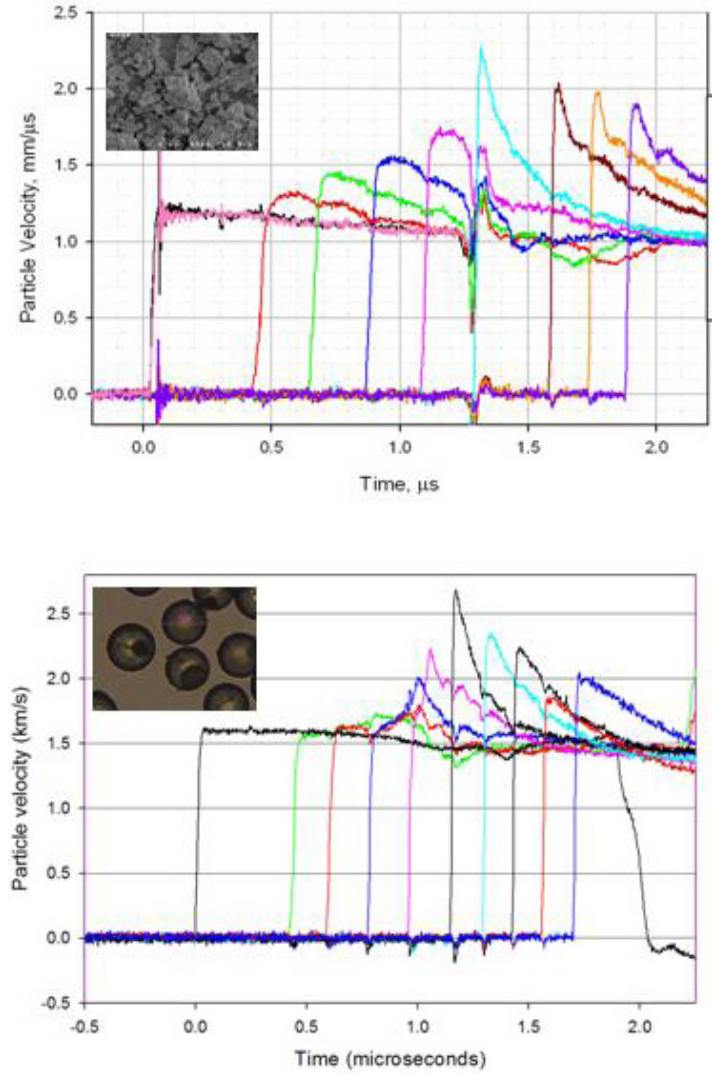


*Figure 2. Gas-gun wave profiles showing heterogeneous vs. homogeneous initiation mechanisms for different size silica beads in gelled nitromethane.*

### Static High Pressure Experiments

Dynamic experiments and reactive chemistry modeling are supported with static high pressure measurements to define the isothermal compression behavior of explosives of interest, as well as seek new phases at high pressures. The isotherms for the explosives nitromethane, trinitrotoluene, [3] triamino-trinitrobenzene, [2] ammonium nitrate, and diaminodiazoxyfurazan were determined using angle-dispersive x-ray diffraction experiments at high pressures at the Advanced Photon Source. Pressure-induced absorbance changes, newly discovered phase transitions at high pressures, and baseline isotherms for validation of density functional theory simulations were revealed.

**Molecular-scale modeling and ReaxFF**

Simulations have been performed on a shocked RDX crystal with the shock propagating along the [100] direction (up = 1 km/s; P= 9.7 GPa). Nanoscale shear bands that nucleate homogeneously and give rise to high local temperatures (due to viscous flow within them) are clearly visible behind the shock front (Figure 3) [4, 5]. Figure 3 also shows the extracted temperatures at 5 nm and 140 nm behind the front. Statistical methods were applied to extract mean temperatures behind the shock front, with temperatures of up to 700-800K observed along shear bands. These 2-D temperature maps will provide input into models at the next length scale. Additional simulations on RDX at this length scale have examined dynamic pore collapse, and shocked bicrystals. In shocked RDX, a stress-induced phase change was found to nucleate at the grain boundary.

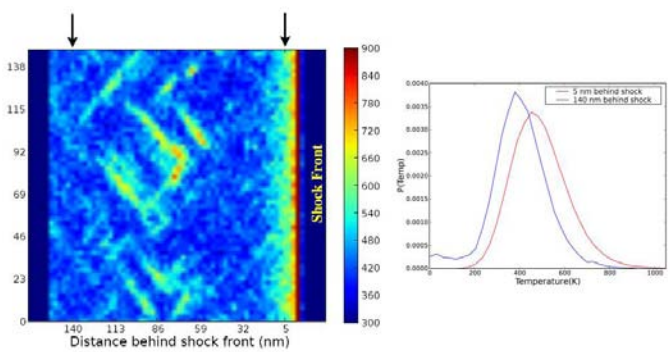


*Figure 3: Simulation showing nanoscale shear bands formed in a shocked RDX crystal, and associated temperatures at two times behind the shock.*

Efforts to validate and assess the ReaxFF force field as applied to TATB and its known graphite/diamond transition, on an isotherm in a HE working fluid have also been performed as a baselining activity for applying the force field to non-ideal CHNO materials.

**Mesoscale Modeling**

At the mesoscale, simulations on a prototypical energetic material, $2AB + A_2 + B_2$, were performed to examine the effects of multiple void collapse events on the chemical kinetics and shock hydrodynamics. Two voids were seeded into a sea of AB molecules, and simulations were performed as the molecules (and voids) were shocked. From the data on reacted molecules, and derived position-time diagrams of stress and temperature, it was found that the initial void collapse induces very little reaction. However, when the shock moves beyond the first collapsed void it is highly curved, and collapses the second void more strongly, leading to far more reaction. The preliminary simulations provide a starting point for Roadrunner-scale simulations planned for FY09-FY10.

**Continuum-level modeling**

We are developing a mathematical framework to capture the physics of hot spot criticality (ignition vs. quenching) based on energy deposited into a condensed phase explosive. The models are formulated for non-ideal equations of state and general reaction kinetics for ideal and non-ideal HE. Cases being examined currently include spatial and temporal length scales of the power deposition such that hot spots evolve according to a balance between compressible and chemical interactions or a balance between thermal conduction and chemical interactions. Two-dimensional high-resolution reactive flow simulations of chemically reactive shock-induced hot-spots in a multi-material HE model are also being conducted.

## Future Work

Research will continue on the ability to prepare and characterize materials with highly tunable and controlled heterogeneities for laser driven and gas-gun shock initiation experiments as outlined above. Simulation, modeling and theory from atomic to micron length scales will continue to be used to develop a physical and chemical based understanding of the role of hot-spots in explosive initiation behavior.

## Conclusion

We have established a strongly synergistic interaction among experiment, simulation, and theory on atomic, nano-, and micron spatial scales to:

Answer fundamental questions about hot spot physics and chemistry as outlined above,

Develop physically-based mesoscale models for thermal and convective evolution, including temperature-dependent chemistry, thermal transport and mechanics, within and among hot spots from defect sources that are controlled and tractable, and

Perform evaluative assessments between observed and calculated shock initiation processes on mesoscopic and continuum scales. Simulations will be based initially on 3-D models that explore the nature of the flow field around one or several inclusions (i.e. on a meso-scale), and subsequently extended to continuum scales for which

direct comparisons will be made to in-situ magnetic gauge records.

To meet these scientific goals, we are studying simplified and controllable materials. We will intentionally introduce "tunable," and well-characterized heterogeneities in simple, but militarily and commercially relevant, energetic materials and logically map out their influence on initiation. We will probe how energy localization occurs, isolate specific features of hot spots, and understand complex interactions among them. Three systems- amorphous, crystalline, and ionic- enable us to isolate, characterize, and probe specific features of explosive sensitization through the controlled incorporation of hot spots.

## References


1. Perry, W. L., T. D. Sewell, B. B. Glover, and D. M. Dattelbaum. Electromagnetically-induced localized ignition in secondary high explosives. To appear in *Journal of Applied Physics.*

2. Stevens, L. L., N. Velisavljevic, D. E. Hooks, and D. M. Dattelbaum. Hydrostatic compression curve for triamino-trinitrobenzene (TATB) determined to 13.0 GPa with powder X-ray diffraction . 2008. *Pyrotechics, Explosives, and Propellants .* **33** (4): 286.

3. Stevens, L. L., N. Velisavljevic, D. E. Hooks, and D. M. Dattelbaum. The high pressure phase behavior and compressibility of 2,4,6-trinitrotoluene (TNT). 2008. *Applied Physics Letters.* **93**: 081912.

4. Cawkwell, M. J., K. J. Ramos, T. D. Sewell, and D. E. Hooks. Homogeneous Dislocation Nucleation and Anomalous Hardening in Cyclotrimethylene Trinitramine. *Physical Review B.*

5. Cawkwell, M. J., T. D. Sewell, L. Zheng, and D. L. Thompson. Shock-induced shear bands in an energetic molecular crystal: Application of shock-front absorbing boundary conditions to molecular dynamics simulations. To appear in *Physical Review B.*

6. Bolme, C. A., S. D. McGrane, D. S. Moore, V. H. Whitley, and D. J. Funk. Single shot Hugoniot of cyclohexane using a spatially resolved laser driven shock wave. 2008. *Applied Physics Letters.* **93**: 191903.


## Publications


Cawkwell, M. J., K. J. Ramos, T. D. Sewell, and D. E. Hooks. Homogeneous Dislocation Nucleation and Anomalous Hardening in Cyclotrimethylene Trinitramine. *Physical Review B.*

Cawkwell, M. J., T. D. Sewell, L. Zheng, and D. L. Thompson. Shock-induced shear bands in an energetic molecular crystal: Application of shock-front absorbing boundary conditions to molecular dynamics simulations. To appear in *Physical Review B.*

Perry, W. L., T. D. Sewell, B. B. Glover, and D. M. Dattelbaum. Electromagnetically-induced localized ignition in secondary high explosives. To appear in *Journal of Applied Physics.*

Stevens, L. L., N. Velisavljevic, D. E. Hooks, and D. M. Dattelbaum. Hydrostatic compression curve for triamino-trinitrobenzene (TATB) determined to 13.0 GPa with powder X-ray diffraction. 2008. *Pyrotechics, Explosives, and Propellants.* **33** (4): 286.

Stevens, L. L., N. Velisavljevic, D. E. Hooks, and D. M. Dattelbaum. The high pressure phase behavior and compressibility of 2,4,6-trinitrotoluene (TNT). 2008. *Applied Physics Letters.* **93**: 081912.

# Design, Synthesis, and Theory of Molecular Scintillators

*Rico Emilio Del Sesto*

20080037DR

## Introduction

The illicit movement of radioactive material, with ever increasing sophistication, has placed stringent requirements on current radiation detector technology. Improvements in total efficiency and energy resolution, combined with reduced detector costs that allow wide deployment, are needed. As a new approach to the development of scintillator materials, this project focuses on designing new materials from the bottom-up, and, through characterization and theoretical modeling, to understand the processes involved in scintillation from the initial incident high-energy gamma or neutron interaction down to the thermalization of secondary charged particles to yield an emission signal for detection. Understanding these processes will allow us to design and optimize materials and predict their behavior for specific applications.

## Benefit to National Security Missions

This project will support the DOE mission of Threat of Weapons of Mass Destruction through enhancement of current capabilities for detecting nuclear threats. Existing scintillators lack characteristics to fully address radiation detector needs. Specifically, it is necessary to have large-volume, low-cost, high-performance materials to satisfy radiation detector requirements.

## Progress

### Approach to Molecular Scintillators

The molecular scintillator is a material which contains molecular units of individual functional components of a scintillator, i.e. the components that 1) interact with incoming radiation, 2) generate excitations, 3) transport and thermalize those excitations, and 4) emit light to provide signal for detection purposes. By compartmentalizing these functions into individual units, structure-property investigations along with theoretical modeling can provide insight into the true mechanism of scintillation. These hybrid inorganic-organic scintillators therefore are capable of combining the high photoelectric absorption of the inorganic material, with the sub-nanosecond light output from the light emitting scintillator, for the next generation of composite radiation detectors.

### Synthesis and characterization of materials for gamma and neutron detection

We have synthesized a series of materials of the class of high-Z particles and clusters for gamma-detection applications, as well as boron clusters for neutron detection. These materials are well studied for other applications. The clusters provide the aforementioned functional units 1 and 2, but are not inherently luminescent at room temperature. Two options to introduce a luminescent unit are organic dyes, or cerium(III) ions due to their high luminescence efficiency and short emission lifetimes. In our attempts to introduce luminescent organic dyes to the clusters, we discovered that the clusters become incompatible with the organic ligands as they tend to oxidize the organic compounds, resulting in charge-transfer species which do not exhibit luminescence. This was confirmed using optical techniques and electron paramagnetic resonance (EPR). The other option of utilizing Ce(III) in the clusters was also attempted. However, similar incompatibilities or highly colored complexes were observed. It has been demonstrated that intramolecular energy transfer from these clusters to an incorporated lanthanide ion can occur, but until recently no examples of Ce(III) existed. We therefore synthesized a Eu(III)-based cluster into several polymers as well as organic liquids, with the total high-Z content at approximately 10% by weight. A polymer containing the Eu-cluster and under UV-irradiation are shown in Figure 1. These materials show very bright emission when exposed to ionizing x-ray radiation, Figure 2, and exhibit light outputs comparable to that exhibited by commercial plastic scintillator. Although the Eu(III) emission has an undesirable lifetime approaching milliseconds, it provides proof of principle of the conversion of ionizing radiation (x-ray) to visible light, utilizing a molecular species which

contains functional units serving the purpose of the different mechanisms in scintillation. Characterization of these materials under gamma irradiation is currently underway.

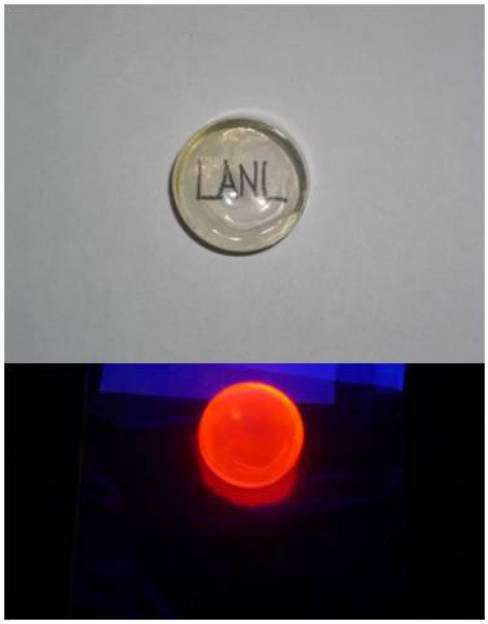


*Figure 1: Structure of Eu(III)-POM cluster; and photograph of a polymer containing these clusters, and under UV-irradiation.*

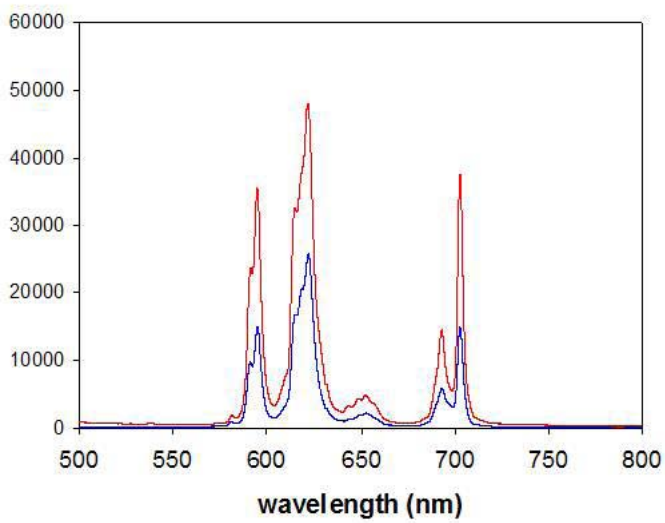


*Radioluminescence spectra of the Eu(III)-POM containing polymer, showing bright emission in response to ionizing radiation.*

We have also synthesized several boron clusters as polymers and liquids for neutron detection applications. Typical organic scintillator dyes were added to the liquids to convert excitations caused by alpha particles (following neutron capture) to a luminescent signal. Initial characterization showed weak response to neutron irradiation, but it appears that solubility of dyes is poor in the liquid matrices. We are currently examining other types of luminescent sites to be utilized for these systems.

Two areas in optical and nuclear spectroscopy capabilities have been of primary focus; combined timing and spectral measurements for scintillators, calibration of photodetectors and calculation of light collection efficiency for precise measurement of scintillator light output. We have procured a system which allows us to measure spectral intensity as a function of time based on a laser excited X-ray tube and streak camera, and have begun commissioning the system. In addition, we implemented the capability to measure gain vs high voltage and quantum efficiency as a function of wavelength for photo-multiplier tubes. These tubes were then used to make absolute light yield measurements on commercial crystals, in preparation for measuring materials developed at LANL. In addition, simulations were carried out to quantify the effects of packaging on light collection efficiency, again with relevance to making absolute light yield measurements.

**Theory and Modeling of molecular scintillators**

The theory and modeling component of this program includes first principle calculations of the electronic structure of the constituent components of the molecular scintillators, and modeling of the dynamics of the excitation generation, excitation transfer between the constituents, and luminescence of the scintillators. The first principle electronic structure calculations provide essential input parameters to the dynamics models. When radiation (gamma rays or neutrons) interacts with the scintillator material, high energy charged particles, such as electrons, are generated. These high energy charged particles generate electronic excitations as they traverse the scintillator material. The electronic excitations are transferred to luminescent centers in the scintillator and light emitted from the luminescent centers are detected by a photodetector indicating the presence of the radiation.

The molecular scintillators under investigation in the program consist of composites of high-Z particles, in which the high energy charged particles generate electronic excitations, and dyes that serve as the luminescent centers. We performed Time Dependent Density Functional Theory (TDDFT) calculations of the electronic structure of both the dyes and the particles or clusters. Calculated optical absorption and emission properties are in good agreement with our experimental observations. Calculated transition energies and dipole strengths play an essential role in the energy transfer modeling. As a specific example, a large Stokes shift was observed in the calculated optical spectra

of the particles and clusters of interest which was consistent with experiment. We have extended our calculations of the optical properties of the scintillator materials to include particles and clusters with a lanthanide ion. We found that, when the influence of the solvent is included in the calculations, a very reasonable energy level diagram is obtained, and consistent with measured absorptions at 333nm (377nm calculated) and 270nm (261nm calculated). We have examined other members in this series, including the cases where the Ln ion is Yb(III), and Eu(III). Current calculations are determining details of the emission spectra and lifetimes of these states.

We have also developed: (a) effective dielectric models for calculation of excitation transition rates and energy loss functions, and (b) rate equations for the calculation of TSL (thermally stimulated luminescense), OSL (optically stimulated luminescence) and PL (photo-luminescense) characteristics in the scintillators. Task (a) is tightly coupled with the first-principles TDDFT efforts of this project. It uses the TDDFT computed excited states, dipole moments and oscillator strengths as input. Task (b) uses the calculated transition rates from task (a) as input. We also developed models for the rate equations using phenomenological transition rates fitted to experiments of known scintillators to benchmark our models. The two parts of task (a) are closely related, because they require the calculation of materials specific dipole moments and oscillator strengths of excited states. We have established an approach for calculating the energy loss function from the electronic structure input parameters.

## Future Work

The synthesis of a series of materials and obtaining structure-property relations in the molecular scintillators are the major task for the upcoming year. We can then begin to understand materials specific processes which are conducive to, or destructive to, the scintillation mechanism. A major challenge for the coming year will be the calculation of higher multipole moments, which are required for the evaluation of the energy loss function. The energy loss function is a central property of the material describing the loss of energy and stopping length of secondary electrons created after the initial excitation with a gamma ray. The model rate equations developed in task (b) will allow us to compare theoretically predicted luminescence properties with experiments. In the coming year, we will compare predictions based on first-principles electronic structure calculations with experiments on the newly synthesized and characterized molecular scintillators. This will enable our team to begin tuning materials properties for emergent luminescense properties of the molecular scintillators.

## Conclusion

We have demonstrated a proof-of-concept in which a material loaded with high-Z molecular clusters with a luminescent site exhibits a response to ionizing radiation. We have also developed theoretical models which will assist in understanding the mechanisms of scintillation in the materials synthesized. This will allow us to continue to develop and optimize new materials which will lead to new radiation detectors.

## Publications

Ortiz-Acosta, D., R. Del Sesto, A. Gaunt, M. Lucero, G. Purdy, B. Bennett, C. Macomber, B. Scott, R. Muenchausen, T. McCleskey, R. Martin, R. Gilbertson , and E. McKigney . Ionic Liquid Polyoxometalates as Light Emitting Materials. Presented at *214th Electrochemical Society Meeting: Molten Salts XVI.* (Honolulu, HI, 12-17 Oct 2008).

continuing project

# Ultrafast Nanoscale XUV Photoelectron Spectroscopy

*George Rodriguez*

20080097DR

## Introduction

This project exploits the coherent properties of short wavelength light and ultrafast short pulse laser technology to convert femtosecond ($10^{-15}$ sec) visible light pulses to the extreme ultraviolet (XUV) soft x-ray portion of the electromagnetic spectrum. Previously only accessible at large synchrotron light facilities, a scaled-down table-top version is now possible through advances in the physics of short pulse laser light-matter interaction for light conversion into the XUV regime. Armed with such a light source, the extremely short wavelength and coherence properties of the light allows us to achieve imaging and time resolutions that approach the intrinsic spatial and time scales of matter, nanometer ($10^{-9}$ m) scale in space and attosecond ($10^{-18}$ sec) scale in time. We will use this unique light source to probe material core level structure and dynamics using a technique called angle-resolved photoelectron spectroscopy (ARPES). In XUV ARPES, extreme ultraviolet light is used to force electrons to be ejected from the material that are subsequently analyzed for their kinetic energy content and angular spatial distribution which provides a detailed signature of material bulk electronic structure and dynamics. Insight into quantum effects and collective particle behavior are thereby provided for complex materials and nanotechnology engineered devices whose emergent properties are critical for understanding function. This project will apply these methods to materials relevant to Laboratory science in actinides, superconductivity, energy conversion, nuclear waste, and sensor technologies.

## Benefit to National Security Missions

The primary scientific motivation underpinning this project is a desire to advance our understanding of the electronic structure and dynamics of complex emergent materials at the nanoscale. Our cross-disciplinary studies will contribute to predictive materials science that supports multiple DOE and NNSA missions including Energy Security, Weapons Physics, Threat Reduction and Nanotechnology.

## Progress

This year, project activities have concentrated on the design, construction, integration, and testing various subsystems that comprise the ultrafast extreme ultraviolet (XUV) photoelectron spectrometer. Initial time-resolved experiments are to begin the second quarter of FY2009. Here we describe the various activities on these sub-systems and planned initial experiments.

Construction and installation of our ultrafast optical light source is complete. An ultrafast 25 femtosecond, 10 kilohertz repetition rate, 1.8 millijoule per pulse Titanium:sapphire laser at 800 nanometers is used to focus into and ionize a noble gas (Ar) contained in a 150 micron hollow core capillary fiber. XUV photons are created via the nonlinear optical high harmonic generation process and a coherent beam containing photon energies from a few eV above 100 eV are generated. The XUV beam output is then directed to a special time-compensated, double-grating, XUV vacuum monochromator required for spectral characterization of the harmonic content and temporal preservation of the XUV pulse. High efficiency throughput is achieved by using grazing incidence metal optics in the monochromator. After the monochromator, the XUV beam is then directed toward a differential vacuum pump line before entering the photoelectron spectrometer. Design, construction and integration of an angle-resolved photoemission spectrometer (ARPES) chamber with the XUV light source are complete. The system is built around the Phoibos 150 analyzer from SPECS, Germany, which is equipped with high sensitivity detector. Other parts include a stainless steel ultra-high vacuum chamber, sample manipulator, gas dosing manifolds, sputtering gun and pumps. Spectral characterization of the XUV source and electron energy-momentum resolution of the spectrometer will be determined by XUV photoemission experiments off a Pt metal surface. These system characterization studies are in progress. The development of the instrument is within one month of the schedule set out in our original proposal.

## Future Work

In the first half of FY2009, we will concentrate on demonstrating our instrument's unique capability as a unique photoemission tool for studying ultrafast dynamics of core level electron dynamics in complex correlated materials with time, energy and momentum resolution. Experimental and theoretical efforts will be focused on studying time-resolved 5*f* electron population dynamics. Using two-photon optical-pump XUV-probe, we will study dynamics of 5*f* "empty" states in the Mott insulator $UO_2$ with attention to understanding relaxation channels. Similarly, optical-pump XUV-probe studies on anti-ferromagnetic $USb_2$ are also desirable since it would be the first study of dispersion kinks and their effects on 5*f* empty states quasiparticle lifetimes and their *k*-space dependence.

In parallel with these activities, design upgrade of the instrument to nanoscale imaging (10's of nm's) will be explored. This will be accomplished by taking advantage of the extremely short wavelength of the coherent XUV light source, with special imaging optics that should provide ultrasharp imaging at the intrinsic focusing limit of the light source. Should the approach be feasible, implementation of this capability will come online in FY2010. With a nanoscale imaging capability, we will then examine 1D confinement electron band structure physics of nanostructures, specifically semiconductor nanowires, especially focusing on the photoelectric conversion energy transport properties of these materials. Additionally, heterogeneity studies will take advantage of the ultrasmall focusing properties of XUV APRPES to probe single-crystallite regions of polycrystalline samples of Ce and U to improve our understanding of Fano resonance mixing of 4*d*-4*f* and 5*d*-5*f* states and to determine *f*-electron orbital distributions in the valence band and the various decay channels present within the resonance. Single grain and orbital identification measurements allow for better comparison with theoretical models that compute spectral densities. In high-temperature superconductors, dynamics of electronic phase separations will be studied with core level sensitivity and high spatial resolution that enables material contrast in complex multi-elemental compounds and alloys.

## Conclusion

This project will aid us in understanding detailed nanoscale quantum properties of materials establishing a basis from which new emergent functional materials may be designed. The DOE Basic Energy Science (BES) or Defense Homeland Security (DHS) Programs could directly benefit from these studies as interest for nanowire-based sensors and devices have applications ranging from ultra-sensitive drug detection chemistry to gas sensing of chemical bio-warfare agents and solar energy conversion. Other mission centric actinide materials science questions will also benefit, enabling a rational design basis for materials that can enhance the US energy security portfolio in superconductivity, nuclear energy, and nuclear waste.

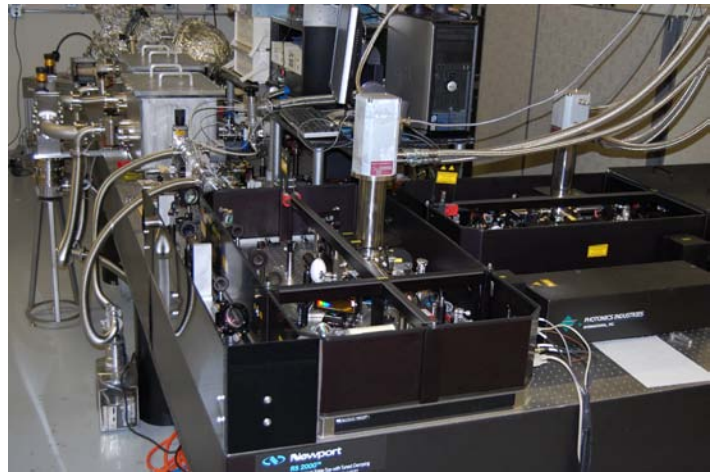


*Figure 1. Photograph of recently constructed ultrafast laser-based coherent XUV source, associated monochromator, and angle-resolved photoemission spectrometer (ARPES).*

## Publications

Kim, K. Y., A. J. Taylor, J. H. Glownia, and G. Rodriguez. Coherent control of THz supercontinuum generation in ultrafast laser-gas interactions. 2008. *Nature Photonics.* **2** (10): 605.

Prasankumar, R. P., S. G. Choi, G. T. Wang, S. T. Picraux, and A. J. Taylor. Ultrafast carrier dynamics in semiconductor nanowires. To appear in *16th International Conference on Ultrafast Phenomena.* (Stresa, Italy, 9-13 Jun. 2008).

Prasankumar, R. P., S. G. Choi, G. T. Wang, S. T. Picraux, and A. J. Taylor. Ultrafast carrier dynamics in semiconductor nanowires. Invited presentation at *Conference on Lasers and Electro-Optics.* (San Jose, CA, USA, 4-9 May 2008).

Prasankumar, R. P., S. G. Choi, S. A. Trugman, S. T. Picraux, and A. J. Taylor. Ultrafast electron and hole dynamics in Germanium nanowires. 2008. *Nano Letters.* **8** (6): 1619.

Rodriguez, G., and K. Y. Kim. THz supercontinuum generation in gas filaments: 'current ' perspective and applications. Invited presentation at *Second International Symposium on Filamentation.* (Paris, France, 22-25 Sep. 2008).

continuing project

# Advanced Fuel Forms with Microstructures Tailored to Naturally Induce Fission Product Separation During Service

*Kurt Edward Sickafus*

20080114DR

## Introduction

Our objective is to investigate key scientific and technological issues underpinning the design of a revolutionary nuclear fuel form possessing desirable attributes of conventional nuclear fuel ($UO_2$ or mixed oxide (MOX) fuel), but with a tailored microstructure that radically eases separation of fission products, drastically reduces separation costs, and substantially mitigates proliferation risks of the separated material. Our advanced nuclear fuel design is based on a dispersion (two-phase composite) nuclear fuel (so-called "dispersion fuel") concept. The goal of this project is NOT to develop a nuclear fuel form that will be readily licensed by the Nuclear Regulatory Commission (NRC). Rather, our goal is to develop the underpinning science to facilitate more rapid evaluation and acceptance of new fuel forms and to demonstrate a LANL institutional capability to deliver innovative approaches to solving complex national problems. This supports DOE's overarching mission: "to advance the national, economic, and energy security of the United States and to promote scientific and technological innovation in support of this mission." Our project promotes a designed merger of two portions of the nuclear fuel cycle, burning and reprocessing (these ordinarily are managed independently).

## Benefit to National Security Missions

This project supports the DOE mission for Energy Security, especially the DOE overarching mission: "to advance the national, economic, and energy security of the Unites States and to promote scientific and technological innovation in support of this mission."

## Progress

Our advanced nuclear fuel design is based on a composite microstructure wherein small fissile material domains (spherical particles or layers) are dispersed in a non-burnable host matrix. Fission products with high kinetic energies form during irradiation and travel about 5-10 microns before stopping in the host matrix. Thus, a natural partitioning evolves between fuel actinides and fission products as this fuel burns. We intend to use a matrix material that can be readily separated from the embedded fissile domain. We have assembled a diverse and qualified team to: 1) fabricate prototype fuel structures; 2) irradiate these structures to simulate their behavior in a reactor and characterize the evolution of key properties such as microstructural changes, thermal conductivity, and solubility; and 3) use theory and atomistic models to optimize fuel chemistry / microstructures.

Initially, our studies focused on $MgO/HfO_2$ composites, wherein MgO represents a chemically-separable host matrix phase, while $HfO_2$ is a surrogate for a fissile, $UO_2$ minority phase. Collectively, these composites have the common feature that both the majority and minority phases are oxides, i.e., ceramic phases. Such composites are often referred to as cercer composites. Since these composites relate most directly to a conventional fuel based on $UO_2$, we believe this part of our project will most likely impact the development of advanced fuels for future thermal, light-water reactors (LWRs).

Our accomplishments on this project are divided into three principal tasks:

### Synthesis & Fabrication

Here, we fabricated model composite samples using three synthesis procedures: 1) conventional bulk processing; 2) thin film growth; and 3) particle coatings based on fluidized-bed chemical vapor deposition (FB-CVD). The conventional ceramic is a sample of composition 90-MgO/10-$HfO_2$. It consists of three phases: MgO, $HfO_2$, and delta ($\delta$)-phase $Mg_2Hf_5O_{12}$. The thin films are multilayers with structures given by $HfO_2$/MgO/$HfO_2$/Si (Figure 1) or $HfO_2$/MgO/$HfO_2$/MgO/$HfO_2$/Si. The particle coatings are MgO coatings of $HfO_2$ particles.

*Figure 1. Schematic drawing of the thin film, tri-layer architecture used for ion irradiation damage studies in this project, in order to simulate a composite (dispersion) nuclear fuel consisting of a fissile minority phase (hafnium oxide, $HfO_2$, used as a surrogate for uranium oxide, UO2) imbedded in a non-fissile majority (matrix) phase (magnesium oxide, MgO, used here).*

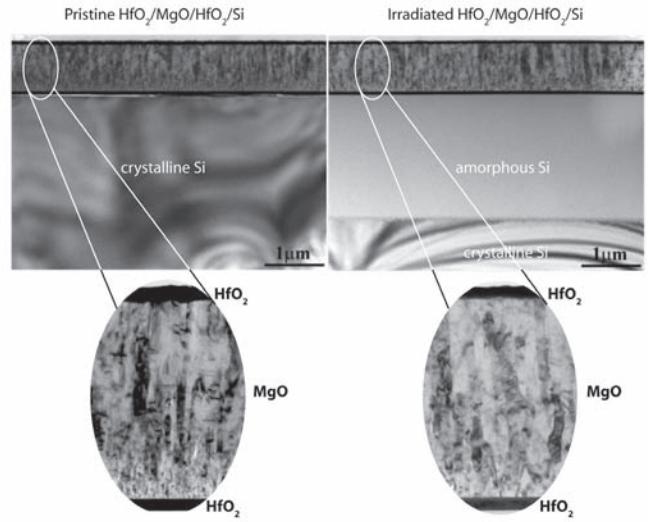


*Figure 2. Cross-sectional transmission electron micrographs obtained from a pristine tri-layer of hafnium oxide/magnesium oxide/hafnium oxide ($HfO_2$/MgO/$HfO_2$) deposited on a silicon (Si) substrate (left-hand micrograph) and an $HfO_2$/MgO/$HfO_2$/Si sample irradiated with 10 MeV gold (Au) ions to a fluence of 5.1•1015 Au/cm$^2$ (right-hand micrograph). The elliptical insets are enlargements of the tri-layer microstructure. The $HfO_2$/MgO/$HfO_2$ tri-layer was not greatly affected by the Au ion irradiation. On the other hand, the crystalline Si substrate was amorphized by the Au ion irradiation across a 2.5 µm thick region following irradiation to the Au ion fluence described above.*

**Irradiation & Characterization**

Here, we irradiated samples with heavy ions (Au) at high energies (10 MeV) at room temperature, to test microstructural stability under extreme environment conditions. We characterized the radiation damage response of our composites using a variety of experimental techniques, including transmission electron microscopy (TEM), X-ray diffraction (XRD), and ion beam analysis (IBA). We find that our composite samples are durable under high-energy, heavy ion irradiation; in particular, they are resistant to radiation-induced amorphization. We found that the conventional ceramic, 90-MgO/10-$HfO_2$, resists amorphization to at least a dose of 100 displacements per atom (dpa) using 10 MeV Au ions, though the $\delta$-$Mg_2Hf_5O_{12}$ component of these samples undergoes an order-to-disorder transformation at a dose of only 1 dpa. The thin film multilayer samples, $HfO_2$/MgO/$_2$Si, showed no significant changes in structure to doses of 3-12 dpa using 10 MeV Au ions (Figure 2). In fact, mixing at the MgO/$HfO_2$ interfaces was almost negligible. We did observe an interesting phenomenon on the surfaces of the irradiated trilayer, $HfO_2$/MgO/$HfO_2$/Si, samples. Using 10 MeV Au ions, we observed radiation-induced "craters" with "spires" protruding from the centers of the craters (Figure 3). These features were observed from relatively low ion fluences ($10^{13}$ ions/cm$^2$) to very high fluences (> $10^{16}$ ions/cm$^2$).

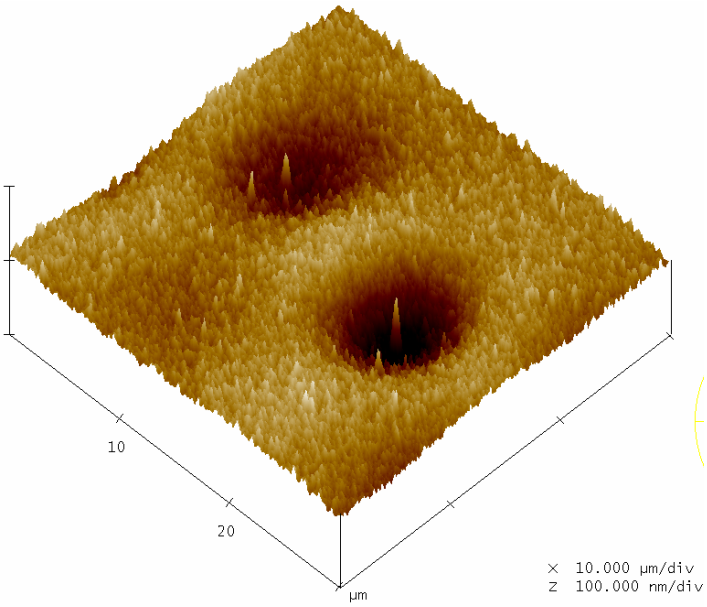


*Figure 3. Atomic force microscopy (AFM) image of the crater/spire features formed on the surface of an $HfO_2$/MgO/$HfO_2$/Si sample after irradiation with 10 MeV Au ions to a fluence of 5.1x10^15 Au/cm2. This is a three-dimensional image in which the surface plane axes (x & y) are shown at 45° with respect to the horizontal (shown in units of 10 µm per division), while the axis normal to the sample surface (z) is shown as a vertical axis (with units of 100 nm per division).*

**Modeling & Simulation**

Here, we examined the role of interfaces on radiation response using atomistic simulation procedures (first principles (e.g., density functional theory (DFT)), molecular statics (MS), and molecular dynamics (MD). Our DFT calculations were used to study the dynamics of fission product (FP) migration and segregation to interfaces in a model $MgO/HfO_2$ composite. We found using DFT that prominent FP species such as Xe, Cs, and Sr, exhibits a strong preference to locate in the $HfO_2$ phase within an $MgO/HfO_2$ composite and if these FP are initially located in the MgO, they readily segregate to the $MgO/HfO_2$ interfaces. In preparation for MD studies of the dynamics of these processes, we developed a model $MgO/HfO_2$ phase boundary using MS, wherein we relaxed the atomic structure at the interface. The geometry of the model interface is (111) MgO / (100) $HfO_2$. Preliminary defect calculations indicate that oxygen vacancies possess energies that are much smaller in the $HfO_2$ layer compared to the MgO layer. These results are significant because they indicate where the fission products will end up in a heterogeneous material. The FPs may not stay where they are originally deposited, but rather migrate to a more energy-favorable location.

## Future Work

Our future plans involve a number of extensions of our past activities:

1. Synthesis & Fabrication. We plan to fabricate new composite samples based on a different surrogate for $UO_2$, namely cerium oxide ($CeO_2$), and alternative matrix oxides, namely calcium oxide (CaO), strontium oxide (SrO), and barium oxide (BaO). In addition to these cercer (ceramic-ceramic) composites, we will also initiate synthesis and fabrication studies on cermet (ceramic-metal) composites, based on zirconium (Zr) metal matrices.

2. Irradiation & Characterization. We will continue to irradiate composite samples using heavy ions (10 MeV Au ions) in the Ion Beam Materials Laboratory (IBML) at Los Alamos National Laboratory (LANL).

3. Modeling & Simulation. We will examine fission product incorporation in $UO_2/MgO$ composites and study the atomic details of radiation damage events at phase boundary interfaces in cercer composites such as $HfO_2/MgO$ and $CeO_2/MgO$.

## Conclusion

We expect to determine whether or not we can create a two-part, nuclear fuel that eases the complexities associated with spent fuel chemical separations processes. This fuel form must not only be easy to separate chemically, but during service as an energy source, it must exhibit both robust and predictable behavior. We will test our advanced fuel materials to ensure that they possess the necessary physical and chemical stabilities. The natural, in-service chemical separations strategy associated with our novel approach will greatly reduce both technological challenges and costs compared to conventional reprocessing. The American taxpayer would benefit with cheaper, cleaner energy.

# Nanoscale Fluctuations in Multifunctional Materials

*Alexander V Balatsky*

20051164DR

## Abstract

This is a project focused on exploring small-scale *fluctuations and inhomogeneities* in organic and inorganic materials. The goal of this project was to develop an understanding of the physics of noise and fluctuations, develop experimental and theoretical tools that would allow predictions, characterization and ultimately design of systems where short scale and time fluctuations are essential. In the work conducted under this proposal we focused on the investigation of materials that falls under these categories: 1) Inhomogeneity and fluctuations in nanoscale systems, like *DNA molecules*, and small *magnetic particles and in mesoscopic magnetic films*. 2) Fluctuations and inhomogeneities at the nanoscale also occur in the bulk when the physical system has some frustration or competition between different states and different interactions. We have looked at collective dynamics in *multiferroics* as a representative of a correlated bulk material.

## Background and Research Objectives

The advantage of studying fluctuations is obvious when one focuses on small length and time scales. Properties of materials at nanoscale are determined by fluctuations. These small-scale fluctuations can occur in artificial structures such as quantum dots and other short length scale systems. We used noise, fluctuations and related short scale inhomogeneities as a tool to reveal the physics of materials. To elucidate the meaning of the noise spectroscopy concept, we point out that the spectrum of excitations and dissipations are closely related through the fluctuation-dissipation theorem, which states that dissipation is caused by the energy being dissipated through excitations of the levels of the given system. On the other hand, at equilibrium any physical system would experience fluctuations. These fluctuations are realized as excitations of the same levels of the system that are involved in dissipation. Hence dissipations and fluctuations contain the same spectroscopic information about the relevant physical system.

Closely related to temporal fluctuations are spatial inhomogeneities. Often spatial inhomogeneities appear at a nanoscale because the size of the objects we study is small. Sometime inhomogeneities reflect frustration due to competing interactions, e.g. competition between qualitatively different ground states. Inhomogeneity reflects short time fluctuations that are "frozen" in a material. Both fluctuations and nanoscale inhomogeneity reflect the same physics that we are trying to uncover in materials and systems of interest.

## Importance to LANL's Science and Technology Base and National R & D Needs

This project is working to develop a fundamental understanding in topics relevant to quantum computing, nanotechnology and spintronics. These technical capabilities are important to the missions of DOE's Office of Science and Nonproliferation programs.

## Scientific Approach and Accomplishments

### Multiferroic functional materials

Our optical studies of low-energy excitations in multiferroic materials led to the following accomplishments:

1. We have completed ultrafast spectroscopic study of multiferroic hexaferrite $Ba_{0.5}Sr_{1.5}Zn_2Fe_{12}O_{22}$ (BSZFO) and detected coherent magnon motion in time domain via transient reflectance. The motion is excited coherently via impulsive thermal modification of the exchange energy, and the time evolution of the magnon coordinate is recorded as a change in reflectance caused by the optical frequency magnetodielectric effect. Transient reflectance provides a sensitive probe of magnetization dynamics in materials with strong magnetodielectric coupling, such as multiferroics, revealing new possibilities for application in spintronics and ultrafast manipulation of the magnetic moment.

2. We conducted Terahertz time domain and far-infrared Fourier-transform spectroscopy on single crystals of multiferroic $HoMnO_3$ in magnetic field, which resulted in the detection of the antiferromagnetic resonance of Mn ion lattice and crystal field excitations of magnetic Ho ions. The measurement is expected to shed light on the possible magnetic coupling between Mn and Ho ions – an important question in the multiferroicity of $HoMnO_3$.

3. We performed Terahertz time domain spectroscopy on single crystals of multiferroic $BiFeO_3$, which resulted in the detection of low-energy magnetic and lattice and, possibly, coupled magnetic-lattice excitations. Reflectance Terahertz spectroscopy measurements were carried out (Figure 1) to distinguish the resonances in magnetic and dielectric parts of the refractive index, without which unambiguous assignment of absorption modes is impossible.

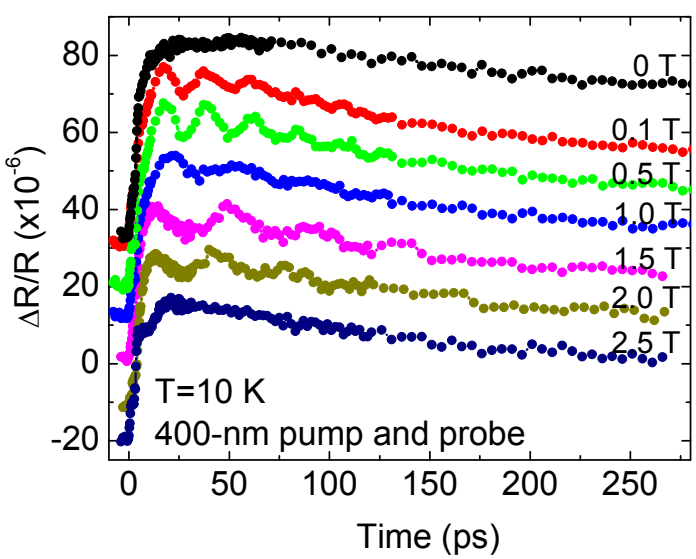


*Figure 1. Transient reflectivity of Ba hexaferrite as a function of field. Observe the appearance of oscillation in the spectra upon increasing the field from zero and the subsequent changes of oscillation frequency.*

We made substantial progress in characterization of multiferroics with optical time domain spectroscopy in the dissipative channel. We did not reach the stage where we could implement noise spectroscopy and nanoscale characterization in multiferroics. Technical demands on development of a new experimental techniques proved to be too high to develop these noise and nanoscale techniques over the span of this projects.

**Noise spectroscopy of small magnetic particles accomplishments**

We built a scanning magneto-optical Kerr microscope to image mesoscopic magnetic films. Preliminary images demonstrate that experiments work, and reveal domain structure in Permalloy films, dots, and squares. We hired Lili Cheng (PhD Columbia U; background in Ferromagnetic Resonance (FMR) of magnetic films) to work on these experiments. An explanation of noise in small magnetic systems is illustrated in Figure 2.

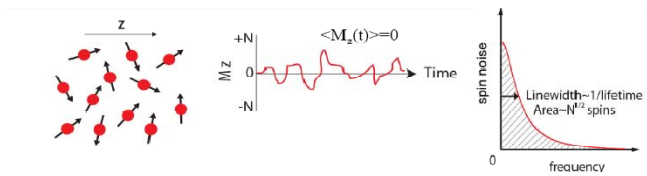


*Figure 2. Explanation of the nature of spin noise.*

In the course of this work we have significantly advanced our instrumentation for spin noise spectroscopy. Our present experimental apparatus uses what is essentially the digital back-end receiver of a radioastronomy telescope. Taking advantage of recent advances in Field Programmable Gate Arrays (FPGAs; "programmable hardware"), we have adapted a high-speed (2GHz) digitizer containing an on-board FPGA processor to compute real-time FFT spectral averaging with a full 1 GHz bandwidth. Doing so avoids the bottlenecks associated with having to transfer large amounts of digitized data over a computer's PCI bus – everything happens directly on the digitizer board. The massively parallel architecture of the FPGA is ideal for this type of application. Using this system we realize a thousand-fold reduction in the data acquisition time required for good data, as compared with commercial swept-scan RF spectrum analyzers.

Using this system we have been able to:

Achieve noise floors of the measured Faraday rotation in the sub-nanoradian range (bear in mind that a nanoradian is the angle subtended by the typical thickness of a human hair, as viewed from a distance of 100 kilometers). This sensitivity is required to measure the extremely tiny signals from free electron spins fluctuating in solid state systems. We have applied our instrument to measure the spin noise of free electrons in gallium arsenide, a prototypical semiconductor. We have measured clean noise spectra in GaAs as a function of electron doping, temperature, laser spot size, and wavelength detuning (Figure 3).

Our interesting finding to date is that the spin noise power, Figure 3, measured as a function of temperature, appears

to extrapolate back to a finite noise signal at zero temperature. We have measured from 30K down to 1.5K, and the trend is linear (expected) but with a nonzero offset (unexpected). This result is against expectation if one considers a sea of electrons as strictly obeying Fermi-Dirac statistics, and may point to interesting electron correlations in n: GaAs beyond the simple Fermi-Dirac statistics.

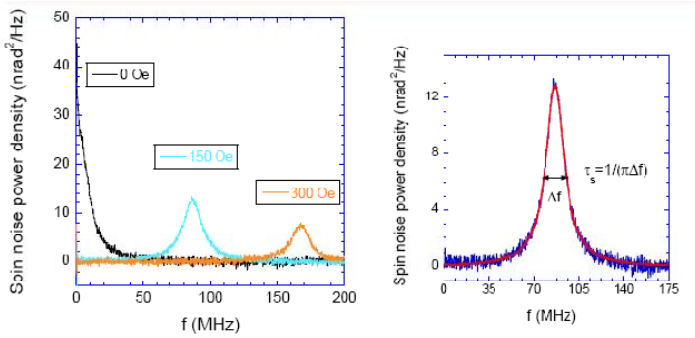


*Figure 3. Measured Spin Noise in 2 Dimensional Eelectron Gas (n doped GaAs) with carrier density n = 10^16/cm^3.*

Using our new apparatus, we anticipate moving to mesoscopic and nanoscale materials systems, such as semiconductor epilayers and quantum dots. Further, we intend to re-visit magnetization noise in ferromagnetic Permalloy metal films for which we have obtained preliminary results. Also of interest are spin noise studies of diluted magnetic semiconductor nanowires (being grown by collaborators at Penn State University), which contain small numbers of Mn atoms. Electron transport through these nanowires may reveal stochastic fluctuations of the Mn spins, which may be detectable using our sensitive instruments.

**Tunneling spectroscopy and DNA nanoelectronics**

The small dimensions of the nanostructured materials pose high demand to the instrumental part of the diagnostics toolkit. The only instrument capable of simultaneous electronic and structural characterization of the nanoscale with atomic resolution is the Scanning Tunneling Microscope (STM). Due to the strong dependence of the current on the tunnel contact area and tip-surface spacing, variations in the surface topography can be mapped with sub-angstrom precision. The major virtue of the STM lies in its ability to probe the electronic structure of the surface with resolution unapproachable by any other method. The combination of two operational regimes allows direct and non-ambiguous analysis of the relationship between atomic structure of the material and its electronic properties. The approach to understand materials at the nanoscale requires the ability to model STM topography and electron tunneling spectra (I/V, dI/dV, etc.), providing wealth of information about electronic structure and function.

At the beginning of this proposal we proposed to explore relations between structure and properties of materials at the nanoscale by probing materials at the nanoscale directly. Our system of choice was a hybrid system material of DNA on carbon nanotubes. As a proof-of-principle we applied our setup to distinguish single DNA nucleotides in the quest for electronic DNA sequencing methods. As a next and more ambitious step we plan to implement inelastic electron tunneling spectroscopy, a new method adding the chemical sensitivity to already exhausting electronic capabilities of our STM. As we discussed in the introduction, dissipative measurement is a counterpart to the noise because of the inherent connection between fluctuations and dissipation.

We created a sophisticated STM instrument providing atomic scale resolution at pA current levels and cryogenic temperature, necessary for DNA immobilization on the metal surface (Figure 4a). We implemented a freeze-dry technique and instrumentation to deposit DNA on the metal surface without subsequent aggregation (Figure 4b). Such method of DNA pulse injection does not induce changes in the surface structure of the metallic substrate, reducing the number of artifacts, usually observed in the STM images.

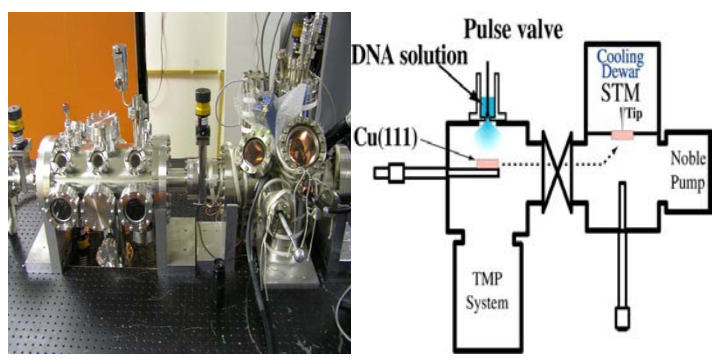


*Figure 4. STM setup layout (a), and (b) schematic drawing of the sample preparation chamber.*

As a proof-of-principle experiments and to test our instrument abilities, we conducted topographical imaging of DNA-wrapped carbon nanotubes (CNT). Figure 5a demonstrates the first images of DNA-CNT constructs ever observed with such high morphological resolution. Our instrument clearly visualizes the periodic wrapping of the CNT by the DNA strand. The coiling period was mathematically extracted from these images, and corresponds very well to the results of molecular dynamics simulations (Figure 5c, d). Currently we are working on uncovering the correlation between the DNA wrapping geometries and structure of the individual CNT using both topographic imaging for structural characterization and

tunneling spectroscopy to extract electronic properties of the material.

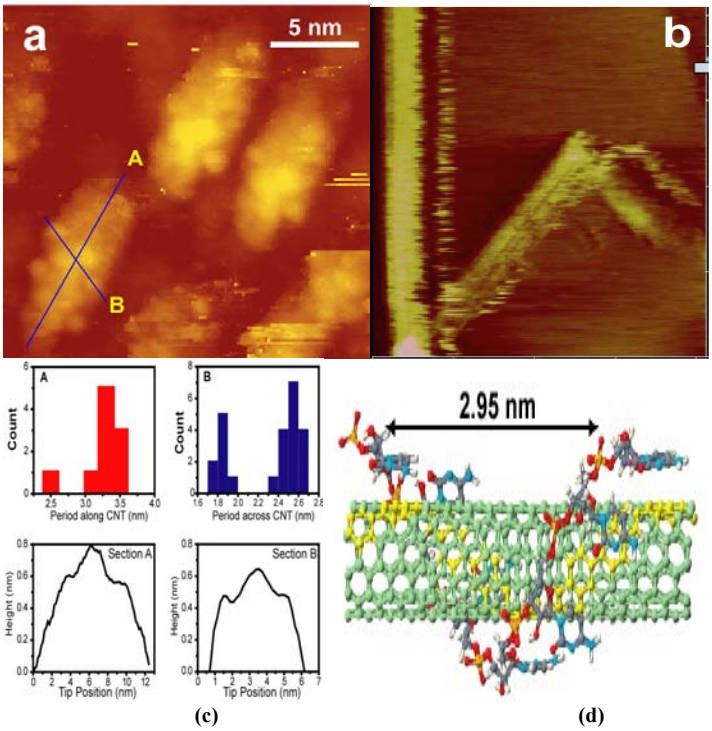


*Figure 5. (a) STM image of the DNA-wrapped carbon nanotubes; (b) STM image of DNA insertion into the nanotube; (c) DNA coiling period statistics extracted from (a); (d) MD calculations of wrapping geometry.*

In conjunction with experimental work we have developed theory of molecular electronic states of DNA bases: A, G, C, and T on surface of Cu (111). We have preformed a comparison of our simulation results of G tunneling spectrum with experimental spectrum obtained by Tanaka's group. We successfully applied developed simulation technique to model geometries of the DNA adsorption onto carbon nanotube surface and resulting electronic properties of such hybrids. An example is shown in Figure. 5d, where period of the DNA coiling has been calculated *ab initio* to be ~3 nm, in excellent agreement with experimental observations (Figure 5 a,c).

Our method can be applied to verification of a recently proposed hypothesis about DNA sequencing using STM technique. The importance of successful genome sequencing cannot be overestimated, as the establishment of a new X-Prize gives proof (the first was offered for the first private space ship): ten million dollars will go to the developers of a sequencing method capable of providing full information on 100 genomes of 6 billion base-pairs length each in 10 days. Development of the proposed STM diagnostic method and its application to the DNA sequencing will be very useful in identifying short DNA fragments and in studies of DNA-pathogen interactions.

**Outcomes**

We secure funding for STM-on-DNA work through National Nanotechnology Enterprise Development Center, and will continue tunneling spectroscopy and electronic structure in DNA and DNA- carbon nanotube composites. Our work in this project has set the stage for us to:

Perform high resolution STM imaging of the geometrical structure of single nucleotides and short single stranded and double stranded DNA molecules.

Conduct spectroscopic studies of the electronic response of DNA-substrate system at cryogenic temperatures.

Perform STM imaging and spectroscopy of DNA-wrapped carbon nanotubes. Investigate changes in the structural and electronic properties of hybrids as a function of the DNA length and composition.

## Publications

Balatsky, A.. Noise spectroscopy. 2007. *SPIE Conference on Noise, May 2007, invited talk.*

Balatsky, A.. DNA Nanoelectronics, invited talk. 2007. *Labs-UNM meeting on Nanobiology.*

Balatsky,I.Vekhter,andJ.-X.Zhu, A. V.. Impurity-induced states in conventional and unconventional superconductors. 2006. *Rev. Mod. Phys.* . **78**: 373.

BalatskyandJ.-X.Zhu, A. V.. Local strong-coupling pairing in d-wave superconductors with inhomogeneous bosonic modes . 2006. *Phys Rev B.* **74**: 094517.

Balatskyetal, A.. STM NMR and nuclear spin noise. 2006. *Phys. Rev. B* . **73**: 184429.

Crooker, S.. Faraday Noise. 2005. *March Meeting, MArch 2005, invited talk.*

Katsuraetal, H.. Voltage dependence of Landau-Lifshitz-Gilbert damping of spin in a current-driven tunnel junction . 2006. *Phys. Rev. B 73, 212501 (2006).* **73**: 212501.

Kilina, S., S. Tretiak, D. Yarotski, J. X. Zhu, N. Modine, A. Taylor, and A. Balatsky. Electronic Properties of DNA base molecules adsorbed on a metallic surface. To appear in *Journal of Physical Chemistry.*

Kilina, S., S. Tretiak, D. Yarotski, J. X. Zhu, N. Modine, A. Taylor, and A. Balatsky. Electronic properties of DNA base bolecules adsorbed on a metallic surface.. 2007. *Journal of Physical Chemistry C.* **111** (2): 14541.

Leeatal, J.. Interplay of electron,Äìlattice interactions and superconductivity in Bi2Sr2CaCu2O81d. 2006. *Nature .* **442**: 546.

Qazilbash, M., M. Brehm, B. Chae, P. Ho, G. Andreev, B. Kim, S. Yun, A. Balatsky, B. Maple, F. Kielmann, and D. Basov. Mott transition in VO2 revealed by infrared spectroscopy and nano-imaging. 2007. *Science.* **318** (12): 1750.

Talbaev, D.. Optical studies of low-energy excitations in multiferroic materials", 22 March 2007, Department of Physics, Rutgers University, invited talk. 2007.

Talbayev, D., A. Balatsky, A. J. Taylor, R. D. Averitt, and T. Kimura. Detection of coherent magnons via transient reflectance in multiferroic Ba0.6Sr1.4Zn2Fe12O22. 2007. *, Conference on Lasers and Electro-optics, Baltimore, MD, USA, May 2007, talk.*

Talbayev, D., A. J. Taylor, R. D. Averitt, and T. Kimura. Detection of coherent magnons via transient reflectance in multiferroic Ba0.6Sr1.4Zn2Fe12O22. 2007. *Strongly Correlate Electrons in Solids, poster.*

Talbayev, D., R. D. Averitt, A. J. Taylor, and T. Kimura. Giant magnetoelastic effect in multiferroic Ba0.6Sr1.4Zn2Fe12O22. 2007. *March meeting of the American Physical Society, Denver, CO, USA, 2007, talk.*

Talbayev, D., R. D. Averitt, A. J. Taylor, and T. Kimura. Giant magnetoelastic effect in multiferroic Ba0.6Sr1.4Zn2Fe12O22. 2006. *ICAM Annual Conference on Frontiers in Complex and Adaptive Matter, Santa Fe, NM, USA, November 2006 talk.*

Talbayev, D., S. A. Trugman, A. V. Balatsky, T. Kimura, A. J. Taylor, and R. D. Averitt. Detection of coherent magnons via ultrafast pump-probe reflectance spectroscopy in multiferroic Ba0.6Sr1.4Zn2Fe12O22 . 2008. *Physical Review Letters.* **101** (3): 097603.

Yarotski, D., A. Balatsky, S. Kilina, A. Talin, S. Tretiak, and A. J. Taylor. Scanning Tunneling Microscopy of DNA-Carbon Nanotube Hybrids.

Yarotski, D. A., S. V. Kilina, A. Talin, S. Tretiak, O. V. Prezhdo, A. V. Balatsky, and A. J. Taylor. Scanning Tunneling Microscopy of DNA-wrapped carbon nanotubes.. To appear in *Nano Letters.*

Yarotski, D., A. V. Balatsky, S. Kilina, A. Talin, J. X. Zhu, S. Tretiak, R. Averitt, and A. Taylor . Scanning Tunneling Microscopy of DNA-carbon nanotube hybrids. 2007. *The 3rd Nanoelectronics and Dynamics of DNA International Workshop, August 26-29, 2007, Honolulu, HI, USA, talk .*

Zhuetal, J. X.. Fourier-transformed local density of states and tunneling into a d-wave superconductor with bosonic modes . 2006. *Phys. Rev. B .* **73**: 014511.

# Structure and Bonding in Actinide Oxides

*David Lewis Clark*

20060019DR


## Abstract

The actinide oxides are of tremendous technological importance in nuclear fuels, environmental transport, nuclear waste management, and corrosion reactions in nuclear weapons. The deceptively simple binary formula of $AnO_2$ (An = actinide element) belies an incredibly complex structural nature, and propensity to form nonstoichiometric phases $AnO_{2\pm x}$. The fundamental physical and chemical properties of actinide oxides that make them so technologically important are governed by hybridization and covalency between the atomic orbitals that make up the metal-oxygen bonds. With recent developments in both theory and spectroscopy, we show that changes in the relative roles of 5*f* and 6*d* atomic orbitals can be experimentally measured, and correlated with the observed trends in structural and physical properties. Understanding the nature of 5*f*-element bonding will provide the key to understanding, predicting, and controlling the complex oxidation behaviors. The work reported here represents the first such study of its kind, and will establish the solid scientific foundation essential for engineered solutions to the wide range of actinide oxide issues in the stockpile, long-term storage, nuclear fuels, and environmental remediation. Finally, it builds an unprecedented competency in materials science of clear benefit to the long-term needs of Los Alamos core programs in nuclear weapons and energy security.


## Background and Research Objectives

The actinide oxides are of tremendous technological importance. They find widespread application as nuclear fuels, in long-term storage of surplus weapon's materials, and they play an important role in environmental actinide migration, and in corrosion reactions in nuclear weapons. The deceptively simple binary formula of $AnO_2$ belies an incredibly complex structural nature, and tendency to form nonstoichiometric phases $AnO_{2\pm x}$ [1]. The actinide series marks the emergence of 5*f* electrons in the valence shell. While the 5*f* electrons clearly participate in the band structure of light actinide metals and some alloys, whether 5*f* electrons participate significantly in covalent bonding in compounds like the actinide oxides is still unclear. Understanding the nature of actinide oxygen bonding will provide the key to understanding, predicting, and controlling the complex oxidation behaviors.

Our research objectives were to establish a new integrated materials chemistry capability at Los Alamos; to determine the structural chemistry of $AnO_{2\pm x}$ systems associated with specific metal oxidation states in light actinides; and to make use of recent advances in theory and spectroscopy to predict and measure the relative contributions of 5*f* and 6*d* atomic orbitals in the different bonding modes identified in $AnO_{2\pm x}$ systems. This work will establish a foundation for developing accurate predictive models for the binary actinide oxides and related compounds that are central to the Los Alamos core mission, and establish new and unique scientific capabilities that will strengthen Los Alamos' role in Office of Science (SC) programs.

## Importance to LANL's Science and Technology Base and National R & D Needs

This work provides technical details on what actinides form $AnO_{2+x}$, the conditions under which they are formed, the nature of the solid state structures, and a detailed understanding of their electronic structure and bonding. This program will supply detailed information about the interrelationships between local structure, chemical bonding, electronic properties, and chemical reactivity in actinide-oxygen systems, thus providing a unique understanding of the physical basis for the observed chemistry and physics of actinide oxides. Such knowledge will directly fuel the development of models for the behavior of oxides in storage environments, corrosion, transportation scenarios, and the environment. The collaborative nature of this approach will extend the Lab's leadership in actinide science, foster the development of new theoretical and spectroscopic techniques, provide critical information to the weapons and environmental management programs

and facilitate the lab goal of becoming the premier actinide materials laboratory in the world. Our scope incorporates state-of-the art Department of Energy (DOE) Office of Basic Energy Sciences (OBES) synchrotron user facilities and collaborations with other national laboratories, universities, and experts from the international actinide science community. Finally, the use of postdoctoral fellows in conducting this research will assist in attracting and training a future generation of actinide scientists to the Laboratory.

## Scientific Approach and Accomplishments

Our approach begins with chemical synthesis of high-purity, well-characterized materials. Actinides were purified by anion exchange chromatography to remove chemical and radiogenic impurities, and then converted to stoichiometric oxides using high temperature tube furnace techniques. All samples were characterized by x-ray diffraction (XRD) prior to use. With high quality samples of stoichiometric $AnO_{2.0}$, we used photoemission spectroscopy (PES) to determine the bound electronic states, and a combination of O K-edge near-edge x-ray absorption fine structure (NEXAFS) and non-resonant inelastic x-ray scattering (NRIXS) to map the unoccupied states above the Fermi level. These were directly compared to the theoretical density of states (DOS) calculated using *hybrid* density functional theory (DFT) with full periodic boundary conditions (PBC). Starting from stoichiometric solids of formula $AnO_{2.0}$, we used pressure-volume-temperature (PVT) and microbalance techniques to perform controlled oxidation with water vapor to generate $AnO_{2+x}$. The local structure of these phases was determined by metal L-edge extended x-ray absorption fine structure (EXAFS) and both x-ray and neutron pair distribution function (PDF) analysis to probe how the interstitial O atoms enter the structure, and what effect it has on existing metal and oxygen atom sites.

Structurally, actinide dioxides form a cubic fluorite-type phase over the composition range of $AnO_x$, where $1.6 < x < 2.0$ for Th – Cf, as illustrated in Figure 1 [2]. The stoichiometric $AnO_{2.0}$ lattice consists of a face-centered cubic (fcc) arrangement of metal atoms in 6-fold "octahedral" sites. Each metal atom is surrounded by 8 O atoms at the corners of a cube, and each adjacent 6-fold octahedral site is vacant (Figure 1). The intermediate phase compositions and structures displaying O/An ratios between 1.6 and 2.0 are realized by omission of O atoms in a periodic array. For the composition range $AnO_x$, where $2.0 < x < 2.25$, x-ray and neutron diffraction reveals a slightly expanded lattice, consistent with the formation of a solid-solution for $AnO_{2+x}$ (U, Pu) [2,3]. The exact position of the extra O atoms has been a topic of debate [4,5,6].

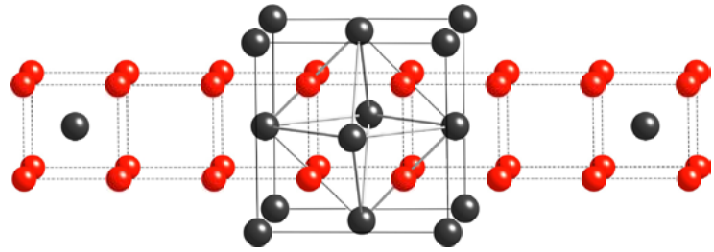

*Figure 1. The solid state structure of $AnO_2$ illustrating the central fcc arrangement of metal atoms (black) with a cube of oxygen atoms (red).*

### Electronic Structure of Stoichiometric $AnO_2$

For many years researchers have been calculating electronic structure in solids using density functional theory (DFT) in the local-spin-density approximation (LSDA). Unfortunately, LSDA often gives incorrect behavior in cases like actinide oxides, where the valence electrons are partially localized. We note that both the LDA and the generalized gradient approximation (GGA) extensions predict $UO_2$ to be a metal, when it is known to be an antiferromagnetic insulator with a gap of 2eV [7]. However, new research has established that hybrid functionals, which include a portion of the exact (Hartree-Fock) exchange interaction, remedy many of these problems, [8] and the introduction of a new screened hybrid DFT by Heyd, Scuseria and Enzerhof (HSE) [9] has extended this approach to metals and insulators [10]. Our recent application of the *hybrid* DFT approach (HSE06) to $UO_2$ gives a magnetic ground state, an insulating gap, and the lattice constant all in good agreement with experiment [11]. Our calculated HSE06 density of states (DOS) for $UO_{2.0}$ is shown in Figure 2.

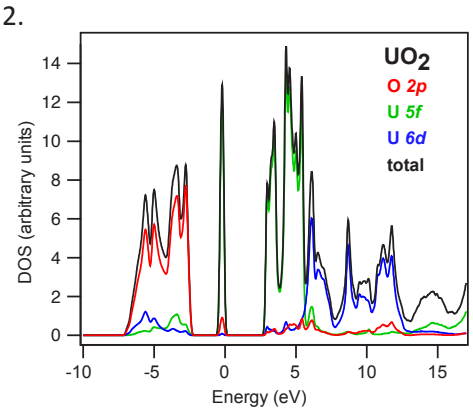


*Figure 2. Calculated total (black) and partial DOS (O 2p red, U 5f green, U 6d blue) for $UO_2$ calculated using the HSE06 functional and scalar relativistic effects.*

The occupied and empty states that are predicted from this new *hybrid* DFT calculation can be compared to experimental photoemission spectroscopy (PES) that can map the filled states, and a combination of oxygen near-edge

x-ray absorption fine structure (NEXAFS) and non-resonant inelastic x-ray scattering (NRIXS) that can map the empty states. With simple analytical functions relating the experimental spectrum to the electronic DOS, there is strong synergy between PES/NEXAFS/NRIXS and electronic structure calculations. Photoemission spectroscopy provides a direct measure of the experimental DOS. Oxygen K-edge NEXAFS and NRIXS measure bound state transitions of O 1*s* electrons into metal-based orbitals that contain O 2*p* character from covalent mixing, and give a direct experimental measure of the O 2*p* DOS [11]. In our studies, the NEXAFS and NRIXS data give nearly identical results, and for brevity we will only show NEXAFS spectra here.

We compare the PES and NEXAFS measurements to our calculation in Figure 3. Overall, the agreement with experiment is quite good. For the photoemission spectra (Figure 3 bottom left) note that the occupied states segregate into a U 5*f* feature near the Fermi energy and a predominantly O 2*p* feature at higher binding energy. Variable photon energy studies clearly identify the O 2*p* and U 5*f* states. Oxygen NEXAFS data are also shown in Figure 3 (bottom right), and these data also compare well to the theoretical values. For the empty levels, NEXAFS data shows two prominent features.

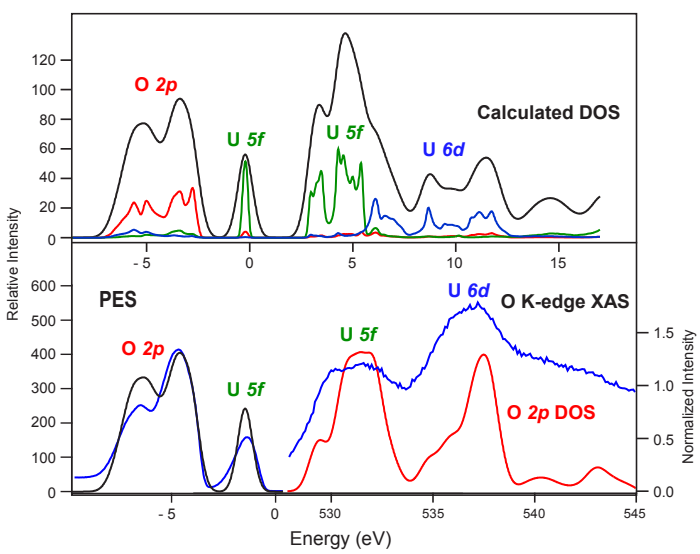


*Figure 3. (Top) Calculated total (black) and partial DOS (O 2p red, U 5f green, U 6d blue) for $UO_2$ calculated using the HSE06 functional and scalar relativistic effects. The total DOS has been given 0.5 eV linebroadening for comparison with experimental data. (Bottom, left) Experimental PES (blue) and calculated spin polarized DOS for $UO_2$ (black). (Bottom, right) Experimental oxygen K-edge NEXAFS (blue) and the calculated spin polarized O 2p DOS for $UO_2$.*

The hybrid DFT calculation tells us that these NEXAFS peaks are associated with the U 5*f* and 6*d* states, and that the general shape and splitting compares quite well with the theory. Of significance is that both experiment and theory indicate that there is significant mixing of O 2*p* character with U 5*f* and 6*d* levels, and therefore greater *f-p* hybridization and dispersion of the energy bands than previously thought. Mulliken population analyses were used to quantify the amount of O 2*p*-U 5*f* mixing, and the result is described in detail in one of our most recent publications [11].

Encouraged by the correlation between theory and experiment, we performed the first systematic study of the electronic properties of the $AnO_2$ series, An=Th–Es, using screened hybrid density functional theory [12]. One might expect later members of the series to show even more localized character as the 5*f* orbital radial extent decreases with increasing *Z*. However, we find two interesting features in the calculations: an An 5*f*–O 2*p* orbital energy degeneracy, which leads to significant orbital mixing and covalency in the intermediate region ($PuO_2$-$CmO_2$), and a strong Hund's rule exchange opposing spin-orbit coupling, which yields an unexpected ground state in $CmO_2$. The calculated electronic structure and DOS is shown in Figure 4 for U, Np and Pu where the convergence of the 5*f* and 2*p* DOS is complete at $PuO_2$.

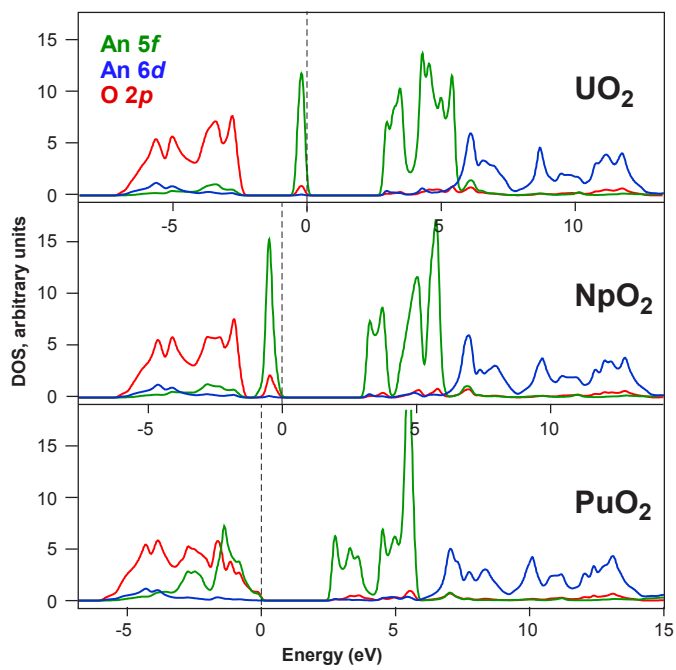


*Figure 4. Theoretical predictions for the partial density of states (O 2p red, An 5f green, An 6d blue) for antiferromagnetic $AnO_2$ where An=U, Np, and Pu, at their respective optimum geometries. Note the merging of An 5f and O 2p DOS upon moving across the series from U through Pu.*

**Nonstoichiometric oxides, $AnO_{2+x}$**

The structure of superstoichiometric oxides with O/An ratio greater than 2 has been the topic debate [4-6]. Neutron diffraction studies on $UO_{2+x}$ were interpreted as suggesting that the excess O atoms do not enter the structure individually, but rather in groups in combination with displaced O atoms and O vacancies in specific, highly ordered arrangements [13,14]. The interstitial O atoms are displaced nearly 1.0 Å from the ideal octahedral site, giving rise to a U-O bond shortening from 2.37 to 2.22 Å. The U atoms remain in their normal fcc positions, and the U-U distances are conserved [4]. This model is appealing because of its compatibility with the fluorite structure (Figure 1) where every anion site, but only every other cation site is filled at integral stoichiometry. Placing the adventitious O in the open cubic holes minimizes the local elastic strain. This mechanism has been corroborated by DFT calculations on $PuO_{2+x}$ that indicate the most stable site for extra O is in these holes [15]. Recent work from our team has demonstrated that this description of $AnO_{2+x}$ is far too simplistic, with the adventitious O incorporated as distinct oxo units that would raise the valence of the U atoms to (VI) [5,16] and Pu atoms to (V) [5,17,18].

We examined U L-edge EXAFS of a large number of samples of $UO_{2+x}$ with $0 < x < 0.2$, and a portion of representative Fourier transform spectra are shown in Figure 5. For $UO_{2.0}$ (x=0) the first peak is the contribution of the eight nearest neighbor O atoms at 2.36 Å, well separated from the more distant second nearest neighbor peak of twelve U atoms at 3.85 Å (the peaks in Figure 5 are all phase shifted to lower R). Regular features from the well-ordered extended structure subsequently continue out through very high distance from the central absorbing atom (not shown in Figure 5). This spectrum is therefore consistent with the crystal structure in Figure 1. However, as x increases to $UO_{2.25}$, the amplitudes of all of the peaks decrease monotonically, indicative of diminished order via displacements of the U and O atoms from their lattice sites coupled to the incorporation of the non-stoichiometric O atoms into interstitial, essentially defect sites. What contradicts the current models in this process is the splitting of the O shell (clearly evident in Figure 5 for $UO_{2.25}$) and the appearance of a short U=O bond distance of 1.74 Å. Diffraction techniques that probe long-range order have never observed this phenomenon in $UO_2$ solids, but the bond distance is similar to those found in discrete U=O bonds in molecular systems which range from 1.74 – 1.80 Å. These results suggest that as the U center becomes partially oxidized in $UO_{2+x}$, there is a strong driving force to form short, strong, covalent U=O bonds. The local structure approach to looking at solids with nominal long-range order is clearly changing the way we think about these materials. During the course of this work, we prepared $UO_{2+x}$ samples using multiple methods to evaluate whether method of preparation could be the result of the discrepancy. We prepared samples using high temperature furnace techniques, low temperature microbalance techniques, and high temperature equilibrium techniques. Samples were also studied by a series of neutron and x-ray PDF measurements. Preliminary analysis of these data shows the possibility of a very unusual result that the x-ray and neutron measurements on the same samples disagree. If this is confirmed, then it will corroborate our recent temperature dependent EXAFS finding that in $U_4O_9$ and $U_3O_7$ the U-O distribution is altered between 50, 100, and 200 K, indicating that the O positions are unusually susceptible to dynamical processes. This work would point to substantial modifications to the phase diagram for $UO_{2+x}$.

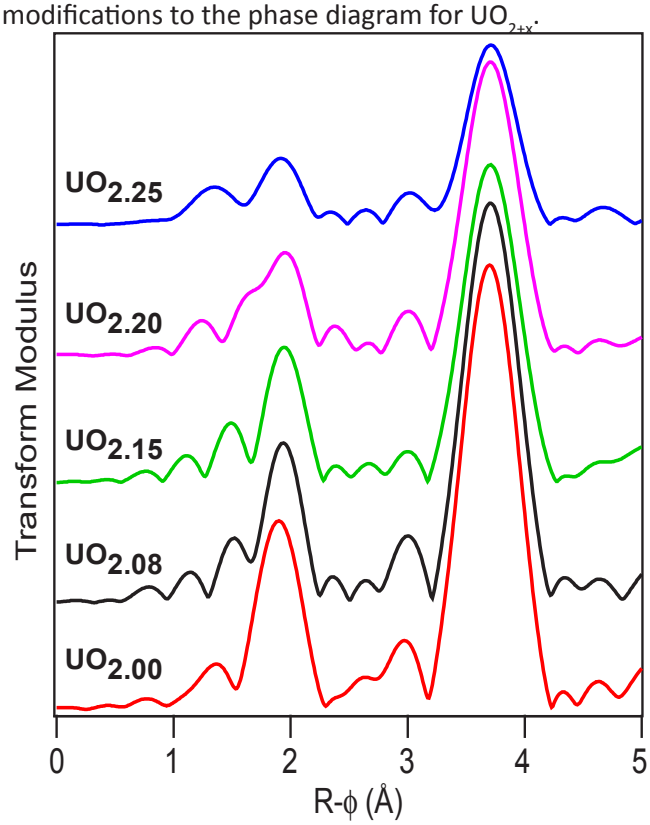


*Figure 5. A comparison of uranium L3-edge EXAFS Fourier transform data on the $UO_{2+x}$ series of compounds where the stoichiometry is carefully controlled between pure $UO_{2.00}$ (bottom) to $UO_{2.25}$ (top) using TGA microbalance techniques. Note that the peaks all occur at lower R values with respect to their true atomic positions due to the EXAFS phase shift (φ, c.a. 0.5 Å).*

This example illustrates our capabilities for careful actinide sample preparation and stoichiometry control in the region of interest between $UO_{2.0}$ and $UO_{2+x}$, and the close integration between *hybrid* DFT calculations, photoemission and NEXAFS to develop a consistent understanding of the electronic structure in cubic $UO_2$. The new O NEXAFS

data clearly show that there is significant covalency in the U-O bonding in $UO_2$, indicating that the U 6*d* contribution is stronger than the U 5*f*, and that the technique shows great promise for extracting the percent contribution of both types of orbitals for comparison with heavier actinides across the series. Our use of U L-edge EXAFS to examine the local structure of the $UO_{2+x}$ series clearly shows that the simple model of incorporation of excess O atoms into octahedral vacancies is incomplete, and reveals the presence of extremely short U(VI)=O bonds at 1.74 Å, similar to the oxo groups formed by discrete molecular complexes.

## References


1. Haire, R. G., and L. Eyring. Comparison of the Binary Oxides. 1994. *Handbook on the Chemistry and Physics of the Rare Earths.* **18**: 413.

2. Clark, D. L., S. S. Hecker , G. D. Jarvinen, and M. P. Neu. Plutonium. 2006. In *The Chemistry of the Actinide and Transactinide Elements.* Edited by Morss, L. R., N. M. Edelstein, and J. Fuger. , third Edition, p. 813. Dordrecht: Springer.

3. Grenthe, I., J. Drozdzynski, T. Fujino, E. Buck, T. E. Albrecht-Schmitt, and S. Wolf. Uranium. 2006. In *Uranium.* Edited by Morss, L. R., N. M. Edelstein, and J. Fuger. , Third Edition, p. 253. Dordrecht: Springer.

4. Allen, G. C., and P. A. Tempest. Ordered Defects in the Oxides of Uranium. 1986. *Proc. Royal Soc. London, Ser. A.* **406**: 325.

5. Conradson, S. D., B. D. Begg, D. L. Clark, C. den Auwer, M. Ding, P. K. Dorhout, F. J. Espinosa-Faller, P. L. Gordon, R. G. Haire, N. J. Hess, R. F. Hess, D. W. Keogh, G. H. Lander, D. Manara, L. A. Morales, M. P. Neu, P. Paviet-Hartmann, J. Rebizant, V. V. Rondinella, W. Runde, C. D. Tait, D. K. Veirs, P. M. Villella, and F. Wastin. Charge Distribution and Local Structure and Speciation in the UO2+x and PuO2+x Binary Oxides. 2005. *Journal of Solid State Chemistry.* **178** (2): 521.

6. Garrido, F., A. C. Hannon, R. M. Ibberson, L. Nowicki, and B. T. M. Willis. Neutron Diffraction Studies of U4O9: Comparison with EXAFS Results. 2006. *Inorganic Chemistry.* **45**: 8406.

7. Frazer, B. C., G. Shirane, D. E. Cox, and C. E. Olsen. Neutron-diffraction study of antiferromagnetism in UO2. 1965. *Physical Review.* **140** (4A): 1448.

8. Prodan, I. D., G. E. Scuseria, and R. L. Martin. Assessment of metageneralized gradient approximation and screened Coulomb hybrid density functionals on bulk actinide oxides. 2006. *Physical Review B: Condensed Matter and Materials Physics.* **73** (4): 045104/1.

9. Heyd, J., G. E. Scuseria, and M. Ernzerhof. Hybrid functionals based on a screened Coulomb potential. 2003. *Journal of Chemical Physics.* **118** (18): 8207.

10. Hay, P. J., R. L. Martin, J. Uddin, and G. E. Scuseria. Theoretical study of CeO2 and Ce2O3 using a screened hybrid density functional.. 2006. *Journal of Chemical Physics.* **125** (3): 034712/1.

11. Roy, L. E., T. Durakiewicz, R. L. Martin, J. E. Peralta, G. E. Scuseria, C. G. Olson, J. J. Joyce, and E. Guziewicz. Dispersion in the mott insulator UO2: a comparison of photoemission spectroscopy and screened hybrid density functional theory. 2008. *Journal of Computational Chemistry.* **29** (13): 2288.

12. Prodan, I. D., G. E. Scuseria, and R. L. Martin. Covalency in the actinide dioxides: Systematic study of the electronic properties using screened hybrid density functional theory. 2007. *Physical Review B: Condensed Matter and Materials Physics.* **76**: 033101/1.

13. M.Willis, B. T.. Structures of UO2, UO2+.chi. and U4O9 by neutron diffraction. 1964. *Journal de Physique (Paris).* **25** (5): 431.

14. M.Willis, B. T.. The defect structure of hyper-stoichiometric uranium dioxide. 1978. *Acta Crystallographica, Section A: Crystal Physics, Diffraction, Theoretical and General Crystallography.* **A34** (1): 88.

15. Petit, L., A. Svane, Z. Szotek, and W. M. Temmerman. First-Principles Calculations of PuO2+x. 2003. *Science.* **301** (5632): 498.

16. Conradson, S. D., D. L. Clark, G. H. Lander, D. Manara, L. A. Morales, J. Rebizant, V. V. Rondinella, and F. Wastin. Local Structure and Charge Distribution in the UO2-U4O9 System. 2004. *Inorganic Chemistry.* **43** (22): 6922.

17. Conradson, S. D., B. D. Begg, D. L. Clark, C. den Auwer, M. Ding, P. K. Dorhout, F. J. Espinosa-Faller, P. L. Gordon, R. G. Haire, N. J. Hess, R. F. Hess, D. W. Keogh, L. A. Morales, M. P. Neu, P. Paviet-Hartmann,

W. Runde, C. D. Tait, D. K. Veirs, and P. M. Villella. Local and Nanoscale Structure and Speciation in the PuO2+x-y(OH)2yzH2O System. 2004. *Journal of the American Chemical Society.* **126** (41): 13443.

18. Conradson, S. D., B. D. Begg, D. L. Clark, C. Den Auwer, F. J. Espinosa-Faller, P. L. Gordon, N. J. Hess, R. Hess, D. W. Keogh, L. A. Morales, M. P. Neu, W. Runde, C. D. Tait, D. K. Veirs, and P. M. Villella. Speciation and Unusual Reactivity in PuO2+x. 2003. *Inorganic Chemistry.* **42** (12): 3715.

## Publications

Bargar, J. R., E. Schofield, A. Mehta, H. Veeramani, K. Ulrich, J. Sharp, R. Bernier-Latmani, D. E. Giammar, S. D. Conradson, and D. L. Clark. Structural identity and reactivity of biogenic UO2. 2008. : GEOC.

Batista, E. R., J. Heyd, R. G. Hennig, B. P. Uberuaga, R. L. Martin, G. E. Scuseria, C. J. Umrigar, and J. W. Wilkins. Comparison of screened hybrid density functional theory to diffusion Monte Carlo in calculations of total energies of silicon phases and defects. 2006. *Physical Review B: Condensed Matter and Materials Physics.* **74** (12): 121102/1.

Boland, K. S., D. L. Clark, S. D. Conradson, X. J. Espinosa-Faller, D. A. Llobett, D. E. Schwarz, and L. E. Wolfsberg. Comparative studies of local structure in UO2+x: A combined neutron diffraction and X-ray absorption study. 2008. *Abstracts of Papers, 235th ACS National Meeting, New Orleans, LA, United States, April 6-10.* : NUCL.

Brown, J. J., J. M. Wills, T. Durakiewicz, M. T. Butterfield, E. Guziewicz, K. S. Graham, J. L. Sarrao, A. J. Arko, E. D. Bauer, D. P. Moore, L. A. Morales, and O. Eriksson. Localized and itinerant states in Pu materials. 2006. *Mat. Res. Soc. Symp. Proc..* **839**: 59.

Burrell, A. K., T. M. McCleskey, P. Shukla, H. Wang, T. Durakiewicz, D. P. Moore, C. G. Olson, J. J. Joyce, and Q. Jia. Controlling oxidation states in uranium oxides through epitaxial stabilization. 2007. *Advanced Materials (Weinheim, Germany).* **19** (21): 3559.

Butterfield, M. T., T. Durakiewicz, I. D. Prodan, G. E. Scuseria, E. Guziewicz, J. A. Sordo, K. N. Kudin, R. L. Martin, J. J. Joyce, A. J. Arko, K. S. Graham, D. P. Moore, and L. A. Morales. A comparison of hybrid density functional theory with photoemission of surface oxides of d-plutonium. 2006. *Surface Science.* **600** (8): 1637.

Conradson, S. D., A. Andersson, K. Boland, D. L. Clark, S. Kozimor, and X. J. Espinosa-Faller. Addressing the structural chemistry of UO2+x and PuO2+x with laboratory and computer experiments. 2008. *Abstracts of Papers, 235th ACS National Meeting, New Orleans, LA, United States, April 6-10.* : NUCL.

Conradson, S. D., A. D. Anderson, D. L. Clark, X. J. Espinosa-Faller, S. Kozimor, R. L. Martin, L. A. Morales, and G. T. Seidler. Structural Chemistry of Pu/UO2+x, 0<x<0.25.. 2008. *Plutonium Futures-The Science, Dijon, France, July 6-11.*

Guziewicz, E., T. Durakiewicz, P. M. Oppeneer, J. J. Joyce, J. D. Thompson, C. G. Olson, M. T. Butterfield, A. Wojakowski, D. P. Moore, and A. J. Arko. Angle-resolved photoemission study of dispersive and narrow-band 5f states in UAsSe. 2006. *Physical Review B: Condensed Matter and Materials Physics.* **73** (15): 155119/1.

Hay, P. J., R. L. Martin, J. Uddin, and G. E. Scuseria. Theoretical study of CeO2 and Ce2O3 using a screened hybrid density functional. 2006. *J. Chem. Phys. .* **125** (3): 034712/1.

Kasinathan, D., J. Kunes, K. Koepernik, C. V. Diaconu, R. L. Martin, I. D. Prodan, G. E. Scuseria, N. Spaldin, L. Petit, T. C. Schulthess, and W. E. Pickett. Mott transition of MnO under pressure: A comparison of correlated band theories. 2006. *Physical Review B: Condensed Matter and Materials Physics.* **74** (19): 195110/1.

LoPresti, V., S. D. Conradson, and D. L. Clark. XANES identification of plutonium speciation in RFETS samples. 2007. *Journal of Alloys and Compounds.* **444-445**: 540.

Peralta, J. E., J. Heyd, G. E. Scuseria, and R. L. Martin. Spin-orbit splittings and energy band gaps calculated with the Heyd-Scuseria-Ernzerhof screened hybrid functional. 2006. *Physical Review B: Condensed Matter and Materials Physics.* **74** (7): 073101/1.

Prodan, I. D., G. E. Scuseria, and R. L. Martin. Assessment of metageneralized gradient approximation and screened Coulomb hybrid density functionals on bulk actinide oxides. 2006. *Physical Review B: Condensed Matter and Materials Physics.* **73** (4): 045104/1.

Prodan, I. D., G. E. Scuseria, and R. L. Martin. Covalency in the actinide dioxides: Systematic study of the electronic

properties using screened hybrid density functional theory. 2007. *Physical Review B: Condensed Matter and Materials Physics.* **76** (3): 033101/1.

Roy, L. E., I. D. Prodan, J. E. Peralta, G. E. Scuseria, and R. L. Martin. Covalency in the actinide dioxides: Systematic study of the electronic properties using screened hybrid density functional theory. 2008. *Abstracts of Papers, 235th ACS National Meeting, New Orleans, LA, United States, April 6-10.* : INOR.

Roy, L. E., P. J. Hay, and R. L. Martin. Revised Basis Sets for the LANL Effective Core Potentials. 2008. *Journal of Chemical Theory and Computation.* **4** (7): 1029.

Roy, L. E., T. Durakiewicz, R. L. Martin, J. E. Peralta, G. E. Scuseria, C. G. Olson, J. J. Joyce, and E. Guziewicz. Dispersion in the mott insulator UO2: a comparison of photoemission spectroscopy and screened hybrid density functional theory. 2008. *Journal of Computational Chemistry.* **29** (13): 2288.

Schofield, E. J., H. Veeramani, J. O. Sharp, E. Suvorova, R. Bernier-Latmani, A. Mehta, J. Stahlman, S. M. Webb, D. L. Clark, S. D. Conradson, E. S. Ilton, and J. R. Bargar. Structure of Biogenic Uraninite Produced by Shewanella oneidensis Strain MR-1. 2008. *Environmental Science & Technology.* : ACS ASAP.

# Dynamics of the Onset of Damage in Metals Under Shock Loading

*Aaron Clyde Koskelo*

20060021DR

## Abstract

Understanding the dependence of shock-induced damage on the material properties and microstructure of metals is essential to predict the behavior of strategically important materials. We seek to correlate the damage with the microstructure by observing dynamically-developed mesoscale defects. During shock loading and unloading these defects may lead to nucleation of microcracks and voids, which then grow and coalesce inducing fracture, fragmentation, and spall.

## Background and Research Objectives

Science-based prediction of damage must consider the effects of microstructure and material state on material behavior. These qualities can vary with differences in material processing or history. The microstructure and material state impact significantly the localization of stress or strain, which initiates the damage accumulation process.

We apply an integrated combination of material synthesis by design, shock/recovery experiments, post-shot metallography, theory, and simulation. Samples are fully characterized before they are shock loaded with laser-driven flyers. Sensitive dynamic interferometry is used to view localized motions at the optically accessible breakout surface. Damage is then analyzed in the recovered specimens. Our goal is to correlate the observed localized displacements and velocities during dynamic loading with the microstructure, damage location and damage character on recovered samples. Results are being used to improve current models of damage.

This work is the first of its kind to correlate dynamic displacement "images" of the breakout surface of polycrystalline materials—with sufficient resolution to see localized deformations and simultaneously enough spatial coverage to collect meaningful statistics— with pre-shot material properties and post-shot damage distribution.

## Importance to LANL's Science and Technology Base and National R & D Needs

We seek an experimentally-derived, physics-based understanding of the role of microstructure on material damage under shock conditions. Our work will result in fundamental advances in the materials science of metals. The capability created can provide the basis for solving problems of programmatic interest. Current production or engineering damage models address continuum-averaged properties, ignoring statistical fluctuations, which may dominate the bulk behavior. Statistics are essential to understand the average macroscopic response given the distribution of microscopic quantities, for nonlinear systems. Knowledge of the statistics provides: 1) a much deeper understanding of the damage process; 2) enables prediction of the likelihood of variability in fracture strength and spall as a function of material properties; and 3) is essential for uncertainty prediction. The ultimate goal for LANL is to estimate the probability of mechanical failure under particular loading conditions, given statistical information on the microstructure.

## Scientific Approach and Accomplishments

Experiments spanning the range from barely incipient spall to nearly full spall were conducted on single crystals, multicrystals and polycrystals, comprising over 270 shots. This data along with our post-shot metallography, pre-shot specimen characterization, and hydrodynamic and molecular dynamic modeling, has provided a significant amount of information. The following pages touch on some of the more import results to date.

Transient Imaging Displacement Interferometry (TIDI) is a very sensitive dynamic displacement measurement tool [1]. Our experiments reveal—for the first time—that a rich range of phenomena occurs when a shock wave reaches the breakout surface. The phenomena include elastic wave scattering from grain boundaries; elastic motion out-of-plane of the grain boundaries

themselves; scattering of the shock wave from surface or near-surface defects after it arrives at the surface; and surface waves generated from scattering from surface defects. Later in the shock-loading profile, waves scattered from buried defects or from dynamically created voids can be observed. The result of all of these sources of dynamic displacement is each transient image of the surface can be quite complex. Fortunately, each of the phenomena has their own length-scale and time dynamics permitting separation of the phenomena in the analysis.

Bowing of the specimen appears as a long-range variation across the image frame and occurs at the beginning of breakout and then subsides. The target bowing is several microns spanning an image region of ~2mm x 2mm. Comparison with "tilt" measurements made with pins on gas gun experiments demonstrate that the tilt seen in our laser-driven flyer experiments is no worse, and perhaps a little better than, the tilt in gas gun-driven flyer shots for the same flyer energies [2].

TIDI, in conjunction with post shot analysis; can reveal the time dynamics of the origin of surface damage. Figure 1 is a post-shot microscopic image of surface damage. The circle in the lower right of the figure damage originating from a terminated twin. The dynamic displacements observed by the TIDI during the shock loading clearly show large distortion of this region early in the shock profile. These dynamic displacements indicate that this type of location is more susceptible to large-motion in the shock-loading and is manifested as permanent damage at the surface [3].

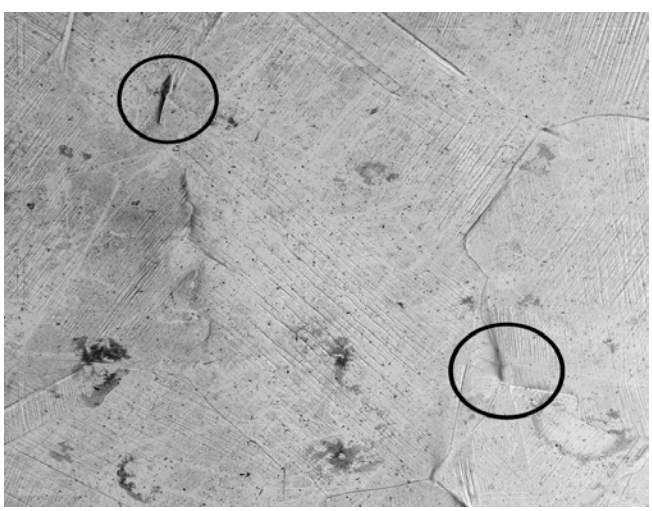

*Figure 1. Microscopic image of the region of damage in a shocked multicrystalline copper specimen.*

Buried triple points also appear to be more susceptible to damage. A three dimensional reconstruction of post-shot sections of a multicrystalline copper target is shown in Figure 2. The grayscale image at the back of the reconstruction is an individual slice of the target. The small black areas are slices through individual voids and coalesced void regions.

As shown in Figure 2, voids nucleate along grain boundaries (intergranular), within grains (transgranular) and at points of intersection between several grains (triple points or quadruple points). The pink dot towards the right of the reconstruction is a void that nucleated at a triple point. The colored regions are three dimensional reconstructions from successive slices through the specimen. To simplify the figure, the grain boundary structure has been removed for these slices but it is clear that some of the coalesced damage is intergranular and some is transgranular.

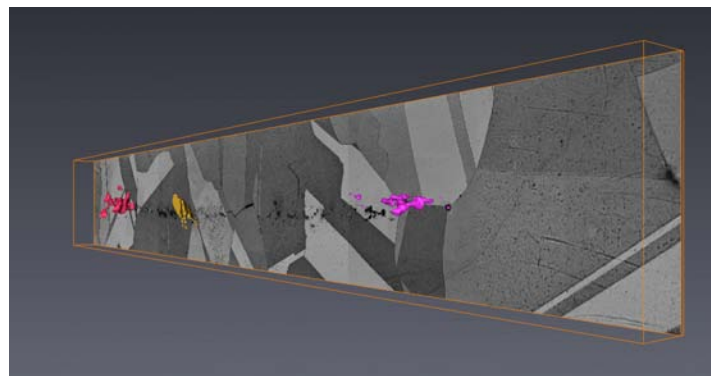

*Figure 2. A three-dimensional reconstruction of spall damage in a shocked multicrystalline copper target. The shock was induced by a laser-driven flyer plate that impacted the target from the bottom. The spall plane is the general line of damage through the midpoint of the target.*

Through analyzing post-shot sections, we are building up a statistical distribution of void nucleation likelihood vs. relative grain mis-orientation. The distribution obtained is the necessary information needed to predict damage in a polycrystalline specimen with a given microstructure. A key observation is that some mis-orientations result in damage away from the general spall plane, i.e. are weaker bonds. An example appears in the upper middle of the grayscale image of Figure 2—an intergranular crack occurred that does not connect with damage at the general spall plane.

**Target with Embedded wire**

With the goal of development of a full three-dimensional model we conducted several shots that could be modeled adequately with a two dimensional hydrodynamic model. The object was to reproduce the dynamic data and predict what the TIDI diagnostic should see. Figure 3 shows a calculation of the displacement wave profile of a copper specimen that contained an embedded tungsten wire well below its surface. The blue line is a cross-section through

the TIDI signature of the embedded wire shot. The other lines are the two dimensional hydrocode calculations as a function of time. The model results are reasonable considering the approximations made.

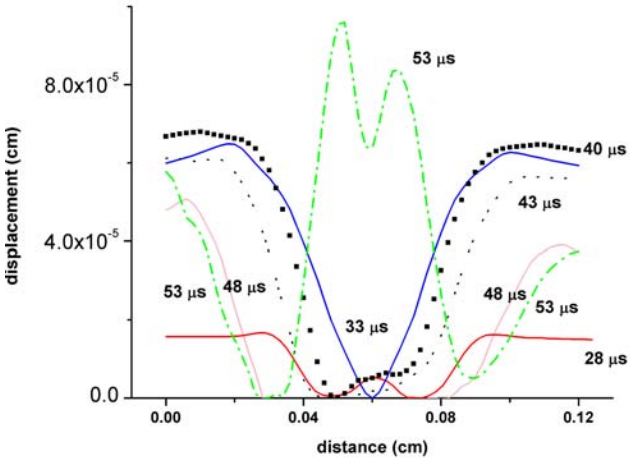


*Figure 3. Comparison of a two-dimensional hydrodynamic model with a TIDI result. The target was polycrystalline copper with a tungsten wire embedded perpendicularly to the shock propagation direction. The base of the TIDI data cross-section lies above the wire and the large displacement wings are caused by the shock propagating around the edges of the wire.*

**Dimples**

The single crystal measurements showed a new phenomenon not seen before. Early in the shock-loading profile, the TIDI images show rapid formation of localized depressions at the surface of the material. These "dimples" are formed once a threshold pressure level is reached. They appear on the compressive part of the wave but as the dimples are depressions, they must be the result of a localized tension-like gradient in the compression wave. Such tension gradients can be created around regions of high dislocation densities or micro-fractures in the material. These regions could be pre-existing in the material or may be stress-induced defects created dynamically by the leading edge of the shockwave. This explanation is compatible with theory by Zubelewicz [4], but has not been previously experimentally observed.

The dimples are crystallographic in origin as different orientations of specimen show characteristic shapes of the dimple. Figure 4 shows a displacement image acquired by TIDI at 88 ns after shock arrival for a <110> single crystal. The color map illustrates the local out-of-plane displacement relative to the average level of the surface. Red signifies a region that is 200 nm above the surface, blue a region that is 200 nm below the surface. The "dimples" are the rectangular blue regions. Neumann's principle suggests that structures created in the <110> geometry should be rectangular in shape as is observed. This is what is observed dynamically with the TIDI and in post-shot microscopic imaging using a VEECO interferometer. The dimples persist and can be clearly identified in the post-shot specimens. Thus the dimples are clearly due to the crystal themselves rather than any unseen subsurface inclusions, which are confirmed from post-shot.

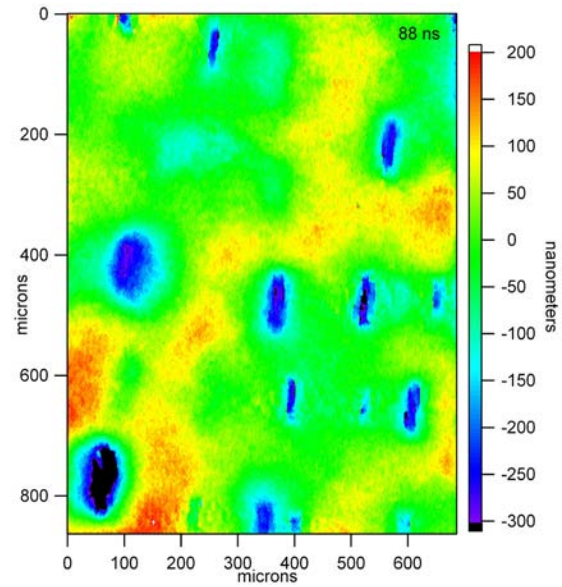


*Figure 4. One frame in a sequence of eight obtained by TIDI during the shock loading of a single copper crystal target. The <110> direction of the copper crystal was parallel with the direction of shock propagaton. The frame has been analyzed to remove the slight bowing in the target.*

**Point VISAR damage model**

Point VISAR has been one of the workhorse diagnostics for over 30 years in the shock-loading community. It measures the back surface velocity as a function of time, shown in blue in Figure 5a. Initially, the surface is at rest. When the flyer hits the front surface of the target, a shock wave is created which then propagates through the target to the back surface. When the wave reaches the back surface, the back surface accelerates. For experiments where the peak shock state is sustained for a period of time, the back surface then travels at a constant velocity. In the figure, this portion of the record is at approximately 25ns. (Because of the type of information sought in this particular experiment, the shock does not have a sustained plateau). The end of the plateau signals the arrival of the release wave originated from the free surface of the flyer. The release decelerates the target back surface and this motion is reflected in the point VISAR trace from 25ns to approximately 100ns.

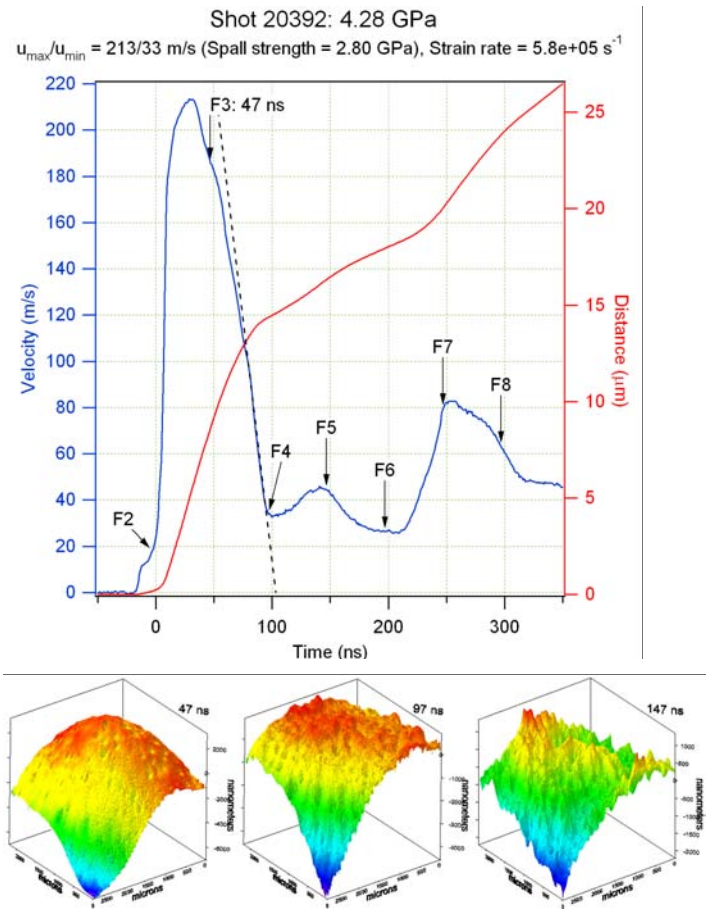


*Figure 5. The graph in the upper part of the figure is the point VISAR record of a shocked single crystal copper specimen. The lower 3-D plots are a sequence of frames from the analyzed TIDI record. The target bowing has not been removed in these plots. The colors range from blue for the smallest out-of-plane displacement and red for the largest.*

The physics underpinning the shape of point VISAR records upon release, particularly under conditions where damage is expected, is not fully understood. We have made hydrocode calculations using our single crystal shot results to parameterize the model. The shapes of the shock rise and the release as far as the plastic yield were well matched, indicating the adequacy of the single crystal plasticity and elastic modeling for the plasticity of the shock rise and the beginning or the release. The slope of the experimental release curve, after plastic yield, was significantly lower than that of the calculation, however. Several model enhancements were tried with only limited success. This lack of agreement indicates that new physical behavior outside the standard modeling used is occurring in the shock release. One possibility is early damage creation upon release. Another is the emergence of some dynamically-created plastic defect upon release.

**Damage development and Spall signature**

TIDI results appear to support strong dynamic plasticity and/or damage early in the first shock-unloading of the surface. Figure 5 shows analyzed diagnostic records of a single-crystal copper specimen oriented with the <110> axis along the shock direction. The purpose of this experiment was to determine the TIDI signature for developing spall. For this experiment, the relative thicknesses of the flyer and target were chosen to move the spall plane to 100 microns of the surface to minimize the effect of dispersion of the waves emanating from any nucleating and coalescing voids. A side-effect of this experiment geometry is to diminish the length of time of the shock plateau as described above but for this experiment, a plateau was not necessary.

The upper plot in Figure 5 shows the point VISAR record from the back surface of the specimen. The blue line is the plot of the surface velocity as a function of time. The arrows labeled F2-F8 are the position in time the TIDI dynamic frames were acquired. Frame 3 is near the point of plastic yield of the copper. The overall curvature is the slight bowing of the target described above. The small, localized depressions in frame 3 are the dimples. In Frame 3, one also sees the beginnings of “pimples”, i.e. regions of small, localized swellings at the surface. The standard deviation of all of these small features is 79 nm in frame 3. By frame 4 this roughening increases to 97 nm and at Frame 5 the roughening has increased to 112 nm. Frame 5 is the position where a compression wave reflected off of a spall plane would reach the back surface. Between frames 3 and 5 is where plastic deformation and void nucleation and growth would occur. Definitive statements relating the reduced slope in the point VISAR record and the correlated increase in back surface roughness seen in both the TIDI and line VISAR to the material response await further analysis of our data and post-shot metallography of the targets.

**Molecular Dynamics Modeling**

We have simulated the spall process of nanocrystalline fcc solid and single crystal Cu under uniaxial loading using the embedded atom method (EAM) potential [5-9]. The simulations reveal heterogeneous nucleation and growth of voids as well as plasticity development where the grain boundaries play a key role. The simulations on single crystal Cu examine the anisotropy in plasticity, spall strength and homogeneous void nucleation, and the results can be compared to our laser experiments and continuum mechanics simulations. The detailed characterization of void nucleation and growth process also allows

a direct comparison with classical nucleation and growth theory for spall.

Other MD results confirm that TIDI measurements are feasible for nanoscale measurements, given sufficiently high signal-to-noise ratio and short wave length for probe lasers; and establish a scale relation jointly with larger-scale experiments [10].

**Conclusion**

In conclusion, we have developed new experimental means to investigate the physics of spall damage formation. The capability is unique in the world, in the combined detail that can be obtained and the number of shots that effectively be conducted. The >270 shots that we obtained have provided information uncovering new or never before observed phenomena such as "dimples" and "pimples" and provided the first dynamic displacement images of damage upon release. The level of detail in our sectioned specimens is also unprecedented. Because of the large number of shots we are able to conduct, we have been able to span the entire range of conditions where voids first begin to form to where full spall occurs. Sectioning the specimens for different shock pressures has clearly revealed where voids originally nucleate. Initial results on statistical distributions demonstrate the importance of triple points and quadruple points. The single crystal target shots conducted also are providing the dynamic plasticity information needed for a fully three dimensional plasticity model. Our two dimensional models reproduce wave propagation reasonably accurately for simple microstructures, as we have demonstrated with a targets with embedded wires. Full three-dimensional models of statistical damage are achievable pending further analysis of our data.

## References


1. Greenfield, S. R., S. N. Luo, D. L. Paisley, E. N. Loomis, D. C. Swift, and A. C. Koskelo. Transient imaging displacement interferometry applied to shock loading. 2007. In *15th American Physical Society Topical Conference on Shock Compression of Condensed Matter.* (Waikoloa, HI, 24-29 June 2007). Vol. 955, p. 1093. USA: American Institute of Physics.

2. Paisley, D. L., S. N. Luo, S. R. Greenfield, and A. C. Koskelo. Laser-launched flyer plate and confined laser ablation for shock wave loading: validation and applications. 2008. *Review of Scientific Instruments.* **79** (2): 023902.

3. Koskelo, A. C., S. R. Greenfield, D. L. Paisley, K. J. McClellan, D. D. Byler, R. M. Dickerson, S. N. Luo, D. C. Swift, D. L. Tonks, and P. D. Peralta. Dynamics of the onset of damage in metals under shock loading. 2007. In *15th American Physical Society Topical Conference on Shock Compression of Condensed Matter.* (Waikoloa, HI, 24-29 June 2007). Vol. 955, p. 557. USA: American Institute of Physics.

4. Zubelewicz, A.. Metal behavior at extreme loading rates: Thermodynamics. 2008. *Physical Review B.* **77** (21): 214111.

5. Zheng, L. Q., Q. An, Y. Xie, Z. H. Sun, and S. N. Luo. Homogeneous nucleation and growth of melt in copper. 2007. *Journal of Chemical Physics.* **127** (16): 164503.

6. An, Q., S. N. Luo, L. B. Han, L. Q. Zheng, and O. Tschauner. Melting of Cu under hydrostatic and shock wave loading to high pressures. 2008. *Journal of Physics: Condensed Matter.* **20** (9): 095220.

7. Luo, S. N., L. B. Han, Y. Xie, Q. An, L. Q. Zheng, and K. W. Xia. The relation between shock-state particle velocity and free surface velocity: A molecular dynamics study on single crystal Cu and silica glass. 2008. *Journal of Applied Physics.* **103** (9): 093530.

8. Luo, S. N., L. Q. Zheng, Q. An, and S. J. Zhao. Tensile failure of single-crystal and nanocrystalline Lennard-Jones solids under uniaxial strain. 2006. *International Journal of Modern Physics C.* **17** (11): 1551.

9. Luo, S. N., Q. An, L. B. Han, K. W. Xia, and W. A. Goddard III. Molecular dynamics simulation of shock-induced spall in Cu at high strain rates. *Journal of Applied Physics.*

10. An, Q., S. N. Luo, S. R. Greenfield, L. B. Han, and W. A. Goddard III. Shock response to material heterogeneity at nanometer scales: Molecular dynamics modeling and implications to measurements. *Applied Physics Letters.*


## Publications


An, Q., S. N. Luo, L. B. Han, L. Zheng, and O. Tschauner. Melting of Cu under hydrostatic and shock wave loading to high pressures. 2008. *Journal of Physics: Condensed Matter.* **20** (9): 095220.

An, Q., S. N. Luo, S. R. Greenfield, L. B. Han, and W. A. Goddard. Shock response to material heterogeneity at nanometer scales: Molecular dynamics modeling and implications to measurements. *Applied Physics Letters.*

Greenfield, S. R., S. Luo, D. L. Paisley, E. N. Loomis, D. C. Swift, and A. C. Koskelo. Transient imaging displacement interferometry applied to shock loading . 2007. In *15th American Physical Society Topical Conference on Shock Compression of Condensed Matter .* (Waikoloa, HI, 24-29 June, 2007). Vol. 955, p. 1093. Melville, NY: American Institute of Physics.

Hashemian, S., S. Digiacomo, P. Peralta, H. D'Armas, S. N. Luo, E. Loomis, D. Paisley, D. Byler, R. Dickerson, and K. J. McClellan. Effects of microstructure on spall damage localization in shock loaded copper multicrystals . 2008. In *137th Annual Meeting and Exhibition of the Minerals-Metals-and-Materials-Society .* (New Orleans, LA, 2008). Vol. I, p. 319. Warrendale, PA: MINERALS, METALS & MATERIALS SOC .

Koskelo, A. C., S. R. Greenfield, S. R. Greenfield, K. J. McClellan, D. D. Byler, R. M. Dickerson, S. N. Luo, D. C. Swift, D. L. Tonks, and P. D. Peralta. Dynamics of the onset of damage in metals under shock loading . 2007. In *15th American Physical Society Topical Conference on Shock Compression of Condensed Matter .* (Waikoloa, HI, 24-29 June, 2007). Vol. 955, p. 557. Melville, NY: American Institute of Physics.

Luo, S. N., D. L. Paisley, R. P. Johnson, T. Shimada, D. D. Byler, E. N. Loomis, S. N. DiGiacomo, B. M. Patterson, K. J. McClellan, R. M. Dickerson, P. D. Peralta, A. C. Koskelo, and D. L. Tonks. Long pulse laser driven shock wave loading for dynamic materials experiments. 2008. In *High-Power Laser Ablation VII.* (Taos, NM, USA, April 20-27, 2008). Vol. 7005, p. 700514. Bellingham, WA, USA: Society of Photo-Optical Instrumentation Engineers.

Luo, S. N., L. B. Han, Y. Xie, Q. An, L. Zheng, and K. Xia. The relation between shock-state particle velocity and free surface velocity: A molecular dynamics study on single crystal Cu and silica glass. 2008. *Journal of Applied Physics.* **103** (9): 093530.

Luo, S. N., L. Zheng, Q. An, and S. Zhao. Tensile failure of single-crystal and nanocrystalline Lennard-Jones solids under uniaxial strain. 2006. *International Journal of Modern Physics C.* **17** (11): 1551.

Luo, S. N., P. D. Peralta, C. Ma, D. L. Paisley, S. R. Greenfield, and E. N. Loomis. Sapphire (0 0 0 1) surface modifications induced by long-pulse 1054 nm laser irradiation. 2007. *Applied Surface Science.* **253** (24): 9457–9466.

Luo, S. N., Q. An, L. B. Han, K. W. Xia, and W. A. Goddard. Molecular dynamics simulation of shock-induced spall in Cu at high strain rates. *Journal of Applied Physics.*

Paisley, D. L., S. N. Luo, D. C. Swift, S. Greenfield, E. Loomis, R. Johnson, P. Peralta, A. Koskelo, and D. Tonks. Experimental method for laser-driven flyer plates for 1-D shocks . 2007. In *15th American Physical Society Topical Conference on Shock Compression of Condensed Matter .* (Waikoloa, HI, 24-29 June, 2007). Vol. 955, p. 1337. Melville, NY: American Institute of Physics.

Paisley, D. L., S. N. Luo, S. R. Greenfield, and A. C. Koskelo. Laser-launched flyer plate and confined laser ablation for shock wave loading: validation and applications. 2008. *Review of Scientific Instruments.* **79** (2): 023902.

Peralta, P., S. Digiacomo, H. D'Armas, S. Hashemian, S. N. Luo, S. Greenfield, E. Loomis, D. Paisley, R. Dickerson, D. Byler, and K. J. McClellan. Microstructural effects on plastic deformation and damage nucleation in shocked Cu multicrystals . To appear in *Symposium on Dynamic Behavior of Materials, TMS Annual Meeting.* (Orlando, Florida, March 2007).

Peralta, P., S. Digiacomo, H. D'Armas, S. Hashemian, S. N. Luo, S. Greenfield, E. Loomis, D. Paisley, R. Dickerson, D. Byler, and K. J. McClellan. Effects of microstructural heterogeneity on deformation and failure of metallic materials under dynamic loading: a multicrystal approach . Presented at *NNSA/SSAA Symposium.* (Washington D.C., Feb. 2007).

Peralta, P., S. Digiacomo, H. D'Armas, S. Hashemian, S. N. Luo, S. Greenfield, E. Loomis, D. Paisley, R. Dickerson, D. Byler, and K. J. McClellan. Microstructural effects on spall damage in shocked Cu multicrystals . To appear in *International Journal of Damage Mechanics.*

Peralta, P., S. N. Luo, R. Dickerson, H. D'Armas, S. Digiacomo, and S. Hashemian. Plasticity and damage characterization in shock loaded Cu multicrystals. To appear in *Plasticity 2007.* (Alaska, June 2007).

Tonks, D. L., D. D. Byler, P. D. Peralta, S. R. Greenfield, S. N. Luo, R. M. Dickerson, S. N. di'Giacomo, K. J. McClellan, and

A. C. Koskelo. Dynamic damage experiments and modeling in shock loaded copper. To appear in *New Models and Hydrocodes for Shock Wave Processes in Condensed Matter.* (Lisbon, Portugal, May 18-23, 2008).

Tonks, D. L., D. L. Paisley, P. D. Peralta, S. R. Greenfield, D. D. Byler, S. Luo, D. C. Swift, and A. C. Koskelo. Spallation damage in copper with columnar grains . 2007. In *15th American Physical Society Topical Conference on Shock Compression of Condensed Matter .* (Waikoloa, HI, 24-29 June, 2007). Vol. 955, p. 605. Melville, NY: American Institute of Physics.

Xia, K., R. Chen, S. Huang, and S. N. Luo. Controlled multipulse loading with a stuffed striker in classical split Hopkinson pressure bar testing. 2008. *Review of Scientific Instruments.* **79** (5): 053906.

Zheng, L., Q. An, Y. Xie, Z. Sun, and S. N. Luo. Homogeneous nucleation and growth of melt in copper. 2007. *Journal of Chemical Physics.* **127** (16): 164503.

# Advanced Actinide Separations in Alkaline Media for Spent Nuclear Fuel and Defense Materials Processing

*Gordon Dennis Jarvinen*

20060088DR

## Abstract

An innovative approach to spent nuclear fuel (SNF) reprocessing could offer tremendous advantages over traditional methods, augmenting our nation's energy portfolio and increasing our energy security. For the past three years, our research team has made significant strides in understanding the fundamental chemical underpinning for a novel SNF reprocessing scheme. This project has provided detailed knowledge of the complexes of key actinide and fission product (FP) elements that form when SNF is dissolved in alkaline solutions, including their solubility, stability, and reaction kinetics. This work has successfully provided the basis for developing a separation technology as a revolutionary alternative to the PUREX process.

## Background and Objectives

The National Energy Policy and LANL Strategic Goals state the critical need for the expansion of nuclear energy to enhance energy security and reduce domestic dependence on foreign oil and fossil fuels. This expansion is hindered by the unresolved problem of SNF accumulation, the high costs of SNF disposal, and proliferation concerns over increased SNF reprocessing. SNF from current U.S. reactors will exceed the legislated capacity of the Yucca Mountain repository by more than a factor of two. Licensing applications for 34 new reactors are expected by 2010 [1].

Originally developed to separate plutonium for the U.S. weapons program, the PUREX process is used to reprocess SNF in large plants in France, the U.K., and Japan. The basis of PUREX is the selective liquid-liquid extraction of Pu and U from SNF dissolved in nitric acid. However, the disposal of the high-level waste resulting from PUREX has still not been successfully accomplished by any nation. In 1996 a National Research Council panel estimated capital costs for a new U.S. PUREX-type plant at $2,000-$7,000/kg-SNF-yr [2]. The panel concluded that such a plant would not be economically viable in the U.S., and innovative approaches to partitioning SNF are needed.

Designing an innovative approach to reprocess SNF is constrained by our understanding of actinide and FP chemistry that was mostly limited to acidic and near-neutral conditions prior to this project. A separation scheme based on the different speciation and solubilities of U, FPs and actinides in oxidative alkaline solutions provides an alternative to the PUREX-type process with reduced costs and enhanced proliferation resistance. Our proposed approach uses peroxide in alkaline media to enhance the dissolution of the uranium oxide matrix of SNF and provides novel routes for selectively partitioning the actinides and FPs. The carbonate-peroxide system has five major benefits over PUREX-type technologies: 1) the efficient removal of the heat-loading isotopes $^{137}$Cs and $^{90}$Sr early in the process, substantially decreasing the footprint for heavily shielded operations and minimizing dose to workers; 2) the high binding affinity of peroxide to control metal separation; 3) a reduction in the number and complexity of the treatment processes; 4) the minimization of secondary organic solvent waste; and 5) the flexible group separation of Np, Pu and Am/Cm resulting in a significant safeguards advantage. Our goal has been to develop a detailed, quantitative, and predictive understanding of the most pertinent molecular processes in alkaline peroxide solutions, whether applied to SNF separations, nuclear weapons materials processing, or actinide release and transport in complex repository or storage environments.

## Importance to LANL's Science and Technology Base and National R&D Needs

This work directly supports LANL's missions of Energy Security and Threat Reduction and addresses the Grand Challenges of the Carbon Neutral Fuel Cycle and Superconductivity and Actinide Science. The revolutionary

separations schemes developed in this project present a novel reprocessing technology that minimizes cost, proliferation risks, and environmental impacts of advanced fuel cycles. Our research is aimed at eventually closing the nuclear fuel cycle and supporting sustainable nuclear energy.

In the DOE's preferred option for transformation of the nuclear weapons complex, LANL will become the "Plutonium Center of Excellence." Fundamental actinide science like that performed in this project is key to maintaining and growing that capability for the DOE and the Nation.

## Scientific Approach and Accomplishments

The development of a revolutionary alkaline process for the separation of SNF requires the efficient dissolution of SNF and separation of key FPs such as Cs, Sr, and the rare earths. Work performed during this LDRD project has focused on structural and thermodynamic characterization of key complexes for the light actinides that form under conditions relevant to alkaline SNF reprocessing. We used a multi-faceted approach to study the fundamental structural, thermodynamic, and kinetic behavior of actinides and fission products in alkaline solutions by drawing on recent advances in actinide diagnostics and theory. Our studies used a variety of spectroscopic tools (e.g., UV-Vis-NIR, FT-IR, RAMAN, NMR, fluorescence, ICP-AES), and single-crystal x-ray diffraction (XRD) studies, combined with theoretical calculations to characterize both solution and solid state species. Most significantly, we have explored the new coordination architectures of novel ternary actinide complexes, integrated with quantum chemical calculations to understand the spectroscopic features and electronic structure of these new compounds.

Our primary focus was the peroxide-carbonate system due to previous understanding of actinide carbonate speciation in solution and solid state. We performed only few studies to explore the feasibility of SNF processing in peroxide-hydroxide solutions, but identified a novel mixed-ligand U(VI) peroxo-hydroxo crystal structure [3]. The following sections briefly describe scientific highlights of our work.

### Dissolution of uranium oxides in peroxide-carbonate solution

Initial work, carried out under the auspices of the Advanced Fuel Cycle Initiative of the DOE, established the enhanced kinetics of $UO_2$ dissolution into a peroxide-carbonate solution [4]. Expanding on this work, we investigated the effects of preparation conditions on the dissolution kinetics of three uranium oxides that are potential feed materials for advanced reprocessing. Nine samples, characterized by powder XRD, BET (surface area), and x-ray photoelectron spectroscopy (XPS), were synthesized over a range of firing temperatures: U(VI) oxyhydroxide "$UO_3$" (350, 400 and 450°C), $U_3O_8$ (700, 900 and 1100°C), and $UO_2$ (500, 700 and 900°C). Dissolution rates decrease at higher firing temperature, which correlates to a decrease in surface area. XPS surface studies showed the presence of U(VI) on the "$UO_3$" surface. The $UO_2$ and $U_3O_8$ solids exhibited a mixture of U(IV) and U(VI) surface species, with increasing fraction of U(IV) with firing temperatures. Insight into the dissolution mechanism in peroxide-carbonate solutions was gained by studying the surface of partially dissolved pellets of $UO_2$ with XPS. Exposure to $H_2O_2$ radically changes the electronic structure of the surface uranium, initiating the oxidative dissolution of $UO_2$ by forming U(VI) peroxo or carbonato species on the surface. Synergistic dissolution occurs in peroxide-carbonate solutions by renewal of active surface sites for enhanced dissolution.

### U-$H_2O_2$-$CO_3^{2-}$ Chemistry

The understanding of uranium speciation is critical to the successful control of dissolution of spent uranium oxide fuel and ultimately fission product separation factors from the actinides because uranium is by far the major component of SNF. Peroxide has proven to be an exceptionally strong ligand for actinide complexation, often out-competing carbonate and hydroxide. The complexity and dynamics of the U(VI)-$H_2O_2$-$CO_3^{2-}$ system are unprecedented in uranium chemistry, and much of this project has focused on determining the structure and thermodynamic parameters for the dominant U(VI) mixed peroxo-carbonate species over a range of reaction conditions.

Figure 1 shows the changes in the absorbance features of the U(VI) tris-carbonato complex, $UO_2(CO_3)_3^{4-}$, upon the addition of $H_2O_2$. The monomeric $UO_2(O_2)(CO_3)_2^{4-}$ species has been isolated and structurally characterized by single crystal XRD studies as $K_4[UO_2(CO_3)_2(O_2)]\bullet nH_2O$ ($n$=1,2.5) [5,6]. The equilibrium constant for the formation of $UO_2(O_2)(CO_3)_2^{4-}$ from the reaction of $UO_2(CO_3)_3^{4-}$, and $H_2O_2$ was unexpectedly large, nearly 100,000.[5] Studies probing the reaction stoichiometry and mechanism suggest that the second dominant solutions species is a novel dimeric U(VI) peroxo-carbonato complex with a proposed formula of $(UO_2)_2(O_2)(CO_3)_6^{6-}$. At lower U(VI) concentrations (< 0.5 mM) the solution speciation favors the formation of only monomeric species; at higher U at least 9 distinct $^{13}$C-NMR resonances illustrate the presence of several other oligomeric species. In the presence of excess peroxide, $^{13}$C-NMR data shows no carbonate complexes, suggesting the formation of the tris-peroxo species, $UO_2(O_2)_3^{4-}$ [7].

Quantum chemical calculations were performed to determine the thermodynamically favored coordination geometry of the peroxo ligand in the dimeric U(VI) peroxo-carbonato solution species. The configuration with the bridging peroxo group aligned perpendicular to the metal-metal axis (*side-on* coordination) is favored over the *end-on* coordination by 26 kcal/mol. The calculated geometries are in good agreement with reported U(VI) structures with *side-on* bonded peroxides. No U(VI) structures with *end-on* coordinated peroxide have been reported. The IR solution spectrum of this complex was also calculated and found to agree well with experimental data.

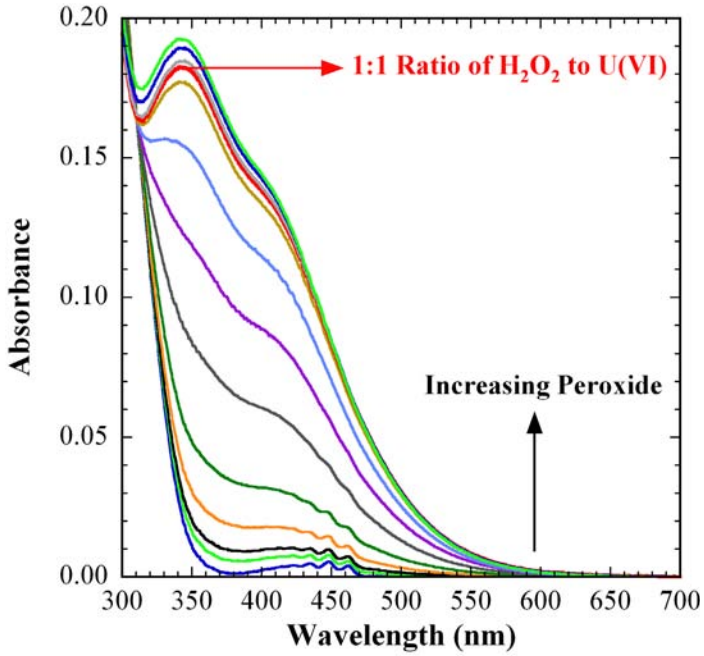


*Figure 1. Spectrophotometric titration of U(VI) with $H_2O_2$ in 0.5 M $K_2CO_3$. The changes in absorbance features are indicative of peroxide complexing with the U(VI) center and displacing a carbonate ligand from $UO_2(CO_3)34$- to form $UO_2(O_2)(CO_3)4$-.*

**Pu-$H_2O_2$-$CO_3^{2-}$ Chemistry**

Aside from the molecular structures of $Pu(CO_3)_5^{6-}$ and $PuO_2(CO_3)_3^{4-}$, little is known about the behavior of Pu in alkaline solutions in single or multi-ligand systems [8]. Small amounts of peroxide have a significant impact on Pu solubility, speciation, and oxidation state stability. While U(IV) is oxidized to U(VI) in the presence of $H_2O_2$-carbonate, Pu(VI) is rapidly reduced to Pu(IV). We have isolated and characterized the molecular structure of $Na_8Pu_2(O_2)_2(CO_3)_6$•$12H_2O$, containing a dimeric anion $Pu_2(O_2)_2(CO_3)_6^{8-}$ with bridging $\mu^2,\eta^2$-$O_2$ ligandsm [9]. This is the first reported crystal structure containing a Pu-peroxide or dimeric Pu complex.

Peroxide titrations of Pu(IV)-carbonate indicate the formation of at least two Pu(IV)- peroxo species. A spectral comparison of the first solution species to $Na_8Pu_2(O_2)_2(CO_3)_6$•$12H_2O$ (Figure 2), suggests that the first complex is the dimeric. This complex forms nearly stoichiometrically, indicating that $Pu_2(O_2)_2(CO_3)_6^{8-}$ is significantly more stable than $(UO_2)_2(O_2)(CO_3)_6^{6-}$. The second Pu(IV) peroxo-carbonato species forms rapidly in the presence of a significant excess of $H_2O_2$ and slowly reverts back to $Pu_2(O_2)_2(CO_3)_6^{8-}$. The first Pu(IV) solution species is stable over a long time period, and its stability is likely controlled by the rate of free $H_2O_2$ decomposition.

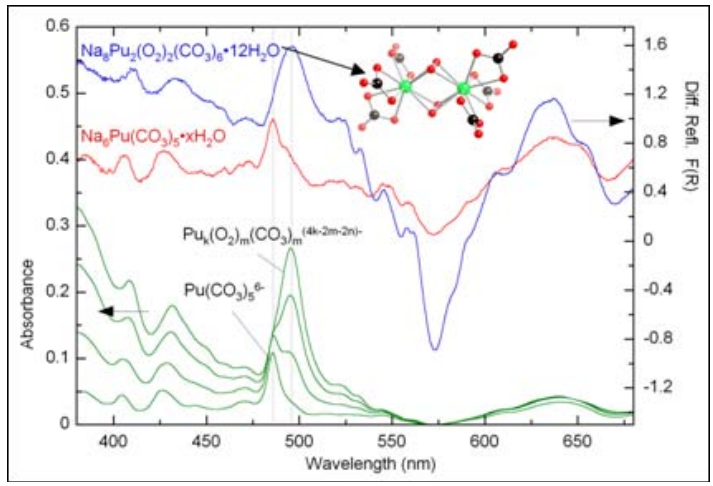


*Figure 2. Spectroscopic comparison showing remarkable agreement of the first Pu peroxo-carbonate solution complex with the solid state structure $Na_8Pu_2(O_2)2(CO_3)6$•$12H_2O$.*

Plutonium exhibits interesting redox kinetics in both carbonate and peroxide-carbonate solutions, with Pu(IV) being the stable oxidation state in the presence of peroxide. When an equal amount of $H_2O_2$ is added to low concentrations of Pu(III) in 2 M $K_2CO_3$, Pu(III) is rapidly oxidized to a mixture of Pu(IV) carbonate and peroxo-carbonate, yet the same oxidation takes in excess of 12 hours in the absence of $H_2O_2$. At 25°C $H_2O_2$ rapidly reduces Pu(VI) to Pu(IV), but cooling the solution has allowed measurement of the redox kinetics and the observation of a blue Pu(VI) peroxo-carbonato intermediate (Figure 3).

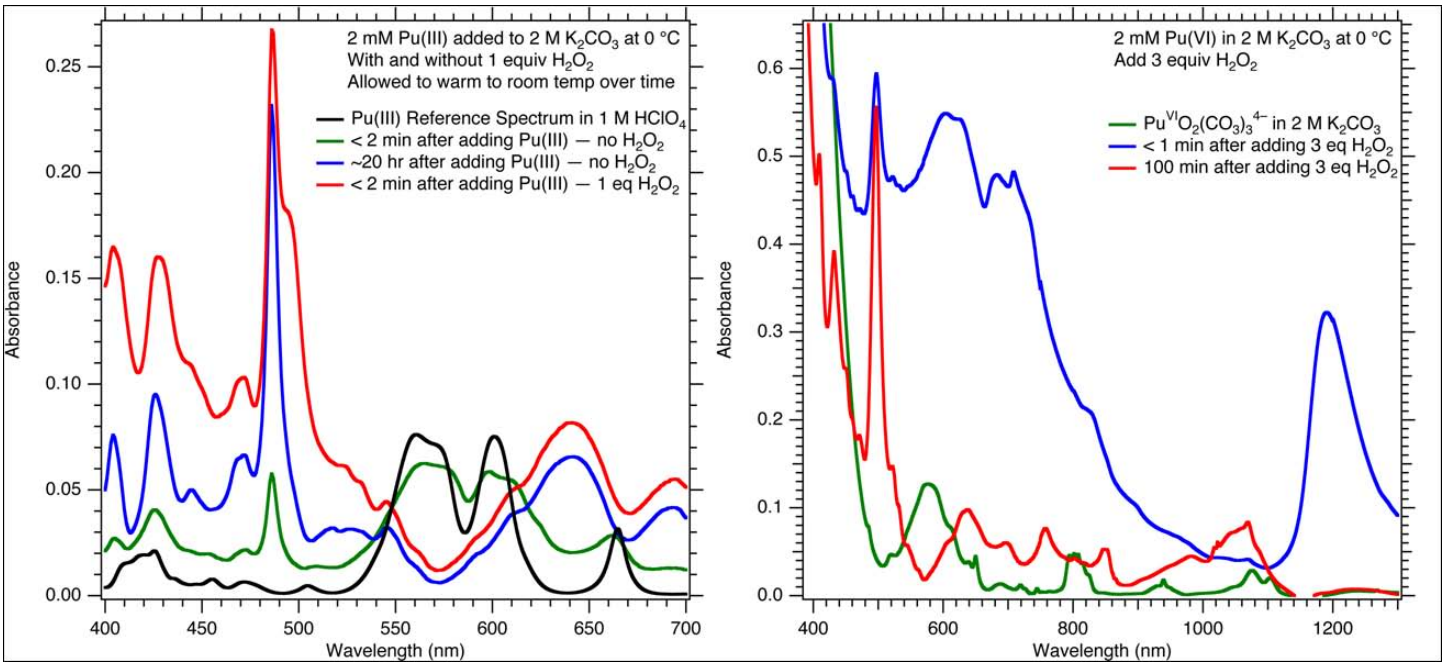


*Figure 3. Plutonium(III) is readily oxidized to Pu(IV) without complexation by $H_2O_2$ (left) while Pu(VI) is reduced to Pu(IV) via a Pu(V) intermediate while forming a competing Pu(VI) peroxo0carbonate complex. (right)*

**Np-$H_2O_2$-$CO_3^{2-}$ Chemistry**

Neptunium in mixed $H_2O_2$-$CO_3^{2-}$ solutions exhibits the most complex redox behavior of the light actinides. For example, $H_2O_2$ oxidizes Np(IV) and reduces Np(VI), with Np(V) being the most stable oxidation state. The rate of peroxide complexation is significantly slower than that for U and Pu, while the decomposition rate is significantly faster. The solubility of Np can be controlled by the $H_2O_2$ concentration, which allows for tunable partitioning of Np.

**Cesium Separation**

The efficient removal of the fission product Cs early in the proposed alkaline separation schemes would be very useful for reducing the gamma shielding requirements and simplifying the radiation damage chemistry. A number of potential absorbents or precipitants for Cs in alkaline solution have been investigated, including the inorganic materials: crystalline silicotitanate IE-911, zeolites IE-95 and A-51, $NaBH_4$, potassium cobalt(II)ferrocyanide (KCFC), and ammonium ferric-hexacyanoferrate (AFCF). Two organic materials, SuperLig 644 and BOBCalixC6, were also tested. The inorganic systems have the advantage of higher radiation resistance relative to the systems containing organic components.

Overall, the ferrocyanides achieved the highest removal of cesium. In sodium carbonate solutions, a number of approaches appear capable of accomplishing removal of Cs to greater than 95% including IE-95, A-51, KCFC, AFCF, tetraphenylborate precipitation, and BOBCalixC6. In $K_2CO_3$ solutions, most of the previous systems are less selective for cesium over potassium, and literature results show that tetraphenylborate is not selective. The most promising candidate in $K_2CO_3$ solutions is AFCF, and it is the only potential candidate from our study for removing cesium from ammonium carbonate solutions.

**Lanthanide (Ln), and Sr/Ba Chemistry**

We have successfully isolated and characterized by single crystal XRD studies molecular structures for the solubility limiting carbonate species across the lanthanide series (except La, Ce, and Pm) [10]. The addition of $H_2O_2$ to lanthanide-carbonate solutions results in the formation of an extremely insoluble peroxo-carbonate complex. Strontium and Ba carbonates are very insoluble, and $H_2O_2$ appears to further decrease their solubility. Our results indicate the feasibility of greater than 95% removal of Ln(III), Sr, and Ba during the initial dissolution step of the alkaline SNF reprocessing scheme.

**Mixed Actinide (An) and An/Ln Chemistry**

The experimental data from the individual actinide systems clearly shows the strong affinity of peroxide towards An(IV) and An(VI) ions, even in the presence of strongly coordinating $CO_3^{2-}$ and $OH^-$ ligands. When $H_2O_2$ is added

to a carbonate solution containing equal concentrations of U(VI) and Pu(IV), Pu(IV) is preferentially complexed. At higher ratios of U:Pu, U(VI) competes with Pu(IV) for peroxide complexation, indicating a higher stability constant for $Pu_2(O_2)_2(CO_3)_6^{8-}$.

Unlike mixed actinide systems, where actinides compete for $H_2O_2$ complexation, peroxide preferentially complexes U(VI) over Ln(III). In general, the lanthanides have shown different solution chemistries than U(VI) and Pu(IV): the solubility of Ln(III) increases at higher carbonate concentrations, while $UO_2(CO_3)_3^{4-}$ decreases; the solubility of Ln(III) in carbonate decreases in the presence of $H_2O_2$ while U(VI) and Pu(IV) solubility increases.

## References


1. Nuclear Power 2010: www.ne.doe.gov/np2010/neScorecard/neScorecard.html. 2008. *DOE Office of Nuclear Energy.*

2. Nuclear Wastes: Technologies for Separations and Transmutation. 1996. *National Academy of Science - Committee on Separations Technology and Transmutation Systems National Research Council.*

3. Zehnder, R., E. Batista, B. Scott, S. Peper, G. Goff, and W. Runde. Synthesis, crystallographic characterization, and conformational prediction of a structurally unique molecular mixed-ligand U(VI) solid, Na6[UO2(O2)2(OH)2](OH)2•14H2O . To appear in *Radiochimica Acta.*

4. Peper, S., L. Brodnax, S. Field, R. Zehnder, S. Valdez, and W. Runde. Kinetic study of the oxidative dissolution of UO2 in aqueous carbonate media. 2004. *Industrial and Engineering Chemistry Research.* **43** (26): 8188.

5. Goff, G., L. Brodnax, M. Cisneros, S. Peper, S. Field, B. Scott, and W. Runde. First identification and thermodynamic characterization of the ternary U(VI) species, UO2(O2)(CO3)24-, in UO2-H2O2-K2CO3 solutions. 2008. *Inorganic Chemistry.* **47** (6): 1984.

6. Zehnder, R., S. Peper, B. Scott, and W. Runde. Tetrapotassium dicarbonatodioxoperoxouranate(VI) 2.5-hydrate, K4[U(CO3)2O2(O2)]•2.5H2O. 2005. *Acta Crystallographica, Section C: Crystal Structure Communications.* **C61** (1): i3.

7. Alcock, N.. Crystal and molecular structures of sodium uranyl triperoxide. 1968. *Journal of the Chemical Society [Section] A: Inorganic, Physical, Theoretical.* **7**: 1588.

8. Clark, D., S. Hecker, G. Jarvinen, and M. Neu. Plutonium. 2006. In *The Chemistry of the Actinide and Transactinide Elements.* Edited by Morss, L., J. Fuger, and J. Katz. Vol. 2, Third Edition, p. 813. Dordrecht, Netherlands: Springer.

9. Runde, W., L. Brodnax, G. Goff, S. Peper, F. Taw, and B. Scott. Synthesis and structural characterization of a molecular plutonium(IV) compound constructed from dimeric building blocks. 2007. *Chemical Communications.* **17**: 1728.

10. Goff, G., M. Cisneros, C. Kluk, K. Williamson, B. Scott, L. Brodnax, and W. Runde. Synthesis, spectroscopy, and structural comparison of Ln(III)(CO3)4 5- in carbonates of the light and heavy rare earth elements. *Inorganic Chemistry.*


## Publications


Gaunt, A. J., S. Reilly, B. Scott, G. S. Goff, L. F. Brodnax, M. Neu, and W. Runde. Advances in the coordination chemistry of the light actinides: U, Np, Pu, and Am. Presented at *Chemistry Capability Review - Los Alamos National Laboratory.* (Los Alamos, Aug. 2007).

Goff, G. S., F. L. Taw, S. M. Peper, L. F. Brodnax, and W. Runde. Characterization of uranium, neptunium, and plutonium complexes in aqueous hydrogen peroxide-carbonate solutions. Presented at *62nd Annual Meeting of the Northwest Region of the American Chemical Society.* (Boise, June 2007).

Goff, G. S., L. F. Brodnax, E. Batista, M. R. Cisneros, F. L. Taw, and W. H. Runde. Computational chemistry as a guide for understanding f-element chemistry in alkaline solutions. Presented at *American Institute of Chemical Engineers Annual Meeting.* (Salt Lake City, 11-15 Nov. 2007).

Goff, G. S., L. F. Brodnax, M. R. Cisneros, F. L. Taw, B. L. Scott, K. S. Williamson, C. A. Kluk, and W. H. Runde. The effect of H2O2 on the chemistry of f-element compounds in the + (III) and (IV) oxidation states in near-neutral and alkaline solutions. Presented at *American Chemical Society National Meeting.* (Boston, 19-23 Aug. 2007).

Goff, G. S., L. F. Brodnax, M. R. Cisneros, F. L. Taw, B. L. Scott, and W. H. Runde. Synthesis and characterization of novel f-element complexes in near-neutral and alkaline solutions. Presented at *American Chemical Society National Meeting.* (Boston, 19-23 Aug. 2007).

Goff, G. S., L. F. Brodnax, M. R. Cisneros, F. L. Taw, K. S. Williamson, and W. H. Runde. Synergistic Chemistry of U(VI) and lanthanide(III) complexes in alkaline carbonate H2O2 solutions. Presented at *American Chemical Society National Meeting.* (Boston, 19-23 Aug. 2007).

Goff, G. S., L. F. Brodnax, M. R. Cisneros, S. M. Peper, K. S. Williamson, C. A. Kluk, B. L. Scott, and W. H. Runde. Solution and solid state chemistry of environmentally relevant actinide and lanthanide complexes in alkaline solutions. Presented at *American Institute of Chemical Engineers Annual Meeting.* (Salt Lake City, 11-15 Nov. 2007).

Goff, G. S., L. F. Brodnax, M. R. Cisneros, S. M. Peper, S. E. Field, B. L. Scott, and W. H. Runde. First identification and thermodynamic characterization of the ternary U(VI) species, UO2(O2)(CO3)24-, in UO2-H2O2-K2CO3 solutions. 2008. *Inorganic Chemistry.* **47** (6): 1984.

Goff, G. S., L. F. Brodnax, M. R. Cisneros, S. M. Peper, S. E. Field, B. L. Scott, and W. H. Runde. First Identification and Thermodynamic Characterization of the Ternary U(VI) Species, UO2(O2)(CO3)24-, in UO2-H2O2-K2CO3 Solutions. 2008. *Inorg. Chem. (Washington, DC, U. S.).* **47** (6): 1984.

Goff, G. S., L. F. Brodnax, M. R. Cisneros, S. M. Peper, S. E. Field, K. S. Williamson, I. May, and W. H. Runde. Development of a novel alkaline based process for spent nuclear fuel recycling. Presented at *American Institute of Chemical Engineers Annual Meeting.* (Salt Lake City, 11-15 Nov. 2007).

Goff, G. S., L. F. Brodnax, M. R. Cisneros, and W. H. Runde. REDOX chemistry of actinides in peroxide-carbonate media: applications to developing a novel process for spent nuclear fule reprocessing. Presented at *American Institute of Chemical Engineers Annual Meeting.* (Salt Lake City, 11-15 Nov. 2007).

Goff, G., F. Taw, S. Peper, L. Brodnax, and W. Runde. Stability and Speciation of Uranium, Neptunium and Plutonium Complexes in Aqueous Hydrogen Peroxide Carbonate Solutions. Presented at *Pu FUTURES The Science 2006.* (Pacific Grove, 9-13 July 2006).

Goff, G., L. Brodnax, M. Cisneros, and W. Runde. Interaction of the Light Actinides with Peroxide: Ternary Actinide Peroxide-Carbonate Complexes in Solution and in Solid State. Invited presentation at *PITTCON 2008.* (New Orleans, LA, 1-7 March 2008).

Long, K. M., G. D. Jarvinen, J. R. FitzPatrick, D. K. Ford, and R. Villarreal. Cesium removal as part of an alkaline separation process for spent nuclear fuel. Invited presentation at *232nd American Chemical Society National Meeting.* (San Francisco, 10-14 Sep. 2006).

Long, K., D. Ford, R. Villarreal, G. Jarvinen, and J. Fitzpatrick. Cesium removal as part of an alkaline separation process for spent nuclear fuel. Presented at *31st Actinide Separation Conference.* (Las Vegas, NV, 11-14 June 2007).

Mullins, D., G. Jarvinen, M. Mayne, D. Ford, K. Long, H. Reichert, P. Palmer, C. D. Tait, D. W. Keogh, and P. Gordon. Crystallization of uranium complexes for partitioning of spent nuclear fuel. 2006. In *Separations for the nuclear fuel cycle in the 21st Century.* Edited by Lumetta, G. J., K. L. Nash, S. B. Clark, and J. I. Freese. Vol. No. 933, p. 183. Washington D. C.: American Chemical Society.

Runde, W., G. Goff, M. Cisneros, L. Brodnax, and S. Reilly. Chemical Behavior of the f-elements in Peroxide-Carbonate Media: Spectroscopic and Structural Characterization of Predominant Complexes in Solution and Solid State. Presented at *Plutonium Futures - The Science 2008.* (Dijon, France, 7-10 July 2008).

Runde, W., G. S. Goff, F. L. Taw, S. M. Peper, L. F. Brodnax, and S. E. Field. Interaction of the light actinides with peroxide: ternary actinide peroxide-carbonate complexes in solution and solid state. Invited presentation at *MIGRATION 2007.* (Munich, 26-30 Aug. 2007).

Runde, W., G. S. Goff, L. Brodnax, J. Fitzpatrick, F. Taw, M. Cisneros, J. D. Farr, E. Batista, and G. Jarvinen. Coordination chemistry of f-elements in alkaline media for advanced processing of spent nuclear fuel. Presented at *Chemistry Capability Review - Los Alamos National Laboratory.* (Los Alamos, Aug. 2007).

Runde, W., L. F. Brodnax, G. S. Goff, S. M. Peper, F. L. Taw, and B. L. Scott. Structural characterization of a molecular plutonium(IV) compound constructed from dimeric

building blocks. 2007. *Chemical Communications.* (17): 1728.

Runde, W., L. F. Brodnax, S. M. Peper, C. Wakefield, and M. Ensor. Effect of Secondary Ligands on the Speciation of Actinides in Carbonate Solutions: Peroxo-Carbonato Pu(IV) and U(VI) Complexes. Invited presentation at *Pacifichem 2005.* (Honululu, 15-20 Decmber 2005).

Taw, F. L., G. S. Goff, S. M. Peper, L. F. Brodnax, E. R. Batista, S. E. Field, C. R. Wakefield, and W. H. Runde. Separation of Uranium from Fission Products in Spent Nuclear Fuel. Presented at *232nd American Chemical Society National Meeting.* (San Francisco, 10-14 September 2006).

Zehnder, R. A., E. R. Batista, B. L. Scott, S. M. Peper, G. S. Goff, and W. Runde. Synthesis, Crystallographic Characterization, and Conformational Prediction of a Structurally Unique Molecular Mixed-Ligand U(VI) Solid, Na6[UO2(O2)2(OH)2](OH)2•14H2O. To appear in *Radiochimica Acta.*

Zehnder, R. A., S. M. Peper, B. L. Scott, and W. H. Runde. Tetrapotassium Dicarbonatodioxoperoxouranate(VI) 2.5-hydrate, , K4[U(CO3)2O2(O2)]•2.5H2O. 2005. *Acta Crystallographica, Section C: Crystal Structure Communications.* **C61** (1): i3.

# Biological Effects of Molecularly Engineered Nanomaterials

*Andrew Paul Shreve*

20060097DR

## Abstract

We have used systematic methods to examine the responses of cells and biomolecular assemblies to synthetically engineered nanoscale materials in order to gain insight into fundamental physical and chemical mechanisms that underlie such effects. Biological, health and environmental effects will ultimately influence all applications of nanoscale materials, and equally important, will also influence societal acceptance of nanotechnology. Thus, the proposed work contributes to the development of fundamental nano-bioscience and also impacts long-term applications of nanomaterials in technologies such as sensor development, energy production and medical treatments. Major results from the project are: 1) an examination of cellular responses to systematically varied fullerene nanoparticles; 2) proteomic and biochemical analysis of protein expression level changes and biochemical signaling pathway activations upon exposure to synthetically engineered carbon nanoparticles; 3) exploration of interaction mechanisms for nanoparticles and biological systems; and 4) development of methods to separate the influence of physical from chemical properties in determining cellular effects of nanomaterials.

## Background and Research Objectives

A scientific and technological revolution is underway, arising from the ability to control and manipulate matter on the nanoscale. However, understanding of the interactions between engineered nanomaterials and biological systems remains primitive. This lack of understanding limits development of nanomaterial applications in the biological arena, and also raises uncertainties about long-term health and environmental effects of nanomaterials [1]. There is enormous interest in such topics because *all applications of nanomaterials will be impacted by their long-term health effects*. Our studies have addressed cellular responses to chemically tailored carbon-based nanoparticles and have explored underlying physical and chemical mechanisms that control the biological interaction of nanoparticles.

Our overall goals were to increase mechanistic understanding of biological and health effects of nanomaterials and to provide a foundation for predictive control of the interface between nanoscale materials and biology. To achieve these objectives, we implemented a research program that has produced significant advances in nanomaterial synthesis, material characterization, assessment of cellular effects induced by systematically varied sets of nanomaterials and exposure levels, elucidation of biochemical responses including up or down regulation of specific protein expression levels upon nanomaterial exposure, study of activation of signaling pathways after exposure of cells to synthetically engineered nanomaterials, and control of nanomaterial interactions with cells and overall biological effects through the use of rational synthesis strategies.

## Importance to LANL's Science and Technology Base and National R & D Needs

There is increasing awareness that much better fundamental understanding of the interaction of nanomaterials with biological systems is needed. This fact has been recognized at the national policy level, as indicated, for example, in multi-agency strategic plans developed as part of the National Nanoscience Initiative (links available at www.nano.gov). Within the multi-agency framework of the NNI, environmental, health and safety aspects of nanomaterials have been specifically addressed as an essential component of NNI's coordinated research framework. At LANL, nanoscience represents an important strategic area that contributes to existing and future programs, for example (bio)threat reduction, energy security efforts, fundamental materials science, the Center for Integrated Nanotechnologies, and intelligence community activities. Overall, the work in this project supports LANL's science and technology base through: 1) development of high-impact science of importance to the laboratory and the nation, 2) addressing technical issues of current and future importance to a broad range of laboratory customers, 3) building new capabilities in multi-disciplinary science, and

4) supporting laboratory missions in energy security, materials science and threat reduction arenas.

## Scientific Approach and Accomplishments

In order to achieve our goals of obtaining an improved systematic understanding of biological effects of engineered nanomaterials, our approach targeted the three key areas of material synthesis, material characterization, and study of cellular responses upon exposure to nanomaterials. Major accomplishments in each of these areas is highlighted in the following sections.

### Synthesis

We used chemical synthetic methods to develop a series of water-soluble fullerenes from three main categories: cationic, anionic and neutral (Figure 1). Such synthetic control has allowed us to investigate the role of charge, surface properties and aggregate size, the latter arising from the fact that various members of the synthesized families of materials demonstrate different propensities for aggregation in aqueous environments. The primary anionic materials studied were so-called tris- and hexa-adducts, where the added three (tris) or six (hexa) groups, presented a di-carboxylic acid moiety from the surface of the fullerene cage. Cationic fullerenes were prepared by attaching ammonium functional groups to the end of the substituents. Neutral fullerene is obtained by connecting two long ethylene oxide chains to the fullerene. Alternatively, water-soluble neutral fullerene was generated by the encapsulation of the fullerene in a cyclodextrin molecule. Overall, our synthetic chemistry approaches demonstrate the successful achievement of tunable solubility, electronic structure, electrochemical properties, aggregation states and, as discussed below, cytotoxicity and other biological responses [2,3].

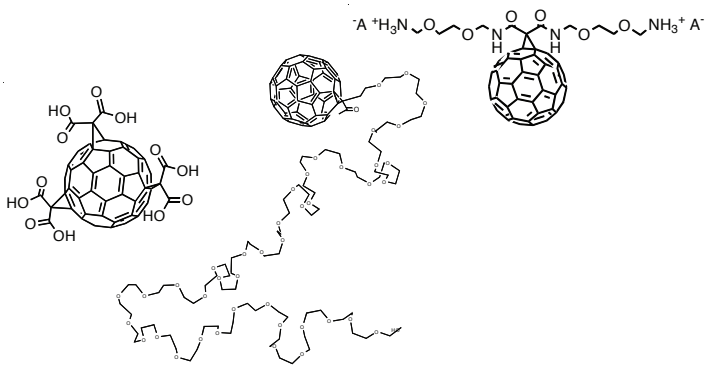

*Figure 1. Examples of fullerene derivatives prepared. On the left is a carboxylic acid derivative (tris substituted), which becomes anionic by deprotonation under most aqueous buffer conditions. In the middle is a neutral fullerene, functionalized with a polyethylene glycol chain. On the right is a cationic fullerene, made by adding amine terminated chains to a carboxylated fullerene.*

We also developed strategies for preparation of different classes of water-soluble fullerene materials by self-assembly based methods (Figure 2) [4]. Here, an important goal was to use the tools of material self assembly to develop a rational design approach toward making water soluble fullerenes with the same size, but different surface functionality, or different size, but the same surface functionality. This set of materials allowed us to differentiate the biological effects originating from aggregation size and surface functionalities. Further, these nanomaterial solubilization strategies allow us to shield the nanomaterials with polymers and charges, thereby controlling their biological effects. Ultimately, such approaches may allow different sized payloads of nanomaterials to be delivered to cells, while also shielding the materials from interaction with non-targeted biological materials. A similar strategy has also been implemented using lipophilic peptides, which afford the possibility of targeting the solublized nanomaterials to specific cells or intracellular structures.

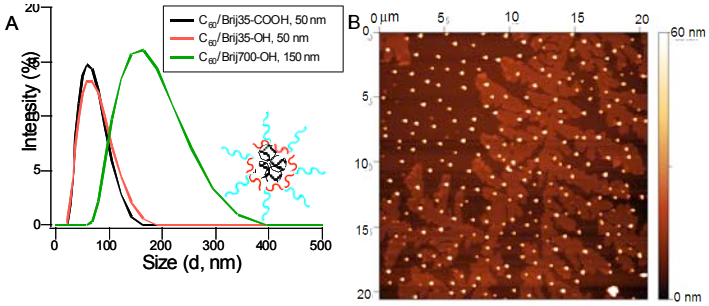


*Figure 2. A schematic of polymer wrapped fullerene materials (inset) and characterization studies of such materials using dynamic light scattering (left) and atomic force microscopy (right) to determine the size distribution of the fullerene/polymer aggregates.*

### Characterization

An important component of our work has been to apply a complete set of characterization tools to understand the chemical and physical properties of the synthesized nanomaterials. Such characterization is essential as a foundation to the ultimate goal of correlating cellular and biological responses with material properties. Characterization efforts have included determination of chemical structure, electronic properties, oxidation and reduction potentials, and solubility of the synthesized materials, and these studies have relied upon techniques such as nuclear magnetic resonance spectroscopy, absorption spectroscopy, electrochemistry, dynamic light scattering and atomic force microscopy. These methods have been applied to both chemically synthesized materials and materials obtained through controlled self-assembly methods. As an example, we used dynamic light scattering and atomic force microscopy to

examine the structure of polymer wrapped fullerenes in aqueous solutions (Figure 2), verifying our aims of producing similar materials that differ either in aggregate size or in the chemical functionalization. These results are closely linked to cellular responses (see below), as studies on these materials indicate that the surface characteristics, but not the size nor toxicity of the fullerene, were the dominant factors for the cellular effects.

**Cellular response**

Our studies of cellular responses induced by fullerene and related nanomaterials targeted several different aspects of biological and biochemical systems. One aspect of our work was focused on overall cellular responses, for example, cell proliferation or cell death through necrosis or apoptosis (programmed cell death) [5,6]. Studies were performed using three relevant cell lines, monocytes (THP1), human skin keratinocytes (HEK), and pulmonary epithelial cells (BEAS-2B), representing immune, dermal and inhalation responses, respectively. As one example of our studies, we examined the responses to three types of fullerenes, underivatized fullerene solubilized by encapsulation in cyclodextrin, and so-called tris- and hexa- substituted carboxylated fullerenes (see above). Comparative analysis of the differential biological responses induced by these molecules included studies of cytotoxicity, generation of reactive oxygen species (ROS), cell proliferation, cell senescence, cell cycle arrest, and immune responses. These studies indicated that significantly different responses are obtained depending on the chemical functionalization of fullerenes in all three cell types examined. For example, depending on the target cell type (immune cell, skin or lung) and the chemical functionalization of the fullerene, the type and extent of induced programmed cell death (apoptosis) was different. Such studies are important because the deregulation of apoptosis has been proposed to contribute to the pathogenesis of many diseases. Even more interesting in terms of cellular responses was the observation that, in immortalized HEK and BEAS-2B cells, tris-$C_{60}$, unlike hexa-$C_{60}$ and cyclodextrin-$C_{60}$, induced premature senescence by inducing cell cycle arrest and preventing cell proliferation. Cellular senescence is the terminally nondividing state that all normal cells enter after a limited number of divisions, and this state has been suggested to be a powerful tumor suppressive mechanism and to contribute to organism aging, as well as serve a general cellular stress response program. The potential ramifications of perturbing cell division and inducing premature senescence in different exposure scenarios may be quite significant, but further understanding of the mechanisms involved in the differential responses observed with chemically distinct fullerenes is still needed.

We also studied the interaction of various polymer wrapped fullerenes with different cells. For some of the polymers studied, we found that the polymer alone, as well as the polymer/fullerene aggregate, both protect cells from apoptosis. On the other hand, other polymers were cytotoxic. Interestingly, larger neutral polymers with substantial polyethylene glycol content seemed to shield the coated nanomaterials from the environment, minimizing cellular effects. Therefore, in these systems, fullerenes were not only solubilized, but also appear to be well protected by polymer coatings.

Other aspects of our work have attempted to address different mechanistic questions related to biological exposure to carbon-based nanomaterials. For example, we explored in some detail the potential for different fullerenes to cause chemical and physical damage to biological membranes. These studies relied upon exposure of fullerenes to model phospholipid membranes under controlled conditions, followed by detailed characterization using techniques such as atomic force microscopy. Studies with different types of fullerenes indicate a complex, differential response, with substantial light-induced membrane damage possible (see Figure 3), depending on lipid or protein composition of membranes and the chemical functionalization of the fullerene materials. Overall, however, it is apparent that a determining factor in controlling membrane damage mechanisms is the degree of interaction between differently functionalized fullerenes and the membrane, which can be controlled through chemical functionalization of the nanoparticles.

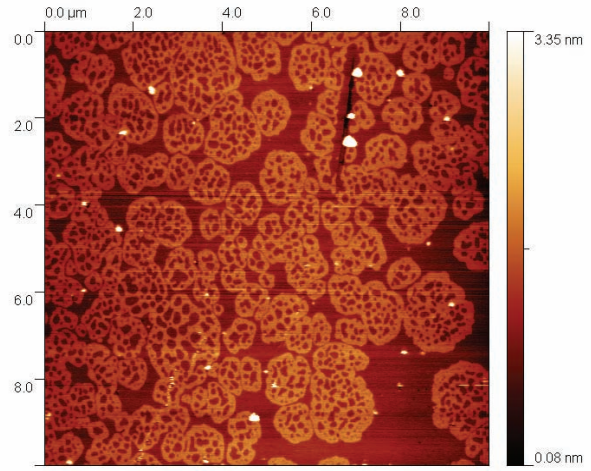


*Figure 3. An atomic force microscopy image of a model phospholipid membrane following fullerene-mediated damage during light exposure. The damage is apparent in the splotchy texture of the regions of the membrane where aggregaged fullerene was present (lighter areas of image). A series of related experiments verified that these types of biological membrane damage processes are correlated with the propensity of any given fullerene derivative to interact with the membrane, which depends upon the nature of chemical functionalization of the fullerene and the composition of the membrane.*

Though most of our studies focused on fullerenes, we also explored how other carbon-based nanomaterials might potentially exert bioactivity with regard to the innate immune system. A mouse macrophage-like cell line (RAW264.7) was exposed to various carbon-based nanomaterials. This cell line is routinely used to model the innate immune system. No gross toxicity was observed when RAW264.7 cells were cultured in the presence of multi-walled carbon nanotubes (MWCNTs) for up to 48 hours. But, upon exposure to MWCNTs, a specific profile of cytokine secretion was induced in this cell type. Cytokines are small proteins that are active in cellular signaling processes. The cytokine profile was observed upon exposure to three different bulk MWCNT preparations that varied by growth method, average dimensions, and residual catalyst content, but not upon exposure to fullerenes or single-walled carbon nanotubes. These data suggest that the MWCNT-induced cytokine profile is unique to MWCNTs and that this profile can be used for biomarkers of MWCNT exposure. The accumulation of a specific profile of cytokines upon MWCNT exposure suggested that a specific pathway of the innate immune system was activated, and our studies have identified one such likely pathway that is similar to the innate immune response upon viral infection [7].

Another important aspect of our work was to develop the capabilities for systematic analysis of protein expression level changes associated with nanomaterial exposure. Such proteomic analysis provides the means to identify cellular signaling and gene regulation mechanisms that might be associated with exposure to different nanomaterials. During the project period, we analyzed effects on THP-1 cells. Proteomic analysis showed changes in expression level of several key proteins. For example, several anti-oxidant proteins were upregulated in response to hexa-carboxy fullerene treatment. Given that the hexa-carboxy fullerenes themselves did not induce reactive oxygen species (ROS), the upregulation of anti-oxidant enzymes points to a role in reduction of basal levels of ROS and ROS-mediated apoptosis. Another important upregulated protein was Interleukin enhancer binding factor 2, part of a dimer that is involved in interleukin-2 expression, which in turn is a key cytokine involved in immune response. The upregulation of this factor suggests that the cell may be potentially manifesting a pro-inflammatory response to these particles. Also upregulated was an enzyme (E2Q) involved in the important ubiquitination process that targets abnormal or short-lived proteins for degradation. Thus, the significant reduction observed in several other proteins could, in part, be a targeted degradation process, indicating the complexity of biological responses that can be elicited by nanomaterial exposure. These and other results from proteomic studies will be described in a forthcoming manuscript.

**Summary**

Overall, our work has addressed the important issue of how to control biological and cellular effects arising from exposure to engineered nanomaterials. An overarching result is that the induced biological responses are quite complex and strongly dependent on the physical and chemical characteristics of the materials, as well as upon dose, exposure time and cell type. Strategies that may limit the biological effects of nanomaterials have been developed, through more general testing is still needed. Fundamentally, achieving a detailed mechanistic understanding of the myriad of biological effects that can be induced by different synthetic nanomaterials remains a daunting task of systems biology, but one that must be successfully addressed to fully enable future applications of nanomaterials in all areas of science and technology.

## References


1. Colvin, V. L.. The potential environmental impact of engineered nanomaterials. 2003. *Nature Biotechnology.* **21**: 1166.

2. Canteenwala, T., W. G. Li, H. L. Wang, and L. Y. Chiang. Low multielectron reduction potentials of emerald green [60]fullerenes. 2006. *Chemistry Letters.* **35**: 762.

3. Wang, C. C., Y. Gao, L. Y. Chiang, and H. L. Wang. Synthesis and characterization of fullerenyl 1,38-bisadduct: C60[-CMe(CO2-Et)2]2. *Organic Letters.*

4. Bao, Y., C. Zhong, G. Montano, R. Iyer, A. P. Shreve, and J. S. Martinez. Differentiating biological effects originating from size and surface characteristics of water soluble fullerenes. *Journal of the American Chemical Society.*

5. Gao, J., H. L. Wang, A. P. Shreve, and R. Iyer. Modulation of gamma-irradiation induced ROS responses by engineered fullerenes in human epidermal keratinocytes. To appear in *Nanomedicine: Nanotechnology, Biology and Medicine.*

6. Houston, K. D., N. H. Mack, S. K. Doorn, and M. S. Park. Identification of biomarkers for multi-walled carbon nanotube exposure. *Nano Letters.*

## Publications

Bao, Y., C. Zhong, G. Montano, R. Iyer, A. P. Shreve, and J. S. Martinez. Differentiating biological effects originating from size and surface characteristics of water soluble fullerenes. *Journal of the American Chemical Society.*

Canteenwala, T., W. Li, H. L. Wang, and L. Y. Chiang. Low multielectron reduction potentials of emerald green [60] fullerenes. 2006. *Chemistry Letters.* **35**: 762.

Gao, J., H. L. Wang, A. P. Shreve, and R. Iyer. Modulation of gamma-irradiation induced ROS responses by engineered fullerenes in human epidermal keratinocytes. To appear in *Nanomedicine: Nanotechnology, Biology and Medicine.*

Houston, K. D., N. H. Mack, S. K. Doorn, and M. S. Park. Identification of biomarkers for multi-walled carbon nanotube exposure. *Nano Letters.*

Martin, R., H. L. Wang, J. Martinez, S. Iyer, G. A. Montano, A. P. Shreve, Y. Bao, C. C. Wang, Z. Chang, Y. Gao, and R. Iyer. Impact of physio-chemical properties of engineered fullerenes on key biological responses. To appear in *Toxicology and Applied Pharmacology.*

Tang, Z., P. A. Padmawar, T. Canteenwala, Y. Gao, E. Watkins, J. Majewski, L. Y. Chiang, and H. L. Wang. Synthesis and characterization of monolayers and Langmuir-Blodgett films of an amphiphilic oligo(ethylene glycol)-C60-hexadecaaniline conjugate. 2006. *Langmuir.* **22**: 5366.

Wang, C. C., Y. Gao, L. Y. Chiang, and H. L. Wang. Synthesis and characterization of the novel 1,38-bisadduct fullerene: C60[CMe(CO2Et)2]2. *Organic Letters.*

# New Classes Of Materials For Gamma-Ray and Neutron Detection

*Darryl Lyle George Smith*

20060136DR

## Abstract

Gamma and neutron detectors play essential roles in approaches to identify special nuclear materials and radiological sources that pose threats as nuclear weapons or radiological dispersal devices. Currently available detectors do not meet all the requirements for many homeland security applications that need large area/volume, rugged, low cost, and fieldable detectors. Recently, there has been dramatic progress in electronic materials research that can be employed to create a new generation of radiation detector materials. In the last decade both organic semiconductors and inorganic quantum-dots have been the focus of intense scientific and technological interest. In this program we demonstrated improved scintillation performance using a composite scintillator consisting of inorganic quantum-dots and an organic semiconductor host. We demonstrated improved light yield from plastic scintillators utilizing a phosphorescent dopant to collect both singlet and triplet excitations. We demonstrated large bulk photoconductive gain, greater than 100, in organic semiconductor photodiodes which showed that these devices are valuable for reading out scintillators used for gamma ray detection.

## Background and Research Objectives

### Gamma Detectors

For nuclear spectroscopy, the standard gamma-detector is the liquid-nitrogen-cooled single crystal Ge detector. This type of detector is excellent for laboratory work, but it is not readily amenable to field applications. Fieldable alternatives, including compressor cooled Ge (CC-Ge), Cadmium-Zinc-Telluride (CZT) and Thallium doped Sodium Iodide (NaI), are available with various performance characteristics. For both CC-Ge and CZT, a major limitation is the small size and great expense of the crystals. For NaI, expense is not as great a problem, but the energy resolution is significantly worse than either CC-Ge or CZT. These detectors are all grown as single crystals, which contributes to their expense. Plastic scintillator detectors are not single crystalline and are much less expensive than any of the spectroscopic detectors but they have very poor energy resolution.

### Thermal Neutron Detectors

Current thermal neutron detectors include gas detectors, scintillators, and semiconductors coated with a thin layer of thermal neutron capturing material (Gd, $^{10}$B, $^{6}$Li). Gas detectors perform well but are expensive and need to be relatively large for good detection efficiency. $^{3}$He proportional counters are the current standard thermal neutron detector. They have been thoroughly optimized and their cost is unlikely to be reduced. Scintillators loaded with neutron absorbers are sensitive to gamma background. Existing solid-state neutron charge collection detection technologies include semiconductors coated with neutron absorbing films. Because the reaction occurs on the surface, the detector collects some variable small fraction of the incident energy, and is therefore sensitive to the gamma-background.

### Fast Neutron Detectors

At present energy resolution for fast neutrons is usually performed using time of flight techniques. These methods work well in a laboratory environment but because of their complexity are not well suited for most field applications. The neutron energy resolution required for practical threat identification is not available using today's liquid scintillator detectors.

## Importance to LANL's Science and Technology Base and National R & D Needs

Because γ-rays and neutrons are sufficiently penetrating to allow detection of nuclear materials at significant distances, γ-ray and neutron detection plays an essential role in approaches to identify special nuclear mate-

rials and radiological sources that could pose an unconventional threat. But the detectors currently used as portal or distributed monitors have limited isotopic identification capability, resulting in excessive false alarms. We investigated materials for three classes of detectors; 1) γ-ray, 2) thermal neutron, and 3) fast neutron detectors. 1) Energy resolving γ-detectors are an important approach to isotope identification, but currently inexpensive γ-detectors that operate at room temperature do not have the energy resolution required for precise and reliable isotope identification. *There is a need for γ-detector materials with good energy resolution that can be fabricated inexpensively and operated at room temperature.* 2) The thermal neutron background is small and detection of significant thermal neutrons is a strong indication of radiological threats. But because the γ-ray background is typically 4-5 orders of magnitude larger that of thermal neutrons, strong discrimination against γ-ray events in thermal neutron detectors is a major challenge. *There is a need for sensitive thermal neutron detector materials with high rejection for γ-ray background events.* 3) Detectors capable of energy resolving fast neutrons would have many applications. For example, fast neutron spectroscopy is a possible method for rapid explosive screening. Currently neutron energy spectroscopy is done using time of flight (TOF) and liquid scintillator approaches. TOF works well in a laboratory environment but because of its complexity is not well suited for field applications. Liquid scintillators suffer from poor energy resolution. *There is a need for energy resolving fast neutron detector materials.*

## Scientific Approach and Accomplishments

### Exciton generation and charge extraction in nanoparticles

Carrier energy in excess of the energy gap ($E_g$) of a bulk-phase semiconductor is efficiently dissipated as heat in the form of phonons. However, provided that at least $1E_g$ of excess energy is present in a carrier (either an electron or a hole) it is also feasible for that carrier to relax to the band edge via excitation of a valence band electron across the energy gap. This process, generically termed "carrier multiplication" (CM), can significantly improve radiation detector performance if it could be made to be efficient. While CM is not efficient in bulk phase semiconductors due to strict requirements of simultaneous conservation of both energy and translational momentum, we have experimentally demonstrated that it becomes efficient in semiconductor nanocrystals (NCs). Specifically, we have developed an ultrafast transient absorption method in which we can directly monitor the production of multiple excitons (electron-hole pairs) following excitation with a single photon of sufficiently high energy. Using this technique we have found that NCs produce multiple excitons (up to 7) in response to excitation in the range of 2.0 to >6.2eV with efficiencies that are limited only by energy conservation. We have shown that this process is broadly general to a variety of NC material systems.

A significant challenge to the utilization of the CM effect in radiation detection is the process of Auger recombination. In this process, which is the inverse of CM, an exciton non-radiatively recombines by transferring its energy to another carrier. Auger recombination typically occurs on time scales of tens to hundreds of picoseconds in NCs. This provides a limit on time available for extraction of multiple carriers or excitons from an excited NC. We have demonstrated that in assemblies consisting of NCs and small molecules the charge can be extracted from a photoexcited NC within ~5ps, which is significantly faster than Auger recombination time. This encouraging result suggests that the CM effect can be utilized in practical radiation detection.

### Modeling electronic processes in nanoparticles

We investigated electron-hole pair generation by energetic charged particles in semiconductor nanocrystals. We are particularly interested in the role of collective excitations such as plasmons on this process. In bulk metals, plasmon generation is the dominant energy loss mechanism for energetic charged particles. The plasmons subsequently decay into electron-hole pairs. The standard theoretical model to describe charged particle energy loss in bulk metals is called the "jellium" model. The properties of charged particle energy loss are described by studying the dielectric properties of this model. There are two basic differences between the well-understood case of bulk metals and the semiconductor nanocrystals that we investigated: a) finite size effects in the nanocrystals, and b) the energy gap in these semiconducting materials. The finite size effects mix longitudinal (such as charged particle) and transverse (such as photon) excitation. To investigate the finite size effects we have studied the dielectric properties of finite sized spheres and ellipses in a jellium like model. The effect of the semiconducting energy gap was incorporated by investigating the "Penn" model which is a generalization of the jellium model introducing an energy gap. We have completed a series of calculations of the dielectric properties of the bulk materials described by the Penn model and will generalized these calculations to finite spheres and ellipses.

We developed a theoretical model for photoluminescense of nanoparticles and identified the nanophosphor YSO:Ce

($Y_2SiO_5$ doped with Ce) as a model system to benchmark our theory. The nano YSO has the potential of increased light output and reduced afterglow over bulk YSO by roughly 50%. Understanding the nature of this increased performance requires modeling of the relaxation processes of the excitations at the $Ce^{3+}$ luminescent site in the presence of traps, such as O vacancies. Defects and traps delay or block the relaxation of an excited Ce site, thus hampering the radiative relaxation process and the measured light output. Most luminescence efficiency models have focused on bulk systems with luminescent sites (donors) on a regular crystal lattice and defects or traps (acceptors) as substitutional or interstitial ions, while nano and bulk YSO:Ce, as well as quantum dots, are in the opposite limit. Our model calculations successfully described the time evolution of the photoluminescense in nano YSO:Ce at room temperature. We identified two characteristic excitation transfer lifetimes with nanosecond dynamics and a very slow afterglow lifetime in the domain of minutes. The nanosecond dynamics of the decay of the photoluminescence signal can be described by a fast (~1 ns) contribution originating from the transfer of a donor to a nearby acceptor and a longer lifetime (~34 ns) that is comprised of a combination of the intrinsic radiative lifetime and donor-donor equilibration.

**Electron beam measurements of radiation detector materials**

To address relevant physical processes in new materials for gamma detection we first had to solve a fundamental technical hurdle. Gammas interact weakly with materials, requiring impractically large test material volume. When gammas interact with materials they produce high energy electrons. By using an electron beam to excite radiation detector test materials, we addressed the essential physics with research scale quantities of material. We have demonstrated this technique on two classes of materials systems: colloidal inorganic quantum dot (qdot)/polymer composites, and metal-organic/polymer composites.

We demonstrated a factor of two improvement in the light yield of a processable scintillator by incorporation of CdSe/ZnS core/shell quantum dots. High energy electrons transfer energy to the detection material via Coulomb interactions that scale with electron density. The energy required to produce an excitation in the qdot (~3 eV) is expected to be much lower than in organic materials (~ 30 eV). We studied a composite scintillator that uses a luminescent polymer as the organic semiconductor host. We measured the optical properties of the composite and demonstrated that Förster excitation transfer occurs from the qdot to the polymer. We demonstrated improved scintillation performance under electron-beam excitation using the cathodoluminescence (CL) attachment of a scanning electron microscope, Figure 1. These scintillation results were interpreted using a theoretical model for the composite-material detector performance.

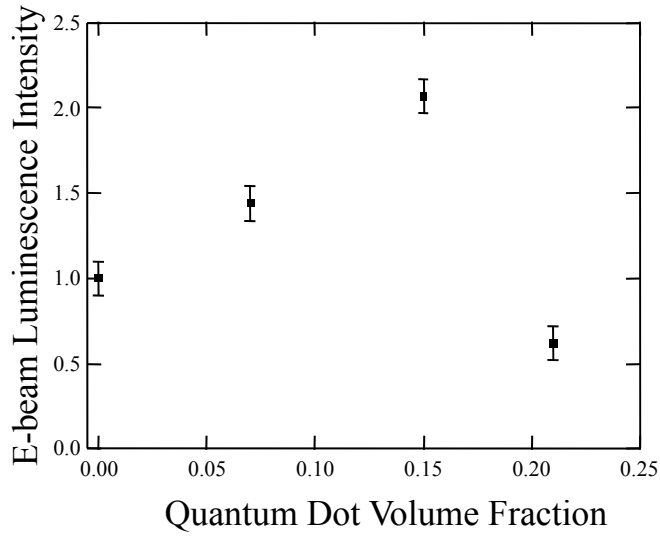


*Figure 1. Cathodoluminescence (CL) intensity as a function of quantum dot fraction, measure relative to CL intensity at quantum.*

We demonstrated large bulk photoconductive gain, greater than 100, in organic polymer diodes. Photoconductive gain was measured in diode structures employing the soluble polymer MEH-PPV as the active layer. The MEH-PPV layer was either undoped or doped by incorporating a soluble C60 derivative or PbSe quantum dots. We determined the spectral response, transient response, and bias dependence of the gain. The photoconductive gain is due to the circulation of hole carriers through the diode in response to electrons trapped in the polymer layer. These results demonstrated that organic polymer diodes are valuable for reading out scintillators used for gamma ray detection.

We demonstrated novel processable scintillators incorporating phosphorescent molecules, with light yields a factor of 3 larger than typical plastic scintillators. We demonstrated improved light yield from plastic scintillators utilizing a phosphorescent dopant to collect both singlet and triplet excitations created by ionizing radiation using poly-vinyltoluene and poly-9-vinylcarbazole doped with an Ir phosphor, Figure 2. The spectral, temporal, and integrated yield responses to pulses of 10 keV electrons were measured as a function of dopant concentration. Both doped plastics yield a maximum light output of 200% of anthracene with decay times of 850 ns. High light yield was obtained for Ir element fractions up to 10 wt %, demonstrating that these scintillators are advantageous for gamma detection.

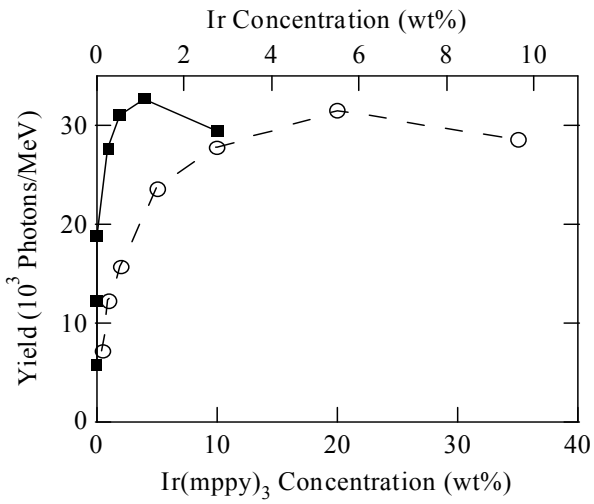


*Figure 2. Yield for PVT and PVK scintillators as function of phosphorescent molecule and Ir wt%.*

**Neutron detector materials**

We evaluated two wide-band-gap lithium-containing materials lithium niobate and lithium tantalate, $LiNbO_3$ and $LiTaO_3$ as thermal neutron detection materials. We used natural lithium materials for convenience, but isotopically enriched $^6$Li can be used when needed. The detector efficiency, which includes allowing for the lithium atoms in the bulk and not on a surface, for thermal neutrons in $LiNbO_3$ is calculated to be above 80% for a thickness 1 mm, which is comparable to a 1 inch diameter $^3$He tube. The possible impact of pyroelectric charge, and its subsequent sparking, was evaluated and found to be negligible for radiation detection applications because we put on metal electrodes and regulate the voltage. Non stoichiometry was found to be a major source of intrinsic point defects. The process of vapor transport equilibration (VTE) is a commercial process to fill the lithium vacancies, and it produces commercially available stoichiometric crystals. Various samples of doped and undoped material have been obtained from different vendors and tested. We found that we could reduce defects with heat treatments in hydrogen or iodine. Electron paramagnetic resonance (EPR), electro and optical absorption, and internal fields measurements have been performed to select samples for photoconductivity and time-of-fight measurements. We submitted an invention disclosure for lithium niobate used as a thermal-neutron detector, and the US DOE accepted it to file for a patent.

**Detector characterization**

We re-evaluated the basis for estimates of the theoretical limit of scintillator performance, based on the theoretical framework adopted in the literature. We found by correcting assumptions for limiting yield and neglect of the Fano factor for scintillators that scintillator performance can be competitive with higher purity Ge performance. In order to achieve this, a low energy/band gap material with minimal energy loss mechanisms must be produced. In addition, high quantum efficiency photo-detectors, such as photodiodes, are necessary to fully exploit the Fano factor. Carrier multiplication in semiconductor nanocrystals will increase the limiting yield, thus improving the Fano factor. An experiment to verify these calculations involves the use of calibrated PMT's with different photo-cathode quantum efficiency in order to measure absolute light yield magnitude and variance. This experiment is being completed under DOE/NA-22 funding. We implemented a Compton coincidence spectrometer to measure scintillator linearity. The novel feature of our spectrometer is the addition of a time resolved capability achieved by digitizing each pulse from the scintillator. A measurement of a solution of semiconductor nanocrystals has been made and analyzed.

## Publications

Alexandrov, B. S., K. D. Ianakiev, and P. B. Littlewood. Branching transport model of alkali halide scintillators. *Journal of Applied Physics.*

Campbell, I. H., and B. K. Crone. Quantum-dot/organic semiconductor composites for radiation detection. 2006. *Advanced Materials.* **18** (1): 77.

Campbell, I. H., and B. K. Crone. Efficient plastic scintillators utilizing phosphorescent dopants. *Applied Physics Letters.* **90** (1): 012117.

Campbell, I. H., and B. K. Crone. Efficient, visible organic light emitting diodes utilizing a single polymer layer doped with quantum dots. 2008. *Applied Physics Letters.* **92** (4): 043303.

Ianakiev, K. D., and B. S. Alexandrov. Temperature behavior of NaI (Tl) scintillation detectors. To appear in *Nuclear Insurmentation and Methods.*

Klimov, V. I.. Mechanisms for photogeneration and recombination of multiexcitons in semiconductor . 2006. *Journal of Physical Chemistry B.* **110** (34): 16827.

Schaller, R. D., M. Sykora, J. M. Pietryga, and V. I. Klimov. Seven excitons at a cost of one: Redefining the limits for conversion efficiency of photons into charge carriers. 2006. *Nano Letters.* **6** (3): 429.

Schaller, R. D., and V. I. Klimov. Non-Poissonian exciton populations in semiconductor nanocrystals via carrier multiplication. 2006. *Physical Review Letters.* **96** (9): 097402.

Sykora, M., M. A. Petruska, J. Alstrum-Acevedo, I. Bezel, T. J. Meyer, and V. I. Klimov. Photoinduced Charge Transfer Between CdSe Nanocrystaline Quantum Dots and Ru-polypyridine Complexes. 2006. *Journal of the American Chemical Society.* **128** (31): 9984.

# Advancing the Chemistry Material Science and Theoretical Understanding of Actinides

*Albert Migliori*

20061471DR

## Abstract

With the NNSA's designation of Los Alamos National Laboratory (LANL) as a plutonium center of excellence, extensive coordination of actinide science, engineering, and manufacturing will be needed. This program will enhance LANL's capabilities in actinide science through creative research in advanced actinide chemistry, actinide materials science, and theoretical understanding of actinide electronic structure. Innovative research has been conducted into new forms of chemical bonding, new kinds of reactivity, and creative new ways to study covalency in actinide bonding that is crucial to advanced fuel cycle research. We also performed state-of-the-art studies on actinide materials properties to gain insight into how strongly correlated electrons impart important properties to actinide materials, and how some new actinide materials can be resistant to radiation damage. All of these areas are important to understanding actinide behaviors in nuclear fuels, nuclear weapons, and environmental behavior in support of DOE and Laboratory missions. This research was conducted entirely by postdoctoral fellows who represent the next generation of actinide scientists and engineers.

## Background and Research Objectives

Knowledge of actinide science continues to be essential to the United States and central to the mission of the DOE and its laboratories, including nuclear weapons, energy security, nuclear safeguards, nonproliferation, environmental restoration, and radioactive waste management. With nuclear weapons technology continuing to play a key role in defense policy for the foreseeable future, knowledge and expertise in the production, processing, purification, characterization, analysis, and disposal of actinide elements is essential to U.S. national security. The purpose of the Seaborg Institute is to provide a focus for actinide science at Los Alamos, to develop and maintain U.S. pre-eminence in actinide science and technology, and to help provide an adequate pool of scientists and engineers with the quality and breadth to meet the challenging and changing needs of the nation. This objective of this research program was to conduct fundamental research in broad areas of theory and modeling, new materials, and actinide chemistry in order to train the next generation of actinide scientists.

## Importance to LANL's Science and Technology Base and National R & D Needs

This project has enhanced our national security mission environment and the evolution of actinide (An) science and technology. The science developed in this project is applicable to national security, stockpile stewardship, reducing global nuclear threats, and can help lead to sustainable nuclear energy. Los Alamos strengths in actinide chemistry, material synthesis, condensed matter physics, complex systems, emergent phenomena, and theory and modeling provide a world-class foundation from which we developed new science. Knowledge and expertise in actinide science is central to the mission of DOE and the NNSA, including national defense, energy security, environmental restoration, and radioactive waste management. By developing new syntheses of novel actinide materials, and understanding how to control material properties and emergent phenomena, researchers can begin to tailor unique properties of actinide materials for new applications. Examples include the development of advanced nuclear fuels, new ways to purify and process Pu, self-healing materials for long-term storage of nuclear wastes, corrosion-resistant alloys for enhanced safety, bioremediation of contaminated sites, and the selective separation of actinides from spent nuclear fuels.

## Scientific Approach and Accomplishments

This project supported only postdoctoral fellows in many areas of actinide science, focusing on the three

main areas of theory and modeling, new materials, and actinide chemistry. We summarize briefly the achievements of many of the postdoctoral fellows working on various subtasks of this project, broken down into the three main areas of focus.

**Theory and Modeling**

Theoretical modeling of nanoscale heterogeneity in Pu/U alloys and oxides, David Andersson, is focused on actinide dioxides derived from the $AnO_2$ fluorite lattice because they are of high technological relevance due to their application in nuclear reactor fuels. Oxidation of $AnO_2$ compounds emerges as a central theme in all use scenarios. The present work used density functional theory calculations to study the oxidation of uranium, neptunium and plutonium dioxides, $AnO_2$ (An = U, Np or Pu), in $O_2$ and $O_2/H_2O$ environments. The calculations demonstrate that the stability of these clusters is an effect of the increased hybridization between actinide ions and excess oxygen ions that is enabled by their particular geometry (Figure 1).

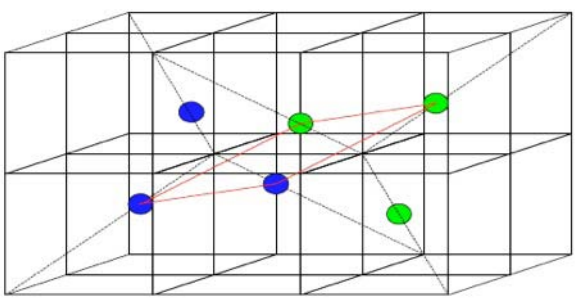

*Figure 1. Green/blue atoms constitute two split di-interstitial O clusters that together form a bound state, the so-called split quad-interstitial. These clusters are the fundamental building block of a range of nano-scale structure patterns in $UO_{2+x}$. The cubes represent the simple-cubic oxygen sublattice in $UO_2$.*

The δ to α transformation pathway in Pu was studied using empirical potentials by Roman Groger. The mechanism responsible for the phase transformation between the high temperature fcc δ phase of Pu and the low temperature monoclinic phase represents an outstanding problem the elucidation of which will significantly contribute to an understanding of the physics of this important metal. This research project used the MEAM (modified embedded atom method) for Pu to investigate which of the intermediate phases is energetically more favorable. This required a new empirical potential that will explicitly account for strong directionality of bonds due to the incompletely filled *f* orbitals.

**Chemistry**

Plutonium biogeochemistry studies by Alison Costello concentrated on the stabilization and potential remediation of Pu contaminated site**s** by a detailed study of the processes and factors affecting Pu speciation and mobilization under environmental conditions. The studies indicate that certain microbes enzymatically reduce Pu(VI)/Pu(V), producing insoluble biogenic plutonium oxides. Characterization of the biogenic $PuO_2$ show the solids are deposited on the cell surface as crystalline nano-particulates and are structurally homologous to synthetic $PuO_2$.

5*f* –Element coordination chemistry was studied by Andrew Gaunt in reference to the key separation problem of the Advanced Nuclear Fuel Cycle, removal of actinides from lanthanides and other fission products. Research focused on isolating a series of actinide complexes that were compared both with each other and to related lanthanide complexes. This research provided an unprecedented systematic study of isostructural trivalent *f*-element complexes with soft donor atom ligands. The results consistently demonstrate shorter An-E than Ln-E bonds and for the first time provide a pattern and trend that supports a modest enhancement of covalency in An(III) vs Ln(III) bonding.

Multiple metal-ligand bonding in the actinides was studied by Trevor W. Hayton. This topic is of great interest because the information uncovered may lead to a better understanding of the nuclear fuel cycle. The task resulted in successful synthesis of the first imido analogues of the uranyl ion (Figure 2). These complexes are true analogues of uranyl; they exhibit a linear N-U-N arrangement, extremely short U-N bonds, and the bis(imido) fragment is difficult to disrupt. This work resulted in a publication in *Science* which was awarded an honorable mention in the *2007 Postdoctoral Prize in Experimental Sciences* competition at LANL.

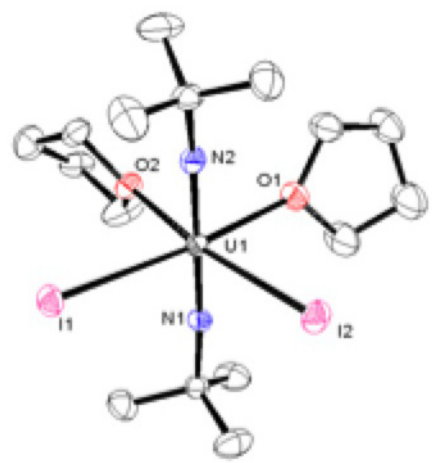


*Figure 2. Solid-state molecular structure of U(NtBu)2I2(THF)2*

Factors affecting the stability of the imido ligand were explored by Robyn Gdula who showed that aromatic groups stabilize the uranium-nitrogen multiple bond, but that aliphatic groups result in reduction to U(V).

The unique bonding in uranium-nitrogen multiple bonds was explored by Liam Spencer who reported the syntheses of

bis(imido) $[U(NR)_2]^{2+}$ and oxo-imido $[U(NR)(O)]^{2+}$ ions which possess many of the bonding features found in $UO_2^{2+}$. His current research with these ions has focused on important questions pertaining to the reactivity of the imido ligands in the $[U(NR)_2]^{2+}$ ion and how this reactivity differs from transition metal imido analogues, and 4) f-orbital communication in dinuclear bis(imido) U(V) complexes. This $f^1$-$f^1$ system displays antiferromagnetic coupling between U(V) centers. This is a rare and important discovery that demonstrates f-electron communication between actinide metal centers.

Peroxide enhanced partitioning of SNF (spent nuclear fuel) in alkaline solutions was studied by George Goff by designing an innovative approach to reprocess SNF. A separations approach based on the different speciation and solubilities would be revolutionary. The approach uses an alkaline carbonate-peroxide system with major benefits over conventional technologies: 1) the efficient removal of the heat-loading isotopes early in the process 2) the high affinity of peroxide to control metal separation; 3) a reduction in the number and complexity of the treatment processes, 4) the minimization of secondary organic solvent waste, and 5) the flexible group separation of Np, Pu and Am/Cm.

Terminal molecular uranium nitrides were explored by Robert Thomson. Uranium nitride $[U{\equiv}N]_x$ is a very promising alternative to uranium dioxide $[UO_2]_x$, which has traditionally been used as the fuel source in nuclear reactors. While the uranyl ion $[O{\equiv}U{\equiv}O]^{2+}$ and uranium imide complexes (U=NR) have been heavily studied, very few uranium nitrides (U≡N) are known, with only one report of a multimetallic molecular system, and no known terminal nitrides. Two main pathways into uranium nitrides are under investigation, one involving azide complexes, and the other employing reactive imides. The first pathway has focused around the generation of well-defined uranium azide complexes ($U\text{-}N_3$) using TMS-F elimination, and the conversion of these azide species ($U\text{-}N_3$) into nitride complexes (U≡N). The second pathway used to access U nitride complexes involves the generation of reactive imide complexes (U=N-R), where the N-R bond can be cleaved under the appropriate conditions.

**Materials**

Magnetoresistance has been studied by Susan Cox in charge-density-wave systems because it is important to improve our understanding of CDWs in uranium. A particular puzzle has been the electrically-insulating phase of colossal magnetoresistance materials. The results show that instead, the electrons collectively form a wave-like entity, known as a charge-density wave (CDW). It was established that the transition in manganites is second order, and is accurately modeled as a Peierls in contrast to the previously accepted picture of charges localized at atomic sites. The effects of disorder on the heat capacity of a charge-density wave have also been seen in U. The work overturns a traditional view, and suggests instead that the transition is driven mainly by a Fermi- surface instability. This result adds to the growing body of evidence that the colossal magnetoresistance present in manganites is driven by the delicate balance between the ferromagnetic and stripe phase.

Strongly correlated electron materials studied by Sonia Francoual in the proximity of a quantum critical point (QCP) give rises to novel ground states such as magnetism, unconventional forms of superconductivity and non Fermi liquid (NFL) behaviors. The actinide alloy $URu_2Si_2$ shows the attributes of quantum criticality. She addresses the consequences of Rhenium doping on the reentrant ordering around the QCP. The experimental approach consists of investigating the magnetization and magnetoresistance properties in $URu_{2-x}Re_xSi_2$ single-crystals at several different values of the Rhenium content at low temperatures in pulsed high magnetic fields.

Actinide dioxide benchmark calculations were made by Lindsay Roy. It was shown that screened hybrid DFT mimics the photoemission spectrum (PES) for $UO_2$. The total and projected density of states are compared with the experimental photoemission spectrum in Figure 3. The peak positions and bandwidths are in good agreement between calculation and experiment.

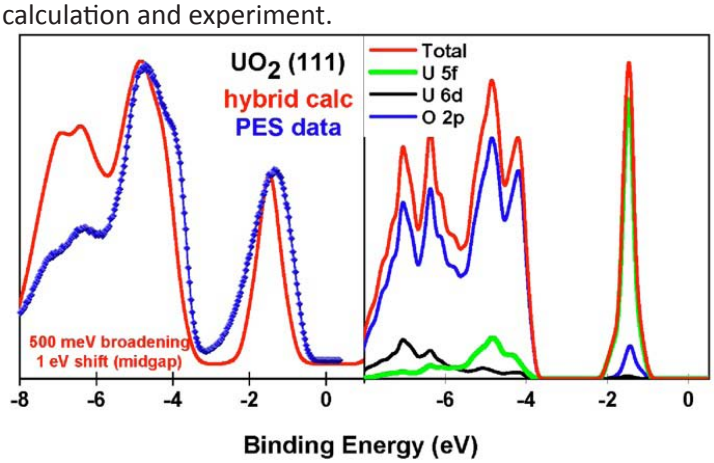


*Figure 3. Experimental PES and the spin polarized DOS for the AFM ground state for $UO_2$ is shown on the left. The right panel depicts the total and partial DOS for $UO_2$ calculated using the HSE functional and scalar relativistic effects.*

Covalency within 4*f*-element complexes was studied by Andrew Sutton. The sharing of two electrons between elements to form a covalent bond is a fundamental concept and the simplest way to envisage a chemical bond. In 4*f*-element chemistry, it has been long believed that bonding is primarily electrostatic with the valence *f*-orbitals being core-like and hence unable to overlap effectively with ligand orbitals. In order to probe the existence and extent of Ln covalency, the aim of this project is to synthesize a range of lanthanide complexes exhibiting a multiple bond to a ligand. A new range of cerium metallocycle complexes have been synthesized and will be used in a comparative oxygen

K-edge XAS study to elucidate the nature of the Ce-O bond.

Thermodynamic measurements of actinides were explored by Yoko Suzuki. Actinides in general have very complicated bonding structures associated with 5 f electrons. Pu is particularly interesting because it goes through many structural phases as temperature increases between 0 to 906 K. Measurements of the temperature dependence of the elastic moduli of alpha and delta Pu show extreme softening on warming by an order of magnitude more than expected for ordinary metals with similar Debye temperatures. Thermal vibrational amplitude, not volume, appears to be a strong candidate for the parameter that drives electron localization.

Radiation damage effects in uranium-bearing δ-phase oxides were studied by Ming Tang. This task involves the synthesis and fabrication of complex ceramic oxide samples, which are fluorite structural derivatives of compounds with stoichiometries near to $M_7O_{12}$, namely, the so-called δ-phase, made from mixtures of uranium oxide (both $UO_2$ and $UO_3$) and sesquioxide compounds such as $Y_2O_3$. Certain δ-phase oxides have been confirmed to be extraordinarily radiation tolerant; in particular, they are especially resistant to amorphization transformations. This task accomplished significant advances regarding investigations of radiation damage effects in fluorite derivative uranium (U) bearing oxides, including: (1) synthesis and fabrication of δ-phase U-bearing oxides ($Y_6U_1O_{12}$, $Gd_6U_1O_{12}$, $Ho_6U_1O_{12}$, $Yb_6U_1O_{12}$, $La_6U_1O_{12}$, $Lu_6U_1O_{12}$) and the RhII-structured compound, $Y_6U_2O_{15}$ and (2) irradiation and characterization of d-$Y_6U_1O_{12}$ and RhII-$Y_6U_2O_{15}$. Experimental results reveal that no irradiation-induced amorphization was observed all these Kr irradiated uranium-bearing δ-phase compounds even at very high radiation dose ~ 50 displacements per atom (dpa), while the tungsten δ-phase compounds became amorphous at the similar irradiation dose. Ultimately, we strive to discover radiation tolerant ceramics unbeknownst to the scientific community and to develop these materials for application in hostile, radiation environments, especially as actinide hosts for advanced nuclear fuels or wastes.

Theoretical study on understanding of bonding interactions was done by Ping Yang. Research focused on theoretical study on understanding of bonding interactions and chemical behavior between actinides using modern density functional theory (DFT) and time-dependent density functional theory (TDDFT). Excellent agreement is obtained between DFT calculated structure and crystal structures for both thorium and uranium fluoroketimides. The theoretically predicted low-lying excited states are consistent with experimental low-temperature luminescence spectroscopic data. This consistency between theory and experiment is also observed in high energy core excitation of various ligands, where the electrons in the inner shell of atoms are excited. The calculations also predicted the antiferromagnetic coupling of a dimeric bis(imido) uranium iodide complex, which was verified by magnetic susceptibility measurements.

## Publications


Andersson, D. A., C. Deo, and B. P. Uberaga. Di-interstitial oxygen clusters and oxygen transport in UO2+x.

Andersson, D. A., J. Lezama, B. P. Uberaga, and S. D. Conradson. Co-operativity among defect sites in AnO2+x and An4O9 (An = U, Np or Pu).

Cantat, T., C. R. Graves, K. C. Jantunen, B. L. Scott, E. J. Schelter, C. J. Burns, P. J. Hay, D. E. Morris, and J. L. Kiplinger. Evidence for the involvement of 5f-orbitals in the bonding and reactivity of organometallic actinide compounds: thorium(IV) and uranium(IV) bis(hydrazonato) complexes. *Journal of the American Chemical Society.*

Chia, E. M., D. Talbayev, B. C. Sales, D. Mandrus, A. J. Taylor, and R. D. Averitt. Coupling between phonons and the hybridization gap in a d-electron Kondo lattice. To appear in *Physical Review letters.*

Chia, E. M., H. J. Lee, N. Hur, E. D. Bauer, T. Durakiewicz, R. D. Averitt, J. L. Sarrao, and A. J. Taylor. Quasiparticle Relaxation across a Spin Gap in the Itinerant Antiferromagnet UNiGa5 . 2006. *Physical Review B.* **74**: 140409R.

Chia, E., H. J. Lee, N. Hur, N. O. Moreno, R. D. Averitt, J. L. Sarrao, A. J. Taylor, and J. -X. Zhu. Quasiparticle dynamics in the spin-density wave state,. *Physical Review letters.*

Chia, E., J. -X. Zhu, D. Talbayev, I. -S. Jo, K. -H. Oh, S. -I. Lee, R. D. Averitt, and A. J. Taylor. Ultrafast observation of a competing order in a high-Tc superconductor. 2007. *Physical Review letters.* **99**: 147008.

Clarke, A.. Shape memory effect deformation structures in a uranium-niobium alloy. 2007. *Actinide Research Quarterly.* **3rd quarter**: 20.

Cox, S.. Heat capacity and the good old days of uranium . 2007. *Actinide Research Quarterly.* **4th quarter**: 12.

Cox, S., E. Rosten, R. D. McDonald, and J. Singleton. Comment on: Pinning frequencies of the collective modes in alpha-uranium . 2007. *Physical Review letters.* **98**: 249701.

Cox, S., J. C. Lashley, E. Rosten, J. Singleton, A. J. Williams, and P. B. Littlewood. Evidence for the charge-density-wave

nature of the stripe phase in manganites. 2007. *Journal Phys Cond Mat.* **19**: 192201.

Cox, S., J. C. Loudon, A. J. Williams, J. P. Atttfield, J. Singleton, P. A. Midgley, and N. D. Mathur. Very weak electron-phonon coupling and strong strain coupling in manganites. 2008. *Phys Rev B.* **78**: 035129.

Cox, S., J. Singleton, R. D. McDonald, A. Migliori, and P. B. Littlewood. Sliding charge density wave in manganites. 200. *Nature Materials.* **7**: 25.

Cox, S., R. D. McDonald, M. Armaniaus, P. Sengupta, and A. Paduan-Filho. Unusual magneto-optical phenomenon reveals low energy spin dispersion in spin-1 Heisenberg antiferromagnetic chain system NiCl2-4SC(NH2)2. 2008. *Phys Rev Lett.* **101**: 087602.

Francoual, S.. The effects of rhenium doping on the temperature-versus-high magnetic field phase diagram of URu2Si2 . 2007. *Actinide Research Quarterly.* **3rd quarter**: 5.

Gaunt, A. J., B. L. Scott, and M. P. Neu. Isolation of a molecular actinide-tellurium bond: Comparison of MIII[N(TePiPr2)2]3 (M = U, La) illustrates bonding differences between 4f and 5f Ions. 2006. *Angewandte Chemie: International Edition.* **45**: 1638.

Gaunt, A. J., B. L. Scott, and M. P. Neu. U(IV) chalcogenolates synthesized via oxidation of uranium metal by dichalcogenides. 2006. *Inorganic Chemistry.* **45**: 7401.

Gaunt, A. J., S. D. Reilly, A. E. Enriquez, B. L. Scott, J. A. Ibers, P. Sekar, K. I. M. Ingram, N. Kaltsoyannis, and M. P. Neu. Experimental and theoretical comparison of bonding differences between An(III) and Ln(III) ions of similar radii in M[(N(EPPh2)2)]3 (M = U, Pu, La, Ce; E = S, Se) and M[N(EPiPr2)2]3 (M = U, Pu, La, Ce; E = S, Se, Te). 2008. *Inorganic Chemistry.* **47**: 29.

Gaunt, A. J., S. D. Reilly, A. E. Enriquez, B. L. Scott, and M. P. Neu. Structural characterization of Pu[N(SiMe3)2]3: a synthetically useful plutonium(III) precursor. 2008. *Inorganic Chemistry.* **47**: 26.

Gaunt, A. J., S. D. Reilly, A. E. Enriquez, T. W. Hayton, J. M. Boncella, B. L. Scott, and M P. Neu. Low-valent molecular plutonium halides . 2008. *Inorganic Chemistry.* **47**: 8412.

Gaunt, A. J., S. D. Reilly, T. W. Hayton, B. L. Scott, and M. P. Neu. An entry route into non-aqueous plutonyl coordination chemistry. 2007. *Chemical Communications.* : 1659.

Gdula, R.. Probing the nature of uranium-ligand multiple bonds. 2007. *Actinide Research Quarterly.* **3rd quarter**: 18.

Goddard, P. A., J. Singleton, C. Maitland, S. J. Blundell, T. Lancaster, P. J. Baker, R. D. McDonald, S. Cox, P. Sengupta, J. L. Manson, K. A. Funk, and J. A. Schlueter. Isotope effect in quasi-two-dimensional metal-organic antiferromagnets. *Phys Rev B.*

Goddard, P. A., J. Singleton, P. Sengupta, R. D. McDonald, T. Lancaster, S. J. Blundell, F. L. Pratt, S. Cox, N. Harrison, J. L. Manson, H. I. Southerland, and J. A. Schlueter. Experimentally determining the exchange parameters of quasi-two-dimensional Heisenberg magnets. 2008. *New Journal of Physics.* **10**: 083025.

Goff, G. S., L. F. Brodnax, M. R. Cisneros, S. M. Peper, S. E. Field, B. L. Scott, and W. H. Runde. First identification and thermodynamic characterization of the ternary U(VI) species, UO2(O2)(CO3)24-, in UO2-H2O2-K2CO3 solutions. 2008. *Inorganic Chemistry.* **47** (6): 1984.

Goff, G. S., M. Cisneros, C. Kluk, K. Williamson, B. Scott, L. Brodnax, and W. Runde. Synthesis, spectroscopy, and structural comparison of Ln(III)(CO3)45- in carbonates of the light and heavy rare earth elements. *Inorganic Chemistry.*

Graves, C. R., A. E. Vaughn, B. L. Scott, E. J. Schelter, J. D. Thompson, D. E. Morris, and J. L. Kiplinger. Probing the chemistry, electronic structure and redox energetics in pentavalent organometallic actinide complexes. *Inorg Chem.*

Graves, C. R., B. L. Scott, D. E. Morris, and J. L. Kiplinger. Tetravalent and pentavalent uranium acetylide complexes prepared by oxidative functionalization with Cu-C⍰C-Ph. 2008. *Organometallics.* **27**: 3335.

Graves, C. R., D. E. Morris, B. L. Scott, and J. L. Kiplinger. Pentavalent Uranium-Imido Complexes. *Inorganic Syn..*

Graves, C. R., D. E. Morris, B. L. Scott, and J. L. Kiplinger. Facile access to pentavalent uranium organometallics: one electron oxidation of uranium(IV) imido complexes with copper(I) salts. 2007. *Journal of the American Chemical Society.* **129**: 11914.

Graves, C. R., E. J. Schelter, T. Cantat, B. L. Scott, and J. L. Kiplinger. A mild protocol to generate mixed-ligand uranium(IV) metallocene complexes using copper(I) iodide. 2008. *Organometallics.* **27**: ASAP.

Graves, C. R., P. Yang, A. E. Vaughn, D. L. Clark, S. D. Conradson, E. J. Schelter, B. L. Scott, J. D. Thompson, P. J. Hay, D. E. Morris, and J. L. Kiplinger. Organometallic uranium(V)-imido halide complexes: from synthesis to electronic structure and bonding. 2008. *Journal of the American Chemical Society.* **130**: 5272.

Graves, C. R., P. Yang, S. A. Kozimor, A. E. Vaughn, D. L. Clark, S. D. Conradson, E. J. Schelter, B. L. Scott, J. D. Thompson, P. J. Hay, D. E. Morris, and J. L. Kiplinger. Systematic studies of organometallic uranium(V)-imido halide complexes. 2008. *Journal of the American Chemical Society.* **130**: 4272.

Groger, R.. Chain-of-states atomistic calculations of the pathways and energetics of structural phase transformations in plutonium. 2007. *Actinide Research Quarterly.* **3rd quarter**: 11.

Groger, R., T. Lookman, and A. Saxena. Atomistic studies of transformation pathways and energetics in plutonium. *Philos Mag.*

Hayton, T. W., J. M. Boncella, B. L. Scott, E. R. Batista, and P. J. Hay. Synthesis and reactivity of the imido analogues of the uranyl ion. 2006. *Journal of the American Chemical Society.* **128** (32): 10549.

Hayton, T. W., J. M. Boncella, B. L. Scott, and E. Batista. Exchange of an imido ligand in bis(imido) complexes of uranium. 2006. *Journal of the American Chemical Society.* **128**: 12622.

Hayton, T. W., J. M. Boncella, P. D. Palmer, B. L. Scott, E. R. Batista, and P. J. Hay. Chemistry: Synthesis of imido analogs of the uranyl ion . 2005. *Science.* **310**: 1941.

Hilton, D. J., R. P. Prasankumar, E. J. Schelter, V. K. Thorsmolle, S. A. Trugman, A. K. hreve, J. L. Kiplinger, D. E. Morris, and A. J. Taylor. Ultrafast spectroscopy of the uranium(IV) and thorium(IV) bis(ketimide) complexes (C5Me5)2An[-N=C(Ph)(CH2Ph)]2 (An = Th, U). 2008. *J Phys Chem A.* **112**: 7840.

Kiplinger, J. L., B. L. Scott, E. J. Schelter, and J. A. Pool Davis Tournear. Sp3 versus Sp2 C-H bond activation chemistry of 2-picoline by Th(IV) and U(IV) metallocene complexes. 2007. *J alloys compd.* **444-445**: 477.

Kiplinger, J. L., J. A. Pool, E. J. Schelter, J. D. Thompson, B. L. Scott, and D. E. Morris. Actinide-Mediated Cyclization of 1,2,4,5-Tetracyanobenzene: Synthesis and Characterization of Self-Assembled Trinuclear Thorium and Uranium Macrocycles. 2006. *Angew Chem Int Ed.* **45**: 2036.

Melfi, P. J., S. K. Kim, J. T. Lee, F. Bolze, D. Seidel, V. M. Lynch, J. M. Veauthier, A. J. Gaunt, M. P. Neu, Z. Ou, K. M. Kadish, S. Fukuzumi, K. Ohkubo, and J. Sessler. Redox behavior of cyclo[6]pyrrrole in the formation of a uranyl complex. 2007. *Inorganic Chemistry.* **46**: 5143.

Roy, L.. Quantum chemistry approaches to actinide electronic structure. 2007. *Actinide Research Quarterly.* **3rd quarter**: 14.

Roy, L. E., P. J. Hay, and R. L. Martin. Revised basis sets for the LANL effective core potentials. 2008. *Journal of Chemical Theory and Computation.* **4** (7): 1029.

Roy, L. E., T. Durakiewicz, R. L. Martin, J. E. Peralta, G. E. Scuseria, C. G. Olson, J. J. Joyce, and E. Guziewica. Dispersion in the Mott insulator UO2: A comparison of photoemission spectroscopy and screened hybrid density functional theory. 2008. *Journal of Computational Chemistry.* **29** (13): 2288.

Runde, W., L. F. Brodnax, G. S. Goff, S. M. Peper, F. L. Taw, and B. L. Scott. Synthesis and structural characterization of a molecular plutonium(IV) compound constructed from dimeric building blocks. 2007. *Chemical Communications.* (17): 1728.

Schelter, E. J., B. L. Scott, J. D. Thompson, D. E. Morris, and J. L. Kiplinger. Toward Actinide Molecular Magnetic Materials: Coordination Polymers of U(IV) and the Organic Acceptors TCNQ and TCNE. 2007. *Inorg Chem.* **46**: 5528.

Schelter, E. J., D. E. Morris, B. L. Scott, and J. L. Kiplinger. Actinide-Mediated Coupling of 4-Fluorobenzonitrile: Synthesis of an Eight-Membered Thorium(IV) Tetraazametallacycle. 2007. *Chem Commun.* : 1029.

Schelter, E. J., J. M. Veauthier, C. R. Graves, K. D. John, B. L. Scott, J. D. Thompson, D. E. Morris, and J. L. Kiplinger. 1,4-dicyanobenzene as a scaffold for the preparation of covalently linked bimetallic actinide complexes exhibiting metal-metal communication. 2008. *Chemistry - A European Journal.* **14**: 7782.

Schelter, E. J., J. M. Veauthier, J. D. Thompson, K. D. John, B. L. Scott, D. E. Morris, and J. L. Kiplinger. 4f-5f Heterotrimetallic Complexes Exhibiting Electrochemical and Magnetic Communication. 2006. *Journal of the American Chemical Society.* **128**: 2198.

Schelter, E. J., P. Yang, B. L. Scott, E. R. Da Re, K. C. Jantunen, P. J. Hay, R. L. Martin, D. E. Morris, and J. L. Kiplinger. Systematic studies of early actinide complexes: thorium(IV) fluoroketimides. 2007. *Journal of the American Chemical Society.* **129**: 5139.

Schelter, E. J., P. Yang, B. L. Scott, E. R. Da Re, K. C. Jantunen, R. L. Martin, P. J. Hay, D. E. Morris, and J. L. Kiplinger. Systematic studies of early actinide complexes: uranium(IV) fluoroketimides. 2007. *Inorganic Chemistry.* **46**: 7477.

Schwarz, D. E.. Structure and bonding in actinide complexes. 2007. *Actinide Research Quarterly.* **3rd quarter**: 27.

Spencer, L.. An investigation of the reactivity of a trans-bis(imido) uranium(VI) complex. 2007. *Actinide Research Quarterly.* **3rd quarter**: 24.

Spencer, L. P., E. J. Schelter, P. Yang, R. L. Gdula, B. L. Scott, J. D. Thompson, J. L. Kiplinger, E. R. Batista, and J. M. Boncella. Antiferromagnetic exchange in a bis(imido) uranium(V) dimeric complex. *Journal of the American Chemical Society.*

Spencer, L. P., P. Yang, B. L. Scott, E. R. Batista, and J. M. Boncella. Uranium(VI) bis(imido) chalcogenate complexes: Synthesis and density functional theory analysis. *Inorganic Chemistry.*

Spencer, L. P., P. Yang, B. L. Scott, E. R. Batista, and J. M. Boncella. Imido exchange in bis(imido) uranium(VI) complexes with aryl isocyanates. 2008. *Journal of the American Chemical Society.* **130**: 2930.

Spencer, L. P., R. L. Gdula, B. L. Scott, J. M. Boncella, and Hayton. T. W.. Synthesis and reactivity of bis(imido) uranium(VI) cyclopentadienyl complexes. To appear in *Chemical Communications.*

Spenser, L. P., P. Yang, B. L. Scott, E. R. Batista, and J. M. Boncella. Imido exchange in bis(imido) uranium(VI) complexes with aryl isocyanates. 2008. *Journal of the American Chemical Society.* **130**: 2930.

Tang, M.. Radiation damage effects in uranium-bearing delta-phase oxides. 2007. *Actinide Research Quarterly.* **3rd quarter**: 16.

Tang, M., J. A. Valdez, and K. E. Sickafus. Ion irradiation damage effects in δ-phase Y6W1O12. 2008. *Journal of Nuclear Materials.* **376**: 247.

Veauthier, J. M., E. J. Schelter, C. N. Carlson, B. L. Scott, R. E. Da Re, J. D. Thompson, J. L. Kiplinger, D. E. Morris, and K. D. John. Direct comparison of the magnetic and electronic properties of samarocene and ytterbocene terpyridine complexes. 2008. *Inorganic Chemistry.* **47**: 5841.

Yang, P.. Theoretical studies of bond-activation chemistry. 2007. *Actinide Research Quarterly.* **3rd quarter**: 2.

Yang, P., B. Spiess, P. P. N. Murthy, and R. E. Brown. Influence of metal cations on intramolecular hydrogen bonding network of phosphorylated compounds. 2007. *Journal of Physical Chemistry A.* **111**: 3602.

Yang, P., E. R. Batista, K. S. Boland, C. J. Burns, C. N. Christensen, D. L. Clark, S. D. Conradson, P. J. Hay, J. S. Lezama, R. L. Martin, D. E. Schwarz, M. P. Wilkerson, and L. E. Wolfsberg. Covalency trends in group IV metallocenes dichlorides. 2008. *Inorganic Chemistry.* **47**: 5365.

Yang, P., E. R. Batista, S. Tretiak, A. Saxena, R. L. Martin, and D. L. Smith. Effect of intra-molecular disorder and inter-molecular electronic interactions on the electronic structure of poly-p-phenylene vinylene (PPV) . To appear in *Physical Review B.*

Yang, P., I. Warnke, P. J. Hay, and R. L. Martin. Density functional theory studies of sp2 and sp3 C-H activation mechanisms by (C5Me5)An(CH3)2 Complexes (An=Th and U). 2008. *Organometallics.* **27**: 1384.

Zehnder, R. A., E. R. Batista, B. L. Scott, S. M. Peper, G. S. Goff, and W. Runde. Synthesis, crystallographic characterization, and conformational prediction of a structurally unique molecular mixed-ligand U(VI) solid, Na6[UO2(O2)2(OH)2](OH)2•14H2O. To appear in *Radiochim Acta.*

deBoissieu, M., S. Francoual, and M. Mihalkovic, et al. Lattice dynamics of the Zn-Mg-Sc icosahedral quasicrystal and its Zn-Sc 1/1 periodic approximant. 2007. *Nature Materials.* **6** (12): 977.

# Improved Length Scaling in Accelerated Molecular Dynamics Methods

*Arthur Ford Voter*

20061423ER

## Introduction

The molecular dynamics method is an extremely powerful tool for studying problems in chemistry, biology, physics, and materials science. Starting only with an interatomic potential describing the forces between atoms, a system is propagated forward in time using Newton's laws, and the true dynamical behavior of the system emerges. This approach is now commonly used to study processes such as fast fracture of a solid, structural fluctuations in a protein, liquid diffusion, fast chemical reactions in solution, and sputtering of a solid surface. A major limitation, however, is that because the equations of motion must be integrated with time steps on the order of femtoseconds (one femtosecond is a millionth of a millionth of a second), the longest time a simulation can run on current computers is typically less than one microsecond. This precludes direct simulation of a vast number of interesting and technologically relevant processes, such as surface diffusion and surface growth, deformation of a surface during manipulation with an atomic probe, thermally activated annealing processes after a radiation damage event or ion implantation, protein folding, grain boundary diffusion, etc. Because we cannot access these longer time scales directly, we typically resort to more approximate models that do not properly incorporate the full complexity of the atom-by-atom interactions and motions, and we have no real error control on the predictions from these higher-level models.

For many systems, the long-time dynamical evolution consists of infrequent events; the system is caught in a single energy basin, wandering around vibrationally millions or billions of times before finding an escape path (e.g., the hop of a surface adatom) that takes it over a barrier to a new energy basin, where it begins vibrating again. Over the last ten years at Los Alamos, we have been developing a new simulation approach that exploits the characteristics of this infrequent-event behavior to reach much longer time scales than one can access using direct molecular dynamics. The key concept in this "accelerated molecular dynamics" class of methods [1] is to let the trajectory find an appropriate way to escape from each basin, but to trick it into doing so more quickly, perhaps at the expense of losing information about the vibrational motion. The result is that the system passes from state to state in a dynamically correct way reaching times of milliseconds, and sometimes even seconds and beyond, with full atomistic fidelity. Interestingly, the transitions the system makes are often much different than we would have expected from our intuition.

A remaining problem with these accelerated molecular dynamics methods is that they are limited to small systems of ~1000 atoms. In this project, we are developing new procedures and algorithms to extend the accessible size scale of these methods so that a much wider range of phenomena can be treated. We are achieving this primarily through spatial parallelization, and we are also exploring other approaches in which we directly modify the algorithms themselves. Our first applications are to the growth of metal films.

## Benefit to National Security Missions

This work advances the state of the art for simulation of processes such as radiation damage in nuclear fuels and nuclear waste, dislocation motion in structural materials, surface growth processing, and fracture, thus contributing to the DOE missions in Energy Security, Nuclear Security, Environmental Responsibility, and Scientific Discovery and Innovation.

## Progress

In the project to develop and apply a spatially parallelized temperature accelerated dynamics (ParTAD), we have now used our new ParTAD method [2] to study the growth of a copper surface from vapor deposition at low temperature [3]. This work is being done in collaboration with Prof. Jacques Amar's group at University of Toledo. X-ray diffraction experiments performed by Miceli's group [4] over the last few years have indicated that for growth below T=~100K, there is a significant strain in the film, which they interpreted as arising from a significant number of bulk vacancies (~2%) incorpo-

rated into the growing film. Combining molecular dynamics deposition simulations (lasting a few ps per deposition) with ParTAD simulations to evolve the system for the much longer time between deposition events, we have been able come much closer to the true experimental deposition conditions than have been possible before now. We employed a much larger system than we could have with regular TAD, and this larger system was necessary to fully understand the morphology of the growing surface. We achieved a deposition rate of 5000 monolayers per second, which is much faster than in the experiment, but is roughly 5 orders of magnitude slower than is possible with a direct molecular dynamics (MD) study, allowing us to study the effect of thermally activated events.

From the films grown using MD+ParTAD, we have simulated the X-ray diffraction patterns for comparison with the experiment, as shown in Figure 1.

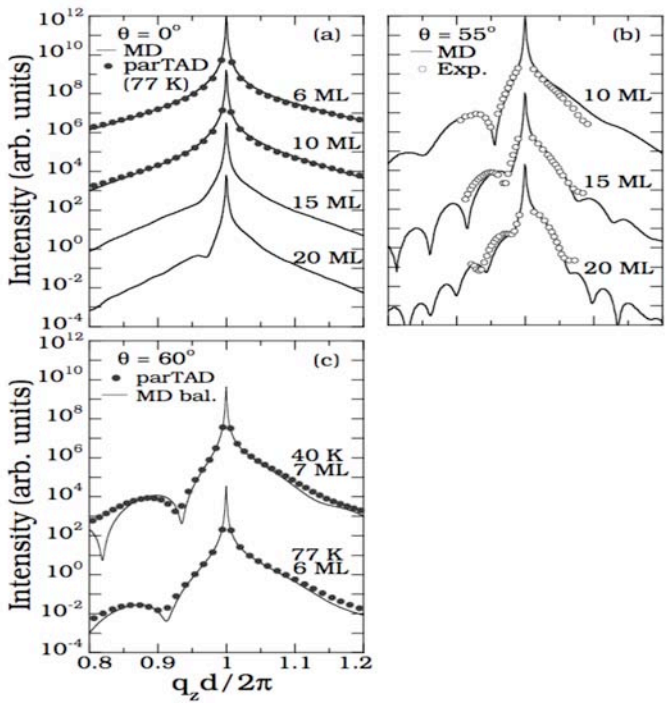


*Figure 1. X-Ray diffraction (XRD) patterns during growth of copper films on Cu(100). a) synthesized XRD spectrum from molecular dynamics (MD) and ParTAD simulations at normal deposition angle. b) Comparison of experimental XRD pattern [4] with XRD pattern predicted from MD at deposition angle (from normal) of 55 degrees. c) Comparison of XRD spectra predicted MD and ParTAD at 60 degrees. The ParTAD films, grown 100,000 times slower, show a softening of the peaks due to the smoothing of the surface caused by the thermal diffusion events during deposition.*

Using direct MD simulations, in which no thermal events have time to occur between successive depositions, we find reflectance oscillations that are in near-quantitative agreement with the experimental pattern (see Figure 1b) when we use a deposition angle of 55 degrees (where zero degrees would be normal deposition). The experimental deposition angle is thought to be close to this value. Comparing the MD simulations with ParTAD simulations, we find that the effect of thermal events, up to a temperature of T=77K, is to slightly soften the reflectance oscillations in the X-ray diffraction spectrum, but the shape is largely unchanged (as shown in Figure 1c).

Perhaps most significantly, as shown in Figure 2, we see an interesting nano-scale roughness in the grown surface, even after just a few (e.g., 7) monolayers, with surprising [100] oriented vertical cliffs (Figure 2d). It appears that this roughness, rather than the incorporation of vacancies into the film, is responsible for the experimentally observed strain in the film. In contrast to the experimental claim of 2% vacancy concentration, we observe a much lower concentration of incorporated vacancies (less than 0.1%). Moreover, we find that if these vacancies are filled in before modeling the X-ray spectrum, the spectrum is essentially unchanged, indicating fairly conclusively that the peaks in the X-ray diffraction spectrum are not due to vacancies.

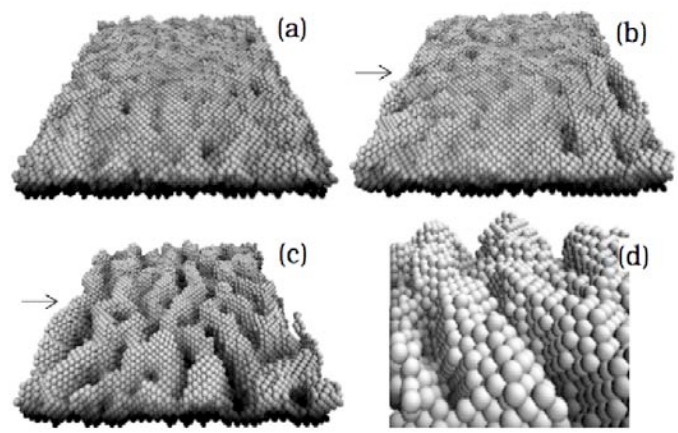


*Figure 2. Surface morphology for copper films grown to 7 monolayer thickness on Cu(100) at T=40K using ParTAD. The deposition rate is 5000 monolayers per second. a) Normal deposition incidence – note the smoothness. b) Deposition angle (from normal) 40 degrees, and c) 60 degrees. Note the increasing nanoscale roughness with increasing deposition angle (arrows show the direction of deposition) and the steep canyon walls at 60 degrees. d) Close-up of c), showing completely vertical cliff walls.*

We have also made further progress on defining a generalized hyperdynamics in which the bias potential is defined locally, thereby allowing arbitrarily large systems to be propagated forward in time. We have developed an algorithmic procedure for this local hyperdynamics and we have implemented it for both model systems and for more realistic embedded atom method (EAM) systems. We have developed an efficient on-the-fly approach for fitting the coefficients that define the bias potential; this refitting needs to be performed each time the system en-

ters a new state. For the three different model systems, we have shown that it gives very accurate results. One of these model-system tests is shown in Figure 3. In our most demanding and precise test, up to a boost factor of 100, it gives rate constants that agree with the exact results (from direct MD) to within 5% or better. Presumably it works well for even larger boosts, but it becomes very expensive to compute the MD results against which we need to compare. We have not yet been able to provide a mathematical proof that the method is valid, but we have a heuristic derivation and we believe the method can be shown to be exact in some limit. A particularly exciting feature of this local hyperdynamics is that it should be easy to implement in the context of large-scale molecular dynamics simulations. For example, on the new Los Alamos Roadrunner system, this could allow us to reach an unprecedented size and time scale of billions of atoms for microseconds.

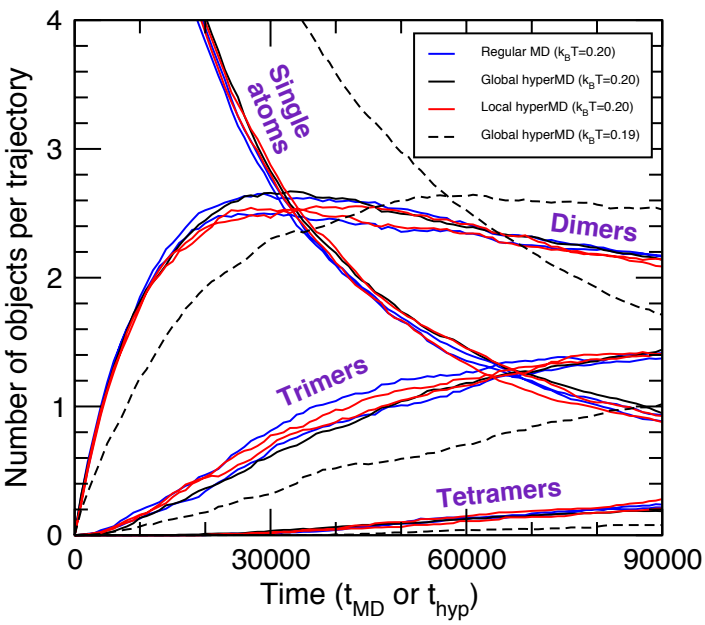


*Figure 3. Test of the local hyperdynamics method for a one-dimensional surface diffusion system in which adatoms that are separate at time zero diffuse and coalesce into larger clusters as the simulation proceeds. The number of clusters of various sizes as a function of time is monitored in the plot. The local hyperdynamics results are in good agreement with the direct MD and global (i.e., regular) hyperdynamics results. To indicate how good this agreement is, the dashed line shows how much the cluster coalescence behavior changes when the temperature is changed by just 5% (from 0.20 to 0.19).*

## Future Work

In the ParTAD project, we have now begun to study low-temperature deposition of copper on silver and silver on copper. We are also beginning to study radiation damage annealing in fcc metals. Time permitting (this project ends partway through fiscal year 2009), we will also investigate this same spatial parallelization approach on the hyperdynamics method.

We will continue to develop and implement the local hyperdynamics method. In particular, we will perform tests on surface-diffusion processes in metals accurately modeled by the embedded atom method (EAM). We continue to seek a rigorous derivation of the method, although it already seems clear that it is powerful enough and accurate enough to be a useful method. Time permitting, we will apply the local hyperdynamics method to large-scale film growth or some other problem where large size and long time are both required.

## Conclusion

We are developing methods that can treat, with full atomistic detail, the dynamics of systems involving many thousands (perhaps millions) of atoms for time scales of microseconds, milliseconds, and beyond. We are achieving this both through spatial parallelization of the existing temperature accelerated molecular dynamics code, and through a redesign of the hyperdynamics algorithm to exploit the local nature of typical thermal transitions in materials. We expect these methods to be powerful for many systems that need to be studied for longer time scales than molecular dynamics can reach and larger sizes than our previous accelerated molecular dynamics methods could reach. We have already applied the spatially parallelized temperature accelerated dynamics approach to reinterpret an experimental study of copper films grown at low temperature, showing that nanoscale roughness, rather than large vacancy concentration, causes the observed features in the X-ray diffraction spectrum.

## References

1. Voter, A. F., F. Montalenti, and T. C. Germann. Extending the time scale in atomistic simulation of materials. 2002. *Annual Reviews of Materials Research.* **32**: 321.

2. Shim, Y., J. G. Amar, B. P. Uberuaga, and A. F. Voter. Reaching extended length scales and time scales in atomistic simulations via spatially parallel temperature-accelerated dynamics. 2007. *Physical Review B.* **76**: 205439.

3. Shim, Y., V. Borovikov, B. P. Uberuaga, A. F. Voter, and J. G. Amar. Vacancy formation and strain in low-temperature Cu/Cu(100) growth. 2008. *Physical Review Letters.* **101**: 116101.

4. Botez, C. E., P. F. Miceli, and P. W. Stephens. Temperature-dependent vacancy formation during the growth of Cu on Cu(001). 2002. *Physical Review B.* **66**: 195413.

## Publications

Shim, Y., J. G. Amar, B. P. Uberuaga, and A. F. Voter. Reaching extended length scales and time scales in atomistic simulations via spatially parallel temperature-accelerated dynamics. 2007. *Physical Review B.* **76**: 205439.

Shim, Y., V. Borovikov, B. P. Uberuaga, A. F. Voter, and J. G. Amar. Vacancy formation and strain in low-temperature Cu/Cu(100) growth. 2008. *Physical Review Letters.* **101**: 116101.

continuing project

# Coulomb Mechanisms for Ion Damage in Insulators in the Electronic Stopping Regime

*Cynthia Jane Reichhardt*

20070156ER

## Introduction

Currently, there is no understanding of the microscopic formation of damage tracks by fission fragments in the electronic stopping regime. This process is important for ceramic fuel materials needed for the President's Global Nuclear Energy Partnership. We are combining theory, simulation, and experiment to study a detailed microscopic mechanism of damage in the electronic stopping regime based on Coulomb explosion processes which result from intense electric fields generated in the ion tracks. Predictions of the theory and of large scale atomistic simulations are being tested through direct experimental investigation of track formation in spinel materials and UO2.

## Benefit to National Security Missions

This project will support the DOE mission in Energy Security and the Office of Science mission in Nuclear Energy by enhancing our understanding of the microscopic mechanism of fission fragment damage in ceramic nuclear fuel materials.

## Progress

The most important accomplishment of the past year is a significant advance in the microscopic theoretical model for latent track formation. A detailed investigation of the lifetime of the charged track generated by the ion revealed that electrons ejected from the track region play an important role in the process of latent track formation. The electrons cause secondary ionization events in the material surrounding the track, resulting in the temporary formation of new scattering centers. As a result, the mean free path of the thermally induced conducting electrons is dramatically reduced on a temporary basis. This permits the charged region at the center of the track to persist for a significantly longer period of time than in a pristine material, and allows latent damage to occur. We are currently calculating theoretical predictions for charge track lifetimes which can be compared with the formation of latent tracks both in the experiments being performed as part of this project and with data from the literature. We stress that this secondary electron damage mechanism has never been considered before, and sheds important new light on the damage process. In our computational modeling efforts, we have performed detailed simulations of spinel and magnesia samples to study the rate at which displacements due to Coulomb explosion processes can occur, as well as the persistence of the latent tracks under thermal annealing. Based on earlier theoretical developments, we have explored the effects of a bond-release mechanism associated with the charged track formation, and showed in simulation that with this mechanism, the amount of latent damage that forms should increase with temperature, in agreement with theoretical predictions. In our experimental efforts, we have fabricated and irradiated both high Z (lutetium oxide) and low Z (scandium oxide) polycrystalline samples, and measured the resulting ion tracks. In both cases, we observe tracks that are approximately ten nanometers in size, but we also find an apparent phase transformation in the lutetium oxide as a result of the irradiation. Based on the recent theoretical predictions, we are now exploring the effects both of temperature and of the preexisting density of scattering centers on track formation. The experimental data is being used in the further development of the microscopic theoretical model.

## Future Work

We intend to develop and study a new model for the detailed microscopic mechanism of ion damage in the electronic stopping regime using a combination of theory, simulation, and experiment. Our approach involves Coulomb explosion processes in the target which occur much faster than phonon time scales. The electric fields generated in ion tracks are extremely intense, and the resulting strong target atom acceleration has not been fully considered in previous work on track formation. We will extend our preliminary theoretical work on calculations of the track charge and charge persistence time to generate a quantitative theoretical model that accepts experimental values as input and contains no free parameters. This model will provide predictions for

the conditions under which damage track formation should occur. The theoretical modeling will be complemented by large-scale atomistic simulations of ion damage processes in insulating materials. Here, the detailed effects of lattice geometry on track formation will be considered. Simulations will be performed both for atomistic potentials and for accurate UO2 potentials. In order to test both the theoretical and numerical work, we will carry out a series of experiments on a series of insulating materials, including spinels and UO2. The samples will be irradiated with swift heavy ions and the damage track structure will be analyzed with TEM and AFM techniques. We will compare the nature of damage tracks formed at different irradiation energies with the predicted damage from the theory and simulations. If our new model successfully passes our tests, it can serve as a foundation point for the development of quantitative, predictive models for radiation damage in insulators, including materials such as UO2.

## Conclusion

To reduce the nation's dependence on foreign oil, it is important to develop alternative energy resources such as nuclear energy. In our work, we will study aging and damage processes that affect ceramic nuclear fuel materials. A better understanding of the damage process will improve our predictive power for the properties of nuclear fuels and could lead to the development of better, more damage resistant fuel materials in the future.

## Publications


Ishimaru, M., Y. Hirotsu, M. Tang, J. A. Valdez, and K. E. Sickafus. Ion-beam-induced phase transformations in delta-Sc4Zr3O12. 2007. *Journal of Applied Physics.* **102**: 063532/1.

Libal, A., C. Reichhardt, and C. J. Olson Reichhardt. Point-defect dynamics in two-dimensional colloidal crystals. 2007. *Physical Review E.* **75** (1): 011403.

Libal, A., C. Reichhardt, and C. J. Olson Reichhardt. Enhancing mixing and diffusion with plastic flow. 2008. *Physical Review E.* **78** (3): 031401.

OlsonReichhardt, C. J., and C. Reichhardt. Viscous decoupling transitions for individually dragged particles in systems with quenched disorder. 2008. *Physical Review E.* **78** (1): 011402.

Reichhardt, C., and C. J. Olson Reichhardt. Disordering transitions and peak effect in polydisperse particle systems. 2008. *Physical Review E.* **77** (4): 041401.

Reichhardt, C., and C.J. O. Reichhardt. Defect fluctuations and lifetimes in disordered Yukawa systems. 2007. *Physical Review E.* **75**: 051407/1.

Reichhardt, C.J. O., C. Reichhardt, and A. R. Bishop. Structure and fragmentation in colloidal artificial molecules and nuclei. 2007. *European Physical Journal E.* **22**: 11.

Rushton, M.J. D., C. R. Stanek, A. R. Cleave, B. P. Uberuaga, K. E. Sickafus, and R. W. Grimes. Simulation of defects and defect processes in fluorite and fluorite related oxides: Implications for radiation tolerance. 2007. *Nuclear Instruments and Methods in Physics Research B.* **255**: 151.

Shen, T. D., S. Feng, M. Tang, J. A. Valdez, Y. Wang, and K. E. Sickafus. Enhanced radiation tolerance in nanocrystalline MgGa2O4. 2007. *Applied Physics Letters.* **90**: 263115/1.

Sickafus, K. E.. Introduction to mathematical models for irradiation-induced phase transformations. 2007. NATO Science Series, Series II: Mathematics, Physics and Chemistry. 235: 321.

Sickafus, K. E., R. W. Grimes, J. A. Valdez, A. Cleave, M. Tang, M. Ishimaru, S. M. Corish, C. R. Stanek, and B. P. Uberuaga. Radiation-induced amorphization resistance and radiation tolerance in structurally related oxides. 2007. *Nature Materials.* **6**: 217.

Tang, M., J. A. Valdez, K. E. Sickafus, and P. Lu. Order-disorder phase transformation in ion-irradiated rare earth sesquioxides. 2007. *Applied Physics Letters.* **90**: 151907/1.

Tang, M., J. A. Valdez, K. E. Sickafus, and P. Lu. Irradiation-induced order-to-disorder phase transformation at different temperatures in Dy2O3. 2007. *JOM.* **59** (4): 36.

Tang, M., J. A. Valdez, and K. E. Sickafus. Ion irradiation damage effects in delta-phase Y6W1O12. 2008. *Journal of Nuclear Materials.* **376** (2): 247.

Tang, M., P. Lu, J. A. Valdez, C. R. Stanek, and K. E. Sickafus. The order-disorder phase transformation in ion-irradiated rare earth sesquioxide Dy2O3. 2007. *Physica Status Solidi C.* **4** (3): 1171.

Uberuaga, B. P., A. F. Voter, K. E. Sickafus, A. Cleave, R. W. Grimes, and R. Smith. Structure and mobility of radiation-induced defects in MgO. 2007. *Journal of Computer-Aided Materials Design.* **14** (SUPPL 1): 183.

Valdez, J. A., Z. Chi, and K. E. Sickafus. Light ion irradiation-induced phase transformation in the monoclinic polymorph of zirconia. 2008. *Journal of Nuclear Materials.* **381** (3): 259.

continuing project

# Synthesis of Nanowire Heterostructures for Strain-Controlled Bandgap Engineering

*Samuel Thomas Picraux*

20070204ER

## Introduction

The goal of this project is to gain a fundamental understanding of the synthesis of epitaxial nanowire heterostructures and their potential for strain-controlled band gap engineering with new electrical, optical, and thermal properties. It is based on our chemical vapor deposition system which has been specifically designed for the catalytic growth of electrically doped semiconducting nanowires and nanowire heterostructures. The small size and high strain of these three-dimensional nanostructures provides a new approach for the rational design of functional materials exhibiting properties not previously attainable. Our studies exploit the unique combination of a new electrically doped silicon-germanium nanowire growth capability, nanoscale microscopy and optical characterization tools, and computational simulations. These materials are anticipated to open the way to new applications in high efficiency thermoelectrics, solar cells, and low power electronic sensing devices. The scientific knowledge gained from this research will enable a new approach to band gap engineering based on heavily strained nanowire architectures.

## Benefit to National Security Missions

This project supports DOE missions in threat reduction, energy research, and nuclear weapons by advancing our fundamental understanding of nanoscale electronic materials for new materials synthesis, chemical and biological sensing, solar energy harvesting, thermoelectric energy conversion, and electronic systems for future low power, miniaturized applications.

## Progress

We have established the conditions for the vertical growth of silicon, germanium, and silicon-germanium alloy nanowires with uniform sidewalls by the vapor-liquid-solid technique using the new LANL cold wall, low pressure chemical vapor deposition system (see Figure 1). Uniform growth with smooth sidewalls is critical in achieving axial heterostructures where the composition of the nanowire is changed from one material (e.g. silicon) to the other material (e.g. germanium). The temperature, pressure, and pre-anneal conditions for nanowire growth have been determined and qualitatively understood. In addition the conditions for the growth of n-type electrically active silicon and germanium nanowires using phosphorous containing molecules as the doping element have been established and optical characterization of excited state carrier lifetimes have been carried out. Publications resulting from these studies include [1-3].

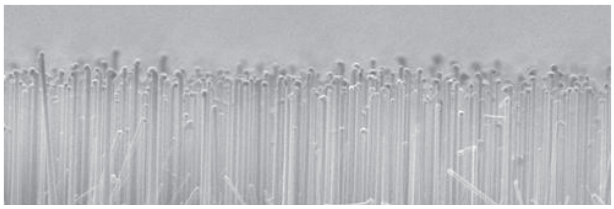

*Figure 1. Dense vertical array of ~40 nm diameter Ge nanowires.*

Methods to synthesize axial silicon/germanium nanowire heterostructures with sharp interfaces are being studied. An in situ optical reflectivity measurement technique has been installed and brought on line which has greatly assisted these studies by directly monitoring the onset of nanowire growth and growth rate, both initially and at the time of heterostructure interface formation. Maintaining uniform growth upon switch-over of the precursor gases at the heterostructure interface has been a critical issue, because the liquid metal seed at the end of the nanowire which controls the growth morphology tends to become unstable with change in the gases. We are making progress in establishing growth conditions to minimize and eventually eliminate this instability of the liquid eutectic seed that lead to subsequent interuption or kinking in the nanowires. We have grown axial heterostructures between pure germanium and silicon nanowires (see Figure 2), as well as between the pure elemental nanowire and silicon-germanium alloy nanowires. Using transmission and scanning electron microscopy techniques we are mea-

suring the composition profile across the heterostructure interface to understand the conditions for achieving the sharpest interfaces. A new theoretical model to describe the interface sharpness of axial heterostructures has been developed and shown to compare well with our initial experimental profiling results. This new model allows us to predict the dependence of the interface sharpness on experimental parameters. The results from this model indicate that the interface sharpness can be significantly increased by reducing the nanowire diameter and lowering the growth temperature.

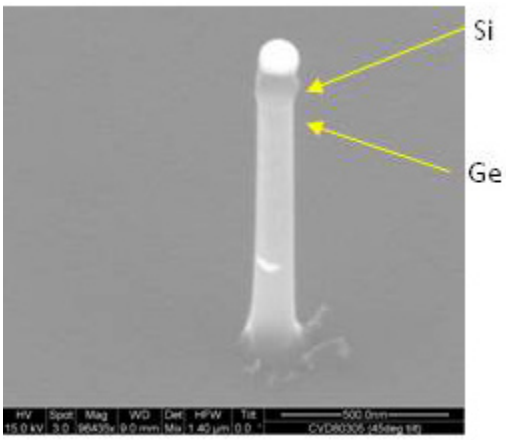


*Figure 2. Vertical silicon nanowire with short axial Si-Ge heterostructure. Light-colored dome on top is the Au growth seed.*

A new molecular dynamics atomistic simulation code has been developed and implemented for predicting the strain distributions near nanowire heterostructures [4]. The code is based on the Modified Embedded Atom Method (MEAM). A MEAM silicon-germanium interatomic potential has been developed and verified based on known materials properties of silicon-germanium alloys as well as those of elemental silicon and germanium crystals. The simulation studies have been applied to silicon/germanium axial heterostructures and the strain distributions determined. It was discovered that localized regions of strain confinement as shown in Figure 3 will occur at the interface even in uniform nanowires with an abrupt composition transition and unanticipated deformations of the interface atoms which varies with nanowire diameter are present. Such molecular dynamics modeling of realistic-sized nanowire heterostructures has not been carried out previously and these results could not have been predicted from previously used continuum modeling approaches.

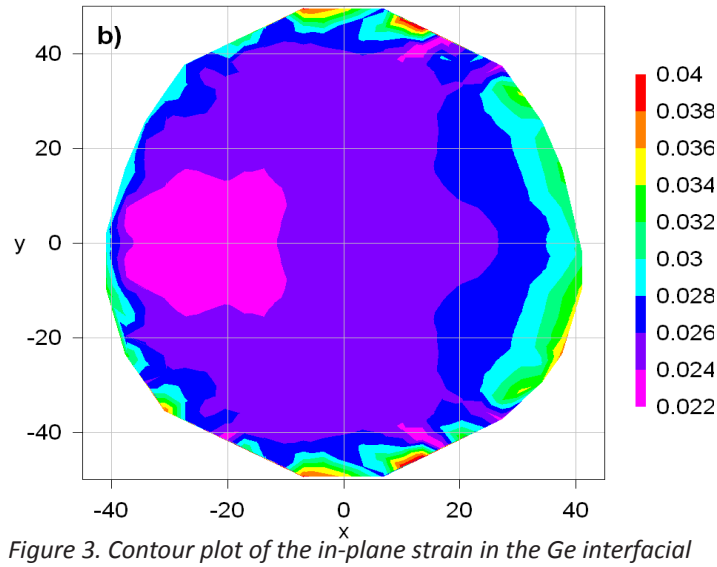


*Figure 3. Contour plot of the in-plane strain in the Ge interfacial layer of a 10 nm diameter Si-Ge axial nanowire heterostructure as determined by molecular dynamics simulations.*

Deformation potential theory has been used to show that large changes in the band gap of the silicon and germanium can be achieved due to the large strains in these nanostructured materials. Also the strain localization along the nanowire near the interface is shown to scale with nanowire diameter. The predictions for the axial case are now being compared to our experiments.

These simulations also allow us to predict the limits of defect free nanowire growth at large diameters for the heterostructured nanowires. For a pure silicon to pure germanium interface, which corresponds to a 4 % lattice mismatch, the axial heterostructure results show this interface to be stable against misfit dislocation formation for nanowire diameters below 70 nm regardless of the nanowire length. This limit falls well within the10 to 50nm diameter region of desired nanowire design. This nanowire stability results from the lack of lateral confinement in these one dimensional structures. Nanowire heterostructures are thus found to have much greater stability than for 2-dimensional silicon-germanium layered heterostructure growth, where dislocation introduction occurs at approximately 1.4 nm layer thicknesses. As a result much greater strains and resulting band gap modifications are shown to be possible in nanowire heterostructures than in conventional layered structures, supporting a key premise of this LDRD project.

## Future Work

To accomplish the objectives of this project we have been systematically exploring silicon-germanium nanowire heterostructures through novel growth strategies, nanowire structure and property characterization, atomistic simula-

tions, and theoretical modeling. Key deliverables of this project include: 1) establish the synthesis of axial silicon-germanium nanowire heterostructures and the degree of sharpness of interfaces; 2) demonstrate methods for selective heterostructure growth of shells over nanowire cores; 3) predict silicon-germanium nanowire heterostructures that will exhibit localized band gaps; 4) establish atomistic simulations of nanowire heterostructure strain distributions; 5) establish the limits of defect free growth of strain achievable in unconstrained nanowire heterostructures; and 6) determine the strain-dependent change in germanium and silicon band gaps for highly strained heterostructures. These objectives are almost complete for the case of axial heterostructures. We are currently finishing up experimental studies of the control of growth morphology during the axial heterostructure growth and establishing the composition profiles across the heterostructure interface as a function of nanowire diameter for comparison with our theoretical predictions. A remaining key objective is to extend these axial nanowire heterostructure studies to the case of core-shell (cylindrical) structures both experimentally and theoretically, and this area will be the primary focus of work for the coming year.

## Conclusion

This project is gaining a fundamental mechanistic understanding of the synthesis of epitaxial nanowire heterostructures and their potential for strain-controlled band gap engineering for the rational design of new functional materials. Specifically, we are using the vapor-liquid-solid growth technique to study the science of synthesizing three dimensional nanowire heterostructures with silicon-germanium as our model system. The studies are exploiting the unique combination of a silicon-germanium nanowire growth capability with our in situ optical probe, electron microscopy-based characterization tools, and theoretical simulations. Our goal is to understand the principles to enable synthesis of sharp nanowire heterostructures, and to design and understand the properties of the resulting new highly strained nanoscale heteroepitaxial materials. We are developing new insight and predictive understanding of the structural limits and electronic properties of these highly strained materials to achieve strain-controlled carrier separation, confinement, and ultra-narrow channel transport . The fundamental knowledge gained from these experiments and simulations will enable rational design of defect-free, 3D nanoscale heterostructures with materials combinations, interfaces, and strain-induced electronic effects not previously accessible. These new materials are of great interest for applications in low power electronics, chemical/biomolecular sensing with near single molecule sensitivity, high efficiency thermoelectric devices, advanced solar cells, and for next generation 3D electronics and flexible electronics.

## References


1. Sierra-Sastre, Y., S. Choi, S. T. Picraux, and C. A. Batt. Vertical growth of Ge nanowires from biotemplated Au nanoparticle catalysts,. 2008. *J. of the Amer. Chem. Soc.*. **130**: 10488.

2. Ingole, S., P. Aella, P. Manandhar, S. B. Chikkannanavar, E. A. Akhadov, D. J. Smith, and S. T. Picraux. Ex-situ doping of silicon nanowires with boron. 2008. *J. Appl. Phys.*. **103**: 104302.

3. Prasankumar, R. P., S. Choi, S. A. Trugman, S. T. Picraux, and A. J. Taylor. Ultrafast electron and hole dynamics in germanium nanowires. 2008. *Nano. Lett.*. **8**: 1619.

4. Swadener, J. G., and S. T. Picraux. Strain distributions and electronic property modifications in Si/Ge axial nanowire heterostructures,. *J. Appl. Phys.*.


## Publications


Ingole, S., P. Aella, P. Manandhar, S. B. Chikkannanvar, E. A. Akhadov, D. J. Smith, and S. T. Picraux. Ex-situ doping of silicon nanowires with boron. 2008. *J. Appl. Phys.*. **103**: 104302.

Ingole, S., P. Manandhar, S. B. Chikkannanavar, E. A. Akhadov, and S. T. Picraux. Charge transport characteristics in boron doped silicon nanowires. To appear in *IEEE Trans. in Nanotech.*.

Pransankumar, R. P., S. Choi, S. A. Trugman, S. T. Picraux, and A. J. Taylor. Ultrafast electron and hole dynamics in germanium nanowires. 2008. *Nano Lett.*. **8**: 1619.

Sierra-Sastre, Y., S. Choi, S. T. Picraux, and C. A. Batt. Vertical growth of Ge nanowires from biotemplated Au nanoparticle catalysts. 2008. *J. of the Amer. Chem. Soc.*. **130**: 10488.

Swadener, J. G., and S. T. Picraux. Strain distributions and electronic property modifications in Si/Ge axial nanowire heterostructures. *J. Appl. Phys.*.

# Synthetic Decoys for Biothreat Agents

*Rashi S Iyer*

20070270ER

## Introduction

As widespread resistance to conventional antibacterial agents continues to pose a major threat, the demand for novel therapeutic approaches to the treatment of infection is increasing. The ability to inhibit bacterial cell-to-cell communication and ensuing virulent gene expression offers a novel treatment strategy. Most microbes require a 'quorate population' to manifest an infection in its target host. Quorum sensing (QS) is triggered by highly specialized molecules synthesized by individual bacteria and is critical for cell-to-cell communication. Many human pathogens, including the Bacillus (anthracis), Pseudomonas, Burkholderia, Salmonella, Staphyloccoci and Yersinia species, regulate expression of virulence factors required for pathogenicity via QS. Given the central role of QS systems in successful bacterial pathogenesis and possibly host cell defense mechanisms, these bacterial-derived chemicals and their molecular targets present an excellent therapeutic opportunity. The overall goal of this project is to design, synthesize and use chemical analogs of QS molecules (mimics) as a therapeutic strategy in microbial infections. We will determine the pathogenic response of the bacteria to these synthetic analogs and investigate the efficacy of the synthetic decoys in attenuating bacterial infection in target host cells.

The synthesis of intelligent QS inhibitors will have a significant impact on both, clinical and agricultural strategies to combat infections. Results from this project will provide targets for drug development [we have a portfolio (already reviewed for significance by TT) of molecular synthesis intellectual property and would place this under that umbrella]. Agencies such as DHS, NIH, NIAID, DOD and CDC have growing interest in the development of novel therapeutics because of its impact on national security and public health, thus we expect future investment in this area. Finally, this project could lead to a patent portfolio with the potential to generate substantial IP licensing.

## Benefit to National Security Missions

This project could tremendously improve our ability to develop an entirely new treatment paradigm for bacterial infection. Improved treatments against bacterial infection directly support biothreat reduction and improving human health, missions particularly relevant to DOE, DHS, NIH, and other government agencies.

## Progress

Our specific goal is to perturb bacterial communication and signaling using synthetic QS analogs, thus providing targeted therapeutic intervention. Towards this goal, we propose to: 1) design and synthesize QS analogs that can act as decoys, 2) determine the pathogenic response of the bacteria to these synthetic analogs, and 3) investigate the efficacy of the synthetic decoys in attenuating bacterial infection in target host cells.

Specific Aim 1: We have successfully synthesized several analogs of AHL molecules that we have determined to be effective in perturbing inter-bacterial QS communication. The bacteria thus far studied to be responsive to our synthetic analogs are, Pseudomonas aeruginosa (PA), Yersinia pestis (YP), Yersinia enetrocolitica (YE) and Burkholderia cepecia (BC). Our submitted patent (AHL-S1207) has been determined to be valuable and we have submitted a new patent disclosure for our new analog (QS0208).

The QS analogs QS0208 significantly inhibited biofilm formation in BC and Yersinia spp. In addition, QS0208 inhibits growth of YP, YE and Y. pseudomonas in biofilm (Figure 1) but not in planktonic growth. Preliminary data indicates that the QS0208 analog may effectively inhibit virulence of all three tested strains of Yersinia, Y. pestis, Y. enterocolitica and Y. pseudomonas.

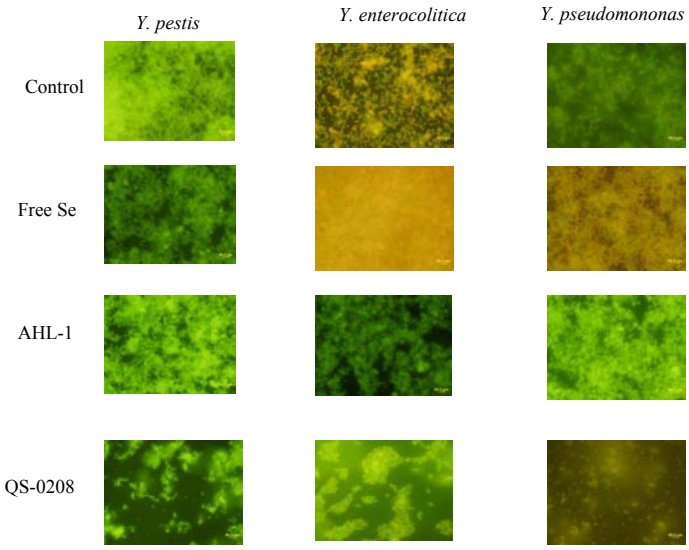


*Figure 1. Effect of QS0208 on biofilm production by Y. pestis, Y. enterocolitica and Y. pseudomonas.*

Specific Aim 2: Using the analogs described above we have examined several virulence and pathogenic responses of PA, YP, YE and BC. We screened the different analogs for effectiveness in shutting down virulent bacterial proteins and correlated the type of virulent response affected by a specific synthetic analogs. The following key parameters were evaluated; growth characteristics of bacterial cultures, twitching-motility and biofilm formation (critical in the infection process), production of pyocyanin (required for pathogenecity) a key virulence factor and protease activity. In this study we have included P. aeruginosa PAO-1 (wild type) and its three mutants JP-1 (-/- C12HSL), PDO-100 (-/- C4HSL) and JP-2 (-/- C12HSL and C4HSL) to observe change in biofilms formation in presence of QS-S analog.

Preliminary data indicates that QS Analog AHL-S1207 may potentially enhance virulence of PA, this is probably due to increased uptake of the QS Analog AHL-S1207 at below threshold concentrations. This function of QS Analog AHL-S1207 can be exploited in two ways:

1. QS Analog AHL-S1207 can potentially be used to 'deceive' bacterial cells to express early virulent genes and pathogenic behavior, thus 'revealing' themselves to host immune cells before they reach a quorate population or result in a biofilm-protected colony.

2. The QS Analog AHL-S1207 can be conjugated to a relevant antibiotic resulting in not only targeted delivery but also enhanced uptake of the antibiotic by PA, increasing efficacy of antibiotics that are currently being used to combat biofilm producing pathogens. In liue of that, we examined the uptake of this analog by bacteria. Here, we conjugated the native AHL molecule to FITC and monitored its bacterial uptake with and without the analog. A decrease in the total uptake of native AHL was observed suggesting that we can use our analog for targeted and enhanced uptake of antibiotics. We have conjugated the antibiotic ciprofloxacin to this analog (Figure 2) and are in the process of determining its uptake by the bacteria. We are currently evaluating the response of Yesrinia and Burkholderia strains to this analog.

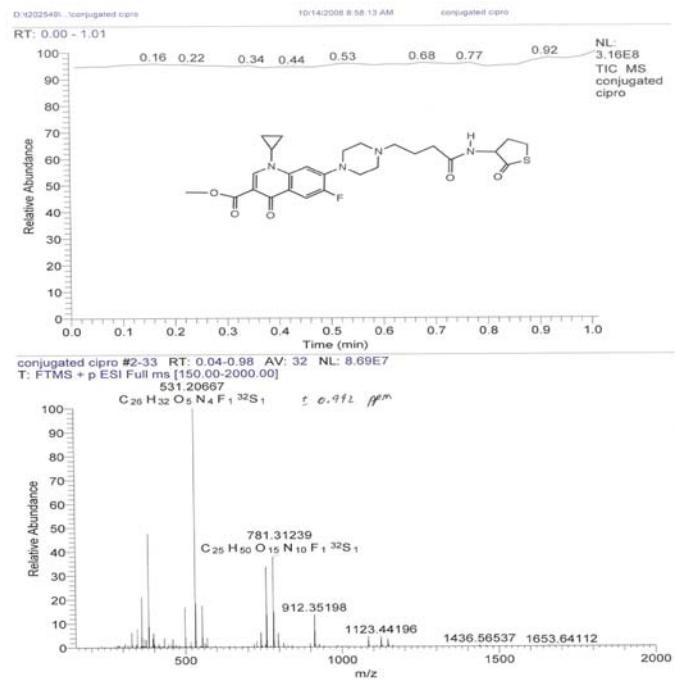


*Figure 2. FTMS and MS of Ciprofloxacin conjugated to AHL-S1207.*

Specific Aim 3: We investigated the ability of the selected synthetic AHL analogs to prevent host infections caused by QS using pathogens. Since, QS0208 effectively inhibited biofilm production and the expression of other virulence factors in PA we set out to determine if QS0208 was effective in preventing *P. aeruoginosa* infection in target host lung epithelial cells. In these experiments cells were either treated with the QS0208 alone, PA alone, and QS0208 pre and post-infection with PA. As expected, significant cell infection and death was observed in the PA-infected cells. In contrast, cells that were exposed to PA and either pretreated or post-treated with QS0208 did not demonstrate any significant cytotoxicity or growth of bacteria. These results clearly indicate that QS0208 can potentially protect target host cells from infection by PA (Figure 3).

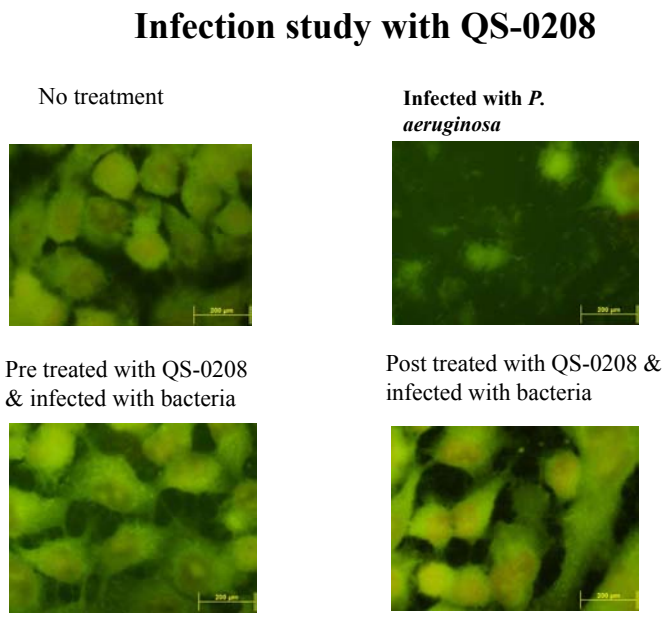


*Figure 3. Effect of QS-0208 on the infection of human lung epithelial cells by P. aeruginosa.*

## Future Work

In many bacterial species, including several biothreat agents, a simple chemical molecule, homo serine lactone, and its acylated form (AHL) is one of the cell-density dependent signal molecules. Critical concentrations of AHL regulate infection, virulence and survival functions. As such, they offer multiple target sites for intervention since the disruption of cell-to-cell communication can be accomplished either by blockade of signal synthesis, by signal molecule degradation, or by inhibition of signal reception. Also, as QS molecules are absent in the host cells, they are ideal drug targets due to the reduced potential for undesired effects. Thus, interference with the bacteria's quorum sensing circuits using synthetic analogs is a potentially effective and targeted therapeutic approach.

The goals of the project are to:

- Design and synthesize QS analogs that can act as inhibitors/decoys.
- Rationally design libraries of QS inhibitors and synthetic derivatives.
- Methodically determine the rate of hydrolysis of AHCL under defined conditions using stable isotope labels and NMR spectroscopy.
- Determine pathogenic expression of the bacteria to these synthetic analogs
- Screen the different analogs for effectiveness in shutting down virulent bacterial proteins
- Correlate the type of virulent response affected by specific synthetic analogs. In this aim we will use synthetic AHL analogs generated in Specific aim 1 and evaluate their ability to interfere with key physiological responses of PA and YP.
- Investigate the efficacy of the synthetic decoys in attenuating bacterial infection in target host cells
- Determine if AHL-analogs are effective in inhibiting PA and YP infection in host cells
- Evaluate and compare the role of AHL molecules and AHL analogs in manipulation of typical host defense responses to promote the survival and virulence of the pathogen.

## Conclusion

Successful completion of our specific aims will provide effective, targeted and relatively non-invasive prophylactic and therapeutic intervention for treatment of infections caused by QS-using pathogens. These include several potential biothreat agents. I Development of analogues of an acylated form of a simple chemical molecule, homo serine lactone, (AHL) will enable us to interfere with disease processes that will have a significant biomedical and agricultural impact. We anticipate that the results will have commercial potential and will actively pursue licensing of developed intellectual property.

## Publications

Ganguly, K., M. Shiflet, P. Silks, S. Iyer, and R. Iyer. Strategies for targeting therapeutics to infectious agents. Invited presentation at *6th International Nanomedicine and Drug Delivery Symposium (NanoDDS'08)* . (Toronto, Canada, 17-20 Oct, 2008).

# Magnetic Resonance Force Microscopy Studies of Ferromagnets on a Nanometer Scale

*Roman Movshovich*

20070330ER

## Introduction

When the size of a ferromagnetic particle is sufficiently reduced, its magnetization can behave as a single large spin that is thermally fluctuating in time between various local ground states (directions of the magnetization). This phenomenon determines the limiting small size of the magnetic particle that can be used in information storage devices, and is called superparamagnetism. The energy barriers between these states depend on several fundamental intraparticle interactions (i.e. electron-electron, electron-lattice, spin-orbit) via the sample's shape, crystallographic, or surface anisotropy. We will use magnetic resonance force microscopy (MRFM) to study the effect of these properties on the superparamagnetic behavior of individual particles. In addition we will implement the Magnetic Force Microscopy (MFM) mode of the operation of our low temperature scanning magnetic probe apparatus. The advantage of this surface magnetic scanning probe is higher spatial resolution that will be used for detailed investigation of the magnetic phenomena (ferromagnetism, vortex matter in superconductors) on the scale down to few tens of nanometers.

## Benefit to National Security Missions

Nanotechnology is a rapidly growing field that impacts much of modern technology. Developing the tools to study nanomaterial properties is crucial for continued advancement of this field. A specific focus of this work is on information storage and retrieval that impacts numerous missions in DOE, DHS, and other government agencies.

## Progress

Significant progress was made during the last year of this project on a number of fronts. MRFM investigations of ferromagnetic films have yielded a number of important results. Investigation of the samples fabricated with optical lithographic techniques where different ferromagnetic films are separated by a distance of a few nanometers demonstrated 1) submicron resolution of the MRFM apparatus; 2) that MRFM can differentiate the material under the tip, i.e. it is material-sensitive. The results of this work have been published [1].

The field profile of a magnetic tip in MRFM has always presented a practical problem: many tips were fabricated by ion beam milling of a larger magnetic particle attached to a micro-mechanical cantilever. As a result of a possible ion beam bombardment damage to the ferromagnetic material of the remaining material, and an irregular shape of the remaining magnetic particle, the field profile, crucial to the analysis of the data and model simulations, was not known. We have approached this problem from two directions. Firstly, the utilization of a regular few-micron size spherical particle on NdFeB, allowed us to model the field of the cantilever as that of a perfect dipole. However, even in that case, uncertainty might exist as to the direction of the magnetic field created by the magnetic tip due to possible microdomain structure, direction of the field due to the crystalline and surface anisotropy. We have developed the experimental approach to characterize spatial distribution of the magnetic field produced by cantilever tip of an arbitrary shape by performing MRFM measurements on a well characterized diphenyl-picrylhydrazyl (DPPH) film. Thereby we were able to map the 3D field profile produced by a Nd2Fe14B probe tip by using the "leading edge" of the MRFM spectra obtained as the sharp edge of the DPPH is approached at different distances from the edge [2].

Our collaboration with the Ohio State University group of Pr. C. Hammel resulted in a demonstration of the direct imaging of the array of the micron-size ferromagnetic particles with Magnetic Resonance Force Microscopy [3]. This work was also was featured in May 26, 2008 issue of Virtual Journal of Nanoscale Science & Technology (http://www.vjnano.org.).

We have performed magnetic resonance force microscopy of a 50 nm thick permalloy film as a function of the probe-sample distance and the angle between

the film plane and the direction of the externally applied magnetic field. At larger angles the multiple resonance modes were observed at small probe-sample distances. Micromagnetic simulations, , which include the inhomogeneous magnetic field of the probe tip, reveal the localized nature of the exited resonance modes [4]. Observation of the localized modes is the first step on the way to spatially resolved ferromagnetic resonance measurements in a continuous ferromagnetic media.

We have implemented the Magnetic Force Microscopy capability to enhance the spatial resolution of magnetic imaging. We built a modular cantilever stage that allows for an easy replacement of the cantilevers. We substituted a commercial MFM cantilever for our home-made MRFM cantilever, and optimized data acquisition software for MFM mode of operation of the apparatus. In addition, we implemented a scanning probe controller, SPM100 from RHK Technology, to use as a part of a dual Magnetic Resonance Force Microscope / Magnetic Force Microscope (MRFM/ MFM) apparatus, and used this apparatus to produce MFM images of the patterned micron-sized squares of ferromagnetic film, and for the first time in our lab, to superconducting vortices in a niobium film. An overview of this dual apparatus and its performance are described in an article that is to be submitted to the Review of Scientific Instruments journal. The dual MRFM/MFM low temperature capability is unique, and enhances LANL's suite of the magnetic scanning probes into the nanometer range.

## Future Work

The objective of this project is to achieve understanding of the phenomena governing behavior of the magnetic nanoparticles and interfaces on nano-scale. We will probe the magnetization and its dynamics in micron and submicron ferromagnetic particles using Magnetic Resonance Force Microscopy (MRFM), and push this capability at LANL to achieve single particle resolution, allowing studies of superparamagnetizm. 1) We will investigate the influence of magnetocrystalline, shape and surface anisotropies on the superparamagnetic transition temperature. 2) We will explore the influence of fabrication methods on the magnetic properties of nanomagnets. 3) We will determine the ultimate practical size and shape of magnetic particles suitable for application as magnetic bits in recording devices. 4) we will perform theoretical studies of magnetic modes in individual particles, and collective modes of densely or sparsely packed particles , as well as 5) develop theoretical tools to understand magnetic phenomena exhibited by nanosize ferromagnetic and ferromagnetic – antiferromagnetic systems in support of experimental data.

The nano- and micro-size magnetic samples will be prepared utilizing both "bottom up", solution/colloidal-based fabrication chemical synthesis (3 to 10 nm size spheres of Co encapsulated in a CdSe shell of variable thickness), and "top down" lithography approaches, including focused ion beam (FIB, down to 20 nm), electron beam lithography (EBL) (down to 50-100 nm), and photolithography (>1mm feature size)

As a part of the exchange bias studies we will implement the scanning capability of MRFM over a large area (cm x cm) to map out the spatial distribution of the exchange field in various bilayer structures. Based on our studies we will propose directions for improvements of GMR read heads. Complementary theoretical component will perform detailed analysis of interaction between the magnetic (ferro and antiferro) modes and the MRFM tip.

We will continue to optimize the Magnetic Force Microscopy mode of operation of the dual MRFM/MFM apparatus to enhance spatial resolution, and utilize the MFM mode to study a variety of the superconducting and magnetic compounds.

## Conclusion

We will investigate large (micron size) magnetic islands with well-defined shape and structure, as well as samples containing a large number of nanometer-size ferromagnets to optimize the Magnetic Resonance Force Microscopy (MRFM) apparatus performance, improve its sensitivity and develop theoretical understanding of anisotropy and magnetostatic energies present in ferromagnetic systems. We will perform studies of single domain nanoparticles and ferromagnetic and superconducting films. We will use samples prepared by chemical synthesis, e-beam thin film deposition, e-beam and ion-beam lithography methods with characteristic sizes down to a few nm. We will implement Magnetic Force Microscopy mode to enhance spatial resolution and use it to investigate a variety of superconducting and magnetic systems.

## References

1. Nazaretski, E., E. A. Akhadov, K. C. Cha, D. V. Pelekhov, I. Martin, P. C. Hammel, and R. Movshovich. Ferromagnetic resonance force microscopy studies of a continuous permalloy-cobalt film. 2008. *Physica Status Solidi A.* **1-4** (205): 1758.

2. Nazaretski, E., E. A. Akhadov, I. Martin, D. V. Pelekhov, P. C. Hammel, and R. Movshovich. Spatial characterization of the magnetic field profile of a probe tip used in magnetic resonance force microscopy. 2008. *Applied Physics Letters.* **92**: 214104.

3. Obukhov, Y., D. V. Pelekhov, J. Kim, I. Martin, E. Nazaretski, R. Movshovich, P. Banerjee, S. An, T. J. Gramila, S. Batra, and P. C. Hammel. Local Ferromagnetic Resonance Imaging with Magnetic Resonance Force Microscopy. 2008. *Physical Review Letters.* **100**: 197601.

4. Nazaretski, E., I. Martin, R. Movshovich, M. Zalalutdinov, D. V. Pelekhov , and P. C. Hammel. 11. Detection of localized excitations in a continuous ferromagnetic film via magnetic resonance force microscopy. *Physical Review Letters.*

## Publications

Mewes, T., C. K. Mewes, E. Nazaretski , and P. C. Hammel. Detection of higher order modulation harmonics in magnetic resonance force microscopy . 2007. *Journal of Applied Physics .* **102**: 033911.

Nazaretski, E., E. A. Akhadov, K. C. Cha, K. Graham, I. Martin, and R. Movshovich. 6. Ferromagnetic resonance force microscopy studies of a continuous permalloy-cobalt film. 2008. *Physica Status Solidi A.* **205**: 1758.

Nazaretski, E., E. Akhadov, I. Martin, R. Movshovich, D. V. Pelekhov , and P. C. Hammel. 9. Spatial characterization of the magnetic field profile of a probe tip used in magnetic resonance force microscopy . 2008. **92**: 214104.

Nazaretski, E., I. Martin, R. Movshovich, M. Zalalutdinov, D. V. Pelekhov , and P. C. Hammel. 11. Detection of localized excitations in a continuous ferromagnetic film via magnetic resonance force microscopy. *Physical Review Letters.*

Nazaretski, E., I. Martin, and R. Movshovich. Ferromagnetic Resonance Force microscopy on a thin permalloy film. 2007. *Applied Physics Letters.* **90**: 234105.

Nazaretski, E., J. D. Thompson, and R. Movshovich. Magnetic resonance force microscopy studies in a thin permalloy film. 2007. *Journal of Magnetism and Magnetic Materials .* **310**: e941.

Nazaretski, E., J. D. Thompson, and R. Movshovich. Temperature-dependent Magnetic Resonance Force Microscopy studies of a thin Permalloy film. 2007. *Journal of Applied Physics.* **101**: 074905.

Obukhov, Y., D. V. Pelekhov, J. Kim, P. Banerjee, S. An, T. J. Gramila, P. C. Hammel, I. Martin, E. Nazaretski, R. Movshovich, and S. Batra. 8. Local Ferromagnetic Resonance Imaging with Magnetic Resonance Force Microscopy. 2008. *Physical Review Letters .* **100**: 197601.

# Controlling Oxidation-States in Actinide-Oxides through Crystal Lattice Pinning

*Quanxi Jia*

20070380ER

## Introduction

The study of oxidation-states of the actinide-oxides, such as uranium- and plutonium-oxides, is of great interest to the U.S. Department of Energy as it addresses the issues of national nuclear security, the safety of the environment, and the safe handling and storage of waste generated by energy and nuclear weapons production. Scientifically, many important aspects of the oxidation kinetics of the materials have not been fully understood. Technologically, actinide materials' long-term storage properties are an area of key importance to the future of nuclear energy and require a good understanding of the chemical interaction between such materials with the environment. Historically, sintered polycrystalline actinide oxides (where the grain boundaries and/or crystallographic imperfections can have a profound effect on the experimental results) have almost always been used exclusively for modeling and understanding such materials. This has been primarily due to limited capabilities to prepare single-crystals with controlled oxidation-states. In this project, we are growing single-crystal like epitaxial actinide-oxides with desired oxidation-states through pinning the crystal lattice. This is the first such attempt in this area of study. Furthermore, we will investigate the physical, electronic, and thermal properties of epitaxial oxides to explore other potential applications of depleted uranium, which DOE currently has huge stockpiles. The success of this project to make epitaxial actinide-oxides easily accessible will place LANL in the forefront of understanding the intrinsic physical properties of actinides. LANL's strategic goals in materials science, energy security, and nuclear weapons will all benefit from this project.

## Benefit to National Security Missions

This project will support the DOE mission in nuclear security, safety of the environment, and the safe handling and storage of waste generated by energy and DOE's nuclear weapons production.

## Progress

In the last year, we have made tremendous progress for this project. Here we highlight the photo-emission measurement of epitaxial UO2 films and their surface stability under normal condicitons.

Epitaxial films, whose crystallographic order is mainly controlled by that of the substrate, have often been adopted as a substitute for single crystals and have been extensively used in the semiconductor industry. For example, epitaxial materials are routinely utilized as active layers to build high performance devices because they exhibit much better physical properties than polycrystaline substrates do. The simplest form of epitaxy is homoepitaxy on which the same material is grown on top of a crystalline source. Heteroepitaxy, on the other hand, is the growth of a given material upon a different substrate. The crystal structure of the substrate can greatly influence the film's preferred crystallographic orientation and structure.

With this in mind, we have tried to "lock in" or "clamp" the lattice of actinide-oxides through epitaxial growth by matching the lattice of the substrate and the film along the interface. For the first time we have found that the lattice matching in heteroepitaxy can stabilize the oxidation state in uranium oxides. In other words, a variety of uranium oxides with controlled phases and controlled oxidation states have been achieved by pinning the crystal lattice in epitaxial films by taking advantage of strong bonding across the interface between the substrate and the film in heteroepitaxy.

It should be pointed out that the epitaxial UO2 and U3O8 films are extremely stable in air. Our x-ray diffraction measurements do not show any noticeable degradation after the films have been exposed to air at room temperature for more than 400 days. This lack of sensitivity to atmospheric conditions may be expected, since the films were formed at 1000 C in an atmosphere of either O2 or air. The extraordinary stability of UO2 films down to a few top-most crystal layers is further confirmed by the lack of significant changes in the valence band structure between the as-deposited and the

sputter-etched surfaces. To test the surface stability of our epitaxial films in environments other than air and/or oxygen, we have performed a controlled H2 dosing experiment with angle resolved photoemission, in order to find the changes in valence band electronic structure introduced by chemisorption of hydrogen. We have started with an epitaxial UO2 film with light Ar sputtering to remove surface adsorbates without changing the structure of UO2 film, and subsequently exposed it to a total dose of 25 Langmuirs and 125 Langmuirs of H2, respectively. For comparision, we have also performed similar experiment on a UO2 single crystal cleaved in vacuum, with H2 dose up to 315L. No changes in valence band have been detected in either case, other than a signal attenuation of the order of 10%, which can be explained by the surface physisorbed hydrogen.

Other important accomplishments are listed here:

1. We have deposited other actinide-oxides films based on this concept. For example, we have demonstrated epitaxial growth of ThO2 film on UO2 using a solution deposition technique.

2. The epitaxial UO2 films have been delivered to other researchers at Los Alamos for further structural and transport studies.

3. We have deposited doped U-oxides for irradiation damage studies.

4. More effort is underway to grow UO3 films based on our lattice engineering concept.

## Future Work

To model and understand the oxidation-states and surface chemistry of actinide-oxides such as uranium-oxides, sintered polycrystalline materials are almost exclusively used due to the limited capabilities to prepare single crystal actinide-oxides with controlled oxidation-states. The use of polycrystalline materials in experiments can create tremendous ambiguity when extracting intrinsic properties of the materials. For instance, experimental results indicate that the kinetic rate of U3O7 formation on UO2 varies when the materials are either powders, polycrystalline pellets, or crystals. Thus it is crucial that high quality single-crystal-like actinide-oxides be prepared for a better understanding of the intrinsic physical properties of actinides as these are fundamental physics and materials issues of great scientific interest.

This project combines the ideas of locking-in or clamping lattice in heteroepitaxy, controlling the oxidation-states in actinide-oxides through pinning the crystal lattice, and growing single-crystal-like actinide-oxide films to make a potential new class of electronic devices using depleted uranium. The detailed research objectives/goals are to:

- Grow epitaxial uranium-oxide films: our goal is to control the phases of oxides since UO2, U3O7, U3O8, and UO3 with different oxidation-states coexist.

- Grow polymorphic uranium-oxides: our goal is to control the crystal structure since, for example, both orthorhombic and hexagonal U3O8 coexist.

- Investigate the physical, electronic, and thermal properties of epitaxial uranium-oxide films with different oxidation-states: our goal is to explore other potential applications of depleted uranium-oxides since DOE currently has huge stockpiles of such oxides.

- Extend our investigation to plutonium-oxides: our goal is to search new area of research involving actinide-oxide surfaces, such as the investigation of the chemical reactivity of the materials.

## Conclusion

The study of oxidation-states of actinide-oxides is of great interest to DOE as it addresses the issues of nuclear security, the safety of the environment, and the safe handling and storage of waste generated by energy and nuclear weapons production. Using our patented polymer-assisted deposition process, we have successfully developed a methodology to control the oxidation-states of actinide-oxides through pinning the crystal lattice. We have also successfully deposited single crystal like epitaxial U- and Th-oxides with controlled crystal structures. Our future work will concentrate on the scientific understanding of the intrinsic properties of actinide-oxides and the growth of other actinide-oxide materials.

## Publications

Burrell, A. K., T. M. McCleskey, P. Shukla, H. Wang, T. Durakiewicz, D. P. Moore, C. G. Olson, J. J. Joyce, and Q. X. Jia. Controlling oxidation states in uranium oxides through epitaxial stabilization. 2007. *Adv. Mater.*. **19**: 3559.

Burrell, A. K., T. M. McCleskey, and Q. X. Jia. Polymer assisted deposition. 2008. *Chem. Comm.* (11): 1271.

Luo, H. M., A. H. Mueller, T. M. McCleskey, A. K. Burrell, E. Bauer, and Q. X. Jia. Structural and Photoelectrochemical Properties of BiVO4 Thin Films. 2008. *J. Phys. Chem. C.* **112**: 6099.

Luo, H. M., Y. Lin, S. A. Baily, H. Wang, M. E. Hawley, T. M. McCleskey, A. K. Burrell, E. Bauer, L. Civale, and Q. X. Jia. Silica Nanoparticles-Oxide Composite Epitaxial Thin Films. 2008. *Angew. Chem. Int. Ed.* **47**: 5768.

# Tunable Infra-Red Chromophores through N-Type Doping of Wide-Gap Semiconductor Nanocrystals

*Sergei A Ivanov*

20070445ER

## Introduction

Colloidal semiconductor quantum dots (QDs) are small, 2-6 nm in diameter, pseudo-spherical crystals of a semiconductor material coated with organic molecules (ligands-surfactants) to protect them from agglomeration, to render them dispersible in solvents, and to passivate (inactivate) their surface from further reactions and defect formation. Binary II-VI semiconductors have the general composition formula AB where A = Zn, Cd, Hg and B = S, Se, Te, and each ion in the lattice forms four bonds to nearest neighbors in tetrahedral fashion, giving rise to either sphalerite-type cubic structure (diamond-like arrangement of atoms alternating cations and anions) or wurtzite-type hexagonal structure. Unlike bulk form of the same semiconductor material, one of the striking properties of ligand-passivated colloidal QDs of II-VI semiconductors is their ability to emit photons in the visible part of electromagnetic spectrum upon excitation with UV light (luminescence).

Synthetic methods for such high-quality QDs of II-VI materials with high uniformity in size and dispersed in water or organic solvents have been well developed, but because of the large energy gap of II-VI semiconductor QDs (gap, Eg, between occupied and unoccupied electron levels), these materials emit light only in visible part of spectrum and are restricted to visible-light applications (e.g., biolabeling, tagging). As such, our ability to tune there optical properties by adjusting the particle size is limited. To use QDs in important applications such as tunable infrared sensors, tunable low-threshold lasers and photovoltaics, one needs QDs with smaller Eg. One of the ways to circumvent the limitation on band-gap tuning would be the doping of II-VI material n-type (introduction of extra electrons into QDs via incorporation of electron-rich ions into QD lattice). This procedure would "convert" II-VI "visible" QDs into IR chromophores (materials that interact with Infra-Red light).

Although QD research has flourished over the last 20 years, approaches to doped QDs are limited to isovalent transition metal (TM) ion doping. The large surface-to-volume ratio for a QD translates into a large portion of dopant present at or near the surface layers, possibly facilitating diffusion of dopant atoms out of the growing QD ("self-purification" process). Tradition high-temperature (lyothermal) syntheses of QDs involve the injection of QD precursors into hot coordinating solvent. High concentrations of QD precursors at high temperature induce formation of critical nuclei (very small clusters of the semiconductor material) followed by nucleation and QD growth at lower precursor concentrations [1]. Incorporation of a dopant in the critical nuclei increases the energy required for nucleation. Therefore, in a lyothermal doping experiment, nucleation of doped crystals might not be competitive with nucleation of pure undoped nanocrystals. As such, successful doping procedures must employ techniques for doped QD growth that do not involve critical nuclei. To this end we will explore two synthetic pathways meeting these requirements: a single source precursor approach [2,3] (Path A) and a QD seed-based approach [4] (Path B) (Figure 1).

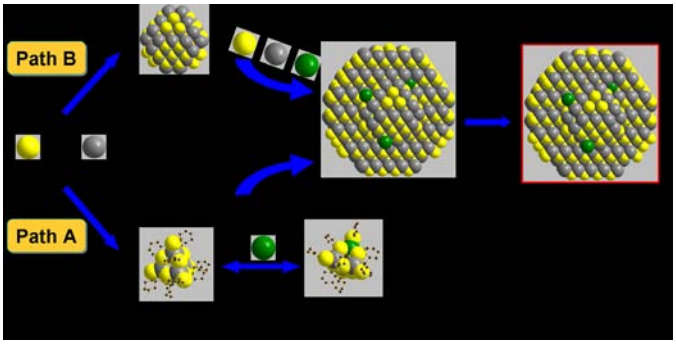


*Figure 1. Two synthetic routes to be explored for the synthesis of doped II-VI semiconductor QDs. Path A involves the synthesis of single-source precursor with consecutive growth of doped charged NC followed by the reduction to neutralize the charge. Path B involves the synthesis of small undoped seed of QD, adsorption of dopant on the surface, shell deposition to incorporate the dopant into interior, and reduction of formed doped charged NC to neutralize the charge.*

## Benefit to National Security Missions

Our goal to develop IR chromophores out of semiconductor QDs will provide critical enabling technology for significant advances in both basic and applied energy sciences, such as a) tunable robust IR sensor systems, b) high-efficiency photovoltaics, c) tunable low-threshold broad band lasers. Robust optical media for use in autonomous sensor systems will support the missions of the DOE and DHS in reducing the threat of weapons of mass destruction and terrorism. Further, an optimized n-doped QD medium comprises an enabling technology for next generation photovoltaics supporting the DOE's Energy Security mission.

Solution of the key issue – stable population of higher electronic levels of a semiconductor QD – would allow doped QDs to make substantial contributions to fundamental nanochemical/nanophysical studies and cutting-edge sensor and energy-capture technologies, providing an important alternative to traditional semiconductor-material dependent applications.

This project supports two core competencies of the Chemistry and Materials -Synthesis (CMS) ER Category. First, if successful, it will provide an enabling technology for the development of next-generation tools for tailoring the electronic properties of materials to control energy transfer (Core: "Functional Design"), which supports the larger missions of Energy Security and Threat Reduction. Second, if successful, it will provide an enabling technology for the control of nanoscale structures of bulk systems (Core: "Nanoscale Synthesis and Assembly"), which supports basic and predictive science goals of the DOE.

## Progress

Out of four semiconductor systems of common II-VI materials, CdS, CdSe, CdTe, ZnSe that are theoretically acceptable for n-doping [5], two systems were experimentally identified as primary for future work, namely CdSe and CdSe, since CdTe is prone to oxidation and its single source precursors are unstable, and ZnSe is less desirable as fewer single-source precursors available. Since indium(III) ionic radius is the closest to that of cadmium among elements of the 13th group of Periodic Table, and relatively stable low oxidation states of indium are accessible in indium compounds, we have identified this element as the most suitable for CdSe and CdS doping.

After the synthesis of multiple single-source Cd-In-S and Cd-In-Se precursors together with several indium complexes we have continued working to identify reaction conditions leading to the incorporation of In into CdS or CdSe QDs via the single-source precursor route (Figure 1). We were able to isolate small Cd-X nuclei from different reactions that lead to the formation of final NC product, but these nuclei did not contain dopant atoms. Originally it was assumed that under conventional lyothermal conditions, the dopants (indium ions) do not incorporate into the NC interior as such process is thermodynamically unfavorable. However, undertaken theoretical investigation of this phenomenon, using small Cd-S clusters as models for real size critical nuclei revealed that both processes, the substitution of $Cd^{2+}$ with $In^{3+}$ on the NC surface and the subsequent reduction (addition of an electron), are thermodynamically *preferred* processes (Figure 2). Finally, one of the reaction conditions was proven to be successful to incorporate $In^{3+}$ ion(s) into CdS NCs (Figure 3) in agreement with theoretical findings.

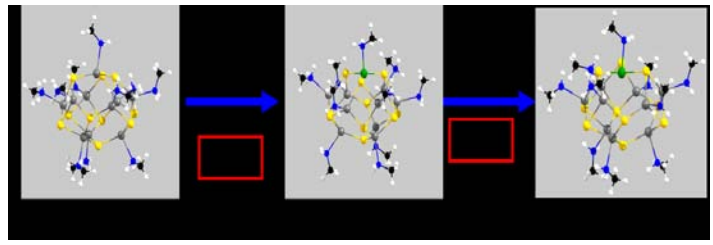

*Figure 2. Calculated free energy change upon replacing one of $Cd_2$+ ions with $In_3$+ in $Cd_{10}S_{10}(NH_2Me)10$ and upon the consecutive reduction of $Cd_9InS10(NH_2Me)10$+ into neutral $Cd_9InS_{10}(NH_2Me)10$. Calculations were conducted at OPBE/LANL2DZ level of theory.*

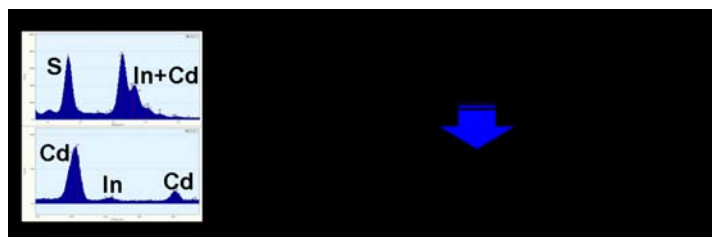


*Figure 3. Main panel shows the reaction schematics that lead to the incorporation of $In_3$+ into CdS NCs. Panel A shows the elemental analysis (EDAX) data confirming the presence of indium in CdS NCs. Panel B reveals the discrepancy between spectroscopically and microscopically (TEM) determined sizes of NCs. The discrepancy was theoretically predicted for CdS NCs with In(3+) incorporated into NC interior.*

In parallel, complementary to conventional lyothermal synthetic conditions, we have started experiments with microwave synthesis of doped QDs, since they require lower temperatures [6] that might facilitate dopant incorporation and deliver the energy directly to the reactants without significant convection heating. Preliminary results of elemental analysis and powder X-ray diffraction indicate that indium atoms can be incorporated into the crystal lattice of CdS NCs, although the degree of incorporation is less than targeted.

We have continued our experiments with dopant adsorption on a surface of small nanocrystal seeds followed by semiconductor shell deposition, which is the second ap-

proach that was proposed. Elemental analysis of In-doped CdSe NCs showed In content less than 0.2% indicating that desirable concentration of the dopant inside of NCs has not yet been achieved. The main obstacle is the stabilization of adsorbed dopant on the surface of the NC seed long enough to overcoat it with a shell of the same semiconductor material.

It appears that the main challenge in NC doping is the dopant annealing out of the nanocrystal during the growth stage due to the close proximity of the NC surface. If that is true, the doping of semiconductor nanowires (NWs) is expected to be easier, as in NWs surface is not as close to the center of NW interior along two dimensions, and even farther removed from the center along the third, NW-growth dimension. We have successfully doped ZnSe NWs with such a conventional dopant as $Mn^{2+}$, although we have not been able yet to compare the doping efficiency with Mn-doped ZnSe QDs.

Finally, to gain an insight into the doping mechanism, we undertook a study of a reverse system, where $Cd^{2+}$ ions are introduced into the lattice of InAs, rather than $In^{3+}$ ions into the lattice of CdX (X = S, Se, Te). Preliminary results again point to the incorporation of the dopant, but optimal conditions for efficient incorporation have not been achieved.

## Future Work

We will continue investigation of the single-source precursor route via slightly modified approach: an incorporation of $In^{3+}$ into NC interior followed by the reduction of doped NC with one electron, formally converting $In^{3+}$ into $In^{2+}$. Since phase separation between CdSe and $In_xSe_y$ is still an issue as we attempt to dope CdSe NCs with $In^{3+}$, further exploration of single-source precursors and growth conditions is needed. One of the impediments to $In^{3+}$ doping of CdS or CdSe NCs can be charge imbalance as we try to replace doubly positive $Cd^{2+}$ with triply positive $In^{3+}$. To address it, $M^{+}$-$M'^{3+}$ charge compensation scheme will be tried. In this approach, $In^{3+}$ dopant ions will be used together with $Cu^{+}$ cations in 1:1 ratio. As $In^{3+}$ and $Cu^{+}$ incorporate into the lattice by replacing two $Cd^{2+}$ ions, the overall charge of the system does not change.

Finally, since the dopant annealing out of the NC interior is still a challenge during synthesis, we will address it by a) continuing the investigation of Microwave-Assisted doping since lower temperatures are needed in this approach; b) doping of semiconductor NWs, since surface influence is diminished compared to QDs and c) continuing theoretical investigation of $In^{3+}$ incorporation into CdS NC interior and studying the inverse doping of InAs with $Cd^{2+}$ to get further insight into the doping mechanism.

## Conclusion

The main conclusion from our work to day has been the demonstration of the successful doping of CdS nanocrystals with $In^{3+}$ experimentally, which was guided by the theoretical justification of thermodynamic favorability of this process.

## References


1. Hollingsworth, J. A.. 'Soft' chemical synthesis and manipulation of semiconductor nanocrystals.. 2004. In *Semiconductor and metal nanocrystals: synthesis, electronic and optical properties..* Edited by Klimov, V. I.. , p. 1. New York: Marcel Dekker.

2. Cumberland, S. L., K. M. Hanif, A. Javier, G. A. Khitrov, G. F. Strouse, and S. M. Woessner. Inorganic clusters as single-source precursors for preparation of CdSe, ZnSe, and CdSe/ZnS nanomaterials. 2002. *Chemistry of Materials.* **14**: 1576.

3. Hanif, K. M., R. W. Meulenberg, and G. F. Strouse. Magnetic ordering in doped Cd1-xCoxSe diluted magnetic quantum dots.. 2002. *Journal of the American Chemical Society* . **124**: 11495.

4. Pradhan, N., D. Goorskey, J. THessing, and X. Peng. An alternative of CdSe nanocrystal emitters: pure and tunable impurity emissions in ZnSe nanocrystals.. 2005. *Journal of the American Chemical Society.* **127**: 17586.

5. Desnica, U. V.. Doping limits in II-VI compounds-challenges, problems and solutions. 1998. *Progress in Crystal Growth and Characterization* . **36**: 291.

6. Gerbec, J. A., D. Magana, A. Washington, and G. F. Strouse. Microwave-enhanced reaction rates for nanoparticle synthesis.. 2005. *Journal of the American Chemical Society.* **127**: 15791.

# Non-Precious Metal Nanocomposites for Fuel Cell Catalysis

*Piotr Zelenay*

20070451ER

## Introduction

Due to its unique electronic and surface properties and resulting ability to facilitate oxygen-oxygen bond splitting, platinum is currently the most active catalyst of oxygen reduction reaction (ORR) in polymer electrolyte fuel cells (PEFCs). The limited resources and high cost of platinum call for the development of less expensive, effective, durable, and easy to manufacture ORR catalysts.

Research in this project focuses on the development of ORR catalysts using two novel approaches. The first approach employs unconventional synthesis to generate highly dispersed metal centers in the coordination environments, known to enhance the ability of these metals to reduce oxygen. This approach involves incorporation of transition metals, e.g., Co, Fe and Cu in matrices of heteroatomic organic polymers, such as polypyrrole. The second approach relies on the modification of electronic and surface properties of carbon-based materials, very poor ORR catalysts in their ordinary form, to create surface sites with significantly enhanced oxygen reduction activity. Unlike in the first approach, relying on the ORR activity of sites specifically containing transition metals embedded into a heteroatomic polymer matrices, in this approach ORR activity can possibly be tied to light elements like nitrogen and carbon. The role of transition metals in this approach is in creating active ORR sites during the heat-treatment step and/or maintaining their activity through interactions with subsurface transition metal species, sufficiently protected to survive the acid leach. The formation of active sites of this type has been typically achieved through the thermolysis of metal-doped organic compounds in the presence of carbon substrate. Both approaches are radically different than those used so far in fuel cell electrocatalysis. If proven successful, this research can greatly facilitate large-scale commercialization of fuel cell power systems for automotive transportation.

## Benefit to National Security Missions

This project supports the DOE mission to protect national and economic security by promoting a diverse supply and delivery of reliable, affordable, and environmentally sound energy and providing world-class scientific research capacity and advancing scientific knowledge.

## Progress

We continued with the development of new non-precious metal catalysts for oxygen reduction reaction. The research focused on strategies for the preparation of nanoporous heteroatomic polymers, incorporation of non-precious metal ORR sites into these polymers as well as determination of active ORR sites and oxygen reduction mechanisms. An emphasis was placed on the determination of active ORR sites and elucidation of structure-activity dependence. For this purpose, extensive electrochemical (fuel cell and/or RRDE) and ex situ spectroscopic (EXAFS, XANES, EPR, XPS) experiments were performed. Two new X-ray absorption techniques were added: an in situ EXAFS/XANES at the transition metal edge and a high-vacuum ex situ EXAFS. While in situ EXAFS/XANES allows for real life studies of the catalytic activity vs. structure relationships, ex situ EXAFS helps to probe the bonding of light elements: nitrogen and oxygen. Whenever possible, the experimental results were complemented by molecular modeling studies employing Parameterized Model 3 (PM3).

The presence of various coordination environments of cobalt in Co/polypyrrole/carbon composites under different fuel cell operating conditions (cell voltage and humidity) was demonstrated using in situ EXAFS. The transitions between these environments were reversible, but relatively slow. No significant changes in catalyst activity beyond those resulting from the cell voltage could be associated with the transitions. In accordance with the in situ EXAFS data, the semi-empirical modeling demonstrated that various ORR sites can exist in Co/PPy/carbon composites and that ORR facilitates their formation and transitions between them. These processes are believed to be responsible for the increase in catalyst activity that always occurs during the initial hours of fuel cell operation in spite of some loss of Co from the catalyst layer. EXAFS and EPR experiments revealed the presence of metallic Co particles in the fresh catalyst and their disappearance during the fuel cell operation. The loss of cobalt from the catalyst layer was

attributed to the dissolution of metallic particles.

Attempts were made to determine the actual oxidation state of active cobalt sites in Co/PPy/carbon composites. The PM3 modeling suggested the presence of mixed valence (3+ and 2+) states with the unpaired spin density delocalized over the polypyrrole backbone, i.e., +3 as the actual oxidation state of metal at fuel cell relevant potentials (Figure 1). The delocalization of free spin in activated catalysts is confirmed by the strong temperature dependence of respective EPR spectra (Figure 2), consistent with "motional narrowing," which is often observed in materials, where the electrons are highly mobile.

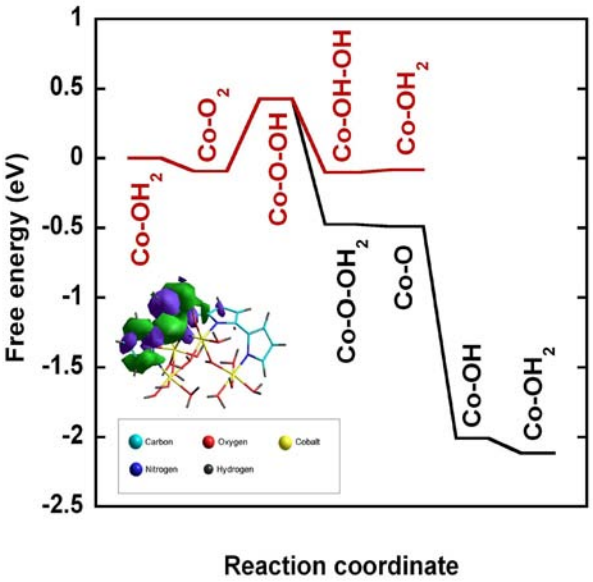


*Figure 1. Free energy diagram for ORR catalyzed by a molecule derived from tetrapyrrole and four Co cations. Stoichiometry of the molecule corresponds to one Co(II) and three Co(III) centers, but free spin density (green and purple) is localized on the ligand (inset).*

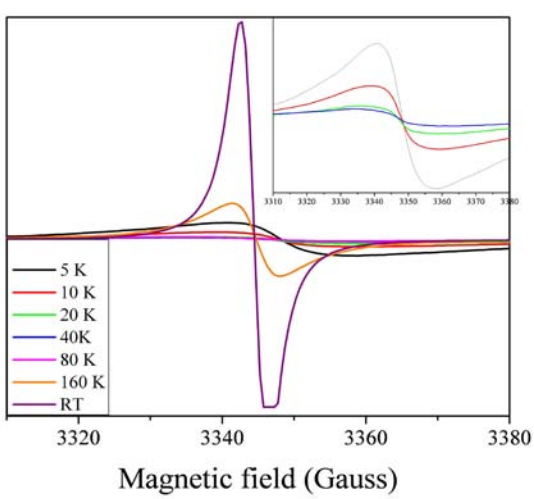


*Figure 2. Temperature effect on EPR spectra of activated Co-PPy-XC72 catalyst. "Motional narrowing" of the EPR signal consistent with unpaired electron of divalent Co donated to the polypyrrole backbone.*

Three new transition metal/polypyrrole/carbon composites containing Fe, Cu and a bimetallic Co+Fe catalyst were synthesized. Their activity was only slightly lower than that of Co/PPy/carbon composites. A new generation of catalysts was developed. These are carbonaceous materials, modified through surface deposition of transition metal/polymer composites, followed by a heat treatment and leaching of any transition metals still remaining on the catalyst surface. More than fifteen different heat-treated catalysts derived from (Fe,Co)/polyaniline, (Fe,Co,Cu)/polypyrrole and (Fe,Co)/cyanamide composites were synthesized and characterized. Pure metal/alloy nanoparticles, oxide-like phases and their combinations were detected by ex situ EXAFS in the heat-treated (Fe+Co)/polyaniline- and (Fe+Co)polypyrrole-based catalysts. The speciation was found to change with the conditions of synthesis and the material composition before the heat treatment. In situ EXAFS at the Co K-edge revealed that metallic nanoparticles are immobile and most likely buried inside the catalyst particles, whereas the spatial distribution of remaining cobalt changes during the fuel cell operation. XPS experiments demonstrated the presence of two different types of potentially active sites in some of the heat-treated (Fe+Co)/polyaniline-based catalysts. While experiments indicate that these sites are associated with the presence of pyridinic and quarternary nitrogen atoms on the catalyst surface, the role of the metal in their activity remains unclear. The (Fe+Co)/polyaniline- and (Fe+Co)polypyrrole-based catalysts are currently studied using ex situ EXAFS at the nitrogen/oxygen absorption edges in an attempt to identify the most active ORR sites.

The most promising heat-treated catalysts were identified. These are polyaniline- and polypyrrole-based materials that contain both Co and Fe and a novel Fe/cyanamide composite that also includes sulfur (Figure 3). The catalytic activity of the latter was attributed to C-N-S surface clusters, based on indirect evidence from XPS and EXAFS measurements.

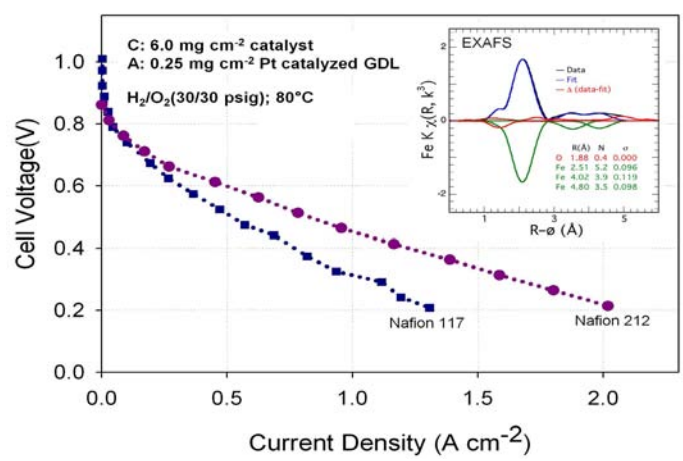


*Figure 3. Fuel cell polarization plots demonstrate good performance of heat-treated ($FeSO_4$ + cyanamide)-based catalyst. The catalytic activity could not be linked to the presence of metallic iron and iron-oxide-like phases indicated by EXAFS results (inset).*

## Future Work

In the upcoming year, we will continue to work on the following tasks:

1. Identification of novel nanocomposite ORR catalysts and viable ways of their synthesis;
2. Determination of active ORR sites and oxygen reduction mechanism on nanocomposite catalysts;
3. Optimization of nanocomposites for maximum catalytic activity
4. Development and optimization of membrane-electrode assemblies (MEAs) for maximum fuel cell performance and durability.

The development and synthesis of ORR-active non-precious catalysts will focus on the incorporation and stabilization of potentially ORR-active sites on 1) nanofibers of heteroatomic polymers, 2) CNT/(heteroatomic polymer) structures, and 3) highly-dispersed carbons, either heat-treated or not. The fundamental kinetic and mechanistic studies of oxygen reduction on non-precious oxygen reduction catalysts (task 2) will utilize a variety of techniques, including EXAFS, XPS, porosimetry, RRDE, and many others. While these techniques have already been quite extensively used to characterize catalysts and determine their active sites, our current understanding of ORR catalysis by these materials suffers from the inherent limitations of many characterization methods, such as XPS), that measure signals from several-nanometer-thick surface layers of materials rather than only from the surface. In order to better characterize surface of catalytically active materials, we will include EXAFS at lower X-ray energies (L-edge) than those used to date (K-edge). If successful, these difficult experiments will greatly improve the understanding of ORR catalysis by non-precious nanocomposites and facilitate the effort to maximize their catalytic activity (task 3).

The development and optimization of membrane-electrode assemblies (task 4) will be continued using the know-how acquired during more than thirty years of fuel cell research at LANL. The work will include optimization of MEA composition and fabrication as well as fuel cell stability testing for at least 300 hours, particularly important for precious-metal-free catalysts.

Before concluding this project, we will create a short-list of methods and materials with the highest activity in oxygen reduction and best stability. We will then perform long-term fuel cell life-testing of the catalysts with start/stop cycling for at least 500 hours. In this phase, we will summarize the mechanistic study of oxygen reduction on (non-precious metal)/(heteroatomic polymer) nanocomposites. Finally, we will define path forward in cathode electrocatalysis research for fuel cells.

## Conclusion

Presented results clearly demonstrate suitability of the approach taken for developing oxygen reduction catalysts for fuel cells. The activity of novel ($FeSO_4$ + cyanamide)-based catalyst is better than published so far for any other precious metal-free ORR catalyst. While much is already known about the origin(s) of catalytic activity of the best performing catalysts and factors affecting their stability, more fundamental studies and extensive characterization are needed to fully understand the ORR on non-precious catalysts and take full advantage of the great potential of these materials.

## Publications

Bashyam, R., C. M. Johnston, S. D. Conradson, and P. Zelenay. Oxygen reduction electrocatalysis on non-precious metal nanocomposites. Invited presentation at *233rd American Chemical Society National Meeting.* (Chicago, Illinois, March 25-27, 2007).

Bashyam, R., C. M. Johnston, S. D. Conradson, and P. Zelenay. Non-precious metal nanocomposite ORR catalysts: RRDE and single fuel cell studies. Presented at *212th Meeting of The Electrochemical Society.* (Washington, DC, 7-12 October 2007).

Bashyam, R., S. Conradson, F. Garzon, J. Chlistunoff, and P. Zelenay. PEFC cathodes based on Co- and Fe-polypyrrole composites. Presented at *9th Gordon Research Conference on Fuel Cells.* (Smithfield, Rhode Island, July 22-27, 2007).

Borup, R., J. Myers, B. Pivovar, Y. S. Kim, N. Garland, D. Myers, R. Mukundan, M. Wilson, F. Garzon, D. Wood, P. Zelenay, K. More, T. Zawodzinski, J. Boncella, J. E. McGrath, M. Inaba, K. Miyatake, M. Hori, K. Ota, Z. Ogumi, S. Miyata, A. Nishikata, Z. Siroma, Y. Uchimoto, and K. Yasuda. Scientific aspects of polymer electrolyte fuel cell durability and degradation. 2007. *Chemical reviews.* **107**: 3904.

Chen, Z., C. Johnston, Y. Yan, and P. Zelenay. Polypyrrole-carbon based non-precious metal nanocomposite electrocatalysts for oxygen reduction reaction at PEFC cathode. Presented at *213th Meeting of The Electrochemical Society.* (Phoenix, AZ, 18-22 May, 2008).

Chlistunoff, J.. Oxygen reduction at transition metal/heteratomic polymer catalysts. Presented at *2008 Mesilla Chemistry Workshop: New Frontiers of Electrocatalysis.* (Mesilla, NM, 9-13 Feb. 2008).

Chlistunoff, J.. Oxygen reduction at transition metal/hetero-atomic polymer catalysts. Invited presentation at *Purdue School of Engineering and Technology, Mechanical Engineering, Indiana University-Purdue University Indianapolis (IUPUI).* (Indianapolis, IN, 3 March, 2008).

Chlistunoff, J., and P. Zelenay. Semi-empirical modeling of Co-polypyrrole composites: oxygen reduction catalysis. Presented at *213th Meeting of The Electrochemical Society.* (Phoenix, AZ, 18-22 May, 2008).

Chung, H., C. Johnston, F. Garzon, and P. Zelenay. A non-precious electrocatalyst for oxygen reduction based on simple heat-treated precursors. 2008. In *214th Meeting of the Electrochemical Society.* (Honolulu, HI, 12-17 Oct. 2008). Vol. 16(2), p. 385. Electrochemical Society Transactions: the Electrochemical Society.

Myers, D., M. Smith, A. J. Kropf, J. Chlistunoff, C. M. Johnston, S. D. Conradson, and P. Zelenay. In situ X-ray absorption and scattering studies of cathode electrocatalysts. Presented at *Progress MEA 2008, First CARISMA International Conference.* (La Grande Motte, France, 21-24 Sept, 2008).

Smith, M., J. Kropf, D. Myers, J. Chlistunoff, C. Johnston, S. Conradson, and P. Zelenay. Non-precious metal nano-composite oxygen reduction electrocatalysts: in situ X-ray absorption spectroscopy studies. Presented at *213th Meeting of The Electrochemical Society.* (Phoenix, AZ, 18-22 May, 2008).

Wu, G., C. Hoon, Z. Lin, K. Artyushkova, F. Garzon, and P. Zelenay. New non-precious catalysts with high ORR performance. Presented at *3rd LANL-AIST-NEDO Workshop on Fuel Cells and Hydrogen Storage.* (San Diego, CA, 8-11 Sept, 2008).

Wu, G., Z. Chen, K. Artyushkova, F. Garzon, and P. Zelenay. Polyaniline-derived non-precious catalyst for the polymer electrolyte fuel cell cathode. 2008. In *214th Meeting of the Electrochemical Society.* (Honolulu, HI, 12-17 Oct, 2008). Vol. 16 (2), p. 159. Electrochemical Society Transactions: The Electrochemical Society.

Zelenay, P.. Alternative catalysts for PEM fuel cells. Invited presentation at *Europacat VIII.* (Turku/Abo, Finland, August 26-31, 2007).

Zelenay, P.. The grand challenge of fuel cell catalysis. Invited presentation at *Lujan Seminar Series on Energy Storage and Energy Materials.* (LANL, July 31, 2007).

Zelenay, P.. Cathode Electrocatalysis: A Great Challenge of Polymer Electrolyte Fuel Cells. Invited presentation at *National Research Council of Canada, Institute for Fuel Cell Innovation.* (Vancouver, Canada, April 7, 2007).

Zelenay, P.. Alternative Oxygen Reduction Catalysts for Polymer Electrolyte Fuel Cells. Invited presentation at *University of Yamanashi (departmental seminar).* (Kofu, Japan, February 5, 2007).

Zelenay, P.. Alternative catalysts for oxygen reduction reaction at the PEFC cathode. Invited presentation at *Los Alamos National Laboratory - NEDO - AIST Workshop.* (Tokyo, Japan, 29 Oct. - 1 Nov. 2007).

Zelenay, P.. Alternative catalysts for oxygen reduction in polymer electrolyte fuel cells. Invited presentation at *Department of Chemistry, University of Tokyo,.* (Tokyo, Japan, 2 Nov. 2007).

Zelenay, P.. Alternative oxygen reduction catalysts for polymer electrolyte fuel cells. Invited presentation at *US-Canada fuel cell workshop.* (Vancouver, Canada, 17-18 March, 2008).

Zelenay, P.. Advances in direct methanol fuel cells at Los Alamos National Laboratory:The formidable challenge of cathode and anode electrocatalysis in DMFCs.. Invited presentation at *Center for Emerging Energy Technologies (CEET) Workshop on 'Spectroscopic methods in structure-to-property correlation for catalysts and electrocatalysts'.* (Santa Fe, NM, 25-26 Sept, 2008).

Zelenay, P., B. Rajesh, J. H. Choi, S. Conradson, and A. Wieckowski. Pt-free electrocatalysts for polymer electrolyte fuel cells. 2006. In *2006 Fuel Cell Seminar Abstracts.* (Honolulu, Hawaii, November 13-17, 2006). Vol. n/a, p. n/a. Fuel Cell Seminar Abstracts: Fuel Cell Seminar.

# Detection of Respiratory Infection by Scent

*Jurgen G Schmidt*

20080317ER

## Introduction

The early detection of epidemic pathogens requires simple, robust and easily deployed assays. While current detection methods rely on rather sophisticated RNA, protein – antibody and laboratory based methods, simpler detection schemes that do not require instrumentation are currently overlooked.

Human preference for visual sensory input biases current detection technologies towards optical read-out of a recognition event, equally discriminatory senses such as olfaction are underutilized in their potential to afford pathogen detection, which is surprising as respiratory infections are located in one of the most ubiquitous sensors available to humans – the nose!

Influenza viridae carry multiple copies of an enzyme - neuraminidase - that cleaves cell surface sialic acids, thus liberating the viral progeny from cell debris. Our project explores the synthesis and biological function of chimeric substrates of sialic acids and odorants. Such substrates will be cleaved by the innate enzymatic activity of the virus and the released odorant stimulates the olfactory receptors to alert the host (Figure 1).

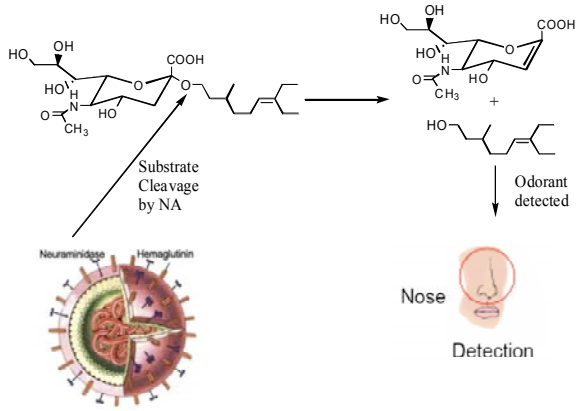


*Figure 1. The detection of respiratory infection by scent: Chimeric odorant sialic acid substrates are cleaved by the innate enzyme activity of influenza to release a scent.*

This detection scheme substitutes instrumentation with the exquisite ability of humans to discriminate and recognize smells for truly fieldable diagnostics. The presence of multiple copies of the enzyme on any viral particle, enzymatic turnover of multiple substrates all combined with the olfactory system amplification may allow detection of viral respiratory infection before a patient becomes aware of symptoms.

Our final goal is to screen a library of such chimeric odorant substrates, optimize the assay and select for molecules that are cleaved differently by viral and bacterial neuraminidases. A discriminatory assay with two easily recognized scents that distinguish bacterial from viral infections can guide the early deployment of medical countermeasures and select the appropriate drugs at an early and most beneficial stage for the patient.

## Benefit to National Security Missions

The proposed research will enable novel detection techniques for emerging health threats. The basic research supports the DOE mission of National Security. In addition this project will further capabilities for Home Land Security in the detection of emerging biothreats.

## Progress

Neuraminidase chimeric substrates for the detection of the presence of viral enzymatic activity require attachment of odorants to neuraminic acid. Neuraminic acids and other sialic acid sugars are among the most challenging starting materials in glycoside chemistry as the anomeric attachment site provides multiple options for unwanted side reactions.

Our first attempts were based on mild additions of aromatic alcohols to the sugar in analogy to reactions reported to generate fluorescent substrates. Standard

glyco-chemistry conditions of phenylthiol activation followed by oxidation to generate a leaving group at the anomeric center, generated elimination side products. We also found that a non anticipated side reaction, the oxidation of double bonds in odorants, occurred that would not allow the use of this commonly found structural feature. Careful screening of methods for sugar-sugar couplings led us to phosphonic acid activation and reaction through anomeric chlorides as alternatives. Among those these two reactions, the method using diethylphosphonate provided the best results for attachment of alcoholic odorants, with products obtained in moderate yields of up to 40% in this challenging coupling step (Figure 2). It is noteworthy that the elimination products obtained in these reactions were recovered and used in a sensor and capturing assay development substituting for very expensive commercial material [1].

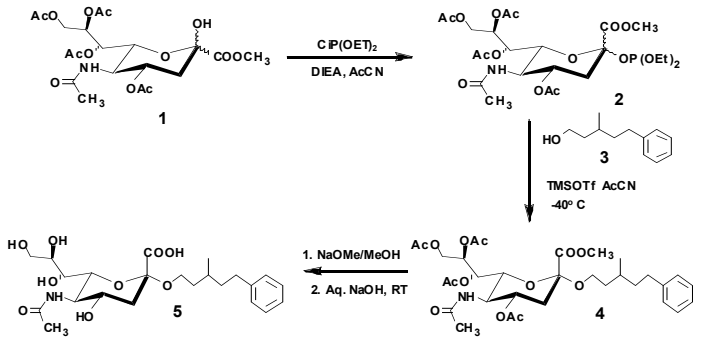


*Figure 2. Synthesis of sialic acid odorant chimera: Suitably protected N-acetylneuraminic acid (1) is reacted with diethylphosphonate to give intermediate (2), which reacts under acid catalysis to form the addition product (4). Deprotection of acetyl and methyl esters gives the chimeric odorant neuraminic acid substrate (5).*

In this funding period we have developed and carefully optimized the chemistry, and tested the method by generating five odorant alcohols attached to neuraminic acids. All compounds were purified and their structure confirmed by $^{1}H$, $^{13}C$ – NMR and mass spectrometry. Our initial evaluation of the substrates for stability in the absence of neuraminidase showed that the odorants are not released by non-specific hydrolysis. We have also confirmed that one can clearly smell and therefore qualitatively observe the presence of the viral enzyme by released scent indicating the turnover of these substrates by the enzyme. Odorant alcohols,however, are soluble in water and generally show low volatility.

Aldehydes, as well as, ketone are commonly found motives in odorants and are generally easier evaporated to produce a scent sensation than alcohols. In this funding period we have begun to investigate the generation of odorant enolates, a ketone or aldehyde equivalent, and are in the process of optimizing their reaction with neuraminic acid. The basicity of the enolate promotes elimination and we are currently screening the available activation chemistries for the sugar to sustain the reaction conditions for enolate - sialic acid chimeric substrates. In addition we have started the design and testing of reactions for carbonate, amine and semi urea attachments of odorants to the neuraminic acid.

On the molecular biology part of the project we have expressed influenza cultures for multiple strains and isolated neuraminidase samples. These isolates are calibrated with a fluorescent enzyme assay to provide neuraminidase activity standardized samples of neuraminidase. Bacterial expression system substitutes for the neuraminidases from highly pathogenic viral subtypes, which cannot be cultured under BSL-2 conditions, are currently established.Future Work

In the next funding period we will establish the mass spectrometry assay for evaluation of relative turnovers among substrates and neuraminidase subtypes. The robust developed chemistry for the attachment of odorant alcohols will be extended to parallel synthesis of alcohol-sialic acid substrate libraries and these products evaluated for structural candidates of discriminatory cleavage by neuraminidases. Specific cleavage over non specific hydrolysis will be optimized by judicious choice of the connection chemistry in the substrates. The development of enolate attachment chemistry provides a valuable new carbohydrate synthetic method we intend to publish.

Our detection approach will combine 4 distinct amplification steps – the presence of multiple neuraminidase copies on a pathogen, the catalytic substrate cleavage, the direct release of the trigger on the sensor and the biological cascade of smell, with a unique pathogen specific event and the exquisite selectivity of olfactory sensing to provide a sensitive, instrumentation free and potentially pre-symptomatic detection scheme. It is therefore our next goal to investigate mass spectrometry sensitivity data that can be indicators to the expected assay sensitivity threshold. Synthetic protocols for the incorporation of a wider range of linkages will be established. We will find critical contacts to the enzyme by Nuclear Magnetic Resonance spectroscopy and modeling. The chemistry for odorant attachment to branched scaffolds and stereoselective attachment chemistry will be developed to enable discriminatory detection among respiratory causative agents, and influence of more complex interfering matrices will be investigated.

## Conclusion

An assay will be developed that specifically detects respiratory infections. We expect to develop chemical entities that are converted by a pathogen specific event to release odorants. This triggers the smell receptors in the nose to allow a "patient" to be alerted of the presence of a pathogen. The exquisite sensitivity and selectivity of olfactory sensing not only provides the means to encode multiple pathogens with different smell, but such an assay will likely allow presymptomatic detection before the onset of other signs of infection.

## References

1. Kale, R. R., H. Mukundan, D. N. Price, J. F. Harris, D. M. Lewallen, B. I. Swanson, J. G. Schmidt, and S. S. Iyer. Development of a carboassay Detection of Influenza virus using capture and reporter biotinylated biantennary S-sialosides. 2008. *Journal of the American Chemical Society.* **130**: 8169.

## Publications

Kale, R.R., H. Mukundan, D. N. Price, J. F. Harris, D. M. Lewallen, B. I. Swanson, J. G. Schmidt, and S. S.Iyer. "Development of a carboassay Detection of Influenza virus using capture and reporter biotinylatedbiantennary S-sialosides". 2008. *Journal of the American Chemical Society*. **130**: 8169.
1.

# Spins in Organic Semiconductors

*Brian Keith Crone*

20080323ER

## Introduction

Today's electronics are based on electron charge. Using electron spin to compliment electron charge in electronics is the basis for a major international research activity called "spintronics." An ideal spintronic device consists of a magnetic contact to inject spin polarized current into the device, an active layer to manipulate the spin polarization, and a magnetic contact to detect the final spin polarization. Organic semiconductors are attractive candidates for the active layer in spintronic devices because they are expected to have much longer spin lifetimes than inorganic semiconductors due to their weak spin-orbit interaction, which is the principal spin de-phasing mechanism in these materials. However, the spin-orbit interaction is also responsible for selection rules that allow optical generation/detection of polarized electron spin distributions, and so these techniques cannot be used in conventional organic semiconductors. Optical injection and detection was essential in the development of electrical spin injection in inorganic semiconductors, and will provide a powerful tool in the development of organic spintronics. The purpose of this work is to develop both optical and electrical methods to inject and detect spins in organic semiconductors and demonstrate the advantages of these materials for spintronic applications. We initially focused on optical spin injection/detection, using organic materials containing a heavy metal atom to increase spin orbit coupling, since it is the most flexible technique. In parallel, we are exploring the use of ferromagnetic insulator based spin filters to electrically inject and detect spins in organic materials. This parallel approach of optical and electrical methods of spin injection will improve our chances of success in this important area of study.

## Benefit to National Security Missions

This project will support DOE missions in basic science and threat reduction by providing the fundamental understanding of spin-based processes in organic materials needed to enable new technologies including quantum information processing and computing. These technologies will support our national security by providing powerful tools for data encryption and decryption.

## Progress

Completed our studies of metal containing organic semiconductors for optical spin injection. We investigated Mg, Zn, and Pt- Octaethylporphyrins (M-OEP). This series was chosen to vary the spin orbit coupling over a wide range (Z=12, 30, and 78). To understand these materials in more detail we performed magnetic circular dichroism (MCD), and CW and time resolved polarized photoluminescence (PL) measurements of these M-OEP materials in an organic host. We measured photoluminescence (PL) of ZnOEP with a short gate on the CCD to look at only singlet emission as well as luminescence with a long 20 ms gate to look at both singlet and triplet emission. The short gate PL shows a broad peak centered at 600 nm due to singlet emission. The long gate PL shows the singlet emission peak, as well as a triplet emission peak centered at 700 nm. This demonstrated that incorporation of spin orbit coupling enables triplet emission, however our attempts to inject and detect spin using time resolved PL in these systems failed. We believe that in these systems there is a delicate balance between having enough spin-orbit coupling to enable triplet emission and hence optical injection, and having too much spin orbit coupling which lowers the spin lifetime in these systems. To understand this balance we are modeling these materials theoretically. Hybrid density functional theory was used to provide quantitative predictions of equilibrium geometries, and optical spectra of platinum poryphyrin (PtP) and the octaethylporphrin derivative (PtOEP). The optical transitions involve transitions to doubly degenerate electronic states that are subject to Jahn-Teller distortions. The potential energy surface (PES) associated with the Jahn-Teller problem was determined by hybrid DFT calculations. Extrema on the PES were characterized as either minima or transition states through the explicit calculation of the vibrational frequencies. The latter also allows us to determine vibrational Huang-Rhys factors for comparison with optical spectra. By explicit calculation of the

intrinsic reaction path connecting the stationary points, we can develop an effective 1-dimensional PES for the pseudo-rotation. This, in combination with the spin-orbit coupling, was used to define an effective vibronic Hamiltonian combining the effects of the JT interaction, the spin-orbit coupling, and the magnetic field. These same calculations will be extended to MgOEP and ZnOEP to gain a better understanding of how to tune the optical properties of metal-organics for efficient spin polarized optical injection and detection.

In parallel to the optical measurements we have also begun fabricating ferromagnetic insulator based spin filters for electrical injection and detection of spins. Currently we are making devices with the structure Al/EuS/Al2O3/Co/Co(1-x)Ox, and Al/EuS/Al2O3/EuS/Co/Co(1-x)Ox. EuS is a ferromagnetic insulator that has different energy gaps for spin up and spin down electrons. It can thus be used as a spin dependent barrier to electron transport. In the first structure, the EuS is used to generate a spin polarized tunneling current, the Al2O3 is a spacer layer to prevent the Co from pinning the magnetization of the EuS, the Co is a ferromagnetic contact, and the Co(1-x)Ox pins the magnetization of the Co. In the second structure the first EuS layer is used for spin injection, and the second for spin detection. Once we have established the device parameters needed for electrical spin injection and detection in this system, we will replace the Al2O3 spacer layer with organic materials to study spin injection and transport in these systems.

## Future Work

The goal of this work is to demonstrate, for the first time, optical generation and detection of spin polarized electron distributions in organic semiconductors, and to then use these techniques to demonstrate and study electrical spin injection and spin dynamics in organic semiconductors. Recent results such as: triplet harvesting in organic light emitting diodes; large magnetoresistances in organic semiconductors; and the report of organic semiconductor spin valves, have highlighted the importance of spin-dependent processes in these materials. Currently spin-dependent processes in organic semiconductors are not well understood. Optical generation/detection of spin polarized electron distributions in inorganic semiconductors has provided a powerful tool for the study of spin dependent processes. Optical spin generation/detection relies on spin-orbit coupling and the resulting optical selection rules. Recent results in our lab on MO molecules, which have a large spin-orbit coupling due to incorporation of heavy-metal atoms, show great promise for the optical generation/detection of spin polarized charges in organic materials. We will investigate the fundamental physical processes needed to achieve first optical and then electrical spin detection/generation in organic semiconductors. In parallel to these efforts we are exploring the use of ferromagnetic insulators for electrical injection and detection of spins in organics. Our specific goals and milestones by fiscal year are:

FY1: Investigate spin dynamics of excitons formed by circularly polarized light in metal organics. Investigate the use of ferromagnetic insulators for spin injection / detection in organics.

FY2: Demonstrate capture of spin polarized charge carriers from an organic matrix onto MO dopants, study the effect of this capture on charge carrier spin polarization, and the polarization of the subsequent light emission. Study the dynamics of spins in organics using ferromagnetic insulator based spin valves.

FY3: Use these techniques to demonstrate and study electrical spin injection and spin dynamics in organic semiconductors.

## Conclusion

The goal of this work is to demonstrate, for the first time, optical generation and detection of spin polarized electron distributions in organic semiconductors, and to then use these techniques to demonstrate and study electrical spin injection and spin dynamics in organic semiconductors. These results will enable organic semiconductor based spintronic devices which are promising candidates for quantum information processing and computing.

# Strain-induced novel physical phenomena in epitaxial ferroic nanocomposites

*Quanxi Jia*

20080394ER

## Introduction

The vast range of structures and properties of composites provides an excellent case platform to investigate novel device functionalities. By combining efforts from both theoretical prediction and experimental verification, we propose to develop a theoretical model for investigating and predicting the magnetoelectric coupling effects on ferroelectric/ferromagnetic epitaxial nanocomposite films. We will also grow epitaxial these nanocomposite films with desired functionalities, and demonstrate a proof-of-principle dual-tuning microwave device. By integrating properties of individual materials, we can overcome the dual problem that single phase materials are rare and only display a very weak magnetoelectric coupling effect at room temperature. We expect the experimental results to open up a wide array of possible applications of these materials. Also, the proposed work holds great promise for enhancing various fundamental and applied studies of functional metal-oxides. This research will ensure LANL's continued leadership in nanotechnology and functional materials. LANL's thrusts in functional materials, nanotechnology, and sensors can all benefit from this project

## Benefit to National Security Missions

This research ties to the mission of DOE Office of Science for fundamental understanding of materials. LANL's thrusts in functional materials, nanotechnology, and sensors will directly benefit from this project

## Progress

In the last review period, we have made tremendous progress in the preparation and characterization of nanocomposite ferroic films using both pulsed laser deposition and polymer-assisted deposition. The following outlines the most important accomplishments and observations.

Two-phase, vertical nanocomposite heteroepitaxial films hold great promise for (multi)functional device applications. In order to achieve practical devices, a number of hurdles need to be overcome, including the creation of ordered structures (and their formation on a large scale), achieving different combinations of materials, and control of strain coupling between the phases. Here we demonstrate major advances on all these fronts: remarkable spontaneously ordered structures were produced in newly predicted compositions, vertical strain was proven to dominate the strain state in films above 20 nm thickness, and strain manipulation was demonstrated by selection of phases with the appropriate elastic modulii. The work opens up a new avenue for strain control in relatively thick films and also promises new forms of ordered nanostructures for multifunctional applications.

An important starting point for our studies was determining which systems have the potential to form clean, nano-composite thin films. Since guidelines to the materials selection of nanocomposites have not been presented before, we developed our own as follows: (i) the chosen phases should both have the potential to grow epitaxially on a given substrate; (ii) the growth kinetics of the individual phases should be similar so that the two phases can both grow with sufficient crystallinity at a chosen temperature; (iii) the two phases of interest should be the most thermodynamically stable when the individual elements are combined; (iv) cations with sufficiently different ionic radii are necessary to minimize intermixing of the phases; (v) for achieving vertical strain control of one phase by another, materials with different elastic constants should be selected.

For this study we grew samples using two materials combinations which satisfied these criteria: $BiFeO_3$ (BFO):$Sm_2O_3$ (SmO). We have observed that there is a reduction in the dielectric loss for the BFO/SmO nanocomposite, compared to the pure films of the two phases. Considering that the dielectric loss for a composite system should be controlled by the phase with higher loss, the result is surprising. Typically, the dielectric loss decreases with decreasing leakage current. We have found that the current perpendicular-to-plane resistivity of different films (SmO, BFO, and BFO:SmO) at a given electric field (SmO is the highest and BFO is the low-

est). If we consider that the BFO and SmO columns in the BFO:SmO nanocomposite film are resistors connected in parallel and because of the highly resistive nature of the SmO, the leakage current will, therefore, be controlled by the BFO. This implies that the leakage current of the BFO in the BFO:SmO nanocomposite film is much lower than that of pure BFO thin film and is indicative of strain control of the dielectric properties. Whilst we cannot rule out the possibility of some Sm substitution in BFO (this is not possible to measure accurately because of the very small size of the nanocolumns), from TEM we did not find any second phases which might form for reasons of mass compensation, i.e. because of displacement of one or both of the cations out of the BFO as a consequence of Sm substitution into it. In addition, previous work on Sm substitution in BFO has shown no systematic evidence for improved dieletric properties. Hence, we believe that in our nanocomposite films, substitution of Sm into BFO may occur but only to a low level.

From theoretical point of view, we have modeled ferroelectric domain structures of (001)c, (101)c, and (111) c epitaxial $BiFeO_3$ thin films using a theoretical approach. We have taken into account long-range elastic and electrostatic interactions. The effects of various types of substrate constraint on the domain morphologies were systematically analyzed. We have shown that domain structures of $BiFeO_3$ thin films could be controlled by selecting proper film orientations and/or substrate constraint.

## Future Work

We will use our theoretical modeling tool to guide our experiments. Three different forms of nanocomposites deposited by either pulsed laser deposition (PLD) or polymer-assisted deposition (PAD) will be investigated. We will also fabricate proof-of-principle dual-tuning microwave devices by utilizing the multifunctional properties of materials.

a) Investigation of the strain effect on the properties of composites using theoretical method: The model, which describes the microstructure using a set of conserved and non-conserved field variables that are continuous across interfacial regions, has recently emerged as a powerful computational approach to modeling and predicting mesoscale (in the range of nanometers to microns) morphological and microstructural evolutions in materials. We will use this approach to simulate the effect of the lattice strain on the properties of nanocomposite films.

b) Growth and characterization of epitaxial nanocomposites: We will investigate three particular epitaxial nanocomposite architectures: the vertically aligned nanocomposite, the layered laminar-like nanocomposite, and the particulate nanocomposite. We will use PLD to grow the first two architectures whereas PAD will be used to construct the particulate nanocomposite.

c) Fabrication of proof-of-principle dual-tuning microwave devices: A tunable microwave device fundamentally operates by changing the microwave propagation factor through physical, electrical, or magnetic means. We will design and fabricate proof-of-principle dual-tuning microwave devices to evaluate the desired functionality of nanocomposites.

Our goals are i) developing a theoretical model for predicting the strain effect on the properties of epitaxial nanocomposite films, ii) growing such epitaxial nanocomposite films with desired functionalities, and iii) developing a proof-of-principle dual-tuning microwave device based on nanocomposites. We seek a fundamental understanding of the relationship between the strain and the physical properties as well as the method to manipulate the strain state in nanocomposites, which are crucial for the application of these materials.

## Conclusion

We have successfully demonstrated the growth of nanocomposite films using pulsed laser deposition. We have also investigated the strain-induced physical phenomena in epitaxial nanocomposites. We will further explore other different forms of nanocomposites proposed in our initial project. We expect to develop a theoretical model to predict the properties of ferroelectric and ferromagnetic nanocomposite films, to have a better fundamental understanding of strain-induced physical phenomena in epitaxial nanocomposite films, to successfully grow epitaxial nanocomposites with complementary functionalities, and to demonstrate proof-of-principle dual-tuning devices using multifunctional epitaxial nanocomposite films.

Toward these goals, we have designed and synthesized a simple elastin domain (short EL, “sEL”) and we are currently evaluating the physical properties of this material. We have shown that this polymer can be displayed on the surface of filamentous phage, which is an exciting result showing us that our simplified experimental plan will work for creating libraries. We found that the expression of this protein, on phage, is nearly that of a highly stable small antibody (D1.3). Further, analysis by western-blotting shows that the expressed protein is of the correct size (Figure 2). We have designed cloning strategies to insert diversity sequences within the simple elastin domain, using methods yet to be implemented for any other project at LANL. Based on ideal physical properties, we have also designed and synthesized an extended elastin sequence (long EL, “lEL”). From this sequence, we have designed a strategy to insert diversity sequences within this polymer. Further, for each elastin polymer we have created controls for

cell binding domains. The design and synthesis of these protein polymers was no small feat. Elastin polymers are repeating units of the same sequence of amino acids. Unfortunately, bacteria do not tolerate highly repeated sequences. To overcome this intolerance, we created a program that randomizes the DNA codons and yet would take into account the codon preferences of E. coli, thus producing a gene sequence that produces our ELPS and is stable in bacteria.

# Genetically Engineered Polymer Libraries

*Jennifer Martinez*

20080395ER

## Introduction

The development of materials with defined biological functionality is a grand challenge in materials chemistry. Unfortunately, the *apriori* design of such biomaterials is difficult, because the complex interaction of proteins and cells with polymers has not been thoroughly defined. These considerations suggest that a combinatorial approach may be an important route toward developing polymers with ideal biofunctionality. Combinatorial chemistry is already of proven value for drug and catalyst discovery. These powerful approaches often start by creating millions of combinatorially synthesized compounds within one reaction vial, and end with identification of lead compounds using highly selective assays. For the approach to be similarly applied to polymer chemistry, methods are needed to: 1) generate diverse libraries, and 2) rapidly identify lead materials based on function and/or physical properties. Traditional combinatorial approaches for creating functional polymers have failed, both because it is difficult to make large synthetic polymer libraries and, most importantly, it is difficult to separate individually reactive polymers from mixtures. These difficulties have led to creation of "spatially resolved libraries", or arrays of individual polymers, but these too have involved limitations in library diversity and size.

*We intend to solve these problems by creating large, diverse libraries of in vivo polymers, displayed in a format that allows rapid identification of functional biomaterials.* We anticipate being able to generate and screen libraries of millions of different compounds from one reaction vial. *In vivo* polymers are genetically engineered protein polymers that are an exciting new class of materials. Protein polymers are designed by recombinant DNA techniques to produce extraordinarily monodisperse products with well-defined molecular weights, stereochemistries, sequences, and biocompatibility; attributes not often attainable by chemical polymerization. While investigators have made significant advances in the use of *in vivo* polymers, no one has of yet made diverse *in vivo* polymer libraries. As a proof of principle for this strategy, we are creating diverse protein polymer libraries individually displayed on the surface of filamentous phage, allowing us to quickly screen from millions of different polymers to identify individual phage that carry biocompatible polymers.

Classes of *in vivo* polymers we are considering for library construction include elastin like polymers (ELPs), silk, and silk-elastin like polymers. Many of these proteins have properties similar to synthetic materials in that they are physically robust, they can be chemically or enzymatically crosslinked, and many have reversible temperature and pH transitions allowing hydrogel or swelled polymer production. These materials have been used as DNA delivery molecules, cell attachment mediums, subcutaneous implants, and as vascular grafts.

## Benefit to National Security Missions

This project will support the DOE mission in Threat Reduction by enhancing our understanding of the rational design of functional nanomaterials for application in chem/biothreat reduction, imaging, and the biosciences missions of the DOE Office of Science. A successful outcome of this new technique will have a profound impact on biomaterials development strategies and more general, combinatorial polymer chemistry. These libraries will greatly facilitate the discovery and production of biopolymers for future application in drug delivery, biocompatible polymers for medicinal implants, and advanced biosensors. This proposal describes a new capability that is leveraging LANL strengths in high-throughput selection, protein production, phage display technology, and polymer characterization.

## Progress

The overall goal of this proposal is to develop diverse polymer libraries and, as a proof-of-principle, to select from those libraries individual polymers that facilitate ECM and cellular interactions, on a long-term path toward building robust biomaterials. Our first library will

be created by inserting diverse recognition elements into elastin like protein polymers (ELPs). This library will be screened *en masse* against fibroblast cells and ECM proteins important for cellular adhesion (Figure 1). Down-selected polymers will be produced recombinantly in bacteria. Mechanical properties of these ELP clones, as monomers or cast films will be investigated (i.e. by contact angle, tensile strength, phase transitions).

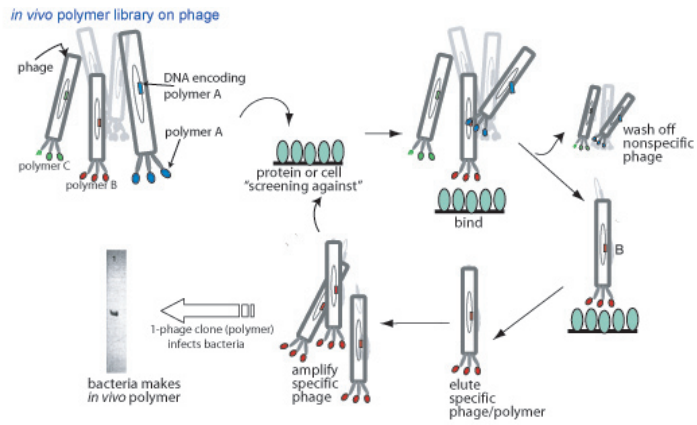


*Figure 1. Flow diagram for selection of in vivo polymers from a phage display library. Phage display is a well established technique at LANL.*

Our goals are :

1. Library creation of elastin like polymers (ELPs) containing diversity domains intermixed with elastin domains. Tasks: a) design and synthesize simple and extended elastin domains; b) design strategies to insert diversity within elastin domains; c) design and synthesize cell binding domains into elastin domains.

2. Display of ELP libraries on the surface of filamentous phage (bacterial virus) and the selection of ELP polymers with affinity toward cells and extracellular matrix proteins. Tasks: a) determine if simple and extended elastin can be displayed by phage; b) determine functionality of elastin while on phage; c) select polymers against proteins and cells.

3. Biocompatibility characterization of the polymers for properties such as cell adherence, spreading, and proliferation. Physical characterization of polymers based on hydrophilicity, tensile strength, and phase transitions. Tasks: as described in goal.

Toward these goals, we have designed and synthesized a simple elastin domain (short EL, "sEL") and we are currently evaluating the physical properties of this material. We have shown that this polymer can be displayed on the surface of filamentous phage, which is an exciting result showing us that our simplified experimental plan will work for creating libraries. We found that the expression of this protein, on phage, is nearly that of a highly stable small antibody (D1.3). Further, analysis by western-blotting shows that the expressed protein is of the correct size (Figure 2). We have designed cloning strategies to insert diversity sequences within the simple elastin domain, using methods yet to be implemented for any other project at LANL. Based on ideal physical properties, we have also designed and synthesized an extended elastin sequence (long EL, "lEL"). From this sequence, we have designed a strategy to insert diversity sequences within this polymer. Further, for each elastin polymer we have created controls for cell binding domains. The design and synthesis of these protein polymers was no small feat. Elastin polymers are repeating units of the same sequence of amino acids. Unfortunately, bacteria do not tolerate highly repeated sequences. To overcome this intolerance, we created a program that randomizes the DNA codons and yet would take into account the codon preferences of E. coli, thus producing a gene sequence that produces our ELPS and is stable in bacteria.

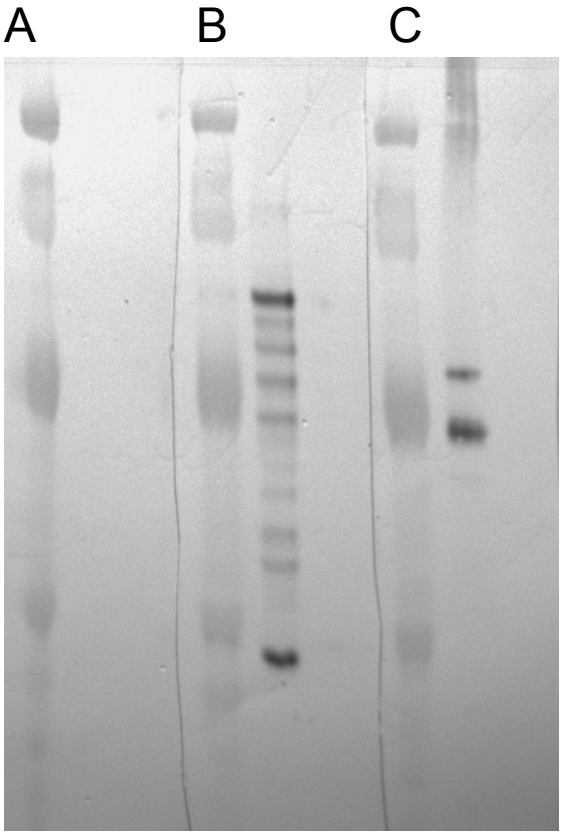


*Figure 2. WESTERN of short ELP (C) as compared to D1.3 (B) on the tip of Protein 3 of M13 phage. Detected with anti-SV5. M13 phage alone do not have SV5, hence they do not appear on the gel (A).*

## Future Work

Now that we have shown we have stable polymer scaffold(s) that can be displayed on the surface of filamentous phage, we will now finish our cloning strategy to generate libraries of diverse sequences (random amino acids and smaller libraries of select amino acids) within the elastin backbone. We will continue to investigate the best expression conditions for production of these polymers. Further, we will begin selection of these libraries against proteins important for the extracellular environmental attachment of cells to biomaterials.

## Conclusion

In vivo polymers are modified versions of elastin and silk, two natural materials that are unrivaled by synthetic materials for elasticity and strength per weight ratios. These polymers can be easily produced in bacteria, with precision unmatched by chemical approaches. We are improving where nature has left off by adding diversity within the polymer scaffold, thus allowing us to generate biocompatible polymers with an ease yet accomplished with synthetic nor engineering strategies. These polymers will be used as the base for future biosensors (i.e. implantable glucose sensors) and vascular grafts.

# Probing Unconventional Superconductivity in Heavy Fermion Thin Films

*Vladimir Matias*

20080519ER

## Introduction

Superconductivity is a physical phenomenon whereby a material loses all resistance to electric current below a certain transition temperature. There are many classes of superconductors, most notably the high temperature superconductors that contain copper oxide with a superconducting transition temperature around 100 K (or about -300 °F). We are exploring the physical nature of superconductivity in a specific class of compounds known as heavy 'fermion' or heavy-electron materials. In these materials conduction electrons are bound to the ionic lattice much tighter than in conventional metals and hence they move as if they were 'heavy.' Typically these materials contain rare earth or actinide elements, such as cerium, and they can exhibit unusual superconductivity that is poorly understood and whose mechanism is still under debate. LANL discovered a plutonium-containing compound in this class of superconductors with a critical temperature of 18 K and the search is still on for even higher transition temperatures. Our project aims to make thin layers of these superconductors for scientific study of their unusual superconductivity. The project combines LANL's advanced thin film technology currently used for high temperature superconductors with the LANL-established expertise in heavy fermion materials to access new physical measurements and shed new light on unconventional superconductivity. We will study the 'heavy-electron' 4*f*-electron systems, specifically, thin films of $CeCoIn_5$ in an 'epitaxial' or single-crystal like form. We intend to use the thin films for model studies of transport across grains within the material. A particular result of this work will be to test the symmetry of superconductivity in these materials, which is presumed to be not spherically symmetric. Furthermore, thin films offer the unique possibility to control the dimensionality of the samples, which will lead to further insight into the spatially inhomogeneous superconducting phases discovered in larger samples of $CeCoIn_5$ [1]. Insights from this work should lead researchers to better understand the limits of superconductivity and how to raise the superconducting transition temperature.

## Benefit to National Security Missions

This project will support the DOE mission in Office of Science by enhancing our understanding of unconventional superconductivity and through the search for new superconducting materials. Superconductivity is potentially a key technology for national energy security and practical superconducting applications are currently being developed by the DOE Office of Electricity.

## Progress

We are attempting two approaches for deposition of "heavy fermion" thin films. One is pulsed laser deposition from a variety of targets and, separately, we are also trying to deposit films by co-evaporation. We modified our vacuum chambers that were mainly used for the deposition of oxide thin films to the needs for growing heavy fermion films. The heavy-fermion compounds, such as $CeCoIn_5$ or $CeIn_3$, are intermetallic systems containing a rare earth (Ce) with a high oxygen affinity. This requires reducing the base pressure in the chambers well below 10E-7 Torr. After careful leak checking and installation of a new bakeout setup we were able to reach base pressures below 10E-8 Torr in both of our vacuum systems. In order to increase the throughput and decrease the number of chamber openings, we use a conveyer belt like sample carrier for single-crystal substrate storage and successive movement into the deposition zone. Up to ten samples can be prepared within one run. Additionally we use a flexible metal tape with a textured MgO layer as a substrate to substitute for single crystals. In the first year of this project we have set up our two deposition systems to be capable of depositing heavy fermion thin films and obtained the necessary materials for deposition. We made our first films of $CeCoIn_5$ and $CeIn_3$ and have encountered a number of issues in deposition that we are currently addressing. The approach we have developed this year for film deposition is to first make the $CeIn_3$ compound and understand how it grows in thin film form. $CeIn_3$ has a similar in-plane lattice parameter to the superconductor $CeCoIn_5$ and also shares many of the same issues in deposition.

For the pulsed laser deposition (PLD), our main approach, the key parameters we are optimizing are substrate temperature and laser energy. For our single-crystal substrates we use mainly MgO and $MgF_2$; the latter has an excellent lattice match to $CeCoIn_5$. The biggest obstacle for depositing epitaxial thin films of $CeCoIn_5$, besides the oxygen affinity of Ce and the low melting point (and relatively high vapor pressure) of In, has been the formation of In droplets at early stages of film growth. We started by investigating possibilities to control the stoichiometry in our films during PLD. We developed a *novel* design for PLD targets based on a ring-area target with concentric rings of Co, Ce, and In. The stoichiometry of the deposit can then be controlled by adjusting the number of laser pulses to each sector of the target. Besides that, we are also preparing films with stoichiometric targets of several different compositions in the Ce-Co-In system. Additionally, we also deposited films in a coevaporation system equipped with *in situ* reflection electron diffraction, known as RHEED. There we optimized conditions for epitaxial Cr buffer layers on MgO for growth of heavy fermion films. These Cr films are extremely smooth and can be epitaxial and as such good buffer layers for growth of $CeCoIn_5$. We also found that the growth conditions for epitaxy by coevaporation seem to require low In content and low deposition temperatures. This is in agreement with recent results by a group in Japan that reported first films of $CeCoIn_5$ [2]. We note that their films are still not epitaxial.

Our PLD results are summarized in Table I. Surprisingly, and in contrast to our first coevaporated films, our best samples to date by PLD were made with In-rich targets and at higher temperatures. Figure 1 shows an x-ray diffraction result from such a film made from a $CeCoIn_{11}$ target. From these results we can see that the films have some epitaxial CeCoIn5 phase, but are not yet single-phase. Figure 2 shows an electron micrograph of this film where we see oriented crystallites within a background matrix. In Figure 3 we show the low temperature electrical transport measurement of the same film indicating the presence of the CeCoIn5 superconducting phase that is not electrically continuous within the film.

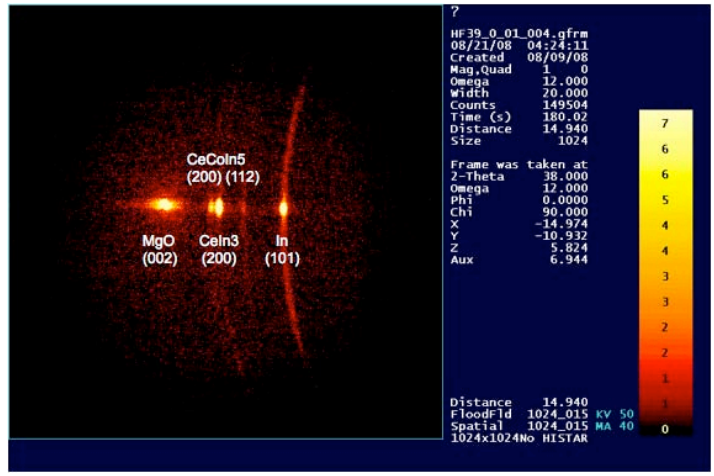


*Figure 1. Image of a two-dimensional x-ray detector from diffraction of a Ce-Co-In film. The result indicates presence of epitaxial $CeCoIn_5$ and $CeIn_3$ phases.*

| Target | Optimum temperatures | Results |
|---|---|---|
| Ce:Co:In ring target allows for atomic layering | ~ 500°C | $CeIn_3$ and $CeCoIn_5$ polycrystalline; some $CeO_2$; excess In droplets |
| Ce-Co-$In_5$ composite target | Low temp 300 – 500°C | Smoother films than atomic layering; In-poor matrix with In-rich droplets |
| Ce-Co-$In_{11}$ composite target | High temp 600 – 700°C | Epitaxial crystallites in In-rich matrix |

*Table 1. Summary of PLD results from the first year of the project.*

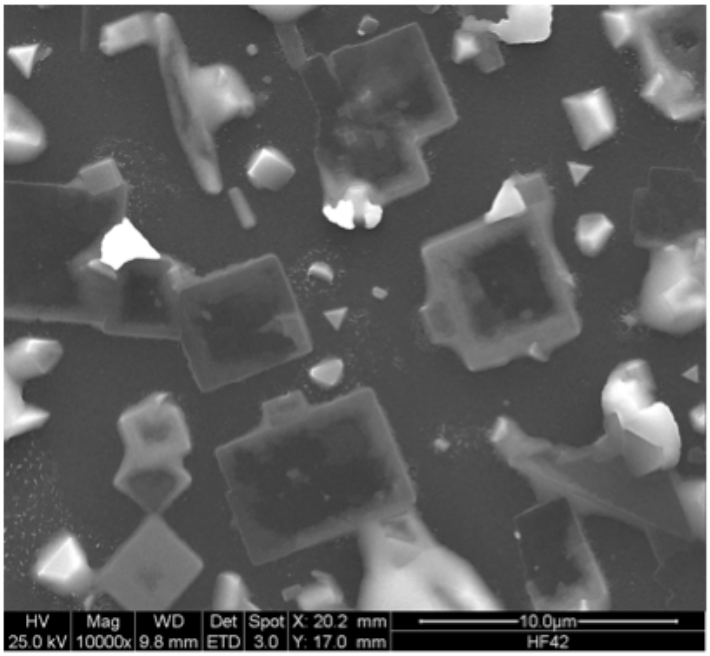


*Figure 2. Secondary electron micrograph of the CeCoIn film shown in Figure 1, with rectangular single-crystalline islands.*

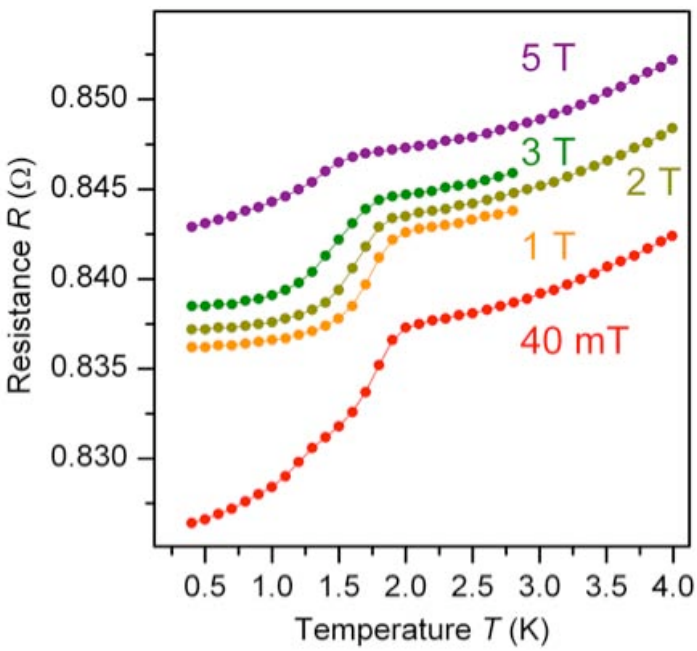


*Figure 3. Electrical transport measurements at low temperature indicating the presence of a superconducting $CeCoIn_5$ phase in the thin film sample.*

## Future Work

The objective of the proposed work is to gain a more thorough understanding of unconventional superconductivity in heavy fermion superconductors (HFS) by studying these materials in thin film form. We will continue to grow the heavy fermion thin films by pulsed laser deposition (PLD) and coevaporation and improve our understanding of the materials science issues in order to perfect them. The goal is to make high-quality single-phase epitaxial films that can be used for study of physical phenomena. In order to probe and possibly clarify the order parameter symmetry in HFS, we will pattern junctions in the films and study transport across grain boundaries. By measuring the low temperature behavior in a magnetic field we will gain new understanding of the inhomogeneous superconducting phase in low dimensionality. Theoretical modeling work will be done in parallel with the experimental work.

## Conclusion

We are studying a class of superconducting materials represented by the compound CeCoIn5 in the form of thin films. We intend to use the thin films for model studies of transport across grains. A result of that will be to test the symmetry of superconductivity in these materials, which are presumed not to be spherically symmetric. This has important implications for determining the physical mechanism that is responsible for superconductivity. So far we are making progress in understanding the materials science necessary to grow these films and we have made epitaxial material, but not yet single phase.

## References

1. Movshovich, R., A. Bianchi, C. Capan, P. G. Pagliuso, and J. L. Sarrao. Possible Fulde-Ferrell-Larkin-Ochinnikov inhomogeneous superconducting state in CeCoIn5. 2005. *Physica B.* **359-361**: 416.

2. Izaki, M., H. Shishido, T. Kato, T. Shibauchi, Y. Matsuda, and T. Terashima. Superconducting thin films of heavy-fermion compound CeCoIn5 prepared by molecular beam epitaxy. 2007. *Applied Physics Letters.* **91**: 122507.

continuing project

# Photocatalytic Materials Based on Quantum Confined Semiconductor Nanocrystals

*Milan Sykora*

20080523ER

## Introduction

The objective of the proposed research is to develop a new class of nanoscale photocatalytic materials, which upon solar irradiation can produce molecular hydrogen via photochemical decomposition of organic substrates or water (Figure 1). The proposed approach is based on exploiting unique properties of semiconductor nanocrystaline quantum dots (NQDs) in assemblies where they are coupled to established molecular redox catalysts. In these photocatalytic assemblies the NQD functions as light harvester and a charge generator, which activates a molecular catalyst via charge transfer (CT). Our first-ever demonstration that molecular catalysts can be effectively sensitized by NQDs demonstrates the feasibility of this approach. The assemblies take advantage of unique properties of NQDs, such as high light harvesting efficiency, size-tunable absorption spectra and redox properties and the ability to convert photon energy to charge with higher than 100% efficiency via the process of carrier multiplication (CM). With the eye towards the practical application of solar hydrogen production the proposed research will lead to development of new nanoscale fabrication methods, an understanding of virtually unexplored interfacial charge transfer at the nanoscale semiconductor-semiconductor and semiconductor-molecule interfaces and generate insights into mechanistic aspects of photocatalytic decomposition of variety of organic substrates and water. The pursuit of these objectives is expected to provide important insights into some of the most intensely studied problems in chemistry.

## Benefit to National Security Missions

This project will support the drive toward national energy security, a key DOE mission. In particular, the work will enhance our understanding of how nanoscale materials can be utilized to improve the efficiencies of the solar energy conversion technologies.

## Progress

During the first year of the project we have made progress on multiple fronts.

### Development of capabilities

During the first year of the project the initial stages were dedicated to staffing and development of technical capabilities. Two very talented postdoctoral associates were recruited and trained to perform research on the project. Also, new instrumental capabilities were developed through acquisition and installation of new instrumentation, which included equipment for measurement of attenuated total reflectance infrared (ATR-FTIR) spectroscopy and a new, state-of-the-art ultrafast transient absorption spectrometer. Acquisition of this instrumentation is not only critical for the success of the project, but it also represents an important expansion of the technical capabilities of the laboratory.

### Technical progress

*Synthesis and characterization of precursor materials*

We have synthesized and characterized numerous materials that are necessary precursors for the construction of photocatalytic and photovoltaic structures. These include light harvesting components - NQDs of various compositions (CdSe, CdS, PbS, PbSe) and various sizes (particle diameter 2 to10 nm), electron transporting components - metal oxide ($MO_x$ = $TiO_2$ and $ZrO_2$) nanoparticles of various sizes (~20-300 nm). We have further synthesized series of Ruthenium polypyridine-based redox catalysts. New synthetic methods were developed to modify catalysts with functional groups necessary for their chemical coupling to the NQDs. The optical and redox properties of these metal complexes were characterized by spectroscopy and electrochemical methods. We have also performed a theoretical study of the effect of the modification of the metal complexes with coupling functional groups on their electronic and optical properties and their charge transfer reactivity. We found, that while the addition

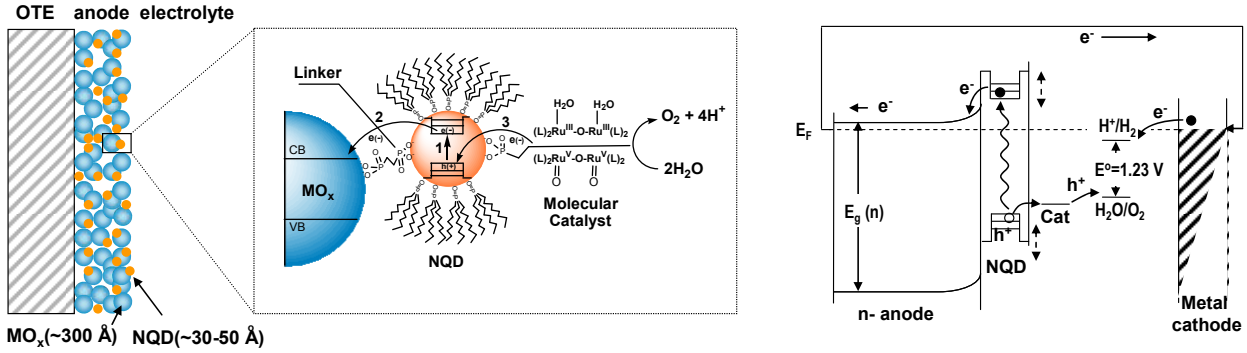


*Figure 1. Left: Schematic diagram of the nanoscale photocatalytic assembly based on coupling of semiconductor NQDs and molecular catalysts. Irradiation of the NQD with visible light leads to generation of one or more electron-hole pairs (1), followed by rapid photoinjection of an electron into the conduction band (CB) of the metal oxide (MOx) (2). This electron is relayed through the external circuit to a metal counter electrode, where it reduces protons to molecular hydrogen. The hole in the valence band (VB) of the NQD is quenched by electron transfer from a molecular catalyst (3). When oxidized (activated) to its active form the molecular catalyst can oxidize the substrate (i.e., organic material or water) generating protons as a byproduct. Although multiple cycles are typically required to oxidize the catalyst to its active form, the number of photons required can be reduced through CM, thus increasing the overall efficiency of the energy conversion process. Right: Energy diagram of the photoelectrolytic cell in which the composite material could be used as a photoanode (Cat is the molecular catalyst). Hydrogen production occurs at a metal (e.g., Pt) cathode. Development of the actual device is not the objective of the current project.*

of carboxyl linking group can affect the optical absorption and emission of the catalysts, it leaves their ionization and electron affinity energies almost unchanged. This strongly indicates that the modification of the catalysts with linking groups is not likely to affect their catalytic activity. The results of the theoretical study are summarized in the publication to be submitted within next few weeks.

*Development of fabrication methods for construction of nanoassemblies*

- Fabrication of NQD/catalyst assemblies: Our initial ATR-FTIR studies indicate that molecular catalysts functionalized with carboxylic acid functionality can be chemically attached to the surface of the NQDs. Two different approaches were developed to study the mechanism and dynamics of the coupling process (Figure 2 a-c). The coupling, during which the functionalized catalysts substitute the original protective ligand layer of NQD, can be achieved through mixing of the NQDs with molecular catalyst in solution or by exposure of NQD film to the solution of catalysts. Our results represent a first ever direct evidence of chemical coupling of molecular catalysts with quantum confined semiconductor nanocrystals. In a separate set of experiments we have developed a procedure, which allows us to determine the exact number of adsorbed catalysts per NQD. The procedure combines steady-state photoluminescence measurements and theoretical isotherm modeling (Figure 2 d). Our preliminary results obtained by this approach suggest that for NQDs with diameter ~5 nm up to seven catalysts can be anchored to the NQD surface. The total amount of the catalysts adsorbed can be controlled by the concentration of the catalyst in solution.
- Chemical coupling of NQD to $MO_x$ surfaces: In our initial set of experiments we have tested two self-assembly procedures for coupling of NQDs to $MO_x$ mesoporous surfaces based on utilization of bifunctional organic linkers. In one approach (method 1) the $MO_x$ is initially functionalized with a bifunctional organic linker. The functionalized mesoporous surface is then exposed to solution of NQDs. In a second approach (method 2) the NQDs are first functionalized with bifunctional linkers via ligand exchange process. The bare mesoporous $MO_x$ surface is then exposed to the solution of functionalized NQDs. Using visible reflectance spectroscopy we have found that both procedures result in efficient NQD/MOx chemical coupling; i.e., significant amount of NQDs can be adsorbed onto the $MO_x$ surface. However, as discussed below the extent of electronic coupling between the NQD and MOx varies between the self-assembly procedures.

**Initial studies of interfacial charge transfer (CT)**

- CT at the NQD/catalyst interface: Building on our progress in the fabrication of the NQD/catalyst nanoassemblies we have performed initial studies of electronic interactions in the CdSe NQD/catalyst structures following photoexcitation by visible and UV radiation. We have found that mechanism of interaction is strongly dependent on the NQD size (i.e., extent of quantum confinement) and the degree of NQD/catalyst electronic coupling (Figure 3). For smaller NQDs (diameter <3.5nm) the dominant mode of interaction is NQD-complex energy transfer, which can occur across the protective ligand layer. The CT is dominant for larger NQDs (>5nm) when the complexes are adsorbed onto

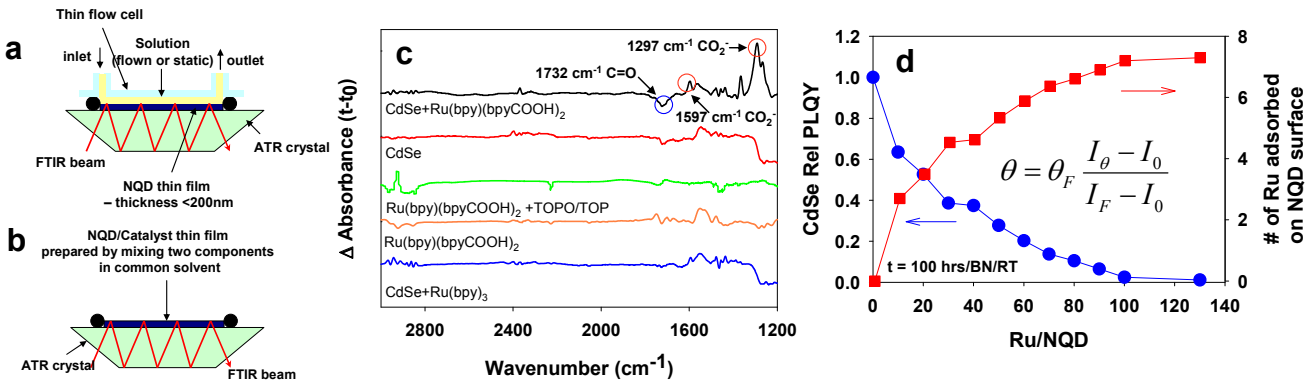


*Figure 2. Preliminary results of NQD surface chemistry studies. (a,b) Two different approaches to monitoring surface exchange chemistry by ATR-FTIR. The FTIR signatures of the original surface ligand and the substituting adsorbate are monitored as function of time. The difference spectra provide information about the mechanism and dynamics of the surface exchange. (c) Difference ATR-FTIR spectra (method B) for the system consisting of NQDs in the presence of Ru metal catalyst functionalized with carboxylic acid group. The deprotonation of the catalyst in the presence of the NQDs , not observed in any of the controls, strongly suggests the adsorption of the catalyst onto the NQD. (d) The PL of the NQD is reduced upon adsorption of the catalyst. The variation in the magnitude of the reduction with catalyst concentration can be used to determine the number of catalysts adsorbed per single NQD and fractional surface coverage (theta).*

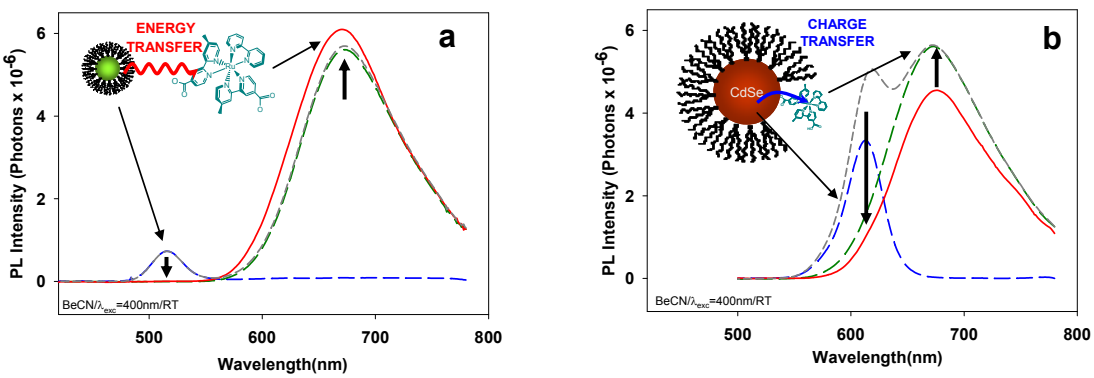


*Figure 3. Preliminary results of steady-state photoluminescence (PL) studies of NQD-catalyst electronic interaction. a) In assemblies consisting of small (less than 2 nm diameter) the reduction of PL of the NQD is paralleled by an increase in the PL of the catalyst, which is an evidence of NQD to catalyst energy transfer. b) In assemblies consisting of large (more than 4 nm diameter) NQDs the reduction of PL of the NQD is paralleled by a decrease in the PL of the catalyst, which indicates the charging of catalyst by NQD to catalyst charge transfer. For the NQD/catalyst assemblies to have utility in practical application the charge transfer has to be the dominant mode of interaction.*

the NQD surface. To best of our knowledge this is a first demonstration of a nanoassembly where the type of electronic interaction (energy vs. charge transfer) depends solely on the size of one of the components. We have initiated quantitative studies of factors that determine the dominance of one or the other interaction process. The understanding of these factors is important from practical standpoint as for the photocatalytic assemblies to be useful in solar energy conversion process the NQD/catalyst interactions must be dominated by charge rather than energy transfer.

- Photoinduced charge separation at the NQD/$TiO_2$ interface: We have performed initial studies of the CT in the NQD/$TiO_2$ assemblies. The results show that at least 30% of NQD excitations lead to charge transfer to $TiO_2$. We find that the efficiency of the CT is strongly dependent on the method used for $MO_x$/NQD coupling. While coupling method 1 yielded the above efficiencies of NQD to $TiO_2$ CT, method 2 yielded efficiencies typically less than 5%. Thus, while the chemical coupling achieved by two methods is comparable, the electronic coupling, dictating the efficiency of interfacial CT is significantly reduced in assemblies prepared by method 2. Further studies are needed to determine the origin of the differences and identification the fabrication process that maximizes the electronic coupling.

## Future Work

Based on our progress during the first year, in second year we will focus on following studies:

1. Fabrication of NQD/catalyst assemblies: Complete the studies of chemical coupling between NQDs and catalysts. Test possibility of NQD-catalyst coupling with functional groups other than carboxylic acid (e.g., phosphonic acid, bipyridyl amine)

2. CT at the NQD/catalyst interface: Identify conditions, which favor CT over ET in NQD/catalyst assemblies. Perform detailed studies of CT in these assemblies in low light intensity (single-exciton) regime. Develop the understanding of the mechanism of interfacial CT and identify the key variables dictating the CT efficiency. Demonstrate control of dynamics of the NQD-catalyst CT.

3. Photoinduced charge separation at the NQD/$TiO_2$ interface: Determine the origin of the differences in CT efficiencies in assemblies prepared by Method 1 and Method 2. Investigate other fabrication processes that will maximize the NQD/$TiO_2$ electronic coupling. Perform detailed studies of CT in NQD/$TiO_2$ assemblies to identify the key variables dictating the CT efficiency. Demonstrate CT efficiencies exceeding 50%.

## Conclusion

In terms of basic science the main objective of the proposed research is improvement of our understanding of how nanoscale materials can be utilized to enhance the efficiencies of the solar energy conversion technologies. The practical objective is a development of a new class of nanoscale materials with potential to produce molecular hydrogen from organic substrates or water upon solar irradiation. These objectives are aligned with DOE's energy security mission as they have potential to reduce our energy dependence on oil and other fossil fuels.

continuing project

# Novel Materials for Gamma-Ray Detection based on Nano-Engineered Semiconductor Nanocrystals

*Richard Daniel Schaller*

20080660ER

## Introduction

In this work, we will the use of semiconductor nanocrystals (NCs) for use as gamma ray detectors. Nanocrystals are nanometer sized crystals of various semiconductors that have a bandgap that differs from the bulk material due to its small size. NCs have many properties that are desirable for gamma-ray detection including large Z for strong interaction with gamma rays, high photoluminescence quantum yields (up to 90%), emission wavelength tunability from the ultraviolet to the infrared, and solution processability. However, some properties of typical NCs are not advantageous for scintillator applications such as a relatively small Stokes shift of the emission (typically ~60 meV or ~20 nm in the visible wavelength range), which causes significant reabsorption of emitted photons in thick solid films. To overcome these problems, we will study NC composite films that are composed of distinct "donor" and "acceptor" NC materials. Wider band gap, high emission quantum yield NC material such as ZnSe or CdSe NCs will generate excitons from high energy particles and act as energy transfer donors while a smaller band gap NC material with a large Stokes shift and high emission quantum yield will act as both an energy transfer acceptor and photon-emitter. Targeted candidate acceptor materials include red- to near-infrared emitting nano-engineered type-II NCs, which emit from a spatially dissociated excitonic state, and indirect gap semiconductor NCs such as silicon. Red- to near-infrared photon emission will help to reduce problems associated with scatter in the solid film. Ratios of donors to acceptors will be guided by modeling to optimize the extent of energy transfer to acceptors and material transparency at the emission wavelength. Photoluminescence excitation and time-resolved emission measurements will be performed to determine rate and extent of energy transfer to acceptors.

## Benefit to National Security Missions

Radiation detection is a key capability in detecting nuclear proliferant materials. This work directly supports nuclear threat reduction and nonproliferation activities that are key mission areas in DOE, DHS, and other government agencies. Semiconductor nanocrystals are good candidates for gamma-ray detectors that are efficient, operate at room temperature, and low-cost

## Progress

During the past year, we have been conducting two types of work. One involves building a pulsed electron gun that will be used to explore the behavior of semiconductor nanocrystals in conditions that mimic excitation with gamma rays. The other involves energy transfer studies between nanocrystals of two different compositions to determine rates of energy transfer and efficiency.

Spent much of last year building an apparatus to excite NC ensemble samples with 1-ps electron pulses of tunable energy (0.5-50keV) and detect the emitted photons with a high time-resolution streak camera (<2ps). Gamma-ray photons cannot be controllably pulsed. However, they do interact with matter to produce energetic secondary electrons (keV-MeV). The secondary electrons produce cascades of lower-energy electrons that eventually generate relatively low-energy material excitations such as proximal electron-hole pairs ("excitons") which can recombine radiatively. However, in addition to exciton formation, electrons can ionize NCs and may also produce multiple excitons within individual NCs. Ionized NCs (containing an uncompensated electron or a hole) cannot emit. A NC that contains both an exciton and an additional charge (a so-called trion) will emit with greatly reduced-efficiency due to unfavorable competition with ultrafast (~5-300ps) nonradiative Auger recombination. Multiple excitons produced within a NC will also emit with reduced efficiency due to Auger recombination. To date, no one has been able to directly measure the branching ratios of material excitations from electron interactions. This transient cathodoluminescence method will allow us to directly measure the low-energy material excitations that result from interactions with energetic electrons. Because it is a transient method, short-lived trions and multiexcitons will be observable and quantifiable due to known spec-

tral and temporal signatures. We will also quantify normally non-emissive, singly-charged NCs by photoexcitation of the sample prior to the arrival of the electron pulse such that transiently emissive trions, in place of ionized NCs, are formed. Direct knowledge of the branching ratios from a survey of several NC samples will be fed back into the synthetic design of the NCs. If ionization is the dominant problem, we will attempt to minimize it via the growth of thick, low-z material shells on high-z NC cores. If we find multi-exciton formation to be the main problem, we can reduce NC size to reduce the energy deposited per NC (electron energy deposition is understood to be a function of path, ~6eV/nm for CdTe, so smaller NCs may equal fewer multi-excitons) such that single excitons are principally formed. At this moment, we have completed construction of the electron gun itself, but the vacuum chamber needed for its operation is still under construction.

Also, we have been performing energy transfer studies of mixed NC films in order to determine the feasibility of this approach for increased Stokes shift such that photoemission may be detected from thick films. Mainly we have been studying CdSe-PbSe films that emit in the near-infrared. We observe fast (<200ps) and efficient energy transfer, though this system is not ideal for scintillation due the inefficiency of near-infrared photodetectors in comparison to visible ones.

## Future Work

We will develop scintillator detector materials composed of mixtures of semiconductor nanocrystals (NCs). NCs have many properties that are desirable for gamma-ray detection including large Z, high emission quantum yields (up to 90%), emission wavelength tunability from the ultraviolet to the infrared, multiple exciton formation, and solution processability. However, there are also detrimental properties of typical NCs for scintillator applications such as a relatively small Stokes shift of the emission (typically ~60 meV or ~20 nm in the visible wavelength range), which causes significant reabsorption of emitted photons in thick solid films. Also, solid films of NCs can have a significant degree of energy transfer which overall decreases emission quantum yield as excitons migrate to any non-emissive NCs that have low-energy defect states. To overcome these two significant problems, we will study NC composite films that are composed of distinct “donor” and “acceptor” NC materials. Wider band gap, high emission quantum yield NC material such as ZnSe or CdSe NCs will generate excitons from high energy particles and act as energy transfer donors while a smaller band gap NC material with a large Stokes shift and high emission quantum yield will act as both an energy transfer acceptor and photon-emitter. Targeted candidate acceptor materials include red- to near-infrared emitting nano-engineered type-II NCs, which emit from a spatially dissociated excitonic state, and indirect gap semiconductor NCs such as silicon. Red- to near-infrared photon emission will help to reduce problems associated with scatter in the solid film. Ratios of donors to acceptors will be guided by modeling to optimize the extent of energy transfer to acceptors and material transparency at the emission wavelength. Photoluminescence excitation and time-resolved emission measurements will be performed to determine rate and extent of energy transfer to acceptors.

## Conclusion

It is expected that semiconductor nanocrystal materials will provide a high detection efficiency, low-cost, scalable gamma ray detector material that is useful for applications such as portal monitoring as well as radiation sensing for materials control and accountability. Such applications are challenging and prohibitively expensive with current materials. Semiconductor nanocrystals are expected to, upon interaction with gamma ray photons, produce excitons that will efficiently produce photoluminescence. This photoemission will be significantly red-shifted with respect to the material absorption feature such that self absorption will not take place significantly.

# Parallel-Replica Dynamics Study of Tip-Surface and Tip-Tip Interactions in Atomic Force MicrosCopy and the Formation and Mechanical Properties of Metallic Nanowires

*Arthur Ford Voter*

20080759ER

## Introduction

Metallic nanowires, with diameters of a few atoms down to even a single atom, will play an important role in future-generation nanodevices, as electrical conductors, and electrical and perhaps mechanical switches. Enabling this technological advance will require that we understand their unique mechanical properties as they are formed and subjected to mechanical stress. Up to now, atomistic simulations aimed at understanding these processes have been necessarily limited to time scales that are thousands or millions of times shorter than experimental time scales. This is because molecular dynamics simulations are limited to times in the nanoseconds, while the relevant atomic force microscope (AFM) experiments require milliseconds to seconds. An example of an AFM experiment [1] in which a metallic nanowire is stretched to failure is shown in Figure. 1.

We have recently developed an accelerated molecular dynamics method called parallel-replica dynamics (Par-Rep) [2], in which time is accelerated through parallelization. By porting the Par-Rep code to the new Roadrunner supercomputer, we will be able to perform the first-ever atomistic simulations of the formation (through AFM tip to surface contact and withdrawal), and tensile test behavior, of metallic nanowires of silver and copper on experimentally accessible time scales of milliseconds. The Par-Rep method gives exact long-time evolution of an infrequent-event system, even one in which the boundary conditions are changing in time. Based on initial benchmark calculations, we expect to achieve a speed of ~0.5 ms of simulation time per wall-clock hour on Roadrunner.

## Benefit to National Security Missions

This project endeavors to develop atomic-scale simulations of materials that will tremendously enhance our basic understanding of materials, and nanomaterials in particular. Such basic understanding of materials and the ability to model novel materials impacts the DOE mission in Scientific Discovery and Innovation, as well as a broad array of other missions important to DOE, DHS, and other government agencies.

## Progress

This project was begun mid-year in FY08. While we wait for the delivery of the Roadrunner computer system, we have begun scoping studies using hyperdynamics simulations in preparation for much more substantial Roadrunner runs. Hyperdynamics [3] is another accelerated molecular dynamics method developed here at Los Alamos. We have performed hyperdynamics simulations on metallic nanowire systems 10 to 20 angstroms in diameter, consisting of roughly 1000 atoms. Because hyperdynamics is not valid for driven systems, we stretch the nanowire quasi-statically, increasing its length by 0.01 angstrom at a time, and then maintaining that length for the duration of the hyperdynamics run until it is time for the next greater length setting. In these simulations we are already observing interesting deformation mechanisms involving formation and passage of partial dislocations.

For example, in order to understand the dependencies of preferred deformation mechanisms on strain rate, we conducted stretching simulations of Ag nanowires at two different stretching velocities, the results of which are shown in Figure 1. The first one used conventional molecular dynamics simulation with a stretching velocity of $10^{-1}$ m/s, and the second one used hyperdynamics with a stretching velocity of $10^{-5}$ m/s. Both simulations were held at a temperature of T=300K. From our results we could clearly see that the formation of stair-rod dislocations is the dominant deformation mechanism at the beginning of the stretching processes. However, in the slow stretching simulation, this stair-rod dislocation could be eliminated by the propagation of another stair-rod dislocation, and in the end we obtained an almost perfect nanowire that was one (002) layer thinner than the initial configuration. We also noticed that the

energy of the nanowire under slow stretching is lower than that under fast stretching, which is not surprising because in the slow stretching simulation the nanowire has more time to relax itself through thermal events. In future runs on Roadrunner at even slower stretching velocities, we anticipate seeing a complete elimination of stair-rod dislocations, allowing the nanowire to become perfect again, but one (002) layer thinner.

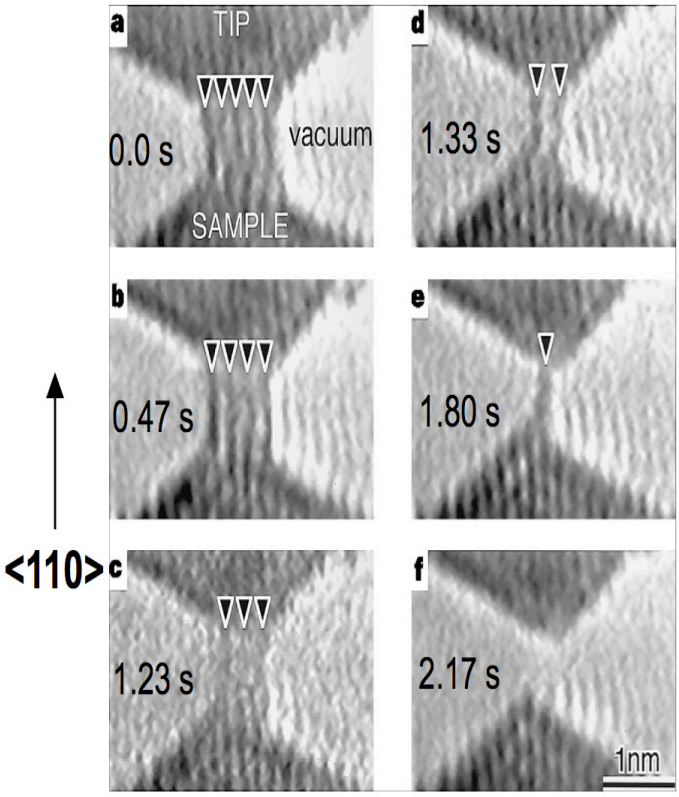


*Figure 1. Series of high resolution transmission electron microscopy (HRTEM) images of gold nanowire as it is stretched. Initially formed using a gold AFM tip, as the tip is withdrawn from the gold sample over a time scale of ~2 seconds, the nanowire thins from five layers to four layers, and so on down to one layer, as indicated by the arrows, before it ultimately breaks completely.*

A key component of this project is the development of a Par-Rep computer program that can exploit the exceptional speed of the Roadrunner architecture. The main Par-Rep program, which can run on normal computer architecturs, has now been developed, and a special force-call subroutine (which evaluates the interatomic forces necessary to perform MD) has been written for the Roadrunner cell architecture. This force routine is extremely fast, taking just 0.3 microseconds per atom.

## Future Work

Our main scientific objective is to resolve in full atomistic detail the processes by which silver and copper nanowires form following tip-to-surface or tip-to-tip contact and how they react to mechanical stress as they are stretched or sheared up to their breaking point. These simulations will be carried out on a time scale accessible to atomic-probe experiments, through the use of the rigorously accurate parallel-replica dynamics method implemented on the Los Alamos Roadrunner supercomputer. Two classes of simulations will be carried out: first, starting from experimentally observed structures, nanowires will be annealed and their mechanical response to strain probed over a range of rates and temperatures; second, nanowires formed starting from clean surfaces and tips will be simulated and their structures and mechanical properties will be compared to experimental ones. We believe we can achieve millisecond simulations of nanowire stretching and breaking using Roadrunner. For the simulations of nanowire formation by tip contact, due to the greater likelihood of too-frequent events, there is a greater risk that we will be limited by algorithmic inefficiency before reaching the millisecond regime. For both cases, simulations at lower temperatures (that are experimentally accessible) will mitigate this inefficiency effect.

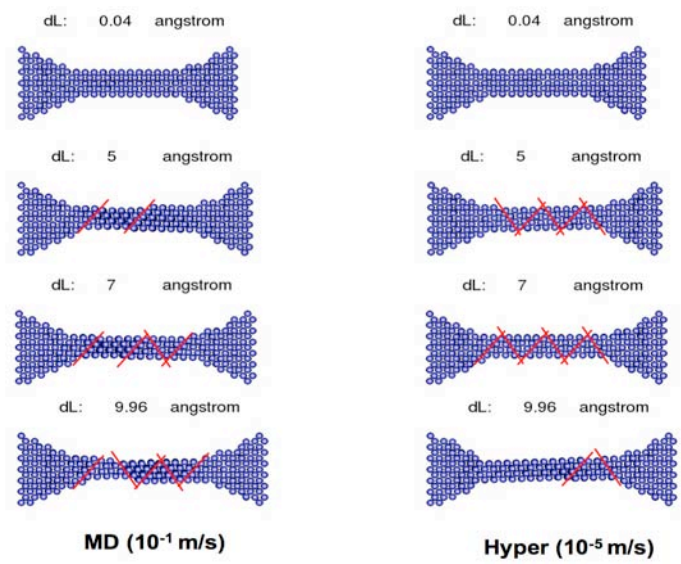


*Figure 2. Results of silver nanowire simulation showing the difference between fast stretching with direct molecular dynamics (MD) and slower stretching with hyperdynamics, as discussed in the text. The nanowire stretched more slowly comes closer to perfect thinning, retaining fewer defects.*

Our computational objective is to port our parallel-replica molecular dynamics code for metal (embedded-atom) systems to Roadrunner. By tuning the parallel-replica algorithm to minimize parallel communication and optimizing the force routine to run as fast as possible on the cell architecture, our goal is to take nearly full advantage of the extreme speed of Roadrunner. Benchmarks we have run using a preliminary version of the force routine, and analysis of issues in parallelizing Par-Rep to 10,000 processors, give us strong reason to believe that we can achieve our goal of a simulation speed of 0.5 milliseconds of simulation per hour of wall-clock time.

## Conclusion

This work will produce a better understanding of the behavior of nanowires, which will find important use in future-generation nanodevices as electrical conductors and switches. Maintaining America's pre-eminence in nanotechnology is important for the economy and for our world standing in technology. The computer program developed for this project will allow direct, accurate simulations of materials dynamical properties on unprecedented time scales, far beyond the scope of this project. This program will thus be a valuable tool for other studies in the future.

## References

Ohnishi, H., Y. Kondo, and K. Takayanagi. Quantized conductance through individual rows of suspended gold atoms. 1998. Nature. **395**: 780.

Voter, A. F.. Parallel replica method for dynamics of infrequent events. 1998. Physical Review B. **57**: 13985.

Voter, A. F.. Hyperdynamics: Accelerated molecular dynamics of infrequent events. 1997. Physical Review Letters. **78**: 3908.

# Hierarchical Assembly of Porous Materials: Obeying Bio-Inspired Allometric Scaling Laws

*Michael Timothy Janicke*

20050506ER

## Abstract

The use of hierarchical porous structures as support materials for catalytic reactions is analogous to the circulatory system in which nutrients are delivered to individual cells via arteries, capillaries and veins. In such a hierarchical system, every fluid element is passed through some capillary to exactly one single site exactly once per pass. By suitably scaling the branching dimensions, the flow-area is conserved, pressure drop is minimal, and diffusion lengths over which activity must occur is reduced to nanometers. With a controlled, graduated set of pores, we can mimic the distribution systems seen in Nature and predicted by Kleiber's Law

## Background and Research Objectives

Nature has provided every living organism an incredible distribution system for transporting nutrients and removing wastes. From insects and shrews to whales and cottonwood trees, every cell in these organisms is connected to an efficient distribution system. Allometric scaling laws in biology have shown that all of these networks are unified in that 1) they are space filling systems that follow fractal-like branching patterns, 2) the final branch of the network (e.g. the capillary in mammalian organisms) is size invariant, and 3) the energy necessary for distribution is minimized. *Every organism has evolved with such an optimal supply network.*

Take for example the mammalian circulatory system. A pulsating heart distributes blood through the aorta to the arteries that are further reduced in diameter until blood enters the capillaries. In the capillaries, the red blood cells transport oxygen and nutrients to the cells before blood is returned through capillaries and the venal system to the heart. Several simple scaling laws almost completely describe the cascade of sizes and lengths for the individual blood vessels in order to satisfy the three requirements described previously (West, GB, *Physica A* 263 (1999) 104-113). Assuming there is a simple bifurcation of each vessel, the cross-sectional areas of the arteries must be conserved as they decrease in radius. This translates to $r_{k+1}/r_k = 2^{-1/2}$ such that a successive artery ($r_{k+1}$) decreases in size at each bifurcation by the inverse of the square root of two. This ensures that the blood cells travel through the system with the same velocity. In effect there is an impedance matching at each level similar to impedance matching in electrical circuits and the blood (or signal) flows without damping. The length of each artery also decreases by a simple relationship, $l_{k+1}/l_k = 2^{-1/3}$ ,and results in space-filling and volume-preserving branching of the blood vessels. Having blood cells travel in the capillaries with the same velocity as those in the aorta would be disastrous, as blood cells must slow down at the cellular level so that nutrients and wastes can diffuse between cells. To satisfy this biological need, smaller blood vessels follow a different scaling law, $r_{k+1}/r_k = 2^{-1/3}$. With this relation, the area-preservation is lost and the blood flow slows down as viscous terms describing the flow begin to dominate and the resistance increases. Thus, the size and length of blood vessels in the mammalian circulatory system can be described naïvely by three scaling laws that determine the radius and length of each vessel.

The aim of this proposed research was to design materials that achieve the same remarkable properties that are observed in natural distribution systems. To achieve this, materials were created by a hierarchical assembly of pores. With such a system, liquids or gases are easily transported to pores with a prescribed radius. This will have phenomenal applications in areas of porous materials, heterogeneous catalysis, and solid-state materials with interesting opto/electronic properties. Take for example a chemical reactor relying on a heterogeneously catalyzed reaction in which these materials will be employed as monolithic catalyst supports. In such a hierarchical system, every fluid element is passed through a capillary to exactly one *single* site exactly

once per pass. By suitably scaling the branching dimensions, the flow-area is conserved, pressure drop is minimal, and diffusion lengths over which activity must occur is reduced to nanometers, the mean path of molecules. The time that a molecule is exposed to the catalyst will be controlled and it can be ensured that each reactant has only a single encounter with a single site or multiple active catalytic sites sequentially. Thus, catalytic processes could be run with greater atom efficiency and less waste from unwanted side reactions. This system is akin to current membrane reactors; however, the materials proposed would have a lower pressure drop through the structure and have the mechanical stability of a monolithic support.

## Importance to LANL's Science and Technology Base and National R & D Needs

The primary DOE mission tie is to energy security. Materials developed within the scope of this project will help the chemical industries lower their energy costs through increased efficiency in processes such as separations. An additional further benefit will be cleaner product streams and less waste. Developing non-linear photonic devices could also greatly impact the solid-state lighting and sensor communities.

## Scientific Approach and Accomplishments

The team took two approaches to assemble structures with hierarchical pore systems. The first was using a 3D printer to develop simple models from computer generated systems. The second was through the synthesis of inverse opal materials with different starting spheres. The latter met with limited success due to cracking of the porous monoliths Figure 1. We discovered that starting with polymer spheres and using silica as the solid support, the spheres could not readily be removed. Pyrolysis and different solvents generally led to deterioration of the solid support. To alleviate this issue, we switched to silica spheres with a titania support. The silica could then be gently removed in a dilute bath of hydrofluoric acid. While we were succeeded with this approach, we could not pursue this for large scale systems due to the use of hydrofluoric acid and we are still looking into different routes to new inverse opals.

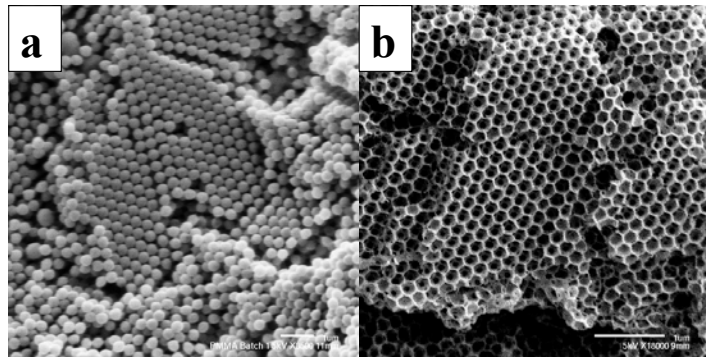


*Figure 1. SEM micrographs of (a) monodisperse polystyrene spheres, the precursor support for inverse opal and (b) a titania inverse opal material. The scale bars are 1μm in both images.*

The first approach, using a 3D printer to generate simple models, was more productive. However, as described below, the team was not able to go beyond simple models to due to the limits in personnel on the team. The printer has since proven to be an excellent tool for developing mock ups for training purposes, items for presentations, and a means to greatly assist our division with printing 3D models of molecules from crystal structures. This offers the chance to handle a visualize molecules that are difficult to portray in two dimensions on paper or a computer screen.

For the project, the team successfully modeled the porous networks for the first time and demonstrated a minimal pressure drop could occur. The results are shown in Figure 2. Presented is a single square channel that is subsequently subdivided into 256 channels. With the velocity magnitude color-coded, it is apparent that the flow in the center of the pores is higher (red represented as a higher flowrate). Thus this obeys the boundary conditions that were imposed with zero velocity at the walls. While this was an unexpected result from the research project, the pressure drop was surprisingly small, only 0.000008 psi. This is exactly predicted by our hypothesis that a porous network obeying the scaling laws from nature would have a minimal pressure drop, much like the blood flowing through the circulatory system. The calculations also demonstrated a key hurdle in the research. In order to develop more complicated systems, very advanced modeling would be necessary. This was outside the scope of the team, and the only known group working on this problem is researchers in Italy modeling the human lung. However, their space filling model for the lung could not be easily adapted to an industrial application where the flow and pores are always in the same direction. This unforeseen obstacle became a real stumbling block for the project; however, while evaluating alternative solutions, which included discussions with

animators at Disney, the group could work on materials applications for this technology.

**Simulation results:**
Boundary condition:
Inlet: 0.01 m/s; Outlet: pressure outlet; wall: non-slip;
Fluid: water;
Mass flow rate: 1.225e-06 kg/s;
Pressure drop: 0.056306127 Pa.

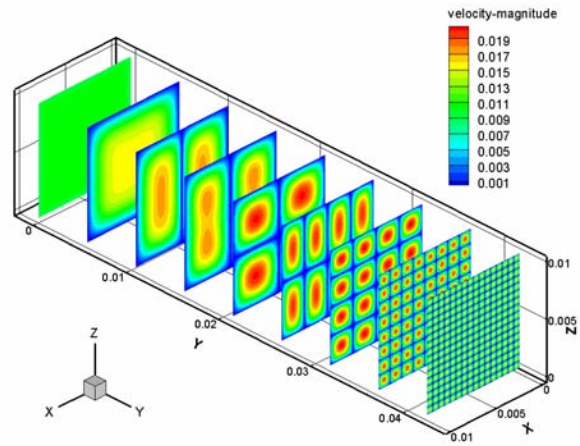


(a) slices on the XZ planes

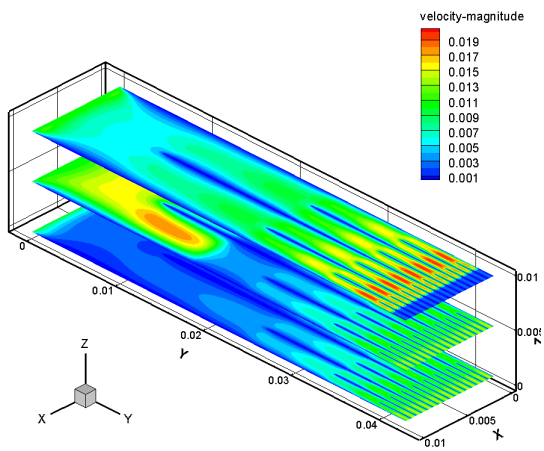


(b) slices on the XY planes

*Figure 2. Two dimensional slices through network showing flow velocities. Dark blue is the slowest moving fluid in the calculation, red is the fastest. As can be seen in the figure, the fluid in the center of the channels is moving the fastest.*

The team redirected its efforts towards complicated porous materials discovery for the DOE complex, namely the high surface area materials aspects of the project. The goal is to meet the needs for radionuclides sequestration for GNEP or other systems demanding highly adsorbent materials. Metal organic frameworks were synthesized and tested for their stability. The literature on this topic is fairly misleading and we discovered this class of compounds would not remain intact for radionuclide trapping. To overcome this obstacle, carbon replicas of highly porous silicates will be explored.

Velocity magnitude (m/s) on the selected slices

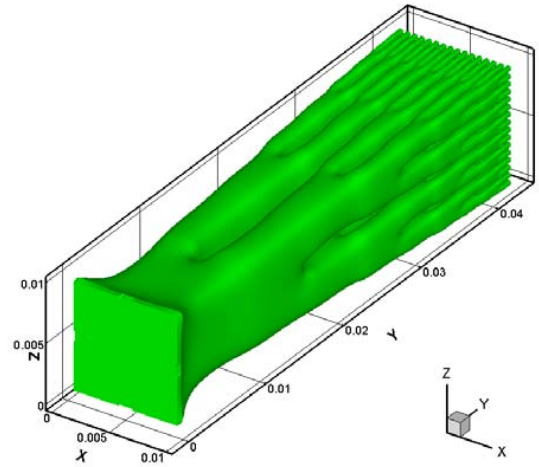

(a) Velocity magnitude = 0.01 m/s

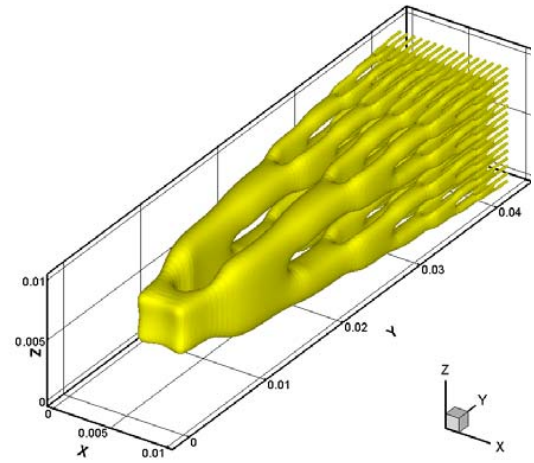

(b) Velocity magnitude = 0.015 m/s

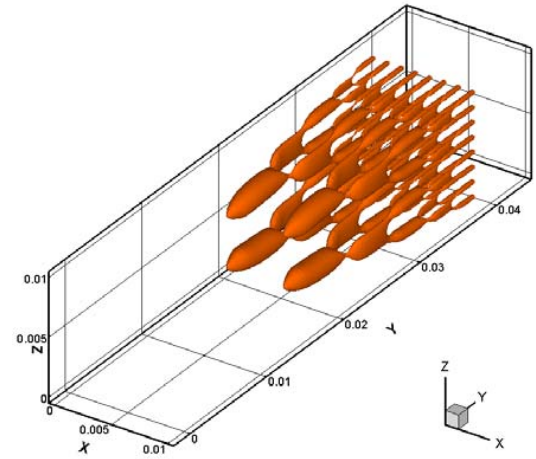

(c) Velocity magnitude = 0.018 m/s

*Figure 3. Three dimensional representation of the flow, differentiated by speed, through the channels. Green is the slowest moving fluid and the smaller subset of the fluid in red is traveling in the center.*

The team also put together several proposals to expand on the foundation of this research. Additionally, a patent disclosure was submitted. The process of filing for a patent is in the early stages and, hence, we are unable to provide many details at this time.

Much of the research for this project is in developing materials having similar transport properties with delivery systems for molecules to and from catalytic sites. With the added possibility to control the time that a molecule is exposed to the catalyst, each reagent molecule will have only a single encounter with a single site or multiple active catalytic sites sequentially. Thus, catalytic processes could be run with greater atom efficiency and less waste from unwanted side reactions. This system is akin to current membrane reactors; however, the materials employed here have a lower pressure drop through the structure and have the mechanical stability of a monolithic support. In order to cover the entire ranges of pore sizes, from cm to nm, a 3-tiered approach is being followed: 1) the assembly of hierarchical pore structures from fundamental polymer chemistry; 2) self-assembly methods such as inverse opal type syntheses; and 3) 3D printing technologies.

In addition to this technology, current discussions are being had with several petrochemical companies in developing carbon dioxide scrubbers based on the development of high surface area materials with a thin layer of adsorbing liquid that can readily trap and release CO2. This work will help American companies stay at the forefront in capturing and sequestering CO2. Funding for this is being applied for from DOE-EERE in collaboration with Chevron as an industrial partner. The goal is to develop new processes with minimal energy costs for carbon dioxide scrubbing from potential waste streams.

**Conclusion**

Taking inspiration from the design of distribution systems in Nature, we seek to create porous systems with the correct fractal dimensions to optimize the transport properties within them. Applications for these new materials range from transferring reactants and products for heterogeneous catalytic reactions to energy harvesting solid-state devices and non-linear optical materials.

# Nanobiomaterials: Building New Nanoarchitectures Using Biomolecular Scaffolds

*Jennifer Martinez*

20060253ER

## Abstract

Few-atom gold nanoclusters exhibit strong size-dependent fluorescence emission. For many applications, these clusters are preferable to quantum dots or organic fluorophores as fluorescent labels. However, the published synthetic procedures to create these nanoclusters involve toxic chemicals, are of low synthetic yield and concurrently produce large nanoparticles. Here, we report methods for the selective synthesis of gold nanoclusters, utilizing physiological temperature, green chemistry, and biological templates.

## Background and Research Objectives

Understanding the molecular basis of life ultimately requires an understanding of the function of individual biomolecules and their assemblies, in the context of a living cell. Ideally we would like to image a single protein molecule within a living cell throughout its lifetime, from expression, to transport, folding, function and degradation. Single molecule measurements have significantly advanced our understanding of the molecular movement, dynamics, and biological function of proteins and other biomolecules. Fluorescence sensing and imaging techniques remain two of the primary methods for *in vitro* detection of molecules in solution, and *in vivo* imaging of cells and cellular processes. Unfortunately, the performance and sensitivity of these laser-induced fluorescence techniques are greatly limited by the utilized fluorescent labels. For instance, organic fluorophores are easily photobleached during the time scale of observation, leading to reduced sensitivity and decreased tracking time of the targets. Relative to conventional organic dyes, semiconductor quantum dots show great promise in biolabeling. Unfortunately, quantum dots have large physical size comparable to proteins and tend to photoblink. All of these challenges require the development of new fluorescent reporters that meet the following requirements: 1) non-toxic to cells and other organisms; 2) smaller than the biomolecules of interest, such as proteins, so that normal biological functions, such as protein-protein interactions, are not disturbed; 3) optimized photophysical properties such as no photobleaching, no photoblinking, short lifetimes and high quantum yields; and 4) facile synthesis and attachment to biomolecules. Each of these attributes is essential for the development of advanced diagnostics and the *in vivo* imaging of cellular processes.

Noble metal nanoclusters may avoid all of these disadvantages when used as fluorescent tags. Few-atom gold nanoclusters are collections of small numbers of gold atoms (<1 nm). Different sized clusters exhibit different emissions. Synthetic issues remain in the production of gold nanoclusters using reported procedures: 1) the use of a toxic inorganic reducing agent ($NaBH_4$); 2) the production of nanoparticles, leading to low yield of nanoclusters; and 3) the reproducible synthesis of size constrained nanoclusters. The overall goal of our work was to explore metal nanocluster architectures and their photophysics to enable the development of new probes for biomolecular sensing and imaging.

## Importance to LANL's Science and Technology Base and National R & D Needs

We expect the results of our work may provide a foundation for the next generation of molecular sensors, based on single molecule sensitivity and molecular specificity of fluorescence. Nanocluster materials are suitable for use in a variety of sensor platforms (microarrays, flow cytometry, waveguides) and applications, including genomic and proteomic analyses and modification of current immunoassay techniques. Imaging biomolecular processes within living cells using metal nanocluster image contrast agents could be a vast improvement over current confocal fluo-

rescence microscopy methods. All of these applications have enormous potential for future support from funding agencies (DARPA, DOE/OBER, DHS/CBNP, NIH/NIBIB).

## Scientific Approach and Accomplishments

The overall goal of this work is to explore metal nanocluster architectures and their photophysics to enable the development of new probes for biomolecular sensing and imaging. The ability to design metal nanocluster architectures with specific emergent photonic properties depends first on the ability to systematically produce clusters and then to select such structures for desired characteristics. We used LANL capabilities in protein folding to guide development of peptide scaffolds, phage display techniques to develop large peptide libraries for high throughput discovery of templating sequences, and hyperspectral fluorescence to screen clusters for photophysical properties. We investigated the use of dendrimers, small organic molecules, polymers, peptides, and proteins as templates.

### Dendrimers

Our laboratory and others had difficulties producing size-constrained nanoclusters utilizing the reported procedures. We developed new approaches for the synthesis of gold nanoclusters. Specifically, we demonstrate the use of physiological temperature (37 °C) and ascorbic acid (vitamin C), a mild biologically derived reductant, for the well-defined synthesis of fluorescent gold nanoclusters using PAMAM dendrimer templates, *without the formation of gold nanoparticles* [1]. Our method produces small blue emissive gold nanoclusters without additional reductant (Figure 1).

Gold nanoclusters with green and red emissions were synthesized using ascorbic acid as reductant. pH stability studies of all gold nanoclusters suggest that they are very stable in a pH range of 6 - 8. This work was the first report of fluorescent gold nanoclusters via a green-chemistry approach, in high yield, and without the formation of gold nanoparticles. We also produced blue clusters using a particle-free method to produce dendrimer-encapsulated gold nanoclusters in high-yield in organic solvent [2]. Proof of concept was demonstrated using OH-terminated poly(amidoamine) dendrimer and $Au(PX_3)_3Cl$ (X = Ph, Me), but the approach can also be extended to the combination of other templates and organic noble metal salts. The synthesis of each (dendrimer nanoclusters by green chemistry and dendrimer nanoclusters in organic solvent) is presented below.

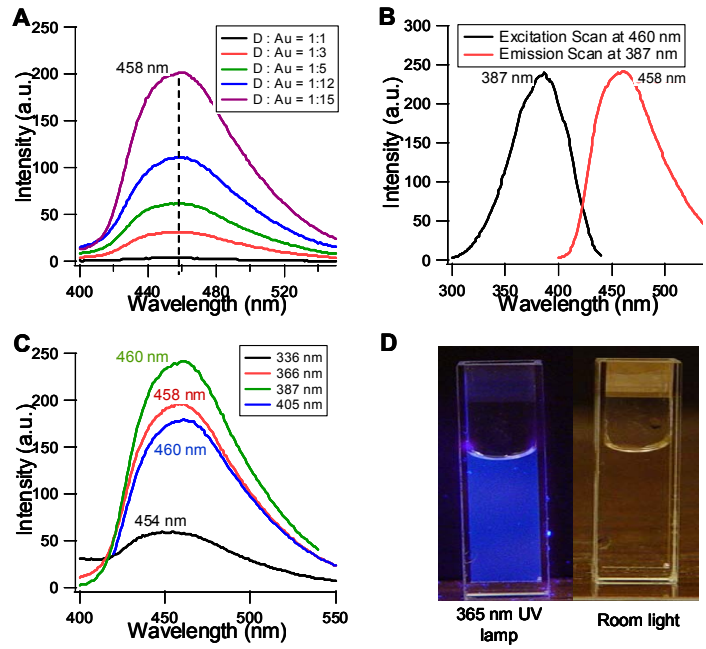


*Figure 1. Photoluminescence properties of Au nanoclusters produced by method A: (A) studies of increasing dendrimer to gold ratios (legend box) excited at 366 nm; (B) excitation/emission scans; (C) emission spectra at different excitation wavelengths (legend box); (D) photography of Au nanocluster solutions produced with method A [intensive blue emission excited with 365 nm light (left) and a clear solution lacking competing nanoparticles with room light illumination].*

*Dendrimer nanoclusters by green chemistry*

Fluorescent gold nanoclusters were synthesized using a hydroxyl-terminated ethylenediamine core, fourth generation, PAMAM dendrimer (G4OH) as template. The gold ions were first sequestered into the dendrimer and then reduced to produce stable dendrimer-encapsulated gold nanoclusters. The sequestration of the gold ions is most likely through the coordination between gold and the tertiary amines at the branch points of the dendrimer molecules. The dendrimer/gold stock solution mixture was stirred in the dark at 4 °C for 24 h to ensure the incorporation of gold ions into the dendrimer. The pre-equilibrated gold/dendrimer stock solution was then either incubated at 37 °C for three days to reach growth equilibrium, or equilibrated with ascorbic acid and gold (1:4 molar ratio of gold to ascorbic acid) at 37 °C for three days, to produce gold nanoclusters with multiple color emissions.

These nanoclusters show strong photoluminescence. Without added reductant the clusters exhibit a maximum emission around 458 nm, which correspond to $Au_8$ nanoclusters based on the spherical Jellium model. A quantum yield of 0.38 is obtained for the blue emitting $Au_8$ nanoclusters; yet, the larger gold nanoclusters show relatively lower

quantum yields ($Au_{13}$, 0.15; $Au_{17}$, 0.12; and $Au_{23}$, 0.09). The preliminary results show lifetimes of nanoseconds for all cluster sizes ($Au_8$, 6.70 ns; $Au_{17}$ 2.45 ns and $Au_{23}$, 2.55 ns). More detailed analysis of lifetimes and studies on photobleaching and blinking are under investigation.

The pH effects on dendrimer-encapsulated gold nanoclusters were studied on two different samples synthesized *with* and w*ithout* ascorbic acid at physiological temperature. These gold nanoclusters are relatively stable at pH 4 - 5 for short periods (up to two days at room temperature); however, prolonged exposure at this pH leads to eventual decrease in fluorescence intensity. In contrast, nearly no change in fluorescence intensity was observed for solutions at pH 7 - 8, suggesting that these nanoclusters are very stable at least for the duration of the test. When the pH value is raised to 10, a decrease in the fluorescence intensity was also observed, but not as significantly as in the acidic solution, indicating that gold nanoclusters are generally more stable in basic rather than acidic solutions.

*Dendrimer nanoclusters in organic solvents*

Previous investigators prepared dendrimer/gold nanoclusters using an unstable gold salt (e.g. $HAuCl_4$) and strong reductant (e.g. $NaBH_4$). This method resulted in formation of large, non-emissive particle byproducts. We developed two strategies to overcome this problem: 1) phosphine-stabilized gold precursors (e.g. $AuPX_3Cl$, X = Me or Ph) were used to improve the stability of the reactant; and 2) heating was applied to provide a mild reducing environment. To facilitate future application in biolabeling, we designed two methods to prepare the gold nanoclusters through fourth generation OH-terminated PAMAM. The first method (A) produced gold clusters in organic medium (e.g. methanol), followed by an evaporation/dispersion process to transfer the product into aqueous medium. The second method (B) utilized a phase transfer technique to synthesize gold clusters directly in aqueous medium (Figure 2).

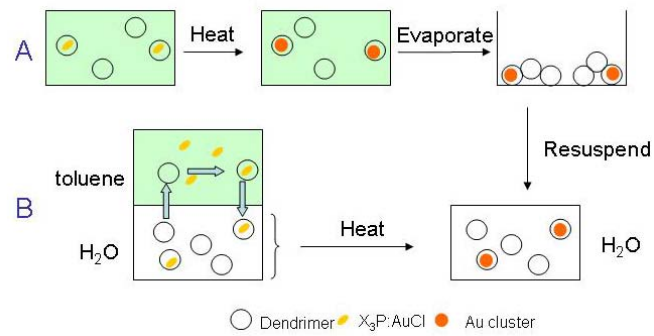


*Figure 2. Schematic representation of gold nanocluster formation for methods A and B. Gold nanoclusters were produced in methanol, followed by solvent evaporation and product resuspension in water (Method A). Gold nanoclusters were produced in a biphasic reaction (Method B).*

The gold nanocluster formation of methods A and B were found to be similar. The products of the reaction were monitored by fluorescence spectroscopy. Minimal dendrimer autofluorescence was detected for G4OH, but a substantial emission peak at 450 nm appeared for samples with addition of Au precursor. We found that the emission intensity increased with both the increase of time and Au/dendrimer ratios of up to 8/1. Based on the maximum excitation/emission, we estimate the size of our nanoclusters to be $Au_8$.

*Polymers*

Recently, the preparation of water-soluble fluorescent silver clusters have been promoted by interaction of silver ions with DNA, dendrimer, polymer microgel, and multiarm star poly(acrylic acid) (PA) systems. Many investigators have emphasized the importance of a “cage effect” for formation of aqueous silver clusters. In all previous work, PA was responsible for binding the silver clusters, while the cage architecture was responsible for stabilizing the PA. PA is a poly-anion multivalent ligand, which has been widely used in stabilizing various types of nanoparticles as well as for drug delivery. We wondered if PA alone could also stabilize fluorescent silver clusters by properly controlling the experimental conditions and size of the polymer, and thus circumventing the complicated process of making “caged” structures. Furthermore, we focused our study on small molecular weight PA, or oligoacrylate (OA), because its molecular weight is comparable to short peptides, and thus opens the possibility for biocompatible routes of fluorescent silver cluster production. We present the synthesis of bright and water-soluble fluorescent silver clusters with diameters of approximately 1 nm, that are solely stabilized by OA [3]. In a typical preparation procedure, OA was added to nanopure water. The mixture was stirred vigorously for at

4 °C, $AgNO_3$ was then added dropwise to the mixture, the solution was then irradiated with 365 nm UV light in the dark at 4 °C. Upon UV irradiation, the fluorescence intensity gradually increased until it reached a maximum after 80 min of UV exposure (Figure 3). The intense fluorescence in our sample came from the UV-reduced silver clusters, which are postulated to be $Ag_n$ (n = 2-8), stabilized by the carboxylate ligands of OA. We reason that the carboxyl groups of the OA have dual functions in the formation of the fluorescent silver clusters. First, some carboxyl groups bind silver ions and subsequently stabilize the silver clusters after UV irradiation. Second, the unbound carboxyl groups are negatively charged and thus prevent self-aggregation.

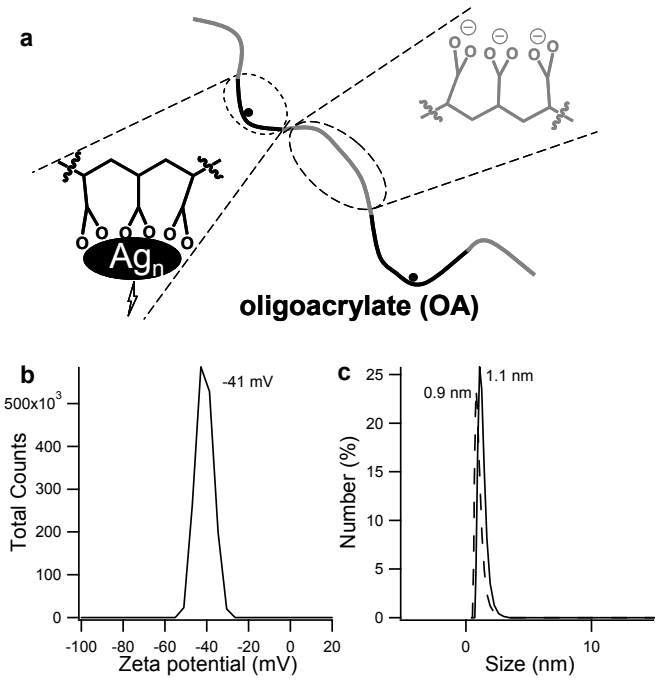


*Figure 3. Proposed fluorescent silver cluster formation mechanism. (b) Zeta potential distribution of silver clusters/OA hybrid. (c) Size distribution of OA (dash line) and silver clusters/OA (solid line).*

*Peptides and proteins*

Biological polymers are similar to organic polymers in that they are composed of repeating blocks of chemical identity. Knowing that organic polymers of identical chemical building clocks can produce clusters, and that nature uses peptides and proteins to template inorganic ions (i.e. metals), we undertook both a rational and combinatorial approach to generate peptide and protein ligands that can template gold clusters.

*High throughput template discovery: combinatorial selection of nanocluster templating peptides*

We used a combinatorial approach to select gold templating ligands from "naïve" (random) phage display libraries. Phage display is a well established technique where random peptides are expressed on the surface of bacterial viruses (phage). Peptide libraries are created by fusing DNA fragments, that encode for peptides, to bacteriophage coat protein genes. The resulting libraries consist of millions of different peptides individually expressed and carried by the phage "vehicles." The benefit of *in vivo* combinatorial selections is that each phage carries one peptide and the DNA that encodes for that sequence, enabling biological production of clones for subsequent selections and screening. This form of combinatorial selection is a powerful method for creating Ag and Au templating peptides by quickly screening millions of different amino acid combinations. Peptides that have specific affinities to inorganic surfaces have been previously selected by phage- or cell-surface display. Substrates such as Au, Ag, $SiO_2$, ZnO, $CaCO_3$, $Cr_2O_3$, $Fe_2O_3$, GaAs, ZnS, and carbon nanotubes have all successfully yielded affinity ligands. Beyond the enhanced sequence diversity, phage display enables the creation of templating sequences that are either cyclic or linear. Linear peptides, with high degree of conformational freedom, mirror the single stranded DNA previously utilized to template silver nanoclusters. Whereas, cyclic peptides may provide a cage-like environment for encapsulation of nanoclusters. After three rounds of selection with both P3 and P8 libraries (peptides on the tip or along the long-axis of phage, respectively) we find roughly 20 peptides that are able to template the formation of gold clusters. These peptides, like dendrimers, show an increased predominance of amine ligands, show a time-dependent cluster formation, and produce a single cluster size. These peptides, when on the long-axis of phage, produce bundles of fluorescent phage that can be visualized by fluorescence microscopy (Figure 4) and by transmission electron microscopy. The peptides are now being cloned into small protein constructs and synthesized as monomeric and polymeric peptides by solid-phase chemistry.

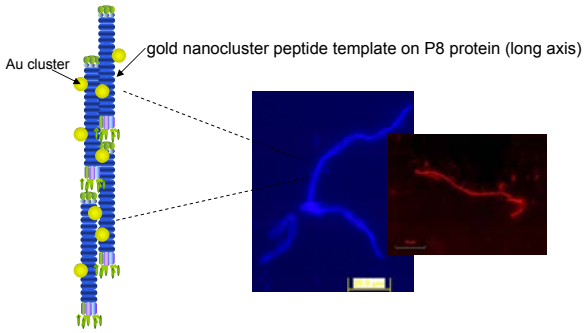


*Figure 4. Fluorescence microscopy images of nanoclusters on P8 peptides of bacteriophage.*

*Maltose binding protein (MBP)*

MBP was selected because it is a proven robust and versatile scaffold for protein engineering design efforts. MBP belongs to a superfamily of transporter proteins that have been evolutionarily adapted to bind to a diverse set of molecular analytes (i.e. sugars, amino acids, DNA, and metal ions). MBP consists of two domains connected by a hinge region, with the ligand-binding site located at the interface of these two domains. Therefore as a rational design strategy for templating nanoclusters with MBP, this ligand-binding site was our initial target region. We have targeted naturally binding amino acid residues and have modified these locations with residues that are rich in hydroxyl, amines, carboxylates, and imidazoles side chains to help coordinate Au and Ag ions which would act as seeds to organize more metal ions within this binding site. In some cases, smaller side chain residues were substituted to help open up the binding pocket to accommodate more metal ions, thereby acting to modulate the internal volume of this binding cavity. Given that the residues that are involved in natural ligand binding span multiple sites (Figure 5), we found that constructs with multiple substitutions served as more promising candidates for templating Ag and Au ions. To ensure that the mutations had minimal perturbations on the overall structure and stability of the protein, RosettaDesign software was utilized before synthesizing the constructs and the resulting constructs were also characterized with biophysical methods (i.e. circular dichroism spectroscopy).

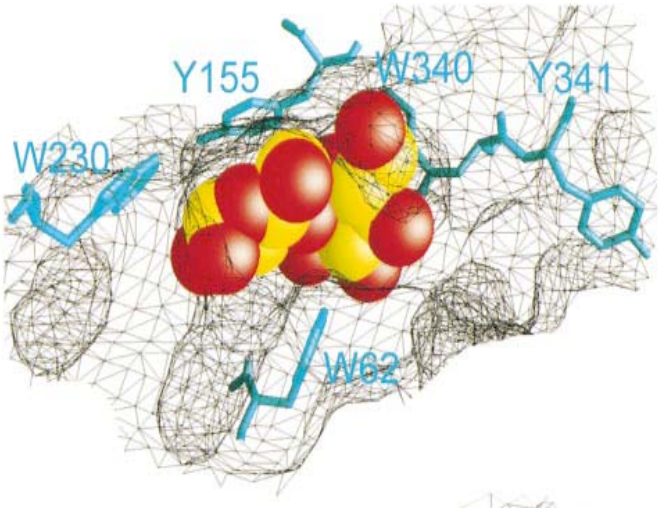


*Figure 5. MBP residues that interacts with maltose.*

## References

1. Bao, Y., C. Zhong, D. M. Vu, J. P. Temirov, R. B. Dyer, and J. S. Martinez. Nanoparticle free synthesis of fluorescent gold nanoclusters at physiological temperature.. 2007. *Journal of Physical Chemistry C.* **111** (33): 12194.

2. Zhong, C., Y. Bao, D. M. Vu, R. B. Dyer, and J. S. Martinez. Fabrication of fluorescent cellular probes: hybrid dendrimer/gold nanoclusters." . 2007. In *Materials Research Society.* (San Francisco, Spring 2007). Vol. 1007, S15 Edition, p. 07. San Francisco: MRS.

3. Zhong, C., Y. Bao, A. M. Dattelbaum, D. M. Vu, J. L. Belyea, R. B. Dyer, and J. S. Martinez. Water-soluble fluorecent silver nanoclusters stabilized with polyacrylate.. *Chemical Communications.*

## Publications

Bao, Y., C. Zhong, D. M. Vu, J. P. Temirov, R. B. Dyer, and J. S. Martinez. Nanoparticle free synthesis of fluorescent gold nanoclusters at physiological temperature. 2007. *Journal of Physical Chemistry C.* **111** (33): 12194.

Zhong, C., Y. Bao, A. M. Dattelbaum, D. M. Vu, J. L. Belyea, R. B. Dyer, and J. S. Martinez. Water-Soluble Fluorescent Silver Nanoclusters Stabilized with Polyacrylate. *Chemical Communications.*

Zhong, C., Y. Bao, D. M. Vu, R. B. Dyer, and J. S. Martinez. Organic synthesis of fluorescent gold nanoclusters. To appear in *Materials Research Society.* (San Francisco, Spring, 2007).

# Understanding the Process of Intercalation Using Stable Isotope Labeled Polyaromatic Hydrocarbons (PAHs) and Oligomeric DNA; the Quantitation of Weak Bonding in DNA.

*Louis A Silks III*

20060317ER

## Abstract

With a view towards better understanding their health risk, the goal of this project was to study, 1) the process of the intercalation of polyaromatic hydrocarbons (PAHs) into oligomeric deoxynucleic acids (DNA), and 2) the effect and extent that soft p———H-X (X = C, N, O) and C-H———O hydrogen bonding interactions have on the structure of the DNA. We focused on the synthesis of the desired PAHs and DNA oligomers, and analysis of the DNA using nuclear magnetic resonance (NMR) spectroscopy. The NMR spectroscopy determines proximity relationships between stable isotopes on the PAH and the labeled DNA base. Study of the DNA bound PAHs provides valuable information on DNA stacking interactions that will also be used to compare with later studies on non-covalently bound PAHs and DNA.

## Background and Research Objectives

PAHs are a general class of aromatic compounds that are environmentally ubiquitous, with significant levels found in air, food, and water. The major sources of PAHs are from the combustion of oil and coal, two of the most abundant energy providers. This class of compounds is extremely structurally diverse, however most incorporate a large planar, π-conjugated, carbon rich area. It was not until the 1930's that the carcinogenic properties of various aromatics were discovered. It has been stated that the majority of PAHs in the air are able to contribute to health risks [1].

The major pathway for PAH carcinogenesis is believed to involve an initial activation (cytochrome P450 for example) and conversion to a reactive epoxide that will then react with DNA thereby causing mutations [2]. Since the majority of PAHs are relatively small, planar molecules, they fit well in between sequential bases within a DNA chain and can stack in these small grooves in a sandwich-type fashion. Once this arrangement is established, reaction to covalently link the PAH to the DNA base is facilitated. The resulting mutations then cause misreading of the DNA, which leads to an induction of tumors. Other pathways have also been shown to be involved in the conversion of healthy cells to tumor cells.[3] Formation of aromatic radical-cations, the formation of aromatic intermediate quinine based molecules, and the formation of benzyl alcohols which undergo intracellular conversion to reactive sulfate esters *all have been shown to attack DNA* [3].

The combination of stable isotopes (SI) with mass spectrometry (MS) and nuclear magnetic resonance spectroscopy (NMR) provides many advantages for structure determination and important dynamic information at much lower concentrations than would otherwise be needed. Spectral overlap, a recurring problem within complex systems due to large amounts of similar resonances, can be reduced with SI labeling and also provide the opportunity to observe targeted weak interactions selectively. Not only does this provide access to local bonding and structure but the determination of the overall solution structure can be obtained using NMR.

During the past 14 years we have been involved in the synthesis and characterization of both uniform and site-specifically-labeled DNA. We have successfully generated nucleosides labeled with $^{2}H$, $^{13}C$, and $^{15}N$ at either or both the deoxyribose portion and/or the base moiety for the purpose of aiding structure determination of complex DNA oligomers. Our experience also includes SI labeling of a wide variety of classes of molecules such as amino acids, carbohydrates and synthons. Many of these have been used in the study of larger biomacromolecular assemblies via NMR, MS, and vibrational spectroscopies. Recently, we have extended our research to the synthesis of $^{2}H$, $^{13}C$ labeled PAHs.

## Importance to LANL's Science and Technology Base and National R & D Needs

This work has given rise to a understanding of complex systems associated with mutations of oligomeric DNA. Understanding complex systems is one of LANL grand challenges, and has applications to our energy and biosecurity missions.

## Scientific Approach and Accomplishments

The first task to be tackled was the synthesis of the chosen PAH. Deciding the placement of the $^{13}C$ atoms was relatively simple. The most favored positions to obtain information about bonding the PAH and the DNA is the terminal position on the ring system. Since the NMR spectroscopy could distinguish each of the labeled carbons we decided that for synthetic simplicity all of those carbons would be labeled in the terminal ring. In addition, benzene where all of the carbon sites are enriched with $^{13}C$ is readily available and not expensive. The synthesis then began (see Figure 1) starting from the 2-nitro-6-methoxy benzoic acid chloride with labeled benzene.

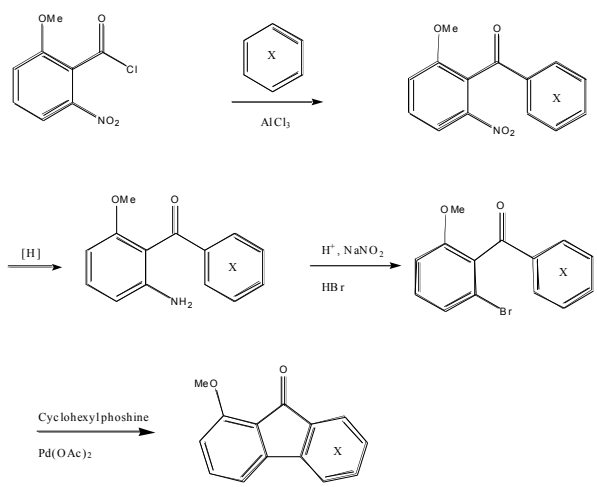


*Figure 1. Synthetic Route to the tricyclic PAH intermediate.*

This Friedels-Craft reaction occurred in high yield to give rise to the benzophenone derivative. Reduction of the nitro group to the amine is accomplished using catalytic hydrogenation. Reaction of the amino with nitrous acid gives rise to an intermediate diazonium salt that is easily substituted by bromide. The bromide serves to activate the carbon position for the annulation reaction. Treatment of the aryl bromide with Pd acetate using cyclohexylphosphine as the ligand afforded the tricycle compound in 89% yield. As with many chemical reactions this process did not work well using the standard literature methods. In fact, using other literature method(s) one product was isolated in 50% yield however, the spectroscopy data was worrisome. Evaluation of a number of other phosphine ligands for the palladium catalyst eventually gave a result that was consistent with the desired structure. The cyclohexyl phosphine complex gave consistent results in terms of yields. Using a number of 2D NMR spectroscopy methods appeared to give results confirming our structural assignment. However, the crystallography rigorously confirmed it. This is illustrated in Figure 2.

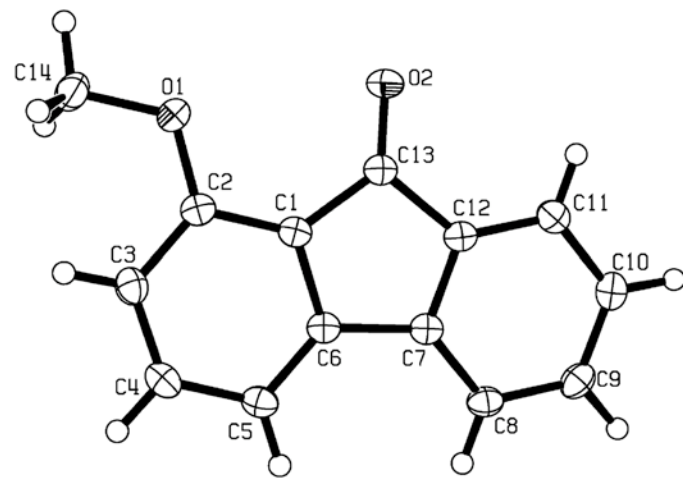


*Figure 2. ORTEP of the key intermediate PAH.*

The PAH was then treated with a diazomethane equivalent to effect a Wolff rearrangement reaction. This gave rise, in high yield, a mixture of regio isomers. This was not relevant considering the next series of chemical reactions removed the hydroxyl group. This was effected by the construction of the triflate, which then undergoes smooth C-O bond reduction with catalytic hydrogenation. Cleavage of the aryl methoxyl methyl group is accomplished using boron tribromide. Remaining to be completed is the establishment of the tether between the DNA base, adenine, and the PAH. Several methods were employed to complete this task. All were successful, however, the most straightforward method was to react the aryl hydroxyl group with ethyl bromo acetate (Figure 3). This occurred quickly and the product could be purified by filtration through silica gel. Reaction of the ester with lithium borohydride smoothly reduced the ester to the primary alcohol. Conversion of this hydroxyl group to the amine was done in two steps. Mitsunobu reaction using phthalimide ($^{15}N$) easily gave rise to the protected amine. Removal of the amine protecting group with hydrazine gave the amine in good overall yield (see Figure 3).

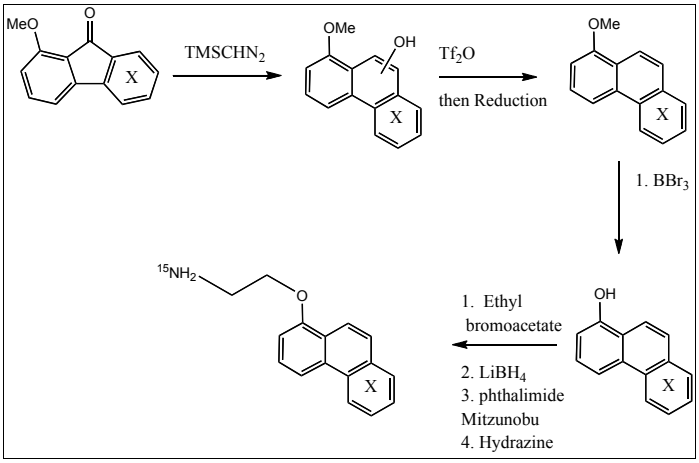


*Figure 3. Synthetic route to the tethered PAH.*

At this point it was decided to test the next series of reactions using a model system. Since the above synthesis was involved and required expensive isotopes, a simpler system was devised to work out the chemistry for the olignucleic acid synthesis. This DNA had one position in the chain that carried an aromatic molecule linked through a 4-atom chain. The synthesis was accomplished by the conversion of a monomeric DNA molecule to one that carried a phenyl ring as illustrated in Figure 4.

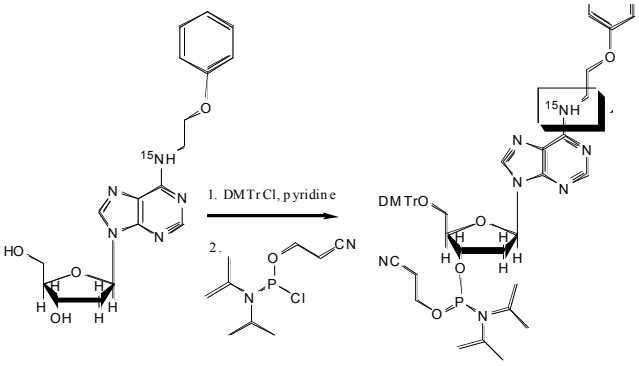


*Figure 4. Synthesis of the PAH phosphoramidite.*

Critical to this series of chemical steps was the discovery that the nitrogen atom at the 6 position of the DNA adenine did not require protection. This masking of the nitrogen is normal protocol to protect it from the oxidation conditions in the solid phase synthesis of the chain of DNA. The DNA were synthesized "DMT on" using a Perkin-Elmer ABI 394 DNA synthesizer using standard phosphoramidite chemistry. The PAH phenyl modified phosphoramidite was placed on port 6 and standard conditions were used for this monomer coupling. Synthesized DNA was deprotected at 50°C for 8 hours and purified using reverse phase oligonucleotide purification columns (Glen Research Poly-Pak II, catalog number 60-3100-01). Single strands were annealed at 95°C and allowed to cool to room temperature. Double stranded DNA was purified by HPLC using a C18 semi-preparative column. Double stranded material was eluted from the column running a 0.1 M Triethylamine acetate (TEAA) pH 7 (Buffer A) to 25% acetonitrile 0.1 M TEAA pH 7 (Buffer B). The duplex DNA was then purified using HPLC methods. This NMR of this duplex has been done. The measurement of the area for the phenyl protons of the tethered group to the DNA indicates the presence of only one phenyl group! This method then paves the way for the construction of a variety of polyaromatic hydrocarbons that are linked to DNA. This will give rise to a better understanding of the interaction of these groups with DNA and by extension should give rise to a better understanding of the role polyaromatic hydrocarbons play in carcinogensis.

In addition, illustrated below is a solution structure of the (+)-cis-anti-benzo[a]pyrene-dA ([BP]dA) adduct opposite dT in a DNA duplex (**1AXV**). This is the same sequence we are using for the phenanthroline DNA (Figure 5).

What remained to be completed is the conversion of the labeled PAH to the deoxyadensine. Reaction of the amine described above with the hypoxanthine deoxyribose under Mitsunobu conditions to give the coupled product. As demonstrated in the model system treatment of the 5' hydroxyl group with dimethoxytrityl chloride will protect this alcohol and allow derivitization of the other 3' hydroxyl group. Reaction with the phosphityl chloride gave rise to the phosphoramite in reasonable yield. This material is now undergoing conversion of the oligomeric DNA for the ultimate NMR studies.

Completion of the NMR data on the labeled PAH DNA duplex will allow for further program development. We plan on submitting these results in a proposal to NIH for further funding of this work. In addition, to help that proposal be successful we plan on submitting further manuscripts for publication. Specifically, the new routes to polyaromatic hydrocarbons are general. That is, it allows for the labeling of a wide variety of structurally different PAH's. This should have wide appeal to the synthetic community. In addition, we envision these compounds to be highly sought after for studies of PAH are in the environment. This leverage could allow for further funding from other sources such as the CDC.

## References

1. G.Harvey, ) R.. Polycyclic Aromatic Hydrocarbons. 1997. By Harvey, R. G.. , p. all. New York: Wiley-VCH.

2. Harvey, R. G.. Polycyclic Aromatic Hydrocarbons: Chemistry and Carcinogenesis. 1991. In *Polycyclic Aromatic Hydrocarbons: Chemistry and Carcinogenesis.* By Harvey, R. G.. , p. all. Cambridge, UK: Cambridge University Press.

3. shalom, y., R. G. Harvey, and J. Blum. Synthesis of nucleoside adducts of highly mutagenic polycyclic aromatic imines . 1999. *Tetrahedron.* **55**: 10231.

4. Harvey, R. G.. Mechanisms of carcinogenesis of polycyclic aromatic hydrocarbons . 1996. *Polycycyclic Arom. Compds..* **9**: 1.

## Publications

"Pete"Silks III, Louis A., David B. Kimball, D. Hatch, M. Shiflett, R. Michalczyk, and E. Moody. Chiral N-Acetyl Selone Promoted Aldol Reactions. To appear in *Synthetic Communications.*

Kimball, D., and L. Silks. Current Progress in the Acetate/Methyl Ketone Aldol Reaction. 2006. *Current Organic Chemistry.* **10** (15): 1975.

Silks, L.. Advances in Asymmetric Synthesis Using Organoselenium Chemistry. 2006. *Current Organic Chemistry.* **10** (15): 1891.

# Development of Redox Affinity Materials for the Separation of Carbon Nanotubes into Pure Chiral Fractions

*Stephen K Doorn*

20060346ER

## Introduction

The remarkable electronic properties of single-walled carbon nanotubes (SWNTs) hold great promise for revolutionary advances in nanoscale electronics, sensors, smart materials, and photonics applications. Attractive characteristics for these applications include near-ideal electronic and thermal conductivities and high quantum yield (~10%) optical emissions in the near-infrared. These properties, however, demonstrate a strong dependence on the specific structure (or chirality) of a given nanotube. The realization of their applications potential has been hindered because nanotubes are produced in a broad range of chiralities that include both metallic and semiconducting types (with a broad range of bandgaps). Thus, one of the true grand challenges of SWNT chemistry is the ability to separate a nanotube sample into pure fractions of a single chirality or electronic type.

A few of the many compelling reasons for producing CNTs of a single chirality include the following: 1) Nanoelectronics applications require SWNTs of known, predictable, and uniform properties. 2) Uniform properties will also be necessary for enabling and optimizing SWNT sensor response. 3) Pure chiralities will also open the door to new applications, such as for bio-imaging and nanoscale tracking needs that require nanoscale particles that act as spectral tags—enabled by the unique spectral signature found for each separate SWNT chirality. The ability to approach these needs through our separations work is tied directly to LANL and DOE goals for developing advanced functional nanomaterials and address specific needs for addressing challenges in threat reduction, bio-sensing, and ultimately in advanced computing architectures.

Past approaches to nanotube separations have been limited by the complexity and scalability of their approach, limitations in terms of structural types accessible, and also by their ultimate scalability [1].

As a basis for separations in our planned approach, we chose an initial strategy that used a newly discovered redox chemistry [2] between SWNTs and organic acceptor molecules. The redox reactivity of the nanotubes is dependent on the nanotube chirality (see, for example, Figure 1). By varying the redox potential of an electron acceptor molecule, we can select which range of nanotube structures will react with the acceptor. Our goal was to create redox-based separations beads whose reactivity would be tuned to selectively bind a desired range of nanotube structures, thus allowing the rapid and highly scalable separation of nanotubes by electronic type.

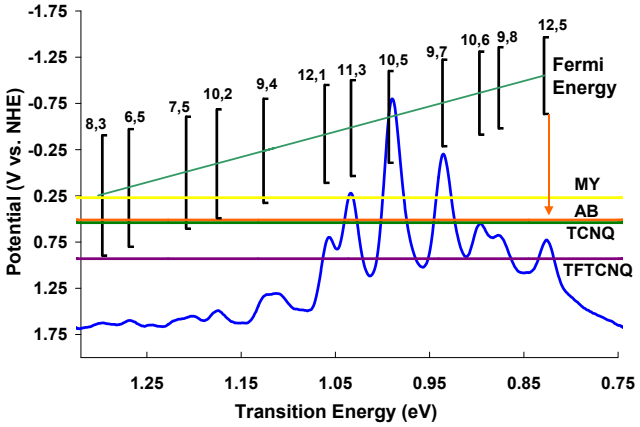


*Figure 1. Plot of relative potential energies of the valence band, conduction band, and Fermi levels of specific nanotube chiralities in relation to reduction potentials (determined by cyclic voltammetry) for the organic acceptor molecules used in this study. The nanotube fluorescence spectrum (785 nm excitation) is superimposed.*

To attain this ultimate goal, we pursued not only the synthesis of such selectively reactive beads, but also other routes to selective nanotube reaction chemistry. Additionally, fundamental redox chemistry was studied and the spectroscopic basis for characterization of separations was defined. As a promising byproduct of the redox studies, we developed a redox-enable optical approach to biosensing as well.

**Project Summary and Results**

*Synthesis and Testing of Redox Affinity Beads*

Our first target for functionalized affinity beads was to synthesize silica beads with azobenzene functionalities, as there are a wide range of azo dyes available to work with. This allows for ease of tuning of their redox characteristics. We took two approaches. The first was to obtain silica beads that are functionalized with reactive organosilanes and to graft the azo dyes of choice directly to the bead. We successfully performed this bead functionalization with phenyl azoaniline. Alternatively, we sought to first functionalize an organosilane with the azo dye. The dye-silane complex was then grafted onto an appropriate silica bead. Synthetic strategy for these functionalizations is depicted in Figure 2. Original silica particles for our studies were 50 micron beads. These were demonstrated to yield low redox reactivity with carbon nanotubes, perhaps due to low absolute loading of the reactive dyes on the particle surface. To overcome this problem, we synthesized nanometer-scale silica particles (100 nm diameters), which were then functionalized with the dyes as described above. Much higher surface loadings of dye were attained. These functionalized particles were then reacted with nanotube solutions, followed by reacting the reacted and unreacted fractions.

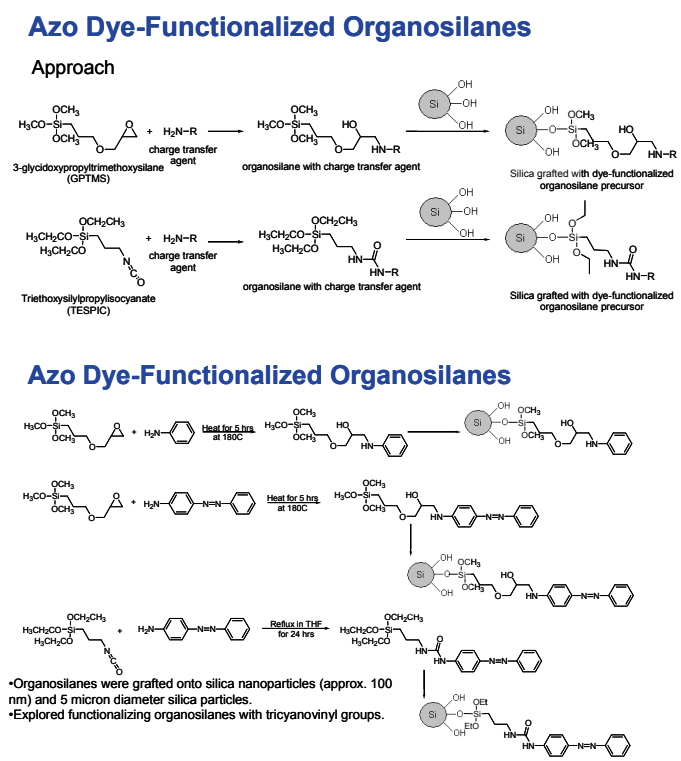


*Figure 2. Synthetic strategy for production of azo dye-functionalized silica beads.*

While the results of the above studies showed some promise in differentiating between nanotube chiralities, we ultimately demonstrated that this first generation of redox affinity beads had insufficient redox power to drive selective reactions with the nanotubes. We next developed a method to functionalize beads with tetracyanoquinone (TCNQ) derivatives, which have the demonstrated redox power to affect most of the chiralities present in our current nanotube samples. The strong electron-withdrawing cyano groups make coupling such derivatives to silica beads via silane chemistry challenging. We pursued a route that made use of recent monosubstitution reactions on TCNQ to provide a long side chain with an appropriate ammine group to react with isocyanate side groups of substituted silanes. While we were able to successfully generate these TCNQ-derivatized beads, we again were unable to generate the desired reactivity between them and our nanotube targets. Simultaneous to this realization, we were obtaining more promising results for nanotube selection based on manipulation of the surfactant chemistry associated with nanotube suspensions. We therefore began to focus our attempts on that approach (see later section on electrolyte manipulation of surfactant chemistry).

*Studies of Redox Reactivity on Carbon Nanotubes*

In addition to developing redox-based separations, we also sought to gain a fundamental understanding of the underlying redox reactions that we would rely on. We designed a series of kinetics experiments in which the redox potentials of the electronic acceptors are varied, without significantly perturbing their structures. This was envisioned to allow us to determine the chirality dependence of kinetic pre-exponential factors needed to understand the nature of charge-transfer complex formation in these systems. We began by studying the Fe, Ru, and Os hexacyanide series. Good data were obtained for the Ferrocyanide reactions with SWNTs, but we found the Ru and Os hexacyanides to rapidly react with water, preventing acquisition of the required data for this series.

We also performed large-scale screening of a variety of metal salt reactions with nanotubes to determine which may be most suitable for mapping nanotube valence band levels. We have investigated a variety of Fe, Mn, Co, Cu, Rh, and Zn salts to determine which have suitable redox potentials, display measurable kinetics, and react with the nanotubes in a largest-to-smallest diameter fashion, indicating that the expected ground-state electron-transfer reactions from the SWNT valence bands are occurring. We are still in the process of identifying a suitably large enough group of reagents to consistently map valence

bands and this will be the topic of a future postdoctoral research project.

*Redox-Based Sensing*

One useful aspect of the redox-based quenching of nanotube fluorescence that we made-use of in our redox studies to measure kinetics is that the quenching is completely reversible: remove the quenching agent, or add a reducing agent and fluorescence response of the SWNTs is returned. While not the focus of the separations aspect of this project, we were able to take advantage of this finding to enable a new approach to SWNT optical sensing. Details of our sensing work are detailed in reference [3].

*Demonstration of Diameter-Selective Manipulation of SWNT Solubilities*

One serendipitous result generated by the previous studies was that we encountered interesting quenching behavior upon addition of sodium perchlorate to our SWNT suspensions. This discovery ultimately has led to our successful approach for nanotube separations described in the next section. We found that its reaction with the SWNT sample resulted in loss of spectral features of certain chiralities, but skipped others of similar diameter. We proceeded to investigate this selective reactivity further and discovered that, by adding appropriate concentrations of electrolytes (including simply NaCl!) to nanotube solutions, their stability can be tuned in a diameter and chirality selective manner thorugh manipulation of the relevant surfactant equilibria (sodium dodecyl sulfate, or SDS, in our case). Precipitation of selected diameter and chirality distributions can be induced by addition of appropriate levels of different valency salts. Recognition of the ability to also affect SDS-nanotube equilibria in a parallel manner via tuning of temperature, we also demonstrated the ability to selectively precipitate nanotubes by lowering of temperature (Figure 3). The results of this study have been published in the Journal of the American Chemical Society [4].

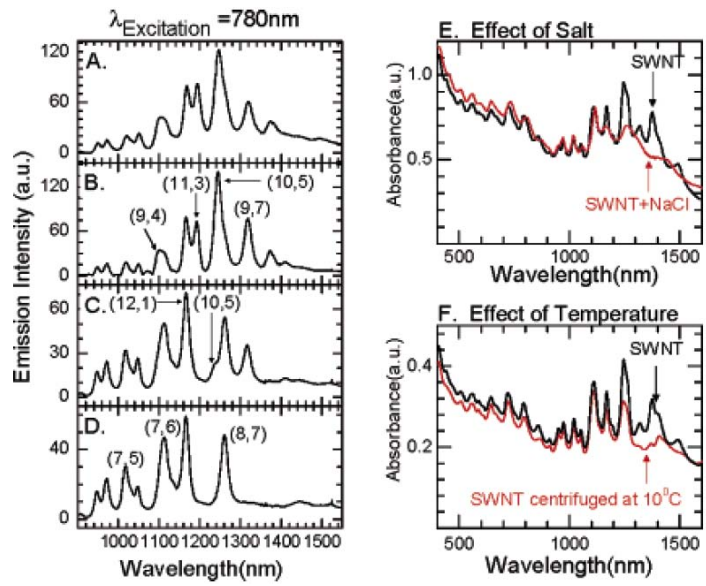


*Figure 3. Spectroscopy of SWNT-SDS dispersions as a function of salt concentration and temperature. A. emission spectrum of the starting SWNT-SDS dispersion; B. same solution in 0.14 M NaCl; C. in 0.43 M NaCl and D. in 0.57 M NaCl; E. absorption spectrum with and without NaCl (0.17 M); F. Change in the absorption spectrum at temperatures below the critical micellar temperature.*

*Density Modulation of Nanotubes for Separations Using Density Gradient Ultracentrifugation*

The above salt-induced precipitation studies led us to study in more depth the fundamental interactions of SDS at the SWNT surface and how they could be tuned via addition of electrolyte. As a reference point for understanding our results, we used previous work done on understanding SDS interactions at graphene surfaces. It had previously been found that SDS will adsorb on graphene as parallel domains of "flat" micelle structures. Addition of electrolyte causes an increase in the packing density of SDS into these structures, which results in a volume increase of the structure from reorientation into a hemi-cylindar [5]. Similar behavior on nanotube surfaces has important implications for their separations based on amplification of their density differences as will be seen below.

In the nanotube case, we found that addition of electrolyte at concentrations below the threshold that would cause SWNT precipitation resulted in an increase in SWNT fluorescence intensity and narrowing of spectral features as electrolyte concentration is increased. We have developed a model for explanation of this behavior based on the above observations and linked to the graphene findings. The spectral behavior with salt addition suggests a decrease in internanotube interactions which might otherwise quench and broaden observed spectra through intertube energy transfer. Our model explains this

decrease in interactions as a result of an increase in surfactant packing density at the nanotube surface. As with graphene, we propose a reorientation of the surfactant structure such that the overall surfactant/nanotube composite experiences a wholesale increase in volume. This volume increase results in a decrease in intertube interactions through the resultant increase in intertube steric repulsions. A significant aspect of this model is that the resultant volume increase results in an overall decrease in density of the composite that should scale with the inherent density of the particular nanotube structure in the absence of a surfactant coating.

We saw an immediate connection between these results and recent developments in separations technology based on density gradient ultracentrifugation. Such an approach is based on the principle that individual components of a mixture, when loaded onto a column of liquid that varies in density along its length, will separate into locations within the column that match their individual densities when subjected to ultracentrifugation. Recent work has shown that these principles can be applied to separation of carbon nanotubes based on differences in their densities. Success so far, however, has been limited to nanotubes that have been suspended with the use of complex, multicomponent surfactant systems. Results also have not been those predicted under the expectation that nanotube density should decrease as their diameters increase. Using the principles of our model for surfactant behavior in the presence of added electrolyte, we have demonstrated that simple addition of NaCl to SDS-suspended nanotubes will result in their fractionation into colored bands following ultracentrifugation in a density gradient (see Figure 4), without the use of any additional cosurfactants.

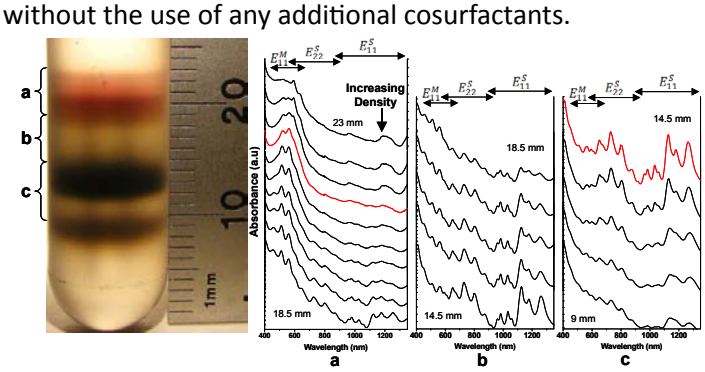


*Figure 4. The results of a density gradient separation on a 1.25% SDS-SWNT dispersion with 91 mM NaCl at 250 C. The photo at left shows fractionation of the initial dispersion into colored bands within the centrifuge tube. Twenty microliter fractions were collected at the same height from 4 tubes and combined. The combined (80 mL) fractions were diluted with 300 mL of 1% SDS/D2O for spectroscopy. Absorbance spectra are shown for fractions collected (a) between 18.5 23 mm (from tube bottom), (b) between 14.5 18.5 mm, and (c) 9 14.5 mm.*

Spectroscopic analysis (Figure 4) of isolated fractions show that nanotubes recovered from the lowest densities of the gradient are highly enriched in metallic nanotubes. Fractions at the highest densities are found to be highly enriched in semiconducting nanotubes. Furthermore, in addition to this demonstrated ability to separate metallic nanotubes from semiconductors, we find that in both cases, the nanotubes separated out according to diameter. The largest diameter nanotubes of either electronic type are found at the lowest densities, with diameters then decreasing as density increases. Additionally, we find that parallel behaviors can be found by adjusting centrifugation temperature without salt, or in combination with salt addition. Lowered temperatures in the absence of NaCl will also result in fractionation into colored bands. It is also found that temperature and salt used in combination can give significant control over resolution of the variable bands found within our separated samples.

In addition to demonstrating our ability to meet our ultimate goal of developing a new approach to nanotube separations, these results validate our model (described above) for surfactant interactions at the nanotube surface. The diameter dependence found in our separations is a direct consequence of the volume change predicted in our model. This volume change will serve as an amplification of the density differences between tubes of different diameter. Separations based on the amplified density differences will follow the density trend expected for unmodified nanotubes. This result is the first demonstration of this trend and is a direct consequence of our ability to make the separation occur with use of only one surfactant component. Additionally, our ability to separate metallic nanotubes from semiconductors demonstrates a fundamental difference in the surfactant behavior at these different surfaces and agrees with our model based on expectations for differences in polarizability between the two electronic families. Finally, the observation of parallel behaviors between salt addition and temperature lowering is a result of an increase in packing density of SDS at the nanotube surface as temperature is lowered. Again, this is in good agreement with the expectations from our model.

There are a number of significant points to be highlighted about our new approach to density gradient separations of SWNTs, including dramatically reduced centrifugation times, and easier post-separation processing which makes the product more amenable to use as a source of metallic and semiconducting material for use in thin film applications [6]. From a theoretical standpoint, the simple SDS/electrolyte system presented here may be more accessible to theoretical modeling than cosurfactant systems for directing further optimization of the separations.

Ultimately, salt enhancement may prove to be of utility in co-surfactant systems as well.

*Fundamental Spectroscopy*

One final aspect of this LDRD project has been the investigation of a number of aspects of the fundamental Raman spectroscopy of nanotube systems. This has been an important part of this effort in that spectroscopic characterization of samples is essential for evaluating the success of the separation and for identifying (see for example Figure 5) and quantifying the different nanotube chiralities present in a given fraction. Some example publications resulting from this aspect of the project are detailed in refs. [7], [8], and [9].

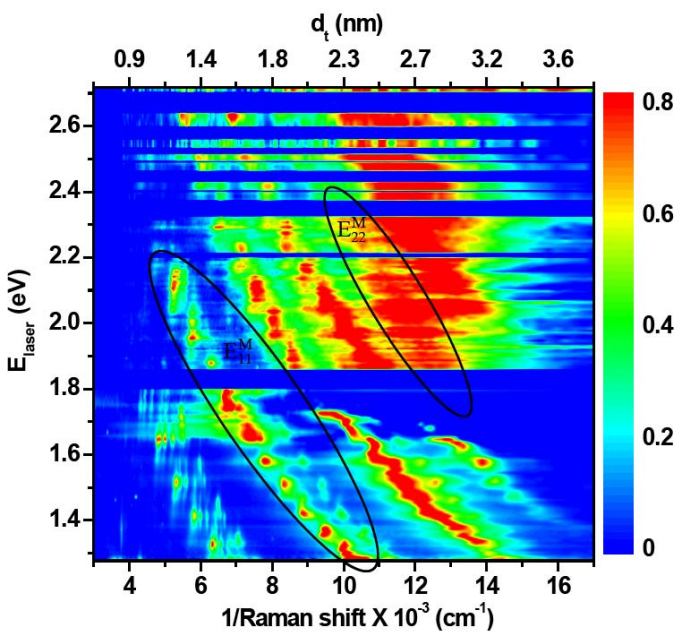


*Figure 5. 2-D Raman excitation map showing the radial breathing mode (RBM) intensity as a function of laser excitation energy and the inverse of the Stokes Raman frequency (proportional to nanotube diameter). Each spectrum composing the plot has been normalized by the strongest peak for better clarity of the RBM resonances. The E11M and E22M features are highlighted.*

**Future Work**

The successful attainment of several of this projects goals has placed us well for follow on research and funding support. The work has resulted in one patent application that we are using to pursue external funding from industrial partners. As part of that effort we have developed a strong interest from Arrowhead/Unidyme and are discussing applications under a non-disclosure agreement. Additionally, we have several envisioned applications of the enriched materials for applications in national security and have generated significant interest in this capability within the defense and national security communities. The purified materials are also serving as the basis for a new effort in reaction chemistry of pure chiralities. The sensing capability enabled by this project is also being continued with Andrew Dattelbaum of MPA-CINT with the development of robust encapsulation materials for real-world bioanalytical applications.

## References


1. Hersam, M. C.. Progress towards monodisperse single-walled carbon nanotubes. 2008. *Nature Nanotechnology.* **3**: 387.

2. O'Connell, M. J., E. E. Eibergen, and S. K. Doorn. Chiral selectivity in the charge transfer bleaching of single walled carbon nanotube spectra. 2005. *Nature Materials.* **5**: 412.

3. Satishkumar, B. C., L. O. Brown, Y. Gao, C. -C. Wang, H. -S. Wang, and S. K. Doorn. Reversible fluorescence quenching in carbon nanotubes for biomolecular sensing. 2007. *Nature Nanotechnology.* **2**: 560.

4. Niyogi, S., S. Boukhalfa, S. B. Chikkannanavar, T. J. McDonald, M. J. Heben, and S. K. Doorn. Selective aggregation of single-walled carbon nanotubes via salt addition. 2007. *Journal of the American Chemical Society.* **129**: 1898.

5. Wanless, E. J., and W. A. Ducker. Organization of sodium dodecylsulfate at the graphite-solution interface. 1996. *Journal of Physical Chemistry.* **100**: 3207.

6. Blackburn, J. L., T. M. Barnes, M. C. Beard, Y. -H. Kim, R. C. Tenent, T. J. McDonald, B. To, T. J. Coutts, and M. J. Heben. Transparent conductive single-walled carbon nanotube networks with precisely tunable ratios of semiconducting and metallic nanotubes. 2008. *ACS Nano.* **2**: 1266.

7. Goupalov, S. V., S. B. Chikkannanavar, and S. K. Doorn. Chirality and excitation dependence of exciton-phonon coupling in carbon nanotubes. 2006. *Physical Review B.* **73**: 115401.

8. Satishkumar, B. C., S. V. Goupalov, E. H. Haroz, and S. K. Doorn. Transition level dependence of Raman intensities in carbon nanotubes: the role of exciton decay. 2006. *Physical Review B.* **74**: 155409.

## Publications

Araujo, P. T., I. O. Maciel, P. B. C. Pesce, M. A. Pimenta, S. K. Doorn, H. Qian, A. Hartschuh, M. Steiner, L. Grigorian, K. Hata, and A. Jorio. Nature of the constant factor between radial breathing mode frequency and tube diameter for single-wall carbon nanotubes. 2008. *Physical Review B.* **77**: 241403(R).

Araujo, P. T., S. K. Doorn, S. Kilina, S. Tretiak, E. Einarsson, S. Maruyama, H. Chacham, M. A. Pimenta, and A. Jorio. Third and fourth optical transitions in semiconducting carbon nanotubes. 2007. *Physical Review Letters.* **98**: 067401.

Doorn, S. K., P. T. Araujo, K. Hata, and A. Jorio. Excitons and exciton-phonon coupling in metallic single-walled carbon nanotubes: resonance Raman spectroscopy. To appear in *Physical Review B.*

Goupalov, S. V., B. C. Satishkumar, and S. K. Doorn. Chirality and excitation dependence of exciton-phonon coupling in carbon nanotubes. 2006. *Physical Review B.* **73**: 115401.

Haroz, E. H., S. M. Bachilo, R. B. Weisman, and S. K. Doorn. Curvature effects on the E33 and E44 exciton transitions in semiconducting wingle-walled carbon nanotubes. 2008. *Physical Review B.* **77**: 125405.

Kilina, S., S. Tretiak, S. K. Doorn, Z. Luo, F. Papadimitrakopoulos, A. Piryatinski, A. Saxena, and A. R. Bishop. Cross-polarized excitons of carbon nanotubes. 2008. *Proceedings of the National Academy of Science.* **105**: 6797.

Luo, Z., F. Papadimitrakopoulos, and S. K. Doorn. Intermediate frequency Raman modes for the lower optical transitions of semi-conducting single-walled carbon nanotubes. 2007. *Physical Review B.* **75**: 205438.

Luo, Z., F. Papadimitrakopoulos, and S. K. Doorn. Bundling effects on the intensities of second order Raman modes in semi-conducting single-walled carbon nanotubes. 2008. *Physical Review B.* **77**: 035421.

Niyogi, S., C. G. Densmore, and S. K. Doorn. Electrolyte tuning of surfactant interfacial behavior for enhanced density-based separations of single-walled carbon nanotubes. *Journal of the American Chemical Society.*

Niyogi, S., S. Boukhalfa, B. C. Satishkumar, T. J. McDonald, M. J. Heben, and S. K. Doorn. Selective aggregation of single-walled carbon nanotubes via salt addition. 2007. *Journal of hte American Chemical Society.* **129**: 1898.

Satishkumar, B. C., L. O. Brown, Y. Gao, C. -C. Wang, H. -L. Wang, and S. K. Doorn. Reversible fluorescence quenching in carbon nanotubes for biomolecular sensing. 2007. *Nature Nanotechnology.* **2**: 560.

Satishkumar, B. C., S. K. Doorn, G. A. Baker, and A. M. Dattelbaum. Fluorescent single-walled carbon nanotube/silica composite materials. To appear in *ACS Nano.*

Satishkumar, B. C., S. V. Goupalov, E. H. Haroz, and S. K. Doorn. Transition level dependence of Raman intensities in carbon nanotubes: the role of exciton decay. 2006. *Physical Review B.* **74**: 155409.

Shreve, A. P., E. H. Haroz, S. M. Bachilo, R. B. Weisman, S. Tretiak, S. Kilina, and S. K. Doorn. Determination of exciton-phonon coupling elements in single walled carbon nanotubes via Raman overtone analysis. 2007. *Physical Review Letters.* **98**: 037405.

# Nanocomposite Thin Films for Surface Assisted Mass Spectrometry

*Andrew Martin Dattelbaum*

20060395ER

## Introduction

For our Laboratory Directed Research and Development-Exploratory Research program we developed the use of nanoporous silica ($SiO_2$) thin films deposited on silicon substrates to characterize the mass of compounds using a laser desorption-ionization mass spectrometry technique. Our technique uses an inexpensive and easily prepared material, nanoporous silica, to 1) hold a sample of interest and 2) help transfer energy from incoming laser light to the sample. This work combined recent advances in nano-bioscience with mass spectrometry techniques to develop a new and versatile platform to characterize a number of biologically relevant molecules, like amino acids and small peptides. We anticipate that the work developed as part of this project will lead to improved methodologies for mass spectrometry analysis of complex chemical and biochemical samples, which will have a significant impact in the areas of drug and catalysis discovery, as well as protein analyses.

## Background and Research Objectives

Mass spectrometry is a technique that is used to measure the mass of molecules. Because mass spectrometry is a sensitive technique it can identify materials in trace amounts, which has made it useful for a variety of applications, including, for example, sensing, water monitoring and forensic analyses on chemical or biological molecules.

One particular type of mass spectrometry uses a laser to help "move" molecules deposited on a surface into a gaseous state where they can be characterized by the mass spectrometry detector. However, the laser can not do all the work and needs help to efficiently get the sample of interest into a gaseous state. Traditionally, samples of interest are mixed with another material, i.e., a "helper" material that strongly absorbs the laser energy. However, the "helper" material can be specific to a class of molecules, meaning that one needs to try a few different "helper" materials for optimal detection when samples contain unknown compounds. In addition, the helper molecule also gets into the detector chamber, and because it is in a high concentration it can overshadow the signal from the compounds one is actually trying to characterize. This is especially troubling when the analyte of interest has a mass close to that of the "helper" molecules used. Therefore, researchers have sought after alternative materials to efficiently promote this technique without a background signal from the "helper" material.

The goal of this project is to develop a thin film that promotes the "movement" of molecules into a gaseous state, without the addition of "helper" molecules, for mass characterization. Specifically, this project will use silica, a robust and chemically inert material, containing nanometer scale pores as the film to improve this mass spectrometry technique. Figure 1 schematically shows how this technique works in practice. The nanoporous silica film acts to 1) hold a sample of interest and 2) help transfer energy from incoming laser light to the sample. The thin film will not move into a gaseous state, so one should be able to characterize a broader range of molecules than currently available, especially low mass compounds. This technique, called surface-assisted laser desorption-ionization mass spectrometry (SALDI-MS), is a unique and useful application of a nanostructured material that could potentially be used to characterize organic and inorganic compounds previously not addressable by traditional LDI-MS.

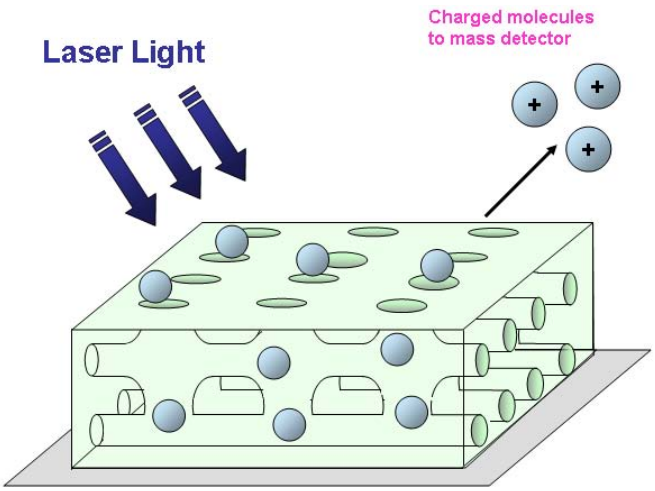


*Figure 1. Schematic representation of the SALDI-MS process using an ordered nanoporous silica thin film to assist in desorption/ionization processes.*

## Importance to LANL's Science and Technology Base and National R & D Needs

Successful development of nanoporous silica on silicon for mass characterization may be beneficial to laboratory programs by readily identifying, and potentially quantifying, newly synthesized organic and inorganic complexes, such as chemical and biological agents, which supports work in threat reduction, actinide chemistry, as well as environmental chemistry. Further, this work generally supports laboratory initiatives in Materials Science and nano-bioscience, including the Center for Integrated Nanotechnologies (CINT), a Department of Energy, Office of Science funded facility.

## Scientific Approach and Accomplishments

Ordered nanocomposite silica thin films for this project were prepared by an evaporation induced self-assembly process [1], which can be accomplished reproducibly at room temperature and under standard atmospheric conditions. The evaporation induced self-assembly process involves vertically pulling a cleaned substrate, such as silicon, at a constant velocity from a solution of ethanol containing a molecule that can condense to form a silica network (silica precursor molecule), as well as a surfactant that can self-assembly into an array of shapes like cylinders. These cylinders can then organize into larger assemblies, like tubes stacked on top of one another, which form the template around which the silica condenses. Film formation occurs as the ethanol solvent evaporates. The thickness of the nanocomposite films prepared in this way was controlled by adjusting the pulling speed of the substrate from a surfactant/silicate solution with slower speeds resulting in thinner more uniform films. Withdrawing cleaned silicon substrates from the surfactant/silicate solution resulted in ordered nanocomposite silica films with thicknesses that increased linearly from ~500 Å (pulling speed at 25 mm/min) to ~1550 Å (pulling speed at 200 mm/min). At faster pulling speeds there is a distinct thickness change, ~20%, from the top to the bottom of the film. However, at deposition speeds of 25 mm/min there is less than a 2% difference in thickness change across the film. The surfactant template was then removed from the film by exposure to deep-UV light (185-254 nm). Removal of the surfactant did not cause the silica framework to collapse. Rather, a nanoporous silica thin film was created.

We have determined the optimal thickness for subsequent SALDI-MS studies. A standard angiotensin peptide was spotted on nanoporous films of various thicknesses. The highest signals and best resolution were obtained for ordered nanoporous silica films that were ~300 Å (pulling speed 25mm/min). As film thickness increased, fewer ions and poorer mass resolution was observed.

An advantage of using deep-UV light to remove surfactant template from the nanocomposite silica films is that the ability to control which regions of the film get exposed to UV light by simple masking techniques. A mask of, for example, chromium patterned on quartz, was used to selectively remove the organic template from the film for the generation of patterned nanoporous silica regions in a field of nanocomposite silica as shown schematically in Figure 2A.

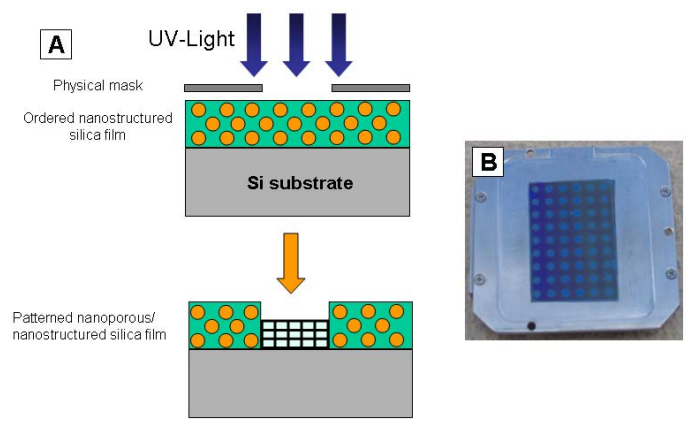


*Figure 2. A) Schematic of the deep-uv exposure technique used to prepare patterned nanostructured-nanoporous silica thin films. B) Optical image of a patterned nanoporous/nanostructured film deposited at a dip-coating speed of 200 mm/min on a silicon substrate that has been fixed on a standard MALDI support. Circles are the nanoporous silica regions and are 1 mm in diameter.*

The thickness of the nanocomposite silica films contracts ~30% upon surfactant removal by deep-UV to ~300 Å and ~950 Å for films withdrawn at 25 and 200mm/min, respectively. The index of refraction also decreases from 1.45-1.46 for the ordered nanocomposite films to ~1.43 for the nanoporous silica films (pores filled with water), consistent with our previous results on thicker ordered nanocomposite silica films [2]. The patterned nanoporous regions are readily distinguishable from the nanocomposite regions, as seen in the digital photograph of a patterned film shown in Figure 2B, due to the changes in thickness and index of refraction upon surfactant removal. Further, because the nanocomposite silica regions contain surfactant molecules, the surface water contact angle (how much water beads up on a surface) is higher, ~42°, than the nanoporous regions, <10°, which do not contain surfactant. The difference in hydrophilicity allows for the corralling and concentration of small volumes of aqueous solutions within the nanoporous regions. Consequently, by patterning the nanocomposite films with deep-UV light we have the ability to spot and analyze more than 50 different samples on a single substrate. The number of spots analyzed could readily be increased using robotic techniques.

Several experiments were performed to determine the optimal manual spotting technique for SALDI-MS characterization of different molecules on the ordered nanoporous silica thin films. These included pipetting different volumes of sample on the nanoporous silica regions and allowing them to 1) dry in air or 2) under a stream of nitrogen. These methods generally resulted in growth of an analyte "film" on the silica surface that limited contact between analyte and the activating nanoporous surface, which resulted in poor mass spectral data. A better spotting method was found by pipetting 1 microliter of sample onto the nanoporous silica, then withdrawing the liquid after 1 min. This allowed the sample time to diffuse into the nanoporous silica film without formation of an analyte film on top of the nanoporous silica.

Using optimal spotting techniques we were able to observe mass spectral data from a variety of small molecules, as seen in Figures 3 and 4. Figure 3 shows a series of mass spectra data for a variety of amino acids, i.e, protein building blocks, which are not generally observable using matrix assisted LDI-MS technique. In addition, we show in Figure 4 the ability to look at single peptides, as well as a mixture of peptides. In Figure 4b, we show that the mass spectrum for a common peptide standard, angiotensin, taken on nanoporous silica has good isotopic resolution, which is comparable to that observed using matrix. However, the current limit of detection for the peptides studied thus far has been less than that observed with matrix.

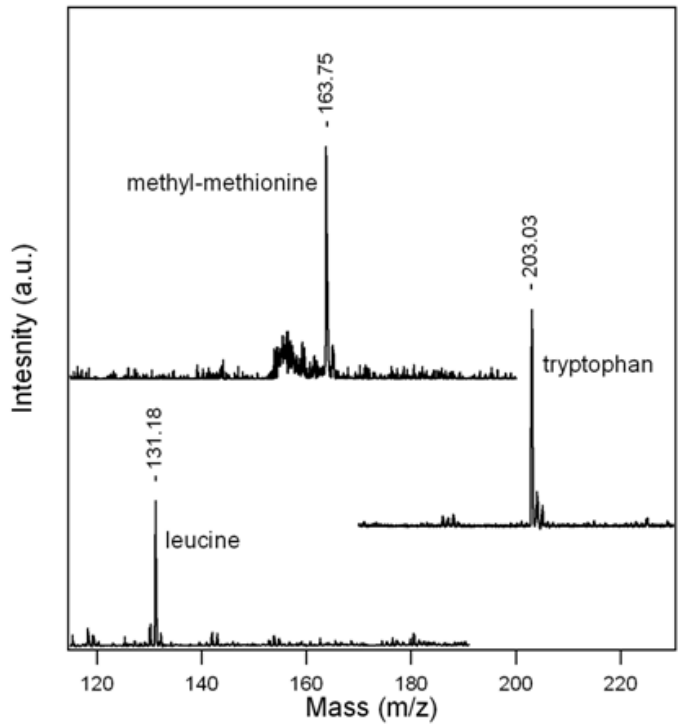


*Figure 3. SALDI-MS analysis of several amino acids on nanoporous silica films. Approximately 10 pmoles of total material is estimated to have been deposited.*

We also made measurements to examine the affects that varying the surfactant used as a template has on the desorption-ionization processes from nanoporous silica thin films. By varying the surfactant used to template, we can control the pore size, as well as the structural order of the silica framework. To date, we have generally used a Brij56™ (Aldrich) surfactant template, which yields a nanoporous silica film with a cubic structure of ~ 2 nm diameter pores. We have also used other surfactants, such as cetyltrimethylammonium bromide (CTAB) and Pluronics P123™ (BASF), which yield smaller and larger pore sizes, respectively, but with a hexagonal silica structure. Films templated by either surfactant have not performed as well as films templated by Brij56, which could be due to the silica structure.

One area where the nanoporous silica films have been successfully utilized by us is the in the identification of siderophores produced by *B. anthracis* and other potentially infective bacteria. Siderophores are small metal chelating metabolites produced by bacteria and secreted into the extracellular medium to scavenge iron that bacteria need for growth. Most siderophores are nonribosomal peptides

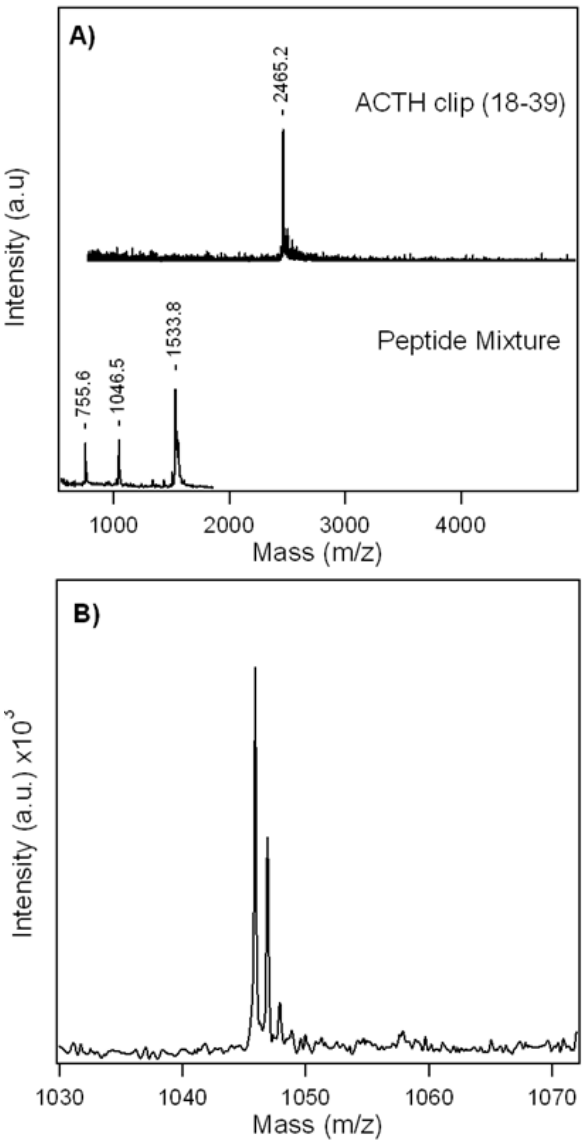


*Figure 4. Analysis of peptides, A) ACTH clip (18-39) and a mixture of peptides, Bradykinin, Angiotensin II and P14R1, on a patterned nanoporous silica film. B) SALDI-MS spectra taken on the same sample of a standard peptide, angiotensin.*

and are structurally diverse. MS fragmentation is the most direct method for structural identification of siderophores, as it provides accurate identification of motifs, and unlike other identification techniques, is not hampered by minor iron (III) contamination, common in siderophore samples. We have analyzed crude siderophore samples from a number of strains of *Bacillus* bacteria for bacillibactin. An example of how SALDI-MS can assist in the structural identification of bacillibactin is shown in Figure 5. Acid hydrolysis of siderophores is commonly used to identify the structural or 'liganding' groups that compose them, and this process, similar to MS/MS methods, is known to easily breakup the siderophore compounds into small identifiable pieces. The acid hydrolysis preparations were analyzed and the fragments that we observed enabled the firm establishment of the structure of this siderophore as shown in the inset. Bacillibactin is a trimer of 2,3-dihydroxybenzoate (DHB)-glycine-threonine monomers. Characteristic fragment ions including those of DHB (1), DHB-glycine (1+2), and DHB-glycine-threonine (3), both in carboxylated and decarboxylated forms, were all clearly visible via the SALDI-MS experiments.

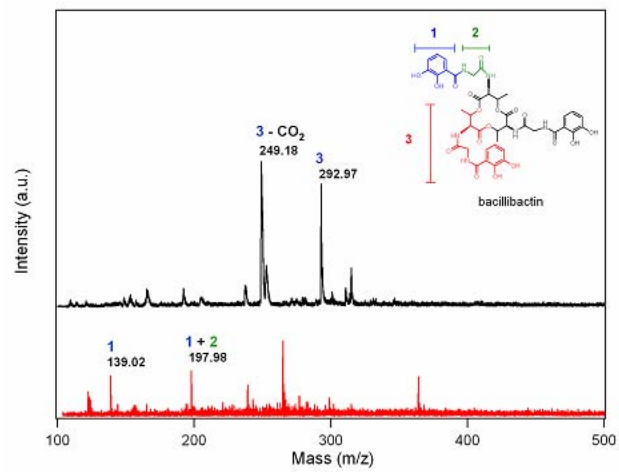


*Figure 5. SALDI-MS of bacillibactin hydrolysate on nanoporous silica films. Subunits 1-3 of bacillibactin were identified by analyzing the hydrolysate in (A) positive or (B) negative ion mode, firmly establishing the identity of this siderophore. Only the peaks used to identify bacillibactin are labeled.*

We have also shown that the ordered nanoporous silica films deposited on silicon require no special handling or storage conditions to maintain their MS ability. We monitored the mass spectrum of angiotensin II spotted on a nanoporous silica film just after it was spotted and then after storing the film for 18 months under ambient conditions in a drawer in the lab. No loss of either intensity or resolution was observed in the mass spectral readings as a result of storage time.

In summary, we have made significant progress towards the specific aims of this LDRD-ER program. We have shown that nanoporous silica films deposited on silicon may be used for the SALDI-MS characterization of small molecules, such as amino acids, peptides and siderophores. We have found that the nanoporous silica samples are stable for over a year, and may be modified to prepare a patterned film suitable for spotting multiple samples for high throughput analyses. However, we were unable to find the right conditions to use this technique as a general platform for large molecule identification, which is currently a limitation of all known SALDI platforms, too. In any event, the results obtained in this project may allow us to attract new programs, especially in the area of threat

reduction, where films that can be used for identification of small molecules then archived for long periods of time are valuable.

## References

1. Lu, Y. F., R. Ganguli, C. A. Drewien, M. T. Anderson, C. J. Brinker, W. L. Gong, H. Soyez, B. Dunn, M. H. Huang, and J. I. Zink. Continuous formation of supported cubic and hexagonal mesoporous films by sol gel dip-coating . 199. *Nature.* **389**: 364.

2. Dattelbaum, A. M., M. L. Amweg, J. D. Ruiz, L. E. Ecke, A. P. Shreve, and A. N. Parikh. Surfactant removal and silica condensation during the photochemical calcination of thin film silica mesophases. 2005. *Journal of Physical Chemistry B.* **109**: 14551.

## Publications

Dattelbaum, A. M., R. K. Hicks, J. S. Shelly, A. T. Koppisch, and S. Iyer. Surface assisted laser desorption-ionization mass spectrometry on nanoporous silica thin films. 2008. *Microporous and Mesoporous Materials.* **114**: 193.

Dattelbaum, A. M., and S. Iyer. Surface assisted laser desorption-ionization mass spectrometry. 2006. *Expert Review of Proteomics.* **3** (1): 153.

# Use of Strain Engineering to Tune the Physical Properties of Nanoscale Metal-Oxide Films

*Quanxi Jia*

20060497ER

## Abstract

Perovskite metal-oxides have become the subject of many theoretical and experimental studies in recent years due to their versatile physical properties and important technological applications. In such complex metal-oxides, the anisotropic lattice-strain caused by the lattice-mismatch between the substrate and the film plays a critical role in their anomalous physical properties. In this project, we used strain engineering to tune the physical properties of nanoscale perovskite metal-oxide films. We conducted a systematic and quantitative analysis of the effects of the anisotropic strain on well controlled and fully strained nanoscale films. We manipulated the lattice-strain either by choosing the substrate material or by inserting a buffer layer or template between the substrate and the film. Our experimental results provide fundamental understanding of the physics of the electron-lattice coupling and the anisotropic properties in perovskite metal-oxides, both of which are fundamental physics and materials issues of great scientific interest. The study also broadens the applications of this class of perovskite metal-oxides.

## Background and Research Objectives

Perovskite oxides films have been regarded as the most promising candidates for next generation electronicdevices because these materials exhibit a wide range of electronic/magnetic properties that conventional metallic elements and covalent semiconductors do not possess. For example, $SrTiO_3$ and $(Pb,Sr)TiO_3$ have been considered for dielectric layers in dynamic random access memories and nonlinear dielectric media in tunable microwave devices. Similarly, the coexistence of distinct multi-functionalities in multiferroic materials such as $DyMnO_3$ makes them the best choice for next generation electronic devices as they offer magnetic and/or electric tuning with much simplified architectures. However, it has been found that the physical properties of such films are quite different from those of their bulk single-crystal counterparts. The strain imposed on the films plays a critical role in their anomalous physical properties. For instance, epitaxial strain can be harnessed to increase the ferroelectric transition temperature by hundreds of degrees and produce room-temperature ferroelectricity in $SrTiO_3$, a material that is not normally ferroelectric at any temperature [1]. Another example includes $BaTiO_3$ where a biaxial strain can result in a ferroelectric transition temperature nearly 500 °C higher than in a bulk single crystal [2]. In such complex metal-oxides, the anisotropic lattice-strain caused by the lattice-mismatch between the substrate and the film plays a critical role in their physical properties. In other words, the strain imposed on the films plays a critical role in their anomalous physical properties. A clear understanding of the relationship between the strain and the physical properties as well as how to manipulate the strain are crucial for the application of these oxides in next generation electronic device

We used strain engineering to tune the physical properties of ferroelectric and ferromagnetic films. These materials were selected due to their interesting structural/physical properties and their technical importance. The main objectives of the study were to 1) construct a theory to make a quantitative and useful connection to experiments, 2) grow well controlled and fully strained nanoscale perovskite metal-oxide films, 3) optimize the substrate and template materials for utmost anisotropic strain effects, 4) characterize the structural and physical properties of fully strained films, and 5) understand the fundamental mechanisms of the lattice-strain and its effects on the tunable properties of nanoscale perovskite metal-oxide films.

## Importance to LANL's Science and Technology Base and National R & D Needs

This project not only provides a better understanding of the fundamental physics and physical chemistry as well as materials issues of metal-oxide films, but also solves technologically important issues related to nanotechnology. It directly impacts LANL's Science and Technology Base in Fundamental Understanding of Materials, linking across length and time scales to achieve multi-scale understanding of properties and phenomena of materials. Furthermore, LANL's thrusts in nanotechnology, sensors for threat reduction, and energy benefit from this project.

## Scientific Approach and Accomplishments

We used ferroelectric and ferromagnetic perovskite as the representative material systems to accomplish our objectives. The following is the detailed description of our scientific approaches.

**Theoretical modeling**

We constructed a theory with two competing order parameters (such as magnetism, and polarization) and a subsidiary order parameter field of strain in order to make quantitative connection to experiments. In thin films where the strain is clamped, this secondary order parameter allows us to tune properties through the phase boundary. We also used theories to predict the temperature dependence of the lattice parameters of ferroelectric films under large biaxial strains.

**Epitaxial growth of fully strained nanoscale perovskite oxide films**

The most important criterion for heteoepitaxy is a moderately small fractional mismatch, $f = (a_f - a_s)/a_s$ in the atomic periodicities of the two materials along the interface, where $a_f$ and $a_s$ represent the atomic spacings along a specific direction in the film and the substrate surface, respectively. The best way to produce large lattice-strains is to choose appropriate substrate materials that have a great lattice mismatch with the films. We used pulsed laser deposition (PLD) to deposit fully strained films on different substrates. PLD is one of the best deposition techniques to grow complex metal-oxides due to its very good control of stoichiometry. The use of much higher oxygen pressure (as high as several hundred mTorr of pure oxygen) during deposition made it possible to avoid oxygen deficiencies commonly observed in the films deposited by sputtering and molecular-beam epitaxy. We found that the control of oxygen content was very critical for our experiment since oxygen vacancies could also introduce strains. To obtain well controlled and fully strained films, we kept the film thickness in the nanoscale range from 10 nm to 50 nm depending on the degree of mismatch between the substrate and the film.

**Optimization of substrate materials and templates for utmost anisotropic strain effects**

We used two different approaches to obtain the utmost anisotropic strain effect. We first used commercial single-crystal $LaAlO_3$, $NdGaO_3$, and $SrTiO_3$ as the substrates. These materials are both structurally and chemically compatible with the films to be deposited. More importantly, they are thermally stable at high deposition temperatures for high-quality epitaxial growth.

**Characterization of the structural properties of fully strained films**

One of the tasks in the study of the anisotropic strain was the qualitative and quantitative characterization of the strain state. We mainly used two different techniques for this purpose: 1) Advanced scanning probes such as scanning transmission electron microscopy (STEM) high-angle annular dark-field (the so-called "Z-contrast") imaging technique and high resolution X-ray diffraction (HRXRD).

**Characterization of the dielectric (ferromagnetic) properties of fully strained nanoscale films**

The ultimate goal of the project was to establish the relationship between the degree of anisotropic strain and the physical properties of the fully strained films. We used a coplanar device structure to evaluate the physical properties of the fully strained nanoscale films. By patterning the contact electrodes along three different crystallographic directions, we could evaluate the anisotropic properties of the films.

We have accomplished our technical objectives through the LDRD ER support. The following highlights our accomplishments. More detailed technical achievements can be found form our technical publications.

The phase-field method, which describes a microstructure using a set of conserved and non-conserved field variables that are continuous across the interfacial regions, has recently emerged as a powerful computational approach to modeling and predicting mesoscale (in the range of nanometers to microns) morphological and microstructural evolutions in materials. We showed that one-unit-

cell-thick $BaTiO_3$ layer in $BaTiO_3/SrTiO_3$ superlattices (see Figure 1) was not only ferroelectric (with ferroelectric transition temperature as high as 250 K) but also polarized the quantum paraelectric $SrTiO_3$ layers adjacent to them. Ferroelectric transition temperature was tuned by about 500 K with varying the thicknesses of the $BaTiO_3$ and $SrTiO_3$ layers, revealing the ferroelectricity was robust in nanoscale system. The theoretical predictions on the ferroelectric transition temperature of the superlattices from the phase field approach were in an excellent agreement with the experimental measurement (see the Figure 2), which evidenced the powerful of the phase field modeling. The modeling showed that the domain formation in ferroelectric layer drastically affect the ferroelectric transition temperature and the induced polarization within the non-ferroelectric layer in a superlattice. Detailed experimental results can be found in our article published in Science. [3].

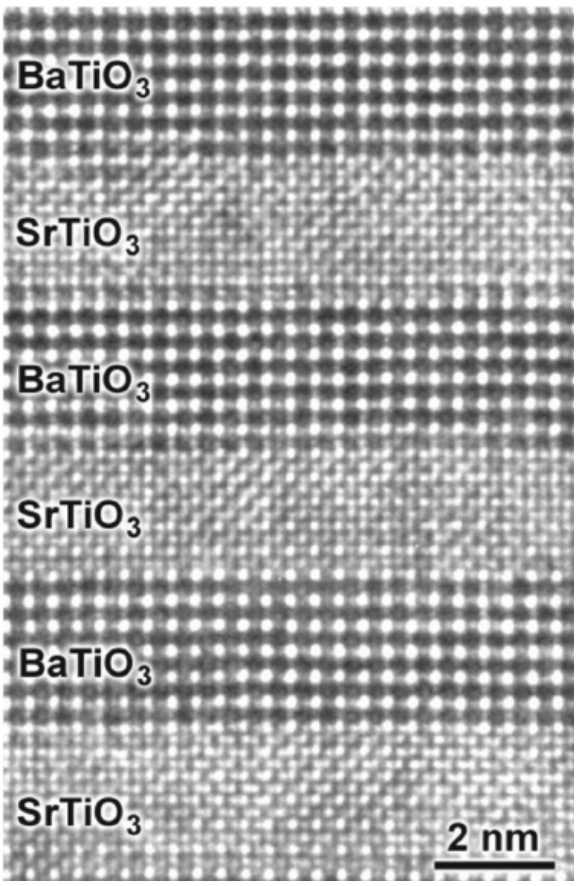


*Figure 1. A high resolution transmission electron microscopy image of a portion of the [($BaTiO_3$)6/($SrTiO_3$)5]20 superlattice. No significant inetrdiffusion of Ba and Sr takes place at the interface.*

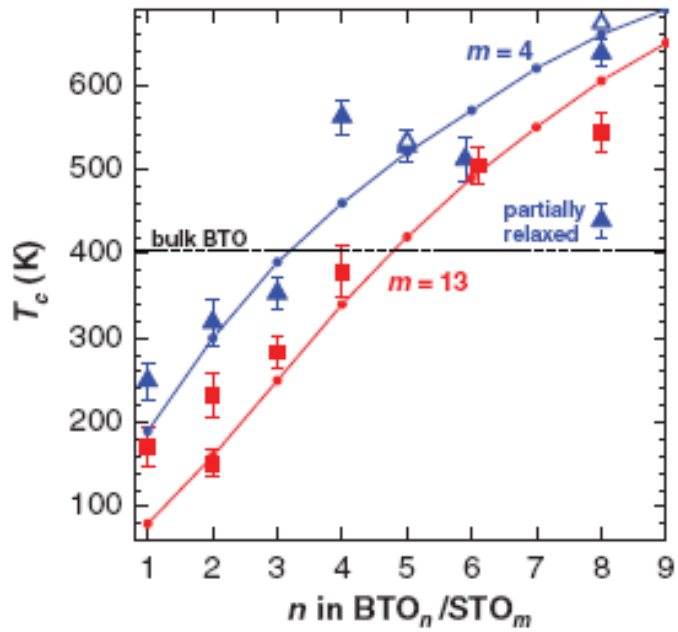


*Figure 2. Dependence of Tc on n and m in superlattices ($BaTiO_3$) n/($SrTiO_3$)m. Blue symbols are for m=4 and red symbols are for m=13 from ultraviolet Raman measurements. Open triangles are from temperature-dependent XRD measurements. Scattered symbols are from experimental measurements. Circles with lines are from phase-field modeling. The black horizontal dash-dotted line shows the Tc in bulk $BaTiO_3$.*

We also used a phase-field model for studying the magnetoelectric coupling effect in epitaxial ferroelectric and magnetic nanocomposite thin films. The model can simultaneously take into account the ferroelectric and magnetic domain structures, the electrostrictive and magnetostrictive effects, substrate constraint, as well as the long-range interactions such as magnetic, electric, and elastic interactions. As an example, we studied the magnetic-field-induced electric polarization in $BaTiO_3$–$CoFe_2O_4$ nanocomposite films. The effects of the film thickness, morphology of the nanocomposite, and substrate constraint on the degree of magnetoelectric coupling were systematically investigated. The simulation illustrated that the magnetic-field-induced electric polarization is highly dependent on the film thickness, morphology of the nanocomposite, and substrate constraint, which provided a number of degrees of freedom in controlling coupling in nanocomposite films. Detailed experimental results can be found in our article published in Appl. Phys. Lett. [4].

The discovery of colossal magnetoresistance in rare-earth manganites of $R_{1-x}A_xMnO_3$ (where R is rare earth and *A* is divalent cation) has triggered enormous studies on these perovskite-based materials over the last decade. However, the intrinsic large magnetoresistance (MR) effect in the perovskite manganites is observed only under high magnetic fields of several teslas at a narrow range of temperatures

around the ferromagnetic-paramagnetic phase transition, which has greatly limited its practical applications. Therefore, it is highly desirable to exploit low field magnetoresistance (LFMR) that can be triggered at an external magnetic field of the order of the coercive field $H_c$. Improvements of LFMR have been achieved either by making the manganites in polycrystalline granular structure or by incorporating other materials to enhance the spin polarized tunneling through grain boundaries. Through various secondary phase attempts using insulators, soft magnetic materials, glass, and other ferromagnetic oxides to make polycrystalline films, many researchers have sacrificed crystallinity and epitaxial orientation to obtain more grain boundaries. It is also hard to achieve uniform properties in randomly oriented polycrystalline films. We successfully deposited well-oriented $(La_{0.7}Sr_{0.3}MnO_3)_{0.5}$:$(ZnO)_{0.5}$ nanocomposite thin films on single crystal sapphires via pulsed laser deposition. The as-grown films and the post-annealed films showed differences in their microstructures. Figure 3 shows the resistivity versus temperature of the as-grown and the post-annealed films in an external magnetic field. The transport measurements were performed along the film surface using the conventional four-probe method, and the magnetic field was applied parallel to the film surface. The magnetoresistance (MR) was also depicted for the as-grown film. The resistivity of the post-annealed film was shown for zero-field only since there was no practical difference at a field of 1 T. It should be noted that an enhanced LFMR of about 12% was achieved in the as-grown films with fine intermixed grains, while a negligible LFMR was observed in the post-annealed films with large single-crystal-like, clearly phase-separated grains. This was superior to that of epitaxial LSMO thin films and was comparable to that of a $La_{0.7}Sr_{0.3}MnO_3$:$Al_2O_3$ composite film ($H$=0.3 T, 77 K) and many of the ceramic bulk composites. Detailed experimental results can be found in our article published in Appl. Phys. Lett. [5].

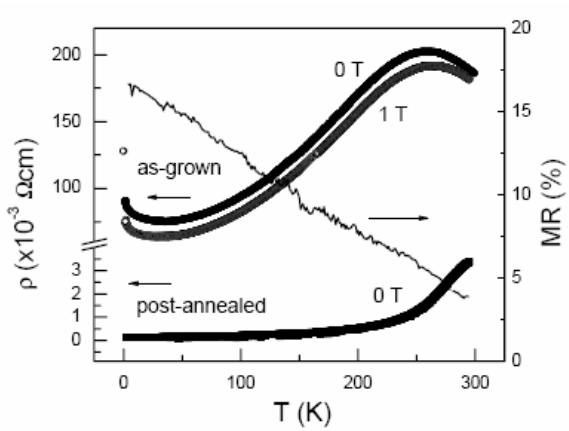


*Figure 3. Resistivity of the as-grown films and the post-annealed films at different fields as a function of temperature. The MR of the as-grown films is also exhibited.*

## References


1. Choi, K. J., M. Biegalshi, Y. L. Li, A. Sharan, J. Schubert, R. Uecker, P. Reiche, Y. B. Chen, X. Q. Pan, V. Gopalan, L. –Q. Chen, D. G. Schlom, and C. B. Eom. Enhancement of ferroelectricity in strained BaTiO3 thin films. 2004. *Science.* **306**: 1005.

2. Haeni, J. H., P. Irvin, W. Chang, R. Uecker, P. Reiche, Y. L. Li, S. Choudhury, W. Tian, M. E. Hawley, B. Craigo, A. K. Tagantsev, X. Q. Pan, S. K. Streiffer, L. Q. Chen, S. W. Kirchoefer, J. Levy, and D. G. Schlom. Room-temperature ferroelectricity in strained SrTiO3. 2004. *Nature.* **430**: 758.

3. Tenne, D. A., A. Bruchhausen, D. L. Kimura, A. Fainstein, R. Katiyar, A. Cantarero, A. Soukiassian, V. Vaithyanathan, J. H. Haeni, W. Tian, D. G. Schlom, C. E. Bom, H. P. Sun, X. Q. Pan, Y. L. Li, L. Q. Chen, Q. X. Jia, and X. X. Xi. Nanoscale Ferroelectricity in BaTiO3/SrTiO3 Superlattices Probed by Ultraviolet Raman Spectroscopy. 2006. *Science.* **313**: 1614.

4. Zhang, J. X., Y. L. Li, F. Zavaliche, Q. X. Jia, D. G. Schlom, R. Ramesh, and L. Q. Chen. Phase-Field Model for Epitaxial Ferroelectric and Magnetic Nanocomposite Thin Films. 2007. *Appl. phys. Lett..* **90**: 052909.

5. Kang, B. S., H. Wang, Y. Li, J. L. MacManus-Driscoll, Q. X. Jia, I. Mihut, and J. B. Betts. Low Field Magnetotransport Properties of (La0.7Sr0.3MnO3)0.5:(ZnO)0.5 Nanocomposite Films Grown via Pulsed Laser Deposition. 2006. *Appl. phys. Lett..* **88**: 192514.


## Publications


Kang, B. S., H. Wang, Y. Li, J. L. MacManus-Driscoll, Q. X. Jia, and I. Mihut. Low Field Magneto-transport Properties of (La0.7Sr0.3MnO3)0.5:(ZnO)0.5 Nanocomposite Films Grown via Pulsed Laser Deposition. 2006. *Appl. phys. Lett..* **88**: 192514.

Lee, J. K., Y. Lin, Q. X. Jia, T. Hochbauer, H. S. Jung, L. Shao, A. Misra, and M. Nastasi. Role of strain in the blistering of hydrogen-implanted silicon. 2006. *Applied Physics Letters.* **89**: 101901/3.

Lee, J. S., B. S. Kang, and Q. X. Jia. Data Retention Characteristics of Bi3.25La0.75Ti3O12 Thin Films on Conductive SrRuO3 Electrodes. 2007. *Appl. phys. Lett..* **91**: 142901.

Lee, J. S., and Q. X. Jia. Epitaxial Growth and Anisotropic Dielectric Properties of La-Doped Bi4Ti3O12 Thin Films. 2007. *Solid State Phenomena* . **124-126**: 7497.

Li, Y. L., H. Y. Hu, D. A. Tenne, A. Soukiassian, D. G. Schlom, L. Q. Chen, X. X. Xi, K. J. Choi, C. B. Eom, A. Saxena, T. Lookman, and Q. X. Jia. Interfacial Coherency and Ferroelectricity of BaTiO3/SrTiO3 Superlattice Films. 2007. *Appl. Phys. Lett..* **91**: 252904.

Li, Y. L., S. Choudhury, J. H. Haeni, M. D. Biegalski, A. Vasudevarao, A. Sharan, H. Z. Ma, J. Levy, V. Gopalan, S. Trolier-McKinstry, D. G. Schlom, Q. X. Jia, and L. Q. Chen. Phase transition and domain structures in strained pseudocubic (100) SrTiO3 thin films. 2006. *Physical Review B.* **73**: 184112/13.

Li, Y. L., S. Y. Hu, A. Soukiassian, D. G. Schlom, X. X. Xi, K. J. Choi, C. B. Eom, A. Saxena, T. Lookman, Q. X. Jia, and L. Q. Chen. Prediction of ferroelectricity in BaTiO3 /SrTiO3 superlattices with domains. 2007. *Appl. Phys. Lett..* **91**: 112914.

Soukiassian, A., W. Tian, V. Vaithyanathan, J. H. Haeni, L. Q. Chen, X. X. Xi, D. G. Schlom, D. A. Tenne, H. P. Sun, X. Q. Pan, K. J. Choi, C. B. Eom, Y. L. Li, Q. X. Jia, C. Constantin, R. M. Feenstra, M. Bernhagen, P. Reiche, and R. Uecker. Growth of Nanoscale BaTiO3/SrTiO3 Superlattices by Molecular-Beam Epitaxy. 2008. *J. Mater. Res..* **23**: 1417.

Tenne, D. A., A. Bruchhausen, D. L. Kimura, A. Fainstein, R. Katiyar, A. Cantarero, A. Soukiassian, V. Vaithyanathan, J. H. Haeni, W. Tian, D. G. Schlom, C. E. Bom, H. P. Sun, X. Q. Pan, Y. L. Li, L. Q. Chen, Q. X. Jia, and X. X. Xi. Nanoscale ferroelectricity in BaTiO3/SrTiO3 superlattices probed by ultraviolet raman spectroscopy. 2006. *Science.* **313**: 1614.

Tian, W., J. C. Jiang, X. Q. Pan, J. H. Haeni, Y. L. Li, L. Q. Chen, D. G. Schlom, J. B. Neaton, and K. M. Rabe. Structural evidence for enhanced polarization in a commensurate short-period BaTiO3/SrTiO3 superlattice. 2006. *Applied Physics Letters.* **89**: 092905/3.

Vasudevarao, A., A. Kumar, L. Tian, J. H. Haeni, Y. L. Li, C. J. Eklund, Q. X. Jia, R. Uecker, P. Reiche, K. Rabe, L. Q. Chen, D. G. Schlom, and V. Gopalan. Mutiferroic Domain Dynamics in Strained Strontium Titanate. 2006. *Phys. Rev. Lett..* **97**: 257602.

Zhang, J. X., Y. L. Li, D. G. Schlom, L. Q. Chen, F. Zavaliche, R. Ramesh, and Q. X. Jia. A phase-field model for epitaxial ferroelectric and magnetic nanocomposite thin films. 2007. *Applied Physics Letters.* **90**: 052909.

Zhang, J. X., Y. L. Li, S. Choudhury, L. Q. Chen, Y. H. Chu, F. Zavaliche, M. P. Cruz, R. Ramesh, and Q. X. Jia. Computer Simulation of Ferroelectric Domain Structures in epitaxial BiFeO3 thin films. 2008. *J. Appl. Phys..* **103**: 094111.

# Improved Molecular Catalysts for Water Splitting

*Reginaldo Cesar Rocha*

20060518ER

## Abstract

In this research project, we integrated experiment and theory into the design, synthesis, and characterization of biomimetic molecular catalysts that can efficiently "split" water into dioxygen and protons - which can be reduced to form molecular hydrogen. Hydrogen is the proposed alternative fuel in the President's Hydrogen Initiative, and deriving hydrogen from water is a promising route to carbon-free renewable energy. In particular, we systematically explored the tunable metal-ligand chemistry and proton-coupled electron transfer reactivity of ruthenium complexes at high-oxidation states to develop a new family of chemically robust, efficient water-oxidation catalysts that exhibited remarkable oxygen-evolving activity from water splitting, with the greatest overall catalytic performance demonstrated to date. The goals and results achieved in this project were an important step toward clean, renewable and economical energy technologies because the complete oxidation of water provides the protons and electrons that are necessary for the production of non-fossil hydrogen fuel from water splitting, which has been a grand challenge in the quest for an artificial photosynthesis.

## Background and Research Objectives

The United States is faced with an immense scientific challenge to secure clean, economically viable energy technologies based on renewable and abundant resources [1]. The world energy consumption rate is estimated to at least double to ~27.5 TW/year by 2050, while the impact of carbon-based pollution on our global climate continues to steadily escalate [2]. In response to an urgent need to safeguard energy security, a national initiative was recently announced as a commitment to a hydrogen-based economy, supporting the research and development necessary to make the transition possible [3].

The heat of combustion of molecular hydrogen ($H_2$) is nearly three times that of gasoline, making $H_2$ an attractive alternative fuel. However, hydrogen does not exist in its pure form on our planet, and its use as a fuel is only viable in the long term if it can be produced from *non-fossil* sources. A promising approach is solar-driven $H_2$ production based on photoelectrochemical devices, in which water is chemically "split" or oxidized into molecular oxygen ($O_2$), and protons and electrons which are further combined to generate hydrogen ($2H^+ + 2e^- \rightarrow H_2$). The realization of efficient water-oxidation catalysis is a chemical transformation of tremendous complexity and remains the bottleneck of $H_2$ production from the overall water "splitting" [$2H_2O \rightarrow O_2 + 2H_2$ (with a free energy difference of +4.92 eV)]. Meeting such a *grand challenge* rests on the chemical manipulation of energy at the molecular level in nanoscale materials [4], and relies on our ability to mimic Nature to split water into its elemental components using bio-inspired catalysts [5].

In natural systems, oxidation of water into dioxygen is catalyzed by the oxygen-evolving complex (OEC), an oxo-bridged $Mn_4Ca$ cluster in photosystem II [6]. Although a variety of manganese complexes have been developed as *structural* models of the OEC, only a few *functional* molecular systems have been capable of carrying out the complete reaction, with the best catalytic performances achieved by complexes of high-valent ruthenium (Ru) with polypyridyl ligands [7]. In this project, we aimed at building upon these foundations by combining experimental and theoretical efforts in order to 1) develop new ligand-bridged ruthenium catalysts with both improved robustness and activity toward water oxidation, and 2) explore both structural and electronic requirements for water-splitting catalysis.

## Importance to LANL's Science and Technology Base and National R & D Needs

The successful development of efficient water-oxidation catalysts represents significant and potentially transformational advancements toward the non-fossil

production of $H_2$ fuel. This research effort therefore supports LANL's missions in energy security by enabling *carbon-neutral renewable energy technologies*, as well as by enhancing the *fundamental understanding of materials*. This work also addresses one of the DOE energy challenges and priorities in the area of *nanoscale catalysts* within the Hydrogen Fuel Initiative [8]. In addition to leveraging existing experimental facilities and expertise, this work can be linked to several LANL institutes and DOE-supported centers, including the Institute for Hydrogen and Fuel Cell Research and the Center for Chemical Hydrogen Storage. Related research is also ongoing in strategically relevant programs across the Laboratory, including nanoscience and nanotechnology as part of the DOE Center for Integrated Nanotechnologies (CINT).

## Scientific Approach and Accomplishments

Research into the development of new water-splitting catalysts based on transition-metal complexes necessitates a diverse effort with synergistic experimental/theoretical approaches to aid rational design, implementation of methods for catalyst evaluation, and optimization of essential components from understanding of structural and electronic requirements for catalytic activity. The selected target chemical compounds described in this report are part of a proposed new generation of water-splitting catalysts based on two high-oxidation-state ruthenium centers (dimers) bridged by electron-rich molecular scaffolds (bridging ligands). This type of complexes exhibits a flexible, dynamic reduction-oxidation ("redox" or electron transfer) chemistry that allows for stepwise proton-coupled electron transfer (PCET) reactions with a 4-electron/4-proton capacity at a single chemical site that satisfies the demand of complete oxidation of water into dioxygen with release of protons and electrons for dihydrogen production. Demonstrated advantages of our approach include facile synthetic preparation of new catalysts with improved structural features, such as added conformational flexibility across the ligand bridging the two active metal sites for favorable and more efficient concerted reactions.

### Design, Synthesis and Characterization

A paradigmatic example of a molecular water-oxidation catalyst is the so-called "blue dimer", which was first introduced by Meyer and co-workers [9]. This complex contains two Ru centers held in close proximity by a bridging oxygen ligand (oxo), and it is capped with two bipyridine ligands on each Ru. Upon activation to the oxidized/deprotonated $O{=}Ru^{V}{-}O{-}Ru^{V}{=}O$ form with a chemical oxidant such as $Ce^{IV}$, the blue dimer has been shown to catalyze water oxidation. However, the rate of water oxidation is slow and only a few catalytic cycles (turnovers) are observed before the highly oxidized catalyst undergoes deactivation by competing reactions and decomposition. More recently, catalytic systems featuring Ru complexes molecularly bridged by electron-rich organic ligands have been devised as a promising approach to address these issues [7]. Of particular relevance to our work is a complex studied by Llobet and co-workers [10]. In this complex, a negatively-charged (i.e. anionic), multi-bonded bridging ligand called "bpp" promotes 1) structural rigidity by locking the two Ru sites at a specific geometric orientation in close proximity, and 2) stabilization of lower oxidation states at the Ru centers and decreased overall molecular charge compared to the blue dimer. This strategy led to a catalyst exhibiting improved activity toward water oxidation and a catalytic turnover number of 18.6 cycles, with an efficiency of 73% with respect to the chemical oxidant ($Ce^{IV}$) used to activate the catalyst.

To narrow in on the structural requirements for a new generation of water-oxidation catalysts based on ligand-bridged complexes, we synthesized and studied a structurally more flexible ruthenium dimer bridged by the pyrazolate ligand, "pyz", and peripherally capped with two bipyridine (bpy) ligands on each metal center. By using the electron-rich pyz ligand, the redox chemistry and stabilization of lower oxidation states (compared to the blue dimer) is similar to Llobet's complex, but with anticipated added flexibility. The structure of the pyz-bridged ruthenium complex with an additional methoxy bridging group between the Ru centers was confirmed and characterized by common structural and spectroscopic methods, including X-ray crystallography (Figure 1), electrospray ionization (ESI) mass spectrometry, and nuclear magnetic resonance (NMR) spectroscopy. The geometry about the Ru centers is a distorted octahedral, with angles between 78° and 98° and between 169° and 175°. The direct Ru–Ru distance (3.72 Å) is nearly identical to that observed for the μ-oxo-bridged blue dimer, but 0.6 Å shorter than that of a related precursor of Llobet's bpp-bridged complex. The Ru–X (X = nitrogen or oxygen) bond distances are consistent with those reported in the literature for related structures, with $Ru{-}N_{pyz}$ (2.076 and 2.074 Å), Ru–O (2.139 and 2.144 Å), and $Ru{-}N_{bpy}$ (2.027–2.063 Å). The electronic properties of this strongly coupled complex were also investigated in detail by cyclic voltammetry, and electronic (visible/near-infrared) and vibrational (infrared) spectroelectrochemistry [11].

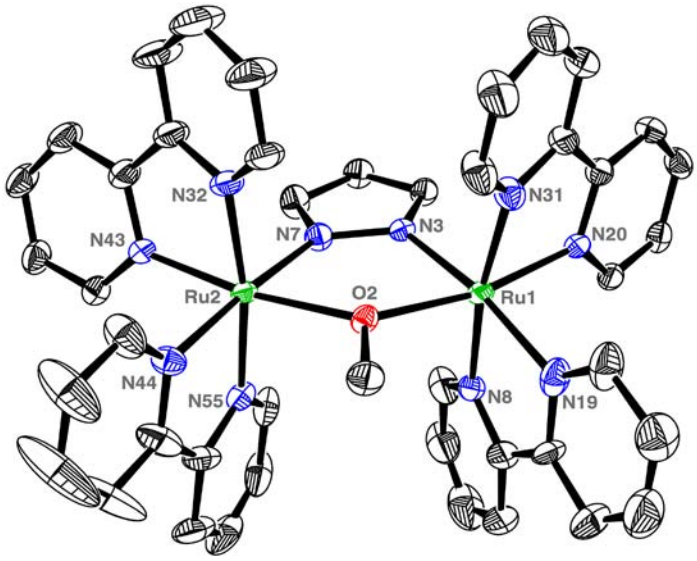


*Figure 1. X-ray crystal structure of the new pyz-bridged Ru dimer prior to replacement of the methoxy group between the metal centers with water ligands. H atoms and counterions are omitted for clarity (thermal ellipsoid plot drawn at 50% probability).*

Dissolution of the methoxy-,pyz-bridged complex (precursor) in water at pH 1 leads to displacement of the methoxy ligand and formation of a "bis-aqua" complex (catalyst), in which both Ru centers are bonded to water molecules, as confirmed by matrix-assisted laser desorption ionization (MALDI) mass spectrometry and NMR spectroscopy.

**Water-Oxidation Catalysis**

The electrochemical potentials involved in the oxidation-reduction processes as well as activation of the synthetic targets for water-oxidation chemistry were assessed by using cyclic voltammetry. For example, the new pyz-bridged Ru complex exhibits a rich electrochemistry (Figure 2) with three reversible oxidation processes (mid-point potentials at +0.47 V, +0.63 V, and +0.75 V vs Ag/AgCl reference electrode). These are coupled one-electron/one-proton processes corresponding to the $Ru^{II}$-L-$Ru^{II}$/$Ru^{II}$-L-$Ru^{III}$, $Ru^{II}$-L-$Ru^{III}$/$Ru^{III}$-L-$Ru^{III}$, and $Ru^{III}$-L-$Ru^{III}$/$Ru^{III}$-L-$Ru^{IV}$ redox pairs, respectively. The fact that three stepwise oxidations were also observed for Llobet's bpp-bridged complex at similar potentials (+0.52 V, +0.60 V, and +0.84 V vs SSCE electrode) supports the notion that these two systems exhibit similar electronic properties, despite the overall molecular structural differences. Evidence for electrocatalytic currents exists above +1.1 V, presumably due to the oxidation of water upon generation of the active $Ru^{IV}$-L-$Ru^{IV}$ state.

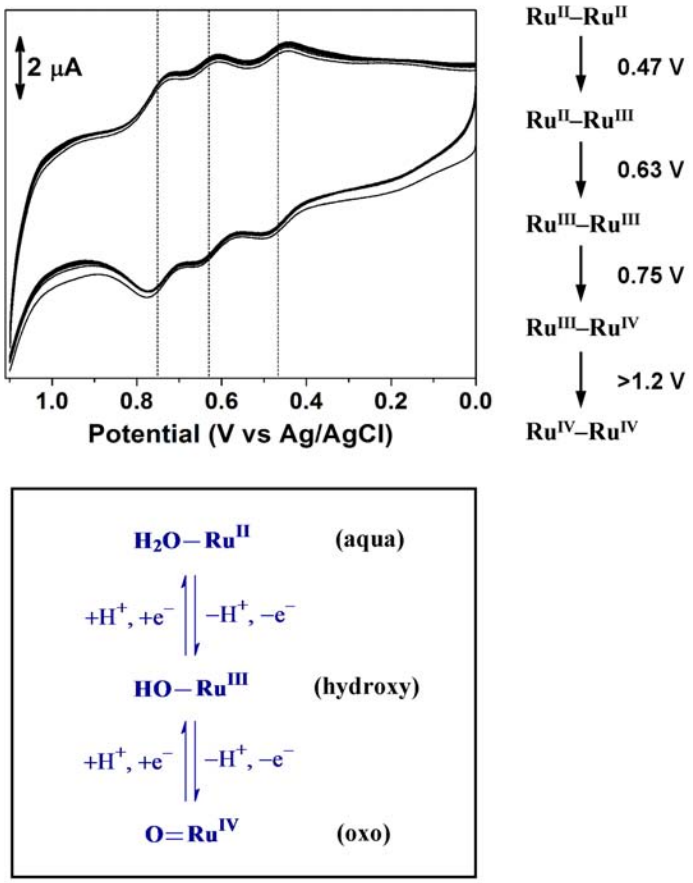


*Figure 2. Cyclic voltammogram of the "bis-aqua" form of the pyz-bridged Ru dimer (acidic aqueous solution at pH 1) with the proton-coupled oxidation-reduction processes noted.*

Addition of excess chemical oxidant ($Ce^{IV}$) to a solution of our new pyz-bridged complex results in the prompt change in the color of the solution from dark orange to yellow, as well as the intense formation of gas bubbles (Figure 3). On the basis of reaction mechanisms previously proposed for the related oxo- and bpp-bridged complexes [9,10], the overall transformation can be interpreted as two main steps: 1) a fast electron-transfer reaction with oxidation of the initial $H_2O$-$Ru^{II}$ species into the O=$Ru^{IV}$ active state, followed by 2) the slower multi-electron catalytic water-oxidation process with $O_2$ evolution and regeneration of the aqua-complex to yield a complete cycle.

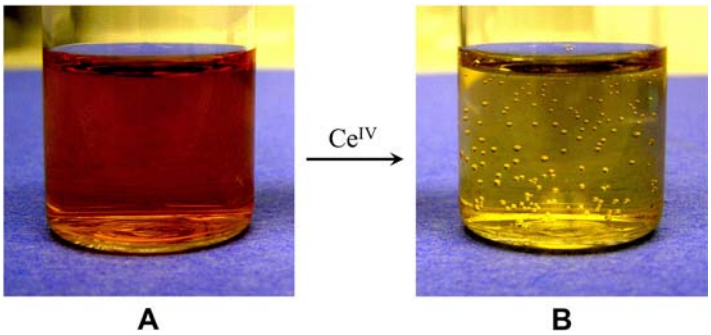


*Figure 3. Photographs of a solution of the new catalyst before (A) and after (B) activation by addition of a chemical oxidant. The intense formation of gas bubbles in B is from the oxidation of water with $O_2$ evolution.*

To quantify the catalytic reaction, oxygen-sensing measurements under controlled conditions using both a Clark-type electrode and a fluorescence-based optical probe were performed for determination of the initial oxygen-evolution rate, $V(O_2)$, at specific catalyst concentrations. All experiments confirmed that the oxidized $O{=}Ru^{IV}{-}L{-}Ru^{IV}{=}O$ species is catalytically active and undergoes four-proton/four-electron reactivity toward complete oxidation of water to give dioxygen. The kinetic analysis for a series of measurements indicated that the $O_2$-evolving reaction is first-order with an unprecedented rate, $k(O_2)$, of 0.28 $s^{-1}$ (Figure 4). This rate constant is 20-100 times greater than those for the highest-performing catalysts previously reported, and reveals that the initial reaction rate for the catalytic water oxidation by the new pyrazolate-bridged dimer is remarkably fast.

In order to estimate the overall catalytic performance of this new system, the reaction was monitored to completion through an integrated approach involving detection of evolved $O_2$ by gas chromatography/mass spectrometry. The plot in Figure 4 shows the amount of $O_2$ generated as a function of time for a typical run. Over 24 catalytic turnovers were measured corresponding to an overall efficiency of > 90% with respect to 100 equivalents of added chemical oxidant (i.e. "catalyst activator"). It is interesting to note that the catalyst remains active for > 40 h, representing improved stability toward deleterious reactions or decomposition.

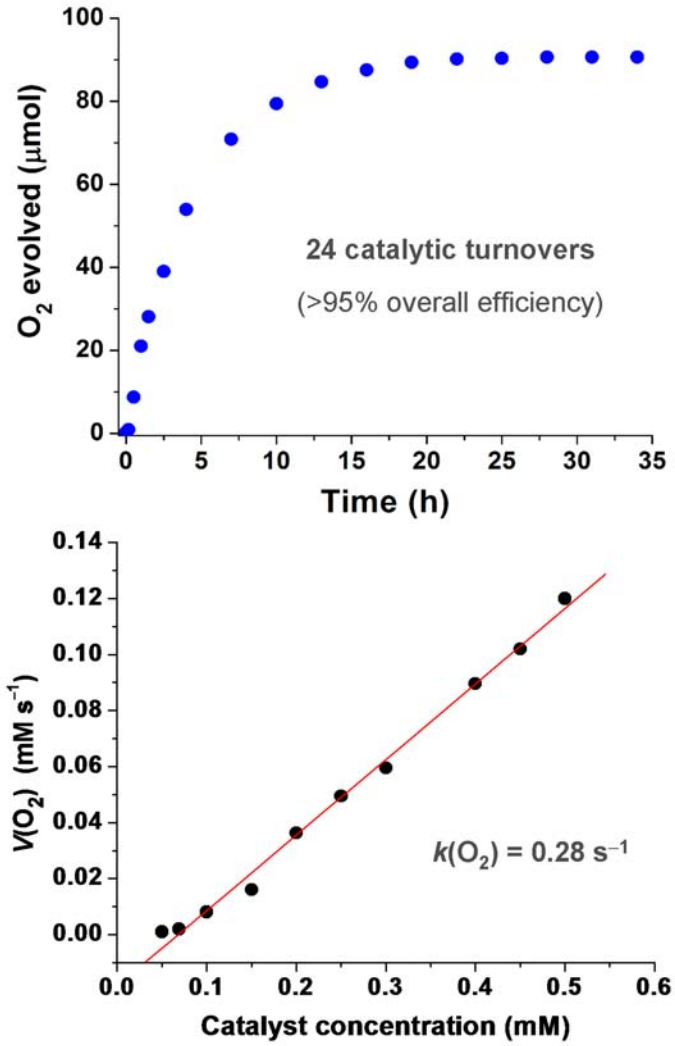


*Figure 4. (bottom) Kinetic analysis using the initial reaction rates $V(O_2)$ at a range of catalyst concentrations to obtain the first-order, $O_2$-evolution rate constant, $k(O_2)$. (top) Determination of turnover numbers from the gas chromatography/mass spectrometry detection of $O_2$ generated over time.*

An advantage contributing to this improved performance is the added geometric flexibility of the Ru chemical sites afforded by the pyrazolate bridge compared to the bpp ligand. Indirect evidence supporting such a difference in conformational flexibility about the bridging ligand comes from the comparison of the relative acidities in the bis-aqua complexes. The fact that the first proton of the water ligands is much more easily removed in the bpp complex (whose acidity is unusually high for this type of systems) is attributed to the structural rigidity promoted by the multi-bonded bridge, which locks the geometry across the two Ru sites with the $H_2O$ ligands in close proximity facing each other. In such a geometrically constrained configuration, the steric repulsion between H atoms facilitates

deprotonation and stabilization of a hydrogen bonding structure of the type H–O×××H–O–H. In contrast, the acid-base behavior of bound water molecules in the pyz-bridged complex is typical of monomeric $Ru^{II}$ complexes [12], indicating that the metal-oxygen sites are allowed to assume a more flexible, cross-bridge relative orientation with two weakly interacting $H_2O$ ligands. As supported by theoretical modeling, such a flexibility should allow for the catalytic sites to adopt optimum configurations "on demand", as dictated by the deprotonation/protonation and oxidation/reduction processes accompanying the course of water-oxidation catalysis, as well as the formation of a water network involving non-coordinated solvent $H_2O$ molecules within the cavity between metal-oxygen bonding sites. This type of transient "suprastructure" must be required on the basis of previous mechanistic studies demonstrating that $O_2$ originates from unbound, solvent water molecules. Ongoing theoretical calculations of these dynamic structural aspects should provide additional insights into the elucidation of molecular requirements for efficient catalysis of water oxidation.

**Theoretical Calculations**

Density functional theory (DFT) calculations [13] were performed to provide insight into catalytic species and reaction pathways. In general, we applied hybrid exchange-correlation functionals (e.g. B3LYP) together with appropriate basis sets for organic fragments and relativistic effective core potentials for transition metals (uncontracted LanL2DZ and associated double-ζ basis set). Solvent effects were included using a dielectric continuum model with the dielectric polarizability of water at room temperature. This approach was successfully employed in the study of the geometric and electronic structure of the bpp-bridged complex (Figure 5), for which we found a stable configuration with two water molecules bound to the two Ru atoms forming a hydrogen-bond network with an H···O distance of 1.81 Å and a Ru–O distance of 2.18 Å for the "donor" water molecule and 2.26 Å for the "acceptor" water. The electronic spectrum of the bis-aqua ($Ru^{II}$-$Ru^{II}$) form of this complex was also elucidated by using density functional linear response theory (time-dependent DFT) [14,15]. The lowest-energy excitations involve charge transfer between the dπ orbitals of the metal centers (with some small amplitude in the bpp bridge) and the π* orbitals on the peripheral tpy ligands.

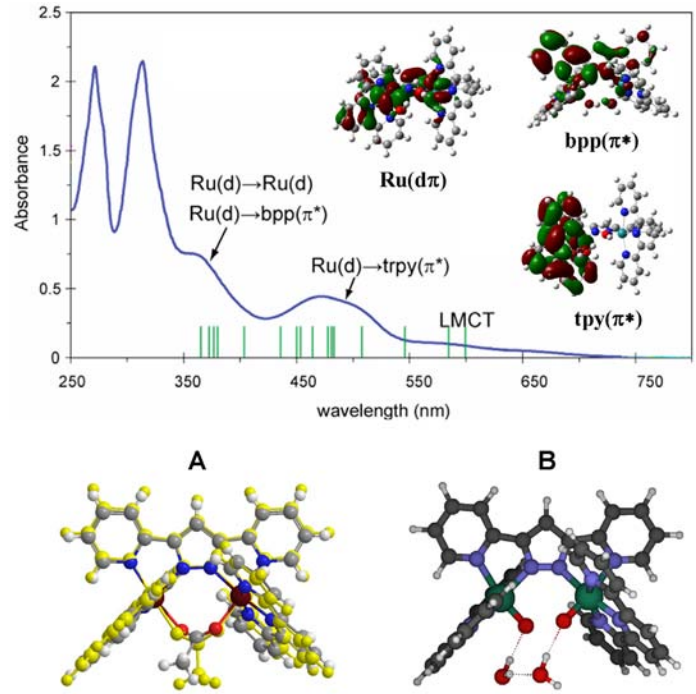


*Figure 5. (top) Electronic absorption spectrum of the bpp-bridged Ru dimer with assignments of molecular orbital transitions from TD-DFT excitations noted. (bottom, A) Overlay of calculated (DFT) and experimental (X-ray) molecular structures of the complex at its resting $H_2O$-Ru(II) state. (bottom, B) Calculated structure of the complex at its active oxo-Ru(IV) state with two solvent water molecules explicitly added; dotted lines indicate hydrogen bonds.*

We have also initiated computational investigations of the thermochemistry of the water-oxidation process by the new pyz-bridged catalyst to derive a detailed understanding of such a complex reaction mechanism using theoretical guidance. The bis-oxo $Ru^{IV}$-L-$Ru^{IV}$ catalytic state with two water molecules in the secondary coordination environment has been computationally explored. For the bpp analogue, we found that the minimum energy arrangement of the water molecules is a hydrogen-bonded architecture with H···O bond distances to the oxy group (Ru=O) of 1.94 and 1.86 Å for the water donor and acceptor, respectively, and an H···O distance of 1.84 Å between the two solvent water molecules. In Llobet's bpp-bridged complex, the calculated O=$Ru^{IV}$ distances are 1.78 Å. This structure allowed us to estimate, theoretically, the thermochemistry for the formation of molecular oxygen. The calculated energy difference between reactants and products was –1.3 eV, confirming that the $O_2$ evolution is energetically favorable following catalyst activation.

We have carried out similar calculations on the pyrazolate-bridged dimer. Our preliminary results revealed that this new catalyst has greater conformational flexibility and a larger three-dimensional coordination volume for incoming solvent water molecules to react with the ruthenium-oxygen chemical sites.

## References


1. "Basic Research Needs to Assure a Secure Energy Future", BESAC Report, 2002.
2. N. S. Lewis, D. G. Nocera, "Powering the planet: chemical challenges in solar energy utilization", *Proceedings of the National Academy of Sciences of the United States of America* **2006**, *103*, 15729-15735.
3. (a) "The President's Hydrogen Fuel Initiative," www.hydrogen.gov; (b) "Basic Research Needs for the Hydrogen Economy", BES Report, 2003.
4. "Nanoscale Research for Energy Needs", BES-NNI Report, 2004.
5. "Basic Research Needs: Catalysis for Energy", BES Report, 2007.
6. K. N. Ferreira, T. M. Iverson, K. Maghlaoui, J. Barber, S. Iwata, "Architecture of the photosynthetic oxygen-evolving center" *Science* **2004**, *303*, 1831-1838.
7. Romero, M. Rodriguez, C. Sens, J. Mola, M. R. Kollipara, L. Francas, E. M. Marza, L. Escriche, A. Llobet, "Ru complexes that can catalytically oxidize water to molecular dioxygen" *Inorganic Chemistry* **2008**, *47*, 1824-1834.
8. "Directing Matter and Energy: Five Challenges for Science and the Imagination", BESAC Report, 2007.
9. F. Liu, J. J. Concepcion, J. W. Jurss, T. Cardolaccia, J. L. Templeton, T. J. Meyer, "Mechanisms of water oxidation from the blue dimer to photosystem II" *Inorganic Chemistry* **2008**, *47*, 1727-1752.
10. C. Sens, I. Romero, M. Rodriguez, A. Llobet, T. Parella, J. Benet-Buchholz, "A new Ru complex capable of catalytically oxidizing water to molecular dioxygen" *Journal of the American Chemical Society* **2004**, *126*, 7798-7799.
11. H. Jude, F. N. Rein, P. S. White, D. M. Dattelbaum, R. C. Rocha, "Synthesis, structure, and electronic properties of a dimer of $Ru(bpy)_2$ doubly bridged by methoxide and pyrazolate" *Inorganic Chemistry* **2008**, *47*, 7695-7702.
12. T. J. Meyer, M. H. V. Huynh, "The remarkable reactivity of high oxidation state ruthenium and osmium polypyridyl complexes" *Inorganic Chemistry* **2003**, *42*, 8140-8160.
13. W. Koch, M. C. Holthausen, "A Chemist's Guide to Density Functional Theory", Wiley-VCH, Weinheim, 2002.
14. M. E. Casida, in "Recent Advances in Density Functional Methods", ed. D. P. Chong, World Scientific, Singapore, 1995.
15. E. R. Batista, R. L. Martin, "On the excited states involved in the luminescent probe $[Ru(bpy)_2(dppz)]^{2+}$" *Journal of Physical Chemistry A* **2005**, *109*, 3128-3133.

# Shedding Light on the Mechanical Unfolding of Individual Proteins

*Peter Marvin Goodwin*

20060593ER

## Abstract

Our goal is to probe the mechanical unfolding of fluorescent proteins using a combination of single-molecule force microscopy and single-molecule fluorescence spectroscopy. We have focused our investigation on understanding the relationship between the fluorescence and folding stability of green fluorescent proteins (GFPs). Combining these two techniques in a single experiment will provide information that spans multiple length scales and timescales. GFPs are excellent model systems that will help us gain a new physical understanding of the interplay between mechanical stress, protein conformation, and the fluorescence emitted by the protein to which this strain is applied. We also expect that this research will generate information that will aid the development of sets of GFP-based 'in vivo' sensors that can report on the magnitude of forces inside of a cell by means of their intrinsic fluorescence. Given their ability to be fused to any biological structure, such sensors would be useful for the measurement of forces generated by intracellular biological processes. Fundamentally, this research aims to improve our understanding of protein folding and unfolding as well as protein function. Proteins are machines that operate at nanometer length scales. Proteins and protein-protein interactions are the primary working examples of nanotechnology in nature. A better understanding of the mechanisms of protein folding/unfolding and function will certainly accelerate the development of man-made, bio-inspired nanotechnologies as well as biotechnology. In a manner similar to the microelectronics revolution of the latter half of the 20$^{th}$ century, such technologies will likely be the 'engines' that drive the economy of the 21$^{st}$ century. As such, it is crucial that the United States maintain a technological lead in these areas.

## Background and Research Objectives

We aim to study the mechanical unfolding of single auto-fluorescent protein molecules using a combination of single-molecule force microscopy and single-molecule fluorescence spectroscopy. Over the past two decades single-molecule fluorescence spectroscopy has matured into a practical tool for the study of chemical and biochemical processes. With AFM-based single-molecule force microscopy it is possible to mechanically unfold proteins and polymers by adhering one end of the polymer to an atomic force microscope (AFM) tip while the other end is attached to a surface[1,2]. The same molecule can be pulled apart over and over again. These molecular "torture rack" measurements have revealed intricate details that would be hidden in ensemble measurements of mechanical deformation. Force spectroscopy permits us to probe mechanical properties of single protein molecules. Fluorescence spectroscopy permits us to probe alterations in the molecule's fluorescence emission induced by changes in the molecule's conformation and environment. When used together on the same protein molecule, these techniques will provide new insights in to the behavior of proteins under mechanical stress. Moreover, if the fluorescence emission of GFP does exhibit good sensitivity to applied force, then it will be possible to develop a GFP-based forced sensor with a fluorescence readout.

## Importance to LANL's Science and Technology Base and National R & D Needs

This research lies at the interface of nanotechnology and biology, a thrust of the DOE-funded Center for Integrated Nanotechnologies. Moreover, the theoretical framework and experimental methods developed herein can clearly be used to study polymers that are not poly-amino acids. The instrumentation and expertise gained through this work will lead to better models of polymers under stress and could potentially lead to more reliable models of polymer aging, both of which have strong tie-ins to other missions of the lab.

We also expect that this research will lead to the development of GFP-based molecular force sensors. For

example, it is known that GFP unfolding forces are strongly dependent on the direction that the force is applied with respect to the GFP β-barrel. We anticipate that engineered GFP mutants with force handles located at different points on the β-barrel can be designed to lose their fluorescence at different pulling forces. In this way, one could create sets of GFP-based 'in vivo' sensors that can report on the intensity of a force at the single molecule level by means of their intrinsic fluorescence. Such 'in vivo' sensors will be invaluable for improving our understanding of force-mediated intracellular processes. An important example of this is mitosis and cytokinesis – the separation chromosomal material between daughter cells during cell division.

Fundamentally, this research aims to improve our understanding of protein folding and unfolding as well as protein function. Proteins are machines that operate at nanometer length scales. Proteins and protein-protein interactions are the prime working examples of nanotechnology in nature. A better understanding of the mechanisms of protein folding/unfolding and function will certainly accelerate the development of man-made, bio-inspired nanotechnologies as well as biotechnology. In a manner similar to the microelectronics revolution of the latter half of the 20$^{th}$ century, such technologies will likely be the 'engines' that drive the economy of the 21$^{st}$ century. As such, it is crucial that the United States maintain a technological lead in these areas.

## Scientific Approach and Accomplishments

### Combined Single-Molecule Force and Fluorescence Spectroscopy

A conceptual setup for combined single-molecule force and fluorescence experiments is shown in Figure 1a. Atomic Force Microscopy (AFM) has the sensitivity to measure force down to ~10 pN (1pN = $10^{-12}$ Newtons). This magnitude of force is approximately a thousand times larger than forces due to thermal agitation (Brownian motion) and approximately a hundred times smaller than the force required to rupture a covalent bond. Proteins mechanically unfold at forces of the order of 100 pN. Deflection, Δ, of the AFM probe cantilever is monitored using the red laser and split photodiode. Force applied by the AFM probe is proportional to the cantilever deflection, Δ, through the cantilever spring constant. Protein fluorescence is excited with the blue laser. Fluorescence emission is collected through the transparent substrate using a high-numerical aperture microscope objective lens. A single-photon counting detector is used to monitor the fluorescence emission of the tethered protein during AFM pulling. Our setup, shown in Figure 1b, is based on a commercial atomic force microscope designed to sit on top of an inverted optical microscope. We modified the optical microscope for ultrasensitive, sample-scanned, confocal fluorescence imaging by addition of a piezoelectric sample scanning stage, laser excitation and a pair of single-photon avalanche photodiode (APD) detectors. The outputs of these detectors are processed by time-correlated single-photon counting (TCSPC) electronics for high (single-photon) detection sensitivity and sub-nanosecond single-photon timing resolution. When used in combination with pulsed laser excitation, TCSPC detection permits the measurement of single-molecule fluorescence lifetimes and can be used to discriminate against background due to prompt, scattered excitation laser light. A demonstration of the atomic force and fluorescence imaging capabilities of this setup is shown in Figure 2.

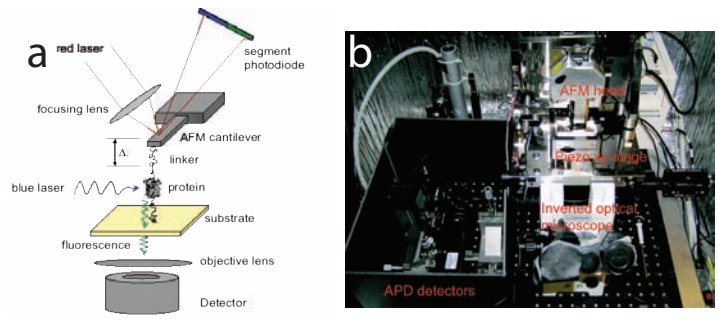


*Figure 1. (a) Conceptual approach to combined single-molecule force and fluorescence microscopy. (b) Setup for combined force and fluorescence microscopy.*

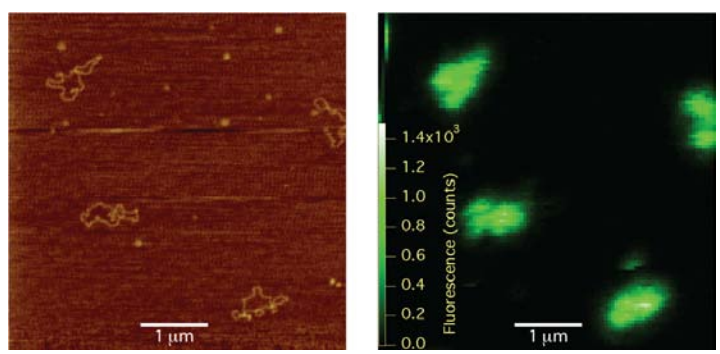


*Figure 2. A pair of spatially-registered AFM height and fluorescence images of double-stranded, circular DNA (pKLAC1, 9091 bp) stained with the fluorescent bisintercalator YOYO-1 on mica. (left) AFM height image of four DNA fragments on mica. The measured height of the DNA above the mica in this image was ~1 nanometer. (right) Fluorescence image of the same region. The diffraction-limited resolution of the fluorescence image prevents one from determining the topology of the DNA fragment (i.e. circular versus linear). In the AFM image the circular conformations of the three fragments that are completely contained in the image are readily apparent.*

### Engineered Fluorescent Protein Constructs for Single-Molecule Force and Fluorescence Experiments

The model system we have chosen for these studies is Green Fluorescent Protein (GFP). The structure of a GFP mutant (super-folder GFP, sfGFP) with enhanced folding stability is shown in Figure 3a. The GFP chromophore is formed auto-catalytically from three amino acid peptides. In GFP's native (folded) state the chromophore is rigidly enclosed inside an eleven-strand β-barrel that protects it from the external environment and renders it intensely fluorescent. If GFP is chemically or thermally denatured (unfolded), fluorescence is lost, but is recovered by refolding the protein.

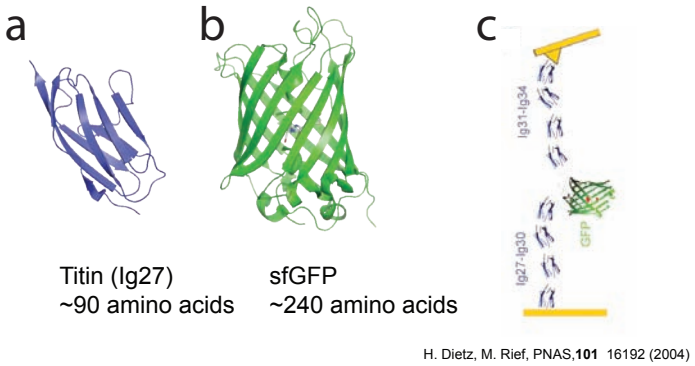


*Figure 3. Structures of a titin (Ig27) subunit (a) and the the super-folder GFP protein (b). Schematic view of the sfGFP-titin construct tethered between a substrate and an AFM tip (c).*

Following earlier work of Dietz and Rief [3] we have engineered a sfGFP-titin construct that is essentially a sfGFP sandwiched between a pair of polypeptides each consisting of four C-N terminal linked human cardiac titin (Ig) modules. The structure of a titin module is shown in Figure 3b. As shown schematically in Figure 3c this construct can be tethered between a substrate and an AFM probe tip. Here the titin modules serve two purposes: 1) as internal controls for the detection of single-molecule unfolding events and, 2) as spacers to reduce quenching of GFP fluorescence by the gold-coated AFM tip and substrate. We have also engineered a second protein construct (sfGFP-ddFLN) using ddFLN modules instead of the titin spacers. The ddFLN1-5 modules serve a similar function as the titin modules in the first construct, but have lower rupture forces, comparable to that of sfGFP and approximately half that of the titin modules. The lower rupture force of the ddFLN modules increases the likelihood of observing the rupture of the sfGFP later in the force-extension curve after non-specific tip-surface interactions have been resolved (tip-substrate separations > ~50 nm).

### Mechanical Unfolding of sfGFP-titin

We have performed single-molecule force-extension (pulling) measurements on titin $(Ig27)_8$ and sfGFP-titin polypeptides bound to gold-coated substrates. The left panel of Figure 4 schematically illustrates the interaction between the AFM tip and the tethered polypeptide during a force-extension measurement. The right panel of Figure 4 shows a force-extension curve obtained during the mechanical unfolding of a single sfGFP-titin polypeptide. The unfolding of the sfGFP module is identified in the force-extension curve based on the characteristic contour length increase (ΔL = 77 nm) of the polypeptide upon unfolding of the sfGFP β-barrel. The unfolding forces and contour length increases we measure for this construct are in good agreement with those reported by Dietz and Rief for a Cycle 3-GFP variant sandwiched between a pair of titin 4-mers [3].

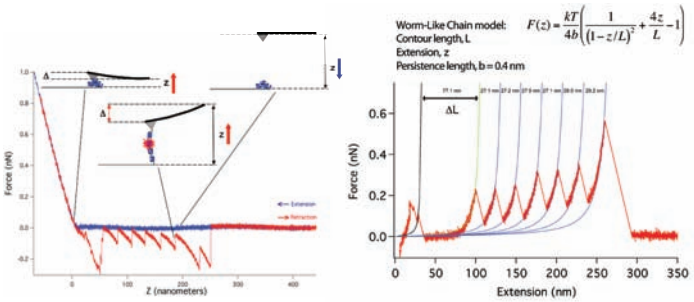


*Figure 4. Left: Approach and retraction force curves recorded during the acquisition and unfolding of titin (Ig27)8 polypeptides immobilized on a gold-coated substrate. Insets show schematically the interaction between the AFM probe tip and a polypeptide tethered to the substrate at different points along the force curves. Right: Force-extension curve measured during the unfolding of a single sfGFP-titin polypeptide immobilized on a gold-coated substrate. Solid black, green and blue curves are WLC fits to entropic extension regions of the data. Blue curves follow the unfolding of individual titin domains, the green curve follows the unfolding of the sfGFP domain.*

### Localization of Individual Fluorescent Polypeptides for Combined Single-Molecule Force and Fluorescence Measurements

In contrast to our preliminary force-extension measurements on high protein coverage substrates, outlined above, our simultaneous single-molecule force and fluorescence experiments will be performed at extremely low protein coverage to eliminate fluorescence background from fluorescent proteins that are not tethered to the AFM tip. Typically, pulling experiments done at high protein coverage are "blind" fishing expeditions in that no effort is made to target a particular surface-immobilized protein with the AFM tip. To work at the low coverage needed for our experiments requires that the protein molecule of

interest be targeted by the AFM tip. We are taking two approaches to this problem. The first relies on localization of the protein on the substrate by fluorescence imaging. The second involves AFM imaging to localize individual, isolated protein molecules on substrate.

To date, we have used fluorescence imaging to localize single sfGFP-titin constructs bound to individual luminescent quantum dots (QDs) immobilized on glass substrates. Due to the limited photostability of GFP, we use QDs to label the sfGFP-titin to eliminate the need to excite the GFP fluorescence during localization. The next step is to demonstrate that we can perform single-molecule force-extension measurements on sfGFP-titin bound to QDs.

We are also pursuing AFM detection of the surface-immobilized sfGFP construct. We intend to use the sfGFP-ddFLN construct for these experiments.

## References


1. Schwaiger, I., C. Sattler, D. R. Hostetter, and M. Rief. The myosin coiled-coil is a truly elastic protein structure. 2002. *Nat. Mater.*. **1** (4): 232.
2. Rief, M., M. Gautel, F. Osterhelt, J. M. Fernandez, and H. E. Gaub. Reversible unfolding of individual titin immunoglobin domains by AFM. 1997. *Science.* **276** (5315): 1109.
3. Dietz, H., and M. Rief. Exploring the energy landscape of GFP by single-molecule mechanical experiments. 2004. *Proc. Nat. Acad. Sci. USA.* **101** (46): 16192.


## Publications


Cotlet, M., P. M. Goodwin, G. S. Waldo, and J. H. Werner. A comparison of the fluorescence dynamics of single molecules of a green fluorescent protein: One- versus two-photon excitation. 2006. *CHEMPHYSCHEM.* **7** (1): 250.

Cotlet, M., P. M. Goodwin, G. S. Waldo, and J. H. Werner. Time-resolved detection of the one- and two-photon excited fluorescence of single molecules of a folding enhanced green fluorescent protein - art. no. 609204. 2006. In *Conference on Ultrasensitive and Single-Molecule Detection Technologies ; 20060121 - 20060124 ; San Jose, CA.* Vol. 6092, p. 9204.

Cotlet, M., S. Habuchi, J. E. Whitier, J. H. Werner, F. C. Schryver, J. Hofkens, and P. M. Goodwin. Single molecule spectroscopic characterization of a far-red fluorescent protein (HcRed) from the anthozoa coral Heteractis crispa - art. no. 609804. 2006. In *Conference on Genetically Engineered Probes for Biomedical Applications ; 20060124 ; San Jose, CA.* Vol. 6098, p. 9804.

Lessard, G., S. Habuchi, J. Werner, P. Goodwin, F. De Schryver, J. Hofkens, and M. Cotlet. Probing dimerization and intraprotein fluorescence resonance energy transfer in a far-red fluorescent protein from the sea anemone Heteractis crispa. 2008. *JOURNAL OF BIOMEDICAL OPTICS.* **13** (3).

# Nanoscale Textured Composite Energetic Materials

*Steven Joseph Buelow*

20060617ER

## Abstract

The goal of this research project was to demonstrate control of the properties of energetic materials via systematic and reproducible tailoring of the material structure at the micron and submicron level. This was accomplished by producing nanoscale structures in "oxidizer" materials and filling them with aluminum "fuel" to produce composite energetic materials. The research proceeded in three phases: developing techniques to fabricate the oxidizer structures, filling the resulting structures with aluminum, and testing the energetic properties of the finished composite materials. The project was successful in producing sub-micron (50-500 nm) structures of nitrocellulose, Teflon, and copper oxide. In addition, Teflon nanostructures were filled with aluminum to produce a composite energetic material. A microheating apparatus was constructed to minimize energy loss while testing the energetic properties of the structures. The project achieved its primary goal, to produce submicron-scale composite energetic materials, and made significant progress toward measuring their properties.

## Background and Research Objectives

Energetic materials (EM) are critical for many military and civilian applications because they compactly store significant quantities of energy that can be quickly released. Familiar uses include gas production for safety devices such as air bags, light for flares, and propellants for firearms and rockets. Compared to other materials, the energy storage densities of common energetic materials such as trinitrotoluene (TNT) are similar to petroleum fuels (roughly 50 to 1000 times better than electrical storage devices such as batteries) while the power densities for energetic materials are generally many orders of magnitude greater than available with either fuels or batteries. Although energetic materials offer many advantages in terms of energy and power storage, their application can be significantly limited by problems associated with controlling their power output and by safety concerns due to sensitivity of the materials to shock, spark, and heat.

Currently, the options to solve these problems are limited. Solutions most often involve the synthesis of new energetic molecules and/or the development of new formulations. Over many years, experiments have empirically shown that the morphology (composition, particle size, and density) of energetic materials on the sub-micron scale can significantly affect initiation and propagation processes [1]. Additionally, experiments at Los Alamos National Lab examining a model nitro-organic compound, polyvinyl nitrate (PVN), indicate that energy transfer processes for initiating reactions occur over similar lengths [2]. These results suggest that controlling the composition and morphology of an energetic material on the sub-micron scale could allow tuning of the rate of energy release and material sensitivity. Although this strategy for control has long been proposed, only recently have the technology tools become available for systematically and reproducibly controlling the structure of energetic materials on this dimension scale.

## Importance to LANL's Science and Technology Base and National R & D Needs

This project produced results relevant to LANL capabilities in Weapons, Threat Reduction, Materials Science, and Chemistry. Many research groups are currently exploring the production and mixing of nanoparticle fuels such as aluminum with nanoparticle oxidizers such as molybdenum oxide [3]. Other efforts are examining the production of monomolecular nanoparticles mixed with low energy binders [4]. Our project is unique. We have developed the tools to reproducibly fabricate well-defined sub-micron composite energetic structures. By demonstrating that these materials can be fabricated in a controlled, reproducible way, we have introduced new opportunities for examining sub-micron scale reaction dynamics and raised the possibility of constructing nearly invisible "explosives on a chip." In addition, the

nanofabrication techniques developed in this project can be applied to other materials to produce a variety of nanoscale devices to further other areas of research at LANL.

## Scientific Approach and Accomplishments

The research efforts of this project were directed in four areas:

- Construction of a thin-film deposition chamber
- Development of nanoscale energetic material fabrication technology
- Nanoscale feature filling to produce composite energetic structures
- Construction of a microheater testing apparatus

The work for this project was performed by a team of LANL staff, technicians, postdoctoral fellows, and students. The team members were Frank Archuleta, Steven Buelow, Mark Hoffbauer, Satish Kasarla, Chandra Savage Marsden, Christopher Martinez, Rhonda McInroy, Jason Stairs, and Todd Williamson. The following is a summary of the results of the research in each of these areas. In addition to the research accomplishments, the results achieved in this project have been used as the basis for a proposal to the Defense Threat Reduction Agency (DTRA) to continue development and testing of these new materials and concepts.

**Construction of a thin-film deposition chamber**

In order to deposit thin metal layers required in various stages of this project, we constructed a high-vacuum chamber (base pressure ~ 5 x $10^8$ Torr) equipped with four magnetron sputtering heads. One sputter source is powered by a DC power supply and includes high-strength magnets for depositing magnetic metals. The other three can use either DC power to sputter metals or an RF generator for non-conducting materials such as ceramics or piezoelectrics. The system includes a load-lock chamber and sample manipulation system to introduce samples without exposing the main chamber to the atmosphere, which keeps oxygen and other contaminants away from sensitive sample materials. Diagnostic equipment including a residual-gas analyzer is used to constantly monitor the system's status, and a deposition controller allows the film thickness and deposition rate to be monitored or controlled. To date, the system has been used to produce high-quality sputtered films of chromel, alumel, stainless steel, aluminum, chromium, copper, niobium, and aluminum oxide ($Al_2O_3$).

**Development of nanoscale energetic material fabrication technology**

The nanoscale texturing process relies on the ENABLE (Energetic Neutral Atom Beam Lithography & Epitaxy) technique [5], which utilizes a collimated beam of neutral oxygen atoms to etch polymeric (organic) material via non-thermal surface reactions. ENABLE is a room-temperature process that is critical for avoiding thermal degradation in delicate materials like nitrocellulose. The ENABLE system won a prestigious 2006 R & D 100 award as one of the most significant new technologies of the year. Initial tests with micron-scale proximity masks demonstrated that ENABLE can effectively produce structures in nitrocellulose and Teflon$^{AF}$ (a spin-coatable form of PTFE) thin films. These polymers etch readily, at rates on the order of 100 nm/min. Producing nanoscale features, however, requires more sophisticated masking techniques, since ENABLE mask layers must maintain their integrity upon exposure to the O-atom beam. In this project, we used electron-beam (e-beam) lithography to produce nanoscale masks for ENABLE etching, as illustrated in Figure 1.

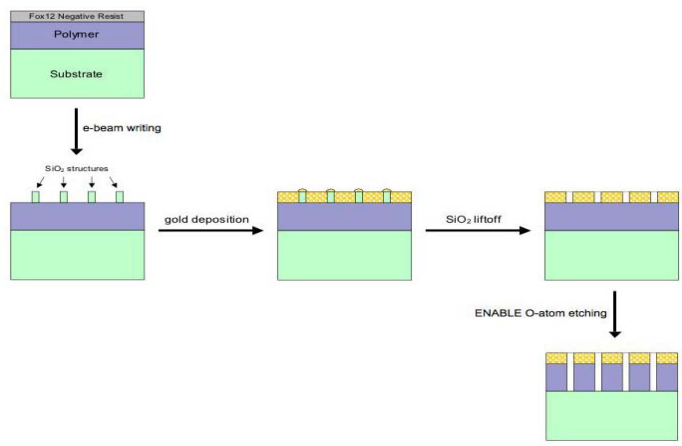


*Figure 1. Illustration of the nanoscale patterning process. The e-beam written structures are transferred into a polymer material (oxidizer) that is then filled with a metal (fuel) forming the nanocomposite energetic material.*

The e-beam lithography was performed at LANL using an electron microscope equipped with an e-beam lithography system that uses either positive or negative e-beam resists to produce feature sizes of <50 nm. Initially, the energetic polymer is spin-coated onto a substrate, typically glass or silicon, to form one to two micron thick films. Then, a negative e-beam resist (Fox 12) is applied with a thickness of ~100 nm. Upon exposure to the electron beam, the polymer chains of the resist cross-link. When the sample is chemically "developed", silicon dioxide ($SiO_2$) patterns are left where the e-beam writing was performed. The resulting $SiO_2$ nanostructures are coated with a thin layer of gold, and the $SiO_2$ is then lifted off, leaving channels

in the gold layer. Finally, the structure is exposed to the ENABLE O-atom beam with a kinetic energy of ~2.5 eV, etching away exposed areas of the polymer and leaving free-standing polymer nanostructures. With this process, we have produced 50-100 nm structures in both PTFE and nitrocellulose, an example of which is shown in Figure 2.

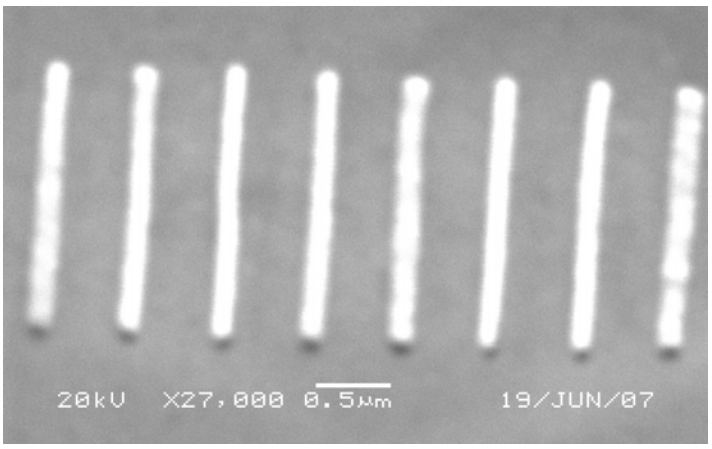


*Figure 2. SEM image of 100 nm channels in nitrocellulose, spaced 500 nm apart. Channel width and spacing can be widely varied, limited only by the resolution of the e-beam.*

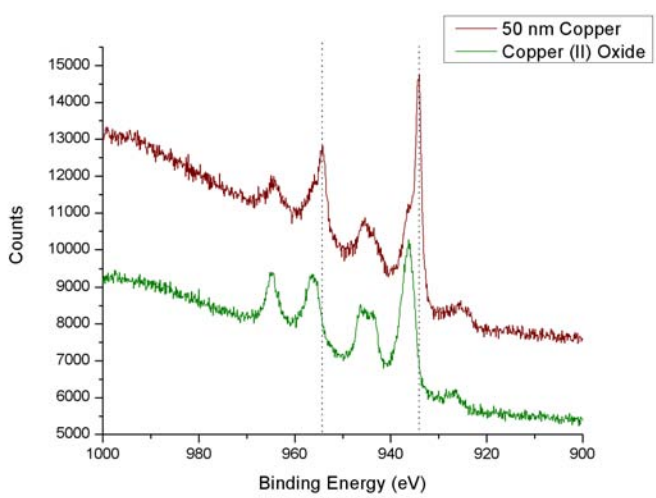


*Figure 3. X-ray photoelectron spectra of thin-film copper (top spectrum) and copper oxidized by the ENABLE beam (bottom), showing complete oxidation of the Cu film.*

With the ENABLE system able to produce both nanoscale structures in polymeric material and directly oxidize metals, it is possible to produce metal oxide nanostructures. If filled with aluminum, these would be essentially "structured nanothermites." Recently, mixtures of copper oxide and aluminum nanoparticles have gained attention for their fast reaction propagation speeds [6]. Producing nanostructured metal oxides employs the same techniques as the polymer nanostructures. First, a polymer template is produced via e-beam lithography. Using the sputter deposition chamber, metal is deposited into the voids of the polymer. The entire assembly is then exposed to the O-atom beam, where the polymer burns away and the metal oxidizes, leaving metal oxide structures. In order to demonstrate the feasibility of this procedure, we have fabricated 100-micron squares consisting of CuO strips 400 nm wide, spaced 100 nm apart. Further research is needed into filling these structures with aluminum and testing their explosive properties, but this work has shown that ENABLE can be a simple, straightforward technique for producing nanopatterned metal oxides.

**Nanoscale feature filling to produce composite energetic structures**

The final step in producing nanocomposite energetic materials involves depositing aluminum metal into the oxidizer (either polymer or metal oxide) structures. This step would appear to be a simple task, but like many nanoscale phenomena, unexpected effects are sometimes observed. After successfully etching 100-nm lines into nitrocellulose and PTFE films deposited on glass substrates, the samples were coated with aluminum using the sputter deposition chamber. The metal coating was stopped at approximately 20% of the polymer thickness, in order to ensure that the metal would be deposited into the bottom of the channels. However, upon examination with a Scanning Electron Microscope (SEM), the lines were raised, as though the metal had piled up over the top of the channels, and the underlying nanoscale channels were not filled. As a test, nitrocellulose and Teflon films were prepared on conducting (doped) silicon substrates, etched and filled as before. This time, the nitrocellulose sample appeared the same but the Teflon sample appeared to have successfully filled the nanoscale channels. Examination by Atomic Force Microscopy (AFM) confirmed that the lines were lower than the surrounding areas, indicating that the aluminum was able to fill in the channels. Figure 4 shows the unfilled nitrocellulose channels (SEM image) and the filled Teflon sample (AFM image). It is not completely clear as to what is affecting the filling process, although electrostatic interactions are suspected. Sputtering occurs in a highly energetic environment involving numerous positively and negatively charged species. Sputter deposition could result in differential surface charging of the polymer nanostructures and substrate surfaces that could repel the sputtered Al ions and prevent them from being deposited into the nanostructures. This assertion is supported by the fact that when the polymers were deposited on non-conductive glass substrates, it was not possible fill the channels. Even though doped silicon substrates are conductive, the nitrocellulose could not be filled. In this case, it is possible that the dipolar nitro ($-NO_3$) groups enhance surface

charging, which serves to efficiently repel the aluminum atoms, forcing them to pile up on the edges of the nanoscale channels. In contrast, the chemically inert $–CF_3$ and $–CF_2$ groups in PTFE would not interact with the aluminum atoms and may impede surface charging, thereby allowing the nanoscale channels to be filled. These results are an interesting example of how forces that are negligible in bulk materials may be important on the sub-micron scale. Clearly it would be worthwhile to further investigate these effects.

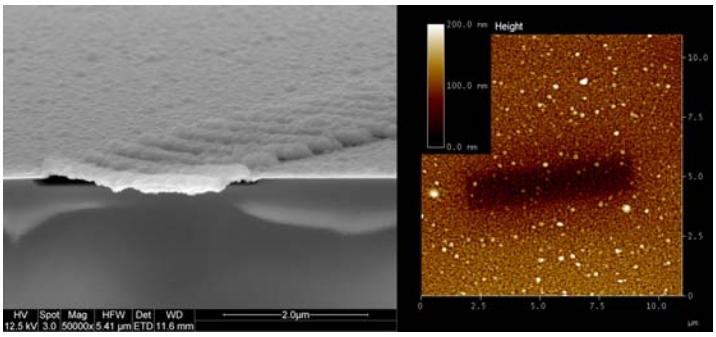


*Figure 4. Results for filling nanoscale channels with Al metal. The SEM image (left) shows the Al overcoating the channels, while the AFM image (right) confirms Al metal successfully deposited into the channels.*

**Construction of a microheater testing apparatus**

The final phase of the project was to measure the energetic properties of fabricated nanostructures. An important aspect of controlling reaction propagation in energetic materials is the ability to add thermal energy to the system. In this phase of the project, we produced thin-film micro-heating assemblies to observe reaction propagation as a function of temperature. Although the idea of thin-film thermocouples is not new [7], we needed to design a microscale thin-film system with a thermocouple and integrated heating wire such that the energetic nanostructures could be deposited on top of the assembly. The assemblies are produced in several steps using the sputter chamber and proximity masks. First, a 200 nm thick chromel heater wire is deposited, followed by a 300-nm insulating layer of $Al_2O_3$. Then, 200 nm chromel and alumel wires were deposited using proximity masks to form a type K thermocouple junction. The entire assembly, shown in Figure 5 (all dimensions in inches), occupies only 0.0625 square inches. Since the structures are so small, the deposition process results in several assemblies on a 1" wafer, as shown in Figure 5 (right). The availability of four sputter heads means that all the materials necessary to fabricate the microheaters are simultaneously present in the chamber, eliminating the need for venting the chamber to change targets. Thus, all of the fabrication steps to produce one set of microheaters can be completed in a day.

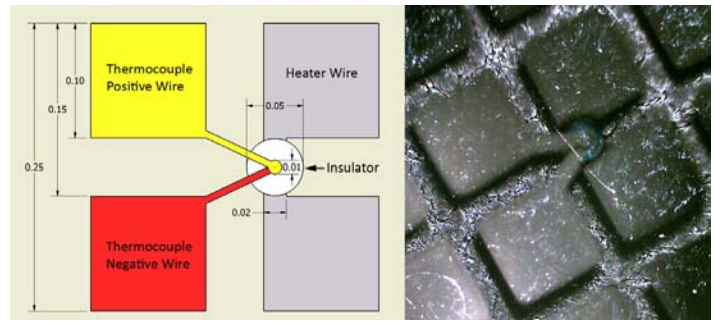


*Figure 5. Diagram and photograph of the thin film microheater assemblies. The left side illustrates the basic parts of the assembly, and the right side is a microscope picture of a completed assembly.*

We have also constructed an apparatus designed to heat the samples and observe the reactions before, during, and after initiation. The sample wafer, containing several heater/energetic material stacks, is mounted on an XY translation stage within a small vacuum chamber. Contact is made with the heater and thermocouple layers via small pins, allowing the sample to be heated while the temperature is carefully monitored. Once the desired temperature is reached, the reaction can be initiated with a laser pulse. The entire process is monitored via a CCD camera that can record video as well as still photographs. Using this system, the thin-film heaters have been operated successfully without the energetic structures, using both direct and pulsed heating. The thermocouples behave as expected, yielding measured temperature changes from heater pulses as short as 10 ms. However, calibration of the thermocouple voltage has been problematic. Initial measurements showed a voltage increase of 0.5 mV for a temperature increase of 10°C, which is approximately the same value as that of a standard type K thermocouple. However, the highest temperature measured in pulsed heating tests was 52°C, above which the heater wire burned through all the layers and shorted out the assembly. It seems unlikely that a 30°C rise in temperature would be enough to melt the heater wire, but more investigation in this area is needed to determine the cause of the problems with the assemblies.

## References

1. Hill, L. G., J. B. Bdzil, W. C. Davis, R. Engelke, and D. L. Frost. Front curvature analysis and detonation shock dynamics calibration for pure and sensitized nitromethane. 1999. *AIP Conference Proceedings.* **505**: 813.

2. McGrane, S. D., D. S. Moore, and D. J. Funk. Shock induced reaction observed via ultrafast infrared absorption in poly(vinyl nitrate) films. 2004. *Journal of Physical Chemistry A.* **108** (43): 9342.

3. Sanders, V. E., B. W. Asay, T. J. Foley, B. C. Tappan, A. N. Pacheco, and S. F. Son. Reaction propagation of four nanoscale energetic composites (Al/MoO3, Al/WO3, Al/CuO, and Bi2O3). 2007. *Journal of Propulsion and Power.* **23** (4): 707.

4. Yang, Y., S. Wang, Z. Sun, and D. D. Dlott. Near-infrared and visible absorption spectroscopy of nano-energetic materials containing aluminum and boron. 2005. *Propellants, Explosives, Pyrotechnics.* **30** (3): 171.

5. Akhadov, E. A., D. E. Read, A. H. Mueller, J. Murray, and M. A. Hoffbauer. Innovative approach to nanoscale device fabrication and low-temperature nitride film growth. 2005. *Journal of Vacuum Science and Technology B.* **23** (6): 3116.

6. Apperson, S., R. V. Shende, S. Subramanian, D. Tappmeyer, S. Gangopadhyay, Z. Chen, K. Gangopadhyay, P. Redner, S. Nicholich, and D. Kapoor. Generation of fast propagating combustion and shock waves with copper oxide/aluminum nanothermite composites. 2007. *Applied Physics Letters.* **91** (24): 243109.

7. Kreider, K. G.. Thin film thermocouples for internal combustion engines. 1986. *Journal of Vacuum Science and Technology A.* **4** (6): 2618.

# Visualization Applied to Electronic Properties of Novel Superconductors

*Alexander V Balatsky*

20061585ER


## Abstract

This project focused on developing visualization as a tool to address electronic, charge and spin inhomogeneity in strongly correlated systems. Primarily, we focused on materials from the Ce-115 family ($CeCoIn_5$ and $CeRhIn_5$). These materials have been characterized using a variety of experimental techniques. Characterization often deals with the multidimensional space of parameters like temperature, pressure, and applied magnetic field. The results found for Ce-115 materials are complicated and require new tools, like 3D visualization to better understand the underlying physics. In order to demonstrate the strengths of the newly developed stereo visualization capability at CINT, we also investigated structural properties of foams and nanostructured particles. By developing this unique scientific visualization capability at the CINT gateway at Los Alamos, scientists have now open access to advanced active stereo three-dimensional visualization tools.


## Background and Research Objectives

We developed 3D visualization as an enabling component of new characterization techniques for the strongly correlated Ce-115 materials, as well as other bulk and nano materials. The objective was to demonstrate the usefulness of 3D visualization for data exploration and analysis. For that purpose, we created a visualization laboratory at CINT with commercially available hardware and open-source software. It became the first visualization laboratory in the unsecure area open to both CINT and LANL users. To develop this visualization tool we used available experimental and theoretical datasets from our collaborators for proof-of-principle demonstrations. By bringing visualization tools and a stereo visualization laboratory in close proximity to scientists, we hope to empower the individual researcher in materials science and nanoscience with unprecedented capabilities to explore complex or multi-dimensional scientific datasets.

In nanoscience, materials science and condensed matter physics researchers are more and more often overwhelmed by the amount or complexity of data produced in table-top experiments or numerical computations. Visualization enhances our ability to see unexpected patterns and correlations in measurements and simulations. The lack of proper visualization can be responsible for our failure to understand the true meaning of our data. This becomes especially important when dealing with a large parameter space of unknowns in experiment or theory, or when quantifying differences between datasets and images.

## Importance to LANL's Science and Technology Base and National R & D Needs

This work allows better understanding of physics and chemistry in actinide-based, heavy-fermion materials and in high-temperature superconductors, as well as in foams, high-energetic explosives, and nanostructured particles. Better knowledge of these materials falls within the grand challenges of actinide research and high-temperature superconductivity as well as fundamental understanding of materials. Creation of a visualization capability in the open area gives uncleared LANL employees and CINT users unprecedented access to top of the line visualization techniques and methods for new ways of exploring complex or large datasets.

## Scientific Approach and Accomplishments

We set up a state-of-the-art stereo visualization laboratory at the CINT gateway at Los Alamos and developed visualization capabilities, which were successfully applied to five scientifically distinct problem sets: (1) compressed foams, (2) scanning tunneling spectroscopy of high-temperature superconductors, (3) multi-dimensional phase diagrams of Ce-115 materials, (4) nuclear magnetic resonance spectroscopy of Ce-115 materials, and (5) depth map and image analysis of SEM datasets of nanostructured particles. Below follows a description of our accomplishments for each of these tasks.

**Study of structural and elastic properties of compressed foams**

We started this project by creating stereo visualizations of the structural and elastic properties of a compressed foam pad simulation by Dr. Scott Bardenhagen (T-14/T-1). The intricate three-dimensional topology of real foams superimposed with simulated components of the stress tensor provides an excellent testbed for advanced stereo visualization. The time evolution of a foam pad during its compression is best studied with 3D visualization tools. Although any physical property can be calculated in a numerical simulation, it is extremely difficult to "see" what is happing inside the foam during compression. From these visualizations we learned that large bubbles and voids in foams collapse first, while smaller voids are more stable and survive up to much higher pressures. This physical behavior leads to an extremely complex spatio-temporal response of foam to external pressures that only materials specific calculations can capture and 3D visualization can faithfully represent. In the future, we hope to compare simulation studies with real-time experiments.

**Scanning tunneling microscopy and spectroscopy of high-temperature copper-oxide superconductors**

In collaboration with the Cornell STM (scanning tunneling microscopy) group of Dr. J.C. Davis, we imaged inelastic scattering processes at the scale of 2-5 nm in superconducting materials with a transition temperature of 76 K. We found that the copper-oxide material $Bi_2Sr_2CaCu_2O_8$ exhibits nanoscale inhomogeneities that correlate with the nanoscale variation of the superconducting gap or strength of the Cooper pairs in the tunneling density of states. This observation opens up new possibilities for the interpretation of the possible mechanisms for high-temperature superconductivity. The observed nanoscale inhomogeneity in the tunneling density of states and in inelastic scattering modes were cross-correlated and indicate the importance of the inelastic electron scattering process in high-temperature superconductors. Figure 1 shows processed data from an STM experiment performed in real space (x-y coordinates) of $Bi_2Sr_2CaCu_2O_8$ with a transition temperature of $T_c$=76 K. The image shown in figure 1 is the corresponding 3D map of the inelastic mode $\Omega$, which provides a visualization of the putative pairing glue of Cooper pairs. The measured inelastic mode is Fourier-transformed and plotted as a function of the two-dimensional momentum space coordinates ($k_x$, $k_y$). The dispersion or $\Omega$-map is recorded as function of energy, that means the external voltage (V) bias between tunneling tip and sample, which is plotted along the vertical axis. The intensity of the color plot is a measure of the strength of the second derivative of the tunneling current with respect to voltage. Surprisingly, the dispersion does not extend to the zone boundaries, but rather is located around the center of the Brillouin zone.

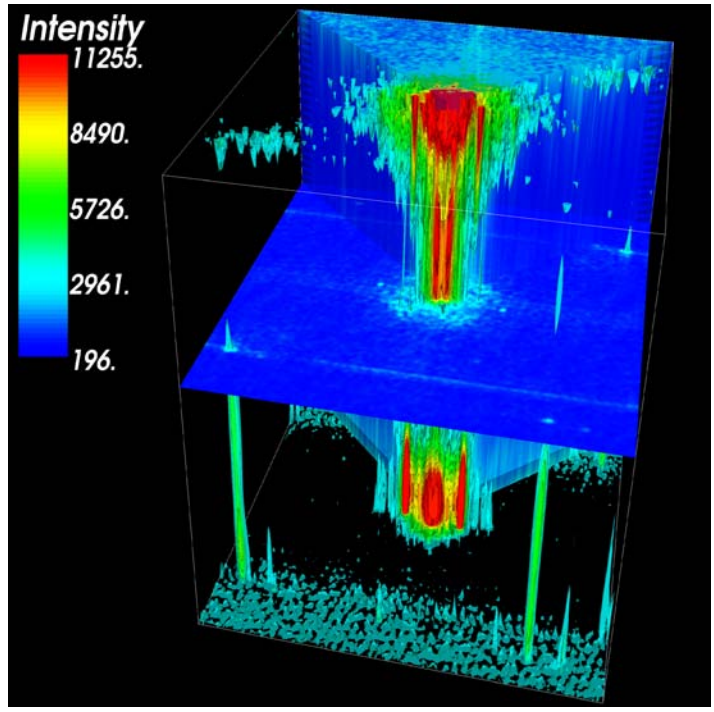


*Figure 1. Processed inelastic tunneling data of the high-temperature copper-oxide superconductor $Bi_2Sr_2CaCu_2O_8$. The funnel shaped object in the center of the image shows the dispersion of the inelastic mode Omega colored by intensity. The dispersion is located around the center of the Brillouin zone. The spikes at the four corners are the Bragg peaks of the underlying crystal structure. The inelastic tunneling signal was acquired over the field of view in x-y real space (48 nm x 48 nm) as a function of bias voltage V (here Z axis). In a second step, the real-space coordinates (x,y) were Fourier transformed to momentum coordinates (kx,ky) to obtain the energy dispersion of the inelastic mode Omega. This mode is due to inelastic scattering of electrons. The coordinates shown in the X-Y plane are momenta kx-ky and the vertical dimension is the mode Omega(kx, ky) shown between 30-80 meV. The image is color coded by the intensity of the mode Omega, that means, by the second derivative of the tunneling current I with respect to bias voltage V.*

**The phase diagram of heavy-fermion superconductor $CeRhIn_5$**

In collaboration with Dr. Tuson Park and Dr. Joe Thompson at MPA-10, we visualized the phase diagram of the heavy-fermion superconductor $CeRhIn_5$. $CeRhIn_5$ phase transitions have been studied before using only 2D plots. Here, by using the newly developed visualization capabilities the scant experimental set of phase transition data points were combined into a single 3D visual model. This model allowed us to explore interactively the phase diagram with its unique phase boundaries. We interpolated the experi-

mental datasets to create smooth and continuous surface boundaries consistent with the laws of thermodynamics and theories of quantum phase transitions. The great advantage of studying these phenomena in $CeRhIn_5$ lies in the facile tunability and accessibility of external parameters like pressure, magnetic field and chemical doping. In Figure 2 we show a comparative visualization of the phase diagram as function of the temperature T (K= Kelvin), pressure P (GPa=Gigapascal) and magnetic field B (T=Tesla).

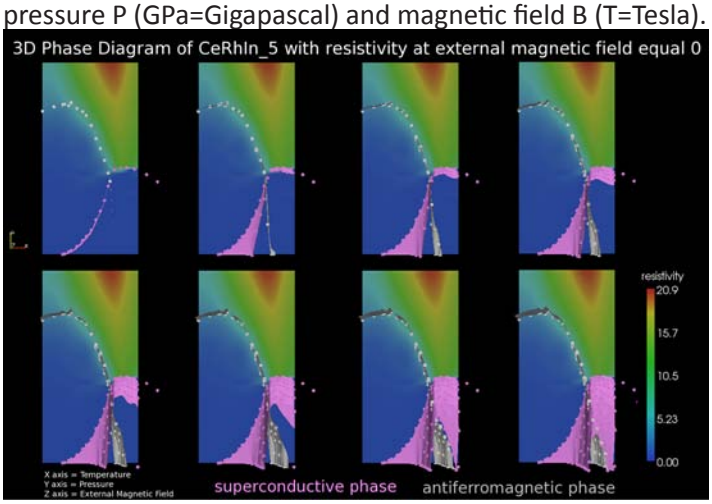


*Figure 2. Comparative phase diagrams for CeRhIn5. The phase transition surfaces are bounded at z=0, that means zero magnetic field, by a plane colored by resistivity (micro-Ohm-cm) versus pressure and temperature. The origin is in the bottom left hand corner of each image. The image series progresses from left to right and top to bottom and shows various outputs of the clip visualization operation that removes data from a (clip) plane. As the clip plane moves through the volume of the phase diagram, one can see how the superconducting (pink) and antiferromagnetic (gray) phase boundaries intersect as the external magnetic field increases in steps of 1.1 T.*

N stands for "normal phase", AFM for "antiferromagnetic" phase, and "SC" for superconducting phase. The color bar gives the zero-field resistivity (in units of micro-Ohm-cm) that goes to zero as the SC region is approached and drops significantly in the AFM region, indicative of the opening of a gap. The cubic and spherical points are the experimentally measured data points extracted from the jumps in the specific heat, and the surfaces were created using interpolation for drawing polygons. The "gray surface" separates the AFM phase from the N phase at high temperatures. The pink surface surrounds the SC region at lower temperatures. The (gray) AFM phase boundary penetrates into the (pink) SC phase boundary, which is typical for competing orders. However, the common region between the AFM and SC boundaries, inside the pink dome, defines the coexistence region of the AFM and SC phases. We also see that the AFM transition temperature decreases with pressure. At T=0 K, the system undergoes a transition as a function of pressure which characterizes the quantum critical region and is thought to be responsible for the anomalous normal state properties. Follow-up measurements are necessary to delineate further the low-field and high-temperature phase boundaries of the AFM and SC phases.

**Indium-NMR spectroscopy of nano-sized droplets in the heavy fermion system $CoCoIn_5$**

In collaboration with Dr. Nicholas Curro (UC Davis) and Dr. Ricardo Urbano (MPA-10), we studied the fundamental interactions and ordering phases in the strongly-correlated heavy-fermion system $CeCoIn_5$ doped with cadmium by using advanced visualization approaches to multi-dimensional NMR spectra. Standard analysis methods of NMR experiments, which integrate out most of the multi-dimensional information of the NMR spectrum, reveal the existence of antiferromagnetic and superconducting order in $CeCoIn_5$, when doped with a few percent of cadmium. For the first time, we applied advanced 3D visualization methods to the NMR spectrum of a strongly-correlated electron system. We used the open-source software tool ParaView to visualize and explore the real and imaginary parts of the measured NMR magnetization as a function of temperature, echo frequency and recovery time. Figure 3 shows the spectral function of $CeCoIn_5$ doped with one percent of cadmium (Cd), which substitutes for indium (In).

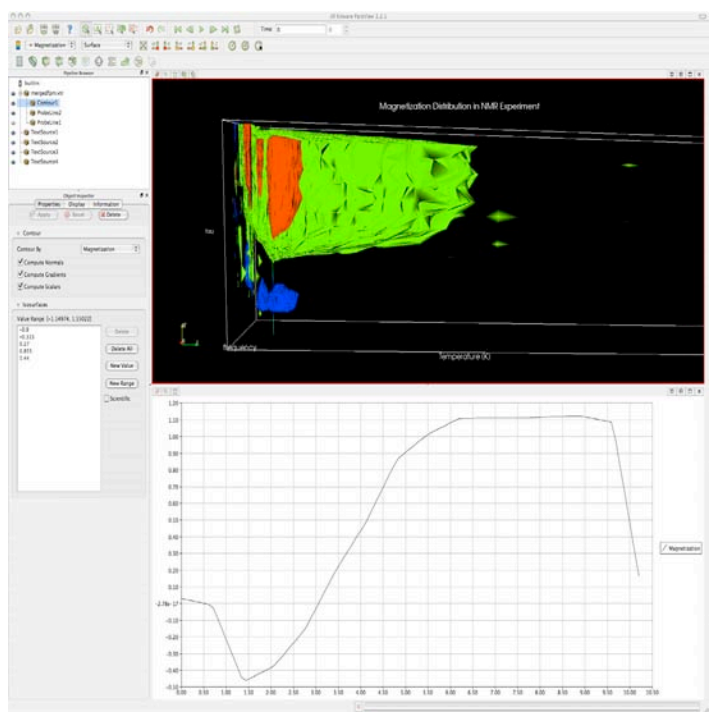


*Figure 3. We used ParaView to create a combined 3D visualization and 2D plot that present the magnetization distribution in an NMR experiment for CeCoIn5 doped with 1% Cd. The 3D window shows a collection of 3D contours of magnetization in arbitrary units [-0.9 (blue), -0.315, 0.27 (green), 0.855 (orange) and 1.44]. The X axis is the normalized NMR frequency, the Y axis is the natural logarithm of the recovery time tau (in units of*

*micro-seconds), and the Z axis is temperature (in units of Kelvin). The plot window below shows the normalized magnetization as a function of log(tau) at fixed temperature (T=2.8 K) and at zero NMR frequency sampling along the probe line shown as a vertical green line, to the left, in the 3D view.*

The obtained result is much more complex than was anticipated. We can clearly identify the precursor of long-range antiferromagnetic order (green contour) as a function of temperature long before its onset (sharp signature in the right orange contour) at 2.8 K. The precursor anomaly extends up to nearly 40 K. Surprisingly, we were able to identify one additional feature in the spectrum at around 2.1 K (middle orange contour) before superconductivity onsets at 1.8 K (left orange contour). Follow-up studies are underway to determine the nature of the spectral signature at 2.1 K as a function of temperature and doping. This newly discovered spectral feature may be due to an inhomogeneous distribution of nanoscale-sized droplets of cadmium clusters, or to an unequal occupation of cadmium on non-equivalent lattice sites of indium, or to the onset of a second antiferromagnetic ordering phase with a uniquely different nesting wave vector connecting different regions of electrons on the complex Fermi surfaces of $CeCoIn_5$. At the moment all these possibilities are being explored further. Visualization has enabled us to see the full content of the NMR spectrum and allowed us to explore in more detail the consequences of the possible formation of nano-sized cadmium droplets in the bulk of the heavy-fermion system $CeCoIn_5$ when doped with cadmium. There is mounting evidence from XAFS that cadmium is neither randomly nor uniformly substituting for indium and more research is required now that we know where to look for its signatures in the NMR spectrum.

**Depth map analysis with scanning electron microscopy**

Scanning electron microscopy (SEM) is a standard imaging tool all the way down to the micro- and nanometer scale for objects with a conducting surface. Nowadays, SEM images can be collected relatively fast and inexpensively compared to other scanning probes. Thus making it an ideal tool for pre-screening or quality assurance of samples. Unfortunately, standard SEM machines take only one image at a fixed viewing angle to measure lateral dimensions, which is not sufficient to provide depth information. In collaboration with Dr. Elshan Akhadov at Sandia National Laboratory and GRA summer student Nathan Brown from Case Western Reserve Universtiy, we developed an efficient approach to extract depth or height information from a stereo-pair of SEM images. Depth analysis, also known as stereogrammetry, in combination with SEM has a long tradition, but was limited to either custom-designed machines or slow depth analysis software. We used a conventional SEM apparatus available at CINT with a rotational sample holder that allows taking images at a minimum of two different viewing angles needed for stereo-pair images. We then performed a depth analysis of the stereo-pair images with a normalized cross-correlation function analyzer programmed on a workstation with a graphics processing unit (GPU) featuring 128 processing elements. Compared to running the same algorithm on a single workstation, we saw roughly a 100 times speed-up. Now we can analyze stereo-pair images almost in real-time within roughly one minute. We found that the limiting factor in speed-up for image analysis is the memory size of the GPU and its registers. Figure 4 shows the processed final result of a depth map for a silver particle with sub-micro-meter resolution. The false color code represents the depth or height information of the micro-meter-sized particle. Figure 5 shows a typical probe line across the 3D image from left to right demonstrating the achieved quantitative height resolution. Resolution limits are due to the electron beam geometry, angle stepping accuracy and pixel resolution of the SEM images. The custom-design of nanostructured silver particles is of great technological interest for developing better surface-enhanced Raman scattering (SERS) techniques, which enable the measurement of the vibrational spectrum of molecules, or the fingerprint of a molecule, with nearly one million times higher signal to noise ratio compared to conventional Raman scattering techniques. We demonstrated that 3D depth analysis of SEM images allows one to perform efficient and quick design tests of nanostructured particles.

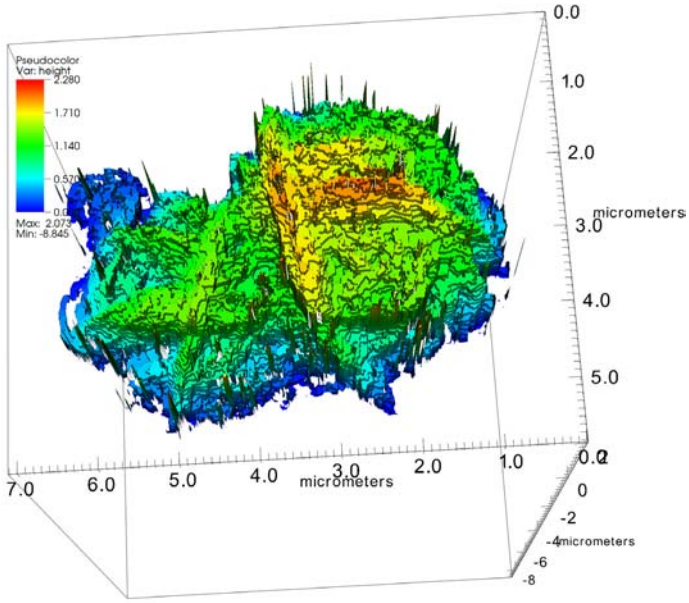


*Figure 4. Reconstructed 3D image of a micro-meter-sized nano-structured silver particle with color-coded height information using the visualization package VisIt. The height information is superimposed onto the 2D SEM image.*

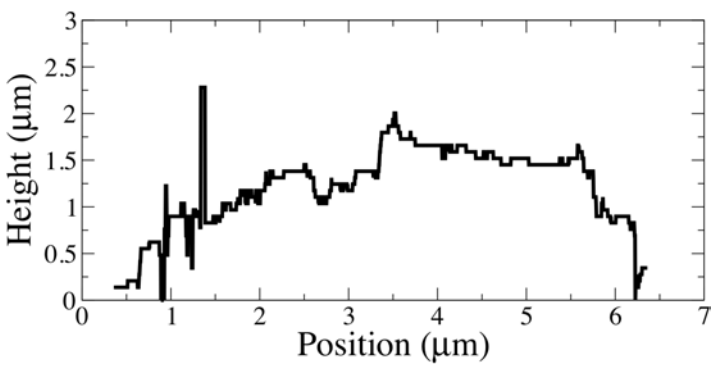


*Figure 5. A typical probe line across the nanostructured silver particle with sub-micro-meter resolution of the particle's height.*

## Publications

Bardenhagen, S. G.. Application of Stereo Visualization Technology to the Study of Foam Morphology and Structural Response (LA-UR-06-7973). Presented at *Supercomputing 06.* (Tampa, FL, 11-17 Nov. 2--6).

Bardenhagen, S. G.. Application of Stereo Visualization Technology to the Study of Foam Morphology and Structural Response. Presented at *Third MPM Workshop (LA-UR-06-7973).* (Albuquerque, NM, 22-23 March 2007).

Brown, N.. Accelerating depth map building with the GPU. Presented at *Salishan Conference on High Speed Computing.* (Gleneden Beach, Oregon, April 21-24, 2008).

Brown, N., and M. C. Cavusoglu. Accelerating depth map building with the GPU. Presented at *Fall Creek Falls 2008.* (Burns, Tennessee, September 7-10, 2008).

Curro, N.. NMR in Strongly Correlated Electron Systems and the 115 Materials. Invited presentation at *Carguese Summer School: 50th anniversary of BCS 'From BCS to Exotic Superconductivity'.* (Carguese, France, July 2007).

Curro, N.. Unexpected Manifestations of Quantum Criticality in a Heavy Fermion Superconductor. Invited presentation at *Colloqium at Rutgers University.* (Rutgers, NH, April 2007).

Curro, N.. Microscopic Inhomogeneity near a Quantum Critical Point. Invited presentation at *Dynamics in Complex Systems III.* (Port Jefferson, May 2007).

Graf, M. J., J. Ahrens, J. Patchett, N. Brown, H. P. Dahal, A. V. Balatsky, D. Modl, L. Monroe, and E. Akhadov. To see is to know: Visualization for materials science and nanoscience. 2008. *SciDAC Review.* (10): 32.

Park, T.. Vanishing energy scale at a quantum critical point in the heavy-fermion superconductor CeRhIn5. Presented at *The International Conference on Strongly Correlated Electron Systems.* (Houston, Texas, 13-18 March 2007).

Park, T.. Probing hidden magnetism and quantum criticality in unconventional superconductors. Invited presentation at *LANL Director's Colloqium.* (Los Alamos, NM, 9 May 2007).

Park, T.. Quantum Criticality in the pressure-induced superconductor CeRhIn5. Invited presentation at *Workshop on 115 Materials: The Rosetta Stone for the Kondo Lattice.* (Aspen, Colorado, 2-5 Aug. 2007).

Park, T.. Is Quantum Criticality a Key to High-temperature Superconductors?. Invited presentation at *US-Korea Conference 2007.* (Washington, DC, 9-12 Aug. 2007).

Park, T., M. J. Graf, L. Boulaevskii, J. L. Sarrao, and J. D. Thompson. Electronic Duality in Strongly Correlated Matter. 2008. *Proceedings of the National Academy of Sciences, USA.* **105**: 6825.

# New High-Nitrogen Polydentate Ligands for Actinide Separations

*David Lewis Clark*

20080717ER


## Abstract

We have examined a new class of ligands (viz., bitetrazole derived ligands) for advanced lanthanide/actinide separations chemistry. Like pyridyl-derived molecules, bitetrazoles are polydentate high-nitrogen content ligands; however, bitetrazoles are water soluble, and are relatively inexpensive and simple to prepare on large scales. This report details our efforts from January 2008 through September 2008. To date, we have prepared and characterized several new lanthanide complexes of bitetrazole derived ligands and examined their separations properties by electronic structure theory calculations. We have shown that these ligands form stable complexes with lanthanides and have good evidence to suggest that these new cost effective ligands will separate actinides from lanthanides.


## Background and Research Objectives

There has been a resurgent interest in actinide chemistry to support nuclear energy production [1]. If the U.S. nuclear energy footprint is to increase, as present trends indicate, improved methods for the treatment of spent nuclear fuel will have to be developed. Indeed, the 2006 report by the US DOE Office of Basic Energy Sciences on *Basic Research Needs for Advanced Nuclear Energy Systems* identified the grand challenge of "*Understanding and Designing New Molecular Systems to Gain Unprecedented Control of Chemical Selectivity during Processing",* and explicitly calls for advanced separations chemistries to be developed that utilize new and novel chemistry agents [2].

After the PUREX or UREX+ processes to extract plutonium and uranium, lanthanide fission products must be separated from minor actinides (Am, Cm). This is an extremely difficult chemical problem, but a revolutionary new approach utilizes polydentate soft donor ligands [3]. The ligands that have shown the most promise fall into two classes of polydentate high-nitrogen content ligands, bis-triazinyl pyridine (BTP) and bis-triazinyl bipyridine (BTBP) as shown in Figure 1.

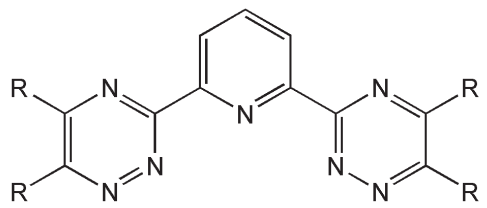

**BTP**
(Bis-triazinyl pyridine)

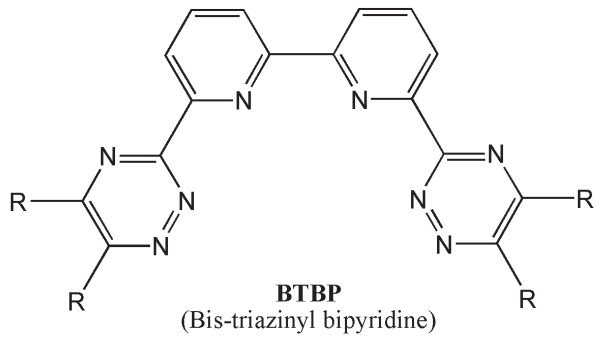

**BTBP**
(Bis-triazinyl bipyridine)

*Figure 1. BTP and BTBP polydentate ligands.*

The use of BTP and BTBP has been shown to dramatically improve separations of transplutonium elements (Am and Cm) from lanthanides (up to $10^7$ enhancements over malonamides). Although these ligands could serve as strong extractants for actinides over lanthanides the disadvantages to their use include the high cost of synthesis, radiation stability, and lack of water solubility. The success of this new approach suggests that other high-nitrogen content polydentate ligands might display similar or even greater separations efficiency for lower cost and greater water solubility. For example, bitetrazole amine (BTA, Figure 2) has been shown to form N-bonded polydentate complexes with a variety of transition metals, including Fe, Cu, Ni, and Co [4]. Although similar in elemental composition to many high-nitrogen explosives, these compounds and their metal complexes are essentially failures in the explosives arena. We propose that because BTA is similar in structure to BTP and BTBP, BTA and its derivatives can be expected to serve as soft donor ligands to f-element

complexes, and may serve as strong extractants for lanthanides and actinides. There are several potential advantages to the use of BTA relative to BTP and BTBP such as the low cost and relatively simple large-scale preparation of the neutral ligand, the ability to form a highly charged species in solution (see Figure 2, deprotonated form), and water solubility which in turn could improve the kinetics of metal complexation. All together, these factors increase the attractiveness of BTA and similar derivatives over BTP and BTBP as actinide/lanthanide chelates and could lead to the development of new state-of-the-art techniques for advanced nuclear energy systems.

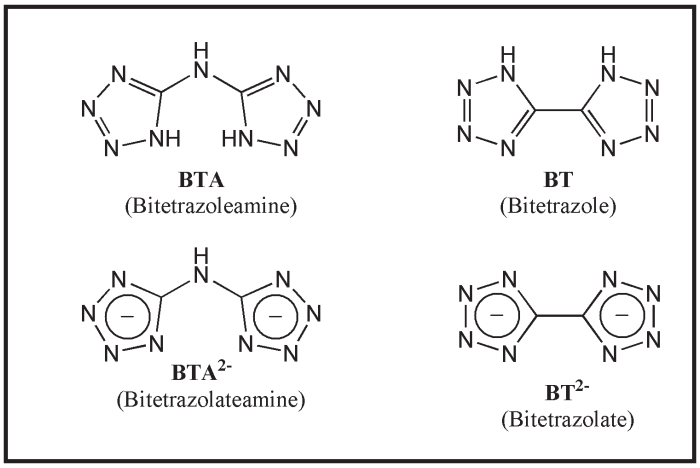


*Figure 2. BTA and BT high nitrogen ligands.*

## Importance to LANL's Science and Technology Base and National R & D Needs

Revolutionary separation processes to partition actinides from lanthanides and other fission products could result from the fundamental knowledge developed through this work. They would lead to improved safety, economics, and proliferation resistance of future plants for partitioning spent nuclear fuel. This includes separation processes for the spent fuel produced by the fast reactor systems that are designed to fission the actinide inventory more effectively than the light water reactors. The increased control of *f*-element coordination chemistry would also be expected to provide new synthetic approaches to prepare more challenging fuel types, such as the transmutation fuels for fast reactors.

## Scientific Approach and Accomplishments

We have examined the fundamental chemistry of the high nitrogen ligands BTA and BT (see Figure 2) with several lanthanides. We have found that these ligands coordinate lanthanide cations well. Indeed, $La^{3+}$, $Ce^{3+}$, $Pr^{3+}$, and $Nd^{3+}$ all form stable complexes with BTA and BT in aqueous solutions under ambient conditions with high yield and purity. An example of the geometry of the formed complexes is shown in Figure 3. These new complexes have been characterized by X-ray crystal diffraction, elemental analysis, FT-IR spectroscopy, and NMR spectroscopy. Additionally, all new complexes were safety tested and do not show any energetic sensitivity towards thermal stress (DSC differential scanning calorimetry) drop weight impact, friction, or spark.

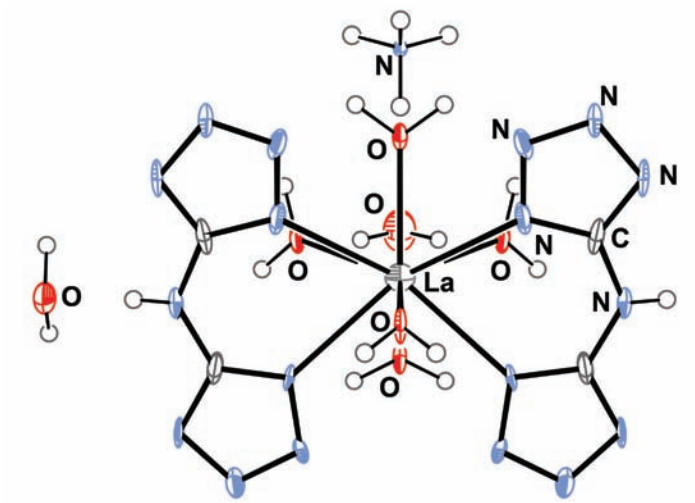


*Figure 3. X-ray crystal structure of $NH_4[La(BTA)2(H_2O)5]\cdot 2H_2O$.*

Density functional theory (DFT) calculations in collaboration with Neil Henson and Rich Martin (T-1) to investigate the electronic structure theory of BT and BTA ligands with lanthanide and actinides. The optimized geometries for Ln(III) complexes that bind two ligands per metal are in good agreement with our crystallographic data suggesting that the DFT models are good and crystal packing has little effect on the preferred structure. The DFT calculations further predict that it is thermodynamically possible to add more than two BT/BTA ligands to an f-element (i.e., actinide or lanthanide) and that the average binding energy for the BT/BTA ligands to the metal is 5-8 times greater than for a water molecule (see Figure 4 as an example for increased BT ligand binding to La). Finally, our calculations also predict that these high nitrogen ligands should effectively separate actinides from lanthanides. More specifically, actinide extraction by BT/BTA is favored over lanthanide extraction by 18-56 KJ/mol, as detailed in Figure 5.

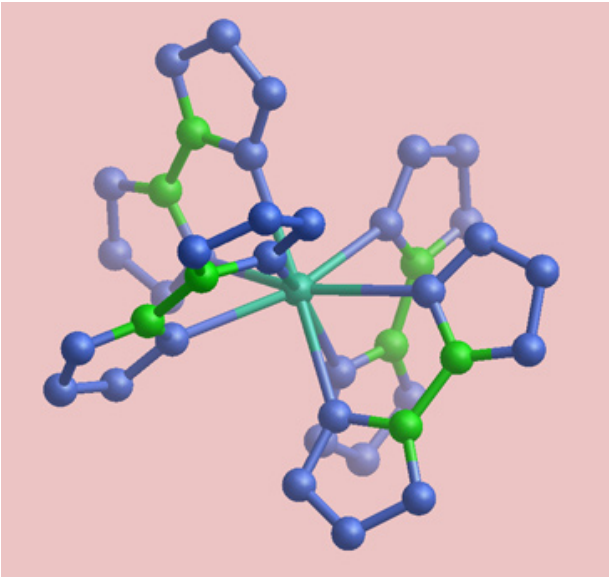

*Figure 4. Calculated structure of La(III) with four BT ligands.*

*Table 1: Calculated thermodynamics for the exchange reaction :*
$[M(H_2O)_9]^{3+} + [M'(BT)_2(H_2O)_6]^+ ?\ [M(H_2O)_9]^{3+} + [M'(BT)_2(H_2O)_6]^+$
*showing enthalpy of reaction (? H) with and without solvent, and free energy of reaction (? G) for lanthanide, La and Ce, and actinide, Am and Cm complexes.*

| M (III) | M' (III) | ΔH (kJmol⁻¹) | ΔH with included solvent field (kJmol⁻¹) | ΔG (kJmol⁻¹) |
|---|---|---|---|---|
| Am | La | -47.1 | -22.9 | -56.0 |
| Am | Ce | -29.0 | -11.0 | -37.9 |
| Cm | La | -25.2 | -8.8 | -36.4 |
| Cm | Ce | -7.1 | +3.1 | -18.3 |
| La | Ce | +18.1 | +11.9 | +18.1 |
| Am | Cm | -21.8 | -14.1 | -19.6 |

*Table 2: Calculated thermodynamics for the exchange reaction :*
$[M(H_2O)_9]^{3+} + [M'(BTA)_2(H_2O)_6]^+ ?\ [M(H_2O)_9]^{3+} + [M'(BTA)_2(H_2O)_6]^+$
*showing enthalpy of reaction (? H) with and without solvent, and free energy of reaction (? G) for lanthanide, La and Ce, and actinide, Am and Cm complexes.*

| M (III) | M' (III) | ΔH (kJmol⁻¹) | ΔH with included solvent field (kJmol⁻¹) | ΔG (kJmol⁻¹) |
|---|---|---|---|---|
| Am | La | -40.8 | -28.3 | -52.7 |
| Am | Ce | -46.2 | -31.1 | -53.3 |
| Cm | La | -32.3 | -24.6 | -43.8 |
| Cm | Ce | -37.7 | -27.3 | -44.3 |
| La | Ce | +5.4 | -2.8 | -0.5 |
| Am | Cm | -8.6 | -3.7 | -8.8 |

*Figure 5. Calculations showing that actinide extraction is favored over lanthanide extractuon for BT and BTA.*

Overall, these results suggest that BTA and BT may serve as excellent chelates for lanthanide/actinide extraction and separation. These ligands are inexpensive and simple to prepare, are water-soluble, and we have shown that they form highly stable lanthanide complexes. The DFT calculations complement our synthetic results and further suggest that BTA and BT will favor actinide (over lanthanide) complex formation. Further study is necessary to validate the DFT calculations with regard to actinide complex formation and lanthanide/actinide separations and to better to define the role these ligands could have in revolutionizing waste remediation techniques.

## References


1. Statistics were provided by the Nuclear Energy Institute, Washington, DC http://www.nei.org (http://www.nei.org). 2007. *Nuclear Energy Institute.*

2. Report of the Basic Energy Sciences Workshop on Basic Research Needs for Advanced Nuclear Energy Systems, July 31 – August 3, 2006. www.sc.doe.gov/bes/reports/files/ANES_rpt.pdf. 2006. *Office of Science.*

3. S.Foreman, M. R., M. J. Hudson, M. G. Drew, C. Hill, and C. Madic. Complexes formed between the quadridentate, heterocyclic molecules 6,6-bis-(5,6-dialkyl-1,2,4-triazin-3-yl)-2,2-bipyridine (BTBP) and lanthanides(III): implications for the partitioning of actinides(III) and lanthanides(III). 2006. *Dalton Transactions.* **13**: 1645.

4. Tappan, B. C., M. H. V. Huynh, M. A. Hiskey, D. E. Chavez, E. P. Luther, J. T. Mang, and S. F. Son. Ultralow-density nanostructured metal foams: combustion synthesis, morphology, and composition . 2006. *Journal of the American Chemical Society.* **128** (20): 6589.

# Integrated Multiscale Simulation for Advanced Nuclear Fuel

*Francis L Addessio*

20080783ER

## Abstract

An effort was pursued to demonstrate the potential of developing a multi-scale, multi-disciplinary approach to provide physicially-based computational models for simulating the thermo-mechanical behavior of nuclear reactor fuels. The tri-structural-isotropic (TRISO) fuel was the focus of this effort. Modeling the response of the TRISO fuel presents a number of technical challenges related to each of the scales and theories as well as the coupling of these diverse disciplines. For example, the details of the gas bubble nucleation and growth within the fuel is poorly understood and requires further investigation. Coupling the radiation field to a material, which is cracking and experiencing debonding between material layers, presents another difficulty that must be considered. Finally, the problem of determining physical properties from ab initio simulations for time- and length-scales that are of interest to the engineering community also remains a challenge.

## Background and Research Objectives

To develop safe energy sources, reduce greenhouse emissions, and control the proliferation of nuclear materials, advanced nuclear reactors are receiving a renewed consideration. The design and analysis of advanced nuclear fuels presents a number of challenges. A reliable, predictive simulation capabilities for describing the behavior of materials under extreme conditions requires basic theory and computational capabilities that are only available at institutions such as the national laboratories. The theoretical and numerical tools, which were utilized in this research, are intended to be sufficiently general and to allow the analysis of a broad spectrum of nuclear power generation problems. However, in an attempt to focus on a representative problem, a Modular Helium-Cooled Reactor (MHR) and the tri-structural-isotropic (TRISO) fuel was considered. In addition to power generation, the TRISO-fueled gas reactor also is a concept that is under consideration for the destruction of spent transuranics (Deep Burn) using a large fractional burnup (more that 70%), which is achieved with a single irradiation. This concept is particularly attractive because the same reactor design can be used for highly efficient power generation and hydrogen production. Deep Burn (DB) rapidly and effectively reduces the inventory of transuranics from spent fuel without the need for repeated recycles, destroys any weapons-usable materials contained in the spent fuel, and precludes the possible weapons use of the residuals.

The TRISO fuel (Figure 1) is a coated particle that is approximately 1 mm in diameter. The fuel core consists of fissile material. The fuel is encapsulated in a porous carbon layer, an inner pyrolytic carbon layer, a silicon carbide (SiC) containment layer, and an outer pyrolytic carbon layer. The purpose of the outer layers is to contain fission products and mitigate thermal-mechanical effects. It has been determined that some of the fission products escape the containment layers during operation. Basic engineering simulations are at a loss to explain the levels of the escaped products. To simulate these processes, a computational effort was pursued. Using first-principles physics, including electronic structure (ES) calculations, molecular dynamics (MD), and accelerated molecular dynamics (AMD) material properties were obtained for extreme conditions. Modeling the nuclear reactions (nuclear burn) provided the temporal production rates of fission products and the ensuing energy production rates. Radiation transport is necessary to model the transport of both small and large mean free path particles under normal operating conditions, including angular dependence, and for transient conditions. The results of these theories are used to develop a fully three-dimensional, physically-based, engineering model to investigate the thermo-mechanical response of the TRISO fuel.

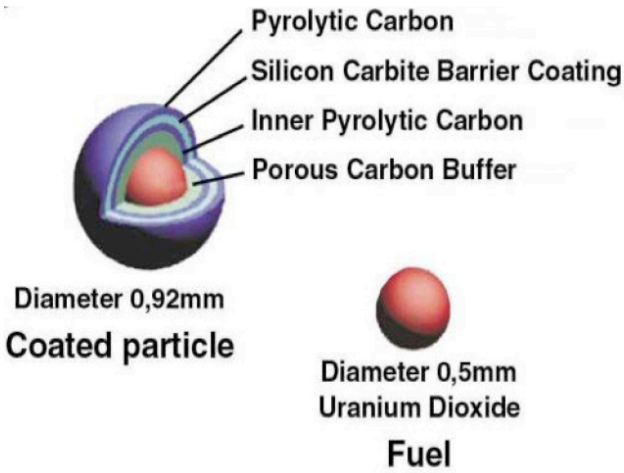


*Figure 1. TRISO fuel particle.*

## Importance to LANL's Science and Technology Base and National R&D Needs

Despite the recent advances in modeling and simulation, accurate predictions for understanding and improving the TRISO fuel system cannot be made. Better models for processes, including the evolution of micro-structure in the presence of radiation, diffusion, and nuclear burn, must be developed. Even partial progress in developing a predictive capability for these phenomena would represent an important benefit for many nuclear energy applications. Various simulation tools reside at different time- and length-scales. The key point is that to make accurate predictions at any of these scales, high quality information must be passed from one level to the next. One of the weak links between scales is between ES and MD methods. ES theories can provide relative energies and activation barriers. Unfortunately, MD simulations using ES forces can only be propagated for a few picoseconds. The standard approach is to construct empirical potentials and to use these faster potentials in MD simulations. Accurately capturing the complexity of the mixture of covalent, metallic, and ionic bonding with an empirical potential is difficult. This is especially true for systems like the multi-component core of a TRISO pellet. Solving this problem, either using new approximate ES methods, a new generation of potentials, use of advanced computer architectures, or novel approaches, represents a research priority. A general solution, perhaps making use of LANL's supercomputing expertise and hardware, would allow the first-ever accurate predictions of fission-product diffusion rates, radiation damage annealing features, and many other properties that require full atomistic detail. This would also enable the use of ES forces with the LANL-developed AMD methods, allowing longer time scales to be accessed. Macro-mechanical capabilities also will require significant improvements to existing numerical and physical models. Currently, for example, the details of the nucleation, growth, and coalescence of gas bubbles within the fuel represents a daunting challenge. Issues related to the damage of the TRISO material layers as well as the debonding between the layers, also will require model development. These phenomena coupled with the diffusion of fission products and the chemical erosion of material layers must be addressed to achieve a predictive modeling capability.

## Scientific Approach and Accomplishments

Continuum simulations were conducted to address the spatio-temporal scales, which are relevant to reactor operations. A three-dimensional approach is necessary to model anisotropic deformations, material properties, and behavior (i.e. the amoeba effect). Two three-dimensional methods were pursued to provide the thermo-mechanical response of the TRISO fuel. Lagrangian approaches were considered because of the relatively small strains and deformations anticipated, the need to consider accurate approaches for modeling gas bubble nucleation and growth, and the need to use physically-based constitutive models. A general formulation must include the effects of creep, conduction, diffusion, chemistry, and irradiation. Inelastic effects such as anisotropic cracking and decohsion between material layers also should be included. In this effort, only thermo-elastic effects and thermal diffusion were modeled. The energy sources were guided by the nuclear burn calculations. They were located at pre-defined hot spots within the fuel in an effort to simulate a non-uniform distribution of heat sources. Best estimates of material properties were obtained from the literature.

One of the computational approaches utilized a Lagrangian finite-element analysis (FEA). This approach used an implicit numerical technique, which allows relatively large time scales to be achieved. Therefore, reactor operational conditions may be addressed using this formulation. In addition to including the effects of the generation of heat, the simulation also included contact with three neighboring fuel particles. The contours of the stress distribution indicated the need to include inelastic effects in future analyses. The second approach that was considered was a material-point method (MPM), which is an advanced version of the particle-in-cell (PIC) technique. This approach utilizes an underlying grid for the solution to the conservation equations and contains a particle field, which intimately communicates with the computational mesh. The constitutive models are embedded on the Lagrangian particle field. The MPM approach is considered to be a viable technique for addressing the bubble nucleation and growth problem. The existing MPM model has an explicit

formulation. Therefore only small time scales, which are relevant to reactor transients, may be addressed. The MPM formulation includes multiple fields and species. This generality will facilitate the ability to track fission products. A distribution of the enthalpy on the material particles is provided in Figure 2. Future considerations include the implementation of advanced constitutive models with improved material properties and a physical and numerical model for the bubble growth problem.

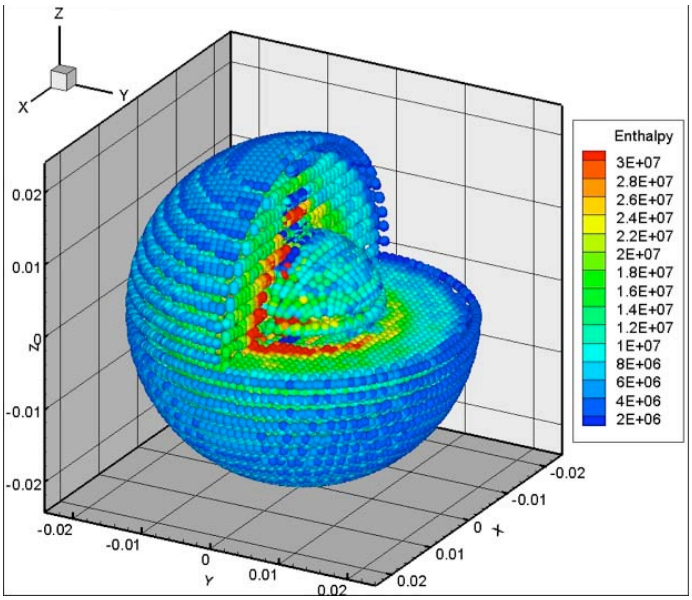


*Figure 2. Explicit MPM simulation.*

The dependence of gas production on details of the fuel composition, reactor configuration, the neutron flux spectrum, and the fuel burn-up were addressed. Three reactor designs were considered: 1) a high-temperature gas reactor (HTGR) with TRISO fuel particles, 2) a modular fast reactor (SMFR) involving a Transuranic (TRU) fuel, and 3) a pressurized water reactor (PWR) with 3% enriched uranium fuel. In comparing the noble gas production across the different reactor designs the power density was fixed at 95W/cc in each case. For all three designs, it was found that Xe was the dominant gas produced. The amount of Xe was very similar for the HTGR and SMFR reactors, but about twice as much Xe is produced in a PWR (Figure 3). The increased production of Xe in the PWR case is caused by the large thermal neutron peak and the corresponding conversion of unstable $^{135}$Xe to stable $^{136}$Xe. The total Kr production is generally only about 20% that of Xe, because of its lower yield as a direct fission product. Of the three reactor designs, the SMFR results in the least amount of Kr, reflecting the smaller yield of Kr from fissioning Pu than $^{235}$U. He production increases significantly with the hardness of the neutron spectrum because there is an increased production of alpha-unstable actinides, particularly the actinides responsible for the main alpha-decay chains of heavy nuclei. In the case of the SMFR the TRU content of the fuel results in the He production exceeding that of Kr. In addition to alpha decay, He production by ternary fission also was taken into account, which turns out to account for about 40% of the He. The temperature gradient across the TRISO fuel also was examined and found to be a strong function of the power. For the upper-end power levels for the TRISO particle design (400mW/particle) the predicted temperature gradient was significant. Finally, the neutron flux in different regions of the TRISO particle was examined. A strong variation with region was observed. In particular, the fast neutron flux is about a factor of two higher in the fuel than in the rest of the particle, while the thermal flux in the fuel is a factor of two lower than in the cladding.

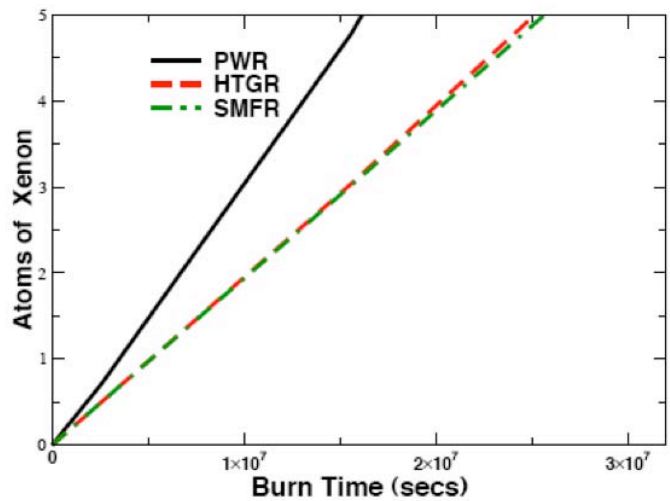


*Figure 3. Xe fission gas production.*

DFT calculations were performed to determine material properties. Urania ($U0_2$) poses a challenge to first-principles methods. The presence of an uranium requires measures to treat the strong electron correlation in the 5f orbitals. The emergence of magnetic structures requires that spin polarization and spin-orbit coupling also be included in the calculations. Urania seldom contains uranium and oxygen in stoichiometric ratios, requiring large unit cells. Calculated elastic moduli agree well with experiment. Calculations of tetragonal distortions result in a value of 2.63 x $10^{12}$ dyne $cm^{-2}$ for the shear modulus c11-c12, which compares favorably to the experimental value of 2.74 x $10^{12}$ dyne $cm^{-2}$. Similarly, calculations with a trigonal distortion lead to a value of 0.61 x $10^{12}$ dyne $cm^{-2}$ for the shear modulus c44, which compares favorably with the experimental value of 0.58 x $10^{12}$ dyne $cm^{-2}$. Figure 4 shows the phonon dispersion of $UO_2$ calculated with and without spin polarization. The acoustic phonon frequencies appear unaffected by magnetic moments, consistent with the elastic moduli results above. The optical phonon frequencies, however, change with the

introduction of magnetic moments and also depend on the relative direction of the moments on neighboring atoms. Calculations for treating the strong electron correlation in the 5f orbitals used the LDA+U method. The effect that varying the Hubbard potential has on the equilibrium volume for $UO_2$ was investigated. The influence of changing the stoichiometry of $UO_{2-x}$ from x=0 to x=0.25 also was considered. Calculations with a larger unit cell will reveal more details of how the influence depends on the value of x. DFT simulations also were performed for SiC. SiC can appear in a wide range of polymorphs, the most common form being a hexagonal crystal structure. The energy differences between the various structures are small. Thermal conductivity of a fuel element's constituents determines how high the operating temperature can be, an important parameter in determining the fuel's efficiency. For a material without dislocations and impurities, the temperature dependence of the thermal conductivity depends on the phonons, which can be readily calculated with DFT. The temperature dependence of the thermal conductivity of 3C-SiC calculated with DFT was in good agreement with measured data. In order to ascertain the behavior of the thermal conductivity with temperature and pressure, the phonon spectra of 3C-SiC was calculated at a sequence of volumes. The calculated phonon density of states (DOS) revealed the expected overall increase in frequencies. The temperature dependence of the thermal conductivity also was evaluated from the phonon DOS for the same sequence of volumes. The thermal conductivity for each volume revealed very little change with pressure.

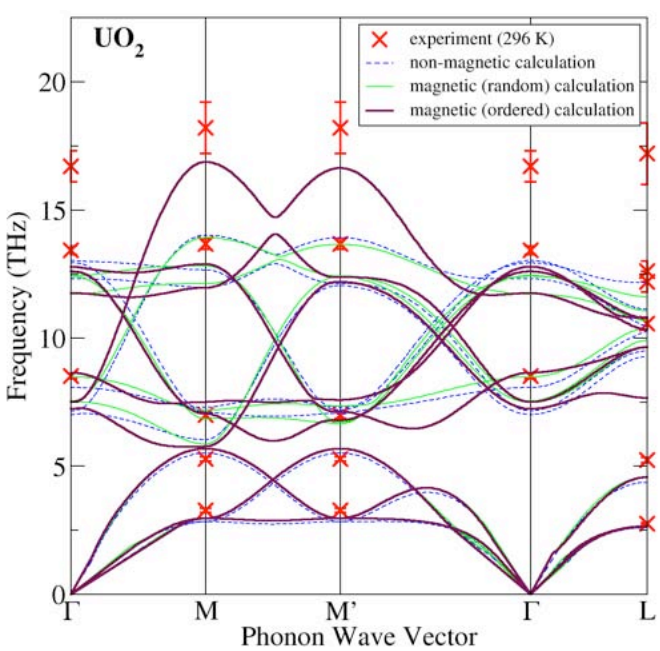


*Figure 4. DFT simulation, phonon dispersion.*

An assessment was made of the approaches for including radiative heat transfer in simulations of a TRISO fuel particle. Issues related to coupling radiation to a Lagrangian continuum description and the integration with materials undergoing progressive damage also were considered. The current method most commonly used for heat transfer simulations are view factors, which consider surface-to-surface radiative heat transfer. Utilizing the time-implicit Monte Carlo (IMC) methods and massively parallel software that are designed for thermal x-ray transport in high energy-density experiments would appear to be excessive. However, the stand-alone IMC analysis has been used to simulate heat transfer in a coal furnace, which is similar to the TRISO fuel problem. Given the number of questions on the behavior of the fuel particle, this approach appears warranted for direct numerical simulations and investigating how the radiative heat transfer interacts with continuum mechanics and material damage models. The IMC software at Los Alamos uses template concepts to allow the same physics coding to run with different meshes. The IMC software has an interface that is used for coupling to hydrodynamics. This approach has shown significant speedups on the Roadrunner architecture. Complementary approaches for neutron transport simulations include deterministic and Monte Carlo solvers. Well-established neutron/gamma transport computational methods are available at the Laboratory. For this application, a multi-geometry, multi-dimensional, multi-group, Sn(discrete-ordinates) deterministic transport approach that uses Adaptive Mesh Refinement (AMR) and is massively parallel is available. This method solves the linear Boltzman transport equation for both static and time-dependent problems in either forward or adjoint mode and allows for anisotropic scattering. The transport iterations are accelerated with diffusion or transport synthetic acceleration. Parallelization is achieved via a two-dimensional spatial decomposition using the KBA sweep algorithm. This approach has been benchmarked for a quarter core model with a mixture of $UO_2$ and MOX fuel assemblies, moderated with water. The assemblies are modeled to the individual pin level. Simulations were able to calculate pin powers that were in excellent agreement with MCNP. The neutron transport capability can run with the hundreds of energy groups and temperature-dependent cross sections that will be required for reactor simulations.

# Lifting the Quantum Critical Conundrum

*Joe David Thompson*

20061383PRD1

## Introduction

All materials undergo some form of phase transition that is induced by raising temperature. A well known example is the solid-liquid transition from ice to water. These classical, thermally-driven phase transitions are well understood, but there is another class of phase transitions that occur at absolute zero temperature and that are not driven by a change in temperature but instead arise because of purely quantum mechanical effects. A zero-temperature magnetic to non-magnetic phase transition induced by a non-thermal variable, such as a change in pressure, is an example of this class of quantum phase transitions. Unlike classical transitions, quantum transitions are not understood nor are the new states of matter that emerge from them. This is the quantum critical conundrum, a fundamental, unsolved problem at the forefront of materials physics. Unlike a thermally induced transition, which changes properties of a material over a narrow temperature interval around the transition, a quantum transition extends its influence over a wide temperature range above absolute zero to create quantum mechanically entangled states of electrons that give materials entirely new functions that could be harnessed for new technologies. Resolving the quantum conundrum is, thus, both a significant scientific and technologically relevant problem.

## Benefit to National Security Missions

Discovering and understanding new states of matter, such as high temperature superconductivity, offers the potential for previously unimagined new energy and sensor technologies relevant to DOE missions. Research in this project has the goal of uncovering the quantum nature of these new states, which is key to realizing new technologies.

## Progress

A commonly assumed theory of quantum criticality in a magnetic system considers the consequences of tuning a magnetic transition to absolute zero temperature. The validity of this theory, however, rests on the nature of the magnetic transition, which is conventionally taken to be a transition that arises from a magnetic instability of itinerant electrons – that is, electronics that roam freely through the material. Though there are a few examples where this theory appears to be consistent with experiments, there are many counter examples where it is unable to account for observations. To account for these discrepancies, a very different theory of magnetic criticality has been proposed in which the magnetic transition is assumed to develop among electrons that are localized. Unfortunately, this type of theory is very difficult and has not been able to calculate many physical properties of materials. Despite this problem, a few basic consequences of this so-called local or Kondo-breakdown type of magnetic criticality are known. These consequences are quite distinct from the commonly assumed form of criticality. In particular, a local quantum phase transition is more 'violent,' creating a change in the number of electronic states that contribute to electrical conduction. This change is not allowed in the more traditional theory. Because of its violent nature, it has been assumed that local quantum criticality would not lead to the spectrum of magnetic and electronic fluctuations that is needed for creating superconductivity. Progress this year has shown that this assumption is not valid.

The strongly correlated electron compound $CeRhIn_5$ is magnetic at atmospheric pressure; its magnetism develops among localized 4f electron on the cerium ion. Previously, we have shown [1] that applying pressure to $CeRhIn_5$ induces a phase of coexisting magnetism and unconventional superconductivity below a critical pressure P1 and that there is a field-induced magnetic quantum transition at a higher pressure P2 inside a purely unconventional superconducting phase. Using specific heat measurements, we have established that superconductivity coexists with localized, magnetic 4f electrons below P1, and that at P1 there is pronounced change in the topology and nature of electronic states that is a continuation of field-induced quantum phase transition at P2. These discoveries were published in the Proceedings of the National Academy of Science [2].

Though important, this study was unable to show definitely the nature of the criticality at P2 and its relationship to pressure-induced superconductivity. From a detailed investigation of the anisotropic electrical resistivity of $CeRhIn_5$ at pressures up to 5 GPa and magnetic fields up to 14 T, we discovered strong evidence that the criticality at P2 is of the local type and that fluctuations associated with local quantum criticality are responsible for superconductivity. In addition, these measurements revealed totally unexpected consequences of local criticality, namely that it induces a very unusual sub-linear temperature dependence to the resistivity, which we showed theoretically is a consequence of the electronic structure of $CeRhIn_5$, and that it induces isotropic scattering of itinerant electrons. This work, recently accepted in the journal Nature [3], represents a major step in lifting the quantum critical conundrum and sets new directions for scientific inquiry.

To understand the relationship between coexisting antiferromagnetism and superconductivity in $CeRhIn_5$, we developed a new capability of field-angle dependent specific heat measurements under pressure. This capability is unique and was used to determine, for the first time in any pressure-induced superconductor, the nature of the superconducting energy gap, in this case for $CeRhIn_5$ [4]. In contrast to some theoretical predictions for the gap structure, these measurements showed that the unconventional gap contained only line nodes, which places new constraints on any theory of gap structure in a phase of coexisting magnetic and superconducting orders.

In the course of this research, the scientific community was surprised by reports of superconductivity near 50 K in two new families of materials, each of which contains layers of FeAs. Like the high-temperature superconductors based on CuO structural units, superconductivity in these new materials is induced by electronic doping that suppresses a magnetic transition. By applying pressure to a new member of these families $CaFe_2As_2$, we have shown for the first time that superconductivity can be induced without electronic doping. This discovery, accepted overnight for publication in the Journal of Physics: Condensed Matter [5], suggests that these new superconductors may be more like $CeRhIn_5$ than the CuO superconductors in which only electronic doping induces superconductivity. In follow-on studies, we have found a complex relationship between pressure-induced superconductivity, magnetism, and crystal structure that suggests superconductivity may be mediated by magnetic excitations within a magnetically frustrated state [6].

## Future Work

This research explores and seeks to understand new states of matter that arise in quantum-critical metals, especially in the context of unconventional superconductivity that develops as a magnetic transition is tuned to absolute zero temperature. Though there has been circumstantial evidence that unconventional superconductivity may be created by an attractive pairing interaction provided by magnetic quantum-critical fluctuations, our recent discoveries of a field-induced magnetic quantum-critical phase inside the unconventional superconducting state of $CeRhIn_5$ now provide very strong evidence for this belief. This result also at least partially lifts the so-called quantum-critical conundrum posed by Laughlin. The generality of this discovery, however, must be established from a set of well-defined experiments in related systems in which it also is believed that quantum-critical fluctuations may mediate unconventional superconductivity. Three classes of unconventional superconductors are well-suited for these purposes: the most widely studied and parental high-Tc compounds $La_{2-x}Sr_xCuO_4$, heavy fermion $CeMIn_5$ (M=Co, Ir, Rh), and the organic superconductors k-(BEDT-TTF)2X. Specific heat effect measurements under high pressures and high magnetic fields are being used as a principal means to locate and explore the quantum criticality as well as to provide key tests of various theoretical models. Other complementary techniques, such as electrical resistivity, magnetic susceptibility, and neutron scattering, will be used as appropriate to provide additional detailed understanding of essential interactions.

## Conclusion

Major scientific directions upon which the future of the country rests include bioscience and its implications for health security, the quantum frontier that encompasses nanoscience and related areas, energy production and conservation, and materials physics from which new technologies and surety of the nuclear stockpile will emerge. These are key missions of the DOE. The research pursued in this project contains elements of the last three directions: a fundamental understanding of materials physics at the intrinsically quantum scale that will underpin new energy technologies and surety of the nuclear stockpile.

## References

1. Park, T., F. Ronning, Y. Q. Yuan, M. Salamon, R. Movshovich, J. L. Sarrao, and J. D. Thompson. Hidden magnetism and quantum criticality in the heavy-fermion superconductor CeRhIn5. 2006. *Nature.* **440**: 65.

2. Park, T., M. J. Graf, L. Boulaevski, J. L. Sarrao, and J. D. Thompson. Electronic duality in strongly correlated matter. 2008. *Proceedings of the National Academy of Science.* **105**: 6825.

3. Park, T., V. A. Sidorov, F. Ronning, J. X. Zhu, Y. Tokiwa, H. O. Lee, E. D. Bauer, R. Movshovich, J. L. Sarrao, and J. D. Thompson. Isotropic quantum scattering and unconventional superconductivity. To appear in *Nature.*

4. Park, T., E. D. Bauer, and J. D. Thompson. Probing the nodal gap in the pressure-induced heavcy-fermion superconductor CeRhIn5. 2008. *Physical Review Letters.* **101**: 177002.

5. Park, T., E. Park, H. O. Lee, T. Klimczuk, E. D. Bauer, F. Ronning, and J. D. Thompson. Pressure-induced superconductivty in CaFe2As2. 2008. *Journal of Physics: Condensed Matter.* **20**: 322204.

6. Lee, H. O., E. Park, T. Park, F. Ronning, E. D. Bauer, and J. D. Thompson. Magnetism, superconductivity and structure in CaFe2As2. *Physical Review Letters.*

## Publications

Jelbert, G., T. Sasagawa, J. D. Fletcher, T. Park, J. D. Thompson, and C. Panagopoulos. Measurement of low energy charge correlations in underdoped spin-glass La-based cuprates using impedance spectroscopy. To appear in *Physical Review B.*

Lee, H. O., E. Park, T. Park, F. Ronning, E. D. Bauer, and J. D. Thompson. Magnetism, structure and superconductivity in CaFe2As2. *Physical Review Letters.*

MenoncaFerreira, L., T. Park, V. A. Sidorov, M. Nicklas, E. M. Bittar, R. Lora-Serrano, E. N. Hering, S. M. Ramos, M. B. Fontes, E. Baggio-Saitovich, H. O. Lee, J. L. Sarrao, J. D. Thompson, and P. G. Pagliuso. Tuning the pressure-induced superconducting phase in doped CeRhIn5. 2008. *Physical Review Letters.* **101**: 0175005.

Nicklas, M., O. Stockert, T. Park, K. Habicht, K. Kiefer, L. D. Pham, J. D. Thompson, Z. Fisk, and F. Steglich. Magnetic structure of Cd-doped CeCoIn5. 2007. *Physical Review B.* **76** (5): 052401.

Park, E., T. Park, J. L. Sarrao, and J. D. Thompson. Evidence for correlation between spin and charge dynamics in La2Cu1-xLixO4. *Journal of Applied Physics.*

Park, T., E. D. Bauer, and J. D. Thompson. Probing the nodal gap in the pressure-induced superconductor CeRhIn5. 2008. *Physical Review Letters.* **101**: 177002.

Park, T., E. Park, H. O. Lee, T. Klimczuk, E. D. Bauer, F. Ronning, and J. D. Thompson. Pressure-induced superconductivity in CaFe2As2. 2008. *Journal of Physics: Condensed Matter.* **20**: 322204.

Park, T., F. Ronning, H. Yuan, M. B. Salamon, R. Movshovich, J. L. Sarrao, and J. D. Thompson. Hidden magnetism and quantum criticality in the heavy fermion superconductor CeRhIn5. 2006. *Nature.* **440**: 65.

Park, T., J. L. Sarrao, and J. D. Thompson. New quantum phase in the heavy-fermion superconductor CeRhIn5. 2007. *Physica C.* **460**: 137.

Park, T., J. L. Sarrao, and J. D. Thompson. Upper critical field scaling near a quantum critical point in the heavy-fermion compound CeRhIn5. 2007. *Journal of Magnetism and Magnetic Materials.* **310**: 712.

Park, T., M. J. Graf, L. Boulaevskii, J. L. Sarrao, and J. D. Thompson. Electronic duality in strongly correlated matter. 2008. *Proceedings of the National Academy of Sciences.* **105**: 6825.

Park, T., V. A. Sidorov, F. Ronning, J. X. Zhu, Y. Tokiwa, H. O. Lee, E. D. Bauer, R. Movshovich, J. L. Sarrao, and J. D. Thompson. Isotropic quantum scattering and unconventional superconductivity. To appear in *Nature.*

Park, T., Y. Tokiwa, E. D. Bauer, F. Ronning, R. Movshovich, J. L. Sarrao, and J. D. Thompson. Normal state properties at a field-tuned quantum-critical point in the heavy-fermion superconductor CeRhIn5. 2008. *Physica B.* **403**: 934.

Pham, L. D., T. Park, S. Marquilon, J. D. Thompson, and Z. Fisk. Reversible tuning of the heavy-fermion ground state in CeCoIn5. 2006. *Phys. Rev. Lett..* **97**: 056404.

# Synthesis of Molecular Actinide Nitrides

*David Lewis Clark*

20061395PRD1

## Introduction

Many of the important properties that make actinide nitrides desirable as fuels are related to their electronic structure, which has been particularly difficult to determine experimentally. In this work, we employ recent developments in electronic structure theory and x-ray spectroscopy to probe how the relative roles of atomic orbitals manifest themselves in the chemical bonding of these fascinating materials. To accomplish this we have focused on development of two synchrotron x-ray experiments: ligand K-edge x-ray absorption spectroscopy (XAS) and non-resonant inelastic x-ray scattering (NRIXS). By combining the intensity data from NRIXS with the energy resolution of XAS, we can determine the roles of 5f and 6d orbitals in metal-ligand bonding, and how they interact with light atoms such as nitrogen to make up metal-nitrogen bonds. Changes in the covalency will result in changes in properties of materials. Electronic structure calculations are used as a guide to develop peak assignments in comparison to the experiments. The combination of these techniques to study light atoms and covalency in actinide materials is unique in the world*. The project goal is to develop new understanding of synthesis and electronic structure in advanced nuclear fuel materials that should make these advanced fuels more accessible for reactor and accelerator based systems.

## Benefit to National Security Missions

The project goal is to develop new understanding of synthesis and electronic structure in advanced nuclear fuel materials. This new understanding should make these fuels more accessible for reactor and accelerator based systems. This work provides a foundation that the DOE can use in meeting its AFCI and GEN4 goals

## Progress

As part of our effort to understand fundamental electronic structure of nitrogen-containing materials, we have developed a unique capability to measure core-electron transitions from nitrogen to empty 5f and 6d orbitals on actinide metal centers (Th, U, Np, Pu). Two approaches have been developed in parallel – ligand K-edge X-ray Absorption Spectroscopy (XAS) and non-Resonant Inelastic X-ray Scattering (NRIXS). Light atom x-ray spectroscopy turned out to be far more complicated than originally envisioned. In ligand K-edge XAS, one can examine bound state transitions in the x-ray absorption spectrum of ligand atoms (N, O, C, etc.) that arise due to covalent mixing between the metal and ligand atom (N, O, etc.). The intensity of the transition provides a direct measure of the relative contributions of 5*f* and 6*d* atomic orbitals in actinide metal-ligand bonding. At the extremely low energies of the first row atoms (N, O), XAS suffers from x-ray self-absorption effects. Another way to obtain the same information is through non-resonant inelastic x-ray scattering (NRIXS). The x-ray scattering is not subject to self-absorption, but does suffer from lower resolution and longer data acquisition time. By combining the intensity data from NRIXS with the energy resolution of XAS, we can determine the roles of 5*f* and 6*d* orbitals in metal-ligand bonding, and how they interact with light atoms such as nitrogen to make up metal-nitrogen bonds. Changes in the covalency will result in changes in properties of materials. Electronic structure calculations are used as a guide to develop peak assignments in comparison to the experiments.

For light atom XAS we developed an Ultra-High Vacuum (UHV) chamber that has been employed at the Stanford Synchroton Radiation Laboratory (SSRL). The experimental chamber is equipped with specialty detectors and safety interlocks for handling radioactive materials that are suitable for UHV operation. For XAS detection, we have utilized photodiode and total electron yield (TEY) detectors to collect both fluorescence yield and photo current, respectively. To handle radioactive materials, we have developed a means to encapsulate samples in a polystyrene/graphite matrix, and coat the surface with 10-12 angstroms of vapor deposited carbon as both

near 400 eV was not reproducible, so we moved to oxygen XAS near 525 eV. We now have excellent XAS data

and theoretical calculations on several oxygen and nitrogen containing compounds. One problem has been the comparison of intensities between fluorescence and total electron yield. Accurate intensity data is key to extracting the percent covalency in the metal-nitrogen or metal-oxygen bond.

An alternate way to obtain accurate intensity information is through a non-resonant inelastic x-ray scattering (NRIXS) experiment, sometimes referred to as x-ray Raman scattering. The x-ray scattering is not subject to self-absorption, but does suffer from lower resolution and longer data acquisition time. We have taken the same suite of compounds to the Advanced Photon Source (APS) at Argonne National Laboratory to study the NRIXS in collaboration with Professor Jerry Seidler (University of Washington). After some effort, we have developed the capability to obtain NRIXS data on the same suite of compounds. To date, we have only completed with NRIXS experiment with a suite of oxygen-containing compounds, but it gives exact intensity data, and has shown that we can rely on the intensities determined by fluorescence yield in the XAS measurement. This represents a major breakthrough. We show a comparison of the NRIXS and TEY data for $NaReO_4$ in Figure 1, where it can be seen that total electron yield gives good intensity data.

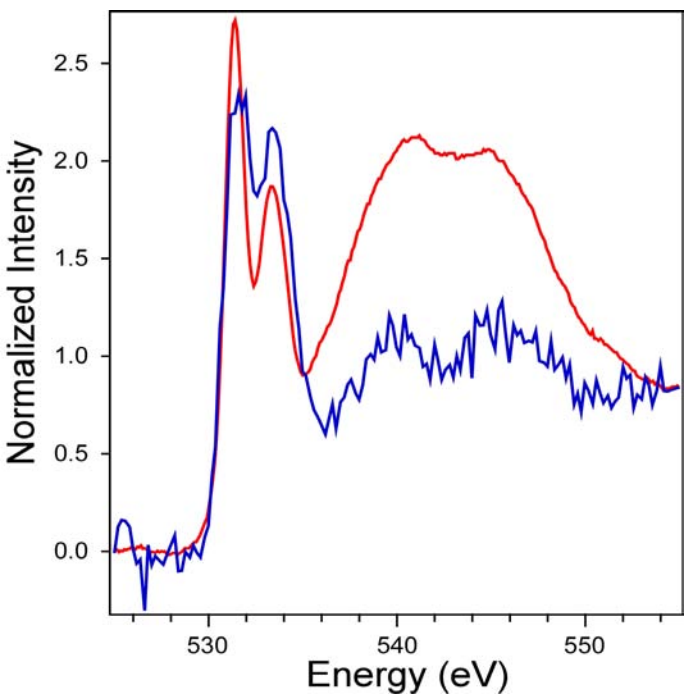


*Figure 1. A comparison of Non-resonant Inelastic X-ray Scattering (blue) and Total Electron Yield (red) detection of the oxygen K-edge for $NaReO_4$.*

## Future Work

By combining the intensity data from NRIXS with the energy resolution of XAS, we can determine the roles of 5f and 6d orbitals in metal-ligand bonding, and how they interact with light atoms such as nitrogen to make up metal-nitrogen bonds. Changes in the covalency will result in changes in properties of materials. Electronic structure calculations are used as a guide to develop peak assignments in comparison to the experiments. We will publish several papers on the development of the capability to perform light atom XAS measurements, and then attempt to obtain reasonable nitrogen spectra this winter.

## Conclusion

The chemical properties of nitrides that make them useful as nuclear fuels are governed by hybridization and covalency between the atomic orbitals that make up the metal-nitrogen bonds within the materials. New approaches to study the covalency in these systems is under development to provide new insights into the nature of bonding, and the factors that control the desirable properties of advanced nitride fuels.

## Publications

Clark, D. L., E. R. Batista, K. S. Boland, C. J. Burns, S. D. Conradson, S. A. Kozimor, P. J. Hay, R. L. Martin, D. E. Schwarz, M. P. Wilkerson, L. E. Wolfsberg, and P. Yang. Applications of X-ray absorption spectroscopy to the electronic structure of actinide ions. 2008. *Abstracts of Papers, 235th ACS National Meeting, New Orleans, LA, United States, April 6-10..* : NUCL.

Clark, D. L., E. R. Batista, K. S. Boland, C. J. Burns, S. D. Conradson, S. A. Kozimor, R. L. Martin, D. E. Schwarz, M. P. Wilkerson, L. E. Wolfsberg, and P. Yang. On the relative roles of 5f and 6d orbitals in uranium metal-ligand bonds. 2008. *Abstracts of Papers, 235th ACS National Meeting, New Orleans, LA, United States, April 6-10..* : INOR.

Conradson, S. D., A. Andersson, K. Boland, D. L. Clark, S. Kozimor, and X. J. Espinosa-Faller. Addressing the structural chemistry of UO2+x and PuO2+x with laboratory and computer experiments. 2008. *Abstracts of Papers, 235th ACS National Meeting, New Orleans, LA, United States, April 6-10..* : NUCL.

Graves, C. R., P. Yang, S. A. Kozimor, A. E. Vaughn, D. L. Clark, S. D. Conradson, E. J. Schelter, B. L. Scott, J. D. Thompson, P. J. Hay, D. E. Morris, and J. L. Kiplinger. Organometallic uranium(V)-imido halide complexes: from synthesis to electronic structure and bonding. 2008. *Journal of the American Chemical Society.* **130** (15): 5272.

Kozimor, S. A., E. R. Batista, K. S. Boland, C. J. Burns, C. N. Christensen, D. L. Clark, S. D. Conradson, P. J. Hay, R. L. Martin, D. E. Schwarz, M. P. Wilkerson, and P. Yang. Covalency trends in metallocene dichlorides (M = Ti, Zr, Hf, Th, U). A chlorine K-edge XAS study. 2008. *Abstracts of Papers, 235th ACS National Meeting, New Orleans, LA, United States, April 6-10..* : INOR.

Kozimor, S. A., E. R. Batista, K. S. Boland, J. M. Boncella, C. J. Burns, D. L. Clark, S. D. Conradson, R. L. Gdula, C. R. Graves, P. J. Hay, J. L. Kiplinger, L. P. Spencer, L. R. Martin, M. P. Wilkerson, L. P. Wolfsberg, and P. Yang. Utilizing oxygen k-edge X-ray absorption spectroscopy to compare covalency for d- and f-block metals. 2008. *Abstracts of Papers, 235th ACS National Meeting, New Orleans, LA, United States, April 6-10..* : NUCL.

Kozimor, S. A., P. Yang, E. R. Batista, K. S. Boland, C. J. Burns, C. N. Christensen, D. L. Clark, S. D. Conradson, P. J. Hay, J. S. Lezama, R. L. Martin, D. E. Schwarz, M. P. Wilkerson, and L. E. Wolfsberg. Covalency Trends in Group IV Metallocene Dichlorides. Chlorine K-Edge X-Ray Absorption Spectroscopy and Time Dependent-Density Functional Theory. 2008. *Inorganic Chemistry.* **47** (12): 5365.

Wilkerson, M. P., J. M. Berg, D. L. Clark, S. D. Conradson, D. E. Hobart, and S. A. Kozimor. Electronic structure measurements of Cs2Np(VI)O2Cl4 using fluorescence emission and ligand k-edge X-ray absorption spectroscopies. 2008. *Abstracts of Papers, 235th ACS National Meeting, New Orleans, LA, United States, April 6-10..* : NUCL.

Yang, P., E. R. Batista, P. J. Hay, R. L. Martin, C. N. Carlson, D. L. Clark, S. D. Conradson, S. A. Kozimor, D. E. Schwarz, and M. P. Wilkerson. Quantification of covalency in An-Cl bonds. 2007. *Abstracts of Papers, 234th ACS National Meeting, Boston, MA, United States, August 19-23..* : NUCL.

continuing project

# Accelerated Molecular Dynamics at Complex Interfaces

*Arthur Ford Voter*

20061524PRD3

## Introduction

This project is aimed at extending the applicability of the accelerated molecular dynamics (AMD) methods recently developed at Los Alamos. These methods offer a way to extend the duration of atomistic simulations of materials by orders of magnitude, e.g., from nanoseconds to milliseconds, and sometimes beyond. However, these AMD methods have not been suitable for treating systems with certain types of complexity, such as a solid surface in contact with a liquid. The reason the AMD approach cannot be directly applied in this case is because in the liquid phase the transitions from one energy basin to another take place extremely rapidly, while the AMD methods can offer speedup when the time between these transitions is very long. In this project, the AMD methods will be generalized, as much as possible, to treat these types of complex systems. This will open the possibility of studying technologically important processes such as corrosion and fuel cell operation at the atomic scale. A more far-reaching goal, if we are successful, will be the ability to treat biological processes such as protein folding and DNA dynamics. In this project we will also focus on finding general algorithmic and numerical improvements that can increase the efficiency of the AMD methods.

## Benefit to National Security Missions

Processes of importance in relation to Energy and Science DOE missions involve complicated dynamical evolution in solid materials, at surfaces, and at the solid-liquid interface. Examples include film growth, stress-corrosion cracking, electrochemical processing, fuel cells, and catalysis. This new methodology will allow the first simulations on the time scale of microseconds and beyond for systems of this type. This project thus benefits DOE missions in Energy Security, Nuclear Security, Environmental Responsibility, and Scientific Discovery and Innovation.

## Progress

This last year has been mainly dedicated to further developments of the accelerated dynamics methodology and software tools. Most notably, we proposed and implemented a self-learning hyperdynamics method, a significant improvement to the original hyperdynamics formalism developed in Los Alamos in 1997 [1]. This new algorithm [2] automatically tunes itself to the system at hand without the user's intervention, yielding optimal performances in a safe and efficient fashion. An example of the power of this approach for surface diffusion processes is shown in Figures 1 and 2. Our method makes the application of accelerated dynamics much easier while providing statistical confidence levels on the quality of the simulation results. The accuracy and efficiency of the method is described in a publication we have submitted [3]. The method has also been showcased at different international and national events throughout the year.

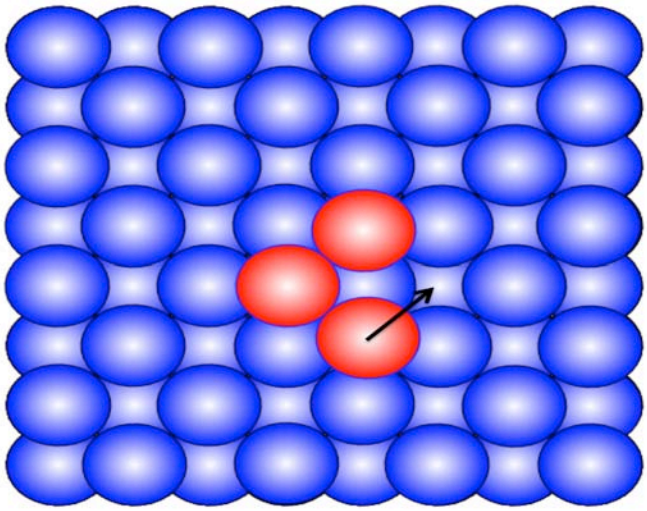

*Figure 1. Silver trimer on Ag(100) surface, showing one pathway for a transition to a new state. The barrier for this pathway is 0.217 eV, and repeated occurrences of this type of mechanism cause the trimer to "spin," a common phenomenon in metallic overlayers on (100) surfaces. This Ag3/Ag(100) system was used for the demonstration of the new self-learning bond boost hyperdynamics method shown in Figure 2.*

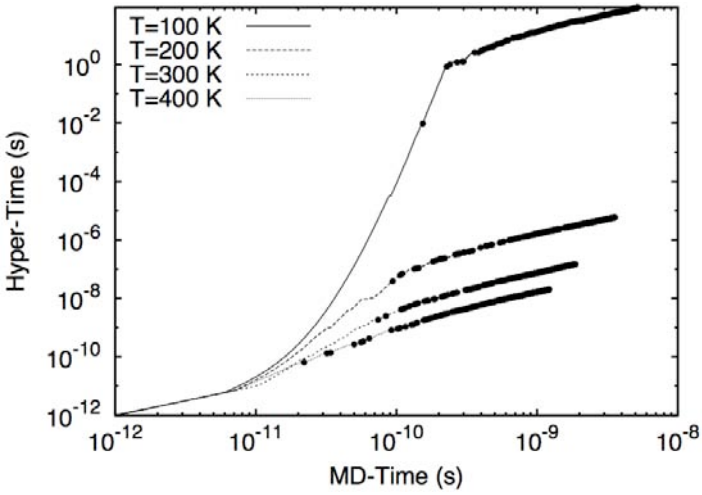


*Figure 2. Evolution of hypertime as a function of molecular dynamics (MD) time for the dynamics of a silver trimer on the Ag(100) surface (see Figure 1), using the new self-learning simplified bond boost bias potential. The filled symbols indicate the times at which transitions occurred. At first, the bias strength is zero, and the hyper-time is the same as the MD time (boost=1). As the algorithm learns about the potential basin, the bias potential turns on and increases in strength. This causes the hyper-time to increase exponentially. In this case, all transitions lead to a symmetry equivalent state, so the self-learning bias strength continues to increase even though transitions are occurring, until it levels out at the maximum safe value. The overall boost factor can become huge when the temperature is low. For example, at T=100K, the second transition occurs at a time of one second, corresponding to a boost factor of almost ten billion compared to normal MD.*

Algorithmic improvements also have been proposed to another accelerated dynamics method, namely the parallel replica method [3], in order to improve it's scaling as the number of processors is increased. Through the use of speculative execution that allow for the overlap of various tasks and more aggressive book-keeping that enable efficient reuse of information within and between simulations, the overhead of the method is significantly reduced. These improvement are particularly important given the increasing availability of massively parallel computing systems.

Both these improvements were integrated into our new computing framework, AMD, yielding a unique capability for long timescale atomistic simulations. Indeed, this framework now enables us to combine the power of both hyperdynamics and parallel replica dynamics into a single hybrid method, opening the door to multiplicative increases in the timescales that can be reached using atomistic simulations.

The aforementioned computational framework also transitioned from development to production during the past year, demonstrating the power of these methods to address technologically relevant material-related problems.

In collaboration with Chun-Wei Pao, we began to apply self-learning hyperdynamics and parallel replica dynamics [3] to the study of the mechanical properties and formation processes of metallic nanowires (funded under a new LDRD-ER project, 20080759ER). These nanostructures are foreseen as playing a major role in the next generation of electronic and nano-mechanical devices. They further offer a unique test bed to probe the nanoscale limit of elasticity and plasticity theories, two questions of considerable fundamental importance. Our simulations provide a unique insight into the behavior of these systems by providing a complete view of their evolution in full atomistic details on length and timescales that approach that of actual probe experiments. Indeed, our simulations are now able to access hundred-fold longer timescales compared to the previous state-of-the-art.

We have also been applying the methods in collaboration with Prof. Ashlie Martini at Purdue University, to study atomic-level stick-slip friction. An example of this kind of simulation is shown in Figure 3. Prof. Martini and Prof. Rob Carpick (a friction-force microscopy experimentalist at University of Pennsylvania) have secured funding from the National Science Foundation, in part based on the power and promise of the accelerated molecular dynamics methods for reaching long time scales so that direct comparisons can be made between simulation and experiment.

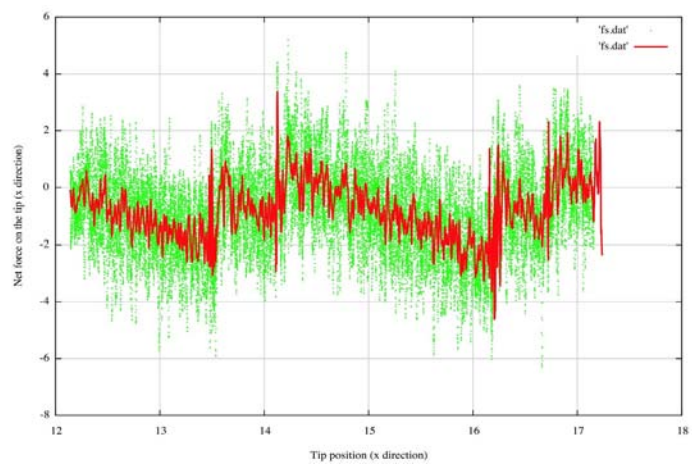


*Figure 3. Force curve showing stick-slip behavior during a driven parallel-replica dynamics simulation of a small atomic force microscope (AFM) tip dragging along a (111) surface. In this case, both the AFM tip and the surface are modeled as copper using an embedded atom interatomic potential. The tip slips from fcc registry to hcp registry and repeats this, spending less time in hcp registry because it is a less stable state (just as it is less stable in the normal crystal stacking). This particular simulation utilized only a few processors, but this type of simulation can be scaled up to thousands of processors to simulate very slow tip velocities if desired.*

The latest algorithmic improvements in the parallel replica dynamics implementation are also being put to the test in a collaboration with John Hamilton at Sandia California, in

a study of silver clusters on the (100) surface of copper. He has discovered that certain magic cluster sizes (e.g., 169 atoms) exhibit ultra fast diffusion with surprisingly complex mechanisms. We are using our AMD tools to help him understand these mechanisms.

## Future Work

Molecular dynamics (MD) has become a powerful tool in chemistry, physics, materials science. Given an interatomic potential, MD gives the dynamical evolution of the system with no prior assumptions about the kinds of reaction mechanisms that might occur. The problem with MD is that it is limited to nanosecond snapshots, while many important processes take microseconds or longer to complete. Accelerated molecular dynamics (AMD) methods, developed by us here at LANL, circumvent this problem for "infrequent" systems. With these methods, we can reach much longer time scales by compressing the time between the infrequent events. A limitation of these AMD methods is that they have only been developed so far for systems with well defined transitions between well-defined states, typically (though not necessarily) involving well-defined barriers. In the present project, we will extend these methods to treat systems that are more complex, and in particular for systems with coexisting liquid and solid phases. At the solid-liquid interface the transitions may still be well defined, but only if one overlooks the coordinates of the atoms in the liquid phase. We will modify the AMD procedures to exploit this concept and hopefully achieve substantial acceleration of the solid-material dynamics. In the case of hyperdynamics, the key will be to base the bias potential purely on the solid coordinates. For parallel-replica dynamics, where detecting transitions is the main requirement, the definition of a transition will exclude the liquid coordinates. Our first tests will be for diffusion on a metal surface in contact with water. A potential hurdle is that the liquid-solid interaction may be too strong to simply ignore the liquid coordinates. As we develop robust procedures, we will extend the simulations to more complex systems, such as electrochemical etching and deposition. We will also seek general algorithmic improvements.

## Conclusion

We are extending the accelerated molecular dynamics approach to treat more complex systems, such as solid-liquid interfaces. This will be achieved for the hyperdynamics and parallel replica dynamics methods, and perhaps for the temperature accelerated dynamics approach as well. The first test application for this project will be diffusion on a metal surface in contact with water or some other liquid. Later applications will include electrochemical deposition. We will also develop general algorithmic and numerical improvements that can increase the efficiency and accuracy of the methods in general. Already the algorithmic improvements are proving valuable in collaborations with theorists and experimentalists at other institutions.

## References

1. Voter, A. F.. Hyperdynamics: Accelerated molecular dynamics of infrequent events. 1997. *Physical Review Letters.* **78**: 3908.
2. Perez, D., and A. F. Voter. Accelerating atomistic simulations through self-learning bond-boost hyperdynamics. *Journal of Chemical Physics.*
3. Voter, A. F.. Parallel replica method for dynamics of infrequent events. 1998. *Physical Review B.* **57**: 13985.

## Publications

Perez, D., and A. F. Voter. Accelerating atomistic simulations through self-learning bond-boost hyperdynamics. *Journal of Chemical Physics.*

# A Chemical Route to Integrate Carbon Nanotubes into Microelectromechanical Systems

*Quanxi Jia*

20061615PRD4

## Introduction

Carbon nanotubes (CNTs) are amongst the strongest known fibers. Carbon nanotubes can undergo large nonlinear deformations or even buckling without permanent damage to the atomic structure, and have demonstrated exceptionally high thermal conductivity. These unique properties allow for many potential nanosystem functions such as large non-linear deflections in nanotube-supported structures, and resonant sensors with molecular level mass sensitivity. However, the electromechanical traits of CNTs have typically been characterized using atomic force microscopy. In this project, we will use microsystem technology as a flexible platform to study the mechanical and electrical properties of CNTs. In other words, we will go beyond the current practice by using microsystem technology to test CNTs for their mechanical deformation and electrical sensing properties.

## Benefit to National Security Missions

This project supports DOE's missions in nanotechnology, energy security, and sensors for threat reduction applications. This work opens the way to the electromechanical characterization of CNTs. It will provide a better understanding of the fundamental physics of novel materials.

## Progress

In the last review period, the director funded postdoc fellow (Guifu Zou) has made tremendous progress. The following highlights our accomplishments. More detailed technical achievements can be found form our technical publications.

We have used a chemical route to connect CNTs to a silicon surface using hydrogen bonds and electrostatic interactions. This connection scheme works at room temperature. In other words, molecular interaction in chemistry provides a simple and flexible route to the integration of CNTs with silicon. We used polyethylenimine (PEI) as a reagent. It is well known that there are many nitrogen atoms in cationic polymers. The positive nitrogen charges facilitate the hydrogen bonding and electrostatic interactions between molecules. Furthermore, PEI is a soluble reagent under physiological conditions. Therefore, this technology can be potentially applied to nano-biomedical therapeutic devices.

The connection between the CNTs and silicon was verified by scanning electron microscopy (SEM). SEM shows an intact CNT fiber, which is 8.2 μm in diameter and 5 cm in length. The CNT fiber appears compact. Dispersed oxidized tips of CNT fiber show the substantial area of contact between the CNTs and the silicon. It should be noted that it is easy to join PEI terminated Si and CNT via electrostatic interactions. SEM clearly shows that many carbon nanotubes around the fiber tip are in good contact with the silicon. Furthermore, the CNT fibers keep their pristine structure and shape. This preservation of CNT integrity is important since it takes a change of only about 1 in 100 carbons along CNTs to substantial change their electrical/optical properties. In addition, the active central parts of CNTs will be perturbed if its surface structure is damaged. Therefore, the Si-PEI-CNT junction that we have developed could supply the basis for linking CNTs to precise locations in electronic, optical, and sensor arrays.

We have also prepared CNT - polymer polyethyleneimine (PEI) composite films by a spin-coated process. This solution is composed of homogeneous long CNTs in water-soluble PEI. Due to long length CNTs and their easy loading in PEI, the CNT/PEI composite films exhibit enhanced conductivity. The conductivity of the composite films steadily improves as the concentration of CNTs increases. However, the conductivity of the composite tends to saturate as the CNTs network becomes increasingly compact. The highest conductivity of the CNT/PEI films is around 43.73 S/cm at CNT concentration of 3%. Furthermore, as-coated CNT/PEI composite films are vulnerable to dissolution in water.

## Future Work

As mechanical elements, carbon nanotubes (CNTs) are amongst the strongest known fibers. CNTs can undergo large nonlinear deformations or even buckling without permanent damage to the atomic structure. They also show exceptionally high thermal conductivity. These unique properties allow for many potential nanosystem functions such as large non-linear deflections in nanotube supported structures and resonant sensors with molecular level mass sensitivity. However, the electromechanical traits of CNTs have typically been measured using atomic force microscope where one applies a force on suspended CNTs while measuring the electrical conductivity. We can go beyond the current achievements by using microsystem technology as a flexible platform for system design to mechanically deform and electrically sense CNTs.

We will use the following chemical route to integrate CNTs into microelectromechanical system and demonstrate our technical concept:

1. In the first instance, CNTs and chips are obtained. The chips are spin coated by polymethyl methylacrylate (PMMA). The spots on the chips to be connected by CNTs are exposed using electron beam lithography.

2. Since the tip of CNTs possesses higher reactivity than their walls, we can easily functionalize the tip of CNTs using chemical methods at room temperature. Similarly, the defined spots for adding CNT on chip can be functionalized through chemical modification. We can easily bond some of the corresponding groups on the surface of polysilicon. Once this has been done, the remaining PMMA is stripped from the chips using acetone in ultrasonic vibration.

3. In the final step, the chip with functionalized spots is immersed in the solution of containing functionalized CNTs. Carbon nanotubes can spontaneously bridge the trench of the chip through bonding effect of two tips of CNTs and two spots of chip under appropriate chemical conditions.

## Conclusion

We have used a chemical route to connection of CNTs to a silicon surface based on hydrogen bonds and electrostatic interactions at room temperature. We have also prepared CNT - polymer polyethyleneimine (PEI) composite films by a spin-coated process. We are currently investigating the use of chemical modification to integrate CNTs into microelectromechanical systems. In addition, we are developing direct and reliable measurement techniques to accelerate the identification of CNTs properties.

## Publications

Zhou, G., M. Jain, H. Yang, Z. Y. Wang, Y. Y. Zhang, D. Williams, and Q. X. Jia. Highly Conducting Water-Soluble Carbon-Nanotube Composite films. *J. Am. Chem. Soc.*

Zou, G., H. yang, M. Jain, H. H. Zhou, D. Williams, M. Zhou, A. K. Burrell, T. M. McCleskey, and Q. X. Jia. Vertical connection of carbon nanotubes to silicon at room temperature using a chemical route. To appear in *Carbon.*

Zou, G., M. Jain, H. H. Zhou, H. M. Luo, S. A. Baily, L. Civale, E. Bauer, T. M. McCleskey, A. K. Burrell, and Q. X. Jia. Ultrathin Epitaxial Superconducting Niobium Nitride Films Grown by a Chemical Solution Technique. To appear in *Chem. Commun..*

Zou, G., M. Jian, H. Luo, T. M. McCleskey, A. K. Burrell, and Q. X. Jia. NbN films by chemical solution deposition. Presented at *APS March meeting.* (New Orleans, 10-14 March, 2008).

# Flexible Plastic Electrodes for Cheap Solar Cells

*Quanxi Jia*

20061630PRD4

## Introduction

Solar cells, which convert light into electrical power, provide for one of the best solutions for our future energy security. However, large-scale electricity production using solar cells remains a dream due to the high cost of fabricating solar cells. One of the expensive components in the solar cells are the electrodes, which are usually made of indium tin oxide (ITO). Due to limited resource of indium on earth, large-scale utilization of ITO will make it even more expensive in the future.

The objective of this project is to develop a cheap, novel carbon nanotube-polymer electrode material to replace the ITO. To accomplish the objectives, we will grow long carbon nanotube (CNT) arrays that are conducive to pulling out thin CNT sheets and to spinning nanotube fibers. We will then develop a method to pull highly oriented, free-standing CNT sheets. Furthermore, we will impregnate the CNT sheets and fibers with a polymer to form conductive CNT-polymer composites for electrode applications.

## Benefit to National Security Missions

This project directly contributes to DOE's mission in energy security by developing a cheap, novel carbon nanotube-polymer electrode material to replace the ITO.

## Progress

We have accomplished our technical objectives through the LDRD PRD support. The following highlights our accomplishments. More detailed technical achievements can be found in our technical publications.

We have grown long CNT arrays up to 4 mm using a chemical vapor deposition (CVD) process. Briefly, Fe/$Al_2O_3$ was used as the catalyst, ethylene served as the carbon source, and Ar with 6% $H_2$ was used to carry the precursor to a tube furnace where the growth took place. The reaction temperature was controlled at 750 C, while the reaction time varied between 15 and 180 min. We have found that the growth of CNTs mainly occurs in the first 90 min, and the further increase of reaction time has little effect on promoting the growth. Particularly, prolonging the time beyond 30 mi) dramatically decreases the spinnability of the CNT arrays, e.g., the spun fibers tend to break during the spinning of CNT arrays with increasing growth times. For instance, long fibers up to meters can be easily spun from the arrays grown in 15 min; short fibers with length of centimeters may be spun from the arrays grown in 40 min but easily break; while only short fiber clumps can be pulled out of the arrays grown in 180 min. This phenomenon may be related to the structure at the top surface of CNT arrays.

We have also developed a process for the synthesis of composite CNT/silica fibers in which CNTs are highly aligned. These composite fibers show much improved mechanical properties and electrical conductivities compared with CNT/silica films, powders or xerogels. The CNT/silica fibers show good tensile strengths due to the formation of cross-linked robust and strong silica networks. In addition, they don't have the drawbacks (e.g., aging and degradation) of CNT/polymer composite fibers and can be used in harsh environments such as high temperatures and strong acids/bases.

Furthermore, we have discovered a new type of carbon material – porous colossal carbon tubes. Compared with carbon nanotubes, colossal carbon tubes have a much bigger size, with a diameter of between 40 and 100 µm and a length in the range of centimeters. Significantly, the walls of the colossal tubes are composed of macroscopic rectangular columnar pores and exhibit an ultra low density comparable to that of carbon nanofoams. The porous walls of colossal tubes also show a highly ordered lamellar structure similar to that of graphite. Furthermore, colossal tubes possess excellent mechanical and electrical properties.

## Future Work

Solar cells, which convert light into electrical power, provide for one of the best potential solutions to the nation's renewable energy needs. However, large-scale electricity production using solar cells remains a dream

due to the high cost of fabricating solar cells. One of the expensive components in the solar cells is electrode, which is usually made of indium tin oxide (ITO). Due to limited resource of indium on earth, large-scale utilization of ITO will make it even more expensive in the future. A good ITO replacement needs to possess the following characteristics: low cost, good conductivity, excellent transparency, and good mechanical integrity.

As this project will be complete at the end of Oct. 2008, we will wrap up this project and explore new funding opportunities to support this effort.

## Conclusion

The goal of this project is to develop a flexible, cheap carbon nanotube-conducting polymer composite film that can replace ITO as electrodes for large-scale solar cell deployments to harvest solar energy. These cheap solar cells will be one of the choices for producing electricity, reducing pollution, and solving the energy crisis in the future.

## Publications

Peng, H. S.. Aligned carbon nanotube/polymer composite films with robust flexibility, high transparency, and excellent conductivity. 2008. *J. Am. Chem. Soc.* **130**: 42.

Peng, H. S., D. Y. Chen, J. Y. Huang, S. B. Chikkannanavar, J. Hanisch, M. Jain, D. E. Peterson, S. K. Doorn, Y. F. Lu, Y. T. Zhu, and Q. X. Jia. Strong and Ductile Colossal Carbon Tubes with Walls of Rectangular Macro-Pores. 2008. *Phys. Rev. Lett..* **101**: 145501.

Peng, H. S., M. Jain, D. E. Peterson, Y. T. Zhu, and Q. X. Jia. Carbon Nanotube/Silica Composite Fibers with Improved Mechanical Strengths and Electrical Conductivities. To appear in *Small.*

Peng, H. S., M. Jain, Q. W. Li, D. E. Peterson, Y. T. Zhu, and Q. X. Jia. Vertically-Aligned Pearl-like Carbon Nanotube Arrays for Fiber Spinning. 2008. *J. Am. Chem. Soc.* **130**: 1130.

Peng, H. S., Y. T. Zhu, D. E. Peterson, and Y. F. Lu. Nanolayeired carbon/silica superstructures via organosilane assembly. 2008. *Adv. Mater.* **20**: 1199.

Peng, H., Y. T. Zhu, D. E. Peterson, and Y. Lu. Nanolayered Carbon/Silica Superstructures via Organosilane Assembly. To appear in *Adv. Mater..*

# Molecular Actinide Alkylidene Complexes

*Jaqueline Kiplinger*

20070525PRD1

## Introduction

Transition metal alkylidene complexes have been shown to decompose polymers to produce gases. Similar transformations could be taking place in waste drums containing actinide materials and could provide an alternative explanation for the generation of gases in storage containers across the DOE complex. This project intends to develop entries into the synthesis of a new class of complexes that possess an actinide-carbon double bond (An=$CR_2$). Although transition-metal complexes possessing the terminal alkylidene functionality (metal-carbon double bond, M=$CR_2$, R = alkyl, aryl) are well documented and widely utilized as reagents in a variety of synthetic transformations, related molecular actinide complexes remain elusive. A particularly interesting and DOE-relevant transformation involves the potential reactivity of alkylidene complexes with polymeric materials.

Based on the unique chemistry exhibited by known uranium imido (metal nitrogen double bond, U=NR) and oxo (metal oxygen double bond, U=O) complexes, the uranium alkylidene (An=$CR_2$) complexes are expected to display chemical behavior that defies prediction. It is likely that these functional groups will be more reactive, which make them attractive targets as reagents to effect new bond-forming and bond-breaking reactions at the actinide metal center. These molecules will open up new frontiers in the understanding of chemical reactivity, improved understanding of covalency, the relative roles of 5f- and 6d-orbitals in chemical bonding, and write a new chapter in modern inorganic chemistry texts..

## Benefit to National Security Missions

The chemistry of the actinide elements is critical to DOE nuclear weapons mission areas (stockpile stewardship, environmental remediation, waste management). Through the synthesis of new actinide compounds this project will provide important information about metal-ligand bonding and improve our ability to reliably predict chemical behavior in a variety of environments. This knowledge will enhance our overall ability to reliably predict the chemical behavior of f-element compounds in applications such as stockpile stewardship, environmental remediation, and waste management within the DOE complex

## Progress

During our efforts to prepare uranium alkylidene complexes (U=$CR_2$) we discovered a general and versatile route for the synthesis of organometallic pentavalent uranium-imido halide complexes by the 1-electron oxidation of tetravalent uranium-imido complexes with copper(I) salts (Figure 1). Although examples of tetravalent and hexavalent uranium compounds are prevalent in the literature, the corresponding U(V) systems are scarce with little accompanying characterization data. As such this discovery was quite exciting as it has enabled a complete study of the electronic structure and bonding in pentavalent uranium systems. From a heuristic perspective, the U(V) oxidation state with its simple $5f^1$ valence electronic configuration remains a highly attractive target. Over the course of this project, a whole suite of U(V) complexes $(C_5Me_5)_2U(=N\text{-}Ar)(X/Y)$ (where X=F, Cl, Br, I; Y=OTf, SPh, SePh, TePh, $NPh_2$, OPh, Me, Ph, C≡CPh, N=$CPh_2$) were prepared. This series includes the first examples of pentavalent uranium with anionic sp, $sp^2$, and $sp^3$ carbon moieties other than carbocyclic ($C_5R_5$, $C_7H_7$, $C_8H_8$) ligands. That a wide range of substituents can be supported within the wedge of these U(V)-imido complexes refutes prior assertions that pentavalent uranium complexes are inherently unstable.

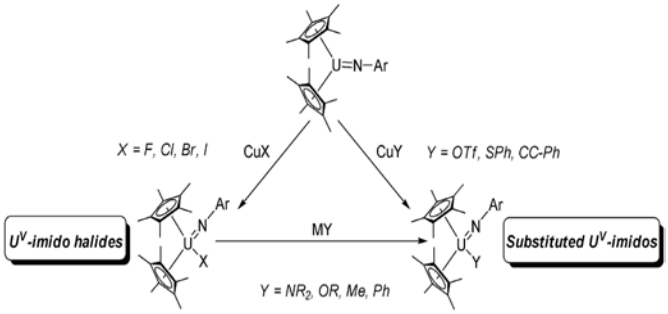


*Figure 1. Path for synthesis of substituted UV-imido complexes.*

The series of $(C_5Me_5)_2U(=N\text{-}Ar)(X/Y)$ (where X=F, Cl, Br, I; Y=OTf, SPh, SePh, TePh, $NPh_2$, OPh, Me, Ph, C≡CPh, $N=CPh_2$) complexes with electronically diverse X/Y ligands and studied using a combination of cyclic voltammetry, UV-visible-NIR absorption spectroscopy, and variable-temperature magnetic susceptibility, which provide a coherent description of the electronic structure of these pentavalent systems and indicate that both the U-X/Y and U=N bonds exhibit covalency. All of the pentavalent uranium compounds exhibit U(VI)/U(V) and U(V)/U(VI) redox couples by voltammetry. The potential separation between these metal-based couples remaining essentially constant at ~1.50 V, but both processes shift in tandem in potential by ~700mV across the series of X/Y ligands. Temperature dependent magnetic susceptibilities are reported for all complexes with $\mu_{eff}$ values ranging from 2.22-2.53 μB. The onset of quenching of orbital angular momentum by ligand fields is observed to occur ~40 K in all cases. There are no significant differences between $\mu_{eff}$ values or temperature dependencies in the magnetic susceptibility based on the identity of the ancillary X/Y ligand. However, an excellent linear correlation was observed between the chemical shift values of the $C_5Me_5$ ligand protons in the $^1H$ NMR spectra and the oxidation potentials of $(C_5Me_5)_2U(=N\text{-}Ar)(X/Y)$, suggesting that there is a common origin – overall σ-/π-donation from the ancillary X/Y ligand to the metal, contributing to both observables. As illustrated in Figure 2, combined, these data confer the following trend in increasing σ/π-donating ability of the X/Y ligand to the $U^V$ metal center: OTf < I < Br < Cl < SPh < C≡CPh < F < [OPh ~ Me ~ Ph] << $NPh_2$ < $N=CPh_2$.

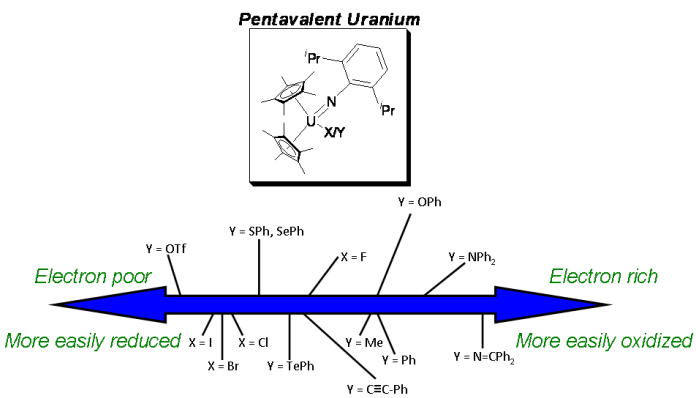


*Figure 2. Showing the effect of ligand substitution (X/Y) on the electronics of the pentavalent $(C_5Me_5)2U(=N\text{-}2,6\text{-}iPr_2\text{-}C_6H_3)(X/Y)$ complexes.*

The electronic spectra are comprised of π-π* and $\pi \rightarrow nb_{5f}$ transitions involving electrons in the metal-imido bond, and metal-centered f-f bands illustrative of the $5f^1$ valence electron configuration. Two distinct sets of bands have been attributed to transitions derived from this $5f^1$ configuration, and the intensities in these bands are increased dramatically over those found in spectra of classical $5f^1$ actinide coordination complexes. Density functional theory (DFT) results for the model complexes $(C_5Me_5)_2U(=N\text{-}Ph)(F)$ and $(C_5Me_5)_2U(=N\text{-}Ph)(I)$ show good agreement with experimental structural and electrochemical data and provide a basis for assignment of spectroscopic bands. The bonding analysis describes multiple bonding between the uranium metal center and imido nitrogen, which is comprised of one σ- and two π-interactions with variable participation of 5f and 6d orbitals from the uranium center. When considered in the broader context of other recent results for organouranium complexes, the results obtained for the $U^V$-imido complexes $(C_5Me_5)_2U(=N\text{-}Ar)(X/Y)$ provide an important bridge between those for $U^{VI}$-imido systems (e.g., $(C_5Me_5)_2U(=N\text{-}Ar)_2$) that have long been regarded as possessing substantial covalency in the metal-ligand multiple bonds and the more recent data for $U^{IV}$-ketimide systems (e.g., $(C_5Me_5)_2U(\text{-}N=C\text{-}Ar_2)_2$) that possess metal-ligand bonding intermediate between single and double bonds based on structural data. All three systems, $(C_5Me_5)_2U(=N\text{-}Ar)_2$, $(C_5Me_5)_2U(=N\text{-}Ar)(X/Y)$, and $(C_5Me_5)_2U(\text{-}N=CAr_2)_2$, exhibit similar experimental hallmarks for covalent metal-ligand bonding. While it is not possible to make quantitative comparisons regarding the degree of covalency from the existing data, the emerging picture is that all three uranium oxidation states are able to support covalent bonding in these organometallic complexes.

The Cu(I)-based oxidation protocol deserves some comment as it has a number of attractive features. Unlike silver- or thallium-promoted oxidations, which are often difficult to predict and control, Cu(I)-salts are inexpensive, readily available, and easily derivatized. Importantly, the copper oxidation protocol avoids the use of silver and thallium salts (RCRA-listed), thereby greatly diminishing the generation of mixed radioactive hazardous waste and potential exposure to highly toxic thallium reagents. Finally, the copper(I)-salts generally give cleaner reactions, and are readily separated from the reaction solution by filtration.

This year we also discovered that the copper(I)-based oxidative functionalization protocol provides a simple and mild method for synthesizing the corresponding U(IV) complexes in good yield (Figure 3). Reaction of the trivalent uranium complexes $(C_5Me_5)_2UI(THF)$, $(C_5Me_5)_2U[N(SiMe_3)_2]$, $(C_5Me_5)_2U(NPh_2)(THF)$ and $(C_5Me_5)_2U(\text{-}O\text{-}2,6\text{-}^iPr_2\text{-}C_6H_3)(THF)$ with copper(I) iodide affords the corresponding tetravalent uranium diiodide, amide-iodide, and aryloxide-iodide complexes $(C_5Me_5)_2UI_2$, $(C_5Me_5)_2U[N(SiMe_3)_2](I)$, $(C_5Me_5)_2U(NPh_2)(I)$ and $(C_5Me_5)_2U(\text{-}O\text{-}2,6\text{-}^iPr_2\text{-}C_6H_3)(I)$, respectively. This protocol was also extended to the synthesis of the alkyl-iodide complex $(C_5Me_5)_2U(CHPh_2)(I)$. The isolation of this complex from the *in situ*-generated trivalent uranium alkyl complex $(C_5Me_5)_2U(CHPh_2)(THF)$ illustrates the synthetic value of this oxidation procedure in those situations where the $U^{III}$ metallocene complex cannot be isolated or is unstable. Over-oxidation and ligand

redistribution are not observed with this Cu-based $U^{III} \rightarrow U^{IV}$ oxidation procedure, making it an attractive synthetic alternative to the existing routes for the preparation of mixed-

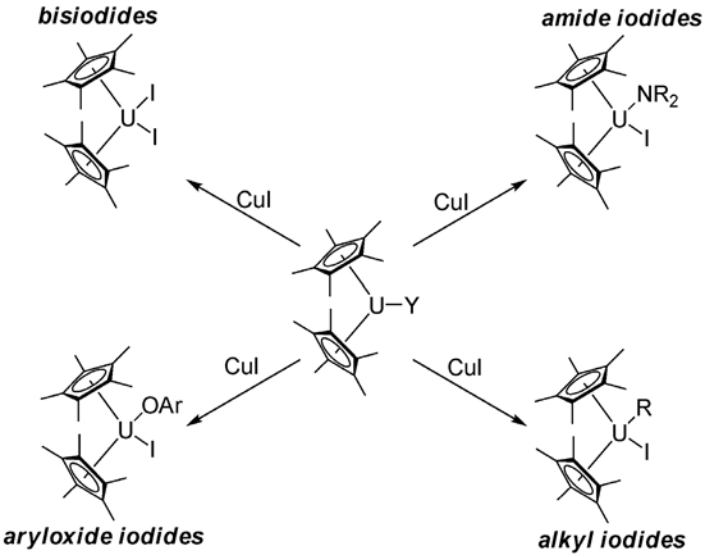


ligand metallocene complexes of the type $(C_5Me_5)_2U(X)(Y)$ (where X = halogen; Y = alkyl, amide, aryloxide, etc.).

*Figure 3. Synthetic procedure for the 1-electron oxidation of organometallic U(III) complexes to their U(IV) counterparts with Cu(I)I.*

## Future Work

This project started in December 2006 and will end at the beginning of December 2008. During the final weeks of this project two additional oxidation papers that deal with gold-oxidation platforms will be completed. The last review of pentavalent uranium chemistry was published in 1969. The impact of the LANL pentavalent chemistry studies has been evidenced by the large number of papers on pentavalent uranium complexes following our initial disclosure. It is now a hot field and accordingly we have been invited to write a review on this body of work, which will also be completed during the final months of this project.

## Conclusion

As evidenced by this project, the DOE complex and LANL clearly benefits from simple exploratory research. The copper(I)-based oxidation chemistry discovered in this project has provided easy chemical control over uranium in oxidation states ranging from U(III) to U(VI). The large range of accessible oxidation states using a single non-toxic reagent is unprecedented and has substantial implications for actinide separations schemes and longer term impact for advance nuclear fuel cycles. Finally, the value of this protocol is being noticed by other groups throughout the chemistry community and has been successfully extended to other uranium chemistry.

## Publications

Cantat, T., C. R. Graves, K. C. Jantunen, C. J. Burns, B. L. Scott, P. J. Hay, D. E. Morris, and J. L. Kiplinger. Evidence for the Involvement of 5f-Orbitals in the Bonding and Reactivity of Organometallic Actinide Compounds: Thorium(IV) and Uranium(IV) Bis(hydrazonato) Complexes.. To appear in *Journal of the American Chemical Society.*

Graves, C. R., A. E. Vaughn, E. J. Schelter, B. L. Scott, J. D. Thompson, D. E. Morris, and J. L. Kiplinger. Uranium(V)-Imido Complexes - Probing the Electronic Structure and Redox Energetics in Pentavalent Organoactinide Complexes. To appear in *Inorganic Chemistry.*

Graves, C. R., B. L. Scott, D. E. Morris, and J. L. Kiplinger. Tetravalent and Pentavalent Uranium Acetylide Complexes Prepared by Oxidative Functionalization with Cu-C⍰C-Ph.. 2008. *Organometallics.* **27**: 3335.

Graves, C. R., B. L. Scott, D. E. Morris, and J. L. Kiplinger. Selenate and Tellurate Complexes of Pentavalent Uranium. *Chemical Communications.*

Graves, C. R., D. E. Morris, B. L. Scott, and J. L. Kiplinger. Facile Access to Pentavalent Uranium Organometallics: One Electron Oxidation of Uranium(IV) Imido Complexes with Copper(I) Salts. 2007. *Journal of the American Chemical Society.* **129**: 11914.

Graves, C. R., D. E. Morris, and J. L. Kiplinger. Pentavalent Uranium-Imido Complexes. To appear in *Inorganic Syntheses.*

Graves, C. R., E. J. Schelter, T. Cantat, B. L. Scott, and J. L. Kiplinger. A Mild Protocol to Generate Uranium(IV) Mixed-Ligand Metallocene Complexes Using Copper(I) Iodide.. 2008. *Organometallics.* **27**: 5371.

Graves, C. R., P. Yang, S. A. Kozimor, A. E. Vaughn, D. L. Clark, S. D. Conradson, E. J. Schelter, B. L. Scott, J. D. Thompson, P. J. Hay, D. E. Morris, and J. L. Kiplinger. Organometallic Uranium(V)-Imido Halide Complexes: From Synthesis to Electronic Structure and Bonding.. 2008. *Journal of the American Chemical Society.* **130**: 5272.

# Superconductivity in Non-Centrosymmetric Materials

*John Singleton*

20070541PRD1

## Introduction

This project investigates materials that show new and unusual types of superconductivity. By using the very high magnetic fields and very low temperatures that are available at the Materials Physics and Applications Division's National High Magnetic Field Laboratory (MPA-NHMFL), the superconductivity can be switched on and off in a controllable manner. This will enable the microscopic properties of the underlying electrons to be uncovered using unique experimental tools designed by Dr Yuan. In this way, the mechanism for superconductivity in these materials will be understood for the first time. This is an important achievement, as it may allow superconductors with desirable properties (e.g. zero resistance at relatively high temperatures, resistance to high magnetic fields) to be designed from scratch. Such discoveries will have an important impact on technologies such as electrical power distribution and transport, and on applications of electromagnets such as MRI; the application of "designer superconductors" could yield greatly increased efficiency, reduced power consumption (important for energy security) and protection against large-scale power outages caused by grid failures.

## Benefit to National Security Missions

This project supports the DOE mission to enhance the nation's fundamental scientific capabilities by improving our understanding of superconductivity. This helps design better practical superconductors, supporting DOE's mission to improve the nation's energy security (i.e. by reducing electrical power consumption). Finally it helps in understanding complex substances such as plutonium.

## Progress

Dr. Yuan has performed a number of influential experiments on exotic superconductors and correlated-electron systems and written several papers. He has also spoken by invitation at a number of international conferences and at overseas universities. The most important results are described below. Several other experiments are in progress and samples of new materials continue to arrive from his network of international collaborators.

1. Very soon after the discovery of the new Fe-based "high-temperature" (RE,La)(O,F)FeAs superconductors in early 2008, Dr Yuan obtained samples and began to investigate their properties using the high-field facilities at MPA-NHMFL. He has mapped out the upper critical field of polycrystals for the first time [1] and has shown that the upper critical field in single crystals is almost isotropic [2] (Figures 1 and 2). The latter result is very strong evidence that the superconductivity is orbitally-limited for all orientations of the field; it sharply distinguishes the new Fe-based superconductors from other exotic materials such as the cuprates and organic metals, where Pauli limiting takes over at certain field orientations. The very important result is being linked to the recently observed Fermi-surface topology [2].

2. Dr Yuan has observed a field-induced Fermi-surface topology change in $CeRhIn_5$ for the first time. This is important evidence about the nature of the field-induced quantum critical behavior in this compound. The result was reported at the American Physical Society March meeting and is being prepared for publication.

3. The unusual layered compound $Na_xCoO_2.H_2O$ was investigated using heat-capacity measurements to reveal the superfluid density and the existence of two separate superconducting states for the first time [3].

4. The triple-layered ruthenate $Sr_4Ru_3O_{10}$ was investigated. Only one ferromagnetic phase was found, and the data meant that it was possible to rule out several previously-proposed antiferromagnetic phase transitions. A magnetic domain model was proposed to account for previously observed magnetotransport and metamagnetic behavior [4].

5. The superconducting order parameter in the non-centrosymmetric superconductors $Li_2(Pd,Pt)_2B$ was

studied using magnetic penetration-depth measurements. The data suggest that an unusual spin-triplet state develops with increasing Pt content due to the broken inversion symmetry [5]. Similar techniques were applied to a number of heavy-fermion superconductors [6].

6. Metallic states close to the quantum phase transition in cubic FeGe were investigated using very high pressures and electrical resistivity. It was found that a pressure of 19 GPa suppressed the long-wavelength helical order, and the observed strong deviations from Fermi-liquid behavior disagree with the standard vision of a quantum critical phase transition [7].

In summary, Dr Yuan is a very energetic and enthusiastic experimentalist. He has developed several collaborations with some of the best sample growers in the world, so that he has access to high-quality samples of the "hottest" materials. Consequently, his work is doing much to raise the international profile of MPA-NHMFL.

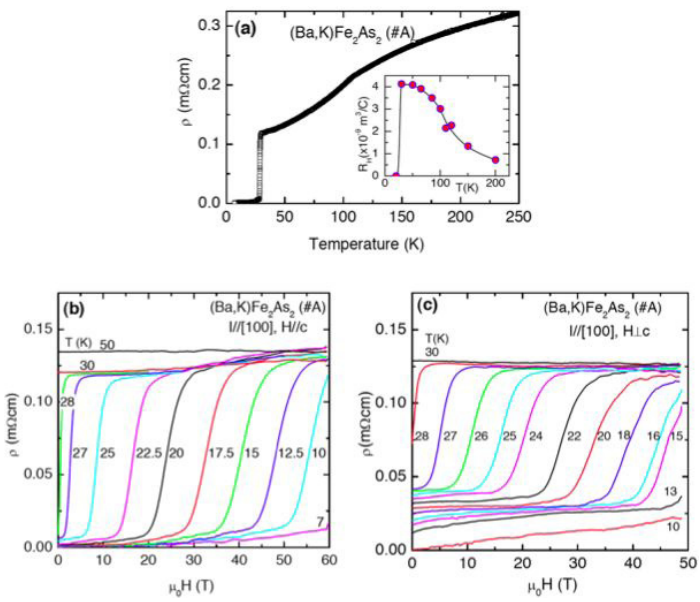


*Figure 1. In-plane electrical resistivity of single crystals of the superconductor (Ba,K)Fe2As2 measured in pulsed high magnetic fields. (a): The temperature dependence of the resistivity ρ(T) at zero magnetic field. Note that there is a weak kink around 108 K in ρ(T) which may correspond to a spin-density-wave or structural transition. The inset shows the temperature dependence of the Hall coefficient RH obtained in pulsed magnetic fields of up to 60T.The field dependence of the resistivity ρ(B) at various temperatures is shown in (a) and (b) for field parallel and perpendicular to the c-axis, respectively.*

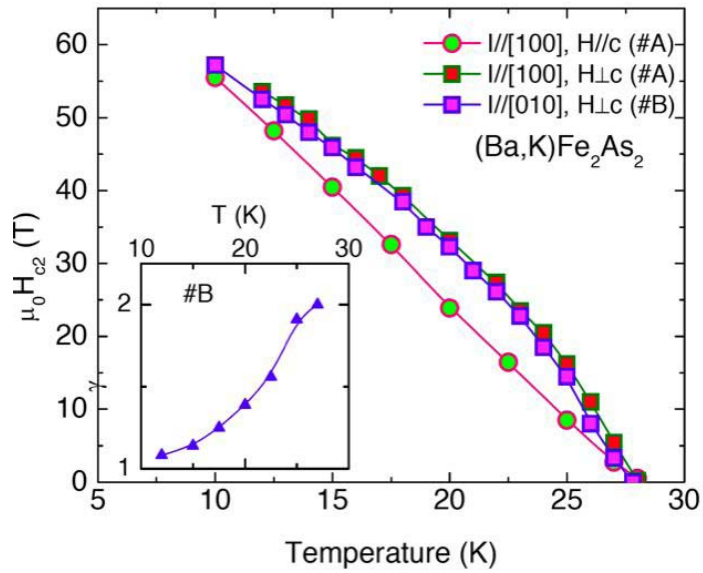


*Figure 2. The upper critical field $Hc_2(T)$ of single crystals of the superconductor $(Ba,K)Fe_2As_2$. The main figure shows Hc2 versus temperature for magnetic field parallel to the c-axis (circles) and perpendicular to the c-axis (squares), in which the critical fields Hc2(T) are determined from the midpoint of the sharp resistive superconducting transitions. Remarkably, the two samples (#A and #B) behave nearly identically despite their different purities. The inset shows the anisotropy parameter =$Hc_2$H¥c /$Hc_2$H //c plotted as a function of temperature. The parameter is about 2 near Tc, a value close to what other groups derived in low-field measurements, but decreases with decreasing temperature and approaches to 1 as the temperature tends to zero, indicating isotropic superconductivity. This is a most surprising finding in a layered material.*

## Future Work

The growth of high-quality single-crystal samples is essential for an understanding of the origin of non-centrosymmetric superconductors. Therefore two new non-centrosymmetric superconductors, LaRhSi and LaIrSi, will be synthesized. Conventional growth techniques are known to produce excellent crystals of these substances. High-magnetic-field quantum oscillation studies (i.e. the de Haas-van Alphen effect) will be carried out in the pulsed-field magnets of MPA-NHMFL. Fields of order 60 T allow quantum oscillations to be seen even in materials that are quite disordered; hence doped alloys of the two materials such as La(Rh,Ir)Si and LaIr(Si,Ge) will also be studied. The measurements will establish both the Fermi-surface topology (necessary to understand the interactions leading to superconductivity) and reveal if there are any spin asymmetries in the Fermi surface. Such spin asymmetries may be important in the competing singlet and triplet pairings that are known to be a feature of non-centrosymmetric superconductors. High-field measurements will also seek exotic superconducting phases, including the helical phase predicted for non-centrosymmetric superconduc-

tors. A further advantage of the doping studies will be an increased understanding of the differing sensitivities of the singlet and triplet pairing states to disorder. In all of this work, the high-field experiments will be backed up by other techniques such as penetration-depth, heat capacity, thermal conductivity, nuclear magnetic resonance and Josephson tunneling, to establish a very complete picture of the unconventional superconductors. Collaborations with theory groups both within LANL and in US universities will examine how theories of electron correlations can describe the experimental data, and thus seek general truths about electron correlations that will assist LANL and the DOE's missions.

## Conclusion

These experiments will establish a leading role for Los Alamos in understanding the microscopic physics of unusual superconductors. The expected results of the measurements include a better knowledge of the interactions between the electrons that give rise to this type of superconductivity. Such interactions are of very general importance, not only in superconductors, but also in unusual metals such as plutonium and its alloys. An understanding of the microscopic theory of the electronic interactions is a great asset in stockpile stewardship. In addition, it will help in designing or predicting better superconducting materials for future use in US industry.

## References


1. Chen, G. F., Z. Li, G. Li, J. Zhou, D. Wu, J. Dong, W. Z. Hu, P. Zheng, Z. J. Chen, H. Q. Yuan, J. Singleton, J. L. Luo, and N. L. Wang. Superconducting Properties of the Fe-Based Layered Superconductor LaFeAsO0.9F0.1-delta. 2008. *Physical Review Letters.* **101**: 057007 1.

2. Yuan, H. Q., J. Singleton, S. Baily, F. F. Balakirev, G. F. Chen, J. L. Luo, and N. L. Wang. Nearly isotropic superconductivity in (Ba,K)Fe2As2. To appear in *Nature.*

3. Mochizuki, M., H. Q. Yuan, and M. Ogata. Specific heat and superfluid density for possible two different superconducting states in NaxCoO2 • H2O. 2007. *Journal of the Physical Society of Japan.* **76**: 023702.

4. Qu, Z., L. Spinu, H. Q. Yuan, V. Dobrosavljevic, W. Bao, J. W. Lynn, M. Nicklas, J. Peng, T. Liu, D. Forbes, E. Flesch, and Z. Q. Mao. Unusual heavy-mass nearly ferromagnetic state with a surprisingly large Wilson ratio in the double layered ruthenates (Sr$_{1-x}$Ca$_{x}$)$_{3}$Ru$_{2}$O$_{7}$. To appear in *Physical Review B.*

5. Yuan, H. Q., M. B. Salamon, P. Badica, and K. Togano. A penetration depth study on the non-centrosymmetric superconductors Li2(Pd1-xPtx)3B. To appear in *Physical Review B.*

6. Steglich, F., C. Geibel, F. M. Grosche, M. Loewenhaupt, O. Stockert, S. Wirth, and H. Q. Yuan. Experimental evidence for unconventional BCS states in heavy-fermion metals . 2008. *Physica B.* **403** (5-9): 968.

7. Pedrazzini, P., H. Wilhelm, D. Jaccard, T. Jarlborg, M. Schmidt, M. Hanfland, L. Akselrud, H. Q. Yuan, U. Schwarz, Y. Grin, and F. Steglich. Metallic state in cubic FeGe beyond its quantum phase transition. 2007. *Physical Review Letters.* **98**: 047204 1.


## Publications


Chen, G. F., Z. Li, G. Li, J. Zhou, D. Wu, J. Dong, W. Z. Hu, P. Zheng, Z. J. Chen, H. Q. Yuan, J. Singleton, J. L. Luo, and N. L. Wang. Superconducting properties of the Fe-based layered superconductor LaFeAsO0.9F0.1-delta. 2008. *Physical Review Letters.* **101**: 057007 1.

Mochizuki, M., H. Q. Yuan, and M. Ogata. Specific heat and superfluid density ofr possible two different superconducting states in NaxCoO2.H2O. 2007. *Journal of the Physical Society of Japan.* **76**: 023702.

Pedrazzini, P., H. Wilhelm, D. Jaccard, T. Jarlborg, M. Schmidt, M. Hanfland, L. Akselrud, H. Q. Yuan, U. Schwarz, Y. Grin, and F. Steglich. Metallic state in cubic FeGe beyond its quantum phase transition. 2007. *Physical Review Letters.* **98**: 047204 1.

Qu, Z., L. Spinu, H. Q. Yuan, V. Dobrosavljevic, W. Bao, J. W. Lynn, M. Nicklas, J. Peng, T. Liu, D. Forbes, and E. Flesch. Unusual heavy-mass nearly ferromagnetic state with a surprisingly large Wilson ratio in the double layered ruthenates (Sr$_{1-x}$Ca$_{x}$)$_{3}$Ru$_{2}$O$_{7}$. To appear in *Physical Review B.*

Steglich, F. C., F. M. Geibel, F. M. Grosche, M. Loewenhaupt, O. Stockert, S. Wirth, and H. Q. Yuan. Experimental evidence for unconventional BCS states in heavy-fermion metals. 2008. *Physica B.* **403** (5-9): 968.

Yuan, H. Q., J. Singleton, S. Baily, F. F. Balakirev, J. L. Luo, and N. L. Wang. Nearly isotropic superconductivity in (Ba,K)Fe2As2. To appear in *Nature.*

Yuan, H. Q., M. B. Salamon, P. Badica, and K. Togano. A penetration depth study on the non-centrosymmetric superconductors Li2(Pd1-xPtx)3B. To appear in *Physical Review B.*

# Multifunctional Copper-Carbon Nanotube Nanocomposites

*Amit Misra*

20070585PRD2

## Introduction

Copper has been used in electrical devices extensively. To improve performance of devices, development of the Cu-based new structures with high strength, good ductility, and conductivity is required. Although processing to reduce the grain size below 100 nm increases the strength of copper, its ductility and electrical conductivity drop considerably. We would like a different way to strengthen copper. Carbon nanotubes (CNTs) possess high elastic modulus, ultrahigh strength, good conductivity, and excellent thermal stability. These novel properties allow CNTs to be an excellent candidate for composite reinforcement – the composite is expected have dramatically better mechanical properties than copper alone. Furthermore, CNT's good thermal and electrical conductivities will minimize the conductivity loss in the nanocomposites. We attempted the synthesis and characterization of CNT-reinforced metallic composites. Previous fabrication techniques involved hot press, plasma spray, hot extrusion, and ball-milling followed by sintering. Obviously, these attempts require high temperatures to obtain fully-dense samples. However, heating not only makes CNTs react with metal matrixes but also increases grain size significantly. As a result, studies of improving both strength and ductility in Cu-CNT composites have not been very successful so far. Here, we are carrying out a novel approach to make high quality multifunctional Cu-CNT nanocomposites by taking advantage of ball milling, powder consolidation, low-temperature annealing, and high pressure torsion at room temperature to avoid coarsening. The designed multifunctional Cu-CNT composites will have an important technological and economic impact by miniaturizing electronic devices. Scientifically, the success of this project will help us understand deformation physics, mechanical behavior, electrical properties, and thermal stabilities of nanocomposites.

## Benefit to National Security Missions

This project will support the DOE mission in basic science and energy security by enhancing our understanding of Cu-carbon nanotube nanocomposites, whose primary application is for electrical power transmission.

## Progress

To efficiently improve mechanical property of Cu-CNT composites, it is desireable that CNTs are much longer than grain sizes so that they can function as the linkage between grains to prevent intergranular fracture. In addition, a good reinforcement effect requires that CNTs can be incorporated into grain interiors. Thirdly, CNTs should also be dispersed into metallic matrices homogenously because clusters of CNTs may cause early fracture due to weak bonding strength between CNTs. Unfortunately, CNTs have a strong tendency to form bundles, and it is difficult to homogeneously disperse CNTs. To overcome this challenge, ball-milling was employed in the current project. The Cu powders (particle sizes: 0.5-1.5µm) with 1wt.% CNTs (length: 20-30µm) were ball milled for up to 5 hrs in an Ar-protected environment. For comparison, Cu powders without CNTs were also ball milled at the same conditions. Scanning electron microscopy (SEM) study shows that after ball milling, the particle sizes increased, which is caused by the cold-welding process during ball milling. Furthermore, particle size depends on the ball milling time. For example, particle sizes are about 8-35µm and 10-50µm after 1hr and 5hrs ball milling, respectively.

A close examination revealed that after 5hrs ball milling, the particle surfaces is clean and smooth. However, there are some fine particles on the surfaces of large particles when the CNTs were added. Furthermore, the analysis found that CNTs were not observed on the particle surfaces, indicating that CNTs have been incorporated into Cu powders during ball milling. The ball milled Cu-CNTs composite powders were compacted into 10mm diameter discs with a thickness of about 1mm in air at room temperature at a stress of about 500MPa. SEM results demonstrate that the discs have many small pores, which is due to a low applied load. Therefore, further processing is required. These discs were subjected to high-pressure torsion (HPT) for two reasons. One, to make samples fully-dense, and other to refine the structures by severe plastic deformation.

The HPT-processed Cu-CNT composites were analyzed by x-ray diffraction (XRD), nanoindenter, and transmission electron microscopy (TEM). The results show that after HPT, the strong (111) texture developed in both Cu and Cu-CNT composites, but, an addition of CNT does not affect the texture intensity. Importantly, no CNT peaks were observed, implying that the CNTs have been incorporated into Cu matrix.

Detailed microstructure analysis for the HPT-processed samples with and without CNTs was conducted by TEM and high resolution TEM (HRTEM). The results demonstrate that all the samples have a nanostructured microstructure and grains exhibited an equiaxed shape. The average grain size is about 22 nm and 29 nm for Cu-CNT composite and Cu, respectively. The grain size distribution of Cu-CNT nanocomposite is apparently narrower than that of pure Cu. It is known that the principle of producing nanostructures by HPT is to form subgrain boundaries via dislocations under severe torsional deformation. These subgrain boundaries then develop into high angle grain boundaries, resulting in grain refinement. With presence of CNTs, the dislocation motion could be inhibited at CNTs. That is, the dislocation accumulation would be enhanced at CNTs. Consequently, an addition of CNTs leads to a further decrease in the grain size and grain size distribution.

Figure 1 displays an HRTEM picture showing CNTs embedded in the Cu matrix. The insert is the HRTEM image of original CNTs. It is worth mentioning that during TEM observations, no CNT agglomeration in the Cu-CNT samples was found, which is critical in obtaining improved performance in CNTs-added composites since CNTs clustering hurts property gains. The flow stress as a function of distance away from the disc sample center was measured for nanostructured Cu and Cu-CNT composite. The results show that the flow stress does not change noticeably with measurement site for both samples, which indicates that the microstructure is approximately uniform. Furthermore, the results demonstrate that the strength of Cu-CNT nanocomposite is higher than that of pure Cu. Such enhancement originates from two aspects. One is grain refinement, and the other is the CNTs reinforcement.

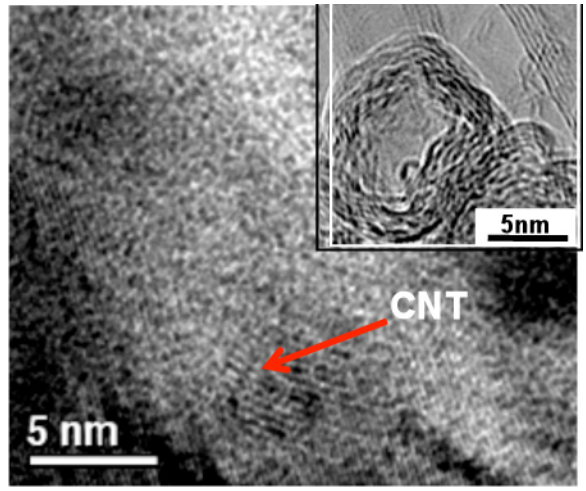


*Figure 1. High-resolution transmission electron microscopy image showing CNTs embedded in Cu matrix. The insert shows the CNTs before insertion.*

The electrical conductivity was also measured on the as-pressed Cu-CNTs composites. These composites have a resistivity of $2\text{-}6.10^{-5}$ Ω.cm. Although it is larger than that of pure Cu ($0.17.10^{-5}$ Ω.cm), it is comparable with that for Ni and Fe (~$0.7\text{-}1.0.10^{-5}$ Ω.cm), and still impressive. Compared with pure Cu, the decreased electrical conductivity of as-pressed Cu-CNTs composites is believed to be mainly due to oxidization, pores (low density), and residual stress. The composite's electrical conductivity would be significantly improved after they are HPT-treated and annealed. Also, in future, the powder consolidation will be performed in glove box to avoid oxidization. In summary, bulk nanostructured Cu-CNTs composite samples have been successfully fabricated via a combination of ball milling, powder consolidation, and HPT. XRD, SEM, TEM and nanoindentation results show that CNTs can be homogeneously dispersed into Cu matrix, which is a key prerequisite to achieve enhanced mechanical and physical properties. Also, it is found that the nanostructured Cu-CNT composite is stronger than pure Cu at the same grain size.

## Future Work

Cu has been widely used in many electrical applications such as the overhead catenary systems (contact and feeder wires) for light-rail transit and coil materials for electromagnets. Nowadays, there are about 6000-miles of light-rail lines worldwide, and replacing these overhead wires will cost more than $1 billion. To improve their service life significantly, Cu conductors with good wear resistance and conductivity are required. Another challenge can be found at the National High Magnetic Field Labs at LANL and Florida is to build electromagnets that can produce extremely high magnetic fields. The limiting factor has been the lack of ultra-strong and conductive wires for building such magnets. To date, attempts to improve the strength

and wear resistance of Cu conductors have not been very successful because they significantly lower the conductivity in most cases. We proposed a novel approach to solve this problem: multifunctional Cu-carbon nanotube (CNT) nanocomposites. The incorporation of ultra-high strength CNTs is anticipated to significantly increase the strength, toughness, thermal stability, and wear resistance of Cu-CNT nanocomposites, while the good conductivity of CNTs will minimize the conductivity reduction in the nanocomposites. Our approach will include:

1. Several methods will be employed to produce CNTs-reinforced Cu nanocomposites, including electro-deposition, severe plastic deformation (SPD), and powder consolidation.

2. The effect of CNTs (volume fraction, length and CNT type) on mechanical properties (strength, ductility and wear resistance), electrical and thermal conductivities, and thermal stability of nanocomposites will be studied.

3. The deformation physics of the Cu-CNT nanocomposites will be studied using scanning electron microscopy, high-resolution transmission electron microscopy, x-ray diffraction, and in-situ deformation-neutron and synchrotron diffractions.

## Conclusion

We expect to successfully fabricate nanostructured Cu-carbon nanotube composites with good wear-resistance, conductivity and high strength. The impact of this work is four-fold: First, it could save billions of dollars annually by prolonging the life of a wide range of components including electrical brushes, switches, and electrical relays. Second, it can be used to make miniature electronic devices, which have great potential for aerospace applications. Third, it could enable the construction of electromagnets that produce magnetic fields much higher than currently possible. Fourth, it will contribute to the understanding of deformation physics, mechanical behaviors, electrical properties, and thermal stabilities of nanocomposites

## Publications

Li, H. Q., A. Misra, and Y. T. Zhu. Fabrication and characterization of nanostructured Cu-carbon nanotube composites. *Composites Part A: Applied Science and Manufacturing.*

# Multiscale Simulations for Cascade Overlap in Irradiated Materials

*Arthur Ford Voter*

20070640PRD2

## Introduction

Study of dynamics of thermally activated phenomena is essential for designing materials with desirable characteristics. However, current materials modeling techniques cannot simultaneously access large length and time scales without making severe approximations that typically corrupt the dynamical evolution. This project addresses these challenges by modifying and building on the characteristics of the temperature accelerated dynamics (TAD) method developed here at Los Alamos. In the TAD method [1], transitions from state to state are made to occur more rapidly by raising the temperature of the system. Although the wrong event sometimes occurs first at higher temperature, the TAD algorithm corrects for this, only allowing the correct events (with a desired confidence) to be accepted. The TAD method gives statistically correct dynamics and it can access large time scales. However, it is limited to small system sizes; e.g., 1000 atoms. We are pursuing two different directions in this project to develop multiscale methods for solid state systems that overcome the materials length and time scale problem with the accuracy of the TAD method. The first approach is to modify the TAD method so that it generates a proper list of reaction processes as it proceeds. This list of processes is then used in the well-known kinetic Monte Carlo (KMC) framework to advance the dynamics. This solves the long-standing problem of how to find a complete (or complete enough with desired confidence) list of rate processes for a given system in a given state. The second approach, which we term "TAD-based KMC", builds on this by generating process lists for small subsets of atoms. The payoff is that this method can be used on extremely large systems, and offers for the first time a KMC method with error control. We are applying these methods to metal and oxide material systems.

## Benefit to National Security Missions

This project will improve our understanding of the complex microstructural behavior of materials under irradiation. This understanding is needed for designing improved nuclear fuels, longer-lasting structural materials, and radiation-resistant matrix materials for long-term waste storage. This project thus contributes to the DOE missions in Energy Security, Nuclear Security, Environmental Responsibility, and Scientific Discovery and Innovation.

## Progress

We have made significant progress this year on the development of advanced forms of the temperature accelerated dynamics (TAD) method for studying long-time dynamics in materials systems. We are pursuing two directions:

1. p-TAD method: A new formulation of the temperature accelerated dynamics (TAD) method called the p-TAD method has been developed, for systematically generating a kinetic Monte Carlo (KMC) process list for a given material system. (A process list is a list of reaction mechanisms, and associated rate constants, for escape from the present state of the system.) The method guarantees that all relevant KMC processes have been detected with a user-specified confidence over large time scales. Generation of such accurate KMC process lists, with error control, is not possible with any other currently available technique. Though the p-TAD algorithm resembles the original TAD algorithm in many ways, the p-TAD method introduces significant improvements to existing TAD method. For example, it offers a more direct way to parallelize the dynamics for small (or large) systems, and it can be made more accurate event by event if desired, because the accurate rate constant is computed at low temperature directly. It also offers the possibility of including quantum dynamical (e.g., tunneling and zero-point) effects. A manuscript describing the p-TAD method will be submitted for publication to the Journal of Chemical Physics shortly.

2. TAD-based KMC method: The TAD-based KMC method (TAD-KMC) is a powerful method developed to simultaneously overcome the length and time scale problem. The method identifies unique local environments, i.e., relative atomic arrangements around each atom, in the material system us-

ing an efficient pattern recognition algorithm. A list of relevant KMC processes is continuously generated with a user-specified confidence for the unique local environments using the p-TAD method described above. Parallel p-TAD calculations are straightforward using multiple processors. KMC process lists from local environments are compiled to generate an on-the-fly master KMC process catalog. Processes are selected using an the efficient n-fold KMC method. Once a KMC catalog is generated, it can be reused for other calculations with the same material at conditions different from ones the catalog was originally generated for. An exciting aspect is that the TAD-KMC scales sublinearly with the number of atoms in the material system, which contributes to its high computational efficiency for large systems. Other important features of the working code developed for this method include, but are not limited to: a) performing p-TAD based on-lattice or off-lattice KMC simulations, as well as their combinations in a spatially adaptive fashion, b) overcoming time scale separation resulting from fast and slow processes, c) compiling KMC catalogs generated from different KMC process list generation methods, d) database management system for efficient storage and retrieval of information, and e) adaptive methods for maximum exploitation of available processors. The code has enabled us to study dynamics of a 50,000 atom metal system over milliseconds with a few hours of computational time using four processors (see Figure 1). The sublinear scaling means that modeling of very large systems, e.g. a million atoms or more, should be possible with relatively modest computational resources. This method is more approximate than a full TAD or p-TAD simulation, due to the environment localization, but it is substantially more accurate than the standard KMC approach that it is meant to compete with, and offers error control for the first time in any KMC method. Figure 2 shows examples of the complicated mechanisms, involving many atoms and sometimes going off lattice, that are allowed to occur naturally as the dynamics progress in a TAD-KMC simulation. A manuscript for publication is current in preparation.

We have also begun developing a new methodology for speeding up either KMC or TAD-KMC simulations in a simple but general way. This “fuzzy superbasin” (FSB) technique builds on the past history of states visited to alter the state-to-state sequence of transitions without modifying the accuracy of the simulation significantly (up to a given confidence level). The FSB technique will help TAD-KMC method reach even longer timescales for given computational resources. We are experimenting with implementation of FSB in the TAD-KMC code, and the time achieved in a test simulation is shown in Figure 3.

*Figure 1. Example of the large system size accessible with the TAD-KMC method. This silver surface diffusion system, consisting of 49,312 atoms, was evolved for milliseconds at T=200K on a four processors.*

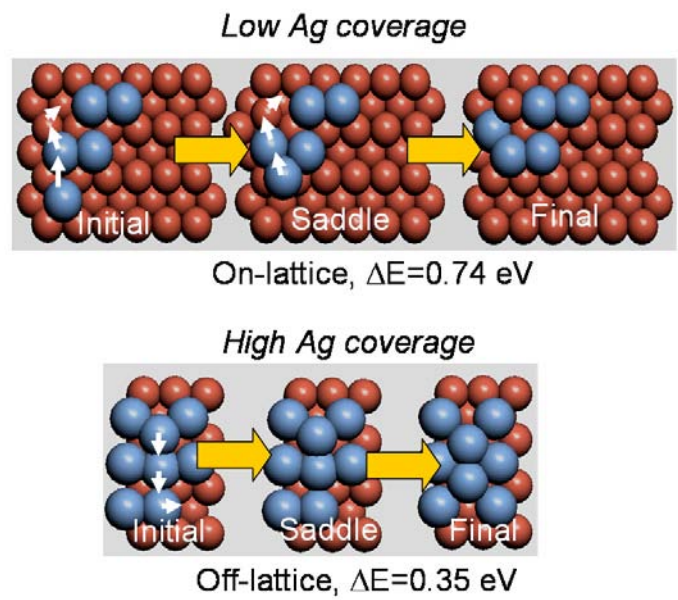


*Figure 2. Mechanisms observed during TAD-KMC simulation of silver adatoms on copper surface [Ag/Cu(100)]. Both panels show moves that are important in the evolution of the Ag overlayer, but which would be omitted from any standard KMC simulation due to their complexity. Top panel: 3-atom concerted exchange move involving two Ag adatoms as well as a Cu substrate adatom that becomes an adatom after the event. Bottom panel: 3-atom concerted move that is off lattice. At high Ag coverages, the Ag film begins to buckle under elastic strain, a feature that is also usually absent in regular KMC models.*

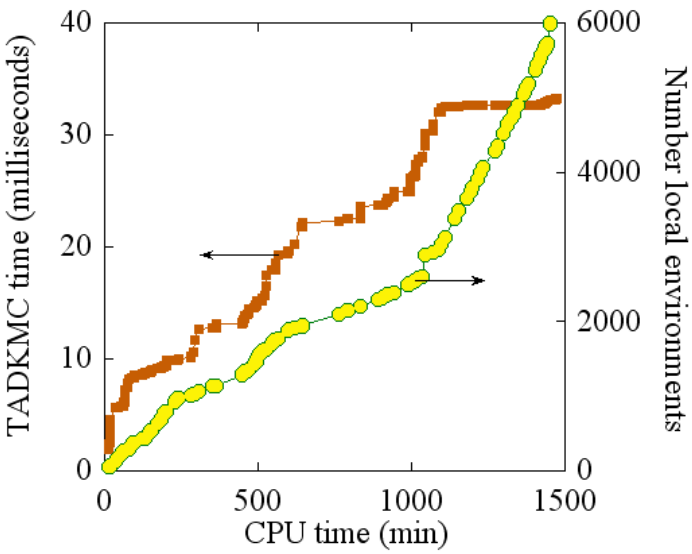


*Figure 3. Time accessed during the simulation of thin-film deposition of silver on a silver surface at T=200K, using TAD-KMC augmented with the fuzzy superbasin (FSB) method. The FSB reduces the total number of transitions while maintaining a desired accuracy in the long-time dynamical outome. Also shown is the number of unique local environment states identified by the TAD-KMC. As states are revisited, TAD-KMC gives a power-law increase in the time with respect to computational time. This effect, also known as the sweeping effect, is observed in all TAD methods.*

## Future Work

Microstructural evolution in a material, especially when driven by irradiation, involves processes on time scales ranging from subpicosecond to seconds and beyond, and length scales from atomic scale to microns (or beyond). No single simulation method can appropriately treat this range of time and length scales. Molecular dynamics (MD) is well suited to the shortest-time processes, including the sub-ps collision cascades, but is hopeless beyond nanoseconds. Accelerated molecular dynamics (AMD) methods, developed here at LANL, are powerful for treating activated processes on much longer time scales. Exactly how long depends on the system, but in favorable cases, AMD simulations can go into seconds and beyond. Kinetic Monte Carlo (KMC) methods, which require known rate constants as input, can go to even longer times (typically many orders of magnitude longer than AMD for the same system) and to much greater length scales. In this project, we are developing a spatial hybrid method that takes advantage of all three of these methods. It will use MD where collision cascades require full trajectory accuracy at the fs time scale and to follow the dynamics into ps until the excess energy has dissipated from the region. It will use our latest AMD methodology in regions where complex defect evolution is occurring, and employ the more cost-effective pure KMC method in regions where the defect dynamics are expected to be simple. The pre-calculated table of rates needed for the KMC will be generated on the fly by the TAD module. The method will employ adaptive meshing and will convert on the fly among the different methods to maintain the maximum speed with the required accuracy. The method will be applied to surface diffusion and growth problems during initial development and testing, and then later to radiation damage in bulk fcc metals described with embedded atom method potentials.

## Conclusion

We are developing a computer simulation approach that combines the best of molecular dynamics, accelerated molecular dynamics, and kinetic Monte Carlo methods, to reach greater time-scales, length scales, and accuracy than has been possible previously. The resulting computer program will be used to study materials under irradiation and other problems. This will offer us a modeling tool that can be used to assist in the design of improved nuclear fuels, improved nuclear structural materials, and materials to contain nuclear waste elements. It can also help in understanding ion implantation and thin film deposition used in semiconductor processing steps, such as for solar cells.

## References

1. Sorensen, M. R., and A. F. Voter. Temperature-accelerated dynamics for simulation of infrequent events. 2000. *Journal of Chemical Physics.* **112**: 9599.

# Ultrafast Non-equilibrium Physics of the Fractional Quantum Hall System

*Antoinette Jane Taylor*

20070654PRD2

## Introduction

We will use ultrafast optical techniques to determine the dynamics of carriers in complex materials whose exotic behavior is dominated by interactions between carriers, in order to understand the underlying physics that determines the properties of these materials. The materials under study include high temperature superconductors, heavy fermion materials, magnetic materials, ferroelectrics, coupled magnetic and electric materials such as multiferroics, nanostructured materials and metamaterials. These materials all exhibit unusual electronic and magnetic properties that are of technological importance for advanced electronic and sensor applications. One of the key open questions in high temperature superconductivity is the nature of the interactions in these materials and the possibility of competing interactions, which will enable advanced technological applications. Ultrafast optical measurements will be used to elucidate the different interactions which should occur on differing timescales, to obtain new information regarding the nature of low-lying singular and collective mode excitations of such complex and nanostructured materials and to explore carrier relaxation of interacting electrons.

## Benefit to National Security Missions

Our new techniques will impact next generation materials and devices, ranging from semiconductors to nanostructures, all of which are important to DOE missions in national security, nanotechnology, and basic science. This project will provide critical information on high-frequency electrical transport, ultrafast optoelectronic or magnetic switching, and broadband, ultrafast photodetectors.

## Progress

Ultrafast optical spectroscopy (UOS) is a powerful technique to study femtosecond dynamics in various systems with very high temporal resolution. In particular, tools in UOS, like all optical pump/probe specstrocopy and four-wave mixing have contributed greatly to our understanding of electron-electron scattering, electron-phonon interactions, etc. in semiconductors, conventional metals and correlated electron materials. Other tools like THz-Time Domain Specstroscopy allow us to directly measure the complex conductivity in correlated electron materials like high-Tc superconductors. Further, by first pumping with optical pulses, and then probing with the far-IR THz pulses, one can measure the ultrafast changes in complex conductivity following optical excitation with picosecond resolution, giving us access to the dynamics of quasiparticles and the superconducting condensate. We are currently building a system capable of pumping with optical or mid-IR pulses, while probing with far-IR THz pulses. By pumping with long wavelength mid-IR pulses, one can excite very low energy excitations in the correlated electron materials and study their effect on the dynamics of correlated electron systems. Over the past few months, we have designed the experimental system allowing us to perform ultrafast pump-probe experiments, where the pump can be optical (400-800 nm) or mid-IR (3-20 microns) and the probe can be optical, mid-IR or far-IR (100-1000 microns). We start with part of a 1-kHz, 3mJ-pulse amplifier system, which is used in combination with a Visible Optical Paramateric Amplifier (OPA) or a midinfrared OPA to generate the pump pulses. The remaining energy in the amplifier pulses is used to generate and then detect few-cycle THz pulses using ZnTe crystals as emitters and detectors. We are currently in the process of aligning the optical experiment.

Metamaterials (materials composed of shaped dielectrics and conductors resulting in specifically designed electromagnetic responses) have generated a lot of interest. They have novel properties like negative refractive index, artificial magnetism, super focusing, etc. Some of the applications in optical communications and data processing require modulation of the electromagnetic properties of the metamaterial, which can be achieved by modulating the optical properties of the constituent dielectrics and conductors. In this project, we study a negative-index metamaterial at near-IR wavelength fabricated with elliptical holes penetrating through the metal/dielectric/metal films. By injecting photoexcited carriers into the dielectric, we alter its optical properties, thereby modulating the electromagnetic response of the metamaterial.

Over the past year, in collaboration with the Center of High Technology Materials, we have fabricated a negative-index metamaterial at 1200nm with elliptical holes in Ag/amorphous-Si/Ag films. Using Fourier Transform IR spectroscopy and Rigorous Coupled Wave Analysis, we have measured and successfully simulated the transmission properties of our sample in the near-IR range (1000nm – 1500nm).

We then set up a pump/probe experiment to study and characterize the modulation of the near-IR transmission properties right after photoexcitation with an optical pulse. In this experiment, we excite the sample with 60 fs, 500 nm optical pump pulses. This excites a large number of photoexcited carriers in the amorphous silicon film. The carriers modify the dielectric properties of the amorphous-Si, effectively making it a conductor and thereby changing the electromagnetic properties of the metamaterial sample. After a short time delay, ranging from 0-20ps, we measure the transmission of a near-IR probe pulse through the sample, thereby directly giving us the modulated transmission properties of our sample in the near-IR. We study the modulation of the transmitted intensity as a function of various experimental parameters, including the wavelength & polarization of the near-IR probe pulse and the intensity and wavelength of the pump pulse. For the highest pump fluence studied, we see sub-picosecond modulation of >25%, suggesting possibilities of terabits per second modulation at telecommunication wavelengths. Current state of the art is limited to 100 gigabits per second modulation using electro-optic modulators due to RC issues. A change from negative to positive induced transmission around the metamaterial resonance can be understood by assuming that photoexcitation makes the $\alpha$–Si dielectric layer conducting, thereby changing from a metamaterial response to limiting the negative permeability and changing the resonance character. At high photoexcitation fluences, for probe wavelengths close to the MM resonance, we see the change in transmission switch from negative to positive within a few picoseconds of photoexcitation, suggesting a dynamic tuning of the metamaterial's resonance frequency.

We also measured the lifetimes of photoexcited carriers in films of amorphous-Si to compare with the modulation times of the transmission of near-IR light in our sample.. The carrier lifetimes in the amorphous-Si films compare well with the modulation times measured on our sample, thereby verifying our understanding of the mechanism behind the modulation.

## Future Work

We will use ultrafast techniques to determine the dynamics of carriers in complex materials whose exotic behavior is dominated by correlations between carriers, in order to understand the underlying physics that determines the properties of these materials. The materials under study include high temperature superconductors, heavy fermion materials, magnetic materials, materials with coupled order parameters such as multiferroics, nanostructured materials and metamaterials. These materials all exhibit unusual electronic and magnetic properties that are of technological importance for advanced electronic and sensor applications. One of the key open questions in high temperature superconductivity is the nature of the interactions in these materials and the possibility of competing orders. Ultrafast optical measurements will be used to elucidate the different interactions which should occur on differing timescales, to obtain new information regarding the nature of low-lying singular and collective mode excitations of such complex and nanostructured materials and to explore carrier relaxation of correlated electrons. Further, the quantum Hall system is a nanostrutured material formed by a two-dimensional electron gas in a large perpendicular magnetic field. Transport measurements have been used to extensively study the ground states of this system, resulting in the well known quantum Hall effects. Linear optical experiments have shed further light on the properties of this fluid and its elementary excitations. However, the above experiments cannot access the coherent ultrafast dynamics. Techniques of ultrafast non-linear optical spectroscopy are ideally suited to study the coherent ultrafast dynamics and will be used to access the coherent ultrafast dynamics of the quantum Hall system. The study of ultrafast dynamics and competing interactions in other nanoscale materials such as quantum wires will also be pursued. These studies will reveal how the underlying ground state correlations affect the ultrafast non-equilibrium properties.

## Conclusion

The non-equilibrium properties of a system are dominated by the interactions between its quasiparticles and collective excitations. On an ultrafast timescale, the scattering of these quasiparticles is a coherent phenomenon, lasting for a finite time interval where standard theories of particle scattering, like the Boltzman approximation and Fermi Golden Rule, fail. The study of ultrafast non-equilibrium physics is thus of fundamental importance. Understanding this early coherent non-equilibrium regime is also essential to building fast, controllable and coherent quantum-devices for the future.

## Publications

Dani, K. M., Z. Ku, P. C. Upadhya, R. P. Prasankumar, S. R. J. Brueck, and A. J. Taylor. Sub-picosecond optical switching with a negative index metamaterial . *Nature Photonics.*

continuing project

# Time-Dependent Density Functional Theory for Ultrafast Optical Phenomena in Strongly Correlated Electron Materials

*Jian-Xin Zhu*

20070690PRD3

## Introduction

Theoretical understanding of the electronic structures of molecules and solids plays a crucial role in the design, synthesis, and improvement of new materials. It is a challenge to find an exact solution to the systems with such a hugh number of degrees of freedom, typically at the order of $10^{23}$ interacting electrons. Density functional theory (DFT) expresses the energy as a functional of the electron density. It is a fast method capable of treating large systems. No other methods can achieve comparable accuracy at the same computational cost. Development of DFT has provided alternative to conventional wavefunction methods. With the rapid advent of reliable density functionals, this theory has become the most popular method in electronic structure calculations of molecules and solids, and has made a notable impact on condensed matter physics, chemistry, and molecular biology. However, since DFT is only designed to describe ground-state properties, time-dependent DFT, which is the most important extension of the static DFT, has been developed and employed to describe the dynamical properties of molecules and solids.

While DFT/TDDFT has achieved practical success in electronic structure calculations of molecules and simple metals, it is inadequate to describe strongly correlated electronic materials, where the Coulomb interaction dominates or competes with the kinetic energy. The competition can generate many such new phases as antiferromagnetism and superconductivity. This project will develop a new theoretical approach for strongly correlated electron material exposed to a time-dependent laser field, from which time-dependent optical conductivity will be formulated. The latter will be used to interpret the ultrafast optical spectroscopy (UOS) on several typical materials. The new method will bridge the theory and the UOS experimental measurement. The UOS is a key experimental technique toward understanding of materials dynamics. In synergy with the DFT, the new approach will also have a predictive power.

## Benefit to National Security Missions

This project will support the DOE missions of the Office of Science by enhancing our understanding of complex materials and their dynamical response. The work will provide a foundation for understanding the electronic excitations and their coupling to other dynamical degrees of freedom like lattice vibrations.

## Progress

In the development and application of DFT, we have completed the following work:

We have tested a non-empirical density functional on jellium, which is a simplified fictional model of metals and a standard testing ground for density functionals, both for bulk and for surface properties. We have calculated the surface properties of jellium in the presence of magnetic fields. The results [1] agree well with those of the highly-accurate but computationally-demanding Quantum Monte Carlo method.

Atomic shell structure, electron pair domains, pi-electron subsystems, etc., are common concepts in descriptive chemistry and play a significant role in modern electronic structure theory. These concepts help us to visualize the bonding between atoms in terms of small groups of localized electrons (e.g. two electrons of opposite spin in a simple covalent bond) and therefore play an important role in predicting new molecular structures and in describing structural changes due to chemical reactions. A precise quantitative description of small groups of localized electrons has been sought for a long time, but none of the solutions proposed so far is completely satisfactory. Recently we have constructed a physically-motivated electron localization function [2,3] in terms of the quantum stress, which can be easily calculated from DFT. With modern visualization techniques for stress fields employed in such diverse fields as engineering, geology, medicine, and biomechanics, we may visualize the process of bond breaking and formation in chemical reactions.

We have found a way to construct [4,5,6] more accurate energy functionals. These high-level energy functionals may solve the problems that commonly-used functionals have encountered in routine electronic structure calculations. Excitation energy of a molecule is a very important quantity in chemistry, and molecular biology. Accurate prediction of this quantity plays a significant role in the study of chemical reaction mechanism. We have tested [7] commonly-used TDDFT methods on the excitation energies of prototype small molecules, for which accurate experimental values are available for comparison. We have found that TDDFT can give an excellent description of excitation energies of molecules. Encouraged by this result, we applied TDDFT to the calculation [8] of absorption spectra of light-emitting organic materials. These organic electroluminescence materials have been used to develop high-performance organic light-emitting diodes and can be employed to fabricate high-resolution, full-color, and flat-panel displays. Our calculations agree with the experimental measurement. This investigation provides a detailed interpretation of experiments and relevant guide for experimentalists to search for luminescent materials with desirable multifunctional properties.

Calculations of the optical conductivity of materials is very useful in the study of interelectronic Coulomb interactions. Many properties of a material are affected by these interactions. Here we have found a new approach to calculate the optical conductivity of strongly correlated electronic materials, in which usual DFT/TDDFT methods fail, due to the strong Coulomb interaction. We have completed the theoretical derivation and analysis and reported our at the 2007 APS March Meeting [9].

## References


1. Tao, J., J. P. Perdew, L. M. Almeida, C. Fiolhais, and S. Kummel. Nonempirical density functionals investigated for jellium: spin-polarized surfaces, spherical clusters, and bulk linear response. 2008. *Physical Review B.* **77**: 245107.

2. Tao, J., G. Vignale, and I. V. Tokatly. Quantum stress focusing in descriptive chemistry. 2008. *Physical Review Letters.* **100**: 206405.

3. Tao, J., I. V. Tokatly, and G. Vignale. Quantum stress focusing in descriptive chemistry. 2008. In *American Physical Society March Meeting.* (New Orleans, March 10-14, 2008). Vol. 53, p. 275. College Park, MD: American Physical Society.

4. Tao, J., J. P. Perdew, V. N. Staroverov, and G. E. Scuseria. Exact-exchange energy density in the gauge of a semilocal density functional approximation. 2008. *Physical Review A.* **77**: 012509.

5. Perdew, J. P., V. N. Staroverov, J. Tao, and G. E. Scuseria. Density functional with full exact ex- change: balanced nonlocality of correlation, and constraint satisfaction. To appear in *Physical Review A.*

6. Tao, J.. Van der Waals-corrected density functional theory. Presented at *Workshop on mathematical and algorithmic challenges in electronic structure theory.* (Minnesota, Sept. 29-Oct. 3, 2008).

7. Tao, J., S. Tretiak, and J. X. Zhu. Excitation energies from a time-dependent nonempirical density functional. 2008. *Journal of Chemical Physics.* **128**: 084110.

8. Tao, J., S. Tretiak, and J. X. Zhu. Absorption spectra of blue-light emitting oligoquinolines from time-dependent density functional theory. To appear in *Journal of Physical Chemistry.*

9. Tao, J., and J. X. Zhu. Optical conductivity in strongly correlated electron materials. 2008. In *American Physical Society March Meeting.* (New Orleans, March 10-14, 2008). Vol. 53, p. 391. College Park, MD: American Physical Society.


## Publications


Perdew, J. P., V. N. Staroverov, J. Tao, and G. E. Scuseria. Density functional with full exact ex- change: balanced nonlocality of correlation, and constraint satisfaction. To appear in *Physical Review A.*

Tao, J.. Van der Waals-corrected density functional theory. Presented at *Workshop on mathematical and algorithmic challenges in electronic structure theory.* (Minnesota, Sept. 29-Oct. 3, 2008).

Tao, J., G. Vignale, and I. V. Tokatly. Quantum stress focusing in descriptive chemistry. 2008. *Physical Review Letters.* **100**: 206405.

Tao, J., I. V. Tokatly, and G. Vignale. Quantum stress focusing in descriptive chemistry. 2008. In *American Physical Society March Meeting.* (New Orleans, March

10-14, 2008). Vol. 53, p. 275. College Park, MD: American Physical Society.

Tao, J., J. P. Perdew, L. M. Almeida, C. Fiolhais, and S. Kummel. Nonempirical density functionals investigated for jellium: spin-polarized surfaces, spherical clusters, and bulk linear response. 2008. *Physical Review B.* **77**: 2454107.

Tao, J., S. Tretiak, and J. X. Zhu. Excitation energies from a time-dependent nonempirical density functional. 2008. *Journal of Chemical Physics.* **128**: 084110.

Tao, J., S. Tretiak, and J. X. Zhu. Absorption spectra of blue-light emitting oligoquinolines from time-dependent density functional theory. To appear in *Journal of Physical Chemistry.*

Tao, J., V. N. Staroverov, G. E. Scuseria, and J. P. Perdew. Exact-exchange energy density in the gauge of a semilocal density functional approximation . 2008. *Physical Review A.* **77**: 012509.

Tao, J., and J. X. Zhu. Optical conductivity in strongly correlated electron materials. 2008. In *American Physical Society March Meeting.* (New Orleans, March 10-14, 2008). Vol. 53, p. 391. College Park, MD: American Physical Society.

# Sensitization of Lanthanide Ion Fluorescence Using Nanocrystal Quantum Dots

*Jennifer Ann Hollingsworth*

20070722PRD3

## Introduction

Once excited, lanthanide ions (Ln's) emit light for long (millisecond) lifetimes. Depending on which lanthanide photoemitter is chosen, light emission can be obtained in the visible and/or the infrared (IR). These characteristics, and especially the long luminescence lifetimes, make Ln's ideal candidates for applications in 1) imaging biological molecules and clinical diagnostics, 2) optical amplification and lasing, and 3) photon up-conversion (lower energy excitation yields higher energy emission). However, Ln's absorb light only weakly, which leads to low emission efficiencies and has prevented their full exploitation in these areas. Further, Ln emission can be "deactivated" (vibrationally quenched) in the presence of common chemicals, especially protic solvents (O-H and N-H bonds). Our work focuses on semiconductor nanocrystal quantum dots (NQDs) as novel sensitizing agents to enhance Ln absorption and protect Ln emission. Characterized by large absorption cross sections over a wide spectral range and tunable color responses, NQDs are predicted to serve as an effective "light antenna" in an NQD-Ln coupled system. Further, it is anticipated that these NQD antenna will then transfer their collected energy to their Ln partners. It has been demonstrated previously that NQDs serve as efficient energy transfer (ET) partners for a variety of materials systems—from other NQDs to dye molecules to transition metal luminescent ions. If successful, by optimizing the chemical coupling strategies for creating Ln-NQD energy transfer pairs, we should facilitate excitation of efficient Ln ion emission and, thereby, contribute to the establishment of a new class of functional fluorophores with utility in key applications from bio-imaging to solid-state lighting.

## Benefit to National Security Missions

This project will support the missions of the DOE Office of Science in advancing fundamental science in support of the national, economic, and energy security of the United States. The resulting scientific understanding will enable technology advances in telecommunications, efficient lighting/lasing, secure printing, optical tags, bioimaging, and radiation detection.

## Progress

Working from the successes of our first-year effort (Eu-doped $In_2O_3$ NQDs) [1], we attempted to prepare additional nanocrystal quantum dot (NQD)-lanthanide (Ln) couples using (1) alternative Ln ions and (2) alternative NQD compositions. We developed synthetic procedures for the preparation of several Ln-doped NQDs – $In_2O_3$:Er, $In_2O_3$:Yb, and $In_2O_3$:Yb,Er. For these, the goal was to obtain near-infrared emission by way of ultraviolet light excitation of the $In_2O_3$ matrix. To date, we have not been able to detect the anticipated infrared emission (i.e., 1540 nm from Er-doped $In_2O_3$ and 980 nm emission from Yb-doped $In_2O_3$). Attempts to characterize these systems using energy dispersive X-ray spectroscopy (EDX) have been inconclusive, implying that doping levels are lower than anticipated based on the reaction chemistries employed. Energetically, the Yb-doped systems were not ideal, as Yb has a unique transition at ~960 nm—considerably red-shifted from the $In_2O_3$ emission. However, Er ions can be excited at 380 nm providing for excellent overlap with $In_2O_3$ emission.

In addition to $In_2O_3$ as an NQD matrix, we attempted an InP matrix. Synthetic procedures were developed for InP:Er, InP:Yb, and InP:Yb,Er Ln-doped NQDs. Similar to the new $In_2O_3$ systems, infrared emission was not apparent for the InP-based materials, and EDX was equally inconclusive.

Up to this point, we had based our choice of NQD largely on whether or not its semiconductor bandgap energy (effectively emission energy) matched an absorbing transition in the Ln. However, given the poor performance of our more recently attempted NQD-Ln systems, we became concerned that NQD semiconductor bandgap energies were perhaps not the the primary factor in determining whether an NQD could efficiently transfer absorbed energy to a Ln dopant. Depending on the mechanism of energy transfer—Forster-like (coulombic interaction) or Dexter-like (electron-exchange interaction)—the bandgap energy overlap may be less important than absolute energy-level overlap, especially of the NQD conduction band energy with the Ln redox potential energy, respectively. We, therefore, compiled

the available data for NQDs and Ln's and determined that if electron-exchange interactions dominated NQD-Ln interactions, then neither $In_2O_3$ nor InP NQDs were ideal candidates for ET-pair systems. Rather, ZnSe was found to be a more ideal matrix, at least for Yb and Eu, and neglecting bandgap overlap with Ln excitation energies.

We therefore prepared ZnSe:Eu and ZnSe:Yb. The Eu version provided the anticipated emission in the red-visible, while the Yb version remained optically silent in the near-infrared. These systems require further optimization, however, by adjusting the Ln content and perhaps incorporating Er, rather than Yb.

We have also initiated work toward our second proposed coupling strategy – chemically linking NQDs with Ln nanophosphors. A recent report in which $LaF_3$:Ln (Ln = Er, Nd, and Eu) nanoparticles were incorporated into an $In_2O_3$ sol gel thin film showed efficient excitation of Er, Nd, and Eu by way of energy transfer from the sol gel thin film matrix to the nanophosphors [2] despite a poor overlap of the $In_2O_3$ conduction band with the redox energies of the former two Ln's. We have synthesized $YVO_4$:Ln nanophosphors to use in our investigations of NQD-Ln nanophosphor coupling chemistry and sensitization efficiencies. These are: $Nd_{0.01}Y_{0.99}VO_4$, $Ho_{0.04}Y_{0.96}VO_4$, $Eu_{0.05}Y_{0.95}VO_4$, and $Er_{0.02}Yb_{0.20}Y_{0.78}VO_4$, where the former three are based on literature preparations and the latter represents new chemistry. In all cases, we were able to obtain spectra of the Ln emissions, ranging from the red-visible to the near-infrared depending upon the specific Ln. These nanophosphors are now being intimately mixed with NQDs in solid-state films in order to obtain sensitization-enhanced Ln emission.

To date, we have prepared thin solid films from mixtures of the Ln nanophosphors ($YVO_4$:Nd and $YVO_4$:Eu) and NQDs (CdSe with emission energies of 586 nm and 520 nm, respectively). The process of thin-film formation entailed mixing the two types of nanomaterials in a concentrated solution, dropcasting a droplet of the solution, and evaporating the solvent to leave a solid film. In contrast with NQDs, $YVO_4$:Ln nanoparticles are water soluble. In order to prepare solution-phase mixtures for dropcasting, we had to modify the surface chemistry of one of the nanomaterials to be compatible with that of the other nanomaterial. We were unsuccessful in rendering the $YVO_4$:Ln nanoparticles soluble in nonpolar solvents. Therefore, we used ligand exchange techniques to render the NQDs water-soluble. The films prepared from such aqueous solutions were subsequently analyzed by spectroscopic techniques, including an investigation of the impact of the relative concentrations of the two species—Ln nanoparticle and NQD—on the efficiency of sensitization.

Here, we provide spectral data for a representative system – $YVO_4$:Nd and 586 nm-emitting CdSe NQDs (Figure 1). The presence of CdSe NQDs provides for enhanced emission at all excitation energies, and it provides for excitation at energies at which the Nd does not possess a transition. Together, these results suggest that we can sensitize Ln-containing nanoparticles, both in terms of increasing the Ln's effective absorption cross section and in expanding the spectral window for excitation. However, photoluminescence excitation spectroscopy (PLE) revealed that these effects of the NQDs are not a result of NQD-Ln energy transfer, but, instead, Ln re-absorption of NQD emission (Figure 2). This result suggests to us that we have likely not achieved intimate mixing of the two nanomaterials systems *at the nanoscale* in the thin solid films as currently prepared. Instead, the $YVO_4$:Nd and CdSe nanomaterials are thought to be spatially segregated within the films, preventing efficient CdSe-$YVO_4$:Nd energy transfer, as energy transfer is a highly distance dependent process.

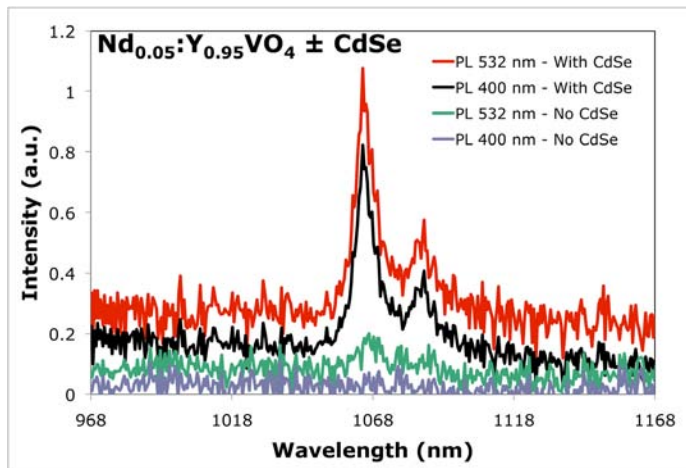


*Figure 1. Photoluminescence (PL) spectra obtained using a Horiba Jobin Yvon NanoLog Spectrofluorometer equipped with an InGaAs array infrared detector; excitation provided by a xenon lamp. Spectra show PL from Nd:YVO4 nanophosphors co-deposited with CdSe nanocrystal quantum dots (NQDs) under 532 nm excitation (red trace) and 400 nm excitation (black trace), as well as PL from Nd:YVO4 nanophosphors in the absence of CdSe NQDs under 532 nm excitation (green trace) and 400 nm excitation (purple trace).*

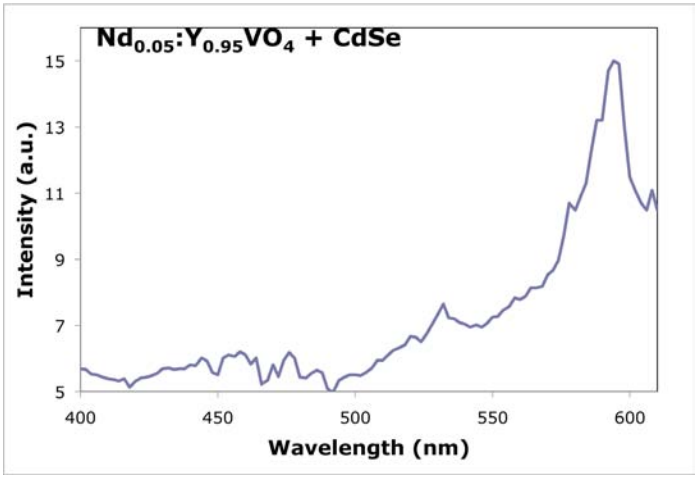


*Figure 2. Photoluminescence excitation spectrum (PLE) for 1066 nm emission from Nd:YVO4 nanophosphors co-deposited with CdSe NQDs revealing excitation through Nd absorption, rather than through CdSe-Nd energy transfer.*

Finally, in addition to attempting to enhance Ln emission from Ln nanophosphors by coupling them to NQDs, we also sought to do so through higher Ln doping concentrations. We successfully modified the literature-reported synthesis chemistry [3] to increase doping levels from 1% to 5% and 10% in the $YVO_4$:Nd system. We observed an ~10-fold increase in emission in increasing the doping level to 5%. In contrast, at 10% loading, Nd-Nd quenching may have been active, as significant additional enhancement was not observed. Thus, a loading of between 5 and 10% may represent an upper loading limit for maximizing infrared emission signal from this system.

## Future Work

In the remaining third of the project, we will focus on achieving truly intimate—at the nanoscale—mixing of our Ln nanophosphors and quantum dots. Our results to date suggest that this may not be possible by creating thin solid films from concentrated solution-phase mixtures of the two nanomaterials. For this reason, we will now increase our efforts toward *direct chemical coupling* of these systems. Initially, we will attempt this by way of electrochemical coupling. We will again modify the surface chemistry of our NQDs such that they are positively charged, rather than negatively charged as they are currently. The Ln nanophosphors are negatively charged. Through an iterative titration process, we will mix solutions of these oppositely charged nanoparticles and record any changes in emission and PLE spectra. Further, we will use dynamic light scattering techniques to observe any changes in particle size resulting from NQD-Ln nanoparticle aggregation. Ln nanophosphors of interest will continue to be Nd:$YVO_4$, Ho:$YVO_4$, EuY:$VO_4$, and ErYb:$YVO_4$, while NQDs under investigation will be the expanded set of $In_2O_3$, InP, ZnSe, and CdSe.

## Conclusion

By chemically coupling nanocrystal quantum dots (NQDs) with lanthanide (Ln) ions, we are combining the best properties of NQDs and Ln's in a single material, essentially creating a new class of fluorophores with specifically designed excitation and emission properties. We are creating these couples by doping Ln ions into NQD matrices, as well as by chemically attaching Ln nanoparticles to NQDs. Such systems should provide great potential for high-efficiency, high-stability, low-toxicity, narrow-band photon sources for a variety of applications ranging from biology (using direct or up-conversion fluorescence) to telecommunications (direct IR fluorescence) to inks for secure printing (up-conversion fluorescence).

## References

1. Vela, J., B. S. Prall, P. Rastogi, D. J. Werder, J. L. Casson, D. J. Williams, V. I. Klimov, and J. A. Hollingsworth. Sensitization and Protection of Lanthanide Ion Emission in In2O3:Eu Nanocrystal Quantum Dots. To appear in *The Journal of Physical Chemistry - C.*

2. Sivakumar, S., F. C. J. M. van Veggel, and M. Raudsepp. Sensitized emission from lanthanide-doped nanoparticles embedded in a semiconductor sol-gel thin film . 2007. *ChemPhysChem.* **8** (11): 1677.

3. Buissette, V., A. Huignard, T. Gacoin, J. P. Boilot, P. Aschehoug, and B. Viana. Luminescence properties of YVO4:Ln (Ln = Nd, Yb, and Yb-Er) nanoparticles. 2003. *Surface Science.* **532-535**: 444.

## Publications

Vela, J., B. S. Prall, P. Rastogi, D. J. Werder, J. L. Casson, D. J. Williams, V. I. Klimov, and J. A. Hollingsworth. Sensitization and protection of lanthanide ion emission in In2O3:Eu nanocrystal quantum dots. To appear in *The Journal of Physical Chemistry - C.*

Vela, J., and J. A. Hollingsworth. Semiconductor nanocrystals: Doped compositions. To appear in *Nanomaterials: Inorganic and bioinorganic perspectives.* Edited by Lukehart, C. M., and R. A. Scott.

# Chemically Synthesized Germanium Nanocrystals for Applications in Solar-Energy Conversion

*Victor Ivanovich Klimov*

20070723PRD3

## Introduction

With increasing concerns regarding elevated levels of carbon dioxide emission, solar radiation is widely considered as the most attractive sustainable, carbon-free energy source. However, current photovoltaic technologies encounter cost and scalability issues and suffer from relatively low efficiencies that are significantly below the limits calculated based on thermodynamic considerations. Currently the photovoltaic (PV) industry is dominated by silicon. This material has an energy gap of ~ 1 eV, which is well suited for single junction devices. However, in order to improve the efficiency of solar cells through the use of, for example, multi-junction tandem architectures or multiple exciton generation (carrier multiplication), one needs materials with a narrow energy gap. One such promising material is germanium (Ge). The applicability of Ge in its traditional "bulk" form in PV technologies is limited because of the indirect character of its energy gap, which leads to low optical absorbtivity. Further, "chemical" factors such as formation of unstable oxides also complicate applications of Ge. The purpose of this project is the development of nanoscale colloidal Ge nanocrystals with enhanced potential for applications in solar cells. Because of quantum confinement, which results in mixing between indirect- and direct-gap minima, Ge nanocrystals are expected to exhibit enhanced absorption cross sections compared to a bulk form of this material. Further, by using appropriate surface termination, we expect to solve the problem of uncontrolled oxidation. In conjunction with our materials work, we will also study electronic and optical properties of engineered nanostructures with focus on their light harvesting ability and carrier multiplication performance.

## Benefit to National Security Missions

This project will lead to the development of novel inexpensive wet-chemistry techniques for the fabrication of Ge nanocrystals. Because of a significant technological potential of these materials in solar energy, this work is directly relevant to the DOE missions in Energy Security.

## Progress

Recently, Ge nanocrystals with good size control have been synthesized by a new plasma method developed by U. Kortshagen and co-workers (R. Gresback et al., Appl. Phys. Lett. 91, 093119, 2007). However, this process is expensive and unscaleable, and the product yield is inherently low. As part of the present project, during the past year we have developed an alternative fabrication route for Ge nanocrystals that relies on colloidal synthesis. Compared to a plasma-based physical synthesis, chemical methods have the greatest potential for scale-up, and yield chemically flexible and processible materials.

In our synthesis, we use germanium diiodide ($GeI_2$) as the germanium precursor at reaction temperature of ~300 degrees C. We have tested various solvents, capping ligands, and reducing agents to establish a set of optimal reaction conditions. In a typical reaction, the mixture of $GeI_2$ and hexadecylamine is transported to a Schlenk line setup without air exposure and heated to 200 degrees C. The solution of n-butyllithium in 1-octadecene is injected into the reaction flask. Then, the reaction mixture is heated to 300 degrees C and held at this temperature for 1 hr under vigorous stirring conditions. Subsequently, the reaction is quenched by removing the heat source and the reaction products are collected in a centrifuge tube. The fabricated nanocrystals were washed with methanol and acetone.

We have also carried out transmission electron microscopy (TEM) studies to characterized sizes and crystallinity of the synthesized nanoparticles (Figure 1A). The high-resolution TEM images demonstrate well-resolved lattice fringes, which is indicative of good crystallinity of the fabricated nanocrystals. The size dispersion of the samples is better than 15%.

Finally, we have examined the chemical and photo- stability of the synthesized particles and also conducted their initial spectroscopic characterization. Specifically, we have investigated photoluminescence of our sam-

ples (Figure 1B). The synthesized particles exhibit infrared emission with quantum yield as high as 10%, which is the highest value (!) reported for these materials so far. Based on the spectral position of the emission peak, we have determined the energy gap as a function of the particle size. Additionally, we have measured single-exciton and multiexciton dynamics. An interesting result of these studies is the observation of very large Auger recombination rates that greatly exceed those of bulk Ge. This observation can be rationalized by taking into account the effects of quantum confinement that remove restrictions due to translational momentum conservation.

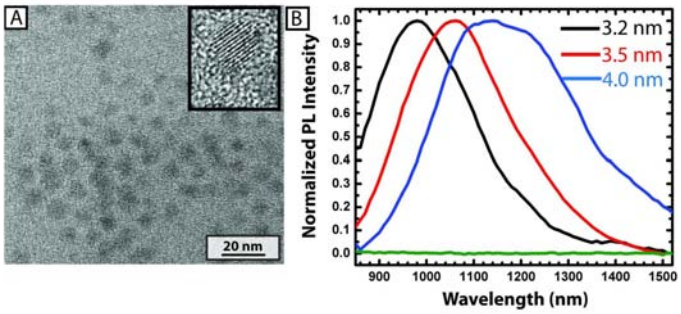


*Figure 1. (A) TEM images of Ge nanocrystals (NCs) of 4.0 nm size whose PL peak centers at 1160 nm (blue curve in Figure 1B). Inset shows high-resolution TEM image of a single Ge NC. The visible lattice spacing matches the Ge (111) d-spacing. (B) Normalized photoluminescence (PL) spectra of Ge NCs of three different sizes.*

## Future Work

In our future work, we will perform comprehensive temporally- and spectrally-resolved photoluminescence and transient absorption (TA) studies of synthesized nanocrystals as a function of their dimensions. Radiative recombination rates will be determined by upconversion or a streak camera with picosecond temporal resolution. These studies will be complemented by investigations of the dynamics of inter- and intraband transitions using temporally and spectrally resolved TA spectroscopy. Due to a multitude of possible transitions, the interpretation of TA spectra can become rather complex. According to our preliminary studies, many of the TA spectra are dominated by photo-induced absorption features due to intraband transitions likely involving multiple band minima. However, by resonantly exciting the zone-center transitions with the largest cross sections, we should be able to assign features arising from different bands. Besides establishing the effects of quantum confinement on the band structure, the assignment of the various transitions to different spectral regions will provide key reference for the study of multi-exciton processes such as Auger-recombination and carrier multiplication.

## Conclusion

As a result of the proposed work, we will develop wet-chemical approaches to high-quality Ge nanocrystals. The developed synthetic routines will allow for accurate control of particle sizes and surface properties. Using optical spectroscopic methods in conjunction with TEM, we will characterize the size dependence of the nanocrystal energy gap. Our spectroscopic work will also provide new insights into the effect of quantum confinement on absorption cross-section and carrier multiplication efficiencies of Ge nanocyrstals.

## Publications

Lee, D., I. Robel, J. M. Pietryga, R. D. Schaller, D. Werder, and V. I. Klimov. Solution-phase synthesis of infra-red emitting germanium nanocrystals. *Journal of American Chemical Society.*

# Molecular Level Investigation of Tunable Energetic Mixtures

*David Steven Moore*

20070766PRD4

## Introduction

Explosive materials (e.g., HMX, PBX) generate rapidly expanding gases, which can cause unnecessary collateral damage. A safer alternative is in intermetallic-forming reactive mixtures, which can undergo ultra-fast shock-induced reactions, releasing significant heat during the formation of solid products, and thereby provide for the controlled defeat of targets. The challenge associated with reactive mixtures has been to determine the molecular-level mechanisms that govern the initiation and kinetics of shock-induced reactions. We are studying the shock-induced initiation of intermetallic reactions through combined laser-driven shock-compression experiments and computer modeling, performed on a range of binary reactive systems, in order to determine the influence of heterogeneity on the molecular-level processes responsible for reaction. Multi-component reactive films (e.g., V/Si, Mo/Si, Al/PTFE) up to 2 µm in thickness will be deposited onto transparent substrates using e-beam deposition and/or spin casting. A novel dynamic masking technique, in which a mask is translated between the source and substrate during deposition, will be employed to construct films with a predefined thickness gradient. This method, performed in forward and reverse mask mode with reactive complements, will be used to fabricate bi-layer films with an internal interface, inclined to the substrate normal by a specified angle. Measures of the total film thickness, roughness, and interface angle, necessary for proper interpretation of results, will be characterized through SEM, AFM, and profilometry. A Ti:sapphire laser system, focused at the substrate/film interface to a spot size of 75 µm, will be used to drive an ultra-fast, supported shock wave (10-20 ps rise-time, >200 ps shocked duration) through the bi-layer. Spatially flat shocks (1-D) will be produced using a field-flattener. Ultra-fast dynamic ellipsometry will be employed at the film/air interface to obtain time- and spatially-resolved surface displacements in a single given experiment, and detect short timescale phase shifts corresponding to the onset of molecular-level reactions. Varying the film species (metals, metalloids, polymers), interface angle during deposition (gradient and non-gradient), and laser-drive energy, will provide great flexibility in further studying the role of heterogeneity in the kinetics of shock-induced reactions at the molecular-level. This experimental work is complemented by multi-scale numerical simulations, used to develop and validate new predictive models for the controlled, ultra-fast initiation of intermetallic reactions.

## Benefit to National Security Missions

The results from this study are directly applicable to threat reduction mission needs, enabling the design of a new class of application-based energetic materials for controlled defeat of targets.

## Progress

Completed addition of the dynamic masking system to our bell jar vapor deposition system necessary to produce multi-component films with a predefined thickness gradient. Have successfully deposited a series of amorphous Si films with a thickness gradient, and characterized their uniformity using SEM.

Produced Al/Si binary films (no gradient at first to capture the response of Si) and have used our Ti:sapphire based laser generated shock system to drive controlled shock waves through them (<10 ps rise time, > 200 ps at constant shock velocity). We measured the shock response of these binary films using ultrafast dynamic ellipsometry (UDE) and found a complex time response. Previous UDE measurements of shocked inert dielectric materials on Al have only shown constant shock and particle velocities. The complex time response is indicated by the time dependent UDE data (i.e., time dependent fringe frequencies). Such complex time response could be due to changes in the particle velocity due to reaction or phase change, or changes in the shocked material index of refraction, also due to reaction or phase change.

Developed two approaches to analyze the time dependent UDE data. One involves a time dependent change in the index of refraction of the shocked material with either sigmoidal or logarithmic approach to a new con-

stant value. The other involves a first order reaction with progress variable, and calculates the time dependent index of refraction. Ellipsometric data are then fit using four variables instead of three, with the fourth describing the time dependent index of refraction. While preliminary analysis indicates better fits to the UDE data (reduced global error) achieved using the time-dependent models, local error in the fringe amplitudes indicates the need for continued work.

We have also produced Mo/Si and V/Si binary films with a sharp (near vertical) step between the two layers. The spatially resolved UDE data are being obtained and will be analyzed using similar tools to those developed for the non-gradient films. Continuum-level simulations of this configuration have been performed using the multi-material Eulerian shock code, CTH, to estimate the magnitude of particle-velocity mismatch at such an interface.

## Future Work

Due to the complex time-dependent UDE response and physical/optical ambiguity of experiments already performed, the following approach is proposed:

-Perform laser-driven shock compression experiments on a single-component system that exhibits a shock-induced structural phase transformation, in order to elucidate the signatures of such time-dependent response in UDE data. We have chosen to investigate single-crystal silicon, which exhibits a polymorphic transformation from the diamond cubic to tetragonal structure above a threshold shock stress of 10 GPa. Silicon samples of the appropriate thickness (1-2 micron) and purity ($\rho$ = 10000 ohm•cm) will be produced through photolithographic microfabrication.

-Develop the technique of femtosecond stimulated Raman spectroscopy (FSRS) for use as a secondary diagnostic in the laser-driven shock experiments. While UDE can supply the details of interface migration and refractive index changes, FSRS can be used to reveal the elimination and formation of vibrational modes associated with the presence of reactants and products, respectively, and their related timescales. Additionally, probing both the Stokes and anti-Stokes Raman transitions can be used to measure temperature, and more completely survey the thermodynamics of ultrafast chemical reactions.

-Perform laser-driven shock compression experiments of binary reactive mixtures, such as V+Si, Mo+Si, and Al+PTFE, in the gradient and step configurations, using the combined diagnostics of UDE and FSRS, to extract the kinetics of ultrafast chemical reactions. Building upon the understanding gained from the investigations of single crystal Si, differentiate between the contributions from phase transformation and chemical reaction in time-dependent UDE data.

## Conclusion

The study will provide the first insight into the critical molecular-level processes responsible for ultra-fast shock induced reactions in multi-component energetic mixtures, and their dependence on system heterogeneity. The results will have a broad impact on conventional reactive material systems, supply the fundamentals to directly manipulate and optimize chemical behavior. This understanding will enable the design of a new class of application-based energetic materials, demonstrating tunable sensitivity, reaction kinetics, and energy yield.

continuing project

# Synthesis, Chemistry and Theoretical Studies of 5*f*-Element Hydride Complexes

*Jaqueline Kiplinger*

20070768PRD4

## Introduction

One of the key missions throughout the DOE Complex as well as the Chemistry, Materials, and Theoretical Divisions at LANL concerns research on the light actinides (Th-Am) to predict *f*-element behavior in a variety of applications such as materials disposition, selective chemical separations, and actinide materials compatibility. Though a key corrosion phenomenon of actinide metals, reaction with hydrogen (hydriding), is a major problem, f-element hydrides surprisingly remain a relatively unexplored.

In this research project we intended to fill this technology gap by developing methods for the preparation of well-defined uranium hydride complexes, studying these systems theoretically using DFT calculations, and exploring their reactivity towards small molecules. In fact, recent studies have shown that actinide hydride complexes can promote remarkable transformations on small molecules and engage in multi-electron chemistry. This work will greatly advance our understanding of the chemical and physical properties of uranium hydrides in addition to providing critical information regarding the interaction of hydrogen with actinide metals. These species are promising materials to access new actinide-based functional groups and materials and provide important information regarding hydriding at the molecular level.

## Benefit to National Security Missions

The chemistry of the actinides is critical to DOE nuclear weapons mission areas (stockpile stewardship, environmental remediation, waste management, materials storage and disposition). By synthesizing new uranium compounds this program will provide important information about bonding and improve our ability to reliably predict chemical behavior in a variety of environments.

## Progress

The bis[2-(diisopropylphosphino)-4-methylphenyl] amido ligand (PNP) **1** is a monoanionic pincer ligand that combines a hard central donor atom (N=amide) with two soft ancillary soft donors (P=phosphine) (Figure 1). Soft donor ligands have been largely ignored as supporting ligands for early actinide chemistry, with the exception of coordination complexes featuring phosphorus and chalcogenide ligands prepared to investigate actinide/lanthanide separation technologies and questions about covalency in “hard-soft” interactions. Given that soft donor ligands provide an excellent opportunity to promote the low valent chemistry of uranium, we initiated a program to develop the coordination chemistry of the robust mono-anionic bis[2-(diisopropylphosphino)-4-methylphenyl]amido or PNP ligand towards the uranium halide complexes, $UCl_4$ and $UI_3(THF)_4$.

This year, several trivalent and tetravalent uranium PNP halide complexes were prepared as potential starting materials for accessing the targeted hydride complex. As depicted in Figure 1, the reaction between (PNP)K (**2**) and one equivalent of $UI_3(THF)_4$ afforded the trivalent halide complex (PNP)$UI_2$(4-$^t$Bu-pyridine)$_2$ (**3**) in the presence of 4-tert-butylpyridine. The same reaction carried out with $UCl_4$ and no donor ligand gave [(PNP)$UCl_3$]$_2$ (**4**), in which the uranium coordination sphere in the (PNP)$UCl_3$ unit is completed by a bridging chloride ligand. When $UCl_4$ is reacted with one equivalent (PNP)K (**2**) in the presence of THF, trimethylphosphine oxide (TMPO) or triphenylphosphineoxide (TPPO), the tetravalent halide complexes (PNP)$UCl_3$(THF) (**5**), (PNP)$UCl_3(TMPO)_2$ (**6**) and (PNP)$UCl_3$(TPPO) (**7**), respectively, are formed in excellent yields.

The bis(PNP) complexes of uranium(III), $(PNP)_2UI$ (**8**), and uranium(IV), $(PNP)_2UCl_2$ (**9**), were easily isolated from the analogous reactions between two equivalents of **6** and $UI_3(THF)_4$ or $UCl_4$, respectively (Figure 2). Complexes **8** and **9** represent the first examples of complexes featuring two PNP ligands coordinated to a

single metal center. Complexes **3**-**9** have been characterized by single-crystal X-ray diffraction and $^{1}H$ and $^{31}P$ NMR spectroscopy. The X-ray structures demonstrate the ability of the PNP ligand to adopt new coordination modes upon coordination to uranium. The PNP ligand can adopt both *pseudo*-meridional and *pseudo*-facial geometries when it is $\kappa^3$-(*P*,*N*,*P*) coordinated, depending on the steric demand at the uranium metal center. Additionally, its hemi-labile character was demonstrated with an unusual $\kappa^2$-(*P*,*N*) coordination mode that is maintained in both the solid-state and in solution. Comparison of the structures of the mono(PNP) and bis(PNP) complexes **3**, **5**, **7**-**9** with their respective $C_5Me_5$ analogues revealed that a more sterically congested environment is provided by the PNP ligand.

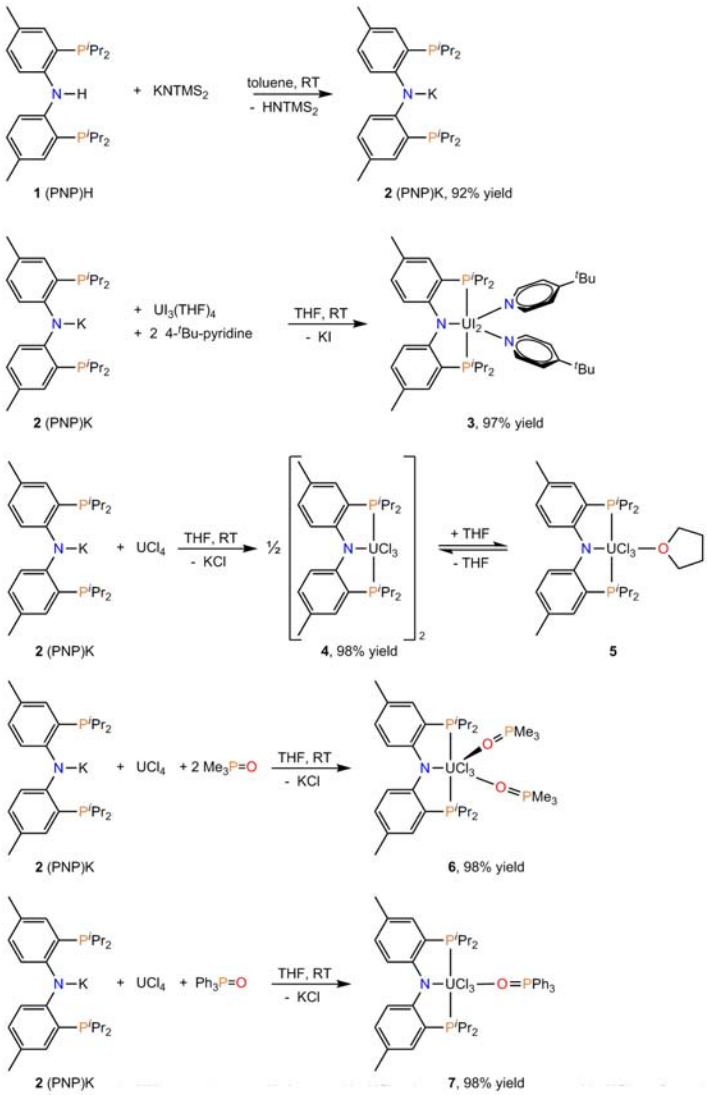


*Figure 1. Synthesis of trivalent and tetravalent uranium mono(PNP) halide complexes.*

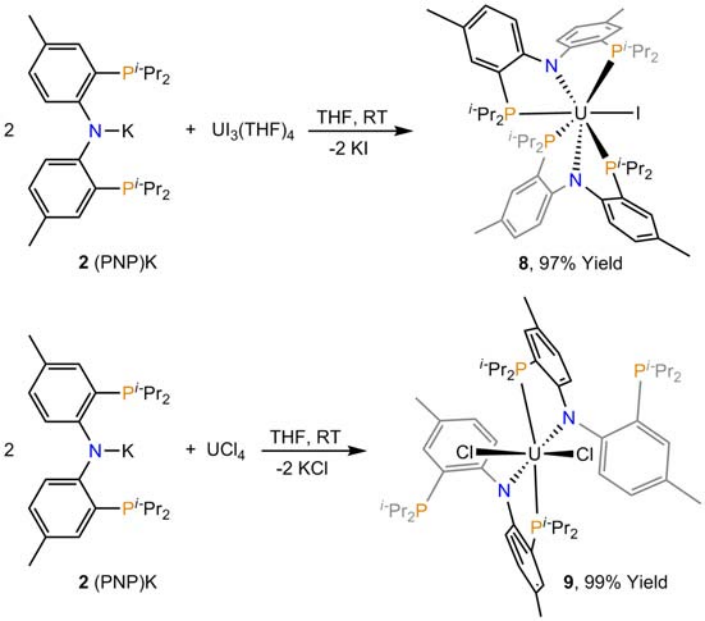


*Figure 2. Synthesis of trivalent and tetravalent uranium bis(PNP) halide complexes.*

The electronic influence of replacing the $C_5Me_5$ ligands with PNP was investigated using electronic absorption spectroscopy and electrochemistry. For **8** and **9**, a chemically reversible wave corresponding to the $U^{IV}/U^{III}$ redox transformation comparable to that for the known $(C_5Me_5)_2U(THF)(I)$ and $(C_5Me_5)_2UCl_2$ was observed. However a ~350 mV shift of this couple to more negative potentials was observed on substitution of the bis($C_5Me_5$) by the bis(PNP) framework, therefore pointing to a greater electronic density at the metal center in the PNP complexes. The UV-visible region of the electronic spectra for the mono(PNP) and bis(PNP) complexes appear to be dominated by PNP ligand-based transitions that are shifted to higher energy in the uranium complexes than in the simple ligand anion (**6**) spectrum, for both the $U^{VI}$ and $U^{III}$ oxidation states. The near IR region in complexes **3**, **5**, **7**-**9** and their $C_5Me_5$ analogues is dominated by *f*-*f* transitions derived from the $5f^3$ and $5f^2$ valence electronic configuration of the metal center. Though complexes of both ligand sets exhibit similar intensities in their f-f bands, a somewhat larger ligand-field splitting was observed for the PNP system, consistent with its higher electron donating ability.

Presumably due to the large size of uranium ions, these complexes show unprecedented binding modes for the PNP ligand set. In transition metal complexes, this ligand is rigorously tridentate $\kappa^3$-(*P*,*N*,*P*) (bound through the one nitrogen atom and the two phosphorus atoms), but for the uranium complex **9** we observe the PNP ligand coordinated to the metal in a bidentate $\kappa^2$-(*P*,*N*) , with one dangling phosphorus.

Exhaustive studies in our labs over the past several months

showed that none of the uranium PNP complexes form stable U-C bonds, which are necessary precursors to a hydride linkage. Nevertheless, preliminary reactivity studies with the trivalent uranium complex $(PNP)_2UI$ (**8**) have demonstrated that the PNP ligand framework can support unusual transformations at the uranium metal center. Reduction of $(PNP)_2UI$ (**8**) with potassium-graphite ($KC_8$) at low temperature (-35 °C) generates a stable uranium(II) synthon (Figure 3). Upon raising the temperature to room temperature, this low valent intermediate oxidatively inserts into one of the P-C bond of the PNP ligand. This intramolecular oxidative addition leads to the formation of complex **10** where a uranium(IV) center is coordinated to one intact PNP ligand, one phosphido group and one reduced PNC ligand. This intramolecular oxidative addition has never been seen before and represents a new chapter in actinide chemistry. Other reaction chemistry demonstrates that the low valent intermediate formally behaves as a uranium(II) synthon. For example, this intermediate has a half-life of 15 minutes at RT and reacts with one equivalent of hexachloroethane ($C_2Cl_6$) yields the uranium(IV) complex **9**. Even more remarkable is that reaction of this low-valent uranium(II) complex with excess pyridine N-oxide leads to the formation of the uranyl complex **11**. This transformation also has never been observed and provides an important missing link between non-aqueous and aqueous actinide chemistry.

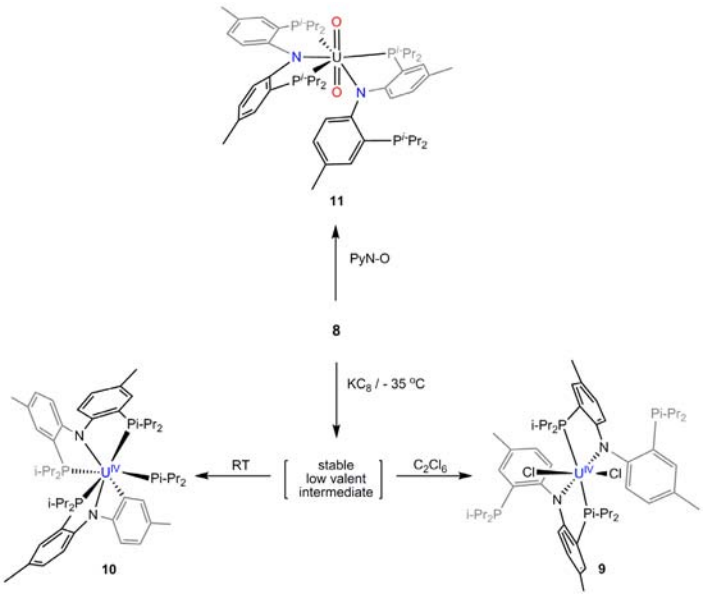


*Figure 3. Reaction chemistry displayed by low-valent PNP-uranium complex (PNP)2UI (8).*

## Future Work

While we are clearly at an early stage, this new uranium system is opening up new frontiers in the understanding of chemical reactivity, and will be writing a new chapter in modern inorganic chemistry texts. The potential of this new system is just being realized, and further studies are certain to have high impact across the actinide chemistry community. Although a terminal hydride complex has not yet been accessible, the reduction of $(PNP)_2UI$ (**8**) allows the formation of a new stable uranium(II) synthon. Future developments will focus on exploiting its unique reactivity to access new functions on uranium, such as terminal sulfide (U=S), selenide (U=Se) and telurido (U=Te) complexes (by the reaction of **8** with phosphine chalcogenide $R_3P$=E). Another important route to explore concerns the ability of complex **8** to access uranium(III) – main group element double bonds, since two "active coordination sites" are available for chemistry on this complex.

## Conclusion

The first uranium(III) and (IV) halide complexes supported by one and two bis[2-(diisopropylphosphino)-4-methylphenyl]amido ligand (PNP) ligands have been synthesized in high yields and fully characterized. The complexes demonstrate that new coordination modes are available for the PNP ligand. The influence of replacing the classic $C_5Me_5$ ligand with PNP on the geometry and electronic structure of the complexes was investigated using X-ray analysis, electronic absorption spectroscopy and electrochemistry. The PNP ligand was shown to provide a more sterically congested environment and greater electronic density at the metal center. Studies aimed at exploiting the novel electronic and geometric features provided by these PNP uranium halide systems are currently underway to support novel structures and promote new reactivities for the actinide series.

## Publications

Cantat, T., B. L. Scott, O. V. Ozerov, D. E. Morris, and J. L. Kiplinger. What a Difference a 5f Element Makes: Trivalent and Tetravalent Uranium Halide Complexes Supported by One and Two PNP Ligands. *Inorganic Chemistry.*

Cantat, T., C. R. Graves, K. C. Jantunen, B. L. Scott, E. J. Schelter, C. J. Burns, P. J. Hay, D. E. Morris, and J. L. Kiplinger. Evidence for the Involvement of 5f-Orbitals in the Bonding and Reactivity of Organometallic Actinide Compounds: Thorium(IV) and Uranium(IV) Bis(hydrazonato) Complexes.. To appear in *Journal of the American Chemical Society.*

Graves, C. R., E. J. Schelter, T. Cantat, B. L. Scott, and J. L. Kiplinger. A Mild Protocol to Generate Mixed-Ligand Uranium(IV) Metallocene Complexes Using Copper(I) Iodide.. 2008. *Organometallics.* **27**: 5371.

# First-Principles-Based Equations of State Including Multi-Phase Chemical Equilibrium

*Milton S Shaw*

20080695PRD1

## Introduction

The goal of the proposed work is to refine and extend computational methods for building an equation of state for chemical explosive detonation products. The principal vehicle for achieving this is the development of a Monte Carlo simulation method specially designed to capture the complexities of chemistry under extreme conditions of temperature and pressure. A very efficient procedure has been implemented for evaluating equilibrium averages with energies derived from quantum chemical calculations in place of approximate functional forms, whereby many steps in a reference system (characterized by a computationally inexpensive "model" potential) are used to generate a single electronic structure configuration. This effectively reduces by up to three orders of magnitude the number of electronic structure calculations required to build ensemble averages. We will also introduce efficient means for accurately describing chemistry at the surfaces of carbon nanoclusters that are known to exist in detonation product fluids.

Replacement of approximate potentials with highly accurate ab initio energy evaluation, especially in the context of Monte Carlo in a reactive ensemble, promises considerable improvement in accuracy over that of previous work and constitutes a significant methodological advance. Namely, it permits evaluation of statistical properties accounting for rare events (in this case, chemical reactions among fluid components) on a highly accurate and reactive potential energy surface, but without actually having to sample those regions of the potential most sensitive to error (i.e., the chemical reaction barrier tops). In addition to enhancing the predictive capability of the Laboratory's continuum detonation models, these developments should be of broad interest to computational scientists in government, industrial, and academic contexts.

## Benefit to National Security Missions

This project will support the DOE/NNSA mission in Nuclear Weapons (Homeland Security and Office of Science) by enhancing our understanding of the extreme pressure and temperature environment occurring in the detonation of chemical high explosives including near-first-principles prediction capability.

## Progress

An existing Monte Carlo simulation code that includes chemical reactivity was adapted (rewritten in Fortran90) for the purposes of this project. Extensive validation studies of the fluid equation of state (EOS) of nitrogen were performed to ensure that the new code reproduces the results of its predecessor. This newly-developed code was extended to include relatively new form of Monte Carlo sampling. In this method, a Markov chain is generated at a prescribed thermodynamic state using a computationally cheap analytic "model potential," with attempted trial moves based on energies obtained from a combination of these and highly accurate electronic structure calculations. The motivation is prediction of the EOS under extreme thermodynamic conditions based on accurate electronic structure energies. Such predictions typically require ~100,000 energy evaluations; this is simply impossible now, and for the foreseeable future, using a brute-force approach. The Monte Carlo method under development allows calculation of meaningful averages based on far fewer expensive electronic structure calculations by generating uncorrelated configurations using a long chain of moves with the reference potential to produce an efficient trial move to be evaluated using quantum chemistry such that the statistical significance of individual electronic structure-based energies is maximized. The specific approach used is based on the formalism of Gelb [1].

We have optimized the Gelb procedure in order to significantly improve its efficiency. This optimization was performed by varying the thermodynamic conditions of the reference system so as to maximize the overlap of its sampled distribution with that of the full system. The advantages of this procedure are substantial, as measured by the average acceptance probability of collective steps in the full system containing a given number of single-particle steps in the reference system. The optimized procedure has been applied to a pair of model potentials meant to roughly approximate nitrogen in the low-temperature, low-pressure region of its shock Hugoniot locus. This primarily methodological discussion is currently being prepared for publication [2].

A careful study was performed to determine what level of electronic structure (quantum chemistry) theory is sufficient for generating accurate nitrogen EOS data. After consideration of other options, we chose to use the Gaussian03 suite of electronic structure codes. In Gaussian03 the basis set is expressed in terms of Gaussian orbitals centered on the nuclear centers. Various flavors of density functional theory, including the generalized gradient approximation (GGA) functionals PBE, BLYP, and exact exchange functions PBE0 and B3LYP, among others, were considered. Ultimately, it was determined that, for the cases of interest to us (molecular fluids at high density), the PBE/6-31G* as implemented within Gaussian03 was the optimal choice. A considerable amount of Monte Carlo sampling at this level of theory and for different values of temperature and pressure have been completed, and some additional sampling is still being performed, using our optimized variant of the Gelb procedure. The results collected so far for the nitrogen Hugoniot are in excellent agreement with the experimental data. This suggests that extensions of the method could be predictive for the complex molecular fluid mixture in chemical equilibrium found in detonation products at pressures around 30 GPa (300,000 bar) and temperatures around 3000 K. The nitrogen results are currently being prepared for publication [3]. An offshoot of this project was the realization that the quantum chemical calculations of atomic forces (easily obtained once the energies have been computed in the Monte Carlo simulations) can be used to predict accurately the shifts in fundamental and “hot band” frequencies of vibrational transitions in diatomic fluids as a function of pressure and temperature. The shifts are found by singular value decomposition of force data to extract the potential parameters that dictate energy level spacing. A journal article describing this technique and its application to fluid nitrogen has been published [4].

## Future Work

The scientific issue addressed will be a highly accurate fundamental theoretical description of the complex fluid mixture at the extreme temperature and pressure that results from detonation of high explosives. The system is a multiphase, chemically reacting mixture of dense molecular fluids and nano-clusters of carbon consisting of about 1000 atoms with an equally reactive surface coupled to the surrounding fluid. Given the limitations of experimental measurements at these extreme conditions, this theoretical approach gives the best opportunity of understanding the underlying physics and chemistry.
The specific tasks are basically the evaluation of potential energy hypersurfaces corresponding to at least 100 molecules, and the evaluation of thermodynamics including equilibrium composition by accurate simulation methods with sufficient speed to be tractable. State-of-the-art density functional electronic structure methods will be used for the energies of fluid configurations as well as for representative segments of carbon nano-cluster surfaces including incorporation of H, N, and O. The thermodynamics simulations will be based on a very efficient implementation of the Monte Carlo method that allows large steps through configuration space that requires only a small number of uncorrelated configuration energies evaluated by the very expensive (due to the large number of atoms) quantum chemistry methods. Of particular importance is the extension of the simulation methods to incorporate the chemical equilibrium composition

Specific goals are:

- Build on the already successful progress to refine the thermodynamic simulation methods required to efficiently sample the equation of state as well as thermodynamic equilibrium of the systems described above.

- Apply these methods to specific simulations that showcase the fundamental chemistry and physics of this complex system and reproduce available experimental benchmarks.

## Conclusion

We have and are continuing to develop improved methods for predicting the pressures, temperatures, and chemical composition of high explosive products of detonation. These are required as input to models of explosive performance and behavior with a wide variety of applications ranging from military defense (NNSA/DoD) to homeland security (DHS). The fundamental methodology, which we will develop, involves intelligently (optimally) combining Monte Carlo simulation techniques with

quantum chemistry, and will be of general use in many situations involving chemically reactive mixtures involving multiple phases, for instance formation of nanocarbon clusters from a reactive fluid.

## References


1. Gelb, L. D.. Monte carlo simulations using sampling from an approximate potential. 2003. Journal of Chemical Physics. 118 (7): 7747.
2. Coe, J. D., T. D. Sewell, and M. S. Shaw. Optimal sampling efficiency in monte carlo simulation with an approximate potential. 2008. In preparation.
3. Coe, J. D., T. D. Sewell, and M. S. Shaw. An efficient monte carlo procedure for describing equilibrium thermodynamics with density functional theory. 2008. In preparation.
4. Coe, J. D., T. D. Sewell, M. S. Shaw, and E. M. Kober. A quantum chemical method for calculating vibrational line shifts in diatomic fluids. 2008. Chemical Physics Letters. 464 (4-6): 265.


## Publications


Coe, J. D., T. D. Sewell, M. S. Shaw, and E. M. Kober. A quantum chemical method for calculating vibrational line shifts in diatomic fluids. 2008. Chemical Physics Letters. 464 (4-6): 265.

Coe, J. D., T. D. Sewell, and M. S. Shaw. Optimal sampling efficiency in monte carlo simulation with an approximate potential. 2008. In preparation.

Coe, J. D., T. D. Sewell, and M. S. Shaw. An efficient monte carlo procedure for describing equilibrium thermodynamics with density functional theory. 2008. In preparation.

# Study of Hybrid Semiconductor/Molecular Systems for Photo-production of Hydrogen

*Andrew Paul Shreve*

20080700PRD1

## Introduction

Charge transfer is one of the basic steps required for solar energy conversion to electricity or chemical fuels. However, optimization of charge-transfer processes in complex composite materials, including molecular light-absorbers and catalysts, remains challenging. There is a need for new studies to provide fundamental knowledge regarding the rates of these processes, and also to address how structural changes in materials can mediate the efficiency of charge transfer. Ultimately, such information will contribute to optimization strategies for systems that use photo-induced catalytic splitting of water for solar production of hydrogen fuel.

## Benefit to National Security Missions

This project supports national needs in energy security, and relates to DOE missions in energy technologies and research by improving fundamental understanding of photo-induced charge separation processes across the interface between molecular catalysts and semiconductor particles. Such hybrid material architectures are expected to provide long-term advantages for solar energy conversion processes.

## Progress

Activities to date have primarily focused on development of spectroscopic instrumentation that will be used for the static and time-resolved experiments that are planned, and on assessment of the performance of the instrumentation. To these ends, a new instrument for time-resolved infrared spectroscopy based on step-scan Fourier Transform infrared spectroscopy has been developed and optimized. From characterization studies to date, the instrument performs better than any similar instrument that has been previously developed. We have initiated studies that use this new instrument to characterize molecular compounds that have been developed for use as light absorbers in solar energy transduction applications. In addition, we have brought on line a new spectrally tunable Raman spectrometer, and have begun measurements of the Raman spectra of similar molecular compounds. The time-resolved infrared spectroscopy and the Raman spectroscopy studies, once performed systematically for a range of compounds, will provide us with important new information regarding strategies to help optimize charge and energy transfer processes in molecular-based solar cell devices.

## Future Work

In the near future we plan to continue exploration of a systematic series of molecular compounds that can be used in light-driven catalysis and charge separation processes. For these compounds, our studies will allow assessment of properties such as charge transfer efficiencies, excited-state lifetimes, structural changes associated with intermediate states, and overall stability. In addition, we will initiate studies in which colloidal semiconductor nanocrystals will be used to transfer electrons or holes into the molecular catalysts and absorbers. The use of semiconductors provides charge separation that is stable long enough to perform subsequent chemistry. However, optimization of charge transfer between the semiconductor and molecular components is crucial in maximizing efficiency. A combination of semiconductors and conjugated chemical links will be tested to determine the most viable combination to yield a highly efficient electron transfer. The work will be separated into two components: 1) The rate of charge transfer will be measured as a function of semiconductor type for specific functionalizations, and 2) Given semiconductors functionalized with different sizes and length of conjugated ligands will be similarly analyzed. In all cases, the spectroscopic tools we have developed to date will be essential for these future studies.

## Conclusion

To produce hydrogen from water in a process driven by light, one must have material components that absorb light and components that catalyze the chemical transformations involved. Since the chemical transforma-

tions require the addition or removal of electrons on the catalysts, the transfer of electrons between the light absorbers and the catalysts must be efficient. We will attempt to better understand the relevant photo-induced electron transfer process by applying static and time-resolved optical spectroscopies to study composite materials in which light absorbers and catalysts are assembled together. Ultimately, such studies will help optimize methods for the solar production of hydrogen.

continuing project

# Structure-Property Relationship for Strained One Dimensional Ferroelectric Nanostructures

*Quanxi Jia*

20080705PRD1

## Introduction

The fabrication of one-dimensional nanostructures involves either bottom-up chemical synthesis or top-down micro/nano-fabrication approaches. We will utilize our unique facilities for materials growth and micro/nano-fabrication to develop high quality ferroelectric nanowires. These nanowires will be characterized with various advanced techniques such as electron microscopy and X-ray/neutron diffraction. We will also establish a nano-manipulation system based on high resolution light microscopy and to develop a piezo-driven flexure stage with a positioning resolution better than 10 nm, which will serve as a general platform to manipulate individual nanowires and apply uniaxial mechanical strain in a well-controlled manner.

## Benefit to National Security Missions

This project supports DOE's mission in Energy Security by exploring energy transfer in nanomaterials. It also support the mission of Office of Science in fundamental science by enhancing our understanding of multifunctionality and ferroelectricity in nanostructured materials. This project will further support Laboratory's thrusts in fundamental understanding of materials

## Progress

The director funded postdoc fellow (Zhaoyu Wang) has made excellent progress for this project even though he just joined LANL six months ago. We have developed processing conditions to grow the ferroelectric films necessary for this project, using polymer assisted deposition. For example, we successfully used polymer-assisted deposition to grow ferroelectric $LiNbO_3$ films. We confirmed that we obtained the desired epitaxial growth, based on structural analysis of the materials. We have also investigated a chemical vapor deposition technique for the growth of nanowires. Furthermore, we have used pulsed laser deposition to grow the ferroelectric films that will be used for the project.

## Future Work

In general, the fabrication of 1D nanostructures involves either bottom-up chemical synthesis or top-down micro/nano-fabrication approaches. We have developed an excellent expertise in fabrication of nanowires, including solution phase methods for III-V compound semiconductor nanowires, CVD synthesis of silicon nanowires, and solid state reaction synthesis of BaTiO3 nanowires. We have also developed the clean room-based micro/nano-fabrication techniques.

We will utilize unique LANL facilities for materials growth and micro/nano-fabrication to grow high quality ferroelectric nanowires. The resulting nanowires will be characterized with various advanced facilities at LANL such as SEM, TEM, AFM, X-ray and neutron diffraction. We also plan to establish a nano-manipulation system based on high resolution light microscopy and to develop a piezo-driven flexure stage for precise positioning, which will serve as a general platform to manipulate individual nanowires and apply uniaxial mechanical strain (that is, stretch the nanowires along their length) in a well-controlled manner. We will integrate an in-situ heating element into the system to study temperature effects. We can then study phase transitions in 1D ferroelectric nanostructure. The dependence of the phase transition temperature Tc (Curie point) on mechanical strain for 1D ferroelectric nanostructures will be revealed. Furthermore, we will develop a Piezoelectric Force Microscopy (PFM) mode of Atomic Force Microscopy (AFM), which will be used to probe ferroelectric and piezoelectric properties of 1D nanostructures under axial strain. By studying nanowires with different diameters, the size effect on the structure and property of strained ferroelectric nanowires will be revealed. To have a better understanding of the experimental results, we will develop theoretical models using classical theories for ferroelectrics, such as phenomenological theory.

## Conclusion

Both chemical solution and physical vapor deposition techniques have been investigated to deposit high quality ferroelectric thin films with desired structural and physical properties. These studies pave the way for the fundamental understanding of the ferroelectric materials and lay the foundation to the fabrication and manipulation of individual ferroelectric nanowires.

continuing project

# Synthesis and Characterization of Novel Metal-Organic Frameworks for Hydrogen Storage

*Amr I Abdel-Fattah*

20080780PRD2

## Introduction

Hydrogen storage is a scientific challenge and the top technical obstacle to the future of hydrogen economy. The development of hydrogen-fueled vehicles requires new materials that can store large amounts of hydrogen molecules at accessible pressure/temperature conditions and are capable of storing and releasing hydrogen efficiently. This work aims at designing, synthesizing and testing novel Metal Organic Frameworks (MOFs) for hydrogen storage and exploring their use in other applications related to environmental and energy problems. The structures, chemical bonding and gas absorption properties of the MOFs are characterized using both single-crystal and powder X-ray diffraction, IR, NMR, SEM, TEM spectroscopes, and surface-area and hydrogen adsorption measurements. Hydrogen binding sites/energies are determined using in-situ high-pressure/low-temperature neutron scattering.

## Benefit to National Security Missions

This project supports the DOE mission in Energy Security and Environmental stewardship by developing novel Metal Organic Frameworks (MOFs) for hydrogen storage and purity. The impact of this project can significantly increase if the concept is successfully utilized for separation science and carbon dioxide ($CO_2$) capture and sequestration. It is also important to other Laboratory missions (e.g., Homeland Security).

## Progress

Postdoctoral Fellow for this project was hired on July 7, 2008. He has completed the required training and work authorization requirements involving safety and security. The following research tasks were accomplished:

### Synthesis of 4,4',4"-benzene-1,3,5-triyl-tribenzoic acid ($H_3BTB$) ligand

The ligand was prepared in two steps form 1,3,5-triphenylbenzene. Benzene-1,3,5-tribenzoic acid ($H_3BTB$) is selected as a novel linker to different metal cations from the following considerations: 1) the large separation of the rigid caryboxylate groups and multiple coordination sites are of benefit for generating nano porous frameworks; 2) the ample phenyl rings can introduce hydrophobic pore surfaces to improve hydrogen sorption selectivity.

### Synthesis of $[Zn_4O(BTB)(H_2O)_2](H_2O)_{3.5}$

The reaction of $Zn(NO_3)_2.6H_2O$ and $H_3BTB$ ligand in DMF under solvothermal reaction created a novel metal-organic framework: $[Zn_4O(BTB)(H_2O)_2](H_2O)_{3.5}$ (1). As shown in Figure 1, MOF 1 exhibits a three-dimensional two-fold interpenetrated porous framework with nano-sized open channels. The window size of open channels is 1.2 nm which is larger than that of the reported MOF-177. Notably, MOF 1 also presents the better stability than those reported for MOF-5 and MOF-177 due to its two-fold interpenetrated nature. The title compound also processes a novel anatase topological structure with $Zn_4O$ clusters and BTB ligands as nodes. It is worth noting that the new MOF 1 is the first case of porous MOF with two-fold interpenetrated anatase mineral topology. The classic mineral topological structure also plays an important role to stabilize its framework. The potential void volume and its accessibility in MOF 1 (how easily guest molecules can be put into the structure from the outside) were calculated by the potential solvent volume module of the Platon procedure. The total potential void volume of the open channels of MOF 1 is estimated to be about 54.8% (12199.0 Å$^3$) of the volume of the unit cell (22241.0 Å$^3$).

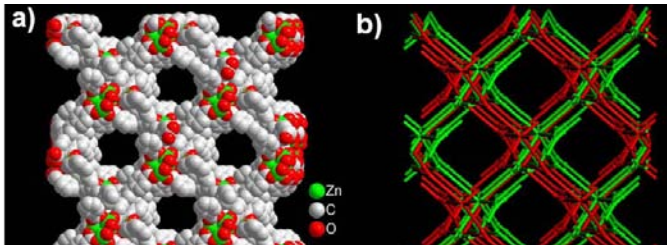


*Figure 1. (a) Two-fold interpenetrated metal-organic framework of $[Zn_4O(BTB)(H_2O)2](H_2O)3.5$ (1) and (b) anatase topological network.*

### Synthesis of $[Ce_4(BTB)_3(OH)_3(H_2O)_4](H_2O)_x$

The reaction of $Ce(NO_3)_3.6H_2O$ and $H_3BTB$ ligand in DMF under solvothermal reaction created a new mesoporous metal-organic framework: $[Ce_4(BTB)_3(OH)_3\text{-}(H_2O)_4](H_2O)_x$ (2). As shown in Figure 2, MOF 2 exhibits a three-dimensional non-interpenetrated mesoporous framework with nano-sized open channel beyond 2 nm. Up to now, only several MOFs with mesoporous structures are reported. Compound used in MOF 2 is also primarily proved to stabilize up to moisture. Notably, the coordinated water molecules to Ce(III) cations present the potential guest coordination sites. The total potential void volume of the open channels of MOF 2 is estimated to be about 72.5% (34258.6 Å$^3$) of the volume of the unit cell (47226.0 Å$^3$).

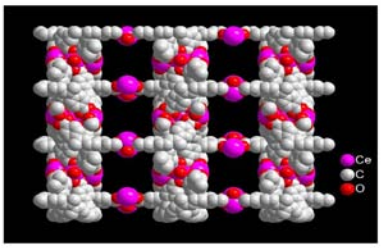


*Figure 2. Mesoporous metal-organic framework of $[Ce_4(BTB)3(OH)3(H_2O)4](H_2O)x$.*

### Synthesis of $ZnNa(BTC)(DMF)(H_2O)_{0.5}$ (BTC = 1,3,5-benzenetricarboxylate)

Reaction of $Zn(NO_3)_2.6H_2O$, NaOH, and $H_3BTB$ ligand in DMF/$H_2O$ under solvothermal reaction resulted in a novel metal-organic framework: $ZnNa(BTC)(DMF)(H_2O)_{0.5}$ (BTC = 1,3,5-benzenetricarboxylate) (3). As shown in Figure 3, MOF 3 exhibits a three-dimensional non-interpenetrated porous framework with nano-sized open channel. There are two types of open channels in MOF 3. The large window size of the open channels is 1.1 nm, and the small one of lower than 0.4 nm. It is most important that MOF 3 is stable with respect to moisture and general organic solvents, such as DMF, CH3CN, MeOH, EtOH and etc. The potential void volume and its accessibility in 3 are estimated to be about 53.6% (4048.3 Å$^3$) of the volume of the unit cell (7551.0 Å$^3$).

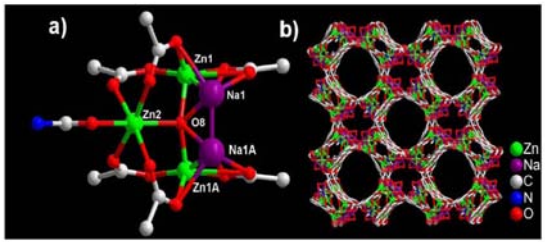


*Figure 3. (a) Molecular building block structure of ZnNa(BTC)(DMF)($H_2O$)0.5 (3) and (b) porous metal-organic network with nano-sized open channels.*

## Future Work

The aim of this work is to design, synthesize and characterize a series of novel MOFs tailored for hydrogen storage. Up to now, three new MOFs have been synthesized and structurally characterized. For the future work, firstly, hydrogen storage capacities of the above three new MOFs will be investigated. Secondly, a number of new MOFs with zeolite-type structures will be designed, synthesized, and characterized. Such framework topologies combine structural features of conventional zeolites, MOFs, and fullerenes, and are thus optimized for gas storage. The integration of nanoparticulates with these frameworks to increase surface area available for the sorption hydrogen molecules will be assessed. The structures, chemical bonding and gas absorption properties of these compounds will be characterized by a variety of techniques including diffraction, spectroscopy and gas absorption surface-area measurements. Hydrogen binding sites and energies will be determined using in-situ high-pressure/low-temperature neutron scattering at Los Alamos Neutron Science Center (LANSCE). Efforts will also be made to integrate neutron diffraction with calorimetry, which will be particularly useful for characterization of MOFs. Valuable information from the theoretical calculations will be used to further optimize the hydrogen storage and sorption/desorption performance of the resulting MOFs.

## Conclusion

In conclusion, three novel MOFs have been synthesized and structurally characterized. Their hydrogen storage capacities are being investigated. A number of new MOFs will further be designed and prepared to optimize the hydrogen storage performance. Through exploring new chemistry and synthetic approaches, our project will produce novel materials that can store large amounts of hydrogen. It is expected to contribute significantly to the utilization of hydrogen in future transport/mobile applications. The results of this research will also provide basis for utilizing similar techniques in environmental and threat-reduction applications. Example of other applications includes actinide separation and storage, which may use the same concept but using Metal Organic Frameworks (MOFs) of larger pore structures.

# Semiconductor Nanowire Heterostructures

*Samuel Thomas Picraux*

20080785PRD3

## Introduction

Semiconductor nanowires are very promising candidates for obtaining properties not currently attainable in electronic, energy harvesting, and sensing devices due to the versatility in their material synthesis and their high surface to volume ratio. These studies of Si/Ge/III-V nanowire structures and their combinations will allow new understanding of nanowire materials growth, device fabrication, property characterization, and analysis and modeling of transport behavior in a variety of device schemes. The work will focus on controlling surface properties through radial heterostructures, overcoming the limits of contact resistance, and integration of nanowires into functional nanosystems.

## Benefit to National Security Missions

This project supports the DOE missions in threat reduction, energy research, and nuclear weapons by advancing our fundamental understanding of nanoscale electronic materials for new materials synthesis, chemical and biological sensing, thermoelectric energy conversion, and electronics systems for future low power, miniaturized applications.

## Progress

The project was initiated on September 15, 2008, the time of Dr. Shadi Dayeh's hiring start date at Los Alamos National Laboratory. Initial efforts focused on learning the operation of the chemical vapor deposition system for the growth of nanowires.

## Future Work

The goal of this project is to gain basic understanding of material properties physics relevant to nanowire device architectures and enable the realization of a new generation of high speed and high performance electronic, optoelectronic, energy harvesting, and sensing devices. These studies of Si/Ge/III-V nanowire structures and their combinations will allow new understanding of nanowire materials growth, device fabrication, property characterization, and analysis and modeling of transport behavior in a variety of device schemes. The work focuses on:

1. Controlling surface properties through radial heterostructures: We will utilize our growth and device expertise in the growth, fabrication and characterization of radial Si/Ge and III-V heterostructure nanowires for surround-gate nanowires FETs to help reduce/eliminate interface states effects. A key advantage of this approach is the ability to modulate the atomic constituents as well as the strain along the channel length of the device to enhance carrier transport, in contrast to standard planar CMOS technology.

2. Overcoming the quantum limit of contact resistance: Attempting to contact NWs by using the same approaches as regular electronics hinders their potential for high-speed operation. This represents the most difficult obstacle to overcome in nanoscale devices (planar and 3D). Engineering multi-probe contacts, within one contact transfer length while being held at the same potential, enable us to overcome the quantum contact resistance limit. We plan to implement this breakthrough at LANL.

3. Full integration into functional systems: To make practical use of NWs, an essential requirement from a circuit design view point is precise location and individual addressing, which requires new growth and device architectures. The selective area growth of Ge and III-V NWs on Si and/or their growth directly on insulator-on-silicon will enable the vertical integration and necessary isolation of the two most promising material systems for high speed p- and n-type devices on standard Si technology, which is not possible in planar Si.

## Conclusion

We will establish synthesis methods for silicon/germanium/III-V nanowires and their combinations in integrated device structures. By understanding how to control surface properties through radial heterostructures,

how to overcome the limits of contact resistance, and how to integrate nanowires into functional nanosystems we will obtain new properties and performance not previously possible. These novel materials are of great interest for applications in energy applications such as a new generation of solar cells, new high performance thermoelectric materials for energy harvesting from heat sources, and new electrical chemical/biomolecular sensing devices with near single molecule sensitivity.

# Size Effects in Nanoscale Ferroelectric Thin Films

*Quanxi Jia*

20051281PRD3

## Abstract

The modern electronic industry demands an ever greater decrease in switching times and length scales, approaching the level of the nanoscale (individual electrons and atoms). In the last several years, ferroelectricity at the nanoscale has emerged as the fertile ground for new physical phenomena and devices. However, shrinking dimensions demands tools capable of not only producing nanoscale ferroelectric materials but also characterizing the properties of ferroelectrics in, for example, ultrathin films and superlattices. The main task of this project is to investigate the influence of size (or film thickness) effects on physical properties in nanoscale ferroelectric thin films

## Background and Research Objectives

Due to the fatigure-free and fast switching speed characteristics, perovskite ferroelectrics have been favorably considered as the materials for nonvolatile ferroelectric random access memory (NvFRAM) devices [1]. On the other hand, a distinctive feature of ferroelectric thin films is the thickness dependent dielectric properties. A number of experimental results have shown that the dielectric constant decreases with film thickness [2-4]. Furthermore, interfaces always play a critical role in controlling the structural and electrical properties in epitaxial ferroelectric films. Both experimental and theoretical works have demonstrated the impact of lateral interface on the physical properties of either single-phase thin films or superlattices [5,6]. The collapse of bulk dielectric behavior in ultra-thin ferroelectric films is usually explained by assuming the existence of "dead layers" or interfacial layers with severely depressed dielectric constant at the electrode/ferroelectric thin film interfaces. However, it makes very difficult to compare and interpret the experimental results from different research groups due to the lack of a systematic investigation to determine the effective thickness and dielectric constant of such an interfacial layer at the electrode/ferroelectric interface.

The objectives of this work are composed of three parts: a) to synthesis high quality nanoscale ferroelectric films; b) to characterize both the structural and electrical properties of ferroelectric materials; and c) to theoretically study the size effect on the ferroelectric properties.

## Importance to LANL's Science and Technology Base and National R & D Needs

This project not only provides a better understanding of the ferroelectricity in nanoscale materials, but also solves technologically important issues related to nanotechnology. It directly impacts LANL's Science and Technology Base in Fundamental Understanding of Materials, linking across length and time scales to achieve multi-scale understanding of properties and phenomena of materials. Furthermore, LANL's thrusts in nanotechnology and energy will benefit from this project.

## Scientific Approach and Accomplishments

Theoretically, we have used theoretical analysis to evaluate the size effects on the physical properties of the ferroelectric materials by combination of Landau-Devonshire theory and first-principle calculation. Experimentally, we have used pulsed laser deposition to grow thin film ferroelectric materials on different substrates so that the lattice strain can be tuned. We have further used different techniques (such as x-ray diffraction, scanning electron microscopy, atomic force microscopy, and transport measurements) to characterize the structural and dielectric properties of the ferroelectric films.

Ferroelectric $BiFeO_3$ (BFO) has been extensively studied since it shows both ferroelectricity with a Curie temperature ($T_C$) of ~1103 K and antiferromagnetic properties with a Neel temperature ($T_N$) of 643 K. Many experimental results show the potential application of BFO thin films for ferroelectric random access memory

(FeRAM) devices. On the other hand, it has been found that the pure BFO usually exhibits a high leakage current that could limit wide applications of this material. Efforts have been made to reduce the leakage current by introducing different kinds of dopants. The origin of the leakage current (or leakage mechanisms) is a critical point to thoroughly solve this problem. However, there are very limited numbers of reports about the leakage mechanisms of BFO in a wide temperature range. In the present work, we have investigated the leakage current density vs. electric field (*J-E*) characteristics of BFO films at temperatures from 80 to 350 K. To our knowledge, it is the first time the leakage mechanisms of BFO films were investigated in this temperature range. We have found that the dominant leakage mechanisms in Pt/$BiFeO_3$/$SrRuO_3$ ferroelectric thin film capacitors are a strong function of temperature and voltage bias. From 80 to 150 K, the leakage currents show bulk-limited the space-charge-limited current (SCLC) behavior in electric fields above onset electric field of the SCLC mechanism for both negative and positive bias resulting in symmetric *J-E* curves (see Figure 1). From 200 to 350 K, the leakage currents show bulk-limited Poole-Frenkel (F-N) emission at an electric field > 45 kV/cm for negative bias. On the other hand, interface-limited F-N tunnelling at electric fields above the onset electric field of F-N tunneling dominants the leakage mechanism for positive bias that results in asymmetric *J-E* curves. Detailed experimental results can be found in our article published in Appl. Phys. Lett. [7].

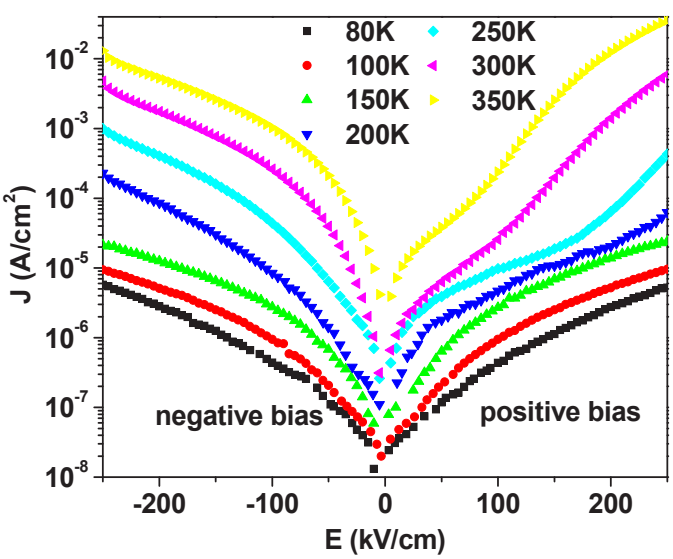


*Figure 1. Typical J-E characteristics of a Pt/BFO/SRO capacitor for both negative and positive bias from 80 to 350 K.*

Recent study has found that highly *c*-axis-oriented $(Bi_{3.15}Nd_{0.85})Ti_3O_{12}$ (BNT) thin films on Pt/$TiO_2$/$SiO_2$/Si substrates exhibit switchable remanent polarization 2*Pr* of over 100 μC/cm² and imprinting-free behavior. These results clearly show that ferroelectric BNT is a very promising candidate for NvFRAM devices. Following the report [8] from Chon *et al*., people have investigated electrical properties of BNT thin films on different bottom electrodes and substrates. On the other hand, a distinctive feature of ferroelectric thin films is the thickness dependent dielectric properties. A number of experimental results have shown that the dielectric constant decreases with film thickness due to the formation of interfacial layer between the ferroelectric and electrode materials. In this study, we have used our analytical approach to evaluate the effective thickness and the dielectric constant of such an interfacial layer through the measurement of the optical refractive index of BNT film and the current-voltage characteristics of a capacitor Pt/BNT/$SrRuO_3$. We have fabricated vertical capacitors having a configuration of Pt/BNT/$SrRuO_3$, where epitxial *c*-oriented BNT films were grown on (001) $SrRuO_3$ (SRO) on (001) $SrTiO_3$ (STO) substrates. We have further fabricated BNT films with different thicknesses ranging from 150 to 350 nm on SRO/STO substrate. The effective dielectric constant of BNT thin films with different thicknesses as a function of frequency is potted in Figure 2. The effective dielectric constant obviously decreases with decreasing BNT thickness. Based on the effective dielectric constant, leakage current, and optical refractive index measurements, the "dead layer" at Pt/BNT interface has been investigated. The thickness and dielectric constant of the dead layer have been estimated to be 19.2 nm and 13.2, respectively. At the same time, the dielectric constant of the bulk BNT layer of 586 has been obtained. Detailed experimental results can be found in our article published in Appl. Phys. Lett. [9].

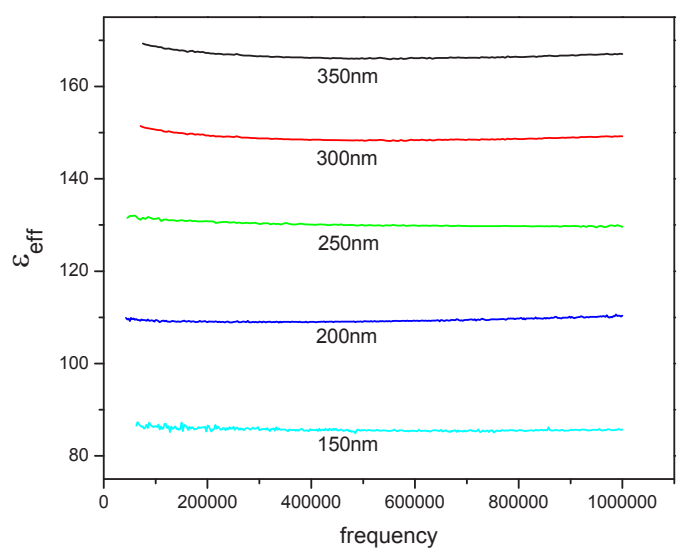


*Figure 2. The effective dielectric constant of BNT thin films as a function of frequency with different thicknesses from 150 to 350 nm.*

Semiconductor devices have been investigated for over 125 years. Around 60 major devices and more than 100 device variations related to them have been found. All these devices can be constructed from a small number of device building blocks. One of these building blocks is the *p-n* junction, which is a key building block for most semiconductor devices, such as the *p-n-p* bipolar transistor. Another building block is the heterojunction, which is the key component for high-speed and photonic device. Recently, *p-n* heterojunctions based on perovskite oxides, which combine the electrical properties of normal *p-n* junctions and the exotic properties of perovskite oxides (such as ferroelectricity and ferromagnetism), have been the subject of intensive theoretical and experimental studies. In our studies, we have selected Nb-doped $SrTiO_3$ (Nb-STO) for the *n*-type semiconductor as STO is a standard substrate for the deposition of perovskite oxides and Nb-STO is a *n*-type semiconductor with an energy band gap of 3.2 eV and an electron affinity of 4 eV. Ferroelectric BFO is chosen as the *p*-type semiconductor for two reasons. Firstly, because BFO has an electron affinity of 3.3 eV and an energy band gap of 2.8 eV, it should form a staggered energy band diagram with Nb-STO. Secondly, BFO is a typical multiferroic material. It is possible to get a BFO/Nb-STO *p-n* heterojunction with both electric and magnetic tunability. We have achieved a large rectifying ratio in a perovskite oxide *p-n* heterojunction by designing energy band structure. For detail, BFO/Nb-STO *p-n* heterojunctions have been fabricated by depositing *p*-type semiconductor BFO films heteroepitaxially on (001) *n*-type semiconductor Nb-STO substrates. Figure 3 shows the *J-V* characteristic of the Pt/BFO/Nb-STO structure at room temperature.

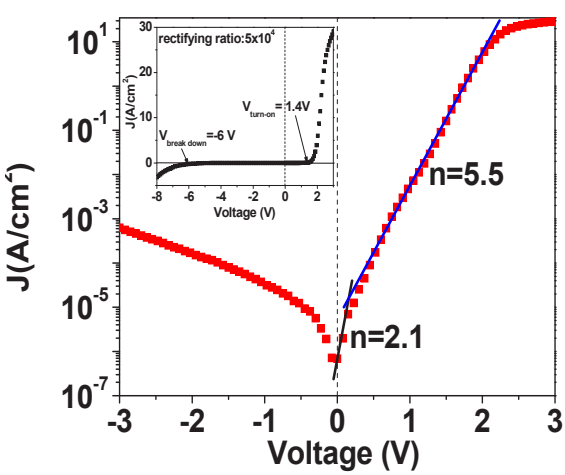


*Figure 3. Rectifying current density vs voltage (J-V) characteristic of BFO/Nb-STO p-n heterojunction at room temperature. At a forward voltage of 0.3-2 V, a high ideality factor of 5.5 is observed. A turn-on voltage of 1.4 V, and a breakdown voltage of -6 V are shown in the inset.*

As predicted, by applying both reverse and forward bias, distinct rectifying behavior is observed. A built-in potential value of 0.6 V was found, in good agreement with the work function difference of BFO and Nb-STO. An ideal turn-on voltage of 1.3 V was determined from a staggered energy band diagram, in good agreement with the experimental value from the *J-V* curve. Based on the results presented here, we believe BFO/Nb-STO *p-n* heterojunctions have a significant potential for oxide electronic applications. Detailed experimental results can be found in our article published in Appl. Phys. Lett. [10].

Recently, composite oxides have been extensively investigated in bulk and thin film forms because of their wide range of applications in microelectronics, magneto electronics, and optoelectronics. Oxide materials in nanocomposite form are particularly appealing as the interaction or coupling between the two constituents can lead to enhanced or new functionalities. In a film-on-substrate geometry, epitaxial composite films can be created in two forms: horizontal and vertical. Nanocomposite films with vertical microstructures such as the nanopillar geometry offer numerous advantages over the conventional horizontal microstructures, such as a larger interfacial area and intrinsic heteroepitaxy in three dimensions. In general, there are two ways to fabricate vertical nanostructures: self-assembly processes and lithography. Self-assembled nanocomposite thin films offer great potential for tailoring the structural and electrical properties. We have fabricated $(BiFeO_3)_{0.5}$:$(Sm_2O_3)_{0.5}$ nanocomposite thin films, where both $BiFeO_3$ (BFO) and $Sm_2O_3$ (SmO) phases are self-assembled into a vertical nano-columnar structure. The dielectric constant of BFO:SmO nanocomposite films is modeled very well by an equivalent parallel circuit. The lower than expected dielectric loss of the nanocomposite is believed to be the result of reduced leakage current density of the BFO phase, both due to the larger interfacial area and greater strain of the phase. The calculated dielectric constant of the nanocomposite from simple parallel circuit model is 92. The difference between the experimental and calculated dielectric constants of BFO:SmO nanocomposite film is about 4%. Thus, the dielectric constant of such a BFO:SmO nanocomposite can be well described by such a simple model. Detailed experimental results have been submitted to in Appl. Phys. Lett. for publication.

## References

1. Araujo, C. A., L. D. McMillan, M. C. Scott, and J. F. Scott. Fatigue-free ferroelectric capacitors with platinum electrodes. 1995. *Nature.* **374**: 627.

2. Abe, K., and S. Komatsu. Measurement and thermodynamic analyses of the dielectric constant of epitaxially grown SrTiO3 films. 1993. *Jpn. J. Appl. Phys. Part 2.* **32**: L1157.

3. Lee, B. T., and C. S. Hwang. Influences of interfacial intrinsic low-dielectric layers on the dielectric properties of sputtered (Ba,Sr)TiO3 thin films. 2000. *Appl. phys. Lett..* **77**: 124.

4. Chen, B., H. Yang, L. Zhao, J. Miao, B. Xu, X. G. Qiu, B. R. Zhao, X. Y. Qi, and X. F. Duan. Thickness and dielectric constant of dead layer in Pt/(Ba0.7Sr0.3)TiO3/YBa2Cu3O7 capacitor. 2004. *Appl. phys. Lett..* **84**: 583.

5. Choi, K. J., M. Biegalshi, Y. L. Li, A. Sharan, J. Schubert, R. Uecker, P. Reiche, Y. B. Chen, X. Q. Pan, V. Gopalan, L. Q. Chen, D. G. Schlom, and C. B. Eom. Enhancement of ferroelectricity in strained BaTiO3 thin films. 2004. *Science.* **306**: 1005.

6. Lee, H. N., H. M. Christen, M. F. Chisholm, C. M. Rouleau, and D. H. Lowndes. Strong polarization enhancement in asymmetric three-component ferroelectric superlattices. 2005. *Nature.* **433**: 395.

7. Yang, H., M. Jain, N. A. Suvorova, H. Zhou, H. M. Luo, P. C. Dowden, R. F. DePaula, D. M. Feldmann, S. R. Foltyn, and Q. X. Jia. Temperature Dependent Leakage Mechanism of Pt/BiFeO3/SrRuO3 Thin Film Capacitors. 2007. *Appl. phys. Lett..* **91**: 072911.

8. Chon, U., H. M. Jang, M. G. Kim, and C. H. Chang. Layered perovskites with giant spontaneous polarizations for nonvolatile memories. 2002. *Phys. Rev. Lett..* **89**: 087601.

9. Yang, H., N. A. Suvorova, M. Jain, B. S. Kang, Y. Li, R. F. DePaula, Q. X. Jia, and C. J. Lu. Effective Thickness and Dielectric Constant of Interfacial Layer at Pt/Bi3.25Nd0.75TiO3/SrRuO3 Interfaces. 2007. *Appl. phys. Lett..* **90**: 232909.

10. Yang, H., H. M. Luo, H. Wang, I. O. Usov, N. A. Suvorova, M. Jain, D. M. Feldmann, P. C. Dowden, R. F. DePaula, and Q. X. Jia. Rectifying Current-Voltage Characteristics of BiFeO3/Nb-doped SrTiO3 Heterojunction. 2008. *Appl. phys. Lett..* **92**: 102113.

## Publications

Kang, B. S., H. Wang, Y. Li, J. L. MacManus-Driscoll, Q. X. Jia, I. Mihut, and J. B. Betts. Low Field Magneto-transport Properties of (La0.7Sr0.3MnO3)0.5:(ZnO)0.5 Nanocomposite Films Grown via Pulsed Laser Deposition. 2006. *Appl. Phys. Lett..* **88**: 192514/3.

Lee, J. K., B. S. Kang, and Q. X. Jia. Data retention characteristics of Bi3.25La0.75Ti3O12 thin films on conductive SrRuO3 electrodes. 2007. *Appl. Phys. Lett..* **91**: 142901.

Luo, H. M., H. Yang, S. A. Baily, O. Ugurlu, M. Jain, M. Hawley, T. M. McCleskey, A. K. Burrell, E. Bauer, L. Civale, T. G. Holesinger, and Q. X. Jia. Self-Assembled Epitaxial Nanocomposite BaTiO3-NiFe2O4 Films Prepared by Polymer-Assisted Deposition. 2007. *J. Am. Chem. Soc..* **129**: 14132.

Yang, H., H. M. Luo, H. Wang, I. O. Usov, N. A. Suvorova, M. Jain, D. M. Feldmann, P. C. Dowden, R. F. DePaula, and Q. X. Jia. Rectifying Current-Voltage Characteristics of BiFeO3/Nb-doped SrTiO3 Heterojunction. 2008. *Appl. Phys. Lett..* **92**: 102113.

Yang, H., H. Wang, H. M. Luo, N. A. Suvorova, M. Jain, D. F. Feldmann, P. C. Dowden, R. F. DePaula, and Q. X. Jia. Epitaxial growth of Sm2O3 thin films on SrTiO3 substrates by pulsed laser deposition . 2008. *Appl. Phys. Lett..* **92**: 062905.

Yang, H., H. Wang, J. Yoon, D. M. Feldmann, P. C. Dowden, J. L. MacManus-Driscoll, and Q. X. Jia. Dielectric Properties of Self-assembled (BiFeO3)0.5:(Sm2O3)0.5 Nanocomposite Films. *Appl. phys. Lett..*

Yang, H., M. Jain, N. A. Suvorova, H. Zhou, H. M. Luo, D. F. Feldmann, P. C. Dowden, R. F. DePaula, S. R. Foltyn, and Q. X. Jia. Temperature-dependent leakage mechanisms of Pt/BiFeO3 /SrRuO3 thin film capacitors. 2007. *Appl. Phys. Lett..* **91**: 072911.

Yang, H., N. A. Suvorova, M. Jain, B. S. Kang, Y. Li, M. E. Hawley, P. C. Dowden, R. F. DePaula, and Q. X. Jia. Effective thickness and dielectric constant of interfacial layers of Pt/Bi3.15Nd0.85Ti3O12/SrRuO3 capacitors. 2007. *Appl. Phys. Lett..* **90**: 232909.

# Fundamental Oxygen Reduction Reaction Studies at High pH

*Brian Pivovar*

20061562PRD3

## Abstract

Polymer electrolyte membrane fuel cells (PEMFCs) have high energy density, high theoretical efficiency, and low emissions, making them promising devices for transportation applications. Despite their advantages, several limitations, including problems associated with water management, prevent widespread commercialization of PEMFCs. In this project, high resolution neutron radiography was used to image water present in PEMFCs during operation under a variety of conditions. The effect of specific operating conditions, including flow direction (co-flow or counter-flow), orientation of the PEMFC with respect to gravity, and simulated anode recycle loop, were examined. Counter-flow operation was found to result in higher water content than co-flow operation, with more uniformly distributed water. Orientation with respect to gravity was also significant, with net water transport observed from the higher side of the cell to the lower side. The higher anode flow rate resulting from the simulated recycle loop facilitated convective removal of liquid water from the anode flow field, leading to lower overall levels of water in the PEMFC. The improved understanding of water distribution during fuel cell operation resulting from this work will aid efforts to effectively manage water in PEMFCs.

## Background and Research Objectives

Effective control of water distribution is a major impediment to implementation of polymer electrolyte membrane fuel cells (PEMFCs). Several important cell parameters, including membrane conductivity and mass transfer resistance within porous electrodes, are intimately linked to water distribution, requiring effective management of water in order to maximize PEMFC performance.

Neutron radiography, performed in situ within an operating PEMFC, is a powerful tool in developing greater understanding of water distribution profiles during cell operation [1]. In particular, the ability to simultaneously correlate water distribution with cell operating conditions and cell performance provides a degree of understanding of water management that is not available with any other existing technique. High resolution imaging of through plane water profiles using a Micro-Channel Plate (MCP) detector with 25 µm resolution produces water profile images in which one can distinguish between water in anode and cathode gas diffusion layers (GDLs), as well as between water in the GDLs above channels and above lands, and water in the channels themselves.

Objectives of this research project were to determine the effects of parameters including flow direction (co-flow vs. counter-flow, illustrated in Figure 1), cell orientation with respect to gravity (illustrated in Figure 2), and anode flow rate (simulated anode recycle) on water distribution, as well as on cell performance.

## Importance to LANL's Science and Technology Base and National R & D Needs

This work supports LANL's science and technology base in the areas of electrochemistry and energy programs. The work supports national R&D needs and the DOE mission of energy security by supporting US energy independence and security, by investigating energy sources that don't rely on imported oil. Furthermore, the development of commercially viable fuel cell technology may become an important part of the US economy.

## Scientific Approach and Accomplishments

Figure 3 illustrates the effect of flow direction (co-flow or counter-flow) on water profiles in various cell components. Significantly more water is present in the membrane electrode assembly (MEA) when a counter-flow configuration is used. The higher water content leads to a lower high frequency resistance (HFR) (0.06 $\Omega$ cm$^2$ for counter-flow vs. 0.09 $\Omega$ cm$^2$ for co-flow) and

*Figure 1. Co-flow and counter-flow fuel cell configurations.*

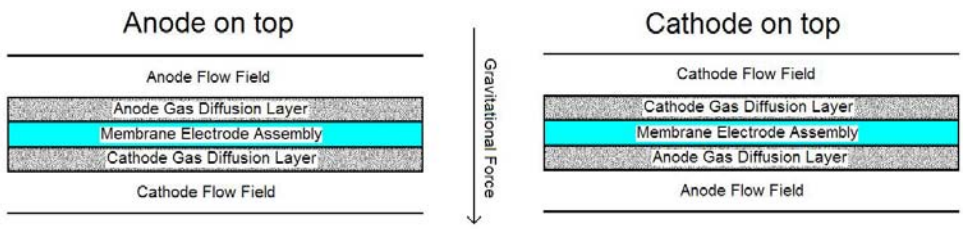


*Figure 2. Fuel cell orientation with respect to gravity. Gravitational force enhances water transport from higher parts of the cell to lower parts.*

improved cell performance (0.10 V at 1.4 A $cm^{-2}$ vs. 0.27 V at 1.5 A $cm^{-2}$). Flow field water content is also plotted in Figure 3, which shows significantly more water in the anode flow fields during counter-flow operation, which under some conditions could lead to problems with flooding. The performance is higher for the counter-flow configuration, though, because under these relatively dry conditions the decrease in ohmic losses more than compensates for any losses that may occur due to flooding.

The effect of gravity on water distribution is shown in Figure 4. Under the conditions employed, the water content in the MEA was lower for the cell with anode on top than in the cathode on top case. Notably, anode GDL water was significantly lower, in the anode on top case, while cathode GDL water was only slightly lower. In order to minimize mass transport losses due to flooding, it is more important to decrease cathode GDL water than it is to decrease anode GDL water, suggesting that putting anode on top may not be an effective way of optimizing water distribution. Both cell orientations produced similar HFRs (0.07 Ω $cm^2$ for the anode on top case vs. 0.06 Ω $cm^2$ for the cathode on top case, but the performance of the cell in the cathode on top was slightly worse because of the overall higher levels of water, including slightly higher water levels in the cathode GDL, which resulted in some losses due to flooding (0.39 V vs. 0.27 V for the anode on top cell). Similar results were observed at lower currents and at higher anode stoichiometries, confirming the effect of gravity on water distribution.

The overall effects of gravity most likely are consequences of the local effects inside the flow fields. Inside the GDLs and the MEA, gravity is unlikely to have a significant effect on water transport, since capillary pressure is the dominant force on liquid water in these components. In

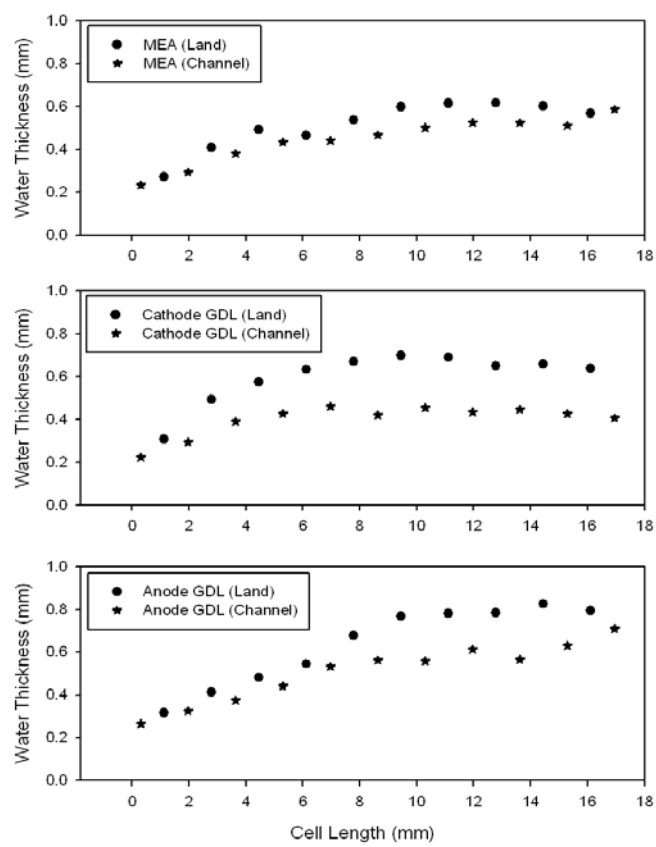


*Figure 3. Average water density under lands and under channels in MEA and GDL layers for a cell operating at 80 ºC, anode stoichiometry = 1.2, cathode stoichiometry = 2, fully humidified anode and cathode feeds, current density = 1.2 A $cm^{-2}$, counter-flow.*

contrast, the larger void dimensions inside the flow fields result in gravity being comparatively more important in controlling the position of water. By placing the anode flow field on top, gravity will tend to force flow field water down to the surface of the GDL, where it can be removed by wicking across to the (relatively dry) cathode side,

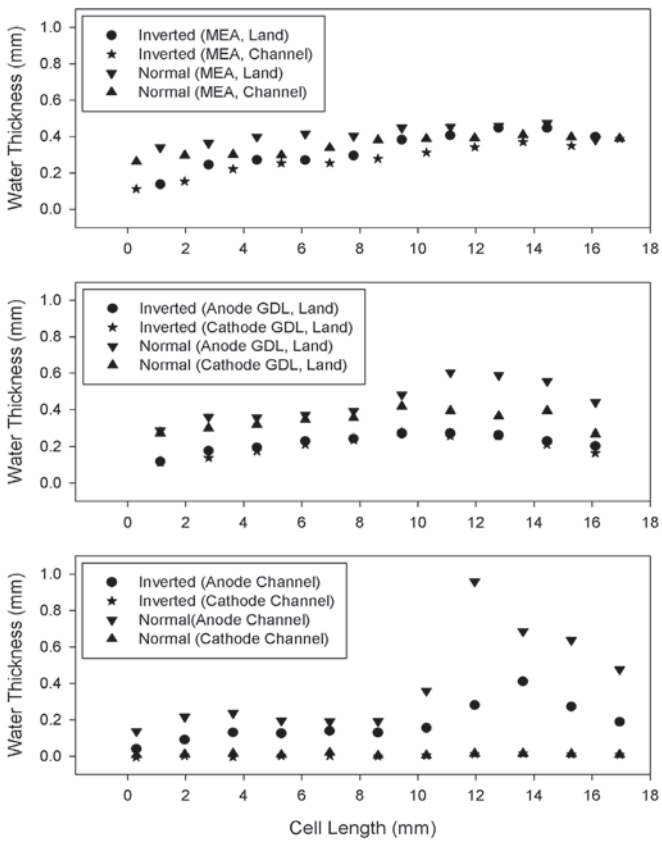


*Figure 4. Effect of gravity on water distribution in a cell operated at 80 ºC, anode stoichiometry = 1.2, cathode stoichiometry = 2, 100% relative humidity (RH) anode feed, 0% RH cathode feed, counter-flow, current density = 1.4 A cm$^{-2}$ for inverted (anode on top) cell and 1.5 A cm$^{-2}$ for normally oriented (cathode on top) cell. Top: MEA. Middle: GDLs. Bottom: flow fields.*

altering the water distribution in all cell components. The much lower anode flow field water content in when the anode is on top (Figure 4) supports this interpretation. These results demonstrate that gravity can have a significant effect on water management in PEMFCs, and that appropriate selection of fuel cell orientation can influence water distribution and cell performance.

Recycling part of the anode outlet gas stream to the inlet can serve both as a way of humidifying the anode inlet, as well as facilitating convective water removal from the anode flow field. In order to simulate the effect of an anode recycle, the anode stoichiometry was increased in some cases from 1.2 to 3.0. The effect of such an increase in anode stoichiometry is illustrated in Figure 5. The increased anode flow rate accelerates removal of liquid water from the anode flow field, leading to a decrease in the anode flow field water content. As a result, transport of generated water from the MEA to the anode flow field is accelerated, leading to a lower MEA water content.

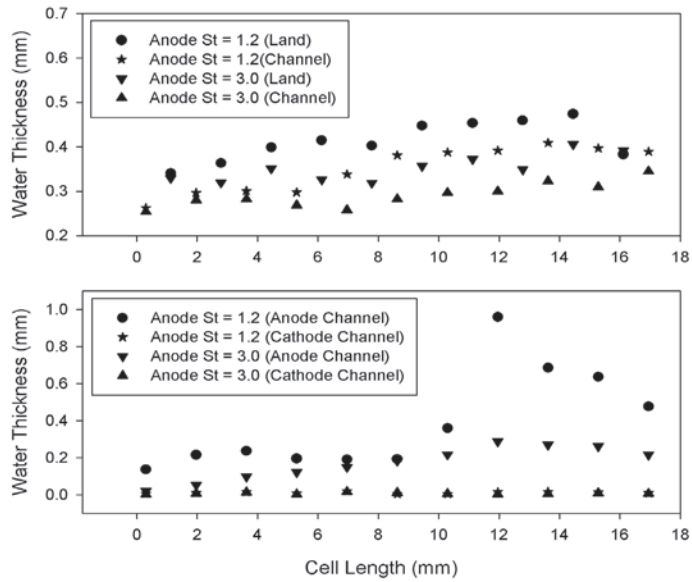


*Figure 5. Effect of simulated anode recycle on a cell operated at 80 ºC, cathode stoichiometry = 2, 100% RH anode feed, 0% RH cathode feed, current density = 1.5 A cm$^{-2}$, counter-flow. Top: MEA. Bottom: flow fields.*

The lower water content leads to a higher HFR (0.08 Ω cm$^2$ at an anode stoichiometry of 3.0 vs. 0.06 Ω cm$^2$ at an anode stoichiometry of 1.2), but the performance stays roughly constant (0.27 V at 1.5 A cm$^{-2}$), likely as a result of decreased anode flooding at the higher stoichiometry. Therefore, incorporation of an anode recycle stream may improve performance in very wet conditions be facilitating convective water removal, though if water removal is too rapid it may result in excessive MEA drying and increased ohmic losses.

Scientific accomplishments resulting from this work are further reported in the technical literature [2].

## References

1. R. Mukundan, J. R. Davey, T. Rockward, J. S. Spendelow, B. S. Pivovar, D. S. Hussey, D. L. Jacobson, M. Arif, R. L. Borup, ECS Trans., 11, 411 (2007).

2. J. S. Spendelow, R. Mukundan, J. R. Davey, T. Rockward, D. S. Hussey, D. L. Jacobson, M. Arif, and R. L. Borup, ECS Trans., 16, 1345 (2008).

# Effects of Length Scale on the Fracture Behavior of Ultra High Strength Nano-composite Materials

*Amit Misra*

20051336PRD4

## Abstract

In recent years, the high strength of nanomaterials has gathered much interest in the materials community. Nanomaterials (polycrystalline and composites) have already been used, largely by the semiconductor community, as critical length scales for chip design have decreased to tens of nanometers. However, to ensure reliability of nanomaterials in almost any application, the mechanisms underlying their structural integrity must be well understood. For these materials to be put into service on a broader scale, not only strength should be considered, but also ductility, toughness, formability, and fatigue resistance. While some progress has been made into constructing models for such deformation mechanisms, little experimental work exists addressing these issues, especially when length scales drop below 10 nanometers. This work forges new inroads into some of these areas by producing stress-strain curves for nanolaminate composites with individual layer thickness of 40 and 5 nm. Nanolaminate composites fabricated via magnetron sputtering comprised of alternating 5 nm thick Cu and Nb multilayers (two relatively soft metals) exhibit strengths on par with tool steel and deformability in compression in excess of 25%.

## Background and Research Objectives

When the sample size, grain size, or domain size becomes comparable with a specific physical length scale such as the electron mean free path, the domain size in ferromagnets or ferroelectrics, the coherence length of phonons, or the correlation length of a collective ground state like superconductivity, then the corresponding physical phenomenon will be strongly affected. Nanocrystals and nanolayered structures offer unique opportunities for tailoring the optical, magnetic, electronic, mechanical and chemical properties of materials. The mechanical properties of materials are enhanced dramatically as the grain size in polycrystalline materials approaches the nanometer scale. Theoretical descriptions and experimental techniques explaining and testing the unique behaviors found at the nanoscale, such as yield strengths close to the theoretically determined maximum for perfect crystals, are really in their infancy.

Metal-based nanolayered composites represent an ideal vehicle for the exploration of the effects of length scales on the plastic deformation and fracture of nanoscale materials since interface structures and layer thicknesses can be precisely tailored using vapor deposition techniques. However, much of the reported results in the literature are hardness data. An estimate of the strength from hardness data corresponds to the flow stress at ~ 7% strain rather than at the usual 0.2% strain, making it difficult to separate the onset of plasticity (i.e., yielding) from the subsequent effect of strain hardening which raises the flow stress. Furthermore, no information about material fracture can be obtained from hardness tests on metals. Ideally, experimental results from a variety of loading configurations, including uniaxial tension, are needed to directly evaluate such quantities as yield strength, strain hardening, and ductility. The key research objectives are to experimentally evaluate the room temperature strength and ductility, via uniaxial tension and compression tests, of metallic nanolaminates.

## Importance to LANL's Science and Technology Base and National R & D Needs

This project supports the Energy Security and the Office of Science missions of DOE through a fundamental understanding of the fracture resistance of high strength nanostructured materials in support of nanoscience research for energy needs. For example, a recent DOE workshop on *Nanoscience Research for Energy Needs* identified the development of "super-strong, light-weight, materials to improve efficiency of cars, airplanes, etc" as one of the research targets in energy-related science and technology where nano-

science can have the greatest impact. Besides energy security, nanostructured strong and light-weight materials will also have a great impact on the design of high performance military platforms with diminished failure rates and lower life cycle costs for national security / defense applications and thermal barrier and wear-resistant nanostructured materials and coatings for aeronautics and space exploration each of these amount to multi-billion dollar industries.

## Scientific Approach and Accomplishments

Some of the challenges in evaluating the stress-strain response of nanomaterials involve the fabrication of flaw-free samples that will reliably give mechanical test data that reflect the bulk material properties independent of geometric effects of sample size or embedded flaws. In this research, magnetron sputtering at the Center for Integrated Nanotechnologies was utilized to fabricate metallic multilayers such that 1) the growth-induced residual stresses and flaws/porosity are minimized, 2) the individual layer thicknesses are well-controlled in the nanometer range, and 3) the overall sample thickness is sufficient to make self-supported foils. This precise control over length scales allows for systematic investigation of the effects of increasing amount of interfacial content on material behavior. Figure 1 is a cross-sectional transmission electron micrograph of a sample with 5 nm layer thickness, although layers of alternating copper (Cu) and niobium (Nb) can be easily varied in thickness to investigate length scales (and accompanying deformation mechanisms) from hundreds of nanometers to ~1 nm in samples with identical chemical composition. The laminar nature of the composites is evident from the micrograph, with the (111) planes of fcc-Cu and (110) planes of bcc-Nb forming the interface between the two phases, as shown in the embedded selected area diffraction pattern.

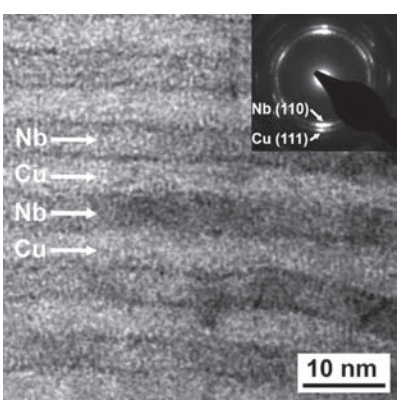


*Figure 1. TEM bright-field micrograph of as-deposited 5 nm Cu/5 nm Nb. Note selected area diffraction pattern showing {111} Cu//{110} Nb fiber texture.*

Once deposited, nanolayered composites can be deformed utilizing a variety of methods, including rolling [2], tension [3], indentation [4] or as in this case, micropillar compression. Focused Ion Beam (FIB) machining has opened opportunities for fabrication of micropillar samples, where a $Ga^+$ ion beam is used to remove material to shape a sample to high precision. [5, 6] The inset scanning electron microscopy (SEM) micrograph in Figure 2 shows such a pillar with nominal dimensions of diameter of 4µm and height of 8µm. The layer direction is perpendicular to the cylinder axis, and several configurations such as larger pillar sizes and different substrates exhibit similar flow behavior. Most of the recent micropillar work in the current body of literature focuses on the effects of sample size (i.e., pillar diameter) on the yield strength of single crystals or nanoporous structures [7-9]. In this study, the critical dimension in the deformation process is not the pillar size, but the layer thickness, and consequently the pillar size is intentionally kept three orders of magnitude larger than the interlayer spacing. As a result, the measured stress-strain curves reflect the mechanical behavior of the Cu/Nb multilayers, independent of the pillar diameter that was varied in the range of 4-8 µm.

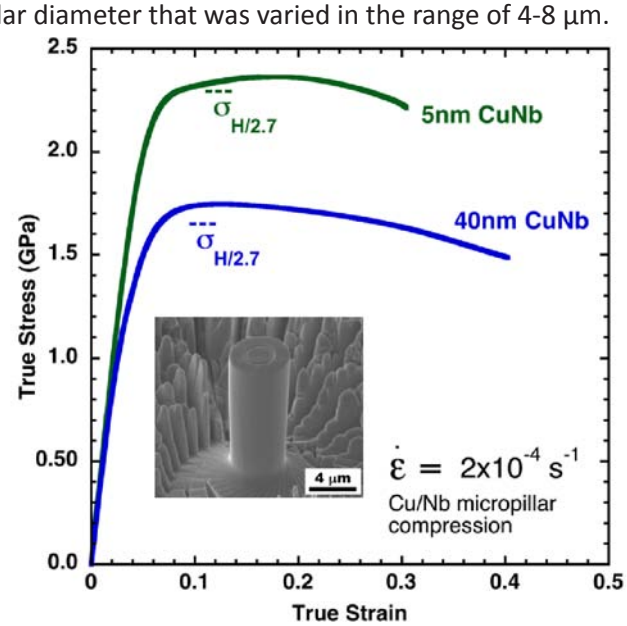


*Figure 2. Compression curves for 40 nm and 5 nm Cu/Nb multilayers. Note the gradual transition between linear elastic and fully plastic yield behavior at flow stresses in excess of 2 GPa. As a comparison, typical strengths for tool steel are on the order of ~2 GPa. Flow stress measurements indicate good agreement with those ascertained via nanoindentation, using a correlation factor of 2.7. Inset: SEM micrograph of micropillar of 5 nm Cu/Nb multilayer in the as-prepared condition. Pillar height is 8 microns, and diameter is 4 microns. Layer interfaces are perpendicular to the cylinder axis.*

The cylinders are compressed at an initial strain rate of $2x10^{-4}$ $s^{-1}$ using a Hysitron Triboindenter nanoindenter

fitted with a 30 µm diameter flat diamond punch while recording load and displacement data. Using this information, stress-strain curves for Cu/Nb multilayers of 5 nm and 40 nm individual layer thickness are calculated using initial pillar dimensions and are shown in Figure 2. These indicate ductility in excess of 25% in the 5 nm case, at which point the sample failed by a shear instability as is evident in Figure 3a. The maximum flow stress is about 2.4 GPa (2400 MPa) and is in good agreement with the strength estimated from nanoindentation measured hardness (σ = Hardness/2.7 as a correlation factor as shown in the plot). Transmission electron microscopy (TEM) results of deformed pillars indicate the presence of a single shear band, the formation and propagation of which could explain the softening effect towards the end of the test. 40 nm Cu/Nb mulitlayers exhibit qualitatively the same behavior, albeit at lower ultimate strength and deformability in excess of 30%. The SEM micrograph of the deformed 40 nm layer thickness pillar (Figure 3b) shows that a shear instability has formed, leading eventually to sample failure, but the pillar has not fractured.

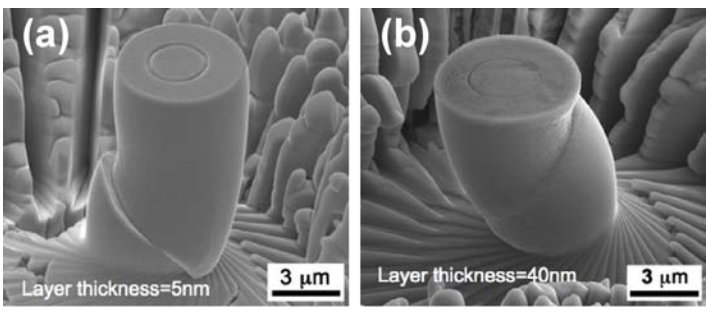


*Figure 3. SEM micrographs of micropillars after compression. (a) 5 nm Cu/Nb multilayer underwent 25% true strain before failing at the shear surface shown. (b) 40 nm multilayer deformed to 35% true compressive strain with failure in shear without fracture.*

As microstructural dimensions such as grain size, or in this study, layer thickness, diminish to below ~10 nm, the fraction of Cu/Nb interface per unit volume of material becomes significant to the point that deformation behavior is dictated by interface properties rather than by the properties of the constituent bulk Cu or bulk Nb. In the 5nm Cu/Nb case, this gives rise to single dislocation deformation mechanisms where the dislocation must cross the Cu/Nb interface. The Cu/Nb interface is unique in that it is incoherent, is resistant to significant interdiffusion even at elevated temperatures, and may have limited shear strength. This limited shear strength can lead to dislocations in Cu being attracted to the interface, where they become trapped due to dislocation core spreading. Very large (~GPa) stresses are required to collapse the core and allow transmission into the adjacent Nb layer, leading to the extreme strengths seen in this material. The flow stresses encountered during micropillar compression of the 5 nm Cu/Nb material are approximately 2.4 GPa, which is on the order of those usually seen in tool steel. This is especially remarkable when one takes into consideration that the yield strengths of pure, single crystal metals such as Cu and Nb are on the order of 10-20 MPa at room temperature. That is, the Cu/Nb nanocomposite exhibits strength of up to two orders of magnitude greater than a rule-of-mixtures calculation between its constituents, while maintaining significant deformability.

## References

1. Mara, N. A., and A. Misra. Deformability of Ultrahigh Strength 5 nm Cu/Nb Nanolayered Composites . 2008. *Applied Physics Letters.* **92** (23): 231901.

2. Misra, A., and R. G. Hoagland. Work Hardening in Rolled Nanolayered Metallic Composites . 2005. *Acta Materialia.* **53** (15): 221.

3. Mara, N. A., and A. Misra. Tensile Behavior of 40 nm Nanoscale Cu/Nb Multilayers . 2008. *Scripta Materialia.* **58** (10): 874.

4. Misra, A.. Structure and Mechanical Properties of Nanolayered Composites. 1998. *Scripta Materialia.* **39** (4-5): 555.

5. Uchic, M. D.. Sample Dimensions Influence Strength and Crystal Plasticity. 2004. *Science.* **305** (5686): 986.

6. Uchic, M. D., and D. A. Dimiduk. A Methodology to Investigate Size Scale Effects in Crystalline Plasticity using Uniaxial Compression Testing. 2005. *Materials Science and Engineering A.* **400** (JUL 25): 268.

7. Volkert, C. A.. Approaching the Theoretical Strength in Nanoporous Au. 2006. *Applied Physics Letters.* **89** (6): 061920.

8. Greer, J. R.. Size Dependence of Mechanical Properties of Gold at the Micron Scale in the Absence of Strain Gradients . 2005. *Acta Materialia.* **53** (6): 1821.

9. Dimiduk, D. M.. Size-affected Single-slip Behavior of Pure Nickel Microcrystals. 2005. *Acta Materialia.* **53** (15): 4065.

## Publications

Aydiner, C., N. A. Mara, and A. Misra. Residual strain and texture in free-standing nanoscale Cu-Nb multilayers . 2007. *Journal of Applied Physics.* **102** (8): 083514.

Mara, N. A., A. V. Sergueeva, A. Misra, and A. K. Mukherjee. High temperature tensile properties-microstructure correlations in Cu/Nb nanoscale multilayers. To appear in *Materials Science and Engineering A.*

Mara, N. A., A. V. Sergueeva, T. Tamayo, X. Zhang, A. Misra, and A. K. Mukherjee. High temperature mechanical properties of Cu/Nb nanoscale multilayers at diminishing length scales. 2007. *Thin Solid Films.* **515**: 3241.

Mara, N. A., D. Bhattacharyya, R. G. Hoagland, and A. Misra. Tensile behavior of 40 nm Cu/Nb nanoscale multilayers. 2008. *Scripta Materialia.* **58** (10): 874.

Mara, N. A., and A. Misra. Deformability of ultrahigh strength 5 nm Cu/Nb nanolayered composites . 2008. *Applied Physics Letters.* **92** (23): 231901.

# Biological and Chemical Sensor Design Using Linearly-Scaled TD-DFT Methods

*Anders Mauritz Niklasson*

20051345PRD4

## Abstract

We propose the development of novel tools to model electronic structures directly from quantum mechanics for the design of advanced biological and chemical sensors. Such a modeling tool is extremely important because of the broad applicability to sensor design and the impact on a variety of national security applications. One advantage of this approach is the computing cost goes up no faster than the number of atoms in the structures that we model. This would enable us to study and design more sensitive sensor systems faster directly from theory. Furthermore, we can optimize or test functionality that cannot be readily accessed in the lab. This will result in better detectors, in a shorter time. The sensor designs will be based on the optical response of materials to epitopes (molecules) that bind to the sensor, and are detected by the way that they modify its optical response. This response will be predicted for various materials directly from the first principles of quantum mechanics.

## Background and Research Objectives

The ability to predict materials properties directly from theory makes it possible to design and tailor properties without costly and time-consuming experiments. Theoretical studies with predicitive power that are directly based on the first principles of quantum mechanics allows for materials design without using empirical data or adjustable parameters. This is, in principle, an extremely powerful approach that undoubtedly will have a major future impact in broad scientific areas of chemistry, materials science and molecular biology. The greatest obstacle preventing current application of science based prediction is the enormous complexity involved in solving the equations that governs the quantum mechanical properties of materials. This proposal will try to overcome some of the computational complexity in the theoretical design of advanced biological and chemical sensors. The key problem is the solution of time-dependent response equations that describe optical properties of materials. Optical response properties are in general much harder to calculate than properties like the molecular structure or forces acting on atoms. The number of arithmetic operations needed on a computer to solve the time dependent response functions typically scales as N^6, where N is the number of atoms or electrons in the system. This strongly limits the size of systems that can be studied. The ultimate goal of this proposal is to overcome the computational N^6 bottleneck and reach a computational cost that scales only linearly with the system size. In practice this is an almost impossible task. However, there are no fundamental limitations in the theory that would prohibit a linear scaling complexity. In fact, in our research we managed to come very close to the ultimate goal!

## Importance to LANL's Science and Technology Base and National R & D Needs

This project supports DOE's mission in threat reduction by enhancing our understanding of fundamental algorithms for electronic structure, with wide applicability to basic research in materials science, chemistry, biology and nanoscience. Our results could be expanded to include the optical properties of plasmas, which are important for NW programs. The ability to extend current first principles electronic structure theory to the study of more complex systems is a key problem to enable predicitive science in many areas of materials science and chemistry, which is of great interest to a broad national and international scientific community.

## Scientific Approach and Accomplishments

Several significant shorter and rather technical accomplishments where achieved during the research. For example, highly accurate electronic structure calculations were performed on Cp and Cp* Ytterbocene-bipyridine complexes to elucidate their electronic properties [4]. However, the major scientific achievement of this research proposal was the development of a novel

approach to solve the time-dependent response problem with a linear scaling computational complexity. We showed that a nonlinear conjugate gradient optimization of a functional description of (optical) excited states is a promising approach to solving response equations with reduced complexity [1,2,3]. This enables excited state calculations of large, complex systems inaccessible to current methods. The excited states of biological molecules and extended, periodic systems are of particular importance in the development and application of sensors and detectors to screen and identify virulent or toxic materials. This research may thus in the near future have a direct impact on improving national security.

## References


1. M. Lucero, A.M.N. Niklasson, S. Tretiak, M. Challacombe, Molecular-orbital-free algorithm for excited states in time-dependent perturbation theory, J. Chem. Phys., Vol. 129, 064114 (2008).

2. M. Lucero, ACS National Meeting Aug 19-23, Boston, MA 2007; Excited States in the Random Phase Approximation: A Molecular Orbital-Free Algorithm. (LAUR# 07-5258)

3. M. Lucero, University of Zurich Dept. of Chemistry, Sep 25, 2007; Excited States in the Random Phase Approximation: A Molecular Orbital-Free Algorithm. (LAUR# 07-5258)

4. M. Lucero, Theoretical Chemistry Symposium, Saarbruken, Germany, Sept 15, 2007; 2'2 Bipyridyl Ytterbocene Complexes: A Molecular Kondo Singlet? (LAUR# 07-6389)


## Publications


Lucero, M., A. M. N. Niklasson, S. Tretiak, and M. Challacombe. Molecular-orbital-free algorithm for excited states in time-dependent perturbation theory. 2008. **129**: 064114.

# Ultrafast Dynamics of Novel Magnetic Materials by Time Domain Spectroscopy

*Antoinette Jane Taylor*

20051347PRD4


## Abstract

New materials with a wide variety of potential applications are continually being developed, but techniques for investigating the underlying dynamics and electronic structures of these materials are often lacking. Understanding of the underlying physics and chemistry of these materials enables us to approach the design of materials with specific properties in a methodical fashion. Without that understanding, it becomes a hit-or-miss endeavor. This project endeavors to develop new tools for investigating the most basic properties of materials, the electronic structure. We use ultrafast optical techniques to determine the dynamics of carriers in materials whose exotic behavior is dominated by correlations between carriers, in order to understand the underlying physics that determines the properties of these materials. The materials under study exhibit unusual electronic and magnetic properties that are of technological importance for advanced electronic applications in, for example, the emerging field of spin electronics. We use femtosecond techniques to obtain new information regarding the nature of low-lying singular particle and collective mode excitations in these materials and are exploring carrier relaxation of correlated electrons.


## Background and Research Objectives

Recently there has been growing interest in "14-1-11" materials due to their rich phase diagram. These materials have the chemical formula $A_{14}MnPn_{11}$ where A is an alkaline or rare earth atom and Pn is a Pnictogen, and exhibit a wide range of behavior, including ferromagnetism, anti-ferromagnetism, the Jahn-Teller effect, and colossal magneto-resistance, and can be found in both metallic and semiconducting phases. $Yb_{14}MnSb_{11}$ is the first ferromagnetic Kondo lattice compound in the underscreened limit. This "Heavy Fermion" behavior, where the effective mass of the carriers is enhanced due to magnetic scattering, originates from the Mn ion and therefore places $Yb_{14}MnSb_{11}$ in a rare group of *d*-electron Kondo compounds. Interestingly the Mn is found in $MnSb_4$ tetrahedra that are Jahn-Teller distorted and about 1 nm apart, meaning the carriers mediate all interactions between the Mn. Therefore, this class of materials provides a bridge between the physics of magnetic molecules and of a coupled lattice of magnetic moments—a connection between molecular and many-body physics. Further, the 14-1-11 system provides a unique opportunity to study the physics of intrinsic colossal magneto-resistance, a property of potential technological importance. Given the ability to tune the properties of these compounds by chemical substitution and strong dependence of carrier dynamics on external magnetic field, the 14-1-11 compounds may also provide excellent magneto-optic materials.

The goal of this project is to use ultrafast spectroscopic techniques to investigate the charge, spin, and vibrational dynamics in these materials over time scales from 10 fs to 1 ns. Specifically, the technique of ultrafast transient optical reflectivity is used to elucidate the overall dynamics of different processes in these materials as a function of temperature, where the dynamics of charges, phonons and spins should occur on different timescales

## Importance to LANL's Science and Technology Base and National R & D Needs

Understanding the physics and chemistry that underlies material properties impacts almost every mission area of the Laboratory. Correlated materials are important to many Department of Energy missions in stockpile stewardship (uranium and plutonium), threat reduction (nonlinear materials for sensor applications), and energy and environment (high temperature superconductors, materials for catalysis). We are studying systems with similar properties that will enable improved understanding of materials for Department of Energy missions.

This research will enable key insights into the physics driving magnetism in Heavy Fermions compounds, as well as insights bridging the physics between f-electron molecules and solids. Further, these studies will yield physics underpinning the properties of novel magnetic materials, important for the emerging field of spintronics, clearly central to future industrial and military needs of the nation.

## Scientific Approach and Accomplishments

The screening of local moments by conduction electrons, termed the Kondo effect has produced a number of surprising results, including heavy Fermion (HF) compounds where the carriers are extremely massive. It has been proposed that coupling between phonon modes and the Kondo effect could manifest new material properties, since strong coupling between magnetism and phonon modes has produced new effects in other systems, such as colossal magnetoresistance and multiferroic behavior in transition metal oxides. However, there have been no observations of coupling between the Kondo effect and an optical phonon mode, in part because it has been unclear how to detect such a coupling.

The lattice plays an important role in the 14-1-11 HF compounds, where various properties can be altered through isoelectronic substitutions. Of particular interest is $Yb_{14}MnSb_{11}$, which is metallic and exhibits ferromagnetic order of the Mn $d^4$ local moment below a Curie temperature $T_C$ of 53 K. A study of its optical conductivity suggested that the Mn *d*shell has a fifth electron that is screened by the Kondo effect. It was argued that the coexistence of ferromagnetism and HF behavior occurs via a distortion of the MnSb4 tetrahedron, motivating us to search for Kondo-lattice coupling in $Yb_{14}MnSb_{11}$ [1].

We demonstrate Kondo-phonon coupling in $Yb_{14}MnSb_{11}$ by simultaneously monitoring the electronic structure and phonon dynamics via ultrafast optical experiments[2]. Specifically, the relaxation time and amplitude of the photoinduced response strongly increase at low temperatures, indicating the presence of a hybridization gap in $Yb_{14}MnSb_{11}$. Furthermore, a softening of a phonon at low temperature is correlated with the development of this HF state. This study therefore provides a blueprint for future examination of Kondo-phonon coupling in other HF compounds [3].

Single crystals of $Yb_{14}MnSb_{11}$ were used in this study. This compound has been well characterized by x-ray diffraction, magnetic susceptibility, electrical resistivity, optical conductivity, specific heat, and x-ray magnetocircular dichroism. The sample in this study provided mirror-like surfaces and therefore time-domain measurements were performed on the as-grown sample. The ultrafast experiments were conducted with a cavity dumped laser producing 50 fs pulse centered at 800 nm with a 2 MHz repetition rate. Comparable results were obtained with a 250 KHz regenerative amplifier (800 nm, 100 fs) coupled to a superconducting magnet, which was used to investigate the effects of magnetic field and fluence.

In the left panel of Figure 1 we plot the photoinduced change in the reflectivity as a function of time at 310 K. After the pump pulse arrives, the induced reflectivity increases indicating a rise in the temperature of the Fermi surface as electron-electron interactions bring the optically excited carriers into equilibrium. We then observe an exponential decay and two exponentially damped oscillatory signals. The exponential decay is due to the carrier and phonon baths coming into thermal equilibrium.

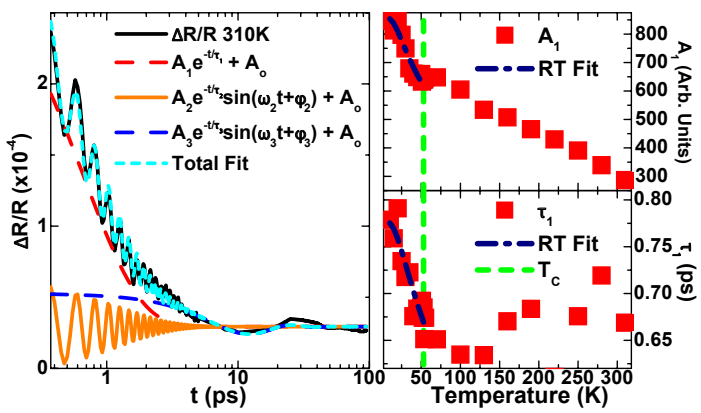


*Figure 1. Left: Pump induced change in reflectivity versus time. Data (black line) are fit with one exponential (red or gray dashed line) and two exponentially damped sinusoidal signals (orange or light gray and dashed blue or lightest gray lines). Right: Amplitude (top) and relaxation time (bottom) of the exponential term versus temperature, point size indicates error bars. The amplitude and relaxation time increase at low temperatures are described via a gap in the density of states for by the Rothwarf-Taylor model (navy or darkest gray dashed line).*

The overall amplitude and decay time of the signal are plotted in the right panel of Figure 1. For $T>T_C$, they follow our expectations for a normal metal, with the decay time nearly temperature independent. However, since the specific heat of the metal is increasing as the sample temperature is raised, the photo-excitation results in a smaller change in the temperature rise of the Fermi surface. Therefore, the amplitude decreases as the sample temperature is raised. Interestingly, the decay time and amplitude increase significantly below $T_C$, as have been observed in superconductors and HF compounds. This is believed to indicate the opening of a gap in the density of

states below $T_c$. Specifically, due to the presence of a gap, the carriers can only relax via emission of high frequency phonons with energy than the gap energy. Since the probability for optical phonons to decay into two phonons of lower energy is fairly small (as opposed to acoustic modes that are much more susceptible to anharmonic affects), it is highly likely that the optical phonon will excite a new electron-hole pair across the gap. This *phonon* bottleneck significantly reduces the transmission of heat from the Fermi surface to the lattice, resulting in an increase in the decay time and amplitude below the transition temperature.

The model of Rothwarf and Taylor (RT) has been very successful in describing the dynamics of superconductors and HF compounds [4]. In the RT approach the quasiparticle and phonon dynamics are described via a set of coupled nonlinear differential equations. The RT equations account for the creation and destruction of electron-hole pairs via emission of high frequency phonons and biparticle scattering as well as a reduction in the number of high frequency phonons via diffusion and anharmonic decay. Recently the RT model has been used to predict the amplitude and decay time of the photoinduced reflectivity, given in Reference [5]. For our data, the results of this analytical form of the photoinduced signal based on the Rothwarf Taylor model are displayed in the right panels of Fig. 1. This fit of the model to our data yields a temperature independent gap of 32 wavenumbers, as compared to previous studies of the optical conductivity, which have found a gap energy of 50 wavenumbers [1]. However, optical conductivity probes the direct hybridization gap (i.e., no change in momentum), whereas the present results are governed by the indirect gap, which should be smaller. Lastly, the application of a 6 T magnetic field, saturating the magnetization did not change the photoinduced reflectivity signal, providing further evidence that the gap is unrelated to the ferromagnetism.

In addition to the relaxation dynamics of the electronic system, the data displayed in Figure 1 also contains information about an optical phonon mode. Specifically, the oscillations in the data result from the coherent generation of optical and acoustic phonons. While there are a variety of proposed mechanisms, it is generally agreed upon that such oscillations are initiated via a Raman process upon optical excitation. The modes are then observed via a Raman shift of the probe pulse, which exponentially decays due to the dephasing of the phonons. As shown in Figure 2, as the temperature is lowered, the optical mode frequency increases while its decay rate decreases. In contrast, for $T<T_c$ the phonon softens and broadens. As discussed later, this low temperature behavior is quite anomalous. Therefore, to confirm that this behavior is intrinsic to the sample and not an artifact of our fitting routine, we subtracted the first term of Equation 1 from the data and then performed a fast-Fourier transform (FFT). The FFT spectra in the top panel of Figure 3 reveal the same trends shown in Figure 2. The center frequency and broadening determined from fits of the FFT data with Lorentzian line shapes are in superb agreement with the results of fitting to the photoinduced signal.

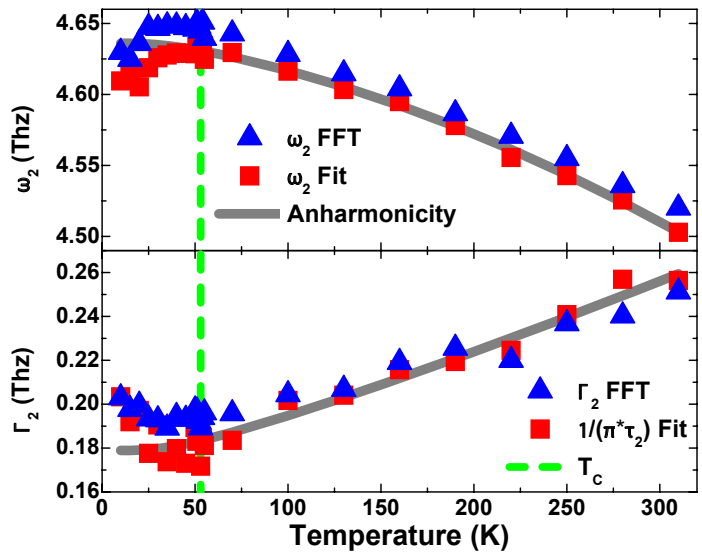


*Figure 2. The phonon mode frequency (top panel) and broadening or damping rate (bottom panel). The mode hardens and sharpens as the temperature is lowered to TC, which is described by anharmonic effects.*

The temperature dependence of the phonon above $T_c$ is similar to anharmonic effects observed in numerous other materials. Specifically, the optical phonon can decay into acoustic modes of lower energy, resulting in a renormalization of its self-energy. Since the likelihood of this decay depends on the occupancy of the phonon density of states, one expects a temperature dependence, which depends on the occupancy of the phonon density of states. The frequency and linewidth for this process are plotted as the solid line in Figure 2 and describe the measured phonon frequency and linewidth well above $T_c$. Nonetheless, these anharmonic effects do not explain the temperature dependence of the phonon mode below $T_c$.

The behavior of the optical phonon below $T_c$ can be understood in terms of magnetically ordered systems using the minimal mean field Hamiltonian for the underscreened Kondo lattice with a phonon. The resultant phonon frequency deviates from the anharmonic phonon frequency described previously by the sum of two terms: one proportional to the ferromagnetic interaction between Mn ions and another proportional to density of Kondo singlets which is basically the density of quasiparticles excited across the hybridization gap and can be determined by the

amplitude of the signal shown in Figure 1. Figure 3 reveals that the phonon continues to soften down to the lowest T. However, the magnetic interaction determined via zero-field cooled SQUID measurements, saturates close to $T_c$, as seen in the gray line in Figure 3, indicating the phonon does not strongly couple to the ferromagnetic order. Nonetheless, the softening of the phonon below $T_c$ follows the temperature dependence of the Kondo singlets, indicating a Kondo-phonon coupling.

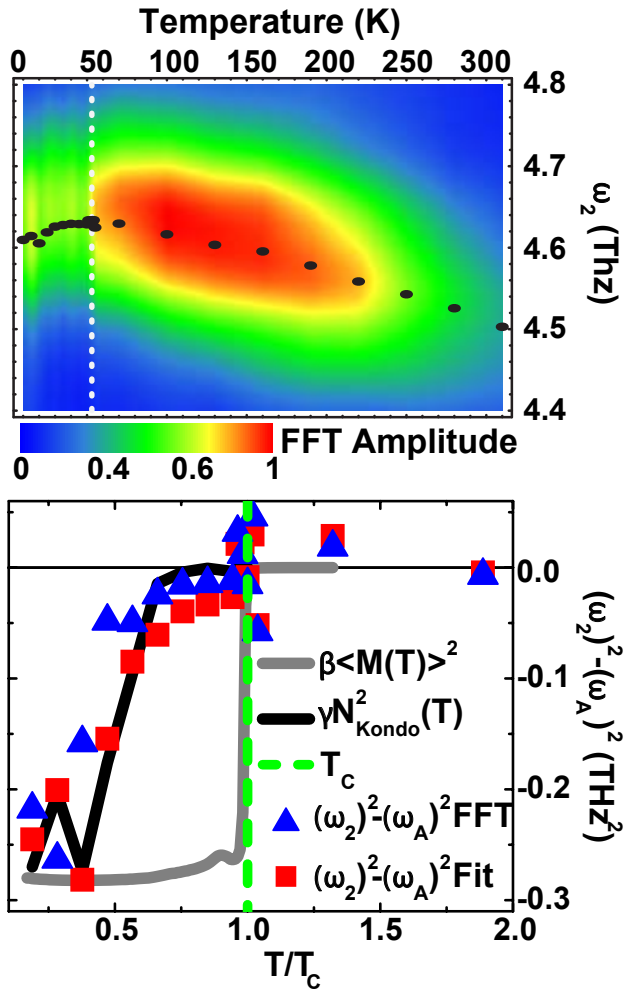


*Figure 3. Top panel: FFT spectrum of data, white dashed line indicates TC and black dots are the center frequency of the phonon mode. Bottom panel: The shift in the phonon frequency after anharmonic effects have been removed. The shift does not appear to result from coupling to ferromagnetic state (gray), but rather via a coupling to the Kondo effect (black line).*

In conclusion, we explored the ultrafast optical properties of $Yb_{14}MnSb_{11}$. Significant changes in the dynamics occur below $T_c$, although they are not connected with the development of the ferromagnetic state. In particular, the amplitude and relaxation time of the electronic response grows significantly at low temperatures, but is not affected by the application of a magnetic field. Furthermore, changes in the frequency of the optical phonon are inconsistent with the temperature dependence of the magnetization. Instead we find that the low temperature enhancement of the photoinduced response and the softening of the phonon result from the development of heavy Fermions and their coupling to the lattice. As expected for a hybridization gap, quantitative analysis reveals the indirect gap probed here is smaller in magnitude than the direct gap determined via optical conductivity experiments [1]. In addition, the softening of the phonon at low temperatures is correlated with the number of heavy quasiparticles. Therefore this is the first demonstration of coupling between the Kondo effect and optical modes, and provides a guide for future studies of Kondo-Phonon coupling effects.

## References


1. Burch, K. S., A. Schafgans, N. P. Butch, T. A. Sayles, M. B. Maple, B. C. Sales, D. Mandrus, and D. N. Basov. Optical study of interactions in a d-electron Kondo lattice with ferromagnetism . 2005. *Physical Review Letters.* **95**: 46401.

2. Demsar, J., J. L. Sarrao, and A. J. Taylor. Dynamics of photoexcited quasiparticles in heavy-electron compounds. 2006. *Journal of Physics of Condensed Matter.* **18**: R281.

3. Burch, K. S., E. Chia, D. Talbayev, B. C. Sales, D. Mandrus, A. J. Taylor, and R. D. Averitt. Coupling between phonons and the hybridization gap in a d-electron Kondo lattice. 2008. *Physical Review Letters.* **100**: 26409.

4. Rothwarf, A., and B. N. Taylor. Measurement of recombination lifetimes in superconductors. 1967. *Physical Review Letters.* **19**: 27.

5. Demsar, J., V. K. Thorsmolle, J. L. Sarrao, and A. J. Taylor. Photoexcited electron dynamics in Kondo insulators and heavy Fermions. 2006. *Physical Review Letters.* **96**: 37401.


## Publications


Burch, K. S., D. B. Shrekenhamer, E. J. Singley, J. Stephens, B. L. Sheu, R. K. Kawakami, D. D. Awschalom, N. Samarth, P. Schiffer, and D. Basov. Impurity band conduction in a high temperature ferromagnetic semiconductor. 2006. *Physical Review Letters.* **97**: 087208.

Burch, K. S., E. E. M. Chia, D. Talbayev, B. C. Sales, D. Mandrus, A. J. Taylor, and R. D. Averitt. Coupling Between An Optical Phonon and the Kondo Effect. 2008. *Physical Review Letters.* **100**: 026409.

Burch, K. S., S. Dordevic, F. P. Mena, D. van der Marel, J. L. Sarrao, J. R. Jeffries, E. D. Bauer, M. B. Maple, and D. N. Basov. On the importance of momentum dependence of the hybridization of local moments and conduction electrons: an optical study of the CeTIn5 (M = Co, Ir, Rh) Kondo lattices. 2007. *Physical Review B.* **75**: 054523.

Bursch, K. S., S. Dordevic, F. P. Mena, D. van der Marel,, J. L. Sarrao, J. R. Jeffries, E. D. Bauer, M. B. Maple, and D. N. Basov. Understanding the optical properties of the 115 family of heavy fermion superconductors. 2007. *Physical Review B.* **75**: 054533.

# High P-T Synthesis of Superhard Carbon Nitride from Graphite-Like Precursors

*Yusheng Zhao*

20061378PRD1

## Abstract

Materials with covalently bonded networks of carbon and nitrogen are generally expected to possess outstanding physical properties such as high bulk moduli and thermal conductivity, superhardness, and wide band gap. The C3N4 composition has attracted special attention because its beta phase, consisting of sp3 carbon and three coordinated nitrogen, has been theoretically predicted to have a bulk modulus or perhaps a hardness rivaling that of diamond, the hardest of the known materials. However, the synthesis of bulk superhard carbon nitride crystallites presents great challenges. Our goal is to use high P-T synthesis to make the novel superhard materials and to understand the related science.

## Background and Research Objectives

Our research makes use of the unique facilities existing at LANSCE, which include instrumentation for large/bulk materials synthesis and in-situ neutron diffraction under high P-T conditions, which is especially needed for structural and bonding character and reaction kinetics studies of materials containing light elements (such as C and N). Sufficiently high pressure is expected to stabilize the denser sp3-bonded phases and also increase the decomposition temperatures of precursor materials. Experiments will be accomplished on a synchrotron x-ray source because of very small sample sizes involved in the high-pressure measurements.

## Importance to LANL's Science and Technology Base and National R & D Needs

Synthesis and characterization of novel superhard materials involves multiple disciplinary scientific andengineering efforts. This project studies ultratough and superhard nanocomposites for advanced technological applications. Our achievements in nano-science and nano-technology, specifically thesuperhard materials in thermo-mechanics advances, will impact DOE's missions in energy, environment, and nation's future economic base.

## Scientific Approach and Accomplishments

To date, the majority of experimental studies in the C-N system have centered on low-pressure thin-film growth. While these studies have led to C-N materials with a wide range of compositions, including a well-defined $C_2N$ phase with some diamond-like properties and a claimed beta-$C_3N_4$ phase with a robust hardness, the uniform tetrahedral sp3 carbon-bonding and superhardness expected for pure beta-$C_3N_4$ have not yet been achieved or proven. Recently, some attentions are focused on using the graphite-like forms of carbon nitride and their derivatives as precursors for the synthesis of superhard C-N materials.

Exploratory efforts have also begun to search for synthesis routes using high pressure and temperature. Both approaches are similar to the way that artificial diamond was first produced from graphitic form of carbon, and they are believed to hold great promises of producing superhard carbon nitrides. However, the kinetics of decomposition of precursors into $N_2$ in such synthesis routes was found to play a dominant role, and the most difficult undertaking is to avoid precursor decomposition below the expected P-T conditions for carbon sp2 to sp3 transformation. We proposed to synthesize the graphite-like carbon nitride precursors using chemical or mechanochemical methods and optimize the graphite-like precursors with enhanced kinetic barriers for decomposition in Large Volume Press.

We have successfully developed solvo-thermal and solvent-free synthesis routes to prepare a number of carbon nitride precursors on the basis of several novel organic-like chemical reactions: (1) $C_3N_3Cl_3$+ $3NaNH_2$,(2) $C_3N_3Cl_3$+ $3NaN_3$, and (3) $C_3N_3Cl_3$+ $NH_4Cl$. Some representative precursors (such as g-$C_3N_4Hx$ and g-$C_6N_9H_3$) were characterized by X-ray/Neutron diffraction, IR spectroscopy and electron microscopy. The as-prepared precursors were identified as graphite-like carbon nitride

nanocrystals. In addition, we have systematically studied the thermal stability of the precursors using Large Volume Press. It was found that the g-$C_3N_4$Hx synthesized via a solvent-free route has higher thermal stability than that synthesized by a solvo-thermal route. The former precursor possesses enhanced kinetic barriers.

We have successfully obtained amorphous hard carbon nitride in the cold-compressed graphite-like carbon nitride nanocrystals g-$C_3N_4$Hx using the high-pressure diamond-anvil-cell (DAC) technique. Our synchrotron X-ray diffraction studies show that crystalline g-$C_3N_4$Hx transforms to an amorphous structure under high compression, which can be quenched to ambient conditions. IR spectroscopy of the quenched samples shows strong peaks related to the vibration of single C-N bonds, indicating the formation of more sp3 bonds and denser carbon nitride structures. These results suggest that the hard phase formed under high pressure. High temperature is expected to overcome the kinetic energy barrier from the amorphous structure to a crystalline superhard phase.

The large volume experiments under high P-T conditions were done to prepare a crystalline superhard phase from amorphous superhard precursors. Experiments in a Large Volume Press were conducted on molecular precursor $C_3N_4H_4$ at LANSCE-LC and NSLS, Brookhaven National Laboratory. These LVP experiments are not very successful because of the incorporation of impurities from the materials surrounding precursors. In the future, we plan to use platinum capsules, which is very stable under high P-T conditions. The precursors will be $C_3N_4H_4$, g-$C_3N_4$Hx, or g-$C_6N_9H_3$. The unwanted hydrogen is expected to diffuse into the platinum capsule, leading to the formation of superhard $C_3N_4$ phase.

# Studies of Sub-Micron Ferromagnetic Particles Using Magnetic Resonance Force Microscopy

*Roman Movshovich*

20061396PRD1

## Abstract

To study magnetic phenomena on submicron scale, we need a suite of tools capable of interrogating individual ferromagnetic sub-micron particles, both their static and dynamic properties. We have developed a dual purpose Magnetic Resonance Force Microscope (MRFM) / Magnetic Force Microscope (MFM) low temperature apparatus and used it study Ferromagnetic phenomena in continuous and patterned thin ferromagnetic films. This project focused on the details of MRFM tip characterization, the magnetic tip – sample interaction, and MRMF imaging capabilities of ferromagnetic films and structures. In particular, we have discovered localized (on the scale of a micron) ferromagnetic resonance modes in thin ferromagnetic films induced by the strongly varying field produced by the MRFM cantilevers. In addition to imaging small ferromagnetic structures, MFM mode of operation allowed us to image magnetic vortices in thin superconducting films, expanding the range of future research opportunities that will be enabled by the MRFM/MFM instrument.

## Background and Research Objectives

When the size of a ferromagnetic particle is sufficiently reduced, its magnetization can behave as a single large spin that is thermally fluctuating in time between various local ground states (directions of the magnetization). This phenomenon determines the limiting small size of the magnetic particle that can be used in information storage devices, and is called superparamagnetism. To study these phenomena, we need a suite of tools capable of interrogating individual ferromagnetic sub-micron particles, both their static and dynamic properties. Evgueni Nazaretski developed a dual purpose Magnetic Resonance Force Microscope (MRFM) / Magnetic Force Microscope (MFM) low temperature-controlled apparatus and used it study Ferromagnetic phenomena in continuous and patterned thin ferromagnetic films. He also initiated studies of the vortex matter in superconducting films using the MFM capability of his apparatus. This project focused on the details of MRFM tip fabrication and characterization, the magnetic tip – sample interaction, and MRMF imaging capabilities of ferromagnetic films and structures. In the past, magnetic resonance investigations of ferromagnetic samples were capable of interrogating only the bulk modes, where all of the sample participated, due to a strong interactions between nearby parts of ferromagnetic material. MRFM is a scanning magnetic probe capable not only of isolating a micron-size of ferromagnetic material and investigating its dynamic properties, but also capable of subsurface investigation of materials, where the resonance conditions are satisfied within the so-called sensitive slice. MRFM investigations on paramagnetic materials led to a great success, ultimately culminating is a single electron spin detection. The goal of our project was to test the material limit of MRFM, i.e. whether MRFM will be capable of investigating ferromagnetic samples on the sub-micron scale, in spite of the strong intra-sample correlations and interactions that are signature of ferromagnetic systems.

## Importance to LANL's Science and Technology Base and National R & D Needs

This project will open a new area of LANL expertise in the forefront of nanotechnology, a field of key national strategic importance. In the future, MRFM will play a stand out role at the Center for Integrated Nanotechnology (CINT) at LANL, recently established and funded by DOE.

## Scientific Approach and Accomplishments

Figure 1 shows a schematic of magnetic cantilever poised over the surface of the sample. This arrangement represents both MRFM and MFM modes of operation. The main difference is in the details of the

construction of the magnetic tip. The field profile of a magnetic tip in MRFM has always presented a practical problem: many tips were fabricated by ion beam milling of a larger magnetic particle attached to a micro-mechanical cantilever. As a result of a possible ion beam bombardment damage to the ferromagnetic material of the remaining material, and an irregular shape of the remaining magnetic particle, the field profile, crucial to the analysis of the data and model simulations, was not known. We have approached this problem from two directions. Firstly, the utilization of a regular few-micron size spherical particle on NdFeB, allowed us to model the field of the cantilever as that of a perfect dipole. However, even in that case, uncertainty might exist as to the direction of the magnetic field created by the magnetic tip due to possible micro-domain structure, direction of the field due to the crystalline and surface anisotropy. We have developed the experimental approach to characterize spatial distribution of the magnetic field produced by cantilever tip of an arbitrary shape by performing MRFM measurements on a well characterized diphenyl-picrylhydrazyl (DPPH) film. Thereby we were able to map the 3D field profile produced by a $Nd_2Fe_{14}B$ probe tip by using the "leading edge" of the MRFM spectra obtained as the sharp edge of the DPPH is approached at different distances from the edge. This method was described in an article "Spatial characterization of the magnetic field profile of a probe tip used in magnetic resonance force microscopy" by E. Nazaretski, E. A. Akhadov, I. Martin, D. V. Pelekhov, P. C. Hammel, and R. Movshovich, *Appl. Phys. Lett.,* **92**, 214104 (2008).

Significant progress was made by Evgueni Nazaretski during this project on a number of fronts. MRFM investigations of ferromagnetic films have yielded a number of important results. Investigation of the samples fabricated with optical lithographic techniques where different ferromagnetic films are separated by a distance of a few nanometers demonstrated 1) submicron resolution of the MRFM apparatus; 2) that MRFM can differentiate the material under the tip, i.e. it is material-sensitive. The results of this work were published in an article "Ferromagnetic resonance force microscopy studies of a continuous permalloy-cobalt film" by E. Nazaretski, E. A. Akhadov, K. C. Cha, D. V. Pelekhov, I. Martin, P. C. Hammel, and R. Movshovich, *Phys. Stat. Sol. A,* 1-4, (2008). This work was featured on the cover of journal where article was published (see Figure 1).

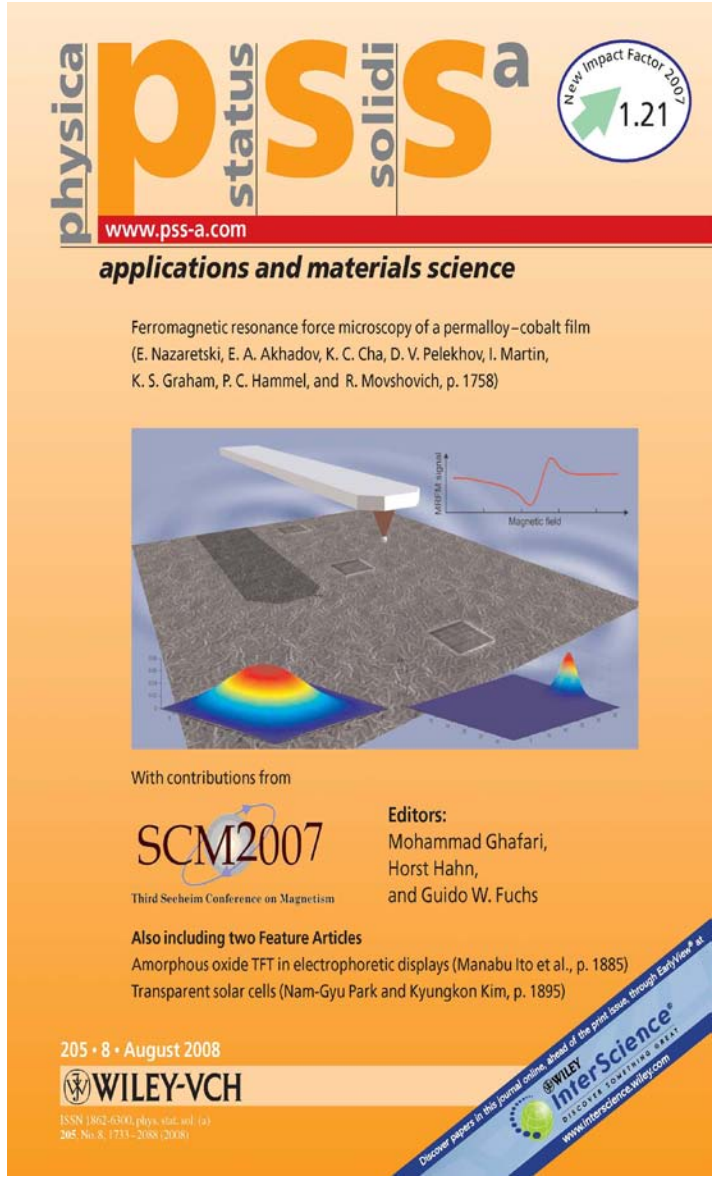


*Figure 1. Schematic of the MRMF/MFM scanning probe over the sample. Magnetic particle is glued to the tip of the cantilever for MRFM mode of operation, or magnetic film evaportated on the tip of the micro cantilever for MFM mode of operation. Sample shown consists of the regular array of squares of magnetic film.*

Dr. Nazaretski received his initial training in the field of MRFM in the laboratory of Pr. Chris Hammel at the Ohio State University. He has continued to strengthen this collaboration over the duration of the PRD project, which has resulted in a number of successful joint projects. Most recent results of this collaboration were published in an article on "Local Ferromagnetic Resonance Imaging with Magnetic Resonance Force Microscopy", Yu. Obukhov, D.V. Pelekhov, J. Kim, P. Banerjee, I. Martin, E. Nazaretski, R. Movshovich, S. An, T.J . Gramila, S. Batra, and P. C. Hammel, *Phys. Rev. Lett.,* **100**, 197601 (2008), which was featured in May 26, 2008 issue of Virtual Journal of Nanoscale Science & Technology, where we demonstrated the

direct imaging of the array of the micron-size ferromagnetic particles.

One of the most fundamental discoveries of this project resulted from the magnetic resonance force microscopy studies of a 50 nm thick permalloy film as a function of the probe-sample distance and the angle between the film plane and the direction of the externally applied magnetic field. At larger angles the multiple resonance modes were observed at small probe-sample distances. Micromagnetic simulations which include the inhomogeneous magnetic field of the probe tip reveal the *localized* nature of the exited resonance modes. The simulations were performed in collaboration with Ivar Martin (T-11, LANL), and Yu. Obukhov and D. Pelekhov, among others, from the group of Pr. Hammel at the Ohio State University. Observation of the localized modes is the first step on the way to spatially resolved ferromagnetic resonance measurements in a continuous ferromagnetic media. These results were submitted for publication in Physical Review Letters, and are at the revision stage at present.

Overall, the project resulted in nine published articles (including one PRL, Ref. [1]), one submitted PRL [6], and five additional articles in preparation. The papers span a wide range from the details of construction [10,11,4,3,2] and principles of operation of the dual MRFM/MFM apparatus to discoveries of the phenomena at the frontiers of magnetism and superconductivity, such as localized ferromagnetic resonance modes in thin films [6] and micron size structures [1].

This project contributed greatly to firmly establishing magnetic scanning probe capability at Los Alamos, with strong connections to both Center for Integrated Nano-Technologies (CINT) and the Superconducting Technologies Center (STC). This project has made strong contributions to several areas of the research at the forefront of magnetism, especially novel phenomena on the micron scale and below.

## References


1. Obukhov, Y., D. V. Pelekhov, J. Kim, P. Banerjee, I. Martin, E. Nazaretski, R. Movshovich, and P. C. Hammel. Local Ferromagnetic Resonance Imaging with Magnetic Resonance Force Microscopy. 2008. *Physical Review Letters.* **100**: 197601.

2. Nazaretski, E., E. A. Akhadov, I. Martin, D. V. Pelekhov, P. C. Hammel, and R. Movshovich. Spatial characterization of the magnetic field profile of a probe tip used in magnetic resonance force microscopy. 2008. *Applied Physics Letters.* **92**: 214104.

3. Nazaretski, E., E. A. Akhadov, K. C. Cha, D. V. Pelekhov, I. Martin, P. C. Hammel, and R. Movshovich. Ferromagnetic resonance force microscopy studies of a continuous permalloy-cobalt film. 2008. *Physica Status Solidi A.* **1-4**: 200723465.

4. Nazaretski, E., D. V. Pelekhov, I. Martin, M. Zalalutdinov, J. W. Baldwin, B. Houston, P. C. Hammel, and R. Movshovich. Ferromagnetic resonance force microscopy in a thin permalloy film. 2007. *Applied Physics Letters.* **90**: 234105.

5. Nazaretski, E., J. D. Thompson, D. V. Pelekhov, T. Mewes, P. E. Wigen, J. Kim, M. Zalalutdinov, J. D. Baldwin, B. Houston, P. C. Hammel, and R. Movshovich. Magnetic resonance force microscopy studies in a thin permalloy film. 2007. *Journal of Nagmetism and Magnetic Materials.* **310**: e941.

6. Nazaretski, E., D. V. Pelekhov, I. Martin, M. Zalalutdinov, D. V. Ponarin, A. Smirnov, P. C. Hammel, and R. Movshovich. Detection of localized excitations in a continuous ferromagnetic film via magnetic resonance force microscopy. To appear in *Physical Review Letters.*

7. Nazaretski, E., D. V. Pelekhov, I. Martin, K. C. Cha, E. A. Akhadov, P. C. Hammel, and R. Movshovich. Localized ferromagnetic resonance force microscopy of permalloy-cobalt films. To appear in *Applied Physics Letters.*

8. Nazaretski, E., I. Martin, K. C. Cha, E. A. Akhadov, and R. Movshovich. 7. Localized ferromagnetic resonance force microscopy of a continuous permalloy-cobalt film . 2007. In *Materials Research Society Fall Meeting 2007.* (Boston, MA, 26-30 Nov. 2007). Vol. 1025E, p. B11. Warrendale, PA,: MRS.

9. Mewes, T., C. K. Mewes, E. Nazaretski , J. Kim, K. C. Fong, Y. Obukhov, D. V. Pelekhov, and P. Wigen. 5. Detection of higher order modulation harmonics in magnetic resonance force microscopy . 2007. *Journal of Applied Physics .* **102**: 033911.

10. Nazaretski, E., J. D. Thompson, R. Movshovich, M. Zalalutdinov, J. W. Baldwin , B. Houston, T. Mewes, D. V. Pelekhov, P. Wigen , and P. C. Hammel. 3. Temperature-dependent Magnetic Resonance Force

Microscopy studies of a thin Permalloy film. 2007. *Journal of Applied Physics.* **101**: 074905.

11. Nazaretski, E., R. Movshovich, T. Mewes, D. V. Pelekhov , and P. C. Hammel. 1. Low temperature magnetic resonance force microscope: design and performance. 2006. *AIP conference proceedings.* **850**: 1641.

## Publications

Mewes, T., C. K. Mewes, and E. Nazaretski . Detection of higher order modulation harmonics in magnetic resonance force microscopy . 2007. *Journal of Applied Physics.* **102**: 033911.

Nazaretski, E., E. A. Akhadov, K. C. Cha, K. Graham, I. Martin, R. Movshovich, D. V. Pelekhov , and P. C. Hammel. 6. Ferromagnetic resonance force microscopy studies of a continuous permalloy-cobalt film. 2008. *Physica Status Solidi A.* **205**: 1758.

Nazaretski, E., E. Akhadov, I. Martin, R. Movshovich, D. V. Pelekhov , and P. C. Hammel. Spatial characterization of the magnetic field profile of a probe tip used in magnetic resonance force microscopy . 2008. *Applied Physics Letters .* **92**: 214104.

Nazaretski, E., I. Martin, and R. Movshovich. Ferromagnetic Resonance Force microscopy on a thin permalloy film. 2007. *Applied Physics Letters.* **90**: 234105.

Nazaretski, E., J. D. Thompson, D. V. Pelekhov, T. Mewes, P. E. Wigen, J. Kim, M. Zalalutdinov, J. W. Baldwin, B. Houston, P. C. Hammel, and R. Movshovich. Magnetic resonance forcemicroscopy studies in a thin permalloy film. (Kyoto, Japan, 26-29 Aug. 2006).

Nazaretski, E., J. D. Thompson, and R. Movshovich. Magnetic resonance force microscopy studies in a thin permalloy film. 2007. *Journal of Magnetism and Magnetic Materials .* **310**: e941.

Nazaretski, E., J. D. Thompson, and R. Movshovich. •Temperature-dependent Magnetic Resonance Force Microscopy studies of a thin Permalloy film. 2007. *Journal of Applied Physics.* **101**: 074905.

Nazaretski, E., R. Movshovich, T. Mewes, D. V. Pelekhov , and P. C. Hammel. 1. Low temperature magnetic resonance force microscope: design and performance. 2006. *AIP conference proceedings.* **850**: 1641.

Obukhov, Y., D. V. Pelekhov, J. Kim, P. Banerjee, S. An, T. J. Gramila, P. C. Hammel, I. Martin, E. Nazaretski, and R. Movshovich. 8. Local Ferromagnetic Resonance Imaging with Magnetic Resonance Force Microscopy. 2008. *Physical Review Letters .* **100**: 197601.

# Interface-Governed Behavior of Nano-Layered Metallic Composites

*Richard Hoagland*

20061438PRD2

## Abstract

We have found the atomic-scale mechanisms whereby interfaces in Cu-Nb multilayer nanocomposites reduce radiation damage. By studying the structure of these interfaces, we have created an analytical model that enables us to propose strategies of informed design of radiation tolerant composite materials for use as structural materials in next generation fission reactors, first wall coatings in fusion reactors, and shielding in space-borne devices. Furthermore, we have carried out high-temperature helium implantation experiments that suggest that distributions of voids and He bubbles created during irradiation may be controlled by tailoring nanocomposite morphology.

## Background and Research Objectives

Nuclear energy—both fission, and in the longer-term, fusion—is carbon neutral and therefore an attractive alternative to obtaining energy from fossil fuels. The operating environment of nuclear reactor components, however, is nothing short of extreme: over time, high levels of sustained irradiation, immersion in corrosive fluids, and temperatures approaching the melting point of some metals cause severe degradation in traditional structural engineering materials. Thus, ensuring that future nuclear reactors are maximally safe, efficient, and reliable entails developing novel classes of materials that are both strong and resistant to the punishing conditions found inside a nuclear reactor.

We take an entirely new approach to developing promising materials for nuclear reactors by considering composites made up of layers of different materials that are only a few dozen atoms thick. The properties of such composites are dominated by the interfaces between the layers, which act as efficient sinks for radiation-induced point defects. Multilayer nanocomposites of Cu and Nb are an example of the successful application of this design strategy: these materials are very strong and at the same time highly resistant to radiation damage.

The goal of this research project was to determine the mechanisms by which interfaces in Cu-Nb multilayer nanocomposites reduce radiation damage and how these mechanisms arise from the atomic-level structure of these interfaces. These insights were then to be used for the development of strategies whereby radiation tolerant materials could be designed by choosing compositions and morphologies that give rise a large volume fraction of radiation damage reducing interface.

## Importance to LANL's Science and Technology Base and National R & D Needs

This project has contributed to several science and technology directions that are strategic to LANL. It has directly addressed the Lab's interests in "energy security" and "carbon neutral energy", specifically in the development of design strategies for novel classes of materials for use in next generation nuclear reactors. This project has also contributed to "fundamental understanding of materials," particularly how complex atomic environments at incommensurate heterophase interfaces lead to unexpected material behaviors. The results of this project have served as the basis for an LDRD-DR proposal that has been endorsed as #1 by MST division in the ongoing 2008 LDRD process. They directly address DOE-OBES's priorities in "Advanced Nuclear Energy Systems" and "Materials Under Extreme Environments" and are expected to have a major long-term impact on LANL's participation in civilian nuclear energy programs—including the Global Nuclear Energy Partnership (GNEP)—as well as the MaRIE signature facility. Opportunities for leveraging the results obtained in this project to develop new shielding materials for space-borne devices are currently being considered in collaboration with ISR division.

## Scientific Approach and Accomplishments

This project was conducted in collaboration with a diverse team of experimentalists and modelers and

has focused on multilayer composites formed by the immiscible elements copper (Cu) and niobium (Nb). It has led to the identification of the mechanisms that account for reduction in radiation damage in the vicinity of Cu-Nb interfaces as well as to the creation of a detailed model of interface behavior that can be used to guide further efforts to develop radiation tolerant materials.

The core studies of this project were carried out using atomistic simulations. The interatomic forces in the Cu-Nb system were modeled using an embedded atom (EAM) potential, which reproduces the immiscibility of Cu and Nb as well as several additional properties—obtained from DFT calculations—describing the interaction between these two elements [1]. Ion collision cascade simulations carried out using this potential have demonstrated that Cu-Nb interfaces do indeed act as sinks for radiation-induced point defects, reducing their average number by nearly 70% within the lifetime of individual cascades [2], as shown in Figure 1.

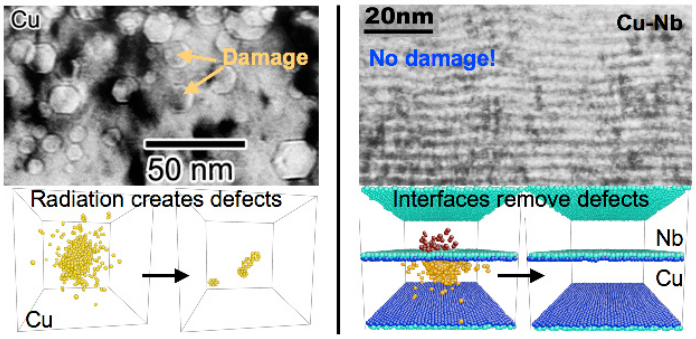


*Figure 1. Effects of He ion radiation on atomic-scale structure. The figure on the upper left shows extensive damage in the form of He bubbles in copper. The bubbles are the result of aggregation of defects produced by damage cascades an example of which appears in the lower left taken from an MD calculation. The figures on the right show the structure of a Cu/Nb multilayer composite (upper) after being exposed to similar radiation. Little or no damage is evident as cinfirmed by MD results (lower) that show defects removed by an interface before they are able to aggregate.*

The long-term effect of point defect migration to Cu-Nb interfaces can be modeled by taking into account several unusual properties of these interfaces, especially their ability to absorb large numbers of vacancy-interstitial pairs and to catalyze their efficient recombination [3, 4]. These properties can be traced back to the ability of Cu-Nb interfaces to exist in several distinct atomic-level structural states that preserve the experimentally-observed Kurdjumov-Sachs orientation relation and differ in density, but are nearly degenerate in energy [1, 3, 4]. This connection between the structure of Cu-Nb interfaces and their properties is exploited to suggest interfaces between other elements that may also reduce radiation damage. Nanocomposites synthesized to contain a large volume fraction such interfaces could be expected to exhibit resistance to radiation damage, like Cu-Nb multilayer nanocomposites.

Finally, we have used helium implantation in MST's IBML to study the behavior of Cu-Nb interfaces at elevated temperatures. These experiments have shown that in addition to reducing radiation damage, Cu-Nb interfaces serve as high diffusivity paths for the implanted He [5]. We also noted an asymmetrical distribution of He-filled voids and bubbles in the Cu and Nb layers, leading us to propose that tailoring of nanocomposite morphologies may be used to control the distribution of such defects in materials subjected to irradiation at elevated temperatures [6].

## References

1. Demkowicz, M.J., and R. G. Hoagland. Structure of Kurdjumov-Sachs interfaces in simulations of a copper-niobium bilayer. 2008. Journal of Nuclear Materials. 372: 45.

2. Misra, A., M. J. Demkowicz, X. Zhang, and R. G. Hoagland. The radiation damage tolerance of ultra-high strength nanolayered composites . 2007. Journal of Metals. 59 (9): 62.

3. Demkowicz, M.J., R. G. Hoagland, and J. P. Hirth. Interface structure and radiation damage resistance in Cu-Nb multilayer nanocomposites. To appear in Physical Review Letters.

4. Demkowicz, M.J., J. Wang, and R. G. Hoagland. Interfaces between dissimilar crystalline solids. To appear in Dislocations in Solids.Edited by Hirth, J.P.

5. Demkowicz, M.J., Y. Q. Wang, R. G. Hoagland, and O. Anderoglu. Mechanisms of He escape during implantation in CuNb multilayer composites. 2007. Nuclear Instrumentation and Methods in Physics Research. 261 (1-2): 524.

6. Hattar, K., M. J. Demkowicz, A. Misra, I. M. Robertson, and R. G. Hoagland. Arrest of He bubble growth in Cu-Nb multilayer nanocomposites . 2008. Scripta Materialia. 58 (7): 541.

## Publications

Hattar, K., M. J. Demkowicz, A. Misra, I. M. Robertson, and R. G. Hoagland. Arrest of He bubble growth in Cu-Nb multilayer nanocomposites. To appear in Applied Physics Letters.

Demkowicz, M.J., Y. Q. Wang, R. G. Hoagland, and O. Anderoglu. Mechanisms of He escape during implantation in CuNb multilayer composites . 2007. Nuclear Instrumentation and Methods in Physics Research. 261 (1-2): 524.

Demkowicz, M.J., J. Wang, and R. G. Hoagland. Interfaces between diccimilar crystalline solids. To appear in Dislocations in Solids, V.14.Edited by Hirth, J.P.

Demkowicz, M.J., R. G. Hoagland, and J. P. Hirth. Interface structure and radiation damage resistance in Cu-Nb multilayer nanocomposites. Submitted to Physical Review Letters.

Demkowicz, M.J., and R. G. Hoagland. Structure of Kurdjumov-Sachs interfaces in simulations of a copper-niobium bilayer. To appear in J. Nuclear Materials.

Demkowicz , M.J., and R. G. Hoagland. Structure of Kurdjumov-Sachs interfaces in simulations of a copper-niobium bilayer. Submitted to Journal of Nuclear Materials.

# Ion Synthesis of Novel SiGe Structures

*Michael Anthony Nastasi*

20061442PRD2

## Abstract

H-induced layer transfer technology, commercially known as ion-cut or Smart-cut™ is a cutting-edge technology that allows total freedom to arbitrarily integrate materials that possess different electronic, magnetic and optical properties. The ability to perform such materials integration will open new possibilities of developing 3-D electronics and novel photonic-electronic devices. Ideally, Smart-cut™ technology can control the thickness of the transferred material by adjusting the energy of the implanted hydrogen ions. However, the radiation damage induced by hydrogen implantation could totally change the properties of the transferred material if the thickness of the transferred layer is less than 100 nm. Recently, our group has successfully developed a novel technique to transfer ultra-thin Si layers(less than 20nm) without ion implantation. In that approach, a highly strained SiGe layer is introduced inside the silicon at a depth below the surface equal to the desired thickness of the transferred layer. That strained SiGe layer will act as hydrogen trapping layer when exposed to a hydrogen plasma, and subsequent H-induced cracking can be guided along this layer parallel to the surface. However, the physical and chemical mechanisms underlying this novel process have not been fully elucidated. The main objective of this project is to improve our scientific understanding of the physical and chemical mechanisms underlying this strain facilitated layer transfer process.

## Background and Research Objectives

The implementation of silicon-on-Insulator (SOI) technology is one of several manufacturing strategies employed to allow the continued miniaturization of microelectronic devices, colloquially referred to as extending Moore's Law. SOI works by placing a thin, insulating layer, such as silicon oxide or glass, between a thin layer of silicon and the silicon substrate. This special structure helps reduce the amount of electrical charge that the transistor has to move during a switching operation, thus making it faster and allowing it to switch using less energy. In recent years, H-induced layer transfer, commercially known as ion-cut or Smart-cut™, has become one of the mainstream technologies for the manufacture of silicon-on-insulator (SOI) wafers. However, the Smart-cut™ process lacks cost efficiency because it requires an expensive ion-implantation step, the cost of which increases with ion dose. In addition, Smart-cut™ technology has difficulty in producing thin layer transfers because of the intrinsic irradiation damage retained in the transferred layer, though there are high demands for ultra-thin SOI with top Si less than 100nm to support the production of fully depleted, complementary metal-oxide semiconductor circuits. Recently, we have successfully developed a thin layer transfer process using strained layers for H trapping. This approach can transfer ultra-thin Si layers(less than 20nm) with very high crystalline quality without hydrogen implantation, and appears to be a promising competitor to Smart-cut™ technology. However, the physical and chemical mechanisms underlying this novel process have not been fully understood.

Our research objective was to understand the physical and chemical physical mechanisms underlying the strain facilitated layer transfer process.

## Importance to LANL's Science and Technology Base and National R & D Needs

The project is closely relevant to the mission of the Laboratory and the DOE. The ability to effectively apply the strain facilitated layer transfer technique to a variety of electronic, magnetic and optical materials will open new possibilities of novel heterogeneous materials integration for the fabrication of next generation sensor and 3-D electronic structures, which have wide potential applications in the areas of nanoscience and nanotechnology, homeland security and energy resources.

## Scientific Approach and Accomplishments

The main objective of this project was to improve our scientific understanding of the physical and chemical mechanisms underlying the strain facilitated layer transfer process. For this propose, the hydrogen trapping phenomena in Si(150nm)/ $Si_{0.80}Ge_{0.20}$ (5nm)/Si substrate during hydrogen plasma treatment was investigated in detail. Scanning electron microscope (SEM) is used to study the evolution of surface morphology during hydrogenation process, and elastic recoil detection (ERD) is utilized to quantify how much hydrogen is trapped. In order to characterize the chemical reaction between the trapped hydrogen and the SiGe layer, infrared spectroscopy (IR), which is very sensitive to Si-H bond, is used.

Figure 1 presents SEM micrographs of the Si/SiGe/Si samples after hydrogenation with different durations between 0.5h and 2.0h. Blisters are formed on all samples after plasma hydrogenation. For the shortest treatment (0.5h), only tiny blisters (~30nm) are detected, as shown in Figure 1(a). As the hydrogenation proceeds, these small blisters grow and coalesce. For a 1h hydrogenation (Figure 1(b)), large blisters, with a diameter generally less than 1um, have developed. The surface for the 1.5h hydrogenation sample (Figure 1(c)) shows a very high density of blisters with blister diameters between 1um and 1.5um. However, the morphology has visibly changed when the hydrogenation is extended to 2h, as shown in Figure 1(d). Many exfoliated huge blisters (~3.5um) surrounded by a scattering of small blisters can be seen. This local exfoliation is due to the built-up molecular hydrogen which promotes crack propagation along the SiGe layer and approximately parallel to the surface.

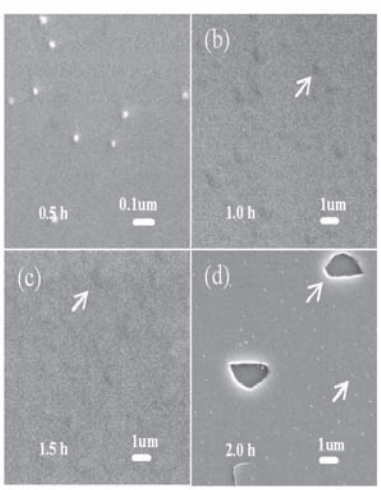


*Figure 1. SEM micrographs from Si/SiGe/Si after plasma-hydrogenation for various durations: (a) 0.5h, (b) 1.0h, (c) 1.5h, and (d) 2.0h.*

Figure 2(a) shows ERD hydrogen depth profiles obtained from hydrogenated Si/SiGe/Si samples. The amount of integrated hydrogen in each peak is plotted as a function of hydrogenation time in Figure 2(b). Figure 2(a) shows that even at the lowest hydrogenation exposure time, the H concentration is well above the solubility limit in Si. The peak H concentration increases with hydrogenation time in the range of 0.5-1.5h. However, the H concentration drops significantly in the 2 h hydrogenated sample because of out diffusion of gaseous $H_2$ from exfoliated blisters along with the loss of bonded hydrogen from inner walls of exfoliated blisters.

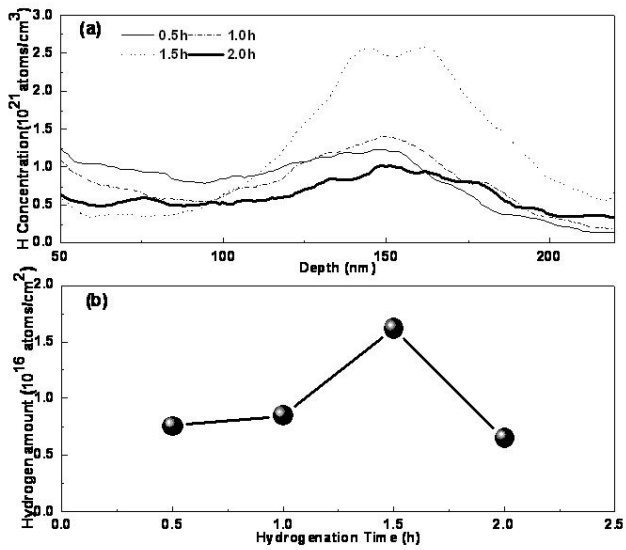


*Figure 2. (a) ERD spectra of hydrogenated Si/SiGe/Si with different durations, and (b) The total amount of trapping hydrogen as a function of hydrogenation time.*

The bonding between H and Si that results during plasma hydrogenation is investigated using IR (Figure 3). Different from the broadband absorption (1800-2300cm$^{-1}$) observed in H-implanted samples, plasma hydrogenated Si/SiGe/Si only shows a narrow absorption region from 2050 to 2150cm$^{-1}$ in Figure 3a, which is indicative of a lack of $V_nH_m$ (V,i.e., Vacancy)and $I_nH_m$ (I, i.e., interstitial) defects. The intensity of the absorption peaks from the 2 h hydrogenation sample is significantly reduced due to the loss of bonded hydrogen following blister rupture. All Si-H bond stretching modes are marked in Figure 3(b). Since (111) platelets form in the near-surface region of hydrogenated Si, the modes at 2063, 2070 and 2082 cm$^{-1}$ are assigned to the unperturbed and perturbed Si-H bond at Si (111) surface. The modes at 2091 and 2099cm$^{-1}$ are assigned to the asymmetric and symmetric stretching modes of a coupled monohydride species $(SiH)_2$ on atomically smooth Si(100) surfaces, and the mode at 2121cm$^{-1}$ is close to the assignment for the asymmetric dihydride stretching motion on atomically rough Si(100) surfaces. It should be noted that the stretching mode for $(SiH)_2$ at 2099cm$^{-1}$

shifts to 2105cm$^{-1}$ for hydrogenation durations of 1h and 1.5h; upon further hydrogenation for 2h, it returns back to 2099cm$^{-1}$. The 2099 to 2105cm$^{-1}$ blue-shift is due to the steric interaction between Si-H bonds and overlying $H_2$ gas. This hypothesis is confirmed by our results which show that the shift from 2099 to 2105 cm$^{-1}$ is strongly correlated with the H content in our samples. For the 0.5h hydrogenated sample, only a small amount of hydrogen has accumulated at the buried SiGe layer. As hydrogenation increases to 1 and 1.5 h, the hydrogen content, and the probability of $H_2$ molecule formation within platelets, also increases. Gaseous $H_2$ inside large platelets or microbubbles will have steric interactions with Si-H bonds on internal (100) surface, and lead to a blue-shift from its relaxed state at 2099 to 2105cm$^{-1}$, as shown in Figure 3. At extended plasma hydrogenation times, microbubbles exploded, gaseous $H_2$ diffuses out though the "popped" blisters, and the mode associated with Si-H bonds on internal (100) surfaces returns back to its unperturbed frequency, i.e., 2099cm$^{-1}$.

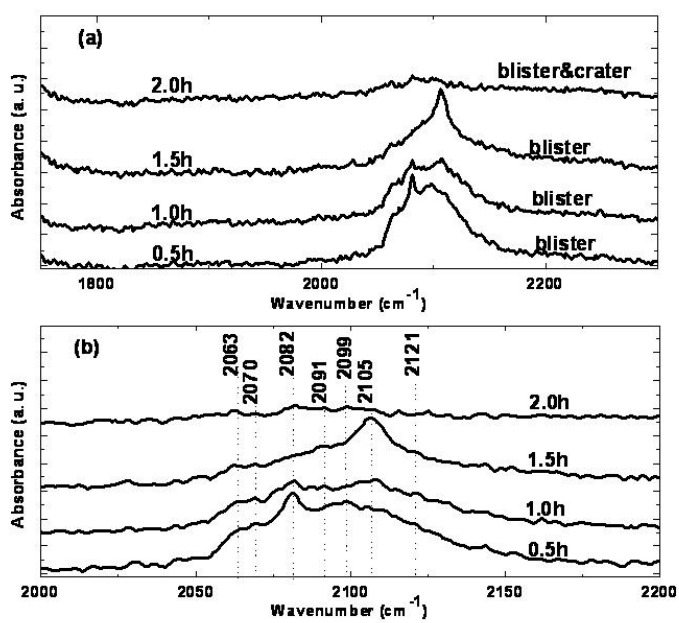


*Figure 3. IR spectra from hydrogenated Si/SiGe/Si with different hydrogenation durations: (a) 1800-2300cm-1; (b) 2000-2200cm-1*

In conventional ion-cut, the defects and the corresponding in plane compressive stress introduced by ion implantation are responsible for hydrogen trapping and platelet nucleation during post implantation annealing. For the plasma-hydrogenation based layer exfoliation process, exfoliation proceeds from the strained SiGe layer, which supplies the needed in-plane-compressive stress for platelet nucleation and H trapping. The state of biaxial compressive stress exists that adds an energetic barrier to any platelet not nucleating in the plane of stress, but does not affect the platelets nucleating with their surface parallel to the Si/SiGe interface , i.e., in the plane of stress. Therefore, a cracking along the SiGe layer, which is parallel to the surface, is formed after long time hydrogenation, thus resulting in the capped Si layer transfer.

Based on the scientific understanding of the physical and chemical mechanisms underlying the strain facilitated layer transfer process, a novel experiment is designed to achieve the successful SiGe layer transfer. $Si_{0.90}Ge_{0.10}$ (200nm)/ $Si_{0.85}Ge_{0.15}$ (5nm)/ Si substrate and $Si_{0.90}Ge_{0.10}$ (200nm)/ $Si_{0.70}Ge_{0.30}$ (5nm)/ Si substrate are grown by molecular beam epitaxy (MBE) technique for SiGe layer transfer study.

Figure 4 shows the surface morphology changes in both two samples after plasma hydrogenation treatment. Blisters are formed on both samples after plasma hydrogenation. For one sample with low Ge concentration (15%) in the buried SiGe layer, the average diameter of the blisters is about 200 nm (Figure 4a). For the other sample with high Ge concentration (30%), the average diameter increases to about 400 nm (Figure 4b). Since the surface blistering behavior has been directly correlated with the cracking formed inside, it is easy to conclude that the strain-facilitated layer transfer technique partly depends on the in plane compressive stress residual in the buried SiGe layer.

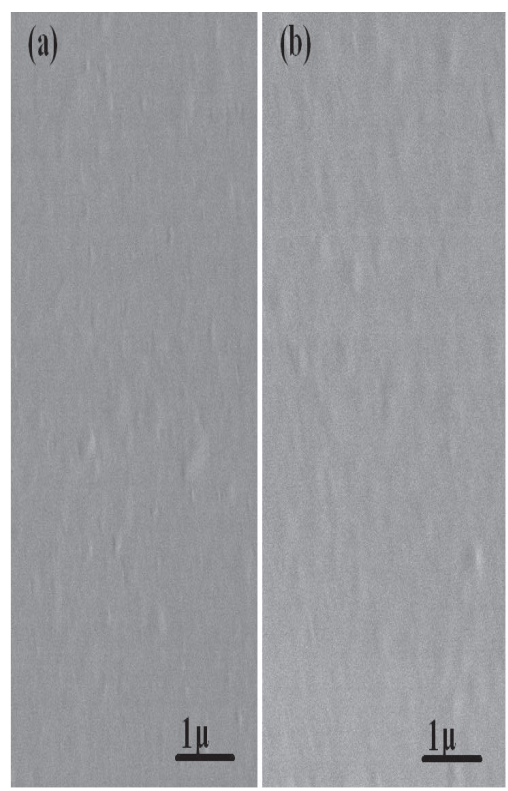


*Figure 4. SEM micrographs obtained from the hydrogenated $Si_{0.90}Ge_{0.10}$/ $Si_{1-x}Gex$/ Si: (a) x=0.15 and (b) x=0.30.*

Figure 5 (a) and (b) shows the hydrogen, germanium and silicon profiles obtained from hydrogenated $Si_{0.90}Ge_{0.10}$ (200nm)/ $Si_{0.85}Ge_{0.15}$ (5nm)/ Si and $Si_{0.90}Ge_{0.10}$ (200nm)/ $Si_{0.70}Ge_{0.30}$ (5nm)/ Si by secondary ion mass spectrometry (SIMS), respectively. A comparison between them shows that (1) the H concentration peaks at the depth of the buried $Si_{1-x}Ge_x$ (where x is equal to 0.15 or 0.30) and (2) the H peak density increases with increasing Ge concentration, i.e., increasing in plane compressive stress.

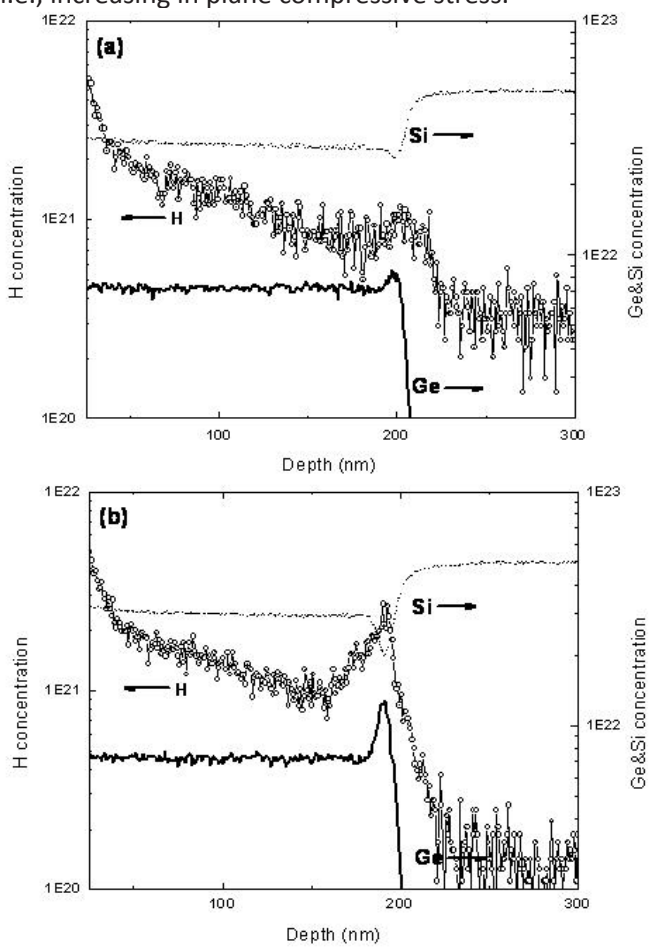


*Figure 5. H, Ge, and Si profiles obtained from the hydrogenated Si0.90Ge0.10/ Si1-xGex/ Si using SIMS: (a) x=0.15 and (b) x=0.30*

Based on these studies and observations we can conclude the following about the the physical and chemical mechanisms underlying strain facilitated layer transfer process: 1) During plasma-hydrogenation, diffusing H is trapped in the region of the SiGe layer and H-platelets are formed; 2) The platelet orientation is controlled by the in-plane compressive stress, which favors nucleation and growth of platelets in the plane of stress and parallel to the substrate surface, and ultimately leads to controlled fracture along the SiGe layer; and 3) the Si/SiGe/Si structure is found to be more efficient in utilizing H for platelet formation and growth compared to H ion implanted Si because there are fewer defects to trap H (e.g. $V_nH_m$ and $I_nH_m$) and therefore, the total H dose needed for layer exfoliation is greatly reduced.

## Publications

Cheng, P., Z. F. Di, M. Nastasi, E. Bruno, M. G. Grimaldi, N. D. Theodore, and S. S. Lau. Effects of hydrogen implantation temperature on InP surface blistering. 2008. *Apllied Physics Letters.* **92**: 202107.

Di, Z. F., Y. Q. Wang, M. Nastasi, F. Rossi, J. K. Lee, L. Shao, and P. E. Thompson. Investigation of stress-induced (100) platelets formation and surface exfoliation in plasma-hydrogenated Si. 2007. *Apllied Physics Letters.* **91**: 244101.

Di, Z. F., Y. Q. Wang, M. Nastasi, L. Shao, and N. D. Theodore. Evidence for ion irradiation induced dissociation and reconstruction of Si-H bonds in hydrogen-implanted silicon. 2008. *Applied Physics Letters.* **93**: 104103.

Shao, L., Z. F. Di, Y. Lin, Q. X. Jia, M. Nastasi, P. E. Thompson, N. D. Theodore, and P. C. Chu. The role of strain in hydrogenation induced cracking in Si/Si1-xGex/Si structures.. 2008. *Applied Physics Letters.* **93**: 041909.

# Searching for New Uranium Based Superconductors

*Joe David Thompson*

20061456PRD2

## Abstract

Superconductivity, a property of materials whose electrical resistance becomes exactly zero below some temperature $T_c$, has important technological applications but also presents significant scientific challenges. In particular, the mechanism that produces superconductivity in some uranium-based materials is believed to be unconventional, and so far only a handful of such examples are known. The goal of this project has been to discover new examples of uranium-based materials that will help develop a more complete understanding of the unconventional superconducting mechanism and of electronic interactions that induce other exotic states in uranium-base materials. In addition, this project has been responsive to discoveries of new, non-uranium based superconductors whose mechanism of superconductivity may be unconventional and whose study benefitted the overall objectives of this project.

## Background and Research Objectives

There are many hundreds of compounds and alloys that become superconducting at temperatures below about 20 K. In each of these, the mechanism that produces superconductivity is well understood: vibrations of the crystal lattice provide an attractive interaction that couples electrons of opposite spin and momentum to create a quantum state in which electron pairs move with exactly zero electrical resistance. These conventional superconductors are extremely sensitive to the presence of magnetic impurities in the material, with a concentration of only 0.1% of magnetic impurities typically being sufficient to destroy the electron pairs and to suppress superconductivity completely. In striking contrast, superconductivity in some uranium-based materials appears to rely on the presence of nearly $10^{23}$ magnetic 'impurities'. The totally unexpected reliance on magnetism has led to the belief that the mechanism of superconductivity in these cases should be unconventional, where now the attractive interaction for creating electron pairs may arise from magnetic 'vibrations' instead of vibrations of the crystal. In the absence of a microscopic theory of unconventional superconductivity, discovering new examples of materials whose superconductivity relies on magnetism is important to guide our understanding of what interactions are important and how they might be controlled.

Like conventional superconductors, unconventional superconductivity seems to be favored by certain crystal structures, one of which is the tetragonal $ThCr_2Si_2$ structure. Another structure type that could be promising is the so-called anti-perovskite structure, which supports conventional superconductivity in $MgCNi_3$ and which is virtually unexplored, with only one reported uranium-based compound $URh_3B_x$ being reported. Adding B to $URh_3$, which is a 'vegetable' with weak electronic correlations, has the effect of narrowing the bandwidth of the uranium 5f-electron band and increasing electron-electron correlations, a situation favorable for unconventional superconductivity, but the crystal structure does not like to be expanded to incorporate the addition of boron atoms, and consequently, the value of x in $URh_3B_x$ is less than 1. If x could be increased to 1, it is possible that the stoichiometric compound $URh_3B$ might be superconducting. One approach to increasing the B content might be to prepare this compound under high-pressure, high-temperature conditions, an initial objective of this project.

During the course of the project, a new family of superconductors was discovered in Japan and pursued aggressively in China. This family of REMXO materials, where RE is a rare earth element, M=Ni or Fe, and X=P or As, forms in a structure closely related to the $ThCr_2Si_2$ structure. Superconductivity develops in these so-called 1-1-1-1 materials at surprisingly high temperatures, approaching 55 K, as magnetic order is weakened by electronic substitutions, for example, by replacing a small amount of O with F. This is very similar to what happens in the well-known high-temperature cuprate

superconductors, which also are unconventional with a mechanism believed to be the same as in unconventional uranium-based superconductors. As a result of this surprising development, this project refocused its attention to these new and related superconductors.

## Importance to LANL's Science and Technology Base and National R & D Needs

This project has addressed one of the Laboratory's strategic challenges, superconductivity and actinide science. In particular, the goals of this project have focused on understanding strong correlations through unconventional superconductivity and exploring the unconventional physical behaviors of 5f-electrons, especially through materials discovery. Though these goals are specific to LANL's science and technology needs, they are equally important to the national need of energy security, which will rely in part on unconventional superconductivity and actinide science.

## Scientific Approach and Accomplishments

Using combinations of materials preparation techniques, including flux growth of single crystals, arc melting and high-pressure, high-temperature synthesis, we were able to prepare $URh_3B_x$ with a larger concentration of B than previously possible. Though x=1 was never reached, the additional B concentration induced weak ferromagnetic order near 16K, a clear signature that the added B decreased the electronic bandwidth of the 5f electrons even further. This situation now is very similar to the case of strongly correlated $UGe_2$, also a weak ferromagnet, that becomes an unconventional superconductor when subjected to pressure. This discovery opens the possibility that $URh_3B_x$ also might superconduct with applied pressure, a possibility that will be pursued by collaborators.

In the course of this work, various attempts were made to grow crystals of this material from fluxes, including Bi flux. The resulting crystals were not $URh_3B_x$ but a new compound $U_3Bi_4Rh_3$, which we found to be a strongly correlated metal with properties indicating that it is very near a zero-temperature ferromagnetic instability, that is, near a ferromagnetic quantum-critical point. This is an exciting discovery because until now there have been no known uranium systems and no known stoichiometric crystals of any type with these properties under ambient conditions. Theoretical models of ferromagnetic quantum criticality predict a very specific response in inelastic neutron scattering experiments, and these predictions are being pursued by UC Irvine and Argonne National Laboratory collaborators who are very excited about this material and the prospects of new physics that it might bring. A natural extension of this discovery was to attempt to prepare crystals in the same structure but with different transition metals replacing Rh. Of various Fe-, Co- and Ni-column elements, only $U_3Bi_4Ni_3$, also a new uranium compound, was stable. In contrast to $U_3Bi_4Rh_3$, $U_3Bi_4Ni_3$ is an insulator with very weak magnetic properties. Our measurement and analysis of its physical properties indicate that the insulating behavior is the result of strong hybridization of uranium's 5f electrons with ligand electrons provided by Ni and Bi. There are very few such examples of this so-called 'Kondo-insulator' behavior, making $U_3Bi_4Ni_3$ another highly interesting discovery of this project.

Though none of these new uranium materials was superconducting, we discovered other new materials that were superconducting and that certainly benefit our general understanding of unconventional superconductivity in uranium-based materials. The first of our new materials is $Mg_{10}Ir_{19}B_{16}$ that becomes superconducting below 4.4 K. Our studies of this compound are consistent with a conventional mechanism of superconductivity; however, what makes the superconductivity particularly interesting is that it appears in this material whose crystal structure lacks inversion symmetry. The conventional theory of superconductivity requires the presence of inversion symmetry, and without it, superconducting electrons should have a distinctly different character. Specifically, electrons that form superconducting pairs are expected to form two, instead of one, superconducting energy gaps below $T_c$ and to have an angular momentum symmetry that is a mixture of 0 and 1, as opposed to only 0 in a conventional superconductor. In general, it is difficult to prove that any superconductor without inversion symmetry meets these expectations, but we have used point-contact spectroscopy to show clearly that there are two superconducting energy gaps in $Mg_{10}Ir_{19}B_{16}$. This result is significant in the context of this project because there is one example of superconductivity in a uranium-based compound that also lacks inversion symmetry, but because of the uranium atom, it has not been possible to make such a clear test of theoretically predicted properties of its superconducting state.
The second discovery is not a single new material that superconducts but is a family of related materials that becomes superconducting. As mentioned earlier, during the course of this project a new series of 1-1-1-1 superconductors was discovered in Asia and the structure of these materials is closely related to the $ThCr_2Si_2$ (1-2-2) structure type that is adopted by the unconventional superconductor $URu_2Si_2$. Because there is an interplay between magnetism and superconductivity in these new materials, as

in unconventional uranium superconductors, we turned attention to searching for new examples and discovered superconductivity in $CaFe_2As_2$ and $BaNi_2As_2$, both of which formed as single crystals in the $ThCr_2Si_2$ structure. $CaFe_2As_2$ orders antiferromagnetically below 170 K but applying a modest pressure to this material suppresses the magnetic ordering temperature and induces superconductivity with $T_c$ greater than 10 K. This sort of response to pressure is very similar to what is found in a few 5f- and several 4f-electron-based unconventional superconductors. On the other hand, there is some form of first-order transition at 130K in $BaNi_2As_2$, perhaps a structural transition, and it becomes superconducting at a much lower temperature of 0.7K. If the transition at 130K is structural and not magnetic, as we suspect, this could account for the very different $T_c$'s in these two materials and imply that magnetism is important for the much higher $T_c$ in $CaFe_2As_2$.

These 1-2-2 and 1-1-1-1 structures can be viewed as layers of $M_2X_2$ atoms separated by a layer of either RE (the 1-2-2 structure) or a layer of $RE_2O_2$ atoms (1-1-1-1 structure). We discovered a new variant on these structures in the form of $La_3Ni_4P_4O_2$, which becomes superconducting at 2.2K. This new material can be viewed structurally as a layered intergrowth of the 1-2-2 and 1-1-1-1 materials. We find no evidence for either magnetism or a structural distortion in this new family member. Though somewhat difficult to prepare, this material could become the prototype for understanding the interrelations between structure, magnetism and superconductivity in all these new superconducting materials.

In summary, though we did not discover new uranium-based unconventional superconductors, this project was quite successful in discovering a number of new uranium and superconducting materials that most certainly have shaped and will continue to shape our understanding of unconventional behaviors of 5f electrons in strongly correlated actinide materials, including superconductors.

## Publications


Baek, S. H., T. Klimczuk, F. Ronning, E. D. Bauer, N. J. Curro, and J. D. Thompson. Low energy spin dynamics at the spin density wave transition in single crystal BaFe2As2: a 75As NMR study. *Physical Review Letters.*

Klimczuk, T., F. Ronning, V. Sidorov, R. J. Cava, and J. D. Thompson. Physical properties of the noncentrosymmetric superconductor Mg10Ir19B16. 2007. *Physical Review Letters.* **99**: 257004.

Klimczuk, T., H. Lee, F. Ronning, T. Durakiewcz, N. Kurita, H. Volz, E. D. Bauer, T. McQueen, R. Movshovich, and J. D. Thompson. Pysical properties of the new Uranium compounds U3Bi4M3 (M=Ni, Rh). 2008. *Physical Review B.* **77**: 245111.

Klimczuk, T., H. W. Zandenberg, Q. Huang, B. Kusz, J. D. Thompson, and R. J. Cava. Spin glass behavior in highly oxygen deficient perovskite BaBi.25Co.75O3-d. *Physical Review B.*

Klimczuk, T., T. M. McQueen, A. J. Williams, Q. Huang, F. Ronning, E. D. Bauer, J. D. Thompson, M. A. Green, and R. J. Cava. Superconductivity in the layered intergrowth compound La3Ni4P4O2. *Physical Review Letters.*

McQueen, T. M., P. W. Stephens, Q. Huang, T. Klimczuk, F. Ronning, and R. J. Cava. Successive orbital ordering in NaVO2. To appear in *Physical Review Letters.*

McQueen, T., Q. Huang, J. W. Lynn, R. F. Burger, T. Klimczuk, B. G. Ueland, P. Schiffer, and R. J. Cava. Magnetic structure and properties of the S=5/2 triangular antiferomagnet alpha-NaFeO2. 2007. *Physical Review B.* **76** (2): 024420.

Park, T., E. Park, H. Lee, T. Klimczuk, E. D. Bauer, F. Ronning, and J. D. Thompson. Pressure-induced superconductivity in single crystal CaFe2As2. 2008. *Journal of Physics: Condensed Matter.* **20**: 322204.

Ronning, F., N. Kurita, E. D. Bauer, B. L. Scott, T. Park, T. Klimczuk, R. Movshovich, and J. D. Thompson. First order phase transition and superconductivity in BaNi2As2 single crystals. 2008. *Journal of Physics: Condensed Matter Physics.* **20**: 342203.

Ronning, F., T. Klimczuk, E. D. Bauer, H. Volz, and J. D. Thompson. Synthesis and proerties of CaFe2As2 single crystals. 2008. *Journal of Physics: Condesned Matter.* **20**: 322201.

Sulkowski, C., T. Klimczuk, R. J. Cava, and K. Rogacki. Effect of substituting Fe and Ru for Ni on the thermopower of MgCNi3. 2007. *Physical Review B.* **76** (6): 060501.

# Multiscale Modeling of Irradiation-induced Defect Processes in High-Cr Ferritic Steels

*Srinivasan G Srivilliputhur*

20061526PRD3


## Abstract

Transition-metal carbides (TMCs) in the Fe-Cr-C ternary system (e.g. $Fe_3C$, $Cr_3C_2$, $Cr_7C_3$, $Cr_{23}C_6$, $Cr_3C$, and CrC) are of great technological significance in the steel and coating industries. Nevertheless, many of their important physical and mechanical properties are largely undetermined in the literature due to experimental difficulties. In this project, we addressed this issue by applying state-of-the-art first-principles density functional calculations to systematically predict the structural, elastic, and electronic properties of these TMCs. By combining a statistical mechanical Wagner-Schottky model with first-principles supercell calculations, the point defect structure in $Fe_3C$ is further investigated. The migration barriers of major point defects in $Fe_3C$ are also determined using the nudged elastic band technique and our results compare favorably with the available experiments in the literature.


## Background and Research Objective

Fe-Cr ferritic/martensitic steels are considered promising candidates for structural applications in future nuclear reactors due to their high strength at elevated temperatures and resistance to radiation damage. Furthermore, Cr additions to ferritic steels are known to provide corrosion resistance for ferritic steels in coolants such as water and lead-bismuth eutectic. Thus, a theoretical investigation of the Fe-Cr-C ternary system would be of both technological and scientific interest. The goal of this project is to use highly accurate first-principles calculations based on density functional theory to predict the structural, elastic, electronic, and defect properties of the technologically important iron and chromium carbides in the Fe-Cr-C system. Aside from their practical importance, results from this project also provide key input to parameterize interaction potentials used by coarser scale computational approaches (e.g. molecular dynamics) for modeling Fe-Cr ferritic/martensitic steels.

## Importance to LANL's Science and Technology Base and National R & D Needs

Steel is a very important structural material in many industrial applications with an annual market of over one billion metric tons. In particular, steel is a major component in the design of nuclear fuel pins. An important understanding of steel at the atomistic scale will thus benefit programs such as the Global Nuclear Energy Partnership (GNEP). This work constitutes an important step in developing a quantitative simulation approach for steel design and evaluation, which can move us past the conventional experimental trial and error approaches of the past 100 years. Overall, this study will greatly benefit the future development and understanding of advanced metallic alloys at LANL.

## Scientific Approach and Accomplishments

### Structural, elastic, and electronic properties of $Fe_3C$

Cementite ($Fe_3C$), which has a complex orthorhombic crystal structure (Figure 1), is one of the most important carbides in steels. In contrast to its technological significance, knowledge of the elastic properties of cementite, critical to understanding the mechanical properties of steels, is quite limited. While polycrystalline bulk cementite has been successfully synthesized through a combination of mechanical alloying and spark plasma sintering, large single-crystal samples are difficult to fabricate. Thus, to date, direct experimental measurements of the single-crystal elastic constants of cementite are still not feasible.

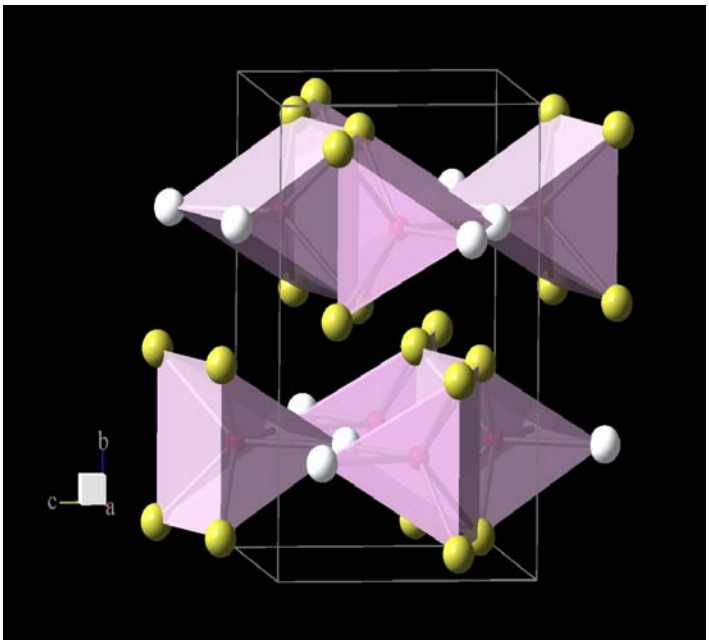


*Figure 1. Crystal structure of cementite. White, yellow, and red spheres represent FeI, FeII, and C atoms, respectively.*

We determine the single-crystal elastic constants of cementite using highly predictive first-principles calculations. Our results show that cementite is elastically stable since its elastic strain energy is positive against any homogeneous elastic deformation. Figure 2 illustrates the directional Young's modulus of cementite calculated using the singe-crystal elastic constants from the present study.

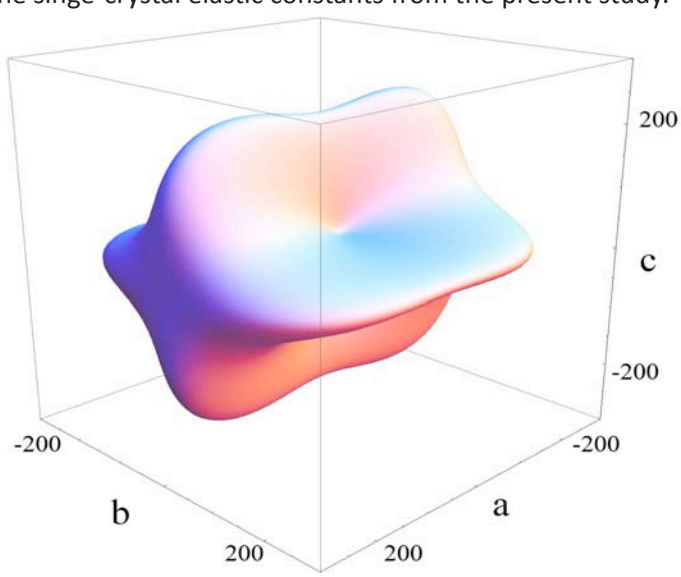


*Figure 2. Representational surface showing the directional dependence of the Young's modulus (in GPa) in cementite.*

For an isotropic system, one would see a spherical shape. In agreement with experiments, Figure 2 shows a considerable deviation in shape from a sphere, thus indicating a high degree of anisotropy in Young's modulus. Remarkably, Figure 2 also directly confirms the experimental observations that the Young's modulus of cementite along the axis is larger than in the directions normal to it.

In addition to the elastic stability criterion, dynamical stability further requires that the phonon spectra of a structure exhibit no imaginary phonon frequencies, the so-called soft modes. A soft mode indicates instability with respect to a particular type of atomic movement, signaling a structural phase transitions. In this study, we have also calculated the phonon dispersion relations for cementite along various high-symmetry directions in the Brillouin zone. Our results show that cementite is also dynamically stable since all phonon frequencies are positive throughout the Brillouin zone.

To investigate the chemical bonding in cementite, we have also calculated its electronic density of states (DOS). Cementite is metallic because of the finite DOS at the Fermi level. Importantly, we see a hybridization between C 2p and Fe 3d states in the energy range from -8 eV to -4 eV below the Fermi level, evidence of covalent bonding between Fe and C atoms. Figure 3(a) shows the charge density distribution in the (010) plane of cementite.

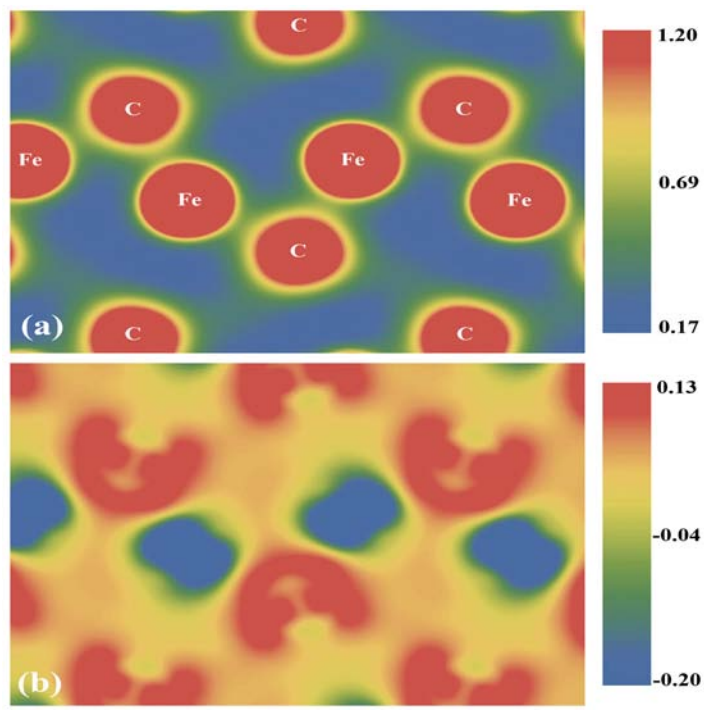


*Figure 3. Plot of (a) total charge density and (b) charge density difference, all in e/Å3, on the (010) plane of $Fe_3C$ containing the nearest-neighbor Fe-C bonds.*

It can be seen that the bonding between Fe and C exhibits some directionality, indicative of covalent bonding. To investigate the charge transfer, we also plot in Figure 3(b) the difference in charge density between $Fe_3C$ compound

and superposition of free atoms in the same plane. Here red color means charge accumulation while blue color means charge depletion. In agreement with the fact that C has a larger electronegativity (2.55) than Fe (1.8), there is clearly a charge transfer from Fe to C atoms, revealing an ionic contribution to the Fe-C bonding. We thus conclude that the bonding in cementite has a complex mixture of metallic, covalent, and ionic characters.

**Point defect thermodynamics and diffusion in $Fe_3C$**

The physical and mechanical properties (e.g., diffusivity, hardness, and ductility) of ordered compounds are strongly affected by the presence of point defects. Despite its technological significance, little is known about the formation and migration properties of point defects in cementite. In fact, it is commonly treated as a stoichiometric line compound in the metastable Fe-C phase diagram. Nevertheless, recent experiments have given clear evidence that cementite does indeed exist at non-stoichiometric compositions. For example, it has been observed that diffusion controlled growth of cementite occurs on the surface of pure iron immersed in a carburizing gas atmosphere, which is only possible if a composition gradient exists within cementite.

We have performed extensive first-principles supercell calculations to understand the point defect structure of cementite. To answer the question "what are the possible interstitial sites for carbon atoms to occupy in the cementite structure?", we have proposed a general computational method to systematically determine interstices in materials with arbitrary symmetry and complexity. This method is based on the simple but unexploited idea that an interstitial atom usually experiences a net repulsive force since its separation from a host lattice atom is usually less than the equilibrium distance. Thus, we can employ a net repulsive pair potential to model interatomic interactions and determine interstitial sites. As shown in Figure 4, our algorithm successfully identified four types of interstitial sites in cementite in addition to the known prismatic ones. Using first-principles calculations on 128-atom supercells, we have obtained the formation enthalpies of cementite containing various types of possible point defects. Our results show that carbon vacancies and octahedral carbon interstitials are the structural defects on the C-depleted ($Fe_3C_{1-x}$) and C-rich ($Fe_3C_{1+x}$) sides of stoichiometry, respectively. For C-depleted cementite, our prediction is in agreement with the experimental observation that the unit cell volume of cementite decreases with decreasing carbon content in $Fe_3C_{1-x}$. In C-rich cementite, an interstitial defect mechanism would indicate that the unit cell volume of $Fe_3C_{1+x}$ increases with increasing x, which is yet to be verified experimentally.

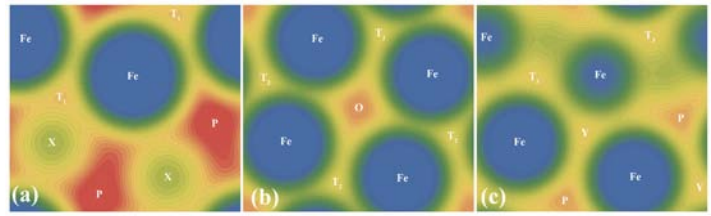


*Figure 4. Contour plots for identifying potential interstitial sites in cementite in different crystal planes. In addition to the known prismatic (denoted P) sites, our algorithm also identified the octahedral (denoted O) and three types of tetrahedral (denoted $T_1$, $T_2$, and $T_3$) interstices in cementite.*

At finite temperatures, entropically-activated thermal defects will also be present in addition to the structural defects. Since single point defects in ordered alloys by themselves are not composition-conserving, thermal defects have to appear in balanced combinations to maintain a constant alloy composition. We investigated the thermal defects in cementite using a combination of the statistical mechanical Wagner-Schottky model and first-principles calculations. Interestingly, while the dominating thermal defects in C-depleted and stoichiometric cementite are found to be carbon Frenkel pairs over the whole temperature range, the major thermal defects in C-rich cementite are strongly temperature-dependent. We found that Interbranch, Schottky, and Frenkel defects dominate successively in the order of increasing temperature.

To understand the diffusion behavior of carbon in cementite, we also determined the minimum energy path and the associated migration barriers for carbon diffusion in cementite using the climbing image nudged elastic band technique. Two relevant diffusion mechanisms are considered in this study: 1) the vacancy mechanism, i.e., jumping of an isolated carbon vacancy between two neighboring prismatic sites (see Figure 5(a)), and 2) the interstitial mechanism, i.e., jumping of an isolated carbon interstitial atom between two neighboring octahedral sites (see Figure 5(b)). Our results show that the migration barrier is essentially independent of jump direction, suggesting that carbon diffusion in cementite is likely to be isotropic. Our calculated migration barrier of carbon interstitials (~2.3 eV) also agrees reasonably well with the experimental values of 1.60-1.92 eV.

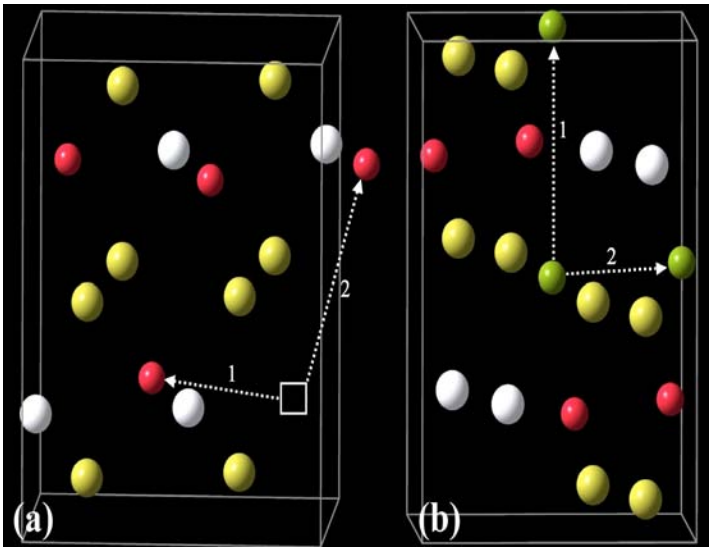


*Figure 5. Illustration of the vacancy (a) and interstitial (b) mechanisms for carbon diffusion in cementite. White and yellow spheres represent FeI and FeII atoms, respectively. Red and green spheres represent carbon atoms occupying prismatic and octahedral interstitial sites, respectively. The empty square represents a carbon vacancy within the prismatic sublattice.*

**Thermodynamic, elastic and electronic properties of chromium carbides**

Chromium carbides are of great technological importance in the cutting tool industries due to their excellent properties such as large hardness, chemical stability, and good wear and oxidation resistance. In the equilibrium Cr-C phase diagram, there are three thermodynamically stable chromium carbides: $Cr_3C_2$, $Cr_7C_3$ and $Cr_{23}C_6$. In addition, a metastable $Fe_3C$-type $Cr_3C$ has been obtained through rapid quenching. A metastable CrC with a rocksalt structure has also been observed using carbon-ion implantation, but is found to be stable only up to ~250°C. In contrast, $Cr_3C$ remains unchanged until the temperature exceeds ~700°C.

We have performed first-principles calculations to understand the thermodynamic stability of these chromium carbides. For $Cr_7C_3$, we consider both the orthorhombic and the hexagonal structures and find the latter to be energetically more stable, which is in agreement with experiments. For $Cr_3C$, its good thermal stability can be understood since it has a negative formation enthalpy that lies only slightly above the ground state convex hull. Finally, our calculations confirm that rocksalt CrC has a positive formation enthalpy and is thus unstable with respect to phase separation into pure Cr and C, which explains its poor thermal stability and difficulties in synthesizing this carbide using conventional methods.

From our calculated single-crystal elastic constants of those chromium carbides, we conclude that all of them are mechanically stable under the ambient condition. To gain insight into the nature of the bonding in chromium carbides, we have calculated their partial electronic DOS. All six chromium carbides are metallic because of the finite DOS at the Fermi level. In all of them, we observe a hybridization between C 2p and Cr 3d states, an evidence of covalent bonding between Cr and C atoms. Our Bader charge density analysis further indicates a charge transfer from Cr to C atoms, revealing an ionic contribution to the bonding. The charge transfer direction is consistent with the larger electronegativity of C (2.55) than Cr (1.6). We thus conclude that, similar to $Fe_3C$, the bonding in chromium carbides has a complex mixture of metallic, covalent, and ionic characters.

## Publications

Jiang, C., Srinivasan G. Srivilliputhur, S. Maloy, A. Caro, and M. Stan. Thermodynamic stability of cementite from first-principles calculations. To appear in *Acta Materalia.*

Jiang, C., Srinivasan G. Srivilliputhur, S. Maloy, and A. Caro. Structural and elastic peroperties of cementite from first-principles calculations.. *Journal of Applied Physics.*

Jiang, C., Srinivasan G. Srivilliputhur, and S. Maloy. The point defect structure of cementite from first-principles calculations.. *Physical Review B.*

Jiang, C., and Srinivasan G. Srivilliputhur. A Universal method to determine intersititals in low symmetry materials. *Scripta Materalia.*

# High Efficiency Carbon Nanotube-$TiO_2$ Nanostructured Solar Cells

*Quanxi Jia*

20061528PRD3

## Abstract

Solar cells, which convert light into electrical power, provide for one of the best solutions for our future energy security. However, large-scale electricity production using solar cells remains a dream due to the high cost of production of large area solar cells. One of the expensive components in the fabrication of solar cells is the electrode, which is usually made of indium tin oxide (ITO). Due to limited resource of indium on earth, large-scale utilization of ITO will make it even more expensive in the future. The objective of this project is to develop a cheap, novel carbon nanotube-polymer electrode material to replace the ITO in the production of solar cells

## Background and Research Objectives

Worldwide energy demand is expected to double within the next fifty years. In order to meet such needs, we must explore other alternatives such as solar energy (a renewable and clean energy), and advance more scientific breakthroughs and technological developments. At the same time, the large-scale use of photovoltaic devices for electricity generation is mainly prohibited by the uneconomic cost/performance ratio. Currently, the conversion of sunlight to electrical power is mainly dominated by photovoltaic devices based on crystal, polycrystalline, and amorphous Si solar cells.
In the fabrication of solar cells, one of the expensive components is the electrode, which is usually made of indium tin oxide (ITO). Due to limited resource of indium on earth, large-scale utilization of ITO will make it even more expensive in the future. Therefore, it is critical to develop new, cheaper electrode materials to replace the ITO. A good ITO replacement needs to possess the following characteristics: low cost, good conductivity, excellent transparency, and good mechanical integrity. Conducting polymers have high transparency and cost two orders of magnitude less than ITO. However, the electronic conductivity and mechanical strength of these conductive polymers need to be further improved. Researchers have tried to incorporate carbon nanotubes (CNTs) into conducting polymers, hoping to simultaneously improve their conductivity and strength. It should be noted that Carbon nanotube (CNT)/polymer composites represent a new direction to these materials [1]. CNTs exhibit excellent mechanical and electrical properties, while polymers provide good flexibility, high transparency, easy processing, and low cost. Three main fabrication approaches (i.e., solution blending, melt blending, and in situ polymerization) have been extensively explored [2]. Unfortunately, advances in processing transparent CNT/polymer composites have been hindered by the aggregation and random dispersion of carbon nanotubes, which results in an extremely low electrical conductivity for composite materials. For example, the conductivity is less than $10^{-6}$ S/cm at room temperature for CNT/poly(methyl methacrylate) nanocomposites synthesized by a melt spinning process [3].

The objective of this proposal is to develop a new approach to solve this problem. In other words, we first pull strong, conducting, and highly transparent CNT sheets directly from long nanotube arrays, and then impregnate the sheet with a conducting polymer to form a *flexible* and *cheap* electrode that can be potentially used for solar cells. The highly oriented nature of the CNT sheets give the electrode both good conductivity and excellent strength, and the small thickness of the CNT sheets gives the electrode superior transparency.

## Importance to LANL's Science and Technology Base and National R & D Needs

This project directly contributes to DOE's mission in energy security by developing a cheap, novel carbon nanotube-polymer electrode material to replace the ITO. It directly impacts LANL's Mission Priorities in energy security. Integration of diverse energy sources underpins the priorities. Furthermore, LANL's thrusts in nanotechnology will benefit from this project.

## Scientific Approach and Accomplishments

Three key steps are involved to accomplish the technological goals: First, grow long CNT arrays that are conducive to pulling out thin CNT sheets. Second, develop a method to pull highly oriented, free-standing CNT sheets that can be scaled up for continuous large-scale productions. Third, impregnate the CNT sheets with a conductive polymer. This can be realized by either passing the continuous CNT sheet through a conductive polymer solution followed by solvent evaporation, or by sandwiching the CNT sheet between two thin conductive polymer sheets. The electrical properties and transparency of the electrodes can be conveniently controlled by tuning structure of such CNT-polymer nanocomposite.

The detailed experimental processes for the synthesis of transparent and flexible CNT/polymer composite films include the following steps. CNT arrays are first grown on silicon by a chemical vapor deposition (CVD) process. Uniform CNT sheets are then pulled out of the arrays and stabilized on glass. Composite films are finally produced by spin-coating or casting polymer solutions onto CNT sheets, followed by evaporation of solvents. Film thickness can be controlled by varying the concentration of polymer solutions and coating times. Transparent and flexible films can be readily peeled off the substrate. For this approach, the fabrication is simple and efficient, and a wide range of polymers and monomers may be used to synthesize functional composite materials. We have used transmission electronic microscopy and scanning electronic microscopy (SEM) to characterize the structural properties of the materials. The electronic conductivity and mechanical property are measured to correlate with the structure of the materials.

A key point for this method is to grow long and spinnable CNT arrays, which produce high-grade sheets. The catalytic iron film on the $Al_2O_3$ buffer layer has been proved to be active for several hours, which is critical for growing long CNT arrays. We synthesized spinnable CNT arrays up to 4 mm using this catalyst system. Figure 1a shows a typical scanning electron microscopy (SEM) image of a CNT array on silicon. Synthesized CNTs are highly aligned and vertical to the substrate. The surface of the array was very clean and smooth. CNT sheets are readily assembled on glass from these high quality CNT arrays as shown in Figure 1b. Both plastic and semiconducting polymers have been studied in this work. Polystyrene (PS), poly(methyl methacrylate) (PMMA), and poly(3-hexylthiophene-2,5-diyl) (P3HT) are purchased from Aldrich. We have also synthesized sulfonated poly(ether ether ketones) (S-PEEK). For PS-, PMMA-, and S-PEEK-derived composite films, they are transparent and show an optical transparency higher than 80% with a thickness of around 5 micrometer. Figure 2 shows the S-PEEK-derived film (around 15 micrometer in thickness) on a labeled paper, and the symbol on the paper can be clearly observed.

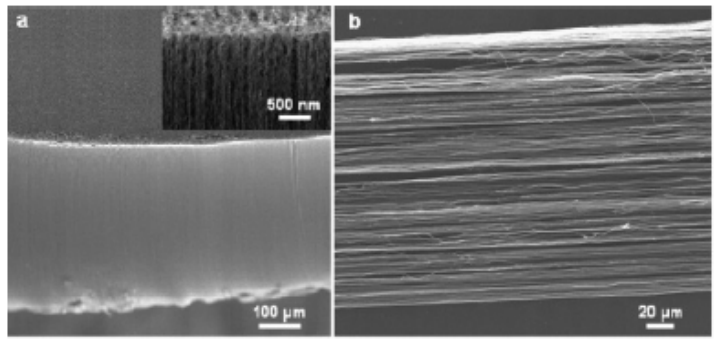


*Figure 1. (a) SEM image of a CNT array (inset: high magnification). (b) SEM image of CNT sheets pulled out of the array.*

*Figure 2. Transparent CNT/S-PEEK composite films on a labeled paper.*

For all studied polymers, their composite films show high conductivities along the CNT-aligned direction. For example, conductivity of S-PEEK-derived films at room temperature is 22 S/cm, approximately the same order of magnitude as films of poly-(3,4-ethylenedioxythiophene) doped with poly(styrenesulfonic) acid. Conductivity can be further increased to 200 S/cm by growing longer spinnable CNT arrays and engineering CNT sheets. Synthesized CNT/polymer films are very stable, and their conductivity keeps constant after being bent many times. Detailed experimental results can be found in our article published in J. Am. Chem. Soc. [4].

## References


1. Xu, M., T. Zhang, B. Gu, J. Wu, and Q. Chen. Synthesis and properties of novel polyurethane-urea/multi-walled carbon nanotube composites. 3540. *Macromolecules.* **39**: 2006.

2. Moniruzzaman, M., and K. I. Winey. Polymer nanocomposites containing carbon nanotubes. 2006. *Macromolecules.* **39**: 5194.

3. Du, F., R. C. Scogna, W. Zhou, S. Brand, J. E. Fischer, and K. I. Winey. Nanotube networks in polymer nanocomposites: Rheology and electrical conductivity. 2004. *Macromolecules.* **37**: 9048.

4. Peng, H. S.. Aligned Carbon Nanotube/Polymer Composite Films with Robust Flexibility, High Transparency, and Excellent Conductivity. 2008. *J. Am. Chem. Soc.* **130**: 42.


## Publications


Li, Q. W., Y. Li, X. F. Zhang, S. B. Chikkannanavar, Y. H. Zhao, A. M. Dangelewicz, L. X. Zheng, S. K. Doorn, Q. X. Jia, D. E. Peterson, P. N. Arendt, and Y. T. Zhu. Structure-Dependent Electronic properties of Carbon Nanotube Fibers. 2007. *Adv. Mater..* **19**: 3358.

Peng, H. S.. Aligned carbon nanotube/polymer composite films with robust flexibility, high transparency, and excellent conductivity. 2008. *J. Am. Chem. Soc..* **130**: 42.

Peng, H. S., D. Y. Chen, J. Y. Huang, S. B. Chikkannanavar, J. Hanisch, M. Jain, D. E. Peterson, S. K. Doorn, Y. F. Lu, Y. T. Zhu, and Q. X. Jia. Strong and Ductile Colossal Carbon Tubes with Walls of Rectangular Macro-Pores. To appear in *Phys. Rev. Lett..*

Peng, H. S., M. Jain, D. E. Peterson, Y. T. Zhu, and Q. X. Jia. Carbon Nanotube/Silica Composite Fibers with Improved Mechanical Strengths and Electrical Conductivities. To appear in *Small.*

Peng, H. S., M. Jain, Q. W. Li, D. E. Peterson, Y. T. Zhu, and Q. X. Jia. Vertically-Aligned Pearl-like Carbon Nanotube Arrays for Fiber Spinning. 2008. *J. Am. Chem. Soc..* **130**: 1130.

Peng, H. S., Y. T. Zhu, D. E. Peterson, and Y. F. Lu. Nano-layeired carbon/silica superstructures via organosilane assembly. 2008. *Adv. Mater..* **20**: 1199.

Zheng, L. X., X. F. Zhang, Q. W. Li, S. B. Chikkannan, Y. Li, Y. H. Zhao, X. Z. Liao, Q. X. Jia, S. K. Doorn, D. E. Peterson, and Y. T. Zhu. Carbon-Nanotube Cotton for Large-Scale Fibres. 2007. *Adv. Mater..* **19**: 2567.

# Theoretical Investigations of Plastic Deformation in Energetic Materials

*Thomas Dan Sewell*

20061639PRD4

## Abstract

The fundamental mechanisms through which the energetic molecular crystal cyclotrimethylene trinitramine (RDX) deforms irreversibly and localizes energy under impact and shock loading have been investigated through a combination of state of the art atomistic simulations and parallel experiments. This work has successfully identified many of the mechanisms that play a role in the response of RDX crystals to extreme loading conditions, including the homogeneous nucleation of dislocations, the formation of amorphous shear bands, and shock and pressure-induced phase transformations. The observation and characterization of the homogeneous nucleation of dislocations in RDX led to the development of a plastic hardening model that explained successfully a set of anomalous experimental results. The formation of amorphous shear bands during shock loading was found to give rise to intense localized heating that may promote the onset to detonation. Furthermore, we were able to predict correctly the crystal structure of a high-pressure polymorph of RDX, thus solving a 30-year-old problem in this material.

## Background and Research Objectives

The initiation of detonation in energetic materials is associated with the formation of 'hot spots' where in spatially localized volumes the temperature and/or stress may significantly exceed the mean values in the material. Hot spots are intimately associated with intense, irreversible deformation due to a heterogeneous defect structure or microstructure. Examples of such defects at the meso- and macroscopic length scales include voids [1] and particle-particle interfaces. Pioneering work by J.J. Dick on the energetic molecular crystal PETN at LANL showed that even in the absence of mesoscopic defects such as voids, initiation sensitivity is still governed by crystal defects [2]. Shock loading experiments on pristine, defect free PETN single crystals led to the hypothesis that molecular-scale crystal defects known as dislocations may play a surprisingly prominent role in initiation sensitivity. Dislocations are line defects in crystals that glide on specific crystallographic planes in response to an applied load and mediate plastic (i.e., irreversible) deformation. It is well known that dislocation motion in crystals facilitates a rapid relaxation of shear stresses. This led Dick to propose that abundant dislocation mediated plasticity upon shock loading leads to insensitive behavior since in the absence of an efficient mechanism for the relaxation of shear stress, molecules would be forced to deform severely, inducing the initial chemical events in the transition to detonation. Hence, the ability to predict anisotropies in the initiation sensitivity of numerous explosives is somewhat surprisingly within the realm of materials science rather than chemistry alone.

The dynamic response of energetic materials at the atomic scale to shock loading is extremely difficult, if not impossible to study experimentally owing to their exceptional brittleness and violent chemical decomposition upon detonation. Thus, atomistic simulations employing an accurate representation of interatomic bonding in these materials are one of the few tools available to access these phenomena on picosecond time scales. Nevertheless, the true potential of atomistic and molecular dynamics simulations can only realized when comparisons with parallel experimental efforts are made. We have taken this approach throughout this project.

Our original aim for this project was *extremely* ambitious since we proposed that we would develop simulation methodologies that would allow the micromechanisms of plastic deformation within complex molecular crystals to be described with the same rigor as those for simple metallic crystals. Over the course of the project, we have demonstrated that this was indeed possible. In particular, we aimed to indentify and characterize, using molecular dynamics simulations and electron structure calculations, the atomic-level

responses of crystallographically oriented RDX single crystals to the propagation of planar shock waves.

## Importance to LANL's Science and Technology Base and National R & D Needs

The development of genuinely predictive thermo-mechanical-chemical models for mechanically anisotropic, molecularly-complex materials requires a detailed understanding of the atomic and molecular scale mechanisms by which such materials deform, react, and/or fail when subjected to harsh mechanical or thermodynamic environments. The need for such understanding is particularly acute when the goal is to understand processes for conditions outside the intervals in calibration space for which experiments exist, or in the neighborhood of material instabilities. While recent advances in computational capability and capacity allow unprecedented simulations of complex material response for complicated materials, true theoretical understanding of molecularly-complex materials requires consideration of degrees of freedom that simply do not exist for the heavily studied cases of simple atomic metals; specifically, non-spherical shapes, intramolecular conformational flexibility, low-symmetry crystal space groups in which orientational order is a factor in addition to simple translational site symmetry, and even chemical transformations. Clearly, many materials relevant to NNSA national defense and energy security missions are subject to these kinds of complications. The fundamental research performed during this Director's Fellowship has contributed significantly to our ability to simulate, assimilate, and understand the physical processes that will dominate the dynamic material response for complicated materials under the kinds of conditions mentioned above. Also, the experimental/theoretical ties established within the framework of this project have already led to significant synergies between atomistic simulation and theory and dynamic experimentation methods, and the expectation is that these synergies will expand in future years.

## Scientific Approach and Accomplishments

We chose to focus the theoretical and simulation work on the energetic molecular crystal RDX since this material is experimentally one of the most studied and best characterized. Furthermore, this approach facilitated a close collaboration between simulation and a concurrent experimental program at LANL [3]. In this manner, predictions arising from the theoretical work could be rapidly investigated in-house, and anomalous experimental results could be dissected using the simulation and modeling tools developed over the course of the project.

Under ambient conditions, RDX, $C_3H_6N_6O_6$, adopts an orthorhombic unit cell with space group *Pbca* that contains eight molecules [4]. An RDX molecule and the 168-atom unit cell of the $\alpha$-RDX polymorph are depicted in Figures 1(a) and 1(b), respectively. In this structure, each molecule adopts a specific conformation, namely, the molecular ring is classified as being in a 'chair' conformation with two nitro groups oriented axially (*A*) to the ring and one equatorially (*E*). This conformation is commonly denoted as *AAE*.

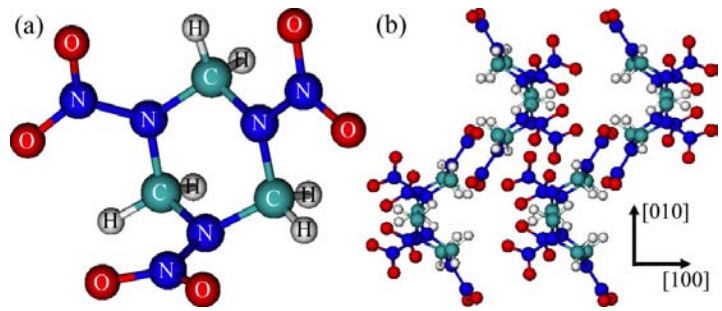


*Figure 1. (a) An RDX molecule, (b) Projection of the alpha-RDX unit cell along [001]*

Large-scale molecular dynamics (MD) simulations were the principal tool employed in the investigation of the micromechanisms of plastic deformation in RDX. The formalism that underlies MD simulations is very straightforward: one integrates numerically the Newtonian equations of motion ($F = ma$) for an ensemble of atoms over time, where the force acting on each atom is given by an interatomic potential (an expression for the total energy of a set of atoms as a function of their coordinates). Despite the apparent simplicity of this method, the simulation of multi-million atom systems with an interatomic potential that describes accurately the bonding within a molecular crystal is extremely challenging. Nevertheless, by utilizing the state-of-the-art, massively parallel MD code LAMMPS (developed at Sandia National Laboratories) [5], a computationally efficient, accurate, and transferable non-reactive molecular potential for nitramines [6], coupled with the outstanding supercomputing facilities available at LANL, we have set a new standard for MD simulations of molecular crystals. Furthermore, we adopted and advanced a new type of boundary conditions for use in MD simulations of shock loading that allows the duration of simulations to be extended significantly for a given number of atoms. This shock front absorbing boundary condition was critical to our ability to track the temporal evolution of relatively slow processes in RDX [7, 8].

A series of large-scale MD simulations were performed for (100) and (111)-oriented RDX single crystals at shock pressures in the range 1.4 to 10 GPa. Owing to the inherent physical anisotropies of RDX, these two orientations led to markedly different mechanical responses. It should be noted that the cases discussed here are almost certainly only a small part of the exceptionally rich physics exhibited by this material. Furthermore, the deformation mechanisms described here can be activated only under extreme loading conditions. Thus, large-scale MD simulations of this type should be considered to be complimentary to all experimental efforts.

In the case of (100)-oriented pristine RDX single crystals, we found no evidence for dislocation-mediated plasticity or polymorphic phase transformations up to shock pressures of 10 GPa. Instead, these crystals deform by the formation and growth of broad, amorphous shear bands at shock pressures greater than about 8 GPa [9]. The role of shear stresses in the formation and evolution of these defects is particularly evident since the shear bands are not aligned with any crystallographic direction in the RDX crystals but instead propagate at approximately 45° to the compressive axis. A snapshot from a large-scale MD simulation containing 10.6 million atoms that illustrates the distribution of shock-induced shear bands is presented in Figure 2.

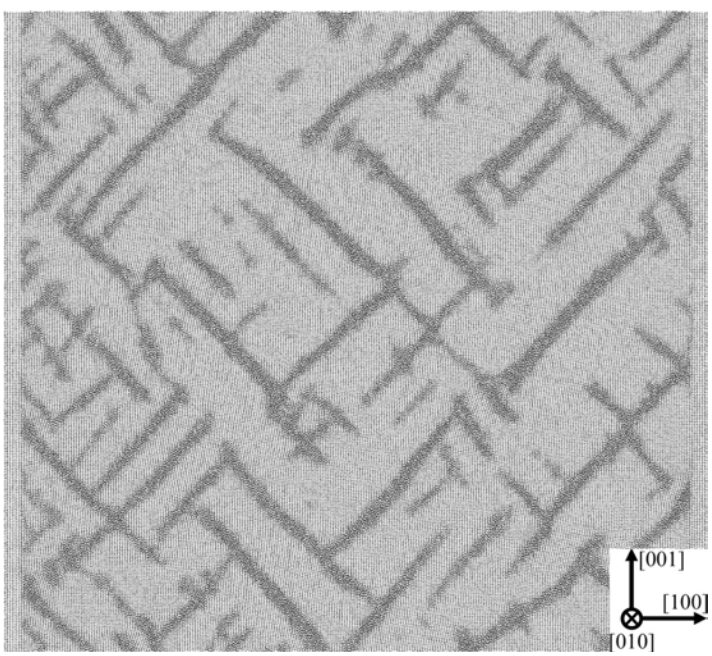


*Figure 2. A projection of the molecular centers of mass following shock loading to 9.7 GPa and application of the SFABC. The shear bands are visible as dark diagonal bands. At maximum compression the cell measures 164 nm x 3.5 nm x 150 nm parallel to [100], [010], and [001], respectively.*

The shear bands that form under shock loading in (100) oriented RDX crystals evolve to a steady-fluctuating state on a time scale that is long relative to the duration of typical MD simulations of shock compression. In order to allow these systems to evolve fully to a steady state, we implemented and refined the shock front absorbing boundary condition method (SFABC) first proposed by Thompson and coworkers [7]. SFABCs allow a simulation cell to be captured at the point of maximum compression in a MD simulation of shock loading and prevent the emission of rarefaction waves from the free surface. By capturing the shock-compressed material in this manner, a subsequent MD simulation can be run, in principle, indefinitely. We propose that the SFABC formalism provides a robust alternative to Hugoniostat approaches, with the additional benefit of providing an exact treatment of phenomena at the shock front [8].

In stark contrast to (100)-oriented crystals, the propagation of planar shock waves normal to RDX (111) resulted in dislocation-mediated plasticity at shock pressures above 1.4 GPa. A series of large-scale MD simulations showed the homogeneous nucleation of partial dislocation loops several nanometers behind the shock front [9]. The dislocations were found to glide only on the (001) plane and possess a Burgers vector of 0.16[010]. Since the displacement mediated by a partial dislocation is not a lattice repeat vector of the crystal, the loops nucleated in our simulations enclose a region of disregistry known as a stacking fault. Hence, above a threshold shock pressure of around 1.4 GPa, the homogeneous nucleation and rapid expansion of partial dislocation loops gives rise to a high density of stacking faults in the material. The stacking faults observed in the simulations were rendered metastable by a change in the conformation of RDX molecules in the two parallel (001)-type planes that define the fault. In particular, full analyses of the conformation of each molecule in the simulations showed that the passage of a partial dislocation causes a change in the orientation of the nitro groups with respect to the molecular from *AAE* to *AEE*, while the conformation of the ring is unaffected. Further investigation showed that a confining pressure of about 1 GPa in addition to a resolved shear stress is required to mediate the *AAE* to *AEE* conformational change. For these reasons, this deformation mechanism cannot be activated under ambient conditions with the loading rates typical of standard laboratory mechanical tests: the observed partial dislocations cannot exist if the stacking fault they create is unstable. In Figure 3 we present a snapshot from a large-scale simulation of the passage of a planar shock wave with shock pressure of 2.2 GPa through a (111)-oriented crystal. In this Figure, only the centers of mass of those

*Figure 3. A projection of the centers of mass of only those molecules that have changed conformation from AAE to AEE after shock loading to 2.2 GPa a (111)-oriented RDX single crystal. The stacking faults are clearly visible as ribbons in this projection.*

molecules that have changed conformation from *AAE* to *AEE* are presented, allowing the stacking faults to be identified clearly in this projection as ribbons.

The abrupt change in deformation mechanism seen during MD simulations of the shock compression of (111)-oriented RDX crystals was found to correlate extremely closely with experimental observations of their elastic-plastic response. A well-defined elastic-plastic structure is seen in flyer plate driven shock wave experiments around 1.25 GPa [9]. However, at 2.25 GPa, the response appears to be almost overdriven [3]. We propose that the plastic hardening caused by the high density of stacking faults created by the homogeneous nucleation of partial dislocations accounts naturally for these otherwise anomalous observations.

The $\alpha$-to-$\gamma$ phase transformation in RDX was first identified by Olinger and coworkers at LANL in the late 1970s by Bridgman anvil cell compression and X-ray diffraction [10]. An abrupt 1.6 % reduction in the volume of the unit cell was recorded at a hydrostatic pressure of 4 GPa. The crystal structure of $\gamma$-RDX was found to remain orthorhombic but with an increase in the *b* lattice parameter and a large decrease in the *c* lattice parameter with respect to the $\alpha$-phase. Recent shock loading experiments suggested that RDX passes through the $\gamma$-phase on route to detonation [11], however the space group and atomic structure of this important polymorph remained unknown for almost 30 years.

A set of MD simulations was designed with the aim of driving $\alpha$-RDX to the $\gamma$-phase. Since the phase transformation is associated with a notable decrease in the *c* lattice parameter, we proposed that shock loading on (001) would promote the transition. Thus, we performed a number of relatively small 1.1 million atom simulations with particle velocities in the range from 175 m/s to 2.5 km/s to map out in detail the Hugoniot for this crystallographic orientation of the shock propagation direction. A kink in the Hugoniot that is indicative of a phase transformation was noted at a shock pressure of about 1.9 GPa, as illustrated in Figure 4. We then extracted a subvolume of material from a shock loading simulation above 1.9 GPa containing around 100000 atoms for further study under hydrostatic pressure. Upon the slow relaxation of hydrostatic pressure we observed a small jump in the unit cell volume and changes in the *b* and *c* lattice parameters consistent with the $\gamma$-phase reverting to $\alpha$-RDX. We then extracted a single unit cell of the suspected $\gamma$-phase and performed a series of highly accurate electronic structure calculations that demonstrated conclusively that this crystal structure is stable at high pressures. Thus, by studying RDX crystals under a variety of loading conditions in system sizes ranging from a million atoms to the electronic level, we were able to produce a prediction for the atomic structure of $\gamma$-RDX. We demonstrated that indeed the crystal structure of $\gamma$-RDX remains orthorhombic, and predicted that the space group changes from *Pbca* to $Pca2_1$ during the transformation with a doubling of the number of unique molecules within the unit cell. Shortly after this work was completed, an experimental team based in the UK published a high-pressure neutron diffraction study that independently confirmed our theoretical prediction [12]. The level of agreement between experiment and theory in this case highlights the exceptional predictive capabilities developed for energetic molecular crystals during the course of the Director's postdoctoral fellowship.

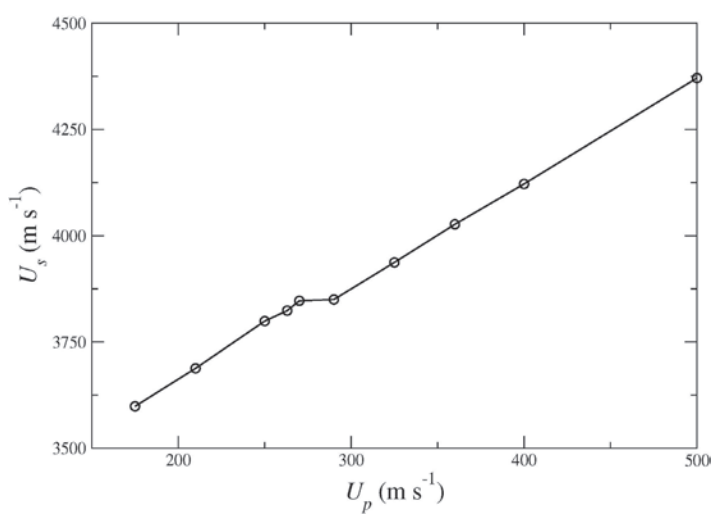


*Figure 4. The theoretical shock velocity vs. particle velocity Hugoniot for (001)-oriented RDX single crystals. The kink in the Hugoniot at a particle velocity of 190 m/s is indicative of a shock-induced phase transformation.*

## References


1. Bowden, F. P., and M. M. Chaudhri. Initiation of explosion in AgN3 and beta-PbN6 single crystals by a collapsing bubble. 1968. *Nature.* **200**: 690.

2. Dick, J. J.. Anomalous shock initiation of detonation in pentaerythritol tetranitrate crystals. 1997. *Journal of Applied Physics.* **81**: 601.

3. Hooks, D. E., K. J. Ramos, and A. R. Martinez. Elastic-plastic shock wave profiles in oriented single crystals of cyclotrimethylene trinitramine (RDX) at 2.25 GPa . 2006. *Journal of Applied Physics.* **100**: 024908.

4. Choi, C. S., and E. Prince. The crystal structure of cyclotrimethylene trinitramine. 1972. *Acta Crystallographica B.* **28**: 2857.

5. Plimpton, S.. Fast parallel algorithms for short-range molecular dynamics. 1995. *Journal of Computational Physics.* **117**: 1.

6. Smith, G. D., and R. K. Bharadwaj. Quantum chemistry based force field for simulations of HMX. 1999. *Journal of Physical Chemistry B.* **103**: 3570.

7. Bolesta, A. V., L. Q. Zheng, D. L. Thompson, and T. D. Sewell. Molecular dynamics simulations of shock waves using the absorbing boundary condition: A case study in methane. 2007. *Physical Review B.* **76**: 224108.

8. Cawkwell, M. J., T. D. Sewell, L. Q. Zheng, and D. L. Thompson. Shock-induced shear bands in an energetic molecular crystal: Application of shock-front absorbing boundary conditions to molecular dynamics simulations. 2008. *Physical Review B.* **78**: 014107.

9. Cawkwell, M. J., T. D. Sewell, K. J. Ramos, and D. E. Hooks. Shock-induced anomalous plastic hardening in cyclotrimethylene trinitramine (RDX). *Physical Review B.*

10. Olinger, B., B. Roof, and H. Cady. The linear and volume compression of beta-HMX and RDX to 9 GPa (90 kilobar). 1978. *Behaviour of Dense Media under High Dynamic Pressures.*

11. Patterson, J. E., Z. A. Dreger, and Y. M. Gupta. Shock wave-induced phase transition in RDX single crystals. 2007. *Journal of Physical Chemistry B.* **111**: 10897.

12. Davidson, A. J., I. D. H. Oswald, D. J. Francis, A. R. Lennie, W. G. Marshall, D. I. A. Millar, C. R. Pulham, J. E. Warren, and A. S. Cumming. Explosives under pressure - the crystal structure of gamma-RDX as determined by high-pressure X-ray and neutron diffraction. 2008. *CRYSTENGCOMM.* **10**: 162.


## Publications


Cawkwell, M. J., T. D. Sewell, K. J. Ramos, and D. E. Hooks. Shock-induced anomalous plastic hardening in an energetic molecular crystal. *Physical Review B.*

Cawkwell, M. J., T. D. sewell, L. Q. Zheng, and D. L. Thompson. Shock-induced shear bands in an energetic molecular crystal: application of shock front absorbing boundary conditions to molecular dynamics simulations. 2008. *Physical Review B.* **78**: 014107.

# Structure and Function of Human Mineralised Tissue

*John G Swadener*

20070565PRD1

## Abstract

Tooth enamel is a hard and stiff biological material that nature has developed into a sophisticated structure to accomplish its function of tearing and chewing food. Certain diseases cause a loss of mechanical strength, which results in loss of tooth function, which can lead to malnutrition. This study examined enamel structure in healthy and diseased tissues and compared test results of mechanical properties to recently developed mathematical models.

## Background and Research Objectives

Tooth enamel is similar to bone in that at the microscopic scale, it is a composite made up of small hard minerals held together by soft collagen molecules. Healthy enamel is composed of approximately 90% mineral, which makes it the hardest and stiffest material in the human body. Unlike bone, enamel is not re-grown, and any damage or disease is likely to be permanent and often leads to tooth loss. Developmental diseases have been reported to lead to below normal enamel mineral content in 19% of children worldwide.

The objective of this study was to assess the structure and mechanical properties of tooth enamel in healthy state and in a state with less than normal mineral content and determine the effect of abnormal mineral content on mechanical properties.

## Importance to LANL's Science and Technology Base and National R & D Needs

This study supported LANL's basic materials science goal by determining the relation between structure at the microscopic scale and mechanical properties of enamel, which are important for tooth function. The results are applicable to tooth diseases, but can be extended to bone and manmade composites as well.

## Scientific Approach and Accomplishments

Human tooth enamel in healthy state and in a state with less than normal mineral content was examined using transmission electron microscopy. The structure for healthy enamel was observed to match previous observations. It is a well-integrated composite of mineral and protein (collagen). In contrast, enamel with below normal mineral content showed marked opacity and a greater number of voids of larger size compared to healthy enamel.

The elastic properties and hardness of the two types of enamel were measured using nanoindentation. Enamel with below normal mineral content was found to have only one fifth the stiffness of healthy enamel, reduced strength, and lower resistance to fracture.

A model to relate structure to mechanical properties in tooth enamel was developed [1] based on a similar model for bone [2]. The model is compared to experimental results as shown in Figure 1 and provides good agreement with the enamel structure orientation. Healthy enamel was found to provide global protection against deformation during dental function. Enamel with below normal mineral content was found to have lower strength and stiffness, which we predict would results in excessive bending during chewing, which would cause teeth to break prematurely.

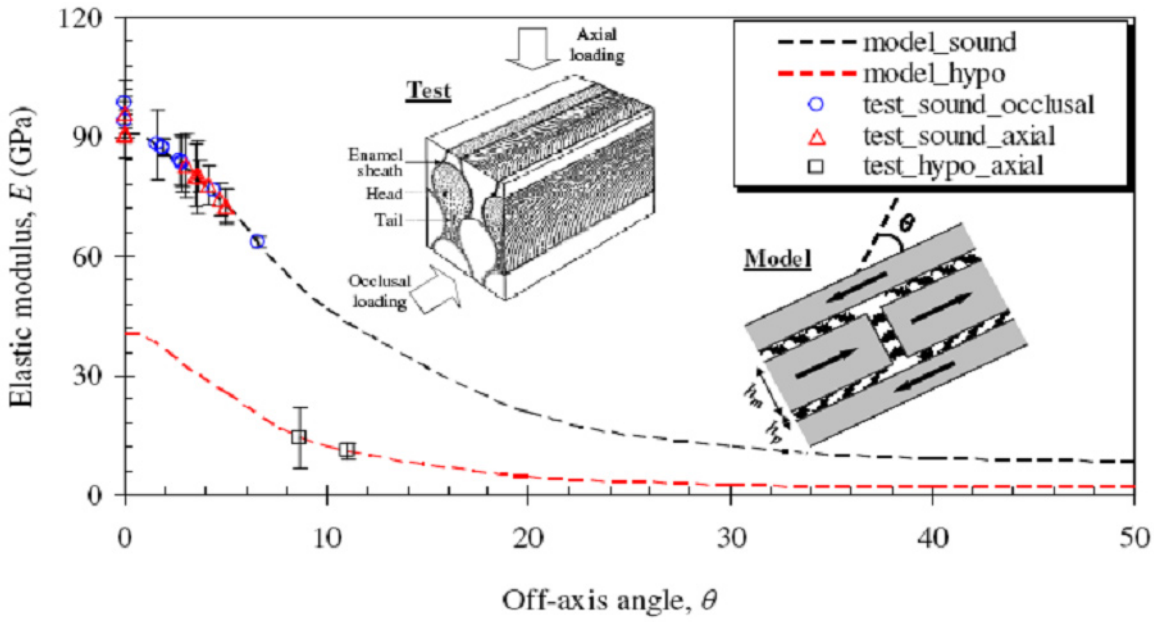


*Figure 1. The elastic modulus (stiffness) of healthy and hypomineralized (below normal) enamel as a function of angle relative to the direction of the enamel rod.*

## References


1. Xie, Z. H., E. K. Mahoney, N. M. Kilpatrick, M. V. Swain, and M. Hoffman. On the structure-property relationship of sound and hypomineralized enamel. 2007. *Acta Biomaterialia.* **3** (6): 865.

2. Ji, B., and H. Gao. Mechanical properties of nanostructure of biological materials. 2004. *Journal of the Mechanics and Physics of Solids.* **52**: 1963.


## Publications

Xie, Z. H., E. K. Mahoney, N. M. Kilpatrick, M. V. Swain, and M. Hoffman. On the structure-property relationship of sound and hypomineralized enamel. 2007. *Acta Biomaterialia.* **3** (6): 865.

# Vibrational Features and Quantum Transport in Molecular Electronics

*Sergei Tretiak*

20070576PRD1

## Abstract

The project focuses on several most challenging problems of molecular electronics and bridge first principle quantum simulations with experimentally measurable quantities. At the fundamental level this work will enable proper description of vibrational features in quantum transport with potential application to diagnostics (identification of molecule and/or chemical paths). Also, it will help to find the roots of discrepancy between different experimental results and will make reliable theoretical predictions (finding important vibrational modes, predicting stability of molecular electronic devices, etc.).

## Background and Research Objectives

The promise of molecular electronics is easily stated: continuing miniaturization will approach the fundamental size limit of Si based electronics in a decade. With fabrication of molecular devices (switches, transistors, biosensors, etc.), questions of properties prediction, diagnostic, stability, and reproducibility become very important. Due to small sizes transport in these structures becomes of essentially quantum nature, and specific vibrational and electronic molecular features are the only footprints indicating presence of the molecule in the device. In order to understand existing experimental data proper first principle description of quantum transport within a wide range of parameters is necessary. Current non-equilibrium descriptions have several shortages. At LANL DIrector funded Postdoctoral Fellow envisions working on the theoretical foundation of molecular electronics. This includes first principle based modeling and analysis of experimentally relevant properties such as I/V (dI/dV and/or d2I/dV2) and noise (and higher moments) curves using nonequilibrium Green,Äôs function (NEGF) approach. Furthermore, we will extend these simulations to incorporate more sophisticated phenomena such as nonequilibrium strongly correlated systems in the intermediate coupling regime, anharmonicities and charge-specific frequencies, vibrational dynamics, and non-Born-Oppenheimer consideration, which can be used for diagnostics and characterization of the device in transition to Coulomb blockade or Kondo, dynamical features of Negative Differential Resistance (NDR), interaction with external laser field, and STM-IETS experiments. As a first step we propose to develop a theoretical scheme to partition the mixed transport situation in the junction into a set of coupled conventional charged states, thus bridging open and isolated system considerations. One can either extend n-projection technique and/or approach by Schoeller et al. to deal with correlation functions, or separate Fock spaces by introducing fictitious chemical potential. In particular, this would allow use of inputs from modern quantum chemical approaches (such as configuration interaction, (time-dependent) density functional theory, etc.) in modeling of molecular transport. To treat large molecules, we will generalize equilibrium linear-scaling methods to transport situation.

## Importance to LANL's Science and Technology Base and National R & D Needs

Apart from expected fundamental achievements, this will boost experimental LANL studies in this area, particularly bridging several CINT thrusts, and enhancing existing theory/experiment LANL programs on nanomaterials research This project supports the DOE missions in Threat Reduction and Energy Security. The work ideally complements and enhances several existing theory/experiment LANL programs on nanomaterials research, and, if realized, will strengthen Complex Electronic Materials and Nanotechnology thrusts in the strategic area of nanoscience.

## Scientific Approach and Accomplishments

This is the final report for this Postdoctoral project. After the first year, the Director-funded Postdoctoral Fellow, Michael Galperin, has joined faculty at UCSD. During his appointment as a Director's Postdoctoral

Fellow he worked on several projects in the field of theoretical description of molecular systems out of equilibrium. In particular, completed projects include:

**Nonlinear transport in molecular junctions**

Strongly correlated resonant transport is an area of importance for building molecular based logic and memory devices. One of physical mechanisms for switching and negative differential resistance proposed by us earlier and developed in several papers is based on electron-slow vibration interaction, leading to formation of dynamic polaron. The mechanism was criticized as an artifact of the treatment by Alexandrov and Bratkovsky in several papers. in this work we developed and published [1] strict mathematical proof of validity of our approach. Moreover, our generalized mathematical scheme, provides isolated molecule results by Alexandrov and Bratkovsky in one limit, and our slow vibration results in another (static limit).

**Optical response of current carrying molecules**

Development of experimental techniques brings this area to the forefront of research. The issueis of importance both due to potential applicability to development of opto-electronic molecular devices, and as a promising diagnostic tool so much needed in molecular electronics. Our effort on this track was twofold. First, we developed and published [2] first non-equilibrium linear response theory capable of dealing with optical response of realistic molecular junctions. This is in contrast to simple model based treatments available in the literature. Second, within simple model approach we developed (to be submitted) a theory of Raman scattering in transport junctions. The issue is of importance due to recent experimental data on simultaneous measurement of conductance and Raman response of molecular junctions, which provide complementary information on the junction characteristics. Interestingly, that non-equilibrium character of the system leads to effects which are not observed in usual (equilibrium) Raman experiments: inverse Raman scattering and  interference effects between different scattering processes. One of the goals for future research is formulation of an approach capable of dealing with the issue in realistic systems.

**Non-equilibrium atomic limit**

Proper theoretical description of strongly correlated transport in molecular systems requires formulation of the theory in the language of many-body molecular states rather than effective single-particle orbitals. This is due to sensitivity of molecular and vibrational structure (especially for small molecules) to change in charging and excitation states of the molecule. This approach also provides possibility to take into account on-the-molecule correlations and incorporate sophisticated quantum chemistry methods into transport calculations (thus bridging between two research communities in quantum chemistry). Besides, optical response of molecular junctions (discussed above) is more convenient to formulate in the language of molecular states (all the standard spectroscopy is formulated this way). The main problem in such description is inability to map non-equilibrium state of the molecule in the junction into set of well-defined charge and excitation states of isolated molecule (absence of proper non-equilibrium atomic limit). During postdoctoral work at LANL we made a first step in development and application of the many-body states approach to inelastic transport in molecular junctions [3].

## References

1. Galperin, M.. Molecular transport junctions: vibrational effects. To appear in *Journal of Physics Condens. Matter.*

2. Galperin, M., and S. Tretiak. Linear optical response of current-carrying molecular junction: A NEGF-TDDFT approach. 2008. *Journal of Chem* Lanthanide Main-Group Element Multiple Bonds

# Lanthanide Main-Group Element Multiple Bonds

*Jaqueline Loetsch Kiplinger*

20070709PRD3

## Abstract

The first example of a lanthanide metal complex featuring a metal-phosphorus multiple bond (Ln=P), or phosphinidene, functional group has been prepared and isolated. The lutetium phosphinidene complex exists as a dimer and possesses bridging phosphinidene groups. Unlike the transition metals and actinides, lanthanide phosphinidenes were an unknown class of compounds until this work. Due to the electronic mismatch between the "hard" lanthanide and the "soft" phosphorus, this new class of molecules is anticipated to provide crucial information concerning the nature of and degree of covalency in Ln metal-ligand bonding, which will enhance our ability to develop 4f-5f element separations schemes for advanced nuclear fuel cycle and waste management efforts within the DOE complex.

## Background and Research Objectives

Transition-metal complexes containing metal main-group element multiple bonds (M=E, E = C, N, O, P) have been of great interest owing to their intriguing bonding properties as well as being implicated as key intermediates in many industrially important processes such as olefin metathesis (catalyzed by alkylidene complexes, M=$CR_2$) and phosphine dehydrocoupling (catalyzed by phosphinidene complexes, M=PR). The *f*-block elements are comprised of both the lanthanides (also known as 4f-elements) and the actinides (also known as the 5f-elements). For the *f*-block elements, actinide complexes containing terminal oxo (U=O), imido (U=NR), and phosphinidine (U=PR) fragments are known; while there have been reports of lanthanide systems with bridging and capping imido units, examples possessing terminal main-group element multiple bonds remain elusive. The goal of this project was to develop methods for synthesizing 4*f*-element complexes containing lutetium-nitrogen (Lu=N), -oxygen (Lu=O), -phosphorus (Lu=P), and –carbon (Lu=C) multiple bonds.

## Importance to LANL's Science and Technology Base and National R & D Needs

The chemistry of the *f*-elements is critical to DOE nuclear weapons mission areas (stockpile stewardship, environmental remediation, waste management). Through the synthesis of new f-element compounds this program will provide important information about metal-ligand bonding and improve our ability to reliably predict chemical behavior in a variety of environments. For example, *f*-block elements containing metal main-group element multiple bonds (M=E, E = C, N, O, P) could be involved in depolymerization chemistry (which would ultimately produce gas) in DOE complex waste containers. Furthermore, complexes such as the lanthanide phosphinidene complexes prepared in this project are anticipated to provide crucial information concerning the nature of and degree of covalency in Ln metal-ligand bonding, which will enhance our ability to develop 4*f*-5*f* element separations schemes for advanced nuclear fuel cycle and waste management efforts within the DOE complex.

## Scientific Approach and Accomplishments

Transition-metal complexes containing metal main-group element multiple bonds (M=E, E = C, N, O, P) have been of great interest owing to their intriguing bonding properties as well as being implicated as key intermediates in many industrially important processes such as olefin metathesis (catalyzed by alkylidene complexes, M=$CR_2$) and phosphine dehydrocoupling (catalyzed by phosphinidene complexes, M=PR). The *f*-block elements are comprised of both the lanthanides (also known as 4*f*-elements) and the actinides (also known as the 5*f*-elements). For the *f*-block elements, actinide complexes containing terminal oxo (U=O), imido (U=NR), and phosphinidine (U=PR) fragments are known; while there have been reports of lanthanide systems with bridging and capping imido units, examples possessing terminal main-group element multiple bonds remain elusive.

The goal of this project was to develop methods for synthesizing 4*f*-element complexes containing lutetium-nitrogen (Lu=N), -oxygen (Lu=O), -phosphorus (Lu=P), and –carbon (Lu=C) multiple bonds. This project only lasted six months, but within this short time period, we successfully synthesized the first lanthanide complex featuring a phosphinidene functional group. As shown in Figure 1, reaction of the bis(alkyl) lutetium(III) complex $(PNP^{iPr})Lu(CH_2TMS)_2$ with 2,4,6-$Me_3$-$C_6H_2PH_2$ ($MesPH_2$) at 80°C resulted in the formation of the lutetium(III) phosphinidene complex as a red colored solid in 52% isolated yield. The $^{31}P\{^1H\}$ NMR spectrum ($C_6D_6$) for the diamagnetic phosphinidene complex exhibits a diagnostic pentet at δ 186.8 ppm coupled to a triplet at δ 18.1 ppm ($^2J_{P\text{-}P}$ = 14.6 Hz) consistent with two bridging phosphinidene units between two $(PNP^{iPr})Lu$ fragments.

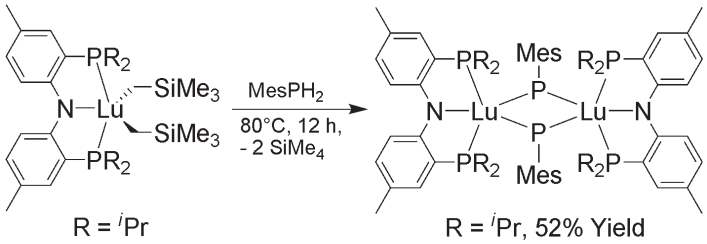


*Figure 1. Synthetic route for preparing the first lanthanide phosphinidene complex.*

The solid-state structure was determined and revealed an asymmetric $Lu_2P_2$ core (Figure 2) for the dimer of the terminal phosphine $(PNP^{iPr})Lu{=}PMes$. The Lu=P bond distances (2.6029(15) Å and 2.5976(14) Å), are shorter than the Lu-P bond distances reported for the few known lutetium phosphide complexes (Lu-$P_{ave}$ = 2.794 Å). This shortening is consistent with multiple bond character between the Lu and P atoms.

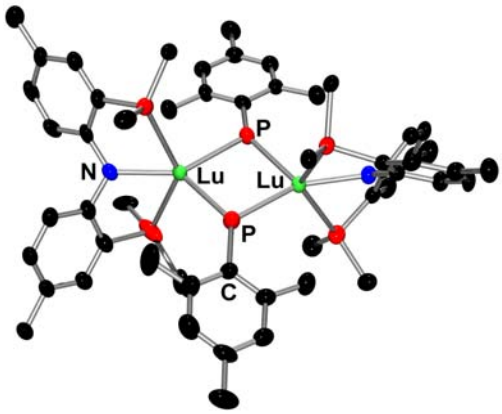


*Figure 2. Molecular structure of the lutetium phosphinidene dimer complex.*

Due to the electronic mismatch between the "hard" lanthanide and the "soft" phosphorus, these 4*f*-element compounds could become a platform for catalytic organophosphorus group-transfer processes and other C–P bond-forming reactions. In preliminary reactivity studies, the dimer complex breaks up and reacts like a terminal phosphinidene, transferring the organophosphorus group Lu=PR') to aldehydes and ketones to make phosphaalkenes, such as $R'P{=}C(C_6H_5)_2$ (Figure 3). This reactivity is similar to known nucleophilic transition-metal phosphinidene systems and suggests that it will be possible to prepare a stable terminal lanthanide phosphinidene for direct comparisons with actinide phosphinidene systems. For example, reaction of with pivalaldehyde affords *E*-MesP=C(H)$^t$Bu (48% yield, $^{31}$P NMR δ 227.1 ppm), and with benzophenone yields $MesP{=}CPh_2$ (72% yield, $^{31}$P NMR δ 234.0 ppm). Concomitant formation of $[(PNP^{iPr})LuO]_x$ is likely, but to date we have not been able to ascertain the fate of the lutetium by-product.

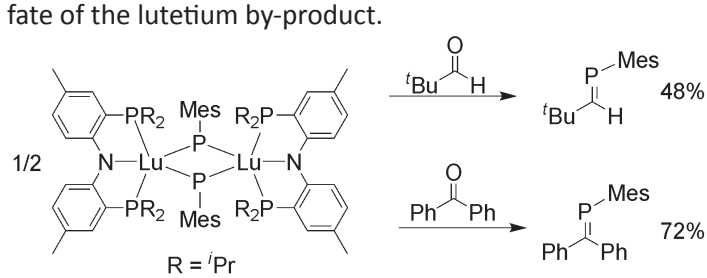


*Figure 3. Reactivity of the lutetium phosphinidene dimer complex with aldehydes (top) and ketones (bottom).*

Attempts to disrupt the dimer and stabilize a terminal phosphinidene using Lewis bases were unsuccessful ($PMe_3$, tmeda, DMAP, or bipyridines) or resulted in decomposition ($O{=}PMe_3$). Kinetic stabilization was also explored using the sterically demanding phosphine, 2,4,6-$^t$Bu$_3$-$C_6H_2PH_2$ ($Mes^*PH_2$). Reaction of a toluene-$d_8$ solution of the bis(alkyl) lutetium(III) complex $(PNP^{iPr})Lu(CH_2TMS)_2$ or $(PNP^{Ph})Lu(CH_2TMS)_2$ with $Mes^*PH_2$ at 80°C for 12 h resulted in quantitative formation of a phosphaindole as determined by $^{31}$P NMR spectroscopy (Figure 4). For transition-metals, the production of the phosphaindole signals the generation of a transient terminal phosphinidene complex, which reacts with a C-H bond on the Mes* *ortho*-$^t$Bu group to give the phosphaindole.

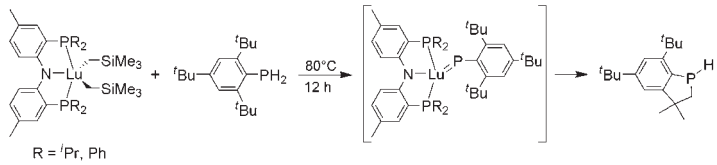


*Figure 4. Generation of a phosphaindole through a transient terminal phosphinidene intermediate.*

The first lanthanide complex featuring a phosphinidene functional group has been prepared and isolated. Although the large ionic radii of the lanthanide ions make it chal-

lenging to introduce enough steric saturation to stabilize a terminal phosphinidene, these results demonstrate that the formation of lanthanide phosphinidenes is possible and that the phosphinidene dimer behaves as a nucleophilic phosphinidene transfer reagent. This new class of molecules is anticipated to provide crucial information concerning the nature of and degree of covalency in Ln metal-ligand bonding, which will enhance our ability to develop 4*f*-5*f* element separations schemes for advanced nuclear fuel cycle and waste management efforts within the DOE complex. Efforts focused on stabilizing a terminal lanthanide-based phosphinidene complex by modifying both the supporting ligand and the substituent on the phosphorus atom will be future objectives in our laboratory.

## Publications

Masuda, J. D., B. L. Scott, K. C. Jantunen, and J. L. Kiplinger. Lutetium Alkyls Supported by a Dearomatized and Functionalized Terpyridine Ligand: Preparation of Fluorinated Anilide Complexes. 2008. *Organometallics.* **27**: 803.

Masuda, J. D., B. L. Scott, K. C. Jantunen, and J. L. Kiplinger. Synthesis, Characterization, and Reactivity of the Thermally Stable Lutetium Tris(alkyl) Complex (tBu2Bipy) Lu(CH2SiMe3)3. 2008. *Organometallics.* **27**: 1299.

Masuda, J. D., K. C. Jantunen, O. V. Ozerov, K. J. T. Noonan, D. P. Gates, B. L. Scott, and J. L. Kiplinger. A Lanthanide Phosphinidene Complex: Synthesis, Structure, and Phospha-Wittig Reactivity. 2008. *Journal of the American Chemical Society.* **130**: 2408.

# Environmental & Biological Sciences

continuing project

# High-Resolution Physically-Based Model of Semi-Arid River Basin Hydrology

*Everett Springer*

20061493DR

## Introduction

Computer simulation models are important tools to address water resources issues that confront today's society. These models allow a water resource manager to test "what if" type of questions and examine the response of surface and subsurface components of the water cycle. In simulating a river basin in regions that are arid or semi-arid, it is important to break the watershed into small parts to more accurately define the response in space and time. Los Alamos National Laboratory (LANL) has used its high performance computing capabilities to develop a hydrologic model of a semi-arid river basin. This model will represent land surface processes on the order of 100 meters providing information at a level of detail that has not been possible for larger river basins. The model will track the surface and subsurface components of the river basin water balance giving a more complete picture of the status of water resources. A key step is developing codes that can be used on parallel computers, which has not been done for large river basin simulations linking surface and groundwater. The parallel computer approach will be able to take advantage of the branching structure of river networks to allocate sections of the river basins to various processors available on the computer. Another contribution will be tools to estimate parameters required for the hydrologic model. The fine spatial grid will require soil properties be estimated for each location, which can number into the millions. We will use available data to train equations that can estimate hydrologic parameters using simpler and easier to obtain information. This approach has the advantage of being applicable to other types of hydrologic models. The model will be tested against observations on a river basin in New Mexico.

## Benefit to National Security Missions

This project will support the DOE missions in Scientific Discovery and Innovation and Environmental Responsibility by enhancing our capabilities to simulate complex environmental systems at resolutions where decision makers can determine impacts of issues such as increased thermoelectric power generation in a region.

## Progress

The newest sequential version of Triangular Irregular Network-(TIN) based Real-Time Integrated Basin Simulator (tRIBS) from New Mexico Tech University (NMT) was integrated with our parallel implementation. The major enhancement to tRIBS was the addition of a snow accumulation and melt routine that created new classes and modified other classes. New code was required for handling "runon" when running in parallel, ordering groundwater flux contributions for repeatable results, and updating of the restart mechanism. Problems were fixed when calculating the voronoi polygon information. An input option and code were added to write out results in binary for visualization. Currently, the NMT benchmarks of a single element (Peacheater basin, Small basin, Puerco basin, and Redondo basin) run correctly for multiple processor runs. The La Jara and Quemazon snow benchmarks have identified a potential bug in the parallel implementation that is being traced.

A critical objective of this project is to assess the importance of coupled surface and subsurface flow in semi-arid regions. To this end we leverage the strengths of two state-of-the-art simulation codes that have previously focused on either surface or subsurface flow. Specifically, state-of-the-art surface flow codes, such as tRIBS, are designed to handle large river basins with significant topographic features while interfacing well with geographic information system (GIS) data. However, the subsurface flow model in tRIBS is highly simplified. In contrast, state-of-the-art subsurface flow codes, such as Finite Element Heat and Mass (FEHM), are well suited for complex subsurface geometries and both saturated and unsaturated flow scenarios, but have either simplified or nonexistent surface flow.

After assessing the tRIBS and FEHM codes and relevant algorithms we determined that the best approach to coupling the codes was at the physical surface of the ground. Previous grid incompatibilities were corrected by adding a surface mesh capability in FEHM with simplified hydrologic routing. The FEHM code uses control volume finite element (CVFE) discretizations. This al-

lows the grid used in tRIBS to be represented exactly in FEHM and greatly enhances the mass conservation of the overall system. The LANL CVFE grid-building code Los Alamos Grid Toolbox (LaGrit), used in conjunction with FEHM, allows the common surface grid (tRIBS' triangular mesh) to be extended in a computationally efficient manner in the subsurface by insuring that the triangular surface mesh forms bases of three-dimensional tetrahedral elements that are then used to represent the subsurface volume. To correctly handle macropore flow correctly, a dual permeability capability was added to the Richards' Equation module in FEHM [1].

The Ponderosa Pine Hillslope site at LANL provides a unique setting in which to validate the tRIBS and FEHM codes through a detailed a detailed surface/subsurface modeling study. In particular, significant differences in snowpack depth and melt conditions at the Ponderosa site during the 1990s generated flow in to distinct regimes, namely dominant surface runoff during years with low snow pack, and significant lateral subsurface flow in years with high snow pack. In addition, the site is well characterized with core samples, infiltration rates, saturation profiles and runoff data [2, 3].

Using the core data and surface elevation data from the Ponderosa site [2], we built a solid earth model that honored the layered stratigraphy, and generated a mesh suitable for flow simulations in FEHM. Using estimates of the layer properties and uniform infiltration on the surface, preliminary simulations of unsaturated flow were conducted. This work positions us to proceed with the final model development, and to conduct calibration and uncertainty studies.

In collaboration with LANL, NMT collaborators began to develop a Ponderosa site specification for tRIBS. Using a similar subsurface stratigraphy, surface elevation data, vegetation maps, and stochastic rainfall they conducted preliminary simulations of surface run-off. This work is a key step in establishing a common model of the Ponderosa site for both FEHM and tRIBS, as well as demonstrating the feasibility of the study.

We continued to collect data for model forcing, model parameters, and model testing for the Rio Ojo Caliente Basin in New Mexico. The University of California at Irvine has generated a set of weather data for the southwestern U. S. on a 4 x 4 km grid [4], and we have extracted the data for the Rio Ojo Caliente. These data will be the model forcing data for our simulations. We are also looking for data to test our simulation results. The Global Land Data Assimilation System (GLDAS) provides distributed data from different land surface models at various resolutions. The highest resolution available is 1/8° for the MOSAIC land surface model, and in Figure 1, the number of cells from MOSAIC that overlay the Rio Ojo Caliente can be seen. Although these grid cells are large compared to the resolution of our models, they do provide us with some distributed data to check our simulations.

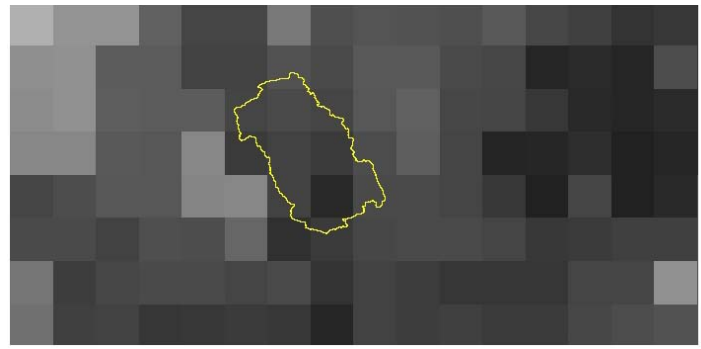

*Figure 1. Rio Ojo Caliente Basin overlaid on 1/8-degree grid cells for MOSAIC Land Surface Model to provide spatial data to check model performance.*

## Future Work

The completion of the benchmark simulations for the parallel version of tRIBS and a series of simulations demonstrating the effectiveness of the parallel implementation on a river basin will complete this parallelization task for this project. The test will involve developing a finer grid representation and simulating the basin response for a given period. We will examine changes in simulation time to determine the effectiveness of the parallel version.

The study of surface/subsurface coupling at the Ponderosa site drives our development of the two state-of-the-art tools, tRIBS and FEHM, towards a common interface at the earth's surface. In FEHM recent developments facilitate the use of a common surface triangulation; in addition, FEHM has a simple surface hydrologic routing capability. Thus, each code can simulate the surface/subsurface flow at the Ponderosa site. However, it is anticipated that the different inputs and resulting flow regimes will play to the strengths of one code versus the other. Thus, we plan to conduct calibration and uncertainty studies of the Ponderosa site for both tRIBS and FEHM independently, and then in a coupled state. Since the lateral subsurface flow is dominated by the flow through macropores [3], we plan to study the impact of the recently developed double-permeability model in FEHM on the calibration and uncertainty. During this work we will develop a common driver for both tRIBS and FEHM that will facilitate sequentially coupling these codes. Data transferred will consist of combinations of head data, saturation (moisture content), and water flux. We anticipate the strength of the surface/subsurface coupling to be different in the wet and dry years, and plan

to explore automatic adjustment of the time step size and the frequency of data passing.

The simulation of the period from 1996 – 2006 for the Rio Ojo Caliente Basin will be completed during the next year. The forcing data will be formatted for tRIBS and additional model parameters will be developed. Data for comparison of the model results will include snow cover, snow water equivalent, soil moisture, and streamflow. Soil parameters will be estimated with help from the Texas A&M collaborator.

## Conclusion

Water resources is a critical issue that confronts many regions of the United States. This effort will develop a tool that will allow simulations to be performed faster while providing more local information on water resources responses. This model will link surface and groundwater systems so a more complete understanding of a basin's water resources is given. Tools will be developed to supply information needed to run the model, and these tools will have applications to other modeling efforts such as weather prediction.

## References

Zyvoloski, G. A., B. A. Robinson, and H. S. Viswanathan. Generalized dual porosity: A numerical method for representing spatially variable sub-grid scale processes. 2008. *Advances in Water Resources.* **31** (3): 535.

Wilcox, B. P., B. D. Newman, D. Brandes, D. W. Davenport, and K. Reid. Runoff from a semiarid ponderosa pine hillslope in New Mexico. 1997. *Water Resources Research.* **33** (10): 2301.

Newman, B. D., A. R. Campbell, and B. P. Wilcox. Tracer-based studies of soil water movement in semi-arid forests of New Mexico. 1997. *Journal of Hydrology.* **196** (1-4): 251.

Li, J., X. Gao, and S. Sorooshian. Model performance of downscaling 1999-2004 hydrometeorological fields to the upper Rio Grande Basin using different forcing datasets. 2008. *Journal of Hydrometeorology.* **9** (4): 677.

## Publications

Dickinson, J. E., S. C. James, S. W. Mehl, M. C. Hill, S. A. Leake, G. A. Zyvoloski, and A. A. Eddebbarh. A new ghost-node method for linking different models and initial investigations of heterogeneity and nonmatching grids. 2007. Advances in Water Resources. 30 (8): 1722.

He, K., L. Zheng, S. Dong, L. Tang, J. Wu, and C. Zheng. PGO: A parallel computing platform for global optimization based on genetic algorithm. 2007. Computers and Geosciences . 33: 357.

Jana, R. B., B. P. Mohanty, and E. P. Springer. Multiscale pedotransfer functions for soil water retention. 2007. Vadose Zone Journal. 6 (4): 868.

Jana, R. B., B. P. Mohanty, and E. P. Springer. Bayesian neural networks for multi-scale soil hydraulic parameter estimation. 2008. Water Resources Research. 44 (8): 1.

Liu, Y., H. Gupta, E. Springer, and T. Wagener. Linking science with environmental decision making: experiences from an integrated modeling pproach to supporting sustainable water resources management, . 2008. Environmental Modelling and Software. 23 (7): 846.

Luo, Y., Z. Lei, L. Zheng, S. Yang, Z. Ouyang, and Q. Zhao. A stochastic model of soil water regime in the crop root zone. 2007. Journal of Hydrology . 335: 89.

Sviercoski, R. F., and B. J. Travis. Analytical effective coefficient for flow equations in porous media by homogenization theory. 2007. In III International Conference in Multiscale Materials Modeling. (Freiburg, Germany, 18-22 Sep. 2006). , p. 885. Stuttgart: Fraunhofer-IRB-Verlag .

Tartakovsky, D. M., A. Guadagnini, and B. Wohlberg. Machine learning methods for inverse modeling. To appear in VI International Conference on Geostatistics for Environmental Applications (geoENV 2006. (Rhodes, , Oct. 2006).

# Rapid Iterative Detection Using Smart Pathogen Signatures

*John Martin Dunbar*

20070010DR

## Introduction

Widespread dissemination of biological pathogens remains a catastrophic threat to humankind and rapid pathogen detection is critical to averting disaster. However, current autonomous detection approaches do not provide rapid detection with sufficient specificity to be of value, which is a critical breach in our nation's defense. To bridge this gap, we are creating a sensor platform that detects and identifies pathogens by rapidly and iteratively performing an assay decision tree based on smart pathogen signatures. This approach eliminates highly complicated microfluidics and parallel assays that inherently fail due to complexity, cross reactivity of reagents, and cost. To achieve this, we will use field gradient-based micromanipulation approaches to develop a programmable sample preparation platform using microspheres as both preparatory 'carrier' surfaces and multiplex assay components. This new preparation and assay approach will be combined with computationally designed 'smart signatures' to perform hierarchical sample interrogation, in which feedback from sample analysis is used to guide further interrogation. Finally, we will integrate our sample preparation and 'smart' assays with cutting edge miniature flow cytometry sensors to detect pathogens of critical importance to aerosol monitoring efforts. Creation and demonstration of this sensor approach will have far reaching impact in the fields of sample preparation and pathogen signature design. Completion of the project would directly fulfill LANL's mission by creating an innovative core sensor platform that will provide early warning of biological weapons and public health threats.

## Benefit to National Security Missions

Completion of the project would directly impact NNSA's threat reduction mission by creating a sensor platform that will provide early warning of biological weapons and public health threats. Furthermore, the basic science developed here will have impact in the fields of sample preparation and pathogen signature design.

## Progress

We advanced the delivery of our major product—an autonomous integrated biosensor—by 7 months and are on track to achieve this goal.

Specific Aim 1: Develop particle manipulation field gradient systems using functionalized and optically encoded microspheres for sample preparation and dynamic assay delivery.

For each process step, we evaluated almost all possible field manipulation techniques in isolated devices. This allowed us to down-select the best fields and devices for use in our prototype biosensor. For example, we successfully built acoustic lysis devices that will be appropriate for the biosensor. Conversely, we abandoned dielectric particle (DEP) positioning because substantial performance and device improvements would be required for practical use. Such field manipulation comparisons are complete for all anticipated process steps. Further, we progressed to validating required field manipulations in microfabricated prototype components (e.g. sample trapping and mixing chamber, lysis chamber) that will be assembled in the biosensor.

We have two very notable accomplishments. First, we developed a general acoustic approach to sample processing for pathogen detection that is adaptable to microfluidics and is capable of lysing cells, spores, and viruses (and demonstrated this in a very quantitative fashion). Lysing – the disintegration of a biological entity in order to analyze its contents – is a highly sought-after goal that will have impact throughout the microfluidic processing field. Second, we have developed an acoustic positioning device that uses square capillaries. This was of critical importance because our original cylindrical flow device for acoustic focusing, which won an R&D100 award in 2007, was ill suited to microfabrication. Square capillaries are compatible with microfabrication. Thus, we can now use acoustic positioning for sample analysis in a microfluidic format.

Specific Aim 2: Develop sets of pathogen signatures for target organisms to provide an iterative set of assays for use with detection platform efforts.

In this aim our technical progress has exceeded our goals. We developed a new type of assay— Multiplexed Oligonucleotide Ligation PCR (MOL-PCR)—to overcome limitations of conventional nucleic acid detection assays. Using this new assay approach, we computationally designed multiple nucleic acid signatures for detection of each of our 4 primary target pathogens, plus 3 additional respiratory pathogens desired by the New Mexico department of Health (NMDH). Some important elements of the computational work are described in a publication (Gans & Wolinsky, 2008). We tested and validated the detection assays with real aerosol samples obtained from the NMDH. We also developed complimentary immunoassays for 2 of the 4 pathogens and are now refining the performance of these assays prior to benchmarking. Deployment of immunoassays and MOL-PCR assays will demonstrate the flexibility of the biosensor platform and also enables detection of intact bacteria or flu virus as well as nucleic acid from lysed bacteria or flu virus. We are currently benchmarking performance of the pathogen detection assays with aerosol samples from the NMDH and are progressing to validating the detection assays with microfabricated components that will comprise the prototype biosensor.

Again, we would like to point out two very significant results. First, we developed a MOL-PCR signature set that can rapidly discriminate F. tularensis tularensis (the most virulent subspecies) from other closely related subspecies—a feat that has been difficult to achieve with conventional assay modalities. Furthermore, we have demonstrated improvements in detection of degraded samples by MOL-PCR, as compared to conventional amplification techniques, which is important because most environmental samples show significant nucleic acid degradation.

Specific Aim 3: Integrate particle manipulation with sensors and process control to create a prototype detection platform to perform assays using smart signatures on pathogens of interest.

Integration of biosensor components with sample assays and development of a control system is proceeding on schedule. We successfully fabricated prototypes of each of the 4 process components needed for the biosensor. Fabrication and basic testing of each component (with microspheres, spores, vegetative cells, virus particles, and protein or DNA) involved multiple iterations (e.g. Figure 1) to achieve acceptable performance characteristics. The most complex component—the thermal cycling unit for nucleic acid detection assays—is in the final stages of iteration and testing. We are progressing to validating performance of each component with representative samples.

The optical detector module is in the final stages of assembly. The general architecture of the prototype biosensor is established (Figure 2). We have a test version of the control software to drive pumps, valves, data acquisition, and iterative sample interrogation. System requirements for power, frequency modulation, and control circuitry are straightforward. We are progressing to fabrication of a custom circuit board for system control.

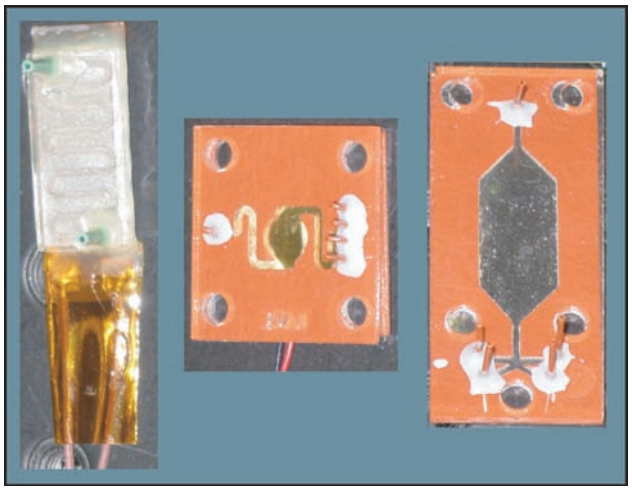

*Figure 1. Fabricated trapping chambers. These are examples of the major versions of fabricated chambers tested for use in the prototype biosensor. Similar design iterations occured for other components of the biosensor.*

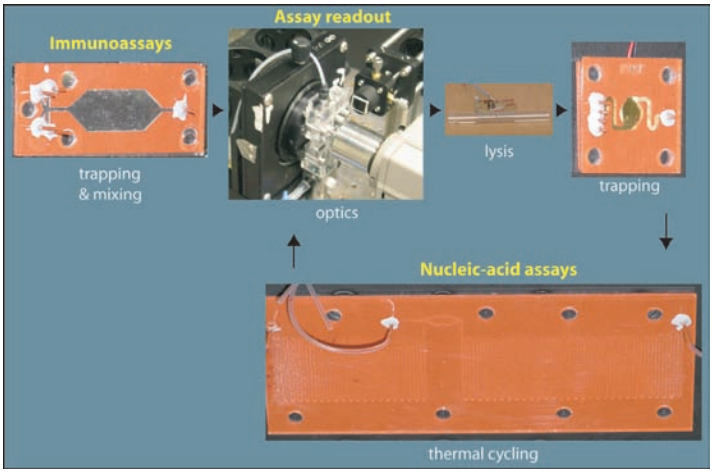


*Figure 2. Biosensor components. The prototype biosensor will contain 4 microfabricated components, as shown, to perform different steps in sample processing and interrogation. The optical detector to readout the results of immuno and nucleic acid detections assays is shown and is in the final stages of assembly and testing. The pump, valves, and tubing to connect the components, and deliver samples and reagents are not shown. The control circuitry (not shown) and software to operate the prototype biosensor are being completed.*

## Future Work

Despite immense national investment in autonomous pathogen sensors, the lack of robust fieldable pathogen detection remains a glaring weakness in the nation's defense against biological weapons. This weakness traces to the use of complex microfluidics and impossibly parallel biochemical assays.

To solve this issue, we are developing technologies to create a robust sensor platform for miniature autonomous pathogen detection. This platform combines force based particle micromanipulation approaches (acoustic, dielectrophoretic and magnetic), with flow cytometry sensors, and assays that use 'smart' pathogen detection signatures. This platform will use a feedback-driven control system based on environmental input and assay results to automate sample preparation, assay chemistry and detection using recursive serial application of a hierarchical decision tree approach. We will demonstrate automated detection of pathogens of concern in aerosol form, including B. anthracis spores and cells, F. tularemia, Y. pestis and influenza virions.

To accomplish our overall goal we have three primary deliverables that are completed or schedule for completion.

**FY2007 and FY2008**

1. An automated field-based sample preparation system.
2. A minimal set of smart pathogen signatures for our organisms of interest.

These goals have been completed.

**FY2008 and FY2009**

1. A prototype demonstration system that weds the sample preparation unit with low cost miniature flow cytometry sensors to perform rapid iterative pathogen assays using a decision tree process.

Success in this final step will be determined as follows:

The system and signatures will be combined to create a prototype system that can detect the test organisms in less than one hour by programmably and autonomously performing immunoassays and nucleic acid assays in fewer than 5 and 15 minutes, respectively.

## Conclusion

This project will develop the technologies to create functional fieldable autonomous sensor systems to detect biological threats. The technologies under development (force-based particle manipulation, microflow detection and pathogen detection signature design) will minimize the need for complex microfluidic circuits and result in robust autonomous sensor systems critical to the nations defense. Once our sensor systems are developed we will integrate our autonomous sample preparation and 'smart' assays to create a system to detect pathogens of critical importance to aerosol monitoring efforts. As such, this effort will directly improve our nation's defense against biological weapons of mass destruction.

## References

1. Gans, J. D., and M. Wolinsky. Improved assay-dependent searching of nucleic acid sequence databases. 2008. *Nucleic Acids Research.* **36**: e74.

## Publications

Gans, J. D., and M. Wolinsky. Genomorama: genome visualization and analysis. 2007. *BMC Bioinformatics.* **8**: 204.

Gans, J. D., and M. Wolinsky. Improved assay-dependent searching of nucleic acid sequence databases. 2008. *Nucleic Acids Research.* **36**: e74.

Habbersett, R. C., M. A. Naivar, T. A. Woods, G. R. Goddard, and S. W. Graves. Evaluation of a green laser pointer for flow cytometry. 2007. *Cytometry Part A.* **71A**: 809.

Mark, J. A., L. D. Green, A. Deshpande, and P. S. White. System integration and development for biological warfare agent surveillance. 2007. *Proceedings of the SPIE.* **6540**: 6540D1.

Naivar, M. A., J. D. Parson, M. E. Wilder, R. C. Habbersett, B. S. Edwards, L. Sklar, J. P. Nolan, S. W. Graves, J. C. Martin, J. H. Jett, and J. P. Freyer. Open, reconfigurable cytometric acquisition system: ORCAS . 2007. *Cytometry Part A.* **71A**: 915.

# A Systematic Strategy for Gene Function Discovery

*Clifford Jay Unkefer*

20070029DR

## Introduction

The most profound outcome of the large-scale genome sequencing effort is the revelation of how little is known about the functions of a very large fraction of genes in every organism sequenced to date. In fact, the fraction of the human genome that has not been assigned function is the same now as when the human genome project began. Even in Escherichia coli K12, our most comprehensively studied bacterium, a fully annotated function cannot be assigned to 43% (1873 of 4359) of its protein-encoding genes. Significantly, there is no functional information for a large fraction (48%) of protein-encoding genes in both A/B listed pathogens and bacteria central to DOE's Genomics:GTL research program. Yet, sequence comparisons have established that most of these genes of unknown function are conserved in hundreds of other organisms, indicating that they have been maintained through evolution and must serve essential functions. We are developing a systematic strategy to discover the function of unknown genes. In contrast to previous efforts that focused on single genes or proteins, we propose a systematic approach to function discovery that utilizes the functional relatedness inherent in the regulation and operation of biochemical pathways. Our approach requires the development of a high throughput screen for identifying the small effector molecules that bind to transcription factors and regulate gene transcription. These effector molecules provide insight into the function of the genes they regulate.

Transcription Factors - Gene transcription, the first step in protein expression, is catalyzed by RNA polymerase that reads along the DNA sequence. Transcription factors are a class of proteins that bind DNA and act in the cell to regulate – that is, turn on or off – the transcription of groups of functionally related genes in a regulon. Genes that encode for transcription factors can be easily recognized based on sequence analysis and identification of the helix-turn-helix motif characteristic of the DNA-binding domain. The binding of the transcription factor to DNA is modulated by the concentration of an effector molecule, which is often a product or substrate of the biochemical pathway encoded by the regulon. When the concentration of the effector is high, the effector/transcription factor-binary complex predominates in solution; the binary complex has high affinity for a specific DNA sequence upstream of the transcribed genes and binding of the binary complex to this site on the DNA blocks RNA polymerase and gene transcription. In this example, the transcription factor acts as a repressor of transcription; in other cases transcription factors can act as activators. Because transcription factors can be identified by their characteristic sequences and they function by binding effectors molecules that are part of the regulated biochemical pathway, transcription factors are a springboard for systematic discovery of the function of all members of a regulon.

## Benefit to National Security Missions

This project directly supports the DOE Office of Science missions in bioenergy by enhancing our understanding of organisms involved in biomass conversion, biofuel synthesis, carbon sequestration, and bioremediation. In addition, this project will provide underpinning science in support of DOE/NNSA and DHS biothreat reduction missions.

## Progress

Our most important progress this year was the development of a Frontal Affinity Chromatography Mass Spectrometry (FAC-MS) approach that rapidly identifies transcription factor (TF) effectors and quantifies their binding to their target transcription factor. In our FAC-MS-based TF effector screening technique, a purified TF is biotinylated and immobilized on avidin-coated beads and packed in a small column. A mixture of potential ligands is continuously infused through the column and into the electrospray mass spectrometer. Molecules in the mixture that do not bind to the immobilized protein immediately elute in the void volume of the column. Active ligands bind to the immobilized protein until the capacity of the column is reached, at which point their

concentrations will increase to their infusion concentrations. The breakthrough volume of bound ligands is related to the protein/ligand binding affinity with tighter binding ligands eluting at larger breakthrough volumes (longer times). Because detection is by mass spectrometry, we can detect ligands at very low concentrations (nM) and obtain structural information on the retained ligands. We use an electrospray Fourier transform mass spectrometer (FTMS) to detect compounds because it measures m/z with ppm accuracy, which allows us to predict the molecular formulae of bound ligands to facilitate their identification. The technology allowed us to discover a set of metabolite effectors that bind to an individual TF. The elution profile for a set of potential effectors for the transcription factor metJ demonstrated binding of several metabolites in the methionine biosynthesis pathway. Adenosine monophosphate (AMP) does not bind to metJ and its elution profile is representative of compounds with low or no affinity for metJ. S-adenosyl methionine (SAM) is known to be an effector for metJ. Our data confirm that SAM binds to metJ. Interestingly, structural analogues of SAM, including S-adenosyl cysteine, S-adenosyl homocysteine, and thiomethyl adeosine, bind to metJ with similar affinity. Sets of metabolite effectors for a single TF were not observed previously because of the lack of an appropriate screening technology. Because structurally related metabolites are often metabolically related compounds as is the case for SAM, S-adenosyl homocysteine, and thiomethyl adeosine, these data will yield important information for gene function discovery.

## Future Work

DNA sequencing has yielded over 440 complete genome sequences of microorganisms. The most profound outcome of this large-scale genome sequencing effort is the revelation that we do not know the function of a very large fraction of the sequenced genes. Gaining clear understanding of the function of the proteins that are encoded by these genes is the next essential goal in achieving a complete understanding of cellular function. Through bioinformatic techniques, stretches of genomes are identified as hypothetical genes or open reading frames (ORFs) that encode proteins. In all sequenced bacteria, the group of homologous ORFs with no assigned function comprises a large fraction (25-45%) of the genome. The fact that sequence homologs have been identified in hundreds of other genomes provides evidence that these ORFs are genes with important functions. For these proteins to be developed as potential targets for broad-spectrum therapeutics or to be exploited for energy production or climate stabilization, detailed functional analysis is essential. In contrast to previous efforts that focused on single genes or proteins, we have developed a systematic approach to function discovery that utilizes the functional relatedness inherent in the regulation and operation of biochemical pathways. We capitalize on the functional significance of transcription factor effectors and the functional relationships of coordinately regulated genes. Characterizing transcription factors will guide our subsequent discovery of the functions of the genes in their respective regulons. We will study the E. coli homologs by producing significant quantities of each encoded protein and use them as ligands on an affinity column with mass spectrometry detection to identify the small metabolites they bind; these metabolites will be potential effectors of the TFs and later the substrates, products and cofactors of enzymes within the pathway. These data will allow assignment of function.

## Conclusion

We will develop and perfect a novel approach to discovery of gene function and will apply this approach to study genes of unknown function from pathogenic and important environmental bacteria. We expect to discover new metabolic pathways, energy transduction mechanisms, regulatory networks and signaling cascades in environmental bacteria that can be manipulated for advancing production of sustainable energy sources and control of global greenhouse gas cycles. In pathogens, we expect to find virulence and antibiotic resistance factors and targets for the next-generation of antibiotics to be used in the fight against man-made or natural health threats.

## Publications

Fox, D. T., K. Hotta, C. C. Browder, C. Kim, P. J. Unkefer, C. J. Unkefer, and A. T. Koppisch. Biosynthesis of the 3,4-Dihydroxybenzoate Moieties of Petrobactin by Bacillus Anthracis. 2008. : NWRM.

Koppisch, A. T., K. Hotta, D. T. Fox, C. E. Ruggiero, C. Kim, T. Sanchez, S. Iyer, C. C. Browder, P. J. Unkefer, and C. J. Unkefer. Biosynthesis of the 3,4-dihydroxybenzoate moieties of petrobactin by Bacillus anthracis. 2008. **73** (15): 5759.

Mu, F., R. F. Williams, C. J. Unkefer, P. J. Unkefer, J. R. Faeder, and W. S. Hlavacek. Carbon-fate maps for metabolic reactions. 2007. **23** (23): 3193.

continuing project

# Host-Pathogen Interactions (Pathomics) in Avian Influenza

*Ruy Miguel Ribeiro*

20070099DR

## Introduction

A pandemic of human H5N1 avian-like influenza could cause many millions of deaths worldwide. We urgently need to understand influenza's potential for human infection, human-to-human transmission, and severity of disease (the "phenotype"). Unfortunately, the knowledge to make these predictions does not exist. We address this deficiency by innovatively combining experimental analyses of molecular markers with new computational tools ("the functional profile"), to ascertain the genomic basis of differences in phenotypes among diverse influenza strains. We are accomplishing this by developing assays based on in vitro infection with different strains of influenza, and searching for host genetic markers in the response to such infections that distinguish between virulent strains and less virulent ones.

Our comparative approach, studying multiple influenza strains, is innovative because we are combining theoretical and experimental tools to the problem of predicting, in a complex system, the outcome of infection. However, this is a high risk scientific goal, because the existence of predictive markers is not a given. However, the potential to develop the knowledge and tools necessary to predict the pandemic potential of any influenza virus is crucial scientific objective, which was validated by our internal and external reviewers during our mid-project review. Moreover, our results will have significant implications for understanding genomic-phenotype relations in other pathogens.

## Benefit to National Security Missions

This project supports the DOE mission in Threat Reduction by lowering the threat from biological weapons of mass destruction, and also the mission of Harnessing the Power of the Living World, as stated by the Office of Science Strategic Plan, by defining and predicting what makes (influenza) viruses pathogenic.

## Progress

We have now completed a set of experiments infecting primary human upper airway epithelial cells, which are the primary site for attachment of influenza A virus, with A/Hong Kong/486/97 (H5N1), RSV (another RNA virus), and appropriate controls for 0, 8, and 24 hour at a low multiplicity of infection. The mRNAs induced by these infections were analyzed by commercial genome microarrays. This work indicated the possibility of the following genes as putative markers for early and high pathogenicity H5N1-specific infection: genes induced by interferons (e.g., IFI, G1P, MX, OAS); chemokine genes (e.g., CXCL, CCL); inflammatory cytokines (e.g., IL1α/β); and anti-viral serum amyloid proteins (e.g., SAA1-4). These results will be confirmed with further experiments (see below). In a parallel approach, we completed a large set of infection experiments of A549 human epithelia cells using influenza strains (A/HK/483/97 (H5N1 – high pathogenicity), A/Sydney/5/97 (H3N2 – medium pathogenicity), A/Beijing/262/95 (H1N1 – medium pathogenicity), and B/Harbin/07/94 (low pathogenicity)) that represent high, medium and low virulence levels. Infected A549 cell samples were collected for two different infection doses (multiplicity of infection of 1 and 4) and six different time points with each influenza strain. Subsequently mRNA expression analysis of 24 host marker candidate genes was conducted on all infection samples along with full controls, using quantitative real time polymerase chain reaction (RT-PCR). We have performed an additional set of infections with a different H3N2 virus to compare variation of gene response within the same subtype of influenza. Further mRNA measurements were done on a second round of experimental in vitro infections with other highly pathogenic viruses A/Vietnam/1203/2004 and A/HK/156/1997. We have also acquired and performed infections with a low pathogenic H5N1 strain (A/Hong Kong/486/97), which is a crucial control for the high pathogenic H5N1 strains. The mRNA from these latter experiments will be processed shortly. All H5N1 infections were done at Lovelace Respiratory Research Institute under Biological Safety Laboratory 3 – BSL3 – conditions.

One of the most novel aspects of this project is the production of truly dynamical time course of cellular infection and genomic expression. The analysis of this type of data is challenging and we are developing permutation/computational methods to analyze this quantitative mRNA expression data. We extended our previous (see last year's report) dendogram clustering analyses and heat maps of gene expression of influenza infection to include data on H5N1 infection at different time points (Figure 1). It is already clear, even in this preliminary analysis, that H5N1 has a different expression profile from other strains. After identifying informative host genes, we are now mapping them onto their respective pathways, to model the gene networks specific to influenza infection. We have availed ourselves of a commercial platform developed by Ingenuity Systems to analyze the relevant pathways identified by genes with altered expression during influenza infection. We will study any differences in pathways involved in low and high virulence influenza infection.

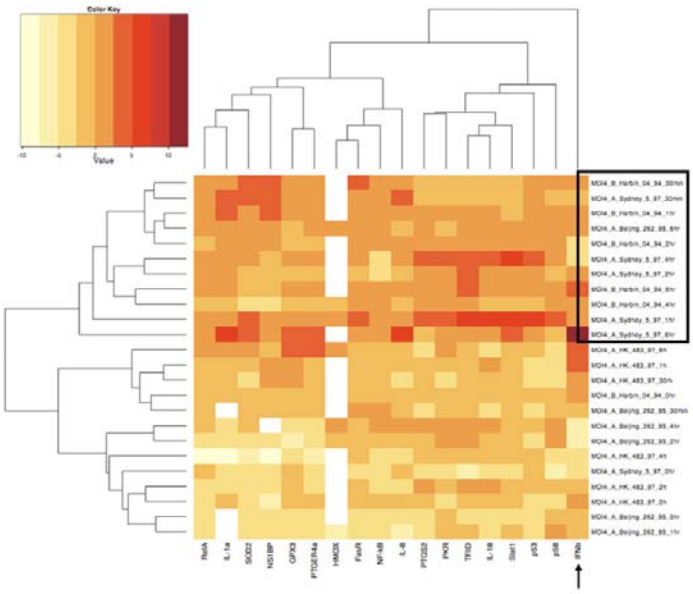


*Figure 1. Clustering of the expression (by RT-PCR) of selected genes after in vitro infection with different influenza strains. Note the clearly stronger expression caused by highly pathogenic H5N1 influenza (highlighted by the box at the top left) compared to H1N1 and H3N2 influenza. The arrow at the bottom indicates the expression of IFNbeta, an important immune response gene, which behaves differently than the other genes.*

The most important genes identified by the theoretical and pathway analyses are the targets for an automated gene discovery processing. The objective of this analysis is, given a target protein, to identify proteins with a similar set of functions. That is, we use information available in public databases (from literature and experimental results) to better characterize the biological function of the genes identified during our work. This is automatically accomplished by BIOGRAM (Biological Graph Metrics), a novel software interface being developed by us to search protein annotations in the Gene Ontology database. An initial version of BIOGRAM was used to score the ~20 proteins in the RT-PCR studies above against a database of ~14,000 human proteins.

Single amino acid changes in the viral genome can have dramatic changes on the influenza viral phenotype. However, those single amino acid changes that have been identified as having effects on phenotype seem to be dependent on the genotypic context in which they occur. We, therefore, believe that it is important to study the interactions and coupling between genotypic changes. In particular, we are interested in the conditions that promote reassortment among the gene segments. We have developed rigorous statistical and computational methods for predicting variation at coupled sites. Our preliminary studies have suggested some functional interactions in the influenza viral nucleoprotein, which may be important for viral fitness.

Non-structural protein 1 (NS1) of influenza A virus is required for virus replication. To better understand the functional role of this molecule, we have engaged in the development of a structural model for the NS1 protein dimer, which is its natural configuration. Based on our model, we have predicted residues important for intermolecular interactions. Moreover, our protein modeling allowed us to discover that there exist similarities between the domain structures of the NS1 protein and host (human) signaling molecules, even though there is a lack of sequence homology. Thus, these similarities could have not been found by sequence analysis. For influenza virus, the minimal replication unit, the viral ribonucleoprotein (vRNP) complex, is comprised of the three-polymerase proteins PB2, PB1, PA and the nucleoprotein NP. A low-resolution structure of the influenza virus polymerase complex by electron microscopy has been published [1]. We are collaborating with those authors to develop a new structure for the NP complex with the observed 9-fold symmetry. We found that a single-stranded RNA in left handed helical conformation wraps around the NP 9mer complex (Figure 2). We are now modeling the structures of the full complex, including PB2, PB1 and PA.

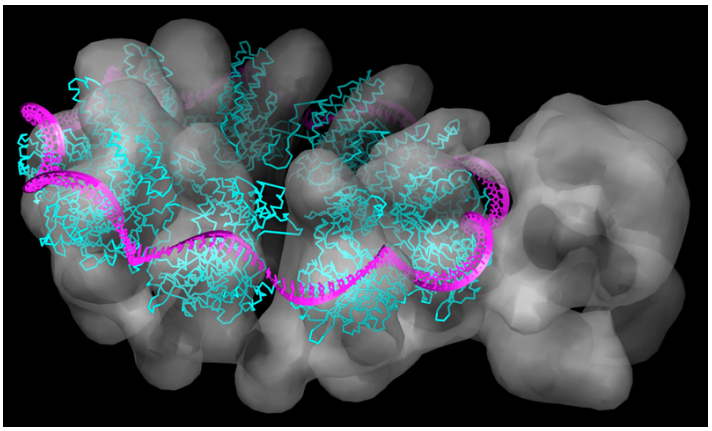

*Figure 2. A low-resolution structure of influenza viral ribonucleoprotein (vRNP) indicated a 9-fold symmetry (shown in the electron microscopy density). We have developed the structure for the NP complex with this 9-fold symmetry (cyan). We then modeled the structure of a single-stranded RNA in left-handed helical conformation wrapped around the NP 9mer complex (magenta).*

At the cellular level, we have developed new models of viral dynamics and are applying them to model in vitro infection (Figure 3). This allows us to estimate critical parameters of viral infection, such as clearance rate and infection rate, and understand the lifecycle of influenza.

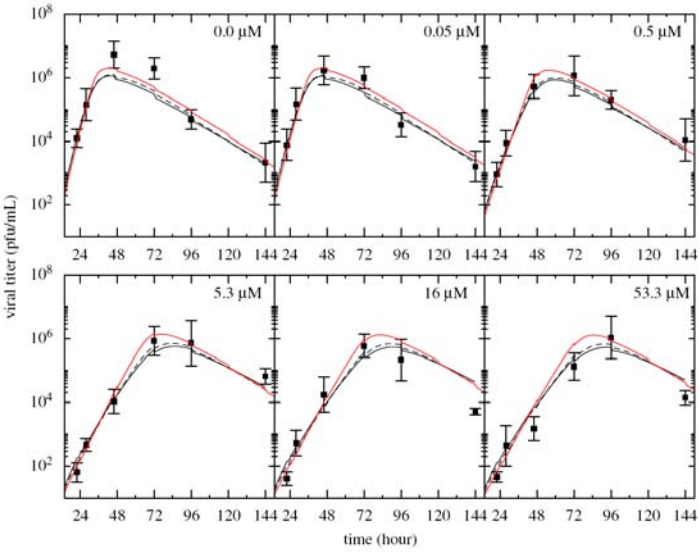


*Figure 3. We have modeled the infectious viral loading in an in vitro infection system, as predicted by three different models of the influenza life-cycle (solid, dashed and red lines).The experimental data (squares) are from experiments performed on MDCK cells at various drug dosages, with each panel corresponding to a different drug concentration.*

We have also studied quantitatively the epidemiology of H5N1 influenza, as well as that of other influenza subtypes. We have developed new methods to quantify transmission parameters, and detect and characterize influenza epidemiology in real time. This may allow to track the changes of an emerging strain, as it mutates and becomes transmissible between humans. (This work resulted in a news story featured in the May 29 edition of The Santa Fe New Mexican: "Scientists examine new way to track outbreaks" by S. Vorenberg.)

## Future Work

We developed a detailed experimental plan to conduct the experiments that are needed to complete our work. This was done taking into consideration the feedback provided by the mid-term review with internal and external reviewers. We are going to finalize the infection experiments with H3N2, H1N1, and H5N1 (low pathogenic) strains of influenza in primary human upper airway epithelial cells for microarray analyses. We are also finishing the infections under BSL3 conditions (at Lovelace) using diverse H5N1 strains in A549 cells. The mRNA of these infections will be analyzed by RT-PCR (and possibly a custom in-house developed microarray). Finally, we will repeat some of the crucial experiments to assess reproducibility.

We will then use the computational techniques that we have been studying to analyze all the data together, looking for the detection signatures of early infection and of pathogenicity. BIOGRAM will be an integral part of this analyses and its continued development is crucial to help us generate new hypotheses for future work. We are also working to integrate our within host approach with our epidemiological results.

## Conclusion

Infectious diseases, such as influenza, kill many thousands of Americans every year, and millions of people worldwide. Understanding how microbes cause disease and which molecular processes influence the severity and virulence of a given pathogen are crucial steps in our attempts to control the devastation caused by infectious diseases. Our work integrating molecular /cellular experiments with state-of-the-art computational and theoretical tools will represent an important step to find the determinants of pathogenicity for human and avian influenza viruses. Continuation of this work will also allow a new paradigm for studying other important human infections, with the aim of developing improved medical diagnosis and interventions.

## References

1. Area, E., J. Martin-Benito, P. Gastaminza, E. Torreira, J. M. Valpuesta, J. L. Carrascosa, and J. Ortin. 3D structure of the influenza virus polymerase complex: localization of subunit domains. 2004. *Proceedings of the National Academy of Sciences of the USA.* **101** (1): 308.

## Publications

Beauchemin, C. A., J. J. McSharry, G. L. Drusano, J. T. Nguyen, G. T. Went, R. M. Ribeiro, and A. S. Perelson. Modeling amantadine treatment of influenza A virus in vitro. 2008. *J Theor Biol.* **254** (2): 439.

Bettencourt, L. M., R. M. Ribeiro, G. Chowell, T. Lant, and C. Castillo-Chavez. Towards real time epidemiology: data assimilation, modeling and anomaly detection of health surveillance data streams. 2007. In *2nd NSF Workshop, Biosurveillance, 2007.* (New Brunswick, NJ, 22 May 2007). Vol. 4506, p. 79. Heidelberg: Springer-Verlag Berlin.

Bettencourt, L. M., and R. M. Ribeiro. Real time bayesian estimation of the epidemic potential of emerging infectious diseases. 2008. *PLoS ONE.* **3** (5): e2185.

Chowell, G., H. Nishiura, and L. M. Bettencourt. Comparative estimation of the reproduction number for pandemic influenza from daily case notification data. 2007. *J R Soc Interface.* **4** (12): 155.

Chowell, G., L. M. Bettencourt, N. Johnson, W. J. Alonso, and C. Viboud. The 1918-1919 influenza pandemic in England and Wales: spatial patterns in transmissibility and mortality impact. 2008. *Proc Biol Sci.* **275** (1634): 501.

Gabbard, J., N. Velappan, R. Di Niro, J. Schmidt, C. Jones, S. Tompkins, and A. Bradbury. A humanized anti-M2 scFv shows protective in vitro activity against influenza. *submitted.*

Zeytun, A., J. C. van Velkinburgh, P. E. Pardington, R. R. Cary, and G. Gupta. Pathogen-specific innate immune response. 2007. *Advances in Experimental Medicine and Biology.* **598**: 342.

# One-Step Biomass Conversion: Looking to Nature for Solutions to Energy Security

*Paul Alfred Langan*

20080001DR

## Introduction

We plan to revolutionize the cost and efficiency of lignocellulosic biomass conversion to sugar. Such a revolution requires a scientific breakthrough, and we look for this breakthrough in nature. We will capture the degradation strategies of the fungi that degrade lignocellulosic biomass. These organisms employ a variety of novel enzymes and cofactors. Our challenge is to optimize these approaches towards industrial application in an accelerated and consolidated biomass conversion process.

## Benefit to National Security Missions

This project will support DOE missions in energy security by dramatically reducing our dependence on imported oil and bring us closer to a carbon neutral fuel cycle.

## Progress

In our Bioreactor and Mass Spectrometry thrust we have cultured P. chrysosporium on poplar at both USDA FPL and LANL. Extracted samples have been subjected to whole degradome surveys at different time points using both GCGC-TOF and FT mass spectrometers. This was aided by establishing a list of compounds identified (~80) and generating spectral libraries of isolated standards for these compounds.

In our Microscopy thrust we demonstrated fluorescence, Raman, and scanning electron microscopy, and microtome procedures developed to prepare our samples. P. chrysosporium has also been cultured at LANL so that its degradative effects can be studied in real time.

In our crystallography thrust X-ray and neutron data have been collected from cellulose and poplar biomass at the Advanced Photon Source at ANL, the ILL and CERMAV in France, and Toledo University. Further proposals for experiments have been accepted for the APS and the ILL that involve an allocation of beam time to this project with a value of around $400K.

In our theory thrust a coarse-grained description of cellulose assembly as a H-Bonding network has been developed. All-atom Replica Exchange Molecular Dynamics simulations of Cellulose oligomers and assembly have been carried out. Large-scale simulations of cellulose micro-fibrils with degrading enzymes have been designed, and we are applying for time on large high performance computers.

In our Protein Science thrust we have formed a collaboration with the group led by Debra Dunnaway-Mariano at the University of New Mexico in order to make more rapid progress. David Fox has been recruited to lead the reorganized LANL part of that collaboration, and has already made significant progress in establishing and testing enzyme assays.

We are on target to meet all project milestones. We have also successfully undergone a first year review of the project. In addition we have presented our results at a number of conferences and have given a number of invited talks. We are also active in writing additional grants and working with program managers towards transition to programmatic funding.

## Future Work

We plan to reverse-engineer the key degradation mechanisms of white rot fungi and optimize them for industrial application in biomass conversion to sugar. In particular this will involve investigating how mediator and mediator-enzyme interactions are used in the initial lignin degradation strategies of fungi and combine them, for the first time, with industrial cellulases to create an accelerated, consolidated biomass conversion process.

Our research plan has been organized into three goal-oriented, but interdependent, sections that address the following three major objectives:

1. Define the key metabolites/mediators/cofactors and enzymes in the fungal degradation of biomass.

2. Characterize the detailed interaction of important metabolites and enzymes with biomass.

3. Combine metabolites with enzymes in a consolidated biomass conversion process.

**Deliverables and Schedule**

We are on track with respect to our proposed schedule of deliverables, which include:

- Culture in the laboratory the Fungal Bioreactor (Years 1-3)
- Carry out Mass Spectroscopy of Degradome (Years 1-3)
- Carry out Spectroscopic Measurements of Bulk Biomass during degradation (Years 1-3)
- Identify key enzymes in degradation (Year 1-2)
- Build, parameterize and simulate atomic models of cell wall components (Year 1)
- Develop a model for identifying key metabolites in the degradome (Year 2)
- Determine the role and relationship between metabolites and enzymes (Year 2-3)
- Carry out structural and spatial measurements of biomass and its degradation (Years 1-3)
- Carry out scattering and diffraction measurements of biomass and its degradation (Years 1-3)
- Extend structural models of cell wall to larger length scales (Year 2-3)
- Develop a model for structural inference of roles of key metabolites and their interactions (Year 3)
- Develop first generation enzyme cocktails for biomass degradation (Year 3)

Our expected accomplishments include characterization of the crucial elements of the fungal-biomass degradome, identification of key metabolites and enzymes in biomass conversion, characterization of the detailed interaction of key metabolites and enzymes with biomass, and development of enzyme and metabolite cocktails for accelerated biomass conversion

## Conclusion

Biofuels are an alternative to conventional energy sources, promising to increase our Nation's energy security by dramatically reducing our dependence on imported oil. They are also better for our environment because they do not introduce fossil carbon into the atmosphere, increasing the greenhouse gas load. Currently, our Nation's bioethanol industry is largely based on the use of starch in grains such as corn that are also needed for food, with the potential to drive up food prices. Biomass, the inedible fibrous material from wood and plant stems, is an abundant alternative source. This project is focused on bringing about the revolution in cost and efficiency of biomass conversion needed to make bioethanol from biomass an economic reality, benefiting our security and our environment.

## Publications

Nishiyama, Y., G. Johnson, A. French, T. Forsyth, and P. Langan. Neutron crystallography, molecular dynamics, and quantum mechanics studies of the nature of hydrogen bonding in cellulose Ib. 2008. *Biomacromolecules.* **9**: 3133.

Nowak-Lovato, K., and K. Rector. SERS Nanosensors for whole cell pH imagery. *Applied Spectroscopy .*

Shary, S., A. Kapich, E. Panisko, J. Magnuson, D. Cullen, and K. Hammel. Differential expression in Phanerochaete chrysosporium of membrane-associated proteins relevant to lignin degradation. To appear in *Applied and Environmental Microbiology.*

Shen, T., and G. Gnanakaran. The stability of cellulose: A perspective from the statistical mechanics of hydrogen bond networks. To appear in *Biophysical Journal.*

Wada, M., L. Heux, Y. Nishiyama, and P. Langan. X-ray crystallographic, scanning microprobe X-ray diffraction, and cross-polarized/magic angle spinning 13C nuclear magnetic resonance studies of the structure of cellulose III(II). To appear in *Biomacromolecules.*

Wada, M., L. Heux, Y. Nishiyama, and P. Langan. X-ray crystallographic and cross-polarized/magic angle spinning 13C nuclear magnetic resonance studies of the structure of the complex of cellulose I with EDA. *Biomacromolecules.*

Wada, M., Y. Nishiyama, H. Chanzy, T. Forsyth, and P. Langan. The structures of cellulose. 2008. *Powder diffraction.* **23** (2): 92.

Wada, M., Y. Nishiyama, H. Chanzy, T. Forsyth, and P. Langan. The structures of celluloses. 2008. *Advances in X-ray Analysis.* **51**: 138.

# Flash before the Storm: Predicting Hurricane Intensification using LANL Lightning Data

*Christopher Andrew Munn Jeffery*

20080126DR

## Introduction

In the wake of the devastating 2005 hurricane season, government agencies, scientific boards and advisory panels have unanimously called for urgent increases in hurricane research and improvements in hurricane forecast accuracy. In coordination with this national agenda, our LDRD project has the following high-profile science & technology objectives:

1. Instrument oil platforms in the northern Gulf of Mexico with LANL's unique 3D total lightning mapping system, capable of remotely probing the violent and opaque hurricane eye-wall.

2. Discover and quantify the dynamics and convective structure of the hurricane eye-wall region as revealed for the first time in the 3D spatial structure, intensity and evolution of the lightning data.

3. Develop a new hurricane model that assimilates this real-time knowledge of eye-wall convective strength, and demonstrate a 50% improvement in 48-hour intensity (wind speed) forecast errors.

The great relevance and timeliness of these objectives is central to the potential impact and high-potential science of this project; our project aligns not only with LANL's "predicting emerging environmental threats" Grand Challenge and energy security priorities, but also with (i) a recent National Science Board report calling for a new national hurricane research initiative; (ii) a recent NOAA science advisory board report advocating "novel methods for data assimilation founded on improved observations of the hurricane". Additionally, the new dual VLF-VHF lightning mapping array that we are building in the Gulf of Mexico, is a new capability that will be of great technological value to the US space-based nuclear denotation monitoring system (USNDS).

## Benefit to National Security Missions

This project supports the Laboratory's Threat Reduction mission by enhancing our understanding of the strength and organization of eyewall convective processes that trigger rapid hurricane intensification, and by developing a new hurricane model to improve forecast accuracy. We contribute to energy security with new tools to anticipate threats to the oil infrastructure. Our detection techniques have application to sensing other signals of national security relevance, such as the electromagnetic pulse from nuclear explosions.

## Progress

Our project has three key components: 1) development of a new dual VLF-VHF "total lightning mapping" array technology, and establishment of a new RF lightning array in the Gulf of Mexico; 2) development of the first-ever hurricane forecast model that includes cloud electrification and lightning prediction; and 3) development of a new data assimilation scheme to ingest lightning data into our unique hurricane forecast model. During year 1 of this project, we focused on tasks 1 and 2, which are required before task 3 can be attempted.

### New Gulf Lightning Array

We built and tested a new dual VLF-VHF lightning mapping technology. This sensor extends LANL's unique VLF technology, which records and transmits over the internet the VLF waveform, and adds a new VHF mapping capability. The new sensor technology is described in detail in Reference [1]. Ten sensor units have been built and tested and 8 of these are currently at host sites in the Gulf. We have also established a new sensor array in the New Orleans area. The array represents a new collaborative effort between LANL, Chevron, Nicholls State University, Louisiana State University, the Port Fourchon Authorities, the Associated Branch Pilots, and the Louisiana Universities Marine Consortium (LUMCON). The location of our sensor array is shown in Figure 1. One of our sensor sites is on a Chevron oil platform (ST-52), 20 miles off the Louisiana coast. As of

July 1st, 2008, 5 of the 8 sensors are currently in operation. The successful operation of the remaining 3 sensors (2 at Chevron sites, 1 at Nicholls) is pending the completion of legal lease agreements, which are currently being negotiated by LANL's legal councsel. Lightning data from hurricane Ike, as recorded by the new array, were presented in December, 2008 at the AGU Fall Meeting [2].

*Figure 1. Image of the Mississippi delta region south of New Orleans. Sensor locations are indicated by blue balloons. From left to right: Nicholls State University, LUMCON, Oil platform ST-52, South Lafourche Airport, Port Fourchon, LSU Agricultural Center, Southwest Pass River Pilot's Station, Venice.*

**New Hurricane Model with Electrification**

We developed the world's first hurricane forecast model with cloud electrification and lightning prediction. This model builds on and extents the cloud electrification parameterizations developed at Oklahoma University (our collaborator) for extra-tropical thunderstorms. We are excited to report that our hurricane model demonstrates the following important physical processes and validates a key scientific hypothesis of our project. We have used our new hurricane model with electrification to compare and contrast the intensification and lightning produced by a sudden burst of intense vertical convection in the eyewall of a simulated hurricane. Comparing the intensification and lightning produces by these eyewall "hot towers" of varying strength, we find that weak hot towers – which produce little intensification – produce negligible lightning, while strong hot towers produce rapid hurricane intensification and trigger a sudden burst of eyewall lightning. This exciting result validates a central scientific hypothesis of our project that a sudden burst of eyewall lightning activity is associated with rapid hurricane intensification. We are currently performing an extended analysis that includes the assessment of a variety of other parameters including aerosol type and concentration, the shape and distribution of the initial hot tower, and vertical wind shear.

PUBLICATIONS: Our project has two finished papers that are currently in the peer-review process: 1) "A Smooth Cloud Model", Reisner and Jeffery, submitted to Monthly Weather Review, and 2) "An analysis of hurricane activity records: 1850-2007", Chylek and Lesins, submitted to Journal of Geophysical Research.

## Future Work

This project is motivated by our remarkable observations of abundant lightning activity in the eyewall of Hurricanes Katrina, Rita and Wilma that coincided with rapid intensification and that were observed by LANL RF sensors sparsely located over the Great Plains and Florida. Intense vortical convective towers in the hurricane eyewall are believed to trigger intensification; the new lightning channel mapping array that we will deploy on oil platforms in the Gulf of Mexico will provide a continuous eyewall monitoring capability that will reveal the formation, merger and decay of these vortical structures as seen in the evolution of their three-dimensional charge structure. We will build a new LANL hurricane model that assimilates our real-time lightning observations and lead the field in achieving success in the national challenge posed by NOAA:

"to demonstrate a 50% improvement in 48 hour hurricane intensity (wind speed) forecast errors using "advanced numerical models, novel methods of data assimilation, and improved observations."

## Conclusion

Our project will perform the first-ever real-time 3D mapping of convective events in the hurricane eyewall using a new lightning remote-sensing capability developed by LANL. We will use this new understanding and remote sensing capability to demonstrate that rapid hurricane intensification, the sudden large-scale transition of violent weather, can be accurately forecast using a novel model that assimilates real-time knowledge of critical small-scale processes--specifically, observations of violent eyewall convection provided by a hurricane lightning imaging system. This new predictive capability of hurricane intensification will save lives and protect infrastructure along the energy critical Gulf coast. Improved capabilities for detecting impulsive electromagnetic signals are relevant for a number of national security missions.

## References

1. Shao, X., J. Harlin, T. Hamlin, D. Suscynsky, and C. Jeffery. Hurricane lightning: a new campaign to investigate hurricane intensification by using lightning observations. Presented at *American Meteorological Society 88th Annual Meeting.* (New Orleans, 20-24, Jan., 2008).

2. Harlin, J., X. Shao, T. Hamlin, T. Light, N. O'Connor, and C. Jeffery. LASA observations of lightning in hurricanes. Presented at *American Geophysical Union Fall Meeting.* (San Francisco, 15-19 Dec., 2008).

## Publications

Chylek, P., and G. Lesins. Multi-decadal variability of Atlantic hurricane activity: 1851-2007. To appear in *Journal of Geophysical Research.*

Harlin, J., X. Shao, T. Hamlin, N. O'Connor, T. Lavezzi, and C. Jeffery. LASA Observations of lightning in hurricanes. Presented at *American Geophysical Union Fall Meeting.* (San Francisco, 15-19 Dec., 2008).

Jeffery, C., and N. Jeffery. Theory and computation of wave-number-2 Vortex Rossby Wave instabilities in hurricane-like vortices. Presented at *Geophysical Turbulence Phenomena.* (Boulder, 27-29 Feb., 2008).

Kao, J., and K. Ide. A reduced Extended Kalman Filter method of data assimilation and parameter optimization. To appear in *Journal of Computational Physics.*

Reisner, J., and C. Jeffery. A smooth cloud model. To appear in *Monthly Weather Review.*

Shao, X., J. Harlin, D. Suszcynsky, and C. Jeffery. Hurricane lightning: a new campaign to investigate hurricane intensification by using lightning observations. Presented at *American Meteorological Society 88th Annual Meeting.* (New Orleans, 20-24, Jan., 2008).

Shao, X., and A. Jacobson. Model simulation of VLF/LF lightning signal propagation over intermediate ranges. *Transactions on Electromagnetic Compatibility.*

# Genomes to Behavior: Predicting Bacterial Response by Constrained Network Interpolation

*John Martin Dunbar*

20080138DR

## Introduction

The DOE Office of Science envisions direct prediction of microbe behavior from a genome sequence, but is stymied by a lack of methods. Consequently, the DOE, DHS, NIH, and IC rely on slow, expensive empirical methods to determine the response of new strains and species to particular stimuli and to identify the genetics underpinning response. For example, knowledge of strain virulence is needed in biothreat risk assessment, but can only be estimated at present through slow and expensive animal studies. Similar hurdles occur in understanding the effectiveness of microbes for bioenergy and waste remediation. This creates an increasingly severe bottleneck as the accumulation of genome sequences (already >1000 partial or complete) greatly outstrips the capacity for experiments to understand them.

To alleviate this bottleneck, we are developing a framework to predict bacterial response to stimuli by constrained extrapolation from experimentally well-characterized model organisms. This project exploits high throughput experimental biology and computation at LANL. As a test system, we are focusing on the genus Burkholderia. This genus contains species that impact biothreat, bioremediation, bioenergy, and public health missions of interest to DOE, DOD, NIH, and the IC.

The impact of our work will be similar to the impact of protein-structure homology modeling, which enables rapid functional analysis and redesign of proteins. The project will lay the foundation for a new kind of homology modeling in which the response networks of model bacteria are experimentally characterized at key intervals across the bacterial domain and are used to interpolate responses from other genome sequences.

## Benefit to National Security Missions

This project supports DOE missions in biothreat reduction, bioenergy, carbon management, and bioremediation by profoundly improving the capacity to decode, harness the capabilities, or assess risks encoded in microbial genomes. This project targets a fundamental bottleneck identified by DOE Office of Science within the Life Sciences.

## Progress

We focused on two major efforts: 1) characterizing stimulus-response pathways in a model organism (Burkholderia thailandensis) and 2) developing a framework to map stimulus-response pathways from the model organism to other genomes. An external 9-member panel reviewed the project in June and concluded the project goal was important & timely, the approaches were sound, and the progress was solid with a good trajectory for success. We have already established a new, high impact experimental technique at LANL, which will facilitate program development. Further, we uncovered a pervasive yet poorly recognized problem in microbial genomics and have developed a solution that has caught the interest of DOE Office of Science OBER.

Regarding first endeavor, "Characterize stimulus-response pathways in the model organism," we are on track to deliver a well-characterized model system, as planned, by month 18. For this goal, we aimed to a) characterize the basic machinery (sensor and response regulator proteins) mediating bacterial response to stimuli and b) measure responses (gene expression patterns) to 20-40 stimuli or growth conditions—a data requirement established by our modeling team.

We developed a new capability at LANL to link stimulus-response machinery (specific sensor and response regulator proteins) to particular stimulus-response pathways. Our model organism contains 22 pairs of sensor-response regulator proteins that are conserved across the Burkholderia genus. To link each pair to a specific stimulus-response, we initially pursued a conventional approach—creation and analysis of defective mutants. However, after the first 5 months, we changed direction to exploit a new, more informative technology with higher scientific impact. We initiated a collaboration

with Dr. M. Bulyk (Harvard Medical School), whose new technology enables more detailed placement of sensor-response regulators within a response network. We successfully cloned half of the response regulators in the model organism for use with Dr. Bulyk's technology. Our focus on response regulator proteins is a new application of Dr. Bulyk's technology, and poses new technical challenges. We made good progress overcoming these challenges. We recently achieved successful assays, but are still refining the performance to improve data quality. This achievement is important; it will allow us to identify the genes controlled by each response regulator in our model organism. Moreover, it is straightforward to apply this to other bacterial species of interest to DOE, such as microbes used for biofuel production.

We completed a large set of planned growth experiments with the model organism. We not only collected RNA samples these experiments, but also metabolite samples, archived to support program development. Affymetrix gene expression microarrays were designed and acquired. The microarrays will be used to analyze the RNA samples, revealing gene expression patterns (i.e. response to stimuli) needed for computational reconstruction of the gene regulatory network.

Regarding our Aim (2) "Develop a framework to extrapolate stimulus-response pathways to other genomes", we have nearly achieved our major year-one milestone—defining the boundaries for extrapolation of behavior. The crux of the problem is to determine the extent of conservation of gene inventory (i.e. the parts list) and gene regulation across sets of increasingly divergent genomes. Our efforts thus far have generated unexpected results with high scientific impact.

For gene inventory comparisons, we developed a parallel computing algorithm to identify functionally orthologous proteins for user-defined groups of species. This flexible software will be exploited in follow-on projects that target other bacteria. Using this software, we found that only about half of the proteins in our model organism have orthologs in the most distant relative within the same genus. This imposes a severe constraint on extrapolation of general behavior beyond the genus level. Results from this analysis (which is beyond the capacity of most university researchers) are now guiding the remainder of the project.

Assessing conservation of gene regulation involves extraction and comparison of intergenic, non-protein coding DNA sequences. To our knowledge, we are the first to attempt such a task on a large scale (i.e. genome-wide and with many genomes). Our unique effort uncovered a significant problem that pervades microbial genomics but is routinely overlooked.

We discovered widespread inconsistencies in the predicted length of orthologous genes among 18 Burkholderia genomes (Figure 1). These inconsistencies represent true uncertainty about the location of the start site for each gene. The extent of these inconsistencies severely impedes comparative studies of gene regulatory elements. Surprisingly, this is a poorly recognized problem. Even more surprising, we were able to devise and implement a relatively simple solution that imposes consistency, and we believe, improves accuracy. DOE Office of Science OBER program managers overseeing genomics-driven research portfolios have expressed keen interest in seeing the completion of our efforts.

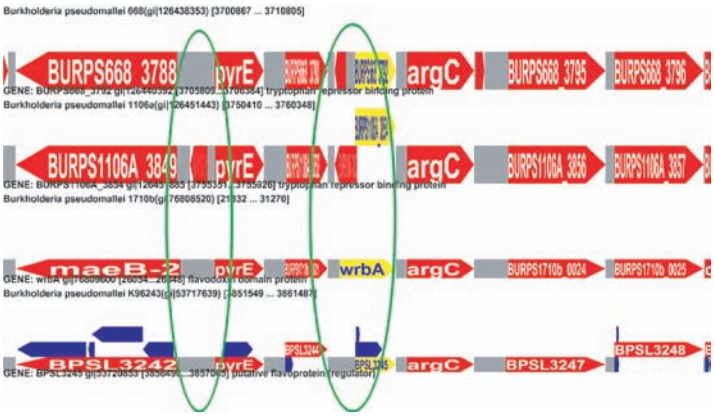


*Figure 1. Genome annotation errors. Shown are orthologous segments from 4 genomes representing different strains of Burkhoderia pseudomallei. The segments have nearly identical DNA sequence, yet predictions of gene lengths differ markedly in each genome. The green circles indicate illustrative examples of the inconsistencies between genomes. The red boxes represent genes. The grey boxes represent the intergenic spaces that control gene regulation. The yellow boxes highlight one particular gene with significant inconsistencies in the predicted start position among genomes. Note that the inconsistencies in the predicted gene start site sometimes abolish the intergenic space. More generally, the pervasive inconsistencies impede extraction of synonymous intergenic regions from different genomes and therefore hinder comparisons of gene regulatory elements.*

On another tack, we used structural modeling and simulations of response regulators in active and inactive states to identify functional sites within these proteins that must be preserved in order to conserve function. Similarly, we exploited LANL's unique capabilities in modeling large protein complexes to obtain a model of a large complex containing DNA, RNA polymerase holoenyzme, and a major response regulator from our model organism. The model enabled us to identify putative protein interaction surfaces (functional submotifs) that must also be preserved across genomes in order to maintain similar behavior. Identification of such functional sites allows us to distinguish functional irrelevant variation in orthologous protein sequences from sequence variation that may impact protein function.

Parallel to these efforts, we continued developing our capability for quantitative modeling of stimulus-response pathways, using two characterized gene circuits as test cases.

The collective efforts during the first 12 months have produced two publications, one manuscript in final stages of editing, and another manuscript in preparation.

## Future Work

Cellular behavior is determined by gene inventory and gene regulation. Gene inventory defines a cell's potential capabilities. Gene regulation determines which capabilities are actually used in various conditions. Recent advances enable reverse-engineering of gene regulatory networks for a single genome. The next logical progression is to translate regulatory networks from one genome to another. For closely related organisms, the elements of a regulatory network can be very similar. This fact motivates our main hypothesis: that the limitations of current approaches can be overcome by determining the regulatory networks for a model organism and then translating them to closely related organisms.

The goal of this project is to develop a capability to predict regulatory networks in new genomes by translating regulatory networks from a model system. We will use fundamental biophysical, biochemical and evolutionary principles to extrapolate the behavior (gene expression) of a well-characterized model bacterium to less well-studied bacteria of interest. This involves a new type of homology modeling, tailored for the key components of regulatory networks, and exploits the high-performance computing and computational biology capabilities at LANL.

We have two primary aims:

1. Provide a detailed experimental characterization and systems-level model of the response of a reference organism to a variety of external stimuli. This is a low risk objective.

2. Extend this model to infer the response networks of organisms with similar genomes. This is a highly innovative component of the project, and builds on our combined expertise in experimental microbial physiology, network reconstruction, structural modeling, and bioinformatics methods. Extending (and validating) pathways from our model system to closely related genomes is a moderate risk objective. As a higher risk objective, we will define the phylogenetic "radius of convergence"—the evolutionary distance over which a response network can be extended.

## Conclusion

This project aims to create a fundamental capability that could transform comparative genomics and reduce the need for experimentation 10 to 100-fold, profoundly cutting costs and accelerating solutions to central problems in biosecurity, bioenergy, carbon management, and bioremediation. We are on schedule to meet our deliverables and have already made very significant findings that have been communicated to DOE Office of Science OBER.

## Publications

Dreisigmeyer, D. W., J. Stajic, I. Nemenman, W. S. Hlavacek, and M. E. Wall. Determinants of bistability in induction of the Escherichia coli lac operon. 2008. *IET Systems Biology.* **5**: 293.

Edwards, J. S., J. R. Faeder, W. S. Hlavacek, Y. Jiang, I. Nemenman, and M. E. Wall. q-bio 2007: a watershed moment in modern biology. 2007. *Molecular Systems Biology.* **3**: 148.

Martin, R. G., E. S. Bartlett, J. L Rosner, and M. E. Wall. Activation of the Escherichia coli marA/soxS/rob regulon in response to transcriptional activator concentration. 2008. *Journal of Molecular Biology.* **380**: 278.

# Complex Biological and Bio-Inspired Systems

*Robert Everett Ecke*

20080673DR

## Introduction

The understanding and characterization of the fundamental processes of the function of biological systems underpins many of the important challenges facing American society, from the pathology of infectious disease and the efficacy of vaccines, to the development of materials that mimic biological functionality and deliver exceptional and novel structural and dynamic properties. These problems are fundamentally complex, involving many interacting components and poorly understood bio-chemical kinetics. We use the basic science of statistical physics, kinetic theory, cellular biochemistry, soft-matter physics, and information science to develop cell level models and explore the use of bio-mimetic materials. This project seeks to determine how cell level processes such as response to mechanical stresses, chemical constituents and related gradients, and other cell signaling mechanisms integrate and combine to create a functioning organism. The research focuses on the basic physical processes that take place at different levels of the biological organism: the basic role of molecular and chemical interactions are investigated, the dynamics of the DNA-molecule and its phylogenetic role are examined and the regulatory networks of complex biochemical processes are modeled. These efforts may lead to the development of bio-sensors to detect hazards from pathomic viruses to chemical contaminants. Other potential applications include the development of efficient bio-fuel alternative-energy processes and the exploration of novel materials for energy usages. Finally, we use the notions of "coarse-graining," which is a method for averaging over less important degrees of freedom, to develop computational models to predict cell function and systems-level response to disease, chemical stress, or biological pathomic agents.

## Benefit to National Security Missions

This project supports Energy Security, Threat Reduction, and the missions of the DOE Office of Science through its far-reaching efforts to accurately model biological systems at the molecular and cellular level. The project's impact encompasses applications to biofuels, to novel sensors and to materials with broad use for energy or threat reduction.

## Progress

The broad, multidisciplinary approach of CNLS offers the unparalleled strength of combining science backgrounds and expertise – a unique and important asset in attacking the complex science of biological organisms. This approach also allows cross-fertilization, with concepts and techniques transferring across field boundaries. This project hen simultaneously and fruitfully investigates bio-complexity at multiple levels, exploring the basic role of molecular and chemical interactions, studying the DNA-molecule dynamics and its phylogenetic role and modeling the regulatory networks of complex biochemical processes.

CNLS researchers are playing a key role in the development of novel methods for simulating rule-based models and in the application of these methods to study cell-surface multivalent ligand-receptor interactions and intracellular signaling events. In particular, we have explored the oligomerization of the linker for activation of T cells (LAT) mediated by the adapter protein Grb2 and the guanine nucleotide exchange factor Sos1. In addition, we have applied traditional simulation methods to study spatiotemporal aspects of cell signaling. Four publications have been prepared on this work.

Single molecule tracking methods are providing a powerful probe of biological systems. Our researchers have analyzed the statistics of the recorded motion of a quantum dot attached to a receptor molecule on the membrane of a living cell. The statistics of the observed trajectories showed that the motion of the receptor is not a free diffusion process. We devised models to explain the receptor's history that give a rare and potentially deeply significant glimpse into the detailed dynamics of specific molecules in a biological organism. These models account for the confinement of the quantum dot by the polymer network on the membrane. Currently the model is being compared quantitatively with the data to obtain the model parameters.

Colloids form an essential building block for self-assembling soft-materials. Our researchers have performed numerical calculations of multilayer charged colloid systems using the generalized random sequential absorption scheme. Depending on the density of the first layer adsorbed on a charged surface, the structure of the multilayers was different. Figure 1 shows a 20-layer system of charged colloid particles. Our calculations are important for understanding and manipulating layer-by-layer growth for preparing nano-structured materials such as separation membranes and optical elements.

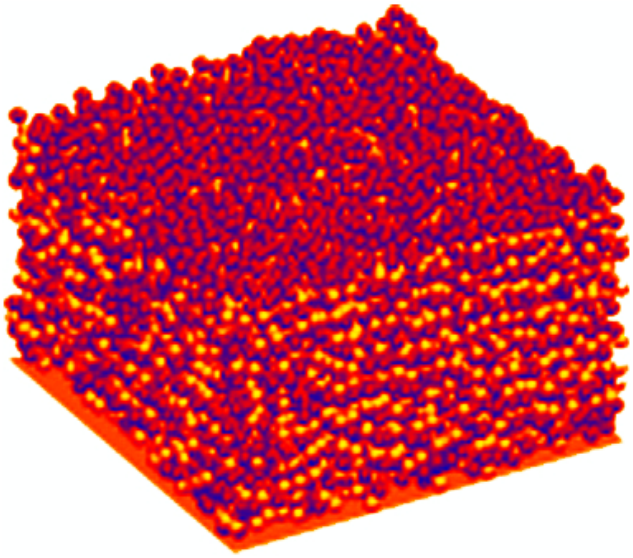

*Figure 1. Topology of colloid particle multilayers composed of twenty layers derived from Monte Carlo simulations. The particles bearing opposite surface charge to the interface (for example positive if the interface is negatively charged) are shown in yellow, whereas the negatively charged particles (same sign of surface charge as the interface) are shown in red.*

Our researchers are investigating scanning tunneling microscope spectra of DNA deposited on a metal surface. Understanding the local electronic properties of DNA bases is crucial in the search for "fingerprints" of the DNA. We have performed sophisticated calculations of the electronic structure of the organic/metal hybrids. We also considered electronic and structural features of the DNA single stranded molecule wrapped on a nanotube.

Our postdocs are exploring theoretical models of transport through the nuclear pore complex, and other selective biological and biologically inspired nano-channels. This year, we have published several papers that connect our theoretical, physics-based model with experimental results on nuclear pore transport. We are also consolidating theoretical and simulation results that describe the polymer filaments involved in the transport through the nuclear pore complex.

In collaboration with researchers at the Scripps Research Institute, we have created an automated procedure to screen cis-antisense pairs in human and mouse genomes from non-coding RNAs. We are now able to screen for microRNAs that are able to bind with high affinity to sense-antisense pairs in the human genome.

## Future Work

We propose to characterize complex biological and soft materials and to study complex biological systems through theoretical, statistical and computational approaches. The objectives pursued by this project are described below:

1. Integrate features at different resolutions to create models of biological systems by incorporating molecular details of cell population dynamics, using atomistic details to inform models for the kinetics of protein-protein interactions, or simplifying models by reducing the detail while preserving the correct physics.

2. Study the mechanisms of innate and adaptive immune responses to infection or vaccination at the molecular level by modeling the responses triggered by cell-surface receptors, such as antigen-recognition receptors, when they bind ligands, and study the molecular mechanisms of virulence factors that interfere in immune response.

3. Explore artificial thin-film materials for purposes such as biosensor design, characterization of membrane-protein interactions, and constructing spatial arrays of proteins and other materials with desired patterns.

4. Develop comprehensive models of cellular systems, such as genome-scale metabolic and genetic regulatory networks in bacteria, for the purposes of metabolic engineering or design of synthetic cellular regulatory systems that yield cells with desired behavioral properties.

5. Pursue studies, particularly of cellular information processing, that take advantage of large datasets and account for stochastic and spatial effects.

6. Apply phenomenological linear and nonlinear strain theory to understand the interplay of interactions that control and optimize virus deformation properties.

7. Develop methods for the theoretical, computational and experimental study of complex biological systems including coarse-graining micro-scale biological details in a manner that preserves observable dynamical quantities.

8. Develop multiscale, tissue-level models based on cell dynamics, cell-cell interactions, and cell-microenviron-

ment interactions, e.g., study bio-film formation, tissue response to viral and bacterial infections, tissue permeability to biological and chemical agents.

9. Use time-dependent density functional theory (DFT) and semi-empirical approaches to model excited-state structure and dynamics. In particular, simulate fluorescence dynamics, fluctuations, and energy transfer involving fluorophores as functions of local protein environment and conformations.

## Conclusion

By building accurate models of how molecular processes interact within a cell to create cell specificity and function, scientists can begin to manipulate those functions for new applications. A specific example is designing an efficient biological biomass conversion process that could help address energy sustainability issues. Other implications of our work include better predictability of the spread of contagious disease and the design of effective vaccines for such diseases. Using these biological systems and their models as a basis, we can design new materials that mimic the function of membranes, vesicles, and muscle.

## Publications

Adamczyk, Z., P. Weronski, and J. Barbasz. Formation of multilayered structures in the layer by layer deposition of colloid particles. 2008. *JOURNAL OF COLLOID AND INTERFACE SCIENCE.* **317** (1): 1.

An, G., J. Faeder, and Y. Vodovotz. Translational systems biology: Introduction of an engineering approach to the pathophysiology of the burn patient. 2008. *JOURNAL OF BURN CARE & RESEARCH.* **29** (2): 277.

Beauchemin, C. A., J. J. McSharry, G. L. Drusano, J. T. Nguyen, G. T. Went, R. M. Ribeiro, and A. S. Perelson. Modeling amantadine treatment of influenza A virus in vitro. 2008. *JOURNAL OF THEORETICAL BIOLOGY.* **254** (2): 439.

Benoit, J., and A. Saxena. Spherical vesicles distorted by a grafted latex bead: An exact solution. 2007. *PHYSICAL REVIEW E.* **76** (4): 041912.

Edwards, J. S., J. R. Faeder, W. S. Hlavacek, Y. Jiang, I. Nemenman, and M. E. Wall. q-bio 2007: a watershed moment in modern biology. 2007. *MOLECULAR SYSTEMS BIOLOGY.* **3**: 148.

Lipniacki, T., B. Hat, J. R. Faeder, and W. S. Hlavacek. Stochastic effects and bistability in T cell receptor signaling. 2008. *JOURNAL OF THEORETICAL BIOLOGY.* **254** (1): 110.

Shen, T., and D. Hamelberg. A statistical analysis of the precision of reweighting-based simulations. 2008. *JOURNAL OF CHEMICAL PHYSICS.* **129** (3): 034103.

Weronski, P., Y. Jiang, and S. Rasmussen. Application of molecular dynamics computer simulations in the design of a minimal self-replicating molecular machine. 2008. *COMPLEXITY.* **13** (4): 10.

Weronski, P., and M. Elimelech. Novel numerical method for calculating initial flux of colloid particle adsorption through an energy barrier. 2008. *JOURNAL OF COLLOID AND INTERFACE SCIENCE.* **319** (2): 406.

full final report

# Rational Vaccine Design: Theory and Experimental Validation

*Bette Tina Marie Korber*

20050155DR

## Abstract

Through this project we have moved our field forward in terms of understanding the basic biology of immune escape in HIV-1 infection, and used this knowledge to rationally design vaccines. HIV is extremely variable and one of the greatest hurdles we face in the HIV vaccine field is making a vaccine that will trigger immune responses against the diverse population of circulating strains. We have developed computational methods for vaccine design and then worked with experimentalists to analyze the data they obtained using our vaccine designs from the first wave of results from animal studies. The first results with our HIV vaccine have been extremely promising, and so our HIV vaccines are being considered for a small human trial, and a series of additional experiments in macaques are underway. Interest in this approach has enabled us to expand our efforts through collaborative studies to Hepatitis C and Ebola vaccine design. We have also studied the impact of variation on protein structure in terms of key antibody binding domains in different HIV subtypes. In parallel, we have developed an interesting new strategy for vaccine delivery, improved vaccine strategies by modeling the temporal relationship of immune responses to HIV vaccines, and developed new methods for assessment of breadth of immune responses. We have also developed methods for Anthrax detection and treatment.

## Background and Research Objectives

With over 33,000,000 current HIV infections, and 3,000,000 new infections a year, HIV/AIDS remains humanity's most serious public health crisis. A vaccine remains elusive, but if achieved, it would be the intervention with the greatest potential to contain this pandemic. A chief obstacle to developing an efficacious vaccine is HIV's diversity – it evolves rapidly within an infected individual, and consequently in infected populations [1]. Worldwide, there are ten major HIV circulating subtypes, grouped by genetic relatedness. The US epidemic is primarily B subtype, while South Africa is C subtype. HIV proteins isolated from people infected with the same subtype differ in about 8-18% of their amino acids. HIV proteins from people infected with different subtypes vary in up to ~35% of their amino acids. We have been working on two classes of HIV vaccine target populations. The first is subtype-specific [2,3], as a successful vaccine may ultimately need to be limited to within-subtype variation. This, however, would require that multiple region-specific vaccines would need to be developed in parallel, making global application of this strategy very expensive. We have also attempted the grander vision of a global vaccine, developing strategies that could potentially provide protection against the spectrum of variation found within the diverse set of all subtypes comprising the global epidemic [4-8].

## Importance to LANL's Science and Technology Base and National R & D Needs

We have made substantial progress toward design and testing vaccine concepts that may be useful for an AIDS vaccine. Preliminary results are promising enough to consider carrying forward into human testing, and to begin development for other pathogens. We have developed theoretical strategies that have allowed us to make progress in understanding the basic biology of immune response to HIV and the nature of immune escape. In the course of these studies developed a new concept for anthrax detection and treatment. Combined, these developments have obvious implications for HIV and Anthrax, but the principles are general and could be applied to other pathogens; thus we have enhanced LANL's ability to respond to either emerging natural pathogens or man made biological weapons, and to protect public health. Our excellent publication record on this DR (47 papers), and national and international collaborations have contributed to LANL's standing in the biological community and our ability to network with other investigators working on public health issues of primary importance.

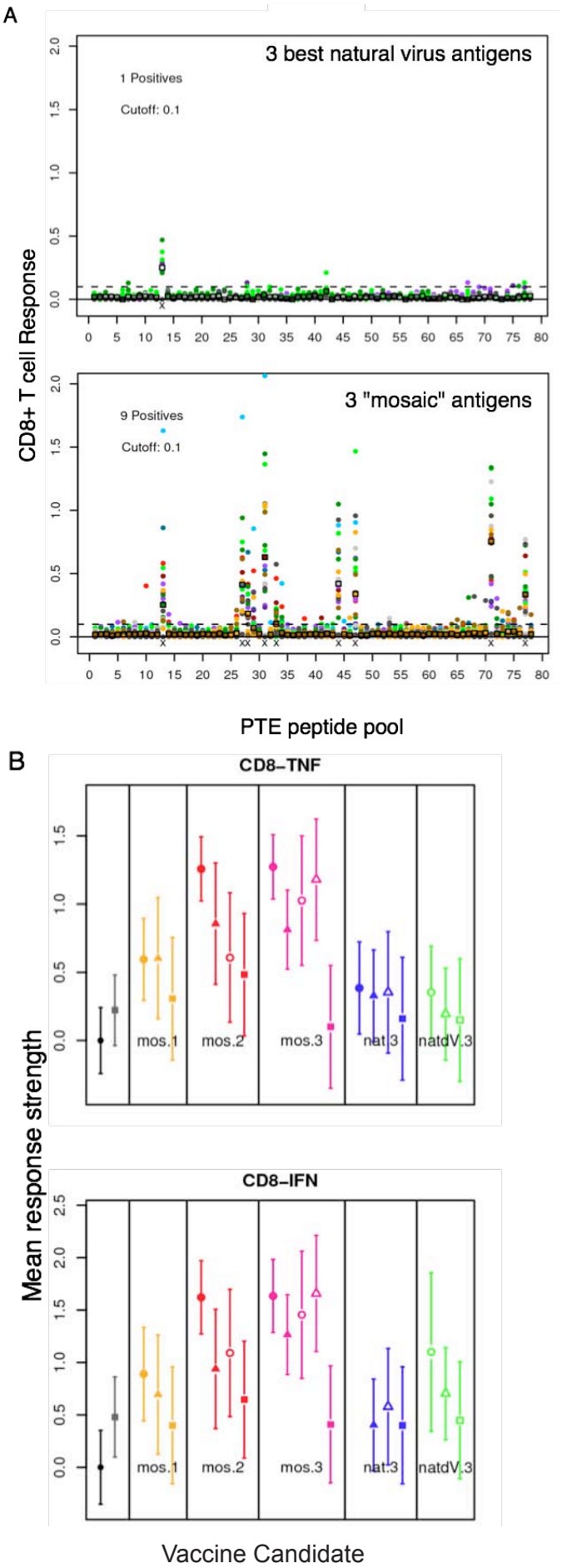


*Figure 1. Comparison of Cytotoxic T cell responses to HIV vaccine antigens in terms of breadth (A) and strength (B) in the first experimental evaluation of mosaic vaccines, performed in mice. CD8+ T cells are part of our immune response to viruses; these cells recognize and kill virally infected cells, i.e. are "cytotoxic" to infected cells, and enable us to clear or control viral infections. γ-interferon is an antiviral protein our body makes to interfere with viral infections, and is used to detect active CD8+ T cell immune responses to vaccines in lab tests. Greater numbers of responses means an enhanced ability to see diverse circulating forms of HIV (A), and greater magnitude of responses means the vaccine response is more intense, thus more likely to confer a protective benefit (B). Panel A represents T-cell responses measured by production of γ-interferon to either a cocktail of 3 natural virus antigens (selected for maximal immune system coverage, above) or to our 3 synthetic 'mosaic' antigens (below). We were able to trigger 9 responses to global variants with mosaics, and 1 response with natural strains. The mosaics are designed based on computational methods developed through this DR. Panel B shows strength values for each of a set of vaccine candidates over a series of tests. Different colors represent different vaccines (mos.1,2,3 are vaccines including 1, 2, or 3 sequences per vaccine; vaccines denoted "nat" are combination of 3 selected intact natural sequences (nat.3) or slightly modified natural strains (natdV.3). Adding more proteins enhances the mosaic response, but 3 natural proteins, comparable to what has been used in vaccine trials to date, is no better than a single mosaic. Within each vaccine, different symbols represent versions of antigens having distinct regions of the proteins deleted to test different design options. Gray bars at left represent negative and positive controls.*

## Scientific Approach and Accomplishments

### The evolution of immune escape

As we began work on vaccine strategies, we simultaneously developed theoretical methods to explore how viral evolution leads to escape from natural human immune responses [9-11]. Through these studies we were able to reject one strategy we had initially considered for vaccine design, that of excluding immune escape variants from vaccines, as we learned this seemingly logical strategy would be counter-productive: an immune escape mutation in one person often is the immunologically susceptible form in another, and immune targets are both complex and dense with extensive overlap [10,11]. Instead we focused on two alternative vaccine approaches: maximizing coverage of natural diversity by a vaccine [6,7], or focusing the vaccine immune response on to the most conserved regions of HIV [8].

**Vaccine concepts**

T-cell immune responses recognize "epitopes" (short, typically 9 amino acid long, contiguous stretches of viral proteins). Our vaccines were computationally designed to maximize population coverage of epitopes, while to package these epitopes in artificial proteins that (aside from increased inclusion of common epitopes) are similar to natural proteins. We employed several different approaches towards these aims. Initially, we designed consensus proteins (built from the most common amino acid found in any position in a protein) or used statistical methods to model the most recent common ancestor of a viral population [2-6]. We then extended these approaches, using a machine-learning algorithm to create small sets of designer proteins that when combined in a vaccine, have the potential to increase the breadth of induced responses [7,12]. We also worked on a vaccine approach that concatenates the most conserved regions of the virus into one amalgamated protein [8]. Recently, we designed a strategy for serial vaccination with distinct artificial proteins that share only the most conserved regions, with variable regions forced to differ to direct vaccine boosting of immune responses to conserved regions, to be presented at the Human Vaccine Trials Network 2008). So we have been attacking this problem from a variety of angles.

**Experimental Validation**

Working with experimentalists at the University of Alabama (who also had support from this project), Duke, Harvard, and the NIH, we have moved from initial theory and design to demonstrating proof-of-concept in animal vaccine studies. Our computer designed ancestral and consensus proteins have turned out to be well expressed, fold properly and are immunogenic vaccines in small animal studies [2-5]. They elicit many more cross-reactive responses than natural strains in mice, and so have been carried forward into macaques [6], the best non-human primate model available for HIV vaccines. Subsequently, our mosaic designs have been synthesized in the lab: these proteins are well expressed, and a first vaccine study has been completed in mice, again showing great promise [12]. Figure1 is representative sample of a large set of experiments from this study; in this case, vaccinating mice with 3 natural strains yielded one response, while vaccinating with 3 mosaic proteins gave rise to 9 responses, and the responses are more intense. More responses mean a greater potential to protect a vaccinated individual from circulating forms of the virus. Two macaque studies mosaic design strategies are currently underway at Harvard.

The promise of the early results with consensus and mosaic strategies in animal studies led the NIH vaccine resources group, together with the GATES foundation, to invite a proposal for a human trial. If funded, we will test the breadth of immune responses induced by: 1) a single natural strain, 2) our consensus design, 3) 3 natural strains, and 4) our 3 protein mosaic design. This proposal (currently under review) was written in collaboration with our colleagues at Duke, Harvard, the NIH, and the Human Vaccine Trials Network.

In the mosaic studies described above, we designed a vaccine with the intent to achieve global protection. We have also designed a more targeted mosaic vaccine for HIV in Asia that will be tested by colleagues in Thailand. Similarly, we have designed a Hepatitis C mosaic vaccine that will be synthesized and tested by the TRANSGENE in France [13], and an Ebola vaccine now under consideration for testing by USAMRID [14]. We are making the design concepts and computer software freely available, but patenting the specific artificial proteins we design, coordinated with our experimentalist colleagues at other institutions who synthesize, express the proteins, and so test the concepts.

**Interpreting vaccine responses**

To assess how cross-reactive an immune response is in terms of protecting against epitope variants from diverse circulating strains, assays need to include the breadth of global diversity. Vaccine induced T-cell responses are generally evaluated with a series of overlapping peptides that, together, span entire proteins. Peptides are mixed with T-cells from vaccinated or infected individuals, to see if the peptides induce the T-cells to respond. To assess how well vaccines elicited responses to a wide range of circulating viruses, we selected 10 contemporary HIV strains that were broadly representative of the global genetic diversity of the virus, each from geographically defined epidemic centers, and designed sets of peptides to reveal how well a vaccine response might react with each of these diverse strains [6]. This was a very expensive strategy as many peptides were required (Table), but it was also illuminating, enabling us to discern a distinct advantage of a consensus vaccine over a natural strain.

**Assessing immune responses in natural infections**

To address detection of responses in natural infection when the infecting strain sequence is unknown, we developed toggle peptides, a concept based on our observation that while HIV is highly diverse, often a given amino acid position is constrained to "toggling" between two or three

dominant amino acids. Toggle peptides incorporate each of the most common amino acids found in variable positions during peptide synthesis. Table 2 compares toggle peptides, an alternative strategy called PTE peptides developed by others [15], and the set of 10 diverse natural sequences used in the consensus vaccine macaque study [6]. Coverage of epitope length fragments by diversity-competent peptide sets (10 natural, PTE, and Toggle) was comparable for all HIV proteins tested and much better than peptide sets based on single sequences (Figure 2), but the toggle peptide strategy requires generation of many fewer peptides (Figure 3). Thus Toggle peptides offer high coverage of diverse sequences, at lower cost. Use of toggle peptides proved experimentally feasible, and allowed better tracking of immune responses as HIV-1 diversifies in individuals and within populations [16].

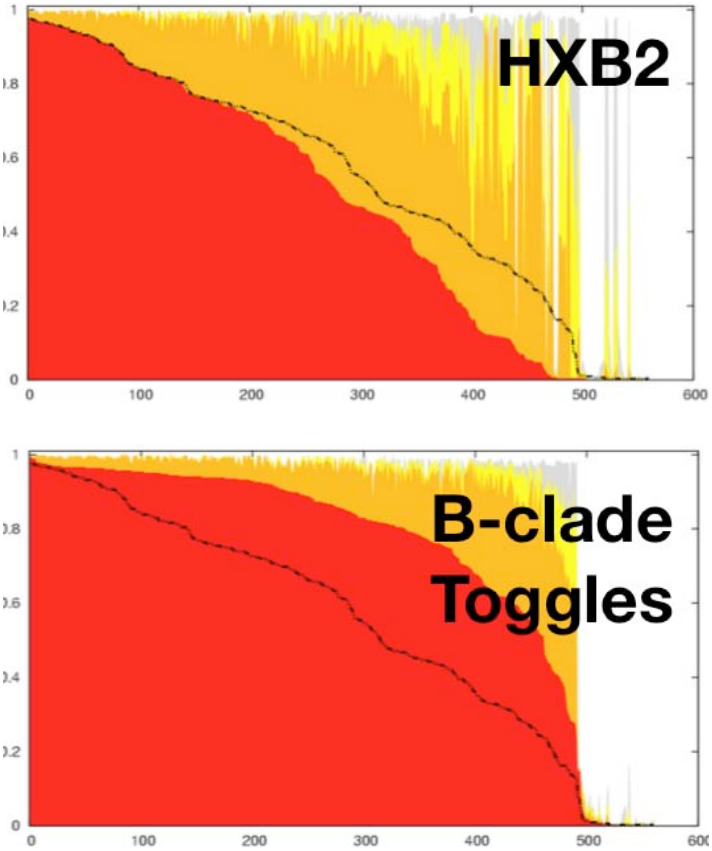


*Figure 3. Figure 2. Nine-mer coverage of aligned B-clade HIV-1 Gag protein data by a traditional peptide set (HXB2, top) and by a set of 12-fold degenerate toggle peptides (bottom). Nine amino acid stretches, or "nine-mers" are the typical length of fragments of HIV proteins that are recognized by T-cell responses in our immune system. X-values represent individual 9-mers in a protein sequence alignment of global sequences, sorted left-to-right by decreasing coverage so that the most conserved nine-mers are at the left, least conserved on the right. If you do not have an exact match in among nine-mer peptides in your experimental system to test the immune response to an infecting strain, a potential immune response is likely to be missed in your assay system, confounding the results and diminishing our ability to understand the natural role of immune protection in HIV infection.The upper bound on coverage by a single sequence (i.e. an ideal protein containing the most common nine-mer at each position) is shown by a dotted line.*

| Gene | HXB2 | consB | consM | B toggles | M toggles | PTE 15% | 10 natural* |
|---|---|---|---|---|---|---|---|
| Gag | 122 | 122 | 122 | 100 | **100** | **454** | **900+** |
| Pol | 248 | 248 | 248 | 200 | **200** | **858** | **1400+** |
| Env | 211 | 207 | 204 | 175 | **175** | **667** | **800+** |
| Nef | 49 | 49 | 49 | 41 | **41** | **206** | **400+** |

*Figure 3. Table summarizing the number of peptides required to test cross-reactivity with diverse strains. 'B' means what you would need to cover just the HIV B subtype for using different peptide design strategies, M means the number needed to cover all circulating forms of the virus. Toggles, PTE and 10 natural protein cover similar highly levels of diversity in immune targets, but the cost of screening experiments directly depends on the number of peptides included, thus toggles are very cost effective.*

**Vectors to deliver viral antigens and testing consensus/ancestral based vaccines**

Throughout this project we have collaborated with Dr. Beatrice Hahn at the University of Alabama, who has tested the immunogenicity of consensus HIV-1 Envelope vaccines both as DNA and Virus Like Particle (VLP) vaccines in guinea pigs. She found that *envelope*-based DNA vaccines induced a very low level neutralizing antibody response, although consensus *envelope* immunogens were at least as good as, and in some instances better than, wild type *envelope* immunogens [2,3]. She also generated recombinant baculovirus (rBV) derived HIV-1 Gag/Envelope VIPs that contained large quantities of Envelope glycoprotein. Enhanced Envy incorporation was achieved by replacing two HIV-1 envelope domains with the corresponding domains of other viruses (MMTV, HA, SP64). All three VLP based immunogens (VLP-HA, VLP-SP64, VLP-MMTV) elicited potent neutralizing antibodies to easy-to-neutralize viruses, although neutralizing antibody responses to more difficult-to-neutralize viruses were low. In summary, given the known advantages of particulate immunogens and their ease of manufacture, rBV derived consensus VIPs merit further evaluation as components of future AIDS vaccines.

**Viral dynamics**

Studies of the kinetics of immune responses to HIV in natural infection and after vaccination were led by Dr.

Alan Per Elson, enabling interpretation of vaccine–induced immune responses and immune responses in acute infection [17-19], and provided information that could ultimately be used to design better vaccine protocols and improved estimations of vaccine impact. Dr. Per Elson's team worked with the Merck AIDS vaccine group to quantify how rapidly T cell levels, after being raised by a vaccine, decline with time. They have also examined new classes of quantitative models of the immune response against HIV and compared these models to data, and modeled the potential of a non-sterilizing vaccine to curb the HIV epidemic [20].

**Protein structure and neutralizing antibody inducing vaccines**

The vaccine successes we have had have all been in the design of T-cell vaccines, but the cross-reactive potential of vaccines designed to elicit neutralizing antibodies is also important, and so far our synthetic vaccines have not elicited potent neutralizing antibodies. Thus we turned our attention to better characterization of the basic biology underlying the breadth of neutralizing antibody responses to HIV. An antibody-based HIV vaccine would ideally neutralize diverse variants, and detailed examination of subtype-specific differences in structure and mutational patterns could inform the design of a polyvalent cocktail with improved cross-reactive breadth. We have been able to apply all-atom molecular dynamics simulations to help define sequence and structural differences in viral glycoprotein gp120 between subtypes B and C in to keys the proteins.

Variation can be dramatically different in the HIV Envelope protein regions in the B and C subtypes in different regions of gp120. Subtype. Such differences could result from the evolution of lineage-specific structural or functional constraints in the proteins that may result in spatially localized differences in neutralizing antibody binding sites. We explored mutational patterns and their structural implications to better understand the effect of immune pressure on viral evolution. Current knowledge of HIV-1 envelope glycoprotein structure and function is largely based on studies of subtype B viruses. In subtype C, the C3 region alpha2-helix is highly variable at the polar face, suggesting it evolves under immune pressure, but maintains its amphipathicity. In the subtype B it is much more conserved and accommodates hydrophobic residues. The V4 hypervariable domain in subtype C is shorter than in subtype B [21], and coordinate patterns in variation and models of structural proximity support close interactions between the two domains [21,22]. We investigated why the subtype C V3 loop domain lacks sites of strong selection analogous to those found in the subtype B, and found the V3 domain may not be solvent-exposed in subtype C and thus excluding it as antibody- target. A cluster of hydrophobic residues flanking the V3 tip of subtype C stabilizing forces may drive this hydrophobic cluster to avoid solvent exposure and antibody accessibility. Experimental results from Dr. Cynthia Derdyn's group at Emory are consistent with the existence of such a hydrophobic cluster [23,24].

**Anthrax rapid response detection and therapy**

After the recent anthrax scare, novel detection and therapeutic agents are being sought to combat the causative agent, *Bacillus anthracis*. Goutam Gupta approached this challenge through the design of a bivalent ligand, which targets the protective antigen, a major toxin of *Bacillus anthracis*. The ligand is a chimeric scaffold, comprised of two toxin-binding domains linked to an antibody frame. It shows efficacy in therapy and diagnosis of anthrax [25,26]. Since the proposed design strategy ensures accelerated and high-yield production in stable and active forms, the chimeric protein provides a viable alternative to conventional antibodies for therapy and detection in bio-threat scenarios. This work was invited for presentation at The World Congress of Vaccines 2008.

## References


1. Korber, B., C. Miller, and T. Leitner. HIV subtypes, antigenic diversity and vaccine design.. To appear in *HIV subtypes, antigenic diversity and vaccine design..* Edited by Koff, W., P. Kahn, and I. Gust.

2. Kothe, D. L., J. M. Decker, Y. Li, Z. Weng, F. Bibollet-Ruche, K. P. Zammit, M. G. Salazar, Y. Chen, J. F. Salazar-Gonzalez, Z. Moldoveanu, J. Mestecky, F. Gao, B. F. Haynes, G. M. Shaw, M. Muldoon, B. T. Korber, and B. H. Hahn. Antigenicity and immunogenicity of HIV-1 consensus subtype B envelope glycoproteins. . 2007. *Virology.* **360** (1): 218.

3. Kothe, D. L., Y. Li, J. M. Decker, F. Bibollet-Ruche, K. P. Zammit, M. G. Salazar, Y. Chen, Z. Weng, E. A. Weaver, F. Gao, B. F. Haynes, G. M. Shaw, B. Korber, and B. Hahn. Ancestral and consensus envelope immunogens for HIV-1 subtype C . 2006. *Virology* . **352** (2): 438.

4. Weaver, E. A., Z. Lu, Z. T. Camacho, F. Moukdar, H. X. Liao, B. J. Ma, T. Kepler, G. J. Nabel, N. L. Letvin, B. T. Korber, B. H. Hahn, B. F. Haynes, and F. Gao. Cross-subtype T cell immune responses induced by an HIV-1

group M consensus Env immunogen. 2006. *Journal of Virology* . **80**: 6745.

5. Liao, H. X., L. L. Sutherland, S. M. Xia, M. E. Brock, R. M. Scearce, S. Vanleeuwen, S. M. Alam, M. Mcadams, E. A. Weaver, Z. Camacho, B. J. Ma, Y. Li, J. M. Decker, G. J. Nabel, D. C. Montefiori, B. H. Hahn, B. T. Korber, G. Gao, and B. Haynes. A group M consensus envelope glycoprotein induces antibodies that neutralize subsets of subtype B and C HIV-1 primary viruses. 2006. *Virology* . **353**: 268.

6. Santra, S., B. T. Korber, M. Muldoon, D. H. Barouch, G. J. Nabel, F. Gao, B. H. Hahn , B. F. Haynes, and N. Letvin. A centralized gene-based HIV-1 vaccine elicits broad cross-clade cellular immune responses in rhesus monkey. 2008. *The Proceedings of the National Academy of Sciences.* **105** (30): 10489.

7. Fischer, W., S. Perkins, J. Theiler, T. Bhattacharya, K. Yusim, R. Funkhouser, C. Kuiken, B. Haynes, N. L. Letvin, B. D. Walker, B. H. Hahn, and B. T. Korber. Designing polyvalent HIV-1 vaccines for optimal coverage of potential T-cell epitopes in diverse global variants . 2007. *Nature Medicine* . **13** (1): 100.

8. Letourneau, S., E. J. Im, T. Mashishi, C. Brereton, A. Bridgeman, H. Yang, L. Dorrell, T. Dong, B. T. Korber, A. J. McMichael, and T. Hanke. Design and pre-clinical evaluation of a universal HIV-1 vaccine. 2007. *PLoS ONE.* **2** (10): e984.

9. Bhattacharya, T., M. Daniels, D. Heckerman, B. Foley, C. Kadie, K. Yusim, B. McMahon, S. Mallal, J. Mullins, G. Learn, B. Walker, and B. T. Korber. Founder effects in the assessment of HIV polymorphisms and HLA allele associations. 2007. *Science* . **315** (5818): 1583.

10. Brumme, Z., C. Brumme, D. Heckerman, B. T. Korber, M. Daniels, J. Carlson, C. Kadie, T. Bhattacharya, C. Chui, J. Szinger, T. Mo, R. S. Hogg, J. S. G. Montaner, N. Frahm, C. Brander, B. D. Walker, and P. R. Harrigan. Indentification of HLA class-I-associated polymorphisms in HIV-1 functional and accessory genes using a population-based, virus lineage-corrected, genetic association approach . 2007. *PLoS Pathogens* . **3**: 94.

11. Rosseau, C. M., M. G. Daniels, J. M. Carlson, C. Kadie, H. Crawford, A. Prendergast, P. Mattews, R. Payne, M. Rolland, D. N. Raugi, B. S. Maust, G. H. Learn, D. C. Nickle, H. Coovadia, T. U'Ndung, N. Frahm, C. Brander, B. D. Walker, P. J. Goulder, T. Bhattacharya, D. E. Heckerman, B. T. Korber, and J. I. Mullins . HLA class I-driven evolution of human immunodeficiency virus type 1 subtype c proteome: immune escape and viral load. 2008. *Journal of Virology* . **82** (13): 6434.

12. Kong, W. P., L. Wu, T. Wallstrom, W. Fischer, Z. Yang, S. Ko, N. Letvin, B. Haynes, B. Hahn, B. Korber, and G. Nabel. Expanded cross-reactive breadth of the T-cell response to mosaic HIV-1 envelope DNA vaccination. *Journal of Virology* .

13. Yusim, K., W. Fischer, H. Yoon, J. Thurmond, P. W. Fenimore, G. Inchauspe, G. Lauer, B. T. Korber, and C. Kuiken. Genotype and global hepatitis C T-cell vaccine sequences optimized to address genetic diversity . *Hepatology* .

14. Fenimore, P. W., W. M. Fischer, C. Kuiken, B. T. Foley, J. R. Thurmond, K. Yusim, H. Yoon, C. Calef, J. Dye, M. Parker, and B. T. Korber. Mosaic proteins for a pan-filoviral cytotoxic T-cell lymphocyte vaccine candidate. *Vaccines* .

15. Li, F., U. Malhotra, P. B. Gilbert, N. R. Hawkins, A. C. Duerr, B. M. McElrath, L. Corey, and S. G. Self. Peptide selection for human immunodeficiency virus type 1 CTOL-based vaccine evolution. 2006. *Vaccine.* **24**: 6893.

16. Frahm, N., D. Kaufmann, K. Yusim, M. Muldoon, C. Kesmir, C. Linde, W. Fischer, T. Allen, B. Li, B. McMahon, K. Faircloth, H. Hewitt, E. Mackey, T. Miura, A. Khatri, S. Wolinsky, A. McMichael, R. Funkhouser, B. Walker, C. Brander, and B. T. Korber. Increased sequence diversity coverage improves detection of HIV-specific T cell responses. 2007. *Journal of Immunology.* **179**: 6638.

17. Wang, Z., B. Metcalf, R. M. Ribeiro, H. McClure, and A. Kaur. Th-1-type cytotoxic CD8+ T-lymphocyte responses to simian immunodeficiency virus (SIV) are a consistent feature of natural SIV infection in sooty mangabeys. 2006. *Journal of Virology.* **80** (6): 2771.

18. Pandrea, I., R. Gautam, R. Ribeiro, J. M. Brenchley, J. Barberscheck, I. F. Butler, T. Rasmussen, P. A. Marx, G. Silvestri, A. A. Lackner, A. S. Perelson, D. C. Douek, R. S. Veazy, and C. Apetrei. Acute loss of intestinal CD4+ cells is not predictive of SIV virulence. 2007. *Journal of Immunology* . **179**: 3035.

19. Davenport, M. P., R. M. Ribeiro, L. Zhang, D. P. Wilson, and A. S. Perelson. A quantitative understanding of the mechanisms and limitations of immune control of HIV. 2007. *Immunology Reviews* . **216**: 164.

20. Ribeiro, R.. HIV epidemiology and the impact of non-sterilizing vaccines . 2006. In *HIV epidemiology and the impact of nonsterilizing vaccines* . Edited by Monaini, R., and R. Dilao. , p. 30. Singapore : World Scientific.

21. Gnanakaran, S., D. Lang, M. Daniels, T. Bhattacharya, C. Derdeyn, and B. T. Korber. Clade specific differences in HIV-1: diversity and correlations in C3-C4 regions of gp120 . 2007. *Journal of Virology* . : 4886.

22. Rong, R., S. Gnanakaran, J. Decker, F. Bibollet, J. Taylor, J. Sfakianos, J. Mokili, M. Muldoon, J. Mulenga, S. Allen, B. Hahn, G. Shaw, J. Blackwell, B. T. Korber, E. Hunter, and C. Derdeyn. Unique mutational patterns in the envelope alpha 2 amphipathic helix and acquisition of length in gp120 hypervariable domains are associated with resistance to autologous neutralization of subtype C human immunodeficiency virus type 1. 2007. *Journal of Virology* . **81**: 5658.

23. Lynch, R. M., T. Shen, S. Gnanakaran, and C. A. Derdeyn. Appreciating HIV-1 diversity: subtypic differences in Env. *AIDS Research and Human Retroviruses.*

24. Lynch, R. M., R. Rong, T. Shen, W. Honnen, J. Mulenga, S. Allen, J. L. Blackwell, S. Zolla-Pazner, A. Pinter, S. Gnanakaran, and C. A. Derdeyn. Conservation of the subtype C Env V3 domain prevents neutralization . *AIDS Research and Human Retroviruses* .

25. Kunkel, M., M. Vuyisich, S. Gnanakaran, G. E. Bruening, A. M. Dandekar, E. Civerolo, J. Marchalonis, and G. Gupta. Rapid clearance of bacteria and their toxins: development of therapeutic proteins. To appear in *Critical Reviews in Immunology* .

26. Vuyisich, M., S. Gnankaran, J. A. Lovchik, R. Lyons, and G. Gupta. A dual-purpose protein ligand for effective therapy and sensitive diagnosis of anthrax.. 2008. *Protein Journal* . **27**: 292.

## Publications

Bhattacharya, T., M. Daniels, K. Yusim, and B. Korber. Founder effects in the assessment of HIV polymorphisms and HLA allele associations.. 2007. *Science.* **315**: 1583.

Brander, C., S. Self, and B. Korber. Capturing viral diversity for in vitro test reagents and HIV vaccine immunogen design. To appear in *Curr Opin HIV AIDS.*

Brumme, Z., C. Brumme, D. Heckerman, B. Korber, M. Daniels, J. Carlson, C. Kadie, T. Bhattacharya, C. Chui, J. Szinger, T. Mo, R. S. Hogg, J. Montaner, N. Frahm, C. Brander, B. Walker, and P. Harrigan. Evidence of Differential HLA Class I-Mediated Viral Evolution in Functional and Accessory/Regulatory Genes of HIV-1.. 2007. *PLoS Pathogens.* **3**: 94.

Davenport, M., L. Zhang, J. W. Shiver, D. Casmiro, R. Ribeiro, and A. Perelson. Influence of peak viral load on the extent of CD4+ T-cell depletion in simian HIV infection. 2006. *Journal of Acquired Immune Deficiency Syndrome.* **41** (3): 259.

Davenport, M., L. Zhang, J. W. Shiver, D. Casmiro, R. Ribeiro, and A. Perelson. Influence of peak viral load on the extent of CD4+ T-cell depletion in simian HIV infection. 2006. *Journal o Acquired Immune Deficiency Syndrome.* **41** (3): 259.

Davenport, M., R. Ribeiro, L. Zhang, D. Wilson, and A. Perelson. A quantitative understanding of the mechanisms and limitations of immune control of HIV. 2007. . *Immunol. Rev.* . **216**: 164.

Fenimore, P. W., W. M. Fischer, C. Kuiken, B. T. Foley, J. R. Thurmond, K. Yusim, H. Yoon, C. Calef, J. Dye, M. Parker, and B. Korber. Mosaic proteins for a pan-filoviral cytotoxic T-cell lymphocyte vaccine candidate. . *Vaccines* .

Fischer, W., H. L. Liao, B. Haynes, N. Letvin, and B. T. Korber. Coping with viral diversity in HIV vaccine design: a response to Nickle et al. . 2008. *Computational Biology* . **4** (1): e15.

Fischer, W., S. Perkins, B. Walker, J. Theiler, T. Bhattacharya, K. Yusim, R. Funkhouser, C. Kuiken, B. Hayes, N. Letvin, and B. Korber. Designing polyvalent HIV-1 vaccines for optimal coverage of potential T-cell epitopes in diverse global variants. 2007. *Nature Medicine.* **13**: 100.

Frahm, N., D. Kaufmann, K. Yusim, M. Muldoon, C. Kesmir, C. Linde, W. Fischer, T. Allen, B. Li, B. McMahon, K. Faircloth, H. Hewitt, E. Mackey, T. Miura, A. Khatri, S. Wolinsky, A. McMicheal, R. Funkhouser, B. Walker, C. Brander, and B. Korber. Increased Sequence Diversity Coverage Improves Detection of HIV-Specific T Cell Responses.. 2007. *J. Immunololgy.* **179**: 6638.

Gao, F., H. X. Liao, B. H. Hahn, N. L. Letvin, B. T. Korber, and B. F. Haynes. Centralized HIV-1 envelope immunogens and neutralizing antibodies. . 2007. *Current HIV Research .* **5** (6): 572.

Gnanakaran, S., D. Lang, M. Daniels, T. Bhattacharya, C. Derdeyn, and B. Korber. Clade specific differences in HIV-1: Diversity and correlations in C3-V4 regions of gp120. 2007. *Journal of Virology.* **J. Virol**: 4886.

Haynes, B., B. Korber, B. Ma, D. Montefiori, T. Wrin, C. Petropoulos, L. Sutherland, R. Searce, and C. Denton. Analysis of HIV-1 subtype B third variable region peptide motifs for induction of neutralizing antibodies against HIV-1 primary isolates. 2006. *Virology.* **345** (14): 44.

Jones, L. E., and A. S. Perelson. Transient viremia, plasma viral load, and reservoir replenishment in HIV-infected patients on antiretroviral therapy. . 2007. *Journal of Acquired Immune Deficiency Syndrome.* **45** (5): 483.

Jones, L., and A. Perelson. Transient viremia, plasma viral load, and reservoir replenishment in HIV-infected patients on antiretroviral therapy.. 2007. *J Acquir Immune Defic Syndr..* **45**: 483.

Kong, W. P., L. Wu, T. Wallstrom, W. Fischer, Z. Yang, S. Ko, N. Letvin, B. Haynes, B. Hahn, B. Korber, and G. Nabel. Expanded cross-reactive breadth of the T-cell response to mosaic HIV-1 envelope DNA vaccination.. *Jounal of Virology.*

Korber, B., C. Miller, and T. Leitner. HIV suptypes, antigenic diversity and vaccine design. . 2007. In *AIDS vaccine development. .* Edited by Koff, W., P. Kahn, and I. Gust. , p. 65. Norfork : Caister Academic Press .

Korber, B., M. LaBute, and K. Yusim. Immunoinformatics comes of age. 2006. *PLOS Computational Biology.* **2** (6): 71.

Kothe, D., B. Haynes, G. Shaw, B. Korber, B. Hahn, Y. Li, J. Decker, F. Bibollet-Ruche, K. Zammit, M. Salazar, Y. Chen, and Z. Weng. Ancestral and consensus envelope immunogens for HIV-1 subtype C. 2006. *Virology.* **79** (2): 438.

Kothe, D., J. Decker, Y. Li, Z. Weng, F. Bibollet, K. Zammit, M. Salazar, Y. Chen, J. Salazar, Z. Moldoveanu, J. Mestecky, F. Gao, B. Haynes, G. Shaw, M. Muldoon, B. Korber, and B. Hahn. Antigenicity and immunogenicity of HIV-1 consensus subtype B envelope glycoproteins. . 2007. *Virology.* **360**: 218.

Kothe, D., Y. Li, J. Decker, F. Bibollet-Ruche, K. Zammit, M. Salazar, Y. Chen, Z. Weng, E. Weaver, F. Gao, B. Haynes, G. Shaw, and B. Korber. Ancestral and Consensus Envelope Immunogens for HIV-1 Subtype C. . 2006. *Virology.* **352**: 438.

Kunkel, M., M. Vuyisich, G. Gnanakaran, G. E. Bruening, A. M. Dandekar, E. Civerolo, J. J. Marchalonis, and G. Gupta. Rapid Clearance of bacteria and thier toxins: development of therapeutic proteins. . 2007. *Critical Reviews in Immunology .* **27** (3): 233.

Letourneau, S., E. J. Im, T. Mashimi, C. Brereton, A. Bridgeman, H. Yang, L. Dorrell, T. Dong, B. Korber, A. J. McMichael, and T. Hanke. Design and pre-clinical evolution of a universal HIV vaccine.. 2007. *Public Library of Science .* **3** (2): e984.

Letourneau, S., E. J. Im, T. Mashishi, C. Brereton, A. Bridgeman, H. Yang, L. Dorrell, T. Dong, B. Korber, A. J. McMichael, and T. Hanke. Design and pre-clinical evaluation of a universal HIV-1 vaccine. . 2007. *PLoS ONE .* **2** (10): e984.

Li, M., J. Salazar, C. Derdeyn, L. Morris, C. Williamson, J. Robinson, J. Decker, Y. Li, M. Salazar, V. Polonis, B. Korber, and D. Montefiori. Genetic and neutralization properties of subtype C human immunodeficiency virus type 1 molecular env clones from acute and early heterosexually acquired infections in Southern Africa. 2007. *j. Virol..* **80**: 11776.

Liao, L., H. Liao, L. Sutherland, S. Xia, M. Brock, R. Scearce, S. Vanleeuwen, S. Alam, M. McAdams, E. Weaver, Z. Camacho, B. Ma, Y. Li, J. Decker, G. Nabel, D. Montefiori, B. Hahn, B. Korber, F. Gao, and B. Haynes. A Group M Consensus Envelope Glycoprotein Induces Antibodies That Neutralize Subsets of Subtype B and C HIV-1 Primary Viruses. . 2006. *Virology.* **353**: 268.

Liu, W., Z. Weng, J. D. Robertson, M. H. Kraus, B. Z. Wang, M. Nathan, P. Pushko, L. Sutherland, B. F. Haynes, G. M.

Shaw, D. C. Montefiori, G. Smith, R. W. Compans, and B. H. Hahn. Non-adjuvanted recombinant baculovirus derived HIV-1 Virus-Like Particles elicit neutralizing antibody responses that are comparable in breadth and magnitude to responses elicited by adjuvanted envelope protein vaccines..

Lynch, R. M., R. Rong, T. Shen, W. Honnen, J. Mulenga, S. Allen, J. L. Blackwell, S. Zoller-Pazner, A. Pinter, S. Gnanakaran, and C. A. Derdeyn. Conservation of the Subtype C Env V3 domain prevents neutralization.. *AIDS Research and Human Retroviruses* .

Lynch, R. M., T. Shen, S. Gnanakaran, and C. A. Derdeyn. Appreciating HIV-1 diversity: subtypic differences in Env.. *AIDS Research and Human Retroviruses* .

Markowitz, M., and A. Perelson. HIV-1 viral dynamics studies in the setting of clinical trials - a window of opportunity. 2007. *J. Infect. Dis.* . **195**: 1087.

Pandrea, I. V., R. Gautam, R. M. Ribeiro, J. M. Brencheley, I. F. Butler, M. Pattison, T. Rasmussen, P. A. Marx, G. Silvestri, A. A. Lackner, A. S. Perelson, D. C. Douek, R. S. Veazy, and C. Apetrei. Acute loss of intestinal CD4+ T cells is not predictive of simian immunodeficiency virus virulence. . 2007. *Journal of Immunology* . **2007** (179): 3035.

Ribeiro, R.. HIV Epidemiology and the Impact of Nonsterilizing Vaccines.. 2007. In *BIOMAT 2006.* Edited by Monaini, R., and R. Dilao. , p. 30. Singapore: World Scientific.

Ribeiro, R. M., M. D. Hazenberg, A. S. Perelson, and M. P. Davenport. Naive and memory cell turnover as drivers of CCR5-to-CXCR4 tropism switch in human immunodeficiency virus type 1: implications for therapy. 2006. *Journal of Virology.* **80** (2): 802.

Rong, L., Z. Feng, and A. Perelson. Mathematical analysis of age-structured HIV-1 dynamics with combination therapy. . 2007. *SIAM J. Appl. Math.* **67**: 731.

Rong, R., S. Gnanakaran, J. Decker, F. Bibollet, J. Taylor, J. Sfakianos, J. Mokili, M. Muldoon, J. Mulenga, S. Allen, B. Hahn, G. Shaw, J. Blackwell, B. Korber, E. Hunter, and C. Derdeyn. Unique mutational patterns in the envelope alpha 2 amphipathic helix and acquisition of length in gp120 hypervariable domains are associated with resistance to autologous neutralization of subtype C human immunodeficiency virus type 1.. 2007. *J. Virol..* **81**: 5658.

Rosseau, C. M., M. G. Daniels, J. M. Carlson, C. Kadie, H. Crawford, A. Prendergast, P. Mattews, R. Payne, M. Rolland, D. N. Raugi, B. S. Maust, G. H. Learn, D. C. Nickle, H. Coovadia, T. U'Ndung, N. Frahm, C. Brander, B. D. Walker, P. J. Goulder, T. Bhattacharya, D. E. Heckerman, B. T. Korber, and J. I. Mullins. HLA class I-driven evolution of human immunodeficiency virus type 1 subtype c proteome: immune escape and viral load.. 2008. *Journal of Virology.* **82** (13): 6434.

Santra, S., B. Korber, M. Muldoon, D. H. Barouch, G. J. Nabel, F. Gao, B. H. Hahn, B. F. Haynes, and N. Letvin. A centralized gene-based HIV-1 vaccine elicits broad cross-clade cellular immune responses in rhesus monkeys. . 2008. *The Proceedings of the National Academy of Sciences* . **105** (30): 10489.

Schneidewind, A., M. A. Brockman, R. Yang, R. I. Adam, B. Li, S. Le Gall, C. R. Rinaldo, S. L. Craggs, R. L. Allgaier, K. A. Power, T. Kuntzen, C. S. Tung, M. X. LaBute, S. M. Mueller, T. Harrer, A. J. McMichael, P. J. Goulder, C. Aiken, C. Brander, A. D. Kelleher, and T. M. Allen. Escape from the dominant HLA-B27-restricted cytotoxic T-lymphocyte response in Gag is associated with a dramatic reduction in human immunodeficiency virus type 1 replication. . 2007. *Journal of Virology* . **81** (22): 12382.

Thurmond, J., H. Yoon, C. Kuiken, K. Yusim, S. Perkins, J. Theiler, T. Bhattacharya, B. T. Korber, and W. Fischer. Web-based design and evaluation of T-cell vaccine candidates.. 2008. *Bioinformatics* . **24** (14): 1639.

Timm, J., B. Li, M. Daniels, T. Bhattacharya, L. Reyor, R. Allgaier, T. Kuntzen, W. Fischer, J. Duncan, J. Schulze zur Wiesch, A. Kim, N. Frahm, C. Brander, R. Chung, G. Lauer, B. Korber, and T. Allen. Human leukocyte antigen-associated sequence polymorphisms in hepatitis C virus reveal reproducible immune responses and constraints on viral evolution.. 2007. *Hepatology.* **46**: 339.

Tuckwell, H. C., P. D. Shipman, and A. S. Perelson. The probability of HIV infection in a new host and its reduction with microbicides. . 2008. *Mathematical Biosciences* . **214** (1-2): 81.

Vuyisich, M., S. Gnanakaran, J. A. Lovchik, R. Lyons, and G. Gupta. A dual-purpose protein ligand for effective therapy and sensitive diagnosis of anthrax. . 2008. *Protein Journal* . **27** (5): 292.

Wang, B. Z., W. Liu, S. M. Kang, C. Huang, L. Ye, Y. Sun, D. Kothe, P. Pushko, T. Dokland, G. Smith, B. H. Hahn, and R. W. Compans. Incorporation of high levels of chimeric

human immunodeficiency virus envelope glycoproteins into virus-like particles. . 2007. *Journal of Virology.* **81**: 10869.

Wang, Z., B. Metcalf, R. M. Ribeiro, H. McClure, and A. Kaur. Th-1-type cytotoxic CD8+ T-lymphocyte responses to simian immunodeficiency virus (SIV) are a consistent feature of natural SIV infection /in sooty mangabeys. 2006. *Journal of Virology.* **80** (6): 2771.

Weaver, E., N. Letvin, B. Korber, B. Hahn, B. Haynes, F. Gao, Z. Lu, Z. Camacho, F. Moukdar, H. Liao, B. Ma, M. Muldoon, J. Theiler, and G. Nabel. Cross-subtype T-cell immune responses induced by a human immunodeficiency virus type 1 group m consensus env immunogen. 2006. *Journal of Virology.* **80** (14): 6745.

Xu, G. Y., M. Lichterfeld, S. Chetty, K. L. Williams, S. K. Mui, T. Miura, N. Frahm, M. E. Feeney, T. Tang, F. Pereyra , M. X. LaBute, K. Pfafferott, A. Leslie, H. Crawford, R. Allgaier, W. Hildebrand, R. Kaslow, C. Brander, T. M. Allen, E. S. Rosenberg, P. Kiepiela, M. Vajpayee, P. A. Goepfert, M. Altfeld, P. J. R. Goulder, and B. D. Walker. Mutually exclusive T-cell receptor induction and differential susceptibility to human immunodeficiency virus type 1 mutational escape associated with a two-amino-acid difference between HLA class I subtypes. . 2007. *Journal of Virology* . **81** (4): 1619.

Yusim, K., W. Fischer, H. Yoon, J. Thurmond, P. W. Fenimore, G. Inchauspe, G. Lauer, B. Korber, and C. Kuiken. Genotype and global hepatitis C T-cell vaccine sequences optimized to address genetic diversity. . *Hepatology* .

# Pathogen Detection Based on Biomodulation

*Basil Ian Swanson*

20060040DR

## Abstract

Autonomous pathogen detection requires very little human intervention and no addition of reagents other than the sample. Furthermore, in a stand-alone format, monitoring air and/or water can occur continuously. A stand-alone instrument must be capable of specific and sensitive detection at the location of interest to avoid the unacceptable time delays associated with the transfer of samples to a central laboratory. With this fact in mind, we undertook the development of the underlying technologies that would permit near real-time, unattended detection with very low reagent stream so that the system could operate for extended periods of time in the field. This goal required the creation of several detection tools, including robust sensing films, stable recognition ligands, robust optical reporters that did not degrade, and a reagent-free transduction approach. These tools will find application in pathogen detection, but can be used for problems in medical diagnostics and the detection of agricultural threats. As they are applied to various detection methods, these tools will ultimately contribute to the development of practical stand-alone detection technologies.

## Background and Research Objectives

The intentional release of pathogens into the environment represents both a military and homeland security threat. Recent funding strategies for the development of detection technologies for pathogens in the environment have been limited to off-the-shelf technologies. As a result, current fielded approaches are little more than sample collectors that require transfer of samples to a reference laboratory for confirmatory analysis. Other approaches under development largely represent miniaturization of current lab-based approaches. Little investment has been made in the underlying science and technology to create new approaches to this difficult problem.

There are several technical barriers to autonomous pathogen detection. First, the large amount of reagents required for conventional lab-based methods is simply impractical for unattended detection over extended periods of time. Second, the poor stability of recognition ligands, especially antibodies, is not suited to real-world conditions where the temperatures encountered and long storage times result in degradation. Third, the sensing films at the interface between the complex samples and the sensor must endure a variety of harsh conditions and resist interference from complex samples. Finally, an autonomous system requires a robust transduction scheme. Optical methods are often used, and the reporters incorporated into a stand-alone platform must resist chemical modification from the sample matrix and alteration due to long-term exposure to excitation sources (typically lasers). Although some progress has been made in addressing the above limitations, the realization of an autonomous detection system remains an unmet challenge.

Overall, the work described below involved creating new tools that solved the limitations outlined above, then integrating them into a practical device for the detection of gene markers and intact pathogens. As you will see, this research team has made considerable progress in the development of novel pieces of the autonomous detection puzzle. These advances should find numerous applications in biological detection in the military, homeland security, and medical sectors.

## Importance to LANL's Science and Technology Base and National R & D Needs

As a National security laboratory, LANL's mission includes addressing the threat of biological weapons. Within this mission space, the detection of purposeful release of biological pathogens into the environment remains a significant problem. However, it should be noted that biological sensors are a dual use technology. The same tools that are developed for pathogen detection can be applied to other civilian areas including medical diagnostics for human diseases and screen-

ing for disease in animal populations (e.g., *M. bovis* in cattle). The research performed in this project has led to the development of several useful tools that will underpin future efforts at the Laboratory to address detection and diagnostic needs, especially detection of human pathogens in remote and/or resource-limited settings.

## Scientific Approach and Accomplishments

### Signal Transduction Based on Biomodulation

The most challenging task in this project was to develop a reagent-free transduction approach where the signal used in detection was not degraded by high, non-specific adsorption of biomolecules from the complex samples encountered in the environment. Our approach was based systematically varying (modulating) the position of a fluorescent dyes attached to the end of a tether. This tether was attached to the surface of a planar optical waveguide, which behaves similarly to an optical fiber—most of the laser light coupled into a waveguide (Figure 1) is contained within the waveguiding material. A small amount, termed the evanescent field, leaks out of the waveguiding layer, with its intensity decaying exponentially as the distance increases from the waveguide surface. The photons in the evanescent field excite the fluorescent dyes in our sensor approach. We rely on the exponential fall-off of this optical field strength to modulate the fluorescence signal. The dye is moved toward and away from the surface by an acoustic field, and the positional modulation of the dye leads to fluctuations in fluorescence intensity (Figure 2). A plot of the response amplitude versus the driving acoustic frequency leads to a unique "frequency spectrum" after a target pathogen binds to the recognition molecule.

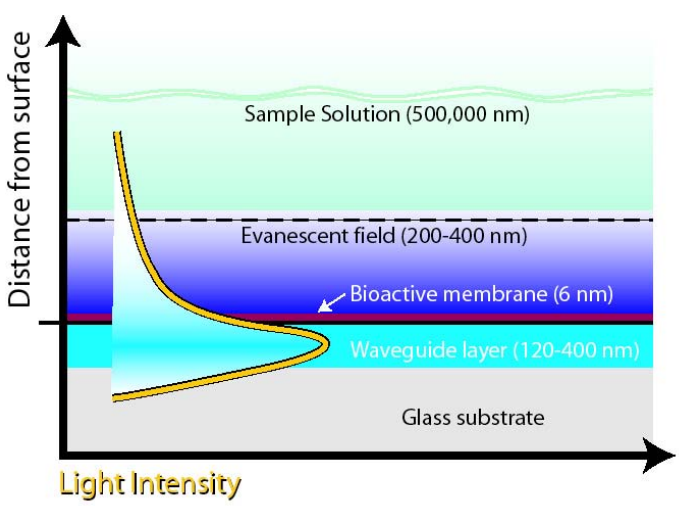


*Figure 1. Planar optical waveguide sensing chip. The evanescent optical field falls off exponentially as a function of distance from the waveguide surface.*

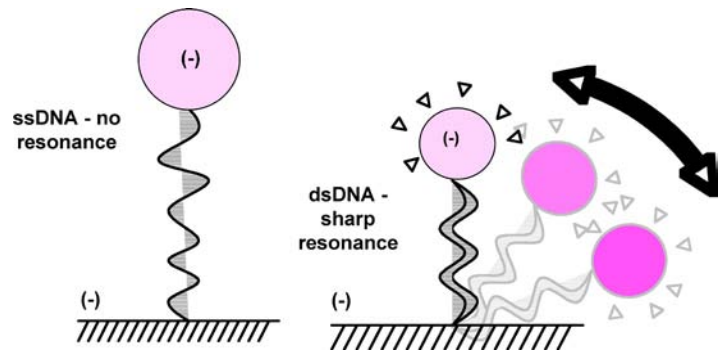


*Figure 2. Positional modulation of a fluorescent dye molecule tethered by single and double stranded DNA. As the dye approaches the waveguide surface, the fluorescence increases (increased color in dsDNA tethered dye) because the dye molecule moves into a brighter portion of the evanescent field.*

Although a number of detection schemes can be executed with this approach, we focused on gene detection. In short, both single stranded and double stranded DNA (ssDNA and dsDNA respectively) linkers have been used to attach dyes to a sensing film (below). In effect, the ssDNA and associated dye follow the movement of the surface. In contrast, dsDNA forms a rigid rod that undergoes harmonic motion relative to the surface under application of the acoustic field. This harmonic motion gives rise to a measurable signal. The frequency spectrum of the dsDNA construct can then be divided by that of the ssDNA frequency response to give spectra as shown in Figure 3. The key observation is that the dsDNA tether gives rise to discrete resonances at~ 10 kHz and 12 kHz that are distinct from that of the ssDNA. Detection of a gene (e.g., ssDNA or mRNA) is possible using this method. Moreover, this same dsDNA construct can be made to detect other pathogen markers (including intact viral particles) by attaching recognition ligands to the dye molecule and measuring spectral changes due to pathogen bindng.

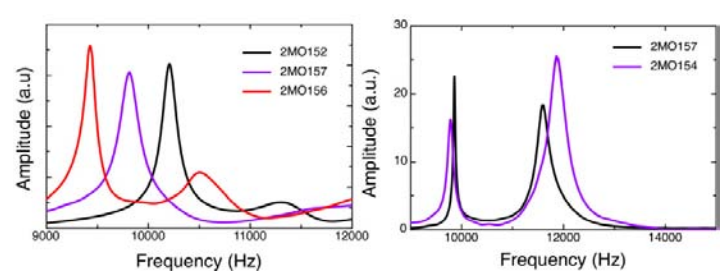


*Figure 3. Typical spectra from a double-stranded DNA linker. The structure in the spectra are similar although shifted in frequency.*

**Robust recognition ligands**

Molecular recognition is at the heart of most phenomena in nature, and is critical in the detection of biological molecules. Typically, the biomolecule (antigen) of interest (e.g., a protein marker that is specific for a pathogen) is recognized and captured by an antibody coupled to the surface of a sensor. The problem with antibodies in autonomous sensing is their lack of stability. Antibodies are proteins that can lose function by denaturing (changing their tertiary structure and therefore losing their functional shape) under a variety of conditions (low or high pH, elevated temperatures etc.). Moreover, as proteins, they are susceptible to degradation by proteases—proteins that cleave particular amino acid sequences. In order to address the inherent instability of antibodies, we have explored the use of alternate recognition molecules—peptides and carbohydrates—which are more stable.

Peptides are typically much smaller than antibodies more stable. Peptides can be synthesized using automated technology, but it is often more efficient to express them in a living system. These recognition agents can be raised against biothreat agents using a technique known as phage display. Phage display technology involves the display of proteins or peptides on the surface of phage particles (viruses that infect bacteria). Traditional peptide phage display libraries are produced using filamentous phage, which produces libraries with five copies each of the selected peptide. Unfortunately, these libraries also exhibit an increased propensity for deletions (phage particles with no displayed peptides). We have created peptide libraries in "helper cells" that allow us to vary between multi-and monomeric display to select ligands with the highest binding affinity. From these results, primary libraries and secondary libraries were selected. Five primary libraries were created in helper cells, consisting of peptides with 6, 10, 12, or 18 amino acids in either cyclic (10, 6) or linear (18, 12, 6) orientation. Each of these primary libraries has also been created as a secondary library in helper cells. Each primary and secondary library was sequenced. These libraries have been screened against influenza virus (serotype H3N1, Port Chalmers strain), to select peptide ligands against this important flu variant.

Carbohydrates represent another class of stable molecules applicable to sensing applications. Often, these molecules determine, or at least participate in, pathogen-host interactions at a cellular level. Influenza, for example, binds to neuraminic acid displayed on cells in the upper respiratory tract; this binding leads to infection of the host. Neuraminic acid binds both hemaglutinin (HA) and neuraminidase proteins on the influenza viral coat, and both proteins are present in multiple copies. This phenomenon enables multivalent binding to several sites simultaneously, and enhances the low binding affinities of single carbohydrate-protein interactions. For sensing applications, this multivalency provides highly efficient capture of the viral particles on a sensing surface. We have prepared multivalent carbohydrate ligands that mimic neuraminic acid in order to develop an "all carbo" assay for influenza. Two of the ligands are depicted in Figure 4. Using these two ligands we were able to demonstrate the strain specific detection of influenza using our waveguide sensor system. This work was published as a communication in the Journal of the American Chemical Society in 2008.

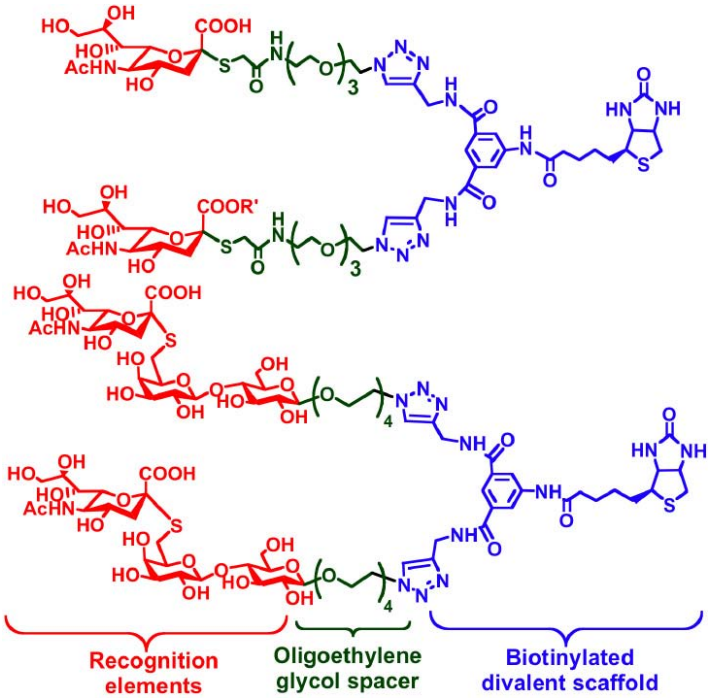


*Figure 4. Two bidentate carbohydrate ligands developed for the detection of influenza.*

**Stable sensing films**

In the past, we have relied on phospholipid bilayers as the interface between the analyte and the sensing surface because they offer superior resistance to non-specific binding. They have limitations, however, including instability to air, detergents, elevated temperature, and high salt solutions. In addition to non-specific binding resistance, this project required a surface that would endure the ionic strength and temperature cycling conditions required for oligonucleotide hybridization. To overcome the disadvantages of lipid bilayers, we developed a stable thin film that effectively resists non-specific binding in a variety of biological assays.

Covalently attached, discrete polyethyleneglycol (PEG)-modified self-assembled monolayers (SAMs) were designed and prepared. These films are formed by the vapor-phase, surface self-assembly of aminopropylsilane, followed by modification with well-defined PEG spacers. The PEG portion of the film acts as a tether between the sensor surface and the reactive portion of the film, and effectively resists non-specific binding. Most of the PEG chains (>99%) end with a chemically and biologically inert methoxy group that effectively blocks unwanted adsorption of molecules. The terminus of a small percentage of the PEG spacers contains a functional group that can be modified in a variety of ways. Testing showed stability to elevated temperature in cell culture media (80 °C for 1h), stability to storage in air for one year, and functional stability in fetal bovine serum, rat urine, and human urine. The films have been successfully used in many different assays from gene to protein and intact virus detection.

Several noteworthy points emerged from our thin-film research. First, the deposition of the self-assembled silane was facilitated through a room temperature, rough vacuum process that required no specialized chemical vapor deposition apparatus. This vapor deposition method allowed dramatic improvements in sensing efficiency, which are detailed in a recent publication (Anderson et al *Langmuir* 2008). Second, the entire thin-film deposition can be completed within two days, which enabled this team to complete a large number of experiments. Taken together, these aspects of this deposition process show our method to be simple, straightforward, and inexpensive, which is a significant improvement over other thin-films and deposition methods present in the current primary literature.

**Robust optical reporters**

Optical sensors have traditionally relied on organic dyes to provide the fluorescence signals used in detection. For applications in autonomous sensing and in the quantitative detection of multiple analytes, it is not possible to use organic dyes because they degrade quickly upon exposure to light. This property, referred to as photobleaching, is especially problematic in the intense optical fields associated with planar optical waveguides. We have pursued two approaches to more robust optical reporters: dye imbedded silica particles and semiconductor quantum dots (QDs).

We have developed several methods to prepare fluorescent silica nanoparticles for use in biomodulation experiments. Encapsulation of fluorescent molecules in silica acts to concentrate the fluorescent molecules in a small region making the fluorescence signal from a nanoparticle more intense (easier to "see") than fluorescence from an isolated, individual molecule. Silica encapsulation also acts as a barrier to prevent the environment from affecting the fluorescence signal emanating from the dye molecules. In addition, we can readily modify the surface of the silica particles to, for example, attach it to a waveguide surface or make it more water soluble.

During the course of this DR, we have encapsulated several inorganic dyes, including ruthenium tris(bipyidine), into silica nanoparticles and studied their fluorescent properties. The ruthenium complexes encapsulated in silica were found to be much more stable than organic dyes, which allow us to monitor them for longer periods of time. We have developed methods to prepare fluorescent silica nanoparticles as small as 25nm in diameter.

In addition to silica encapsulated dyes, we have worked toward a reporter-ligand scaffold based on chaperonin protein-QD conjugates. Robust ligand scaffolds based on chaperonin proteins can be engineered to bind to semiconductor quantum dot (QD) reporters in their central pores while carrying multivalent recognition ligands on the solvent exposed position for target binding. Chaperonins are composed of 14-18 protein subunits called heat shock proteins (HSP60). One family of HSP60, originating from the *Sulfolobus shibatae*, can self-assemble into a double-stacked ring structure with a ~ 6 nm size central cavity. Such proteins are robust—they can tolerate high temperature, low pH, organic solvent treatment, and protease digestion without losing their biological functions. The binding affinity of protein to reporter QD was measured and found to be quite high (K d ~ 0.1 nM). Recognition ligands were introduced onto the chaperonin scaffolds by site-directed mutagenesis and chemical modification. The results demonstrated that our ligand-chaperonin-QD conjugates bind specific target molecules efficiently with high optical and physical stability. In addition to their application in sensing, these conjugates may find use as "stealthy" delivery vehicles to deliver both imaging and therapeutic agents to cancer tumors.

## Publications

Anderson, A. S., A. M. Dattelbaum, G. A. Mantano, D. N. Price, W. K. Grace, J. S. martinez, J. G. Schmidt, K. M. Grace, and B. I. Swanson. Preparation, Characterization, and Use of Modified Self-Assembled Thin-Films for Biomarker Detection. Presented at *Detection Technologies 2007.* (San Diego, 1-2 Nov. 2007).

Anderson, A. S., A. M. Dattelbaum, G. A. Montano, J. G. Schmidt, J. S. Martinez, W. K. Grace, K. M. Grace, and B. I.

Swanson. Functionalized waveguides for biological assays. 2007. In *Materials Research Society.* (Boston, 29-1 Nov. 2006). , p. 35. Warrendale, PA: Mat Res. Soc. Symp. Proc..

Anderson, A. S., A. M. Dattelbaum, G. A. Montano, W. K. Grace, J. S. Martinez, J. G. Schmidt, K. M. Grace, and B. I. Swanson. Preparation and use of modified self-assembled thin films for detection of Bacillus anthracis protective antigen. Presented at *Mat. Res. Soc..* (Boston, Nov, 2006).

Anderson, A. S., A. M. Dattelbaum, G. A. mantano, D. N. Price, W. K. Grace, J. S. Martinez, and J. G. Schmidt. Functional PEG-Modified Films for Biological Detection. 2008. *Langmuir.* **24** (5): 2240.

Kale, R. R., H. Mukundan, A. S. Anderson, R. M. Vermillion, B. I. Swanson, J. G. Schmidt, and S. S. Iyer. Detection of intact influenza virus using biotinylated biantennary S-sialosides. 2008. *Journal of the American Chemical Society.* **130** (26): 8169.

Mukundan, H., H. Xie, A. S. Anderson, W. K. Grace, J. E. Shively, and B. I. Swanson. Optimizing a Waveguide-based Sandwich Immunoassay for Tumor Biomarkers. To appear in *Bioconjugate Chemistry.*

Mukundan, H., H. Xie, W. K. Grace, J. S. Martinez, N. Hartman, and B. I. Swanson. A Mmtichannel waveguide for quantitative and rapid detection of antigens in quadruplicate. *Analytical Chemistry.*

Mukundan, H., J. Kubicek, D. Price, A. Anderson, J. Martinez, W. K. Grace, R. Cho, S. Y. Eum, S. H. Hwang, S. K. Park, L. Via, C. Barry, and B. I. Swanson. : Sensitive Detection of Tuberculosis-Specific Markers in Patient Urine using a Waveguide-based Optical Biosensor. Invited presentation at *Immunodiagnosis of Tuberculosis .* (Virginia Beach, Sept. 2008).

Mukundan, H., J. Kubicek, D. Proce, A. Anderson, W. K. grace, R. Cho, L. Via, C. Barry, and B. I. Swanson. Sensitive Detection of Tuberculosis-Specific Markers in Patient Urine using a Waveguide-based Optical Biosensor. Presented at *Keystone Symposium.* (Bangkok, Oct. 2008).

Mukundan, H., W. K. Grace, J. Shively, and B. Swanson. Waveguide-based optical biosensor for the early sensitive detection of breast cancer markers. Presented at *American Society for Clinical Oncology.* (San Francisco, Sept. 2007).

Swanson, B. I.. Biological sensors based on biomimetic approaches and nanobio materials. Invited presentation at *US/EU NanoBio Materials Conference.* (Ispra, Italy, 2-4 June 2008).

Swanson, B. I.. Reagent-free sensors for pathogen detection. Invited presentation at *DTRA Maui Meeitng.* (Maui, June 2007).

Xie, H., H. Mukundan, W. K. Grace, J. S. Martinez, and B. I. Swanson. Quantum dots for multiplex detection of B. anthracis lethal toxin components in single mode planar optical waveguides. *Angewante Chemie.*

Xie, H., M. Cotlet, Y. F. Li, J. Trent, and B. I. Swanson. Chaperonin proteins scaffolds for quantum dots and target-binding ligands. Presented at *Mat. Res. Soc..* (San Francisco, 17-21 Mar. 2008).

Xie, H., Y. F. Li, H. K. Kagawa, J. D. Trent, M. Cotlet, and B. I. Swanson. An intrinsically fluorescent recognition ligand scaffold based on chaperonin protein and semiconductor quantum dot conjugates. To appear in *Small.*

Xie, H., Y. F. Li, M. Cotlet, J. D. Trent, and B. I. Swanson. Engineering of chaperonin protein templates for encapsulation of quantum dots. *ChemBioChem.*

Xie, H., Y. Li, J. Trent, and B. I. Swanson. Interaction of the engineered chanperonin proteins with water-soluble quantum dots. Presented at *Am . Chem. Soc. National Meeting.* (Chicago, Mar. 2007).

# Computational Methods for Protein Function Inference

*Michael E Wall*

20060700DR


## Abstract

Genome projects have greatly accelerated the rate at which genetic information is becoming available for a wide variety of organisms. However, little is known about how to decode this information and use it to understand how an organism works and what its capabilities are. The purpose of this project is to use information from genetic sequences, protein structures and biological databases to computationally predict and understand the mechanisms of the functions of proteins. The methods will support genome-wide analysis of the functions of proteins and protein networks and will enable prediction of the capabilities of emerging pathogens.


## Background and Research Objectives

More-than a decade after the publication of the Haemophilus influenzae genome sequence in 1995 (which marked the beginning of the era of shotgun sequencing), there are now over 300 complete bacterial sequences deposited at the Institute for Genome Research (TIGR). The rate of appearance of new microbial genome sequences now approaches one per day, increasing manifold our breadth of knowledge about microbes. How has the depth of knowledge increased over a similar period?

Consider Escherichia coli K12, the most comprehensively studied bacterium. A fully annotated function cannot be assigned to 43% (1873 of 4359) of E. coli's protein-encoding genes. Furthermore, no functional information has been derived from homology for 34% (1482 of 4359) of the E. coli genes. The state of knowledge of the E. coli genome is essentially the same as that in 1997 when the genome sequence first was published [1]. Like E. coli, the fraction of the human genome that has not been assigned function is the same now as when the human genome project began. In addition, there is no functional information for a large fraction (25-48%) of protein-encoding genes in both A/B listed pathogens and bacteria central to DOE's biotechnology goals. Structural genomics efforts are helping to address the gap between sequence and function through genome-wide determination of the structures of proteins of unknown function. However, even with these structures in hand, researchers are currently lacking the computational methods that would enable the functions of proteins to be inferred from their sequence and structure. New methods are required to fully leverage the structure databases for increasing our knowledge of protein function.
The overall goal of this project is to develop computational methods that can be used to help fill the gap between information about protein sequence and protein function. Our efforts are focused on making full use of structure databases for prediction of protein function. Our goal is addressed through achieving the following objectives:

1. Develop bioinformatics resources that integrate information about protein sequence, structure, and function.
2. Develop and validate methods and software for predicting protein function from protein sequence and structure information.
3. Make methods and results publicly available via the web and other means.

## Importance to LANL's Science and Technology Base and National R & D Needs

The methods we develop contribute to prediction of the capabilities of microbes of interest to DOE and DHS. Our methods will be useful for developing engineered microbes that can be precisely controlled to produce biofuels or degrade environmental waste, helping to increase Energy and Environment security. They will also be useful for predicting and defeating the capabilities of emerging pathogens in Threat Reduction.

## Scientific Approach and Accomplishments

Our overall approach is to develop informatics resources and computational tools for prediction of protein function. The project leverages the expertise of members in databases and bioinformatics; protein structure and dynamics; and, in the early stages of the project, text analysis.

**Develop bioinformatics resources that integrate information about protein sequence, structure, and function**

We have integrated diverse information about proteins in a relational database. The database includes publicly available information about sequence, structure, and function, and also includes unique data sets (e.g. functional site predictions) generated by the project. We have also revised and maintained SchemaTrans software to facilitate the importing of diverse kinds of data (C Egner, JD Cohn, LA-CC-05-103). The database has been brought to other projects (e.g. LDRD and Intelligence Community programs), has been offered as a resource on proposals (e.g. NIH R01).

**Develop and validate methods and software for predicting protein function from protein sequence and structure information**

We developed an original method called Dynamics Perturbation Analysis (DPA) to predict small-molecule binding sites in proteins using analysis of protein dynamics, and tested the method using hundreds of protein-ligand structures from a docking test set [2]. We developed an accelerated method called Fast DPA for making high-throughput predictions [3], and applied it to predict functional sites for ~50,000 proteins in SCOP [4], a library of protein domain structures (JD Cohn, D Ming, ME Wall, in preparation). We also investigated the consequences of the underlying theoretical foundation of the method for thermodynamic models of ligand binding [5].

We applied DPA to protein structures predicted by ROBETTA [6] for the CASP 8 structure prediction experiment; CASP is evaluating our predictions and we expect to hear results of our performance in October 2008. The effort to predict functional sites for predicted structures will continue after the project ends and is the focus of ongoing program development efforts with Richard Bonneau (NYU), a well-known structure prediction expert who co-authored ROBETTA.

We built on DPA to develop a method to evaluate and optimize coarse-grained models of proteins, and used the method to improve the popular Elastic Network Model of protein vibrations [7]. To further our coarse-grained modeling capabilities, we developed software for simulating a popular nonlinear, coarse-grained simulations of protein dynamics, and used the software to discover and model patterns in the complex energy landscapes of proteins [8]. To better understand why DPA works so well using coarse-grained models, we performed a detailed comparison of protein vibrations using 20 proteins, and found that coarse-grained models and all-atom models respond in a remarkably similar way to perturbations (D Ming, ME Wall, in preparation). We also began developing nonequilibrium statistical mechanics methods for coarse-grained modeling of nonlinear protein dynamics with unprecedented accuracy (M Anghel, D Ming, ME Wall, in preparation).

In an exciting recent development, we have developed a DPA-based method for automatically predicting allosteric linkages in proteins. We do this by indirectly addressing the following central question: By how much does the affinity of a compound for the active site change when an allosteric effector binds to a regulatory site? Because the answer to this question is currently out of reach computationally, we define a related problem that we can solve on a single workstation in about a minute per protein using a highly simplified model of the protein and its interactions. The first results we obtained using the method are illustrated in Figure 1. Our method has great potential for predicting a large number of new targets for drug design and we have therefore submitted an invention disclosure through LANS. The Laboratory is currently assessing the commercial potential of our technology for patenting and technology maturation, and we are also submitting an NIH exploratory research proposal to further develop the method.

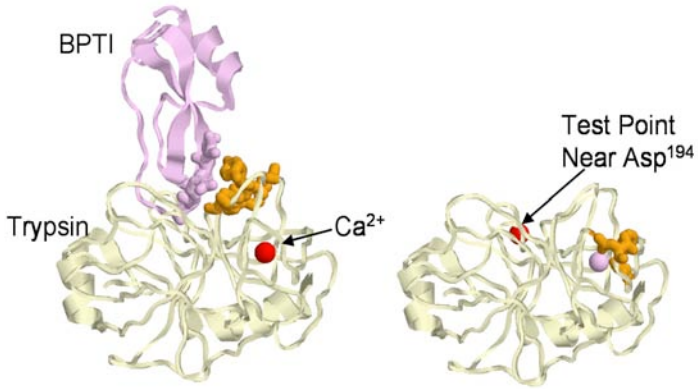


*Figure 1. Prediction of allosteric linkage in trypsin, in which this enzyme changes shape and activity due to molecular binding at a site other than the enzymatically active one. Left panel. The interaction between $Ca^{2+}$ (red) and trypsin (yellow) is modeled and used to predict a regulated site (orange) known to interact with BPTI (purple). Right panel. Interactions with the $Asp^{194}$ catalytic residue (red) are predicted to control the activity residues (orange) that interact with the $Ca^{2+}$-ion (purple).*

We also developed methods for combinatorial optimization of protein structures for protein structure prediction [9]. In addition, we modified our previously published software for protein structure comparison [10] so that it could be applied to predict genome-wide functional assignments for yeast [11]; this method is now widely used and is even being applied to 150 genomes in one of the largest computational biology efforts worldwide (R. Bonneau, NYU).

In other related work, we developed test sets for reverse engineering of metabolic networks from metabolomic data [12]; performed normal mode analysis of Argonaute, the catalytic engine of RNA interference [13]; developed a machine learning method to predict protein function from protein structure (J Howse, JD Cohn, CEM Strauss, ME Wall, in preparation); developed a method for fast estimation of protein configurational entropy (I Nemenman, CEM Strauss, ME Wall, in preparation); released and documented methods and LUNUS software for diffuse scattering from protein crystals (http://lunus.sf.net) [14]; and developed text-based methods for protein function inference [15, 16]. The text analysis expert has moved to University of Colorado and is submitting a NIH R01 grant on novel text analysis methods in collaboration with the PI of the LDRD project.

**Make methods and results publicly available via the web and other means.**

We developed a server to implement protein function inference methods on the web, and have made available predictions of functional sites for 50,000 protein structures (http://pfig.lanl.gov). We have also developed a bootable CD that assembles an *ad hoc* cluster of computers on a local network for running ROBETTA structure prediction and function annotation software [6], satisfying the demands of many Universities and commercial users.

Overall, the project was highly productive, yielding 12 publications, 5 publications in preparation, 1 software package developed (Fast DPA), and 2 invention disclosures (Prediction of Protein Functional Sites Using Fast Dynamics Perturbation Analysis, IDEA 07-186; Method to Predict Allosteric Linkages in Proteins, IDEA 08-251). The project also generated significant external visibility for LANL, not only through numerous invited and contributed presentations, but also by helping to establish the highly successful q-bio Conference on Cellular Information Processing (http://q-bio.org) through project-related efforts of members Ilya Nemenman and Michael Wall, who were co-organizers of the 2007 and 2008 conference [17]. (The organizers, including Nemenman and Wall, submitted a NIH R13 conference grant application to support future q-bio conferences, and NIH expects this grant to be funded in time for the 2009 conference.)

## References


1. Blattneretal., F. R.. The complete genome sequence of Escherichia coli K-12. 1997. *Science.* **277** (5331): 1453.
2. Ming, D., and M. E. Wall. Interactions in native binding sites cause a large change in protein dynamics. 2006. *Journal of Molecular Biology.* **358**: 213.
3. Ming, D., J. D. Cohn, and M. E. Wall. Fast dynamics perturbation analysis for prediction of protein functional sites. 2008. *BMC Structural Biology.* **8**: 5.
4. Murzin, A. G., S. E. Brenner, T. Hubbard, and C. Chothia. SCOP: a structural classification of proteins database for the investigation of sequences and structures. 1995. *Journal of Molecular Biology.* **247**: 536.
5. Wall, M. E.. Ligand binding, protein fluctuations, and allosteric free energy. 2006. In *AIP Conference Proceedings.* (Zaragoza, Spain, 8-11 Feb 2006). Vol. 851, p. 16. Melville, New York: AIP.
6. Chivian, D., D. E. Kim, L. Malmstrom, P. Bradley, T. Robertson, P. Murphy, C. E. Strauss, R. Bonneau, C. A. Rohl, and D. Baker. Automated prediction of CASP-5 structures using the Robetta server. 2003. *Proteins.* **53** (Suppl 6): 524.
7. Ming, D., and M. E. Wall. Allostery in a coarse-grained model of protein dynamics. 2005. *Physical Review Letters.* **95**: 198103.
8. Ming, D., M. Anghel, and M. E. Wall. Hidden structure in protein energy landscapes. 2008. *Physical Review E.* **77**: 021902.
9. Wolpert, D. H., C. E. Strauss, and D. Rajnarayan. Advances in distributed optimization using probability collectives. 2006. *Advances in Complex Systems.* **9**: 383.
10. Ortiz, A. R., C. E. Strauss, and O. Olmea. MAMMOTH (matching molecular models obtained from theory): an automated method for model comparison. 2002. *Protein Science.* **11**: 2606.
11. Malmstrom, L., M. Riffle, C. E. Strauss, D. Chivian, T. N. Davis, R. Bonneau, and D. Baker. Superfamily assignments for the yeast proteome through integration of structure prediction with the gene ontology. 2007. *PLoS Biology.* **5**: e76.

12. Nemenman, I., G. S. Escola, W. S. Hlavacek, P. J. Unkefer, C. J. Unkefer, and M. E. Wall. Reconstruction of metabolic networks from high-throughput metabolite profiling data: in silico analysis of red blood cell metabolism. 2007. *Annals of the New York Academy of Sciences.* **1115**: 102.

13. Ming, D., M. E. Wall, and K. Y. Sanbonmatsu. Domain motions of Argonaute, the catalytic engine of RNA interference. 2007. *BMC Bioinformatics.* **8**: 470.

14. Wall, M. E.. Methods and software for diffuse X-ray scattering from protein crystals. To appear in *Methods in Molecular Biology.*

15. Maguitman, A. G., A. Rechtsteiner, K. Verspoor, C. E. Strauss, and L. M. Rocha. Large-scale testing of bibliome informatics using Pfam protein families. 2006. *Pacific Symposium on Biocomputing.* **2006**: 76.

16. Verspoor, K., J. D. Cohn, S. Mniszewski, and C. A. Joslyn. A categorization approach to automated ontological function annotation. 2006. *Protein Science.* **15**: 1544.

17. Edwards, J. S., J. R. Faeder, W. S. Hlavacek, Y. Jiang, I. Nemenman, and M. E. Wall. Q-bio 2007: a watershed moment in modern biology. 2007. *Molecular Systems Biology.* **3**: 148.

## Publications

Edwards, J. S., J. R. Faeder, W. S. Hlavacek, Y. Jiang, I. Nemenman, and M. E. Wall. Q-bio 2007: a watershed moment in modern biology. 2007. *Molecular Systems Biology.* **3**: 148.

Maguitman, A. G., A. Rechtsteiner, K. Verspoor, C. E. Strauss, and L. M. Rocha. Large-scale testing of bibliome informatics using Pfam protein families. 2006. *Pacific Symposium on Biocomputing.* **2006**: 76.

Malmstrom, L., M. Riffle, C. E. Strauss, D. Chivian, T. N. Davis, R. Bonneau, and D. Baker. Superfamily Assignments for the Yeast Proteome through Integration of Structure Prediction with the Gene Ontology. 2007. *PLoS Biology.* **5** (4): e76.

Ming, D., J. D. Cohn, and M. E. Wall. Fast dynamics perturbation analysis for prediction of protein functional sites. 2008. *BMC Struct Biol.* **8**: 5.

Ming, D., M. Anghel, and M. E. Wall. Hidden structure in protein energy landscapes. 2008. *Physical Review E.* **77** (2 Pt 1): 021902.

Ming, D., M. E. Wall, and K. Y. Sanbonmatsu. Domain motions of Argonaute, the catalytic engine of RNA interference. 2007. *BMC Bioinformatics.* **8**: 470.

Ming, D., and M. E. Wall. Allostery in a coarse-grained model of protein dynamics. 2005. *Physical Review Letters.* **95**: 198103.

Ming, D., and M. E. Wall. Interactions in native binding sites cause a large change in protein dynamics. 2006. *Journal of Molecular Biology.* **358**: 213.

Nemenman, I., G. S. Escola, W. S. Hlavacek, P. J. Unkefer, C. J. Unkefer, and M. E. Wall. Reconstruction of metabolic networks from high-throughput metabolite profiling data: in silico analysis of red blood cell metabolism. 2007. *Annals of the New York Academy of Sciences.* **1115**: 102.

Verspoor, K., J. Cohn, S. Mniszewski, and C. Joslyn. A categorization approach to automated ontological function annotation. 2006. *Protein Science.* **15** (6): 1544.

Wall, M. E.. Ligand binding, protein fluctuations, and allosteric free energy. 2006. *AIP Conference Proceedings.* **851**: 16.

Wall, M. E.. Methods and software for diffuse X-ray scattering from protein crystals. To appear in *Methods in Molecular Biology.*

# Functional Proteomics Studies of Bacillus Anthracis

*Ryszard Michalczyk*

20060437ER

## Introduction

In Bacillus anthracis, as in most bacteria, the function of majority of the 3025 genes is completely unknown. In this project we are addressing a detailed understanding of the structure, function and interactions of native B. anthracis proteins. We are generating mutants of B. anthracis lacking the genes of interest and compare them with the wild-type bacteria. We are expressing and purifying the proteins of interest to analyze their structure. Subsequently, we will compare their structural homology with known proteins to identify functional relationships. In parallel, we will investigate their biological role by preparing gene knock-out mutants and assessing the effects of these deletions on the growth of B. anthracis and protein expression patterns. This research forms a basis for analysis of possible function and interactions of these proteins with biological targets. The results will lead to a better understanding of the biology of this pathogen and possibly to new therapeutics and vaccines against anthrax infection – steps critical to reducing the threat posed by B. anthracis.

Combination of molecular biology methods to generate knock-out mutants, comparative proteomics to assess gene expression changes, and structural biology (NMR) methods to characterize protein structure, together with bioinformatics methods for structural comparisons and function elucidation constitutes state of the art approach to deducing functions of proteins potentially important to anthrax pathogenesis. The potential payoff of identifying high value targets against anthrax is high.

## Benefit to National Security Missions

Our research is directly related to biothreat reduction, an important national security mission area for DOE, DHS, and other agencies. The project is also relevant to the goals of DOE's Genomes to Life mission that endeavors to understand the function of genes.

## Progress

Generation of knock-out mutants suffered setbacks – the standard knock-out protocol and two modifications we designed and tried so far have been unsuccessful due to a large number of false positives. We have designed a new approach in which an endonuclease gene, activated by nutrient depletion, destroys the cloning vector following recombination. This approach eliminates false positives and we are confident it will lead to desired mutants. The knock-out plasmid necessary for this approach is in the final stages of construction.

Proteins pXO1-166 and -137 have been cloned and expressed in E. coli. Work on increasing yield and solubility of pXO1-137 is in progress. Proteins pXO1-190 and pXO1-138 suffered setbacks in cloning – all products obtained so far contained mutations. Another round of cloning and verification is in progress. Expression of the remaining proteins in E. coli resulted in insoluble products. With addition of GST-tag to the N-terminus of the proteins, which normally increases protein solubility improved soluble expression, however, the yields of soluble products were not sufficient. Although refolding of insoluble proteins yielded soluble products, it is not certain that the proteins re-folded to their native structures and there are no activity tests that can be used to assess that fact. Additional expression attempts in ArcticXpress cells were also unsuccessful. It is possible that these proteins are toxic to the host or severely alter host metabolism. To this end we are progressing on two fronts. First is to use E. coli cell-free expression system in which cell survival is not required for protein production. Trials in a commercial cell-free system are in progress with various expression tags and induction conditions being assessed. Second approach is to use self-induction system which has been used previously to produce toxic proteins [1]. Initial trials in this system appear promising. Additional trials, possibly including re-cloning as secreted proteins, are planned as a back-up strategy.

Protein pXO1-166 has been purified to homogeneity and obtained in milligram quantities (~4 mg/L of culture). The protein has been identified as protective anti-

gen repressor (PagR) important in regulation of expression of protective antigen which is a part of the three-protein toxin system [2]. Purification was achieved using standard chromatographic methods on two ion-exchange columns. The protein has been subjected to initial biochemical characterization. Protein is a dimer in solution, MW = 23 kDa, and is very basic with pI = 9.6. Circular dichroism spectra indicate presence of secondary structure (~50% alpha-helix) – analysis agrees well with theoretical predictions. Protein is thermally stable with midpoint unfolding transition temperature of 71 deg. C and is stable for at least a month. Initial NMR spectra indicate presence of a stable tertiary structure and hydrophobic core rendering it suitable for structural studies (Figure 1).

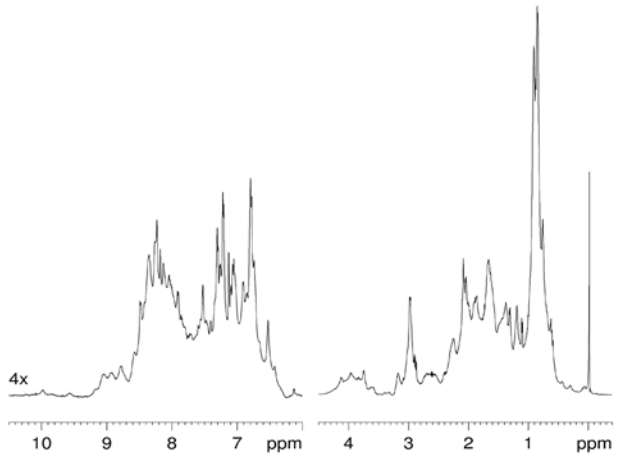


*Figure 1. 1H NMR spectrum of protein pXO1-166 showing good dipersion of resonances and indicating the presence of a folded protein core. The vertical scale in the right panel (6-10.5 ppm) was expanded 4-fold for better visualization.*

Growth in 13C/15N-labeled media has been performed and and isolation of labeled protein is in progress, to be immediately followed by NMR experiments. In addition, we have characterized binding of PagR to three DNA promoters from Bacillus anthracis (Figure 2). The binding is similar for all three sequences with affinities ranging from 19 to 43 nM. We have also determined that binding of the protein to DNA involves one contact per monomer between the protein and DNA phosphate groups. We are attempting to identify the consensus DNA binding sequence for PagR by truncating the promoter sequences studied to identify the core binding site which can then be used to screen anthrax genome for other promoters regulated by this protein.

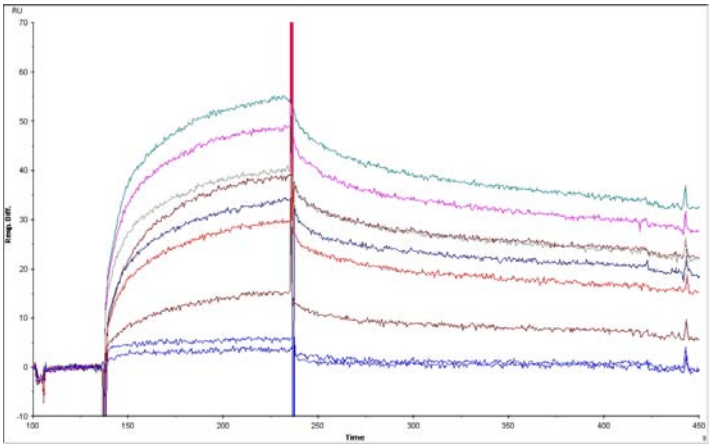


*Figure 2. Binding of pXO1-166 to DNA promoter for protective antigen gene measured by surface plasmon resonance. Association time was 100s, dissociation time 180s. Concentrations of protein used were 10nM, 50nM, 100nM, 200nM, 300nM, 400nM, 500nM, 600nM and 700nM.*

Overall, we have obtained good preliminary data and moved the project forward to the point where further experiments should be more successful. We are also ready to progress to structure determination stage of the project for pXO1-166 and pXO1-137.

## Future Work

Our research addresses a central challenge in pathogen biology: understanding the role of proteins in bacterial pathogens. In Bacillus anthracis, as in most bacteria, the function of majority of the 3025 genes is unknown. Characterizing protein structure and changes in cellular physiology that result from gene inactivation provide vital insights to their general role and specific function. We are working to clone 6 genes encoding B. anthracis proteins from pathogenicity island that are implicated in pathogenesis, express the proteins in E. coli, characterize their biochemical properties and three-dimensional solution structure.

Subsequently, we will compare their structural homology with known proteins to identify functional relationships. In parallel, we are investigating their biological role by preparing gene knock-out mutants and assessing the effects of these deletions on the growth of B. anthracis and protein expression patterns. Elucidating the roles of these proteins will also enable assignment of putative functions to their homologs in other bacterial pathogens.

In the nearest future we will finish the construction of our new knock-out plasmid tool and generate knock-out mutants lacking genes of interest. We will produce extracts from wild-type and knock-out strains for determination of

differential protein expression under growth conditions stimulating pathogenicity. We will also begin NMR structural work on proteins pXO1-166 and pXO1-137 leading to tertiary structure determination. Simultaneously, we will continue expression trials of the remaining proteins to produce soluble products suitable for NMR. We will characterize the stability and secondary structure of these proteins and subsequently follow with structure determination.

Results of this research will form a basis for further functional proteomics studies of B. anthracis. Analysis of protein expression patterns and structural studies of the proteins potentially involved in pathogenesis will increase our knowledge of the biology of anthrax. The results will be applied to identification of biological pathways in which these proteins are involved and to the search for inhibitors of these processes. The methods used will be extended to additional genes of B. anthracis and other pathogens.

## Conclusion

We will clone genes encoding B. anthracis proteins of unknown function that are implicated in pathogenesis, express the proteins in E. coli, and characterize their three-dimensional structure. We will compare their structural homology with known proteins to help identify their function. We will investigate their biological role by preparing gene knock-out mutants and assessing effects of these deletions on the growth of B. anthracis and protein expression patterns. The results will lead to a better understanding of the biology of anthrax and possibly to new therapeutics and vaccines against anthrax infection – steps critical to reducing the anthrax threat.

## References

Studier, F. W.. Protein production by auto-induction in high density shaking cultures. 2005. *Protein Expression and Purification.* **41**: 207.

Mignot, T., M. Mock, and A. Fouet. A plasmid-encoded regulator couples the synthesis of toxins and surface structures in Bacillus anthracis. 2003. *Molecular Microbiology.* **47** (4): 917.

# Drug Binding and Catayltic Mechanism in DHFR

*Paul Alfred Langan*

20070131ER

## Introduction

Understanding the relationship between the function of biologically active molecules and their structure is at the heart of designing new drugs and understanding the function in the body. This proposal utilizes a combination of techniques to investigate drug binding and catalytic mechanisms of dihydrofolate reductase (DHFR). DHFR is one of the most important targets for anti-cancer therapy and for the development of antimicrobial agents. Recently, DHFR has emerged as a new target against a number of debilitating bacterial-derived afflictions, including tuberculosis and anthrax. We are seeking to fully understand the complete configuration of hydrogen for the first time in a reductase enzyme, verifying the catalytic mechanism and bridging the gap between structure and function to elucidate a metabolic process crucial to life. While the results of this work will be far-reaching, we will exploit results specifically to enhance target-drug interactions by the design of new mechanism-based inhibitors against cancer and anthrax.

## Benefit to National Security Missions

This project supports the national security mission of biothreat reduction important to DOE, DHS, and other government agencies. Furthermore, understanding of the catalytic mechanisms and how we might custom design drugs, we will impact the health and welfare of our nation.

## Progress

We have optimized a Sumo expression system with D2O and algal hydrolysate (normal incubation). We grew different strains of algae using normal incubators and generated different bacterial growth media from the hydrolysates. We found that there were differences in the amounts of protein expression with different hydrogenous hydrolysate. One of the best performers was chlorella. We have now been able to grow chlorella routinely on 90% and above D2O so we can perdeuterate large quantities of protein for crystallization trials. We tested using the Protein Production robot for E. coli fermentation with D2O and hydrolysate but we found (with a number of different proteins; DHFR, HIV protease and MSOX) that there was no real gain in using the robot rather than a regular incubator. We have sent the various algal hydrolysates for analysis of amino acid/sugar profile in order to explain the different performances of the different cultures. The Mass spec analysis will be carried out at B8 LANL TA35. We have also carried out mass spec analysis of the vairous perdeuterated proteins we have produced from our hydrolyzate to ensure full perdeuteration. This work was carried out at B8 in TA-43. This work has been entirely conducted at LANL and a number of publication reporting the results are in preparation. We have already solved the X-ray structure of baDHFR, a major milestone for year 3 and we have determined high resolution X-ray structures of the various ecDHFR complexes, using data collected at the Advanced Photon Source at Argonne National Laboratory. We have also collected X-ray data from perdeuterated ecDHFR to confirm that it has the same structure as the hydrogenous (regular) form of the protein.

## Future Work

In the remaining period of this project our focus will be on growing further large crystals and collecting neutron data sets from crystals of complexes of ecDHFR, and determining their neutron structures, having already determined their X-ray structures. Our collaborators in CWRU have produced a number of large crystal of ecDHFR complexes for neutron crystallography measurements and we have data collection from a ternary complex scheduled at LANSCE. A postdoc will come to LANL to be trained in neutron data collection from CWRU. Our remaining efforts will depend on postdocs Zoe Fisher and also David Fox, two new postdocs associated with this project after the departure of postdoc Leighton Coates for a position at the SNS at ORNL. Zoe Fisher will primarily be involved in data collection and David Fox on protein expression. Specifically we hope to determine the neutron structure of DHFR with MTX and NADPH bound and also DHFR with folate and NADPH bound. The anticipated outcome of this work will be

knowledge of the complete configuration of hydrogen for the first time in a reductase enzyme, verifying the catalytic mechanism and bridging the gap between structure and function to elucidate a metabolic process crucial to life. The results will be exploited to enhance target-drug interactions by the design of new mechanism-based inhibitors against cancer and anthrax.

**Milestones**

Year 2-3: Neutron data collection from ecDHFR complexes; structure determination and modeling; start high yield production of perdeuterated baDHFR; Write NIH grant application for future work on B. anthracis.

## Conclusion

Dihydrofolate reductase (DHFR) is an essential enzyme conserved across species that is a multi-million dollar drug target against cancer and microbes. Recently DHFR has emerged as a new target against a debilitating bacterial-derived afflictions, including tuberculosis and anthrax. We propose to develop new innovative strategies that will enhance our understanding of the catalytic mechanism of the enzyme DHFR from E. coli and enable drug design with B. anthracis DHFR, providing the nation with unique capabilities to address present future needs in health, welfare and biothreat reduction.

## Publications

Bennett, B., A. Gardberg, M. Blair, and C. Dealwis. On the determinants of amide backbone exchange in proteins: a neutron crystallographic comparative study. 2008. *Acta Crystallographica* . **D64**: 764.

Bennett, B., H. Xu, R. Simmerman, R. Lee, and C. Dealwis. Crystal structure of the anthrax drug target, bacillus anthracis dihydrofolate reductase . 2007. *Journal of Medicinal Chemistry.* **50** (18): 4374.

Blakeley, M., P. Langan, N. Niimura, and A. Podjarny. Neutron Protein Crystallography: Opportunities, challenges and limitations. 2008. *Current Opinion in Structural Biology* . **18**: 593.

Langan, P., M. Mustyakimov, Z. Fisher, A. Kovalevskyi, A. Valone, M. J. Waltman, P. Adams, P. Afonine, B. Bennett, C. Dealwis, C. Unkefer, and B. P. Schoenborn. Protein structures by spallation neutron crystallography. 2008. *Journal of synchrotron radiation.* **25**: 215.

Liu, X., L. Hanson, P. Langan, and R. Viola. The Effect of Deuteration on Protein Structure: A High Resolution Comparison of Hydrogenated and Perdeuterated Haloalkane Dehalogenase. 2007. *Acta Crystallographica.* **D63**: 1000.

# Substrates for the Detection and Differentiation of Influenza Viridae

*David Bryan Kimball*

20070148ER

## Introduction

Human respiratory viruses, such as influenza A, B, and C, respiratory syncytial virus (RSV) and human rhinovirus (HRV) account for millions of infections in the US each year and continue to be a leading cause of death. Although new antiviral drugs for the treatment of influenza have become available recently, their usefulness depends entirely on an early diagnosis (within the first 2 days of infection). More than 150 human cases of transmission of avian flu strain H5N1, an emerging threat, have been reported since 2004. New methods to detect, monitor and differentiate these viruses are needed to enable an effective and efficient response. The common receptor motifs found on influenza viridae are an enzyme – neuraminidase, with 9 subtypes and a binding receptor hemaglutinin with 6 subtypes. Previous pandemic influenza outbreaks were associated with H1N1 (Spanish, 1918), H2N2 (Asian, 1957) and H3N2 (Hong Kong, 1968) antigenic determinants of influenza A. We propose to take advantage of this commonality by synthesizing the structures recognized by influenza strains (sialic acids), modified such that after the virus binds to and cleaves the receptor the products and ratios will be easily detectable and distinguishable using mass spectrometry (MS). Unlike other methods for influenza detection, time resolved MS signatures obtained will distinguish all subtypes, including newly emerging strains and co-infections, in a single assay that will take hours rather than days or weeks. It will also be a functional assay capable of directly measuring the virulence of the sample infection. Finally, a key aspect will be the ability to do rapid large scale, automated testing using currently available MS equipment.

## Benefit to National Security Missions

This project will further basic science progress in the detection of pathogens and contribute to our portfolio of focused measurements and analysis of biological systems. The technology will allow monitoring of emerging threats by infectious agents and therefore supports biothreat reduction mssions of DOE, DHS, and other agencies.

## Progress

The critical step in the first year of this LDRD research project was to provide substrates for neuraminidase and hemaglutinin of Influenza viridae. The synthesis of labeled compounds generally requires additional effort to optimize reaction yields and economically introduce the expensive stable isotope into the final products. We explored multiple reported synthetic options and combined them with novel synthetic approaches to provide an efficient path for generating all proposed structural variants of neuraminidase substrates.

The main goal of this project during the past year was to perform final optimization on the synthesis of differently 13C labeled 2,3- and 2,6-sialyl lactose and to produce useful amounts of each (>100 mg). These two initial influenza viral enzyme substrates allow our MS-based assay to be developed. Concurrently, preliminary work on conditions for the MS-based assay was to be developed using neuraminidase and 2,6-sialyl lactose. In short, both substrates are now in hand, only awaiting final deprotection steps, and initial MS conditions have been obtained for assay development.

The most efficient route to labeled sialyl lactose, with any regiochemistry, requires extensive protective group chemistry on each of the three main components: sialic acid, galactose, and glucose. No commercial sources are available for lactose with any 13C enrichment. Thus, 13C enriched lactose must be synthesized prior to coupling to a sialic acid moiety. This is most readily accomplished using enriched glucose or galactose, both of which are available commercially. We selected enriched glucose since it is available in more numerous enrichment patterns as well as being generally less expensive. This was an important consideration, as the total synthesis of (M+6)lactose ready for coupling to a sialic acid totaled 12 steps and a combined yield of close to 17%. Optimizing our reaction conditions to 12 steps and 17% overall yield was a significant success, since alternate routes evaluated in year 1 were far less efficient. In addition, for subsequent coupling to a suitably prepared sialic acid moiety, other routes produced

lactose moieties with protecting groups that did not give appreciable yields of the desired sialyl lactose product. Optimization of each step is often a complex synthetic process involving numerous side by side reactions with slight variations in reaction conditions. This also necessitates multiple purifications to verify which conditions give the best yield and extensive characterization of all intermediates for each route.

Finding the correct conditions which allow a purified enzyme to function while providing a matrix conducive to MS analysis was nontrivial. This is a necessary step, however, since it is much more complicated and dangerous to work with viral samples. Successful utilization of purified neuraminidase, analogous to viral surface neuraminidase, requires specific buffering conditions for enzymatic activity to be observed. Unfortunately, many of these buffers result in salt conditions which hinder MS detection and analysis of both the substrate as well as cleavage products. After numerous trials, however, the combination of enzyme activity with subsequent detection of starting materials and products was accomplished. Rough detection limits were also extrapolated.

In order to validate the enzyme kinetics under conditions which facilitate MS experiments, we recently purchased an Ocean Optics fluorimeter. The kinetics of the commercially available neuraminidases is calibrated using a substrate having a fluorescent target bound to sialic acid. Since we have modified the enzyme solution, we must now verify the turnover rate known in the literature using established fluorimetry procedures. Linking MS-based enzyme turnover analysis to more traditional fluorimetry-based analysis will be a key validation of our method. The modular nature of the Ocean Optics fluorimeter makes it ideal for this type of routine analysis, since a higher power LED with a very narrow wavelength window can be used to increase sensitivity when quantification of a particular absorption within the sample is required.

## Future Work

With the success of our synthetic methods, we are now poised to characterize the functional differences between purified enzymes specific for one type of sialyl lactose linkage over another using MS. We are collaborating with a source capable of providing us with viral binding protein (hemagglutinin) so that we are able to increase the complexity of our MS experiments for more accurate assay development (more comparable to real world samples). We further intend to provide our CDC contacts with both substrates and preliminary MS results so that large scale sampling can begin.

So far, our synthesis has focused on cleavable substrates which will provide mass differentiated products on exposure to an enzyme. In order to further differentiate time resolved mass spectral profiles for different viral samples, we will also explore substrates which contain a sialyl lactose linkage that resists cleavage. Sulfur based linkages are known to resist enzyme cleavage and thus we can use these substrates as competitive inhibitors. With our synthesis of sialyl lactose substrates optimized, minimal alterations are necessary to generate the S-linked substrates.

## Conclusion

This project takes advantage of substrate selectivity by synthesizing the structures recognized by influenza strains (sialic acids), modified such that after the virus binds to and cleaves the receptor the products and ratios will be easily detectable and distinguishable using sensitive mass spectrometry. The final result of this project will be a multi-substrate panel assay capable of detecting, quantifying, and differentiating influenza strains regardless of whether they are known or novel. Large scale sample testing can show geographic viral phenotype drift and the emergence of antiviral drug resistance.

# Magnetic Turbulence and Kinetic Dissipation in Solar Wind and Solar Corona Plasmas

*Hui Li*

20070170ER

## Introduction

Understanding the electromagnetic medium that impinges upon and surrounds the earth are crucial to virtually every aspect of space flight from space craft and sensor design to safety considerations in manned space flight. Furthermore, the ionic medium impacts all manner of communications and sensing systems. During the past forty years, spacecraft measurements in the solar wind indicate that this medium is turbulent, with large-amplitude, broadband fluctuations of magnetic fields and plasma velocities. The observations further show that long-wavelength fluctuations of the inertial range and short-wavelength fluctuations of the so-called "dissipation range" have distinctly different properties. Although there has been substantial progress in the theoretical understanding of the inertial range through the use of fluid theories such as magnetohydrodynamics (MHD), there has been much less progress in the interpretation of the short-wavelength regime, in part because collisionless dissipation (which is not included in fluid theories) appears to play a fundamental role in the physics.

Particle-in-cell (PIC) computer simulations are the tools necessary to address the full physics of short-wavelength plasma turbulence. We propose to carry out the first-ever PIC simulations that self-consistently capture both the cascade and kinetic dissipation of turbulence in magnetized, collisionless plasmas such as the solar wind. This will be possible through the use of LANL's supercomputing resources such as the Roadrunner machine and the Laboratory's high performance VPIC simulation code. If our proposed research is successful, LANL will become a world leader in plasma turbulence research, with further applications to laboratory plasmas, planetary magnetospheres, and astrophysical plasmas.

## Benefit to National Security Missions

This project will improve our understanding of solar wind magnetic fluctuations and the space environment that affects NNSA's missions in non-proliferation. Furthermore, Laboratory competencies in Basic Energy Science in fundamental plasma research will be strengthened in support of multiple energy and national security missions in DOE and other government agencies.

## Progress

We have carried out the first particle-in-cell (PIC) simulations of the cascade of whistler turbulence. The simulations show a spectral anisotropy which is consistent with the preference for cascade in directions perpendicular to the background magnetic field predicted by fluid theories of whistler turbulence. Our new results show for the first time that whistler turbulence spectra become more anisotropic with increasing fluctuation energy, that magnetic compressibility is substantial for whistler turbulence, and that whistler turbulence preferentially heats electrons in directions parallel and anti-parallel to the background magnetic field.

Used PIC simulations of the electron/electron instability to demonstrate that the enhanced electric field fluctuations from this instability not only slow down the electron beam driving the instability but also scatter the electrons to relatively large pitch-angles relative to the background magnetic field. We have quantified this result, providing predictions that can be tested using solar wind observations of suprathermal electrons associated with solar electron bursts.

Developed model and algorithm for calculation of linear tearing modes in resistive MHD and two fluid models. This algorithm is general and can be used for calculation eigenmodes in different plasmas. The approach was applied for calculation of tearing modes in RFP like plasma in slab geometry. The results of resistive MHD and two fluid models were compared with the two fluid effects identified. The two fluid effects are strong in RFP

plasma. The developed method of calculation of modes in two fluid model is used for comparison of tearing modes calculated in two fluid and fully kinetic PIC models. The result shows that fully kinetic tearing modes in RFP plasma are similar to the ones calculated in the two fluid model meaning that kinetic effects due to large ion Larmor radius in RFP does not influence significantly tearing modes in RFPs.

Additional result in PIC simulations of tearing modes is that secondary instability with large wave numbers is found wich can make contribution to ion heating in RFPs at reconnection events. So far, we have had 10 refereed publications, numerous talks and poster presentations at various meetings.

## Future Work

Decades of spacecraft measurements of the magnetic fluctuations suggest that the solar wind is turbulent. There is, however, no satisfactory understanding of the origin and properties of the short wavelength turbulence, which is believed to provide a continuous heating of the solar wind. A comprehensive understanding of these long-standing problems requires treating turbulence and dissipation together, which has not been possible thus far.

We will carry out the first-ever particle-in-cell (PIC) simulations that self-consistently capture both the cascade and the kinetic dissipation of magnetic turbulence in collisionless plasmas. This is made possible by the LANL's supercomputing resources and our high-performance PIC codes. We expect for the first time to extract detailed information on both the fluctuating fields (specifically, the types of waves which persist and their spectral dependence on wavenumber and anisotropies) and the particles (specifically, whether electrons or protons are heated and their velocity-space signatures). The short-wavelength turbulence regime in the solar wind extends from the spectral break point near where the wavelength corresponds to the ion inertial length to much shorter wavelengths near the electron inertial length. The PIC simulations are used to follow the nonlinear flow of this energy self-consistently, including the development of magnetic turbulence and its dissipation on particles. We plan to investigate three distinct approaches: a) injecting ensemble of waves; b) injecting MHD turbulence; and c) generating turbulence self-consistently through a global instability.

The simulation box will be made large enough to enable the turbulent cascade to carry field energy to shorter wavelengths where dissipation becomes appreciable. Simulation results will be compared against solar wind and solar corona observations from various spacecraft available to LANL.

We will perform PIC simulations of tearing modes in reversed field pinch experiments to understand the secondary instability with large wave numbers and their implications for ion heating in the experiments.

## Conclusion

We expect to build a self-consistent theory on the origin and dynamics of solar wind magnetic turbulence. Our proposed simulations will achieve a new interpretation of short-wavelength solar wind turbulence and will provide a catalog of particle signatures of magnetic dissipation for use in identification of that process in terrestrial and other planetary magnetospheres as well as in the solar wind. We will perform study of secondary instabilities found in PIC siulations and their relation to ion heating in reversed field pinch experiments. We expect our results to be applicable in systems such as laboratory fusion experiments, and astrophysical disks/jets.

## Publications

Gary, S. P., S. Saito, and H. Li. Cascade of Whistler Turbulence: Particle-in-Cell Simulations. 2008. *Geophysical Research Letters.* **35**: L02104.

Gary, S. P., and S. Saito. Broadening of solar wind strahl pitch-angles by the electron/electron instabilities: particle-in-cell simulations. 2007. *Geophysical Research Letters.* **34**: L14111.

Saito, S., S. P. Gary, H. Li, and Y. Narita. Whistler turbulence: Particle-in-cell simulations . 2008. *Physics of Plasmas .* **15**: 102305.

Saito, S., and S. P. Gary. Whistler scattering of suprathermal electrons in the solar wind: particle-in-cell simulations. 2007. *J. Geophysical Research.* **112**: A06116.

Saito, S., and S. P. Gary. Whistlers are not created equally: scattering of strahl electrons in the solar wind via particle-in-cell simulations. 2007. *Geophysical Research Letters.* **34**: L01102.

Saito, S., and S. P. Gary. Energy dependence of perpendicular scattering for electron beams by the electron/electron instability in solar electron bursts. To appear in *Physics of Plasmas .*

Svidzinski, V. A., and H. Li. Calculation of resistive MHD and two fluid tearing modes by example of RFP-like plasma. 2008. *Physics of Plasmas.* **15**: 052106.

Svidzinski, V., H. Li, and B. Albright. Particle in cell simulations of tearing modes in reversed-field-pinch-like plasma. *Physics of Plasmas* .

Svidzinski, V., V. Mirnov, and H. Li. m=1 ideal kink modes in a line-tied screw pinch with finite plasma pressure . 2008. *Physics of Plasmas* . **15**: 092106.

# Understanding a Killer: A Predictive Model of Tumor Development

*Yi Jiang*

20070180ER

## Introduction

The project aims to develop a comprehensive modeling tool for the study of biophysical and biochemical mechanisms underlying tumor growth. Our study focuses on how the local cellular microenvironment influences cell physiology and cell behavior changes, and how such cell level changes influence tumor growth dynamics. The modeling tool we have been developing is a novel cell-based, multiscale modeling framework, which incorporates intra-cellular, cellular, and extra-cellular level descriptions. At the intra-cellular level, we model the signaling pathways and protein regulatory networks for cells. At the cellular level, we use a cellular Potts model that describes cells with extended cell shape and volume, and cell-cell interactions and behaviors with effective energies and constraints. At the extra-cellular level, we use diffusion-reaction type of continuous equations for the chemical dynamics in the extra-cellular environment. The three level models are closely integrated and feedback on each other to form a complete multiscale framework. We use this framework to model the three stages of tumor growth: avascular (before blood vessel) tumor growth, tumor induced angiogenesis (growth of new blood vessels), and vascular tumor growth. In additional to help better understand the tumor biology, this model can potentially help to predict effects of chemo- and radio- therapies on tumor growth, and suggesting new therapeutic strategies.

## Benefit to National Security Missions

This project supports the better understanding the biophysical processes of pathology that will directly impact the goal of improving human health. The methods developed here will also lay the groundwork to improve biothreat reduction. These areas of research directly impact missions of DOE OBER, NIH, DHS, and other government agencies.

## Progress

Continued to develop our predictive tumor models on the three phases of tumor development: the avascular tumor growth, tumor induced angiogenesis, and vascular tumor growth.

For avascular tumor growth modeling, after we have completed the parallelization of our avascular tumor codes in the first year of the LDRD project, we focused on applying this model to investigate the mechanisms underlying the tumor growth saturation. In particular we investigated the effects of cell shedding, growth inhibitors, mechanics, on cell cycle arrest and death. We are in the process of summarizing these results into a paper.

For tumor-induced angiogenesis, we developed a two-dimensional model of tumor angiogenesis. The model not only produces realistic sprout morphologies, but also generates more complicated processes including branching and anastomosis that occur in tumor angiogenesis. In the past year, we have further developed the angiogenesis model to correctly model cell retraction, which allowed for quantitative comparisons of cell migration speed with experiment. We have also investigated the detailed mechanisms of cell-matrix interactions in angiogenesis. In particular we focused on the matrix topography on the sprout morphology and migration speed. We showed that there is an optimal matrix density that facilitates fastest sprout extension, and that matrix alignment influence sprout extension speed. This work has been submitted to PLoS Computational Biology. In addition, we have also started the development of intracellular regulatory networks for vascular endothelial cells. The intracellular network involves the receptor tyrosin kinase and integrin signaling pathways and their cross-talks (Figure 1).

In order to model vascular tumor growth, we have implemented both the blood flow and rheology in a realistic tumor vasculature, following the Pries mode. Our model solves coupled differential equations for flow and transport (Hb, oxygen and glucose) in blood vessels, while in the tissue external to blood vessels it converts to reactive particles to transport oxygen and glucose and messenger molecules. We have initiated collaboration with Prof. T. Secomb (U. Arizona), an expert in the field of vasculature adaptation. We have obtained several blood vessel network reconstructions from Prof. Secomb. We are using these reconstructions to model blood flow in realistic networks. In particular, we are focusing on the role of tumor blood vessel leaki-

ness on the chemical distribution in tumor and the results vascular tumor growth (Figure 2).

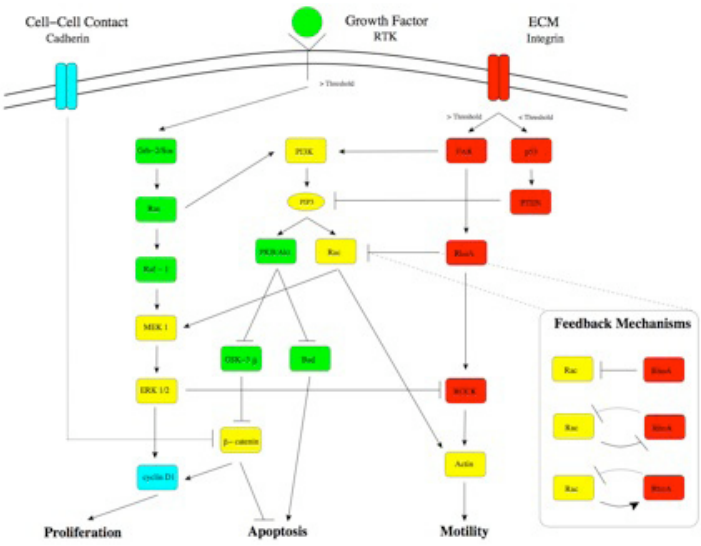


*Figure 1. Model of Receptor Cross-talk During Angiogenesis. Reduced signal transduction network linking external stimuli to a cell's internal decision making machinery and cell phenotype. This network highlights the relationship between growth factor, integrin, and cadherin receptors, allowing for cross-talk between the three to ultimately decide the cell's fate. An arrow between nodes signifies activation and a hammerhead indicates an inhibitory effect. The inset shows different feedback scenarios between Rac1 and RhoA supported by experimental evidence. We investigate the implications of each of these feedback loops on cell behavior.*

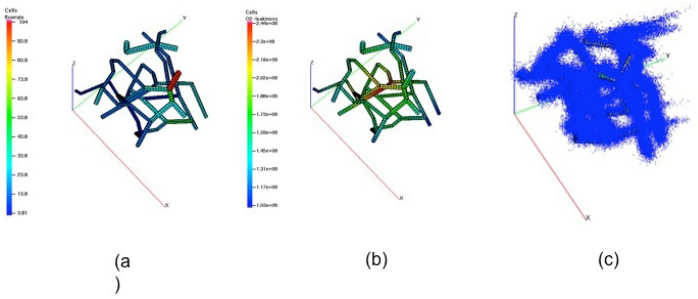


*Figure 2. Color-coded images of flowrate (a), oxygen vessel wall permeability (b) and a snapshot of glucose diffusing out from vessels (c). Vasculature is from rat brain tissue reconstruction. In (a), flow rate is a strong function of vessel segment radius, as well as of arterial vs. venous pressure difference, and hematocrit. In (b), leakiness is assumed a function of location of tumor relative to vessel segment; a 150 micron diameter tumor is assumed present in the center of the box. In (c), glucose is being consumed at different rates depending on the tissue type – normal vs. tumor (quiescent, proliferating, necrotic). Verification and validation comparisons with various experimental data are in progress.*

On the experimental side, in order to provide more comprehensive data for model development, we have finished complete spheroid growth curves for four different cell lines under standard culture conditions in the previous year. We also completed spheroid growth curves under 5-times increased glucose concentration, which should have the effect of increasing the hypoxic fraction and thereby raising the expression of HIF-1α. We have found that spheroids from each of the four cell lines grew to larger saturation sizes in the increased glucose concentration, as would be expected due to the decrease in central necrosis. However, the presence or absence of HIF-1α had no effect on most of the spheroid growth parameters. These results have very interesting implications for the role of HIF-1α in regulating tumor development, as it would appear that this cell survival protein actually has little impact on spheroid growth dynamics (Figure 3). In addition, we have a second complete set of spheroid growth curve measurements of the same cell types under altered nutrient supply conditions. These data will provide a valuable resource for further refinement of the mathematical model. It is worth pointing out that these complete spheroid growth experiments are not simple to perform. Thus, these data will represent a very valuable resource for the future of our mathematical model development. We have also continued to provide more measurements for the mathematical model, including the cell shedding from the spheroid surface. We have made some measurements of cell shedding in large spheroids near saturation, but the data have yet to be analyzed. We have also just received an extensive set of histology slides prepared by an outside company, which we will use to directly measure the amount of central necrosis as a function of spheroid size.

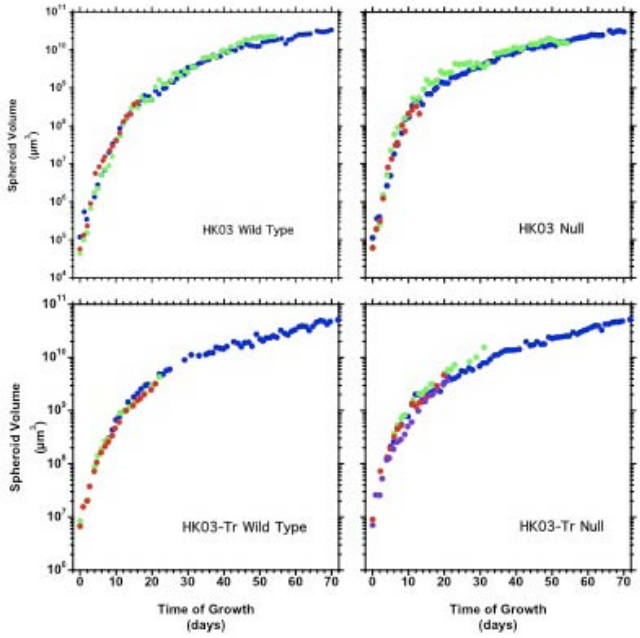


*Figure 3. Growth curves of spheroids expressed as the total spheroid volume as a function of time in culture in standard medium (5.5 mM glucose, 0.28mM oxygen). Points represent means of 25 measurements; different colors represent repeated, independent cultures.*

## Future Work

This project seeks to provide a comprehensive and predictive model for tumor development and chemotherapy based on quantitative experiments. We have developed a state-of-the-art integrated model that includes a cellular model for cell dynamics (cell growth, division, death, and cell adhesion), an intracellular protein regulatory network for cell cycle control, and extracellular reaction-diffusion chemical dynamics. This model has produced excellent results for initial avascular tumor development. We plan to build on the initial success of our cellular model for solid tumor growth and:

- Optimize the model to simulate the complete, realistic range of time and length scales of avascular tumor growth and validate this expanded model with an extensive set of existing and new experimental data;
- Extend the model to study the initiation of angiogenesis and resulting changes in tumor growth, simulating a crucial step in tumor progression;
- Incorporate a data-based network of blood vessels within the solid tumor, simulating tumors at advanced stage;
- Model the effects of chemotherapy at different stages of tumor development (avascular, angiogenic development, and advanced disease).

Besides supporting the Lab's science-based prediction goal, this research will provide novel modeling methods that are applicable to many national defense related biological problems, e.g. progression of disease in humans.

## Conclusion

The project will produce a comprehensive and predictive, multiscale cell model for tumor growth. The model can be used to generate and test hypotheses in tumor biology and development, which will have important application to basic cancer research, as well as to study therapeutic effects on tumor growth. We anticipate that this project will produce several novel predictions about the microenvironmental regulation of tumor growth and angiogenesis, which will provide the basis for future experimental and modeling work. Finally, the project will develop an integrated, multiscale model framework that will be applicable to other problems e.g. disease progression in humans.

## Publications

Bauer, A. L., T. L. Jackson, and Y. Jiang. A cell-based model exhibiting branching and anastomosis during tumor-induced angiogenesis. 2007. *Biophysical Journal.* **92**: 3105.

Jiang, Y.. A multiscale, cell-based framework for modeling cancer development. 2007. In *Lecture Notes in Computer Science.* Edited by Shi, Y., G. v. Albada, J. Dongarra, and P. Sloot. Vol. 4487, p. 770. Springer: Springer.

Jiang, Y.. Understanding a killer: a predictive model for tumor development. 2006. *Contemporary Mathematics.* **410**: 173.

# An Experimental and Theoretical Framework for Reactive Micromixing

*Amr I Abdel-Fattah*

20070267ER

## Introduction

Coupled small-scale mixing and chemical reactions (i.e., reactive micromixing) is an important process underpinning many seemingly different applications. This project aims at improved quantitative understanding of reactive micromixing in systems of varied complexities and seeks feasible techniques for enhancing mixing in microscopic systems, i.e., those with a low Reynolds number (Re). Our approach to achieving these goals is to study mixing in the presence and absence of chemical reaction processes, reactive and nonreactive micromixing respectively, at the microscopic scale through a series systematic laboratory experiments in well-characterized systems having increased complexities. In parallel, the Lattice Boltzmann Method (LBM) is utilized to simulate the experiments under similar conditions. The results of both experiments and simulations are compared and then used to modify and validate existing models at different scales. Several seemingly different applications can benefit from the results of this project. Examples include- a) industrial: such as organic synthesis, combustion, polymerisation, precipitation and fermentation; b) environmental: such as the fate of transport of contaminants in, and remediation of, subsurface media and groundwater aquifers; c) medical, biomedical and pharmaceutical: such as the design, development and use of microfluidic devices for patient diagnosis, patient monitoring, blood analysis, drug delivery, drug discovery, and microscale flow cytometers for cancer cell detection; d) homeland security and threat reduction: such as the design and use of chemical, nuclear and biological sensors; e) engineering and technological: such as chemical and nuclear reactors, micromixers, micron-scale supersonic nozzles, ink-jets, micro-machined electrophoretic channels for DNA fractionation and polymerase chain reaction (PCR) chambers for DNA amplification, and the membraneless H-filters that separate and filter particles by size without a membrane; and f) domestic applications: such as surface cleaning, fabric care, cosmetics, and painting.

## Benefit to National Security Missions

This project supports the DOE missions in Threat Reduction and Energy Security and Science missions by improving our quantitative understanding of reactive-micromixing and its integration into larger-scale systems for environmental and energy sciences and applications. In microscopic systems such as microfluidics, this improved understanding is essential for the design and validity of chem-bio sensors. Other applications include: biological and chemical sensors and microreactors; oil recovery and fuel cells; subsurface remediation and contaminant transport.

## Progress

In the past year (second year of the project) we designed, synthesized, and tested several porous micromodels with different geometry. One of our main goals was to run experiments and LBM simulations at very low flow rates, i.e., low Pe. We modified and validated the experimental setup until stable and reproducible results were obtained at very low injection rates (down to 2 micro-liters/hour).

Microscopic visualization non-reactive micromixing experiments were conducted at different injection rates (i.e., different Peclet numbers, Pe) in the porous micromodels of cylindrical, elliptical, and heterogeneous grains. The experiments used fluorescence dye as a nonreactive agent in de-ionized water. The experiments were performed at different values of Pe ranging from 100 down to two. The results lead to quantitative understanding of nonreactive micromixing in a uniform porous medium of cylindrical grains and provided the first comprehensive data set on transitional micromixing, before and after reaching steady state; reported data in the literature is limited to steady-state conditions [1]. The concentration profile across the advancing interface between the fluorescence dye solution and de-ionized water enabled the characterization of the interfacial micromixing. The experimental Pe was obtained as the number of channel widths it took the system to reach full mixing. Performing Lattice Boltz-

mann (LB) simulations at the experimental Pe resulted in transient and steady-state concentration profiles qualitatively very closely matching the experimental profiles (Figure 1), thus establishing a higher level of confidence in our LB simulations. The LBM simulation results, however, showed a higher rate of mixing (~ 4 times). This was attributed to the dimensionality differences (3D vs. 2D) between the simulations and the actual micromodels used in the experiments. The results of these experiments are being documented in a manuscript for publication and a conference presentation.

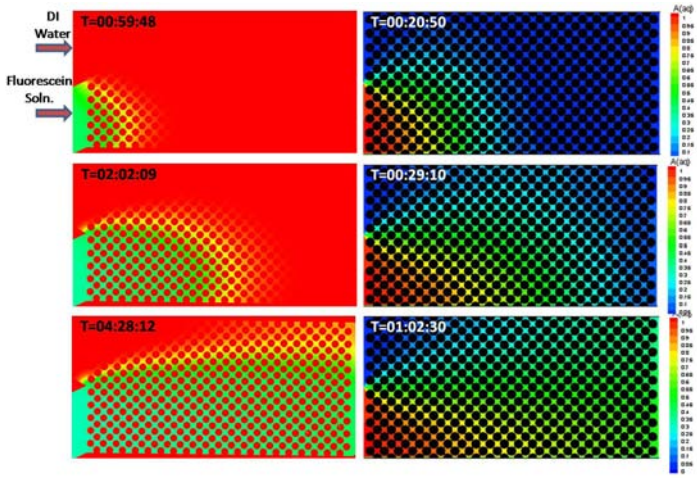


*Figure 1. Experimental (left) and LBM simulation (right) results of a non-reactive micromixing experiment employing de-ionized water and fluorescein solution at Pe ~ 2. Micromodel used: staggered array of cylindrical grains of diameter 600-µm, height 35-µm, porosity = 0.38.*

A set of reactive micromixing experiments was also started. In these experiments, two reacting solutions – one with free Ca+ ions and the other is a calcium ion indicator (Oregon 5N BAPTA), were introduced parallel to each other into the micromodel at a very low flow rate (4 microlters/hr). The calcium indicator reacted with the free Ca+ ions in a 1:1 molar ratio and correspondingly its fluorescent intensity was increased approximately by 6 times. It is important to note that the ratio of the molecular diffusion coefficients of the indicator (OG5N) and the calcium ions is about 2.2 times. Two sets of experiments were performed - one with equimolar concentration of the two species ([Ca], [OG5N] = 30 uM) and the other to have a concentration gradient ([Ca] - 100 uM, [OG5N] - 50 uM). LBM simulations were performed using the experimentally measured Pe. Selected experimental results are shown Figure 2 and corresponding LBM simulation results are shown in Figure 3. As these two figures indicate, there is a good qualitative agreement between the experimental and LBM simulation results. Again, the mixing rate obtained from the LBM simulations was at least 20 times higher than that suggested by the experimental results.

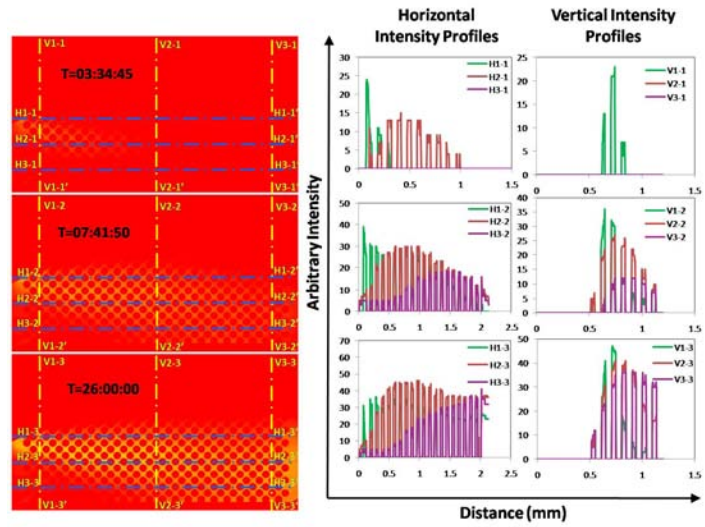


*Figure 2. Experimental results of a reactive micromixing run using a 100 mM Ca+ ions solution and a 50 mM OG5N calcium ion indicator at Pe ~ 2. Micromodel used: staggered array of cylindrical grains of diameter 600-µm, height 35-µm, porosity = 0.38.*

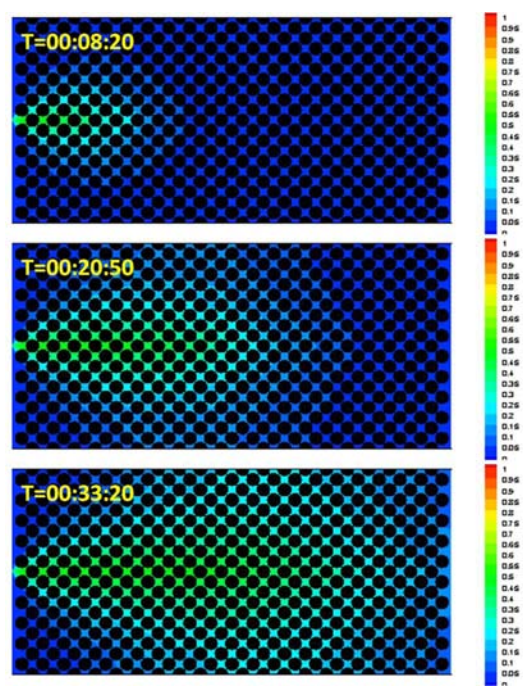


*Figure 3. LBM simulation results for the experimental run presented in Figure 2 of reactive micromixing using a 100 mM Ca+ ions solution and a 50 mM OG5N calcium ion indicator at Pe ~ 2. Micromodel used: staggered array of cylindrical grains of diameter 600-µm, height 35-µm, porosity = 0.38.*

We explored a technique for enhancing micromixing in low Reynolds-number (Re) systems, similar to our system, using "peristalsis." Peristalsis is responsible for transporting urine in the ureter and chime in the gastro-intestinal tract in physiological flows. Our work intended to enlighten the existing knowledge of peristaltic flows through the incorporation of solid particle transport. We performed

theoretical and computational studies on the transport of macroscopic solid particles by peristalsis using the LBM to investigating the mechanisms and conditions by which "peristalsis" can enhance mixing in these systems. In our system, a peristaltic flow occurs when a tube or channel with flexible walls transports the contained fluid, and in this case also the immersed particle, by progressing a series of contraction or expansion waves along the length of those walls. In these computational experiments, we systematically studied how changes in both the geometrical and physical parameters of the system affect the associated particle transport. We have also investigated the particle response to the peculiar phenomenon of "trapping" where a region of re-circulating fluid moves with the wave as a result of a large wall deformation. The particle is seen to enter this region and adopt a path following the closed streamlines, thus being transported at the speed of the wave, maximizing the transport. We have submitted a manuscript reporting our findings to "Physics of Fluids."

## Future Work

This project studies the extent and rate of micromixing, with/without chemical reactions, in systems of increased chemical and physical heterogeneity, and explores techniques for incorporating micromixing in large-scale transport problems and for enhancing mixing in microscopic systems. Experimental and modeling efforts will be carried out in parallel to achieve the project's goals. Experiments performed in micro-channels with well defined geometries will provide unique data for numerical modeling, and model results will subsequently be verified against results from macroscale systems. Microscopic-scale experiments will employ video microscopic visualization system unique to LANL and appropriate fluorescent reaction indicators to quantify mixing and chemical reactions in T-shaped microreactors. Two different solutions will be injected at the same time and rate through the microreactor's two opposite arms to flow alongside each other in its main channel. The extent of mixing will be measured and characterized in terms of parameters such as Peclet number and species concentration distribution/evolution across/downstream the channel. Experiments will be repeated in the same microreactor after packing its main channel with beads of different size, shape and surface reactivity to alter the system's chemical and physical heterogeneity. Results of the microscopic experiments will be simulated using a Lattice Boltzmann (LB) approach to regenerate the experimental results and then create numerical results at a wider parameters range. The LB technique makes very few assumptions about the system's chemistry and physics and should accurately reproduce the experimental results. These results will be further verified against additional microscopic experiments at selected parameter values. The Peclet number and other measured parameters will be used to characterize mixing occurring at the macroscopic-scale which are critical in determining an upscaling scheme for larger scale applications. An apprach for enhancing mixing in the micromodels based on peristalsis, acoustic stimulations, and electrokinetics will be explored and evaluated.

## Conclusion

We performed experimental and computational studies on micromixing in systems of different geometries at low Pe conditions. Our results represent the first comprehensive data set on transitional micromixing, before and after reaching steady state. Qualitative agreement between experimental and LBM simulation results was obtained for both reactive and non-reactive micromixing conditions. A technique for enhancing micromixing by peristalsis in the presence of macroscopic solid particles was investigated. This study led to the conditions under which enhanced micromixing can be reached.

The main expected results of our work are: 1) quantitative understanding of reactive/nonreactive-micromixing phenomena; 2) better integration of micromixing in macroscopic systems; and 3) an approach for enhancing mixing in microscopic scale systems. Important applications to the scientific community and the public include: a) Energy and Industrial: fuel cells, oil recovery, organic synthesis, combustion, polymerization, fermentation; b) Environmental and Water Security: groundwater remediation, subsurface contaminants transport, desalination; c) Medical: microfluidic devices for patient diagnosis/monitoring, blood analysis and cancer cells detection, drug efficiency; d) Homeland Security and Threat Reduction: enhanced chemical, nuclear, and biological sensors and micro-reactors, MEMS, micromixers, membrane-less filters for separation processes

## References

1. Willingham, T. W., C. J. Werth, and A. J. Valocchi. Evaluation of the effects of porous media structure on mixing-controlled reactions using pore-scale modeling and micromodel experiments. 2008. *Environmental Science Technology.* **42** (9): 3185–3193.

## Publications

Connington, K., Q. Kang, H. Viswanathan, A. I. Abdel-Fattah, and S. Chen. Peristaltic particle transport using the Lattice Boltzmann method. *Physics of Fluids.*

continuing project

# Subsurface Transport Parameter Estimation with Multiscale, Multiobjective Optimization

*Andrew Victor Wolfsberg*

20070441ER

## Introduction

A significant challenge in contaminant transport modeling is to obtain a mechanistic understanding of transport parameter scaling that accurately addresses the combined influence of physical and chemical heterogeneities at different scales. Although millions of dollars are spent each year for regulatory-driven investigations to characterize risk associated with contamination in groundwater, there remains no practical theory to integrate laboratory-scale data in field-scale predictions for resource analysis, risk assessment, or remedial design. This project is endeavoring to develop a upscaling methodology to provide a theoretical and practical link between controlled experimental results at scales increasing from the laboratory bench to the multi-kilometer field scale at which resource assessment and remediation is actually conducted. We develop and test the upscaling methods for prescribing appropriately scaled parameters in numerical models of fluid flow and contaminant migration in saturated fractured media (Figure 1).

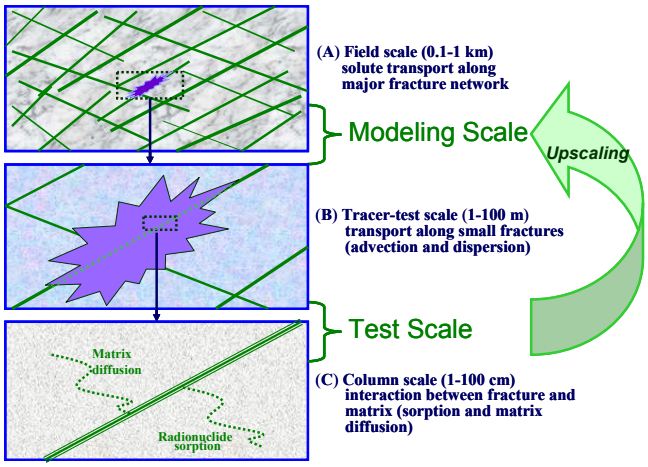


*Figure 1. Spatial hierarchical scales of fractured rock to show the gap between test scale and the modeling scale [1].*

## Benefit to National Security Missions

This project supports the DOE/NNSA missions in environment, energy, and science by enhancing our understanding of subsurface fluid and contaminant migration processes and subsurface property structures. High performance computing, new mathematical theories, and DOE/NNSA site data sets enable development of these methods to improve accuracy in important resource assessments.

## Progress

Progress in the first two years of the project has been made in six primary areas, which are described below:

1. Development of fracture network with a multi-scale transition probability model: To test concepts of parameter scaling from bench-scale fractured-rock column experiments to fracture network characterization, we have developed a multi-scale transition probability model to simulate the geometry of fracture network systems and at the same time to upscale the fracture apertures and fracture block proportions (see Figure 2). Flow and reactive solute transport in the upscaled fracture network are simulated with a novel generalized dual-porosity model, which enables highly efficient and accurate simulations of diffusive concentration fronts moving between fractures and matrix material. The developed methodologies will have broad applications for modeling flow and reactive solute transport in the fractured rocks.

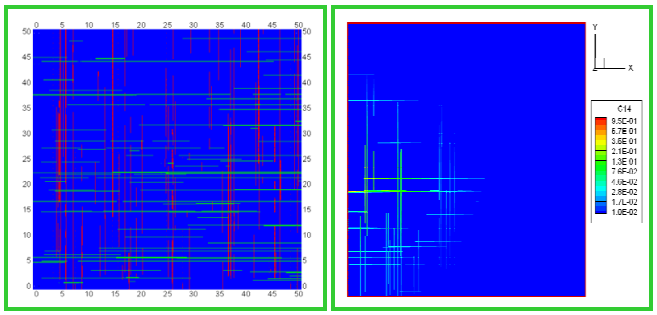

*Figure 2. A fracture network system created with multiscale transition probability models (left) and the simulated contaminant distribution in the fracture network (right).*

2. Development and testing of simultaneous inverse models for characterizing single fracture laboratory experimental parameters: Working with a novel data set developed at LANL for a series of laboratory column transport experiments, we have developed a simultaneous inversion methodology for parameter estimation from multiple experiments. Two inverse methods were developed, compared, and contrasted, one a global search algorithm and the other a local gradient-based search algorithm. Our results demonstrate that the global search method provides greater accuracy and quantification of the estimation uncertainty, but at a higher computational cost. Two papers have been prepared on this subject [1, 2]. Professional talks on this subject have been given at The American Geophysical Union meeting and at the Geological Society of America meeting.

3. Development and testing of mathematical upscaling formulations: Following the parameters estimation from the laboratory scale studies, we have developed a multi-modal spatial random function that upscales the critical transport parameters for fracture aperture, matrix diffusion, and solute sorption coefficient for field-scale simulation. The effective field-scale parameters are related to their geometric mean, variance, integral scale and domain size. Their values increase with their integral scales and are much larger than their geometric means. This has led to a publication in geophysical Research Letters [3].

4. Development of a stochastic inverse methodology for identifying subsurface material structure with limited hydrologic and geologic data: Upscaling laboratory parameters to the field scale requires knowledge of subsurface material structure. Therefore, using a field-scale groundwater model and associated head observations and geologic information from boreholes, we solve the inverse problem for the stochastic parameters in the transition probability model and generate the material distribution necessary for upscaling transport parameters. These results provide insight regarding material proportions, mean lengths of features, and their roles in controlling fluid flow. A paper is published in a peer reviewed journal on this aspect of the project [4].

5. Development of numerical models for upscaling processes and parameters for networks of connected discrete fractures: At the field scale, predictive models are resolved at scales much larger than that of a single fracture. Thus, any grid block in a model is characterized by multiple interacting fractures. Therefore, we have developed a discrete fracture network modeling system for the purpose of estimating effective fracture parameters for any grid block in a fieldscale model. Our first result has been to estimate the effective fracture aperture for a sub-grid-block system of parallel, but not identical, fractures. With this methodology, the upscaled single, effective fracture aperture reproduces the same flow dynamics as the group of smaller fractures. The next step is to combine the effective fracture aperture with the effective matrix diffusion coefficient to ensure mass transfer from fractures to matrix is preserved in the upscaled material properties. We are also using this network model to investigate interference between fractures via diffusion in the matrix material separating them. New models using inverse Laplace Transform solutions for transport in fractured media and superposition concepts are being invoked to solve, via inversion, fracture interaction parameters applicable at larger scales.

6. Development of analytical solutions for upscaling sorption coefficients in saturated fractured rock system: We have developed a scaling methodology to upscale matrix sorption coefficients for fractured-rock systems by characterizing both the tortuosity field (physical heterogeneity) and retardation factor field (chemical heterogeneity) in the rock matrix. We compute the effective tortuosity with a conservative tracer. Then, using a sorbing tracer, we derive the equations for upscaling the sorption coefficients in a saturated, fractured rock system (see Figure 3). The derived upscaling equations for the sorption coefficients are verified with Monte Carlo simulations, which are based on a generalized dual-porosity model to enable highly efficient and accurate numerical simulations of diffusive concentration fronts moving between the fractures and matrix material [5]. Two more papers have being prepared from this area of study [6].

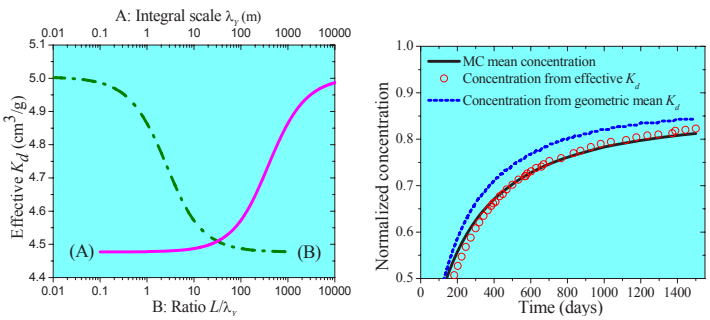


*Figure 3. Effective sorption coefficient (left) and the comparison of the concentration breakthrough curves computed from the effective KBdB, geometric mean KBdB and the Monte Carlo simulations (right).*

## Future Work

The goal of this research project is to integrate components of multiobjective optimization theory, multimode spatial statistics and upscaling algorithms, and hierarchical transition probability models to identify and then account for complex physical and chemical processes at increasing scales for subsurface flow and contaminant transport simulation. The next phase of this project will involve integrating the upscaling theory developed in Year 1 and 2 with observations at both the laboratory and the field scale. We will extend the derived upscaling methods for heterogeneous fracture apertures and reaction coefficients in fracture rock, and verifying the upscaling equations with MC simulations. This extension should allow for effective parameters for flow, matrix diffusion, and solute retention via reactions with immobile minerals to be developed for complex fracture networks. We anticipate applications of this theory and methodology to DOE/NNSA sites such as the Los Alamos site and the Nevada Test Site as well as in emerging alternative hydrocarbon extraction investigations such as those associated with oil shale extraction from induced fractured media. Although programs at these sites cannot always develop new theories, they often employ the most recent developments in computational subsurface science, thus enabling applied programmatic growth. We expect two more papers will be completed in the last year.

## Conclusion

The physical and chemical heterogeneities of matrix properties are a source of reactive transport parameter scale dependence in solute migration models. Results to date indicate that model parameters estimated from centimeter-scale experiments can not be directly used for field-scale simulation. However, the laboratory-scale values, when considered in conjunction with field-scale variability of material properties, leads to mathematical formulations for estimating effective values at increasing scales. Key parameters affecting solute migration in fractured rock systems include the matrix diffusion coefficient, the fracture aperture, and the effective block porosity. We have scaled each of these individually with the transition probability theory developed in this project and are now developing scaling algorithms to solve their scaled dependence simultaneously. The scientific results from this study will provide a theoretical and practical link between controlled experimental results obtained at the laboratory bench scale to the field scale at which risk assessment and contaminant remediation are actually conducted.

## References


1. Wolfsberg, A., Z. Dai, J. Vrugt, and P. Reimus. Inverse Modeling of Colloid-facilitated Plutonium Transport in Fractured Tuffaceous Rock. *J. of Contaminant Hydrology.*

2. Dai, Z., A. Wolfsberg, Z. Lu, and R. Ritzi. Representing Aquifer Architecture in Macrodispersivity Models with an Analytical Solution of the Facies Transition Probability Matrix. 2007. *Geophys. Res. Lett..* **34** (L20406): 1.

3. Dai, Z., A. Wolfsberg, Z. Lu, and P. Reimus. Upscaling matrix diffusion coefficients for heterogeneous fractured rocks. 2007. *Geophys. Res. Lett..* **34** (L07408): 1.

4. Harp, D., Z. Dai, A. Wolfsberg, J. Vrugt, B. Robinson, and V. Vesselinov. Aquifer structure identification using stochastic inversion. 2008. *Geophys. Res. Lett..* **35** (L08404): 1.

5. Dai, Z., A. Wolfsberg, Z. Lu, and H. Deng. Scale dependence of sorption coefficients for contaminant transport in saturated fractured rock. *Geophys. Res. Lett..*

6. Dai, Z., A. Wolfsberg, Z. Lu, and H. Deng. Identifying sorption processes and parameters for radionuclide transport in fractured rock. To appear in *J. of Stochastic Environmental Research and Risk Assessment.*


## Publications


Dai, Z., A. Wolfsberg, A. Lu, and P. Reimus. Upscaling matrix diffusion coefficients for heterogeneous fractured rocks. 2007. *Geophysical Research Letters.* **34** (7): L07408;1.

Dai, Z., A. Wolfsberg, Z. Lu, and H. Deng. Scale dependence of sorption coefficients for contaminant transport in saturated fractured rock. *Geophys. Res. Lett..*

Dai, Z., A. Wolfsberg, Z. Lu, and R. Ritzi. Representing aquifer architecture in macrodispersivity models with an analytical solution of the transition probability matrix. 2007. *Geophysical Research Letters.* **34**: L20406;1.

Harp, D., Z. Dai, A. Wolfsberg, J. Vrugt, B. Robinson, and V. Vesselinov. Aquifer structure identification using stochastic inversion. 2008. *Geophys. Res. Lett..* **35** (L08404): 1.

# Identifying High Risk Species Critical for the Emergence of Pandemic Influenza

*Jeanne Marie Fair*

20080230ER

## Introduction

It is estimated that some 40 million Americans would become infected if a pandemic emerges from avian influenza (A/H5N1) and over 700,000 people will need hospitalization in such a scenario. The most critical mitigation for stopping the emergence of the highly pathogenic avian influenza into human populations in the pandemic form is to detect and control H5N1 in avian populations. However, management of highly pathogenic influenzas in wild and domestic animal populations requires a better understanding of the determinants of host range. Missing at the moment is critical data that can lead to which avian species should be under surveillance. To answer this question we are investigating the major host range determinant for influenza which is the binding site for the virus, sialic acid, which varies between mammals and bird cell membranes. The specific hypothesis behind the research is that the characterization of sialic acid of species in each order in the Class Aves can be used as a phylogenetic guide map to host range for influenza and that data can then be used to guide surveillance efforts for strains of concern for influenza. This hypothesis is based on the following observations. First, that to gain entrance into cells, human influenza viruses bind preferentially to sialic acid containing N-acetylneuraminic acid α2,6-galactose (SA α2,6Gal) linkages while avian and equine viruses bind preferentially to those containing N-acetylneuraminic acid α2,3-galactose (SA α2,3Gal) linkages. Second, that it has also been recently discovered that chickens and quail have human α2-6 receptors in their lungs as well. And third, viruses isolated from distinct bird species differ by their recognition of the oligosacchride receptors in the corresponding bird species.

## Benefit to National Security Missions

Management and detection of highly pathogenic influenzas in wild and domestic animal populations require a better understanding of the determinants of host range. There has been a very large multi-agency effort for monitoring for influenza in the wild birds for the last five years that will be difficult to be sustainable. Disease detection of pathogens crossing our borders must be based a strong scientific foundation that provides the focus to be effective in monitoring for diseases.

## Progress

A sample and analysis database is in development and is a relational database programmed in Microsoft structured query language (MsSQL) (Figure 1). It will be housed on a LANL MsSQL Server and accessible to multiple users on and off campus depending on access privileges. The database will be capable of tracking molecular to landscape scale data and will interact with a geographic information system (GIS) in order to accommodate spatial analyses. Certain data standards are being developed in collaboration with the Wildlife Disease Information Node of the National Biological Information Infrastructure. The database will contain information on the bird collection, specimen type, sialic acid (Sia) content analysis as well as spatial and geographical identification of Sia types in tissue sample. The materials and methods leading to the database inputs will also be contained within the database. This tool will allow fluid communication between internal collaborators as well as external colleagues in the field of Avian Research. Also, the database can be easily adapted and applied to other species and issues of concern that may arise in the future.

A spatial model is being developed to investigate the spatial dynamics of sialic acid distribution in the respiratory and digestive tract of birds. Currently, it is not known whether a difference in relative abundance of specific sialic acid types among different animal species affects the potential of influenza viruses to evolve in the host and we have no baseline readings of sialic acid amounts in various bird species to determine which birds should be under surveillance. Development of this spatial model for both tracts will be performed by

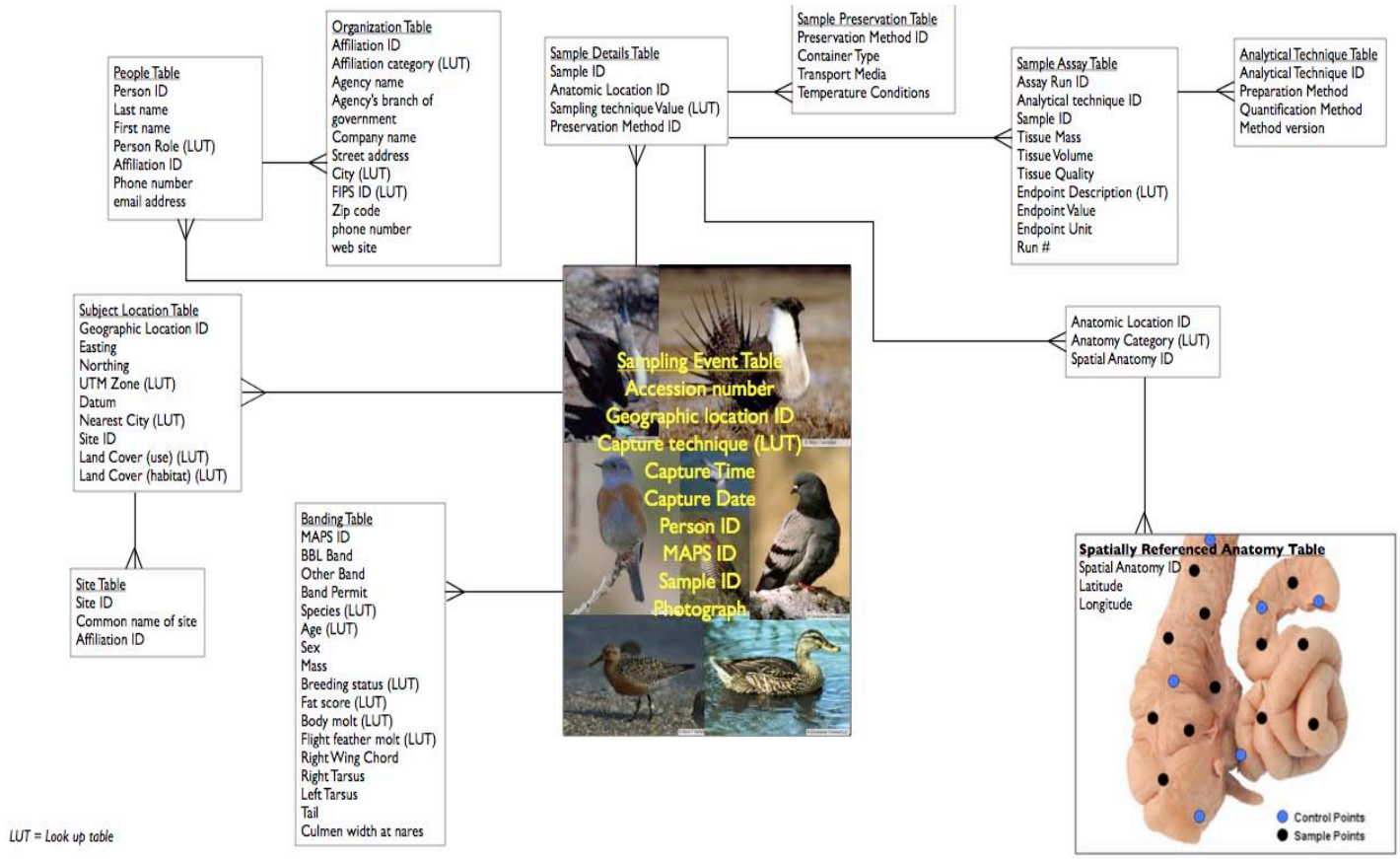


*Figure 1. Initial data model for the avian science SQL relational database.*

digitally photographing the sample tissues and creating a digital surface mosaic from the images. Sialic acid concentrations will then be completed for the two tracts and the distribution of concentration of Sia and subtype visualized as a surface mosaic to show sialic acid differences along the length of each tract. A high-resolution camera has been purchased and tripod apparatus has been configured to enable photographing of dissected avian specimens collected in the field. We are beginning to attain 5-10 samples per Species from all Avian Families. Initial test photographs of specimens will be used to prototype GIS processing techniques to ortho-rectify photographs to local coordinate system to accurately map physiological control points and samples taken from the specimens collected (Figure 1). Variation in Avian RBC Sia subtypes is being assessed along a phylogenetic gradient using a DNA-DNA hybridization-based taxonomy developed by Sibley and Ahlquist (1995) (Figure 2). This will be compared to variation in each anatomic tract and may be used as a non-lethal indicator of the sialic acid bond ratio within a species.

Measuring sialic acid requires a series of steps including the homogenization of tissue and/or lysis of red blood cells, release of bound Sialic acid via Sia-to-galactose bond cleavage and then quantification. However, methods to measure total sialic acid differ from those used to measure the relative abundance of specific glycosidic linkage types (α2-3 and α2-6). The former can be performed through non-specific cleavage of the glycosidic bond linking Sia to underlying cell surface glycans by acid hydrolysis, whereas the latter relies on bond-specific breakage by enzymes with known activities (Figure 3).

The isolation and quantitation of Sia in red blood cells (RBCs) has been initiated. Prior to the measurement of RBC-bound Sia, RBC ghosts must be prepared to remove hemoglobin by lysis, and the resulting lysate treated so as to inactivate native sialidases and preserve Sia's chemical structure. Using several protocols, we have successfully isolated and detected unbound pigeon Sia by mass spectrometry (MS). Most recently, we attained an estimate of approximately 50 µM total Sia from rock pigeon RBCs. Our instrument of choice for the new higher throughput and more sensitive method for Sia quantification from avian specimens was a Thermo Finnigan LCQ Deca XP mass spectrometer, which is connected to a front end Surveyor

HPLC system with automated sample handling. This liquid chromatography based system is well suited for analysis of carbohydrate targets and numerous samples can be analyzed in a short time with full automation.

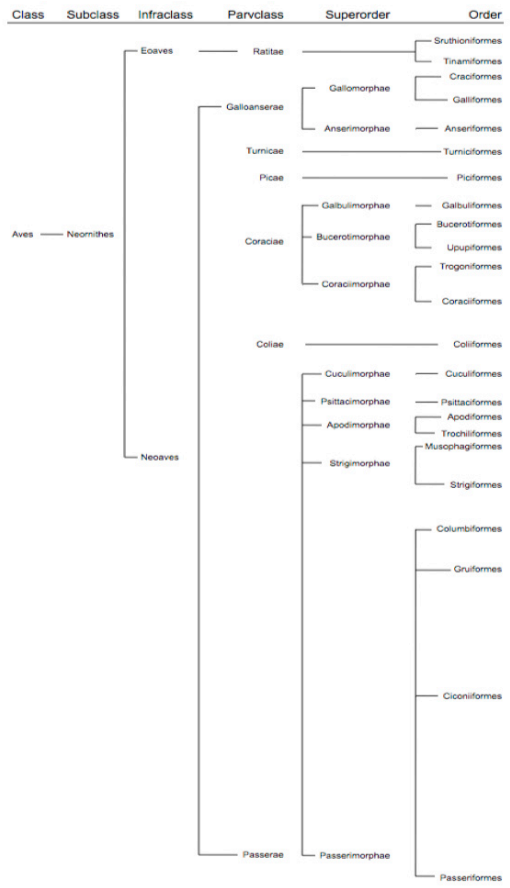


*Figure 2. DNA-DNA hybridization based avian phylogenetic tree for all avian Orders.*

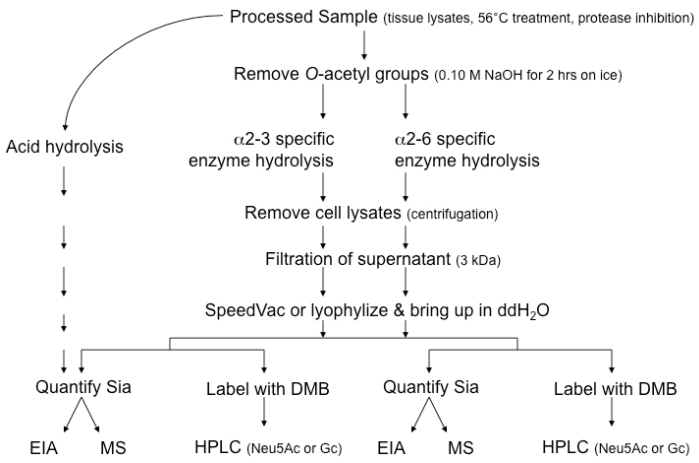


*Figure 3. Flow chart of sialic acid characterization and quantification in avian tissues.*

## Future Work

For samples acquisition, we set up collaborations with numerous zoos, including the Wildlife Conservation Society in New York and the St. Louis Zoo, as well as the Wisconsin Department of Natural Resources and U.S. Fish and Wildlife Service. The zoos are currently collecting blood samples from highly exotic bird species. We have obtained samples from wild waterfowl in New Mexico through collaboration with New Mexico State University. We also set up a successfully funded collaboration with the leading Sia laboratory in the world at University of California San Diego to continue this work through the Los Alamos and University of California research program.

We plan to further characterize Sia variation in our focal species in order to hone HPAI surveillance and response efforts. This work will determine which life-history stages these species would most likely be susceptible to influenza infection. We have also begun a relationship with the U.S. Department of Agriculture's Southeast Poultry Research Laboratory in Athens, GA to attain inactivated LPAI and HPAI H5N1 virus isolates for studies aimed at determining whether the focal species' in this project differ in their lymphocyte proliferation response to either of these antigens. We predict that the differences between species will be greater when testing the lymphocyte response to LPAI than HPAI based on differential mortality in HP but not LPAI.

## Conclusion

With the initial successes in rock pigeon sialic acid measurements, a new state of the art mass spectrometer, and new collaborations with UCSD, USDA and several state and Federal wildlife organizations, we expect rapid progress in sample acquisition and analysis for the upcoming year of this project. Due to the immensity of the survelliance challenge, current influenza surveillance systems for birds may easily miss influenzas of concern in asymptomatic populations. We hope that the new data compiled in this project will help focus influenza surveillance efforts.

## References

1. Sibley, C., and J. Ahlquist. Phylogeny and classifications of birds.. 1990.

2. Reuter, G., and R. Scheuer. Determination of sialic acids. 1994. In *Methods in Enzymology..* Edited by Lennarz, W., and G. Hart. , p. 168. San Diego, CA: Academic Press.

3. Warren, L.. The thiobarbituric acid assay of sialic acids. . 1959. *Journal of Biological Chemistry.* **234**: 1971.

4. Crook, M., M. Hag, and P. Tutt. Evaluation of three assays for the determination of serum total sialic acid.. 1993. *Clinical Biochemistry.* **26**: 449.

## Publications

Fair, J., K. McCabe, Y. Shou, and B. Marrone. Immunophenotyping of Chicken Peripheral Blood Lymphocyte Subpopulations: Individual Variability and Repeatability. . 2008. *Veterinary Immunology and Immunopathology.* **In Press**: In Press.

# The Effect of Acoustical Waves on Stick—Slip Behavior in Sheared Granular Media: Implications for Earthquake Recurrence and Triggering

*Paul Allan Johnson*

20080268ER

## Introduction

Dynamic earthquake triggering remains a compelling mystery: how do transient seismic waves with micrometer displacements trigger earthquakes, often with failure occurring long after the waves have passed? How can triggering take place at distances of hundreds of kilometers, from the earthquake generating the seismic waves? We are addressing how triggering takes place; however the work will also lead to a new understanding of the importance of seismic energy on earthquake physics and more generally, there will be broad impact on unexpected material failure induced by moderate-amplitude sound. To address our goals and simultaneously test a model we recently developed [1], we are conducting laboratory studies of stick—slip in granular media and its response to applied acoustic waves. In preliminary studies, we used glass beads to simulate granular fault zone wear material (gouge), sheared under constant normal stress while subject to acoustic waves. We observed evidence for triggered "earthquakes" when applied sound-wave amplitudes exceeded several microstrain. We were surprised to also observe significantly delayed "earthquakes" relative to those observed without wave perturbation (increased recurrence), as well as strain memory of the sound perturbation in the granular material. These phenomena persisted despite the severe material reset that takes place during a large "earthquake". We will determine how and why these phenomena occur and place them in the context of real earthquakes, as well as other failure scenarios including avalanches, landslide and failure of incipient damage in the presence of moderate amplitude sound.

## Benefit to National Security Missions

There is a large class of diverse applications of this work that include predicting unexpected breakdown behavior. This project will support the DOE missions in Science by enhancing our understanding of earthquake prediction, and Nuclear Weapons by enhancing our understanding of small amplitude vibration on incipient damage in components.

## Progress

In addition to very small amplitude wave displacements that cause triggering, earthquake nucleation depths are of order 10-20 km, and thus static overburden might be expected to prohibit triggering by seismic wave stress perturbations (~100000 Pa). To better understand the physics of dynamic triggering as well as the influence of dynamic stressing on earthquake recurrence, we conducted laboratory studies of stick—slip in granular media with and without applied acoustic vibration. Glass beads were used to simulate granular fault zone wear material, sheared under constant normal stress, while subject to transient or continuous perturbation by acoustic waves. We found that small magnitude failure events, corresponding to triggered aftershocks, occur when applied sound-wave amplitudes exceed several microstrain. These events were frequently delayed and/or occur as part of a cascade of small events. Vibrations also cause large slip events to be disrupted significantly in time relative to those without wave perturbation. The effects are observed for many large-event cycles after vibrations cease, indicating a strain memory in the granular material. Figure 1 illustrates the disruption in the stick-slip recurrence due to vibration, and compares it to an experiment where no vibration was applied. Dynamic stressing of tectonic faults may play a similar role in determining the complexity of earthquake recurrence.

Laboratory studies of granular friction have emerged as a powerful tool for investigating tectonic fault zone processes and earthquake phenomena including post-seismic slip, interseismic frictional restrengthening, and earthquake nucleation. In this work, we explore experimentally the effects of dynamic loading on stick—slip behaviour and speculate how our results impact understanding of earthquake processes, in particular, dynamic earthquake triggering and stick—slip recurrence. Dynamic earthquake triggering involves seismic waves from one earthquake promoting or inhibiting failure on faults they disturb. Dynamic triggering has been clearly documented in a few cases far from an earthquake

source, at distances much greater than the fault radius of the triggering source1 (outside the traditional 'aftershock zone'), and mounting evidence suggests it commonly occurs near the earthquake source.

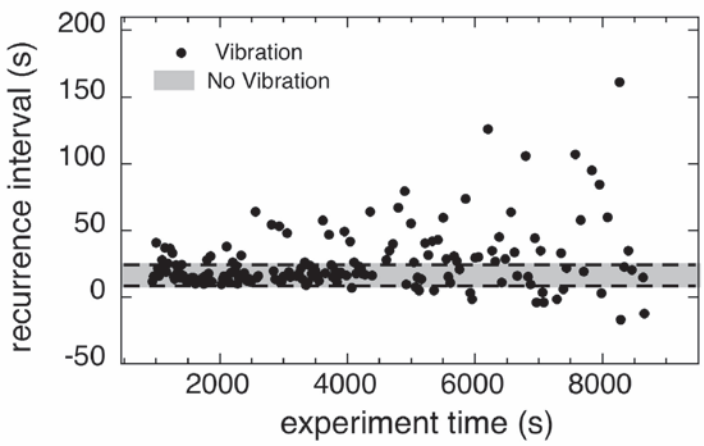


*Figure 1. Recurrence versus experiment time for runs with vibration (solid circles) and without. The shaded region and dashed lines show the mean recurrence interval of +-1 standard deviation. Data trend removed. Compared to the non-vibration experiments, both the scatter and average recurrence interval increases progressively in experiments with vibration.*

The origin of dynamic earthquake triggering by transient seismic waves is a complex problem. Our results show that granular-friction processes are consistent with two of as yet unexplained observations in earthquake seismology: 1) small amplitude waves can trigger failure both immediately and delayed failure relative to the strain transient, and 2) earthquake recurrence patterns are complex. Understanding the role of vibration-induced disruption of earthquake recurrence could have significant implications for seismic hazard assessment and reliable forecasting of earthquakes.

These observations were described in a paper published in the Journal Nature, in January 2008 [2].

## Future Work

Our goal is to unravel how dynamic earthquake triggering takes place, by employing laboratory studies of stick-slip and observational studies of earthquakes. The work will have direct impact on other avalanche –type behavior (see below).

Our hypotheses are,

- Dynamic waves trigger earthquakes due to nonlinear softening-to-weakening, both in the laboratory and in the Earth, due to the nonlinear response of the fault gouge, given certain conditions (critical state, shear weakness and/or low effective pressure, elevated strain); toward that goal we are working on the nonlinear elastic response of granular media, and have recently published a paper on this topic (3,4).
- Strain memory is responsible for delayed triggering in the lab and in the Earth, and for disrupted recurrence in the lab, and potentially in the Earth;
- The origin of behaviors is explained by the micromechanics of the medium—the force chains—and that these processes may be widespread (sound induced crack failure, landslides, avalanche).

Our tasks are to, 1) test the hypotheses in laboratory and model stick-slip studies, and 2) inspect seismic data for observations that may support or refute the hypotheses. Whether or not the processes are nonlinear in origin, our ultimate objective is to understand the role of dynamic waves on earthquake processes, and apply what we learn to a scope of problems that are related to catastrophic breakdown due to moderate amplitude sound. Without such tools we have no hope of predicting earthquakes (a very hard problem in any case) or understanding when cracks in a component may breakaway due to the presence of sound. Each task will be considered met with a series of peer-reviewed journal publications submitted. In addition, we add the task of looking for applications of interest to DOE, in particular, to issues related incipient damage where components may be in the presence of moderate amplitude sound.

## Conclusion

Triggering is an intriguing scientific question that confounds, and we find that the effects of acoustics on faulting in the laboratory create many other questions as well. Our work will tell us what effect seismic waves generated by one earthquake have on a fault located nearby or far away. We already have evidence that the effects could be significant, and that seismic waves may strongly effect time-dependent earthquake forecasting, a primary goal of seismologists. Ultimately, predictive models used in earthquake prediction will surely have to include earthquake triggering and wave effects on fault recurrence and memory.

## References

1. Johnson, P. A., and X. Jia. Nonlinear dynamics, granular media and dynamic earthquake triggering. 2005. *Nature.* **473**: 871.
2. Johnson, P. A., H. Savage, M. Knuth, J. Gomberg, and C. Marone. The effect of acoustic waves on stick-slip behavior in sheared granular media: implications for earthquake recurrence and triggering. 2008. *Nature.* **451**: 57.

3. Brunet, T., X. Jia, and P. A. Johnson. Transitional, elastic-nonlinear behaviour in dense granular media. 2008. *Geophysical Research Letters.* **35**: L19308.

4. Guyer, R., and P. A. Johnson. The nonlinear mesoscopic elasticity class.

## Publications

Brunet, T., X. Jia, and P. A. Johnson. Transitional, elastic-nonlinear behaviour in dense granular media. 2008. *Geophysical Research Letters.* **35**: L19308.

Guyer, R., and P. A. Johnson. The nonlinear mesoscopic elasticity class.

Johnson, P. A., H. Savage, M. Knuth, J. Gomberg, and C. Marone. The effect of acoustic waves on stick-slip behavior in sheared granular media: implications for earthquake recurrence and triggering. 2008. *Nature.* **451**: 57.

# Developing a Remote Sensing of the Solar Surface

*Joseph Eric Borovsky*

20080321ER

## Introduction

Understanding the solar wind that impinges upon and surrounds the Earth is crucial to virtually every aspect of space flight from spacecraft and sensor design to safety considerations in manned space flight. Furthermore, the solar-wind interaction impacts all manner of communications and sensing systems. The ultimate goal of this LDRD/ER Project is to develop a new research area connecting the physics of the solar surface with the physics of the solar wind, thereby advancing the understanding of both.

This LDRD/ER Project has three research objectives:

- Survey the properties of the solar wind that emanates from different features on the sun. This will provide a large body of information about the sources of the solar wind.
- Map the magnetic flux tubes measured by the ACE spacecraft to their specific regions of origin on the solar surface. This will provide a large body of information about the origin of structure in the solar wind, about the predictability of patterns in the solar wind, and about the properties of important magnetic-flux concentrations that escape from the sun.
- Develop a technique to use existing solar-wind instruments to make remote measurements of the time-dependent dynamics of the magnetic flux concentrations as they escape from the sun.

## Benefit to National Security Missions

This project will enhance our understanding of the solar wind and its impact on the space environment, which affects space-based platforms and sensors. This project will support the missions in Threat Reduction and treaty verification important to DOE, DHS, and other government agencies.

## Progress

In this LDRD project, criteria for discerning flux-tube discontinuities in the solar wind were explored. It was decided that the most-reliable criteria is a combinations of large change in the magnetic-field direction and large shift in the flow-velocity vector. These most-reliable criteria have been implemented by researchers at the University of New Hampshire on entire ACE data set for the ACE-spacecraft data server. The number of flux tubes per 1 hour data interval will be an available product.

In this project, work progressed on the statistical matching of measured solar-wind discontinuities in the plasma properties versus the magnetic-field properties versus the energetic-particle properties. Plasma and field properties show more correlations than combinations involving energetic particles. This is consistent with reconnection acting near the sun to re-map the solar-wind flux tubes into the solar surface.

An examinations of regions around the heliospheric current was commenced using the ACE data set to discern Alvenic interfaces from Alfven waves. These regions are of note because of the large fluctuations in the solar-wind magnetic field and the regions are of particular interest because of the historical belief by the magnetospheric community that these regions have large-amplitude Alfven waves which anomalously drive activity at Earth. Discerning the difference in these regions proves particularly difficult.

The investigators have begun to introduce zero-crossing methods into solar-wind data analysis. Zero-crossing methods come from the experimental fluid-turbulence community: the methods are based on a statistical analysis of the time intervals between subsequent crossings of a measured quantity through the origin. The methods are powerful and very intuitive, particularly for a medium such as the solar wind that is comprised of flux tubes plus turbulent fluctuations. Techniques have been developed for automatically finding and removing walls of solar-wind flux tubes. The techniques will be tested and refined soon. Indications are that the same

zero-crossing methodology can be used to simultaneously analyze the properties of the solar-wind flux tubes, the solar-wind MHD turbulence, and the relationship between the two.

To provide leadership to the solar-wind research community, a session on this LDRD topic entitled "Origin of structure in the solar wind" was organized at the 2008 NSF SHINE Workshop, a session entitled "Small-Scale Structure in the Solar Wind and Its Effect on Earth" was organized at the joint GEM-SHINE Workshop, and a CSSE Workshop in being organized in Santa Fe for October 6-10, 2008. Invited talks were presented on this LDRD work at two international conferences and a third invitation has been accepted, and a poster was presented at the NSF SHINE Workshop. One paper has been published: J. E. Borovsky, Flux tube texture of the solar wind: Strands of the magnetic carpet at 1 AU?, J. Geophys. Res., 113, doi:10.1029/2007JA012684, 2008 and another paper has been submitted.

## Future Work

This project has three research objectives.

- Survey the properties of the solar wind that emanates from different features on the sun. In particular the central portions of off-equatorial and equatorial coronal holes and coronal-hole edges will be compared. This will involve coordination of the ACE spacecraft data with models of where the solar wind originates from the solar surface. The goal will be to obtain a large data base of coordinated solar-wind properties and solar source locations. This objective will provide a large body of information about the sources of the solar wind.

- Map the magnetic flux tubes measured by the ACE spacecraft to their specific regions of origin on the solar surface. This will also involve coordination of the ACE spacecraft data with models of where the solar wind originates from the solar surface. The goal will be to obtain a large data base of solar-wind flux-tube properties and their solar source locations. This objective will provide a large body of information about the origin of structure in the solar wind, about the predictability of patterns in the solar wind, and about the properties of important magnetic-flux concentrations that escape from the sun.

- Develop a technique to use existing solar-wind instruments to make remote measurements of the time-dependent dynamics of the magnetic flux concentrations as they escape from the Sun. This will involve detailed and statistical comparisons of the locations of solar-wind discontinuities seen in the magnetic-field measurements, in the plasma measurements, and in the energetic-electron measurements. Displacements of the various discontinuities represents the amount of magnetic-field reconnection near the sun. The goal will be a statistical picture of the reconnection rate in chromospheric structures.

## Conclusion

We expect that this project will provide bodies of information about the sources of the solar wind and about the origin of structure in the solar wind, about the predictability of patterns, and about the properties of important magnetic-flux concentrations that escape from the sun.

We expect to develop a technique to use solar-wind instruments to make remote measurements of the dynamics of the flux concentrations as they escape from the sun.

The ultimate goal of this project is to develop a research area connecting the physics of the solar surface with the physics of the solar wind.

## Publications

Borovsky, J. E.. Flux tube texture of the solar wind: Strands of the magnetic carpet at 1 AU?. 2008. *Journal of Geophysical Research.* **113**: A08110.

Borovsky, J. E., and S. P. Gary. On viscosity and the Reynolds number of MHD turbulence in collisionless plasmas: Coulomb collisions, Landau damping, and Bohm diffusion. To appear in *Physics of Plasmas.*

# A New Approach to Unravel Complex Microbial Community Processes

*Cheryl Rae Kuske*

20080464ER

## Introduction

Soil organic matter is the largest pool of terrestrial carbon on Earth. Soil microbiota (bacteria, fungi, microfauna) are responsible for stabilization and release of this pool via complex decomposition processes. Although key to carbon flux in terrestrial ecosystems, microbial decomposition is one of the major unknowns for prediction of carbon sequestration, ecosystem responses to climate change, and contaminant mitigation. Our project aims to provide an in situ assessment of microbial decomposition of different carbon sources using a unique Tunable Diode Laser Spectroscopy (TDL) system, and parallel identification of the active microbial participants using stable isotope probing (SIP) and metagenomic analysis of the microbial community. This combination of new techniques is being applied to different soil types to identify key players in the decomposition of simple and complex substrates, and in situ field surveys at LANL's woodland observatory. Scientific contributions from this project will include:

- Multi-scale demonstration of a suite of novel approaches to identify connections between soil microbial community composition, activity and metabolic processes,
- New insights into fundamental decomposition processes, and
- Determination of temperature and moisture effects on microbial community structure, metabolism and ecosystem carbon sequestration.

## Benefit to National Security Missions

This project endeavors to develop new technology and a comprehensive understanding of carbon cycling in soils. Soil carbon is among the largest sources of $CO_2$ input to global atmospheric $CO_2$, and is released into the air by complex microbial communities that reside in the soil. Microbial decomposition processes also affect movement of organic pollutants and toxic metals in soils, supporting missions in DOE/SC, and other government agencies.

## Progress

### Method Development

Our research has progressed in both laboratory and field experiments, primarily toward development of experimental systems to mesh the respiration and microbial community composition measurements. First, we established a soil microcosm system through which we can incubate soils under different conditions, and take measurements of the microbial community biomass and composition, as well as decomposition rates ($CO_2$ production) and carbon sources used ($\delta^{13}C$ of $CO_2$). Specific challenges included developing a simple 'jar' system that could be replicated, that could be plumbed for sensitive TDL measurements without leaking, and that could be sampled over time for community analysis. We are in the final stages of development and calibration of this system.

Second, we established experimental parameters for stable isotope probing (SIP), where a $^{13}C$-labled carbon substrate is used to identify the active populations capable of degrading that substrate in a background of complex soil microbial community. We determined ultracentrifugation criteria to effectively separate $^{13}C$ and $^{12}C$ microbial DNA and the process is working well with experimental controls. In addition, we conducted baseline SIP experiments with LANL woodland observatory soil using $^{13}C$-labeled carbon simple substrate (acetate) to generate experimental controls and to determine the response of soil microbial communities over a period of ca. two weeks. As expected, a very wide variety of soil microbes were able to use a simple labeled carbon substrate. The range of buoyant density of the collective genomes of the soil organisms precluded separation of the $^{13}C$ labeled DNA from $^{12}C$ DNA in the complex soil mixture using simple substrate, but the analytical methods are working and will be applied to the complex carbon experiments described below.

**Microcosm Experiments: Decomposition of Complex Soil Carbon**

The carbon substrates that accumulate in soils are predominantly complex cellulosic compounds derived from plant material. They are a critical and major pool of carbon in the terrestrial carbon cycle. These complex carbon substrates sequester carbon in soils; their decomposition is mediated by a less diverse group of soil microorganisms and occurs more slowly. One avenue of our analysis of decomposition in soils will continue with a focus on these complex substrates that represent rate-limiting steps in soil carbon cycling and are a key missing element in our ability to monitor or predict carbon dynamics in terrestrial ecosystems.

We are generating $^{13}C$-labeled complex cellulosic substrates via plant cell culture at LANL to use as substrates for SIP experiments of soil decomposition. We needed to develop this capability in house because these substrates are either not available commercially, or are prohibitively expensive. While generating the $^{13}C$ substrates, we conducted a series of soil microcosm experiments to test the ability of soil microbial communities to decompose xylan and cellulose. Soils from a natural arid land (our TA-51 field site) and a Michigan agricultural soil were compared under oxic (aerated) and hypoxic (oxygen limited) conditions that are typical in soils. Preliminary comparisons indicate that members of the phylum Acidobacteria are abundant in the soils (ca. 20% of the composition) and respond to additions of complex carbon substrates, especially under hypoxic conditions in the agricultural soils. These experiments are being used as a basis for more rigorous studies that integrate microbial community responses and rates of $CO_2$ emission when $^{13}C$-labeled carbon substrates are decomposed in soils.

**Field Studies**

We are beginning DNA-based microbial community and $\delta^{13}C$ flux measurements in soils at the TA-51 field site. Soil samples differing in carbon composition have been collected from the root zones of dead and live pinyon and the microbial community is being profiled. In parallel, we have developed and tested an accurate flip-top (open and close) chamber to conduct TDL measurements of $CO_2$ flux without perturbing the ambient $CO_2$ concentration and $\delta^{13}C$ flux. To date, we have proven that our chamber makes extremely accurate and precise measurements of both $CO_2$ flux and its $\delta^{13}C$ composition in a lab setting using an artificial matrix column, and will be putting this chamber into the field setting in year two of the project. The results of this effort are now in review at Global Change Biology. [Powers, H.H., J. Hunt, D.T. Hanson, N.G. McDowell. A dynamic soil chamber system coupled with a tunable diode laser for online measurements of $\delta^{13}C$ and $\delta^{18}O$ of soil respired $CO_2$. Global Change Biology, in review].

## Future Work

In year two, we will continue soil microcosm experiments with two major objectives:

- Determine the dominant, active microbial participants responsible for degradation of complex cellulosic carbon substrates in different soils.
- Determine the extent to which pulses of $CO^2$ that are rapidly released from soil following a wetting event are mediated by microbial activity.

We will also continue field site surveys to (3) determine similarities or differences in total microbial communities in soils with different dominant carbon sources, in association with dead or live pinyon. In parallel, determine the rate of $CO_2$ flux from root zone soils over natural seasonal temperature and moisture gradients.

## Conclusion

Assessing the relative contribution of different soil microorganisms to decomposition in parallel with undisturbed metabolism measurements has been a major goal of soil science for over five decades. We expect to refine parallel measures of the process (using a novel tunable diode laser) and active microorganisms (SIP/metagenomics). Deliverables include peer-reviewed manuscripts that link soil decomposition processes with the dominant microbial communities responsible for those processes, and information that will aid development of more defined models of soil microbial decomposition.

## Publications

Powers, H. H., J. Hunt, D. T. Hanson, and N. G. McDowell. A dynamic soil chamber system coupled with a tunable diode laser for online measurements of delta13C and delta18O of soil respired CO2. *Global Change Biology.*

# Nonequilibrium Mechanics of Geomaterials

*James Alan Tencate*

20080603ER

## Introduction

Work by Los Alamos researchers during the past decade has pioneered a new direction in the study of non-linear-elastic, dynamic behavior in materials. Certain materials display surprisingly large nonlinearities, which include conditioning and memory effects, appearing at wave strains smaller than parts per million---disturbances equivalent to seismic waves far from an earthquake epicenter. The materials relax in a very peculiar way over very long durations after the wave disturbance, a nonequilibrium phenomenon termed "slow dynamics." The uniformity of these behaviors over a wide variety of complex materials promises a new era in understanding and characterizing their mechanical behavior. Geomaterials are prototypes for these (apparently) unrelated solids that include granular materials, sintered and damaged metals, some ceramics, and even high explosives. Though there are some clues as to the processes leading to the bulk behavior, the microphysics of the nonequilibrium behavior of slow dynamics remains unknown. We plan a new generation of experiments, which will redefine the field. We also propose a joint experimental and theoretical effort to develop an overarching description valid for these common yet unusual materials. Our framework employs a mesoscale description of a free-energy landscape (i.e., fluctuating potential barriers) of the dynamical behavior. Achievement of a predictive capability will have a major impact on diagnostics of materials, and on earthquake mechanics, and seismic wave propagation.

## Benefit to National Security Missions

This project will primarily support the DOE/NNSA mission in Science by greatly enhancing our understanding and ability to model consolidated, cemented materials, from geomaterials to explosives. The project will also support the missions of science for Nuclear Weapons (explosives) and Energy Security (oil- gas-bearing reservoir rocks and CO2 sequestration).

## Progress

Our work to date has primarily concentrated on experiments---although work is proceeding at a somewhat slower pace on the theoretical front as well. Two competing theories are currently used to describe the dynamical behavior of poorly cemented materials, one is a purely phenomenological model frequently used to describe any generalized hysteretic system (called a Preisach model). The limitations of the Preisach model to describe experiments on poorly cemented granular systems like rocks has never been explored (or challenged) until now. Moreover, the ability of such a model to extrapolate and predict behavior at higher frequencies (e.g., seismic frequencies) has been proposed but is still unknown experimental territory. Experiments are rare and all are qualitative. Two sets of experiments have been completed this past year. The first set is a suite of measurements to explore the limitations of Preisach model with varying rate stress-strain measurements. In fact, we discovered that the hysteresis loops, loops seen in rocks since the beginning of the last century is, in fact, not repeatable but is rate dependent. This is not a surprising result in, say hysteresis in magnetism but has not been observed or reported in rocks and furthermore, has been found to occur at a very accessible (experimentally) time scale. For example, a very long measurement (over a weekend) is sufficient for a typical sandstone sample to completely lose its hysteresis in a repeated stress-strain measurement. Indeed, the remaining stress-strain curve is purely nonlinear. What we have done, in fact, is to remove the time dependent, nonequilibrium behavior of the rock's dynamics and isolated just its nonlinearity, at least at these low frequencies. This result can be seen in the plot shown in Figure 1. The area of the hysteresis loop was plotted as a function of measurement rate for a wide range of rates. As can be seen on the plot, very slow sweeps show no hysteresis; the sample is essentially only nonlinear and the nonequilibrium effects are no longer evident. These results were presented at two conferences this summer (end of June, early July) and a paper on these results has been submitted to Geophysical Research Letters and is currently in review.

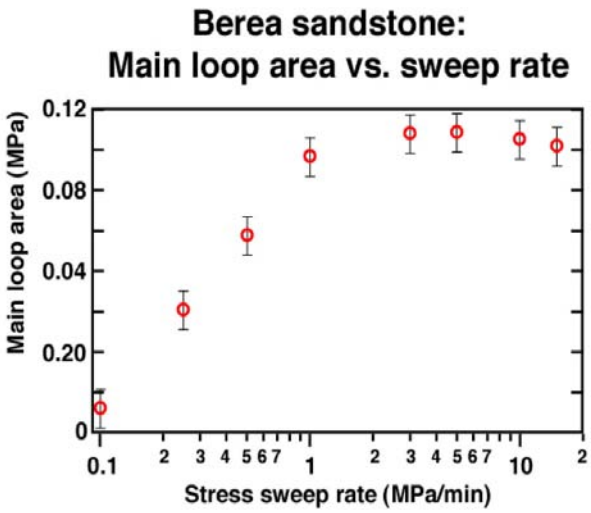


*Figure 1. Area of hysteresis loops as a function of measurement rate. Very slow rates yield curves which have no area and thus elastic aftereffect has essentially erased the memory of the stress history of the sample.*

At the higher end of the frequency scale, namely kHz frequencies where "slow dynamics" appears, separating the nonequilibrium behavior from the nonlinear behavior has been more of a challenge. These frequencies are interesting because many rock properties are often obtained at higher frequencies (e.g., a resonance frequency taken on a core sample to determine modulus and wavespeed). A very long duration experiment in a very thermally stable environment has been performed where the sample was disturbed as little as possible during measurements and, in contrast, like the very long stress-strain measurements, the sample's stiffness was also measured at a very slow rate to allow it to come to a new quasi-equilibrium during every measurement point. Experiments continue with other samples and different times. Experiments of a colleague in Sweden—in fact, one of us was asked and participated as an Opponent in his dissertation committee this fall—will complement our results next year. In fact, we are in discussions about transitioning his experiments to Los Alamos for further research.

Work is also progressing on the theoretical front, to determine what "slow dynamic" information can be gleaned from past published results. Most of this published data is qualitative and rates are often not specified but some information is there. Developing a mesoscale description of a free-energy landscape (i.e., fluctuating potential barriers) of the dynamical behavior observed has begun as well.

## Future Work

Certain materials display huge nonequilibrium/nonlinear behaviors, appearing at wave strains smaller than parts per million---disturbances equivalent to waves far from an earthquake. The materials relax over long durations after the wave disturbance, a nonequilibrium phenomenon termed "slow dynamics." This past year's experimental work has focused on the very slow, "quasi-static" stress strain measurements; this upcoming year's work is focused at experiments with waves in the kHz frequency range. The nature of nonequilibrium nonlinear dynamics and the generic behavior of slow dynamics across many complex geomaterials promise a new era in understanding these materials. Currently, no fundamental explanation of this nonequilibrium phenomenon has been developed, very few quantitative experiments have ever been done at these higher frequencies. A new generation of slow dynamics experiments is being started and a joint experimental and theoretical effort to develop a description valid for these common materials are planned. The theoretical framework employs a mesoscale description of a free-energy landscape (i.e., fluctuating potential barriers) of the behavior. Previous experiments, which we hope to improve upon this year, have been carried out in the regime where both Landau nonlinearity and nonequilibrium effects coexist. Initial dynamic experiments will isolate Landau nonlinearity (nonequilibrium effects are locked out) for materials with different physical origins for nonequilibrium/nonlinearity: sandstones (grain cementation), limestones (twinning), granites (cracks), and mock explosives (cracked grains). Experiments exploring the role of thermal relaxation in nonequilibrium slow dynamic behavior will follow. New frequency/time domain methods will isolate nonequilibrium behavior, e.g., slow measurements to freeze nonequilibrium effects, fast measurements to avoid their onset. These experiments provide information about energy scales and can distinguish between competing theoretical explanations of power-law relaxation. Describing the Landau nonlinearity with nonequilibrium dynamics via effective field theories is another key aspect. Nonlinear wave equations with relaxation phenomena will be derived from the nonequilibrium equation of state following a Landau-Ginzburg approach. Predictions will be compared to experimental observations. The addition of self-consistent stochastic forcing to the model will then be used to study slow dynamics.

## Conclusion

This work will lead to an increased understanding of how materials like oil- and gas-bearing rocks and explosives react to wave excitation. Nonequilibrium statistical mechanics has never been used to describe these materials; it will provide a robust description and model of the dynamics. Current models for these materials are not unique: every rock requires another model. Slow dynamics occur as a result of the way these materials are cemented. Understanding will help predict porosity/permeability in reservoir rocks (CO2 sequestration) and crack density (for explosives) and yield improved models of wave propagation for earthquake and man-made explosion forensics.

## References

1. Claytor, K. E., J. R. Koby, and J. A. TenCate. Limitations of Preisach Theory: Elastic aftereffect, congruencem and end point memory. To appear in *Geophysical Research Letters.*

# Evolution and Function of Microbial Signatures

*Murray Alvin Wolinsky*

20080618ER

## Introduction

The primary goal of this proposal is to develop the science underlying microbial signatures. For us, signatures are relatively short nucleic acid sequences that can be used to identify bacteria or viruses of interest. Signatures are of great practical importance in medical diagnostics, biodefense, microbial forensics and related disciplines, but they also pose fundamental scientific questions pertaining to evolution, functional organization, microbial diversity and speciation, which have been inadequately addressed [1].

Currently the most successful techniques for identifying useful nucleic acid detection or diagnostic signatures rely on an computational comparison of the sequences for target groups of interest with the sequences for all background organisms. Any differences which appear between the target sequences and the background sequences represent potentially useful signatures.

For microbes, it turns out that "blind" methods of signature identification -- that rely on no biological information concerning role or function of these sequences -- work as well as or better than more traditional methods which employ such information. Since roles are not needed to identify signatures, this has led to a lack of interest in the biological significance of these signatures: essentially signatures are treated as random or meaningless elements that happen to perform well in specific assays.

This work aims at trying to understand the biological significance of these signature elements "after the fact": knowing that these signatures distinguish target groups of interest from background groups, what can we learn about their roles and distribution [2]?

This work has the potential to shed light on the definition of microbial species is a (which is a matter of controversy) and to develop new methods for predicting sequence function.

## Benefit to National Security Missions

Better understanding of microbial signatures supports biothreat reduction and basic bioscience missions in DOE, DHS, and other government agencies. The work will develop a scientific basis for understanding how the evolution of pathogens (that occurs naturally or by manipulation for use as bioweapons) may impact our techniques for their detection.

## Progress

We have just completed an important part of one of our core goals for this effort: specifically, we have generated the empirical distribution of all 15-mer signatures and conserved elements for all publicly available bacterial sequenecs. Once we have analyzed this distribution and are confident that it is correct, we will generate similar empirical distributions for other length scales (as well as similar distributions for amino acid sequences). Our efforts for the upcoming year are expected primarily to focus on analysis and modeling of these distributions, with particular attention on comparing model fits using different models of speciation that have been proposed in the literature (and that may be improved on as a result of this work).

More concretely, given a tree (phylogeny) that contains the sequences of all fully-sequenced bacteria in Genbank (approximately 700 at present), we want to compute two sets of information for each group (at each of the approximately 1400 nodes): we want the number of conserved sequences (i.e., those present in every organism at or below this node) and we want the number of signatures -- sequences that are conserved and unique to this node (i.e, sequences which are present in every organism at or below this node but which are present no where else). An attempt at a graphic presentation of this goal is depicted in Figure 1.

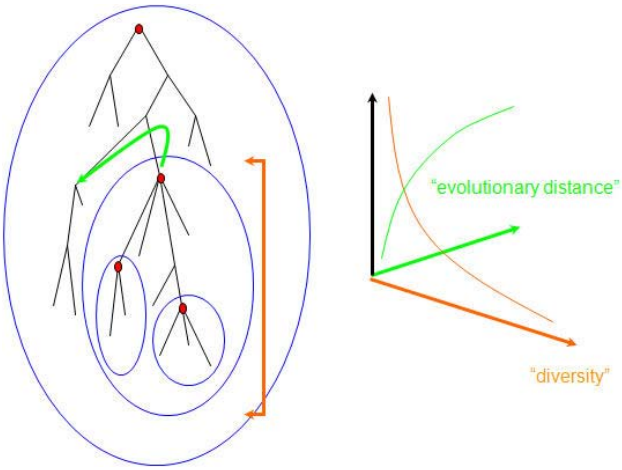


*Figure 1. A key goal is relating the empirical distribution of signatures to phylogenetic properties of the taxa groups of interest. Specifically, we expect that the most critical modeling parameters are likely to be evolutionary depth at a given node (shown in orange) and nearest distance to remainder of tree (shown in green).*

These distributions are the key object of interest for this work -- it was the lack of such distributions and of any theoretical expectations regarding them that motivated the initial proposal and that remain of key interest.

In order to generate these distributions, two things are necessary -- 1) an authoritative and comprehensive tree of all sequenced microbes and 2) computational algorithms to calculate the distributions of interest for this tree. Substantial progress has been made on both tasks. Extensive discussions led to the necessity of computing a new tree suitable for our purposes: this tree must be comprehensive, have good evolutionary branch lengths (for future modeling applications), and be both published and publicly available. Work with Ben McMahon in T10 has recently led to the development of a suitable tree. A draft publication is expected shortly.

Initial work has also been performed on a third task -- that of obtaining "null" models for expectations of these signatures using random or standard evolutionary models. We expect to focus on these methods once the empirical signature distributions become available.

A novel idea has emerged during the course of the investigations of the first year – namely, that the k-mer distributions can be used themselves to create novel, genome-wide phylogenies of the bacteria. If maximum-likelihood methods are used to generate these phylogenies, then, among other benefits, it will be possible to get direct estimates of rates of lateral transfer of k-mers at different length scales. If funding permits, we would like to study this idea over the next year.

This work has also contributed to the development of two proposals for outside funding for related (but distinct) investigations. A proposal to the DHS on "Forensic Signatures for Rapidly Evolving RNA Viruses" was submitted and accepted: work on that effort is expected to start this year. A second proposal was submitted to the NIAID on "Rapid, Low Cost, and Detailed Respiratory Infection Point of Care Diagnostics." Information on the status of that proposal will not be available until January 2009.

Finally, revisions and updates to a paper on signature distributions in Yersinia pestis, one of the motivating studies for this work [3], is in progress and expected to be submitted this fiscal year.

In brief, we have 1) developed and are preparing for publication a novel comprehensive tree of microbes needed to make further progress on this effort, 2) produced and are testing initial code for the computation of signature distributions, 3) procued the first empirical distribution of 15-mer signatures and conserved elements for all nodes of a comprehensive microbial tree, 4) contributed to two proposals on related areas (one of which has been funded, the other pending), and 5) are continuing to revise a publication on signature distributions in Y. pestis.

For the second year of this effort, our main goald are to verify and complete accurate empirical distributions for all microbes on the new phylogeny and to obtain at least preliminary modeling results for these distributions.

## Future Work

We intend to answer the following questions:

- Can the distributions of microbial signatures (short nucleic acid sequences) be predicted?
- Do signatures support a coherent definition of microbial species? What are the implications of signature distribution for microbial diversity?
- How are signatures related to regulation and function?
- Can robustness of signatures be predicted?

We will develop computational tools that:

- Identify functional signatures
- Produce more robust signatures

A major task will be to develop mathematical models that predict number of signatures and compare with computational "measurements" on microbial populations. Specifically, by choosing a broad class of microbes (e.g., Proteobacteria) and counting signatures, and then progressing to smaller sub-groupings and counting signatures, we will

get empirical signature distributions that can be compared to theoretical models. If we get good fits, we will obtain values for microbial evolutionary speciation rates and for total microbial population sizes. Thus our methods may furnish independent ways of estimating microbial biodiversity.

We will also study how these distributions are affected by signature lengths. Do the features of the distributions of signature counts remain fixed or are there signature lengths for which these distributions show marked changes? Answering this question will shed light on whether microbial species constitute a meaningful and discrete level of biodiversity.

Current year (2008-2009): Understand the distribution of microbial signatures

- Ensure that we have a comprehensive (containing all relevant species) microbial phylogeny with accurate branch lengths (completed).
- Determine the empirical distribution of signatures as a function of signature size and correlate with the size scales of functional elements (still in progress)
- Analyze implications of results on definitions of microbial species.
- Model signature evolution and compare with distributions of number of signatures

Final year (2009-2010): Characterize our empirical signatures regarding function using modeling, literature and bioinformatics methods.

- Identify methods to predict lateral gene transfer and study effects on signature robustness.
- Develop methods to predict signature robustness and thereby acquire the ability to prioritize signatures

## Conclusion

The results of this research are expected to have practical benefits in terms of improved signatures for public health and biodefense use. This work will lead to better and more reliable detection of threat agents and thereby help limit their potential damage. It will also lead to improved scientific models of microbial speciation (and its interpretation) and an improved characterization of microbial diversity. This increased scientific knowledge can be expected to enhance our understanding of, and abilities to coexist with and benefit from our biological environment.

## References

1. Gans, J., M. Wolinsky, and J. Dunbar. Computational improvements reveal great bacterial diversity and high metal toxicity in soil. 2005. *Science.* **309**: 2018.
2. Hubbell, S.. The Unified Neutral Theory of Biodiversity and Biogeography. 2001.
3. Chain, P., E. Carniel, F. Larimer, J. Lamerdin, and P. Stoutland. Insights into the evolution of Yersinia pestis through whole-genome comparison with Yersinia pseudotuberculosis.. 2004. *Proceedins of the national Academy of Sciences.* **101**: 13826.

## Publications

Stubben, C., M. Duffield, I. Cooper, D. Ford, J. Gans, A. Karlyshev, B. Lingard, P. Oyston, A. de Rochefort, J. Song, R. Titball, B. Wren, and M. Wolinsky. Steps toward broad-spectrum therapeutics: discovering virulence-associated genes present in diverse human pathogens . *Proceedings of the national Academy of Sciences.*

# Coupling of Genetics and Metabolism and the Orgin of Life

*Hans Joachim Ziock*

20080716ER

## Introduction

The goal of this project is to demonstrate in an artificial process the most important capability of any living system, namely the use of external energy and resources to replicate its information system (in our case, a nucleic acid polymer, i.e. DNA). This is a problem that Nature must have solved in order for life to emerge. To address this problem, the project seeks to modify and adapt an experimentally proven light-driven information-metabolic process that we previously developed. The modification consists of adapting the existing photo-chemically driven process to one capable of reproducing a longer strand of DNA from smaller "building block" sections of DNA, thereby enabling the reproduction of the information-metabolic complex itself. The process we are pursuing is far simpler than any such process in modern life and unique from any other being pursued by the scientific community at large.

On the science side, the assembly and demonstration of such an information reproduction system would represent a significant advance in the study of the emergence of life. On the application side, the demonstration of a simple, non-enzymatic enabled, direct, and switchable light-driven DNA ligation [polymerization of short DNA single strands (oligomers) or nucleotides resulting in DNA replication] would potentially have an extraordinary impact in biochemistry and therapeutics.

## Benefit to National Security Missions

This project supports the DOE/NNSA mission of supporting US leadership in science and technology. By the end of the project we will have developed a technique for using light to drive and control DNA replication, the critical step in developing light controlled therapeutics and self-healing organic nanomaterials.

## Progress

The first year of effort has been devoted to establishing the DNA-container association for the protocell that we hope to eventually build. This association is a critical aspect of the protocell development and is a necessary first step in the reproduction of the information component of a self-contained system. Furthermore, it is absolutely essential for this to occur in any process involving the coupling of the genetics and metabolism and claiming to be related to the origin of life. Our "container" consists of small vesicles constructed of fatty acid molecules, which when they reach a critical concentration form cell-like bilayer structures. Fatty acid molecules have a water-loving end and an oil ("fat")-loving hydrophobic end. As such, when introduced into water, the molecules tend to form sheets that are two molecules thick (i.e. bilayers), with the water loving ends of the molecules associating with the water and the oil loving ends facing each other yielding an oily interior to the bilayer sheet. (The most stable configurations for fatty acids are small spherical water-filled bilayer compartments called vesicles, as they do not expose any of the oil ends to water. See Figure 1.) The roles of the container for the protocell are to collocate the various components of the protocell in a common location and give it identity. Furthermore the collocation greatly increases the local concentration of reactants associated with a protocell's life cycle and hence in theory also the rate of reactions associated with its replication.

By attaching oil-loving tails to our information/metabolic complex the goal is to enhance the tendency for the metabolic and information complex to be associated with the container. We have experimentally demonstrated that such an association does in fact occur and does so very strongly (Figure 2). At the same time we needed to demonstrate that the association does not seriously hinder or preclude our desired chemical reactions in which the underlying information/metabolic complex plays the enabling role. Figure 3 shows show experimental results related to this where me measured the time dependence of the extent of reaction for several different configurations of the information/metabolic complex system that we have produced and for two different starting scenarios. The left half of the figure follows the reaction starting at a point when no vesicles were present, while for right half of the figure vesicles were present from the outset. All these steps were carried out during and confirmed in the first 10 months of

funding. (Our project effectively started in January 2008 and hence this report only reflects 10 months of effort.)

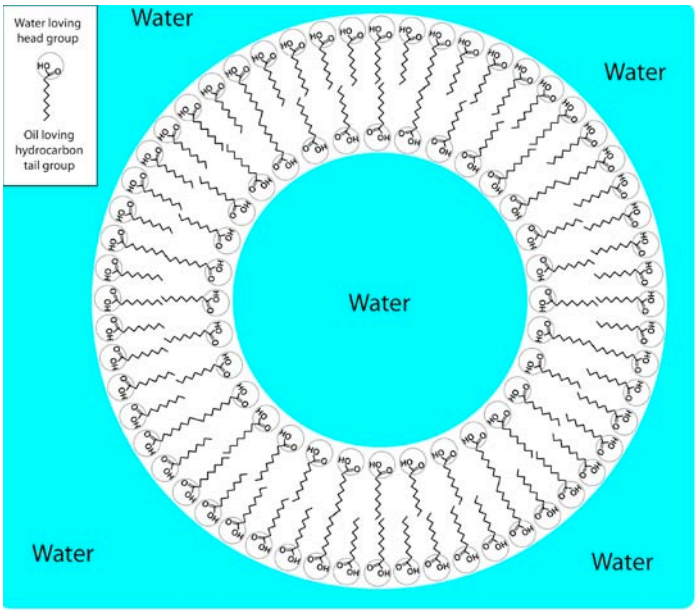


*Figure 1. A cross section of a vesicle that is made of a double layer of amphiphile molecules. As shown, an amphiphile molecule has a water loving polar end that likes to interact with water, and a hydrocarbon end that "hates" water and hence tries to avoid contact with it. The result is a bilayer structure as shown. To avoid exposure of the ends of a bilayer sheet to water, the bilayer wraps itself into a sheet as shown in the 2D image, or for the 3D world, into a spherical vesicle. Typically the diameter of the interior water volume is far larger than the thickness of the bilayer wall, and thus the figure is not to scale.*

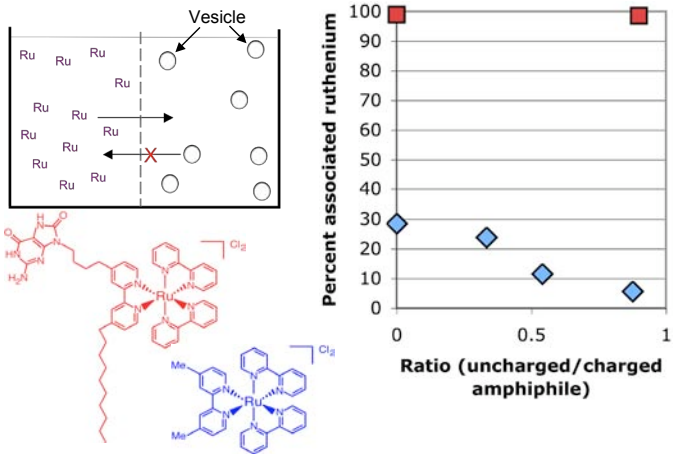


*Figure 2. The association with vesicles of two versions of the information/metabolic molecule (one with and one without the attachment of an oil loving tail). The measurement is done using a dialysis cell where a semi-permeable membrane divides the cell into two halves. The pores of the membrane are sufficiently large to allow the information/metabolic molecules to freely pass, but too small to allow the vesicles to pass. The two halves of the cell are filled respectively with an information/metabolic molecule and a vesicle containing solution. At a later time, the concentrations of the information/metabolic molecule in the two halves of the cell are determined from which the association strength can be determined. By varying the ratio of uncharged to charged amounts of molecules comprising the vesicles, one can determine the extent of the association due to charge versus that due to an affinity for "oil."*

The work undertaken involved the development of a new diagnostic/measurement process of sufficient precision for our needs. This was required produce quantifiable and repeatable results that were absolute in nature as opposed to the qualitative of the initial measurements in our preceding work. The new process relies on the use of High Performance Liquid Chromatography (HPLC) coupled with wavelength resolved light absorbance. Furthermore, considerable effort went into tuning the process to allow clean and individually identify of our unique reactants and reaction products. Careful calibrations of the measurement technique with the chemical compounds in question were carried out in order to yield absolute (as opposed to relative) measurements of the reactions being investigated. Loose associations that formed between the various reacts and reaction products meant that these calibrations were far from straight forward.

Some of our earlier work had shown that about 20–30% of our information/metabolic complex without oil-loving tails associated with the bilayers. This fragile association was due to a weak attraction between the positively charged information/metabolic complex and the negatively charged vesicles. When an oil-loving tail was added to create the new complex, the association increased to almost 100%. This resulted in a several-fold increase in the number of complex molecules associated with the protocell.

The work showed that when using our metabolic/information complex with an attached oil-loving tail, the reaction rate increased significantly (greater than a factor of 6 at equal concentrations) compared to that for the complex without the tail. Furthermore, when the concentration of the complex with the tail was lowered by a factor of 10 relative to the complex without the tail comparable reaction rates were still achieved. These results conclusively showed that not only did the metabolic/information complex continue to function when bound to a vesicle with an oil-loving tail, but that in fact worked far. A comparison of the left and the right halves of Figure 3 shows that this is true both went vesicles are initially present (right half) and when they are not initially present (left half). The accelerated rate seen for the latter case is believed to be due to the existence of very small pure oil-like structures inherent for the reactant that our metabolic process converts into the material that makes up the vesicles. As such, even with no vesicles initially present, there is a limited preexisting association between the reactants that results an enhanced production rate for the molecules that eventually

self-assemble to form the vesicles. Our investigations also showed that there is a significant association between the vesicles and the reactants that are subsequently converted into vesicle material by the metabolic reaction.

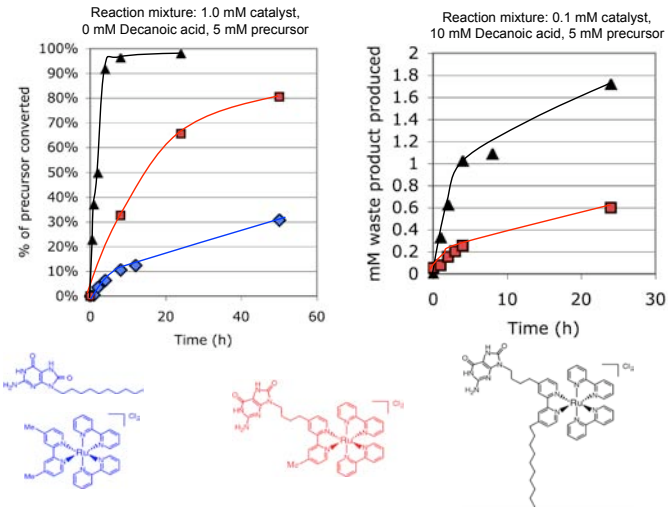


*Figure 3. The extent of conversion at different times of the precursor of the vesicle building blocks into actual building blocks for different versions of the information/metabolic molecule. The left half shows the results when no vesicles are initially present (although they do begin to form when ~ 50+ % of the reaction is complete). Three different versions of information/metabolic complex are shown: blue – the two components of the information/metabolic complex are not chemically bound, but both associate to some extent with our oil-like and/or vesicle structures due to either a charge interaction or an oily tail; red–the two components are chemically linked and interact to a limited extent due to charge; and black – a chemically linked information/metabolic complex with a chemically attached oil loving tail. The right half shows the results for the case when vesicles are already present at the start of the experiment. The two curves have the same coding as for the left half.*

Finally, as preliminary work for future project work associated with the reproduction of the information/metabolic complex, vesicle stability was studied as function of temperature. Higher temperatures will be used in the future to melt double-stranded into single-stranded DNA molecules that are the templates for the DNA replication. The experiments showed that the vesicles were sufficiently stable at the temperatures needed to melt the DNA so as to not present a problem.

## Future Work

Having now established the required strong association between the different components of our future photocell without a disruption of their function, as well as the desired temperature stability of the system required for replication of the information component of the protocell, our next step is to modify the various components to enable the reproduction of the metabolic/information complex by the system as a whole.

Currently our metabolic/information molecule is a ruthenium tris-bipyridine derivatized with a single nucleobase. In the next step, this single nucleobase will be replaced by a DNA strand to meet the more standard definition of an information molecule. Attaching the DNA strand will be achieved by standard bioconjugate chemistry. By varying the DNA sequence, we will prove the specificity of the information content for metabolic reactions. That is, some strands will yield a functional metabolic complex and others won't.

The next step is information replication using the well-known complementarity of DNA bases. A short single-stranded DNA template and 2 oligomers (even shorter DNA single-stands) which are complementary to the different halves of the DNA template will be provided. One oligomer will be chemically activated, while the other has a protecting group attached. The oligomers will spontaneously base-pair with the template, but must still be bonded end-to-end to form a continuous complementary strand. Our metabolic/information molecule will be used to link the two oligomers, thus replicating the template information. Another copy of the metabolic/information complex will absorb light energy and then use that energy to cleave the protecting group, allowing that oligomer to react with the activating group of the other oligomer yielding a continuous strand. Showing this light driven/controlled replication of the DNA is our final task.

## Conclusion

Learning and understanding how nature was first able to replicate information is fundamental to understanding life's origins and life's march to ever increasing complexity/capability. This is something that science has tried to discover throughout the ages. On the applied side, the demonstration of a method allowing one to artificially harvest light energy and applying it to reproducing the information system itself is the first step in the development of truly capable self-repairing materials and light switchable and controlled therapeutics. Imagine a nano-treatment system that could be switched on in specific locations or that's able to reproduce itself when needed.

## Publications

A.Monnard, P., M. S. DeClue, and H. Ziock. Amphiphile nanostructures as model for artificial cell-like entities. 2008. *Current Nanoscience.* **4**: 71.

DeClue, . S., P. - A. Monnard, J. A. Bailey, S. E. Maurer, G. E. Collis, H. - J. Ziock, S. Rasmussen, and J. M. Boncella.

Nucleobase mediated, photocatalytic vesicle formation from ester precursor molecules . To appear in *Journal of the American Chemical Society.*

Rasmussen, S., J. A. Bailey, J. M. Boncella, L. Chen, G. Collis, S. Colgate, M. S. DeClue, H. Fellermann, G. Goranovic, Y. Jiang, C. Knutson, P. - A. Monnard, F. Mouffouk, P. Nielsen, A. Sen, A. Shreve, A. Tamulis, B. Travis, P. Weronski, J. Zhang, X. Zhou, H. Ziock, and W. H. Woodruff. Assembly of a minimal protocell. To appear in *Protocells: Bridging Nonliving and Living Matter.* Edited by Rasmussen, S., M. A. Bedau, L. Chen, D. Deamer, D. C. Krakauer, N. H. Packard, and P. F. Stadler.

Tamulis, A., V. Tamulis, H. Ziock, and S. Rasmussen. Influence of water and fatty acid molecules on quantum photo-induced electron tunneling in self-assembled photosynthetic centers of minimal protocells. 2008. In *Multiscale Simulation Methods for Nanomaterials.* Edited by Ross, R. B., and S. Mohanty. , First Edition, p. 9. Hoboken, N.J: Wiley.

Zhou, X., Y. Jiang, S. Rasmussen, and H. Ziock. A method to bridge different-level coarse-grained models by estimating free energies of high-dimensional conformations: jump-in-sample simulations. 2008. *The Journal of Chemical Physics.* **128** (17): 174107.

# New Frontiers in Viral Phylogenetics

*Tanmoy Bhattacharya*

20080733ER

## Introduction

The genetic sequence of any organism is a blueprint for its development and of its strategies for survival and combat: the knowledge of the RNA sequence of rapidly mutating viruses like HIV therefore gives us enormous insights into how the virus manages to spread and evade both the immune system and medical interventions against it. The problem is, of course, the backdrop of vast amount of variation that is of little functional significance against which the interesting patterns need to be discriminated statistically. This background variation is, moreover, not random; since the strains of the virus are related by common descent, there are genealogical patterns imprinted on them too. It has become clear in recent work that a successful deciphering of the genetic correlates of viral escape strategies need us to be able to first reconstruct the phylogenetic history of the viral strains being studied.

For hundreds of strains of viruses, we had solved this problem before by parallelizing the maximum likelihood algorithms; and that had allowed us to answer questions about the population biology of the viruses. But such a number of sequences has too little statistical power to answer the questions we are asking today, questions about virus adaptation in individual hosts that are essential for intervention in the disease course. Before the advent of the modern era of petaflop computing, it was considered impossible to do a proper analysis with the thousands of sequences that are needed instead. The fundamental problem is that the set of evolutionary histories to search over is a huge discrete space, increasing faster than exponentially in the number of sequences, and the evaluation of the likelihood of the history is expensive. Even a parallel implementation guided by excellent heuristics ultimately runs across fundamental compute power limitations, requiring a impressionistic search of the space that, in the past, have been seen to lead to biased results.

In this project we planned to take that crucial enabling step of implementing the required algorithms on the highly heterogeneous computers that currently provide the largest available computational power, and that are likely to become more common in the future. If successful, we reasoned, this would open up huge vistas, and would already be applicable to a systematic quest for the events that underlie the invasion of a HIV-naive body by the viruses; a field where experimentalists are accumulating vast amounts of data in search of useable patterns.

## Benefit to National Security Missions

Emerging pathogens and ways to deal with them is a central mission for the DOE Office of Science, and is an underpinning to biothreat reduction (DHS). Other federal agencies like NIH are also interested in the problem, and this proposal builds a capability that can help bridge the interests of NIH and DHS. It also contributes to understanding how to map interesting problems on to the new and emerging computer architectures that can translate to other projects.

## Progress

In this first year of the work, we benchmarked the tasks that were necessary to adapt maximum likelihood (ML) phylogenetics code of Bhattacharya, Olsen, and Felsenstein, to efficiently use the Roadrunner supercomputer at Los Alamos. The existing ML program developed by our group had in the past been used with a messaging passing software called MPI. This was used to distribute the task of evaluating the likelihood of candidate histories (family trees) to different `nodes', each of which evaluated the likelihood using a serial procedure. The Roadrunner supercomputer, although vastly more powerful than these previous computers, is a very different architecture, whose heterogeneity required us to exploit parallelism also at a smaller scale in order to see its true potential. This task of initial assessment and benchmarking was completed and formed the basis of the subsequent restructuring. We found that we needed to adapt the code to consider individuals, and their parents, and their grandparents, etc., one at a time using the Cell synergistic processor, rather than considering it as the `node' in the previous code that evaluated entire histories at once.

This has meant `taking apart' the program in a detailed way and putting it back together into a multi-level parallel algorithm that maps on to this machine and other anticipated parallel-within-parallel machines. The task of high level restructuring of the code to split apart the tasks that need low-level parallelization, and implementation of these low-level tasks on the Cell processor, is complete. The primary bottleneck that we eliminated in this process was the slowdown in the propagation of probability information through a candidate history (a tree). We now use the on-chip direct memory access (DMA) features of Roadrunner's Cell processor to move the data between `workers' that map on to on-chip processes in the current architecture. Since these tasks form the inner core, and almost the entirety of the floating point load, of the calculation, we further hand-coded these workers to use the Cell's vectorization instructions.

The restructured the ML code now performs five separate 'core' numerical functions on the Cell synergistic processor units, driven by the control logic on the PPE. In order of computational expense, these calculations are node vector merging, vector multiplication, branch smoothing, node evaluation, and tip calculation. All of these operations involve intensive transfer of data, and push the Cell memory flow controller to its limit. Nonetheless, the most expensive calculation keeps the SPU processors doing useful work 90% of the time. Currently, the full code, involving the other four less compute-intensive parts don't scale as well, but we still see 40% utilization for typical data sets.

## Future Work

The major remaining secondary bottleneck is in the code that accepts the candidate history and does the final calculations needed to score it. This requires a simple restructuring that will require only a week's work to implement. We will then adapt the code to run under DaCS that control the Cell blades, and provide the overall control logic of user interaction; a task that we estimate will take about a month. In parallel, we are investing the use of improved instrumentation techniques that are evolving at IBM and LANL to help optimize the single-processor -parallelized code. We also will look at improving the algorithm of the tree proposal heuristic, as we have evidence that a naïve parallelization of the current algorithm will not scale for very large datasets; especially since we now have a higher-performance tree evaluator.

Depending on the actual deployment of the complete Roadrunner at Los Alamos, we will then employ the developed codes to help solve some of the issues arising in other projects in HIV biology that we are also working on. Phylogenetic inference is an essential tool in many studies in the life sciences through which we have been able to address fundamental research problems and gain understanding of the biology of the HIV virus. Maximum likelihood (ML) methods are powerful tools for such analyses, but computational resources limit us to heuristic searches for the genealogical history that maximizes the likelihood score. Markov Chain Monte Carlo (MCMC) methods for obtaining molecular phylogenies have been advocated as a better strategy for defining phylogenetic relationships because they properly sample the set of credible histories and models of evolution. These methods, however, are even more computationally challenging than the classical ML strategies we have employed, and neither of these approaches can currently be applied to the large data sets being generated to have sufficient statistical power to answer questions of biological interest. The various biology projects had therefore proposed to use sub-optimal, but then feasible, methods to solve these problems.

Once this code is developed, however, we shall be free of many of those constraints. Initially, we shall apply it to data sets of HIV sequences that have been generated by our colleagues in the CHAVI collaboration. The fundamental question we would like to answer is whether there are sequence features that occur repeatedly during HIV evolution: such features are likely to be indicative of adaptations that the virus needs to survive and multiply, and are worthy targets of vaccines and therapeutics. We also plan to investigate briefly whether an architecture such as roadrunner would permit an efficient implementation for an MCMC approach to evaluating phylogenies, and whether our current code can form the core of such further development.

## Conclusion

The study of rapidly mutating viruses got a boost with the development of rapid sequencing technology to determine the sequence from thousands of viruses circulating in the body. Understanding how the diversity amongst these viruses changes over time can inform on issues like the development of drug resistance and escape from immune pressure. The viral strains, however, are obviously not independent as assumed in other such large data sets, but related by common descent. This project aims to develop the computational tools for analysis of such data, and apply it to a particularly interesting question relevant to HIV vaccine design. The initial work of mapping the problem on to the new architecture is complete, and the code development and debugging is expected to be complete before the new machine is deployed and ready for application to the biological process of interest.

# Cellulosomes in Action: Peta-Scale Atomistic Bioenergy Simulations

*Kevin Yosh Sanbonmatsu*

20080755ER

## Introduction

Biomass ethanol, based on all plant and tree parts, has the potential to satisfy 30% of our transportation fuel demand, unlike corn-based ethanol, which is expected to be insufficient. Biomass energy production requires the breakdown of plant and tree fiber. Current industrial fiber breakdown processes are not efficient. Bacteria, however, have devised ways to break down fiber extremely efficiently. Our goal is to understand how bacteria break down fiber and ultimately use this knowledge to make industrial fiber processing more efficient. Bacteria use a suite of nanomachines called cellulosomes. The nanomachines act like molecular paper shreaders, shreading away sheets of plant fiber, hopping from point to point on the sheets. During the process, the sheets are transformed into blobs of fiberous chunks, capable of being converted into ethanol. A problem is that midway through the shreading process, the blobs get in the way. We will study how the nanomachines are able to navigate through this dense medium of fiber blobs that exists during the break down of fiber sheets.The RoadRunner supercomputer will be used to simulate the process of cellulosome migration through partially processed plant fiber, shedding light on one of the key bottlenecks in biomass ethanol production. We will address the following questions:

- What parts of the cellulosome machine interact with what parts of cellulose?
- How do these interactions differ between the crystal-like phase, the partially degraded phase and the amorphous phase of degradation?
- How does the presence of several cellulosomes affect this process?

## Benefit to National Security Missions

Our simulation is directly relevant to national energy security, a key DOE mission. This work is also important to identify steps toward producing renewable carbon neutral energy, another important DOE mission.

## Progress

The goal of our project is to improve our understanding of the process of cellulose degradation using large-scale molecular dynamics simulations by leveraging the speed-up obtained with RoadRunner. We have ported individual pieces of the molecular dynamics software to the RoadRunner architecture. We are currently integrating and testing on RoadRunner nodes. Our current goal is to finish the port by October 20 for the SuperComputing 2009 conference in Austin, TX. We have ported the code to the AMD component of RoadRunner and to the power processing unit (PPU) and synergistic processing unit (SPU) components of RoadRunner, individually. That is, we now have working versions of the code that run independently on the AMD processor and on the power processing unit (PPU) and synergistic processing unit (SPU) of the cell broadband engine (CBE) of RoadRunner. Now, we are constructing infrastructure for these components to interact.

In detail, our molecular dynamics code has been modified to support the IBM Data Communication and Synchronization (DaCS) libraries for accelerating its nonbonded calculations on the cell processors. The modifications include launching the cell processes, overhaul of the memory subsystem to support aligned buffers, minimalist on demand direct memory access (DMA) transfers, and the initial port of the water-water nonbonded kernel on the cell broadband accelerator. The framework is in place to enable the rapid addition of additional nonbonded kernels on the CBE.

With respect to modeling, we have created structural models of the cellulosome and of the processive exocelluase. We have constructed an initial starting configuration of the processive exocellulase docked to cellulose sheets, caught in middle of the processing a strand of cellulose.

## Future Work

Our immediate goal is to perform reduced model simulations of the movement of the exocellulase during cellulose processing for the November 2008 conference.

In the winter we will set up the initial structure for all-atom explicit solvent dynamic simulations. Following this, we will perform the simulations on RoadRunner.

We will address the question: What parts of the cellulosome machine interact with what parts of cellulose?

## Conclusion

The molecular dynamics simulation program will be adjusted and optimized to run on the Roadrunner computer. The cellulosome/cellulose complex will be simulated to understand the process of cellulose degradation.

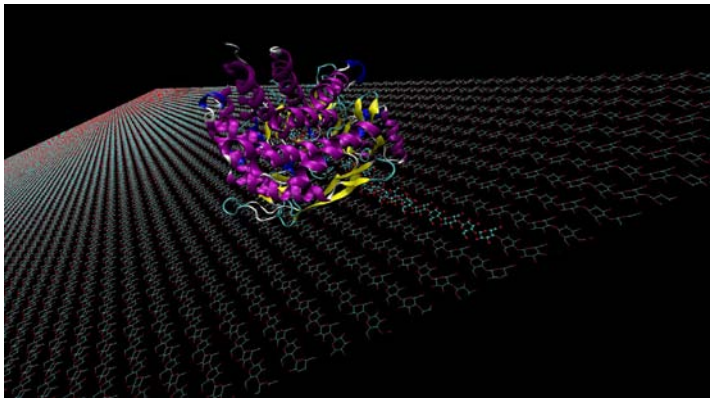

*Figure 1. Cellulosome binding to cellulose. Molecular model used in the simulations of cellulosome-cellulose interaction.*

full final report

# Testing Embedded Model Assumptions of Stable Isotopic Dynamics with Continuous Sampling: Are Modelers' Assumptions of the Global Carbon Cycle Correct?

*Nathan Gabriel Mcdowell*

20050323ER

## Abstract

We tested the three fundamental assumptions about isotopic composition of carbon dioxide central to global carbon cycle models: 1) assimilation, 2) respiration, and 3) storage. The three assumptions discount fundamental interactions with water limitations for terrestrial vegetation, which are particularly pronounced in drylands. Previous studies have been unable to test the assumptions because technological limitations precluded acquisition of necessary high-frequency, continuous measurements of stable isotopes and associated ecosystem carbon and water fluxes. We employed a revolutionary new technology, Tunable Diode Laser Spectroscopy, for rapid, near real time analysis of atmospheric carbon dioxide for testing our primary hypotheses. This system was used to generate the longest continuous record of biosphere-atmosphere isotopic $CO_2$ exchange in the world, and was employed to investigate model assumptions at unparalleled frequencies. The impact of our work is high. We have given more than 20 invited presentations on our work and have published 20 peer-reviewed articles. Our results are likely to alter how the global carbon cycle is understood and modeled, simultaneously contributing to LANL and DOE foci on climate and $CO_2$.

## Background and Research Objectives

Through continuous monitoring of atmospheric carbon dioxide at Moana Loa, Charles Keeling produced arguably the most important environmental finding of the 20th century—unequivocal evidence of rising carbon dioxide and strong suggestive evidence of anthropogenic-caused global warming. Scientists now are challenged to predict the global carbon cycle, the terrestrial component of which is the most uncertain component-the "missing" sink. Central to addressing this challenge are isotopically-constrained models of the global carbon cycle. The underlying constraints in these models are based on few data, requiring modelers to make three critical but untested assumptions about fluxes and storage of carbon isotopes. We have tested the three fundamental assumptions about isotopic composition of carbon dioxide central to these models: 1) assimilation, 2) respiration, and 3) storage. The three assumptions discount fundamental interactions with water limitations for terrestrial vegetation, which are particularly pronounced in drylands. Previous studies have been unable to test the assumptions because technological limitations precluded acquisition of necessary high-frequency, continuous measurements of stable isotopes and associated ecosystem carbon and water fluxes. We have addressed these issues with a revolutionary new instrument for continuous stable isotopic composition, co-located with an array of carbon and water flux towers and detailed soil-plant water data.

Our specific research objectives were to determine mechanisms regulating isotopic exchange of 1) foliage, 2) soils, 3) ecosystems, and lastly, to 4) determine the ability of carbon cycle models to capture temporal dynamics of the isotopic exchange between ecosystems and the atmosphere.

## Importance to LANL's Science and Technology Base and National R & D Needs

The results of this project have already had a major impact on how the global carbon cycle is understood and modeled, simultaneously contributing to LANL and DOE foci in Climate and $CO_2$. We have developed $CO_2$-isotopic monitoring technology into a world leading capability. This ER supported the development of LANL's Tunable Diode Laser Facility. Our facility has generated the longest continuous record of biosphere-atmosphere $CO_2$-isotopic exchange in the world, and has generated the only publications regarding high

frequency isotopic exchange of foliage, soils, and ecosystems, and the only high frequency test of model predictions of isotopic exchange. We are being solicited by other national labs and academic institutions for collaborations, thus providing more evidence of the value of LDRD's investment to LANL's reputation and standing. We are now poised to apply our technology and skills to 1) monitoring of $CO_2$ emissions worldwide, and 2) quantifying climate impacts on regional ecosystems.

## Scientific Approach and Accomplishments

Our approach was broad, including empirical, experimental, field, lab, and model based analyses. We maintained a long term observation platform of $CO_2$ isotopes for quantifying pattern and for comparison to models. We conducted field and lab based tests of the mechanisms regulating leaf and soil isotopic exchange. Each of these efforts yielded peer-reviewed publications. We now know that climate has a profound impact on ecosystem carbon storage, ecosystem hydrology, and their respective isotopic tracers. As a result of our work, the isotopic composition of $CO_2$ can be used to trace impacts on carbon cycling and hydrology at ecosystem and regional scales. The listed publications demonstrate each of these results.

## References

1. McDowell, N., and E. Al. Measuring and modeling the stable isotope composition of biosphere-atmosphere CO2 exchange: where are we and where are we going? . 2008. *EOS.* **89**: 94.

## Publications

Barbour, M., G. Farquhar, D. Hanson, C. Bickford, and H. Powers. A new measurement technique reveals temporal variation in delta 18O of leaf respired CO2. 2007. *Plant, Cell and Environment.* **30**: 456.

Barbour, M., N. McDowell, G. Tcherkez, C. Bickford, and D. Hanson. High frequency measurements reveal rapid post-illumination changes in the carbon isotope composition of leaf-respired CO2. 2007. *Plant, Cell and Environment.* **30**: 469.

Bickford, C., D. Hanson, and N. McDowell. High resolution field measurements of diurnal carbon isotope discrimination and internal CO2 conductance in a semi-arid species, Juniperus monosperma . *Plant Cell and Environment.*

Breshears, D., N. McDowell, K. Goddard, K. Dayem, S. Martens, and C. Meyer. Drought recovery via foliar absorption of intercepted rainfall bypasses soil water uptake. 2008. *Ecology.* **89**: 41.

Breshears, D., O. Meyers, C. Meyer, F. Barnes, C. Zou, C. Allen, N. McDowell, and W. Pockman. Tree die-off response to global-change-type drought: mortality insights from a decade of plant water potential measurements. . To appear in *Frontiers in Ecology and Environment.*

Engel, S., H. Lease, N. McDowell, and B. Wolf. Resource use by a grasshopper community quantified using tunable diode laser spectroscopy to measure breath d13C. *Rapid Communications in Mass Spectrometry.*

Flexas, J., M. Ribas-Carlo, D. Hanson, J. Bota, B. Otto, J. Cifre, N. McDowell, H. Medrano, and R. Kaldenhoff. Tobacco aquaporin NtAQP1 is involved in mesophyll conductance to CO2 in vivo. 2006. *Plant Science.* **48**: 427.

Hanson, D., C. Bickford, K. Brown, H. Powers, and N. McDowell. Real-time measurement of photosynthetic carbon isotope fractionation using a tunable diode laser: Insights into on-line estimation of mesophyll conductance. To appear in *Plant, Cell and Environment.*

Hanson, D., C. Bickford, K. Brown, H. Powers, and N. McDowell. Real-time measurement of photosynthetic carbon isotope fractionation using a tunable diode laser: Insights into on-line estimation of mesophyll conductance. To appear in *Plant, Cell and Environment.*

Hanson, D., C. Bickford, K. Brown, H. Powers, and N. McDowell. Real-time measurement of photosynthetic carbon isotope fractionation using a tunable diode laser: Insights into on-line estimation of mesophyll conductance. *Plant, Cell and Environment.*

Kolb, T., and N. McDowell. Forty years of research at the Fort Valley Experimental Station. 2008. *USDA Forest Service.*

McDowell, N.. Measuring and modeling the stable isotope composition of biosphere-atmosphere CO2 exchange: where are we and where are we going?. 2008. *EOS.* **89**: 94.

McDowell, N., B. Bond, N. Phillips, and M. Ryan. Mechanisms linking increased tree size to hydraulic-induced photosynthetic constraints: a global meta-analysis.. *Size*

*and age related changes in tree structure and function.* Edited by Meinzer, R., and U. Niinemets.

McDowell, N., H. Adams, J. Bailey, M. Hess, and T. Kolb. Homeostatic maintenance of ponderosa pine gas exchange in response to stand density changes. 2006. *Ecological Applications.* **16** (3): 1164.

McDowell, N., H. Adams, J. Bailey, and T. Kolb. The response of ponderosa pine growth efficiency and leaf area index to a forty-year stand density experiment. 2007. *Canadian Journal of Forest Research.* **37**: 343.

McDowell, N., L. Marshall, and C. Allen. Growth, carbon isotope discrimination, and mortality across a ponderosa pine elevation transect. *Global Change Biology.*

McDowell, N., S. White, and W. Pockman. Transpiration and stomatal conductance across a steep climate gradient in the southern Rocky Mountains. . To appear in *Ecohydrology.*

McDowell, N., and E. Al. Tansley Review: Mechanisms of plant survival and mortality during drought: why do some plants survive while others succumb?. 2008. *New Phytologist.* **178**: 719.

Newman, B., B. Wilcox, S. Archer, D. Breshears, C. Dahm, C. Duffy, N. McDowell, F. Phillips, B. Scanlon, and E. Vivoni. The ecohydrology of arid and semi-arid environments: a scientific vision. 2006. *Water Resources Research.* **42**: W0632.

Powers, H., J. Hunt, D. Hanson, and N. McDowell. A dynamic soil chamber system coupled with a tunable diode laser for online measurements of d13C and d18O of soil respired CO2. *Global Change Biology.*

Slutzky, S., C. Meyer, D. Breshears, P. Rich, A. White, and N. McDowell. Understory vegetation response to climate and piñon mortality in four piñon –juniper woodlands. . *Ecosystems.*

Uehlein, N., O. Beate, D. Hanson, N. McDowell, and R. Kaldenhoff. Function of aquaporins as chloroplast gas pores challenges the concept of membrane CO2 permeability. . To appear in *Plant Cell.*

# Nascent Protein Folding Inside the Tunnel of the Ribosome: Cotranslational Folding

*Kevin Yosh Sanbonmatsu*

20060230ER

## Abstract

Protein folding is a fundamental step in gene expression, completing the flow of information from DNA to protein as specified by the central dogma of molecular biology. In the cell, proteins do not fold independently, but begin the folding process during protein biosynthesis inside the ribosome. Until recently, it has not been possible to study protein folding inside the ribosome in atomic detail due to the lack of structural data. However, the determination of the atomic structure of the large ribosomal subunit allows us to address this investigate this important process in atomic detail. This structure has revealed the existence of a long, narrow tunnel inside the ribosome through which the newly forming protein must travel in order to move from the site of protein manufacturing to the external environment. We will implement a novel method of molecular dynamics simulations (the growing polypeptide simulation method) to study the mechanism of nascent peptide folding and movement through the ribosomal tunnel, as well as the effects of antibiotics on this process.

## Background and Research Objectives

Ribosomes are large ribonucleoprotein complexes responsible for protein synthesis. Because the ribosome is one of the most highly conserved complexes in biology, molecular mechanisms in one ribosome often operate across all kingdoms of life. Many regions of the ribosome are 100% conserved across all organisms (the so-called 'universal' rRNAs). Each ribosome contains a small subunit, responsible for decoding the information on the messenger RNA, and a large subunit, responsible for adding each amino acid to the newly synthesized, nascent protein and for assisting in protein folding. In particular, the large ribosomal subunit contains a long 'tunnel' extending from the peptidyl transferase center, where each amino acid is added, to the exterior solvent face of the ribosome. The nascent protein advances through the tunnel as it is manufactured and is thought to be partially folded by the time it exits the ribosome.

The problem of nascent protein movement through the ribosomal tunnel is analogous to pushing a strand of yarn through a straw. The nascent protein is 'pushed' from behind by the addition of new amino acids. Because the ribosome tunnel is charged and highly non-cylindrical, it is not clear how the nascent protein can not only move past the charged tunnel walls, but also navigate through the tunnel's circuitous pathway, which has many protuberances and indentations.

Approximately 50% of the antibiotics used in the clinic target the ribsome. The macrolides represent a large class of ribosome antibiotics, which normally inhibit peptidyl transferase or physically narrow the tunnel, blocking the nascent protein. Recent x-ray structures have determined the binding sites of several macrolides and other antibiotics to the large ribosomal subunit.

The goals of our project are to 1) characterize the folding of short proteins and simulate the ribosome tunnel, 2) simulate the movement of a newly manufactured protein through the ribosome tunnel and 3) simulate antibiotics interacting with the ribosome.

## Importance to LANL's Science and Technology Base and National R & D Needs

Simulating matter at the atomic level of detail has a vast number of applications. Understanding how matter behaves at this level allows us to more carefully control the matter. Applications include nanotechnology and biotechnology. The ribosome is one of the only existing molecular computers. This molecular machine performs a look-up table operation. Thus, understanding the ribosome at the atomic level may lead to the development of nanocomputers and smart materials that can adapt to their environment. Because the ribosome is

the target of about 50% of the antibiotics used today in US hospitals, this study sets the stage for computational drug design of novel ribosome antibiotics. Important ribosome antibiotics are used to treat Anthrax and Plague. In addition, antibiotics used together in combination therapy target the ribosomes of MRSA (methicillin resisitant staph bacteria). Our study has pioneered simulations of ribosome antibiotics and the large-scale simulation of nanoscale biological systems. This is a critical area of technology to keep the US competitive in computational biology, nanotechnology and biomedicine.

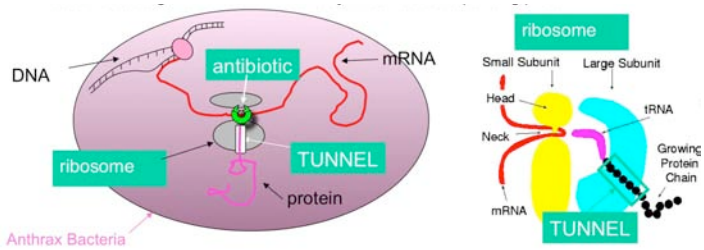


*Figure 1. Schematic of the manufacturing of protein by the ribosome. The ribosome binds to genetic instructions and assembles proteins based on these instructions. Antibiotics act like monkey-wrenches and gum up the ribosomes harmful bacteria.*

## Scientific Approach and Accomplishments

Our approach uses computer simulations to understand a critical molecule important to all living systems called the ribosome. The ribosome, which is responsible for implementing the genetic code in every organism, happens to be a quite large molecule compared to other molecules that have been studied. This molecule acts like a protein factory, reading genetic instructions and fabricating corresponding proteins. The ribosome is composed of approximately 250,000 atoms. We use Newton's laws of motion to simulate the dynamics of the ribosome in atomic detail. To accurate simulate the ribosome, one must also simulate the molecules in the ribosome's environment that are close by. These molecules mainly consist of water, potassium, chrorlide, and magnesium. The environment plays a crucial role in the inner workings and machinery of the ribosome and must be modeled accurately. The minimum number of water molecules required to accurately simulate the ribosome is approximately 800,000. Our full simulations of the entire ribosome included 2.64 million atoms and is the largest calculation completed to date in the field of computational biology.

An important part of ribosome mechanism is the transport of the protein from the manufacturing site to solution environment. The protein is assembled deep inside the ribosome. A tunnel burrowing through the ribosome exists to transport the spaghetti-like protein from the inner depths of the ribosome to the water solution outside of the ribosome. The specific goal of our project was to simulate this process. To do this, we developed a new technique where we effectively add building blocks of the protein (amino acids) by using the computer simulation to push the protein from behind. In this manner, one can study how the protein is able to worm its way through the tunnel and escape from the ribosome. We were able to isolate the parts of the ribosome's tunnel that are tricky to navigate.

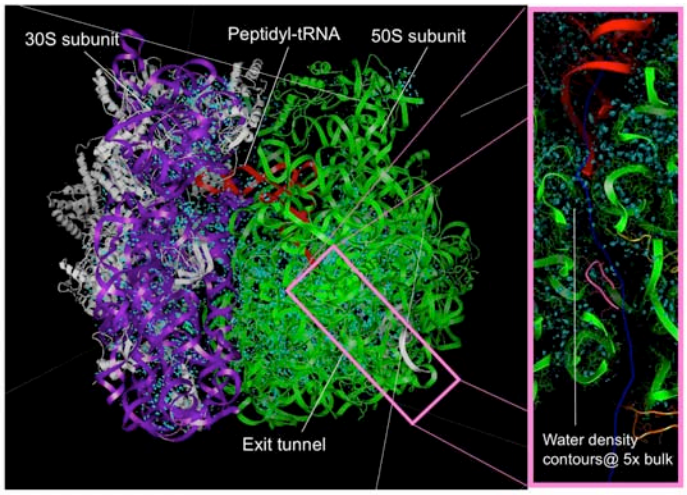


*Figure 2. Structure of the ribosome. The ribosomal exit tunnel transports the newly assembled protein from the center of the ribosome to the water solution outside.*

The second major accomplishment of the project was to simulate antibiotics interacting with the ribosome. We developed techniques to design force fields that describe the interaction between the antibiotic and its target, the ribosome. We were able to simulate the process of drug binding and performed the longest, most intensive simulation of drug binding to date. Our simulation revealed a new way of thinking about drug binding. Before our work, textbook descriptions of drug binding modeled the process in two separate states: 1) the drug not bound to its target, and 2) the drug bound to its target. We found that there is a continuum of states: first the drug binds to a landing zone near its target. Next, the drug crawls along the ribosome until it finds the target. We are working with the tech-transfer department to patent our findings.

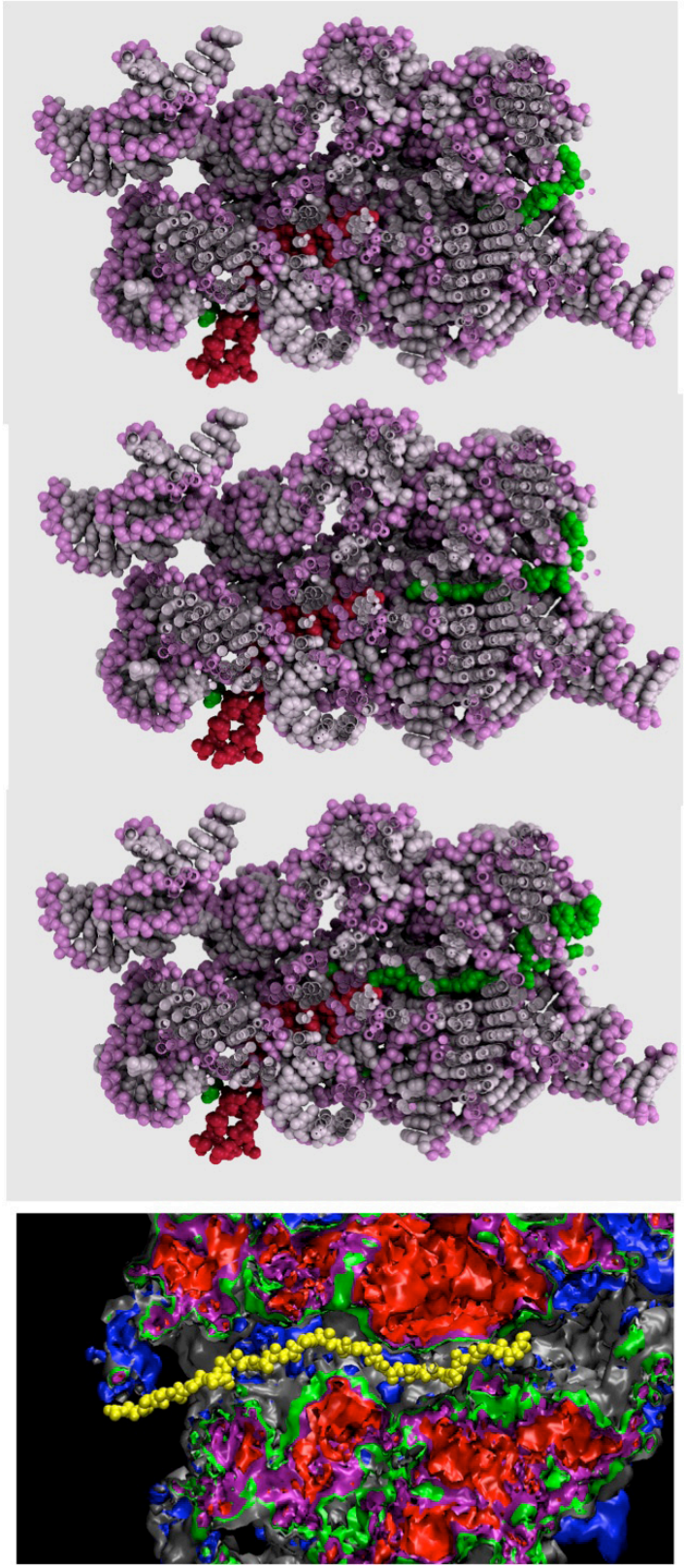

*Figure 3. Simulating the transport of the newly manufactured protein from the center of the ribosome to the external solution environment. Top three panels show the growing protein as it moves out of the ribosome. Bottom panel shows the electric field (electrostatic potential isosurface) of the tunnel of the ribosome.*

## References


1. Ramakrishnan, V., and P. B. Moore. Atomic structures at last: the ribosome in 2000. 2000. *Current Opinions in Structural Biology.* **11** (2): 144.
2. Sanbonmatsu, K. Y., and C. S. Tung. High performance computing in biology: multimillion atom simulations of nanoscale systems.. 2007. *Journal of Structural Biology.* **157** (3): 470.


## Publications


Munro, J. B., A. C. Vaiana, K. Y. Sanbonmatsu, and S. C. Blanchard. A new view of protein synthesis: mapping the free energy landscape of the ribosome using single-molecule FRET.. 2008. *Biopolymers.* **89** (7): 565.

Sanbonmatsu, K. Y.. Alignment/misalignment hypothesis for tRNA selection by the ribosome. 2006. *Biochimie.* **88**: 1053.

Sanbonmatsu, K. Y.. Energy landscape of the ribosomal decoding center. 2006. *Biochimie.* **88**: 1075.

Sanbonmatsu, K. Y., S. Joseph, and C. S. Tung. Simulating movement of tRNA into the ribosome during decoding. 2005. *Proceedings of the National Academy of Sciences, U S A..* **102**: 15854.

Sanbonmatsu, K. Y., and C. S. Tung. High performance computing in biology: Multimillion atom simulations of the ribosome. 2007. *Journal of Structural Biology.* **157**: 470.

Sanbonmatsu, K. Y., and C. S. Tung. Large-scale simulations of the ribosome: a new landmark in computational biology. 2006. *Journal of Physics.* **46**: 334.

Vaiana, A., and K. Sanbonmatsu. Entropy Shuttling Facilitates Drug Dissociation From the Ribosome. To appear in *Journal of the American Chemical Society.*

# Multigene Correlations and Their Implications for Cardiovascular Disease

*Rajan Gupta*

20060340ER

## Abstract

Cardiovascular disease is the number one killer in the United States and therefore a public health priority. A number of genetic, environmental and lifestyle factors contribute to cardiovascular health. Clinicians and geneticists are constantly discovering additional genes and other factors with possible links to cardiovascular disease. Getting quantitative results with robust validation, however, is a growing algorithmic and computational challenge. Our goal is to develop statistical tools to extract multigene and gene-environment interactions that clinicians can use for early intervention with respect to vascular disease and better adapt therapy to an individual patient's needs and conditions.

## Background and Research Objectives

Establishing statistically significant correlation between multiple genes and a disease is a very challenging problem. For example, one of the motivations of the Human Genome project states "Scientists believe single nucleotide polymorphisms (SNP) maps will help them identify the multiple genes associated with such complex diseases as cancer, diabetes, vascular disease, and some forms of mental illness. These associations are difficult to establish with conventional gene-hunting methods because a single altered gene may make only a small contribution to the disease." Today about 2 million SNPs have been identified and hundreds if not thousands are believed to be implicated in increased risk for vascular disease. Which genes contribute individually or in concert becomes an increasingly difficult clinical and computational problem as the number of known SNPs grows, requiring sampling of thousands of patients to get statistically significant results.

Our goal was to achieve the following three main research objectives: To adapt methods from machine learning and information theory to study correlations between multiple variables; to develop efficient Markov Chain Monte Carlo methods to establish the statistical significance of observed correlations; and to provide an efficient implementation of these algorithms on parallel supercomputers and to develop a user friendly interface that allows simultaneous analysis using different algorithms to cross-check the results. Since different methods of assessing multigene interactions have different inherent assumptions and are sensitive to different aspects of the interaction, our analysis will have smaller dependence on assumptions.

## Importance to LANL's Science and Technology Base and National R & D Needs

Cardiovascular disease is the number one killer in the United States and therefore a public health priority. A number of genetic, environmental and lifestyle factors contribute to cardiovascular health. Clinicians and geneticists are constantly discovering additional genes and other factors with possible links to cardiovascular disease. The challenge is to quantify possible correlations, not only when factors are individually implicated but when a significant effect is present if a set of factors act in concert. Our goal is to use multiple tests from machine learning and information theory to identify the minimum sets of salient combinations and predictor functions that can be rigorously tested by cross-validation.

This project requires developing novel mathematical approaches for analysis. In addition, the extremely large number of possible interactions (gene-gene and gene-environment) presents a computational challenge that demands the use of high performance parallel computers. The development of effective mathematical approaches, as proposed, will yield incredible benefits to biological science and medicine: First, the identification of gene interactions will help enormously to define interactive pathways of macromolecules. This is particularly important as the complexity of molecular crosstalk in signaling pathways and in transcriptional networks is becoming appreciated. Furthermore, it is likely that

most human chronic disease involves the interaction of a number of genomic determinants. Thus, the prediction of risk will be greatly improved, allowing the early detection of a predisposition to a given disease, allowing for timely preventive measures. Lastly, the appreciation of gene-gene interaction effects will allow the understanding of the individuality of the genomic basis of a patient's disease, providing a basis for individualization of treatment. The resulting mathematical algorithms and computational capability can be generalized to any arena of biology or human disease. They are most likely to benefit multi-factorial

disorders like those involving the cardiovascular system, neurodegenerative disorders, metabolic problems such as diabetes, and even ageing itself.

## Scientific Approach and Accomplishments

The main analysis approach we have focused on identifies the sets of inputs that interact and on quantifying the interaction using techniques from information theory; specifically those of mutual and interaction information. In this approach information of a distribution is defined, following Shannon [1, 2], as the negative of the entropy: $-\Sigma pi \log pi$. This definition can be interpreted as the expected amount of information, on an additive scale, that a measurement will provide: thus, for traits that are very common or very rare, we assign small information because we are virtually certain of its value anyway, and a measurement is unlikely to increase our knowledge except on rare occasions. If two random variables (*e.g.,* the output and the input) are such that the knowledge of one does not change the probability distribution of the other, we call them statistically independent. It is easy to see that in this case the information of their joint distribution is the same as the sum of the information of the marginals. The difference of these, $-\Sigma pi\bullet \log pi\bullet - \Sigma p\bullet j \log p\bullet j + \Sigma pij \log pij$, where $pi\bullet + \Sigma j\ pij$ and $p\bullet j + \Sigma i\ pij$ denote the marginals, is a non-negative quantity called the mutual information [1, 2] and measures the correlation between the two variables. The advantage of this measure of statistical non-independence is its non-parametric nature: it is independent of the coding scheme used (*i.e.,* the labels *i* and *j* above need not be thought of as having numerical values), and it makes no assumption about the normality of the distributions. Because of the same reason, it cannot take advantage of order relations amongst the input states and only answers the question as to whether a combinatorial partitioning method would find a significantly predictive partitioning. Thus, for example, it can equally well identify an heterozygous advantage as it can the effect of a dominant or recessive gene, but, because of its generality, its statistical power is less than methods which assume, *a priori,* an additive response from the alleles. Nevertheless, it is often the case that the lack of systematic errors from improper assumptions outweighs the smaller statistical power. Mutual information is a standard method not only for its traditional role in establishing correlations [3], but also for a vast array of other tasks like finding covarying genetic markers [4], functional genomic clustering [5] and as a distance measure for gene clustering [6].

When there are two causative factors, one can form the mutual information between the output variable and the joint state of the two inputs, and consider its relation to the mutual information between the dependent variable and each of the inputs separately. In the presence of linkage disequilibrium between the two traits, their joint distribution is less informative than the sum of their individual distributions, and hence, the mutual information of the result with the joint could be smaller than the sum of the mutual information with the individual variates.

Contrariwise, different combinations of alleles might each work synergistically, in which case neither input has a significant predictive value, but the joint mutual information is high. The difference between the mutual information with the joint state of the inputs, and the sum of the mutual information with each trait, is called the three-way interaction information. For fixed marginal distributions, its value is minimized either at the boundaries of the probability space (*i.e.,* for some probability becoming zero), or when the logistic regression is linear. Because of this, the significance of the deviation of the interaction information from its minimum possible value at fixed marginals can be used as a measure of the interaction amongst the factors.

To obtain this significance, one can use a randomization test in which the output labels are shuffled keeping the marginals the same: such a scheme is statistically valid if no cell contains very small number (of the order of 10) of observations. We implemented this randomization test using Markov Chain Monte Carlo to evaluate significance of the interaction information.

The calculation of the mutual and interaction information is straightforward; the computational power is needed for determining the significance. Randomizing large data sets maintaining the marginals is computationally intensive. We perform this by conceptually presorting the data so that all the elements that contribute to the counts in the same cell of the contingency table are consecutive. A set of *d* sequences, where *d* is the number of input factors is then selected for output-label swapping with another such set. An accept/reject step allows the swapping only if the marginals would stay unchanged. In fact we find that an

MCMC algorithm described in terms of increments and decrements of counts in the cells, without any reference to the original data, can generate the final probability distribution. The probabilities of the elementary moves and the change in the interaction information arising from the move can be calculated relatively easily. The available parallelism can be used to run multiple chains simultaneously and reduce the error in the estimation of the null distribution.

This null distribution is then be used to assign a *p* value to the assertion that the observed interaction information is larger than expected in a random assortment with the same marginals. Significance will be assigned after correcting this for multiple tests by the Bonferroni method [7].

We developed and optimized a code to run on serial machines capable of calculating mutual and interaction information for any set of factors, or scan all possible combinations of factors. It also performs randomization test using Markov Chain Monte Carlo to evaluate significance.

The first data set we analyzed was a large kindred set (60 patients) with familial-combined hyperlipidemia (above normal lipids including cholesterol). We found hypercholesterolemia (high cholesterol) associated with a mutation (called E270K) in a gene for a receptor of low density lipid (LDL). This gene plays a role in the metabolism of cholesterol and this association was known previously. We also detected a correlation between high cholesterol and a mutation (called I269N) in the gene for a protein called melanocortin 4 receptor (MC4R). This protein is not known to play a role in cholesterol metabolism and the correlation is thus unexpected. This dataset had been studied extensively by our colleagues at UCSF and the new finding was therefore a confirmation of the power of interaction information methods.

The second set we analyzed using our novel entropy-based algorithm to calculate correlations between genes and lipids consists of 714 subjects and contains information on behaviors (for example the use of tobacco and alcohol), lipid profiles and genotypes at 170 sites for Single Nucleotide Polymorphisms (SNPs). These locations were again selected because of previous studies on Coronary Artery Disease (CAD) and this set had been studied extensively by our UCSF collaborators. Previously well documented single-gene associations, such as between lipid levels and the mutations in the gene for the protein called APOE held true in our analysis. We further confirmed the association between high density lipids (HDL) and the mutation called (SNP: rs6083; N215S) in the hepatic lipase (LIPC) gene.

Our analyses uncovered several previously unknown associations as well. The most notable was the association between LDL-Cholestrol and a polymorphism (rs5174; R893Q) in the gene called LRP8. The discovery of a new gene in the regulation of LDL levels was considered sufficiently important that our UCSF collaborators analyzed a second cohort of 738 subjects for confirmation. This required very significant effort of our UCSF colleagues and the new data became available only in August 2008. The previously observed statistically significant contribution was confirmed in this second cohort by the binary regression method and, more significantly, by our interaction information methods. However, the cholesterol levels in subjects with only one chromosome carrying the mutation (heterozygotes) were inconsistent. In one case the single copy of the mutation was providing protection whereas in the other cohort, the heterozygotes had high cholesterol.

The publication of our results has been put on hold pending resolution of this contradictory observation. Our UCSF colleagues are resequencing the first cohort in house as that data sample had previously come from an outside vendor. Our codes and suite of analysis is ready and we can finish the project with minimal further investment of time once those data are available.

We have also started a preliminary analysis of gene-gene interactions for these data sets. Our preliminary study shows that for most of the (170 X 170) combinations, many cells contain very small number (less than 10) observations. We are working with our cardiologist colleagues at UCSF to understand how to reduce the dataset without introducing bias. Based on these analyses, Dr. Kane at UCSF has submitted a proposal to UCOP Lab Fee RFP for a much larger study.

The methods developed in this study can be applied to a number of similar studies. In particular they are being applied to the analysis of HIV for the vaccine design program lead by Bhattacharya and Korber at LANL.

## References


1. Shannon, C. E.. A Mathematical Theory of Communication. 1948. *The Bell Systems Technical Journal.* **27**: 379.

2. Shannon, C. E.. A mathematical Theory of communication II. 1948. *The Bell Systems Technical Journal.* **27**: 623.

3. Klus, G. T., A. Song, A. Schick, M. Wahde, and Z. Szallasi. Mutual information analysis as a tool to assess the role of aneuploidy in the generation of cancer-

associated differential gene expression patterns. 2001. *Pac Symp Biocomput.* : 42.

4. Korber, B. T., R. M. Farber, D. H. Wolpert, and A. S. Lapedes. Covariation of mutations in the V3 loop of human immunodeficiency virus type 1 envelope protein: an information theoretic analysis.. 1993. *Proc Natl Acad Sci USA.* **90**: 7176.

5. Butte, A. J., and I. S. Kohane. Mutual information relevance networks: functional genomic clustering using pairwise entropy measurements. 2000. *Pac Symp Biocomput.* : 418.

6. Zhou, X., X. Wang, E. R. Dougherty, D. Russ, and E. Suh. Gene clustering based on clusterwide mutual information.. 2004. *J Comput Biol.* **11**: 147.

7. Bland, J. M., and D. G. Altman. Multiple significance tests: the Bonferroni method. 1995. *British Medical Journal.* **310**: 170.

full final report

# Quantifying the Role of the Cold Plasmasphere in the Loss of the Electron Radiation Belts

*Joseph Eric Borovsky*

20060360ER

## Abstract

One of the outstanding issues in magnetospheric physics and space-weather forecasting is: What causes the intensity of the electron radiation belt to decay? Researchers hypothesize that two mechanisms could be important. One mechanism is associated with the distortions of the magnetosphere during geomagnetic storms. The other mechanism is precipitation of relativistic electrons from the magnetosphere into the atmosphere catalyzed by the presence of cold plasma (the plasmasphere) in the magnetosphere. Via data-analysis and computer simulations, the effects of cold plasma on the dynamics of the magnetosphere are explored, with particular emphasis on the effects that the cold plasma has on the electron radiation belts.

## Background and Research Objectives

The relativistic electrons that are trapped in the Earth's magnetic field form an important population of particles for magnetospheric physics. These relativistic electrons form the inner and outer electron radiation belts. The outer belt is very dynamic, with the number density of relativistic electrons varying with time by several orders of magnitude. These outer-belt relativistic electrons are of great concern to the operators of spacecraft in geosynchronous orbit because they can wreck havoc on spacecraft electronics, sometimes causing catastrophic damage to very valuable space assets. They are sometimes referred to as "killer electrons".

A second population of particles in the magnetosphere that is important for the radiation belts and important for this research project is the Earth's plasmasphere. The plasmasphere is cold plasma that sometimes builds up to high densities in the dipole magnetic field lines of the magnetosphere; the cold plasma comes from outgassing of the ionosphere.

It is believed that two mechanisms are important for the loss of these relativistic electrons: drift out of the magnetosphere and pitch-angle scattering by plasma waves into the atmosphere. The plasma waves that scatter the relativistic electrons are believed to live in the cold plasma of the plasmasphere.

The overarching research objective of this project is to confirm that relativistic-electron precipitation into the atmosphere is catalyzed by cold plasma in the magnetosphere and to quantify that process. As this project evolved, the newly discovered effect of the plasmaspheric plasma on solar-wind/magnetosphere coupling was uncovered and the exploration and quantification of that effect was added as a second research objective.

## Importance to LANL's Science and Technology Base and National R & D Needs

Los Alamos National Laboratory has a programmatic mission to measure and understand the radiation environment at geosynchronous orbit for satellite-based sensors operating there. This project will enable LANL personnel to better understand the factors that influence this radiation environment and to better predict this radiation environment. A critical skill that this project will develop is the ability to understand the decay of the Earth's radiation environment.

## Scientific Approach and Accomplishments

1. In a data-analysis study of the cold plasma and energetic particles of the magnetosphere, a decay in the intensity of the outer electron radiation belt was observed during geomagnetically calm intervals before geomagnetic storms [1]. This decay was associated with the buildup of plasmaspheric plasma in the magnetosphere during the calms before the storms.

2. In a data-analysis study that spanned several solar cycles, 27-day repeating high-speed-stream storms were demonstrated to be a more effective source of energetic-electron events than are nonrepeating coronal-mass-ejection-driven storms [2].

3. In a solar-wind/magnetosphere data-analysis study, the reduction of solar-wind/magnetosphere coupling was statistically associated with the occurrence of plasmaspheric drainage plumes in the magnetosphere [3]. This supported our hypothesis that dense plasmasphere plasma mass loads reconnection between the solar wind and the magnetosphere on the dayside.

4. Our hypothesis that reconnection could be mass loaded by dense plasma was explored and confirmed using a series of two-dimensional MHD computer simulations of the reconnection of asymmetric plasmas [4]. These simulations were followed up for the more-complicated case of driven reconnection [5].

5. Using three-dimensional MHD computer simulations of the solar-wind-driven magnetosphere, a very clear demonstration was presented that plasmaspheric drainage plumes mass load dayside reconnection and reduce solar-wind/magnetosphere coupling [6].

6. Using the 3D MHD computer simulations, solar-wind magnetosphere coupling was explored and quantified. The main findings of this were (i) that solar wind electric field does not control the rate of reconnection at the dayside magnetosphere [6] and (ii) that a solar-wind/magnetosphere coupling formula was derived and tested [7].

7. Using superposed-epoch data analysis techniques, the hypothesis that radiation-belt dropouts are associated with the occurrence of plasmaspheric drainage plumes was confirmed [8]. It was further found that radiation belt dropouts are associated with a combined occurrence of plasmaspheric drainage plumes and superdense plasma sheets.

8. The origins of the superdense plasma sheet and the plasmaspheric drainage plumes in the solar wind were explored via superposed data analysis [8,9,10]. The superdense plasma sheet has its origin in compressed slow wind at the leading edge of corotating interaction regions and the plasmaspheric drainage plume is caused by a magnetic sector reversal in the corotating interaction region.

9. The properties of plasmaspheric drainage plumes during high-speed-stream-driven storms were statistically explored and the properties of drainage plumes (durations, widths, mass transport rates, etc.) were quantified [11].

10. Via this LDRD project, a workshop on plasmaspheric drainage plumes was organized in Taos, New Mexico, October 9-13, 2006 (see [12] for a published write up), a conference on high-speed-stream-driven storms was organized in Ambleside, England, September 2-7, 2007 (see (13] and [14] for write ups), and a workshop on high-speed-stream-driven storms was organized in Santa Fe, New Mexico, July 23-25, 2008.

## References


1. Borovsky, J. E., and J. T. Steinberg. The 'calm before the storm' in CIR/magnetosphere interactions: Occurrence statistics, solar-wind statistics, and magnetospheric preconditioning. 2006. *Journal of Geophysical Research.* **111**: 102309.

2. Borovsky, J. E., and M. H. Denton. The effect of plasmaspheric drainage plumes on solar-wind/magnetosphere coupling. 2006. *Geophysical Research Letters.* **33**: L20101.

3. Borovsky, J. E., and M. H. Denton. The differences between CME-driven storms and CIR-driven storms. 2006. *Journal of Geophysical Research.* **111**: A07S08.

4. Borovsky, J. E., and M. Hesse. The reconnection of magnetic fields between plasmas with different densities: Scaling relations. 2007. *Physics of Plasmas.* **14**: 102309.

5. Birn, J., J. E. Borovsky, and M. Hesse. Properties of asymmetric magnetic reconnection. 2008. *Physics of Plasmas.* **15**: 032101.

6. Borovsky, J. E., M. Hesse, J. Birn, and M. M. Kuznetsova. What determines the reconnection rate at the dayside magnetosphere?. 2008. *Journal of Geophysical Research.* **113**: A07210.

7. Borovsky, J. E.. The rudiments of a theory of solar-wind/magnetosphere coupling derived from first principles. 2008. *Journal of Geophysical Research.* **113**: A08228.

8. Borovsky, J. E., and M. H. Denton. Relativistic-electron dropouts and recovery: A superposed-epoch study of the magnetosphere and the solar wind. To appear in *Journal of Geophysical Research.*

9. Denton, M. H., and J. E. Borovsky. The superdense plasma sheet in the magnetosphere during high-speed-stream-driven storms: Plasma transport timescales. To appear in *Journal of Atmospheric and Solar-Terrestrial Physics.*

10. Denton, M. H., and J. E. Borovsky. Superposed epoch analysis of high-speed-stream effects at geosynchronous orbit: Hot plasma, cold plasma, and the solar wind. 2008. *Journal of Geophysical Research.* **113**: A07216.

11. Borovsky, J. E., and M. H. Denton. A statistical look at plasmaspheric drainage plumes. 2008. *Journal of Geophysical Research.* **113**: A09221.

12. Goldstein, J., J. Borovsky, J. Foster, and D. Carpenter. Formation, dynamics, and impact of plasmaspheric plumes. 2007. *Eos Transactions of the American Geophysical Union.* **88** (23): 247.

13. Denton, M. H., J. E. Borovsky, R. B. Horne, R. L. McPherron, S. K. Morley, and B. T. Tsurutani. High-speed solar wind streams: A call for key research. 2008. *Eos Transactionsl of the American Geophysical Union.* **89** (7): 62.

14. Denton, M. H., J. E. Borovsky, R. B. Horne, R. L. McPherron, S. K. Morley, and B. T. Tsurutani. Introduction to Special Issue on high speed solar wind streams and geospace interactions (HSS-GI). To appear in *Journal of Atmospheric and Solar-Terrestrial Physics.*

## Publications

Birn, J., J. E. Borovsky, and M. Hesse. Properties of asymmetric magnetic reconnection. 2008. *Physics of Plasmas.* **15**: 032101.

Borovsky, J. E.. The rudiments of a thoery of solar-wind/magnetosphere coupling derived from first principles. 2008. *Journal of Geophysical Research.* **113**: A08228.

Borovsky, J. E., M. Hesse, J. Birn, and M. M. Kuznetsova. What determines the reconnection rate at the dayside magnetosphere?. 2008. *Journal of Geophysical Research.* **113**: A07210.

Borovsky, J. E., and J. T. Steinberg. The 'calm before the storm' in CIR/magnetosphere interactions: Occurrence statistics, solar-wind statistics, and magnetospheric preconditioning. 2006. *Journal of Geophysical Research.* **111**: A07S10.

Borovsky, J. E., and M. H. Denton. The differences between CME-driven storms and CIR-driven storms. 2006. *Journal of Geophysical Research.* **111** (A07S08): 1.

Borovsky, J. E., and M. H. Denton. The effect of plasmaspheric drainage plumes on solar-wind/magnetosphere coupling. 2006. *Geophysical Research Letters.* **33** (20): L20101.

Borovsky, J. E., and M. H. Denton. Relativistic-electron dropouts and recovery: A superposed-epoch study of the magnetosphere and the solar wind. To appear in *Journal of Geophysical Research.*

Borovsky, J. E., and M. H. Denton. A statistical look at plasmaspheric drainage plumes. 2008. *Journal of Geophysical Research.* **113**: A09221.

Borovsky, J. E., and M. Hesse. The reconnection of magnetic fields between plasmas with different densities: Scaling relations. 2007. *Physics of Plasmas.* **14**: 102309 .

Denton, M. H., J. E. Borovsky, R. B. Horne, R. L. McPherron, S. K. Morley, and B. T. Tsurutani. High-speed solar wind streams: A call for key research. 2008. *Eos Transactions of the American Geophysical Union.* **89** (7): 62.

Denton, M. H., J. E. Borovsky, R. B. Horne, R. L. McPherron, S. K. Morley, and B. T. Tsurutani. Introduction to Special Issue on high speed solar wind streams and geospace interactions (HSS-GI). To appear in *Journal of Atmospheric and Solar-Terrestrial Physics.*

Denton, M. H., and J. E. Borovsky. The superdense plasma sheet in the magnetosphere during high-speed-stream-driven storms: Plasma transport timescales. To appear in *Journal of Atmospheric and Solar-Terrestrial Physics.*

Denton, M. H., and J. E. Borovsky. Superposed epoch analysis of high-speed-stream effects at geosynchronous orbit: Hot plasma, cold plasma, and the solar wind. 2008. *Journal of Geophysical Research.* **113**: A07216.

Goldstein, J., J. Borovsky, J. Foster, and D. Carpenter. Formation, dynamics, and impact of plasmaspheric plumes. 2007. *Eos Transactions of the American Geophysical Union.* **88** (23): 247.

# Non-blinking and Robust Quantum-Dot Fluorophores for Applications in Biology

*Jennifer Ann Hollingsworth*

20060581ER

## Abstract

We have investigated a new nanocrystal quantum dot (NQD) architecture based on an inorganic shell approach to address two intrinsic flaws (blinking and environmental sensitivity) limiting NQD applications. Success was achieved in both aims and demonstrated in stability and room- and low-temperature fluorescence spectroscopy studies, where emission behavior of individual NQDs was emphasized. Our successful efforts provide enabling technologies for fundamental biochemical/biophysical research, medical diagnostics, biosensors, and efficient solid-state lighting.

## Background and Research Objectives

Fluorophores are biological tags that can be used to track single biomolecules or image entire cells, glowing when interrogated by a light beam. Semiconductor nanocrystal quantum dots (NQDs) are near-ideal fluorophores for applications from basic molecular biology to integrated biosensors. NQDs have broadband absorption, narrow and tunable emission, exceptional brightness, and survive bright light (resist photobleaching). They are small enough to be used in the study of living cells. Despite these advantages over traditional techniques (e.g., organic dyes), the use of NQDs is limited by two factors: 1) sensitivity to the environment and 2) fluorescence intermittency (blinking).

Specifically, NQD optical properties are frustratingly sensitive to their surface chemistry and chemical environment. The coordinating organic ligands used to passivate the NQD surface during growth are retained following preparation and are strong contributors to such ensemble NQD optical properties as quantum yields (QYs) in emission. Unfortunately, ligands are labile and can become uncoordinated from the NQD surface and, as organic molecules, they can be damaged by exposure to the light sources used for NQD photoexcitation. Ligand loss through physical separation or photochemistry results in uncontrolled changes in QYs and, in the case of irreversible and complete loss, in permanent "darkening" or photobleaching. In addition, NQDs are characterized by significant "blinking" (fluorescence intermittency) at the single NQD level. While a precise mechanism has yet to be universally accepted, blinking is generally considered to arise from an NQD charging process in which an electron (or a hole) is temporarily lost to the surrounding matrix or captured to surface-related trap states. When charged, the NQD is vulnerable to highly efficient and non-radiative ("dark") Auger processes, where energy that is supplied to the NQD is transferred to the free electron or hole rather than used by the NQD to produce light. Thus, NQD emission turns "off" when the NQD is charged and turns "on" again when NQD charge neutrality is regained.

We proposed to develop a novel NQD architecture – a graded inorganic shell applied to the optically active NQD core – that aimed to solve these problems. Through the thick, graded-shell approach we hoped to reduce the efficiency of the Auger process. In this case, even if the NQD became charged, the "dark" process of Auger would be inactive, allowing excited-state electron-hole recombination to produce light. Alternatively, in the event that Auger processes remained active, we hoped to provide sufficient physical separation between the optically active NQD core and the NQD surface to isolate the excitonic wavefunction from the instabilities associated with changing NQD surface chemistry and environment. In this way, we aimed to enhance the robustness of NQDs to environmental effects and to eliminate NQD blinking. Importantly, others have previously reported the use of so-called "antiblinking reagents" to suppress blinking. Such reagents likely serve as charge mediators or charge compensators [1, 2]. In contrast, our "all-inorganic" approach was to create a fundamentally unique NQD architecture that is structurally more akin to physically grown epitaxial QDs, for which optical properties are stable and blinking is not observed [2].

## Importance to LANL's Science and Technology Base and National R & D Needs

Optimized NQD optical markers comprise an enabling technology for advanced bioimaging and single-biomolecule-tracking capabilities that support the DOE's Science Strategic Goal. In this area, the technology will support fundamental biochemical/biophysical studies, as well as medical diagnostics. Further, robust optical markers for use in autonomous environmental pathogen sensor systems will support DOE missions in homeland security, reducing the threat of weapons of mass destruction and terrorism. The results from this study will also impact Energy Security in the area of efficient solid-state lighting.

## Scientific Approach and Accomplishments

### Biocompatibility studies

Early on in this effort, we assessed the biocompatibility of NQDs in terms of their impact on biomolecular function. Specifically, we investigated an important case study of biomolecular activity, namely, the polymerization of tubulin "monomers" into microtubule biopolymers. We attached NQDs directly to the tubulin and studied polymerization kinetics and maximum NQD-tubulin ratios allowed for the tubulin to remain active toward polymerization. We compared the effect of coupling to tubulin amine sites vs. tubulin carboxylic acid sites. For coupling to amine surface sites, we found a limiting stoichiometry of 1 NQD per 6 tubulin and observed a 5-fold increase in the critical tubulin concentration required for onset of robust polymerization. In other words, NQD coupling to the tubulin amine sites deleteriously impacted polymerization kinetics. This was likely through interference with a critical GTP binding site. In contrast, small molecules, such as biotin or organic dyes, bound in this fashion to tubulin did not appreciably alter polymerization kinetics. We attempted to circumvent this problem by coupling NQDs to *pre-formed* microtubules by way of their amine sites, followed by depolymerization to create NQD-tubulin conjugates indirectly. Since these conjugates were prepared from viable microtubule polymers, they should have comprised only conjugates whose NQDs were bound through non-GTP-interfering amine sites. In conclusion, we observe that sensitivity of the biomolecular process, namely polymerization, to choice of NQD conjugation strategy suggests that use of NQDs as biomolecular labels for studying active processes must take into account the potential for NQD size and/or charge to influence the process being studied. These results were reported in [3]. Further, as part of this effort, we have also investigated the degree of clustering in core/multishell NQDs using a novel optical method to quantitatively determine clustering [4]. This component of the effort was relevant for biological applications and blinking studies in that clustering can cause unwanted cytotoxic effects and can interfere with data interpretation, respectively.

### Environmental sensitivity and blinking studies

The majority of our efforts have focused on addressing the dual aim of achieving environmentally robust and non-blinking NQDs. Initially, we attempted to finesse the energetics of the NQD core/graded-multishell systems, i.e., we attempted to create smooth potential energy gradients from NQD core to outer shell surface by using complicated (core)/shell structure, such as (A) (CdSe)/2CdS/$Zn_{0.13}Cd_{0.87}S$/$Zn_{0.49}Cd_{0.51}S$/ $Zn_{0.8}Cd_{0.2}S$/2ZnS and (B) (CdSe)/11CdS/2$Zn_{0.13}Cd_{0.87}S$/2$Zn_{0.49}Cd_{0.51}S$/2$Zn_{0.8}Cd_{0.2}S$/2ZnS. It was thought that the presence of a smooth energy gradient from NQD core out to NQD surface would significantly reduce the efficiency of the Auger process and, thereby, prevent blinking. Further, we hypothesized that even if the NQD core wavefunction still extended to the NQD surface, the effects of surface-related charging would be minimized by reducing the efficiency of the "darkening," Auger processes. However, although the thinner graded shell structures [e.g., (A) above: 7 shell monolayers] provided ultra-high emission efficiencies (QYs >90%), blinking statistics were not significantly altered. In contrast, the thicker graded shell structures [e.g., (B) above: 19 shell monolayers] provided markedly suppressed blinking behavior (see below), but QYs in emission were a low 9% on average. Interestingly, our best results to date have been with far simpler (core)/shell systems.

Earlier this year, we reported for the first time that the key optical properties—QY, photobleaching and blinking—can be rendered independent of NQD surface chemistry and chemical environment by growth of a very thick and *simple* inorganic shell [2]. Specifically, starting with 3-4 nm NQD CdSe cores (Figure 1), we grew the particles to a size of 15-20 nm by sequentially applying monolayers of CdS shells (Figure 1). We also reported the more complex shell structure discussed above as "B." In both case, the shell layers of CdS, ZnS, or CdxZnyS alloys were grown onto CdSe cores using modified literature procedures based on a successive ion layer absorption and reaction (SILAR) method. The growth of nominally 18-19 monolayers of shell material (calculated based on the amount of shell-precursor added) was conducted over a period of five days with reasonable control over size dispersity (Figure 1) and retention of a regular, faceted particle shape. We named these NQDs "giant" NQDs (g-NQDs).

g-NQD absorption spectra are dominated by the CdS shell material. This is not unexpected as, at these sizes, the shell:core volume ratio is approximately 100:1. However, a much smaller but separate absorption feature occurs clearly at ~620 nm and represents the absorption onset of the core CdSe. This feature exhibits spectral fine structure that is indicative of a narrow size dispersion and shows that the CdSe has remained intact despite the very long reaction times. Further, it is this CdSe core that provides the PL. No emission is observed from the g-NQD shell.

With g-NQDs, we have succeeded in creating truly environmentally robust NQDs. g-NQDs are uniquely insensitive to changes in ligand concentration and identity, and the chemical stability afforded by the g-NQDs clearly surpasses that of the standard multi-shell and core-only NQDs. Specifically, we observed that upon precipitation from growth solution and re-dissolution in hexane, the QYs for g-NQDs did not change (±5%; Figure 1). In contrast, QYs for standard multi-shell NQDs dropped by approximately 30% (Figure 1), while those for core-only samples dropped by more than 80% (Figure 1).

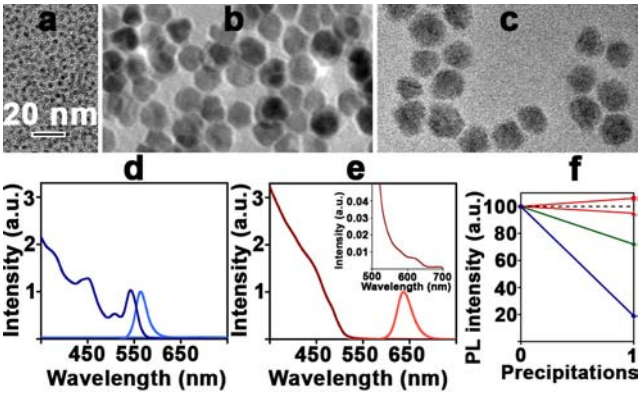


*Figure 1. Transmission electron microscopy (TEM) images for (a) CdSe NQD cores, (b) CdSe/19CdS g-NQDs, and (c) CdSe/11CdS-6CdxZnyS-2ZnS g-NQDs. (d) Absorption (dark blue) and PL (light blue) spectra for CdSe NQD cores. (e) Absorption (dark red) and PL (light red) spectra for CdSe/19CdS g-NQDs (inset: absorption spectrum expanded to show contribution from core). (f) Normalized PL compared for growth solution and first precipitation/re-dissolution for CdSe/11CdS-6CdxZnyS-2ZnS and CdSe/19CdS g-NQDs (red), CdSe/2CdS-2ZnS and CdSe/2CdS-3CdxZnyS-2ZnS NQDs (green), and CdSe core NQDs (blue). Dashed line indicates no change.*

Further, we observed no change in QY upon transfer to water using a standard ligand exchange procedure (replacing as-prepared ligands with mercaptosuccinic acid). Finally, we have also ligand exchanged the g-NQDs with pyridine, drop-cast a thin, solid films of g-NQDs, and subsequently subjected the film to vacuum and elevated temperature to assess the impact of thermal exposure and ligand loss on photoluminescence. We confirmed that compared to traditional multi-shell NQDs, g-NQDs are robust to these effects (Figure 2). In addition to the discussed applications in the biological sciences, this result has important implications for applications in optoelectronics, such as light-emitting diodes and single-photon light sources.

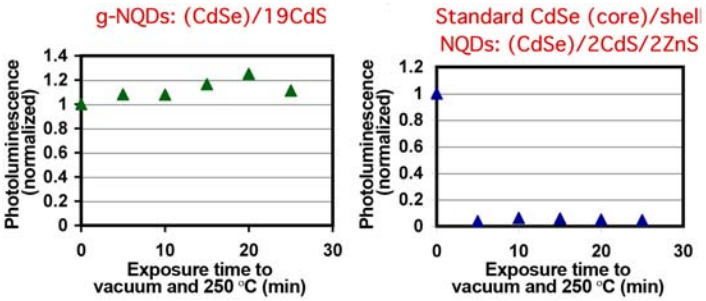


*Figure 2. Stability study to assess the relative robustness of g-NQDs compared to traditional multi-shell NQDs as a function of temperature and time. The results further demonstrate that g-NQDs are insensitive to surface chemistry, as in this experiment surface capping ligands are first replaced with pyridine and then largely removed through heating under vacuum in the solid state.*

Perhaps more remarkably still, the g-NQDs are stable under continuous laser illumination at a single QD level. Specifically, freshly diluted g-NQD solutions were dispersed onto clean quartz slides. Samples were irradiated for several hours at a time over several days. Photobleaching was not observed. This result stands in stark contrast with those obtained for control samples. Namely, core-only samples, as well as the thinner multishell samples, photobleached (complete absence of PL) within 1 s, and commercial NQDs (Qdot®655ITK™) faded to half their original intensity within ~15 min (Figure 3).

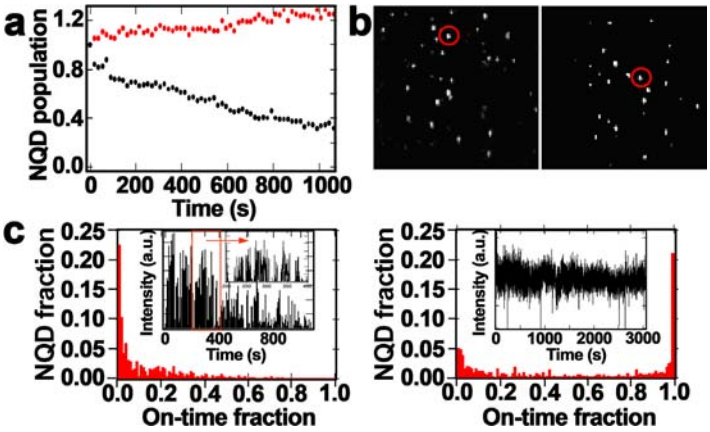


*Figure 3. Single-NQD emission studies. (a) Photobleaching study: Emitting NQD fraction over time: commercial NQD, Qdot®655ITK™ (black); g-NQD CdSe/19CdS (red). (b) Fluorescence image showing individual NQDs 'lighting up' under laser excitation. (c) Blinking study: On-time histograms of commercial NQDs (left) and CdSe/19CdS g-NQD (right) showing the fraction of NQDs as a function of time spent 'on'. Insets in (c) show fluorescence time traces of the circled NQDs in (b).*

Under these continuous excitation conditions, significantly suppressed blinking behavior was observed for 19-shell g-NQDs vs. control samples (Figure 3). Typical of classically blinking NQDs, >70% of the Qdot®655ITK™ NQDs have on-time fractions (fraction of total observation time that a single-NQD is "on") of <0.2. In contrast, >20% of the g-NQDs are non-blinking—have an on-time fraction of >0.99—and >40% of these NQDs have an on-time fraction of >0.8 over the 54 minutes of observation time. More recently, we have improved blinking statistics further, where 40% of the g-NQDs never turn off during the observation time of 54 min. In addition, we have investigated shell thickness dependence on g-NQD blinking behavior and have found that significantly suppressed blinking is observed at as few as 9 monolayers of CdS shell, allowing for smaller overall g-NQD sizes and simplified preparations.

Blinking behavior can be different depending upon the timescale used to make the observations. Our first measurements were all conducted using an effective observation time of ~200 ms. While at this scale we saw significant blinking suppression (see above), the question remained whether blinking was continuing but simply at shorter timescales. Such "fast" blinking would not be detected using our original measurement approach but would affect some potential applications in biology and optoelectronics if it existed. For this reason, we have also studied blinking at the fast timescales of 10 and 1 ms. Again, we saw conclusive evidence for non-blinking g-NQDs over our long observation time of 54 min (Figure 4).

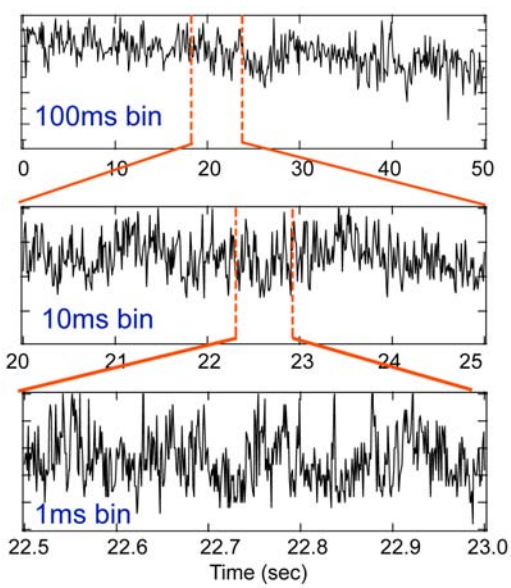


*Figure 4. Unprecedented suppression of blinking at all timescales: (top) 100 ms, (middle) 10 ms, and (bottom) 1 ms. Here, no 'off-period' was observed for CdSe/19CdS g-NQDs at any timescale over the 54 minute observation period.*

In addition to enhanced robustness and suppressed blinking, one of our original aims was to reduce the efficiency of the "dark" Auger processes. Recent intriguing evidence suggests that Auger recombination is effectively inactive in at least some fraction of the g-NQDs. Namely, in low-temperature photoluminescence spectra of traditional NQDs, only the emission from the lowest exciton state and its phonon replica are observed (Figure 5). This is due to the strong quenching of bi-exciton and higher order multi-exciton emission by very fast (efficient) Auger recombination as excitation pump intensities are increased. In stark contrast, in the case of some g-NQDs, biexciton and higher-order multiexciton emission is observed (Figure 5). This is the first evidence of multiexiton emission in standard, non-time-resolved photoluminescence spectroscopy dominating over single-exciton emission. This result indicates that Auger is suppressed to the point that the Auger recombination rate is comparable to the radiative recombination of multi-excitons.

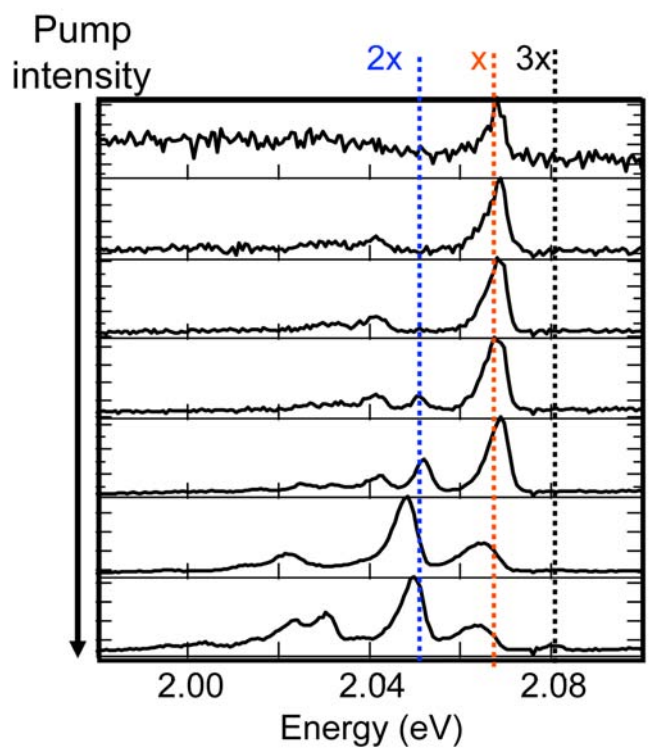


*Figure 5. Unprecedented multiexiton emission dominating single-exciton emission in non-time-resolved photoluminescence spectroscopy. Emission peaks from bi-exciton ('2x'), tri-exciton ('3x'), and higher order multi-exciton complexes emerge as pump intensities are increased.*

Finally, we have also investigated new g-NQD-enabled physics at the ensemble level. Here, we observed amplified spontaneous emission (ASE) at pump fluences 1-2 orders of magnitude lower than those required for traditional NQDs. This result, coupled with unusually long gain

lifetimes for g-NQDs, implies that g-NQDs could exhibit ASE when pumped with continuous-wave lasers rather than exclusively with pulsed lasers. Together, these results suggest that g-NQDs will enable new, low-energy lasers coupled with all the benefits of traditional NQDs, such as color-tunability and facile chemical processing.

**Conclusions and future work**

As a result of this LDRD ER project, we have developed a new class of NQD that possesses unique chemistry and physics for enabling multiple key technologies from fundamental biology to biosensing to efficient lighting. Three additional manuscripts are currently in progress [i.e., 1) shell-thickness dependence/expanded spectral window study, 2) fast-blinking/Auger study, and 3) ASE/lasing study].

In follow-on projects, we will attempt to understand why some g-NQDs are non-blinking, while others still blink, as well as why some exhibit multiexciton emission and others do not. Subtle structure-function relationships likely lie at the heart of the answer to this problem. High-resolution transmission electron microscopy analyses conducted as part of this study have already shown that the g-NQDs are not uniform [2], but correlating these non-uniformities back to function will require further effort. To this end, we will develop a more precise understanding of the sub-structure of the g-NQD and will correlate these structural features with optical properties at the single-NQD level. This knowledge will serve as valuable feedback to enable improved synthetic methods for optimizing g-NQD behavior and generalizing the g-NQD approach to new compositions and new spectral windows for enhanced application potential. Furthermore, through existing (NIH) and potential new funding (e.g., SISGR DOE) sources, we will emphasize the development of g-NQD science for mission-relevant applications (e.g., supporting medical diagnostics and solid-state lighting, respectively). Finally, through a CINT project, we are demonstrating utility for single-particle tracking within cells using streptavidin-conjugated g-NQDs (collaborator: Professor Lidke, UNM).

## References


1. Jeong, S., M. Achermann, J. Nanda, S. Ivanov, V. Klimov, and J. Hollingsworth. Effect of the thiol-thiolate equilibrium on the photophysical properties of aqueous CdSe/ZnS nanocrystal quantum dots. 2005. *Journal of the American Chemical Society.* **127**: 10126.

2. Chen, Y., J. Vela, H. Htoon, J. Casson, D. Werder, D. Bussian, V. Klimov, and J. Hollingsworth. ”Giant” multishell CdSe nanocrystal quantum dots with suppressed blinking. 2008. *Journal of the American Chemical Society.* **130**: 5026.

3. Jeong, S., and J. Hollingsworth. Polymerization of nanocrystal quantum dot-tubulin bioconjugates. 2006. *IEEE Transactions on Nanobioscience: Special Issue on Colloidal Quantum Dots for Biomedical Applications.* **5**: 239.

4. Bussian, D., A. Malko, H. Htoon, Y. Chen, J. Hollingsworth, and V. Klimov. Quantum optics with nanocrystal quantum dots in solution: quantitative study of clustering. To appear in *Journal of Physical Chemistry C.*


## Publications


Bussian, D., A. Malko, H. Htoon, Y. Chen, J. Hollingsworth, and V. Klimov. Quantum Optics with Nanocrystal Quantum Dots in Solution: Quantitative Study of Clustering. To appear in *Journal of Physical Chemistry C.*

Chen, Y., J. Vela, H. Htoon, V. Klimov, and J. Hollingsworth. ‘Giant” multishell CdSe nanocrystal quantum dots with suppressed blinking. 2008. *Journal of the American Chemical Society.* **130**: 5026.

Jeong, S., and J. Hollingsworth. Polymerization of nanocrystal quantum dot-tubulin bioconjugates. 2006. *IEEE Transactions on Nanobioscience: Special Issue on ‘Colloidal Quantum Dots for Biomedical Applications.* **5**: 239.

# Acoustic Effects on Microscopic and Core-Scale Colloid Interactions and Porous Fluid Transport

*Peter Morse Roberts*

20060607ER


## Abstract

Acoustic and elastic stress (seismic) waves cause significant changes in the behavior of solid, liquid and gas transport in porous media. Examples of useful applications include removal of micro-contaminants (e.g., bio-threat agents) from surfaces, micro-fluidic particle manipulation, improved efficiency of colloid deposition and assembly on surfaces, increased domestic oil and gas production, and enhanced contaminant extraction from groundwater aquifers. If this phenomenon can be harnessed reliably, it will have profound impacts on LANL, DOE and DoD energy, national security and environmental stewardship missions, including Bio-Threat Reduction, Energy Security and Environmental Management programs. This project focused on exploratory experimental investigations on the coupling of acoustic and elastic waves to immiscible 2-phase porous flow and to the interactions of micron-size particles (colloids) with liquid, gas and solid interfaces in unsaturated, non-aqueous or hydrophobic porous systems. The major research goal was to identify acoustically induced colloid interactions and enhanced fluid flow as a major, multi-scale mechanism for altering colloid and fluid transport in porous media. To achieve this goal, two major scale-dependent categories of experiments were performed. Micro-scale experiments focused on probing the physical parameters and processes controlling acoustic coupling to colloidal mobility, wettability alteration and multiphase fluid displacement. Core-scale experiments focused on characterizing the resulting bulk mass transport properties of stimulated colloids in a natural porous medium.


## Background and Research Objectives

Natural and artificial acoustic and elastic stress perturbations are known to cause significant changes in multiphase fluid flow behavior in porous media [1, 2]. Acoustic excitation can also cause sub-pore size particles (colloids) to become mobilized and expelled from fluid filled pores [3, 4]. If these phenomena can be harnessed, it should be possible to use stress waves to control the movement of fluids and colloids in beneficial ways. The coupled stress/flow phenomenon is controlled by a suite of diverse physical mechanisms that can operate over scale lengths ranging from the molecular to the global. Numerous mechanisms have been identified but their relative importance is unknown. Two poorly understood mechanisms in particular warrant exploratory research. These are 1) stress-induced colloid mobilization and 2) acoustic alteration of wettability. The dynamics (movement and interaction) of colloids can strongly affect bulk fluid flow in porous media, primarily by altering either the average pore or pore-throat cross-sectional diameter. Similarly, the preference (wettability) of a porous matrix to attract one immiscible fluid phase over another (e.g. oil vs. water) strongly affects the mobility of the two phases. Currently there are not enough experimental data to answer three major questions about these two important mechanisms: What is the nature of coupling between stress oscillations and colloidal forces (e.g., van der Waals, electric double layer, structural, and steric forces), pore fluid displacement, and interactions with surrounding solid interfaces? What is the magnitude of colloid behavior perturbations and wettability alteration required to cause observable changes in porous mass transport behavior? What is the contribution of the coupled stress/colloid mechanism to the enhanced flow phenomenon, relative to the altered wettability mechanism? This project sought to find clues for answering these questions by performing exploratory laboratory experiments on porous systems comprised of mixed hydrophilic/hydrophobic components using both aqueous and non-polar liquids. Three main hypotheses were tested: 1) Pressure and/or stress oscillations couple with the physicochemical forces that control colloid interactions with surrounding interfaces (e.g., solid-liquid and gas-liquid interfaces) to induce attachment and detachment events that are influenced by

adjustable physicochemical parameters. 2) These oscillations also interact directly with the pore matrix and fluids to induce enhanced 2-phase fluid (e.g., oil and water) flow. 3) Part of the coupling between acoustics, colloids and immiscible fluid displacement is due to induced wettability changes.

## Importance to LANL's Science and Technology Base and National R & D Needs

If the phenomenon of acoustically-coupled colloid/gas/fluid interactions can be understood and harnessed reliably, it will lead to advances in the ability to control porous mass transport in the Earth. Thus, this research impacts LANL and DOE needs in Energy Security, Bio-Threat Reduction, Environmental Management and fundamental Office of Science research.

## Scientific Approach and Accomplishments

Two unique experimental laboratory facilities developed at LANL were used in this project. The first is a specialized "Dynamic Core Flow Stimulation System" (DCFSS), which is used to investigate the effects of low-frequency mechanical stress oscillations on fluid, gas and colloid transport behavior in porous core samples (see Figure 1). The second is the "Automated Video Microscopic Imaging and Data Acquisition System" (AVMIDAS), which is used for real-time microscopic visualization of colloid behavior in glass flow cells (see Figure 2). The DCFSS has been used in the past to observe bulk mass transport properties for single-phase and 2-phase fluid-only transport through various porous rocks during stress stimulation. It has also been used for studying the transport of aqueous hydrophilic colloid suspensions through hydrophilic porous media. For this project modifications were made to allow gas to be injected and hydrophobic materials to be studied. Numerous improvements were made to the AVMIDAS facility. Capabilities such as high-resolution imaging, reflected and transmitted light, and fluorescence and DIC microscopy were added to the system. These enhanced capabilities enable better visualization and simultaneous quantification of the behavior of a wider range of colloid types, sizes, and surface characteristics. A new interchangeable flow cell was also designed and manufactured. The cell allows the utilization of any flat surface in the experiments, regardless of its opaqueness or roughness. New image processing and data extraction routines were also developed that improved the quality of the data and provided insightful information on the observed particle behaviors. In addition to the DCFSS and AVMIDAS systems, a new apparatus was procured for this project to measure wettability changes induced by acoustic excitation. The VCA Optima XE Surface Analysis System (SAS), manufactured by AST Products Inc., is an automated analytical instrument to perform contact angle and surface tension measurements of liquids and to calculate the surfaces energies of various surfaces. The instrument is equipped with a motorized syringe for precise dispensing of liquids and a CCD camera that captures live images and video, which are analyzed using included software. The instrument is being used to study surface wettabilities of different coated surfaces and the effect of acoustics on contact angle. Recently, the instrument has been upgraded to incorporate a heated environmental chamber and a tilting base assembly used for making dynamic (advancing and receding) contact angle measurements.

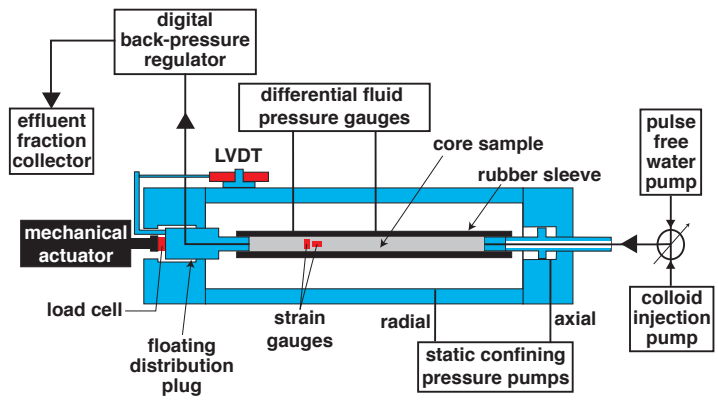


*Figure 1. Schematic diagram of DCFSS apparatus used for low-frequency dynamic stress, porous transport stimulation experiments.*

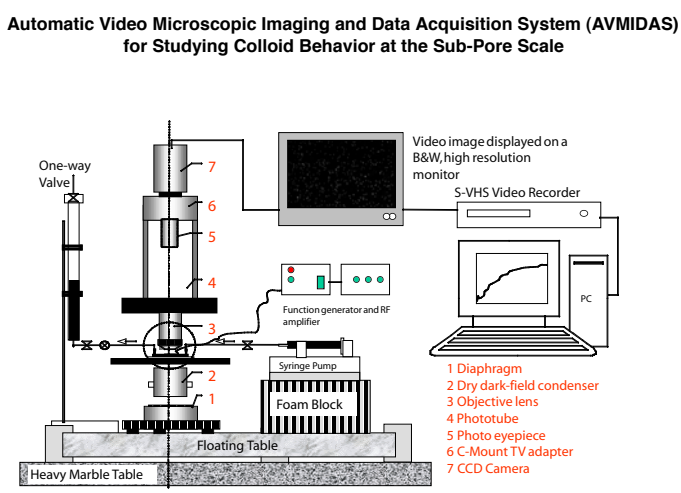


*Figure 2. Schematic of AVMIDAS apparatus used for visualizing and quantifying microscopic colloid behavior and immiscible fluid displacement.*

A series of experiments were performed in each of the two facilities above to investigate the acoustically induced

colloid mobilization and altered wettability mechanisms. The following summarizes three key experimental observations selected from the suite of results obtained.

An experiment was performed in the DCFSS to study the influence of fluid ionic strength and gas (air) injection on the ability of low-frequency mechanical stress to liberate solid colloids trapped in the porous matrix of a Fontainebleau sandstone core. Initial flushing of the core with 0.1 M NaCl solution was performed to remove or stabilize any pre-existing in-situ particles. Polystyrene microspheres, 1 micron in diameter, were then suspended in 0.1 M NaCl solution and injected into the core at a flow rate of 0.1 mL/minute. Effluent samples exiting the core were collected continuously and analyzed for produced microsphere concentration during the entire experiment. The results are shown in Figure 3.

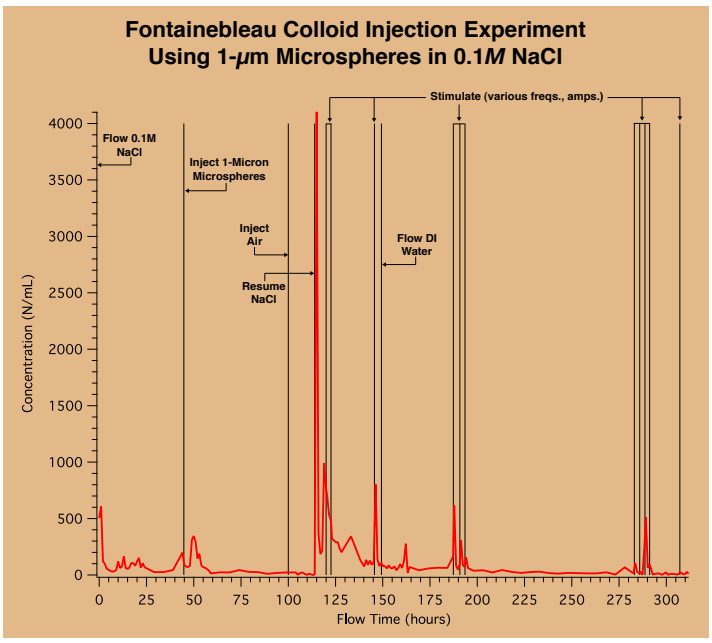


*Figure 3. Effluent microsphere concentration vs. time during flow of either fluid or air for Fontainebleau microsphere injection experiment. Experimental events, including microsphere and air injection, NaCl and DI water flow, and episodes of dynamic stress stimulation, are indicated by labeled red lines.*

A small concentration peak followed by a tail-off was observed after the microspheres were injected. After the background concentration stabilized, air was injected into the core for approximately 12 hours and then flow of pure 0.1 M NaCl solution was resumed to flush any microspheres released by the air. The large peak immediately after NaCl flow was resumed shows that air injection was highly effective at releasing trapped microspheres. Dynamic stress stimulation was then applied to the core at frequencies below 50 Hz, but had little effect on the decay rate of the effluent microsphere concentration. However, a large peak was observed when stress stimulation was applied after the background concentration had once again leveled off. Next, flow of deionized water was initiated. The lower ionic strength should release more microspheres, but this was not observed. However, when additional stress stimulation was applied, significant new concentration peaks were observed at certain frequencies and amplitudes. The results demonstrate that air injection has a profound effect on colloid release, but dynamic stress induced release is strongly inhibited at high ionic strength.

Using the SAS with an acoustic transducer attached to the wetting surface, direct measurements were made of the acoustically induced change in contact angle of a water droplet on a glass surface (see Figure 4). Shown are captured images of the droplet profile excited at different ultrasonic frequencies and the resulting contact angle made with the glass surface. As a result of droplet resonance, the contact angle is significantly reduced at specific acoustic frequencies. This implies that acoustics can dynamically change the wettability of a surface to specific liquids. In this case the wettability of water to glass increased. This mechanism has potential for explaining laboratory and field observations that indicate stress stimulation may temporarily alter a formation's wettability, allowing for enhanced immiscible displacement.

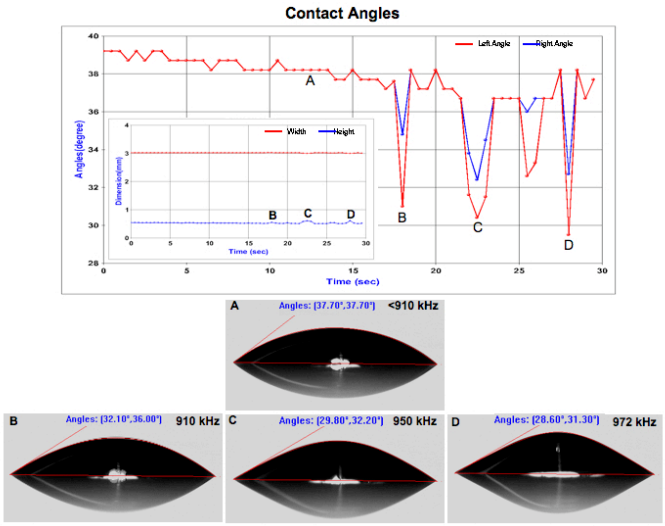


*Figure 4. Contact angle measurements of a water droplet on a glass surface excited at different acoustic frequencies. Droplet resonance at 910 kHz (B), 950 kHz (C) and 972 kHz (D) reduce the contact angle and effectively increase the wettability.*

AVMIDAS was used in experiments to visualize immiscible displacement of a non-polar liquid by water in an artificial porous media consisting of closely packed 1-mm diameter borosilicate beads. This process is analogous to so-called "water flood" field operations for enhanced recovery of

depleted oil reservoirs. A single layer of beads was sandwiched between two glass plates and the edges were sealed with epoxy. Inlet/outlet fluid ports were installed at the left and right edges of the resulting cell. The beads were then saturated with decane. Figure 5 (top) shows a bright-field microscopic image of the decane-saturated bead pack. The field of view is approximately 1 cm X 0.4 cm. A mixture of water and fluorocene was then injected at a constant flow rate of 1mL/hour into the left side of the cell to displace the decane. A snapshot dark-field image of the displacement at roughly 50% water saturation is shown in Figure 5 (center).

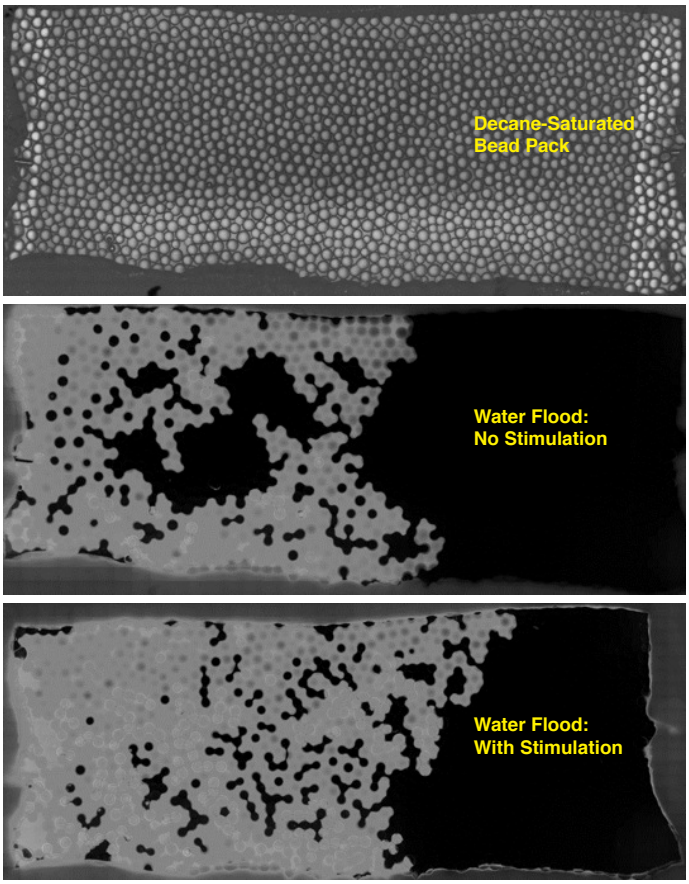


*Figure 5. Microscopic images of immiscible displacement (water flood) experiments in a borosilicate bead pack. Top: bead pack initially saturated with decane. Middle: Displacement of decane by water injection in the absence of fluid pressure stimulation at 50% water saturation. Bottom: Displacement of decane by water injection with fluid pressure oscillations at 50% water saturation.*

Black regions correspond to decane-saturated beads and light gray regions show where the water/fluorocene mixture has invaded. Notice the large connected regions where the decane has been left behind by the water injection. This is typical of behavior exhibited by oil reservoirs, where 30-50% of the in-place oil is usually bypassed by water flood operations. After cleaning the bead pack thoroughly and re-saturating with decane, the same experiment was repeated at a higher flow rate of 6 mL/hour with similar results. Large patches of unswept decane were again left behind, indicating that trapping cannot be overcome by increasing constant-rate fluid velocity alone. Next, the experiment was repeated again, but this time fluid pressure oscillations were imposed during water injection. The resulting displacement at 50% water saturation is shown in Figure 5 (bottom). The majority of the previously bypassed decane was displaced. A likely explanation is that a threshold of shearing force on the decane must be overcome before it can be detached from the host beads. Under constant-rate flow this threshold cannot be overcome. Fluid pulsations produce higher instantaneous pressure transients that are capable of delivering the additional shear force required to detach the decane in the previously unswept regions.

The experiments performed by this project have provided unique fundamental data about the importance of several different mechanisms for coupling dynamic stress to colloid mobility and multiphase porous fluid transport. We have demonstrated that the presence of gas enhances colloid detachment in porous systems containing high ionic strength fluids. Because dynamic stress mobilization of colloids is inhibited at high ionic strength, the presence of gas in the system is a likely means for increasing the effectiveness of seismic stimulation in high salinity reservoirs. In multiphase immiscible fluid systems, we now have direct evidence that low-frequency pressure oscillations enhance the release of non-polar liquids from a porous matrix when water is attempting to displace it. We have also seen that acoustics can dynamically alter a formation's wettability. The information gained by this project will be useful for improving the effectiveness of seismic stimulation applications over a wide range of physicochemical conditions that are typically encountered in field situations.

## References

1. Beresnev, I. A., and P. A. Johnson. Elastic-Wave Stimulation of Oil Production: A Review of Methods and Results. 1994. *Geophysics.* **59**: 1000.

2. Roberts, P. M., I. B. Esipov, and E. L. Majer. Elastic Wave Stimulation of Oil Reservoirs: Promising EOR Technology?. 2003. *The Leading Edge.* **22** (5): 448.

3. Venkitaraman, A., P. M. Roberts, and M. M. Sharma. Ultrasonic Removal of Near-Wellbore Damage Caused by Fines and Mud Solids. 1995. *Society of Petroleum Engineers, Drilling & Completion Journal.* **10** (3): 193.

4. Roberts, P. M.. Laboratory Observations of Altered Porous Fluid-Flow Behavior in Berea Sandstone

Induced by Low-Frequency Dynamic Stress Stimulation. 2005. *Acoustical Physics.* **51** (1): 160.

## Publications

Abdel-Fattah, A. I., and P. M. Roberts. Colloid Deposition and Removal at an Acoustically Stimulated Surface. 2006. In *Proceedings, 7th International Electrokinetics Conference (ELKIN).* (Nancy, France, 25-29 Jun. 2006). Vol. 7, p. 42. France: ELKIN.

Abdel-Fattah, A., S. Tarimala, P. Roberts, and R. Ibrahim. Acoustically-Induced Microparticle Orbiting and Clustering on a Solid Surface: Origin and Implications. 2008. In *Proceedings, Particles 2008 Conference.* (Orlando, 10-13 May 2008). Vol. I, p. 1. Orlando: Nanoparticles.org.

Roberts, P. M., A. I. Abdel-Fattah, and J. A. TenCate. Acoustic coupling to colloid interactions at solid/liquid interfaces under varying physicochemical conditions (invited). 2006. In *Proceedings, 11th International Workshop on Nonlinear Elasticity in Materials (IWNEM).* (Sorrento, Italy, 4-9 June 2006). Vol. 11, p. 1. Italy: IWNEM.

Roberts, P. M., A. I. Abdel-Fattah, and J. A. Tencate. Acoustic Stimulation of Colloid Behavior at the Pore and Core Scales. 2006. In *Eos, Transactions of the American Geophysical Union, 2006 Fall Meeting.* (San Francisco, 11-15 Dec. 2006). Vol. 87(52), p. H51F0537. Washington, DC: AGU.

Roberts, P. M., R. H. Ibrahim, and A. I. Abdel-Fattah. Stress/Strain Cycling Effects on Colloid Transport in a Synthetic Porous Medium. 2007. In *Eos, Transactions of the American Geophysical Union, 2007 Fall Meeting.* (San Francisco, 10-14 Dec. 2007). Vol. 88(52), p. H51G0858. Washington, DC: AGU.

Roberts, P. M., and A. I. Abdel-Fattah. Pore-Scale Acoustic Effects on Colloid Interactions at Solid/Liquid Interfaces under Varying Physicochemical Conditions. 2005. In *Eos, Transactions of the American Geophysical Union, 2005 Fall Meeting.* (San Francisco, 5-9 Dec. 2005). Vol. 86(52), p. H33A1380. Washington, DC: AGU.

# Complex Dynamical Climate Systems Analysis

*Gerald Leroy Geernaert*

20060686ER


## Abstract

The ER project goal was to address nonlinear interactions among processes that regulate and/or perturb the earth's climate system. Interactions included dynamical, physical, biogeochemical, and anthropogenic forcings; and specific tasks addressed coupled climate modeling, carbon cycle science, geophysics of carbon sequestration, aerosol and cloud influences on radiative balance, eco-hydrology, and paleoclimatology.


## Background and Research Objectives

The project was built on broad objectives to advance climate predictability using hindcasted data sets (paleoclimatology) and improve our understanding and parameterizations of processes that improve our ability to advance future climate predictions.

## Importance to LANL's Science and Technology Base and National R&D Needs

DOE leads the nation in providing affordable and clean energy to all US economic and national security sectors. This project underpins this DOE core mission, by providing the science needed to assess climate impacts on energy security, and making the best possible climate predictions that will affect future energy and national security. It also helps define the needs and designs for next generation infrastructures as well as the appropriate technology needed to sequester carbon dioxide on a large scale.

## Scientific Approach and Accomplishments

### Paleoclimate change with advanced isotope sampling

The objective of this task was to advance hindcast simulations of earth's climate with the use of newly developed isotopic measurements collected in the Valles Caldera, with a focus on very high temporal resolution precipitation variability and ecological feedbacks. Using an 80 m core, measurements of organic content, Pb abundance (indicators of dry/wet conditions), C/N ratios (e.g., $^{13}C$ and $^{15}N$), and the D/H ratio of *n*-alkanoic acids (and leaf wax) on lacustrine sediments from the Valles Caldera, New Mexico, formed the basis of this work. The climatic record obtained from the Caldera bog site, initially spanning the last 13,000 calendar years before present (YBP) revealed pronounced changes in environmental conditions that were in agreement with the pollen record (Anderson et al., 2008). Periods of wetter climate were observed during the period 13,000-9,000 YBP and over the last 6,000 YBP while a pronounced dry period was observed ca. 9,000-6,000 cal YBP; these basic patterns corroborated other records of drier climate in the Southwest during this period. During wetter periods, enhanced aquatic and terrestrial productivity was evident by increasing C/N ratios, and $^{15}N$ signatures indicative of aquatic and terrestrial organic matter sources. Similarly, before ca. 10,000 YBP, $^{13}C$ signatures suggested enhanced aquatic productivity though the relatively lower signatures observed yet could also indicate the presence of C4 plants surrounding the bog. During the dry period, significantly low C/N ratios suggested intense decomposition in agreement with the observed higher $^{15}N$ signatures. The return to wetter conditions and the establishment of the modern mixed conifer after 6,000 YBP was evident by increasing C/N ratios and $^{15}N$ and $^{13}C$ signatures in the range of values observed in terrestrial and aquatic plants.

We also performed compound-specific analyses on lacustrine sediments spanning ~350 ky to 552 ky before present, i.e., extending over numerous glacial cycles. A new technique for paleotemperature was applied particularly to this section of the core, i.e., the "MBT" molecular proxy. The results indicated the occurrence of mega-droughts during interglacial periods that may be excellent analogs to drought conditions predicted for the southwestern United States, as a result of human-induced climate change. Furthermore, the observed systematic hydrogen isotopic changes throughout the

deep core correspond to variations of summer precipitation. As a consequence of our study, it is now suspected that there have been systematic variations of the dynamical interactions between southwest monsoonal circulations, El Nino oscillations, and midlatitude jets.

**Interactions between ecological processes and regional climate change**

This task's objective was to test mechanisms at the leaf, soil and ecosystem level by which climate and physiology regulate the carbon and oxygen isotope composition of CO2 exchanged between the biosphere and the atmosphere. This objective was tested using high frequency Tunable Diode Laser Spectroscopy measurements of the isotopic composition of CO2 exchange from these tissues, ancillary measurements of physiology, climate, and tissue isotopic composition (via mass spectrometry), and via model analyses using high resolution ecosystem-isotope process models. Numerous control processes operating in plant canopies were documented, with particular effort to parameterize the internal conductance in semi-arid species, mesosphyll conductance, stomatal conductance, and transpiration rates for various gases.

**Mixed phase clouds and climate change**

Mixed phase clouds pose a major problem in understanding climate and climate change of polar regions. This task was designed to develop a satellite based method for retrieval of mixed phase clouds and to improve our ability to model their development and lifetime. There were four key accomplishments of this task First, the daytime and nighttime cloud phase detection (water cloud, ice cloud, or a mixed phase cloud) was developed using the near infrared and thermal infrared spectral bands. The verification was performed by application of the developed algorithm to the NASA MODIS (Moderate Resolution Imaging Spectro-radiometer) images of hurricane Katrina and images of storm clouds over the Indian Ocean. Second, we studied the effect of aerosols on regional climate, with a study of aerosol advection on microphysical properties of water and ice clouds over the Indian subcontinent and adjacent ocean. In contrast to our expectations, we found that air pollution aerosols over the seas adjacent to India lead to larger, rather than smaller, ice crystals. We built a simple model that overcame this surprise, by examining the heterogeneous ice nucleation on black carbon or mineral dust. Third, in a study of the Arctic clouds, a cloud microphysics parameterization was developed and tested against Arctic data collected during 1997 and 1998. We determined that the ice nucleation number concentration is the controlling factor of the overestimation of monthly mean ice water path originally produced by previous model. Fourth, a newly developed cloud phase algorithm was modified and applied to detect melt areas of the Greenland ice sheet. Using the algorithm, we found that the ice sheet melt area increased drastically during the late 1990s and early 2000s; however, the melting was even more extensive during 1930s and 1940s.

**Atmospheric surface and boundary layer storm dynamics**

Surface and boundary layer theory is unable to address highly heterogeneous and accelerating flows. We developed a generalized surface layer theory, for inhomogeneous conditions, that can be applied to bulk parameterizations of momentum, heat, and mass exchange. In addition, we advanced modeling of fire propagation using nonlinear feedbacks, and advanced the physics of hurricane storms, with particular attention to the air-sea interaction physics and cloud microphysics.

**Ocean modeling and climate simulation**

The first task focused on the development and application of an upper ocean model, for use in global climate simulations. During the first two years of this project, the model was developed and successfully implemented as a second level version of the Parallel Ocean Program model; sea ice and land surface components were subsequently added, and it was run in a coupled mode with an atmospheric model. Key results of this task were: (a) the new model framework is able to produce a stable climate within a few decades, with many aspects of climate comparable to that obtained using a full-depth ocean model after a long spin up time. Moreover, there is no long-term drift in the UOM solutions (Zhao et al. 2008a) as was more commonplace among previous versions of upper ocean models used elsewhere. Model simulations demonstrated that a doubling of atmospheric carbon dioxide indicate the distinctive roles of the abyssal ocean in participating interannual variability and global warming response. Specifically, the deep ocean is now confirmed to have only a minor effect on the upper ocean short-term climate variabilities. However, it plays a more substantial role, particularly in the Southern Ocean and North Atlantic, when radiative forcing ultimately changes the deep ocean state (Zhao et al. 2008a). During the third year of this ER, preliminary results (Zhao et al. 2008b) show that changing diapycnal diffusivities in the tropics may have a global influence by atmospheric teleconnections, and this suggests that a range of climate sensitivities may come from uncertainties in ocean model parameters. In addition, the advanced upper ocean modeling was used during year 3 to demonstrate that the Agulhas Retroflection, can act as a stabilizing process for the Meridional Overturning Circulation in the Atlantic.

## Publications

Anderson, R. S., R. B. J ass, C. D. Allen, L. M . Cisneros-Dozal, and J.. L. Toney. Development of the mixed conifer forest in northern New M  exico and its relationship to H  olocene environmental change.. 2008. *Q  uaternary Research.* **6  9** (2): 26  3.

Anderson, R. S., R. B. Jass, J. L. Toney, C. D. Allen, L. M. Cisneros-Dozal, M. Hess, J. Heikoop, and J. Fessenden. Development of the mixed conifer forest in northern New Mexico and its relationship to Holocene environmental change.. 2008. *Quaternary Research.* **69** (2): 263.

Barbour, M. M., D. T. Hanson, G. Tcherkez, BC. B. Bickford, and N. G. McDowell. High frequency measurements reveal rapid post-illumination changes in the carbon isotope composition of leaf-respired CO2. To appear in *Plant, Cell and Environment.*

Barbour, M. M., G. D. Farquhar, D. T. Hanson, C. B. Bickford, H. H. Powers, and N. G. McDowell. A new measurement technique reveals temporal variation in d18O of leaf respired CO2. To appear in *Plant, Cell and Environment.*

Barbour, M. M., N. G. McDowell, G. Tcherkez, C. Bickford, and D. Hanson. High frequency measurements reveal rapid post-illumination changes in the carbon isotope composition of leaf-respired CO2. *Plant, Cell and Environment.*

Breshears, D. D., N. G. McDowell, K. L. Goddard, K. E. Dayem, S. N. Martens, and C. W. Meyer. 2008 Drought recovery via foliar absorption of intercepted rainfall bypasses soil water uptake. 2008. *Ecology.* **89**: 41.

Breshears, D. D., O. B. Myers, C. W. Meyer, F. J. Barnes, C. B. Zou, C. D. Allen, N. G. McDowell, and W. T. Pockman. Tree die-off in response to global-change-type drought: mortality insights from a decade of plant water potential measurements.. *Frontiers in Ecology and Environment.*

Chylek, P., M. Dubey, U. Lohmann, V. Ramanathan, G. Lesins, J. Hudson, G. Altmann, and S. Olsen. Aerosol indirect effect over the Indian Ocean. 2006. *Geophysical Research Letters.* **33**: L06806.

Chylek, P., M. K. Dubey, and J. Dozier. Remote sensing of Greenland ice sheet using multispectral near-infrared and visible radiances.. 2007. *J. Geophys. Res..* **10** (1029): 112.

Chylek, P., S. Robinson, M. Dubey, M. King, Q. Fu, and W. Clodius. Comparison of near infrared and thermal infrared cloud phase detection. To appear in *Journal of Geophysical Research.*

Cisneros-Dozal, L. M., J. Heikoop, Y. Huang, J. L. Toney, J. M. Heikoop, J. Fessenden, and P. Meyers. Climate change during the Holocene and late Pleistocene in northern New Mexico inferred from organic carbon, δ13, δ15N and Pb abundance.. *Geophysical Research Letters.*

Flexas, J., M. Ribas-Carbo, D. T. Hanson, J. Bota, B. Otto, J. Cifre, N. G. McDowell, H. Medrano, and R. Kaldenhoff. Tobacco aquaporin NtAQP1 is involved in mesophyll conductance to CO2 in vivo. To appear in *Plant Science.*

Geernaert, G. L.. A note on the evaporation duct height for inhomogeneous conditions in coastal zones. To appear in *Journal of Applied Meteorology and Climatology.*

Hanson, D. T., C. Bickford, K. Brown, H. Powers, and N. G. McDowell. Real-time measurement of photosynthetic carbon isotope fractionation using a tunable diode laser: Insights into on-line estimation of mesophyll conductance. To appear in *Plant, Cell and Environment.*

Yuan, J., Q. Fu, and N. McFarlane. Test and improvements of GCM cloud parameterication. To appear in *Atmospheric Research.*

# Solid Earth Geoscience: Transient & Steady-State Earth Processes

*Claudia Johnson Lewis*

20060688ER

## Introduction

The ER project goal was to address fundamental scientific questions in seismology, hydrology, dynamic Earth processes, and structural geology (how rocks deform and why) using observational, experimental, numerical, and theoretical techniques. The objectives were to enhance our basic understanding of fundamental processes that control natural hazards, natural resources (including water and energy), and the environment and to develop new instrumental and modeling capabilities and expertise.

## Tie to DOE Missions

This project supports the DOE and LANL missions of solving national problems in energy, environment, infrastructure and health security. It also supports the DOE priorities of ensuring the integrity and safety of the country's nuclear weapons and ensuring that safety legacies of the cold war do not impede future national security missions.

### Hydrothermal Activity in Water Moons and the Parent Bodies of Meteorites

Carbonaceous chondrites are meteorites that contain high levels of water and organic compounds, indicating they have not undergone significant heating since they were formed. They are therefore thought to represent the solar nebula from which our solar system condensed. In order to unlock information about conditions in the early solar system, the goal of this task was to develop a computer code incorporating chemical reactions and chemical transport to numerically model the early evolution of planetary bodies.

We successfully simulated hydrothermal circulation in carbonaceous chondrite parent bodies of different radii, chemical isotope $^{26}$Al concentrations, and permeability. Additionally, we implemented water-rock chemical interactions by coupling two computer codes (dubbed MAGHNUM and PHREEQC). MAGHNUM simulates freezing, thawing, and transport of water and solutes. PHREEQC is used to simulate the geochemical reactions. The coupled computer code tracks changes in permeability, porosity, and the distribution of different minerals with time and determines the role that flow patterns and flow rates have in controlling water-rock interactions. An exciting outcome of this project is that some early planetary bodies appear to have been quite heterogeneous in their chemical and mineralogical composition, raising the possibility that these bodies may have been the source of many different kinds of meteorites previously thought to have been derived from distinct sources.

In addition, we used the code to investigate hydrothermal circulation and water-rock reactions in the interior of Europa, a moon of Jupiter, and Enceladus, a moon of Saturn. The results of the numerical simulations for the thermal evolution of Enceladus support the idea that it is a differentiated planetary body with a large rock-metal core (like Earth) surrounded by a liquid-ice water shell. Differentiation of Enceladus into layers and the existence of liquid water have important implications for explaining its ongoing internal activity. A layer of liquid water could provide a source for the water-vapor plume detected by the Cassini robotic spacecraft mission at Enceladus' south polar region. Our thermal evolution model further suggests that the interior of Enceladus has been altered through hydrothermal activity and water-rock reactions. These results represent important advances in understanding the distribution of water on other planets and their moons, as water is a crucial ingredient for life.

### Coupled Process Modeling of Subsurface Formation of Karst

This task tackles numerical modeling of complex hydrologic-geologic systems in order to illuminate natural processes of dissolution and precipitation of importance to energy development and carbon sequestration. "Gradient reaction" systems are those where flow rates

are slow enough that flowing aqueous solutions are locally saturated with respect to mineral phases. Dissolution or precipitation in such systems can be sustained where there is a gradient of mineral solubility along flow paths. The solubility gradient typically results from a salinity or thermal gradient. In this task, we investigate thermal gradients and their influence on solubility in forming subsurface karst, which are areas of erosional features in limestone. This is the first time that gradient reactions in heterogeneous media or fractures of variable width (or aperture) have been considered.

Because the rate of alteration due to aqueous reactions is proportional to the local fluid flux in gradient reaction systems, preferential flow paths experience preferentially higher rates of dissolution (or precipitation), and thus enlarge at a faster rate (dissolution case) or seal at a faster rate (precipitation case). We considered the case where aperture variability is described as a random field and solved the problem of reactive alteration of heterogeneous media under gradient reaction conditions in a conductive heat transfer regime. Dissolution leads to elongated preferential flow channels aligned with the solubility and hydraulic gradient, whereas precipitation leads to elongated precipitate bodies perpendicular to the solubility and hydraulic gradient.

We defined an approach for initial implementation of coupled problems in a finite element heat and mass transfer model (FEHM). Since FEHM was developed for porous media rather than discrete fractures, re-definition of several variables was required to mimic a fracture – some of these re-definitions are generic to other potential applications of FEHM to discrete-fracture systems, and as such will enhance the capabilities of FEHM. The critical component of this work was the incorporation of buoyant convective flow in the fracture and its consequences on pattern formation.

This research has provided significant new insights into the rich variety of behavior emerging from coupling between reactive alteration and non-isothermal flow (where temperature does not remain constant, including the case of buoyant convection) in geologic flow systems. Our results apply in a number of gradient reaction systems: karst systems formed below the Earth's surface by dissolution of calcite; sealing of fractures in hot-dry-rock geothermal systems as a result of cooling with precipitation of silica; and formation and emplacement of ocean-bed methane hydrates with precipitation.

**Nonlinear Dynamics in Earthquake Strong Ground Motion**

The dynamic response of rocks and sediments to earthquakes, which is highly dependent on individual localities, strongly controls the amount of damage to structures. Sediments can amplify ground motion at a site if seismic waves are trapped between sediment layers near the Earth's surface. However, simple linear scaling may not accurately predict strong ground motion from large earthquakes, the topic investigated in this task. At larger strains (larger earthquakes), laboratory studies show a reduced (nonlinear) amplification of ground motion. We conducted field and laboratory experiments using a large vibrator truck typically used in oil exploration to characterize changes in material stiffness with duration of shaking in granular materials and natural sediments. We compared these data to laboratory-scale results to understand nonlinear response to strong ground motion. Our goal was to test new techniques for measuring ground shaking towards clarifying nonlinear dynamics in Earth materials.

Measurements of nonlinear soil response under natural conditions are critical to understanding soil behavior during earthquakes. Sites overlying soil have a profound effect on ground motion during earthquakes due to their low wave speeds (seismic waves propagate slowly through soil), layered structure, and nonlinear material properties. In field experiments, we observed the *in situ*, nonlinear response of a natural soil formation using measurements obtained immediately adjacent to a large vibrator truck. The vibrating source generates a steady-state wavefield in the soil formation at a range of discrete source frequencies and amplitudes. Accelerometers within the source provide an estimate of the source output to the soil. Steady-state amplitude ratios are computed between the receivers and the source, and between adjacent receiver pairs within the array. We find that both sets of amplitude ratios show dramatic decreases in peak frequency as the source amplitude is increased. These peak frequency shifts are qualitatively similar to the nonlinear soil response observed for laboratory samples under resonance conditions, in which rock samples are made to oscillate at their natural frequency. Amplitude ratios between adjacent receiver pairs suggest the nonlinear soil response persists across the receiver array and is not limited to the source-soil contact region. The magnitudes of the observed peak shifts appear to depend on their frequency, a proxy for depth, which is consistent with the dependence of soil nonlinearity on confining pressure observed in laboratory experiments. Our determination of significant nonlinearity in these experiments is good news in that the amplifying effects of sediments subjected to strong ground motion are apparently not as great as implied by weak-motion studies.

In companion work, propagation of "Rayleigh waves" from the vibrator source was studied. Rayleigh waves are seismic waves that propagate along the surface of the Earth, resulting from interaction between the P- and S-waves that travel through the Earth's inner layers; Rayleigh waves are responsible for almost all the destruction associated with earthquakes. In our experiments, we found that as the force load of the shaker increased, the Rayleigh wave phase velocity decreased by as much as 30% at the highest frequencies used (up to 30 Hz), in agreement with what was observed in the resonance experiments described above. The greatest change in velocity occurred nearest the surface, within the upper 4 m. Our results suggest that it may be possible to characterize nonlinear soil properties *in situ* using a non-invasive field technique, making seismic hazard evaluation and engineering design faster and less expensive.

**Evolution of Fault-Bounded Relay Zones during Continental Extension**

The primary objective of this task was to better characterize the evolution of fault relay zones in continental rifts by integrating three-dimensional fault geometries, kinematics (a description of the path the rocks took during deformation) determined from paleomagnetic and structural techniques, and overall stress distributions from modeling using finite element techniques. Important objectives were to develop more accurate inputs for geologic framework models of rift margins that will allow hydrologists to better model fluid flow in the shallow crust and for geologists and seismologists to better define earthquake hazards.

Relay zones transfer displacement between two overlapping faults by tilting and rotating the fault-bounded blocks. With increasing displacement, adjoining faults eventually link together. The primary objective of this task was to determine the temporal and spatial distribution of the rotational component of deformation (i.e., rotations of crustal blocks about a vertical-axis) in the relay zones that form the diffuse boundary between two major extensional basins in the Rio Grande rift: the Albuquerque and San Luis basins. Vertical-axis rotations of the crust are best assessed by comparing the magnetization directions of rocks to the Earth's magnetic field direction at the time when the rocks acquired their magnetic signature. In this area of the Rio Grande rift, ignimbrite sheets of the more than 2 million-year-old Bandelier Tuff (erupted explosively from the Valles Caldera in the Jemez Mountains) were mapped in detail and correlated using new geochemical data. As ignimbrites cool after eruption, they acquire a stable magnetization that typically changes little with vertical-axis rotation. We obtained new paleomagnetic data from Bandelier Tuff exposures (401 specimens). Our data show no statistically significant vertical-axis block rotations in the Jemez Mountains and therefore suggest that the termination of fault linkage and relay zone development between the Albuquerque and San Luis basins took place before Bandelier Tuff volcanism or more than 2 million years ago.

In addition, we used a commercial finite element analysis program called "MARC" to develop a nonlinear model of the interaction between a pair of extensional faults and its influence on the structural evolution of the relay zone. The model uses simple fault geometries and isotropic material properties, and models the faults as frictional sliding surfaces; known displacements for the Pajarito fault system, the local boundary of the Rio Grande rift, have been used to impose boundary conditions for the model. The modeling demonstrates that even under orthogonal extension and overall plane-strain deformation (two-dimensional strain), the relay zone evolves in a complex manner.

The model results suggest that displacement of material particles in a relay zone deviates from the regional transport direction (i.e., transport resulting from plate tectonic interactions) and that the relay zone undergoes non-coaxial deformation, in which the principal strain directions are not parallel to the principal stress directions throughout the period of deformation. The model-derived minimum compressive stress directions within the relay zone are oblique to the regional extension direction throughout the deformation, as they would be in the simpler case of coaxial deformation. This suggests that oblique structures may develop to accommodate the regional extension in the same episode of deformation rather than forming in a distinct stage. Vertical-or oblique-axis rotation is not necessarily predicted by simple extension, yet is important in understanding earthquake risk, evolution of crustal basins and their filling sediments, and possible fluid-flow pathways.

## Publications

Blair, M. W., E. G. Yukihara, R. Kalchgruber, and S. W. S. McKeever. "Investigating the effect of low ambient temperatures on the luminescence process," Radiation Measurements. . *Radiation Measurements.*

Blair, M. W., R. Kalchgruber, E. G. Yukihara, and S. W. S. McKeever. "Low temperature effects on the OSL process of Martian simulants." . Invited presentation at *Fourth New World Luminescence Dating and Dosimetry Workshop.* (Denver, CO, 2006).

Blair, M. W., R. Kalchgruber, S. W. S. McKeever, E. R. Benton, D. K, Reust, and C. J. Wilson. "A Potential Extra-Terrestrial Application for OSL Dating: Developing Techniques for In-Situ Dating on Mars," . Invited presentation at *9th International Conference "Methods of Absolute Chronology.* (Gliwice, Poland, 2007).

Blair, M. W., R. Kalchgruber, and S. W. S. McKeever. "Developing luminescence dating for extraterrestrial applications: characterization of martian simulants and minerals,". 2007. *Radiation Measurements .* (42): 392.

Brown, S., K. Karlstrom, E. Kirby, W. Ouimet, M. Dillon, C. Cox, D. Newell, M. De Moore, J. van Wijk, and D. Coblentz. Hypothesis for epeirogenic uplift above the Jemez lineament: Is Neogene doming recorded by river profiles and terraces? . To appear in *Amer. Geophys. Union Fall meeting.* (San Francisco, CA, Dec 15-19, 2008).

Chaudhuri, A., H. Rajaram, H. Viswanathan, and G. Zyvoloski. Reactive Alteration of Fractures and Resulting Transitions in Fluid Flow and Heat Transfer Regimes. *Geophysical Research Letters.*

Chaudhuri, A., H. Rajaram, and H. Viswanathan. Stochastic Analysis of Precipitation/Dissolution and Aperture Alteration in Variable Aperture Fractures Under Gradient-Reaction Conditions. Invited presentation at *American Geophysical Union, Fall Meeting.* (San Francisco, December 10-14, 2007).

Coblentz, D., J. van Wijk, W. S. Phillips, K. Karlstrom, and C. Chase. The Geodynamic Origins of Western U.S. Topography: Correlations and Speculations. To appear in *Amer. Geophys. Union Fall meeting.* (San Francisco, CA, Dec 15-19, 2008).

Donohoo-Hurley, L., J. W. Geissman, P. J. Fawcett, T. Wawrzyniec, and F. Goff. A 200 kyr lacustrine record from the Valles Caldera: Insight from environmental magnetism and paleomagnetism.. 2007. *Geology of the Jemez Montians Region II.*

Ebinger, C., E. Beutel, and J. van Wijk. Concentration of Extensional Stress By Magma Bodies Responsible for Recurring Magmatism in the East African Rift. To appear in *Amer. Geophys. Union Fall meeting.* (San Francisco, CA, Dec 15-19, 2008).

Fawcett, P. J., J. Heikoop, F. Goff, R. S. Anderson, L. Donohoo-Hurley, J. W. Geissman, G. WoldeGabriel, C. D. Allen, C. M. Johnson, S. J. Smith, and J. Fessenden-Rahn. Two Middle Pleistocene Glacial-Interglacial Cycles from the Valle Grande, Jemez Mountains, northern New Mexico. 2007. *New Mexico Geological Society Guidebook, 58th Field Conference, Geology of the Jemez Mountains Region II.*

Geernaert, G.. Recent developments in surface layer theory for inhomogeneous conditions over the ocean: turbulence, fluxes, and profiles.. 2007. In *In Turbulence and Nonlienar Processes in Astrophysical Plasmas.* . Edited by Shaikh, D., and G. Zank. , p. 382. New York: AIP.

Gomberg, J., and P. A. Johnson. Dynamic triggering of earthquakes. 2005. *Nature.* **473**: 830.

Goteti, R., G. Mitra, A. Sussman, and C. Lewis. Insights into mechanical evolution of relay zones in extensional tectonic settings using three-dimensional finite element modeling. Invited presentation at *Geol. Soc. Amer. Annual Meeting.* (Denver, CO, Oct 28-31, 2007).

Goteti, R., and G. Mitra. Three-dimensional finite element modeling to understand the role of fault interaction in the evolution of relay zone structures: Implications for the Cenozoic Rio Grande rift. To appear in *Geological Society of America Abstracts with Programs.* (Phildelphia, PA, Oct 2006).

Goteti, R., and G. Mitra. Role of Fault Interactions in the Evolution of the Rio Grande Rift of North-Central New Mexico: Insights from Numerical Experiments. *Geol. Soc. Amer. Special Paper.*

Goteti, R., and G. Mitra. Three-dimensional finite element modeling to understand the role of fault interaction in the evolution of relay zone structures: Implications for the Cenozoic Rio Grande rift. Invited presentation at *Geol. Soc. Amer.* . (Phildelphia, PA, Oct 22-25, 2006).

Goteti, R., and G. Mitra. Role of Fault Interactions in the Evolution of the Rio Grande Rift of North-Central New Mexico: Insights from Numerical Experiments. To appear in *Geol Soc. Amer. Annual Meeting.* (Houston, TX, Oct 5-9, 2008).

Johnson, C. M., P. J. Fawcett, and A. S. Ali. Geochemical Indicators of Redox Conditions as a Proxy for mid-Pleisto-

cene Climate Change From a Lacustrine Sediment Core, Valles Caldera, New Mexico. 2007. *New Mexico Geological Society Guidebook, 58th Field Conference, Geology of the Jemez Mountains Region II.*

Kalchgruber, R., E. R. Benton, G. O. Sawakuchi, M. W. Blair, and S. W. S. McKeever. The Luminescence Efficiency of Cosmic Radiation at the Surface of Mars and in the Martian Regolith – A Study with Quartz and Regolith Simulants. Invited presentation at *15th Solid State Dosimetry Conference.* (Delft, The Netherlands, 2007).

Kalchgruber, R., M. W. Blair, S. W. S. McKeever, E. R. Benton, D. K. Reust, and B. N. Strecker. An innovative approach to in-situ dating of geomorphological features on Mars. 2007. *Planetary and Space Science 55.* : 2203.

Kalchgruber, R., M. W. Blair, S. W. S. McKeever, E. R. Benton, D. K. Reust, and B. N. Strecker. The Challenges of In-Situ Luminescence Dating of Sediments on the Surface of Mars. Presented at *15th Solid State Dosimetry Conference.* (The Netherlands, 2007).

Kalchgruber, R., S. W. S. McKeever, M. W. Blair, E. R. Benton, and D. K. Reust. A Prototype Instrument for In Situ Luminescence Dating of Sediments on Mars. Invited presentation at *7th International Conference on Mars.* (Pasadena, CA, 2007).

Kalchgruber, R., S. W. S. McKeever, M. W. Blair, S. Doe, D. K. Keust, S. Gupta, and B. N. Strecker. Development of a luminescence dating device for in situ dating of geomorphological features on Mars. Invited presentation at *Workshop on Surface Ages and Histories: Issues in Planetary Chronology.* (Houston, TX, 2006).

Karlstrom, K. E., L. J. Crossey, J. Coblentz, and J. W. van Wijk. Model for Tectonically driven incision of the <6 Ma Grand Canyon. Geology.

Karlstrom, K., w. Ouimet, D. Coblentz, and J. van Wijk. Colorado River system of the southwestern U.S.: analysis of the longitudinal profile, differential incision, and hypothesis for dynamic uplift and rapid incision in the last 6 Ma. To appear in *Amer. Geophys. Union Fall meeting.* (San Francisco, CA, Dec 15-19, 2008).

Lawrence, Z., P. Bodin, C. Langston, F. Pearce, J. Gomberg, P. Johnson, F. Y. Meng, and T. Brackman. Induced Dynamic Nonlinear Ground Response at Garner Valley, California, Bull. 2008. *Seismol. Soc Amer.* : 1412.

Mason, S., A. J. Sussman, C. J. Lewis, J. N. Gardner, E. Schultz-Fellenz, and J. Geissman. New Paleomagnetic Data from the Quaternary Bandelier Tuff: Implications for the Tectonic Evolution of the Rio Grande Rift.. To appear in *Amer. Geophys. Union Annual Meeting.* (San Francisco, CA, Dec 15-19, 2008).

McDowell, N. G., D. Baldocchi, M. M. Barbour, C. Bickford, M. Cuntz, D. T. Hanson, A. Knohl, H. H. Powers, T. Rahn, J. Randerson, W. J. Riley, C. Still, K. Tu, and A. Walcroft. Measuring and modeling the stable isotope composition of biosphere-atmosphere CO2 exchange: where are we and where are we going? . 2008. *EOS.* (AGU 89): 94.

McDowell, N. G., H. D. Adams, J. D. Bailey, and T. E. Kolb. The response of ponderosa pine growth efficiency and leaf area index to a forty-year stand density experiment.. 2007. *Canadian Journal of Forest Research.* **37**: 343.

McDowell, N. G., S. A. White, and W. T. Pockman. Transpiration and stomatal conductance across a steep climate gradient in the southern Rocky Mountains. . To appear in *Ecohydrology.*

McDowell, N. G., and L. Marshall. Growth, carbon isotope discrimination, and mortality across a ponderosa pine elevation transect. . *Oecologia.*

Mosar, J., S. Cloetingh, and J. van Wijk. Mantle controls on landward basin migration at rifted margins: example from the Mid-Norwegian margin.. *special issue of Tectonophysics.*

Newman, B. D., B. P. Wilcox, S. Archer, D. D. Breshears, C. N. Dahm, C. J. Duffy, N. G. McDowell, F. M. Phillips, B. R. Scanlon, and E. R. Vivoni. The ecohydrology of arid and semi-arid environments: a scientific vision.. 2006. *Water Resources Research.* : 42.

Ogden, D. E., G. A. Glatzmaier, and K. H. Wohletz. Effects of vent overpressure on buoyant eruptions columns: Implications for plume stability. 2008. *Earth Planet. Sci. Letter.* (113): 283.

Ogden, D. E., K. H. Wohletz, G. A. Glatzmaier, and E. E. Brodsky. Numerical simulations of volcanic jets: Importance of vent overpressure.. 2008. *J. Geophys. Res..* **113**: B02204.

Palguta, J., G. Schubert, and B. J. Travis. Hydrothermal Circulation in Icy Bodies. Presented at *The 5th Astrobiology Science Conference.* . (Houston, TX, 2008).

Palguta, J., and B. J. Travis. Hydrothermal convection and aqueous alteration in carbonaceous chondrite parent bodies.. 2006. *Bull. Amer. Astron. Soc.* : 38.

Pearce, F.. Nonequilibrium Nonlinear Dynamics in Earth Materials: Application to Strong Ground Motion Site Characterization. Presented at *10th Workshop on Nonlinear Elasticity in Materials.* (Sorrento, Italy, July 2006).

Pearce, F.. In Situ Nonlinear Resonant Ultrasound Spectroscopy (NRUS) Using a Large Vibrator Truck: Innovation in Nonlinear Acoustics. Presented at *Innovation in Nonlinear Acoustics.* (State College, PA, July 18-22, 2006).

Pearce, F.. In Situ Nonlinear Resonant Ultrasound Spectroscopy (NRUS) Using a Large Vibrator Truck: Innovation in Nonlinear Acoustics. Presented at *Innovation in Nonlinear Acoustics.* (State College, PA, July 18-22, 2006).

Pearce, F., P. Bodin, Z. Lawrence, J. Gomberg, F. Yuh Meng, and P. A. Johnson. In Situ Nonlinear Soil Response applying an Active Source. Presented at *12th International Workshop on Nonlinear Elasticity.* (Corsica, France, June 2007).

Pearce, F., P. Bodin, Z. Lawrence, J. Gomberg, F. Yuh Menq, and P. A. Johnson. Inducing In Situ, Nonlinear Soil Response Applying an Active Source. To appear in *J. Geophys. Res.* .

Pearce, F., P. Bodin, Z. Lawrence, J. Gomberg, F. Yuh Menq, and P. A. Johnson. In Situ Measurement of Nonlinear Soil Response Applying an Active Source. Presented at *11th International Workshop on Nonlinear Elasticity.* (Sorrento, Italy, June 2006).

Pearce, F., Z. Lawrence, J. Gomberg, F. Yuh Menq, and P. A. Johnson. In Situ, Nonlinear Soil Response applying an Active Source: Application to Local Site Characterization?. Presented at *3rd International Symposium on "Effects of Surface Geology on Seismic Motion.* (Grenoble, France, August 2006).

Peron-Pinvidic, G., J. van Wijk, D. Shillington, and L. Gernigon. Role of magmatism in continental lithosphere extension.. To appear in *Tectonophysics Special Issue.*

Rajaram, H., and B. Andre. Modeling the Early Evolution of Hypogene Karst Systems by Dissolution and Fracture Growth in Hydrothermal Systems, Society of Industrial and Applied Mathematics . Presented at *Mathematical and Computational Issues in the Geosciences.* (Santa Fe, New Mexico, March 19-22, 2007).

Schubert, G., J. D. Anderson, B. J. Travis, and J. Palguta. Enceladus: Present internal structure and differentiation by early and long term radiogenic heating.. 2007. *Icarus 188.* : 345.

Sine, C., D. Wilson, W. Gao, S. P. Grand, R. Aster, J. Ni, and S. W. Baldridge. Mantle structure beneath the western edge of the Colorado Plateau. 2008. *Geophys. Res. Letter.* **35**: l10303.

Sussman, A. J., C. J. Lewis, S. Mason, B. Oliva-Urcia, J. N. Gardner, J. Geissman, and E. Schultz-Fellenz. Paleomagnetism and Stratigraphic Correlations of Quaternary Bandelier Tuff Cooling Units, Jemez Mountains: Implications for the Tectonic Evolution of the Rio Grande Rift. *Geol. Soc. Amer. Special Paper.*

Sussman, A., B. Oliva, C. J. Lewis, R. Soto, R. Goteti, and G. Mitra. Vertical-axis rotations associated with relay ramps in the Rio Grande rift, New Mexico. To appear in *Geological Society of America Abstracts with Programs.* (Philacelphia, PA, Oct 2006).

Sussman, A., B. Oliva, C. J. Lewis, R. Soto, and R. Goteti. Vertical-axis rotations associated with relay ramps in the Rio Grande rift, New Mexico. Presented at *Geol. Soc. Amer..* (Phildelphia, PA, Oct 22-25, 2006).

Travis, B. J., J. Palguta, and G. Schubert. . Hydrothermal circulation in Europa's mantle: Implications for seafloor plume generation, ice shell thickness, and surface geology. *Icarus.*

Uehlein, N., O. Beate, D. Hanson, N. G. McDowell, and R. Kaldenhoff. Function of aquaporins as chloroplast gas pores challenges the concept of membrane CO2 permeability. . To appear in *Plant Cell.*

Wang, X., J. F. Ni, R. Aster, E. Sandvol, D. Wilson, C. Sine, S. Grand, and S. W. Baldridge. Shear wave splitting and mantle flow beneath the Colorado Plateau and its

boundary with the Great Basin. To appear in *Bull. Seis. Soc. Am.* .

White, T. D., and G. WoldeGabriel. Asa Issie, Aramis and the origin of Australopithecus. 2006. *Nature 440.* : 883.

Wilson, J. E., L. B. Goodwin, and C. J. Lewis. Alteration and cementation of deformation-band faults in the Bandelier Tuff, Los Alamos, NM: A record of vadose-zone flow and transport. 2006. *Journal of Geophysical Research.* **111**: B09201.

WoldeGabriel, G., J. Heikoop, F. Goff, D. Counce, P. J. Fawcett, and J. Fessenden-Rahn. Appraisal of post-South Mountain volcanism lacustrine sedimentation in the Valles Caldera using tephra units. 2007. *New Mexico Geological Society Guidebook, 58th Field Conference, Geology of the Jemez Mountains Region II.*

WoldeGabriel, G., W. K. Hart, P. R. Renne, and Y. Haile-Selassie. Geology of the Adu Asa Formation, SW Afar Rift Western margin Monograph. Edited by White, T..

Zhao, B.. The impact of Reduced Mixing in the Tropics on Simulated Global Climate Change in Response to Doubled CO2 Forcing. To appear in *J. Physical Oceanography.*

Zhoa, B.. Climate Simulation Using an Upper-Ocean Model in CCSM3. To appear in *Physical Oceanography.*

vanWijk, J. W., J. van Hunen, and S. Goes. Small-scale convection during rifting: evidence from the Rio Grande rift. . 2008. *Geology 36.* : 575.

vanWijk, J., J. van Hunen, and S. Goes. Small scale convection during continental rifting: evidence from the Rio Grande rift. Presented at *SSA Meeting.* (Santa Fe, NM, 2008).

vanWijk, J., J. van Hunen, and S. Goes. Small scale convection during continental rifting; evidence from the Rio Grande rift. To appear in *SSA Meeting.* (Santa Fe, New Mexico, August 2008).

vanWijk, J., and J. Van Hunen. Lithosphere-mantle interactions during rifting and continental breakup. To appear in *Geomod Conference.* (Italy, July 2008).

vanWijk, J., and J. van Hunen. Lithosphere-mantle interactions during rifting and continental breaku. 2008. *Bollettino di Geofisica 49.* **2**: 342.

vanWijk, J., and J. van Hunen. Lithosphere-mantle interactions during rifting and continental breakup. Presented at *Geomod Conference.* (Italy, 2008).

vanWijk, J., and J. van Hunen. Mantle-lithosphere interactions in continental rift zones. Presented at *EGU Meeting.* (Vienna, 2008).

# A Strategy for Effective Antibiotic Delivery

*Srinivas Iyer*

20061494ER

## Abstract

The overarching goal of this Laboratory Directed Research and Development-Exploratory Research (LDRD-ER) program was to initiate efforts towards developing a novel approach to deliver therapeutics to bacteria. Antibiotic drugs have long been relied upon as the primary treatment for bacterial infections. However, these drugs are usually delivered to the whole body and while they do reach areas where the therapeutic effects are needed, they also exert their action on other tissues. This results in several problems: inefficient systemic delivery that requires much higher doses, unwanted side-effects on uninfected areas and, frequently, the emergence of antibiotic resistance. In addition, several strong antibiotic compounds cannot be used in a non-targeted approach. Hence, there is tremendous need to improve the activities of available antimicrobial agents and this is best done by precise targeting. Targeting in this context refers to delivering the drug where it needed while ensuring that surrounding areas are not affected. Given the above, we chose to employ a Trojan Horse approach, which could potentially subvert natural bacterial mechanisms.

## Background and Research Objectives

Our primary approach was based on the iron acquisition process in bacteria. All bacteria need iron for survival. Given prior expertise and data within our group on the anthrax causing bacterium *B. anthracis*, we designed our strategy around this organism. Iron is a requisite mineral for the proliferation of *B. anthracis*, as well as other bacteria; however, in spite of the abundance of iron in the environment, it is not readily available to bacteria. Further, iron balance within a mammalian host is tightly regulated. A common strategy employed by bacteria to solubilize and sequester iron is the biosynthesis and secretion of small sized, high-affinity iron binders termed siderophores. A considerable amount of research, by others, and us has been performed on the mechanisms *B. anthracis* uses to obtain sufficient iron from the host to support its astoundingly rapid growth during infection. These studies identified a unique siderophore [1], since then shown to be produced by many other bacteria as well [2]. In the typical scenario, bacteria produce and release siderophores into the surrounding milieu and then re-ingest siderophores after they have captured iron from their environment. The precise mechanism by which the complex enters the cell and releases iron is not completely understood, however several theories have been put forward. In general, it is thought that proteins on the surface of the bacterial cell recognize iron-bound siderophore and help internalize them. Our premise was that attachment of an antibiotic to such a siderophore would enable the "targeted" delivery of these compounds to bacteria alone since siderophores are not taken up by the host cells. The key challenge in such an approach is to devise appropriate attachment strategies and the bulk of our effort was spent on doing this and studying the interaction of these complexes with model membranes. In addition, knowledge of specific proteins on the surface of the bacterial cell that may be involved in such uptake would be highly beneficial, so that we could understand how the uptake process occurs and consequently influence the design of the attached molecules. While the complexity of this whole approach far surpasses possible achievement in a short time, we believe this project has laid the necessary foundation for follow-up studies in order to achieve our long-term goals. Results from our work thus far under the auspices of this LDRD project are discussed later in this document.

## Importance to LANL's Science and Technology Base and National R & D Needs

This project will enhance the nation's health security by significantly advancing research to support more effective clinical intervention. Institutionally, developing new biomedical research and capabilities addressing threats posed by pathogens (existing / emerging

/ bioengineered) support LANL's roles in the DOE Threat-Reduction Mission. This project has set the stage for further experimentation that could potentially lead to the development of a new capability, attracting new sponsors. There is growing interest in this topic from agencies such as the NIH and DOD because of its impact both on national security and public health, thus we expect future investment in this area of research from these agencies. Finally, the development of a candidate molecule may have the potential to generate substantial IP licensing

## Scientific Approach and Accomplishments

The overall approach we used had three major components: 1) Studying interactions of siderophores with model membranes in order to investigate interactions 2) Attachment of a model siderophore to a model antibiotic and testing efficacy in inhibiting B. anthracis growth and 3) Examining bacterial cell surface proteins that may play a role in uptake of complexes.

The interactions of siderophores with model membranes were studies using a synthetic lipid monolayer as a part model of the cell membrane. These experiments were done at the LANL LANSCE Lujan Center. A Langmuir-Blodgett trough was prepared that essentially allows the measurement of perturbations of the surface area of the monolayer upon addition of components. Results showed an increase in total area as seen in Figure 1, indicating that the siderophore was inserting into the membrane.

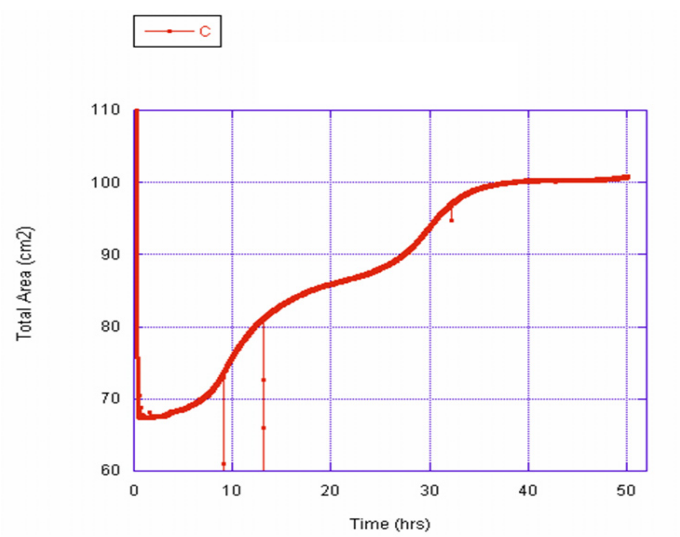


*Figure 1. Petrobactin (1 mg/mL) in solution in water was injected into a LB trough under a DDPE monolayer. Increase in surface area of the monolayer is seen.*

Additional experiments using authentic bacterial membranes in a different format where we tried to replicate the whole bilayer were attempted but were not conclusive as protruding proteins prevented the formation of a uniform bilayer on the quartz crystals we were using. This is an area we wish to investigate more closely in the future in follow-up projects. In this regard, the availability of beam time has been most helpful.

The attachment of siderophore to ampicillin was done using desferrioxamine, a commercially available siderophore to investigate the possibility of generating suitable conjugated molecules. The conjugation strategy employed a standard and commercially available method, hence facilitates reproduction. Thus desferrioxamine was coupled to the conventional antibiotic ampicillin. The formation of the conjugate was tested by analyzing the product by mass spectrometry in our laboratory. The results indicated that the product forms but that there were also other reaction components present. Several efforts to separate these components were made, however we were unable to obtain completely pure fractions. Nevertheless, we proceeded with testing the attached molecules. Testing of these conjugates with cultures of B. anthracis were disappointing in that, we did not see a huge increase in bacterial death with the conjugate over that of free antibiotic alone. This is partly because in this case ampicillin alone also worked very well since at higher concentrations of both antibiotic and conjugate, complete inhibition was observed. Nevertheless as seen in Figure 2, there was a promising finding that at a 0.312 microgram antibiotic equivalent, the inhibition of bacterial growth mirrored that of antibiotic alone.

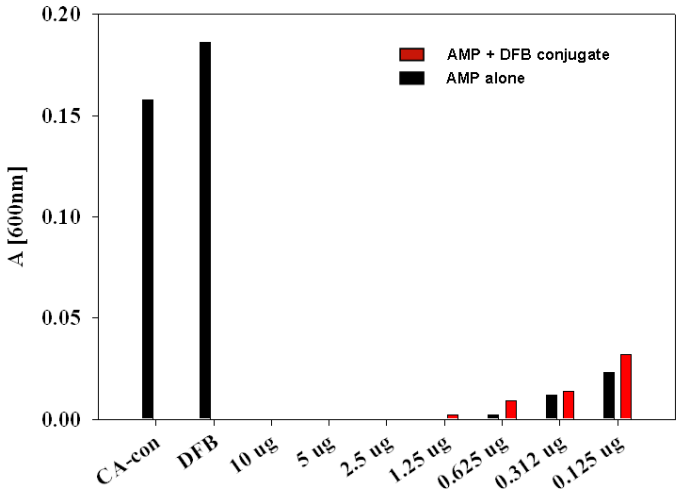


*Figure 2. B. anthracis was grown in CA incomplete media. Absorbance at 600 nM indicating kive cells was measured for control (media alone), DFB (siderophore alone) and varying concentrations of ampicillin and estimated concentrations of DFB-Ampicillin conjugate. Both treatments appear to inhibit bacterial growth effectively.*

This result has been viewed in the context that we still do not have a means to accurately quantify total conjugate amount. Thus the amount stated here is a close estimate and allays any fear we originally had that the conjugation process may affect the efficacy of antibiotic. These results set the stage for future studies using a variety of siderophore and antibiotic combinations to determine the possibility of generating a compound that could be universally applied.

The results of proteomic examination to understand cell surface proteins have identified several proteins that are produced by the bacteria in low iron growth conditions. Our assumption is that these proteins play an important role in the bacterial response to these conditions. Our goal in future studies will be to examine these results from a structural perspective in order to understand whether they may play a role in uptake of the complexes we generate. In addition, we will propose the design of targeted approaches to tease out only transport related proteins.

In conclusion, significant effort was made in this project to lay the framework for long-term antibiotic development. The progress made here provides much needed preliminary data that we need to design appropriate larger and longer term investigations, which we will propose to other agencies.

## References

1. Koppisch, Andrew T., Cindy C. Browder, Amanda L. Moe, Jacob T. Shelley, Blaine. A. Kinkel, Larry E. Hersman, S. Iyer, and Christy E. Ruggiero. Petrobactin is the primary siderophore synthesized by Bacillus anthracis str. Sterne under conditions of iron starvation.. 2005. *BioMetals.* **18**: 577.

2. Koppisch, Andrew T., Suraj S. Dhungana, Karen K. Hill, Hakim H. Boukhalfa, Henry S. Heine, Leslie A. Colip, Raymond B. Romero, Yulin Y. Shou, Lawrence O. Ticknor, Babetta L. Marrone, Larry E. Hersman, Srinivas S. Iyer, and Christy E. Ruggiero. Petrobactin is produced by both pathogenic and non-pathogenic isolates of the Bacillus cereus group of bacteria.. 2008. *Biometals.* **21**: 581.

## Publications

Ganguly, K., A. T. Koppisch, C. E. Ruggiero, and S. Iyer. Siderophore-antibiotic conjugates: promising antimicrobials. Presented at *The Fourth International Nanomedicine and Drug Delivery Symposium* . (Omaha NE, Oct 8-10.06).

Ganguly, K., M. Ollivault-Shiflett, R. Michalczyk, C. Ruggerio, A. T. Koppisch, T. Sanchez, P. Silks, R. Iyer, and S. Iyer. Strategies for targeting therapeutics to infectious agents. Presented at *Bio-Security Science Workshop sponsored by the LANL Center for Bio-Security Science (CBSS).* (Los Alamos, NM, December 13-14' 07).

# Trapping Rare Culture Mutations for Bioweapon Attribution and Forensics

*John Martin Dunbar*

20061517ER


## Abstract

This high-risk, 1.7 year (5/2006 - 2/2008) project aimed to reproduce and improve a facile technology for detection of spontaneous mutations in cell cultures. Such a technology would be transformative for the biotechnology sector. Applications include genetic screening in public health, engineering organisms for energy production, and microbial forensics. For biothreat reduction, the technology would fill a significant gap by enabling "barcoding" of biological cultures such that every batch could be uniquely identified.

Our central approach focused on establishing a published in vitro assay using the MutS protein for mutation detection. The MutS protein is a natural detector of DNA mutations in cells. The central challenge of this project was to reproduce performance described in a remarkable 2004 research report from China. The first year of the project was devoted to establishing the assay system. We abandoned plans to improve the system during the second year, as the Chinese results were not reproducible, nor ultimately credible.

We redirected our focus to a) improve quantification of MutS-DNA binding in order to assess the general feasibility of mutation detection and b) evaluating other possible mutation detection strategies. We concluded that a MutS-based technology for general detection of mutations is not feasible; this conclusion is bolstered by recent discussions with 2 companies that separately attempted to develop similar MutS-based technology. We usefully narrowed the scope of possibilities for general mutation detection and are attempting to pursue two other detection strategies through other agencies.


## Background and Research Objectives

Detecting mutations is a cornerstone of modern biology and bioforensics. As a population of cells grows, mutations arise naturally or through artificial induction. The most important question in countless medical, biotechnology, and forensics applications is where do the mutations occur? Identifying mutations that perturb biological systems illuminates how the systems function. More generally, mutations provide genetic signatures useful for bioforensics.

To discover where mutations occur, the most effective technology is DNA sequencing. Unfortunately, sequencing remains expensive and can only detect the numerically dominant genotype. For many applications, the mutations of greatest interest are "rare". Developing technology for general detection of "rare" mutations has been a biotechnology goal for over a decade [1]. However, the challenge of fishing mutated DNA from a large sea of normal DNA continues to be a technology gap.

Detecting rare, spontaneous mutations in bacterial or viral cultures for forensics is particularly challenging. Consider a typical 1 milliliter bacterial culture grown overnight to a density of $10^7$ cells/ml. With a standard mutation rate, more than $10^5$ mutants are expected to exist, but the parental strain (the dominant genotype) outnumbers mutants by at least 1000:1 (Figure 1). This high ratio of normal DNA to mutant DNA increases the difficulty of detecting the mutations.

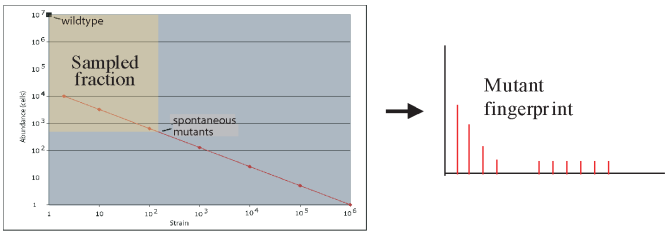


*Figure 1. Idealized ranked abundance distribution of mutants expected in a 24 hour bacterial culture. The parental strain is ranked 1, and all mutants arising by point mutation are ranked 2 to 10^5. Summing the abundance of every strain in the sample provides the total number of cells/ml. The point mutation frequency is assumed to be about 10^-9 bp/generation. The most abundant mutations in a sample provide a unique fingerprint, or barcode, of a culture. Culture barcodes can be used for sample matching and, in the nonproliferation arena, tracking "sublots" of material that is distributed between labs from a larger batches of parent material.*

If rare mutations in a culture could be detected, they would provide a genetic barcode of the culture. The relative abundance of mutants in a culture reflects the order in which mutations arise. Because mutation is a stochastic process, the order in which mutations arise differs every time a population of cells is grown. Therefore, a unique barcode is created in every batch of cells. Furthermore, the barcode evolves as a culture grows. Barcode evolution occurs because of natural selection. Beneficial mutations will disproportionately increase in abundance during culture growth. Identifying beneficial mutations can provide clues about how a culture was produced. Thus, an effective mutation detection technology would provide valuable forensic information that can be used for applications in nonproliferation and attribution.

A 2004 Chinese research report [2] indicated feasibility of a facile technology for detection of rare mutations in bacterial genomes. Spurred by the report, this project focused on two objectives.

1. Establish a published technology at LANL for detection of rare mutations.
2. Improve detection sensitivity, if possible, to enable batch typing of bacterial and viral cultures.

## Importance to LANL's Science and Technology Base and National R & D Needs

A facile technology to detect numerically rare mutations in cell cultures would transform LANL's experimental biology capabilities and would advance the biothreat reduction mission. Mutational analysis is a cornerstone of modern biology. Biological systems either improve or become defective (i.e. lose function) as a result of mutation. The positive and negative perturbations caused by mutations inform our understanding of how biological systems work. Consequently, development of techniques to mutate biological systems in ways that are amenable to subsequent characterization has been central to biological research for the past 70 years but has only succeeded for a few model organisms. A facile technology for genome-wide detection of mutations would enable easy characterization of mutations in any organism, and thus would have broad impact.

## Scientific Approach and Accomplishments

Our initial approach focused on reproducing a published technology for detection of rare mutations in bacterial cultures. In 2004, a Chinese research group described an *in vitro* method that enabled detection of 2 point mutations responsible for antibiotic resistance in a pathogenic strain of *Pseudomonas aeruginosa* [2]. This report was exceptional and unique in reporting successful scanning for point mutations throughout a bacterial genome.

The Chinese method involved creation of heteroduplexes (a double-stranded DNA molecule containing a mismatch) and fishing out the heteroduplexes with a thermostable version of the MutS protein. Heteroduplexes are created by melting a pool of double stranded DNA and then cooling the DNA to permit re-anneal. During re-annealing, some single stranded DNA containing a mutation inevitably anneals with complementary DNA that does not contain a mutation. This creates a double stranded DNA molecule containing a mismatch and is referred to as a heteroduplex. DNA molecules that are perfectly matched are called homoduplexes.

Our key technical challenge in adapting the Chinese method for a bioforensics application was to demonstrate an additional 1000-fold increase in heteroduplex detection sensitivity. In the Chinese report, the ratio of homoduplex: heteroduplex was ~20,000:1. For an overnight bacterial culture containing spontaneous mutants, the ratio would be at least 20,000,000:1. With this ratio, clean separation of heteroduplex DNA from homoduplex DNA would be more challenging. It is generally believed that MutS binds with low affinity to homoduplex DNA and "slides" along the DNA scanning for mismatches. If mismatches exist, MutS stops at the mismatch site and forms hydrogen bonds with the mismatched nucleotides [5]. Clean extraction of heteroduplex DNA depends on efficiently removing the background of homoduplex DNA bound with low affinity to MutS. This problem is similar to the selection of a few useful antibodies in phage display libraries that typically contain a large background (e.g., $10^6$) of non-specific binders—an area of expertise for Dr. Peter Pavlik, a former LANL who was co-investigator and the primary technical expert for this project.

**Components for initial approach**

Our initial approach included the 3 components below, which were successfully completed over a 9-month period.

1. To enable careful, systematic studies of heteroduplex capture, we created a set of test DNAs for routine production of defined homoduplex: heteroduplex mixtures (ranging from 1:1 to 1,000,000:1 ratios). We chose a 400 bp fragment from a gene in E. coli. We created and confirmed 3 mutated fragments containing a point mutation in the middle of the fragment. With this collection of 4 *E. coli* fragments, we could

produce heteroduplexes representing every possible mismatch.

2. To enable heteroduplex capture, we constructed and purified 4 different versions of the thermostable MutS protein (NCBI D63810, TTHMUTS). The versions differed in length and were coupled to different C-terminal peptide tags that facilitate purification/immobilization. We placed the purification and immobilization tags on the C terminus such that the N-terminal DNA binding domain of the MutS protein would be oriented outwards, maximizing DNA capture.

3. We successfully purified all 4 versions of the MutS protein, but the full-length versions routinely precipitated from solution, presumably owing to tretramer formation. Truncation of the C terminus eliminates tetramer formation and has been shown in multiple reports to be irrelevant for DNA binding *in vitro*. We purified a truncated MutS to near homogeneity (Figure 2) and used it for most experiments. This version of the protein had a biotin tag enabling immobilization of the protein on different surfaces.

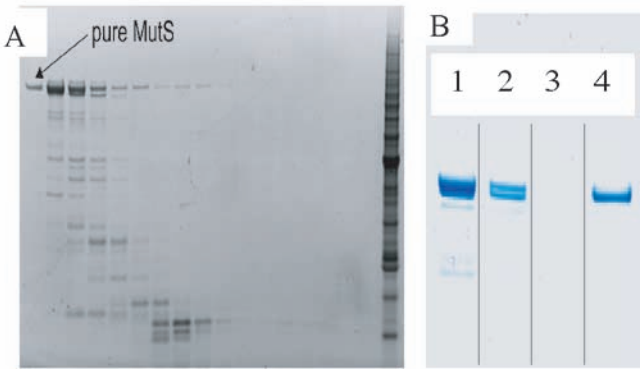


*Figure 2. MutS purification and immobilization. Panel A. Typical purification results. Panel B. Immobilization on magnetic beads. 1) MutS + Streptavidin Beads, 2) MutS that did not bind to the Beads, 3) beads washed to remove unbound MutS, 4) the amount of MutS captured by the beads.*

4. To enable quantification of heteroduplex recovery, we created real-time qPCR assays. In most of the anticipated capture experiments, the heteroduplex DNA would be too dilute to measure by any method except qPCR. Therefore, we created qPCR assays to detect the wildtype or the mutated base in each of the 4 E.coli gene fragments that we developed in component 1. These assays were rigorously tested and successfully validated.

After completing the components above, we began heteroduplex capture studies. We used a robotic system to automate the capture assays and to improve data quality.

**MutS capture assay**

We began with the simplest test: capture of pure heteroduplex compared to parallel capture of pure homoduplex. We created a relatively pure heteroduplex fraction by using a strand-directed enzymatic procedure to specifically degrade one strand of each duplex fragment (from component 1 above). The heterologous single stranded DNAs were mixed 1:1 to create heteroduplex. Based on the 2004 Chinese report, which described clean heteroduplex capture from a mix containing about 1 heteroduplex per 20,000 homoduplexes, we expected no residual homoduplex in our control assay. Yet, we routinely observed homoduplex capture. Moreover, homoduplex capture was nearly equal to heteoduplex capture.

Figure 3 shows typical results from a series of these experiments. The quantity of DNA was carefully monitored at every step. We included additional controls in many experiments to rule out other potential artifacts. In these experiments, we visualized the DNA directly instead of by qPCR because the quantity of DNA was sufficiently high. In Figure 3, a slight enrichment of heteroduplex is apparent relative to captured homoduplex, but the enrichment factor is small. We repeated this experiment a number of experiments with different permutations including use of different protein preps, wash conditions, an input DNA. *None of our experiments demonstrated significant discrimination of heteroduplex DNA over homoduplex DNA.*

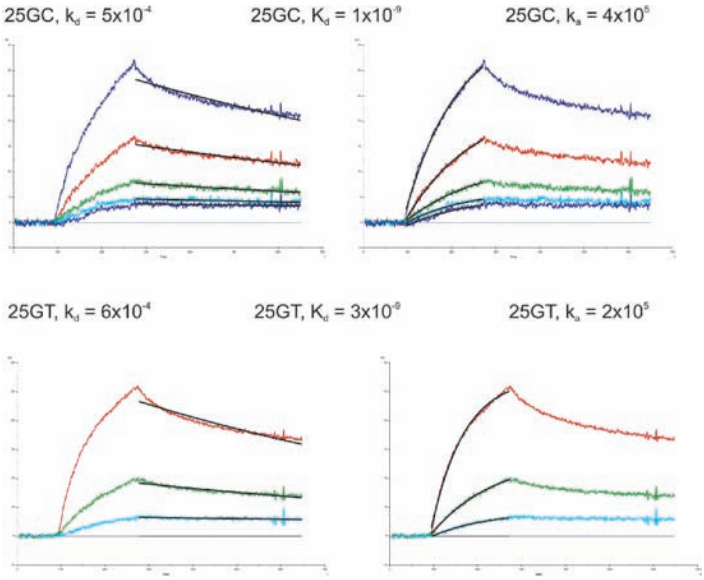


*Figure 3. Kinetic data for binding of 25bp hetero and homoduplexes to surface-immobilized Tth MutS. Different colors represent various concentrations of DNA used, while black lines are the best fits for the experimental data.*

**Kinetic analysis**

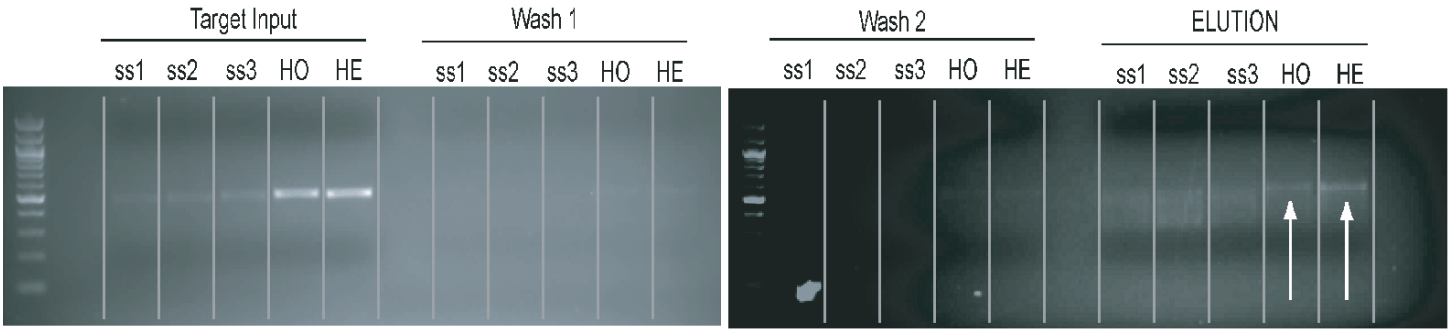


*Figure 4. Quantification of DNA capture and loss in 5 parallel MutS binding assays. The bands in each lane are DNA. ss1-3 = single stranded DNA. HO = homoduplex. HE = heteroduplex.*

Surface plasmon resonance (SPR) is a well-known analytical method for studying biomolecular interactions. We employed an SPR-based instrument to measure the kinetic parameters of MutS-DNA interactions. We also switched to using synthetic DNA oligos, 25nucleotides long, in order to eliminate any doubts about the double stranded DNAs used for capture. After immobilizing the MutS on the surface of the chip, we flowed 25bp DNA heteroduplexes and homoduplexes over the chip for MutS binding. Initial experiments did not show a significant difference in binding of MutS to hetero versus homoduplex.

We selected two particular DNA substrates and performed a number of additional studies. It has been reported numerous times that MutS binds G:T mismatches better than any other, so we compared the MutS binding to a 25bp DNA containing a G:T mismatch and another DNA containing a G:C base pair. As shown in Figure 4, both the association ($k_a$) and dissociation ($k_d$) rate constants, as well as the equilibrium binding constants ($K_d$) for the two substrates were very similar.

**Comparison with E.coli MutS**

For comparison, we bought a commercial stock (GeneCheck, Inc) of E.coli MutS immobilized on beads, and we assessed DNA binding using a flow-cytometry assay. For this study, we prepared 41bp-long synthetic DNAs with both ends blocked by the protein streptavidin. Enhanced discrimination of end-blocked hetero vs. homoduplex DNAs by MutS has been reported [6,7]. Our DNAs were fluorescently labeled so the amount of fluorescence per bead reflected the amount of DNA captured by MutS. Assays were performed in triplicate. Like our thermostable MutS, the *E. coli* MutS showed only a small enrichment of heteroduplex over homoduplex.

**Agreement with literature**

We carefully assessed our results relative to published studies. The small number of reports describing MutS activity *in vitro* have conflicting data, even when identical methods were employed. There is agreement that shorter DNA fragments (like we used) are preferred, but fragments of 16-6400bp have been used successfully as MutS substrates [8,9]. Many reports agree that the on-rate for MutS-DNA is independent of the type of DNA and instead the off-rates differ. Wide discrepancies occur in reported heteroduplex enrichment factors (Figure 5). The most frequently observed range of enrichment is 2 to 20-fold, similar to our results. This range is inadequate for genome-wide mutation scanning. Two reports of heteroduplex enrichment >1000-fold appear to be outliers. The 2004 Chinese report describing 20,000-fold enrichment is an extreme outlier, and nothing is apparent in the methodology that would account for exceptional performance. We conclude that the Chinese report is not credible. Based on our observations, MutS is untenable as a core platform for genome-wide mutation detection. Personal communications from the technical representatives at the companies GeneCheck and CodonDevices, which have attempted to exploit MutS for mutation detection, support our conclusion. The consensus is that MutS is not robust for *in vitro* mutation detection.

**Other approaches to culture barcoding**

We experimentally tested a culture-based approach to barcode bacterial cultures. This approach used negative selection to eliminate dominant genotypes from a culture. Ideally, a handful of resistant mutants would remain and could be characterized to create a barcode. This approach as been used routinely to obtain spontaneous antibiotic resistant mutants. We attempted to find conditions for negative selection that would act on a larger number of genetic loci than antibiotics do, providing a more robust barcode. We tested conditions including extremes of pH,

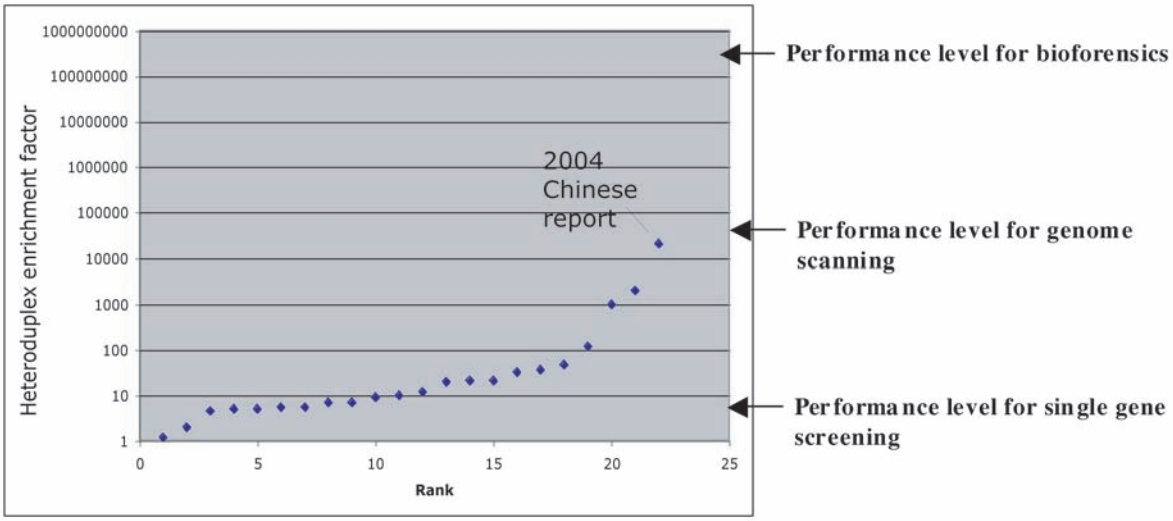


*Figure 5. Heteroduplex enrichment factors in published studies [2, 5-20] of MutS in vitro mutation detection.*

salt, detergent, alcohol, osmolarity, and nitrate concentrations. This approach was unsuccessful. Cultures responded either in a binary fashion (either lack of inhibition or complete inhibition), or showed promising responses that were difficult to reproduce in independent trials.

**Accomplishments**

1. We successfully assessed two strategies for bioforensics mutation detection (MutS capture vs selective culturing). We narrowed the scope of possibilities for strategies to detect rare mutations. Results from this project will improve proposals to external agencies by providing preliminary data and by focus effort on 2 remaining conceptual approaches for detection of rare mutations.

2. This project facilitated retention of 1 staff scientist (the PI) who rejected an external job offer in order to pursue this project.

3. This project enabled a strategic hire / postdoc conversion. B division managers selected Momo Vuyisich, a postdoc in 2007, as a strategic hire. His expertise was an ideal match for this project. He began working on this project in its 12$^{th}$ month as part of a strategic hiring plan. Ten months after Momo's conversion to staff, he succeeded in landing a ~1M external grant to develop assays for detection of genetic variation in biothreat agents.

## References


1. Taylor, G. R., and J. Deeble. Enzymatic methods for mutation scanning. 1999. *Genetic Analysis.* **14**: 181.

2. Wang, J., and J. Liu. Directly fishing out subtle mutations in genomic DNA with histidine-tagged Thermus thermophilus MutS. 2004. *Mutation Research.* **547**: 41.

3. Natrajan, G., M. H. Lamers, J. H. Enzlin, H. H. K. Winterwep, A. Perrakis, and T. K. Sixma. Structures of Escherichia coli DNA mismatch repair enzyme MutS in complex with different mismatches: common recognition mode for diverse substrates.. 2003. *Nucleic Acids Research.* **31**: 4814.

4. Blackwell, L. J., K. P. Bjornson, D. J. Allen, and P. Modrich. Distinct MutS DNA-binding modes that are differentially modulated by ATP binding and hydrolysis. 2001. *Journal of Biological Chemistry.* **276**: 34339.

5. Carr, P. A., J. S. Park, Y. Lee, T. Yu, S. Zhang, and J. M. Jacobsen. Protein-mediated error correction for de novo DNA synthesis. 2004. *Nucleic Acids Research.* **32**: e162.

6. Allen, D. J.. MutS mediates heteroduplex loop formation by a translocation mechanism. 1997. *EMBO Journal.* **16**: 4467.

7. Takamatsu, S., R. Kato, and S. Kuramitsu. Mismatch DNA recognition protein from an extremely thermophilic bacterium,Thermus thermophilus HB8. 1996. *Nucleic Acids Research.* **24**: 640.

8. Schofield, J. J., S. Nayak, T. H. Scott, C. Du, and P. Hsieh. Interaction of Escherichia coli MutS and MutL at a DNA mismatch. 2001. *Journal of Biological Chemistry.* **276**: 28291.

9. Tachiki, H., R. Kato, and S. Kuramitsu. DNA binding and protein-protein interaction sites in MutS, a mismatched DNA recognition protein from Thermus thermophilus HB8. 2000. *Journal of Biological Chemistry.* **275**: 40703.

10. Bi, L. J., Y. F. Zhou, X. E. Zhang, J. Y. Deng, Z. P. Zheng, B. Xie, and C. G. Zhang. A MutS-based protein chip for detection of DNA mutations. 2003. *Analytical chemistry.* **75**: 4113.

11. Biswas, I., and P. Hsieh. Identification and characterization of a thermostable MutS homolog from Thermus aquaticus. 1996. *Journal of Biological Chemistry.* **271**: 5040.

12. Bjornson, K. P., J. Blackwell, H. Sage, C. Baitinger, D. Allen, and P. Modrich. Assembly and molecular activities of the MutS tetramer. 2003. *Journal of Biological Chemistry.* **278**: 34667.

13. Jiricny, J., S. Su, S. G. Wood, and P. Modrich. Mismatch-containing oligonucleotide duplexes bound by theE. coli mutS-encoded protein. 1988. *Nucleic Acids Research.* **16**: 7843.

14. Lebbink, J. H., D. Georgijevic, G. Natrajan, A. Fish, H. H. Winterwerp, T. K. Sixma, and N. D. Wind. Dual role of MutS glutamate 38 in DNA mismatch discrimination and in the authorization of repair. 2006. *EMBO Journal.* **25**: 409.

15. Sachadyn, P., A. Stanislawska, and J. Kur. One tube mutation detection using sensitive fluorescent dyeing of MutS protected DNA. 2000. *Nucleic Acids Research.* **28**: e36.

16. Schofield, M. J., F. E. Brownewell, S. Nayak, C. Du, E. T. Kool, and P. Hsieh. The Phe-X-Glu DNA Binding Motif of MutS. 2001. *Journal of Biological Chemistry.* **276**: 45505.

17. Selmane, T., M. J. Schofield, S. Nayak, C. Du, and P. Hsieh. Formation of a DNA mismatch repair complex mediated by ATP. 2003. *Journal of Molecular Biology.* **334**: 949.

18. Stanislawska-Sachadyn, A., P. Sachadyn, R. Jedrzejczak, and J. Kur. Construction and purification of His6-Thermus thermophilus MutS protein. Protein expression and purification. 2003. *2003.* **28**: 69.

19. Wagner, R., P. Debbie, and M. Radman. Mutation detection using immobilized mismatch binding protein (MutS). 1995. *Nucleic Acids Research.* **23**: 3944.

20. Whitehouse, A., J. Deeble, R. Parmar, G. R. Taylor, A. F. Markham, and D. M. Meredith. Analysis of the mismatch and insertion/deletion binding properties of Thermus thermophilus, HB8, MutS. 1997. *Biochemical and Biophysical Research Communication.* **233**: 834–837.

# Experimentally Constraining Climate Forcing by Black Carbon Deposition on Snow

*Manvendra Krishna Dubey*

20080766ER


## Abstract

Los Alamos deployed the world's first 3-laser photoacoustic instrument on an aircraft to measure the optical properties of aerosol pollution in the atmosphere over the Arctic in spring 2008. We measured very dark, soot and organic aerosols that have a warming effect on climate and not the standard cooling effect that is associated with sulfate aerosols that have a cooling effect. Real time satellite data assimilated transport models indicate that this pollution was imported from Chinese dust storms and Siberian fires as well as from Eurasian energy sectors. Our wavelength dependent optical properties are used to diagnose the soot, dust, sulfate and organic components of this complex soup of pollutants. We use our optical observations to estimate a direct radiative forcing by pollution of the order of 10 to 30 of W $m^{-2}$. This forcing by aerosols is much larger than that by greenhouse gases. Our results underscore the need to accurately treat long-range pollution transport in models to simulate the observed rapid melting of the Arctic ice sheet.


## Background and Research Objectives

The Arctic is a beacon of global change. Recent observational trends show a rapid melting of the Arctic ice sheets, with the possibility of an ice-free Arctic within our lifetime. This would abruptly tip our planet to a new climate state with extreme impacts, underscoring the urgency of the problem. The Arctic has warmed twice as fast as the global mean in the last century, and the anthropogenic greenhouse gas forcing only accounts for about half of the observed Arctic warming. The Arctic vortex serves as an atmospheric receptor of air pollution from northern mid-latitude continental areas, as manifested by the thick aerosol layers. This Arctic Haze is a regular and sustained regional winter and springtime feature. Emission sources that contribute to it include anthropogenic black carbon (BC) and sulfate, smoke from massive boreal fires and dust from desert regions. These regional haze perturbations trigger unique regional responses, such the darkening of ice by deposition of BC, which promotes the melting of ice sheets. Recent climate simulations suggest that regional Arctic pollution is responsible for half of the observed Arctic warming, with ice darkening by BC contributing 30%. However, there are substantial uncertainties in our ability to quantify and predict these regional Arctic forcing and impacts. To better quantify the role of aerosols pollution (warming or cooling?) in Arctic warming we performed airborne measurements of aerosol absorption and scattering using LANL's state of the art 3-laser photo-acoustic spectrometer during the month of April 2008.

## Importance to LANL's Science and Technology Base and National R & D Needs

Achieving energy security and ensuring the sustainability of the earth system is an emerging mission at LANL. Focusing on Arctic change is appropriate since it is the canary for the climate-change coalmine, where the first signals are emerging and the impacts are expected to be most dramatic.

## Scientific Approach and Accomplishments

Los Alamos National Laboratory deployed the world's first 3-laser photoacoustic and nephelometer instrument on a Canadian Convair-580 aircraft in April 2008. Our instrument measured aerosol absorption, scattering and single scatter albedo of aerosol pollution at 405, 532, and 781 nm , which span the solar spectrum. The single scatter albedo is the ratio of the scattering to the sum of scattering and absorption and determines how light or dark the aerosols are, which in turn determines if they cool or warm the climate. For example pure soot is dark with a SSA of about 0.3, thus warming climate while sulfate aerosols are highly scattering

with a SSA of close to 1, thus cooling climate. There were 42 complementary measurements of cloud microphysics, aerosol chemistry, and ice composition. On numerous flights we intercepted and interrogated pervasive pollution layers above Alaska. The absorption and scattering signals occurred in layers from 1 to 6 km above the surface and were as large as 30 to 200 Mm $^{-1}$ (Figure 1) .

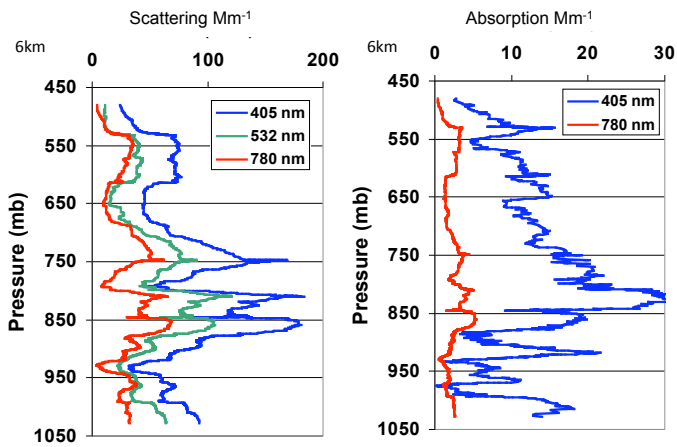


*Figure 1. Vertical profiles of aerosol scattering (left) and absorption (right) measured by our airborne 3 laser photoacoustic instrument at 405 (blue), 532 (green) and 781 nm (red) above Alaska in April 2008. Note the dark absorbing layers on the right that are from soot and organic aerosols that cause warming, which could be contributing to the melting the Arctic ice.*

These large values are typical of polluted urban environments, and our data provides evidence of this widespread pollution over the Arctic in early spring. Alternating light and dark aerosol layers with single scatter albedo ranging from 0.7 to 0.95 were evident, and they extended over large regions. Real time satellite data assimilated transport models indicate that this pollution was imported from Chinese dust storms and Siberian fires as well as Eurasian sulfate. Our wavelength dependent optical properties are used to diagnose the soot, dust, sulfate, and organic components of this complex soup of pollutants. We are testing the fidelity of our diagnostics by analyzing chemical compositions from a single particle laser ablation spectrometer instrument developed by Pacific Northwest National Laboratory. Our optical observations imply a direct radiative forcing by aerosol pollution of the order of 10 to 30 W m $^{-2}$ for this region (Figure 2). This is much larger than the greenhouse forcing and needs to be considered to accurately simulate the observed rapid melting of the Arctic ice sheet. Our new aerosol process level findings are now being incorporated in next generation climate models to better predict the future impacts of energy policies on our earth system.

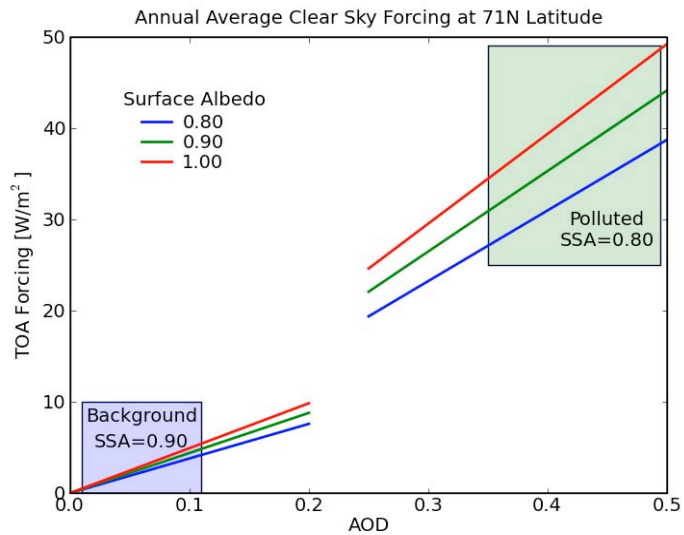


*Figure 2. Top of the atmopshere radiative forcing (warming effect) as a function of aerosol optical depth (AOD, column attenuation of sunlight at surface) above Alaska. Our results constrain the radiative forcing by aerosols to be of order 10s of W/m2 on annual average using our measured values (polluted box). This regional forcing by Arctic Haze is much greater than the global average forcing by anthropogenic greenhouse gases.*

## Publications

Dubey, M. K., and C. Mazzoleni. The Indirect and Semidirect Field Campaign over Alaska in 2008. Invited presentation at *Cloud Modeling for Climate Workshop.* (Toulouse, France, 2-4 June 2008).

# Modeling Influenza Infection and the Early Immune Response

*Alan S Perelson*

20080771ER

## Abstract

Upon their entry, respiratory pathogens such as influenza A virus and *Streptococcus pneumoniae* target epithelial cells (EC) in the lung. However, it is not known how dendritic cells (DC), which are some of the earliest players in the immune response to infection, play a role in countering infection. The goal of this pilot project is to develop a cell model of EC and DC (EC:DC) that can be used to study infection by influenza A virus and *Streptococcus pneumoniae* with emphasis on examining (i) the induction of host factors that are specifically induced upon infection of EC only in the presence of DC and (ii) the effect of DC on the expression of viral factors that support viral growth and infection. It is encouraging to note that preliminary studies demonstrate the feasibility of a (EC: DC) model for influenza infection. Detailed measurements using this cellular system open the possibility of experiment-based deterministic and stochastic models for describing the balance between infection as determined by viral growth and the immune response as determined by the expression of key host factors.

## Background and Research Objectives

Respiratory pathogens pose great threats to public health and national security. The 2001 attack by deadly inhalation anthrax caused terror throughout the nation and tremendous economic damage. Early detection of infection and design of countermeasures require a thorough understanding of the events in the early immune response that determine whether the pathogen successfully infects a person or is eliminated. Experiment based modeling provides a framework for describing the balance between viral growth and clearance by early immune response.

## Importance to LANL's Science and Technology Base and National R & D Needs

A multidisciplinary team of experimentalists and theoreticians has been assembled to model a very important yet unexplained aspect of infection, i.e. the balance between successful pathogen growth and clearance, which is determined by the failure or success of the early immune response. This balance is determined by the interplay of key pathogen virulence factors and host response markers involved in early immune defense. Success of this work lies in our ability to quantitatively make these measurements, which will position LANL to develop a more comprehensive model of respiratory infection that rely on more exhaustive measurements of extracellular protein levels, intracellular mRNA based on a reliable cellular system of infection.

## Scientific Approach and Accomplishments

In order to quantitatively characterize the balance between viral growth and host defense, we have designed an experimental system of infection comprised of small airway epithelial cells (SAEC) and immune dendritic cells (DC) that are recruited to the sites of infection. The roles of DCs however, have previously been ignored in cell models of infection. Using this cell model, we have determined the expression of (i) key viral factors such as viral nuclear protein (NP), viral matrix protein (M1), and influenza A nonstructural protein 1 (NS1) that are critical to viral growth and (ii) host cytokines and chemokines that are critical to early immune defense.

### Cell Model for Infection

In preliminary experiments, we have cultured primary human SAECs in the presence or absence of DCs at a ratio of 10:1. Cells were infected with H1N1 influenza A virus (IAV, A/BJ/26/95) at multiplicity of infection (MOI) of 2 for 0, 6 hrs (representing beginning of rep-

lication) and 24 hrs (where viral markers are detectable). Cell free supernatants were then tested for release of cytokines that are implicated in host defense to influenza A virus.

### Quantitative Measurements of Secreted Factors

In preliminary experiments, no TNFα, MIP1α, and MIP1β and very low levels of IFNα and β were detectable in the supernatants up to 24 hours (data not shown). Significantly, 6 hours post infection, influenza A virus inhibited IL6 release from epithelial cells, which could be restored by the presence of DCs (Figure 1). These results suggest that the interplay between SAEC and DCs could modulate the host immune response to IAV.

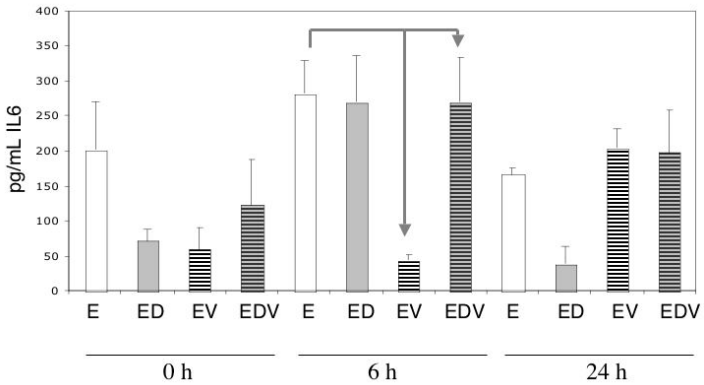


*Figure 1. Inhibition of IL6 release from influenza infected epithelial cells is restored by presence of dendritic cells at 6 h (ELISA data).*

### Quantitative Measurements of Gene Expression

We have performed real-time PCR analysis for viral RNA of NS1, NP, M1 and host response genes IL6, IL8, IL10, IL18, TNFα, IFNα, IFNβ, MIP1α and MIP1β. Figure 2 shows the fold change in expression of the viral genes that code for NP, M1 and NS1. At 6h, most viral gene expression is lower in host cells in the presence of DCs. DCs also impact the gene expression of host defense molecules as seen in Figure 3. In co-culture, MIP1α and β expression are induced. Similar induction occurs in epithelial cells alone in response to influenza A. DCs are able to induce IL8, IL10, MIP1α and β gene expression at 6 hours post infection. DCs can also inhibit influenza A virus mediated TNF and IFNβ expression at 6 and 24 hours respectively (Figure 4). While these results are reporters of host response, they point to a need for mechanistic studies examining these responses.

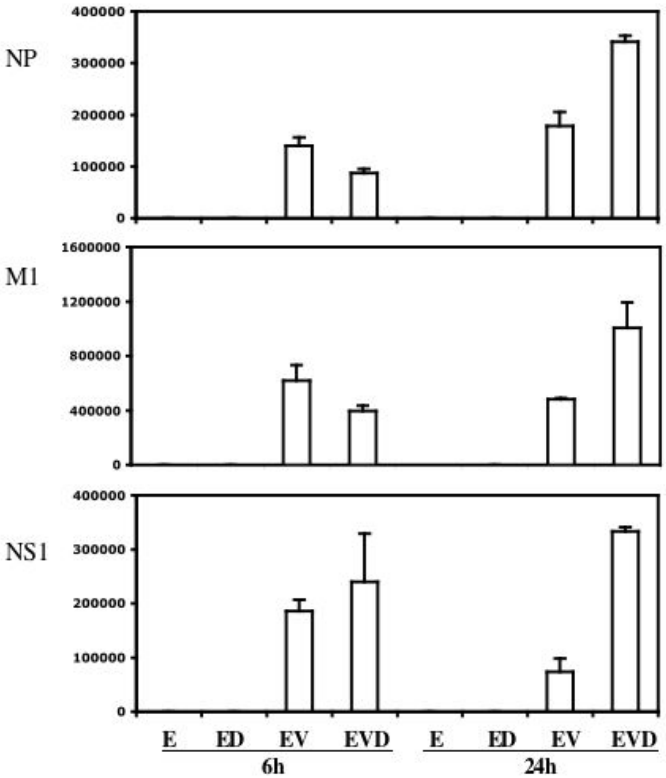


*Figure 2. Gene expression of viral markers is altered in the presence of dendritic cells (RT-PCR analyses).*

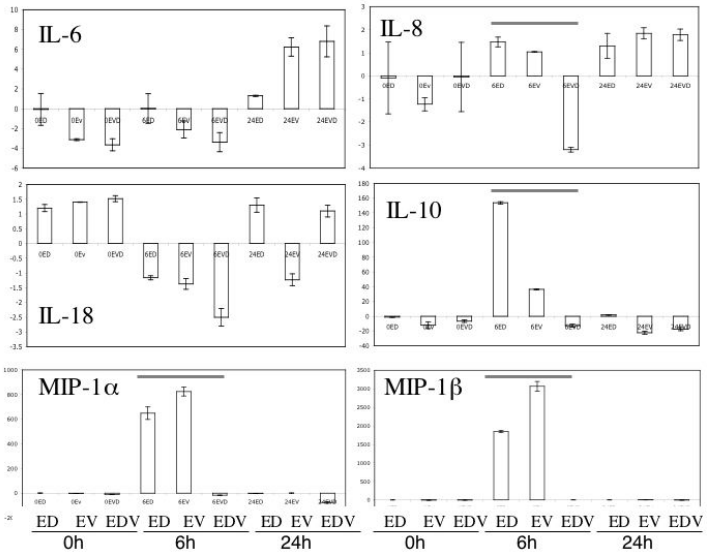


*Figure 3. DCs impact gene expression of host defense molecules (RT-PCR analyses).*

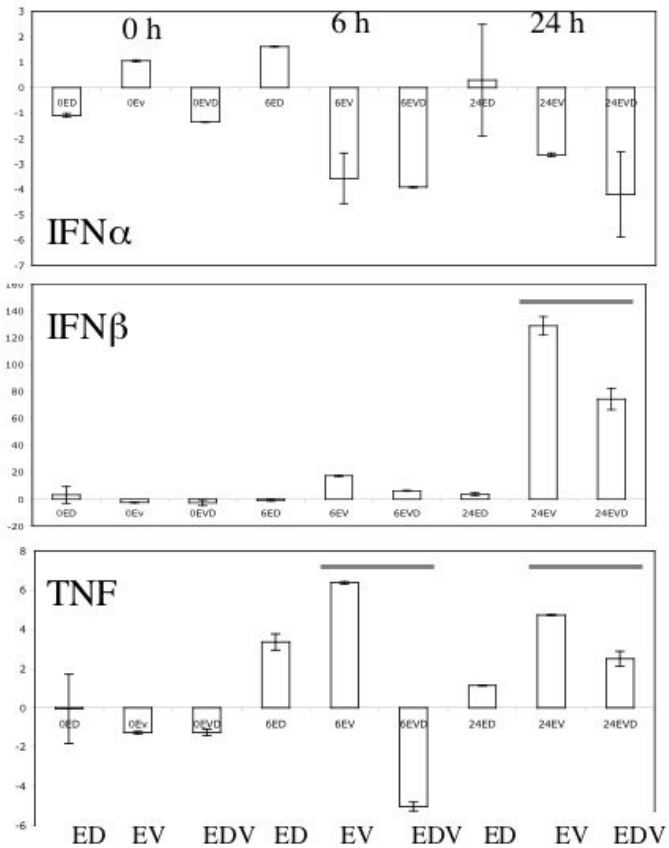


*Figure 4. DC play a role in inhibition of influenza mediated TNF and IFNb expression at 6 and 24 h respectively (RT-PCR).*

**Measurements of Surface Expression and Intracellular Protein**

We have performed flow cytometric analyses for three cell surface host cytokine receptors: IFN$\alpha/\beta$ receptor, TNF receptor and the IL6 receptor (data not shown). These receptors are upregulated in response to release of cognate cytokines. Interestingly, while no marked changes in surface expression of IFN $\alpha/\beta$ receptor are observed after 6-24 h of infection, surface expression of the IL6 receptor is slightly upregulated at 24 hours only in cultures containing DC's. Follow up experiments validating this observation are on going.

Measurements of the levels of influenza protein NS1 were made from these cells at 24 h (Figure 5). Contrary to gene expression data of NS1 (Figure 3), DC containing samples show inhibited levels of NS1 protein expression. Whether this is a consequence of inhibition of protein translation remains to be determined. Furthermore, these results remain to be validated by western blotting and in replicate experiments.

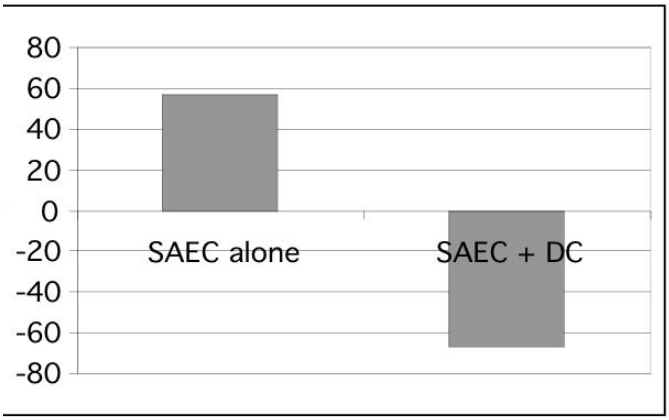


*Figure 5. Intracellular protein levels of NS1, meaured by flow cytometry, are inhibited in the presence of DCs.*

**Mathematical modeling of early infection**

When influenza is first encountered there is the possibility that the infection is cleared due to random events rather than an explicit host defense. For example, if only one or a few infectious viral particles are inhaled by a host, these particles could be cleared from the body before they infect any cells. The same type of event could occur in cell culture, as we have previously shown that influenza A virus in culture loses infectivity with a half-life of about 6.6 hours [1]. Thus if small amounts of virus are used these virions could lose their infectivity before they infect a cell. Even if the input virus infects some cells, this infected cell might die before they release any virus. Thus, it is possible at low doses that infection simply dies out. Thus, to distinguish true host defense from random occurrences we have been building a stochastic simulation model of early infection. This model could have general applicability many infections and could help establish the threshold of infectious agents needed to random events in the establishment of infection. For example, after the anthrax attacks in Washington, DC there was great interest in determining the minimum number of bacteria needed to establish infection.

Our model considers target cells (i.e., EC), infected cells, and virions, which we denote T, I, and V, respectively. There are approximately $10^8$ epithelial cells in the upper airways of a human that could be the targets of infection. At the earliest times during infection, few of these will become infected and thus our model holds the target cell number constant. This is an approximation that can be relaxed in later work.

We let $n_v$ and $n_I$ represent the number of virions (virus particles) and infected cells respectively, kT is the rate at which virions infect target cells, c is the rate at which virions are cleared, is the average rate at which infected cells die and

N is the average number of virions produced by an infected cell. The model is described in the following table:

| Process | Change in $(n_v,n_I)$ | Rate |
|---|---|---|
| Infection of a cell by a virus | $(n_v,n_I)$ to $(n_v-1,n_I+1)$ | $kTn_v$ |
| Clearance of a virion | $(n_v,n_I)$ to $(n_v-1,n_I)$ | $cn_V$ |
| Production of a virion | $(n_v,n_I)$ to $(n_v+1,n_I)$ | $\delta Nn_I$ |
| Infected cell death | $(n_v,n_I)$ to $(n_v,n_I-1)$ | $\delta n_I$ |

A key dimensionless quantity is the reproductive ratio, $R_0$, which is approximately the number of new infected cells created by each infected cell. Deterministic models predict infection for $R_0>1$ and clearance (in which the infection dies out) for $R_0<1$, where the reproductive ratio is given by:

$$R_0 = NkT/(kT+c)$$

When the number of infectious virions and infected cells is very small, the certainty of the deterministic dynamics gives way to fluctuations and uncertainty. Thus stochastic clearance of the virus can occur when $R_0>1$.

From the model in Table 1 one can compute the probability, $\Pi$, that an infection that starts with $n_v(0)$ virus particles is totally cleared, i.e., leads to $n_v=0$ and $n_I=0$, when $R_0>1$. The formula we have derived for this is

$$\Pi=\rho^{n_v(0)}$$

where $\rho= 1- (R_0-1)/N$. This implies that the probability of infection is $1-\rho^{n_v(0)}$. To see the implications of this consider an example where $R_0=5$ and N=10. Then, $\rho=0.4$ and the probability of infection is 0.6, 0.84, 0.9898, and 0.9999 for $n_V(0)$= 1, 2, 5 and 10 respectively. Here we are assuming that all viral particles are infectious, so the value of N is rather small. An infected cell may produce thousands of viral particles but typically only a few of these are infectious. The calculation above shows that for these parameter values the probability of infection is essentially one when 10 or more infectious viral particles initiate the infection. Having a formula allows one to compute the probability of clearance for other parameter values. Clearly, when $R_0$ is larger than 5 it will be harder to clear the infection when the same number of virus particles initiate the infection. Further work will need to be done to understand the number of virus particles one might inhale when a person is in close contact with an infected person.

There are also a number of other things that we can calculate with our model that should be of interest to the biodefense community. For example, the model can be used to predict, given an initial infection with $n_v(0)$ virions, how long it will take for the number of virus particles to reach some threshold of detectability. All instruments and assays will only be able to detect that a person is infected if the number of virus particles is above some threshold. Given that threshold we could estimate a probability distribution of detecting that a person is infected. This should be important for early detection of infection. Similarly, the immune system will not detect that a person is infected until some other threshold of virus and/or infected cells is reached. As in the experiments described above, once dendritic cells enter the lung and interact with virus, various cytokines are secreted. These cytokines interact with other cells and generate the symptoms of influenza. Thus, another avenue of applicability is trying to predict when infection could be diagnosed via symptoms as a function of the number of virions that initiate infection and the number of dendritic cells that enter the lung.

**Summary**

We have established a human primary cell model consisting of epithelial cells, which are the targets of influenza infection, and dendritic cells, which are immune cells that are recruited to sites of infection in the lungs. We have made preliminary quantitative measurements on gene and protein levels of intracellular, secreted and surface expressed host defense cytokines, their receptors and specific influenza virulence factors such as NS1. Our preliminary data suggest a role for dendritic cells in host defense to influenza A virus infection. Furthermore, we have developed a mathematical model of early infection that provides insight into the probability of a person being successfully infected after inhaling a small number of infectious virus particles. Other applications of the model might be useful for the biodefense community. In addition, this pilot project has allowed us to establish an influenza work area, biosafety level two, in the Biosciences Division. Personnel have been trained in handling of influenza and approval has been obtained from the LANL Institutional Biosafety Committee for use of primary human cells and cell lines along with influenza A viruses (IBC99, submitted May 28, 2008, approved August 6, 2008).

Theoretical results of this project have been incorporated into an NIH proposal as preliminary work and a draft manuscript is in preparation. The work also resulted in a follow-up idea paper and “quad-chart” that has been discussed with DoD program managers.

## References

1. A.Beauchemin, C. A., J. J. McSharry, G. L. Drusano, J. T. Nguyen, G. T. Went, R. M. Ribeiro, and A. S. Perelson. Modeling amantadine treatment of influenza A virus in vitro.. 2008. *Journal of Theoretical Biology.* **254** (2): 439.

# Ultra Deep Sequencing of HIV Acute Infection Sample to Determine Nature of Transmitted Virus and Understand Immune Escape

*Bette Tina Marie Korber*

20080774ER

## Abstract

We initiated a project tailored to address one of the most pressing questions in HIV research while learning how to implement and move forward with cutting edge sequence technology; the progress we have made in the arena has enabled us to hit the ground running with a biosecurity HIV-TB DR proposal starting October 1, 2008. The open biological question we are in the process of resolving is whether or not a single virus is successfully transmitted and establishes transmission, or if multiple viruses are transmitted, with one competing most successfully and so dominating in acute viremia. This question bears on vaccine design, immune evasion, accrual of drug resistance at the population level, and basic viral biology. We completed the sequencing for a single patient over time, and have made progress on a second patient. In particular in the case of the first patient we have made significant progress with analysis. We have begun to develop error correction codes to experimental error in these experiments, and through detailed analysis of our initial dataset we have discovered that to optimize this procedure we need to go back to the raw data from the 454 sequencer. We are still in the process of sorting out the best statistical means for contending with error. We have also learned about the biology of infection and the progression of mutations in the first individual studied over time in very early infection; now with 1000 fold greater sensitivity than before, we have learned the a single strain establishes infection.

## Background and Research Objectives

During the course of infection, HIV evolves rapidly to evade ongoing immune responses, and to occupy new target cell populations, all the while maintaining viral fitness. Consequently, there can be over 10% variation between Envelope proteins within a single chronically individual. In contrast, in most new infections only a single, uniform viral population is observed. Most sexual encounters with an HIV infected individual do not result in transmission, so clearly there are natural barriers, leading to the hypothesis that certain phenotypic characteristics of the virus may be associated with successfully transmitted virus. If such characteristics could be defined, it may help us narrow the target for vaccine design. The NIH has invested in a very large multinational effort, called CHAVI (http://www.chavi.org/), to gather and characterize acutely infected patients samples to better understand the events surrounding HIV transmission and early infection. Bette Korber leads a small team in T-10 whose role in CHAVI is to provide analysis of the HIV sequence data collected in the project. Using traditional sequencing methods, our colleagues have explored HIV sequence diversity in acutely infected individuals. With these methods it is feasible to sequence roughly 50 HIV genes per sample, and our first two CHAVI papers are in press describing and modeling observed HIV variation in 102 acutely infected people. We are now beginning to analyze the impact of the initial immune response against the virus on viral evolution, and a number of samples taken serially over the first weeks to months of infection are currently being characterized. Sequences from the earliest samples initially exhibit a small number of scattered mutations relative to the sample consensus, consistent with a simple Poisson model of mutation under no selection. Then suddenly, about 2 months in, mutations can begin to appear in a very focused region of the virus, and the mutated viruses rapidly begins to replace the initial virus; as it turns out, such mutations are usually escape mutations that can mapped to CTL (cytotoxic T lymphocyte) epitopes. CTL epitopes are the small stretches of viral protein that are recognized by receptors on host immune cells, enabling them to specifically kill HIV infected cells. An example of this type of immune escape pattern is shown in the enclosed figure. Because of our analysis role in CHAVI, we have worked to help define and analyze these samples, and thus our CHAVI colleagues are willing to share these samples, (a very precious resource, as HIV acute infection cases are

very hard to come by), with us for further characterization. In return we offer a novel research capability to them to address our pressing question, through LANL's role in the Joint Genome Initiative (JGI, http://www.lanl.gov/orgs/b/b6/b6index.shtml), ultra-deep sequencing, as well as a theoretical team uniquely suited to rapidly analyze this the new kind of data.

Ultra-deep sequencing takes advantage of the same 454 sequencing methodology that has enabled JGI to very rapidly march through the complete sequences of many bacterial genomes. This experimental method has mainly been applied to assembling massive full length genomes, but it can alternatively be applied to sampling "deeply" (upwards of 100,000 sequences) from a single sample. Currently, only very short regions of interest of about 220 bases are feasible. The analysis challenges are daunting, including alignment issues with complex patterns of insertions and deletions, phylogeny, dealing with error, visualization methods, and statistical interpretation.

## Importance to LANL's Science and Technology Base and National R & D Needs

This work addresses the laboratory mission in Science Programs and relates to the Grand Challenges in Complex Systems Information Science and Technology. Its an investment in resources had could be part of the spectrum of capabilities in our new biosecurity facility. We are already expert in rapidly sequencing bacterial genomes with this methodology, but this will allow us to expand into the arena of amplicon sequencing, and new and critical application of these methods.

## Scientific Approach and Accomplishments

The Broad Institute sequencing facility at MIT, in collaboration with a group at Harvard, recently sequenced up to 130,000 HIV sequences per sample from four chronic patients, spanning a drug resistance mutation in the HIV V3 region. Not knowing quite where to begin with interpreting this mountain of sequences, they sent these sequences to the analysis team at LANL and asked if we could help. We made significant headway with a first available ultra-deep sequence set, and discovered two important things: first, over the short stretch analyzed (~40 amino acids) the diversity was immense, with over 1,000 variants in a single sample; second, the drug resistant forms were present in the pre-therapy samples, but in some cases at a very low frequency such that they would not have been detected using conventional strategies. These rare forms rapidly came to dominate later samples after selective pressure was applied through therapy. This work was initiated prior to the DR, but was brought to completion through the DR in its early months; it is currently under review at PLoS Genetics.

With the resources provided by this interim funding, we have been able to work closely with the JGI 454 sequencing team at Los Alamos and our collaborators at the University of Alabama, to develop a improved protocols for amplicon sequencing from the ground up, including exploring of strategies to increase experimental yield. The transitional funding also provided the resources to greatly improve our analysis strategies relative to our first study. We developed a suite of error correcting codes and applied to our first pass at a single patient, the acute infected patient SUMA from the University of Alabama cohort. Further error correcting codes are in progress. We have obtained ~500,000 sequences from SUMA, spanning three short regions of the genome, at 3 time points. Figure 1 illustrates the phylogenetic tree of the TAT gene fragment, Figure 2 of the REV gene fragment, and shows their evolution over time.

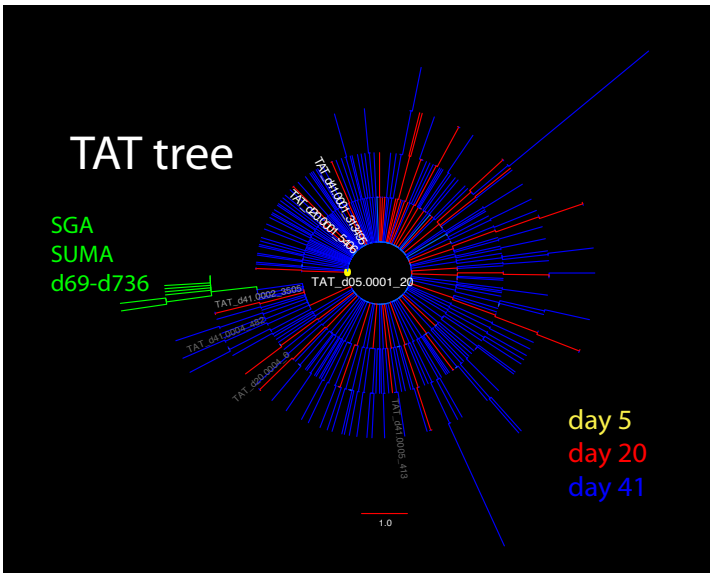


*Figure 1. Phylogenetic tree illustrating the evolution of the Tat gene fragment in early infection. Each unique form of the 454 sequences is represented by a colored line; yellow is the first time point, red and blue the next two time points. The length of the each unit line segment is indicative of 1 mutation in the fragment. Green lines represent sequences identified as immune escape forms isolated from later time points (day 69 through 736). Common sequences are named and marked by how many times there were found in a sample, following the underscore. The first time point only gave us 20 sequences, however the third time point gave ~~>300,000, and we in the process of working out what gave rise to such different yields.*

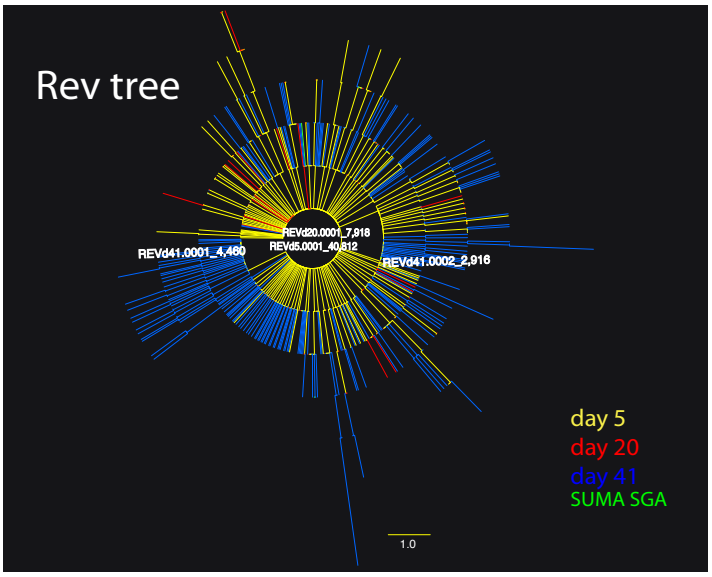


*Figure 2. Phylogenetic tree illustrating the evolution of the Rev gene fragment in early infection. See figure 1 for details.*

Modeling of the expected number of mutations that could accrue in early infection indicates that only a single virus was transmitted. We found evidence for selection earlier than previously thought, meaning an earlier initiation of the immune response than could be detected by conventional means. The earliest escape mutations were found at very low levels in the first sample, and later escape mutations were not present at all until later time points, suggesting base mutations rates may play a role in the order of immune escape, an idea we will follow up on. Trouble shooting these experiments has required us to use more experimental resources than anticipated; while our original plan was to sequence four individuals, we now hope to examine three for our first publication, and finishing this study as our first accomplishment under the new DR. Thus the work for two papers is underway, one will be our analysis protocol for amplicon sequencing of HIV and other variable pathogens, the other will be a biology paper about the nature of early HIV infection and immune escape.

# Climate Change Forecasts Using Ensemble Forecasting Games

*Marian Anghel*

20080779ER

## Abstract

One of the grand challenges facing the geosciences today is to provide accurate predictions of future climate changes along with quantifications of prediction uncertainties. Traditionally, the spread of results from an equally weighted ensemble of climate models was used as a subjective indicator of the range of uncertainty in climate forecasts [1]. To improve these forecasts, the variations in quality between models must be included.
Unfortunately, due to the complexity of the climate system the traditional approaches to addressing modeling uncertainties face conceptual difficulties that make them almost impossible to apply in practice. By contrast, in this project, we investigate an ensemble forecasting approach based on a game theoretical forecasting paradigm centered on the model of prediction with expert advice. Forecasting is defined as a repeated game played between the forecaster, advised by an ensemble of experts (climate models), and the environment, i.e. the climate, generating an observed outcome sequence. Unlike classical forecasting methods, this approach is devoid of any probabilistic assumptions about the climate system. Hence, it avoids the trap of making questionable and often unnecessary assumptions.

## Background and Research Objectives

Climate is defined as the mean physical state of the climatic system, which is composed of five intimately interconnected components: atmosphere, hydrosphere, cryosphere, lithosphere, and biosphere. Because future climate may be very different from the observational record, the primary tool for assessing climate changes are large computer models that attempt to accurately simulate the complex nonlinear and multi-scale interactions among the components of the climatic system. These coupled atmosphere-ocean general circulation models (AOGCMs) are driven by a number of forcing agents, including greenhouse gases produced by human activities, aerosols, changes in the sun's energy, or changes in land use. The process of tuning model parameters involves subjective judgment and is not guaranteed to identify the optimum location in the model parameter space. Typically, the future projections are based upon initial conditions extracted from the end of the simulations of the 20th century and upon a number of standard scenario simulations providing a range of plausible estimates for the future climate forcings.

Due to the complexity of the climate system the traditional Bayesian approach to ensemble forecasting faces conceptual difficulties that makes it almost impossible to apply in practice. By contrast, the paradigm of prediction with expert advice avoids these pitfalls while proposing to answer a different, but fundamental question: Given the observations of historical climate, and given the available climate models (experts), what combination of ensemble models has the best forecasting skill? Since the application of the paradigm of prediction with expert advice to the problem of climate change forecasting has never been attempted before, the research objectives set for this project are as follows:

1. Define simple nonlinear models that have similar behavior to the complex climate models of interest, and apply the proposed game theoretic techniques to forecast their evolution. The goal is to gain an understanding of the proposed prediction algorithm and its forecasting performance, and to compare this approach to more traditional model selection techniques.

2. Using the insights learned from forecasting the evolution of these simple models to build weighted forecasting ensembles using AOGCMs as experts. Leading modeling centers around the world that participate in the Program for Climate Model Diagnosis and Intercomparison (PCMDI) provides these AOGCMs. For this task, we will use the modeling outputs of this multi-model ensemble and the record of past climate observations in order to construct weighted forecasting ensembles for each global climate variable.

## Importance to LANL's Science and Technology Base and National R & D Needs

This project supports the DOE Office of Science mission in biological and environmental research by enhancing our ability to make the best possible estimates of climate change and its uncertainties based on past climate observations and available climate models.

Moreover, the research undertaken in this project is relevant to the Laboratory mission in Energy Security and the more specific Energy Security goal of mitigating the impacts of energy demand growth. The forecasting approach investigated in this project provides a methodology that will improve our ability to predict climate change impacts at global and regional scales and will provide decision makers with improved estimates of the quality of those projections.

Furthermore, the same ensemble approach can be used to determine the best model parameterization or, when alternative models or even modeling paradigms are available, the best multi-model description for generic complex systems. Relevant applications include infrastructure modeling, the estimation of accurate interatomic potentials for nonequilibrium molecular dynamics simulations, subgrid scale parameterization of turbulence, or multiscale materials modeling. In all these cases both structural and parametric uncertainty can be investigated using a grand ensemble (an ensemble of ensembles) in which, for each model structure (parameterization scheme), an ensemble of models can be generated to explore parametric uncertainty.

## Scientific Approach and Accomplishments

We will address the problem of predicting a sequence of future events based on a sequence of past observations. The forecasting methodology we propose to solve this classical sequential decision problem uses the paradigm of prediction with expert advice [3, 4]. Prediction with expert advice is based on the following protocol for sequential decision making [5]: the decision maker is a forecaster whose goal is to predict an unknown sequence describing thefuture evolution of a dynamical system. For climate, we can, for example, predict the evolution of various climate variables (surface air temperature, average ocean level, precipitation patterns, etc) . The forecaster computes his prediction in a sequential fashion, and his predictive performance is compared to that of a set of reference forecasters that we call experts. For climate predictions each expert is identified with a member of the multi-model ensemble (AOGCMs). More precisely, at each time step the forecaster has access to the set of expert predictions provided by each member of the multi-model ensemble. On the basis of the experts' predictions, the forecaster computes his own guess for the next outcome, which is a weighted average of the predictions provided by the experts. After the forecast is computed, the true outcome is revealed. The predictions of the forecaster and experts are scored using a nonnegative loss function. The loss can, for example, estimate the departure of the predicted climate variable from its observed value or from its average climate value. Based on the estimated losses the forecaster updates the weights on each expert by taking into account the forecasting skill of each expert. This forecasting skill is measured by the cumulative loss of the experts, which is computed by summing the expert losses up to this round of the game. The forecaster will increase the weights of the experts with small cumulative loss by choosing, for example, weights that are monotonically decreasing as a function of the expert's cumulative loss. In this way, the forecaster gives more weights to the experts that predict well, thus increasing his own forecasting skill as the game progresses.

We have applied this prediction paradigm to build forecasting ensembles for a simple, nonlinear, surrogate "climate" model and for a small ensemble of AOGCMs from the PCMDI ensemble.

We have devised a simple "climate" model which uses a Lorenz dynamical system driven by a periodic forcing term [6]. The parameters of the Lorenz system are chosen to guarantee the system's weak synchronization to the periodic forcing, and hence quasi-periodicity, thus allowing the definition of seasons, while the underlying motion still remains chaotic. Using this simple model we have used the three coordinates of the underling Lorenz model to define quasi-periodic climate variables and we have applied the paradigm of forecasting with expert advice for a wide range of scenarios and ensembles. It should be pointed out that would not have been possible had we only worked directly with the climate data and models available to us. The nonlinear evolution of this simple model, as shown in Figure 1, exhibits a similar behavior to the monthly evolution of the average surface temperature computed by an AOGCM.

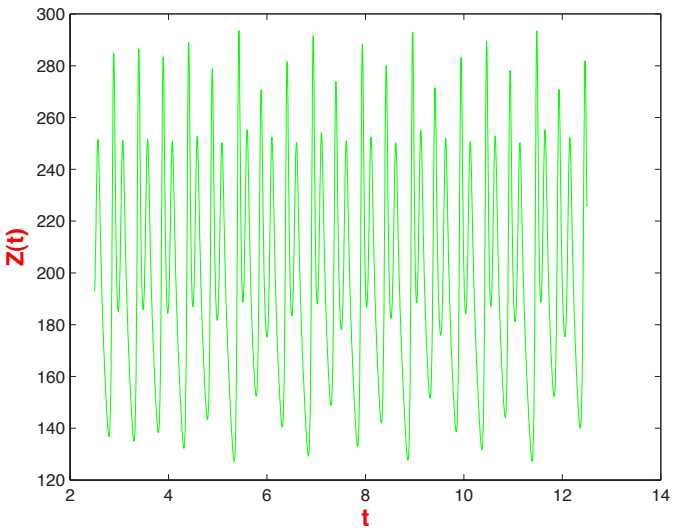


*Figure 1. The evolution of one coordinate of the driven Lorenz model. This is a quasi-periodic, chaotic system that offers a simple surrogate for more complex climate models. Indeed, this coordinate offers a good approximation to the nonlinear evolution of the surface air temperature shown in Figure 2.*

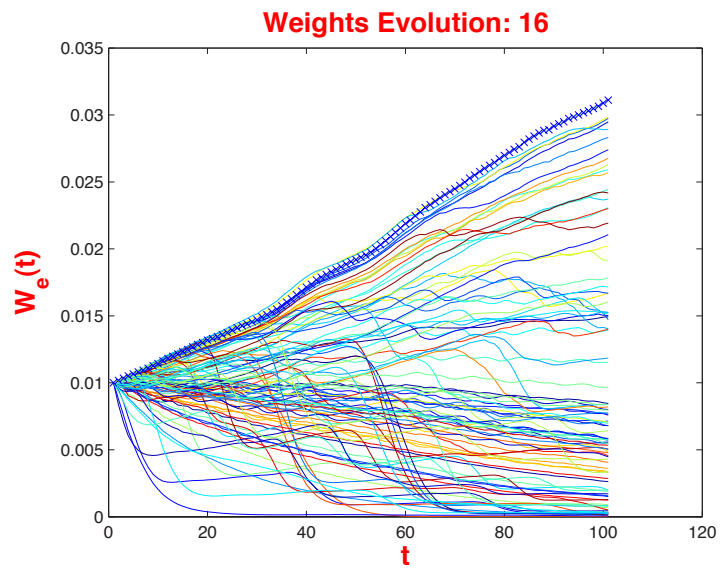


*Figure 2. Evolution of the ensemble weights during a forecasting game played every year during a one hundred year forecasting interval. The ensemble has one hundred members (experts) and the weights are equal at the beginning of the forecasting game. After playing the game for one hundred years, the spread in weights among the members of the ensemble is considerable. The best experts have considerably larger weights than the worst experts.*

Using this model, we have checked the influence of uncertainty in model parameters, initial conditions, or in the length of playing the forecasting game, on the forecasting skill of the ensemble. Our goal was to compare the forecasting performance of the weighted prediction algorithm with the forecasting performance of the equally weighted algorithm.

This approach has allowed us to infer the following insights. First, the weights of the experts evolve considerably during the forecasting game, as shown in Figure 2. Therefore, making forecasts using an equally weighted ensemble is suboptimal. Indeed, in Figure 3 we show how the weighted ensemble – blue line- and the best expert – red line – outperform the equally weighted ensemble – green line. The forecasting performance is the absolute relative forecasting error averaged over a one hundred year forecasting period.

Furthermore, the uncertainties in model parameters have a significantly larger influence in the evolution of the expert weights than the uncertainties in initial condtions. Second, an ensemble tuned to specific climate variables, for example by defining a loss function that only measures the performance of forecasting the climate for a specific season, outperforms the ensemble tuned to forecast global observables. In this case the loss function measures the performance of forecasting the climate for **all** seasons. Third, the learning rate, which measures how fast the expert weights are adjusted during the game plays a significant role in designing a good forecasting ensemble and has to be chosen carefully.

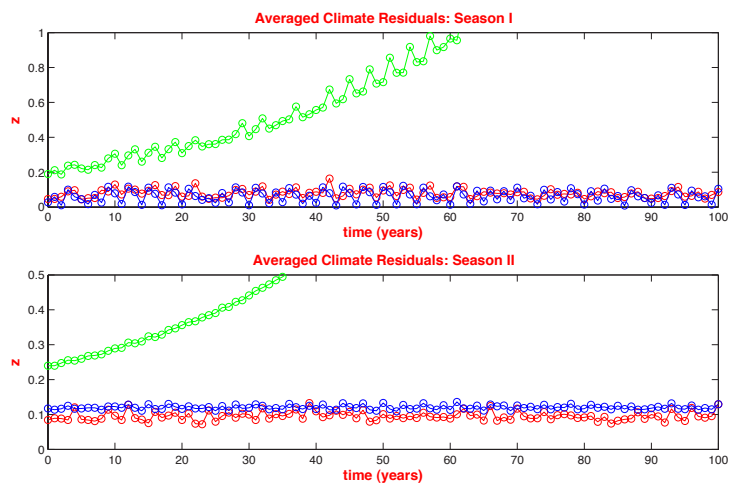


*Figure 3. Comparison between the performance of the equally weighted ensemble (green line), the weighted ensemble (blue line), and the best expert (red line) at the end of the forecasting game. In this case, the weighted forecaster, as well as the best forecaster, as computed using the forecasting with expert advice paradigm, significantly outperforms the equally weighted ensemble. The forecasting performance is the absolute relative forecasting error averaged over a one hundred year forecasting period. The 'climate' variable used is the z coordinate of the driven Lorenz model. Each member of the ensemble has different model parameters and initial conditions. We plot the forecasting performance for predicting 'season' one - top plot- and for predicting 'season' two - bottom plot.*

Finally, using the insights gained from building ensembles to forecast the behavior of the simple driven Lorenz model described above, we have started to experiment with ensemble design for climate change forecats. Due to the significant difficulties in processing the large and complex model outputs generated by the AOGCMs archived by the PCMDI project, we have only used a twenty member ensemble. Furthermore, we have only been able to apply the forecasting paradigm to estimate the weights of the models for estimating the evolution of the surface air temperature. For this climate variable we have used its averaged values - averaged over space (the surface of the Earth) and time (annual averages)- and its evolution is shown in Figure 4 for the twenty member ensemble. To score the performance of the ensemble we have used the observational data provided by PCMDI starting from 1958 and shown in blue circles in Figure 4. We have only applied the forecasting game for the period 1958-1990 and we have used the model weights at the end of this period to make ensemble predictions covering the period from 1991 to 1999. The evolution of the weights for this twenty model ensemble is shown in Figure 5. We notice that during the evolution of the game two dominant experts have emerged, as expected from an analysis of Figure 4. At the end of the game, one of these experts has a weight of one and the ensemble has collapsed. As a result we lose the ability to estimate the forecasting uncertainty as encoded in the spread of the ensemble forecasts. Before we can draw any definitive conclusions more forecasting experiments using the complete set of AOGCMs are necessary.

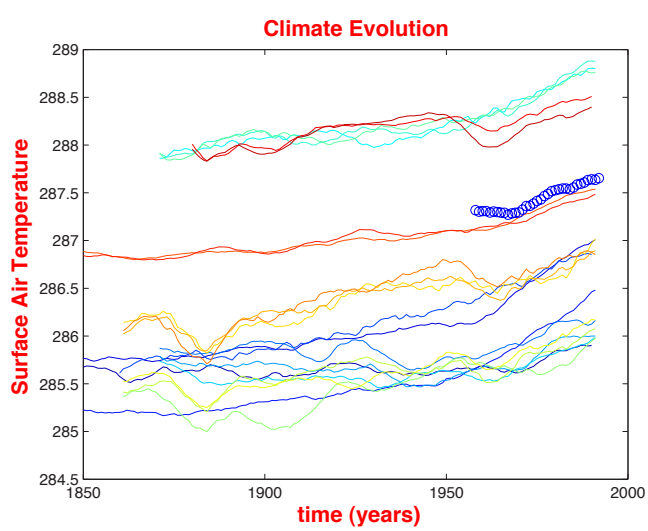


*Figure 4. The evolution of the surface air temperature - averaged over space (the surface of the Earth) and time (annual averages) - in twenty atmosphere-ocean general circulation models (AOGCMs). The blue circles represent the evolution of observational data for the period 1958-1999.*

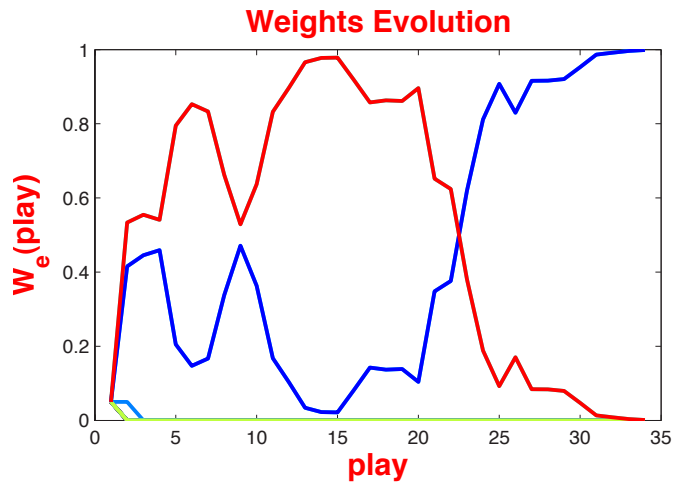


*Figure 5. The evolution of model (expert) weights for an ensemble of AOGCMs. The ensemble only includes twenty models and it was used to predict the evolution of the surface air temperature. The observational data used to score the experts' performance covers only the time interval from 1958 to 1990. Each model was initially assigned equal weights. During the forecasting game, two models have emerged with dominant weights. At the end of the game, one of these models has a weight of one and completely dominates the ensemble.*

## References

1. The Physical Science Basis. 2007. *IPCC Forth Assessment Report.*

2. Global Climate Projections. 2007. *IPCC Forth Assessment Report.*

3. Cesa-Bianchietal, N.. How to use expert advice. 1997. *Journal of the ACM.* **44**: 427.

4. Vovk, V.. A game of prediction with expert advice. 1998. *Journal of Computer and System Sciences.* **56**: 153.

5. Cesa-Bianchi, N., and G. Lugosi. Prediction, Learning, and Games. 2006.

6. Parketal, E. H.. Phase synchronization in the forced Lorenz system. 1999. *Physical Review E.* **60**: 6627.

continuing project

# Creating a Mathematical Foundation for High-Dimensional Search and Optimization Algorithms to Solve Complex Nonlinear Models

*Bruce Alan Robinson*

20070560PRD1

## Introduction

Numerical simulation models, along with theory and experiments, have become fundamental tools for understanding complex nonlinear systems. Most systems that we care about for any number of missions, from nuclear weapons to the Earth's climate system, are both complex and nonlinear. However, successful application of complex models is not straightforward: many of the parameters and internal states in these models require calibration/updating before meaningful predictions and uncertainty estimates can be made. Global optimization algorithms based on evolutionary search are increasingly being used for estimating parameters and states in these models. Many recent studies, including my own research using environmental models, have demonstrated that hybrid and adaptive methods that extract information from the sampling history to continuously update the state of the model are dramatically more efficient than more traditional static methods. However, the field of optimization relies on heuristic approaches to test for efficiency, rather than more formal theoretical approaches. This calls into question the validity of hybrid and adaptive search and optimization methods for solving high-dimensional state and parameter estimation problems. A sound mathematical foundation, combined with testing on canonical search problems and real-world applications, is essential for advancing the field of optimization beyond its current state, and for solving emerging mission-relevant problems.

In this project, we are: 1) developing formal convergence proofs of hybrid and adaptive search methods for the solution of nonlinear single and multi-objective optimization problems, 2) continuing the development of hybrid and genetically adaptive search methods, and 3) applying these methods to environmental and other modeling problems of strategic importance to the Laboratory. This research is enabled by the opportunity to collaborate with world-class theoretical and numerical analysts and physical scientists at LANL, a large selection of mission-relevant models and emerging problems to choose from, and the excellent parallel computing facilities at LANL.

## Benefit to National Security Missions

The methods developed are integral to the advancement of the science and development of next-generation environmental models in many programs tied to the DOE energy security mission, including groundwater resource, contaminant transport, oil and gas, nuclear waste disposal, and carbon sequestration applications.

## Progress

In the past year, we have developed a novel concept of genetically adaptive multimethod search that significantly enhances the efficiency of single and multiobjective evolutionary optimization, and have developed the mathematical foundation and numerical implementation of a novel Markov Chain Monte Carlo (MCMC) algorithm (Differential evolution adaptive Metropolis, or DREAM) for computationally efficient posterior inference in a Bayesian framework. The algorithmic advances have been accepted / published in applied mathematical journals, and the usefulness and applicability of these methods has been demonstrated by application to various sampling and inverse problems in different fields of studies. We are currently extending the mathematical and numerical advances developed within this project to particle filtering approaches for combined parameter and state estimation.

In the area of applications, the project's advances in parameter estimation and uncertainty estimation have led to significant contributions in hydrologic modeling and hydrologic laboratory and field methods. For instance, in one study, we demonstrated that only a very limited number of discharge observations is needed to appropriately calibrate streamflow forecasting models, that data of throughfall contain insufficient information to parameterize canopy interception models appropriately, that water uptake by plant roots is difficult to estimate in the presence of significant uncertainty associated with the hydraulic properties of the soil, and that most of the uncertainty in streamflow forecasting is due to uncertainty with the observed rainfall data. The project has also

placed LANL at the center of the current debate on the most appropriate methods for uncertainty estimation in hydrology. Particularly, there is strong disagreement whether an uncertainty framework should have its roots within a proper statistical (Bayesian) context, or whether such a framework should be based on a different philosophy and implement informal measures and weaker inference to summarize parameter and predictive distributions.

On one study, we compared a formal Bayesian approach with a more common, but less formal approach for assessing uncertainty in conceptual watershed modeling. Our results demonstrated that formal and informal Bayesian approaches have more common ground than the hydrologic literature and ongoing debate might suggest. The main advantage of formal approaches is, however, that they attempt to disentangle the effect of forcing, parameter and model structural error on total predictive uncertainty. This is key to improving hydrologic theory and to better understand and predict the flow of water through catchments.

Another study considered application of MCMC simulation to parameter inference in the Sacramento Soil Moisture Accounting (SAC-SMA) model, a lumped conceptual watershed model that describes the transformation from rainfall into basin runoff using six state variable reservoirs. This model is extensively used by the National Weather Service for flood forecasting throughout the United States. Inputs to the model include mean areal precipitation (MAP) and potential evapotranspiration (PET) while the outputs are estimated evapotranspiration and channel inflow. This real-world study poses an interesting challenge for MCMC samplers due to the complexity of the model's response surface. Figure 1 illustrates the evolution of the sampled values of the UZTWM parameter, representing the upper zone tension water maximum storage, as function of the number of SAC-SMA model evolutions using the a) classical random walk Metropolis (RWM), b) delayed rejection adaptive Metropolis (DRAM) [1] (c), differential evolution-Markov chain (DE-MC) [2], (d) DREAM, and (e) Shuffled Complex Evolution (SCE-UA) [3] global optimization algorithms. The bottom panel (Fig. 1f) depicts the evolution of the mean root mean square error (RMSE) value derived with the various methods. First, note that DREAM exhibits superior performance. The $N$ = 13 chains have converged to a limiting distribution within 40,000 SAC-SMA model evaluations with a good mixing of the individual trajectories. Second, DREAM achieves a significantly lower RMSE than its counterpart of approximately 13.70 ($m^3/s$) separately derived with the state-of-the-art SCE-UA algorithm. This analysis shows that SCE-UA has converged prematurely to a sub-optimal region in the parameter space, contradicting many published studies in the literature that have shown that SCE-UA is a reliable and efficient optimizer of nonlinear watershed models. These results suggest that DREAM enhances the efficiency of MCMC simulation, and simultaneously estimates values of the SAC-SMA model parameters that improve the reliability of flood forecasts.

Finally, in the past year, the Postdoctoral PI has organized 7 topical sessions at various (inter)national conferences, and has given 10 invited talks and seminars. In addition, 17 papers have been published or are in press, and four papers are currently in review.

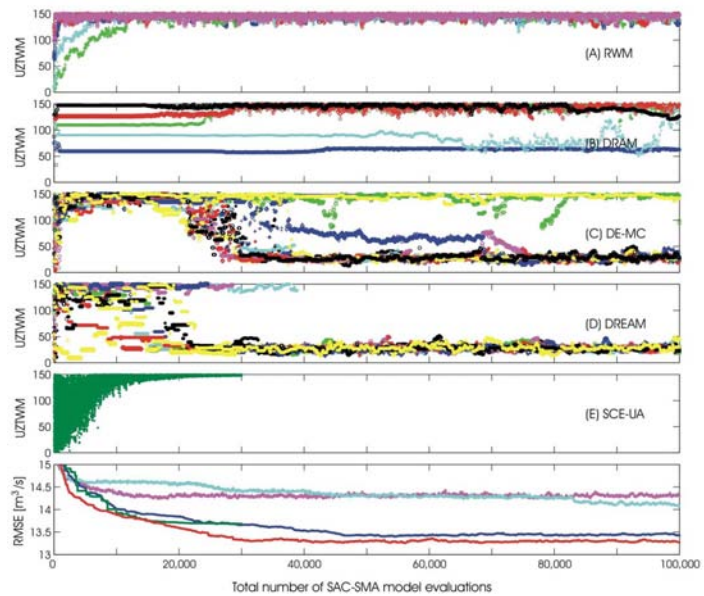


*Figure 1. Our DREAM algorithm provides both rapid convergence of model parameters to stable values, and smaller errors with respect to the real world. Evolution of sampled values of the upper zone tension water maximum storage (UZTWM) parameter (in mm) with the (a) RWM, (b) DRAM, (c) DE-MC, (d) DREAM Markov chain Monte Carlo sampling schemes, and (e) SCE-UA global optimization algorithm. Each trajectory in panels (a)-(d) is coded with a different color and symbol. The lines in the bottom panel (f) depict the evolution of the mean Root Mean Square Error value derived with the RWM (purple), DRAM (cyan), DE-MC (blue), DREAM (red), and SCE-UA (green) algorithms.*

## Future Work

Numerical simulation models, along with theory and experiments, have become fundamental tools for the understanding complex nonlinear systems and science based decision making. However, the usefulness and applicability of numerical system models is increasingly being held back by problems with parameter and state estimation. A sound mathematical foundation, combined with testing on canonical search problems and real-world applications, is essential for advancing the field of optimization beyond its current state, and solve emerging mission-relevant problems. More detailed technical descriptions of the three tasks are as follows:

1. Extension of the work to very high dimensional problems using dimensionality reduction: Despite the exceptional progress made, the very nature of high-performance computing model applications are that they consist of an extraordinary number of degrees of freedom, or unknown parameters that can, in principle, be adjusted to optimize the model. This situation calls for a new approach to systematically reduce the dimensionality of these large-scale simulation models. By merging dimensionality reduction methods with our new optimization algorithms, we anticipate being able to expand the applicability of our research to a much broader range of models.

2. Improving computational efficiency: Our MCMC method can be improved by incorporating new ideas that enable us to reduce the number of Markov chains that are initiated, and by modifying the algorithm to enhance its performance in high-performance computing platforms.

3. Applications: Work will continue to apply the methods to environmental and other modeling problems of strategic importance to the Laboratory. Applications of interest to LANL and other scientists include those in the fields of ecology, hydrology (vadose zone and aquifer), hydrogeophysics, and soil physics.

This work is methodological in nature, designed to advance the field of optimization, and will allow us to solve currently intractable nonlinear parameter and state estimation problems. This research is enabled by the opportunity to collaborate with world-class theoretical and numerical analysts and physical scientists at LANL, a large selection of mission-relevant models and emerging problems to choose from, and the excellent parallel computing facilities at LANL.

## Conclusion

This work is answering general, methodological questions on the science of optimization and mathematical model development. The methods developed in this project are being applied to natural systems models to provide insights about scientific questions of environmental interest. In each of these applications, we are collaborating with LANL scientists acquiring large, spatially distributed data sets and developing complex computer models of these natural systems. Thus, by acting as a catalyst to push the frontiers of science in these ongoing projects, we are contributing to the Laboratory's efforts in energy security and complex natural systems.

## References

Haario, H., M. Lane, A. Mira, and E. Saksman. DRAM: efficient adaptive MCMC. 2006. *Statistics and Computing.* **16**: 339.

TerBraak, C.. A Markov chain monte carlo version of the genetic algorithm differential evolution: easy Bayesian computing for real parameter spaces. 2006. *Statistics and Computing.* **16**: 239.

Duan, Q., V. K. Gupta, and S. Sorooshian. Effective and efficient global optimization for conceptual rainfall-runoff models. 1992. *Water Resources Research.* **28**: 1015.

## Publications

Behrangi, A., B. Khakbaz, J. A. Vrugt, Q. Duan, and S. Sorooshian. Comment on: Dynamically dimensioned search algorithm for computationally efficient watershed model calibration' by Bryan A. Tolson and Christine A. Shoemaker. 2008. Water Resources Research. 43: W01413.

Blasone, R. S., J. A. Vrugt, H. Madsen, D. Rosbjerg, G. A. Zyvoloski, and B. A. Robinson. Generalized likelihood uncertainty estimation (GLUE) using adaptive Markov Chain Monte Carlo sampling. 2008. Advances in Water Resources. 31: 630.

Clark, M. P., A. G. Slater, D. E. Rupp, R. A. Woods, J. A. Vrugt, H. Gupta, T. Wagener, and L. Hay. Framework for understanding structural errors (FUSE): a modular framework to diagnose differences between hydrological models. 2008. Water Resources Research. 44: W00B02.

Dane, J. H., J. A. Vrugt, and E. Unsal. AMALGAM optimization of equivalent capillary models of soils using observed air permeability data and high performance computing. Water Resources Research.

Elkington, R., S. C. Dekker, and J. A. Vrugt. Multiobjective optimality of a combined photosynthesis and soil water balance model using AMALGAM evolutionary search. Plant, Cell & Environment.

F.terBraak, C. J., and J. A. Vrugt. Differential evolution Markov chain with snooker updater and fewer chains. To appear in Statistics and Computing.

Feyen, L., J. A. Vrugt, B. Nuallin, J. van der Kniff, and A. de Roo. Parameter optimization and uncertainty assessment for large-scale stream flow forecasting. 2007. Journal of Hydrology. 332: 276.

Feyen, L., M. Khalas, and J. A. Vrugt. Semi-distributed parameter optimization and uncertainty assessment for large-scale streamflow simulation using global optimization. 2008. Hydrological Sciences Journal. 53 (2): 293.

Harp, D. R., Z. Dai, A. V. Wolfsberg, J. A. Vrugt, B. A. Robinson, and V. V. Vesselinov. Aquifer structure identification using stochastic inversion. 2008. Geophysical Research Letters. 35: L08404.

Hinnell, A. W., T. P. A. Ferre, J. A. Vrugt, S. Moysey, J. A. Huisman, and M. B. Kowalsky. Improved extraction of hydrologic information from geophysical data through coupled hydrogeophysical inversion. Water Resources Research.

Koller, J., Y. Chen, G. D. Reeves, R. H. W. Friedel, T. E. Cayton, and J. A. Vrugt. Identifying the Radiation Belt Source Region by Data Assimilation. 2007. Journal of Geophysical Research - Space Physics. 112: A06244.

Stauffer, P. H., J. A. Vrugt, H. J. Turin, C. W. Gable, and W. E. Soll. Untangling diffusion from advection in unsaturated porous media: experimental data, modeling and parameter uncertainty assessment. To appear in Vadose Zone Journal.

Tittonell, P., M. T. van Wijk, M. C. Runo, J. A. Vrugt, and K. E. Giller. Analyzing trade-offs in resource and labor allocation by smallholder African farmers using inverse modeling techniques. 2007. Agricultural Systems. 95: 76.

Vereecken, H., J. A. Huisman, H. Bogena, J. Vanderborght, J. A. Vrugt, and J. W. Hopmans. On the value of soil moisture measurements in vadose zone hydrology: a review. To appear in Water Resources Research.

Vrugt, J. A.. Comment on: How effective and effcient are multiobjective evolutionary algorithms at hydrologic model calibration?. 2007. Hydrology and Earth System Sciences. 11: 1435.

Vrugt, J. A., B. A. Robinson, and J. M. Hyman. Self-adaptive multimethod search for global optimization in real parameter spaces. To appear in IEEE Transactions on Evolutionary Computation.

Vrugt, J. A., C. G. H. Diks, and M. P. Clark. Ensemble Bayesian model averaging using Markov chain Monte Carlo sampling. To appear in Environmental Fluid Mechanics.

Vrugt, J. A., C. J. F. ter Braak, C. G. H. Diks, D. Higdon, B. A. Robinson, and J. M. Hyman. Accelerating Markov chain Monte Carlo simulation from self adaptive differential evolution with randomized subspace sampling. To appear in International Journal of Nonlinear Sciences and Numerical Simulation.

Vrugt, J. A., C. J. F. ter Braak, H. V. Gupta, and B. A. Robinson. Equifinality of formal (DREAM) and informal (GLUE) Bayesian approaches in hydrologic modeling?. To appear in Stochastic Environmental Research and Risk Assessment.

Vrugt, J. A., C. J. F. ter Braak, H. V. Gupta, and B. A. Robinson. Reply to comment by Keith Beven on equifinality of formal (DREAM) and informal (GLUE) Bayesian approaches in hydrologic modeling?. To appear in Stochastic Environmental Research and Risk Assessment.

Vrugt, J. A., C. J. F. ter Braak, M. P. Clark, J. M. Hyman, and B. A. Robinson. Treatment of uncertainty in hydrologic modeling: doing hydrology backwards with Markov chain Monte Carlo simulation. To appear in Water Resources Research.

Vrugt, J. A., J. van Belle, and W. Bouten. Pareto front analysis of flight time and energy use in long distance bird migration. 2007. Journal of Avian Biology. 38: 432.

Vrugt, J. A., P. H. Stauffer, T. Wohling, B. A. Robinson, and V. V. Vesselinov. Inverse modeling of subsurface flow and transport properties using recent advances in global optimization, parallel computing, and sequential data assimilation. 2008. Vadose Zone Journal. 7 (2): W00B02.

Vrugt, J. A., and B. A. Robinson. Treatment of uncertainty using ensemble methods: Comparison of sequential data assimilation and Bayesian model averaging. 2007. Water Resources Research. 43: W01411.

Vrugt, J. A., and B. A. Robinson. Improved evolutionary optimization from genetically adaptive multimethod search. 2007. Proceedings of the National Academy of Sciences of the United States of America. 104: 708.

Wohling, T., J. A. Vrugt, and G. F. Barkle. Comparison of three multiobjective optimization algorithms for inverse

modeling of vadose zone hydraulic properties. 2008. Soil Science Society of America Journal. 72: 305.

Wohling, T., and J. A. Vrugt. Combining multi-objective optimization and Bayesian modeling averaging to calibrate forecast ensembles of soil hydraulic models. To appear in Water Resources Research.

vanWijk, M. T., and J. A. Vrugt. Significant tradeoff in the prediction of water and carbon fluxes. Global Change Biology.

# The Role of NS1 in Disrupting Immune Responses During Influenza Infection: A Modeling and Experimental Approach

*Alan S Perelson*

20070645PRD2

## Introduction

Seasonal influenza kills 36,000 people each year in the United States. Pandemics, or global epidemics, can kill far more. The world currently faces the threat of a severe pandemic from a strain of influenza known as H5N1. This strain has infected more than 385 people to date, with a mortality rate of 60%.

Influenza interacts with many facets of the immune system. In order to infect cells, it must escape destruction by small proteins that are secreted by cells in the nose, throat, and lung. Once inside cells, influenza makes a particular protein that inhibits the host immune response and thereby can cause severe disease. H5N1, in addition, triggers an over-reaction by the immune system by setting off excessive activity of a different protein on the surface of cells that signals danger. H5N1 also triggers increased production of other proteins that may amplify this excessive danger signal. This over-reaction of the immune system is a common cause of death due to the H5N1 influenza virus.

Little is known about these interactions between influenza and the immune system. We propose to redress these gaps in knowledge in a quantitative way, and then based on experimental findings to develop mathematical models to describe each system. The experiments for this study will be conducted using lung cells in culture infected with contemporary strains of human seasonal influenza.

The ultimate goal of this work is to understand how influenza subverts the immune response in order to generate a successful infection. If these mechanisms can be quantitatively elucidated, then new treatments might be designed. Further, we may be able to better understand why strains such as 1918 flu and H5N1 are so deadly.

## Benefit to National Security Missions

This project will support the DOE mission in reducing biological threats - influenza is on the list of identified threat agents. It will also support the missions of DHS and NIH in responding to biological threats.

## Progress

This project involves both experimental and theoretical components. In order to carry out experiments a variety of training requirements have had to be met. All LANL-wide required training, plus seven additional courses have been taken. Four more courses still need to be completed.

Experiments will be conducted in the lab space of Ahmet Zeytun, under an Institutional Biosafety Committee (IBC) protocol of Anu Chaudhary and Ahmet Zeytun. This required writing a new protocol, which will allow new BSL-2 work with influenza. This protocol has been approved, and subsequently, we have also achieved approval of the new BSL-2 room for influenza work and an IWD for the work as well. After some of the theoretical work described below is completed, experiments will begin.

On the theoretical side, we have been developing an epidemiological model of influenza infection, with which we can examine the effects of antiviral therapy for both prevention and treatment, using any combination of three drugs, such as oseltamivir and zanamivir, neuraminidase inhibitors, and amantadine, an M2 channel blocker. For both amantadine and, increasingly, oseltamivir, antiviral resistance has appeared; resistance to zanamivir, which is much less commonly used, has yet to develop on a significant scale. Thus, there is considerable interest in whether combination therapy consisting of both amantadine and oseltamivir could still be effective, and whether more widespread use of zanamivir could slow down the development of resistance to any or all of these drugs. The model allows the emergence of flu strains resistant to any of the drugs alone or in

combination. The model also follows the spread of resistant virus through the population. The surprising result, thus far, is that combination therapy, while blunting an influenza epidemic, may also lead to the rapid emergence of strains resistant to any two drugs used for treatment. The model is currently being explored for predictions of which combinations of drugs used for prevention and treatment will minimize both the numbers of cases and the development of drug resistance, over the short and long terms. This work should be completed and submitted for publication soon.

We have also been working on viral dynamic modeling in which basic ordinary differential equation models of viral growth within a single host are developed and the effects of antiviral treatment included in the model. Thus, while our epidemiological modeling considers populations of people and the spread of virus between them, this type of model examines only a single person with infection spreading between cells in that person. Ultimately, multiscale models in which both single people and populations are modeled need to be developed. The equations in the viral dynamic model are nonlinear and we have been develping numerical methods of solution. The goal of this work is to develop realistic models that can then be used to interpret data and estimate model parameters. Preliminary work is ongoing and results are promising.

## Future Work

Seasonal influenza kills 36,000 people each year in the United States. Pandemics can kill far more. The world currently faces the threat of a severe pandemic from a strain of influenza known as H5N1. This strain has infected more than 385 people to date, with a mortality rate of 60%.

In order to infect cells, influenza must escape destruction by antimicrobial peptides (AMPs), among other barriers. Inside cells, influenza makes a protein called NS1 that inhibits the host immune response and thereby causes severe disease. H5N1, in addition, can trigger an often fatal over-reaction of the immune system by signaling through a cell surface receptor called TLR4. H5N1 also causes increased production of proteins called SAA, which may amplify TLR4 signaling.

Little is known about these interactions between influenza and the host. We propose to redress these gaps in experimental knowledge in a quantitative way, and then based on experimental findings to develop mathematical models to describe the kinetics relevant to each system.

In the experimental component, lung cells in culture will be infected with a strain of seasonal influenza, and the kinetics of the production and activities of these host and influenza molecules will be measured, using techniques such as quantitative RT-PCR. Based on the data, mathematical models will be developed to describe the kinetics of AMP and viral production, NS1 production and its interaction with host proteins, and SAA production and TLR4 signaling. Fitting the models to data will allow estimation of model parameters.

The ultimate goal of this work is to understand how influenza subverts the immune response in order to generate a successful infection. If these mechanisms can be quantitatively elucidated, then new treatments might be designed. Further, we may be able to better understand why strains such as 1918 flu and H5N1 are so deadly.

## Conclusion

Influenza infection has caused tens of millions of deaths. There is a chance that bird flu (H5N1) may start a new global pandemic. This work will elucidate some of the basic mechanisms used by influenza to defeat the host immune defenses. If we can better understand how influenza proteins, such as NS1, interact with host proteins to turn off host cell defenses we may be able to develop new drugs that will be able to better protect us against influenza infection.

# Photodegradation of Leaf Litter in Water-Limited Ecosystems

*Thomas A Rahn*

20070688PRD3

## Introduction

Recent research has revealed a new role for sunlight in the terrestrial carbon cycle: photodegradation in semi-arid environments may account for up to 60% of plant litter decomposition (Brandt et al., 2007). This process likely results in emission of carbon dioxide, a greenhouse gas, and volatile organic compounds (VOCs), which impact troposphere ozone concentrations and contribute to secondary aerosol production. Furthermore, cloud cover and UV-B, both of which are predicted to change with shifts in climate, likely influence this process

Photo-degradation of organic matter can occur by direct or indirect processes. Direct photo-degradation occurs when a molecule absorbs light and undergoes a reaction resulting in its chemical transformation. Indirect photo-degradation is the process whereby a photo-excited molecule will react with constituents of the system such as water or oxygen to produce reactive intermediates, such as the hydroxyl radical which can, in turn, react with and breakdown molecules unable to undergo direct hoto-degradation. Resolving the dominant mechanism will provide critical constraints on the process and is therefore a key step in placing plant photo-degradation in the context of the global carbon cycle. For example, if photochemically produced reactive oxidants are important in plant photo-degradation, the pool of photo-labile carbon is significantly larger than if the process were limited to molecules that undergo direct photo-degradation, due to the strong reactivity of oxidants such as the hydroxyl radical with a wide-range of organic molecules. The objective of this study is to quantify the role of direct vs. indirect photo-degradation in the production of carbon dioxide and VOCs from plant litter found in water-limited ecosystems.

## Benefit to National Security Missions

This project will support LANL's mission of energy security and DOE's Office of Science mission in Biological and Environmental Research by advancing monitoring, mitigation, and verification technologies for Carbon Sequestration Science, in particular, terrestrial carbon sequestration.

## Progress

This project called for exposing plant material to ultraviolet (UV) radiation in a controlled environment over a range of temperatures and pressures with subsequent analysis of reaction products by various trace gas analyzers employed in our laboratory. In the first nine months of this project, we assembled the requisite materials required to perform the experiments including UV source, UVA and UVB filters and photometers and a specially made quartz reaction vessel with a water-cooled jacket. The system has been tested without plant material to test air tightness; background signals resulting from the O-ring materials have been resolved. We have quantified the photochemical release of $CO_2$ from dried leaf litter of 10 tree and grass species prevalent in major biotic zones of New Mexico, including its isotopic signature. Emitted $CO_2$ and its isotopic signature were measured using a tunable diode laser (TDL) to assess the pool of photochemically-labile plant matter ($\delta^{13}C$-$CO_2$) in a given sample and to assess the source of the oxygen ($\delta^{18}O$-$CO_2$). The cumulative $CO_2$ released upon exposure of 0.1-0.3 g of dried leaf litter to three hours of simulated sunlight ranged from 300-900 ng $CO_2$ per g of carbon in the dried litter. Generally, the isotope $^{13}C$-$CO_2$ was depleted (4-7 ± 2‰) with respect to the leaf litter sample. The isotope $^{18}O$ had a similar abundance to atmospheric $O_2$, suggesting that the oxygen in the emitted $CO_2$ originated from the atmosphere.

Examples of $CO_2$ emitted and its isotopic content are shown in Figure 1 for an oak leaf. In this example, a sample of oak leaf was exposed to UV radiation for a period of 3 hours, after which the chamber air was purged and introduced to the TDL instrument. The pulse of $CO_2$ is shown in Figure 1A . Integration of this peak yields the rate of photochemically induced carbon loss. The $^{13}C$ and $^{18}O$ content of the released $CO_2$ are shown in panels B and C. The isotopic values are deter-

mined from the average for the period over which the $CO_2$ concentration exceeds 200 ppm, the lower limit for which isotopic results are valid.

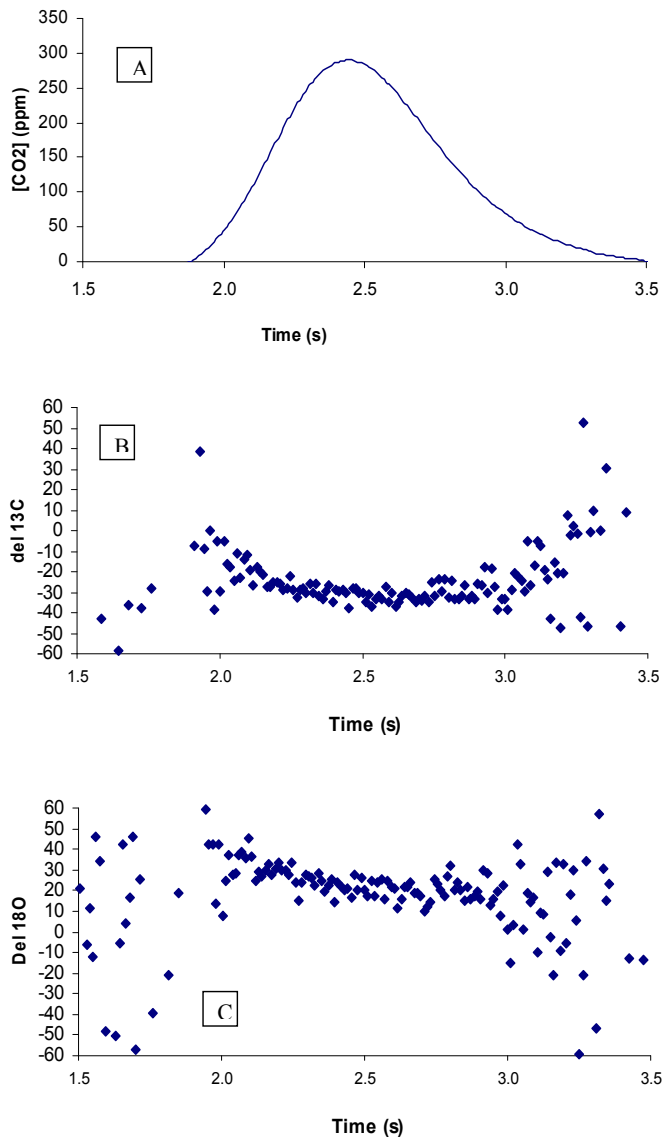


*Figure 1. $CO_2$ and its isotopic content emitted from oak leaf material exposed to three hours of simulated sunlight. See text for more detail.*

## Future Work

Future work will continue to explore and quantify the amount of carbon released as $CO_2$ during these processes. In addition, we will begin to quantify emission of other carbon containing species such as methane, carbon monoxide and VOCs. We also will introduce various oxygen bearing radical species to our simulator and begin to explore the relative influence of direct and indirect processes.

## Conclusion

This project will resolve whether photodegradation of plant material is a direct or an indirect process (or a combination of both) and investigate the processes which plant directly oxidizes material in the presence of sunlight. The results will provide much needed information on the role of abiotic plant decomposition in the carbon cycle of arid lands.

## References

1. Brandt, L. A., J. Y. King, and D. G. Milchunas. Effects of ultraviolet radiation on litter decomposition depend on precipitation and litter chemistry in a shortgrass steppe ecosystem. 2007. *Global Change Biology.* **13**: 2193.

# Pore-Scale Modeling of Multiphase Flow and Reaction in Charged Porous Media

*Qinjun Kang*

20070760PRD4

## Introduction

Multiphase flow and reaction in charged porous media are ubiquitous in energy and environmental sciences research and pose a formidable challenge. In the present scenario of a global concern over energy security and environmental issues, the physics of transport and reaction encompassing multiple length scales prevalent in natural and synthetic porous media is poised to play a key role. Two critical research needs of prominent national and global importance within the broad spectrum of energy and environmental issues include sequestration of carbon dioxide ($CO_2$), a greenhouse gas, and clean energy harvesting via a sustainable hydrogen energy economy. CO2 sequestration involves transport and reaction physics in geologic porous media, while hydrogen energy involves complex, electrochemical reaction coupled multi-physical transport phenomena in fuel cells comprising of varied synthetic porous media. However, the inherently complex morphology of such porous media coupled with multi-physical (physico-electro-chemical), reactive (chemical/electrochemical) transport and interfacial processes catering over multiple length scales (nano/micro/meso/macro) makes this problem notoriously difficult and consequently poses several open questions of fundamental and scientific interest. In this project, we intend to develop for the first time a comprehensive pore-scale modeling framework involving multiphase (air/water), reactive (chemical/electrochemical) transport and interfacial processes in the presence of electrical charge in the sub-micron and micron length scales in porous media. The overriding objective of this project is to develop a science-based approach toward fundamental understanding of the underlying transport and reaction in charged porous media and answer some of long-standing questions in the broad spectrum of energy and environmental research, including subsurface contaminant migration, geological CO2 sequestration, and fuel cell technology.

## Benefit to National Security Missions

This project will support the DOE/NNSA missions in Energy Security, Environmental Quality, and the missions of the Office of Science by enhancing our understanding of underlying multiphase flow and reaction in porous media at the pore scale in the presence of charged surfaces.

## Progress

A key focus of this project since its inception in January, 2008, has been on pore-scale, multiphase transport in micro-porous media with relevance in the energy and environmental research. A pore-scale formalism encompassing a microstructure reconstruction model and a two-phase lattice Boltzmann (LBM) model has been developed in order to study the profound structure-wettability-transport interplay prevalent in the micro-porous (porous composite and fibrous) structures in the emerging field of electrochemical energy conversion devices, specifically in the polymer electrolyte fuel cells for automotive power. This is the first attempt to understand the two-phase (air/water) behavior and interfacial dynamics including droplet formation, flooding front formation and propagation and two-phase regime transition dynamics (capillary fingering to stable displacement) in the fuel cell micro-porous structures which exhibit strong capillary dominated transport. The details of this study are furnished in a journal article [1], which is currently under review.

Another fundamental study has been conducted using the two-phase lattice Boltzmann model to study the droplet motion and dynamics on a wettability graded channel wall with different hydrophilic and hydrophobic surface patterning. This study is perceived as a pore-scale prototype numerical experiment to understand the strong coupling between droplet motion and wetting characteristics depending on the capillary number, a measure of the relative importance of the surface forces. A fundamental understanding of capillarity-

wettability interplay is imperative to potential two-phase regime exploitation (e.g. capillary fingering, viscous fingering, stable displacement) in the emergent engineering (e.g. energy, microfluidics) applications. A journal manuscript detailing the findings from this study is currently under preparation.

In order to study the electrochemistry-coupled transport mechanisms in porous structures, a direct numerical simulation (DNS) model based on fine-scale computational fluid dynamics (CFD) formalism has been developed. The DNS model solves the species and charge transport along with interfacial electrochemical kinetics directly on top of the porous microstructure. Recent work is specifically directed toward the development of surface complexation reactions between the aqueous and solid phases in a porous structure. Concurrently, work is underway to develop an integrated formalism encompassing the LBM for solving multiphase flow and the DNS model for solving transport which is envisioned to provide a coherent description of coupled mutiphysical transport in charged porous media. In this regard, an improved lattice Boltzmann formalism for studying two-phase transport is also currently under development which would relax some of the present numerical restrictions (e.g. high density ratio). Recent efforts have been presented in the CMWR conference [2] and the CEKA annual meeting [3].

As a precursor to the pore-scale modeling of transport in charged porous media, a theoretical study has been performed to study the electrochemistry and electrokinetic effects on transport in catalytic porous structures. A specific study in the context of fuel cell electrodics encompassing electrochemical reaction, electromigration, electrostatics and charge accumulation along with species transport has been conducted. This study presented in the ELKIN2008 conference on non-linear electrokinetics in the context of electrochemical energy systems research was a unique contribution. In particular, this work has direct implications in decontamination of porous structures. A manuscript on the theoretical study of electrochemistry and electrokinetics in catalytic porous structure is currently under preparation. This further emphasizes the multidisciplinary nature of the research scope addressed through this project.

## Future Work

We will continue the work to develop a comprehensive pore-scale modeling framework for investigating transport in the presence of charged mineral surface in porous media based on the Lattice Boltzmann (LB) method. Specifically, the future work will involve: 1) the development of an innovative model to account for electric double layer effects on transport in single aqueous phase, multicomponent systems; and 2) the extension of the model to multiphase systems with high density and viscosity contrast. The proposed research will be based on our existing expertise in both electrochemistry and thermal-fluid sciences and experience with the LB method.

## Conclusion

Accounting for electrochemical processes in multiphase flow and reaction is critical to understanding colloid facilitated transport of radionuclides. This project will enable a science-based approach toward fundamental understanding of the underlying transport and reaction mechanisms for the migration of radionuclides involving heterogeneous surface reactions with minerals. A computer code on this subject will be developed to model these processes and research results will be published in leading journals. This project will have direct implications in a broad spectrum of environmental and energy research, including subsurface contaminant migration, $CO_2$ sequestration in geologic formations, and fuel cell technology.

## References

1. Mukherjee, P. P., C. Y. Wang, and Q. Kang. Mesoscopic modeling of two-phase behavior and interfacial dynamics in polymer electrolyte fuel cell porous materials. *Journal of the Electrochemical Society.*

2. Mukherjee, P. P., M. Wang, Q. Kang, and P. C. Lichtner. Pore-scale modeling of transport in charged porous media. Presented at *Computational Methods in Water Resources XVII International Conference.* (San Francisco, CA, 6-10, July 2008).

3. Mukherjee, P. P., M. Wang, Q. Kang, and P. C. Lichtner. Modeling of transport in charged porous media. Presented at *5th Annual Meeting of Center of Environmental Kinetics Analysis (CEKA).* (Pennsylvania State University, 22-24 Oct. 2008).

## Publications

Mukherjee, P. P., C. Y. Wang, and Q. Kang. Mesoscopic modeling of two-phase behavior and interfacial dynamics in polymer electrolyte fuel cell porous materials. *Journal of the Electrochemical Society.*

Mukherjee, P. P., M. Wang, Q. Kang, and P. C. Lichtner. Pore-scale modeling of transport in charged porous media. Presented at *Computational Methods in Water Resources XVII International Conference.* (San Francisco, CA, 6-10, July 2008).

Mukherjee, P. P., M. Wang, Q. Kang, and P. C. Lichtner. Modeling of transport in charged porous media. Presented at *5th Annual Meeting of Center of Environmental Kinetics Analysis (CEKA).* (Pennsylvania State University, 22-24 Oct. 2008).

# Modeling Fast Basal Sliding of Ice Sheets for Climate and Sea Level Prediction

*William Henry Lipscomb*

20070765PRD4

## Introduction

Recent observations show that outlet glaciers and ice streams in Greenland and West Antarctica have accelerated and thinned dramatically, with atmospheric and oceanic warming the likely cause. Given the potential catastrophic impacts of rapid sea level rise, it is critical to predict how ice sheets will respond to future climate warming. This is not yet possible because fundamental physical processes are not represented in ice-sheet models and are only beginning to be understood. The goal of this project is to improve ice sheet models by including realistic treatments of 1) subglacial hydrology that can evolve in response to changes in the overlying ice sheet, and 2) basal sliding in regions underlain by deformable subglacial "till." These processes are crucial for predicting the evolution of ice streams and outlet glaciers, which can flow 10 to 100 times faster than ice that is frozen to the bed. The new process models will be implemented in a state-of-the-art ice-sheet model (GLIMMER), the ice-sheet component of the Community Climate System Model (CCSM). This model will be used by glaciologists and climate modelers worldwide for regional studies and global climate projections. In particular, model results from GLIMMER and CCSM will be incorporated in the reports of the Intergovernmental Panel for Climate Change (IPCC), which won the 2007 Nobel Peace Prize for its role in educating the world about the risks of climate change. The most recent IPCC assessment report specifically noted the need for better ice sheet models.

## Benefit to National Security Missions

This project supports the DOE mission of the Office of Science by enhancing our understanding of physical processes that control the response of ice sheets to climate change.

## Progress

The postdoc Stephen Price has ported a state-of-the-art ice sheet modeling code from the University of Bristol to LANL and has 1) continued his work on general model development, and 2) started model development specific to his LANL project.

General model development, which is necessary to apply the model towards the specific project goals but is also necessary to use the model for any large-scale predictive simulations, has included the following:

- The addition of a stable ice-thickness evolution solver for predicting changes in ice sheet geometry over time. Additional work has been done with U.K. colleagues to include a more accurate, stable, and efficient thickness evolution scheme. The new scheme is currently being tested and will be applied toward model experiments to be presented at the 2008 Fall meeting of the American Geophysical Union (AGU; see below).
- The addition of the ability to simulate regions of floating ice (e.g. ice shelves or ice tongues), which are fully coupled to land-bound, grounded ice. Previously, this improvement applied only to ice shelves with a simplified shelf-front geometry. As of October 2008, this scheme has been generalized to apply to ice shelves with arbitrary horizontal dimensions.
- The addition of a freely moving grounding line (the point of transition/coupling between grounded and floating ice). Work is underway to verify that modeled grounding line migration—which is known to be highly susceptible to numerical artifacts—is consistent with benchmarking experiments.
- Changes required so that the model will compile and run on numerous platforms and give identical results.
- Modifications in the current "higher-order" momentum balance solver so that it will compile and run within the GLIMMER ice sheet model, which currently uses an oversimplified momentum balance solver. GLIMMER has been coupled to CCSM, and the addition of a higher-order solver will allow for much more realistic simulations of ice sheet flow and evolution.

Model development specific to the goal of improving the simulation of regions of fast sliding in ice sheets includes the following:

- The addition of a simple iteration to approximate glacier sliding over a "plastic bed." That is, below some yield stress, no sliding occurs, and at the yield stress, sliding occurs such that basal shear stress remains at the yield stress. Initial tests suggest that this iteration, which is straightforward to implement and computationally inexpensive, may be adequate for capturing the large-scale behavior of ice streams sliding over a plastic bed (which occurs in numerous locations in Antarctica). Further testing is needed to determine whether this treatment will be adequate in the long term.

- Work with colleagues at the University of Cambridge on incorporating a basal-processes model into the code. The basal processes model takes information on basal hydrology (e.g. how wet the bed is) and known subglacial-interface properties (e.g. whether the interface is bedrock or soft, weak, moldable till) and provides the larger model with an estimate for the required yield stress. Initial experiments from the coupled ice sheet / basal-processes model will be presented at the 2008 Fall AGU meeting.

- An initial tuning of basal sliding parameters for the Greenland ice sheet. This is a necessary step in obtaining a reasonable initial condition from which predictive runs of Greenland's future mass balance will start. Figure 1 compares the modeled ice sheet surface velocities ("model") to the observation-based velocity field ("observations") used to tune the model sliding parameters. Work is underway to use this model state as an initial condition from which to conduct a range of perturbation experiments, exploring the short-term response of the Greenland ice sheet to environmental forcing (i.e., sea level contribution during the next several decades).

Price has given presentations discussing the goals and progress of his work to the Climate, Ocean and Sea Ice Modeling (COSIM) group and the T-3 (Fluid Dynamics and Solid Mechanics) Group at LANL. He presented his work to the larger climate modeling community at the annual Community Climate System Model workshop in Breckenridge, Colorado, in June 2008. He presented his research and led a breakout session at the August 2008 LANL workshop, "Building a next-generation community ice sheet model." He is co-author of the workshop report (a summary of which has been submitted to *Eos*, the journal of AGU transactions), and he is leading a focus group on ice sheet hydrology that emerged from the workshop. In September he presented results from model experiments on grounding line migration at the international Forum for Research into Ice Shelf Processes (FRISP) meeting in Derbyshire, U.K. In November he gave a summary of his earlier work at the National Academy of Sciences 2008 *Kavli Frontiers of Science* Symposium. In December, he will be co-author on two presentations at the annual AGU meeting in San Francisco. One will summarize model experiments exploring the evolution of an idealized 3D ice sheet/stream/shelf system coupled to the basal processes model discussed above. The second will present initial progress towards coupling the ice sheet/stream/shelf model to the LANL HYPOP ocean circulation model. He is a co-author of two papers published this year in the *Journal of Glaciology* [1, 2].

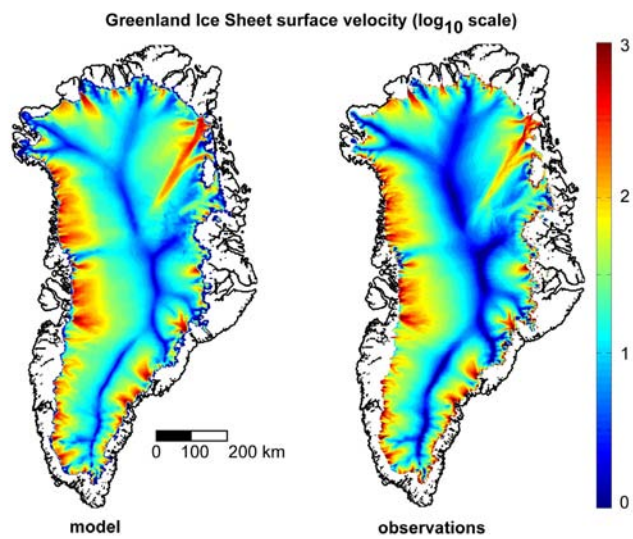


*Figure 1. (a) Modeled surface velocities of the Greenland ice sheet, using a new model with a higher-order stress balance. (b) 'Balance' velocities based on the observed surface mass balance. Velocities are plotted on a logarithmic scale; the numbers on the color scale correspond to the logarithm (base 10) of the velocity in m/s.*

## Future Work

Ice sheets will likely be primary contributors to 21st century sea level rise, but estimates of these contributions are poorly constrained because essential physical processes that control ice sheet outflow on yearly to decadal time scales are missing from predictive ice sheet models. The goal of this project is to develop improved models of subglacial hydrology and basal sliding for ice sheet and climate studies. During the coming year, generic sliding laws and a plastic-bed sliding law will be added to the GLIMMER ice sheet model, and the model will be tested using standard benchmarks. Using modern-day maps of subglacial properties (e.g., basal traction and basal water-layer thickness), empirical relationships will be defined to link sliding parameters with the subglacial water system. The improved basal boundary conditions will be used to perform simple applications. A subglacial water model will then be added

to GLIMMER, and the evolution of subglacial water will be linked to the evolution of sliding parameters. The improved model will be applied to outlet glaciers in Greenland and to ice streams in the Amundsen and Ross Sea embayments of West Antarctica in order to better understand the cause and future course of changes in those regions. This research will result in an ice sheet model with more accurate and realistic basal boundary conditions, which are necessary for predicting the response of the Greenland and Antarctic ice sheets to climate changes. The model will be incorporated in CCSM and will be used by glaciologists and climate modelers worldwide for regional studies and global climate projections.

## Conclusion

The desired outcome of this effort is a next-generation ice sheet model that can be used to predict the rate of sea level rise associated with the potentially rapid retreat of the Greenland and West Antarctic ice sheets. As underscored by the recent assessment report of the Intergovernmental Panel for Climate Change, current ice sheet models are too crude to simulate rapid dynamic changes in ice outflow. Since rapid sea level rise could have huge socioeconomic impacts, improved ice sheet models are essential for evaluating risks associated with climate change.

## References

1. Price, S. F., A. J. Payne, G. A. Catania, and T. A. Neumann. Seasonal acceleration of inland ice via longitudinal coupling to marginal ice. 2008. *Journal of Glaciology.* **54** (185): 213.

2. Catania, G. A., T. A. Neumann, and S. F. Price. Characterizing englacial drainage in the ablation zone of the Greenland ice sheet. 2008. *Journal of Glaciology.* **54** (187): 567.

## Publications

Catania, G. A., T. A. Neumann, and S. F. Price. Characterizing englacial drainage in the ablation zone of the Greenland ice sheet. 2008. *Journal of Glaciology.* **54** (187): 567.

# Modeling the Immune Response to Pathogens

*Alan S Perelson*

20070781PRD4

## Introduction

Combating infectious disease demands a comprehensive approach, which requires understanding the mechanisms of pathogenesis and host-pathogen interactions on multiple scales – from pathogen cell invasion all the way to the host immune response. It also calls for fast and efficient methods of pathogen detection. Our research has focused on two aspects of the problem. The main research direction has dealt with the understanding the kinetics of the immune response to pathogens. The second focused on the understanding of the mechanisms by which the cell regulates transport of matter into and out of the cell nucleus, which is pertinent to viral replication, and development of the methods for pathogen detection.

### Kinetics of immune response

The immune system protects higher organisms from infection by pathogenic microorganisms. For intracellular pathogens, such as viruses and certain types of bacteria, cytotoxic T lymphocytes (CTL), are the primary means of defense. After activation by encounter with an antigen, T cells proliferate at a rapid rate and differentiate into CTLs, which then kill infected cells. The magnitude, the duration and the rapidity of the T cell response dictate the clinical course and the eventual outcome of the infection. The factors that determine the kinetics of T cell response are still poorly understood. Discriminating between different mechanisms and models of the kinetics of the immune response requires development of a quantitative conceptual framework that, in particular, allows quantitative estimation of the kinetic parameters pertinent to T cell activation, such as birth and death rates during different phases of the response. Our goal is to develop models of the kinetics of the T cell response and validate them by comparing with the experimental data.

### Mechanisms of selective transport through nano-channels and of nucleocytoplasmic exchange

Functioning of living cells requires selective transport of molecules into and out of the cell nucleus. This transport is also important for the replication of many viruses, such as influenza, that replicate in the nucleus. It occurs through Nuclear Pore Complexes (NPC) - channels that are able to selectively transport only certain molecular species into the nucleus, while effectively filtering out others, even very similar ones. Moreover, NPCs can selectively transport their specific molecules in the presence of vast amounts of non-specific competitors. Strikingly, transport through the NPC occurs without direct input of metabolic energy and without transitions from an 'open' to a 'closed' state during the transport event. Other biological channels function in a similar way. In addition, mechanisms of selectivity operational in such channels hold a great potential for applications in nano-technology and nano-medicine, which recently has lead to design artificial selective nano-channels. In particular, such channels can (and have been) used for pathogen detection. Precise mechanisms and conditions of selective transport through such selective nano-channels are still unknown.

## Benefit to National Security Missions

This project will support the DOE mission in threat reduction by enhancing our understanding of the body's ability to fight natural and engineered threat pathogens and will contribute to development of new methods of pathogen detection.

## Progress

### Combining quantitative experiments and modeling to understand kinetics of immune response

Using the theory of branching processes, we have designed theoretical tools that provide a general framework for quantitative understanding of T cell kinetics (Figure 1). Together with experimental collaborators at the Sloan Kettering Memorial Cancer Center, New York, we performed quantitative experiments in order to quantify the *in vivo* kinetics of T cell activation, proliferation and decline during the acute response to an intracellular bacterial infection. The experiments used T cells from a transgenic mouse model, developed by Dr. Alena Gallegos in the laboratory of Dr. Eric Pamer.

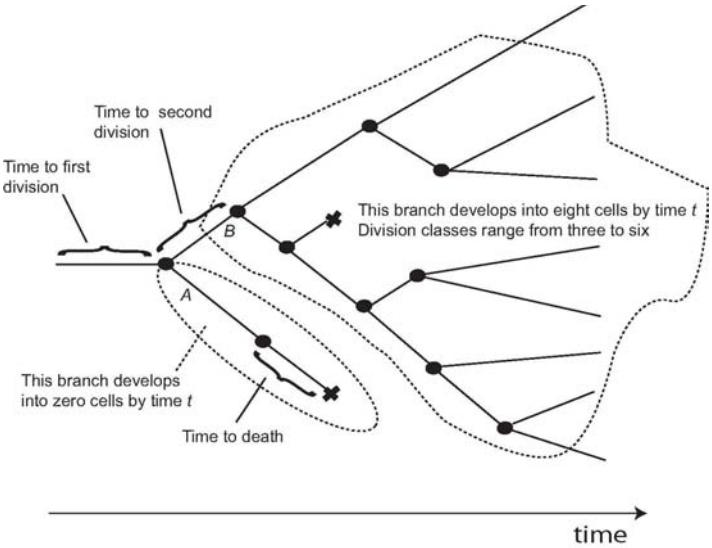


*Figure 1. Schematic illustration of the process of lymphocyte expansion and contraction represented as a branching process.*

In particular, in the first stage of the project, we have focused on the application of our theoretical tools to the analysis of the CFSE labeling experiments. CSFE is an intracellular dye that dilutes approximately two-fold every time a cell divides, which experimentally allows to measure the number of cells that have divided *n* times at a given time *t.* From comparison with the theoretical predictions of our model, we have extracted the kinetic parameters such as the birth and death rates of the lymphocytes (Figure 2).

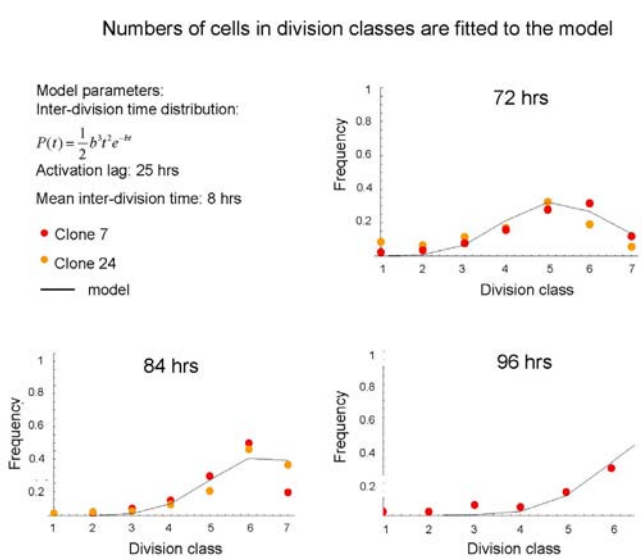


*Figure 2. Estimated kinetic parameters of T cell expansion are obtained from the fit of the theoretical model to the experimental data.*

Our theory has also helped to address experimental challenges. One current difficulty is obtaining well resolved labeling data *in vivo,* which is very noisy. Potentially, many factors can contribute to the noise in vivo experiments, including the small numbers of labeled cells. Building upon the analytical theory, we have developed an agent-based simulation of the process of activation, proliferation and death of lymphocyte populations. Using simulations, we have established that the major factor determining the level of noise is the initially wide distribution of the amount of CFSE in labeled cells. This lead us to use an instrument called a fluorescently activated cell sorter (FACS), to pre-sort cells over their CFSE count, prior to the experiment, in order limit the noise. Also, using available data on the estimated division rates, we ran simulations in order to determine the time points that provide most information for the estimation of the kinetic parameters. This resulted in well-resolved CFSE data that is amenable to quantitative analysis.

Altogether, using insight obtained from the theory, together with Dr. Alena Gallegos in Pamer's lab, we have collected sufficiently well time resolved data on lymphocyte proliferation, suitable for quantitative analysis. The data is currently being analyzed in order to extract the birth and death rates of the lymphocytes in different division classes, as shown in Figure 2. To the best of our knowledge, this is the first time a study of such magnitude and scope has been attempted.

**Nano-channels and nucleo-cytoplasmic exchange**

We have developed a theoretical model to explain the mechanisms of selectivity of transport through biological and artificial nano-channels, which contains only two essential ingredients: - i) transient trapping of the cargoes inside the channel (e.g. due to transient binding to moieties inside the channel) ii) competition between the transported molecules for the limited space inside the channel (Figure 3).

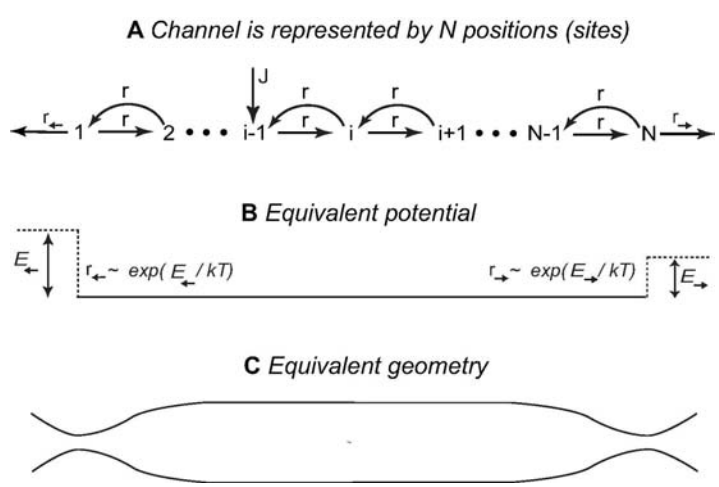


*Figure 3. Representation of the transport through a channel in terms of random hopping with exclusion.*

Parts of the work have been done in a close collaboration with the experimental colleagues at Rockefeller University who have been working on implementation of the concepts in a real nano-molecular filter.

The theory provides a mechanism for selectivity based on the differences in the kinetics of transport through the channel between different molecules, provides a basis for understanding the mechanisms of nucleo-cytoplasmic exchange, and provides a blueprint for future creation of ever more selective artificial nano-channels. The theoretical predictions explain well previous experimental results and have been verified in ongoing experiments at the Rockefeller University [1-2].

## Future Work

**Kinetics of the immune response**

We propose to elucidate the mechanisms involved in the T cell response via a new generation of theoretical models and concepts informed by quantitative experiments. As a part of this program we shall continue developing quantitative methods (both experimental and computational) to measure the pertinent kinetic parameters.

In parallel, we shall examine several models of the T cell activation. In particular, we will examine a model in which an initial brief encounter with the antigen starts an intracellular, genetic, or epigenetic differentiation process, which leads to rapid proliferation followed by equally rapid cell death (a 'program'). A second model will examine global feedback through where T cell death is regulated through a soluble molecule that is secreted by the expanding T cells themselves. Thus, as the T cell population gets large, the concentration of this molecule will increase and provide a feedback leading to the population contraction. These and other models will be formulated and tested against experimental data. Understanding quantitatively the immune responses to intracellular pathogens could profoundly affect disease treatments.

**Understanding the mechanisms of viral entry and design of efficient bio-sensors for pathogen detection.**

Due to the lack of space, we cannot elaborate on the future research in this direction. In one sentence, we shall build upon the theory we have developed to further our understanding of mechanisms of viral entry to the nucleus, and to design efficient molecular nano-sorters and bio-sensors.

## Conclusion

This research will enhance our knowledge of how the immune system fights intracellular pathogens, such as viruses and certain bacteria, and will enhance our abilities in pathogen detection. We expect to learn in detail how the immune response develops in the presence of a pathogen and how it is ultimately shut off as the pathogen is eliminated. If the immune response is not properly shut off then autoimmune disease could result. We also expect to learn about the details of mechanisms of viral entry to the nucleus and use the learned mechanisms for the design of efficient bio-sensors for pathogen detection.

## References

1. Zilman, A., S. Di Talia, B. T. Chait, M. P. Rout, and M. O. Magnasco. Efficiency, selectivity and robustness of nucleo-cytoplasmic transport. 2007. *PLoS Computational Biology.* : e125.

2. Zilman, A.. Effects of inter-particle interactions on selective transport through narrow channels: theory versus experiment.. To appear in *Biophysical Journal.*

## Publications

Jovanovic-Talisman, T., J. Tetenbaum-Novatt, A. S. McKenney, A. Zilman, R. Peters, M. P. Rout, and B. T. Chait. Artificial nano-channel that mimics the nuclear pore complex.. To appear in *Nature.*

Zilman, A.. Effects of inter-particle interactions on selective transport through narrow channels: theory versus experiment.. To appear in *Biophysical Journal.*

Zilman, A., J. Pearson, and G. Bel. Effects of jamming on transport times through nano-channel.. *Physical Review Letters.*

Zilman, A., S. Di Talia, B. T. Chait, M. P. Rout, and M. O. Magnasco. Efficiency, selectivity and robustness of nucleo-cytoplasmic transport.. 2007. *PLoS Computational Biology.* : e125.

Zilman, A., S. Di Talia, T. Jovanovic-Talisman, B. T. Chait, M. P. Rout, and M. O. Magnasco. Enhacement of transport selectivity through nano-channels in the presence if non-specific competition.. *Proceeedings of the National Academy of Sciences USA.*

# Spectroscopic Studies and Photonic Applications of "Giant" Nanocrystal Quantum Dots

*Victor Ivanovich Klimov*

20080703PRD1

## Introduction

Nanocrystal quantum dots (NQDs) are nanosized semiconductor crystals that show high photoluminescence quantum yields. The color that they emit can be tuned by adjusting the size of the dot, because of an effect called quantum confinement. Based of these properties, nanocrystals are attractive materials for applications in areas such as optical amplification and lasing [1]. However, the practical utilization of nanocrystals in lasing is complicated by their low stability at the high excitation intensities required to obtain optical gain and fast carrier nonradiative losses resulting from multiexciton Auger recombination.

Recently, we have developed a new type of composite core-shell NQDs that comprise a small quantum-confined core of CdSe overcoated with a very thick shell (up to 20 monolayers) of a wider gap material such as CdS [2]. The overall size of these composite particles is quite large (10 – 20 nm), therefore, they have been dubbed "giant" quantum dots (g-NQDs). Compare to traditional dots, g-NQDs show greatly increased absorption cross-sections, enhanced emission efficiencies, and improved photostability. Our initial studies also indicate that they exhibit reduced rates of Auger recombination, in which energy flows through other paths and is unavailable for lasing. All of these properties are beneficial for photonic applications, especially, in lasing technologies. The goal of this project is to evaluate the potential of g-NQDs in optical amplification and lasing through comprehensive studies of their electronic and optical properties conducted in conjunction with microstructural characterization and theoretical modeling of electronic states and carrier relaxation dynamics.

## Benefit to National Security Missions

This work can potentially enable novel types of compact, tunable lasers, providing thus a contribution to several technologically important areas such as optical amplification, fiber optics, telecommunication, and remote sensing. All of these areas are of significant interest to the DOE Office of Basic Energy Sciences.

## Progress

During the past year, we have studied single- and multi-exciton recombination dynamics in g-NQDs comprising a 5-nm CdSe core overcoated with 11 or 19 monolayers of CdS (Figure 1a). These studies indicate an increased radiative decay time compared to traditional nanocrystals (up from ~20 ns to ~60 ns). Further, we observe an approximately three-fold lengthening of Auger lifetimes compared to standard NQDs emitting at the same wavelength. The latter is a quite promising result from the perspective of lasing applications, because Auger decay represents a major factor that limits optical gain lifetimes in these structures.

We have also tested te optical-gain performance of g-NQDs by analyzing pump intensity onsets for amplified spontaneous emission (ASE) and ASE spectral properties. We observe that the ASE threshold drops down to just a few tens of microjoules per centimeter squared, which is one to two orders of magnitude lower than for standard, core-only nanocrystals (Figure 1b). We also observe other unusual optical-gain behaviors for these structures such as multi-band ASE spectra, in which the band-edge emission co-exist with higher-energy stimulated emission features due to transitions involving excited electronic states (Figure 1c). The overall spectral range of optical amplification in g-NQD samples extends over more than 500 meV. ASE with such a large spectral width has never been previously observed for any other types of optical gain media. The large spectral width of the optical gain can be used to produce lasing materials with a continuously tunable emission color.

To elucidate unusual optical-gain properties of g-NQDs, we have conducted effective-mass modeling of their electronic structures. The results of these calculations indicate that these nanocrystals belong to quasi-type-II structures, in which spatial distributions of electron and hole wave functions differ significantly from each other. The reduced spatial electron-hole overlap may explain the reduction in the rates of both single-exciton radiative decay and Auger recombination. These properties coupled with enhanced absorption cross-sections likely

result in the observed reduction in the ASE threshold and extension of the optical-gain spectral range.

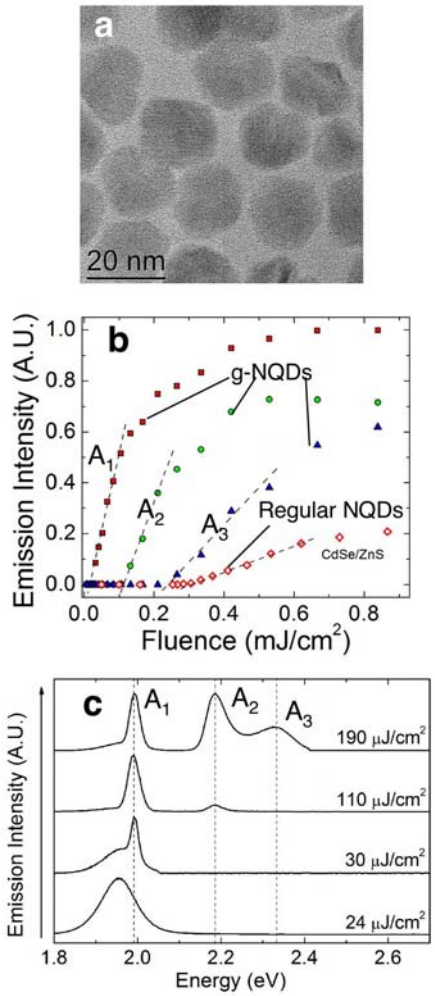


*Figure 1. (a) A transmission micrograph of g-NQDs comprising a 5 nm CdSe core overcoated with 19 monolayers of CdS. (b) The development of amplified spontaneous emission (ASE) in a g-NQD sample within three different spectral bands (labeled in panel c) as a function of pump fluence, in comparison to data for a regular core-only NQD sample. (c) The ASE spectra of g-NQD as a function of pump fluence.*

## Future Work

In our future work, we will conduct detailed studies of single and multiexciton dynamics in g-NQD as a function of "geometrical" (e.g., core size and shell width) and "electronic" (e.g., band offsets at the core/shell interface) parameters. This experimental work will be performed in conjunction with theoretical studies of electronic structures and carrier relaxation behaviors, conducted using effective mass approximation and perturbation approaches. In addition to ensemble spectroscopic methods, we will also utilize single-nanocrystal spectroscopies involving micro-photoluminescence and photon-correlation measurements. These studies will help us to distinguish between spectroscopic signatures of single- and multiexciton states and clarify the role of Coulomb effects in multiexciton dynamics. We will also study lasing performance of g-NQDs by combining them with various optical microcavities including photonic structures. As a result of these efforts, we will attain a better understanding of factors that control optical-gain spectral characteristics and relaxation dynamics, which will help in practical utilization of g-NQDs in lasing technologies.

## Conclusion

Our research is expected to lead to understanding of electronic structures and carrier relaxation behaviors in a recently developed, new type of nanocrystalline materials - giant NQDs. One anticipated result of our work is the understanding the role of Auger processes in recombination of multiexciton states. Since stimulated emission from multiexcitons dominates the optical-gain properties of nanocrystals, this work will help us to evaluate the potential of g-NQDs in lasing technologies. An expected practical outcome of this project is the demonstration of highly efficient, color-tunable lasing structures based on chemically synthesized nanoparticles.

## References

1. Klimov, V. I., A. A. Mikhailovsky, S. Xu, A. Malko, J. A. Hollingsworth, C. A. Leatherdale, H. J. Eisler, and M. G. Bawendi. Optical gain and stimulated emission in nanocrystal quantum dots. 2000. *Science.* **290**: 314.

2. Chen, Y. F., J. Vela, H. Htoon, J. L. Casson, D. J. Werder, D. A. Bussian, V. I. Klimov, and J. A. Hollingsworth. 'Giant' multishell CdSe nanocrystal quantum dots with suppressed blinking . 2008. *Journal of American Chemical Society.* **130**: 5026.

## Publications

Garcia-Santamaria, F., Y. Chen, R. D. Schaller, J. A. Hollingsworth, and V. I. Klimov. Multi-frequency, low-threshold amplified spontaneous emission from giant quantum dots. To appear in *2008 Fall Meeting of the Materials Research Society.* (Boston, MA, 1 - 5 December 2008).

# Modeling Control of Viruses by Immune Responses

*Alan S Perelson*

20080726PRD2

## Introduction

Humans during their lifetime encounter many pathogens. The immune system is responsible for clearance of these pathogens from the host. Clearance of intracellular pathogens, such as viruses, is mainly achieved by a special population of immune cells, CD8 T-cells that can kill pathogen-infected cells. Although for several viruses the importance of CD8 T cells in pathogen clearance has been established, many quantitative properties of the infection, such as the growth dynamics of the pathogen, and the dynamics of pathogen clearance by the CD8 T-cell response, are unknown in detail. This project aims to provide basic information about these dynamic processes.

## Benefit to National Security Missions

This project will support the DOE mission in threat reduction / WMD nonproliferation by enhancing our understanding of virus infections and the immune response to them. It is important to support other missions of the laboratory as well (e.g., Homeland Security), but not to the exclusion of the DOE mission.

## Progress

Postdoc appointment did not begin until September 2008. Thus, little progress so far. Nonetheless, one part of the proposal was on estimating the killing efficacy of CD8 T cells - T cells that control growth of viral infections in mice and humans. We have started a collaboration with the lab of Prof. Aron Lukacher (Emory University, Atlanta, GA) to measure the killing efficacy of CD8 T cells following a polyoma virus (PyV) infection of mice. Polyoma virus establishes a chronic infection in mice and our study will be the first one to quantify the killing efficacy of CD8 T cells during a chronic viral infection.

Preliminary results suggest that the killing efficacy of CD8 T cells specific to one epitope of PyV during the acute phase of the infection is very similar to previous estimates of the killing efficacy of CD8 T cells specific to a different virus, lymphocytic choriomeningitis virus. Also, during the chronic phase of the infection, CD8 T cells appear to maintain their killing efficacy, which is surprising given that it is believed that T cells generally loose their effector functions during chronic viral infections. We are currently discussing the possibility of additional experiments to test specific predictions of our model.

## Future Work

The proposed research is aimed at developing novel mathematical models describing the dynamics of viruses and CD8 T cell responses that can control viral growth. The developed models will be tested against data on the dynamics of viral infections and the host's CD8 T cell responses. The models will improve our fundamental understanding of how viral infections are fought. Specifically, we will investigate the growth kinetics of simian immunodeficiency virus (SIV) in sooty mangabeys (SM) the natural hosts of the virus and rhesus macaques (RM). Data for this project are available through a collaboration with Dr. G. Silvestri (Univ. Penn.). Many vaccines against HIV that stimulate CD8 T cells are currently being tested in RM. Many studies have shown, such vaccines fail to provide sterilizing immunity (i.e., cannot prevent viral growth in vaccinated hosts). Via a collaboration with D. Barouch (Harvard), we will investigate using mathematical models potential reasons for the failure of such vaccines by analyzing data on the dynamics of SIV and CD8 T cell responses in RM from vaccine trials. This analysis will allow us to estimate the in vivo efficacy of CD8 T cells in controlling viral growth in nonhuman primates. Furthermore, using available data on in vivo killing of virus-infected cells by CD8 T cells in mice during an acute viral infection (i.e., an infection that is cleared from mice within ten days or so), we will develop a quantitative framework to estimate the per capita killing efficacy of CD8 T cells in vivo. The developed models will be also applied to estimate the killing efficacy of CD8 T cells during a chronic viral infection of mice (i.e., an infection that is not cleared); the data for the analysis will be supplied by J. Wherry (Wistar Institute).

## Conclusion

Viruses infect us from time to time and cause disease and possibly death. Viruses, such as HIV and influenza, are of great concern. This project is aimed at developing a quantitative understanding of how the cell-mediated immune response fights such viruses. Currently, no approved vaccine is based on stimulating a cell-mediated immune response, although such responses in many infections are the body's main mechanism of clearing a viral infection. By improving our understanding of such responses this projects aims to bring us closer to being able to develop vaccines that stimulate cell-mediated immune responses.

# Multi-scale Analysis of Multi-physical Transport Processes of Electroosmosis in Porous Media

*Qinjun Kang*

20080727PRD2

## Introduction

Electrokinetic phenomena, such as electrophoresis and electroosmosis, were discovered nearly 200 years ago, and have had a wide range of applications in many fields ever since. However, simulation and analysis of these phenomena is a great challenge because of the multi-scale and multi-physics nature of the problem. None of the existing (macroscopic, mesoscopic, or microscopic) methods can individually solve this multi-scale multi-physical transport problem accurately with present-day computers. This problem will be further complicated if chemical reactions occur in the bulk fluid or at the fluid-solid interface. In this project, we will develop a comprehensive numerical framework to investigate electrokinetic flow coupled with reactive transport in porous media. We approach this problem in three stages by: 1) developing an innovative model for coupled electrokinetic flow and reactive transport in porous media, accounting for multi-physical transport processes, including fluid flow, electric potential distribution, ion convection and diffusion, as well as chemical reaction; 2) performing nano to micro upscaling analysis of these multi-physical transport processes; and 3) validating the numerical model through theoretical analysis and available experimental data.

The successful accomplishment of the proposed research will provide 1) an improved understanding of the multi-physical electrokinetic transport phenomena coupled with chemical reaction in micro/nanofluidic devices, 2) innovative techniques to bridge atomistic modeling based on first principals with mesoscale modeling based on statistical-analysis, and 3) a better understanding of the effect of nanoscale structures on the microscale devices.

This research will have direct implications in a broad spectrum of research relevant to LANL missions, including new energy exploitation (fuel cells and biofuels), fossil energy prospecting (oil and gas), environmental protection (decontamination of radionuclides in solids), biological applications (enzymatic analysis, DNA analysis, and proteomics), and biomedical applications (clinical pathology and bio-smoke alarm).

## Benefit to National Security Missions

This project will support the DOE/NNSA missions in Energy Security, Environmental Quality, and the missions of the Office of Science by enhancing our understanding of multi-physical (hydro-, thermo-, and electro-dynamic) transport processes of electroosmosis in natural porous media.

## Progress

Significant progress has been made in the past six months. Particularly, 1) we developed a multi-lattice Boltzmann method (LBM) framework to solve the strongly coupled nonlinear governing equations, 2) implemented a comprehensive boundary condition for electrokinetic nanoflows in silicon or glass channel, and, for the first time 3) investigated the problem of electrokinetic transport in microchannel with random roughness has been investigated.

At the pore scale (from microns to centimeters), the Poisson-Boltzmann (PB) model is available to describe electrokinetic transports within the electric double layer (EDL) for slowly-moving flows; however, when the scale goes down to submicrons or nanometers, the Boltzmann distribution assumption may break down due to the overlap of EDLs. Another factor that may invalidate the PB model is the heterogenous charge of surfaces. These factors can not be accounted for in the popular Poisson-Boltzmann model. The appliability of the Poisson-Boltzmann model is not only a fundamental problem in physics but also of significant importance for engineering applications. To investigate this problem, we introduced a more fundamental model, the Poisson-Nernst-Planck (PNP) model, without any ion distribution hypothesis. In this model, the fluid flow, electric transport, ion diffusion and convection, chemical regulation and energy transport are strongly coupled together. This model poses great challenges to numerical solutions, especially at micro- and nano-scales and for complex geometries.

Over the past few months, we developed a coupled

Lattice Boltzmann model framework to solve the coupled governing equations. The governing equation for each transport process is solved by a lattice Boltzmann model, and the entire process simulated through an iteration procedure. After validation, this method is used to study the applicability of the Poisson-Boltzmann model for electrokinetic flows in microchannels. The results show that for homogeneously charged long channels, the Poisson-Boltzmann model is applicable for a wide range of electric double layer thickness. For the electric potential distribution, the Poisson-Boltzmann model can provide good predictions until the electric double layers fully overlap, meaning that the thickness of the double layer equals the channel width. For the electroosmotic velocity, the Poisson-Boltzmann model is valid even when the thickness of the double layer is ten times the channel width. For heterogeneously charged microchannels, a higher zeta potential and an enhanced velocity field may cause the Poisson-Boltzmann model to fail to provide accurate predictions. The ionic diffusion coefficients have little effect on the steady flows for either homogeneously or heterogeneously charged channels. However the ionic valence of the solvent has remarkable influence on both the electric potential distribution and the flow velocity, even in homogeneously charged microchannels. Both theoretical analyses and numerical results indicate that the valence and the concentration of the counter-ions have a stronger influence than more obvious factors like the Debye length, the electrical potential distribution, and the ions transport. Our results may significantly improve the understanding of the electrokinetic transport characteristics in microchannels.

The surface charge may lead to chemical reaction and colloidal characteristics on the solid surfaces, depending on the pH value of the solution, the surface charge density, and temperature et al. This phenomenon is more important for nanoscale electrokinetic flows, especially in silicon and glass channels. The boundary condition caused by such reactive surfaces is also nonlinearly coupled among several equations. We have developed an efficient iteration algorithm and code to solve the boundary condition.

Due to its complexity, electrokinetic transport in microchannels with random roughness has never been investigated before. We have developed a numerical tool to model the electrokinetic transport in microchannels with random roughness. The three-dimensional microstructure of the rough channel is generated by a random generation-growth method with three statistical parameters to control the number density, the total volume fraction and anisotropy characteristics of roughness elements. The governing equations for the electrokinetic transport are then solved by a high-efficiency lattice Poisson-Boltzmann method in complex geometries. The effects from the geometric characteristics of roughness on the electrokinetic transport in microchannels are thereby modeled and analyzed. For a given total roughness volume fraction, a higher number density leads to a lower fluctuation due to the random factors. The electroosmotic permeability increases with the roughness number density, nearly as a logarithmic law for a given volume fraction of roughness, but decreases with the volume fraction of roughness for a given roughness number density. When both the volume fraction and the number density of roughness are given, the electroosmotic permeability is enhanced by increase of the characteristic length along the external electric field direction or decrease of the length of the direction of across the channel. For a given microstructure of rough microchannel, the electroosmotic permeability decreases with the Debye length. Compared with the corresponding flows in a smooth channel, the rough surface may enhance the electrokinetic transport when the Debye length is smaller than the roughness characteristic height under the assumption of constant zeta potential for all surfaces. The present results may improve the understanding of the electrokinetic transport characteristics in microchannels.

We are confident that our methods are the most advanced numerical techniques to investigate electrokinetic flows at the micro and nano scales. We expect that these new developments will lead to a series of high impact papers in peer reviewed journals. In fact, within our first six months, we have finished two manuscripts for high-impact journals.

## Future Work

The immediate next step is to integrate the comprehensive boundary conditions we proposed into the multi-LBM frame work to investigate the electrokinetic nanoflows. Future work will involve 1) developing innovative models for reproducing the multi-scale random microstructures of porous media through new numerical models to reflect the macroscale statistical information obtained from measurements; 2) performing micro->meso->macro upscaling analysis of multi-physical transport processes of electroosmosis in the porous structures, including fluid flow, electric potential distribution, ion convection and diffusion; and 3) developing a novel hybrid model to integrate the models for different scales so that the important information at the small scale can be captured without resolving the small scale in the entire computational domain.

## Conclusion

This project will enable a science-based understanding of electroosmosis, a phenomenon discovered nearly 200 years ago, and having had a wide range of applications in many fields since then. Particularly, the successful accomplishment of the proposed research will provide 1) an improved understanding of multi-physical transport phenomena of electroosmosis through multi-scale structures

of porous media, and 2) innovative techniques to bridge atomistic modeling with mesoscale modeling based on statistical-analysis and continuum modeling. This project will have direct implications in a broad spectrum of energy and environmental research, including new energy exploitation (fuel cells and biofuels), fossil energy prospecting (oil and gas), environmental protection (decontamination of radionuclides in solids), biomedical engineering applications, and novel materials design.

## Publications

Mukherjee, Partha P., M. Wang, Q. Kang, and P. C. Lichtner. Pore-Scale modeling of transport in charged porous media. Presented at *Computational Methods in Water Resources XVII International Conference.* (San Francisco, CA, 6-10, July 2008).

Wang, M., Q. Kang, and N. Pan. Thermal conductivity enhancement of carbon fiber composites. 2009. *Applied Thermal Engineering.* **29**: 418.

Wang, M., and Q. Kang. Modeling electrokinetic flows in microchannels using coupled lattice Boltzmann methods. *Journal of Computational Physics.*

# Fluvial Geomorphic Response to Permafrost Thawing: Implications for the Global Carbon Budget and Arctic Hydrology

*Cathy Jean Wilson*

20080788PRD3

## Introduction

Permafrost covers 24 percent of the exposed land mass in the Northern Hemisphere. The presence of permafrost serves to impede the flow of water from the surface to the subsurface controlling the balance between surface water runoff, lake volumes and groundwater flow into rivers. Studies of arctic lake distributions and base flows in arctic rivers indicate that global warming and permafrost degradation may already be having detectable impacts on the both surface and subsurface hydrology in arctic watersheds. Largely unstudied to date, however, is the feedback between permafrost distribution and the morphology and mobility of arctic river systems. Understanding the behavior of these river systems is critical to understanding the linkages and feedbacks between oceanic, atmospheric and terrestrial systems to global climate change.

Rivers are the key arteries that link terrestrial source areas (floodplains and hillslopes) to ocean sinks. Rivers also control both the sequestration and remobilization of carbon, nutrients and sediments within the large percentage of the arctic located in terrestrial lowlands. Estimates suggest that up to 1,200 Gt of carbon are presently trapped in permafrost with a large percentage of that fraction located in lowland areas. If permafrost degradation and/or warming of surface waters results in an increase in arctic river mobility, through increase bank erosion, much of the carbon presently frozen in floodplains may be mobilized. This carbon may rapidly oxidize or methylate and be released to the atmosphere. Alternatively, it may be flushed to the oceans where it could dramatically alter ocean geochemistry or be sequestered by deposition.

Changes in river mobility may also provide an additional feedback in the thawing of lowland permafrost. At present, most models of permafrost melting focus on the effects of increased air temperatures on the permafrost in near surface layers. It is well documented, however, that permafrost is substantially more degraded or entirely absent directly beneath rivers. An increase in the rate that rivers traverse their floodplains could greatly increase the degradation of permafrost to depths greater than currently anticipated. The role of groundwater flow through partially frozen soils is another critical aspect of permafrost dynamics largely overlooked in present warming models.

## Benefit to National Security Missions

This work allows us to begin to quantify global atmospheric loadings of Carbon in the form of methane or $CO_2$ for input into Global Climate Change models. Reducing uncertainty in climate predictions through better data and models is a central goal of the DOE Office of Science BER climate change mission.

## Progress

Our project commenced at the beginning of August 2008. In that time we have had two main focuses: 1) the development of remote sensing methodologies and data sets for the quantification of arctic river mobility, and 2) the development and application of coupled heat and fluid flow models to explore the processes governing thermal erosion of river banks and the coupling of surface and groundwater systems in permafrost dominated arctic watersheds. In both initiatives, we are leveraging existing LANL technologies and expertise to explore a critical and new component in the coupling of atmospheric and oceanic models of climate change to terrestrial processes.

Our preliminary GIS analysis of maps of existing global permafrost distributions and digital elevation models (used to identify rivers and floodplains) indicates that approximately 50% of North American and 40% of Asian permafrost lies in lowland areas bounding arctic rivers. Our initial remote sensing analysis has focused on a subset of North American floodplains located in Alaska

for which there is publically available aerial photographs and satellite imagery from the late 1970s to the present day.

Using the LANL's GeniePro, an adaptive, automated extraction technology for the analysis of remote sensing data, we have begun to analyze the Yukon Flats region of Alaska. Preliminary results indicate that GeniePro is a very effective tool for identifying and quantifying the boundaries of both river channels and lakes. Through ongoing collaborations with members of the International, Space, & Response (ISR) Division we are working on refining techniques for feature extraction with GeniePro, developing new strategies for precise image registration, and implementing algorithms for the discretization and quantification of spatial and temporal changes in river channels and lakes.

## Future Work

Through an additional collaboration within the Earth & Environmental Science (EES) Division we will use the "Maghnum" numerical model developed by Bryan Travis to model thermodynamic and groundwater interactions between arctic rivers and permafrost-rich floodplains. Maghnum is a coupled heat, fluid and vapor flow model with the capability of modeling the dynamics of freezing and melting of water ice. Maghnum was originally developed to examine Martian dynamics and our project represents a new application of this technology. Initial efforts with Maghnum suggest that it is extremely well suited to studying permafrost dynamics. Additional modifications to the existing code, to be implemented in the coming year, will involve developing numerical approaches for adjusting model boundary conditions to incorporate river bank erosion in order to quantify dynamic feedbacks between rivers and floodplains.

In addition our collaborations across LANL, we are actively engaged in developing collaborations with researchers at the University of Alaska, Fairbanks (UAF), Idaho State University (ISU) and the University of Pennsylvania. UAF researchers have extensive expertise and data resources (both in field studies and remote sensing) regarding permafrost dynamics and observations on changes in permafrost distribution in response to global climate change. Researchers at UPenn and ISU have funded field programs to examine river dynamics in response to changes in arctic river flow and sediment loading.

## Conclusion

Through these collaborations we will be able to leverage LANL's remote sensing and modeling expertise to gain data to test our analysis and calibrate our models. It is anticipated that these initial collaborations will serve as the foundation for future proposals to expand our research both geographically and in overall focus. We believe our initial focus on floodplain dynamics and development of the Maghnum code will allow for the expansion of our project to examine watershed scale processes. This work will be an important advancement in the coupling of terrestrial hydrological processes to both atmospheric and oceanic models looking in order to predict the fate of carbon under a changing global climate.

# Determinaing the Mechanisms of Enzymes Xylose Isomerase and HIV Protease Using Neutron Crystallography

*Paul Alfred Langan*

20080789PRD3

## Introduction

Understanding the structure of proteins and how they work is central to drug design. Most modern-day medicines are small organic molecules that block the activity of a specific enzyme that is essential for the infectious agent's proliferation. These medicines bind to a site in the enzyme that blocks the molecule involved in the infectious process from binding, or that prevents the reaction from proceeding. X-ray crystallography provides information on structure for drug design but less on the reaction mechanism. Most mechanisms involve the transfer of hydrogen (H), but mobile H atoms are invisible to X-rays. Neutrons can be used to determine the location and movement of H during a reaction. We propose to develop neutron crystallography techniques to derive the mechanisms of the enzyme D-xylose isomerase (XI) and apply those techniques to determine the mechanism and design more effective drugs for HIV-1 protease PR. We expect to established strategies for using this information in drug design. Modern-day drug design relies on a collection of different tools and the impact of generating a new tool and new ideas for structure-assisted drug design efforts would undoubtedly by great.

## Benefit to National Security Missions

The enzymes involved in this project are important for bioenergy and energy security. Rational drug design is important for biothreat reduction. Understanding enzyme mechanism is an important fundamental science mission.

## Progress

Although this project has just started (August 4th 2008) the postdoc, Andrey Kovalevsky, has already made significant contributions towards both of the main aims. In particular, he has grown a number of large crystal of XI with various ligands bound and data collection has already begun.

## Future Work

XI catalyzes the inter-conversion of aldo-sugars D-xylose or D-glucose to the keto-sugars D-xylulose and D-fructose, respectively, by using a divalent catalytic metal such as Mg2+. The reaction proceeds through several H transfer stages. We plan to obtain structures of XI in complex with substrates, substrate intermediates and substrate products so that I can map out the movement of H during the reaction and determine the detailed mechanism. A key strategy is inhibiting the protein (so that the substrates are unchanged) with nickel and cadmium metals (in place of Mg) and we have already shown that this works in preliminary X-rays studies at LANL on XI with a glucose substrate. We plan to use a crystallization robot in B division, the deuteration laboratory and PCS at LANSCE to grow large deuterated crystals of complexes and to collect neutron crystallography data. A crystallization robot has not been used before to optimize crystal size for neutron crystallography and new strategies will be developed. The presence of metals will allow structures to be determined in a new way using anomalous scattering methods.

The positions of H atoms in the active site of PR are believed to be crucial for its mechanism. Our goal is to exploit the strategies developed above to deuterate PR, obtain crystals and determine neutron structures for a) ligand-free (native) PR; b) PR complexed with an engineered substrate that could be trapped as a reaction intermediate; c) PR complexed with clinical drugs. We already have considerable experience with PR and drug design. We will express, purify and crystallize wild-type and mutant enzyme in the native and substrate- or inhibitor-complexed forms, collect neutron diffraction data at PCS, refine and analyze structures. We will then develop a strategy for exploiting this new information on mechanism and H location in rational drug design.

## Conclusion

We expect to obtain detailed information on the mechanisms of XI and PR within a two-year framework, a leap forward in our understanding of how enzymes work on the molecular level. We also expect to established strategies for using this information in drug design. Modern-day drug design relies on a collection of different tools and the impact of generating a new tool and new ideas for structure-assisted drug design efforts would undoubtedly be great.

## Publications

Kovalevsky, A., A. Katz, H. Carrell, L. Hanson, M. Mustyakimov, S. Fisher, L. Coates, B. Schoenborn, G. Bunick, J. Glusker, and P. Langan. Hydrogen location in stages of an enzyme-catalyzed reaction: time-of-flight neutron structure of D-xylose isomerase with bound D-xylulose.. 2008. *Biochemistry.* **47**: 7595.

# Exploring the Membrane Penetration Machinery of Bacterial Toxins

*Jaroslaw Majewski*

20061387PRD1

## Abstract

The membrane is also the gateway to the cell. It governs what passes in and out of the cell by controlling its composition of lipids and membrane proteins. There is no doubt that further advancements in membrane science will be essential to the medical fields. Our work focuses on providing new insights into membrane structure (including lateral structure, *ie.* lipid rafts or domains) by spotlighting membrane-toxin interactions and development of higher resolution structure determination techniques.

## Background and Research Objectives

Cells are highly organized with many functional units or organelles defined by one or more membranes. Inter-cellular interactions are very important communication systems for organisms. They are responsible for hormone secretion, immune response, and many other key aspects of an organism's survival. The membrane is the medium for which all of these inter-cellular interactions take place. At least 30% of the genome encodes for membrane proteins and at least 50% of all drugs target membrane proteins. The membrane is also the gateway to the cell. It governs what passes in and out of the cell by controlling its composition of lipids and membrane proteins. There is no doubt that further advancements in membrane science will be essential to the medical fields. Our work focuses on providing new insights into membrane structure (including lateral structure, *ie.* lipid rafts or domains) by spotlighting membrane-toxin interactions and development of higher resolution structure determination techniques. Likewise, the engineering of bio-membrane-based sensors requires that their properties on a solid support be known. Specifically, we have explored the membrane penetration mechanism of cholera toxin and botulinum neurotoxin (the most potent toxin known). Through these investigations we anticipate to find evidence supporting the significant role of lipid rafts during toxin-membrane interactions that are essential for membrane penetration. Once the membrane penetration mechanisms of these toxins are well understood, a mimetic mechanism may be utilized to bioengineer drug delivery methods to transfect cells with a desired drug or genetic therapy. Following the mission of national security, it is imperative that we establish rapid and accurate toxin-detection schemes to protect the public.

## Importance to LANL's Science and Technology Base and National R & D Needs

The research area of low dimensional advanced material structures (soft condensed matter) is of extreme current interest in the fields of physics, chemistry, medicine, and biology (including threat reduction problems). Specifically, this project focuses on the structure of bio-membranes and their interactions with proteins (toxins). Improving the knowledge of bio-membranes fits within DOE's Mission because understanding their behavior elucidates details in membrane interactions within an organism, aiding basic science which directly translates to technological developments which use membranes as platforms sensors that take advantage of nanotechnology.

## Scientific Approach and Accomplishments

### Toxin-Membrane Interactions

The main focus of this research project has been to study the binding and membrane penetration mechanisms of cholera toxin and botulinum neurotoxin using scattering techniques, fluorescence microscopy, and a Langmuir trough. We have been able to establish, through scattering measurements, that these toxins are able to induce phase transitions in the lipid membranes that can initiate the intoxification process. Recently, we have been able to clarify the role of pH dependence on toxin structure and membrane penetration.

### X-ray Studies at the Solid-Liquid Interface

This project has heavily concentrated on technique development to use x-ray reflectivity and grazing incidence

diffraction techniques to study single bilayer membranes, with full hydration, on a solid support. Previously, measurement of these samples was confined to neutron reflectivity. The role of interactions with the substrate with the biomembrane was elucidated and quantified. We have been able to characterize a single bilayer of DPPC, the hydrogen atom of phospholipids.

## The Role of Cholesterol in Membrane Defects

The Smith-Lemli-Opitz syndrome (SLOS) is an often lethal birth defect resulting from mutations in the gene responsible for the synthesis of 3-hydroxy-steroid$^{7}$-reductase (DHCR7), the enzyme that catalyzes the reduction of the double bond at carbon-7 on 7-dehydrocholesterol (7-DHC) to form unesterified cholesterol. The incidence of SLOS is on the order of 1:20,000–1:70,000 and is more common in individuals of European heritage. For comparison, the three most common autosomal recessive genetic conditions in childhood are commonly listed as cystic fibrosis (1:2,500), phenylketonuria (1:14,000), and galactosemia (1:40,000). Newborns with SLOS have specific facial abnormalities and often suffer cleft palate, congenital heart disease, genitourinary abnormalities, and syndactyly. In addition, they typically demonstrate mental retardation and brain abnormalities and are characterized further by an almost uniform failure to thrive. It is hypothesized that the deficiency in cholesterol biosynthesis and subsequent accumulation of 7-DHC in the cell membrane leads to defective composition, organization, dynamics, and function of the cell membrane. Tulenko *et al* have demonstrated, using x-ray diffraction and other techniques, that increased 7-DHC and reduced cholesterol content leads to abnormal membrane fluidity and atypical membrane organization.

Preliminary studies using x-ray reflectivity and grazing incidence diffraction of model monolayers containing 7-DHC, prepared to mimic SLOS membranes, revealed atypical membrane organization when compared to equivalent membranes containing cholesterol instead of 7-DHC. In addition, monolayers composed of real cell membrane extracts from SLOS children have been measured. GIXD reveals a significant decrease in lateral order when 7-DHC is present in the membrane relative to when cholesterol is present. This trend is observed in both the model membranes and membranes from real cell extracts. From reflectivity, membranes containing 7-DHC also are thinner by approximately ~4Å.

## Scattering Studies of Cell Extracts

Using Surface Science to Construct a Better Model Membrane: Membrane fusion is a critical and recurring cellular event. Although ubiquitous, the fusion process is complex, varies with cell or membrane type and thus presents challenges to isolating the fusion machinery *in vivo*. Cell membranes are multi-component structures but typically studied model membranes consist of only one or two lipid classes. Intracellular vesicle interactions, in particular phagosome-lysosome interactions, offer the opportunity to study membrane fusion *in vivo* and *in vitro* thereby making development of an accurate membrane model feasible. To construct a model of the phagosome-lysosome system, we have been studying phagosomal extracts derived from beads phagocytosed by J774 cells. We have completed preliminary work investigating the behavior of monolayers and bilayers derived from the cell extracts utilizing the Langmuir-Blodgett trough, fluorescence microscopy and AFM. To our knowledge, the use of GIXD to study the in-plane and out-of-plane structure of cell extracts has not been reported in the literature. Therefore, it is extremely advantageous to perform an in-depth structural study of cell membrane extracts via GIXD.

## Exploring the Structure of Cushioned Lipid Bilayers

Solid supported lipid bilayers have been heavily studied for the past three decades. There are two main methods used to form the supported bilayer – vesicle self-assembly and LB and LS deposition. Vesicle self-assembly takes advantage of the instability of small uni-lamellar vesicles with substrate contact to form a supported membrane. LB and LS methods are more cumbersome, but have the advantage of being able to control the composition of the inner and outer leaflet independently and, if deposited at high surface pressures, typically yield more tightly packed bilayers. Although useful for many biophysical studies, the close proximity of the solid support hinders the investigation of integral membrane proteins (IMPs) as interactions with the substrate can greatly alter the IMPs' conformation and render it un-functional. The primary strategy for increasing the spacing between the substrate and bilayer is creation of a water rich polymer spacer or tether region to cushion the bilayer. These ultrathin polymer layers are intended to mimic the generic role of the extracellular matrix or the cytoskeleton.

The structure of the cushioned bilayer system is frequently characterized using fluorescence microscopy (FM) and fluorescence recovery after photobleaching (FRAP), surface plasmon resonance (SPR), and ellipsometry to demonstrate that the substrate is well covered by the bilayer **and that the lipid bilayer retains fluidity.** A major hurdle is that

FM and FRAP are relatively poor structural characterization tools due to limited resolution. We would like to take advantage of using neutron reflectivity (NR) measurements which have the ability to characterize a complete range of structures, from patching to complete based on the density of the bilayer as well as the spacing between the substrate and the lipid bilayer. The use of NR in tandem with x-ray reflectivity (XR) and grazing incidence x-ray diffraction (GIXD) will be used to characterize the structure of the lipid bilayer and cushion will enable a greatly improved understanding of these hybrid systems.

The majority of cushioned bilayer systems that have been described in the literature utilize adsorbed polymer layers, grafted polymers, or lipopolymer tethers. In all cases, the polymer layer acts as a hydrophilic, deformable and mobile substrate upon which the bilayer membrane rests. Each method has been demonstrated to yield reasonably complete bilayers, as established primarily by FM and FRAP. Grafted polymers typically take advantage of thiol or silane coupling depending on the substrate chemistry. All previous NR measurements of cushioned bilayers involve thiols, which couple to metal surfaces such as gold or silver. The scattering from relatively thick metal layers unfortunately swamps the signal from the subsequent organic layers deposited on top of the metal film. As a result, our studies of grafted systems will be limited to silanes which are effective couplers to oxide surfaces such as glass, silicon with its native oxide layer, and quartz. A number of silanes have been used to anchor polymer cushions or tethers to substrates to cushion lipid bilayers. In general, the thickness of the cushion can be tailored by the molecular weight of the PEG polymer chain as well as its grafting density. A number of other grafting motifs have been used including the addition of lipid or lipid-like anchors at the distal end of the polymer chain to enhance coupling between the polymer cushion and supported lipid bilayer. For example, a number of groups have created cushioned bilayers by simple incorporation of PEG lipid conjugates. Cremer and co-workers have demonstrated that cushioned membranes can be formed by mixing in a small fraction of PEG-lipid (e.g. 2000 MW PEG – DSPE) and vesicle incubation or Langmuir-Blodgett deposition. On the other hand, Hristova and coworkers have found that the bilayer deposition method is critical and that the length or grafting density of PEG-lipids used does not directly impact the diffusion of small proteins incorporated into the membrane. A missing piece of information in both of the above studies is the actual structure of the cushioned membrane complex that is formed. In both cases, no structural characterization was conducted; only FM and FRAP measurements were used. Part of the challenge is the difficulty in obtaining reliable and high resolution measurements of the structure of bilayer cushioned membranes in water with techniques such as SPR and ellipsometry. We further suggest that FM and FRAP are relatively poor characterization tools due to limited resolution.

We plan to measure silane-based polymer cushioned lipid bilayers as a function of the PEG length, PEG-lipid cushioned complexes, and bilayers formed on deposited polymer layers at the quarz/water and silicon/water interface. For example, cellulose polymer cushions deposited by Langmuir-Blodgett deposition have been used to reconstitute integrins into lipid bilayers. The unique aspect of this project will be some of the first structural characterization afforded by NR measurements. Once well-characterized samples are available that consistently yield cushioned bilayers, their application in biosensor technologies will be greatly increased.

## Publications

Miller, C. E., J. Majewski, E. Watkins, and T. L. Kuhl. Probing the Local Order of Single Phospholipid Membranes Using Grazing Incidence X-ray Diffraction. To appear in *PRL.*

Miller, C. E., J. Majewski, E. Watkins, and T. L. Kuhl. Part I: An X-ray Scattering Study of Cholera Toxin Penetration and Induced Phase Transformations in Lipid Membranes. To appear in *Biophysical Journal.*

Miller, C. E., J. Majewski, K. Kjaer, M. Weygand, R. Faller, S. Satija, and T. L. Kuhl. Neutron and X-ray scattering studies of cholera toxin interactions with lipid monolayers at the air-liquid interface.. 2005. *Colloids and Surfaces B.* **40**: 159.

Miller, C. E., J. Majewski, R. Faller, S. Satija, and T. L. Kuhl. Cholera toxin assault on lipid monolayers containing ganglioside GM1. 2004. *Biophysical Journal .* **86**: 3700.

Miller, C. E., J. Majewski, T. Gog, and T. L. Kuhl. Grazing incidence diffraction of cadmium arachidate multilayers at the solid-liquid interface.. 2005. *Zeitschrift Fur Kristallographie.* **220** (12): 987.

Miller, C. E., J. Majewski, T. Gog, and T. L. Kuhl. Characterization of biological thin films at the solid-liquid interface by X-ray reflectivity.. 2005. *PRL.* **94** (23): 238104 .

Miller, C. E., J. Majewski, and D. Busath. Integration of Ganglioside GT1b Receptor into DPPE and DPPC Phospholipid Monolayers: An X-ray Reflectivity and Grazing Incidence Diffraction Study. *biophysical Journal.*

Miller, C. E., J. Majewski, and T. L. Kuhl. Characterization of single biological membranes at the solid-liquid interface by X-ray reflectivity.. 2006. *Colloids and Surfaces A* . **284**: 434.

Miller, C. E., J. Majewski, and T. L. Kuhl. Part II: Diffraction from 2D Cholera Toxin Crystals Bound to their Receptors in a Lipid Monolayer. To appear in *Biophysical Journal.*

# Numerical Techniques of Rifting and Passive Margin Formation: The Role of Mantle Plumes

*David Coblentz*

20061388PRD1

## Abstract

Since the 1970s the concept of mantle plumes has been used to explain hot spot volcanism located within the tectonic plates (such as the Hawaii-Emperor island chain) and more recently to explain anomalous magmatic activity (for example in continental rift zones) that has major climatic and biotic implications. Because there is growing evidence to suggest that the mantle plume idea does not explain magmatic and volcanic (and related seismic) activity in most continental rift zones, we test other possible causes. In this project, we investigate the origin of volcanism in continental rift zones by using and developing numerical modeling techniques.

## Background and Research Objectives

The outermost part of the Earth from the surface to about 200 km depth is called the lithosphere. This is the solid outer layer of the Earth, consisting of the crust and the rigid uppermost part of the mantle. It is broken up into tectonic plates or lithospheric plates (Figure 1 inset). These tectonic plates move with respect to one another; they either collide at convergent boundaries, or spread apart at divergent boundaries, or move parallel to each other at transform boundaries. The lithospheric plates are not totally rigid; they deform internally, for example to form rift zones where the lithosphere is extended. Such continental rift zones will eventually result in the formation of divergent plate boundaries and passive margins. The lithospheric plates move on top of a lower viscosity layer, the asthenosphere. The asthenosphere flows like a liquid on geological time scales. Below the asthenosphere the mantle material is more rigid again.

The inner part of the Earth, below the mantle, is the core. Many scientists believe that mantle plumes are formed at the core-mantle boundary. These mantle plumes would be an effective manner to transport heat toward the surface of the Earth (the Earth is cooling). Upon arrival at the surface of the Earth, the mantle plume high temperatures would result in massive melting of rocks, resulting in volcanism and the formation of large igneous provinces on Earth- the mantle plume theory. Whether mantle plumes exist or not is however a topic of debate [2]. There are many indications that mantle plumes exist, coming for example from seismic tomography [3]. Seismic tomography reveals seismic wave velocity anomalies there where mantle plumes are expected, indicating that warm mantle material is transported toward the surface of the Earth, in agreement with the mantle plume theory. There are however just as many indications that mantle plumes might not exist, or at least not exist in the form that the mantle plume theory predicts. For example, the mantle plume theory predicts that the surface of the Earth would be elevated above a mantle plume, but this has not been observed.

Another point of discussion is what, if any, influence mantle plumes would have on plate tectonics and the lithosphere. When mantle plumes are formed deep in the Earth they are expected to move upwards toward the base of the lithosphere. Arrived at the surface (or at the base of the lithosphere), their high temperatures would result in melting of rocks, and scientists have suggested that their arrival might result in the formation of continental rifts, and eventually passive margins and divergent plate boundaries. If this is the case, then there should be a relation between divergent plate boundaries, passive margins, huge amounts of magmatism (i.e., large igneous provinces), and mantle plumes. Figure 1 shows a map of the Earth with the large igneous provinces on Earth, the mantle plumes, and some of the volcanic divergent plate boundaries. In some places such a relation seems to be present (such as the northern North Atlantic), in other places the relation does not exist; divergent plate boundaries have been formed without magmatism (southern north Atlantic), or volcanic provinces are not related to mantle plumes or divergent plate boundaries (Siberia).

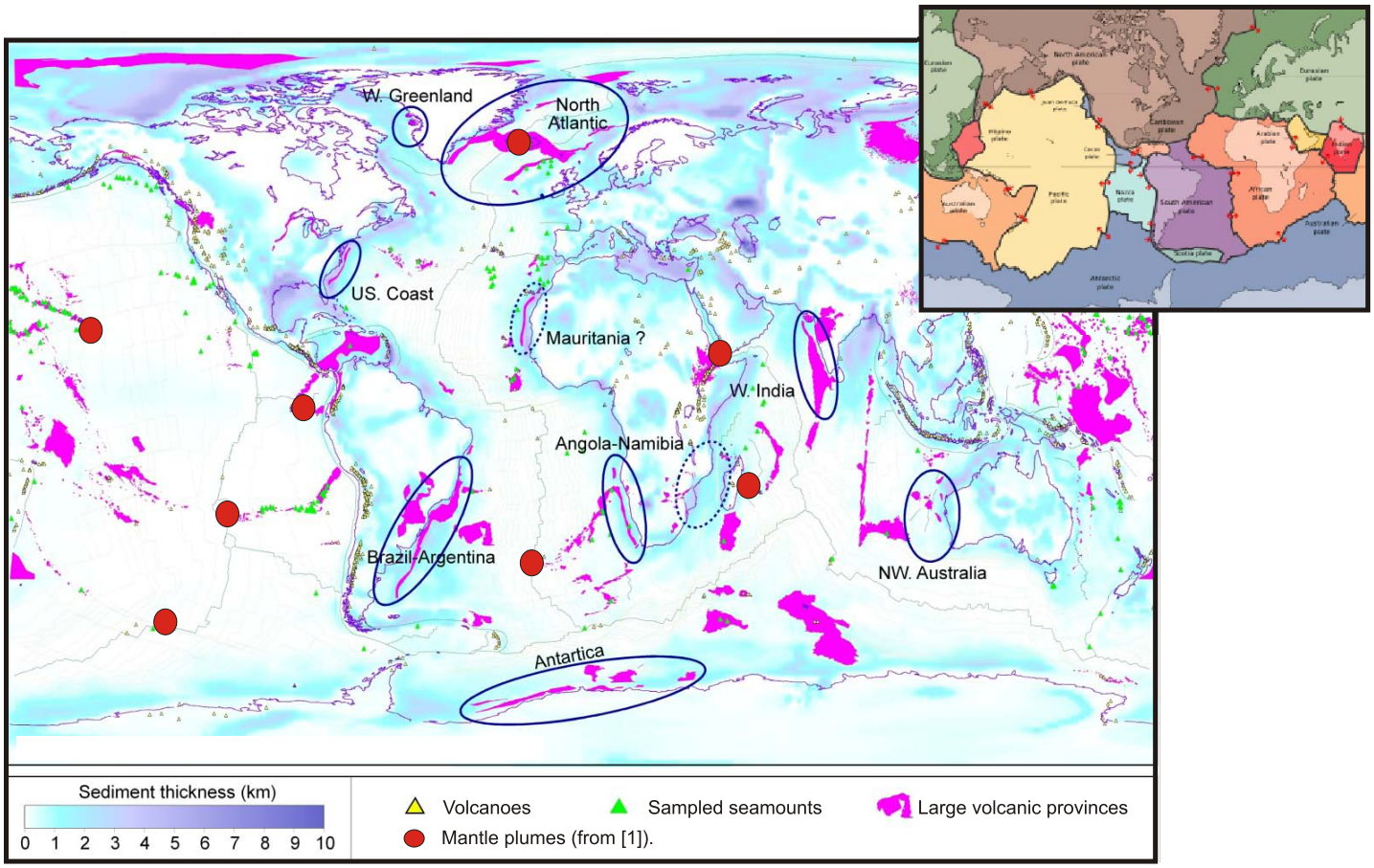


*Figure 1. World map, showing the relation between excess volcanism (large volcanic provinces) and mantle plumes. Large volcanic provinces (magenta), mantle plumes as proposed by [1] (red), volcanic rifted margins (encircled blue). The blue shading on the map is the sediment thickness. Map modified from L. Gernigon (Norwegian Geological Survey). Inset: major tectonic or lithospheric plates, shown in different colors.*

The focus of this research is the relation between continental rifts and the formation of divergent plate boundaries, magmatism, surface uplift, and mantle plumes. Divergent plate boundaries form after a period of rifting, or extension and thinning of the lithosphere. We develop and use numerical models to study rifting of the lithosphere, and the relation with the underlying asthenosphere. Model predictions of temperature are translated into synthetic seismic wave velocity structures that are then compared with seismic tomography. After developing the models, we have applied them to continental rift zones such as the Rio Grande rift, the East African Rift, the West Antarctic rift zone and the northern North Atlantic volcanic province. We have also applied the models to intercontinental magmatism that is not related to rifted lithosphere: the Colorado Plateau region in the southwestern US.

**Observations**

*West Antarctic Rift system*

The Transantarctic Mountains are a major mountain belt bisecting the Antarctic continent (Figure 2A) [4]. The mountain range is located on the tectonic boundary between non-cratonic West Antarctica and cratonic East Antarctica. Cratonic lithosphere is very old, strong, cold and thick lithosphere, and it has therefore other deformation characteristics than normal lithosphere. The Transantarctic Mountains belong to the longest mountain ranges on Earth; the range has a length of 3500 km and mountain peaks over 4 km high. The range follows the West Antarctic rift system along its entire length, but a possible relation between the formation of the mountain range and the rift system is unclear. Recent seismic tomography studies in Antarctica give constraints on the mantle structure beneath the area. Using numerical models, we find an explanation for uplift of the Transantarctic Mountains that are supported by the recent seismic tomography.

*The Rio Grande Rift zone*

Recent seismic imaging across the Rio Grande Rift in the southwestern US revealed unexpected structures in the underlying mantle [6]. A low seismic wave velocity anomaly is present below the rift, while high velocity

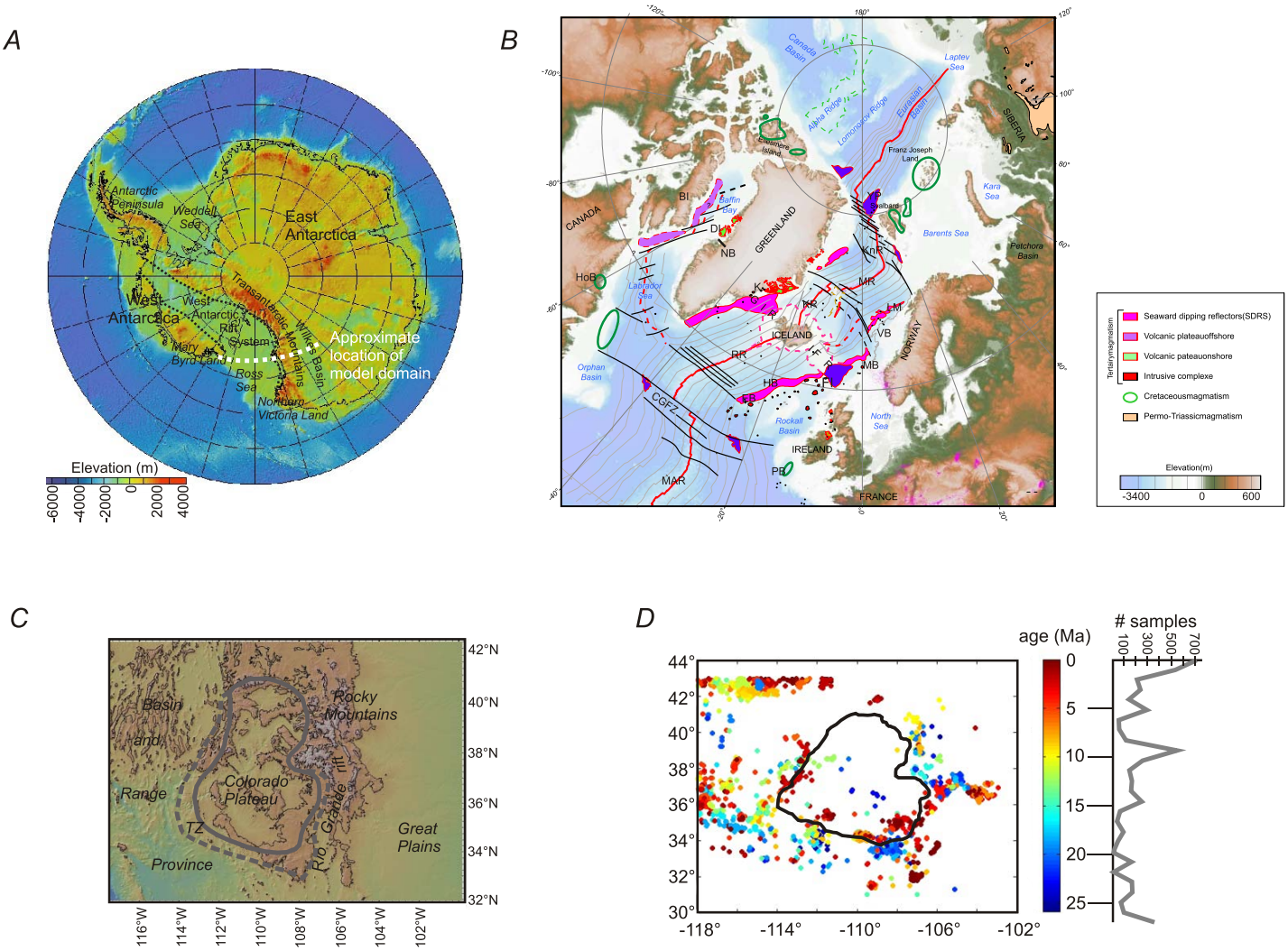


*Figure 2. A) West Antarctic Rift study area, showing the main geological structures and topography. The West Antarctic Rift is flanked by an elongated mountain range, the Transantarctic Mountains. We show in our numerical models that these geological structures are related to each other. B) The North Atlantic Igneous Province, with volcanic passive margins, Iceland, intrusive and extrusive magmatic complexes, and the divergent plate boundary (Mid-Atlantic spreading ridge). Here, the Iceland mantle plume is thought to be responsible for formation of this volcanic province and breakup of the continents and formation of the divergent plate boundary. C) Southwestern US study area with the Colorado Plateau and the Rio Grande rift indicated. D) Same study area as shown in C), the colored dots show the location and timing of magmatism. Yellow and red colors show recent magmatism, blue colors are older magmatic centers. Note the limited amount of magmatism inside the Colorado Plateau.*

structures are found beneath the rift flanks [7]. Such a low seismic wave velocity anomaly beneath the rift indicates higher than normal temperatures, and is often interpreted to result of a (small) mantle plume. However, there is only moderate magmatic activity in the Rio Grande rift (Figure 2C and D), which is not in agreement with a mantle plume. We have modeled the formation of the Rio Grande rift, and calculated from the model predicted temperature structure the corresponding synthetic seismic wave velocity anomaly. As a first, this synthetic seismic wave velocity structure was compared to tomographic data to explain the structures in the seismic tomography.

*Colorado Plateau*

The Colorado Plateau is a major tectonic and physiographic province centered on the Four Corners region of the southwestern United States noted for its tectonic stability relative to its neighboring provinces (Figure 2C). The Plateau has behaved as a coherent block across much of Phanerozoic time, during which it has been seemingly impervious to the Mesozoic compression and Cenozoic extension and magmatism that sculpted the adjacent Basin and Range province and Rio Grande rift zone (Figure 2C, D). A recent pulse of magmatism is observed around the edges of the Colorado Plateau. This is intraplate volcanism,

not related to plate boundaries or continental rift zones. We show with numerical models that this magmatism can be explained by upwelling mantle material at the edges of the Plateau [9].

*Volcanic rifts and mantle plumes*

Figure 1 shows that many volcanic rifted margins or continental rift zones are related to mantle plumes. Based on this observation, it has been suggested that mantle plumes might be responsible for continental breakup. Two areas on Earth where this hypothesis can be tested are the East African Rift system, and the northern part of the North Atlantic (Figure 1). In a review manuscript we have tested the mantle plume hypothesis for formation of the volcanic North Atlantic. We have used numerical models to study the problem in the East African Rift system.

## Importance to LANL's Science and Technology Base and National R & D Needs

This project supports the DOE by providing world-class scientific research needed to ensure the success of DOE missions in national and energy security and advance the frontiers of knowledge in physical and computational sciences.

## Scientific Approach and Accomplishment

### Newly developed numerical models of mantle flow beneath continental rifts

We have modified a finite element code for upper mantle flow to include a high-viscosity lithosphere and visco-plastic rheology. A visco-plastic rheology realistically describes deformation of the lithosphere. With this model, we are able to study both flow in the mantle and asthenosphere, and deformation of the lithosphere. A detailed model description can be found in [7].

### Updating the technique for synthetic seismic velocity structures

The method we use to convert a given thermal structure as a function of pressure/depth and composition into seismic velocity and density consists of three components: (1) calculation of the phase diagram which provides the mineral proportions and mineral composition, (2) calculation of the mineral elastic parameters and density at the desired pressure-temperature conditions, and averaging of the mineral properties according to their proportions from step 1, (3) addition of the dispersive effects on velocity of anelasticity.

We updated our previous approach [8], see for a detailed description [7].

### Results

*The West Antarctic Rift and Transantarctic Mountains*

We used numerical models [4] to study the formation of the West Antarctic rift zone. The numerical models included the strong cratonic lithosphere of East Antarctica. The models suggest that uplift of the Transantarctic Mountains is related to formation of a small crustal root beneath the range (visible in Figure 3A) and the formation of the adjacent West Antarctic Rift system. Upon extension of the lithosphere, the rift is formed at the boundary between cratonic East Antarctica and non-cratonic West Antarctica. Figure 3A shows an excellent agreement between our numerical models and tomographic data.

*The Rio Grande Rift zone*

Recent seismic imaging across the Rio Grande rift revealed a low seismic wave velocity anomaly below the rift and high velocity structures below the western Great Plains. They have previously been interpreted to result from compositional, temperature or melt contributions. We performed a dynamic test of these interpretations using a lithosphere-upper mantle model (Figure 3B). The models show that the formation of the Rio Grande rift zone could not have started as long as the lithosphere of the western US was under compression from the Late Cretaceous-Early Tertiary low-angle subduction of the Farallon plate. When the state of stress changed to wide-spread extension in the Basin and Range area in the Oligocene, formation of the Rio Grande rift was facilitated west of the edge of the Great Plains craton where the lithosphere became weakened by thermal erosion. The low seismic wave velocity that is present beneath the Rio Grande rift can to a large extent be explained by passive upwelling normal temperature asthenosphere, allowing the presence of small amounts of melt only. The fast anomaly beneath the western Great Plains can be explained thermally as cold downwelling lithosphere, destabilized by small-scale convection.

*Magmatism and the Colorado Plateau*

We propose small-scale edge-driven convection, induced by variations in lithosphere thickness imposed by Cenozoic extension on both sides of the Plateau, as the source of magmatism. The cold temperature regions in the numerical models correspond well with the imaged seismic tomographic structures by the RISTRA seismic experiment[10].

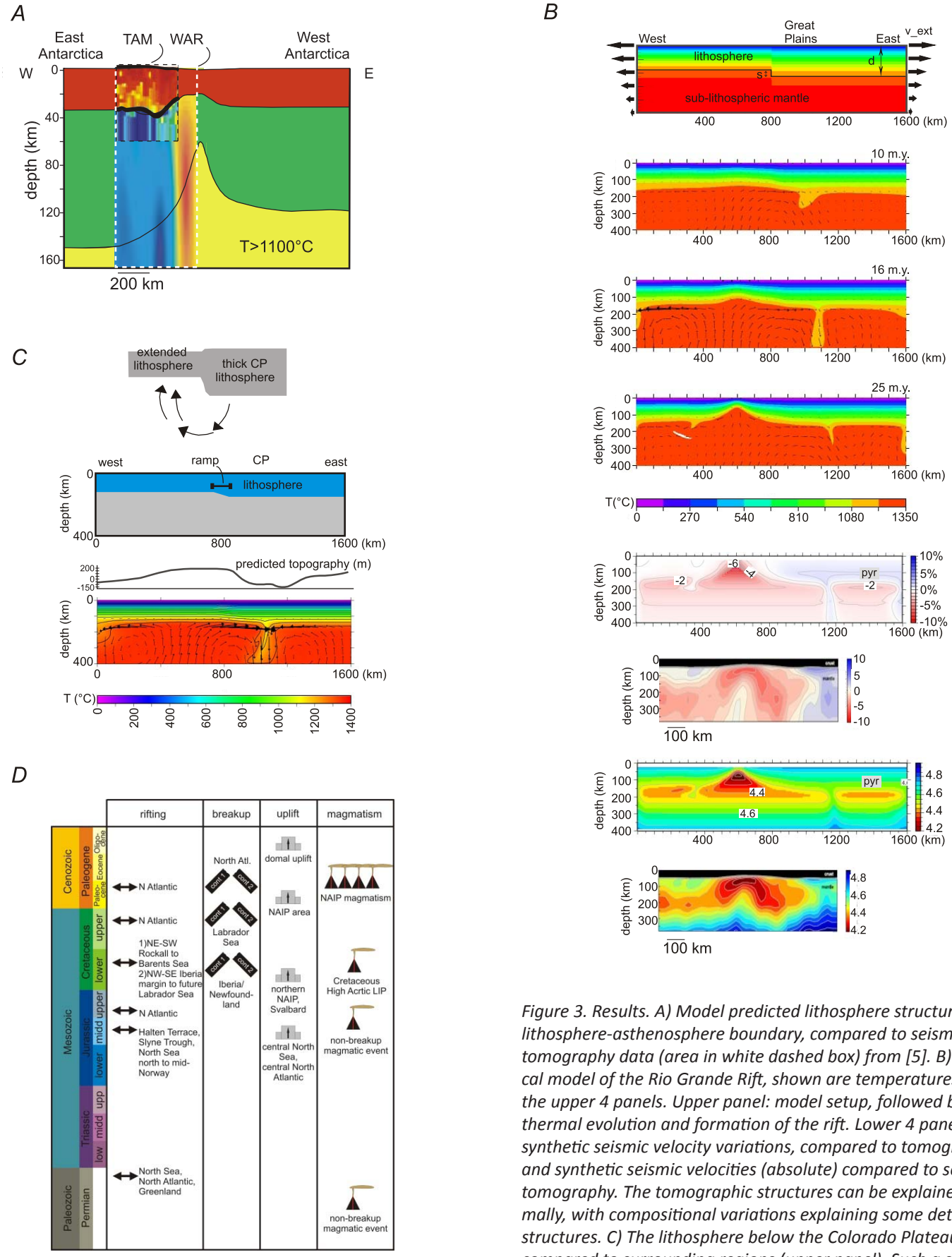


*Figure 3. Results. A) Model predicted lithosphere structure and lithosphere-asthenosphere boundary, compared to seismic tomography data (area in white dashed box) from [5]. B) Numerical model of the Rio Grande Rift, shown are temperatures in the upper 4 panels. Upper panel: model setup, followed by the thermal evolution and formation of the rift. Lower 4 panels: synthetic seismic velocity variations, compared to tomography, and synthetic seismic velocities (absolute) compared to seismic tomography. The tomographic structures can be explained thermally, with compositional variations explaining some detailed structures. C) The lithosphere below the Colorado Plateau is thick compared to surrounding regions (upper panel). Such a step in lithosphere thickness is included in our numerical models (middle panel). It causes convection whereby the upwelling mantle*

*material results in magmatism along the edges of the Colorado Plateau. D) Tectonic history of the North Atlantic volcanic province, including uplift of the surface, magmatism, and the timing of continental breakup. Such a detailed reconstruction [2] clarifies the relation between mantle plumes, volcanism and the formation of divergent plate boundaries.*

Numerical geodynamic modeling corroborates this hypothesis and offers an explanation for the differential uplift along the Plateau margins that is consistent with the geochronologically constrained inward CP edge migration of volcanic centers and asthenospheric finite strain inferred from seismic anisotropy.

These modeling results and seismic observations suggest that Colorado Plateau lithosphere is being destroyed by entrainment in small-scale edge-driven convection at both edges imaged by RISTRA (Figure 3B). We suggest that rapid Miocene extension and asthenospheric upwelling beneath the Basin and Range province (Figure 2C) emplaced a temperature jump at the Basin and Range-Colorado Plateau boundary that initiated the current convective system. The convection is removing parts of the Colorado Plateau lithosphere along its western edge, and is responsible for a magmatic/volcanic front migrating towards its interior.

*Volcanic rifts and mantle plumes*

The mantle plume concept is currently being challenged as an explanation for North Atlantic Igneous Province formation. Alternative models have been suggested, including delamination, meteorite impact, small-scale rift-related convection, and chemical mantle heterogeneities. We review available datasets on uplift, strain localization, age and chemistry of igneous material, and tomography for the North Atlantic Igneous Province, and compare them with predictions from the mantle plume and alternative models [2]. The mantle plume concept is quite successful in explaining formation of the North Atlantic Volcanic Province, but unexplained aspects remain. Delamination and impact models are currently not supported. Rift-related small-scale convection models appear to be able to explain volcanic rifted margin volcanism well. However, the most important problem that non-plume models need to overcome is the continuing, long-lived melt anomaly extending via the Greenland-Faeroe Ridges to Iceland.

In the East African Rift system, we find that the magma resulting from the Afar mantle plume has intruded the lithosphere and caused rift segmentation [10]. This explains the architecture of the rift.

## References


1. Courtillot, V., J. Davaille, J. Besse, and J. Stock. Three distinct types of hotspots in the Earth's mantle. 2003. *Earth and Planetary Science Letters* . **205**: 295.

2. Meyer, R., J. W. Wijk, and L. Gernigon. The North Atlantic Igneous Province: a review of models for its formation. 2007. *Geological Society of America Special Paper "The origins of melting anomalies: plumes, plates and planetary processes".* **430**: 525.

3. Montelli, R., G. Nolet, F. S. Dahlen, G. Masters, R. E. Engdahl, and S. Hung. Finite-frequency tomography reveals a variety of plumes in the mantle. 2004. *Science* . **303**: 338.

4. Van-Wijk, J. W., J. F. Lawrence, and N. W. Driscoll. Formation of the Transantarctic Mountains related to extension of the West Antarctic Rift system. 2008. *Tectonophysics* . **458**: 117.

5. Lawerence, J. F., D. A. Wiens, A. A. Nyblade, S. Anandakrishan, P. Shore, and D. Voigt. Upper mantle thermal variations beneath the Transantarctic Mountains inferred from teleseismic S-wave attenuation. 2006. *Geophysical Research Letters.* **33**: 23.

6. Gao, W., S. Grand, W. S. Baldridge, D. Wilson, M. West, J. Ni, and R. Aster. Upper mantle convection beneath the central Rio Grande Rift imaged by P and S wave tomography. 2004. *Journal of Geophysical Research* . **109**: doi:10.1029/2003JB002743.

7. VanWijk, J. W., J. van Hunen, and S. Goes. Small-scale convection during continental rifting: Evidence from the Rio Grande Rift. 2008. *Geology* . **136**: 575.

8. Goes, S., R. Govers, and P. Vacher. Shallow mantle temperatures under Europe from P and S wave tomography. 2000. *Journal of Geophysical Research* . **105**: 11153.

9. VanWijk, J. W., S. Baldridge, J. van Hunen, D. Coblentz, R. Aster, J. Ni, and S. Grand. Mantle upwelling at the western and southern margins of the Colorado Plateau: an explanation for Neogene magmatism. *Geology* .

10. Corti, G., J. W. Van Wijk, S. A. P. L. Cloetingh, and C. Morley. Tectonic inheritance and continental rift architecture: numerical and analogue models of the East African Rift System. 2007. *Tectonics* . **26**: doi:10.1029/2006TC002086.

## Publications

Beutel, E., C. Ebinger, and J. van Wijk. Concentration of extensional stress by magma bodies responsible for recurring magmatism in the East African Rift. *Journal of Geophysical Research.*

Corti, G., J. van Wijk, S. Cloetingh , and C. Morley. Tectonic inheritance and continental rift architecture: numerical and analogue models of the East African Rift System . 2007. *Tectonics* . **26**: 1.

Corti, G., and J. W. Van Wijk. Modeling the architecture of the East African Rift System. Invited presentation at *European Geophysical Union Meeting.* (Vienna, April 2006).

Karlstrom, K., E. Crow, L. Crossey, D. Coblentz, and J. W. van Wijk. Model for tectonically driven incision of the <6 Ma Grand Canyon. To appear in *Geology.*

Lawerence, J., J. van Wijk, and N. Driscoll. Tectonic implications for uplift of the Transantarctic Mountains, in Antarctica: A Keystone in a Changing World . *USGS Open-File Report* .

Meyer, R., J. van Wijk, and L. Gernigon. The North Atlantic Igneous Province: a review of models for its formation . 2007. *Geological Society of America Special Paper* . **430**: 525.

Péron-Pinvidic, G., J. van Wijk, D. Shillington, and L. Gernigon. Role of magmatism in continental lithosphere extension . *Tectonophysics* .

VanWijk, J. W.. Geodynamic models of lithosphere deformation. Invited presentation at *MYRES Meeting.* (Italy, July 2006).

VanWijk, J. W.. Mantle flow beneath rift zones. Invited presentation at *Upper Mantle Imaging Conference.* (Woods Hole, MA, July 2006).

VanWijk, J. W., R. Meyer, and L. Gernigon. North Atlantic Igneous Province: A review of models for its formation. To appear in *North Atlantic Igneous Province: A review of models for its formation.*

VanWijk, J. W., and D. K. Blackman. Oblique extension of slow-spreading ridges. Invited presentation at *European Geophysical Union Meeting.* (Vienna, April 2006).

VanWijk, J. W., and G. Corti. Numerical and analogue models of oblique extension: application to the East African Rift. Invited presentation at *MYRES Meeting.* (Italy, July 2006).

VanWijk, J., S. Baldridge, J. van Hunen, D. Coblentz, R. Aster, J. Ni, and S. Grand. Mantle upwelling at the western and southern margins of the Colorado Plateau: an explanation for Neogene magmatism. *Geology* .

VanWijk, J., and L. Gernigon. North Atlantic Igneous Province formation: An interdisciplinary geophysical and geochemical review. Invited presentation at *European Geophysical Union Meeting.* (Vienna, April 2006).

vanWijk, J., J. van Hunen, and S. Goes. Small-scale convection during rifting: evidence from the Rio Grande ri. *GEology.*

vanWijk, J., J. van Hunen, and S. Goes. Small-scale convection during rifting: evidence from the Rio Grande rift . 2008. *Geology.* **36**: 575.

vanWijk, J., R. Aster, S. Grand, D. Coblentz, J. Ni, and S. Baldridge. Lithospheric erosion and edge driven convection at the margins of the Colorado Plateau. *Nature.*

vanWijk, J., and D. Blackman. Development of en echelon magmatic segments along oblique spreading ridges . 2007. *Geology.* **35**: 599.

vanWijk, J., and L. Gernigon. Discussion on "Mechanisms of crustal growth in large igneous provinces: the North Atlantic Province as a case study '. To appear in *Geological Society Special Paper* .

# Measurements of Absorption and Scattering by Aerosols: How do they Offset Global Warming?

*Manvendra Krishna Dubey*

20061397PRD1

## Abstract

Humankind's fossil energy emissions have increased greenhouse gases and air-pollution that have together warmed our global climate by 0.6 C over the anthropocene (preindustrial to present). The additional +2.6 W/m$^2$ heat trapped (positive radiative forcing) by anthropogenic greenhouse gases is well quantified. The net cooling (negative radiative forcing) by air-pollution, principally small particles called aerosols that scatter away sunlight is substantial but ill quantified with a range of -2.4 to -0.6 W/m$^2$. Therefore the net societal radiative forcing of 0.6 to 2.4 W/m$^2$ while positive is uncertain by a factor of 4, limiting our ability to predict climate change. The problem arises due to the complex nature of aerosols, for example sulfate aerosols scatter sunlight to cool climate while black carbon (soot) aerosols absorb sunlight to warm climate. In reality light and dark aerosols transform and mix in the atmosphere, and the optical properties of this mixed aerosol determines their net radiative forcing. A key observational gap has been our limited ability to measure light absorption by aerosol. Current methods collect particles on substrates and monitor light attenuation. We have developed and applied a new photo-acoustic method to measure light absorption by aerosols directly without any substrate. Our photo-acoustic field data show that the substrate-based methods suffer from severe artifacts and can overestimate light absorption under polluted conditions.

## Background and Research Objectives

The cooling by aerosols by pollution has offset about half the warming by greenhouse gases over the industrial era. However, this masking effect of aerosols is uncertain by a factor of 4 and limits our ability to simulate the past warming and predict future climate change. This uncertainty arises due to the complex and dynamic chemical, physical and optical properties, and often competing of aerosols on our radiation budget and climate. For example, sulfate aerosols scatter sunlight cooling the air while black carbon particles absorb sunlight to warm the air. Real atmospheric aerosols are mixtures of these aerosol types with a varied degree of mixing with a range of optical properties, which can cause cooling or warming. Therefore, reliable measurements of optical measurements over a range of aerosol conditions are essential to quantify the aerosol climate forcing. Unfortunately, the community has been confined to the use of filter-based instruments that are known to have large artifacts that have to be carefully corrected for and have associated uncertainties. Our project has made a quantum leap in measurement technologies to measure aerosol optical properties and applied them to quantify the aerosol radiative forcing in a variety of regimes; urban, remote, cloudy and Arctic to fill this gap.

## Importance to LANL's Science and Technology Base and National R & D Needs

Achieving energy security and ensuring the sustainability of the earth system is an emerging mission at LANL. Our project better defines the past and current climate forcing by aerosol pollution from societal fossil energy use activities. Specifically it enables the diagnosis of past observed warming and retrieves more accurate estimates of climate responses to past forcings. This is critical to forecast future warming by greenhouse gases.

## Scientific Approach and Accomplishments

*Climate sensitivity*, the ratio of warming to radiative forcing, which determines the vulnerability of our Earth system to human activity and natural variability, *remains ill constrained* and uncertain by a factor of 2 to 4. Accurate determination of this parameter is essential to inform energy policy for effective transition to a carbon neutral economy. The forcing by anthropogenic greenhouse gases is well quantified. The large uncertainty in *climate sensitivity* arises from incomplete knowledge of forcing by aerosols. Quantifying the role of aerosols poses a challenge because of their complex

composition, short lifetime, heterogeneous distributions, ability to absorb and scatter solar and terrestrial radiation, and their effects on clouds. Furthermore, aerosol induced weakening of the hydrological cycle is a key water sustainability issue for the 21st century. Our project made quantum leaps in optical instrumentation to measure in situ the absorption and scattering.

We helped develop and deploy a new photoacoustic instrument, which measures both absorption and scattering in situ without using the substrate collection that is employed in conventional methods (e.g. Particle Soot Absorption Photometer or PSAP). We deployed our instrument for numerous DOE, NOAA and NSF campaigns. The regions sampled ranged from remote to urban and include Mexico City, Alaska, California, Houston, Oklahoma, Colorado and Korea. Our field data clearly showed that conventional filter based (e. g. PSAP) methods can systematically overestimate aerosol absorption by a factor of 2 to 3 particularly in polluted urban environments (Figure 1).

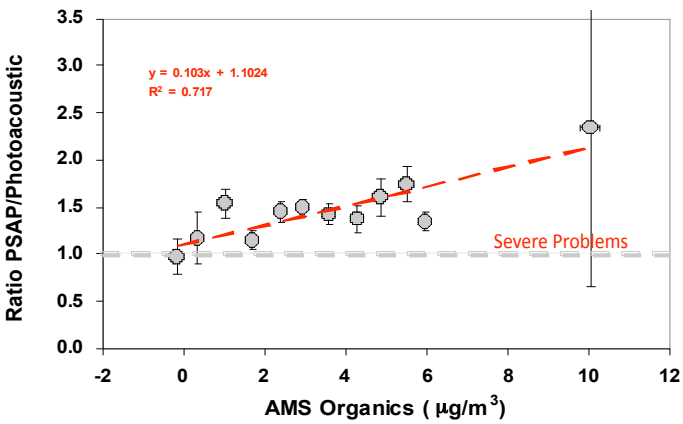


*Figure 1. Ratio of conventional filter based (PSAP) absorption and our photoacoustic absorption made above Houston as a function of organic aerosols. Numbers greater than 1 clearly show that traditional filter methods have a systematic high bias of PSAP under polluted conditions and should be treated with caution. Our does not use any substrate and is reliable.*

Based on this finding DOE's ARM project has funded us to deploy a new 3-laser photoacoustic instruments at their Southern Great Plains site to correct their conventional PSAP data set. Our advances included the deployment of the world's first 3 laser photoacoustic instrument to measure aerosol absorption and scattering at 405 (blue), 532 (green) and 781 (red) nanometers, spanning the solar spectrum. We have demonstrated that this instrument can discriminate dust from soot – both are absorbing aerosols. Furthermore our field campaigns were successfully integrated to glean process-level information on aerosol physical-chemical transformations in the atmosphere as they age and effect clouds. We highlight the following results from field campaigns:

1. We observed a *dark aerosol plume within a marine stratus cloud* in California during a field campaign in 2005. Our analysis shows that soot, when mixed with sulfate, is effectively scavenged by cloud drops. This alters cloud reflectivity, and needs to be considered in climate models. We also demonstrated that in aged plumes soot, sulfate and salt are internally mixed and result in high single scatter albedo, which is independent of the cloud water (Figure 2).

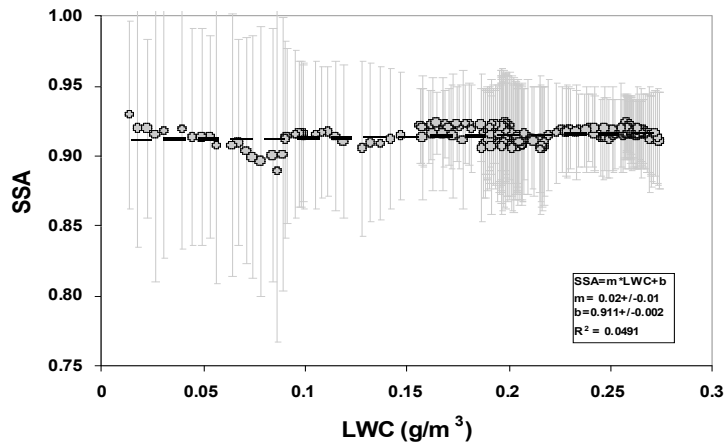


*Figure 2. Single scatter albedo (SSA), a measure of the aerosol darkness ( 1 is light sulfate, 0.3 is dark soot) versus the cloud water in a polluted cloud off the coast of California indicating that soot, sulfate and salt are internally mixed so that their SSA is independent of cloud water.*

2. We measured diurnal profiles of aerosol absorption and scattering in Mexico City. We discovered a *large photochemical production of organic aerosols* in the afternoon, which is missing in current models. We also measured changes in absorption by soot and linked it to boundary layer dynamics and changes in the shape of soot aggregates (fractal morphology) (Figure 3). We integrated a wealth of data to estimate the *net radiative forcing by pollutants and greenhouse gases for a megacity, a new metric to guide policy.*

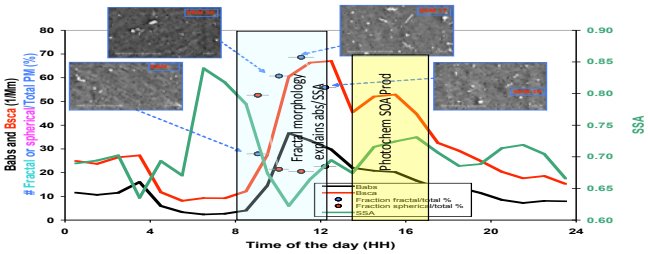


*Figure 3. Diurnal profiles of optical properties and soot morphology measured at Picos Tres Padres about 1 km above Mexico City in 2006. The secondary organic aerosol scattering peak in the afternoon and the late morning absorption peak, are new processes that are not resolved in current climate models.*

3. We discovered that *cloud processed aerosols are darker* above Houston and Oklahoma (Figure 4). This could result from selective scavenging of sulfate and/or reducing the size of the aerosols. These new mechanisms are now being incorporated in global models to better quantify the role of aerosol pollution in climate change.

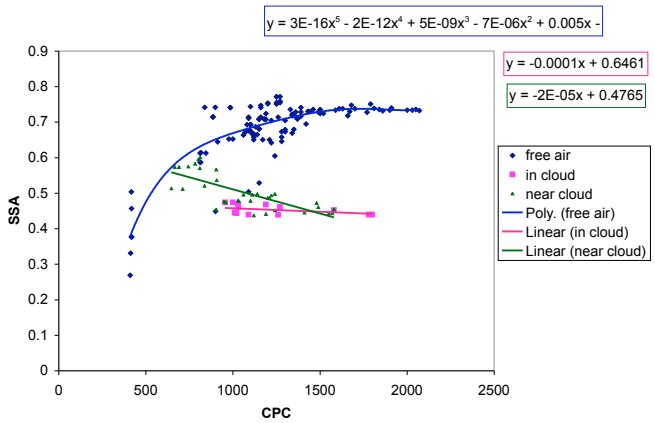


*Figure 4. Observed single scatter albedo (a measure of the aerosol darkness) versus condensation particle counts over Houston for cloud free, near cloud and in cloud air showing the darkening (lower SSA) of aerosols by cloud processes. These details are not resolved in current climate models and can be very important.*

Our new aerosol process level findings are now being incorporated in next generation climate models to better predict the future impacts of energy policies on our earth system.

## Publications


Herndon, S. C., T. B. Onasch, E. C. Wood, J. H. Kroll, M. R. Canagaratna, M. A. Zavala, W. B. Knighton, C. Mazzoleni, M. K. Dubey, R. Seila, B. de Foy, J. Fast, L. T. Molina, C. E. Kolb , and D. R. Worsnop. The correlation of secondary organic aerosol with photochemical ozone in a megacity outflow. *Geophysical Research Letters.*

Mazzoleni, C., M. Dubey, P. Chylek, and P. Arnott. In Situ Measurements of Absorbing Aerosols from Urban Sources, in Maritime Environments and during Biomass Combustion. Presented at *American Geophysical Union.* (San Francisco, 11-15 December 2006).

Mazzoleni, C., P. Arnott, M. Dubey, P. Chylek, J. Seinfeld, R. Flagan, T. Rissman, H. Jonsson, S. Murphy, and A. Sorooshian. In-cloud measurements of absorbing aerosols during the Marine Stratus Experiment, CA 2005. *Atmospheric Chemistry and Physics.*

Mazzoleni, C., H. D. Kuhns, J. Witt, N. Nussbaum, H. Moosmuller, O. Chang, G. Parthasarathy, S. K. Nathagoudenpalayam, G. Nikolich, and J. G. Watson. A real world case study of tailpipe emissions for school buses using a 20% biodiesel blend. 2007. *Science of the Total Environment.* **385** (1-3): 146.

Mazzoleni, C., M. Dubey, R. Chakrabarty, H. Moosmüller, P. Chylek, T. Onash, M. Zavala, S. Herndon, and C. Kolb. Diurnal Evolution of Aerosol Optical Properties and Morphology at Pico Tres Padres, Mexico City. Presented at *IUGG 2007 meeting.* ( Perugia, Italy, 2-13 July 2007.).

Mazzoleni, C., M. K. Dubey, P. Arnott, P. Chylek, and J. Seinfeld. Insights from insitu measurements of black carbon during the Marine Stratus Experiment. 2005. In *American Geophysical Union (EOS Transactions).* (San Francisco, 4-9 December 2005). Vol. 86(52), p. A31B. Washington DC: AGU.

Olsen, S. C., M. K. Dubey, C. Mazzoleni, P. Chylek, Y. Zhang, J. T. Randerson, and L. Horowitz. Estimates of Megacity Radiative Forcing. *Science.*

# Fluorescence Lifetime Spectroscopy by Flow Cytometry

*James Paul Freyer*

20061468PRD2

## Abstract

We have constructed and tested an improved phase-sensitive flow cytometer (PSFC) system for measuring a variety of fluorescence kinetic parameters. This improved system includes use of a LANL-developed digital data acquisition system to record and process data from the analog detectors. The PSFC has been applied to measurements of autofluorescence lifetimes of cells, measurement of fluorescence lifetimes of novel fluorescence proteins and separation of spectrally-overlapping fluorophores. We have also developed a novel, completely digital approach to acquiring phase-sensitive data that should allow relatively simple addition of this technology to any commercial flow cytometer, considerably extending the impact of this work.

## Background and Research Objectives

Fluorophores are excitable molecular species that emit light after they absorb light, which is useful for several analytical biology applications. The basis of phase-sensitive flow cytometry is the use of a modulated laser beam: essentially the laser is turned off and on very rapidly so that the sample is exposed to a time varying optical excitation. This means that the fluorescence emitted by the sample is also modulated, varying from a maximum at the peak excitation to zero when the beam is off. However, emission of a fluorescence signal is time-delayed relative to the excitation, since it takes a finite time (referred to as the fluorescence lifetime) for the excited state of the fluorophore to decay and emit the fluorescence photon. Typically, the laser modulation is a sine wave with a frequency in the range of 10-50 MHz. The fluorescence emission will also be a sine wave, but the emitted light is phase-shifted due to the delay induced by the fluorescence lifetime. Measurement of this phase shift provides a means of directly measuring the fluorescence lifetime of the fluorophore being excited. A robust phase-sensitive flow cytometry - fluorescence activated cell sorting (PSFC-FACS) system may have several positive, and perhaps global, outcomes for analytical biology and every-day engineering applications. Currently FACS is a commercially available technology that is used world-wide on the benches of thousands of biochemistry labs. Our current PSFC system, which analyzes biological materials as they flow past a sensor, can be improved in several aspects. To-date, PSFC measurements 1) have only been demonstrated over a narrow range of fluorophore lifetimes, 2) are restricted to single-exponential fluorescent decay measurements and to a limited extent, bi-exponential decay, and 3) lack translation to a FACS system.

The primary objective of this research was to improve the techniques used to measure phase-sensitive fluorescence parameters by flow cytometry, with the end goal of constructing a new PSFC that is simpler to operate and has better phase discrimination. A second goal was to demonstrate the application of this technology to several relevant biological problems, including the reduction of autofluorescence background, the separation of spectrally-overlapping fluorophores and the measurement of fluorescence lifetimes of engineered fluorescent proteins. A final goal was to implement a completely digital approach to measuring phase information in flow cytometry.

## Importance to LANL's Science and Technology Base and National R & D Needs

This project supports the National Flow Cytometry Resource, an NIH-funded national biomedical technology resource dedicated to the development, application and dissemination of new flow cytometry instrumentation and techniques. The instrumentation developed out of this work is important to the national biomedical community due to its wide applicability in a variety of fluorescence measurement problems, including: separation of overlapping fluorophores; reduction of autofluorescence background; and direct quantification of fluorescence lifetime. Potential research and clinical applications include: improved measurement of dim fluorescence signals (important in many immunostaining techniques); improved separation of overlapping fluorophores (important in immunostaining and multiplex-

ing methods); improved engineering of novel fluorescent proteins (important as ligands for labeling a variety of cells and cellular constituents); and improved detection of cellular processes (important in ligand binding and measurement of molecular environments). The successful development of a digital system for measuring phase parameters in flow cytometry also has considerable importance in technology transfer, as this would allow simple addition of this parameter to existing commercial instruments.

## Scientific Approach and Accomplishments

Our initial approach involved making hardware improvements to the existing phase-sensitive cytometer, which had originally been developed by Steinkamp and colleagues. As described below, one of the improvements was to use the Open Reconfigurable Cytometry Acquisition System (ORCAS), a digital data acquisition system developed by the flow cytometry team at LANL, to collect the signals from the analog phase processing electronics on the original instrument. About halfway through this project, we hit upon the idea of using the signal processing capabilities of ORCAS to directly extract the phase information from the digitized output of the photomultiplier tubes used to detect the fluorescence signals. This improvement bypasses the analog processing components, resulting in a simpler, cheaper and more precise collection of phase information. Concurrent with these technical developments, we have demonstrated the application of the PSFC to several different types of fluorescence measurements.

### Original PSFC Improvements

The original PSFC instrument used analog radio-frequency (RF) components to both modulate the laser and to collect and process the fluorescence signals, as illustrated in Figure 1. A continuous-wave laser was modulated by inserting an electro-optical modulator (EOM) in the light path prior to sample excitation. We have made several improvements to this system that have markedly improved its performance. The first improvement was the use of the ORCAS digital data system to digitize the outputs from the analog RF components. This allowed for improved signal collection and decreased noise. The ORCAS system was also used to do some of the calculations required for extracting fluorescence lifetimes (e.g. ratios of the sine and cosine of the modulated signals) in digital space instead of by using separate analog components. The second major improvement was the installation of a newer solid state laser diode that could be directly modulated. Not only did this result in an improved depth of modulation compared to the EOM (i.e. "off" was truly off), but also any of several different diodes could be placed in the same housing to obtain a wide variety of excitation wavelengths. We also made other improvements in the flow cell, photo-multiplier tubes (PMTs) and light scatter detector (used as a trigger for the fluorescence signal as well as a non-phase shifter reference signal). Over the first year of the project all of these upgrades were installed and tested, and several different types of phase-sensitive fluorescence measurements were made (described in section 3.3 below).

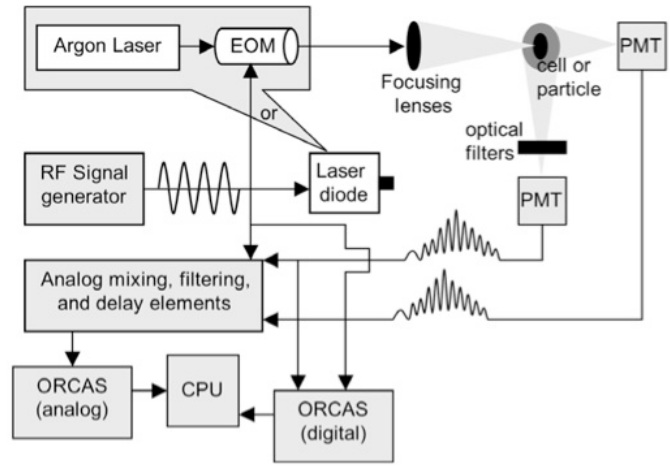


*Figure 1. Schematic diagram of the redesigned PSFC instrument, illustrating the optical and electronic components. Note the original signal path through the analog components and the new path directly into ORCAS.*

### Digital Phase Measurement

We have recently demonstrated the ability to acquire fluorescence lifetime without analog hardware. As illustrated in Figure 1, the outputs of the PMTs and the reference signal are run directly into ORCAS. The methods to bypass the analog mixing, delaying, and filtering steps include directly capturing the correlated modulated fluorescence signals and reference sinusoidal signals directly by the ORCAS system. The signals are then sorted and post-processed to determine the average lifetime shifts. Fitting routines such as fast Fourier Transform filtering are used to acquire the phase shift and amplitude of the correlated waveforms. The phase shift between the reference sine wave and modulated pulse is directly proportional to the fluorescence lifetime of the sample. Figure 2 provides the results from preliminary measurements using scattering beads, Flow-Check microspheres and CHO cells stained with ethidium bromide for total DNA content. Waveforms were collected directly into ORCAS, and subsequently with the traditional analog phase system at the same frequency. Our data suggest that one can easily acquire digital lifetime values similar to the analog system, but without any of the RF analog hardware. Combined with the use of a directly modulated solid-state laser, this new development will allow the addition of fluo-

rescence lifetime capabilities to an existing flow cytometer with very little modification or expense. Optimization is still ongoing to decrease variation in waveform fitting and in the frequency response of the ORCAS system.

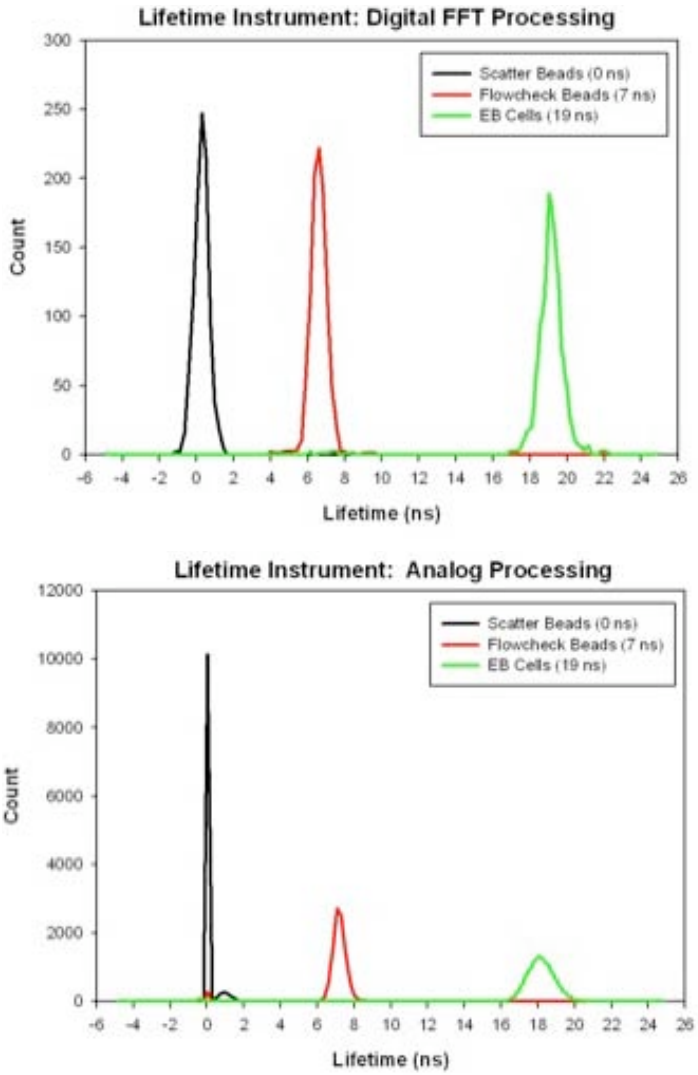


*Figure 2. Comparison of fluorescence lifetimes measured with the analog components (top) and the new digital processing method (bottom).*

**PSFC Applications**

We have used the improved PSFC instrument to make several types of fluorescence measurements that demonstrate the power of this technology for a variety of biomedically-relevant applications. We will discuss three of these briefly below: 1) measurement of the endogenous fluorescence lifetimes of cells; 2) measurement of the fluorescence lifetimes of engineered fluorescent proteins; and 3) use of a fluorescence lifetime signal to separate multiple fluorophores with overlapping emission spectra.

**Endogenous fluorescence lifetimes**

In a first application for developing phase-sensitive technology, we have acquired the average lifetime of intrinsic fluorophores from viable cell samples: these data have been published recently in a Proceedings paper. This project is motivated by the need to acquire statistically significant values of bulk autofluorescence lifetimes at wavelengths used in typical cytometry applications. The identification of the average lifetime from endogenous species, which are ubiquitous to cells, is the first step towards assays and applications that easily separate autofluorescence noise from dim fluorescence tags. In addition to reducing the autofluorescence noise floor in cytometry, lifetime measurement may also provide information about how the endogenous species emission may or may not impact emission from extrinsic tags. Finally, combined spectral and autofluorescence information on unstained cells can provide information about the endogenous molecular species that fluoresce in cells, and may allow the label-free separation of different cell types or physiological alterations. Two cell types, one non-tumorigenic and one tumorigenic, were measured over a wide range of excitation wavelengths. A lifetime 'spectrum' was ultimately acquired from the average lifetime results, as shown in Figure 3. It is clear from these data that the average autofluorescence lifetimes of cells vary across the excitation spectrum, over a range from 2-10 ns. An interesting finding of this work was that the autofluorescence lifetimes of proliferating and quiescent cells differed significantly at 488 nm excitation: we are following up this observation with measurements on other cells types.

**Lifetimes of fluorescent proteins**

Intrinsically fluorescent proteins have become invaluable tools for the labeling of cells and cellular constituents. There is considerable effort both within LANL and externally to develop novel fluorescent protein reagents. We have demonstrated the ability to measure the fluorescence lifetime of cells expressing fluorescent proteins, as illustrated in Figure 4. It is clear from these data that we can easily resolve even relatively small differences in fluorescence lifetime (<1 ns). One important application of this technology that we are working towards is the ability to sort cells based on lifetime measurements: this would allow the screening of different fluorescent proteins to select for those with long lifetimes (which translates into increased fluorescence intensity). A second application is the ability to separate bound from unbound fluorescent proteins, based on a change in lifetime upon binding: this would allow the detection of specific binding of a protein ligand in a high background of unbound ligand (which would eliminate the need for washing steps to remove unbound protein).

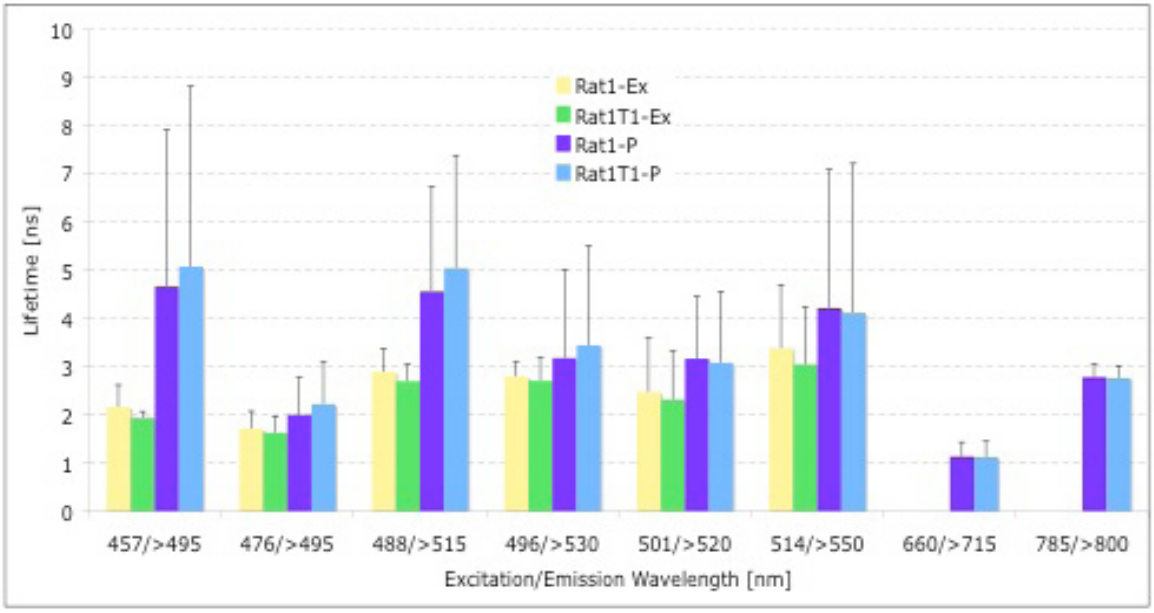


*Figure 3. Fluorescence lifetime values for two different cell lines (Rat1 and Rat1-T1) in two different growth stages (Ex: exponentially growing; P: plateau non-growing) at eight different excitation/emission wavelengths. Values are means and standard deviations for 3-5 different experiments.*

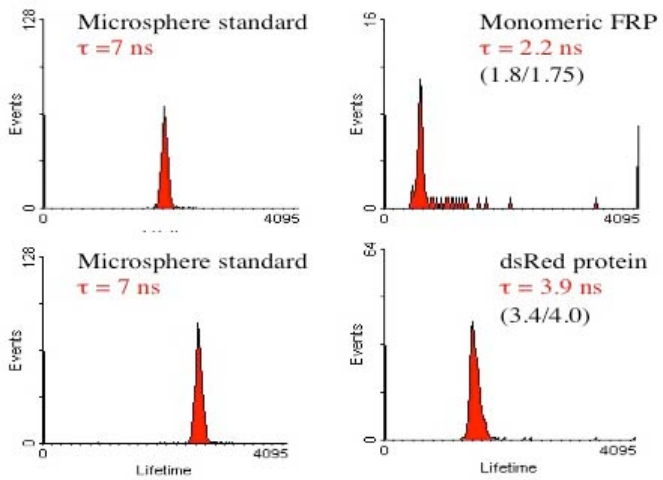


*Figure 4. Fluorescence lifetime histograms for control microspheres (left panels) and cells expressing two different fluorescent proteins (right panels). Numbers in red are lifetime values obtained with the PSFC instrument, while numbers in black represent measurements on a fluorescence lifetime spectrometer.*

## Separation of fluorophores

In order for lifetime measurements to contend with intensity-based multiplexing and provide solutions for the complex cytometry assays, we have proposed several applications that involve multiplexing based on lifetime. Recently, using combinations of fluorescence microspheres, we demonstrated that we could separate populations based on nanosecond lifetime changes or less. Figure 5 is the first example in which a mixture of four bead populations with similar intensities were separated in spite of having highly overlapping spectral emissions. All populations were separable without gating, compensation, or other methods, even though all data were collected in the same fluorescence emission channel. The average lifetime of each microsphere type was exploited to collect the 2-D histograms, showing clearly defined populations. We have also demonstrated the ability to separate overlapping fluorescence emissions using a technique referred to as "phase-filtering": the fluorescence of one fluorophore in a mixed sample is basically removed by filtering out phase shifts of a certain magnitude. Applications of this technique include reducing nonspecific dye binding fluorescence and autofluorescence background interferences for Raman scattering applications.

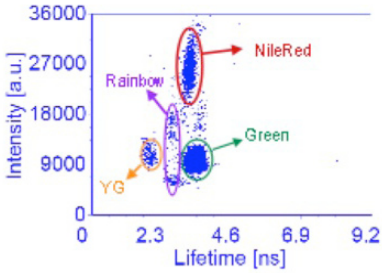


*Figure 5. 2-D scatter plots of fluorescence intensity versus fluorescence lifetime for four different types of microspheres (indicated by the different colored labels) measured together in a single sample. Note the ability to separate different microspheres with the same fluorescence intensity (and emission wavelength) using the fluorescence lifetime parameter.*

## Publications

Goddard, G. R., J. P. Houston, J. C. Martin, and S. W. Graves. Cellular discrimination based on spectral analysis of intrinsic fluorescence. 2008. In *SPIE Proceedings.* (San Jose, 19-24 Jan. 2008). Vol. 6859, p. 85908. Bellingham, WA: SPIE.

Houston, J. P., M. Naivar, J. C. Martin, S. Carpenter, G. Goddard, and J. P. Freyer. Endogenous fluorescence lifetime of viable cells by flow cytometry. 2008. In *SPIE Proceedings.* (San Jose, 19-24 Jan. 2008). Vol. 6859, p. 85908. Bellingham, WA: SPIE.

Sevick-Muraca, E. M., R. Sharma, J. C. Rasmussen, M. V. Marshall, J. A. Wendt, H. Q. Pham, E. Bonefas, J. P. Houston, L. Sampath, K. E. Adams, D. Blanchard, R. E. Fisher, S. Chiang, R. Elledge, and M. E. Mawad. Imaging of lymph flow in breast cancer patients after microdose administration of a near-infrared fluorophore - feasibility. 2008. *Radiology.* **246** (3): 734.

Sharma, R., W. Wang, J. Rasmussen, A. Joshi, J. P. Houston, K. Adams, A. Cameron, S. Ke, M. Mawad, and E. Sevick. Quantitative imaging of lymph function. 2007. *American Journal of Physiology: Heart and Circulation.* **292**: H3109.

# Information Science & Technology

# The Physics of Algorithms

*Michael Chertkov*

20070063DR

## Introduction

Many problems in information processing that are important at Los Alamos are computationally complex at a fundamental level: algorithms guaranteed to find the best solution require an exponentially large amount of time, making them completely impractical.

This project was proposed not to solve a specific problem in a long-standing and established field, but rather to develop a new interdisciplinary field that has been coming into existence over the past five years in the international science arena. The main objective has been to apply methods from statistical physics to develop heuristic algorithms that rapidly find good solutions. By providing a solid theoretical basis for these heuristics, statistical physics methods enable one to mathematically quantify their performance in high-reliability applications, and to systematically design improvements. Specific goals have included testing and verifying these general purpose algorithms on a wide range of applications, such as communication and routing on networks, developing multi-objective optimization schemes to minimize path length and energy consumed, extending coding theory to deal with a network of communicating agents, etc.

There are three key steps in the research approach: (a) State the problem in terms of optimization and/or inference and/or learning, (b) Develop and extend a heuristic algorithm, and (c) Analyze the algorithm.

The project proposed using a unified set of approaches, including belief propagation, finite size scaling, and series expansions, to develop general algorithms that benefit a wide range of LANL applications, such as network monitoring, data reconstruction, and logistical problems. Furthermore, the algorithmic problems envisioned, such as community detection, are essential to a wide array of challenges in network science, including biological networks and adversary social networks. The proposal aimed at complementing recent network research, with the larger goal of developing a capability at LANL in the physics of algorithms broadly applicable to modern challenges in information technology.

## Benefit to National Security Missions

This project supports the DOE mission in Treat Reduction and Nuclear Weapons by enhancing our understanding, developing and constructing new algorithms for wireless sensor networks, community detection in adversary social networks, resource allocation in parallel computing architectures and contributing to verification and validation of LANL critical software.

## Progress

In the course of our research, we have developed the following algorithms and mathematical results:

- A general framework, called Loop Calculus, for expressing exact statistical inference in terms of the result of a computationally feasible Belief Propagation algorithm in the general case of a q-ary alphabet. A further result is the discovery of a new class of graphical models that, in spite of containing many loops, are solved exactly by an algorithm of the Belief Propagation type.
- A novel algorithmic approach, Quantum Belief Propagation, for performing calculations in quantum systems and in classical systems in continuous time. In particular, this leads to a new numerical technique for implementing belief propagation with high accuracy in systems with time dependence
- A study of the phase structure of Graph Bisection over randomgraphs, suggesting the unusual scenario that the problem's solution space undergoes a clustering phase transition (``replica symmetry breaking'') within its over constrained region. Further work has applied this study to graphs more closely reflecting real network data, namely Geographical Threshold Graphs that capture key features of wireless networks while allowing a tunable topology.
- A novel algorithm for community detection and clustering based on belief propagation. This algo-

rithm appears to run in nearly linear time on graphs with the small-world structure characteristic of social and technological networks

- A ranking algorithm that allows inference based on data that may contain systematic errors, such as upsets that occur in competitions. Statistical physics methods including scaling techniques, random-walk analysis, and Monte Carlo simulations were used to establish the algorithm and test its performance.
- Structural properties of networks with addition and deletion of nodes using kinetic theory. This models information networks such as the internet and communication networks such as cell phones and sensor networks. Analytical solutions have been obtained for network properties including the number of dangling nodes and the diameter
- Study of the growth in the number of pareto-optimal paths in the problem of multi-objective optimization for different classes of graphs with randomly assigned edge weights. The distribution of the number of paths is found to be independent of the distribution of weights under certain conditions, and satisfies some interesting scaling properties.
- A formalism for implementing belief propagation on discrete optimization problems with global constraints.
- A graph reduction approach that takes network data and generates an ensemble of smaller graphs that are statistically similar. Applied to a real internet graph, this approach produces networks with features closely resembling snapshots of the (smaller) internet from several years earlier.
- A study of how synchronization of a network of identical oscillators is affected when adding, removing, and moving single edges in the network. This suggests specific strategic rewiring schemes: a greedy approach based on the Laplacian eigenvectors of the network, for instance, can be better than methods targeting the nodes of largest and smallest degree.
- Routing algorithms for effective information diffusion in ad hoc networks and sensor networks was developed.
- A study of the nonmetric traveling salesman problem, relating the ``cavity method'' from statistical physics to a specific implementation of the belief propagation algorithm was conducted. This provided one of the most competitive algorithms for the nonmetric problem.
- A Locally Minimum Cost Forwarding game was studied. Results included a heuristic game theoretic routing protocol that finds Nash equilibria whose efficiency appears to be within a constant factor of optimal.
- 
- A packet routing approach based on ETOP has been implemented and evaluated, and an in-depth analysis shows why paths selected by ETOP improve TCP performance.
- A multi-radio network model was developed. Such networks promise to offer super-linear throughput improvements through the use of multiple-path combinations.
- A study of the problem of placing additional nodes owned by a single profit-maximizing entity into an existing network is shown to be NP-hard. A number of polynomial-time heuristics are proposed for finding non-optimal but satisfactory solutions.
- A non-equilibrium spin-flip process underlying performance of the random edge simplex algorithms was analyzed. We showed that this process exhibits aging, rejuvenation, spatial and temporal correlations. We characterized algorithmic performance to high accuracy using monte carlo simulations, approximate theoretical techniques, and series extrapolation.

## Future Work

In addition to continued progress on areas discussed above, expected new research include:

- A host of novel inference algorithms based on Belief Propagation and Loop Calculus that achieve efficient and asymptotically optimal tracking of small identical objects immersed in a stochastic environment, e.g. turbulent flows.
- The application of recently developed approximate inference algorithms to multi-target tracking in a smoothing framework. The smoothing approach is expected to yield results superior to (popular) forward filtering alone.
- A new approach to reconstructing phylogenetic trees, given characters of a set of related organisms. This is a classic problem of great importance in biology, which has not yet been explored using physics-based techniques.
- A new class of approximate inference methods, blending recently developed variational combinatorial ap-

proaches from the graphical model literature with multi-scale approaches in statistical physics. These methods will be applied to structured problems, such as inference, optimization and learning for computer graphics as well as two- and three-dimensional image recognition.

- Application of results in clustering and community detection to other systems, further addressing foundational questions of what makes specific classes of problems computationally hard.
- New methods coupling theory and simulation for the analysis and optimization of routing protocols within realistic ad-hoc networks, such as Wireless Sensor Networks.
- Development and application of Belief Propagation related algorithms to solving network min-max interdiction models.
- New non-equilibrium approaches to sampling from a given multivariate distributions via Markov Chain Monte Carlo methods that preserve locality but explicitly break the common assumption of detailed balance.
- Algorithms for studying jamming in materials, such as how to pack a disordered arrangements of spheres in 2D. The goal is to develop effective algorithms for packing beyond the cover density of 0.95 that recent work in this project has achieved.
- Studies of communication and simulation of networks, specifically focused on designing more efficient and scalable peer-to-peer and sensor networks.

## Conclusion

This project was proposed not to solve a specific problem in a long-standing and established field, but rather to develop a new interdisciplinary field that has been coming into existence over the past 5 years in the international science arena. The main objective has been to apply methods from statistical physics to develop heuristic algorithms that rapidly find good solutions. By providing a solid theoretical basis for these heuristics, statistical physics methods enable one to mathematically quantify their performance in high-reliability applications, and to systematically design improvements. Specific goals have included testing and verifying these general purpose algorithms on a wide range of applications, such as communication and routing on networks, developing multi-objective optimization schemes to minimize path length and energy consumed, extending coding theory to deal with a network of communicating agents, etc.

The project proposed using a unified set of approaches, including belief propagation, finite size scaling, and series expansions, to develop general algorithms that benefit a wide range of LANL applications, such as network monitoring, data reconstruction, and logistical problems. Furthermore, the algorithmic problems envisioned, such as community detection, are essential to a wide array of challenges in network science, including biological networks and adversary social networks. The proposal aimed at complementing recent network research, with the larger goal of developing a capability at LANL in the physics of algorithms broadly applicable to modern challenges in information technology.

## Publications

Antal, T., D. ben-Avraham, E. Ben-Naim, and P. L. Krapivsky. Front Propagation in Flipping Processes. 2008. *Journal of Physics A.* **41**: 465002.

Bardonjic, M., A. Hagberg, and A. G. Percus. Giant Component and Connectivity in Geographical Threshold Graphs. To appear in *Proceedings The 5th Workshop On Algorithms And Models For The Web-graphs (WAW2007).* ( , ).

Bardonjic, M., A. Hagberg, and A. G. Percus. Combinatorial Analysis of Geographical Threshold Graphs. Presented at *The 8th Latin American Theoretical Informatics Symposium, 2007 .* ( , 2008).

Ben-Naim, E., M. Hastings, and D. Israelevitz. Statistics of partial minima. 2007. *Journal of Physics A: Mathematical and Theoretical.* **40** (47): F1021.

Ben-Naim, E., and N. W. Hengartner. Efficiency of Competitions. 2007. *Phys. Rev. E.* **76**: 026106.

Ben-Naim, E., and P. L. Krapivsky. Addition-Deletion Networks. 2007. *J. Phys. A.* **40**: 8607.

Ben-Naim, E., and P. L. Krapivsky. Condensates in Driven Aggregation Processes . 2007. *Phys. Rev. E.* **75**: 011103.

Ben-Naim, E., and P. L. Krapivsky. Phase Transition with Non-Thermodynamic States in Reversible . 2008. *Phys. Rev. E .* **77**: 061132.

Boettcher, S., B. Goncalves, and H. Guclu. Hierarchical Regular Small-World Networks. 2008. *Journal of Physics A.* **41**: 252001.

Bokolamulla, D., T. Aulin, and A. Hansson. Low-complexity iterative detection based on limited bi-directional search. 2006. *IEEE Proceedings -- Communications.* **153**: 933.

Bradonjic, M., A. G. Percus, and V. P. Roychowdhury. Topology Control with Geographical Threshold Graphs. 2007. *LAUR pending.*

Bradonjic, M., A. Hagberg, and A. G. Percus. The structure of geographical threshold graphs. To appear in *Internet Mathematics .*

Bradonjic, M., T. Mueller, and A. G. Percus. Coloring geographical threshold graphs. 2008. *LA-UR08-5098.*

Chernyak, V., and M. Chertkov. Loop Calculus and Belief Propagation for $q$-ary Alphabet: Loop Tower. To appear in *IEEE ISIT 2007, arXiv:cs.IT/0701086.* (Nice, June 20-26, 2007).

Chernyak, V., and M. Chertkov. Fermions and Loops on Graphs. I. Loop Calculus for Determinant. *JSTAT.*

Chernyak, V., and M. Chertkov. Fermions and Loops on Graphs. II. Monomer-Dimer Model as Series of Determinants. *JSTAT.*

Chertkov, M.. Exactness of Belief Propagation for some Graphical Models with Loops. 2008. *JSTAT.* **P**: 10016.

Chertkov, M., L. Kroc, and M. Vergassola. Belief Propagation and Beyond for Particle Tracking. 2008. *LA-UR-08-3645.*

Chertkov, M., V. Chernyak, and R. Teodorescu. Belief Propagation and Loop Series on Planar Graphs. 2008. *JSTAT.* **P**: 05003.

Eidenbenz, S., A. Hansson, V. Ramaswamy, and C. Reidys. On a new class of load balancing network protocols. To appear in *Advances in Complex Systems.*

Eidenbenz, S., L. Anderegg, P. Widmayer, and L. Peeters. Optimal node placement in a selfish network. To appear in *ALGOSENSORS 2007.* ( , 2007).

Eidenbenz, S., N. Hengartner, G. Jakllari, S. Krishnamurthy, and M. Faloutsos. End-to-end routing metric. To appear in *IEEE INFOCOM 2008.* ( , 2008).

Eidenbenz, S., and S. Kakumanu. Local heuristics for multi-radio networks. 2007. *LAUR pending.*

Ercal-Ozkaya, G., S. Eidenbenz, A. Meyerson, and A. Percus. On a Locally Minimum Cost Forwarding Game. 2007. *LA-UR-07-6304.*

Goncalves, B., G. Istrate, A. G. Percus, and S. Boettcher. The core peeling algorithm for graph bisection: an experimental evaluation. 2006. *LA-UR 06-6863.*

Guclu, H., and M. Yuksel. Limited Scale-Free Overlay Topologies for Unstructured Peer-to-Peer Networks. To appear in *IEEE Transactions on Parallel and Distributed Systems .*

Gutfraind, A., A. Hagberg, D. Israelevitz, and F. Pan. Interdiction of a Markovian Evader. Presented at *ALENEX09.* (ALENEX09, 2009).

Gutfraind, A., A. Hagberg, and F. Pan. Optimal Interdiction of Unreactive Markovian Evaders. *SIAM Journal of Optimization.*

Hagberg, A., D. Shult, and P. J. Swart. Exploring network structure, dynamics, and function using NetworkX. To appear in *SciPy2008.* (Pasadena, Aug 2008).

Hagberg, A., and D. A. Shult. Network Resistance to Synchronization. 2007. *LA-UR Pending.*

Hagberg, A., and D. Shult. Rewiring networks for synchronization. 2008. *Chaos.* **18**: 037105.

Hansson, A., and C. Reidys. A sequential dynamical systems framework for congestion-aware routing. To appear in *Canadian Discrete and Algorithmic Mathematics Conference.* (Banff, Canada, May 2007).

Hastings, M.. Quantum Belief Propagation. 2007. *Phys. Rev.B.* **76**: 201102.

Hastings, M.. Inference from Matrix Products: A Heuristic Spin Glass Algorithm. 2008. *Physical Review Letters.* **101**: 167206.

Hastings, M., E. Ben-Naim, and D. Izraelevitz. Statistics of Partial Minima. 2007. *Journal of Physics A.* **40**: F1021.

Istrate, G., S. Kasiviswanathan, and A. G. Percus. The cluster structure of minimum bisections of sparse random graphs. 2007. *LA-UR 06-6566.*

Istrate, G., S. Kasiviswanathan, and A. G. Percus. The cluster structure of minimum bisections of sparse random graphs. 2006. *LA-UR 06-6566.*

Krishnamurthy, V., M. Faloutsos, M. Chrobak, J. H. Cui, L. Lao, and A. G. Percus. Sampling large internet topologies for simulation purposes. 2007. *Computer Networks.* **51**: 4284.

Nassr, M., J. Jun, S. Eidenbenz, A. Hansson, and A. Mielke. Scalable and reliable sensor network routing: Performance study from field deployment. To appear in *IEEE Conference on Computer Communications (INFOCOM).* (Anchorage, AK, May 2007).

Percus, A. G.. The traveling salesman problem and kth-nearest neighbors. 2006. *LA-UR 06-6896.*

Percus, A. G., G. Istrate, B. Goncalves, R. Z. Sumi, and S. Boettcher. The peculiar phase structure of random graph bisection. To appear in *Journal of Mathematical Physics.*

Percus, A. G., G. Istrate, S. Kasiviswanathan, S. Boettcher, N. Hengartner, and B. Goncalves. Belief propagation for graph bisection. 2006. *LA-UR 06-6868.*

Ramaswamy, V., A. Hansson, and S. Eidenbenz. A probabilistic congestion aware routing protocol for wireless sensor networks. To appear in *International Conference on Distributed Computing in Sensor Systems.* (Santa Fe, June 2007).

Ramaswamy, V., A. Hansson, and S. Eidenbenz. COBRA: A multi-path adaptive local load sensing routing protocol for wireless sensor networks. 2007. *Technical Report LA-UR-07-2905.*

Rani, D., H. Guclu, and M. Yuksel. Ad Hoc Limited Scale-Free Models for Unstructured Peer-to-Peer Networks. To appear in *IEI P2P.* (Aahen, Germany, 2008).

Turitsyn, K., M. Vucelja, and M. Chertkov. Irreversible Monte Carlo Algorithms for Efficient Sampling. *Physical Review Letters.*

Wang, C., J. D. Hyman, A. G. Percus, and R. Caflisch. Parallel tempering for the traveling salesman problem. 2008. *LA-UR 08-5100.*

Yanmaz, E., and H. Guclu. Improving Event Coverage in Wireless Sensor Networks. Presented at *Infocom 2009.* (Rio de Jeneiro, Brazil , April 2009).

# Automated Change Detection in Remote Sensing Imagery

*James Patrick Theiler*

20080040DR

## Introduction

Our aim is to identify meaningful changes that have occurred in scenes that have been imaged multiple images. The repeated images are typically taken at different times, possibly with different instruments, and inevitably under different conditions. Real changes in the scene from one image to the next are hidden by a profusion of incidental differences, caused by variations in illumination, calibration, or atmospheric distortion. The central effort in this project is the development of a statistical methodology to distinguish these pervasive but incidental differences from the less common but more interesting actual changes that have occurred in the scene. This effort builds on a machine learning framework that was developed at Los Alamos and elsewhere, and that provides a formal mathematical basis for identifying what is anomalous in a dataset.

The motivation for this project is the burgeoning accumulation of image data and the limited resources available to examine it. These data potentially contain important nuggets of useful information, but those nuggets are hidden among the raw terabytes of background clutter. What automated change detection can provide is a way to cull through the massive quantity of imagery that may be coming into a facility, and chip out a small number of the most anomalous changes. At this point, a professional analyst can decide which changes provide actionable information and/or merit further investigation.

## Benefit to National Security Missions

This project will support the DOE missions in nonproliferation and national security by developing the technology to enhance an analyst's ability to identify new and/or changed sites from broad area search imagery. Our tools also provide benefit to a range of DoD and other national security stakeholders, many of whom are dependent on remote imagery to carry out missions ranging from counterterrorism to urban warfare. Furthermore, our techniques rely on innovative statistical estimation tools, and this supports DOE's broader scientific mission.

## Progress

### Software development

A revision-controlled software repository has been set up; the software consists of a coherent set of matlab routines that implement a suite of existing and newly developed change detection algorithms, along with support tools that enable comparisons of the different algorithms under different conditions.

### Simulation framework

The ultimate test of a change detection algorithm is performance in the field: how well does it find real changes in real images? While this project continues to employ real data collections, it is important to recognize the difficulties in using this data for extensive quantitative comparisons. We have developed (and implemented as part of our software repository) a simulation framework that provides unlimited test imagery with perfect ground truth for a broad but controlled range of normal and anomalous changes. This allows us not only to employ statistically meaningful quantities of data, but to tease apart the various aspects of the data for which one or another algorithm might exhibit particular sensitivity. While the results of these simulations are not a good way to judge the expected false alarm and detection rates that might be expected in real field situations, they do provide a consistent, objective, and statistically powerful way to compare the relative performance of different algorithms. The framework has two components: one for producing "pervasive differences" over the whole image, and one for producing the "anomalous changes." A variety of options exist for either component which provides flexibility for the simulation. This framework was applied to an extensive set of comparisons of a quadratic family of change detection algorithms [1].

### New algorithms

The first major result of this project was the development of a new algorithm which explicitly optimizes the change detection performance under some broad

assumptions about the nature of anomalous change [2] and the more restrictive assumption that the data distribution is Gaussian. In a survey article [1], we showed that a number of standard algorithms [3,4,5] that have been used for hyperspectral change detection can be expressed as special cases in a family of quadratic covariance-based algorithms. The new algorithm that we developed, called "Hyper", belongs to this class as well, but unlike the standard algorithms, its quadratic coefficient matrix has negative as well as positive eigenvalues -- this leads to hyperbolic (rather than ellipsoidal or cylindrical) boundaries. As well as comparing algorithms in this class analytically, the survey paper also performed a series of empirical comparisons with real data (but simulated anomalies) comparing the performance of the various algorithms. Figure 1 [1] shows ROC curves for seven different detectors. ROC (Receiver Operating Characteristic) quantifies the tradeoff between sensitivity and false alarms; our algorithms far outperform the standard algorithms.

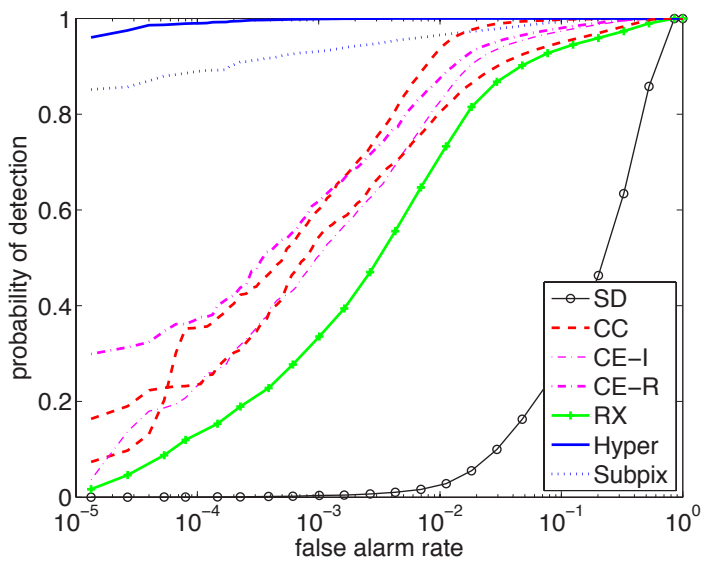


*Figure 1. ROC curves for seven different anomalous change detectors: simple difference (SD), chronochrome (CC), standard covariance equalization (CE-I), optimized covariance equalization (CE-R), Mahalanobis distance (RX), our new algorithm (Hyper, based on hyperbolic boundaries), and a subpixel variant of Hyper (Subpix). Both the pervasive difference (in this case, multiplicative noise) and the anomalous changes (full pixels) were simulated, but the original data was from a real hyperspectral image. Our Hyper and Subpix far outperform the five more conventional approaches [1].*

Using the same real data and simulated anomalies, we investigated dimension reduction schemes for anomalous change detection and we discovered that usual standby -- principal components analysis – is substantially outperformed by canonical components analysis (CCA) [1].

We developed a variant of Hyper that is optimized for finding subpixel anomalous changes. The smaller the anomalous change, the harder it will be to detect, and this applies for any algorithm, but the subpixel anomalous change detection algorithm was found to perform better than the competitors when the change was smaller than a pixel [6]. Figure 2 shows the subpixel-optimized algorithm outperforming all of the other quadratic algorithms, including Hyper, when the simulated anomaly was much smaller than a pixel.

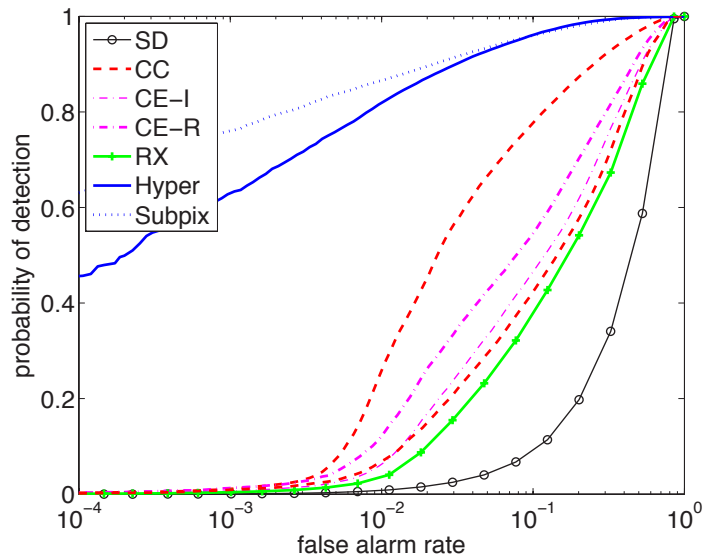


*Figure 2. Same as Figure 1, except the simulated anomalous changes are at the subpixel level and are therefore more subtle. Again, our algorithms substantially outperform prior approaches.*

**Spatial aspects**

Much of the direct change detection effort in the first year emphasized pixel-wise change detection in hyperspectral imagery. However, spatial correlations and spatial structure are important aspects of imagery, and are particularly important in panchromatic imagery since there is so little spectral information in the individual pixels. We have investigated image interpretation at larger scales than a pixel using hierarchical segmentation approaches [7,8,9,10].

Although the newly developed framework for anomalous change detection promises a greater robustness to misregistration errors (because those errors are pervasive and so their effects can, in principle, be learned) [11], we also want to achieve better image-to-image registration in the first place. One approach for doing that is by rapidly finding uniquely identifiable "interest points" in images [12]; by finding and correlating these points in pairs of raster images, we will be able to accurately and rapidly align the two images with each other.

High-cadence wide-angle imagery (eg, video) provides a new set of change detection challenges. Here, there

are many images, and the aim is either to find a single "ephemeral" image [work in progress], or to find and track moving objects [13].

**Data acquisition**

In addition to existing datasets that were available in-house, and that we have used for developing software and theory, we also acquired some new datasets to assist in further development and validation.

From an external collaborator (Steven Adler-Golden), we acquired some time sequence datasets that have previously been used for detecting anomalous time sequences in the imagery. From other colleagues (Joseph Meola, Michael Eismann), we obtained a dozen hyperspectral (visible to near infrared) image cubes taken of the same outdoor scene, at various times of the day, and at various times of the year [14]. In some of the images, a small number of actual changes were introduced (some folded tarps placed on a grassy hillside).

Our main data collect, however, was in-house. We have acquired two sets of data (hyperspectral in the long-wave infrared) from the ORCAS sensor. The first set was very noisy, but with bad pixel mitigation developed for the AVEX project, they were good enough for "viewgraph quality" results. A second set has been collected which is much less noisy, and we will be using that as part of our studies.

## Future Work

Because any algorithm, ours included, benefits when the two images are more nearly identical, we will develop a scheme for generating an image processing pipeline that more nearly equalizes the two images. The early efforts in this area will be based on manual preprocessing, but over the course of the project, we will automate the pipeline selection process.

We are also starting to investigate a new class of algorithms which are optimized for a broader family of distributions than the Gaussian. These "elliptically contoured" distributions have the same second moments as corresponding multivariate Gaussians, but have fatter tails that more accurately reflect the statistics of real data. The mathematics is a little more complicated, but we have identified specific cases with closed form solutions. We have already shown how to do this for target detection [15]; and preliminary experiments with anomalous change detection also suggest better performance on more realistic backgrounds than the corresponding Gaussian-based algorithms.

A further extension, which makes no assumptions at all about the background distribution, employs a support vector machine to "learn" to find anomalous changes. Preliminary experiments have been performed which indicate that (at least for the case in which the data were appropriately dimension reduced) the SVM provided better performance than any of the competing algorithms. The SVM is also the most computationally expensive algorithm, and further efforts are being made to streamline the algorithm as it is applied in the anomalous change detection scenario.

## Conclusion

This project has begun to develop a practical set of tools that implement some innovative algorithms for detecting small but real changes in a scene, based on two (or more) remote sensing images taken of the scene. These algorithms have been designed to be insensitive to the kinds of pervasive differences -- such as scene illumination or sensor calibration (brightness, focus, contrast) -- that tend to occur over large parts of the iamge, and that do not correspond to actual or interesting changes in the scene. This will ultimately enable the development of systems that cue professional image analysts to likely change sites.

## References


1. Theiler, J.. Quantitative comparison of quadratic covariance-based anomalous change detectors. 2008. *Applied Optics.* **47**: F12.

2. Theiler, J., and S. Perkins. Proposed framework for anomalous change detection. 2006. In *ICML Workshop on Machine Learning Algorithms for Surveillance and Event Detection.* (Pittsburgh, PA, 29 June 2006). , p. 7. Pittsburgh, PA: ICML.

3. Schaum, A., and A. Stocker. Long-interval chronochrome target detection. 1998. *Proc. ISSSR (International Symposium on Spectral Sensing Research).* : 0.

4. Schaum, A., and A. Stocker. Hyperspectral change detection and supervised matched filtering based on covariance equalization. 2004. *Proc. SPIE.* **5425**: 77.

5. Nielsen, A. A., K. Conradsen, and J. J. Simpson. Multivariate alteration detection (MAD) and MAF post-processing in multispectral bi-temporal image data: new approaches to change detection studies. 1998. *Remote Sensing of the Environment.* **64**: 1.

6. Theiler, J.. Subpixel anomalous change detection in remote sensing imagery. 2008. In *IEEE Southwest Sympsoium on Image Analysis and Interpretation.* (Santa Fe, 24-26 March 2008). , p. 165. New York: IEEE.

7. Loss, L. A., G. Bebis, M. Micolescu, and A. Skurikhin. Investigating how and when perceptual organization cues improve boundary detection in natural images. To appear in *IEEE Computer Society Conference on Computer Vision and Pattern Recognition (CVPR).* (Anchorage, AK, 23-28 June 2008).

8. Prasad, L., and S. Swaminarayan. Hierarchical image segmentation by polygon grouping. To appear in *IEEE Computer Society Conference on Computer Vision and Pattern Recognition (CVPR).* (Anchorage, AK, 23-28 June 2008).

9. Skurikhin, A. N.. Proximity graphs based multi-scale image segmentation. To appear in *International Symposium on Visual Computing.* (Las Vegas, NV, 1-3 December 2008).

10. Skurikhin, A. N., and P. L. Volegov. Object-oriented hierarchical image vectorization. To appear in *International Conference on Geographic Object Based Image Analysis (GEOBIA).* (Calgary, Canada, 6-7 August 2008).

11. Theiler, J.. Sensitivity of anomalous change-detection to small misregistration errors. 2008. *Proc. SPIE.* **6966**: 69660X.

12. Rosten, E., R. Porter, and T. Drummond. Faster and better: a machine learning approach to corner detection. *IEEE Transactions on Pattern Analysis and Machine Intelligence (PAMI).*

13. Porter, R., A. Fraser, R. Loveland, and E. Rosten. A recurrent velocity filter for detecting large numbers of moving objects. 2008. *Proc. SPIE.* **6969**: 69690C.

14. Eismann, M. T., J. Meola, and R. C. Hardie. Hyperspectral change detection in the presence of diurnal and seasonal variations. 2008. *IEEE Transactions on Geoscience and Remote Sensing.* **46**: 237.

15. Theiler, J., and B. R. Foy. EC-GLRT: Detecting weak plumes in non-Gaussian hyperspectral clutter using an elliptically-contoured generalized likelihood ratio test. To appear in *International Geoscience and Remote Sensing Symposium (IGARSS).* (Boston, MA, 6-11 July 2008).

## Publications

Foy, B. R., J. Theiler, and A. M. Fraser. Hyperspectral target detection using machine learning in a reduced dimensional space. 2008. *LA-CP-08-0026.*

Loss, L. A., G. Bebis, M. Nicolescu, and A. Skurikhin. Investigating how and when perceptual organization cues improve boundary detection in natural images. 2008. In *2008 IEEE Computer Society Conference on Computer Vision and Pattern Recognition Workshops (CVPR Workshops) ; 23-28 June 2008 ; Anchorage, AK, USA.*

Porter, R., A. Fraser, R. Loveland, and E. Rosten. A recurrent velocity filter for detecting large numbers of moving objects. 2008. *Proc. SPIE.* **6969**: 69690C.

Prasad, L., and S. Swaminarayan. Hierarchical image segmentation by polygon grouping. 2008. In *2008 IEEE Computer Society Conference on Computer Vision and Pattern Recognition Workshops (CVPR Workshops) ; 23-28 June 2008 ; Anchorage, AK, USA.*

Rosten, E., R. Porter, and T. Drummond. Faster and Better: a machine learning approach to corner detection. *IEEE Transactions on Pattern Analysis and Machine Intelligence (PAMI).*

Rosten, E., and R. Loveland. Camera distortion self-calibration using the plumb-line constraint and minimal Hough entropy. *Machine Vision and Applications.*

Skurikhin, A. N.. Proximity graphs based multi-scale image segmentation. Presented at *International Symposium on Visual Computing.* (Las Vegas, NV, 1-3 December 2008).

Skurikhin, A. N., and P. L. Volegov. Object-oriented hierarchical image vectorization. To appear in *International Conference on Geographic Object Based Image Analysis (GEOBIA).* (Calgary, Canada, 6-7 August 2008).

Theiler, J.. Quantitative comparison of quadratic covariance-based anomalous change detectors. 2008. *Applied Optics.* **47**: F12.

Theiler, J.. Sensitivity of anomalous change-detection to small misregistration errors . 2008. *Proc. SPIE.* **6966**: 69660X.

Theiler, J.. Subpixel anomalous change detection in remote sensing imagery. 2008. In *IEEE Southwest Sympsoium on Image Analysis and Interpretation.* (Santa Fe, 24-26 March 2008). , p. 165. New York: IEEE.

Theiler, J., and B. R. Foy. EC-GLRT: Detecting weak plumes in non-Gaussian hyperspectral clutter using an elliptically-contoured generalized likelihood ratio test. To appear in *International Geoscience and Remote Sensing Symposium (IGARSS).* (Boston, MA, 6-11 July 2008).

# Information Science and Technology: Metagenomics

*Nicolas W Hengartner*

20080662DR

## Introduction

Metagenomics is the science of analyzing microbial DNA fragments from environmental samples with aim of determining which organisms compose the community, the relative and absolute abundance of each species, and ultimately, what the community is doing. Sequencing environmental samples enables the discovery of new species of bacteria and possibly new enzymes because most bacteria (99%) do not grow in the laboratory and cannot be sequenced using the traditional shotgun method.

New ideas are needed to analyze shotgun DNA sequencing of environmental samples because the traditional methods for assembly and annotation fail for the following reasons: 1) the coverage of any species other than the most common is likely to be significantly less than one, and 2) classification of individual reads to phylogeny (binning) is error prone in the presence of yet unknown species. As a consequence, the DNA reads (which are limited to a few dozen base pairs) are likely impossible to assemble into a full sequence, making gene identification and determining what the community does, nearly impossible.

This project develops novel information science to analyze metagenomic data by assigning phylogeny and function to individual reads. The enabling idea is that pressures from natural selection forces essential peptide substrings to remain conserved over very large evolutionary distances. By discovering such conserved regions, we have the possibility of developing local signatures for particular functions. That such an approach is plausible can be guessed by looking at multiple sequence alignments for the rna-polymerase.

We proposed to develop information science and technology tools based on these shared sequences. This involves (1) developing fast algorithms to identify all such sequences using the 690+ fully sequenced bacterial and archeal genomes, (2) develop algorithms to organized the found shared sequences into paragenomic sequences (that characterize phylogeny) and orthogenomic sequences (that characterize function) and search metagenomic reads for these signatures, (3) develop statistical analyses to ascertain the uncertainty of the attribution, and (4) develop statistical analysis tools of the signatures to perform comparative metagenomic analysis.

## Benefit to National Security Missions

This project will support the DOE and NNSA missions in Energy Security by enhancing our understanding of the response of the environmental microbial community (microbiome) to changing climate, and to understand the flow of energy and matter between the microbiome and the environment.

## Progress

We developed tools to investigate the prevalence of shared kmers (amino acid sequences of length k) between two genomes. We found that about a third of the genes from distantly related species had shared 10-mers of amino acid, in which 10 amino acids in a row were identical. The number of shared k-mers increased with decreasing genetic distances between the species. But even in the limit of closely related species, there are genes that did not have shared 10-mers. This analysis provides evidence that the analysis of shared kmers can tell us about gene function.

After one year, we have nearly completed the indexing tool that is at the hart of our ability to index all the known genomes and metagenomic samples, and produces lists of shared k-mers at a number of organizational levels: genes, chromosomes, species, samples. Figure 1 shows the match between k-mers in selected proteobacteria, compared to the genome of Burkholderia. The challenge was to make this computationally tractable. The latest benchmarks indicate that we will be able to index all 690+ completed bacterial genomes, and identify all the shared pairwise k-mers in about one week on a two-processor desktop. With the ability of identifying all the shared kmers between any two species, we are now ready to investigate genomic organizations of the shared kmers, attributing each shared k-mer to either function or phylogeny. This information

will feed into the modeling and analysis we are developing in the subsequent phases of the project.

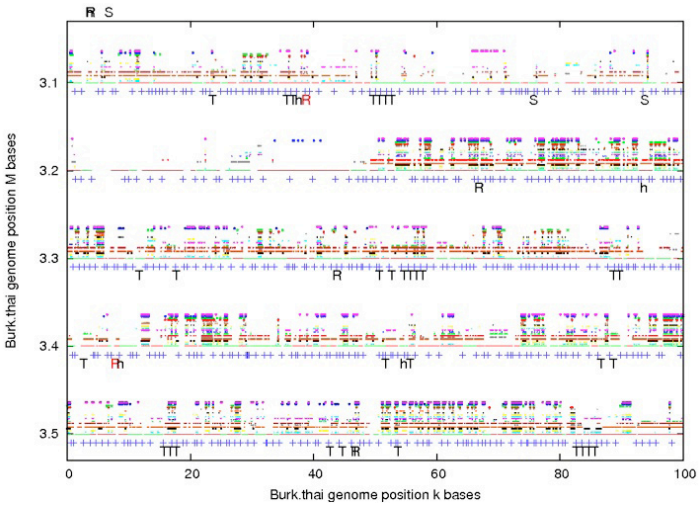


*Figure 1. Position of along the genome of 10-mers that are shared between the genome of Burkholderia (position on the x axis) and selected proteobacteria (on the y axis).*

We developed visualization of shared k-mers that relate them to their position in the genome. Our aim is to use the relationship of multiple shared k-mers to positions within their respective genomes to help develop automatic identification of operons. Figure 2 shows how the length distribution between runs of shared sequences inform us about both phylogeny and function.

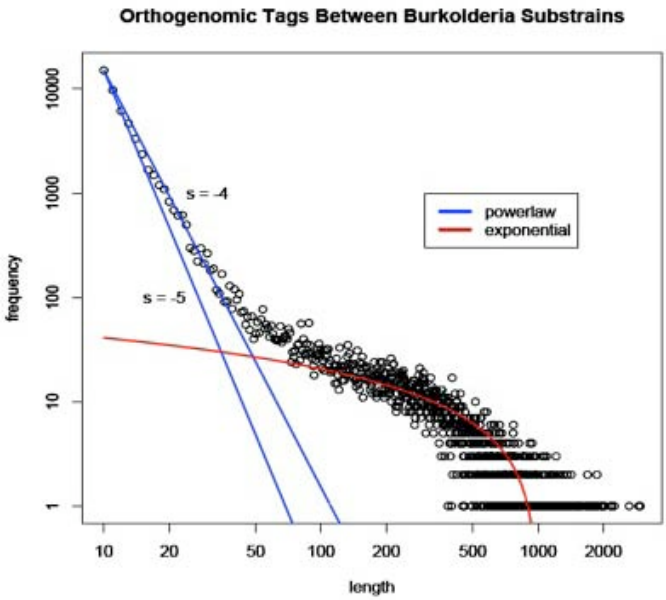


*Figure 2. Length distribution of shared maximal runs of shared sequences on a log-log scale. Note the powerlaw decay for small degree (exponent between 3 and 5) and the geometric decay for large runs. The ratio of these distributions is a good measure for the phylogenetic distance between two bacteria.*

Parallel to this effort, we have developed a fragment recruitment tool that, based on early successes, is being considered for integration into the JGI metagenomics toolbox. We are proceeding with enhancing the tool and developing a webserver that will allow internal (and hopefully external) users to access the tool. Figure 3 shows the result of fragment recruitment from nearby species to the genome of Candidatus Pelagibacter ubique HTCC1062. The quality of the recruitment decreases rapidly for more distant phyla. We have a draft paper describing our tool and another second draft paper that applies the tool to do visual exploratory data analysis of metagenomics data.

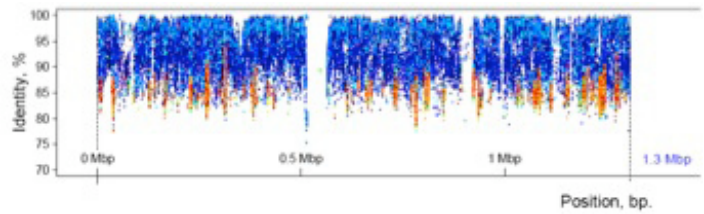


*Figure 3. Example of fragment recruitment tool for a near neighbor of Candidatus Pelagibacter ubique. The x-axis denotes position within the genome and the y-axis indicates the level of similarity between the read and the genome.*

## Future Work

In metagenomics, DNA is sequenced from environmental samples containing communities of interdependent organisms. The fundamental question is to identify what signal the sequencing data contains, and how to extract it. The information science challenge is on how to organize and structure the metagenomics data to enable us to leverage past knowledge on sequenced genomes and other metagenomics data. The information technology challenge is to make our endeavor computationally efficient, so that analysis can be run on a desktop instead of a supercomputer. To that end, we are carrying out the following tasks:

Task 1: Develop a data management and organization tool for generating shared k-mers from all the fully sequenced genomes that is computationally tractable.

Task 2: Validate information content of shared k-mers by comparing classification of genes/organisms based on shared k-mers with classical bio-informatics methods such as Blast and COG. Use results to quantify uncertainty.

Task 3: Develop analysis tools for understanding genome organization and evolution based on shared k-mers using notions of paragenomic and orthogenomic sequence tags and position of joint occurrences of tags within multiple genomes.

Task 4: Develop statistical methods and visualization tool to support scientific discoveries.

Task 5: Develop binning tools that can be integrated with the JGI genomics toolbox.

## Conclusion

We will develop methods for extracting information and knowledge from massive amounts of data from sources that directly impact the mission of the DOE. We aim to develop a new paradigm for the analysis of metagenomic data that focus information extraction of unassembled DNA reads. To do so, we will develop data management and organization tools based on short DNA sequence indexing, develop statistical methods for information extraction, and thereby support scientific discoveries and inferencing.

# Statistical Physics of Networks, Information and Complex Systems

*Robert Everett Ecke*

20080671DR

## Introduction

In this project we explore mathematical methods and concepts of statistical physics that are finding abundant applications across the scientific and technological spectrum from soft condensed matter systems and bio-informatics to economic and social systems. Our approach exploits the considerable similarity of concepts between statistical physics and computer science, allowing for a powerful multi-disciplinary approach that draws its strength from cross-fertilization and multiple interactions of postdocs with different backgrounds. The work on this project takes advantage of the newly appreciated connection between computer science and statistics and addresses important problems in data storage, decoding, optimization, the information processing properties of the brain, the interface between quantum and classical information science, the verification of large software programs, modeling of complex systems including disease epidemiology, resource distribution issues, and the nature of highly fluctuating complex systems. Common themes that the project has been emphasizing are (i) neural computation, (ii) network theory and its applications, and (iii) a statistical physics approach to information theory. The project's efforts focus on the general problem of optimization and variational techniques, algorithm development and information theoretic approaches to quantum systems. These efforts are responsible for fruitful collaborations and the nucleation of science efforts that span multiple divisions such as EES, CCS, D, T, ISR and P.

## Benefit to National Security Missions

This project supports the DOE mission in Energy Security and Nuclear Non-Proliferation by developing novel information science tools to understand communication, sensing, and interactions in complex networks such as the internet or energy distribution system. It will also support programs in Threat Reduction and Homeland Security, for example by understand social networks.

## Progress

Evidence of the progress of this project can be found in the ample science publications that have resulted directly or indirectly from work on this project. Network theory, graph theory and the statistical physics description of classical information science have introduced new paradigms and have opened up novel strategies to tackle problems that were previously beyond the scope of a scientific description. The applications of the new mathematical network and graph theory descriptions reach beyond the field of information theory and have contributed to a wide variety of fields that deal with complexity, coherent behavior, networks and information flow such as bio-informatics, epidemiology, quantum information science and many-body physics. This project has successfully exploited the multi-disciplinary make up of the center for nonlinear studies (CNLS) to combine expertise in statistical physics, network theory, graph theory, computer science, disordered systems and library sciences to give fundamental and broad contributions to information science, broadly defined. Below, we highlight a select number of contributions that have been made by CNLS postdocs working on this project.

A crucial challenge in estimating and measuring quantities pertains to answering two questions: how accurate we can expect the estimate to be and with how much confidence we can trust the obtained values. The framework of Bayesian inference provides a systematic approach to this class of problems. This technique was discovered to be closely related to network theory and the calculation of weighted counting is related to the calculation of a partition function. Participants in this project have developed a novel loop-calculus method to approximate the partition function in a controllable and systematic manner.

Much of scientific computing and analysis relies on optimization techniques. Rigorous mathematical studies have revealed the speed and efficiency of specific optimization methods and criteria exist to determine which method works best depending on the circumstances

and boundary conditions. Motivated by the abundance of optimization methods, this project has explored a new strategy for optimization -- one that combines multiple methods. The potential for speed-up and the advantages of combining multiple optimization techniques is remarkable, and the study of speed up and optimal strategies for how to combine the methods has been studied in the context of earth sciences and geophysics.

The use of the world-wide web, the increased memory of computers and the increased efficiency of inter-computer communications is suggesting new paradigms for computer usage and scientific computing. One computing strategy alternative to the usual architecture of scientific computing that has been considered in this project, is to 'farm out' calculations to different web-users and have the calculations performed by the structure that stores data. In addition to increasing the effective memory and data-storage, this scheme would allow calculations to be performed by data-storage hardware. Does the advantage of limitless computing space make up for the reduction in speed? This question, the schemes for realizing this new computing strategy, the mathematical description of its operation and the new prospects they bring with them are being considered in this project, using the expertise and background of library sciences.

The theorems of network theory and the insights from graph theory are finding a fertile ground in a host of fields that deal with complex behavior and effects of disorder. In the areas of biology and epidemiology, it has opened up opportunities to describe phenomena and general behavior that could not be described previously. In the project, participants have applied the concepts and descriptions of networks to bring new insights into the general trends in the problems of describing the spread of disease.

An important area of information theory seeks to optimize ways of searching for information. CNLS researchers have investigated the gain of exchanging information between more than one searcher. Suppose two autonomous agents (say, mobile robots) are searching for a source of radiation. A recent paper in Nature showed that searching based on maximizing information ("infotaxis") can be more effective than a standard gradient search. Preliminary results (see attached figure) show that, using this formalism, it is possible to have synergetic coordination between multiple searchers and that deliberately synergetic motion may lead to more efficient searches. In Figure 1, the color map shows the redundancy (blue) or synergy (red) of an arrangement of searcher locations. The source (black dot) emits particles that have an angular correlation (2 particles are always emitted in opposite but random directions) and the location of one searcher (green dot) is fixed. The grid shows the synergy or redundancy of the arrangement as a function of positions for a second searcher. When the searchers are close together they are competing for the same particle (redundancy), but if they are on opposite sides of the source they increase the chances of each getting a particle (synergy). This thinking might be used to optimize searches for nuclear materials.

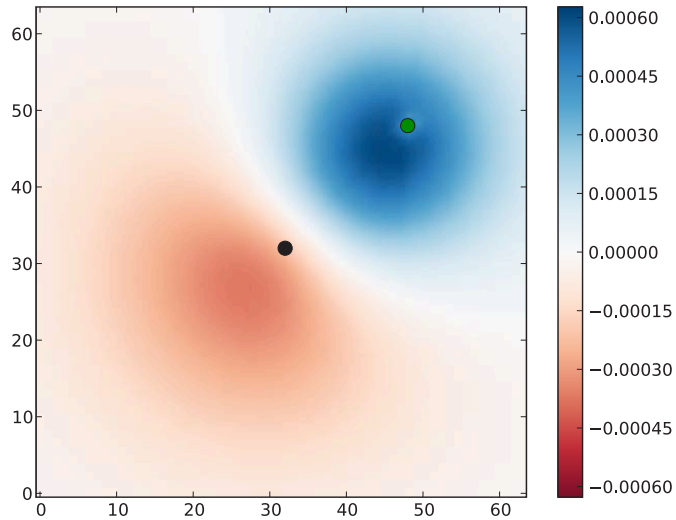


*Figure 1. Multiple, coordinated searchers can have synergetic coordination that may lead to more efficient searches. The colormap shows the redundancy (blue) or synergy (red) of an arrangement of searcher locations. The source (black dot) emits particles that have an angular correlation (2 particles are always emitted in opposite but random directions) and the location of one searcher (green dot) is fixed.*

## Future Work

Mathematical methods from graph theory and network theory and concepts of statistical physics are enriching the breath and impact of information theory. Conversely, information theoretic approaches are impacting the fields of neural computation, epidemiology, data processing, statistical non-equilibrium, and quantum physics. This project takes advantage of the newly appreciated connections and the intriguing prospects offered by the multi-disciplinary symbiosis to address important problems in data transmission and storage, decoding, optimization, the information-processing properties of the brain, the interface between quantum and classical information, verification of large software programs, modeling of complex systems including disease epidemiology, resource distribution issues, and the nature of highly fluctuating complex systems.

We will continue with the development and application of a set of theoretical and computational methods to address important problems of national interest:

- Develop systematic approaches to finding computationally efficient methods that optimize the performance of classes of problems such as data transmission. We will find the most efficient way to transmit data reliably with minimum energy cost for a network of generalized transmitter/receiver units with information processing at each node.

- Explore concepts of classical information theory applied to the coupling of quantum information systems in which quantum entanglement is limited by the spatial separation of nearby quantum states.

- Investigate the optimal method for relating two images with common features, e.g., groups of particles such as in fluid tracking methods or in feature recognition systems.

- Develop functional physiologically-inspired models of neural computing that account for essential details in performing realistic computational functions and that are missing from artificial-neural-network approaches to machine-learning.

- Investigate connections between data acquisition, processing, analysis and prediction applied to complex systems.

- Investigate network concepts applied to problems in infectious disease, social behavior and population dynamics.

## Conclusion

The ability to organize, manipulate and optimize the transmission, reception and processing of information underpins much of the national infrastructure, the information based economy and many features of national security. Our research efforts address problems in the organization and processing of information applied to efficient communication under constraints of error tolerance, bandwidth, or power consumption (as in distributed sensor systems). Another important application is understanding how diseases spread and, thus, how strategies for containing them can be developed. A third research goal seeks to further our understanding of how the brain converts visual stimuli to achieve a successful, efficient and sophisticated system of image processing and recognition.

## Publications

Bettencourt, L. M., V. Gintautas, and M. I. Ham. Identification of functional information subgraphs in complex networks. 2008. *PHYSICAL REVIEW LETTERS.* **100** (23): 238701.

Bianconi, G., N. Gulbahce, and A. E. Motter. Local structure of directed networks. 2008. *PHYSICAL REVIEW LETTERS.* **100** (11): 118701.

Bianconi, G., and N. Gulbahce. Algorithm for counting large directed loops. 2008. *JOURNAL OF PHYSICS A-MATHEMATICAL AND THEORETICAL.* **41** (22): 224003.

Burr, T. L., and G. Chowell. Signatures of non-homogeneous mixing in disease outbreaks. 2008. *MATHEMATICAL AND COMPUTER MODELLING.* **48** (1-2): 122.

Chertkov, M., V. Chernyak, and R. Teodorescu. Belief Propagation and Loop Series on Planar Graphs . 2008. *Journal of Statistical Mechanics.* : P05003.

Chertkov, M., and M. G. Stepanov. An efficient pseudo-codeword search algorithm for linear programming decoding of LDPC codes. 2008. *IEEE TRANSACTIONS ON INFORMATION THEORY.* **54** (4): 1514.

Chowell, G., L. M. Bettencourt, N. Johnson, W. J. Alonso, and C. Viboud. The 1918-1919 influenza pandemic in England and Wales: spatial patterns in transmissibility and mortality impact. 2008. *PROCEEDINGS OF THE ROYAL SOCIETY B-BIOLOGICAL SCIENCES.* **275** (1634): 501.

Devetak, I., and J. Yard. Exact cost of redistributing multipartite quantum states. 2008. *PHYSICAL REVIEW LETTERS.* **100** (23): 230501.

Hayden, P., M. Horodecki, A. Winter, and J. Yard. A decoupling approach to the quantum capacity. 2008. *Information Dynamics and Open Systems.* **15** (1): 7.

Lopez, E., R. Parshani, R. Cohen, S. Carmi, and S. Havlin. Limited path percolation in complex networks. 2007. *PHYSICAL REVIEW LETTERS.* **99** (18): 188701.

Miller, J. C., and J. M. Hyman. Effective vaccination strategies for realistic social networks. 2007. *PHYSICA A-STATISTICAL MECHANICS AND ITS APPLICATIONS.* **386** (2): 780.

Mineev, M., M. Putinar, and R. Teodorescu. Random matrix theory in 2D, Laplacian growth, and operator theory . 2008. *Topical Review, Journal of Physics A: Mathematical Theory.* **41**: 263001.

Motter, A. E., N. Gulbahce, E. Almaas, and A. Barabasi. Predicting synthetic rescues in metabolic networks. 2008. *MOLECULAR SYSTEMS BIOLOGY.* **4**: 168.

Nuno, M., T. A. Reichert, G. Chowell, and A. B. Gumel. Protecting residential care facilities from pandemic influenza. 2008. *PROCEEDINGS OF THE NATIONAL ACADEMY OF*

*SCIENCES OF THE UNITED STATES OF AMERICA.* **105** (30): 10625.

Rodriguez, M. A.. Grammar-Based Random Walkers in Semantic Networks. 2008. *Knowledge-Based Systems.* **21** (7): 727.

Rohlf, T., N. Gulbahce, and C. Teuscher. Damage spreading and criticality in finite random dynamical networks. 2007. *PHYSICAL REVIEW LETTERS.* **99** (24): 248701.

Santhi, N.. On Algebraic Decoding of q-ary Reed-Muller and Product Reed Solomon Codes . *IEEE Transactions on Information Theory.*

Smith, G., and J. Yard. Quantum communication with zero-capacity channels. 2008. *SCIENCE.* **321** (5897): 1812.

Srinivasan, R., R. Pepe, and M. A. rodrigues. A Comparison Between Ethnographic and Clustering-Based Semi-Automated Techniques for Cultural Ontologies. *Journal of American Society for Information Science and Technology .*

Wocjan, P., and J. Yard. The Jones polynomial: quantum algorithms and applications to quantum complexity theory. 2008. *Quantum Information and Computation.* **8**: 0147.

Yard, J., I. Devetak, and P. Hayden. Capacity theorems for quantum multiple access channels: classical-quantum and quantum-quantum capacity regions. 2008. *IEEE transactions on Information Theory.* **54** (7): 3091.

# Information Science and Technology: Streaming Data

*Sarah Ellen Michalak*

20080729DR

## Introduction

Information Science and Technology is an emerging domain in which LANL has many strategic interests such as metagenomics, bioinformatics, cyber security, and more broadly the visualization and analysis of massive real-time streaming data. Recent years have seen an explosion in the size of datasets. As we have become adept at capturing and archiving massive amounts of data, we have outpaced our ability to effectively analyze it. This DR is developing new capabilities to analyze and visualize enormous data streams in near real-time. Through the use of specialized computer hardware as well as advanced statistical and visualization algorithms, we are developing the capabilities needed to regain control over previously overwhelming amounts of information. This capability is especially important due to the LANL's roles in threat reduction. Cyber-security, bioinformatics, and near-space astronomy are all sources of massive streams of data which must be analyzed in real time to detect any and all threats.

## Benefit to National Security Missions

We must analyze the people, materials, and vehicles that pose a threat, in environments ranging from urban warfare to near-Earth space. This requires real-time processing and fusion of multiple data streams as enabled by methods such as those being developed under this proposal. Applications will speak to Threat Reduction and Global Security missions.

## Progress

Our research focuses on the challenging streaming data problem of real-time, full-sky transient detection using measurements from radio telescopes. This work is motivated by the Long Wavelength Array (LWA), which is being built in southern New Mexico. The LWA will enable scientists to investigate the lowest frequencies (10-88 MHz), which have not yet been fully explored. Our work is not part of the mainstream of the LWA project, but the LWA and other radio telescopes offer an ideal data stream to test novel information science approaches.

Via our research, we have developed key pieces of a system that would enable real-time detection of radio transients, specifically:

- Processing (correlation) of incoming measurements
- Analysis of correlated data to identify transient events of interest
- Storage of data identified to be of interest
- Images of the sky

The first step in transient detection is to process the raw data. This processing is referred to as "correlation." Our correlation research has investigated full-sky aperture synthesis using FX correlation. At a high level, an FX correlator first applies a Fourier transform to the data ("F") followed by a multiply-accumulate ("X") to extract the signal from the antenna measurements.

For this work, we have focused on the measurements received by a single station of the LWA, which contains 256 dual-polarized antennas. With this data, the correlation problem has a complexity of order $N^2$ [O(N^2)], where N equals the number of antennas (256). Specifically, there are 32,640 pairs of antennas whose measurements must be correlated in real time for each frequency channel of interest. For this work, we are considering 65,536 frequency channels, resulting in over 8.5 billion (=4x32,640x65,536; the factor of "4" accounts for the dual-polarization) pairs of measurements that must be simultaneously processed in real time. With these specifications, the calculation requires 61.3 Tflops and 256 GB/s bandwidth for incoming antenna data and 64 GB/s bandwidth for outgoing visibility product data. To our knowledge, an FX correlator at this scale has not been previously attempted, nor has an FX correlator using 256 antennas and any number of frequency channels.

Detailed designs and implementations have been completed to help determine the base performance of the F and X parts of the FX correlator algorithm using standard processors. We implemented several versions

of the X part of the algorithm starting with a basic serial implementation followed by a threaded version and finally an MPI version. An optimized FFT algorithm (FFTW) for the F part of the FX correlator algorithm was also implemented on a standard architecture. We investigated a matrix transpose that needs to occur between the F part and the X part of the algorithm in order to obtain greatly improved performance. This effort was undertaken to investigate computation and communication scaling issues. Analysis of this work generated performance metrics that were used to compare the results of cutting-edge hybrid computing approaches to more conventional approaches.

We produced a hybrid implementation of the X part of the FX algorithm that uses cell processors and Opteron processors in combination and is approximately 30x faster than a conventional approach. The "F" portion (polyphase filter banks and FFT) was implemented on cell processors, with a resulting 18x speed-up over a conventional approach. In addition to the performance (speed of computation) gains, the hybrid approach is cheaper, uses less energy, and requires less space compared to a conventional approach. These are key features given the limited space and power at the LWA site. Because of these power and space constraints, the FX correlator for the LWA will likely operate on 128 frequency channels. A joint NSF proposal with UNM has been submitted that would provide funding for implementing an all-sky correlator for the LWA based on the advances that we have made.

Once the data have been correlated, they next need to be mined for transient events. We wrote software that reads quadrature-sampled antenna data, converts each antenna signal to a complex Fourier spectra, applies phase shifts that are a function of frequency and the desired viewing direction, and combines the spectra using a correlator array. The result of the processing is a time-varying spectra showing deviations from background energy from a specified direction in space. This allows visual search of the data for interesting signals. In the coming two years, this work will be extended to include the development of algorithms for automated transient detection and then the porting of these algorithms to the real-time setting.

Technology for storing the data temporarily while it is mined for transient events is required. We have developed a flexible ring buffer architecture that provides time to decide whether data is important before it is either written out for analysis or discarded. This ring buffer architecture is novel, since it uses disk rather than memory, and incorporates reliability mechanisms to guard against disk failures. A prototype ring buffer system has been developed for proof of principle, with testing and related improvements the current focus of this work. Because we use disk rather than memory, we can store orders of magnitude more data than conventional ring buffers.

Visualization of the data requires converting a noisy raw image to something useful and clean. We have investigated how the performance of one of the canonical algorithms for this procedure, the CLEAN algorithm, could be enhanced via use of GPUs and other emerging architectures. An end-to-end implementation of CLEAN has been developed so that appropriate architectural choices can be made.

## Future Work

FY09 efforts will focus on the development of automated transient-detection algorithms and related visualization and enhancements to the ring buffer architecture that will permit storage of data identified to be of interest. In FY10, the transient detection algorithms and visualization methods will be ported to the real-time setting via use of emerging hardware.

As this project develops key pieces of a real-time transient detection system, we are exploring how this technology might be brought to fruition so that it can enable astronomical research. As mentioned above, an NSF grant proposal was submitted that would provide student funding to implement a real-time all-sky correlator at the LWA site. Collaborations with individuals at UC-Berkeley, the Allen Telescope Array and the National Radio Astronomy Observatory are also being investigated.

## Conclusion

We will develop methods for extracting information and knowledge from massive amounts of data from sources that directly impact the mission of the DOE by developing new methods designed for real-time streaming visualization and data analysis. The capabilities developed here will have applications across LANL's Threat Reduction and global security mission. Many important threat detection problems, from those in cyber security domains to near-space object tracking, can be greatly augmented by the technology we are developing. With our new methods the amount of time required to identify threats within massive streams of data may be drastically reduced, ultimately enabling real-time detection.

# New Approach to Bayesian Inference Under Modeling Uncertainty

*Nicolas W Hengartner*

20070172ER

## Introduction

Complex systems are naturally described in terms of related subsystems and components. In many examples, information and data is acquired at the component level, and one wished to make inference about the whole system and relevant sub-systems. A mathematical method called "Bayes nets" provides a mathematical framework for rolling-up component level data to make system level inferences. This approach requires the modeler to specify the relationships between components, subsystems and full system using conditional distributions. In practice, these relationships may be only partially known. The first objective of this research is to investigate how second order probabilities are useful for vague specifications of these relationships and to develop numerically efficient algorithms for propagating the associated uncertainties.

Computational efficiency is a prerequisite for the second phase of this project, which is to develop a principled framework for data marshaling. Simply stated, we want to use our knowledge of the uncertainty to help identify the value of future measurements. If successful, this research will provide the means to optimize how one can most efficiently collect data with the aim of answering questions of interest. This work will impact a broad range of work that requires careful and efficient design of measurement systems to answer specific questions or to measure specific quantities from an experiment or system.

## Benefit to National Security Missions

This work makes fundamental contributions to the science underlying ubiquitous sensor networks. The research is directly relevant to the treat reduction and nuclear weapons missions by enhancing our ability to extract information from noisy or corrupted data and is applicable to intelligence gathering, nuclear event attribution, and weapons reliability analysis.

## Progress

It is common for experts to summarize their knowledge of uncertainty about a particular phenomena by specifying means and variances of observable and unobservable variables. Thus it is essential to be able to develop flexible models for second order probabilities that can be specified by means and variances. In the first year of this project, we have developed and implemented a methodology for specifying joint the distribution of multinomial probabilities using mixtures of Dirichlet distributions. This results of this research have recently been published in a refereed journal.

The second year was devoted to developing the framework and computationally tractable models for uncertainty quantification in the presence of second order probability. Our research has uncovered an attractive second order probability model for which system inference is amendable to an analytical solution in special cases, and simple yet surprisingly good approximations in general. We also have extended the work from the first year and now have uncovered a model that fits arbitrary mean and variance specification (subject only to the natural constraint) for multinomial probabilities. Two papers exposing the results of our second year are in draft form.

One of our investigators, Andrew Fraser, published a book Hidden Markov Models and Dynamical Systems, that describes many of the mathematical tools that are required in the current line of investigation. Figure 1 shows the cover page of that book.

This project also enabled an international collaboration with Prof. Eric Matzner-Lober, with whom we have developed novel nonparametric bias reduction techniques that we expect will be useful in exploring high dimensional data.

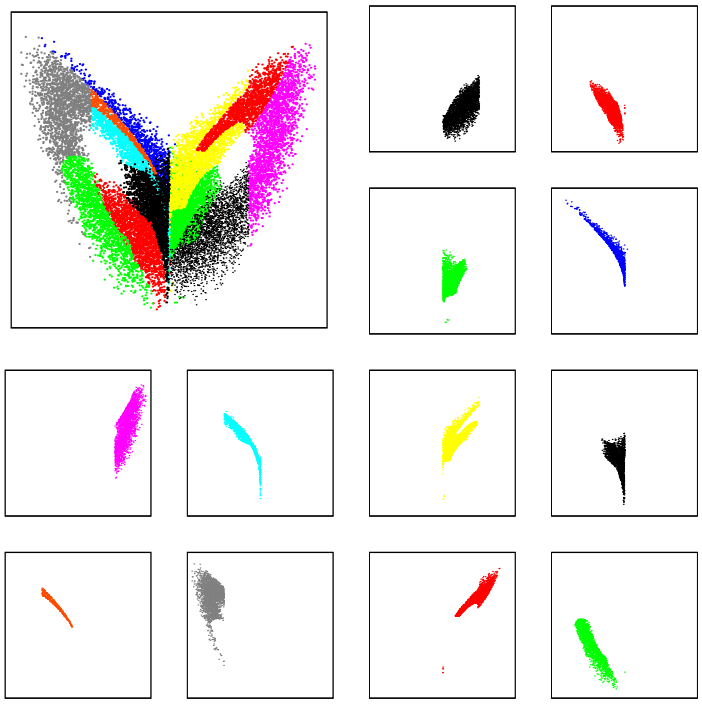

*Figure 1. Cover of "Hidden Markov models and dynamical systems" by A. Fraser.*

Finally, we have started work on maximum entropy sampling, a general paradigm that will serve as our foundation for planned work on data marshaling scheduled in the third year. The preliminary results of that research have been presented at an invited talk at the Joint Statistical Meeting this summer.

## Future Work

The Bayes network methodology is a powerful approach to modeling relationships between experimental variables by using probabilistic relationships to relate observable and inferred variables.

The goal of this research is the development of Bayesian statistical models that contain, embedded within the model itself, information about the accuracy of modeling parameters, and permit propagation of this uncertainty to the inferences generated. Currently, such a confidence analysis is performed numerically, which can be computationally prohibitive as the number of parameters increases, or when the computation of a single model instance is expensive.

A preferable approach is to propagate the modeling confidence assessment as an integral aspect of the Bayesian probability propagation itself. This demands attention to the representation of the modeling uncertainty. In this project we will investigate new approaches for modeling probability uncertainties based on polynomial models.

Task 1: Extensions to multi-valued Bayes nets: In previous work we restricted our attention to the binary variable problem. We will investigate the extension of this approach to the more general case when multi-level random variables are involved.

Task 2: Prototype implementation: To compare our approach with others numerically, we will build a prototype software system that will implement the algorithms developed under this project.

Task 3: Comparison to classical approaches, computational complexity, and validation: We will examine the computational complexity of our approach as a function of the fidelity with which the distributions are modeled. Finally, stochastic simulations can be used to validate our implementation.

Task 4: Develop a framework for data marshaling that uses the derived uncertainty quantification at the system level to help identify the value of specific future observations.

## Conclusion

Most scientific and engineering applications depend on inferring relationships from data. This inference is often based on models that may or may not be accurate. The effect of these modeling uncertainties is currently addressed by using many different models and comparing the results across models to see where the inference uncertainties occur. This is slow and inaccurate. We are developing mathematical tools that allow a user of these models to understand and quantify the effect of modeling uncertainties on inferences in an efficient and accurate fashion.

## References


1. Fraser, A. L.. Hidden Markov models and dynamical systems. 2008.

2. Hengartner, N., and E. Matzner-Lober. Asymptotic unbiased density estimators. To appear in *ESAIM.*

3. Cornillon, P. A., N. W. Hengartner, and E. Matzner-Lober. Recursive Bias Estimation for high dimensional regression smoothers. *Journal of the Royal Statistical Association, Series B.*

4. Burr, T., N. Hengartner, E. Matzner-Lober, and L. Rouviere. Smoothing low resolution spectral data. *IEEE Transaction on Nuclear Science.*

## Publications

Burr, T., N. Hengartner, E. Matzner-Lober, and L. Rouvier. Smoothing low resolution spectral data. *IEEE Transaction on nuclear sciences.*

Burr, T., N. Hengartner, E. Matzner-Lober, and L. Rouviere. Bias reduction in action. To appear in *Joint Statistical Association Meeting.* (Denvers, July 28 - Aug 5, 2008).

Cornillion, P. A., N. Hengartner, and E. Matzner-Lober. Recursive bias estimation for high dimensional regression smoothers. *Journal of the Royal Statistical Society, Series B.*

Fraser, A. L.. Hidden Markov models and dynamical systems. 2008.

Hengartner, N., and E. Matzner-Lober. Unbiased density estimation. To appear in *ESAIM.*

Izraelevitz, D., H. Martz, D. Leishman, and W. Gibson. On representing second-order uncertainty in multi-state systems via moments of mixtures of Dirichlet distributions. To appear in *Journal of Statistical computing and simulations.*

# Sharp characterization of minimizers (typically) involving interfaces in images

*Pieter Johan Swart*

20070187ER

## Introduction

The need to understand image and video data for a range of applications has mushroomed in the last few years. Imaging data in the medical, security, strategic, intelligence, industrial, and scientific communities have grown out of the ubiquity of exponentially increasing streams of image and video data. By some estimates, as much as 70-80% of such data goes un-analyzed. Our work creates new abilities to understand precisely how important new image processing methods work and what we can know from the output of those methods. Are the observed features, extracted from the raw images reliable? Can we make careful scientific inferences reliably? We are also generating new algorithms that expand the information we extract from the images. While this work demands deep insights from intricate mathematical areas, it has already begun delivering concrete, practical results that improve our ability to analyze images and extract information in the presence of noise.

## Benefit to National Security Missions

Analysis of image and video data for "value" is a critical component to rapid data assessment and analysis. Numerous missions related to threat reduction, weapons data analysis, nonproliferation, and basic science is directly impacted by this work. Missions relevant to DOE, DHS, and other government agencies will be enhanced.

## Progress

In 1992, Rudin, Osher, and Fatemi suggested using the total variation (TV) seminorm for regularization when denoising images. This approach revolutionized the field of image denoising, infusing the field with many new ideas from variational analysis and nonlinear analysis as well as new algorithms. The resulting Rudin-Osher-Fatemi TV regularized denoising algorithm is the classic approach for achieving this. Compared to other methods, this approach to denoising by finding a minimizer to a variational problem is powerful, but not well-understood by the image processing community (given that it relies on rather deep results from the theory of Geometric Measure Theory) and rather expensive to compute in practice. The precise nature of the minimizers is an intricate mathematical problem that we have solved by finding a new mathematical description. The goal of this LDRD-ER is the generation of new insights into the Total Variation (TV) regularized functionals and especially the development of new fast new algorithms used to compute their minimizers.

In the first year of the project, we have made an exciting new discovery connecting the "flat norm" from geometric measure theory to the L1TV functional form used in image analysis. This discovery is now being rapidly leveraged to provide us with new methods to describe and understand shape and image data, explore the statistics of shapes, and greatly generalize the L1TV functional to data previously beyond its domain. By the second year of this project we have gained significant understanding into this new approach and has developed numerical implementations to test this. The underlying mathematics of our approach is rather novel, and therefore does not have a long history of algorithm development. In the third year of this project we will continue with the underlying mathematical analysis, but much of the emphasis will shift to speeding up the numerical methods, with careful testing and comparison with other methods, and with comparisons on more challenging data sets than classic benchmarks.

One goal of this project has been to use these insights to generate whole families of exact solutions to these variationals. Furthermore, we have been developing hybrid methods to generate numerical solutions for any input data while maintaining very careful control on errors.

Over the past year we have used insights from geometric analysis to a) generate a precise characterizations of such minimizers, b) careful estimates of the accuracy of algorithms designed to compute minimizers, c) hybrid algorithms based on a) and b), and d) generalizations of the existing L1TV and L2TV functionals useful for data

driven-analysis of scientific images. We are now working on the application of the newest insights to real data and shape challenges, and developing faster algorithms for the practical implementation of these ideas. In addition to the publications lead by Vixie, Allard, and Esedoglu, we have several papers in preparation describing the above results. For example, the review paper by Bill Allard in the SIAM Journal Of Mathematical Analysis, as well as the follow-up versions II and III, clearly lays out the mathematical foundation of this approach. We are working, in collaboration with Vixie, Allard, Esedoglu and postdoc Simon Morgan, on followup papers to the original Vixie and Morgan paper that appeared in the journal Abstract and Applied Analysis.

This year has also seen the change in PI from Kevin Vixie to Pieter Swart, when Vixie left LANL to join Washington State University. We have worked very hard to build a working collaboration between Vixie, Esedoglu and Allard, so as to assure that this change will not seriously affect the successful completion of the initial goals of this project.

## Future Work

This approach is not limited to 2D images, but can be extended to regularize higher dimensional data sets, such as 3D geometric shapes or structures in hyperspectral datasets. This analysis is being explored in recent work by Eseduglo and Elsey.

We plan a workshop and more applied review papers to disseminate these results, as well as continuing careful numerical testing of these methods in the application domain. The deeper mathematical work will continue as well. The multiscale signature that immediately resulted from the discovery by Vixie and Morgan is being applied to shape recognition and other related shape tasks.

On another related front, we are extending the theoretical results and the flat norm to the case in which the surface energy term is anisotropic. This is useful both because one of the fastest methods for L1TV is a graph cut method, and this algorithm uses an anisotropic approximation of the TV term. Moreover, there are also many important physical applications in which the surface energies are anisotropic. For example, in the solution of micromechanical continuum models in metallic alloys, this is usually the case. This work has both a computational thread and a theoretical, geometric measure theory thread. An example of work here is the realization that we can compute the anisotropic weights in a simple, semi-analytic way. Other pieces include the very recent characterization of minimizing sets with anisotropic energies to be something like the best approximation of the input sets by an appropriately scaled Wulff shape (a shape which characterizes the anisotropic surface energy).

Other research threads include more mundane, but important comparison of methods for the computation of the L1TV functional at a wide range of parameter values. As mentioned above, this will open up applications to sets with codimension > 1 and to sets that are not boundaries. A somewhat surprising example of an unusually thin minimizer was recently found and this is being written up.

We have come to the point where the third year will be dominated by computational work, even though there will be a very strong theoretical component that continues. We expect that the groundwork laid this year and the previous year will yield a large number of applied publications and new algorithms for the flat norm.

## Conclusion

We are confronted with an ever-increasing tidal wave of data. A large fraction of this data consists of images of every conceivable type. The thorough analysis of this flood of images is rapidly becoming one of our most challenging scientific problem. Increasingly, inferences from this data need to be accompanied by rigorous quantification of uncertainty. This requires fully characterized image analysis methods. This is precisely what we will deliver. The work has the potential to significantly impact on every challenge requiring image analysis with quantified uncertainty.

## Publications

Allard, W. K.. Total variation regularization for image denoising I: Geometric theory. 2007. *SIAM Journal on Mathematical Analysis.* **39** (4): 1150.

Allard, W. K.. Total variation regularization for image denoising III: Examples..

Allard, W. K.. Total variation regularization for image denoising II: Examples. .

Elsey, M., and S. Esedoglu. Analogue of the total variation denoising model in the context of geometry processing.

Morgan, S. P., and K. R. Vixie. L1TV computes the flat norm for boundaries. 2007. *Abstract and Applied Analysis.* **2007**: Article ID 45153.

Vixie, K. R.. Some properties of minimizers for the Chan-Esedoglu L1TV functional. 2007. *http://arxiv.org/abs/0710.3980.*

# Instabilities Driven Turbulence and Mixing in Convergent Geometries

*Daniel Livescu*

20070195ER

## Introduction

Many of the flows of interest for the Laboratory involve species with different molecular masses and occur in the presence of a constant or time varying acceleration. The acceleration generates differential body forces, leading to instabilities, which grow in time so that the resulting flow ultimately becomes turbulent. In many situations such flows occur in convergent geometries (e.g. cylindrical or spherical). Examples include Inertial Confinement Fusion targets, laser induced launching of a flyer plate, stellar pulsations, or supernova explosions. Fundamental turbulence studies and high resolution simulations of these flows in Cartesian geometry only recently have started to be performed and there is no such study in convergent geometries. Moreover, early time analytical studies are almost entirely confined to immiscible fluids and incompressible flows with very few studies addressing the case of variable density or compressible flows and none the miscible case.

We are developing a multi-pronged, multi-investigator research program to improve the computational and modeling capabilities for instability-driven flows in convergent geometries and advance the understanding of the mathematics and physics characterizing turbulence generated in such conditions. Our study is providing analytical results for early time (linear and non-linear) growth, new tools for mixing description, fundamental turbulence studies, a turbulence modeling methodology and Direct Numerical Simulations data.

## Benefit to National Security Missions

The project supports the DOE mission in Nuclear Weapons and Office of Science missions in Fusion Energy Sciences and Advanced Scientific Computing Research by advancing our understanding of the instability-generated turbulence in convergent geometries using theory and large scale, high performance computational tools.

## Progress

The tasks for this project are being accomplished as proposed. Thus, the first analytical study of early time gravitational instabilities growth in cylindrical geometries has been finalized and the results submitted for journal publication [1,2], presented at several scientific meetings, and published in conference proceedings [3,4]. Among the new, unexpected findings are: 1) the non-uniqueness of the compressible to incompressible limit, 2) large differences between explosion (gravity acting outward) and implosion (gravity acting inward) compared to the Cartesian geometry, and 3) qualitative differences between the 2-dimensional circular case compared to the 3-dimensional case.

A study of instability driven mixing in variable density turbulence has been finalized and the results documented in two journal publications [5,6] and presented at several conferences [7, 8, 9, 10]. For this study, the largest fully resolved simulations of homogeneous two fluid mixing have been performed. The results revealed an asymmetry in the mixing process, with the pure light fluid mixing faster than the pure heavy fluid. None of the mixing metrics usually used by models can capture this asymmetry and thus new metrics have been proposed. In addition, bounds on the fluid composition based on low order moments of the density probability density function have been analytically derived. These bounds can be used as realizability conditions or to describe the mixing state in low dimensional modeling. Another unexpected finding was the persistent anisotropy of the smallest scales of motion due to buoyancy, despite the intermediate scales becoming nearly isotropic. This is contrary to the usual universality assumption on the decoupling and independence of the small scales of motion from the large scales and has important consequences on the popular large eddy simulations turbulence modeling approaches.

To perform direct numerical simulations (such that all relevant scales of motion are accurately solved) of the turbulence generated by acceleration driven instabilities in convergent geometries a new, high-performance

high-accuracy code has been developed. The code solves the compressible Navier-Stokes equations and species transport equations in cylindrical and spherical geometries using a sixth order compact finite differences scheme with error behavior close to that of a spectral scheme. The numerical singularities at the origin and on the theta=0 plane are avoided by appropriate coordinate transformations and using an even number of points in theta and r directions. In this approach, there is no loss of accuracy near the origin and no regularization condition is needed. Thus, the code allows flow and non-zero gradients at the origin. The code has been verified and low resolution parameter studies are under way [4].

## Future Work

For this project, we are conducting a multi-pronged research program to improve the computational and modeling capabilities for instability-driven flows in convergent. The following tasks are planned for FY09:

- Extend our early time instability studies to situations of interest to supernovae by including in the analysis: a) spherical geometry effects and b) non-uniform equilibrium temperature.
- Investigate if the mixing asymmetry we found in buoyancy driven flow is a general feature or principle of multi-material turbulent mixing.
- Perform petascale Direct Numerical Simulations of instability driven turbulence and mixing. The database will be used for understanding the nature of mixing and turbulence characteristics and as a verification tool for multiphysics, low resolution codes.
- Examine turbulence characteristics and extend analytical turbulence closures to include non-homogeneities. This will enhance our predictive tools and allow the development of improved low dimensional models using a science-based approach.

## Conclusion

- For the flow generated by Rayleigh-Taylor instability between miscible fluids in convergent geometries the project is providing:
- First analytical studies of early stages instability growth, necessary for code verification.
- First fundamental turbulence study and new modeling techniques, necessary for improved predictive capabilities.
- A high performance (petascale) Direct Numerical Simulations code and first such simulations. The DNS results can also be used for verifying multiphysics low resolution simulation codes.

The results are important for scientific advancement and enhancing our understanding of the universe (e.g. turbulence, supernova explosions) and improving our predictive capabilities in areas as inertial confinement fusion and atmosphere dynamics.

## References


1. Yu, H., and D. Livescu. Rayleigh-Taylor instability in cylindrical geometry with compressible fluids. 2008. *Physics of Fluids.* **20** (10): 104103:1.
2. Livescu, D.. Comment on 'Compressibility effects on the Rayleigh-Taylor instability of three layers' [Phys. Fluids 19, 096103 (2007)]. 2008. *Pysics of Fluids.* **20** (2): 029103:1.
3. Yu, H., and D. Livescu. Linear Analysis of Rayleigh-Taylor Instability between Immiscible Compressible Fluids in Cylindrical Geometry. 2007. In *61 Meeting of the Division of Fluid Dynamics, American Physical Society.* (Salt Lake City, 22-24 November 2007). Vol. 52, 17 Edition, p. 253. Bulletin of the American Physical Society: APS.
4. Yu, H., and D. Livescu. Compressible Rayleigh-Taylor instability in cylindrical geometry. To appear in *11 International Workshop on the Physics of Compressible Turbulence.* (Santa Fe, 14-18 July 2008).
5. Livescu, D., and J. R. Ristorcelli. Variable density mixing in buoyancy generated turbulence. 2008. *Journal of Fluid Mechanics.* **605**: 145.
6. Livescu, D., J. R. Ristorcelli, R. A. Gore, S. H. Dean, W. H. Cabot, and A. W. Cook. High-Reynolds number Rayleigh-Taylor turbulence. To appear in *Jornal of Turbulence.*
7. Livescu, D., and J. R. Ristorcelli. Mixing characteristics in buoyancy driven turbulence," in Advances in Turbulence XI. 2007. In *Advances in Turbulence XI.* Edited by L.M.Palma, J. M., and S. Lopez. Vol. 117, 544 Edition, p. 546. Oporto, Portugal: Springer.

8. Livescu, D., and J. R. Ristorcelli. Variable-Density Mixing in Buoyancy-Driven Turbulence. 2007. In *61 Meeting of the Division of Fluid Dynamics, Americal Physical Society.* (Ssalt Lake City, 22-24 November 2007). Vol. 52, 17 Edition, p. 287. Bulletin of the American Physical Society: APS.

9. Livescu, D., J. R. Ristorcelli, and R. A Gore. High-Reynolds number Rayleigh-Taylor turbulence. To appear in *11 International Workshop on the Physics of Compressible Turbulent Mixing.* (Santa Fe, 14-18 July 2008).

10. Livescu, D., and J. R. Ristorcelli. Molecular mixing and the mix parameter in variable density buoyancy driven turbulence. To appear in *11 International Workshop on the Physics of Compressible Turbulent Mixing.* (Santa Fe, 14-18 July 2008).

## Publications

Livescu, D.. Comment on 'Compressibility effects on the Rayleigh-Taylor instability of three layers' [Phys. Fluids 19, 096103 (2007)]. 2008. *Physics of Fluids.* **20** (2): 029103:1.

Livescu, D., J. R. Ristorcelli, R. Gore, S. Dean, W. Cabot, and A. Cook. High Reynolds number Rayleigh-Taylor turbulence. *Journal of Turbulence.*

Livescu, D., J. R. Ristorcelli, and R. A. Gore. High-Reynolds number Rayleigh-Taylor turbulence. To appear in *11 International Workshop on the Physics of Compressible Turbulent Mixing.* (Santa Fe, 14-18 July 2008).

Livescu, D., and J. R. Ristorcelli. Variable density mixing in buoyancy driven turbulence. 2008. *Journal of Fluid Mechanics.* **605**: 145.

Livescu, D., and J. R. Ristorcelli. Variable density mixing in buoyancy driven turbulence. 2007. In *APS DFD07.* (Salt Lake City, 19-21 Nov. 2007). Vol. 52, 17 Edition, p. 253. Salt Lake City: APS.

Livescu, D., and J. R. Ristorcelli. Mixing characteristics in buoyancy driven turbulence. 2007. In *Advances in Turbulence XI.* Edited by L.M.Palma, J. M., and S. Lopez. Vol. 117, p. 544. Oporto, Portugal: Springer.

Livescu, D., and J. R. Ristorcelli. Molecular mixing and the mix parameter in variable density buoyancy driven turbulence. To appear in *11 International Workshop on the Physics of Compressible Turbulent Mixing.* (Santa Fe, 14-18 July 2008).

Mohd-Yusof, J., and D. Livescu. Turbulence direct numerical simulations on RoadRunner. Presented at *Supercomputing07.* (Reno, 10-16 Nov. 2007).

Yu, H., and D. Livescu. Compressible Rayleigh-Taylor instability in cylindrical geometry. 2007. In *APS DFD07.* (Salt Lake City, 19-21 Nov. 2007). Vol. 52, 17 Edition, p. 287. Salt Lake City: APS.

Yu, H., and D. Livescu. Rayleigh-Taylor instability in cylindrical geometry with compressible . 2008. *Physics of Fluids.* **20** (10): 104103:1.

Yu, H., and D. Livescu. Compressible Rayleigh-Taylor instability in cylindrical geometry. To appear in *11 International Workshop on the Physics of Compressible Turbulent Mixing.* (Santa Fe, 14-18 July 2008).

# Moment-Based Interface Tracking for Multi-Material Flows

*Rao Veerabhadra Garimella*

20070202ER

## Introduction

Accurate tracking of material interfaces is an important aspect of many simulations necessary for our national energy and security goals. For example, the National Ignition Facility at LLNL attempts to initiate fusion in a BB-sized target filled with hydrogen fuel with the help of 192 giant laser beams directed into a gold capsule (hohlraum) enclosing the fuel. This process is called Inertial Confinement Fusion or ICF. The intense heat generated by the lasers will cause the outer layer of the fuel pellet to explode, generating a reactionary shock wave that drives the remaining material towards the center of the pellet. To design and understand this experiment, it is critical to simulate and understand how the different materials travel after the ablation of the external layer.

In our LDRD project, we will advance the state-of-the-art for multi-material gas dynamics simulations by introducing an innovative method to track material interfaces in gas dynamics or hydrodynamics simulations. This method, called the Moment-of-Fluid (MoF) interface reconstruction technique was recently invented at LANL. Unlike previous methods, which only tracked the volumes of different materials in computational cells, the MoF method also tracks the centroids of the materials in the cells. This leads to a more accurate and more efficient tracking of material interfaces in simulations like ICF. The higher fidelity of simulations made possible by this new method is expected to better our understanding of the phenomena that occur in such applications.

## Benefit to National Security Missions

This project supports the DOE/NNSA mission in Science and National Security by developing a more accurate method of tracking multi-material interfaces in hydrodynamic simulations for many mission relevant applications such as ICF.

## Progress

In the first year we implemented the Moment-of-Fluid (MOF) interface tracking method and moment update procedures in Qacina, an incompressible flow solver developed by Mark Christon. This year we completed the coupling between MOF and Qacina by accounting for the different material densities in mixed cells in the momentum (not moment) update equations (Variable Density Momentum Update). This involved solving a pressure-poisson equation as part of the momentum update. We also made the code multi-threaded so that we could run larger simulations. Finally, we enhanced the code so that we can now do multi-material (more than two materials per mesh cell) interface reconstruction based on the MOF method [1].

With the completion of the coupling between Qacina and MOF, we conducted convergence studies showing that, when coupled with a flow solver, MOF maintains a second order rate of convergence. For the convergence study we used the vortex-in-a-box test case where an initially circular blob of material is deformed into a spiral using an initial velocity given by an analytical expression (Figure 1). We also conducted tests of a bubble of light material rising in a fluid of denser material (without surface tension effects) and compared it with VOF type methods (1st order Youngs and 2nd order Swartz methods). Finally, we have simulated the collision of two bubbles of different density, one rising and one falling (Figures 2 and 3). In all these tests, we see that the MOF method captures small features like thin filaments better than traditional interface reconstruction methods. These tests have also revealed the critical effect of divergence error in the implementation of MOF methods in incompressible flow solvers. In order for the moment update method to produce accurate reference centroids, the flow solver must be able to maintain extremely low divergences (below 1e-10). Failure to do so introduce centroid errors and consequently, chatter in the reconstructed interfaces.

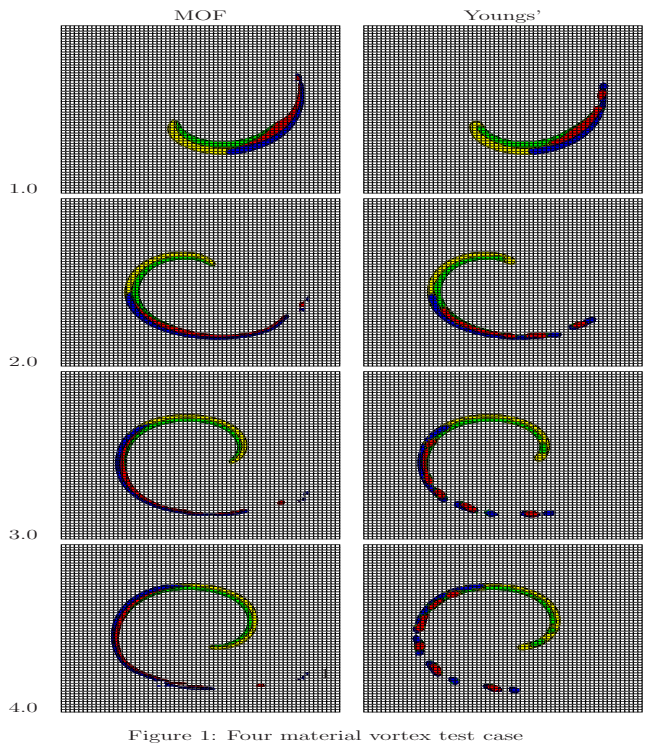


*Figure 1. Simulation of the vortex-in-a-box test with an initially circular four material blob. Notice how the MOF method maintains the filaments and the relative positions of the materials much better than a traditional Youngs method.*

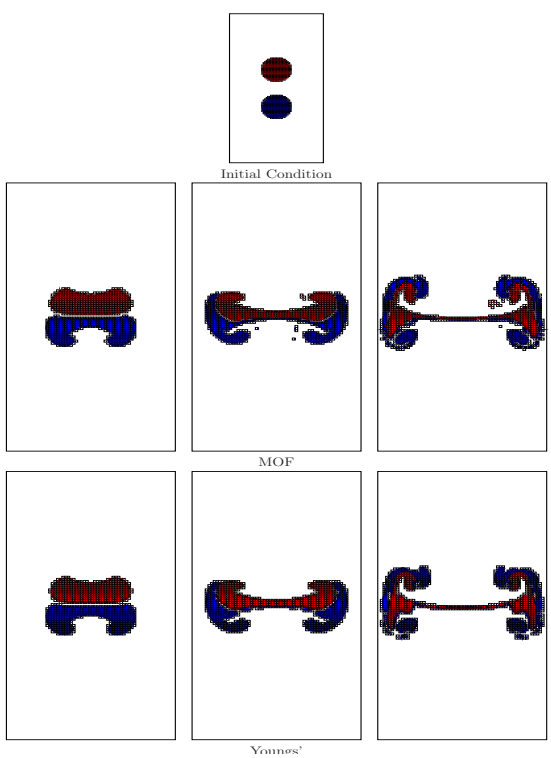


*Figure 2. Simulation of the collision of two bubbles. The background fluid density is 1.0, the top (red) bubble is of density 1.5 (causing it to drop) and the bottom (blue) bubble is of density 0.5 (causing it to rise). Again, notice how the MOF method maintains better coherence of filaments.*

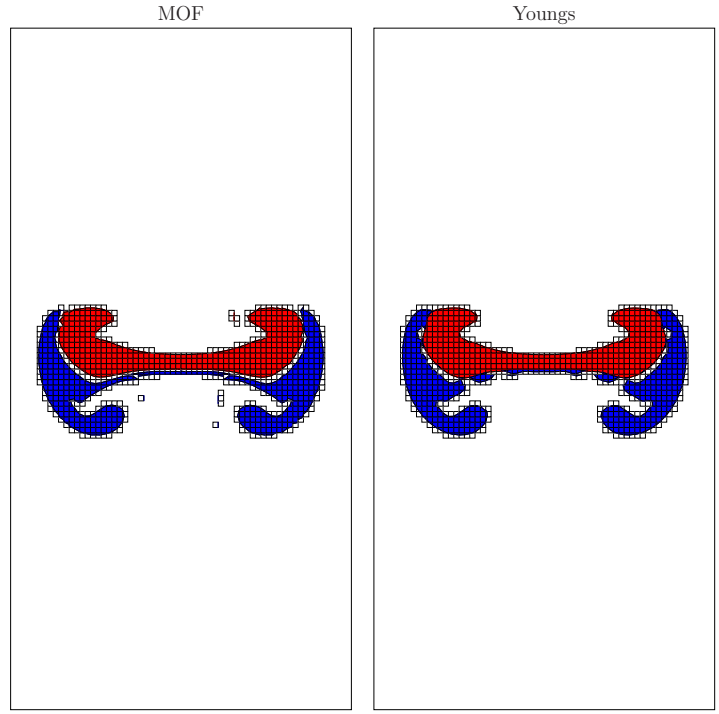


*Figure 3. Closeup view of the collision of two bubbles showing better handling of filaments by MOF.*

In addition to the above studies, we have developed a simple error estimator for MOF reconstructions based on the discrepancy of reference and reconstructed centroids (Milestone 1, Year 1).

Also, we have developed two new curvature estimation methods for MOF (Milestone 2, Year 1). The first method is based on using the error estimate for the MOF reconstruction to estimate the curvature of the interface. The second method is based on fitting a circle to the volume fraction and moment data. Unfortunately, both methods do not show the level of accuracy or the convergence rate we expected. We have investigated other methods based on volume fractions alone for tackling the problem - of the four methods investigated, only the height function approach gives convergent curvature estimates with second-order accuracy. However, the height function approach has been restricted so far to only uniform structured meshes only. Our team has extended the method to non-uniform structured meshes while maintaining order convergence. We are planning to generalize the method to unstructured meshes and test whether it will maintain the accuracy it shows on structured meshes.

Based on the curvature estimation methods, we plan to put a surface tension model in the Qacina code to conduct more realistic simulations of the bubble rise problem.

We have presented our work (both results from our simulations and the curvature estimation methods) at two separate talks at the internationally renowned SIAM Annual Meeting in San Diego in July 08 and are preparing a paper on our results. Two other papers are also in preparation discussing the curvature estimation methods developed and tested this year.

## Future Work

In the coming year, we will work on the following topics:

- Extension of the height function method to unstructured meshes
- Incorporation of surface tension into Qacina
- Conformal adaptive refinement of quadrilateral meshes driven by MOF error estimates developed in Year 1, Milestone 1
- Investigate alternative moment update schemes that are less sensitive to divergence
- Study issues of moment update in 3D

## Conclusion

This project will develop a new method of tracking multi-material interfaces in hydrodynamics simulations necessary for many applications related to national security and energy resource utilization. This is an innovative method that promises to significantly improve the accuracy of interface tracking and as a result, increase the fidelity of complex hydrodynamic simulations such as ICF simulations.

At the end of the project, we expect to have fully developed, mature, and efficient interface tracking technology that will be ready for direct incorporation into major hydrocodes at LANL and other DOE codes.

## References

1. Dyadechko, V., and M. Shashkov. Reconstruction of multi-material interfaces from moment data. 2008. *Journal of Computational Physics.* **227** (11): 5361.

## Publications

Dyadechko, V., and M. J. Shaskov. Reconstruction of Multi-material interfaces from moment data. 2008. *Journal of Computational Physics.* **227** (11): 5361.

# Hyperbolic Polynomials Approach to Approximate Counting and Lower/Upper Bounds in Combinatorics, Statistical Physics and Computational Geometry

*Leonid Gurvits*

20070243ER

## Introduction

Many important problems in physics, geometry, engineering, and mathematics involving counting, or estimating to a certain accuracy, the number of objects with a given property, whether these be ways of covering a surface with small molecules of given types, paths visiting every point in a network, or more abstract mathematical objects. This project pursues a new approach to such problems, that involve constructing a multi-variable polynomial, such that a particular coefficient of the polynomial is proportional to the number of objects to be counted [1]. In many important cases this polynomial is positive hyperbolic (a notion originating in the theory of partial differential equations [2]). Hyperbolic polynomials are a deep mathematical structure underlying, and generalizing, some of the mathematics most fundamental to operations research (in particular, convex optimization and linear programming for resource allocation and system design) and to quantum physics (positive semidefinite matrices, which represent the states, and also the dynamical evolution, of quantum systems). We are further developing the theory of hyperbolic and related polynomials, and applying it to the approximation of counting problems, obtaining upper and lower bounds on the number of objects to be counted. We are also applying this theory to the theory of optimization over convex sets associated with hyperbolic polynomials. Besides these applications, the project is yielding fundamental advances in mathematics based on hyperbolic polynomials.

## Benefit to National Security Missions

This project supports a tremendously wide variety of mission areas by enhancing our understanding of and ability to solve a wide variety of computational problems in physics and engineering. For example, problems of partial differentiation supporting the Nuclear Weapons mission, and understanding code-breaking threats important to DHS missions are impacted.

## Progress

This project has yielded many accomplishments over the past year. In a paper published in Electronic Journal of Combinatorics, the proofs of the celebrated Schrijver-Valiant conjecture and generalized van der Waerden conjecture were unified and dramatically simplified using stable polynomials (closely related to hyperbolic polynomials). This advance could pave the way to a proof of an even broader generalization, also with applications to approximate counting problems. It has been nominated for the American Mathematical Society's Delbert Ray Fulkerson prize. The paper "Polynomial time algorithms to approximate mixed volumes within a simply exponential factor", an important application of the project's methods to a problem of computational geometry, was accepted by the Journal of Discrete and Computational Geometry. A short proof, based on the mixed volume, of Liggett's theorem on the convolution of ultra-logconcave sequences was accepted by the Journal of Combinatorial Theory.

The project introduced two new classes of polynomials, generalizing the stable polynomials: Alexandrov-Fenchel and Strongly Log-Concave polynomials, and generalized aspects of the theory of stable and hyperbolic polynomials to these classes, including the inequalities involved in approximate counting problems. This work has been presented at MTSN 2008 (Matrix Theory, Networks, and Systems) at Virginia Tech.

Two new issues broached this year were: spectral theory for the convex cones associated with homogeneous polynomials, and the systematic description of their dual cones. We have established that the noncommutative spectral theory for convex cones developed by Alfsen and Shultz in the 1970s [3] can sometimes, but not universally, be applied to hyperbolicity cones and their duals. When it applies, it should allow the development of new and more efficient, interior-point and primal-dual algorithms for efficient optimization over such cones (a vast generalization of the linear and semidefinite programming problems which are ubiquitous in applications).

Several important publications have also resulted from earlier years' work on this project. Gurvits' work with student Alex Olshevsky on stability testing for matrix polytopes has appeared in IEEE Transactions on Automatic Control. [4] Gurvits' work with Shmuel Friedland, "Lower bounds for partial matchings in regular bipartite graphs and applications to the monomer-dimer entropy" has appeared in the journal Combinatorics, Probability, and Computing [5].

## Future Work

We will continue to pursue our unifying approach to approximate counting and upper and lower combinatorial bounds based on properties of positive hyperbolic (and related) multivariate polynomials. Expected applications include still tighter lower/upper bounds on the k-dimensional monomer-dimer entropy and related quantities, derandomization of Markov Chain Monte Carlo algorithms approximating the permanent of non-negative matrices, algorithms approximating the number of perfect matchings in non-bipartite graphs, even better algorithms for approximating/bounding the mixed volume of convex sets, fast algorithms for highly mixed partial differentiation of stable black boxes with many inputs, and better understanding of NP-hardness.

Continued work based on applying spectral theory to hyperbolicity cones may yield important mathematical advances, including generalizations of Kostant's celebrated theorem on the convexity of the moment map, and hyperbolicity-cone generalizations of important linear algebra theorems concerning eigenvalues (e.g. Lidskii's theorem). Since homogeneous cones associated with Lie groups (of automorphisms of the cone) are all hyperbolicity cones, these may have important applications in Lie theory. The work may also provide an approach to proving or disproving the generalized Lax conjecture and analogues, concerning the representability of hyperbolicity cones in terms of the much better-understood positive-semidefinite matrix cones (as "slices" of these cones, or by other means). This would be of great significance to the optimization community.

Major tasks include:

- Further study the possibility and limitations of applicability of our approach to approximating the number of perfect matchings in non-bipartite graphs.
- Study the applicability of our approach to approximating the mixed volume of convex sets and the connections to computational algebra (solution of systems of polynomial equations).
- Study other, hopefully better, convex relaxations of the logarithm of the corresponding coefficient in generating polynomials.
- Study various models of random positive hyperbolic polynomials and the corresponding random analogues of the Van der Waerden and Schrijver-Valiant conjectures.
- Connect our approach with quantum search algorithms and quantum linear optics algorithms.
- Extend our approach to other problems such as factorization (important in the theory of Bayesian networks).
- Look for additional classes of multivariate polynomials, which also allow fast coefficient determination.

## Conclusion

We aim to produce algorithms enabling computers to be programmed to solve, or approximately solve, important classes of problems in mathematics, physics, chemistry, geometry, and engineering. One of these problems is computing the partition function of certain physical systems, which gives the thermodynamical properties of such systems, helping us understand the properties of materials. The algorithms we aim for could also help efficiently take highly mixed derivatives of polynomials and other functions, potentially helping in fast computer solution of partial differential equations used to describe many physical and nonphysical systems, such as the behavior of fluids, plasmas, and the climate. So far, the project has yielded both major mathematical advances such as the unified and generalized Schrijver-van der Waerden/Valiant type bounds and the introduction of new classes of tractable polynomials, and applications of these advances in improved approximation algorithms, for example for mixed volume computation in geometry and for the monomer-dimer problem relevant to chemical and materials problems.

## References

1. Gurvits, L.. Hyperbolic polynomials approach to van der Waerden/Schrijver-Valiant like conjectures: sharper bounds, simpler proofs and algorithmic applications. 2006. In *STOC'06. Proceedings of the 38th Annual ACM Symposium on Theory of Computing* . (Seattle, 23-26 May 2006). , p. 417. USA: ACM SIGACT.

2. Atiyah, M. F., R. Bott, and L. Garding. Lacunas for hyperbolic differential operators with constant coefficients. 1970. *Acta Mathematica.* **124**: 109.

3. Alfsen, E. M., and F. W. Shultz. Non-commutative spectral theory for affine function spaces on convex sets. Memoirs of the American Mathematical Society, Vol. 6, No. 172.. 1976.

4. Gurvits, L., R. Shorten, and O. Mason. The stability of switched positive linear systems. 2007. *IEEE Transactions on Automatic Control.* **52** (6): 1099.

5. Friedland, S., and L. Gurvits. Lower bounds for partial matchings in regular bipartite graphs and applications to the monomer-dimer entropy. 2008. *Combinatorics, Probability, and Computing.* **17** (3): 347.

## Publications

Barnum, H.. Semidefinite programming characterization and spectral adversary method for quantum complexity with noncommuting unitary queries. 2007. In *Algorithms and Complexity for Continuous Problems.* (Dagstuhl, Germany, 24-29 Sept. 2006). Vol. 06391, p. Electronic. Dagstuhl, Germany: IBFI.

Friedland, S., and L. Gurvits. Lower bounds for partial matchings in regular bipartite graphs and applications to the monomer-dimer entropy. 2008. *Combinatorics, Probability and Computing.* **17** (3): 347.

Gurvits, L.. Van der Waerden / Schrijver-Valiant-like conjectures and stable (aka hyperbolic) homogeneous polynomials:  one theorem for all . 2008. *Electronic Journal of Combinatorics.* **15** (1): R66.

Gurvits, L.. Polynomial time algorithms to approximate mixed volumes within a simply exponential factor. 2007. *Electronic Colloquium on Computational Complexity.* **TR07**: 037.

Gurvits, L.. A short, based on the mixed volume, proof of Liggett's theorem on ultra-logconcave sequences. To appear in *Journal of Combinatorial Theory.*

Gurvits, L., R. Shorten, and O. Mason. The stability of switched positive linear systems. 2007. *IEEE Transactions on Automatic Control.* **52** (6): 1099.

Gurvits, L., and A. Olshevsky. Stability testing of matrix polytopes. 2007. In *European Control Conference, 2007.* (Kos, Greece, July 2007). , CD-ROM  Edition, p. 3919. Saint Martin d'Heres, France: European Union Control Association.

continuing project

# Excited States and Optical Response of Nanosized Molecules at Linear Scaling Numerical Cost

*Sergei Tretiak*

20070256ER

## Introduction

The project aims to develop theoretical methods and numerical algorithms allowing computation of excited state properties of large molecular systems at linear scaling cost. These algorithms will permit calculation of excited states and optical responses directly from first principles, and will be implemented into the LANL-developed software. Development of such capabilities will lead to several breakthroughs in numerical algorithms/quantum chemical modeling providing vast improvements over existing approaches. This project will strongly contribute to several fields: 1) Computational science: we will provide a first of its kind iterative algorithm combining Krylov subspace solvers and sparse matrices schemes; 2) Molecular modeling: our research will create a practical scheme for fast O(N) calculation of molecular excited states - a major breakthrough in the computational chemistry; 3) Materials science and nanotechnology: applications of our methodology will elucidate the fundamental trends governed by quantum-mechanics, which in turn dictate the electronic properties of large molecular systems. The outcome will have immediate technological implications, and, more generally, offer valuable guidance for synthesis and experiment, while providing insight into the nature and behavior of excitations in soft optical materials such as conjugated organics. These cutting edge computational capabilities will find broad applications in numerous programs at LANL as well as general scientific community.

## Benefit to National Security Missions

The computational tools created will provide powerful predictive simulations for several classes of complex systems, including Nuclear Weapons and Threat Reduction activities, and will play an important role in the design and optimization of new materials and devices. This work benefits missions relevant to DOE, DHS, and other government agencies.

## Progress

Our article on the benchmark results of our developed conjugated gradient algorithm in application to the model system (chain of hydrogens) have been published in the Journal of Chemical Physics [1]. Over the past year we have extended our prototype 'orbital free' code for calculating excited states to real molecular systems. This code now includes four optimized algorithms, namely modified Lanczos, Arnoldi, Davidson, and Rayleigh quotient iterative procedures. These procedures have been modified from their original parent techniques applicable to the Hermetian eigen-problems only, so that they are able to deal with the J-symmetric structure of the RPA eigen-equation. All algorithms work in the representation-independent (i. e. orbital-free) framework. Conventional orbital based algorithms for solving the time-dependent Self-Consistent Field (TD-SCF) equations restrict the solution subspace to a particle-hole and hole-particle (ph-hp) symmetry by construction. In an orbital independent formulation, we impose this ph-hp symmetry by using the occupied subspace projector, the idempotent ground state density matrix. The algorithms also utilize indefinite inner product for ortho-normalization of excitation vectors and 'Wilkinson shift' methodology for obtaining many excited states. Their convergence is ensured by application of the Thouless variational principle. Consequently, all these approaches are readily transferrable for a linear-scaling implementations of both Hartree-Fock and Kohn-Sham self-consistent field theories for the calculation of excitation energies and frequency-dependent molecular responses, by solving the RPA (non-Hermitian) and CIS (Hermitian) eigenvalue equations in the molecular orbital-free framework. All developed numerical approaches have been thoroughly tested with respect to the imposed numerical noise to address linear-scaling conditions, see Figure. 1. Convergence behavior and stability has been numerically benchmarked for computations of excited states of realistic molecular systems (conjugated polymers and carbon nanotubes), see Figure. 2. We found that algorithm convergence critically depends in the quality of to the initial guess.

Consequently, we have developed a ladder of improving approximations for the initial guesses. Finally, we explored several implementations on numerical pre-conditioners allowing accelerating algorithmic convergence. The results allows to single out the most efficient procedure – namely modified Davidson algorithm - suitable for large-scale calculations of electronic excitations in the time-dependent perturbation theory in the linear scaling regime. To summarize, during the second year we have followed the outlined milestones of the project and finalized the prototype code containing four distinct routines for 'orbital free' calculations. The second manuscript summarizing our numerical studies has been submitted to the Journal of Chemical Physics [2]. We have transferred the developed routines into the LANL-developed MONDO-SCF suite and currently we are fine-tuning the code. Recently we have obtained first proof of principles of the linear scaling excited state calculations, see Figure. 3.

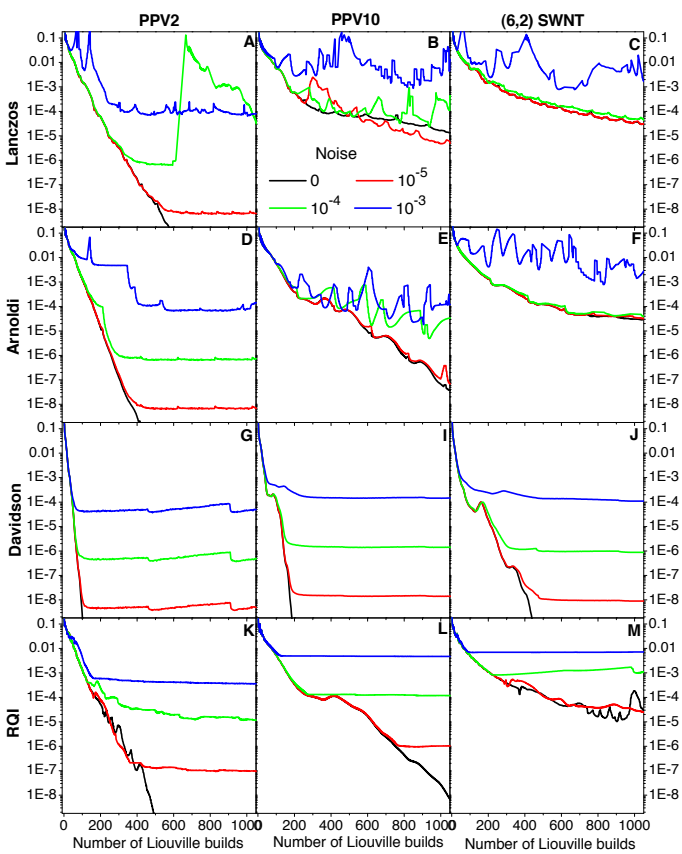


*Figure 1. Convergence rates of the first excited state in the presence of numerical noise in the RPA method. The same random guess is used in all calculations. The horizontal axis (number of Liouville builds) shows the associated numerical expense.*

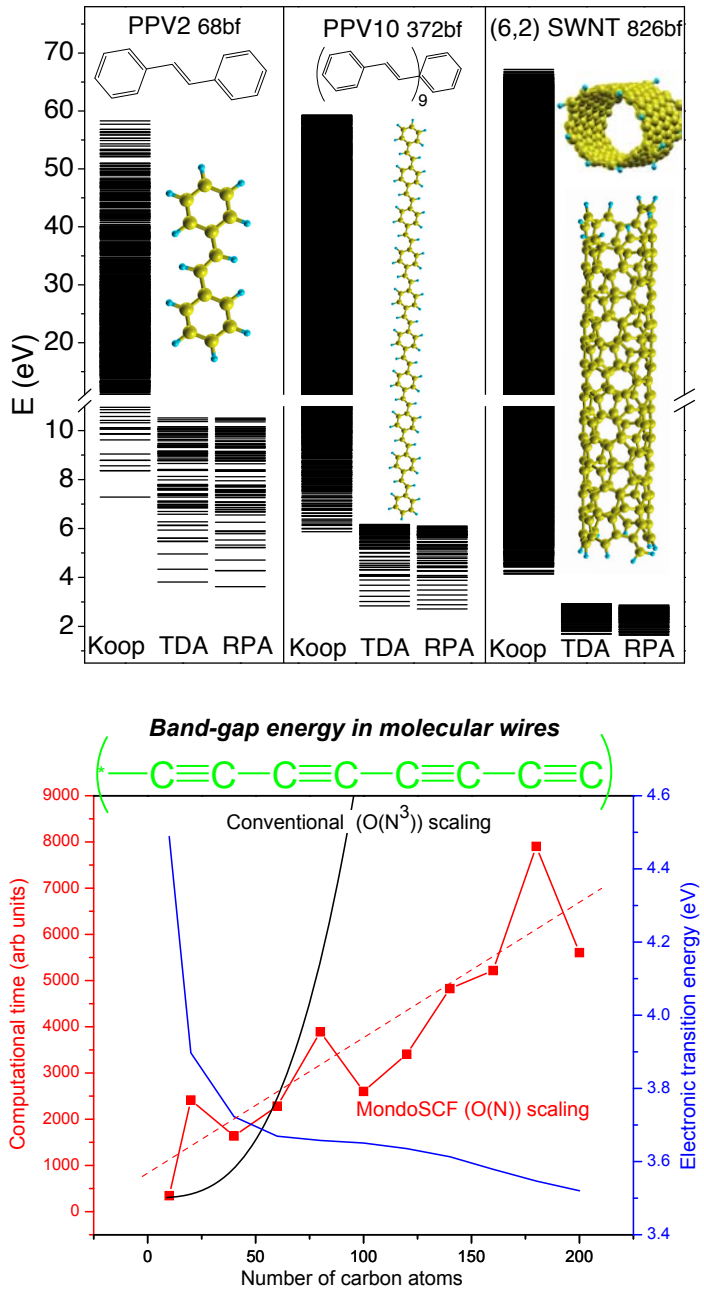


*Figure 3. The RQI algorithm has been programmed into LANL developed MondoSCF package and proof-of principles excited state calculations in the linear scaling regime is demonstrated.*

## Future Work

Currently the most advanced first principle calculations of excited states (such as time-dependent density functional theory, TDDFT) require O(N^3) computational effort, N being the number of atoms in the molecule. Typically this limits the calculations to few excited states of molecules up to ~100 atoms in size. The proposed work aims to overcome these limitations by developing stable and efficient algorithmic procedures for finding a partial eigenspectrum of a tetradic (N^2xN^2) non-Hermitian, non-sparse Liouville matrix at O(N) (linear) computational cost. This will be

achieved by simultaneous application of two techniques: Krylov subspace eigensolvers (producing O(N^6) to O(N^3) reduction) and sparse matrix methods (permitting an additional O(N^3) to O(N) deduction). We intend to deliver a complete set of theoretical tools for rapid calculations of excited states and optical properties in large molecular systems. These algorithms will be integrated into LANL-developed MondoSCF software suite. The developed tools will achieve O(N) scaling regime when computing excited state properties as a function of molecular size N. This project will strongly contribute to several fields: 1) Computational science: we will provide a first of its kind iterative algorithm combining Krylov subspace solvers and sparse matrices schemes; 2) Molecular modeling: our research will create a practical scheme for fast O(N) calculation of molecular excited states - a major breakthrough in the computational chemistry; 3) Materials science and nanotechnology: applications of our methodology will elucidate the fundamental trends governed by quantum-mechanics, which in turn dictate the electronic properties of large molecular systems. The outcome will have immediate technological implications, and, more generally, offer valuable guidance for synthesis and experiment, while providing insight into the nature and behavior of excitations in soft optical materials such as conjugated organics. These cutting edge computational capabilities will find broad applications in numerous programs at LANL as well as general scientific community.

## Conclusion

Successful completion of the proposed research will permit, for the first time, a practical computational approach to optical properties and enable theoretical spectroscopy of nano-sized systems boosting computationally treatable molecules to 1000-10000 atoms range. In the course of the project massively parallel MondoSCF program package will be substantially improved. The applications undertaken in the project are expected to result in a fundamental understanding of electronic processes in functional matter (such as photo-sensing, photo-labeling, light harvesting and bio-functionalities), provide novel design strategies for new electronic materials, and foster integration and improvements in experimental LANL research in nanoscience.

## References

1. Lucero, M. J., A. M. Niklasson, S. Tretiak, and W. M. Challacombe. Molecular-Orbital-Free Algorithm for Excited States in Time-Dependent Perturbation Theory. 2008. *Journal of Chemical Physics.* **129**: 064114.

2. Tretiak, S., C. M. Isborn, A. M. Niklasson, and W. M. Challacombe. Representation independent algorithms for molecular response calculations in time-dependent self-consistent field theories. To appear in *Journal of Chemical Physics.*

## Publications

Lucero, M. J., A. M. Niklasson, S. Tretiak, and W. M. Challacombe. Molecular-Orbital-Free Algorithm for Excited States in Time-Dependent Perturbation Theory. 2008. *Journal of Chemical Physics.* **129**: 064114.

Tretiak, S., C. M. Isborn, A. M. Niklasson, and W. M. Challacombe. Representation independent algorithms for molecular response calculations in time-dependent self-consistent field theories. To appear in *Journal of Chemical Physics.*

# Agent-Based Modeling and Simulation of Cellular Signaling Systems

*William Scott Hlavacek*

20070416ER

## Introduction

Proteins in cellular regulatory systems, because of their multicomponent composition, can interact in a combinatorial number of ways to generate myriad protein complexes, which are highly dynamic. This feature of protein-protein interactions has been called combinatorial complexity [1], and is recognized as a major barrier to understanding cell biology. The problem of combinatorial complexity is alleviated by using a rule-based computational approach to model protein-protein interactions [2]. In this approach, proteins and protein complexes are represented as structured objects (graphs) and protein-protein interactions are represented as (graph-rewriting) rules that operate on these objects to modify their properties, consistent with transformations mediated by the interactions being represented. Rules can serve as definitions of individual reactions or entire reaction classes, and they can be used as generators of reactions. The assumption underlying this modeling approach, which is consistent with the modularity of regulatory proteins, is that interactions are governed, at least to a first approximation, by local context that can be captured in simple rules (e.g., by the availability of binding sites on two binding partners). Rules can, in principle, be used to generate reaction networks that account comprehensively for the consequences of specified protein-protein interactions. However, the size of a rule-derived network can severely challenge conventional methods for simulating reaction kinetics. This project is aimed at developing new methods for simulating rule-based models that imply large-scale chemical reaction networks and then using these methods to gain insights into the complex systems that cells use to make decisions in response to environmental stimuli.

## Benefit to National Security Missions

This project can broadly impact the field of simulating biomolecular interactions that are immediately relevant to missions in DOE/SC and NIH. A predictive understanding of cellular regulation is important, for example, for the engineering of microbes for useful purposes that can impact environmental science, threat reduction and other mission areas.

## Progress

The key accomplishments are development of two novel algorithms that enable the simulation of rule-based models that cannot otherwise be simulated. We have also started to apply these methods to study cellular systems.

The first method developed is an agent-based method in which 1) a time increment is sampled from an exponential distribution, 2) a rule is selected from among a weighted list of rules, just as reactions are sampled in the well-known Gillespie's method, and 3) the selected rule is used to generate a reaction event (i.e., to select reactants to participate in a type of reaction defined by the selected rule). Reaction network generation is avoided entirely. In a first application of the method, we used it to study multivalent ligand-receptor binding, obtaining results that are relevant for a number of experimental systems that have been studied in the laboratory of our collaborator, Dr. Richard G. Posner (Translational Genomics Research Institute, Phoenix). The method has been reported in Physical Review E [3]. Two manuscripts reporting applications of the method are being prepared for submission. We are now working on extensions of the method that will allow for incorporation of geometric constraints on the formation of molecular complexes. Preliminary results have been obtained for complexes that form in two dimensions (i.e., on a cell surface) and we expect to generalize the approach to three dimensions in the coming year of the project.

The second method developed as part of this project, also an agent-based method, is a generalization of a method, implemented in software called StochSim, which was developed by Morton-Firth and Bray [4]. The generalized method can be used to model a much greater variety of molecular interactions than the original and we have implemented the method in general-purpose software called DYNSTOC. A manuscript about the method and software has been submitted to Bioinformatics [5].

Now that appropriate methods and software tools have been developed for simulating large-scale rule-based models, we have started to build such models. We are

building a large model for signal-transduction events mediated by the receptor tyrosine kinase EGFR, which plays an important role in many cancers. We have also started to build a model for metabolism in the bacteria Escherichia coli that accounts for the fates of every carbon atom of metabolites in enzyme-catalyzed reactions. We expect to be able to apply our novel simulation tools to the study of these systems to obtain insights into the molecular mechanisms of cancer and into how metabolism might be reengineered for useful purposes. The models that we are pursuing would represent breakthroughs in the fields of computational systems biology and metabolic engineering.

## Future Work

There is strong motivation to better understand the processes of cellular signaling, in which protein interactions play a central role. Indeed, we would like to make accurate predictions about the functional roles of proteins and the effects of modifying protein interactions in particular systems. Our ability to make such predictions is a measure of our basic understanding of molecular cell biology and a range of practical consequences may stem from an improved capability to rationally manipulate cellular regulatory systems on the basis of predictive mathematical models. Current models of signaling systems are far from capturing all of the relevant mechanistic details necessary to make accurate predictions, in part because it is difficult to account for the enormous number of post-translational modifications and protein complexes that can be generated by interactions among even small sets of proteins. Our main goals are 1) to develop a representational framework suitable for concisely capturing site-specific details about protein interactions while accounting comprehensively for the possible consequences of protein interactions and 2) to develop novel discrete-event simulation methods that take advantage of this representational formalism and overcome the problem of simulating the large-scale chemical reaction networks that characterize the dynamics of protein interactions. Proteins will be modeled as abstract computing devices, termed molecular finite state automata (MFAs), and their interactions will be represented as molecular event classes, which will define how the states of MFAs are altered by interactions. To accomplish our goals, we will develop MFA descriptions for the human proteome based on information stored in electronic databases, develop and test models for particular systems that are difficult to simulate using conventional methods, and comparatively evaluate the efficiency the new event-driven simulation methods that we contemplate. We will also perform the largest simulation of the dynamics of a signal-transduction system to date.

## Conclusion

The expected results of this project include a formal language for representing proteins and protein interactions, which play a central role in regulating cellular activities, and novel methods for simulating the large-scale chemical reaction networks that characterize the dynamics of protein interactions. These methods are required to obtain system-level predictions about the dynamical behavior of cellular signaling systems, molecular changes of which are responsible for a variety of diseases, including cancer. Predictive models of these systems may eventually enable the engineering of microbes for useful purposes, such as bioenergy production, environmental remediation, and microbial carbon cycling.

## References


1. Hlavacek, W. S., J. R. Faeder, M. L. Blinov, A. S. Perelson, and B. Goldstein. The complexity of complexes in signal transduction. 2003. *Biotechnology and Bioengineering.* **84**: 783.

2. Hlavacek, W. S., J. R. Faeder, M. L. Blinov, R. G. Posner, and M. Hucka. Rules for modeling signal-transduction systems. 2006. *Science's STKE.* **2006**: re6.

3. Yang, J., M. I. Monine, J. R. Faeder, and W. S. Hlavacek. Kinetic Monte Carlo method for rule-based modeling of biochemical networks. 2008. *Physical Review E.* **78**: 031910.

4. Morton-Firth, C. J., and D. Bray. Predicting temporal fluctuations in an intracellular signaling pathway. 1998. *Journal of Theoretical Biology.* **192**: 117.

5. Colvin, J., M. I. Monine, J. R. Faeder, W. S. Hlavacek, D. D. Von Hoff, and R. G. Posner. Simulation of large-scale rule-based models. 2008. *Los Alamos Technical Report LA-UR-08-04860.*


## Publications


Colvin, J., M. I. Monine, J. R. Faeder, W. S. Hlavacek, D. D. Von Hoff, and R. G. Posner. Simulation of large-scale rule-based models. 2008. *Los Alamos Technical Report LA-UR-08-04860.*

Yang, J., M. I. Monine, J. R. Faeder, and W. S. Hlavacek. Kinetic Monte Carlo method for rule-based modeling of biochemical networks. 2008. *Physical Review E.* **78**: 031910.

# Fast Approximation Algorithms for Systems of Linear Inequalities

*Donald Rhea Hush*

20070421ER

## Introduction

Computational modeling is rapidly becoming ever more central to developing and refining our understanding of the physical world. The efficiency with which those computational models can solve the complex problems of the physical world depend on the efficiency of the algorithms used to express physical parameters and solve complex mathematical problems.

This project will develop computer algorithms for the following core problem in computer science: given a collection of red and blue dots scattered randomly on a piece of paper, position a line that best separates the red and blue dots. In higher dimensions, where we seek a "hyperplane" that best separates the red and blue dots, this problem is notoriously difficult. At the same time however, it is well known that the computational bottleneck for many important applications can be traced to this red-blue dot problem. Examples of such applications include identifying the smallest subset of genes that exhibit a coordinated response to a particular stimuli, determining the primary suppliers and consumers in large networks of individuals or institutions that are connected by the flow of money or information, and detecting anomalies on a computer network. This project promises to produce practical algorithms that produce near optimal solutions for the red-blue dot problem in very high dimensions and with a very large number of red and blue dots, and therefore promises to make significant advances in several important applications.

## Benefit to National Security Missions

This project enhances our understanding of how to solve the computational problem of automatic analysis and screening of large amounts of data. Such solutions will impact many important and diverse applications including threat reduction and intelligence missions of DOE, DHS, and other government agencies.

## Progress

Algorithm development is divided into five tasks:

1. Develop a rigorous understanding of a class of red-blue dot distributions that admit computationally efficient solution algorithms.

2. Design a surrogate optimization problem whose solutions are (with high probability) good approximate solutions of the class of red-blue dot problems determined in task one.

3. Design a solution method for this surrogate problem. Here we adopt a novel approach that decomposes the surrogate optimization problem into a nesting of two optimization problems: a large convex problem nested inside a small non-convex problem.

4. Design and analyze algorithms for the nested optimization problems. First we will develop and analyze algorithms for the large convex problem, making sure that they will scale to very large problem sizes. Then we will develop algorithms for the small non-convex problem, with the goal of striking an optimal balance between the computational efficiency and the accuracy of the approximate solution.

5. The last task is to perform extensive testing of our algorithms on both synthetic and real data.

In this second year we completed tasks one through three, made significant progress on task 4, and began work on the final task five. More specifically we finalized the following work from year one:

- Characterize distributions that admit efficient algorithms.

- Design a surrogate optimization problem based on this characterization.

Most of our work this year went into tasks three and four where we completed the design of several candi-

date optimization problems, developed and analyzed numerous (new) algorithms for these optimization problems, and performed numerous lab experiments to identify the fastest and most robust algorithm in practice. Finally, as part of our initial work on task five we tested our algorithms with data sets up to 100,000 data points (red and blue dots) and 100 dimensions and verified that the algorithms produced near-optimal solutions.

## Future Work

In our final year we plan to complete tasks four and five. More specifically we plan to develop a streamlined implementation of our algorithm that uses optimized data structures to make the most efficient use of both time and memory. Finally, we plan to apply this algorithm to data from numerous applications including network monitoring for cybersecurity, high precision machining for manufacturing, and activity monitoring for situational awareness.

## Conclusion

We expect this project to produce new algorithms for a core problem in computer science that appears frequently in practice, and is solved very poorly by existing algorithms. Indeed, we expect to produce the first practical algorithms that scale to very large problem sizes and promise near optimal solutions. This will substantially advance our problem solving capabilities for applications such as the development of regulatory network models in genomics, the analysis of organizational networks (e.g. people-to-people networks) for national security, and the analysis of surveillance imagery for threat reduction.

## References

1. Scovel, C., D. Hush, and I. Steinwart. Approximate duality. 2007. *Journal of optimization theory and applications.* **135** (3): 429.

## Publications

List, N., D. Hush, C. Scovel, and I. Steinwart. Gaps in support vector optimization. 2007. In *Lecture Notes in Computer Science.* Vol. 4539, p. 336. Berlin:Heidelberg: Springer.

Scovel, C., D. Hush, and I. Steinwart. Stability of unstable learning algorithms. 2007. *Machine Learning.* **67** (3): 197.

Scovel, C., D. Hush, and I. Steinwart. Approximate duality. 2007. *Journal of optimization theory and applications.* **135** (3): 429.

# Minimal Description of Complex Shapes with Applications to Experiments and Validationof Large-Scale Codes

*Mark B Mineev*

20070483ER

## Introduction

Computational modeling and simulation has become a cornerstone of many fields of science. This is especially true of weapons physics where experimental testing is largely prohibited by treaties. Hence, advances in understanding of weapons physics can only come through computational modeling of the physics. This project will develop the mathematical tools needed to model fluid dynamics which will impact both weapons physics and the broader field of fluid dynamics.

The project is devoted to a recently found and developed (partially by us) powerful methods of modeling the complex shapes dynamics occurring in various processes including those in unstable fluid interface dynamics and highly stressed materials under extreme loads - these processes belong to those at the core mission of LANL. In short we are applying a deep mathematical structure lying behind the nonlinear dynamics of complex shapes to various physical processes and obtain closed form solutions which excellently approximate complex shapes dynamics. We also address the minimal description concept for complex interfaces using our algorithms and modern mathematical theories, such as quadrature domains, closely related to the approaches we exploit in the project.

Our work is expected to significantly facilitate complex calculations, provide validation of large scale codes existing at LANL, and save a great deal of computational volume because for closed form solutions computer need much less information to deal with.

## Benefit to National Security Missions

This work is closely tied to nuclear weapons physics, a key NNSA mission, through the validation of codes with experimental data (obtained previously or with sub-critical experiments). Furthermore, through recovering real images from incomplete data, and obtaining description of unstable interfaces will impact DOE, DHS and other government agency missions.

## Progress

Here are key accomplishments made within framework of the project during this year:

Based on our very recent discoveries, we have written and published a review "Random Matrices, Laplacian Growth, and Operator Theory" in the Journal of Physics A [Ref. 1]. In this work we have addressed and significantly clarified our recent results in the major themes of this ER project devoted to new powerful analytic approximation techniques based on the quadrature domains, Pade approximations, Hankel matrices, and the Schwarz-function. This constitutes a critical milestone within a major task #1 (see the technical description) and opens a road for development an algorithm to process a wide class of complex images evolution. This review is on the top cited/downloaded work of all phys/math publications 2008, based on weekly citation reports (please see nph-abs_connect.htm).

We have extended the complex interface dynamics theory to arbitrary elliptic operators governing the domain evolution. This problem was critical to solve for elucidation of the mathematical structure hidden behind the unstable fluid/fluid interfaces where ideal (inviscid) liquids are involved. These processes address such phenomena as the Rayleigh-Taylor, Richtmyer-Meshkov, and Kelvin-Helmholtz instabilities, which are tightly related with one of LANL core mission in hydrodynamics. This work entirely fulfills FY08 part of the major goal #2 of the project (see the technical description) of revealing an analytic structure in these instabilities beyond perturbative level [Ref. 2]. We have significantly developed the technique based on the recently discovered (by us) multi-cut dynamics solutions of unstable interface dynamics. Specifically, we have revealed key analytic time-dependent properties of Riemann surfaces within this class of dynamics, and have demonstrated that this class exhausts all possible solutions of 2D interface dynamics, so that all previously known solutions are limits and reductions of this multi-cut dynamics. This work presents a new powerful

mathematical device to process and solve a wide variety of complex image evolutions and presents a milestone of the project indicated as a major task #4 in the technical description [Abanov et al., to be submitted to Physica D (Nonlinear Phenomena)].

We have completed the analysis of the stochastic model of growth initiated last year, and obtained a probability measure for growing contours. Thus, we are prepared to write a numerical code to compare these findings with real multi-scale experiments and codes. This addresses the key goal #3 indicated in the technical description of the project, namely to elucidate global universal fractal statistics in stochastic growth related to unstable 2D evolutions of complex shapes [Mineev-Weinstein and Gruzberg., to be submitted to J. of Statistical Physics].

In addition to the theoretical advances reported above, we (jointly with the experimental collaborators from the Center for Nonlinear Dynamics, U. of TX), completed a big work on the dynamics of harmonic moments for unstable interfaces, driven by external sources and isotropic surface tension. This work (taken about two years) fully confirmed all our previous conjectures of infinitely many conservations laws lying behind these complex nonlinear processes. This work constitutes an experimental component of the major task #3, which addresses universal statistical features of evolution of complex fluid/fluid interfaces. The paper is prepared for a submission for publication into a Phys. Rev. E (Nonlinear Phenomena) [Leshchiner et al., to be submitted to Phys. Rev. E].

PDF files of all five works (published, submitted, and to be submitted) are available upon request. In short, we have successfully resolved the key issues outlined in the project for this year. Based on the results described in the above, we started to translate the key theoretical results into MatLab-based codes. This enables us to work with our experimental collaborators on the testing of our predictions.

## Future Work

Our project contains four major tasks:

1. Using the power of the Hankel-Toeplitz Matrices, the theory of the Markov moments, the generalized Pade approximation technique, and the concept of minimal length description, to develop an algorithm for image processing of arbitrarily complex shapes and to establish interconnections with quadrature domains - a new powerful tool for analytical approximations.

2. Using our recent preliminary results and powerful analytical structure, lying behind a broad class of interface dynamics, to obtain analytic solutions for free boundary motions in such processes as the Rayleigh-Taylor, the Richtmyer-Meshkov, and the Kelvin-Helmholtz instabilities beyond a perturbative level.

3. Using recent experimental and theoretical discoveries in stochastic two-dimensional growth to elucidate structure and universal statistical distributions for global geometric characteristics of fractal-like complex shapes that have been observed in experiments.

4. Using the so-called multi-cut solutions for the Laplacian growth, which we have recently discovered, to build up a universal mathematical device to address numerous broad classes of nonlinear interface dynamics. The major principle, which is expected to help in reaching this goal, is a switch from singly-connected conformal mappings, which were mostly used so far, to double-connected ones (an annulus geometry).

## Conclusion

Our proposed work in unstable fluid interfaces addresses core issues of the LANL mission in weapon physics: our success in this direction constitutes considerable progress in one of the most notoriously unstable and unpredictable processes that scientists and engineers face in this mission. Also the proposed work on minimal description of complex images should benefit LANL simulations and experiments by providing verification and validation with useful physically meaningful metrics. This testing is expected to save considerable computational effort and help in assuring the quality of large scale simulation codes.

## References


1. Mineev-Weinstein, M., M. Putinar, and R. Teodorescu. Random Matrices in 2D, Laplacian Growth, and Operator Theory (Review). 2008. *Journal of Physics, A, Math. Theor.*. **41**: 263001.

2. Mineev-Weinstein, M., D. Khavinson, and M. Putinar. Planar Elliptic Growth. To appear in *Journal of Complex Variables and Operator Theory.*


## Publications


Abanov, A., M. Mineev-Weinstein, and A. Zabrodin. Self-similarity in Laplacian Growth. 2007. *Physica D.* **235**: 62.

Abanov, A., M. Mineev-Weinstein, and A. Zabrodin. Cut Dynamics in Laplacian Growth. *Physica D (Nonlinear Phenomena).*

Crowdy, D., M. Mineev-Weinstein, and M. Putinar. Preface. To appear in *Compl. Anal. Oper. Theory.*

Leshchiner, A., M. Thrasher, M. Mineev-Weinstein, and H. L. Swinney. Dynamics of Harmonic Moments in Laplacian Growth. *Phys. Rev. E.*

Mineev-Weinstein, M., D. Khavinson, and M. Putinar. Planar Elliptic Growth. To appear in *Journal of Complex Variables and Operator Theory.*

Mineev-Weinstein, M., M. Putinar, L. Sander, and A. Zabrodin. Preface. 2007. *Physica D.* **235**: vii.

Mineev-Weinstein, M., M. Putinar, and R. Teodorescu. Random Matrices in 2D, Laplacian Growth, and Operator Theory (Review). 2008. *Journal of Physics, A, Math. Theor..* **41**: 263001.

Mineev-Weinstein, M., and I. Gruzberg. Planar Stochastic Laplacian Growth. *J. of Statistical Physics.*

continuing project

# Conconvex Compressed Sensing

*Rick Chartrand*

20080128ER

## Introduction

The project will develop techniques that allow images or other signals to be reconstructed from much less data than are currently regarded as necessary. Whenever measurements are expensive, dangerous, or simply unavailable in large quantities, what would seem to be an impossible reconstruction task can become completely feasible. A typical example would be medical image reconstruction from a few X-rays, instead of a high-dose CT scan. The success of the project depends on fundamental advances in mathematics, in particular relating to difficult optimization problems that are widely regarded as intractable, yet appear to be solvable using surprisingly simple algorithms.

By considering the reconstruction results in reverse, we find that a small number of very simple measurements can serve as a lossless compression of the original signal. By using random measurements, compression can be done without needing to perform expensive computations that are infeasible for large datasets, or impossible in the case of streaming data where one does not have the data in hand to compute with. The mathematical results have the potential of demonstrating that simple, nonadaptive measurements can compress nearly as well as the most expensive, clever, fully-adaptive technique possible, even when those techniques are entirely infeasible. This can allow a small fraction of a streaming dataset to be stored and/or processed, with guaranteed fidelity of information.

## Benefit to National Security Missions

This project will enhance our ability to maximize the information recovered from the fewest data, which has many applications, including 3-D image reconstruction, streaming data analysis, and sensor network information retrieval. These missions are particularly relevant to DOE, NIH, the intelligence community, and other government agencies.

## Progress

One of the key accomplishments has been the development of an algorithm that converges much more quickly than the previously-used gradient descent method [1]. One of its crucial advantages is that it works without user supervision, allowing increased automation for more numerical testing of performance and investigating theoretical issues [2]. This algorithm is also more flexible than those appearing in the literature, allowing for signals that are sparse in any of a greater variety of ways, and easily adapting to the case of noisy measurements [3]. This new algorithm is also more easily studied theoretically, having more easily characterized behavior [4].

Much progress has been made on the primary theoretical endeavor of the project. This concerns proving that the algorithm is able to compute the global minimum of a nonconvex optimization problem. A consequence of the nonconvexity is that there is a huge number of local minima, and any reasonable algorithm could be expected to become stuck in any of them, instead of finding the global minimum. Yet, numerically we observe our algorithm to find the global minimum, without explicitly attempting to do so. But without theoretical justification for this, many in the research community remain skeptical of the nonconvex approach. A successful proof will bring great notoriety to LANL's efforts in this key area of information science, and lead to papers with many citations. Our work thus far has greatly improved our understanding of the theoretical issues, to the point that we can now say that we understand why the algorithm is as successful as it is. We have many partial results, but difficult details remain to be overcome before we can have a complete proof. National Academy members are starting to enter this area, but we are close to a proof and expect to be first to obtain one.

Our connection to the University of Chicago radiology department has led to our methods being applied to the diagnosis of breast cancer using tomosynthesis instead of CT [5], where a few X-rays are used instead of an X-ray from every angle. The reduction in dose is

significant, and preliminary tests show the ability of small microcalcifications to be resolved.

## Future Work

Our project addresses the issue of reconstructing signals (including images, network states, signals of any other form) from severely underdetermined linear systems. The method is to exploit the sparsity or compressibility of essentially all useful signals. This is currently done in the recent body of work known as "compressive sensing." This project explores the use of a nonconvex variant of these methods, which appears to allow successful reconstruction using even fewer measurements than the methods in the literature.

A major near-term objective is the development of rapidly-converging algorithms that are efficient enough to be used in very large-scale problems.

We will seek to prove that local minimization algorithms will converge to the global minimum of the optimization problem central to this project. This is observed in practice, but given the nonconvex nature of the problem, the proof is highly nontrivial. Given that a closely-related problem is known to be NP-hard, success will be a considerable accomplishment. The approach will exploit the relationships between sparsity and orthogonality in very high dimensional spaces. The goal is a theorem specifying conditions for convergence.

We will explore various applications. Central among these is medical imaging, where radiation dose and scantime are issues. High-quality 3-D reconstructions from EEG may be possible for the first time. Characterizing the extent to which nonadaptive dimension reduction for hyperspectral imaging and streaming data results from our approach will be a byproduct of the above theoretical work. New collaborations with University of New Mexico researchers may lead to the development of new compressive imaging systems, and methods for computing the radiation profiles needed to deliver a precision radiation dose to cancer patients undergoing radiation therapy, which would likely lead to patents and NIH funding of continued research.

## Conclusion

As scientific computations grow larger, it will become impossible to keep up with the increase in data, unless we learn how to process information as efficiently as possible. This project will help describe the theoretical limits on how much information is actually necessary, and how to attain those limits.

In another direction, the ability to learn more from fewer measurements will allow discovery of threats using fewer resources. Medical diagnoses may be possible using much less radiation than current X-ray procedures. New scientific applications may arise in situations where it is now infeasible to acquire enough data.

## References


1. Chartrand, R., and W. Yin. Iteratively reweighted algorithms for compressive sensing. 2008. In *33rd International Conference on Acoustics, Speech, and Signal Processing* . (Las Vegas, 31 Mar. - 4 Apr. 2008). , p. 3869. Piscataway: IEEE.

2. Saab, R., R. Chartrand, and O. Yilmaz. Stable sparse approximations via nonconvex optimization. 2008. In *33rd International Conference on Acoustics, Speech, and Signal Processing.* (Las Vegas, 31 Mar. - 4 Apr. 2008). , p. 3885. Piscataway: IEEE.

3. Chartrand, R.. Nonconvex compressive sensing and reconstruction of gradient-sparse images: random vs. tomographic Fourier sampling. 2008. In *IEEE International Conference on Image Processing.* (San Diego, 12-15 Oct. 2008). , p. 1. Piscataway: IEEE.

4. Chartrand, R., and V. Staneva. Restricted isometry properties and nonconvex compressive sensing. 2008. *Inverse Problems.* **24** (035020): 1.

5. Sidky, E. Y., I. Reiser, R. M. Nishikawa, X. Pan, R. Chartrand, D. B. Kopans, and R. H. Moore. Practical iterative image reconstruction in digital breast tomosynthesis by non-convex TpV optimization. 2008. In *SPIE Medical Imaging.* (San Diego, 16-21 Feb. 2008). Vol. 6913, p. 691328. Bellingham: SPIE.


## Publications


Chartrand, R.. Nonconvex compressive sensing and reconstruction of gradient-sparse images: random vs. tomographic Fourier sampling. 2008. In *IEEE International Conference on Image Processing.* (San Diego, 12-15 Oct. 2008). , p. 1. Piscataway: IEEE.

Chartrand, R., W. Yin, and IEEE. Iteratively reweighted algorithms for compressive sensing. 2008. In *33rd IEEE International Conference on Acoustics, Speech and Signal Processing ; 20080330 - 20080404 ; Las Vegas, NV.* , p. 3869.

Chartrand, R., and V. Staneva. Restricted isometry properties and nonconvex compressive sensing. 2008. *INVERSE PROBLEMS.* **24** (3).

Saab, R., R. Chartrand, O. Yilmaz, and IEEE. Stable sparse approximations via nonconvex optimization. 2008. In *33rd IEEE International Conference on Acoustics, Speech and Signal Processing ; 20080330 - 20080404 ; Las Vegas, NV.* , p. 3885.

Sidky, E. Y., I. Reiser, R. M. Nishikawa, Xiaochuan Pan, R. Chartrand, D. B. Kopans, and R. H. Moore. Practical iterative image reconstruction in digital breast tomosynthesis by non-convex TpV optimization. 2008. In *Medical Imaging 2008: Physics of Medical Imaging ; 18-21 Feb.* ( 2008 ; San Diego, CA, USA). Vol. 6913, p. 691328.

# Foundations for Practical Pattern Recognition Systems

*Reid Buchanan Porter*

20080182ER

## Introduction

The goal of this project is to improve learning algorithms for practical pattern recognition systems. Our approach is based on a novel combination of techniques from nonlinear signal processing and computational learning theory. This approach can improve performance and provide a better understanding of discrete pattern recognition systems. Discrete pattern recognition systems are designed using computational primitives that can be implemented exactly and efficiently on a digital computer (e.g. logical operations such as AND, OR, etc.), whereas continuous pattern recognition systems are designed using computational primitives that can only be approximated by the digital computer and are often computationally expensive (e.g. real-valued multiplication, exponentiation, etc.). As our world becomes more digital, the design of discrete pattern recognition systems becomes more important. However, discrete pattern recognition systems lack the firm mathematical foundation and performance guarantees enjoyed by continuous pattern recognition systems, which limits their usefulness in operational environments.

By exploring several new mathematical approaches, this project aims to develop a deeper understanding of discrete pattern recognition systems, thereby exposing their strengths and weaknesses, and providing valuable insight into the operational scenarios where they will be most effective. With this understanding this project also aims to develop new algorithms, which are more robust to operational scenarios and therefore more effective in real world environments. This project is focused on developing theorems and algorithms and is applicable to a wide range of pattern recognition applications. At the same time, the project has identified several specific applications relevant to threat reduction that it will use to develop, test and validate the work performed throughout the project.

## Benefit to National Security Missions

Pattern recognition systems allow computers to filter large quantities of data and highlight data that is most important to human users. This project will help these systems process more data in less time and make fewer mistakes. These advances will help the US government to better exploit the vast quantities of intelligence information being acquired, and provide defense organizations with increased information to quickly identify and diffuse threats. These advances will also help reduce the cost of managing, and exploiting intelligence information.

The applications that this project targets are directly relevant to the NNSA mission area of nonproliferation and include: the detection and classification of electromagnetic pulses from space, and in the identification and classification of proliferation signatures in satellite imagery and video, and the classification and characterization of special nuclear materials from spectroscopy as well as chemical and physical analysis.

## Progress

The fundamental pattern recognition problem is to build a model of some desired behavior by generalizing from a finite collection of examples of this behavior. Successful solutions to this problem find applications in nearly all aspects of computational science, including bio-informatics, signal processing, computational chemistry and data mining. Although the optimal behavior is well defined it typically cannot be achieved in practice due to a lack of information and resources. There are three sources of error (deviation from optimal): representation, estimation and computation. The representation error is due to the mismatch between our choice of model class and the true underlying behavior. The estimation error is due to the fact that we have only a finite number of examples of the desired behavior. The computation error reflects the lack of optimality due to limited computational resources (i.e. the resources needed to both produce and implement the model).

This past year we focused on learning discrete classifiers for two-class classification with independent and identically distributed (IID) examples. Our first accomplishment was to investigate and develop new algorithms for optimal dyadic decision trees (DDT). Dyadic decision trees provide a solution method that exactly minimizes complexity-penalized misclassification loss. This loss can be linked to estimation error, which means the approach is consistent (with infinite samples the method approaches optimal) and provides better visibility and control than many other approaches. This project developed solutions that yield faster run times, use less memory, and simplify the user interface compared to existing methods. Specifically we have transformed the traditional bottom-up (dynamic programming) algorithm into a top-down (memorized) algorithm, which allowed us to add a "look-ahead pruning" heuristic that significantly improved the run time and memory usage. We also replaced the typical "dynamic dictionary" data structure with a "universal hash table" which further improved the run time. Finally, we developed an efficient and automated algorithm for selecting the tuning parameters, which lead to a simpler user interface and low error rates. Figure 1 provides examples of some of the performance improvements we obtained.

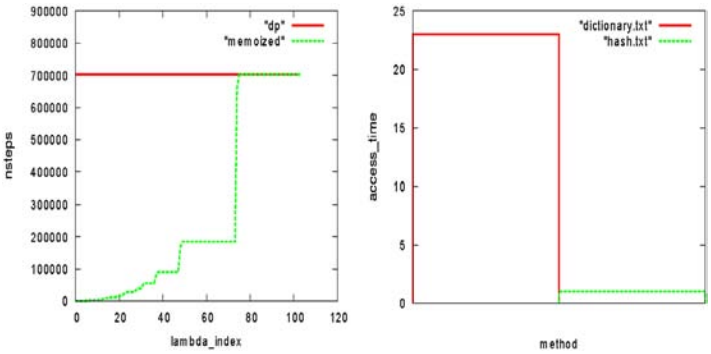


*Figure 1. Left) The number of training steps used in the traditional dynamic programming (dp) method compared to the new memoized algorithm for various values of lambda (tuning parameter), and Right) the total access time in seconds for the traditional dictionary method compared to the new hash table method, showing further reduction in computation time.*

Dyadic decision trees control representation, estimation, and computational errors through an efficient optimization of complexity penalized misclassification loss. While this appears to work well on general purpose computers for problem sizes up to fifteen to twenty dimensions, it does not explain the performance of other pattern classification tools which use a convex surrogate for misclassification loss and scale to much higher dimensions. Our second main accomplishment was to develop a framework for discrete pattern classification based on the Stack Filter model class that may address some of these questions. Stack Filters are defined as the class of functions that commute with thresholding, and can be generalized to include all discrete mappings, e.g., the class of decision trees. These properties may provide a way to understand how a wide range of loss functions affect representation, estimation and computation errors for discrete classifiers. We call this framework, Ordered Hypothesis Machines (OHM). This year we developed a representation for the framework that increases the size of the model class (leading to arbitrarily low representation error) but does not increase the size of the optimization problem used in training (reduced computational error). We also developed software implementations for several loss functions as well as exhaustive and greedy learning algorithms. We have applied OHM to several synthetic and benchmark datasets and have obtained promising results in reasonable time, e.g., comparable performance to the dyadic decision tree approach.

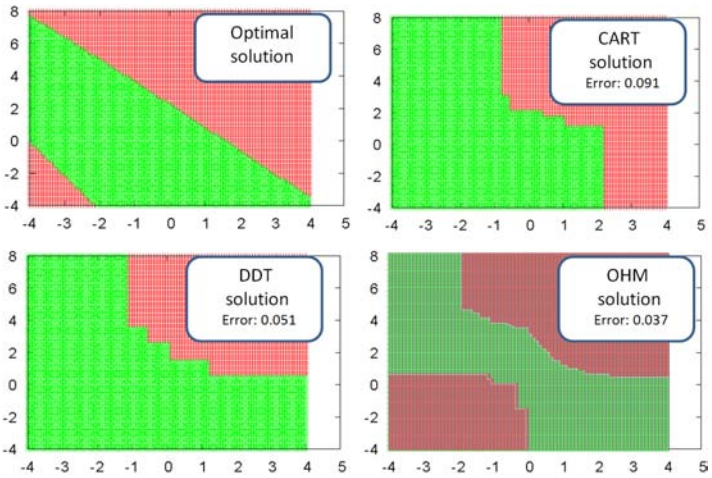


*Figure 2. Decision surfaces and error estimates obtained for (top left) the optimal classifier, (top right) the standard Classification and Regression Tree (CART) algorithm, (bottom left) the new optimal Dyadic Decision Tree (DDT) classifier and, (bottom right) the new Ordered Hypothesis Machine (OHM) classifier.*

A third direction that was investigated concerned morphological associative memories. While not directly related to our previous directions, associative memories have important applications in image and video processing and historically have been an important topic in research fields related to the stack filter framework we are developing. Several associative memories were investigated, and implemented, and several significant properties were observed. For example, depending on the type of noise (additive or subtractive) and the type of operators used (max or min), the memories are extremely tolerant to noise and allow stored patterns to be reconstructed with random noise levels up to more than 95% (Figure 3). We have found that these memories are not only extremely robust to input noise but also to noise added to the stored patterns. This suggests that there is a high redundancy in storing the patterns, and that the way the memory is build can potentially be optimized.

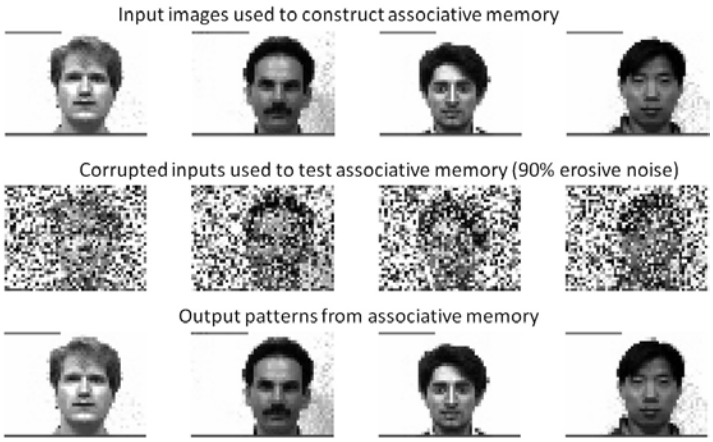


*Figure 3. An example of the unique properties of Morphological Associative Memories. Images corrupted by certain types of noise can be perfectly restored even when 90% of the input pixels are corrupt.*

## Future Work

In the short term our immediate goal is to prepare publications based on the work described. We will submit a journal article on the dyadic decision tree work and a peer reviewed conference paper on the Stack Filter classification work. We expect these tasks to be completed in the first quarter of financial year 2009. Additional algorithm work in these areas will include:

- Improving the scalability of the dyadic decision tree work by investigating median tree representations as well as developing greedy learning algorithms based on the "look-ahead pruning" idea.

- Further investigation and analysis of the stack filter classification framework to determine its utility in understanding discrete pattern classification algorithms in general.

In the coming year we will also begin applying and adapting our techniques to practical pattern applications of interest to NNSA and others. These more practical problems lead to variations of the two-class pattern recognition problem that we plan to investigate. Specific examples include:

- Sequential labeling: In many applications an end user is more willing to provide labeled examples to the learning system one at a time, rather than providing all examples up front. Recent theoretical results also show learning some classes of discrete models may in fact be easier when examples are selected sequentially, compared to the IID case. We will investigate these results and plan to develop algorithms and software to support a user-interactive method of model design.

- Application-level metrics: We have also found that in many applications the user productivity is the main metric of performance. This is related to the detection rate and false alarm rate of the pattern recognition system but not directly. We plan to reexamine our learning algorithms in this light and investigate opportunities for optimization.

## Conclusion

Continued work on this project will produce new learning algorithms, which can simultaneously address estimation, representation and computation errors for discrete model classes. Algorithms produced during the projects first year are all ready providing better solutions for problems in which decision trees are currently used. As we move forward this project aims to provide justification for using discrete model classes in new application domains, and provide solutions with measurable advantages in real world applications.

# Multilevel Adaptive Sampling for Multiscale Inverse Problems

*John David Moulton*

20080300ER

## Introduction

Characterizing uncertainty in physical systems, based only on limited and indirect data, is critical to applications such as groundwater management and tomographic imaging. For decision making, a description of the uncertainty regarding the underlying system state (e.g., the boundary of a contaminant plume), as opposed to a single "best estimate", is required because decisions must account for a realistic range of plausible states. Statistical inference through the Bayesian framework provides a powerful approach with a solid theoretical foundation for this type of analysis. Specifically, uncertainty quantification in this setting is achieved through sampling the posterior probability distribution in order to approximate various integrals, such as the mean and variance of the system state. While in recent years significant progress has been made in the development of sampling techniques, efficient sampling of high-dimensional spaces, typical of complex multiscale forward models, remains elusive. In particular, applications are often forced to restrict their analysis to linearized and over-simplified reduced forward models, and to limit sensitivity and optimization studies.

Although analogous issues have been addressed by robust multilevel solution algorithms, the potential synergy with statistical sampling has been overlooked. Multilevel solution algorithms achieve optimal algorithmic scaling by combining corrections from coarsened representations (reduced dimension models), with a simple fixed-point iteration. The robustness of these algorithms relies on the accuracy of the coarsened representations and is achieved through important multiscale concepts such as variational coarsening. We will build on these multiscale modeling concepts to drive the development of new efficient multilevel sampling algorithms that will significantly improve the efficiency of the Bayesian approach. We will focus on tomographic problems in which the forward model is multiscale diffusion, such as Electrical Impedance Tomography (EIT), as success in this fundamental setting will provide insight that is applicable to a wide range of applications.

## Benefit to National Security Missions

Advances in the efficient solution of inverse problems, particularly those that characterize the subsurface environment, play a significant role in much of science from calculating contaminant plumes to medical imaging. This work is relevant to many missions in DOE and other government agencies including nuclear weapons diagnostics and climate modeling.

## Progress

In this research we consider steady-state electrical impedance tomography (EIT) as a canonical inverse problem in which the forward model is multiscale diffusion. Here the problem is to recover the spatially-dependent conductivity inside an object given data on its boundary in the form of the potential, which is measured for a prescribed pattern of applied boundary currents (fluxes). The mathematical model that maps the state (i.e., conductivity) to the measured data (i.e., potential and flux) is referred to as the forward model. In this statistical framework, solving the inverse problem corresponds to quantifying statistics about the posterior distribution of the state (i.e., conductivities) conditioned on the measurements. We calculate these statistics over the posterior distribution using a Markov chain Monte Carlo (MCMC) procedure. However, due to the high computational cost of the forward model many practitioners do not consider the full Bayes formulation, and limit their analysis to computing the maximum a posterior (MAP) estimate, or consider a linearized forward model. The objective of this research is to develop adaptive multilevel sampling techniques that facilitate the efficient analysis of the full forward model.

We consider a stylized EIT problem on a two-dimensional square discretized on an orthogonal grid with bilinear finite elements. The conductivity is discretized on the same grid. To develop the concepts that we need to integrate the components of a multilevel iterative solver (e.g., multigrid) into a multilevel sampling algorithm we considered multilevel approximations to the forward map in the Delayed Acceptance Metropolis-Hastings (DAMH) proposed in [1]. This algorithm

rigorously supports the use of a state-dependent approximation by creating a two-stage acceptance procedure that may be characterized by a modified proposal distribution. In this initial work we consider computing approximations by limiting the number of V-cycles and altering the cycle-parameters of the black box multigrid (BoxMG) algorithm [2]. We demonstrate the effectiveness of this approach for a binary conductivity reconstruction problem with a state dependent approximation based on the solution at the previous state and a reduced convergence tolerance [4]. In addition, for a gray-scale conductivity reconstruction we consider a multilevel augmented posterior based on a two levels of approximation [3]. Specifically, the approximation was made state-independent by using an initial guess set by a previously computed mean and either two V-cycles or a single V-cycle. In this latter case we find only a marginal increase in autocorrelation length, which is more than offset by gains in overall computational efficiency.

Significant progress on adaptive techniques for MCMC sampling has been made as well. This aspect of sampling will be critical to the efficiency at each level of the multilevel sampler, as well as the overall efficiency. The slow convergence of MCMC sampling is frequently caused by an inappropriate selection of the proposal distribution used to generate trial moves in the Markov Chain. In recent work we showed that significant improvements to the efficiency of MCMC simulation could be made by using a self-adaptive Differential Evolution learning strategy within a population based evolutionary framework [5]. This scheme, entitled DiffeRential Evolution Adaptive Metropolis or DREAM, runs multiple different chains simultaneously for global exploration, and automatically tunes the scale and orientation of the proposal distribution during the search. Ergodicity of the algorithm is proved, and various examples involving nonlinearity, and multimodality show that DREAM is generally superior to other adaptive MCMC sampling approaches. The DREAM scheme significantly enhances the applicability of MCMC simulation to complex, multimodal search problems.

## Future Work

This initial integration of multigrid components with the MCMC sampling in EIT improves overall computational efficiency. However, at present sampling and approximation is still driven at the finest scale, and hence, gains in overall efficiency are limited. We are currently developing a multilevel sampling strategy that builds posterior distributions up from coarse scales to the finest scale. This sampling strategy will work directly with the weights of the discrete forward model; leveraging a hierarchical view of the Dirichlet-to-Neumann map to improve scalability of the sampling algorithm. In addition, we will study the efficiency of the new advanced single-scale samplers, such as DREAM, in this multilevel setting. To further enhance the performance of DREAM we will explore particle filtering as a means to reduce the ensemble size for sequential posterior exploration, as well as multi-try Metropolis sampling in a parallel setting.

## Conclusion

The overarching goal of this research is to deliver a new level of efficiency and scalability to the Bayesian framework for uncertainty quantification in complex multiscale applications. Thus far, we have developed a delayed acceptance (DAMH) algorithm for a stylized EIT problem that leveraged components of a robust variational multigrid algorithm. In addition we have developed a multiresolution augmented posterior MCMC scheme for this application. This initial integration of multigrid components with MCMC sampling has improved the performance of Bayesian inference for this class of high-dimensional problems. In addition, we further advanced the theoretical foundation of the DREAM sampling algorithm.

## References


1. Christen, J. A., and C. Fox. Markov chain Monte Carlo using an approximation. 2005. *Journal of Computational and Graphical Statistics.* **14**: 795.

2. Dendy, J. E.. Black Box Multigrid. 1982. *Journal of Computational Physics.* **48**: 366.

3. Higdon, D., C. S. Reese, J. D. Moulton, J. Vrugt, and C. Fox. Posterior exploration for computationally intensive forward models. To appear in *Posterior exploration for computationally intensive forward models.* Edited by Meng, X. L., A. Gelman, and G. Jones.

4. Moulton, J. D., C. Fox, and D. Svyatskiy. Multilevel approximations in sample-based inversion of the Dirichlet-to-Neumann map. 2008. *Journal of Physics: Conference Series.* **124**: 012035.

5. Vrugt, J. A., C. J. F. terBraak, C. G. H. Diks, D. Higdon, B. A. Robinson, and J. M. Hyman. Accelerating Markov chain Monte Carlo simulation from self adaptive differential evolution with randomized subspace sampling. To appear in *International Journal of Nonlinear Sciences and Numerical Simulation.*

## Publications

Higdon, D., C. S. Reese, J. D. Moulton, J. Vrugt, and C. Fox. Posterior exploration for computationally intensive forward models. To appear in *The Handbook of Markov Chain Monte Carlo.* Edited by Meng, X. L., A. Gelman, and G. Jones.

Moulton, J. D., C. Fox, and D. Svyatskiy. Multilevel approximations in sample-based inversion of the Dirichlet-to-Neumann map. 2008. *Journal of Physics: Conference Series.* **124**: 012035.

Vrugt, J. A., C. J. F. terBraak, C. G. H. Diks, D. Higdon, B. A. Robinson, and J. M. Hyman. Accelerating Markov chain Monte Carlo simulation from self adaptive differential evolution with randomized subspace sampling. To appear in *International Journal of Nonlinear Sciences and Numerical Simulation.*

# Adaptive Algorithms for Inverse Problems in Imaging

*Brendt Egon Wohlberg*

20080341ER

## Introduction

Image data are ubiquitous, occurring in such diverse fields as experimental physics, biology, geosciences, non-proliferation surveillance, and medical diagnosis. The family of problems including denoising, blur removal, resolution enhancement, and inpainting represent an important part of the analysis of such data. Solving such problems effectively requires some form of model of the data so that it can be distinguished from the degradation to be removed. These models are usually simplified representations designed by mathematical analysis, and cannot accurately represent all of the properties of complex data, such as images of natural scenes, radiological images, etc. In this project, in contrast, we learn appropriate data models from large sets of examples of the problem domain data, promising more accurate reconstructions and also the ability to adapt to new types of data (e.g. from a specialized scientific instrument), with unusual properties that are not compatible with the assumptions made by standard approaches for these kinds of problem. The general approach is motivated by a geometric view of the problem, distinguishing between the full space of all data that can possibly be represented, and the much smaller space of uncorrupted example data. Within this view, the desired reconstruction is achieved by finding a representation, which is close both to the measured data and the space of uncorrupted data.

## Benefit to National Security Missions

Image analysis and related data plays an important role of a number of DOE missions, including Nuclear Weapons (e.g., proton radiography of dynamics experiments) and Threat Reduction (e.g. satellite and airborne imagery). Advances in image analysis are also relevant to many government agencies.

## Progress

The majority of effort to date has been expended on understanding fundamental components of the problem, primarily the numerous issues surrounding the construction of a reliable estimate of a local tangent plane to the manifold of image blocks, and significant progress has been made in understanding technical issues such as:

- Choice of image block size, based on computational experiments, as well as by theoretical analysis of the implications of a Gaussian noise model;
- Effects of the size and composition of the training data set;
- Number of neighboring training blocks to utilize in constructing the estimate of the local tangent plane;
- Effective methods for estimating a local tangent plane from the selected neighbor blocks in the training data;
- Effects of varying noise levels on the other problem parameters;
- Exploiting the structure of the training data in estimating parameters required by the tangent plane estimation techniques; and
- Approaches to assembling a set of overlapping denoised image blocks into a single coherent estimate of the denoised image in its entirety.

Based on these results, we have designed a denoising algorithm, which estimates noise-free versions of each image block by projection into the local tangent plane constructed via a sparse representations in terms of its nearest neighbors in the training data. This initial algorithm has a denoising performance which is already superior to the highly regarded Total Variation regularization method, and competitive or superior (depending

on specific test) to the state of the art Non-Local Means method.

We have recently begun to work on the more challenging problems of single-image superresolution (estimating a higher resolution version of a low resolution image) and inpainting (estimating missing regions of an image). Initial inpainting results, employing a simple approach inspired by our general geometric framework, are very promising, and already competitive with the state of the art on small test problems.

A paper on parameter selection issues was presented at the IEEE Southwest Symposium on Image Analysis and Interpretation (March 2008), and work on algorithms for local linear and quadratic approximations to a manifold characterized by sampled data was presented at the SIAM Conference on Imaging Science (July 2008). A paper on related adaptive image reconstruction methods, work on which was partially supported by this LDRD project, has been accepted for publication in IEEE Transactions on Image Processing, and two additional papers (one of which is on the inpainting results) are currently under review for presentation at the 2009 IEEE International Conference on Acoustics, Speech, and Signal Processing.

## Future Work

Research over the following year will concentrate on the following aspects of the problem:

- Develop tools for understanding and exploiting the geometry of the manifold of image blocks;
- Understand and exploit the relationship between sparse optimization methods and the geometric (manifold) view of the space of image blocks;
- Continue to develop the denoising algorithm, and understand how the very successful methods using example blocks from the image to be denoised (such as Non-Local Means) fit within our geometric framework;
- Develop a superresolution algorithm based on our framework, and extend the simple framework for inpainting.

We will endeavor to make an initial public release of our experimental code, and shall continue to give priority to publication of the results of our research.

## Conclusion

This proposal promises to advance the state of the art in solving a wide variety of problems in the analysis of image and other data. First, by learning the models instead of constructing approximations by mathematical analysis, the increased accuracy of the models is expected to deliver better performance when applied to the removal of noise, blur, etc. Second, the availability of an automated procedure for deriving a data model provides flexibility in addressing new types of data, making it possible to rapidly address such problems in the context of niche data, which have not received much research attention.

Progress after the initial year of this project, together with the rapid growth of similar ideas in the external research community, provide evidence for the great potential of these methods.

## Publications

Lin, Y., and B. Wohlberg. Application of the UPRE method to optimal parameter selection for large scale regularization problems. 2008. In *IEEE Southwest Symposium on Image Analysis and Interpretation.* (Santa Fe, NM, 24 - 26 Mar. 2008). , p. 89. New York: IEEE.

Rodriguez, P., and B. Wohlberg. Efficient minimization method for a generalized total variation functional. To appear in *IEEE Transactions on Image Processing.*

Wohlberg, B.. Inpainting with sparse linear combinations of exemplars. Presented at *International Conference on Acoustics, Speech, and Signal Processing.* (Taipei, Taiwan, 19 - 24 Apr. 2009).

Wohlberg, B., and P. Rodriguez. An l1-TV algorithm for deconvolution with salt and pepper noise. Presented at *International Conference on Acoustics, Speech, and Signal Processing.* (Taipei, Taiwan, 19 - 24 Apr. 2009).

# Stochastic Transport on Networks: Efficient Modeling And Applications to Epidemiology

*Ilya Mark Nemenman*

20080391ER

## Introduction

A variety of problems of relevance to biosecurity, public health, and basic science research can be viewed as special cases of a general problem of studying stochastic transport on networks. Examples include:

- Epidemilogy, where diseases spread by random interaction events among humans and/or animals tied into social and/or agricultural networks,
- Basic biochemical processes, relevant for cancer and other molecular diseases, where the response of an organism to external stimuli, such as pathogen invasions, are governed by complex stochastic dynamics on cellular regulatory and metabolic networks, and many others.

Such stochastic processes on networks are notoriously difficult to study in detail computationally. The best algorithms involve simulation of the underlying processes event by event, which becomes computationally prohibitive when the number of possible events is astronomically large, as it is for contacts among people in a general population, or for biochemical transformations. This project is designed to create novel algorithms, based on disparate tools from physics, computer science, and information theory, to simulate these stochastic interaction events fast and rigorously. The general idea being pursued revolves around coarse-graining stochastic events, so that entire spread of an epidemics or multiple chemical reactions can be modeled as a series of complex, macroscopic steps.

## Benefit to National Security Missions

This project supports DOE and DHS missions in bio-security by developing advanced tools for understanding of progression of epidemics. Furthermore, the project supports the DOE Energy security mission by enhancing the understanding of biochemical networks, an essential component for biofuels development. Finally, the project supports the basic scientific research mission of LANL and DOE by providing a new level of understanding of complex stochastic processes.

## Progress

The project has contributed to the following publications:

- A Mugler, E Ziv, I Nemenman, C Wiggins. Serially-regulated biological networks fully realize a constrained set of functions. IET Systems Biology 2:313, 2008.

  One of important questions in the program of coarse-graining stochastic kinetics is: what effect, if any, does the underlying network topology have on the measurable properties of the transport? In this paper, we used computational simulations of stochastic biochemical networks to provide an answer to this question. We found that the network topology constrains the measurable properties to a certain allowable class, but the topology provides almost no constraints within the class.

- D Dreisigmeyer, J Stajic, I Nemenman, W Hlavacek, and M Wall. Determinants of bistability in induction of the Escherichia coli lac operon. IET Systems Biology 2:293, 2008.

  The relation between the network structure and the measurable transport behavior has been investigated in this paper in the context of the bacterial gene regulation, namely the E.coli lac operon. Conclusions similar to Ref. 1 above have been made, further supporting the hypothesis of a weak, but nonzero link between the network topology and its function.

- C Teuscher, I Nemenman, F Alexander. Novel computing paradigms: Quo vadis? Physica D 237:v–viii, 2008.

  This paper was an editorial reviewing the emergent

field of non-traditional computing, where analysis of systems can be performed not on traditional digital machines, but on different architectures, suited a lot better to simulate and analyze, in particular such massively distributed processes as the network stochastic transport.

- J Edwards, J Faeder, W Hlavacek, Y Jiang, I Nemenman, and M Wall. q-bio 2007: a watershed moment in modern biology. Mol. Syst. Biol. 3:148, 2007.

- I Nemenman, W Hlavacek, J Edwards, J Faeder, Y Jiang, M Wall. Editorial: Selected papers from the First q-bio Conference on Cellular Information Processing. IET Systems Biology 2:203, 2008.

  These two publications summarize the involvement of the project's PI in organization of the series of International q-bio Conferences on Cellular Information processing. The conference and the affiliated Summer School have been attracting over 200 researchers to New Mexico in the last years, and have turned Aug, 2008; and multiple independent participants have called the conference their "intellectual home", "watershed moment in modern biology", and "premier conference in the field." The conference advances basic and applied science in the field of relevance to LANL, DOE, and the nation as a whole, and firmly establishes LANL/DOE as a leader in this important field.

- NA Sinitsyn and I Nemenman. Universal geometric theory of mesoscopic stochastic pumps and reversible ratchets. Phys. Rev. Lett. 99:220408, 2007.

  In this work, we have shown that methods, well developed in quantum and statistical physics, can be used to analyze stochastic transport properties in various kinetic networks, including: biochemistry, stochastic ratchets (e.g., molecular motors), and epidemiology (namely, the SI model of epidemic spread).

- Submitted manuscript: NA Sinitsyn, N Hengartner and I Nemenman. Coarse-graining stochastic biochemical networks: quasi-stationary approximation and fast simulations using a stochastic path integral technique. Submitted, 2008.

  In this work, currently under a consideration for a publication at PNAS, we have shown that kinetic networks can be coarse-grained, so that a dynamics of the relevant degrees of freedom can be modeled without a laborious study of internal, irrelevant degrees of freedom, and yet preserving information (such as higher cumulates of stochastic transport currents) about these internal, eliminated structure.

Figures from these papers:

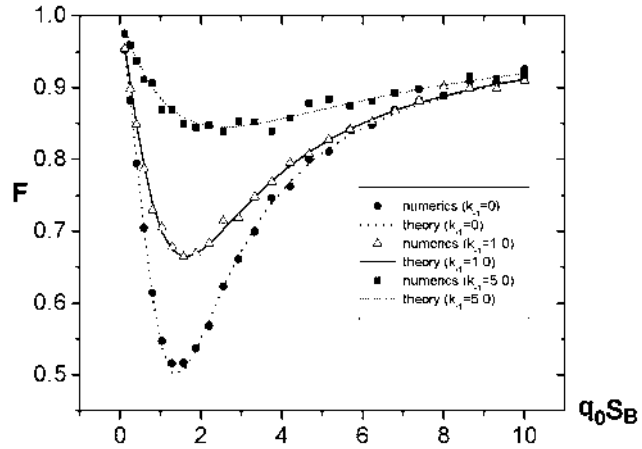


*Figure 1. Comparison of a full stochastic simulation of the Fano factor of a two-step enzymatic pathway (dots, takes hours of simulations) with an analytical coarse-grained treatment of Reference [7] as a function of various kinetic parameters. A complete agreement is clearly seen.*

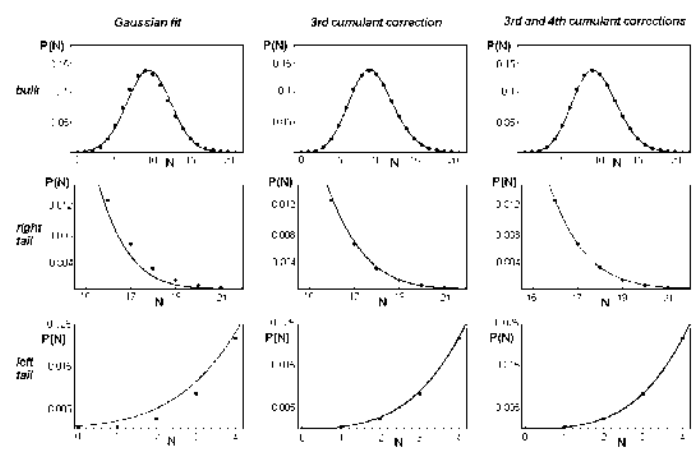


*Figure 2. The coarse-graining technique discussed in Reference [7] allows for simulations of kinetic networks without keeping track of microscopic internal states details, but still preserving the effect of these states on observable variables. In this figure, we show how the technique allows to preserve higher order cumulants of the stochastic transport through an enzymatic pathway, and how preservation of progressively higher order cumulants allows one to get results that approximate detailed simulations with progressively higher details.*

## Future Work

The goal of this project is to perform physics-inspired "coarse-graining," such that the properties of many of the microscopic nodes in a network are "integrated out," and only large-scale observable dynamics is modeled. Three manuscripts are currently in preparation, addressing this problem from different angles.

- With collaborators at Columbia University, we are completing a study of evolvability of stochastic biochemical networks by answering the question: how much modification to the network structure is required to force the network to perform a certain observable functional behavior. This work will be completed in the next year of the project.
- With students from the q-bio summer school, described in [4, 5] above, we have been able to use the methods introduced in [6, 7] to perform coarse graining of a handful of traditional kinetic schemes that exist in the context of SI and SIR epidemiological models and multistep biochemical reactions. This work has been invited for a publication at the q-bio special issue of IET Systems Biology and will be published over the next year.
- Most importantly, the study in [7] has suggested that some aspects of stochastic transport are universal, and depend very weakly on the details of the involved kinetic network diagram. If proven true, this will represent a paradigm shift and a major simplification in our attempts to understand and model transport networks, since observable quantities would depend only on a handful easily measurable parameters rather than on the entire set of microscopic details. This possibility will be the main research direction for the project in the upcoming year.

## Conclusion

This project is developing advanced tools for understanding, computer simulations, and prediction of transport phenomena in complex network. These networks include biochemical networks (relevant for bioengineering and biomedicine), social networks (relevant for epidemiology), and potentially maybe even infrastructure networks (relevant for Homeland Security applications). All of these fields are of a critical importance to the nation, and we are on track to make essential contributions to them.

## References


1. Mugler, A., E. Ziv, I. Nemenman, and C. Wiggins. Serially-regulated biological networks fully realize a constrained set of functions. 2008. *IET Systems Biology.* **2**: 313.
2. Dreisigmeyer, D., J. Stajic, I. Nemenman, W. Hlavacek, and M. Wall. Determinants of bistability in induction of the Escherichia coli lac operon. 2008. *IET Systems Biology.* **2**: 293.
3. Teuscher, C., I. Nemenman, and F. Alexander. Novel computing paradigms: Quo vadis? . 2008. *Physica D.* **237**: v.
4. Edwards, J., J. Faeder, Y. Jiang, I. Nemenman, W. Hlavacek, and M. Wall. q-bio 2007: a watershed moment in modern biology. 2007. *Mol. Syst. Biol..* **3**: 148.
5. Nemenman, I., W. Hlavacek, J. Edwards, J. faeder, Y. Jiang, and M. Wall. Editorial: Selected papers from the First q-bio Conference on Cellular Information Processing. 2008. *IET Systems Biology.* **2**: 203.
6. Sinitsyn, N., and I. Nemenman. Universal geometric theory of mesoscopic stochastic pumps and reversible ratchets. 2007. *Phys. Rev. Lett..* **99**: 220408.
7. Sinitsyn, N., N. Hengartner, and I. Nemenman. Coarse-graining stochastic biochemical networks: quasi-stationary approximation and fast simulations using a stochastic path integral technique. *Proc. Natl. Acad. Sci. (USA).*


## Publications


Dreisigmeyer, D., J. Stajic, I. Nemenman, W. Hlavacek, and M. Wall. Determinants of bistability in induction of Escherichia coli lac operon. 2008. *IET Systems Biology.* **2**.

Edwards, J., J. Faeder, W. Hlavacek, Y. Jiang, I. Nemenman, and M. Wall. q-bio 2007: a watershed moment in modern biology. 2007. *Mol. Syst. Biol..* **3**: 148.

Mugler, A., E. Ziv, I. Nemenman, and C. Wiggins. Serially-regulated biological networks fully realize a constrained set of functions. 2008. *IET Systems Biology.* **2**.

Nemenman, I., W. Hlavacek, J. Edwards, J. Faeder, Y. Jiang, and M. Wall. Editorial: Selected papers fromthe First q-bio Conference on Cellular Information Processing. 2008. *IET Systems Biology.* **2**.

Sinitsyn, N., N. Hengartner, and I. Nemenman. Coarse-graining stochastic biochemical networks: quasi-stationary approximation and fast simulations using a stochastic path integral technique. *Proc. Natl. Acad. Sci. (USA).*

Sinitsyn, N., and I. Nemenman. Universal geometric theory of mesoscopic stochastic pumps and reversible ratchets. 2007. *Phys. Rev. Lett.* **99**: 220408.

Teuscher, C., I. Nemenman, and F. Alexander. Novel computing paradigms: Quo vadis?. 2008. *Physica D.* **237**: v.

# Critical and Crossover Behaviors at Jamming Transitions

*Charles Reichhardt*

20080448ER

## Introduction

In this project we will develop a fundamental understanding of the jamming process in granular materials. These seemingly simple materials, which include dry sand and powders, exhibit flow behavior far different from ordinary solids, liquids, and gases. Understanding the peculiar behavior of granular materials is vital for predicting and controlling them under a variety of industrial, civil engineering and scientific conditions. Jamming plays an important role in determining the behavior of a granular medium. When the grains are widely separated or slowly moving, they can flow in a manner similar to a fluid, but when the grain separation decreases or the grain speed increases, the grains suddenly jam and resist further motion in an abrupt transition to a solid state. The fluid to solid transition associated with jamming is extremely poorly understood but is essential for any application of granular materials. For example, granular media forming a levy is normally in a solid state, but it can unjam in a catastrophic transition to a fluid state which causes the levy to fail. In contrast, when granular media is flowing, such as when a mold for a highly-filled polymer-based explosive is filled, a sudden transition into the solid state can interfere with the filling process. We are studying the jamming process and the transition between fluid and solid states and working to apply powerful concepts from statistical physics which have been successful in describing ordinary solids and liquids. If we can identify universal behaviors associated with the jamming transition, this will permit us to control the failure of materials and will also enhance our understanding of how and when complex materials fail. This would have a profound implact on the materials science, industrial, infrastructure, and national security needs of the nation.

## Benefit to National Security Missions

Jamming underlies numerous physical problems including oil exploration, aging, material failure, pollutant propagation in porous media, solid waste transportation and storage, weapons manufacturing, plastic-based-explosives, and characterization of materials out of equilibrium. DOE missions relevant to this research include energy and environmental research, weapons physics, materials science, modeling and simulation.

## Progress

Developed a simulation code that can accommodate complicated grain geometries such as dimers and trimers. We are examining the effect of different shape ratios of the granular media particles to determine whether the same universal behavior appears irrespective of shape. We have also explored the effect of quenched disorder on jamming and found evidence that disorder should be added as a fourth axis to the proposed jamming phase diagram. This result suggests that jamming also occurs in pours media. Our major result is that due to the increasing length scale that forms in the system as jamming is approached, when the length scale of the porous media matches that of the granular media the system will jam. This implies that jamming can occur at much lower densities in porous media. When the density of the quenched disorder is sufficiently high, a percolation transition occurs and the system is always jammed. We also find a jamming transition at low granular density when every minimum in the quenched disorder landscape traps a granular particle. We have begun to study the dynamics of the system as jamming is approached, and we observe diverging fluctuations in the velocities. As a result, the nature of the velocity power spectrum changes dramatically near jamming. To better understand how universal the jamming transition is, we have begun a study of a system containing periodic arrangements of obstacles. We find a jamming transition in the case when the granular particles have a dimer structure. This jamming occurs only for certain directions of load, which may indicate that this is a new type of directional jamming or anisotropic jamming.

## Future Work

We propose to investigate critical behavior and intermittent dynamics at and near jamming transitions, and address the following questions: Is critical behavior

universal to jamming phenomena? Does the nature of the criticality change for different amounts of disorder or varied particle interactions? How does a continuum description of the medium break down near jamming or yielding transitions? Using simulations and experiments in conjunction with scaling theory, we will determine whether jamming phenomena in a broad class of systems exhibit critical behavior. We will develop models with controllable amounts of disorder which can be realized in experiments on collections of grains. We will study jamming transitions for elongated and irregular particles by moving a probe particle through the system as the density or the disorder is increased, and we will use scaling theories to analyze the data. We will also investigate the crossover to the jammed state by studying fluctuations of the surrounding bath of particles and showing how these fluctuations become relevant as the jamming transition is approached. We will perform a series of experimental measurements using high accuracy imaging techniques to identify the dynamics and locations of the particles. This will allow the validation of the theory and simulation results. Preliminary experimental data agrees well with our recent simulations. An understanding of when the discreteness of the particles changes the qualitative behavior of the response of the system as the jamming transition is approached will be profoundly useful for understanding the conditions under which multiscale simulation models break down.

## Conclusion

- We will make several predictions for a continuous phase transition with critical behavior for the simple disk system, and test them experimentally.
- We will determine if a similar phase transition occurs in more complicated particle geometries and for varied densities to confirm the existence of universal behaviors near jamming.
- We will investigate the nature of the fluctuations as the jamming transition is approached to understand if moving or flowing states exhibit critical behavior away from jamming.
- We will seek to understand the consequences of critical behavior for the dynamics near jamming and the unjamming process.

## Publications

Libal, A., C. Reichhardt, and C. J. Olson Reichhardt. Enhancing mixing and diffusion with plastic flow. 2008. *Physical Review E.* **78** (3): 031401.

Mangan, N., C. Olson Reichhardt, and C. Reichhardt. Reversible to irreversible flow transitions in periodically driven vortices. 2008. *Physical Review Letters.* **100** (18): 187002.

Reichhardt, C., and C. J. Olson Reichhardt. Disordering transitions and peak effect in polydisperse particle systems. 2008. *Physical Review E.* **77** (4): 041401.

Reichhardt, C., and C. J. Olson Reichhardt. Moving vortex phases, dynamical symmetry breaking, and jamming for vortices in honeycomb pinning arrays. To appear in *Physical Review B.*

Wan, M. B., C. J. Olson Reichhardt, Z. Nussinov, and C. Reichhardt. Rectification of swimming bacteria and self-driven particle systems by arrays of asymmetric barriers. 2008. *Physical Review Letters.* **101** (1): 018102.

# Time-reversible Born-Oppenheimer Molecular Dynamics

*Anders Mauritz Niklasson*

20080562ER

## Introduction

The ability to analyze and study materials properties directly from the fundamental laws of quantum mechanics provides an enormous scientific and technological opportunity, but it is also a great challenge that requires a number of simplifications and approximations of the underlying theoretical description to enable practical simulations. Among various theoretical methods, Born-Oppenheimer molecular dynamics has emerged as one of the most important techniques. Born-Oppenheimer molecular dynamics simulations based on self-consistent density functional theory, where the nuclear cores are assumed to evolve surrounded by an electronic cloud that always is in ground state (self-consistent) equilibrium for each new nuclear configuration, are indispensable in a large number of scientific areas that employ atomistic simulation. In many ways Born-Oppenheimer molecular dynamics can be seen as the gold standard of molecular dynamics simulations. However, challenges in nanoscience, biofuels and actinide chemistry, for example, require significant algorithmic improvements to allow simulations of much larger size and complexity than previously possible.

In this project we will explore and develop general ab initio molecular dynamics technologies based on the new opportunities provided by the time-reversible loss-less integration approach to Born-Oppenheimer molecular dynamics that recently was invented at LANL by the proposal authors [1]. Our findings will form the basis for high-performance ab initio molecular dynamics schemes that are significantly better suited to tackle present and future challenges in computational materials science. This research is at the very forefront of a highly competitive field of research that is expected to have a significant impact over a broad area of scientific disciplines.

## Benefit to National Security Missions

The direct or indirect applications of Born-Oppenheimer molecular dynamics range from the problem of high-temperature stabilization of d-Pu to the folding structures of protein molecules in human cells, all issues with close ties to the DOE missions in Nuclear Weapons, Threat Reduction, and Office of Science, which will benefit from enhancing our fundamental understanding of materials. Our work will provide molecular dynamics simulation tools that overcome some significant shortcomings of Born-Oppenheimer molecular dynamics. These problems include a high computational cost, numerical instabilities, and a systematic drift in the total energy. We hope our work will evolve to a new generation of high-performance molecular dynamics simulation methods based on the first principles of quantum physics.

## Progress

The first year of this project has been highly successful. The key initial discovery was an extended Lagrangian generalization of time-reversible Born-Oppenheimer molecular dynamics (TR-BOMD) [2]. The new formulation enables the application of higher-order symplectic or geometric integration schemes that are stable and energy conserving even under incomplete self-consistency convergence. It was demonstrated how the accuracy is improved by over an order of magnitude compared to previous formulations at the same level of computational cost. Figure 1 shows how the accuracy is improved, as measured by the amplitude of the energy oscillations, at he same level of computational cost. In the original proposal, higher-order symplectic integration was considered a high-risk possibility that was expected only in the last year of this project. The new formulation has opened a whole new set of opportunities that will be followed up by further studies.

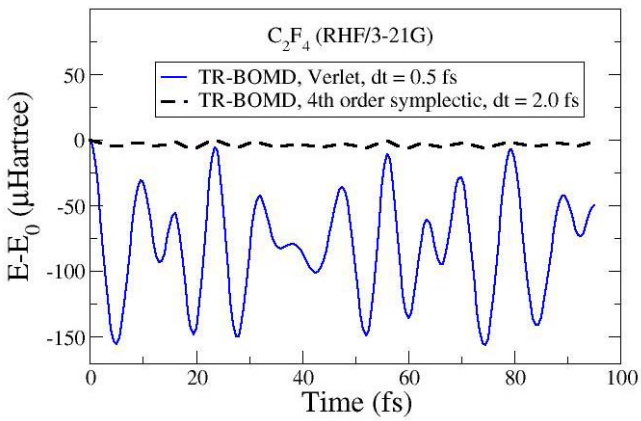


*Figure 1. Total energy fluctuations for conventional TR-BOMD based on the Verlet integration and for a higher-order symplectic integration scheme derived from the extended Lagrangian formulation of TR-BOMD. At the same level of computation cost the accuracy, as measured by the amplitude of the oscillations, is improved by over an order of magnitude.*

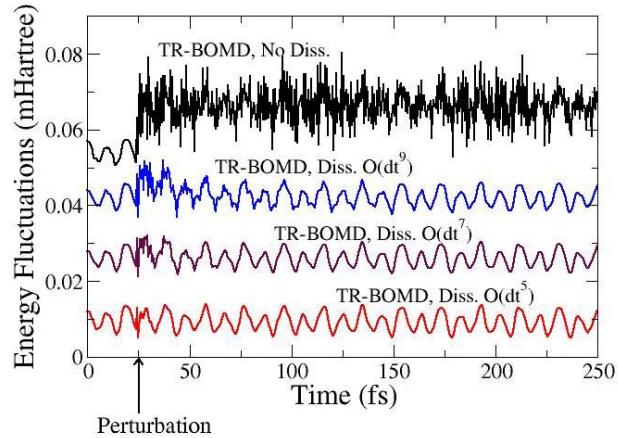


*Figure 2. The effect of an artificial (very large) perturbation in a water simulation, with and without dissipation. The different dissipation terms break the time-reversal symmetry at various higher-order in the time step dt.*

In reduced complexity calculations that are necessary in studies of very large systems, consisting of thousands of atoms, the level of numerical approximations may cause small errors. In an exactly time-reversible scheme all these errors will propagate and never disappear. Eventually an accumulation of errors may create fluctuations that may lead to instabilities and divergence. By introducing dissipation that removes numerical noise this problem can be avoided. We have performed an analysis of the fluctuation and dissipation properties of TR-BOMD and developed a Langevin-like dynamics for the electronic degrees of freedom that automatically removes noise while keeping the energy stable. Figure 2 shows the effect of various dissipation terms on an artificial perturbation. The ability to suppress numerical noise while keeping the energy stable should enable an efficient and accurate linear scaling TR-BOMD for studies of very large complex systems, which is one of the goals of this project.

If wavefunctions are used to represent the propagation of the electronic degrees of freedom an arbitrary phase occurs, since the energy is invariant under rotations of the wavefunctions. We have managed to generalize the Lagrangian description of TR-BOMD to overcome this problem. This enables implementation in a very broad class of electronic structure methods based on plane-wave or wavelet representations as well as methods based on some highly efficient direct energy minimization techniques.

In a generalization to a non-orthogonal representation for the electronic degrees of freedom we discovered a new form of fictitious ``Pulay force'' that is driven by the change in the basis set that follows the evolution of the nuclear degrees of freedom. Instead of being caused by the gradient with respect to position of the basis set, as in the original Pulay force, the new force arises from the second-order time derivative of the non-orthogonal wavefunction representation.

## Future Work

We are currently performing several implementations of our recent findings in state-of-the-art electronic structure codes that are used at LANL. These codes include MondoSCF, Quickstep (part of CP2K) and VASP. An implementation in a self-consistent tight-binding code has been started in collaboration with Prof. Karplus research group at Harvard University and an implementation in Quantum Espresso is discussed with Prof. Holmstrom at Universidad Austral in Chile. We are also performing a systematic study of various higher-order geometric integration schemes and their optimization for TR-BOMD. During the remaining part of this project we also hope to develop efficient

linear scaling TR-BOMD, implement a novel hybrid Monte-Carlo sampling method for calculations of thermodynamic properties, and perform preliminary studies of applications beyond regular Born-Oppenheimer molecular dynamics, including finite electronic temperatures, non-adiabatic dynamics and response.

## Conclusion

We have made some very promising initial discoveries that have opened doors to new highly efficient and accurate computational methods to study materials properties directly from the fundamental principles of quantum mechanics. Some of these methods are currently being implemented in electronic structure codes used at LANL and they will be ready for applications very soon. Further developments, in particular towards linear scaling TR-BOMD, look very promising.

## References

1. N.Niklasson, A. M., C. J. Tymczak, and M. Challacombe. Time-reversible Born-Oppenheimer molecular dynamics. 2006. *Physical Review Letters.* **97** (12): 123001/1.

2. N.Niklasson, A. M.. Extended Born-Oppenheimer molecular dynamics. 2008. *Physical Review Letters.* **100** (12): 123004.

## Publications

N.Niklasson, A. M.. Extended Born-Oppenheimer molecular dynamics. 2008. *Physical Review Letters.* **100** (12): 123004.

# Implicit Adaptive Mesh Refinement: A Magnetohydrodynamics Application

*Bobby Philip*

20050315ER

## Abstract

Science-based predictive capability is LANL's primary national security goal. True predictive capability demands high confidence in simulations when experimental data is lacking, and requires both high-fidelity physics models and high-quality numerical approximations of these models. We addressed the latter for multi-physics simulations by developing methods that control both time and space errors. We controlled the time errors with high-order implicit time integration, and the space errors with adaptive mesh refinement. To ensure efficiency, we used physics-based preconditioners implemented with optimal multilevel solvers. To demonstrate the effectiveness of our approach, we explored novel magnetic reconnection studies at realistic regimes of electrical resistivity.

## Background and Research Objectives

There is an increasing emphasis in the scientific computing community (and particularly at LANL) on the predictive capability of numerical simulations. There are two fundamental sources of errors in numerical simulations: 1) modeling errors and 2) numerical errors intrinsic to the temporal and spatial discretization. Predictive capabilities require controlling both types of errors. However, these error sources often interact in the course of a given simulation, making it impossible to discern which source is polluting the numerical solution the most.

The main goal of this project was to develop and demonstrate a numerical approach that effectively controls discretization error without sacrificing algorithmic efficiency. Strict control of discretization error helps isolate modeling errors, eliminating the ambiguity. This required developing numerical algorithms that combined high-order implicit time integration with spatial adaptive mesh refinement (AMR). Implicit time integration allowed us to control temporal errors. AMR methods are used to provide tight spatial error control while resolving relevant length scales by locally increasing grid resolution, focusing computing resources on the regions of the problem that require them.

This project set out to answer three major questions. Firstly, the combination of implicit methods and AMR techniques in complex physics models is a newly emerging research area that has barely been explored. Successful demonstration of our implicit AMR implementation helped resolve crucial issues that arise in combining AMR and implicit time integration. By providing answers to these crucial issues we have advanced the state of the art. Secondly, we demonstrated how an important class of highly efficient solution methods (referred to as Newton-Krylov methods in the literature) could be implemented on AMR grids. The combination of these solution methods and AMR had never previously been attempted for complex multi-physics problems, and a successful demonstration would be considered to be a significant advance for AMR methods. Thirdly, the capabilities of the resulting solver were demonstrated using the magnetohydrodynamics (MHD) equations. MHD is a macroscopic description of the motion of electrically conducting fluids in the presence of magnetic fields. Recent, first-of-a-kind results on the problem of magnetic reconnection [4] in MHD were demonstrated in realistic regimes. Such regimes are inaccessible without an efficient, adaptive implicit solver of the type we have successfully developed.

## Importance to LANL's Science and Technology Base and National R & D Needs

This effort is tied to DOE weapons, science and energy resource missions. Our methods will lead to deeper understanding of magnetic reconnection, with applications in space weather and design of fusion-based power generation systems. The Fusion Simulation Project has identified our approach as an essential capability for success of their efforts.

## Scientific Approach and Accomplishments

To achieve our research objectives we built upon the Structured Adaptive Mesh Refinement Application Infrastructure (SAMRAI) developed at LLNL for AMR and the Portable, Extensible Toolkit for Scientific computation (PETSc) developed at ANL for nonlinear solvers. We also developed a framework that allowed us to explore formulations and solution ideas rapidly. Existing solution methods in SAMRAI were generalized and deployed in our problems. To combine AMR with implicit time integration we developed a time integration framework on AMR grids that would allow us to study different time integration schemes and the interaction of time integration and AMR grids.

The effectiveness of this strategy became clear in the very first year of this project when it was discovered that a well-known model formulation (the primitive variable formulation) of resistive MHD was unsuitable for AMR. This was due to the presence of third-order derivatives in the model equations. Extensive tests led to the discovery that these high order derivatives introduced error on AMR grids that led to time integration schemes failing dramatically. These issues are discussed in our preliminary report [1]. While the model formulation issue was unexpected and not a focus of our research, it did allow us to inform the scientific community of these issues. With a suitable model formulation for our problem (described in references [1,2]) we were able to concentrate on the major research goals for our project.

As mentioned earlier our target application area was resistive MHD. Three challenging problems were selected from the MHD literature.

The first problem was the tearing mode problem of [4]. Figure 1 shows the current in a fully evolved tearing mode problem on AMR grids. The second problem considered was the island coalescence problem, where two magnetic islands (current channels) attract and reconnect. In resistive MHD, during the reconnection process, a thin, elongated current sheet forms at the reconnection site, which governs the reconnection rate, and therefore the global dynamics [5]. Figure 2 shows a plot of the current in an island coalescence calculation on AMR grids. The third problem was a tilt mode calculation [6]. Figure 3 shows the current in a fully evolved tilt mode calculation on AMR grids.

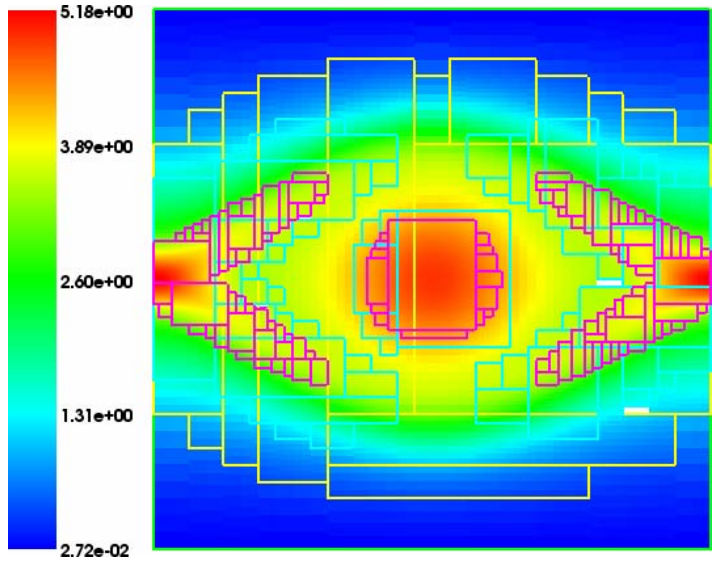


*Figure 1. Time snapshots of current for the tearing mode problem at t=200.*

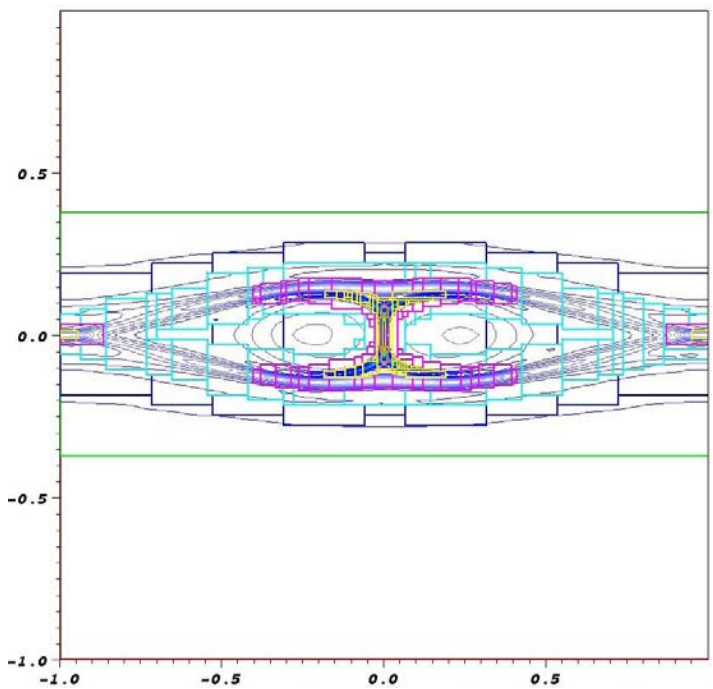


*Figure 2. Snapshots of the current at the peak of the reconnection during the coalescence process.*

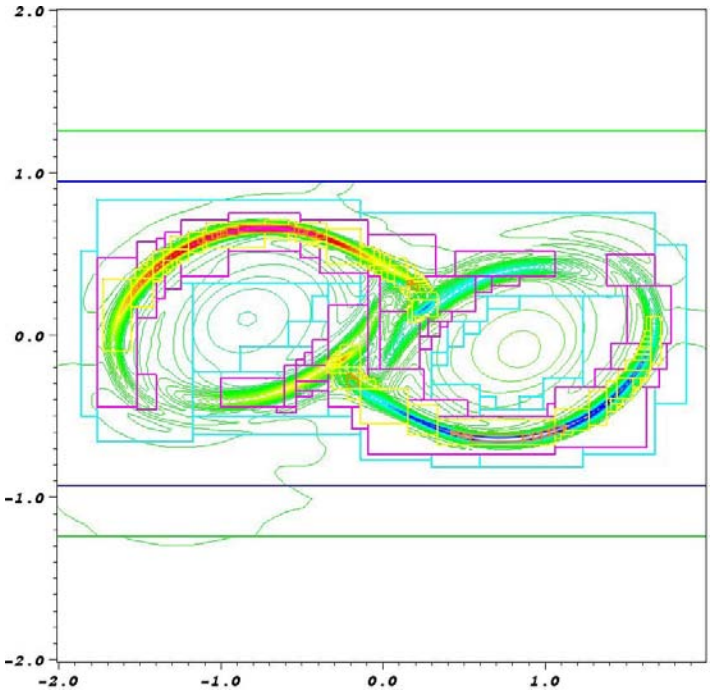


*Figure 3. Current during the evolution of the tilt instability*

Using the three model problems above we successfully demonstrated implicit time integration on AMR grids. A critical part of this demonstration was to characterize how to avoid discretization errors on AMR grids, and how to combine implicit temporal integration schemes with AMR to avoid error propagation throughout the domain. During time integration on AMR grids it is necessary to change the spatial regions where high grid resolution is present in response to evolving solution features that need to be resolved accurately. This involves changing the AMR grid in a process called regridding. Once regridding occurs it is necessary to transfer data from the AMR grid prior to regridding onto the new AMR grid present after regridding before the simulation can continue. A common approach is to use linear interpolation to transfer data. However, linear interpolation is not suitable for all problems. Figure 4 depicts the error in the current on a SAMR grid after one regrid operation at t = 2.5 and subsequent time-stepping using Crank-Nicolson (CN) and quadratic interpolation at coarse-fine interfaces up to t = 42.5. Linear interpolation was used to transfer data from the old to the new grid hierarchy during regrid. The concentration of discretization errors at coarse-fine interfaces introduced during regridding is evident, despite the fact that quadratic interpolation was used at coarse-fine interfaces during the time evolution. Furthermore, the particular time integration scheme used in this case preserves the memory of generated errors, even if the location of the coarse-fine interfaces changes. Errors are concentrated at grid boundaries, as shown by the stairstep features in Figure 4. Once generated during regridding, these errors remain for the rest of the calculation. The previous examples illustrate potential sources of error that can accumulate due to a combination of a poor temporal integrator and low-order interpolation during regridding, even if higher-order interpolation is used at coarse-fine interfaces. Low-order interpolation generates spatial errors that are not damped in time by the temporal scheme. Coarse-fine errors mostly disappear when sufficiently high-order interpolation is used (both at regrid operations and subsequently during time evolution) in combination with a robustly damping temporal scheme. We were pleased to show that using cubic interpolation at the time of regrid, quadratic interpolation between regrid operations, and an appropriate time integrator causes these artifacts to disappear.

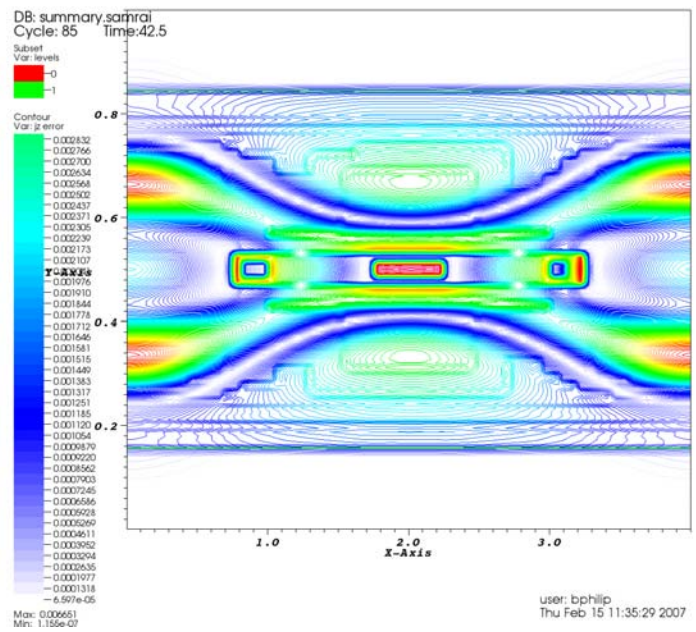


*Figure 4. Error in current at t=42.5 after several regridding operations.*

The purpose of grid adaptation is to minimize the number of degrees of freedom required for a given simulation, while being compatible with a given numerical error level. In practice, the expectation is that the overall numerical error of the simulation does not increase due to the introduction of AMR. Otherwise, it defeats the purpose of using such schemes in the first place. We use the island coalescence problem to characterize the generation and temporal propagation of errors in our implementation. We focus on two main aspects of error generation in SAMR: 1) the treatment of coarse-fine interfaces at patch boundaries, and 2) the placement of patches. The former is fundamentally a spatial discretization issue, whereas the latter is related to error estimation. Figure 5 depicts several time histories of error propagation in AMR simulations featur-

ing different base grids and levels of refinement. The error is obtained with an exact error detector, which compares the AMR solution with a 1024x1024 reference solution. The figure shows the volume weighted l2-norm of the error (which approximates the L2-norm). We have used a fixed timestep in the calculation to isolate spatial errors. The time history of the numerical error mimics the evolution of the physical instability (i.e., exponential growth followed by nonlinear saturation). The point of this plot is to establish that the error is fundamentally a function of the finest resolution employed, and not a function of the base grid size or the number of levels of refinement. For instance, the 64b3l, 128b2l, and 256b1l simulations feature the same error (time histories are actually superimposed), while using different base grid refinements and number of grid levels. The same is true for 64b4l, 128b3l, 256b2l, and 512b1l (although error differences are more noticeable due to the log scale of the plot). Another side point from this figure is the impact that adding a level of refinement has on the overall error of the computation: the error decreases by a factor of four on average, similar to the error reduction that would be obtained by uniform refinement.

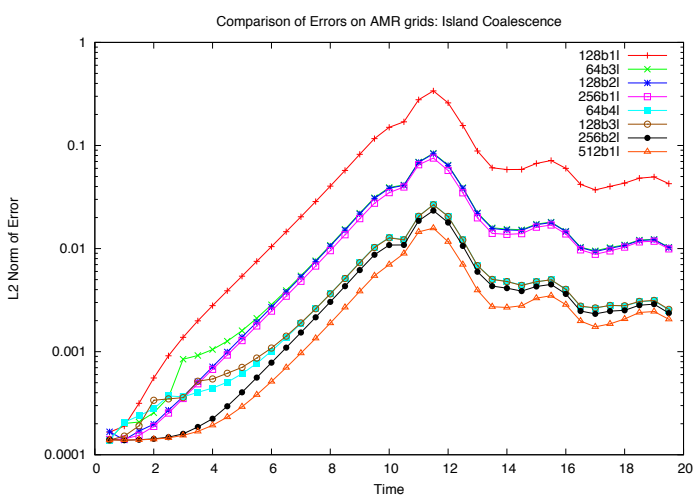


*Figure 5. Time histories of numerical errors for the island coalescence problem with various base grids and levels of refinement. The convention in the legend is nbml, which denotes an nxn base grid with m levels of refinement.*

Having established the correctness of our simulations and characterized the nature and evolution of temporal and spatial error in implicit time integration on AMR grids we also provide details on the cost savings associated with such an approach.

In general, algorithmic scalability of a PDE solver numerical algorithm requires that work per iteration be proportional to the problem size and that the number of iterations be independent of the problem size. In the context of AMR, however, it is difficult to test for scalability directly by performing grid convergence studies, because the problem size is difficult to predict a priori when one changes base grids and levels of refinement for a given simulation. To overcome this limitation, in this work we follow two figures of merit to characterize algorithmic performance in an AMR context. The first one is the same as in single-grid approaches, and measures algorithmic performance under uniform grid refinement. The second one is AMR-specific, and measures the effect on performance of changing coarse-grid resolutions and AMR levels of refinement for a fixed maximum resolution. We define an AMR solver to be equivalent-to-uniform-mesh if the AMR solver performance depends only on the maximum effective resolution (i.e., solver performance is independent of base grid refinement and the number of refinement levels). Furthermore, we define an AMR algorithm to be scalable if it scales under uniform-grid refinement, and if it features equivalent-to-uniform-mesh performance. This equivalent-to-uniform AMR solver performance is obtained for significantly less computational effort and memory storage than uniform grids would require. For example, uniform 512x256 grid tearing mode runs on average required a total wall-clock time of 29900 seconds, while the equivalent AMR calculation with a 64x32 base grid and 4 levels of refinement only requires 17% of that time on average (timings obtained on a MacBook Pro with a 2.33 GHz Intel Core 2 Duo processor, 2 GB of RAM, running Mac OS X 10.4.10.). Furthermore, on average, the 64x32 run with 4 levels of refinement required only 14% of the number of degrees of freedom of a uniform 512x256 run. Note that the strong correlation between the reduction in degrees of freedom and the reduction in CPU time is also a consequence of the equivalent-to-uniform property of our AMR implementation. Similar results both in solver performance as well as time and memory savings were obtained for island coalescence model problems. In the case of the tilt mode problem as evolving features in this problem are extremely small compared to the domain size, this AMR calculation on average only required 0.36% of the degrees of freedom of a uniform grid calculation (a uniform grid calculation would have required 67108864 degrees of freedom, which corresponds to a 4096x4096 uniform grid with 4 unknowns per grid cell). This example serves to illustrate the significant savings that AMR can provide over uniform grid calculations. We note that the relatively small number of degrees of freedom enabled us to perform this calculation on a workstation, while a parallel machine would have been required to perform the uniform-grid calculation.

The project also led to the development of new multiscale solver ideas detailed in Reference [3].

The success of our project led to further program development. It formed the basis of one SciDAC II proposal and one Office of Science multiscale proposal. Unfortunately these have not been successful. It also led to a summer project by a DOE Computational Science Graduate Fellow (CSGF), Mark Berrill from Colorado State University. The project also led to a collaboration with the University of Colorado at Boulder on numerical methods for MHD, involving the Ph.D. student James Adler.

## References


1. Philip, B., M. Pernice, and L. Chacon. Solution of Reduced Resistive Magnetohydrodynamics using Implicit Adaptive Mesh Refinement. 2007. In *Domain Decomposition Methods in Science and Engineering XVI.* Edited by Keyes, D., and O. Widlund. , p. 725. New York: Springer-Verlag.

2. Philip, B., L. Chacon, and M. Pernice. Implicit Adaptive Mesh Refinement for 2D Reduced Resistive Magnetohydrodynamics. 2008. *Journal of Computational Physics.* **227** (20): 8855.

3. Philip, B., and T. Chartier. Adaptive Algebraic Smoothers. *SIAM Journal on Scientific Computing.*

4. Knoll, D., and L. Chacon. Coalescence of magnetic islands, sloshing, and the pressure problem. 2006. *Physics of Plasmas.* **13**: 32307.

5. Richard, R. L., R. D. Sydora, and M. Ashour-Abdalla. Magnetic reconnection driven by current repulsion. 1990. *Physics of Fluids B.* **2**: 488.

6. Chacon, L., D. Knoll, and J. Finn. An implicit, nonlinear reduced resistive MHD solver. 2002. *Journal of Computational Physics.* **178**: 15.


## Publications


Philip, B., L. Chacon, and M. Pernice. Implicit Adaptive Mesh Refinement for 2D Reduced Resistive Magnetohydrodynamics. 2008. *Journal of Computational Physics.* **227** (20): 8855–8874.

Philip, B., M. Pernice, and L. Chacon. Solution of reduced resistive magnetohydrodynamics using implicit adaptive mesh refinement. 2006. In *16th International Conference on Domain Decomposition Methods.* (New York, 12-15, Jan. 2005). Vol. 55, p. 725. New York: Springer-Verlag.

Philip, B., and T. Chartier. Adaptive Algebraic Smoothers. *SIAM Journal on Scientific Computing.*

# Automatic Video Analysis Integrating Depth, Shape, Texture and Color

*Garrett Kenyon*

20060268ER

## Abstract

Understanding how biological systems represent and process information has long been thought to hold the key to designing more powerful computer algorithms. Work supported under this LDRD-ER project resulted in significant advances in our understanding of how biological neural circuits represent and process information.

## Background and Research Objectives

Biological computation is very different from conventional digital computing. Perhaps the most essential difference arises from the distinction between discrete vs. continuous time. In digital systems, information is represented as a string of logical bits, either 0 or 1, and processing occurs during discrete clock cycles, so that the inputs to any computational element are always present on the same clock cycle. In biological neural circuits, information is represented by strings of action potential spikes, which are similar to logical bit but are distributed continuously in time, so that the relative timing of such spike events provides an additional mechanism for coding information. The major focus of this LDRD-supported research effort was to examine how biological neural systems might utilize the relative timing of action potential spikes to represent and process information.

## Importance to LANL's Science and Technology Base and National R & D Needs

America's national security increasingly depends on advances in information technology. Smart sentries, for example, which were able to detect suspicious or threatening behavior against an enormous background of innocuous events, would be of extraordinary benefit to homeland security, intelligence and military applications. The only existing systems capable of reliably detecting "abnormal" or suspicious behaviors are biological organisms. Thus, by seeking to understand the computational principles that govern the operation of biological neural systems, this LDRD-supported research was designed to enable fundamental contributions to America's national security.

## Scientific Approach and Accomplishments

All research conducted under the auspices of this LDRD-ER project was performed using computer simulations of synaptically connected spiking neurons. Supported research may be divided into five categories: 1) Neural Coding, 2) Dendritic Processing, 3) Synaptic Plasticity, 4) High-Performance Neural Simulations, and 5) Biologically-Inspired Distributed Sensors (BIDS).

*Neural Coding*

Research was conducted to investigate how the relative timing of spike among fibers in the optic nerve could be used to encode novel types of information. This research can be further subdivided into four separate projects:

*See Globally, Spike Locally*

In the first year of support, work was completed on a project to investigate how retinal output cells whose axons make up the optic nerve might employ oscillatory spike timing to encode global topological aspects of stimuli to which they are responding. Our results showed that while the mean firing rates of individual neurons could be used to encode the local image intensity at each pixel, temporal oscillations in the firing rates of individual neurons could be used to indicate the presence of a large feature to which individual neurons were responding.

*Number Sense*

In the first year of support, work was also completed on a project to investigate how retinal output neurons might use stimulus-specific oscillations to encode numerosity. Neurons responding to the same object

tend to oscillate in phase with each other, whereas the phase relationship between neurons responding to different objects tends to vary randomly over time. We reasoned that the oscillatory power per spike, measured across the entire visual scene over several hundred milliseconds, should scale as the inverse square root of the number of distinct objects in the scene, regardless of the relative positions, shapes or sizes of the objects in question, and thus should encode the abstract concept of numerosity. Our results showed that such an encoding mechanism is consistent with behavioral experiments in which monkeys were trained to detect changes in the numerosity of randomly generated computer displays.

*Resonance*

In the first year of support, work was completed on a project that investigated whether very small, rapid eye movements, referred to as ocular tremor, could augment the information conveyed by retinal oscillations by tapping into a high-frequency resonance present in the inner retina.

*Extreme Synergy*

In the final two years of support, considerable effort was devoted to an analysis of how retinal output neurons might encode information far more efficiently by using relative spike timing. The dramatic conclusion of this research was that in order the fully decode the local pixel intensity, it may be necessary to consider not only the firing rate of each neuron individually, but to also consider the pairwise correlations between each neuron and all of its neighbors. This hypothesis, which we term Extreme Synergy, asserts that local pixel information can be distributed across a large neighborhood of similarly activated surrounding cells, thereby greatly reducing the number of spikes required to convey the same total amount of visual information.

**Dendritic Processing**

A major research project was undertaken throughout the period of support to better understand the role of dendritic morphology in the integration of synaptic information. The conclusion of this study, described in the abstract cited below, is that individual biological neurons contain, within their elaborate dendritic structures, extensive networks of interconnected logical units, and thus that each neuron is in fact a network unto itself.

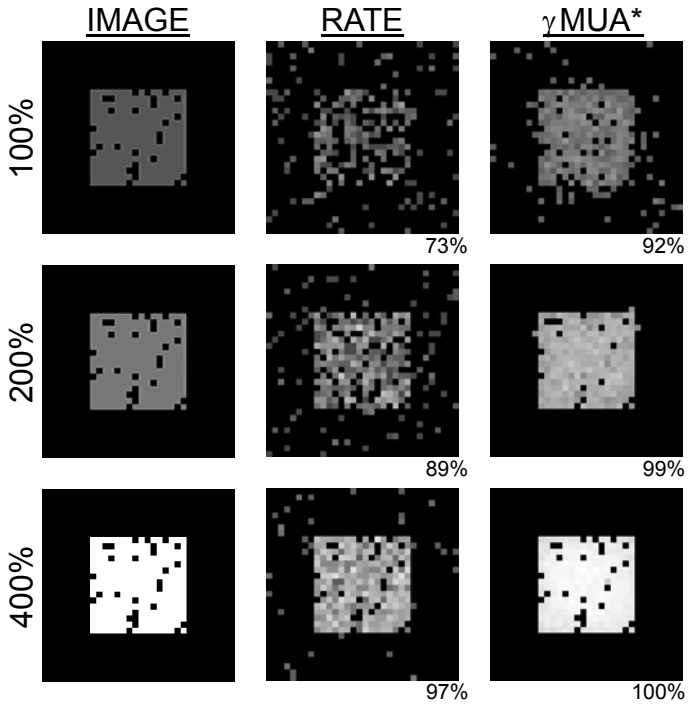


*Figure 1. Extreme Synergy*

**Synaptic Plasticity**

Funds were also used to support the preparation of a manuscript describing how unsupervised plasticity rules could act to maintain long-term memories at biological synapses despite ongoing random changes in individual synaptic strengths due to both intrinsic and extrinsic sources of noise.

**High-Performance Neural Simulations**

Major effort was expended during the third year of the project to develop high-performance neural simulation software that could execute efficiently on hybrid architectures such as the Roadrunner supercomputer. A simplified model of the primary visual cortex was implemented using integrate-and-fire neurons whose synaptic interactions were governed by a cocircular geometric construction. This summer, the resulting software, called PetaVision, became the first scientific simulation to achieve a sustained performance of 1 Petaflop.

**Biologically-Inspired Distributed Sensors (BIDS)**

The principles of biological computation discovered, in part, through research supported by this LDRD project were applied to the design of a new type of wireless sensor network, termed BIDS, which stands for Biologically-Inspired Distributed Sensors. Wireless sensor networks have been proposed as a possible technology

for the automated monitoring of large, remote regions, such as national borders. Due to the size and remoteness of such applications, the individual sensors must be very cheap and able to operate continuously on very low power. Wireless networks based on spiking neurons represent a novel solution for meeting the low-cost and low-power required for deployment across large, remote areas. A patent application is being prepared based on BIDS technology and several supporting research projects have been published.

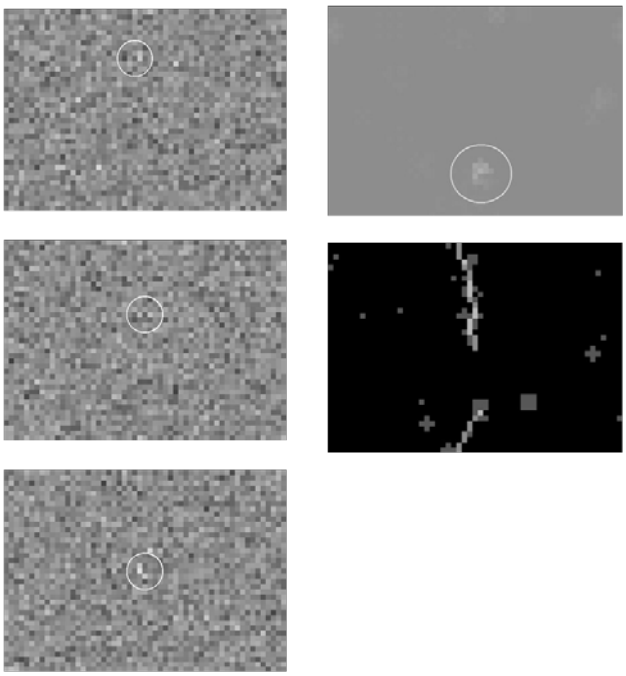

*Figure 2. BIDS*

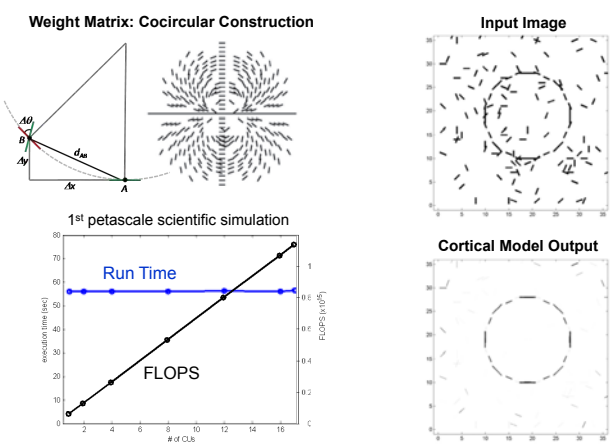


*Figure 3. PetaVision.*

### Review Articles

This LDRD research project was used to support the preparation of an encyclopedia article describing the use of computational models to study cellular and synaptic phenomena in the vertebrate retina.

## References

1. Nugent, M. A., R. Porter, and G. T. Kenyon. Reliable storage at unreliable synapses: Using separable environments to stabilize long-term memories. 2008. *Physcia D.* **237** (9): 1196.

2. Kenyon, G. T.. Extreme Synergy: Spatiotemporal Correlations Enable Rapid Image Re-construction from Computer Generated Spike Trains. To appear in *Journal of Vision.*

## Publications

Allegretti, D. G., G. T. Kenyon, and W. Priedhorsky. Cellular automata for distributed sensor networks. 2008. *International Journal of High Performance Computing Applications.* **21** (2): 167.

Allegretti, D. G., and G. T. Kenyon. Tracking with Context-Aware Distributed Networks. *Journal of Parallel and Distributed Computing.*

Kenyon, G. T.. Theoretical and Computational Neuroscience: Retinal Models. To appear in *New Encyclopedia of Neuroscience.* Edited by Squire, L..

Kenyon, G. T.. Extreme Synergy: Spatiotemporal Correlations Enable Rapid Image Re-construction from Computer Generated Spike Trains. To appear in *Journal of Vision.*

Miller, J. A., K. S. Denning, J. S. George, D. W. Marshak, and G. T. Kenyon. A high frequency resonance in the responses of retinal ganglion cells to rapidly modulated stimuli: A computer model. 2006. *Visual Neuroscience.* **23** (5): 779.

Miller, J. A., and G. T. Kenyon. Extracting number selective responses from coherent oscillations in a computer model. 2007. *Neural Computation.* **19** (17): 1766.

Nemzek, R., G. T. Kenyon, A. Koehler, D. M. Lee, W. Priedhorsky, and E. Y. Raby. SNM-DAT: simulation of a heterogeneous network for nuclear border security. 2007. *Nuclear Instruments and Methods In Physics Research Section A: Accelerators, Spectrometers, Detectors and Associated Equipment.* **579** (1): 414.

Nugent, M. A., R. Porter, and G. T. Kenyon. Reliable storage at unreliable synapses: Using separable environments to stabilize long-term memories. 2008. *Physcia D: Unconventional Computing.* **237** (9): 1196.

Rasmussen, C., G. Kenyon, C. Ferenbaugh, J. Galbraith, S. Swaminarayan, P. Datta, C. Wright, and S. Zucker. Petascale Computing: A Big Brain for Big Bird. Presented at *Supercomputing 2008.* (Austin, TX, 2008).

Stephens, G. J., S. Neuenschwander, J. S. George, W. Singer, and G. T. Kenyon. See globally, spike locally: Oscillations in a retinal model encode large visual features. 2006. *Biological Cybernetics.* **95** (4): 327.

# Automated Induction of Templates for Extracting Information from Text

*Cornelia Maria Verspoor*

20060270ER

## Abstract

The availability of digitized textual information has increased dramatically. The large volume of information now available has created problems for effective management of that information. The field of information extraction has developed in partial response to these problems, developing applications that search for specific types of information through manual definition of linguistic patterns. In this research, we explore methods for automatically tackling the search for information in text and enabling text understanding at a deeper level. We have produced a novel unsupervised learning approach to the problem of word sense disambiguation, and explored formal methods for inducing semantic hierarchies from text. Both of these results have an important impact on text understanding.

## Background and Research Objectives

This work aims to vastly extend what information computers will be able to extract from text and will support rapid retargeting of information extraction systems from one domain to another. We have explored a data-driven paradigm in computational linguistics, in which machine learning is used to tackle deeper language understanding (word sense disambiguation) and formal methods are used to infer hierarchical concept hierarchies from text.

## Importance to LANL's Science and Technology Base and National R & D Needs

This work facilitates rapid development of information extraction systems sensitive to terminology in particular domains. It has broad application for intelligence analysis, bioinformatics, and any field with large quantities of textual data sources. At LANL, it could provide access to weapons physics information that is essentially inaccessible in our archives.

## Scientific Approach and Accomplishments

The accomplishments are first listed, and the primary results are elaborated on in the following text.

1. We have developed core infrastructure software within an open source text processing architecture (called UIMA, or the Unstructured Information Management Architecture, from IBM, or International Business Machines, Inc.) to support linguistic analysis, specifically statistical analysis, part-of-speech tagging, shallow parsing, gazetteer matching, and semantic abstraction, which has been used to drive analysis of important key phrases in documents.

2. We designed an unsupervised learning approach for semantics-enhanced language models utilizing the Expectation-Maximization algorithm, and published the methods as well as experiments on word sense disambiguation of corpus data.

3. We designed an approach to semantic ontology induction from text through application of Formal Concept Analysis to linguistic properties of the text.

4. We have designed an unsupervised learning approach to identification of multi-word expressions utilizing a network representation of text sequences inspired by related work in biological sequence analysis, and have begun preliminary experiments on corpus data. This work was not completed.

5. We have integrated collocation (phrase) extraction with latent semantic analysis and have done preliminary assessment of whether this results in more coherent semantic clusters; using mutual information derived phrases the results were not promising, using a different statistical measure (Pearson's chi-squared independence) the results were more promising. While we experimented with this we were unable to obtain significant publishable results.

**Semantics-enhanced language models**

An N-gram language model aims at capturing statistical syntactic word order information from corpora. Although the concept of language models has been applied extensively to handle a variety of NLP problems with reasonable success, the standard model does not incorporate semantic information, and consequently limits its applicability to semantic problems such as word sense disambiguation. We propose a framework that integrates semantic information into the language model schema, allowing a system to exploit both syntactic and semantic information to address NLP problems. Furthermore, acknowledging the limited availability of semantically annotated data, we discuss how the proposed model can be learned without annotated training examples. We reported in our publication (Lin and Verspoor 2008) on a case study showing how the semantics-enhanced language model can be applied to unsupervised word sense disambiguation with promising results.

Syntax and semantics are two major aspects of language use. Syntax refers to the grammatical structure of a language whereas semantics refers to the meaning of the symbols arranged with that structure. To fully comprehend a language, a human must understand its syntactic structure, the meaning each symbol represents, and the interaction between the two. In most languages, syntactic structure conveys something about the semantics of the symbols, and the semantics of symbols may constrain valid syntactic realizations. As a simple example: when we see a noun following a number in English (e.g. "*one book*"), we can infer that the noun is countable. Conversely, if it is known that a noun is countable, a speaker of English knows that it can plausibly be preceded by a numeral. It is therefore reasonable to assume that for a computer system to successfully process natural language, it has to be equipped with capabilities to represent and utilize both the syntactic and semantic information of the language simultaneously.

The n-gram language model (LM) is a powerful and popular framework for capturing the word order information of language, or fundamentally syntactic information. It has been applied successfully to a variety of NLP problems such as machine translation, speech reorganization, and optical character recognition. An n-gram language model utilizes conditional probabilities to capture word order information, and the validity of a sentence can be approximated by the accumulated probability of the successive n-gram probabilities of its constituent words W1 … Wk.

As powerful as a traditional n-gram LM can be, it does not capture the *semantic* information of a language. Therefore it has seldom been applied to semantic problems such as word sense disambiguation (WSD). To address this limitation, in this paper we propose to expand the formulation of a LM to include not only the words in the sentences but also their semantic labels (e.g. word senses). By incorporating semantic information into a LM, the framework is applicable to problems such as WSD, semantic role labeling, and even more generally machine translation and information extraction – tasks that require both semantic and syntactic information to be solved.

Figure 1(a) is a general finite state representation of a sentence of four words (W1…W4) connected through a bigram LM. Each word can be regarded as a state node and the transition probabilities between states can be modeled as the n-gram conditional probabilities of the involved states (here we assume the transition probabilities are bigrams). In fact each word in a sentence has a certain lexical meaning (sense or semantic label, Si) as represented in Figure 1(b). Conceptually, for each word-based finite state representation there is a dual representation in the semantics (or sense) domain, as shown in Figure 1(c). A *semantics-based LM* (or SLM) like Figure 1(c) records the order relations between meanings. Alternatively, one can combine both representations into a hybrid language model that captures both the word order information and the word meaning, as demonstrated in Figure 1(d). Figure 1(d) represents a *word-sense LM* (or WSLM), a semantics-enhanced LM incorporating two types of states: word symbols and their semantic labels. The intuition behind WSLM is that when processing a word, people first try to recognize it's meaning (i.e. $P(S_n|W_n)$), and based on that predict the next word (i.e. $P(W_{n+1}|S_n)$). Figure 1(e) is the same as Figure 1(d) except that the bigram probabilities are replaced by trigrams. It embodies the concept that the next word to be revealed depends on the previous word together with its semantic label, and the meaning of the current word depends on not only the word itself but the meaning of the previous word.

The major reason for the success of a LM-based approach to NLP problems is its capability of predicting the validity of a sentence. In Figure 1(a), we can say that a sentence "W1W2W3W4" is valid because P(W2|W1)*P(W3|W2)*P(W4|W3) is relatively high. Similarly given that the semantic labels of each word in the sentence are known, the probabilities P(S2|S1)*P(S3|S2)*P(S4|S3) can be applied to assess the semantic validity of this sentence as well. Furthermore, we can say that a word sequence together with its semantic assignment (interpretation) is valid based on

a WSLM if the probability of P(S1|W1)*P(W2|S1)*…*P(W4|S3)*P(S4|W4) is high. We can therefore use a semantics-enhanced LM to rank possible interpretations for a word sequence.

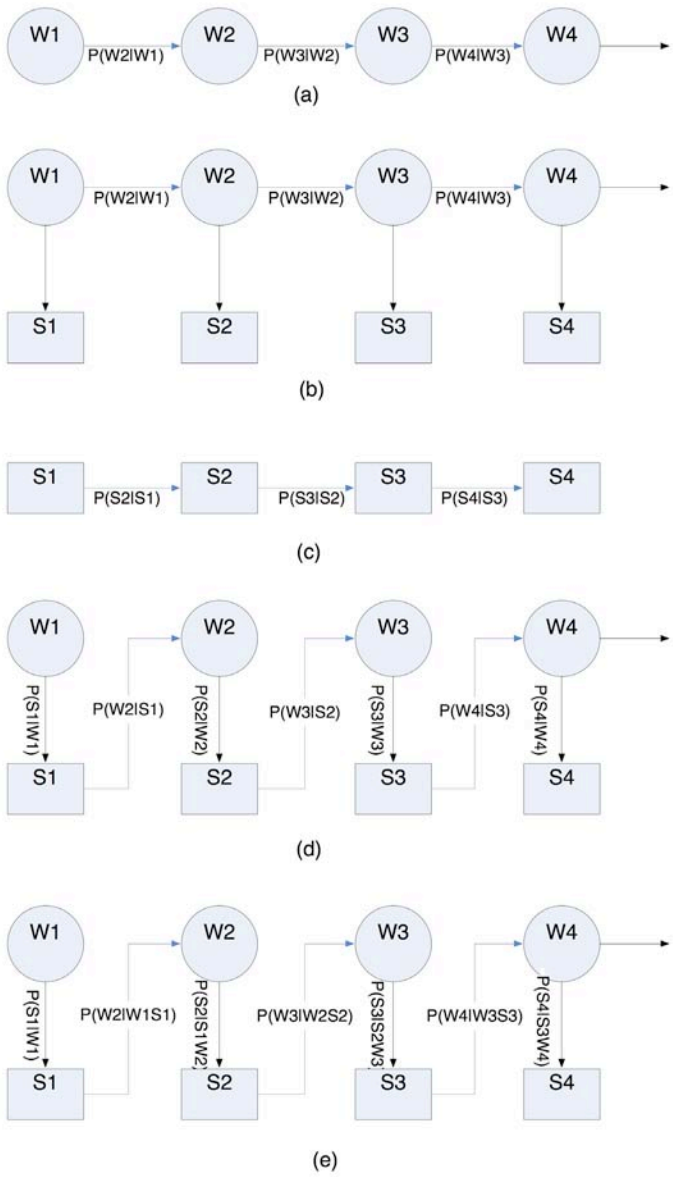


*Figure 2. (a) A typical finite-state, bigram LM representation of a sentence. (b) Each word in the sentence has a certain meaning (or semantic label). (c) A semantic-based language model. (d) a hybrid LM integrating word and sense information. (e) Like (d) except that a trigram model is used.*

There are three major contributions in our paper. First we proposed a framework that enables us to incorporate semantics into a language model. Second we showed how such model can be learned efficiently (O(nb2) in time) in an unsupervised manner. Third we demonstrated how this model can be used to perform the word sense disambiguation (WSD) task and how additional knowledge can be exploited to improve the performance of the model on the task. Our experiments also suggest that WSD can be a suitable platform to evaluate the semantic language models.

**Ontology induction from text**

The central mechanisms to represent organized knowledge, and the cores of real-world ontologies, are semantic hierarchies: mathematically ordered typing structures relating terms or concepts of a domain within semantic relations like subsumption (taxonomic, "is-a", generality relations) and composition (meronomic, "has-part", part-whole relations). The vast increase of computational information in science has resulted in a proliferation of ontologies of increasing size, in areas ranging from bioscience to the military and intelligence communities to the World Wide Web. Successful ontologies like the GO (http://www.geneontology.org) and Wordnet (http://wordnet.princeton.edu) have grown to be very large, with over 20K and 150K nodes respectively. The automated creation and management of large ontologies is a critical need since such ontologies in turn provide the foundation for understanding of linguistic data and inference over extracted knowledge.

Source information for ontology induction could be user elicitation, structured data, or other sources, but one prominent and obvious source is text. Ideally, lexical and linguistic information can be gleaned from texts in a way to automatically or semi-automatically determine subsumptive and meronomic relations among terms and concepts. Research in ontology construction from text draws on a number of strategies. Following the distributional similarity hypothesis terms are semantically similar if they share linguistic contexts like co-occurrence with the same terms, or occur in the same syntactic relation to a term. Thus agglomerative clustering of terms can be accomplished based on using similarity of term usage vectors capturing the linguistic contexts of the term. Alternatively, particular phrasal structures can be identified that stereotypically distinguish specific from general terms, and can be captured by schemata or templates such as "X, Y, and other Z" (e.g. "Cats, dogs, and other animals") . Finally, methods from order and lattice theory, specifically Formal Concept Analysis (FCA), can be employed to discover inherent relations between objects described through a set of attributes. FCA is a discrete math method for representing the set of sub-relations present in an overall binary relation (say, among lexical terms) in the context of their hierarchical structure, and thus yields natural semantic hierarchies from term relations.

Our approach extends the intuition of the distributional similarity hypothesis to assert a **Distributional Generality Hypothesis**, that *semantic generality of terms, as represented by hierarchical relations among them, can be determined from the analysis of their shared linguistic contexts.* In particular, to the extent that the more general a term is, the more contexts it can be used in, then we aim to show that the distribution of nouns with respect to the verbs they are arguments of, and *vice versa*, is an important source of information about term generality that can be used to construct a semantic hierarchy of relations among terms. Our publication (Joslyn et al 2008) reports on some initial research results supporting a future overall methodology towards the semi-automatic construction of semantic hierarchies from term relations extracted from text. Specifically, we describe our formal method for hierarchy construction, selection and processing of a test corpus for extracting verb-noun pairs from natural language, measurement and filtering of the resulting verb-noun term matrices for density optimization, and finally look at the resulting semantic hierarchies produced by FCA.

## Publications


Abi-Haidar, A., J. Kaur, A. Maguitman, P. Radivojac, A. Rechtsteiner, K. Verspoor, Z. Wang, and L. M. Rocha. Uncovering protein-protein interactions in the bibliome. 2007. In *Proceedings of Second BioCreative Challenge Evaluation Workshop.* (Madrid, Spain, April 23-25, 2007). , p. 247. ISBN 84-933255-6-2: .

Abi-Haidar, A., J. Kaur, A. Maguitman, P. Radivojac, A. Rechtsteiner, K. Verspoor, Z. Wang, and L. M. Rocha. Uncovering protein interaction in abstracts and text using a novel linear model and word proximity networks. 2008. *Genome Biology.* **9** (Suppl 2): S11.

G.Gessler, D. D., C. A. Joslyn, K. M. Verspoor, and S. E. Schmidt. Deconstruction, Reconstruction, and Ontogenesis for Large, Monolithic, Legacy Ontologies in Semantic Web Service Applications. 2006. *Los Alamos Unclassified Release report.*

Gessler, D., K. Verspoor, C. Joslyn, B. Koester, and S. Schmidt. Integrating semantic data sources for disease-implicated gene discovery. 2007. In *Rocky Mountain Bioinformatics Conference.* (Snowmass, CO, Nov 30 - Dec 2, 2007). , p. 4. Colorado: ICSB.

Joslyn, C. A., K. M. Verspoor, and D. D. G. Gessler. Knowledge integration in open worlds: Utilizing the mathematics of hierarchical structure. 2007. In *the First IEEE International Conference on Semantic Computing.* (Irvine, CA, September 17-19, 2007). , p. 105. Piscataway, NJ: IEEE Computer Society.

Joslyn, C., D. D. G. Gessler, S. E. Schmidt, and K. M. Verspoor. Distributed Representations of Bio-Ontologies for Semantic Web Services. 2006. In *The Joint BioLink and BioOntologies Special Interest Group of the Intelligent Systems for Molecular Biology Conference.* (Fortaleza, Brazil, 6-10 Aug, 2006). , p. 1. International Society for Computational Biology.

Joslyn, C., P. Paulson, and K. Verspoor. Exploiting term relations for semantic hierarchy construction. 2008. In *2008 IEEE International Conference on Semantic Computing.* (Santa Clara, California, 4-7 Aug 2008). , p. 42. California: IEEE Computer Society.

Lin, S.. Modelling, Searching and Explaining Interesting Instances in Multi-Relational Network. 2006. *PhD dissertation, University of Southern California.*

Lin, S. d., and K. Verspoor. Learning Semantics-Enhanced Language Models Applied to Unsupervised WSD. 2007. *LAUR 07-0618.*

Lin, S., and K. Verspoor. A semantics-enhanced language model for unsupervised word sense disambiguation. 2008. In *Computational linguistics and intelligent text processing.* Vol. 4919, p. 287. Berlin/Heidelberg: Springer.

Verspoor, K.. Semantics, Text, and a Cure for Cancer. Invited presentation at *Recent Advances in Natural Language Processing.* (Borovets, Bulgaria, September 27-29, 2007).

# Monte Carlo Estimation of Eigenvalues of Ultradimensional Matrices and Continuous Operators

*James E Gubernatis*

20060272ER


## Abstract

Our objective was to develop new numerical methods, suitable for Monte Carlo implementation, that enable the computation of multiple eigenvalues and eigenvectors of very large matrices and continuous operators. By "very large " we mean matrices so large that available computer memory is insufficient not only for storing them but also for storing any one of their eigenvectors. Such problems are common in science, engineering, and mathematics. We started by implementing our original algorithm deterministically (non Monte Carlo), discovered a numerically more stable version, and successfully benchmarked it for a variety of matrices. Then, we moved to Monte Carlo implementations. Here, we benchmarked the algorithm on a non-trivial problem from statistical mechanics. Next, we moved from matrices to continuous operators. Here, we focused on problems where the two largest eigenvalues are very close in value. The challenge was not the estimation of the eigenvalues but instead the efficient estimation of the eigenvectors. Drawing on several simple benchmark problems used for nuclear reactor design, we demonstrated a nearly hundredfold improvement in the convergence to the eigenvectors. Key to this was the development of new means for sampling eigenvector components of mixed sign. Besides the new methods for multiple eigenpair determination, we also developed a new sampling method, the sewing algorithm, that enables the Monte Carlo sampling of states from a very large system from those of a much smaller one.


## Background and Research Objectives

Finding the eigenvalues and eigenvectors, that is, the eigenpairs, of matrices and continuous operators is a ubiquitous problem in science, engineering, and mathematics. In some cases, only the few largest or smallest eigenpairs are needed. While this seemingly simplifies the problem, these cases are too often so complex that available computer memory is insufficient to store even one eigenvector. Standard eigenpair computational methods must be replaced by Monte Carlo methods. Our objective was producing and benchmarking Monte Carlo algorithms to compute the two largest or smallest eigenpairs of these challenging problems.

**What are eigenvalues and eigenvectors?**

Most of computational science, engineering, and mathematics replaces the basic additions, subtractions, multiplications, and divisions of numbers by related operations on large collections of numbers simultaneously. Matrices and continuous operators are two classes of mathematical objects used in such operations. These objects typically have the property that after operating on some group of numbers, say 1, 2 and 3, a new group, say 2, 4, and 6, is produced. Some groups are special, as in this contrived example, by having the new components related to the old by a common multiplication factor. In this example, each component of the new group is a factor of 2 times the corresponding component of the old group. The group (1, 2, 3) and the common factor 2 are said to be an eigenvector and eigenvalue of the matrix or operator. In general, a matrix or continuous operator has many eigenpairs.

**Why bother computing eigenvalues and eigenvectors?**

While sounding very abstract, the eigenvalue and eigenvector concept is in fact very useful. A physical system usually exists in one eigenvector or in a combination of several eigenvectors of the matrix or operators that determine its behavior. A simple example is a guitar. When one string is fretted and plucked, the resulting sound comes from a specific eigenvector of the operator representing the string. When the stings are chorded and strummed, the sound is that of several specific eigenvectors. A less obvious example is a nuclear reactor. In its design, the distribution of neutrons in it is tuned to represent the eigenvector whose largest eigenvalue is 1. The significance of 1 is

the production of neutrons in the reactor is balanced by their loss. If the eigenvalue were greater than 1, too many neutrons are being produced and meltdown could occur; if less than 1, too few neutrons are being produced and shutdown could occur.

**Why just two eigenpairs?**

The nuclear reactor example is also one for which knowing only the two largest eigenpairs suffices. The division of the second largest eigenvalue by the largest is called the dominance ratio, and this ratio is an indicator of the stability of the reactor design. Being close to 1 means reactor might take a long time to reach its intended operating state; then reactor designers must address this possibility when designing reactor control systems. Another example for which knowing only two eigenpairs suffices comes from statistical mechanics. The two largest eigenvalues of something called the transfer matrix of a physical system provides all necessary information about the equation of state of the system, for example, information about whether a solid, liquid, or gaseous phase exists as temperature and pressure are varied, and also provides important information about microscopic details of these phases.

**Why Monte Carlo?**

Monte Carlo is a simulation method that enables reliable estimates of solutions to a problem without the need to solve all the details. It does this by successively generating different parts of the solution, that is, samples of the solution, and estimating the solution from an average of the samples. With this approach we can obviate the storage problem associated with our eigenvectors.

The power iteration method [1] is the standard technique used to find the largest eigenvalue of a matrix and the accompanying eigenvector. This is the method we will build upon. In it, one starts with a guess of the eigenvector and then repeatedly multiplies this guess by the matrix (or operator) of interest. Eventfully the result is a vector proportional to the eigenvector associated with the eigenvalue of largest magnitude. Simple procedures allow the estimation of this eigenvalue. A simple arithmetic shift of the matrix allows the determination of the eigenpair associated with the smallest eigenvalue. Monte Carlo methods for the estimation of the largest or smallest eigenpair always use some form of the power iteration method. For example, the power iteration method has been used in reactor design simulations for decades. How do we generalize this method to find the two dominant eigenpairs simultaneously and how do we give this generalization a Monte Carlo expression are the two questions our research sought to answer.

## Importance to LANL's Science and Technology Base and National R & D Needs

We considered a generic problem in physics, chemistry, engineering, and mathematics. Our success is an enabling technology independent of a specific application. The most obvious impact areas are the computation of ground and excited states of atoms, molecules, solids, and nuclei, improved search engines of databases, more efficient equation of state calculations in statistical mechanics, and more efficient nuclear reactor simulations.

## Scientific Approach and Accomplishments

We began by implementing several of our previously proposed techniques [2,3] and then studied their effectiveness for small matrices whose eigenpairs were available by conventional numerical methods or exact methods. These problems benchmarked our procedures. The general strategy of these procedures is as follows [5]: If one considers multiple sub-groupings of the components of an eigenvector, the essence of its being an eigenvector is that the ratio of the information contained in each sub-group after and before the application of the matrix to the vector is the eigenvalue. The normal power iteration method considers just one group (all the components at once). If one constrains it by maintaining the ratio for two, three, etc. sub-groups, one can then obtain two, three, etc. eigenpairs [2,3]. Our initial procedures worked in many cases but through these simple deterministic (non Monte Carlo) studies we discovered how to make them more stable numerically [4].

The success achieved deterministically is illustrated in Figure 1 [4]. Here, we found the second largest eigenpair of the matrix obtained from the discretization of the one-dimensional Laplacian operator $d^2/dx^2$, shifted so the lowest eigenvalue is 0. Discretization converts this continuous operator into a matrix. As illustrated by the figure, the second eigenvalue approaches 0 as the order (size) of the matrix becomes very large. The figure demonstrates excellent agreement of the computed value with the analytically obtained value. The absolute value of the difference between the exact and computed values shows agreement up to roughly the number of significant digits possible with double precision arithmetic. Equally impressive results were found for deterministic computations of eigenpairs of the Hamiltonian matrix of the one-dimensional Hubbard model [5] and for the transfer matrix of the two-dimensional Ising model [6].

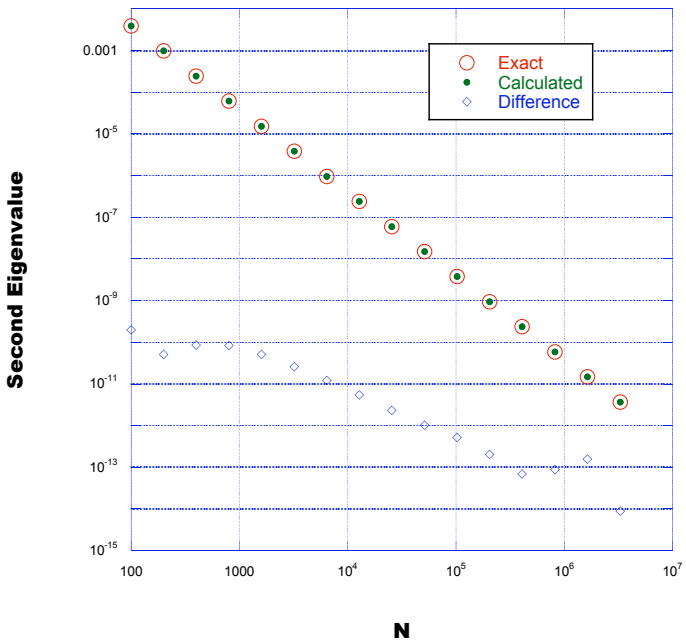


*Figure 1. The second smallest eigenvalue of the matrix representing the discretization of the one-dimensional gradient operator on a circle as a function of the order of the matrix. The values obtained by our modified power method are compared with the exact values. Also shown are the absolute values of the difference between the two values. The order of the largest matrix was 3,276,800.*

Next, we developed a Monte Carlo implementation of our method [7] and studied two specific problems. One was larger-sized transfer matrices of the two-dimensional Ising model [6]. We revisited this problem because Onsager [8] in his celebrated work on the two-dimensional Ising model generated exact expressions for all the eignevalues of the transfer matrix for any system size, no matter how large, so we had benchmarks. We first developed our Monte Carlo techniques for several modestly-sized systems, for which computer memory was adequate. In the process, we refined our Monte Carlo techniques. For example, we successfully implemented [7] a pair-wise component cancellation technique [9] to improve our calculation of the second eigenvector. We also discovered a simple analytic requirement for the convergence of the simulation that supplements the monitoring of the value of eigenvalue [7].

The basic computational operation in the power iteration method is the multiplication of a vector by a matrix. How this operation is sampled and estimated by a Monte Carlo method is reasonably well developed. To compute more than the dominant eigenpair for large-sized transfer matrices, we now had to address a new Monte Carlo challenge. Deterministically the matrix-vector multiplication engages all components of the vector and enables them all to contribute to a single component of the new vector. In a Monte Carlo implementation only a sample of the components of the vector are known. With only a sample, the likelihood of any two components of the old vector contributing to the same component of the new vector is vanishingly small, but such multiple contributions are necessary for an accurate sampling of the new vector, especially for the second eigenvector whose components must have mixed signs. Accordingly, the Monte Carlo procedure must have a part that promotes such multiple contributions. For the transfer matrix problem we found the one used in the original study [1,2] of our methods worked.

Our results for the larger-sized transfer matrix problem are shown in Table 1 [7]. It shows comparisons between Onsager's exact results and our Monte Carlo estimates for the transfer matrix for a square lattice of size *m* x *m* with m varying by a unit of 8 up to 48. The agreement of our Monte Carlo results with the exact results is excellent. The order of the matrix is $2^m$. For the matrix representing the 48 x 48 lattice the order was one thousand times one billion. This is huge. On a single computer processor we accurately obtained the two largest eigenvalues for this matrix in two days. The order of this matrix was a million times larger than ones previously studied. Previous studies obtained just the largest eigenvalue, and the computations required two weeks on a parallel computer.

The significance of increasing the lattice size by steps of eight is the following: To sample from such large systems we devised a new algorithm that builds the samples for the large systems, for which we cannot store an eigenvector, from successive samples of a small system, for which we can. We can easily store the eigenvectors for a system of size *m*=8, and thus used it to sample those of size 16, 24,

| Matrix | $v_1$ (Onsager) | $v_1$ | $v_2$ (Onsager) | $v_2$ |
|---|---|---|---|---|
| $2^{16} \times 2^{16}$ | $2.93297 \times 10^6$ | $2.93307 \pm 0.00008 \times 10^6$ | $2.79225 \times 10^6$ | $2.79482 \pm 0.00010 \times 10^6$ |
| $2^{24} \times 2^{24}$ | $4.95473 \times 10^9$ | $4.95480 \pm 0.00020 \times 10^9$ | $4.79510 \times 10^9$ | $4.79502 \pm 0.00029 \times 10^9$ |
| $2^{32} \times 2^{32}$ | $8.39316 \times 10^{12}$ | $8.39311 \pm 0.00049 \times 10^{12}$ | $8.18959 \times 10^{13}$ | $8.18807 \pm 0.00061 \times 10^{13}$ |
| $2^{40} \times 2^{40}$ | $1.42333 \times 10^{16}$ | $1.42333 \pm 0.00007 \times 10^{16}$ | $1.39565 \times 10^{17}$ | $1.39558 \pm 0.00008 \times 10^{17}$ |
| $2^{48} \times 2^{48}$ | $2.41504 \times 10^{19}$ | $2.41522 \pm 0.00019 \times 10^{19}$ | $2.37584 \times 10^{19}$ | $2.37481 \pm 0.00054 \times 10^{19}$ |

*Table 1. Estimates of the two dominant eigenvalues $\nu_1$ and $\nu_2$ and their errors of the transfer matrix for variously sized lattices. Also given for each lattice size is Onsager's exact result.*

etc. We call this new algorithm the sewing algorithm [10]. It should have applicability to problems other than the specific ones we considered.

The final class of problem we considered was determining the eigenpairs of a continuous operator without discretizing the operator, that is, without creating a matrix. The benchmarks we chose where drawn from nuclear reactor design problems that had dominance ratios near unity [3]. For these benchmarks, the standard power iteration method for the dominant eigenpair converges rapidly to the eigenvalue. The difference between using our method, which gives two eigenpairs, and the standard power iteration method, which gives just one, lies in how fast they converge to the eigenvectors. The convergence of the standard method is slow for dominance ratios near unity. We achieved a significant speed up. We illustrate this in Figure 2 [11]. Here we plotted the relative entropy versus iteration (cycle) number. Relative entropy is a quantity that provides a global figure of merit of the convergence of our eigenvector estimates to the exact answer [12,13]. To provide an "exact" answer we computed the eigenvector though exceptionally long Monte Carlo simulations. The relative entropy is zero if the results of shorter runs approach the exact answer; otherwise, it is a negative number. The plots thus show how rapidly our method evolves to the answer. From them we see that the standard power iteration method (green line) rises slowly and relatively smoothly to zero in about 400-450 cycles. The red and blue lines show the results of our new method for relative entropy for the dominant and second eigenvector. (For the second eigenvector we had to extend the definition of relative entropy.) They both rise to zero in about 5 cycles. The ragged structure is indicative of statistical independence between successive cycles and thus indicates an extra benefit, a facilitation of the estimation of confidence intervals of the results. The illustrated efficiency was achieved in part by replacing the scheme to promote component cancellation with a new scheme. The old scheme promoted point-wise cancelation; the new promotes region-wide cancellations.

Word of our results has generated several collaborations. We are presently collaborating with N. Kawashima (Institute of Physics, University of Tokyo), J. Doll (Department of Chemistry, Brown University), and M. Troyer (Institute for Theoretical Physics, Eidgenössische Technische Hochschule, Switzerland) on the scaling dependence of critical phenomena in the two-dimenional Ising model in the presence of a magnetic field, comparative efficiency of Monte Carlo algorithms used in chemical physics, and gap estimation in quantum magnets.

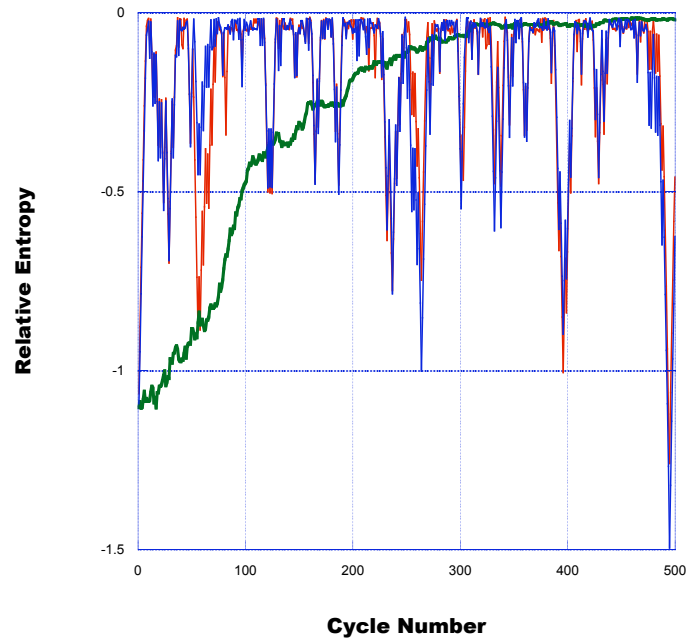


*Figure 2. Convergence of the eigenfunctions for Problem 1 of [12] as a function of the iteration cycle number as measured by the relative entropy and computed by Monte Carlo implementation of the standard and our modified power method. The green line is the fundamental mode computed by standard power method. The red and blue lines are the fundamental and second eigenfunctions computed by our modified power method. Besides converging faster, our method displays a high degree of statistical independence between results from different cycles. This is indicated by the spiky structure after convergence is reached.*

## References

1. Wilkinson, J. H.. 1965.

2. Booth, T. E.. Power Iteration for the Several Largest Eigenvalues and Eigenfunctions. 2006. *Nuclear Science and Engineering.* **154**: 48.

3. Booth, T. E.. Computing the higher k-Eigenfunctions by Monte Carlo Power Iteration: a Conjecture. 2003. *Nuclear Science and Engineering.* **143**: 291.

4. Gubernatis, J. E., and T. E. Booth. Multiple Extremal Eigenvalues by the Power Method. 2008. *Journal of Computational Physics.* **227** (19): 8508.

5. Montorsi, A.. The Hubbard Model. 1992.

6. Thompson, C. J.. 1972.

7. Booth, T. E., and J. E. Gubernatis. Monte Carlo Determination of Multiple Extremal Eigenvalues. *Physical Review E.*

8. Onsager, L.. Crystal Statistics. I. a Two-Dimensional Model with an Order-Disorder Transition. 1944. *Physical Review E.* **65**: 117.

9. Arnow, D. M., M. H. Kalos, M. A. Lee, and K. E. Schmidt. Green's Function Monte Carlo for Few Fermion Problems. 1982. *Journal of Chemical Physics.* **77**: 5562.

10. Booth, T. E., and J. E. Gubernatis. Sewing Algorithm. To appear in *Computer Physics Communications.*

11. Booth, T. E., and J. E. Gubernatis. Improved Criticality Convergence Via a Modified Power Iteration Method. To appear in *Transactions of the American Nuclear Society.*

12. Ueki, T., F. B. Brown, D. K. Parsons, and D. E. Kornreich. Autocorrelation and Dominance Ratio in Monte Carlo Criticality Calculations. 2003. *Nuclear Science and Engineering.* **145**: 279.

13. Ueki, T.. Information Theory and Undersampling Diagnostics for Monte Carlo Simulation of Nuclear Criticality. 2005. *Nuclear Science and Engineering.* **151**: 283.

## Publications

Booth, T. E., and J. E. Gubernatis. Monte Carlo Determination of Multiple Extremal Eigenpairs of Very Large Matrices with Application to the Transfer Matrix of the Two-Dimensional Ising Model. *Physical Review E.*

Booth, T. E., and J. E. Gubernatis. Sewing Algorithm. To appear in *Computer Physics Communications.*

Booth, T. E., and J. E. Gubernatis. Multiple Extremal Eigenpairs of Very Large Matrices by Monte Carlo Estimation. 2008. *LA-UR-08-0043.*

Booth, T. E., and J. E. Gubernatis. Improved Criticality Convergence Via a Modified Monte Carlo Power Iteration Method. To appear in *Transactions of the American Nuclear Society.*

Gubernatis, J. E., and T. E. Booth. Multiple Extremal Eigenpairs by the Power Method,. 2008. *Journal of Computational Physics.* **227**: 8508.

# New Method for Complex Contingency Analysis

*William Henry Press*

20060302ER

## Abstract

The extraction of coherent information from large, sparse tables of experimental outcomes, and more generally of high dimensional data, is a major challenge in data mining and knowledge discovery. Application areas include exploring the dependencies between nuclear test yield discrepancies and weapons design choices, ensuring the confidentiality and security of government databases, and correlating disease states with multiple genetic features. This project has developed principled statistical methods for the analysis of such data for several application area of interest to DOE: genomics and biology, multi-stage searches for rare events, and energy spectrum estimation for radio-isotope identification.

## Background and Research Objectives

Many complex experiments produce data in which the meaning or experimental outcome is hard to decipher. Often this is because the numbers of input variables and of possible outcomes are both large. Examples include correlating cancer diagnoses with multiple genetic features, predicting ozone concentrations at a specific location from multiple relevant atmospheric time series, or exploring the dependencies between nuclear tests yield data and weapons design choices.

The challenge with the statistical analysis of high dimensional data is referred to as the curse of dimensionality. The mathematical difficulties are that (random) points in high dimensions are far apart from one another, and that modeling high dimensional data requires one to do multiple hypothesis testing. Researchers are rightly suspicious of any finding where the observer has tried so many different hypotheses that one might appear correct by chance.

This project is developing new computational methods and analyses to understand the results of complex data in an objective and statistically sound way.

## Importance to LANL's Science and Technology Base and National R & D Needs

Many DOE missions involve experiment and/or observation that produce high dimensional data of the type addressed by this project. Due to its intrinsic sparseness, the analysis of high dimensional data must take advantage of known constraints implied by its context. As such, we have developed data analysis methods in four general application areas: 1) methods for finding over-expressed peptides from DNA data, 2) analysis methods enabling proteomic mass spectroscopy to help identify protein function, 3) improving the searches for rare events, such as the detection of a terrorist, using sampling techniques that are better than "profiling," and 4) developing statistical estimation tools for the energy spectrum of particles emitted by radio-isotopes from low resolution detectors that ultimately enable better identification of the radiation source.

All these problems are relevant to the DOE mission of the laboratory. The data analysis and algorithmic capabilities we have developed in the course of this project will help us better meet the future mission needs of LANL.

## Scientific Approach and Accomplishments

This project has made significant contribution to four data problem.

1. How to find over and under expressed peptides from genomics data? The problem is both statistical and algorithmic; as one needs to explore the space of all short peptides, which is huge, and for each peptide, test if it might be over or under represented when compared to a baseline model.

2. What do proteins do? While we can now sequence entire genomes cheaply, understanding the genetic language remains a challenge. To help understand

the function of genes, one complements DNA with other experiments. For this effort, we considered experiments relying on mass spectroscopy.

3. Finding an "evildoer" has often been seen as finding a needle in a haystack. While simple visual inspection might be indeed daunting, one can improve ones chances by using a magnet, or for that matter, other techniques to identify a smaller subset of items worth further investigation. We explored how best to use pre-screening.

4. The energy spectrum of particles emitted from radioisotopes serves as a fingerprint of that source. But estimation of that spectrum with low-resolution detectors over short time intervals is dominated by the sampling noise. Smoothing of the spectrum can reduce the noise at the cost of increased bias. We have developed techniques that have the potential to substantially reduce the bias where it matters (at the peaks and valleys) while marginally impacting the spectrum at other locations, thus potentially improving radioisotope identification.

**Analysis of genomic sequence data**

Understanding the meaning of DNA sequence data by classifying and interpreting regions of DNA sequences remains a major challenge in biology. State-of-the-art models use hidden Markov models to classify DNA regions into coding/non-coding regions and into Clusters Of Genes (COGs).

Dr. Press has improved upon these techniques by developing a Markov tree model, which was published as an LA-UR web note [1], and a significant application to a study of the human genome was published in the prestigious journal Genetics [2].

The approach relies on analyzing contiguous strings of DNA, called k-mers, to identify particular strings of interest. For both genomics and text-based intelligence data, "strings of interests" are those that are either over-represented or under-represented with respect to a "random assembly" baseline. It is easy to see why an excess of joint occurrences of the words "twin towers" and "jihad" in intercepted communications might raise suspicions. Similarly, nullomers defined as k-mers of DNA that do not occur in DNA coding have been linked to possibly lethal peptides. A difficulty with systematically identifying over- and under expressed strings is the need to search over large sets of strings and perform multiple statistical tests of hypothesis. Fast algorithms that enable timely exploration of huge sets of hypothesis have been produced using optimized variable-length polygraphic trees.

The needs to explore large hypothesis space for relating multiple risk factors to genotype has lead Dr. Press to develop a new and fast transform method to efficiently characterizes a large data set based on single-factor and multi-factor risks. The method, which is related to the Fast Hadamar Transform, has a broad range of applications and has been published in Proceedings of the National Academy of Sciences [3]. An unexpectedly powerful outcome is that the technique can be used for nonlinear and robust statistics, with which we hope to pursue intelligence-related applications. For example, the method can be applied to image analysis (see Figure 1) where the fast "median Radon transform" can find a very faint linear feature in a background that is confused by point sources:

Figure 1a shows an almost invisible line that is four pixels wide and whose intensity is half a standard deviation above the background noise, whose distribution has a propensity of generating large outliers. The faint line in Figure 1a) is revealed by the discrete median Radon transform as the blob of points in Figure 1b. Using the median over the mean makes the procedure less sensitive to the outliers. Transforming Figure 1b back into image space using the inverse discrete Radon transform produces Figure 1c. This procedure has achieved two goals: it has revealed the faint line in Figure 1a and has eliminated many of the outliers at the cost of introducing faint lines.

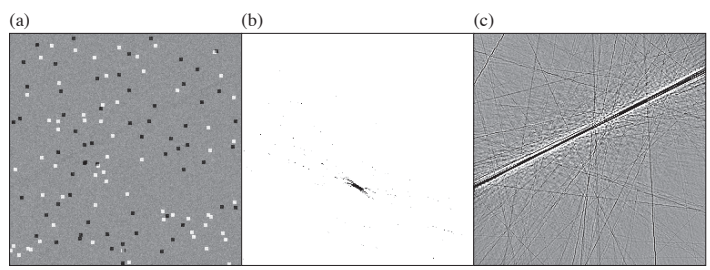


*Figure 1. The 'fast median radon transform' can find a very faint linear feature in a background that is confused by point sources. Panel (a) contains a faint line (one half standard deviation from the background noise) that is four pixel wide. Furthermore, the noise is characterized by having some severe outliers (the back and white dots). Panel (b) shows the result of the discrete median transform of the image in panel (a). The concentration of points seen in the center are related to the faint line. Indeed, taking the inverse Radon transform, one sees in panel (c) the faint line emerging. In addition, the technique has also removed the outliers, at the cost of introducing some faint lines.*

Figure 2 shows the reconstruction of a photograph entirely from the median (not sum) values along projections (this is interesting mostly because it is visually so striking).

*Figure 2. Practical performance of the fast median radon transform to reconstruct a noisy image. Original image was transformed using the median discrete Radon transform and transformed back using a traditional inverse Radon transform. Expect that both the discretization and regularization of the inverse lead to smearing. The absence of smearing in the reconstruction demonstrate that the method has very low distortion.*

**Decoding Shotgun Proteomic Mass Spectra by Sequential Statistical Models**

Shotgun mass spectrometry tries to identify hundreds or thousands of simultaneously expressed proteins from some tens of thousands of measured, generally rather noisy, peptide spectra. The challenge is that there are many more proteins than observations. To get around this problem, it is customary to use dimensionality reduction techniques to make the number of free parameters commensurate with the number of observations. Most existing data reduction algorithms compare (typically by convolution) each spectrum against every possible peptide in a theoretical library. Limitations on library size severely constrain these algorithms. Dr. Press has developed a different approach, in which the problem is parsed into a succession of increasingly specific hypotheses, and a verifiable statistical model is constructed. The resulting models answers questions about:

- With what probability are ion fragments of specified mass present in the spectrum?
- What are the most likely amino acid sequences, given these ions?
- Using only fast hash-table lookup, which of these sequences occur in the reference proteome?
- With what probability is any given protein detected?

The combination of these ideas, none of them completely new, yields a versatile pipeline, easily modified for new challenge problems, for example the systematic detection of post-translational modifications across the whole proteome.

**Strong Profiling Is Not Mathematically Optimal for Discovering Rare Malfeasors**

The use of profiling by ethnicity or nationality to trigger secondary security screening is a controversial social and political issue. Overlooked is the question of whether such actuarial methods are in fact mathematically justified, even under the most idealized assumptions of completely accurate prior probabilities, and secondary screenings concentrated on the highest-probability individuals. Dr Press has demonstrated that strong profiling (defined as screening at least in proportion to prior probability) is no more efficient than uniform random sampling of the entire population, because resources are wasted on the repeated screening of higher probability, but innocent, individuals. A mathematically optimal strategy would be ``square-root biased sampling,'' the geometric mean between strong profiling and uniform sampling, with secondary screenings distributed broadly, though not uniformly, over the population. Square-root biased sampling is a general idea that can be applied whenever a ``bell-ringer'' event must be found by sampling with replacement, but can be recognized (either with certainty, or with some probability) when seen. The results of this research will appear in the Proceedings of the National Academy of Sciences [4], and has been preliminary selected for press coverage (by PNAS) when it is published.

**Nonparametric bias correction.**

In high-dimensional nonparametric smoothing, sparseness of the covariates, often referred too as the curse of dimensionality, forces one to use very large smoothing parameters to control the noise in the estimate at the cost of increased bias. Much attention has been given to select optimally the smoothing parameter from the data. Inspired by the boosting algorithm used in machine learning, Dr. Hengartner et al. have focused on iterative refinement of the nonparametric smoother via successive bias corrections. By selecting judiciously the number of bias correction steps, we obtain smoothers that in well-known test data sets (Los Angeles Ozone data) and simulated data sets, over 20% improvements in the prediction error over the current best algorithms. The reason why we get such good performance is that the iterative bias corrected smoother adapts to the local smoothness of the regression function, which is often smoother than stipu-

lated by the model. That work has been submitted for publication to the Annals of Statistics [5].

The ideas of iterative bias correction have nice statistical properties. In Hengartner et al. [6,7], we show that multiplicative bias correction in both nonparametric density estimation and nonparametric eliminates asymptotically the bias without increasing the asymptotic bias. Multiplicative bias correction methods are particularly suitable for the estimation of energy spectrum of radio-isotopes, with the latter being useful for identification and characterization of the source. Figure 3 gives an example of the improvement one multiplicative bias correction step produces. That work has been submitted for publication in IEEE transaction on nuclear science [8].

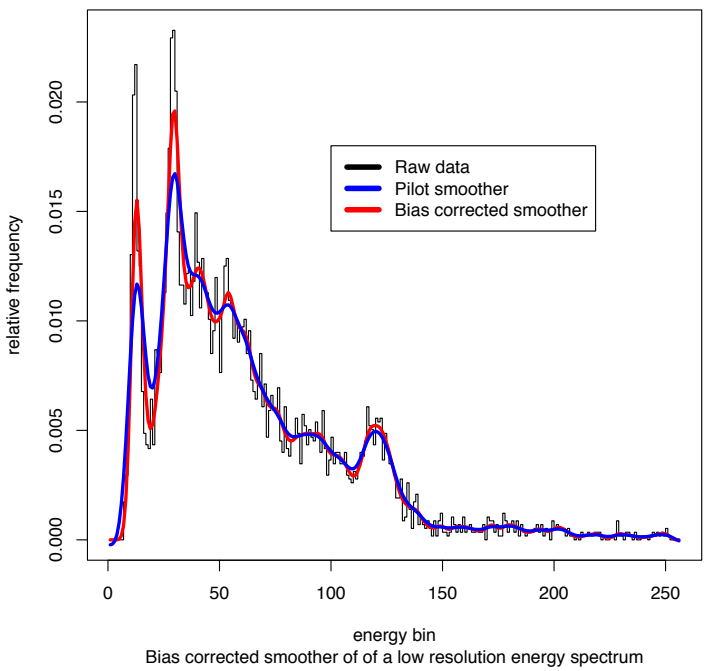


*Figure 3. Energy spectrum from a low resolution NaI detector to be used as a signature by which the source radio-isotope is identified. The black line shows the raw counts, which due to small sample Poisson statistics, is intrinsically noisy. The blue line is a classical nonparametric smoother of the raw data. It is significantly less variable than the raw data but under estimates the peaks and over estimates the valleys. The red line shows the bias-corrected smoother. Notice how it more aptly estimates the peaks and valleys with minimal change otherwise. Since radio-isotopes are identified based on the size and locations of peaks, using the bias-corrected smoother will improve identification.*

## References


1. Press, W.. Reconstructing the full internal state of a molecular phylogenetic tree with arbitrary branch-dependent substitution probabilities. 2006. *LA-UR 065816.*

2. Press, W., and H. Robins. Isochores exhibit evidence of gene interacting with large-scale genomic environment. 2006. *Genetics.* **174**: 1029.

3. Press, W.. Discrete Radon transform has an exact, fast inverse and generalizes to operations other than sums along lines. 2006. *Proceedings of the National Academy of Sciences.* **103**: 19249.

4. Press, W.. Bias beats profiling: an optimal strategy for detecting rare events. To appear in *Proceedings of the national academy of sciences.*

5. Hengartner, N., E. Matzner-Lober, and P. A. Cornillion. Recursive Bias Estimation for high dimensional regression smoothers. *Annals of Statistics.*

6. Hengartner, N., and E. Matzner-Lober. Asymptotic unbiased density estimation. To appear in *ENSAIM.*

7. Hengartner, N., E. Matzner-Lober, L. Rouviere, and T. Burr. Multiplicative bias corrected nonparametric smoothers with application to nuclear energy spectrum estimation. *Technometrics.*

8. Burr, T., N. Hengartner, E. Matzner-Lober, S. Myers, and L. Rouviere. Smoothing low resolution spectral data. To appear in *IEEE transaction on nuclear sciences.*


## Publications


Burr, T., N. Hengartner, E. Matzner-Lober, S. Myers, and L. Rouviere. Smoothing low resolution spectral data. To appear in *IEEE transaction on nuclear sciences.*

Hengartner, N., E. Matzner-Lober, L. Rouviere, and T. Burr. Multiplicative bias corrected nonparametric smoothers with application to nuclear energy spectrum estimation. *Technometrics.*

Hengartner, N., E. Matzner-Lober, and P. A. Cornillon. Recursive bias estimation for high dimensional regression smoothers. *Annals of Statistics.*

Hengartner, N., and E. Matzner-Lober. Asymptotic unbiased density estimation. To appear in *ESAIM.*

Press, W.. Bias beats profiling: an optimal strategy for detecting rare events. To appear in *Proceedings of the national academy of sciences.*

Press, W. H.. Reconstructing the Full Internal State of a Molecular Phylogenetic Tree with Arbitrary, Branch-Dependent Substitution Probabilities. 2006. *LA-UR 065816.*

Press, W. H.. Maximizing the Information Rate from Single-Molecule, Motion-Based DNA Sequencing Using RNA Polymerase. 2006. *LA-UR 065815.*

Press, W. H.. Discrete Radon transform has an exact, fast inverse and generalizes to operations other than sums along lines. 2006. *Proceedings of the National Academy of Sciences.* **103**: 19249.

Press, W. H., and H. Robins. Isochores Exhibit Evidence of Genes Interacting with the Large-scale Genomic Environment. 2006. *Genetics.* **174**: 1029.

Robins, H., and W. H. Press. Human microRNAs target a functionally distinct population of genes with AT-rich 3' UTRs. 2005. *Proceedings of the National Academy of Sciences.* **102** (43): 15557.

# Energy Distributions in Granular Flows

*Eli Ben-Naim*

20060305ER

## Abstract

This goal of this project was to investigate how energy is distributed in driven granular media. By analyzing how energy dissipation and energy injection counterbalance, this project provided quantitative understanding of the nonequilibrium nature of granular flows. Our mathematical modeling and simulation effort filled significant existing gaps in the theory, and answered important open questions raised by recent empirical observations. Modeling dynamical properties of nonequilibrium systems arises in LANL programs such as materials modeling, material packing, fluid instabilities, and multiscale modeling. Combining theoretical analysis, large-scale computation, and image analysis of experimental data, we determined how energy propagates in dilute and dense granular media. The following research projects were carried out.

1. Cascade dynamics was analyzed in spatially extended systems using asymptotic analysis and large-scale Molecular Dynamics simulations with rare but powerful energy injection.

2. Typical and extremal velocity statistics of driven granular systems with rotational motion and viscous damping was quantified using exact solutions and Monte Carlo simulations of the kinetic theory.

3. Onset criteria for the transition from stable to unstable flow and the development of stream instabilities in the flow of thin granular layers down an inclined plane were determined experimentally and understood using continuum theory.

This research produced needed granular flow models and advanced our understanding of the statistical mechanics of nonequilibrium systems.

## Background and Research Objectives

Granular media such as rocks, sand, and dust are ensembles of solid, weakly deformable, macroscopically-sized particles that interact via energy dissipating collisions in dilute settings and via contact forces in dense settings. Granular flows conserve mass and momentum, but they do not conserve kinetic energy. This fact has deep consequences. Most notably, the energy distribution does not adhere to the equilibrium Maxwell-Boltzmann distribution law.

This project developed mathematical and computational models that describe energy propagation and transfer in driven granular media. The theoretical framework used was primarily kinetic theory, and the overall goal of the project was to extend this framework to situations where rotational motion is dominant or where the granular media is immersed in a fluid environment. Another important goal is to study how energy cascades from large scales to small scales and how it cascades in space.

This research project combined theory, computation, and experiment to produce validated, predictive theoretical models. The theoretical methods include extreme statistics analysis and asymptotic methods, the computational techniques include direct molecular dynamics and Monte Carlo simulations, and the experimental studies will utilize high-speed video imaging to characterize particle velocities.

## Importance to LANL's Science and Technology Base and National R & D Needs

Granular flow underlies numerous industrial processes including transport, processing, and packing of granular products such as grains, pellets, and pills and natural processes such as propagation of sand dunes and some volcanic flows. Recently developed experimental characterization and theoretical modeling techniques

have significantly advanced our ability to model granular materials to the point that accurate measurements and quantitative predictions can be made. This project focuses on the role of energy dissipation, a defining feature of granular flows. This research quantified how energy is distributed in granular media using analytic theoretical techniques, advanced simulation methods, and experimental characterization.

Granular flow and packing is important for oil exploration, propagation of pollutants in porous media, transportation and storage of solid waste, weapons manufacturing and plastic-based-explosives, characterization of materials out of equilibrium. Hence, this research is relevant to several DOE missions including energy and environmental research, weapons physics, materials science, and modeling and simulation.

This project developed long term theoretical, computational, and experimental capabilities in granular flow and kinetics at Los Alamos National Laboratory. The project, through a significant number of visible theoretical and experimental investigations positioned Los Alamos in a competitive place in the rapidly growing area of research in granular physics. This research is widely supported by a number of national agencies such as the NSF, NASA, and DOE. The result of this project is that Los Alamos is viewed as a leader in theoretical and experimental modeling of granular flow and granular kinetics. Also, this project established numerous national and international collaborations with colleagues in academia, industry, and other national laboratories.

## Scientific Approach and Accomplishments

The work on this project included theoretical, computational, and experimental studies of granular flows and driven granular systems. The major focus was on solutions of the kinetic theory of driven granular systems and experimental characterizations of granular flows down an inclined plane. The key accomplishments are detailed in what follows.

**Discovery of singular energy distributions in driven and undriven granular flows**

We have developed a comprehensive kinetic theory that accounts for both the linear and rotational degrees of freedom. The primary feature of granular particles, energy dissipation through inelastic collisions is shown to result in significantly different energy statistics compared with ideal gases (reference 1). The energy is not partitioned equally among the different degrees of freedom. Instead, the partition of energy between rotational and linear motion follows a nonuniform distribution. We have discovered that this distribution has singularities and that special ratios of rotational-to-linear energy are preferred. This is a fundamental consequence of the nonequilibrium nature of granular matter and granular flows.

These discoveries are made possible through analysis of extremely energetic particles. Extreme statistics are given by a linear kinetic theory, that we developed, using a geometric representation of the velocities of the particles in a higher dimensional space. Analysis of this kinetic theory was performed through a combination of advanced theoretical and computational methods. The Monte Carlo simulation techniques used allow us to resolve the velocity distribution down to one in 100 trillion particles.

We also performed large scale molecular dynamics simulations of granular systems driven through rare but powerful injection of energy. These numerical simulations confirm the predictions of our theory qualitatively and quantitatively. In particular, the cascade picture where energetic particles transfer their energy to slower particles was confirmed numerically.

**Development of a kinetic theory for the energy distribution of sheared dense suspensions**

We have developed a kinetic theory for granular particles in a fluid. This theory accounts for dissipation thorough viscous damping as well as random forcing (reference 2). The equations for various quantities such as the Fourier transform of the velocity distributions were solved analytically and many characteristics of the form of the energy distributions were established through exact solutions and Monte Carlo simulations. Predictions of this theory were first verified against results of experiments involving driven granular media in fluids. Then, the theory was applied for explaining the results of large scale Lattice Boltzmann simulations of sheared dense suspensions where solid particles are immersed in a fluid. We have found that the velocity distribution have generic exponential tails, in contrast with the Gaussian tails expected in equilibrium. The theory provides understanding of the mechanism underlying the deviation from equilibrium distribution and was validated by the large scale simulations up to one in one million particles.

**Discovery of an exact solution of the kinetic theory of driven granular rods**

Another major achievement of this project is the discovery of an exact solution for the kinetic theory of a gas of inter-

acting vibrated granular rods. This mathematical framework takes advantage of the discrete Fourier spectrum of the angular distribution of rod orientation. We found that the angular distribution is related to iterated partitions of the integer numbers. This theory fully characterizes the phase transition from an ordered state at low driving to a disordered state at high driving. This kinetic theory represents an alternative framework for describing synchronization processes and it demonstrates the role of dissipation in nonequilibrium gases, the key theme of this project. Moreover, the mathematical solution methods can be applied to a general class of equations that involve convolution, including for example aggregation processes. This theory has a broad range of applicability for nonequilibrium phase transitions with relevance to granular particles, microtubules and molecular motors.

**Experimental characterization of granular flows**

We studied experimentally granular flow on an inclined plane. The system consists of a rough incline varying in length from 1 to almost 3 meters. Granular materials included glass beads, salt, sand, and copper particles of different shapes. For the first class of particles we sieved the particles into size distributions to determine the size dependence of phenomena we studied.

First, we determined the phase diagram of flowing granular material on a rough inclined plane as a function of plane angle. Below the angle of repose for bulk materials, there is no flow. At somewhat higher angle, there is intermittent or steady flow provided the layer thickness is large enough. The steady flow is unstable with respect to lateral variations in velocity and thickness at still higher angles. Finally, there is a liquid-gas transition of the layer where it essentially evaporates leaving no well defined layer provided the inclination angle is high enough. We discovered that contrary to theoretical predictions, air plays a negligible role in any measured property of the flow except when the layer evaporates. Even in this latter case the effects are minimal. Our work was the first to present an overall phase diagram of flow on a rough inclined plane.

Furthermore, flow on an inclined plane has become a standard system for understanding the complex constitutive relations (rheology) of granular materials. A very effective phenomenology was previously developed in which the depth-average velocity of the layer is scales as the three-half power of the layer thickness with a coefficient that depended on the details of the layer thickness where flow stops (for a particular angle). This power law dependence is consistent with a stress-strain rate condition postulated by Bagnold. We undertook a careful and extensive re-evaluation of this phenomenology for eight different materials and a variety of mean sizes. We found that the existing phenomenology works well for glass beads and sand provided the particle size was less than or comparable to the surface roughness. Nevertheless, the relationship between velocity and height could be improved by a correction suggested from kinetic theory. For copper particles, however, the existing scaling law was not a satisfactory description for the results, with velocity scaling linearly with the height. This result remains unexplained theoretically.

Finally, in the intermittent regime of flow, avalanches form with surprising properties. In a comprehensive investigation of avalanche properties, we showed how one can understand avalanches as falling into one of two classes. For smooth, spherical particles, avalanches are governed by a condition at the front where the material in front of the avalanche collapses. The avalanches in this case have a particle velocity less than the front velocity, are relatively slow and can be described quite well by a depth-averaged approach that yields a Burgers equation shock profile to reasonable accuracy. In contrast to the theory, however, the avalanches do not decay but sustain a compact and localized form, reminiscent of a solitary structure. We also explored quantitatively the extent to which this latter observation is verified. For irregular particles or particles with a high inter-particle friction coefficient, more potential energy is built up before the layer starts to avalanche. The resulting avalanches have more inertia and are higher and faster than corresponding avalanches in glass bead systems. This latter type of avalanche is a cascading flow where grains move faster than the front in a motion similar to a cresting, breaking wave on a beach. Indeed the theory for the two is very similar. Despite the remarkably good agreement between theory and experiment, there are some gaps in the theory that still need to be addressed.

**Conclusion**

Quantitative understanding of the non-equilibrium nature of granular flows was developed by analyzing how energy dissipation and energy injection counterbalance. This project combined theoretical, computational, and experimental studies to produce validated, predictive models of granular flows. This project further developed the standard theoretical framework, kinetic theory, to situations where rotational motion dominates, and situations where the granular media is immerse in a fluid environment. Also, the propagation of energy from large to small scales was quantified. The results of this research significantly advanced our understanding of systems driven out of equilibrium and it contributes to better granular flow models.

## References


1. Ben-Naim, E., and J. Machta. Stationary States and Energy Cascades in Inelastic Gases. 2005. *Phys. Rev. Lett..* **94**: 138001.

2. Kohlstedt, A., K. Snezhko, M. Sapozhnikov, I. Aranson, J. Olafsen, and E. Ben-Naim. Velocity Distributions of Granular Gases with Drag and with Long-Range Interactions. 2005. *Phys. Rev. Lett..* **95**: 068001.


## Publications


Ben-Naim, E., B. Machta, and J. Machta. Power-law velocity distributions in granular gases. 2005. *Phys Rev E.* **72**: 021302.

Ben-Naim, E., and A. Zippelius. Singular energy distributions in driven and undriven granular media. 2007. *J. Stat. Phys..* **129**: 677.

Ben-Naim, E., and J. Machta. Stationary States and Energy Cascades in Inelastic Gases. 2005. *Phys. Rev. Lett..* **94**: 138001.

Ben-Naim, E., and P. Krapivsky. Alignment of Rods and Partition of Integers. 2006. *Phys Rev E.* **73**: 031109.

Ben-Naim, E., and P. Krapivsky. Condensates in driven aggregation processes. 2007. *Phys. Rev. E.* **75**: 011103.

Borozsonyi, T., T. Halsey, and R. Ecke. Avalanche dynamics on a rough inclined plane. 2008. *Phys. Rev. E.* **78**: 011306.

Borozsonyi, T., and R. Ecke. Rapid Granular Flow on a Rough Incline: Phase Diagram, Gas Transition, and Effects of Air Drag. 2006. *Phys. Rev. E.* **74**: 061301.

Borozsonyi, T., and R. Ecke. Flow rule of dense granular flows down a rough incline. 2008. *Phys. Rev. E.* **76**: 031301.

Daya, Z., E. Ben-Naim, and R. Ecke. Experimental characterization of vibrated granular rings. 2006. *Eur. Phys. Jou. E..* **21**: 1.

Harting, J., H. Herrmann, and E. Ben-Naim. Non-equilibrium velocity distributions in sheared hard-sphere suspensions. 2008. *EPL.* **83**: 30001.

Herrmann, H., J. Harting, M. Hecht, and E. Ben-Naim. Simulation of Dense Colloids. 2008. *Brazi. Jour. Phys..* **38**: 37.

Libal, A., C. Reichhardt, and C. J. O. Reichhardt. Realizing colloidal spin ice on arrays of optical traps. 2006. *Phys. Rev. Lett..* **97**: 228302.

Reichhardt, C., and C. J. O. Reichhardt. Stripes, clusters, and nonequilibrium ordering for bidisperse colloids with repulsive interactions. 2007. *Phys. Rev. E.* **75**: 040402.

# A Faster Multipole Method

*Michael S Warren*

20060350ER

## Abstract

Fast multipole methods (FMM) have become an ubiquitous tool for the simulation of physical systems with long-range interactions. Since their introduction they have been applied to a vast range of problems, but limitations in the algorithms are impeding progress in areas as diverse as biology, materials science and astrophysics. We have made considerable progress in creating a novel parallel adaptive FMM by combining a number of techniques, which have been discussed in the literature, but have not been combined or fully exploited in any existing method.

## Background and Research Objectives

Fast multipole methods have become a fundamental element in the study of complex physical systems, in part because they are inherently adaptive and do not require the imposition of a lattice. Because interactions occur between each pair of bodies (particles, atoms or other discrete entity) in an N-body simulation, the computational work scales asymptotically as N squared. The FMM allows N-body simulations to be performed on arbitrary collections of bodies in time much less than N squared. FMM scaling is usually quoted as being of order N or order N log N. The technique uses a truncated expansion to approximate the contribution of many bodies with a single interaction. The basic idea of an N-body algorithm based on a truncated series approximation is to partition an arbitrary collection of bodies in such a manner that the approximation can be applied to the pieces, while maintaining sufficient accuracy in the force (or other quantity of interest) on each particle.

Fast multipole algorithms that use adaptive tree data structures are also referred to as treecodes. By their nature, treecodes are inherently adaptive and are most applicable to dynamic problems with large density contrasts, while fast multipole methods have been mostly non-adaptive and applied to fairly uniform problems needing high accuracy. This distinction is for the most part artificial, as the same mathematical and performance analysis can be applied to both.

## Importance to LANL's Science and Technology Base and National R & D Needs

A significantly faster multipole method will allow us to push the envelope of biomolecular simulation to 100 million atoms, enabling the study of small and medium sized viruses, as well as complexes of proteins, and enable larger simulations using gravitational N-body methods to probe the nature of dark energy. The multidisciplinary expertise and high-performance computing capabilities at Los Alamos make this one of the few, if not the only, institution in the world with the capability to tackle these problems. While special-purpose fast multipole methods are proliferating in a number of application areas, we have developed a general solution that will enable scientists to tackle the most formidable problems in a wide range of relevant application areas.

For several decades, molecular dynamics (MD) simulations have been an important tool in statistical mechanics, with applications ranging from equation of state calculations, to non-equilibrium behavior such as transport coefficients. Short-range potentials can be naturally computed with order N cost (even for many-body potentials) if the range of the potential is much shorter than the size of the simulation box, since each atom only interacts with a small number of neighbors. However, for charged systems, e.g. ionic solids, where Coulombic interactions are unavoidable, the FMM has become the tool of choice.

Computational methods have been used in biology for sequence analysis (bioinformatics), all-atom simulation (molecular dynamics), and more recently for modeling biological networks (systems biology). Of these three techniques, all-atom molecular dynamics simulation is the most computationally demanding, with respect to compute load, communication speed, and memory

load. Because of this heavy compute load, biomolecular simulations have been limited to relatively small systems such as single proteins or complexes of a small number of proteins, which are a simplified model system of a realistic environment within the cell. The bottleneck in these calculations is the long-range force calculation. These forces are essential for accurate dynamics due to the large number of charges typically present. One example is DNA, which contains two negatively charged phosphates for each pair of bases that establish the genetic code. In solution, positive ions such as sodium and potassium interact to neutralize these charges over large scales, but a reasonable solution to their dynamics requires accurate computation of the Coulombic interactions over significant distances.

## Scientific Approach and Accomplishments

Our primary objective is the development of a method which can simulate systems over ten times larger than the current state-of-the-art, while staying within a reasonable allotment of supercomputer time (on the order of a million processor hours per year per application). We have developed multipole acceptance criteria and error analysis combined with the pseudo-particle approach to compute fewer interactions faster, while maintaining acceptable accuracy; We have also optimized the implementation of the algorithm to account for the limitations inherent in modern computing architectures (both at the microprocessor level, and the parallel system level), including the implementation of the most important parts of the code on the new Roadrunner computer system at Los Alamos.

Consider a configuration of sources as in Figure 1. The sources are contained within a ``source'' cell of radius bmax, while the field is evaluated at separation D from x0, the center of ``sink'' cell. We use a bound on the error in terms of properties of the source cell, the sink cell, and the separation between them, and it can be used to decide, dynamically, when the multipole approximation is accurate enough to be used between a pair of cells. The error bound is essentially a precise statement of several intuitive ideas. Interactions are more accurate when:

1. The interaction is weak, or it is well-approximated by its lower derivatives.
2. The sources are distributed over a small region.
3. The field is evaluated near the center of the local expansion.
4. More terms in the multipole expansion are used.
5. The truncated multipole moments are small.

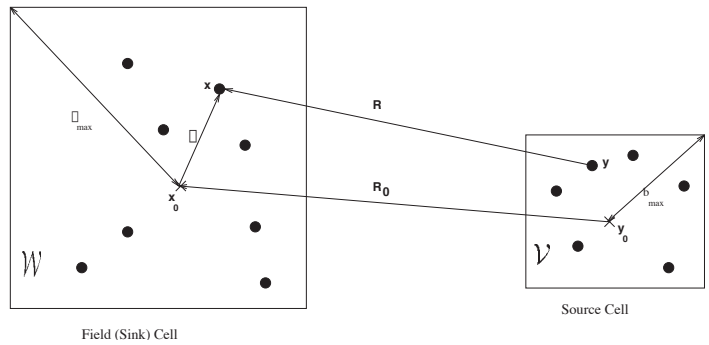


*Figure 1. An illustration of the relevant distances used in the error bound equation.*

We contributed a benchmark for gas-dynamics including gravity to a publication describing our smoothed particle hydrodynamics (SPH) code [1]. Improving upon our already state-of-the-art performance, we have also completed implementing a pseudo-particle method up to quadrupole order, along with associated implementation of flexible periodic boundary conditions. The performance of the pseudo-particle method is substantially better than either the monopole or quadrupole method at equivalent accuracy, although the exact factor depends on the definition of accuracy used. Even further performance improvements were gained via updating the assembly language implementation of the inner force-interaction loop for gravity for the x86_architecture. The assembly language routines typically offer a 10x speedup over high-level languages like C and FORTRAN [2].

We implemented the pseudo-particle method to quadrupole order, and investigated efficient approaches for higher orders. We also implemented periodic boundary conditions with support for large aspect ratios. Figure 2 represents a ``light-cone'' of large scale structure calculated with these new boundary conditions.

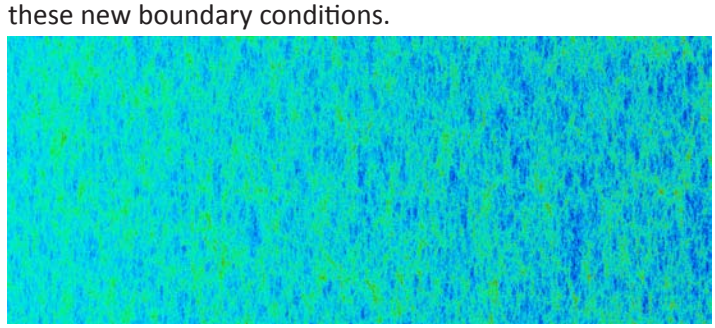

*Figure 2. This image represents the evolution of dark matter in the Universe. The large aspect ratio of the computational volume was enabled by new code implemented as part of this project. This 'light cone' graphically demonstrates the increased clustering of dark matter over time, with less clustering on the left hand side of the image. Due to the time it takes light to travel from one side of the volume to the other, we are able to look back in time to see structure in the Universe as it appeared billions of years ago.*

Several virus systems were investigated for feasibility of large-scale simulation. The criteria for simulation were the size of the resulting system, availability of structure, and impact to the understanding of viral function. The four most promising systems are (1) T4 bacteriophage (1000 Angstrom length, 15 million atoms), (2) HK97 bacteriophage (500 Angstrom diameter, 20 million atom system), (3) polio virus (300 Angstrom diameter, 10 million atom simulation) and (4) phi29 virus (200 Angstrom diameter, 3 million atoms). Simulations of the T4 bacteriophage will elucidate the mechanism of phage docking to the host cell by studying conformational changes in the stalk of the phage particle. Simulations of HK97 will study the affect of viral RNA on the structural stability of the surrounding capsid. Simulations of the polio virus will examine deformation of the host membrane due to viral entry. Simulations of phi29 will study the mechanism of viral genome packaging inside the capsid. We have performed feasibility studies to determine which system is most amenable to molecular dynamics simulations.

To establish a baseline for large-scale simulations of biomolecular systems, scaling studies of the NAMD (NAnoscale Molecular Dynamics, developed at the University of Illinois) code on the were performed for several systems of different size, including the ribosomal decoding center (16,300 atoms), transfer RNA (57,300 atoms), apoa1 (92,200 atoms), f1ATPase (328,000 atoms), small ribosomal subunit (1,070,000 atoms), intact ribosome (2,030,000 atoms) and ribosome with extended mRNA (2,640,000 atoms). Scaling improves dramatically for larger system sizes with 85% efficient scaling for the largest system. The 'turn-over' point, beyond which systems show improved speed with the number of processors, is approximately 100,000 atoms. The dynamic load-balancing in NAMD significantly improves scaling efficiency. The results were published in the Journal of Physics and the Journal of Structural Biology (see [3] and [4]).

Work on the materials aspect of the problem has gone towards constructing a test system composed of an ionic crystal (ammonium perchlorate) for benchmarking against the LAMMPS (LArge-scale Atomic/Molecular Massively Parallel Simulator) MD code developed at Sandia. We are also investigating the structure of LAMMPS to evaluate the best interface for implementation of the new multipole method cleanly within its current design. We also implemented Lennard-Jones interactions within the HOT framework, and tested the parallel implementation against LAMMPS as well as developing file translation routines to convert to and from LAMMPS format.

We developed large-scale test problems and run them with GROMACS (GROningen Machine for Chemical Simulations, a molecular dynamics simulation package originally developed at the University of Groningen). Familiarity with GROMACS was established as a prelude to using its biological interaction routines. Benchmarks and tests have been developed concurrently and will provide a means to verify the accuracy of the code, before attempting more demanding simulations. We further tested and optimized scaling of GROMACS on 15,000 , 1M, 2M and 18M atom systems. An example of a system used to test and evaluate different algorithms is the satellite tobacco mosaic virus, shown in Figure 3.

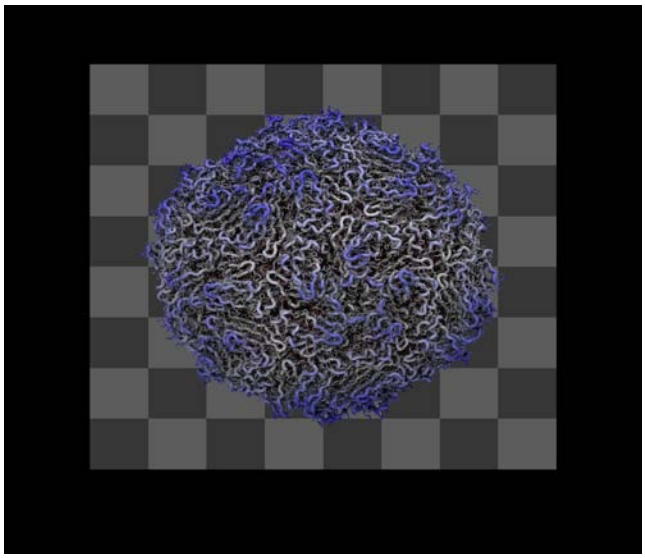

*Figure 3. Atomic structure of the satellite tobacco mosaic virus. The three-dimensional structure of this virus is well characterized by x-ray crystallography. The icosahedral plant virus consists of 60 identical protein subunits which encapsulate the ~1000 base RNA genome. This virus represents an ideal test system for large-scale biomolecular simulations. We have performed preliminary simulations of the virus with GROMACS using approximately 18 million atoms. The protein backbone atoms are represented by tube rendering while amino acid side chains are represented by bond rendering. Atoms are color-coded according to the distance from the center of the capsid, with dark blue furthest away from the center, and light blue, white and pink/red successively closer to the center.*

We ported code to the AMD opteron component of RoadRunner and to the power processing unit (PPU) and synergistic processing unit (SPU) components of RoadRunner, individually and implemented an abstraction that allows us to offload computation to the Cell processor.

For biological systems, we implemented the highest-use kernel (water-water) based on work at UNC and modified GROMACS to support the IBM Data Communication and

Synchronization (DaCS) libraries for accelerating its nonbonded calculations on the Cell processors. These modifications include launching the Cell processes, overhaul of the memory subsystem to support aligned buffers, minimalist on demand direct memory access (DMA) transfers, and the initial port of the water-water nonbonded kernel on the Cell broadband accelerator. The framework is in place to enable the rapid addition of additional nonbonded kernels on the Cell processor. Additionally, the gravity kernel was ported to the cell processor, obtaining over 60% of peak performance.

When preparing a large-scale molecular dynamics (MD) simulation of polymeric materials, one faces the significant challenge of creating the realistic input for the software. While excellent automated tools exist for the actual MD computations, creating the initial model representation can require substantial amounts of time and manual effort from the user. This process entails specifying particle coordinates, atom types, chemical bonds, valence angles, and torsional constraints. Commercial simulation packages often include so-called "builders" that aid in this process and can accommodate the import of standard file types, such as protein data base (pdb) files. However, these commercial packages present drawbacks to users that may wish to modify or augment the capabilities of the MD code since the source is not readily available. Moreover, these builders typically lack the ability to construct elaborate mesoscale models. Fortunately, freely available open source codes are becoming more robust and competitive compared to their commercial counterparts. Sandia National Laboratory's LAMMPS MD code is an excellent example of this class of software and presents particular interest to this effort. Because of its versatility and excellent performance, LAMMPS also finds use at LANL in several different programs. However, LAMMPS does not include a builder capability, thus hindering our efforts to employ it in large-scale simulations of polymeric and biological materials of interest in the context of this LDRD.

To remedy this, we have developed a standalone builder for large-scale MD simulations entitled "Bob". The central tenet driving Bob's design is that building a complicated polymer simulation should be easy for the user. Though still under development, the present version enables the user to create a simulation box with a variety of molecular species in a simple script. Presently, several coarse-grained models of polymers can be specified, including linear chains, star-branch polymers, dendrimers, and networks. All-atom models are accommodated via a homopolymerization function that reads in a monomer file containing the chemical details; all the user need do is specify the number of chains and degree of polymerization required. The code will also read in existing LAMMPS data files, permitting the addition of new species. For example, Figure 4 contains an image of a build produced by Bob of an organic crystal surrounded by polymer. The crystal was previously prepared using commercial tools commonly used for the creation of small molecule builds. The polymer was added by Bob.

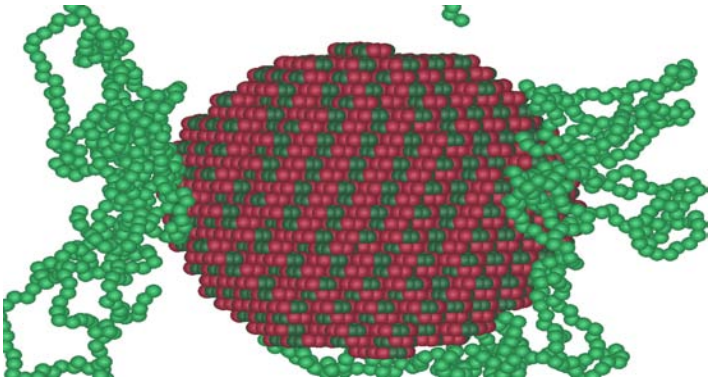

*Figure 4. An image of an organic crystal with united atom polymer chains produced by the initial conditions builder (Bob) developed during our project.*

More recent efforts are focused on adding the ability to read pdb files. As in the case of the all-atom polymers, the approach is to construct monomer files containing the chemical details for the protein amino acids. A simple solvation function that places SPC model water molecules around the polymer has already been implemented. Once the pdb module is completed and the code has undergone substantial internal vetting, it will be released as an open source product. Moreover, this software will continue to find use in new efforts beginning in FY09, including large-scale atomistic simulations of lipid membranes with nanoparticles.

Capabilities developed during this research were essential to enabling a new project on Roadrunner "Cellulosomes in Action: Peta-Scale Atomistic Bioenergy Simulations."

## References


1. Fryer, C. L., G. Rockefeller, and M. S. Warren. SNSPH: a parallel three-dimensional smoothed particle radiation hydrodynamics code. 2006. *Astrophysical Journal.* **643**: 292.

2. Warren, M. S., and J. Wofford. Astronomical data analysis with commodity components. 2007. *International Conference for High Performance Computing, Communications and Storage (SC'07).*

3. Sanbonmatsu, K. Y., and C. S. Tung. Large-scale simulations of the ribosome: a new landmark in computational biology. 2006. *Journal of Physics: Conference Series.* **46**: 334.

4. Sanbonmatsu, K. Y., and C. S. Tung. High performance computing in biology: multimillion atom simulations of nanoscale systems. 2007. *Journal of Structural Biology.* **88**: 470.

## Publications

Abate, A., S. Bridle, L. F. A. Teodoro, M. S. Warren, and M. Hendry. Peculiar velocities into the next generation: cosmological parameters from large surveys without bias from non-linear structure. 2008. *Monthly Notices of the Royal Astronomical Society.* **389**: 1739.

Fryer, C. L., G. Rockefeller, and M. S. Warren. SNSPH: a parallel three-dimensional smoothed particle radiation hydrodynamics code. 2006. *Astrophysical Journal.* **643** (1): 292.

Huff, E., A. E. Schulz, M. White, D. J. Schlegel, and M. S. Warren. Simulations of baryon oscillations. 2007. *Astroparticle Physics.* **26**: 351.

Sanbonmatsu, K. Y., and C. S. Tung. Multimillion atom simulations of the ribosome. 2007. *Journal of Structural Biology.* **88**: 470.

Sanbonmatsu, K. Y., and C. S. Tung. Large-scale simulations of the ribosome: a new landmark in computational biology. 2006. *Journal of Physics: Conference Series.* **46**: 334.

Tinker, J. L., A. V. Kravtsov, K. Abazajian, M. S. Warren, G. Yepes, S. Gottlober, and D. E. Holz. Toward a halo mass function for precision cosmology. *Astrophysical Journal.*

Warren, M. S., K. Abazajian, D. E. Holz, and L. Teodoro. Precision determination of the mass function of dark matter halos . 2006. *Astrophysical Journal.* **646** (2): 881.

Warren, M. S., and J. Wofford. Astronomical data analysis with commodity components. 2007. *International Conference for High Performance Computing, Communications and Storage (LA-UR 07-5543).*

Wetzel, A. R., A. E. Schulz, D. E. Holz, and M. S. Warren. Close pairs as proxies for galaxy cluster mergers. 2008. *Astrophysical Journal.* **683**: 1.

full final report

# Novel Physics Inspired Approach to Error-Correction

*Michael Chertkov*

20060473ER

## Abstract

Modern technologies heavily rely on a wide range of error-correcting mechanisms to circumvent their inherent unreliability and to ensure faithful transmission, processing and storage of information. There has been a great deal of research activity in coding theory in the last half a century that has culminated in the recent discovery of coding schemes that approach reliability limit. One of the main obstacles for wider use of these new codes is that due to complex behavior of their decoding algorithms no systematic methods which would allow characterization of the Bit-Error-Rate are known. This is especially true at the high values of the Signal-to-Noise-Ratio where many systems operate. A new generation of communication systems in which extremely low BER are required (e.g., ~1 error per 10^12 bites in optics communications) is creating new challenges for error-correction technology. One of the main obstacles for implementing efficient codes is the emergence of the so-called error-floor, which is essential slow-down of the BER decay with the SNR increase. For most of the applications/channels this effect was neither formulated analytically nor understood numerically, while the current Monte-Carlo simulation approach is not practical when the target is less than 10^(-8:-9) for BER requiring a large number of simulations.

This project develops a physics inspired approach for the calculation of extremely low post error correction Bit-Error-Rates, thus offering a comprehensive tool for quantitative comparison of competitive coding/decoding schemes. In addition, the approach offers new insights into the mechanisms of coding/decoding BER control/optimization.

We develop computational toolbox to describe statistics of rare events for modern error-correction schemes. We address the problem of how to evaluate BER in critical applications where it must be extremely low, while experimental and brute-force numerical approaches are prohibitively expensive or impossible. The ability to find the most probable noise configuration of the channel noise that causes an error-correction scheme to fail provides a way to estimate the actual performance of the scheme. These results will help to distinguish good codes from bad ones and to see where bad codes need improvement/correction.

## Background and Research Objectives

Classic information theory [1] gives a theoretical foundation, but not quite a practical solution, on how to realize an error control system through coding. The high SNR (low noise) regime is of particular interest because of a special feature of the modern codes achieving the limit of reliable transmission, which is referred to as an error floor. Error floor is a phenomenon of an abrupt degradation of the coding scheme performance, measured by BER, from the so-called water-fall regime of moderate SNR to the absolutely different error-floor asymptotics achieved at high SNR. Typical BER values are $10^{-12}$ for an optical communication system, $10^{-15}$ for hard drive systems in personal computers and as small as $10^{-18}$ for storage systems used in banks and financial institutions. However, direct numerical methods, e.g. Monte Carlo, cannot be used to determine BER below $10^{-9}$.

The problem is really generic and it also emerges in various information technology, computer science and reliable/security communication applications across many Divisions and Programmatic efforts at LANL. Thus the task of addressing the domain of extremely low BER is very relevant in connection with the current architecture of supercomputers at DOE complex, in which many processors with large on board caches are strung together. The development of computationally efficient error-correcting codes with high Signal-to-Noise-Ratio (SNR) will have a significant impact on our computational ability. But for this to happen, we need first to develop methods to evaluate the post error-correction BER in high SNR environments. Another LANL relevant task is in developing Low-Density-Parity-Check (LDPC) codes, that may be, e.g., applied to securing classical

key-distribution channel in the quantum-cryptography test bed experiment.

To address the challenge we suggest in-house LANL-developed physics-inspired approach that, according to our pilot research, should ultimately solve the problem of the error-floor analysis. The method is coined instanton, after a theoretical particle developed in quantum physics that lasts for only an instant, occupying a localized portion of space-time. Statistical physics applies the notion of instanton to a microscopic configuration which, in spite of its rare occurrence, contributes most to macroscopic behavior of the system. Our instanton is the most probable configuration of the noise that causes a decoding error.

Let us consider a model of a general communication system with error correction. Data originating from an information source are parsed into fixed length words. Each word is encoded into a longer codeword and transmitted through a noisy channel (e.g., radio or optical link, magnetic or optical data storage system, etc.). The decoder tries to reconstruct the original codeword using the knowledge of the noise statistics and the structure of the code. Error resilience is achieved at the expense of introduced redundancy, and the information theory gives conditions for the existence of finite redundancy error correction codes. However it does not give a method for realizing decoders of low complexity. In general there is no better way to reconstruct a codeword that was most likely transmitted then to compare likelihoods of all possible codewords. However, this Maximal Likelihood (ML) algorithm becomes intractable already for codewords that are tens of bits long.

Novel exciting era has started in the coding theory with the discovery of Low-Density Parity-Check (LDPC) [2,3]. These codes are special not only because they can ideally achieve the virtually error-free transmission limit, but mainly because a computationally efficient, so-called iterative, decoding was readily available. When operating at moderate noise values these approximate decoding algorithms show an unprecedented ability to correct errors, the remarkable feature that attracted a lot of theoretical attention. It is believed that the error floor is a fundamental consequence of iterative decoding, and that the approximate algorithms mentioned above are incapable of matching the performance of ML decoding in reducing errors beyond the error-floor threshold. The importance of error-floor analysis was recognized on the early stages of the turbo codes revolution, and it soon became apparent that LDPC codes are also not immune from the error-floor deficiency. The most noticeable approache to the error-floor analysis problem proposed so far was a heuristic approach of the importance sampling type [4], utilizing theoretical consideration developed for a typical randomly constructed LDPC code performing over the very special binary-erasure channel.

Our approach to the error-floor analysis is different. We suggest an efficient calculation scheme, which is ab-initio by construction, i.e. the scheme requires no additional assumptions (e.g. no sampling). This is one of the rare situations when simultaneous development of theoretical and numerical approach is not only useful but is proven to be of a great value for cross-fertilization of the ideas. Finally, the numerical instanton scheme we propose to develop is generic, as it bears restrictions neither to the channel no to decoding types.

This proposal will address the following fundamental problems of coding theory: 1) developing computationally tractable approach to estimating BER for various practical schemes, e.g. LDPC codes decoded iteratively; 2) designing new high-performance realistic (finite word length) codes; 3) finding optimal (fast and/or efficient/cheap) ways to decode a given code.

Currently, the major stumbling block in this line of research is our inability to accurately estimate the post error-correcting BER for realistic codes in low noise channels. Our proposed research will solve this problem by developing both the theoretical underpinnings and the associated numerical and simulation tools necessary to produce reliable estimates for very small, $10^{-15}$ or smaller post error-correcting BERs.

Finding a good finite length coder/decoder is an application specific task. The quality of a coder/decoder depends on both the level and type of dependency structure of the noise in the channel. Indeed, past experiences suggest that good codes for one type of channel (for example metro-area optical networks) may not be suitable for another type (such as open-space communications). The reason is simple: the channel specific noise structure depends crucially on the application. This dependency of the coder/decoder on the application specific noise structure is another extremely important, but only marginally developed, subject that be investigated under this proposal.

Our approach has two components:

First, we characterize analytically (or semi-analytically) extremal noise configurations producing the largest after error-correction bit error rate using saddle-point approximations, which are also known as optimal fluctuation or instanton calculus in statistical physics.

Second, we plan to apply the method to developing new and improving existed coding/decoding schemes.

Our R&D goal is to contribute solving the following fundamental tasks in coding theory: (i) developing computationally tractable approach to estimating BER for various practical schemes, e.g. LDPC codes decoded iteratively; (ii) designing new high-performance realistic (finite word length) codes; (iii) finding optimal (fast and/or efficient/cheap) ways to decode a given code.

## Importance to LANL's Science and Technology Base and National R & D Needs

The project is important for development of high speed supercomputer links and lines capable to transmit securely and reliably large amount of data. Other area of current research at LANL which benefits from the project is the development of efficient algorithmic solutions for computationally hard tasks. This interdisciplinary research in the field of a new generation of error-correction codes utilizes the tools of modern statistical physics, information theory and computer science. It is of both fundamental scientific and practical importance. The results of the proposed research will find applications/customers in Homeland Security, Threat Reduction and the ASCI (supercomputers) programs. It will further stimulate important new developments in the following areas that are relevant for LANL/DOE interests and expertise: Information science, High speed data processing, Fast manipulation of large amounts of information, Fine time resolution of ultra-fast/optical processes, moving, storing and processing large amounts of data generated by supercomputer facilities, and Reliable and secure communication of various sorts (wireless, satellite, cable, etc).

## Scientific Approach and Accomplishments

The results of our research are poised to make a substantial impact on the areas of high speed data transmission, data processing and information theory. We develop the following set of methods which should create a major breakthrough in informatics and the estimation of errors remaining after correction.

- A major product of the research is the creation of the Instanton/Pseudo-codeword-search toolbox capable of optimizing error correction performance, thereby helping in the design of new codes/decoders applicable to a broad range of modern technologies. We illustrated performance of the instanton-pseudo-codewords technique on examples of Additive-White-Gaussian-Channel, Binary Symmetric Channel and Channel with Inter-Symbol Interference. The approach was successfully tested on variety of medium-to-large-size Low Density Parity Check Codes.

- We also developed a new theoretical technique, coined Loop Calculus, which allows to relate efficient but suboptimal decoding schemes, such as Belief Propagation and Linear Programming decoding, to the optimal Maximum Likelihood and Maximum Aposteriori decoding. Combination of the Instanton/Pseudo-codeword search approach and the Loop Calculus technique suggests an improved decoding scheme, capable of reducing the error-floor caveat of the graph-based codes.

- We suggested a novel code-construction technique which guarantees an improved performance in the error-floor domain (of large signal-to-noise ratios) while keeping the same performance in the water-fall domain (of-small-to-moderate signal-to-noise ratios). The construction was tested for Low-Density-Parity Check Codes of medium size performing over Additive-White-Gaussian and Binary-Symmetric Channels.

- Algebraic codes are the most widely deployed class of error correction codes. They are attractive because of their provably good worst case performance guarantees. However decoding techniques for these classes of codes have not benefited from the huge advances being made in iterative decoding techniques for sparse graphical codes and low density parity check codes. The reason for this is the dense nature of the parity checks associated with the common algebraic codes. We have developed a variety of techniques which can efficiently transform a dense code representation to a sparse graphical form. We leveraged on these techniques to propose new decoding algorithms for general linear codes.

- Product code constructions are widely used in satellite communication and optical-fiber backbones. Iterative decoders have been proposed for such codes based on variants of the Belief propagation algorithm. We have recently proposed an accurate and tight theoretical analysis of such a general recursive product code decoder. This provides for the first time ever a tight theoretical guarantee on the performance of a general product code decoder.

## References


1. Shannon, C. E.. A mathematical theory of communication. 1948. *Bell System Technical Journal* . **27**: 379.
2. Gallager, R. G.. Low density parity check codes. 1963.
3. Richardson, T., and R. Urbanke. The renaissance of Gallager's low-density parity-check codes. 2003. *IEEE Communications Magazine* . **41**: 126.
4. Richardson, T.. Error Floors of LDPC Codes. Invited presentation at *2003 Allerton Conference.* (Allerton, Illinois, September 2003).


## Publications


Anguita, J. A., M. Chertkov, B. Vasic, and M. A. Neufeld. Bethe-Free-Energy Based Decoding of Low-Density Parity-Check Codes on Partial Response Channels. *IEEE Journal of Selected Areas in Communications.*

Chertkov, M.. Reducing the Error Floor. To appear in *Information Theory Workshop '07 on 'Frontiers in Coding'.* (Lake Tahoe, 2-6 Sep, 2007).

Chertkov, M., and M. Stepanov. An efficient pseudo-codeword-search algorithm for linear programming decoding of LDPC codes. To appear in *IEEE Transactions on Information Theory +arXiv:cs.IT/0601113+ LAUR-06-0124/06-6751.*

Chertkov, M., and M. Stepanov. Pseudo-codeword Landscape. To appear in *Proceedings of IEEE ISIT 2007.* (Nice, June 20-26, 2007).

Chertkov, M., and M. Stepanov. Searching for low weight pseudo-codewords. To appear in *2007 Information Theory and Application Workshop, proceedings.* (San Diego, CA, Jan 26-Feb 2, 2007).

Chertkov, M., and V. Chernyak. Loop calculus in statistical physics and information science. 2006. *Physical Review E + cond-mat/0601487 + LAUR-06-0443.* **73**: 065102.

Chertkov, M., and V. Chernyak. Loop series for discrete statistical models on graphs. 2006. *Journal of Statistical Mechanics + cond-mat/0603189 + LAUR-06-1221.* **P06**: P06009.

Chertkov, M., and V. Chernyak. Loop calculus helps to improve belief propagation and linear programming decodings of low-density-parity-check codes. To appear in *44th Allerton Conference on Communication, Control, and Computing + cs.IT/0609154 + LAUR-06-6751.* (Allerton, IL, 27-29 Sep. 2006).

Chilappagari, S. K., M. Chertkov, M. Stepanov, and B. Vasic. Instanton-based Techniques for Analysis and Reduction of LDPC Error-floors. *Special issue of IEEE JSAC on Capacity Approaching Codes.*

Chilappagari, S. K., M. Chertkov, and B. Vasic. Provably Efficient Instanton Search Algorithm for LP-decoding over the BSC. *Submitted to IEEE IT.*

Santhi, N.. The Secant Method Decoder. Invited presentation at *LANL CNLS Workshop on Algorithms, Inference and Statistical Physics.* (Santa Fe, May 1-5, 2007).

Santhi, N.. On Algebraic Decoding of $q$-ary Reed-Muller and Product Reed Solomon Codes. To appear in *ISIT 2007.* (Nice, June 20-26, 2007).

Santhi, N.. Weighted Maximum Likelihood Decoding of (3,3)-LDPC codes is NP hard. Presented at *IEEE ISIT 2008.* (Toronto, July 2008).

Santhi, N., M. Chertkov, and A. Hansson. Least Contradictory Tree Scheduling, Radial Scaling and Gap Amplification for Improved Loopy Belief Propagation. Presented at *IEEE ISIT 2008.* (Toronto, July 2008).

Stepanov, M., and M. Chertkov. Instanton analysis of Low-Density-Parity-Check codes in the error-floor regime. To appear in *ISIT (International Symposium of Information Theory) + arXiv:cs.IT/0601070+LA-UR-06-0126.* (Seattle, 9-14, July 2006).

Stepanov, M., and M. Chertkov. Improving convergence of belief propagation decoding. To appear in *44th Allerton Conference on Communication, Control, and Computing + cs.IT/0607112 + LAUR-06-5058.* (Allerton, IL, Sep 27-Sep 29, 2006).

# Simulation and Modeling of the Quantum Response

*Anders Mauritz Niklasson*

20060551ER


## Abstract

We have explored and developed computational simulation techniques that are based on highly efficient recursive formulations of quantum mechanical problems for the calculation of basic materials properties. Such problems include materials response to various perturbations, for example, energy response due to external or internal perturbations, including energy gradients or the nuclear forces. These properties are all required in studies of predictive quality that employ atomistic simulation that are based directly on the first principles of quantum mechanics. The main goal of this exploratory research proposal was the development of new general electronic structure technologies for quantum response calculations that combine a very high accuracy with a low computational cost. This would allow detailed theoretical studies of systems with a large number of atoms beyond the reach of current methods with new algorithms that can take full advantage of increases in computer capacity.


## Background and Research Objectives

Almost any material properties such as the hardness of a diamond, the color of gold, the crystal structure of iron at the center of earth, or the folded protein structure of hemoglobin in human blood, can in principle be determined directly from theory based on the first principles of quantum mechanics. The only obstacle to predict these properties is the enormous computational complexity required in solving a set of quantum mechanical equations that were formulated already over 80 years ago. Despite the enormous increase in computer power during the last 60 years, we are still far from predicting many important problems directly from theory. One fundamental problem can be traced back to history. When scientist like Heisenberg, Schrodinger, and Dirac first proposed quantum mechanics, electronic computers did not exist. The original formulations of quantum mechanics therefore evolved in the framework of fairly simple analytical techniques that were available at the time to perform calculations. Many of the first descriptions of quantum mechanics are still used today, despite the fact that they are not very well adapted to modern computing. One particular problem that has been addressed during the last 10 years is the increase in computational complexity as a function of system size. Traditional quantum mechanical calculations (including a number of sophisticated approximations) typically require a computational cost that scales with the cube (~N^3) of the system size (N). Thus, to perform calculations of a system that has ten times as many atoms requires a computational cost that is one thousand times larger! For most calculations based on the first principles of quantum mechanics this has prohibited studies of systems larger than a few hundred atoms. This is clearly insufficient for many interesting problems in chemistry, materials science, and molecular biology. However, by reformulating the basic quantum description in the calculation of materials properties it is sometimes possible to overcome this computational bottleneck. Recently it has become possible to calculate certain materials properties with a cost that scales only linearly (~N) with the system size, N. Figure 1 shows the schematic picture of the required cost for various scaling of the computational cost.

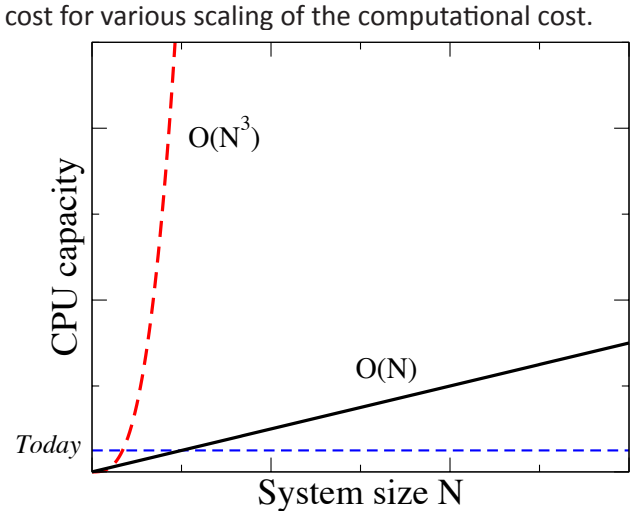


*Figure 1. The required computational capacity or cost for a given size of a calculation for a conventional method, O(N^3), in comparison to the proposal linear scaling methods, O(N). The blue dotted line shows the current (hypothetical) computational capacity.*

Despite a significant increase in CPU capacity, traditional methods that scale cubically, O(N^3), will not be able to treat much larger systems than today. Only with the new linear scaling methods, O(N), is it possible to significantly extend the reach of quantum theory and take full advantage of increased computer capacity.

The purpose of this research proposal is to explore some new opportunities given by efficient new recursive formulations, made by the investigators, for linear scaling calculations of quantum response properties. Such properties include materials response to various perturbations, for example, energy response due to external or internal perturbations, including energy gradients or the nuclear forces. In particular nuclear forces and the corresponding molecular dynamics are of key importance in simulations of materials properties. The idea is to explore and develop new algorithms that are well adapted to modern computing, which will allow the extension of highly accurate quantum mechanical simulations to larger and more complex problems for which conventional methods fail.

## Importance to LANL's Science and Technology Base and National R & D Needs

The ability to simulate larger, more complex materials systems directly from the first principles of quantum mechanics, without using empirical adjustable parameters, is pivotal in a truly predictive science. Many problems of interest, for example, matter under extreme conditions at high temperatures and pressure, details of important mechanisms of interactions, or specific chemical reaction paths, are often very hard or even impossible to study in laboratory experiments. The new techniques developed in this proposal will thus have a direct impact on predictive and basic materials science at LANL, ranging from nanotechnology to molecular biology.

First principles electronic structure theory that allows for theoretical investigations and predictions of materials properties is a rapidly growing field of science with great potential in wide areas of research ranging from chemistry and nanotechnology to molecular biology. The problem of extending current state-of-the-art methods to the study of larger and more complex systems is therefore of great interest to a broad national and international scientific community. The ability to provide some significant new developments in the area of reduced complexity electronic structure theory would therefore further strengthen the leadership in materials science at LANL and attract scientific talent worldwide.

## Scientific Approach and Accomplishments

### Matrix-Matrix multiplications on parallel machines

To enable high-performance numerical calculations that can reach close to 100% efficiency on a modern computer platform, we must avoid performing floating-point operations on individual numbers separately. Instead large matrices of numbers are manipulated simultaneously. One key operation utilized in this research proposal is sparse matrix-matrix multiplication, when a major part of all the numbers in the matrices are zero. To this date, a substantial amount of research effort has gone into parallel sparse matrix-vector multiplications. Sparse parallel matrix-matrix multiplications has been given much less attention. This lack of research made it necessary for us to investigate parallel sparse matrix-matrix multiplications in greater detail. Current state-of-the-art data formats for sparse matrices employ packing of the matrix data to achieve a high degree of compression. However, these storage formats have some disadvantages and perform poorly for certain matrix operations, as for example insertion of matrix elements. Another disadvantage is that as matrix elements are added to the sparse matrix, the performance of the matrix multiplication using these compressed formats degrades rapidly. Our goal was to develop a simple, yet powerful sparse matrix storage format that gives a high degree of compression of the matrix data, provides fast insertion of matrix elements, and allows for fast and efficient data distribution of partial matrix data for parallel operations. The matrix-matrix product based on this format should have competitive performance across a wide range of sparsity levels, so that it can be a real alternative to existing, well-established matrix formats. We investigated the simple division of the sparse matrix into submatrix blocks, which has many of these features, including high level of data compression and good data division into chunks which can be easily distributed in a parallel computation. We were able to show how the ordering of the submatrix blocks in memory affects the performance of the matrix multiplication [7]. We are currently developing these ideas further and hope to soon have a matrix-matrix multiplication with competitive performance.

### Large scale electronic structure calculations, a new record with over 10,000 atoms!

One highly efficient reduced complexity algorithm we have developed within this research proposal is based on a direct energy minimization of the total energy with respect to the single-particle wavefunctions that describe the quantum states of the electrons. By performing an optimi-

zation of the electronic states, not one by one, as in more conventional calculations, but for all at the same time in a quantum bundle, utilizing some efficient recursive techniques proposed by the PI, it was possible to reach a very high computational efficiency [5]. This approach, in its current implementation, is not a linear scaling algorithm. Its main cost is dominated by a quadratic scaling O(N^2), but with a fairly small computational overhead. With this novel scheme we managed to perform a record calculation where we calculated the electronic structure at a very high degree of accuracy for a system of a DNA fragment containing over 10,000 atoms.

**Linear scaling response theory for non-orthogonal basis sets**

The most efficient quantum mechanical calculations of materials properties are based on a local description of the electronic states that govern the specific features of the system. When the atoms move due to a perturbation, the frame for this local description follows the atoms. This specific effect has to be included in quantum response calculations. By utilizing a recursive update technique (recently proposed by the PI for a specific congruence transformation of the quantum mechanical eigenvalue problem) it was possible to include this specific response effect in reduced complexity calculations that scale only linearly with the system size [1]. The proposed linear scaling technique allows for calculations of both low and high-order response functions.

**Hierarchical decomposition of the congruence transformation**

A recursive linear scaling algorithm for the inverse factorization of (Hermitian positive definite) matrices of numbers was proposed [2]. This algorithm and the related mathematical theory was developed to make it possible to utilize computations on parallel platforms. The mathematical technique is quite novel, for example, using modern modularity concepts in network theory used social science and information theory, and the results are of high potential impact in large scale calculations that can take advantage of future computational standards with teraflop capacity that are beyond even current state-of-the-art reduced complexity algorithms.

**Time-reversible Born-Oppenheimer molecular dynamics**

Molecular dynamics simulations, based on the first principles of quantum mechanics, are indispensable in a large number of scientific areas that employ atomistic simulation. However, challenges in nanoscience, biofuels and actinide chemistry, for example, require significant algorithmic improvements to allow simulations of much larger size and complexity than previously possible. Born-Oppenheimer molecular dynamics, where the dynamics is driven by forces calculated in a rigorous way from the electronic structure at each instantaneous nuclear configuration, is currently the gold standard of atomistic simulations. However, Born-Oppenheimer molecular dynamics has several severe fundamental shortcomings, including a high computational cost and an unphysical systematic drift in the energy because of broken time-reversal symmetry in the underlying propagation of the electronic degrees of freedom. These problems have been well known for the last 30 years, but they have been considered to be impossible to overcome. In our exploratory work on the electronic response in molecular simulations we unexpectedly managed to remove the fundamental problems with the broken time-reversal symmetry and reduce the high cost associated with Born-Oppenheimer molecular dynamics [3,4]. This was achieved with a surprisingly simple technique based on additional auxiliary approximate electronic degrees of freedom, which is propagated in parallel with the exact electron density. This research resulted in the funding of a separate research proposal and further studies were therefore not continued within this proposal during the last year. However, despite being completely unexpected, it is by far the most successful and important outcome of this ER project.

**Reduced complexity calculations at finite electronic temperatures**

At finite electronic temperatures the electronic configurations has to be described by an ensemble of electronic states that on the average are fractionally occupied. This is in contrast to conventional electronic structure theory that assumes a zero-temperature approximation where the electronic states are either fully occupied or unoccupied. The zero-temperature approximation in particularly helpful in reduced complexity calculations, since the integer occupation of the electronic states simplifies the calculations. To enable reduced complexity calculations also at finite electronic temperatures we proposed a highly efficient recursive scheme for calculating the fractionally occupied electronic states at finite temperatures [6].

**Nuclear forces at high-temperatures**

A finite electronic temperature modifies the forces acting on the atoms. One of the contributions to the force acting on each atom in a molecular dynamics simulation is fictitious and due to the adaptive form of the electronic description that follows the atoms as they move. This is the famous Pulay force that was derived almost 40

years ago. The original expression for the Pulay force is unfortunately valid only at zero electronic temperature. Alternative expressions valid at finite temperature are not well suited (or impossible) to use in connection to reduced complexity algorithms, where the computational cost scales only linearly with the system size. Thanks to one of the recursive formulations forming the basis for this ER proposal it was possible to derive a very simple and computationally efficient form of the Pulay force that is valid also at finite temperatures [6]. This generalized Pulay force expression solved a key problem in high-temperature atomistic simulations for large complex systems.

## References


1. N.Niklasson, A. M., and V. Weber. Linear scaling density matrix perturbation theory for basis-set-dependent quantum response calculations: an orthogonal formulation. 2007. *Journal of Chemical Physics.* **127** (6): 064105.

2. Rubensson, E. H., N. Bock, E. Holmstrom, and A. M. N. Niklasson. Recursive inverse factorization. 2008. *Journal of Chemical Physics.* **128** (10): 104105.

3. N.Niklasson, A. M., C. J. Tymczak, and M. Challacombe. Time-reversible Born-Oppenheimer molecular dynamics. 2006. *Physical Review Letter.* **97** (12): 123001/1.

4. N.Niklasson, A. M., C. J. Tymczak, and M. Challacombe. Time-reversible ab initio molecular dynamics. 2007. *Journal of Chemical Physics.* **126** (14): 144103.

5. Weber, V., J. VandeVondele, J. Hutter, and A. M. N. Niklasson. Direct energy functional minimization under orthogonality constraints . 2008. *Journal of Chemical Physics.* **128** (8): 084113.

6. N.Niklasson, A. M.. A note on the Pulay force at finite temperatures. *Journal of Chemical Physics.*

7. Bock, N., E. H. Rubensson, P. Salek, A. M. N. Niklasson, and M. Challacombe. Cache oblivious storage and access heuristics for blocked matrix-matrix multiplication. *Computer Physics Communications (LA-UR-08-05038).*


## Publications


N.Niklasson, A. M.. A note on the Pulay force at finite temperatures. *Journal of Chemical Physics.*

N.Niklasson, A. M., C. J. Tymczak, and M. Challacombe. Time-reversible Born-Oppenheimer molecular dynamics. 2006. *Physical Review Letters.* **97** (12): 123001.

N.Niklasson, A. M., C. J. Tymczak, and M. Challacombe. Time-reversible ab initio molecular dynamics. 2007. *Journal of Chemical Physics.* **126** (14): 144103.

N.Niklasson, A. M., and V. Weber. Linear scaling density matrix perturbation theory for basis-set-dependent quantum response calculations: An orthogonal formulation . 2007. *Journal of Chemical Physics.* **127** (6): 64105.

Rubensson, E. H., N. Bock, E. Holmstrom, and A. M. N. Niklasson. Recursive inverse factorization. 2008. *Journal of Chemical Physics.* **128** (10): 104105.

Weber, V., J. VandeVondele, J. Hutter, and A. M. N. Niklasson. Direct energy functional minimization under orthogonality constraints. 2008. *Journal of Chemical Physics.* **128** (8): 084113.

# Statistics for the Engineering and Physical Sciences

*Christine Michaela Anderson-Cook*

20060697ER


## Abstract

Two major statistical research areas were explored in this project: Computer Models as Alternatives or Complements to Physical Models, and Performance Assessment of Complex Systems without Conventional Testing. In the first, computer modeling based on the underlying science can often be more cost-effective and explore a wider range of possible input combinations than collecting empirical data for understanding highly complicated relationships. We have developed new tools to collect better data, to assess the potential benefit of the data to be collected before new resources are spent, and to integrate results from physical testing and computer simulation. In the second area, data at the full-system and component levels of a complex system have been integrated to improve the overall precision of reliability estimates. We have developed methodology to assess the added benefits in terms of improved prediction of system reliability if supplementing existing models with alternate measures of aging and usage are added to the model. The relative improvement can then be compared to the incremental cost of this additional data to assess the broader advantages of additional explanatory variables.


## Background and Research Objectives

The goals of the project were to develop complementary methodologies to enhance the ability to estimate performance and reliability over a broad range of conditions. With specialized tools for flexible data types and strategies for efficient and cost-effective data collection, it is possible to both improve the quality of our modeling as well as the per observation utility of data collected. This increase in efficiency can improve both the accuracy and precision of our estimates.

Several different statistical research areas were explored as part of the "Statistics for the Engineering and Physical Sciences" project. Quantitative, graphical and qualitative tools were developed that built on the criteria of good designed experiments in Myers and Montgomery [1]. By considering multiple objectives for an experiment, we can find a data collection strategy that balances good performance for a variety of criteria and makes our designed experiment more robust to unforeseen complications and changes in our understanding of the system. These tools facilitate more precise comparisons between data collection strategies focused on good estimation and prediction, both when a model form for the underlying relationship between inputs and the response is known and unknown. In addition, specific methodology was developed to compare designs under a variety of potentially plausible model forms. As well, analysis tools for several specialized situations were developed to make maximal use of information gained during a single experiment or during sequential experimentation. Finally, new methodology was developed to facilitate better prediction of system reliability by synthesizing information from multiple data sources, where possible contradictions existed between these sources.

## Importance to LANL's Science and Technology Base and National R & D Needs

Developing and refining tools for modeling, model assessment and analysis of computer models and complex systems will facilitate more precise and robust assessment of the nuclear stockpile and improve the precision of surveillance estimates for the annual assessment by using all available information in a more cohesive manner, thus advancing DOE's mission in these areas. By better understanding the trade-offs between different data collection strategies, both for what type of data to collect and also which combinations of inputs to consider, better choices can be made about how to spend available budgets to get a best collection of data for the desired purposes of the experiments.

## Scientific Approach and Accomplishments

In exploring the two broad research areas, a number of themes were identified for further development. A major thrust was to examine the assessment of designed experiments through quantitative, graphical and qualitative measures [2]. In this research, formal criteria for what constitutes a good collection of data for a specific objective were identified. By considering good estimation and prediction in conjunction with ease of implementation, robustness to unexpected experimental occurrences and model misspecification and the design stage, the likelihood of good results from the analysis can be greatly improved. Which types of data and which combinations of inputs should be collected are dependent on the goals of the experiment. Typically two major priorities of experiments are good estimation of the model parameters and good prediction of new responses at input combinations not collected as part of the designed experiment. Graphical tools were developed for evaluation of prediction for split-plot experiments [3, 4], a category of experiments where some of the inputs are costly-to-change, and hence dictate the run order and experimental constraints under which data are collected. In addition, a case study illustrated the new methodology and demonstrated the detailed comparison of data collection alternatives for an engineering example [5]. Additional tools were developed for specialized situations involving non-normally distributed responses [6] and for designed experiments with a large number of input factors [7]. By understanding the trade-offs between optimizing various prediction and estimation criteria, an engineer or scientist can make more informed decisions about which data should be collected in a designed experiment. This will lead to higher quality of prediction for future responses and more accurate and precise characterization of the underlying relationship between the response and the inputs that influence it.

A second area of research was to consider the effect of model misspecification on quality of estimation and prediction. Often researchers do not know the true underlying form of the relationship connecting the response of interest and the inputs, but do have intuition about one of several functional forms that might be appropriate for approximating the relationship well. In these cases, it is important to determine which collection of data to obtain taking into account the model uncertainty that is present. Historically, the approach to selecting a designed experiment involved specifying a single model, and then choosing an optimal design based on this model being correct. If the model later turned out to be incorrect, then little could be done to improve how well the chosen designed experiment would predict and estimate. By focusing on the prediction variance, bias and the mean squared error of different response surface designs which assume first or second order models, we can quantitatively assess their relative robustness to model misspecification. As part of this project, new graphical tools were created to compare alternative designed experiments to see how well they would perform under a variety of types of model misspecification [8]-[9]. Frequently, a design can be selected that performs well over several potential models under consideration, while not being optimal for any of them. This is a good choice when model uncertainty exists, since good performance across a range of plausible models is preferable to a design that performs superbly for one model but poorly for another.

A third area considered was the development of new statistical tools for analyzing non-standard responses. In some experiments, the goal of the experiment is to predict an optimal combination of inputs, which will lead to ideal response values. If the response of interest is not a mean or variance, specialize tools are needed to find the optimal combination. New methodology was developed to use a Bayesian analysis to estimate optimal combinations of input factors to maximize the proportion of high quality product in an engineering manufacturing setting [10]. This methodology incorporated the non-normal nature of the response as well as the uncertainty in the estimation of the model parameters. In addition, graphical tools were developed which shown how robust different combinations of inputs are to variability in some of the uncontrollable input factors [11]. This helps the researcher to know what realistic production distributions of responses might be expected outside of laboratory conditions in a less controllable production environment.

Finally, research was conducted in the area of estimation and prediction for reliability of complex systems. While systems may have been designed to have either a series or parallel structure, in practice there may be dependencies between components or connectivity issues that cause the assumed relationships to be no longer be correct. For example, consider a population of complex systems, such as car engines, kitchen appliances, or rockets. The engineers who design the system intend for it to have a series structure. However, there are a number of ways that this might not be the correct structure once the system is built and data are being collected. 1) During production connectivity issues between components might mean that it is possible for two components to each work separately, but not work when combined together. 2) If the performance of one component depends on receiving the correct signal or power supply from another component, we may observe apparent failures of some components even when

that component is actually working. 3) The component level tests may be incorrectly calibrated relative to the demands on that component during the full system test. For example, it might be that a component will pass the component level test, but the system level test could fail because the component cannot perform adequately. Hence before we confidently use component level test data to estimate system reliability, it would be beneficial to assess the compatibility of the different data sources. A formal test was developed to assess whether data from different levels of the system are consistent with the assumed model form [12]. Finally, it is often possible to have several input factors which are thought to influence changes in the reliability of the complex system. For example, the aging of the system is commonly important for predicting changes in reliability. In addition, different measures of usage may also drive changes in performance. However, it can be potentially detrimental to include some of these measures into our statistical model when they are not influential for prediction, particularly if they are highly correlated. New methodology was developed to compare several models based on different numbers of input variables to find a model which predicts best in a user-specified region [13]. A key feature of this research has been strategies for appropriately specifying a viable region in the input space over which we should consider doing prediction. Often with correlation between input measures, some regions of a spherical or cuboidal region are not sensible given the observed data from which the analysis was performed. This methodology can help improve prediction, but also help guide which future data should be collected based on cost and quality of prediction.

By combining tools for good analysis and data collection in the areas of computer experiments and for modeling complex systems, we can better understand the implications of model uncertainty, and we will be better able to estimate a wide variety of behaviors for the response without as much costly physical or full-system data. This will mean that systems can be understood and explored under a broader range of operational conditions in a more timely and cost-effective manner.

## References


1. Myers, R. H., and D. C. Montgomery. Response surface methodology: process and product optimization using designed experiments. 2002.

2. Anderson-Cook, C. M., C. M. Borror, and D. C. Montgomery. Response surface design evaluation and comparison (with discussion). To appear in *Journal of Statistical Planning and Inference* .

3. Liang, L., C. M. Anderson-Cook, T. J. Robinson, and R. H. Myers. Three-dimensional variance dispersion graphs for split-plot designs. 2006. *Journal of Computational and Graphical Statistics* . **15**: 757.

4. Liang, L., C. M. Anderson-Cook, and T. J. Robinson. Fraction of design space plots for split-plot designs. 2006. *Quality and Reliability Engineering International* . **22**: 275.

5. Parker, P. A., C. M. Anderson-Cook, and T. J. Robinson. Robust split-plot designs. 2008. *Quality and Reliability Engineering International* . **24**: 107.

6. Ozol-Godfrey, A., C. M. Anderson-Cook, and T. J. Robinson. Fraction of design space plots for generalized linear models. 2008. *Journal of Statistical Planning and Inference* . **138**: 203.

7. Li, J., L. Liang, C. M. Borror, C. M. Anderson-Cook, and D. C. Montgomery. Graphical summaries to compare prediction variance performance for variations of the central composite design for 6 to 10 factors. To appear in *Quality Technology and Quantitative Methods.*

8. Anderson-Cook, C. M., C. M. Borror, and B. Jones. Graphical tools for assessing the sensitivity of response surface designs to model misspecification. To appear in *Technometrics.*

9. Ozol-Godfrey, A., and C. M. Anderson-Cook. Fraction of design space plots for examining mixture design robustness to measurement errors. 2007. *Journal of Statistics and Applications* . **1**: 171.

10. Robinson, T. J., C. M. Anderson-Cook, and M. S. Hamada. Bayesian analysis of split-plot experiments with non-normal responses for evaluating non-standard performance criteria. To appear in *Technometrics.*

11. Abraham, A., T. J. Robinson, and C. M. Anderson-Cook. A graphical approach to robust design. To appear in *Quality Technology and Quantitative Methods.*

12. Anderson-Cook, C. M.. Evaluating the series or parallel structure assumption for system reliability. To appear in *Quality Engineering.*

13. Pintar, A., and C. M. Anderson-Cook. Model selection from the perspective of prediction. 2008. *Los Alamos Technical Report LA-UR 08-05666.*

## Publications

Abraham, A., T. J. Robinson, and C. M. Anderson-Cook. A graphical approach to robust design. To appear in *Quality Technology and Quantitative Methods.*

Anderson-Cook, C. M.. Design of experiments: A single experiment or sequential learning. 2007. *Quality Progress.* (March): 71.

Anderson-Cook, C. M.. Evaluating the series or parallel structure assumption for system reliability. To appear in *Quality Engineering.*

Anderson-Cook, C. M.. More is Better. 2008. *Quality Progress.* (March ): 55.

Anderson-Cook, C. M.. More is not always better: Quality and lower dependence trump quantity. To appear in *Quality Progress.*

Anderson-Cook, C. M.. Assessment of Experimental Designs. 2007. In *Encyclopedia of Statistics in Quality and Reliability.* , p. 121. New York: Wiley.

Anderson-Cook, C. M., C. M. Borror, and B. Jones. Graphical tools for assessing the sensitivity of response surface designs to model misspecification. To appear in *Technometrics.*

Anderson-Cook, C. M., C. M. Borror, and D. C. Montgomery. Response surface design evaluation and comparison (with discussion). To appear in *Journal of Statistical Planning and Inference .*

Li, J., L. Liang, C. M. Borror, C. M. Anderson-Cook, and D. C. Montgomery. Graphical summaries to compare prediction variance performance for variations of the central composite design for 6 to 10 factors. To appear in *Quality Technology and Quantitative Methods.*

Liang, L., C. M. Anderson-Cook, T. J. Robinson, and R. H. Myers. Three-dimensional variance dispersion graphs for split-plot designs. 2006. *Journal of Computational and Graphical Statistics .* **15**: 757.

Liang, L., C. M. Anderson-Cook, and T. J. Robinson. Fraction of design space plots for split-plot designs. 2006. *Quality and Reliability Engineering International .* **22**: 275.

Liang, L., C. M. Anderson-Cook, and T. J. Robinson. Cost penalized estimation and prediction evaluation for split-plot designs. 2007. *Quality and Reliability Engineering International .* **23**: 577.

Ozol-Godfrey, A., C. M. Anderson-Cook, and T. J. Robinson. Fraction of design space plots for generalized linear models. 2008. *Journal of Statistical Planning and Inference .* **138**: 203.

Ozol-Godfrey, A., and C. M. Anderson-Cook. Fraction of design space plots for examining mixture design robustness to measurement errors. 2007. *Journal of Statistics and Applications .* **1**: 171.

Parker, P. A., C. M. Anderson-Cook, T. J. Robinson, and L. Liang. Robust split-plot designs. 2008. *Quality and Reliability Engineering International .* **24**: 107.

Pintar, A., and C. M. Anderson-Cook. Model selection from the perspective of prediction. 2008. *Los Alamos Technical Report LA-UR 08-05666.*

Robinson, T. J., C. M. Anderson-Cook, and M. Hamada. Bayesian analysis of split-plot experiments with non-normal responses for evaluating non-standard performance criteria. To appear in *Technometrics.*

# Integrated Feature Vector for Human Pathogen Characterization

*H Helen Cui*

20080769ER

## Abstract

Pathogen characterization has remained a major challenge in infectious disease research and the biothreat defense field. High costs, ethics and time constraints prohibit extensive cellular experiments and animal tests when we face an unknown pathogen, whether it is due to natural cause or malevolent intent. Improving currently existing pathogen detection technologies is an important mission for both public health and biothreat defense communities. In this pilot study, we examined a new computational approach to establish rapid and accurate characterization of human bacterial pathogens. Combining advanced bioinformatics, machining learning technology, and LANL's high performance computing, we developed a new feature selection algorithm to identify a small set of protein features to form a human bacterial pathogen feature vector. Our feature vector approach and the classification techniques have demonstrated a promising capability to rapidly predict the human pathogenic nature of a bacterium. This exploratory study provided a proof-of-principle for establishing an analytical capability that can be critical to both preventing biological threat proliferation and reducing public health consequences.

## Background and Research Objectives

An infectious disease results from the exposure of the susceptible hosts to pathogenic microbial agents, due to a natural outbreak or man-made release. While traditional pathogenic microorganisms are still the significant threats to public health and national security, emerging and engineered pathogens have also become a major concern. Microbial evolution and changes in our social and physical environment (*e.g.,* wars, climate changes) continue to drive the emergence of previously unknown infectious diseases. The rapid development of biotechnology and recent successes in synthetic genomics has made it clear that the appearance of genetically modified or engineered pathogens is only a matter of time. Early detection and characterization of the pathogen responsible for a disease outbreak, along with effective countermeasures, will enable the mitigation of the effects from potential pandemic spread. However, rapid and accurate detection and characterization of pathogens, especially previously unknown pathogens, has remained a major challenge to the public health and biothreat defense communities.

High throughput sequencing has been producing a tremendous amount of nucleotide sequence data, and providing gene inventory and associated protein annotation information for many organisms. For example, GenBank has collected sequences, submitted by laboratories throughout the world, for more than 100,000 distinct organisms, and this collection is growing at an exponential rate, doubling every 10 months. If used effectively, the existing, ever-growing volume of diverse data (*e.g.,* genomics, proteomics, and metabolomics, *etc*) can become an extremely valuable resource for pathogen characterization by means of bioinformatics and computational biology.

The main objective of this pilot project is to test if we could extract a set of features that uniquely represents human bacterial pathogens from the existing huge volume of bacterial genomic and proteomic data, with combined bioinformatics and machine learning technologies. The success of the pilot project will provide a proof-of-principle for a direct means for bacterial pathogen characterization, and a technical ground for a new area of pathogen detection research and technology development.

## Importance to LANL's Science and Technology Base and National R & D Needs

The US government, including the Department of Homeland Security and Department of Defense, has made huge investments in infectious disease detection and prevention. Los Alamos National Laboratory

has been one of the national key assets contributing its broad range of technical expertise to support this mission. Various Laboratory Directed Research and Development (LDRD) projects have developed specific virulence and pathogen species markers using advanced experimental and computational tools. In November 2006, two scientific research areas were identified as part of the LANL Complex System Grand Challenges: *Protecting the population from natural, emerging and engineered pathogens,* and *Creating algorithms and architectures with the computational ability of natural systems.*

More recently, the Department of Energy's National Nuclear Security Administration (NNSA) has stated that NNSA will bring our science, technology and engineering enterprise to bear on solving large, urgent national security challenges, including biological threats. The broad range of research and development activities at the national labs will continue to ensure that the nation is equipped to deal with technology surprises and anticipate new national security threats. The objectives and technical approaches of this project are well aligned with our mission goals to address these challenges.

Currently, different technologies are being developed to characterize pathogens at the sequence, molecular, biochemical, physiological or clinical levels. Epidemiological aspects of infectious diseases and biothreat proliferation related activities are also being monitored and studied. The results from these studies have become the foundations for advanced detection assay design and new medical countermeasure development, for both public health protection and biothreat defense. One of the most important requirements in biothreat nonproliferation is to provide high-fidelity analyses to assess Biological Weapons Convention (BWC) compliance and to attribute the use of BW in suspicious outbreaks throughout the world. Despite the pressing needs, currently there is no effective methodology that combines integrated analyses of large volume of existing disparate data with targeted experimental procedures, to rapidly and accurately characterize problems we may face and to determine the appropriate responses. It is essential for these analyses to be timely and accurate, and capable of predicting the pathogenic nature of previously unknown microbial organisms.

The development of robust pathogen detection assays requires the identification of a minimal set of proteins or DNA sequences that confer pathogenic phenotypes. Current methods for designing DNA pathogen detection assays focus on the identification of DNA signatures that are unique and conserved among a specific set of pathogens. The signatures that reside within known virulence associated genes are preferred for robust detection. These signatures are then used in biochemical detection assays (*e.g.*, as a PCR primer or TaqMan probe). However, there are a number of problems with the current assay design approaches. First, ascertaining the functional relevance of the genomic regions targeted by a particular detection assay is often difficult due to the high fraction of hypothetical genes in bacterial genomes. Second, current detection assays are typically specific to pathogens that have been collected in strain libraries – which represent only a tiny fraction of the diversity that exists in nature. In addition, recent advances in next generation sequencing technologies suggest that the days of performing traditional biochemical detection assays are limited. In the future, one can imagine that microbes can be detected by performing real time metagenomic sequencing and assembly of all genomes present in a biological sample. The detection of known (*i.e.,* sequenced) pathogens can then be as simple as a database search using the Basic Local Alignment Search Tool (BLAST, a technology will be referred later in this study), or related sequence comparison tools. However, the identification of novel emerging or engineered pathogens (*i.e.,* not previously sequenced) will still be a major challenge.

Our project takes a new approach that utilizes LANL's technical expertise in bioinformatics and information sciences, high performance computing, and knowledge in infectious diseases to address the great challenges in infectious disease early detection and prevention. The methods and algorithms developed in this project can potentially establish a new capability to predict pathogenic nature of a newly found bacterium, provide additional technical approaches for pathogen early detection and characterization, and therefore enhance the current capability to protect the population from natural, emerging and engineered pathogens.

## Scientific Approach and Accomplishments

Our hypothesis is that the problem of pathogen detection may be computationally posed as a classification problem and solved by using machine learning techniques (*e.g.*, support vector machines). Given the ever-increasing volume of complete microbial genomic sequences, one may be able to computationally extract distinctive features that can be used to classify microorganisms, for example, to classify pathogenic vs. non-pathogenic bacteria. The presence and absence of these features in a known or unknown bacterium can then become a direct indication of its pathogenic nature.

With a short term, small amount of LDRD reserve funding in FY08, we have taken a first step to test this hypothesis,

searching for features (or selected protein sequences in this study) that can automatically separate human pathogens from all other bacteria that are not human pathogens.

In May 2008, we downloaded all 679 completely sequenced bacterial genome sequences from the National Center for Biotechnology Information (NCBI). We manually labeled each bacterial strain as either a "human pathogen" (*e.g., Y. pestis*, *B. anthracis*, etc.) or "not a human pathogen" (*e.g., X. fastidiosa*, *X. citri*, etc.), genomes belonging to species of ambiguous pathogenicity were ignored. Manual classification was made by expert decision based on available literature. To account for variations of pathogenicity between strains of a species, each individual strain was classified.

Next, we applied the advanced bioinformatics technology to analyze the similarities of bacterial sequences. We started with the proteomes (*i.e.*, all protein sequences) of all the completely sequenced bacterial genomes analyzed above. A BLAST comparison of all proteins (both from human pathogens and not human pathogens) was processed to quantify and score the degree of sequence similarity between every possible pair of proteins. A total of approximately 2.2 million protein sequences were processed for sequence similarity scoring. Because of the massive volume of the data, LANL high performance computing resource, Turquoise Linux Cluster (TLC), was used to accelerate the data processing.

To search for a set of human pathogen features from the new proteomic data obtained in the previous step, we developed a new feature selection algorithm (tentatively named *Minimal Entropy Search Algorithm)* to select a small subset of proteins (*i.e.*, features) whose presence or absence most accurately predicts membership in the set of human pathogens, for example, to select a few dozens of features from a couple of million protein sequences (Figure 1). The algorithm minimizes *overall* randomness of the similarity scores for each protein. Those protein sequences that show high probabilities to be present or absent in human pathogens were chosen as the features.

We then developed a classification algorithm to mathematically and automatically separate the human and not-human pathogens using the selected features as inputs to the computational classifiers. Several classifiers are available for this application. In this study, we decided to adapt a cutting-edge classification technique called *Support Vector Machines* (SVMs). SVMs were introduced by Vapnik and his colleagues for solving two-class pattern recognition problem [1,2]. Three unique advantages make SVMs a must-try in classifications (Figure 2): 1) It provides a *margin*, instead of a strict line to separate two different classes; 2) It minimizes the possibility of over-fitting the training data and provides model stability for future applications; and 3) It uses *kernel*s (transformations) to provide non-linear classifications for better classification accuracy.

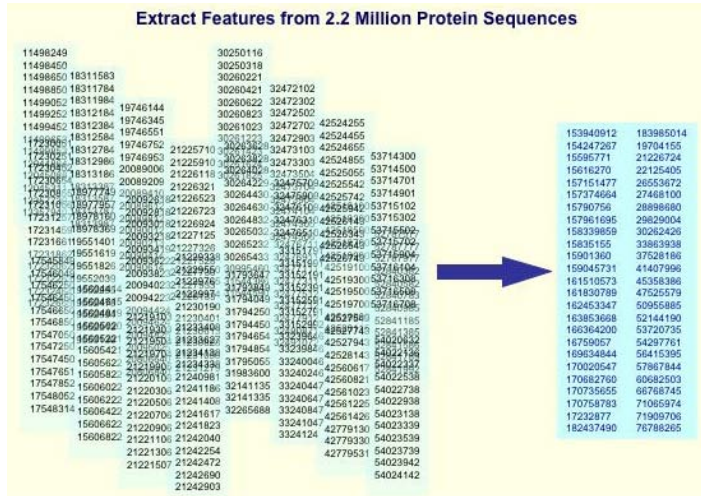


*Figure 1. Conceptual scheme of a feature vector. A subset of protein sequences are extracted from a potential 2.2 million feature space. The presence of feature vector in a bacterium represents the membership of human pathogens.*

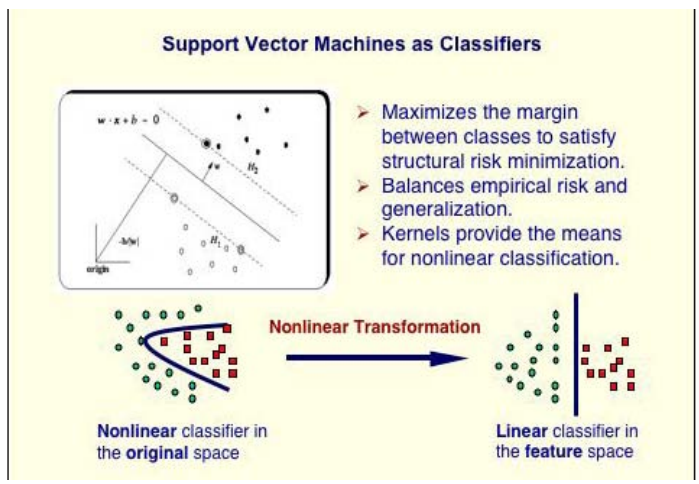


*Figure 2. The support vector machines. The figure illustrates the major benefits of SVMs, and non-linear transformation for pathogen classification.*

Using the *Minimal Entropy Search* algorithm we developed, we were able to select 50 protein sequences from a pool of 2.2 million. These 50 protein sequences form a feature vector (i.e., a group of features) whose presence or absence most accurately predicts membership in the set of human pathogens. With these 50 features and the support vector machine as the classifier [3], an 86% overall classification accuracy was achieved when separating human pathogens from the other bacteria. The classification

accuracy was validated using 5-fold cross validation, that is, the data set was divided into five subsets; each time, one of the subsets was held out as the test data and the rest was used as training data set. While further improvement of accuracy and understanding of the biological mechanisms of these features is desirable, the 86% overall prediction accuracy proves that it is feasible to use the methodology we have developed to select features to separate human pathogens from other bacterial microorganisms.

This short term project proved a significant concept, that is, combining advanced bioinformatics, machining learning technology, and high performance computing power, it is feasible to automatically classify microbial organisms with specified criteria. Previous efforts have used machine learning techniques to infer the biological function of hypothetical proteins; however, this is the first attempt, to the best of our knowledge, to automatically classify all bacterial human pathogens from complete whole genome sequences, without using the known pathogenic markers.

This project also provided a basic understanding for developing novel approaches to detect and characterize previously unknown microbes. Many current detection assay designs focus on the DNA or protein signatures in known pathogens. Our work is focused on developing the next generation of pathogen detection platforms: detection assays that will not rely on any known DNA signatures, but instead metagenomic sequencing and assembly of unknown samples, followed by an automatic protein sequence-based pathogen classification algorithm. Our method employs machine learning techniques to identify proteins that are both positively and negatively correlated with pathogenicity. It is a bottom-up, thorough and rapid approach, which has allowed us to generate promising preliminary results in a short period of time with a limited funding. This new approach can potentially provide a novel path for more effective pathogen early detection and characterization, and therefore enhance the current capability to protect the population from natural, emerging and engineered pathogens. This project leads to a new research redirection to develop direct means for bacterial pathogen characterization, and a technical ground for a new area of pathogen detection research and technology development.

We intend to continue to refine the feature selection process, further improve the prediction accuracy, and explore the application of this technology to characterize other pathogenic entities such as viruses. Our method establishes a general framework for answering genome-based classification questions, and may allow us to classify genomes by categories that are relevant to different national health security needs, including plant pathogenicity, antibiotic resistance and genetic engineering of microbial organisms. It is also important to understand the mechanisms of why some seemingly basic, non-virulence related proteins are selected as classification features. These studies can potentially provide a new approach to substantially advance our biothreat detection capability.

## References


1. Cortes, C., and V. Vapnik. Support-vector network. 1995. *Machine Learning.* **20**: 273.

2. Vapnik, V.. Statistical learning theory. 1998.

3. Chang, C. C., and C. J. Lin. LIBSVM: a Library for Support Vector Machines. 2001. *http://www.csie.ntu.edu.tw/~cjlin/libsvm/.*

# Towards Human Level Artificial Intelligence: A Cortically Inspired Semantic Network Approach to Information Processing and Storage

*Luis Bettencourt*

20080724PRD2

## Introduction

The research goals of this LDRD will be achieved by implementing our best understanding of neural computational primitives - the underlying mechanisms of the brain - on the fastest computers in the world. Unique to our project, all of this will be realized from a computer science/algorithmic perspective different from that of the older neural network researchers of the past. This research is cutting edge in the fact that it is focused on developing algorithms to synthesize network (graph) structures that compute in a manner similar to natural cortical networks. This research is high risk in that many solutions been proposed in the neural network paradigm of artificial intelligence research with modest results. However, even partial success will be significant for advancing brain understanding and inspiring new application algorithms, and substantial success would be revolutionary. Methods for large-scale graph storage and querying will be developed, methods for multi-relational (semantic) network analysis will be developed, and methods for encoding computational processes within a graph structure will be developed.

## Benefit to National Security Missions

Nuclear nonproliferation and energy security are all challenged by massive volumes of heterogeneous data that overwhelm human analysis. The same is true across the DoD and homeland security missions. Success will advance the areas of complex systems, distributed sensing in natural and social environments, and information science and technology.

## Progress

There have been eight publications [1-8] with respect to this LDRD project. Here we highlight briefly several off these results. References [3, 5] provide the technical mechanisms by which multi-relational (semantic) networks can be traversed in a "meaningful" way. In short, the random walk algorithms of single-relational networks have been generalized to support the graph structure being studied in this LDRD project.

In addition there have been several other papers that are currently in peer-review with respect to this project or have recently appeared. Reference [7] is concerned with identifying redundant informational structures in the cortical tissue of mice. With respect to a multi-relational (semantic) modeling of this phenomena, creating/identifying redundant computing graph patterns will prove promising. This is analogous to identifying when two pieces of software perform the same operation (similar to a commuting diagram in category theory). How these redundant structures are identified can be accomplished through the formalisms presented in [1,5,8] where algebraic structures are presented that can be used to determine (algebraically) when two paths through a multi-relational (semantic) network are the 'same.' That is, while two paths may appear different, they may in fact, through the axioms of the algebra, represent the same information.

Future directions include the further development of the algebra described in Reference [8] for constructing and analyzing complex, multi-relational networks. The benefit of this direction is that a formal mathematical system exists for identifying isomorphic (structure preserving) mappings between different graph patterns. With respect to patterns that "compute", finding redundant computing patterns (or patterns of computing that are the same at a higher level) will prove exciting and useful. Furthermore, a greater understanding of the theory of categories and abstract algebra will aid in this research push. For this reason, resources are currently being allocated to learning the appropriate branches of mathematics that will yield the greatest return on investment.

## Future Work

In a 2001 Scientific America article, Tim Berners-Lee (the inventor of the World Wide Web) defined the Semantic Web as "an extension of the current web in which information is given well-defined meaning, better enabling computers and people to work in cooperation." However, the Semantic Web is more general than this application-specific definition as it is a general-

modeling substrate that can be used to model many types of system—conceptual, physical, virtual, etc. This point was made salient in Dr. Rodriguez's doctoral thesis where he developed a new theory for embedding general-purpose computers within this distributed network substrate. Previous to this conceptual advance, the Semantic Web was solely considered a space where the structure of the world could be modeled, not its process.

One of the "hard" problems of modern neuroscience is specifying how the human neocortex computes at the various levels of abstraction (i.e. molecular, cellular, network, etc.). While seemingly a difficult problem, our hypothesis is that the cortical algorithm is not difficult to understand and, ultimately, simulate for the purpose of yielding cortical-based artificial intelligence. It is the area of "cortical computing" that Dr. Rodriguez will tackle during his Postdoctoral work at the Los Alamos National Laboratory. This research goal will be achieved through the abstraction and implementation and integration of neural computational primitives proposed in the neuroscience literature. However, given his area of expertise, all of this will be realized from a computer science/algorithmic perspective different from that of the older neural network researchers of the past or of explicit simulations of neurons and synapses. Working with others at the CNLS, experiments will be conducted with both designed and self-organized large-scale, cortically inspired networks that actively learn patterns in temporally and spatially changing signals and apply them to modern day large-scale graph substrates such as the Semantic Web.

## Conclusion

This research aims at creating a new generation of synthetic computational systems capable of open-ended artificial learning and prediction such that eventually, large-scale artificial cortical networks may match and surpass the reasoning abilities of the human brain. Other expected results include formal methods (both computational and algebraic) for analyzing and creating multi-relational (semantic) graph structures, methods for storing and querying large-scale graph structures, and methods for creating computational primitives that can be represented as a graph.

## References


1. Rodriguez, M. A., A. Pepe, and J. Shinavier. The Dilated Triple. To appear in *Emergent Web Intelligence.* Edited by Chbeir, R., A. Hassanien, A. Abraham, and Y. Badr.
2. Srinivasan, R., A. Pepe, and M. A. Rodriguez. A Comparison Between Ethnographic and Clustering-Based Semi-Automated Techniques for Cultural Ontologies. To appear in *Journal of the American Society for Information Science and Technology.*
3. Rodriguez, M. A., J. Bollen, and H. Van de Sompel. Automatic Metadata Generation using Associative Networks. To appear in *ACM Transactions on Information Systems.*
4. Rodrigues, M. A., and A. Pepe. On the Relationship Between the Structural and Socioacademic Communities of a Coauthorship Network. 2008. *Journal of Informetrics.* **2** (3): 195.
5. Rodriguez, M. A.. Grammar-Based Random Walkers in Semantic Networks. 2008. *Knowledge-Based Systems.* **21** (7): 727.
6. Rodriguez, M. A., and J. Geldart. An Evidential Path Logic for Multi-Relational Networks. *Association for the Advancement of Artificial Intelligence.*
7. Ham, M. I., V. Gintautas, M. A. Rodrigues, R. Bennett, C. L. Santa Maria, and L. M. A. Bettencourt. Density-Dependence of Functional Spiking Networks in Vitro. *Journal of Neural Computation.*
8. Rodriguez, M. A., and J. Shinavier. Exposing Multi-Relational Networks to Single-Relational Network Analysis Algorithms. To appear in *ACM SIGIR.* (Boston, 19-23 July 2009 ).


## Publications


Ham, M. I., V. Gintautas, M. A. Rodriguez, R. Bennett, C. L. Santa Maria, and L. M. A. Bettencourt. Density-Dependence of Functional Spiking Networks in Vitro. *Journal of Neural Computation.*

Rodrigez, M. A., A. Pepe, and J. Shinavier. The Dilated Triple. To appear in *Emergent Web Intelligence.* Edited by Chbeir, R., A. Hassanien, A. Abraham, and Y. Badr.

Rodriguez, M. A.. Grammar-Based Random Walkers in Semantic Networks. 2008. *Knowledge-Based Systems.* **21** (7): 727.

Rodriguez, M. A., J. Bollen, and H. Van de Sompel. Automatic Metadata Generation using Associative Networks. To appear in *ACM Transactions on Information Systems.*

Rodriguez, M. A., and A. Pepe. On the Relationship Between the Structural and Socioacademic Communities of a Coauthorship Network. 2008. *Journal of Informetrics.* **2** (3): 195.

Rodriguez, M. A., and J. Geldart. An Evidential Path Logic for Multi-Relational Networks. *Association for the Advancement of Artificial Intelligence.*

Rodriguez, M. A., and J. Shinavier. Exposing Multi-Relational Networks to Single-Relational Network Analysis Algorithms. To appear in *ACM SIGIR.* (Boston, 19-23 July 2009 ).

Srinivasan, R., A. Pepe, and M. A. Rodrigez. A Comparison Between Ethnographic and Clustering-Based Semi-Automated Techniques for Cultural Ontologies. To appear in *Journal of the American Society for Information Science and Technology.*

# Finite State Projection for Accurate Solution of the Master Equation

*Ilya Mark Nemenman*

20080730PRD2

## Introduction

Life is uncertain, and the future often unfolds not according to a predetermined path, but in unpredictable directions. These wanderings are called "stochastic processes", and although they have an element of chance, their unfolding can be described mathematically by the effects of one or more random variables. Such stochastic processes are a cornerstone of a variety of subjects, from statistical physics to control theory. Lately they are becoming more and more prominent in systems biology as well, where they describe biochemical reactions, genetic evolution, or host-pathogen interactions. The most common tool to describe stochastic events has always been the master equation. Contrary to its simple name, the master equation is, in fact, a system of infinitely many ordinary differential equations, and hence it is very difficult to solve.

In his preceding work, Dr. Munsky has suggested a way of truncating the size of the master equation system by inventing the Finite State Projection (FSP) algorithm, which automatically selects which of the equations in the system need to be preserved, and which need to be ignored. The method is having a large impact already.

Still, a big hurdle remains: in many biochemical systems, the number of participating chemical species is huge, often many millions or more. This makes the master equation becomes even more complex: it is now a very large system of infinite systems of ordinary differential equations. In these situations, the FSP algorithm cannot achieve the required computational simplifications anymore. The goal of this project, therefore, is to make the FSP approach work even in these extremely complicated cases by developing a method for selection of the "relevant" degrees of freedom using control theory and information theory techniques.

## Benefit to National Security Missions

This project will support the DOE mission in Threat Reduction and Basic Science. The stochastic analysis tools will impact myriad fields in science, medicine, and industry. Stochastic models are used in projects throughout LANL and DOE: genomics, fluid dynamics models, global climate dynamics, social interaction and epidemiological models, and material science models.

## Progress

Dr. Munsky started his appointment at LANL in July 2008. Over the three months of this newly initiated project, he has completed a publication of his prior work [1], which deals with calculations of escape rates for multistable kinetic systems using the FSP method. He has also had a paper accepted [2] at the IEEE Conference on Decision and Control, a premier conference in the field, which deals the identifiability of stochastic kinetic systems.

## Future Work

With the PI of the project, Dr. Nemenman, and additional LANL collaborators, Drs. Hengartner, Bel, and Sinitsyn, Dr. Munsky has noticed that stochastic properties of large biochemical kinetic systems exhibit curious universal behavior, which can be characterized by just a handful of parameters. If confirmed, this observation can lead to a solution to the main question posed in this research project by identifying a small number of relevant characteristics of a kinetic system, and thereby suggesting FSP-based methods for fast, reliable, low-dimensional and low-parameter methods for simulations of such systems. It is expected that the next year of the research will revolve around analyzing this intriguing possibility.

## Conclusion

In this research, Dr. Munsky is extending the FSP approach to efficiently and accurately handle a vast range of complex stochastic systems that cannot be analyzed with any existing approach. New algorithms developed here would allow computational analysis of diverse biological systems, from models of genetic interactions in cancer development, to understanding the spreads of epidemics. In addition to practical utility, the work is bound to uncover the beautiful mathematical structure behind dynamics of stochastic kinetic networks, which is of interest on its own.

## References

1. Munsky, B., and M. Khammash. Transient analysis of stochastic switches and trajectories with applications to gene regulatory networks. 2008. *IET Systems Biology.* **2**: 323.

2. Munsky, B., and M. Khammash. Using noise transmission properties to identify stochastic gene regulatory networks. To appear in *46th IEEE Conference on Decision and Control.* (Cancun, Mexico, Dec, 2008).

## Publications

Munsky, B., and M. Khammash. Transient analysis of stochastic switches and trajectories with applications to gene regulatory networks. 2008. *IET Systems Biology.* **2**: 323.

Munsky, B., and M. Khammash. Using noise transmission properties to identify stochastic gene regulatory networks. To appear in *46th IEEE Conference on Decision and Control.* (Cancun, Mexico, Dec, 2008).

# Statistical Physics of Optimization

*Michael Chertkov*

20080787PRD3

## Introduction

In many areas of science, from computer science and information theory to engineering and statistical physics, as well as in biology or social sciences, optimization problems are widespread and important. Optimization typically involves a large number of variables, e.g. particles, agents, cells or nodes, and a cost function depending on these variables, such as energy, measure of risk or expenses. Optimization problems which belong to the so-called NP-complete class are particularly difficult, it is believed that the number of operations required to minimize the cost function is in the most difficult cases exponential in the system size. However, even in an NP-complete problem the practically arising instances might, in fact, be easy to solve.

In this project we will address the following fundamental questions which concern general combinatorial optimization setting: How to recognize if an NP-complete problem is typically hard and what are main reasons for this? How to find an approximate solution of a hard problem? Answering these questions is crucial for developing new efficient algorithms for hard problems, and it is also relevant for designing secure cryptographic systems. Another comprehensive question addressed in this project is: How to correct errors when information is sent via a noisy communication channel? Specifically, we will aim to develop virtually non-existent theory of nonlinear codes based on the recent progress achieved in related discipline of combinatorial optimization.

## Benefit to National Security Missions

Our goal is to use statistical physics models to predict, understand and improve communication mechanisms. Our methods will enable communication protocols required to work with yet unseen amounts of data. This project will support DOE mission in National Security by enhancing understanding of new principles for Information Communication and Storage.

## Progress

The Postdoc was hired on September 2, 2008. During the first month she made progress on two specific problems --- first the learning of flow parameters based on particle tracking, and second the study of the analysis of planted ensemble of constraint satisfaction problems.

The problem of particle tracking consists of inferring parameters of the system, such as the diffusion constant, based on two consecutive photographs of the system of moving particles. It was previously realized in LANL that the belief propagation algorithm approximates very precisely the desired quantities. We developed an exactly solvable model of this problem in which the belief propagation algorithm is exact and compared quantitatively the performance of the algorithm on this model and on the data generated in a realistic way. The results are very promising. And presently we aim to apply our method to real experimental data.

Some important application of constraint satisfaction problems, e.g. benchmarking or in cryptography, require instances which surely do have at least one solution. A common way to generate such instances is to start with a solution and add only constraints which are not violated by this solution. This is called the planted ensemble. We studied the random planted ensemble and for a first time we quantified the region of parameters in which the problem is algorithmically hard if we do not reveal any information about the planted solution. We also found some interesting connections to the physics of structural glasses where the planted solution acts as the crystalline ordered state.

## Future Work

Optimization is fundamental in many areas of science, from computer science and information theory to engineering and statistical physics, as well as to biology or social sciences. Optimization typically involves a large

number of variables, e.g. particles, agents, cells or nodes, and a cost function depending on these variables, such as energy, measure of risk or expenses.

In this project we will apply concepts from the statistical physics of disordered systems to problems of computer science, information theory and artificial intelligence. Insights coming from models and methods of statistical physics will be fruitful in these domains and will bring novel predictions, understanding and practical results. In particular, We plan to study error-correcting codes. Linear codes are the best known codes achieving this task. The linearity of the codes is not needed a priori, but almost always assumed for simplicity. We will challenge this concept and consider nonlinear codes based on the locked constraint satisfaction problems mentioned above, as these may be significantly better than their linear counterparts. We also want to address packet-based communication over the noisy Internet. To deal with realistic structured graphs and networks, We plan to combine mean field and perturbative techniques with loop calculus, a new theoretical framework developed recently. We also plan to extend our recent understanding of static optimization problems to the analysis of more challenging dynamical problems that arise in adapting environments, by developing new dynamical models and techniques necessary to fully exploit the huge amount of data collected in modern molecular biology, social sciences, etc. We intend to develop better inference models allowing for accurate learning of relevant parameters and rules in the data. This research will combine physics-based ideas with learning and inference methods from artificial intelligence.

## Conclusion

We apply concepts from the statistical physics of disordered systems to problems of computer science, information theory and artificial intelligence. We study error-correcting codes. We consider nonlinear codes based on the locked constraint satisfaction problems mentioned above, as these may be significantly better than their linear counterparts. We will address packet-based communication over the noisy Internet. We combine mean field and perturbative techniques with loop calculus, a new theoretical framework developed at Los Alamos. We extend recent understanding of static optimization problems to the analysis of more challenging dynamical problems that arise in adapting or competing environments.

full final report

# Self-Organizing Wireless Ad-Hoc and Sensor Networks with Functional Guarantees

*Sami Ayyorgun*

20061624PRD4

## Abstract

In this project, the focus has been on the design and analysis of self-organizing wireless ad-hoc and sensor networks. Due to lack of a centralized controller in these networks, they inherently need to have some self-organizing features. The sensor network environment is a highly dynamic (e.g., due to node failures, mobility of nodes, or time-varying nature of the wireless channels), and it is desirable that the network adapts to the topology changes and function properly even if some of the nodes themselves cannot function anymore.

Considering applications such as biological and chemical hazard detection, or assistance in evacuation of survivors, our objective has been to analyze and improve the behavior of self-organizing wireless networks in terms of certain desired performance metrics such as connectivity, energy efficiency, delay, security, longevity, and event detection capability.

## Background and Research Objectives

Wireless sensor networks have found various application venues in environmental monitoring, health monitoring, and target tracking in hostile situations to name a few. Especially in the case of monitoring physically inaccessible or dangerous areas for humans to enter, such as wildfire tracking, glacier or volcano monitoring, liveliness detection in emergencies or hazardous material tracking, the use of wireless sensor networks is expected to increase tremendously. Due to the inaccessibility of the geographical areas in these applications, the sensor nodes need to be either airdropped,d forming a static network, and/or deployed using mobile robots (which might be overlaid on top of a static network). Optimizing the connectivity, coverage, energy, delay, security, longevity, and self-organization aspects of such wireless ad hoc and sensor networks is critical. Battery lifetime presents a major challenge to success, so it is essential that we optimize the performance of the network for a given consumption of energy.

## Importance to LANL's Science and Technology Base and National R & D Needs

This project supports the DOE/NNSA missions in nonproliferation, threat reduction (counter terrorism), and homeland security by enhancing our understanding of how to develop and use self-organizing wireless sensor networks towards these missions.

## Scientific Approach and Accomplishments

Our research falls under two separate thrusts: First, we have introduced a routing protocol for efficient data dissemination. In this work, the focus has mainly been on the design and impact of mobility on the topology, connectivity, security, and event detection capability of wireless sensor networks. Secondly, we have introduced a novel stochastic communication scheme called BSTeR (read as "booster"), which stands for "Boost by Smart Transmit-power Random-variables". BSTeR is a self-organizing scheme which breaks the coupling among many performance metrics (including energy, delay, longevity, etc.) for the first time in the literature.

In what follows, we summarize the accomplishments under these two separate research thrusts.

### Impact of Mobility

First, we proposed a topology-dependent mobility model to improve the connectivity of a static wireless network overlaid by a small-size mobile network. The model takes into account the degree of the nodes in the network and it is assumed that a mobile node moves toward higher degree nodes with a higher probability. We studied the performance of the model in the presence of node failures and it is shown that adding a few mobile nodes to the wireless network is very beneficial and the deployed network can continue to operate even with more than 30% node failure.

Next, we have investigated the impact of mobility on the security of a hybrid (i.e., static and mobile) and pure mobile wireless sensor network. With the emergence of

computer worms that can spread over air interfaces, wireless ad hoc and sensor networks can be vulnerable to node compromises even if the deployed network is not connected to the backbone. Depending on the physical topology of the wireless network, even a single infected node can compromise the whole network. We have shown that the epidemic spread threshold and size depend on the physical topology of the underlying wireless network as well as the mobility model employed by the infected mobile nodes. More specifically, our results show that in a fully-connected wireless network targeted attacks are more effective, whereas for a random topology random attacks can be sufficient to compromise the whole network.

Finally, we examined the impact of mobility on the event detection performance of wireless networks. If the event to be detected by the sensor network is of time-critical nature, the coverage of the network should be sufficiently high to be able to respond to the detected event in a timely manner; such as wildfire monitoring or liveliness detection under rubble in case of an earthquake, where the emergency personnel work against the clock. In such cases, we have found out that using a mobile sensor network would be highly beneficial both in terms of event detection and utilization of the available system resources. To this end, we have proposed a coverage-based, cooperative mobility model to improve event coverage in wireless sensor networks without prior knowledge of the physical topology and by using only local topology information. An empirical study is conducted to test the performance of the proposed model, where a finite-duration, stationary (such as a live person under rubble) or mobile event (such as a moving target) is assumed to occur at a random location in the geographical area to be monitored. It is shown that the coverage-based mobility model consistently results in a better performance than the other mobility models and the desired event detection probability can be achieved by the minimum number of nodes estimated by the analysis.

**Self-organizing Stochastic Communications Paradigm**

We have introduced a stochastic communication scheme called BSTeR (read as “booster”), which stands for “Boost by Smart Transmit-power Random-variables.” In this scheme, we have the transmit power of each node n be determined by a random variable $P_n$. These transmit-power random variables are independent, but their Probability Mass Functions (PMFs) are calculated intelligently so as to yield concurrent performance gains. More specifically, we formulated a set of Linear-Programming problems and solved them to calculated these PMFs. We have shown that the BSTeR scheme provides significant performance gains concurrently over many metrics; including connectivity, energy, delay, longevity, security, and energy-delay relation. No other protocol in the literature was able to achieve this.

We submitted an Invention Disclosure to the TT Division for this novel scheme being introduced.

Towards developing the underpinnings of a proof-of-concept design of the BSTeR scheme, we have developed a realistic power-model for the sensor nodes (TelosB) that we have in the testbed (that we have built). We had conducted experiments which have validated the model. One interesting observation that we have verified is that the energy consumption (not the radiated energy but instead the energy consumed by the electronics) varies as $d^{gamma}$ where gamma is not necessarily greater than 2 (where d is the distance between the transmitter and receiver). This is due to the amplifier nonlinearities at the nodes. This observation has pointed out a failure in conventional thinking regarding the energy-distance relation that is ubiquitous in the literature.

Towards developing the underpinnings of a proof-of-concept design of the BSTeR scheme, we have developed a highly energy-efficient sleep-wakeup algorithm (called PowerNap) for controlling the on/off status of all the transmitter-receiver pairs. We have proved that PowerNap is self-stabilizing, in that the protocol is resilient to packet losses in recovering its state-space. We had implemented this protocol on the testbed (that we have built). Our results indicate that PowerNap’s performance is about 90% close to the theoretical limit of sleep-wakeup efficiency.

Using Markov chains, we had calculated the probability that a node would be involved in communications in the BSTeR scheme. However, incorporating these probabilities for coming up with more efficient dynamic load-balancing schemes (in the form of LP optimization) has proved to be difficult.

We had presented the BSTeR scheme in the Plenary Session of the IEEE International Conference on Mobile Ad-hoc and Sensor Systems (MASS) in 9/29--10/2 in Atlanta (GA), which has been nominated for the best-paper award. The presentation is very well received, resulting many invited technical talks (e.g. from Telcordia, NASA JPL, et.c) and further inquiries (e.g. from IBM Zurich) about this self-organizing communication scheme.

Should further funding become available, we would investigate the following:

- Incorporate link unreliabilities into the network model, and find efficient transmit-power random variables for the BSTeR scheme.
- Incorporate the probability that any given node would be involved in communication in BSTeR scheme, and find efficient transmit-power random variables for the BSTeR scheme.

- Demonstration of the overall system design for a chosen specific application of interest, which would yield concurrent performance gains.

In summary, this project has developed many algorithms that govern the desired, as well as the observed, characteristics of man-made or natural self-organizing wireless networks. In particular, we have shown the impact of mobility on the performance of wireless sensor networks, which has provided great insight into fault-tolerant network design. Secondly, our work on stochastic communication for wireless adhoc/sensor networks, namely the BSTeR scheme, has been received as signaling a paradigm in this field. This work has provided a seminal insight into designing wireless adhoc/sensor networks by de-coupling the dependencies among many performance metrics for the first time in the literature.

## References


1. Ayyorgun, S., J. Ai, and S. Shankar. Towards a Self-organizing Stochastic Communications Paradigm for Wireless Adhoc/Sensor Networks. 2008. In IEEE Intl. Conference on Mobile Adhoc and Sensor Systems. (Atlanta, Sept. 29--Oct. 2). Vol. I, First Edition, p. 1. Atlanta: IEEE.

2. Yanmaz, E.. Impact of Topology-dependent and independent Mobility Models on the Connectivity of Wireless Networks. 2008. In IEEE Sarnoff. (Princeton, March 30-April 1). Vol. I, First Edition, p. 1. Princeton: IEEE.

3. Yanmaz, E., and T. Karrels. A Multi-tracking Wireless Ad hoc Routing Protocol. 2008. In IEEE International Wireless Communications and Mobile Computing Conference. (Crete Island, 6-8 Aug 2008). Vol. I, First Edition, p. 1. New York: IEEE.

4. Yanmaz, E.. Impact of Mobility Pattern on Epidemic Propagation in Wireless Networks. 2008. In IEEE International Symposium on Personal, Indoor and Mobile Radio Communications. (Cannes, 15-18 Sept. 2008). Vol. I, First Edition, p. 1. New York: IEEE.

5. Yanmaz, E.. Epidemic Propagation in Overlaid Wireless Networks. To appear in IEEE Global Telecommunications Conference. (New Orleans, Nov. 30-Dec. 4 2008).


## Publications


Ayyorgun, S., J. Ai, and S. Shankar. Towards a Self-organizing Stochastic-Communications Paradigm for Wireless Adhoc/Sensor Networks. 2008. In *IEEE International Conference on Mobile Ad-hoc and Sensor Systems.* (Atlanta, Sept. 29--Oct. 2 2008). Vol. I, First Edition, p. 1. Atlanta: IEEE .

Yanmaz, E.. Mobility, Failure, and Self-organization in Wireless Networks. 2007. *Los Alamos National Laboratory.*

Yanmaz, E., and T. Karrels. Routing Protocols in Wireless Ad hoc Networks. 2007. *Los Alamos National Laboratory.*

# Physics

continuing project

# Beyond the Neutrino Matrix

*Andrew Hime*

20070003DR

## Introduction

The discovery of solar and atmospheric neutrino oscillations has opened new questions and opportunities at the intersection of nuclear and particle physics, astrophysics, and cosmology. A diverse experimental program, supported by theory, aims to seek out the dark matter in the universe, elucidate the fundamental properties of neutrinos and their interactions with matter, the role they play in stellar evolution, and in ultimately shaping the universe we observe today. A major effort involves the design and construction of a detector capable of utilizing, interchangeably, targets of liquid argon and liquid neon. At the 360 kg scale this detector will serve in a competitive search for dark matter and seed the design of a massive (10 to 100 ton) detector capable to detect dark matter and, simultaneously, the low-energy neutrinos from the sun. The project also supports, in part, complementary research and development for a detector in search of neutrinoless double beta decay and the antineutrino phase of the MiniBooNE program. A theoretical component to the project provides computational support directly relevant to this experimental program as well as in interpreting the experimental data provided world-wide in the context of fundamental theories beyond the Standard Model

## Benefit to National Security Missions

This project will support a DOE mission of the Office of Science to obtain a fundamental understanding of the universe through the elucidation of neutrino properties and the search for cosmological dark matter. The development of novel and ultra-sensitive radiation detectors builds capabilities for new detectors for nuclear threat detection.

## Progress

Significant progress has been made in the design and realization of the Mini-CLEAN detector. A conceptual design for the detector is complete, including a detailed background model indicating that the experiment can reach the desired level of sensitivity for a competitive direct dark matter search.

A full engineering design for the Mini-CLEAN detector is under completion and major procurements have begun. A strong, international collaboration of ~75 people has been formed consisting of 15 institutions in the US and Canada, consisting of students, post-doctoral associates, technicians, engineers and scientific staff at the level of ~35 FTE [~8 FTE at LANL]. A major milestone was met in FY08 with the completion of the engineering design, mechanical drawings, and failure mode analysis of the outer vacuum containment vessel for the Mini-CLEAN detector. This component of the detector was successfully sent out for bid and is now under fabrication.

The experiment has been approved for installation at SNOLAB and a technical and safety review is planned for early in the new calendar year. SNOLAB has agreed to contribute significant underground infrastructure to the project, including a large water shield, platform and overhead crane, and cleanroom. This allows the LANL team to focus its resources on the final design, engineering, and procurement of the central detector that we aim to complete by the end of the project. In addition to the engineering program, LANL has also constructed a series of test-benches to measure and optimize components of the optical modules central to the detector concept. The design of these optical modules is novel and we have begun to construct a dedicated prototype for testing at cryogenic temperatures before finalizing the design. In FY08, significant work was done to simplify the design of the acrylic light guides and photomultiplier tube coupling which maintains the prerequisite light yield for the detector but reduces engineering complexity and, ultimately, cost.

Several complementary efforts have seen progress with respect to development for the Majorana neutrinoless double beta decay program. Our program, unique to LANL's LANSCE facility, has seen measurements of critical (n, n`) gamma reactions on isotopes of lead, copper, and germanium that, hitherto missing from the nuclear data base, provide cross-section measurements critical to the development of ultra-sensitive searches for neutrinoless double beta decay experiments and of general interest to the "low-background" scientific community.

Several publications are underway or anticipated from this effort, including a new study at LANSCE's "IceHouse" neutron beam to better quantify cosmogenic production of Ge-68. In addition, we constructed, and successfully operated, a dedicated detector to study alpha contamination on the surface of Ge detectors as well as a mechanical test cryostat, the so-called "canary-cage", to test the mechanical, thermal, and electronics design for the baseline Majorana detector.

The MiniBooNE collaboration continued to record data in anti-neutrino mode. The "box" has been opened on the blind data set, the results from which will be announced before the end of this calendar year. A comparison between data from this phase and the previous neutrino phase is critical in determining whether or not the low-energy anomaly present in the neutrino data set is indicative of new physics. In this regard, a new method to search for CP and CPT violation by comparing neutrino data to anti-neutrino data has been developed in collaboration with groups at Alabama and Florida. The accelerator neutrino team wrote a White Paper on a future OscSNS experiment at ORNL that could obtain the world's best sensitivity to neutrino oscillations in the mass region above 0.1 $eV^2$. In addition, a study was performed indicating that a new experiment at FNAL, moving the present detector to a new location, would increase the neutrino event rate by about a factor of six relative to the present configuration, and could determine if Mini-BooNE's low-energy excess is due to neutrino oscillations in only an additional year of data taking.

On the theory front work continued to study short-range correlations in nuclear double beta decay, comparing various approaches to reduce uncertainties in the nuclear matrix element. Predictions were also made for the Mini-BooNE results on the assumption of consistency with those from LSND and KARMEN and the possible existence of sterile neutrinos or CP violation. These studies confirm that the MiniBooNE results might reflect the existence of new physics. We find that, within these models, it is possible to reconcile Mini-BooNE/LSND with KARMEN or the solar/atmospheric neutrino results, but not with both. Additional investigations were made of coherent neutrino oscillations in supernovae, indicating the important role that neutrino-neutrino interactions can play. Additional investigations of the effects of supernova neutrino density and the expected signal in terrestrial detectors could have impact on planning for future neutrino detectors.

Following a mid-term review of this LDRD project, we received valuable endorsement for the project and guidance from the review panel with respect to focusing the final year of the project towards the successful construction of the Mini-CLEAN detector whilst maintaining a pertinent theory component and coming to a natural closure of the Mini-BooNE program in FY09. In addition, collaborators on this project submitted a new FY09 proposal that would be dedicated to the double beta program at LANL. This proposal was positively endorsed and funded in the competitive peer reviewed LDRD process. In FY09 we intend to redirect resources to bolster the dark matter program and to facilitate major procurements towards the construction of the Mini-CLEAN detector.

## Future Work

The technical program for the direct detection of dark matter focuses on a detailed engineering design for the Mini-CLEAN detector in parallel with detailed Monte Carlo simulations, test-benches and prototyping at the Laboratory to optimize this design with respect to scientific reach. With the outer vacuum/containment vessel now under fabrication, we will finalize the technical drawings for the inner vessel (IV) and optical cassettes central to the Mini-CLEAN detector. Coming to closure on the IV design and mechanical drawings are critical elements to ensure that procurement of these items can be made in FY09, as are the completion of R&D tests for the optical cassettes, and finalization of their engineering and mechanical drawings. A major goal for FY09 will be sending out the IV and optical cassette design for bid and fabrication. Major procurements will also be made in FY09 to complete fabrication and testing of the PMT array, electronics & DAQ systems, vacuum and purification systems for the Mini-CLEAN detector.

Analysis of antineutrino data from the MiniBooNE experiment to test the LSND evidence for neutrino oscillations is now completed and complemented by theoretical calculations of neutrino cross-sections relevant to MiniBooNE. This information will be used to mark out the most productive path to understanding the low-energy anomaly uncovered by the Mini-BooNE data.

Fundamental theory efforts consider neutrino mixing in a model constrained by the experimental data, illuminating further questions of quark-lepton and family symmetry that are essential to further progress towards the long-sought goal of the grand unification of all forces. We are seeking a relation between neutrino mass, dark matter and dark energy as a function of time in the expansion of the Universe.

## Conclusion

Data from the antineutrino phase of MiniBooNE has been obtained and analyzed. Comparison of these results to those previously obtained from the neutrino will be critical

in assessing the origin, and future steps, to understanding the low-energy excess observed in MiniBooNE.

Significant progress was made in the development of the Majorana project and a new FY09 LDRD-DR was awarded for a dedicated double beta decay program at LANL. This new grant bolsters the future of this program at LANL and allows critical funds to be redirected to the design and construction of the Mini-CLEAN detector through this existing project in FY09. We will face an ambitious schedule in FY09 to ensure completion of the engineering design, mechanical drawings, and procurement of all major subsystems for the Mini-CLEAN detector.

A highly complementary theory component continues to lend support to the experimental neutrino program and fundamental insight into understanding the plethora of data in the context of theories within and beyond the standard model.

## Publications


Aguilar-Arevaloet.al., A. A.. Search for electron neutrino appearance. 2007. *Physical Review Letters.* **98**: 231801.

Aguilar-Arevaloet.al., A. A.. Measurement of muon neutrino quasi elastic scattering on carbon. To appear in *Physical Review Letters.*

Avigninone, F. T., S. R. Elliott, and J. Engle. Double beta decay. To appear in *Reviews of Modern Physics.*

Avignone, F. T., S. R. Elliott, and J. Engle. Double Beta Decay, Majorana Neutrinos and Neutrino Mass. 2008. *Reviews of Modern Physics.* **80**: 481.

Duan, H., G. M. Fuller, J. Carlson, and Y. Z. Qian. Analysis of collective neutrino flavor transformations in supernovae. 2007. *Physical Review.* **D75**: 125005.

Duan, H., G. M. Fuller, J. Carlson, and Y. Z. Qian. Neutrino mass hierarchy and stepwise spectral swapping of supernova neutrino flavors. To appear in *Physical Review Letters.*

Duan, H., G. M. Fuller, J. Carlson, and Y. Z. Qian. Flavor evolution of the neutronization neutrino burst from an O-Ne-Mg core-collapse supernovae. To appear in *Physical review Letters.*

Duan, H., G. M. Fuller, J. Carlson, and Y. Z. Qian. Flavor Evolution of the Neutronization Neutrino Burst from an O-Ne-Mg Core-Collapse Supernovae. 2008. *Physical Review Letters.* **100**: 021101.

Duan, H., G. M. Fuller, J. Carlson, and Y. Z. Qian. Neutrino Mass Hierarchy and Stepwise Spectral Swapping of Supernovae Neutrino Flavors. 2007. *Physical Review Letters.* **99**: 241802.

Duan, H., G. M. Fuller, and J. Carlson. Simulating Nonlinear Neutrino Flavor Evolution. To appear in *Computational Science and Discovery.*

Friedland, A.. The Impact of Neutrino Magnetic Moments on the Evolution of Massive Stars. *Astrophysical Journal.*

Gehman, V. M., and S. R. Elliott. Multiple isotope comparison for determining neutrinoless double beta decay mechanisms. To appear in *Nuclear Instruments and Methods.*

Goldman, T., G. J. Stephenson, and B. H. J. McKellar. Multichannel oscillations and relations between KARMEN, LSND and MiniBooNE. 2007. *Physical Review.* **D75**: 091301.

Guiseppe, V., S. R. Elliott, A. Hime, D. M. Mei, and D. Perepelitsa. Neutron Inelastic Scattering in Natural Pb as a Background in Neutrinoless Double Beta Decay Experiments. *Physical Review C.*

Lippincott, W. H., K. J. Coakley, D. Gastler, A. Hime, E. Kearns, D. N. McKinsey, J. A. Nikkel, and L. C. Stonehill. Scintillation Time Dependence and Pulse Shape Discrimination in Liquid Argon. 2008. *Physical Review C.* **78**: 035801.

Mei, D. M., A. Hime, Z. B. Yin, and L. C. Stonehill. A Model of Nuclear Recoil Scintillation Efficiency in Noble Liquids. 2008. *Astroparticle Physics Journal.* **30**: 12.

Mei, D. M., S. R. Elliott, A. Hime, V. M. Gehman, and K. Kazkaz. Neutron inelastic scattering processes as background for double beta decay experiments. 2008. *Physical Review C.* **77**: 054614.

# Dark Energy and the Cosmic Web

*Katrin Heitmann*

20070005DR

## Introduction

The project focuses on the characterization of dark energy as derived from the large-scale distribution of galaxies in the Universe. In particular, it uses weak lensing, baryon acoustic oscillations, and clusters of galaxies measurements as probes of dark energy. In order to use these three probes very accurate high-performance simulations have to be carried out. A major thrust of this project is the development of a framework to combine a small number of very costly and very accurate cosmological simulations with observations of these three probes and to derive constraints on dark energy from this. The first – highly non-trivial – step is to show that the required accuracy level of 1% can be obtained in these simulations, then a suite of simulations has to be carried out which will lead finally to the desired constraints on dark energy. The project builds on Los Alamos strengths in three areas to achieve these goals: high-performance computing, verification & validation, and quantification of margins and uncertainties. During the first two years of the project the first two tasks have been successfully completed and the framework to combine data and simulations has been demonstrated to work with simulated data. During the last year the focus of the project will be on the combined data analysis.

## Benefit to National Security Missions

This project addresses two top Office of Science priorities: dark energy and supercomputing. This project targets robust knowledge extraction from large datasets using a combination of simulations and sophisticated data analysis, relevant to Quantification of Margins & Uncertainties for the weapons program. Our supercomputing supports techniques relevant to threat reduction.

## Progress

We have made significant progress in demonstrating that we can measure the dark matter power spectrum from our simulations at the 1% accuracy level out to wavenumbers k ~ 1h/Mpc. The power spectrum (and the related correlation function) is the most important cosmological statistic to learn about dark energy from baryon acoustic oscillations and weak lensing. Its precise prediction over a range of cosmologies is a cornerstone for the success of large-scale structure based probes of dark energy.

In order to show that the required accuracy has been attained, we proceeded in three steps. (i) A major code comparison study was carried out, the Cosmic Code Comparison Project. This project led to an invited paper for the inaugural issue of a new journal Computational Science and Discovery [1]. As part of the verification and data analysis work, new tools were implemented into ParaView, a visualization tool in part developed at Los Alamos. The broader goal of this part of the effort is to develop a general analysis framework which is able to cope with very large cosmological simulations in efficient ways. In addition, two more visualization papers were published [2,3]; we have received an invitation for a contribution to a special edition of IEEE Computer Graphics and Applications [4]; and two more papers are in preparation. (ii) We carried out a comprehensive cosmological initial condition verification program. One major result here was that the formation of structures will be suppressed if the simulation is started at too low a redshift [5]. (iii) After performing a set of final tests we started to carry out a large suite of cosmological dark matter simulations. This suite encompasses 32 cosmological models (the model selection is based upon our new cosmic calibration framework) and 21 realizations for each model; resulting in 672 simulations. This suite of simulations will be immensely valuable for a large number of projects. It has been completed recently and is currently analyzed.

An additional major component of the project is the development of a new simulation code that can take advantage of emerging hybrid architectures such as Roadrunner, the new supercomputer at Los Alamos. The code is under test right now. Due to this work a new LDRD project has been initiated.

Significant progress was made in the area of determining the mass function of dark matter halos. We studied the connection between different dark matter halo definitions. This project is extremely important to overcome problems in connecting observations of clusters of galaxies to simulations [6].

An observational component of our project deals with a special sub-population of groups of galaxies, the so-called fossil groups. So far only 15 fossil groups have been detected. We have discovered two new fossil groups and a system that might be in the pre-fossil group stage, leading to a publication [7]. A second paper on fossil groups is nearing completion. Several new fossil groups have been identified in the 400d survey. This new sample allows a controlled study of fossil groups in the optical and x-ray. Another observational component of the project deals with constraining dark energy from clusters of galaxies. One paper is currently under review [8], two more are in preparation. A theoretical study related to cluster masses has revealed important new insights on the normalization of the power spectrum [9].

Based on the cosmic calibration framework, which is being developed as part of this project [10], we have investigating questions about efficient covariance calculations [11]. In a different area, we are working with researchers from the University of Chicago and Simon Fraser University on determining reliable photometric redshifts for upcoming surveys such as the Dark Energy Survey and the Large Synoptic Survey Telescope. Such an effort is crucial for the success of these missions.

As a supplementary part of this project, cosmological shocks in adaptive mesh refinement simulations and the acceleration of cosmic rays have been investigated and a paper on the results has been accepted for publication [12].

## Future Work

We will investigate the nature of dark energy by studying 1) the expansion history of the Universe, and 2) the evolution of structure in the Universe. Structure in the Universe forms by gravity-driven amplification of primordial density fluctuations, leading to the complex distribution of mass as traced by the distribution of galaxies, the cosmic web. The intrinsic geometry of the web defined by dark matter and galaxies, and the properties and evolution of its structural components, such as galaxy clusters, are the twin information reservoirs for dark energy. They provide data on the evolution history of the Universe and the growth rate of structure formation, essential for distinguishing dark energy from modified gravity. The key to optimally and robustly extracting the encoded information is an integrated theory, simulation, and analysis program that puts the available observational datasets to full use. In this project we target baryon acoustic oscillations, galaxy clusters, and gravitational lensing as the prime data sources. The complementary nature of these probes provides essential cross-checks on the results obtained. These structure formation-based methods are sensitive in different ways to the dark energy equation of state and modifications of gravity. We will perform state-of-the-art high-performance simulations specifically targeted at these three probes and investigate and identify possible systematic problems. This is crucial for the design of next-generation dark energy observational missions. The theoretical component of the proposal lies in parameterizing and proposing new dark energy models and predictions for modified gravity, the simulation component in taking these models and generating predictions to compare to observational data, and the analysis program in developing the tools necessary for this essential last step. Two crucial components of the project are statistical analysis and visualization, where we dramatically impact and extend the frontier in combining information from large datasets and expensive simulations.

## Conclusion

Less than ten years have passed since the astonishing discovery of a mysterious agent driving an accelerated expansion of the Universe. This discovery has been hailed as the harbinger of a revolution in fundamental physics. Why is there so much excitement? Simply because no fundamental understanding exists. Cosmic acceleration demands completely new physics and challenges basic notions of quantum theory and general relativity. We will advance our understanding of dark energy with a powerful integrated approach which combines data, sophisticated theory, and world-leading simulations. We will precisely characterize dark energy and determine whether general relativity needs modification on cosmological scales.

## References


1. Heitmann, K., Z. Lukic, P. Fasel, S. Habib, M. S. Warren, M. White, J. Ahrens, L. Ankeny, R. Armstrong, B. O'Shea, P. Ricker, V. Springel, J. Stadel, and H. Trac. The cosmic code comparison project. To appear in *Computational Science and Discovery.*

2. Anderson, E., C. Silva, J. Ahrens, K. Heitmann, and S. Habib. Provenance in comparative analysis: A study in cosmology. 2008. *Computing in Science and Engineering.* **10**: 30.

3. Haroz, S., K. L Ma, and K. Heitmann. Multiple uncertainties in time-variant cosmological particle data.

2008. In *IEEE Pacific Visualization Symposium.* (Kyoto, Japan, 4 - 7 March, 2008). , p. 207. Kyoto: Piscataway, NJ, USA, IEEE.

4. Haroz, S., and K. Heitmann. Seeing the differences between cosmological simulations. 2008. *IEEE Computer Graphics and Applications.* **28**: 37.

5. Lukic, Z., K. Heitmann, and S. Habib. The halo mass function: High redshift evolution and universality . 2007. *Astrophysical Journal.* **671**: 1160.

6. Lukic, Z., D. Reed, S. Habib, and K. Heitmann. The structure of halos: Implications for group and cluster cosmology. To appear in *Astrophysical Journal.*

7. Voevodkin, A., C. Miller, K. Borozdin, K. Heitmann, S. Habib, P. Ricker, and R. Nichol. X-ray observations of optically selected giant elliptical-dominated galaxy groups. 2008. *Astrophysical Journal.* **684**: 204.

8. Vikhlinin, A., R. A. Burenin, H. Ebeling, W. R. Forman, A. Hornstrup, C. Jones, A. V. Kravtsov, S. S. Murray, D. Nagai, H. Quintana, and A. Voevodkin. Chandra cluster cosmology project II: Samples and X-ray data reduction . *Astrophysical Journal.*

9. Evrard, A. E., J. Bialek, M. Busha, M. White, S. Habib, K. Heitmann, M. Warren, E. Rasia, G. Tormen, L. Moscardini, C. Power, A. R. Jenkins, L. Gao, C. S. Frenk, V. Springel, S. D. M. White, and J. Diemand. Virial scaling of massive dark matter halos: Why clusters prefer a high normalization cosmology . 2008. *Astrophysical Journal.* **672**: 122.

10. Habib, S., K. Heitmann, D. Higdon, C. Nakhleh, and B. Williams. Cosmic calibration: Constraints from the matter power spectrum and the cosmic microwave background. 2007. *Physical Review D.* **76**: 083503.

11. Schneider, M. D., L. Knox, S. Habib, K. Heitmann, and D. Higdon. Simulations and cosmological inference: A statistical model for power spectra means and covariances. 2008. *Physical Review D.* **78**: 063529.

12. Skillman, S. W., B. W. O'Shea, E. J. Hallman, J. O. Burns, and M. L. Norman. Cosmological shocks in adaptive mesh refinement simulations and the acceleration of cosmic rays.

## Publications

Anderson, E., C. Silva, J. Ahrens, K. Heitmann, and S. Habib. Provenance in comparative analysis: A study in cosmology . 2008. *Computing in Science and Engineering.* **10** (3): 30.

Bashinsky, S.. Mapping cosmological observables to the dark kinetics. *Astrophysical Journal.*

Evrard, A. E., J. Bialek, M. Busha, M. White, S. Habib, K. Heitmann, M. S. Warren, E. Rasia, G. Tormen, L. Moscardini, C. Power, A. R. Jenkins, L. Gao, C. S. Frenk, V. Springel, S. D. M. White, and J. Diemand. Virial scaling of massive dark matter halos: Why clusters prefer a high normalization cosmology . 2008. *Astrophysical Journal.* **672**: 122.

Habib, S., K. Heitmann, D. Higdon, C. Nakhleh, and B. Williams. Cosmic calibration: Constraints from the matter power spectrum and the cosmic microwave background. 2007. *Physical Review D.* **76**: 083503.

Haroz, S., K. Ma, and K. Heitmann. Multiple uncertainties in time-variant cosmological particle data . 2008. In *IEEE Pacific Visualization Symposium.* (Kyoto, 4-7 March 2008). , p. 207. Kyoto: Piscataway, NJ, USA : IEEE.

Haroz, S., and K. Heitmann. Multiple uncertainties in time-variant cosmological particle data. 2008. *IEEE Computer Graphics and Applications.* **28** (5): 37.

Heitmann, K., Z. Lukic, P. Fasel, S. Habib, M. S. Warren, M. White, J. Ahrens, L. Ankeny, R. Armstrong, B. W. O'Shea, P. M. Ricker, V. Springel, J. Stadel, and H. Trac. The cosmic code comparison project. To appear in *Computational Science and Discovery.*

Li, C., D. E. Holz, and A. Cooray. Direct reconstruction of the dark energy scalar-field potential. 2007. *Physical Review D.* **75**: 103503.

Lukic, Z., D. Reed, S. Habib, and K. Heitmann. The structure of halos: implications for group and cluster cosmology. To appear in *Astrophysical Journal.*

Lukic, Z., K. Heitmann, S. Habib, S. Bashinsky, and P. M. Ricker. The halo mass function: High redshift evolution and universality. 2007. *Astrophysical Journal.* **671**: 1160.

Schneider, M. D., L. Knox, S. Habib, K. Heitmann, D. Higdon, and C. Nakhleh. Simulations and cosmological inference: A statistical model for power spectra means and covariances. 2008. *Physical Review D.* **78**: 063529.

Skillman, S. W., B. W. O'Shea, E. J. Hallman, J. O. Burns, and M. L. Norman. Cosmological shocks in adaptive mesh refinement simulations and the acceleration of cosmic rays. To appear in *Astrophysical Journal.*

Vikhlinin, A., R. A. Burenin, H. Ebeling, W. R. Forman, A. Hornstrup, C. Jones, A. V. Kravtsov, S. S. Murray, D. Nagai, H. Quintana, and A. Voevodkin. Chandra cluster cosmology project II: samples and X-ray data reduction . *Astrophysical Journal.*

Voevodkin, A., C. Miller, K. Borozdin, K. Heitmann, S. Habib, P. Ricker, and R. Nichol. X-ray observations of optically selected giant elliptical-dominated galaxy groups. 2008. *Astrophysical Journal.* **648**: 204.

# High-Current, High-Energy, Laser-Driven Ion Accelerators: An Enabling and Revolutionary Scientific Research Tool

*Juan Carlos Fernandez*

20070023DR

## Introduction

This project aims to extend the scientific understanding in relativistic laser-matter interactions to develop a revolutionary class of ion beams, driven by high-energy short-pulse lasers. Specifically, we intend to demonstrate efficient conversion of laser energy into ion beams. Based on encouraging initial simulation results, we hope to gain the understanding and control required to produce nearly monoenergetic ion beams, with the ability to control the ion energy over a range of up to hundreds of MeV/nucleon. This project is at the cutting edge of relativistic laser-matter interactions, plasma physics, massive multi-scale simulations and advanced accelerator development. This project also has the secondary goals of optimizing beam performance and assessing the suitability of these beams for two missions: a high-power C-ion beam in the 30-40 MeV/nucleon range, the energy suitable for fast ignition, and; a high-energy C-ion beam of >100 MeV/nucleon, as required for cancer therapy. We pursue these goals by means of a research program that integrates theory, modeling, laser development and experiments. The modeling is done primarily with the VPIC code running in the LANL Roadrunner supercomputer architecture [1, 2]. The experiments are done on the LANL Trident laser, one of the premier intermediate scale HEDP facilities in the world. In order to exploit these novel acceleration mechanisms, ultrathin targets (30 nm) and laser pulses with unprecedented contrast (about $10^{10}$) must be used. This is because stronger prepulses would destroy such thin targets prior to the arrival of the main pulse that drives the ion acceleration. As part of this project, a new and elegant pulse cleaning scheme to achieve the required contrast has been invented at LANL and fully implemented on Trident [3]. That makes Trident the high-energy laser system with the cleanest short-pulse in the world right now, and the only one capable of shooting targets in the range of 100 nm down to 3 nm, as demonstrated experimentally. Diamond-like C films (in thicknesses ranging from 3 – 60 nm) have been successfully fabricated and fielded as laser targets on Trident experiments. A large suite of massive simulations (some already completed) is used to guide the experimental work. Initial experimental campaigns have been deployed on Trident in FY08, where C-ion energies of up to 400 MeV have been observed. A more definitive experimental exploration of the scheme and validation of our understanding and modeling are planned for FY09.

## Benefit to National Security Missions

Laser-matter interactions are important to the DOE Science mission. Energetic-ion interactions with dense plasmas are an important problem in High Energy Density Physics, supporting the Science and Nuclear-Weapons missions. Energetic ions might enable the "fast ignition" scheme on the National Ignition Facility, which impacts the Energy and Weapons missions of the DOE. Highly compact accelerators could provide new means to probe for nuclear materials, with benefit to nuclear nonproliferation and counter-nuclear smuggling (homeland security).

## Progress

At the end of FY08 (two-thirds into the project duration), this project can list significant accomplishments.

- There has been significant progress in scoping out advanced acceleration mechanisms (the originally conceived one, and a new candidate), with C as the chosen ion species, using a large number of massive, state-of-the-art simulations with the VPIC code in 1, 2 and 3D [2]. A typical VPIC 3D simulation features solid-density targets, using 14 billion cells and 21 billion particles, performed with 4096 processors on the base (un-accelerated) system of Roadrunner.

- There has been significant progress in understanding theoretically the physics operative in the Break-Out Afterburner (BOA) novel acceleration mechanism [4]. BOA requires a thin target (in the tens of nm range), and a laser intensity that is sufficiently high (> $10^{20}$ W/cm$^2$). Under those conditions, after an initial phase of the more familiar target-sheath

normal acceleration (TNSA) based on the electrostatic field from laser-driven charge separation, BOA sets in. The laser penetrates and heats the bulk of the thin targets, also aided by the effect known as relativistic transparency (the plasma frequency decreases when the electrons are relativistic). As the result, the laser ponderomotive force both heats the electrons volumetrically and imparts on them a large directed velocity, relative to the ions. That condition leads to a very fast growing instability, known as the Buneman instability, which transfers energy from the electron drift to the ions, resulting in dramatic ion acceleration. Initially, the ion gains energy as a nearly monoenergetic beam. As seen in simulations, if the laser pulse continues long enough, the ions continue to gain energy, but the energy distribution spreads due to spatial spreading of the electrons and other effects. As we gain more understanding, we are learning that the ion energy and the beam energy distribution depend on many parameters in ways that we do not fully understand yet: target thickness, laser pulse duration, temporal and spatial shape of the laser pulse, and laser intensity. The better understanding required to optimize properly both ion energy and energy spread, remains as the main scientific thrust in the remainder of this project. Due to the ultra-thin targets required, and thus the ultra-high laser-pulse contrast required, Trident is the only laser in the world where BOA can be studied.

- We have also begun exploring other concepts that promise high-energy ion beams, especially the so-called Radiation Pressure Acceleration (RPA) [5]. This scheme requires similar target thicknesses and intensities as BOA, provided a circularly polarized laser pulse at nearly normal incidence is used. Contrary to a linearly polarized-beam, a circularly polarized beam mostly pushes the electrons longitudinally, rather than heating them. The ponderomotive push is so strong that the electron population gets pushed ahead of the ions, creating a huge charge- separation electric field. If the laser continues to drive the plasma, that field can accelerate the ions to ? GeV and beyond. We have implemented a circularly polarized beam on Trident, where, again, due to the small target thickness and thus the high pulse contrast required, it is the only laser where RPA can be studied presently. A number of VPIC simulations have indicated the quantitative requirements for the process to work, and initial experiments on Trident have been conducted.

- We have obtained and fielded on Trident the ultra-thin (3 – 60 nm) diamond-like C foils required by these advanced ion-acceleration schemes. These targets have been fabricated, characterized and provided to us by our collaborators at the Ludwig Maximilians Universität (LMU) in Munich. The fabrication method is based on vapor deposition. We have also endorsed an SBIR proposal by Applied Diamond Inc., which would create a domestic industrial supplier of these thin films in the US. Moreover, we have also located a source of similarly thin graphitic C films, sold by the TRIUMF accelerator group in Canada. The project PI has actually seen and manipulated sample foils fabricated by that group.

- We have devised an elegant scheme to reach the laser-pulse contrast ratio (> $10^{10}$ ) required to shoot such targets, named SPOPA (Short Pulse Optical Parametric Amplification) [3]. This work is being patented and will be published subsequently. This accomplishment is critical, because when using thin targets, the prepulse associated with conventional laser technology would destroy the target much before the high-intensity part of the pulse arrives. This scheme has been implemented on Trident, and its ability to drive ion beams successfully, at full laser energy, has been demonstrated on C targets as thin as 3 nm. There is no instrument yet that is capable of measuring such high laser-pulse contrast, so we estimated the contrast by looking at the survivability of targets under low energy Trident pulses, as surrogates for prepulses in a full energy shot. We have tested both ps prepulses due to multiple reflections from optics in the amplifier chain, and amplified spontaneous emission (ASE) pedestals of order  ns, on which the main pulse sits. As a result of this study, we have bounded the “prepulse” level to less than $< 5 \times 10^{-10}$ for ps prepulses, and $< 2 \times 10^{-12}$ for ASE pedestal. This is an astonishing level of performance.

- Prior to availability of fully amplified SPOPA pulse on Trident, we have fielded successfully full system shots with thin targets at the $10^{10}$ contrast level, using 2 plasma mirrors in sequence.  In spite of the known, relatively high energy losses with plasma mirrors, we believe we have delivered up to 40 J on target using this technique. The results are consistent with our expectations that the targets with thicknesses of 10 nm and above survive the pre-pulse hydrodynamic shock. C ions with energy of up to 200 MeV energies were observed, as shown in Figure 1, which shows the C-ion energy spectrum with 40 J laser energy on target, a thin (60 nm) DLC foil, (with C ion energies of up to 200 MeV), compared to the C spectra from a thin C-layer on a Pd substrate (black squares) [6], and from a 5 micron DLC target (green rectangles).

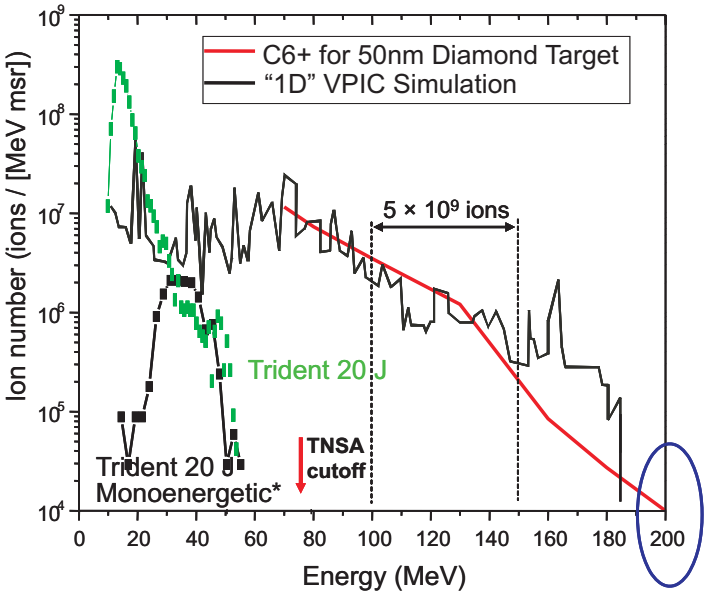


*Figure 1. Carbon ion spectra from the Trident 0.5 ps laser pulse on a 50 nm diamond-like carbon (DLC) target. The black line is the prediction from a VPIC simulation, the red is the data. Note the much better performance compared to two other targets. One is a thin C film on a Pd foil [6], and the other is a 5-micron DLC target. The TNSA prediction for the maximum C energy is 75 MeV, showing other processes are operative.*

- Once the fully amplified SPOPA pulse was available on Trident, we fielded successfully full system shots with thin targets, using various target thicknesses, down to 3 nm. Pulses of up to 90 J were delivered to these targets. Both proton and C beams were observed. C ions with energy of up to 400 MeV energies were observed in this initial attempt.

- Circularly-polarized full energy short pulses have been demonstrated on Trident, a key capability required to study the RPA ion-acceleration mechanism.

- We have developed the concept of FI based on these laser-driven ion beams. Using integrated calculations with the LASNEX code, we have designed an integrated FI proof of principle experiment to demonstrate modest fusion gain, suitable for Omega EP or for NIF/ARC [7]. This design would work equally well with a variety of ion species. A collaboration with Prof. Honrubia and Dr. Temporal at the Univ. Politecnica de Madrid has extended our understanding of the requirements for ion-driven FI, just presented at the IAEA Fusion Conference in Geneva, October 2008. These results are summarized in Figure 2 and 3. Figure 2 shows three specific target plasmas that could be ignited by a laser-driven ion beam. Figure 3 shows the minimum total energy of a C ion beam to ignite, as a function of ion energy. It is seen that the optimum ignitor-beam C-ion energy , for the realistic target calculated self consistently with the LASNEX hydrocode [8], lies at 35 MeV/nucleon, where a 12 kJ beam energy is required. These results are presented in the conference proceedings [9].

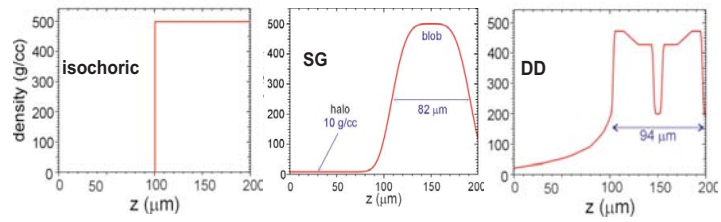


*Figure 2. Three DT fuel assemblies studied for Fast Ignition (FI): Left, ideal isochoric sphere at 500 g/cc; Middle, a super Gaussian (SG) profile; Right, a direct-drive implosion using 485 kJ of laser energy.*

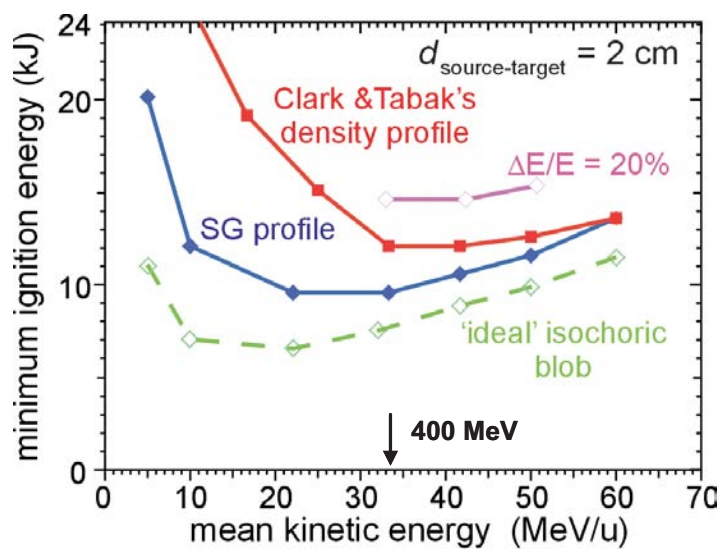


*Figure 3. Minimum beam energy (kJ) necessary to ignite the various DT fuel assemblies shown in Figure 2, versus ion-energy per nucleon. The minimum is around 400 MeV for C ions.*

- TNSA-based proton acceleration remains important for the community and as a viable candidate for FI, which only requires moderate energy protons. On that front, this project is delivering important, if unanticipated, results. Based on Trident experiments, we are developing a consistent picture of how proton acceleration performance can be improved by two main factors: better laser-pulse contrast and better target morphology. Morphology improvements have been explored using novel targets featuring a cone & "pizza-top" geometry at the 30 TW level, which gives higher proton acceleration performance: higher conversion efficiency of the laser to the ion beam, and higher peak energy (> 30 MeV versus 20 MeV for flat foils) [10]. For a given laser energy, proton acceleration on Trident using flat foils often outperforms the results from other lasers, perhaps due to better pulse contrast. E.g., on a Trident shot (a 10micron Mo foil target, a laser energy on

target of 87 J, a pulse length of 660 fs [132 TW] and a laser intensity of $5x10^{19}$ W/cm$^2$) a TNSA proton beam on Trident has been produced with a high-energy cut-off just above 50 MeV. This comes close to the best performance of lasers worldwide. The mighty Nova PW laser, now decommissioned, achieved just 58 MeV at four times the energy and 6 times the intensity.

- We have successfully demonstrated the manipulation and focusing of laser-produced proton beams using miniature quadrupole magnetic lenses, provided to us by our collaborators at the Max Planck Quantum Optics & LMU in Munich. This was accomplished on experiments on Trident in the Fall of 2007 and on Z-beamlet in December 2007 [11].

## Future Work

This project has a primary motivation of developing a revolutionary ion beam technology based on the "laser-plasma afterburner" concept. This high-risk, high payoff goal depends, of course, on whether the initial modeling turns out to be right, and whether the desired level of performance can be actually realized with the performance available on Trident. The scientific deliverable is a validated theory and modeling capability that allows us to ascertain what experimental conditions are needed to achieve the performance desired. Specific questions involve how the various ion beam characteristics depend on laser and target parameters.

Based on the accomplishments to date, we intend to deliver, by the end of this project, the validated theory and modeling necessary to guide us to our goals, by means of a research program that integrates theory, modeling and experiments. The remaining broad tasks include: 1) perform the suite of simulations corresponding to the laser pulses that can be delivered by the improved Trident, to the DLC targets that have been developed. 2) Compare those simulations to the results from preliminary experiments in FY08. 3) If the agreement is not acceptable, understand the discrepancy and modify the models accordingly. Otherwise, assuming good agreement, refine our theoretical models, to provide guidance on how to optimize performance within the scope of the targets that we may be able to fabricate, and the available performance on Trident. 4) Use that understanding to run specific simulations to design optimized experiments for FY09. 5) Field those experiments and validate our theory and modeling capability. 6) Use that validated predictive capability to specify what is necessary to reach the ion-beam parameters required by each of our three identified stakeholders: boost, FI and cancer therapy.

## Conclusion

Our primary goal is to develop a revolutionary class of ion beams, driven by high-energy short-pulse lasers. Specifically, we intend to validate our theoretical and computational models on relativistic laser-matter interactions, the best in the world, with experiments using the unique capabilities of the LANL Trident laser. That validated capability will be used to understand what laser and target parameters are necessary to demonstrate high-efficiency conversion of laser energy into nearly monoenergetic ion beams, and the simultaneous ability to control the ion energy over a range of up to hundreds of MeV/nucleon. We are well on our way to deliver the required understanding. A new scheme to produce ultra-high contrast laser pulses has been invented and implemented on Trident. The ultra-thin targets in the range necessary for the BOA and RPA mechanisms have been produced and successfully fielded on Trident. Laser-driven C beams, with a high-energy cutoff of 400 MeV, have been already produced on Trident.

## References


1. Bowers, K. J., B. J. Albright, L. Yin, B. Bergen, and T. J. T. Kwan. Ultrahigh performance three-dimensional electromagnetic relativistic kinetic plasma simulation. 2008. *Physics of Plasmas.* **15**: 055703.

2. Yin, L., B. J. Albright, B. M. Hegelich, K. J. Bowers, K. A. Flippo, T. J. T. Kwan, and J. C. Fernandez. Monoenergetic and GeV ion acceleration from the laser breakout afterburner using ultrathin targets. 2007. *Physics of Plasmas.* **14**: 056706.

3. Shah, R. C., R. P. Johnson, T. Shimada, K. A. Flippo, J. C. Fernandez, and B. M. Hegelich. High-temporal contrast using low-gain optical parametric amplification. *Optics Letters.*

4. Albright, B. J., L. Yin, K. J. Bowers, B. M. Hegelich, K. A. Flippo, T. J. T. Kwan, and J. C. Fernandez. Relativistic Buneman instability in the laser breakout afterburner. 2007. **14**: 094502.

5. L.Robinson, A. P., M. Zepf, S. Kar, R. G. Evans, and C. Bellei. Radiation pressure acceleration of thin foils with circularly polarized laser pulses. 2008. *New Journal of Physics.* **10**: 013021.

6. Hegelich, B. M., B. J. Albright, J. Cobble, K. Flippo, S. Letzring, M. Paffett, H. Ruhl, J. Schreiber, R. K. Schulze, and J. C. Fernandez. Laser acceleration of quasi-monoenergetic MeV ion beams. 2006. *Nature.* **439**: 441.

7. Fernandez, J. C., B. J. Albright, K. A. Flippo, B. M. Hegelich, T. J. T. Kwan, M. J. Schmitt, and L. Yin. Progress on ion based fast ignition. 2008. *Journal of Physics: Conference Series.* **112**: 022051.

8. Clark, D., and M. tabak. A self-similar isochoric implosion for fast ignition. 2007. *Nuclear Fusion.* **24**: 1147.

9. Fernandez, J. C., J. J. Honrubia, B. J. Albright, K. A. Flippo, D. C. Gautier, B. M. Hegelich, M. J. Schmitt, M. Temporal, and L. Yin. Progresson the development of ion-based fast ignition. To appear in *IAEA Fusion Conference 2008.* (Geneva, 13-18 October).

10. Flippo, K. A., E. d'Humieres, S. A. Gaillard, J. Rassuchine, D. C. Gautier, M. Schollmeier, F. Nurnberg, J. L. Kline, J. Adams, B. Albright, M. Bakeman, K. Harres, R. P. Johnson, G. Korgan, S. Letzring, S. Malekos, N. Renard-LeGalloudec, Y. Sentoku, T. Shimada, M. Roth, T. E. Cowan, J. C. Fernandez, and B. M. Hegelich. Increased efficiency of short-pulse laser-generated proton beams from novel flat-top cone targets. 2008. *Physics of Plasmas.* **15**: 056709.

11. Schollmeier, M., S. Becker, M. Geissel, K. A. Flippo, A. Blazevic, S. A. Gaillard, D. C. Gautier, F. Gruner, K. Harres, M. Kimmel, F. Nurnberg, P. Rambo, U. Schramm, J. Schreiber, J. Schutrumpf, J. Schwarz, N. A. Tahir, B. Atherton, D. Habs, B. M. Hegelich, and M. Roth. Controlled Transport and Focusing of Laser-Accelerated Protons with Miniature Magnetic Devices. 2008. *Physical Review Letters.* **101**: 055004.

## Publications

Albright, B. J., L. Yin, K. J. Bowers, B. M. Hegelich, K. A. Flippo, T. J. T. Kwan, and J. C. Fernandez. Relativistic Buneman instability in the laser breakout afterburner. 2007. *Physics of Plasmas.* **14**: 094502.

Albright, B. J., M. J. Schmitt, J. C. Fernandez, G. E. Cragg, I. Tregillis, L. Yin, and B. M. Hegelich. Studies in capsule design for mid-Z ion-driven fast ignition. 2008. *Journal of Physics: Conference Series.* **112** (2): 022029 .

Bowers, K. J., B. J. Albright, L. Yin, B. Bergen, and T. J. T. Kwan. Ultrahigh performance three-dimensional electromagnetic relativistic kinetic plasma simulation (invited). 2008. Physics of Plasmas. **15** (5): 055703.

Fernandez, J. C., B. J. Albright, K. A. Flippo, B. M. Hegelich, T. J. Kwan, M. J. Schmitt, and L. Yin. Progress on ion based fast ignition. 2008. *Journal of Physics: Conference Series.* **112** (2): 022051.

Fernandez, Juan C., J. J. Honrubia, B. J. Albright, K. A. Flippo, D. C. Gautier, B. M. Hegelich, M. J. Schmitt, M. Temporal, and L. Yin. Progress on the development of ion-based fast ignition. To appear in *22nd IAEA Fusion Conference.* (Geneva, Switzerland, 13-18 October 2008).

Flippo, K. A., E. d'Humieres, S. A. Gaillard, J. Rasuchine, M. Schollmeier, B. Albright, M. Bakeman, T. E. Cowan, D. C. Gautier, K. Harris, R. P Johnson, S. Letzring, F. Nurnberg, M. Roth, J. C. Fernandez, and B. M. Hegelich. Increased efficiency of short-pulse laser generated proton beams from novel flat-top cone targets (invited). 2008. *Physics of Plasmas.* **15** (5): 056709.

Flippo, K., B. M. Hegelich, B. J. Albright, L. Yin, D. C. Gautier, S. Letzring, M. Schollmeier, J. Schreiber, R. Schulze, and J. C. Fernandez. Laser-driven ion accelerators: spectral control, monoenergetic ions and new acceleration mechanisms. 2007. *Laser and Particle Beams.* **25** (1): 3.

Fuchs, J., Y. Sentoku, E. d'Humieres, T. E. Cowan, J. Cobble, P. Audebert, A. Kemp, A. Nikroo, P. Antici, E. Brambrink, A. Blazevic, E. M. Campbell, J. C. Fernandez, J. C. Gauthier, M. Geissel, M. Hegelich, S. Karsch, H. Popescu, N. Renard-LeGalloudec, M. Roth, J. Schreiber, R. Stephens, and H. Pepin. Comparative spectra and efficiencies of ions laser-accelerated forward from the front and rear surfaces of thin solid foils. 2007. *Physics of Plasmas.* **14**: 053105.

Gautier, D. C., K. Flippo, J. C. Fernandez, B. M. Hegelich, and J. Fuchs. Time resolved analysis of the expansion of isochoricly heated thin foils. 2007. In *2007 IEEE Pulsed Power Plasma Science Conference.* (Albuquerque, NM, USA, 17-22 June 2007). Vol. ISBN 978-1-4244-0913-6, p. 610. Piscataway, NJ, USA: IEEE.

Harres, K., M. Schollmeier, E. Brambrink, P. Audebert, A. Blazevic, K. Flippo, D. C. Gautier, M. Geissel, B. M.

Hegelich, F. Nurnberg, J. Schreiber, H. Wahl, and M. Roth. Development and calibration of a Thomson parabola with microchannel plate for the detection of laser-accelerated MeV ions. 2008. *Review of Scientific Instruments.* **79** (9): 093306.

Hegelich, B. M.. Ultra-high intensity laser acceleration of ions to MeV/nucleon energies. 2007. In *2007 IEEE PARTICLE ACCELERATOR CONFERENCE.* (Albuquerque, NM, USA, 25-29 June 2007). Vol. ISBN 978-1-4244-0916-7, p. 2512. Piscataway, NJ, USA: IEEE.

Schollmeier, M., K. Harres, F. Nurnberg, A. Blazevic, P. Audebert, E. Brambrink, J. C. Fernandez, K. A. Flippo, D. C. Gautier, M. Geissel, B. M. Hegelich, J. Schreiber, and M. Roth. Laser beam-profile impression and target thickness impact on laser-accelerated protons. 2008. *Physics of Plasmas.* **15** (5): 053101.

Schollmeier, M., M. Roth, A. Blazevic, E. Brambrink, J. A. Cobble, J. C. Fernandez, K. A. Flippo, D. C. Gautier, D. Habs, K. Harres, B. M. Hegelich, T. Hessling, D. H. H. Hoffmann, S. Letzring, F. Nurnberg, G. Schaumann, J. Schreiber, and K. Witte. Laser ion acceleration with micro-grooved targets. 2007. *Nuclear Instruments and Methods in Physics Research A.* **577**: 186.

Schollmeier, M., S. Becker, M. Geissel, K. A. Flippo, A. Blazevic, S. A. Gaillard, D. C. Gautier, F. Gruner, K. Harres, M. Kimmel, F. Nurnberg, P. Rambo, U. Schramm, J. Schreiber, J. Schutrumpf, J. Scharwz, N. A. Tahir, B. Atherton, D. Habs, B. M. Hegelich, and M. Roth. Controlled transport and focusing of laser-accelerated protons with miniature magnetic devices . 2008. *Physical Review Letters.* **101** (5): 055004.

Shah, R. C., R. P. Johnson, T. Shimada, K. A. Flippo, and J. C. Fernandez. High-temporal contrast using low-gain optical parametric amplification. *Optics Letters.*

Yin, L., B. J. Albright, B. M. Hegelich, K. J. Bowers, K. A. Flippo, T. J. T. Kwan, and J. C. Fernandez. Monoenergetic and GeV ion acceleration from the laser breakout afterburner using ultrathin targets (invited). 2007. *Physics of Plasmas.* **14** (5): 056706.

# Cold Atom Surface Imaging

*Eddy Marcel Elvire Timmermans*

20070028DR

## Introduction

This project exploits the laser-like coherence of cold atom Bose-Einstein condensate (BEC) systems for developing a coherent optics technique that can image the fields and forces near surface structures. The project also aims at exploring the exquisite sensitivity of BEC's to external forces to observe and probe the quantum fluctuation-induced forces, Casimir-Polder forces, that are experienced by atoms near surfaces and sensitive to geometrical structures as well as to the material composition of the surface. The coherent BEC optics technique could give an imaging method that has access to the ten nanometer scale resolution that is currently hard to handle with current surface miscroscopy techniques. The Casimir-Polder forces play an important role in nanotechnology and are difficult to measure with non-trivial geometries.

The participants of this project focus on quantum fluctuations relevant to the near-surface physics that plays a crucial role in nanotechnology; they propose ultra-sensitive probes and explore limitations and realizations of such probes and they develop cold atom optics with Bose-Einstein condensates (BEC's) for the demonstration and development of a novel surface microscopy. The theoretical and experimental work has been organized around three closely related focal points: 1) near-surface quantum fluctuation physics, 2) ultra-sensitive quantum probes, and 3) slow matter wave holography. The coordination of theory and experiment and the interplay of multiple areas of expertise – surface, solid state and many-body physics, classical and quantum optics, as well as cold atom physics – is creating a unique, highly visible project that optimizes the advantages of the Los Alamos National Laboratory science environment.

## Benefit to National Security Missions

This project supports the DOE mission in basic science by developing cold atom systems, of fundamental interest, into practical sensing and microscopy technologies, which can probe, condensed matter surfaces in novel length scales. The results can enhance the LANL capabilities in material science and quantum information. Advances in sensing have potential benefit to multiple missions, including homeland security, support to DoD, and nuclear nonproliferation.

## Progress

In addition to developing a new capability that we suggest will be useful to the laboratory in the near future, the project is producing a number of scientific products: novel concepts for cold atom and quantum physics and tools for experimental, numerical and mathematical use. Among the concepts, we cite the use of phase separated Bose-Einstein condensates (BEC's) to create a high-sensitivity weak force probe, the development of a perturbation approach to calculate Casimir forces (caused by quantum field vacuum fluctuations constrained by boundary conditions of the surface) for geometrical surface structures, the creation of macroscopic Schrodinger cat states in first-order quantum phase transitions and the use of freely expanding BEC's to image external potentials and fields holographically. The tools that are being developed include a mathematical framework to understand the effects of quantum evolution in many-body systems and the development of an efficient non-linear Schrodinger equation solver to simulate BEC-dynamics.

Dalvit and Da Rosa have developed methods to calculate Casimir forces for atoms near geometrical surface structures – a corrugated surface in one case and a wedge in another. Mozyrsky has developed a general non-equilibrium Green function framework to account for the relaxation of the BEC near the surface as a function of systems. Timmermans showed that the tun-

ability of trapping frequencies of trapped phase separated BEC's can nearly cancel the buoyancy and trapping force experienced by a phase separated bubble immersed in an immiscible, larger trapped BEC. This device, a BEC-level (analogous to the spirit'-level device in building) yields a hypersensitive weak force detector. Estimates of the experimental accuracies suggest a sensitivity that could allow Casimir force measurements as far away from the surface as 50 or 80 micron. By superimposing a shallow double well-potential experienced by the bubble, one can also create a many-body Schrodinger cat state - a superposition of two states in which the entire bubble resides either in one well or in the other well (surface tension could preclude states in which the bubble gets divided between both wells). Mozyrsky has shown that the zero temperature phase separation in mixtures of fermions and bosons, which is a first-order quantum phase transition, can spontaneously create many-body Schrodinger cat states in which the system can oscillate between a separated and non-separated phase. Cucchietti proposed and studied the detection of critical points of quantum phase transitions with a Loschmidt echo, taking advantage of the sensitivity of the systems near criticality. The efficiency of quantum probes depends sensitively on quantum effects in its time evolution. Berman, partly in consultation with Dalvit and Timmermans, has developed a novel mathematical framework for treating quantum effects in many-body dynamics.

The experimental component of the project focused on matter wave holography and on applying the BEC oscillator technique to surfaces that modify the Casimir-Polder interaction. In the second year of the project, the laboratory work was aimed towards a first demonstration of matter wave holography. This experiment would record a slice of the interference pattern resulting from scattering a Bose-Einstein condensate off a complex potential painted by a rapidly-rastered laser beam. Rather than work in 3D and image a slice of the interference pattern, we have decided to use a cylindrically-focused red-detuned laser beam to form a light sheet trap which confines all of the atoms to a horizontal plane. We now have in place a sophisticated computer-controlled deflection system that allows us to create completely arbitrary 2D potentials on top of the light sheet that can serve as the scatterer. Superimposed on the sheet is a tightly-focused red-detuned beam, which propagates vertically, forming an "optical tweezer" (below left) within the light sheet. The tweezer traps a few thousand condensate atoms. The tweezer beam is controlled by our deflection system, so it can be rapidly switched from forming a single beam trap to painting a complex potential. Figure 1 illustrates this capability by showing measured and calculated interference patterns in the density of atoms that were initially contained in two, three of four potential wells painted by our technique, and were released when all trapping potentials were switched off. We can also switch off the tweezer beam only to allow the BEC to expand in the plane and then image (through the sheet) the fringes produced when the expanding condensate scatters off the painted potential. The images below show observed and computed matter wave interference patterns for the expansion and overlap of two, three, and four tweezers respectively, demonstrating that our imaging system has sufficient resolution to resolve the interference fringes. We have also been able actually create and manipulate condensates in time-averaged potentials with various shapes. This new result assures us that the system will also be able to make smooth and well-controlled potentials to serve as the first holographic imaging targets, the goal we are currently pursuing. In the other experimental thread, we have designed, in consultation with Dalvit and with our fabrication colleagues at Sandia National Laboratory, a patterned surface that can be placed inside the vacuum system near the BEC. Fabrication of this chip was recently completed at Sandia. Figure 2 shows one of the fabricated surfaces, characterized by Marilyn Hawley in MST-8.

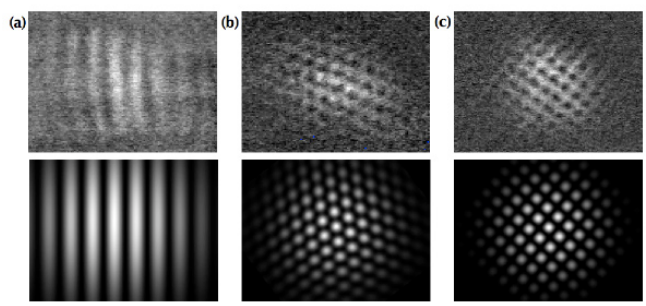


*Figure 1. Observed and Simulated interference patterns of falling Bose-Einstein condensates (BEC's) initially trapped in two, three and four potential wells. For the observed patterns shown in the upper images, the BECs were trapped by painted potentials.*

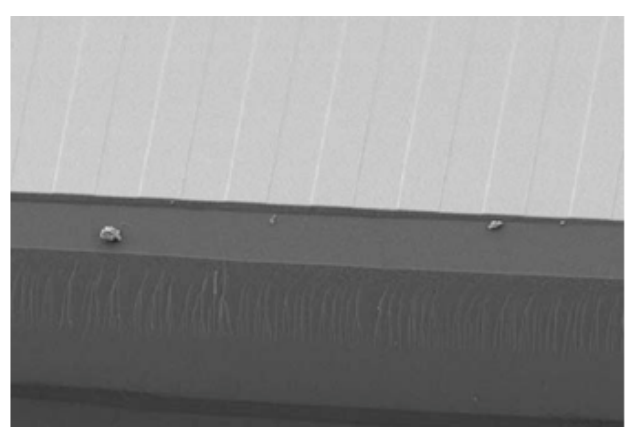

*Figure 2. Image of a surface structures fabricated at Sandia. Surfaces such as these will be used to measure the modification of the Casimir force experienced by atoms near geometrical structures.*

With thirteen publications in print, four of which appeared in Physical Review Letters, the project has had high-profile output during the first two years of its duration. The visibility of the project has lead to eleven invited talks, half of which where delivered at international venues, mostly at high-profile workshops and conferences. The project's work has been featured the popular literature – Dalvit was asked to prepare a contribution to the Science and Technology Section of 'the Economist', and Timmermans' work on phase separated BEC's for weak force measurement was featured in Physics World and in the Virtual Journal of Nanoscale Science & Technology.

## Future Work

This project will exploit the exquisite sensitivity of cold atom Bose-Einstein condensates (BEC's) to external forces and fields for the development of a new surface microscopy and surface probe. The long-term aim towards which this project will work is the production of BEC-devices that sense weak forces as well as measure electric and magnetic fields near physical surfaces on length scales that are inaccessible to current surface technology. Specifically, the prospective BEC-technology promises the imaging of surface fields with a variable in-plane resolution that can be tens of nanometers, the measurement of all three vector components (in-plane as well as out-of-plane) of these fields, and the measurement of vacuum fluctuation forces near engineered surface structures with topologies or surface compositions relevant to nanotechnology.

To achieve these goals, we will proceed along two different lines (a) for the slow matter wave holography work and (b) for the vacuum fluctuation force measurements. To achieve BEC-holography (a), we will first develop the theoretical description of slow matter holography, then test the description with simulations, which will also help with designing the first experiments that we will undertake to demonstrate the holographic imaging technique, scattering the BEC from a well-defined laser-induced external potential. A next step could be the imaging of an electric field near a `tip', before proceeding with full surface measurements. To measure the electromagnetic vacuum forces with a BEC-oscillator (b), we will design a highly stable optical/magnetic trap that brings the BEC close to the surface and gives the ability to accurately determine the BEC-distance from the surface. While this trap is being constructed and tested, we will design and order the relevant surface structures from Sandia National Laboratory, as well as perform theoretical calculations to estimate the outcome of the measurements and help with the surface structure design.

## Conclusion

This project is laying the groundwork for a novel surface technology that will complement existing surface microscopes. Bose-Einstein condensate (BEC) based holography will probe surfaces with an in-plane resolution on a novel magnification scale, ranging, for instance, from ten to a hundred nanometers, a magnification that is currently not generally available in surface microscopy, and will measure all three components of electric and magnetic fields. The BEC pendulum will measure the electromagnetic vacuum fluctuation induced forces, which are weak on a microscopic scale, but dominate at the sub-micron scale of current nanotechnology.

## Publications

A.R.Dalvit, D., P. A. Maia Neto, A. Lambrecht, and S. Reynaud. Probing quantum vacuum geometrical effects with cold atoms. *Physical Review Letters.*

Berman, G. P., D. A. R. Dalvit, and F. Borgonovi. Quantum dynamical effects as a singular perturbation for observables in open quasi-classical nonlinear mesoscopic systems. To appear in *Chaos, Solitons and Fractals.*

Berman, G. P., D. A.R. Dalvit, G. V. Schlyapnikov, N. Tarkhanov, and E. M. Timmermans. On the stability of a Bose-Einstein condensate trapped in a one-dimensional toroidal geometry. *International Journal of Theoretical Physics.*

Berman, G. P., G. L. Celardo, F. M. Izraelev, and V. G. Zelevinsky. Transition from isolated to overlapping resonances in the open system of interacting fermions. 2008. *Physics Letters B.* **659**: 170.

Berman, G. P., and N. Tarkhanov. Quantum dynamics in the Fermi-Pasta-Ulam problem. 2006. *International Journal of Theoretical Physics.* **45**: 1865.

Bhongale, S., and E. Timmermans. BEC-level for measuring small forces. *Physical Review Letters.*

C.N.Mendes, T., F. S.S. Rosa, A. Tenorio, and C. Farina. Dispersion forces between an atom and a perfectly conducting wedge. *Journal of Physics A.*

Celardo, G. L., F. M. Izrailev, V. G. Zevelinsky, and G. P. Berman. Open system of interacting fermions: statistical properties of cross-sections and fluctuations. 2007. *Physical Review E.* **76**: 031119.

Merkli, M., I. M. Sigal, and G. P. Berman. Decoherence and thermalization. 2007. *Physical Review Letters.* **98**: 130401.

Merkli, M., I. M. Sigal, and G. P. Berman. Resonance theory of decoherence and thermalization. 2008. *Annals of Physics.* **323**: 373.

S.S.Rosa, F., T. N.C. Mendes, and C. Farina. Spontaneous emission of an atom near a wedge. *Journal of Physics A.*

Solenov, D., and D. Mozyrsky. Kinetics of the phase separation transition in cold-atom boson-fermion mixtures. 2008. *Physical Review Letters.* **100**: 150402.

Zurek, W. H., F. M. Cucchietti, and J. P. Paz. Gaussian decoherence and Gaussian echo from spin environments. 2007. *Acta Physica Polonica B.* **38** (5): 1685.

# Multiscale Modeling of Strongly Interacting Systems

*Robert Everett Ecke*

20070505DR

## Introduction

This project focuses on the most challenging and, arguably, relevant class of many-body systems: systems that are intractable by brute force-methods because their physics depends intrinsically and crucially on the role of interactions and correlations and/or on the interplay of multiple length and/or time scales. The list of problems that fall within this category -- turbulence in fluids, disordered systems, classical and quantum phase transitions, quantum chromodynamics (in the high-energy limit), conventional and high temperature superconductivity -- illustrate their ubiquity in nature, their relevance and the central role they have played in the development of science. The complexity that follows from the intertwining of scales and the nonlinearity that results from the inclusion of inter-particle interactions and correlations places the description of this physics among the most challenging focal points of science. In addition to focusing on fundamental, frontier physics, this project also impacts practical engineering areas and contributes to core missions of the laboratory.

The participants of this project further the understanding of the strength of materials including elastic and plastic material response, fluid turbulence and mixing, macroscopic quantum systems: superconductors and Bose-Einstein condensates, optimization of designing nanotechnological devices and mathematical physics of multi-scale problems.

## Benefit to National Security Missions

This work supports the DOE mission in Nuclear Weapons by enhanced understanding of fluid turbulence and greater capabilities to model the dynamics of materials. It also supports the DOE Energy Security mission through new methods and approaches in the areas of superconductivity and nano science and technology.

## Progress

In the past year, this project has spawned a number of new insights by exploring intriguing prospects of new technologies (such as cold atom physics and nanotechnology), by employing non-equilibrium transport approaches to quantum problems, by applying Ginzburg-Landau free-energy approaches to the description of plasticity in martensitic phase transformations, by transferring techniques across fields (such as between nonlinear physics and many-body quantum physics) and by exploiting the power of novel numerical techniques (turbulence). This multi-disciplinary approach provides a powerful strategy to bring fundamental advances and provides different angles of attack to the description of multi-scale systems. Below, we provide a few selected highlights of CNLS postdoc research that illustrates the advantages of such multi-disciplinary approach.

The recent reports of an observed anomaly in the torsion balance measurements of superfluid helium under high pressures have sharply increased the interest in a predicted supersolid phase (a phase in which the same matter exhibits solid and superfluid behavior). Participants in this project have shown that the analogue of such supersolid state can be created in a spin 1 Heisenberg spin system of high anisotropy. This intriguing result may fuel new experiments in strongly correlated electron matter and/or in cold atom optical lattice experiments.

The increased access to and control over ultra-small surface structures that is provided by nanotechnology is leading to the creation of complex structures such as micro and nano electromechanical devices, molecular electronic circuits and nano-scale superconducting wires. One effort in this project has aimed at providing a combined analytical/numerical approach to optimize the design of complex nanoscale devices. A recent calculation determined the optimal characteristics of a superfluid wire at a surface to provide minimal overall resistance.

Cold atom technology is now creating and probing superfluid fermion systems that have not been accessible to table top experiments previously but are expected to occur in matter under extreme conditions: for instance, the experimental study of polarized fermion superfluids

may be relevant to the superfluid structure inside neutron stars and to quantum chromodynamics in the high baryon density limit. One effort at CNLS suggests that an exotic form of superfluidity, in which the superfluid order parameter in equilibrium exhibits a double time dependence which reverses sign under the exchange of the time variables. This odd-frequency pairing mechanism, initially proposed by Berezinsky and studied as a candidate theory to explain high temperature superconductivity, might now be realizable in cold atom mixtures of quantum degenerate mixtures of fermion and boson gases.

Fluids mix by the continuous stretching and folding of material elements under the action of the fluid velocity field. As in many chaotic dynamical systems there is exponential growth or decay of perturbations in the flow. In one study of a periodically-forced quasi-two-dimensional fluid, we should how the average exponential growth, i.e, the rate of stretching of the field or the Lyapunov exponent, increased smoothly as a function of increasing forcing. The full spatial stretching field can be obtained for this experimental system and is shown in Figure 1. This represents the first calculation of high-resolution stretching fields from experimental data.

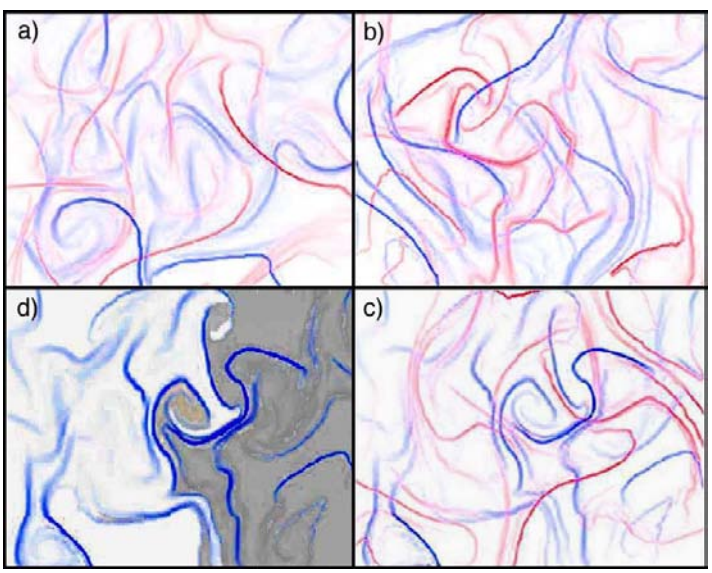


*Figure 1. Stretching fields of periodically-forced 2D turbulence with red (blue) indicating forward (backward) in time fields: a) periodic flow for Reynolds number Re = 8, b) turbulent flow Re = 108), c) same as in b) but one period later, d) reverse stretching fields for field shown in b) with virtual dye placed in the flow and advected by the velocity fields to demonstrate how lines of large stretching affect mixing of the fluid.*

The discovery that certain classes of non-linearly coupled oscillators spontaneously synchronize has found many applications in nature and techniques from nonlinear dynamics, statistical physics and network theory have greatly enriched the action range of nonlinear physics. One of he CNLS postdocs working in the framework of this project has discovered that the Kuramoto model of nonlinearly coupled oscillators, which has been used to illustrate synchronization, can be reformulated as a linear coupling problem, which allows the exact solution of classes of Kuramoto models that were previously not soluble and which gives novel insight into the dynamics of the synchronization transition.

## Future Work

In this project, we study a select group of multi-scale physics problems that are amenable to similar theoretical and computation treatment. The development and application of theoretical and computational multi-scale methods will address some of the most challenging problems faced by LANL and the DOE. Wherever possible, we compare and contrast our results with physical experiment.

Our specific objectives for this project are to:

- Use coarse graining/filtering to derive efficient computational models of turbulent flows including methods such as large-eddy simulation and Lagrangian-averaged approaches. Apply these techniques to turbulent flows with reduced dimensionality owing to rotation, magnetic field or stratification, to magneto-hydrodynamic systems, to flows where density fluctuations drive turbulence, and to turbulent fluids involving chemical reactions. Compare with results from turbulence phenomenology and statistical hydrodynamics.

- Understand and predict the behavior of systems far from thermodynamic equilibrium, e.g., systems driven by an external force such as fracture dynamics, experiencing a sudden change in their environments, or transitioning from one meta-stable or long-lived state to another. Derive well-parameterized evolution equations for mesoscopic non-equilibrium dynamical processes progress and validate the equations and their solutions against experiment. Develop highly accurate and efficient computational methods that bridge the many relevant space and time scales. Investigate nonlinear elasticity in a wide variety of materials of interest to LANL.

- Investigate how the properties of the quantum critical point determine the high temperature structure of unconventional superconductors such as heavy Fermion superconductors and possibly high-Tc superconductors. Explore some of the implications of these theoretical ideas to on-going experimental efforts at LANL and elsewhere.

- Expand on the discovery that specific non-Hermitian

Hamiltonians provide physically allowable descriptions of the real world. Apply these ideas to problems in the fundamental nature of matter and to condensed matter systems where experimental confirmation of non-Hermitian quantum mechanics might be possible.

## Conclusion

In this project, we expect to achieve the following goals:

- Develop fundamental understanding of fluid turbulence and mixing by combining new experiments, enhanced numerical simulations and novel theory and translate these advances into practical turbulence models for weapons and/or climate programs.
- Investigate properties of materials subjected to high strain through experiment and numerical simulation to produce better dynamic fracture models with application to dynamic materials in weapons and geophysics.
- Explore fundamental and applied aspects of superconductivity and superfluidity with applications to developing novel superconductors and to unraveling and exploiting the relationship between superfluidity, superconductivity, and Bose-Einstein condensates via cold atom physics.
- Our work on using effective field theories and effective action descriptions will increase the understanding of the dynamics and structure of quantum phase transitions. Our studies of Feshbach resonance physics will allow cold atom systems to explore the physics of effective nuclear Skyrme-like interactions in cold atom matter.
- A platform of skillfully combined analytical and numerical techniques will provide a useful framework to optimize the design of nanostructures and exploit the prospects of nanoplasmonics. By mining and refining the capabilities of numerical tools such as Time-dependent density functional tools, quantum chemistry methods will give detailed spectroscopic information for use in nano-technology and its use in DNA-studies.
- By combining multiple optimization methods, CNLS research is designing a new class of optimization techniques that will greatly speed up optimization algorithms in a wide variety of science fields.

## Publications


Badaeva, E., and S. Tretiak. Two photon absorption of extended substituted phenylenevinylene oligomers: A TDDFT study. 2008. *CHEMICAL PHYSICS LETTERS.* **450** (4-6): 322.

Bandi, M. M., J. R. Cressman, and W. I. Goldburg. Test of the fluctuation relation in Lagrangian turbulence on a free surface. 2008. *JOURNAL OF STATISTICAL PHYSICS.* **130** (1): 27.

Bandi, M. M., and C. Connaughton. Craig XY distribution and the statistics of Lagrangian power in two-dimensional turbulence. 2008. *PHYSICAL REVIEW E.* **77** (3): 036318.

Ben-Naim, E., and A. Zippelius. Singular energy distributions in driven and undriven granular media. 2007. *JOURNAL OF STATISTICAL PHYSICS.* **129** (4): 677.

Ben-Naim, E., and P. L. Krapivsky. Phase transition with nonthermodynamic states in reversible polymerization. 2008. *PHYSICAL REVIEW E.* **77** (6): 061132.

Bender, C. M.. Making sense of non-Hermitian Hamiltonians. 2007. *Rpts. Prog. Phys..* **70** (6): 947.

Bender, C. M., and D. W. Darg. Spontaneous breaking of classical PT symmetry. 2007. *Journal of Mathematical Physics.* **48** (4): 042703.

Bender, C. M., and H. F. Jones. Interactions of Hermitian and non-Hermitian Hamiltonians. 2008. *JOURNAL OF PHYSICS A-MATHEMATICAL AND THEORETICAL.* **41** (24).

Bender, C. M., and J. Feinberg. Does the complex deformation of the Riemann equation exhibit shocks?. 2008. *JOURNAL OF PHYSICS A-MATHEMATICAL AND THEORETICAL.* **41** (24).

Berti, S., A. Bistagnino, G. Boffetta, A. Celani, and S. Musacchio. Two-dimensional elastic turbulence. 2008. *PHYSICAL REVIEW E.* **77** (5): 055306.

Bhongale, S. G., and E. Timmermans. Phase separated BEC for high-sensitivity force measurement. 2008. *PHYSICAL REVIEW LETTERS.* **100** (18): 185301.

Borzsonyi, T., T. C. Halsey, and R. E. Ecke. Avalanche dynamics on a rough inclined plane. 2008. *PHYSICAL REVIEW E.* **78** (1): 011306.

Cassidy, A., I. Grigorenko, and S. Haas. Formation of collective excitations in quasi-one-dimensional metallic nanostructures: Size and density dependence. 2008. *PHYSICAL REVIEW B.* **77** (24): 245404.

Chertkov, M., C. Connaughton, I. Kolokolov, and V. Lebedev. Dynamics of energy condensation in two-dimensional turbulence. 2007. *Physical Review Letters.* **99** (8): 084501.

Chertkov, M., I. Kolokolov, and V. Lebedev. Strong effect of weak diffusion on scalar turbulence at large scales. 2007. *PHYSICS OF FLUIDS.* **19** (10): 101703.

Connaughton, C., R. Rajesh, and O. Zaboronski. Constant flux relation for aggregation models with desorption and fragmentation. 2007. *PHYSICA A-STATISTICAL MECHANICS AND ITS APPLICATIONS.* **384** (1): 108.

Demsar, K., J. Stare, and J. Mavri. Structure and vibrational dynamics of hydrogen bond in hydrogenbissulfate anion in the gas phase and in the solid state: A computational study. 2007. *JOURNAL OF MOLECULAR STRUCTURE.* **844**: 215.

Fransson, J.. Detection of exchange interaction in STM measurements through Fano-like interference effects. 2007. *Physical Review B.* **76** (4): 045416.

Fransson, J.. Subnanosecond switching of local spin-exchange coupled to ferromagnets. 2008. *PHYSICAL REVIEW B.* **77** (20): 205316.

Fransson, J., and A. V. Balatsky. Surface imaging of inelastic friedel oscillations. 2007. *Physical Review B (Condensed Matter and Materials Physics).* **75** (19): 195337.

Fransson, J., and A. V. Balatsky. Exchange interaction and Fano resonances in diatomic molecular systems. 2007. *Physical Review B.* **75** (15): 153309.

Fransson, J., and J. Zhu. Spin dynamics in a tunnel junction between ferromagnets. 2008. *NEW JOURNAL OF PHYSICS.* **10**: 013017.

Frisch, U., S. Kurien, R. Pandit, W. Pauls, S. S. Ray, A. Wirth, and J. -Z. Zhu. Hyperviscosity, galerkin truncation, and bottlenecks in turbulence. 2008. *Physical Review Letters.* **101** (14): 144501.

Fujita, K., I. Grigorenko, J. Lee, W. Wang, J. X. Zhu, J. C. Davis, H. Eisaki, S. Uchida, and A. V. Balatsky. Bogoliubov angle and visualization of particle-hole mixture in superconductors. 2008. *PHYSICAL REVIEW B.* **78** (5): 054510.

Graf, M. J., A. V. Balatsky, Z. Nussinov, I. Grigorenko, and S. A. Trugman. Torsional oscillators and the entropy dilemma of putative supersolid 4He. To appear in *Journal of Physics and Chemistry of Solids.*

Grigorenko, I.. Analytical solution for optimal squeezing of wave packet of a trapped quantum particle. 2008. *JOURNAL OF CHEMICAL PHYSICS.* **128** (10): 104109.

Grigorenko, I., A. Balatsky, and S. Haas. Optimal control of electromagnetic field by metallic nanocrystals. 2008. *New Journal of Physics.* **10**: 043017.

Grigorenko, I., J. -X. Zhu, and A. Balatsky. Optimization of the design of superconducting inhomogeneous nanowires. 2008. *Journal of Physics: Condensed Matter.* **20**: 195204.

Grigorenko, I., S. Haas, A. Balatsky, and A. F. Levi. Optimal control of electromagnetic field using metallic nanoclusters. 2008. *NEW JOURNAL OF PHYSICS.* **10**: 043017.

Groger, R., T. Lookman, and A. Saxena. Defect-induced incompatibility of elastic strains and dislocation behavior within a Landau theory of martensitic phase transformations. To appear in *Physical Review B.*

Groger, R., T. Lookman, and A. Saxena. Mesoscopic description of martensitic phase transformations mediated by dislocations using the Landau-Ginzburg theory. To appear in *Proceedings of Multiscale Materials Modeling.* (Tallahassee, 27-31 Oct. 2008).

Groger, R., and V. Vitek. Explanation of the discrepancy between the theoretical and measured yield stresses in body-centered cubic metals. 2007. *Philosophical Magazine Letters.* **87**: 113.

Gurvitz, S. A.. Quantum mechanical approach to decoherence and relaxation generated by fluctuating environment. 2008. *PHYSICAL REVIEW B.* **77** (7): 075325.

Haack, J. R., and C. D. Hauck. Oscillatory behavior of asymptotic-preserving splitting methods for a linear model of diffusive relaxation. To appear in *Kinetic and Related Models.*

Hauck, C. D., C. D. Levermore, and A. L. Tits. Convex duality and entropy-based moment closures: Characterizing degenerate densities. 2008. *SIAM JOURNAL ON CONTROL AND OPTIMIZATION.* **47** (4): 1977.

Hauck, C. D., and R. B. Lowrie. Temporal Regularization of the P_N Equations. To appear in *SIAM Journal of Multiscale Modeling and Analysis.*

Jeffery, N., and B. Wingate. The importance of tilted rotation in nonhydrostatic ocean modelling. *Journal of Physical Oceanography.*

Kilina, S., E. Badaeva, S. Tretiak, A. Saxena, A. Piryatinski, and A. R. Bishop. Bright and Dark Excitons in Semiconductor Carbon Nanotubes. *Journal of Physical Chemistry and Chemical Physics.*

Kilina, S., E. R. Batista, P. Yang, S. Tretiak, A. Saxena, R. L. Martin, and D. L. Smith. Electronic structure of self-assembled amorphous polyfluorenes. 2008. *ACS NANO.* **2** (7): 1381.

Kilina, S., S. Tretiak, D. A. Yarotski, J. X. Zhu, N. Modine, A. Taylor, and A. V. Balatsky. Electronic properties of DNA base molecules adsorbed on a metallic surface. 2007. *Journal of Physical Chemistry C.* **111** (39): 14541.

Kilina, S., S. Tretiak, D. A. Yarotski, J. Zhu, N. Modine, A. Taylor, and A. V. Balatsky. Electronic properties of DNA base molecules adsorbed on a metallic surface. 2007. *JOURNAL OF PHYSICAL CHEMISTRY C.* **111** (39): 14541.

Kilina, S., S. Tretiak, S. K. Doorn, Z. Luo, F. Papadimitrakopoulos, A. Piryatinski, A. Saxena, and A. R. Bishop. Cross-polarized excitons in carbon nanotubes. 2008. *PROCEEDINGS OF THE NATIONAL ACADEMY OF SCIENCES OF THE UNITED STATES OF AMERICA.* **105** (19): 6797.

Kilina, S., and S. Tretiak. Excitonic and vibrational properties of single-walled semiconducting carbon nanotubes. 2007. *ADVANCED FUNCTIONAL MATERIALS.* **17** (17): 3405.

Klein, W., H. Gould, N. Gulbahce, J. B. Rundle, and K. Tiampo. Structure of fluctuations near mean-field critical points and spinodals and its implication for physical processes. 2007. *Physical Review E.* **75** (3): 031114.

Lakshmanan, M., and A. Saxena. Dynamic and static excitations of a classical discrete anisotropic Heisenberg ferromagnetic spin chain. 2008. *PHYSICA D-NONLINEAR PHENOMENA.* **237** (7): 885.

Law, K. J., P. G. Kevrekidis, D. J. Frantzeskakis, and A. R. Bishop. Emergence of unstable modes in an expanding domain for energy-conserving wave equations. 2008. *PHYSICS LETTERS A.* **372** (5): 658.

Mangan, N., C. Reichhardt, and C. J. Reichhardt. Reversible to irreversible flow transition in periodically driven vortices. 2008. *PHYSICAL REVIEW LETTERS.* **100** (18): 187002.

Maniadis, P., T. Lookman, E. M. Kober, and K. O. Rasmussen. Stress distributions in diblock copolymers. 2007. *Physical Review Letters.* **99** (4): 048302.

Mrovec, M., R. Groger, A. Bailey, D. Nguyen-Manh, C. Elsasser, and V. Vitek. Bond-order potential for simulations of extended defects in tungsten. 2007. *Physical Review B.* **75**: 104119.

Nunner, T. S., N. A. Sinitsyn, M. F. Borunda, V. K. Dugaev, A. A. Kovalev, A. Abanov, C. Timm, T. Jungwirth, J. Inoue, A. H. MacDonald, and J. Sinova. Anomalous Hall effect in a two-dimensional electron gas. 2007. *PHYSICAL REVIEW B.* **76** (23): 235312.

Pomeau, Y., M. Le Berre, P. Guyenne, and S. Grilli. Wave-breaking and generic singularities of nonlinear hyperbolic equations. 2008. *NONLINEARITY.* **21** (5): T61.

Pomeau, Y., and D. C. Roberts. Hydrodynamic boundary condition for superfluid flow. 2008. *PHYSICAL REVIEW B.* **77** (14): 144508.

Pomeau, Y., and D. Roberts. Casimir Friction I: Friction of the vacuum on a spinning dielectric. To appear in *Modern Encyclopedia of Mathematical Physics.* Edited by Arefeva, I., and D. Sternheimer.

Pomeau, Y., and D. Roberts. Casimir Friction II: Casimir effect on drag in zero temperature superfluids. To appear in *Modern Encyclopedia of Mathematical Physics.* Edited by Arefeva, I., and D. Sternheimer.

Pomeau, Y., and D. Roberts. On the hydrodynamic boundary condition for superfluid flow. 2008. *Physical Review B.* **77**: 144508.

Pryadko, L. P., and P. Sengupta. Second-order shaped pulses for solid-state quantum computation. 2008. *Physical Review A.* **78**: 032336.

Roberts, D., and R. Teodorescu. A linear path toward synchronization: Anomalous scaling in a new class of exactly solvable Kuramoto models. To appear in *European Physical Journal.*

Santamore, D. H., and E. Timmermans. Fermion-mediated interactions in a dilute Bose-Einstein condensate. 2008. *PHYSICAL REVIEW A.* **78** (1): 013619.

Schmidt, P., I. Grigorenko, and A. F. Levi. Design of resonators using materials with negative refractive index. 2007. *JOURNAL OF THE OPTICAL SOCIETY OF AMERICA B-OPTICAL PHYSICS.* **24** (11): 2791.

Sebastian, S. E., N. Harrison, P. Sengupta, C. D. Batista, S. Francoul, E. Palm, T. Murphy, H. A. Dabkowska, and B. D. Gaulin. Fractalization drives crystalline states in a frustrated spin system. To appear in *Proceedings of the National Academy of Science.*

Sengupta, P., A. Raghavan, and S. Haas. Disorder-enhanced phase coherence in trapped bosons on optical lattices. 2007. *New Journal of Physics.* **9** (4): 103.

Sengupta, P., and C. Batista. Spin supersolid in anisotropic spin-one Heisenberg chain. 2007. *Physical Review Letters.* **99** (21): 217205.

Sengupta, P., and C. Batista. Ground state and thermal transitions in a Field-induced spin-Supersolid phase. 2008. *Journal of Applied Physics.* **103**: 07C709.

Sengupta, P., and C. D. Batista. Field-induced supersolid phase in spin-one Heisenberg models. 2007. *Physical Review Letters.* **98** (22): 227201.

Sengupta, P., and L. Pryadko. Quantum degenerate Bose-Fermi mixtures on 1-D optical lattices. 2007. *Physical Review B.* **75**: 132507.

Sengupta, P., and S. Haas. Quantum glass phases in the disordered Bose-Hubbard model. 2007. *Physical Review Letters.* **99** (5): 050403.

Sherrington, D.. A simple spin glass perspective on martensitic shape-memory alloys. 2008. *JOURNAL OF PHYSICS-CONDENSED MATTER.* **20** (30): 304213.

Sinitsyn, N. A.. Reversible stochastic pump currents in interacting nanoscale conductors. 2007. *PHYSICAL REVIEW B.* **76** (15): 153314.

Sinitsyn, N. A.. Semiclassical theories of the anomalous Hall effect. 2008. *JOURNAL OF PHYSICS-CONDENSED MATTER.* **20** (2): 023201.

Sinitsyn, N. A., V. V. Dobrovitski, S. Urazhdin, and A. Saxena. Geometric control over the motion of magnetic domain walls. 2008. *PHYSICAL REVIEW B.* **77** (21): 212405.

Sinitsyn, N. A., and A. Saxena. Geometric phase for non-Hermitian Hamiltonian evolution as anholonomy of a parallel transport along a curve. 2008. *JOURNAL OF PHYSICS A-MATHEMATICAL AND THEORETICAL.* **41** (39): 392002.

Sinitsyn, N. A., and J. Ohkubo. Hannay angle and geometric phase shifts under adiabatic parameter changes in classical dissipative systems. 2008. *JOURNAL OF PHYSICS A-MATHEMATICAL AND THEORETICAL.* **41** (26): 262002.

Stare, J., J. Panek, J. Eckert, J. Grdadolnik, J. Mavri, and D. Hadzi. Proton dynamics in the strong chelate hydrogen bond of crystalline picolinic acid N-oxide. A new computational approach and infrared, Raman and INS study. 2008. *JOURNAL OF PHYSICAL CHEMISTRY A.* **112** (7): 1576.

Tao, J., G. Vignale, and I. V. Tokatly. Quantum stress focusing in descriptive chemistry. 2008. *PHYSICAL REVIEW LETTERS.* **100** (20): 075325.

Tao, J., J. P. Perdew, L. M. Almeida, C. Fiolhais, and S. Kummel. Nonempirical density functionals investigated for jellium: Spin-polarized surfaces, spherical clusters, and bulk linear response. 2008. *PHYSICAL REVIEW B.* **77** (24): 245107.

Tao, J., V. N. Staroverov, G. E. Scuseria, and J. P. Perdew. Exact-exchange energy density in the gauge of a semilocal density-functional approximation. 2008. *PHYSICAL REVIEW A.* **77** (1): 012509.

Twardos, M. J., P. E. Arratia, M. K. Rivera, G. A. Voth, J. P. Gollub, and R. E. Ecke. Stretching fields and mixing near the transition to nonperiodic two-dimensional flow. 2008. *PHYSICAL REVIEW E.* **77** (5): 056315.

Vrugt, J. A., B. A. Robinson, and J. M. Hyman. Self-adaptive multimethod search for global optimization in real parameter spaces. To appear in *IEEE Transactions on Evolutionary computations.*

Wu, C., S. V. Malinin, S. Tretiak, and V. Y. Chernyak. Multiscale modeling of electronic excitations in branched conjugated molecules using an exciton scattering approach. 2008. *PHYSICAL REVIEW LETTERS.* **1** (5): 057405.

Wöhling, T., J. A. Vrugt, and G. F. Barkle. Comparison of three multiobjective optimization algorithms for inverse

modeling of vadose zone hydraulic properties. 2008. *Soil Science Society of America Journal.* **72**: 305.

Yarotski, D., S. Kilina, S. Tretiak, A. Balatsky, O. Prezhdo, and A. J. Taylor. Scanning tunneling microscopy of DNA-wrapped carbon nanotubes. *Nano Letters.*

Yu, H., J. Zhang, and N. Li. Lattice Boltzmann simulation of mass transfer in thermally driven cavity flows. 2008. *PROGRESS IN COMPUTATIONAL FLUID DYNAMICS.* **8** (1-4): 206.

Yu, H., N. Li, and R. E. Ecke. Scaling in laminar natural convection in laterally heated cavities: Is turbulence essential in the classical scaling of heat transfer?. 2007. *Physical Review E.* **76** (2): 026303.

Yu, H., and S. S. Girimaji. Study of axis-switching and stability of laminar rectangular jets using lattice Boltzmann method. 2008. *COMPUTERS & MATHEMATICS WITH APPLICATIONS.* **55** (7): 1611.

continuing project

# Development of a Magnetically Driven Target for Thermo-Nuclear Burn Studies (*U)

*Robert Gregory Watt*

20070518DR

## Introduction

This LDRD project is developing a magnetically driven cylindrical confinement system for the creation of a small region of material existing under extreme conditions. Using a low cost multi-MA electrical current source, an Al cylinder will be driven radially inward until it impacts on a series of nested, less massive Au shells whose purpose is to provide a very high velocity inner most Au shell. Figure 1 shows a conceptual model of such a system. The velocity of this last shell will be at a level where further impact on an object in the center will produce a region in which material conditions are sufficient for many types of physics studies not currently possible in the laboratory. One of the experimental packages that might be placed in the central void is a cylindrical ICF target consisting of a Au pusher and a frozen DT core inside the pusher. This target is used in the project as a design tool. Other applications would use different central objects. The system being developed in this LDRD project has a broad range of potential applications. The system utilizes the fact that in a planer geometry the final velocity of a small mass impacted by a much larger mass can exceed the impact velocity by as much as a factor of two in a single collision. It is possible to use several sequential collisions to produce an object moving much faster than the original source object. A cylindrical geometry further enhances this multiplication due to radial convergence of sequential shells. In a cylindrical geometry, this process can use an Al shell imploding at several km/sec, using multiple cylindrical collisions, and produce a Au shell imploding at a velocity in excess of 100 km/sec. Figure 2 is the velocity vs. time plot for a 4 shell, 3 collision system showing how such a system works. In addition to creating a high energy density platform for boost physics studies in the central region of the final Au shell, such a system provides a cylindrical configuration for the study of nuclear fusion. The conditions achieved would be similar to those created in a spherical capsule at the National Ignition Facility under the Inertial Confinement Fusion program, and could provide an inexpensive complement to the study of fusion at large laser facilities.

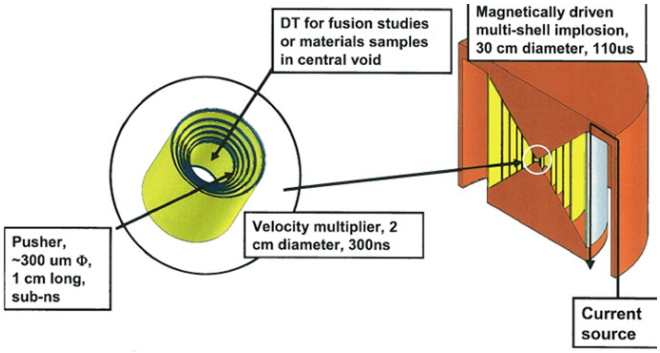


*Figure 1. A conceptual model of a current driven Al shell imploding a series of sequential Au velocity multiplication layers. The final layer in an ICF contest would comprise the Au pusher used to crush and heat frozen DT inside.*

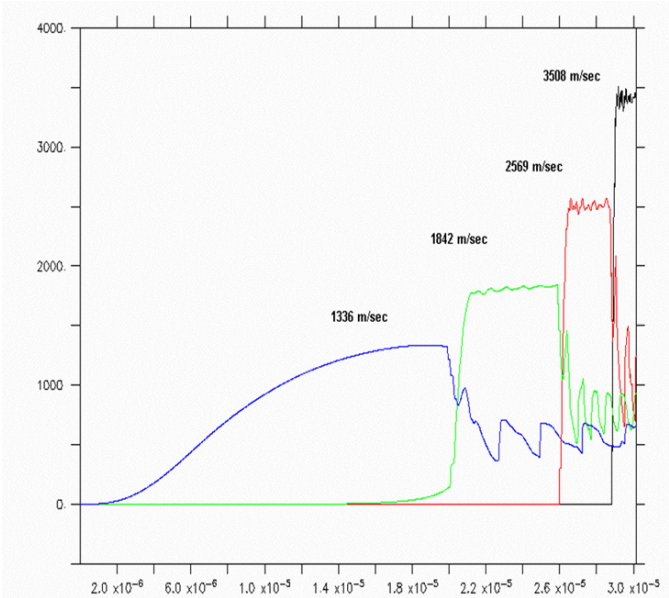


*Figure 2. Velocity vs. time plots for 4 shells of sequentially smaller mass, showing how velocity multiplication works in a cylindrical geometry.*

## Benefit to National Security Missions

Without going into undue detail, the intent of this project is to explore a high-risk concept to benefit NNSA/DP programs.

## Progress

The LDRD project has been effectively broken into two sequential phases. The first phase was the study of drive mechanisms and velocity multiplication, potential failure mechanisms, and the initial engineering conceptual design of a system capable of achieving the necessary energy content in the inner most Au shell. The second phase is to take the knowledge gained and experimentally confirm operation of the system. Once the system operation has been confirmed in this LDRD project, the system would be used for physics studies in follow on work.

In phase one we have now completed the initial evaluation of system performance, stability, and effectiveness. The results of a large number of simulations using a variety of different codes have lead us to the conclusion that a system using an explosively driven pulsed power generator (a 1.4 meter long Ranchero generator at Firing Point 88 at LANL ) producing a 40 MA current pulse should suffice to drive the experiments. An Al liner containing approximately 4 MJ of kinetic energy will be used to drive a nested Au cylinder system to create an innermost Au multiplier shell moving at 100-200 km/sec for impact on a central experimental region. Critical to operation of the system as planned is the ability to drive the Al to velocities in excess of 10 km/sec, stably increase successive Au multiplier shell velocities to extreme values, and ultimately create the desired conditions for impact on a cylindrical experimental package. The calculated maximum Al driver velocity on impact with the Au multiplier in simulations is presently somewhat less than the 20 km/sec desired and needs further study to couple more efficiently into the higher density Au. Optimization of the driven liner plus coupling layers is underway. Assuming the Au multiplier starts at around 20 km/sec upon driver impact, velocity multiplication within the Au cylinder system has been shown to reliably give a 10x increase over the driver velocity. The observed efficiency of multiplication is somewhat less than the ideal level, resulting in less multiplication than is potentially possible. The margin with which a 20 km/sec initial velocity multiplier can achieve the desired 200 km/sec final velocity will increase with further refinements, but is currently adequate with a simple cushion between the aluminum and gold. The multiplier has been shown to be stable with respect to instability growth from surface perturbations, plastic cushion non-uniformity, and cylindrical axis centering errors. The required tolerances will be well within the current state of the fabrication art at LANL. The final velocity achieved appears in simulations to be adequate to create the conditions we desire. As a figure of merit, in a cylindrical inertial confinement fusion (ICF) context, the system is capable of burning a 172 micron diameter, 1 cm long frozen deuterium-tritium fuel load, producing of order $10^{15}$ DT neutrons/cm of length in the absence of significant instability growth, given 200 km/sec at the pusher-fuel interface. The system thus appears to satisfy the requirements of the original LDRD proposal, as evidenced by temperatures and pressures at the center of the system suitable to probe the physical regime of ICF.

A review of the project at the 16 month point concluded that it was sufficiently promising to continue into the experimental phase. As a result, detailed engineering is underway for the Ranchero current source and all the system components needed to couple that generator into the Al load within which will reside the Au multiplier system. Diagnostics have been identified and demonstrated in other applications that are adequate to determine system operation. Initial tests of generator function and the extremely high current density joints needed to couple the generator to the Al liner are expected in the fall of 2008, with the initial test of an Al driver coupled to several internal shells expected in early 2009. As of the date of this annual report, simulations of the system still undergoing optimization indicate a final velocity achieved at the pusher fuel interface of an ICF load just under 100 km/sec, which is adequate for initial experiments in several venues. The achieved velocity is expected to improve significantly with further optimization in the drive section of the system.

Results to date in this work have been reported in the Proceeding of Megagauss XII, several open presentations, and several classified conference proceedings, as well as in a classified mid-term review document (see Publications below).

## Future Work

Applications of this platform cover many areas of high energy density physics and materials science. Classified applications are discussed in several documents in the vault. ICF applications have been discussed but are not currently funded. Verification and optimization of the system will continue through the end of project in Feb. 2010.

## Conclusion

Results to date have been promising and experimental verification should be forthcoming in the next 18 months. Initial system function verification using a static load assembly driven by an explosive pulsed power generator creating a 40 MA current pulse is expected by January 2009. Operation into an imploding Al liner with several subsequent shells is expected by summer 2009.

## Publications

Atchison, W., A. Kaul, C. L. Rousculp, and R. G. Watt. Optimization of a Ranchero driven high energy liner driver system (U) . To appear in *MegaGauss XII.* (Moscow, Russia, 13-18 July 2008).

Colgate, S., R. G. Watt, W. Atchison, and C. Rousculp. Equilibrium ignition by a cold adiabat: ICF via multi-collision velocity multiplication (U) LA-UR-08-06915. 2008. *Presentation to be given at Sandia National Laboratory, Nov. 6, 2008.*

Guzik, J., R. G. Watt, W. Atchison, and S. Colgate. An LDRD project to develop a fusion target driven by velocity multiplication using colliding shells (U) LA-CP-08-01191. To appear in *NECDC 2008.* (Livermore, Ca., 20-24 Oct. 2008).

Sgro, A. G.. Studies of a magnetically driven liner for TN burn (U) LA-CP-08-. To appear in *NECDC 2008.* (Livermore, Ca., 20-24 Oct. 2008).

Watt, R. G., W. Atchison, and S. Colgate. LDRD 20070518-dr midterm review: a project to develop a magnetically driven target for thermo-nuclear burn studies (U) LA-CP-08-00675. 2008. *Presentation to LANL LDRD Office, May 22, 2008.*

Watt, R. G., W. Atchison, and S. Colgate. LDRD 20070518-DR Development of a Magnetically Driven Target for Thermo-nuclear Burn Studies (U) LA-CP-07-1593. To appear in *NEDPC 2007.* (Los Alamos, NM, 22-26 Oct. 2007).

Watt, R. G., W. Atchison, and S. Colgate. Development of a Magnetically Driven Target for Thermo-nuclear Burn Studies (U) . To appear in *JOWOG37 2008.* (Los Alamos, NM, 11-14 Feb. 2008).

# Prompt and Radiochemical NTS Diagnostics and New Measurements (U)

*David J Vieira*

20080009DR

## Introduction

This R&D project will advance our understanding of weapons performance through the refined analysis of existing underground test data, improved explosion code calculations, and new nuclear cross section measurements. The main thrust is to combine neutron pinhole images and refined arsenic radiochemical diagnostic information to provide new constraints on weapons code simulations to advance our understanding of key performance processes.

## Benefit to National Security Missions

This project will support the DOE/NNSA mission in stockpile stewardship by enhancing our understanding of weapons performance. This work builds upon, enhances, and brings together several essential Laboratory core capabilities to focus on a long standing problem that currently limits our simulation codes from being fully predictive.

## Progress

Significant progress has been made during the first year of this three year Laboratory Directed Research and Development (LDRD) project. Much of the work is of a classified nature and details cannot be given here, however, the following unclassified summary of our accomplishments is provided.

This project involves the non-trivial production of radioactive targets; the undertaking of three very challenging nuclear cross section measurements; a reliance on nuclear theory to predict nuclear cross sections for other reactions that can not be measured; a re-analysis of prompt and radiochemical diagnostics from past underground nuclear tests; and weapons code simulations for a selected set of Nevada Test Site (NTS) events.

During the past year, updated explosion code calculations on three of the four selected NTS events have been performed and contrasted to prompt and radiochemical diagnostic data. The PINEX (PINhole EXperiment) movie images for one of these events have been updated and contrasted to the simulations. Important differences were noted and they point the way for further investigation. A re-analysis of reaction-in-flight and total neutron, time-integrated PINEX images have been done for another NTS event and a refinement of this work and its extension to a second NTS event is currently in progress.

A preliminary arsenic production and destruction cross section network that is needed to interpret the 73As/74As radiochemical diagnostic has been prepared and the first explosion code simulation using this new library has recently been performed. These initial results are of high interest and we are pursing further calculations, re-examining all of the radiochemical diagnostic results, and studying all of the effects that contribute to and/or modify the 73As/74As “radchem” results. Refined Hauser-Feshbach calculations of many of the cross sections that cannot be measured are also being undertaken.

## Future Work

To further improve the arsenic production/destruction network, we are undertaking a set of new cross section measurements. In particular, we are planning to make the following three measurements: 1) $^{74}$As(n,p); 2) $^{73}$As(n,2n); and 3) $^{73}$As(n,g). All of these measurements are challenging since they involve the preparation and complications of doing measurements with radioactive targets of $^{7}$4As($t_{1/2}$=18 d) and $^{73}$As($t_{1/2}$=80 d). Related to the production of these isotopes, we have performed test runs at the Isotope Production Facility (IPF) at the Los Alamos Neutron Scattering Center (LANSCE). Curie amounts of activity can be prepared via (p,xn) reactions at the IPF facility using its 250 microA (up to 100 MeV) proton beam with radiochemical processing of the irradiated target at our TA-48 hotcell facility. Two targets,

one germanium and the other selenium, have been irradiated and assayed in separate test runs to provide production data. The radiochemistries for extracting arsenic from these irradiated targets was developed and based on the production rates and ease in doing the chemical separations in a hotcell, the germanium target was selected as the best production target. In September and October 2008, a germanium target encapsulated in niobium was run for 20 days, but two days before it was to be removed, the front niobium window failed and all of the $^{73}$As and $^{74}$As that had been produced was lost to the cooling water system. The IPF is designed to handle such target failures, so this was not a safety incident, but this has delayed our experiment measurement program. We are not planning the next irradiation using an Inconel-encapsulated germanium target for May-July 2009.

Of the measurements mentioned above, the first experiment planned is the $^{74}$As(n,p) cross section measurement using the Lead Slowing-Down Spectrometer (LSDS) at the Weapons Neutron Research (WNR) are at LANSCE. In this experiment a 1 µA, 20 Hz proton beam that has been accumulated in the Proton Storage Ring (PSR) of the LANSCE accelerator is delivered to a tungsten target to produce spallation neutrons. These spallation neutrons evolve into a large lead cube that surrounds the target where the neutrons are down scattered inefficiently through several neutron-lead interactions, effectively accumulating a large neutron flux (~10,000x gain) in the lead spectrometer. This property enables the measurement of neutron-induced, charged-particle-out reactions with small samples (down to the 10 ng level). Thus by placing a ~1 microg (~100 mCi) sample of $^{74}$As inside a proton detector that in turn is placed inside the LSDS, we plan to measure the $^{74}$As(n,p) cross section for the first time.

During the past year, we performed a test run on the LSDS using various samples and detector systems. Since the neutron flux is so high inside the LSDS, radiation damage of silicon-based detectors was found to be a problem. Although gas ionization counters work well for the detection of fission fragments in the LSDS, the range of the 5-MeV protons emitted in the desired exothermic reaction is too long without going to a highly pressurized system. Thus we explored using CVD (chemical vapor deposition) diamond detectors. Good results were obtained with polycrystalline diamond detectors in detecting fission fragments with no significant radiation damage found during the course of a 5-day test run. Improved energy resolution is possible using single crystal CVD diamond detectors and we are currently testing these detectors off-line. Another LSDS run will be scheduled in 2009 to coincide with the production of the $^{74}$As target.

The $^{73}$As(n,2n)$^{72}$As experiment is planned to be performed at the Triangle University Nuclear Laboratory (TUNL) on the campus of Duke University. This is a relatively straightforward activation measurement provided that a sufficiently pure $^{73}$As target can be made. We will use a lead attenuator between the irradiated target and the germanium counter to reduce the sensitivity to low-energy gamma-rays emitted by the $^{73}$As target ($E_g$ =53 keV). We will also need to wait for the $^{74}$As present in the target to decay down to an acceptable activity level that does not overwhelm the gamma counting system. This work will be done with our collaborators from Duke / North Carolina State / the University of North Carolina and Lawrence Livermore National Laboratory. Our University collaborators are supported through a Stewardship Science Academic Alliance (SSAA) grant.

Finally, we will undertake the $^{73}$As(n,gamma) measurement using the DANCE (Detector for Advanced Neutron Capture Experiments) at LANSCE using the same set of targets produced for the TUNL measurement. To this end we have fabricated a machinable tungsten gamma-ray attenuator that will surround the radioactive target. We will test this tungsten attenuator in December 2008.

This LDRD project was reviewed at the Weapons Science Capability Review that was held in Los Alamos, May 5-8, 2008. This review committee consisted of experts from several Universities, Lawrence Livermore National Laboratory, NNSA/SAIC, and was chaired by Roy Schwitters (U. Texas at Austin). The committee gave this project high marks, as exemplified by this excerpt taken from the unclassified report. “This work is first rate. The project is well integrated between theory, simulation, and experiment. The committee was impressed with the quality of the science presented. This project is exactly what is needed to advance the state of predictive capability in Laboratory codes.”

# Global Monitoring of the Sky with Thinking Telescopes: Finding and Interrogating Cosmic Explosions

*W Thomas Vestrand*

20080039DR

## Introduction

We are capitalizing on the exciting opportunities for discovery enabled by our path-finding "Thinking" Telescope project by further developing this revolutionary technology and expanding into a distributed network with unprecedented capability. This telescope network will be the world's most advanced network of robotic instruments and will be the first that is capable of accurately localizing optical transients as short as a minute and making a series of interrogating follow-up observations while they are still bright. A revolutionary aspect of our system is that it is a coordinated network of intelligent software agents conducting sky monitoring and transient recognition on a global scale. This allows the monitoring and response instruments to feed observations back to a hierarchical decision engine, pose new questions for interrogation, conduct triage, and optimize the network hardware configuration for real-time knowledge extraction. Our global network of sky sentinels and rapid response telescopes will observe the full night sky searching for optical transients, simultaneously monitor more than 10 million celestial persistent sources and autonomously recognize anomalous behavior, select targets for detailed interrogation, and make real-time, follow-up observations—all without human intervention.This challenging goal is only within our reach because of significant LANL achievements in robotic instrumentation, distributed networks, artificial intelligence, advanced database technology, and time-domain astrophysics.

## Benefit to National Security Missions

This project will support DOE missions by developing a new paradigm employing robotic, distributed, instrumentation for situational monitoring. The tools and methodologies developed will have general applicability to areas of Defense, Intelligence, and Homeland Security, and have direct applicability to specific problems in Space Situational Awareness and ubiquitous sensing.

## Progress

There has been three key accomplishments that are having a significant scientific impact.

The first accomplishment is our detection of a "naked eye" gamma-ray burst (GRB; Figure 1). On March 19, 2008, a little after midnight local time, we detected a flash of light from a gamma-ray burst (GRB080319b) that reached a peak apparent magnitude of 5.3 magnitude while the gamma-rays were being emitted. The absolute magnitude of this flash that occurred at a redshift of z = 0.9, Mv =- 38.6, makes it the most luminous optical transient ever detected by mankind. Our Thinking Telescopes (TT) system made observations that include measurements of location before the GRB burst and during the exceptionally bright flash as well as simultaneous multi-color observations in V,R, I band of the late phases of the flash and early afterglow. Our observations were made with seven different telescopes in our Thinking Telescope system (Figure 2) and provide an unmatched observational record of optical emission from this amazing GRB.

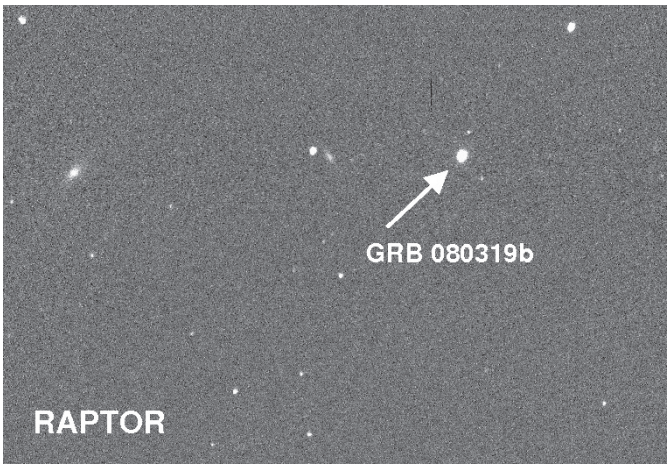


*Figure 1. The 'naked eye' gamma-ray burst. This image from one of our RAPTOR telescopes shows the fading optical afterglow from this explosion that formed a new black hole at a distance of 7.5 billion light years from earth.*

*Figure 2. A panoramic view of some of the robotic RAPTOR telescopes in our Thinking Telescopes autonomous network.*

The extremely bright prompt optical emission we measured from GRB080319b revealed features that are normally not detectable in gamma-ray bursts. We found the optical and gamma-ray variability during the explosion were correlated, but the optical flux is much greater than can be reconciled with a single emission mechanism and a straightforward extrapolation of the flat gamma-ray spectrum. This extreme optical behavior is best understood as synchrotron self-Compton model (SSC) in which optical seed photons are produced as synchrotron radiation and Compton scattered to gamma-ray energies by the same population of energetic electrons. After a gradual onset of the gamma-ray emission, there is an abrupt rise of the prompt optical flux suggesting that variable self-absorption dominates the early optical light curve. Our simultaneous multi-color optical light curves following the flash show spectral evolution consistent with a rapidly decaying red component due to large angle emission and the emergence of a blue forward shock component from interaction with the surrounding environment. While providing little support for a reverse shock that dominates the early afterglow, these observations strengthen the case for the universal role of the SSC mechanism in generating gamma-ray bursts. Our TT system also persistently monitored the burst location for several hours before the gamma-ray burst. Those measurements rule out the presence of optical precursor for 30 minutes prior to the gamma-ray burst down to a flux limit of 0.5 Jy, or just 2.5% of the peak flux--the strongest limits yet obtained.

Another key scientific accomplishment came from our study of the early afterglows from all known GRB for which the distance is known. After correcting to a standard fiducial distance (z=2), we found that the temporal behavior of the early optical afterglows can be divided into four morphological classes: fast-rising with an early peak, slow-rising with a late peak, flat plateaus, and rapid decays since first measurement. The fast-rising optical afterglows display correlations among peak flux, peak epoch, and post-peak power-law decay index that can be explained with a structured outflow seen off-axis, but whether the optical emission comes from a reverse or a forward shock cannot be determined. We found the afterglows with plateaus and slow rises may be accommodated by the same model, if the observer location are farther off to the side than for the fast-rising afterglows, or alternatively could be due to a long-lived injection of energy and/or ejecta in the blast-wave. The exciting conclusion is: if better calibrated with more afterglows, the peak flux -- peak epoch relation exhibited by the fast and slow-rising optical light-curves could provide a way to use these afterglows as standard candles for studying the very early universe. A standard candle is a source of known brightness, which can be used as a rule to measure the distance to far-off parts of the universe.

Our system also has the capability to monitor variations in nearby celestial objects (Figure 3). For example, one such scientific accomplishment was our unique observations of an outburst of optical emission from Comet Holmes. Our persistent monitoring cameras in the Thinking Telescopes network measured an amazing increase in the brightness, from fainter than 10th magnitude to nearly 2nd magnitude in just a single night (This is an increase of almost 2000 times!). The Thinking Telescopes measured the comet's brightness every 20 seconds throughout the night, revealing the development of a giant gas and dust cloud that was blown off the surface of the comet detail.

*Figure 3. A comet as imaged by one of our wide-field, persistent monitoring, telescopes.*

## Future Work

We are developing wide field sky monitors and several new fast response telescopes for deployment in a global grid. This grid will be the world's most powerful for exploring the critical first minutes of a gamma-ray burst (GRB) and other fast optical transients. This global network, with its autonomous interrogation capability, will enable real-time marshaling of assets to observe important transients as well as recognize and truncate responses for uninteresting events.

We will develop a generic messaging protocol for operating heterogeneous telescope networks enables high availability. The network will include redundant computing resources and fail-over conditions. We will develop controls/network topologies with multiple feedback paths which provide a high degree of fault tolerance and allow system recovery without human intervention. We will systematically examine sensor networking issues common to ubiquitous sensing systems, with a view to reusable solutions. By testing a fully integrated system under field conditions, we will develop techniques for robust operation with a data that are intermittent and of varying quality—experience essential for building practical systems of any kind.

To maximize scientific yield, we will construct Decision Engines that continuously cross-correlate the data stream with context information and have the ability to immediately command an optimized follow-up response. We will develop architecture capable of handling the optimization problems specific to a fully networked and globally distributed environment. The global context information will include both static and dynamic external data (e.g. archival catalogs and alert feeds from space-based instruments), and the metadata describing the state of the system itself. Time-sensitive and otherwise critical information is organized into "events" that can be efficiently passed between the nodes of the network. Events represent the most important states and state transitions that characterize both the monitored objects and system components.

## Conclusion

We will make the first simultaneous multi-color observations of prompt optical emission while the gamma-rays are being emitted by Gamma Ray Bursts (GRBs). Our telescopes, the world's most powerful for exploring those critical first minutes, allow us to probe the nurseries of the first black holes. We will make the first comprehensive search for GRB Precursors, Orphans, and other Transients. We expect to discover "orphan" GRBs, extreme flares and novae, constrain the frequency of GRB precursors, find unpredicted encounters with nearby solar system objects, and find the nearby supernovae needed to calibrate estimates of dark energy in the universe.

## Publications

Hoffman, D., T. Harrison, and J. Coughlin et al. New Beta Lyrae and Algol candidates from the Northern Sky Variability Survey. 2008. *Astronomical Journal.* **136** (3): 1067.

Kumar, P., and A. Panaitescu. What did we learn from gamma-ray burst 080319b?. 2008. *Monthly Notices of Royal Astronomical Society.* **391** (1): L19.

Panaitescu, A.. X-ray flares, plateaus and chromatic breaks of GRB afterglows from up-scattered forward-shock emission. 2008. *Monthly Notices of Royal Astronomical Society.* **383** (3): 1143.

Panaitescu, A., and W. T. Vestrand. Taxonomy of gamma-ray burst optical light curves: identification of a salient class of early afterglows. 2008. *Monthly Notices of Royal Astronomical Society.* **387** (2): 497.

Perley, D., J. Bloom, and N. Butler et al. The troublesome broadband evolution of GRB 061126. 2008. *Astrophysical Journal.* **672** (1): 449.

Vestrand, W. T., H. Davis, and J. Wren et al. Autonomous global sky surveillance with real-time robotic follow-up: night sky awareness through Thinking Telescopes technology. To appear in *Advanced Maui Optical and Space Surveillance Technologies Conference.* (Maui, 14-16 Sept. 2008).

White, R., H. Davis, W. T. Vestrand, and P. Wozniak. Distributed intelligence in an astronomical distributed sensor network. 2008. *Astronomische Nachrichten.* **329** (3): 278.

White, R., and A. Allan. An overview of the heterogeneous telescope network system: concept, scalability and operation. 2008. *Astronomische Nachrichten.* **329** (3): 232.

Wozniak, P., W. T. Vestrand, and A. Panaitescu et al. Gamma-Ray Burst at the extreme: 'the naked eye burst' GRB 080319B. To appear in *Astrophysical Journal.*

continuing project

# Carrier Multiplication in Nanoscale Semiconductors for High-Efficiency, Generation-III Photovoltaics

*Victor Ivanovich Klimov*

20080057DR

## Introduction

The solution to the global energy challenge requires revolutionary breakthroughs in areas such as the conversion of solar energy into electricity. One such breakthrough is high-efficiency generation of multiple electron-hole pairs (excitons) from absorption of single photons, which is known as carrier multiplication. For more than 20 years it has been recognized theoretically that such a process has the potential to significantly increase the power conversion efficiency of photovoltaic devices, by yielding an increased photocurrent for the same photovoltage. In 2004, using a novel experimental approach, we discovered that semiconductor nanocrystals, in distinction from bulk materials, undergo this process very efficiently within the range of solar photon energies. Here, we conduct theoretical and experimental studies of the fundamental physics of carrier multiplication and relevant phenomena (e.g., charge and exciton extraction from the nanocrystals) with the goal to develop novel principles, materials, and architectures for making use of this process in practical photovoltaic technologies. Specifically, to identify the factors that control the energy onset and the efficiency of multiexciton generation, we perform detailed studies of the carrier-multiplication mechanism. Further, we test the carrier multiplication performance of elongated nanocrystals (quantum rods) and quantum wires because these two types of nanostructures have good transport properties and are readily incorporated into devices, which could simplify practical realization of photovoltaics utilizing multiexciton generation. Finally, we investigate energy- and charge-transfer processes in engineered energy-gradient structures in the context of extraction of multiple charges produced via carrier multiplication from the nanocrystals.

## Benefit to National Security Missions

This project directly supports the DOE mission in Energy Security, specifically, in areas of alternative energy sources and energy efficiency. The proposed studies also address several critical research areas relevant to LANL challenges in "Carbon-Neutral Energy" and "Design, synthesis and properties of photoactive nanostructures."

## Progress

The key accomplishments in this project during the review period are 1) the first observation of carrier multiplication in photoluminescence of PbSe nanocrystals using a femtosecond up-conversion experiment, 2) the development of a new model of carrier multiplication, which considers the process of photostimulated generation of biexcitons from vacuum, and 3) the first comparative study of multiexciton dynamics in nanocrystals of direct- and indirect-gap semiconductors.

### Carrier multiplication signatures in photoluminescence and transient absorption

In most of the published reports, carrier multiplication was probed with femtosecond transient absorption, which allowed detection of multiexcitons based on their fast Auger recombination dynamics [1, 2]. In this project, we investigate carrier multiplication in PbSe nanocrystals by applying time-resolved photoluminescence and transient absorption. Both techniques show clear signatures of carrier multiplication with efficiencies that are in good agreement with each other. Nanocrystals of the same energy gap show moderate batch-to-batch variations (within ~30%) in apparent multiexciton yields and larger variations (up to a factor of 3) due to difference in sample conditions (stirred vs. static solutions). These results indicate that nanocrystal surface properties may affect the carrier multiplication process. They also point toward potential interference from "extraneous" effects such as photoionization that can distort the results of carrier multiplication studies.

Multiexciton yields measured under conditions when "extraneous" effects are suppressed via intense sample stirring and the use of extremely low pump levels (0.02 - 0.03 photons absorbed per particle per pulse) indicate that both the electron-hole creation energy and the carrier multiplication threshold in nanocrystals are

reduced compared to those in bulk solids (Figure 1). These results indicate a confinement-induced enhancement in the carrier multiplication process in nanocrystalline materials, which might make possible more efficient photovoltaic cells.

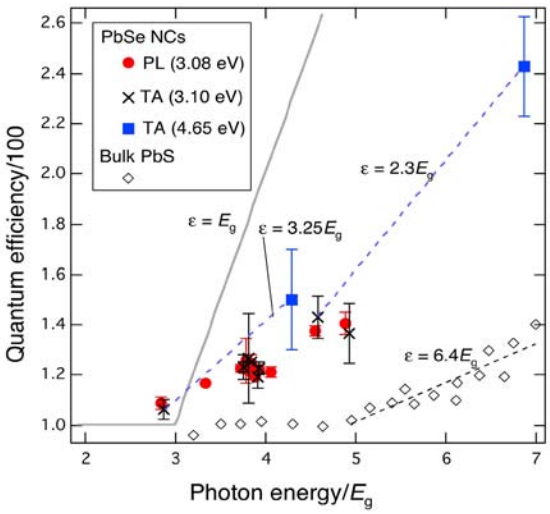


*Figure 1. Quantum efficiencies of photon-to-exciton conversion derived for PbSe nanocrystals (stirred samples) from time-resolved photoluminescence, PL (red circles; excitation at 3.08 eV) and transient absorption, TA (black crosses correspond to excitation at 3.10 eV and blue squares 4.65 eV). Black diamonds are data for bulk PbS. Gray solid line is the "ideal" QE line, which corresponds to the electron-hole creation energy, e, equal to the energy gap. The slope of the dashed lines was used to evaluate the electron-hole creation energies for nanocrystals (indicated in the figure).*

### Carrier multiplication mechanism

In this project, we have also analyzed a physical mechanism for photogeneration of multiexcitons by single photons, which involve intraband optical transitions within the manifold of biexciton states. In this mechanism, the virtual biexciton is generated from the nanocrystal vacuum by the Coulomb interaction between two valence-band electrons, which results in their transfer to the conduction band. The virtual biexciton is then converted into a real, energy-conserving biexciton by photon absorption on an intraband optical transition. The proposed mechanism is inactive in bulk semiconductors because momentum conservation suppresses intraband transitions. However, it becomes highly efficient in the case of zero-dimensional nanocrystals, where quantum confinement results in relaxation of momentum conservation, which is accompanied by the development of strong intraband absorption. Our calculations show that the efficiency of the carrier multiplication channel mediated by intraband optical transitions can be comparable to or even greater than that for impact-ionization-like processes mediated by interband transitions.

### Mechanisms for multiexciton decay: Auger recombination in nanocrystals of direct- and indirect-gap semiconductors

Practical utilization of carrier multiplication in solar-energy conversion technologies requires detailed understanding of mechanisms for carrier recombination in both single- and multiexciton regimes. Whereas the intrinsic channel for single-exciton recombination in nanocrystals is radiative decay, multiexicon decay is dominated by the nonradiative Auger recombination [3]. To understand the influence of quantum confinement on Auger decay rates, we have performed side-by-side studies of Auger recombination in nanoparticles of several different compositions including Ge, PbSe, InAs, and CdSe. We have observed that the only factor that has a significant affect on the measured recombination rates is the size of the nanocrystals – but not the details of the material's electronic structure. Most surprisingly, comparable rates are measured for nanocrystals of direct- and indirect-gap semiconductors despite a dramatic (four-to-five orders of magnitude) difference in respective bulk-semiconductor Auger constants (Figure 2). We explain this unusual observation by the lack of translation motion in these ultrasmall particles, which eliminates the need for meeting the momentum conservation requirement, which is the major reason for the difference in Auger decay rates in the direct- and indirect-gap semiconductors.

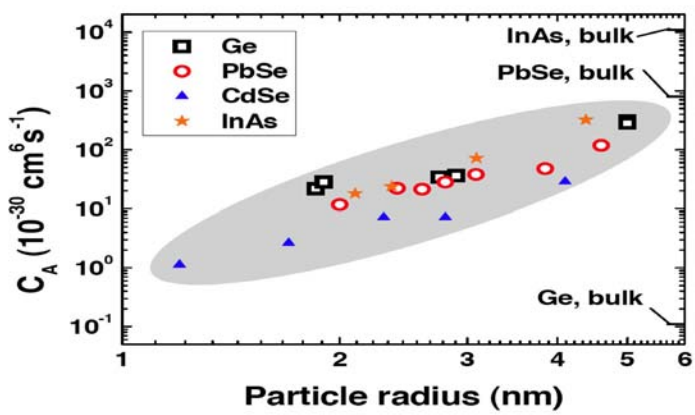


*Figure 2. Universal size dependence of Auger constants in semiconductor nanocrystals. When plotted as a function of nanocrystal radius, the Auger constants (CA) for nanocrystals of both direct- and indirect-gap semiconductors show a similar cubic size dependence.*

## Future Work

We plan a combination of theoretical and experimental studies of the fundamental physics of carrier multiplication, which can help in practical realization of the benefits of this process in solar-energy conversion technologies. In order to better utilize the available spectrum of solar energies for multiexciton generation, it is desirable that the carrier multiplication onset energy is minimal and that

the efficiency of this process above the onset is as large as is allowed by energy conservation. However, at present the factors that control the carrier multiplication threshold as well as its efficiency are not known, which is largely because of poor understanding of the mechanism for multiexciton generation in nanomaterials. In our future work, we plan to elucidate this mechanism by conducting side-by-side studies of multiexciton generation for the regimes of hot-electron and hot-exciton injection.

Further, we will study the impact of material dimensionality on the carrier multiplication process. Specifically, we will try to determine whether high multiplication efficiencies are unique to zero-dimensional nanocrystals or can also be obtained in other nanomaterials such as one-dimensional quantum wires. Because of their good charge transport properties nanowires can be incorporated into devices more readily than nanocrystals.

Finally, we will address the issue of extraction of multiple charges produced via carrier multiplication from the nanocrystals. Specifically, we will develop energy-gradient architectures, which will allow us to quickly separate excitons spatially through the energy transfer process. We will also study hybrid structures, in which monolayers of nanocrystals are assembled at the interface between electron and hole transporting layers. Alternatively, established electron (metal oxides) and hole transporters (organic polymers) will be used in an arrangement where the offsets of conduction and valence bands will provide the driving force for charge separation.

## Conclusion

Large exciton multiplicities produced by carrier multiplication can be exploited to increase the efficiency of photovoltaic cells. In the case of a traditional photoexcitation process (one exciton per absorbed photon), the detailed-balance power conversion efficiency of a single-junction solar cell can reach approximately 31% [4]. Using carrier multiplication one can surpass this limit. Specifically, in the case of a two-energy-gap multiplication threshold (minimal value as defined by conservation of energy), the power conversion efficiency increases to 42% [5]. Practical implementation of carrier multiplication, however, faces a number of challenges. Some of these challenges (of both fundamental and applied character) are being addressed in the present project. We expect that as a result of our work, we will understand the fundamentals of carrier multiplication (with the intent of optimization of its efficiency) and develop proof-of-principle device architectures that implement carrier multiplication for producing increased photocurrent.

## References


1. Schaller, R. D., and V. I. Klimov. High efficiency carrier multiplication in PbSe nanocrystals: Implications for solar-energy conversion. 2004. *Physical Review Letters.* **92**: 186601.

2. Ellingson, R., M. C. Beard, J. C. Johnson, P. Yu, O. I. Micic, A. J. Nozik, A. Shabaev, and A. Al. Efros. Highly efficient multiple exciton generation in colloidal PbSe and PbS quantum dots. 2005. *Nano Letters.* **5**: 865.

3. Klimov, V. I., A. A. Mikhailovsky, D. W. McBranch, C. A. Leatherdale, and M. G. Bawendi. Quantization of multiparticle Auger rates in semiconductor quantum dots. 2000. *Science.* **287**: 1011.

4. Shockley, W., and H. J. Queisser. Detailed balance limit of efficiency of p-n junction solar cells. 1961. *Journal of Applied Physics.* **32**: 510.

5. Klimov, V. I.. Detailed-balance power conversion limits of nanocrystal-quantum-dot solar cells in the presence of carrier multiplication. 2006. *Applied Physics Letters.* **89**: 123118.


## Publications


Durach, M., A. Rusina, V. I. Klimov, and M. I. Stockman. Nanoplasmonic renormalization and enhancement of Coulomb interactions. 2008. *New Journal of Physics.* **10**: 105011.

Klimov, V. I., J. A. McGuire, R. D. Schaller, and V. I. Rupasov. Scaling of multiexciton lifetimes in semiconductor nanocrystals. 2008. *Physical Review B.* **77** (19): 195324.

McGuire, J. A., J. Joo, J. M. Pietryga, R. D. Schaller, and V. I. Klimov. New aspects of carrier multiplication in semiconductor nanocrystals. To appear in *Accounts of Chemical Research.*

Pietryga, J. M., D. J. Werder, D. J. Williams, J. L. Casson, R. D. Schaller, V. I. Klimov, and J. A. Hollingsworth. Utilizing the lability of lead selenide to produce heterostructured nanocrystals with bright, stable infrared emission. 2008. *Journal of American Chemical Society.* **130** (14): 4879.

Pietryga, J. M., K. K. Zhuravlev, M. Whitehead, V. I. Klimov, and R. D. Schaller. Evidence for barrierless Auger recombination in PbSe nanocrystals: A pressure- dependent study of transient optical absorption. To appear in *Physical Review Letters.*

Sykora, M., L. Mangolini, R. D. Schaller, U. Kortshagen, D. Jurbergs, and V. I. Klimov. Size-dependent intrinsic radiative decay rates of silicon nanocrystals at large confinement energies. 2008. *Physical Review Letters.* **100** (6): 067401.

# Probing Physics Beyond the Standard Model through Neutron Beta Decay

*Alexander Saunders*

20080116DR

## Introduction

This project explores for Physics Beyond the Standard Model by using neutron beta decay in three ways, each at the cutting edge of the field. First, it uses ultra-cold neutrons, neutrons that have such low temperature that they can be stored for hundreds of seconds in material bottles, to measure the neutron lifetime. This lifetime, with a value of about 15 minutes, is only known to about one second. Unfortunately, existing experiments disagree at the six second level. The present work is unique in using a gravito-magnetic trap (Figure 1) to store the ultra-cold neutrons while they decay, thus eliminating the leading uncertainties in previous work. Second, this project intends to establish the technology that will be used for the next generation of neutron beta decay correlation experiments, which measure the correlations between the outgoing particles from neutron decay and the original polarization of the neutron. Previous experiments have detected only the outgoing beta particle, with rough energy calibration; the result of the present work will be a new generation of experiments that measure the outgoing electron and proton in coincidence, with unprecedented energy resolution. Finally, we will advance the theory of neutron beta decay in two ways: first, by linking low energy neutron experiments to high energy kaon decay experiments that follow similar decay processes, and second, by exploring the impacts that different values of the decay correlations and neutron lifetime can have on the new physics emerging beyond the standard model.

## Benefit to National Security Missions

This project will support the DOE mission in Nuclear Physics by enhancing our understanding of physics beyond the standard model. This project will provide measurements of neutron properties, a main goal of the DOE Nuclear Physics Long Range Plan. Fundamental nuclear science underlies the weapons program and nuclear threat reduction.

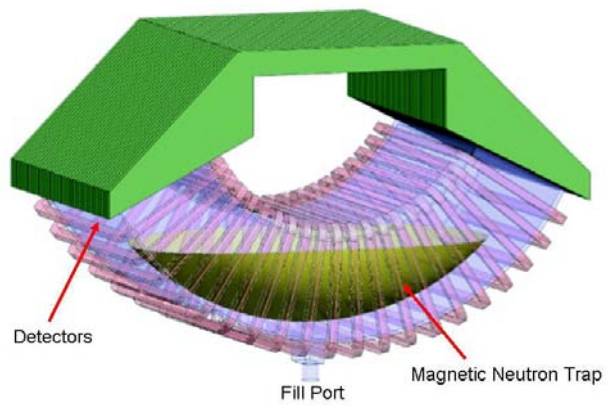


*Figure 1. Schematic of the neutron lifetime experiment. Neutrons are filled into the experiment through the bottom fill port, then trapped by the magnetic trap. The electrons from the decaying neutrons are detected by wire chambers at each end of the trap.*

## Progress

Progress has been made on all three main goals of the project. The first goal is developing and building a prototype experiment that will measure the neutron lifetime. The ultimate goal of the full experiment is to measure the neutron lifetime to a precision better than any previous experiment (<1 s), and with entirely unique systematic uncertainties. The goal of this part of the LDRD project is to build and test a prototype, which will make a measurement of the neutron lifetime to about the 10 second level or better. The experiment is based on storing ultra-cold neutrons (UCN) in a gravito-magnetic trap[1]; that is, a trap which is closed on the bottom and sides by an array of permanent magnets and on the top by gravity. Since UCNs rise about one meter in the earth's gravity field, the scale of the trap is about one meter high by one meter wide by two meters long. The magnetic trap and its support structure are now under construction: acquisition and fabrication of the parts and raw materials are complete and final assembly is in progress. The vacuum canister that surrounds the whole experiment is complete and delivered, and is now in the process of being leak tested

before installation of the experiment. We expect to take first data with the experimental apparatus during the second year of the LDRD project.

At the same time, we have made progress on the development of future neutron beta decay correlation experiments. We have designed and worked with the manufacturer to construct the first large-area ion-implanted silicon detectors for neutron beta decay studies. We currently have working prototypes of detectors with a thickness of 0.5 mm. We are currently testing the critical properties of these detectors, including entrance window thickness, energy resolution, and rise time. 1.0 mm thick detectors have been constructed and are being tested for basic operation by the manufacturer before shipping. 1.5 and 2.0 mm detectors will be attempted in the next year. Detectors of at least 1.5 mm thickness are required to determine the energy of all electrons from neutron beta decay.

We have explored improved measurements of neutron decay correlations using UCNs and the silicon detectors being developed in this project. The most promising appear to be the parameters b and B. b is the Fierz interference term in the neutron decay that distorts the shape of the electron spectrum, if scalar or tensor interactions due to physics beyond the Standard Model interfere with the vector or axial vector interactions in the Standard Model.

B is the correlation between the neutron spin and the momentum of the anti-neutrino. Although the anti-neutrino is not detected, there is enough kinematic information to extract B from the neutron spin-proton momentum correlation C. Because the proton mass is much greater that that of the other two decay particles, it carries very little kinetic energy from the decay, but substantial momentum. To good approximation, the electron and anti-neutrino share the kinetic energy from the decay. For low electron energy, the neutrino carries most of this energy. For momentum to be conserved, the proton must be emitted opposite to the anti-neutrino. Therefore, C = -B as E_e approaches zero and B can be extracted from the decay data for low electron energy. Since we are only interested in the low-energy portion of the spectrum for this measurement, full thickness silicon detectors may not be required, making a measurement of B possible in the near future. There is recent interest in precision measurement of B, as it has been shown to be sensitive to certain classes of supersymmetric extensions to the Standard Model[2].

Finally, we have begun our theoretical investigations of the consequences of the next generation of neutron beta decay experiments. The theory effort in this LDRD-DR project has two main goals, aimed to assess the impact and significance of the proposed experimental effort. The goals are: 1) Reduce the theoretical uncertainty on Delta = ($|V_{ud}|^2$ + $|V_{us}|^2$ + $|V_{ub}|^2$ - 1) below the 0.001 level. This entails a better understanding of the uncertainty in extracting $V_{us}$ from kaon semileptonic decays (K -> Pi l nu), and 2) Investigate the effects of TeV-scale new physics scenario on violations of the quark-lepton weak universality (which would imply delta not equal to 0). Below, we review progress achieved in both items one and two during the first year of this LDRD-DR project.

1. Reducing theoretical uncertainties We have focused on the cleanest source of information on $V_{us}$ , namely the kaon semileptonic decays K -> Pi l nu (where l denotes an electron or muon). Here theory input is needed to pin down the size of electromagnetic corrections and effect of second order SU(3) flavor symmetry breaking (due to mass splitting among s-quark and u-quark) in the K -> Pi matrix element of the weak vector current. In this first year we have completed the analysis of electromagnetic corrections, which has led to a publication [3] in collaboration with Dr. Maurizio Giannotti (LANL T-2 postdoc) and Prof. Helmut Neufeld (University of Vienna, Austria).

2. Probing physics beyond the Standard Model Whether or not a significant deviation of Δ from zero is observed (or signals of non V-A interactions appear in the correlation measurements), beta decays will provide unique information on the nature of physics beyond the Standard Model, i.e. on new particles and interactions existing above the electroweak scale (~100 GeV ). Quantitatively, the size of non-standard effects that are being probed by the current CKM unitarity tests is at the level of alpha/Pi $(M_W/M_{new})^2$ , which corresponds to the mass range 100 GeV < $M_{new}$ < 1 TeV that will be directly accessible at the Large Hadron Collider (CERN). Therefore, beta decays have the potential to constrain couplings and mixing patterns for new particles discovered at the LHC.

During this first year we have joined the FlaviaNet Working Group on Kaon Decays, an international effort based at the Frascati Laboratory in Italy (INFN). The aim of this Working Group is to compile and update a database with all relevant experimental and theoretical results in kaon physics. Within this collaboration, we have produced a first publication [4] summarizing the status of CKM unitarity tests as of January 2008. Using theoretical input from lattice QCD (whose uncertainty is under scrutiny, see item (1) above), the status of Vud and Vus is summarized in Figure 2 [4]. Using this, in [4] we have derived stringent constraints on the parameter space of the two-Higgs doublet extension of the standard model, see Figure 3.

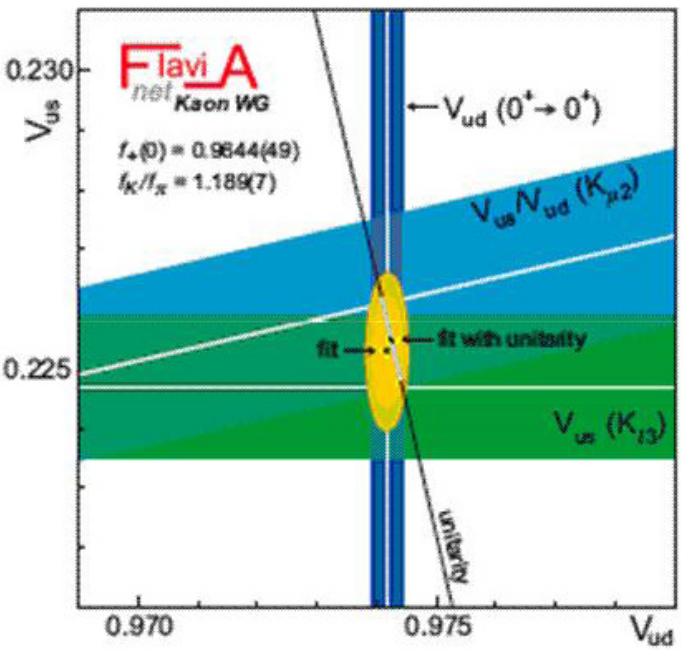


*Figure 2. Results of fits to Vud, Vus and Vus/Vud [4]. The theoretical input on form factor and ratio of decay constants is from lattice QCD.*

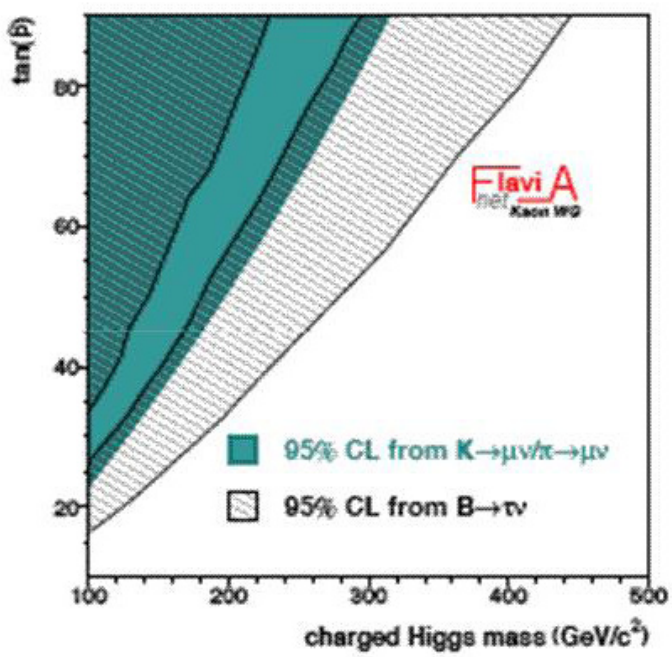


*Figure 3. Excluded region in the plane of charged Higgs mass vs tan(beta) (ratio of two neutral Higgs vacuum expectation values).*

## Future Work

In the remaining two years of this project, we intend to bring to conclusion all three parts of this project. First, we will complete a prototype measurement of the neutron lifetime using our revolutionary magnetic ultra-cold neutron trap. Second, we will establish the optimal approach to next-generation experiments measuring the neutron beta decay parameters, and demonstrate our silicon detectors, which will likely be used for these experiments. Finally, we will complete our investigations into the theory of neutron beta decay, including pushing down the theoretical uncertainties in the decay process and studying the impact of more precise measurements on the Standard Model of Nuclear and Particle Physics.

## Conclusion

Relying on LANL traditional capabilities and strengths, this program of neutron decay experiments and theoretical support will:

- Result in a world-class measurement of the neutron lifetime during the project and justify future programmatic funding of asymmetry measurements;
- Significantly improve our knowledge of light quark (up and down) mixing induced by weak interactions, and as a consequence, put stringent constraints on or detect the presence of a fourth generation of quarks, the violation of quark-lepton universality (due to supersymmetry or extra-dimensions), or the presence of new gauge bosons.

## References

1. Walstrom, P. D., J. D. Bowman, S. I. Penttila, C. Morris, and A. Saunders. A magneto-gravitational trap for absolute measurement of the ultra-cold neutron lifetime . To appear in *Nuclear Instruments and Methods in Physics Research, A.*

2. Profumo, S., M. J. Ramsey-Musolf, and S. Tulin. Supersymmetric contributions to weak decay correlation coefficients. 2007. *Physical Review D.* **75** (7): 075017.

3. Cirigliano, V., M. Giannotti, and H. Neufeld. Electromagnetic effects in Kl3 dec. 2008. *Journal of High Energy Physics.* **11**: 6.

4. Cirigliano, V.. Precision tests of the Standard Model with leptonic and semileptonic kaon decays. 2008. *The FlaviaNet Working Group on Kaon Decays.*

## Publications

Cirigliano, V.. Precision tests of the Standard Model with leptonic and semileptonic kaon decays. 2008. *The Flavia-Net Working Group on Kaon Decays.*

Cirigliano, V., M. Giannotti, and H. Neufeld. Electromagnetic effects in Kl3 decays. 2008. *Journal of High Energy Physics.* **11**: 6.

Walstrom, P. L., J. D. Bowman, S. I. Penttila, C. Morris, and A. Saunders. A magneto-gravitational trap for absolute measurement of the ultra-cold neutron lifetime. To appear in *Nuclear Instruments and Methods in Physics Research, A.*

continuing project

# Cosmic Explosions Probing the Extreme: X-Ray Bursts, Superbursts, and Giant Flares on Neutron Stars

*Sanjay Reddy*

20080130DR

## Introduction

Explosions on neutron stars (x-ray bursts, superbursts and giant-flares) provide a window to observe phenomena in extreme environments and probe the fundamental nature of matter at the most extreme density. One of the goals of this project is to develop the theory and simulation tools need to model the outer 1 km of the neutron star (neutron star crust) where these explosive phenomena are expected to occur. We will use these tools for detailed astrophysical simulations of neutron star bursts and flares, to directly confront the observed light-curves. The other major goal of the project is to develop computer programs and to use existing computer codes to simulate hydrodynamics and radiation transport to accurately predict light curves to study a wider class of cosmic explosions, especially supernovae, both thermonuclear and core-collapse. In this report we describe progress made on both fronts. First, we briefly outline our research in the past year that has addressed several important issues about the physical processes and the properties of matter in the neutron star crust.

## Benefit to National Security Missions

This project involves the modeling of multi-scale (explosive) phenomena in extreme environments. The underlying nuclear, plasma and atomic physics, and the computational techniques for radiation hydrodynamics, are relevant to Department of Energy missions, especially the nuclear weapons mission.

## Progress

Thermal conductivity, neutrino and nuclear reactions in the crust play a critical role in the thermal evolution of accreting neutron stars. They are responsible for setting the temperature profiles in the crust and in turn determine where explosive nuclear burning that powers x-ray bursts and superbursts can occur [1]. We have already made key contributions to all of these areas:

- Reddy and collaborators showed that a new mechanism for heat conduction exists in the inner crust, wherein heat is carried by superfluid neutrons rather than electrons [2] (see Figure 1 where the new mode of conduction labeled "sPh": is shown to be more effective, at times, than electron conduction);
- Gupta, Moller and Kawano showed that a new set of nuclear reactions in which excited nuclear states emit neutrons fundamentally changes the nuclear flows and energy release, leading to robust heating at shallower depth [3];
- Steiner and Reddy showed that neutrino cooling in the inner crust, where neutrons are superfluid, is strongly suppressed due to Cooper pairing correlations and the superfluid gap [4]. These new ingredients are now being incorporated in numerical simulations of the cooling of accreting neutron stars to ascertain if the temperature in the crust is large enough to account for the observed thermonuclear explosions.

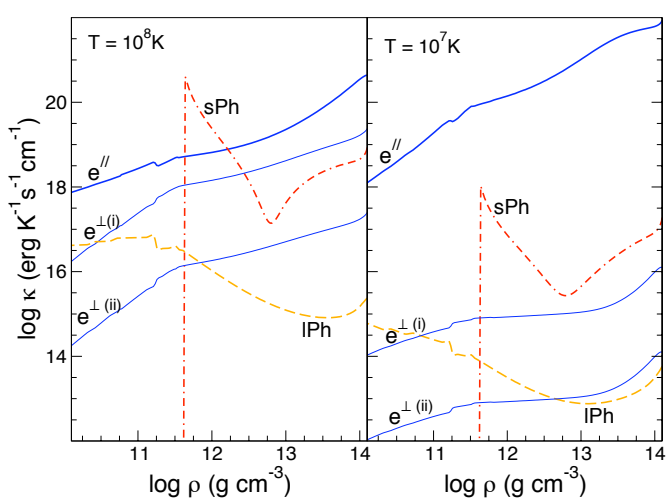


*Figure 1. Superfluid heat conduction (red, dashed) can compete with electron conduction (blue) both parallel and transverse to the magnetic field.*

One of the key ingredients in modeling the neutron star crust is the superfluid behavior of low-density neutron matter in the inner crust. As mentioned earlier the pairing gap and the resulting superfluid behavior particularly impact neutron star cooling. The only accurate method to compute these quantities is the Quantum Monte Carlo method that requires a large-scale computational effort. During the past year Carlson and collaborators have carried out these Quantum Monte Carlo calculations for neutron matter and tested their methods by comparing to similar strongly interacting Fermion cold atom experiments [5]. These calculations represent the state of the art and predict a significantly larger superfluid gap than those obtained using diagrammatic techniques.

Giant flares are powered by the enormous magnetic fields ($10^{14}$ – $10^{15}$ G) characteristic of Magnetars (magnetized neutron stars). In the standard scenario, the mechanism for energy release and storage depends on the mechanical properties of the solid neutron star crust [6]. The breaking of the neutron star crust is expected to trigger the giant flare, yet very little is known about the mechanical properties of the crust. Modeling these dense ionic solids where the electrons are both relativistic and extremely degenerate requires large-scale molecular dynamics (MD) simulations involving $10^5$-$10^6$ ions. Jerome Daligault, Kai Kadau and Mike Warren have developed computer programs to perform these large-scale MD simulations to predict how the crust would respond and break due to the large (magnetic) stresses. We are currently in the process of running a suite of simulations that will be reported shortly. Richard Epstein, Hui Li & Steve Price have proposed an alternate mechanism, where thermo-resistive instabilities in the crust trigger large-scale magnetic field reorientation and power the observed magnetar flares. This instability occurs because of the increase of ohmic resistance with temperature in neutron star crusts. They have computed eigenmodes for thermal perturbations and shown that stars with ~$5\times10^7$ K interiors, typical for neutron stars of age $10^4$ years, exhibit thermo-resistive instabilities.

The supernova light curve task focuses on modeling emission (both spectra and light-curves) of cosmic explosions. Here there are 5 key focus areas: 1) studying progenitors, 2) modeling light-curves with existing or easily developable technologies, 3) atomic opacity studies, 4) porting techniques to Roadrunner and 5) preparing new techniques. During the first year, a series of pilot studies focused on proving the techniques outlined in our proposal to learn if new capabilities were necessary to produce our intended results.

To study the emission from cosmic explosions, we must understand the environments through which the explosion propagates. Our project has led several efforts in studying supernova progenitors by modeling the white dwarf mergers. In the merger process, material is ejected into the surrounding medium. It is this material that the subsequent explosion collides with, producing additional emission. In our progenitor studies, we have also begun studying the formation rates of various supernova progenitors with C. Belczynski (Oppenheimer Fellow) and his student Ashley Ruiter (currently at Harvard).

We seek to model the photon emission from these explosions. This year we completed a suite of 1-dimensional simulations using an enhanced RAGE code (we added a discrete ordinate method to model gamma-ray transport). Using the TOPS monochromatic opacities, we were able to calculate the first supernova spectra that are based on from radiation hydrodynamics codes (see Figure 2). This success marked the completion of the major milestone for the 1st year of this proposal. Its completion allowed us to focus on projects to succeed in the milestones of year 2 (which include multi-dimensional calculations and more complex transport schemes for the thermal transport). We ran into a number of technical issues with transport and with our opacities, which we discuss below.

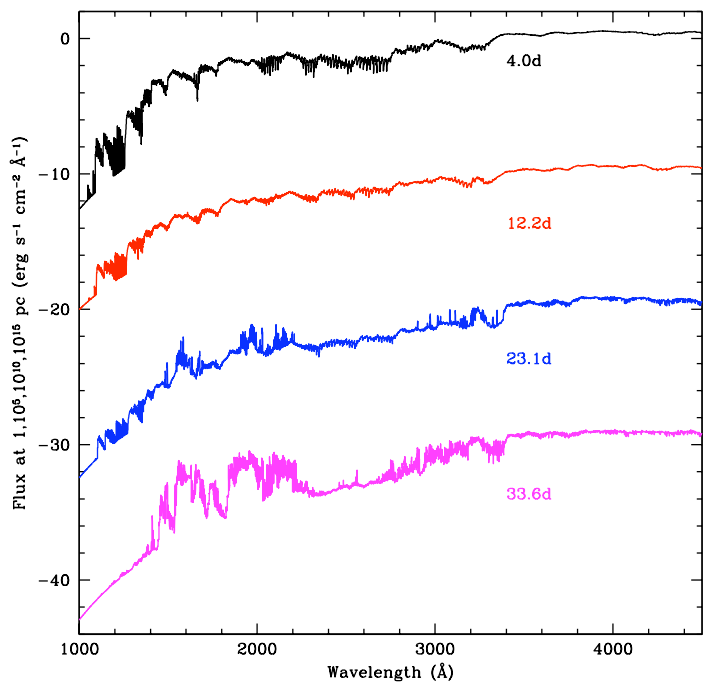


*Figure 2. Photon flux vs energy for a type Ib supernova (exploding Wolf-Rayet Star) at 4 different times during the explosion. This theoretical curve shows detailed spectral features. By matching this structure to an observed spectrum, we can determine yields and explosion energies.*

Supernovae create some conditions that were not considered by the TOPS opacity database. We have worked closely with the opacity team to correct for these differences in our supernova calculations. As a result, we have identified

many of the problems we need to pursue in years 2 and 3. One major project will be the inclusion of opacities for matter that is out of local thermodynamic equilibrium (NLTE). Although a full study of NLTE opacities is beyond the scope of this project, we hope to make some serious progress into our understanding of what we need to do regarding NLTE by the end of this proposal. We will gauge the importance of NLTE by doing some focused problems.

Another part of this project was to make our transport methods more accurate. Here we have focused on Implicit Monte Carlo (IMC). In the first year of this proposal, we outlined what we needed to implement IMC into the RAGE-style hydrodynamics. We began work on a code termed "Cassio" which will have this transport feature. In addition, this technique has been modified to run on the Roadrunner hybrid architecture. At the same time, we would like to move to 3-dimensional calculations to better study asymmetric explosions. We ran a first test model in year 1 and it is now being used to test the new Roadrunner machine. We plan to be running these calculations by the second half of year 2.

This calculations discussed are building upon work done with the RAGE code. This will allow us to attack a number of applications. But to truly attack a wide number of cosmic explosions, we need a relativistic code. As originally proposed, our project planned to develop this code by the end of year 2 and run it in year 3. At our actual level funding, we plan to complete development of the code in year 3 and have our first test runs in year 3. This year we have completed the analysis and physics discussions, and can begin to develop the code.

## Future Work

We propose to develop a model for the neutron star crust which incorporates: (1) heat deposition due to electron capture, and nuclear and pycnonuclear reactions, (2) heat transport due to the flow of degenerate electrons in a strongly interacting multi-component plasma, (3) neutrino cooling due to weak interactions in dense matter. To address how magnetic fields can power giant flares we will simulate the evolution of magnetic fields in the crust. We will explore a new class of resistive MHD instabilities as a trigger for the outburst, as suggested by recent observations. In this context, we will also study the coupling between magnetic modes and crustal modes to explain the quasi-periodic oscillations observed in giant flares. In the context of supernova light curves, our quantitative models of explosions and light curves will be used to extract information about supernova dynamics, nucleosynthesis and asymmetries.

## References


1. Cumming, A., J. Macbeth, J. J. M. in 't Zand, and D. Page. Long type I x-ray bursts and neutron star interior physics. 2006. *Astrophysical Journal.* **646**: 429.
2. Aguielra, D., V. Cirigliano, J. Pons, S. Reddy, and R. Sharma. Superfluid heat conduction and the cooling of magnetized neutron stars. To appear in *Physical Review Letters.*
3. Gupta, S., T. Kawano, and P. Moller. Neutron reactions in accreting neutron stars: a new pathway to efficient crust heating. To appear in *Physical Review Letters.*
4. Steiner, A., and S. Reddy. Superfluid response and the neutrino emissivity of neutron matter. To appear in *Physical Review C.*
5. Gezerlis, A., and J. Carlson. trongly paired fermions: Cold atoms and neutron matter. 2008. *Physical Review C.* **77**: 032801(R).
6. Duncan, R., and C. Thompson. Formation of very strongly magnetized neutron stars - Implications for gamma-ray bursts. 1992. *Astrophysical Journal Letters.* **392**: L9.


## Publications


Aguilera, D., V. Cirigliano, J. Pons, S. Reddy, and R. Sharma. Superfluid heat conduction and the cooling of magnetized neutron stars. To appear in *Physical Review Letters.*

Fryer, C. L., and S. Diehl. On the road to understanding Type Ia progenitors: Precision simulations of double degenerate mergers. 2008. In *Hydrogen-Deficient Stars ASP Conference Series.* (Eberhard Karls University, Tübingen, Germany, 17-21 September, 2007). Vol. 391, p. 335. San Francisco: Werner and Thomas Rauch. .

Fryeretal., C. L.. Constraints on Type Ib/c supernovae and gamma-ray burst progenitors. 2007. *The Publications of the Astronomical Society of the Pacific.* **119** (861): 1211.

Gezerlis, A., and J. Carlson. Strongly paired fermions: Cold atoms and neutron matter. 2008. *Physical Review C.* **77**: 032801(R).

Gupta, S., T. Kawano, and P. Moller. Neutron reactions in accreting neutron stars: a new pathway to efficient crust heating. To appear in *Physical Review Letters.*

Liu, S., Z. H. Fan, C. L. Fryer, J. M. Wang, and H. Li. Stochastic electron acceleration in shell-type supernova remnants. 2008. *Astrophysical Journal.* **683**: L163.

Steiner, A., and S. Reddy. Superfluid response and the neutrino emissivity of neutron matter. To appear in *Physical Review C.*

Young, P. A., and C. L. Fryer. The local environments of long-duration gamma-ray bursts. 2007. *Astrophysical Journal.* **670**: 584.

continuing project

# Novel Signatures of Beyond the Standard Model at the Large Hadron Collider

*Rajan Gupta*

20080661DR

## Introduction

A new era in our understanding of the basic constituents and forces of nature will begin when the Large Hadron Collider (LHC) at CERN, Geneva, starts taking data in 2009. It will explore the energy range up to a few TeV where current experiments and theory suggest that new physics must appear. The key unanswered questions of physics beyond the standard model are the origin of the scale of electroweak symmetry breaking and the nature and mass of the Higgs boson, the particle responsible for giving mass to all elementary particles. What we do know is that this physics must cause phenomena that occurs below a few TeV. This is precisely the energy range that the LHC will probe. Equally important, the physics that stabilizes the Higgs under quantum corrections, of which broken supersymmetry is the leading candidate, must also appear at the same scale.

The signal of new physics, however, is very likely to be buried in background of known phenomena. Elucidating possible production and decay mechanisms of Higgs bosons and supersymmetric particles are crucial to uncovering new phenomena. This proposal will develop an understanding of Higgs bosons and supersymmetric particles and devise strategies for their detection and analysis as a function of their possible masses. We will explore in detail the possibility of light right-handed neutrinos into which the Higgs particles will decay, and supersymmetry breaking mediated by a combination of gauge fields and gravity. Developing the capability to lead in this area is central to Beyond The Standard Model Grand Challenge.

The Standard Model has been developed over the past three decades and there are no particle physics experiments that disagree substantially with any of its predictions. Yet there is still something fundamentally missing. Despite the common theoretical framework the Standard Model provides for describing three of the gauge forces observed in nature, it does not adequately explain why two of gauge bosons (W and Z) are massive.

Another gap in the Standard Model is the Higgs mechanism, which gives particles mass - the simplicity of the Higgs mechanism belies some troubling aspects of its dynamics. The mechanism does not explain why the Higgs boson condenses - it is purely descriptive; the condensation is put into the theory by humans. Also troubling, the quantum mechanical interactions the Higgs boson has with itself and fermions, especially the top quark, cause its mass to diverge as its ``size'' is sent to zero. Something must exist in Nature – outside of the Standard Model - to cancel this divergence if the Higgs boson exists at the TeV scale.

Supersymmetry is a strong candidate for new physics at the LHC because it can potentially solve these problems of the Higgs. It is the unique extension of the Poincare symmetry, and predicts the presence of a superpartner with a different spin for each particle. It is analogous to the successful prediction of special relativity that there exists an anti-particle with an opposite charge for each particle. The null observation of superpartners suggests that our vacuum is not supersymmetric, i.e., the vacuum distinguishes bosons and fermions, while keeping special relativity as a good symmetry. The realization of such a vacuum where the space-time symmetry is partially broken has not been easy; a complicated structure has been necessary for supersymmetric models to be realistic.

Since there are, in general, many speculative models that provide mechanisms that solve the problems of mass, scientists would like to know which of these, if any, are favored by the new discoveries, and which are not.

Graesser and Kitano are developing techniques to find and interpret the new particle physics discoveries. Discoveries at the LHC are not an end, but a beginning: once a discovery has been established, what is it? What are the new particles; what are their masses; what are

their quantum numbers; and what are their interactions with other particles? The last two questions are difficult to determine experimentally, but they are also the most relevant for identifying the new physics.

## Benefit to National Security Missions

Physics beyond the Standard Model is one of the five Grand Challenges that define the science mission of LANL. The work of Kitano and Graesser in understanding supersymmetry, the Higgs boson and signatures of novel events at the LHC are core areas of this grand challenge. Their work is also aligned with the highest priority areas of the High Energy program of the DOE Office of Science as documented in the 2008 HEPAP P5 report.

## Progress

Supersymmetric models have many new particles and therefore a complicated spectrum. When superparticles are produced at a collider they quickly decay to Standard Model particles and other superparticles. This cascade decay ends when a stable superparticle is produced. In many models this particle is electrically and color neutral, so it escapes the detector, undetected. The production of superpartners at the LHC then leads to events with many Standard Model particles and two superparticles (dark matter candidates) that escape the detector.

In LA-UR- 08-04335, Graesser and Rutgers University collaborators J.Shelton and S.Thomas focus on such decay chains, and examine the correlations between the energy-momenta of muons and electrons. The theoretical distributions for these quantities provide important information such as the spins of the intermediate particles and their interactions. They have found different patterns can be obtained under different hypotheses about the underlying particle spectrum and interactions between the new particles, which can then be used to confirm or falsify different hypotheses.

Graesser and Shelton have completed a follow-up study (LA-UR 08-07771, arXiv:0811.4445). They focus on events containing taus and leptons, and on events containing b-quarks and leptons. They find that distributions formed from b-quarks and leptons are sensitive to the spectrum of stops and also sbottoms. They further propose to use signed b-quarks as a tool to further discriminate sbottom and stop contributions, and to also experimentally confirm the hypothesis. This can be done with a realistic signing rate for the charge of the b-quark.

This preprint also examines distributions formed from pairs of taus or a tau with an electron or muon. They find features that are strongly correlated with whether the sleptons and staus involved in these processes have the same-handedness or opposite-handedness. Further, a precision measurement of these distributions could in principle tell us the separate handedness of the sleptons and taus. Such results would provide valuable information about the interactions between the new particles, which would allow us to discriminate or favor specific models. Similar conclusions are obtained for distributions involving two taus. We have also suggested algorithms for fitting tau-tau and lepton-tau distributions.

In LA-UR-08-3550, Graesser, Friedland (LANL) and Giannotti (LANL) investigate theoretical properties of ``unparticles'', recently proposed by Georgi at Harvard [1]. Unparticles have attracted significant theoretical attention since they have curious theoretical properties and can be produced at the LHC. Our work uses AdS/CFT to clarify a number of confusions in the literature, and has implications for signals at the LHC.

## Future Work

- Investigate b-l correlations further by using a Monte Carlo event generator for a few representative supersymmetry parameter points. Graesser will collaborate with Shelton (Rutgers U.).

- Implement non-standard decays of the Higgs boson to right-handed neutrinos into event generators such as PYTHIA or MadEvent/MadCalc. These processes have been proposed by Graesser in previous publications. Investigate the discovery potential of Tevatron (at Fermilab) or LHC and identify most important channels for discovery.

Recently, there has been progress in the study of supersymmetry breaking [2]. Model building is simplified once we allow for our universe to be in a meta-stable vacuum, rather than the true vacuum. With M.Ibe at SLAC, Kitano has proposed a new class of supersymmetric models [Phys. Lett.B663:242 246,2008,Phys.Rev.D77:075003,2008]. In these models, a new force operating at a short-distance scale creates a meta-stable non-supersymmetric vacuum. The dynamics also contains a mechanism for directly giving masses to the superpartners. It was possible to perform a reliable calculation of the mass spectrum by using the effective description of the theory by composite fields, thanks to our understanding of the non-perturbative dynamics of supersymmetric theories.

In gauge-mediation models [3] (GM), the spectrum of the superpartners can be calculated with only a few parameters. An interesting possibility, which is often realized in

GM models, is that the stau is the next-to-lightest superpartner. In this case, the lifetime of the stau can be very long. For collider physics, such a long-lived particle is useful in studying new-physics events because its charge and momentum can be directly measured just like the muon. Once we have such a particle, various precision tests of supersymmetry can be done at the LHC, which are usually thought to be difficult.

In this long-lived stau scenario, Kitano has proposed a search strategy of lepton flavor violation at the LHC [JHEP 0803:023,2008]. It was shown that the decay of the neutralino into a stau and a muon is sensitive to the flavor mixing parameters in the supersymmetric standard model. He also performed a study of Drell-Yan production of superparticles in this scenario and found various measurements such as masses, spins, parity and CP asymmetry are possible at the LHC [JHEP 0811:045,2008] by looking at angular and energy correlations of decay products.

Supersymmetry also provides a dark matter candidate. In collaboration with H.Murayama (UC Berkeley) and M.Ratz (Technische Universitat Munchen), Kitano proposed a cosmological scenario where the baryon asymmetry and dark matter of the universe are both generated from a single scalar condensation in the early universe [Phys.Lett. B669:145-149,2008]. Not only is this a realistic scenario, it explains one of the puzzling features of the universe, namely that the energy densities of baryons and dark matter are similar to each other. Such a consistent framework will be an important input to LHC physics.

## References


1. Georgi, H.. Unparticle Physics . 2007. *Physical Review Letters.* **98**: 221601.
2. Intriligator, K. A., N. Seiberg, and D. Shih. Dynamical SUSY breaking in meta-stable vacua. 2006. *Journal of High Energy Physics .* **0604**: 021.
3. Dine, M., A. Nelson, and Y. Shirman. Low-energy dynamical supersymmetry breaking simplified. 1995. *Physical Review D.* **51**: 1362.


## Publications


Ibe, M., and R. Kitano. Minimal direct gauge mediation . 2008. *Physical Review D.* **77**: 075003.

Ibe, M., and R. Kitano. Sweet spot supersymmetry and composite messengers . 2008. *Physics Letters B.* **663**: 242.

Kitano, R.. Study of chargino-neutralino production at hadron colliders in a long-lived slepton scenario. 2008. *Journal of High Energy Physics .* **11**: 045.

Kitano, R.. A clean slepton mixing signal at the LHC. 2008. *Journal of High Energy Physics .* **03**: 023.

Kitano, R., H. Murayama, and M. Ratz. Unified origin of baryons and dark matter . 2008. *Physics Letters B.* **669**: 145.

# High-Precision Spectroscopic Search for Variation of the Fine-Structure Constant

*Justin Roald Torgerson*

20080663DR

## Introduction

The discovery of time variation of a fundamental constants would fundamentally change the way we interpret nature and the universe around us. It is well known that our currently accepted physical theories possess too many "fundamental" constants; that is, there are too many parameters which we cannot calculate and, taken together, overdefine the scales of mass, charge, distance, time, etc. It is therefore conclusive that our current physical theories are, at best, incomplete. Data from astrophysical sources have been analyzed to imply that the Fine Structure Constant (α) was smaller in the distant past compared with its current value. The Fine Structure Constant is ubiquitous in physics, setting for example the size of the atom and the rate of nuclear reactions.

We are developing an experimental apparatus capable of searching for modern-day variation of α with unprecedented sensitivity. Our technique will use two optical frequency standards (laser sources locked accurately to narrow transitions in atomic ions) which will be compared through a femtosecond laser-based frequency comb (FLFC). The femtosecond laser will be referenced to an optical frequency standard locked to a transition in singly-ionized ytterbium ($Yb^+$) and some light from the FLFC will be frequency multiplied by a factor of four, then used to drive a narrow transition in trapped, doubly-ionized ytterbium ($Yb^{2+}$). In this way, the FLFC becomes the second optical frequency reference. Measurements of the FLFC's frequency offset and repetition rate in this "locked" state are sufficient to determine a possible time variation of α at a rate of one part in $10^{18}$ per second. In addition to possibly changing the way we view nature, this experiment will perfect the technique of optical atomic spectroscopy with light generated directly from a FLFC.

We are also working in parallel with collaborators at the University of California, Berkeley (UCB) to search for time variation of alpha by taking advantage of two nearly degenerate states in atomic dysprosium (Dy) that are also highly dependent upon the value of alpha. In this experiment, the energy levels are so close that transitions between them can be make with a radio-frequency (rf) source that can be compared to a laboratory cesium clock. This differs dramatically from the trapped-ion experiment in that the comparison of frequencies is straightforward. However, the systematic effects that can limit the sensitivity are less understood so that neither experimental approach possesses a clear advantage over the other.

## Benefit to National Security Missions

The primary research proposed here directly supports the Grand Challenge of "Beyond the Standard Model" and is directly relevant to DOE, Office of Science missions. The intellectual merit of this project rests upon the implications of a nonzero variation of α on physics and metrology. Variation of α would play a crucial role in the development of an ultimate unified theory of Nature. In metrology, such a variation would signify a fundamental limit for the stability of next-generation atomic clocks and, thus, inevitably alter the definition of the second.

LANL's work on $Yb^{2+}$ is also of interest to the National Institute for Science and Technology (NIST), since it can be the basis for a new optical frequency standard of exceptional stability, which can be important for both national security and information security as advocated by NIST. Clocks of sufficient accuracy could be used for navigation, the detection of underground facilities, and the detection of massive smuggled objects, impervious to any shielding. Our technique for spectroscopy with light generated directly with a FLFC opens a new paradigm in optical spectroscopy since nonlinear optics and a FLFC can be used to generate nearly any color of light: a serious limitation for many transitions of interest in the science community.

## Progress

Our most exciting progress this year has been the trapping of isotopically pure $^{174}Yb^{2+}$ in an rf Paul trap. This is the first time in history that this ion has been trapped and cooled and also the first time that any doubly-ionized atom has been trapped in a Paul trap. We subsequently reduced the temperature of the $Yb^{+}/Yb^{2+}$ dual-species ion cloud by direct laser cooling of $Yb^{+}$, which then cooled the $Yb^{2+}$. We have now begun a series of investigations that will allow us to create an optical frequency standard based upon the trapped $Yb^{2+}$. Our short-term goal is to develop direct laser cooling of the $Yb^{2+}$ by driving the cooling transition at 252nm with a laser source that we previously constructed.

Direct laser cooling of the $Yb^{2+}$ also requires several "re-pump" sources to drive the population out of metastable energy levels that lie below the excited state of the cooling transition and become populated over time. Figure 1 shows a schematic of some of the energy levels of $^{174}Yb^{2+}$. Of particular interest is the $^3P^o_2$ state that can be populated after a few hundred milliseconds. While this is a long time compared to the 230ns lifetime of the $^3P_1$ state that populates it, it is still short on a laboratory time scale and makes the ion difficult or even impossible to detect depending upon the experimental arrangement.

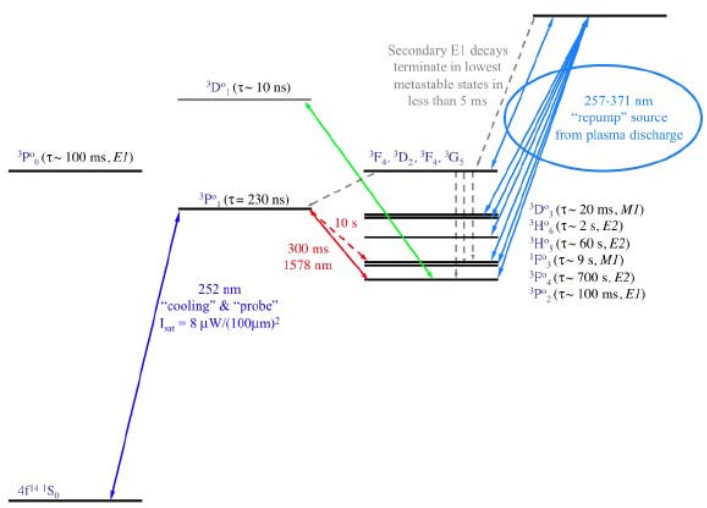


*Figure 1. Partial Energy Level Diagram for Yb III: The cooling and interrogation transition is at 252 nm. When the ion is in the upper state accessed by this transition, the ion can decay into several lower states which are long-lived through either radiative decay or collisions with residual gas atoms in the vacuum. With the plasma-repump source and either the 501nm source (green line) or 1578nm source all the population can be returned to the ground state and the ion will again fluoresce at 252nm.*

We have completed the construction of the three repump sources which we will need to depopulate the metastable states, including the problematic $^3P^o_2$ state, under various conditions. Two of the sources are based on tunable external cavity diode lasers at 1578nm and 1002nm with the latter being frequency-doubled to 501nm. Both of these systems are tunable over the necessary range of ~100GHz and supply 1-2mW of power at the final wavelengths; about 100 times more than the required 10mW.

The third repump source is a high-current plasma discharge of Yb/Kr and will only be necessary for long interrogation times (tens of minutes) and for initial searches for the cooling transition near 252nm. There are six energy levels below the $^3P_1$ excited state of the cooling transition and four of them can only be populated efficiently through collisions with background gas (or buffer gas). Since a plasma discharge can, in principle, be made to produce many lines specific to Yb, $Yb^{+}$ and $Yb^{2+}$, the spectral density of these lines will be of order $10^5$-$10^6$ times higher than an LED or other lamp source. We are currently installing our first version of this source will begin to use it immediately.

We have also investigated collisional decay channels in $^{174}Yb^{+}$ not previously studied as illustrated in Figure 2. It is important for us to understand the various mechanisms that can cause decay in the excited states of $Yb^{+}$ upon which one of our optical frequency standards will be based. For a reliable optical frequency standard, knowledge of the long-term behavior of $Yb^{+}$ is necessary. Even small amounts of residual gas can occasionally move population from the useful cooling and clock state to two other metastable states. We have largely concluded this study and have been able to, respectively measure and put an upper limit on the collisional cross-sections for the two dominant collisional decay channels involving these transitions. These studies have also allowed us to develop techniques that we will use with $Yb^{2+}$ once we have identified the cooling transition and are directly laser-cooling $Yb^{2+}$ as well.

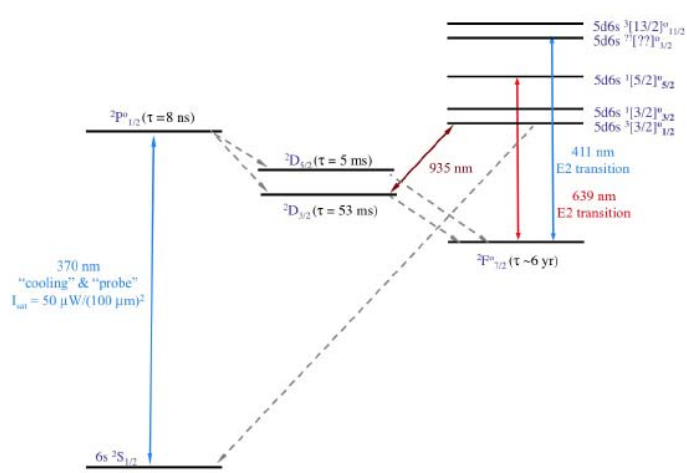


*Figure 2. Partial Energy Level Diagram for Yb II: The cooling and interrogation transition is at 370nm. There are several parasitic decays that can occur that are all driven by collisions with residual background gas (grey dashed lines). We have studies these in detail by measuring the decay of fluorescence at 370nm under various background gas pressures and laser intensities and building an accurate mathematical model of the fluorescence/decay process.*

We acquired apparatus for, and have begun construction of the frequency-quadrupled femtosecond frequency comb for direct spectroscopy of the $Yb^{2+}$ "clock" transition at 221nm. We anticipate having the frequency comb operational in the next few months and the frequency-quadrupling operational shortly thereafter.

We have also worked closely with our collaborators at UCB on our second search for time variation of α based on nearly-degenerate levels in atomic dysprosium. Last year, we reported our first limit on variation of α, (da/dt)/α<$4\times10^{-15}$/yr [1] from this experiment. This result itself is limited by several technical systematic problems from our imperfect apparatus and our time this year has been spent constructing a new measurement apparatus with more ideal properties such as a better vacuum, magnetic shielding and more homogeneous electric fields in the test region of the apparatus. Figure 3 shows a schematic of the new apparatus that we have constructed and are in the process of testing.

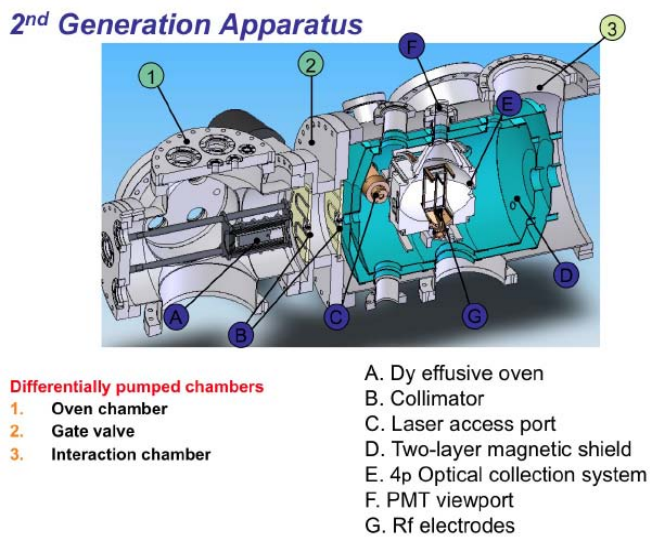


*Figure 3. Cut-away schematic of the new version of the dysprosium apparatus: We now have the capability to operate the experiment at low temperature, with high magnetic shielding and with homogeneous electric and laser fields.*

## Future Work

We will extend our work with single trapped ytterbium ions to create two optical frequency references based on field-insensitive transitions in ytterbium. Our work with $Yb^{2+}$ represents the first trapped-ion investigation with a doubly-charged species and opens a new paradigm for trapped-ion laser spectroscopy studies as well as optical frequency standards. We will perform high resolution spectroscopy on $Yb^{2+}$ with light synthesized directly from the frequency comb with a resolution of $5\times10^{-14}$ which is 50 times better than the current state-of-the-art comb as defined by our NIST collaborator and one of our postdoctoral researchers. Our advantages in this aspect of the experiment are gained through our use of a narrow transition of a trapped ion and elimination of a noisy amplification process. Through the high sensitivity of $Yb^{+}/Yb^{2+}$ transitions to α, this provides a sensitivity to fractional changes in α of ~$10^{-15}$ which is approaching the best laboratory limits.

Our second proposed effort involves measuring rf electric-dipole transition frequencies between nearly degenerate opposite-parity levels in atomic dysprosium. Our measurements on dysprosium at UC Berkeley have allowed investigation of systematic uncertainties and have solidified the design criteria for a dysprosium-base search for α-variation. We will complete the assembly and characterization of the apparatus and expect to reach a sensitivity of (da/dt)/α~$1\times10^{-16}$/yr within the next two years.

## Conclusion

Both of experimental efforts discussed above can each provide a factor of ~100 improvement over the current best experimental results for variation of the fine structure constant, α. These experiments have the potential to achieve this sensitivity with only one year of averaging compared to the current best measurement that averaged over six years of data [2]. Furthermore, in contrast to the current best measurement, the levels that are being compared are electronic levels, which allows for α-variation to be deduced without assumptions regarding the variation of other fundamental constants.

## References

1. Cingoz, A., A. Lapierre, A. -T. Nguyen, N. Leefer, D. Budker, S. K. Lamoreaux, and J. R. Torgerson. Limit on the Temporal Variation of the Fine-Structure Constant Using Atomic Dysprosium. 2007. *Physical Review Letters.* **98**: 040801.

2. Fortier, T. M., N. Ashby, J. C. Bergquist, M. J. Delaney, S. A. Diddams, T. P. Heavner, L. Hollberg, W. M. Itano, S. R. Jefferts, K. Kim, F. Levi, L. Lorini, W. H. Oskay, T. E. Parker, J. Shirley, and J. E. Stalnaker. Precision Atomic Spectroscopy for Improved Limits on Variation of the Fine Structure Constant and Local Position Invariance. 2007. *Physical Review Letters.* **98**: 070801.

full final report

# New Approaches to Quantum Computing and the Dynamics of Quantum Phase Transitions

*Wojciech Hubert Zurek*

20060039DR

## Abstract

A quantum phase transition is a discontinuous change of the properties of a quantum system that occurs as a consequence of a continuous change of its Hamiltonian. Bose-Einstein condensates (BECs) offer clean and elegant examples of quantum phase transitions, including especially the insulator-superfluid transition. This project studies the dynamics of quantum phase transitions in Bose-Einstein condensates and explores the utility of phase-transition dynamics for quantum computation. As with the usual (thermodynamic) phase transitions, most work on quantum phase transitions has focused on equilibrium behavior. However, the dynamics of phase transitions is a rich problem of obvious fundamental interest, with applications that span the range from low temperature physics to cosmology. More importantly, a thorough understanding of quantum phase transition dynamics in general, and in BECs in particular, is necessary to implement quantum computation in BECs. We will also use feedback from the BEC studies to develop powerful nonstandard approaches to quantum computing, including topological QC and adiabatic QC, and to study decoherence in quantum phase transitions. LANL has a unique combination of theoretical and experimental capabilities to study quantum phase transitions in BECs and to become a leader in this emerging field.

## Background and Research Objectives

The goal of this project is to develop and test new approaches to quantum computation by studying the nonequilibrium dynamics of quantum phase transitions, especially those in ultracold gaseous Bose-Einstein condensates (BECs). A typical quantum phase transition (QPT) is a discontinuous change of the character of the ground state of a quantum system as a consequence of a continuous change of its Hamiltonian.

Our program focuses on the dynamics of the Mott insulator-superfluid transition in a BEC, because this QPT is essential for proposed BEC QC designs and because BEC is a clean, experimentally accessible system for QPTs and information processing. Specific objectives include:

- Characterize the dynamics of quantum phase transitions (e.g., investigate their role in the formation of topological defects, and explore topological control of quantum states in the BEC setting).
- Investigate the suitability of BECs for quantum information processing (e.g., study utility of entanglement and large-scale quantum superpositions left behind by a QPT).
- Develop and evaluate nonstandard quantum information processing strategies, including in particular adiabatic and topological quantum computation that can be modeled using BECs.
- Study decoherence in the BEC setting. Investigate its implications for fundamental physics (condensed matter, etc.). Assess limitations it imposes on information-processing strategies.

These aims are interconnected: they involve generally applicable theory closely tied to experiments. Our proposed implementation of the Mott QPT is discussed further in the Scientific Approach section below. In essence, we aim to understand how a single condensate wavefunction with coherent phase throughout forms out of several pre-existing pieces, and how it can be coherently manipulated. Such manipulations are interesting because they can be used to process information. For instance, a superfluid-insulator QPT transforming a single BEC superfluid into a million-particle “insulator” with exactly one atom per site performs the initialization of a BEC QC. Besides such standard QC strategies (analogous to classical computing but with quantum logic gates that use qubits), our experiment will let us explore nonstandard QC.

For example, in adiabatic QC the system starts in an

easily accessible ground state of a standard Hamiltonian, which is then smoothly changed to one whose ground state encodes the answer to a problem. Remarkably, it has been shown to be equivalent to standard QC. Topological QC is another relevant nonstandard strategy. The key idea is that topological defects can be manipulated to implement QC with the advantage of being more robust to environmental perturbations than conventional qubits.

## Importance to LANL's Science and Technology Base and National R & D Needs

Understanding the dynamics of quantum phase transitions is of fundamental interest; applications range from low temperature and condensed matter physics to cosmology. Most importantly for LANL's strategic priorities, a thorough understanding of QPT dynamics in BECs is necessary for implementing quantum information processing in this promising setting. Quantum techniques are the most general means known to promote—or for adversaries to jeopardize—security (quantum crypto key distribution, and breaking public key cryptography with quantum computers are concrete examples), so pursuing BEC quantum information processing also contributes to LANL's strategic goal of becoming a Preferred Laboratory for Defense. Moreover, since computer components are rapidly shrinking towards the size of single atoms, quantum computing (QC) will become a required technology for cutting-edge computation, a critical lab capability.

## Scientific Approach and Accomplishments

The research program has three inter-connected components. Wojciech Zurek leads the effort directed at developing the theory of non-equilibrium quantum phase transitions. Malcolm Boshier leads the effort to build the tools for the experimental realization and verification of these ideas. Howard Barnum leads the team looking at the connection of these two threads to information theoretic aspects of quantum information processing.

We first discuss the accomplishments of the theory component. Extensive studies of the dynamics of a quantum phase transition of cold atoms in a periodic potential were performed by Damski, Zurek, Cucchietti and Dziarmaga (external collaborator) and published in Physical Review A [1]. They explain how the correlations between atoms arise during a transition from the insulator to the superfluid phase. The scaling of the asymptotic value of atom-atom correlations with the rate at which the height of the periodic potential is ramped down was found. Different analytical approaches were developed and numerically verified. This study is relevant to a number of current experiments where BECs are placed in a standing laser field producing a periodic potential.

We have studied the formation of entanglement in a quantum phase transition in a quantum Ising model. The results [2] show that the basic mechanism responsible for the formation of defects in phase transitions explains the reach of entanglement in chains of spins described by the quantum Ising model. It is suggestive (but far from established) that this result will generalize to other quantum phase transitions.

Formation of a single Bose-Einstein condensate (BEC) with a torus topology from a collection of initially disconnected BEC "pools" was studied by Dziarmaga, Meisner, and Zurek [3]. The transition that occurs in this setting has a different character than the "usual" second order phase transitions. In particular, one starts the quench that induces the transition at the critical point. In spite of that, we were able to produce a simple and compelling model of this process that seems to accord rather well with numerical simulations of the discrete version of the Gross-Pitaevskii equation. We expect that its key prediction – scaling of the typical velocity of the superflow in the final torus with the rate of quench – will be soon tested experimentally in Boshier's laboratory.

Damski and Zurek have studied extensively dynamics of quantum phase transitions in a ferromagnetic Bose-Einstein condensate, i.e., a cold cloud of spin-1 atoms. Such a condensate is considered as one of the most relevant systems for investigations of dynamics of quantum phase transitions. Indeed, it is easily experimentally accessible and its parameters are well controlled in temporal and spatial domains. Three papers have been written on the subject.

The first one [4], describes dynamics of magnetization during a symmetry breaking quantum phase transition taking place from the unmagnetized (polar) phase to the magnetized (broken-symmetry) phase. In particular, time and length scales for the creation of magnetic topological defects were found using various theoretical approaches. A quantum version of the Kibble-Zurek approach known from classical phase transitions was developed and successfully applied to this problem. Analytical predictions have been found to be in full agreement with numerics. Experimentally relevant quench parameters have been determined as well.

The second paper [5] describes the transition in the opposite direction, i.e., from the magnetized to the unmagnetized phase. Here all the details of condensate dynamics near a critical point were unraveled and the Kibble-Zurek-like theory was fully verified. Condensate dynamics after the quench ends were also described in an effort to provide easily experimentally measurable signatures of the non-equilibrium dynamics during a quantum phase transition. In particular, (an)harmonic oscillations of magneti-

zation were predicted with the amplitude and/or period carrying crucial information about dynamics near a critical point. Excellent agreement was found again between analytical calculations and numerical simulations.

The third paper [6] describes a quantum phase transition induced by a spatial variation of the external magnetic field imposed on the condensate. Here the novel Kibble-Zurek-like theory developed within this LDRD project [7] was used. It was found that the condensate magnetization is non-trivially affected by the gradient field around the critical point on the length scale depending on the critical exponent nu of the condensate. In addition to showing how the quantum phase transition can be induced in space, this work suggests a new promising way for the measurement of the spatial critical exponent "nu". As before, both analytical and numerical simulations were found to be in agreement.

Zurek has also studied (alone, as well as in collaboration with colleagues, including Robin Blume-Kohout) various processes that transfer information between quantum systems. This led to several papers [8,9] that elucidate the nature of quantum jumps as well as studies of the so-called quantum Darwinism that sheds new light on the way in which classical reality of our everyday experience arises within our quantum Universe.

The experimental effort in Boshier's laboratory focuses on building a flexible experimental system, which can create and manipulate BECs in arbitrary dynamic potentials. This is a challenging task because the extremely delicate nature of ultracold BECs imposes stringent requirements on the smoothness and stability of potentials, which confine them. We have recently shown that an extension of the scheme that we originally proposed, based on painting time-averaged optical dipole potentials, provides a robust and straightforward way to create and manipulate BECs in complex, arbitrary and dynamic potentials. Here the optical dipole potential is a focused, off-resonant laser beam, which exerts a force on atoms through the interaction of the non-uniform laser field and the atomic polarizability. This demonstration represents the first realization of such a broad and general capability, and a paper describing the technique is now in preparation.

Figure 1 (a) shows the additions made to our existing BEC machine to allow for manipulating BECs in painted potentials. The optical trap is a combination of a static horizontal light sheet (which supports atoms against gravity and provides tight confinement in the vertical direction) and the rapidly-moving tightly-focused laser beam, which paints the potential on top of the sheet. The painting is controlled by a sophisticated computer system which permits arbitrary scan patterns of a few seconds duration. As long as the scanning frequency (several kHz) is faster than the trapping frequencies (several 100's of Hz) the condensate sees the time-averaged potential. Condensates are created in the combined optical trap by transferring a very cold atomic cloud from the magnetic trap of the original machine and then evaporating by lowering the optical trap intensity to allow the hottest atoms to escape. Figure 1 (b-e) show in-situ absorption images of complex BECs created with this system.

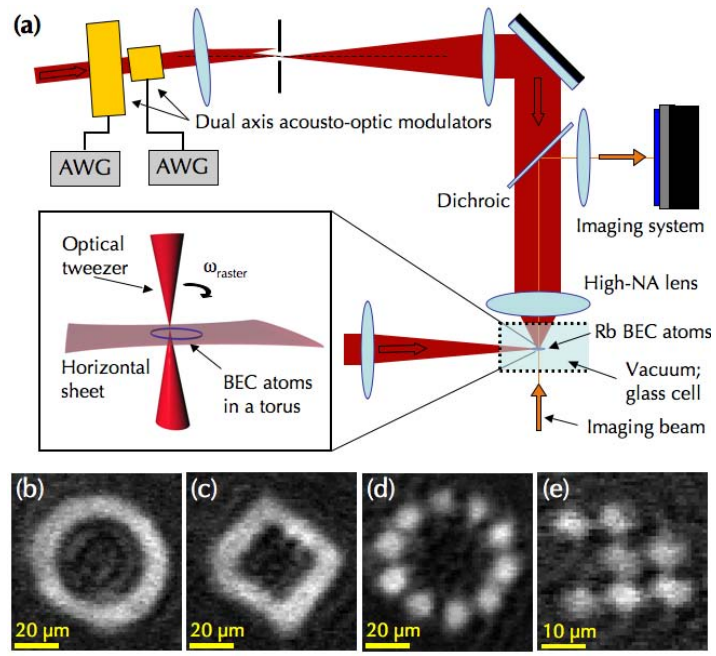


*Figure 1. (a) shows the setup for creating and manipulating BECs in painted dynamic and arbitrary potentials. (b)-(e) show in-situ absorption images of BECs in a variety of static geometries, none of which have been realized previously in the laboratory.*

For the specific experiment of studying the BEC QPT predictions we wanted to create a ring of independent BECs, reconnect them into a single toroidal geometry at variable rate, and then make a measurement of winding number. Figure 2 shows that we now have the tools to perform this process. Further, since the individual BECs can be created from a single toroidal BEC, there exists the possibility of preparing them with known phases. As an aside, it may now also be possible to probe carefully the predictions of the KZ theory for the BEC phase transition by creating BECs in a large ring and measuring the winding number statistics as a function of the quench time.

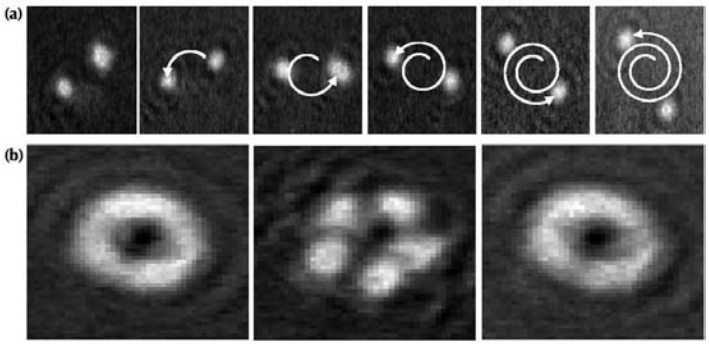


*Figure 2. Examples of time-dependent manipulation of a BEC in a painted potential. (a) shows two condensates made to orbit each other with increasing separation. The lower sequence (b) realizes the dynamics required to test the predictions of the theory component of this project for the results of a non-equilibrium quantum phase transition.*

Finally, we summarize the accomplishments of the information theoretic thread. In a paper in Physical Review Letters, Barnum and collaborators showed that some quantum computations using Lie-algebraic gates could be efficiently simulated classically [10]. These include gates implemented using the interactions of certain solvable condensed-matter physical models (such as the quantum Ising model interactions) which exhibit quantum phase transitions, strongly suggesting that not all systems supporting phase transitions are usable for universal quantum computation. Barnum also formulated a lower bound method for quantum query complexity with arbitrary unitary queries, a problem closely related to parameter estimation, in terms of semidefinite programming [11].

In a paper in Physical Review Letters, and follow-on papers in Physical Review A, Boixo and collaborators demonstrated advantages for quantum parameter estimation obtained with long-range interactions, with multibody interactions, and with entangled states in both closed and open-system scenarios. A major result is that---with multibody interactions---the quantum "Heisenberg limit" of 1/N, for using an N-body system with single-body interactions to measure a parameter, can be surpassed (although a generalized version of the Heisenberg limit involving the total action of the estimation process, in units of Planck's constant, is still respected) [12]. Another major, and somewhat surprising, result is that with multibody systems, a quantum advantage can be gained even without using initial entanglement [13,14].

As part of this work, Boixo and collaborators showed how such estimation procedures may be experimentally realized using BECs (leading to an invited presentation by Boixo at a major international cold-atom physics conference). Boixo and collaborators also showed that mixed-state quantum computation with a fixed number of pure qubits resembles standard quantum computation in providing fast parameter estimation in many cases, but unlike standard quantum computation it cannot speed up Grover's "search" problem [15]. Boixo and a collaborator showed that a well-known multi-qubit entanglement measure, that has been shown to signal quantum phase transitions in a variety of systems including spins, has an operational interpretation as a measure of the usefulness of a multipartite state for precision estimation of the level of "depolarizing noise" acting independently on each spin [16].

As part of the project's push toward investigating new approaches to quantum computation, including adiabatic computation, Barnum, Boixo, and collaborators investigated the possibility that adiabatic quantum computation could be used to speed up classical "simulated annealing" processes. This led to a measurement-based version of an adiabatic process, using the "Zeno effect" of quantum measurement to keep the system following the ground state of a sequence of different Hamiltonians. When applied to a sequence of "quantum coherent random walks" corresponding to the stochastic transition matrices of a classical simulated annealing algorithm, the procedure allows one to prepare a quantum superposition of all the ground states of the classical problem, allowing one to achieve the effect of classical simulated annealing algorithms, but with computational cost scaling inversely with the square root of the gap of the classical transition matrices, rather than with the inverse gap as in simulated annealing [17]. They have begun work on versions of this algorithm having improved performance in other parameters, and applications to genuine continuous-time evolution adiabatic theorems and computation.

## References

1. Cucchietti, F. M., B. Damski, J. Dziarmaga, and W. H. Zurek. Dynamics of the Bose-Hubbard model: transition from a Mott insulator to a superfluid. 2007. *Physical Review A.* **75** (2): 023603.

2. Cincio, L., J. Dziarmaga, M. M. Rams, and W. H. Zurek. Entropy of entanglement and correlations induced by a quench: Dynamics of a quantum phase transition in the quantum Ising model. 2007. *Physical Review A.* **75** (5): 052321.

3. Dziarmaga, J., J. Meisner, and W. H. Zurek. Winding up of the wave-function phase by an insulator-to-superfluid transition in a ring of coupled Bose-Einstein condensates. 2008. *Physical Review Letters.* **101**: 115701.

4. Damski, B., and W. H. Zurek. Dynamics of a quantum phase transition in a ferromagnetic Bose-Einstein

condensate. 2007. *Physical Review Letters.* **99** (13): 130402.

5. Damski, B., and W. H. Zurek. How to fix a broken symmetry: quantum dynamics of symmetry restoration in a ferromagnetic Bose-Einstein condensate. 2008. *New Journal of Physics.* **10** (4): 045023.

6. Damski, B., and W. H. Zurek. Quantum phase transition in space. 2008. *arXiv:0809.2877.*

7. Zurek, W. H., and U. Dorner. Phase transition in space: how far does a symmetry bend before it breaks?. 2008. *Philosophical Transactions of the Royal Society A.* **366**: 2953.

8. Blume-Kohout, R., and W. H. Zurek. Quantum Darwinism: Entanglement, branches, and the emergent classicality of redundantly stored quantum information. 2006. *Physical Review A.* **73** (6): 062310.

9. Zurek, W. H.. Quantum origin of quantum jumps: Breaking of unitary symmetry induced by information transfer in the transition from quantum to classical. 2007. *Physical Review A.* **76** (5): 052110.

10. Somma, R., H. Barnum, E. Knill, G. Ortiz, and L. Viola. Eff cient solvability of Hamiltonians and limits on the power of models of quantum computing. 2006. *Physical Review Letters.* **97**: 190501.

11. Barnum, H.. Semidefinite programming characterization and spectral adversary method for quantum complexity with noncommuting unitary queries. To appear in *Algorithms and Complexity for Continuous Problems.* (Dagstuhl, 24-29 September 2006).

12. Boixo, S., S. T. Flammia, C. M. Caves, and J. M. Geremia. Generalized limits for single-parameter quantum estimation. 2007. *Physical Review Letters.* **98**: 090401.

13. Boixo, S., A. Datta, S. T. Flammia, A. Shaji, E. Bagan, and C. M. Caves. Quantum-limited metrology with product states. 2008. *Physical Review A.* **77** (1): 012317.

14. Boixo, S., A. Datta, M. J. Davis, S. T. Flammia, A. Shaji, and C. M. Caves. Quantum metrology: dynamics versus entanglement. 2008. *Physical Review Letters.* **101**: 040403.

15. Boixo, S., and R. Somma. Parameter estimation with mixed-state quantum computation. 2008. *Physical Review A.* **77**: 052320.

16. Boixo, S., and A. Monras. Operational interpretation for multipartite entanglement. 2008. *Physical Review Letters.* **100** (10): 100503.

17. Somma, R., S. Boixo, H. Barnum, and E. Knill. Quantum simulations of classical annealing processes. 2008. *Physical Review Letters.* **101**: 130504.

## Publications

Barnum, H.. Semidefinite programming characterization and spectral adversary method for quantum complexity with noncommuting unitary queries. 2006. In *Algorithms and Complexity for Continuous Problems.* (Dagstuhl, 24-29 September 2006). , p. p. Dagstuhl: IBFI.

Barnum, H., J. Barrett, M. Leifer, and A. Wilce. Generalized no-broadcasting theorem. 2007. *Physical Review Letters.* **99** (24): 240501.

Barnum, H., O. C. Dahlsten, M. Leifer, and B. Toner. Nonclassicality without entanglement enables bit commitment. To appear in *2008 IEEE Information Theory Workshop (ITW).* (Porto, Portugal, 5-9 May 2008).

Blume-Kohout, R., and W. H. Zurek. Quantum Darwinism: Entanglement, branches, and the emergent classicality of redundantly stored quantum information. 2006. *Physical Review A.* **73**: 052113.

Blume-Kohout, R., and W. H. Zurek. Quantum Darwinism in quantum Brownian motion: the vacuum as a witness. 2008. *arXiv.*

Boixo, S., A. Datta, M. J. Davis, S. T. Flammia, A. Shaji, and C. M. Caves. Quantum metrology: dynamics versus entanglement. 2008. *Physical Review Letters.* **101**: 040403.

Boixo, S., A. Datta, S. T. Flammia, A. Shaji, E. Bagan, and C. M. Caves. Quantum-limited metrology with product states. 2008. *Physical Review A.* **77** (1): 012317.

Boixo, S., S. T. Flammia, C. M. Caves, and J. M. Geremia. Generalized limits for single-parameter quantum estimation. 2007. *Physical Review Letters.* **98**: 090401.

Boixo, S., and A. Monras. An operational interpretation for multipartite entanglement. 2008. *Physical Review Letters.* **100** (10): 100503.

Boixo, S., and R. D. Somma. Parameter estimation with mixed-state quantum computation. 2008. *Physical Review A.* **77** (5): 052320.

Cincio, L., J. Dziarmaga, M. M. Rams, and W. H. Zurek. Entropy of entanglement and correlations induced by a quench: Dynamics of a quantum phase transition in the quantum Ising model. 2007. *Physical Review A.* **75**: 052321.

Cucchietti, F. M., B. Damski, J. Dziarmaga, and W. H. Zurek. Dynamics of the Bose-Hubbard model: transition from

Mott insulator to superfluid. 2007. *Physical Review A.* **75**: 023603.

Cucchietti, F. M., J. P. Paz, and W. H. Zurek. Decoherence from spin environments. 2005. *Physical Review A.* **72** (5): 052113.

Cucchietti, F. M., S. Fernandez-Vidal, and J. P. Paz. Universal decoherence induced by an environmental quantum phase transition. 2007. *Physical Review A.* **75**: 032337.

Dalvit, D., J. Dzarmaga, and W. H. Zurek. Predictability sieve, pointer states, and the classicality of quantum trajectories. 2005. *Physical Review A.* **72** (6): 62101.

Damski, B., and J. Zakrzewski. The Mott insulator phase of the one dimensional Bose-Hubbard model: a high order perturbative study. 2006. *Physical Review A.* **74**: 043609.

Damski, B., and W. H. Zurek. Adiabatic-Impulse approximation for avoided level crossings: from phase transition dynamics to Landau-Zener evolutions and back again. 2006. *Physical Review A.* **73** (6): 063405.

Damski, B., and W. H. Zurek. Dynamics of a quantum phase transition in a ferromagnetic Bose-Einstein condensate. 2007. *Physical Review Letters.* **99**: 130402.

Damski, B., and W. H. Zurek. How to fix a broken symmetry: quantum dynamics of symmetry restoration in a ferromagnetic Bose-Einstein condensate. 2008. *New Journal of Physics.* **10** (4): 045023.

Damski, B., and W. H. Zurek. Quantum phase transition in space. 2008. *arXiv:0809.2877.*

Dziarmaga, J., J. Meisner, and W. Zurek. Winding up of the wave-function phase by an insulator-to-superfluid transition in a ring of coupled Bose-Einstein condensates. 2008. *Physical Review Letters.* **101**: 115701.

Friedland, S., and L. Gurvits. Lower bounds for partial matchings in regular bipartite graphs and applications to the monomer-dimer entropy. 2008. *Combinatorics Probability and Computing.* **17** (3): 347.

Gurvits, L., R. Shorten, and O. Mason. On the stability of switched positive linear systems. 2007. *IEEE Transactions on Automatic Control.* **52** (6): 1099.

Gurvits, L., and A. Olshevsky. Stability testing of matrix polytopes. To appear in *European Control Conference 2007.* (Kos, Greece, 2-5 July 2007).

Larson, J., B. Damski, G. Morigi, and M. Lewenstein. Mott-insulator states of ultracold atoms in optical resonators. 2008. *Physical Review Letters.* **1** (5): 050401.

Martin, I., and W. H. Zurek. Measurement of energy eigenstates by a slow detector. 2007. *Physical Review Letters.* **98**: 120401.

Somma, R., H. Barnum, E. Knill, G. Ortiz, and L. Viola. Efficient solvability of Hamiltonians and limits on the power of models of quantum computing. 2006. *Physical Review Letters.* **97**: 190501.

Somma, R., S. Boixo, H. Barnum, and E. Knill. Quantum simulations of classical annealing processes. 2008. *Physical Review Letters.* **101**: 130504.

Toscano, F., D. A. R. Dalvit, L. Davidovich, and W. H. Zurek. Sub-Planck phase-space structures and Heisenberg-limited measurements. 2006. *Physical Review A.* **73**: 023803.

Viola, L., and H. Barnum. Entanglement and subsystems, entanglement beyond subsystems, and all that. 2006. In *Foundations of Quantum Information and Entanglement.* (Boston, 23-24 March 2006). , p. p. Boston: Cambridge University Press.

Zurek, W. H.. Quantum origin of quantum jumps: breaking of unitary symmetry induced by information transfer in the transition from quantum to classical. 2007. *Physical Review A.* **76** (5): 052110.

Zurek, W. H., F. M. Cucchietti, and J. P. Paz. Gaussian decoherence and gaussian echo from spin environments. 2007. *Acta Physica Polonica B.* **38** (5): 1685.

Zurek, W. H., and U. Dorner. Phase transition in space: how far does a symmetry bend before it breaks?. 2008. *Philosophical Transactions of the Royal Society A.* **366**: 2953.

# Heavy Quarks as a Probe of a New State of Matter

*Patrick Lee Mcgaughey*

20060049DR

## Abstract

Intriguing evidence exists that a new state of matter (the quark-gluon plasma or QGP) is formed in collisions of heavy ions at the Relativistic Heavy Ion Collider (RHIC). We have developed a unique experimental capability for the direct identification of heavy quarks that will be used to accurately determine the properties of the QGP. We have constructed a silicon micro-vertex detector (SVD) that can measure heavy quarks produced in nuclear collisions. In parallel, we have developed new capabilities in theory and simulation to interpret future heavy quark data.

## Background and Research Objectives

The quark-gluon plasma is the state of matter in the early universe prior to the phase transition into protons and neutrons. Heavy quarks (charm and beauty) are the cleanest probes in the laboratory quest for the QGP. We have developed a silicon vertex detector to identify these heavy quarks. We have developed many of the theoretical tools necessary for the interpretation of the future data, including lattice and non-equilibrium field theory calculations. A pressing question we have addressed is: What is the mechanism of energy loss for heavy quarks in the plasma? Upcoming data and corresponding theoretical calculations of these processes will allow us to determine the physical properties of the QGP.

## Importance to LANL's Science and Technology Base and National R & D Needs

The primary focus of this proposal was to exploit an exciting opportunity in the basic physics of nuclear matter at the extremes of high temperature and density. The experiments at RHIC are among the highest priorities of the national nuclear physics program. Heavy quark measurements have the unique ability to isolate signatures specific to the QGP from background processes. We have constructed a silicon micro-vertex detector with state-of-the-art position resolution, speed and power consumption to make these heavy quark measurements. Integrating an SVD with the forward arm of the PHENIX detector will ensure a leadership role for LANL in this flagship of the national nuclear physics program. Development of the theory and simulation of matter under extreme non-equilibrium conditions met LANL's strategic goal of predictive modeling of complex systems. Pushing the state-of-the-art in lightweight, silicon technology is the next frontier for nuclear verification and non-proliferation applications.

## Scientific Approach and Accomplishments

### Theory

*Equilibrium and Non-Equilibrium Field Theories*

To study the non-equilibrium evolution of the QGP from first principles of the theory of strong interactions known as quantum chromo-dynamics (QCD), sophisticated theoretical techniques to add the contributions of the different sub-processes that affect a physically measurable quantity are necessary. We have developed a method of re-summing those contributions within a theoretical framework known as the Hard Thermal Loop approximation and assuming that the interactions between the constituents of the plasma are weak. In quantum field theory particles are able to emit and re-absorb other particles (called virtual particles). This property determines their behavior in physical processes. We carried out the complete analysis for the properties of the electron given by the emission of up to two virtual particles when this electron propagates in a high-temperature electro-magnetic plasma. The relevant emission and absorption processes, graphically expressed as diagrams, are shown in Figure 1.

This work opens the way to a systematic and independent computational approach to the re-summation of sub-processes in both the electromagnetic theory and the theory of the strong nuclear force. We will now be able to capture the hydrodynamic and dissipative processes in the quark-gluon plasma from first principles. Future work may explain why the QGP appears to be-

have more like a liquid than a gas of free particles. In our approach we will also be able to calculate the Equation-of-State of the plasma above the critical temperature and compare it to lattice simulations described in the next section.

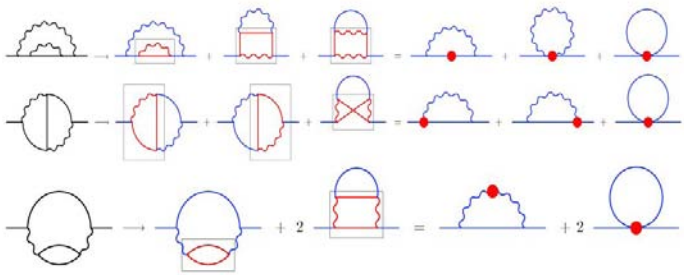

*Figure 1. Two-loop fermion self-energy diagrams, showing the hard thermal loop (red, boxed), the soft loop (blue), and the contraction to effective one-loop processes.*

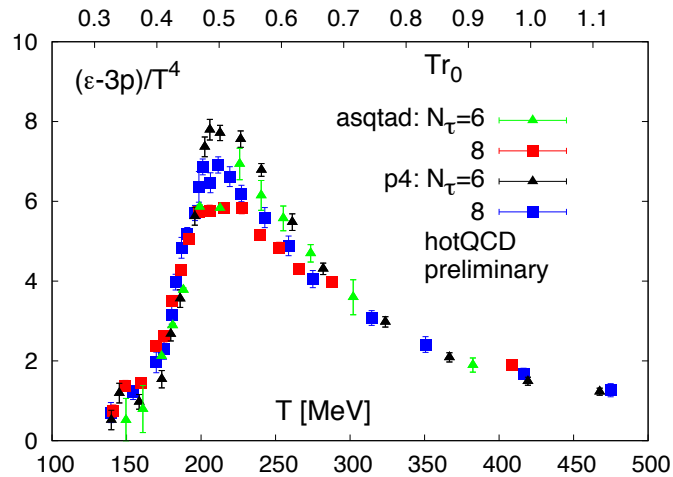


*Figure 2. Preliminary results for the QCD Equation of State as a function of temperature in MeV and in units of r0.*

*The QCD Equation-of-State from Lattice simulations*

The analysis of the data coming from RHIC has relied on relativistic hydrodynamics simulations. The results suggest a strongly-interacting plasma with very small viscosity. A crucial ingredient of this analysis is the characterization of its Equation-of-State (EoS) over the temperature range relevant to RHIC and LHC energies. The only way to calculate the EoS from first principles is via numerical Lattice QCD simulations. We have initiated and co-lead a US-wide "HotQCD" collaboration of experts working on QGP properties. Our HotQCD collaborative effort will extend well beyond the term of this project.

We obtained high-statistics results for two different ways of approximating the continuous strong interaction theory on a discrete lattice. In our approach it was very important to be able to have enough lattice steps in the "time" direction, since they determine the accuracy of the calculations. Our lattices were state-of-the-art with temporal extent $N_t$ = 6 and 8. As shown in Figure 2, we find that the two approximations give consistent results and estimate that the EoS obtained on $N_t$ = 8 lattices represents the actual continuum value to better than 20% uncertainty over the temperature range relevant for RHIC and LHC. This precision has already reached a stage where these lattice estimates of the EoS should be used in the phenomenological analysis of RHIC data. A related quantity of high interest in heavy ion physics is the transition or "critical" temperature from particles to a QGP and the nature of this phase transition. Previous calculations have found a type of transition known as "rapid crossover". We confirmed this finding and all of our studies produced an estimate of the critical temperature in the range of 185-195 MeV.

**Novel approach to heavy particle attenuation in the QGP:**

One of the outstanding theoretical puzzles in heavy ion physics has been the large 4-fold suppression, $R_{AA}$ ~ 1/4, in the production rate of electrons coming from the decay of massive particles (known as *D*-mesons and *B*-mesons) carrying the exotic quantum numbers called "charm" and "beauty", respectively. We identified the lack of proper treatment of the time that such particles take to form and the naïve application of energy loss approaches developed to describe the attenuation of light particle production in strongly-interacting plasmas as the leading source of this discrepancy. We proposed a novel mechanism of heavy particle suppression based on their dissociation when they collide with the constituents of the quark-gluon plasma. We showed that our results not only provide a solution to the above theoretical puzzle but they can also be used to assess the QGP properties, such as the time during which this new state-of-matter exists, its temperature, and its density. Our approach allowed for an improved description of the large attenuation of the decay electrons from heavy particles produced in reactions with gold nuclei at RHIC as shown in Figure 3.

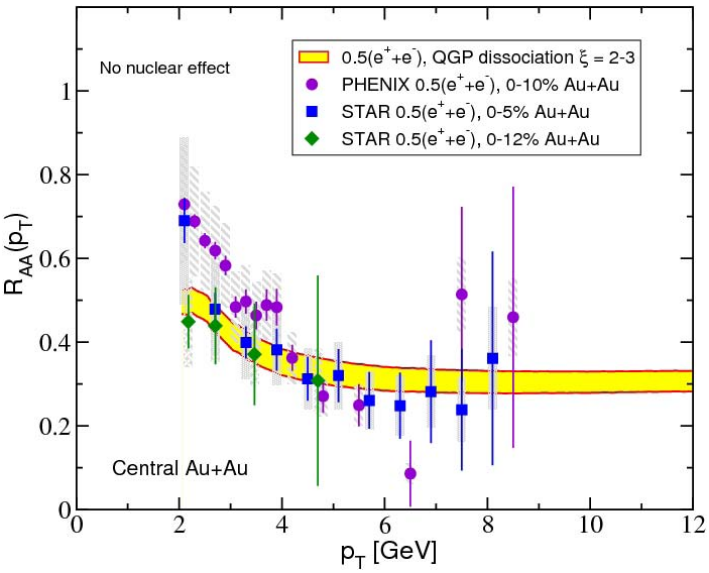


*Figure 3. Suppression of electron production from QGP-induced dissociation of heavy mesons compared to experimental data.*

The new theory that we developed makes unique experimentally testable predictions, namely, the suppression of the "beauty" particles is comparable to that of the "charm" particles. Alternative theoretical models, such as particle diffusion in the plasma, have always had problems with describing the suppression of the "beauty" particles since they are, on average, four times as heavy as the "charm" particles. We verified numerically and independently that the diffusion mainstream approach has difficulty in producing *B*-meson suppression. As a result, two different theoretical paradigms have been now presented to the experimental community and the main difference is the relative degree to which the "beauty" particles are attenuated relative to the "charm" particles. The detector technology developments described below will allow direct and unambiguous measurements of *B* and *D*-mesons, thereby identifying the correct mechanism for the suppression of their production rate in the QGP and, consequently, yield a correct assessment of the QGP properties.

## Experiment

*Silicon micro-vertex detector construction*

We have completed the design and construction of a silicon micro-vertex detector that can be used to detect heavy quark decays. Three detector stations were designed that are compatible with the PHENIX detector at RHIC. Each station consist of two identical planes mounted vertically offset to each other to allow for complete tracking coverage. Each plane has ten pixel detector modules, approximately 1 by 8 cm, mounted on a cooled support plane. The entire detector consists of about 1.4 million pixels. The steps required to construct the detector were: silicon pixel detector procurement, readout chip procurement, hybridization, module production, plane production and assembly.

The silicon detectors used were the ATLAS silicon pixel sensors. We obtained and tested a total of 25 silicon wafers, each of which contains 6 detectors. The detectors are readout using the custom FPIX2.1 chip. It incorporates a dead-time free readout by continuously processing all of the detector hits in real time. 10 wafers of readout chips were tested, each containing 138 FPIX chips.

The electrical connection of the readout-chips with the silicon sensor (called hybridization) was performed by solder bump bonding 8 readout chips to each sensor. 90 of these hybrids were produced and tested. A custom flexible kapton circuit board was used to connect the signals from the hybrids to the detector planes. The hybrids were assembled to form a detector module by precisely gluing each hybrid onto the kapton and wire-bonding the electrical connections. The resulting detector modules were also tested.

An assembled pixel plane is shown in Figure 4. One side of the printed circuit board holds all of the electronic components as well as the cooling lines. The other side (shown) holds 10 detector modules. The development of the pixel plane was rather challenging, given the large number of signal lines and wire bond pads.

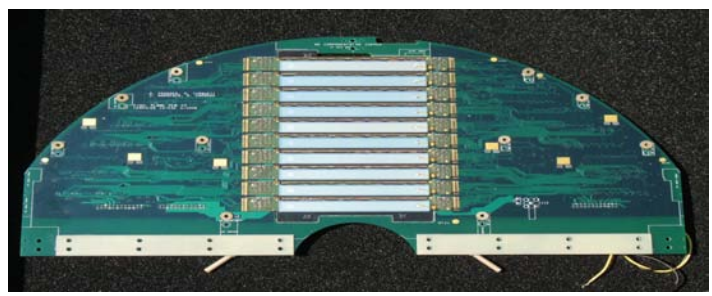

*Figure 4. A photograph showing an assembled pixel detector plane, which contains approximately 160,000 pixel detector elements.*

To date we completed the production and testing of all detector modules and 3 of the detector planes have been produced. The remainder will be completed during the next few months.

*Readout Electronics*

The data from the readout chips goes through two stages of electronics before reaching a data acquisition system. The first stage is located next to the vertex detector. It collects the digital data from the detector, serializes it and sends it out over optical fiber. The first stage has been

designed, is currently being constructed, and will be tested in the near future.

A second stage of electronics will reside inside the experiment's counting house. It retrieves the optical fiber data, buffers it until an experimental trigger occurs, then sends the data to the experiment's data acquisition system. The second stage conceptual design is complete and construction is expected to begin early 2009.

*Detector Performance Simulations*

Simulations of the silicon micro-vertex detector were carried out in order to optimize its performance in Au+Au collisions at RHIC. Since the capabilities of this high-resolution device are in large part determined by how much multiple scattering particles of interest undergo, it was important to simulate not only the detector itself, but also its surroundings, in as much detail as possible.

The detector was simulated using the GEANT-3 software package. The simulations showed, as expected, that the tracking resolution strongly depends on the track momentum. The track resolution needs to be good enough to reject backgrounds caused by decays of pions or kaons and background tracks that come directly from the event vertex. We obtained a distance of closest approach resolution of about 100 µm, which is sufficient for this task. Thus, the micro-vertex detector would allow us to directly distinguish between models of heavy quark propagation in the quark-gluon plasma, as demonstrated in Figure 5.

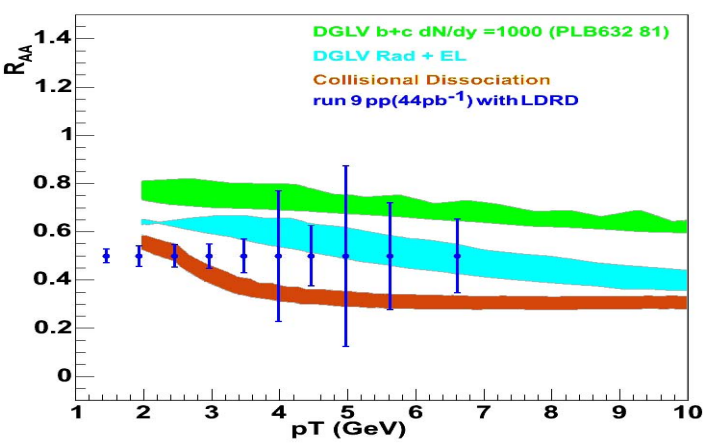


*Figure 5. Simulated sensitivity of the pixel detector compared to theoretical calculations of heavy quark suppression in the quark-gluon plasma.*

*Follow-on Project - The Forward Vertex Tracker*

Based upon the knowledge and expertise gained during this LDRD DR project, we developed a proposal for a much larger vertex detector that would cover the entire acceptance of the PHENIX muon arms at RHIC: "Proposal for a Forward Silicon Vertex Tracker (FVTX) for the PHENIX Experiment." The DOE has approved and funded this ~$5 million project, which began in mid FY08.

## $Z^0$+jet: A New Probe for the Quark Gluon Plasma

High transverse momentum jets are a key measurement in the study of the quark-gluon plasma, which will be created in abundance at the Large Hadron Collider (LHC) in Geneva. The dimuon decay of a high transverse momentum $Z^0$ particle associated with a hadronic jet is a unique probe which, based upon energy conservation between the $Z^0$ and jet, can provide a precise measurement of the energy loss of particles in the plasma. This would allow for a direct determination of the opacity of the QGP.

We have studied the production rates and the detector response for $Z^0$ decays to muon pairs. The results show that Compact Muon Solenoid (CMS) detector is very efficient at identifying the $Z^0$, with high purity and good resolution up to very high transverse momentum. This work has been published in a dedicated section of the official CMS Heavy Ions Physics Technical Design Report, an important achievement since only the analyses included therein will have guaranteed CMS analysis resources.

Work has continued on studying the detector response for heavy-ion collisions. Our emphasis has been on finalizing the software infrastructure required for analyzing the signal and backgrounds of the dimuon measurement. Tracks that come from the jet that balances the $Z^0$ and are detected in the silicon tracker are key to this analysis. We organized a meeting in CERN to assess the tracker performance in the heavy-ion environment and to establish the future improvements and developments needed. After discussion with the experts, we have implemented and tested the final missing piece, the Monte-Carlo matching for muons. A hit-by-hit track-matching algorithm, suitable for the high-density track environment of heavy-ion collisions, is now in place and ready to use.

We have also begun trigger studies to determine what the performance of the existing CMS muon triggers will be and how they will influence the rates of the dimuon signal. Future developments in this area are necessary and will be continued.

The status of this project, which is recognized as an official CMS analysis and included in the list of on-going analyses, was presented during several group and collaboration meetings. The full results of our project will be presented in a detailed analysis note, which is now in preparation.

A follow up proposal entitled the "First Unambiguous Measurement of Jet Fragmentation and Energy Loss in the Quark-Gluon Plasma" was submitted and approved for FY09 LDRD ER funding. With the completion of the LHC expected shortly, we plan to formally join the CMS experiment and begin data taking in 2009. The physics goal is to make the first direct measurement of in-medium jet fragmentation, which will allow for a precise determination of the plasma properties in a new and unexplored energy regime corresponding to even earlier times in the evolution of our universe.

## Publications


Brooks, M.. Technical Design Report of the Forward Silicon Vertex Tracker (FVTX), Proposal to the Department of Energy . 2007. *PHENIX Collaboration / Experiment at Brookhaven National Laboratory.*

Butsyk, S.. Heavy Flavor Measurements with FVTX Upgrade Detector. Presented at *American Physica Society Division of Nuclear Physics Meeting.* (Newport News, Oct. 2007).

Butysk, S.. Forward Pixel-Based Vertex Detector for PHENIX. Presented at *IEEE Nuclear Science Symposium.* (San Diego, Oct. 2006).

Carrington, M. E., and E. Mottola. Gauge invariance of the static fermion mass beyond hard thermal loops. 2007. In *International Conference on Strong & Electroweak Matter 2006.* (Upton, NY, May 2006). Vol. A, 275 Edition, p. 142c. Holland: Nuclear Physics.

Gupta, R.. Toward a precise determination of Tc with 2+1 flavors of quarks. 2007. In *Lattice 2007.* (Regensburg, July 2007). Vol. I, 1 Edition, p. 179. Trieste: Proceedings of Science.

Gupta, R.. The QCD EoS from simulaitons on BlueGene L supercomputers at LLNL and NYBlue. 2008. *LA-UR-08-06482.*

Kapustinsky, J., J. G. Boissevain, M. Brooks, S. Butsyk, G. Cardoso, D. Chrisitan, B. Cole, G. Grim, R. Gupta, B. Knapp, G. J. Kunde, S. Kwan, D. Lee, M. Leitch, M. Liu, E. Mannel, P. McGaughey, E. Mottola, A. Purwar, W. Sondheim, M. Turqueti, H. Van Hecke, I. Vitev, X. Wang, D. Winter, and W. Zajc. A pixel-based tracker to probe the quark-gluon plasma at PHENIX. To appear in *Frontier Detectors for Frontier Physics.* (Pisa, Italy, May 21-27, 2006).

Kunde, G.. CMS physics technical design report: Addendum on high density QCD with heavy ions . 2007. *Journal of Physics.* **G** (34): 2307.

Kunde, G.. Probing the Quark-Gluon Plasma with Jets in CMS at the LHC. Invited presentation at *High-pT physics at LHC International Workshop.* (Jyvaskyla, Mar. 2007).

Kunde, G.. A New Probe for the QGP at the Large Hadron Collider. Invited presentation at *Nuclear Winter Dynamics 2007.* (Big Sky, Feb. 2007).

Kunde, G.. The Inclusive Forward Vertex Detector for PHENIX. Presented at *IEEE Nuclear Science Symposium.* (Honolulu, Oct. 2007).

McGaughey, P.. Heavy quark detection with a forward silicon micro-vertex detector in the PHENIX experiment. 2006. In *Particles and Nuclei International Conference.* (Santa Fe, NM, Oct. 2005). Vol. 842, First Edition, p. 1079. Melville, NY: American Institute of Physics.

Mironov, C.. Probing the Quark-Gluon Plasma with Z0-Tagged Jets in CMS. Invited presentation at *Quark Matter 2006 international conference.* (Shanghai, Nov. 2006).

Mironov, C., P. Constantin, and G. J. Kunde. Dilepton Tagged Jets. 2007. *European Physics Journal.* **C** (49): c19.

Mironov, C., and G. Kunde. The CMS Experiment at the LHC. 2008. *Joutnal of Instrumentation.* **3**: S08004.

Mottola, E.. Gauge Invariance of the Static Fermion Mass Beyond Hard Thermal Loops. 2007. *Nuclear Physics.* **A** (275): 142c.

Mottola, E.. Beyond Hard Thermal Loops: Fermion Self-Energy in Hot QED. Invited presentation at *From RHIC to LHC: Achievements and Opportunities.* (Seattle, Oct. 2006).

Mottola, E.. Beyond HTL's: Resummation in Equilibrium and Non-Equilibrium Gauge Theor ies. Invited presentation at *Nonequilibrium Dynamics in Particle Physics and Cosmology.* (Santa Barbara, Feb. 2008).

Vitev, I.. Recent PQCD calcuations of heavy quark production . 2006. *Journal of Physics.* **G** (32): S317.

Vitev, I.. Non-Abelian energy loss in cold nuclear matter. 2007. *Physical Review.* **C** (75): 064906.

Vitev, I.. Collisional dissociation of heavy mesons in dense QCD matter. 2007. *Physics Letters.* **B** (649): 139.

Vitev, I.. Open charm tomography of cold nuclear matter.

2006. *Physical Review.* **D** (74): 054010.

Vitev, I.. Novel heavy flavor suppression mechanisms in the QGP. 2007. *Journal of Physics.* **G** (34): s769.

Vitev, I.. PQCD approach to parton propagation in matter. 2007. *Nuclear Physics.* **A** (783): 31.

Vitev, I.. Recent PQCD calculations of heavy quark production. 2006. *Journal of Physics.* **G** (32): S317.

Vitev, I.. Collisional dissociation of heavy mesons in the QGP. Invited presentation at *International 2007 RHIC & AGS Users Meeting.* (New York, Jun. 2007).

Vitev, I.. Predictions for the LHC: from photons to heavy quarks.. Invited presentation at *Last Call for LHC Predictions international workshop.* (Geneva, May 2007).

Vitev, I.. Self-consistency of jet quenching calculations at the LHC. Invited presentation at *High pT at the LHC international workshop.* (Jyvaskyla, Mar. 2007).

Vitev, I.. Open charm and bottom production and suppression in dense matter. Invited presentation at *Selected Topics on Heavy Flavor Production in High-Energy Collisions.* (Beijing, Nov. 2006).

Vitev, I.. Open charm tomography of cold nuclear matter. Invited presentation at *ISMD 2006 international conference.* (Partay, Sept. 2006).

Vitev, I.. Theoretical Developments in Heavy and Light Flavor Energy Loss. 2008. *Journal of Physics G.* **35** (1): 104011.

vanHecke, H.. The FVTX detector in PHENIX. Presented at *American Physica Society Division of Nuclear Physics Meeting.* (Newport News, Oct. 2007).

full final report

# DREAM: A Dynamic Radiation Environment Assimilation Model to Understand Acceleration, Transport, and Losses in Natural and HANE-Produced Radiation Belts

*Geoffrey D Reeves*

20060060DR

## Abstract

The Dynamic Radiation Environment Assimilation Model (DREAM) was developed at Los Alamos National Laboratory to assess, quantify, and predict radiation hazards in the space environment: both the natural environment and the anthropogenic environment produced by high altitude nuclear explosions. DREAM was initially developed as a basic research activity to understand and predict the dynamics of the Earth's Van Allen radiation belts but has also now been tested and validated for application to space weather forecasting and space situational awareness. DREAM uses Kalman filter techniques to assimilate data from space environment instruments with a physics-based model of the radiation belts. DREAM can assimilate data from a variety of types of instruments and data with various levels of resolution and fidelity by assigning appropriate uncertainties to the observations. Data from any spacecraft orbit can be assimilated but DREAM was designed to utilize and extend space environment information from the US nuclear detection system (USNDS) systems at geosynchronous and GPS orbits. With those inputs, DREAM can be used to predict the radiation belt environment at any satellite. We report here on an end-to-end test of DREAM in which we predict the environment in a highly-elliptical polar orbit.

## Background and Research Objectives

DREAM uses observations of the space radiation environment and sophisticated numerical data assimilation models to 1) produce accurate specifications of the space environment in the Van Allen radiation belts, and 2) illuminate and understand physical processes that cannot be derived from observations or models alone.

### Introduction to the Radiation Belts

The Earth's radiation belts (sometimes called the Van Allen belts) were discovered just over 50 years ago by James Van Allen's experiment on Explorer 1, the first US satellite in orbit. Ever since then, the radiation belts have been a scientific puzzle as well as an extreme hazard to the safe and reliable operation of satellites. The radiation belts are composed of energetic electrons and protons that are trapped in the Earth's magnetic field (the "geomagnetic field"). The radiation belt electrons and protons have energies that are high enough (millions of electron volts – MeV) that they penetrate through the metal shielding of satellites much like X-rays penetrate through non-metallic objects. In the process the electrons and ions can do significant damage to satellites, to space instruments, or to astronauts. Compromises must be made between spacecraft operational lifetime, cost, reliability, and the possible consequences of spacecraft failure. These are just some of the reasons why our technology-dependent society increasingly needs to understand the radiation belts, the risks they pose, and how to minimize those risks. This is the goal that motivated the development of the Dynamic Radiation Environment Assimilation Model – DREAM.

The intensity of the radiation belts is constantly changing because they respond (through a complex series of interactions) to activity on the sun. An example of these changes for three different electron energies is shown in Figure 1, which illustrates about 500 days of satellite observations with intensity shown in color as a function of radial distance from the center of the Earth and time. Changes in intensity by more than a factor of 1,000 are common. The challenge for the DREAM project was to develop a model that can reproduce and explain not just the average conditions but also all the variability.

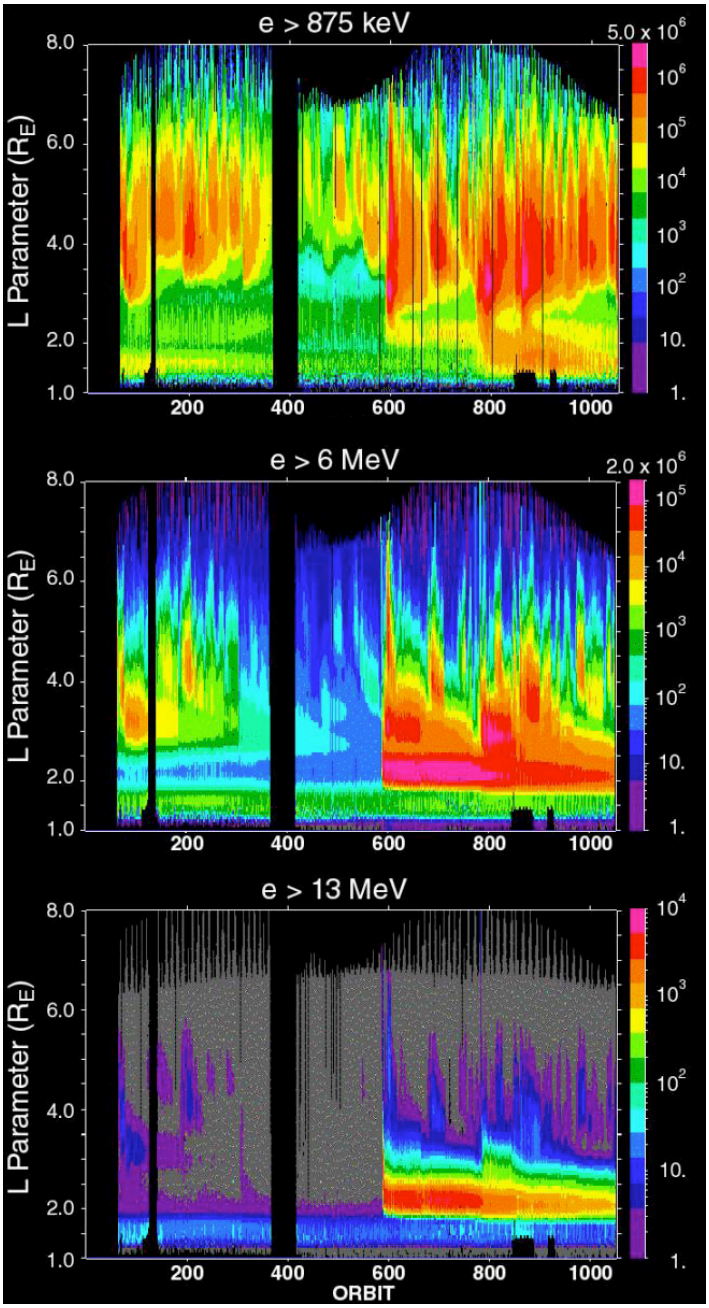


*Figure 1. The Earths radiation belts are highly variable in time, energy, and spatial distribution. This figure shows electron fluxes as a function of geocentric distance (LL in Earth Radii and orbit number for three energies. Data are from the CRRES satellite and cover approximately 500 days in 1990-1991.*

## Importance to LANL's Science and Technology Base and National R & D Needs

Los Alamos' mission in space began in the early 1960s with the signing of the limited nuclear test ban treaty and the need for technologies that could verify compliance as well as detect and characterize any treaty-violating nuclear tests. The space environment monitoring program began almost immediately afterwards when scientists realized the tremendous impact of the space environment on satellite systems.

There is virtually no national security system that does not depend crucially on the reliable operation of satellites in space. The impacts of the space environment are becoming more important as circuits get smaller, electronic devices strive for denser and denser memory storage, and computational needs get every more demanding. The national need for understanding and predicting the effects of "Space Weather" is increasing as fast as our more well-known dependence on computer and internet technologies.

Fortunately, we now have opportunity and tools that we need to advance our understanding of the space environment and its effects, not just incrementally, but dramatically. It is only quite recently that we have had the necessary components: new data, new theories, the DREAM data assimilation model, and the required computational resources. This is the ideal role for LDRD: national security programs that identify a compelling need – a research base that applies cutting-edge research to complex problems – and development of new capability to enhance the performance and reliability of the next generation of space systems.

## Scientific Approach and Accomplishments

The Earth's radiation belts present a difficult set of challenges to space physicists and modelers. The volume is enormous and the observations from satellites are very sparse. Many processes operate simultaneously: the Earth's magnetic field deforms and distorts; electrons and ions are injected into the system from other parts of space; various processes energize those particles and move them around the system; and other processes remove particles from the radiation belts by ejecting them out of the system or scattering them down into the atmosphere. The intensity of the radiation belts is a delicate balance among all these competing processes [1, 2].

### Data Assimilation and Magnetic Coordinates

One of the most sophisticated and successful tools for developing very accurate models of very complex systems is data assimilation. Data assimilation combines limited observations with physical models using techniques, such as Kalman filtering that optimize the accuracy of the assimilation model output. Both the physical models and the observations are assumed to have uncertainties and generally the assimilation model output is neither completely consistent with the equations of the physical model or completely consistent with the data inputs but, rather, produces an output is optimized to minimize internal inconsistencies.

Even though the radiation belts are extremely variable, assimilative modeling is helped by the fact that there are strong correlations among fluxes measured at different locations. These correlations exist because the Earth's magnetic field guides the motion of charged particles (electrons and protons). Charged particles gyrate in circles around a particular magnetic field line. They also bounce back and forth along a magnetic field line between magnetic mirror points (Figure 2). This means that the particles measured at any point on a field line can be specified by the distribution of particles at the magnetic equator. We label that point by the parameter "L" which is measured in units of Earth radii (1 $R_E$ = 6370 km).

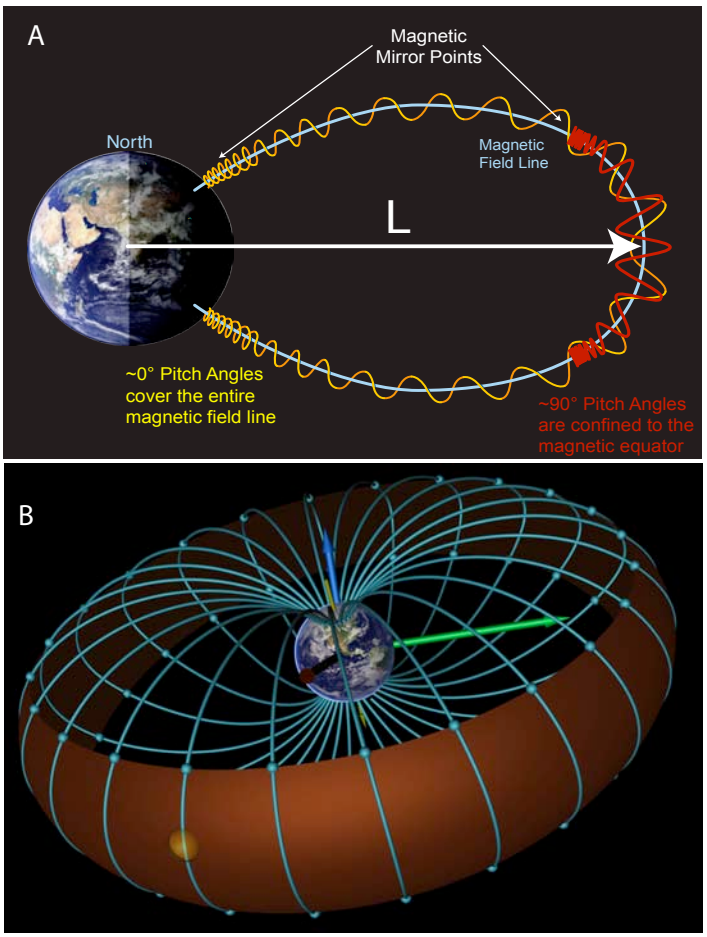


*Figure 2. Motion of charged particles and the definition of "L". (A) Electrons and positive ions will gyrate around the magnetic field and will bounce along the field between magnetic mirror points which are determined by the local magnetic field strength and the particle's pitch angle. Therefore it is convenient to label any point on a magnetic field line with the same value of "L" which is defined as the radial distance to the magnetic equator and is measured in units of Earth radii (RE). (B) Motion of charged particles on a "drift shell". This figure illustrates magnetic field lines and mirror points (blue) and the drift motion of charged particles around the Earth along a trajectory that traces a surface called a "drift shell". The magnetic field and drift shells change and are distorted by solar and geomagnetic activity.*

The Earth's magnetic field also causes charged particles to drift azimuthally around the Earth. As particles bounce and drift they follow a surface called a "drift shell" (Figure 2B). The geomagnetic field and the drift shell are distorted by solar activity and by internal electric currents. The distortion is most extreme during geomagnetic storms. A significant accomplishment of the DREAM program was the development of a sophisticated module that self-consistently calculates the distortion of the magnetic field due to ring current and plasma pressures during storms [3]. This model was the first of its kind and, in itself, an important scientific advance.

Physical modeling of the radiation belts first requires converting electron or ion flux at a into a coordinate system defined by the gyration, drift, and bounce motion of those particles. DREAM uses the radial diffusion equation to quantify particle transport. We use energy diffusion or phase space assimilation to represent processes that accelerate particles to higher energies. We allow particles to be lost out of the system by specifying the dynamic boundary of the magnetosphere. We apply different losses to the atmosphere in two different regions. Inside the high density plasmasphere (L ≈ 2-4) we use a constant 10-day lifetime and outside the plasmasphere we use an activity-dependent lifetime parameterized by the Kp index. The plasmasphere and its boundary are specified by a dynamic model that is also parameterized by Kp. The physical model and details of the assimilation can be found in [4-10].

***DREAM Results***

We describe here a test case that uses space environment instruments from the USNDS program to calculate the global, three-dimensional, time-dependent radiation environment. The data that we assimilate in this example come from the LANL Synchronous Orbit particle Analyzers (SOPA) detectors on three geosynchronous satellites and from the Burst Detector Dosimeter (BDD IIR) on GPS-Navstar41. The data that we use to test and validate our global prediction comes from 1 MeV electron measurements from the Comprehensive Energetic Particle and Pitch Angle Distribution (CEPPAD) experiment on NASA's POLAR satellite. It is important to emphasize that data from the POLAR satellite are not used in the assimilation in any way and that POLAR is in a vastly different orbit from the input data sets.

We compare the predicted 1 MeV flux at POLAR using three different radiation belt models: DREAM, CRRESELE, and AE8. The AE8 model is the accepted international standard model. AE8 is not a time-dependent model but there are slightly different versions for solar maximum or solar minimum. This study uses AE8min. The CRRESELE model is based on observations taken in 1990-1991 by the joint USAF-NASA Combined Release and Radiation Effects Satel-

lite (CRRES). It is a time-dependent model that is parameterized by geomagnetic activity (Kp).

Figure 3 shows the results of our calculations for 2005. The top panel shows the 1 MeV electron fluxes measured by the POLAR satellite (in electrons/cm$^2$/s/sr/keV). The fluxes are observed to vary considerably both as a function of time and location. As expected, the peak of the electron belt is typically observed between L=4-5 with a steep drop-off in flux at higher L. Fluxes varies in response to geomagnetic activity (bottom panel). Geomagnetic activity is measured by two indices: Kp and Dst - with the strongest activity indicated when they deviate from zero.

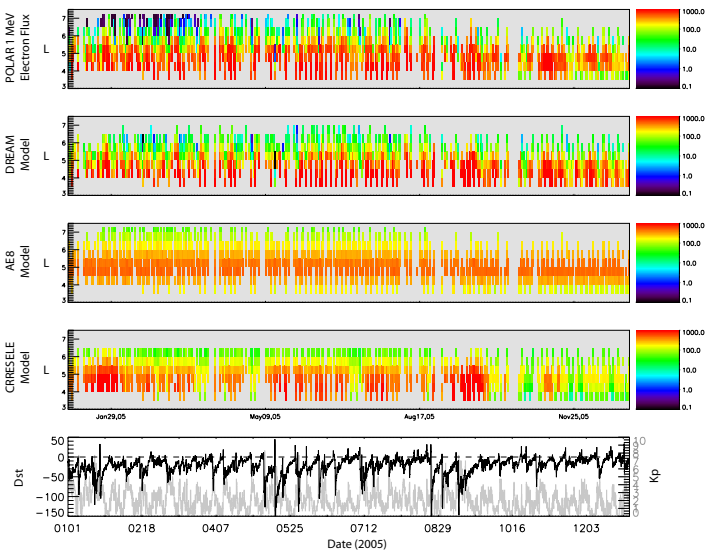


*Figure 3. DREAM model results. The top 4 plots all show 1 MeV electron flux (color-coded with units of #/cm2/s/sr/keV) as a function of time and L (radial distance from the center of the Earth in units of RE = 6370 km). Data are binned in 1-day, 0.5 L intervals. From top to bottom the panels show flux measured by the POLAR satellite, flux predicted by the DREAM model, the AE8min model, and the CRRESELE model. The bottom panel shows geomagnetic activity measured by Kp (gray) and Dst (black). High levels of activity are indicated by large positive values of Kp and by large negative values of Dst. Data are for the year 2005.*

The next three panels show the results from the three models: DREAM, AE8, and CRRESELE. All three models provide global specification of 1 MeV electron flux but model results are only plotted in bins where POLAR observations are available for direct comparison. As noted, the AE8 model shows no variation because it is an average, static model. The CRRES model, by design, scales with geomagnetic activity (Kp averaged over 15 days) and shows a reasonable correlation with POLAR observations. The DREAM model shows the most variation both in time and L and has the best correlation with the POLAR observations. While this is to be expected from a data assimilation model, the ability of DREAM to reproduce the fluxes at POLAR using very limited

**Metrics for Prediction and Validation**

Now we turn to metrics that can be used to validate our results and provide quantitative comparisons. In this section we evaluate the ability of the models to reproduce average conditions and their ability to predict variations. First we look at the average fluxes. Figure 4 shows the electron flux as a function of L averaged over a full year – 2005, the same interval shown above. All three plots show, in black, the average profile of 1 MeV electron flux as a function of L measured by POLAR. The mean of the log(flux) is the solid curve and the standard deviation around the mean is shown with dotted curves.

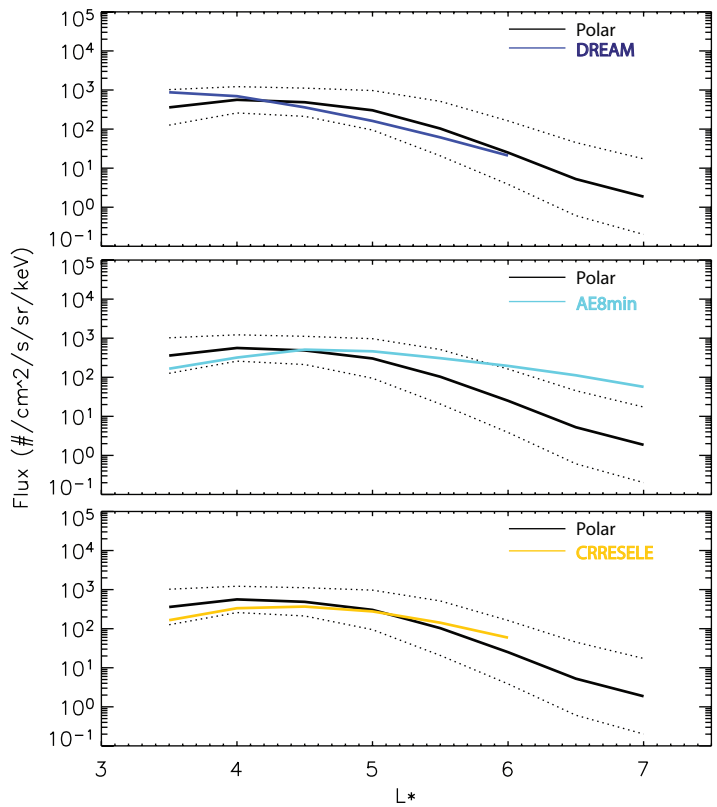


*Figure 4. Average flux values predicted by the models. Each panel shows the average and standard deviation of fluxes measured by POLAR as a function of L (geocentric radius). The average fluxes predicted by the DREAM, AE8, and CRRESELE models reproduce the average observations reasonably well with the exception of AE8 at high L values.*

As one would hope, all three models are able to reproduce the average conditions with some degree of accuracy but where the DREAM data assimilation really shows its utility is in predicting the variation around the mean. A standard metric for measuring the ability to track variations is the prediction efficiency, PE. Prediction efficiency measures the differences between the model and actual observations normalized to the difference between the

actual observations and the average of those observations. Prediction efficiency is defined such that a value of 1 indicates that the model exactly predicted the measurements at each observation time. A value of 0 indicates that the model predictions were as good as, but no better than, just guessing the average. Values below zero indicate that the predicted values are actually worse than guessing the average. In the stock market, 0 would be like the prediction efficiency on a buy-and-hold strategy, positive values would represent successful market timing, and negative values would represent unsuccessful market timing.

Figure 5 shows the prediction efficiency for DREAM, AE8, and CRRESELE. The AE8 model is the accepted, standard average values. If those averages were right the prediction efficiency would be 0, but, as we saw in Figure 4 the AE8 averages are only correct at L=4.5. At all other points the average is wrong so the prediction efficiency is negative. The CRRESELE model has an output that is scaled by geomagnetic activity but the fact that the prediction efficiency is negative at all L indicates that the variations are at the wrong times or are of the wrong magnitude. In contrast the DREAM model is positive across all L, indicating that it predicts much of the observed variation with the right timing and the right magnitude. Our goal in the future is approach a perfect prediction efficiency of 1.

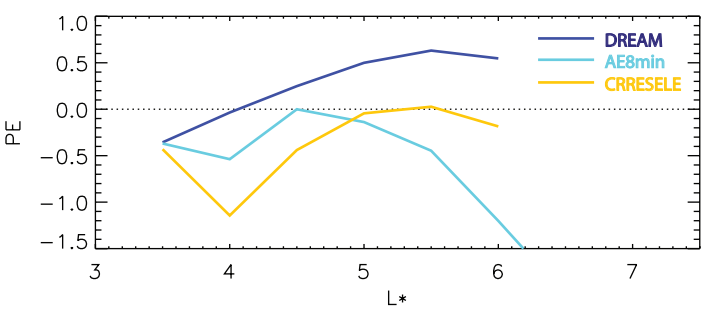


*Figure 5. The prediction efficiency, PE (defined in the text), tests the ability of the model to predict the variation of fluxes around the mean. A prediction efficiency of 1 is perfect agreement at all times. Prediction efficiencies less than or equal to zero do not provide useful predictions of the time variation of the observations.*

### Conclusions

This report highlights the primary result from the Dynamic Radiation Environment Assimilation Model – the ability to predict the complex dynamics of the Earth's radiation belts using a new assimilative model and space environment observations from Los Alamos' USNDS instruments. These predictions are tangible, measurable, and show more than an order of magnitude improvement in our ability to predict that hazardous space environment. The results presented here, though, do not reflect all of the accomplishments of the LDRD-DR project. Along the way, we developed a variety of numerical algorithms that are the first of their kind, one of which has been submitted for a US patent. We have developed new physical insight into the processes that control the radiation belts; proving, for example, that resonant wave-particle interactions are the dominant process for accelerating radiation belt electrons to relativistic energies [7]. We have developed a sophisticated set of coupled models that describe inner magnetospheric dynamics from thermal to relativistic energies while, at the same time, providing a means of predicting the distortion of the magnetic field during geomagnetic storms, the regions where wave production produces acceleration or scattering into the atmosphere, the rates of escape of radiation belt electrons from the magnetosphere to the solar wind, and many others. Currently the NNSA office of Nuclear Nonproliferation is supporting future development of DREAM and its transition to operations for national security space programs.

## References

1. Reevesetal., G. D.. Acceleration and loss of relativistic electrons during geomagnetic storms. 2003. *Geophysical Rseearch Letters.* **30** (10): 1529.

2. Reevesetal., G. D.. Current understanding of radiation belt dynamics and challenges for the future. To appear in *Space Weather.*

3. Zaharia, S.. Self-consistent modeling of magnetic fields and plasmas in the inner magnetosphere: Application to a geomagnetic storm. 2006. *Journal of Geophysical Research.* **111** (A11S14): doi:10.1029/2006JA011619.

4. Shprits, Y. Y., and R. M. Thorne. Time dependent radial diffusion modeling of relativistic electrons with realistic loss rates. 2004. *Geophysical Rseearch Letters.* **31** (L08805): doi:10.1029/2004GL019591.

5. Chenetal., Y.. Multi-satellite Determination of the Relativistic Electron Phase Space Density at Geosynchronous Orbit: Methodology and Initial Results During Geomagnetic Quiet Times. 2005. *Journal of Geophysical Research.* **110** (A10210): doi:10.1029/2004JA010895.

6. Chenetal., Y.. Multisatellite determination of the relativistic electron phase space density at geosynchronous orbit: An integrated investigation during geomagnetic storm times. 2007. *Journal of Geophysical Research.* **112** (A11214): doi:10.1029/2007JA012314).

7. Chen, Y., R. H. W. Friedel, and G. D. Reeves. The Energization of Relativistic Electrons in the Outer Van Allen Radiation Belt.. 2007. *Nature Physics.* **3** (9): 614.

8. Koller, J., R. H. W. Friedel, and G. D. Reeves. Radiation

Belt Data Assimilation and Parameter Estimation. 2005. *Los Alamos National Laboratory Technical Report, LA-UR-05-6700.*

9. Kolleretal., J.. Identifying the radiation belt source region by data assimilation. 2007. *Journal of Geophysical Research.* **112** (A06244): doi:10.1029/2006JA012196.

10. Kolleretal., J.. Radiation Belt Data Assimilation with an Ensemble Kalman Filter.. 2007. In *4th Space Weather Symposium.* (San Antonio, TX, 14-18, Jan, 2007). Vol. , Edition, p. . San Antonio: .

## Publications

Chen, Y., G. D. Reeves, and R. H. W. Friedel. The Energization of Relativistic Electrons in the Outer Van Allen Radiation Belt. 2007. *Nature Physics.* **3** (9): 614.

Chen, Y., R. H. W. Friedel, G. D. Reeves, T. G. Onsager, and M. F. Thomsen. Multi-satellite Determination of the Relativistic Electron Phase Space Density at Geosynchronous Orbit: Methodology and Initial Results During Geomagnetic Quiet Times. 2005. *J. Geophys. Res..* **110**.

Chen, Y., R. H. W. Friedel, and G. D. Reeves. Phase space density distributions of energetic electrons in the outer radiation belt during two Geospace Environment Modeling Inner Magnetosphere/Storms selected storms. 2006. *J. Geophys. Res..* **111** (A11S04).

Chen, Y., R. H. W. Friedel, and G. D. Reeves. Multisatellite determination of the relativistic electron phase space density at geosynchronous orbit: An integrated investigation during geomagnetic storm times. 2007. *J. Geophys. Res..* **112** (A11214).

Gary, S. P., H. Saito, and H. Li. Cascade of whistler turbulence: Particle-in-cell simulations. 2008. *Geophys. Res. Lett..* **35** (L02104).

Gary, S. P., and S. Saito. Broadening of solar wind strahl pitch-angles by the electron/electron instability: Particle-in-cell simulations, Geophysical Research Letters. 2007. *Geophys. Res. Lett..* **34** (L14111).

Horne, R. B.. Acceleration of Killer Electrons. 2007. *Nature Physics.* **3** (9): 590.

Jordanova, V. K.. Modeling geomagnetic storm dynamics: New results and challenges. 2007. *J. Atmos. Solar Terr. Phys..* **69**: 56.

Jordanova, V. K., M. Spasojevic, and M. F. Thomsen. Modeling the electromagnetic ion cyclotron wave induced formation of subauroral proton arcs. 2007. *J. Geophys. Res..* **112** (A08209).

Jordanova, V. K., Y. Miyoshi, S. Zaharia, M. F. Thomsen, G. D. Reeves, D. Evans, C. Mouikis, and J. F. Fennell. Kinetic Simulations of Ring Current Evolution During the Geospace Environment Modeling Challenge Events. 2006. *J. Geophys. Res..* **111** (A11S10).

Koller, J., Y. Chen, G. D. Reeves, R. H. Friedel, T. E. Cayton, and J. A. Vrugt. Identifying the radiation belt source region by data assimilation. 2007. *J. Geophys. Res..* **112** (A06244).

Lavraud, B., V. K. Jordanova, and M. F. Thomsen. Modeling the effects of local time variation of plasma sheet properties on proton ring current energy and peak location. 2008. *J. Geophys. Res..* **113** (A05215).

Lavraud, B., and V. K. Jordanova. Modeling the effects of cold-dense and hot-tenuous plasma sheet on proton ring current energy and peak location. 2007. *Geophys. Res. Lett..* **34** (L02102).

Maget, V., S. Bourdarie, D. Boscher, and R. H. Friedel. Data assimilation of LANL satellite data into the Salammbô electron code over a complete solar cycle by direct insertion. 2007. *Space Weather.* **5** (S10003).

Miyoshi, Y. S., V. Jordanova, A. Morioka, M. F. Thomsen, G. D. Reeves, D. Evans, and J. Green. Observations and modeling of energetic electron dynamics during the Oct. 2001 storm. 2006. *J. Geophys. Res..* **111** (A11S02).

Pulkkinen, T. I., N. Ganushkina, E. Tanskanen, M. Kubyshkina, G. D. Reeves, M. F. Thomsen, C. T. Russell, H. J. Singer, J. Slavin, and J. Gjerloev. Magnetospheric Current Systems During Stormtime Sawtooth Events. 2006. *J. Geophys. Res..* **111**.

Reeves, G. D., R. H. W. Friedel, J. Koller, Y. Chen, S. Zaharia, V. K. Jordanova, and Y. Y. Shprits. Initial results from the Dynamic Radiation Environment Assimilation Model (DREAM). 2007. *J. Atmos. Solar Terr. Phys..*

Saito, S., and S. P. Gary. All whistlers are not created equally: Scattering of strahl electrons in the solar wind via particle-in-cell simulations. 2007. *Geophys. Res. Lett..* **34** (L01102).

Saito, S., and S. P. Gary. Whistler scattering of suprathermal electrons in the solar wind: Particle-in-cell simulations. 2007. *J. Geophys. Res..* **112** (A06116).

Shprits, Y. Y., D. Kondrashov, Y. Chen, R. M. Thorne, M. Ghil, R. H. Friedel, and G. D. Reeves. Reanalysis of relativistic radiation belt electron fluxes using CRRES satellite data, a radial diffusion model, and a Kalman filter. 2007. *J. Geophys. Res..* **112** (A12216).

Shprits, Y. Y., R. M. Thorne, R. Friedel, G. D. Reeves, J. Fennell, D. N. Baker, and S. G. Kanekal. Outward radial diffu-

sion driven by losses at the magnetopause. 2006. *J. Geophys. Res.*. **111**.

Tu, W., X. Li, Y. Chen, and G. D. Reeves. Storm-Dependent Radiation Belt Dynamics. 2007. *Geophys. Res. Lett.*.

Vapirev, A. E., and V. K. Jordanova. Calculation of bounce-averaged velocities and hydrogen densities for a storm-time magnetic field. 2007. *Geophys. Res. Lett.*. **34** (L10103).

Varotsou, A., D. Boscher, S. Bourdarie, R. B. Horne, N. P. Meredith, and R. H. Friedel. The Salammbo 3D radiation belt physical model: test simulations including electron-chorus resonant interactions. 2007. *J. Geophys. Res.*.

Varotsou, A., R. H. Friedel, G. D. Reeves, B. Lavraud, R. M. Skoug, T. E. Cayton, and S. Bourdarie. Relativistic electron flux rise times during the recovery phase of geomagnetic storms as measured by NS41 GPS satellite. 2007. *J. Atmos. Solar Terr. Phys.*.

Winske, D., and S. P. Gary. Hybrid simulations of debris-ambient ion interactions in astrophysical explosions. 2007. *J. Geophys. Res.*. **112** (A10303).

Zaharia, S.. Improved Euler potential method for three-dimensional magnetospheric equilibrium. 2008. *J. Geophys. Res.*. **113** (A08221).

Zaharia, S., J. Birn, and C. Z. Cheng. Toward a global magnetospheric equilibrium model. 2005. *J. Geophys. Res.*. **110**.

Zaharia, S., M. F. Thomsen, J. Birn, M. H. Denton, V. K. Jordanova, and C. Z. Cheng. Effect of Storm-Time Plasma Pressure on the Magnetic Field in the Inner Magnetosphere. 2005. *Geophys. Res. Lett.*. **32**.

Zaharia, S., V. Jordanova, M. F. Thomsen, and G. D. Reeves. Self-consistent modeling of magnetic fields and plasmas in the inner magnetosphere: Application to a geomagnetic storm. 2006. *J. Geophys. Res.*. **111**.

Zaharia, S., V. K. Jordanova, M. F. Thomsen, and G. D. Reeves. Self-consistent geomagnetic storm simulation: The role of the induced electric fields. 2007. *J. Atmos. Solar Terr. Phys.*.

# Mix Processes in Inertial Confinement Fusion

*Anna Catherine Hayes-Sterbenz*

20060081DR

## Abstract

Understanding mix in Inertial Confinement Fusion (ICF) experiments at the National Ignition Facility requires the diagnosis of charged particle reactions within an imploded target. Radiochemical diagnostics of these reactions are currently under study by scientists at Los Alamos and Lawrence Livermore National Laboratories. Measurement of these reactions requires assay of activated debris and tracer gases from the target. Presented below is an overview of the prompt Radiochemistry diagnostic development efforts, including a discussion of the reactions of interest as well as the progress being made to collect and count activated material

## Background and Research Objectives

The National Ignition Facility (NIF) is expected to drive deuterium-tritium (DT) filled inertial confinement fusion (ICF) capsules to thermonuclear ignition by compressing DT spheres from 2 mm in diameter to approximately 100 microns in diameter. The ignition and burn of the capsule are likely to be adversely affected by hydrodynamic mixing of the DT fuel with shell material, which must be understood and controlled. There are a number of reasons to expect that mix at the NIF will be complicated and difficult to control. The convergence ratios (~30:1) required for ignition pose a challenge for direct simulations of instability growth arising from asymmetries and capsule non-uniformities. Within a reasonable range of mix parameters, substantial mix can occur, with ignition failure as a possible outcome. Understanding the source of any failure is critical, as attempts to achieve ignition by increasing the laser power will result in laser damage. Furthermore, in the event full ignition is achieved, the scientific focus at NIF will move to the detailed exploration of key unanswered questions in thermonuclear burn, the role of hydrodynamic mixing being one of these central questions.

The central objective of this project is to develop a mix diagnostic for NIF based on radiochemical measurements of reactions between charged-particles from the fuel with the shell material. Energetic charged particles have limited range in a NIF capsule due to energy losses from collisions with free electrons. The stopping power, dE/dx, is a function of electron density and temperature, as well as the charged-particle energy E. The limited range of these particles implies their reaction rates with shell ions are strongly dependent on the spatial overlap between the shell material and the charged particle source. To a good approximation, significant reaction rates will occur only where both the charged-particle source and the shell material are brought into close proximity, within a stopping length. If the shell material is closely mixed with the fuel, the number of reactions is enhanced by the ratio of the mixing length (the thickness of the mixing region) to the stopping length in the unmixed fuel.

## Importance to LANL's Science and Technology Base and National R & D Needs

NNSA has set a major scientific milestone of attempting fusion ignition with energy gain at NIF in 2010. Mix physics is inherently interesting, both in the ICF context and in laboratory's weapons program. Understanding the detector material response to the extreme radiation flux is directly relevant to the physics targeted by the MaRIE facility

## Scientific Approach and Accomplishments

We have been developing a mix diagnostic, commonly referred to as β-Mix', which endeavors to measure the reaction of high-energy (knock-on) tritons with the shell material. The reactions are chosen to produce β–emitters. Knock-on tritons are produced by collisions with 14 MeV neutrons traversing the capsule. The number of knock-on tritons scales with the neutron fluence. Most of these knock-on tritons simply thermalize, while some will fuse with deuterium, but a significant fraction will react with shell material. The triton stopping length in the DT plasma is relatively short, so only knock-on tritons near shell material, e.g. the fuel/shell interface, undergo a t+shell reaction. The neu-

trons probe the full ρr of the capsule and the production of knock-on tritons is not complicated by the DT burn wave. The long range of the neutrons and the higher density of the fuel in the cold regions mean that β–Mix is primarily a probe of mix in the *outer-regions* of the capsule. The enhancement of the t+shell reactions is determined by the overlap (physical co-location) of the shell material with the fuel, burning or not.

The expected signals for β–Mix show more than an order of magnitude enhancement of the number of β–reactions produced when shell/fuel mix occurs. For these calculations we have assumed uniform atomic mix into a mixing length of 4 microns. We have also examined other mix models, including strongly wrinkled shell/fuel interfaces and chunk mix. In the latter two models the enhancement (relative to the no-mix case) was about a factor of two, reflecting the typical increase in the surface area of the shell material exposed to the energetic triton fluence. In general, we find that all reactions show most sensitivity to atomic-like mix, where the enhancement is proportional to the mixing strength. Using the Scannapieco and Cheng model, with the mix parameter tuned to reproduce Omega ICF yields, the enhancement factor turns out to be about 50 for NIF. A typical predicted overlap of the shell material with the DT fuel, using the Scannapieco and Cheng model, is shown in Figure 1. The value of the Scannapieco and Cheng mix model parameter used in these calculations was $\alpha$=0.06, where $\alpha$ is the ratio of the enhancement to the collisional mean free path of a particle to the dynamic mixing length in a multifluid system.

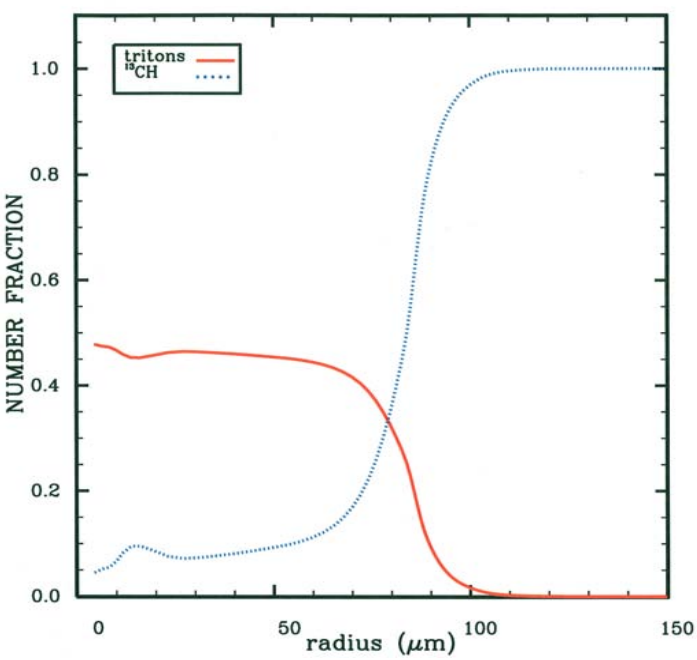


*Figure 1. The atomic mix model predicted overlap of the shell material (13C) and the tritons from the fuel.*

Diagnosing mix in an ICF experiment, requires the following simplified process flow:

1) Collect and count activated debris products, 2) Correct for experimental efficiencies and reaction cross sections, and 3) Interpret the correlated reaction data set to infer mix.

The second and third tasks occur ``offline'' and rely on established techniques developed by Nuclear Chemistry and Physics, including independent experimental data, e.g., reaction cross sections. The primary technical challenges for developing a prompt radiochemical diagnostic for the NIF, are the collection and assay of activated target debris in an extremely harsh environment.

Figure 2 illustrates a simplified view of the environmental issues effecting debris collection during ICF implosions. Shortly after bang time, materials within the target chamber are exposed to three distinct energetic wavefronts: a ``radiation'' wavefront, generated by laser matter interactions and bang-time reactions within the target, an ``ablation'' wavefront of material driven from the target by the laser or radiation drive, and finally, a ``disassembly'' wavefront of material which remained with the target through bang-time and subsequent disassembly. It is the disassembly material that carries the mix signals to be diagnosed.

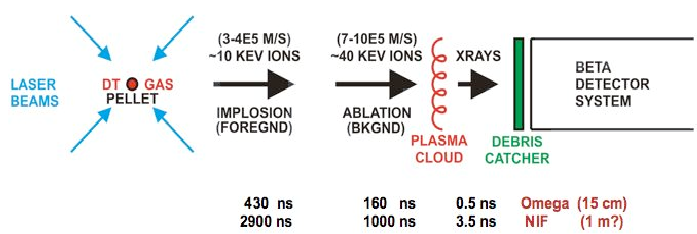


*Figure 2. Three distinct wavefronts of energy propagate from imploded targets in ICF experiments, including radiation from the target, ablated material from the target, and finally the disassembled target debris, which contains the signals of interest for radiochemical diagnostics. The time of arrival of the wavefronts shown are for the Omega target chamber, where the debris collector was at 15 cm; at NIF the debris collector may be as far as 5 m.*

For indirect drive experiments at the NIF, the radiation wavefront produced by laser matter interactions with the target is expected to exceed about 1-2 J/cm$^2$ at the target chamber wall, five meters from target chamber center. The surfaces of materials exposed to nanosecond scale pulses of 100 eV X-rays, or 10 KeV ions, with energy densities above 1 J/cm$^2$ will readily ablate. This results from the short range, O(100) nm, and short duration, O(1) ns, of the radiation, producing temperatures in the range of a few eV in the volume of deposition. This ablation is illustrated in Figure 3 by the ``plasma cloud.'' To test these concepts,

experiments were performed in Jan. 2007 with the Omega laser. Foils were located 15 cm from a directly driven CH target and exposed to the fluence of X-rays and ions produced by the imploding the target. Figure 4 shows post-shot results of titanium alloy foils (Ti 90%, Al 6%, Va 4%) exposed to $D_2$ filled targets. The targets were driven by 23 kJ of 351 nm laser energy for 1 ns. The foils were originally flat and the dark border on the edge of the foil indicates where the mechanical support frame protected the foil from exposure to the experiment. Results from optical profilometry at the boundary between the exposed and unexposed regions of the foil indicate that 160 nm of material was removed from the surface during these shots. The calculated incident energy on the foil is approximately 12 eV per liberated foil ion.

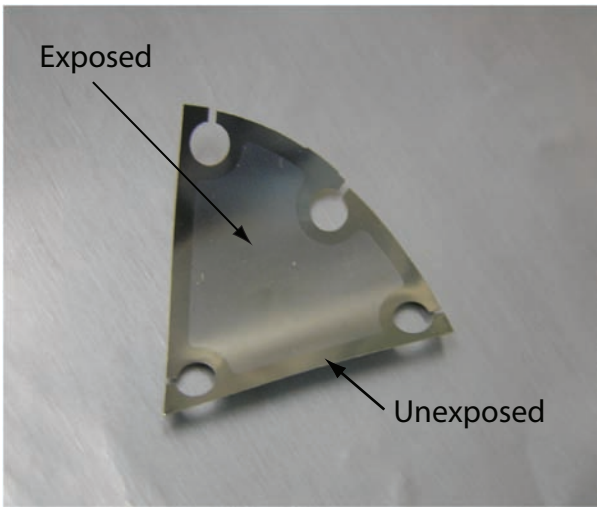


*Figure 3. Titanium alloy (Ti64) foils exposed to debris from a direct drive experiment using D_2 filled CH targets at the Omega laser.*

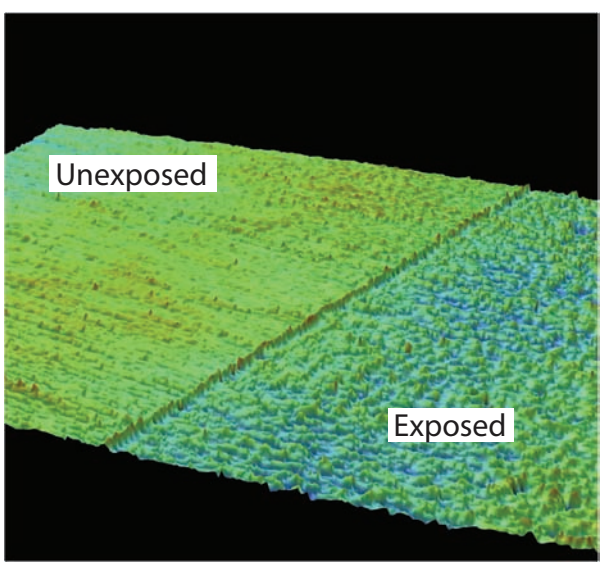


*Figure 4. Surface profilometry of the foil shown in Figure 3. The average material removed from the foil surface was measured to be 160 nm of material.*

This ablated plasma cloud poses a significant technical challenge for direct debris collection via ``implantation,'' particularly when the transport time of the disassembly material to the collector is short compared to the dispersal time of the ablated plasma. The stopping range of normally incident $^{13}C$ atoms impinging solid Ti is approximately 23 nm and 90 nm for 10 and 40 keV ions, respectively, which is less than the 160 nm of ejected material. Therefore, direct collection of the target disassembly debris is not possible when the sum of the radiation and ablation wavefront energy densities is above 1 J/cm$^2$. For experiments using the Omega laser, this issue may be addressed by moving to larger distances from the target to reduce the incident fluence to tolerable levels.

To gain understanding of these issues, experiments were performed at the Repetitive High Energy Pulsed Power Facility (RHEPP-1) at Sandia National Laboratory. Ion beams with energy densities from 1-10 J/cm$^2$ were used to ablate the surface of different material shapes and compositions to address the issues relevant for debris collection in ICF experiments. The primary diagnostic for these experiments was a 9-frame, framing camera. Results from a typical experiment are shown in Figure 5.

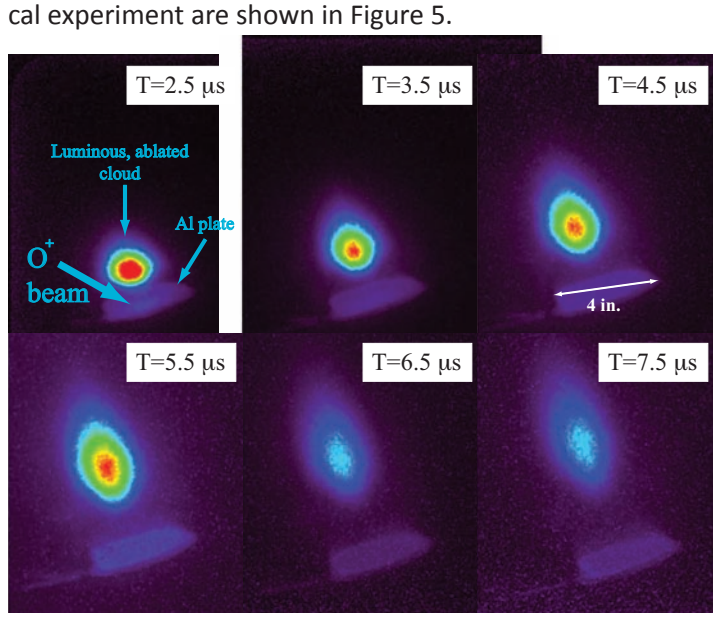


*Figure 5. Experiments to study debris dynamics using the RHEPP1 facility at Sandia National Laboratory. An 8 J/cm2 O2 beam was used to generate a hot plume of Al ions that were imaged with a framing camera at the times indicated.*

Here a luminous (few eV) ablation cloud is emitted by a target impinged with 6 J/cm$^2$ ion beam. The six images show the clear propagation of the plume created by a 700 kV, 100 ns, $O_2$ ion beam striking an 1100 series Al target. The times indicated are relative to when the $O_2$ beam struck the target. The ion beam strikes the target at roughly a 45$^o$ angle from the left, as indicated in the figure. From this experiment and others, it is clear that the ablated

cloud moves normal to the target surface, with some lateral dispersion for flat or convex shapes. Measurements of the luminous centroid indicate that material is moving at a collective velocity of 1.12 microns *normal* to the target. In ICF experiments with reflectors positioned tens of centimeters from the target, the time scale for ablation will be relatively short when compared to the transit times for the ablated plume. Thus, it should be possible to use the plume as an entrainment and transport mechanism for material carrying mix signatures. Further experimental results show the plume shape and density may be altered by the geometry of the target; thus, focusing of the ablation plume to enhance collection and transport may be possible.

Future experiments on Omega are needed to understand the dynamics of these phenomena in greater depth as well as in an ICF environment where the power density is much higher and the depth of energy deposition is much shorter.

## Publications

Bradley, P. A., A. C. Hayes, R. S. Rundberg, G. Jungman, B. Mihaila, and J. C. Solem. Exploring the possibilities of radiochemistry on the national ignition facility . 2005. In *International Conference on Nuclear Data for Science and Technology.* (Santa Fe, 26 Sept.-1 Oct. 2004). Vol. II, First Edition, p. 1486. New York: AIP.

Grim, G.. Inertial confinement fusion burn diagnostics at Los Alamos National Laboratory. To appear in *Inertial Fusion Science and Applications 2007.* (Kobe, 20-23 April 2007).

Grim, G., P. Bradley, T. Bredeweg, A. Keksis, M. Fowler, A. Hayes, G. Jungman, R. Rundberg, D. Vieira, and J. Wilhelmy. Prompt Radiochemistry at the NIF. 2008. *Review of Scientific Instruments.* **37**: 70.

Hayes, A. C., G. Jungman, J. C. Solem, P. A. Bradley, and R. S. Rundberg. Prompt beta spectroscopy as a diagnostic for mix inignited NIF capsules. 2006. *Modern Physics Letters A.* **21**: 1029.

Hayes, A. C., G. Jungman, P. A. Bradley, G. P. Grim, J. B. Wilhelmy, R. S. Rundberg, and A. Obst. Mix Diagnostics for NIF. To appear in *Nuclear Explosive Design Physocs Conference (NEDPC 2007).* (Los Alamos, 21-26 Oct 2007).

Hayes, A. C., G. Jungman, and P. A. Bradley. Claculation of Charged-particle Transport for NIF Mix Diagnostics. To appear in *Nuclear Explosive Computer Design Conference (NECDC) 2006.* (Los Alamos, 23-27 Oct. 2006).

Hayes, A., and G. Jungman. Radiochemistry cross-section sensitivity studies. 2005. In *ILWOG/Nuclear Data Meeting.* (Los Alamos, May 2005). Vol. I, First Edition, p. LA. Los Alamos: Alamos National Lab.

continuing project

# Experimental Study of Driven Magnetic Relaxation in a Laboratory Plasma

*Scott Chia Hsu*

20061435ER

## Introduction

This is an exploratory experimental project to form novel plasma equilibrium states that takes advantages of resonant effects to efficiently couple power from a plasma gun power source into the magnetic fields of the plasma. The improved efficiency would allow for higher current multiplication, i.e., a higher plasma current for a given plasma source current. If this is successful, then we can potentially harness this effect to create plasma states suitable for compact pulsed neutron sources or even magnetic fusion energy. These states are similar to a "spheromak" plasma, which has been studied for more than 20 years, but offer potential benefits over the spheromak in terms of formation efficiency, stability, and confinement of heat in the plasma (which is needed for fusion energy applications).

## Benefit to National Security Missions

This project enhances our fundamental understanding of science important to fusion energy, an important mission area in the DOE Office of Science. Our work will provide validation experiments for computational codes to be used for the International Thermonuclear Reactor (ITER), and an ideal testbed for exploring predictive science methodology.

## Progress

In the past year, our primary accomplishments were in three areas. First, we completed all the necessary new hardware and preparations/modifications of an existing experimental facility. The major new hardware includes a coaxial gun plasma source (125 kJ, 10 kV, 150 kA), a magnetic coil set for producing a vacuum "bias" magnetic field needed by the plasma source, a custom-made fast gas puff valve system (~10^20 atoms in <100 us), and the custom-made power supplies that power each system. In short, we now have a new and unique operational plasma physics experiment capable of addressing many basic plasma science questions. Second, we addressed and overcame several facility requirements in the course of obtaining IWD approval for operation. These requirements were not foreseen and fell onto this project to resolve. The first issue: building electrical ground was questioned by the cognizant electrical safety officers. It was beyond the ability of this project to permanently resolve this issue, and thus we finally proposed a fix that satisfied the ESO's concerns for safety. This fix involved running hard ground wires from all the experimental hardware (vacuum chamber, capacitor bank room, and control racks) to a single ground point at the facility electrical panel. The second issue related to fire protection in a screen room that housed the main capacitor banks. Due to the short time remaining on the project, we finally negotiated a temporary solution for having fire extinguishers available and fire extinguisher training for the PIC, while plans are made to install fire protection sprinklers in the screen room. In all, addressing these facility-related issues delayed the IWD approval by about 6 months, and thus while we were ready to energize our new hardware systems in October 2007, we were not able to do so until late spring 2008. The third accomplishment was the assembly of a 48 channel miniature magnetic probe array that will be the primary experimental diagnostic. This probe measured the in situ magnetic field at 16 spatial positions and utilizes miniature commercial inductor chips soldered to twisted pair thin gauge insulated magnet wire. The assembly was an extremely labor-intensive job. In addition, a digital acquisition system using a LABVIEW interface and MDSPlus data storage/retrieval was developed for the experiment. We have tested all the hardware systems successfully, and experimental campaigns have begun and will continue for the duration of the project. We are hopeful that the major milestone for the project will be fulfilled by the end of project in January 2009, i.e., the determination whether we can easily form the predicted novel relaxed plasma states by exploiting resonances in the coupling between power source and plasma.

## Future Work

We will perform plasma experiments to create and characterize driven magnetically relaxed plasmas. The experimental setup will have simple geometry to facilitate data interpretation and comparisons with nonlinear magnetohydrodynamic (MHD) simulations. We

have developed experimental/hardware resources making use of existing systems at Los Alamos supplemented by some new hardware. Our system is centered around a planar coaxial source integrated into a cylindrical flux-conserving boundary. The coaxial source is powered by a capacitor bank (approximate values 8 mF, 10 kV, 150 kA, 125 kJ) that is capable of creating and sustaining the plasma for a resistive decay time (~0.5 ms), such that we can observe and study driven plasma relaxation. A substantial portion of the hardware for the capacitor bank was available at no cost.

Initial experimental campaigns will scope out the operational regimes afforded by our source and power supply. In parallel, we are developing plasma diagnostics including magnetic probe arrays (for characterizing magnetic topology/equilibrium), electrostatic probes (for characterizing plasma density, temperature, flows, and electric potential), and an imaging camera (for surveying the global dynamics of the plasma evolution). When the experimental apparatus is running the research plan will be as follows:

1. Create/characterize magnetically relaxed states as a function of the source current-to-flux ratio, a key parameter in determining the nature of the relaxed state.

2. Study global instabilities which facilitate plasma evolution toward relaxed states.

3. Study microinstabilities/fluctuations which give rise to large scale electric field sustaining the plasma in the relaxed states.

4. Study magnetic energy spectrum as function of spatial wavenumber.

## Conclusion

We expect to experimentally create and characterize driven magnetically relaxed plasmas and answer the question whether theoretically predicted novel relaxed states can be created in the laboratory, and whether we can exploit resonant effects to couple power efficiently into the magnetic fields of a magnetically confined plasma. If so, this could be a promising new direction for spheromak research. We also expect to perform detailed measurements of the plasma dynamics that allow the plasma to reach a relaxed state and for the plasma to transition between relaxed states. This work will provide fundamental advances in plasma science and make progress toward a unified description of magnetically-relaxed plasmas both in laboratory and astrophysical settings. It could lead to novel fusion configurations and pulsed neutron sources and help answer longstanding puzzles in astrophysics.

A natural sponsor for follow-on work is the DOE Office of Fusion Energy Sciences (OFES), and specifically their "Innovative Confinement Concepts" (ICC) research portfolio. However, this ICC program will undergo a program review in FY09, and we will await the outcome of that review before formulating a strategy for selling this project to OFES.

## Publications

Hsu, S. C., and X. Z. Tang. A proposed experiment to study relaxation formation of a spherical torus with a plasma center column. 2007. *Journal of Fusion Energy.* **26** (1/2): 85.

continuing project

# Beta Decay of Polarized Radioactive Atoms in an Optical Tweezer

*Xinxin Zhao*

20070160ER

## Introduction

The "Standard Model" is a widely accepted theory that describes our understanding of matter and radiation. The Standard Model quantitatively predicts a vast array of observables by which the model can be tested. If observables are different from those predicted by the Standard model, it signifies the existence of physics "beyond the Standard Model," providing a new breakthrough in our understanding of the Universe.

Recent advancements in atom trapping have resulted in exciting scientific breakthroughs in atomic, molecular and optical physics with several Nobel Prizes awarded. At Los Alamos, we have developed a unique combination of capabilities that enable us to efficiently trap and cool radioactive isotopes and utilized them to study nuclear physics. Radioactive atoms confined in an optical dipole trap have many intrinsic advantages for fundamental symmetry experiments, providing a highly polarized, point-like sample with minimal perturbation from the environment, which can be well characterized. This would be an ideal system for studying parity violating beta-decay of spin-polarized $^{82}$Rb ($t_{1/2}$ =75 sec) atoms. $^{82}$Rb was chosen because it is easy to laser cool and trap, it decays through pure Gamow-Teller transitions and we have reliable supply because it is a key biomedical radioisotope produced at LANL. We plan to first trap $^{82}$Rb in our high efficiency magneto-optical trap (MOT), and use an optical tweezer to transport the atoms to a science chamber where we will polarize the $^{82}$Rb atoms/nuclei and measure the beta asymmetry positron-spin (A) and recoil-spin correlations for a 0.1% test of Standard Model predictions. Once developed, this approach can be applied to other research opportunities in the area of ultra-cold strongly coupled plasma physics and quantum control/quantum information science.

## Benefit to National Security Missions

This project contributes to our basic understanding of forces and processes in the universe governed by the "Standard Model," and impacts basic understanding of physics, a key DOE mission. The technical spin-offs support the NNSA mission of thread reduction in ultra-sensitive detection of radioactive materials.

## Progress

We have completed the study of loading radioactive $^{82}$Rb in the optical dipole and published a paper titled "Trapping radioactive $^{82}$Rb in an optical dipole trap and evidence of spontaneous spin polarization" in Physical Review A Rapid communication. Following on the observation of the evidence of spontaneous spin polarization, we made resolved Zeeman spectroscopy measurement for the population of the spin states. We found that atoms are indeed polarized (80%) in the stretched state and 20% in the anti-stretched state. To have more control on the sample polarization and to measure it with an uncertainty of better than 1%, we have setup and demonstrated the optical pumping of atoms in the dipole trap. We use a circularly polarized light for the optical pumping beam and align the optical pumping beam in the direction of the optical pumping magnetic (B) field. We improved the polarization of the optical pumping laser beam to better than 99%. To have better control of optical pumping B field, we need to minimize the residue magnetic (B) field, we have setup a Faraday rotation experiment to measure the residue magnetic field in situ and just recently observed the Faraday rotation signal of the cold atoms in an YAG laser dipole trap as shown in Figure 1.

The Faraday rotation signal provides a powerful tool for in situ measurement of the magnetic field inside the vacuum chamber. The "frequency of oscillation" is a precise measure of the B field, while the amplitude is related to the sample polarization. This allows us to minimize the residue field with compensation coils while monitoring the oscillating Faraday signal. With three pairs of coils already in place (very crude at this point), we can now lower the residue field to 14 mG, this reduces the uncertainty of the optical pumping B field to less than 1%. We should be able to reduce this uncertainty by more than an order of magnitude with improved compensating coils. Because the amplitude of the Faraday signal is related to the polarization of the

sample, Faraday rotation measurements also provide a powerful tool to study the dynamics of decoherence and the evolution of the sample polarization in the dipole trap. We have made preliminary measurement of the coherence time of polarized atoms in the YAG trap, and found that the spin relaxation is suppressed by over an order of magnitude over the rate set by the far-off resonance scattering. We also found that the spin polarization is further enhanced and reinforced when the two-body collision loss rate of the mixed spin states is greater than the one body trap loss. These advancements are an important step towards a new generation of precision beta decay correlation measurements with polarized atoms. This work is in progress and we expect to finish up the measurement and submit a paper titled "Polarized atoms in an optical dipole trap." this year.

We presented our work at the 2008 American Physical Society, Division of Atomic, Molecular and Optical Physics meeting (DAMOP) at State College, Pennsylvania in May and the 2008 International Conference on Atomic Physics meeting (ICAP) at Storrs, CT in July.

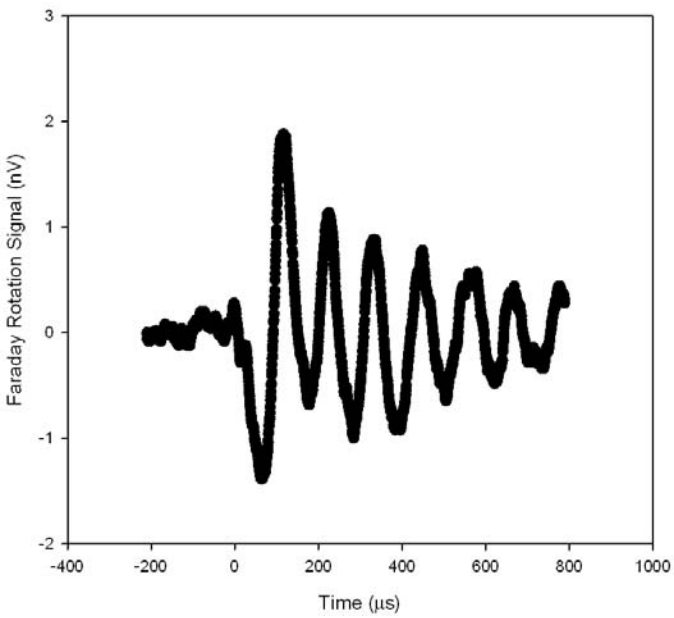


*Figure 1. Faraday rotation signal of linearly polarized probe beam (900 MHz off resonance) passing through a cloud of spin polarized atoms in a YAG laser optical dipole trap. The oscillation is due to the spin of the polarized atoms processing around the residue magnetic field, while the decay of the amplitude is due to the residue magnetic field gradient in this case.*

## Future Work

We plan to transfer radioactive 82Rb atoms from a magneto-optical trap (MOT) to an optical tweezer and transport these atoms to a science chamber where high precision beta-recoil measurement can be carried out.

We expect to "shuttle" about 100,000 $^{82}$Rb atoms with near unity efficiency to the science chamber in a few seconds. We will then polarize the atoms into a stretched state with an optical pumping beam in a uniform magnetic field. We plan to map out the beta-spin and recoil-spin correlations by rotating the direction of the magnetic field. These numbers are sufficient to obtain the necessary accumulation of statistics for a high-precision (0.1%) experiment and represent an improvement over the state-of-the-art by an order of magnitude. Unlike all previous beta-asymmetry experiments, an optical tweezer is an ideal clean environment. Many systematic effects are eliminated or minimized, such as backscattering from substrate, detector acceptance and depolarizing effect of the inhomogeneous magnetic field, and the beta decay of unpolarized nuclei lost to the walls of the vacuum chamber. This new proposed approach for the measurement of the positron-spin and recoil-spin correlation function in $^{82}$Rb beta decay would open a new frontier for fundamental symmetry work involving pure Gamow-Teller transitions. Once successful, other lighter radioactive isotopes such as $^{8}$Li could be explored. The combination of these new generation experiments can open a new window in the search for physics beyond the Standard Model.

## Conclusion

Laser cooled and trapped radioactive atoms would open a new frontier for fundamental symmetry research. These new generation experiments can open a new window in the search for physics beyond the Standard Model.

## Publications

Feldbaum, D., H. Wang, J. Weinstein, D. J. Vieira, and X. Zhao. Trapping radioactive 82Rb ion an optical dipole trap and evidence of spontaneous spin polarization. 2007. Physical Review A Rapid Communication. **76**: 051402(R).

continuing project

# Nano-Engineered Casimir Forces

*Diego Alejandro Roberto Dalvit*

20070163ER

## Introduction

The project aims at harnessing quantum vacuum forces via nano-engineering of the geometry and material composition of micro- and nano-electromechanical systems. Casimir forces, due to quantum vacuum fluctuations, are the main interactions between bodies in the micro and nano scales, and offer potential applications to nanotechnology, such as non-contact force transmission and frictionless bearings. However, due to their typical attractive nature, they also pose severe limitations to nanomachines, as their moving parts stict together due to these forces.

In this project we aim at understanding, both theoretically and experimentally, the possibility of Casimir repulsion by engineering the geometry and composition of metamaterials, that are artificial structures with designer electromagnetic response. By designing these structures with nanoscales features it is possible to endow them with non-trivial magnetic response in the infrared and optical part of the electromagnetic spectrum, which is a pre-requisite for obtaining Casimir repulsion.

We are studying the conditions under which quantum vacuum repulsion with metamaterials is feasible, including different theoretical aspects such as metallic-based and dielectric-based metamaterials, effects of optical anisotropy, dissipation, and magneto-dielectric response. We are also designing and fabricating metamaterials with the required characteristics for Casimir repulsion, including split-ring resonators and fishnet arrays at the nanoscale. Finally, part of this project involves the measurement of Casimir forces at micron separations with ultrasensitive torsional balances, and at sub-micron separations with micro-electromechanical systems.

The success of this project will represent a landmark in the quest for harnessing quantum vacuum fluctuations, with several potential applications in nanotechnology.

## Benefit to National Security Missions

This project supports the DOE/Office of Science missions by enhancing our understanding and control of vacuum-mediated forces, and will have a strong impact on programmatic missions in the fields of nanotechnology, precision measurement, and quantum science and technology.

## Progress

Made significant progress in the understanding the basic theoretical aspect of quantum vacuum repulsion with metamaterials. Based on a generalization of the Lifshitz theory, which is the main ingredient to compute Casimir forces between real materials, we have calculated Casimir forces involving magneto-dielectric and possibly anisotropic metamaterials, focusing on the possibility of repulsive forces. We have found that Casimir repulsion decreases with magnetic dissipation, and even a small conductivity (Drude) background in metallic-based metamaterials acts to make attractive a Casimir force that would otherwise be predicted to be repulsive. We have shown that the sign of the force also depends sensitively on the degree of optical anisotropy of the metamaterial, and on the form of the frequency dependency of the magnetic response. These results have been published in " Casimir-Lifshitz theory and metamaterials", F.S.S. Rosa, D.A.R. Dalvit, and P.W. Milonni, Physical Review Letters 100, 183602 (2008).

In the recent months, we have continued to study Casimir interactions with metamaterials, and focused our attention on forces between metals and magneto-dielectric metamaterials and on the possibility of inferring magnetic effects by measurements of these forces. We have analyzed metamaterials including structures with uniaxial electric and biaxial magnetodielectric anisotropies, as well as structures with isolated metallic and dielectric properties that can be described in terms of filling factors and a Maxwell Garnett approximation. The elimination of reduction of Casimir stiction by appropriate engineering of metallic-based metamaterials, or the indirect detection of magnetic contributions, appears to be challenging, as small background

Drude contributions to the permittivity act to enhance attraction over repulsion, as does magnetic dissipation. In dielectric-based metamaterials the magnetic properties of polaritonic crystals, for instance, appear to be too weak for repulsion to overcome attraction. However, we expect that experiment involving metamaterials can show a significant reduction of the Casimir force between bulk materials.

Using electromagnetic simulations, we are designing an optimum metamaterial to exhibit the Casimir effect in the near-infrared. We have also devised a procedure for fabrication small enough features for metamaterials in this wavelength range. As a result we have published two papers: "Effects of microstructure variations on macroscopic terahertz metafilm properties", J.F. O'Hara, A.K. Azaf, H.T Chen, A.J. Taylor, and E. Smirnova, Active and Passive Electronic Components 2007, 49691 (2007); "Optically thin terahertz metamaterials", R. Singh, E. Smirnova, A.J. Taylor, J.F. O'Hara, and W. Zhang, Optics Express 16, 6537 (2008).

In joint work with our external experimental collaborator Prof Steve Lamoreaux from Yale University, we have also studied Casimir interactions between semiconductor materials. We have developed a new theory of Casimir interactions that take into account drifting of carriers in these materials, and we have derived the corresponding frequency-dependent dispersion relations that describe a crossover between Lifshitz results for dielectrics and for good conductors. In the quasi-static limit, relevant for large separations (above 2 microns), our calculated reflection amplitudes account for charge (Debye) screening present in conducting surfaces with small density of charges. This work has been published in Physical Review Letters 101, 163203 (2008).

In joint work with Prof. Roberto Onofrio at Dartmouth College we have performed precision electrostatic calibrations in the sphere-plane geometry and observed anomalous behavior. Namely, the scaling exponent of the electrostatic signal with distance was found to be smaller than expected on the basis of the pure Coulombian contribution and the residual potential found to be distance dependent. We argue that these findings affect the accuracy of the electrostatic calibrations and invite reanalysis of previous determinations of the Casimir force. This work was published in Physical Review A 78, Rapid Communications, 020101 (2008).

We have also studied the possibility of Casimir repulsion between media separated by fluids. Using an exact numerical method for finite nonplanar objects, we demonstrated a stable mechanical suspension of a silica cylinder within a metallic cylinder separated by ethanol, via a repulsive Casimir force between the silica and the metal. We investigate cylinders with both circular and square cross sections, and show that the latter exhibit a stable orientation as well as a stable position, via a method to compute Casimir torques for finite objects. Furthermore, the stable orientation of the square cylinder is shown to undergo an unusual 45 degrees transition as a function of the separation length-scale, which is explained as a consequence of material dispersion. This work is in press in Physical Review Letters, arXiv:0807.4166.

## Future Work

In the near future, we plan to apply these results on Debye screening to an ongoing experiment of the Casimir force between pure germanium plates, that is expected to probe for the first time temperature corrections to the Casimir force between bulk systems.

We also plan to investigate ways to engineer the Casimir force in different geometries and with various designed materials in order to achieve strongly modified vacuum forces. Our tasks will be: i) modeling and simulation of engineered Casimir forces with different geometries and materials; (ii) design and fabrication of artificial materials, such as sub-wavelength aperture arrays and split ring resonators, with tailored electromagnetic response in the infrared and optical region of the electromagnetic spectrum; and (iii) detection of Casimir forces between artificial materials with ultra sensitive microcantilevers and torsion pendulums. The final goal is to demonstrate control of nano-engineered Casimir forces, and to perform the first experimental demonstration of strongly modified vacuum forces reaching the crossover to repulsion.

## Conclusion

The expected results of this project are the modeling and simulation of vacuum-mediated forces for different geometries and composition of designed materials, the fabrication of engineered nanomaterials with tailored electromagnetic response (such as plasmonic and metamaterials), and the experimental detection of such forces between these type of materials using ultra precise measurement techniques with microcantilevers and torsion pendulums. We expect to demonstrate, for the first time, strongly modified and repulsive Casimir forces, which will have applications for nanotechnology, engineered materials, and precision metrology.

## References

1. S.Rosa, F. S., D. A. R. Dalvit, and P. W. Milonni. Casimir-Lifshitz theory and metamaterials. 2008. *Physical Review Letters.* **100**: 183602.

2. S.Rosa, F. S., D. A. R. Dalvit, and P. W. Milonni. Casimir Interactions for Anisotropic Magnetodielectric Metamaterials. 2008. *Physical Review A.* **78**: 032117.

3. O'Hara, J. F., A. K. Azaf, H. T. Chen, A. J. Taylor, and E. Smirnova. Effects of Microstructure Variations on Macroscopic Terahertz Metafilm Properties. 2007. *Active and Passive Electronic Components.* **2007**: 49691.

4. Singh, R., E. Smirnova, A. J. Taylor, J. F. O'Hara, and W. Zhang. Optically Thin Terahertz Metamaterials. 2008. *Optics Express.* **16**: 6537.

5. R.Dalvit, D. A., and S. K. Lamoreaux. Contribution of Drifting Carriers to the Casimir-Lifshitz and Casimir-Polder Interactions with Semiconductor Materials. 2008. *Physical Review Letters.* **101**: 163203.

6. Kim, W. J., M. Brown-Hayes, D. A. R. Dalvit, J. H. Brownell, and R. Onofrio. Anomalies in Electrostatic Calibrations for the Measurement of the Casimir force in a sphere-plane geometry. 2008. *Physical Review A, Rapid Communications.* **78**: 020101.

7. Rodriguez, A. W., J. N. Munday, J. D. Joannopoulos, F. Capasso, D. A. R. Dalvit, and S. G. Johnson. Stable suspension and dispersion-induced transitions from repulsive Casimir force between fluid-separated eccentric cylinders. To appear in *Physical Review Letters.*

## Publications


Brown-Hayes, M., J. H. Brownell, D. A. R. Dalvit, W. J. Kim, A. Lambrecht, F. C. Lombardo, F. D. Mazzitelli, S. M. Middleman, V. V. Nesvizhevsky, R. Onofrio, and S. Reynaud. Thermal and dissipative effects in Casimir physics. 2006. *Journal of Physics A.* **39**: 6195.

Chen, H. T., J. F. O'Hara, A. J. Taylor, R. D. Averitt, C. Highstrete, M. Lee, and W. J. Padilla. Complementary planar terahertz metamaterials. 2007. *Optics Express.* **15** (3): 1084.

Kim, W. J., M. Brown-Hayes, D. A. R. Dalvit, J. H. Brownell, and R. Onofrio. Anomalies in electrostatic calibrations for the measurement of the Casimir force in a sphere-plane geometry. 2008. *Physical Review A, Rapid Communications.* **78**: 020101.

Kim, W. J., M. Brown-Hayes, D. A. R. Dalvit, and R. Onofrio. Status report on the measurement of the Casimir force in a cylinder-plane geometry. To appear in *Recontres de Moriond.* (La Thuile, Italy, 11-18 March, 2007).

Mazzitelli, F. D., D. A. R. Dalvit, and F. C. Lombardo. Exact zero-point interaction between cylinders. 2006. *New Journal of Physics.* **8**: 240.

O'Hara, J. F., A. K. Azaf, H. T. Chen, A. J. Taylor, and E. Smirnova. Effects of Microstructure Variations on Macroscopic Terahertz Metafilm Properties. 2007. *Active and Passive Electronic Components.* **2007**: 49691.

R.Dalvit, D. A., and S. K. Lamoreaux. Contribution of drifting carriers to the Casimir-Lifshitz and Casimir-Polder interactions with semiconductor materials. 2008. *Physical Review Letters.* **101**: 163203.

Rodriguez, A. W., J. N. Munday, J. D. Joannopoulos, F. Capasso, D. A. R. Dalvit, and S. G. Johnson. Stable Suspension and Dispersion-Induced Transitions from Repulsive Casimir Froce between fluid-separated Eccentric Cylinders. To appear in *Physical Review Letters.*

S.Rosa, F. S., D. A. R. Dalvit, and P. W. Milonni. Casimir-Lifshitz theory and metamaterials. 2008. *Physical Review Letters.* **100**: 183602.

S.Rosa, F. S., and D. A. R. Dalvit. Casimir interactions for anisotropic magnetodielectric metamaterials. 2008. *Physical Review A.* **78**: 032117.

Singh, R., E. Smirnova, A. J. Taylor, J. F. O'Hara, and W. Zhang. Optically Thin Terahertz Metamaterials. 2008. *Optics Express.* **16**: 6537.

Spagnolo, S., D. A. R. Dalvit, and P. W. Milonni. Van der Waals interactions in a magneto-dielectric medium. 2007. *Physical Review A.* **75**: 052117.

# Understanding Dynamical Diversity of Extrasolar Planets

*Hui Li*

20070171ER

## Introduction

The discovery of 170 extrasolar planets in the past decade has stimulated an explosive growth in studying the basic processes that regulate planet-system evolution. At least two fundamental mysteries have emerged. One is that proto-planet embryos that are formed farther out in protoplanetary disks could migrate towards their central stars through tidal interactions with their nascent gaseous disks. This seriously limits the time available for these embryos to grow into giant planets, contrary to the discoveries of many giant planets both in our Solar system and many extra-solar planet systems. Another mystery is how the orbital evolution of proto-planets/embryos produces the observed large diversity in semi-major axis and eccentricity distributions, which are completely different from solar system planets. Our models, run on supercomputers, will address these mysteries.

## Benefit to National Security Missions

The proposed research will push the limits of supercomputing and help to establish the Laboratory as a leading institution in computational protoplanetary research. Protoplanetary science is becoming a major research area in astronomy. We can make an immediate impact in this field and enhance the DOE mission in basic science.

## Progress

We have completed the implementation of two different types of isothermal disks, one with constant sound speed and one with constant aspect ratio. These differences have an impact on how waves are damped in the disk, consequently affecting the migration of protoplanets. We have also implemented multiple planet capability so that we can study the migration of multiple planets, which is more consistent with observations. In addition, we have completed implementing disk self-gravity in our 2D hydrodynamics code. This implementation is extremely efficient, and we have shown it gives nearly a factor of 100 speed-up over the traditional tree-code approach in disks. Such a unique and efficient disk self-gravity scheme has allowed us to make hundreds of runs (instead of tens of runs we had expected). This code is probably the fastest code in the community on studying disk self-gravity in planet-disk interactions. A detailed description of the disk self-gravity scheme and implementation on parallel computers has been accepted to Astrophysical Journal Supplements.

We have performed hundreds of 2D hydrodynamic simulations to study the migration of proto-planets in gaseous disks, using our newly developed planet-disk code with disk self-gravity. One important result we found is that disk self-gravity actually accelerates the migration of proto-planet embryos. There has been some confusion in the community prior to our study whether disk self-gravity will speed up or slow down the migration. Our results (along with another team) have clearly resolved this confusion. We have summarized these results in a paper and submitted to a refereed journal.

Another important result is that, for nearly inviscid disks, we discovered a new phenomenon, which could be a solution to a long-standing problem in proto-planet migration. The embryos of proto-planets were thought to migrate too fast towards their parent stars so that they could not survive in their nascent disks long enough to form giant planets (contrary to the observed existence of giant planets). We found that the density distribution around the planet embryos can be modified strongly and the traditional theory for migration does NOT apply. The density distribution around the planet is changed in such a way that the total net torque on the planet is greatly reduced, hence slowing down or completely stopping the planet migration. Through extensive simulations, we have surveyed the planet mass and disk parameters to determine the critical planet embryo masses above, which they can survive in the disk. We expect this result will have an important impact in addressing this long-standing mystery. We have written up this key result and have been accepted to Astrophysical Journal Letters.

We have finished the linear theory analysis of the Rossby vortex instability associated with a dip/gap in disks. This work is based on our previous work on understanding the secondary instability in disks. This instability explains why we have seen vortices in our planet migration simulations. These results have been written up and submitted to Astrophysical Journal.

In addition, we have studied the protoplanet migration in turbulent disks, where the disk turbulence is produced by its own self-gravity. It is believed that, at least for some disks, the disks can be quite massive so that the disk is inherently unstable. Once the disk becomes turbulent, the traditional analysis on planet-disk tidal interactions is no long applicable. Our simulations indeed show that planet migration shows a much larger diversity than the migration in regular (non-turbulent) disk flows. We believe that this offers some insight into understanding the observed diversity in orbital parameters of extra-solar planets.

## Future Work

The discovery of 170 extrasolar planets in the past decade has stimulated an explosive growth in studying the basic processes that regulate planet-system evolution. Planets can interact gravitationally with their nascent gaseous disks by driving tidal waves. When these waves dissipate (e.g., via shocks), it gives rise to angular momentum exchange between the planet and the disk. When the angular momentum of the planet changes, it migrates radially, i.e., by moving towards (or away from) the central star. Such a migration threatens the planet's survivability. The observed extra-solar planets show that: a) a good fraction of the proto-planets can survive; b) but they have a vast diversity in semi-major axis and eccentricity distributions, which are completely different from solar system planets.

To address the observed dynamical diversity of extrasolar planets and their migration, we will focus on three new, yet critical aspects: 1) the role of the newly discovered secondary instability; 2) the role of the disk self-gravity; and 3) the role of multiple embryos. This will be achieved by performing large-scale, high-resolution planet-disk simulations and by conducting analytic studies of the flow stabilities. We plan to answer three key questions raised by observations: 1) Is Type I migration indeed too fast or could it be alleviated by including these new processes? 2) Could the secondary instability drive eccentricities of the planets? 3) What are the semi-major axis and eccentricity distributions of the multiple embryo systems from the planets and disk interactions? The proposed simulations will push the limits of supercomputing. They contain a spatial scale separation of ~ 1000 and long integration times. This requires a series of modifications (including adding self-gravity) to our existing codes.

## Conclusion

We propose a comprehensive theoretical and computational study of the orbital evolution of both single and multiple protoplanets/embryos in gaseous protoplanetary disks. We will investigate our newly discovered instability, associated with the disk's potential vorticity profile, affects protoplanetary evolution. This instability produces vortices that cause the torques on the protoplanet/embryo to experience large changes. We will also examine the effects of disk self-gravity and the effect of having more than one protoplanet, neither of which have been well studied. Our simulations will push the limits of supercomputing.

## Publications

Li, H., S. Lubow, S. Li, and D. Lin. Type I Planet Migration in Nearly Laminar Disks. To appear in *Astrophysical Journal Letters.*

Li, S., M. J. Buoni, and H. Li. A fast potential and self-gravity solver for disks. To appear in *Astrophysical Journal Supplements.*

Yu, C., H. Li, S. Li, I. Dobbs-Dixon, and D. Lin. Dynamics of Type I migration of protoplanets. *Astrophysical Journal.*

Yu, C., H. Li, and S. Li. Vortex Instability Associated with Gaps in Disks. *Astrophysical Journal.*

# Probing Correlated Electron Behavior via Direct Uranium-235 Nuclear Magnetic Resonance

*Eric Dietzgen Bauer*

20070188ER

## Introduction

The fundamental understanding of the emergent behavior resulting from strong correlations between electrons that are responsible novel forms of matter such as magnetism and superconductivity is one of the grand challenges in modern condensed matter physics today. Uranium and uranium compounds are prototypical examples of such materials, and these systems often exhibit exotic forms of magnetic and superconducting order at low temperatures. By using Nuclear Magnetic Resonance (NMR) techniques, we will detect the U resonance of compounds enriched with U-235. This work will offer new insight into the behavior of the correlated electrons in the exotic ordered states. This project will support the DOE and LANL missions in the fundamental understanding of materials at the atomic scale and of exotic superconductivity, by enhancing our understanding of the complex interactions between electrons in uranium based compounds. This project will also support the mission of threat reduction by developing new techniques for detecting enriched uranium.

## Benefit to National Security Missions

This project will support the DOE mission of the Office of Science, basic energy sciences, by enhancing our understanding of the complex interactions between electrons in uranium based compounds. This project will also support the mission of threat reduction by developing new techniques for detecting enriched uranium.

## Progress

The compound USb2 is an itinerant magnet, in which the magnetism results from partial filling and overlap of the energy bands with primarily f- and d-character, rather than arising from the interaction of localized uranium magnetic moments tightly bound to their atomic cores. We have investigated this compound using both U-235 and Sb-121 NMR. We have succeeded in observing the U-235 NMR signal (a first for Los Alamos National Lab, and the first observation of the U-235 signal in the United States) due to the large internal magnetic field of 277 Tesla in the magnetic state. We successfully obtained the nuclear relaxation rates T1^-1 and T2^-1 of 235^U of this itinerant antiferromagnet — the first ever direct information about the nuclear relaxation processes in a uranium intermetallic compound. Comparison of these U-235 results to the detailed temperature dependence of the Sb-121 NMR is in progress to shed light on the low temperature behavior of this system.

The URu2Si2 system is one of the most interesting and challenging correlated electron system as it exhibits a highly unusual ordered state at low temperature, with a yet-unidentified order parameter despite 25 years of intense research. By doping the pure compound with a few percent of Rh, it has been found that a new large-moment phase is stabilized in which antiferromagnetism with a large ordered moment coexists with the hidden order parameter. In an initial attempt to find the U-235 signal, we learned that the U-235 signal in a 2%-Rh doped URu2Si2 sample is too weak to be observed directly, and instead have focused our attention on a series of samples of 238^U(Ru1-xRhx)2Si2 to determine the nature of the hidden order phase. Our results [1] indicate that this large moment antiferromagnetic phase is not a true thermodynamic phase that competes with the hidden order phase, but rather an artifact of the intrinsic inhomogeneity that develops as a result of doping. Our 29^Si NMR spectra clearly reveal an inhomogeneous coexistence between the hidden order component and the large moment antiferromagnetism. These results contrast with recent neutron scattering data, which suggested a new thermodynamic phase. In collaboration with A. Balatsky (T-11), we hypothesize that the Rh dopants locally suppress the hidden order parameter, and that the antiferromagnetism arises as a secondary effect in regions where the hidden order is suppressed.

Motivated by our discovery of a new compound U3Bi4Ni3, in which the physical properties are reminiscent, though not entirely conclusive, of Kondo insulating behavior, we performed 209^Bi NMR/NQR measurements to determine if the insulating behavior arises from hybridization of local 5f electrons and conduction electrons (Kondo insulator), or if it is a simple band effect. The presence of temperature independent energy gap deduced from these NMR/NQR experiments of approximately 50 meV, consistent with recent photoemission measurements and electrical resistivity, together with the temperature dependence of Knight shift, provides strong evidence for Kondo insulating behavior in U3Bi4Ni3 arising from strong correlations between the conduction electrons and the uranium local moments.

## Future Work

Understanding the subtleties of correlated electron behavior that give rise to unusual properties is one of the grand challenges of modern condensed matter physics. One important class of materials with strongly correlated electrons is the set of uranium-based heavy-fermion compounds with exotic ground state order, such as coexisting superconductivity and magnetism, or "hidden" order. To probe these unusual ground states, a suite of experimental techniques can be applied to investigate the bulk thermodynamic, magnetic and electronic responses of these systems. However, there are few techniques that can probe the physics of these systems on a microscopic scale. In the remainder of this project, we will continue to develop and implement a new method, direct Nuclear Magnetic Resonance (NMR) of the U-235 nuclei, which will enable, for the first time, the direct study of the nature of the 5f electrons that are responsible for the heavy-fermion state and the unusual ordered states that evolve from it. NMR provides detailed microscopic information about the static and dynamic magnetic and electronic degrees of freedom at a particular site in the unit cell. Since the naturally occurring isotope of uranium, U-238, is NMR-inactive, such information has not been previously available.

Measuring the NMR directly at the U site will enable us to learn about not only the degree of hybridization of the 5f electrons across a broad class of correlated f-electron materials, but also to probe the dynamics of hidden order, quadrupolar order, magnetism and superconductivity at a microscopic level. In order to accomplish these goals, we intend to synthesize, characterize, and look for the NMR signal in several U-based compounds, including both metallic and insulating antiferromagnets. If the NMR signal can be found, we will fully characterize the NMR response. These data will then be compared with bulk measurements and NMR of the ligand sites.

We will continue our efforts on understanding the hidden order state in URu2Si2. In this material, pressures of up to 15 kbar stabilize an antiferromagnetic state with a large effective moment of 0.7 Bohr magnetons. This large moment may be large enough to slow the U-235 nuclei down in this material allowing observation of the U-235 signal directly. If successful, these results would be the first-ever microscopic measurement of the uranium nuclei in URu2Si2 and would lend valuable insight into the nature of the hidden order phase that has perplexed the scientific community for over a quarter-century.

Investigating a number of different strongly correlated uranium materials with a variety of distinct ground states will not only yield valuable information about the microscopic behavior of uranium in these compounds, it will also stretch the limits of this new and powerful technique. In contrast to investigating the itinerant antiferromagnet in USb2 and the hidden order state in URu2Si2, we will cast our net even further and attempt to observe the U-235 signal in a superconductor U6Fe. Again, the spin relaxation decreases exponentially in the superconducting state, making it possible to observe directly the U-235 signal. If we are successful in finding the U-235 signal in the conventional superconductor U6Fe, in which the glue that binds superconducting electron pairs is comprised of tiny lattice vibrations, (or phonons), this technique will be applied to unconventional superconductors such as UPd2Al3 where the mechanism of electron pairing is still not known.

## Conclusion

This project will enhance our basic understanding of the fundamental properties of strongly correlated electrons. Fifty years ago, the forefront of condensed matter physics was research the strange behavior of semiconductors. As a result of fundamental inquiries about the physics of the electrons in these materials, new technologies such as the transistor, the integrated circuit, and the modern computer were eventually developed. Today, modern condensed matter physicists are investigating the emergent behavior of new materials, such as superconductors and heavy fermions. A secondary benefit of this work may also be new technology for detecting enriched uranium.

## References

1. Baek, S. H., N. J. Curro, M. J. Graf, A. V. Balatsky, E. D. Bauer, J. C. Cooley, and J. L. Smith. Locally probing the hidden order in URu2Si2 by impurity doping. *Nature Physics.*

## Publications

H.Baek, S., N. J. Curro, M. J. Graf, A. V. Balatsky, E. D. Bauer, J. C. Cooley, and J. L. Smith. Locally probing the hidden order in URu2Si2 by impurity doping. *Nature Physics.*

Baek, S. H., N. J. Curro, E. D. Bauer, J. L. Smith, and J. Cooley. 235Uand 121Sb NMR Investigation of an itinerant antiferromagnet, USb2. 2008. *Physica B.* **403**: 850.

continuing project

# Cold Atom Quantum Liquid Mixtures

*Eddy Marcel Elvire Timmermans*

20070234ER

## Introduction

At sufficiently low temperatures, fluid systems exhibit quantum behavior and their dynamics cannot be described by Newton's equations. Collisionless Fermi-fluid dynamics and long-range laser-like phase coherence have been studied in table-top experiments with helium liquids. However, strong interaction effects preclude quantitatively accurate first principle descriptions and these experiments do not give insight into the behavior of quantum liquids in regimes that are not as accessible such as the heavy fermion systems and high T_c superconductors of condensed matter physics and the quantum fluids in the interior of neutron stars modeled in astrophysics. Quantum phase transitions in which the system abruptly changes its qualitative structure at zero temperature as a parameter of the system, such as the strength of the inter-particle interactions, is varied, are expected to play an important role in all three of the above named examples. In spite of the great interest into these phenomena, a general theoretical description that captures all of the physics of these phenomena remains an outstanding challenge. Employing atoms that have been cooled to nanoKelvin temperatures, the lowest temperature range ever reached in fluid systems, provides a new technology that can directly study such quantum phase transitions in a highly accessible and controllable environment.

In particular, mixtures of cold atom quantum degenerate gas systems can emulate the many-body behavior of interesting quantum liquid mixtures. The effects that are caused by mediated interactions also provide the prospect of studying correlations in regime in which the inter-particle interactions remain relatively weak. Hence, the inter-particle interactions can still be understood from first principles and the correlation effects that become particularly prominent near quantum critical points are due to quantum entanglement and not to strong interaction effects. These mediated interactions have a finite range and the introduction of finite range physics suggests that many more interesting many-body systems can be simulated than with the contact interactions that have currently been available in cold atom traps. Our studies have revealed interesting mediated interactions effects near the phase separation transition of boson-fermion mixtures and mixtures of Bose-Einstein condensates (BEC's). The nucleation process that causes the phases to separate in the fermion-boson mixture is a many-body macroscopic tunneling process, which suggests that such cold atom mixtures could give the first clean observations of macroscopic quantum tunneling. Our work on describing near-equilibrium BEC-dynamics as a field theory also gives us a new handle on understanding the phonon radiation caused by accelerating impurity atoms (Bremstrahlung) and suggests the cold atom prospect of exploring optics-like phenomena such as superradiance.

## Benefit to National Security Missions

This project supports the DOE mission of basic science and explores the prospect of ultra-high resolution sensors. Our many-body studies involve phenomena that play a crucial role in low temperature material and actinide science, and explore quantum information prospects. These studies also reveal prospects for sensors that could measure weak external forces.

## Progress

In the first two years of this project, the participants have discovered how and why mean-field descriptions of quantum degenerate fermion-boson gas mixtures fail near the first order quantum phase transition that causes the mixture to phase separate. In addition to providing a significant correction to the densities at which the phase separation takes place, the studies also show the culprit to be fermion-mediated interactions that counteract the short distance boson-boson repulsions and cause an overall attraction which tends to break up the BEC. On the mixed phase side, the mediated interactions become longer and longer ranged near the phase separation point and they also cause the compressibility of the boson gas to diverge. Exactly how the range and the compressibility diverge is difficult to determine, but its scaling coefficients, which

could be measured experimentally, could provide one of the first measurements of quantum scaling. We have studied the equation of state of the mixed phase and pointed out the qualitative differences of its predictions for the density profile in inhomogeneous traps with the predictions of mean-field theory. The phase separation can set in at densities below the values at which the system becomes mechanically unstable. The mechanical instability causes the phases to separate into chunks of roughly the same size and is known from finite temperature (ordinary) phase separation transitions as 'spinodal decomposion'. Below the line of spinodal decomposition, the phase separation can happen as the result of a process that overcomes the free energy barrier that separates the two minima of the transition. At finite temperature, this process is caused by thermal activation - local collision processes push the system over the barrier - but at sufficiently low temperatures, the system has to quantum tunnel through the barrier. We have explored the prospect of studying this type of macroscopic quantum tunneling in cold atom systems. We have also studied the near-equilibrium dynamics of a BEC in the presence of impurity atoms that move while being embedded in the BEC. The description we developed of the BEC-response (involving the creation and annihilation of phonon modes) emphasizes the analogy with field theory in general and with electromagnetism in general. This description is particularly illuminating in understanding the reason for why accelerating impurities cause phonons to radiate in a process that is closely analogous to the emission of Bremstrahlung of accelerating charges. This study allows us to qualitatively predict the energy loss of cold atoms that are being cooled at velocities below the critical velocity for BEC-superfluidity (sub-sonic cooling), so that we can show how effective subsonic cooling can be if the experimentalists insert an optical potential in the cold atom trap in an effort to cool impurity atoms down to lower temperatures than currently reached with sympathetic cooling. This treatment also reveals the finite system limitations of cold atom physics in studying fundamental superfluid phenomena such as the predicted Casimir-like drag and the study of self-localized BEC polarons.

## Future Work

Cold atom mixtures provide unprecedented prospects for the study of quantum liquid physics: Quantum phase transitions such as phase separation, mean-field collapse and magnetic instabilities can be accessed in a controlled manner by tuning Hamiltonian parameters continuously. The mediated interactions which cause the phase separation of the traditional condensed low temperature helium-3 and helium-4 fluids can be varied and, perhaps, used for gate operations in quantum information experiments. The self-localization induced by increasing the interaction of a single impurity atom with the boson atoms of a Bose-Einstein condensate (BEC) can finally allow cold atom experimentalists to localize and transport atoms inside a BEC, suggesting new studies of superfluidity, light localization, the Unruh effect and, perhaps, the creation of a quantum register of movable cold atom qu-bits.

This project will then aim at answering the following questions: How do the relevant many-body quantities scale in the second-order phase transitions of cold atom mixtures and how do these findings compare to the 'standard' (and, often differing) quantum phase transition descriptions? How does the critical impurity-boson interaction strength for self-localization scale as a surrounding BEC-mixture is brought close to phase separation, and what happens to its effective mass? Can we exploit the long range of quantum critical fluctuations to induce anisotropic and/or exotic forms of fermion superfluidity? Can a self-localized BEC-polaron have spin so that it can be used as a movable qubit in quantum information experiments? How can phase separated BEC's improve the sensitivity of weak-field BEC sensors?

To achieve these goals, this project develops many-body descriptions of the cold atom physics, tests some of the predictions by numerical simulations, and explores the similarity and differences with standard many-body systems that may undergo similar many-body phenomena.

## Conclusion

The theoretical studies of this project will reveal how cold atom experiments can test the scaling hypothesis and the description of quantum phase transitions. We will explore how quantum criticality (the nearness of a quantum phase transition) can affect the mediated interactions in a quantum liquid mixture and how it can affect the single particle properties of impurity atoms embedded in the cold atom quantum liquids. This project will also test the use of quantum phase transition instabilities in cold atom quantum liquid mixtures to significantly improve the resolution of cold atom trap sensors.

## Publications

Cucchietti, F. M., B. Damski, J. Dziarmaga, and W. H. Zurek. Dynamics of the Bose-Hubbard Model: Transition from Mott insulator to Superfluid. 2007. *Physical Review A.* **75**: 023603.

Cucchietti, F. M., S. Fernandez-Vidal, and J. P. Paz. Universal Decoherence induced by an Environmental Phase Transition. 2007. *Physical Review A.* **75**: 032337.

Kalas, R., A. Balatsky, and D. Mozyrsky. Odd-frequency pairing in binary boson-fermion cold atom mixtures. *Physical Review A.*

Mozyrsky, D., I. Martin, and E. Timmermans. Coherent Mesoscopic tunneling in Boson Fermion Mixtures. 2007. *Physical Review A.* **76** (5): 051601(R).

Santamore, D., and E. Timmermans. Fermion mediated interactions in a dilute Bose-Einstein Condensate. 2008. *Physical Review A.* **78**: 013619.

# Investigation of Energetic Ion Generation and Transport in Ultra-Intense Laser-Matter Interaction

*Brian James Albright*

20070235ER

## Introduction

Intense particle beams are important components of a host of applications, including fast ignition inertial confinement fusion, high energy density physics, warm dense matter, novel nuclear physics studies, and hadrontherapy of tumors. However, tailoring these intense particle beams for specific applications requires that we understand the physics of their generation, something that, until recently, has been simply intractable with computing resources at hand.

When ultra-intense lasers interact with thin, solid targets, enormously intense particle beams can be generated. This technique is known as "laser-ion acceleration." The objective of this work is to combine state-of-the-art modeling capability, the world's fastest supercomputers, and theory acumen to the problem of understanding the fundamental properties of laser-ion accelerators.

The work we are doing in this project in the area of fast ignition laser fusion alone promises to revolutionize the way we approach inertial confinement fusion experiments. Integrated design calculations of ion driven fast ignition, which we did as part of the proposed work, have shown the feasibility of achieving fast ignition via less stringent design requirements than traditional fast ignition--and without the need for a reentrant cone. [1] While much work remains to be done to bring this technology to fruition, it has the potential to deliver cheap, carbon-neutral energy to the grid in the next 20 years.

A payoff of the project is to better validate the VPIC code [2], which can be leveraged onto other projects in the future and can help cement Laboratory leadership in areas of high energy density physics, plasma physics, and high performance computing.

## Benefit to National Security Missions

The project supports mission areas in both nuclear weapons and fusion research. Fundamental research to enable laser-generated ion beams to study warm dense matter and high energy density physics supports the NNSA nuclear weapons mission. Laser-ion accelerators can also directly impact the DOE mission in fast ignition inertial confinement fusion.

## Progress

We have fulfilled the following objectives:

- VPIC Diagnostic Development: Teaming with CCS-2 and X-3 staff, we have implemented implement readers for VPIC three-dimensional data output on Paraview and Ensight Gold software. Application of this work to the specific problem of laser-particle acceleration has been supported by this project. Work done as part of this project will be showcased in the LANL and ASC booths at the upcoming Supercomputing 2008 conference in Austin.

- Two- and three-dimensional studies of laser-particle acceleration physics have been conducted on the Redtail quad-q system. These studies have been hampered somewhat by competition for resources and their status is, as yet, incomplete. We have worked to ensure stability of MPI and I/O subsystems; for the most part, I/O has proven to be, generally, robust, however we are working with LANL HPC staff to isolate existing problems with MPI. Our LPI runs are proving to be invaluable to them, as they serve as an aggressive test of the subsystems.

  Our work has established the viability of various approaches to particle acceleration and our three-dimensional studies, the first of their kind, have shown that the so-called relativistic ponderomotive acceleration mechanism, which utilizes a circularly polarized laser, can lead to ion beam properties that are superior to linearly polarized systems (like the laser break-out afterburner). Moreover, we have discovered that there is a transition from RPA- to BOA-like acceleration in longer pulse durations.

We have verified theoretical models of laser absorption physics in these regimes and have supported experiments on the Trident laser this Spring that showed, for the first time, the efficacy of tailoring the laser absorption physics to the target composition and thickness. We also have uncovered the essential physics that governs BOA performance for a given system—namely, the importance of having the burn-through occur when the laser intensity is at its maximum. This work will be reported in a Phys. Rev. Letter (submitted).

- We have executed some of the first-ever integrated modeling of particle beam transport and deposition into compressed ICF cores. This work has been shown at the prestigious American Physical Society and International Fusion Sciences and Applications meetings and has been documented in refereed journal articles.

- Implementation and verification of collision models in VPIC has completed. This work will be integral to validation of VPIC reflectivity with experimental data in the coming year and it represents the first time in the community that these models have been applied to large-scale PIC simluations of collisional laser-plasma interaction. This work directly applies to the third task of the proposal, involving the which we expect to complete this next fiscal year.

- LANL staff on the proposal have visited IBM Poughkeepsie to do the first-ever science runs on Roadrunner examining 3D laser-plasma interaction physics, the key elements of which can be used to run high-resolution calculations of laser-ion acceleration. A series of Gordon Bell simulation runs were done and on 17 connected units of Roadrunner (12240 Cell chips, 6120 dual-core Opteron chips), the calculation sustained in excess of 374.25 TFlop/s and used one trillion simulation macroparticles and 42 TBytes of RAM (more than 4 times the aggregate data in the Library of Congress). Our Gordon Bell Prize submission is one of the finalists. While not one of the initial goals of the project, harnessing the power of petascale computing for future work was an objective added in the past FY which we have run to completion.

- We have documented our results in a Gordon Bell simulation paper and will showcase our results at the American Physical Society and ACM Supercomputing Meetings. We have been invited to give numerous high-profile invited and plenary talks, including a Gordon Bell Prize Finalist talk at the ACM Supercomputing Meeting in Nov. 2008; two invited talks at the American Physical Society Meeting in Nov. 2008; an invited talk and an invited plenary talk at the 13th Advanced Accelerator Concepts Workshop in July, 2008; an invited "visionary" plenary talk at the High Energy Density Physics Symposium in November 2008, and two invited talks at the American Geophysical Union. Also, an invited plenary talk was given at the Los Alamos Computer Science Symposium and the Salishan Conference on High Performance Supercomputing. Approximately 40 contributed talks on these topics were given by the team and collaborators.

- One of our team (L. Yin) won the prestigious APS Katherine Weimer career award, in part for her contributions to this LDRD project. Several of us on the team received a LANL Distinguished Performance Award for work within this project's scope.

- We have documented our work in several refereed journals; please see the accompanying list of articles for details.

- A final topic of note is that we were able to recruit two postdocs to LANL to work with us on short-pulse laser-matter interaction and to take over for the last postdoc hired on this project (G. Cragg), who has since moved on to a position with the Naval Research Laboratories. Both should begin within the next year.

## Future Work

We will pursue three theoretical and particle-in-cell modeling thrusts pertaining to the physics of short-pulse laser-particle accelerators. Each will extensively use the unique simulation capability VPIC that the researchers maintain. VPIC is a state-of-the-art ab initio particle-in-cell plasma simulation code with unsurpassed speed and scalability. VPIC enables fully kinetic simulations in 2D and 3D of semi-collisional plasma kinetics of a scale never before attempted; this is vital to informing the theory and uncovering the underlying physics.

Task 1: Understand the physics of the conversion of ultra-intense lasers on target foils 10s of microns in thickness. Laser deposition onto pre-formed plasma (from finite laser pedestal) can lead to several complicated, competing physics processes, including self-generated magnetic fields, ponderomotive and wakefield acceleration, wave breaking, resonant absorption, and vacuum heating. We will perform detailed simulations and analysis to examine which processes dominate, and in which regimes; we shall provide concrete recommendations for how to optimize laser deposition for laser-particle accelerator applications.

Task 2: Understand the physics of the penetration and propagation of charge-neutral laser-accelerated ion beams into dense plasma media with steep density gradients. This is key to utilization of laser-ion accelerators in warm-dense-matter and high-energy-density experiments, as well as fast ignition inertial confinement fusion. Collective

beam-plasma instabilities (simulated for the first time in this work in the relevant dense-plasma regimes) will be assessed for whether they dominate the beam energy deposition in dense plasma media. In so doing, the feasibility of fast ignition ICF will be informed.

Task 3: Understand electron acceleration and transport kinetics (specifically, filamentation instability) in laser-driven targets. Filamentation, having collisional and collisionless manifestations, can affect both laser-ion accelerators and "traditional" fast ignition ICF operation. Application of collision-modeling capability in VPIC will enable this study and motivate paths forward for FI and HEDP application of ion beams.

## Conclusion

The physics of ion acceleration from the interaction of ultra-intense short pulse lasers with thin (10+ micron) targets is poorly understood on fundamental grounds, despite their great promise to impact and even revolutionize several areas of science, including nuclear weapons physics and fast ignition inertial confinement fusion. Our work will apply state-of-the-art laboratory simulation capability and analytic theory to improve our understanding of the generation of these beams and, perhaps most importantly, to their transport into dense plasma media. This will enable wider application of this emerging technology and improved utilization of DOE short-pulse laser facilities.

## References


1. Albright, B. J., M. J. Schmitt, J. C. Fernandez, G. E. Cragg, I. Tregillis, L. Yin, and B. M. Hegelich. Studies in capsule design for mid-Z ion-driven fast ignition. 2008. *Journal of Physics Conference Series.* **112**: 022029.

2. Bowers, K. J., B. J. Albright, L. Yin, B. Bergen, and T. J. T. Kwan. Ultra high performance three-dimensional electromagnetic relativistic particle-in-cell simulation. 2008. *Physics of Plasmas.* **15**: 055703.


## Publications


Albright, B. J., L. Yin, Kevin J. Bowers, B. M. Hegelich, K. A. Flippo, T. J. T. Kwan, and J. C. Fernandez. Relativistic Buneman instability in the laser break-out afterburner. 2007. *Physics of Plasmas .* **14**: 094502.

Albright, B. J., L. Yin, Kevin J. Bowers, B. M. Hegelich, K. A. Flippo, T. J. T. Kwan, and J. C. Fernandez. Relativistic Buneman instability in the laser break-out afterburner. 2007. *Virtual Journal of Ultrafast Science.* **6**: 10.

Albright, B. J., M. J. Schmitt, J. C. Fernandez, G. E. Cragg, I. Tregillis, L. Yin, and B. M. Hegelich. Studies in capsule design for mid-Z ion-driven fast ignition. 2008. *Journal of Physics Conference Series.* **112**: 022029.

Bowers, K. J., B. J. Albright, B. Bergen, L. Yin, K. J. Barker, and D. J. Kerbyson. 0.374 pflop/s trillion-particle kinetic modeling of laser plasma interaction on Roadrunner. To appear in *2008 Association of Computing Machinery/Institute for Electrical and Electronic Engineers Conference on Supercomputing.* (Austin, Texas, USA, 17-22 Nov. 2008).

Bowers, Kevin J., B. J. Albright, L. Yin, B. Bergen, and T. J. T. Kwan. Ultra high performance three-dimensional electromagnetic relativistic particle-in-cell simulation. 2008. *Physics of Plasmas .* **15**: 055703.

Cragg, G. E., and A. K. Kerman. Coherent decay of Bose-Einstein condensates. 2007. *Physical Review Letters.* **98**: 080405.

Cragg, G. E., and A. K. Kerman. Independent pair approximation for attractive Bose condensates. 2007. *Physics Letters A.* **371**: 7.

Fernandez, J. C., Brian J. Albright, Kirk A. Flippo, Bjorn M. Hegelich, Thomas J. T. Kwan, Mark J. Schmitt, and L. Yin. Progress on ion based fast ignition. 2008. *Journal of Physics Conference Series.* **112**: 022051.

Flippo, K., B. M. Hegelich, B. J. Albright, L. Yin, D. C. Gautier, S. Letzring, M. Schollmeier, J. Schreiber, R. Schulze, and J. C. Fernandez. Laser-driven ion acceleators: spectral control, monoenergetic ions and new acceleration mechanisms . 2007. *Laser and Particle Beams.* **25** (1): 3.

Flippo, K., E. d'Humieres, S. A. Gaillard, J. Rassuchine, M. Schollmeier, F. Nurberg, J. Adams, B. Albright, M. Bakeman, D. C. Gautier, N. R.-L. Galloudec, K. Harris, R. P. Johnson, J. L. Kline, G. Korgan, S. Letzring, S. Makelos, T. Shimada, M. Roth, T. E. Cowan, J. C. Fernandez, and B. M. Hegelich. Increased efficiency of short-pulse laser generated proton beams from novel flat-top cone targets. 2008. *Physics of Plasmas .* **15**: 056709.

Henig, A., D. Kiefer, C. Gautier, K. Flippo, S. Letzring, R. Johnson, T. Shimada, L. Yin, B. J. Albright, J. Fernandez, K. Markey, M. Zepf, V. Kh. Liechtenstein, S. G. Rykovanov, H. C. Wu, J. Shreiber, D. Habs, and B. M. Hegelich. Enhanced

laser-driven ion acceleration in the relativistic transparency regime. *Physical Review Letters.*

Kline, J. L., D. S. Montgomery, R. A. Hardin, K. A. Flippo, T. Shamada, R. P. Johnson, L. Yin, H. A. Rose, and B. J. Albright. Investigation of laser plasma instabilities using picoseconds laser pulses. 2008. *Journal of Physics Conference Series .* **112**: 022042.

Lemons, D. S., B. J. Albright, D. Winske, Kevin J. Bowers, and W. Daughton. Collision models for plasma simulation codes (U). To appear in *Proceedings of the Nuclear Explosives Design Physics Conference.* (Los Alamos, NM, 22-26 Oct. 2007).

Lemons, D. S., W. Daughton, D. Winske, and B. J. Albright. Small-angle Coulomb collision model for PIC codes. To appear in *Journal of Computational Physics.*

Yin, L., B. J. Albright, Kevin J. Bowers, B. M. Hegelich, K. A. Flippo, T. J. T. Kwan, and J. C. Fernandez. Monoenergetic and GeV laser ion acceleration from the laser breakouit afterburner using ultrathin targets. 2007. *Physics of Plasmas .* **14**: 056706.

# New States of Matter in Stars, Nuclei and Cold Atoms

*Sanjay Reddy*

20070276ER

## Introduction

While physics has advanced by leaps and bounds over the past 100 years, there still exist many states of matter that are poorly understood, or are yet to be discovered. This project endeavors to identify and characterize a new state of matter that is formed at low temperature when two species of Fermions that attract one other strongly are combined. When the densities of these species are equal, matter in known to exhibit either superfluid or superconducting behavior where macroscopic flows of either matter or electric currents occurs without dissipation. Since no two fermions can occupy the same quantum state (Pauli principle), even at low temperature fermions occupy states of increasing energy. Those with the highest energies (called the Fermi energy) tend to be very sensitive to interactions. Even a weak attractive interaction will cause fermions to pair up with other fermions with similar energy. Such pairs are called Cooper pairs and the properties of such systems are well known in the context where the interaction is weak, as in electron superconductivity in solid-state physics and liquid helium in low-temperature experiments, since the nobel prize winning work of Bardeen, Cooper and Schrieffer (1957). However, 50 years later we still know very little about the preferred state of matter when the densities of interacting fermions differ and when the interaction between the fermion species is strong. It is not known if such a state should have novel superfluid properties that will manifest quantum mechanical behavior at the macroscopic scale.

Asymmetric states of fermion matter at low temperature are difficult to engineer and control in the laboratory, but they occur inside nuclei and dense nuclear and quark matter. Their properties play a key role in diverse phenomena ranging from nuclear reactions in the laboratory to astrophysical observations of neutron stars. Although there has been a sustained theoretical effort to address these questions experimental input has been lacking. Recent progress in trapping and cooling fermion atoms in atom traps has opened new avenues to create and manipulate asymmetric states of fermionic matter [1]. These experiments provide the primary motivation for our theoretical work. We have developed and tested theoretical tools needed to describe many fermion cold atom systems. In our study we combine large-scale computational methods such as Quantum Monte Carlo (QMC), analytic methods based on quantum field theory, and recent experimental observations to explore the nature of the superfluid state when the interactions between fermions are strong. The methods and insights gained in this study impact our understanding of analogous asymmetrical Fermi systems such as neutron-rich nuclei and dense matter inside neutron stars. The results of our study have already provided quantitative information about the superfluid nature of neutron mater inside neutron stars and about the role of fermion pairing inside nuclei. It also provides a benchmark for theories of strongly interacting Fermi systems in general.

## Benefit to National Security Missions

Cold and dense nuclear matter is expected to be both superfluid and superconducting and our proposed research on strongly interacting 2-component Fermi systems directly address key questions relating to our understanding of “Nuclear Materials Under Extreme Conditions” - a high priority goal of the Office of Science.

## Progress

Research performed during the past year has addressed key questions relating to the nature of strongly coupled Fermi systems. Some of this research has been published in peer-reviewed journals. Below we summarize the research conducted and completed in the past year:

### Superfluid gap

The most important physical quantity that characterizes the strength of a superfluid Fermi system is called the gap. It is the minimum energy required to excite a fermion from the quantum ground state and is related to the binding energy of the Cooper pair. The variation of

the gap with the strength of the interaction is a critical input that affects the behavior of both symmetric and asymmetric states of fermion matter. Any theory that hopes to describe strongly interacting Fermi systems should be able to predict the gap in the symmetric state with high precision. Yet, until recently a comparison between theory and experiment did not exist. It had been difficult to extract the gap in the strong coupling regime from cold-atom experiments due to ambiguities in interpreting the experimental measurement. In a recent article, published in the Physical Review Letters, we have shown that an unambiguous extraction of the gap from the experimental measurement of the density profiles in the atomic trap containing $^6$Li atoms is possible [2]. In these experiments $^6$Li atoms in two different hyperfine states are trapped and cooled below the superfluid transition. Below a critical temperature experiments observe a phase-separation between a nearly symmetric superfluid state in the center and a highly asymmetric normal state in the exterior. Our study showed that the density profile of the atoms in the transition region is exponentially sensitive to the gap. This feature is shown in Figure 1, where even a small variation in the value of the gap significantly changes the polarization at the superfluid-normal interface. We exploited this sensitivity to extract the gap for first time from the experimental results published [1]. When the scattering length is tuned to be infinite, we found that the gap is ~0.45(5) E_F where E_F is the Fermi energy.

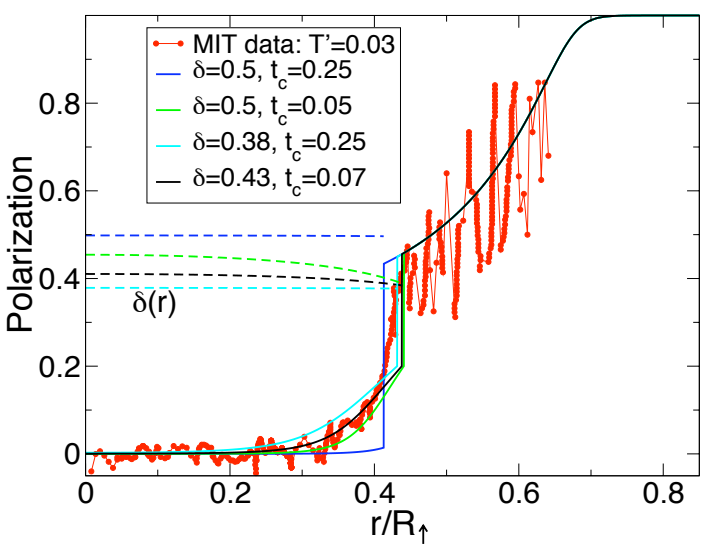


*Figure 1. The polarization density as a function of the distance from the center of the trap. The phase boundary between normal and superfluid matter occurs at r/R ~0.4. The profile is very sensitive to the assumed value of the gap.*

**Equation of state and gap in cold-atoms and neutron matter**

We have completed large-scale numerical calculations using the Quantum Monte Carlo method to calculate the thermodynamic properties and superfluid gap in Fermi systems with short-range interactions. The method and results are equally applicable to both $^6$Li atoms in a terrestrial atomic trap and neutron matter inside neutron stars because the fundamental interactions in these systems are very similar. Our results for the cold-atom systems were tested directly with measurements from cold atom experiments. The excellent agreement found here especially in the regime where the interaction is strong provides for the first time an experimentally tested theory to describe neutron matter inside neutron stars [3]. This striking comparison between the equation of state and the superfluid gap in cold-atom systems and neutron matter is shown in Figure 2.

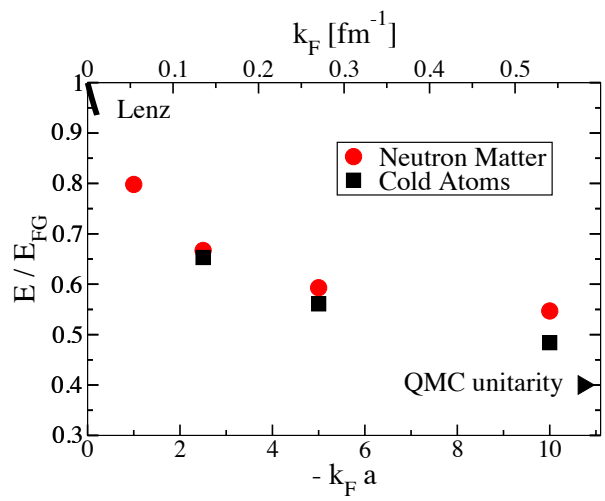


*Figure 2. The ratio of the energy per particle in the interacting system to its value in the non-interacting fermi gas is plotted as function of density for cold atom systems and neutron matter. At unitarity when the scattering length is infinite, experiment finds this ratio to be ~ 0.40(5) - in good agreement the QMC result.*

**Ground state of asymmetric fermi systems in weak coupling**

Analytic methods can be applied to Fermi systems when the interaction strength is weak. Here approximate methods such as mean field theory where quantum fluctuations of the normal and superfluid density are ignored are expected to provide an accurate description. We have performed an extensive analysis of a two-component Fermi system within mean field theory [4]. At finite temperature we show that Cooper pairs can form even though they may not exist at zero temperature due to thermal smearing

of the occupation levels of the fermions. We also analyze the role of instabilities in the homogenous phase at finite asymmetry and find that novel superfluid states such as those predicted by Ferrel, Fulde, Larkin and Ovchinnikov [5] are likely. These states of matter are heterogeneous and can be crystalline with regions where the gap alternates between a maximum and a minimum value. Our paper identifies for the first time regions in the temperature – number asymmetry parameter space where experiment can hope to probe heterogeneous phase of superfluidity.

## Future Work

We are now in the process of adapting our numerical methods (QMC) to study asymmetric systems. One particular goal will be to study systems with moderate asymmetries since these are regions where novel superfluidity is most likely to appear [3]. Our predictions will be tested against results for the density profiles and the electro-magnetic response from cold-atom experiments in asymmetric systems. Since these experiments are yet to discover a new state of matter, we expect that our study will help these experiments identify robust signals for novel superfluidity. We are also studying fermion systems where the masses of the interacting fermions are chosen to be very different in anticipation of cold atom experiments in which a mixture of $^{6}$Li and $^{40}$K atoms are trapped and cooled to low temperatures. We are also working on extending our QMC methods to apply to asymmetric neutron-rich matter and simple low energy models for dense quark matter. We will calculate response and transport properties in strongly coupled superfluid phases. We will extend QMC algorithms to study finite temperature aspects.

## Conclusion

Our study has focused on the development and testing of theories and numerical methods such as quantum Monte Carlo (QMC) to describe strongly interacting Fermi systems. Comparisons to cold atom experiments have validated our QMC numerical method. We have demonstrated that we can provide a quantitative description of: (i) symmetric superfluid matter, (ii) superfluid states with small asymmetry, and (iii) normal state with extreme asymmetry. We are now in process of developing theory and numerical methods to study states with intermediate asymmetry in order to help identify a novel heterogeneous states of superfluid fermionic matter. We are also applying our techniques to study analogous systems such as dense nuclear and quark matter under extreme conditions of relevance to the astrophysics of neutron stars and supernova.

## References


1. Shin, Y., C. H. Schunck, A. Schirotzek, and W. Ketterle. Phase diagram of a two-component Fermi gas with resonant interactions. 2008. *Nature.* **451** (7179): 689.
2. Carlson, J., and S. Reddy. The superfluid gap in strong coupling. 2008. *Physical Review Letters.* **100**: 150403.
3. Gezerlis, A., and J. Carlson. Strongly paired fermions: Cold atoms and neutron matter. 2008. *Physical Review C.* **77** (3): 032801(R).
4. Sharma, R., and S. Reddy. A mean field analysis of pairing in asymmetric fermi systems at finite temperature. To appear in *Physical Review A.*


## Publications


Alford, M. G., M. Braby, S. Reddy, and T. Schafer. Bulk Viscosity due to Kaons in Color-Flavor-Locked Quark Matter. 2007. *PHYSICAL REVIEW C.* **75**: 055209.

Carlson, J., and S. Reddy. The superfluid gap in strong coupling . 2008. *PHYSICAL REVIEW LETTERS.* **100**: 150403.

Gezerlis, A., and J. Carlson. Strongly-Paired Fermions: Cold Atoms and Neutron Matter. 2008. *Physical Review C.* **77** (3): 032801(R).

Sharma, R., and S. Reddy. A mean field analysis of pairing in asymmetric Fermi systems at finite temperature. To appear in *PHYSICAL REVIEW C.*

continuing project

# Ultra-Low Field Resonant Absorption Magnetic Resonance Imaging of Neural Activity

*Petr Lvovich Volegov*

20070349ER

## Introduction

Currently, there is no method that can directly measure and unambiguously localize brain activity. Functional magnetic resonance imaging (fMRI) detects blood flow and oxygenation changes that are associated with increased neural activity. Thus, fMRI is really only an indirect measure of neural activity, and therefore, the fMRI signal is not necessarily co-located or linearly correlated with the neural response. On the other hand, electro-/magneto-encephalography (EEG/MEG) detects the electric/magnetic fields outside the head that are produced by neural activity within the brain. Although, EEG/MEG has good temporal resolution (~ms), it has poor spatial resolution due to the ill-posed inverse problem of localization. Thus, a technique that combines the advantages of both of these methods would produce a quantum leap in our understanding of neuronal processing.

We propose to demonstrate the feasibility of using a resonant absorption mechanism for direct neural imaging (DNI) in the human brain with magnetic resonance imaging (MRI) techniques at ultra-low fields (ULF, 1-100 microTesla). MRI spatially encodes the nuclear magnetic resonance (NMR) signature of nuclei in a volume of interest. The NMR signal arises from a population of polarized spins precessing about an orienting magnetic field with a characteristic Larmor frequency. The NMR signal decays with time as transitions between spin states occur and as the spin population dephases. Resonant absorption occurs when the frequency of an external magnetic field matches the Larmor frequency, resulting in dramatically increased transition probability.

We hypothesize that when the spin precession frequency of a population of nuclei overlaps with frequency bands of brain activity, resonant absorption will lead to greatly enhanced probability of spin state transitions and more rapid NMR signal decay. This is made possible because neural activity occurs largely in the frequency band below 2kHz and the Larmor frequency for protons at ULF is ~42 to 4200Hz.

## Benefit to National Security Missions

The technique of ultra-low field MRI being developed here, because of the ability to detect and differentiate a vast array of materials, has direct application to NNSA and DHS missions, including Threat Reduction, by developing technologies to detect nuclear materials and/or other threat materials.

## Progress

We have explored our hypothesis with several first-principal demonstration experiments. As reported previously [1], we performed several current phantom experiments to determine the correct measurement field for detecting currents in the range of neurally-generated currents. The current phantoms consisted of 1% NaCl, with approximately 0.5g/l $CuSO_4$. We applied three different waveforms: a DC current, a modulated sinc pulse, and a pseudo-random waveform. Using these current waveforms, we detected a current of approximately 10 µA which generated a field of 20 pT in a voxel of 3 mm x 3 mm x 2mm. This 20 pT magnetic field is in the range of magnetic fields due to neural currents. In addition, we observed signal enhancement for waveforms that had an "on-resonance" frequency component. However, because our imaging capabilities were not functional at the time, we were not able to conclusively determine the spatial location of the enhanced signal.

Therefore, we have developed a multiple echo protocol for generating magnetic resonance images at ultra-low fields. These MRI techniques are the necessary prerequisites for refining the protocols to elicit the direct neuronal images. The details of the techniques are included in [2]-[4]. An example of the level of resolution we are achieving now in comparison with commercial high field MRI is given in Figure 1.

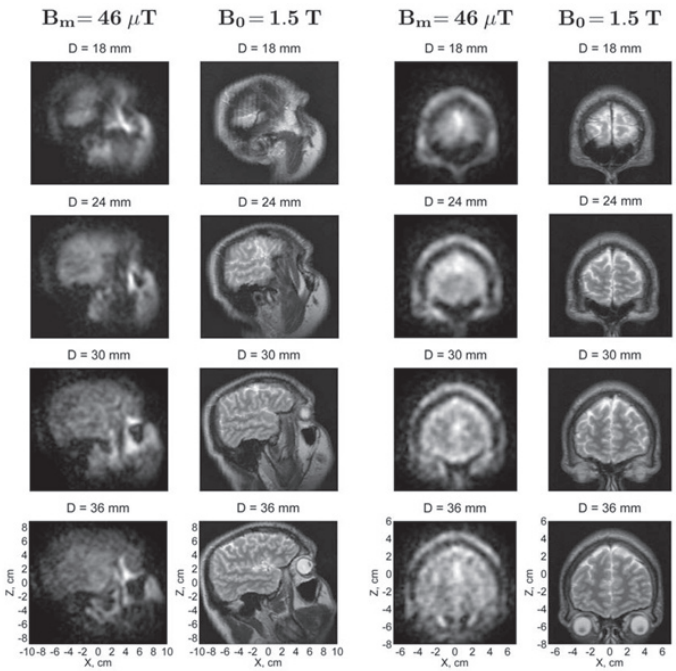


*Figure 1. First images of the human brain by ULF MRI compared to images by 1.5 T MRI [2].*

Using this protocol, we have performed some additional phantom experiments. We detected a phase change in the MRI signal that was localized to the position of the current in the phantom. However, calculations done in support of these experiments revealed that the voxel size was much larger than the optimum voxel size. Thus, we are planning future experiments with a more appropriate voxel size to correct for this. More phantom experiments to further explore the resonant mechanism are also being planned.

With respect to building realistic neural source models, we have constructed a library of neurons consisting of the major cell types found in the cerebral cortex. To ensure that the neurons are as realistic as possible, we investigated the effects of changing the distribution and composition of these conductances on the firing patterns of the neurons and adjusted them to match experimental data. Using anatomical and electrophysiological data, we connected these neurons in such a way as to produce neurons with functional receptive fields. This network of neurons was given realistic input to produce firing patterns that were consistent with experimental data. An example of these currents for a single neuron is shown in Figure 2.

Furthermore, we derived the theoretical time evolution behavior of the proton spin in the presence of a generalized time-varying perturbing magnetic field (i.e., from the neuronal currents). This has revealed the additional resonant absorption effect that we hypothesized. The perturbing magnetic field will not only change the MRI signal phase and amplitude (which are the effects utilized in high field MRI studies), but it will enhance the change in the MRI signal amplitude if it has time-harmonic components that overlap with the Larmor frequency from the applied measurement field. Indeed, because the frequency content of activated neurons is on the order of 100-1000Hz, the measurement field must be of ultra-low field strength in order to achieve this overlap. We have used this derivation to write a 3D Finite Difference Time Domain code that is capable of calculating the MRI signal from arbitrary time-varying current waveforms throughout time. Preliminary results suggest that this resonant absorption effect could cause significant changes in the MRI signal. The results of a set of simulations for a single-frequency sine waveform are shown in Figure 3. A characteristic resonance curve is observed when the frequency of the sine wave passes through the "on-resonance" condition. Further studies to explore this more deeply will be forthcoming.

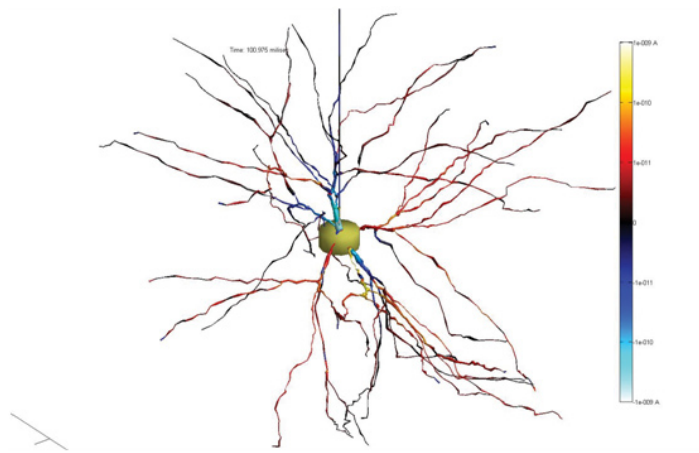

*Figure 2. Calculated currents for a single neuron at one moment in time due to a realistic stimulus.*

*Figure 3. Calculated MRI signal phase change for a sine current waveform with a frequency equal to some percentage of the Larmor frequency.*

Finally, we have investigated various stimulation protocols for human DNI experiments. We are exploring two different stimuli that produce activity in two different brain regions, visual and somatosensory cortex. We are looking at several different visual stimulation protocols, including circular and square sinusoidal gratings, circular checkerboards and natural images. With somatosensory stimuli, we are looking at high frequency activation of touch receptors, which have been shown to drive activity in the somatosensory cortex at a particular frequency and which could potentially produce resonance at a higher and more easily detected frequency.

## Future Work

As mentioned in the previous section, we constructed computational models of each of the major cell types found in cerebral cortex. To build on this work, we plan to use these models in conjunction with our Finite Difference Time Domain code to construct statistical profiles of the temporal and spatial distribution of the magnetic field for each class of neurons. We will use these statistical models of magnetic fields as the basis for a large-scale model of magnetic fields in a section of the brain.

We are also planning several future experiments to investigate neural activity in multiple experimental paradigms. We will focus on brain regions with high frequency neural activity that would require higher measurement fields to satisfy the resonance condition. While most neural activity is less than 100 Hz, some areas such as the hippocampus and somatosensory cortex produce oscillations in the 200-300 Hz range, with some reports of up to 700 Hz oscillations. Also, each action potential is itself a high frequency event that could potentially produce the perturbations of the spins in the surrounding extracellular fluid necessary for DNI.

Another experimental system we plan to explore is the retina. The retina has some unique advantages for DNI. It has a highly organized, laminar structure and it can be removed with all of its intrinsic connections intact. Removal allows direct experimental access to the tissue without any intervening bone or connective tissue. Our plan is to stimulate the retina with light flashes while simultaneously recording both electrical potentials using a multi-electrode array and directly measuring neural activity. By measuring electrical activity, we will fine-tune the measurement magnetic field.

Finally, we will use a combined experimental and computational approach to detect the temporal and spatial evolution of epileptic seizures. The protocol we will use has been used for many years to study epilepsy: intraperitoneal injections of kainic acid to induce acute seizures in rodents. Epileptic seizures are characterized by high-amplitude, high frequency neural activity. Also, the neurons participating in the seizure fire synchronously. The combination of high amplitude currents generated by synchronously firing neurons in a large portion of the brain will produce a very large signal, making an animal model of epilepsy an ideal platform for investigating DNI. To help guide experiments, we will use a computational model of epilepsy. A biologically realistic model will allow us to determine the distribution of magnetic fields and to optimize imaging parameters.

## Conclusion

We expect to develop a new approach, ultra-low field MRI that will enable the direct imaging of neural activity in the human brain. This new technique can lead to new methods of studying brain function and illnesses that is a quantum leap over any existing technique. We believe this technology will directly benefit health care and the ability to robustly detect brain patterns. Thus, it will aid not only in furthering our understanding of how the brain works in general, but also in understanding and diagnosing various neurological disorders. Finally, the development of ultra-low field MRI has farther-reaching applications to homeland security. Our progress so far has taken us a great deal further towards developing this important technology.

## References


1. KrausJr, R. H., P. Volegov, A. Matlachov, and M. Espy. Towards direct neural current imaging by resonant mechanisms at ultra-low field. 2008. *NeuroImage.* **39**: 310.

2. Zotev, V S., A. Matlashov, P. Volegov, I. M. Savukov, M. Espy, J. C. Mosher, J. J. Gomez, and R. H. Kraus Jr. Microtesla MRI of the human brain combined with MEG. 2008. *Journal of Magnetic Resonance.* **192**: 197.

3. Zotev, V. S., P. L. Volegov, A. N. Matlashov, M. A. Espy, J. C. Mosher , and R. H. Kraus Jr. Parallel MRI at microtesla fields. 2008. *Journal of Magnetic Resonance .* **192**: 197.

4. Espy, M., M. Flynn, J. Gomez, C. Hansen, R. Kraus, P. Magnelind, K. Maskaly, A. Matlashov, S. Newman, M. Peters, H. Sandin, I. Savukov, L. Schultz, A. Urbaitis, P. Volegov, and V. Zotev. Applications of ultra-low field magnetic resonance for imaging and materials studies. To appear in *IEEE Trans. Appl. Supercond.*

## Publications

Espy, M., M. Flynn, J. Gomez, C. Hansen, R. Kraus, P. Magnelind, K. Maskaly, A. Matlashov, S. Newman, M. Peters, H. Sandin, I. Savukov, L. Schultz, A. Urbaitis, P. Volegov, and V. Zotev. Applications of ultra-low field magnetic resonance for imaging and materials studies. To appear in *IEEE Trans. Appl. Supercond.*

Flynn, M. C., P. Volegov, J. Mosher, A. Matlashov, M. Espy, and R. H. Kraus, Jr.. Simulation of magnetic fields for direct neuronal imaging. To appear in *Society for Neuroscience.* (San Diego, CA, 2-7 Nov. 2007).

Kraus,Jr., R. H., P. Volegov, A. N. Matlachov, and M. Espy. Toward direct neuronal current imaging by resonance mechanisms at ultra-low field. 2008. *NeuroImage.* **39** (1): 310.

Volegov, P., H. Sandin, V. Zotev, M. Flynn, K. Maskaly, A. Matlashov, J. Mosher, M. Espy, and R. Kraus Jr. Direct Neuronal Imaging by Ultra Low Field MRI. Invited presentation at *the 14th Annual Meeting of The Organization for Human Brain Mapping.* (Melbourne, Australia, 15-19 June 2008).

Volegov, P., V. Zotev, M. Espy, M. Flynn, J. Gomez, C. Hansen, R. Kraus Jr, P. Magnelind, K. Maskaly, A. Matlashov, S. Newman, M. Peters, H. Sandin, I. Savukov, L. Schultz, and A. Urbaitis. Concurrent Ultra Low Field MRI and Brain Function Measurements. Invited presentation at *16th International Conference on Biomagnetism.* (Sapporo, Japan, 25-29 Aug. 2008).

Zotev, V., A. Matlashov, P. Volegov, I. Savukov, M. Espy, J. Mosher, J. Gomez, and R. Kraus Jr. Microtesla MRI of the human brain combined with MEG. 2008. *Journal of Magnetic Resonance .* **194**: 115.

Zotev, V., P. Volegov, A. Matlashov, I. Savukov, T. Owens, and M. Espy. SQUID-based Microtesla MRI for In Vivo Relaxometry of the Human Brain . To appear in *IEEE Trans. Appl. Superconduct.*

Zotev, V., P. Volegov, A. Matlashov, M. Espy, J. Mosher, and R. Kraus Jr. Parallel MRI at microtesla fields. 2008. *Journal of Magnetic Resonance .* **192**: 197.

continuing project

# Unique Observations of Nature's Largest Explosions

*W Thomas Vestrand*

20070382ER

## Introduction

The goal of this project is to build the world's fastest robotic telescope and to use it to make unprecedented cosmic cinematography of explosive phenomena in the universe. The key technical objective is to field new technology cameras that will be capable of imaging fast varying optical flashes with much greater temporal resolution than is possible with conventional astronomical cameras. The key scientific goal is to study the brief flashes of light emitted when some of the very first super-massive stars in the universe collapsed to form black holes. Since these flashes of light typically last less than a minute, we need to deploy these imagers on ultra-fast slewing telescopes that can point to any direction in the sky and begin the cinematography in less than ten seconds. By studying the explosion thorough its flash of visible light and the interaction of the explosive ejecta with its surrounding material through the visible afterglow light, we will obtain new information about nature's largest explosions since the big bang as well as probe the early universe and its properties the in era before our solar system was formed.

## Benefit to National Security Missions

This project will construct and operate autonomous robotic instrumentation capable of interrogating fleeting cosmic explosions that can occur at any time and in direction of the sky. The development of expertise with autonomous robotic instrumentation is essential for building next generation instrumentation to support the DOE's Threat Reduction mission.

## Progress

An important scientific achievement this year was our commissioning of the RAPTOR-T system (see Figure 1) for making simultaneous multi-color observations of gamma-ray bursts (GRBs) and our collection of the first measurements of burst colors during the critical first minute of a GRB. The telescope is composed of four high-end COTS optical tube assemblies that are co-aligned and co-located on a single rapidly slewing mount. Each of the four tube assemblies is a 0.41-meter f/10 Cassegrain telescope employing a different clear/VRI broad-band filter. Together these four co-aligned tube assemblies yield an effective aperture for RAPTOR-T of 0.82-meter. An advantage of this approach is the much more compact size of the telescope for a given focal ratio. This in turn translates into a lower moment of inertia and makes it much easier to achieve the extremely rapid slewing speeds needed to begin observations of GRB optical emission in less than 10 seconds after a GRB trigger. The RAPTOR-T servo motors and drive system has been significantly scaled up to achieve the same slewing speed and settling specifications as the previous generation of our mounts—able to be on a burst location and begin observations in as little as six seconds after the GRB trigger. No other telescope with an effective aperture as large as RAPTOR-T is capable of observing prompt optical emission from GRBs and measuring the spectral energy distribution within ten seconds of the GRB trigger. We have already begun making GRB observations with this system and during the coming year we expect to determine definitely the radiation mechanism for the optical emission from GRBs.

*Figure 1. The RAPTOR-T rapid response telescope that is capable of simultaneous multi-color imaging anywhere in the visible sky in less than 10 seconds.*

During the last year we have also made very significant progress on the path to bringing together new robotic telescope and fast cadence imaging camera technologies that will give us a unique capability for exploring

the ultra-fast variability of astrophysical transients. We completed the construction and deployment of a new robust 0.5-meter Ritchey-Chrétien telescope and the associated robotic enclosure. The telescope, called RAPTOR-Z, is capable of slewing speeds greater than 100 degrees/second and accelerations greater than 100 degrees/second/second. In practice, this means that the telescope can typically be on target and making observations in less than five seconds after a receipt of a transient localization anywhere in the visible sky. Construction was also completed on the robotic enclosure that houses the telescope. We developed a new system of sensors to monitor power grid status, temperature, humidity, and other weather conditions and integrated them with enclosure controls to enable the enclosure to protect autonomously the safety of the housed telescope.

We also completed testing of an Electron Multiplication Charge Coupled Device (EMCCD) camera for deployment on the RAPTOR-Z telescope. Custom driver software was developed, integrated with our RAPTOR data acquisition system, and successfully tested. The ability of these EMCCD to operate at very high frame rates, without the penalty of high read noise suffered by conventional CCDs, will allow us to make observations of GRBs with an unprecedented combination of temporal resolution and sensitivity.

## Future Work

The key technical goal of this project is to upgrade the RAPTOR-T telescope system and operate it with cameras capable of the fast cadenc needed for exploring the spectral and temporal properties of the optical emission during the critical first few minutes after the onset of a GRB. Since most GRBs last less than a minute, this means we will need to deploy new fast cameras that are capable of making sensitive optical observations that can take several exposures every ten seconds. We are purchasing and deploying fast Electron Multiplying CCD (EMCCD) cameras that have at least a 1Kx1K format, better than 50% quantum efficiency across the BVRI wavelength range, exceptionally fast readout times (>3MHz), and readout noise of <10 e. A photometry/astrometry pipeline and new data acquisition software will be written to analyze the data collected by these cameras.

Our key scientific tasks are:

- Collect simultaneous 4-color (BVRI) observations of GRB optical emission light-curves starting at ~6 seconds with a few second cadence for more than 30 GRBs .
- Use the 4-color, fast-cadence, optical measurements collected during the first minutes to separate intrinsic variations from extrinsic variations generated by variable extinction and dissect the light curve into the prompt and early afterglow components.
- Use the derived intrinsic spectral variations to constrain the fundamental parameters of the relativistic bulk flow and the derived extrinsic variations to constrain the properties of the dust screen and the extinction curve.
- Construct photometric redshifts, quickly identify high-z GRBs while they are bright, and publically release the information by Internet through the GCN, so that they can be used as cosmological beacons to probe the properties of intergalactic gas.
- Use multi-color observations of early optical emission to study the reverberation signal with the goal of probing the star formation environment in the early universe.

## Conclusion

We will collect observations of optical light starting at 6 seconds from GRBs to study the reverberation signal with the goal of probing the star formation environment in the early universe. These measurements will be used to distinguish intrinsic from extrinsic variations generated by variable extinction and to dissect the light curves into prompt and early afterglow components. We will thereby constrain the parameters of the relativistic flow and the dynamic dust screen. We will also identify very distant GRBs, while they are bright, to use as cosmological beacons for probing the properties of intergalactic gas.

## Publications

Panaitescu, A., and P. Kumar. A unified model for the gamma-ray and prompt optical emissions of GRB 990123. 2007. *Monthly Notices of Royal Astronomical Society.* **376**: 1065.

Perleyetal, D. A.. The troublesome broadband evolution of GRB 061126: Does a grey burst imply grey dust?. 2008. *Astrophysical Journal.* **672** (1): 449.

Ruiz-Velascoetal., A. E.. Detection of GRB 060927 at z = 5.47: Implications for the use of gamma-ray bursts as probes of the end of the dark ages. 2007. *Astrophysical Journal.* **669** (1): 1.

White, R. R., W. T. Vestrand, J. Wren, and P. R. Wozniak. Using distributed sensor network architecture to link heterogeneous astronomical assets. 2008. *Astronomische Nachrichten.* **329** (3): 278.

White, R. R., and A. Allen. An overview of the heterogeneous telescope network concept, scalability and operations capability and distributed architecture. 2008. *Astronomische Nachrichten.* **329** (3): 232.

Yostetal, S.. Exploring broadband GRB behavior during gamma-ray emission. 2007. *Astrophysical Journal.* **657** (2): 925.

Yostetal, S. A.. The dark side of ROTSE-III prompt GRB observations. 2007. *Astrophysical Journal.* **669** (2): 1107.

# Electron-Neutrino Correlation in Neutron Beta Decay

*Wesley Scott Wilburn*

20070488ER

## Introduction

Precision studies of neutron properties are important ways to look for new physics and test new theories. The current Standard Model of nuclear and particle physics provides a framework for all of nuclear and particle physics and includes very precise predictions for how the neutron decays through emission of an electron and a neutrino (beta decay). These predictions, for example the probability that the electron or neutrino is emitted in the same direction as the neutron spin, or the probability that the electron and neutrino are emitted in the same direction, can be tested by precise experiments. Differences between the predicted and measured results would indicate the discovery of new, "Beyond the Standard Model" physics. For these reasons, the neutron acts as an important laboratory for nuclear and particle physics. To measure these decay parameters with the required precision, sufficient neutrons must be available to provide adequate statistics. The Spallation Neutron Source, currently being commissioned in Oak Ridge Tennessee, will provide an intense beam of neutrons suitable for such experiments. In addition, false effects (systematic errors) must be reduced to very low levels. One such effect is imperfect knowledge of the neutron polarization. This project will study the feasibility of reducing all such systematic errors to the required level of precision and prove that a precision neutron decay experiment can be conducted that is an order of magnitude more precise than previous experiments.

## Benefit to National Security Missions

Testing a model that describes the most basic properties of matter is a core DOE mission. Furthering our understanding of these properties of matter also impacts other mission areas including nuclear weapons and fusion research. Finally, particle detectors developed here will impact the threat reduction missions of DOE and DHS.

## Progress

The project has made major project on three fronts: demonstration of a new precision neutron polarization technique, further analysis of systematic errors, and conceptual design of the experiment.

Precision neutron polarization at the 0.1% level is a key requirement for precision neutron decay experiments. Our design relies upon the unique interaction of neutrons with polarized helium-3 gas. Circularly polarized laser light produces atomically polarized rubidium, which spin-exchanges with helium-3 to produce nuclear-polarized helium-3. Cold neutrons passing through the polarized helium-3 are absorbed with high probability if their spins are opposite to the helium-3, and with much lower probability if theirs spins are the same as the helium-3. This produces a high neutron polarization, and gives a powerful method of measuring the neutron polarization, since the interaction between the neutrons and helium-3 is understood to a few parts in 10^5. In principle, the neutron polarization can be determined with this technique with a precision of less than the required 0.1%. What limits the actual precision of this technique are neutron backgrounds, electronic noise, and other practical matters.

We improved the previously constructed experiment at LANSCE to test this technique consisting of a polarized helium-3 cell with neutron transmission monitors, plus a neutron polarization analyzer, a spin flipper, and an additional transmission monitor to check the polarization with an independent technique. The second of three planned runs was conducted during the 2008 LANSCE run cycle. While the results are still being analyzed, we believe they are significantly better than the statistically and systematically limited precision of 0.7% obtained in the first run in 2007. A third run will be conducted during the 2009 LANSCE run cycle to address any remaining questions. In addition we definitively answered a question from previous experiments about the mechanism for depolarization of helium-3 by intense neutron beams. This result has been published. in the journal Physical Review Letters.

An experiment at the 0.1% precision level requires careful control of systematic effects that can result in an incorrect measurement. We have carefully investigated several such effects and presented the findings in a 98 page beam time proposal to the Spallation Neutron Source (SNS) Fundamental Neutron Physics Beamline (FnPB) Physics Review and Advisory Committee (PRAC). Systematic effects that have now been analyzed include: neutron depolarization effects, electric and magnetic field inhomogenieties, electron and proton backscattering from detector surfaces, detector timing and energy resolution, proton scattering from residual gas, and electron trapping by Penning traps. In total, 18 separate potential systematic effects are analyzed in this document. As an example, proton scattering from residual gas is analyzed to show that the 10^-8 mbar vacuum planned for the spectrometer will be sufficient to meet the goals of the experiment.

The conceptual design of the experiment has advanced. The charged-particle detector design has improved, and a mounting and cooling scheme for the detectors has been engineered and is under construction.

## Future Work

The field of fundamental neutron physics aims to answer important questions concerning the Standard Model (SM) of the electro-weak interaction. Particularly exciting is the possibility of exploring new physics, such as new quark generations or additional electro-weak gauge bosons. Unlike high energy physics, where direct production of new particles is emphasized, high-precision neutron experiments at low energies look for very small effects due to a coupling of undiscovered massive particles to light quarks. The information obtained in these measurements is usually complementary to that obtained in direct searches. Precision measurements of neutron beta decay provide a sensitive test of the Standard Model. One parameter is the correlation between the outgoing electron and proton momenta that is sensitive to the ratio of axial to vector coupling constants.

Previous determinations of this ratio in neutron decay have focused on measuring the correlation between the neutron spin and electron momentum. These experiments have been limited in precision primarily by two effects: large backgrounds and uncertainty in neutron polarization. Our approach addresses the first of these limitations by observing coincidences between the decay proton and electron in high-quality silicon detectors, greatly reducing the background. The second limitation is addressed by a new precision neutron polarimetry technique, and additionally by also measuring a neutron decay parameter that does not depend upon neutron polarization..

The work to be completed during this project includes completion of a conceptual design, modeling of important parameters of the spectrometer, and simulation of the charged particle transport. In addition, we will perform R&D for the detector system and develop a data acquisition system.

## Conclusion

We expect to prove the feasibility of the neutron decay experiment, answer all significant technical questions, and be ready to propose a construction project. We will have shown that the detectors work properly, that a suitable spectrometer magnet can be constructed, and that a neutron beam with the required properties can be produced. In addition, we will have shown that the data collected can be properly analyzed.

## Publications

Alarcon, R., S. Balascuta, S. Baessler, E. Frlez, D. Pocanic, L. Barron-Palos, J. D. Bowman, T. V. Cianciolo, S. I. Penttila, K. P. Rykaczewski, G. R. Young, J. R. Calarco, F. W. Hersmann, V. Cirigliano, A. Danagoulian, T. Ito, A. Klein, J. Ramsey, W. S. Wilburn, T. E. Chup, M. Sharma, C. Crawford, T. R. Gentile, M. Gericke, A. Micherdzinska, S. Page, G. L. Greene, and R. K. Grzywacz. Precise measurement of neutron decay parameters - The abBA experiment. 2008. *Beam Time Request to SNS FNPB Proposal Review Advisory Committee.*

Sharma, M., E. Babcock, K. H. Andersen, L. Barron-Palos, M. Becker, S. Boag, W. C. Chen, T. E. Chupp, A. Danagoulian, T. R. Gentile, A. Klein, S. Penttila, A. Petoukhov, T. Soldner, E. R. Tardiff, T. G. Walker, and W. S. Wilburn. Neutron beam effects on spin-exchange-polarized 3He.. 2008. *Physical Review Letters.* **101** (8): 083002.

# Experimental and Computational Studies of Magnetic Bubble Expansion as a Model for Extra-galactic Radio Lobes

*Scott Chia Hsu*

20070506ER

## Introduction

This is a collaborative project between LANL and the University of New Mexico, supported by LDRD and the NSF/DOE Partnership in Basic Plasma Science. We are trying to develop better understanding and insight into the evolution of immense extra-galactic structures known as "radio lobes" (because we observe these structures from ground-based telescopes in the radio frequency spectrum). These radio lobes are believed to be "blown up" by the expansion of magnetized plasmas born from accretion disks near the centers of galaxies. The expansion is governed by rich plasma physics phenomena that develop such as shocks, magnetic reconnection, and angular momentum transport from the lobes to the intergalactic medium. We are studying the model problem of a magnetized plasma expanding into a background plasma in the laboratory, and we are running coordinated numerical simulations to uncover the details of these plasma physics phenomena which we believe govern the evolution of radio lobes.

## Benefit to National Security Missions

This project supports the DOE missions in fundamental science and science-based prediction of complex systems. There is secondary support for Office of Science mission of Fusion Energy Sciences, by contributing basic understanding of complex plasma physics phenomena.

## Progress

In the past year, we have finished preparations for starting up the laboratory experiments (at UNM) and have already achieved first plasma, and we have finished running the first set of computer simulations which will guide the initial experiments.

The preparations involved adding hardware systems to an existing laboratory experiment HelCat at UNM, including 1) a new pulsed coaxial gun and associated power system for generating the magnetized bubble plasmas, 2) an external magnetic coil to provide an initial magnetic field in the system, 3) fast custom gas valves for puffing in gas that will be ionized to form the plasma, and 4) a magnetic probe that will take in situ measurements of local magnetic field inside the plasma.

The numerical simulation work involved adapting a pre-existing magnetohydrodynamic (MHD) computer code to the geometry and conditions of the UNM experiment and running relevant simulations to predict the experimental evolution. The results have been written up, and have been accepted for publication in the July 2008 issue of Physics of Plasmas, a top peer-reviewed plasma physics research journal. The title of this publication is "Ideal magnetohydrodynamic simulation of magnetic bubble expansion as a model for extragalactic radio lobes" by W. Liu, S. C. Hsu, H. Li, S. Li, and A. G. Lynn. Key findings of the simulation work include the identification of shock formation when the bubble propagates into the background plasma, and that the bubble develops asymmetries about its propagation axis due to reconnection and inhomogeneous angular momentum transport due to the background magnetic field. These results will help guide the initial experiments at UNM.

A second paper related to the theory of magnetic bubble expansion in the astrophysical context (W. Liu et al.) has just appeared online in Astrophysical Journal Letters.

## Future Work

This project is motivated by exciting recent work in plasma-astrophysics, which has proposed a picture of galaxy evolution depending on plasma physics. This picture highlights energy flow in the life cycle of active galaxies, showing that at each step, magnetic energy features prominently in the large-scale evolution of the galaxy. These steps are as follows:

1. Magnetic turbulence leads to angular momentum transport allowing matter to accrete inward in a gravitational potential, leading to the formation of a super-massive black hole.

2. Magnetic energy is amplified via a dynamo effect in the surrounding accretion disk, converting mechanical energy to magnetic energy.

3. Magnetic helicity injection organizes the magnetic fields into jets which transport magnetic energy onto extra-galactic scales.

4. The energy/plasma carried far away by the jet reach equilibrium with the inter-galactic medium, forming extra-galactic "radio lobes" which are thought to be gigantic relaxed plasmas.

This project involves laboratory plasma experiments and MHD numerical simulations to help address outstanding issues related to the third/fourth steps above that cannot at present be resolved from numerical computation or astronomical observations alone. The experiments will study the relaxation of a magnetized plasma bubble as it expands into and reaches equilibrium with a lower pressure background. Experimental data will provide insights into this process and data for validating sophisticated computations being carried out in this field. Key nonlinear plasma physics questions to be addressed include:

- How much flux conversion occurs within the bubble during expansion?
- How much plasma heating/acceleration occur within the bubble due to reconnection, and what fraction goes to ions versus electrons?
- If the bubble has net angular momentum, how does it evolve and how much is transferred to the background plasma?

Experiments will be conducted on the HELCAT experimental facility at University of New Mexico (with involvement from LANL staff) and numerical simulations at LANL.

## Conclusion

This project will combine laboratory experiments (conducted at UNM) and numerical simulations to study how a magnetized plasma bubble expands into a lower density background plasma as a way to gain insight into the structure and formation of extra-galactic radio lobes. The primary scientific objectives of the project are to characterize and understand the underlying nonlinear plasma physics of the expanding magnetized plasma bubble, providing experimental data and numerical simulation results on bubble formation, expansion, and relaxation.

## Publications

Liu, W., H. Li, S. Li, and S. C. Hsu. Long-term evolution of magnetized bubbles in galaxy clusters. 2008. *Astrophysical Journal Letters.* **684**: L57.

Liu, W., S. C. Hsu, H. Li, S. Li, and A. G. Lynn. Ideal magnetohydrodynamic simulation of magnetic bubble expansion as a model for extragalactic radio lobes. 2008. *Physics of Plasmas.* **15**: 072905.

# Precision Cosmology and the Neutrino Sector

*Salman Habib*

20080031ER

## Introduction

The fundamental constituents of nature – the elementary particles – and their interactions with each other were described for many years by a very successful paradigm referred to as the Standard Model (SM). Excitingly, recent experiments and observations have shown that the SM provides only a very partial description of the make-up of the Universe. Solid -- now overwhelming -- evidence for what is termed Beyond Standard Model (BSM) physics first came from cosmological observations and terrestrial neutrino experiments. Cosmological observations of distances to exploding stars called supernovae, of the motion of stars and gas clouds in galaxies, and of the distortion of galaxy images by an analog of optical lensing due to gravity, all show that 80% of the mass in the Universe resides in a mysterious form of matter – so-called dark matter – that finds no place in the SM. In the SM, there exists a class of enigmatic, weakly interacting class of particles termed neutrinos, assumed to be massless. However, experiments have shown that in fact neutrinos do have mass and can change from one type of neutrino into another and back, a process called neutrino oscillations.

It turns out that cosmology and the neutrino sector are intimately related, providing complementary information about each other. Cosmology provides the best-known limits on the sum of all neutrino masses, currently very difficult to constrain with terrestrial experiments. In addition, cosmological observations can probe new aspects of neutrino physics such as the existence of new types of neutrinos that have no SM interactions, the hypothesized sterile neutrinos. In this project, we conduct an integrated research program that connects experiments, observations, and theory, to shed light on the neutrino mass, the effective number of neutrinos, and the existence of sterile neutrinos. The sterile neutrino could be a candidate for the dark matter particle; one of our aims is to investigate this possibility.

## Benefit to National Security Missions

This project will support the DOE Office of Science (HEP/NP) mission by enhancing our understanding of the neutrino sector and its connection to cosmology using ground-based and satellite observations. Because the project develops and uses high-performance computing tools and advanced statistical methods for data analysis and for combing theoretical results with this analysis, it also ties in to corresponding aspects of NNSA threat reduction and stockpile stewardship programs.

## Progress

Cosmological constraints on neutrino properties can be extracted from two sources: 1) analysis of small temperature fluctuations in the cosmic microwave background, the residual light left over from the primordial fireball (often referred to as the Big Bang), and 2) from observations of how mass is distributed in the Universe. The Planck satellite, to be launched in 2009, will provide important cosmic microwave background data for constraining the neutrino sector. Using a new statistical analysis technique that we have developed, called ``cosmic calibration”, we have worked on building an accurate method to predict the small temperature fluctuations that will be observed by Planck. The method works over two ranges corresponding to large and small spatial scales on the sky. This work has now been completed, more than achieving the required target. A paper is under preparation.

A typical analysis of observational data can involve hundreds of thousands of associated theoretical simulations to find out which model best describes the data. This process can become very expensive if a large number of parameters have to be determined at high precision. We replace the simulation runs by a very fast ``look-up’’ technique called emulation, that allows many different analyses with many different assumptions. Thus, the emulators will be very useful for extracting scientific information from Planck data and for optimizing the process for doing so.

The effect of neutrinos on the distribution of matter in the Universe is very difficult to calculate accurately. This is because neutrinos have small masses and appreciable velocities at the start of the numerical simulation that must be performed for determining their effect on the distribution of the rest of the matter. These simulations have two species of particles, the neutrinos and the dark matter, both evolving under the influence of gravity in an expanding Universe. The small masses of neutrinos lead to artifacts arising from numerical effects due to their interactions with the much heavier dark matter simulation particles. We have found that all neutrino simulations to date have been contaminated by these problems to a significant extent. We have found that the best way to get around this problem is to fix the number of simulation particles so that all the particles in the simulation have the same mass (this means that there will be many more dark matter particles than neutrino particles). This makes the simulations accurate, however, the required number of particles is now very large and requires a significantly more complex simulation code. A new high-performance code that will serve to minimize these problems is almost complete. This code will function as a new module in the Roadrunner Universe simulation framework now being written to run on the world's fastest computer (Roadrunner at Los Alamos). A new routine that will work with sterile neutrinos will also be part of this code. The code itself and results from it will be presented in two publications.

Sterile neutrinos -- depending on their mass -- suppress the formation of structure in the cosmological mass distribution at small length scales. Such a suppression can be detected using observations from galaxy surveys of the Universe such as the Sloan Digital Sky Survey (SDSS). We are working on a new analysis of SDSS data. Coupled with this analysis is an improvement in the numerical simulations that avoids artifacts produced by not having enough simulation particles.

## Future Work

Precision cosmology provides key observational probes of the neutrino sector. Cosmological observations can be very sensitive to the neutrino mass, while terrestrial experiments strongly constrain the mass differences, but provide less stringent constraints on the absolute mass. Cosmology also provides constraints on the existence of possible additional types of neutrinos that have no conventional Standard Model interactions, the sterile neutrinos.

This proposal takes an integrated approach to addressing three problems we believe to be the most promising scientifically as well as timely in terms of upcoming observations and experimental results. These are the total neutrino mass, the number of neutrino species, and constraints on the sterile sector. The analysis requires significant advances in theoretical predictions for the effects of neutrinos on the microwave background (high-resolution data from Planck and polarization results from ground-based observation) and large scale structure (results from galaxy surveys, weak gravitational lensing, and analysis of the quasar Lyman-alpha forest), and in combining observational and experimental data with results from large-scale simulations to yield the required constraints with robust error bounds. As a consequence of some recent work at Los Alamos, we are in an excellent position to achieve mass limits of order .05 eV, constrain the number of neutrino species within +/- .2, and to confirm or exclude sterile neutrinos as a warm dark matter candidate.

## Conclusion

The Standard Model (SM) of particle and nuclear physics is one of the crowning scientific achievements of the last century. Despite its successes, the SM is incomplete. The dominant components of the Universe -- dark energy and dark matter -- are not included in the SM. Nonzero neutrino masses also provide compelling evidence for physics beyond it. Significantly, cosmology and neutrino physics are themselves inextricably connected. We expect to attain significantly improved constraints on the sum of neutrino masses, the number of neutrinos, and how structure formation in the Universe is influenced by the neutrino sector.

# Finding the First Cosmic Explosions

*Daniel Holz*

20080080ER

## Introduction

The goal of this project is to determine whether the very first stars in the Universe can be directly observed. Although our understanding of cosmology on the largest scales and at the earliest times is secure, we have a shaky understanding of how we go from small density perturbations at very early times to the rich structure we see today. In particular, the process of galaxy formation is still quite mysterious. The key component of this process is the formation of stars. In this project we are exploring whether it is possible to directly image the very first stars to form in the Universe, and thus test a key underpinning of cosmology.

In the first year we have generated many of the components essential to addressing the key elements of this proposal. We have estimates of the event rates of the first generation of stars, as well as preliminary lightcurves of the stars themselves. We have also developed initial results for the lensing distributions at high redshifts. These three components are now in the process of being combined into a robust pipeline, specifically addressing whether the first generation of stars can be directly imaged.

## Benefit to National Security Missions

Large-scale computer simulations are being used to study the basic science of stellar evolution. Current hydrodynamic codes are used and tested in astrophysical environments, contributing to the verification and validation effort. Techniques being developed to simulate and predict observational data may contribute to threat reduction missions.

## Progress

The very first stars in the universe end their lives in the most powerful thermonuclear explosions in all of nature (Figure 1). Although these events are intrinsically extraordinarily bright, we have yet to observe them. These stars, a critical underpinning of our cosmological model, are only known to exist on paper and in large computer simulations. In this project, we are developing an approach to directly observe these events, thereby either confirming a pillar of cosmology, or revolutionizing our understanding of star formation.

*Figure 1. An infrared image of NGC 1260, produced using adaptive optics at the Lick Observatory. The bright fuzzy dot is supernova SN 2006gy, the most energetic stellar explosion ever recorded. It is thought to be the death of a massive star, and could be representative of the type of supernovae expected from the very first generation of stars in the Universe.*

Current simulations of the formation of the first stars in the universe suggest that these stars were extremely massive, some hundred times more massive than typical stars today. These stars formed from primordial matter, consisting of only hydrogen and helium, at a time when the universe was less than 1% of its current age (just a few 100 million years after the Big Bang). They likely lost little mass in their evolution, and ended their lives in immensely powerful thermonuclear explosions (that were up to a factor of 100 times more powerful than Type Ia supernovae, the tremendously bright cosmological standard-candles). Direct observation of the death throes of one of these first stars continues to elude us. Although they are a critical underpinning of modern cosmology, clear confirmation of their existence is wanting. While we have a mature theoretical

edifice describing the collapse of the very first structures in the universe, and the subsequent birth of the first stars, we have neither direct nor circumstantial evidence that these processes actually did not occur, nor that this first generation of stars ever existed.

We are exploiting gravitational lensing, a uniquely powerful tool to probe the high-redshift universe (Figure 2). The gravitational effects of matter near the line-of-sight to a distant object impacts the observed brightness and shape. In extreme cases, this lensing can cause tremendous increases (>100X) in the apparent brightness of a distant source. In addition, as the sources move to higher redshifts, the likelihood for these strong lensing effects increases. Gravitational lensing offers the possibility of transforming the death of a first star at the very edge of the universe into an event easily observable by modern surveys. Most lensing studies to date have focused on sources at low redshifts (z<5), since it has not been thought that there would be significant numbers of bright, compact sources at much higher redshift. In this project we are extending lensing calculations to very high redshifts.

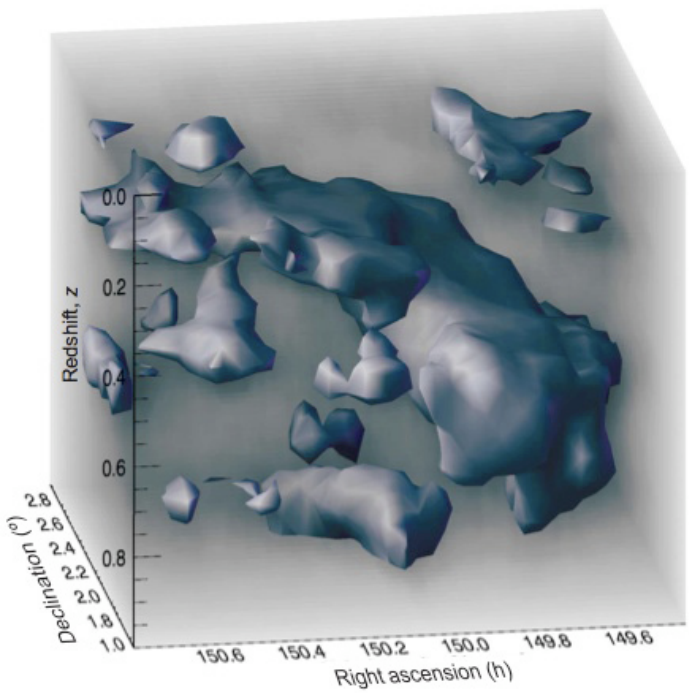


*Figure 2. Large-scale three-dimensional distribution of dark matter, as determined by weak gravitational lensing. This map was generated by the COSMOS group, using an unprecedented 575 pointings of the Hubble Space Telescope (Massey et al. 2007). The map loses signal at redshift z ~ 1. We are interested in lensing magnification effects out to z ~ 20.*

This project relies on two major areas of expertise at LANL:

- Simulation of the first generation of stars.
- Calculation of gravitational lensing from large-scale structure.

On the simulation side, a number of different codes are being utilized. Brian O'Shea is using ENZO, Alex Heger is using KEPLER, and Dan Whalen is using ZEUS-MP. Each of these codes has been significantly developed to be able to address the problem of the first generation of stars, which are found in unusual environments when compared to stars "today". Although preliminary results are in 1D, the next phase of the project will generalize these results to 2D (and, in some cases, 3D).

The calculation of gravitational-lensing effects is being done with the SUM code developed by Daniel Holz. This code is being significantly generalized and extended to be able to calculate effects to very high redshifts (z>15). The code now incorporates a range of models for the matter distribution in galaxy and galaxy clusters in the Universe, including isothermal spheres and Navarro-Frenk-White profiles. In addition, the code takes advantage of the recent developments at LANL in determining an accurate mass function for dark matter halos.

This project has made significant progress in its first year. There are three major calculations, which need to be performed:

- The event rate of Pop III supernovae.
- The lightcurves of Pop III supernovae.
- The gravitational lensing distributions at high redshift.

Preliminary estimates of all three of these quantities are now available.

Brian O'Shea has produced event rates, taking simplified models of stellar "self-quenching", and neglecting the presence of metal-enriched stars. These results show a range of possible event rates, peaking at values of 1e-6 SNe/Mpc^3/year. These high event rates indicate that Pop III SNe is likely to occur during any reasonable survey mission (Figure 3).

Both Alexander Heger and Dan Whalen have produced preliminary lightcurves, using different codes with different approximations. In particular, Heger has produced over 1000 lightcurves, varying parameters such as the mass of the progenitor star and the energy of the explosion. This constitutes far-and-away the largest set of lightcurves in existence. Using the luminosity and radius, we will be able to infer the effective temperature of the supernovae, and thus estimate the colors of these first objects. This is pre-

cisely the information we need to determine what would be seen in telescopes. Although these first results are rudimentary, they establish a baseline. Thus at the end of the first year we have now made significant progress, with robust estimates of how often the first cosmic explosions happen, and at what distances. In addition, we now know how bright these explosions are, and how their brightnesses evolve, as well as the colors. This latter information is particularly important, as these objects happen at high redshift (>10), and thus only "blue" objects will remain in the optical band. To estimate whether a first supernova will be seen, we need to know not only how bright it will be, but also what color the light will be, so we can identify the instruments to use to detect them.

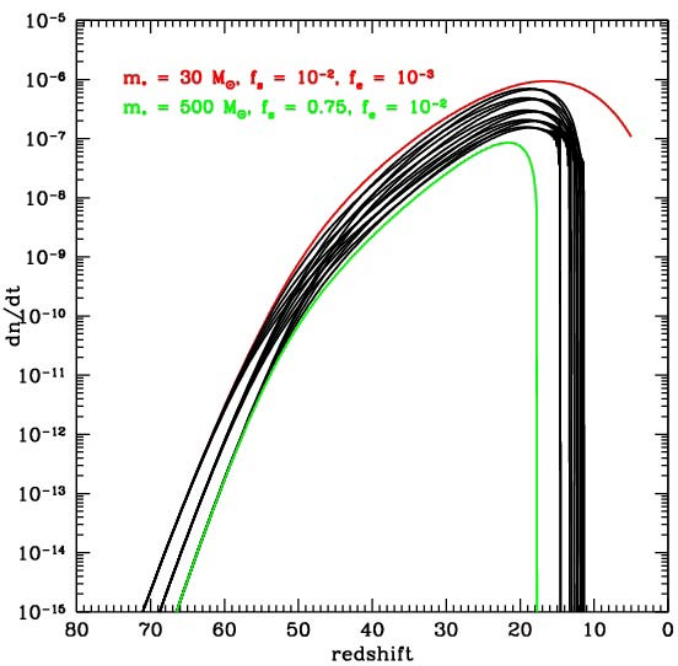


*Figure 3. Preliminary plots for the event rate of Pop III supernovae, as a function of mass of the progenitor stars. The rate is in units of # per cubic Mpc per year.*

Daniel Holz has made significant progress on the gravitational lensing calculations. We have taken the stochastic universe method (SUM) cosmological lensing code, and generalized it in two important ways. First, we have accounted for the distribution of masses of galaxies (and galactic halos) in the Universe. To do this we have incorporated the Los Alamos mass function, which was published in 2006 by Warren, Abazajian, Holz, & Teodoro. This mass function is good to 5%, and is the definitive result to date. In addition, we have incorporated the Navaro, Frank, & White halo mass distribution into the code. Previously the SUM approach relied on isothermal spheres. The NFW description is expected to be a more accurate approach. The SUM code now produces results for the gravitational lensing out to redshift of ~5, which is significantly higher than has ever been achieved previously. We are in the process of further refining this code, and intend to push it out to redshift ~20, the distance at which the very first cosmic explosions are thought to occur.

## Future Work

As discussed in detail in the previous section, tremendous progress has already been made in the two major components of this proposal:

- Simulation of the first generation of stars.
- Calculation of gravitational lensing from large-scale structure.

Both of these steps will now be generalized and refined, including a transition from 1D to 3D for the simulations, and an extension from redshift ~5 to redshift greater than 10 for the lensing calculations. Once this has been accomplished, we will be able to incorporate everything into a robust pipeline, and definitively address the key questions of the proposal: can we directly image the first stars?

## Conclusion

In summary, we are slightly ahead of the schedule found in the proposal, and expect to have initial results for detectability of the first cosmic explosions in the coming year. This project has already made significant strides, producing preliminary values for all three of the key quantities (SN event rates, SN lightcurves, and lensing distributions). We have also produced 7 papers on our ongoing work. Over the coming year all three of the key results will be refined and generalized. In addition, these will be incorporated to make the first estimates of what might actually be seen from Earth. By the end of the coming year we expect to have initial values for the likelihood of directly observing the death throes of one of the very first stars in the Universe.

## Publications

Heger, A., and S. Woosley. Nucleosynthesis and evolution of massive metal-free stars. Astrophysical Journal.
Hu, W., D. Holz, and C. Vale. CMB cluster lensing: cosmography with the longest lever arm. 2007. Physical Review D (Rapid Communications). 76 (12): 127301.

Joggerst, C., S. Woosley, and A. Heger. Mixing in zero and solar metallicity supernovae. To appear in Astrophysical Journal.

Lai, D., M. Bolte, J. Johnson, S. Lucatello, A. Heger, and S. Woosley. Detailed Abundances for 28 Metal-poor Stars:

Stellar Relics in the Milky Way. 1524. Astrophysical Journal. 681: 2008.

Sarkar, D., A. Amblard, D. Holz, and A. Cooray. Lensing and supernovae: quantifying the bias on the dark energy equation of state. 2008. Astrophysical Journal. 678: 1.

Tinker, J., A. Kravtsov, A. Klypin, K. Abazajian, M. Warren, G. Yepes, S. Gottlober, and D. Holz. Toward a halo mass function for precision cosmology. To appear in Astrophysical Journal.

Woosley, S. E., S. Blinnikov, and A. Heger. Pulsational pair instability as an explanation for the most luminous supernovae. 2007. Nature. 450: 390.

# Materials and Device Optimization Towards Room Temperature Spin-Transport Through Single-Walled Carbon Nanotubes

*Stephen K Doorn*

20080164ER

## Introduction

Controlling and manipulating electron spin for information processing adds new dimensionality to electron function that promises quantum leaps in computing capability through higher device densities and dramatically decreased power consumption. The challenge of realizing room-temperature spintronics boils down to that of controlling the mechanisms for loss of spin information. Carbon nanotubes are uniquely promising for meeting this challenge, due to their low spin-orbit coupling and structural perfection. These characteristics will promote long spin lifetimes and spin-diffusion lengths. Our approach to developing nanotubes as spin-transport materials is to focus on the following specific areas: 1) Maximize spin-polarization of the electrodes through improvements in domain structure via advances in epitaxial materials synthesis. 2) Maximize spin-injection into the nanotubes through engineering of the electrode/nanotube interfacial composition and interaction. 3) Minimize spin loss through minimizing spin scattering in the nanotube by use of suspended CVD-grown single-walled structures that eliminate defect scattering sites.

## Benefit to National Security Missions

This project directly addresses DOE's goals of developing advanced functional nanomaterials. Additionally, our approach is aligned with needs for developing new materials and technologies for enabling next-generation computing capability.

## Progress

This first year of the project has been a capability-building year. We have built a new capability for coordinated efforts in nanotube synthesis, magnetic thin-film development, nanotube device fabrication, and nanotube characterization. The year has also produced some unexpected personnel challenges. Our original intention was to work with Yuntian Zhu of MST-STC to provide the long single walled carbon nanotubes required for our device studies. Yuntian has since left LANL. We filled this hole in capability by developing our own synthesis apparatus and by leveraging past collaborative efforts with Prof. Jie Liu of Duke University. Additionally, the original postdoc intended for this project (Sandip Niyogi) also left LANL. We have since hired a new postdoc to take his place.

### CVD Capability for synthesis of long SWNTs

For our first generation of devices, we have been obtaining SWNTs from Jie Liu (Duke University). These are originally grown as relatively dense parallel arrays of nanotubes using a quartz substrate. The nanotubes follow the crystal planes during growth, thus resulting in their highly parallel nature. We transfer these tubes to the silicon substrates useful for our measurements by coating the parallel array with PDMS, lifting of the array, redepositing it on silicon, then dissolving away the PDMS. The SWNTs are then left in a pristine state on the desired silicon substrate. We have performed AFM on the test samples to evaluate the effectiveness of the PDMS removal step. Some residue has been left behind and we are currently evaluating the ability to remove the remaining residue through a combined sonication/solvent wash. Sonication conditions must remain gentle to prevent simultaneous removal of the nanotubes from the substrate. In order to not be reliant on an external collaboration as a source for our nanotubes, we have also proceeded with building an identical capability at LANL. To date we have set up the required apparatus (see Figure 1). This consists of a tube furnace coupled to the necessary mass-flow controllers required to generate the nanotube growth catalyst, followed by introduction of a carbon source (ethanol in our case) to generate the desired SWNTs.

*Figure 1. New C-CDE capability for performing CVD growth of SWNTs.*

**Device Fabrication**

For our first-generation device, we have devised a multi-step fabrication procedure as follows. A pattern consisting of locations for registry marks, trenches, ferromagnetic electrodes, and gold connecting electrodes was designed using AutoCAD (Figure 2). Patterning of silicon substrates with native oxide layer was done using e-beam lithography (in collaboration with Elshan Akhadov at Sandia). First, the registry marks for all subsequent patterning were etched into the substrate. This step was followed by etching a series of trenches (~200 nm deep, 1 um wide) over which our nanotubes would be deposited. The substrates (7 in total) were then shipped to Duke University, where Jie Liu's group deposited the parallel nanotube arrays. The samples were returned to Sandia, where they were then patterned for ferromagnetic electrode deposition ($La_{0.7}Sr_{0.3}MnO_3$, or LSMO, in this case). Our next step will be the deposition of the electrodes, followed by patterning and deposition of the gold contact electrodes. At this point the samples will be ready to be evaluated for magneto-transport characteristics. In addition to the LSMO electrodes, two substrates are being set aside for Co deposition for comparisons.

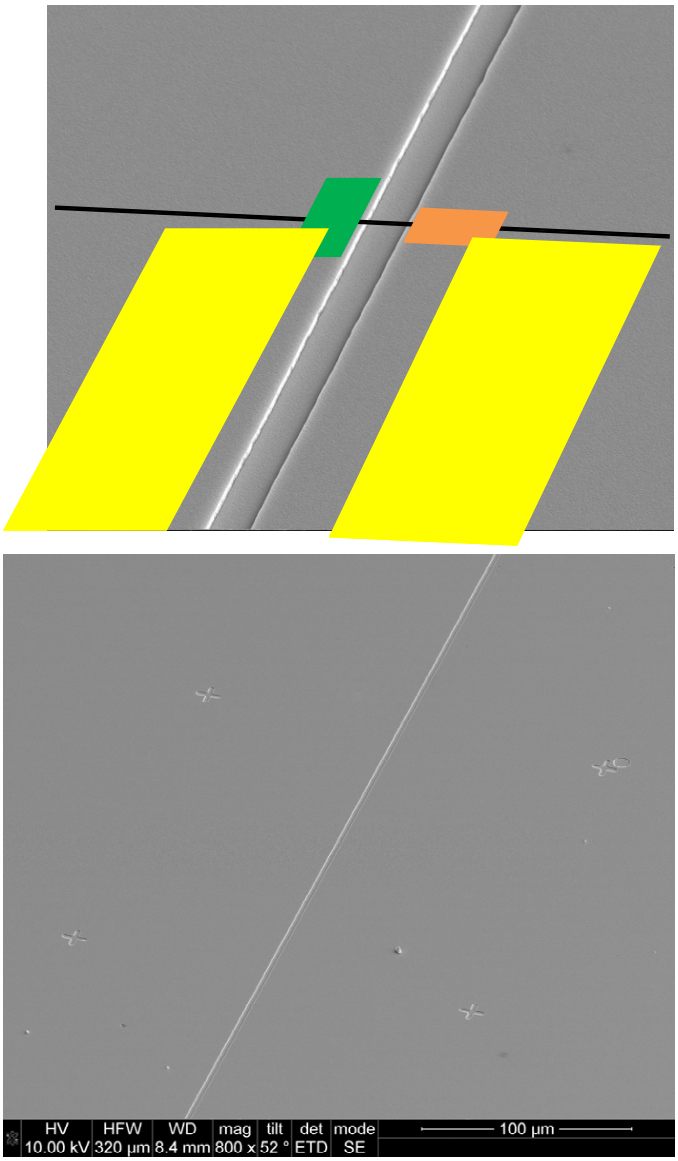


*Figure 2. a) Pattern used for guiding device fabrication (top) showing ferromagnetic electrodes (green and orange), gold contacts (yellow) and nanotube (black) over trench. b) Current stage of first-generation device: registry marks plus trenches etched in silicon substrate (bottom).*

**LSMO Film development**

Silicon with native oxide is a new, untried, substrate for LSMO deposition, so prior to the deposition of these electrodes we must first evaluate the optimum growth conditions for suitable high quality films. Lowest-T depositions compatible with good magnetic properties (minimal domain appearance) are necessary to prevent degradation of our nanotubes and the patterning mask. The deposition apparatus for this particular material was developed over the past year and is now complete (see Figure 3). It is currently undergoing some simple tests, after which we intend to begin a parameter study for optimal growth of the LSMO films.

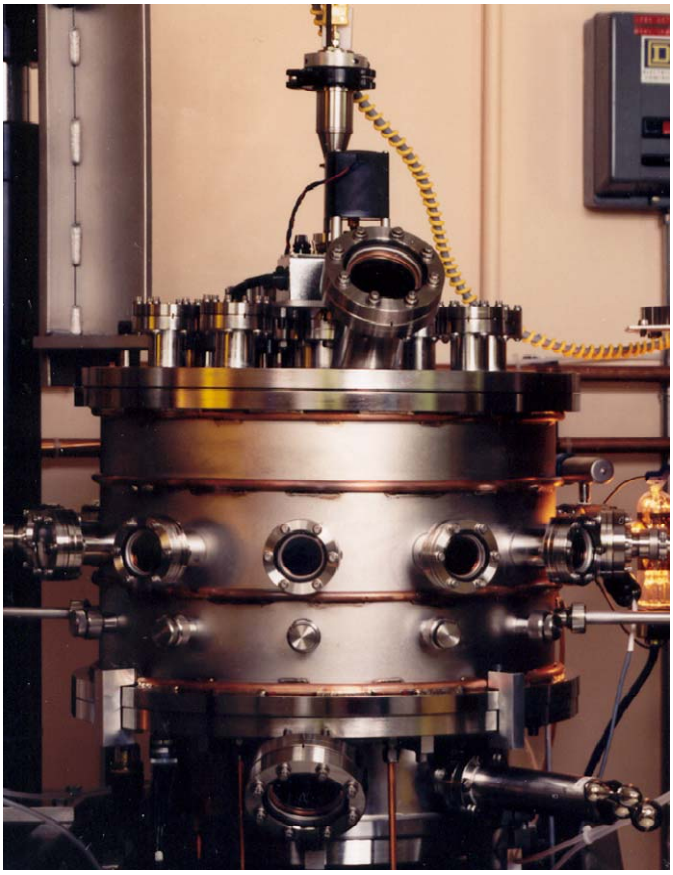

*Figure 2. Epitaxial deposition chamber for growth of LSMO thin film electrodes*

**Nanotube Defect Characterization**

A critical aspect of our project is the evaluation of sources for spin scattering in our devices, which would ultimately limit the degree of spin-transport we are able to attain. Sources we are currently interested in evaluating are substrate-nanotube interactions and also defect sites within the nanotubes. Defect sites will be evaluated in two ways. The first is via Raman spectroscopy and the second is via transport measurements. We are establishing an advanced capability to perform such measurements. Transport measurements will include STM surface potential capability, which provides an ultimate resolution of defect sites and looks at direct conductance transversely through the tube walls and provides high spatial resolution of defect sites (which will limit observed conductance). Another approach will be the use of local conductance measurements, in which a bias voltage is applied along the length of a tube via an AFM tip. To date we have generated the appropriate substrates and electrode structures to pursue these measurements. We have also developed a powerful new single-tube Raman capability in collaboration with Han Htoon of MPA-CINT. This new instrument is a Raman microscope coupled to both a tunable laser excitation source and tunable detection. This highly versatile system will allow us to probe defect structure (through its effects on nanotube phonon modes) for a wide range of nanotube diameters and chiralities. To date, in addition to establishing this new capability, we have also demonstrated the ability to obtain spectra of single-tube device structures. This Raman approach will be our workhorse method for evaluating defect effects on transport in our working devices.

## Future Work

Our current focus is completion of the first generation device so we can proceed to magneto-transport measurements, coupled to an evaluation of how transport is affected by nanotube defect structure and substrate interactions. Spin-scattering effects will be probed by intentionally introducing defects into the nanotube structure via e-beam irradiation or chemical etching of the tubes. Optimization of ferromagnetic film growth will also proceed in the next year. As our CVD system is now online, we will also be developing protocols for synthesis of appropriate nanotubes to enable our device fabrication and measurements. We anticipate that these areas will be completed within the current fiscal year.

## Conclusion

In the first year of this project we have established both internal and external sources for the carbon nanotube transport channels to be used in our investigations. Furthermore, we now have in place the necessary device fabrication capability and are well-along the path to having our first functioning test devices. We have also established instrumentation and techniques for advanced ferroelectric film growth and defect characterization. We are well placed for performing our first spin-transport measurements in the first half of the second year and anticipate developing second generation devices and probing fundamental scattering measurements in FY09.

continuing project

# The First Precise Determination of Quark Energy Loss in Nuclei

*Ivan Mateev Vitev*

20080201ER

## Introduction

Precise theoretical and experimental determination of the stopping power of materials for electrons was one of the great early successes of the classical and quantum theories of electro-magnetic interactions. Today, its practical applications range from medical imaging to national security applications, such as proton and muon radiography. In contrast, very little is known about the stopping power of nuclear matter for strongly interacting particles, such as quarks. It is widely recognized in the nuclear and particle physics communities that progress in this area is urgently needed. It will have immediate impact on our understanding of the fundamental forces in nature and the interpretation of the data coming from the current and future heavy ion experiments (areas of basic research where the US has made large strategic investments). This project embraces the unique opportunity to make the first precise determination of quark energy loss in large nuclei using as a platform upcoming experiments at the Fermilab and JPARC facilities in the US and Japan, respectively. It is based on a synergy of novel theoretical techniques (first ever calculation of initial-state energy loss), improvements in detector technology (design and deployment of readout electronics) and development of software simulation packages (optimization of the experimental setup for the breakthrough measurements). We expect that the successful completion of this project will lead to the determination of the shortest radiation length (a fundamental characteristic of the strength of particle-matter interactions) ever measured in nature.

## Benefit to National Security Missions

This project will support DOE's mission in Science by enhancing understanding of "Nuclear Matter in Extremis," a primary goal of the Office of Science and LANL's Beyond the Standard Model capability. Technology developed will support National Security areas of Threat of Weapons of Mass Destruction and Detection of Nuclear Materials.

## Progress

Theory: We have completed the theoretical derivation of the stopping power of cold nuclear matter for particles of "color" charge, such as quarks and gluons. We used a formal recurrence relation approach to multiple parton scattering to find the complete solution to the problem of medium-induced gluon emission from partons propagating in such medium. The differential bremsstrahlung spectrum, where Landau-Pomeranchuk-Migdal quantum-mechanical destructive interference effects are fully accounted for, was calculated for three different cases: 1) a generalization of the incoherent Bertsch-Gunion solution for asymptotic on-shell jets, (2) initial-state energy loss of incoming jets that undergo hard scattering, and 3) final-state energy loss of jets that emerge out of a hard scatter. Our analytic solutions were given as an infinite opacity series, which represents a cluster expansion of the sequential multiple scattering. These new solutions allowed, for the first time, direct comparison between initial- and final-state energy loss in cold nuclei. We demonstrated that, contrary to the naive assumption, energy loss in cold nuclear matter can be significant. Numerical results to first order in opacity showed that, in the limit of large jet energies, initial- and final-state energy losses exhibit different path length dependences, linear versus quadratic, in contrast to earlier findings. In addition, in this asymptotic limit, initial-state energy loss was found to be considerably larger than final-state energy loss, as shown in Figure 1.

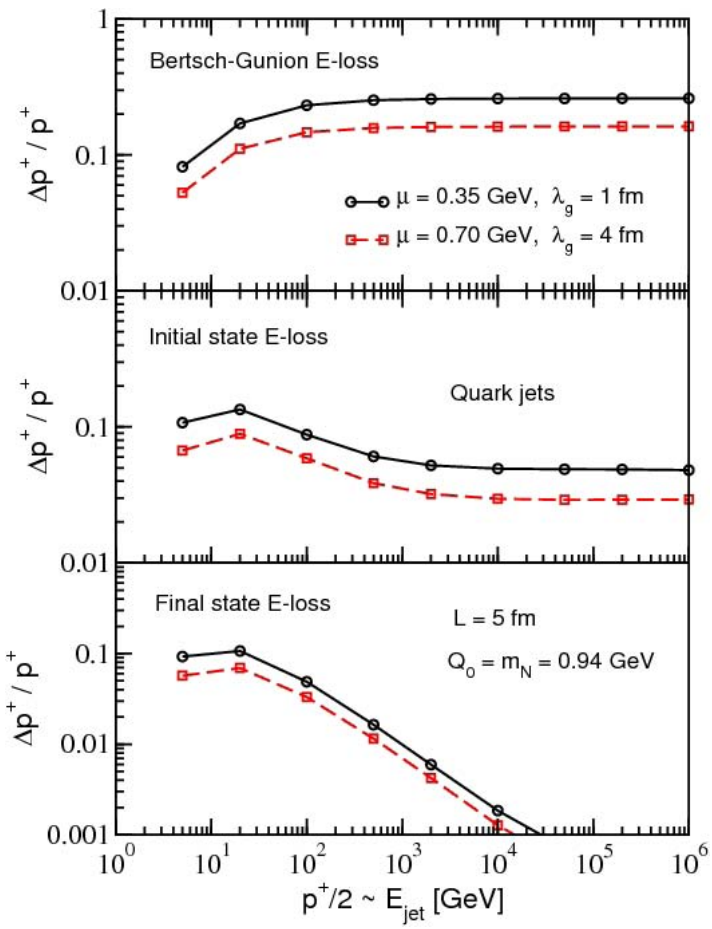


*Figure 1. Comparison of the fractional energy loss for 3 different energy loss regimes in cold nuclear matter. The middle panel represents the case pertinent to the Drell-Yan process in proton-nucleus collisions.*

We are also in the process of finishing a next-to-leading order code for Drell-Yan production.

Hardware (muon ID): We have completed the basic design and construction of a muon identifier for the E906 experiment. The identifier will have two horizontal and two vertical detector layers, each with an area of ~250 * 250 cm. The identifier is composed of aluminum drift tubes that will provide both good position resolution and track matching to the Station 3 drift chambers. Each detector layer is constructed of two staggered rows of 2" diameter tubes. This arrangement provides for excellent efficiency with reasonable channel count. The identifier has been instrumented with Nanometrics N-277 amplifier / discriminator electronics with emitter-coupled logic outputs. The outputs were digitized using CAEN VME-based time-to-digital converters controlled by the PC-DAQ data acquisition system developed by Dr. Gary Hogan.

768 drift tubes were assembled and successfully tested using an argon-isobutane (70:30) gas mixture with a high voltage setting of +2300V. Final data taking and analysis were completed with vertical cosmic ray muons, see Figure 2, at the LANSCE facility by Dr. J. Andrew Green. A position resolution of ~300 microns was obtained, together with a muon detection efficiency of over 99%. The maximum drift time was ~1.6 microsecond. This level of performance is more than adequate for the E906 experiment. The detector layers were then disassembled and placed into storage, ready for shipment to FNAL.

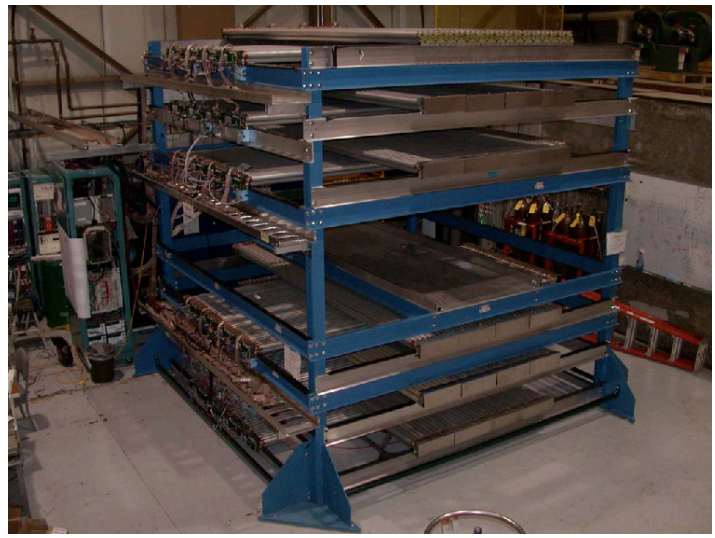

*Figure 2. Cosmic ray test setup for the muon identifier elements at Los Alamos Neutron Scattering Center. The support structure is shown in blue and the 2" drift tubes are silver.*

The commercial readout electronics used on the tracker were found to suffer from significant channel-to-channel crosstalk and are prone to oscillate. We designed and deployed a complete set of replacement electronics employing modern components with low voltage differential signaling outputs. These include a new amplifier / discriminator, time-to-digital converter and programmable high voltage supply. A novel feature of this new readout system is that we used universal serial bus interfaces (USB) to perform all of the communication and detector readout, which greatly decreased the total cost and complexity. More than 4000 channels of the new electronics have been built and tested, providing high efficiency with a near zero noise rate. The final choice of electronics installed in E906 will depend upon the design of the experiment's data acquisition system, which is presently underway.

Simulation: We have developed an event generator simulation package for fixed target p+p and p+n collisions based on PYTHIA and ROOT libraries from CERN. We have generated 100 Million Drell-Yan events in p+p collisions at beam energy of 120 GeV that we expect to have at the E906 experiment at Fermilab. The full simulated events have been analyzed to study the kinematic distributions of the muon pairs produced in the Drell-Yan process. To study the backgrounds, 10 Million of minimum biased and charm quark events were also generated and analyzed. Initial study

showed that we can clearly identify the Drell-Yan signal from other backgrounds in the di-muon channel, and there is a clear correlation between high mass di-muon rapidity and the initial quark's momentum (or the x1 parameter), which is very important for the proposed quark energy loss study, see Figure 3.

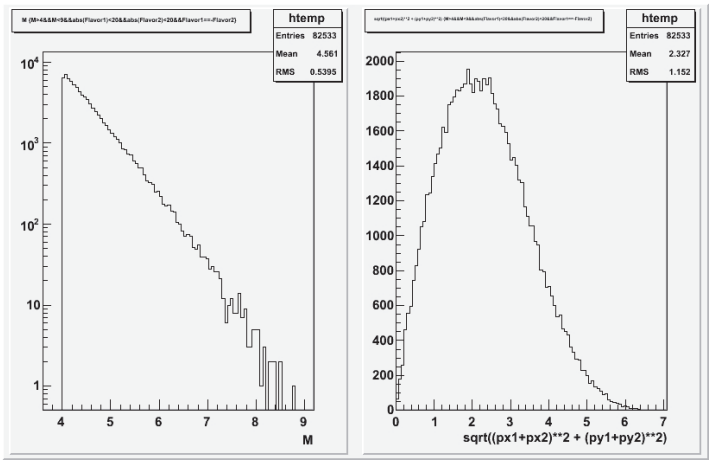


*Figure 3. DY to di-muon simulations, corresponding to about 5% of the expected p+p statistics. The left-hand plot shows the di-muon mass distribution, the right hand plot shows the dimuon transverse momentum distribution.*

In next a few months, we will implement the theoretical energy loss calculations into our simulation to study experimental sensitivity to the determination of quark energy loss parameters and publish our results.

## Future Work

The biggest gap in our knowledge of nuclear reactions in extremis is the stopping power of cold nuclei for quarks and gluons. The goal of this LDRD ER project is to successfully complete a joint theoretical and experimental initiative and provide the first precise determination of the stopping power of cold nuclear matter for strongly interacting particles.

The theoretical derivation of the radiative energy loss of quarks and gluons in nuclear matter has been completed and published. We will soon produce a next-to-leading order code for Drell-Yan, the specific physics process of interest. We employ the collinear factorization scheme of perturbative Quantum Chromodinamics to calculate the differential cross sections and will carry out comparison to existing Drell-Yan data. We are also in the process of generalizing this code to the case of large nuclei so that important many-body effects, such as isospin, the Cronin effect, nuclear shadowing and our derived radiative energy loss can, be seamlessly incorporated.

We are still scheduled to begin running in January of 2010 and E906 is now decoupled from the Tevatron running. Currently the collider run extends into 2010. We are awaiting a schedule from Fermilab concerning when they can install the magnet and beam line. Due to the "continuing resolution" recently passed by Congress, our starting date will likely slide. Our plan is still to install the muon detector at Fermilab by the end of this year. In the coming a few months, we will perform an electrical continuity test of all of the anode wires and check that all of the readout electronics are working with an external pulser. After the completion of the electrical tests, the proportional tubes will be shipped to Fermilab for installation in the experimental hall.

In January of 2010 we will host an E906 software meeting at LANL where we will distribute the software from our previous experiment. We will also present a series of tutorials on the function and operation of the software, with the goal of preparing collaboration members to write a new particle tracker for E906 in the "C" language.

## Conclusion

We provided consistent theoretical derivation of the stopping power of nuclear matter for strongly interacting particles. Work has begun on identifying signature observables that can be used to experimentally determine the energy loss of these particles in nuclear matter. We have started adapting instrumentation developed for homeland security to instrument an experiment at either Fermilab or JPARC to carry out the pivotal measurements of energy loss. Simulation software development for this project is under way. This software will also be useful for future heavy-ion research. Successful completion of this work will enhance our understanding of nuclear matter under extreme conditions, such as in the early universe.

## Publications

Liu, M.. Future high energy dimuon experiments at Fermilab and JPARC. Invited presentation at *LBL seminar.* (Berkeley, CA, 2007).

McGaughey, P.. E906 muon identifier status. Invited presentation at *E906 Collaboration Meeting at Fermilab.* (Batavia, IL, 20-21 June 2008).

Vitev, I.. Non-Abelian energy loss in cold nuclear matter. 2007. *Physical Review C.* **75**: 064906.

Vitev, I.. Theoretical developments in heavy and light flavor energy loss. 2008. In *Quark matter 2008.* (Jaipur, India, 4-10 February). , p. 104011. Journal of Physics G: IOP.

Vitev, I.. The first precise determination of quark energy loss in nuclei. Invited presentation at *E906 Collaboration Meeting at Fermilab.* (Batavia, IL, 20-21 June 2008).

Vitev, I., and B. Zhang. A Systematic study of direct photon production in heavy ion collisions. To appear in *Physics Letters B.*

Zhang, B., and I. Vitev. Direct photon production in d+A and A+A collisions at RHIC. To appear in *Hot Quarks 2008.* (Estes Park, CO, 17-23 Aug. 2008 ).

# Entanglement in Quantum Ground States

*Matthew B Hastings*

20080342ER

## Introduction

This project studies the nature of ground states in quantum systems from the point of view of quantum entanglement. The idea of quantum entanglement is behind the rapidly developing fields of quantum computing and quantum key distribution. Quantum computers that take advantage of entanglement may be able to perform computations that are not tractable on a classical computer. Within the field of quantum computing, the study of quantum entanglement involves looking at very carefully engineered states, which are created by carefully controlling the system. On the other hand, this project looks at the kind of quantum entanglement, which is present in naturally occurring systems. We consider the entanglement in ground states of local quantum systems. This offers two possible rewards. First, certain naturally occurring ground states, like those in the quantum Hall effect, have nontrivial entanglement that can be used to do quantum computation, without requiring the careful control required by other approaches. This approach, called topological quantum computation, is a possible very robust approach to quantum computation. Second, many other naturally occurring ground states have fairly simple entanglement, and can well be described classically. Then, it should be possible to develop novel algorithms to model the ground state and dynamics of these systems using existing classical computers. This can lead to new advances in materials.

## Benefit to National Security Missions

This project supports the DOE Office of Science Mission in Basic Energy Sciences by enhancing our understanding of ground state properties of quantum systems such as in materials science and quantum chemistry, and by enhancing our understanding of which systems are useful for building a quantum computer.

## Progress

Constructed explicit bounds on entanglement entropy for ground states general quantum systems in one dimension, and also provided bounds for the entanglement entropy for quantum systems in thermal states [2]. This accomplishes one of the FY08 milestones "Determine bounds on entanglement entropy such as area laws for quantum systems". We have also made progress on proving the ability to represent the ground state of such Hamiltonians as matrix product states, which provides part of one of the FY09 milestones. In addition, we have been studying dynamics in these systems. In many cases, when a quantum system is perturbed, the perturbation leads to an increase in entanglement entropy with time. The increase in entanglement entropy with time makes it difficult to simulate these systems. We have developed a novel algorithm, called the "light-cone method", that increase the range of times over which some of these systems can be studied, and applied it to study of dynamics relevant to cold atoms. On the system sizes studied, the light-cone algorithm is roughly 1000 times faster than competing algorithms, with roughly 1000000 less memory usage. This permits the study of dynamics in systems in cases [8], which are completely intractable by competing approaches. We have begun a collaboration with Ulrich Schollwock, a professor at Technical University of Aachen and an expert on numerical techniques, to combine some of these ideas with competing approaches to develop even more efficient algorithms for the dynamics.

Developed a novel algorithm to find matrix product representations for quantum systems in thermal states, called "Quantum Belief Propagation" . This algorithm has been tested against competing algorithms and exact results, and is highly accurate at high temperature and very fast. It has been applied to study of very large system sizes in disordered systems, a case not tractable by other methods. We have also begun to collaborate on this algorithm with David Poulin, who is currently a professor at University of Sherbrooke, and who independently developed very similar ideas,

creating separately a similar algorithm. We are working on extensions of the algorithm to higher dimensions, and have initial results for the two dimensional Heisenberg model. If successful on this model, we hope to apply it to models such as the Hubbard model.

Finally, we have studied different topologically distinct phases of free fermion systems [3], working towards one of the FY10 milestones "Determine possible phases of systems with a matrix product representation". We are currently trying to extend this approach to more complicated interacting systems.

Additional work on related projects has included introducing the idea of quantum expanders [7] and resolving the famous additivity conjecture in quantum information theory [9].

## Future Work

We will study entanglement in quantum ground states, with applications to topological quantum computing. The locality of interactions in physical quantum systems means in many cases that correlations and entanglement are short-ranged, restricting the type of entanglement compared to an arbitrary excited state. This enables us to accurately represent the ground state by a class of states called matrix product states, in which the entanglement is carried by a small number of auxiliary bond variables. Topological quantum computation is a concept for building a quantum computer using certain systems, which are topologically ordered, having degenerate ground states, which are protected against decoherence due to topological properties. Computation is performed by operations such as moving particles around each other. We have the following major objectives: (1) characterize ground states of local quantum Hamiltonians, using matrix product states and determine which of these states are useful for topological quantum computation (2) determine the robustness of these phases against perturbations such as disorder found in real-world systems. We will perform the following tasks: (1) determine bounds on ground state entanglement entropy, compare to area laws; (2) compute explicit matrix product operator representations for quantum Hall states and other related systems; (3) using locality properties of the Hamiltonian, determine robustness of the ground state against external perturbations and determine change in matrix product state representations; (4) determine ability to represent the ground state of an arbitrary local Hamiltonian using matrix product state; and (5) compute topological properties of entanglement entropy in matrix product states and use to study topological order in the ground state, characterizing the usefulness for topological quantum computation. Obtaining these goals will lead to new ways of building quantum computers and will advance our understanding of the fundamental nature of materials, especially strongly correlated materials and non-Fermi liquid materials.

## Conclusion

Topological quantum computing is a proposed method for doing quantum computation that avoids problems with decoherence that currently are preventing other approaches from working. We will characterize which physical systems, such as quantum Hall systems, are useful for topological quantum computing. This work will be based on a representation of the ground state using a class of states called "matrix product states". We will determine how accurately matrix product states represent physical ground states, in particular in systems with disorder. This work will also benefit our fundamental understanding of materials and simulation of quantum systems.

## References


1. Wolf, M. M., F. Verstraete, M. B. Hastings, and J. I. Cirac. Area laws in quantum systems: mutual information and correlations. 2008. *Physical Review Letters.* **100**: 070502.

2. Hastings, M. B.. Topology and phases in fermionic systems. 2008. *JSTAT.* **01**: L001.

3. Hastings, M. B.. Observations outside the light-cone: algorithms for non-equilibrium and thermal states. 2008. *Physical Review B.* : 144302.

4. Hastings, M. B., and A. W. Harrow. Classical and quantum tensor product expanders. *QIC.*

5. Hastings, M. B., and L. S. Levitov. Synchronization and dephasing of many-body states in optical lattices. *Physical Review Letters.*

6. Hastings, M. B.. A Counterexample to additivity of minimum output entropy. *Nature Physics.*


## Publications


Chertkov, M., R. Teodorescu, and V. Chernyak. Belief propagation and loop series on planar graphs. 2008. *Journal of Statistical Mechanics.* (P05): 003.

Chertkov, M., and V. Chernyak. Fermions and loops on graphs. I. loop calculus for determinant. 2008. *arXiv:0809.3479.*

Chertkov, M., and V. Chernyak. Fermions and loops on graphs. II. monomer-dimer model as series of determinants. 2008. *arXiv:0809.3481.*

Hastings, M. B.. Topology and phases in fermionic systems. 2008. *JSTAT.* **01**: L001.

Hastings, M. B.. Observations outside the light-cone: algorithms for non-equilibrium and thermal states. 2008. *Physical Review B.* **77**: 144302.

Hastings, M. B.. A counterexample to additivity of minimum output entropy. *Nature Physics.*

Hastings, M. B., and A. W. Harrow. Classical and quantum tensor product expanders. *QIC.*

Hastings, M. B., and L. S. Levitov. Synchronization and dephasing in many-body states in optical lattices. *Physical Review Letters.*

Wolf, M. M., F. Verstraete, M. B. Hastings, and J. I. Cirac. Area laws in quantum systems: mutual information and correlations. 2008. *Physical Review Letters.* **100**: 070502.

# CP-violating Moments of Atoms and Nuclei

*Anna Catherine Hayes-Sterbenz*

20080424ER

## Introduction

The "Standard Model" is a widely accepted theory that describes our understanding of matter and radiation. The existence of and precise magnitude of the electric dipole moment (EDM) is a test of some of the most basic underpinnings of the Standard Model. If and EDM is found, it signifies the existence of physics "beyond the Standard Model," providing a new breakthrough in our understanding of the Universe.

A permanent electric dipole moment (EDM) of a physical system requires time-reversal (T) and parity (P) violation. Experimental programs are currently pushing the limits on EDMs in atoms, nuclei, and the neutron to regimes of fundamental theoretical interest. The Standard Model (SM) predicts values for the EDMs in these systems that are too small to be detected in the foreseeable future, and hence a measured nonzero EDM is an unambiguous signal for a new source of CP violation and for physics beyond the SM. In this project we are calculating the magnitude of PT-violating EMDs in light and heavy nuclei and determining the expected sensitivity of such a measurement to the underlying PT-violating iterations. We are examining the complementarity of measurements in nuclei to those for the neutron in terms of their sensitivity to different components of the PT-violating interaction.

## Benefit to National Security Missions

This project will contribute to our basic understanding of forces and processes in the universe governed by the "Standard Model." It directly addresses issues in the LANL "Beyond the Standard Model" Grand Challenge and impacts basic understanding of physics that underlies nuclear weapons, a key DOE mission.

## Progress

A new experimental scheme for measuring Electric Dipole Moments (EDMs) of nuclei, stripped of their atom electrons, in a magnetic storage ring suggests that EDMs in light nuclei could be measured to an accuracy of $10^{27}$ e cm. Unlike searches for CP-violating moments of the nucleus through measurements of atomic EDMs, a measurement for a stripped nucleus would not suffer from a suppression of the signal though atomic Schiff screening. For this reason, the latter could represent about an order of magnitude better sensitivity to the underlying PT-violating interaction than the present limit on the neutron EDM.

It's small magnetic anomaly makes $^3$He is an ideal candidate for a high precision EDM measurement in a magnetic storage ring. We examined the nuclear structure issues determining the EDM of 3He and calculated the matrix elements of the relevant operators using the no-core shell model. The calculations represent an exact solution of the 3-body problem using several nucleon-nucleon interactions, complemented with three-body forces.

There are two possible sources of an EDM in 3He, one from an EDM of the individual nucleons and a second from a PT-violating nucleon-nucleon force. For the latter we use a one-meson-exchange model, including pi, rho, and omega meson-exchange.

We solved the three-body problem for the ground state of 3He by direct diagonalization of the effective Hamiltonian in a harmonic oscillator basis. To calculate the EDM requires high accuracy excited states of 3He in the continuum. For this we used a variation of the Podolsky method, which required including 40 harmonic oscillator shells to achieve convergence. In this way, we obtained an accurate description of the continuum, as demonstrated by a comparison between the calculated and measured photo-absorption cross section for 3He.

We examined results using different nuclear forces, including the CD BONN and Argonne V18 potentials. For the nucleonic contribution to the 3He EDM we found very similar results for the isoscalar and isovector EDMS from these different nucleon-nucleon potentials.

In the case of the contribution to the EDM from the PT_violating nucleon-nucleon interaction, we found that pion-exchange dominated. The PT-violating pion-

exchange potential also gave very similar results for the different nuclear potentials examined.

The rho- and omega-exchange contributions to the EDM we found to be at most 10% of the pion-exchange. This suppression was due to the very short-range nature of rho- and omega-exchange. This short-range behavior also resulted in more model dependence in the calculated contributions of these terms to the EDM, and these terms could only be calculated within 50%.

Finally, we compared the EDM of 3He with that expected for the neutron and deuteron. For the latter we used the one-pion loop expression in the chiral limit. We concluded that a measurement of 3He would provide complementary information to the neutron and deuteron and would be especially sensitive to the isotensor pion PT-violating coupling. Thus, assuming that similar sensitivities could be reached in these three measurements, stringent limits on the three pion-nucleon PT-violating coupling constants (isoscalar, isovector and isotensor) could be set from a measurement in all three systems.

## Future Work

In this project we will quantify the magnitude of CP-violating moments of those atoms and nuclei of experimental relevance and relate these to the elecri dipole moment (EDM) of the neutron. A new experimental scheme for measuring EDMs of nuclei (stripped of their atomic electrons) in a magnetic storage ring suggests that the EDM of the deuteron and of 3He could be measured to an accuracy of better that 10^-27 e cm, which is an order of magnitude better that the present limit on the neutron EDM. The LANL neutron EDM experiment, aimed at measuring d_n to an accuracy of $10^-28 e cm, requires that the measurement be made with respect to the atomic EDM of 3He. The 3He acts as a polarizer and co-magnetometer in the experiment and thus a rigorous theoretical verification that the EDM of 3He is not a significant (unknown) systematic background to the measurement is crucial. To address these issues we will calculate the first fully quantum-mechanical atomic and nuclear CP-violating moments of 3He, 225Ra, and 199Hg. These calculations will allow new measurements in atoms, nuclei, and the neutron to provide stringent limits and tests of non-Standard Model theories of the origin of CP-violation.

In the coming year we will determine the nuclear CP-violating moments of 3He. This will allow us to quantify the contribution of 3He as a background to LANL's EDM measurement. In the second year we will determine the expected signal for a magnetic storage ring measurement of the EDM of 3He, and compare it with that expected for the proton and the deuteron. In the third year we will carry out detailed shell model and Nilsson model calculations for CP-violation in heavy atoms. We will quantify the relative merits of measuring atomic EDMs in deformed nuclei as opposed to spherical nuclei.

## Conclusion

This project will determine the magnitude of the cp-violating moments of both atoms and nuclei and the relative merits of present and proposed experimental programs to search for these moments. These results will provide crucial input and support for the national experimental program to search for electric dipole moments in fundamental systems.

## Publications

Hayes, A. C., and J. L. Friar. Sensitivity of nuclear transition frequencies to temporal variation of the fine structure constant ot the strong interaction. 2007. *Physics Letter B.* **650**: 229.

Stetcu, I., C. P. Liu, J. L. Friar, A. C. Hayes, and P. Navratil. Nuclear Electric Dipole Moment of 3He. 2008. *Physics Letters B.* **665**: 168.

# Ultrafast Nanoplasmonics for Photonics and Quantum Control at the Nanoscale

*Anatoly V Efimov*

20080473ER

## Introduction

This project addresses fundamental scientific aspects of generating, manipulating, controlling and using visible electromagnetic fields (light) on the nanoscale. Our approach will be to design metallic nanostructures optimized for localization of these fields. Localization of light on the nanometer scale is of critical technological importance for connecting the field of photonics, which underpins communication technologies with nanoelectronics that enables future information technologies. Our specific challenge is to learn how to manipulate these fields, not only spatially, but also, and most importantly, temporally. The temporal aspect in local field design is extremely important for ultrafast processes in nature and technology, such as controlling molecular dynamics, steering chemical reactions, selective sensing, signal processing and communication. Thus, femtosecond optical pulses are used in our experiments to excite and measure the ultrafast dynamics of the localized fields. It is important to realize that femtosecond time scales are characteristic to many processes in nature, such as fundamental vibrations in molecules and crystals, isomerization reactions responsible for vision and energy transfer between mesosystems. Generating an understanding of and experimentally controlling the temporal profile of the localized electromagnetic fields is the cutting-edge challenge in modern science addressed in this project.

## Benefit to National Security Missions

This project will support the DOE missions of the Office of Science and contribute to Threat Reduction and Energy Security missions by enhancing our understanding of the fundamental behavior of electromagnetic fields (light) localized to the nanoscale as well as their interactions with quantum systems for sensing and communications applications.

## Progress

Theoretical: In contrast to all previous models describing behavior of local plasmonic fields, e.g. on a nanoantenna, we developed a fully quantum model in the linear nonlocal response approximation to calculate both spatial and temporal distribution of the broadband plasmonic field excited by the external spatially uniform, but temporally shaped electromagnetic radiation. The direct problem of finding localized field given the external field, and the inverse problem of computing the external field starting with the desired local control field are solved. In our work we proved that even in a quantum regime a realistic metallic nanostructure acts as a linear filter to the incoming external field, thus proving the general possibility of (temporal) control of the local electromagnetic field by sculpting the external field. For a given spatial location on or near a nanostructure the complex profile of an external field can be simply and uniquely computed from the desired local field complex amplitude profile in temporal or spectral domains (inverse problem). Importantly, this finding negates the necessity of finding the local field profile with computationally expensive iterative search algorithms (e.g. Genetic Algorithm.) This is a pioneering development since quantum control with surface plasmons has not been addressed so far. Publication is being prepared.

### Experimental

First-generation samples of metallic waveguides were prepared. These include wedge waveguides and channel waveguides manufactured by FIB on a metal-coated GaAs substrate. Metal wall quality presents a problem of large scattering leading to high loss. Alternative sample preparation techniques are being worked on and include nanoimprint lithography and direct laser writing. In parallel, metal strip waveguide samples embedded in polymer were prepared by our collaborators in U. Denmark. These samples show lower loss, due to decreased scattering and relaxed confinement due to scale.

Broadband spectral interferometry system based on supercontinuum generation in a bismuth-oxide step index fiber was developed for the phase-sensitive detection of plasmon-polariton modes outcoupled from plasmonic waveguides. The system was tested on dielectric waveguides and found capable to measure optical dispersion (0.05 rad phase noise) in 500 nanometer spectral window around 1500 nm, an important telecom wavelength range. Sensitivity of the FTIR spectrometer is an issue for plasmonic waveguides. Spectrometer upgrades are pursued.

Initial experiments on local plasmon field control were performed on subwavelength aperture array samples containing nanoholes of different shapes and sizes. Temporal shaping of the incident femtosecond laser pulse was preformed using home-build liquid-crystal spatial light modulator pulse shaper. Both linear transmission and surface second harmonic were adaptively optimized with a learning algorithm. It was found that at ~100 fs pulse duration the residual phase effects were dominant over plasmon localization and control could not be reliably detected. After theoretical analysis of the results it was determined that excitation pulses with durations comparable to relaxation times of plasmonic excitation (~10 fs) on the metal nanostructure are required for robust plasmonic field localization control. Thus, the 10 fs laser system is currently being fitted and optimized for further experiments.

## Future Work

Having established the general applicability of plasmonic nanostructures for control of the local field distribution in time, our future work will focus on experimental demonstration of control and investigation of potential applications toward control of quantum systems' dynamics using resonantly enhanced and spatially confined electromagnetic fields. To this end further and more systematic work on sample preparation will be performed.

Plasmonic waveguides of various geometric configurations will be prepared and investigated. These will be studied for broadband optical light coupling, propagation loss, degree of subwavelength confinement and most importantly there linear (dispersion) properties will be investigated from the point of view of femtosecond science. For example, discovery of anomalous dispersion in certain waveguide configurations will open up the possibility of soliton formation and propagation. Additionally, propagation loss compensation with distributed amplification will be addressed using recent developments in high optical gain materials.

Further, nonlinear propagation regimes in plasmonic waveguides will be investigated using spectroscopy of the outcoupled light. High degree of field confinement in the plasmonic nanocircuits may allow efficient nonlinear interaction to be realized in the future signal processing elements, something that was never successfully demonstrated in the integrated optical designs. Nonlinear coupling in plasmonic nanostructures may finally allow a practical realization of an optical transistor, which is not based on a bulk and narrowband interferometric schemes of the past.

Finally, we plan to begin a series of quantum control experiments using metallic nanostructures and analyte mixtures in liquid and solid forms, as well as on the surface. Initial experiments shall include an attempt to control molecular vibration dynamics of analyte systems in contact with the nanostructure using temporally shaped external femtosecond pulses with the wavelength in the vicinity of the plasmon resonance via the impulsive stimulated Raman scattering mechanism. We will compare the control efficiency as a function of pump wavelength proximity to the resonance wavelength. The control efficiency is expected to be enhanced many orders of magnitude, similar to surface-enhanced Raman scattering (SERS) efficiency enhancement observed previously.

## Conclusion

This project will attempt to advance the field of plasmonics by developing the science and technology for excitation, shaping and detection of broadband plasmonic fields bound to metallic nanostructures for the purpose of controlling the behavior of individual quantum systems and their interactions. Nanoplasmonics is an active area of study because of its importance for sensor applications in defense, security and medicine. This work will advance the current state of the art by focusing on the temporal aspect of the plasmonic fields and may lead to novel technologies and devices beyond sensors and towards control of nanoscale quantum systems.

# Probing physics beyond the Standard Model with supernovae

*Alexander Friedland*

20080636ER

## Introduction

The current theoretical understanding of matter is encoded in the so-called Standard Model (SM), which describes a large body of experimental data from atomic energy scales up to the current energy frontier of a few hundreds of GeV. Despite its successes, the SM is known to be incomplete.

The overarching goal of this project is to investigate the sensitivity of astrophysical systems to novel effects beyond the Standard Model. We specifically focus on core-collapse supernovae – the final stage in the evolution of massive stars -- and their progenitor stars. In these systems, we identify cooling and transport processes that would receive additional contributions in various proposed scenarios of new physics and compute the effects of the new physics on the evolution of each system considered.

## Benefit to National Security Missions

This project will support the DOE Office of Science missions in High Energy Physics and Nuclear Physics. In High Energy Physics, it will contribute to our understanding of the fundamental interactions. In Nuclear Physics, it will advance our understanding of hot, dense nuclear matter in astrophysics, fundamental symmetries, and neutrinos.

## Progress

In the course the first year of the project, we have pursued three physical scenarios in which new physics can affect stellar objects.

One such new physics scenario involves a class of models in which photons can escape into extra dimensions. Models of this kind have been actively discussed in the literature over the last ten years and motivated the latest round of orthopositronium decay experiments. Orthopositronium is a bound state of an electron and its antiparticle and normally decays to three photons. The prediction of the extra-dimensional models we considered is that some of the decay could involve new particles living in the fifth dimension. We realized that in this framework there would be an additional strong energy loss channel for many astrophysical systems. We considered the effect on cooling of core-collapse supernovae (as well as on red giant and horizontal branch stars). We found that the resulting astrophysical bounds on these scenarios are much more stringent (by orders of magnitude) than what can be feasibly achieved in the laboratory. The paper with the bounds has already been accepted and published in Physical Review Letters [1].

Another kind of analysis involved astrophysical bounds on the neutrino magnetic moment. Although neutrinos have no electric charge, in many extensions of the Standard Model they can couple to photons via the magnetic moment interaction. We explored, for the first time, the effect the magnetic moment would have on the evolution of massive stars. Contrary to the prevailing wisdom in the field, we found this effect is very significant, in some cases spectacular. In particular, we found that not only does the threshold masses for forming core-collapse supernovae change, but also a new kind of supernova (a white dwarf explosion inside a massive star) appears. The paper with these results has been submitted to the Astrophysical Journal [2].

Our main effort over the past year has been invested in the development of a computer model of a cooling protoneutron star (the object formed after the collapse of the iron core of the massive star) that incorporates new neutrino interactions. It can be thought of as “a particle physicists supernova model”, as it does not model the visible explosion (the hydrodynamics effects are left out), but aims to retain the physics relevant to the total energy balance, cooling time scales, and neutrino fluxes. The ultimate goal is to identify robust signatures of new physics -- such as novel interaction that can change neutrino flavor (neutrinos are known to come in three flavor states: electron, muon, and tau).

Our preliminary estimates indicate that a supernova could be orders of magnitude more sensitive to these flavor-changing effects than terrestrial experiments. In

addition to placing limits on new physics, our model should give useful predictions for the neutrino signal from a supernova within the Standard Model scenario.

To implement this program, we are building a numerical code describing the cooling of the protoneutron star during approximately 50 seconds following the core collapse. At the first stage, we are working to include all relevant effects of known physics. The code is being extensively tested in this mode, before new physics is added. The results obtained at this stage are expected to be useful by themselves: they will yield a reference prediction of the time evolution of the neutrino spectra of all flavors. The accuracy of this prediction should rival those published in the literature. They may also lead to improved understanding of neutrino decoupling and spectra formation.

We currently have the following:

- A code describing the diffusion of neutrinos in the protoneutron star as a function of time, within the framework of known physics. The different neutrino flavors are not yet separated in this code. The transition between the diffusion regime and the free-streaming regime is done with a flux-limiter prescription – there is no intermediate regime where mu and tau neutrinos are transported out of thermal equilibrium with the matter. The radial grid is adjusted manually.

- A separate code computing the neutrino diffusion coefficients, which are then fed into the first code. This second code includes the Standard Model scattering and absorption processes for the conditions of the supernova. It incorporates neutrino-nucleon scattering, including weak magnetism effects, and neutrino-electron scattering. The code is designed to yield separate predictions for the electron neutrino, electron antineutrino, and mu and tau neutrinos and antineutrinos. The effects of strong interactions between nucleons are included in the mean-field framework. Work is in progress on incorporating the chemical composition of the medium.

- A third code modeling the transport of neutrinos close to the neutrino sphere by the Monte Carlo method. This code computes the transmission coefficient as a function of the neutrino energy. For the moment, it has simplified scattering cross sections. The realistic cross sections computed by code 2 are yet to be included.

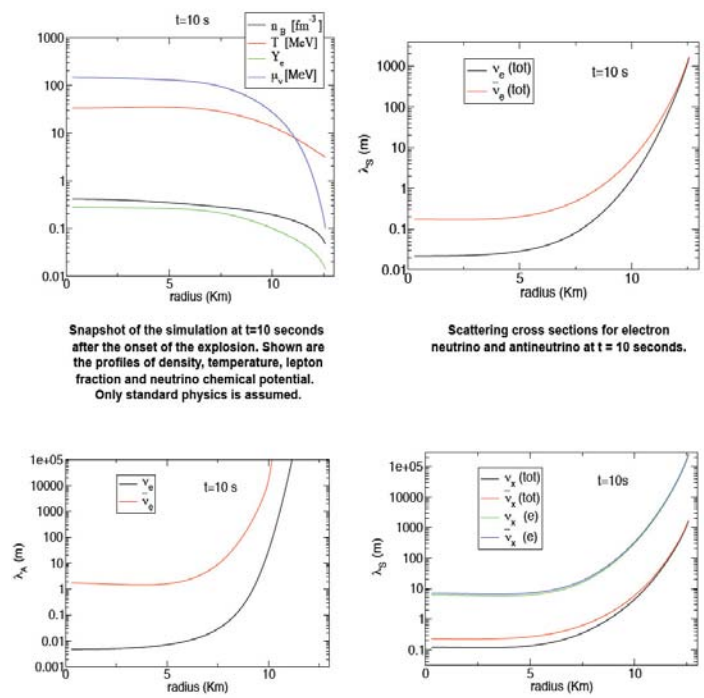


*Figure 1. Snapshots of the simulation at t=10 seconds after the onset of the explosion. Shown are the profiles of density, temperature, lepton fraction and neutrino chemical potential, as well as the mean free paths for the neutrinos of all flavors.*

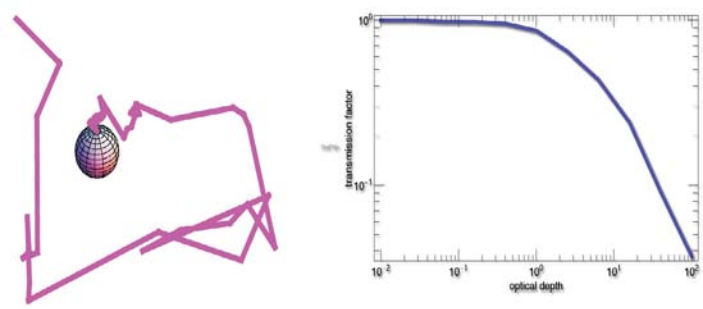


*Figure 2. We model the transport of neutrinos close to the neutrino sphere by the Monte Carlo method. The left panel shows the snapshot of a representative neutrino trajectory. The right panel shows the transmission coefficient computed by the Monte Carlo code as a function of the neutrino energy.*

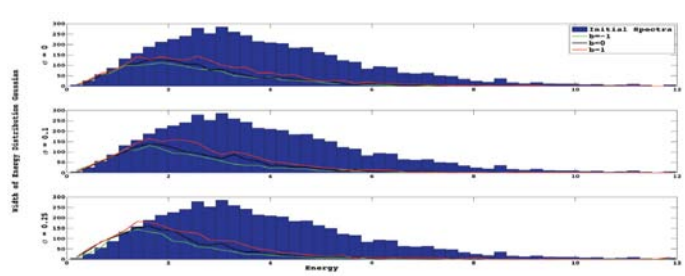

*Figure 3. Spectra of emitted neutrinos computed by the Monte Carlo Code, compared to the thermal input spectra. The recoil exchange of energy is varied. Preliminary results.*

## Future Work

- Finalize the neutrino opacity code, by including in it processes like neutrino bremsstrahlung and pair annihilation, or prove that these processes are not important anywhere inside the PNS.
- Split the diffusion code in different flavor bins (treating the electron and non-electron flavors separately).
- Investigate the possibility of automatic radial grid adjustment from within the code.
- Model the region where muon and tau neutrinos fall out of thermal equilibrium with matter and undergo multiple neutral current collisions with nucleons with small (but non-negligible!) recoil. Incorporate neutrino-electron scattering in this regime – the analysis we did earlier this year indicates that these interactions also play an important role in exchanging energy. A possible scenario is to extract a numerically efficient prescription from the Monte Carlo code and implement it as an addition to the diffusion code.
- Connect this model to the diffusion code on one side and the free-streaming limit on the other. The results obtained at this point will be published on their own.

Moreover, in the process of developing the Monte Carlo code we are finding potentially interesting new effects in neutrino decoupling and spectra formation, which have apparently been overlooked in the literature. The effects have to do with how energy is deposited in the layer close to the neutrinosphere (the region in the collapsed star where neutrinos become freesteaming). Previous Monte Carlo studies considered the decoupling in a putative, unchanging profile. We observe, however, that the strong energy dependence of the neutrino cross sections, combined with the energy exchange via nuclear recoil, may imply the muon and tau neutrinos effectively heat the medium as they decouple. The heating changes the medium, which in turn affects how neutrinos scatter and decouple. The investigation of these effects – an unexpected bonus as compared to our original plans – is currently in progress.

## Conclusion

In the first year of the project, we have investigated three different ways of testing physics beyond the standard model with supernovae and their progenitor stars. In the first case, we have found that supernovae and stars are significantly more sensitive to a class of models with extra dimensions than existing or planned laboratory experiments. In the second case, we found that the hypothetical neutrino magnetic moment can have dramatic effects on the evolution of supernovae progenitors, including an appearance of a totally new class of supernova explosions.

Finally, we have been developing “a particle physicist’s supernova model” that will provide a unique way to test new neutrino interactions. Considerable progress has been made, as outlined above. The ultimate goal will be to identify robust signatures of new physics in supernova explosions that are larger than the inherent uncertainties of the simulations. In addition to placing limits on new physics, our model will give useful predictions for the neutrino signal from a supernova within the Standard Model scenario. Such predictions will be crucial for the next round of large water Cherenkov neutrino detectors that are in the planning stage in Japan, Europe, and particularly in the US in connection with the National Underground Science Laboratory.

## References

1. Friedland, A., and M. Giannotti. Astrophysical bounds on photons escaping into extra dimensions. 2008. *Physical Review Letters.* **100**: 031602.
2. Heger, A., A. Friedland, M. Giannotti, and V. Cirigliano. The Impact of Neutrino Magnetic Moments on the Evolution of Massive Stars. *Astrophysical Journal.*

## Publications

Friedland, A., and M. Giannotti. Astrophysical bounds on photons escaping into extra dimensions. 2008. *Physical Review Letters.* **100**: 031602.

Heger, A., A. Friedland, M. Giannotti, and V. Cirigliano. The Impact of Neutrino Magnetic Moments on the Evolution of Massive Stars. *Astrophysical Journal.*

continuing project

# Three-Dimensional Dynamics of Magnetic Reconnection in Space and Laboratory Plasmas

*William Scott Daughton*

20080735ER

## Introduction

Magnetic reconnection is a basic plasma process in which magnetic field energy is rapidly converted into kinetic energy, including both high-speed flows and heating of the plasma. Scientists believe this process plays a fundamental role in planetary magnetospheres, solar flares and laboratory fusion machines. However, many questions regarding the basic physics of magnetic reconnection remain poorly understood. Researchers have put forward a variety of simplified models to explain some of the main features, but these models rely upon a variety of uncontrolled approximations and many questions remain highly controversial. In particular, one of the most longstanding issues is the role of plasma instabilities in controlling the three-dimensional (3D) structure and time evolution of the reconnection process. This project will address this question using the particle-in-cell (PIC) simulation technique that describes the reconnection physics at the most basic level without making any approximations. In the past, this kinetic simulation approach has been limited by the extreme computational requirements necessary to resolve all space and time scales. This project will overcome these limitations by combining three unique innovations: (1) the plasma simulation code VPIC which has been carefully optimized to exploit the new Roadrunner petaflop supercomputer, (2) an open boundary model that will permit the simulations to more realistically describe large-scale systems in nature and (3) a careful validation of the simulation results against the Magnetic Reconnection eXperiment (MRX). The specific research tasks include implementing both the open boundary model and the experimental boundary conditions for MRX into the VPIC code. When the Roadrunner machine becomes operational in early 2009, a series of large-scale simulations will be performed using both the open-boundary model and the experimental conditions for MRX. These 3D simulations will be nearly 100 times larger than any previous study of this type. The scale of these simulations will be sufficient to allow plasma instabilities to develop within the reconnection layer and thus provide a definitive 3D description of the dynamics.

## Benefit to National Security Missions

This project will support the DOE mission in Nuclear Weapons by enhancing our understanding of high temperature plasmas and exploiting the new hybrid computing technology on Roadrunner. It supports the energy mission by advancing our understanding of fusion machines, and nuclear nonproliferation by better tools to understand risks to satellites.

## Progress

Recent two-dimensional (2d) kinetic simulations [1] using boundary conditions appropriate for MRX have uncovered a large discrepancy between the experimental measurements of the reconnection layer and the simulations. In particular, the thin current sheet measured within the experiment is a factor of ~(3-5) times larger than predicted by the 2D collisionless simulations. The two leading possibilities to explain this discrepancy are weak binary collisions and 3D effects such as current aligned plasma instabilities. This project is presently examining both of these possibilities. To begin with, the experimental boundary conditions necessary to describe the driven reconnection process in MRX have been implemented within the VPIC code and carefully benchmarked against the previous 2D results, as illustrated in Figure 1. This comparison has confirmed the basic discrepancy [1] regarding the thickness of the electron layer. In order to examine the influence of binary collisions, a well-known collision model [2] has been implemented within the VPIC code and benchmarked against a variety of simple analytic test problems. For example, the electrical resistivity arising from election-ion collisions is thought to play an important role in the dynamics of reconnection. As illustrated in Figure 2, we have demonstrated that the collision model within VPIC recovers the classic theoretical prediction [3] for the electrical resistivity of fully ionized plasmas. These types of detailed benchmarks provide evidence that Coulomb collisions are correctly modeled within the fully kinetic VPIC simulations, and have allowed us to confidently proceed to our primary goal of understanding the re-

connection process in MRX. In this regard, we have started performing 2D semi-collisional simulations of MRX using a range of collision frequencies appropriate for this experiment. The introduction of Coulomb collisions modifies the structure of the reconnection layer in a number of important ways. However, the thickness of the current sheet within the reconnection layer is only increased by ~50% at most, which is still much thinner than the experimentally measured layer thickness in MRX. At the present time, we do not believe that Coulomb collisions can fully explain the experimentally measured layer thickness [1] and thus it is important to consider 3D processes as we more forward.

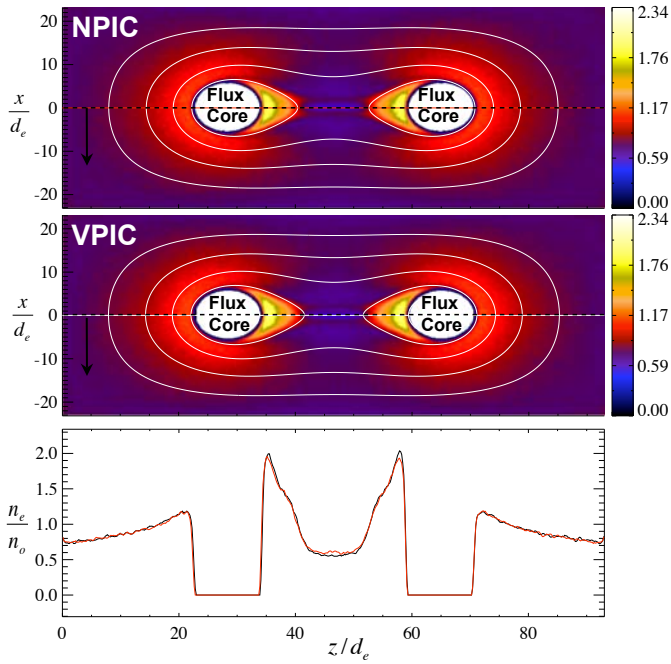


*Figure 1. In order to test the MRX boundary conditions, extensive cross-verification simulations have been performed between NPIC in Reference [1] and the VPIC code used in this project. This example compares the plasma density at the same simulation time along with the magnetic flux surfaces. Despite large differences in numerical methods, the agreement between the two codes is excellent for all cases considered.*

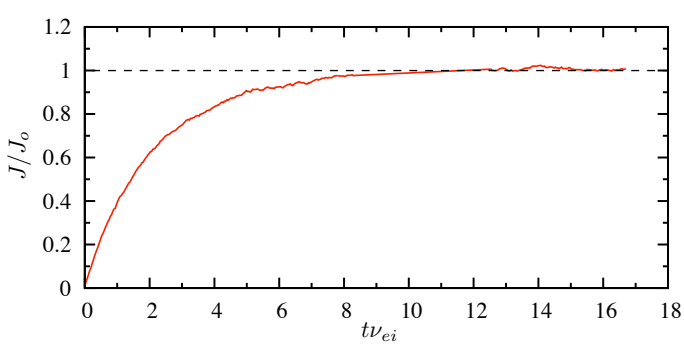


*Figure 2. Example resistivity benchmark showing current as a function of time between two parallel plates with an applied electric field. The parameters are for hydrogen at temperature T = 20 eV. The saturation current J_o is in excellent agreement with Spitzer theory [3].*

In preparation for the Roadrunner Science campaign in 2009, we have started a limited number of 3D simulations on the Yellowrail and Redtail clusters (same base system as Roadrunner). These initial 3D simulations are in the collisionless limit, with the goal of testing the boundary conditions and identifying plasma instabilities that might influence the structure and dynamical evolution of the reconnection layer. In order to allow these simulations to fit on the available clusters, it is presently necessary to reduce the separation between the ion and electron scales by employing an artificial electron to ion mass ratio $m_i/m_e$=100. The example simulation illustrated in Figure 3 was performed on the Redtail cluster using 1024x96x2048 cells with ~40 billion computational particles. The electron current sheet that forms between the flux cores in Figure 3 is unstable to a current driven instability that produces strong fluctuations in the electric field as shown in the bottom panel.

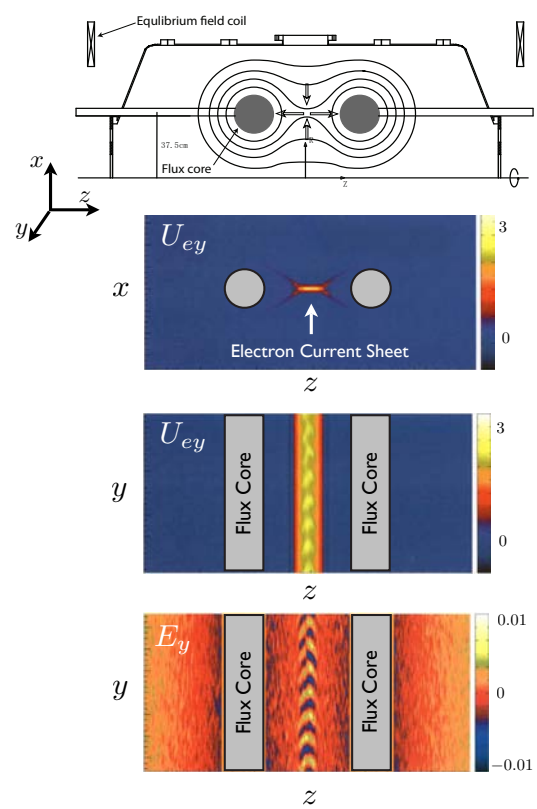


*Figure 3. Initial example of a 3D VPIC simulation with boundary conditions relevant to model MRX. A schematic of the experiment is shown in the top panel, while the next two panels show the electron fluid velocity normalized to the electron thermal speed. The thin electron-scale current sheet is unstable to current driven instability that strongly influences the electron flow (2nd to bottom) due to the electric field fluctuations (bottom panel).*

These electric field fluctuations strongly perturb the electron flow within the layer, but at the present time it remains unclear what influence this instability has on the overall reconnection dynamics. We are presently working

out a theoretical description of the instability in order to better understand how it scales with the plasma parameters. The large increase in computing power from Roadrunner, will allow us to study the dynamical evolution over a more realistic range of parameters. This particular science problem is now fully ready to exploit the Roadrunner machine when it becomes available in 2009.

## Future Work

The second main science goal of this project is to implement open boundary conditions into the VPIC code in order to better understand the dynamics of magnetic reconnection in large open systems that occur in Nature. This approach [4] allows both plasma and magnetic flux to enter and exit the system in a manner that effectively mimics a much larger system. We are presently implementing these boundary conditions within VPIC and will begin testing this model by early 2009. The results obtained with VPIC will be first carefully benchmarked against recently published 2D results [4] and then we will proceed to larger-scale 3D simulations using Redtail. These large calculations will be used to ensure that the diagnostics, I/O and MPI subsystems are all working properly in preparation for the Roadrunner science campaign in 2009.

## Conclusion

This project will contribute to the predictive understanding of magnetic reconnection in high temperature plasmas by including 1) realistic boundary conditions, 2) influence of weak binary Coulomb collisions, and 3) complex 3D effects such as plasmas instabilities. The ability to predict this complex behavior of magnetic reconnection has practical applications for a wide range of applications such as laboratory fusion machines and the plasma environment around the Earth where communication satellites play a crucial role in modern society.

## References


1. Dorfman, S., W. Daughton, V. Roytershteyn, H. Ji, Y. Ren, and M. Yamada. Two-dimensional fully kinetic simulations of driven magnetic reconnection with boundary conditions relevant to the Magnetic Reconnection Experiment. 2008. *Physics of Plasmas.* **15**: 102107.

2. Takizuka, T., and H. Abe. A binary collision model for plasma simulation with a particle code. 1977. *Journal of Computational Physics .* **25**: 205.

3. Spitzer, L.. Physics of fully ionized gases. 1956.

4. Daughton, W., J. Scudder, and H. Karimabadi. Fully kinetic simulations of undriven magnetic reconnection with open boundary conditions. 2006. *Physics of Plasmas.* **13**: 072101.


## Publications


Dorfman, S., W. Daughton, V. Roytershteyn, H. Ji, Y. Ren, and M. Yamada. Two-dimensional fully kinetic simulations of driven magnetic reconnection with boundary conditions relevant to the Magnetic Reconnection Experiment. 2008. *Physics of Plasmas.* **15**: 102107.

Yin, L., B. J. Albright, Kevin J. Bowers, W. Daughton, T. J. T. Kwan, J. Margulies, E. M. Nelson, and H. Karimabadi. New insights into collisionless magnetic reconnection enabled by ultra-high performance three-dimensional kinetic simulations. 2008. *IEEE Transactions on Plasmas Science.* **36** (4): 1110.

Yin, L., W. Daughton, H. Karimabadi, B. J. Albright, Kevin J. Bowers, and J. Margulies. Three-dimensional dynamics of collisionless magnetic reconnection in large-scale pair plasmas. 2008. *Physical Review Letters.* **101**: 125001.

continuing project

# The Roadrunner Universe

*Salman Habib*

20080743ER

## Introduction

Dark matter and dark energy are the dominant components of the Universe, though poorly understood and largely unobserved. Their ultimate nature, however, remains mysterious, especially so of the dark energy. Ambitious ground and space-based missions investigating different aspects of the "Dark Universe'' constitute a national and international investment measured in billions of dollars. The discovery potential of almost all of these missions relies crucially on theoretical modeling of the large scale structure of the Universe. The Roadrunner Universe project will carry out the largest high-resolution simulations of the distribution of matter in the Universe, resolving for the first time galaxy scale mass concentrations over observational volumes representative of state-of-the-art sky surveys. A key aspect of the project will be a major simulation suite covering over thirty different cosmologies, an essential resource for interpreting next-generation observations. This effort represents an approximately two to three orders of magnitude improvement over the largest current equivalent. The resulting database will become an essential component of Dark Universe science for years to come. The Roadrunner Universe project will implement a hierarchical grid/particle algorithm that optimally matches physical aspects of the simulation to the corresponding hybrid architecture of Roadrunner, making aggressive use of the Cell BE engine. In order to handle the enormous simulation database, a dedicated analysis and visualization software framework will be developed. Running also on Roadrunner, this framework will extract science products from the simulations, in both static and "on the fly'' modes, as well as filter the raw output into a manageable datastream.

## Benefit to National Security Missions

This project will significantly impact DOE missions including the Sloan Digital Sky Survey-III, especially the Baryon Oscillation Spectroscopic Survey. The two longer-term major missions this work will support are the Joint Dark Energy Mission (JDEM) and the Large Synoptic Survey Telescope (LSST). Our statistical methods apply to weapons reliability and data mining for Threat Reduction, relevant missions in DOE, DHS, and other government agencies.

## Progress

The basic tasks in the Roadrunner Universe Project break down into two components: the simulation code itself and the associated analysis framework. The framework is particularly important since the outputs from the simulation runs will be so large that a major part of the analysis must be performed in real time.

The work on the simulation code itself proceeds in three steps: 1) complete a version of the medium-resolution part of the code that will run on the Opteron layer using the particle overloading idea invented for this project, 2) extend this version so that the particles live on the Cell BE layer, while the density grid stays on the Opteron layer, 3) add the short-range force solver to the Cell BE medium resolution layer. Currently, we have almost completed step (1) in this process by a complete rewrite of the original particle-mesh code MC^2 (Mesh-based Cosmology Code) in a way that will allow a better match to the Roadrunner architecture. In addition, the original MC^2 code will provide a very important validation check during the porting to Roadrunner. Because communication is such a performance hit on Roadrunner we have worked on techniques to reduce it as much as practicable. For example, by implementing optimally filtered gradients in Fourier space we can eliminate the boundary communication that would be required to do the gradients via finite-differencing. Various pieces of step (2) have also been implemented. The particle deposition and interpolation steps are now running on the Cell BE with good performance. Additionally, the communication between the Opteron and Cell layers is also being optimized. Finally, for the short-range solver, we investigated various options, and decided to use a direct particle-particle force solve since this method has the simplest data structure and provides the most performance on the Cell architecture. Other techniques, such as a tree-based algorithm, are very difficult to implement efficiently on the Cell.

The analysis and visualization framework is also a complex piece of algorithm and software development. We have chosen to break up the analysis framework into two pieces: parts that are easy to do on the Opteron layer and parts that must involve the Cell layer. Here, we have decided to do as much of the analysis as possible on the Opteron layer, since analysis costs less than the simulation and we would like the analysis toolkit to be as general as possible. However, there are problems such as the determination of correlation functions, that must involve both layers. We are taking a hybrid approach to these problems. For example, the correlation function will be computed in two ways, on longer scales, via a grid-based spectral method on the Opteron layer, and then a matched direct particle-particle computation on the Cell layer will provide the small-scale information. Currently work is ongoing on a fast parallel FOF (friends-of-friends) halo finder -- the serial version has been validated and has excellent performance. The parallel version of the FOF finder exploits the particle overloading data structure intrinsic to the design of the code. In addition, methods for merger-tree analysis of dark matter halos are also being developed.

## Future Work

The decade-old discovery of cosmic acceleration and confirmed evidence for the existence of "dark energy'" represents one of the greatest mysteries in all of physical science. This discovery adds to the overwhelming observational evidence for "dark matter'', dominating any form of matter seen in a laboratory. The combined "dark sector'', of which little is known aside from its existence, comprises more than 95% of the Universe. Cosmological parameters are now known at the level of 5-10%, and next-generation experiments aim to reduce this to 1%!

The DOE/NASA/NSF Dark Energy Task Force (DETF) studied the requirements and prospects for both near and longer-term dark energy probes. This project will carry out very large volume simulations of the Universe in order to faithfully represent and investigate structure formation over observationally relevant scales being targeted by next-generation surveys, as outlined by the DETF. Doing this, while truly capturing galaxy-scale dark matter concentrations, has never before been accomplished. Our simulations will be the first to achieve this target.

The volume, accuracy, and mass and force resolution of the simulations have been designed to optimally impact all three structure formation-related Dark Universe probes. They will provide excellent coverage for baryon oscillations and cluster surveys, with sub-percent accuracy over all scales relevant to baryon acoustic oscillation (BAO) surveys. The high dynamic range ensures that weak lensing surveys can use our results down to scales where gas physics becomes important and must be modeled separately.

A fundamental goal of precision cosmology is the accurate determination of cosmological parameters. This requires a template of predictions against which observations may be compared, a daunting task given the large number of cosmological parameters. A recent breakthrough by us allows a finite number of large-scale simulations to achieve this task; the project will thus create the world's first high-resolution "cosmic emulator''.

## Conclusion

The results from this project will further our understanding of two of the most outstanding problems in all of physical science: dark energy and dark matter. The simulations performed in this project will not only be the largest ever run, but will be targeted at improving the design of future cosmological surveys and interpreting the results obtained from theses surveys. The project includes the development and application of advanced statistical methods and new ways of analyzing very large datasets. These techniques, along with new methods for programming next-generation computers, have applications going far beyond the specific domain of the project.

# Implicit Monte Carlo Calculations of Supernova Light-Curves

*Aimee L Hungerford*

20080744ER

## Introduction

In this project we will complete the first 2-dimensional simulation of a core-collapse supernova light-curve using the Roadrunner machine. Supernovae are important to a wide range of astrophysical and physics fields; they are the sites of compact object (neutron star, black hole) formation and are the primary source of enrichment of heavy elements in the universe. They are likely sources of cosmic rays and could induce further star formation. There intense emission make supernovae ideal probes of the early universe and cosmology. The NASA/DOE Joint Dark Energy Mission is likely to use supernovae to probe the nature of dark energy. In addition, supernovae are produced under intense conditions (reaching densities well above nuclear densities and temperatures ranging from 100 MeV to a few Kelvin). Supernovae provide an ideal testbed for nuclear and particle physics as well as general and special relativity.

The importance of supernovae in such a wide range of astrophysical and physical fields makes understanding supernova light-curves an extremely active field. The data set with the most potential for diagnosing these cosmic explosions remains the optical light (as opposed to neutrinos, gravitational waves or high energy gamma rays). Unfortunately, our best diagnostic also requires the most complicated physics software to accurately model how the explosion mechanism is reflected in this light. But by taking advantage of LANL's computing power and expertise in computational science (namely radiation hydrodynamics) and atomic processes, we have already taken the lead in theoretical aspects of this field. Simulations of one-dimensional light-curves using a preliminary version of the RAGE plus IMC code package Cassio are already underway.

## Benefit to National Security Missions

This project supports the DOE mission in Nuclear Weapons by enhancing our understanding of numerical simulation for complex multiphysics systems. Numerical radiation hydrodynamics is a key competency for the stockpile stewardship mission of LANL. This project represents cutting-edge research into current issues for radiation-hydrodynamics of complex astrophysical systems.

## Progress

Since the start of this project, members of our team have altered the communication libraries for the cell version of our implicit Monte Carlo (IMC) code to work with the available libraries on the developmental Roadrunner machine. An improvement in code performance was observed in moving to the developmental machine as compared to the cell simulator environment. Figure 1 shows the performance improvement from the cell accelerators using both the cell simulator environment and the actual Roadrunner developmental machine. A code performance enhancement from factor of 7 speed-up to factor of 8 speed-up is evident for the test problem.

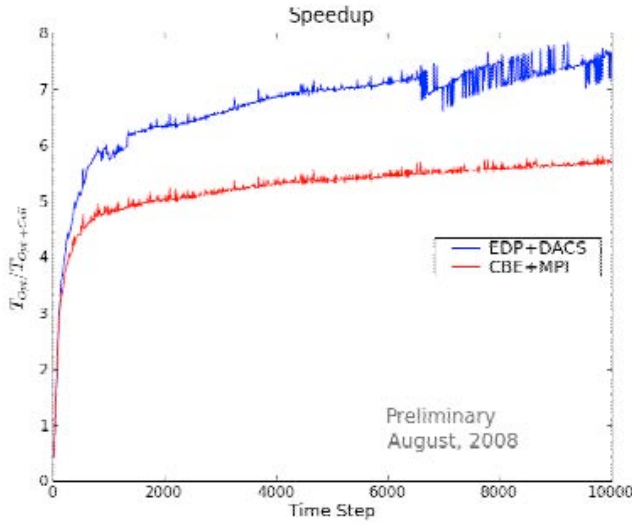


*Figure 1. Roadrunner assessment IMC code performance as implemented on the cell simulator environment (red line) and the developmental Roadrunner cluster (blue line). Plotted is the enhancement due to cell acceleration as a function of cycle.*

This project will ultimately put together transport in multi-angle, multi-energy group and multi-space dimensions. Our process for getting ready for the ultimate simulation has been to explore combinations of these three to test if there are obstacles with combining them for the supernova regime. Along these lines, we have run the following simulations with our preliminary version of Cassio:

- 1 spatial dimension, gray, flux-limited diffusion
- 1 spatial dimension, multigroup, flux-limited diffusion
- 2 spatial dimensions, gray, flux-limited diffusion
- 1 spatial dimension, multigroup, implicit Monte Carlo transport

The flux-limited diffusion simulations have been completed with capability that exists in the RAGE code alone and is work that has been done alongside the Cosmic Explosions LDRD-DR effort. Early on, issues arose with the multi-group flux-limited diffusion calculations and our team put forth the effort to understand whether these arose due to the wide temperature ranges specific to the supernova regime. We discovered that a portion of the challenges with multigroup were ameliorated by a more appropriate choice of tabular opacity parameters. Figure 2 shows the radiation energy density versus radius for various groups in the early phases of our multigroup flux-limited diffusion calculation. However, at later times there remain challenges with multigroup flux-limited diffusion that seem to originate from issues with the diffusion algorithm itself. These should not affect our Roadrunner work as we will be running primarily with the IMC radiation treatment rather than diffusion.

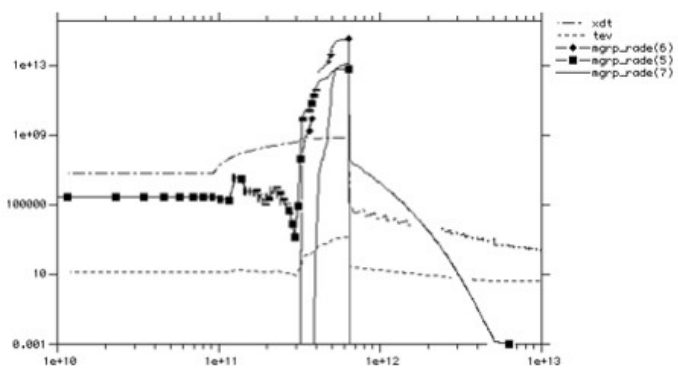


*Figure 2. Radiation energy density for 3 energy groups from a one dimensional multi-group flux-limited diffusion calculation with the RAGE code. The spectral peak occurs between 1 and 10 keV for this phase of the calculation in which material temperatures are roughly 1 keV. This is consistent with thermal radiation which is expected at this early phase of the calculation.*

The IMC simulation in 1 spatial dimension has also uncovered some unforeseen challenges. The IMC method is notoriously slow to achieve a solution for regions of high optical depth. The method is often supplemented by an analytical random walk step in order to accelerate precisely these regions. For the supernova regime, we find that the random walk algorithm, as implemented in Wedgehog IMC, does not help for the unique scattering conditions in the supernova. Our team has added a mild alteration to the random walk algorithm in order to handle the extremely large optical depths present in our supernova setups.

Finally, we have overcome some of the challenges in bringing the interface functionality (between the hydrodynamics and radiation packages in Cassio) to a state of readiness for porting to the Roadrunner machine.

## Future Work

While we have identified and overcome several stumbling blocks along the way to a Roadrunner compatible IMC radiation-hydrodynamics code for supernova simulation, there are steps remaining before the start of the open science computing allocation on Roadrunner next year. The cell version of the IMC has yet to be run in conjunction with the hydro code. As we complete the final steps in polishing the interface functionality between the radiation and hydro packages, we will then be ready to swap out the base version of the IMC package for the cell optimized version. Additionally, there are capabilities in the base version of the IMC package that we have altered to enable efficient simulation of the supernova problem. These capabilities must be included in the cell-optimized version of the IMC code. Finally, we must verify that the run time performance seen from the IMC test problem on the cell architecture is achievable with the physical conditions in supernovae. Additional enhancements in the parallel efficiency of the hydrodynamics code are planned once we have the full code operational on the developmental machine.

## Conclusion

This project will advance both our understanding of the fundamental physics at work in the most dynamic explosions in our universe today, and the feasibility of attacking grand challenge problems like this using the latest in computational technology. This work aims to find the best way to put petaflop technology to use on solving a problem with cosmic relevance. The stunning discovery that our universe is expanding and accelerating in its expansion, was first shown by blindly using observed properties of supernovae. A solid physics basis for understanding why those properties hold is the ultimate goal of our simulation work.

# Instabilities Driven Reacting Compressible Turbulence

*Daniel Livescu*

20080747ER

## Introduction

Turbulence is a complex phenomenon that is common to many processes in physics from the cosmic scale of astrophysical explosions to the global scale of environmental and weather phenomena and to the microscopic scale of chemical reaction dynamics. The study of fluid turbulence is one area that is likely to benefit from petascale computing, where very large scale computations can bring the insight and indicate the appropriate modeling paradigms for the routine coarse mesh calculations needed in applications. Large scale simulations of canonical incompressible turbulent flows have been performed and advanced our understanding of the turbulence phenomena. As a result, several modeling approaches now work reasonably well for coarse mesh simulations of these simple flows, even though a complete parameterization of turbulence still eludes us. In many important applications, however, fluid turbulence is accompanied by complicating physics: compressibility, exothermic reactions, and differential accelerations. In many situations such flows occur in convergent geometries (e.g., cylindrical or spherical). Examples include Inertial Confinement Fusion targets, laser induced launching of a flyer plate, stellar pulsations, or supernova explosions. Fundamental turbulence studies and high resolution simulations of these flows have not been performed and the appropriate modeling paradigms are not known.

We will advance our understanding of turbulence and turbulent mixing beyond the standard configurations, by performing the first (very large) Direct Numerical Simulations of instabilities driven reacting compressible turbulence in Cartesian and convergent geometries with different configurations of fuel (well-stirred and two-component). The work will set the state-of-the-art for the numerical methods and algorithms for accurate flow calculations on heterogeneous computer architectures and will fill a gap in our knowledge of the physics of turbulent multi-fluid reacting flows. The parameters for the reacting simulations are chosen to be relevant to burning in Type I X-ray bursts and Type Ia supernovae and allow to determine effective flame propagation speeds.

## Benefit to National Security Missions

Developing a petascale computational capability in fluid turbulence modeling will impact a wide variety of physics investigations from astrophysics and nuclear weapons physics to plasma physics of fusion energy and climate modeling. This work will benefit relevant mission areas in DOE and other government agencies.

## Progress

The CFDNS code has been ported to the Roadrunner architecture and low resolution simulations to probe parameter values and physical configurations are under way. We tested the algorithms and scaling on the full machine when it was assembled at the IBM site in June 2008. Among the advances made to the-state-of-the-art numerical methods used in the Roadrunner version are a vectorized serial tridiagonal solver which takes full advantage of the Cell architecture and achieves approx. 40 times speed-up compared to similar Opteron code [1] and new parallel algorithms for solutions to tridiagonal systems. This speed-up for the serial tridiagonal solver is achieved by exploiting the memory bandwidth of the Cell's Element Interconnect Bus and the SPEs' independent memory controllers. Since most of the computational time is spent calculating solutions to tridiagonal systems, this is the part, which was highly optimized. Thus, the new parallel algorithm maintains the performance of the serial solver [2]. Other advances deal with optimizing the flow of data on heterogeneous architectures for memory intensive applications.

The parameters for the high resolution simulations to be performed on Roadrunner are being determined using preliminary low resolution calculations on institutional computing resources. To ensure the soundness of the final simulations, the preliminary results are being subjected to the scrutiny of the scientific community [3].

## Future Work

Rayleigh-Taylor instability (RTI), which occurs at the interface between a heavy fluid overlying a lighter fluid, is of fundamental importance in a multitude of applications ranging from inertial confinement fusion, to combustion, and to astrophysics. RTI plays a crucial role in flame propagation in Type Ia supernovae and possibly the development of ignition bubbles for detonation.

It also determines the time-scale of mixing and burning and hence the rise time of burst in helium-ignited Type I X-ray bursts. Thus, RTI is the dominant acceleration mechanism for the flame since the burning is controlled by the fluid motion mixing the fuel with hot ashes, rather than by thermal conduction. Type Ia supernovae have received much attention recently, due to their use as standard candles in cosmology. Yet, the mechanism for explosion is not fully understood, in particular the detonation initiation.

We will perform the first DNS of instabilities driven reacting compressible turbulence with different configurations of fuel (well-stirred and two-component). The work will set the state-of-the-art for the numerical methods for accurate flow calculations on heterogeneous computer architectures, will fill a gap in our knowledge of the physics of turbulent reacting flows, and will find the appropriate modeling paradigms for such flows. The parameters for the reacting simulations are chosen to be relevant to Type I X-ray bursts and Type Ia supernovae and allow to determine effective flame propagation speeds.

**Tasks:**

- Verify and validate the Roadrunner implementation of the CFDNS code.
- Perform the first Direct Numerical Simulations of instabilities driven, compressible reacting turbulence in Cartesian and spherical geometries. The Cartesian reacting simulations will be performed at conditions relevant to Type I X-ray bursts and Type Ia supernovae.
- Provide the first instability growth and turbulence characteristics studies under these complex conditions.

## Conclusion

We will perform the largest simulations to date of turbulent flows consisting of:

- Nonreacting compressible Rayleigh-Taylor instability
- One-component reacting compressible Rayleigh-Taylor instability relevant to type Ia supernovae
- Two-component reacting compressible Rayleigh-Taylor instability relevant to type I X-ray bursts

The computations will also be the first Direct Numerical Simulations (such that all scales of motion are accurately computed) of these problems. Thus, the project will provide the first evidence of turbulence characteristics beyond the standard configurations, a database for testing astrophysics codes, and will examine the initiation of supernovae and of X-ray bursts initiation.

## References


1. Mohd-Yusof, J., D. Nehal, and D. Livescu. Roadrunner: Compressible Turbulence Simulation. Presented at *International Conference for High Performance Computing, Network, Storage, and Analysis.* (Reno, 10-17 November 2007).

2. Mohd-Yusof, J., D. Livescu, T. Kelley, M. Petersen, and D. Nehal. Roadrunner application: Simulation of Compressible Turbulence. To appear in *International Conference for High Performance Computing, Network, Storage, and Analysis.* (Austin, 10-17 November 2008).

3. Livescu, D.. Plans for Unstable Flame Calculations on Roadrunner. Invited presentation at *ASC Computational Astrophysics Consortium Meeting.* (Stanford, 7-9 April 2008).


## Publications


Livescu, D.. Plans for Unstable Flame Calculations on Roadrunner. Invited presentation at *ASC Computational Astrophysics Consortium Meeting.* (Stanford, 7-9 April 2008).

Mohd-Yusof, J., D. Livescu, T. Kelley, M. Petersen, and D. Nehal. Roadrunner application: Simulation of Compressible Turbulence. To appear in *," International Conference for High Performance Computing, Network, Storage, and Analysis.* (Austin, 10-17 November 2008).

Mohd-Yusof, J., D. Nehal, and D. Livescu. Roadrunner: Compressible Turbulence Simulation. Presented at *," International Conference for High Performance Computing, Network, Storage, and Analysis.* (Reno, 10-17 November 2007).

# Saturation of Backward Stimulated Scattering of Laser In The Collisional Regime

*Lin Yin*

20080761ER

## Introduction

This project aims to develop the world's first truly first-principles model of laser-plasma interaction (LPI) in laser-driven hohlraums (fusion capsules or cavities). [1]. The proposed work uses the Roadrunner petaflop supercomputer and applies the state-of-the-art VPIC kinetic plasma simulation code, recently adapted to run efficiently on Roadrunner. The objective is to develop a validated predictive capability for LPI that will enable more successful experimental designs in inertial confinement fusion (ICF) experiments.

Success of this project will have several prospective payoffs: First, it directly supports the achievement of fusion ignition on the National Ignition Facility, which has manifold tie-ins into high-profile, exciting science, including carbon-neutral energy production, high energy density physics, laboratory astrophysics, and weapons science.

Moreover, by learning to control LPI, we can guide the search for new, high gain, high efficiency operating regimes for NIF ignition (including fast ignition) that simply cannot be attempted now because our understanding of the basic nonlinear physics of LPI is incomplete and phase space is simply too large to sample experimentally in an economical way.

Finally, a high-risk/high-reward application of LPI is in novel plasma gain media (so-called Raman amplifiers) to generate extremely high power, short pulse lasers. If demonstrated experimentally, these new amplifiers could enable short pulse laser intensities and energy densities inaccessible today without going to very large, expensive facilities. Potential applications include fast ignition inertial confinement fusion, novel high fluence ion beams for nuclear physics studies, and hadrontherapy of tumors.

## Benefit to National Security Missions

This project supports the nuclear weapons mission in two ways:

1. Laser Plasma Interaction science underpins high energy density and boost physics experiments at the National Ignition Facility.
2. Improved verification and validation of the VPIC plasma code on Roadrunner supercomputer will improve modeling of processes in nuclear weapons.

## Progress

- VPIC Diagnostic Development: Teaming with CCS-2 and X-3 staff, we have implemented readers for VPIC three-dimensional data output. These readers enable manipulation and analysis of data both on Paraview and Ensight Gold (the preferred format for ASC data).
- Two-dimensional and some three-dimensional studies of LPI physics have been conducted on the Redtail quadq system. These studies have been hampered somewhat by competition for resources and their status is, as yet, incomplete. We have worked to ensure stability of MPI and I/O subsystems; for the most part, I/O has proven to be, generally, robust, however we are working with LANL HPC staff to isolate existing problems with MPI. Our LPI runs are proving to be invaluable to them, as they serve as an aggressive test of the subsystems.
- Work has started on modifying our existing collision models to implement novel collision models [2] into VPIC [3] that are suitable for laser-plasma interaction studies. This work will be integral to validation of VPIC reflectivity with experimental data in the coming year and it represents the first time in the community that these models have been applied to large-scale PIC simulations of LPI. Collisional effects on SRS saturation and hypotheses of the proposal have been confirmed by 2D simulations.

- LANL staff on the proposal have visited IBM Poughkeepsie to do the first-ever science runs on Roadrunner examining 3D LPI physics in NIF-like plasma conditions. A series of Gordon Bell simulation runs were done and on 17 connected units of Roadrunner (12240 Cell chips, 6120 dual-core Opteron chips), the calculation sustained in excess of 374.25 TFlop/s and used one trillion simulation macroparticles and 42 TBytes of RAM (more than 4 times the aggregate data in the Library of Congress). Our Gordon Bell Prize submission is one of the finalists in the "Peak Performance" category.
- We have initiated discussions with T- and P-Division theory and experimental colleagues to isolate the best experiments and simulation diagnostics for LPI validation.
- We have documented our results in a Gordon Bell simulation paper and will showcase our results at the American Physical Society and ACM Supercomputing Meetings. We have been invited to give numerous high-profile invited and plenary talks, including an anticipated Gordon Bell Prize Finalist talk at the ACM Supercomputing Meeting in Nov. 2008; two invited talks at the American Physical Society Meeting in Nov. 2008; an invited talk and an invited plenary talk at the 13th Advanced Accelerator Concepts Workshop in July, 2008; an invited "visionary" talk at the High Energy Density Laboratory Physics Symposium in November 2008.

## Future Work

The VPIC code [3] is a state-of-the-art, fully relativistic, explicit, charge-conserving, electromagnetic, particle-in-cell kinetic plasma modeling code developed at LANL. VPIC has been converted to run on the hybrid Roadrunner architecture and served as one of the key codes during the Roadrunner Phase 3 acceptance. Access to 6.7M hours on the full Roadrunner system during the initial "Stabilization and Integration" phase of its deployment at LANL. This time will be spent using VPIC to perform kinetic plasma modeling of laser-plasma interaction (LPI) to study the nonlinear kinetics of stimulated Ramanand stimulated Brillouin scattering in the collisional regime. These calculations

are important from a basic physics standpoint and they are relevant to upcoming fusion ignition experiments on the National Ignition Facility.

Tasks for this project are:

1. Further VPIC diagnostic development,
2. Relevant, smaller-scale two-dimensional (2D) simulations on quadq on Redtail to isolate the key collisional physics and gain confidence in vital subsystems such as MPI and I/O,
3. Prepare relevant scientific calculations for a LANL Gordon Bell Prize submission in late Spring, 2008,
4. Perform verification and validation studies of LPI in the collisional regime with large-scale 3D simulations on Roadrunner.

Goals (corresponding to the aforementioned tasks):

1. Ensure that the diagnostics are in place to operate in the challenging environment of the full Roadrunner deployment in the yellow (with thin access to archival subsystems).
2. Shake down existing hardware and subsystems to maximize chances of success on the full Roadrunner system
3. Plan for the largest-scale PIC calculations ever performed and gain international recognition for LANL's leadership in high performance computation.
4. Ensure that the science results we obtain can be trusted.

Work will be documented in papers (including a Gordon Bell paper to Supercomputing conference) and scientific journals.

## Conclusion

We expect two key things to result from this study. The first is to illuminate the underlying nonlinear physics of laser-plasma instabilities (LPI), a problem of critical importance to the success of fusion ignition on the National Ignition Facility, paying special attention to the role of binary collisions in the physics. The second is to use this understanding to identify plasma parameter regimes which are relatively safe from LPI and to pose possible mitigation strategies to avoid their effects. This is an important basic science study directly related to mitigation of risk on a multi-billion dollar experiment.

## References

1. Yin, L., B. J. Albright, K. J. Bowers, W. Daughton, and H. A. Rose. Saturation of backward stimulated scattering of laser in kinetic regime. 2007. *Physical Review Letters.* **99**: 265004.
2. Lemons, D. S., W. Daughton, D. Winske, and B. J. Albright. Small-angle Coulomb collision models for PIC codes. To appear in *Journal of Computational Physics.*

3. Bowers, K. J., B. J. Albright, L. Yin, B. Bergen, and T. J. T. Kwan. Ultra high performance three-dimensional electromagnetic relativistic particle-in-cell simulation. 2008. *Physics of Plasmas* . **15**: 055703.

## Publications

Bowers, K. J., B. J. Albright, B. Bergen, L. Yin, K. J. Barker, and D. J. Kerbyson. 0.374 pflop/s trillion-particle kinetic modeling of laser plasma interaction on Roadrunner. To appear in *Proceedings of the 2008 ACM/IEEE Supercomputing Conference.*

# Physics of Astrophysical Jets

*Hui Li*

20051169ER

## Abstract

Astrophysical jets are energetic outflows of magnetic fields and relativistic plasmas with gigantic dimensions and astonishing powers. Observations suggest that they are powered by supermassive black holes at the centers of galaxies, but their formation, propagation and dissipation are poorly understood. We have conducted three dimensional (3-D) magnetohydrodynamic (MHD) studies, guided by astronomical observations and laboratory plasma experiments. These simulations help us to achieve a more fundamental understanding of the key physical processes governing these objects.

This project has established the Laboratory as one of the leading institutions in understanding astrophysical jets and has improved the Laboratory's competencies in basic research and computer simulation. The physics behind the MHD simulations and the computational simulation of those processes have created new capabilities germane to the Laboratory's key programs

## Background and Research Objectives

Astrophysical jets span an enormous range of spatial and temporal scales. Magnetic fields are believed to have a pivotal role in determining the jet production, propagation, and termination as the jets evolves in different astrophysical environments. Furthermore, such systems have intricate dissipation processes by producing the radiation we observe; yet they are amazingly stable by maintaining their global structures over extremely large distances.

To obtain a basic physical understanding of such systems, we adopted several approaches, which include analytical study of the stability of a magnetic helix, 2D/3D magnetohydrodynamics simulations of large-scale structures of astrophysical jets and lobe formation, and laboratory experiments of the production of astrophysical magnetic fields. Part of the study relied on the state-of-the-art supercomputing facilities available at the Laboratory. Understanding the stability and transport in such systems will help us gain better understanding of magnetic fusion experiments and vice versa. Our project fostered strong cross discipline collaboration between laboratory plasma physics research and astrophysics research.

We built a comprehensive understanding about the production, propagation and dissipation of astrophysical jets, and related them to laboratory studies of magnetic fusion experiments such as reversed field pinch and spheromak. Our theoretical and simulation studies were guided by laboratory experiments and astronomical observations.

## Importance to LANL's Science and Technology Base and National R & D Needs

This project supports DOE programs and core competence development in large scale computing. The proposed research established LANL as one of the leading institutions in understanding astrophysical jets and added an important part to the LANL's science portfolio in basic research and computer simulation. It also provided a vehicle to maintain and grow important core capabilities and acted as a driver for science applications in understanding the hydrodynamic and MHD high speed flows, shocks and instabilities. Comparisons with astrophysical observations and laboratory experiments improved our ability in building predictive modeling capabilities, which are germane to the Laboratory's key programs.

## Scientific Approach and Accomplishments

We have performed extensive 3D MHD simulations on the formation of astrophysical jets, utilizing LANL's Institutional Computing machines, such as PINK and COYOTE. We have gained a new understanding on how radio lobes of extra-galactic radio galaxies are formed through the interaction between the magnetically dominated jets and the background plasma, plus the jet's instability. We have successfully demonstrated, for the first time, that a magnetically dominated energy injection can naturally lead to a collimated outflow (jet) and form large radio lobes. This approach is fundamentally different from the previous models, which are mostly

the hydrodynamical jets [1]. Specifically, we have made progress in the following areas:

**Understanding the global morphology of astrophysical jet-lobe structures**

Astrophysical jets are observed to have a collimated jet-body plus large lobes at the end of jets. This underlying physics reason for this morphology has been the subject of intense studies. Using a new approach to modeling the magnetically dominated outflows from active galactic nuclei, we study the propagation of magnetic tower jets in gravitationally stratified atmospheres (such as a galaxy cluster environment) at large scales (more than tens of kiloparsecs) by performing three-dimensional MHD simulations. We find that as the magnetic energy is injected into a small central volume over a finite amount of time, the magnetic fields expand down the background density gradient, forming a collimated jet and an expanded ``lobe'' due to the gradually decreasing background density and pressure. Both the jet and lobes are magnetically dominated. This agrees with the observations quite well. These simulations help us understand the physical processes of lobe formation and expansion. Figure 1 shows our 3D MHD modeling of a jet/lobe system in galaxy clusters [2].

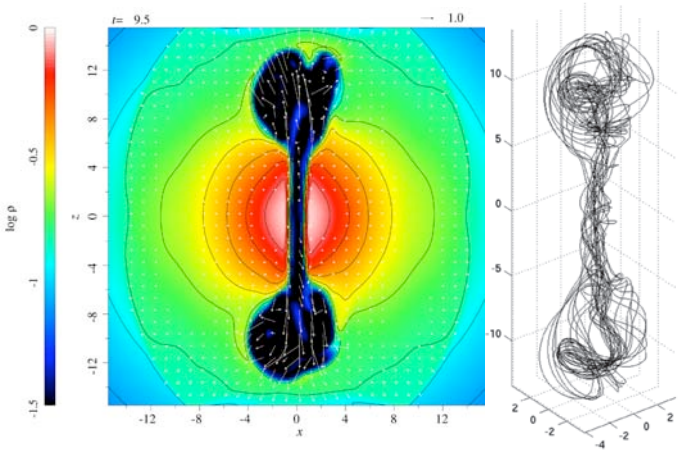


*Figure 1. The structure of a magnetically dominant jet/lobe system in a galaxy cluster. (left) Density distribution of the jet/lobe (black region indicates low density) and the background cluster medium (red/yellow/green). (right) The corresponding magnetic field lines for the jet/lobe system.*

**Understanding the stability properties of ``magnetic tower'' jets**

In addition to the jet-lobe morphology, the astrophysical jets often show global instabilities that represent as wiggles, kinks, and hot-spots. Motivated by the results from nonlinear numerical simulations, we have performed linear stability studies of magnetic structures. We developed a new method for studying linear stability of kink-like modes in a cylinder with line-tied boundary conditions, mimicking the situation of the jets. The method was applied to a special equilibrium magnetic field configuration. We showed that our method reproduces results previously found at some limiting cases. Again, through comprehensive 3-D MHD simulations, we find that, because the jets in our model are carrying large amounts of electric currents, it is naturally expected that the jet-lobe will be unstable to the current-driven instabilities (CDI). As CDI develops, it gradually "kinks" the jet into having wiggles and hot-spots. This result is again supported by the observations of jets with wiggling structures [3]. By comparing the non-linear simulations with linear theories, we then mapped the parameter spaces where the astrophysical jets could become unstable [4]. The effects of boundary conditions and the background pressure conditions are also considered [5,6].

**Comparing with astronomical observations**

Recent X-ray and radio observations of astrophysical jets in galaxy clusters reveal the dynamical interaction between outbursts of supermassive black hole activities and the background intragalactic medium such as X-ray cavities and corresponding radio bubbles. These observations provide an important test environment for our new modeling. Our simulation results show the magnetically dominated lobes expand subsonically, which should be observable in some observations. The tower jet, which possesses a highly wound helical magnetic field, is subject to the non-axisymmetric modes of the current-driven instability to form the wiggles. We have examined the jet of a famous radio galaxy, Hercules A, with our magnetic tower jet model. By using our numerical results, we have confirmed that the jet/lobe transition, the wiggling, and the projected magnetic field distributions associated to the source. They are qualitatively consistent with the real radio observations. To confront our magnetically dominated jet model with observations, we conducted an extensive survey of 64 cavities in the X-ray halos of clusters, groups and normal elliptical galaxies, using data from collaborator D. Rafferty (Penn State University). We showed that the evolution of the size of the cavities as they rise in the X-ray atmosphere is inconsistent with the standard model of pure adiabatic expansion of purely hydrodynamic models. We also noted that the majority of the observed bubbles should have already been shredded apart by Rayleigh-Taylor instabilities if they were of purely hydrodynamic nature. Instead we found that the data agrees much better with our model where the cavities are magnetically dominated and inflated by a current-dominated magneto-hydrodynamic jet model. These results have considerable impact on the energy budget associated with active galactic nucleus feedback. Figure 2 shows the comparison between our models and the observations [7].

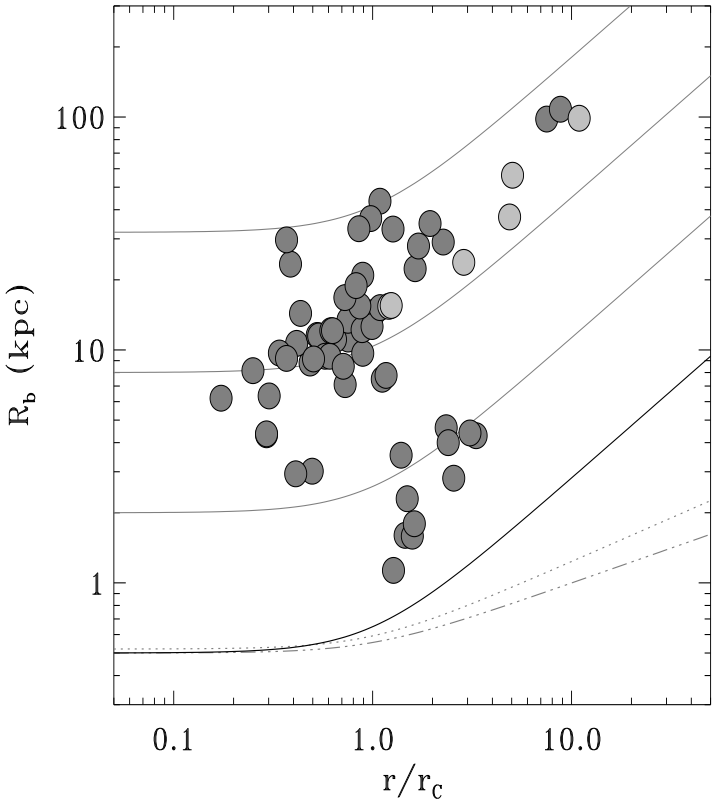


*Figure 2. The size distribution of X-ray bubbles as a function of their distance to the galaxy cluster center (circles). The solid lines show the expectation from our magnetic model whereas dotted and dashed lines show the expectation from hydrodynamic models.*

## References


1. Li, H., and e. al. Modeling the Large-Scale Structures of Astrophysical Jets in the Magnetically Dominated Limit. 2006. *Astrophysical Journal.* **643**: 92.

2. Nakamura, M., H. Li, and S. Li. Structure of Magnetic Tower Jets in Stratified Atmospheres. 2006. *Astrophysical Journal.* **652**: 1059.

3. Nakamura, M., H. Li, and S. Li. Stability Properties of Magnetic Tower Jets. 2007. *Astrophysical Journal.* **656**: 721.

4. Evstatiev, E. G., G. L. Delzanno, and J. M. Finn. A new method for analyzing line-tied kink modes in cylindrical geometry. 2004. *Physics of Plasmas .* **13**: 072902.

5. Delzanno, G. L., E. G. Evstatiev, and J. M. Finn. The role of resistivity on line-tied kink modes in cylindrical geometry. 2007. *Physics of Plasmas.* **14**: 070702.

6. Finn, J. M.. Magnetic reconnection - Null point. 2007. *Nature Physics (News and Views).* **2**: 445.

7. Diehl, S., H. Li, and C. Fryer. Constraining the Nature of X-Ray Cavities in Clusters and Galaxies. 2008. *Astrophysical Journal.* **687**: 173.


## Publications


Delzanno, G., E. Evstatiev, and J. M. Finn. Resistive effects on line-tied magnetohydrodynamic modes in cylindrical geometry. 2007. *Physics of Plasmas.* **14** (9): 092901.

Delzanno, G., E. Evstatiev, and J. M. Finn. Line-tied kink modes in cylindrical equilibria with magnetic shear. 2007. *Physics of Plasmas.* **14** (7): 072902.

Delzanno, G., E. G. Evstatiev, and J. M. Finn. The role of resistivity on line-tied kink modes in cylindrical geometry. 2007. *Physics of Plasmas.* **14** (7): 070702.

Diehl, S., H. Li, C. Fryer, and D. Rafferty. Constraining the Nature of X-ray Cavities in Clusters and Galaxies. 2008. *Astrophysical Journal.* **687**: 173.

Diehl, S., M. Nakamura, H. Li, and D. Rafferty. X-ray Observables of Magnetically Dominated Cavities in Clusters. 2007. *Proceedings of 'Extragalactic Jets: Observations and Theory from Gamma-ray to Radio' (astro-ph/0711.0331).*

Evstatiev, E. G., G. L. Delzanno, and J. M. Finn. A new method for analyzing line-tied kink modes in cylindrical geometry. 2006. *Physics of Plasmas.* **13**: 072902(1.

Finn, J. M.. Magnetic reconnection: null point. 2006. *Nature Physics (News and Views).* **2**: 445.

Finn, J. M., G. Lapenta, and H. Li. Similarity Solutions for Magnetic Bubble Expansion. 2004. *Physics of Plasmas .* **11**: 2082.

Kronberg, P. P.. Magnetic Fields in Galaxy Systems, Clusters and Beyond. 2005. In *Cosmic Magnetic Fields.* Edited by Wielebinski, R., and R. Beck. , p. 9. Heidelberg: Springer Verlag.

Kronberg, P. P.. Energy and Magnetic Field beyond Clusters: Expectation and Evidence. 2005. In *The Magnetized Plasma in Galaxy Evolution.* Edited by Chyzy, K., K. Otmianowska-Mazur, M. Soida, and R. J. Dettmar. , p. 239. Krakow: Jagiellonian University.

Kronberg, P. P.. Extragalactic Radio Sources, IGM Magnetic Fields, and AGN-based Energy Flows. 2006. *AN-Astronomical Notes.* **327**: 517.

Kronberg, P. P., R. Kothes, C. J. Salter, and P. Perillat. Discovery of New Faint Radio Emission on 8° to 3' Scales in the Coma Field, and Some Galactic and Extragalactic Implications. 2007. *Astrophysical Journal.* **659**: 267.

Li, H., G. Lapenta, J. M. Finn, S. Li, and S. A. Colgate. Modeling the Large-Scale Structures of Astrophysical Jets in the Magnetically Dominated Limit. 2006. *Astrophysical Journal.* **643**: 92.

Nakamura, M., H. Li, S. Diehl, and S. Li. Numerical Modeling of AGN Jets: Formation of Magnetically Dominated Lobes and Stability Properties of Current-carrying Jets. 2007. *Proceedings of 'Extragalactic Jets: Observations and Theory from Gamma-ray to Radio' (astro-ph/0707.1537).*

Nakamura, M., H. Li, and S. Li. Structure of Magnetic Tower Jets in Stratified Atmospheres. 2007. *Astrophysical Journal.* **652**: 1059.

Nakamura, M., H. Li, and S. Li. Stability Properties of Magnetic Tower Jets. 2007. *Astrophysical Journal.* **656**: 721.

Nakamura, M., I. Tregillis, H. Li, and S. Li. Modeling of Herc A Using MHD Jet Models. 2008. *Astrophysical Journal.* **686**: 843.

Pariev, V. I., S. A. Colgate, and J. M. Finn. A magnetic alpha-omega dynamo in AGN disks. II. Magnetic field generation, theories, and simulations . 2007. *Astrophysical Journal.* **658**: 129.

Xu, Y., P. P. Kronberg, S. Habib, and Q. W. Dufton. A Faraday Rotation Search for Magnetic Fields in Large Scale Structure. 2006. *Astrophysical Journal.* **637**: 19.

# Chemical Thermoacoustics

*Drew Adam Geller*

20060321ER

## Abstract

Thermoacoustics is a rapidly developing, relatively new field of energy conversion, which harnesses the oscillations of temperature, heat flux, pressure, and motion in intense sound waves. In the project described here, we have advanced the quantitative science of this phenomenon in new directions, laying the groundwork for understanding it in chemically reacting gas mixtures, by modeling the relevant aspects of the thermoacoustic mixture-separation and power-consumption/production processes (analytically when possible, numerically when necessary), by building experimental hardware, by checking the models against the experiments, and by iterating toward better understanding.

When this work is complete, we and others will be ready to use thermoacoustics to separate the components of chemically reacting gas mixtures, with hardware for which materials requirements will be minimal, capital costs will be low, environmental impact of fabrication will be low, and lifetime will be long. Potential applications include direct solar hydrogen production from water near 2300°C, production of hydrogen from nuclear energy, zero-emission coal, and other industrial hot-gas separations.

## Background and Research Objectives

Mixture separation is one of the great technological challenges, pervading the energy, chemical, and materials-processing industries. Impurities must be removed from feedstocks, contaminants must be removed from effluents, and products must be separated from one another after synthesis. The challenge is so diverse that dozens of different separation methods are in widespread use in industry.

Semi-permeable membranes are, in principle, the most efficient and hence the most obviously attractive mixture separators. (When liquid and vapor coexist, distillation is also an efficient option.) However, sometimes the desired equilibrium of the chemical reactions involved in an industrial process demands elevated temperatures, so membrane materials are limited and may be threatened by the reactivity of the mixture. Such elevated-temperature reactions include the "shift-conversion" reaction $CO + H_2O \leftrightarrow CO_2 + H_2$ and the "steam reforming" reaction $CH_4 + H_2O \leftrightarrow CO + 3H_2$, which are used in hydrocarbon-based hydrogen production, and the removal of sulfur compounds (e.g., $H_2S$, COS, $SO_2$) from hot gas streams that are predominantly CO and $CO_2$ in zero-emission-coal concepts. The S-I cycle for nuclear or solar thermal hydrogen production also needs improved high-temperature separation of $SO_2$ from $O_2$ and $H_2O$ and separation of $H_2$ from HI and $I_2$. In these reactions, even temperatures of only 500°C are challengingly "high" with respect to the practical use of current membranes. Other reactions involving hot separations include direct thermal dissociation of water, ammonia synthesis from nitrogen and hydrogen, and some of the intermediate steps in the production of nitric acid from ammonia.

Thermoacoustics could be extremely useful for hot-gas separations—especially for the mixtures of interest in hydrogen production, because most of these mixtures involve constituents with large ratios of molecular masses (e.g., $O_2/H_2$, $I_2/H_2$), which yield powerful and efficient thermoacoustic separations. However, the practical potential of thermoacoustics for hydrogen production cannot be realized without first establishing a much stronger scientific foundation, which has been the purpose of the work described here.

In thermoacoustic mixture separation, an acoustic wave traveling in a gas mixture in a tube carries the lighter component of the mixture parallel with the wave propagation and drives the heavier component anti-parallel to it. This process is the result of properly time-phased oscillating radial thermal diffusion and oscillating axial viscous motion, which depend on the thermal and viscous boundary conditions imposed on the sound wave by the solid wall of the tube. Basically, the two components of the mixture take turns being partially

immobilized in the viscous boundary layer near the wall of the tube, so the oscillating axial motion outside of the boundary layer carries light-enriched gas in one direction and heavy-enriched gas in the other direction. (Figure 2 in *Phys. Rev. Lett.* **85**, 1646–1649 (2000) gives the clearest qualitative explanation of this process.) Remarkably, this simple acoustic phenomenon was not discovered until 1998, when Los Alamos postdoc Phil Spoor noticed slightly anomalous behavior in a coupled pair of thermoacoustic engines that used a helium–xenon mixture. In the decade since then, the Los Alamos thermoacoustics team has developed an accurate quantitative theory of the process in nonreacting binary mixtures under the simplest circumstances. Starting from the most fundamental thermodynamic and hydrodynamic equations, we derived analytical solutions for the microscopic behavior of all variables of interest with respect to the two spatial dimensions perpendicular to the acoustic-propagation direction, and then performed numerical integrations along the direction of propagation. Our initial experiments with a helium–argon mixture in a short tube confirmed those calculations. We then designed a longer apparatus to achieve an isotope enrichment. In an 8-foot length of 3-mm tubing, we separated neon, a mixture of $^{22}$Ne and $^{20}$Ne, to create 1% isotope-fraction differences from end to end; and we separated a 50–50 helium–argon mixture into 70% helium at one end, 70% argon at the other.

However, our understanding at that time was completely inadequate for any quantitative evaluation of the potential of thermoacoustics in multi-component, reacting gas mixtures. In such mixtures, acoustic power will indeed produce mixture separation, but the physics was beyond the state of the art at that time because these mixtures have more than two components and have oscillating chemical reactions at the acoustic frequency. (For example, at 2200°C, partially dissociated $H_2O$'s reactions need only a millisecond to reach 90% of equilibrium concentrations.) Thus, the primary research objective of the work described here has been to create basic, quantitative understanding of the important thermoacoustic mixture-separation physics in multi-component, chemically reacting gases, through coordinated theory and experiment, so that rational designs of candidate separation schemes can be evaluated and undertaken in the future.

## Importance to LANL's Science and Technology Base and National R & D Needs

Thermoacoustic separation appears well suited to elevated-temperature, chemically reacting separations, including direct solar hydrogen production from water near 2300 C, production of hydrogen from nuclear energy, zero-emission coal, and other industrial hot-gas separations. Other applications include the separation of the hydrogen isotopes used in fusion research and nuclear weapons

## Scientific Approach and Accomplishments

Even though we are ultimately interested in high-temperature mixtures, we have conducted most of our experiments near room temperature, to keep the cost of this research low.

1. Non-reacting mixtures with 3 or more components. We are building upon our previous two-component analytical theory to accommodate mixtures with three components in which the high- and low-mass components have much lower concentrations than the mid-mass component, and we are hopeful that results without limitations on concentrations and for four or more components can also be obtained. We are well along in the design of an experiment to confirm our theory with experiments with He/Ne/Ar and possibly H2/He/Ne/Ar.

2. Superimposed steady flow. Before this project, our previous experiments had used batch-mode separation only, and our previous theory had assumed zero net mole flux. In the course of this project, we developed a theory for thermoacoustic mixture separation with superimposed steady and oscillating flows, and confirmed the theory by experiment with He/Ar. This work has been published as a peer-reviewed full-length article in the Journal of the Acoustical Society of America [1], and the theory has been incorporated into our publicly shared thermoacoustic software package DeltaEC (Design Environment for Low-amplitude ThermoAcoustic Energy Conversion) [2] and its documentation.

3. Gas mixtures with oscillating chemical reactions. Oscillating endothermic-exothermic chemical reactions add new sources of oscillating molar density, entropy, temperature, and concentration gradients to thermoacoustics. We have begun our theoretical analysis by studying two components mixtures before proceeding to three components. For the experiments, we plan to use mixtures that equilibrate rapidly at an easily accessible temperature: hydrogen + iodine + hydrogen iodide at several hundred degrees C.

4. Simultaneous axial temperature gradients and axial concentration gradients. In concepts for high-temperature thermoacoustic separators, other thermoacoustic processes such as the production of acoustic power will occur along with the separation in regions with axial temperature gradients. We have developed a theory for this complicated situation, by analytically integrating the

relevant hydrodynamic, thermodynamic, and mass-diffusion equations across the cross-section of the separation duct and numerically integrating those results along the length of the duct. We have confirmed our theory with experiments in He/Ar in a convenient temperature range near and above room temperature. A full article describing the theory and experiments has been submitted to the Journal of the Acoustical Society of America [3], and the theory has been incorporated into the next version of our publicly shared thermoacoustic software package DeltaEC and its documentation, scheduled for release in the fourth quarter of 2008.

## References


1. Swift, G. W., and D. A. Geller. Continuous thermoacoustic mixture separation. 2006. *Journal of the Acoustical Society of America.* **120** (5): 2648.

2. Ward, W. C., J. P. Clark, and G. W. Swift. Design environment for low-amplitude thermoacoustic energy conversion. 2008. *http://www.lanl.gov/thermoacoustics/DeltaEC.html.*

3. Geller, D. A., and G. W. Swift. Thermoacoustic mixture separation with an axial temperature gradient. *Journal of the Acoustical Society of America.*


## Publications


Geller, D. A., and G. W. Swift. Thermoacoustic mixture separation with an axial temperature gradient. *Journal of the Acoustical Society of America.*

Swift, G. W., and D. A. Geller. Continuous thermoacoustic mixture separation. 2006. *Journal of the Acoustical Society of America.* **120** (5): 2648.

# The S-Process in the Sm-Eu-Gd Region - A Probe for Stellar Mixing

*Aaron Joseph Couture*

20060357ER

## Abstract

Nearly all of the chemical elements are synthesized in stars. One of the principal mechanisms for such synthesis is neutron capture, which makes successively heavier elements, and the rates for synthesis of an element and its isotopes depend on nuclear information. We used unique capabilities at Los Alamos in intense neutron sources and a powerful detector array to measure neutron capture rates on radioactive nuclei, which provide stringent tests of astrophysical models. Further, a new theoretical and computational collaboration was created to investigate the stellar nucleosynthesis to probe convection in quiescent and explosive nucleosynthesis scenarios. Finally, theoretical improvements were made both in the models for predicting neutron capture rates and in the model parameters.

## Background and Research Objectives

Nuclear astrophysics is concerned with the physical processes that are responsible for the origin of the elements. The vast majority of elements are made in stars. The abundance distribution of elements in the sun and on earth are the result of a complex history of galactic chemical evolution. Ultimately, astronomers will be able to reconstruct the sequence of events that lead from the Big Bang and its pristine initial abundance configuration of He and H through the formation of the first and following generations of stars, each of which taking the ejecta of the previous generation as a starting generation for a new stellar life cycle.

An important step in solving this grand problem is to elevate the simulations of nuclear production processes in stars to a new quantitative level. The fundamental problem is that multi-dimensional effects of stellar mixing associated with the physics of convection, rotation, and magnetic fields cannot be fully captured in simulations for sufficiently long stellar evolution times. The explosive and dynamic terminal phases of stellar evolution, in particular supernovae, are accessible to direct numerical simulation, and this technique has resulted in very much improved understanding of these events. However, dominating effects in such simulations, like asymmetries related to rotation, or the density stratification of the stellar envelope at the time of the explosion, depend on the initial model. The initial model in turn is the end point of the long quiescent stellar evolution phase, and it depends on how accurately nonlinear and generically multi-dimensional processes that determine stellar mixing can be accounted for in these very long-lasting evolution phases. Current models cannot account for stellar mixing associated with the range of physical processes involved with sufficient accuracy. This severely impedes the ability of astronomers to take full advantage of a new generation of observational data that is now becoming available.

In order to provide the simulated stellar abundance data sets that are needed to interpret the abundance data from new observations in a larger astrophysical context, the physics of mixing has to be better accounted for. One strategy is numerical multi-dimensional simulations that target short phases of characteristic sections of a star, with the assumption that meaningful information about stellar mixing can be extracted and included in the efficient spherically symmetric simulations used for abundance simulations. The goal of our exploratory research is to establish a new method of validation and verification for this approach. With our approach we will be able to measure the mixing and thermodynamic conditions deep inside the star where the elements are produced. We will achieve this goal by using the fact that for some radioactive isotopes in a neutron rich environment the nucleosynthesis path depends on the temperature dependent interplay of neutron capture and beta-decay.

## Importance to LANL's Science and Technology Base and National R & D Needs

Past nuclear weapon tests rely on theoretical estimated reaction rates. This project supports NNSA's mission by developing the means to replace those data with experimentally determined values whenever possible or at least to improve the accuracy of the theoretical estimates. The knowledge and expertise developed in this project will allow direct measurement on most of

the crucial capture reactions on unstable nuclei. Further, the improved knowledge about convection will help us to understand dynamic processes in nuclear devices.

## Scientific Approach and Accomplishments

Experimentally, our first major effort was to develop a technique to evaluate the feasibility of neutron capture measurements on unstable isotopes with modern neutron time of flight facilities such as the Detector for Advanced Neutron Capture Experiments (DANCE) at the Los Alamos Neutron Science Center (LANSCE) [1]. We developed a model of DANCE in the GEANT3 [2] simulation package from CERN. We evaluated the expected s-process branchings under a variety of astrophysical scenarios in order to determine which radioactive isotopes could play a role as branch points, and thus determined the isotopes for which neutron capture cross sections were needed. The response of the DANCE instrument to samples of each branch point isotope were then simulated in order to determine what size of sample material and what neutron flux would be required to perform measurements on these branch point isotopes [3]. These tools can easily be applied to other problems of interest to Los Alamos and have already been employed for planning neutron capture cross section measurements on $^{244}$Cm for the Advanced Fuel Cycle Initiative and on As isotopes for the weapons program.

Based on these simulations, we determined the optimum sample mass for a measurement of the neutron capture cross section on $^{152}$Eu, a critical branch s-process branch point. The reaction network around $^{152}$Eu is shown in Figure 1. Because some key personnel left Los Alamos over the course of the project, we had to change our plans for sample production. It was not possible to make the sample in-house. Instead, we took advantage of a collaboration with Idaho National Laboratory to acquire the sample of $^{152}$Eu. The resulting sample consisted of 6 micrograms of $^{152}$Eu in a matrix of ~40 micrograms of $^{151}$Eu and ~40 micrograms of $^{153}$Eu. This corresponded to an activity of 30 MBq, or 30 million decays per second, all of which produced high energy gamma rays, which could be detected by DANCE. The measurements took place in December 2006 and December 2007. The first series of measurements focused primarily on the development of the techniques needed to perform a measurement on such a high rate sample. The second measurement series focused on acquiring the necessary data to extract the capture cross section of $^{152}$Eu(n,γ). We used the total reaction energy information as well as the excellent time resolution of DANCE in order to differentiate neutron capture from natural radiodecay as well as differentiate neutron capture on the stable isotopes from neutron capture on $^{152}$Eu. This represents the first ever measurement of neutron capture on $^{152}$Eu. The data from this will be fed into theoretical nuclear model calculations to improve the accuracy of calculated neutron capture rates on unstable isotopes as discussed below. Further, it will be fed into stellar s-process models to provide an additional constraint on the mixing mechanism in Asymptotic Giant Branch stars.

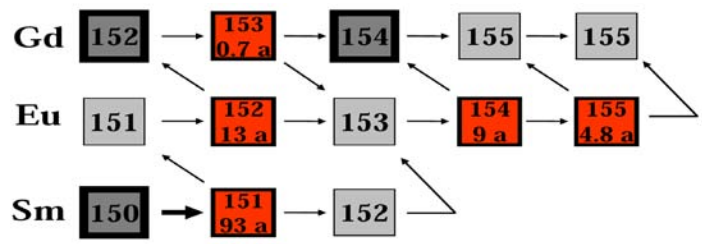


*Figure 1. The s-process path in the Sm-Eu-Gd region. The isotopes in red boxes are radioactive with their half-lives and represent branch points in this region. Samarium-150, Gd-152, and Gd-154 are all s-only isotopes, which make neutron capture cross sections on Eu-152 and Eu-154 even more important.*

In parallel, we worked to improve theoretical model calculations of neutron radiative capture process. These calculations are still unsatisfactory to predict unknown reaction rates for nucleosynthesis network calculations because the model parameters have uncertainties and the model itself has some deficiencies due to approximations made. The model parameters—nuclear level densities, gamma-ray strength functions, giant-dipole resonance parameters, and the optical model potential—are often estimated phenomenologically or obtained by microscopic models. The uncertainties on these parameters propagate to the calculated capture cross sections, and it is often said that the current quality of the capture calculation is ±50% when no experimental information is available.

The model calculation gives a reasonable excitation function (capture cross sections as a function of incident neutron energies). Once careful experimental data from advanced experimental facilities such as DANCE became available, we are able to adjust our calculations to the data and extrapolate the model prediction to obtain a Maxwellian averaged cross section for the s-process. Our effort included both improvement of the capture reaction calculations, and refinement of the model parameters.

The nuclear level density can be obtained from different methods, spanning from phenomenological systematics to *ab initio* methods. Since the s-process network calculations are very sensitive to the capture rate, it requires very accurate capture rate estimates, and phenomenological extra- or interpolation of level densities often gives better results for nuclei in the valley of stability [4].

The Gilbert-Cameron-type (GC) level density parameters obtained from the experimental average s-wave resonance spacing values are converted into the asymptotic level den-

sity parameters $a^*$ with the KTUY05 shell correction and pairing energies [5]. This procedure washes out the shell structure in the level density parameters. The $a^*$ parameter obtained is now expressed with a simple function of mass number $A$.

The other important model parameters have also been studied, and we concluded that phenomenological model parameters available in literature are in sufficient quality. The gamma-ray strength function at low energies was tested by calculating gamma-ray energy spectra from the $^{59}$Co(p,2γ) reaction with the Monte Carlo Hauser-Feshbach method [6].

We have developed a new technique to calculate the direct/semi-direct cross section based on the Hartree-Fock BCS (HF-BCS) theory [7]. The single-particle wave function is given by the deformed HF-BCS calculation and decomposition into spherical HO basis to obtain appropriate angular momentum coupling. In this method the spectroscopic factor can be related to single-particle occupation probabilities. A benchmark calculation for the neutron capture reaction on $^{238}$U was performed. The DSD is the dominant process in this energy range, and our calculation agrees the experimental data very well.

A statistical model calculation for deformed nuclei where strongly coupled channels exist is one of the long-standing problems in the Hauser-Feshbach theory. This is particularly important for neutron capture calculations for rare earth elements like Eu as they are often very deformed. Kawai, Kerman, and McVoy (KKM) calculated an energy-averaged S-matrix element [8] in the coupled-channels formalism, and recently we showed the effect of nuclear deformation on the compound cross section by solving the KKM theory numerically [9].

The nuclear deformation effect is also important to calculate the inverse process of the compound reactions. The coupled-channels method gives an S-matrix element, which is no longer diagonal. Instead of having the transmission coefficient, we can construct a Satchler's penetration matrix from the S-matrix. This yields correct penetration probabilities for the inverse channels. In this coupled-channels Hauser-Feshbach framework (CCHF), we calculated neutron capture cross sections and compared with the DANCE data of $^{241}$Am and $^{237}$Np in the fast energy region. The calculated $^{241}$Am capture cross section is shown in Figure 2 [10].

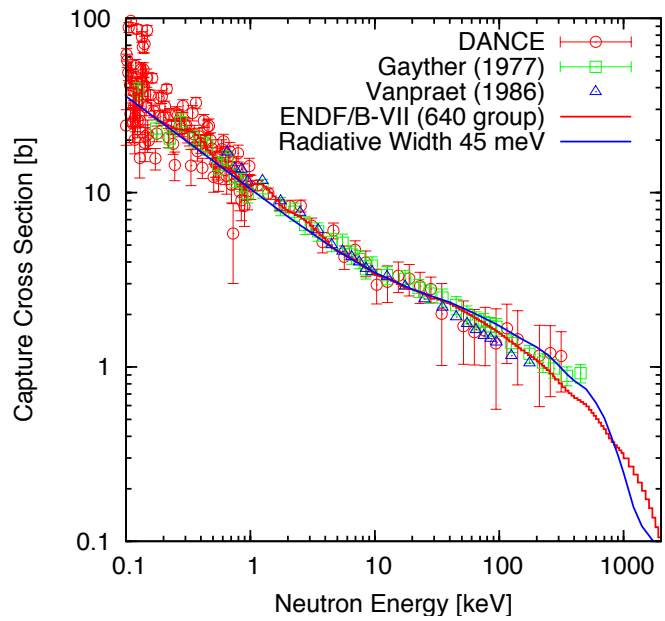


*Figure 2. Comparison of calculated capture cross section on Am-241 with the DANCE experimental data. The red curve is the evaluated cross section in ENDF/B-VII.0 and the blue curve is the present calculation. These two curves coincide up to 20 keV, and our new results give higher cross sections above this energy.*

The astrophysical and stellar modeling effort in this project at LANL has led to the formation of a new international group of collaborators (*NuGrid*) interested in quiescent nucleosynthesis during normal stellar evolution, explosive nucleosynthesis in supernova explosions, or nuclear reaction during the dynamic phase of stellar mergers or their remnants.

As part of this effort, we are on the path to produce high-precision, three dimensional, smooth particle hydrodynamic (SPH) simulations of double-degenerate mergers with various mass ratios. We are carrying out a detailed verification and validation effort. Particular emphasis is put on the initial condition setup, and the choice of the equation of state, which we find to strongly affect the dynamics of the merger. Our goal is to implement more realistic equations of state to use a stellar evolution model, and to follow dynamically important nuclear reactions and their energy input in the simulations directly. As part of the *NuGrid* collaboration, we will also use new post-processing tools to follow the evolution of SPH particles with a complete nuclear network, and use this output to validate our simulations with abundance measurements observed in R Coronae Borealis (RCB) stars [11].

Double-Degenerate (DD) mergers are an alternative to the single-degenerate progenitor scenario for type 1a supernovae (SN) that has recently received a surge in attention [12,13]. In this process, two white dwarfs (WD) merge, pushing one of them over the Chandrasekhar limit, which

causes it to contract and explode. The main advantages of this model are that the predicted rate of DD mergers is consistent with the observed SN rate, in contrast to many other SN1a progenitor models. While this DD merger scenario was ruled out early on [14], promising new results have shed a new light on this paradigm, opening up small windows of opportunity for SN1a as a result of DD mergers [13].

We use the self-consistent field method to setup up our initial conditions. This method was first developed by [15] and employed by [16], [17] and [18]. It iteratively solves the equilibrium configuration for unequal mass close binaries in co-rotation. Its biggest advantage is that initial conditions are in perfect equilibrium, imposing very few artifacts in the simulations due to an imprecise initial setup. Its main drawback at the moment is that one is bound to choose a rather simple equation of state to produce polytropes, though work is underway to generalize this method for a more realistic equation of state. In order to be able to model a rather gentle Roche lobe overflow correctly with a particle based method like SPH, we have developed a new SPH particle setup method that allows us to increase the resolution in the outer layers, while keeping an optimal distribution of particles. Figure 3 shows an example setup for a *q=1.3* mass ratio binary. The accretor is set up with a constant particle density on the left, while the donor on the right (filling 99.7\% of its Roche lobe) has an 8x higher resolution in its outer layers.

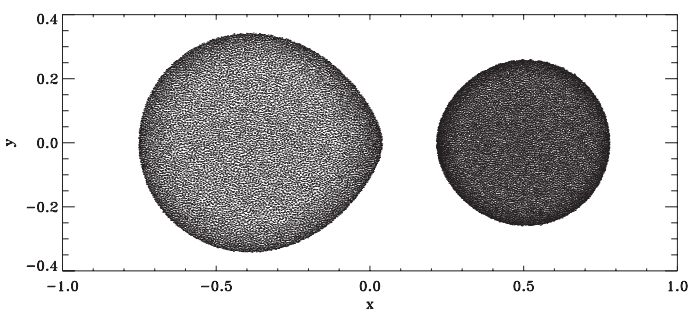


*Figure 3. Initial condition setup for a q=1.3 mass ratio white dwarf binary system*

We also note a strong difference in behavior for corotating vs. non-corotating systems. Non-corotating systems tend to transfer a significant fraction of the orbital angular momentum into spinning up stars. This results in the orbit shrinking, bringing the star into deeper Roche lobe contact and artificially shortening the merger time scale. For more details, refer to [19].

To understand the effects of the equation of state and shocks in particular on the dynamics of the merger, we have conducted various runs with different equations of state but otherwise identical initial conditions. Figure 4 shows the time evolution of a DD merger between two polytropes with a mass ratio of *q=1.3*. This sequence shows the crucial 1.5 orbits where the most dynamic phase of the actual merger takes place (starting at around 9.5 orbits). This run assumes an ideal gas equation of state and includes shocks, which can be easily seen as strong density discontinuities in the snapshots. Note that the remnant settled into an almost spherically symmetric configuration, and is differentially rotating, with a fast rotating core and a hot envelope. At the end of our simulation, the extent of the halo is around 100 solar radii, and is still expanding. However, we do emphasize that the actual behavior may very well quantitatively differ when a more realistic equation of state is employed.

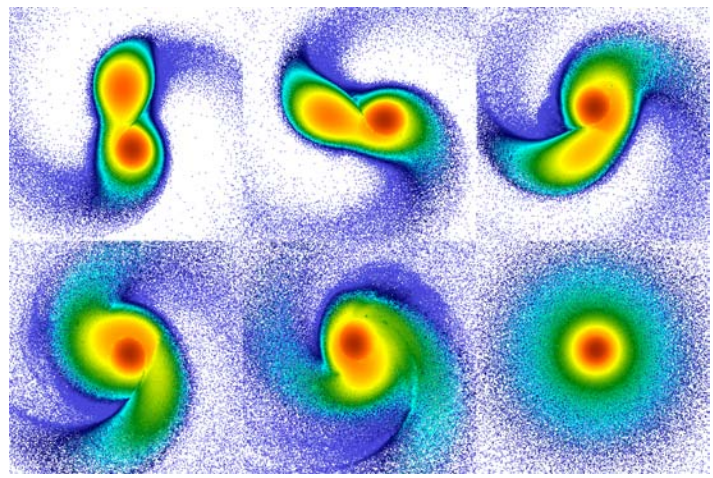

*Figure 4. SPH simulation of the q=1.3 merger simulation with an ideal gas equation of state. The figure shows a time sequence starting at the onset of the merging process after about 9.5 orbits. Note the importance of the strong shocks. The last panel shows the core of the relaxed merger remnant (~16 orbital periods).*

## References

1. Heil, M., R. Reifarth, M. M. Fowler, R. C. Haight, F. Kaeppeler, R. S. Rundberg, E. H. Seabury, J. L. Ullmann, J. B. Wilhelmy, and K. Wisshak. A 4pi BaF2 detector for (n,gamma) cross-section measurements at a spallation neutron source. 2001. *Nuclear Instruments and Methods in Physics Research A`*. **459**: 229.

2. GEANT--Detector Description and Simulation Tool. 1993. *CERN Program Library Long Writeup W5013.*

3. Couture, A., and R. Reifarth. Direct measurements of neutron capture on radioactive isotopes. 2007. *Atomic Data and Nuclear Data Tables.* **93**: 807.

4. Kawano, T., S. Chiba, and H. Koura. Phenomenological nuclear level densities using the KTUY05 nuclear mass formula for applications off-stability. 2006. *journal of Nuclear Science and Technology.* **43**: 1.

5. Koura, H., T. Tachibana, M. Uno, and M. Yamada. Nuclidic mass formula on a spherical basis with an improved even-odd term. 2005. *Progress in Theoretical Physics.* **113**: 305.

6. Kawano, T.. Statistical model calculations for neutron radiative capture process. Presented at *Workshop on Statistical Nuclear Physics and its Applications in Astrophysics.* (Athens, 8-11 July 2008).

7. Bonneau, L., T. Kawano, T. Watanabe, and S. Chiba. Nucleon direct-semidirect radiative capture with Skyrme-Hartree-Fock-BCS bound states . 2007. *Physical Review C.* **75**: 054618.

8. Kawano, T., L. Bonneau, and A. Kerman. Effects of direct reaction coupling in compound reactions. 2007. In *International Conference on Nuclear Data for Science and Technology.* (Nice, 22-27 April 2007). , p. 041. NICE: EDP Science.

9. Jandel, M., T. A. Bredeweg, E. M. Bond, M. B. Chadwick, R. R. Clement, A. Couture, J. M. O'Donnell, R. C. Haight, T. Kawano, R. Reifarth, R. S. Rundberg, J. L. Ullmann, D. J. Vieira, J. B. Wilhelmy, J. M. Wouters, U. Agvaanluvsan, W. E. Parker, C. Y. Wu, and J. A. Becker. Neutron capture cross section of 241Am . 2008. *Physical Review C.* **78**: 034609.

10. Clayton, G. C., T. R. Geballe, F. Herwig, C. Fryer, and m. Asplund. Very large excesses of 18O in hydrogen-deficient carbon and R Coronae Borealis stars: Evidence for white dwarf mergers. 2007. *Astrophysical Journal.* **662**: 1220.

11. Saio, H., and K. Nomoto. Off-center carbon ignition in rapidly rotating, accreting carbon-oxygen white dwarfs. 2004. *Astrophysical Journal.* **615**: 444.

12. Yoon, S. C., P. Podsiadlowski, and S. Rosswog. Remnant evolution after a carbon-oxygen white dwarf merger. 2007. *Monthly Notices of the Royal Astronomical Society.* **380**: 933.

13. Nomoto, K., and Y. Kondo. Conditions for accretion-induced collapse of white dwarfs. 1991. *Astrophysical Journal.* **367**: L.

14. Hachisu, I.. A versatile method for obtaining structures of rapidly rotating stars II--Three dimensional self-consistent field method. 1986. *Astrophysical Journal Supplement.* **62**: 461.

15. Motl, P. M., J. E. Tohline, and J. Frank. Numerical methods for the simulation of dynamical mass transfer in binaries. 2002. *Astrophysical Journal Supplement.* **138**: 121.

16. R.D'Souza, M. C., P. M. Motl, J. E. Tohline, and J. Frank. Numerical simulations of the onset and stability of dynamical mass transfer in binaries. 2007. *Astrophysical Journal.* **643**: 381.

17. Motl, P. M., J. Frank, J. E. Tohline, and M. C. R. D'Souza. The stability of double white dwarf binaries undergoing direct-impact accretion. 2007. *Astrophysical Journal.* **670**: 1314.

18. Fryer, C. L., and S. Diehl. On the road to understanding type Ia progenitors: Precision simulations of double degenerate mergers. 2008. In *Hydrogen-Deficient Stars.* (Tuebingen, 17-21 September 2007). Vol. 391, p. 335. San Francisco: Astronomical Society of the Pacific.

## Publications

Baker, J., C. McGrath, T. Hill, R. Reifarth, and F. Tovesson. Actinide targets for neutron cross section measurements. 2008. *J. Radioanalytical Nucl. Chem.* **276** (2): 555.

Bonneau, L., T. Kawano, T. Watanabe, and S. Chiba. Nucleon direct-semidirect radiative capture with Skyrme-Hartree-Fock-BCS bound states. 2007. *Physical Review C.* **75**: 054618.

Chia, S., H. Koura, T. Hayakawa, T. Maruyama, T. Kawano, and T. Kajino. Direct and semi-direct capture in low-energy (n,gamma) reactions of neutron-rich tin isotopes and its implications for r-process nucleosynthesis. 2008. *Physical Review C.* **77**: 015809.

Couture, A., and R. Reifarth. Direct measurements of neutron capture on radioactive isotopes. 2007. *Atomic Data and Nuclear Data Tables.* **93**: 807.

Dashdorj, D., G. E. Mitchell, T. Kawano, J. A. Becker, U. Agvaanluvsan, M. B. Chadwick, J. R. Cooper, M. Devlin, N. Fotiades, P. E. Garrett, R. O. Nelson, C. Y. Wu, and W. Younes. Neutron induced inelastic cross-sections of 150Sm for E_n= 1--35 MeV. 2007. *Nuclear instruments and Methods in Physics Rresearch B.* **B261**: 948.

Dashdorj, D., T. Kawano, P. E. Garrett, J. A. Becker, U. Agvaanluvsan, L. A. Bernstein, M. B. Chadwick, M. Devlin, N. Fotiades, G. E. Mitchell, R. O. Nelson, and W. Younes. Effect of preequilibrium spin distribution on 48Ti + n cross sections. 2007. *Physical Review C.* **75**: 054612.

Diehl, S., C. Fryer, M. Bennett, F. Herwig, R. Hirschi, A. Hungerford, G. Magkotsios, M. Pignatari, G. Rockefeller, F. Timmes, and P. Young. NuGrid: Toward High-Precision Simulations of Double Degenerate Mergers. To appear in *Nuclei in the Cosmos X.* (Mackinac island, 27 July-1 Aug 2008).

Diehl, S., C. Fryer, and F. Herwig. The Formation of Hydrogen Deficient Stars through Common Envelope Evolution. 2008. In *Hydrogen Deficient Stars.* (Tuebingen, 17-21 Sept. 2007). Vol. 391, p. 221. San Francisco: AStronomical Society of the Pacific.

Diehl, S., and G. Rockefeller. A New Optimal Initial Conditions Scheme for Smooth Particle Hydrodynamics. *Monthly Notices of the Royal Astronomical Society.*

Esch, E. I., R. Reifarth, E. M. Bond, T. A. Bredeweg, A. Couture, S. E. Glover, U. Greife, R. C. Haight, A. M. Hatarik, M. Jandel, T. Kawano, A. Mertz, J. M. O'Donnell, R. S. Rundberg, J. M. Schwantes, J. L. Ullmann, D. J. Vieira, J. B. Willhelmy, and J. M. Wouters. Measurement of the 237Np(n,gamma) cross section from 20 meV to 500 keV with a high efficiency, highly segmented 4pi BaF_2 detector. 2008. *Physical Review C.* **77**: 034309.

Fryer, C., and S. Diehl. On the Road to Understanding Type Ia Progenitors: Precision Simulations of Double Degenerate Mergers. 2008. In *Hydrogen Deficient Stars.* (Tuebingen, 17-21 Sept. 2007). Vol. 391, p. 335. San Francisco: AStronomical Society of the Pacific.

Herwig, F., S. Austin, and J. Lattanzio. Nuclear reaction rate uncertainties and astrophysical modeling: Carbon yields from low-mass giants. 2006. *Physical Review C.* **73**: 025802.

Hirschi, R., S. Diehl, M. Bennett, C. Fryer, F. Herwig, A. Hungerford, G. Magkotsios, M. Pignatari, G. Rockefeller, F. Timmes, and P. Young. NuGrid: s-process in massive stars. To appear in *Nuclei in the Cosmos X.* (Mackinac island, 27 July-1 Aug 2008).

Hungerford, A., S. Diehl, M. Bennett, C. Fryer, F. Herwig, R. Hirschi, G. Magkotsios, M. Pignatari, G. Rockefeller, F. Timmes, and P. Young. NuGrid: Difficulties in Probing Nuclear Physics: A Study of 44 Ti and 56 Ni. To appear in *Nuclei in the Cosmos X.* (Mackinac island, 27 July-1 Aug 2008).

Jandel, M., T. A. Bredeweg, E. M. Bond, M. B. Chadwick, R. R. Clement, A. Couture, J. M. O'Donnell, R. C. Haight, T. Kawano, R. Reifarth, R. S. Rundberg, J. L. Ullmann, D. J. Vieira, J. B. Wilhelmy, J. M. Wouters, U. Agvaanluvsan, W. E. Parker, C. Y. Wu, and J. A. Becker. Neutron capture cross section of 241Am. 2008. *Physical Review C.* **78**: 034609.

Johnson, J., F. Herwig, T. Beers, and N. Christlieb. A search for nitrogen-enhanced metal-poor stars. To appear in *Astrophysical Journal.*

Kawano, T., M. B. Chadwick, P. Talou, and P. G. Young. Nuclear Reaction Data for Nuclear Technologies and Applications. 2008. In *international Workshop on Compound-Nuclear Reactions and Related Topics.* (Fish Camp, CA, 22-26 October 2007). Vol. 1005, p. 17. Melville: AIP.

Kawano, T., S. Chiba, and H. Koura. Phenomenological Nuclear Level Densities Using the KTUY05 Nuclear Mass Formula for Applications Off-Stability. 2006. *Journal of Nuclear Science and Technology.* **43**: 1.

Mertz, A., T. Bredeweg, A. Couture, M. Jandel, R. Haight, J. O'Donnell, R. Reifarth, R. Rundberg, J. Tesmer, J. Ullmann, I. Usov, D. Vieira, Y. Wang, and J. Wouters. Characterization of the neutron beam profile at DANCE. 2006. *LANL internal report.*

Reifarth, R., M. Heil, C. Forssen, U. Besserer, A. Couture, S. Dababneh, L. Doerr, J. Goerres, R. C. Haight, F. Kaeppeler, A. Mengoni, S. O'Brien, N. Patronis, R. Plag, R. S. Rundberg, M. Wiescher, and J. B. Wilhelmy. The 14C(n,gamma) cross

section between 10 keV and 1 MeV. 2008. *Physical Review C.* **77**: 015804.

Reifarth, R., U. Agvaanluvsan, A. Alpizar-Vicente, T. Bredeweg, E. Esch, U. Greife, R. Haight, R. Hatarik, F. Herwig, J. O'Donnell, R. Rundberg, J. Schwantes, J. Ullmann, D. Vieira, and J. Wouters. Neutron capture rates on radioactive nuclides - DANCE. 2006. *New Astronomy Reviews.* **50**: 644.

Rockefeller, G., S. Diehl, M. Bennett, C. Fryer, F. Herwig, R. Hirschi, A. Hungerford, G. Magkotsios, M. Pignatari, F. Timmes, and P. Young. NuGrid: Nucleosynthetic Yields from Collapsars. To appear in *Nuclei in the Cosmos X.* (Mackinac island, 27 July-1 Aug 2008).

Sivarani, T., T. Beers, P. Bonifacio, P. Molaro, R. Cayrel, F. Herwig, M. Spite, and B. Plez. First stars X. The nature of three unevolved Carbon-Enhanced Metal-Poor stars. 2006. *Astronomy & Astrophysics.* **459** (1): 125.

Ueta, T., A. Speck, R. Stencel, F. Herwig, R. Gehrz, R. Szczerba, H. Izumiura, and A. Zijlstra. Detection of a far-infrared bow shock nebula around R Hya: the first MIRIAD results. 2006. *Astrophysical Journal.* **648**: L39.

Werner, K., and F. Herwig. The elemental abundances in bare planetary nebula central stars and the shell burning in AGB stars. 2006. *Publications of the Astronomical Society of the Pacific.* **118**: 183.

Wouters, J., A. Alpizar-Vicente, T. Bredeweg, E. Esch, R. Haight, R. Hatarik, J. O'Donnell, R. Reifarth, R. Rundberg, and J. Schwantes. Acquisition - Analysis system for the DANCE BaF2 gamma-ray calorimeter. 2006. *IEEE Transactions on Nuclear Science.* **53**: 880.

# Role of Electrostatic Forces in Space and Astrophysics

*Gian Luca Delzanno*

20060399ER


## Abstract

This project has been devoted to study the role that electrostatic fields play in plasmas as mediator between small and large scales and its importance in the self-organization of large scale systems. We have focused on space and astrophysical plasmas and specifically considered the process of conversion of magnetic energy into kinetic energy of the plasma particles and heat (this process is commonly referred to as magnetic reconnection) and the interaction between small bodies immersed in plasmas. The project has been very multidisciplinary and has included theoretical modeling, state-of-the-art numerical simulations and an experimental activity. Our findings have confirmed that indeed electrostatic fields play a critical role in the micro-macroscopic coupling in plasmas. This can be considered a paradigm shift since previously the consensus was that electrostatic fields are shielded away from the bulk of the plasma and cannot play any major role in it.

Our work supports DOE's strategic science mission. We investigate fundamental processes related to astrophysical systems, but as a paradigm of many other systems crucial in national security work. Furthermore, the understanding of the near Earth environment is crucial for studies aimed at threat reduction and homeland defense. Last but not least, the project constitutes a step forward toward predictive capabilities in plasmas, which, for instance, are relevant for achieving fusion energy, a very important goal for the nation and the world


## Background and Research Objectives

The aim of the project was to investigate a new possibility: that electrostatic fields play a crucial role in the self-organization of large scale systems.

The project involved two distinct aspects:

1. The role of electrostatic fields in the conversion of magnetic energy into kinetic (both the ordered energy of flows and particle fluxes and the disordered energy of heat) in processes developing in the solar system and in astrophysical plasmas and termed "magnetic reconnection."

2. The role of electrostatic forces arising from the interaction of small bodies immersed in ionized nebulae in the protosolar and protoplanetary systems. These forces were always considered repulsive due to the fact that all objects share the same sign of charge. However, thanks to our recent discovery the force might, in certain conditions to be explored, become attractive.

Our findings confirmed and enlarged our initial view points. The electrostatic fields indeed play a crucial role in both situations. In the section 'Scientific Approach and Accomplishments' we list the key findings for each of the two aspects.

## Importance to LANL's Science and Technology Base and National R & D Needs

This project has fundamental relevance for LANL and DOE missions as it moves forward in enabling true physics-based predictive capabilities. A fundamental goal of the project has been to understand micro-macro coupling and how the small scale microphysics organize to affect large scale system processes. This goal is broader than just space and astrophysics. Similar effects are present in any type of plasmas and in other materials.

The physics-based predictive modeling of plasmas in general and of burning plasmas specifically requires addressing the issue of how to represent the micro-macro coupling in simulations. A practical example of spin off of the present work with programmatic relevance is the study of shocks in plasmas and the presence of induced electrostatic turbulence that self-

organizes in a large scale electric field. These results are applicable to laser-plasma interaction.

Understanding the near Earth environment is also relevant for threat reduction and homeland defense studies.

The present project also directly impacts some of the laboratory strategic goals (grand challenges): Section 3 'Fundamental understanding of materials', Section 4 'Carbon Neutral Fuel Cycle Team Report', and Section 5 'Complex Systems'. Particularly, pathways to fusion energy are relevant to investigations of a carbon neutral fuel cycle that is an increasingly urgent goal for our nation and the world.

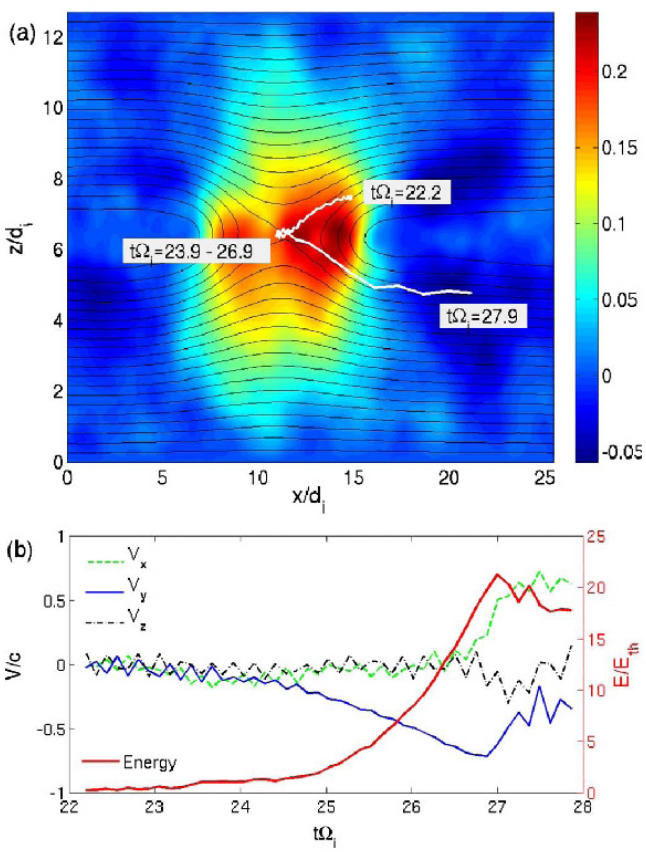


*Figure 1. Electric field superimposed on a trajectory (panel a) and energy increase (panel b) for a region of magnetic reconnection where magnetic energy is converted to kinetic energy. From Reference 1.*

## Scientific Approach and Accomplishments

This project has been very multidisciplinary, including theoretical modelling, state-of-the-art numerical simulations and experiments. Numerical simulations have been conducted mainly with existing tools but, when needed, we have also developed new, innovative tools. Experiments have been conducted in the RSX (Reconnection Scaling eXperiment) device.

With regard to the role of the electrostatic field in magnetic reconnection, the main accomplishments are:

- We investigated the statistical distribution of the plasma particles in reconnection regions, tracking the energy transformations from magnetic to kinetic. We produced a detailed comparison of findings in satellite data and in our simulations, arriving at a complete and self-consistent model of specific events observed in the Earth environment. The role of electrostatic forces have been identified, its origin tracked and its effects verified, in complete agreement with out original viewpoint [1].

- We studied the processes of self organization and in particular the role of electrostatic fields in the processes of coalescence of flux ropes. We discovered a new regime where the system evolution becomes invariant to the change of a number of macroscopic drivers proving that the microscopic physics, thanks to the role of the electrostatic field becomes enslaved to the requirements of the macroscopic drivers [2].

- An approach to track the evolution of high energy particles, in multiple scales systems such as those under investigation was derived in the special relativity limit using a new approach to the implicit moment method [3, 4, 5].

- The rate of the energy conversion was studied and it was demonstrated that the cause for the onset of the conversion resides on a self-reinforcing runaway mechanism produced by the electrons and mediated by the electrostatic fields [6].

- A direct comparison of the predictions of the old paradigm based on anomalous collision processes and our new model based on the role of the electrostatic field was conducted proving the inadequacy and the inconsistencies of the old paradigm [7].

- The expansion of the reconnection processes and the roles of flows and electrostatic fields were studied in 3D fully kinetic simulations, investigating the role of the coupling of large scales and small scales mediated by electric fields [8].

- Besides focusing on the fundamental physics of magnetic energy conversion in reconnection processes

we also investigated its application to specific astrophysical processes, namely the jets emitted from the accretion disks around supermassive black holes in AGN [9] and the processes relevant to the formation of the solar wind [10].

With regard to the role of electrostatic forces arising from the interaction of small bodies in plasmas, the main accomplishments are:

- The experimental investigation thanks to collaboration with P-24 of the motion of objects immersed in a plasma, highlighting the role of electrostatic and drag forces [11].

- The prostellar and proplanetary nebulae are magnetized as suggested by models and confirmed by observation, it is therefore crucial to investigate the process of interaction between the particle and the plasma in a magnetized plasma. We considered both the process of charging and shielding, providing an analysis of the force field around an object immersed in a magnetized plasma [12].

- Similarly, the plasma in protostellar and protoplanetary nebulae is weakly magnetized and an investigation of the effect of neutral collisions is key to our understanding of the processes. We developed a new computational tool based on a montecarlo collision package added to our DEMOCRITUS plasma code. The process of charging and shielding in a collisional plasma was studied and the force field computed [13].

- We investigated the temporal evolution of the force field around an object immersed in a plasma discovering a new effect that leads to the cyclical chaotic fluctuation of the force field with cyclical times of reduced repulsion or even repulsion followed by attraction [14].

- Based on our previous work we have a detailed understanding of the conditions needed for the new attractive electrostatic force. The following step has been to investigate in details the conditions in protostellar nebulae by modelling the interaction of radiation from nearby stars with the gas in a nebulae. We have identified the regions where the attractive force is present, proving that indeed our proposed mechanism is possible (paper in preparation).

With regard to the experimental campaign conducted to verify the premises of the project, the main accomplishments are:

- We have investigated experimentally with the RSX device the evolution of the kink instability carrying out for the first time a direct investigation of the role of the electrostatic field. We discovered that the electrostatic field is indeed, as we proposed, the main driver of the plasma motion, despite the electromagnetic nature of the kink instability [15].

- Magnetic flux tubes or flux ropes in plasmas are important in nature and the laboratory. Axial boundary conditions strongly affect flux rope behavior, but this has never been systematically investigated. We discussed new data and theory that demonstrate how external boundary geometry can be employed to stabilize the kink mode, and provide a laboratory “dial” between two different mathematical boundary conditions. We experimentally and theoretically demonstrate for the first time axial boundary conditions (BC) that are continuously varied between ideal magnetohydrodynamic (MHD) non-line-tied and line-tied. The flux rope displacement BC is increasingly constrained from non-line-tied (free) to line-tied (fixed), and is consistent with the kink instability threshold [16, 17].

- We have experimentally described the collisions between flux ropes and whether they merge or coalesce, which prior to this has only been computationally modeled. This may provide a logical framework for three dimensional spontaneous onset of magnetic reconnection [18].

- A laboratory example of impulsive onset of magnetic reconnection has been shown. How the onset and cessation of magnetic reconnection events abruptly comes to pass has been a long standing question. We show a three dimensional laboratory example of the onset and stagnation of Sweet-Parker type magnetic reconnection that is self consistently driven by magnetohydrodynamic attraction and collision of magnetized, parallel current (flux) ropes. The mutually attracting flux rope plasmas advect oppositely directed magnetic fields towards each other, accompanied by the annihilation of magnetic flux. When the inflow speed increases past the Sweet-Parker speed, the magnetic flux arrives faster than flux annihilation can process it. This is a threshold for magnetic flux and pressure pile up around the reconnection region, accompanied by changes in the magnetic topology. The piled up fields generate forces that react back on the incoming flux ropes to stall the inflow and thus the reconnection process [19].

- A three dimensional probe positioner has been designed, installed and is in use to explore three dimensional volumes of plasma with good spatial resolution [20].

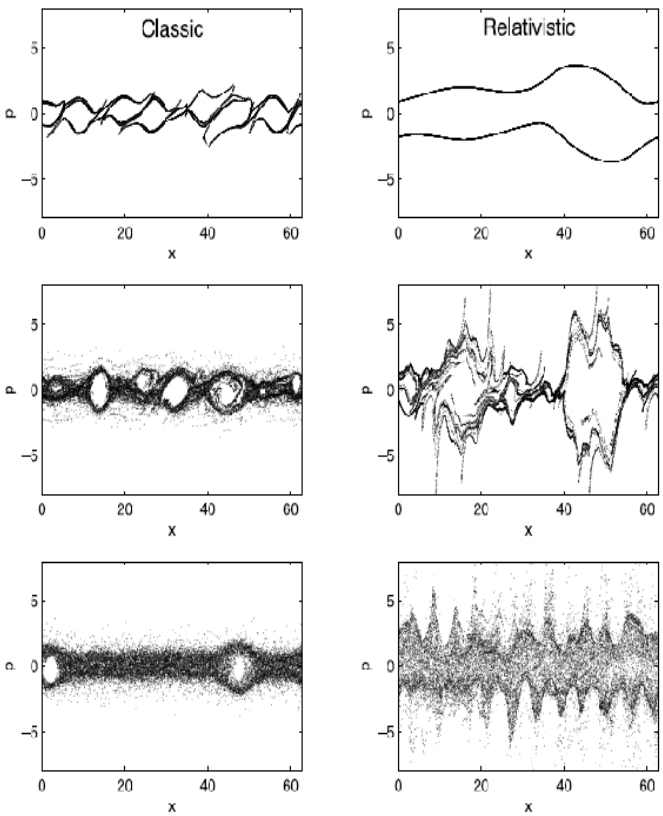


*Figure 2. Starting from the same initial condition (top panel ), the classical (left panel ) and relativistic (right panel ) systems evolve differently in the phase space (x, p space). From top to bottom successive times are shown. The energies reached in the relativistic case are largely superior. From Reference 21.*

In the process of execution of the project we made two unanticipated new discoveries, related to the role of the electrostatic fields:

- The anomalous acceleration of high energy particles in relativistic systems where electrostatic fluctuations become highly effective in the relativistic Minkowski spacetime: the deposited heat remains trapped by the inability of particles to diffuse aways at speed exceeding the speed of light. A runaway process ensues where particles become highly energetic and their distribution becomes a power law. This finding has profound implication for our understanding of high energy particles in the cosmos, and in particular for the ultra high energy cosmic rays [21].

- The role of the electrostatic field in self-organizing the microscopic physics emerged in one unexpected area: the evolution of shocked collisionless plasmas where electrostatic fields become the dominant mechanism that determines the shock profile and the particle acceleration at the shocks. This too has profound implication to astrophysical as well as laboratory plasmas [22].

Finally we organized a special session on the role of electrostatic fields in laboratory, space and astrophysical plasmas at the 2006 AGU Fall Meeting in San Francisco, a meeting attended by over 13,000 people, including former Vice President Albert Gore. We are also organizing a special section on magnetic reconnection in space and astrophysical plasmas at the 2008 AGU Fall meeting in San Francisco.

The project has also produced six Master's Degree theses. Four postdocs were involved at various stages during the development of the project. Two have been converted to Limited Term Staff Member positions at LANL, one has recently obtained a position at the University of Colorado.

## References

1. Wan, W., G. Lapenta, G. L. Delzanno, and J. Egedal. Electron acceleration during guide field magnetic reconnection. 2008. *Physics of Plasmas.* **15**: 032903.

2. Wan, W., and G. Lapenta. Micro-macro coupling in plasma self-organization processes during island coalescence. 2008. *Physical Review Letters.* **100**: 035004.

3. Lapenta, G., J. U. Brackbill, and P. Ricci. Kinetic approach to microscopic-macroscopic coupling in space and laboratory plasmas. 2006. *Physics of Plasmas.* **13**: 055904.

4. Noguchi, K., C. Tronci, G. Zuccaro, and G. Lapenta. Formulation of the relativistic moment implicit particle-in-cell method. 2007. *Physics of Plasmas.* **14**: 042308.

5. Brackbill, J. U., and G. Lapenta. Magnetohydrodynamics with implicit plasma simulation. 2008. *Communications in Computational Physics.* **4**: 433.

6. Wan, W., and G. Lapenta. Electron self-reinforcing process of magnetic reconnection. 2008. *Physical Review Letters.* **101**: 015001.

7. Innocenti, M. E., and G. Lapenta. Momentum creation by drift instabilities in space and laboratory plasmas. 2007. *Plasma Physics and Controlled Fusion.* **49**: B521.

8. Lapenta, G., D. Krauss-Varban, H. Karimabadi, J. D. Huba, L. I. Rudakov, and P. Ricci. Kinetic simulations of X-line propagation in 3D reconnection. 2006. *Geophysical Research Letters.* **33**: L10102.

9. Li, H., G. Lapenta, J. M. Finn, S. Li, and S. A. Colgate. Modeling the large scale structures of astrophysical jets in the magnetically dominated limit. 2006. *Astrophysical Journal.* **643**: 92.

10. Lapenta, G., and A. L. Restante. Blob formation in the solar wind: role of converging flows and viscosity. To appear in *Annales Geophysicae.*

11. Ticos, C. M., Z. Wang, G. L. Delzanno, and G. Lapenta. Plasma dragged microparticles as a method to measure plasma flows. 2006. *Physics of Plasmas.* **13**: 103501.

12. Patacchini, L., I. H. Hutchinson, and G. Lapenta. Electron collection by a negatively charged sphere in a collisionless magnetoplasma. 2007. *Physics of Plasmas.* **14**: 062111.

13. Rovagnati, B., M. Davoudabadi, G. Lapenta, and F. Mashayek. Effect of collisions on dust particle charging via particle-in-cell Monte-Carlo collision . 2007. *Journal of Applied Physics.* **102**: 073302.

14. Rovagnati, B., G. Lapenta, and F. Mashayek. Dynamic nature of the ion wake in dusty plasmas. 2008. *Physics Letters A.* **372** (38): 5991.

15. Intrator, T. P., I. Furno, D. D. Ryutov, G. Lapenta, L. Dorf, and X. Sun. Long-lifetime current-driven rotating kink modes in a non-line-tied plasma column with a free end. 2007. *Journal of Geophysical Research.* **112**: A05590.

16. Furno, I., T. P. Intrator, D. D. Ryutov, S. Abbate, T. Madziwa-Nussinov, A. Light, L. Dorf, and G. Lapenta. Current driven rotating kink mode in a plasma column with a non-line-tied free end. 2006. *Physical Review Letters.* **97**: 015002.

17. Sun, X., T. P. Intrator, L. Dorf, I. Furno, and G. Lapenta. Transition of MHD kink stability properties between line-tied and non line-tied boundary conditions. 2008. *Physical Review Letters.* **100**: 205004.

18. Sun, X., T. P. Intrator, L. Dorf, I. Furno, and G. Lapenta. Relationship between flux rope merging, bouncing and onset threshold for 3D Sweet-Parker reconnection. *Physical Review Letters.*

19. Intrator, T. P., X. Sun, G. Lapenta, R. M. Kulsrud, I. Furno, and L. Dorf. Experimental onset threshold and magnetic pressure pileup for 3D Sweet-Parker reconnection. *Nature Physics.*

20. Intrator, T. P., X. Sun, L. Dorf, I. Furno, and G. Lapenta. A three dimensional probe positioner. To appear in *Review of Scientific Instruments .*

21. Lapenta, G., S. Markidis, and A. Marocchino. Relaxation of relativistic plasmas under the effect of wave-particle interactions. 2007. *Astrophysical Journal.* **666**: 949.

22. Lapenta, G., and J. King. Study of current intensification by compression in the Earth magnetotail. 2007. *Journal of Geophysical Research.* **112**: A12204.

## Publications

Amatucci, W. E., W. Scales, E. Thomas, and G. Lapenta. Dusty plasmas in Colonial Williamsburg. 2007. *IEEE Transactions On Plasma Science.* **35** (2): 253.

Brackbill, J. U., and G. Lapenta. Magnetohydrodynamics with implicit plasma simulation. 2008. *Communications in Computational Physics.* **4**: 433.

Camporeale, E., G. L. Delzanno, W. Daughton, and G. Lapenta. New Approach for the study of linear Vlasov stability of Inhomogeneous Systems. 2006. *Physics of Plasmas.* **13** (9): 092110.

Delzanno, G. L., L. Chacon, J. M. Finn, Y. Chung, and G. Lapenta. An optimal robust equidistribution method for two-dimensional grid adaptation based on Monge-Kantorovich optimization. To appear in *Journal of Computational Physics.*

Delzanno, G. L., and J. M. Finn. The effect of line-tying on tearing modes. 2008. *Physics of Plasmas.* **15**: 032904.

Evstatiev, E. G., R. A. Nebel, L. Chacon, J. Park, and G. Lapenta. Space charge neutralization in inertial electrostatic confinement plasmas. 2007. *Physics of Plasmas.* **14** (4): 042701.

Finn, J. M., G. L. Delzanno, and L. Chacon. Grid generation and adaptation by Monge-Kantorovich optimization in two

and three dimensions. To appear in *Proceedings of the 17th International Meshing Roundtable.*

Furno, I., T. P. Intrator, D. D. Ryutov, S. Abbate, T. Madziwa-Nussinov, A. Light, L. Dorf, and G. Lapenta. Current-driven rotating-kink mode in a plasma column with a non-line-tied free end. 2006. *Physical Review Letters.* **97** (1): 015002.

Furno, I., T. P. Intrator, G. Lapenta, L. Dorf, S. Abbate, and D. D. Ryutov. Effects of boundary conditions and flow on the kink instability in a cylindrical plasma column. 2007. *Physics of Plasmas.* **14** (2): 022103.

Innocenti, M. E., and G. Lapenta. Momentum creation by drift instabilities in space and laboratory plasmas. 2007. *Plasma Physics and Controlled Fusion.* **49**: B521.

Intrator, T. P., I. Furno, D. D. Ryutov, G. Lapenta, L. Dorf, and X. Sun. Long-lifetime current-driven rotating kink modes in a non-line-tied plasma column with a free end. 2007. *Journal of Geophysical Research-Space Physics.* **112** (A5): A05S90.

Intrator, T. P., X. Sun, G. Lapenta, R. M. Kulsrud, I. Furno, and L. Dorf. Experimental onset threshold and magnetic pressure pileup for 3D Sweet-Parker reconnection. To appear in *Nature Physics.*

Intrator, T. P., X. Sun, L. Dorf, I. Furno, and G. Lapenta. A three dimensional probe positioner. To appear in *Review of Scientific Instruments .*

Jacobs, G. B., J. S. Hesthaven, and G. Lapenta. Simulations of the weibel instability with a high-order discontinuous galerkin particle-in-cell solver. 2006. *Collection of Technical Papers - 44th AIAA Aerospace Sciences Meeting.* **19**: 14189.

Lapenta, G.. Self-feeding turbulent magnetic reconnection on macroscopic scales. 3008. *Physical Review Letters.* **100** (23): 235001.

Lapenta, G., D. Krauss-Varban, H. Karimabadi, J. D. Huba, L. I. Rudakov, and P. Ricci. Kinetic simulations of x-line expansion in 3D reconnection. 2006. *Geophysical Research Letters.* **33** (10): L10102.

Lapenta, G., I. Furno, T. Intrator, and G. L. Delzanno. Kink instability of flux ropes anchored at one end and free at the other. 2006. *Journal of Geophysical Research-Space Physics.* **111** (A12): A12S06.

Lapenta, G., J. U. Brackbill, and P. Ricci. Kinetic Approach to microscopic-macroscopic coupling in space and laboratory plasmas. 2006. *Physics of Plasmas.* **13** (5): 055904.

Lapenta, G., S. Markidis, and A. Marocchino. Relaxation of relativistic plasmas under the effect of wave-particle interactions. 2007. *Astrophysical Journal.* **666** (2): 949.

Lapenta, G., and A. L. Restante. Blob formation in the solar wind: role of converging flows and viscosity. To appear in *Annales Geophysicae.*

Lapenta, G., and J. King. Study of current intensification by compression in the Earth magnetotail. 2007. *Journal of Geophysical Research.* **112**: A12204.

Li, S.. Modeling the large-scale structures of astrophysical jets in the magnetically dominated limit. 2006. *Astrophysical Journal.* **643** (1): 92.

MacDonald, E. A., K. A. Lynch, M. Widholm, R. Arnoldy, E. M. Klatt, P. M. Kintner, and G. Lapenta. In Situ Measurement of Thermal Electrons on the SIERRA Nightside Auroral Sounding Rocket. To appear in *Journal of Geophysical Research.* **111** (A12): 1.

Marocchino, A., G. Lapenta, E. G. Evstatiev, R. A. Nebel, and J. Park. Two-dimensional electron-electron two-stream instability of an inertial electrostatic confinement device. 2006. *Physics of Plasmas.* **13** (10): 102106.

Noguchi, K., C. Tronci, G. Zuccaro, and G. Lapenta. Formulation of the relativistic moment implicit particle-in-cell method. 2007. *Physics of Plasmas.* **14** (4): 042308.

Patacchini, L., I. H. Hutchinson, and G. Lapenta. Electron collection by a negatively charged sphere in a collisionless magnetoplasma. 2007. *Physics of Plasmas.* **14** (6): 62111.

Rovagnati, B., G. Lapenta, and F. Mashayek. Dynamic nature of the ion wake in dusty plasmas. 2008. *Physics Letters A.* **372** (38): 5991.

Rovagnati, B., M. Davoudabadi, F. Mashayek, and G. Lapenta. Effect of ion-neutral collisions on the charging of a dust particle. 2007. *Collection of Technical Papers - 45th AIAA Aerospace Sciences Meeting.* **14**: 9705.

Rovagnati, B., M. Davoudabadi, G. Lapenta, and F. Mashayek. Effect of collisions on dust particle charging via particle-in-cell Monte-Carlo collision. 2007. *Journal of Applied Physics.* **102** (7): 073302.

Sun, X., T. P. Intrator, L. Dorf, I. Furno, and G. Lapenta. Transition of MHD kink stability properties between line-tied and non line-tied boundary conditions. 2008. *Physical Review Letters.* **100**: 205004.

Sun, X., T. P. Intrator, L. Dorf, I. Furno, and G. Lapenta. Relationship between flux rope merging, bouncing and onset threshold for 3D Sweet-Parker reconnection. To appear in *Physical Review Letters.*

Ticos, C. M., Z. H. Wang, G. L. Delzanno, and G. Lapenta. Plasma dragged microparticles as a method to measure plasma flows. 2006. *Physics of Plasmas.* **13** (10): 103501.

Wan, W., G. Lapenta, G. L. Delzanno, and J. Egedal. Electron acceleration during guide field magnetic reconnection. 2008. *Physics of Plasmas.* **15**: 032903.

Wan, W., and G. Lapenta. Micro-macro coupling in plasma self-organization processes during island coalescence. 2008. *Physical Review Letters.* **100**: 035004.

Wan, W., and G. Lapenta. Electron self-reinforcing process of magnetic reconnection. 2008. *Physical Review Letters.* **101**: 015001.

Wan, W., and G. Lapenta. Evolutions of nonsteady state magnetic reconnection. To appear in *Physics of Plasmas.*

# Detecting Spinons with the Wiedemann-Franz Law

*Filip Ronning*

20060407ER


## Abstract

Newly discovered materials (e.g. high temperature superconductors) suggest that a basic tenant of condensed matter physics, that electrons are fundamental particles which carry both spin and charge, may fail completely. Theory indicates that the low energy behavior may be described by electrons breaking apart into spinless charged particles (called holons), and chargeless spin particles (called spinons). This fractionalization can be detected by measuring a violation of the Wiedemann-Franz law, which equates thermal conductivity to charge conductivity through fundamental constants. We have measured the Wiedemann-Franz law (WFL) in a variety of novel systems, which have been conjectured to possess a fractionalization of the electron, in an effort to explore these theoretical ideas and provide experimental data proving or constraining the theoretical concepts.


## Background and Research Objectives

Violations of the WFL are few and far between. Superconductors, because they are perfect charge conductors and perfect thermal insulators, are the one well known case to cause a violation both theoretically and experimentally. More recently, the WFL has been violated in the *normal* (non-superconducting) state of the electron-doped cuprate $Pr_{2-x}Ce_xCuO_4$ and in the heavily underdoped hole-doped cuprate $YBa_2Cu_3O_{7-\delta}$ [1, 2]. These results raise the possibility that an additional excitation may exist which has zero charge, i.e. that spinons form in the normal state of the cuprates.

Spinons are special spin excitations which carry no charge. Figure 1 gives the basic idea of how spin-charge separation in one-dimension leads to the fractionalized excitations known as spinons and holons. Consider first in (a) a hypothetically ordered one-dimensional (1-D) antiferromagnet-meaning that the spins of neighboring electrons are pointed in opposite directions. (b) A combined spin and charge excitation can be added by removing one electron with charge -*e* and spin ½. (c) Allowing electrons to hop from occupied to the unoccupied neighboring site creates, after some hops, a domain wall in the spin order. This is the topological excitation known as a spinon, which carries spin ½ and charge 0. Meanwhile, the holon, with charge *e* and spin 0, has separated itself from the spin excitation. The charge excitation can carry both heat and charge, and thus will satisfy the WFL; whereas, the spinons are excitations with zero charge, and thus their presence will produce a violation of the Wiedemann-Franz law [3]. This expectation still awaits experimental verification in a one-dimensional system, where spinons are theoretically well established.

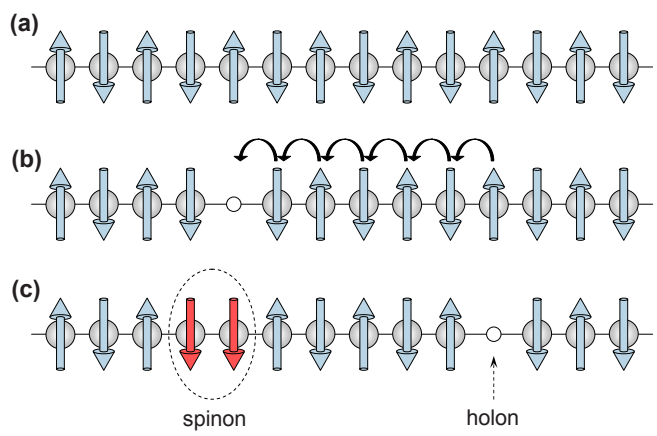


*Figure 1. Illustration of how the spin and charge degrees of freedom can become separated.*

In contrast to our understanding of 1-D systems, the theory of quantum critical points (defined below) in higher dimensions is at a complete loss. Recent theories argue that spinons should also be expected at a quantum critical point [4]. In fact, the physics of quantum critical points and 1-D systems are strongly related. A quantum-critical point (QCP) is a phase transition at T = 0 K whose behavior is dictated solely by quantum fluctuations. Experimentally, a phase, such as antiferromagnetic order, can be tuned to a quantum-critical point by a number of different parameters, but pressure, magnetic field, and chemical doping are by far the most common. As the transition is tuned toward T=0, the diverging fluctuations control the properties of the material not only in the immediate vicinity of the quantum-critical point but also far from T=0. For instance, in

high $T_c$ cuprates it is believed to be relevant to 1000 K. It was supposed to be straightforward to extend the highly successful theories of classical phase transitions to the quantum regime by considering temporal correlations [5]. However, there does not appear to be any system with all of the resulting experimental consequences expected from this theory. Further, there are literally hundreds of systems which appear close to a quantum critical point [6]; that is, they deviate qualitatively from Fermi-liquid theory. Unfortunately, the detailed responses in each system, such as the temperature dependence of various observables, are sufficiently different that no generalities can be drawn about the experimental consequences of a quantum-critical point. This situation is in stark contrast to that of classical, thermally-driven phase transitions in which predicted physical properties are material independent. Consequently, it is far from obvious that an appropriate theory of quantum criticality is known at all, and theory is desperately searching for guidance. What is crucially needed are measurements of very fundamental properties that will both constrain and guide the development of a theory of quantum-phase transitions with the generality and predictive power of the theory of classical phase transitions. Our measurements provide such a test.

In addition, the violations of the WFL in high $T_c$ cuprates provide some guidance as to where else one might expect to find spinons [1, 2]. The results on the cuprates strongly suggest that an additional excitation must exist which has zero charge, and thus indicate that some form of spin-charge separation or spin-liquid state occurs in the normal state of the cuprates. A spin-liquid state is a state with short range spin correlations, but lacks long range order at T=0, often as a result of strong frustration between various spin-exchange interactions. Theoretically, it has been shown that spin-liquid states with spinon excitations are possible and may even be energetically favorable under certain conditions in 2-D [7]. Thus, measuring thermal and charge conductivity in systems better established as spin liquid states, will shed further light on the nature of the ground state observed in high $T_c$ cuprates.

Our research objective was to explore a variety of one (Copper pyrazine dinitrate and $NaV_2O_4$), two (Sm(La,Sr) $CuO_4$ and $La_{1.2}Sr_{1.8}Mn_2O_7$), and three ($CeCoIn_5$ and $Sr_3Ru_2O_7$) dimensional systems to determine whether a violation of the Wiedemann-Franz law exists, and whether such behavior can indeed be attributed to spinon excitations. In addition, we attempted to develop the so-called 3-omega technique for measuring thermal conductivity so that similar measurements of the Wiedemann-Franz could be performed under pressure.

## Importance to LANL's Science and Technology Base and National R & D Needs

Complexity in electronic structure of strongly correlated electron systems is the basis for future energy and sensor technologies and may play a critical role in NNSA's nuclear stockpile stewardship. Our objectives will help provide a fundamental understanding of these materials, for developing successful theories and a means for developing new technologies.

## Scientific Approach and Accomplishments

To identify the observation of spinons in one dimension using thermal transport we were severely limited by material issues. No solid state system is truly one-dimensional. There is always some finite interchain coupling, which at low enough temperatures will lead to higher-dimensionality physics. To accurately study the WFL in the T=0K limit, temperature-dependent transport properties must be measured to at least 300mK, preferably lower. Thus, to verify the expected violation of the Wiedemann-Franz law in a true one-dimensional system, one must first find a system that does not order at low temperatures due to the interchain coupling. Copper pyrazine dinitrate [$Cu(C_4H_4N_2)(NO_3)_2$] is precisely such a system: a quasi-one-dimensional magnet which shows no ordering down to at least 100mK [8]. Furthermore, the specific heat shows this material has the T-linear term expected for spinons. Our measurements of thermal conductivity are in fact suggestive of a T-linear contribution to the thermal conductivity at the lowest temperatures. However, we had severe difficulties in getting reproducible results, especially with regards to the magnitude of the T-linear term. We attribute this issue with the occurrence of microcracks upon cooling the sample. Microcracks change the geometric factor, which converts the measured conductance into conductivity, by an unknown amount. Consequently, we conclude that while an organic material such as Copper pyrazine dinitrate would appear ideal for studying the thermal transport of spinons, material issues preclude an accurate study. In an attempt to find a scond suitable material we explored the oxide $NaV_2O_4$, while quasi-1D metallic conduction was found at low temperatures, we did not find any evidence for spinon transport [9]. We are unaware of any other quasi 1-D material which does not order down to 100mK.

In two dimensions, we have used heat capacity to probe the compound Sm(La,Sr)CuO4. The way the Sm spins are arranged on a square planar layered structure with a lack of ordering down to 50mK suggests that there is enough frustration to produce a spin liquid state. From heat capacity we indeed find evidence for a strongly frustrated system, however a spin liquid state at the lowest temperatures was not found [10]. We also studied $La_{1.2}Sr_{1.8}Mn_2O_7$

(LSMO), a 2D ferromagnet, to elucidate the origin of the WFL violation in the cuprates. By measuring a disordered system such as manganin it became apparent to us that disorder could mimic a violation of the WFL. The low T resistivity of LSMO is similar both in magnitude and anisotropy as in the underdoped cuprates where a violation has been observed. We show that the WFL is satisfied in LSMO [11], which further supports the notion that the violation in the cuprates originates from spinon conduction. Furthermore, our measurements on LSMO provide the first demonstration of heat transport by 2D magnons (another type of spin excitation) in a metallic system.

In 3 dimensions we have explored the notion that a quantum-critical point may give rise to exotic particles by studying $Sr_3Ru_2O_7$ and $CeCoIn_5$. Both systems possess a magnetic field tuned QCP, and our measurements show that both $Sr_3Ru_2O_7$ [12] and $CeCoIn_5$ [13] satisfy the Wiedemann-Franz law at the QCP. One possibility for the lack of spinons observed at these QCP is that the magnetic field which produces the QCP, also localizes the spinons so that they may not transport heat. Hence, we also attempted to develop a technique to measure thermal conductivity under pressure at low temperatures.

The conventional steady state approach to measuring thermal conductivity is not appropriate for high pressure studies because the pressure transmitting medium shorts out any attempt to set up steady state thermal gradients. By using a so called “3-omega” technique this problem is overcome [14]. This technique has been successfully applied to measure thermal conductivity under pressure at high temperatures [14]. The key technical difficulty to overcome at low temperatures results from the fact that the magnitude of the signal, is proportional to dR/dT, the first derivative of the resistance with respect to temperature, of the thermometer which must be directly evaporated onto the sample. To prevent our intermetallic samples from degrading the evaporation could not be performed above 300 deg C. This proved to be a strong liability for our thermometers. Growths of $SrRuO_3$ and $PrBa_2Cu_3O_{7-\delta}$ under various conditions proved not to have the necessary thermometer characteristics at low temperatures. We conclude that it will be exceedingly difficult to find an oxide material which will be useful to act as a thermometer for the “3-omega” technique for measuring thermal conductivity.

In conclusion, we have measured the Wiedemann-Franz law in 1-, 2-, and 3-dimensional systems. The lack of violations observed provides strong constraints to theories working on strongly correlated electron systems including the high temperature superconducting cuprates.

## References


1. Hilletal., R. W.. Breakdown of Fermi-liquid theory in a copper-oxide superconductor . 2001. *Nature.* **414**: 711.
2. DoironLeyraud, N.. Onset of a Boson Mode at the Superconducting Critical Point of Underdoped YBa2Cu3Oy. 2006. *Physical Review Letters.* **97**: 207001.
3. Kane, C. L., and M. P. A. Fisher. Thermal Transport in a Luttinger Liquid. 1996. *Phyical Review Letters.* **76**: 3192.
4. Senthil, T., M. Vojta, and S. Sachdev. Weak magnetism and non-Fermi liquids near heavy-fermion critical points. 2004. *Physical Review B.* **69**: 035111.
5. Hertz, J. A.. Quantum Critical Phenomena. 1976. *Physical Review B.* **14**: 1165.
6. Stewart, G.. Non-Fermi-liquid behavior in d- and f-electron metals. 2001. *Review of Modern Physics.* **73**: 797.
7. Lee, S. S., and P. A. Lee. U(1) Gauge Theory of the Hubbard Model: Spin Liquid States and Possible Application to κ-(BEDT-TTF)2Cu2(CN)3 . 2005. *Physical Review Letters.* **95**: 036403.
8. Hammar, P. R.. Characterization of a quasi-one-dimensional spin-1/2 magnet which is gapless and paramagnetic for gμBHJ and kBTJ . 1999. *Physical Review B.* **59**: 1008.
9. Yamaura, K.. NaV2O4: A Quasi-1D Metallic Antiferromagnet with Half-Metallic Chains. 2007. **99**: 196601.
10. Ronning, F.. Magnetic Excitations of the 2-D Sm Spin Layers in Sm(La,Sr)CuO. 2007. *Journal of Magnetism and Magnetic Materials.* **310**: e392.
11. Ronning, F.. Thermal Conductivity of La1.2Sr1.8Mn2O7. *Nature Physics.*
12. Ronning, F.. Thermal Conductivity in the Vicinity of the Quantum Critical End Point in Sr3Ru2O7 . 2006. *Physical Review Letters.* **97**: 067005.
13. Paglione, J.. Nonvanishing Energy Scales at the Quantum Critical Point of CeCoIn5. 2006. *Physical Review Letters.* **97**: 106606.
14. Chen, F.. Thermal conductivity measurement under hydrostatic pressure using the 3 omega method. 2004. *Review of Scientific Instruments.* **75**: 4578.

## Publications

Hawthorn, D. G., S. Li, M. Sutherland, E. Boaknin, R. W. Hill, C. Proust, F. Ronning, M. Tanatar, J. Paglione, D. Peets, R. Liang, D. Bonn, W. N. Hardy, N. Kolesnikov, and L. Taillefer. Doping dependence of the superconducting gap in Tl2Ba2CuO6+delta from heat transport.. 2007. *Physical Review B.* **75**: 104518.

Paglione, J., M. A. Tanatar, D. G. Hawthorn, F. Ronning, R. W. Hill, M. Sutherland, L. Taillefer, and C. Petrovic. Non-vanishing energy scales at the quantum critical point of CeCoIn5. 2006. *Physical Review Letters.* **97**: 106606.

Ronning, F., C. Capan, N. O. Moreno, J. D. Thompson, L. N. Bulaevskii, R. Movshovich, and D. van der Marel. Magnetic excitations of the 2-D Sm spin layers in Sm(La,Sr)CuO4. 2007. *Journal of Magnetism and Magnetic Matter.* **310**: e392.

Ronning, F., N. Kurita, R. Movshovich, K. McClellan, N. Hur, and I. Vekhter. Low temperature thermal conductivity of La1.2Sr1.8Mn2O7. *Nature Physics.*

Ronning, F., R. W. Hill, M. Sutherland, D. G. Hawthorn, M. A. Tanatar, J. Paglione, L. Taillefer, M. J. Graf, R. S. Perry, Y. Maeno, and A. P. Mackenzie. Thermal conductivity in the vicinity of the quantum critical end point in Sr3Ru2O7. 2006. *Physical Review Letters.* **97**: 067005.

Yamaura, K., M. Arai, A. Sato, A. B. Karki, D. P. Young, R. Movshovich, S. Okamoto, D. Mandrus, and E. Takayama-Muromachi. NaV2O4: A quasi-1D metallic antiferromagnet with half-metallic chains. 2007. *Physical Review Letters.* **99**: 196601.

# Amplification of Surface Plasmons by Stimulated Emission from Semiconductor Nanocrystals

*Victor Ivanovich Klimov*

20060494ER

## Abstract

Metal nanostructures allow the versatile manipulation of light via control of resonances associated with collective electron oscillations known as surface plasmons (SPs). Interest in metal nanostructures has grown tremendously in the context of emerging applications in nanoplasmonics, where SPs play a role of electrons in traditional electronic circuits. One serious problem restraining the applicability of plamonic devices is strong attenuation of plasmons that limits their propagation length to a few micrometers. A possible solution to this problem is the development of methods for SP amplification. This project focused of studies of the fundamental physics of SP amplification using semiconductor nanocrystals (NCs) as active plasmon emitters. As part of our synthetic effort, we fabricated hybrid structures, in which a metal nanoparticle is overcoated with a thin silica shell followed by a dense monolayer of NCs. We characterized these structures using various spectroscopic methods including a new near-field single-particle technique, which provides information on both the spectrum and the phase of plasmon oscillations. By using series of hybrid nanostructures of controlled geometries and compositions, we studied interactions of SPs with NCs as a function of spectral positions of the plasmon and NC electronic resonances as well as spatial separation between the metal and the semiconductor components. We also theoretically analyzed these interactions within a newly developed Green's function formalism. The work conducted in this project provides guidelines for a rational design of NC/metal structures, which yields high plasmon emission rates together with reduced SP damping.

## Background and Research Objectives

Optical responses of metals are dominated by collective electron oscillations known as surface plasmons (SPs). These oscillations greatly enhance an electric field in vicinity of a metal surface (so called "field-enhancement" effect), which has been widely utilized to increase the sensitivity of spectroscopic analytical techniques [1] dealing with detection of small amounts of various bio- and chemo-species. Most recently, significant interest in SPs has been generated in the context of applications of nanoscale metal structures in nanoplasmonics, where SPs are utilized to carry, store, and process information. These would be an alternative to conventional silicon electronics. A serious problem in nanoplasmonics is rapid attenuation of SPs, which limits their propagation length to a few micrometers. A possible solution to this problem is through the development of active devices such as SP amplifiers and coherent SP sources ("plasmon lasers"). This proposal focuses of both fundamental and practical aspects of SP amplification in nanoscale structures that employ semiconductor nanocrystals (NCs) as active plasmon emitters.

The theoretical background for our work has been laid by pioneering theoretical studies of Bergman and Stockman that established principles of SP amplification [2]. This work demonstrated that SPs can be treated in terms of damped bosons, and hence, the formalism previously developed for photons can be transferred to the SP system. Semiconductor NCs represent a promising system for realization of ideas of plasmonic gain. They are characterized by strong emitting dipoles and tunable emission wavelengths that can be matched to the SP resonance by simply adjusting NC size. Further, using relatively simple colloidal chemistry NCs can be conjugated to metal surfaces, which should provide strong electronic coupling of the NC electronic excitations to the SP dipole.

The research objective of this project was to build experimental and theoretical foundation for studies of the problem of SP amplification in hybrid semiconductor/metal structures that comprise semiconductor NCs. Our specific goals included: 1) the development of synthetic procedures for fabricating well defined semiconductor/metal structures in which interactions

between NCs and SPs can be controlled via simple colloidal chemistry; 2) the development of spectroscopic techniques for resolving SP resonances in individual nanostructures, which would allow reliable detection of both spectral and phase characteristic of plasmon oscillations; and 3) the development of a theoretical approach for treating interactions between NC excitations and SP resonances.

## Importance to LANL's Science and Technology Base and National R & D Needs

Strong enhancement of local fields associated with SPs has been widely applied in chemo/bio sensing technologies. In recent nanoplasmonic applications, SPs have been utilized to carry, store, and process information. The potential of SPs in various applications can be greatly enhanced through the development of methods for plasmon amplification, which could potentially solve the problem of rapid damping of electronic excitations in metals. This project focused on the development and fundamental studies of active structures built of nanoscale metal particles and semiconductor NCs that could potentially serve as SP-gain species. The conducted work is relevant to LANL interests in both world-class fundamental science (physics of hybrid plasmon-exciton interactions) and strategic applications (ultrasensitive bio- and chemo-sensing and new plasmonic circuitry). This project also addresses the dynamic and exciting new field of Nanoscience, the strategic importance of which to the LANL mission was recognized by establishment of the DOE Center for Integrated Nanotechnology (CINT).

## Scientific Approach and Research Accomplishments

### Synthesis of hybrid semiconductor/metal nanostructures

In this project, we developed and studied spectroscopically well-defined hybrid structures that consisted of a metal core overcoated with a silica ($SiO_2$) shell, followed by a dense monolayer of CdSe NCs [3]. The dielectric silica spacer of a controlled thickness provided a simple means for tuning interactions between the NCs and the metal nanoparticle. To illustrate this tunability, we demonstrated switching between NC emission quenching and enhancement by varying the silica shell thickness. Synthetic procedures developed by us employed a final step of self-assembly of NCs onto the silica shell performed via simple titration of the NC solution with pre-fabricated core/shell Au/$SiO_2$ particles. This approach allowed us to perform an accurate quantitative analysis of the effect of the SPs in the metal on dynamics of electronic excitations in the NCs.

Hybrid gold/silica/CdSe-NC superstructures were synthesized via a multi-step procedure, which involved synthesis of gold nanoparticles, gold-particle surface activation, silica-shell deposition, modification of the silica surfaces with $-NH_2$ groups, and final self-assembly of CdSe NCs onto the particle surfaces (Figure 1A). Gold nanoparticle seeds (15 nm in diameter) were prepared according to the standard sodium-citrate reduction method. A seeded growth method was applied to prepare larger partilces (up to 45 nm in diameter). To deposit a silica shell, we used a modified version of the procedure reported previously [4]. We found that (3-mercaptopropyl)trimethoxysilane (MPTMS) was better suited for surface activation of gold nanoparticles than (3-aminopropyl)trimethoxysilane (APTMS) (originally used in ref. 4) because of stronger binding of the –SH groups to the gold surfaces. The use of MPTMS also allowed us to reduce the yield of pure silica particles produced by homogeneous nucleation and structures that comprised multiple Au cores.

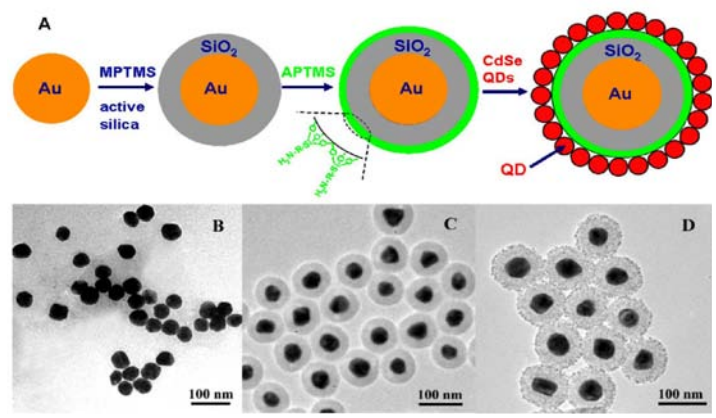


*Figure 1. (A) Multi-step synthesis of hybrid Au/$SiO_2$/CdSe-NC nanostructures. (B) TEM images of synthesized gold cores, (C) core/shell gold/silica nanoparticles, and (D) final hybrid Au/$SiO_2$/CdSe-NC nanostructures (NC diameter is 6.0 nm).*

The silica-coated nanoparticles were treated with APTMS (a silane coupling agent), which reacted with the surface silanol groups to produce silica surfaces functionalized with $-NH_2$ groups. Finally, the surface-modified nanoparticles were dispersed in a tetrahydrofuran (THF) solution of CdSe NCs synthesized via a high-temperature pyrolysis method. Because of strong binding interactions between the CdSe NCs and the $-NH_2$ ligands, the NCs self-assembled onto the surface of the silica shell, resulting in the targeted hybrid gold/silica/CdSe-NC superstructures. Figure 1 shows an example of transmission electron microscopy (TEM) images of gold-core nanoparticles (B), gold/silica core/shell structures (C), and final hybrid gold/silica/NC nanocomposites (D). In this example, the gold-core diameter $D \approx$ 45 nm, and the silica-shell thickness $H \approx 24$ nm. While the

gold cores have irregular shapes, the gold/silica structures are nearly spherical and highly monodisperse (4% size dispersion). CdSe NCs form uniform dense monolayers on all of the Au/$SiO_2$ particles. TEM images indicate that our synthesis does not produce such byproducts as plain silica particles or particles comprising multiple Au cores, while such byproducts are difficult to avoid using APTMS as an activator of gold surfaces.

**Near-field detection of surface plasmons in individual nanoparticles**

An important component of our project was the development of experimental methods for reliable detection of the spectral shape of SP resonances, because this shape is expected to be strongly affected by interactions with electronic excitation in NCs. Specifically, stimulated emission of plasmons by NCs would lead to reduction in SP damping, and hence, narrowing of the plasmon resonance. In the case of macroscopic ensembles of metal particles, a significant contribution to the measured SP broadening comes from size, and especially, shape nonuniformity. Therefore, in order to reliably measure intrinsic SP linewidths we have developed a new near-field spectroscopic technique, which provides single-nanoparticle sensitivity in studies of plasmon oscillations [5].

In this method, a femtosecond white light continuum transmitted through a sub-wavelength aperture of a near-field scanning optical microscope (NSOM) is used to selectivly excite SP modes in individual nanoparticles. In addition to high ~50-nm spatial resolution, this technique provides phase sensitivity, which allows for precise determination of both SP resonance energies and linewidths. An important feature of this method is that together with spectroscopic information it provides information on sample morphology, which allows us to directly relate the measured SP response to particle's geometrical parameters such as its size and shape.

Figure 2 provides an example of application of this NSOM techniques to studies of SPs in atomically flat gold nanoparticles displayed in panel (A). Panels (B) and (C) show near-field images recorded for small and large nanoparticles, respectively, while panels (D) and (F) display corresponding transmission spectra recorded in the near-field configuration. Small particles exhibit a single, near-center minimum in the transmission geometry indicating dominance of a single SP mode. Larger particles show more complex transmission patterns due to excitation of multiple plasmon modes. Interestingly, near-field extinction spectra of nanoparticles [red line in (D)] deviate significantly from those of extended gold films [black line in (D)], indicating importance of SP resonances. One effect of SPs is the development of interference features [shown in (E)] due to coherent superposition of the near-field probe emission and the emission re-radiated by oscillating dipoles associated with different SP modes. In an example in panel (E), the interference spectrum exhibits a zero-crossing at 2.05 eV, which provides a precise measure of the SP-resonance. Further, the separation between the zero-crossing point and the spectral maximum at 2.2 eV represents an accurate measure of the intrinsic SP linewidth.

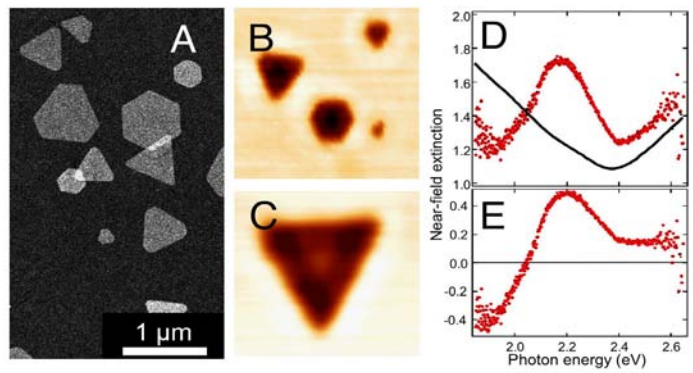


*Figure 2. Scanning-electron microscopy (A) and optical near-field (B) images of flat gold nanoparticles of different dimensions and shapes. Spatial distribution of light intensity in (B) reflects the distribution of surface-plasmon (SP) modes. The near-field extinction spectrum of the nanoparticle in the upper-left corner of (B) is displayed in panel (D) by the red line, and it is compared to the extinction spectrum of bulk gold shown in black. Strong difference between these two spectra is due to excitation of the SP resonance in the nanoparticle. The field re-radiated by the SP dipole experiences coherent superposition with the field emitted by the near-field probe, which produces a characteristic interference feature displayed in panel (E).*

**Effect of surface plasmons on multiparticle Coulomb interactions**

Optical as well as SP gain in NCs relies on emission from multiexciton states. Therefore, the development of practical approaches for SP amplification requires detailed understanding of the effect of a proximal metal on Coulomb electron-electron interactions. In this project, we have developed Green's function formalism for describing "plasmon-dressed" Coulomb interactions [6]. We illustrated this formalism by analyzing dressed electron-electron interactions for an important example of metal-dielectric nanoshells that exhibit a reach resonant behavior in both the magnitude and phase. We further applied our new theoretical approach to describing the nanoplasmonic renormalization of Coulomb interactions for a NC placed in vicinity of a plasmonic nanoshell.

The plasmonic renormalization of the Coulomb interaction is illustrated in Figure 3, which shows the results of calculations for a NC located at the "North Pole" of a silver nanoshell (marked by arrow) with aspect ratio of 0.9 (the latter value is the ratio of the shell radius to its thickness). For this nanoshell, the lowest dipole SP resonance is at 1.60 eV. In the case of low-energy detuning from this resonance (1.5 eV; Figure 3A), the computed renormalization factor (defined as the ratio of the electric field amplitude with and without SP renormalization) indicates strong dielectric screening (i.e., field reduction; indicated by blue color) in the region near the NC. On the opposite side of the nanosphere, there is a "mirror image"of the dressed interaction potential oscillating in phase (as indicated by the red color) with the applied field. This shows that the nanoplasmonic effects greatly extend the range of the dressed Coulomb interaction. This is due to the delocalization of the dipole eigenmode, which defines the nanoplasmonic effects in this spectral region.

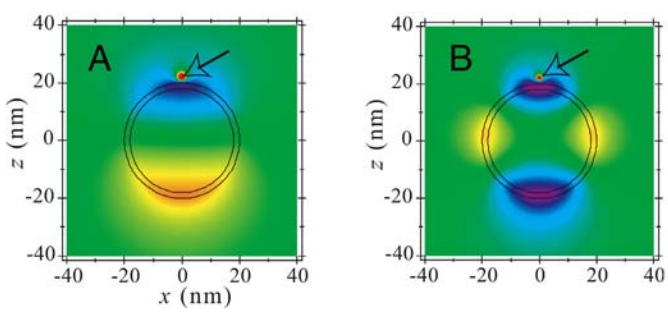


*Figure 3. SP renormalization factor of the "dressed" Coulomb interaction for a NC located at the "North Pole" a silver nanoshell (marked by arrow) with aspect ratio of 0.9. Calculation are conducted for energies 1.5 eV (A) and 1.61 eV (B) that below and above the SP resonance, respectively. The magnitude of the renormalization factor is shown by color-coding; red and blue colors corresponds to in-phase and out-of-phase oscillations, respectively.*

Interestingly, the situation changes dramatically for energy 1.61 eV, which is slightly above the dipole resonance (see Figure 3B). In this case, the SP renormalization results in dynamic *anti*-screening (field enhancement) in the vicinity of the NCs. The renormalized potential oscillates in phase with the bare Coulomb potential, as indicated by the red color of the cloud around the arrow. There is also a very strong interaction potential on the diametrically opposite side of the nanoshell, which oscillates out of phase (shown by blue).

**Summary**

In this project, we have addressed several theoretical and applied aspects of the problem of exciton-SP interactions in the context of plasmon amplification. Specifically, we have developed a multi-step synthesis of hybrid superstructures that comprise gold cores and dense layers of CdSe NCs separated by a silica shell. Quantitative spectroscopic studies of these structures indicate strong interactions between SPs excited in the metal core and NC excitons. We have further demonstrated that this architecture allows for versatile control of NC-SP coupling through control of the metal-core size and the thickness of the dielectric spacer. These results indicate large promise of these superstructures as model systems for studies of SP gain in the configuration where the metal core serves as a plasmonic nanocavity while NCs act as active plasmon emitters.

Further, we have developed a spectroscopic near-field technique for analyzing the SP response in individual nanostructures. We have demonstrated the applicability of this technique for highly accurate measurements of both the position and the width of the SP resonances in individual metal nanoparticles. This capability is an extremely useful tool for detecting the effect of SP amplification based on changes in attenuation of plasmon oscillations. Our studies also demonstrate the feasibility of spectrally resolved imaging of SP modes in individual nanoparticles. This capability can be utilized in studies of giant-field enhancement effects as well as in such practical application as single-molecule spectroscopy and sensing. Further, the ability to directly correlate the SP response with the particle geometry, demonstrated here, can be extremely useful for benchmarking various theoretical approaches developed for treating nanoscale plasmonic systems.

Finally, we have developed a novel Green's function formalism for the quantitative analysis of plasmonic renormalization of Coulomb carrier-carrier interactions that needs to be accounted for in the problem of SP optical gain. One important result our theoretical modeling is high spectral sensitivity of this renormalization. An interesting feature of this effect is that it can be utilized for controlling Auger recombination rates that define the lifetime of the SP gain. Specifically, by tuning NC emission to the red of the SP resonance one can obtain efficient suppression of Auger recombination through effective screening of the Coulomb interaction by out-of-phase plasmon oscillations

## References


1. Raether, H.. Surface Plasmons . 1988.
2. Bergman, D. J., and M. I. Stockman. Surface plasmon amplification by stimulated emission of radiation: quantum generation of coherent surface plasmons in nanosystems. 2003. *Phys. Rev. Lett..* **90** (2): 027402.
3. Liu, N. G., B. S. Prall, and V. I. Klimov. Hybrid gold/silica/nanocrystal quantum-dot superstructures: Synthesis and analysis of semiconductor-metal interactions. 2006. *J. Am. Chem. Soc..* **128**: 15362.
4. Liz-Marzan, L. M., M. Giersig, and P. Mulvaney. Synthesis of nanosized gold-silica core-shell particles. 1996. *Langmuir.* **12** (18): 4329.
5. Achermann, M., K. L. Shuford, G. C. Schatz, D. H. Dahanayaka, L. A. Bumm, and V. I. Klimov. Near-field spectroscopy of surface plasmons in flat gold nanoparticles. 2007. *Opt. Lett..* **32** (15): 2254 – 2210 .
6. Durach, M., A. Rusian, V. I. Klimov, and M. I. Stockman. Nanoplasmonic renormalization and enhancement of Coulomb interactions. To appear in *New J. Phys..*


## Publications


Achermann, M., K. L. Shuford, G. C. Schatz, D. H. Dahanayaka, L. A. Bumm, and V. I. Klimov. Near-field spectroscopy of surface plasmons in flat gold nanoparticles . 2007. *Opt. Lett..* **32** (15362): 2254.

Durach, M., A. Rusian, V. I. Klimov, and M. I. Stockman. Nanoplasmonic renormalization and enhancement of Coulomb interactions. To appear in *New J. Phys..*

Liu, H. G., B. S. Prall, and V. I. Klimov. Hybrid gold/silica/nanocrystal quantum-dot superstructures: Synthesis and analysis of semiconductor-metal interactions. 2006. *J. Am. Chem Soc. .* **128** (15362): 15362.

# Exploring the Darkness: Cosmic Voids

*Katrin Heitmann*

20060495ER


## Abstract

One of the most striking features of the universe is the presence of large, almost empty regions - the cosmic voids. Since their discovery, tremendous advances in determining the make - up of the Universe have been made. In contrast, the secrets of the dark sector - of dark matter and dark energy - have yet to be revealed. Cosmic voids provide a means to simultaneously challenge and explore the Standard Model of Cosmology, including the evolution of the dark sector. In this project we have studied the formation and evolution of voids, investigated possible dark matter candidates which could explain the darkness of voids, i.e. why are not more dwarf galaxies found inside voids, and the dependence of the properties of voids on cosmological parameters.


## Background and Research Objectives

The detailed distribution of mass in the Universe is only now being revealed by astronomical surveys such as the Sloan Digital Sky Survey (SDSS). To gain a richer and ultimately profound understanding of cosmological structure, a deep and contiguous 3-D map of the Universe is required, and this is what SDSS has provided over the last decade. Some of the most striking objects in this 3-D map are very large, highly underdense, and very underluminous regions -- the cosmic voids. Each void is a miniature "universe," with the same structural elements as the large-scale galactic distribution, but at lower density. This ensemble of universes is a unique resource for advancing our understanding of the Universe as a whole. Although voids fill at least half of the observed volume, the study of voids remains in its infancy. This is because voids are complex structures, and a major study demands a combination of large-volume observations, targeted analysis methods, and state-of-the-art simulations. In this project, voids have been investigated qualitatively and quantitatively based on high-performance simulations.

The significance of this project is underscored by the fact that an astonishing 99.6% of our Universe is apparently dark, dominated by mysterious dark energy and dark matter components. Although the precise nature of the dark sector is unknown, cosmologists are confident that a consistent framework for understanding the Universe exists. This confidence rests on the success of general relativity and the paradigm of gravitational structure formation. Just as the cosmic microwave background is the key evidence for cosmological expansion, the large-scale distribution of matter is the ultimate touchstone for structure formation theory. Since much of our knowledge of the dark Universe rests on this theory, developing methods for testing its validity has the highest priority in cosmology. Cosmic voids provide a way to explore the dark sector of the Universe as well as testing our models and theories for structure formation.

In order to make progress on both fronts – exploring the nature of the dark Universe and advancing our understanding of large-scale structure formation, we identified four key questions. 1) What is the best way to define voids? It is often assumed that voids are spherical structures with constant, large underdensities. This assumption is too crude, however, and all of the information about the structure of voids is lost. Developing a robust definition of voids is therefore a crucial first step. 2) How do voids form and evolve? The answer to this question will be important for our understanding of large-scale structure formation. 3) Why are voids deficient of dwarf galaxies? The answer to this question holds new information about the nature of dark matter or dark energy – or both. 4) How do the properties of voids depend on cosmology? By characterizing void properties as a function of cosmological parameters, voids could be a new powerful probe of cosmology.

During the project we have made progress on answering all of these four questions, and in the following we summarize our accomplishments.

## Importance to LANL's Science and Technology Base and National R & D Needs

This project targets two of DOE's top science priorities: dark energy and supercomputing. State-of-the-art high-performance simulations have been carried out to understand cosmic voids. The evolution and structure of cosmic voids depend strongly on the nature of the dark energy in the Universe. The project also addresses one of the Scientific Grand Challenges recently established at Los Alamos National Lab: Beyond the Standard Model to Understand the Universe: Dark Energy, Dark Matter, Cosmology, and Stellar Evolution.

## Scientific Approach and Accomplishments

During the first year of the project one major focus was to find the answer to our first question: What is the best way to define voids? After studying different possible definition of voids, the conclusion was reached that a density threshold method would be the most conservative way of defining voids. In detail, the global distribution and morphology of dark matter voids in a cold dark matter universe including dark energy have been studied using density fields generated by N-body simulations [1]. Voids were defined as isolated regions of the low-density excursion set specified via density thresholds, the density thresholds being quantified by the corresponding filling factors, i.e., the fraction of the total volume in the excursion set. The work encompasses a systematic investigation of the void volume function, the volume fraction in voids, and the fitting of voids to corresponding ellipsoids and spheres. Figure 1 shows a void region identified in the simulation and the corresponding best-fit ellipsoids. The relevance of the percolation threshold to the void volume statistics of the density field both in the high redshift, Gaussian random field regime, as well as in the present epoch has been established. By using measures such as the Inverse Porosity, the quality of ellipsoidal fits to voids was characterized, finding that such fits are a poor representation of the larger voids that dominate the volume of the void excursion set.

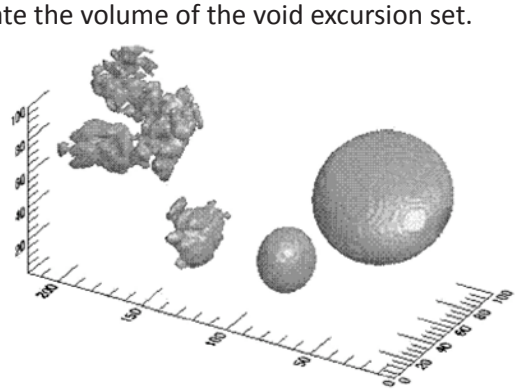

*Figure 1. Simulated voids and the corresponding best-fit spheres.*

Work on answering the third question (Why are voids deficient of dwarf galaxies?) was initiated in the first year and continued through the second year. One of the greatest mysteries concerning voids is their apparent emptiness and darkness. Conventional cold dark matter models predict a large number of faint galaxies in voids; an order of magnitude more than are actually observed. A possible solution to this problem would be a warm dark matter component, which would suppress structure formation in voids. A possible candidate is the so-called sterile neutrino. In Abazajian and Koushiappas [2] a comprehensive analysis of constraints on the sterile neutrino as a dark matter candidate was carried out. (This paper has become a standard reference in the field and has gained in only two years 50 citations.) The minimal production scenario with a standard thermal history and negligible cosmological lepton number is in conflict with conservative radiative decay constraints from the cosmic X-ray background in combination with stringent small-scale structure limits from the Lyman-alpha forest. It was shown that entropy release through massive particle decay after production does not alleviate these constraints. It was further shown that radiative decay constraints from local group dwarf galaxies are subject to large uncertainties in the dark matter density profile of these systems. Within the strongest set of constraints, resonant production of cold sterile neutrino dark matter in non-zero lepton number cosmologies remains allowed is therefore still a viable solution to the missing dwarf problem in voids. Following up on this work, even tighter constraints on sterile neutrinos have been derived from the radiative decay of sterile neutrino dark matter. The limit on the mass for the sterile neutrino is < 2.9 keV. The results are reported in [3].

Another explanation for the darkness of the voids is that observations are not able to detect dwarf galaxies in voids because they are so faint. Part of the research in the last two years was focused on finding new ways of detecting very dark dwarf galaxies. One possibility is to investigate gamma ray fluxes from known dwarf galaxies around the Milky Way and by using kinematic data from these dwarf galaxies, to constrain the properties of their dark matter halos. By understanding the properties of these dwarf galaxies, one can make predictions for the galaxy population in voids and how faint they might be. If it turns out that relatively massive dark matter halos can host very dim galaxies, then this could be the key to the puzzle: although a large number of dark matter halos might exist in voids, the tiny galaxies that they produce would be too faint to find. This work has been published in [4,5,6]. Koushiappas won the Leon Heller Publication Award for his publication [4] in 2008.

Another focus of our research in the second and third year has been on the question about the formation and evolution of voids and the cosmic network as a whole. The large-scale structure of the Universe, as traced by the distribution of galaxies, is made up of three major components: voids, filaments, and clusters. Figure 2 shows the large-scale structure elements from a simulation. We have studied how the cosmic structure has its origin in the properties of the initial density field (nature) and how its contrast is then amplified by the nonlinear evolution (nurture). A percolation-based analysis was combined with N-body simulations of the gravitational instability. A percolating region in a simulation is defined as a region connecting one side of the box to the opposite side without any interruption. Particles in an initial percolating region were identified and their evolution was followed to the final state. It was found that the initial single percolation region fragments, in the course of gravitational evolution, into more than 25,000 isolated regions, however, practically all of them end up back inside the percolating region in the final state. This leads to the conclusion that most of the large-scale structure, and specifically large regions such as voids, was imprinted already in the initial conditions of the Universe. Figure 3 shows the percolating region at 50 (in blue) and the distribution of the dark matter from these regions in their final position (yellow). A paper describing these results has been submitted to Physical Review Letters [7].

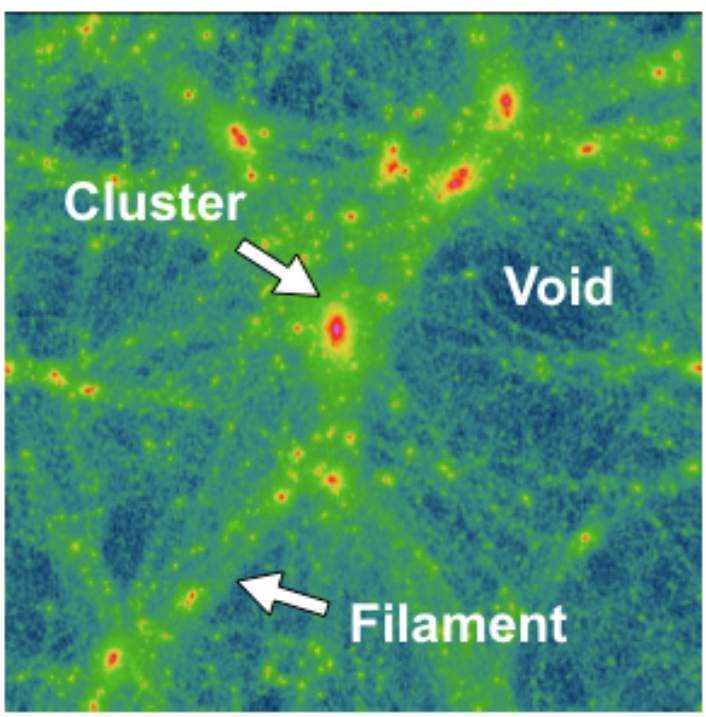


*Figure 2. The large-scale structure elements in the Universe: Filaments, clusters, and voids.*

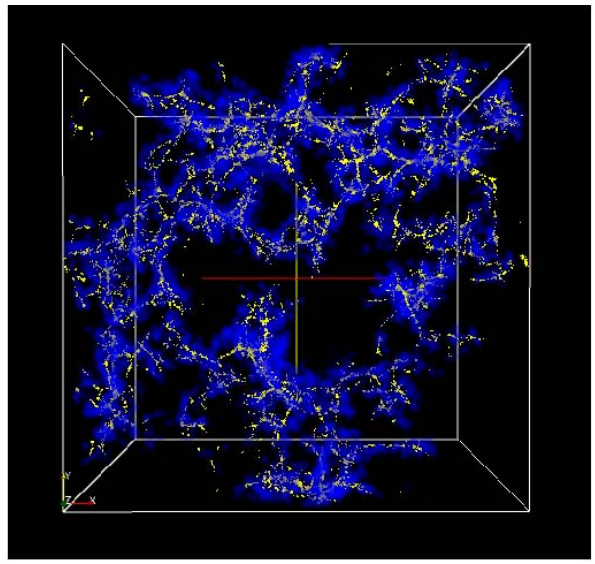

*Figure 3. Percolating region in the initial conditions (blue) and after forward-mapping into the final position (yellow).*

During the second and last year a large suite of cosmological simulations encompassing 32 different cosmological models has been carried out to study the dependence of the properties of voids on cosmological parameters. An additional parameter was implemented into the existing particle mesh code to enable the modification of the dark energy equation-of-state parameter w. The volume fraction per overdensity interval as a function of density was measured, and a small but detectable dependence of these void properties on the underlying cosmology. The results will be reported in Physical Review D soon (the departure of Koushiappas to a new faculty position at Brown University three months before the end of the project slowed down the write-up process of the paper).

As part of the LANL involvement in the Sloan Digital Sky Survey, a number of SDSS efforts were supported. Specific activities included monthly observing runs at the US Naval Observatory (Flagstaff, AZ) to enhance the network of photometric standard stars and to obtain data on selected open clusters. Continued support of the SEGUE spectroscopic target selection was carried out. Data analysis for low-mass and metal-poor cool stars and for the open cluster survey was performed. Continued controls engineering support of the Telescope Performance Monitor system was provided. The network of photometric standard stars was enhanced and data on selected open clusters was obtained. SDSS multi-epoch photometry was analyzed to map the southern extent of the 25 Ori group and to characterize its pre-main-sequence population. These activities led to several SDSS publications: [8], [9], [10], [11], [12], [13].

Overall, the project led to 12 papers, published in peer review journals (one more paper is currently under review),

which were cited 865 times so far and eight invited and seven contributed presentations at international conferences and Universities.

## References


1. Shandarin, S., H. Feldman, K. Heitmann, and S. Habib. Shapes and Sizes of Cosmic Voids. 2006. *Monthly Notices of the Royal Astronomical Society.* **367** (4): 989.

2. Abazajian, K., and S. Koushiappas. Constraints on sterile neutrino dark matter. 2006. *Physical Review D.* **74**: 023527.

3. Abazajian, K., M. Markevitch, S. Koushiappas, and R. C. Hickox. Limits on the radiative decay of sterile neutrino dark matter from the unresolved cosmic and soft X-ray backgrounds. 2007. *Physical Review D.* **75**: 063511.

4. Koushiappas, S.. Proper motion of gamma-rays from microhalo sources. 2007. *Physical Review Letters.* **97**: 191301.

5. Strigari, L., S. Koushiappas, J. S. Bullock, M. Kaplinghat, J. D. Simon, M. Geha, and B. Williams. The most dark matter dominated galaxies: predicted gamma-ray signals from the faintest Milky Way dwarfs. 2008. *Astrophysical Journal.* **678**: 614.

6. Strigari, L., S. Koushiappas, J. Bullock, and M. Kaplinghat. Precise constraints on the dark matter content of Milky Way dwarf galaxies for gamma-ray experiments. 2007. *Physical Review D.* **75**: 083526.

7. Shandarin, S., S. Habib, and K. Heitmann. Origin of the cosmic web: Nature vs nurture. *Physical Review Letters.*

8. Adelman-McCarthyetal, J.. The fourth data release of the Sloan Digital Sky Survey. 2006. *Astrophysical Journal Supplement.* **162**: 38.

9. Gunnetal, J.. The 2.5 m telescope of the Sloan Digital Sky Survey. 2006. *Astronomical Journal.* **131**: 2332.

10. Harrisetal, H.. The white dwarf luminosity function from the Sloan Digital Sky Survey imgaging data. 2006. *Astronomical Journal.* **131**: 571.

11. McGehee, P. M.. The southern flanking fields of the 25 Orionis Group. 2006. *Astronomical Journal.* **131**: 2959.

12. Rodgeretal, C. T.. Improved u'g'r'i'z' to UBVR_CI_C transformation equations for main sequence stars. 2006. *Astronomical Journal.* **132**: 1629.

13. Silvestrietal, N.. A catalog of spectroscopically selected close binary systems from the Sloan Digital Sky Survey. 2006. *Astronomical Journal.* **131**: 1674.


## Publications


Abazajian, K., M. Markevitch, S. M. Koushiappas, and R. C. Hickox. Limits on the radiative decay of sterile neutrino dark matter from the unresolved cosmic and soft X-ray backgrounds. 2007. *Physical Review D.* **75**: 063511.

Abazajian, K., and S. M. Koushiappas. Constraints on sterile neutrino dark matter. 2006. *Physical Review D.* **74**: 023527.

Adelman-McCarthy, J. K., M. A. Agueros, S. S. Allam, K. S. J. Anderson, S. F. Anderson, J. Annis, N. A. Bahcall, I. K. Baldry, J. C. Barentine, A. Berlind, M. Bernardi, M. R. Blanton, W. N. Boroski, H. J. Brewington, J. Brinchmann, J. Brinkmann, R. J. Brunner, T. Budavari, L. N. Carey, M. A. Carr, F. J. Castander, A. J. Connolly, I. Csabai, P. C. Czarapata, J. J. Dalcanton, M. Doi, F. Dong, D. J. Eisenstein, M. L. Evans, X. Fan, D. P. Finkbeiner, S. D. Friedman, J. A. Frieman, M. Fukugita, B. Gillespie, K. Glazebrook, J. Gray, E. K. Grebel, J. E. Gunn, V. K. Gurbani, E. de Haas, P. B. Hall, F. H. Harris, M. Harvanek, S. L. Hawley, J. Hayes, J. S. Hendry, G. S. Hennessy, R. B. Hindsley, C. M. Hirata, C. J. Hogan, D. W. Hogg, D. J. Holmgren, J. A. Holtzman, S. Ichikawa, Z. Ivezic, S. Jester, D. E. Johnston, A. M. Jorgensen, M. Juric, S. M. Kent, S. J. Kleinman, G. R. Knapp, A. Y. Kniazev, R. G. Kron, J. Krzesinski, N. Kuropatkin, D. Q. Lamb, H. Lampeitl, B. C. Lee, R. F. Leger, H. Lin, D. C. Long, J. Loveday, R. H. Lupton, B. Margon, D. Martinex-Delgado, R. Mandelbaum, T. Matsubara, P. McGehee, T. A. McKay, A. Meiksin, J. A. Munn, R. Nakajima, T. Nash, E. H. Neilsen, H. Newberg, P. R. Newman, R. C. Nichol, T. Nicinski, M. Nieto, A. Nitta, W. O'Mullane, S. Okamura, R. Owen, N. Padmanabhan, G. Pauls, J. Peoples, J. R. Pier, A. C. Pope, D. Pourbaix, T. R. Quinn, G. T. Richards, M. W. Richmond, C. M. Rockosi, D. J. Schlegel, D. P. Schneider, J. Schroeder, R. Scranton, U. Seljak, E. Sheldon, K. Shimasaku, J. A. Smith, V. Smolcic, S. A. Snedden, C. Stoughton, M. A. Strauss, M. SubbaRao, A. S. Szalay, I. Szapudi, P. Szkody, M. Tegmark, A. R. Thakar, D. L. Tucker, A. Uomoto, D. E. VandenBerk, J. Vandenberg, M. S. Vogeley, W. Voges, N. P. Vogt, L. M. Walkowicz, D. H. Weinberg, A. A. West, S. D. M. White, Y. Xu, B. Yanny, D. R. Yocum, D. G. York, I. Zehavi, S. Zibetti, and D. B. Zucker. The fourth data release of the Sloan Digital Sky Survey. 2006. *Astrophysical Journal Supplement.* **162**: 38.

Gunn, J. E., W. A. Siegmund, E. J. Mannery, R. E. Owen, C. Hull, R. F. Leger, L. N. Carey, G. R. Knapp, D. G. York, W. N. Boroski, S. M. Kent, R. H. Lupton, J. E. Anderson, J. Annis,

J. C. Barentine, L. M. Bartoszek, S. Bastian, S. B. Bracker, H. J. Brewington, C. I. Briegel, J. Brinkmann, Y. J. Brown, M. A. Carr, P. C. Czarapata, C. C. Drennan, T. Dombeck, G. R. Fedrerwitz, B. A. Gillespie, C. Gonzales, S. U. Hansen, M. Harvanek, J. Hayes, W. Jordan, E. Kinney, M. Klaene, S. J. Kleinman, R. G. Kron, J. Kresinski, G. Lee, S. Limmongkol, C. W. Lindenmeyer, D. C. Long, C. L. Loomis, P. McGehee, P. M. Mantsch, E. H. Neilsen, R. M. Neswold, P. R. Newman, A. Nitta, J. Peoples, J. R. Pier, P. S. Prieto, A. Prosapio, C. Rivetta, D. P. Schneider, S. Snedden, and S. Wang. The 2.5 m telescope of the Sloan Digital Sky Survey . 2006. *Astronomical Journal.* **131**: 2332.

Harris, H. C., J. A. Munn, M. Kilic, J. Liebert, K. A. Williams, T. von Hippel, S. E. Levine, D. G. Monet, D. J. Eisenstein, S. J. Kleinman, T. S. Metcalfe, A. Nitta, D. E. Winget, J. Brinkmann, M. Fukugita, G. R. Knapp, R. H. Lupton, J. A. Smith, and D. P. Schneider. The white dwarf luminosity function from Sloan Digital Sky Survey imaging data. 2006. *Astronomical Journal.* **131**: 571.

Koushiappas, S. M.. Proper motion of gamma-rays from microhalo sources. 2006. *Physical Review Letters.* **97**: 191301.

Koushiappas, S. M.. Detecting the dark matter via the proper motion of gamma-rays from microhalos. 2007. In *1st GLAST Symposium.* (Stanford, Palo Alto, 5-8 Feb. 2008). Vol. 921, p. 142. AIP Conf. Proc.: Springer.

McGehee, P. M.. The southern flanking fields of the 25 Orionis Group. 2006. *Astronomical Journal.* **131**: 2959.

Rodgers, C. T., R. Canterna, J. A. Smith, M. J. Pierce, and D. L. Tucker. Improved u'g'r'i'z' to UBVR_CI_C transformation equations for main sequence stars. 2006. *Astronomical Journal.* **132** (3): 989.

Shandarin, S., H. Feldman, K. Heitmann, and S. Habib. Shapes and sizes of voids in the LCDM universe: Excursion set approach. 2006. *Monthly Notices of the Royal Astronomical Society.* **367** (4): 1629.

Shandarin, S., S. Habib, and K. Heitmann. Origin of the Cosmic Web: Nature vs Nurture. *Physical Review Letters.*
Silvestri, N. M., S. L. Hawley, A. A. West, P. Szkody, J. J. Bochanski, D. J. Eisenstein, P. McGehee, G. D. Schmidt, J. A. Smith, M. A. Wolfe, H. C. Harris, S. J. Kleinman, J. Liebert, A. Nitta, J. C. Barentine, H. J. Brewington, J. Brinkman, M. Harvanek, J. Krzesinki, D. Long, E. H. Nielsen, D. P. Schneider, and S. A. Snedden. A catalog of spectroscopically selected close binary systems from the Sloan Digital Sky Survey. 2006. *Astronomical Journal.* **131**: 1674.

Strigari, L. E., S. M. Koushiappas, J. S. Bullock, and M. Kaplinghat. Precise constraints on the dark matter content of Milky Way dwarf galaxies for gamma-ray experiments. 2007. *Physical Review D.* **75**: 083526.

Strigari, L., S. M. Koushiappas, J. S. Bullock, M. Kaplinghat, J. D. Simon, M. Geha, and B. Williams. The most dark matter dominated galaxies: predicted gamma-ray signals from the faintest Milky Way dwarfs. 2008. *Astrophysical Journal.* **678**: 614.

# Quantum Nondemolition Detection of Photons

*Michael David Di Rosa*

20060558ER

## Abstract

At first glance, optics appears as a natural platform on which to invent and build the technologies required for quantum-information processing (QIP). Photons, for instance, can store and carry quantum information with excellent fidelity and immunity from environmental noise. They are among the most durable registers of quantum information and also its fastest conveyor, providing a quantum wiring that delivers information at literally light speed. Another speed to consider is how fast a chosen route can go from laboratory demonstration to reliable device, a pace usually tied to the availability of technical resources. In this regard we note that photonics is a highly developed technology with an abundance of commercial products and decades of research in quantum optics to draw from. The most successful QIP venture to date, quantum key distribution (QKD), owes its ascent partly to present-day photonics and optical-communication hardware.

Attempts to step beyond QKD and devise more sophisticated yet practicable optics-based quantum processors, such as quantum computers, have foundered on the fact that photon-photon interactions are negligibly weak. While the inertness of photons makes them robust carriers of quantum information, it also raises a corollary problem of using photons to compose quantum gates. Because photons do not interact, there is essentially no chance of changing the state of a photon based on the states of other coincident photons and thus constructing a logic operation. There are, however, other ways to construct purely optical quantum gates without requiring impossibly strong photon interactions, at least theoretically. A supposed special device that counts single photons without destroying them—a so-called quantum nondemolition (QND) detector—and allows them free passage for continued use provides the key. Assuming this device were possible, quantum-logic gates that use and manipulate photons could be built compactly and operate at speeds far higher than those of any other quantum-logic architecture proposed to date. The wealth of today's photonics technology will be at the disposal of optics-based QIP, once the link of QND detection is demonstrated.

If realized experimentally, such QND measurements could revolutionize the approach and appeal of quantum computing with advantages in raw computational speed and new architectures. The repeated use of information-bearing photons, for example, could simplify algorithms for error correction and fault tolerance. The technology for QND measurements can also be used to construct an entangled photon source and a fully-deterministic Bell-state analyzer which, in turn, can be used to build a QKD device that delivers information faster and over greater distances than does the QKD algorithm of current practice.

The theoretical inclusion of a QND photon counter in quantum-logic constructs happened recently and not by accident. Several years ago, the quantum-optics community relayed an intriguing prospect for a QND photon detector that struck QIP theorists as adaptable if not critical to photonic logic. In our research, we undertake the QND detector concept and show by way of an archetypal system how quantum coherences can be manipulated for QND measurements. The approach is new, affords photon-number resolution, and represents a significant simplification over former photon QND demonstrations that pass atoms through ultrahigh-finesse microwave cavities. Because our method can be readily integrated with existing photonics technology, we believe it will have profound implications for scalable quantum computing and QKD

## Background and Research Objectives

The architecture of quantum-information processing (QIP) is naturally suited to the use of light. Photons, for example, are especially resistant to the environmental couplings that intervene in QIP and render further quantum calculations impossible. The development of all-optical quantum computation has nonetheless been

hindered by the lack of a nonlinear operation that allows two photons (two qubits) to interact with high probability. Realizing the rarity of photon-photon interactions, Knill *et al*. [1] examined the prospects for computing with linear optics and standard detectors. Powerful quantum gates, they found, were possible but overly complex to build. Nemoto and Munro [2], however, saw the middle ground of small nonlinear interactions—interactions neither infinitesimally weak nor impossibly strong as required for efficient photon-photon couplings—as an untapped resource for scalable optical quantum computation. Small nonlinearities, for example, while unsuitable for photon entanglement could be used to make photon-number-resolving detectors that neither destroyed the photon(s) nor affected the information (such as polarization) it carried as a qubit. In effect, the detector is transparent. Such quantum nondemolition detectors have long been theorized as possible through four-wave mixing and the optical Kerr effect [3, 4], both of which occur in most media. Because QND detectors appeared possible through these non-exotic interactions, Nemoto and Munro went on to suppose their eventual existence and showed how QND detectors plus common optics could make simple, scalable logic gates for quantum computing [2].

Historically, cross-Kerr nonlinearities have been considered extremely weak, perhaps even too weak to make a practical QND device. That changed, however, with the introduction of coherent phenomena generally known as electromagnetically-induced transparency (EIT). Schmidt and Imamoglu [5] have theoretically shown that Kerr nonlinearities can be augmented through EIT coherences to a point sufficient for performing QND measurements. Our research identifies a physical match to the theoretical template of Schmidt and Imamoglu within a four-level system in atomic mercury, in which we will show three important advances in QND measurements: 1) photon-number resolution (as necessary for quantum-logic gates), 2) the unimpeded transmission of counted photons for re-use in computations, and 3) the use of optical-wavelength photons. These advances bring QND logic to existing photonics technology, a compatibility that could be exploited later at LANL for first demonstrations of purely photonic quantum-logic gates and quantum teleportation.

The overarching goal is the demonstration of QND measurements of single photons through the cross-phase modulation (XPM) inherent in Kerr media. In itself, a QND measurement is not unique. Nogues *et al.* in 1999 [6] used the extremely strong couplings between matter and radiation within a special microwave cavity built of superconducting niobium mirrors kept at 1 K to detect the presence (or absence) of one microwave within the cavity. The cavity was essentially a near-perfect "photon trap" and an elemental component of the technique. The use of such super cavities in optics-based quantum computing, however, appears unlikely. The photons are trapped in the cavity by design, their number beyond one is not easily established, and it is unlikely the photons could be switched in and out of these cavities on demand for reuse in a series of computations. A significant change in the approach to QND detection is thus needed for photonics-based QIP to proceed.

## Importance to LANL's Science and Technology Base and National R & D Needs

The project supported DOE missions in National Security and may lead to spin-off technologies useful for quantum encryption, quantum-key distribution, and detection of faint light levels. As a project in basic quantum optics, the research also fulfills the Office of Science mission of the DOE. A prime objective was to place LANL at the forefront of a new and promising route to scalable quantum computing, a priority area of research cited under Complex Systems of the Laboratory's strategic investment plan. The project supported the Laboratory's research goals of exploiting quantum systems for new forms of simulations, communications, and sensing, the latter area being relevant to cited investment areas of both Complex Systems and Ubiquitous Sensing. Beyond the project's near-term motivation of enabling quantum computing lies the far-reaching potential QND measurements have for uncovering faint signals and perturbations. Extensions of this work into new generations of detectors of national security import are conceivable.

## Scientific Approach and Accomplishments

We built a novel QND detector from the giant Kerr nonlinearity theoretically identified by Schmidt and Imamoglu [5]. Photons are still detected through transduction, though the process is quite different from the usual conversion (destruction) of photons into electrons. Instead, the presence of a photon induces a measurable phase shift in a coincident laser beam. The optical phenomenon by which one laser beam traversing a medium induces a phase shift on another and overlapping beam is the essence of cross-phase modulation and is well known. The challenge, however, was to produce this effect when only a few photons—the ones we counted—are available for inducing a phase shift in the overlapping beam.

The Kerr medium we chose is atomic mercury, and the energy levels involved as well as the quantum-coherent

mechanisms that tailor the medium for a QND measurement have been discussed previously [7, 8]. We thus omit those details and instead describe the overall design of our experiment, as shown in Figure 1. Within the Kerr medium, three laser beams overlap: a signal beam, a probe beam, and a drive beam. The signal beam contains the one to several photons to be counted, and the drive beam is needed as part of a quantum-coherence scheme that enhances the Kerr nonlinearity. The number of signal photons and probe-beam photons that enter the Kerr medium emerge unchanged by the interaction. The polarization of the signal-beam photon(s) is also unchanged by the Kerr medium, an important feature because optical qubit information is often encoded in polarization. The phase of the probe beam, however, is shifted by an amount proportional to the number of photons. In this way, the photon-number state of the signal beam is conveyed nondestructively by XPM to the phase of the probe beam.

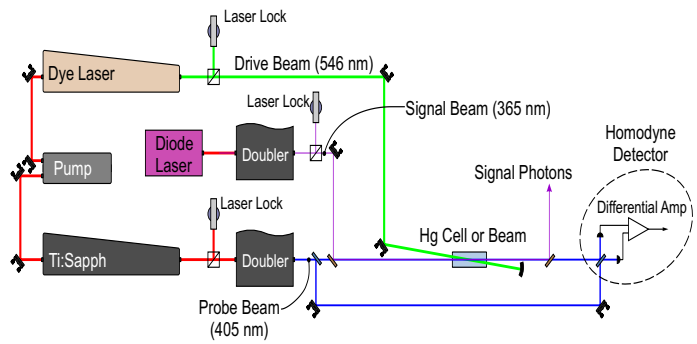


*Figure 1. Schematic design for a QND photon detector. The interaction within the Kerr medium between the signal beam (of zero to several photons) and the probe beam is enhanced significantly by the overlap of a drive beam. By XPM, the probe-beam phase is changed in proportion to the photon number of the signal beam. A balanced homodyne detector measures the phase shift of the probe beam. Neither the signal beam nor the probe beam is absorbed in the process.*

The broader view of Figure 1 now becomes one of an interferometer that measures the phase of the probe beam accumulated through the Kerr interaction. In the path of the probe beam are two beamsplitters. The first reflects 50% of the probe light toward the Kerr medium. The remaining 50% transmits through this beamsplitter, avoids the Kerr medium, and becomes the local oscillator (LO) input to a balanced homodyne detector [9]. Within the homodyne detector, a second 50/50 beamsplitter recombines the LO and the Kerr-affected probe beam for their interferometric measurement on two detectors. The detector signals are sent to a differencing junction, and the output constitutes the homodyne measurement. When the LO light and phase-shifted probe light interfere constructively at one detector, they interfere destructively at the other, giving rise to a difference signal that depends on the phase induced in the probe beam during the Kerr interaction. Three continuous-wave lasers are used in the experiments, and we developed an economical and effective means for locking and adjusting the output frequency of each [10].

Our research included a full quantum-optical simulation of the system. Figure 2 summarizes the simulations in a graph showing the real and imaginary susceptibilities of our chosen Kerr medium at the laser frequency of the probe beam. The black and red traces give the susceptibilities in cases without and with an overlapping signal beam, respectively. Recall that the real and imaginary susceptibilities determine the refractive index (*i.e.*, the phase shift) and absorption loss of light. In essence, Figure 2 shows how the material responds in the presence of signal photons and how the probe beam is accordingly affected. Without signal photons, and with the probe beam tuned precisely to an atomic resonance (a frequency of zero detuning from resonance in Figure 2), the probe beam experiences neither phase shift nor absorption. When the weak signal is present, the susceptibilities are seen to shift slightly toward higher frequencies. The absorption is negligible while the phase of the probe beam shifts to values easily measured by the homodyne circuit (diagrammed in Figure 1). Theory shows that the absorptions of probe-beam and signal-beam photons are correlated. Because practically no probe-beam absorption occurs, signal photons pass through the medium without loss while imparting their presence and number in the phase-shift of the probe beam.

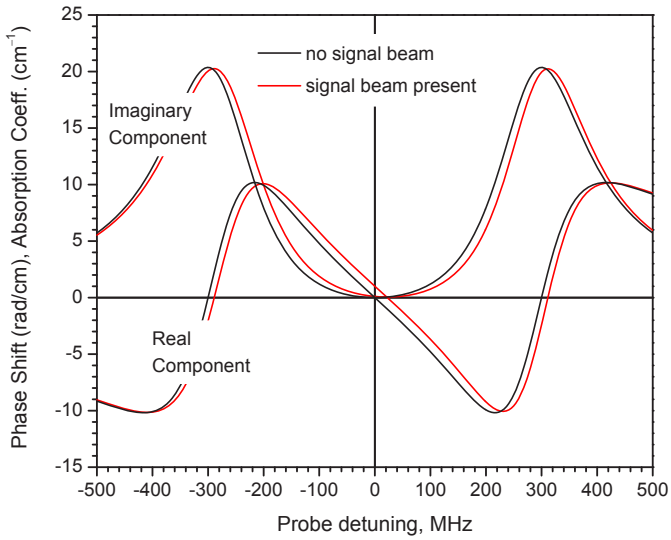


*Figure 2. Kerr-medium response at the probe-beam frequency to the presence of signal photons. The real and imaginary susceptibilities yield the phase-shift and absorption, respectively, undergone by the probe beam. Absorption is zero or negligible independent of signal photons, but the phase shift induced by signal photons is easily measured. No probe-beam absorption indicates no absorption of signal photons, either.*

We embarked on a challenging research program and showed, in computation, that a QND photon counter useful for optics-based quantum information processing can be made. Our work in both theory and computation led to two patent disclosures and forthcoming papers [11-13] related to and extending the QND work. The experimental challenge inspired a novel concept in locking the frequency of lasers [10]. As implied by Figure 1, the needed experiments are equipment intensive, as are many first demonstrations that push technical boundaries. The wherewithal for that demonstration was built from the ground up over the course of the program and is now complete. Owing to the LDRD program, we have in hand theoretical proof for both our QND concept and related new ideas in quantum optics, significant experimental resources, and new experimental techniques. We look forward toward plying these resources in the persistent need identified by LANL and outside agencies to advance quantum information processing and quantum optics in applications of national interest.

## References


1. Knill, E., R. Laflamme, and G. J. Milburn. A scheme for efficient quantum computation with linear optics. 2001. *Nature.* **409**: 46.
2. Nemoto, K., and W. J. Munro. Nearly Deterministic Linear Optical Controlled-NOT Gate. 2004. *Physical Review Letters.* **93**: 250502.
3. Milburn, G. J., and D. F. Walls. State reduction in quantum-counting quantum nondemolition measurements. 1984. *Physical Review A.* **30**: 56.
4. Imoto, N., H. A. Haus, and Y. Yamamoto. Quantum nondemolition measurement of the photon number via the optical Kerr effect. 1985. *Physical Review A.* **32**: 2287.
5. Schmidt, H., and A. Imamoglu. Giant Kerr nonlinearities obtained by electromagnetically induced transparency. 1996. *Optics Letters.* **21**: 1936.
6. Nogues, G., A. Rauschenbeutel, S. Osnaghi, M. Brune, J. M. Raimond, and S. Haroche. Seeing a single photon without destroying it. 1999. *Nature.* **400**: 239.
7. DiRosa, M. D.. Quantum nondemolition detection of photons (invited). . *Eighth Annual Southwest Quantum Information and Technology Workshop (Albuquerque, NM, 17-19 Feb. 2006).*
8. Mertes, K. M., D. H. Bradshaw, and M. D. Di Rosa. Quantum Nondemolition Detection of Photons through an Enhanced Cross- Kerr Interaction. . *Tenth Annual Southwest Quantum Information and Technology Workshop (14-17 February 2008).*
9. Yariv, A.. Quantum Electronics. 1989.
10. Tonyushkin, A. A., A. D. Light, and M. D. Di Rosa. Phase-locked scanning interferometer for frequency stabilization of multiple lasers. 2007. *Review of Scientific Instruments.* **78**: 123103.
11. Bradshaw, D. H., and M. D. Di Rosa. When the refractive index and group index depend on time as well as space (in preparation). *Physical Review A.*
12. Bradshaw, D. H., and M. D. Di Rosa. The effect of dispersion and the vacuum noise of an optical cavity mode (in preparation). *Physical Review A.*
13. Bradshaw, D. H., M. D. Di Rosa, D. V. Seletskiy, and M. Sheik-Bahae. Design of a simple nano-scale metallic optical cavity for rapid single photon emission (in preparation). *Optics Letters.*

## Publications

Bradshaw, D. H., M. D. Di Rosa, D. V. Seletskiy, and M. Sheik-Bahae. Design of a simple nano-scale metallic optical cavity for rapid single photon emission (in preparation). *Optics Letters.*

Bradshaw, D. H., and M. D. Di Rosa. When the refractive index and group index depend on time as well as space (in preparation). *Physical Review A.*

Bradshaw, D. H., and M. D. Di Rosa. The effect of dispersion and the vacuum noise of an optical cavity mode (in preparation). *Physical Review A.*

DiRosa, M. D.. Quantum nondemolition detection of photons (invited). Invited presentation at *Eighth Annual Southwest Quantum Information and Technology Workshop.* (Albuquerque, NM, 17-19 Feb. 2006).

Light, A. D., and M. D. Di Rosa. Phase-locked scanning interferometer for frequency stabilization of multiple lasers. Presented at *Eighth Annual Southwest Quantum Information and Technology Workshop.* (Albuquerque, NM, 17-19 Feb. 2006).

Mertes, K. M., D. H. Bradshaw, and M. D. Di Rosa. Quantum Nondemolition Detection of Photons through an Enhanced Cross-Kerr Interaction. 2008. *Southwest Quantum Information and Technology Tenth Annual Meeting.*

Tonyushkin, A. A., A. D. Light, and M. D. Di Rosa. Phase-locked scanning interferometer for frequency stabilization of multiple lasers. 2007. *Review of Scientific Instruments.* **78**: 123103.

Tonyushkin, A. A., and M. D. Di Rosa. Phase-locked scanning interferometer for frequency stabilization of multiple lasers. Presented at *2007 Meeting of the Divison of Atomic, Molecular, and Optical Physics of the American Physical Society.* (Calgary, Alberta, Canada, 4-9 June 2007).

# Manipulation and Control of Electron Spins in Semiconductors with Strain Engineering

*Darryl Lyle George Smith*

20060589ER

## Abstract

Manipulation and control of the electron spin in semiconductors is central to the operation of a new generation of "spintronic" devices having the potential to overcome the power consumption and speed limitations of conventional electronics, and which are also promising candidates for the physical implementation of quantum information processing and computing ideas. To date, efforts to manipulate electron spin in semiconductors have concentrated on the use of magnetic fields, which couple directly to electron spin, but which also lead to strong spatial spin dephasing. Using scanning Kerr microscopy, we have demonstrated that controlled application of strain can be used to manipulate and control electron spin in semiconductors. This approach to spin manipulation has many advantages compared with traditional methods based on magnetic fields (e.g., it solves the strong spatial spin dephasing problem). In this program, we utilized a closely coupled experimental/theoretical program to demonstrate that strain engineering can effectively manipulate electron spin in semiconductor structures.

## Background and Research Objectives

Non-equilibrium, electron-spin-based phenomena in semiconductors are currently of great technological and fundamental scientific interest [1]. Commercially available devices based on the manipulation of electron spin in metallic magnetic structures, such as the giant magneto resistance (GMR) read heads now used on all computer hard drives, are revolutionizing information storage technology. Operation of semiconductor devices based on electron spin require: 1) establishment of a non-equilibrium spin-polarized electron distribution in the semiconductor; 2) transport of the electron spin distribution across the semiconductor structure; 3) manipulation and control of the electron spin distribution; and 4) detection of the electron spin distribution. Recently, there has been rapid progress on items 1), 2) and 4) on this list. The effective manipulation and control of spin is currently a major bottleneck to the implementation of spin-based semiconductor devices. Until very recently, only spin manipulation by magnetic fields had been demonstrated. Magnetic fields couple directly to electron spin by the Zeeman effect. In semiconductors like GaAs that do not have a center of inversion, there is also a coupling between electron spin and strain that arises because of the spin-orbit interaction and unlike spin-magnetic field coupling depends on electron velocity. *The fact that spin-strain coupling depends on the electron velocity, and strain-magnetic field coupling does not, is crucial in determining the different effects that magnetic fields and strain fields have on electron spin distributions.* Prior to our work, the coupling between strain and electron spin was known in principle, but there had been very few experimental investigations of the consequences of this coupling and little appreciation of its potential importance in spin-based semiconductor devices.

Scanning Kerr microscopy is an experimental technique used to acquire 2D images of spin-polarized conduction electrons in semiconductors [2]. The images can be used to reveal the spatial dependence of spin diffusion/drift in the presence of applied electric, magnetic, and strain fields [3]. In scanning Kerr microscopy, spatial images electron spin populations are acquired by measuring the Kerr rotation imparted on a linearly-polarized probe laser beam that is reflected from the semiconductor surface, and raster-scanned. Spin populations can be generated optically by the absorption of circularly polarized light utilizing optical selection rules [3] and electrically by injection from a ferromagnetic contact utilizing spin dependent tunnel barriers [4]. These spin-polarized electrons drift/diffuse laterally away from their point of generation. Kerr microscopy

images of a spin population in GaAs can then be used to study the transport and time evolution properties of non-equilibrium spin populations generated by the optical generation or electrical injection.

## Importance to LANL's Science and Technology Base and National R & D Needs

The ability to manipulate and control the electron spin degree of freedom in semiconductors is central to the operation of a new generation of semiconductor "spintronic" devices that have the potential to overcome the power consumption and speed limitations of conventional electronic circuits, and which are promising candidates for the physical implementation of quantum information processing and computing ideas. Semiconductor devices utilizing electron spin require transport of spin-polarized electrons from one location in the device to another, and a means to manipulate the electron spin orientation. To date, most effort on electron spin manipulation in semiconductors has concentrated on the use of magnetic fields. Magnetic fields couple directly to electron spin, but as was discussed in the Background section, magnetic fields lead to a strong spatial dephasing of electron spin in semiconductors because of the random walk nature of electron transport in these materials. We have used scanning Kerr microscopy to demonstrate that application of strain can be used to manipulate and control electron spin in semiconductors. The use of strain to manipulate electron spin has many advantages compared with traditional methods based on magnetic fields. For example, we have shown that because of the way strain couples to spin, spatial electron spin coherence is maintained much better in strain fields than in magnetic fields. In these experiments, we investigated the effect of strain/spin coupling in the case of bulk semiconductors in which the strain was spatially uniform and temporally static. In this program we engineered strain with both nanometer-scale spatial resolution, and with ultrafast temporal resolution. We employed a closely coupled experimental/theoretical program to demonstrate that strain engineering can be used effectively for controlled electron spin manipulation in semiconductor structures. This work coupled strongly with research at CINT both at LANL and Sandia.

## Scientific Approach and Accomplishments

### Manipulating and Imaging Optically Generated Spin Populations

Using scanning Kerr microscopy, we directly acquire two-dimensional images of spin-polarized electrons flowing laterally in epilayers of n-type GaAs. Optical injection provided a local dc source of polarized electrons, whose subsequent drift and/or diffusion is controlled with electric, magnetic, and - in particular - strain fields. Spin precession induced by controlled uniaxial stress demonstrates the direct k-linear spin-orbit coupling of electron spin to the shear components of the strain tensor. To understand these experimental results we constructed a spin-drift-diffusion model to describe spin-polarized electron transport in zincblende semiconductors in the presence of magnetic fields, electric fields, and strain. We presented predictions of the model for geometries that correspond to optical spin injection from the absorption of circularly polarized light, and for geometries that correspond to electrical spin injection from ferromagnetic contacts. Starting with the Keldysh Green's function description for a system driven out of equilibrium, we construct a semiclassical kinetic theory of electron spin transport in strained semiconductors in the presence of electric and magnetic fields. From this kinetic theory we derive spin-drift-diffusion equations for the components of the spin density matrix for the specific case of spatially uniform fields and uniform electron density. We solved the spin-drift-diffusion equations numerically and compare the resulting images with scanning Kerr microscopy data of spin-polarized conduction electrons flowing laterally in bulk epilayers of n-type GaAs. The spin-drift-diffusion model accurately described the experimental observations. We contrast the properties of electron spin precession resulting from magnetic and strain fields. Spin-strain coupling depends linearly on electron wave vector and spin-magnetic field coupling is independent of electron wave vector. As a result, spatial coherence of processing spin flows is better maintained with strain than with magnetic fields, and the spatial period of spin precession is independent of the applied electrical bias in strained structures whereas it is strongly bias dependent for the case of applied magnetic fields.

### Manipulating and Imaging Electrically Injected Spin Populations

We directly imaged electrical spin injection and accumulation in the gallium arsenide channel of lateral spin transport devices which have ferromagnetic (Fe) source and drain tunnel barrier contacts. Emission of spins from the source is observed, and a region of spin accumulation is imaged near the ferromagnetic drain contact. Both injected and accumulated spins have the same orientation (antiparallel to the contact magnetization), and we show that the accumulated spin polarization flows away from the drain (against the net electron current). The electrical conductance can be modulated by controlling the spin

orientation of electrons flowing through the drain. Using both spin imaging and local Hanle effect studies, we investigate the drift and diffusion of electrically-injected spins in lateral Fe/GaAs spin-detection devices, both within and outside of the current path. We used first principle electronic structure calculations of the Fe/GaAs interface to explain these experimental observations. A minority-spin resonant state at the Fe/GaAs (001) interface is predicted to reverse the spin polarization with the voltage bias of electrons transmitted across this interface. Using a Green's function approach within the local spin-density approximation, we calculated the spin-dependent current in a Fe/GaAs/Cu tunnel junction as a function of the applied bias voltage. We found a change in sign of the spin polarization of tunneling electrons with bias voltage due to the interface minority-spin resonance. This result explains the experimental data on spin injection in Fe/GaAs contacts and on tunneling magnetoresistance in Fe/GaAs/Fe magnetic tunnel junctions. We also investigated the magnetic structure on the Fe (001) surface and theoretically studied scanning tunneling spectroscopy using a spin-polarized tip (SP-STM). We showed that minority-spin surface states induce a strong bias dependence of the tunneling differential conductance which largely depends on the orientation of the magnetization in the SP-STM tip relative to the easy magnetization axis in the Fe (001) surface. We proposed to use this effect in order to determine the spin character of the Fe (001) surface states. This theoretical technique can also be applied also to other magnetic surfaces in which surface states are observed.

**Measurements of Effects of External Fields on Spin Lifetimes**

In n-type GaAs epilayers doped near the metal-insulator transition, we studied the evolution of the electron spin lifetime as a function of applied lateral electrical bias. The spin lifetimes were measured via the Hanle effect using magneto-optical Kerr rotation. At low temperatures (less than 10K, where electrons are partially localized and the spin lifetime is greater than 100 ns at zero bias), a marked collapse of the spin lifetime was observed when the applied electric field exceeded the donor impact ionization threshold of 10 V/cm. A steep increase in the concentration of delocalized electrons – subject to the Dyakonov-Perel spin relaxation mechanism – accounts for the rapid collapse of spin lifetime and also strongly influences electron spin transport in this regime. In electron-doped GaAs, we used scanning Kerr-rotation microscopy to locally probe and spatially resolve the depolarization of electron spin distributions by transverse magnetic fields. The shape of these local Hanle-effect curves provided a measure of the spin lifetime as well as spin transport parameters including drift velocity, mobility, and diffusion length. Asymmetries in the local Hanle data were used to reveal and map out the effective magnetic fields resulting from strain due to spin-orbit coupling.

**Electrical Detection of Spin Populations**

Using Fe/GaAs Schottky tunnel barriers as electrical spin detectors, we showed that both the magnitude and sign of their spin-detection sensitivities are widely tunable with voltage bias applied across the Fe/GaAs interface. Electrons with fixed spin polarization in GaAs can be made to induce either positive or negative voltage changes at spin-detection electrodes, and some detector sensitivities can be enhanced over ten-fold with applied bias. This tenability derives from the interplay between two physical processes: 1) the bias dependence of the tunneling spin polarization (a property of the Fe/GaAs interface), and 2) the bias dependence of spin transport in the semiconductor, which can dramatically enhance or suppress spin-detection sensitivities. We demonstrated that the bias dependence of spin-polarized tunneling in combination with electric-field driven spin transport can be used to control the sensitivity of spin-detection in lateral Fe/GaAs structures. By tuning the voltage bias applied across a Fe/GaAs detector, we controlled both the magnitude and sign of its spin-detection sensitivity. Experiments revealed that spin detection sensitivity can differ significantly from the polarization of the tunneling current, due to spin drift and diffusion effects in the semiconductor channel. Finally, we showed that in multi-terminal devices a spin-detector's sensitivity can be controlled – and optimized – independently from the details of spin injection at a source electrode, providing much freedom and flexibility in device design. We presented a theoretical model that describes electrical spin-detection at a ferromagnet/semiconductor interface. We showed that the sensitivity of the spin detector has strong bias dependence which, in the general case, is dramatically different from that of the tunneling current spin polarization. We showed that this bias dependence originates from two distinct physical mechanisms: 1) the bias dependence of tunneling current spin polarization, which is of microscopic origin and depends on the specific properties of the interface, and 2) the macroscopic electron spin transport properties in the semiconductor. Numerical results show that the magnitude of the voltage signal can be tuned over a wide range from the second effect which suggests a universal method for enhancing electrical spin-detection sensitivity in ferromagnet/semiconductor tunnel contacts. Using first-principles calculations we examine the particular case of a Fe/GaAs Schottky tunnel barrier and found very good agreement with the experimental measurements. We also predicted the bias

dependence of the voltage signal for a Fe/MgO/GaAs tunnel structure spin detector.

**Calculations of Strain Induced Spin Splittings in GaAs**

We used a recently developed self-consistent GW approximation to present first principles calculations of the conduction band spin splitting in GaAs under [110] strain. The spin orbit interaction is taken into account as a perturbation to the scalar relativistic Hamiltonian. These are the first calculations of conduction band spin splittings under deformation based on a quasiparticle approach; and because the self-consistent GW scheme accurately reproduced the relevant band parameters. This approach was demonstrated to be a reliable predictor of spin splittings in a variety of semiconductors.

## References


1. Zutic, I., J. Fabian, and S. Das Sarma. Spintronics: fundamentals and applicarionds. 2004. *Reviews of Modern Physics.* **76** (2): 323.
2. Kato, Y., R. C. Myers, A. C. Gossard, and D. D. Awschalom. Coherent spin manipulation without magnetic fields in strained semiconductors . 2004. *Nature.* **427** (6969): 50.
3. Crooker, S. A., and D. L. Smith,. Imaging spin flows in semiconductors subject ot electric, magnetic and strain fields. 2005. *Physica Review Letters.* **94** (23): 236601.
4. Smith, D. L., and R. N. Silver. Electrical spin injection into semiconductors. 2001. *Physical Review B.* **64**: 045323.


## Publications


Chantis, A. N., D. L. Smith, J. Fransson, and A. V. Balatsky. Detection of the spin character of Fe(001) surface states by Scanning Tunneling Microscopy: A theoretical proposal. *Phys. Rev.*

Chantis, A. N., M. Cardona, N. E. Christensen, D. L. Smith, M. van Schilfgaarde, T. Kotani, A. Svane, and R. C. Albers. Strain-Induced Conduction Band Spin Splitting in GaAs from First Principles Calculations. To appear in *Phys. Rev..*

Crooker, S. A., E. Garlid, A. N. Chantis, D. L. Smith, K. S. M. Reddy, Q. Hu, T. Kondo, C. J. Palmstrom, and P. A. Crowell. Bias-controlled sensitivity of ferromagnet/semiconductor electrical spin detectors . *Phys. Rev. Lett..*

Crooker, S. A., M. Furis, X. Lou, P. A. Crowell, D. L. Smith, C. Adelmann, and C. J. Palmstrom. Optical and electrical spin injection and spin transport in hybrid Fe/GaAs devices. 2007. *Journal of Applied Physics.* **101**: 081716.

Furis, M., D. L. Smith, S. A. Crooker, and J. L. Reno. Bias-dependent electron spin lifetimes in n-GaAs and the role of donor impact ionization. 2006. *Applied Physics Letters.* **89**: 102102.

Furis, M., D. L. Smith, S. Kos, E. S. Garlid, K. S. M. Reddy, C. J. Palmstrom, P. A. Crowell, and S. A. Crooker. Local Hanle-effect studies of spin drift and diffusion in n:GaAs epilayers and spin-transport devices . 2007. *New Journal Physics .* **9**: 347.

Hruska, M., S. Kos, S. A. Crooker, A. Saxena, and D. L. Smith. Effects of strain, electric, and magnetic fields on lateral electron-spin transport in semiconductor epilayers. 2006. *Physical Review B.* **73**: 075306.

Hruska, M., S. Kos, S. A. Crooker, A. Saxena, and D. L. Smith. Modeling spin-polarized electron transport in semiconductors for spintronics applications. 2007. *Computing in Science and Engineering .* **9**: 46.

Lou, X. H., C. Adelmann, S. A. Crooker, E. S. Garlid, J. Zhang, K. S. M. Reddy, S. D. Flexner, C. J. Palmstrom, and P. A. Crowell. Electrical detection of spin transport in lateral ferromagnet-semiconductor devices. 2007. *Nature Physics* . **3**: 197.

Lou, X., C. Adelmann, M. Furis, S. A. Crooker, C. J. Palmstrom, and P. A. Crowell. Electrical detection of spin accumulation at a ferromagnet-semiconductor interface. 2006. *Physical Review Letters.* **96**: 176603.

# Structure and Evolution in Cosmology and Astrophysics

*Richard Ira Epstein*

20060685ER

## Abstract

This project is focused on observing and modeling the astronomical systems to unravel the most pressing problems in cosmology and astrophysics. For example, recent observations have shown that the overall universe is expanding ever more rapidly. This accelerating expansion is ascribed to a new, poorly understood field that permeates all space called "dark energy". Our research will use theoretical models and observations to elucidate the properties and consequences if dark energy. Our specific tasks will examine early galaxy formation and clustering and high-energy emission from distant objects.

## Background and Research Objectives

The high redshift Universe at redshift 10 - 20 is where the frontiers of cosmology and astrophysics meet. In coming years, new observations targeting the epoch of reionization and beyond will vastly increase our knowledge of the pre-reionized universe. This era is known as the ``dark ages'', because photons from this epoch cannot reach us today. In order to shed light onto the dark ages we have to understand the formation of the first bright objects, the first stars and the first galaxies. To understand these epochs it is necessary to examine in detail the complex baryonic processes that regulate the evolution of galaxies, with an eye toward making predictions of their observable properties for upcoming ground- and space-based observatories such as the Thirty Meter Telescope and the James Webb Space Telescope.

To interpret the dynamics of the early universe, one needs to explore optimal ways to study the dark energy. This involves a range of issues, including specific observational approaches as well as theoretical underpinning of the dark energy. It is also important to investigate the formation and evolution of galaxies at cosmological epochs that are only now being probed observationally. Specifically, one of our goals is to investigate feedback processes (e.g. supernova explosions, metal enrichment, energy from cosmic rays and active galactic nuclei) using the cosmological AMR code Enzo. Another of our goals has be to develop innovative gamma-ray instruments that can be used to study the formation of the elements in the universe. These devices may also have importance for medical and homeland security applications.

## Importance to LANL's Science and Technology Base and National R & D Needs

This work can lead to the development of instruments and computational capabilities for NNSA's nuclear nonproliferation mission objectives. For example, we will develop innovative gamma-ray instruments that can help detect and identify sensitive nuclear materials. The science ties to missions of DOE OS.

## Scientific Approach and Accomplishments

We have explored the importance of gravitational lensing on Type Ia supernova distance measurements. We analyzed gravitational lensing as a potential systematic. We show that for sufficiently large fields, and for sufficiently large datasets, the errors due to gravitational lensing can be controlled. We have also explored a further systematic, having to do with the currently favored model of Type Ia supernovae, which describes them as a two-population family. We find that the post-calibration systematic between different families must be controlled to a few percent. These results can easily be generalized to more sophisticated models of the supernova population.

We have also investigated different ways to parameterize the dark energy, advocating a multi-parameter, model independent approach. We showed that this approach can be used to directly reconstruct the dark energy scalar-field potential in a model-independent fashion. We have also shown that this approach can lead to precision determination of 3 or more dark

energy parameters from future surveys. This result has garnered a fair share of attention, as it goes against "conventional wisdom."

The high redshift Universe at redshift 10 - 20 is where the frontiers of cosmology and astrophysics meet. In coming years, new observations targeting the epoch of reionization and beyond will vastly increase our knowledge of the pre-reionized universe. This era is known as the ``dark ages'', because photons from this epoch cannot reach us today. In order to shed light onto the dark ages we have to understand the formation of the first bright objects, the first stars and the first galaxies. We have modeled the formation and evolution of the dark matter structures in which stars and galaxies form, and quantified their numbers and distribution throughout the history of the universe. We have discovered clues from the halo mass function that the mechanisms of halo formation have important differences at high redshifts. This work provides an essential connection between observable galaxies and the fundamental properties of dark matter. We have measured the clustering properties of halos likely to host stars and galaxies at redshifts of 10 and higher. This work provides a crucial link between the halo clustering strength, which is expected to be measured in upcoming observations.

We have investigated feedback processes (e.g. supernova explosions, metal enrichment, energy from cosmic rays and active galactic nuclei) using the cosmological AMR code Enzo. Results have been obtained for simulations looking at the highest-redshift structure formation - examining the formation and evolution of Population III stars and their effects on a second generation of structure formation. We have implemented the Biermann Battery into simulations of Population III star formation within an MHD framework. We find that the Population III stars formed including this effect are both qualitatively and quantitatively similar to those from hydrodynamics- only (non-MHD) cosmological simulations. We observe peak magnetic fields of ~$10^9$ G in the center of our star-forming halo at z ~ 17.55. The magnetic fields created by the Biermann Battery effect are predominantly formed early in the evolution of the primordial halo at low density and large spatial scales, and then grow through compression and by shear flows. The fields seen in this calculation are never large enough to be dynamically important, and should be considered the minimum possible fields in existence during Population III star formation, and may be seed fields for the stellar dynamo or the magnetorotational instability at higher densities and smaller spatial scales.

We have examined the transition between Population III (metal free) stars and Population II (metal enriched) stars, and have discovered that there are three modes of metal-enriched star formation in the early universe. One mode, occurring when there is a very low level of metal content in the gas, is virtually indistinguishable from primordial star formation. For metallicities well above the critical value, efficient cooling rapidly lowers the gas temperature to the temperature of the cosmic microwave background (CMB). The gas is unable to radiatively cool below the CMB temperature, and becomes thermally stable. For high metallicities, 0.3% that of the sun, this occurs early in the evolution of the gas cloud, when the density is still relatively low. The resulting cloud-cores show no fragmentation, forming only massive stars. If the metallicity is not vastly above the critical value, the cloud cools efficiently but does not reach the CMB temperature, and fragmentation into multiple objects occurs.

An additional exploration of the Population III to II transition involves the detailed exploration of the chemical-thermal-dynamical evolution of gas in an evolving Pop III supernova remnant within the HII region formed by that star. A range of plausible explosion energies and host halo masses were considered, and the remnant was evolved from the initial free expansion phase (~10 AU) to extremely late stages of evolution (tens of millions of years later). We find that if the star ionizes the halo, the ejecta strongly interacts with the dense shell swept up by the H II region, potentially cooling and fragmenting it into clumps that are unstable to gravitational collapse. If the star fails to ionize the halo, the explosion propagates metals out to 20 - 40 pc and then collapses, enriching tens of thousands of solar masses of primordial gas, in contrast to previous models that suggest such explosions 'fizzle'. Rapid formation of low-mass stars trapped in the gravitational potential well of the halo appears to be inevitable in such circumstances. Consequently, it is possible that far more stars were swept up into the first galaxies, at earlier times and with distinct chemical signatures, than in present models. Upcoming measurements by JWST and ALMA may discriminate between these two paradigms.

Our work on cosmological hydrodynamics has three components: 1) cluster physics, 2) the structure and mass distribution of group and cluster-scale dark matter halos, and 3) code validation studies to characterize the accuracy of simulation methods. The initial work was focused on cluster physics using the FLASH code and to extending FLASH's capabilities via subgrid modeling (intra-cluster light as an example). Because of difficulties with FLASH performance in dealing with large-scale cosmological simulations at the time, we switched to using the LANL MC^2 code. Using these simulations, we carried out the best-characterized and detailed study so far of the time evolution of the

halo mass function, all the way from high redshift (z=30), to the present. The essential result is that the halo mass function follows a "universal" form to a very high degree of accuracy (roughly 5%) even though its value changes by orders of magnitude as a function of evolutionary epoch. In order to obtain results at the percent level of accuracy, error control in cosmological simulations has to be taken to a previously unattained level. The LANL group has coordinated a world-wide code validation effort to improve simulation standards. The latest work consists of analyzing the structure of halos, showing that halo masses given by the two most commonly used halo definitions can in fact be connected by a mapping formula, provided halo concentrations are known. In addition, this work showed that major halo substructure is cosmology-dependent (perhaps in a universal manner) and this feature can be used as a cosmological test. Observations of clusters are now being analyzed (by us and elsewhere) to see whether current catalogs are already good enough for this type of analysis.

We have developed a background rejection technique that improved the sensitivity of Milagro gamma ray observatory by a factor of two, Milagro made several important discoveries. The sources we detected nearly doubled the number of TeV sources in the Northern hemisphere. All three of our discovered sources have been confirmed by other experiments: one by the HESS experiment and two by the Tibet air shower array. One of our candidate sources has been confirmed by the Tibet experiment. Prior to this work the future of all-sky TeV gamma-ray detectors was uncertain, the results were of limited significance - marginal detections of previously known TeV sources such as the Crab Nebula. Now, the future of such detectors is on a firm foundation and there is widespread support within the broader community to develop the next generation instrument, known as HAWC. On the scientific front, this work has made Milagro the most sensitive gamma-ray detector above ~10 TeV in energy, enabling us to hunt for the elusive sources of cosmic rays. We have measured the spatial distribution of the Galactic diffuse gamma-ray emission at unprecedented energies near 20 TeV and detected an excess of this emission from the Cygnus Region of our Galaxy - perhaps indicating the presence of cosmic-ray accelerators in this region.

We developed a new approach to gamma-ray optics based on channeling in waveguides made from multilayered structures consisting of alternating thin-film layers of a high-density reflecting material and a low-density spacer material. These structures can act as planar waveguides for gamma rays with energies between ~ 100 keV and a few MeV. We showed channeling of 122 keV gamma rays in flat and curved waveguide structures composed of a high-density gold-palladium alloy film and a low-density polymer film. These results establish the feasibility of using gamma-ray waveguides to construct concentrating optics. To demonstrate channeling, we fabricated two 4 cm by 3 cm thin-film multilayer structures on silicon substrates. One consists of ten alternating layers of 40 nm thick sputter-deposited gold-palladium and 4 micron thick spin-coated UV curable polymer film. A second similar structure consists of 30 pairs of gold-palladium layers and 1.2 micron thick polymer layers. The Au-Pd layers serve as reflectors while the low-density polymer keeps the Au-Pd layers separated, smooth, and parallel. In a curved waveguide the gamma rays can be deflected up to twice the critical angle per reflection. To see the effects of multiple reflections we set up a gamma-ray detection system, which only measures gamma rays, deflected by more than several time the critical angle. Using this procedure maximum deflections of 5.8 times the critical angle in one wave guide and in the first waveguide (4 micron thick polymer) and 6.3 time in second waveguide (1.2 micron thick polymer).

## Publications


Abdo, A. A.. TeV Gamma-Ray Sources from a Survey of the Galactic Plane with Milagro. 2007. *Astrophysical Journal Letters.* **664**: L91.

Abdo, A. A.. Discovery of TeV Gamma-Ray Emission from the Cygnus Region of the Galaxy. 2007. *Astrophysical Journal Letters.* **664**: L33.

Abdo,etal., A.. Milagro constraints on very high energy emission from short-duration Gamma-Ray Bursts. 2007. *Astrophysical Journal.* **666**: 361.

Abdo,etal., A.. TeV gamma-ray sources from a survey of the galactic plane with Milagro . 2007. *Astrophysical Journal Letters.* **664**: 91.

Abdo,etal., A.. Discovery of TeV gamma-ray emission from the Cygnus Region of the Galaxy . 2007. *Astrophysical Journal Letters.* **658**: 33.

Bloser,etal., P.. The MEGA Project for medium energy gamma-ray astronomy. 2006. *Chin. J. Astron. Astrophys. Suppl..* **6**: 388.

Chao, L., D. E. Holz, and A. Cooray. Direct reconstruction of the dark energy scalar-field potential. 2007. *Physicval Review D.* **75**: 103503.

Cooray, A., D. E. Holz, and D. Huterer. Cosmology from supernova magnification maps. 2006. *Astrophys. J. Lett.* **637** (L77): 37.

Cooray, A., D. Huterer, and D. E. Holz. Problems with pencils: lensing covariance of supernova distance measurements. 2006. *Phys. Rev. Lett. .* **96** (021301): 23.

Duan, H., G. M. Fuller, J. Carlson, and Y. Z. Qian. Flavor Evolution of the Neutronization Neutrino Burst from an O-Ne-Mg Core-Collapse Supernovae. 2008. *Phys. Rev. Lett.* (211): 100.

Duan, H., G. M. Fuller, J. Carlson, and Y. Z. Qian. Analysis of Collective Neutrino Flavor Transformations in Supernovae. 2007. *Phys. Rev.* **690**: D75.

Fan, S., S. Liu, J. Wang, C. L. Fryer, and H. Li. Stochastic Acceleration in the Western Hotspot of Pictor A. 2008. *The Astrophysical Journal (Letters).* **673**: L139.

Hao, S., H. Li, D. C. Collins, S. Li, and M. L. Norman. Formation of X-Ray Cavities by the Magnetically Dominated Jet_Lobe System in a Galaxy cluster. 2008. *Ap.J.* **681**: L. 61.

Heitmann, K., Z. Lukic, S. Habib, and P. M. Ricker. Capturing Halos at High Redshifts. 2006. *Astrophys. J. Lett..* **L85**: 642.

Huaiya, D., G. M. Fuller, J. Carlson, and Y. Z Qian. Neutrino Mass Hierarchy and Stepwise Spectral Swapping of Supernovae Neutrino Flavors. 2007. *Phys. Rev. Lett..* **99**: 87.

Huang, L., L. Siming, S. Shen, M. J. Cia, H. Li, and C. L. Fryer. Linearly and Circularly Polarized Emission in Sagittarius A. 2008. *The Astrophysical Journal (Letters).* **676**: L119.

Li, C., D. E. Holz, and A. Cooray. Direct reconstruction of the dark energy scalar-field potential. 2007. *Phys. Rev. D .* (103503): 75.

Lui, S., L. Qian, X. Wu, C. L. Fryer, and H. Li. The Nature of Linearly Polarized Millimeter and Submillimeter Emission in Sagittarius A. 2007. *The Astrophysical Journal (Letters).* **668**: L127.

Lukic, Z., K. Heitmann, S. Habib, S. Bashinsky, and P. M. Ricker. The Halo Mass Function: High Redshift Evolution and Universalit. 2007. *Astrophys. J. .* **671**: 1160.

Reed, D., F. Governato, T. Quinn, J. Stadel, and G. Lake. The age dependence of galaxy clustering. 2007. *Monthly Notices of the Royal Astronomical Society.* **378**: 777.

Reed, D., F. Governato, T. Quinn, J. Stadel, and G. Lake. The Age Dependence of Galaxy Clustering. 2007. *Monthly Notices of the Royal Astronomical Society.* **378** (7772): 160.

Reed, D., R. Bower, C. S. Frenk, A. Jenkins, and T. Theuns. The Halo Mass Function from the Dark Ages through the Present Day. 2007. *Monthly Notices of the Royal Astronomical Society.* **374** (2): 20.

Sarkar, D., A. Amblard, A. Cooray, and D. E. Holz. Implications of two Type Ia supernova populations for cosmology. 2008. *Astrophys. J. Lett.* **684** (L13): 85.

Sarkar, D., A. Amblard, D. E. Holz, and A. Cooray. Lensing and supernovae: quantifying the bias on the dark energy equation of state. 2008. *Astrophys. J.* **678** (L13): 63.

Siming, L., F. Zhong-Hui, L. Christopher, C. L. Fryer, J. Wang, and H. Li. Stochastic Electron Acceleration in Shell-Type Supernova Remnants. 2008. *The Astrophysical Journal (Letters).* **683**: L163.

Sullivan, S., A. Cooray, D. E. Holz, and J. Cosmology. Narrowing constraints with type Ia supernovae: converging on a cosmological constant. 207. *Astropart. Phys.* **08** (4): 099.

Sullivan, S., A. Cooray, and D. E. Holz. Narrowing constraints with Type Ia supernovae: converging on a cosmological constant. 2007. *Journal of Cosmology and Astroparticle Physics.* **09**: 4.

Sullivan, S., D. Sarkar, S. Joudaki, D. E. Holz, and A. Cooray. Beyond two dark energy parameters. 2008. *Phys. Rev. Lett.* **100** (241302): 123.

Tournear, D. M., M. A. Hoffbauer, E. A. Akhadov, A. T. Chen, S. J. Pendleton, T. L. Williamson, K. C. Cha, and R. I. Epstein. Gamma Ray Waveguides. 2008. *Applied Physics Letters.* **92** (153502-1): 80.

Tournear, D., R. I. Epstein, and R. M. Kippen. Gamma-ray channeling in layered structures. 2004. In *IEEE Nuclear Science Symposium Conference.* (San Francisco, CA, 2004). Vol. 7, R4-2 Edition, p. 4282. New York, NY: IEEE.

Wunderer,etal., C. B.. The ACT Vision mission study simulation effort. 2006. *New Astron. Rev.* **50**: 608.

Xu, H., D. C. Collins, M. L. Norman, S. Li, and H. Li. A Cosmological AMR MHD Module for ENZO. Presented at *AIP Conf. Proc. 990.* (San Diego, CA, 2008).

full final report

# Supersymmetry Breaking in Various Dimensions

*Tanmoy Bhattacharya*

20060694ER

## Abstract

The Standard Model of particle physics is an extremely successful theory except that, absent new interactions, it is unstable due to quantum corrections. Most plausible possibilities for new physics invoke a 'supersymmetry' between particles with different spins. Since no such symmetry is observed in nature, explanations of this kind need to 'break' the symmetry maintaining its nice properties. A particular class of theoretical ideas to address this is called higher dimensional broken supersymmetry and all models incorporating it predict new interactions possibly observable in upcoming experiments. Accurate predictions from these theories have, however, been difficult to obtain because they required yet-to-be-developed 'nonperturbative' techniques. The aims of this proposal were four-fold: to develop new models of supersymmetry breaking, to develop nonperturbative methods for studying these models, to determine the experimental implications of these models, and to study cosmological features that could generically constrain entire classes of these models. In this report, we describe the progress that was made in each of these four fronts.

## Background and Research Objectives

Particle physics today finds itself at an odd juncture: the entire suite of experiments that have been performed seem to be explained admirably well by a theory which we call the Standard Model of particle physics; and, yet, this theory has a number of rather disconcerting features. For one, it has a number of parameters whose values seem arbitrarily selected from an extremely large range of possible magnitudes. Furthermore, quantum effects make a large hierarchy of magnitudes extremely difficult to maintain: in these theories, a natural situation would be one where all these parameters are similar in magnitude.

For these reasons, it has long been thought that the Standard Model is just an approximation to a more complete theory that would explain and stabilize the magnitudes of these parameters. Most of these extensions involve a symmetry called supersymmetry that link properties of particles with different spins. It has long been known that particles with a spin of half a unit, called fermions, can have a property called chirality that make them better behaved in quantum theory. As supersymmetry links particles of different spins, it can stabilize the entire theory, including the interactions of the spinless particles called scalars, by using the chirality of the fermions.

The problem with these ideas has been twofold. First, it has been difficult to come up with complete 'nonperturbative' definition of interacting chiral theories in anything but two dimensions, and lacking such a fundamental definition, concrete calculations in these extended theories turn out to be near impossible. Second, naïve implementations of supersymmetry lead to manifestly absurd theories with particles of different spins having equal masses, a situation not observed experimentally. This consequence can be avoided by carefully constructing theories that realize the supersymmetry in a hidden or 'broken' fashion. This is a difficult task, but recent advances have shown that the problem becomes easier if we describe our four dimensional (with three space and one time dimensions) world as a higher dimensional universe in which the other dimensions cannot be sampled at low energies, either due to strong forces or due to quantization effects.

Given this scenario, a large amount of experimental effort is focused at discovering hints about these manifold ideas that go beyond the Standard Model. In this project, we participated in this grand adventure by developing explicit theories of broken supersymmetry and studying them to see what kind of experimental signatures they produce. We also spent a substantial fraction of our time trying to define interacting theories of chiral fermions that can be used for nonperturbative calculations. Finally, we noticed that most supersymmetric theories, irrespective of the details of their construction, contain extra scalars and nonstandard interactions of fermions that are too weak to affect terrestrial experiments but have large cosmological and astrophysical effects. With this in mind, we studied

these cosmological implications with an eye to providing bounds on these that are independent of other details of the theories in which they reside.

## Importance to LANL's Science and Technology Base and National R & D Needs

The high-energy physics component of the mission of the DOE's Office of Science consists primarily of understanding the nature of elementary particles, their properties, and interactions beyond the current standard model. To this end, the DOE supports experimental efforts that push the 'intensity frontier', most notably at Fermilab and the Large Hadron Collider. The research conducted here contributes to the theoretical arm of that program by constructing theoretical models as well as providing input as to which extensions of the standard model are testable at these facilities, and which are better constrained through cosmological observations. The DOE Office of Science has also committed itself to supporting particle physics research on the 'energy frontier' using astrophysical and cosmological tools, and this research directly addresses that.

## Scientific Approach and Accomplishments

In this project, we constructed [1] an explicit new model of physics beyond the standard model. This involved standard ideas from supersymmetry, but evaded a long-standing problem of a 'little hierarchy' between two important parameters in the supersymmetric electroweak sector. This hierarchy was problematic due to quantum corrections to the mass of the Higgs' boson, and we found a novel means of suppressing these corrections. The theory also turned out to hint at a bigger structure where all interactions seem to unify into a simple non-hierarchical structure when viewed at the so-called Planck scale, the natural energy scale of gravitational effects.

We also investigated a different class of supersymmetric models that are best described as a thin slice of a five-dimensional universe with a constant space-time curvature. When this slice is thin, momentum quantization guarantees that it is indistinguishable from a four-dimensional world at low energies. The supersymmetry in this universe can, however, be broken by effects occurring on the boundaries of the slice, and this kind of model has long been known to have attractive phenomenological features. The problem arises with the thickness of the slice: even at low energies, the thickness can fluctuate in response to four-dimensional dynamics and appear as an extra light scalar particle called the radion. We found [2] that quantum effects can actually suppress these oscillations, and made predictions about the masses of new particles, called graviphotons, that arise from this construction.

In addition to these explicit constructions, we studied the general problem that these supersymmetric theories contain heavy modes, called moduli, that can decay into lighter particles. In particular, one set of light modes, called gravitini, form the supersymmetric partners of the quanta of gravitation that couples to all energy equally. These decays can, therefore, not be suppressed by tuning the details of the theory and can reheat the early universe and lead to contradiction with current cosmological observations. We found [3] general conditions under which the kinematic suppression of these decays would make them consistent with known observations and hence admit them as viable theories.

On a similar line, we questioned whether extra dimensions could become observable in astrophysical phenomena even when they do not have direct implications for terrestrial experiments. We found a particularly promising example in plasmon oscillations that can lose energy into higher dimensions and hence decay faster than expected. These, we found [4], provide bounds better than terrestrial experiments by six orders of magnitude! Partly because of these calculations, experimental plans to search for extra dimensions using orthopositronium decays, planned or ongoing in Europe, US and Japan, were modified or discontinued as being unpromising.

Scalars that arise generically in these supersymmetric theories also turn out to have properties very similar to previously postulated scalar particles called axions. As part of a separate project, we were studying the effect of axions on the substructure of galactic halos and participating in the Axion Dark Matter Experiment searching for cosmological signatures of axions. As part of this project, we extended those efforts [5] to include searches for these scalars that arise in supersymmetric theories, especially those formulated in higher dimensions. The main technical challenge was to simulate the evolution of galaxies as the matter collapses into caustic rings; and study effects of relativistic matter like axions and neutrinos on this in fall. In a separate study [6], we showed that previous results on axion masses and the Peccei-Quinn scale did not properly take into account primordial magnetic fields and, hence, could not be used to rule out these models. We also discussed [7] how far the chiral anomalies in the standard model affect the detectability of axion-like particles in laboratory experiments.

Generic features of higher dimensional supersymmetric models not only involve extra scalar particles, but they also include extra interactions of the chiral fermions of the Standard Model. Since one set of these particles, the neutrinos, are otherwise weakly interacting, the modifications in their interactions due to the extensions of the Standard Model can have interesting consequences. We studied these [8] and found that they can change the evolution of

energy contained in a supernova and, under right conditions, can lead to supernovae with features qualitatively different than known before. Extra neutrino interactions with scalars were also found to distort the cosmic microwave background [9]; and we showed that previous ideas that extra interactions at high redshift would act like dark energy without leaving any other signature on the cosmic microwave background were ill founded. Investigations of extra interactions that could convert neutrino flavor in terrestrial experiments were also carried out [10].

While studying these theories, we discovered that vector particles in higher dimensional theories were not properly treated in previous work, leading to a confused discussion in the literature. Our work [11] provided an intuitive explanation of the tensor structure of these propagators and resolved the previous controversies.

A large part of the effort in this project was expended in developing a rigorous definition of interacting chiral theories, so that future calculations can reach higher precision than has so far been possible. This has been a long standing problem: all known rigorous definitions of quantum field theories in four and higher dimensions are given as limits of quantum theories on finite discretized space-time volumes, but due to the Nielsen-Ninomiya theorem [12], chiral fermions do not exist on such discretized spaces. Progress in implementing chiral fermions was made when it was realized that in odd-dimensional space-times, the chiral symmetry is actually related to a space rotation that was known to be recovered as a symmetry when the discretization effects disappeared in the limit. The problem, however, remained that this construction led to a structure in which both chiral partners of a fermion arose from the same underlying structure and, therefore, continued to interact identically: a theory that differentiated in their interaction structure could not be constructed this way.

When such a theory is placed in a slice of a five-dimensional world, the boundaries of the slice necessarily break the symmetry under spatial rotations. This leads to chiral edge states appearing at the boundaries of the slice, and if one can arrange matter density to be different at the two edges in the five-dimensional world, one could envisage a world in which the two chiralities behaved differently. In particular, previous attempts [13] tried to remove one of the two chiralities by making it heavy using the famous Higgs' mechanism to happen preferentially at one edge. This construction, however, failed to give a chiral gauge theory. If one allowed the gauge field to fluctuate along the fifth dimension, the matter density repelled it from the edge and gave it a mass comparable to the heavy modes in the theory unlike a gauge theory with massless gauge bosons. If one constrained the gauge field to be held constant in the fifth dimension and the couplings between the Higgs' field and the fermions was weak, quantum corrections led to a theory in which the gauge boson and the wrong chirality fermion got masses of the same magnitude, and so one could either remove both or neither. On the other hand, when the coupling was made strong, it led to a situation in which the fermion at the edge disappeared and a new chiral fermion appeared in the bulk: in effect, the edge just shifted inwards from where the matter density lay.

Our previous contribution to this field lay in understanding that these considerations change considerably when the five-dimensional universe has a strong space-time curvature. In particular, we had studied an anti-de-Sitter space-time that has a constant negative curvature, or a constant cosmological gravitational field. In such a world, the gravitational red shift results in mass and energy scales at different parts of the space time being exponentially different and the effect of a localized Higgs' field is vastly different on a gauge field and a fermionic field. In particular, we noticed that in these space-times, we could allow the gauge field to be repelled away from an edge and yet not gain too much mass due to the red-shift effect. The fermion field, however, remains compressed near the edge and retains the Higgs' mass as in the flat world. Taking the limit of an infinite curvature in an infinitely thin slice, we showed that [14] one could obtain a chiral gauge theory provided the quantum effects remained in control. This last caveat, unfortunately, could not be avoided without expensive computer simulations that we could not perform.

We, therefore, now chose to investigate the similar situation in a two-dimensional world embedded as a slice of a three-dimensional anti-de-Sitter universe. In this case, the limits lead to a weakly interacting three-dimensional theory that can be investigated by analytical series expansions without requiring computer simulations. Our investigations revealed [15] that the mechanism proposed does lead to a chiral gauge theory in this case, and strongly suggests that the four-dimensional case of interest would work similarly.

These investigations also pointed a new direction for further research. Lüscher had already pointed [16] out that the Nielsen-Ninomiya theorem could be evaded by implementing not the chiral symmetry, but rather a different one that reduced to the chiral symmetry when the discretization was removed. The higher-dimensional construction in a slice leads our edge states to possess this symmetry, and we showed that this is sufficient to lead to a construction of interacting chiral fermions. These developments show the way for a future simpler construction and our presentations at conferences have been appreciated in the field; but further work will be needed to establish the usefulness of these techniques.

## References


1. Csaki, C., Y. Shirman, and J. Terning. A simple model of low-scale direct gauge mediation. 2007. *Journal of High Energy Physics.* **JHEP0705** (5): 099.

2. Katz, A., Y. Shadmi, and Y. Shirman. Supersymmetry breaking and the radion in AdS(4) brane worlds. 2007. *Physical Review.* **D75** (5): 055008.

3. Dine, M., R. Kitano, A. Morisse, and Y. Shirman. Moduli decays and gravitinos. 2006. *Physical Review.* **D73** (12): 123518.

4. Friedland, A., and M. Giannotti. Astrophysical bounds on photons escaping into extra dimensions. 2008. *Physical Review Letters.* **100** (3): 031602.

5. Duffy, L. D., and P. Sikivie. The caustic ring model of the Milky Way halo. 2008. *Physical Review.* **D78** (06): 063508.

6. Campanelli, L., and M. Giannotti. Primordial magnetic fields and the Peccei-Quinn scale. 2006. *arXiv:astr-ph/0611207.*

7. Friedland, A., and M. Giannotti. The impact of neutino magnetic moments on the evolution of massive stars. 2008. *arXiv:0809.4703 [astro-ph].*

8. Friedland, A., K. M. Zurek, and S. Bashinsky. Constraining models of neutrino mass and neutrino interactions with the Planck satellite. 2007. *arXiv:0704.3271 [astro-ph].*

9. Friedland, A., and C. Lunardini. Two modes of searching for new neutrino interactions at MINOS. 2006. *Physical Review.* **D74** (3): 033012.

10. Friedland, A., M. Giannotti, and M. Grasser. Comments on the Proca equation in Randal Sundrum II background, and unparticles. 2008. *Los Alamos Report LA-UR 08-3550.*

11. Nielsen, H. B., and M. Ninomiya. Absence of neutrinos on a lattice, 1. Proof by homotopy theory. 1981. *Nuclear Physics.* **B185** (1): 20.

12. Kaplan, D. B.. A method for simulating chiral fermions on the lattice. 1992. *Physics Letters.* **B288** (3-4): 342.

13. Bhattacharya, T., C. Csaki, M. R. Martin, Y. Shirman, and J. Terning. Warped domain wall fermions. 2005. *Journal of High Energy Physics.* **JHEP0508** (8): 061.

14. Bhattacharya, T., M. R. Martin, and E. Poppitz. Chiral lattice gauge theories from warped domain walls and Ginsparg-Wilson fermions. 2006. *Physical Review.* **D74** (8): 085028.

15. Luescher, M.. Exact chiral symmetry on the lattice and the Ginsparg-Wilson relation. 1998. *Physics Letters.* **B428** (3-4): 342.


## Publications


Bhattacharya, T., M. R. Martin, and E. Poppitz. Chiral lattice gauge theories from warped domain walls and Ginsparg-Wilson fermions. Presented at *The XXIV International Symposium on Lattice Field Theory.* (Tucson, Arizona, July 23-28).

Bhattacharya, T., M. R. Martin, and E. Poppitz. Chiral lattice gauge theories from warped domain walls and Ginsparg-Wilson fermions. 2006. *Physical Review.* **D74** (8): 085028.

Campanelli, L., and M. Giannotti. Primordial magnetic fields and the Peccei-Quinn scale. 2006. *arXiv:astro-ph/0611207.*

Dine, M., R. Kitano, A. Morisse, and Y. Shirman. Moduli decays and gravitinos. 2006. *Physical Review.* **D73** (12): 123518.

Duffy, L. D.. Dark Matter Caustics. Presented at *Cosmo 08.* (Madison, WI, 25-29 Aug. 2008).

Duffy, L. D.. Dark matter caustics in the Milky Way halo. Presented at *Santa Fe Cosmology Workshop.* (Santa Fe, NM, 30 Jun. - 18 Jul. 2008).

Duffy, L. D.. The caustic ring model of the Milky Way halo. Presented at *The Dark Side: 2.* (Ann Arbor, MI, 27 May - 14 Jun. 2008).

Duffy, L. D.. The high-resolution search for axions in galactic halo substructure. Presented at *American Physical Society's Division of Nuclear and Particle Physics Meeting.* (Nashville, TN, 25-28 Oct. 2006).

Duffy, L. D., and P. Sikivie. The caustic ring model of the Milky Way halo. 2008. *Physical Review.* **D78** (6): 063508.

Friedland, A., K. M. Zurek, and S. Bashinsky. Constraining models of neutrino mass and neutrino interactions with the Planck satellite. *Physical Review.*

Friedland, A., and M. Giannotti. Astrophysical bounds on photons escaping into extra dimensions. 2008. *Physical Review Letters.* **100** (3): 031602.

full final report

# The Secret Life of Quasiparticles

*Stuart Alan Trugman*

20061402ER

## Abstract

We investigate how an electron moves through a system of atoms that are free to vibrate. The electron organizes a cloud of displaced atoms (phonons) around it, forming a composite object called a polaron quasiparticle, which can move, but is heavier than an electron. Using quantum mechanics for both the electron and the phonons, we have calculated the properties of the quasiparticle, how it forms from a bare electron that is injected by a laser beam or by tunneling from a metallic tip, and how it interacts with ultrafast laser probes

## Background and Research Objectives

The behavior of noninteracting electrons and phonons is considered to be understood. What happens, however, when electrons and phonons interact, as they do in real materials? Over 50 years ago, Lev Landau first proposed that the electrons change into "quasiparticles". Quasiparticles behave in some ways like bare (noninteracting) electrons, but other properties are different, such as their mass, which depends on the strength of the interactions. As quasiparticle research progressed, it became common not to attempt to calculate the quasiparticle properties from first principles, but instead to take them from experiment. The quasiparticle phenomenology then tells how the system responds to perturbations that vary slowly in time and space.

In this project, we have moved beyond these historically limiting constraints. We have recently made advances in calculating the dynamics of interacting quantum systems, enabling investigations that were previously impossible. Using this innovative approach, we have made progress toward calculating, measuring, and controlling the dynamics of these systems with a specific focus on the dynamical interactions between electrons and quantum phonons.

By organizing the many-body Hilbert space in an efficient, recursive manner, we have recently developed algorithms that are many orders of magnitude more powerful than those previously available. We can now accurately compute the quasiparticle mass and internal structure. This, however, only explains how the system responds to very weak (sometimes unphysically weak) and very slow perturbations. Quasiparticles are more interesting and complex than bare particles. How they respond to stronger or higher frequency perturbations, which can break them apart, or how they dynamically form from bare particles injected by tunneling or by photon absorption, was previously unknown.

We have calculated how a polaron quasiparticle (plus other excitations) form in real time and real space when a bare electron is injected optically or by a tunneling event into a system with electron-phonon coupling. In addition, we have calculated how a polaron quasiparticle responds to an AC driving field that is not slow: the quasiparticle can access internal excited states, and can fall apart, emitting pieces of itself (phonons), at particular driving frequencies. These calculations are based on another advance, treating the entire system, including the phonons, fully quantum mechanically. Previous approaches had been based on the assumption that it is 1) intractable to treat the phonons quantum mechanically in these situations, and 2) unnecessary to do so, because phonons are heavy and slow compared to electrons, and based on the Born-Oppenheimer approximation, can be treated semiclassically. We have shown that not only is it possible to calculate with fully quantum phonons, but it is necessary to do so. Semiclassical approximations get the polaron formation time wrong, especially starting from a wide initial electron wavepacket.

These calculations are relevant to a number of experiments and emerging technologies, including two-photon photoemission experiments, ultrafast optical pump-probe experiments, time resolved STM (scanning tunneling microscopes), and to nanotechnology, including the conductivity of a single molecule. Experiments were performed by our colleagues at CINT (the Center for Integrated Nanotechnolgies), the NHMFL (National High Magnetic Field Laboratory), and elsewhere. The polaron quasiparticle itself is a spontaneously self-orga-

nized nanostructure, an electron carrying with it a compact phonon cloud, that can be moved with an electric field or trapped in place, with a mass that can be varied by many orders of magnitude in a controllable way.

## Importance to LANL's Science and Technology Base and National R & D Needs

This research impacts a number of fields in science and technology. Understanding and controlling polaron tunneling and transport are basic science issues affecting the DOE's energy security and nanotechnology missions. This work also has implications for sensor applications to support Homeland Security, and impacts the fields of chemistry (Creutz-Taube ions), biomolecules, and quantum information.

## Scientific Approach and Accomplishments

We have calculated in real space and real time how a polaron quasiparticle dynamically forms from a bare electron that is injected optically, by two-photon photoemission, or by a time-resolved scanning tunneling microscope. (The first two experiments have been done, the last is planned.) The bare particle can also be an exciton, an electron-hole bound state that is coupled to phonons. The calculation includes fully quantum phonons, which are required to obtain the correct polaron formation dynamics. The results are compared to fast optical experiments at LANL and elsewhere in the US and Japan.

In the calculation, we turn the initial wave function loose in an enormous fully quantum many-body Hilbert space of well over a million basis states, and use the time dependent Schrodinger equation to numerically time evolve it essentially without approximation [1]. This is made possible, in part, by a sparse representation of the electron-phonon interaction, meaning that the basis is chosen so that each basis state interacts with only a few others. The resulting dynamics are unconstrained by any a priori notion of how polarons should form. One output of the calculation is an animated movie. Four snapshots from the movie are shown in Figure 1. An initial bare electron wave packet is launched to the right as shown in panel (a). In panel (b) the electron is not yet dressed by phonon excitations and thus is moving roughly as fast as the free electron (dashed line). In panel (c) after an elapsed time of one phonon period, the electron density consists of two peaks. The peak on the right (black arrow) is essentially a bare electron. The peak on the left is a polaron wave packet moving more slowly. As time goes on, the bare electron peak decays and the polaron peak grows. Some phonons are left behind (blue line), mainly near the injection point. These phonons are of known phase with displacement shown in red. Some phonon excitations travel with the polaron (magenta). Finally, a coherent polaron wave packet is observed when the polaron separates from the uncorrelated phonon excitations.

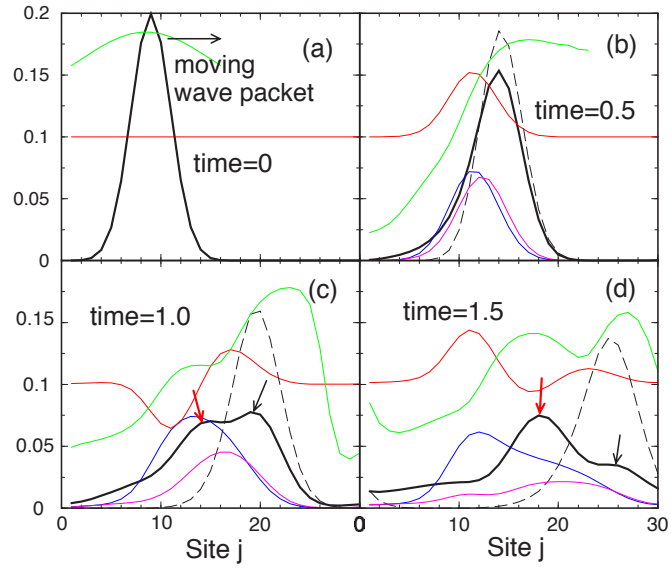


*Figure 1. Snapshots from a movie of polaron formation. The calculation is performed on a 30-site periodic lattice. Time is measured in phonon periods. Black: the electron density. Blue: the phonon density. Red: the lattice displacement X. Green: the velocity. Magenta: the expectation of the electron density times the phonon density on the same site. Dashed: the (noninteracting) free electron wave packet for reference. The red and green curves have been offset by 0.1.*

In another project, we worked with CINT (Center for Integrated Nanotechnologies) users Prof. Holger Fehske and PhD student Andreas Alvermann (Greifswald, Germany) to calculate polaron quasiparticle properties in anisotropic systems. We begin with an electron coupled to phonons in a 1d chain. The 1d chain is duplicated, until copies fill three dimensional space. As yet, the chains do not communicate, so the physics is still 1d. Then we slowly turn on hopping between the chains. To move from one chain to another, the polaron must leave behind the phonon cloud it has carefully organized on the first chain, hop across to a second chain, and then organize a new phonon cloud there. Because of the awkwardness of this process, the polaron effective mass increases more perpendicular to the chains than parallel to them [2]. (A larger mass in a given direction corresponds to greater difficultly moving in that direction.) The hopping between the chains is slowly increased until it becomes as large as the hopping along the chains (see Figure 2). At this point, the system has become an isotropic 3d solid. In this way, we are able to interpolate continuously between dimensions 1 and 3. One motivation for doing this is that it was previously speculated that polaron physics is qualitatively different in 1d and 3d. One can see from Figure 2, however, that the

behavior changes continuously. In contrast to almost all other accurate numerical techniques, the variational method we use does not have finite size effects: the chains are infinite rather than chopped off, and extend to infinity in the transverse direction as well. This work has applications to systems that integrate many nanowires.

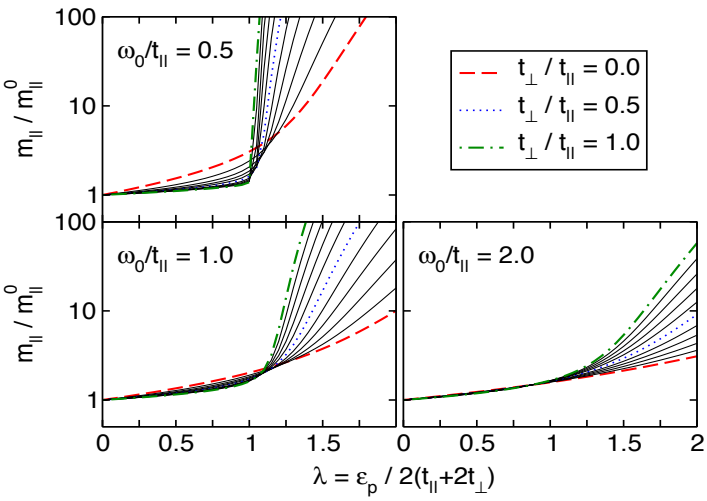


*Figure 2. Polaron mass for different anisotropy and phonon frequencies as indicated. In each panel, eleven curves for the ratio of perpendicular hopping to parallel hopping equal to 0.0, 0.1, …, 1.0 in steps of 0.1 are shown. The mass is plotted on a log scale. The electron-phonon coupling increases along the x-axis. Dimensions 1 and 3 become increasingly similar as the phonon frequency increases.*

Professor Fehske and I also addressed another outstanding problem in quasiparticle dynamics. When a polaron or another quasiparticle is perturbed by a slowly oscillating electric field, its AC conductivity is controlled by the renormalized polaron mass: it moves just like a heavy version of the electron. The mass can increase by several orders of magnitude, as seen in Figure 2. What if the AC electric field is rapidly rather than slowly oscillating? Previously, quasiparticle theory did not cover this case, and the answer was unknown. We have numerically calculated the AC conductivity at increasing frequencies using a variational method, again with fully quantum phonons and electron, as shown in Figure 3. The conductivity contains a good deal of structure, as the quasiparticle is shaken so rapidly that it begins to fall apart, emits pieces of itself (free phonons), and accesses internal excited states (bound states of the polaron and excited phonons) [3].

In the last completed project, we have extended our quasiparticle theory from its original context of electron-phonon interactions to include interactions of electrons and spin-flips in a 3-dimensional antiferromagnet. This work was motivated by some very interesting de Haas-van Alphen measurements of the heavy fermion compound CeIn3 done at the National High Magnetic Field Laboratory (NHMFL) at Los Alamos by experimentalists from Los Alamos, Cambridge University (UK), and Kobe and Shizuoka Universities (Japan). The de Haas-van Alphen measurements map out the Fermi surface of a metal, specifically, the extremal cross sections of the Fermi surface in the plane perpendicular to the applied magnetic field. The measurements were initially quite puzzling. They seemed to show a low density of holes collecting not at the center of the Brillouin zone, and not at the corner, but in very anisotropic pancake shaped pockets halfway between the origin and the corner in the <111> and symmetry-related directions. These pancakes appear to migrate toward the origin and merge there as the magnetic field is increased to about 40 T (tesla). This behavior is completely unexpected in the standard Kondo lattice theory of heavy fermions, but we realized that this is how a small density of holes that are self-doped into an antiferromagnetic lattice of Ce ions should behave.

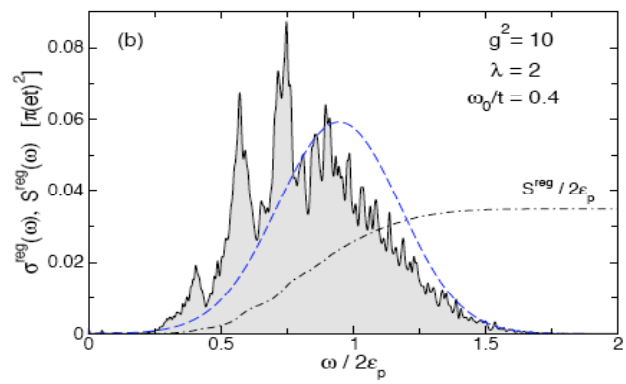


*Figure 3. The optical conductivity of the 1D Holstein polaron at zero temperature is shaded grey. Results are obtained by a variational exact diagonalization method. The dashed blue line is an approximate analytic theory, which has some resemblance to the numerically exact conductivity for the parameters shown (but less so at other phonon frequencies, not shown).*

In an antiferromagnet, there are two interpenetrating sublattices, A and B, with the A sublattice containing up spins, and the B sublattice down spins. As a hole hops from one sublattice to another, it transfers a spin to the "wrong" sublattice without changing its spin orientation. Further hops result in a nontrivial quasiparticle: a hole surrounded by a cloud of spin-flips moving through an antiferromagnet. The cloud of spin-flips can be treated analogously to the cloud of phonon excitations, with some modifications. For example, a single site can host multiple phonon quanta, but only a single spin-flip. The calculated dispersion of the spin polaron is such that its energy minimum is halfway to the zone boundary in the <111> direction, where it forms pancake shaped hole pockets, as observed in the experiments. As the magnetic field increases, the background antiferromagnet cants or tilts, with an increasingly large ferromagnetic z component of spin in addition to the staggered xy component. As the ferromagnetic

component grows, the pancakes migrate toward the origin, undergoing a Lifshitz transition where they touch and the topology changes, consistent with the de Haas-van Alphen measurements [4,5]. This is shown in Figure 4.

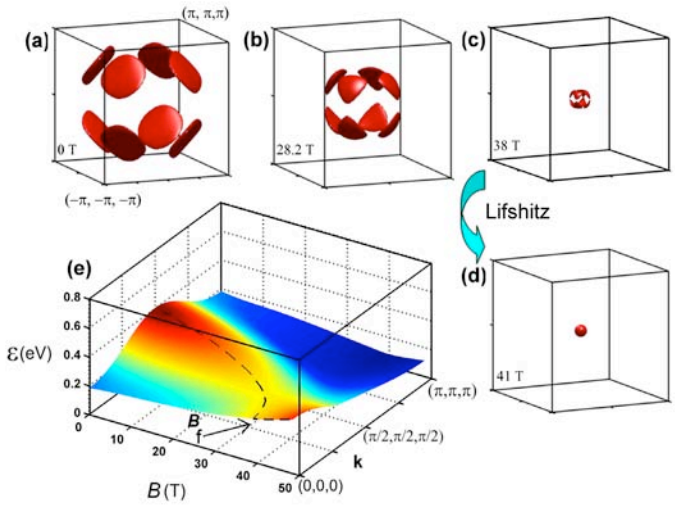


*Figure 4. Fermi surface and f-electron dispersion of CeIn3. (a-d) Theoretical f-hole Fermi surface topologies at different magnetic fields simulated using a strong coupling Hubbard model with parameter U/t = 8. A Lifshitz transition is indicated in the vicinity of 40 tesla. (e) Calculation of the dispersion along the <111> direction using the strong coupling Hubbard model. The dispersion maximum, and hence the hole pocket location, migrates from momentum (pi,pi,pi)/2 to (0,0,0) following the dotted line, as the antiferromagnetic background is polarized by the magnetic field. Band flattening near the dispersion maximum at Bc ~ 40 T is responsible for the divergent effective mass and the Lifshitz transition.*

In addition to the completed projects described above, there are several promising incomplete projects arising from this LDRD. We hope to find other funding so that they may continue. One project is with Prof. Michael Galperin at UC San Diego, in which we are investigating the correlations between successive electrons that inelastically tunnel through a molecule with electron-phonon coupling.

There are also suggestions that quasiparticles may change their properties dynamically, and that it may be possible to control this. While tunneling through a barrier, a polaron may drag its heavy phonon cloud through, or it may instead shed its phonons, move quickly through as a light object, and reorganize the phonons at the far end. A polaron captured by an impurity appears to be heavier near the center and lighter in the tails, and similarly for bipolarons in superconductors. Polarons can bind additional (thermal) phonons, so that it may be possible to move packets of heat with an electric field, with applications to thermoelectric devices.

## References


1. Ku, L. C., and S. A. Trugman. Quantum dynamics of polaron formation. 2007. *Physical Review B.* **75**: 014307.

2. Alvermann, A., H. Fehske, and S. A. Trugman. Solution of the Holstein polaron anisotropy problem. To appear in *Physical Review B.*

3. Fehske, H., and S. A. Trugman. Numerical solution of the Holstein polaron problem. 2007. In *Polarons in advanced materials.* Edited by Alexandrov, A.. , p. 393. Dordrecht, Netherlands: Springer.

4. Sebastian, S. E., N. Harrison, M. Jaime, V. Fanelli, T. Ebihara, C. D. Batista, S. A. Trugman, T. Murphy, E. Palm, and H. Harima. Heavy holes - precursor to superconductivity in antiferromagnetic CeIn3. *Proceedings of the National Academy of Sciences.*

5. Harrison, N., S. E. Sebastian, C. D. Batista, and S. A. Trugman. How do holes get heavy and superconduct?. 2008. In *Strongly Correlated Electronic Systems (SCES).* (Houston, 13-18 May, 2007). Vol. 403, p. 977. Amsterdam: Physica B.


## Publications


Alvermann, A., H. Fehske, and S. A. Trugman. Solution of the Holstein polaron anisotropy problem. To appear in *Physical Review B.*

Fehske, H., and S. A. Trugman. Numerical solution of the Holstein polaron problem. 2007. In *Polarons in advanced materials.* Edited by Alexandrov, A.. , p. 393. Dordrecht, Netherlands: Springer.

Harrison, N., S. E. Sebastian, C. D. Batista, and S. A. Trugman. How do holes get heavy and superconduct?. 2008. In *Strongly Correlated Electronic Systems (SCES).* (Houston, 13-18 May, 2007). Vol. 403, p. 977. Amsterdam: Physica B.

Hilton, D. J., R. P. Prasankumar, S. A. Trugman, A. J. Taylor, and R. D. Averitt. On photo-induced phenomena in complex materials: probing quasiparticle dynamics using infrared and far-infrared pulses. 2006. *Journal of the Physical Society of Japan.* **75**: 11006.

Ku, L. C., and S. A. Trugman. Quantum dynamics of polaron formation. 2007. *Physical Review B.* **75**: 014307.

Sebastian, S. E., N. Harrison, M. Jaime, V. Fanelli, T. Ebihara, C. D. Batista, S. A. Trugman, T. Murphy, E. Palm, and H. Harima. Heavy holes - precursor to superconductivity in antiferromagnetic CeIn3. *Proceedings of the National Academy of Sciences.*

full final report

# Steps Toward Practical Quantum Information Processing

*Malcolm Geoffrey Boshier*

20080710ER

## Abstract

Quantum mechanical entanglement provides ways of solving problems, which have no efficient classical method of solution. This includes factoring of large numbers, a task whose assumed difficulty underpins public-key cryptographic systems. This important application is one example of the power of quantum computing. The use of controllable quantum systems as quantum simulators for calculating the properties and evolution of complex quantum systems is another. Quantum entanglement is also employed in the emerging field of quantum metrology, where a system is placed into a an exotic quantum state which has a sensitivity to some external force (such as gravity or magnetic fields) which is greater than can be achieved with even the most perfect classical system. This project addressed several aspects of the grand challenge of understanding and exploiting entanglement to make quantum computing and other forms of quantum information processing both practical and useful.

## Background and Research Objectives

Quantum mechanical entanglement provides ways of solving problems, which have no efficient classical method of solution. This includes factoring of large numbers, a task whose assumed difficulty underpins public-key cryptographic systems. This important application is one example of the power of quantum computing. The use of controllable quantum systems as quantum simulators for calculating the properties and evolution of complex quantum systems is another, first suggested by Feynman many years ago and now coming within reach of state of the art experiments. Quantum entanglement is also employed in the emerging field of quantum metrology, where a system is placed into an exotic quantum state that has a sensitivity to some external force (such as gravity or magnetic fields) greater than can be achieved with even the most perfect classical system.

This project addressed several aspects of the grand challenge of making quantum computing, and other forms of quantum information processing, both practical and useful. It has two main components.

The first is work towards demonstrating a prototype quantum simulator, a kind of analog quantum computer that can simulate otherwise intractable many-body systems and answer questions about statistical physics. Strings of trapped ions can simulate interacting spin systems and, with two internal states of the ion corresponding to spin-up and spin-down, laser beams making state-dependent forces on the ions can be used to engineer effective spin-spin interactions between neighboring ions. The short-term aims are to demonstrate an effective spin-spin interaction between two ions and to develop methods for creating arrays of ions that can simulate solid lattices. Long-term goals include using the quantum simulator to investigate the behavior of candidate hamiltonians (the formal quantum mechanical way of describing a system of atoms or other particles), which might explain high-temperature superconductivity.

The second thread is largely theoretical. It addresses the important question of just where the power of quantum computing comes from. It also seeks new quantum algorithms for an important class of problems in the mathematical theory of knots. It involves research on network quantum information theory, quantum conditional information, and their roles in understanding and computational modeling of complex quantum systems. Finally, it strives to deepen our understanding of quantum-mechanical entanglement, the unique property of quantum systems which is believed to be the source of the power of quantum computing and of other quantum technologies, and to search for new ways to exploit it in practical devices.

## Importance to LANL's Science and Technology Base and National R & D Needs

The common thread that ties together the components of this project is "information": quantum information science provides completely new approaches to the challenges of securing, acquiring, and processing information. The killer application for the field of quantum information science is factoring large numbers on a

quantum computer. The prospect of using a quantum computer in this way to crack public key cryptography drives a substantial investment in quantum computing by the intelligence community. If quantum computers can be built, it is clearly in the national interest that we be the first to do so, and if quantum computing is impossible or even constrained due to some fundamental physical law it is also important that we know that first. This is one factor driving research in the area of quantum entanglement. Another is that entangled systems have other useful applications besides quantum computing. Their delicate nature, which is a big engineering challenge to exploiting them in quantum computers, also makes them exquisitely sensitive detectors of many important forces and fields. This "quantum metrology" aspect of entanglement is important to National needs and to the LANL mission in sensing.

Although realizing practical quantum computation will take many years, the exciting prospect of solving otherwise intractable problems using controllable quantum systems – quantum analog computing - is becoming possible now. As Feynman noted many years ago, it is essentially impossible to simulate even a modest quantum system on a classical computer (e.g., the world's most powerful supercomputer, LANL's "Roadrunner", will be able to deal with only around 40 particles). The reason is fundamental: the amount of information contained in a quantum system increases exponentially with the number of particles in the system. In contrast to the demanding requirements of large quantum computers, systems of just 100 qubits can form useful quantum simulators. Feynman's original idea of simulating the physics of a quantum system on another (controllable) quantum system would be of direct interest for many-body quantum mechanics issues such as equation of state in extreme conditions, high temperature superconductivity, etc. pursued in Los Alamos because of their obvious national importance. They also help solve the engineering problems facing practical quantum computation.

## Scientific Approach and Accomplishments

When assessing the accomplishments of this project it should be remembered that this project was for less than one year at a funding level of around 50% of a standard ER project.

### Quantum Simulation

Cold-trapped ions are widely regarded as the most accomplished technology of the many possibilities known for constructing a quantum computer. They are also an ideal candidate system for simulating interacting spin systems. With two internal states of the ion corresponding to spin-up and spin-down, it has recently been shown [1] that laser beams making state-dependent forces on the ions can be used to engineer effective spin-spin interactions between neighboring ions. LANL scientists John Chiaverini and Warren Lybarger have just proposed an improved implementation of this idea [2], and detailed how to realize a 2D array of trapped ions (Figure 1). The technology could also be extended to ladders of ions arranged around a ring (Figure 2). A set of interacting spins in this topology is interesting because it can be shown to be equivalent, via a mathematical transformation named for Jordan and Wigner, to the Hubbard-type models, which may provide the elusive fundamental explanation of the phenomenon of high-temperature superconductivity.

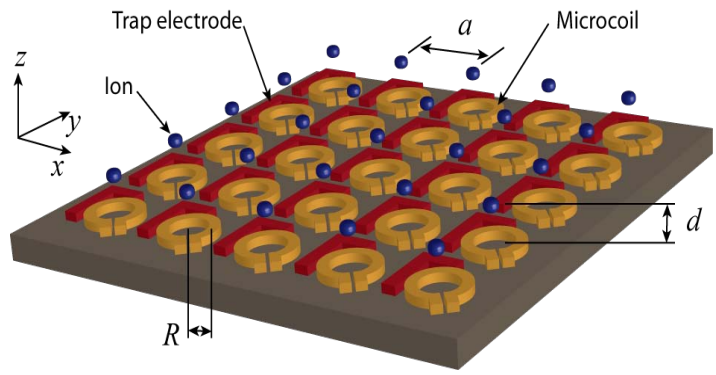


*Figure 1. Rendering of section of surface trap array and microcoils. Leads are not shown, and the electrodes shown are only a representative subset of those required. Ions may be trapped directly above loops, or trap electrodes and coils may be offset so ions can be trapped above any point in a microcoil unit cell.*

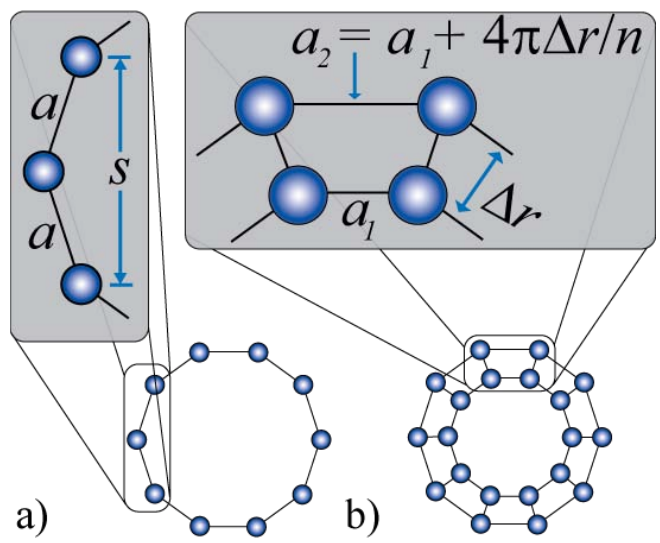


*Figure 2. The trapped ion technology of Figure 1 can be adapted to realize (a) ring and (b) ladder geometries with periodic boundary conditions.*

Work performed under this project is advancing the development of this new ion trapping technology. Graduate student Paul Blackburn developed a new experimental control and data acquisition software system for the main experiment, including enhancement of the control hardware and logic. These improvements have already been

proven to provide a more stable and more easily adaptable experimental control system in LANL work toward quantum simulation of condensed matter systems using trapped ions.

### Quantum Entanglement and QIP Theory

The quantum information theory thread led by Jon Yard research explores how quantum physics changes fundamental notions of information and computation. Quantum particles carry a different type of information than the usual kind that flows through today's computers and networks. Quantum information, as it is called, behaves in different ways than familiar classical information, and a deeper understanding of its properties leads the way towards dramatic advances in computational power as well as in unconditionally secure communication. A basic concern is protecting quantum information from noise. A noisy quantum process can be viewed as a communication channel (Figure 3). Prior to this project, Yard made fundamental contributions to the theory of asymptotically perfect error correcting codes for point-to-point [3] and network [4] communication. The ultimate limit for correcting errors from a given channel is called the capacity of the channel.

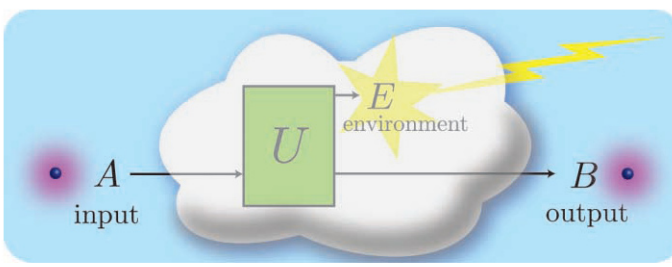


*Figure 3. Representation of a quantum channel. A channel reversibly transfers the state of a physical system in the laboratory of the sender to the combination of the system possessed by the receiver and an environment that is inaccessible to the users of the channel. Discarding the environment results in a noisy evolution of the state. The input and output denote separate places in space and/or time, modeling, for example, a leaky optical fiber.*

While it is not yet known how to compute the capacity from a description of a given channel, Yard made the startling discovery [5] that there are pairs of channels, each having zero capacity for communication which, when combined, nonetheless allow for noiseless communication. His results uncover a rich structure in the theory of quantum communication which had not been anticipated and deepen the relationship between quantum cryptography and quantum coherence, while giving new hope for protecting quantum systems from noise which was previously thought to be too strong. Yard has also made fundamental discoveries regarding how quantum information can be moved around within collections of quantum systems [6], proving the existence of optimal codes for the compression of quantum data which make use of quantum mechanical side information at the encoder and decoder.

Besides communication, another reason for protecting quantum data from noise is so that it can be used inside of a computer. Such a quantum computer, whose constituents remain in quantum superposition throughout a computation, could perform calculations, which would otherwise be intractable on a conventional computer. A central task is thus to determine the power of quantum computers by designing new programs, or algorithms, to be run on them. To this end, Yard has developed a new algorithm for solving certain problems in topology on such a computer [7] while giving new insights into the theory of quantum and classical computation in general.

### External Collaborators

The project supported short visits by several external collaborators, all-working with LANL scientists to better connect theory and experiment in quantum information processing.

Professor Augusto Smerzi of the University of Trento (Italy) is collaborating with Lee Collins and other colleagues at LANL to investigate practical applications of ultracold atom systems to quantum technologies such as high-precision measurement. Ultracold gases, especially when chilled below their critical temperature, provide a new arena for testing fundamental concepts such as superfluidity and phase transitions and for exploring applications to a broad set of fields from quantum information to geophysics. As atoms are cooled, they begin to exhibit quantum mechanical properties such coherence and entanglement. In the former, the atomic wave functions overlap, and a system of millions of atoms suddenly behaves as one entity, the Bose-Einstein condensate. The gaseous BECs lend themselves to intricate manipulation with external fields and to detailed imaging. The other property, entanglement, allows systems to exist in arbitrary superpositions of states unlike in classical systems. Various mechanisms such as interferometers operating with light (photons) generally have a sensitivity related to 1/sqrt($N$) where $N$ represents the number of particles. However, the entanglement in ultracold atomic systems yields a drastic improvement to $1/N$, the so-named Heisenberg limit. While photon numbers far exceed those for atoms, the inverse-$N$ dependence implies that quantum devices such as interferometers are now reaching sensitivities comparable to the best optical devices. As the number of experimentally trapped atoms continues to rise, the prospects appear propitious for atom optical devices to become the measuring instruments of choice in many areas. The means of achieving these levels of precision has been a primary goal of this collaboration.

The ability to manipulate the BEC with various fields per-

mits the design of quantum devices in analogy with many currently-operating systems. For example, the superconducting quantum interference device (SQUID), which measures very small changes in the magnetic flux through superconducting loops, has an extensive range of uses from biomedical scans to detecting gravitational waves. An analogous system might be constructed from BECs by confining the superfluid in a toroidal geometry. Due to the superfluid nature, a current or circulation in such a loop, once started, would persist undiminished for very long times. However, until recently, no effective procedure existed for initiating such currents. This situation has changed with the demonstration by the NIST group that a Gauss-Laguerre light beam, produced by a particular twisting of wave fronts, can impart angular momentum directly to a toroidal BEC, thus generating a persistent current. Placing barriers within the torus to modulate flow produces a configuration similar to a SQUID. This may, given the properties of the ultracold system, lead to sensitivities beyond current superconducting devices. An experimental BEC research group at LANL led by Malcolm Boshier has also just demonstrated a new technology for confining and manipulating BECs using focused laser beams, which could be applied to these ideas to realize practical measuring instruments.

In the work supported by this project, we have investigated both analytically and numerically several promising 1D models of a flow in a superfluid over a barrier. This has lead to several interesting findings concerning the nature of the process such as the identification of a class of stable solutions and the development of solitons in response to gradual changes in the height and width of the barrier. Such studies have lead to the construction of more realistic models in 2D and the 3D toroidal geometries. Initial, large-scale computational studies in 2D have confirmed that many of the basic 1D findings have direct analogues. Other phenomena such a vortex formation remains strictly a multi-dimensional effect, whose full realization requires 3D simulations. We have developed very powerful, highly-parallel computer methods to address these cases. We expect several papers to arise from this recent work.

In a related thread, Professor Matt Davis from the University of Queensland recently visited LANL to further our collaboration on a project involving drag forces in superfluids. It is widely accepted that a superfluid flow exhibits a critical velocity below which an object immersed in the flow would feel no force despite the fluid's movement. However, this mechanism ignores the presence of quantum fluctuations, which, there is reason to believe, can produce a drag force on an immersed object and thus affect the critical velocity. It is precisely this effect that Matt Davis and LANL's David Roberts have studied during his visit to LANL. Much progress was made in simulating this drag effect in dilute condensates using a quantum simulation technique that approximates the quantum fluctuations by Wigner noise. Although there are still various problems that need to be resolved, publication of the results in Physical Review is expected before the end of the year.

Finally, Professor Juan Pablo Paz from the University of Buenos Aires is working with the LANL group of Wojciech Zurek on the important issue of the effect of a system's environment on quantum entanglement in that system, using the theory of decoherence pioneered by Zurek.

## References


1. Porras, D., and J. I. Cirac. Effective Quantum Spin Systems with Trapped Ions. 2004. *Physical Review Letters.* **92**: 207901.

2. Chiaverini, J., and W. E. Lybarger Jr.. Laserless trapped-ion quantum simulations without spontaneous scattering using microtrap arrays . 2008. *Physical Review A.* **77** (2): 022324.

3. Hayden, P., M. Horodecki, A. Winter, and J. Yard. A decoupling approach to the quantum capacity. 2008. *Information Dynamics and Open Systems.* **15** (1): 7.

4. Yard, J., I. Devetak, and P. Hayden. Capacity theorems for quantum multiple access channels: classical-quantum and quantum-quantum capacity regions. 2008. *IEEE Transactions on Information Theory.* **54** (7): 3091.

5. Smith, G., and J. Yard. Quantum communication with zero-capacity channels. 2008. *Science.* **321**: 1812.

6. Devetak, I., and J. Yard. Exact cost of redistributing multipartite quantum states. 2008. *Physical Review Letters.* **100**: 230501.

7. Wocjan, P., and J. Yard. The Jones polynomial: quantum algorithms and applications to quantum complexity theory. 2008. *Quantum Information and Computation.* **8**: 147.


## Publications


Devetak, I., and J. Yard. Exact cost of redistributing multipartite quantum states. 2008. *Physical Review Letters .* **100** (23): 230501.

Smith, G., and J. Yard. Quantum communication with zero-capacity channels. 2008. *Science.* **321**: 1812.

Wocjan, P., and J. Yard. The jones polynomial: quantum algorithms and applications in quantum complexity theory. 2008. *Quantum Information and Computation.* **8** (1-2): 147.

# Trapped-ion Quantum Simulations of Condensed-Matter Systems for Understanding of Novel Materials

*John Chiaverini*

20080720ER

## Abstract

The simulation of interacting quantum systems is generally intractable using classical computers as the required resources scale exponentially with system size. Many condensed matter physics problems require understanding of these types of problems, however, for application of correlated electron and spin behavior to novel material design as well as for the description and manipulation of quantum phase transitions, route to fundamental understanding of coherent material properties. The future of energy security depends in part on devising new materials with desirable behaviors. Use of a controllable quantum system to emulate the typically inaccessible materials themselves allows one to bypass the exponential difficulties. In our effort to pioneer the use of trapped ions for quantum simulations, we have developed a trap-array structure with on-chip delivery of radio-frequency (RF) control fields. This will enable large arrays of trapped-ion "spins" for the simulation of quantum magnetic systems while eliminating the largest fundamental source of error in standard schemes for trapped-ion quantum processing. These advances should also lead to reductions in the errors in two-quantum-bit "gates" for quantum computing with trapped ions.

It should be pointed out that this was a project that was funded for the 9 month period Jan-Sep 2008 only, with funds approximately equivalent to one year at the standard LDRD ER level, not the typical 3-year ER funding level.

## Background and Research Objectives

Quantum computers promise dramatic speedups over classical computers for tasks such as factoring and search. However, a quantum computer capable of outperforming a classical model at these tasks will require thousands of qubits (quantum bits) and hundreds of thousands of individual operations. Alternately, there are problems for which an exponential gain can be obtained using a system of tens of qubits. Such problems are quantum simulations of interacting quantum systems, as described here.

To take one example, high-temperature superconductivity (HTS) may lead to room temperature resistance-free current transport and other efficiency gains of national energy security interest, if only its mechanisms are more fully understood; at present, there is no successful theory for HTS behavior. Many models have been suggested, but only those with a high degree of symmetry or those related to previously solved problems can be made predictive. Exact solutions for large numbers of interacting quantum particles are difficult to acquire, and therefore many plausible models cannot be practically explored. The direct investigation of a larger selection of models will be enabled by quantum simulation. As long as the proposed Hamiltonian can be mapped onto a lab Hamiltonian, the former's exact quantum evolution can be reproduced. One model suggested to explain HTS is the Hubbard model, which consists of fermions that can tunnel between sites and interact with each other. The Hubbard model is not solvable in two dimensions for arbitrary interactions. However, through mapping of this hopping-fermion model to an interacting spin Hamiltonian [1], it can be emulated in a collection of trapped ions manipulated by laser beams.

The use of quantum methods for computing was originally suggested to solve this type of problem [2]. The density matrix for an N-spin-1/2 interacting system contains 2^2N complex elements. This exponential scaling limits (classical) supercomputers to exact simulation of 30--40 spins. Nature, however, is not bothered by exponential complexity, and so the use of an accessible quantum system to tackle such a problem can provide a large speedup. By mapping the problem to be solved onto interactions between individual trapped ions, we can provide insight into condensed-matter systems which cannot be easily and cleanly manipulated.

Atomic ions are one of the most advanced systems for quantum information processing [3], and pairs of their

internal electronic levels are perfect spin-1/2 analogs. Ions are trapped by electromagnetic fields and are typically manipulated using laser beams. The ions' shared external vibrational states in the trap are used to couple different ions' internal states. Traps currently in use are one-dimensional arrays containing a few ions (see Figure 1), but such designs may enable basic-level simulations of interacting spin Hamiltonians through application of fields to bring about state evolution and subsequent state determination. Hamiltonian parameters can be adjusted via laser frequency and intensity, easily-controlled experimentally [4].

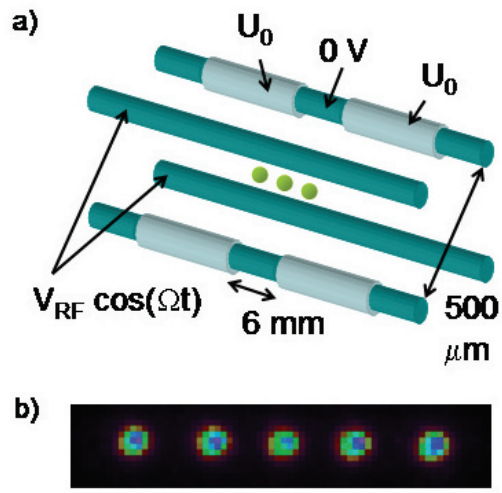


*Figure 1. Standard ion trap structure and trapped ions. (a) Drawing of macroscopic linear quadrupole RF Paul trap for electromagnetic confinement of ions showing typical scale and voltages applied. (b) Ion fluorescence image. Five ions are held in a trap like that depicted in (a). The distance between ions is approximately 10 micrometers, and the false colring represents fluorescence level from black up to blue.*

Currently, it is difficult to realize large-scale quantum simulations in the lab for two reasons, one technological and one fundamental. First, with macroscopic traps as described above, it is impossible to form the large arrays that would allow simulations of systems inaccessible with classical simulations. Second, there are fundamental sources of error (described below) in the standard method for bringing about interactions that are sufficiently large that simulations using hundreds of spins would not faithfully reproduce the behavior of the system of interest. Below we describe the method we have developed to address both of these problems using a novel surface-electrode trap array with integrated delivery of RF fields for the on-chip production of spin-spin interactions.

## Importance to LANL's Science and Technology Base and National R & D Needs

This research lies at the center of the second S&T priority under the Complex Systems Grand Challenge in the FY09 LDRD-DR Strategic Plan ("Exploiting quantum systems: computations, simulations, ..."). It also has a connection with the "Information Science" Grand Challenge and LANL's mission to remain at the forefront of computing and algorithmic technologies. Direct simulations of quantum systems will not get easier with time despite Moore's law. The exponential nature of the problem makes it imperative to develop new methods, and quantum processing is one technology that can address the problem. Our work overlaps with the "Fundamentals of Materials" Grand Challenge: The methods we have developed will be capable of simulating or emulating behavior of matter starting from the most fundamental (quantum) level. The DOE Office of Science Basic Energy Sciences program is also recognizing the importance of this new research area to condensed matter physics, especially in regards to quantum emulation as a tool for basic understanding of condensed matter.

High-fidelity multi-qubit quantum operations with errors below the fault-tolerance threshold will be necessary for any large-scale quantum processor hoping to, e.g., factor large numbers faster than a classical computer. This application to cryptography is of obvious interest to for adversarial communication intercept. However, this type of quantum control would also make a great impact on quantum information science in general, including possible uses in other quantum algorithms and quantum repeaters for secure communication. An additional, very relevant area that could be expanded with improved manipulation of quantum entanglement, as described here, is quantum-enhanced measurement (QEM). QEM could enable quadratic or better enhancements in electromagnetic sensing precision with comparable resources to standard measurement methods. Our research impacts quantum information science by increasing our understanding of quantum systems that are of the size and that have architectures suitable for useful quantum information processing (QIP). QIP has an immediate interest for LANL and DOE because of its significance for homeland security and threat reduction. The research described here aligns well with the goal of the Quantum Institute to build up our quantum information processing architecture to position LANL to become a major player in these applications of quantum information processing.

## Scientific Approach and Accomplishments

The largest fundamental error, at the few-percent level, affecting the best present multi-qubit quantum operations [5] is due to the use of lasers to apply an optical force to trapped ions dependent on their internal electronic states. These forces are typically brought about using two-photon Raman transitions that couple to quantum states (long-lived levels) virtually through short-lived electronic states, as shown in Figure 2. The lasers are detuned from resonance with these intermediate states, but even at gigahertz and terahertz detunings, the scattering probability from these levels is large enough to cause qubit errors at the per-

cent level [6]. The use of these intermediate levels leads to a fundamental limitation in current two-ion interaction. This limitation is such that for simulations of hundreds of spins, most experimental "runs" of the simulation would be faulty, even not considering all other error sources.

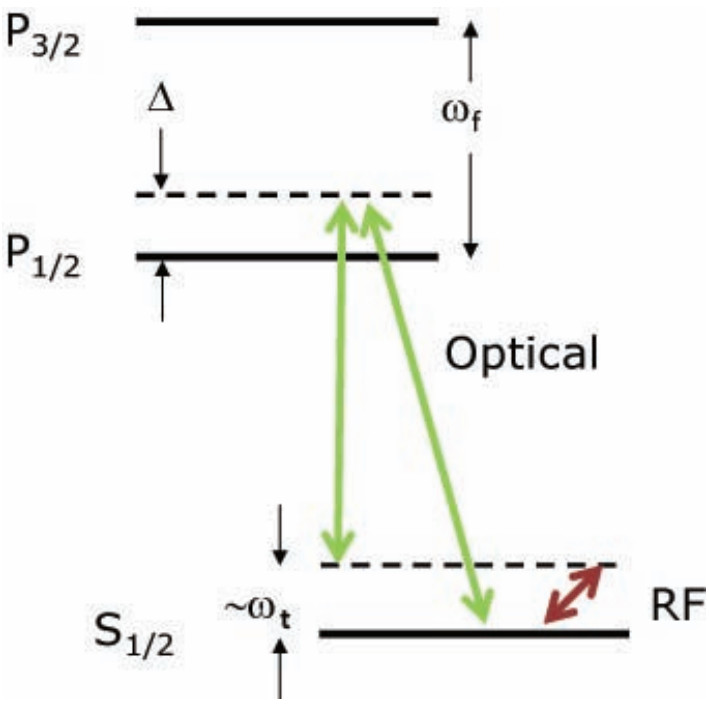


*Figure 2. Optical and alternative RF excitation for two-qubit gates. Ion electronic levels are depicted as Black lines, and colored lines represent applied electromagnetic control fields (green for the optical Raman scheme and red for RF excitation). The S level is a long-lived qubit state, and the P levels are short-lived intermediate levels. The detuning [Delta] from resonance and fine structure splitting [omega]f are depicted, and [omega]t is the trap frequency.*

Multi-ion spin-spin interaction may be brought about without the use of lasers to create forces on the ions---applied RF radiation near the ions' trap frequency can also produce forces, if the RF fields have appreciable spatial gradients [7] compared to the ions' wave-packet extents (10's of nanometers) in the harmonic trapping potential (see Figure 2). The use of direct RF fields does not require coupling to short-lived intermediate levels, almost completely eliminating the error due to spontaneous photon scattering described above. RF wavelengths are long (meters) however, so gradients must be introduced. These gradients can be produced by means of microfabricated coils which, due to their sub-wavelength extent, will produce nearby fields that vary rapidly in space. These coils can be integrated with surface trap electrodes such that the electrodes required for both trapping ions and for bringing about interactions between pairs of ions will be part of the same modular structure [8] (see Figure 3). RF fields applied to the coils beneath each ion produce a large-gradient field at the ion's position, which can produce a state-dependent force. If these fields vary in time near the trap frequency, the ions' vibrational motion is excited dependent on their state, leading to a gate similar to the controlled-phase gate (which is equivalent to a spin-spin interaction), as in the current optical case.

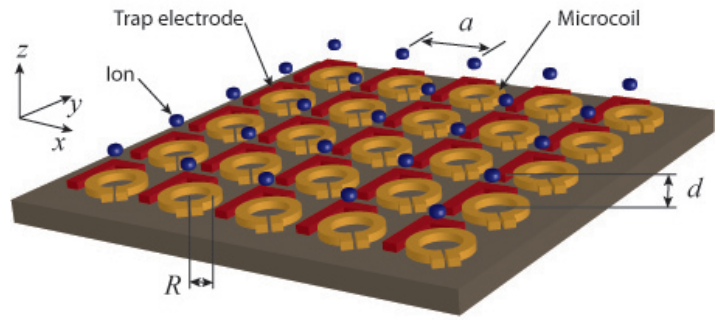


*Figure 3. Rendering of section of surface trap array and microcoils. Leads are not shown, and the electrodes shown are only a representative subset of those required. Ions may be trapped directly above loops, or trap electrodes and coils may be offset so ions can be trapped above any point in a microcoil unit cell. Possible values for the dimensions are coil radius R = 5 micrometers, ion-surface distance d = 5 micrometers, and inter-ion distance a = 15 micrometers.*

Using this scheme, we calculate that we can produce spin-spin interactions at the kilohertz scale with devices at easily accessible scales and realistic applied RF power. This kilohertz interaction is to be compared with the many-millisecond to second scales for quantum level coherence demonstrated in trapped-ion systems. To get a reliable simulation of an interacting spin system, we must be able to let the system evolve under these interactions for a time that would allow us to see the interactions take place, and with kilohertz rates, the required timescale is approximately 1 ms. We can also bring about global spin rotations, which simulate the effect of spins in an external magnetic field. Microwave fields produced uniformly across the array can bring these rotations about with rates comparable to or faster than that for the spin-spin interactions. The combination of these two parts of the simulation, the local spin-spin interaction and the global spin-field interaction, will allow for understanding of the competing interactions present in many solid-state systems. These are the properties that make them technologically and fundamentally interesting and useful, and these are the fundamental behaviors that we hope to elicit in our much more controllable system of an array of trapped ions.

What's more, these surface-electrode trap arrays can be fabricated with standard microfabrication techniques, using optical photolithography, standard metal deposition and etching, and electroplating. The scales required are well above the resolution limits, and error in the lithography, small to begin with, are transmitted to the fields above at a greatly reduced level, making the system robust to technical uncertainties in fabrication. Simpler surface-

electrode traps have been demonstrated previously [9], and the RF coils used here can benefit from the long history of technology designed for nuclear magnetic resonance excitation with magnetic coils. Since the ion array layout is controlled by the surface electrode structure, we can produce any array desired, not just the square lattice depicted above. For instance, there are many interesting array symmetries that produce quantum behaviors that are poorly understood, such as spin glasses and geometric frustration that can be found in lattices with triangular or hexagonal symmetries. These problems could be addressed in our system with only a minor modification to the array design. Similarly, defects and pinning of the lattice can be introduced intentionally so that the effects of these ever-present imperfections in real materials may be more systematically studied.

In addition to the quantum emulation work described here, this technology may also benefit quantum computing two-qubit gate fidelity, since the spontaneous photon scattering described above is a limiting factor for these operations in trapped ions, as well. Using gates brought about with RF fields, these operations should become fault-tolerant, allowing arbitrarily long quantum algorithms when error correction is used. Such arrays may also find use in a related but complementary form of quantum processing known as on-way quantum computing (OWQC) or measurement-based quantum computing [10]. OWQC can perform any algorithm that a standard quantum computer can, but it involves only measurements and single-bit rotations after an initial, one-time multi-qubit operation. The arrays described here could allow for this initial entangling operation using the RF interactions, and then all subsequent steps are much easier individual qubit rotations and measurements [8].

In short, on-chip delivery of RF control fields to ions held in an array by microfabricated surface traps will enable advances in many areas of the quantum information processing field. We hope to be able to follow on to the research conducted here and build these devices in the near future. Our first goal will be to produce spin-spin interactions between a few ions without the use of lasers. Then we will move onto larger arrays to attack condensed matter models inaccessible using direct classical computer simulation. This will open up new opportunities for modeling of the solid state, eventually allowing the design of novel materials from the fundamental level up.

## References


1. Batista, C. D., and G. Ortiz. Generalized Jordan-Wigner transformations. 2001. *Physical Review Letters.* **86**: 1082.
2. Feynman, R. P.. Simulating physics with computers. 1982. *International Jounral of Theoretical Physics.* **21**: 467.
3. Wineland, D. J., M. Barrett, J. Britton, J. Chiaverini, B. DeMarco, W. M. Itano, B. Jelenkovic, C. Langer, D. Leibfried, V. Meyer, T. Rosenband, and T. Schaetz. Quantum information processing with trapped ions. 2003. *Philosophical Transactions of the Royal Society of London A.* **361**: 1349.
4. Porras, D., and J. I. Cirac. Effective Quantum Spin Systems with Trapped Ions. 2004. *Physical Review Letters.* **92**: 207901.
5. Leibfried, D., B. DeMarco, V. Meyer, D. Lucas, M. Barrett, J. Britton, W. M. Itano, B. Jelenkovic, C. Langer, T. Rosenband, and D. J. Wineland. Experimental demonstration of a robust, high-fidelity geometric two ion-qubit phase gate. 2003. *Nature.* **422**: 419.
6. Ozeri, R., W. M. Itano, R. B. Blakestad, J. Britton, J. Chiaverini, J. D. Jost, C. Langer, D. Leibfried, R. Reichle, S. Seidelin, J. H. Wesenberg, and D. J. Wineland. Errors in trapped-ion quantum gates due to spontaneous photon scattering. 2007. *Physical Review A.* **75**: 042329.
7. Mintert, F., and C. Wunderlich. Ion-Trap Quantum Logic Using Long-Wavelength Radiation. 2001. *Physical Review Letters.* **87**: 257904.
8. Chiaverini, J., and W. E. Lybarger Jr.. Laserless trapped-ion quantum simulations without spontaneous scattering using microtrap arrays. 2008. *Physical Review A.* **77**: 022324.
9. Seidelin, S., J. Chiaverini, R. Reichle, J. J. Bollinger, D. Leibfried, J. Britton, J. H. Wesenberg, R. B. Blakestad, R. J. Epstein, D. B. Hume, W. M. Itano, J. D. Jost, C. Langer, R. Ozeri, N. Shiga, and D. J. Wineland. Microfabricated Surface-Electrode Ion Trap for Scalable Quantum Information Processing. 2006. *Physical Review Letters.* **96**: 253003.
10. Raussendorf, R., and H. J. Briegel. A One-Way Quantum Computer. 2001. *Physical Review Letters.* **86**: 5188.


## Publications


Chiaverini, J., and W. E. Lybarger Jr.. Laserless trapped-ion quantum simulations without spontaneous scattering using microtrap arrays. 2008. *Physical Review A.* **77**: 022324.

continuing project

# Ultrafast Phenomena: Short-Pulse laser Interactions with Atoms and Molecules

*Lee A Collins*

20061600PRD4

## Introduction

The aim of this project is the theoretical and computational study of the interaction of ultrashort laser pulses with atoms and molecules as well as the behavior of composite materials under extreme conditions. With the duration of electromagnetic pulses reaching the fundamental time period of electron motion, we have reached a critical threshold for probing, manipulating, and understanding the basic interactions and processes that govern matter at the atomic scale. For example, experiments have recently observed in "real" time (~attoseconds) the migration of electrons from conduction bands to the surface and the jumping of electrons from different sites within a molecule. Such ultrafast exchanges hold substantial promise for assembling new nano-materials and altering fundamental electronic mechanisms that govern the outcome of intricate quantum mechanical events. A thorough knowledge of the simplest of these mechanisms is required in order to piece together more complicated systems. Therefore, we begin our studies with simple systems in order to explicate the basic mechanics. This study in turn requires the development of sophisticated computational techniques to solve the basic underlying quantum mechanical equations. In addition, we perform a complementary study on more extended systems such as mixtures of atoms in the warm, dense matter regime, typical of planetary interiors and inertial confinement fusion capsules. Our goal again concentrates on the understanding of basic quantum mechanical interactions as a means of extracting certain prescriptions for determining the properties of the composite from the pure atomic constituents. Such rules have extensive application in the modeling of macroscopic phenomena.

## Benefit to National Security Missions

The ability to probe material properties on the time scale of atomic motion promises better understanding of basic materials from the solid to the plasma state. Our probes will greatly improve our fundamental knowledge of important materials, impacting DOE missions from materials for energy to sensors for threat reduction.

## Progress

This fiscal year has marked a time of concerted progress on the basic elements of the project and has witnessed four publications and four manuscripts in the submission process to high-profile, peer-reviewed research journals such as Physical Review as well as an invited talk at the annual meeting of the Division of Atomic, Molecular, and Optical Physics of the American Physical Society.

Several areas in regards to the interaction of atoms and molecules with intense and ultrashort laser fields have received particular attention including the double photoionization of Helium and the Hydrogen molecule. The first investigations have focused on small two-electron systems since they provide an effective testbed for more complicated targets, for cleanly resolving basic interactions and mechanisms, and for comparisons with experiments. They also provide the simplest systems for the study of correlation, which arises solely through quantum mechanical effects, and can dramatically alter certain processes from a classical or perturbative picture. For Helium, our studies have disentangled very complicated cross sections in terms of sequential and nonsequetial processes in regards to whether the system absorbs two photons simultaneously or one after the other. The knowledge of such fundamental internal processes is essential to understanding the means of manipulating and controlling atoms, molecules, and nanosystems by external electric and magnetic fields. In addition, the formalism has been expanded to determine not only the distribution of the electrons but also of the recoiling ion. This full characterization of the kinetic and spatial distributions of the final states of the particles can be directly compared to elaborate experiment results from sophisticated detectors, giving a complete view of the photoionization process that allows separation of the various competing mechanisms. All these intricate comparisons arise from our

ability to solve the time-dependent Schrodinger equation that describes the quantum mechanical nature of these systems. To this end, we have improved our finite-element discrete variable representation program by extensions to massively-parallel constructions and more accurate temporal propagators. The program scales linearly on parallel platforms over hundreds of processors.

A related set of calculations focuses on the Hydrogen molecule. An interesting speculation has arisen in these ultrashort interactions as to whether the ejected electron in passing between the nuclear centers can undergo interference much as in the famous double-slit experiment by Young with light. Our theoretical results have placed distinct limits on this mechanism and questioned this interpretation of recent experiments at low photon energies. We have also devised elaborate visual display packages that permit a clear examination of the complicated spatial probability distributions that describe the exiting particles.

In a related study, we have applied density functional theory approaches to atomic mixtures such as Lithium Hydride (LiH) in the warm, dense matter regime. This regime covers such areas as planetary interiors, White Dwarf surfaces, inertial confinement fusion (ICF) capsules, and high energy density physics (HEDP) devices such as Z-pinch machines. We use the large-scale quantum simulation techniques to test various mixing rules devised to combine pure atomic properties to form those of the composite. These rules provide extensive information for many data bases used to model macroscopic phenomena. We found that in some regimes, these rules can have substantial errors for the equation-of-state and opacities.

## Future Work

The advent of ultrashort laser pulses has revolutionized the study of basic material properties, both static and dynamical. The short time scale permits probing of the motion of atoms within molecules, chemical reactions, and structure changes. This feature of the pulse can also be used to produce high intensities in which the strength of the laser field exceeds that binding the atomic particles. In such cases, interesting new phenomena arise such as high harmonic generation, which has in turn been employed to generate attosecond (10^-18s) pulses on the time frame of electron motion. To explore such rapid and strong interactions requires treating the full three-dimensional time-dependent Schrödinger equation that describes the intricate quantum mechanical processes, since perturbation approaches fail in these regimes. We shall develop a highly-scalable technique for solving this massive problem by merging several powerful schemes. The spatial component will be treated by a discrete variable representation (DVR) within finite elements. This permits a very flexible spanning of space occupied by the complicated wavefunction solution while utilizing the highly-efficient and accurate DVR scheme to minimize the number of points within an element. A real space product approach assures a systematic and rapid propagation of the temporal component. Initial tests on small atomic systems indicate a robust procedure that gives linear scaling out to a thousand nodes. However, to address the wide variety of systems under current experimental investigation will require large-scale extensions to treat more complex systems, principally to merge atomic and molecular structure capabilities (e,g. density functional theory) with the temporal and gridding techniques. Studying attosecond imaging techniques for complicated systems, ultrafast manipulation procedures for chemical processes, and the effects of correlation in time-evolving cases give but a few of the potential applications.

## Conclusion

We expect to develop efficient, parallel algorithms to solve the time-dependent quantum mechanical equations that describe the interaction of radiation with matter. Such massively-parallel approaches are essential to describe the large temporal and spatial domains covered by such cases. We shall employ the techniques to study attosecond pulse interactions with atoms and molecules in order to image and follow the underlying electronic motion, which should yield a better understanding of basic structure and dynamics of basic material systems.

## Publications

Horner, D. A., C. W. McCurdy, and T. N. Rescigno. Triple differential cross sections and nuclear recolil in two-photon double ionization of helium. To appear in *Physical Review A.*

Horner, D. A., J. D. Kress, and L. A. Collins. Quantum molecular dynamics simulations of warm dense lithium hydride: examination of mixing rules. 2008. *Physical Review B.* **77**: 064102.

Horner, D. A., S. Myabe, T. N. Rescigno, C. W. McCurdy, F. Morales, and F. Martin. Classical two-slit interference effects in two-photon double ionization of molecular hydrogen at high energies. To appear in *Physical Review Letters.*

Horner, D. A., T. N. Rescigno, and C. W. McCurdy. Decoding sequential versus non-sequential two-photon double ionization of Helium using nuclear recoil. 2008. *Physical Review A.* **77**: 030703(R).

Horner, D., F. Morales, T. Rescigno, F. Martin, and C. McCurdy. Two-photon double ionization of helium above and below the threshold for sequential ionization. 2007. *Physical Review A.* **76**: 030701.

Horner, D., W. Vanroose, T. Rescigno, F. Martin, and C. McCurdy. Role of nuclear motion in double ionization of molecular hydrogen. 2007. *Physical Review Letters.* **98**: 073001.

Kress, J., L. Collins, S. Mazevet, and D. Horner. Quantum molecular dynamics simulations of optical reflectivity of shock-compressed Tin. 2007. *American Institute of Physics Proceedings.* **995**: 1433.

Vanroose, W., D. Horner, F. Martin, T. Rescigno, and C. McCurdy. Double photoionization of aligned molecular hydrogen. 2006. *Physical Review A.* **74**: 052702.

Yip, F., D. Horner, C. McCurdy, and T. Rescigno. Singlr and triple differential cross sections for double ionization of H-. 2007. *Physical Review A.* **75**: 042715.

# Gamma-Ray Bursts and Gravitational Waves from Compact Mergers

*Christopher Lee Fryer*

20070574PRD1

## Introduction

The two main thrusts of this project are to study the progenitors of gamma-ray bursts and supernovae, and to study sources of gravitational wave emission.

The primary progenitors of both gamma-ray bursts and type Ia supernovae are binary star systems. In this project, we are modeling the populations of these systems to determine their formation throughout the history of the universe. By comparing these results to observations, we can probe the early universe and help devise better experiments to study dark energy. We are using a Monte-Carlo population synthesis code on LANL and New Mexico (Encanto) computers to run these calculations.

We are also modeling the sources of gravitational wave emission as part of his work as a Laser Interferometric Gravitational-Wave Observatory (LIGO) member. This work leads much of the general relativity work done at the laboratory into a focus that is closer to that of mainstream science.

## Benefit to National Security Missions

This project takes full advantage of the computational and physics expertise developed at the national laboratories as part of their mission in nuclear weapons. It has direct relevance to DOE Office of Science missions such as SNAP (Supernova/Acceleration Probe) and may impact LANL's "Beyond the Standard Model" Grand Challenge.

## Progress

We focused much of the work on the study of gamma-ray bursts (GRBs) progenitors at high redshift, as these GRBs hold the most promise as probes of the early universe. We have studied the formation processes for population III (first generation of) stars. But we have also studied the role of a number of additional binary effects, published in a series of papers in the Astrophysical Journal.

An example of this work is the study of a twin population of massive stars. There is some evidence that massive stars are born in binaries where the masses of the two stars in the binary are nearly equal. But most of this evidence did not arise from observations of binaries themselves (which suggests the opposite) but the argument that these binaries can better explain the population of double neutron stars and also gamma-ray burst progenitors. The question we worked to solve is: how do such binaries affect the double neutron star and gamma-ray burst populations? Surprisingly, it had less effect than had been previously assumed, arguing that these twins are unlikely to really exist. This work has been submitted to the Astrophysical Journal.

Another example of this work is our study of neutron star birth masses. This project takes full advantage of the supernova expertise at Los Alamos and will produce a new set of birth neutron star masses to be used by the greater population synthesis community.

We are also working on a study of type Ia supernova progenitors. This work ties directly into LANL's work on the Destiny Joint Dark Energy Mission. For this work, LANL is using Advanced Simulation and Computing (ASC) codes to model type Ia Supernova emission to be used in designing the Joint Dark Energy Mission (JDEM) satellite. The spectra and light curves of supernovae depends sensitively on the surrounding environment and, as a result, on the progenitor. Our work thus far provides the first step in this study - the characteristics of the progenitor.

We are currently working with New Mexico State University and Harvard's Center for Astrophysics to do the first complete study of type Ia progenitors. We will then couple these results to hydrodynamic studies of white dwarf mergers to produce detailed environments around type Ia supernovae, ultimately producing light-curves for these events. The crucial aspect of this study is to determine if there is a population of type Ia progenitors that are rare at low redshift, but more common at the high redshifts probed by the Joint Dark Energy Mission. If this progenitor has light curves that do not

follow the peak brightness/width relationship of low redshift supernovae, they may add a systematic error to the observations at these redshifts, hampering the success of the Joint Dark Energy Mission. If this is the case, we will determine if we can pinpoint some spectral feature that can be used by this mission to remove these progenitors. We have begun much of the work for this project in the past year and hope to finish many results in the next year

## Future Work

The primary issue with gamma-ray burst progenitors for short-duration bursts is the evolution of binaries. This also dominates many of the uncertainties in determining the signals from these binaries with respect to gravitational waves. Our project will focus on this binary evolution. The goal of this project is to first revamp our binary population synthesis code by developing better physics codes to determine the parameters in this code: advanced stellar evolution models developed at LANL taking advantage of detailed models of mixing, binary merger calculations using the LANL-developed Smooth Particle Hydrodynamics (SNSPH) code, using the latest developments in nuclear physics to revamp our understanding of neutron stars. After developing the tools and running them to revamp the binary evolution code, we will then begin an intensive study of these binaries focusing on the observational implications of such physics-based calculations including both gamma-ray bursts and gravitational wave detections.

## Conclusion

This project will rule out many of the proposed gamma-ray burst progenitors allowing theorists to focus on the few remaining progenitors for detailed numerical study. These massive explosions play such an important role in our understanding of the universe from large-scale cosmology (these bursts are so powerful that they can be observed in the early universe and hence can be used as standard candles) to our understanding of the Earth (it has been proposed that a gamma-ray burst, not an asteroid, caused the extinction of the dinosaurs). By understanding their progenitors, we make all of these broader studies tractable.

## Publications

Belczynski, K., K. Z. Stanek, and C. L. Fryer. Short-Hard Gamma-Ray Bursts in Young Host Galaxies: the Effect of Prompt Twins. *Astrophysical Journal.*

Belczynski, K., R. O'Shaghnessy, V. Kalogera, F. Rasio, R. Taam, and T. Bulik. The lowest-mass stellar black holes: catastrophic death of neutron stars in gamma-ray bursts. To appear in *Astrophysical Journal.*

Belczynski, K., and R. Taam. The most massive progenitors of neutron stars: CXO J164710.2-455216. *Astrophysical Journal.*

Bulik, T., K. Belczynski, and A. Prestwich. IC10 X-1: the immediage progenitor of a double black hole binary. *Astrophysical Journal.*

Fragos, T., V. Kalogera, K. Belczynski, G. Fabbiano, D. W. Kim, N. J. Brassington, L. Angelini, R. L. Davies, J. S. Gallagher, A. R. King, S. Pellegrini, G. Trinchieri, S. E. Zepf, and A. Zezas. Models for Low-Mass X-Ray Binaries in the Elliptical Galaxies NGC3379 and NGC4278: Comparison with Observations. *Astrophysical Journal.*

Linden, T., J. F. Sepinsky, V. Kalogera, and K. Belczynski. Probing Electron-Capture Supernovae: X-ray Binaries in Starbursts. *Astrophysical Journal.*

Ruitter, A. J., K. Belczynski, M. Benacquista, and K. Holley-Bockelmann. The Contribution of Halo White Dwarf Binaries to the LISA Signal. *Astrophysical Journal.*

# Theoretical and Experimental Investigation of Relaxation Mechanisms in Ultra-low Field NMR for Magnetic Resonance Imaging

*Michelle A Espy*

20070626PRD2

## Introduction

The aim of the project is to investigate new techniques and basic science of ultra-low field (ULF) nuclear magnetic resonance, NMR, and magnetic resonance imaging, MRI. The advantage of ULF is simplicity in generating fields, new contrast features, new information about dynamics, and possibility to develop inexpensive, portable MRI scanners, to supplement high field MRI scanners widely employed in medical hospitals and research facilities. The last point is particularly significant because if ULF MRI scanners are developed, this can lead to a revolution in MRI technology and medical diagnostics. The atomic magnetometer (AM) is the key for such revolutions, because AMs are non-cryogenic, maintenance-free, and inexpensive. So far MRI with an atomic magnetometer has not been demonstrated, and the important goal of this project is such demonstration and the development of applications based on it. The behavior of MRI parameters such as T1 (longitudinal relaxation) and T2 (transverse relaxation) contrast enhancement is another important goal for the project. Such contrast enhancement is one of advantages of ULF MRI, with possibilities for applications in cancer diagnostics. For example, to enhance contrast gadolinium based compounds are injected, but at ULF MRI similar contrast can be achieved without injection of gadolinium. Our group works on the detection of liquid explosives for department of homeland security and on the detection of enrichment of uranium, both methods closely relevant to LANL missions which rely on ULF NMR/MRI. The present technology is based on SQUID (superconducting quantum interference device) magnetometers, which require liquid helium. However, similar experiments can be conducted with atomic magnetometers with benefit of non-cryogenic operation, simplifying deployment of ULF NMR systems in real life applications.

## Benefit to National Security Missions

This work could impact DOE missions including counter proliferation because ultra-low field NMR can detect U235 inside metal containers (lead), energy missions through the potential ability to detect and log oil reserves, and support for DHS missions through the ability to detect explosives, even inside other containers.

## Progress

This year was extremely productive: we were able to obtain the first MR image with an atomic magnetometer (Figure 1) and submitted the results to Physics Review Letters [1]; we also recorded the first brain image at ultra low field using SQUIDs, and the results are published in JMR [2]. The work on the analysis of 3He NMR signal at ULF NMR continued and the paper was published in JMR [3]. The system for NMR/MRI with an atomic magnetometer has been built and is under investigation. Initial results are obtained and optimization plan is designed to improve the sensitivity and practical applicability of the techniques based on the atomic magnetometer. We plan to conduct various ULF MRI experiments with the atomic magnetometer: first MRI of the human hand; first brain MRI with an atomic magnetometer, investigate applications to food inspection, security (detection of explosives), and to explore basic science of ULF MRI. The work has revolutionary value and further progress can lead to the development of new MRI techniques, widely applicable in healthcare, industry, security and military.

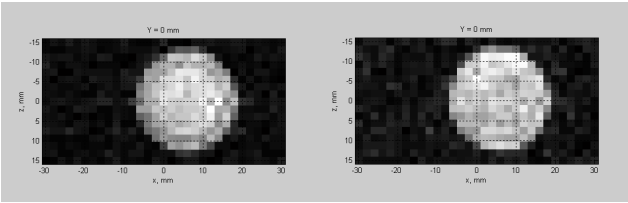


*Figure 1. MRI obtained with SQUID (left) and atomic magnetometer (right) at 3.2 kHz. Resolution is 2 mm, acquisition time is 12 minutes.*

In addition to the above spectacular achievement, we have done work on analysis of theoretical aspects of ULF MRI relaxation. For example, the relation between relaxation and dynamics was explored for potential applications in the studies of proteins, fuel cells, diffusion. We have also looked at the possibility of the magic angle rotation of the magnetic field (not the NMR sample as in conventional methods), which should enable the applications in solid state ULF NMR, completely new unexplored dimension of NMR. For example, it is impossible to rotate a human subject even at low frequency, but the field can be rotated at a kHz rate and NMR lines can be significantly narrowed and the signal enhanced. Finally, we have measured T1 and T2 of the human brain at ultra-low frequencies for the first time [4].

## Future Work

The effort will continue to investigate nuclear magnetic resonance NMR relaxation mechanisms in ultra-low (micro-Tesla) magnetic fields, with emphasis on improving our imaging contrast. Contrast mechanisms are due to fluctuations caused by thermal motion of molecules. The main application of this research is in ultra-low-field (ULF) MRI (magnetic resonance imaging) and spectroscopy. The differences in relaxation times at ULF may enable new methods for imaging and material differentiation that cannot be realized at high fields (~Tesla). In all applications relaxation times are of great importance. The challenge of this research is the signal is much smaller than in conventional NMR, thus the most sensitive magnetic detectors and shielding have to be used. For example, relaxation times and mechanisms in ULF are not known even in simple substances.

Apart from imaging contrast, we also desire to improve imaging resolution and signal-to-noise ratio. These will be important steps both for developing a research tool and demonstrating practical applications of the technology.

### Proposed Work

Measure relaxation times for various substances and analyze relaxation mechanisms. In conjunction with experimental work, current theories of relaxation time will be extended to formulate an understanding of the relationship between relaxation times and applied magnetic field strength. The difference in relaxation time (T1, longitudinal/T2, transverse, or "contrast") between different tissue types is a powerful tool in modern clinical MRI. Currently, it is a baffling mystery why different closely related materials (e.g. healthy and tumor tissue) have significantly different relaxation times.

We plan to extend our measurements from phantoms to biological objects including in vivo imaging with ~ 1mm spatial resolution.

### Impact of Work

The result will be: 1) the measurements of relaxation times; 2) the development of theory of relaxation in low field; 3) demonstration of MRI with an atomic magnetometer; 4) applications in cancer diagnostics; 5) other applications in areas such as security, food inspection (the content of metal containers, such as canned food, can be analyzed without opening using ULF NMR), and geology. In the long term, this research can result in the development of portable inexpensive ULF MRI scanners for medical diagnostics with benefits to millions of people for whom such diagnostics will be accessible.

## Conclusion

We anticipate that understanding NMR relaxation mechanisms at ultra-low fields will enable us to improve medical imaging manifold. This is particularly important for people who can not be imaged in traditional MRI systems. This work will also tremendously enhance our ability to detect and differentiate materials. Ultra-low field NMR is particularly unique in the ability to make such measurements inside metal containers. This has a variety of national security applications and non-defense applications (such as food inspection).

## References

1. Savukov, I. M., V. S. Zotev, P. L. Volegov, M. A. Espy, A. N. Matlashov, and R. H. Kraus, Jr.. In situ MRI with an atomic magnetometer. To appear in *Physical Review Letters.*

2. Zotev, V. S., A. N. Matlashov, P. L. Volegov, I. M. Savukov, M. A. Espy, J. C. Mosher, J. J. Gomez, and R. H. Kraus, Jr.. Microtesla MRI of the human brain combined with MEG. 2008. *Journal of Magnetic Resonance.* **194**: 115.

3. Savukov, I. M., A. Matlashov, P. Volegov, M. Espy, and M. Cooper. Detection of 3He spins with ultra-low field nuclear-magnetic resonance employing SQUID's for application to a neutron electric dipole moment experiment. 2008. *Journal of Magnetic Resonance.* **195**: 129.

4. Zotev, V. S., P. L. volegov, A. N. Matlashov, I. M. Savukov, T. Owens, and M. A. Espy. SQUID-based microtesla MRI for in vivo relaxometry of the human brain . To appear in *IEEE Transactions on Applied Superconductivity.*

## Publications

Savukov, I.. Atomic Magnetometers. To appear in *Multi-disciplinary University Research Initiative.* (Boulder, CO, July 18-20).

Savukov, I.. Applications of atomic magnetometers to MEG and NMR. To appear in *International Brain Mapping Intraoperative Surgical Planning Society.* (Washington, DC, Sept 6-8, 2007).

Savukov, I. M., V. S. Zotev, P. L. Volegov, M. A. Espy, A. N. Matlashov, and R. H. Kraus, Jr. . In situ MRI with an atomic magnetometer. To appear in *Physical Review Letters.*

Savukov, I., A. Matlashov, P. Volegov, M. Espy, and M. Cooper. Detection of 3He spins with ultra-low field nuclear-magnetic resonance employing SQUID's for application to a neutron electric dipole moment experiment. 2008. *Journal of Magnetic Resonance.* **195**: 129.

Zotev, V. S., A. N. Matlashov, P. L. Volegov, I. M. Savukov, M. A. Espy, J. C. Mosher, and R. H. Kraus, Jr.. Microtesla MRI of the human brain combined with MEG. 2008. *Journal of Magnetic Resonance.* **194**: 115.

Zotev, V. S., P. L. Volegov, A. N. Matlashov, I. M. Savukov, T. Owens, and M. A. Espy. SQUID-based microtesla MRI for in vivo relaxometry of the human brain. To appear in *IEEE Transactions on Applied Superconductivity.*

# Noise in Biochemical Networks: Rigorous Analysis with Field-Theoretic Tools

*Ilya Mark Nemenman*

20070649PRD2

## Introduction

Various problems in diferese fields, from statistical physics to cellular regulatory networks, involve analysis of stochastic properties in transport phenomena on a variety of networks. This analysis is usually very difficult due to the intrinsic stochastic nature of the processes, which necessitates their computational modeling in a computationally prohibitive event-by-event fashion.

In this project, Nikolai is developing ways to transplant the tools that have proven to be effective in mesoscopic condensed matter physics into the realm of stochastic processes on networks. If successful, many decades of successful work in one field will come to bear fruits in another, allowing fast and efficient simulations and analysis of the processes, and impacting a variety of fields, from basic biomedical sciences, to biosecurity and energy security.

A critical notion in the work is the geometric phase, a common property of quantum and mesoscopic systems, but previously unseen in the stochastic domain. In the course of the project, we have discovered the phase in certain biochemical processes, and it is expected that similar results will hold in arbitrary systems. The phase will be the main conduit for connections between mesoscopic quantum systems and the stochastic transport on networks.

## Benefit to National Security Missions

The project will develop predictive capabilities applicable to the biosciences mission of DOE, specifically for bioenergy research; advance the scientific understanding of basic biochemical processes of interest to DOE bioenergy mission and will be useful for threat reduction applications in the context of host-pathogen interactions, supporting DOE and DHS missions.

## Progress

This project has discovered the geometric phase in classical stochastic systems. More specifically, suppose that, in a stochastic system, one changes certain kinetic rates with time. This happens, for example, in cells due to the natural time of day variations, and in epidemiological networks due to the variation of the infection rates in the course of the year. It turns out that the stochastic nature of the processes results in the contribution to the transported amounts in these networks, which would not be expected from a pure deterministic treatment. This contribution, as we have discovered, is a precise analogue of the Berry (or geometric) phase in quantum mechanics, but this is the first time such an effect has been found in a non-quantum system. The finding is quite remarkable: in particular, it has been believed that, to find details of a macroscopic structure of a network, one should be able to conduct experiments that are able to track all of the aspects of its stochastic dynamics. In contrary, we have found that much of this information is available through the geometric phase observation in a bulk, mean-value experiment, provided the experiment traces responses to temporal perturbations. These results are expected to be used to uncover properties of ion channels in neurons in a collaboration with the NIH group of Dr. Sergey Bezrukov; a recent trip to NIH has started the collaboration. Similarly, these results seem to be important for a burgeoning field of nonequlibrium statistical physics, such as applications of the theory of stochastic ratchets to molecular motors, etc. A collaboration with Chris Jarzynski (University of Maryland) has been initiated.

Since the start of the project, the funding has been used in the following research projects.

Refs (Sinitsyn and Nemenman, 2007 and Sinitsyn and Nemenman, 2007a) were the original works where the geometric phase in stochastic kinetics has been noted, and the tools developed in the context of the quantum-mechanical Berry phase were used to solve a variety of problems in chemical kinetics, nonequilibrium statistical physics, and mathematical epidemiology.

In (Sinitsyn and Ohkubo, 2008; Sinitsyn, Dobrovitski, et al., 2008; Sinitsyn, 2007; Sinitsyn and Saxena, 2008) Nikolai SIntsyn further developed the theory of the geometric phase in statistical physics problems, and related the phenomenon to geometric phases in classical and

quantum mechanics, using the latter two to help with solutions of important applied problems, such as the motion of magnetic domain walls.

Refs (Sinitsyn, 2008; Nunner et al, 2007; Borunda et al, 2007) have studied, in particular, geometric effects in traditional condensed-matter problems of relevance to nanotechnology.

Applications of the geometric phase to nonequlibroum statistical physics problems have revealed an important question: under which conditions does a small, periodic perturbation of a system result in an nonzero current through it? This question was answered fully in (Chernyak and Sinitsyn, 2008).

The developed theory also also to derive coarse-grained, simple tools for simulation of stochastic kinetic networks and for reverse-engineering the underlying kinetic diagram based on mesoscopic experimental data, and this was competed as well (Sinitsyn, Hengartner, and Nemenman, in press; de Ronde et al., in press).

## Future Work

The work on this project continues to address the three specific aims postulated in the original proposal:

1. Analytical derivation of coarse-grained descriptions of long time scale signal processing dynamics in a set of basic building blocks of biochemical reaction networks, such as Michaelis-Menten reaction, Hill allosteric reaction, signaling cascades, multiple covalent modifications hypercubes, etc.

2. Creation and dissemination of rigorous numerical algorithms and software for efficient simulations of the aforementioned “building blocks” reactions in the context of a large whole-cell biochemical network.

3. Creation of tools for inference of the underlying kinetic scheme from experimental fluctuations data.

All of these specific outcomes are essential stepping stones on the way to understanding and manipulating dynamical properties of biochemical signaling networks, such as those involved in diseases, bioremediation, or bioenergy production.

Importantly, a new practical application has emerged and will be investigated in the remaining half year of the project. Namely, existence of the geometric phase and the ability to evaluate it analytically and numerically allows for creation of control theory for stochastic systems, where small molecular copy number fluctuations are not avoidable. Dr. Sinitsyn has suggested that this can be used for optimal design of biochemical batteries, where periodic perturbations of the system, such as F1ATPase, can be used to design a high efficiency, optimized devicetransforming electrical energy into a chemical storage, and vice versa. This possibility needs to be explored in detail due to its obvious importance for the Nation.

## Conclusion

We expect to complete the analysis of a variety of small biochemical reaction networks, which form basic building blocks of all concerted interactions among molecules in a cell. Effects of the noise coming from the small number of molecules on the ability of these networks to function reliably will be analyzed, and efficient simulation software will be developed. This will be an essential first step for understanding and manipulating many biochemical signaling networks, involved, for example, in energy production and diseases, such as cancer, and may eventually lead to breakthroughs on both of these fronts. Emerging understanding can help us design better molecular machines, such as a chemical battery, described above.

## Publications

Borunda, M., T. Nunner, T. Luck, N. Sinitsyn, C. Timm, J. Wunderlich, T. Jungwirth, A. MacDonald, and J. Sinova. Absence of skew scattering mechanism in two dimentional systems: a test of anomalous Hall effect theory. 2007. *Phys. Rev. Lett..* **99**: 066604.

Chernyak, V., and N. Sinitsyn. Pumping-Restriction Theorem for stochastic networks. 2008. *Phys. Rev. Lett..* **101**: 160601.

Nunner, T., N. Sinitsyn, M. Borunda, A. Abanov, C. Timm, T. Jungwirth, J. Inoue, V. Dugaev, A. MacDonald, and J. Sinova. Anomalous Hall effect in two-dimensional electron gas. 2007. *Phys. Rev. B.* **76**: 235312.

Sinitsyn, N.. Semiclassical theories of the anomalous Hall effect. 2008. *J. Phys.: Cond. Matt..* **20**: 023201.

Sinitsyn, N.. Reversible stochastic pump currents in interacting nanoscale conductors. 2007. *Phys. Rev. B.* **76**: 153314.

Sinitsyn, N., A. MacDonald, T. Jungwirth, V. Dugaev, and J. Sinova. Anomalous Hall effect in 2D Dirac band: link between Kubo-Streda formula and semiclassical Boltzmann equation approach. 2007. *Phys. Rev. B.* **75**: 045315.

Sinitsyn, N., N. Hengartner, and I. Nemenman. Coarse-graining stochastic biochemical networks: quasi-stationary

approximation and fast simulations using a stochastic path integral technique. *Proc. Natl. Acad. Sci. (USA).*

Sinitsyn, N., V. Dobrovitski, S. Urazhdin, and A. Saxena. Geometric control over the motion of magnetic domain walls. 2008. *Phys. Rev. B.* **77**: 212405.

Sinitsyn, N., and A. Saxena. Geometric phase for non-Hermitian Hamiltonian evolution as anholonomy of a parallel transport along a curve. 2008. *J. Phys. A: Math. Theor..* **41**: 392002.

Sinitsyn, N., and I. Nemenman. Universal geometric theory of mesoscopic stochastic pumps and reversible ratchets. 2007. *Phys. Rev. Lett.* **99**: 220408.

Sinitsyn, N., and I. Nemenman. The Berry phase and the pump flux in stochastic chemical kinetics. 2007. *EPL.* **77**: 58001.

Sinitsyn, N., and J. Ohkubo. Hannay angle and geometric phase shifts under dissipative evolution. 2008. *J. Phys. A: Math. Theor..* **41**: 262002.

deRonde, W., B. Daniels, A. Mugler, N. Sinitsyn, and I. Nemenman. Mesoscopic statistical properties of multistep enzyme-mediated reactions. To appear in *IET Syst. Biol..*

# Detecting the Highest Energy Gamma-Rays and Neutrinos to Determine the Origin of Cosmic Rays

*Brenda L Dingus*

20070658PRD2

## Introduction

Los Alamos National Laboratory has developed the world's most sensitive observatory of very high energy gamma rays from astrophysical sources. The data from this observatory, called Milagro and located at LANL, is being examined for transient sources and for correlations of these transient events with other observatories such as the IceCube neutrino detector located at the South Pole. In order to detect transient sources, Monte Carlo simulations of the various changes in the detector configuration must establish the stability of the Milagro observatory over the eight years of operation. In addition, this project uses these detailed simulations to design a future observatory, High Altitude Water Cherenkov (HAWC), which will be over an order of magnitude more sensitive than Milagro. The HAWC observatory will discover new sources of gamma rays and monitor known transient sources to understand the highest energy particle accelerators in the Universe. These astrophysical particle accelerators include supermassive black holes at the center of active galaxies, the remnants of supernova explosions, and rapidly spinning neutron stars. The gamma rays from these sources are direct probes of the physical mechanisms in these extreme laboratories that can't be duplicated on Earth.

## Benefit to National Security Missions

This project supports the missions of the Office of Science by enhancing our understanding of high energy physics in extreme astrophysical environments, which cannot be reproduced in laboratories on Earth. This project will also support other missions through developing competency in experimental collection and analysis of large data sets.

## Progress

The analysis task of directly comparing transient Milagro sources with measurements from other experiments (particularly neutrino telescopes) has been the primary focus for the first year of Dr. Pretz' postdoctoral appointment. He has worked on understanding what free parameters need to be modeled in Monte Carlo simulations in order to adequately model Milagro's performance across time. Milagro has a large eight-year dataset of over 100 TBytes and the configuration and setup of the experiment has changed through time. The most important instabilities are 1) periodically one of the 728 photomultiplier (PMT) detector elements will fail and temporarily 15 other elements will not be operational, 2) during the winter, the Milagro pond accumulates snow on the cover increasing the low energy threshold, and 3) the calibration of the detector is updated periodically that has resulted in systematic changes.

Through Dr. Pretz's work, we understand the importance of accounting for both outages and changing calibrations of the PMTs in Milagro. This is particularly important at high energies where Milagro's measurements are of the most value. Dr. Pretz has made make corrections in the data accounting for the time-dependent numbers of dead and re-calibrated PMTs, and formed new figures of merit based on these much more stable and better modeled parameters. Folding this information into the Monte Carlo simulation for the experiment yields much better agreement between simulation and data. This agreement is especially important for transient observations since we are looking for changes in the sources on the same timescale as changes in our detector. Others in the Milagro collaboration have also used this new understanding to resolve a major disagreement in the measured cosmic-ray energy spectrum over time. We are now in the process of publishing this work.

Dr. Pretz's has helped keep the Milagro experiment working until its decommissioning this summer. He has taken shifts and worked to repair the experiment when it is periodically down. He has maintained the Milagro computer cluster at LANL and worked to further develop the core Milagro software. He also mentors a Milagro student Grant Christopher from New York University who is using the Milagro data to study the Sun's

magnetic field. Dr. Pretz has given several talks about the Milagro experiment at conferences as well.

In addition to this work on Milagro, Dr. Pretz has contributed to LANL's efforts on the HAWC project, the next generation detector based on the Milagro observatory. He has performed tests on the HAWC test tank at the Milagro site. He has assisted with construction and first testing of a PMT test setup at LANL. This setup will eventually be used to test all of the Milagro PMTs for HAWC. He has worked with the HAWC software group in the design of the HAWC software, prototyping the HAWC software framework, and is engaged in development of the HAWC Data Acquisition system.

## Future Work

Cosmic rays are a population of energetic nuclei that continuously strike the atmosphere. Cosmic rays are observed by the secondary air shower that results when cosmic rays interact in the atmosphere. The fundamental question -- where do cosmic rays come from -- has not been conclusively answered. The energy of individual cosmic rays is enormous, with > 1 Joule in a single particle. The sources of these particles must be among the most extreme environments in the universe allowing us to probe physics beyond the standard model in environments that can never be reproduced on Earth.

A source of cosmic rays should be a source of neutrinos and gamma rays due to cosmic-ray interactions in the source. Because gamma rays and neutrinos are neutral they will reach us through the galactic magnetic field undeflected and still point back to their source. A gamma-ray signal, by itself, is ambiguous as to whether cosmic rays or electrons are being accelerated, and a neutrino signal is difficult to see over the atmospheric neutrino background.

The Milagro gamma-ray detector at LANL has been run in coincidence with the partially completed IceCube neutrino detector since 2006. The detectors are both wide field observatories, and resolve much of the same area of the sky. Furthermore, they have comparable energy response and angular resolution. We will use the two detectors together to probe transient sources for gamma-ray and neutrino signals. Having performed the first analysis of the 2006 IceCube data, we are uniquely suited to carry out this work at LANL working with the Milagro team. Additionally, we will use our experience from working with Milagro to optimize the design of the upcoming High Altitude Water Cherenkov (HAWC) detector for the detection of transient gamma-ray sources.

## Conclusion

Cosmic rays are energetic particles that account for a large fraction of the energy in our galaxy. The sources of cosmic rays must be powerful particle accelerators. Man-made accelerators have yet to achieve the energetics of nature. Nature's accelerators are likely to be the most extreme objects in the Universe, such as black holes ejecting jets of plasma at nearly the speed of light or the densest stars rotating with periods of a fraction of a second. Understanding these extreme sources pushes our understanding of basic physics and cosmology beyond the standard model.

## Publications

Abdo, A.. Discovery of localized regions of excess 10-TeV cosmic rays. To appear in *Physical Review Letters.*

# Anti-Neutrino Oscillation and Cross Section Measurements at MiniBooNE

*Geoffrey Blount Mills*

20070701PRD3

## Introduction

Neutrinos, the most enigmatic of the fundamental particles found in nature, remain one of the last gaps in our understanding of particle masses. This project is at the forefront of neutrino oscillation physics, which has provided the only window available to experimentally explore neutrino mass. It provides a setting to explore the fundamental properties of neutrinos and their propagation over a distance of 550 meters and with an energy range of 100-2000 MeV, which corresponds to oscillations of neutrinos with a mass-squared difference of ~0.5 eV^2.

While it it generally thought that the neutrino oscillations observed in solar and atmospheric neutrinos are due primarily to active neutrino oscillations, the sterile components of neutrinos may play an important role at mass-squared differences in the range of ~0.5 $eV^2$ (sterile neutrinos are a hypothetical neutrino that do not interact via any of the fundamental interactions of the Standard Model except gravity). Furthermore, the long baseline experiments currently under construction will benefit greatly from knowledge of neutrino and anti-neutrino cross sections in the 100-2000 MeV neutrino energy range.

The discovery of evidence for light sterile neutrinos would have a profound impact on the standard model of particles, the standard model of cosmology, and models of super nova explosions. Indeed, the explanation of our very existence, i.e. why the universe is devoid of anti-matter may lie in the understanding of CP violation in neutrino oscillations.

This project supported special analyses of neutrino experimental data that were not part of the mainline Office of Science experiments.

## Benefit to National Security Missions

This project directly supports the DOE mission in the Office of Science by measuring antineutrino cross sections and searching for anti-neutrino oscillations and physics beyond the Standard Model. Furthermore, the neutrino detector technologies also support the DOE missions in threat reduction.

## Progress

The project has again shown substantial progress over the past year. This last year saw the conclusion of the neutrino-mode and antineutrino-mode operations of the SciBooNE experiment, a collaboration of a number of Japanese institutions and US institutions. SciBooNE operated in the Booster Neutrino Beam (BNB) at Fermi National Laboratory. It was located nearer to the primary proton target than MiniBooNE at a distance of roughly 150 meters and thus enjoys a much larger flux of neutrinos. SciBooNE is much smaller than MiniBooNE and offers a more highly segmented sensitive detector volume that allows for the separation of nuclear fragments and outgoing leptons in the final state of the neutrino reaction.

The analysis of the SciBooNE neutrino and antineutrino data has yielded critical information about the reactions of neutrinos and antineutrinos on carbon nuclei and free protons as reported in the first SciBooNE paper [1] on coherent pion production in charged current neutrino interactions. The paper addresses to what extent the nucleons inside a nucleus, in this case carbon, behave coherently or behave individually (resonantly) when a charged pion is produced in the reaction. The somewhat unexpected result is that they appear to behave primarily as individuals in a resonant fashion without significant contribution from coherent amplitudes. Figure 1 demonstrates this effect by plotting the distribution in the square of the four-momentum transferred to the nucleus by the neutrino, $Q^2$. Charged current (CC) reactions which are coherent show a smaller $Q^2$ than do incoherent processes because the nucleus recoils as a The results of this work have been presented at invited talks at numerous conferences [4,5].

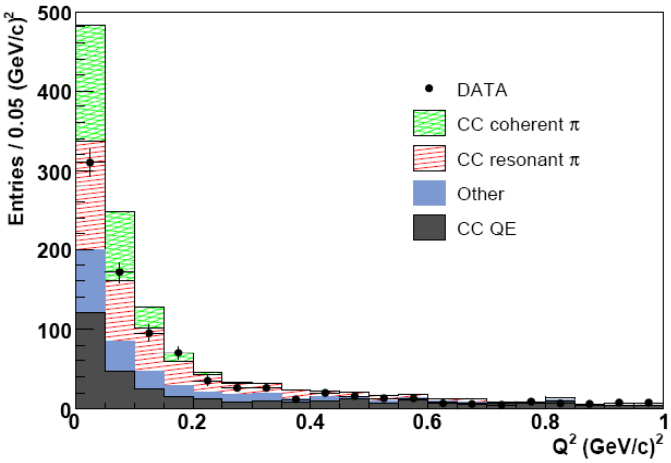


*Figure 1. The above graph from reference 1 shows the distribution of SciBooNE events that contain solely a charged muon and a charged pion in the final state. The quantity Q2 is the four-momentum squared transferred to the nucleus by the neutrino. Q2 is a convenient variable since it differentiates between coherent and resonant pion production. The back circles are the measured SciBooNE data, the shaded regions are the predictions of the MiniBooNE simulation where CC refers to "charged current" and QE refers to "quasi elastic." The graph demonstrates the SciBooNE conclusion that there is very little coherent amplitude present in the data.*

## Future Work

The remainder of this project will be spent on further analysis of the MiniBooNE and SciBooNE data in order to further determine neutrino and antineutrino cross sections. SciBooNE will be able to reconstruct the recoiling proton in quasi elastic neutrino reactions that will provide vital information for neutrino-nucleus reaction models. Those models will have far reaching implications for future neutrino oscillation experiments.

## Conclusion

The science proposed in this project will measure fundamental properties of neutrino interactions. Neutrinos are unique particles in nature and may one day explain the origins of the universe we live in. In addition, they may one day provide capabilities in technologies we have yet to imagine, such as interstellar space travel or future energy sources based on their unique interaction characteristics. For example, neutrinos may travel in spacetime dimensions outside the ones we are accustomed to.

## References

1. Hiraideetal., K., and T. SciBooNE-Collaboration. Search for Charged Current Coherent Pion Production on Carbon in a Few-GeV Neutrino Beam. To appear in *arXiv:0811.0369, [hep-ex] (submitted to Physical Review D).*

2. Aguilar-Arevaloetal., A. A., and T. MiniBooNE-Collaboration. Measurement of Muon Neutrino Quasielastic Scattering on Carbon . 2008. *Physical Review Letters.* **100** (1): 032301.

3. Zeller, G. P.. Low Energy Neutrino Cross Sections from K2K, MiniBooNE, SciBooNE, and MINERvA . (Christ Church, New Zealand, June, 2008).

4. Zeller, G. P.. . 2007. In *proceedings of the 5th International Workshop on Neutrino-Nucleus Interactions in the Few-GeV Region .* Edited by Zeller, G. P., J. G. Morfin, and F. Cavanna. Vol. 1, 1 Edition, p. 1. Washington, D.C: AIP.

## Publications

Hiraideetal, K., and T. SciBooNE-Collaboration. Search for Charged Current Coherent Pion Production on Carbon in a Few-GeV Neutrino Beam. To appear in *Physical Review D.*

MiniBooNE-collaboration, T.. Measurement of Muon Neutrino Quasi-Elastic Scattering on Carbon. To appear in *Physical Review Letters.*

# Phase Transitions in Quantum Systems and Quantum Information

*Wojciech Hubert Zurek*

20070705PRD3

## Introduction

Even small and smooth changes in the parameters of a physical system can, under some circumstances, lead to dramatic changes in its properties. Such critical phenomena are known as classical phase transitions when triggered by the change of the temperature, e.g., the melting of ice and the demagnetization of a magnet by heating to a high temperature. Quantum phase transitions [1], on the other hand, happen at absolute zero and are triggered by a change in parameters of the system's Hamiltonian. A famous example is the superfluid-insulator phase transition of ultra-cold atoms in optical lattices – laser induced egg carton-like traps [2]. It is important to characterize various phase transitions. For example, the Landau theory deals with the second order classical phase transitions by making use of the local order parameter and symmetry breaking [3]. We are developing novel approaches to quantum phase transitions by borrowing physical notions from quantum information science. Two concepts in particular, fidelity [4] and decoherence, can be utilized to characterize quantum critical phenomena with "intrinsic" and "external" dynamics, respectively. This research should lead to developing fidelity as a useful tool for other relevant instances, including even the classical phase transitions (e.g., normal-superfluid transition). It will be also applicable to the study of quantum computing [5], where fidelity should be a good way to estimate probability of errors. Moreover, the analogy between so-called adiabatic quantum computing and quantum phase transitions is very close, and my research results will be directly relevant for evaluating various implementations and strategies. Another research direction is the study of effects of the interaction between a quantum critical system and its external surrounding systems [6]. We are developing a theory for detection of quantum phase transitions in terms of quantum decoherence (the loss of fragile coherence properties) of its external system.

## Benefit to National Security Missions

This project will support the missions of the Office of Science by enhancing our understanding of materials and our comprehension of complex natural systems. It will also support the Intelligence mission of the Laboratory by bringing the encryption-breaking power of quantum computing one step closer to reality.

## Progress

### Quantum fidelity approach to thermal phase transitions

Quantum fidelity is a tool borrowed from quantum information science to characterize quantum phase transition, which occurs at absolute zero. Previously we and our collaborators generalized this essential quantum mechanical notion to finite-temperature thermal state [7]. In the last year, we studied the thermal phase transition with generalized fidelity, and established the connection between the generalized fidelity and traditional criteria, such as susceptibility and specific heat. This exploration enables us to understand the mechanism of generalized fidelity to thermal phase transition and its limitation. Moreover, the deviation of fidelity from traditional criteria at low temperature, especially at zero temperature, highlights the quantum to classical transition of the system. We use this method to predict the thermal phase transition in Lipkin-Meshkov-Glick model -- a well studied model in nuclear physics (Figure 1).

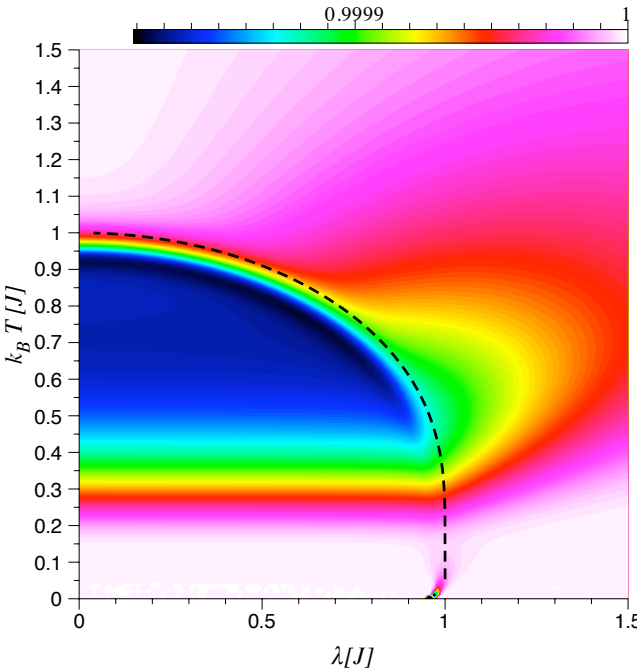


*Figure 1. We develop a new technique to detect the phase boundary of quantum matter, in analogy to the pressure/temperature line along which ice melts into water. This technique is much simpler than any previous methods, and do not need any prior knowledge about the matter. This figure is an illustration of our method. The black dashed line is the phase boundary according to previous, tedious calculation, while the (black) minimum of the colored contours plot represents the boundary detected by our new technique. The two results are similar, and we understand the difference, which arises from the small sample that we model.*

**Finite-temperature footprint of quantum criticality**

Genuine quantum phase transitions occur at absolute zero. However, these transitions also influence to the properties of the system at finite temperature. To experimentally verify the properties of a quantum phase transition system, we must study its footprint at finite temperature. Motivated by the quantum-classical mapping in statistical mechanics [1], we find the finite-temperature scaling behavior of magnetic susceptibility of 1D quantum Ising chain. We also reveal the relation between the magnetic susceptibility and geometric phase [8], which has been extensively studied in quantum phase transition system. Moreover, our study indicates the thermodynamic observable – magnetic susceptibility – can be used to witness the macroscopic entanglement in many body systems.

**Decoherence induced by the quench dynamics across a quantum critical point**

Decoherence is used to explain the quantum-classical transition. It is believed that the occurrence of decoherence in a quantum system due to the coupling of the central system and its ubiquitous macroscopic environment. In this study, we find a new mechanism –the quantum criticality—which also enhances the decoherence process. This study brings new insights into the understanding of quantum dynamics in complex systems.

**Non-equilibrium statistical mechanics at nanoscale and quantum thermodynamics**

There are tremendous advances in non-equilibrium statistical mechanics both theoretically and experimentally during the last ten years [9, 10, 11]. These studies focus on the fluctuations of thermodynamic observables. We study the work fluctuations of a simple quantum two-level system by the method that we developed in quantum thermodynamics. We rigorously prove from the microscopic point of view the convergence of the amount of work in different realizations in an isothermal process. We point out that this new mechanism is different from usual case – thermodynamic limit. Besides, we verify the validity of a formulation of the second law – minimal work principle. These results let us understand the fluctuations in work output of a nanoscale motor (Figure 2).

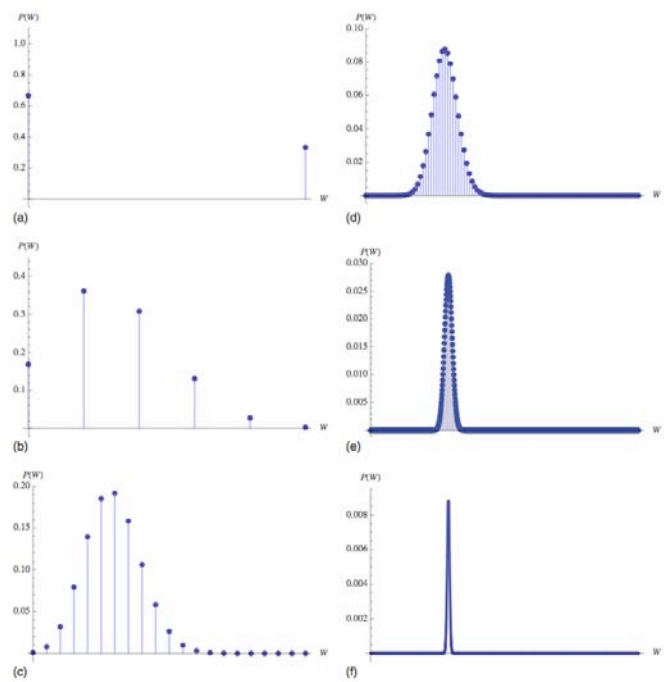


*Figure 2. The distribution of work done by a microscopic system, for operation times that range from short (a) to long (f). For a macroscopic system, the amount of work done by a motor is not controlled by quantum effects, which is why automobiles operate smoothly. However, for a microscopic system, quantum fluctuations will be appreciable. That means motors of nanometer size will not be able to work smoothly as our car. Instead, they will jump up and down during the operation. Our study showsd that even for a motor of nanometer size, as long as it operates slowly, can work smoothly (narrow distribution).*

**Quantum thermodynamic cycle and quantum heat engines**

Heat engines usually use a macroscopic classical fluid, such as a classical ideal gas as the working substance, and the underlying theory – thermodynamics – usually deals with system of macroscopic size. We consider instead a heat engine using a single-particle quantum system as the working substance, and study what remains of thermodynamics in the extreme limit of small systems having a few degrees of freedom. We make a quantum mechanical extension of thermodynamics to the single-particle system and reproduce the result of thermodynamics for macroscopic system. Meanwhile we establish the one-to-one mapping between a single particle in a 1D box and classical ideal gas, and a single particle in a 1D harmonic potential with single mode photon gas in a cavity [12]. Our study lays the foundation for future single-molecule machines (Figure 3).

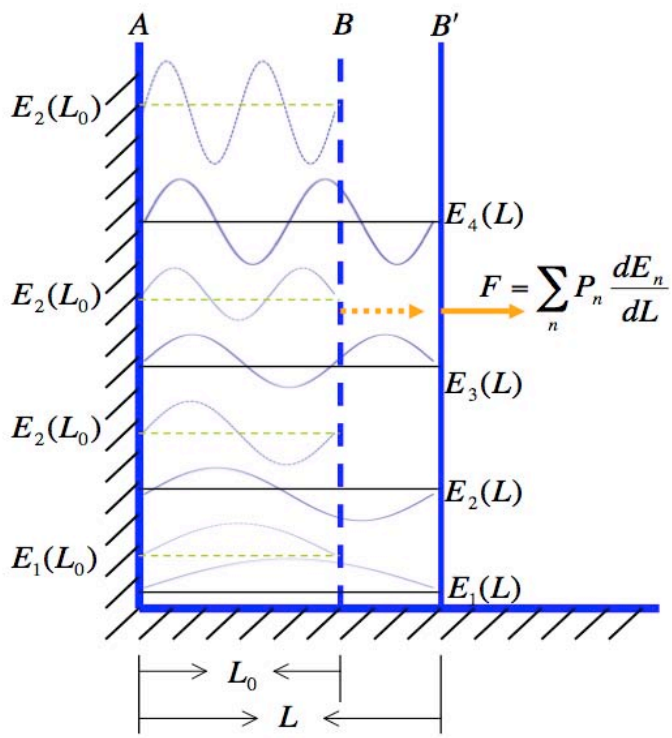


*Figure 3. The piston in a motor is usually driven by the pressure of high temperature gas inside the cylinder. Here we designed a new concept cylinder. The piston is driven not by the collision of gas molecules. Instead, the piston is driven by the pressure of radiation or matter waves. When the radiation is very strong, the pressure can be powerful enough to drive a piston.*

**Quantum Darwinism for mixed state environment**

Quantum Darwinism, is a theory developed from quantum decoherence theory [13]. It aims to provide a thorough understanding of the emergence of macroscopic classical world from the microscopic world governed by the counter-intuitive quantum mechanics [14]. Previous studies of quantum Darwinism focuses on pure environment state, and static systems. In our recent work, we consider the dynamics of quantum Darwinism. These studies demonstrate how the information about the pointer observable of the system is abundantly stored in the environment. We also consider the general case of the environment -- mixed-state environment, and study how the mixedness of the environment influences the storage of information in the environment.

## Future Work

We will develop novel approaches to quantum phase transitions using physical notions from quantum information science. Two concepts in particular - fidelity and decoherence - will be utilized to characterize quantum critical phenomena with intrinsic and external dynamics, respectively.

A second direction is to study the quench dynamics of a quantum phase transition system and its relation to the experimental feasibility of the adiabatic quantum computation. In an adiabatic quantum computation experiment, the Hamiltonian is required to change so slowly that quantum adiabatic condition can be satisfied. However, it is usually very difficult to estimate whether a quench process is reliably adiabatic. We will consider a quench forward and then backward scheme. Through comparison with its initial state, we can tell whether the forward process is a reliable for adiabatic quantum computation. In addition, we can experimentally evaluate the minimum energy gap through this way.

## Conclusion

The research will result in the development of novel methods for understanding quantum phase transitions, using powerful concepts from the field of quantum information. If successful it will add significantly to our understanding of several important classes of materials. In addition, the research will result in a greater understanding of quantum computing, especially the thermodynamic aspect of quantum computation, such as energy dissipation. The taxpayer should care because the realization of the end technological goals would revolutionize computing and materials science.

## References


1. Sachdev, S.. Quantum Phase Transition. 1999.
2. Greiner, M., O. Mandel, T. Esslinger, T. W. Hansch, and I. Bloch. Quantum phase transition from a superfluid to a Mott-insulator in a gas of ultracold atoms. 2002. *Nature.* **415**: 39.
3. Landau, L. D., and E. M. Lifshitz. Statistical Physics. 1980.
4. Zanardi, P., and N. Paunkovi. Ground state overlap and quantum phase transitions. 2006. *Physical Review E.* **74**: 031123.
5. Nielsen, M. A., and I. L. Chuang. Quantum Computation and Quantum Information. 2000.
6. Quan, H. T., Z. Song, X. F. Liu, P. Zanardi, and C. P. Sun. Decay of Loschmidt echo enhanced by quantum criticality. 2006. *Physical Review Letter.* **96**: 140604.
7. Zanardi, P., H. T. Quan, X. G. Wang, and C. P. Sun. Mixed-state fidelity and quantum criticality at finite temperature. 2007. *Physical Review A.* **75**: 032109.
8. Zhu, S. L.. Geometric phases and quantum phase transitions. 2008. *International Journal of Modern Physics B.* **22**: 561.
9. Jarzynski, C.. Nonequilibrium equality for free energy differences. 1997. *Physical Review Letter.* **78**: 2690.
10. Crooks, G. E.. Nonequilibrium measurements of free energy differences for microscopically reversible Markovian systems. 1998. *Journal of Statistical Physics.* **90**: 1481.
11. Bustamante, C., J. Liphardt, and F. Ritort. The nonequilibrium thermodynamics of small systems. 2005. *Physics Today.* **54** (7): 43.
12. Scully, M. O., M. S. Zubairy, G. S. Agarwal, and H. Walther. Extracting Work from a Single Heat Bath via Vanishing Quantum Coherence. 2003. *Science.* **299**: 862.
13. Zurek, W. H.. Decoherence and the Transition from the Quantum to the Classical. 1991. *Physics Today.* **44** (10): 36.
14. Zurek, W. H.. Decoherence, einselection and the quantum origins of the classical. 2003. *Review of Modern Physics.* **75**: 715.


## Publications

Quan, H. T.. Finite-temperature scaling of magnetic susceptibility in XY spin chain. To appear in *Physical Review B.*

Quan, H. T.. Quantum thermodynamic cycles and quantum heat engines (II). *Physical Review E.*

Quan, H. T.. Decoherence induced by the quench dynamics across a quantum critical point. *Physical Review A.*

Quan, H. T., S. Yang, and C. P. Sun. Microscopic work distribution of small system in quantum isothermal process. 2008. *Physical Review E.* **78**: 021116.

Quan, H. T., and F. M. Cucchietti. quantum fidelity and thermal phase transition. To appear in *Physical Review E.*

# Detecting Dark Matter with Cryogenic Liquids

*Andrew Hime*

20070751PRD4

## Introduction

Detecting dark matter in the laboratory has rapidly ascended to become a top priority in the fields intersecting the boundaries of nuclear and particle physics, astrophysics, and cosmology. The proposed CLEAN (Cryogenic Low Energy Astrophysics with Noble liquids) experiment will directly search for dark matter particles in our galactic halo by looking at scintillation light in a cryogenic liquid target. Both liquid argon and liquid neon targets are under study due to their low intrinsic radioactivity, high scintillation yield, and unique ability to distinguish the signal of interest from unbiquitous electron and gamma ray background. This project focuses upon the development of a full Monte Carlo package to simulate the detector response and to optimize its design. This simulation package will be critical for the design and construction of prototype detectors at the 100 to 1000 kg scale and ultimately afford the design of a massive (10 to 100 ton) detector capable of the direct detection of dark matter and low-energy neutrinos from the sun.

## Benefit to National Security Missions

This project will support the DOE Office of Science missions in basic research to elucidate fundamental properties of neutrinos using the sun as a unique astrophysical source and in novel detectors for low-energy solar neutrinos and cosmological dark matter in the universe. We also build capabilities to detect nuclear threats.

## Progress

A flexible and detailed software simulation code is of critical need in order to optimize the design of the CLEAN detector. This project allows LANL to lead this effort in developing and coordinating a full simulation and analysis package for CLEAN that encompasses the salient microphysics of scintillation light production, propagation, and detection. The simulation, with its internal microphysics calibrated by experimental data, will then be used in the design of CLEAN detectors at various target mass scales relevant to the direct detection of WIMP dark matter and low energy solar neutrinos.

A GEANT4-based simulation code has been written and benchmarked against experimental data in hand from existing prototype detectors and additional optical measurements that have been made in the Laboratory. This code has proven critical in understanding the optical properties of the CLEAN detector and our ability to reconstruct events in position and in energy. The results of these simulations have allowed us to optimize the design of the optical cassettes that are a novel and central component of the Mini-CLEAN detector.

Significant progress has been made on position and energy reconstruction algorithms that are critical for separating signals of interest from radioactive backgrounds in the CLEAN detector concept. Detector optical effects, such as Rayleigh scattering of ultraviolet light and absorption of ultraviolet light from detector surfaces have been successfully implemented into the code. Preliminary versions of this code indicate a 10 to 20% improvement in rejection of backgrounds from the edge of the detector. A variation is in progress, which uses more of the waveform information from the photomultiplier tubes to improve background rejection by a factor of five or more.

Increasing software quality has been a second focus. Automated testing and verification of the simulation and analysis software, allowing us to identify problems that appear as new code is added and old code is changed, has been successfully implemented. This has proven to be valuable for ensuring the physics that we simulate does not change due to subtle bugs.

The software and analysis package under development through this project is now the accepted platform for the institution-wide CLEAN collaboration. Stan Seibert has also taken the lead role coordinating the movement of software updates between the CLEAN and the SNO+ collaborations, who have adopted the CLEAN simulation package as well. Although in the early stages, this cooperation between the two experiments has already

resulted in the exchange of useful features developed by both groups.

As members of the SNO collaboration, we are also engaged in a reanalysis of data taken during the experiment's first two phases of operations. This analysis effort is being led by Stan Seibert at LANL, and promises to maximize the sensitivity of the SNO data with respect to our previous discovery of neutrino oscillations in the Sun and the general resolution of the solar neutrino problem. This effort is near completion and we expect to publish the results early in the new calendar year.

## Future Work

In the next year, effort will be split between software development and two R&D projects now being constructed. The first R&D test setup will allow us to measure the wavelength-shifting properties of TPB, an organic compound that converts ultraviolet light to visible light. TPB is a critical component of the CLEAN design, and we need to understand its conversion efficiency as a function of UV wavelength in greater detail. Toward this end, we have obtained a UV deuterium lamp source and will be using it to illuminate acrylic disks coated with TPB and measuring the emitted visible light. This work will be generally useful to other noble liquid scintillator experiments, so we will be submitting these results for publication in 2009.
The second R&D project is a prototype for testing the PMT and acrylic waveguide cassette design that will be used in the Mini-CLEAN assembly. This liquid argon system is currently being designed with help from Andrew Mastbaum, an undergraduate student who will be leaving in December. Stan Seibert will be taking over management of the system, and use it to test the optics of the cassette with liquid argon scintillation light. Results from both the UV lamp and the cassette system will be fed back into the material properties used by the simulation to improve the accuracy of our model. This will allow us to better test and improve our reconstruction algorithms in preparation for data from the Mini-CLEAN experiment and in optimizing the design of the full-scale CLEAN experiment.

## Conclusion

The design of a CLEAN (Cryogenic Low Energy Astrophysics with Noble liquids) detector for dark matter and solar neutrinos requires a flexible and detailed simulation software package to ensure that the scintillation light detection and event reconstruction afforded by the design can meet its scientific goals. Significant progress has been made to establish a realistic simulation package that incorporates the microphysics of scintillation light production, propagation, and detection using targets of liquid argon and liquid neon. Development of the simulation will continue with emphasis turning to its calibration against data obtained from a series of experiments conducted at the Laboratory during the course of this project.

# The Dynamics of Dark Energy

*Katrin Heitmann*

20070775PRD4

## Introduction

Dark energy is one of the central topics of research in cosmology today. Type Ia supernovae provided the first evidence for its existence: In the late nineties it was found that distant supernovae appear fainter than expected, implying that the expansion of the universe is accelerating. In a matter-dominated universe, objects attempt to gravitate towards each other, and the expansion rate decreases with time. Thus the observations imply that some sort of energy other than matter is dominant at present -- this is the `dark energy.'

The project covers several aspects of the theory and observations of dark energy. Given the massive amount of data expected in the near future, a major part of this work will be to formulate a consistent statistical approach towards the reconstruction of cosmological parameters from data. It has been shown that different cosmological observations are sensitive to different combinations of the parameters, and have different biases and assumptions built into the observations. Hence it is necessary to find an optimal and unbiased way of extracting information from all the available data.

Only now is reliable data on the total energy density of the universe (obtained from the ages of clusters of galaxies) becoming available. Combined with probes of the matter density, this can directly constrain the dark energy density -- potentially more powerfully than supernovae, which measure only the integration of the energy density. Probes of the mass distribution such as weak lensing and baryon acoustic oscillations provide another effective data dimension. Incorporating this further information will lead to much stronger constraints on the nature of dark energy than is possible at present.

## Benefit to National Security Missions

The project targets two of the top priorities of the DOE mission: understanding the nature of dark energy and high-performance computing. In addition, the project is relevant for the threat reduction arena in providing new techniques to extract information from diverse and very large data sets.

## Progress

Together with researchers from UC Santa Cruz, we have begun to investigate two different strategies for constraining the equation of state of dark energy w from supernova data. One strategy is based on a parametric fit to the data from which the variation of the dark energy parameter w with time can be derived. The other strategy is non-parametric and is based on a neural network approach. Both methods have been tested on simulated data with special emphasis on the robustness of the methods with respect to measurement errors. The major conclusion that has been reached is that supernova data are too noisy for this approach. In order to obtain constraints on the dark energy equation of state, the second derivative needs to be evaluated. This turns out to be a very unstable process with the noisy data that is available. Therefore a completely different strategy has been followed recently.

The second strategy is based on the idea of modeling the equation of state itself with different assumptions:

- w being constant
- w having a weak time dependence which can be expressed via a Taylor expansion of w with respect to the cosmic acceleration parameter a
- modeling w via a Gaussian process model, therefore parameter free.

The next step is then to include the data in this process and evaluating the probability that w is in fact constant or time dependent. A set of simulated data has been produced which is based on a model with w=constant but not necessarily equal tos -1 (which is the value for the standard cosmological constant). A second simulated data set for a dark energy quintessence model has been generated. These models lead to a small time dependence in w. The analysis framework has been tested

with the w=-1 models and has been proven to work. The next step is now to investigate how robust the predictions are and how they improve if 1) the number of data points is increased, and 1) the error bars of those data points are decreased. In addition, questions about systematic errors will be investigated.

The framework has been used to analyze currently available supernova data. The results point to several difficulties with the real data sets, which are under closer investigations right now. The first results of this work have been presented at the UCSC Departmental Poster and Research Day.

Another line of investigations has been started investigating the possibility of early dark energy. This project has been started with researchers from UC Irvine, a UCOP proposal has been submitted. The idea here is to find out if large scale structure probes of dark energy allow us to put constraints on a particular class of dark energy models. The first necessary steps for this project have been initiated: the growth function, which describes the growth of structure in the Universe has been implemented for early dark energy models and can now be used to run large scale structure simulations of this scenario.

## Future Work

This projects targets the dynamics of dark energy. In the last decade, the richness and quality of observational data has steadily improved, and so has the evidence for dark energy. Very little is known, however, about its physical nature -- it could be a new form of energy but could also arise from a modification of general relativity. With next-generation supernova surveys, as well as other complementary observations such as weak gravitational lensing and galaxy clustering, a large amount of data will become available in the near future. It is imperative to formulate powerful techniques to shed light on the enigma of dark energy using these datasets. The main goal of this project is to obtain methods for extracting the maximum information from the data currently available to us, and to develop new techniques for future datasets.

A major part of the project will be to formulate a consistent statistical approach towards the reconstruction of cosmological parameters from data. It has been shown that different cosmological observations are sensitive to different combinations of the parameters, and have different biases and assumptions built into the observations. Hence it is necessary to find an optimal and unbiased way of extracting information from all the available data. The growth of cosmological perturbations as probed by both weak-lensing and supernovae will be studied to pinpoint and explore the exciting possibility of non-standard gravitational behavior of the universe on large scales. Since the two datasets approach the reconstruction of the same quantity through different methods, this yields a strong cross-check on the systematics of both experiments. The study of modified gravity models involves developing correct linear and non-linear perturbation theories and applying those to the available data. This would result in strong constraints on non-standard models of dark energy.

## Conclusion

The project will lead to new insights into the nature of dark energy by combining different cosmological probes, namely supernova measurements, baryon acoustic oscillations, cosmic microwave background observations, and weak lensing. Only by combining these probes is it possible to distinguish dark energy from a modification of general relativity on very large scales. The project will lead to a new statistical framework which will incorporate these different probes as well as systematic measurement errors. Understanding the nature of dark energy is one of the most important tasks in physics today and this project will lead to an important contribution.

# Dynamics of Quantum First Order Phase Transitions

*Dima V Mozyrsky*

20080689PRD1

## Introduction

We investigate the kinetics (i.e. dynamics) of phase transitions in atomic mixtures at ultralow (a few nano-Kelvin) temperatures. Initially we are focusing on the phase separation transition, when the system of two species splits into two (or more) phases —for example, one of the atomic species is expelled from the mixture of two species. The transitions of this type are typically discontinuous (i.e. the so-called first order transitions) and, as a result, their dynamics is controlled by the process called nucleation, that is, spontaneous formation of microscopic nuclei of the new stable phase in the middle of the unstable (or metastable) old phase. For example, in case of a mixture containing two different types of atoms, tiny droplets of the phase containing only a single species of the atoms start to emerge. Similarly, small (i.e. microscopic) crystals of ice start to appear in the middle of supercooled water when it starts to freeze. While in the latter case the dynamics of the nuclei, i.e., the crystals of ice, is governed by the thermal (or classical) fluctuations, the dynamics of the cold atomic mixtures is controlled by the quantum fluctuations, - most of the thermal fluctuations are "frozen out" at nano-Kelvin temperatures. State-of-the-art cold atom traps provide an excellent opportunity to measure this phenomenon. We will also study the possibility to control such transitions by external radiation as well as additional atomic species. Apart from advancements in understanding, observation, and measurement of quantum phase separation in cold atoms, this investigation will, hopefully, shed some light onto unconventional mechanisms of high-temperature superconductivity, which, in certain cases, appear to be closely related to the transitions of this sort.

## Benefit to National Security Missions

The project will support the DOE mission by enhancing our understanding of fundamental properties of complex systems. These areas of research constitute two major grand challenges pursued by the Los Alamos National Laboratory. Quantum systems may lead to new means of sensing and computing for missions such as Threat Reduction.

## Progress

The postdoc has been developing calculation framework to evaluate observable quantities such as, for example, nucleation rate—the number of droplets of a single species emerging from the mixture per unit time. Our results indicate that there are two distinct regimes of nucleation realized at different densities:

1. At the lowest densities sufficient to trigger the phase separation (just above the phase separation line in the phase diagram) the droplets are well defined;

2. At large densities distinct droplets do not form—one of the species is gradually expelled from significant volume of the mixture.

We have found that the dynamics of the separation strongly depends on the degree of interaction within the system. Observable nucleation is predicted in strongly-interacting and confined mixtures. In addition, the nucleation rate is very sensitive to the mass ratio of atoms of the two species. This enforces stringent requirement on experimental design. Measurements on expansion of externally created droplets are recommended as a first and relatively easy step in experimental verifications of our results.

## Future Work

Further work will be focused at two directions:

1. We will investigate cold atom mixtures which more closely resemble novel high-temperature magnetic superconducting materials. Based on our understanding of quantum phase separation we believe that in certain regimes superconductivity in such mixtures may be based on unconventional odd-frequency mechanism, where correlations between particles are not instantaneous, but are "extended" in time. Research in this direction will contribute to laboratory and nation-wide effort in the field of high-temperature superconductors.

2. We will investigate the opportunity to control the

phase separation dynamics externally (in particular by laser fields and by atoms of other species). This direction of research should bring understanding of how to appropriately design cold atom mixtures to utilize their quantum properties in sensing applications.

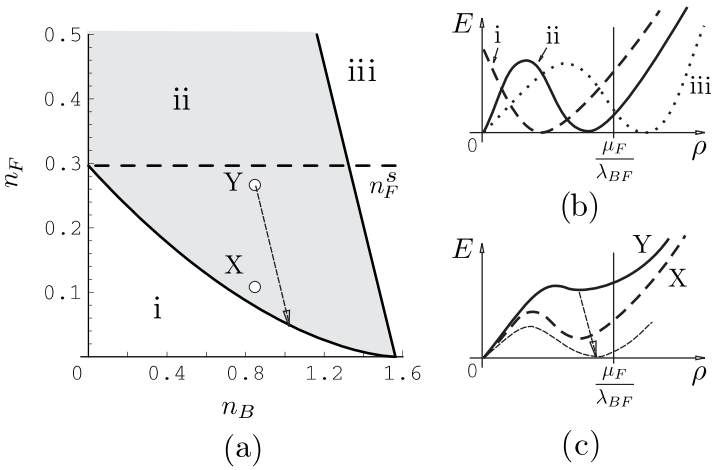


*Figure 1. The phase diagram of two-component cold atom mixture featuring quantum nucleation transition (density of each component is in natural units of the system). Three phases are possible: mixture, coexistence of mixture and pure component of one of the species (fermions), complete spatial separation of the two components. During the nucleation the remaining mixture drifts to the lower portion of the diagram (as shown by the arrow). All phases can be deduced from the equilibrium energy density of the system, as shown on right insets.*

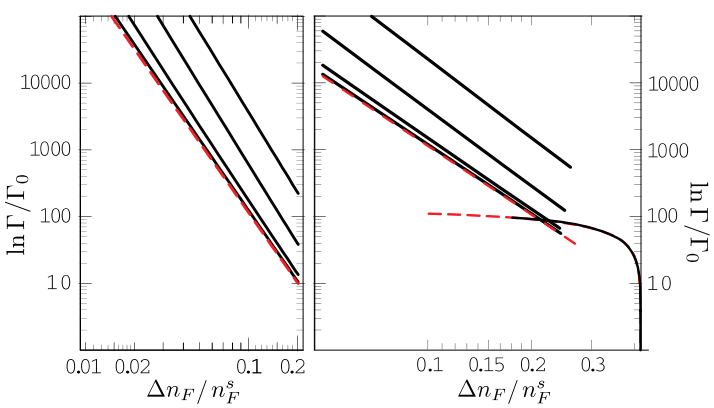


*Figure 2. Nucleation rate as a function of density variation for various mass ratios. Species with comparable masses produce much greater exponents resulting in extremely low (unobservable) nucleation rates. Highly-interacting system is shown on the left plot; on the right plot interaction is lower by the order of magnitude.*

## Conclusion

Understanding of the dynamics of quantum phase transitions may answer a number of fundamental questions. These questions range from evolution of the universe at its early stages to problems of cluster dynamics in magnetic systems. Contemporary cold atom systems, such as atoms or molecules confined in magnetic or optical traps, provide a perfect setup where such transitions can be observed and controlled with a desired accuracy. The work will set up the theoretical framework for the description of the dynamics of the first order phase transitions in these systems, guiding experimental effort in this direction. It will support National security mission by providing insight in fundamental properties of these systems to be used in sensing applications and beyond.

## Publications

Solenov, D., and D. Mozyrsky. Kinetics of the phase separation transition on cold-atom boson-fermion mixtures. 2008. *Physical Review Letters.* **100**: 150402.

Solenov, D., and D. Mozyrsky. Quantum nucleation and macroscopic quantum tunneling in cold-atom boson-fermion mixtures . 2008. *Physical Review A.* **78**: 053611.

# Nonequilibrium Quantum Phase Transitions

*Eli Ben-Naim*

20080723PRD2

## Introduction

To quote from Wikipedia, "a quantum phase transition (QPT) is a phase transition between different quantum phases (phases of matter at zero temperature) ... The transition describes an abrupt change in the ground state of a many-body system due to its quantum fluctuations." Quantum phase transitions are poorly understood. The goal of the present project is to develop a firm theoretical foundation for quantum phase transitions. As applications of nanotechnological devices controlled by quantum behavior multiply and diversify, this understanding is increasingly important.

Our project comprises two complementary subjects. The first is developing an understanding of quantum synchronization, in which different regions of a material spontaneously lock into the same quantum phase. Not only will this be of fundamental interest in itself, but, more importantly, it will have strong implications for decoherence, the mechanism which connects the quantum and classical worlds, and will help to bridge the gap between classical and quantum physics. Moreover, a fleshed-out theory of quantum synchronization may have direct practical applications such as interpreting and understanding the spectrum of molecules such as polyethylene, disordered superconductor films, and the quantum behavior observed in collective atomic recoil lasing.

The second subject is quantum drag, which will give us a new fundamental understanding of superfluidity. The phenomenon of superfluidity is one that we have known of for over half a century, yet it remains enigmatic in many respects. As the key to numerous applications, both current and future, such as atom lasers, precision clocks, and gyroscopes, it is of great importance that we move towards a more precise grasp of the physics underlying superfluidity.

## Benefit to National Security Missions

This work supports the energy security mission as it leads to better fundamental understanding of superconductors, materials that have zero resistance. These materials' potential energy applications include efficient electric power transmission and power storage devices, and sensors for threat reduction. This also supports LANL's competencies in quantum science and nanotechnology.

## Progress

We made significant progress in calculating the drag experienced by an impurity of any strength moving through a quasi 1-D Bose-Einstein condensate (BEC). Not only have we been the first to show that such a force exists in this geometry, but we have been able to calculate the force's dependence on velocity and impurity strength. We expect to publish our results in the next couple of months. We have also been in contact with ultracold atom experimentalist Peter Engels from the University of Washington who has expressed an interest in looking for this effect in his BEC experiments in quasi-1d geometries.

We have also made some progress in simulating this drag effect in dilute condensates using a quantum simulation technique that approximates the quantum fluctuations by Wigner noise. This approaches the problem from a new perspective. We expect to finish this project before the end of the year. Most importantly, experimentalists at LANL led by Malcolm Boshier have expressed interest in looking for this effect; our detailed numerical simulations will be invaluable for that endeavor. We remain in constant contact with the ultracold experimentalists at LANL discussing possible future experiments (such as vortex tunneling in condensates).

In a related project, we have formulated the problem of Casimir drag in superfluids in the context of a fermionic system: a drag force is caused by the scattering of quantum fluctuations within a flow of superfluid fermions. Here, the problem has many new physical effects and promises to be important for current fermionic experiments. We have also made progress in calculating the static Casimir effect in a BCS superfluid (the standard model of superconductors), the existence of which demonstrates the important implications of quantum fluctuations in these systems.

Experimentalists at Lancaster University working with $He_3$ have recently expressed interest in our recent work of the reformulation of the hydrodyamic boundary condition for superfluid flow. We remain in contact.

We have recently finished calculations of realizing supersolids, a controversial new form of matter, in dilute Bose-Einstein condensates using impurity fields. We have made some progress with framing the problem of quantizing the Kuramoto self-synchronization model and have also made some progress towards solving it. One of the more significant strides we have made is the successful embedding of this dissipative system within a Hamiltonian formalism, a crucial first step towards developing a general quantized model of synchronization.

Other projects involve the evolution of scientific ideas, in collaboration with Mark Herrera (undergraduate who I mentored at CNLS) and Natali Gulbahce (UCSF), and prediction of yeast growth rates from gene expression data (see submitted paper below).

## Future Work

Much ongoing experimental and theoretical effort is being directed at quantum phase transitions (QPTs), phase transitions induced by quantum rather than thermal fluctuations. QPTs are widely held to be the key to understanding enigmatic material phenomena such as high-Tc superconductivity, and the quantum critical point at which the QPT occurs is believed to determine the properties of the system at much higher temperatures and organize the phase diagram. To date the focus has been mainly on equilibrium QPTs; nonequilibrium QPTs – QPTs occurring in externally driven systems – remain largely unexplored. However, recent advances in the field of ultracold atomic gases make it possible to conduct systematic experimental study of nonequilibrium quantum dynamics, and the onus is now on theory to keep abreast.

This project addresses this need by constructing a coherent theoretical framework for nonequilibrium QPTs through a two-pronged approach, each centered on a different phenomena.

**Quantum Synchronization**

This project aims to develop a broadly applicable and informative model of nonequilibrium QPTs; this is possible because the quantum critical point is insensitive to microscopic detail and permits generalization. The starting point will be the classical Kuramoto model, which is the archetypal model of driven self-synchronizing systems (e.g. Josephson junction arrays and collective atomic recoil lasing) and one of few tractable models able to describe nonequilibrium classical phase transitions. Building upon recently generalized theoretical results, this project goal is to quantize the Kuramoto model to obtain an analogous model for quantum systems.

**Quantum Drag**

As a complementary bottom-up approach, this project will focus on the Casimir drag effect, where scattering quantum fluctuations induce a zero-temperature reversible conversion between normal fluid and superfluid – a process that can be thought of as a nonequilibrium QPT. This project will determine the characteristics of this QPT and its critical point through individual theoretical research.

## Conclusion

This project will construct a theoretical framework of nonequilibrium Quantum Phase Transitions. This research holds great potential for science and technology because such phase transitions involve significant quantum-level events that have a direct macroscopic effect and, as such, lend themselves to myriad applications in the rapidly expanding field of nanotechnology.

This project will also build an understanding of superfluidity that has the accuracy needed to turn the new dilute ultracold atom systems into applications such as atom lasers, precision clocks, and gyroscopes as well as prompt a review of our fundamental notions about areas of science related to superfluidity.

## Publications

Pomeau, Y., and D. C. Roberts. On the hydrodynamic boundary condition for superfluid flow. 2008. *Phys. Rev. B.* **77**: 144508.

Roberts, D. C.. Solving the Kuramoto model of a self-synchronizing, finite population of glob ally coupled oscillators. 2008. *Phys. Rev. E.* **77**: 03114.

Roberts, D. C., and R. Teodorescu. A linear path toward synchronization: Anomalous scaling in a new class of exactly solvable Kuramoto models. To appear in *European Physical Journal.*

Roberts, D. C., and R. Teodorescu. A linear path towards self-synchronization: Analysis of the fully locked transition of the Kuramoto model. 2008. In *First International Workshop on Nonlinear Dynamics and Synchronization INDS'08.* (Klagenfurt, Austria, 18-19 July, 2008). , p. 184. Germany: Shaker Verlag.

Ruderfer, D. M., D. C. Roberts, E. O. Perlstein, S. L. Schreiber, and L. Kruglyak. Predicting individual drug response in a panel of 104 genotyped and expression-profiled yeast strains. . *PLOS genetics.*

# Dissipation and Decoherence in Complex Many-Body Systems

*Wojciech Hubert Zurek*

20080728PRD2

## Introduction

We are examining several issues related to decoherence in many-body quantum systems. Quite generally, investigating quantum systems takes an exponential amount of resources. However, recent progress in simulation techniques has come from incorporating ideas from the quantum information community into computational algorithms. These techniques have enabled a large and interesting category of quantum systems to be investigated on a classical computer with resources that are only polynomial (rather than exponential) in the size of the system. We are applying these novel methods to simulate the time-dependent evolution of quantum systems. Two of our immediate goals are to study the dynamics of quantum phase transitions that are starting to be examined experimentally in, e.g., Bose-Einstein condensates (BEC's), and to understand the behavior of nonequilibrium nanoscale systems, e.g., electronic transport in molecular systems. In the process of investigating these systems, we expect to improve and generalize these novel methods to increase both their scope and the size of the systems (i.e., to 100-10,000 particles/atoms/molecules) they are able to tackle.

## Benefit to National Security Missions

This project will support the missions of the Office of Science by enhancing our understanding of materials and comprehension of complex natural systems. This work will also support the Homeland Security and Threat Reduction missions of the Laboratory by bringing the encryption breaking power of quantum computing one step closer to reality and by developing an understanding of biomolecular detection with nanoscale electronic sensors.

## Progress

Quantum Phase Transitions and Decoherence – We are examining how quantum systems behave when driven through a phase transition in the presence of decoherence. In particular, in the absence of decoherence, topological defects are generated – i.e., these are features of the quantum state that can not be changed with local perturbations to the state of the system and are therefore "protected" from local decoherence (a feature that is necessary in quantum computing). However, when driving the system, superpositions of defects are also created. We find that these superpositions are actually extraordinarily sensitive to local noise and will collapse essentially instantaneously from a coherent quantum state to an incoherent mixture of states with a single topological defect that remains protected. This finding sheds light on a fundamental issue in the dynamics of quantum phase transitions and also on what types of states might be useful for quantum computing. In addition, we are continuing the development of an efficient numerical technique for studying the dynamics of 100's of spin-1/2 qubits in order to understand how information spreads into an environment when a system decoheres. This work supports the LANL mission of gaining a fundamental understanding of materials and of complex natural systems.

Nanoscale electronic sensors – We have been investigating the behavior of nonequilibrium systems at the nanoscale. In particular, we have examined two issues: the effect of noise on the ability to detect biomolecules with electronic sensors and how ionic transport occurs through nanopores. The former is in particular regard to a proposal for rapid DNA sequencing using transverse electronic transport measurements and nanopores. Previously, we have shown that the electronic current allows for the efficient detection of a DNA base in a sequence in the presence of structural fluctuations and water, but in the absence of other sources of noise such as ionic fluctuations. As a first step to incorporate these other sources of noise, we have investigated the effect of strong white noise. We found that the efficient distinguishability of the bases is not influenced by white noise unless it is unrealistically strong, thus reaffirming that electronic transport might serve as a process for rapid DNA sequencing. Also having to do with nanopores, we have investigated how ions move from bulk into a nanopore to create an ionic current. This is process that occurs in natural (biological ion channels) as well as artificial systems (synthetic nanopores, e.g.,

made for sequencing and molecular detection). We have proposed a particular functional form of the energetic barrier for ionic transport based ON molecular dynamics simulations. This form of the energetic barrier predicts, for instance, that there should be a precipitous drop in ionic current when the radius of the nanopore is shrunk below the radius of the first hydration layer of the ions. Further, we propose an experiment to test our proposal that will help procure an understanding of the operation of nanopores and, in particular, of biological ion channels. This research will help the development of nanopore-based electronic sensors that will create new possibilities for ubiquitous sensors, and thus this work addresses the LANL mission of Threat Reduction. As well, such sensors open up new avenues for investigation into the complex interface between solids, liquids, and biomolecules, and increase our understanding of how materials behave at the nanoscale. The work has resulted in two articles in preparation.

Simulation techniques for decohering and dissipating quantum systems – An ongoing project of ours is the development efficient simulation techniques for "open" quantum systems, e.g., nanoscale systems interacting with external probes and their environment. This work recently resulted in an article "Finite representations of continuum environments," which appeared in the Journal of Chemical Physics in September. In this work, we examined how different portions of the environment influence the dynamics of a system and used this knowledge to create a novel representation of the environment for numerical simulations. The latter significantly reduces the computational cost necessary to accurately simulate the dynamics of quantum systems in contact with their environment. Over the past few months, we have made further progress in understanding how optimal the construction above is and also how to extend it to truly many-body quantum systems. The influence of this work is wide-ranging: it increases our ability to simulate quantum systems in realistic situations and thus greatly increases our ability to make science-based predictions on issues ranging from high-temperature superconductivity (how the environment impacts the transition temperature, for instance) to DNA sequencing with nanoscale electrodes (see above). This work thus supports the strategic thrust of science-based prediction, as well as provides a computational basis for further investigation into threat reduction, complex systems, and materials.

## Future Work

For our future research we will investigate a several issues revolving around dissipation and decoherence (D&D) in complex physical systems. Building on our past research on the efficient representation of partially entangled states, we will develop an innovative computational method that can simulate the dynamical behavior of thousands of atoms or particles as it interacts with the outside world. Using this method along with analytical techniques, we will investigate several distinct but interrelated issues involving D&D in complex many-body systems. For all these issues, our current understanding is hampered by the lack of accurate methods to study D&D. In particular, we will:

- calculate physical characteristics of dissipative materials relevant to superconductivity and evaluate the possibility of engineering a dissipative transition to create a room-temperature superconductor;
- simulate the precise behavior of decoherence in (solid-state) architectures for quantum computing and delineate approaches for suppressing and correcting for decoherence; and
- simulate electronic transport across molecules in the presence of strong D&D (including "colored" noise) in order to assess the effect of the aqueous environment on practical application of nanoscale electronic sensors, and more generally to study open scientific issues and challenges at the interface between solids, liquids, and biomolecules.

## Conclusion

This research has increased our understanding of decohering and nonequilibrium systems, and more generally of complex systems and materials at the nanoscale. Further, the work has resulted in a greater knowledge of systems useful for quantum computing and also in the setting of the theoretical basis nanoscale, biological/single-molecule sensors. The future work will result in the development of novel simulation techniques for driven, nonequilibrium, and dissipative quantum and nanoscale systems. The realization of the end technological goals could revolutionize computing and medical treatments, giving us increased security and health.

# Strongly Coupled Fermion Systems: From Atomic Gases to Dark Matter

*Sanjay Reddy*

20080731PRD2

## Introduction

The underlying scientific issue that our research addresses is to better understand the nature of matter. Although the Standard Model of particle physics can, in principle, predict the properties of all matter on earth, in practice, even approximately computing the properties of a proton comprising only three quarks is a Herculean computational challenge. Our innovative approach is to combine computer simulations (Monte-Carlo), experiments, and analytic techniques to understand systems of many fermions. Universality in the underlying theory allows these results to be applied to many systems, from cold-atoms and superconductors, to nuclear matter, stellar matter, and possibly even the elusive dark-matter.

## Benefit to National Security Missions

Our research on strongly interacting Fermi systems ties in well with Office of Science missions relating to nuclear physics, astrophysics and condensed matter physics. The results of this work will enhance our ability to model superfluid and superconducting matter in both the terrestrial and astrophysical context.

## Progress

The project began August 2008 when the postdoctoral candidate M. Forbes arrived. He is currently working on the ground state of system of heavy Fermions in a background of light Fermions.

## Future Work

The main goal is to combine experiment, numerical, and analytic results to develop a density functional theory (DFT) that quantitatively describes two-component cold-atom gases. Once this DFT is verified with cold-atom systems, it can be applied to other systems such as nuclear matter and quark matter.

A subset of the following tasks will establish this theory: 1) Validate that the DFT can describe finite systems using Monte-Carlo (MC) simulations. 2) Investigate the importance of gradient corrections to the DFT using MC simulations of deformed traps. 3) Apply the DFT to calculate properties of inhomogeneous systems including 4) Crystalline LOFF states, 5) Surface tensions of phase boundaries, and 6) other finite size effects. 7) Extend the model to capture the effects of temperature on the gap and pseudo-gap. 8) Apply these models to nuclear and astrophysical systems.

The second goal is to confirm or rule out our proposal that dark matter consists of quark anti-matter nuggets. This includes 1) improving the quantitative accuracy of the emission calculations to provide detailed predictions with which to better test the theory. 2) Working with other astrophysicists to compile tests of our current proposal from existing data. 3) Search for additional observational evidence to confirm or rule out the proposal. 4) Solidify the formation mechanism. 5) Investigate how the phenomenology of these objects might constrain the many-body properties of quark matter. 6) Investigate alternative explanations for some of the anomalous emissions we presently attribute to dark matter. Finally, a related task is to investigate additional astrophysical phenomena to determine additional signatures for pairing and exotic many-body physics from astrophysical objects.

## Conclusion

We will develop many-body techniques to accurately compute the basic properties of matter relevant to cold atom experiments and nuclei. This is a prerequisite for finding new applications of certain materials, and for calculating properties of exotic nuclei and nuclear matter that cannot easily be studied in experiments. We will then apply these methods to predict properties of matter in the astrophysical context, shedding light on some of the great mysteries of the universe, including the nature of the mysterious dark-matter that forms most of the mass of the universe, but which has yet to be directly observed.

# Matter and Light

*Katrin Heitmann*

20080786PRD3

## Introduction

Cosmology relies on melding diverse measurements to understand the composition and evolution of the Universe. Microwave background observations showed that the Universe is flat, but studies of the clustering of matter found only one-third of the matter required. Famously, supernovae observations then showed that dark energy provided the missing energy density, bringing all measurements into concordance. This project is aimed at future surveys that will measure the distribution of galaxies in the Universe with very high accuracy. From these measurements, new cosmological constraints will be derived and these will advance our understanding of the fundamental constituents of our Universe: dark matter and dark energy.

Current and near-future galaxy surveys probe such huge volumes and such a large range of distance scales that it is a computational "grand challenge'' to compare our theoretical understanding of galaxy clustering with the surveys. It is vital to develop efficient statistical and numerical techniques that can enable the making of such comparisons.

## Benefit to National Security Missions

The project targets two of the top priorities of the DOE mission: understanding the nature of dark energy and high-performance computing. In addition, the project is relevant for the threat reduction arena in providing new techniques to extract information from diverse and very large data sets.

## Progress

The postdoc supported by this project, Adrian Pope, was hired on 9/29/2008. During the last two weeks he completed all necessary training. Initial discussions on new projects have been started.

## Future Work

Our measurements of large-scale structure statistics from large-volume cosmological surveys are becoming so good that a new generation of matching theoretical tools must be developed. In principle, N-body simulations provide detailed views of the clustering of dark matter, but the volumes and resolution necessary to mimic large surveys make it prohibitive to produce a large suite of N-body simulations covering a range of different cosmological parameters. The cosmic calibration project initiated at Los Alamos National Laboratory by Habib, Heitmann, and Higdon is an important step in using a limited number of large-scale simulations to predict large-scale structure statistics with high precision. During this project the framework will be extended and developed in an important new direction: modeling the effects of galaxies as biased tracers of matter when predicting the shape of the galaxy correlation function and other large-scale structure statistics.

An important challenge with large surveys is to estimate the covariance between different length scales in a large-scale structure measurement. Using N-body simulations for this task is inherently inefficient because a large-volume, high-resolution simulation has a small amount of information about large scales and over-calculates information about small scales -- ideally one wants to access a similar amount of information on all scales. During this project new methods will be developed that efficiently balance the information on all scales.

Ultimately this machinery will be used to measure the three-point galaxy correlation function from the Sloan Digital Sky Survey Luminous Red Galaxy sample. An accurate measurement of this correlation function will yield crucial information about the amplitude of matter fluctuations and the bias of galaxies. Without an accurate model and covariance matrix we cannot learn about cosmology from the raw correlation function.

## Conclusion

Our current understanding of the Universe relies heavily on measurements of its large-scale structure as probed by the clustering of galaxies. These studies are complicated by the fact that the luminous baryonic matter in galaxies (stars, gas) is only a tracer for the dark matter, whereas theoretical models directly predict the clustering properties of dark matter. This project will focus on understanding the connection between light and matter. This will be a crucial step for interpreting new cosmological observations and obtaining constraints on dark energy. The project will lead to new insights about the evolution and content of the Universe.

# High Energy Particles in Astrophysical Outflows

*Christopher Lee Fryer*

20051222PRD3

## Abstract

Plasmas are the most common phase of matter in the universe and rich carriers of waves from low frequency magneto-hydrodynamic (MHD) waves to high frequency kinetic waves. Understanding the resonant interactions of these waves with charged particles plays essential roles in our exploration of many phenomena in nature, especially in solar and high energy astrophysics, where the generation and transport of high energy particles are dominated by electromagnetic interactions. In this two-year project we studied these waves in a range of astrophysical problems from solar flares to active galactic nuclei to supernovae and gamma-ray bursts. This has led to a fruitful collaboration involving a number of students and with academic institutions across the world.

## Background and Research Objectives

The origin of the cosmic rays is one of the top 10 "unsolved mysteries" in physics. Cosmic rays arise from particles accelerated to ultra-relativistic speeds. Such particles are produced in the most energetic sites in the universe. Cosmic explosions produce the most energetic of these sites. LANL has a long history in modeling and observing supernovae and gamma-ray bursts. What we have not developed is the theory to tie these explosion models with the observations. In part, this is because particle acceleration is a very difficult phenomenon to model. It involves strong, often relativistic shocks with strong magnetic fields. The state of the art in academia is to use parameterized models to move from the shock physics to the creation of accelerated particles.

This project was based on a fellowship bringing Siming Liu to Los Alamos National Laboratory for two years. Siming is an expert in these parameterized models and, for LANL to make the first step bridging theory and observation, we needed to learn these models. Siming ultimately stayed an additional 9 months and is now continuing to work with us from the University of Glasgow where he has a research position. The goal of this project was to bring in expertise on particle acceleration at LANL to better tie LANL's theory efforts in active galactic nuclei, supernovae and gamma-ray bursts to observations of these phenomena. Siming's expertise in particle physics and wave phenomena was ideally suited to make this bridge. But to do this, we had to move from his expertise in particle acceleration in solar flares to the fields studied at LANL.

The first step was to have Siming teach LANL scientists the parameterized models in the problem of solar physics. Our plan was to educate his hosts, Fryer and Li, in the current state of models so that we can better apply this physics to more LANL relevant models. Particle acceleration in solar flares is what powers the high-energy particles in the solar wind, an important aspect of satellite physics. LANL has worried about this from the receiving end for its satellites, but not so much in the production side.

A second step was to attack a problem that both sides knew reasonably well – the supermassive black hole at the center of the Milky Way. The supermassive black hole at the center of our own Galaxy is the best-studied black hole in the universe. Understanding it provides information allowing us to explain a host of astrophysical objects thought to be produced by black holes. It is also one of the best probes of high-energy physics we have available to us (producing much more energetic conditions than those produced by the Large Hadron Collider). This study easily led into studies of active galactic nuclei.

Finally, we planned to study the particle acceleration in supernova and gamma-ray burst shocks to tie our explosion models to the observations. The goal of this project was to develop the framework to tie our theory to the observations, allowing us to more easily attract funds for NASA and NSF funded missions.

## Importance to LANL's Science and Technology Base and National R & D Needs

To start to attract money outside of NNSA, LANL needs to make its science more relevant to a broader set of scientists. One way to do this is to bring in experts to help LANL scientists do this work. This project did exactly this. We brought in Siming as an expert under the postdoctoral fellow program and worked intensely on a number of projects, both teaching Siming the science strengths at LANL and having him teach us about particle acceleration. We now have a suite of powerful tools to tie our theory to observations, both allowing us to collaborate more fully with LANL-based observational projects and to develop collaborations outside of LANL.

Here, we'll briefly outline some of the spin-offs. First, by reinvigorating LANL research on solar flares and particle acceleration in solar flares, LANL is in a better position to help this crucial effort in national defense.

But the broader work, studying particle acceleration with Siming has allowed LANL to develop an entire program on particle acceleration that has strong ties to NASA and DOE Office of Science goals. Siming's move to the University of Glasgow allows us to broaden our collaboration base and we are now working closely with scientists in the United Kingdom. We expect Siming to send us a string of graduate students to work jointly with us on these topics.

The tools we have developed are ideally suited for NASA missions such as GLAST and NSF missions like HAWC, opening up the possibility of receiving funds for this projects.

## Scientific Approach and Accomplishments

During Siming's time at LANL, we have published seven joint refereed papers and thirteen publications in total [1-13], many of which are published in the Letter part of the Astrophysical Journal (the equivalent of physical review letters for astrophysicists). Most of the papers focused on work studying the Galactic Center where we had the most initial overlap, but we managed to learn both about solar particle acceleration and active galactic nuclei.

But the primary accomplishment of this project was to tie our theory work in stellar explosions to observations. In this sense, this project has been a phenomenal success. Figure 1 shows images of our current fits of our theoretical models of high-energy emission from supernova remnants. The fit is of flux versus photon energy. Not only had this object not been explained previously, but no team had used detailed stellar explosion models in their fits. This is a prime example of how careful explosion models, coupled with accurate physics, can truly explain the high-energy spectra we observe [13].

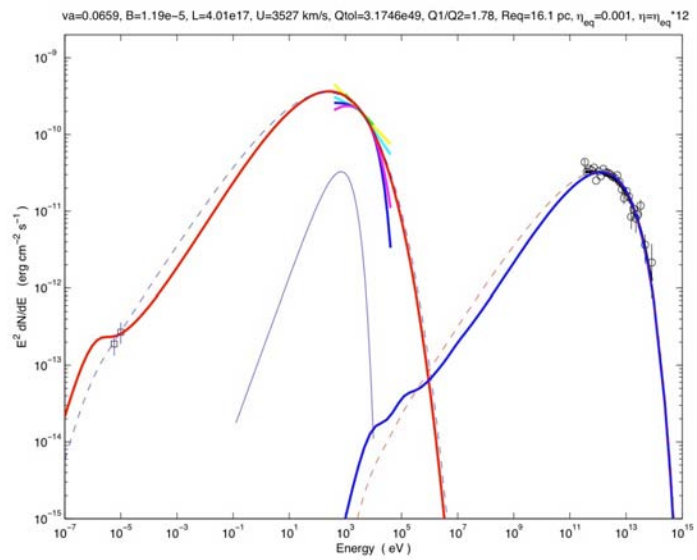


*Figure 1. Flux versus photon energy to the Cassiopeia A supernova remnant. The close fit between our models and measurements speaks to the accuracy of our coupled stellar explosion and particle acceleration models.*

Another success of this project is the career of Siming. He has moved on to a research position at the University of Glasgow and has a faculty position offer back in China. He plans to continue his collaborations with LANL scientists and we see this collaboration bringing us a string of bright researchers over the course of the next few years (hopefully to continue for decades).

Finally, the project of particle acceleration has motivated LANL scientists to develop a grass-roots effort to produce more realistic models of this process. By combining our newly gained understanding of this process with the computational excellence at LANL, we can take this particular field to a new level of sophistication.

## References

1. Liu, S., V. Petrosian, M. Melia, and C. Fryer. Testing the Stochastic Acceleration Model for Flares in Sagittarius A*. Invited presentation at *36th Cospar Meeting.* (Beijing, China, 16-23 July, 2006).

2. Liu, S., V. Petrosian, F. Melia, and C. Fryer. A Testable Stochastic Acceleration Model for Flares in Sagittarius A*. 2006. *Astrophysical Journal Letters.* **648**: 1020.

3. Chan, C., S. Liu, C. Fryer, D. Psaltis, F. Ozel, G. Rockefeller, and F. Melia. MHD Simulations of Accretion onto Sgr A*: Quiescent Fluctuations, Outbursts, and Quasi-Periodicity. To appear in *Astrophysical Journal.*

4. Fryer, C., S. Liu, G. Rockefeller, A. Hungerford, and G. Belanger. Probing the Density in the Galactic Center Region: Wind-blown Bubbles and High-Energy Proton Constraints. 2007. *Astrophysical Journal.* **659**: 389.

5. Liu, S., C. Fryer, and H. Li. Black Hole Accretion in Low States: Electron Heating. To appear in *Astrophysical Journal Letters.*

6. Bittner, J., S. Liu, C. Fryer, and V. Petrosian. Correlation between Flux and Spectral Index during Flares in Sagittarius A*. 2007. *Astrophysical Journal Letters.* **661**: 863.

7. Liu, S., L. Qian, X. Wu, C. Fryer, and H. Li. The Nature of Linearly Polarized Millimeter and Submillimeter Emission in Sagittarius A*. 2007. *Astrophysical Journal Letters.* **668**: 127.

8. Liu, S., Z. Fan, J. Wang, C. Fryer, and H. Li. Stochastic Particle Acceleration in the Hot Spots of FRII Radio Galaxies. 2007. In *American Astronomical Society Meeting.* (Austin, TX, 7-11, Jan. 2008). , p. 118.05. BAAS: AAS.

9. Liu, S., L. Huang, Z. Shen, M. Cai, H. Li, and C. Fryer. Polarimetric Imaging of the Relativistic Accretion Flow in Sagittarius A*. 2007. In *American Astronomical Society Meeting.* (Austin, TX, 7-11, Jan. 2008). , p. 118.07. BAAS: AAS.

10. Fan, Z., S. Liu, J. Wang, C. Fryer, and H. Li. Stochastic Acceleration in the Western Hot Spot of Pictor A. 2008. *Astrophysical Journal Letters.* **673**: 139.

11. Jian, Y., S. Liu, V. Petrosian, and C. Fryer. Cascade and Damping of Alfv'{e}n-Cyclotron Fluctuations: Application to Solar Wind Turbulence Spectrum. *Astrophysical Journal Letters.*

12. Huang, L., S. Liu, Z. Shen, M. Cai, H. Li, and C. Fryer. Linearly and Circularly Polarized Emission in Sagittarius A*. 2008. *Astrophysical Journal Letters.* **676**: 119.

13. Liu, S., Z. Fan, C. Fryer, J. Wang, and H. Li. Stochastic Electron Acceleration in Shell-Type Supernova Remnants. 2008. *Astrophysical Journal Letters.* **683**: 163.

## Publications

Bittner, J. M., S. Liu, C. L. Fryer, and V. Petrosian. Correlation between Flux and Spectral Index during Flares in Sagittarius A*. 2007. *Astrophysical Journal.* **661**: 863.

Fryer, C. L., S. Liu, G. Rockefeller, A. Hungerford, and G. Belanger. Probing the Density in the Galactic Center Region: Wind-Blown Bubbles and High-Energy Proton Constraints. 2007. *Astrophysical Journal.* **659**: 389.

Liu, S., C. Fryer, and H. Li. Black Hole Accretion in Low States: Electron Heating. *Astrophysical Journal.*

Liu, S., F. Melia, V. Petrosian, and M. Fatuzzo. Stochastic Acceleration in the Galactic Center HESS Source. 2006. *Astrophysical Journal.* **647** (2): 1099.

Liu, S., L. Qian, X. Wu, C. Fryer, and H. Li. The Nature of Linearly Polarized Millimeter and Submillimeter Emission in Sagittarius A*. 2007. *Astrophysical Journal Letters.* **668**: 127.

Liu, S., V. Petrosian, F. Melia, and C. L. Fryer. A Testable Stochastic Acceleration Model for Flares in Sagittarius A*. 2006. *Astrophysical Journal.* **648** (2): 1020.

# The Neutrino Matrix and Beyond

*Andrew Hime*

20051243PRD3

## Abstract

This Postdoctoral Research and Development (PRD) project resulted in significant enhancement of LANL research in the area of particle astrophysics, specifically focusing on WIMP dark-matter detector development as well as understanding of the properties of solar neutrinos. The PRD work was primarily centered on development of the DEAP/CLEAN dark-matter detector program, and resulted in a publication on the pulse-shape discrimination capabilities of liquid argon scintillation detectors and another publication in preparation on the liquid argon nuclear-recoil quenching factor. A secondary component of the PRD work involved the Sudbury Neutrino Observatory (SNO) and included writing and publication of a lengthy technical paper about the SNO $^3$He proportional counters, as well as hardware work and contributions to analysis of the data from the third phase of SNO. In addition to the benefits of the research performed under this PRD project, the project served as an effective recruiting tool, since the postdoctoral researcher is now a LANL staff member.

## Background and Research Objectives

Understanding the dark matter that makes up the vast majority of the matter density of the universe is one of the most important pursuits of modern science. A favored hypothesis is that the dark matter consists of Weakly Interacting Massive Particles (WIMPs), which interact only gravitationally and through the weak interaction. These WIMPs could be directly detected through weak-interaction-mediated nuclear recoils in a massive, ultra-pure, underground detector. Current-generation WIMP detectors have masses on the order of 10 kg, and have only placed limits of about $10^{-43}$ cm$^2$ on the WIMP-nucleon interaction cross-section. Development of next-generation WIMP detectors with dramatically larger target masses is being vigorously pursued by the low-energy particle astrophysics community and is crucial for directly detecting WIMP dark matter.

LANL is leading a significant effort to develop a conceptually simple, scalable, and economic next-generation WIMP detection technology based on noble liquid scintillators. Noble liquids, such as argon and neon, scintillate brightly in the extreme ultraviolet in response to the passage of fast charged particles. A nuclear recoil induced by a WIMP would produce a bright flash of scintillation light in a noble liquid scintillation detector, and this light can be wavelength-shifted to the visible and read out by an array of photomultiplier tubes (PMTs). Although electron-recoil background events induced by beta decays and gamma rays also produce scintillation light in noble liquids, the time profile of the electron-recoil events is dramatically different than for nuclear-recoil events, allowing highly efficient rejection of the electron-recoil backgrounds. This PRD project focused on hardware development and analysis of data from prototype noble liquid scintillation detectors for this effort.

This WIMP detector development effort strongly leverages LANL's existing capabilities in low-background particle detection that stem from the Sudbury Neutrino Observatory (SNO). SNO was a $10^6$-kg heavy-water Cherenkov detector designed to study the properties of solar neutrinos. The SNO experiment consisted of three phases of data taking, starting in 1999 and ending in 2006. A significant secondary component of this PRD project consisted of hardware, analysis, and publication writing work for the third phase of the SNO experiment, in which $^3$He proportional counters were used to detect neutrons liberated by neutrino interactions with deuterium in the heavy water.

## Importance to LANL's Science and Technology Base and National R & D Needs

LANL's position at the forefront of neutrino physics dates back to the Nobel Prize winning 1956 detection of the neutrino by Frederick Reines and Clyde Cowan. Since then, LANL scientists have played significant roles in a number of important experimental efforts

in neutrino physics. A hallmark of experimental neutrino physics is conceiving of a measurement so difficult that it borders on the absurd, and then turning that idea into a successful experiment. This spirit of meeting impossible challenges pervaded Reines's thinking when he first set his mind to experimental detection of the neutrino that had to exist to save conservation of energy in beta decay. And this same spirit has driven decades of successful experiments since then. One of the most recent among these was the SNO experiment, which had radio-purity requirements that bordered on the impossible and which ended up solving the long-standing Solar Neutrino Problem.

The next great challenge in low-background particle detection is direct detection of WIMP dark matter. Now that neutrinos are beginning to be well understood, many scientists at LANL and elsewhere are turning their attention to an even more difficult challenge. The WIMP-nucleon interaction cross section is known to be even smaller than the cross sections involved in neutrino interactions, so detectors must be even more sensitive and backgrounds reduced even further in order to be successful. LANL's leadership in the field of WIMP dark matter detection provides a continuation of the spirit of tackling nearly impossible challenges that has existed here since the early days of the laboratory's history.

Identifying dark matter is consistently mentioned as one of the most important scientific research areas by studies and panels tasked with prioritizing national R & D needs. Here at LANL, dark matter and neutrino research is part of the Beyond the Standard Model Grand Challenge and is essential to maintaining and strengthening LANL's science and technology base. Research in the area of low-background particle detection has consistently provided an excellent recruitment tool that brings some of the best and the brightest young scientists into LANL. This work is an essential part of the basic science that is the cornerstone of the LANL LDRD program.

## Scientific Approach and Accomplishments

The DEAP/CLEAN detector development program at LANL is a comprehensive effort to develop a conceptually simple, scalable, and economic next-generation WIMP detection technology based on noble liquid scintillators. Most proposed next-generation WIMP dark matter detectors use technology that is complicated and not easily scaled to the very large detector sizes that are likely to be required to identify dark matter. The DEAP/CLEAN concept consists simply of a large tank of noble liquid viewed by PMTs. This avoids the technical challenges inherent in other WIMP detectors, such as growing of a large array of solid-state detectors for the CDMS concept, or drifting an ionization signal across a large detector for the XENON concept. While the DEAP/CLEAN concept is relatively simple compared to other proposed WIMP detectors, it still presents a significant R&D challenge. Some of the major R&D efforts were part of this PRD project, including characterizing PMTs for use at cryogenic temperatures, understanding background rejection capabilities in noble liquids, and studying the response of noble liquids to nuclear recoil signals characteristic of WIMP interactions.

A major component of this PRD project was detector development and prototyping work for the DEAP/CLEAN program. Two test stands, one at room temperature and one at cryogenic temperatures, were developed for characterization of PMTs and light guides that will be used in DEAP/CLEAN WIMP detectors. Measurements of quantum efficiency, reflectivity, and other PMT properties made using the room-temperature PMT test stand provided critical input to detector design. The cryogenic PMT test stand was developed under this PRD project and now is in use for studies of PMT operating properties as a function of temperature.

Analysis of data from prototype DEAP/CLEAN detectors comprised a significant part of this PRD project. One major analysis effort was to understand the pulse-shape discrimination capabilities of liquid argon for rejection of electron-recoil backgrounds caused primarily by beta-decay of cosmogenic $^{39}$Ar in the target material. While this analysis was lead by collaborators at Yale University, significant essential contributions were made through this PRD project. A paper detailing pulse-shape discrimination in liquid argon was produced and published in Physical Review C, volume 78, number 3.

Another major analysis effort under this PRD project was measurement of the quenching of the scintillation light produced by nuclear recoils in liquid argon compared to the light produced by electron-recoil events of the same deposited energy. It is critical to understand the relative response of the detector to nuclear and electron recoils since the signals of interest in a liquid-argon WIMP detector are nuclear recoils, but the detector would be calibrated with sources that produce electron recoils and the primary background is an electron recoil signal. Measurements of neutron-induced nuclear recoils at a number of different recoil energies were performed in order to characterize the scintillation response of liquid argon as a function of nuclear recoil energy. Although the measurements were performed at Yale University, the analysis was led at LANL as part of this PRD project. A paper presenting the results of this analysis is in preparation and the results have been presented at conferences.

In addition to the noble liquid WIMP detector development work that formed the core of this PRD project, a significant amount of effort was focused on the SNO experiment, which completed its third and final phase of data-taking halfway through this PRD project. For the third phase of SNO, an array of $^3$He proportional counters known as Neutral Current Detectors (NCDs) was installed in SNO's heavy water to detect neutrons liberated by neutrino interactions with deuterium. A great deal of expertise on the SNO NCDs was brought to this PRD project, particularly in the areas of hardware and intrinsic radioactive backgrounds. This expertise allowed high-impact contributions to be made to the SNO project under this PRD project without detracting from the DEAP/CLEAN work that was the primary component of the PRD project.

One major result of the SNO aspect of this PRD project was the writing, editing, and publication of a lengthy technical article on the SNO NCDs, published in Nuclear Instruments and Methods in Physics Research A, volume 579, pages 1054 – 1080. This paper describes the design, construction, installation, and characterization of the NCDs, discusses the electronics and data acquisition system, and considers event signatures and backgrounds in the NCDs. Writing and editing of the paper was performed under this PRD project. The paper was accepted without revisions by the journal.

Another contribution of this PRD project to the SNO experiment was in background analysis for the NCD-phase SNO results, published in Physical Review Letters, volume 101, article 111301. A significant potential background in that solar neutrino flux measurement was introduced by the presence of a radioactive hotspot on one of the NCDs. A series of measurements of the hotspot was performed after decommissioning of the SNO detector, in order to identify and quantify the hotspot. One of the measurements involved analysis of time correlations between alpha decays from the hotspot, and was performed under this PRD project. The characterization of the hotspot that resulted from these measurements reduced the systematic uncertainty on the NCD-phase flux result from 4% to well under 1%. Details of the hotspot analysis will be published in a paper that is currently in preparation.

In addition to the direct impacts of the research performed under this PRD project, the project provided other benefits to LANL. One goal of the LANL postdoctoral program, and particularly the LDRD PRD program, is to recruit and retain promising young scientists at the laboratory. This PRD project clearly served as an effective recruiting tool, since the postdoctoral researcher is now a LANL staff member.

## Publications


Lippinicott, H., D. McKinsey, J. Nikkel, A. Hime, L. C. Stonehill, D. Gastler, E. Kearns, and K. Coakley. Scintillation Time Dependence and Pulse Shape Discrimination in Liquid Argon. 2008. *Physical Review C.* **78**: 0.35801.

O.Collaboration, S. N.. An Array of Low-Background 3He Proportional Counters for the Sudbury Neutrino Observatory. 2007. *Nuclear Instruments and Methods A.* **579**: 1054.

O.Collaboration, S. N.. An Independent Measurement of the Total Active 8B Solar Neutrino Flux Using an Array of 3He Proportional Counters in the Sudbury Neutrino Observatory. 2008. *Physical Review Letters.* **101**: 111301.

Stonehill, L. C.. Testing of Materials and Components at Cryogenic Temperatures for a Noble Liquid Dark Matter Detector. Presented at *IEEE Nuclear Science Symposium.* (Honolulu, HI, Oct. 29 - Nov. 2, 2007).

Stonehill, L. C.. Quenching of Nuclear Recoil Scintillation Signals in Liquid Argon. Presented at *Meeting of the American Physical Society.* (Jacksonville, FL, Apr. 14 - 17, 2007).

Stonehill, L. C.. Noble Liquid Scintillation Detectors for Low-Energy Particle Astrophysics. Presented at *IEEE Nuclear Science Symposium.* (San Diego, CA, Oct. 30 - Nov. 2, 2006).

Stonehill, L. C.. Alpha Backgrounds in the SNO 3He Proportional Counter Arra. Presented at *Meeting of the American Physical Society.* (Dallas, TX, Apr. 22 - 25, 2006).

full final report

# A Multiscale Approach to Modeling Continental Rift Tectonics

*Carl Walter Gable*

20051286PRD3

## Abstract

The evolution of the Earth's surface is intimately linked to processes in its interior. In fact, the oceanic crust and continents are the upper thermochemical boundary layer of the Earth's convecting mantle. We are employing multiple computational techniques to explore the feedback between continents and the mantle. At global scales, we model convection using the high resolution, 3D spherical finite element (FEM) mantle convection code Terra. We added continents to Terra using a Lagrangian particle-in-cell (PIC) technique that permits the tracking of characteristics at sub-grid scales. Further insight into local-scale processes occurring in rifting margins, namely the advection of heat and mass through magmatic systems, is then looked at using the multi-material, multi-phase finite volume code Truchas. The goals of this project include furthering our understanding of the links between the thermal evolution of the mantle on a continental scale and the transport of that heat to surface through systems at the scale of volcanoes.

## Background and Research Objectives

Continents episodically cluster together to form supercontinents, ultimately breaking up in association with intense magmatic activity. The breakup of Pangea, the last supercontinent, was accompanied by the emplacement of the largest known continental flood basalt (CFB), the Central Atlantic Magmatic Province (CAMP), which caused massive extinctions at the Triassic-Jurassic boundary (Figures 1,2). These eruptions suggest that mantle temperature is a function of continent size, with anomalously high temperatures developing beneath supercontinents. However, a quantitative understanding of how continent size and fundamental flow features inside the Earth modulate mantle temperature is lacking.

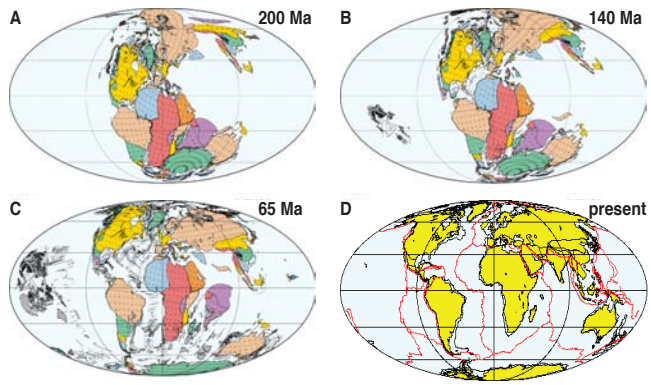


*Figure 1. Plate reconstructions from the time of Pangea, 200 million years (m.y.) ago, until today.*

Most of the Earth's volcanism occurs where planar magma-filled fractures intersect the surface. Such eruptions can span all scales, from meter wide basaltic dikes, to mid-ocean ridge plate formation zones, to giant feeders of flood basalts (Figure 2). The behavior of fissure eruptions depends on a combination of factors including the thermal and mechanical properties of the intruded rock, magma source volume and pressure, initial dike dimensions, and magma rheology. Quantitative information on the detailed evolution of these channels is lacking, in part due to insufficient numerical tools. Using a new multi-material, multi-phase fluid dynamics model we are developing better constraints on fundamental aspects of fissure events, such as the influence of system geometry and relationships between timing and magma volume, that could help guide future observations of catastrophic eruptions, hone volcanic hazards assessments, and push the capabilities of magma dynamics models.

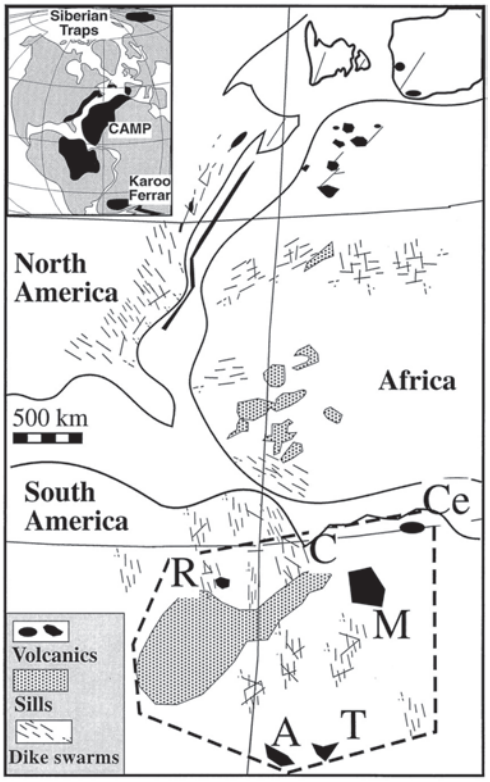


*Figure 2. Location map of the Central Atlantic Magmatic Province (CAMP) in a Pangea reconstruction at 200 m.y. ago, also showing the Siberian and Karoo-Ferrar continental flood basalt provinces in the inset. The area presently recognized as being part of CAMP is shown by a dashed contour, with sample sites indicated: R, Roraima; M, Maranhao; C, Cassiporee; Ce, Ceara; A, Anari; and T, Tapirapua.*

## Importance to LANL's Science and Technology Base and National R & D Needs

Our work directly addressed several of the *LDRD Strategic Investment Priorities* for Earth, Space, and Environmental Sciences (ESE). Specifically, our models represent advances towards the Solid Earth Geophysics *Key Capabilities* of "Understanding the Earth via state of the art measurements and geologic models of the crust, mantle and core" and "Computational advances in forward and inverse modeling of deformation behavior of Earth materials including tectonic (slow)" processes. The proposed study also seeks to better constrain the physics behind natural events that significantly alter the Earth's climate. Our results will therefore have relevance on long time scales for understanding the Climate and Environmental Systems *Key Capability* of "Advanced simulations of global processes, including climate change and ocean circulation" as well as the *Core Competency* "Knowledge of the ability of the environment to accept and retain man-made and natural emissions and pollutants such as $CO_2$."

In addition to furthering key capabilities in ESE, this study falls generally under the *Grand Challenge* category of "Complex Systems." Great interest lies in understanding the impact of energy choices on climate and the environment. An important step in characterizing anthropogenic climate change is to understand fluctuations in the natural system that occurred before human intervention. CFBs associated with the breakup of supercontinents represent a significant type of natural forcing that we should consider in the big picture of global change.

## Scientific Approach and Accomplishments

The physical viability of supercontinent cycles depends on the heat budget of the Earth's interior. As a first step at investigating the influence of supercontinents on the mantle, a study was therefore undertaken to investigate the conditions favoring supercontinent formation. Phillips and Bunge [1] used Terra models to show that periodic supercontinent cycles are unlikely to occur if an upper limit on heat flow out of the Earth's core is adopted. Regular supercontinent cycles do occur in idealized models with three continents and a mantle heated purely from within (Figure 3). In a model incorporating six continents and strong mantle plumes this regularity is broken and supercontinents form only sporadically. Better constraints on the strength of mantle plumes could therefore help further support or confound the notion of a theoretically plausible periodic supercontinent cycle. This study was extended to address the influence of supercontinental heating on the stability of the Earth's rotation axis [2].

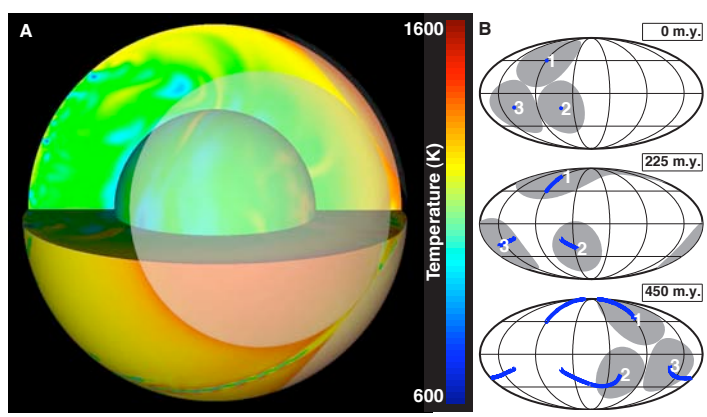


*Figure 3. A model with three continents and a purely internally heated mantle. Each continent covers 10% of the surface, similar to present day Asia. A, A snapshot of temperature in the mantle. Continents are shown as transparent caps. Red is hot (upwellings beneath continents) and blue is cold (downwellings away from continents). The outer surface corresponds to 100 km depth. B, Continent locations (gray circles) and drift paths (blue lines) for excerpts from the model. At 0 m.y. the continents are grouped into a supercontinent. By 225 m.y. the continents have dispersed. They reaggregate by 450 m.y. to form a second supercontinent.*

Following up on these studies Phillips and colleagues demonstrated that supercontinental aggregation could lead to large-scale melting without the involvement of mantle plumes [3]. In fact, the aggregation of a supercontinent like Pangea could lead to mantle warming of up to 100 °C and hence extensive volcanism in the style of the CAMP even in the absence of mantle plumes (Figure 4). This warming was shown to reflect an increase in the dominant wavelength of mantle convection in response to the formation of a large, rigid continent. The supercontinent attenuates the smaller-scale flow features that are prevalent during periods when the continents are dispersed, eliminating the most efficient modes of removing heat from the Earth's interior. This premise was further extended to investigate the likelihood of supercontinent induced heating during the early history of the Earth [4].

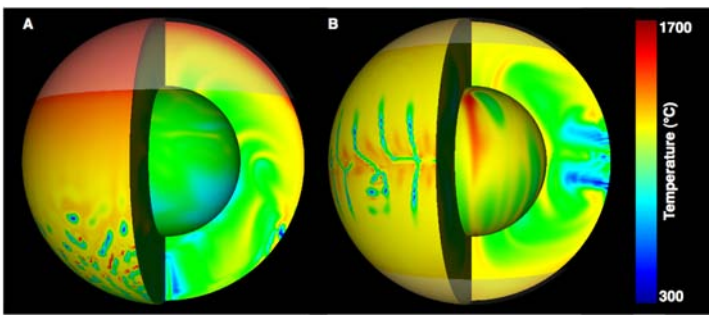


*Figure 4. Temperature field snapshots for models with (A) a supercontinent and (B) two antipodal continents. The mean temperature at base of the continental thermal boundary layer in (A) is 1614 ºC (red), while in (B), it is only 1475 ºC (yellow). Translucent caps denote continent locations. Linear features on planetary surfaces delineate regions of cold, subducting material.*

To address the modes of heat transport from beneath continents to volcanoes at the surface, we developed quantitative models of the behavior of fissure-style volcanic eruptions. Such events, in which magma propagates through the crust via planar fractures, constitute a primary mode of magma transport in the Earth. However, the way in which fissure eruptions evolve varies considerably. Some cease shortly after initiation, others show focusing of magma into localized, cylindrical conduits, and still others maintain their planar pathways for millions of years. The critical parameters that govern these different behaviors are not well constrained partially due to a lack of sophisticated numerical tools capable of addressing this fully three dimensional (3D) problem. We expanded the capabilities of the Los Alamos National Laboratory 3D metallurgy software Truchas for application to magma dynamics in order to address these problems.

Truchas solves for conservation of mass, momentum, and energy for multi-material, multi-phase systems. While the basic physics governing metal casting (Truchas' developed purpose under the Department of Energy's Accelerated Strategic Computing Initiative) and the "casting" of molten rock in the Earth are closely related, differences in material properties and problem scales do present challenges in applying this tool to a new genre of systems. Magmas can have viscosities that are many orders of magnitude larger than metals in typical Truchas simulations. LANL casting operations are characterized by centimeter scale molds and durations of seconds, but volcanic systems contain dikes that are meters wide by kilometers tall with eruption time scales of days, to months, to years. These differences test the generality of Truchas' numerical algorithms. Support from members of the Truchas Team in the Computer and Computational Sciences Division (James Sicilian and Mark Christon) helped to insure the success of modifications and additions necessary to make the code robust over a wider parameter range.

A study on melting and solidification of magma in continental dikes led to a paper addressing the duration of the most recent rhyolite eruption in the Valles caldera, New Mexico [5]. This work is currently being extended to look at magma transport beneath the Southwestern Nevada volcanic field (SNVF). The SNVF, surrounding Yucca Mountain, boasts 17 volcanoes that have erupted over the past 5 million years. Geochemical analyses of the volcanic deposits suggest that magmas rose from great depth in the upper mantle (roughly 50 km) directly to the surface. Volume estimates for the volcanic deposits and the mapped surface expressions of the feeder channels suggest that such magmas would have traveled in isolated batches, not in open conduits connecting the source to the surface. Whereas the open conduit model essentially mimics the well-studied physics of channel flow, modeling of finite pulses of magma required a new conceptual model to represent the physics associated with ascent in a closed box.

We developed an approach that models magma ascent in the reference frame of the ascending dike (Figure 5). Preliminary results suggest that stirring associated with shear flow of the magma with respect to the walls can significantly increase the solidification rate, which will affect how geochemical interpretations for the SNVF lavas agree with physical constraints. We anticipate a paper that highlights our novel modeling approach and evaluates the physical validity of geochemical interpretations made for the SNVF.

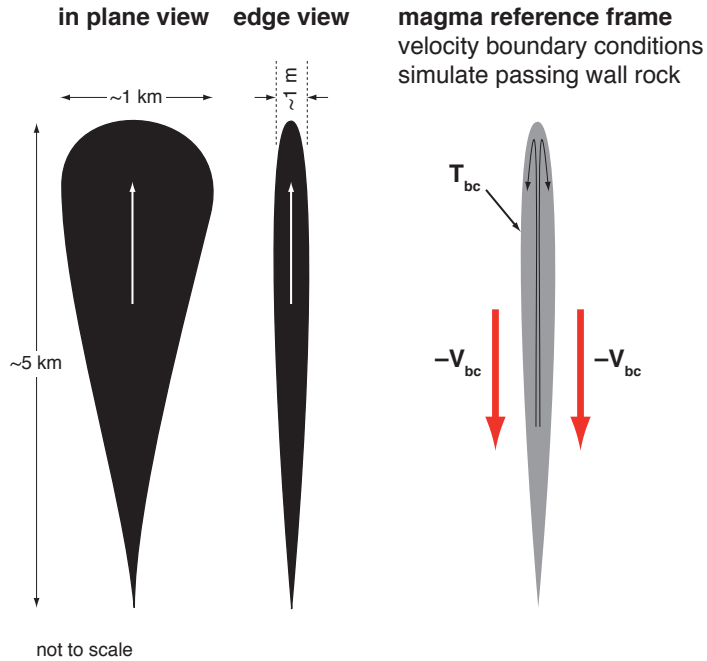


*Figure 5. Schematic view of an isolated, ascending magma pulse. Left, outline of the dimensions of the problem. Right, conceptual approach of modeling the ascending pulse in the reference frame of the propagating dike tip as applied with the modified Truchas code.*

As a result of this work, improvements to Truchas include a more general implementation of the solution for multiple phase changes, a correction to the way in which enthalpy is computed for fluid inflow conditions, the introduction of an Arrhenian temperature dependent viscosity formulation, development of a matrix pre-conditioner to improve convergence of the linear viscous solution, correction to an algorithm that initializes model temperatures, correction to the calculation of the viscous stress gradient, and modification of the treatment of solid materials to facilitate modeling in the fluid reference frame with phase changes. These technical developments have improved the robustness of Truchas for its programmatic applications in manufacturing associated with nuclear weapons and fuels, while fostering a new collaboration between computational and Earth scientists.

## References

1. Phillips, B. R., and H. P. Bunge. Supercontinent cycles disrupted by strong mantle plumes. 2007. *Geology.* **35** (9): 847.

2. Phillips, B. R., H. P. Bunge, and K. Schaber. True polar wander in mantle convection models with multiple, mobile continents. To appear in *Gondwana Research.*

3. Coltice, N., B. R. Phillips, H. Bertrand, Y. Ricard, and P. Rey. Global warming of the mantle at the origin of flood basalts over supercontinents. 2007. *Geology.* **35** (5): 391.

4. Coltice, N., H. Bertrand, P. Rey, F. Jourdan, B. R. Phillips, and Y. Ricard. Global warming of the mantle beneath continents back to the Archean. To appear in *Gondwana Research.*

5. Phillips, B. R., W. S. Baldridge, C. W. Gable, and J. M. Sicilian. Duration of the Banco Bonito rhyolite eruption, Valles caldera, New Mexico, based on magma transport modeling. 2007. *New Mexico Geological Society Guidebook, 58th Field Conference.* : 382.

## Publications

Coltice, N., B. R. Phillips, H. Bertrand, Y. Ricard, and P. Rey. Global warming of the mantle at the origin of flood basalts over supercontinents. 2007. *Geology.* **35** (5): 391.

Coltice, N., H. Bertrand, P. Rey, F. Jourdan, B. R. Phillips, and Y. Ricard. Global warming of the mantle beneath continents back to the Archean. To appear in *Gondwana Research.*

Phillips, B. R., H. P. Bunge, and K. Schaber. True polar wander in mantle convection models with multiple, mobile continents. To appear in *Gondwana Research.*

Phillips, B. R., W. S. Baldridge, C. W. Gable, and J. M. Sicilian. Duration of the Banco Bonito rhyolite eruption, Valles caldera, New Mexico, based on magma transport modeling. 2007. *New Mexico Geological Society Guidebook, 58th Field Conference.* : 382.

Phillips, B. R., and H. P. Bunge. Supercontinent cycles disrupted by strong mantle plumes. 2007. *Geology.* **35** (9): 847.

full final report

# Quantum Fluctuations of Event Horizons

*Emil Mottola*

## Abstract

Because of the enormous gravitational redshift near the event horizon of a black hole (a finite region from which light cannot escape), black holes provide a unique window into the quantum domain. The redshift of short wavelengths into longer ones acts as a kind of "magnifying glass'' of physics near the horizon. We have studiedquantum fluctuations of event horizons in a new and much more detailed way, and done cutting edge research on a new approach to reconciling quantum physics with gravitation.

## Background and Research Objectives

This project was aimed at a new and deeper understanding of quantum effects in gravity, with implications for the past and future history of the universe, its large scale structure and origin of dark energy today. A systematic approach to the quantitative study of the spacetime fluctuations induced by quantum fields in an evaporating black hole within the framework of stochastic gravity has been pioneered. The central object of interest is the noise kernel, which is the symmetrized two-point quantum correlation function of the stress tensor operator. As a concrete example it has been applied to the study of the spherically-symmetric sector of metric perturbations around an evaporating black hole background geometry. For macroscopic black holes those fluctuations have been found to grow and eventually become important when considering sufficiently long periods of time (of the order of the evaporation time), but well before the Planckian regime is reached.

The assumption of a simple correlation between the fluctuations of the energy flux crossing the horizon and far from it, which was made in earlier work on spherically-symmetric induced fluctuations, has been carefully scrutinized and found to be invalid. Our analysis suggests the existence of an infinite amplitude for the fluctuations when trying to localize the horizon as a three-dimensional hypersurface, as in the classical case, and, as a consequence, a more accurate picture of the horizon as possessing a finite effective width due to quantum fluctuations. This is supported by a systematic analysis of the noise kernel in curved spacetime smeared with different functions under different conditions. This case study shows a pathway for probing quantum metric fluctuations near the horizon and understanding their physical meaning.

## Importance to LANL's Science and Technology Base and National R & D Needs

This is a basic research project on fundamental questions of gravitation and dark energy in astrophysics and cosmology, one of the areas of fundamental physics of interest to DOE Office of Science.

## Scientific Approach and Accomplishments

Dr. Roura has computed the correlation functions for the primordial metric fluctuations and their power spectrum in inflationary cosmological models driven by an inflaton field, based on the Einstein-Langevin equation, which emerges in the framework of stochastic semiclassical gravity. He showed with Prof. Verdaguer that the correlation functions for the metric perturbations that follow from the Einstein-Langevin formalism coincide with those obtained with the usual quantization procedures when the scalar field perturbations are linearized. His method has been explicitly applied to a simple model of chaotic inflation consisting of a Robertson-Walker background, which undergoes a quasi-de-Sitter expansion, minimally coupled to a free massive quantum scalar field. The technique based on the Einstein-Langevin equation can deal naturally with the perturbations of the scalar field even beyond the linear approximation, as is actually required in inflationary models, which are not driven by an inflaton field, or when calculating corrections due to non-linear quantum effects in the usual inflaton driven models.

Dr. Roura has also applied the study of the stress-tensor quantum correlation function to the study of the spherically-symmetric sector of metric perturbations around an evaporating black hole background geometry. For macroscopic black holes he finds that those fluctuations grow and eventually become important when considering sufficiently long periods of time (of the order of the evaporation time), but well before the Planckian regime is reached. His analysis suggests the existence of an infinite amplitude for the fluctuations when trying to localize the horizon as a three-dimensional hypersurface, as in the classical case, and, as a consequence, leads to a more accurate picture of the horizon as possessing a finite effective width due to quantum fluctuations. This case study shows a pathway for probing quantum metric fluctuations near the horizon and understanding their physical meaning.

A third achievement has involved clarifying and providing a solid basis for the analysis of the quantum backreaction from nonconformal fields in de Sitter spacetime. A number of studies in the literature had found large infrared backreaction effects due to the one-loop vacuum polarization of nonconformal fields, leading to significant deviations from de Sitter spacetime. By explicitly calculating the closed-time-path effective action and solving the backreaction equations governing the dynamics of the mean geometry, it has been shown that the contribution from local terms proportional to the logarithm of the scale factor, responsible for the substantial deviations found in earlier studies, are cancelled by the contribution from nonlocal terms, which had been neglected in those studies. The semiclassical de Sitter solution has then been found to be stable under isotropic perturbations. Furthermore, the explicit semiclassical solutions obtained provide the right background geometry where the properties and effects of quantum metric fluctuations should be studied.

## Publications

Fleming, C. H., B. L. Hu, and A. Roura. Solutions to Master Equations of Quantum Brownian Motion in a General Environment with External Force. 2007.

Hu, B. L., and A. Roura. Fluctuations of an evaporating black hole from back reaction of its Hawking radiation: Questioning a premise in earlier work. 2007. *Int. J. Theor. Phys.* **46**: 2204.

Hu, B. L., and A. Roura. Metric fluctuations of an evaporating black hole from back reaction of stress tensor fluctuations. 2007. *Phys. Rev. D.* **76**: 124018.

Roura, A.. Quantum horizon fluctuations of an evaporating black hole. 2007. *J. Phys. A.* **40**: 7075.

Roura, A., E. Verdaguer, and G. Perez-Nadal. Stability of de Sitter spacetime under isotropic perturbations in semiclassical gravity . 2008. *Phys. Rev. D.* **77**: 124033.

Roura, A., E. Verdaguer, and G. Perez-Nadal. Backreaction from non-conformal quantum fields in de Sitter spacetime. 2008. *Class. Quant. Grav..* **25**: 154013.

Roura, A., and E. Verdaguer. Cosmological perturbations from stochastic gravity. 2008. *Phys. Rev. D.* **78**: 064010.

# Three-dimensional Magnetic Reconnection Experiments

*Thomas P Intrator*

20061475PRD2

## Abstract

Magnetic reconnection underlies magnetic activity in many space weather processes, including the solar corona (coronal mass ejections from the Sun, solar flares and many others) and magnetospheric substorm. Magnetic reconnection is also a key process in laboratory plasmas. In laboratory, not only experiments are especially designed to investigate this process but also important multinational endeavors such as ITER have to contend with the physics of reconnection (e.g. in sawtooth crashes and tearing modes). Most theoretical, computational and experimental work on magnetic reconnection starts with boundary conditions or initial conditions where steady reconnection is the goal by design. But in nature and the laboratory the onset of reconnection is usually driven naturally by some evolution of plasma mediated forces and reconnection has the freedom of developing either quasi-statically or intermittently. The initiation is frequently observed to be explosive. Nature seems to display both behaviors: recent papers have observed both types of behaviors, steady and intermittent, both in simulation and in observations (in space and in laboratory). Space and laboratory reconnection data can advance the current understanding of the conditions leading to steady or unsteady reconnection. What are the conditions leading to the onset of reconnection? And what are the processes leading to its (permanent or temporary) reduction or suspension? Recent experiments and simulations are starting to crack this problem.

## Background and Research Objectives

The relaxation and self-organization of plasmas with embedded magnetic fields and currents is an important feature for many solar, space, astrophysical, and fusion plasmas. Frequently the evolution of global structure is tied to the microphysics of how magnetic energy is coupled to particle energy, and the three-dimensional structure of magnetic fields. Part of this story includes magnetic reconnection, which is the fundamental process in a conducting plasma where magnetic field lines of opposite polarity are broken and "reconnected" into a new configuration, leading to the conversion of magnetic field energy into plasma kinetic and thermal energy. Magnetic reconnection plays an important role in the solar corona, the earth's magnetosphere, and interactions between the two ("space weather"), and is gaining acceptance as an essential process in galaxy evolution (e.g., accretion disks, jets, radio lobes). The effects of the third dimension are unknown. Successful 3D reconnection experiments such as we have carried out at LANL have advanced our understanding of reconnection in natural settings.

## Importance to LANL's Science and Technology Base and National R & D Needs

Magnetic reconnection is the fundamental process in the physics of fusion energy devices, the solar corona, the earth's magnetosphere, and interactions between the two ("space weather"), and astrophysical plasmas. This has strong ties to fusion energy science, which is a mission of DOE, as well as understanding the operational environment of NNSA's counterproliferation space assets.

## Scientific Approach and Accomplishments

There have been 3D and 2D "spontaneous" reconnection experiments that included significant externally programmed magnetic drive and X-line geometry. However internal forces during magnetic self-organization have been shown to be important for large-scale systems [Wan2008]. Here we show a laboratory example of three dimensional (3D) Sweet-Parker type magnetic reconnection that is impulsively initiated between two freely moving parallel current flux ropes that attract each other so that they force oppositely directed magnetic fields together. As 3D kink instabilities grow, the flux rope collision and flux annihilation region becomes a 3D patch of reconnection.

The unique laboratory experiment at LANL is called the Reconnection Scaling Experiment (RSX). A schematic of the Reconnection Scaling Experiment (RSX) is shown in Figure 1. Two plasma guns generate two hydrogen plasma current channels, embedded in a background magnetic guide field.

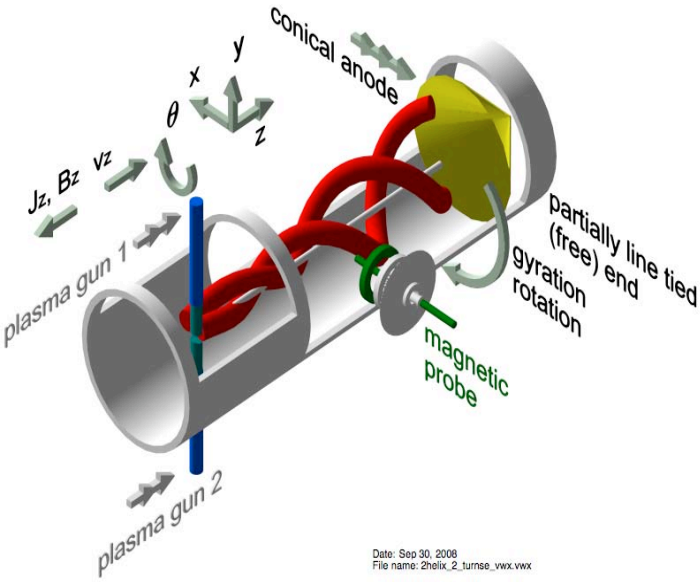


*Figure 1. Schematic of the RSX experiment showing coordinate system and geometry (single arrows), two plasma guns (double arrows) that insert radially but create axial flux ropes, two kinking flux ropes, external conical anode (triple arrow) that allows adjustable axial boundary condition, fiducial line (fictitious and for reference only) at the vessel z axis, and magnetic probe inserted through a 3D probe positioner.*

A paper [1] "Transition of MHD kink stability properties between line-tied and non line tied boundary conditions" by authors: X. Sun, T. P. Intrator, L. Dorf, I. Furno, and G. Lapenta, has been published in *Physical Review Letters*. Magnetic flux tubes or flux ropes in plasmas are important in nature and the laboratory. Axial boundary conditions strongly affect flux rope behavior, but this has never been systematically investigated. We discussed new data and theory that demonstrate how external boundary geometry can be employed to stabilize the kink mode, and provide a laboratory "dial" between two different mathematical boundary conditions. We experimentally and theoretically demonstrate for the first time axial boundary conditions (BC) that are continuously varied between ideal magnetohydrodynamic (MHD) non-line-tied and line-tied. The flux rope displacement BC is increasingly constrained from non-line-tied (free) to line-tied (fixed), and is consistent with the kink instability threshold. This may be useful beyond the usual theoretical expectations. This may turn out to be important for solar, space, and astrophysical situations.

A paper [2] has been written that experimentally describes the collisions between flux ropes and whether they merge or coalesce, which prior to this has only been computationally modeled. This may provide a logical framework for three-dimensional spontaneous onset of magnetic reconnection. This has been submitted to *Physical Review Letters*.

We have submitted a paper [3] to *Nature- Physics* that outlines a laboratory example of impulsive onset of magnetic reconnection. In many space, astrophysical and laboratory plasmas, magnetic reconnection converts magnetic energy into particle thermal and flow energy during unsteady, impulsive, explosive events. How the onset and cessation of these events abruptly comes to pass has been a long-standing question. We show a three dimensional laboratory example of the onset and stagnation of Sweet-Parker type magnetic reconnection that is self consistently driven by magnetohydrodynamic attraction and collision of magnetized, parallel current (flux) ropes. The mutually attracting flux rope plasmas advect oppositely directed magnetic fields towards each other, accompanied by the annihilation of magnetic flux. When the inflow speed increases past the Sweet-Parker speed $v_{SP} = v_A / S^{1/2}$, where $v_A$ is the Alfven speed and S is the Lundquist number for the reconnection layer, the magnetic flux arrives faster than flux annihilation can process it. This is a threshold for magnetic flux and pressure pile up around the reconnection region, accompanied by changes in the magnetic topology. The piled up fields generate forces that react back on the incoming flux ropes to stall the inflow and thus the reconnection process.

A three-dimensional probe positioner has been designed, installed, and is in use to explore three-dimensional volumes of plasma with good spatial resolution. This paper [4] has been accepted and will appear in Review of Scientific Instruments in 2008.

A paper [5] that discusses the long lifetime and apparently stabilized kink unstable flux rope has been published in Journal of Geophysical Research. It shows experimental measurements of the electrostatic electric field that is part of the 3D self-organization of the flux rope, which is the quantum of MHD. The twist which is the spin of the current rope on its own axis rotates in the opposite direction to the write which is a 3D helical gyration of the flux rope as it corkscrews like a barber pole shape. Ideally, the twist plus the writhe total to a constant. The twist appears to be consistent with a drift Alfven wave and drift driven by a radial E field crossed with the axial B field. The writhe is the signature of the kink instability itself. The twist and writhe couple the electron and ion dynamics.

## References


1. Sun, X., T. P. Intrator, L. Dorf, I. Furno, and G. Lapenta. Transition of MHD kink stability properties between line-tied and non line tied boundary conditions. 2008. *Physical Review Letters.* **100**: 205004.

2. Sun, X., T. P. Intrator, L. Dorf, and G. Lapenta. Relationship between flux rope merging, bouncing and onset threshold for 3D Sweet-Parker reconnection. *Physical Review Letters.*

3. Intrator, T. P., X. Sun, G. Lapenta, I. Furno, and L. Dorf. Experimental onset threshold and magnetic pressure pileup for 3D Sweet-Parker reconnection. *Nature -Physics.*

4. Intrator, T. P., X. Sun, L. Dorf, I. Furno, and G. Lapenta. A three dimensional probe positioner. To appear in *Review of Scientific Instruments .*

5. Intrator, T. P., I. Furno, D. D. Ryutov, G. Lapenta, L. Dorf, and X. Sun. Long-lifetime current-driven rotating kink modes in a non-line-tied plasma column with a free end. 2007. *Journal of Geophysical Research-Space Physics .* **112**: A05S90.


## Publications


Furno, I., T. Intrator, and D. D. Ryutov. Current-driven rotating-kink mode in a plasma column with a non-line-tied free end. 2006. *Physical Review Letters.* **97** (12006): 015002.

Intrator, T. P., I. Furno, D. D. Ryutov, G. Lapenta, L. Dorf, and X. Sun. Long lifetime current driven rotating kink modes in a non line-tied plasma column with a free end. 2007. *Journal Geophys Res. - Space Physics.* **112**: A05S90.

Intrator, T. P., X. Sun, G. Lapenta, I. Furno, and L. Dorf. Experimental onset threshold and magnetic pressure pileup for 3D Sweet-Parker reconnection.. *Nature Physics.*

Intrator, T. P., X. Sun, L. Dorf, I. Furno, and G. Lapenta. A three dimensional probe positioner. To appear in *Review of Scientific Instruments .*

Sun, X., T. Intrator, L. Dorf, and G. Lapenta. Flux rope coalescence, bouncing, and spontaneous magnetic reconnection. *Physical Review Letters.*

Sun, X., T. P. Intrator, L. Dorf, I. Furno, and G. Lapenta. Transition of MHD kink stability properties between line-tied and non line tied boundary conditions. 2008. *Physical Review Letters.* **100**: 205004.

# Theoretical Studies of Cold Atom Fermi-liquids and Bose-Einstein Condensates on Chips

*Eddy Timmermans*

20061558PRD3

## Abstract

In this project, we have developed a cluster expansion for calculating the ground state energy of a mixture of fermionic and bosonic atoms that interact through short-range interactions. This system, which can be created and controlled in ultra-cold atom traps exhibits a quantum phase transition and promises an interesting new avenue of research for cold atom physics. We discovered how and why the mean-field description breaks down qualitatively near the spinodal decomposition line, and how a cluster expansion method can calculate the higher order contributions in the limit of low BEC-density. We developed a Thomas-Fermi treatment to study the effects on the atom trap density profiles, which can be measured accurately with current cold atom technology. This study suggests intriguing new prospects for cold atom studies of many-body physics in general and of quantum phase transition physics in particular.

## Background and Research Objectives

We have studied the ground state energy of a homogeneous mixture of a cold atom mixture of a Bose-Einstein condensate (BEC) of single spin component, neutral bosonic atoms and a normal (i.e. non-superfluid) Fermi-liquid of ultra-cold fermionic atoms. This system can undergo phase separation transitions such as observed in condensed, low temperature helium-3/helium-4 mixtures. We studied the mixture near the phase transition that brings the system from a homogeneous mixture to a spatial configuration in which part of space is occupied by fermions only that have separated from the fermion-boson mixture. The transition boundary of the phase diagram can be crossed in cold atom experiments by increasing the strength of the fermion-boson interactions in a magnetically controlled Feshbach resonance. The latter cold atom technique gives rise to the highly unusual knob of varying inter-particle interactions by varying the strength of a near-homogeneous, external magnetic field near specific values. Mathematically, the variation of the magnetic field knob near the phase separation transition controls the value of a Hamiltonian parameter that suddenly alters the nature of the ground state, so that the anticipated cold atom fermion-boson phase separation phenomenon is a quantum phase transition that can be studied in an unusually accessible, controllable many-body system.

The ability to gradually and accurately steer a many-body quantum system along a predetermined trajectory of its phase diagram, crossing phase boundaries at will illustrates the unprecedented advantages that the cold atom laboratory has to offer to study many-body physics. In heavy fermion systems and high $T_c$ superconductivity – phenomena that are expected to be caused by the nearness of a second-order quantum phase transition (called "quantum criticality") – the variation of Hamiltonian parameters are difficult to control reliably and the measurement of the specific consequences of direct interest are often even more difficult to carry out. In sharp contrast to the strongly correlated electron materials, the cold atom technology also offers a degree of experimental accessibility that is unusual in many-body physics. At the nano Kelvin energy and temperature range reached by laser cooling, the many-body quantum physics manifests itself at the micron length scale and the millisecond time scale. Micron scale physics can almost be imaged directly by visible light and the optical technology allows manipulations on the nanosecond time scale. Cold atom physics then provides an unusual and intriguing window on many-body physics that are typically relevant to inaccessible and hard-to-control physical systems. In addition to quantum critical systems, some of the fermion-boson physics is relevant, for instance, to neutron star physics, in the regions below 'neutron-drip' in which neutrons move between protons that are arranged in a Coulomb lattice. The neutrons than interact with the vibration modes of the proton Coulomb lattice, which are

phonons, similar to the interaction of the fermionic atoms with the low-lying excitations of the BEC of cold atoms. Another example of a relevant system is the condensed, low temperature mixture of helium-3/helium-4 mixtures that exhibited the phenomenon of phase separation. While these studies revealed the importance of mediated interactions, strong interactions and finite-range-interactions effects preclude a first-principles understanding of this mixture. Hence, cold atom physics promises to shed light on the many-body structure of systems that are inaccessible or not available for tabletop experimentation. While the cold atom systems do not resemble the strongly correlated electron materials in detail, their study can still reveal general properties relevant to the latter systems. For instance, if quantum phase transitions exhibit scaling, as has been postulated, than cold atom measurements can possibly reveal the scaling properties of all transitions of systems in the same universality class.

The objectives of this project were partly determined by the previous work that was published on the description of the ultra-low temperature fermion-boson mixtures with short-range interactions. First, we wanted to explore the breakdown of the mean-field approximation that has been successful in describing most cold atom experiments, as the interactions tend to be weak. However, the competition of a weak interaction with a correlation-induced interaction can invalidate the mean-field description, which fails to pick up the correlations. In the case of the fermion-boson mixtures, we found that it is the competition of the fermion-mediated and hard-sphere boson-boson interactions that causes the spinodal decomposition that causes the fermion-boson mixture to separate into regions of approximately equal size. Secondly, we wanted to explore the explicit connections with quantum phase transitions. In the fermion-boson mixture, we found that, contrary to the mean-field description, the boson compressibility diverges near the spinodal decomposition instability. This type of behavior is reminiscent of critical opalescence in ordinary (finite temperature) phase transitions and the power law of its divergence will provide one of the critical exponents of the relevant scaling dynamics. On a more practical side, the diverging compressibility would make the density profile of a BEC trapped in a BEC-CHiP-arrangement near a surface in a fermion-boson mixture ultra-sensitive to the tiniest variations of the potential of the surface. Hence the BEC-density profile could image the potential surface very accurately with micron scale resolution. This surface imaging scheme has been demonstrated with single BEC's, but we note that the BEC-mixtures could yield order of magnitude improvements in the sensitivity of the surface probe.

## Importance to LANL's Science and Technology Base and National R & D Needs

In the long term, cold atom physics is of strategic interest to the laboratory and can provide the nation with unique and relevant science resources in the areas of threat reduction (TR) and information science and technology (IS&T). The cold atom systems are created with scalable technology so that atom traps and their control knobs will be miniaturized (efforts in this direction are under way) to yield easy-to-handle devices that could be cold-atom based surface microscopes, ultra-high resolution sensors of magnetic or gravity fields, gyroscopes and interferometers. The exquisite sensitivity of ultra-cold atoms, their quantum coherence properties under the proper experimental conditions and the fact that they are amenable to the ultra-precise techniques of optics (in particular laser-based optics) lead to estimates of the accuracy of such devices that are comparable to or exceed the accuracy of the commercially available, often larger and more difficult to transport versions of the above named devices. The combination of atom-optical technology with the convenience of condensed matter surface physics also promises a convenient architecture for the implementation of quantum information protocols.

In the short term, cold atom physics offers the prospect of unprecedented access to interesting parameter regions and unsolved problems of quantum many-body physics. The boson-fermion mixture studies of this project have addressed fundamental issues relevant to astrophysics (neutron star physics), condensed matter and materials science (quantum phase transitions). In particular, the insights into the correlation physics that drives the fermion-boson phase separation transition suggests new avenues for cold atom explorations of quantum phase transition physics, as well as to a theoretical framework for attacking the unsolved problem of describing quantum phase transitions. The project has therefore contributed to the goals of materials science, which has been targeted by the 'complex transition' as a focal point for Los Alamos science, as well as to the goals pursued by the study of strongly correlated (*f*-electron) materials, which is a Los Alamos grand challenge area.

## Scientific Approach and Accomplishments

Deborah Santamore worked with me for one year and a few months on this project as a postdoctoral Los Alamos Director's fellow before she took a job on the faculty of Temple University in Philadelphia. Some of the results of this work have been published in a long paper in Physical Review A [1]. In addition, we are writing up two

shorter, joint papers that report on other aspects of our findings. The project considered cold atom mixtures of a Bose-Einstein Condensate of bosonic (integer spin) atoms overlapping with a Fermi-fluid of fermionic (half integer spin) atoms. All fermionic atoms and all bosonic atoms are assumed to occupy the same spin state so that they are indistinguishable and exhibit spin statistics. The system is at a very low temperature, although the temperature is assumed to exceed the critical temperature for p-wave fermion pairing that can be induced by the boson mediated interactions. These conditions are realistic for current cold atom experiments. In this project we have developed a cluster expansion of the zero-temperature equation of state – the ground state energy of the homogeneous mixture at fixed boson and fermion densities. The cluster expansion allowed us to study higher order correlations of the system in the low BEC density-limit near the transition point for the phase separation transition. The specific phase separation phenomena of interest here is similar to the phase separation observed in low temperature condensed helium-3/helium-4 mixtures: above a specific fermion concentration or density, the system can reach a lower energy (or free energy) by rearranging its atoms spatially, creating spatial regions in which only fermion atoms reside. The temperature in the condensed helium-3/helium-4 mixtures is still sufficiently high to describe that phase transition as an ordinary finite temperature transition driven partly by the entropy of the system. In contrast, the cold atom mixtures can be brought to zero-temperature conditions at which the system can only nucleate by means of macroscopic many-body tunneling and the dynamics of the phase transition is driven only by the interactions and depends on the variation of a Hamiltonian parameters that can be controlled by experiment: the phase transition is a quantum phase transition (albeit a first order one). The results of our calculations show how and why the mean-field description fails in describing the physics near the transition point. The mean-field description had previously been used in determining the quantitative conditions for which the inhomogeneous trap system would exhibit phase separation. To describe the inhomogeneous trap density profiles, we developed an improved Thomas-Fermi description from the equation of state. These studies allowed us to zoom in on the striking experimental signatures that can be used to observe the failure of the mean-field description in the boson density profile and to observe the effects of the boson-mediated fermion-fermion interactions in the density imprint of a smaller BEC emerged in a larger, trapped fermion system.

The cluster expansion that we developed in this project is a generalization of the Goldstone diagram technique to calculate the many-body energy in an all-fermion system. The inclusion of the boson degrees of freedom in the boson-fermion mixture need to be handled with care. Previously published studies missed out on the dominant perturbation contribution because they excluded contributions that correspond to zero-momentum transfer processes. The correct treatment, as we show, can be obtained from a careful treatment of the large system limit. This analysis results in a boson compressibility that diverges as the mixture approaches the line of spinodal decomposition from the homogeneous mixture side, as shown inFigure 1.

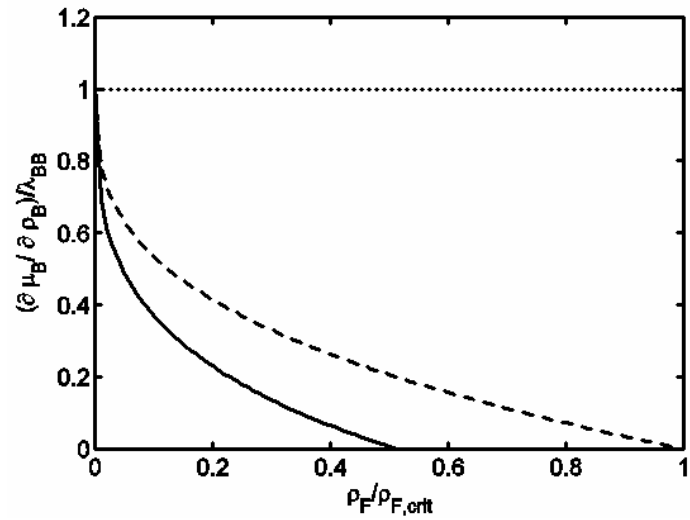


*Figure 1. Graph of the inverse boson compressibility (arbitrary units) as a function of the fermion density. The dotted line shows the inverse boson compressibility obtained from the mean-field description; the dashed line shows the inverse compressibility calculated in second order perturbation theory; the full line shows the result from the infinite series summation.*

Calculating up to second order, we found that the divergence is caused by the fermion-mediated boson-boson interactions and that the mechanical instability that signals spinodal decomposition occurs at the same value of the fermion density as in the mean-field description. However, in the presence of a quantum phase transition, we should not trust low order perturbation theory to give quantitatively accurate values. A general diagrammatic analysis rapidly becomes intractable, but in the limit of low BEC-densities (so low that the BEC coherence length significantly exceeds the average fermion-fermion distance) only a limited class of diagrams survive that we can add to all orders. These diagrams are shown in Figure 2. The result of this infinite series summation gives a fermion density at which the spinodal decomposition sets in that is $(4/5)^3$ approximately equal to 0.5. Hence, correct perturbation treatment shows that the mediated interaction causes the compressibility to diverge and higher order calculations show that the boundaries of the phase diagram can be substantially affected by higher order correlations. In the region where higher order corrections are less important

we can study the effects of boson mediated interactions in a Hartree-Fock approximation. This study links the boson-fermion mediated interactions to a Yukawa interaction model for fermion-fermion attraction. Our study revealed that if the fermions and bosons have comparable masses that retardation significantly alters the equation of state, giving fermion-fermion interaction energies that could differ by a factor of two. The term that is affected by the retardation is the exchange energy. We have shown that a striking example of the boson-mediated interaction can be found in the density profile of a cold atom fermion system where the fermions overlap with a small BEC. We developed a Thomas-Fermi treatment to study the effects of the mediated interactions and the diverging boson compressibility on the atom trap density profiles which can be measured accurately with current cold atom techniques. The divergence of the compressibility gives striking effects on the BEC density profile as the BEC shrinks markedly and the BEC-density derivative is proportional to the compressibility.

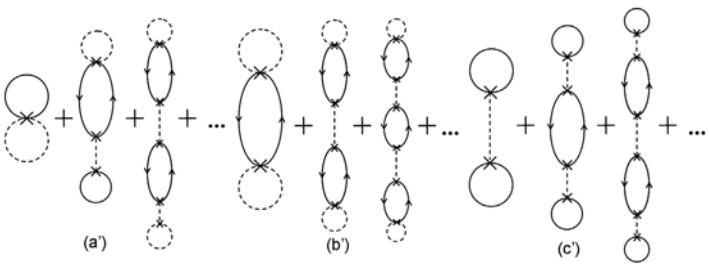


*Figure 2. Goldstone diagrams representing the infinite series summation carried out to calculate the ground state energy of a homogeneous fermion-BEC mixture with short-range interparticle interactions in the low BEC-density limit.*

## References

1. Santamore, D., and E. Timmermans. Fermion-mediated interactions in a dilute Bose-Einstein condensate. 2008. *Physical Review A.* **78** (1): 013619.

## Publications

Santamore, D., and E. Timmermans. Fermion-mediated interactions in a dilute Bose-Einstein condensate. 2008. *Physical Review A.* **78** (1): 013619 .

# Search for Temporal Variation of the Fine Structure Constant

*Justin Roald Torgerson*

20061563PRD3

## Abstract

The possibility of fundamental constants varying in both space and time would definitely imply new physics beyond the Standard Model and lend support for various theories constructed to unify gravity with other forces. Variation of nongravitational constants would, in addition, violate Einstein's Equivalence Principle. Recently, evidence for temporal variation of the fine-structure constant ($\alpha = 2\pi e^2/hc$, where e is the electron charge, h is Plank's constant and c is the speed of light), a dimensionless quantity characterizing the strength of the electromagnetic interaction, was found from analyses of quasar absorption spectra [1]. The result is controversial since other groups, using different data and methods, claimed zero variation. This has generated much motivation for performing laboratory measurements, which are controllable, reproducible, and do not rely on numerous assumptions.

This work supports a larger project to measure α-variation using optical frequency standards by investigating novel ideas regarding the production and spectroscopy of $Yb^{2+}$. There are several promising avenues of investigation for production of trapped $Yb^{2+}$ which we must consider since $Yb^{2+}$ has not been trapped previously. Moreover, these investigations require a stable, turn-key source of neutral Yb and $Yb^{+}$ that are the focus of much of the work discussed. Spectroscopy of trapped $Yb^{2+}$ is also novel and laser sources and techniques must be developed to succeed with this experimental effort. This project pursued a novel approach to the production of $Yb^{2+}$ using a 252 nm laser.

## Background and Research Objectives

The basic underlying assumption of all currently successful theories, from Newtonian gravity to the Standard Model, is that fundamental constants (FCs) do not vary in space or time. It is, of course, natural to question the validity of this assumption and experimentally test it. Any result showing variation would definitely signify new physics beyond what is already known. Furthermore, such variation would violate Einstein's Equivalence Principle (EEP) and therefore be forbidden by general relativity (and all other metric theories of gravity). Thus, testing this assumption could constrain numerous theories aimed at unifying gravity with the other forces.

In addition, recent discoveries in astrophysics and cosmology continue to provide ample motivation to look for FC-variation. These discoveries include the determination that the cosmic microwave background has an unexpected large-scale structure, that the expansion of the universe is still accelerating, and that it mostly contains dark energy and dark matter. Theories to explain these and other observations lead to the possibility and even predict variation of fundamental constants.

Of particular interest among FCs are the dimensionless coupling constants that determine the strength of the fundamental forces. Of these, the coupling constant of the electromagnetic force, the fine-structure constant (α), has received considerable attention. Currently, the evidence for variation of α is inconclusive. The data come from observational measurements collected from ancient sources from which α-variation can be deduced. So far, most of the data suffer from relatively low sensitivity and/or systematic effects which limit their results.

Several astrophysical searches and analyses of the Oklo natural fission reactor phenomenon have reported results which could be interpreted as a linear change of $(d\alpha/dt)/\alpha$ ⍰ $10^{-16}$–$10^{-17}$ $yr^{-1}$ . However, other astrophysical searches have come to opposite conclusions and the most recent Oklo analysis is consistent with no change with a tighter limit. On the other hand, it has been argued that these results may be in agreement if a nonlinear variation of α, in space and/or time, is assumed. Finally, it is worth noting that these observational measurements are dependent upon models and assumptions that cannot be fully verified at present.

Laboratory measurements are only beginning to place similar limits on α-variation. However, laboratory measurements offer numerous advantages. They can be repeated under controlled conditions and do not rely on as many assumptions to complicate the interpretation. Moreover, laboratory experiments can be sustained for only a few years, but can utilize methods which provide much higher sensitivity and in systems which have larger inherent sensitivities to changes in α than those available in observational searches.

The larger experiment that this work supported is a search for time variation of alpha with optical frequency references based upon transitions in $Yb^+$ and $Yb^{2+}$ ions. The particular transitions we have selected in $Yb^+$ and $Yb^{2+}$ are insensitive to most external perturbations and possess narrow linewidths that can be excited by a stabilized laser source of the appropriate wavelength. The requirements for the linewidths of these laser sources is extremely tight but feasible: less than 1 Hz linewidths are required but, this requirement is still ten times larger than the current state-of-the-art of about 100 mHz. The requirements for the stability of the ions are equally restrictive and we require that the ions are trapped and cooled to a few 10's of microKelvin. This last requirement has driven much of the work, which was performed under the postdoctoral LDRD project reported here.

## Importance to LANL's Science and Technology Base and National R & D Needs

The intellectual merit of this project rests upon the implications of a nonzero variation of α on physics and metrology. Variation of α would play a crucial role in the development of an ultimate unified theory. In metrology, such a variation would signify a fundamental limit for the stability of next-generation atomic clocks and, thus, inevitably alter the definition of the second.

Historically, LANL has been known for excellent work in atomic spectroscopy and continues to support a broad range of work in the field from optical cooling and trapping to spectroscopy of rare, short-lived isotopes with unique properties. The work supported by this postdoctoral LDRD grant, extends and supports these technological and scientific efforts at LANL. For example, this work includes one of only two ion-trapping efforts at LANL and our expertise in laser technology and laser frequency stabilization have been requested numerous times to aid other experimental efforts at LANL. The possibility of such postdoctoral fellowships such as the one reported on here, was also important to attract young talent such as Li-Bang Wang who was its recipient.

This project enabled a strengthening of collaboration with the National Institute of Science and Technology (NIST) Time and Frequency Standards Group and further allowed us to bring technology developed there to LANL. In particular, Li-Bang and I were able to travel to NIST several times to construct and evaluate femtosecond laser oscillators to determine their adequacy for our future needs. We now have a femtosecond-laser oscillator and associated optics and electronics and are using them to develop a frequency-quadrupled optical frequency comb; a key element of our comparison of optical transition energies in $Yb^+$ and $Yb^{2+}$ ions.

LANL's work on $Yb^{2+}$ is also of interest to NIST, since it can be the basis for a new optical frequency standard of exceptional stability. The primary research proposed here directly supports the Grand Challenge of "Beyond the Standard Model" and is directly relevant to DOE, Office of Science missions. The ion-trapping technology is relevant to trace species detection for counterterrorism and nuclear nonproliferation.

## Scientific Approach and Accomplishments

The postdoctoral research project this past year has allowed Li-Bang Wang to investigate several ideas that were not parts of the original concept for our search for α-variation with optical frequency references. These include a clever scheme to stabilize the photo-ionization laser in resonance with a transverse-illuminated effusive oven source of ytterbium, saturated absorption spectroscopy of $Yb^+$ ions in a pass-through hollow cathode source to stabilize the main $Yb^+$ interrogation laser, previously untested ion trap geometries, and intra-laser-cavity frequency doubling which resulted in a more efficient frequency-quadrupled laser at 252 nm.

The photoionization laser stabilization technique resulted in our ability to consistently and without much effort load isotopically pure samples of $^{174}Yb^+$ ions. This is important since only one isotope, $^{171}Yb$, possesses the required nuclear spin (I=1/2) required for our search for alpha-variation. Our work with $^{174}Yb$ can be easily extended to $^{171}Yb$ with the addition of a frequency modulation technique to mix the F=3 and F=4 hyperfine levels of the $^{171}Yb$ ground state. Photoionization is also important because it allows us to eliminate several deleterious effects caused by excessive motion of the trapped ions due to the build-up of charges near the trapped ions. Electron-impact ionization is the most common method employed to produce

ions near an ion trap. However, the excess electrons cause potentials on the insulating surfaces within the ion trap and prevent us from cooling the ions below a few milliKelvin.

The basic principle of photoionization is shown in Figure 1. A single laser source at 399 nm illuminates Yb atoms travelling transverse to the beam and is excited with two successive photon absorptions to a state in which the valence electron is no longer bound to the $Yb^+$ ion. The separation between transition frequencies for the six stable isotopes of Yb is only a few GHz and a slight misalignment of the laser beam and oven source of ytterbium atoms or a drift in laser frequency is enough to blend the transitions and destroy the isotope selectivity of the process. The problem of laser drift can be eliminated by fixing the laser frequency relative to a reference frequency that is well known. However, the most common references use molecular iodine or methane and these molecules do not possess any transitions below 500 nm. Li-Bang solved this problem by referencing the laser to the fluorescence from a collimated oven source of neutral ytterbium which he illuminated transverse to its motion to provide the required stability of a few MHz. Figure 2 illustrates the success of this technique which provides nearly 100% isotope selectivity for loading $^{174}Yb^+$ ions into the trap [2].

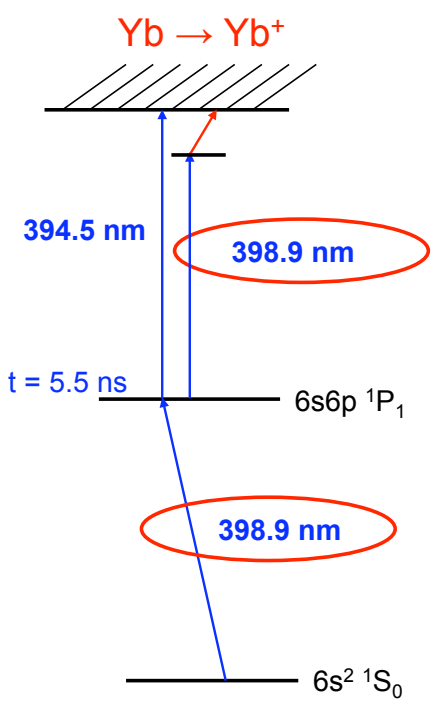


*Figure 1. Partial energy-level diagram for neutral ytterbium. Isotope selectivity is due entirely to the resonance of the 398.9 nm laser with the single P level shown. While it appears that a second 399 nm photon is not enough to effect photoionization, interaction of the excited atom with the trapping field of ~2000 V/cm is sufficient to remove the valence electron.*

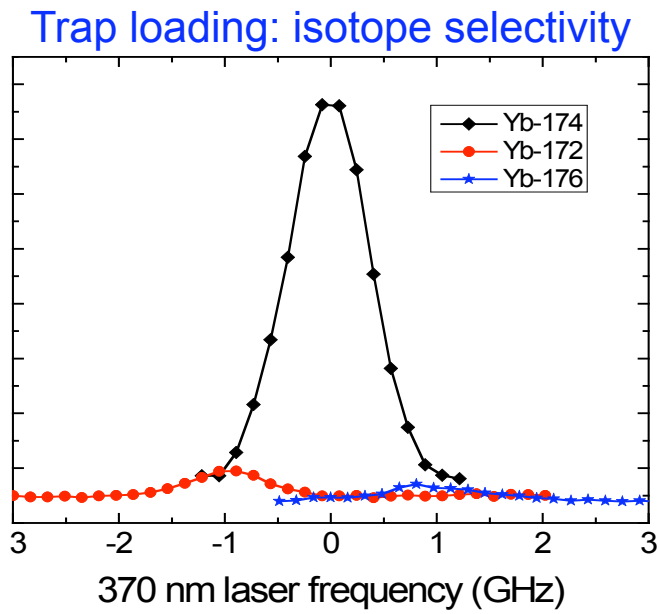


*Figure 2. Singly-ionized ytterbium fluorescence in the ion trap as a function of photoionzation laser frequency. Zero frequency is taken to be the frequency for which loading Yb-174 is most efficient. When positioned at zero frequency, the isotope selectivity for Yb-174 is better than 97%.*

Many of the requirements for this experiment are interdependent and another example of this is related, again, to the isotope selectivity of the ion trapping process. For the ions to avoid perturbation by changes in the laboratory environment, the ion trap must be well shielded from outside electromagnetic fields. This requirement for shielding is also true for photoionization process to be isotope selective. This is true because the ytterbium beam source is not tightly collimated due to the space requirements inside the vacuum system that holds the trap. Therefore, some of the atoms have a component of their motion towards or away from the photoionization laser beam and this causes a shift in the frequency of the light they absorb. This shift is several GHz; enough to prevent photoionization from being isotope selective unless the trap is carefully designed. In particular, it is important for the trapping fields to fall off quickly so that ions created away from the center of the trap are not captured. For most fields of concern to us, the converse is also true: if the fields from the trap fall off quickly, fields from the laboratory outside the trap will be shielded away from the ions within it.

Li-Bang's experimentation with new trap geometries also aided this work and allowed us to design a trap whose rf trapping field falls off rapidly enough to maintain the isotope selectivity selectivity allowed by the stabilized laser source. Previous trap geometries were far too open and caused Stark and collisional shifts of the ytterbium and reduced the isotope selectivity so that we could not separate $^{171}Yb$, $^{172}Yb$ and $^{174}Yb$ atoms.

After this fruitful work with isotope-selective loading of ions into the trap, our efforts were given to the next task of automating the process of $Yb^+$ ion cooling. Li-Bang's efforts to stabilize the 370 nm $Yb^+$ cooling and interrogation laser have resulted in its almost turn-key operation. This is important to the long-term success of the experiment and Li-Bang's method is sufficiently accurate and reproducible to be used without major modification for the lifetime of the experiment. Saturated absorption is not a new technique, but a highly optimized optical system must be used to generate a usable signal from a hollow cathode source. A hollow cathode lamp provides an electrically and motionally noisy environment, yet their availability and reasonable cost make them appealing for use as optical references for ions. Our frequency-locking signal possesses a signal/noise of greater than 30 and represents a tour de force success for this work [3]. Figures 3 and 4 show a diagram of the apparatus and the resulting signal respectively.

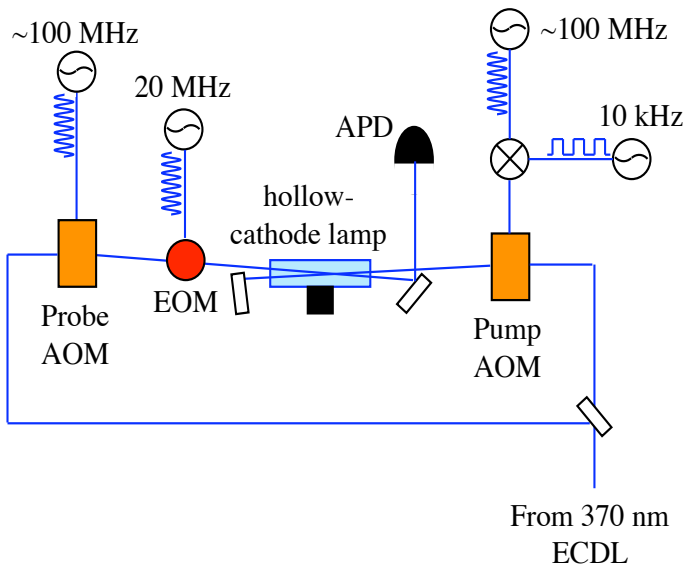


*Figure 3. Schematic diagram of the saturated absorption apparatus used to reference the 370 nm cooling laser to single-ionized Yb. AOM and EOM are acoustooptic and electrooptic modulators, APD is an avalanche photo-diode detector and the laser source at 370 nm is an external cavity diode laser (ECDL).*

We were also able to try a potentially better technique to construct a laser to excite the $Yb^{2+}$ ions once they are trapped. Laser-driven resonance fluorescence is the most sensitive technique to determine that an ion is contained within an ion trap. However, the strongest transition that is accessible with current laser technology is about 20 times weaker than the transition we used in $Yb^+$ at 370 nm, and is deep in the ultraviolet region at 252 nm. The most common scheme for generating tunable coherent light in the deep-uv is to frequency-quadruple readily available near-ir diode or Ti:Sapphire lasers with two steps of frequency-doubling. The frequency-doubling stages involve external resonant cavities that are required to increase the intensity of light incident upon a nonlinear crystal. These cascaded doubling cavities produce enhanced amplitude noise from both amplitude and frequency noise of the master laser and can prevent us from seeing the signal from weakly emitting $Yb^{2+}$ ions. The technique, which we employed, was to modify a commercial Ti:Sapphire laser by replacing several of the optical elements with custom optics and to insert a carefully arranged potassium-niobate crystal within the modified cavity. We followed this configuration with a single external enhancement cavity as the final stage of frequency-doubling. Our calculations showed that this technique was feasible, which disagreed with the manufacture's analysis of the same problem. We succeeded and were able to eliminate one of the external doubling stages and its associated electronics which has resulted in a significantly lower noise and more stable output of several milliWatts at 252 nm [4].

*Figure 4. Absorption of a single 370 nm laser beam (red) and saturated absorption of two counter-propagating beams (blue) for the same ytterbium hollow-cathode lamp. Note the greater detail*

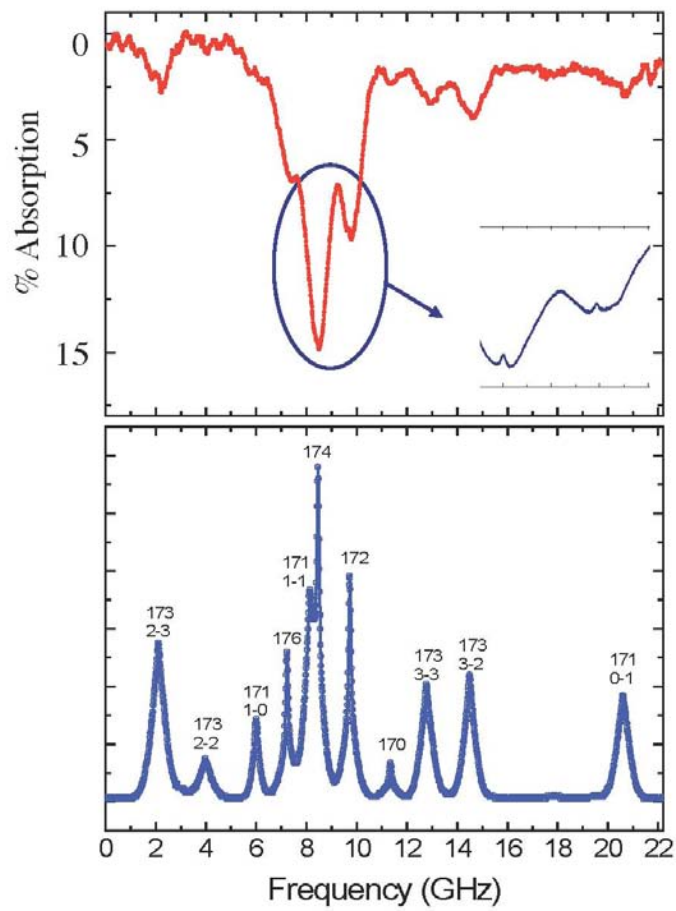


*and narrower features in the saturated absorption spectrum.*

In conclusion, this postdoctoral project has provided Li-Bang with the opportunity to explore several ideas

outside the main course of our experimental efforts, which have improved our chances for success. The most significant of these ideas have been techniques for frequency stability of our specific laser sources for which simple references do not exist, improved ion trap designs and understanding and a better technique for frequency quadrupling of a commercial narrow-linewidth Ti:Sapphire laser source. Li-Bang left us in January of this year to take a position at National Tsing-Hua University – one of Taiwan's top research universities.

## References


1. Murphy, M. T., J. K. Webb, and V. V. Flambaum. Further evidence for a variable fine-structure constant from Keck/HIRES QSO absorption spectra . 2003. *Monthly Notices of the Royal Astronomical Society.* **345**: 609.

2. Wang, L.- B., A.- T. Nguyen, M. M. Schauer, and J. R. Torgerson. Efficient photoionization loading of ytterbium and indium ion traps. Presented at *38th Annual Meeting of the Division of Atomic, Molecular, and Optical Physics .* (Calgary, Alberta, Canada, 5-9 June 2007).

3. Schauer, M. M., J. Danielson, D. Feldbaum, A.- T. Nguyen, L.- B. Wang, X. Zhao, and J. R. Torgerson. Trapping and spectroscopy of singly- and doubly-charged ytterbium ions. To appear in *Physical Review A.*

4. Wang, L.- B., D. Feldbaum, J. Ogren, and J. R. Torgerson. DUV laser source for laser cooling and spectroscopy of doubly-ionized ytterbium. To appear in *Reviews of Scientific Instruments.*


## Publications


Schauer, M. M., A.- T. Nguyen, L.- B. Wang, J. Danielson, D. Feldbaum, X. Zhao, and J. R. Torgerson. Trapping and spectroscopy of singly- and doubly-charged ytterbium ions. To appear in *Physical Review A.*

Wang, L.- B., A.- T. Nguyen, M. M. Schauer, and J. R. Torgerson. Efficient photoionization loading of indium and ytterbium ion traps. Presented at *38th Annual Meeting of the Division of Atomic, Molecular, and Optical Physics .* (Calgary, Alberta, Canada, 5-9 June 2007).

Wang, L.- B., D. Feldbaum, J. Ogren, and J. R. Torgerson. DUV laser source for laser cooling and spectroscopy of doubly-ionized ytterbium. To appear in *Reviews of Scientific Instruments.*

# Quantum Fluctuations in Bose-Einstein Condensates

*Eli Ben-Naim*

20070573PRD1

## Abstract

High precision frequency standards such as atomic clocks are critical for applications of great national significance such as the satellite GPS system. Another emerging technology is computing, using inherently quantum mechanical devices, i.e., quantum computing. Such applications require highly accurate theoretical understanding and descriptions of macroscopic quantum states. This theoretical project explores an important quantum mechanical effect that has been largely overlooked to date that impacts systems important for quantum computation and atomic clocks.

## Background and Research Objectives

Superfluidity continues to fascinate physicists many decades after its discovery in 1938. It is widely accepted that a superfluid flow exhibits a critical velocity below which an object immersed in the flow would feel no force despite the fluid's movement. However, this mechanism ignores the presence of quantum fluctuations which, there is reason to believe, can produce a drag force on an immersed object and thus affect the critical velocity. Inspired by the work of Hendrik Casimir who showed that quantum fluctuations produce a force in a perfect electromagnetic vacuum, our early work shows that the scattering of quantum fluctuations should produce a slight damping force on an idealized object in a slow-moving infinitely extended dilute Bose-Einstein condensate [1]. Dilute BECs are a recently discovered form of matter that have superfluid behavior and provide a convenient medium in which to investigate quantum fluctuations because, compared to superfluid Helium, they are both better understood theoretically and more easily manipulated experimentally.

Our proposed "Casimir-drag" force may underlie the discrepancy that exists between theory and experiment in superfluid Helium. However, while the existence of a Casimir-drag force has the potential to explain the observed critical velocity and may even improve understanding of superfluid turbulence, it raises a number of fundamental questions about the basic nature of superfluidity, such as how persistent currents can exist and how fluctuations can dissipate energy. This research project addressed these apparent paradoxes.

## Importance to LANL's Science and Technology Base and National R & D Needs

This work supports the threat reduction mission and has applications in areas such as encryption and secure computing via the connections with quantum computation. Further application in precision time standards are central to systems of national importance such as the GPS network. It supports core LANL competencies in theoretical physics, nanoscience and nanotechnology.

## Scientific Approach and Accomplishments

This project produced progress in two areas: Casimir drag force and phase transitions in synchronization as detailed below.

**Casimir drag force induced by quantum fluctuations.**

We had significant progress in calculating the drag experienced by an impurity of any strength moving through a quasi 1-D Bose-Einstein condensate (BEC). Not only have we been the first to show that such a force exists in this geometry, but we have been able to calculate the force's dependence on velocity and impurity strength as detailed in a forthcoming publication. We contacted ultracold atom experimentalists from the University of Washington who has expressed an interest in looking for this effect in his BEC experiments in quasi-1d geometries.

We also have progress in simulating this drag effect in dilute condensates using a quantum simulation

technique that approximates the quantum fluctuations by Wigner noise. This computation approaches the problem from a new perspective and we expect to finish this project before the end of the year. Most importantly, experimentalists at Los Alamos have expressed interest in looking for this effect and these detailed numerical simulations will be invaluable for that endeavor.

In a related investigation, we have formulated the problem of Casimir drag in superfluids in the context of a fermionic system: a drag force is caused by the scattering of quantum fluctuations within a flow of superfluid fermions. Here, the problem has many new physical effects and promises to be important for current fermionic experiments. We have also made progress in calculating the static Casimir effect in a BCS superfluid (the standard model of superconductors), the existence of which demonstrates the important implications of quantum fluctuations in these systems.

Finally, we investigated Casimir drag forces induced by quantum fluctuations in a moving superfluid scattering off a potential well. In particular, we advanced beyond initial calculations in an idealized system towards a more experimentally realizable geometry. In particular, our research posits the hydrodynamic boundary condition for a superfluid in a realistic container with rough walls, a result that can be applied directly to experiment. For a given superfluid flow, this boundary condition describes how the scattering of quantum fluctuations generates a temperature difference between the material wall and the superfluid, resulting in the conversion of some normal fluid at rest along the boundary even when the boundary is held at zero temperature. These ideas that were published recently in Phys. Rev. B have already generated interest among experimentalists at Lancaster University working with He3.

Our results also cast the Casimir-drag effect as a nonequilibrium quantum phase transition. It is a phase transition in the sense that superfluid is converted reversibly into normal fluid. This phase transition is driven by quantum rather than thermal fluctuations. Quantum phase transitions are significant for a number of reasons. For instance, since quantum-level events thereby can have a direct macroscopic effect, phase transitions have great potential for use in future technological applications. Furthermore, quantum phase transitions are widely held to be the key to understanding enigmatic properties such as high-temperature superconductivity. To date the focus has been largely on equilibrium quantum phase transitions; their nonequilibrium counterparts remain elusive. However, recent advances in the field of ultracold atomic gases now make it possible to conduct precise experimental study of nonequilibrium quantum dynamics and there isa pressing need for theory to keep abreast.

**Phase transition in synchronization**.

To understand nonequilibrium phase transitions, we considered the paradigmatic transition from an unsynchronized state to a synchronized one in a system of coupled oscillators using the classical Kuramoto model. This model describes numerous phenomena in a wide range of fields, from Josephson junctions and atomic recoil to populations of flashing fireflies and the synchronized action of cardiac pacemaker cells. We have generalized the classical results of the Kuramoto model and showed that using complex variables, the nonlinear coupling mechanism can be replaced by an ordinary linear coupling. This is a significant theoretical simplification as it enables a direct solution of the underlying linear equations. We have used these equations to study static and dynamic characteristics of the transition from anon-synchronized state into a synchronized state.

Furthermore, we have made some progress with framing the problem of quantizing the Kuramoto self-synchronization model and have also made progress towards solving it. One of the more significant strides we have made is the successful embedding of this dissipative system within a Hamiltonian formalism, a crucial first step towards developing a general quantized model of synchronization.

Finally, we extended our previous results on the linear reformulation of the Kuramoto model. We are in the process of generalizing the linear reformulation too much larger classes of intra-system couplings by applying spectral theory to the problem of synchronization.

## References

1. Roberts, D. C., and Y. Pomeau. Casimir-like force arising from quantum fluctuations in a slow-moving dilute Bose-Einstein condensate. 2005. *Phys. Rev. Lett.* . **95**: 145303.

## Publications

Perlstein, E. O., D. M. Ruderfer, D. C. Roberts, S. L. Schreiber, and S. L. Schreiber. Genetic basis of individual differences in the response to small molecule dru gs. 2007. *Nature Genetics.* **39**: 496.

Pomeau, Y., and D. Roberts. On the hydrodynamic boundary condition for superfluid flow. 2008. *Phys. Rev. B.* **77**: 144508.

Pomeau, Y., and D. Roberts. Casimir Friction I: Friction of the vacuum on a spinning dielectric. To appear in *Modern Encyclopedia of Mathematical Physics.* Edited by Arefeva, I., and D. Sternheimer.

Pomeau, Y., and D. Roberts. Casimir Friction II: Casimir effect on drag in zero temperature superfluids. To appear in *Modern Encyclopedia of Mathematical Physics.* Edited by Arefeva, I., and D. Sternheimer.

Roberts, D.. Solving the Kuramoto model of a self-synchronizing, finite population of glob ally coupled oscillators.. 2008. *Phys. Rev. E.* **77**: 03114.

Roberts, D. C., and R. Teodorescu. A linear path towards self-synchronization: Analysis of the fully locked transition of the Kuramoto model.. 2008. In *First International Workshop on Nonlinear Dynamics and Synchronization INDS'08.* (Klagenfurt, Austria, 18-19 July, 2008). , p. 184. Germany: Shaker Verlag.

Roberts, D. C., and R. Teodorescu. A linear path toward synchronization: Anomalous scaling in a new class of exactly solvable Kuramoto models.. To appear in *European Physical Journal.*

Roberts, D., and A. Newell. Finite-time collapse of N classical fields described by coupled nonlinear Schrodinger equations. 2007. *Phys. Rev. E.* **74**: 047602.

# Technology

continuing project

# Image Reconstruction with Time-Reversal Mirrors

*Paul Allan Johnson*

20060046DR

## Introduction

Conventional seismic imaging relies on determining time delays and amplitude changes from one or more sources to one or more receivers, and then inverting for the velocity or attenuation structure. Normally, just the compressional (P) wave is used, but occasionally the shear (S) wave is used as well. Remarkably, all of the remaining wave energy rattling around the system, known as the "coda" in seismology and acoustics, is thrown away in conventional imaging, yet the coda contains almost all of the wave source and scattering-source information! If that information in the waveform could be used, we could obtain the complete transfer function between the sources and the receivers, as well as characterize individual sources.

Our work is focused on applying *elastic-wave time reversal* to imaging real and virtual sources (wave scatterers). The work is revolutionizing imaging itself while simultaneously developing the means to learn about the characteristics of a complex source like an earthquake or a virtual source (scatterer) like a disbond in a part. Of note is that the method we are developing may be the only means to reliably locate recently discovered earthquakes known as "non-volcanic tremor," that have long duration signals. The implications of locating tremor in regards to earthquake prediction may be significant.

We have the means to image "around corners" for instance, because we use all of the waveform. The idea proposed here has never before been conceived of nor attempted. The approach we take is to use the concept of the Time Reverse Mirror. The Time Reverse Mirror is a simple and ingenious way to recreate from measured signals a virtual source (e.g., a scatterer like a pit anomaly) or a real source (e.g., an earthquake). The Time Reverse Mirror can be understood as follows: imagine filming a pebble dropped into a pond of water. Ripples emanate outward from the pebble, a "real" wave source. A rock reed from the pond is a "virtual" source that scatters the waves. Stop the movie some time after the scattering took place, and run it backwards to the time when waves intersect the reed; then to the time when the pebble impacts the surface. We can "reconstruct" each of the two sources by freezing the movie at different times. This analogy describes the idea behind the time reversal mirror technique. Figure 1 shows an example of applying time reversal in an aluminum plate in order to image the original source. The large peak shows the spatial extent of the time-reverse focus. Time reversal works because the wave equation does not depend on whether the wave propagates forward or backwards in time. This is called reciprocity. We are advancing the Time-Reversal Mirror method to develop a universal high-resolution image reconstruction approach, and integrate it with sophisticated image analysis.

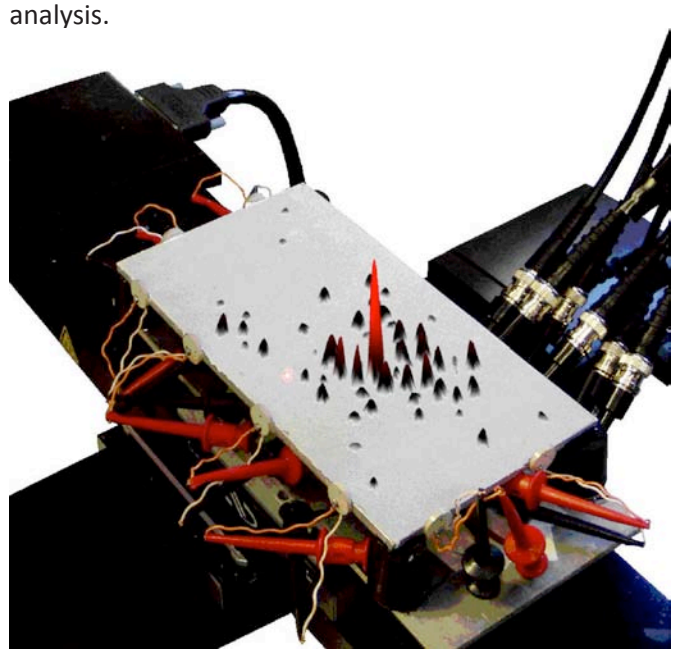

*Figure 1. Photograph of a rectangular aluminum plate used in a Time Reversal study. The overlaid peaks on the plate display the velocity magnitude from actual measurements. The overlay-image was taken at the time of focus and the large-amplitude peak corresponds to the original source location. The smaller peaks are coherent wave energy that is associated with the focus [1].*

## Benefit to National Security Missions

The impact on the primary DOE missions of ensuring the safety and reliability of the U.S. nuclear deterrent, improving the nation's energy security, and enhancing the nation's fundamental scientific capabilities will be enormous, by detecting anomalies in weapons, discrim-

inating nuclear explosions from earthquakes, and answering fundamental science questions about earthquakes.

## Progress

We have made significant advances in the area of this research in the past year. We have established ourselves as the world leaders in studies and applications of time reversal to solids (including Earth), as well as in applications. Our efforts in combining time reversal and elastic nonlinear behavior of solids, termed "Time Reversal Nonlinear Elastic Wave Spectroscopy" originated at LANL, and are resulting in new and useful applications for damage diagnostics (e.g., Figure 2). Since we began our work, numerous groups in the US and Europe are following suite.

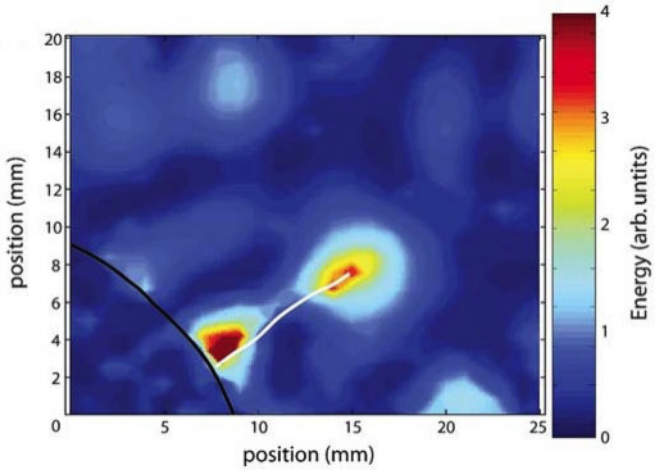


*Figure 2. Time Reversal Nonlinear Elastic Wave Spectroscopy (TRNEWS) result in a cracked metal sample. In the forward propagation when the waves intersect the crack, elastically-nonlinear-generated frequencies are created. In this case, the source signals, input outside the image area, were comprised of two frequencies. Upon interaction with the crack, a wave at the difference frequency was created. The wave field was detected outside the image area, time reversed, band-pass filtered at the difference frequency, and emitted. The signals coalesce at the origin of the difference frequency, the crack, as shown by the bright spots. The white line approximates the crack while the black curve is the edge of the sample (a steel bearing cap) [2].*

Our project addresses strategic goals of the Lab in several areas. It is already being applied to diffusion bond quality in the weapons program, with a deliverable diagnostic and imaging device slated for 2010. Support is coming from Enhanced Surveillance (Campaign 8). In addition, exploratory work is being carried out in the area of Rendersafe, with funds from NN20. This work is a direct result of the DR funding. We see other potential areas that we are in the process of developing, including locating underground structures and sending audio signals that can be localized spatially and temporally. Spin off work for imaging in Earth will be funded by Chevron (CRADA funds in negotiation). Further, we see potential applications in medicine and potential funding via sources such as NIH.

Developments that were not apart of the original proposal include the idea of combining elastic nonlinearity with time reversal In addition, our work in medical applications to bone and dental implants with the Medical Acoustics Laboratory of University of Paris 6 (P. Laugier) is another unanticipated area that we believe holds great promise in regards to development of applications and for follow-on funding (NIH is the target).

Specific accomplishments include the following. First, we have developed TR NEWS, Time Reversal Nonlinear Elastic Wave Spectroscopy diagnostic and imaging methods for nondestructive evaluation of components. We are developing Time Reverse migration imaging, both linear and nonlinear, for 2-D applications to nondestructive evaluation and extension to 3-D (work in progress). We discovered that time reversal can be applied to locating what is termed non-volcanic tremor sources—both earthquake tremor and we believe man-made tremor such as in a buried structure. These sources are very hard (nearly impossible) to reliably locate [especially depth] with existing methods. We have discovered unexpected potential developments in medicine, especially to applications of bone diagniostics related to osteoporosis diagnosis. These developments are evidence that we are now clearly established as the world leaders in this area.

In summary, our key accomplishments include device development for inspecting diffusion bonds; the development of 2-D unique and effective 2-D imaging methods for nondestructive evaluation applications, and the potential to take them to 3-D; and the other applications described above (medicine, application to tremor).

## Future Work

Our future work in this area will be to continue to develop applications that can be used in the weapons program and nondestructive evaluation. We will seek future funds from LDRD to work on the location of long-duration signal sources such as tremor and those emanating from underground structures. Potentially important medical applications may follow from this work, primarily for imaging bone integrity, important for diagnosing osteoporosis and monitoring healing from bone fracture. We will seek NIH and or DOE funds for this work.

## Conclusion

Successful completion of the research will establish Los Alamos and collaborators as the world leaders in nonlinear and linear dynamics combined with time reversal mirrors in solids. We address a number of strategic challenges in-

cluding: three-dimensional, non-destructive evaluation of weapons components developing the means to decrease the discrimination threshold between nuclear and non-nuclear events. In addition, applications to interrogate industrial components for damage will be enormous, as well as applications to imaging fractures in C02 reservoirs (the primary means of C02 escape), and imaging fractures in oil reservoirs.

## References


1. Anderson, B., M. Griffa, C. Larmat, T. J. Ulrich, and P. A. Johnson. Time Reversal. 2008. Acoustics Today. 4: 5.
2. Ulrich, T. J., P. A. Johnson, and R. A. Guyer. Interaction Dynamics of Elastic Waves with a Complex Nonlinear Scatterer Applying the Time Reversal Mirror. 2007. Physical Review Letters. 98: 10430.


## Publications


Anderson, B., M. Griffa, C. Larmat, T. J. Ulrich, and P. Johnson. Time reversal. To appear in Acoustics Today. 4: 5.

Anderson, B., T. J. Ulrich, M. Griffa, P. Y. LeBas, M. Scalerandi, and P. Johnson. Experimental identification of Masked Sources Using the Selective Source Reduction (SSR) Method. To appear in Journal of Applied Physics.

Griffa, M., R. Guyer, T. J. Ulrich, B. Anderson, and P. Johnson. Investigation of the robustness of Time Reversal Acoustics in solid media through the reconstruction of temporally symmetric sources. To appear in J. Physics D: Applied Physics.

Griffa, M., R. Guyer, T. J. Ulrich, B. Anderson, and P. Johnson. Investigation of the robustness of Time Reversal Acoustics in solid media through the reconstruction of temporally symmetric sources. 2008. Journal of Physics D. 41: 85415.

Guyer, R., and P. Johnson. The nonlinear mesoscopic class of materials.

Johnson, P.. Imaging Mechanical Defects: Time Reversal Nonlinear Elastic Wave Spectroscopy (TR NEWS) and Time Reversal Imaging Methods. To appear in McGraw Hill 2009 Yearbook of Science & Technology.

Larmat, C., J. P. Montagner, M. Fink, and J. Tromp. Time reversal location of glacial earthquakes. Journal of Geophysical Research. 113: B09314.

Muller, M., D. Mitton, M. Talmant, P. Laugier, and P. Johnson. Nonlinear ultrasound can detect accumulated damage in human bone. 2008. Journal of Biomechanics. 41: 1062.

Muller, M., T. J. Ulrich, M. Talmant, P. Laugier, and P. Johnson. Assessment of damage in cortical bone using nonlinear acoustic techniques, in, Biomedical applications of vibration and acoustics for imaging, characterization and diagnostics. Edited by Al-Jumaily, A..

Ulrich, T. J., A. Sutin, R. Guyer, and P. Johnson. Time reversal and nonlinear elastic wave spectroscopy TR NEWS techniques. 2008. International Journal of Nonlinear Mechanics. 43: 209.

Ulrich, T. J., A. Sutin, T. Claytor, P. Pappin, P. Y. LeBas, and J. TenCate. The time reversed elastic nonlinearity diagnostic applied to evaluation of diffusion bonds. 2008. Applied Physics Letters. 93: 151914.

Ulrich, T. J., A. Sutin, and P. Johnson. Imaging nonlinear scatterers applying the time reversal mirror. 2006. Journal of the Acoustical Society of America. 119: 1514.

Ulrich, T. J., M. Griffa, and B. Anderson. Symmetry-based imaging condition in time reversed acoustics. 2008. Journal of Applied Physics. 104: 064192.

Ulrich, T. J., P. A. Johnson, and R. A. Guyer. Investigating Interaction Dynamics of Elastic Waves with a Complex Nonlinear Scatterer Applying the Time Reversal Mirror. 2007. Physical Review Letters. 98: 10430.

Ulrich, T. J., P. Johnson, M. Muller, D. Mitton, M. Talmant, and P. Laugier. Application of nonlinear dynamics to progressive fatigue damage in human cortical bone. To appear in Applied Physics Letters. 91: 213901.

Ulrich, T. J., and P. A. Johnson. Imaging and characterizing damage using time reversed acoustics. To appear in Review of Progress in Quantitative Nondestructive Evaluation. (Oregon, 30 July-4 Aug. 2006).

# Construction and Use of Superluminal Emission Technology Demonstrators with Applications in Radar, Astrophysics, and Secure Communications

*John Singleton*

20080085DR

## Introduction

The project demonstrates that sources of electromagnetic radiation, such as radio waves, can be made to be superluminal, that is travel faster than the speed of light. Although this may sound like science fiction, no laws of physics are in fact being broken; the source consists of a wave-like disturbance in a special antenna made of alumina, and it obeys the principles of Relativity and Electromagnetism. Most people will be familiar with the idea of a sonic boom, an intense burst of sound encountered some distance from a high-performance airplane that accelerates through the sound barrier. This occurs because the airplane overtakes the sound waves that it has emitted, pushing them together to make the "boom". In the same way, our superluminal source overtakes its own radio waves (which travel at the speed of light), producing an "electromagnetic boom;" a region of very tightly-focused and powerful radio waves. This effect has many potential applications, including medicine (focussing beams to kill tumors), radar, long-range communications (e.g. with distant space probes) and security (e.g. disabling stolen cars without harming people in and around them). In addition to building three superluminal technology demonstrators, the current project looks at the very difficult mathematics of the electromagnetic boom (e.g. how to predict and control it) and ties superluminal emission to astronomical phenomena. We have recently shown that pulsars, neutron stars that emit pulses of radiation seen by astronomers on Earth, are natural superluminal sources; using our mathematical models, we are able to predict all of the properties of their radiation. The models are now being turned to other space phenomena such as gamma-ray bursts and Quasars.

## Benefit to National Security Missions

This project supports the DOE mission in nonproliferation by providing secure, low-power surveillance and monitoring technologies. Superluminal sources are also relevant to secure communications, radar and directed-energy applications. They provide insights into the basic principles that govern the Universe, supporting Office of Science missions.

## Progress

Technology Demonstrator 1 (TD-1), a 125 mm radius, full-circle machine, is under construction (Figure 1a). A full electromagnetic modeling has been performed for the 72-element antenna of this machine, and the individual elements (Figure 1b) have been shown to perform very well over a 30-40 percent bandwidth (the antenna design is being written up for a technical publication). This means that with minimal adaption, the same elements will be usable in the second technology demonstrator, a linear accelerator design. The first nine elements of TD-1's antenna array have been fabricated (Figure 1c) and are being used in an 8-element array (one ninth of the final machine) that enables control software and detector protocols to be tested. The other 63 antenna elements (plus several spares) are in production.

The analog/digital control circuitry for TD-1 has been designed, protyped and tested within ISR-6 using demonstrator boards (Figure 2a). Having shown that the concept is successful, the control circuits are now being mass-produced on circuit boards (Figure 2b). Use of broad-band components and two standard, computer-programmable master oscillators means that the control circuits are very adaptable; they are capable of controlling the planned second and third technology demonstrators without further modification. This is a considerable advance on original expectations; it was thought that separate control systems would be needed for each machine. In addition, it points towards the feasibility of eventually mass-producing superluminal technology.

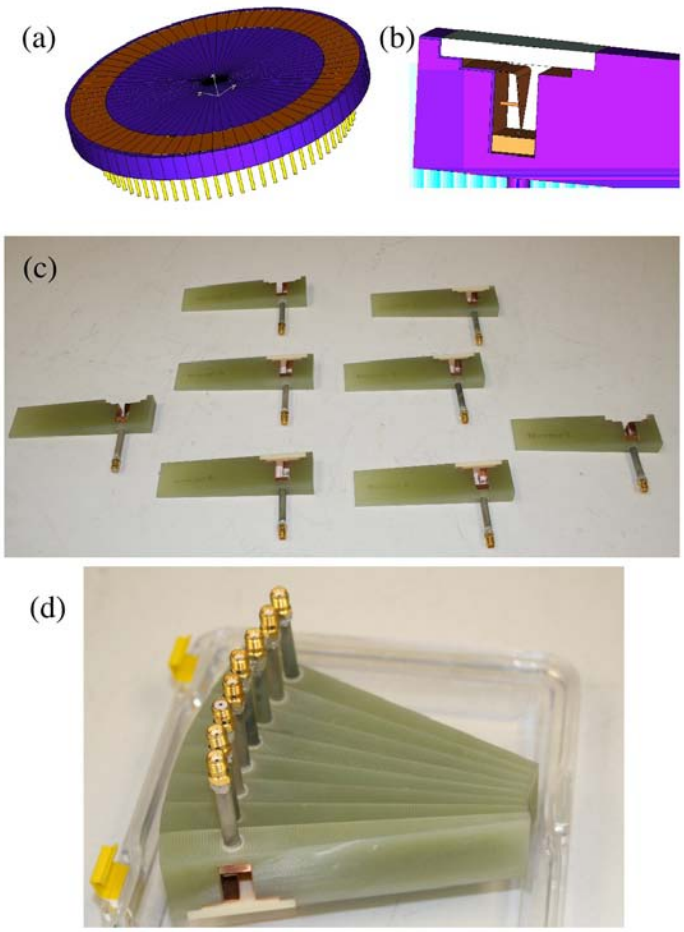


*Figure 1. (a) Overview of the antenna array for Technology Demonstrator 1. There are 72 elements, each with a coaxial connection (yellow) to its individual control module. The elements are machined from the composite material G10 (purple) and the active region that contains the superluminal polarization current is alumina (brown). (b) Enlargement of one of the 72 elements, showing the triangular impedance-matching transition from antenna to coaxial cable. (c) Eight of the first nine elements to be manufactured (currently undergoing detailed testing). (d) The elements arranged in the arc of a circle.*

The antenna mount (with full tilt and pan) for the first two technology demonstrators has been acquired, installed and tested. The detector antennas and remote positioning unit for experiments with all three technology demonstrators have been acquired, integrated, tested and installed in the anechoic chamber at ISR-6. Control software for the antenna mount and detector positioning has been made and tested; it is being integrated with the software to control the antenna electronics.

The mathematical /computational work associated with the project has yielded several important discoveries about the control of superluminal sources and their applicability to astronomical objects [1-4]. Very soon after the discovery of pulsars, it was realized that the very stable periodicity of the mean profiles of their pulses could only result from a source that rotates, and which therefore possesses a rigidly rotating radiation distribution. In Reference [4], we showed that this source rotation, in combination with superluminal emission, can explain not only the periodicity of the pulses, but also the detailed frequency dependence of the emitted radiation. By inferring the values of two adjustable parameters from observational data (values that are consistent with those of plasma frequency and electron cyclotron frequency in a conventional pulsar magnetosphere), and by mildly restricting certain local properties of the source, it is possible to account quantitatively for the emission spectrum of the Crab pulsar over 16 orders of magnitude of frequency [4] (Figure 3a). This is the first time in the forty-year history of pulsars that a single model has succeeded in predicting observational data over more than a very narrow frequency band. Several talks on related topics have been given at an astrophysical conferences.

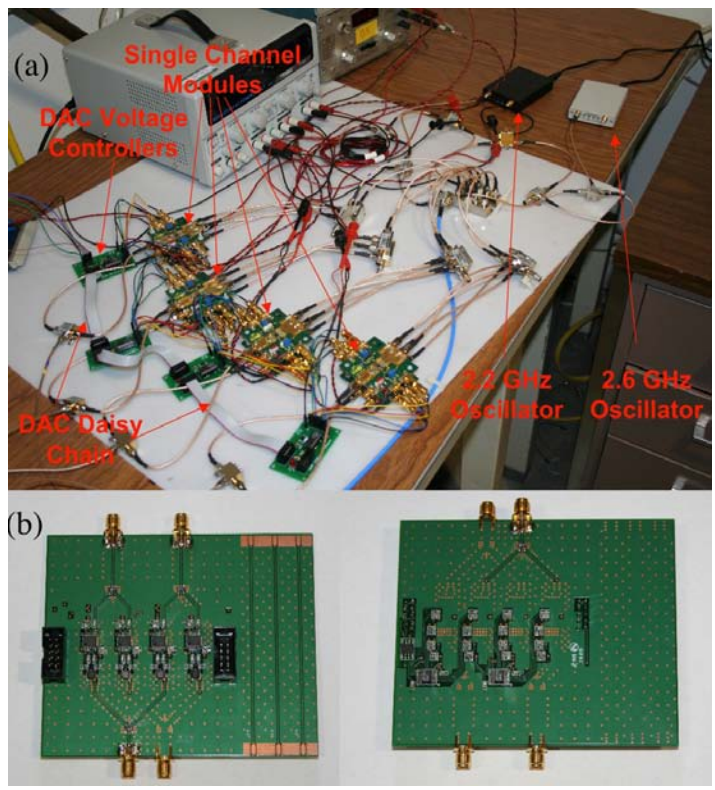


*Figure 2. (a) Prototype control circuits for the 72-element Technology Demonstrator 1 under test. The digital to analog converters (DAC) set the voltages that determine the phase of the signals sent to the antenna array (and therefore the speed of the polarization current). Four single-channel control modules built from Analog Devices demonstration boards are shown, as are the two master oscillators. Eight of these prototype modules are being used with eight of the antenna elements shown in Figure1 as a test array. (b) Production versions of the control modules for the 72 element Technology Demonstrator 1, built on four-layer circuit boards.*

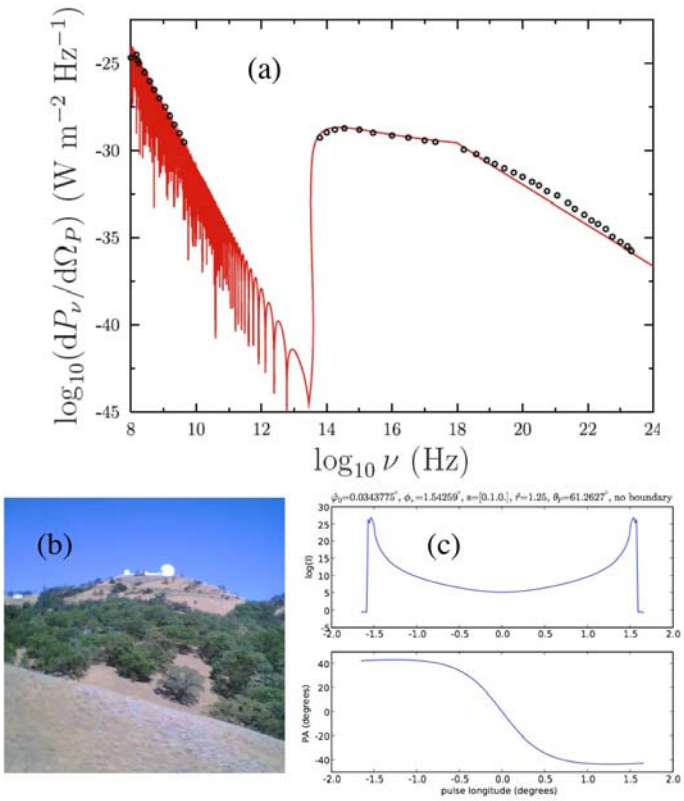


*Figure 3. (a) Superluminal model of the emission spectrum of the Crab pulsar (curves), plotted over 16 orders of magnitude of frequency. Using only two adjustable parameters determined from GHz data, the model reproduces astronomical observations (points) over the complete frequency range shown. (b) The Lick Observatory, where a high-speed detector has been set up to record pulse structure within the afterglows of gamma-ray bursts. (c) Numerical calculations of the intensity and position angle (PA- a measure of polarization) from an extended, rotating, superluminal source. The double-peak nature of the intensity and the 90 degree swing in PA closely resemble astronomical observations.*

The computational results suggest that superluminal sources are also involved in phenomena such as gamma-ray bursts. To check this hypothesis, a high-speed detector has been set up at the Lick Observatory (Figure 3b) to study the temporal features present in the afterglows of gamma-ray bursts. The detector is presently under test and should be in use by early 2009.

Numerical simulations have now been extended from point-like, rotating superluminal sources to sources that are extended in the azimuthal direction, which will be the case in the real world. Encouragingly, this has produced simulated intensity and polarization data that are very similar to astronomical observations from pulsars [5]. This work is still under development.

White papers are being presented to various defense agencies, NASA and DOE IN (via LANL contacts) to publicize eventual applications of superluminal technology. In this context, we have submitted a patent application for superluminal radar [6].

## Future Work

Superluminal sources are exceptional in that the radiation received from them can contain contributions from more than one retarded time. Moreover, when a superluminal source accelerates, contributions from an extended period of source time can arrive simultaneously at an observer.

The technology demonstrators (TD1-3) will explore these issues and study communication, radar, astrophysics and directed-energy applications of superluminal sources. TD1 will animate a polarization current around a circular dielectric and will be a 72-element device with a radius of 125 mm operating at 2.4 GHz. It will modulate the emitted signal at the rates required for communication and radar applications. Its compactness, also demonstrating the scalability of the technology for future field applications, means that experiments can be performed in the LANL RF anechoic chamber. This will be invaluable for verifying the numerical models of superluminal emission that form an important part of the project.

For directed energy applications, a linear acceleration of the polarization current is more fruitful, as it will produce energy concentration at a point; elsewhere, energy concentration will be small, reducing collateral damage. TD2 is therefore a low-power linear accelerator, using the same modules as TD1; it will be used to study energy concentration in the anechoic chamber. Later, the feasibility of constructing a high-power device (TD3) employing kV electronics will be assessed.

The wave fronts emitted by sources that travel faster than light are unlike the radiation generated by any other known emission mechanism. Initial results suggest that superluminal emission is an important process in the observable universe, occurring, for example, in pulsars and nuclear explosions. In addition to simulating communications and radar applications of superluminal sources, numerical computations will model the electromagnetic radiation from astrophysical objects such as pulsars. By comparing these to observational data it may be possible to deduce the internal structure of pulsars.

## Conclusion

The new method for generating radio waves, superluminal emission, is an almost completely unexplored technological field. It has potential applications in secure communication, radar, electronic countermeasures, electronic weapons and long-range, low-power transmission. To develop these applications, three prototype transmitters, each designed to exploit a particular property of superluminal emission, will be constructed using the electronics expertise at LANL. These compact machines will be used as technology demonstrators for radar, communications and directed-energy, and to verify the computer models of superluminal emission. They will also be used to explore possible spin-off technologies in areas such as medical diagnostics and therapy.

## References


1. Ardavan, H., A. Ardavan, J. Singleton, J. Fasel, and A. Schmidt. Fundamental role of the retarded potential in the electrodynamics of superluminal sources. 2008. Journal of the Optical Society of America A (Optics, Image Science and Vision) . 25 (3): 543.
2. Ardavan, H., A. Ardavan, J. Singleton, J. Fasel, and A. Schmidt. Spectral properties of the nonspherically decaying radiation generated by a rotating superluminal source. 2008. Journal of the Optical Society of America A (Optics, Image Science and Vision) . 25 (3): 780.
3. Ardavan, H., A. Ardavan, J. Singleton, J. Fasel, and A. Schmidt. Morphology of the nonspherically decaying radiation generated by a rotating superluminal source. 2008. Journal of the Optical Society of America A (Optics, Image Science and Vision) . 25 (9): 2167.
4. Ardavan, H., A. Ardavan, J. Singleton, and M. R. Perez. Mechanism of generation of the emission bands in the dynamic spectrum of the Crab pulsar. 2008. Monthly Notices of the Royal Astronomical Society. 388 (2): 873.
5. Schmidt, A., H. Ardavan, J. H. Fasel, J. Singleton, and A. Ardavan. Occurence of concurrent orthogonal polarization modes in the Lienard-Wiechert field of a rotating superluminal source. 2007. Proceedings 363 WE Heraeus Seminar, MPE-Report . 291: 124.
6. Singleton, J., H. Ardavan, and A. Ardavan. Apparatus and method for phase fronts based on superluminal polarization current. 2008. United States of America Patent 12/191,148.


## Publications


Aradavan, H., A. Aradavan, J. Singleton, and M. R. Perez. Mechanism of generation of the emission bands in the dynamic spectrum of the Crab pulsar. 2008. Monthly Notices of the Royal Astronomical Society. 388 (2): 873.

Ardavan, H., A. Ardavan, J. Singleton, J. Fasel, and A. Schmidt. Fundamental role of the retarded potential in the electrodynamics of superluminal sources. 2008. Journal of the Optical Society of America A (Optics, Image Science and Vision) . 25 (3): 543.

Ardavan, H., A. Ardavan, J. Singleton, J. Fasel, and A. Schmidt. Spectral properties of the nonspherically decaying radiation generated by a rotating superluminal source. 2008. Journal of the Optical Society of America A (Optics, Image Science and Vision) . 25 (3): 780.

Ardavan, H., A. Ardavan, J. Singleton, J. Fasel, and A. Schmidt. Morphology of the nonspherically decaying radiation generated by a rotating superluminal source: reply to comment. 2008. Journal of the Optical Society of America A (Optics, Image Science and Vision) . 25 (9): 2167.

Ardavan, H., A. Ardavan, J. Singleton, J. Fasel, and A. Schmidt. Response to comment on method of handling the divergences in the radiation theory of sources that move faster than their own waves. Journal of Mathematical Physics.

Middleditch, J.. Pulsars, cosmology and science with giant telescopes. Invited presentation at Science with giant telescopes. (Chicago, 15-18 June 2008).

Middleditch, J., and M. R. Perez. The Kinematics of the SN 1987A Beam/Jet(s). 2008. Bulletin of the American Astronomical Society . 40 (2): 206.

Middleditch, J., and M. R. Perez. The SN 1987A Beam/Jet and Its Associated Mystery Spot. 2008. Bulletin of the American Astronomical Society . 39 (4): 742.

Perez, M. R., B. McCollum, M. E. van den Ancker, and M. D. Joner. The enigmatic young object: Walker 90/V590 Monocerotis. 2008. Astrnomy and Astrophysics. 486 (2): 533.

Schmidt, A., H. Ardavan, J. Fasel, M. Perez, and J. Singleton. Superluminal emission processes as a key to understanding

pulsar radiation. 2008. Bulletin of the American Astronomical Society . 39 (4): 917.

Singleton, J.. Lawbreakers? Superluminal sources in the laboratory and as a model for pulsars. Invited presentation at 23rd Annual New Mexico Symposium. (Socorro, October 2007).

Singleton, J., A. Schmidt, J. Fasel, H. Ardavan, A. Ardavan, and M. R. Perez. Polarization currents that travel faster than the speed of light in vacuo: laboratory demonstrations and a model for pulsar observational data. 2008. Bulletin of the American Astronomical Society . 39 (4): 950.

# Science-Based Prediction and Control of Complex Manufacturing Processes

*Matthew Thomas Bement*

20060079DR

## Abstract

The main objective of this project is to improve part quality by understanding and ultimately controlling how a manufacturing process affects a part's performance. At a high level, achieving this objective requires coordinated advances in the areas of 1) metrology, 2) signal processing, 3) predictive modeling, 4) pattern recognition, and 5) control theory. More specifically, the two manufacturing processes of precision turning and friction stir welding were selected as case studies to demonstrate advances in each of these areas. In addition to generating fifteen publications and one patent disclosure, the results of this project will have a measurable impact on how critical parts at Los Alamos National Laboratory are machined.

## Background and Research Objectives

The key scientific "Grand Challenge" in this work is to develop a comprehensive unified view of manufacturing processes as ensembles of interacting non-linear dynamical systems, which has thus far not been accomplished. By fundamentally understanding and ultimately controlling how a manufacturing process affects a part's performance, it is expected that part quality can be significantly improved. While the applicability of this approach is broad, this project focused on precision turning and friction stir welding as two prototypical manufacturing operations.

The unified framework consists of five discrete scientific disciplines. 1) The first discipline is metrology, which is used to identify and measure key in-process physical behaviors using novel sensor networks that will collectively have data rates in the gigabyte per second range. Examples included high-speed optical and thermal imaging, acoustic emission, and inexpensive, robust thin film piezoelectric patches for strain measurements. Such ubiquitous sensing has previously not been applied in the manufacturing arena due to the extreme challenges in processing such large data sets in real-time. 2) Signal processing must then be employed to reduce the data stream dimensionality using innovative feature extraction techniques that are also guided by physics-based understanding of process dynamics and stability. Examples include image processing and frequency domain features such as relative peak heights at resonant frequencies. 3) The next discipline is science-based predictive modeling for the purpose of creating interrelated physics-based process models that capture the dynamical behavior and underlying stability of a given manufacturing process. An example is the construction of a first-principles based "inverse" model to infer material condition based on video, temperature, and acoustic data collected during machining. 4) The discipline of pattern recognition provides the essential link between the extracted features and metrics of part quality. 5) Control theory is then employed to develop and implement advanced, non-traditional process control and optimization methods such as adaptive control for the purpose of controlling, in real-time, not just process parameters, but part quality itself.

Advances in each of these five areas as they pertain to the case studies of precision turning and friction stir welding are presented in Section 3 below.

## Importance to LANL's Science and Technology Base and National R & D Needs

The successful execution of this project will enable critical weapons components manufactured throughout the NNSA's nuclear weapons complex to be produced more cost effectively and with higher quality than is currently possible. By furthering efforts to understand, monitor and control the physical mechanisms that lead to defects, poor part quality, and ultimately poor or unacceptable part performance, this project supports DOE's advanced manufacturing and rapid technology responsiveness priorities.

## Scientific Approach and Accomplishments

As stated in Section 1, precision turning and friction stir welding were chosen as the two case study processes. Thus, the approach and accomplishments associated with each case study will be discussed below.

### Precision turning

The main purpose of this project is to improve part performance by understanding and ultimately controlling how a manufacturing process affects a part's performance. There are many aspects of performance that may be of interest in a general situation. One aspect of a metal part's performance that is relevant to LANL/NNSA is its behavior under explosive loading. It is well known that surface finish as well as spatial variations in microstructure (e.g. grain size) plays significant roles in the dynamic behavior of an explosively driven metal. In current practice, surface finish measurements are collected, though only after a part has been machined. Traditional measurement of microstructure variations over an entire finished part is typically not practical or even possible. Thus, in order for a part's quality to be improved, estimates of surface finish and microstructure variations need to be made in real-time.

Surface finish is at least partially due to relative motions between the cutting tool and the part. Thus, it is desirable to first estimate the motions of both the tool and the part. This was accomplished in the first year of the project through a series of experiments. The experimental setup included a novel, workpiece-mounted accelerometer. In a paper documenting results from this set of experiments [1], it was shown that dynamic information from the workpiece propagates to the cutting tool more consistently in the tangential cutting direction than in the radial cutting direction. In addition, trajectories in the state space comprised of workpiece acceleration in the radial and tangential cutting directions were investigated, and it was graphically shown that stable cutting results in relatively high dimensional dynamics and unstable cutting results in relatively low dimensional dynamics.

Unstable cutting, also known as chatter, is characterized by large relative displacements between the cutting tool and workpiece and is particularly detrimental to surface finish. While chatter is a well known phenomenon, the actual transition from stable to unstable cutting has not been previously modeled in a geometrically rigorous manner. Consequently, a study of this transition was conducted and is documented in [2].

With a model of dynamics that influence surface finish, it is then desirable to improve surface finish. A prototype actuator, shown in Figure 1, was developed to allow high bandwidth tool motion for the purpose of reducing tool/workpiece relative motion. When an adaptive control scheme was used to control this actuator, a significant increase in the stable depth of cut was observed [3]. This has important benefits for improving productivity without sacrificing surface finish.

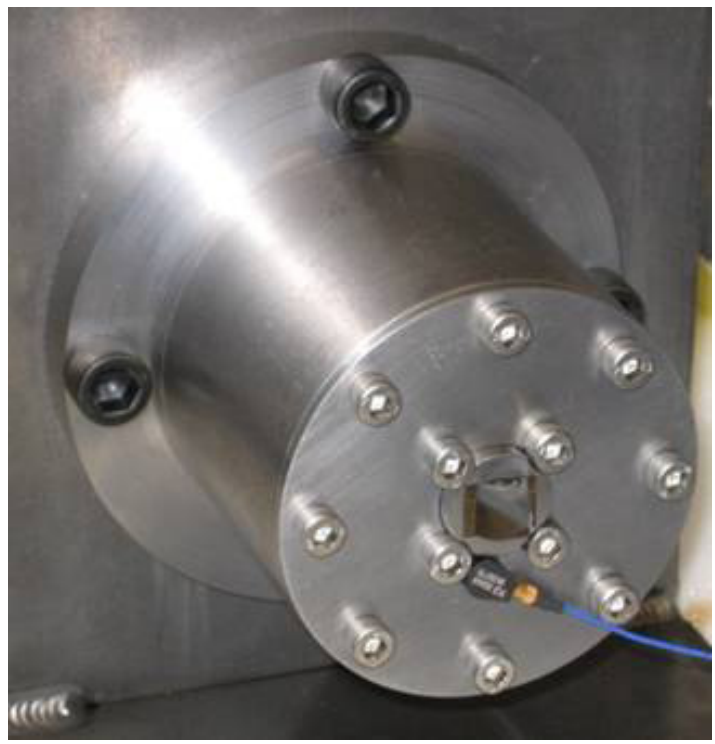

*Figure 1. High bandwidth actuator*

As stated above, variations in the workpiece microstructure can also be important for a part's performance. By the time a part is at the point in its manufacturing process where it is ready for machining, it is not reasonable to expect to somehow control its bulk microstructure via the machining process. However, it is reasonable to expect that the machining process could adapt to spatial variations in microstructure, provided such variations could be estimated. That is, if the spatial variations could be estimated during roughing cuts, then it may be possible to make very small, spatially varying changes to the part's dimensions during a finish cut. These spatially varying dimensional changes would be designed to offset or counter the spatially varying microstructure that would otherwise have an undesirable effect on the part's hydrodynamic behavior. While prescribing the dimensional changes necessary to offset spatially varying microstructure was beyond the scope of this project, multiple studies were carried out to

demonstrate the capability of detecting these variations during cutting.

More specifically, a series of experiments were performed in which cuts were performed on steel and aluminum workpiece materials which had a variety of microstructures. Hundreds of gigabytes of data were ultimately obtained from these experiments using a large array of sensors. Specifically, tool acceleration, cutting force, acoustic emission, and high-speed video (4000 frames/sec) data were collected. Analysis of the video data was particularly of interest. Fundamentally, it was observed that softer material (corresponding to a larger grain size) produced a thicker chip. This effect can in fact be predicted using physics based modeling (see Figure 2). Because the depth of cut and cutting speed are constant, the mass flow rate of the chip must be constant. Consequently, a thicker chip corresponds to a slower chip.

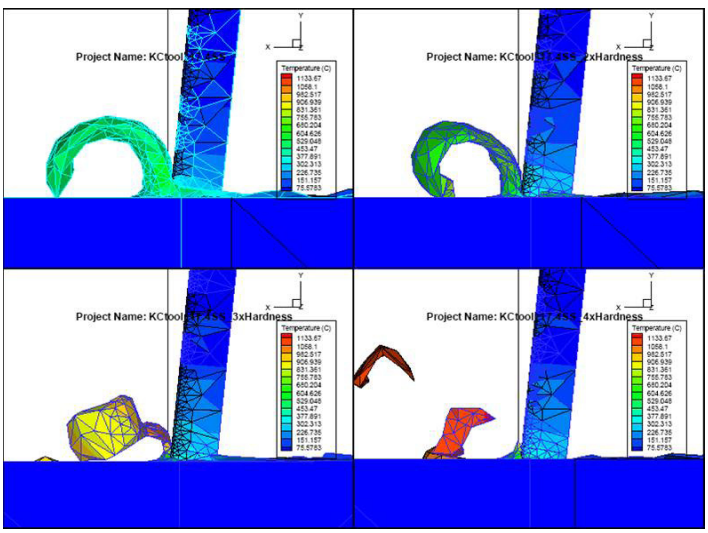

*Figure 2. Effect of hardness on chip thickness*

Through the use of automated image processing of the high-speed video and the development of an automatic classifier [4], it was found that chip velocity and, consequently, local workpiece hardness could be assessed with high accuracy. In addition, an effort was undertaken to determine the feasibility of implementing this classification scheme in real-time. Using a new reconfigurable processor, it was demonstrated that the classification could be done in real-time and with an acceptable power and physical footprint (less than a standard PC) [5]. This novel use of high-speed video represents an important, non-contact, large stand-off material characterization capability that is particularly valuable for monitoring the machining of hazardous or high precision components, as it does not require any modification of an existing, qualified process.

Finally, it is worth noting that based on the successes demonstrated in this project in the areas of modeling, monitoring, and control of the precision turning, a new precision turning center and glovebox being installed for plutonium machining at TA-55 has been designed to accommodate data acquisition capabilities similar to those used in the above mentioned experiments (e.g., cutting force, tool acceleration, high speed video).

**Friction stir welding**

In friction stir welding, a cylindrical, shouldered tool with a profiled pin (typically helical threads) is rotated, then plunged into the joint line of the rigidly abutted weld material and is then translated along the joint line (see Figure 3). Frictional heat generated between the tool pin, shoulder and the material of the workpiece causes the latter to reach a viscoplastic state that allows the traversing of the tool along the weld line. For friction stir welding to be widely adopted, it must be able to be reliably carried out by industrial robots. This requirement comes with many challenges due to the forces involved, as well the potential for defects. Two significant types of defects include joint gap defects and seam tracking defects. Both of these types of defects were studied.

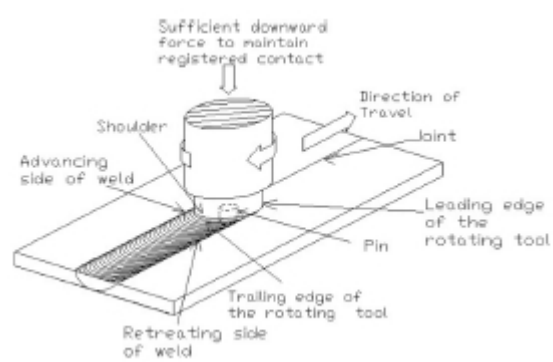


*Figure 3. Friction stir welding process*

As its name implies, joint gap defects occur when there is a gap in the joint to be welded (usually due to inadequate joint preparation). For certain weld types (e.g., lap welds), these gaps can not be seen visually before or after the weld, though they can cause significant degradation in the bond quality. Consequently, it is important to be able to automatically detect such gaps during the welding process, particularly as industrial robots perform more of these welds.

Therefore, a series of experiments was conducted with an instrumented spindle to determine if the measured welding forces and torques could be used to detect the

presence of joint gaps. The Fourier transform of the measured forces and torques was then calculated, thereby transforming signals which are functions of time to signals which are functions of frequency. These transformed, frequency dependent signals were then "binned" (similar to a histogram) by frequency, and these bins were used as the input features to train a support vector machine for classification of the presence of gaps. Using this classifier, it was determined that gaps larger than 0.003" could be reliably detected [6]. Such an automated defect detection capability represents an important contribution to the advancement of automated friction stir welding.

Seam tracking defects often occur in a weld known as a blind T-joint (see Figure 4), which is particularly important for airframe manufacturing. In this weld, a horizontal member is welded to a vertical member. This is a challenging weld, because the weld joint and vertical member is not visible during the welding process. As a result, it is possible that the tool might not stay aligned and centered over the vertical member as the weld progresses. If this happens, the bond quality of the weld may be compromised. Thus, it is desirable to be able to automatically detect and correct misalignments in the tool path.

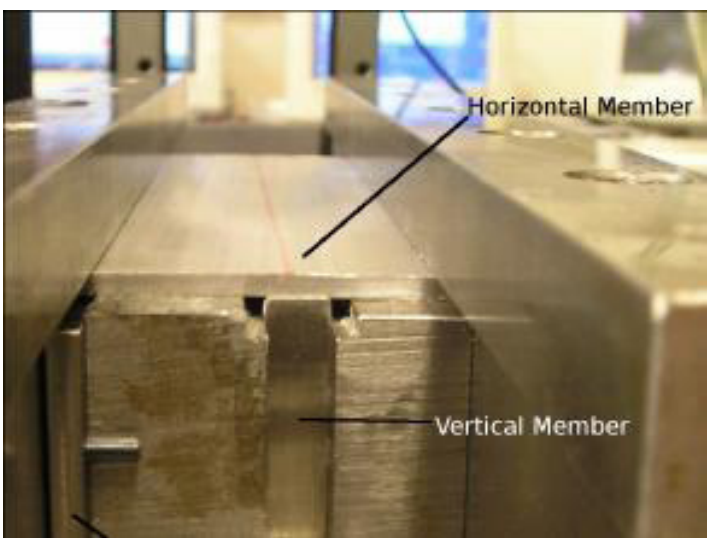


*Figure 4. T-joint*

The first step is to develop techniques for determining the position of the welding tool with respect to the weld seam during the welding process. As established through an experimental study, and as shown in Figure 5, there is a strong correlation between axial force and weld offset position. Similar correlations are observed for other measured forces and torques [7]. These correlations suggest that it should indeed be possible to not only detect misalignment in real time, but to develop a controller which can react to minimize the misalignment. Unfortunately, even in a weld with no offset, there is enough variation in these measured quantities that the controller might incorrectly react to correct a non-existent offset.

The solution to this problem lies in making the controller react to relative changes in the measured forces and torques rather than absolute changes. To accomplish this, the weld tool is "weaved" back and forth by a small amount as the weld progresses. This has been previously demonstrated to have no adverse affect on weld quality, and it provides the controller with a localized version of the data shown in Figure 5. This method is relative, in that it compares the relative axial load of two locations in the weld, rather than a function based on absolute values of axial force. This reduces sensitivity to changes in the process such as changes in tools, tool wear, weld parameters, etc.

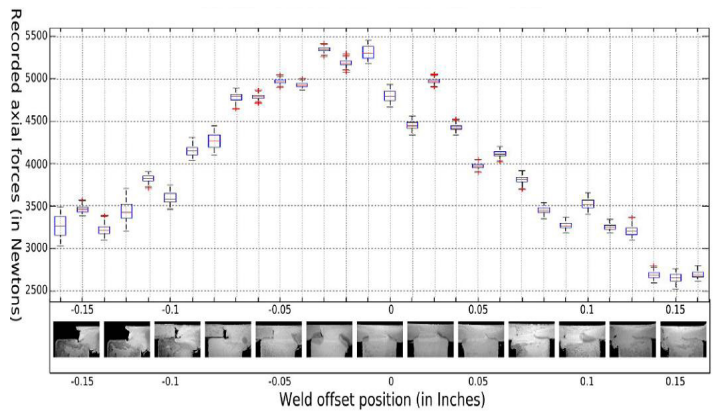


*Figure 5. Effect of offset on axial force*

The center of the weave motion is then moved in the direction with the higher axial force. In this way, the tool is moved to maintain a maximum axial force, and in doing this maintains a good weld position. Experimental results have demonstrated that joints with serious misalignment can still be welded reliably with this novel control method. This monitoring and control system, for which a patent has been submitted, represents a key advance to the state of the art in automated friction stir welding.

## Summary

In summary, through the use of the two case studies of precision turning and friction stir welding, coordinated advances were made in the areas of 1) metrology, 2) signal processing, 3) predictive modeling, 4) pattern recognition, and 5) control theory. In addition to generating 15 publications and 1 patent disclosure, the results of this project will have a measurable impact on how critical parts at Los Alamos National Laboratory are machined in the future.

## References


1. Cardi, A. A., H. A. Firpi, M. T. Bement, and S. Y. Liang. Workpiece dynamic analysis and prediction during chatter of turning process. 2008. *Mechanical Systems and Signal Processing.* **22** (6): 1481.

2. Cardi, A. A., M. T. Bement, and S. Y. Liang. A geometrically comprehensive approach to modeling dynamic cutting forces in turning: Application to regenerative chatter. To appear in *2008 International Conference on Manufacturing Science and Engineering.* (Evanston, IL, 7-10 Oct. 2008).

3. Radecki, P. P., W. A. Kruse, A. J. Welsh, E. A. Moro, G. Park, and M. T. Bement. Improving a turning process using piezoelectric actuators and ultrasonic assisted machining. To appear in *2009 International Modal Analysis Conference.* (Orlando, FL, 2-9 Feb. 2009).

4. Hush, D. R., M. T. Bement, and T. K. Wong. Inferring hardness from high-speed video of the machining process. To appear in *2008 International Conference on Manufacturing Science and Engineering.* (Evanston, IL, 7-10 Oct. 2008).

5. Cash, W., S. Schnelle, S. Lee, J. Frigo, and M. T. Bement. A reconfigurable hardware application for the machining of metal parts. To appear in *2008 International Modal Analysis Conference.* (Orlando, FL, 4-9 Feb. 2008).

6. Fleming, P., D. Lammlein, D. Wilkes, K. Fleming, T. Bloodworth, G. Cook, A. Strauss, D. DeLapp, T. Lienert, M. Bement, and T. Prater. In-process gap detection in friction stir welding. 2008. *Sensor Review.* **28** (1): 62.

7. Fleming, P. A., D. H. Lammlein, D. M. Wilkes, G. E. Cook, A. M. Strauss, D. R. DeLapp, and D. A. Hartman. Misalignment detection and enabling of seam tracking for friction stir welding. *Science and Technology of Welding and Joining.*


## Publications


Cardi, A. A., M. T. Bement, and S. Y. Liang. Workpiece dynamic analysis and prediction during chatter of turning process. 2008. *Mechanical Systems and Signal Processing.* **22** (6): 1481.

Cardi, A. A., M. T. Bement, and S. Y. Liang. Workpiece dynamics during stable cutting in a turning operation. To appear in *International Journal of Manufacturing Research.*

Cardi, A. A., M. T. Bement, and S. Y. Liang. A geometrically comprehensive approach to modeling dynamic cutting forces in turning: Application to regenerative chatter. To appear in *2008 International Conference on Manufacturing Science and Engineering.* (Evanston, IL, 7-10 Oct. 2008).

Cash, W., S. Schnelle, S. Lee, J. Frigo, and P. Graham. A reconfigurable hardware application for the machining of metal parts. To appear in *International Modal Analysis Conference.* (Orlando, FL, 4-8 Feb. 2008).

Crawford, R., G. E. Cook, A. M. Strauss, M. A. Stremler, and D. A. Hartman. Experimental defect analysis and force prediction simulation of high weld pitch friction stir welding. To appear in *Science and Technology of Welding and Joining.*

Crawford, R., T. Bloodworth, G. E. Cook, A. M. Strauss, and D. A. Hartman. High speed friction stir welding process modeling. To appear in *Internation Friction Stir Welding Symposium.* (Montreal, Canada, 10-13 Oct. 2006).

Espinoza, A. A., L. J. Mayer, P. V. Oberlin, and M. T. Bement. Design and evaluation of a piezoelectric actuator for turning. To appear in *International Modal Analysis Conference.* (Orlando, FL, 19-22 Feb. 2007).

Fleming, P. A., D. H. Lammlein, D. M. Wilkes, G. E. Cook, A. M. Strauss, D. R. DeLapp, and D. A. Hartman. Misalignment detection and enabling of seam tracking for friction stir welding. *Science and Technology of Welding and Joining.*

Fleming, P. A., D. M. Wilkes, G. R. Shearer, T. J. Lienert, M. Bement, and e. t. al. Fault detection and in-process control of friction stir welding. To appear in *AeroMat.* (Baltimore, MD, 25-28 Jun. 2007).

Fleming, P., D. Lammlein, D. Wilkes, K. Fleming, T. Bloodworth, G. Cook, A. Strauss, D. DeLapp, T. Lienert, M. Bement, and T. Prater. In-process gap detection in friction stir welding. 2008. *Sensor Review.* **28** (1): 62.

Hush, D. R., M. T. Bement, and T. K. Wong. Inferring hardness from high-speed video of the machining process. To appear in *2008 International Conference on Manufac-*

*turing Science and Engineering.* (Evanston, IL, 7-10 Oct. 2008).

Lammlein, D. H., T. J. Lienert, M. Bement, and e. t. al. Implementation of a Bellville spring stack opposed shoulder and retractable tool pin design in the FSW of closed contours. To appear in *AeroMat.* (Baltimore, MD, 25-28 Jun. 2007).

Park, G. H., M. T. Bement, D. A. Hartman, N. Tolk, and R. Smith. The use of active materials for machining processes: A brief review. 2007. *International Journal of Machine Tool and Manufacture.* **47** (15): 2189.

Prater, T. J., T. S. Bloodworth, P. A. Fleming, and e. t. al. Friction stir welding of aluminum, titanium, and aluminum metal matrix composites using a diamond coated molybdenum tool. To appear in *AeroMat.* (Baltimore. MD, 25-28 Jun. 2007).

Radecki, P. P., W. A. Kruse, A. J. Welsh, E. A. Moro, G. Park, and M. T. Bement. Improving a turning process using piezoelectric actuators and ultrasonic assisted machining. To appear in *2009 Internation Modal Analysis Conference.* (Orlando, FL, 2-9 Feb. 2009).

# Cerium-Doped Glass Scintillators

*Markus Peter Hehlen*

20070134ER

## Introduction

Gamma-ray scintillators are materials that emit light when exposed to gamma rays. Such radiation is emitted by Special Nuclear Materials (SNM) and other radioactive materials that are indicative of nuclear fuels cycle processes or that pose a threat to national security. Efficient gamma-ray scintillators are the key element in devices that detect, identify, and track nuclear material; and they are an essential component of our homeland defense and nonproliferation infrastructure. Sensitive gamma-ray spectrometers are needed to detect/identify nuclear material at the ports of entry, along borders, and in densely populated areas. Such spectrometers become cost-prohibitive when they have to build on conventional scintillator crystals which are expensive and difficult to grow and handle. This project addresses this critical material limitation. We will explore and develop cerium-doped sulfide glass as a novel, versatile gamma-ray scintillator material. The use of glass instead of crystals can significantly reduce cost, allow casting into large scintillator elements, enable easy integration with cost-effective photo-diodes, while still offering high energy resolution. Glasses have a disordered atomic structure and, in contrast to crystals, may have more degrees of freedom to form defects during the gamma-ray scintillation process. The formation of such defects can degrade the scintillation performance. Sulfide glasses have not been studied for this application before. In contrast to common oxide and fluoride glasses, the chemical bonding in sulfide glasses is covalent and thus more rigid and less prone to defect formation. Moreover, the covalency of the chemical bonding can be fine-tuned by adding glass modifiers. We will exploit this property to maximize the gamma-ray scintillation yield and to demonstrate the potential of in this new class of radiation-detection materials.

## Benefit to National Security Missions

This project will support the NNSA mission in Defense Nuclear Nonproliferation by enhancing our understanding of detecting the proliferation of nuclear/radiological weapons of mass destruction and illicit nuclear materials trafficking. The project will conduct applied research to develop a superior scintillator material that contributes to strengthening our national security infrastructure.

## Progress

The successful completion of our first technical objective in the first year of the project provided a new baseline material: cerium-doped gallium-sodium-sulfide (GNS:Ce) glass. This material was the starting point to address the second technical objective in FY08, which was to gain a fundamental understanding and performing a systematic optimization of the photo-luminescence and scintillation processes in this new material. The key highlights of FY08 are:

- Completed the optimization of glass composition and basic fabrication method.
- Demonstrated scintillation in cerium-doped sulfide glass for the first time.
- Preparing a patent application that covers the composition of these new scintillators.

In more detail, the technical achievements of FY08 include:

- Optimizing the band gap of the material was found to be essential. The energy of the 5d emitting state of the cerium chromophore must be below the band edge in order for quenching processes to be suppressed and cerium quantum yield to be high. A high chromophore quantum yield is one critical requirement for an efficient gamma-ray scintillator. We identified cesium chloride (CsCl) as an important modifier in GNS glass. CsCl is ionic and can penetrate the glass network by breaking up some of the Ga-S bonds. Replacement of some of the covalent Ga-S bonds by ionic Ga-Cl bonds decreases the average covalency of chemical bonding and causes a blue-shift in the band edge energy of the glass (Figure 1). This blue shift is substantial, and our GNS glass doped with 20% CsCl has the largest

badgap of any sulfide glass reported to date (~3.2 eV). Such a large band gap puts the conduction band above the emitting 5d state of cerium and thus suppresses quenching - i.e. enhances the quantum yield - of the cerium 5d state. As a result, these materials emit bright green when excited optically in the violet. This constitutes the first-ever demonstration of efficient emission by cerium in a sulfide glass.

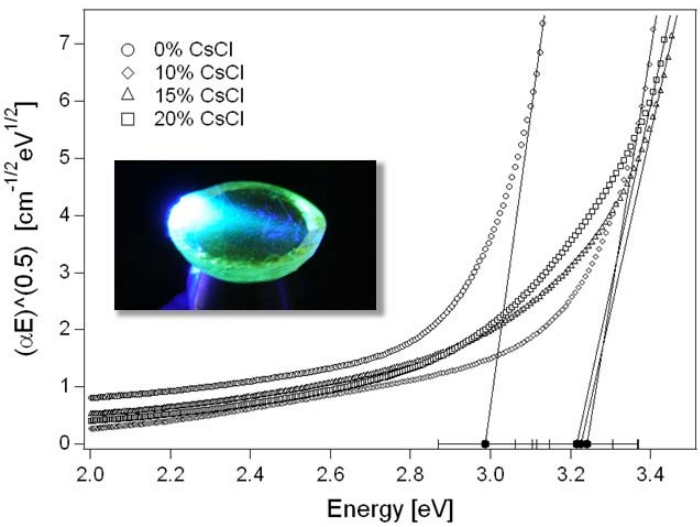


*Figure 1. Band gap energy in gallium-sodium-sulfide (GNS) glass for different CsCl concentrations. CsCl is ionic and penetrates the covalent gallium-sulfide glass network, decreasing the average covalency and increasing the band-edge energy to 3.2 eV. The picture shows the bright green emission from a GNS:Ce glass excited with blue light at room temperature.*

- A detailed analysis of the optical properties of GNS:CsCl samples showed that the actual CsCl content was substantially lower than expected. We found that CsCl has a substantial vapor pressure and is partially lost from the batch during glass melting in our inert-atmosphere furnace. Earlier studies of similar materials reported in the literature omitted this effect and consequently lacked accuracy. We succeeded in measuring the actual cesium content with high precision via energy-dispersive X-ray spectroscopy using facilities at the LANL Center for Integrated Nanotechnologies (CINT). Based on these results we were able to modify our glass fabrication procedure in such a way that the resulting CsCl-doped GNS glasses had the desired target composition to within the experimental error (Figure 2). This represents the first stoichiometrically correct series of CsCl-doped GNS glasses, and our results will clarify and correct several erroneous reports in the literature.

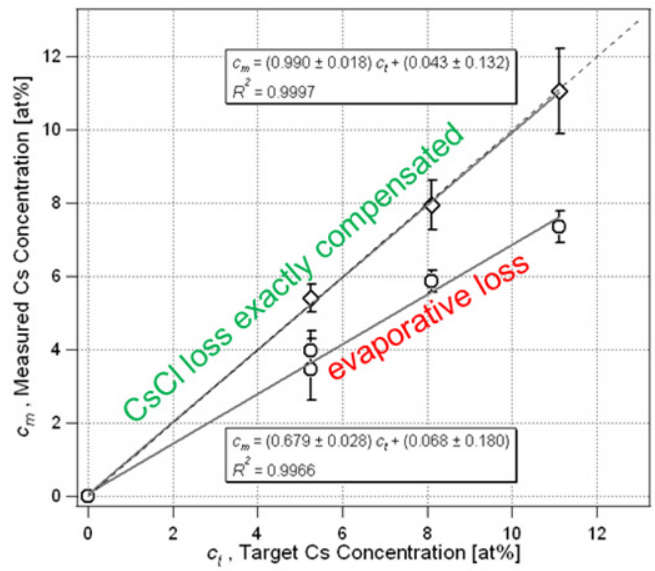


*Figure 2. Measured Cs+ concentration as a function of target Cs+ concentration for two different fabrication methods. High CsCl vapor pressure causes unacceptable evaporative losses in the original fabrication method (circles). The improved fabrication methods compensates for these losses and yields glasses with the correct composition (diamonds).*

- A detailed spectroscopic study of GNS glasses doped with CsCl and cerium revealed the interplay between the optical transitions of cerium and the band excitation of the glass. For this study several sample series with different cesium and cerium content were fabricated using the modified glass-fabrication procedure. All glass samples were ground and polished to optical-quality discs. The extensive spectroscopic study included measurements of photoluminescence (PL), photoluminescence excitation (PLE), absorption, and X-ray excited photoluminescence (XPL) spectra as a function of temperature between 300 and 10 K (Figure 3). Detailed analysis of this extensive data set and the preparation of several publications are currently underway.

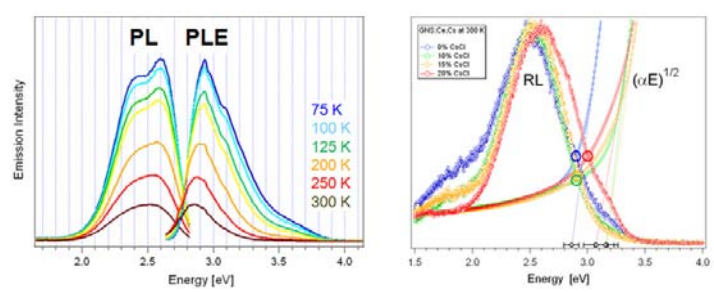


*Figure 3. LEFT: Photoluminescence (PL) and photoluminescence excitation (PLE) spectra of GNS:Ce glass at different temperatures. GNS:Ce emits efficiently in the green spectral region when excited in the blue/UV. RIGHT: First ever demonstration of scintillation (RL=radioluminescence) in cerium-doped sulfide glasses. Scintillation emission below the band gap is observed when exciting the glass with 25 keV X-rays at room temperature.*

- The most recent XPL measurements are particularly exciting since they show that the samples emit a bright green scintillation light when excited by X-rays at ~25 keV (see Figure 3). This indicates that these glasses can be efficient gamma-ray scintillators. Further XPL and gamma-scintillation measurements are currently being performed. These preliminary scintillation results indicate that optimum scintillation performance can be achieved by adding just enough CsCl to sufficiently blue-shift the band edge but not too much CsCl to maintain a high degree of covalency in the chemical bonding. Upcoming experiments will find that optimum CsCl concentration and quantify the gamma-scintillation performance of this new material.

## Future Work

The goal of the project is to deliver a proof-of-concept glass scintillator suited for integration into next-generation gamma-ray sensors. Cerium-doped chalcogenide glasses are a novel class of materials. We took an initially broad view of this compositional space and subsequently identified and focused on a few select materials for further development towards mission-relevant applications. The usefulness of these glasses is determined by their gamma-ray scintillating performance, the chemical and mechanical durability of the glass matrix, and the scalability of the material to the sizes required by advanced device architectures. We have now achieved two out of the three main objectives: 1) to develop the conceptual material design and 2) to optimize the scintillating performance of candidate materials.

The next step, and the focus of FY09 activities, is to explore material scalability. Larger-volume samples of the highest performing GNS:Ce glass will be explored to identify a fabrication process that yields high-quality scintillating elements while maintaining scintillating performance. This effort will establish whether the material is scalable for future integration into practical gamma-ray sensors.

Successful completion of the three main objectives would constitute a breakthrough in gamma-scintillator technology and offer a scintillator material that is directly applicable to critical homeland-security systems.

## Conclusion

The project exploits the excellent gamma scintillating performance of cerium and combines it with a chemically and mechanically versatile chalcogenide glass matrix to create a unique scintillator material. A range of glass compositions have been systematically studied for their scintillating properties, promising candidate materials were down selected, and their scintillating performance was optimized. We expect to produce efficient scintillating glass elements and to gain an understanding of the underlying scintillating mechanisms. The successful completion of the project would constitute a breakthrough in gamma-scintillator technology and offer a scintillator material that is directly applicable to critical homeland-security systems.

# Nano-Structured Foams for Hydrogen Storage

*Erik Paul Luther*

20070173ER

## Introduction

Hydrogen is a candidate energy carrier for applications such as zero emission vehicles. One of the main barriers to using hydrogen in automotive applications is safe storage. This project is investigating novel materials to store hydrogen. These materials must store large amounts of hydrogen quickly and repeatedly and release them in a controlled manner. This research has developed a new method of creating metal foams which have never been used for hydrogen storage. Foams are expected to adsorb and desorb hydrogen quickly due to the tremendous amount of surface exposed to the hydrogen gas.

The process for creating metal foams has no parallel. A foam with nanometer size pores is made by an extremely rapid burning of a starting material. There is no obvious limit to the size or shape of the foam that can be created in this manner. As a rapid, large scale production method for making nanomaterials, there is no equal. Due to the nature of this process, many aspects are uncertain. This research seeks to understand and control the process such that it can be used for the intended application.

Success in this area will enable rapid refueling of vehicles which is critical to consumer acceptance of hydrogen as a replacement for hydrocarbon fuels.

## Benefit to National Security Missions

This project supports U.S. energy security and supports basic understanding of materials, both of which are key DOE missions. With the extremely high surface areas and flexibility in materials that can be accessed by this technique, a truly unique method for hydrogen storage may be achieved.

## Progress

Work this year has focused on synthesis of new precurors and preparation techniques for precursors. Experiments aimed at the synthesis of two component alloys that are known to adsorb hydrogen were also conducted. Hydrogen sorption studies of palladium foam continued to supply data for a developing model for the kinetics of hydrogen uptake of foams.

The main goal of this project is to produce novel foams that would be capable of rapid uptake of hydrogen. Lithium nitride has been reported as a candidate storage material with high hydrogen storage capacity. By producing lithium nitride in foam form, improved sorption kinetics were anticipated due to high surface area, nanosized grains and pores and fast heat conduction. Numerous metal foams, some with high nitrogen content, have been produced to date including iron, cobalt, nickel, titanium, palladium, and zirconium all produced by burning metal bi(tetrazolo)amine precursors. Previously, LiBTA (lithium bi(tetrazolo)amine) was produced for the combustion synthesis of lithium nitride foam. Unfortunately, this precursor and all of the lithium compounds synthesized to date, lithium bitetrazole (BT), bi(tetrazolo)amine (BTA), and bistetrazolylaminotetrazine (BTATz), have failed to support combustion.

Various synthesis techniques for lithium compounds have been attempted but these materials show little response to ignition at atmospheric or elevated pressures, waters of hydration were the suspected cause. Drying the materials did not improve the combustion properties, suggesting that the water of hydration was too tightly bound, and three new synthesis routes were attempted, two non-aqueous. Recently, a new high-temperature dehydration procedure was found, and the LiBTA dehydrated, but self-propagating combustion still failed.

It is believed that MgN foams and/or lithium containing MgN foams will have interesting hydrogen storage properties. MgBTA salt was produced, and based on Mg high affinity for nitrogen, it is believed that in the combustion of this material MgN will be formed. Like many of the BTA salts, it was discovered that the MgBTA is hydrated, having approximately 1.5 $H_2O$ per MgBTA. This hydrate suffers from the same combustion problems as the LiBTA hydrate, however unlike the LiBTA, once dehy-

drated burns quite well.

Compacts of dehydrated MgBTA were pressed and ignited in a nitrogen atmosphere. These were found to burn poorly. It is known that magnesium is readily oxidized by nitrogen; therefore, it was expected that Mg powder would burn in atmosphere upon ignition. As a consequence, dehydrated MgBTA was mixed with Mg powder. It was hypothesized that the Mg powder would burn creating enough heat to help combust the MgBTA that would supply nitrogen gas to serve as the foaming or blowing agent. This material was found to burn quite well in a nitrogen atmosphere yielding a monolithic foam. The foam appears relatively coarse; however, characterization has yet to be completed. Depending on the results, optimization of this foam will be attempted.

$LaNi_5$ is a well known, well characterized hydrogen storage material. Attempts to synthesize this alloy in order to compare the kinetics of hydrogen uptake of bulk versus foam material were made. Lanthanum bi(tetrazaolo)amine was synthesized as a component in FY07 and recently was subjected to the drying procedure. Unexpectedly, the complex was stable after loss of all water.

The combustion properties of the anhydrous $La(BTA)_2(NH_4)$ were much improved as evident by small-scale screening. In this period we produced enough of the anhydrous material for formulation with NiBTA with the goal of producing $LaNi_5$. In FY07 we reported the synthesis of two complexes of NiBTA, one that is the $NiBTA(NH_3)_5$ complex, and one that is $Ni(BTA)_2(NH_4)_2$, the former having no useful combustion properties, and the latter with poor, but usable combustion properties. Recently, it was also discovered that the $Ni(BTA)_2(NH_4)_2$, also contains two waters of hydration, and after dehydration, the combustion properties are much improved. The two anhydrous precursors were mechanically mixed, pressed and combusted under nitrogen. The result was a good burn that resulted, unfortunately, in a powder not a monolithic foam. The powder will be characterized as it is expected to be porous. Depending on these results, additional compositions will be made in an attempt to vary the burn rate, which is believed to strongly influence the formation of the monolith.

Attempts to synthesize $Fe_xTi_y$, another hydrogen storage alloy, were also made. $Ti(BTA)_2$ was synthesized and formulations of TiBTA/FeBTA were produced at various ratios to produce $Fe_xTi_y$ foams. These formulations produced a low-density foam that was flaky and not a single monolith. Initial characterization has indicated that contrary to expectations, the iron and titanium has segregated as opposed to alloying. It is currently being analyzed for structure, purity and hydrogen uptake. New methods of mixing the component precursors will be attempted to promote alloying.

In order to model numerically the hydrogen absorption in palladium foams we are building on our previous work regarding the kinetics of oxygen removal from ceria (M. Stan et al, J. Appl. Phys. 95 (2004) 3358). We have developed a computer implementation of a chemical diffusivity model which takes into account the composition dependence of the diffusion coefficient and activation energy. Simulations for a variety of geometries and boundary conditions are being performed. In support of this work we have collected considerable hydrogen absorption/desorption data on Pd foam. This data will be compared with uptake on foils and powders. Initial experiments suggest that hydrogen uptake in the foam is considerably faster than in the foil although the maximum uptake is lower. The model will tell us if the increased rate is simply a function of geometry or if there are additional physical or chemical factors influencing the rate.

## Future Work

Our research will provide insight into a new materials synthesis procedure we discovered. That process yields metal foams of the lowest density and highest surface area known to the authors. We will pursue the following research goals: A) A variety of new nanostructured metal/metal nitride foams will be produced extending the method to ceramic materials. B) Additional understanding of the chemistry of precursor materials synthesis will be gained. C) Additional synthesis of foams will yield new knowledge of how the foams are formed. D) Hydrogen storage materials will be produced which have the promise of meeting near term FreedomCar goals. E) Thermodynamic properties will be modeled. F) Kinetics of hydrogen sorption/desorption will be determined.

The hydrogen sorption/desorption behavior of the ceramic foams will be studied with the following six step model in mind: 1) Molecular gaseous hydrogen diffusion to the material, 2) Molecular adsorption to the surface, 3) Dissociation, 4) Absorption, 5) Diffusion within the material, 6) Hydride reaction.

## Conclusion

This project will investigate hydrogen storage. The United States economy is highly dependent on foreign sources of oil. Reducing our dependence on foreign oil is a key national security issue. Although fuel efficiency is being improved by more wide spread use of hybrid vehicles, a major shift from non-renewable petroleum based fuels to renewable fuels such as hydrogen is necessary. Depending on the production method, hydrogen will curtail our need for foreign oil and greatly reduce the emission of carbon dioxide into the atmosphere. At the very least, it centralizes production of emissions making them easier to scrub or sequester.

## Publications

Tappan, B., S. Steiner, A. Mueller, B. Scott, and E. Luther. Combustion synthesis of ultralow-density nanoporous gold foams. *Chemistry of Materials.*

# Nano-Composite Scintillator for Neutron Capture Measurements

*Ernst Ingo Esch*

20070176ER

## Introduction

We are investigating the feasibility of nano-composite materials as detector material for neutron capture experiments. Several areas of research require the measurement of neutron-induced reaction rates for isotopes with short half-lives. This necessitates detection systems that can handle higher count rates and have faster recovery times. Presently available materials are either not suitable or cannot be produced in volumes necessary to absorb the full energy of the gamma-ray that is produced when a neutron is absorbed. Within this project we will investigate scintillators material embedded in a matrix of low-cost material for gamma-ray detection in a neutron environment with the goal to establish an inexpensive way produce the detectors with the desired properties. These materials will be tested for their chemical and physical properties and finally assembled as a detector. In parallel simulations to understand and predict the material behavior will be performed. The assembled prototype detector is then tested by placing it into an intense neutron environment produced by the Los Alamos Neutron Science Center. Both model predictions and detector performance will be studied.

## Benefit to National Security Missions

Detecting nuclear particles and reactions is central to a broad array of missions from basic nuclear physics and nuclear weapons to nuclear power to nonproliferation. These represent core mission areas for DOE NNSA and Office of Science, DHS, and other government agencies.

## Progress

The work to date can be described as a parallel effort of material-science/chemistry, physics properties, and beam physics:

### Chemistry

Since CeF3 was the most promising material as single crystal, it was the first nano composite to be manufactured. C-SIC fabricated $CeF_3$ and other possible nano composite scintillator materials. We loaded different nano material into different matrices. Electron paramagnetic resonance spectroscopy (EPR) provided direct information on the Ce-ion lattice local structure. Ordering and morphology on multiple length scales was observed using X-ray diffraction (XRD), transmission and scanning electron microscopy (EM) and atomic force microscopy (AFM). Optical characterization consisting of absorption, photoluminescence (PL), radioluminescence (RL), and diffuse reflectance were used to determine particle sizes. The initial experiments measured the optical absorption in transmission to ascertain the absorption bands associated with the Ce ion. Also, to verify particle size, a model to fit Raleigh scattering has been generated and successfully employed.

### Physics properties

We conducted physics properties measurement in our laboratory by measuring the sample response to gamma sources of different energies. From the gamma response spectra we were able to determine the light yield, resolution, and the peak-to-compton-ratio. Each sample of nanoparticles was dispersed in a liquid matrix to improve light transmission. In parallel we are constructing a GEANT4 simulation to simulate these detector materials in a DANCE like configuration. In order to be able to run the codes in a timely manner, we upgraded an existing Beowulf cluster.

### Beam Physics

Several weeks of beam time has been allocated at the Los Alamos Neutron Science Center (LANSCE) for testing of a first prototype of the nanocomposite gamma-detector. A detector prototype will be placed in a beam of neutrons in order to study the basic properties of the generated signals. Other possible tests include studying the response in terms of timing properties, signal characteristics, and the ability to distinguish neutron signals from other types of radiation. The LANSCE facility provides pulsed beams of neutrons with a range of energies, and the so-called neutron time-of-flight method can be used to measure neutron capture cross-sections. This has the advantage that the detector response can

also be studied as a function of incident neutron energy. Preparations for running these tests at LANSCE have been done by configuring a flight path to accommodate the experiment, and calibrating a neutron flux monitor to be used as a reference.

As an addendum, it should be mentioned that this LDRD/ER proposal was one of the trigger points for the accelerator community to invite the PI for a plenary session talk at the International Conference on the Application of Accelerators in Research and Industry.

## Future Work

We plan to investigate the feasibility of nano-composite materials as gamma-ray detector material for neutron capture experiments. Stewardship, technological and astrophysical programs require neutron induced reaction rates for isotopes with half-lives down to a few days. In order to investigate the desired neutron capture rates, higher neutron fluxes than currently usable are necessary. This necessitates detection systems that can handle higher count rates and have faster recovery times. Presently available materials are either not suitable or cannot be produced in volumes necessary for a calorimetric detection. Recent research at LANL has shown that nano-composites embedded in a matrix of secondary material might offer a viable replacement to mono-crystalline material. This would allow the cost-effective production of detectors with the desired material in large volumes. Within this project we will investigate the most promising candidate ($CeF_3$) as a nano-composite for gamma-ray detection in a neutron environment.

In the first year we will develop nano particle $CeF_3$ and characterize its optical properties. We will also investigate other nano material suitable for use as a detector material and optimize the optical and radiation response of the material. Additionally we will explore matrix materials to find the best detector/matrix candidate.

In the second year we will disperse the nano material in the matrix, optimize the composite and measure it's properties. The data will be used to benchmark the detector simulations. We will manufacture several detector elements of the most promising material with volumes of a few cubic centimeters.

In the third year the different detector elements will be characterized and tested for their neutron radiation hardness. This will take place either at the neutron facilities available at the Los Alamos Neutron Science Center (LANSCE). Additionally we will simulate complex experimental setups for neutron capture experiments with radioactive samples.

## Conclusion

We plan to investigate the feasibility of nano-composite materials as gamma-ray detector material for neutron capture experiments. Stewardship, technological and astrophysical programs require neutron induced reaction rates for isotopes with half-lives down to a few days. This project seeks to enable the cost-effective production of detectors with the desired material properties in large volumes. Within this project we investigate the most promising candidate. We will produce, characterize and optimize the material, build a proto-type detector, and measure its neutron sensitivity and gamma-detection properties. Parallel simulations will eventually determine the use of this material in systems with hundreds of detector units.

continuing project

# From Novel Principles to Novel Device Structures for High-Efficiency Generation of Solar Electricity

*Victor Ivanovich Klimov*

20070338ER

## Introduction

Semiconductor nanocrystals (NCs) are promising materials for the realization of low-cost, high-efficiency photovoltaics (PV). They can be synthesized and processed via solution-based techniques readily applicable to the fabrication of large-area devices including solar cells. NCs also exhibit a number of unique physical properties that can benefit PV applications. For example, the NC-size-controlled energy gap can be used to tailor the absorption spectrum for the best match to the solar radiation spectrum. Further, one can boost power conversion efficiency via NC-specific processes such as generation of multiple charges by single photons (carrier multiplication) and/or hot-electron extraction in the presence of a "phonon bottleneck" in intraband relaxation. The first practical step toward utilization of the unique properties of NCs in the PV technologies could be through their integration into traditional semiconductor thin-film devices. The goal of this project is the development of a new type of hybrid solar cells that combine NCs and semiconductor charge-extraction layers. In our initial proof-of-principle studies, we will target devices comprising CdSe NCs and amorphous silicon. Eventually, we will extend this work to NCs of narrow-gap materials such as PbSe, PbS, and InAs that will be combined with charge-transport layers made of germanium and possibly silicon-germanium alloys. The use of these materials will allow us to increase the power conversion efficiency through improved coverage of the solar spectrum, and perhaps, multiexciton generation via carrier multiplication. The anticipated product of this project is a high-efficiency, thin hybrid solar cell fabricated via simple wet-chemistry procedures and traditional thin-film technologies.

## Benefit to National Security Missions

This project involves the development of new types of photovoltaic structures based on semiconductor nanocrystals. This work is relevant to DOE missions in both world-class fundamental science and energy security missions. Successful implementation of new strategies outlined in this proposal will yield technologies relevant to DOE missions in Energy Security.

## Progress

During the review period, we have demonstrated for the first time functional PV structures that combine colloidal NCs with amorphous silicon. These devices show good PV performance (EQEs up to ~4% and IQEs up to ~10%), which can be further improved through optimization of the photoconductivity of the NC layer and the refinement of a-Si fabrication procedures. Below, we describe in greater detail our fabrication procedures and results of device characterization.

### Fabrication of hybrid PV structures

The fabricated devices (Figure 1a) comprise a layer of pyridine-capped CdSe NCs sandwiched between indium tin oxide (ITO) and a-Si. To grow an a-Si layer on top of an NC film, we have used either electron-beam (e-beam) evaporation or radio-frequency (rf) magnetron sputtering; both of these methods allow encapsulation of the NCs without adversely affecting their physical properties. The thickness of the a-Si layer was typically between 50 and 100 nm. For photocurrent measurements, the structure was completed with an Al electrode. These devices showed stable PV performance in air under ambient conditions.

We have performed transmission electron microscopy (TEM) characterization of the fabricated structures (Figures 1b-d). The high-resolution TEM images show resolvable lattice fringes of CdSe NCs, which indicates that the NC integrity is preserved during silicon film growth. The latter is also confirmed by spectroscopic studies (Figures 1e-f). Specifically, optical absorption measurements show that the lowest-energy, 1S absorption feature of the NCs is preserved in the final device structure. Further, NC photoluminescence although quenched, is still observable following silicon deposition.

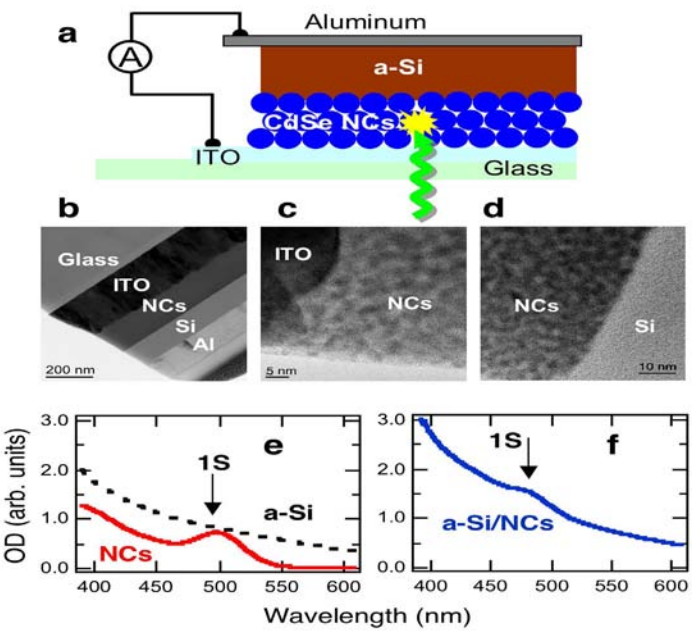


*Figure 1. Hybrid a-Si/NC PV structures: TEM and spectroscopic characterization. (a) Schematic of the PV device. (b) A cross-sectional TEM image of the PV structure. (c) and (d) High-resolution TEM images of the ITO/NC and the NC/a-Si interfaces, respectively. (e) The absorption spectra (in terms of optical density, OD) of the NC and a-Si films separately deposited on glass slides. (f) The absorption spectrum of the hybrid a-Si/NC structure.*

**Characterization of PV performance**

To study electronic interactions at NC/Si interface, we have analyzed the PV response of devices fabricated using NCs of two different sizes (energy gaps 2.5 and 2.1 eV) that correspond to two different injection regimes (Figure 2a). For larger-gap (>2eV) NCs electrons can transfer from the NCs to Si while the direction of transfer is opposite in the case of NCs with a smaller gap (<2eV). Since these structures are composed of thin layers of undoped materials, their operation is similar to that of, for example, thin-film polymer PV cells. If such devices are under short-circuit conditions, the Fermi levels in the electrode materials come to equilibrium, which results in the buildup of an internal electric field. In the case of ITO and Al, this field provides a driving force that directs electrons toward the Al electrode, while holes are directed to the ITO contact (Figure 2b).

To analyze the performance of our PV devices, we use external and internal quantum efficiencies (EQE and IQE, respectively) that are calculated as the ratio of a spectrally resolved photocurrent (measured as the number of charges extracted from the cell under short-circuit conditions) to the number of either incident (EQE) or absorbed (IQE) photons. The EQE is determined by the performance of a PV device at all stages of the photo-conversion process from light harvesting to charge separation, carrier transport, and collection at the electrodes. On the other hand, the IQE characterizes processes internal to a PV device separating them from its light harvesting ability.

As expected based on the "energetics" at the Si/NC interface, the devices that comprise NCs with the 2.5-eV energy gap show a good PV response (EQE of ~4%), which mimics the NC absorption spectrum (Figure 2c). The EQE values are greatly reduced (down to less than 0.1%) in the devices made of the NCs with energy gap of 2.1 eV (Figure 2d). In this case, the lowest NC electron level is below the a-Si conduction band edge, which inhibits electron injection into the silicon layer. These results indicate the possibility of obtaining good electronic coupling between NCs and Si, and also demonstrate our ability to control the charge flow at the NC/Si interface through the quantum-size effect.

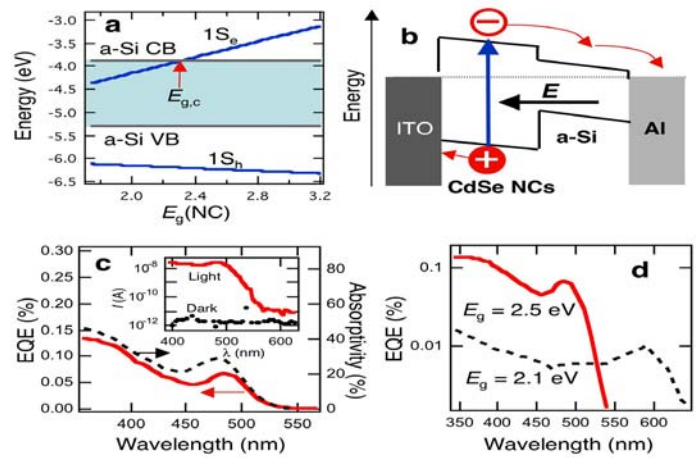


*Figure 2. The effect of NC size on the PV performance of a-Si/NC structures. (a) The size-dependent energies of the NC 1S electron and hole levels (blue lines) plotted as a function of the NC energy gap in comparison to the band-edge positions of a-Si (grey lines); all energies are measured versus vacuum. Eg,c is the critical NC gap; sufficiently small NCs with Eg > Eg,c can inject a photoexcited electron into a-Si. (b) Schematics of energy structures in a PV device operating under short-circuit conditions; the horizontal arrow shows the direction of the internal electric field, E. (c) The EQE spectrum (solid red line) of the PV device fabricated using NCs with energy gap of 2.5 eV in comparison to the NC absorption spectrum measured in terms of percentage of absorbed photons (dashed black line). Inset: The spectral dependence of the photocurrent (solid red line) and the dark current (black circles). d, Comparison of PV performance (in terms of EQE on a log scale) of the devices fabricated using NCs with energy gaps of 2.5 eV (solid red line) and 2.1 eV (dashed black line).*

Because of the small thickness of these structures, they do not absorb all incident light. Therefore, the IQE values for them can be much greater than the EQE values. For example for the device with 4% EQE, the IQE is greater than 10%. This relatively high value shows that these first-generation hybrid structures show quite efficient performance with regard to extraction of charges from the NCs and their collection at the electrodes.

## Future Work

In the above proof-of-principle study, the PV response was entirely due to the NCs, while the a-Si film played a role of charge-separation/transport element. On the other hand, interesting opportunities are provided by structures, in which the PV response is due to light absorption in both the NCs and a bulk-semiconductor layer. This type of performance is expected, for example, for devices made of a-Si and infrared (IR) absorbing PbS NCs. According to a diagram in Figure 3, electrons photogenerated in PbS NCs can be transferred into amorphous silicon and then collected at the Al electrode. Further, the alignment of the valence-band states at the PbS NC/a-Si interface favors hole transfer from silicon into NCs followed by collection at the ITO electrode. Thus, this structure is expected to show photocurrent due to both a-Si and the NCs.

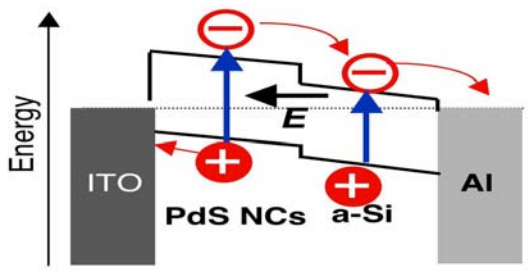


*Figure 3. Schematics of energy structures in a PbS NCs/a-Si PV device operating under short-circuit conditions; the horizontal arrow shows the direction of the internal electric field. Charges generated in both NCs and a-Si can contribute to photocurrent.*

An immediate advantage of these structures compared to traditional a-Si cells is the IR extension of their operational range due to efficient absorption of IR photons in PbS NCs. Additional improvements can be expected from multiexciton generation via carrier multiplication. However, because of a high three-energy-gap onset in lead-salt NCs, the benefits from carrier multiplication in this specific case are not expected to be large. To take advantage of this phenomenon, we will use NCs made of materials with very dissimilar electron and hole masses (e.g., InAs or InSb), for which the onset for multiexciton generation is expected to approach two energy gaps.

## Conclusion

To summarize, during the past year, we have demonstrated for the first time functional PV structures that combine colloidal NCs with amorphous silicon. These devices show good PV performance (EQEs up to ~4% and IQEs up to ~10%), which can be further improved through optimization of the photoconductivity of the NC layer and the refinement of a-Si fabrication procedures. A further increase in the performance is also possible through the realization of tandem structures, in which the PV response is due to light absorption in both the NCs and the bulk-semiconductor layer. These devices will provide high power-conversion efficiency in combination with low fabrication costs allowed by wet-chemistry procedures and traditional thin-film technologies.

## Publications

Jiang, X. M., R. D. Schaller, S. B. Lee, J. M. Pietryga, V. I. Klimov, and A. A. Zakhidov. PbSe nanocrystal/conducting polymer solar cells with an infrared response to 2 micron. 2007. *J. Mater. Res.*. **22** (8): 2204.

Klimov, V. I.. Detailed-balance power conversion limits of nanocrystal-quantum-dot solar cells in the presence of carrier multiplication . 2006. *Appl. Phys. Lett.*. **89** (12): 123118.

Klimov, V. I.. Spectral and dynamical properties of multiexcitons in semiconductor nanocrystals . 2007. *Annu. Rev. Phys. Chem.* **58**: 635.

McGuire, J. A., J. Joo, J. M. Pietryga, R. D. Schaller, and V. I. Klimov. New aspects of carrier multiplication in semiconductor nanocrystals. To appear in *Accounts of Chemical Research.*

Sun, B., A. T. Findikoglu, M. Sykora, D. J. Werder, and V. I. Klimov. Hybrid photovoltaic devices based on semiconductor nanocrystals and amorphous silicon . To appear in *Nature Nanotechnology.*

# X, Gamma, Alpha : Ultra-High Resolution Spectroscopy

*Michael W Rabin*

20070367ER

## Introduction

We are making, testing, and using microcalorimeter nuclear spectrometers of very high spectral resolution for detecting enriched uranium, the analysis of environmental samples, and for application in nuclear forensics and nuclear inspections. Superconducting materials are an almost ideal choice for radiation absorbers in microcalorimeters because of their unique thermal properties. We have produced the first microcalorimeter array spectrum of special nuclear material and the first splitting of the major Pu peaks in an alpha-particle energy spectrum.

## Benefit to National Security Missions

This project directly supports the Threat Reduction mission of the DOE through development of powerful technology for detecting and assaying nuclear materials. Our work supports international nuclear safeguards and nuclear forensics to prevent the misuse of nuclear materials.

## Progress

We have started the characterization of the next generation of x and gamma-ray detector chips. These chips are optimized to have increased dynamic range and excellent linearity up to 200 keV. The new approach consists of detector elements with multiple epoxy posts surrounding the transition-edge sensor (TES). This is in contrast to the old approach, which had a single SU8 post attached directly to the TES element, resulting in mechanical and chemical stress on the TES. The distributed nature of the mounting posts also reduces the dependence of the response on the photon interaction position in the tin absorber. Consequently, the absorber size has been increased from 1 $mm^2$ to 2.25 $mm^2$, which results in increased detection efficiency. While the layout of the next-generation chip allows for 66 individual pixels, it is intended to be read out in two banks of 32 pixels each; the two remaining pixels are kept as spare. Using a flip-chip bonder for simultaneous absorber attachment, we achieved 100% yield for this chip (Figure 1). Experiments indicate that 55 of the 66 pixels are active. With this chip, we have observed excellent linearity up to 129 keV, a marked improvement over the first-generation chip. The observed energy resolutions for individual pixels of the next-generation chip have ranged between 50 and 100 eV at 100 keV at low event rate. An X- and gamma-ray spectrum of special nuclear material demonstrating this new chip's performance is shown in Figure 2 [1].

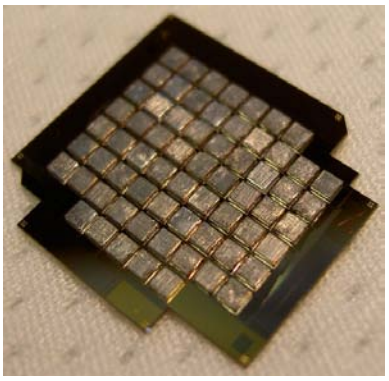

*Figure 1. Sixty-six pixel gamma-ray chip. Each pixel is an individual transition-edge sensor microcalorimeter detector with a tin absorber.*

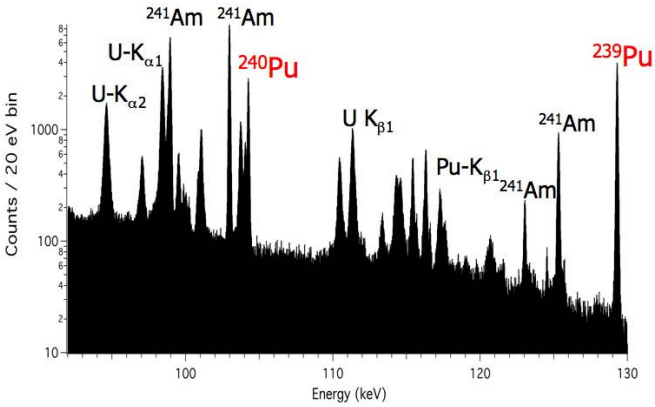


*Figure 2. X- and gamma-ray spectrum of plutonium using chip shown in Figure 1. Thirty-one pixels were operated simultaneously using time-division multiplexing; of those pixels, data were combined after calibration from twenty-one pixels.*

Plutonium data from the spectrometer have been analyzed with standard isotopic analysis code used by the International Atomic Energy Agency (IAEA) and developed at Los Alamos. With some modification to a standard parameter sets without modification of the computational kernel, we obtained isotopic abundances that are in reasonable agreement for $^{240}$Pu content with both measurements with high-purity germanium detectors and the declared values. These initial findings and the analysis required to produce them illustrate the issues regarding the application of standard codes to microcalorimeter data, e.g. the need for new models for peak tailing and for summing data from multiple pixels each with different inherent energy resolution [2].

Well-validated Monte Carlo simulation codes are important for the interpretation of measured data, for studying application scenarios, and for guiding future sensor arrays and associated cryostat technology. GEANT4 low-energy EM simulation code was implemented to assess its effectiveness at replicating measured data from our detector system. We found that GEANT4 reproduced all measured spectral features and detection efficiencies with good accuracy. We used the validated simulation to quantify gains in detection efficiency that could be realized with large arrays, an optimized cryostat, and alternate absorber materials. We demonstrated that microcalorimeter arrays could eventually be competitive with planar germanium detectors with respect to detection efficiency in the 100 keV regime, while simultaneously providing more than an order of magnitude improvement in energy resolution [3].

Limitations in alpha spectral resolution affect nuclear materials accounting, international nuclear safeguards, the detection of nuclear smuggling, and other activities that require rapid and accurate analysis of nuclear materials. However, the strongest alpha peaks of $^{240}$Pu and $^{239}$Pu are separated by only 11.6 keV and cannot by resolved by Si detectors. Microcalorimeters can dramatically streamline nuclear forensic analysis by eliminating elemental separation of mixed actinide samples and providing, at the same time, isotopic information that presently is determined by mass spectrometry. To demonstrate this point, we have used a microcalorimeter to unambiguously measure the $^{239}$Pu and $^{240}$Pu isotopic fractions in a mixed-isotope Pu sample (Figure 3). The microcalorimeter spectrum is fit with five peaks consisting of two left-handed exponentials convolved with a Gaussian instrumental response to yield a $^{240}$Pu/$^{239}$Pu atomic ratio of 0.128 ± 0.007, in good agreement with the known ratio of the sample, which is 0.135 ± 0.001. The clear peak separation gives confidence that there is no unrecognized systematic error in the fitting. In contrast, values for the $^{240}$Pu/$^{239}$Pu atomic ratio extracted from the Si data are prone to error. The results determined using the Si detector are systematically low for three standard line shape models, and strangely high for the fourth, whereas values from the microcalorimeter are similar for all of the line shape models and cluster tightly around the known value. This analysis captures the limitations of existing alpha detectors for determining $^{239}$Pu/$^{249}$Pu ratios: measurements of moderate accuracy are possible, but the risk of unrecognized systematic error prevents the use of alpha spectrometry for precision isotopics. This limitation is clearly overcome by microcalorimeter detectors [4].

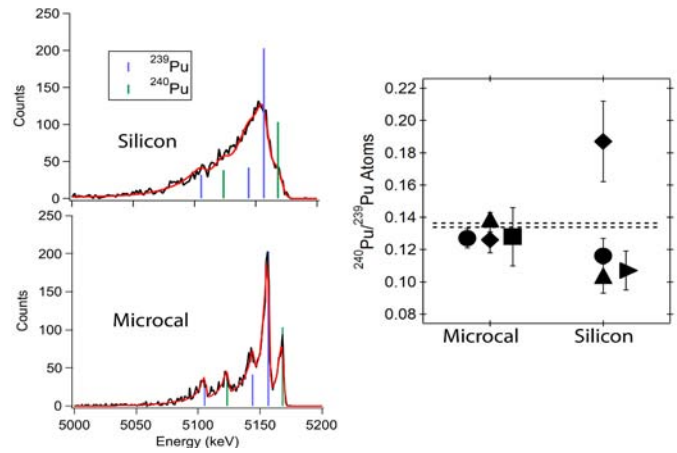


*Figure 3. Alpha particle energy spectra from plutonium and analysis. Upper left panel shows results from conventional silicon detector, data are in black and a fit is shown in red; the major peak for Pu-240 is not resolved. Low left panel shows results from same sample using microcalorimeter detector; the major Pu-240 is now clearly resolved. Right panel shows analysis to determine isotopic ratio; the microcalorimeter results cluster closely around the known value (dashed lines).*

We continue to explore absorbing materials with improved efficiency over Sn. The ideal absorber combines high atomic number, low heat capacity per volume, and good thermalization properties. Good thermalization implies the fast and efficient conversion of photon energy to heat that can be measured with a thermometer. The atomic number (50) and heat capacity of Sn are only intermediate. However, its thermalization properties are excellent and consequently it has been the only absorber to produce high quality results at gamma-ray energies. In the proceeding year, we built and tested gamma-ray detectors with two new absorbers: high purity Tantalium (Ta) and Lead Tungstate ($PbWO_4$). Neither of these materials performed acceptably. The Ta device showed a very small pulse height and very long pulse response, indicating either an anomalous heat capacity or long-lived athermal excitations. The $PbWO_4$ showed signal-to-noise ratios as good as $10^3$ in individual pulses, but enormous variation in response from pulse to pulse. This variation could be caused by material inhomogeneity, but other explanations are possible. In order to determine the temperature-dependent heat capacity of prospective absorber materials, we also built a dedicated sample box for heat capacity measurements. The sample box contains wiring and fixturing to measure the heat capacity of two samples per cooldown. Initial test results with Sn samples were

promising and measurements will continue after a redesign to improve measurement accuracy below 200 mK.

## Future Work

We will develop new microcalorimeters and the associated nuclear applications. We will characterize and use nuclear microcalorimeter spectrometers of amazing spectral resolution for nuclear forensics, detecting enriched uranium, the analysis of environmental samples, and nuclear inspections. We have completed all the initial characterization of a complete X and gamma ray microcalorimeter spectrometer operating now at LANL. We anticipate completing fabrication of an a reconfigured array of X/gamma pixels with 64 TES sensors, and will move toward integration of four such chips into the spectrometer, giving us 256 pixels and approximately the same detection area as commercial a planar Ge spectrometer. We will use the completed instrument for several crucial nuclear measurements, directly comparing the results with models. In parallel with detector fabrication and characterization we will model the application of microcalorimeters to a range of measurement problems. Modeling results can be compared to actual measurement results using source materials present at LANL.

Superconductors are an almost ideal choice for particle absorbers in microcalorimeters because of their low heat capacity and small (milli-eV) bandgap. Increased effort on higher efficiency absorbers is planned for FY09. Our limited results on Ta to date are consistent with cycles of quasiparticle recombination and recreation by pair-breaking recombination phonons. Our results also indicate that these effects are more severe in pure Ta. As a result, we are particularly interested in measurements on high-defect-density ("dirty") superconducting materials where the quasiparticle lifetime is expected to be shorter. Tests on other candidate materials are also planned, including HgCdTe, which has worked well at X-ray energies.

We will develop a microcalorimeter whose size and absorber are optimized for alpha particle detection. To evaluate the performance of the microcalorimeter detectors for alpha spectrometry, small area Pu sources will be prepared. We will continue the improvement of sample preparation techniques based on simplified electrochemistry, concentrating efforts on reduction of energy broadening ("straggle") and chemical yield (crucial to analysis of trace samples).

## Conclusion

We expect to have a complete, quantitative performance assessment of a 256-pixel microcalorimeter array for X and gamma ray spectrometry, including new measurements of fundamental X and gamma ray spectral features, e.g. peak centers, widths, and shapes. We also expect to demonstrate quantitative alpha spectrometry for Pu isotopes for direct comparison to conventional technology. We will apply this new instrument to problems directly related to nuclear forensics, law enforcement support, and international nuclear safeguards.

## References


1. Bacrania,etal, M. K.. Large-area microcalorimeter detectors for ultra-high-resolution x-ray and gamma-ray spectroscopy. *IEEE Transactions on Nuclear Science.*

2. Karpius,etal, P. J.. A First Application of the FRAM Isotopic Analysis Code to High-Resolution Microcalorimetry Gamma-ray Spectra. *IEEE Transactions on Nuclear Science.*

3. Hoover,etal, A. S.. Simulating the response of ultra-high energy resolution X- and Gamma-ray microcalorimeter detectors. 2007. In *IEEE Nuclear Science Symposium and Medical Imaging Conference 2007.* (Honolulu, Hawaii, 15-21 Nov. 2007). Vol. I, p. 847. Los Alamitos, CA: IEEE.

4. Horansky,etal, R. D.. Superconducting calorimetric alpha particle sensors for nuclear nonproliferation applications. 2008. *Applied Physics Letters.* **93**: 123504.


## Publications


Doriese, W. B., J. N. Ullom, J. A. Beall, W. D. Duncan, L. Ferreira, G. C. Hilton, R. D. Horansky, K. D. Irwin, J. A. B. Mates, C. D. Reintsema, L. R. Vale, Y. Xu, B. L. Zink, M. W. Rabin, A. S. Hoover, C. R. Rudy, and D. T. Vo. 14-pixel, multiplexed array of gamma-ray microcalorimeters with 47 eV energy resolution at 103 keV. 2007. *Applied Physics Letters.* **90**: 193508.

Rabin, M. W., A. S. Hoover, C. R. Rudy, S. P. Lamont, D. M. Tournear, D. T. Vo, J. A. Beall, W. B. Doriese, W. D. Duncan, L. Ferreira, G. C. Hilton, R. D. Horansky, K. D. Irwin, G. C. O'Neil, C. D. Reintsema, J. N. Ullom, L. R. Vale, K. Chesson, and B. L. Zink. Microcalorimeter Nuclear Spectrometers. 2006. In *IEEE Nuclear Science Symposium 2006.* (San Diego, CA, Oct 2006). Vol. 1, p. 544. New York: Nuclear Science Symposium Conference Record, 2006.

continuing project

# A Novel Approach to Manufacturing Ultra-Tall Carbon Nanotube Forests

*Quanxi Jia*

20070368ER

## Introduction

This project will explore the growth of ultra-tall (10-30 mm) carbon nanotube forests (arrays) at fast production speeds. Such ultra-tall nanotube forests offer the only pathway to effective utilization of extremely high-strength nanotubes for many important applications from next-generation aerospace structures to personnel armor. In this project, we will use an innovative approach to grow ultra-tall nanotube forests, based on unique LANL expertise and facilities. We will design and fabricate a unique chemical vapor deposition (CVD) system that will allow for base-growth of nanotube forests to lengths 10 times greater than are presently possible, while at the same time maintains a fast growth rate. The synthesized nanotubes will be characterized using several state-of-the-art techniques available at LANL. In addition, the project will also help us to understand how the substrate and buffer layer affect the nucleation and growth physics of nanotube forests. We envision this research to be the first step towards commercial production of carbon nanotubes that can be used for countless structural and electronic applications.

In details, we will use the catalytic CVD method to grow ultra-tall carbon nanotube forests at high production speeds. This process involves the following steps: `) deposit a buffer layer on a Si substrate, 1) deposit a catalyst film, 3) nucleate catalyst particles, 4) grow nanotube forests in a CVD chamber under appropriate processing parameters including flowing hydrocarbon gas, temperature, time etc. We will use the following R&D approaches to solve the five outstanding issues encountered during the growth of nanotube forests:

1. Optimize and control catalyst size,
2. Keep catalyst particles in an optimum environment,
3. Deliver the hydrocarbon gas to the catalyst particles,
4. Avoid the formation of amorphous carbon, and
5. Determine the optimum processing temperature and hydrocarbon gas partial pressure.

## Benefit to National Security Missions

This project supports DOE Office of Science missions in nanotechnology. Carbon nanotubes are currently at the frontier of materials science. Synthesis of long carbon nanotube forests will make it possible to develop a whole new class of advanced materials for applications ranging from aerospace to personnel armor.

## Progress

In the last year, we have made tremendous progress for this project. For example, we have optimized the processing conditions to grow long carbon nanotube (CNT) forest; we have also studied the CNT surface termination on the spinnability of the CNT forest. Here we highlight the surface termination on the spinnability of CNT forest.

Carbon nanotubes (CNTs) have been extensively studied recently due to their unique structure and excellent mechanical, electrical, and chemical properties. Numerous promising applications of CNTs have been reported. To exploit their excellent properties for more practical applications, it is desirable to assemble individual CNTs into macroscopic fibers. This approach enables CNTs to be highly aligned and physically attached in the resulting fibers. Therefore, it is promising to produce high-strength CNT fibers. Early results have shown that the long array greatly improves the fiber's performance, so the common thinking is to improve the spinnability of synthesized long arrays. Unfortunately, most reported long CNT arrays are not spinnable.

We have grown long CNT arrays up to 5 mm using a chemical vapor deposition (CVD) process. Briefly, Fe/$Al_2O_3$ was used as the catalyst, ethylene served as the carbon source, and Ar with 6% $H_2$ was used to carry the precursor to a tube furnace where the growth took place. The reaction temperature was controlled at 750 °C, while the reaction time varied between 15 and 180 min. We have found that the growth of CNTs mainly occurs in the first 90 min, and the further increase of reaction time has little effect on promoting the growth. Particularly, the prolonged time (> 30 min) dramatically

decreases the spinnability of the CNT arrays, i.e., the spun fibers tend to break during the spinning of CNT arrays with increasing growth times. For instance, long fibers up to meters can be easily spun from the arrays grown in 15 min; short fibers with length of centimeters may be spun from the arrays grown in 40 min but easily break; while only short fiber clumps can be pulled out of the arrays grown in 180 min. This phenomenon may be related to the structure at the top surface of CNT arrays.

Our systematic investigation on the processing-structure-spinnability relationship shows that the top surface plays a key role in determining the spinnability of long CNT arrays. CNT arrays grown in 30 min with clean top surfaces are spinnable, while those grown beyond 30 min are non-spinnable. Scanning electron microscopy (SEM), transmission electron microscopy (TEM), and Raman characterizations confirm that the CNT arrays with prolonged growth times have a disordered top layer with a mixture of amorphous carbon, graphite, and CNTs. This carbon mixture deteriorates the spinning ability of synthesized arrays. Spun CNT fibers show excellent mechanical strengths and electrical conductivities.

## Future Work

Carbon nanotubes are the strongest materials ever discovered by mankind. However, this extremely high strength has yet to be utilized, because there is currently no technology to produce carbon nanotubes in long length and large quantity. This project seeks to overcome these obstacles. The significance of ultra-tall carbon nanotube forests (or arrays) derives from the tremendous impact they will have on science and technology in many advanced applications. Ultra-tall carbon nanotube forests will enable an entirely new and revolutionary class of advanced materials that are ultra-strong and lightweight.

We will grow ultra-tall (10-30 mm) carbon nanotube forests (arrays) at fast production speeds. We will use an innovative approach to grow ultra-tall nanotube forests, based on unique LANL expertise and facilities. We will design and fabricate a unique chemical vapor deposition system that will allow for base-growth of nanotube forests to lengths 10 times greater than are presently possible, while at the same time maintains a fast growth rate. The synthesized nanotubes will be characterized using several state-of-the-art techniques available at LANL. In addition, the project will also help us to understand how the substrate and buffer layer affect the nucleation and growth physics of nanotube forests. We envision this research to be the first step towards commercial production of carbon nanotubes that can be used for countless structural and electronic applications.

It is the objective and goal of this project to solve the aforementioned five outstanding issues so as to manufacture ultra-tall carbon nanotube forests at high production speed. A secondary but equally important goal is to understand how the substrate and buffer layer affect the nucleation and growth physics of the carbon nanotube forests.

## Conclusion

We have systematically investigated the processing-structure-spinnability relationship and the CNT surface termination on the spinnability of the CNT forest. We will continue to develop cutting-edge technology for synthesizing ultra-tall carbon nanotube forests (10-30 mm tall) for specific applications. In addition, we will further study the substrate/buffer layer and catalyst interactions so that we have a better understanding of the nucleation and growth physics of carbon nanotube forests. We believe that this project will result in an enabling technology for the large-scale commercial production of carbon nanotube forests.

## Publications

Li, Q. W., Y. Li, X. F. Zhang, S. B. Chikkannanavar, Y. H. Zhao, A. M. Dangelewicz, L. X. Zheng, S. K. Doorn, Q. X. Jia, D. E. Peterson, P. N. Arendt, and Y. T. Zhu. Structure-Dependent Electronic Properties of Carbon Nanotube Fibers. 2007. *Adv. Mater* . **19**: 3358.

Usov, I. O., Y. Q. Wang, Q. W. Li, Y. T. Zhu, R. F. DePaula, and P. N. Arent. Impurity Elements Study of Carbon Nanotubes Fabricated by Chemical Vapor Deposition. 2007. *Nuclear Inst. And Methods in Physics Research.* **261**: 574.

Wang, Z. L., D. W. Tang, X. B. Li, X. H. Zheng, W. G. Zhang, L. X. Zheng, and Y. T. Zhu. Length-Depedent Thermal Conductivity of an Individual Single-Wall Carbon Nanotube on Substrate. 2007. *Appl. Phys. Lett..* **91**: 123119.

Wang, Z. L., D. W. Tang, X. Zheng, W. Zhang, and Y. T. Zhu. Length-dependent Thermal Conductivity of Single-wall Carbon Nanotube: Prediction and Measurements. 2007. *Nanotechnology.* **18**: 475714.

Yao, Y. G., Q. W. Li, J. Zhang, L. Y. Jiao, Y. T. Zhu, and Z. F. Liu. Temperature Mediated Growth of Single-Wall Carbon Nanotube Intramolecular Junctions. 2007. *Nat. Mater..* **6**: 283.

Zhang, X. F., Q. W. Li, T. G. Holesinger, P. A. Arendt, J. Y. Huang, T. G. Clapp, R. F. Depaula, X. Z. Liao, Y. H. Zhao, L.

# Optical, Electronic, and Magnetic Doping of ENABLE Grown Semiconducting Films

*Mark Arles Hoffbauer*

20070436ER

## Introduction

The growth of uniform alloys of semiconducting thin film materials and their controlled doping is central to the fabrication of optoelectronic devices. In spite of their tremendous potential for solid state lighting and photovoltaic energy harvesting, there are still significant technical challenges related to producing high-quality InGaN-related materials that are efficient, reliable, and inexpensive. Forming uniform alloys of Ga nitride related materials containing substantial amounts of In is a difficult challenge, limiting the potential uses of these materials for photovoltaic (PV) and light emitting diode (LED) applications. Achieving high-quality p-type doped InGaN semiconducting films (especially with In-rich InGaN alloys) and doping with unconventional materials such as magnetic atoms, nanocrystals, and other species are particularly difficult.

The lack of control of film uniformity and the dopant's lattice position and chemical environment often require thermal processing steps that limit the alloy composition and/or dopant materials to those that are thermally stable. For example, the desire to exploit InGaN for widely tunable PV and LED applications is severely hampered by clustering of In at concentrations greater than about 20%, preventing the formation of uniform alloys of In-rich InGaN. Similarly, the clustering of magnetic dopant atoms (e.g. Co and Mn) has severely hindered the development of GaN-based above room-temperature dilute magnetic semiconductor materials for spintronic applications. This difficulty has inhibited the development of an entire new field of spin-based devices for a host of applications including quantum computing. At LANL we recently developed a new type of LED that used GaN-based semiconducting thin films to encapsulate optically active nanocrystalline moieties by growing a thin film of semiconducting GaN over a layer of nanocrystals. However, the resulting LEDs showed low light emission efficiency due to the delicate nature of the nanocrystals and relatively poor semiconductor film quality that combined to impose large barriers for injecting charge into the embedded nanocrystals.

Common techniques for incorporating In, dopant atoms, and/or other species into GaN-related thin films during growth have proved difficult due to clustering and phase segregation caused by high growth temperatures, e.g. In clustering in In-rich InGaN. We are developing novel solutions to these problems by combining energetic neutral atom beam lithography & epitaxy (ENABLE, a novel low-temperature film growth technology recently developed at LANL) with various growth and doping schemes. Our results are producing improved optoelectronic materials with novel electronic, optical, and structural properties for energy security applications ranging from efficient full-spectrum white LEDs and PV devices to advanced chemical sensors.

## Benefit to National Security Missions

Electronic and photonic materials support the national energy security and threat reduction missions of DOE with applications ranging from efficient solid state lighting to photovoltaic electrical energy production and advanced sensor development. This project will improve the properties of doped semiconducting materials for these applications.

## Progress

To date, our focus has been on improving the quality of our GaN and InGaN thin film growth. Particular attention is being placed on tunable-bandgap InGaN mixed alloy films since they serve as models for growing uniform alloy films and for incorporating dopants in a controlled manner. By accurately controlling film stoichiometry during growth, the material properties of our ENABLE-grown GaN semiconducting films have been vastly improved, with X-ray diffraction results comparable to the best reported in the literature for GaN grown on heteroepitaxial substrates. Notably, our photoluminescence (PL) measurements show large improvements in intensity, exceeding those observed for commercially available GaN materials. High-quality InN semiconducting films have been grown and optimized, yielding device-quality electronic and optical results comparable to the best report-

ed to date by other growth techniques. We have also grown mixed InGaN alloy films at low temperatures over the full In-rich to Ga-rich composition ranges showing excellent uniformity and no evidence of clustering or phase segregation [1] as confirmed by x-ray diffraction (XRD) results shown in Figure 1. In addition, Figure 2 shows results for exceptionally bright PL that confirms the expected bandgap emission for InGaN films of varying stoichiometry. Our PL and XRD results are practically impossible to achieve by conventional growth techniques, making our InGaN films amongst the best ever reported and opening up the possibility of using these device-quality materials in high-efficiency, full-spectrum lighting and PV applications.

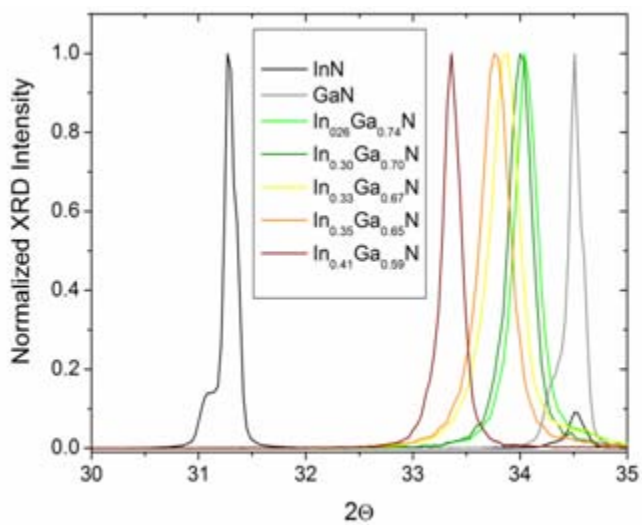


*Figure 1. XRD data for InN, GaN, and InxGa1-xN films of vary-ing composition indicated in the figure caption and color coded according to their peak photoluminescence. In all cases the films show uniform compositions and single phase material with no appreciable segregation.*

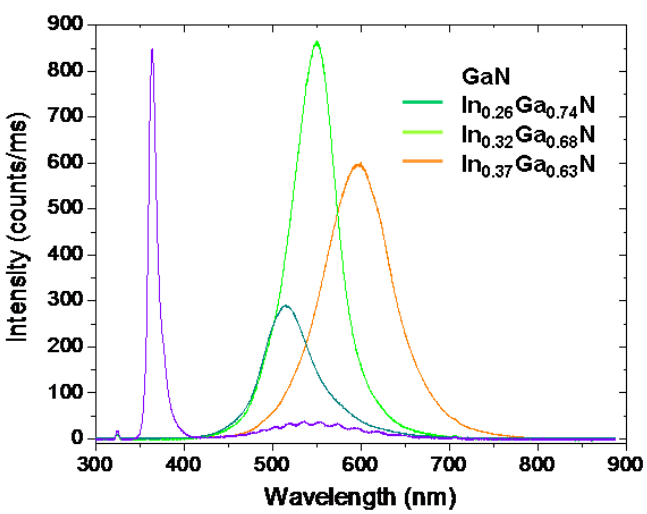


*Figure 2. PL from ~1 µm thick InGaN films grown by ENABLE on sapphire at ~750°C. The intensities are absolute counts for GaN and for three InGaN compositions yielding dark green, yellow-green, and red-orange emission.*

We recently installed a Mg dopant source into the ENABLE system and have confirmed the controlled incorporation of Mg as a dopant into GaN films. The PL signature of the dopant indicates that a substantial fraction of the Mg is active as a dopant without needing the thermal activation step common to other doping schemes. We have also studied the properties of nanocrystalline CdSe materials encapsulated by a GaN film as a basis for placing these nanocrystalline materials directly into the lattice of GaN thin films. To date, these studies have focused on the survivability of sub-monolayer coverage's of CdSe nanocrystals when covered by a GaN film.

We are presently working on lowering the background carrier concentration in our GaN and InGaN films—a necessary step before being able to confirm electrically active p-type doping of these materials. Another dopant source is being installed on the ENABLE system for operation with multiple dopant materials for controlled n- and p-type doping and for magnetically active dopants. This source will allow us to fabricate quantum well structures and to incorporate magnetic dopants into films. We plan to integrate other dopant sources into the ENABLE system that will allow multiple materials to be directly incorporated into films as they are growing, with particular interest in imbedding CdSe nanocrystals into GaN films with the goal of ultimately being able to observe PL from single CdSe nanocrystals.

## Future Work

Future work will further develop techniques for addressing the thermal stability problems associated with growing uniform alloys and doping of GaN-based semiconductors by combining low-temperature ENABLE film growth with doping by thermal, aerosol, and/or electrospray techniques. Our future goals are to 1) development optimized growth strategies for forming uniform InGaN alloys over the full In compositional range with excellent electronic and optical properties for PV and LED device applications, 2) optimize the film growth and doping processes for fabricating devices structures, and 3) fully optimize the electronic and optical properties of doped films and demonstrate prototype device fabrication. These efforts will focus on targeting high-efficiency, full-spectrum PV and LED devices and their applications.

## Conclusion

ENABLE has previously been used to demonstrate growth of high-quality undoped GaN-related films at low temperatures. The goal of this project is to combine low-temperature film growth by ENABLE with a wide variety of doping techniques for incorporating thermally sensitive and/or fragile materials into semiconducting films. The resulting materials are expected to have improved optical and

electronic properties, leading to novel devices for a wide variety of applications important to solid state lighting and photovoltaic energy production.

## References

1. Williamson, T. L., M. A. Hoffbauer, K. M. Yu, L. A. Reichertz, M. E. Hawkridge, R. E. Jones, N. Miller, J. W. Ager III, Z. Liliental-Weber, and W. Walukiewicz. Highly Luminescent InGaN Thin Films Grown Over the Entire Composition Range by Energetic Neutral Atom Beam Lithography & Epitaxy (ENABLE). *Physica Status Solidi c.*

## Publications

AgerIII, J. W., L. A. Reichertz, K. M. Yu, W. J. Schaff, T. l. Williamson, M. A. Hoffbauer, N. M. Haegel, and W. Walukiewicz. InGaN/Si Heterojunction Tandem Solar Cells. 2008. In *33rd IEEE Photovoltaic Specialists Conference.* (San Diego, CA, May 11–16, 2008). Vol. , Edition, p. . : .

Miller, N., R. E. Jones, K. M. Yu, J. W. Ager, Z. Lilental-Weber, E. E. Haller, W. Walukiewicz, T. L. Williamson, and M. A. Hoffbauer. Low-temperature grown compositionally graded InGaN films. 2008. *Physica Status Solidi c.* **5**: 1866.

Reichertz, Lothar A., Kin M. Yu, Y. Cui, Michael E. Hawkridge, Jeffrey W. Beeman, Z. Liliental-Weber, Joel W. Ager III, W. Walukiewicz, William J. Schaff, Todd L. Williamson, and Mark A. Hoffbauer. InGaN Thin Films Grown by ENABLE and MBE Techniques on Silicon Substrate. 2008. *Materials Research Society Symposium Proceedings.* **1068**: xxx.

# Terahertz Generation Harnessing the Two-Stream Instability

*Kip A Bishofberger*

20080210ER

## Introduction

The terahertz regime of the electromagnetic spectrum is situated between traditional high-frequency microwave and extremely far-infrared light. Both producing and detecting terahertz waves has been both difficult and the focus of significant efforts world-wide. Because of the very specific absorption and transmission properties of terahertz radiation, there are potentially many high-impact applications including medical imaging, secure or covert communication, and cloaking.

High-power sub-millimeter and terahertz-frequency sources have remained an elusive target of physicists and engineers over the past many years. While lasers and microwave circuitry have conquered higher and lower frequencies, this missing band has a vast range of scientific, commercial, and military applications. A group at LANL has shown that a particular instability in a particle beam, a phenomenon well-known and strongly avoided by most accelerator laboratories, can actually be harnessed, controlled, and utilized to produce high-power terahertz radiation. Simulations predict that this experiment could break open the barrier to this band of frequencies, opening the door to future applications.

## Benefit to National Security Missions

This project has the potential to impact a broad range of missions including threat reduction (e.g. imaging and communication technologies), supporting the INTEL communicty (secure or covert communication, covert imaging, etc.), to improving human health (DOE/SC, NIH) through enabling new medical imaging technoogies.

## Progress

The project was proposed to have simultaneous experimental and theoretical explorations of the two-stream phenomena and microwave amplification. On both sides, we have made significant strides and have created a clear path forward to the completion of this research.

First, the theoretical understanding of the two-stream instability is much better understood. We brought in a graduate student from the University of New Mexico who is experienced with theoretical and computational modeling of beam dynamics. Within the first two weeks of his arrival, he was successfully running simulations of the dynamics involved. By using an established beam-simulation code, we are quickly exploring the parameter space through which the amplification process can be successful.

These simulations are crucial, as they model the full three-dimensional aspects of the beams, whereas our previous simulations employed a simpler one-dimensional description. The three-dimensional results indicate that the necessary beam conditions are somewhat different than we originally expected: for example, the energy difference between the two beams needs to be slightly smaller than originally believed, and the bandwidth of oscillations is not as flat as we originally expected. These findings are actually excellent news, as we wish to have the beam energies very similar, and for an oscillator experiment, the desired frequency can be selected and amplified more efficiently. We believe that experimental results will verify these findings and will generate the microwave amplification according to our theoretical models.

Second, we have successfully modeled the experimental setup. This process was more difficult than originally expected, as the beam currents warranted a modified beamline than originally described. Instead of using a dipole magnet to coalesce two electron beams into one, we are simply steering the two beams into a solenoid magnet, and the radial magnetic field merges the two beams together. This new design is actually simpler than the original, reducing the number of beamline elements, complexity, weight, and overall length. Simplifications like this make the experimental design even more robust than in our original proposal and provide additional tuning flexibility (beam energies, for example). Perfecting the beamline design took a few months of work, but we have purchased most of the parts necessary to build the experiment, on target with the end of the fiscal year. With a simple setup, we

anticipate producing experimental results very early in the next year.

As a measure of our achievements, we invite the reader to read our reviewed journal article, "Compact two-stream generator of millimeter- and submillimeter-wave radiation," that was published in Physics of Plasmas, July (vol.15, #7). Of course the theoretical and experimental modeling has produced more results than just that, and we have tabulated this progress at several conferences: IVEC, ICOPS, SRSSS, and later this year, FEL and LINAC. Our heavily attended talks and posters have brought significant attention to the prospects of our ideas and the cutting-edge science here at LANL.

On a second front, we are awaiting notice from Tech Transfer about the possibilities of patenting this device. Finally, we are personally also very excited about the collaboration with University of New Mexico and the inclusion of the finest graduate students; we enjoy providing them with one-of-a-kind research topics (the types that LANL can provide but universities cannot) while simultaneously utilizing their creative, dedicated, and enthusiastic labors to formulate a full understanding of the unique research we are developing.

In all, our project has already produced significant (and published) results, has simplified the requirements for further developments, and is on track towards completing the novel and cutting-edge goals within our timeline. We are extremely pleased with our progress over the past year.

## Future Work

We plan to test a new concept to generate high-power sub-millimeter and terahertz-frequency radiation. Such a source has been a challenging goal in recent history, while the applications of such a device continue to grow. This experiment will use the Two-Stream Instability, a well-known phenomenon that can easily occur in accelerator-physics laboratories around the world. Previously avoided in accelerator-based experiments, we have successfully simulated the instability and shown that it can be utilized to generate and amplify sub-millimeter and terahertz-frequency radiation in a reliable and efficient manner.

It is important to note that such research can be immediately utilized in a variety of scientific, commercial, and military applications. In particular, Threat Reduction has desired efficient, adaptable devices in this frequency range for remote sensing, communications, and imaging applications. Terahertz radiation is seen as a vital tool: it combines the penetrating power of microwaves with the high resolution of IR and visible imaging. We look forward to developing such a device for such applications.

The full proposal can be split into three main thrusts:

- Experimental demonstration of the concept at approximately 100 GHz.
- Nonlinear analysis and numerical simulations of the interaction at 1 THz.
- Construction and demonstration of a 1-THz prototype.

We foresee the first two goals occurring somewhat simultaneously, as each will foster progress in the other. By the end of the experiment, we predict that we will have a working prototype of a one-terahertz source utilizing a new physics technique and directly applicable to a variety of applications.

## Conclusion

This experiment is an attempt to build a high-power sub-millimeter and terahertz radiative source using a well-known physics phenomenon. This compact device, loosely similar to a laser, is predicted to produce a beam of this radiation which is applicable to numerous scientific, commercial, and security-based military applications. For example, this frequency range can be used for extremely high-bandwidth communications (such as a super-charged internet). This type of source could imagine the contents of shipping containers arriving daily at American ports. It is capable of detecting specific environmental hazards. Like lasers today, terahertz sources could be ubiquitous in countless future applications.

# Nano-Fission-Material based Neutron Detectors

*Ernst Ingo Esch*

20080221ER

## Introduction

Neutron detectors are among the best sensors for detecting proliferant nuclear materials, however high-efficiency neutron detectors are among the most challenging nuclear particle detectors to design and produce. This project endeavors to investigate the feasibility of nano-composite fission materials mixed into regular organic scintillator to study the idea of a solid state fission detector for neutron measurements. The principal thrust of this project is to produce a low-hazard, fast, and rugged neutron-detector that might be able to replace the current "$^3$He" workhorse. The approach for the project is to generate nanoparticles from fissionable material and then binding them into an organic scintillator. Once a neutron induces fission in the nanoparticle, the fission fragments have enough energy to leave the nanoparticle and deposit most of their energy in the organic scintillator. The energy deposited in the scintillator creates scintillation light, which can then be used to identify the neutron interaction. In the project we are propsing to manufacture the fissionable nanoparticles and mix them into a feasible organic scintillator. The resulting detector material will then bee examined for its chemical and physical properties. In parallel a computer simulation of the energy transfer and reactions in the material will be generated to understand these processes. Finally a prototype test will be conducted by exposing the detector to neutrons from a Los Alamos Neutron Science Center beam line.

## Benefit to National Security Missions

Neutron detectors are a foundational technology to reducing the threat of nuclear proliferation and detecting the threat of rogue nuclear weapons. This project directly supports nonproliferation and threat reduction missions in the DOE, DHS, and other government agencies. Finally, this work could yield detectors to better safeguard nuclear materials.

## Progress

The work to date can be described a s a parallel effort of material-science/chemistry, physics properties, and beam physics:

### Chemistry

The syntheses of uranium nanoparticles have been reported using harsh thermal techniques such as hydrothermal syntheses[1], sputtering[2], and laser ablation [3]. In the context of producing uranium nanoparticles to serve as fissionable material in gamma and neutron detectors, such specialized techniques are not feasible to produce material in a cost-efficient and large-scale manner. Thus, we are exploring new ways to synthesize these materials that would allow for economic scale-up while still maintaining precise control of chemical properties and morphology.

Our approach focuses on the synthesis of air- and water-stable uranium complexes formed under ambient conditions. Known uranium compounds such as $UO_2(NO_3)_2{\cdot}H_2O$, $UO_2Cl_2{\cdot}H_2O$, $UO_2(OH)_2{\cdot}H_2O$, $UO_2(O_2){\cdot}H_2O$, $Na_4UO_2(O_2)_3{\cdot}H_2O$, $Na_4UO_2(CO_3)_3{\cdot}H_2O$, and $Na_6(UO_2)_3(CO_3)_6{\cdot}H_2O$ have been synthesized in the bulk form. In order to control particle size, these complexes are redissolved in the presence of a capping ligand such as oleic acid, polyethylene glycol, tributylphosphate, or trioctylphosphine oxide. Currently, we are working to optimize solvent conditions, stoichiometry, and temperature control to allow for capping ligand binding and precipitation of uranium nanoparticles. We will continue to explore other uranyl complexes with water-soluble ligands such as phosphates and sulfates, in addition to targeting organic solvent-compatible uranium complexes such as $UO_2Cl_2(amide)_2$. Among our arsenal of uranium compounds and capping ligands, we expect to find the optimal permutation to form uranium nanoparticles in a cost-efficient and scalable manner.

### Physics properties

An instrument to measure the linearity of the signal response has been designed and procurement is in pro-

cess. Also, data acquisition and electronics for light-output and light quenching has been outlined and is currently in the process of being ordered. Another ongoing activity for the nanomaterial fission neutron detector is to develop the capabilities need for accurate simulations of the proposed design. The main task is to verify the accuracy of the fission model in the GEANT4 software package, which is a Monte Carlo simulation code commonly used in nuclear and high energy physics. Certain problems with fission observables being generated in the code have been identified, and are being corrected. In the next step the detector geometry and properties will be modeled in GEANT4 in order to predict its performance. For this endeavor we are able to use an existing processor farm that had been purchased for a different project.

**Beam Physics**

Two weeks of beam time has been allocated at the Los Alamos Neutron Science Center (LANSCE) for testing of a first prototype of the nanomaterial fission neutron detector. A detector prototype will be placed in a beam of neutrons in order to study the basic properties of the generated signals. Other possible tests includes studying the response in terms of timing properties, signal characteristics, and the ability to distinguish neutrons from other types of radiation. The LANSCE facility provides pulsed beams of neutrons with a range of energies, and the so-called neutron time-of-flight method can be used to determine the neutron energy for each signal from the detector. This has the advantage that the detector response can be studied as a function of incident neutron energy. Preparations for running these tests at LANSCE have been done by configuring the 4FP90L flight path to accommodate the experiment, and calibrating a neutron flux monitor to be used as a reference.

## Future Work

Within the proposed project, we want to synthesize fissionable nanoparticles and load them into a plastic scintillator matrix. We will investigate the physical properties of the detector material and find the optimal parameters for particle size and loading ratio and matrix type. In parallel with current R&D, in Los Alamos aimed at nanocomposite scintillators for gamma detection, our goal is to manufacture nanomaterials in quantities large enough to build and characterize fission detectors.

In the first year we will develop nano-fission particles (oxides of $^{209}$Bi, $^{197}$Au and $^{181}$Ta) and load them at different mass fractions into different existing scintillator matrix materials and characterize their optical properties. We will also systematically optimize the optical and radiation response of the material. In parallel we will simulate energy deposition and quenching in the loaded matrix material.

In the second year we will continue dispersing nano-fission material in the matrix,

extending to actinide nanoparticles (oxides of $^{235}$U and $^{238}$U), systematically optimize the composite and measure the optical and gamma-ray detection properties of the composite. The data will be used to benchmark the detector simulations. At the end of the second year we will manufacture several detector elements large enough to be used as fission flux monitors from the most promising material with volumes of order tens of cubic centimeters.

In the third year the different detector elements will be characterized and the prototype will be tested for its neutron beam response. This will take place either at the WNR or at the Lujan Center.

## Conclusion

The resulting detector technology will enhance our capability for detecting nuclear threats from special nuclear material. The detector material will be able to detect neutrons over a wide range energies, unlike $^{3}$He tubes, ideally suiting this technology for nonproliferation purposes and nuclear research. Rugged, cost effective material with large volumes and therefore large efficiency can be used i.e. in portal monitors to counter nuclear smuggling. Easily operable detectors can be used in neutron beam measurements in basic and applied science experiments.

## References


1. Wang, Q., G. D. Li, S. Xu, J. X. Li, and J. S. Chen. . 2008. *Journal of Materials Chemistry.* **18** (10): 1146.
2. Meshakin, V. I., and A. P. Budnik. . 2007. *Atomic Energy.* **103** (2): 605.
3. Trelenberg, T. W., S. C. Glade, J. G. Tobin, and A. V. Hamza. . 2006. *Surface Science.* **600** (11): 2338.

# Efficient Structures for Low-Energy Acceleration of Light Ions

*Sergey S Kurennoy*

20080228ER

## Introduction

Compact ion accelerators are important and enabling technologies for a variety of applications including medical therapy, imaging, and active interrogation. For example, a compact accelerator delivering deuterons with energies of a few MeV can serve as a mobile intense neutron and gamma source for interrogation of special nuclear materials.

The project aims to develop novel room-temperature accelerator structures for low-energy charged particles. We suggested using the H-mode resonator cavities that are about ten times more efficient at the beam velocities around a few percent of the speed of light compared to the usual drift-tube linear accelerator (DTL). However, keeping the beam transverse size small to avoid losses is inherently difficult in H-cavities compared to the DTL where the beam focusing is usually achieved with electromagnetic quadrupole magnets placed inside its large drift tubes. Inserting permanent-magnet quadrupoles (PMQ) inside the H-cavity small drift tubes solves the focusing problem without reducing the accelerating efficiency [1]. The high efficiency of the H-mode accelerator with PMQ beam focusing opens up a new option of using small inexpensive radio-frequency (RF) generators as its power source instead of usual large and expensive RF klystrons. Such high-efficiency H-PMQ accelerator structures for low-energy light ions have multiple applications, either in stand-alone accelerators or as a part of the front end in ion linear accelerators.

Designing such accelerators for considerable ion-beam currents requires a careful balance of beam-physics and engineering considerations. We plan to achieve this balance by combining electromagnetic 3-D modeling with beam dynamics simulations and engineering thermal-stress analysis.

## Benefit to National Security Missions

This project will support the DOE missions of Treat Reduction, Non-Proliferation, Homeland Security, and the Office of Science research missions, by providing high-efficiency accelerators of light ions. For example, a compact 4-MeV deuteron accelerator [3] can drive a mobile intense neutron and gamma source for interrogation of special nuclear materials.

## Progress

Significant progress has been made in developing room-temperature H-mode accelerator structures with PMQ beam focusing for low-energy ions. Following our research plan, we developed an interface for transferring data between our 3-D electromagnetic (EM) code, MicroWave Studio (MWS), and engineering codes, COSMOS and ANSYS. This allowed us to perform iterative EM-engineering analysis and show the effectiveness of water cooling the H-mode structures with cooling channels located in the vanes supporting the H-structure drift tubes (DTs). The temperatures of PMQ, as well as the structure stresses, remain well within the acceptable range [2], see Figure 1. This proves feasibility of room-temperature H-PMQ accelerator concept since in effective H-mode structures there can be no cooling channels inside DTs while the PMQ temperatures should be kept below 150-200° C.

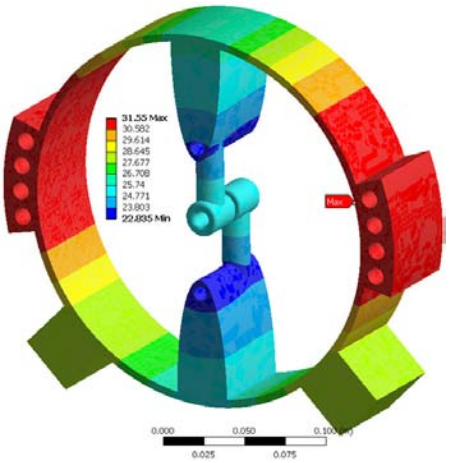


*Figure 1. Temperature distribution in a regular IH structure with two cooling channels in the vanes at the nominal 10% duty. No cooling in the outer manifolds is needed here. The geometrical beta is 0.04, and the accelerating gradient is 2.5 MV/m.*

We performed beam-dynamics analysis of the inter-digital H-mode (IH) structures using the envelope code TRACE 3-D and proved the concept of the transverse beam focusing using permanent-magnet quadrupoles of reasonable strength [2, 5]. Our analysis showed that good results for the particular application, a 1-4 MeV IH-PMQ deuteron accelerator with 50-mA beam current, can be achieved with PMQ installed only in every third drift tube (DT), see Figure 2, which gives a significant cost saving due to a reduced number of the required PMQs.

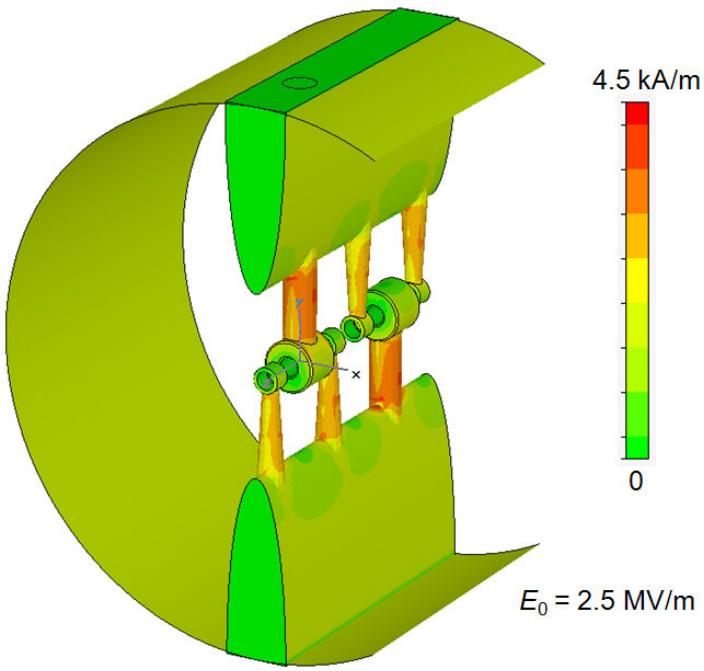


*Figure 2. Surface current magnitude in the modified IH1-3 structure (the cavity wall is partially cut for better view). The empty drift tubes are reduced in size to increase the structure efficiency.*

Using EM modeling with MWS, a systematic study of the IH-structure EM parameters was performed in the beam velocity range of interest, from 3.3 to 6.5 percent of the speed of light, that corresponds to the deuteron beam energies from 1 to 4 MeV. Based on this reference data, a few preliminary designs of the compact 1 to 4 MeV IH-PMQ deuteron accelerator were completed and compared [5]. The accelerator total length is about 1.5 m, with the cavity inner radius below 15 cm; it will include 38 to 40 DTs. For the nominal duty factor of 10%, the power dissipated in the cavity walls will be below 2.5 kW, which is significantly smaller than the power put into the beam, 15 kW. The study also revealed that the maximal electric fields at a fixed average accelerating field in the IH structure become rather high near its high energy end increasing the danger of sparking. Two IH-structure improvement options were explored: increasing the gaps between the DTs and using DTs of different sizes depending on whether they house PMQ or not - larger DTs with PMQ and slim short empty ones. Both of these options reduce the maximal electric field and simultaneously increase the structure efficiency [2, 4, 5]. We are developing a procedure to transfer 3-D EM fields in H-mode structures computed by the MicroWave Studio to the multi-particle tracking code Parmela. This will allow us to perform detailed multi-particle beam-dynamics simulations using the realistic fields from 3-D EM analysis. Such an analysis is required to compare the beam properties for different H-mode structures, with different beam focusing schemes, to select the best accelerator design.

Our project to date resulted in three invited talks, four conference publications [1-4], and four technical notes, see [5]. They generated certain interest to the IH-PMQ accelerator technology from industry and medical-accelerator projects. We are now in the process of formalizing a CRADA agreement with AccSys Technology Inc (Pleasanton, CA) that is interested in acquiring our H-mode linac technology for medical applications.

## Future Work

We are developing novel room-temperature accelerator structures for low-energy protons or deuterons by combining H-mode resonator cavities and a strong transverse beam focusing using permanent-magnet quadrupoles (PMQ). Our research includes designing high-efficiency multi-cell H-cavities, studying beam dynamics in the cavities with PMQ focusing and optimizing the beam quality, and developing cost-efficient cooling and fabrication methods for such structures. Achieving a balance of the structure efficiency, beam quality, and thermal management requires multiple iterations of electromagnetic modeling (EM), beam dynamics (BD), and engineering thermal-stress analysis (EA). We are developing an efficient interface between the available EM, BD, and EA codes to facilitate the process.

Our R&D goals for the second year of the project are as follows:

- Develop an effective EM-BD interface to perform multi-particle beam dynamics simulations using realistic 3-D EM fields calculated by the MicroWave Studio. This will allow us to iterate the structure design to optimize the beam quality, as well as to analyze the structure sensitivity to fabrication errors for establishing the manufacturing tolerances.
- Design the front and end cells of the accelerator tank. Develop RF power input and tuning mechanisms.
- Based on these results, finalize the design of the IH-structure cold model (full- or half-size aluminum model tested at low RF power; one possible version is shown in Figure 3) and prepare its drawings.

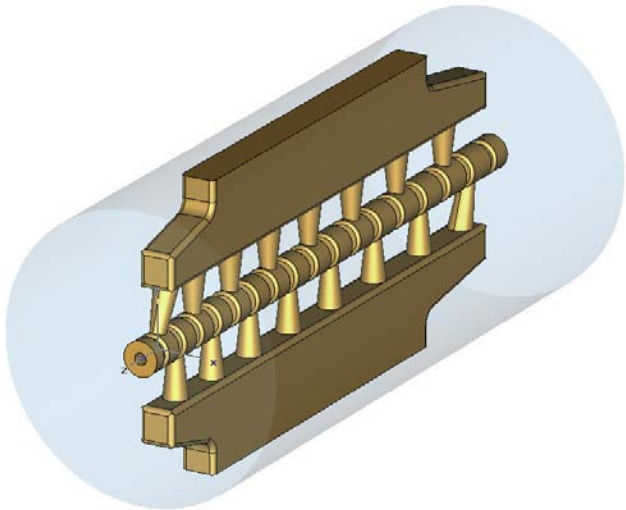

*Figure 3. MWS model of a short IH-structure (52 cm) with gradually increasing cell lengths. The outer cavity wall is removed to show the end-cell design.*

## Conclusion

We expect that our research will produce the following results:

- A conceptual design of novel high-efficiency room-temperature accelerating structures for light ions in the low-beam-velocity range, based on H-mode cavities with a strong transverse beam focusing by permanent-magnet quadrupoles, which can be used in multiple applications;
- An effective interface between the codes for a combined Electromagnetic-Beam-dynamics-Engineering analysis that will also be useful for various accelerator projects at LANL or other labs;
- A tested cold model of H-PMQ accelerating structure that confirms our design and fabrication concepts.

Among many possible applications of room-temperature H-PMQ structures, two deserve our special attention. One is a compact 4-MeV deuteron accelerator for homeland defense (an intense neutron and gamma source for interrogation of special nuclear materials). Another application could be a cost-effective replacement of the aging DTL in the LANSCE linear accelerator.

## References


1. Kurennoy, S. S., L. J. Rybarcyk, and T. P. Wangler. Efficient accelerating structures for low-energy light ions. 2007. In *Proceedings of Particle Accelerator Conference 2007.* (Albuquerque, NM, USA, 25-29 June 2007). , p. 3824. New York, NY: IEEE.

2. Kurennoy, S. S., S. Konecni, J. F. O'Hara, and L. J. Rybarcyk. IH accelerating structures with PMQ focusing for low-energy light ions. 2008. In *Proceedings of European Particle Accelerator Conference 2008.* (Genoa, Italy, 23-27 June 2008). , p. 3428. Geneva, Switzerland: European Physical Society .

3. Kurennoy, S. S., J. F. O'Hara, and L. J. Rybarcyk. Compact linac for deuterons. To appear in *42nd ICFA Advanced Beam Dynamics Workshop on High-Intensity, High-Brightness Hadron Beams.* (Nashville, TN, USA, 25-29 Aug. 2008).

4. Kurennoy, S. S., J. F. O'Hara, E. R. Olivas, and L. J. Rybarcyk. Efficient low-beta H-mode accelerating structures with PMQ focusing. To appear in *XXIV Linear Accelerator Conference (Linac08).* (Victoria, BC, Canada, 29 Sep. - 3 Oct. 2008).

5. Kurennoy, S. S.. IH accelerating structures with PMQ focusing. 2008. *Los Alamos National Laboratory Report LA-UR-08-03795.*


## Publications


Kurennoy, S. S.. IH accelerating structures with PMQ focusing. 2008. *Los Alamos National Laboratory Report LA-UR-08-03795.*

Kurennoy, S. S., J. F. O'Hara, E. R. Olivas, and L. J. Rybarcyk. Efficient low-beta H-mode accelerating structures with PMQ focusing. To appear in *XXIV Linear Accelerator Conference (Linac08).* (Victoria, BC, Canada, 29 Sep. - 3 Oct. 2008).

Kurennoy, S. S., J. F. O'Hara, and L. J. Rybarcyk. Compact linac for deuterons. To appear in *42nd ICFA Advanced Beam Dynamics Workshop on High-Intensity High-Brightness Hadron Beams.* (Nashville, TN, USA, 25-29 Aug. 2008).

Kurennoy, S. S., L. J. Rybarcyk, and T. P. Wangler. Efficient accelerating structures for low-energy light ions. 2007.

In *Proceedings of Particle Accelerator Conference 2007.* (Albuquerque, NM, USA, 25-29 June 2007). , p. 3824. New York, NY: IEEE.

Kurennoy, S. S., S. Konecni, J. F. O'Hara, and L. J. Rybarcyk. IH accelerating structures with PMQ focusing for low-energy light ions. 2008. In *Proceedings of European Particle Accelerator Conference 2008.* (Genoa, Italy, 23-27 June 2008). , p. 3428. Geneva, Switzerland: European Physical Society.

# Compact Millimeter Wave Spectrometer Based on a Channel Drop Filter

*Lawrence M Earley*

20080409ER

## Introduction

Terahertz and millimiter-wave devices are proving to have many important applications from sensing and imaging to communication. Among the greatest impediments to exploiting this regime of the electromagnetic spectrum are the difficulties in building sources with sufficient power and sensors with the necessary sensitivity suitable for practical applications.

In this project, we have designed and are constructing a novel passive mm-wave spectrometer based on photonic crystals (PCs), which are periodic arrays of tiny rods. There is a need for a compact wide-band versatile and configurable mm-wave spectrometer for applications in mm-wave communications, radio astronomy, and radar receivers for remote sensing and nonproliferation. We have designed different PCs spectrometers working in the frequency range from 90 to 300 GHz. The spectrometer operating at 250 GHz can be employed in remote sensing missions for detection of methyl chloride. The primary objective of the research is to develop a fabrication technique for the photonic crystal spectrometers at mm-waves, and test proof-of-principle spectrometers. We consider the Micro-Electro-Mechanical Systems (MEMS) technology for fabrication, which involves etching the structure on a silicon wafer. Fabrication of a mm-wave photonic crystals is at the cutting-edge of MEMS technology, in particular, it pushes the limits of the etching process. However, MEMS is the very high potential technology for fabrication of the devices at mm-waves to fill the so-called “terrahertz gap”, where the conventional fabrication techniques are not applicable. Therefore, exploring and advancing the limits of MEMS technology is of the great importance. Creation of a novel ultra-compact, wide-band, configurable, and easy to operate under all weather conditions mm-wave spectrometer would enable Laboratory missions in both national security and basic research and directly addresses the laboratory grand challenge “Detection of nuclear materials (Ubiquitous sensing).”

## Benefit to National Security Missions

This project, through the development of a new mm-wave spectrometer, will impact a broad range of technical problems including sensing, and communication. These technical areas are crucial for supporting threat reduction, nuclear material detection, and other missions important to DOE, DHS, and other government agencies.

## Progress

The project has made significant progress up to date in two areas. The first area was fabrication of a 98 GHz structure with a MEMS process, studying the limitations of the MEMS process, and testing the 98 GHz filter at the laboratory. The second area was designing the alternative configurations of the structure to simplify fabrication and expand the covered frequency range.

We have studied fabrication of a 98 GHz version of the structure with a MEMS process. The MEMS fabrication process consists of four stages. The first stage is the fabrication of thick high-resistivity silicon wafers. The second stage is the creation of a thermal oxide mask on top of the wafer. The third stage is etching of the wafers to create the periodic pattern. And the fourth stage is the gold-plating of the structure and bonding it with the metallic plates. The first two stages of fabrication were successful. However, once the etched sample structures (Figure 1) were studied, it was found that the process pushes the limits of the existing technology. The rods in the structure that were initially designed to be 1000 micro-meters high have suffered undercuts once the length reached 650 micro-meters (Figure 2). Therefore we had to limit the height of the rods to 500 micro-meters. This expected to result in some additional losses in the experiment. Indeed, very high losses were observed during the laboratory testing. In addition, it was discovered that the undercuts were present even in the 500 micro-meters structure, and the shapes and positions of the undercuts were very random. This severally degraded the performance of the structure, which constituted the filter. Therefore we have concluded that

the MEMS process is more applicable at higher frequencies. Thus for the next two years we are planning to shift the main focus of the project to 300 GHz instead of further pursuing fabrication of 98 GHz structures.

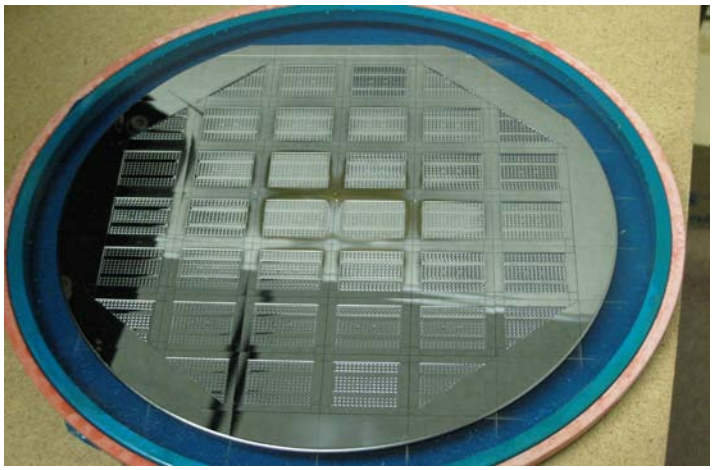

*Figure 1. PBG structures etched on a silicon wafer.*

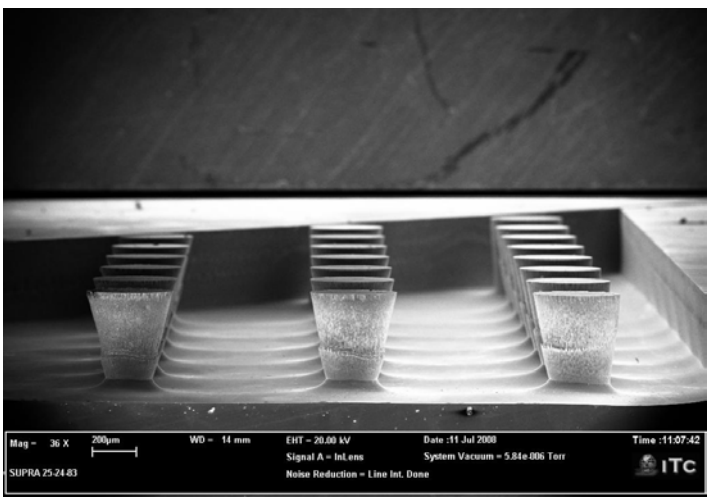


*Figure 2. Cross-sectional view of the posts in the PBG structure. The undercut etching is clear.*

nvestigation of novel photonic crystal configurations became particularly important once the limits of the etching process at the frequency of 98 GHz were established. We have proposed a novel idea that the crystals with metallic rods will be more appropriate for fabrication of the filters at the frequency of 100 GHz and below. Metallic filters are easier to fabricate at lower frequencies using conventional machining, however they may be more sensitive to losses and machining tolerances. A design of the metallic filter was prepared and fabricated in a conventional machine shop (Figure 3) and initial tests in the mm-wave laboratory look very promising: the right frequency is being filtered and the losses are low. To conduct the final tests we now need to manufacture some additional connecting components. Those components are currently in the machine shop.

The results of this work were reported at the 33rd International Conference on Infrared, Millimeter, and Terahertz Waves in Pasadena, CA [1].

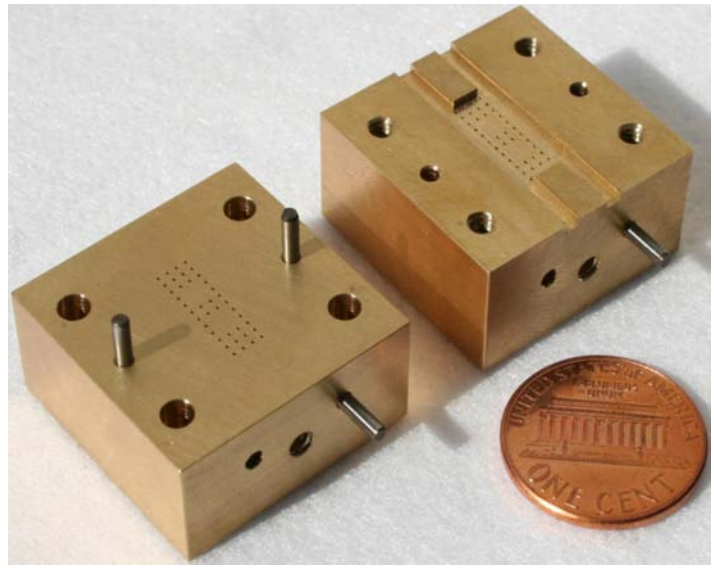


*Figure 3. A photograph of the disassembled copper channel-drop-filter.*

## Future Work

Based on the progress up to date the work plan for the FY 2009 was modified as follows:

1. Redesign the filter to operate at the frequency of around 300 GHz. The new design will not be a simple scaling, since the dimensions of waveguides conventionally used at 300 GHz do not scale from the dimensions of standard waveguides used at 100 GHz.

2. Fabricate the 300 GHz sample and test it. We will conduct the upgrade to the existing mm-wave measurement system at ISR-6, because of the projected increase of the need of 300 GHz measurements.

3. Finish fabrication of the components for the metallic filter operating at around 100 GHz, test it, and study different tuning concepts to compensate for conventional machining tolerances. Tuning will enhance the performance of the filter.

The successful completion of this project will yield a unique and ultra-compact mm-wave device for rapid and highly accurate passive remote detection. The spectrometer will be wide-band, real time, easy-to-operate and easy-to-transport, and may be employed for detection of nuclear materials even under adverse weather conditions.

## Conclusion

At the end of this project there will exist a new electronic device that will be capable of enhancing several national security missions. This new device will be a small and lightweight spectrometer that can be used for detection of nuclear material and be used by our military forces in radar and secure communications. The new device will allow improved nuclear material detection and make our military systems more secure with better performance.

## References

1. Smirnova, E. I., L. M. Earley, C. E. Heath, and D. Yu. Shchegolkov. Design and fabrication of a 100 GHz channel-drop filter. 2008. In *33rd International Conference on Infrared, Millimeter, and Terahertz Waves.* (Pasadena, CA, 15-19 Sept. 2008). , p. 1175. Online: IEEE.

## Publications

Smirnova, E. I., L. M. Earley, C. E. Heath, and D. Yu. Shchegolkov. Design and fabrication of a 100 GHz channel-drop filter. 2008. In *33rd International Conference on Infrared, Millimeter, and Terahertz Waves.* (Pasadena, CA, 15-19 Sept. 2008). , p. 1175. Online: IEEE.

# Novel High Performance Terahertz Metamaterial Photonic Devices

*John F O'Hara*

20080414ER

## Introduction

The control of electromagnetic (EM) waves influences nearly every aspect of our lives, from communications with cell phones, radios, and fiber optics to simply capturing a photograph with a camera. Technological advances have made it possible to control EM waves of nearly every type including radio waves, microwaves, infrared, visible, and ultraviolet light, and x-rays. There is one notable exception: terahertz (THz) waves. Terahertz science has been pursued heavily since the early 1990's in an effort to overcome this hurdle. Still, practical devices suitable for controlling THz waves simply do not exist and THz technology has consequently failed to graduate into real-world usability. Despite this, THz science remains an important pursuit since there are many promising THz applications including: covert identification of chemical and biological agents, security screening where THz is used to see inside of closed packages, ultra-broadband communications, and even environmental and quality control. The problem is that natural materials are suitable to control almost all EM waves except THz. Our project is to create new materials that control THz waves very well; these are called tunable metamaterials. Metamaterials are engineered materials that allow designers to control EM waves in numerous ways. We combine natural materials (e.g. metals, insulators, and semiconductors) to create metamaterials that are specifically tuned for THz control. Furthermore, they can be manipulated real-time to actively adjust this control, something very few natural materials can do. This cutting-edge approach offers unprecedented levels of both THz/material interaction strength and functional versatility. In short, metamaterials provide a method of controlling THz in ways not previously possible.

## Benefit to National Security Missions

This represents a major impact to THz science, engineering, and technology, but it also offers fundamentally new science opportunities.
This project serves as a benefit to national security in several ways. It enhances our fundamental understanding of materials, creates new capabilities in sensing, and opens the door for new threat reduction technologies by improving our ability to use this unique (and largely unused) portion of the electromagnetic spectrum. Due to the fundamental but applied nature of this work, it broadly supports numerous important mission areas for DOE, DOD, DHS, and other government agencies. In fact, the work is currently soliciting interest from external government agencies.

## Progress

There has been excellent progress so far on this project, mainly in modulation of freely propagating THz waves. Modulation of freely propagating waves is the backbone of myriad technologies, such as radar, communications, and imaging. Therefore any THz modulation technology is a very important step forward. So far we have demonstrated numerous state-of-the-art performances for THz modulators. First, we have demonstrated fast amplitude modulation of freely propagating THz waves with modulation depths up to ~50% (previous comparable technologies reached only ~3% modulation depth) and at speeds up to 2 MHz [1]. Further, we have shown that our modulating devices operate over a wide frequency range despite the fact that they are tuned to operate at a single frequency. This fortunate but unexpected result stems from the fact that metamaterials manipulate THz waves simultaneously in many ways, a fact we can exploit for improving THz technology. This work is currently in the publication process.

We have also found another approach that enables extremely high-speed modulation of freely propagating

THz waves. This technique uses metamaterials to control the polarization of THz waves in conjunction with a special THz generator. In this method the generator emits two separate THz waves, each one having a different polarization and each one controlled by a user-provided electronic signal. Polarization-sensitive metamaterials convert these two waves into a single modulated wave that can carry the information provided by the user. This modulation method takes advantage of the extremely rapid switching times of THz photoconductive sources and therefore provides a path forward for THz-based high-speed wireless communications. We believe this work may enable secure, giga-bit per second wireless communication systems suitable for an office environment, for example. We have also successfully demonstrated a metamaterial that allows THz waves to be frequency modulated by laser light. Frequency modulation is important because it's the basis for numerous technologies including FM radio, modern radar, and many digital communication links. In fact, it is one of the core concepts in modern technology; but it has never before been demonstrated in THz waves. In this work, metamaterials were designed with special semiconductor components. The semiconductors act like miniature switches that, when illuminated by laser light, change the electronic structure of the metamaterial. Essentially the semiconductors act like weights added to a clock's pendulum. When weight is added to a pendulum it swings more slowly, or equivalently its resonance frequency is lowered. Similarly, when our semiconductors are illuminated, they lower the metamaterial's resonance frequency, thus modulating the frequency at which the material and THz waves interact. These important results were published in the prestigious Nature Photonics Journal [2].

Finally, we have begun designing special THz lenses suitable for focusing freely propagating THz waves. Based on numerous studies, we have determined that very thin metamaterials can be used to achieve the same focusing behavior as a traditional thick lens. Such an approach has the benefit of producing extremely lightweight and compact lens designs. In addition metamaterials enable even greater performance gains. For example, metamaterial lenses can be modified so that they cannot reflect any THz waves and therefore do not waste any THz energy in doing their job. This is all comparable to making eyeglasses in which the lenses are paper-thin, flat, and invisible but still correct the wearer's vision. We are also exploring active lenses that change their focal length at the user's demand by employing some of the concepts explained previously. This is comparable to eyeglasses that change their prescription with the flick of a switch. These devices are not only important for making compact and high-performance THz technology. They also serve to advance metamaterial science in general and our work may someday serve as a model for novel optical technologies that utilize metamaterial concepts.

## Future Work

Our future tasks will be to complete the several ongoing studies involving THz modulation, high-speed communication via polarization-sensitive metamaterials, and creating the metamaterial THz lenses. This should bring us nearly to the end of this LDRD project, however, the research is proving to be very fruitful and we expect numerous additional developments as we continue.

We have developed new devices for manipulating freely propagating terahertz waves. These devices include frequency and amplitude modulators, high-speed communication components, and focusing devices, all of which did not previously exist or were extremely immature THz technologies. Most of our work has been experimentally demonstrated and the remaining is in development. Our new devices all utilize metamaterials concepts to overcome the weaknesses inherent in natural materials with respect to controlling THz waves. Most of our devices also utilize novel concepts that permit a user to actively control the performance of the device. This work represents fundamentally new advances in manipulating terahertz waves. This is increasingly interesting for myriad homeland security and/or defense related missions as it represents a unique and untapped technology.

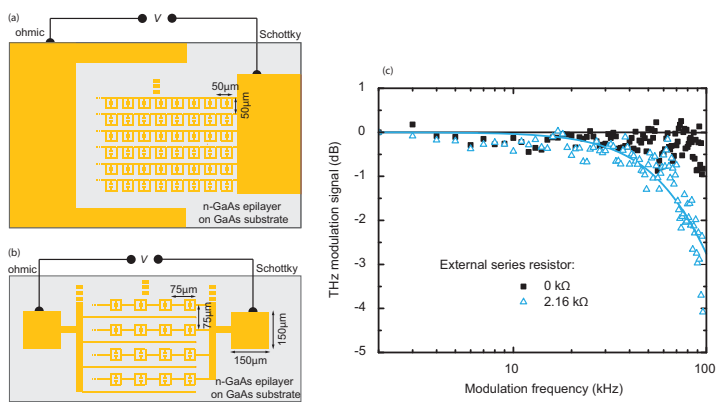


*Figure 1. Electrically modulated metamaterials. (a) original design, (b) improved high-speed design, (c) measured modulation for high-speed design. Black squares show modulation occurs beyond 100 kHz.*

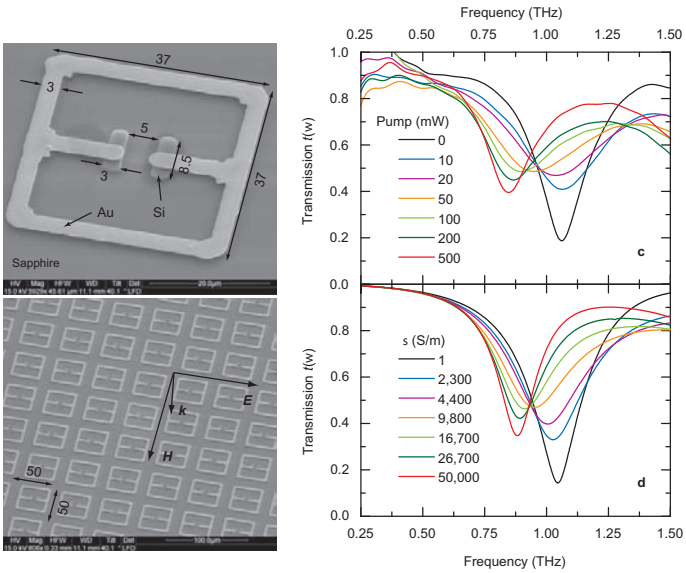


*Figure 2. Frequency tunable THz metamaterial. (a) and (b) show metamaterial components highlighting the semiconductors that tune the observed behavior. (c) and (d) show measured and simulated response. The resonant dip in transmission is shifted to lower frequency when the metamaterial is illuminated by 10's-100's of milliwatts of laser power.*

## References


1. Chen, H. T., S. Palit, T. Tyler, C. M. Bingham, J. M. Zide, J. F. O'Hara, D. R. Smith, A. C. Gossard, R. D. Averitt, W. J. Padilla, N. M. Jokerst, and A. J. Taylor. Hybrid metamaterials enable fast electrical modulation of freely propagating terahertz waves. 2008. *Applied Physics Letters.* **93**: 091117.

2. Chen, H. T., J. F. O'Hara, A. K. Azad, A. J. Taylor, R. D. Averitt, D. B. Shrekenhamer, and W. J. Padilla. Experimental demonstration of frequency-agile terahertz metamaterials. 2008. *Nature Photonics.* **2**: 295.


## Publications


Azad, A., H. Chen, E. Akhadov, N. Weisse-Bernstein, A. Taylor, and J. O'Hara. Multi-layer planar terahertz electric metamaterials on flexible substrates. 2008. In *Conference on Quantum Electronics and Laser Science Conference on Lasers and Electro-Optics, CLEO/QELS 2008 ; May 4-9 2008 ; San Jose, CA, United States.*

Chen, H., A. Azad, D. Shrekenhamer, W. Padilla, R. Averitt, A. Taylor, and J. O'Hara. Frequency tunable terahertz metamaterials. 2008. In *Conference on and Quantum Electronics and Laser Science Conference Lasers and Electro-Optics, QELS 2008 ; May 4-9 2008 ; San Jose, CA, United States.*

Chen, H., J. O'Hara, A. Azad, A. Taylor, R. Averitt, D. Shrekenhamer, and W. Padilla. Experimental demonstration of frequency-agile terahertz metamaterials. 2008. *NATURE PHOTONICS.* **2** (5): 295.

Chen, H., S. Palit, T. Tyler, C. Bingham, J. O. Zide, J. O'Hara, D. Smith, A. Gossard, R. Averitt, W. Padilla, N. Jokerst, and A. Taylor. Hybrid metamaterials enable fast electrical modulation of freely propagating terahertz waves. 2008. *APPLIED PHYSICS LETTERS.* **93** (9): 091117.

O'Hara, J., E. Smirnova, A. Azad, H. Chen, and A. Taylor. A circuit model for terahertz metafilms and effective medium implications. 2008. In *Conference on Quantum Electronics and Laser Science Conference on Lasers and Electro-Optics, CLEO/QELS 2008 ; May 4-9 2008 ; San Jose, CA, United States.*

Padilla, W. J., Hou-Tong Chen, J. F. O'Hara, A. J. Taylor, and R. D. Averitt. Opto-electronic control of terahertz metamaterials. 2007. In *Photonics: Design, Technology, and Packaging III ; 5 Dec.* ( 2007 ; Canberra, ACT, Australia). Vol. 6801, p. 68010H.

# Accuracy of Laser-Induced Breakdown Spectroscopy for Trace Detection

*Roger Craig Wiens*

20080718ER

## Introduction

Laser-induced breakdown spectroscopy (LIBS) is a technique that is used to determine elemental compositions of samples at some distance (up to tens of meters) with no sample preparation. Laser pulses focused on the target produce plasma "sparks" composed of material ablated from the target. Each element present in the sample produces light at unique wavelengths. By measuring the optical spectrum of the emitted light (the color) from the sparks, the elemental composition can be determined. However, looking at just one emission peak for a given element turns out not to be very accurate. This project explores the application of data mining techniques that use all wavelengths for each element, allowing many peaks to be interrogated simultaneously. In effect, we go from one data point per element, to 6,000 channels per element, using a group of techniques classified as multivariate analysis (MVA).

We have started with two types of MVA. One, called principal components analysis (PCA), simply groups samples by spectral characteristics, starting with the strongest correlation (principal component), second strongest, third strongest, etc. We can use this analysis to determine if a new sample is similar to previous samples, or has significant differences.

A second and more powerful MVA technique is partial least squares (PLS). As used here, PLS quantitatively determines the compositions of samples analyzed by LIBS. It does this by being given the elemental composition of a "training set" of standards similar to the unknowns. It determines the correlations among all 6000 channels and uses that information to determine the composition of the unknown sample.

Preliminary results indicate that these MVA techniques will significantly increase the accuracy of the LIBS technique, but there are a lot of details that need to be understood. Key aspects are how to correct for the effects of sample-to-instrument distance, how many standards are needed for this type of analysis, and how close the standards need to match the sample in composition.

## Benefit to National Security Missions

The main set of standards used for this project is geological in nature. However, the applications extend to all uses of LIBS. The project will support the DOE mission by significantly improving the accuracy of LIBS for use in carbon sequestration, chem-bio detection, potential for IED detection, and nuclear materials detection.

## Progress

### Preliminary Analyses

A number of geologic standards were selected and obtained. These include samples from all three classes of rocks, focusing on both igneous and sedimentary samples. The standards include a number of different basalts and olivine-rich standards, several gypsum standards, and a number of stream sediments. These are mostly in the form of powders, but we are also using a few glasses for basaltic standards and several ceramics for sedimentary standards. In contrast to mineralogical methods such as x-ray diffraction, LIBS does best with mineralic mixtures, as are encountered by the LIBS laser beam in remote LIBS experiments. We are also considering standards that would be useful for programmatic applications.

Prior to having the above standards in hand, we investigated some data taken earlier at several different distances. Three data sets were investigated. The first data set was used mostly to determine accuracies and precisions at two and five meter stand-off distances with a limited set of standards. We are still analyzing this data set for the relations between the signal-to-noise ratio (SNR) and the accuracy and precision of the results.

A second set of data was used for PCA analyses. One key issue is the effect of varying the distance to samples/standards. Can one analyze a set of standards at one distance and apply the data correctly to an unknown sample at another distance? How does this degrade the accuracy, and are there ways to correct for it? The data set consisted of laser-induced breakdown spectroscopy

(LIBS) measurements made at 4, 6.5, and 9 m on a set of nine standards. Five replicate analyses were made on each standard at each distance. The results were normalized, so that the primary distance effect, that of overall intensity, would be removed. The results were analyzed by the Unscrambler PCA program. The first two principal components had relatively little distance effect, successfully grouping the five replicate analyses from each standard into respective tight clusters independent of distance. However, if one zoomed in on the individual clusters, one could still see a distance effect which appeared to incorrectly assign higher silicon abundances to measurements taken at greater distances. Higher principal components all had strong distance effects. Wavelength channels that had a strong weighting in the higher PCs were identified.

The PCA program was then run with distance as one of the components. The first principal component now corresponded to the instrument-to-sample distance. The correlations of each wavelength channel with distance were noted, and the spectra were corrected by adding or subtracting a factor obtained by multiplying the distance by each channel's distance correlation coefficient. The result was then fed back into the PCA program with the distance coefficient as a cross-check. The distance correlation had indeed been removed. The results were then used in the PLS program to see if quantitative uncertainties were reduced by the distance correction. The results clearly needed further correction, which we believe is the result of the baseline, described in the next paragraph.

A third data set was investigated to determine whether baseline corrections improve the statistics. Background subtractions for LIBS involve taking spectrometer exposures of identical duration to the LIBS exposures, only without the laser. However, in addition to emission peaks, LIBS produces a continuum that the typical background subtraction does not remove. This can be removed by flattening the baseline. It was noted in the PCA plots that much of the distance correlation was the result of differing black body intensities. We have now produced a routine to flatten the baseline after background subtraction and before entering the data into the multivariate routines.

### Data Collection

At this point in time, the larger group of standards were obtained and pressed into pellet targets. The group consists of nearly seventy standards, as compared with less than ten used in the above study.

The standards were run at 1.5, 3.5, and 5.5 meters from the instrument. The complete set of standards was used in the 3.5 meter set-up, while the 1.5 and 5.5 meter arrangements used a subset of thirty standards. Each standard was analyzed in five separate spots, each spot being a collection of fifty laser shots and spectra. Background spectra (50 each) were taken to correspond with each standard. The fifty shots per spot will be averaged, but the fact that we have separate spectra means we will be able to check for trends within the data from each spot, such as if the laser was heating up, defocusing, etc. In total, we have collected some 37,000 spectra.

In addition to the data set, we now have the tools to begin analyses, consisting of automated background subtraction, baseline removal, averaging, and signal-to-noise determination, prior to using the multivariate analysis techniques

## Future Work

Armed with the database and tools described above, we are set to study in greater detail the application of multivariate analysis to LIBS. The accuracy of LIBS is hindered by chemical matrix effects in which the abundances of some elements adversely affect the relationship between abundances and emission line intensities of other elements. We will apply MVA in various contexts of LIBS analyses to understand its strengths and characteristics in terms of accuracy, detection limits, types of training sets needed, environmental constraints, and applicable types of samples.

We propose the following specific tasks:

- Finishing the distance correction. We are currently in the middle of this study, as described above.
- Benchmarking of statistical improvements using MVA. Determine the signal to noise ratio (SNR) needed to obtain ±10% accuracy and precision for both univariate and multivariate cases. We expect the result will show that accurate analyses can be made with lower effective SNR, increasing the distance at which analyses can be made. We propose to also investigate detection limits as a function of stand-off distance and to investigate whether a training data set taken at one distance and/or detector noise level is applicable to a range of distances and/or detector noise levels.
- Exploring ranges of calibration sets. We propose to address the following questions: How widely applicable is a given training set? How do we extend the analysis to minor and trace elements and what samples are used in the training set. What is the right balance and breadth of standards that are needed to cover a given set of samples?
- Interpretation of principal component analysis (PCA) results: How does the addition of different standards and/or samples alter the axes of PCA plots? How easy is it to relate the principal components to elemental compositions?

- Diverse applications. We propose to apply MVA to some of the following: explosive detection, chem-bio agent detection, and nuclear material identification.

## Conclusion

We expect to significantly improve the accuracy and detection limits of LIBS, a rapidly growing analytical technique that has applications in many areas including homeland security, nuclear threat reduction, defense, manufacturing process control, the mining industry, and space exploration.

## Publications

Clegg, S. M., R. C. Wiens, J. E. Barefield, E. Sklute, and M. D. Dyar. Quantitative remote laser induced breakdown spectroscopy by mutivariate analysis.. To appear in *Spectrochimica Acta B.*

# Development of an Engineering Model for Rubber Elasticity

*David Edward Hanson*

20060226ER

## Abstract

The goal of this research has been to discover the molecular basis of rubber elasticity and to develop molecule-specific models useful to the engineering community. Using molecular dynamics simulations of isolated polybutadiene chains, we tested the mechanism assumed to give rise to the elastic force by the classical (entropic) theory of rubber elasticity. We compared the snap-back velocity calculated from these simulations with experimental measurements on bulk rubber samples and found that the simulation gave a velocity about two orders of magnitude less than the experimental value. From this, we established that classical elasticity theory must be, at best, incomplete. We identified one elasticity mechanism that is operative at moderate to high tensile strains by performing quantum chemistry calculations on single rubber molecules as they are extended from their equilibrium conformation to the rupture limit. We find that chain rupture occurs at a tensile force of ~7 nN at a strain greater than 40%. This relatively large rupture strain implies that dominant enthalpic chain stretching must commence well before tensile failure occurs.

## Background and Research Objectives

Classical rubber elasticity theory [1] had its origins in the 1930's and it has remained an area of active research to this day. It attempts to relate the retractive force in elastomers, e.g., rubber, to the change in conformational entropy of the individual polymer chains that comprise the cross-linked network. The putative mechanism that produces the retractive force is the tendency for the polymer chains to seek conformations with more probable (higher entropy) end-to-end distances in response to random thermal collisions. We shall refer to this process as 'thermal collapse'. The chain is assumed to be isolated but the theory is thought to apply to melt systems as well. Because the theory is formulated from within the framework of thermodynamics, it does not explicitly include time, and it is not possible to apply it to kinetic processes. For example, the theory says nothing about how fast a polymer chain should retract from an extended conformation when one end is released, a situation that occurs when a stretched elastomer is suddenly released from tension. It is obvious that the retraction velocity of the network chains is a consequence of the elasticity and must be at least as fast as the bulk material. Experiments performed as early as 1944 [2] show that the retraction velocity of a rubber sample, abruptly released from tension, can be as high as 100 m/s. Furthermore, these experiments clearly establish that the retraction propagates as a wave along the sample, starting at the tip, with points along the sample remaining at rest until the retraction wave has passed. We tested this mechanism with molecular dynamics simulations and investigated other elastic processes using quantum chemistry methods.

## Importance to LANL's Science and Technology Base and National R & D Needs

At LANL, elastomers are widely used in nuclear weapons, and the question of how long term aging affects their elastic properties is important for predicting the stockpile lifetime. Moreover, the lab faces the prospect of having to replace some elastomers that are no longer being produced and whose composition is unknown or proprietary. Consequently, improving our understanding of elasticity will benefit LANL as well. The fields of biology and nano-technology could also benefit from the ideas and methodology that we will develop. This work will reinvigorate the polymer science of elasticity and LANL is in a strong position to assume a leadership role by virtue of our strength in computational chemistry, molecular simulation and large scale computing.

## Scientific Approach and Accomplishments

To test the viability of the thermal collapse molecular mechanism, we performed molecular dynamics simulations on isolated polybutadiene on chains containing

96, 148 and 200 carbon atoms at temperatures of 150K, 298K and 600K. The simulations were performed with a commercial software package, Accelrys/Materials Studio [3] with the Compass [4] all-atom force field at three temperatures: 150K, 298K and 600K. These simulations whose trajectories are shown in Figure 1 allowed us to study the retraction velocity of a free end of an idealized network chain from extended conformations in response to thermal collisions. We then compared the average snap-back velocity calculated from these simulations, shown in Figure 2, with experimental measurements on bulk rubber samples. Over the range of chain lengths, extension ratios and temperatures simulated, we found that the average retraction velocity of a free end seen in the simulations is about two orders of magnitude less than the experimental value. Had we performed a more faithful (but computationally intractable) simulation that included surrounding material, the retraction velocity would have been several orders of magnitude slower. A paper describing these results has been submitted to the journal Polymer.

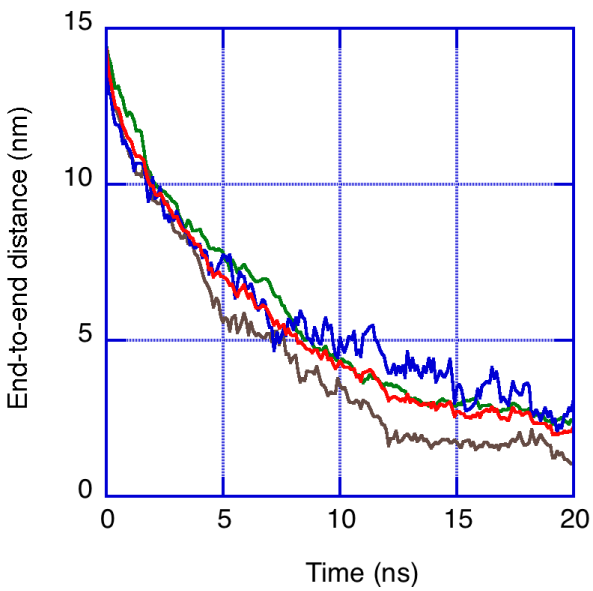


*Figure 1. End-to-end distance vs. time for 148-carbon chain at three temperatures, 150K (blue), 298K (tan), 600K (green) and average (red).*

Motivated by the discrepancy between the classical theory and the MD simulations, we chose next to investigate the behavior of rubber polymers at extensions approaching bond rupture. We performed quantum chemistry Density Functional Theory calculations for single molecules of (cis1,4) polyisoprene and polybutadiene as they are extended from their equilibrium conformation towards the dissociation limit. Isoprene differs from butadiene in that one hydrogen atom in each 4-carbon unit is replaced by a pendant methyl group (C24 and C32 in Figure 1). If one defines a coordinate for extension as the distance between the two terminal carbon atoms of an oligomer of butadiene, then a reaction path can be defined by optimizing all remaining coordinates under the constraint of a fixed extension. One intuitively expects a bond rupture to involve breaking a C-C bond and the generation of two weakly coupled fragments. We define this transition is that point along the extension curve at which an open shell solution lies lower in energy than the restricted, closed shell, solution.

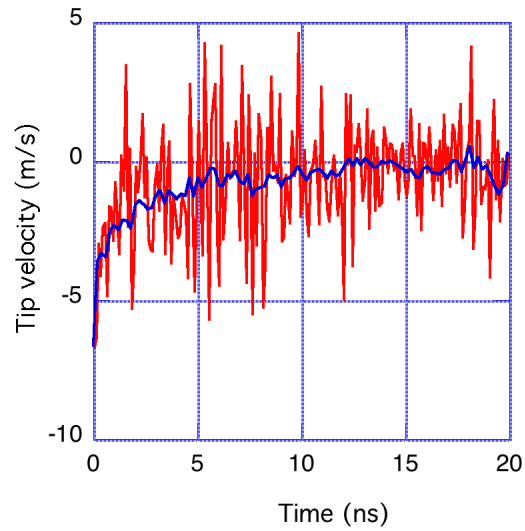


*Figure 2. Radial velocity of the free end with respect to fixed end computed as the numerical derivative of the end-to-end distance averaged over 5 MD runs (solid red), and numerically smoothed data (solid blue).*

Using the Gaussian03 [5] suite of electronic structure codes, the optimized electronic ground state energy at each point along the extension curve was computed. As a compromise between network chain fidelity and computational feasibility, we chose model systems containing one, two or three isoprene units. The isoprene molecule is shown in Figure 3. Two extra C atoms were added at the ends (C1 and C2), one necessary to include 4 bonds for each isoprene unit, and an additional C to enforce symmetry and reduce end effects. The equilibrium conformation was obtained by optimizing the electronic energy, allowing all atoms to move. Using this equilibrium as the initial state, a scan of the potential energy was performed by moving the end carbon atoms away from one another in steps of 0.05, 0.1 or 0.15 Angstrom, depending on the number of isoprene or butadiene units in the molecule. The end atoms, C1 and C2, were kept fixed during optimization at each end-to-end distance. The tensile forces as a function of extension for polyisoprene, shown in Figure 4, were calculated by numerically differentiating the energy profile. Due to the extra end carbon atom in our models, there is some ambiguity in the end-to-end length for a

section of the molecule comprising two isoprene units. There is also some uncertainty in the fraction of the total potential energy associated with their energy. Since the extra bond is a double bond, it tends to stretch less and store less energy than the single bonds in the chain, and we estimate that the energy error introduced by the extra carbon atom is less than 5%. Rupture occurs at a tensile force/ strain of 6.8 nN/ 45% for isoprene and 7.2 nN/ 42% for butadiene and these values are consistent with previous calculations [6]. A paper describing these results has been submitted to The Journal of Chemical Physics.

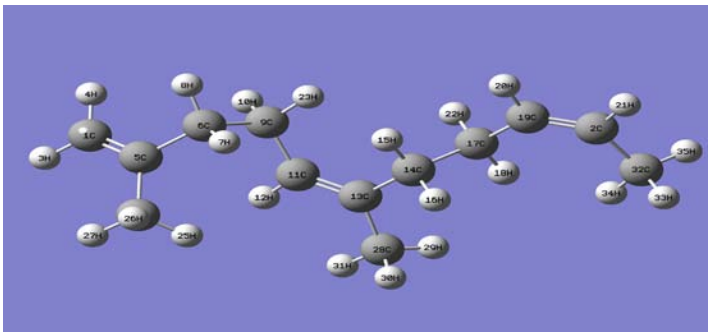

*Figure 3. Initial conformation of double isoprene molecule with additional end carbon atoms. Atoms C24, C 28 and 32C are in pendant methyl groups*

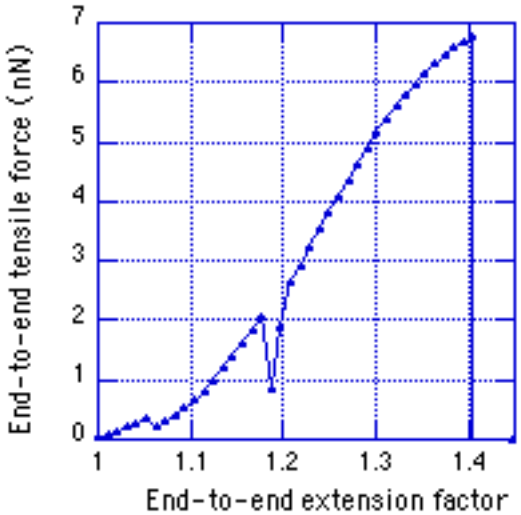


*Figure 4. Tensile force for 2-unit isoprene molecule vs extension factor. Discontinuities are due to bond re-orientation.*

Knowing the failure mechanism in a single rubber molecule provides insight into the failure process of a bulk sample. As the sample is stretched, some network paths must become taut from one end of the sample to the other. And, a chain cannot rupture until the sample is stretched by an additional ~40% after it is taut. If an isoprene sample fails at an extension ratio of 7.5 (typical), then the last chains that ruptured must have commenced stretching at an extension factor of 5.2 (7.5 divided by 1.45). But the failure of a single chain cannot cause catastrophic failure. Since the cross links of a rubber network each nominally contain four chains (tetrafunctional), the network remains intact for a single chain failures; the two remaining chains at a crosslink node can become taut upon further extension. Consequently, at least two chains emanating from a crosslink must rupture before the last chain can fail in the vicinity of that crosslink. This suggests that enthalpic stretching, accompanied by rupture, must begin at even lower extensions, perhaps at or before $\lambda$ ~3.6 (5.2 divided by 1.45). Exactly how the rubber network readjusts the load-bearing paths as chains fail is a topic for continuing research. From numerical simulations of a network, we know that the distribution of network path lengths across a sample is very broad with a peak many times the sample width. Only the shortest paths are the ones that can become load bearing upon tensile strain, and it is their distribution that we are interested in. We investigated two (constant chain length) biasing algorithms to study short network paths from the origin to a plane at the opposite edge of the sample. The algorithms are applied at each tetrafunctional network node to define the next node in the path across the network. The algorithms are: 1) choose the next network path node as the one closest to the opposite side and, 2) at each node, throw out the 'worst' node (the one furthest from the opposite side) and choose randomly between the two remaining. Our numerical simulations reveal that both algorithms yield very narrow distributions with centers at 1.64 and 3.28 times the sample width, respectively. For a real network, these factors must be multiplied by the ratio of the average chain length between nodes to the node separation distance. We have only just begun to apply this analysis to real rubber networks to explain the tensile stress versus strain-to-break over the last half of the extension curve, but the preliminary results are promising. Scaling the integral of the chain force extension curve over a constant path length distribution, yields a stress curve qualitatively the same as experiment. Unfortunately, the experimental record is not complete enough to allow quantitative comparisons.

## References

1. G.Treloar, L. R.. The physics of rubber elasticity. 1975.
2. Mrowca, J.. Retraction of stressed rubber. 30. *Physical Review.* **66**: 1944.
3. Sun, H.. Accelrys Discover Materials Studio. 2006.

4. Sun, H.. Update with correct title before submitting report. 1998. *Journal of Physical Chemistry B.* **102** (38): 7338.

5. Gaussian03. 2004. commercial: software.

6. Beyer, M. K.. The mechanical strength of a covalent bond calculated by density functional theory. 7307. *Journal of chemical physics.* **112** (17): 2000.

# MRI in Microtesla Magnetic Fields with Simultaneous MEG

*Michelle A Espy*

20060312ER

## Abstract

We have developed an instrument that extends magnetic resonance imaging (MRI) into a new regime using ultra-low magnetic fields (ULF). We have successfully demonstrated a multi-modality instrument for studying brain function that has, for the first-time, allowed MRI information to be acquired simultaneously with direct high temporal resolution measurements of neuronal function provided by magnetoencephalography (MEG). MEG data provides no anatomical information and is subject to an ill-posed inverse problem for source localization. While functional MRI (fMRI) has been increasingly applied to the study of brain function, it suffers from the fundamental limitations that neuronal function is inferred from indirect hemodynamic or metabolic information with poor temporal resolution (~1 sec). Our instrument has shown that the same sensors can be used to simultaneously acquire MRI and MEG data, capitalizing on the strengths of both modalities while pushing the technology and applications for both MRI and MEG into a totally new regime. The instrument has had applications far beyond brain imaging alone, enabling portable, low-cost MRI without superconducting magnets, permitting a truly open design, and allowing novel imaging sequences. The ULF MRI instrument we have designed has enabled imaging objects inside metallic containers, essentially eliminating susceptibility artifacts, and possibly allow for contrast mechanisms not realized at high fields. Such a tool is now being applied to LANL mission-relevant applications including a multi-million dollar project in ULF MRI to detect liquid explosive, and non-proliferation monitoring of UF6. Finally, the potential to directly image physiological currents by ULF MRI is an exciting prospect, without the inherent ambiguity of the inverse problem, which would represent a totally new functional imaging modality, and our work on this project has significantly leveraged progress in this area.

## Background and Research Objectives

While the ultra-low field (ULF) magnetic resonance imaging (MRI) instrument developed here has a vast array of potential applications, we focused largely on functional brain imaging where our group is a recognized world leader. The primary objective of the work, to demonstrate detection of anatomical (MRI) and functional (magnetoencephalography or MEG) brain imaging was accomplished [1] and results are shown in Figure 1. The impact of the work is reflected in publications in the scientific literature, popular press, the cover of the Journal of Magnetic Resonance, and an editorial in Nature [2] on the importance of the work referenced throughout this report. More telling, work from this project was singled out as the impetus for a multi-million euro, multi-national European effort [3]. The progress in ULF MRI arising from this proposal has been readily applied to numerous other biological and non-biological problems from low-cost, small footprint anatomical imaging and imaging of subjects that are not candidates for high-field (such as those with medical implants or metal from injuries) to inspection and detection and imaging of special nuclear materials through metallic enclosures [4], and detection and classification of materials such as liquid explosives.

MEG is a non-invasive technique that measures magnetic fields outside the head that are the direct consequence of neuronal activity in the living brain. MEG uses superconducting quantum interference device (SQUID) sensors to measure the extraordinarily these low level magnetic fields, usually in the range from $10^{-15}$ to $10^{-12}$ T. While other functional imaging modalities such as functional MRI (fMRI) depend on the relatively slow and indirect hemodynamic response of the brain to *infer* function, MEG (and electroencephalography or EEG) measures the electromagnetic fields arising directly from the neuronal currents with sub-millisecond temporal resolution.

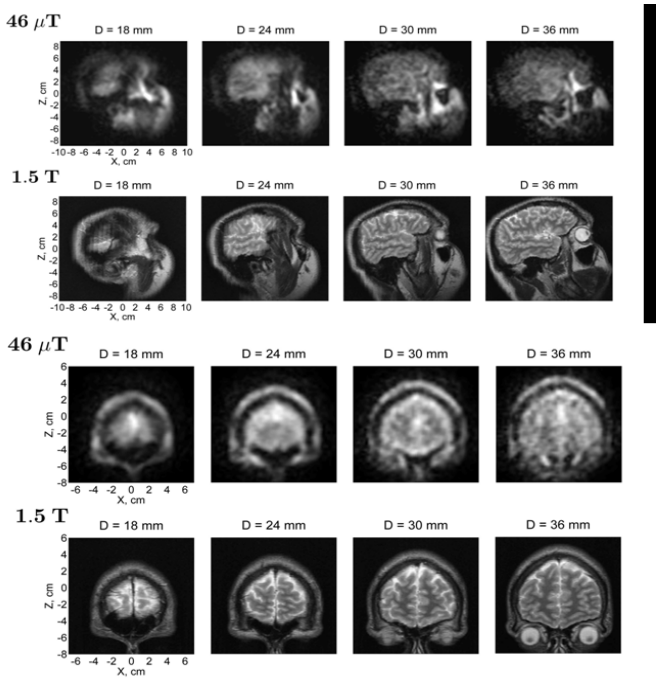


*Figure 1. Human brain images recorded at 46 microTesla compared to images of the same subject acquired at 1.5 Tesla. The data presented are for slices through the brain. 'D' refers to slice depth relative to SQUID position above the head. 7-channel auditory MEG data (not shown) were acquired in the same session.*

The inverse problem of source localization from MEG (and EEG) is ill posed. That is, there is no exact solution when transforming recorded MEG data to the exact location of sources in the brain. Determining the source region requires models of source current distribution, geometry and inhomogeneous conductivity within the head volume conductor. Neural electromagnetic data are often combined with anatomical or functional tomographic data obtained with high field MRI and fMRI, both to constrain the inverse problem (e.g. limiting sources to cortical surfaces) and to provide the anatomical structure onto which the functional sources are projected.

MEG and MRI data are taken with two completely separate instruments because the SQUIDs cannot operate in the large magnetic fields (up to 15 orders of magnitude larger than an MEG signal) required by high field MRI systems. Acquisition of data from two separate instruments necessitates using data fusion techniques to integrate and superpose the two data sets, called 'coregistration', in an accurate and meaningful way. The error for co-registering the MRI/MEG data is commonly 5 mm and is the leading source of error in MEG source localization to anatomical structure. *Simultaneous anatomical MRI with MEG greatly benefits the MEG community as the anatomical and functional information could be acquired in a single instrument.*

We successfully demonstrated an instrument capable of acquisition of MRI and MEG data in the same system, as the magnetic fields required for ULF MRI ($10^{-3}$ to $10^{-5}$ Tesla) imaging are now compatible with SQUID sensors. Moreover, the same SQUID sensors used to detect the MEG signal are the detector of choice for measuring the MR signal, as the SQUID has unrivaled sensitivity and a response that is independent of frequency. While it is unlikely that the best ULF MRI resolution will match that of modern high-field (4 T or more) anatomical imaging, in most functional imaging applications the ~ 1 mm spatial resolution we demonstrate is sufficient. In cases where higher resolution is desired, a multi-point surface fit of lower-resolution ULF MRI to high-resolution high-field MRI can be used. Moreover, ULF images are free of artifacts (e.g. magnetic susceptibility) that limit high field images. ULF MRI also benefits the high-field MRI community by providing a calibration for the susceptibility distortions of any given sample that can be used to correct the high field MRI. Combining dynamic anatomical imaging with electrophysiological information may also prove valuable in cardiac studies. Ultimately, low-field MRI may lead to direct imaging of the magnetic fields from neural currents by observation of a change in the MR frequency, phase or relaxation (see for example [5]). We ourselves are investigating this area with promising initial results [6]. Realizing tomographic imaging of bioelectric sources by ULF MRI, combined with the high temporal resolution of MEG would represent an entirely new imaging modality revolutionizing functional imaging. Additional motivation for low field MRI is the prospect of a reduced cost and smaller MRI instruments by removing the requirement for large permanent or massive superconducting magnets. Between 1 – 5% of all high field MRI scans are interrupted due to subjects experiencing claustrophobia within the closed magnet bore. Millions of people with *in vivo* metal from medical procedures, implants, or injuries cannot be imaged at high field because of RF induced heating or interference. There would be no such difficulty imaging these people at ULF. Low-field methods even enable imaging using the Earth's magnetic field, ~50 μT, for a variety of applications including geophysical NMR measurements to characterize subsurface water, hydrocarbon deposits, or pollutant plumes (see for example [7] and references therein). *In contrast to high field systems, measurement fields at ULF are not required to be highly homogeneous to achieve narrow NMR line width* allowing the possibility of very narrow NMR lines with high signal-to-noise. Susceptibility artifacts due to coupling between the applied field and different sample materials, a principal source of noise in functional MRI, are significantly reduced at ULF. The absence of such artifacts may provide opportunities for novel forms of

functional imaging. The observation that relaxation times in tumor samples measured *in vitro* was different than for normal tissue was a major impetus in introducing MR methods to medicine. However the ability to separate benign from malignant tissue has yet to be achieved. It is possible that we can manipulate relaxation contrast at ULF to provide significant contrast not realized at high fields. We have already demonstrated the acquisition of NMR signals through conducting containers up to several millimeters thick [7], a consequence of the low Larmor frequencies at ULF. This has lead to LANL mission-relevant applications like in-situ detection and imaging of special nuclear materials and non-destructive inspection and detection of liquid explosives, applications that could not be realized with high-field systems.

I*n this work we successfully developed a novel SQUID-based instrument for simultaneous acquisition of the world's first MEG and MRI data at ultra-low fields* [1]. We demonstrated ULF MRI approaches including image contrast not available at high fields, reduced susceptibility artifacts, open system design, multiple sensors for imaging acceleration [8] and the capability to measure samples inside metallic containers and/or containing metallic objects [6]. A significant goal was the measurement of simultaneous MEG/MRI of sufficient quality to be the basis for a proposal to outside agencies (e.g. NIH) for continued funding. This work did indeed lead to an NIH grant as well as a major project with the Department of Homeland Security. We have built an instrument that is both robust and portable, and sufficiently generic to explore the many other potential applications of ULF NMR and MRI.

## Importance to LANL's Science and Technology Base and National R & D Needs

- The development of an instrument capable of simultaneous bioelectric (MEG) and anatomical measurements has been a major advance to the neuroimaging community and will help validate functional studies based on hemodynamic responses (fMRI).
- ULF MRI and MEG open up the potential for *directly* imaging neuronal currents, considered by many to be the 'holy grail' of neuroimaging.
- ULF MRI alleviates many practical disadvantages of high field systems (e.g. ability to image people with metallic implants, reduced system size and cost), thereby benefiting millions more people than current MRI.
- Low frequency and *ex-situ* imaging is a major benefit for detecting samples located inside metallic containers. This has been important for the detection of SNM that has been shielded and homeland security applications in detection of liquid explosives In both applications both the ability to provide chemical information though metals and the practical merits of a system without very large magnetic fields have been crucial. There are also applications in non-destructive evaluation/flow based systems, and *ex-situ* measurements such as resource exploration and environmental monitoring.
- The novel SQUID operating techniques have benefited the applied superconductivity community and our demonstration of iarray-based MRI, with novel field and gradient capabilities has benefitted the entire NMR/MRI community.
- More direct applications of this particular proposal will include developing the neuroscience underpinnings to help the war-fighter of the future better process information, neural-inspired devices, portable battle-field MRI, and possibly better measures of understanding human-intelligence and motivation.
- The sensitivity of ULF MRI to a novel "slow" regime of molecular dynamics will provide new diagnostics relevant to Biosecurity initiatives (conformational dynamics associated with antiviral drug resistance) and Energy Security (kinetic studies of enzymes involved in biomass conversion and water diffusion kinetics of proton exchange in fuel cells).

## Scientific Approach and Accomplishments

SQUID sensors are needed for ULF MRI to compensate for the small sample polarization and detection efficiency. The SQUID is a magnetic flux-to-voltage converter of exquisite sensitivity with a response that is independent of frequency. The primary limitation to ULF MRI is low signal to noise ratio because of the small sample polarization at low fields. In addition to ultra-sensitive detectors (such as SQUIDs) signal can also be increased by prepolarizing techniques, where the sample is polarized at a higher field independent of the measurement step (i.e. Bp ~ mT). The MRI measurement is then performed at a lower field, Bm ~ microTesla. SQUIDs are also the only detectors presently capable of bioelectric measurements such as MEG. The MEG/MRI signals are easily separable since the MRI signal is found in a very narrow frequency window and can be tuned (by choice of Bm) to be above the typical MEG band-

width (DC to few hundred Hz). We utilized a 7-channel SQUID-based array of 2nd order axial gradiometers and designed a magnetic field system capable of generating pre-polarizing fields on the order of ~ 50 mT with measurement fields easily adjusted between 10-100 microTesla. [1,8,9,10]. Figure 2 presents the system hardware.

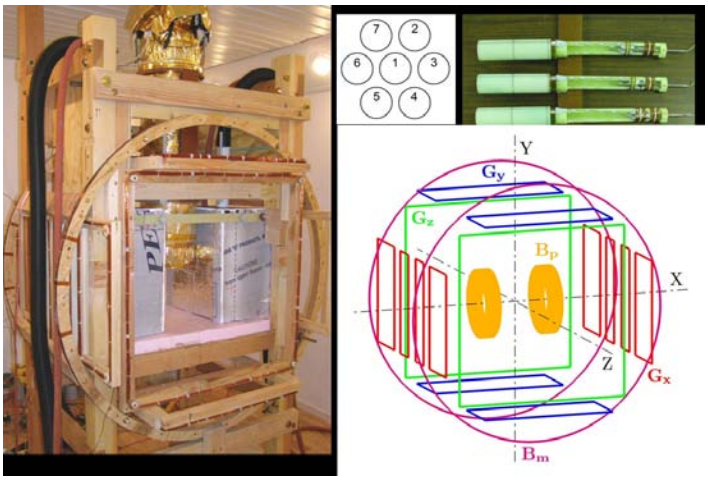


*Figure 2. Clockwise from left: Photograph of 7-channel ULR MRI system used in this work, SQUID sensor pattern, three of the seven gradiometers, schematic of MRI cois. Bp and Bm refer to polarization and measurement fields respectively. Gx,Gy,Gz refer to magnetic field gradients.*

At the same time we developed the computational and analytical tools to optimize 1) array design for noise-cancellation, 2) pulse sequences, 3) models of instrument performance, and 4) algorithms for data acquisition and analysis. Figure 3 presents the pulse sequence design.

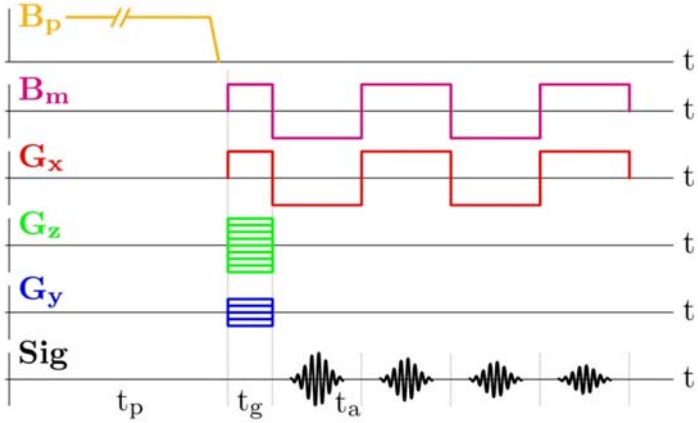


*Figure 3. Pulse sequence used to produce ULF MRI images. Field labels refer to magnetic coils shown in Figure 2.*

While the majority of our studies were conducted within magnetically shielded enclosures, we also were able to demonstrate noise-cancellation methods using reference channels and computational methods such as beam forming techniques to reduce the effects of ambient noise and minimize the type of external shielding required. Another impediment to ULF MRI has been the relatively long imaging times. Lower strength magnetic fields generally must be accompanied by comparably lower gradient fields for imaging. This limits the width of the spectral content of the signal, and increases the required acquisition time. We developed methods to correct the effects of concomitant gradients that inevitably arise when generating the desired gradients for spatial encoding [8]. Our system design has relied n the use of conventional Golay and Maxwell gradient coil designs, but with open coil design (see Figure 2). An important component of system design was development of algorithms to analyze the data and reconstruct images such as those shown in Figures 1 and 4.

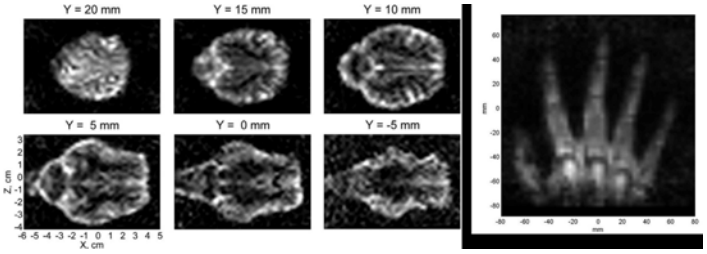


*Figure 4. Left: Images of a preserved sheep brain acquired at 46 microTesla. Y represents distance from the SQUID sensor. Right: Images of the human hand at 46 microTesla.*

We also developed electronics optimized for array based ULF MRI system using SQUIDs [9]. Our prepolarizing technique utilizes magnetic fields that are relatively large and rapidly changing in amplitude for a SQUID. We have already developed and implemented a method that allows the SQUIDs to survive the prepolarizing pulse for single channel axial gradiometers whereby we are able to start data acquisition a few milliseconds after the prepolarizing pulse ends. It was also necessary to investigate new dewar materials to decrease the SQUID recovery time, and our experience from this work has lead to the design of a dewar with noise lower than the intrinsic SQUID noise (< 0.4 fT). We also studied first and second-order axial gradiometers as potential sensors for an ULF MRI system. Our research has recently evolved into two new system designs shown in Figure 5.

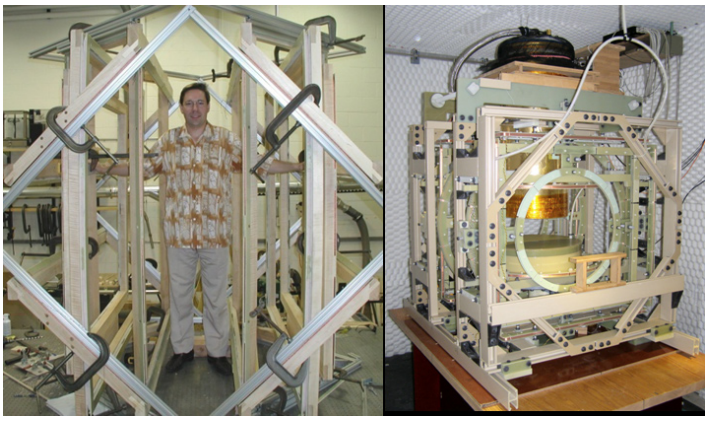

*Figure 5. Left: Next generation gradient coils for whole-body imaging. Right: The 7-channel ULF MRI system designed for homeland security applications. The coils and design are modeled after the original system shown in Figure 2.*

In summary, we have developed and demonstrated the world's first instrument capable of acquiring both MEG and MRI. We have leveraged this research to numerous follow-on applications relevant to LANL and the nation.

## References


1. Zotev, V., A. Matlashov, P. Volegov, I. Savukov, M. Espy, J. Mosher, J. Gomez, and R. Kraus. Microtesla MRI of the human brain combined with MEG. 2008. *Journal of Magnetic Resonance.* **194** (1): 115.

2. Pruessmann, K.. News and views. 2008. *Nature.* **455**: 43.

3. Highlights: Microtesla MRI of the Human Brain with simultaneous MEG. 2008. *European Superconductivity News Forum http://www.ewh.ieee.org/tc/csc/europe/newsforum/highlightsZotevH14.html.*

4. Magnelind, P., A. Matlashov, P. Volegov, and M. Espy. Ultra-low field NMR of UF6 for 235U detection and characterization. To appear in *IEEE Transactions on Applied Superconductivity.*

5. Xiong, J., P. Fox, and J. Gao. Directly mapping magnetic field effects of neuronal activity by magnetic resonance imaging. 2003. *Human Brain Mapping.* **20**: 41.

6. Kraus, R., P. Volegov, A. Matlashov, and M. Espy. Toward direct neural current imaging by resonant mechanisms and ultra-low field. 2008. *Neuroimage.* **39** (1): 310.

7. Matlashov, A., P. Volegov, M. Espy, J. George, and R. Kraus. SQUID detected NMR in microtesla magnetic fields. 2004. *Journal of Magnetic Resonance.* **170** (1): 1.

8. Zotev, V., P. Volegov, A. Matlashov, M. Espy, J. Mosher, and R. Kraus. Parallel MRI at microtesla fields. 2008. *Journal of Magnetic Resonance.* **192** (2): 197.

9. Zotev, V., A. Matlashov, P. Volegov, A. Urbaitis, M. Espy, and R. Kraus. SQUID-based instrumentation for ultra-low-field MRI. 2007. *Superconducting Science and Technology.* **20** (11): S367.

10. Zotev, V., A. Matlashov, P. Volegov, J. Sandin, M. Espy, J. Mosher, A. Urbaitis, S. Newman, and R. Kraus. Multi-Channel SQUID System for MEG and Ultra-Low Field MRI. 2007. *IEEE Transactions on Applied Superconductivity.* **17** (2): 839.


## Publications


Espy, M., M. Flynn, J. Gomez, C. Hanson, R. Kraus, P. Magnelind, K. Maskaly, A. Matlashov, S. Newman, M. Peters, H. Sandin, I. Savukov, L. Schultz, A. Urbaitis, P. Volegov, and V. Zotev. Applications of ultra-low field magnetic resonance for imaging and material studies. To appear in *IEEE Transactions on Applied Superconductivity.*

Kraus, R., M. Espy, A. Matlachov, J. Mosher, A. Urbaitis, P. Volegov, and V. Zotev. SQUID-based Direct Measurement of Neural Currents by Nuclear Magnetic Resonance. To appear in *IEEE Transactions on Applied Superconductivity, 2006 Applied Superconductivity Conference.* (Seattle, WA, 27 Aug - 1 Sept, 2006).

Matlachov, A., P. Volegov, M. Espy, J. Mosher, V. Zotev, A. Urbaitis, and R. Kraus. Multi-channel SQUID MEG System Compatible with Ultra-Low Field MRI. To appear in *IEEE Transactions on Applied Superconductivity, 2006 Applied Superconductivity Conference.* (Seattle, WA, 27 Aug - 1 Sept, 2006).

Zotev, V., A. Matlachov, P. Volegov, M. Espy, J. Mosher, S. Newman, and R. Kraus. Multi-Sensor system for simultaneous ultra-low field MRI and MEG. To appear in *Biomagnetism: Proceedings of the 15th International Conference on Biomagnetism.* (Vancouver, BC Canada, 21 - 25 August, 2006).

Zotev, V., A. Matlashov, P. Volegov, A. Urbaitis, M. Espy, and R. Kraus. SQUID-based instrumentation for ultra-low field

MRI. 2007. *Superconducting Science and Technology.* **20** (11): 367.

Zotev, V., A. Matlashov, P. Volegov, H. Sandin, M. Espy, J. Mosher, A. Urbaitis, S. Newman, and R. KRaus. Multi-channel SQUID system for MEG and ultra-low field MRI. 2007. *IEEE Transactions on Applied Superconductivity.* **17** (2): 839.

Zotev, V., A. Matlashov, P. Volegov, I. Savukov, T. Owens, and M. Espy. Human brain imaging by SQUID-based microtesla MRI and MEG. To appear in *IEEE Transactions on Applied Superconductivity.*

Zotev, V., A. Matlashov, P. Volegov, M. Espy, H. Sandin, J. Mosher, A. Urbaitis, S. Newman, and R. Kraus. Multi-sensor system for simultaneous ultra-low-field MRI and MEG. 2007. *International Congress Series.* **13** (A): 631.

# Seeing Undetectable Cancers with Time-Reversed Ultrasound

*Lianjie Huang*

20060318ER


## Abstract

The breast cancer death rate in the United States has changed little since the 1930s, despite increased routine screening using X-ray mammography since 1960s. Although early cancer detection is the key to reducing mortality, no reliable medical imaging tools are currently available for detection at its earliest, most curable stages. We developed a vastly improved, high-resolution ultrasonic cancer-imaging methodology. The new imaging methods we developed included: ultrasound breast reflection imaging using time-reversed ultrasound, bent-ray and waveform ultrasound tomography, wave-theory-based ultrasound reflection imaging, and super-resolution ultrasound imaging. We applied our new methods to in vivo clinical ultrasound breast data acquired using a ring transducer array at Karmanos Cancer Institute. The dramatically improved image quality and resolution enable us to detect tiny, currently undetectable, early-stage and thus more treatable cancers.


## Background and Research Objectives

Breast cancer is the most frequently diagnosed cancer in U.S. women. It accounts for nearly one out of three cancers diagnosed in U.S. women. More than 200,000 women and 1,500 men in the U.S. learn that they have breast cancer each year --- up from about 100,000 two decades ago, according to the American Cancer Society. X-ray mammography is presently the only routine screening tool available for breast cancer detection. However, the effectiveness of X-ray mammography is currently being hotly debated. Early cancer detection is the only know means for reducing cancer mortality. Clinical studies have shown that ultrasound imaging has tremendous potential to detect small, early-stage cancers that cannot be detected by X-ray mammography. Compared to X-ray mammography, ultrasound imaging is a safe (without ionizing radiation), comfortable (without compression), and portable imaging modality. However, current state-of-the-art ultrasound cancer imaging produces low-resolution and noisy (full of speckle) images, which greatly limit its capability to detect cancers.

The primary research objective of this project is to significantly improve ultrasound image resolution and quality in order to detect currently undetectable tiny breast cancers. We address this challenge by increasing data acquisition aperture using a full-aperture ring transducer array for breast imaging, and by accounting for ultrasound scattering from breast heterogeneities during image reconstruction. We demonstrate using the in vitro and in vivo ultrasound breast data that our new ultrasound imaging technology greatly reduces image noise and improves image resolution. It has tremendous potential to be used for breast cancer screening.

## Importance to LANL's Science and Technology Base and National R & D Needs

The increased breast ultrasound image quality and resolution enable us to detect currently undetectable, earliest-stage and thus more treatable breast cancers, and ultimately, reduce cancer mortality. The high-resolution imaging methodology we developed has also great potential for applications in other fields, such as nondestructive evaluation and underground imaging. This research addresses an urgent national need in developing alternative, more effective breast cancer screening tool.

## Scientific Approach and Accomplishments

Ultrasound image resolution is a function of data acquisition aperture. In collaboration with Karmanos Cancer Institute, we make use of a full-aperture ring transducer array for breast imaging. The breast is immersed into a water tank, encircled by the ring transducer array consisting of 256 elements of transducers. The ring array is translated vertically to scan 50-80 slices of ultrasound data for whole breast tomography. We further improve ultrasound image quality and resolution by accounting for ultrasound scattering from breast heterogeneities, which result in ultrasound speckle (noise) in current clinical ultrasound.

We developed several novel image reconstruction algorithms for high-resolution ultrasound imaging. We

conducted ultrasound tomography using correct ultrasound ray paths that are bent instead of straight like X-ray [1, 2, 3, 4]. This significantly reduces artifacts of ultrasound breast images and enhances image resolution. To further improve image resolution, we made use of waveform tomography that uses entire ultrasound waveforms for image reconstruction [5]. Ultrasound tomography provides a heterogeneous background for ultrasound reflection imaging to account for ultrasound scattering. We developed a time-reversal ultrasound imaging algorithm using a numerical scheme to solve acoustic wave equation, which governs ultrasound wave propagation in the heterogeneous breast [6]. To enhance computational efficiency of wave-based ultrasound reflection imaging, we developed ultrasound reflection image reconstruction algorithms using primary ultrasound reflection signals [7, 8]. In addition, we investigated the spatial sampling requirement for the ring array, and developed a diffraction tomography and a super-resolution imaging algorithm that can provide one order of magnitude better details than conventional ultrasound imaging [9, 10, 11, 12, 13].

We applied our novel ultrasound image reconstruction algorithms to in vivo ultrasound breast data acquired using a ring transducer at Karmanos Cancer Institute. An example of in vivo whole breast ultrasound tomography is shown in Figure 1. The breast cancer is shown in red with higher sound speeds compared to the surrounding tissues. Our in vivo applications demonstrate that our novel image reconstruction algorithms can provide ultrasound breast images with much higher resolution and quality than current clinical ultrasound, and that they have tremendous potential for reliable breast cancer detection and diagnosis.

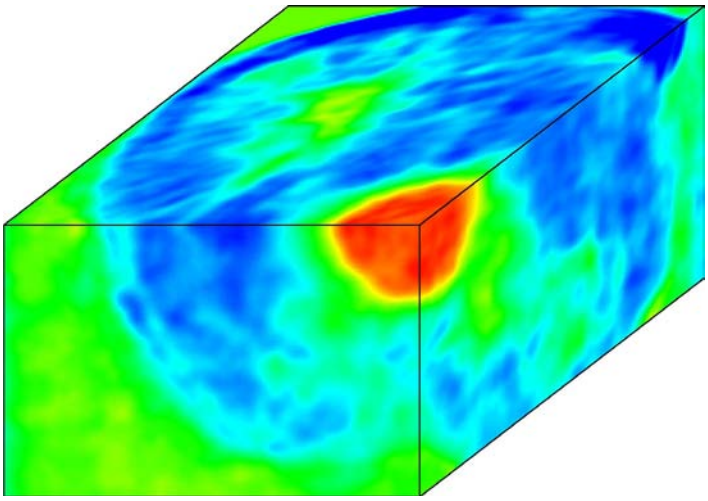

*Figure 1. In vivo whole breast ultrasound tomography image showing a breast cancer with red color (Data from Karmanos Cancer Institute).*

## References


1. Quan, Y., and L. Huang. Sound-speed tomography using first-arrival transmission ultrasound for a ring array. 2007. In *SPIE Medical Imaging 2007.* (San Diego, CA, 17-22 Feb. 2007). Vol. 6513, p. 651306. Bellingham, Washington: SPIE.

2. Li, C., L. Huang, N. Duric, H. Zhang, and C. Rowe. An improved automatic time-of-flight picker for medical ultrasound tomography. To appear in *Ultrasonics.*

3. Li, C., N. Duric, and L. Huang. Clinical breast imaging using sound-speed reconstructions of ultrasound tomography data. 2008. In *SPIE Medical Imaging 2008.* (San Deigo, CA, 16-21 Feb. 2008). Vol. 6920, p. 692009. Bellingham, Washington: SPIE.

4. Li, C., N. Duric, and L. Huang. Comparison of ultrasound attenuation tomography methods for breast imaging. 2008. In *SPIE Medical Imaging 2008.* (San Deigo, CA, 16-21 Feb. 2008). Vol. 6920, p. 692015. Bellingham, Washington: SPIE.

5. Pratt, R. G., L. Huang, N. Duric, and P. Littrup. Sound-speed and attenuation of the breast tissue using waveform tomography of transmission ultrasound data. 2008. In *SPIE Medical Imaging 2008.* (San Diego, CA, 16-21 Feb. 2008). Vol. 6510, p. 65104S. Bellingham, Washington: SPIE.

6. Huang, L., N. Duric, and P. Littrup. Breast imaging with time-reversed ultrasound. 2006. In *SPIE Medical Imaging 2006.* (San Deigo, CA, 11-16 Feb. 2006). Vol. 6147, p. 156. Bellingham, Washington: SPIE.

7. Huang, L., and Y. Quan. Ultrasound pulse-echo imaging using the split-step Fourier propagator. 2007. In *SPIE Medical Imaging 2007.* (San Diego, CA, 17-22 Feb. 2007). Vol. 6513, p. 651305. Bellingham, Washington: SPIE.

8. Huang, L., K. M. Hanson, Y. Quan, C. Li, and N. Duric. Globally optimized Fourier finite-difference method for ultrasound breast imaging. 2008. In *SPIE Medical Imaging 2008.* (San Diego, CA, 16-21 Feb. 2008). Vol. 6920, p. 6920007. Bellingham, Washington: SPIE.

9. Simonetti, F., L. Huang, and N. Duric. On the spatial sampling of wave fields with circular ring apertures. 2007. *Journal of Applied Physics.* **101**: 083103.

10. Simonetti, F., L. Huang, N. Duric, and O. Rama. Super-resolution ultrasound tomography: A preliminary study with a ring array. 2007. In *SPIE Medical Imaging 2007.* (San Diego, CA, 17-22 Feb. 2007). Vol. 6510, p. 65103F. Bellingham, Washington: SPIE.

11. Simonetti, F., L. Huang, N. Duric, and O. Rama. Imaging beyond the Born approximation: An experimental investigation with an ultrasonic ring array. 2007. *Physical Review E.* **76**: 036601.

12. Simonetti, F., L. Huang, and N. Duric. Frequency diversity in breast ultrasound tomography. 2008. In *SPIE Medical Imaging 2008.* (San Diego, CA, 16-21 Feb. 2008). Vol. 6913, p. 6913E. Bellingham, Washington: SPIE.

13. Simonetti, F., and L. Huang. From beamforming to diffraction tomography. 2008. *Journal of Applied Physics.* **103**: 103110.

## Publications

Duric, N., C. Li, C. Glide-Hurst, P. Littrup, L. Huang, J. Lupinacci, S. Schmidt, R. Rama, L. Bey-Knight, and Y. Xu. Breast imaging with ultrasound tomography: Clinical results at the Karmanos Cancer Institute. 2008. In *The 2008 International Conference on Biomedical Engineering and Informatics.* (Sanya, Hainan, China, 28-30 May 2008). Vol. 2, p. 713. Washington, DC: IEEE Computer Society.

Duric, N., C. Li, P. Littrup, C. Glide-Hurst, L. Huang, J. Lupincacci, S. Schmidt, R. Rama, L. Bey-Knoght, and Y. Xu. Multi-model breast imaging with ultrasound tomography. 2008. In *SPIE Medical Imaging 2008.* (San Diego, CA, 16-21 Feb. 2008). Vol. 6920, p. 69200O. Bellington, Washington: SPIE.

Duric, N., P. Littrup, C. Glide-Hurst, C. Li, L. Huang, R. Pratt, Y. Quan, and F. Simonetti. Detection of Breast Cancer with Ultrasound Tomography. Presented at *49th AAPM Annual Meeting.* (Minneapolis, Minnesota, 22-26 July 2007).

Goulding, N. R., J. D. Marquez, E. M. Prewett, T. N. Claytor, L. Huang, and B. R. Nadler. Ultrasonic imaging techniques for breast cancer detection. To appear in *International Modal Analysis Conference XXV.* (Florida, 2007).

Goulding,, N. R., J. D. Marquea, E. M. Prewett, T. N. Claytor, L. Huang, and B. R. Nadler. Ultrasonic Imaging Techniques for Early Breast Cancer Detection. To appear in *Review of Progress in Quantitative Nondestructive Evaluation.* (Denver, CO, July, 2007).

Huang, L., K. Hanson, Y. Quan, R. Pratt, C. Li, N. Duric, and P. Littrup. Ultrasound Reflectivity Imaging with a Split-Step Fourier Propagator for Cancer Detection and Diagnosis in Heterogeneous Breasts. Presented at *49th AAPM Annual Meeting.* (Minneapolis, Minnesota, 22-26 July 2007).

Huang, L., K. M. Hanson, Y. Quan, C. Li, and N. Duric. Globally optimized Fourier finite-difference method for ultrasound breast imaging. 2008. In *SPIE Medical Imaging.* (San Deigo, CA, 16-21 2008). Vol. 6920, p. 6920007. Bellingham, Washington: SPIE.

Huang, L., M. Fehler, N. Duric, and P. Littrup. Applications of acoustic-wavefield downward continuation to geophysical and medical imaging. 2006. In *The 151st Meeting of the Acoustical Society of America (ASA).* (Providence, Rhode Island, 5-9 June 2006). Vol. 119, p. 3214. New York: The Journal of the Acoustical Society of America.

Huang, L., N. Duric, and P. Littrup. Breast imaging with time-reversed ultrasound. 2006. In *SPIE Medical Imaging 2006: Ultrasonic Imaging and Signal Processing.* (San Diego, CA, 11-13 Feb 2006). Vol. 6147, p. 156. Bellingham, Washington: SPIE.

Huang, L., Y. Quan, C. Li, N. Duric, and K. M. Hanson. Ultrasound pulse-echo imaging with an optimized propagator. 2008. In *The 2008 International Conference on Biomedical Engineering and Informatics.* (Sanya, Hainan, China, 27-30 May 2008). Vol. 2, p. 281. Washington, DC : IEEE Computer Society.

Huang, L., Y. Quan, N. Duric, and C. Li. Ultrasonic reflection imaging with a heterogeneous background for breast cancer detection and diagnosis. 2006. In *The 4th Joint Meeting of the Acoustical Society of America and the Acoustical Society of Japan.* (Honolulu, Hawaii, 28 Nov.-2 Dec. 2006). Vol. 119, p. 3214. Honolulu, Hawaii: The Journal of the Acoustical Society of America.

Huang, L., and Y. Quan. Ultrasonic reflection imaging by inward continuation of ultrasonic wavefields using the split-step Fourier propagator. 2007. In *SPIE Medical Imaging 2007: Ultrasonic Imaging and Signal Processing.* (San Diego, CA, 17-22 Feb. 2007). Vol. 6513, p. 651305. Bellingham, WA: SPIE.

Li, C., L. Huang, N. Duric, H. Zhang, and C. Rowe. An improved automatic time-of-flight picker for medical ultrasound tomography. To appear in *Ultrasonics.*

Li, C., N. Duric, and L. Huang. Calibration of Bent-Ray Ultrasound Tomography and Its Application to Breast Cancer Detection and Diagnosis. Presented at *49th AAPM Annual Meeting.* (Minneapolis, Minnesota, 22-26 July 2007).

Li, C., N. Duric, and L. Huang. Clinical breast imaging using sound-speed reconstructions of ultrasound tomography data. 2008. In *SPIE 2008.* (San Diego, CA, 16-21 Feb. 2008). Vol. 6920, p. 692009. Bellingham, Washington: SPIE.

Li, C., N. Duric, and L. Huang. Comparison of ultrasound attenuation tomography methods for breast imaging. 2008. In *SPIE Medical Imaging 2008.* (San Diego, CA, 16-21 Feb. 2008). Vol. 6920, p. 692015. Bellingham, Washington: SPIE.

Li, C., N. Duric, and L. Huang. Breast imaging using transmission ultrasound: reconstructing tissue parameters of sound speed and attenuation. 2008. In *The 2008 International Conference on Biomedical Engineering and Informatics.* (Sanya, Hainan, China, 27-30 May 2008). Vol. 2, p. 708. Washington, DC: IEEE Computer Society.

Pratt, R. G., L. Huang, and N. Duric. Sound-speed and attenuation imaging using waveform tomography of transmission ultrasound data. 2007. In *SPIE Medical Imaging 2007: Physics of Medical Imaging.* (San Diego, CA, 17-22 Feb. 2007). Vol. 6510, p. 65104S. Bellingham, WA : SPIE.

Quan, Y., and L. Huang. Sound-speed tomography using first-arrival transmission ultrasound for a ring array. 2007. In *SPIE Medical Imaging 2007: Ultrasonic Imaging and Signal Processing.* (San Diego, CA, 17-22 Feb. 2007). Vol. 6513, p. 651306. Bellingham, WA: SPIE.

Simonetti, F., L. Huang, N. Duric, and O. Rama. Super-resolution ultrasound tomography: A preliminary study with a ring array. 2007. In *SPIE Medical Imaging 2007: Physics of Medical Imaging.* (San Diego, CA, 17-22 Feb. 2007). Vol. 6510, p. 65103F. Bellingham, WA, USA: SPIE.

Simonetti, F., L. Huang, N. Duric, and O. Rama. Imaging beyond the Born approximation: An experimental investigation with an ultrasonic ring array. 2007. *Physical Review E.* **76**: 036601.

Simonetti, F., L. Huang, and N. Duric. On the spatial sampling of wave fields with circular ring apertures. 2007. *Journal of Applied Physics.* **101**: 65103F.

Simonetti, F., L. Huang, and N. Duric. Frequency diversity in breast ultrasound tomography. 2008. In *SPIE Medical Imaging 2008.* (San Diego, CA, 16-21 Feb. 2008). Vol. 6913, p. 6913E. Bellingham, Washington: SPIE.

Simonetti, F., L. Huang, and N. Duric. Transmission and reflection diffraction tomography in breast imaging. 2008. In *The 2008 International Conference on Biomedical Engineering and Informatics.* (Sanya, Hainan, China, 27-30 May 2008). Vol. 2, p. 723. Washington, DC: IEEE Computer Society.

Simonetti, F., and L. Huang. From beamforming to diffraction tomography. 2008. *Journal of Applied Physics.* **103**: 103110.

# Surface Enhanced Raman (SERS) Based Flow Cytometry Detection

*Stephen K Doorn*

20060386ER

## Abstract

New advances in high throughput bioanalytical methods are required to address rapidly emerging needs for bio-threat detection, disease diagnosis, and new drug discovery. Flow cytometry approaches to these needs requires the use of spectral barcodes, or tags, for the detection and identification of targeted analytes using advanced multiplex techniques [1]. Such multiplexing is becoming increasingly important in bio-forensics and biothreat detection in that each requires rapid identification of agents and materials with high confidence/no false positives. We developed molecular spectroscopic barcodes that may provide a large library of unique signatures for flow-based analysis. Our unique signatures are based on nanoparticles that emit bright surface enhanced Raman (SERS) signals from glass-encapsulated surface-bound dye molecules for detection and identification. We also designed and developed the Raman-based instrumentation required for measurement of these tags in flow.

We met nearly all the goals we outlined in our original proposal. We have successfully developed a range of bright Raman spectral tags based on different nanoparticle architectures. The project has generated significant interest in the use of our spectral tags in security-related tagging applications.

## Background and Research Objectives

Rapid bioanalysis has become increasingly reliant on the use of so-called "smart signatures" that are essentially multiple responses that when combined together unambiguously identify a target agent. Simultaneous identification of the large number of such signatures required necessitates an advanced degree of multiplexing capability. Current approaches to multiplexing with fluorescent dyes are limited in the multiplexing "space" they can attain due to their broad, overlapping spectral responses. What is required is an orders of magnitude increase in capability that can only be obtained through use of narrower spectral signatures such as those found in Raman spectra.

The success of this project was dependent on development of appropriate SERS-active particles that emit the necessary brightness to be detected at rapid flow rates. We took three separate routes to design of these particles. These approaches seek to optimize particle brightness through control of plasmon resonance energies and through introduction of enhanced electromagnetic field locations (hot spots) through controlled particle aggregation. The project also required the development of first-ever Raman detection capability coupled to flow cytometry. The detection end incorporates two important innovations, both designed to reduce background autofluorescence from biosamples: incorporation of full-spectral phase-sensitive detection and use of excitation wavelengths in the red.

## Importance to LANL's Science and Technology Base and National R&D Needs

This project directly addresses DOE's goal of developing advanced functional nanomaterials. DOE is also interested in materials that function at the nano-bio interface. Our SERS materials will functionalize to bioanalytes at the nanoscale. We also address DOE's needs for development of new and sensitive methods and instrumentation for bioanalysis. On the national security side, we have generated strong interest from NA22 and NA24 in the potential use of our tags as signatures for authentication.

## Scientific Approach and Accomplishments

### Nanoparticle Development

Our core approach has been to generate SERS-active spectral tags through controlled aggregation of individual ~60 nm gold and silver nanoparticles. The basic aggregate geometry is to add a SERS-active dye molecule to the nanoparticle surface and functionalize them with an amino or mercapto silane, which will ultimately be used for initiating the growth of a stabilizing glass shell over the particle architecture. Production of these aggregates thus requires an understanding

and control over the competing surface equilibria of the dye and silane to create both bright and stable tags. For gold, the presence of the dye molecule also promotes aggregation of the particles and we have carried out an extensive study aimed at understanding and controlling the aggregation chemistry to optimize particle brightness. Our approach was to use metal-mediated fluorescence quenching of SERS dyes to measure surface areas occupied by both dyes and silanes, followed by examioning the obtainable SERS intensities as a function of both silane and dye loading. The result was the development of an aggregation "phase diagram" that demonstrates as dye surface concentration increases, SERS signal increases as a result of aggregate formation. At some peak concentration, further increases in dye disrupts aggregates and decreases SERS signal. Dye aggregation power can further be adjusted by degree of silane coverage. These results form the basis for rationally designing and controlling aggregated particles for the cytometry application. We have demonstrated the ability to glass-coat the aggregates and have performed studies that helped us balance the competing chemistries, for both amino and mercapto silanes. We currently find that the mercapto silane-based coating results in more stable particles.

In addition to the gold cores, we have pursued silver-based tags as a potentially brighter signature. We have developed a route to controlled aggregation of silver particles using salt additions. The salt aggregation approach was found necessary after we discovered that dye-induced aggregation was not extensive for silver. The aggregation chemistry was developed in parallel with a first-time demonstration of silver glass-coating chemistry. The resultant tags are

Are typically a factor of 10 or more brighter than our gold tags. Additionally, use of silver and control over its aggregation state allows us to tune the resonant plasmon frequencies throughout the visible and near-IR spectral regions. A schematic of the synthetic approach to both the Au and Ag-based spectral tags is shown in Figure 1. Details of their synthesis and characteristics are given in references [1] and [2].

We have also demonstrated the ability to obtain strong SERS signals from glass-coated aggregates with the use of a broad range of dyes. We currently have a multiplexed tag library of 90 dyes. Figure 2 shows a number of representative examples of the varying fingerprint spectra obtainable with this library. Given this large number of dyes, analytical approaches must be developed for rapid recognition of the different spectral signatures. To meet this need we have been applying a principle components analysis approach to defining the "barcodes" available from individual dyes. This recognition effort is also important in that we are using it to direct how we might make different combinations of the 90 different tags to exponentially expand the attainable signatures.

Plasmon resonance tunability has significant potential for allowing optimization of our SERS intensities, so this has been a further area of study. To that end, we have developed a capability for synthesis of glass-core/gold-shell particles with demonstrated SERS activity. By varying the relative thickness of the shell with respect to the diameter of the core, the plasmon resonance can be continuosly tuned from the visible into the near-IR, giving great versatility in useable excitation wavelengths. We have also synthesized related particles: hollow shell gold nanoparticles. These particles also have tunable plasmon resonances and their hollow nature provides an additional route for physical manipulation for flow analysis, which we are now investigating.

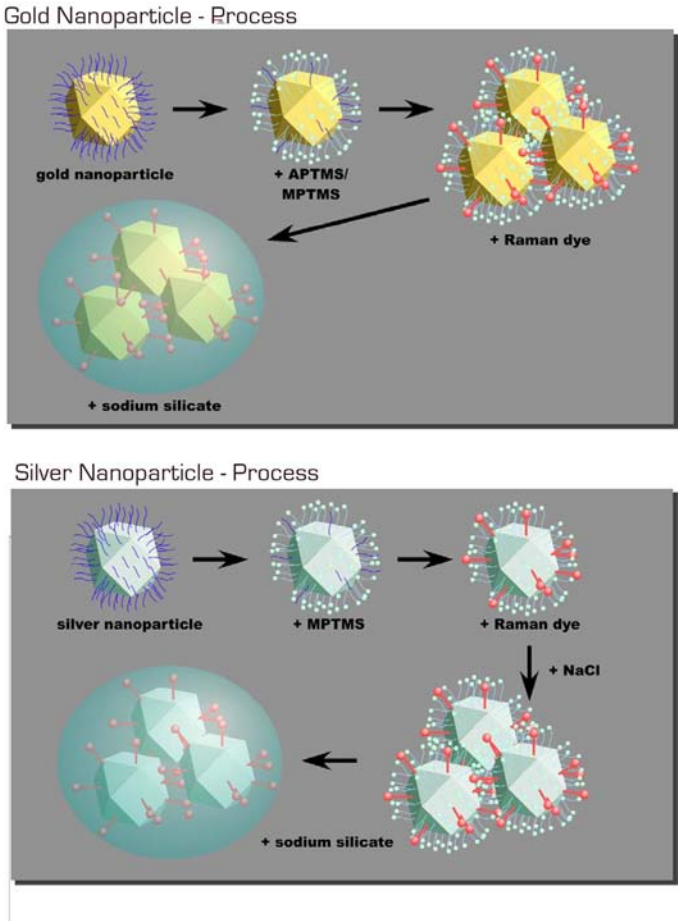


*Figure 1. Scheme of synthetic plan for generating gold and silver nanoparticle SERS spectal tags with glass coating for flow cytometry applications.*

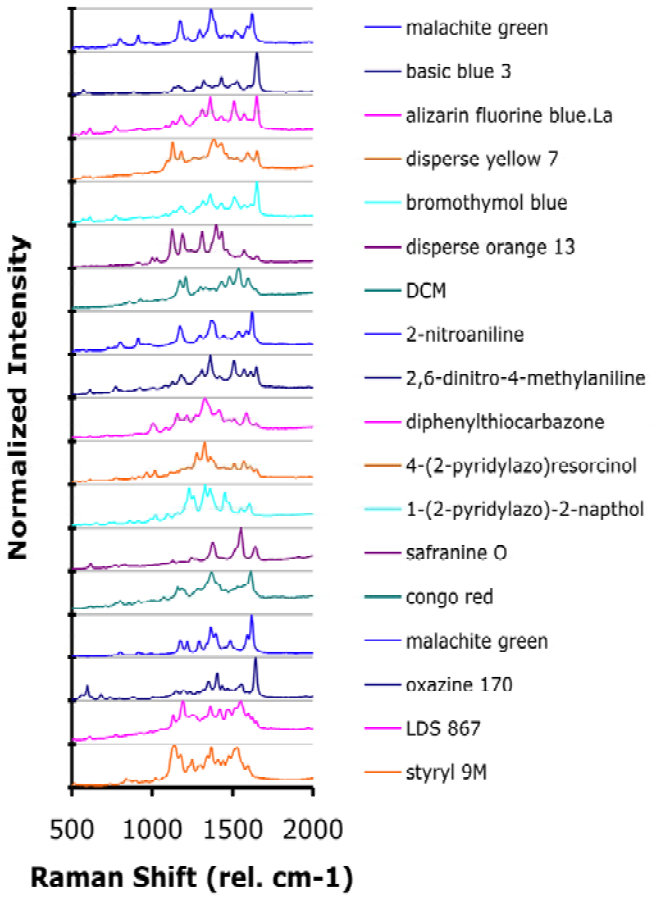


*Figure 2. Representative SERS fingerprint spectra for 18 different dye-tagged silver nanoparticle spectral tags.*

An extension of the nanoshell work includes generating particles that are labeled with a fluorescent dye. Plasmon absorbances in the nanoshell may be used to enhance the fluorescence emission of the particles if the relative geometries of the various particle components are chosen properly. We are currently investigating the possibility of fluorescently labeling the $SiO_2$ core prior to encapsulating with the Au shell. A dye can be incorporated into the $SiO_2$ particles by first functionalizing an amine reactive dye with an amine terminated silane. This reaction yields a dye that readily incorporates into the $SiO_2$ matrix as the glass core particles begin to form, and does not affect the subsequent functionalization steps required for Au shell growth. These hybrid fluorescent/SERS active particles are currently being tested in our flow cytometry test bed for simultaneous fluorescence and Raman detection. One final variation on the nanoshell work is our current effort at hybridizing magnetic nanoparticles with plasmonic/SERS functionality. The combined magnetic/SERS functionality will provide a route to new modes of particle manipulation for both advanced flow techniques and for tuning interparticle interactions for studying the fundamentals of SERS hotspot generation. These efforts have also successfully led to a new LDRD project aimed at combining plasmonic behavior in a photonic lattice in an approach that will be enabled by these magnetic core particles. The variety of nanoparticle types we have developed are illustrated in Figure 3.

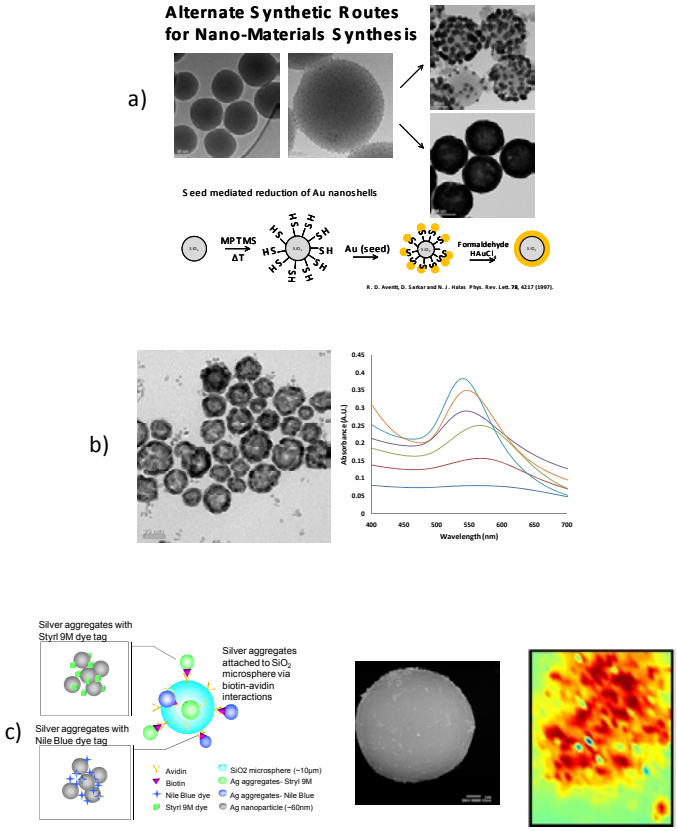


*Figure 3. Examples of additional nanoparticle spectral tag development. a) scheme for production of and transmission electron microscope (TEM) images of particles along pathway to synthesis of silica-core/gold-shell SERS tags. b) TEM image of hollow gold nanoshells and plasmon spectra demonstrating tunability of resonance. c) Depiction, TEM image, and SERS spectral image of a SERS multiplexed tag particle.*

To make the above particle types functional for bioanalytical applications requires conjugation to bioreceptor ligands. We have generated the capability to conjugate both biotin and carboxylate functional groups on the glass-coated surfaces of our SERS tags. Carboxylated tags in particular will allow binding to ammine groups, facilitatin the use of the tags for protein-based assays. The biotin functionalities have facilitated the performance of in-flow tests of the tags by binding them to support beads via the biotin-avidin interaction. This interaction has also been used as route to developing a higher degree of multiplexing capability as well.

Our spectral signatures can be multiplexed to a much higher degree by combining muliple dyes on a given tag—with the combined signatures effectively generating a new unique tag. Doing this at the single nanoparticle level

is difficult because of the same competing surface chemistries that were encountered in optimizing the glass-coating chemistry. Our approach is to instead combine different nanoparticle tags onto a single support particle via the biotin-avidin binding chemistry. We have demonstrated this ability and have also shown that the resulting spectral signatures are simple linear combinations of individual spectra, determined by the starting ratio concentrations of tag mixtures we use to generate the final encoded beads. Example nanoparticle structures and spectra from this approach are shown in Figure 3.

**Development of a Full-Spectral Detection Capability for Flow Cytometry**

In parallel to the particle development, it is necessary to create new instrumentation capable of in-flow, full-spectral detection with a sensitivity capable of measuring individual tags in the 10s to 100s of microsecond transit times typically used in flow cytometry. The full-spectral goal is required in order to exploit all the detail available within our Raman fingerprint signatures. To date, we have designed and built a system capable of measuring spectra from 1-6 tags passing through the interrogation volume in a 25 μs transit time. Our system (schematically depicted in Figure 4) is constructed around a BD FACSCalibur optical platform flow chamber and fluorescence/light scatter collection optics. Crossed cylindrical lenses are used to focus laser excitation to an ellipse approximately 50 mm wide by 12 mm high. Collected signal is focused onto a Holospec HS-f/2.2-Vis spectrograph, which disperses the light over the face of a thermo-electrically cooled electron multiplied 1600x200 pixel Andor Newton CCD array. The light is incident on approximately 75% of the height of the CCD to assure efficient light collection. The columns of the CCD chip are summed vertically on-chip to increase effective pixel size, and thereby collection efficiency. The CCD array is interfaced directly to a data acquisition program. Our CCD array was chosen for its inherent quantum efficiency, which exceeds 80% for the wavelength region of 500 to 800 nm and low noise characteristics of less than 10 e-/pixel/exposure.

Previous Raman flow cytometry measurements, while showing the feasibility of making such measurements in flow [4], were limited in ability to resolve single spectral tag particles. Through use of serial dilution studies on our spectral tags, we have demonstrated the ability to isolate the signature from as few as 1-2 tags per triggered event (in experimentally relevant microsecond timescales). An example spectrum from one such event is shown in Figure 5 and indicates the degree of detail and signal to noise obtainable with our instrumentation. An overlay of 100 individual events (also in Figure 5) indicates that spectra from individual tags are relatively uniform. Similarly, we have demonstrated the ability to simultaneously measure fluorescent tags generated in our core-shell approach and are able to trigger data acquisition from such events. In continuing work, we will be focusing on improving our spectral resolution to take full advantage of the detailed signatures of our tags and combine the full spectral capability with our development of phase sensitive rejection of background signals.

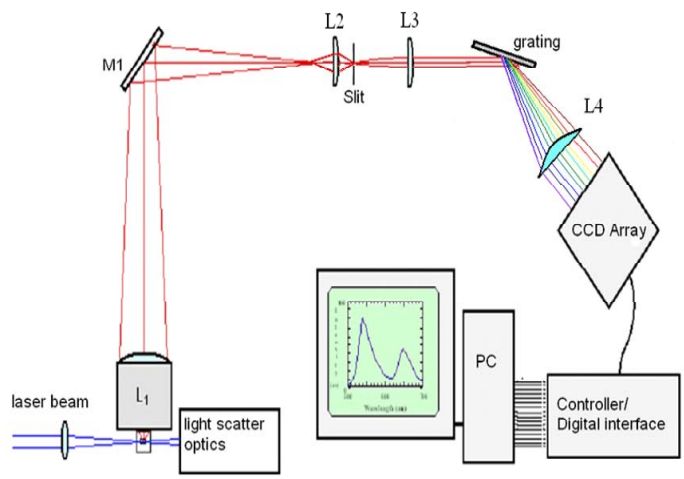


*Figure 4. Schematic depiction of the Raman Flow Cytometer. Laser excitation is focused onto the sample in flow, with SERS signal being collected by lens L1, transferred to spectrograph (grating and lens L4) and imaged at EMCCD array.*

**Phase Sensitive Background Rejection**

We have also developed a Phase-Sensitive Flow Cytometry (PSFC) system that measures radio-frequency modulated fluorescence from cells, beads, or other particles as they rapidly pass through a tightly focused laser source. Background autofluorescence can thus be rejected from signals of interest using this approach. In this system, particles are syringe pump injected at a flow rate of 5 to 50 microliters/min and subsequently hydrodynamically focused within a standard flow cytometry chamber. Typically, thousands of particles/minute are passed through the laser beam at this rate. The PSFC is designed to collect frequency-domain data based on a homodyne mixing platform in which a modulated, phase-shifted reference signal is mixed at the same frequency as the detected fluorescence signal. An argon-ion laser with an electro-optic modulator (or a NIR laser diode) is modulated by a Hewlett Packard frequency synthesizer that generates a 1-MHz to 1-GHz input signal. Phase-shifted and amplitude-attenuated fluorescence is emitted from the cell or particle and focused at 90° from excitation onto the window of a photomultiplier tube (PMT). Through modulation of the laser frequency and comparison to two 90 degree out-of-phase reference sig-

nals, the collected fluorescence signals are processed in the frequency-domain and allow for phase-filtering of different signal components. For example, a sample with two unique lifetimes can be discriminated by nulling the phase shift of one signal to home in on the second component's lifetime. We have demonstrated nulling of signals associated with lifetimes of 3.5 and 5 ns. Particle sensitivities are now at 200 particles (as determined by fluorescence calibrations on serially diluted particles) with the PMT system. We anticipate approaching single-tag sensitivities by moving to the EMCCD detection. Additionally, our next immediate step will be to move to demonstration of discrimination of Raman from fluorescence backgrounds and finally coupling capability to excitation and acquisition sources of the full-spectral cytometer.

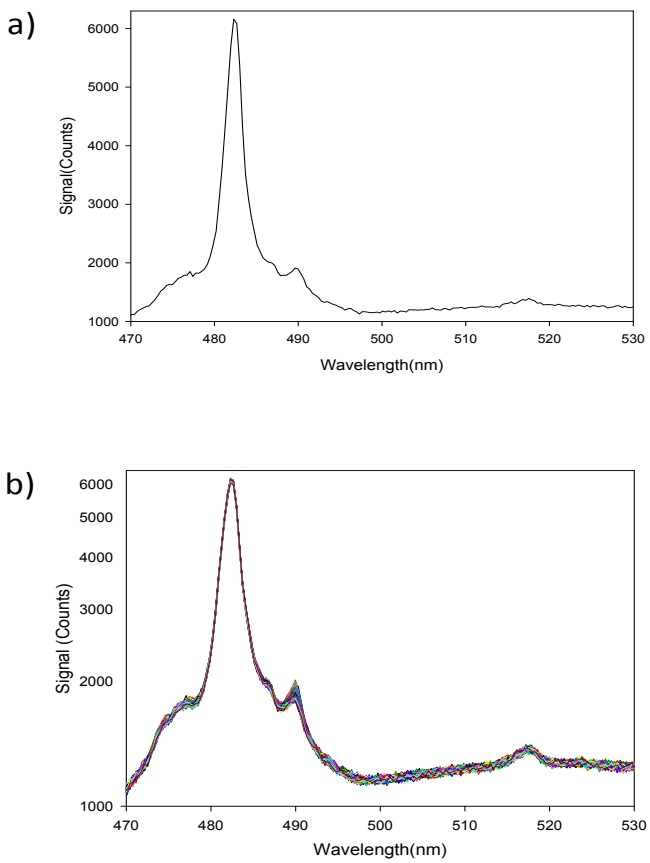


*Figure 5. a) SERS spectrum obtained in flow of a single nanoparticle spectral tag. b) Overlay of 100 spectra from separate SERS tag particles. Demonstrates uniformity in spectral signatures obtainable from individual tags.*

In summary, we have met nearly all the goals we outlined in our original proposal. Our bright Raman spectral tags have allowed us to develop the full-spectral in-flow detection instrumentation required to start incorporating the tags into real bioanalytical applications. As a result of the efforts within this project, this capability is recognized as an important future growth area for LANL's NIH Flow Resource. The resource will be helping to support final development of the full-spectral instrumentation. In particular, we will be working with the Resource to integrate the phase sensitive filtering with the Raman detection capabilities. Additionally, the project has generated significant interest in the use of our spectral tags in security-related tagging applications. As one example, we have generated strong interest from NA22 and NA24 in the potential use of our tags as signatures for authentication and seals and anticipate this as a future funding source. Finally, this effort has also provided a solid foundation for pursuing further studies on plasmonic-based sensing and materials. We have used some of our particle developments to serve as the core of a new LDRD effort starting this year aimed at integrating plasmonic functionality with photonic lattices.

## References

1. Nolan, J. P., and L. A. Sklar. Suspension array technology: evolution of the flat-array paradigm. 2002. *Trends in Biotechnology.* **20**: 9.

2. Brown, L. O., and S. K. Doorn. Optimization of the preparation of glass-coated, dye-tagged metal nanoparticles as SERS substrates. 2008. *Langmuir.* **24**: 2178.

3. Brown, L. O., and S. K. Doorn. A controlled and reproducible pathway to dye-tagged, encapsulated silver nanoparticles as substrates for SERS multiplexing. 2008. *Langmuir.* **24**: 2277.

4. Watson, D. A., L. O. Brown, D. F. Gaskill, M. Naivar, S. W. Graves, S. K. Doorn, and J. P. Nolan. A fow cytometer for the measurement of Raman spectra. 2008. *Cytometry.* **73A**: 119.

## Publications

Brown, L. O., and S. K. Doorn. Optimization of the preparation of glass-coated, dye-tagged metal nanoparticles as SERS substrates. 2008. *Langmuir.* **24**: 2178.

Brown, L. O., and S. K. Doorn. A controlled and reproducible pathway to dye-tagged, encapsulated silver nanoparticles as substrates for SERS multiplexing. 2008. *Langmuir.* **24**: 2277.

Diebold, E. D., N. H. Mack, S. K. Doorn, and E. Mazur. Femtosecond laser nanostructured substrates for surface-enhanced Raman scattering. To appear in *Langmuir.*

Watson, D. A., L. O. Brown, D. F. Gaskill, M. Naivar, S. W. Graves, S. K. Doorn, and J. P. Nolan. A flow cytometer for the measurement of Raman spectra. 2008. *Cytometry.* **73A**: 119.

# Processing of Ultra-High Strength Electrical Conductors using a Novel Nano-Twinned Structure

*Amit Misra*

20060392ER


## Abstract

Traditional engineering approaches to develop high strength materials always result in poor electrical conductivity. We have developed a physical vapor deposition based processing approach to produce metals such as copper that exhibit over an order of magnitude increase in mechanical strength with insignificant loss in electrical conductivity. These materials have a unique structure composed of a layered arrangement of nanometer spaced boundaries known as twin boundaries where the twinned portion of the crystal is a mirror image of the parent crystal. This report describes the first ever attempt of controlled processing of metals having parallel-oriented, nano-twinned structures. The findings of this research will have significant impact in the manufacturing of multi-functional materials for a variety of mechanical, electrical and nuclear engineering applications such as high-strength electrical conductors for high field magnets and power transmission lines; high-strength, high corrosion or erosion resistance materials, etc.


## Background and Research Objectives

Engineering applications involving high-field magnets and electrical power transmission are central to critical LANL missions of energy security, weapons, and homeland defense. These applications require multi-functional materials that possess both high mechanical strength and high electrical conductivity. Unfortunately, the material properties of high electrical conductivity and high mechanical strength have opposing requirements. The best electrical conductors are very pure metals, e.g., aluminum (Al), copper (Cu), silver (Ag) since any impurity atoms, and other lattice defects such as dislocations, stacking faults and grain boundaries scatter electrons and result in lower conductivity. However, pure metals tend to be mechanically very soft, with the exception of carefully synthesized "perfect crystals" in the form of thin whiskers that due to their limited shapes and sizes and high production costs are not suitable as engineering materials.

Metallurgists have developed a number of practical methods to improve the strength of metals, such as adding impurity atoms (solid-solution strengthening), cold working (creation of stored dislocations via plastic deformation), grain size refinement and composites. A common feature in all these strengthening methods is the addition of point, line or planar defects in the material that cause strengthening by resisting the motion of dislocations but also serve as scattering centers for electrons, thereby reducing the electrical conductivity.

This exploratory research is built upon a LANL discovery [1] of nanotwinned structure in certain face-centered cubic (fcc) metals processed via sputter deposition. Twin boundaries are a special kind of low-energy, high-symmetry grain boundaries such that the twinned portion of the crystal is a mirror image of the parent crystal. While twins have been reported before in shock-loaded [2], vapor-deposited [3] and electrodeposited materials [4], the novelty of the structure discovered by us are: (i) average twin spacing of only 2-4 nm, and (ii) preferred orientation such that all twin planes are normal to the growth direction [5]. This property enables tailoring the orientation of the microstructure to the desired direction of highest conductivity.

The key objectives of this research are to explore: (i) experimentally and theoretically, the processing and material parameters that produce layered, nanotwinned structures in metals, and (ii) the correlations between the nanotwinned structures and the electrical and mechanical properties.

## Importance to LANL's Science and Technology Base and National R & D Needs

This project supports the following missions. (i) The LANL grand challenge on *Fundamental Understanding of Materials*, specifically the "*ability to design, assemble and fabricate materials and material systems with specific functionality*"; (ii) DOE's energy security

mission. A recent Office of Science report on *Nanoscience Research for Energy Needs* specifically cites "*power transmission lines capable of 1 gigawatt transmission*", and "*super-strong, light-weight materials to improve efficiency of cars, airplanes, etc*" as key technological challenges in energy security where nanoscience can have the greatest impact.

## Scientific Approach and Accomplishments

### Synthesis and Microstructures

High deposition rate (around 3 nm/s) magnetron sputtering was used to synthesize Cu foils with total thickness ranging from 1 to 30 micrometers. Transmission electron microscopy (TEM) was used to characterize the microstructure of the as-deposited Cu foils. As shown in the cross-section TEM image in Figure 1a, along with the corresponding selected area diffraction pattern in the inset, sputter-deposited Cu exhibits a {111} fiber texture along the growth direction and an average columnar grain size that varied from 43 to 80 nm with deposition rates from 1.8 to 3 nm/s, respectively. Figure 1a also shows an extremely high density of planar defects within the columnar grains.

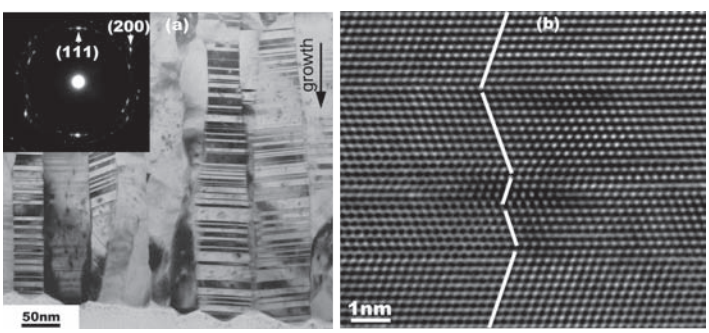


*Figure 1. (a) Bright field transmission electron microscopy (TEM) image and (b) high-resolution TEM image showing the nanotwinned structure of sputter deposited copper.*

High-resolution TEM (HRTEM) imaging of these planar defects revealed these to be {111} twin interfaces separated by a few nanometers (Figure 1b). Most growth-induced twin interfaces are parallel to the film surface. Some planar faults were identified to be stacking faults. Statistical measurement of the twin thickness and spacing from several TEM images indicate that the average twin thickness is 4 nm, whereas the average spacing between adjacent twins is also on the same order, about 5 nm. Overall the size distribution was very narrow for both twin thickness and spacing, with very few twins exceeding 10 nm dimensions. In a different approach, we synthesized epitaxial nanotwinned Cu films on hydrofluoric acid cleaned silicon substrates. In these films, the column boundaries shown in Figure 1a did not exist, so the Cu matrix was essentially single crystalline. The polycrystalline films with nanometer-scale columns are referred to as nanocrystalline (nc) nanotwinned (nt) Cu and the epitaxial Cu films with nanotwins are referred to as epi-nt Cu.

Several uni-axial tensile tests were performed on free-standing 20 micrometers thick nc, nt Cu foils. The results were very reproducible and the average value of the ultimate tensile strength was 1.2 GPa, over an order of magnitude higher than bulk single crystal pure Cu. The hardness, as measured by nanoindentation, was 3.5 GPa. In spite of the ultra high tensile strength, the fracture surface of nanotwinned Cu showed typical ductile dimples as examined by scanning electron microscopy. Most dimples had diameters of one micron or less, much larger than the columnar grain diameters of around 40-80 nm.

Twin boundaries with spacing on the order of a few nanometers pose a significant barrier to the transmission of dislocations. Molecular dynamics (MD) simulations were performed to study the interaction of glide dislocations with a twin boundary in a fcc crystal modeled with embedded-atom-method potentials (Figure 2a). Under applied pure shear, Figure 2b, a resolved shear stress of 1.7 GPa is needed to transmit a glide dislocation across the twin interface onto the complementary {111} glide plane in the neighboring crystal, leaving behind a residual dislocation at the twin boundary. In a different simulation (Figure 2c), the slip transmission was studied under tensile loading.

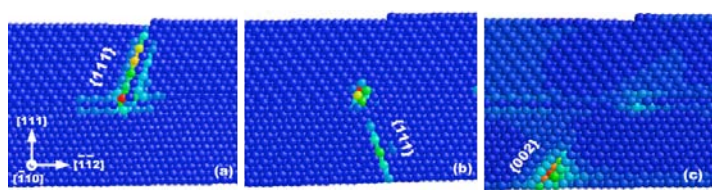


*Figure 2. Molecular dynamics simulation of the transmission of a single glide dislocation across a symmetric (111) twin boundary. (a) A glide dislocation is introduced on one side of the twin boundary without any applied stress. (b) The model is subject to stresses such that when the resolved shear stress on the dislocation exceeds 1.7 GPa, the dislocation moves away from the twin interface. A partial dislocation remains at the interface. (c) In response to a biaxial stress (in a plane parallel to the interface) that exerts a resolved shear stress of 3 GPa, a dislocation moves away from the twin interface into the lower grain on a {200} plane, leaving a partial dislocation at the interface.*

For applied tension parallel to the interface, the force acting on a glide dislocation has the wrong sign to move it away from the boundary on the {111} slip plane in the

adjacent crystal. Thus, slip is observed to transmit onto the {200} plane, a non-typical glide plane in fcc, at a resolved shear stress of approximately 3 GPa. MD simulations thus indicate that the inherent strength of the twin interface to the transmission of single dislocations is rather high. A single dislocation was considered in this simulation since a dislocation pile-up is unlikely at twin lamellae thickness of 5 nm or less. The simulations shown in Figure 2 compute an upper bound estimate of the barrier strength of twin boundaries to slip transmission in the absence of dislocation pile-ups.

Thermal stability of nano-twinned Cu was investigated using high-vacuum annealing up to 800 °C for 1 hour. Average twin lamellae thickness increased gradually from approximately 4 nm for as-deposited films to slightly less than 20 nm after annealing at 800 °C. The average columnar grain size, on the other hand, increased rapidly from approximately 50 nm for as-deposited to 500 nm for Cu annealed at 800 °C. Figure 3 shows the cross-section TEM images of annealed samples. Note the twin lamellae thickness of approximately 20 nm and the column width on the order of 500 nm in a sample annealed at 800 °C. High-resolution imaging of the column grain boundary showed that the twins in the adjacent grains are misoriented by a small angle of 9°. Overall there is a much higher driving force to reduce the large energy of the high-angle columnar grain boundaries than the low-energy coherent twin boundaries.

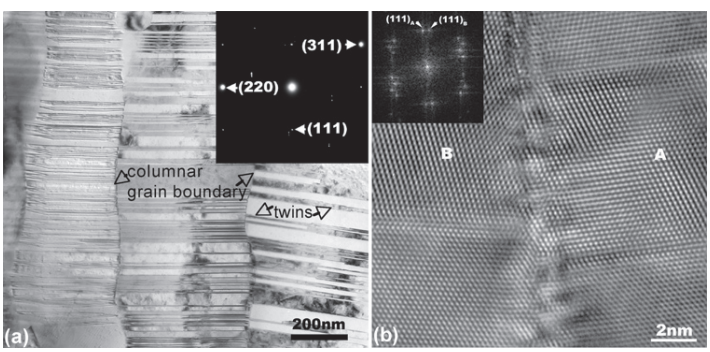


*Figure 3. (a) TEM image showing that the nanotwinned structure in Cu is retained even after annealing at 800 °C for 1 hour. The vertical boundaries represent columnar grains. (b) High-resolution TEM image showing that the nanotwins labeled A and B in adjacent columnar grains are misoriented by a small angle of 9°. The insets in (a) and (b) are the corresponding selected area diffraction patterns.*

The mechanical and electrical properties of the annealed films were characterized and correlated with the columnar grain size and twin lamellae thickness. In spite of an order of magnitude increase in the columnar grain size, the annealed films retained a high hardness of 2.2 GPa, reduced from 3.5 GPa in the as-deposited state. The high hardness of the annealed films is interpreted in terms of the thermally stable nanotwinned structures. In other words, the twin boundaries present strong barriers to slip transmission, and as long as the twin lamellae thickness is on the order of a few to a couple tens of nanometers to suppress dislocation pile-ups, the high hardness of nanotwinned materials will be maintained. The room temperature electrical resistivity of nanotwinned Cu dropped from 28 microOhm-cm in the as-deposited state to 3.7 microOhm-cm after 800 °C anneal. This shows that the high-angle column grain boundaries are strong scattering sites for electrons, and so a reduction in the number of these boundaries leads to lower resistivity. Electron scattering is weak at low-angle coherent twin boundaries, so in spite of nanometer-spaced twins, there is low contribution to resistivity from twins. The effects of annealing on the twin and column dimensions, electrical resistivity and hardness are summarized in Figure 4.

| Nanotwinned Cu | Avg lamellar thickness, nm | Hardness, GPa | Resistivity, μΩ cm | Avg grain size, nm |
|---|---|---|---|---|
| As deposited | 4.4 | 3.8 | 28 | 43 |
| Annealed 200°C-1hour | 7.1 | 3.4 | 17.9 | 125 |
| Annealed 400°C-1hour | 7.7 | 3.3 | 7.5 | 232 |
| 600°C-1hour Annealed | 9.5 | 2.9 | 4.9 | 320 |
| 800°C-1hour Annealed | 16.3 | 2.4 | 3.7 | 544 |

*Figure 4. Summary of the effects of annealing on the twin and column grain dimensions, electrical resistivity and hardness.*

The epi-nt Cu films exhibited the best combination of high strength and high electrical conductivity. At 300 K, the resistivity of epi-nt Cu films (1.7 microOhm-cm), with an average twin spacing of 16 nm, was only 10% higher than the resistivity of oxygen-free high-conductivity Cu (1.58 microOhm-cm). By comparison the strength of over 1000 MPa of epi-Cu was over an order of magnitude higher than bulk oxygen-free high-conductivity Cu (< 100 MPa). Overall, the epitaxial nanotwinned Cu films possess the highest ratio of the mechanical strength to electrical resistivity at 300 K in metals.

## References


1. Zhang, X., A. Misra, and R. G. Hoagland. Nanoscale-twinning-induced strengthening in austenitic stainless steel thin films. 2004. *Applied Physics Letters.* **84** (7): 1096.

2. Murr, L. E.. Contribution of deformation twins to yield stress. 1978. *Scripta Metallurgica.* **12** (11): 1031.

3. Yu, D., and F. Spaepen. The yield strength of thin copper films on Kapton . 2004. *Journal of Applied Physics.* **95** (6): 2991.

4. Shen, Y. F., L. Lu, and K. Lu. Tensile properties of copper with nanoscale twins. 2005. *Scripta Materialia.* **52** (10): 989.

5. Zhang, X., A. Misra, and R. G. Hoagland. Enhanced hardening in Cu/330 stainless steel multilayers by nanoscale twinning. 1004. *Acta Materialia.* **52** (4): 995.


## Publications


Anderoglu, O., A. Misra, F. Ronning, M. F. Hundley, and X. Zhang. Epitaxial nanotwinned Cu films with high strength and high conductivity. 2008. *Applied Physics Letters.* **93** (8): 083108.

Anderoglu, O., A. Misra, F. Ronning, and X. Zhang. Microstructures and electrical properties of epitaxial nanotwinned Cu films. *Journal of Applied Physics.*

Anderoglu, O., X. Zhang, and A. Misra. Thermal stability of sputtered Cu films with nanoscale growth twins . 2008. *Journal of Applied Physics.* **103** (9): 094322.

Misra, A.. Twinning in nanometals. 2008. *JOM- A Publication of the Minerals, Metals and Materials Society.* **60** (9): 59.

Zhang, X., A. Misra, M. F. Hundley, and R. G. Hoagland. Thermal stability of sputter-deposited 330 austenitic stainless-steel thin films with nanoscale growth twins. 2005. *Applied Physics Letters.* **87** (23): 233116.

Zhang, X., A. Misra, and R. G. Hoagland. Effects of deposition parameters on residual stresses, hardness and electrical resistivity of nanoscale twinned 330 stainless steel thin films. 2005. *Journal of Applied Physics.* **97** (9): 094302.

Zhang, X., O. Anderoglu, R. G. Hoagland, and A. Misra. Nanoscale growth twins in sputtered metal films. 2008. *JOM- A Publication of the Minerals, Metals and Materials Society.* **60** (9): 75.

Zhang, X., O. Anderoglu, and A. Misra. Influence of deposition rate on the formation of growth twins in sputter-deposited 330 austenitic stainless steel films . 2007. *Applied Physics Letters.* **90** (15): 153101.

Zhang, X., and A. Misra. High-strength sputter-deposited Cu foils with preferred orientation of nanoscale growth twins. 2006. *Applied Physics Letters.* **88** (17): 173116.

# Stabilization of Hydrogen Clathrates: Engineering a Solution to Hydrogen Storage

*Yusheng Zhao*

20060416ER


## Abstract

Ever-increasing fossil energy consumption and associated global environmental concerns have provoked intensive searches for alternative energy resources including hydrogen. A major challenge for using hydrogen is to develop suitable materials to store it under a variety of application conditions. One class of promising materials is novel inclusion compounds that consist of three-dimensional frameworks of hydrogen-bonded $H_2O$ molecules (hydrate clathrate) or metal cations and organic linkers (metal-organic frameworks) with hydrogen molecules trapped inside their cages. We have constructed a high-pressure low-temperature apparatus for synthesis of hydrates in the laboratory and have developed an extremely fast way to synthesize hydrogen clathrate in a matter of minutes, with excellent reversibility. We have investigated the dynamics of hydrogen in the ternary clathrate formed from water, THF, and hydrogen using neutron scattering. Moreover, we have designed and synthesized a number of new metal-organic frameworks (MOFs) with novel cage/channel-topologies for hosting large quantities of hydrogen. We applied shape-, size-, and bonding-selectivity rules to separation/capture of hydrogen and by-product gases (such as $CO_2$, $H_2S$ and $NO_x$) associated with fossil fuel use. Our studies have provided important insights into effective separation and encapsulation, storage capacity, phase stability and engineering kinetics of formation and degassing of these materials, which are critical issues in tackling the top technological challenges facing the hydrogen economy.


## Background and Research Objectives

Alternative energy resources including hydrogen are becoming increasingly important for the future economy. A major challenge for using hydrogen is to develop suitable materials to store it under a variety of conditions, which requires systematic studies of the structures, stability, and kinetics of various hydrogen-storing compounds. The recent discovery of hydrogen-containing clathrate hydrate presents a completely new technological means for hydrogen storage [1-2]. The ice-like polyhedral framework of clathrate hydrate can hold substantial amounts of guest molecular hydrogen. We have designed an extremely fast way for the clathrate synthesis to induce complete hydrogen hydrate formation in a matter of minutes, with excellent reversibility [3]. The high energy content and fast kinetics are advantages that make hydrogen clathrate an excellent candidate material for hydrogen storage. However, the pure hydrogen clathrates occur only at low temperatures or/and high pressures. One aim of this project is to synthesize hydrogen clathrates at larger scales and at practical temperature/pressure conditions. Another aim is to explore design and synthesis of another type of framework materials, MOFs, for hydrogen storage. In this work, we have employed multiple experimental techniques such as chemical synthesis, neutron diffraction, thermal and gas adsorption analyses, to tackle the related issues in a comprehensive and integrated manner.

## Importance to LANL's Science and Technology Base and National R & D Needs

This project directly addresses LANL's mission in Nation Energy Security via providing underpinning science and technology for hydrogen economy and related environmental issues. This work is also tied to the lab's grand challenge in "*Fundamental Understanding of Materials*" through enhancing the *"ability to design, assemble and fabricate materials with special functionality."*

## Scientific Approach and Accomplishments

### Hydrate Clathrates

To utilize clathrates for hydrogen storage and other applications, we have constructed and tested a high-pressure low-temperature system for synthesis of hydrate clathrates in the laboratory. This apparatus can be used to prepare clathrate samples in large quantities and with various gas molecules such as hydrogen and carbon dioxide. The samples can then be loaded into pressure cells for neutron diffraction experiments. Com-

pared to *in situ* synthesis in the neutron beam, this method reduces the time needed in the neutron beam, and, additionally, portions of the samples can be used for other analyses such as scanning electron microscopy, mass spectrometry, IR and Raman spectroscopy and X-ray diffraction. A methane–ethane clathrate sample has been prepared using this apparatus over 26 h with a temperature range of 254–290 K and a pressure range of 20–35 MPa. The sample was then measured at the HIPPO (high-pressure preferred orientation) beamline of Los Alamos Neutron Science Center (LANSCE) at 200 K and ambient pressure. The obtained neutron diffraction data was analyzed using the Rietveld method (Figure 1), yielding lattice parameters, atomic position, atomic displacement parameters and methane/ethane ratio. The gas concentrations (methane 82.93 wt%, ethane 17.07 wt%, normalized) were also measured by gas chromatography, which varied slightly from the initial gas of 80 wt% methane and 20 wt% ethane [4].

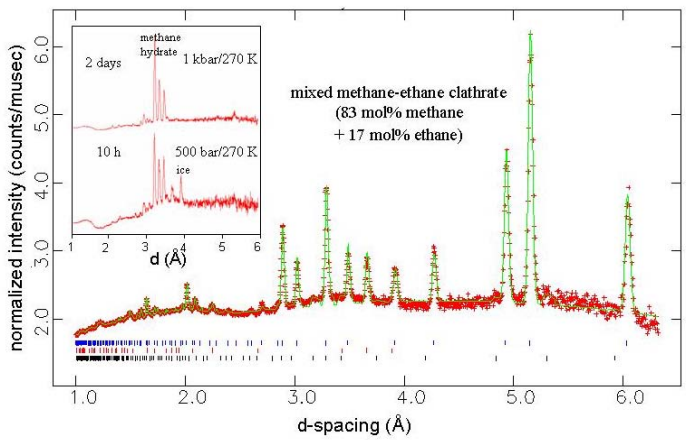


*Figure 1. Fitted neutron diffraction pattern of a mixed methane–ethane sI clathrate (82.93 wt% methane and 17.07 wt% ethane) with minor sII phase and D2O ice. Data are shown as red plus signs, and the green curve is the best fit to the data. Tick marks below the pattern show the positions of allowed reflections (blue, sI phase; red, ice; black, sII phase). P-T, pressure-temperature. (Inset) Neutron patterns of methane clathrate formed from ice and D2 in situ in the Al pressure cell. Note that formation of methane clathrate was not complete even after 10 h at 500 bars and 270 K, indicating sluggish formation kinetics compared with hydrogen clathrate.*

Although pure hydrogen clathrate can only exist at low temperatures or/and high pressures, addition of certain molecules such as tetrahydrofuran (THF) can extend its stability to ambient conditions [5, 6], a key step toward practical applications. We have investigated the dynamics of hydrogen in the deuterated ternary clathrate formed from water, THF, and hydrogen, using inelastic neutron scattering [7]. The results show that the quantum rotor states are only perturbed to a small extent upon adsorption, while the translational quantum states are significantly modified by confinement in the clathrate cage. More specifically, the adsorbed hydrogen has three rotational excitations at about 14 meV in both energy gain and loss. These transitions could be unequivocally assigned since there was residual orthohydrogen at low temperatures, resulting in an observable J = 1→0 transition at 5 K. A doublet in neutron energy loss at about 28.5 meV is interpreted as J = 1→2 transitions. In addition to the transitions between rotational states, there are a series of peaks that arise from transitions between center-of-mass translational quantum states of the confined hydrogen molecule. A band at approximately 9 meV can be unequivocally interpreted as a transition between translational states, while broad features at 20, 25, 35, and 50-60 meV are also interpreted to as transitions between translational quantum states.

**Meta-organic frameworks**

To develop other framework materials for hydrogen storage, we have synthesized a number of metal-organic frameworks (MOFs) using various organic ligands and hydrothermal/solvothermal methods. High-quality crystals of these compounds were grown, and their structures were solved with single-crystal X-ray diffraction (XRD). One of the new MOFs we synthesized is a helical double-layered Co(II)-organic framework comprised of [CoII4(*m3*-OH)$_2$] clusters linked by an asymmetric flexible ligand 3,4-PBC (Figure 2) [8]. This novel cobalt(II)-organic framework with the formula $[Co_2(OH)(3,4\text{-PBC})_3]_n$ was prepared via reaction of CoO with an unsymmetrical pyridylbenzoate ligand, 3-pyrid-4-ylbenzoic acid (3,4-PBC). Specifically, CoO (18.7 mg, 0.25 mmol) and 3-pyrid-4-ylbenzoic acid (99.6 mg, 0.5 mmol) were put into $H_2O$/dimethylformamide (4/4 mL) in a 23 mL Parr Teflon-lined stainless steel vessel and were heated at 105 °C for 72 h. Single-crystal XRD reveals that this compound crystallizes in the monoclinic space group $P2_1/c$. Its structure and composition were further confirmed by powder XRD, elemental analysis, infrared (IR) spectroscopy, and thermogravimetry analysis (TGA). X-ray crystallographic analysis shows that, in the asymmetric unit of this MOF, there are two $Co^{II}$ atoms, three 3,4-PBC ligands, and one $\mu_3$-OH group (Figure 2). O7 is coordinated to three Co atoms and has a bond valence sum of 0.95 based on the bond lengths of Co-O [1.9950(9), 2.0621(9), and 2.1824(9) Å]. This value suggests that O7 may combine with H, forming a hydroxyl group, which is consistent with the strong OH stretching found in the IR spectrum. In this structure, two different types of Co atoms can be distinguished, Co1 and Co2. Co1 is coordinated by three carboxylate O atoms [O4, O(5a), and O1], one N atom from four 3,4-PBC ligands, and two $\mu_3$-OH groups, forming a distorted $CoO_5N$ octahedron, while Co2 is ligated by three 3,4-PBC O atoms, one 3,4-PBC N atom, and one $\mu_3$-OH group to fur-

nish a distorted $CoO_4N$ trigonal bipyramid. The bond angles between the cis ligands and the Co1 center range from 82.99(4) to 97.77(4)°, whereas the bond angles between the cis ligands and the Co2 center range from 84.43(4) to 127.43(3)°. The Co-O and Co-N distances are all within the normal range found in other reported experiments. In addition to its structural novelty, this phase exhibits a significant overall antiferromagnetic behavior as revealed by our magnetic susceptibility measurements.

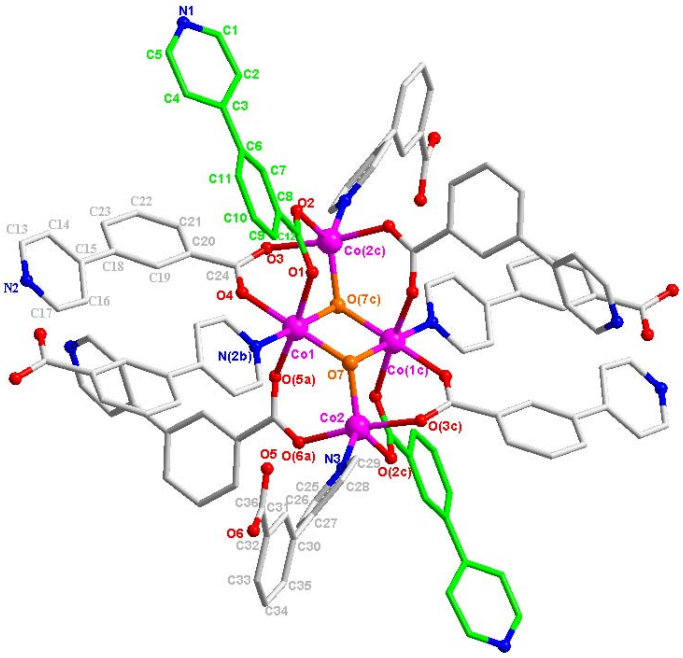


*Figure 2. Coordination environments of the CoII ions in [Co2(OH)(3,4-PBC)3]n.*

Other MOFs we have newly designed include 1) two copper(II)-organic frameworks, synthesized using 3-pyrid-4-ylbenzoic (3,4-PBC) and 3-pyrid-3-ylbenzoic (3,3-PBC) acid, which have a 2-fold helical square grid network and a double-stranded chain structure, respectively; 2) Two supramolecular isomers of cobalt-organic frameworks, assembled by a flexible pyridylbenzoate ligand (3,3-PBC), with different torsion angles between the pyridine and benzene rings in the ligand; 3) A series of microporous frameworks composed of rare earth metal ions and the benezentricarboxylate ligand; 4) A 3-dimensional framework with large pores consisted of $Eu^{3+}$ and the long-bridging ligand, dipenyldicarboxyalte, where the $Eu^{3+}$ ions are bridged by the carboxylate groups, forming $[Eu(COO)_2]_n$ chains. In particular, we successfully synthesized a porous rare-earth metal-organic framework, $Y(BTC)(H_2O)\cdot 4.3H_2O$ (H3BTC = 1,3,5-benzenetricarboxylate), using the solvothermal reaction. The dehydrated sample exhibits permanent porosity, selective gas adsorption, and good $H_2$ adsorption ability. We used powder neutron diffraction to demonstrate for the first time direct structural evidence that an optimal pore size (around 6 Å) strengthens the interactions between $H_2$ molecules with pore walls, which thereby allows for enhancing hydrogen adsorption from the interaction between hydrogen molecules with the pore walls rather than with the open metal sites within the framework.

## References


1. Mao, W. L., H. K. Mao, A. F. Goncharov, V. V. Struzhkin, R. J. Hemley, M. Somayazulu, and Y. Zhao. Hydrogen clusters in clathrate hydrate. 2002. *Science.* **297**: 2247.

2. Lokshin, K. A., Y. Zhao, D. He, W. L. Mao, H. K. Mao, R. J. Hemley, M. V. Lobanov, and M. Greenblatt. Structure and dynamics of hydrogen molecules in the novel clathrate hydrate by high pressure neutron diffraction. 2004. *Physical Review Letters.* **93**: 125503.

3. Lokshin, K. A., and Y. Zhao. Fast synthesis method and phase diagram of hydrogen clathrate hydrate. 2006. *Applied Physics Letters.* **88**: 131909.

4. Zhao, Y., H. Xu, L. L. Daemen , K. Lokshin , K. T. Tait , W. L. Mao, J. Luo, R. P. Currier , and D. D. Hickmott . High-pressure/low-temperature neutron scattering of gas inclusion compounds: progress and prospects. 2007. *Proceedings of the National Academy of Sciences.* **104**: 5727.

5. Florusse, L. J., C. Peters, J. Schoonman, K. Hester, C. A. Koh, S. F. Dec, K. N. Marsh, and E. D. Sloan. Stable low-pressure hydrogen clusters stored in a binary clathrate hydrate. 2004. *Science.* **306**: 469.

6. Lee, H., J. W. Lee, D. Y. Kim, J. Park, Y. T. Seo, H. Zeng, I. L. Moudrakovski, C. I. Ratcliffe, and J. A. Ripmeester. Tuning clathrate hydrates for hydrogen storage. 2005. *Nature.* **434**: 743.

7. Tait, K. T., F. Trouw , Y. Zhao , C. M. Brown, and R. T. Downs . Inelastic neutron scattering study of hydrogen in d(8)-THF/D2O ice clathrate. 2007. *Journal of Chemical Physics .* **127**: 134505.

8. Luo, J., Y. Zhao, H. Xu, T. L. Kinnibrugh, D. Yang, T. V. Timofeeva, L. L. Daemen, J. Zhang, W. Bao, J. D. Thompson, and R. P. Currier. A novel helical double-layered cobalt(II)-organic framework with tetranuclear [CO4(mu(3)-OH)(2)] clusters linked by an unsymmetrical pyridylbenzoate ligand . 2007. *Inorganic Chemistry.* **46**: 9021.

## Publications

Lokshin, K., and Y. Zhao. Fast synthesis method and phase diagram of hydrogen clathrate hydrate. 2006. *Applied Physics Letters.* **88** (13): 131909.

Luo, J., Y. Zhao, H. Xu, T. L. Kinnibrugh, D. Yang, T. V. Timofeeva, L. L. Daemen, J. Zhang, W. Bao, J. D. Thompson, and R. P. Currier. A novel helical double-layered cobalt(II)-organic framework with tetranuclear [CO4(mu(3)-OH)(2)] clusters linked by an unsymmetrical pyridylbenzoate ligand . 2007. *Inorganic Chemistry.* **46**: 9021.

Tait, K. T., F. Trouw, Y. Zhao, C. M. Brown, and R. T. Downs. Inelastic neutron scattering study of hydrogen in d(8)-THF/D2O ice clathrate. 2007. *Journal of Chemical Physics.* **127** (13): 134505.

Zhao, Y., H. Xu, L. L. Daemen, K. Lokshin, K. T. Tait, W. L. Mao, J. Luo, R. P. Currier, and D. D. Hickmott. High-pressure/low-temperature neutron scattering of gas inclusion compounds: Progress and prospects. 2007. *Proceedings of the National Academy of Sciences.* **104**: 5727.

# Generation, Detection, and Manipulation of a Single Magnetic Spin

*Scott A Crooker*

20060542ER

## Abstract

Driven by the need for ever-increasing storage density in today's hard-disk industry, and the desire for ever-increasing sensitivity in magnetic-resonance imaging, the number of magnetic moments (*i.e.*, spins) involved in a measurement necessarily becomes smaller and smaller. However, this trend clearly cannot continue indefinitely -- ultimately the limit of a single quantum-mechanical spin will be reached. At present, however, the direct measurement of the magnetization from a *single* spin is a tremendously daunting proposition, as conventional techniques (*e.g.*, NMR) lack the required sensitivity by many orders of magnitude. Nonetheless, from viewpoints of both fundamental precision measurement as well as basic science, detection of a single quantum-mechanical spin represents a truly landmark achievement of modern measurement, and further, is directly germane to recent ideas and schemes for future implementation of quantum computation. This LDRD ER project embarked on a three-step route towards this goal, wherein we 1) Fabricated nanometer-scale material systems (semiconductor nanocrystals) which readily permit inclusion of single magnetic atoms, and further, also allow for simple read-out of the atom's spin via *optical* (rather than *magnetic*) means. 2) Detected these spins using established techniques at LANL for high-resolution single-molecule luminescence (PL) spectroscopy, and 3) Manipulated these spins using applied magnetic fields, and directly measured the influence on the band structure of the electrons and holes in the nanocrystal.

## Background and Research Objectives

Detection of the magnetic field from small numbers of magnetic atoms or nuclei represents a significant measurement challenge. Present-day MRI scanners and commercial NMR instruments can only detect as few as ~$10^{12}$ polarized nuclear spins, and commercial electron spin resonance spectrometers can detect down to ~$10^7$ $\mu_B$ (the Bohr magneton, $\mu_B$, is the magnetic moment of a single electron). Cutting-edge detectors employing, *e.g.*, cryogenic dc SQUID magnetometers can achieve sensitivities of ~$10^3$ $\mu_B$. The detection of a *single* spin with magnetic moment of order 1 $\mu_B$ remains, therefore, considerably beyond the sensitivity of these technologies. In fact, only very recently has magnetic detection of a single spin been reported (in this case using specialized nano-mechanical cantilevers, millikelvin temperatures, and hours of data collection).

This ER program proposed to circumvent the extreme sensitivity that is required for direct detection of a single spin's magnetic field, and exploit a well-known coupling in magnetically-doped semiconductors, wherein the spin orientation of magnetic atoms has a profound influence on the semiconductor's radiative transitions. In this way, we use *optical* means to detect the *magnetic* spin state of single magnetic atoms. Study of these "diluted magnetic semiconductors" (DMS) dates back to the 1970s (examples include $Zn_{1-x}Mn_xSe$ or $Cd_{1-x}Mn_xTe$). Typically, magnetic manganese atoms, which have a total spin $\boldsymbol{S}=5/2$, are introduced with concentration x=0 to ~50%. Electrons (and holes) in the host semiconductor interact with the local spins of the embedded Mn atoms, through a strong spin-spin exchange interaction of the form $J_{ex}\boldsymbol{S\sigma}$ where $\boldsymbol{S}$ is the spin of the Mn atom, $\sigma$ is the spin of the electron (and/or hole), and $J_{ex}$ is the interaction strength. Of course, in bulk DMS materials, the mobile electrons and holes "see" the combined influence of many thousands of Mn atoms, so that interaction energy depends on the *average* projection of the Mn ensemble magnetization, $\langle \boldsymbol{S}_z \rangle$, along the axis defined by $\boldsymbol{\sigma}$ (chosen to be *z*). Naturally, this projection averages to zero in the absence of an aligning magnetic field. With a magnetic field, the net effect of the exchange interaction is to shift the bandgap of the semiconductor by huge amounts (up to ~100 meV) as the Mn spins become aligned and $\langle \boldsymbol{S}_z \rangle \gg 0$. Thus, photoluminescence (PL) emitted by the semiconductor shifts by many nanometers in response to the average spin of the Mn ensemble. Indeed, these PL

spectral shifts are often used in bulk DMS materials to measure of the average Mn spin orientation $<S_z>$ .

It therefore follows that if electrons and holes in a semiconductor can be forced to interact strongly with one (and only one) Mn atom, then the spectra of the emitted luminescence will reveal the spin projection $<S_z>$ of that single Mn atom, even in zero magnetic field. This scenario, however appealing, is not realistic for bulk DMS materials. Even if it were feasible to introduce a single Mn atom into a crystal of bulk semiconductor, it would be impossible to coerce the mobile electrons and holes to remain in the immediate vicinity of this Mn atom, and not wander off elsewhere in the crystal.

Nonetheless, the principle of the idea remains valid. We therefore proposed to realize this ideal scenario by foregoing the notion of bulk materials and exploiting established capabilities at LANL for fabrication of semiconductor nanocrystals, into which we will introduce single magnetic Mn atoms using proven chemistry methods. The full, zero-dimensional quantum confinement of electrons and holes within a nanocrystal ensures a strong and enduring coupling between electrons (and holes) and the local embedded Mn spin. To detect the spin state of a single Mn spin, it is necessary that we selectively measure the PL from a *single* nanocrystal. This can be achieved using established techniques for single-nanocrystal microscopy (already in regular use in our laboratories). Finally, manipulation and control of these single Mn atoms will be accomplished using a combination of magnetic fields, and techniques for spin manipulation in NMR and electron paramagnetic resonance (radio-frequency and microwave radiation).

## Importance to LANL's Science and Technology Base and National R & D Needs

Detection and manipulation of magnetization form the cornerstones of today's vast hard-disk magnetic storage industry. Similarly, detection and manipulation of atomic and nuclear magnetic moments are the basis of modern magnetic resonance technologies such as MRI, NMR, and electron spin resonance. Driven by the desire and need for ever-increasing storage densities (for hard drives), and ever-increasing sensitivity and resolution (*e.g.*, for MRI), the number of magnetic moments (*i.e.*, spins) involved in a measurement necessarily becomes smaller and smaller. Obviously this trend cannot continue indefinitely -- ultimately we will reach the limit of a single quantum-mechanical spin. At present, however, the direct measurement of the magnetization from a single spin is a tremendously difficult proposition, due to the extreme sensitivity required (conventional NMR methods lack the required sensitivity by almost 12 orders of magnitude!). Nonetheless, from viewpoints of both fundamental measurement as well as basic science, detection of a single quantum-mechanical spin represents a truly landmark achievement of modern measurement, and directly supports the recently announced LANL initiatives in Nanoscience, and in Materials Science.

## Scientific Approach and Accomplishments

### Direct observation of exciton fine structure in individual CdSe nanocrystal quantum dots

The first task in this ER program was to demonstrate that we could study individual semiconductor nanocrystal quantum dots. This was accomplished using a home-built cryogenic microscope (which was later incorporated into a high-field magnet; see below). The first experiment focused on nonmagnetic CdSe nanocrystals. We reported polarization-resolved, low-temperature, high-spectral-resolution studies of the photoluminescence from individual CdSe nanocrystal quantum dots (NQDs). The spectra reveal a 'fine structure' splitting of the bright exciton state in a subset of the studied NQDs. The two fine structure states are spectrally separated by an energy of up to 3 meV depending on NQD size and are characterized by linearly (and orthogonally) polarized emission dipoles. The average splitting scales approximately with inverse NQD volume, consistent with an anisotropic electron-hole exchange interaction which can result from a breakdown of cylindrical symmetry in some of the NQDs. This work [3] was published in *Physical Review B.*

### Anomalous circular polarization and Zeeman effect in individual CdSe nanocrystals

The next step was to perform single-nanocrystal spectroscopy in a high magnetic field, to attempt to resolve the Zeeman (spin) splittings within individual nanocrystals. A Zeeman splitting between otherwise degenerate spin eigenstates under applied magnetic fields is a fundamental quantum mechanical effect that has been studied in many different quantum systems ranging from atoms and molecules to electron-hole excitations (excitons) in both bulk and nanostructured semiconductors. Recently, a significant research effort has focused on field-dependent spin phenomena in semiconductor quantum dots (QDs), motivated by a desire to understand the fundamental spin structure of QD electronic states and by potential technological applications in solid-state spintronics and quantum information processing.

In this part of the ER program, we study for the first time polarized PL from individual CdSe NQDs at low temperatures and in magnetic fields to 5 T. The unusually strong

anisotropic exchange splitting $\Delta_{XY}$ found in many NQDs dramatically modifies the magneto-PL polarization of the emitting "bright" exciton. We observe two distinctly different and systematic behaviors: In all NQDs exhibiting small $\Delta_{XY}$ (<0.5 meV) we observe a traditional $\sigma^{\pm}$-polarized Zeeman doublet, from which we measure, for the first time, the exciton g-factor of single nanocrystals. In contrast, all NQDs exhibiting large $\Delta_{XY}$ (>1 meV) show a highly anomalous PL polarization wherein the lower-energy PL peak becomes circularly polarized with increasing B while the higher energy peak remains linearly polarized. We show that strong mixing between the emitting and absorbing bright-exciton states, which results from anisotropic exchange interactions in these NQD, accounts for this effect. This work [2] is presently under review at *Physical Review Letters*.

**Tunable magnetic exchange interactions in Mn-doped ZnSe/CdSe nanocrystals**

In parallel with the above two experimental microscopy challenges, we also developed the techniques to grow semiconductor nanocrystals that are doped with single magnetic atoms. We then studied ensembles of these magnetically-doped nanocrystals in high magnetic fields, to study their influence on the band structure of the electrons and holes in the nanocrystal itself. Magnetic doping of semiconductor nanostructures is actively pursued for applications in magnetic memory and spin-based electronics. Central to these efforts is a drive to control the interaction strength between carriers (electrons and holes) and the embedded magnetic atoms. In this respect, colloidal nanocrystal heterostructures provide great flexibility via growth-controlled 'engineering' of electron and hole wavefunctions within individual nanocrystals. In this last part of the ER program, we have demonstrated a widely tunable magnetic sp-d exchange interaction between electron-hole excitations (excitons) and paramagnetic manganese ions using 'inverted' core-shell nanocrystals composed of $Mn^{2+}$-doped ZnSe cores overcoated with undoped shells of narrower-gap CdSe. Magnetic circular dichroism studies reveal giant Zeeman spin splittings of the band-edge exciton that, surprisingly, are tunable in both magnitude and sign. Effective exciton g-factors are controllably tuned from -200 to +30 solely by increasing the CdSe shell thickness, demonstrating that strong quantum confinement and wavefunction engineering in heterostructured nanocrystal materials can be utilized to manipulate carrier-$Mn^{2+}$ wavefunction overlap and the sp-d exchange parameters themselves.

Traditionally, embedding paramagnetic atoms into low-dimensional semiconductor structures requires molecular-beam epitaxy or chemical vapor deposition techniques. In parallel however, advances in colloidal chemistry have recently allowed magnetic doping of semiconductor nanocrystals (NCs), providing an alternative and potentially lower-cost route towards magnetically active quantum dots. With a view towards enhancing carrier-paramagnetic atom spin interactions, colloidal NCs typically generate stronger spatial confinement of electronic wavefunctions compared to their epitaxial counterparts, which is thought to enhance *sp-d* exchange coupling even for a single magnetic dopant atom.

While magnetically-doped monocomponent NCs are well established, wavefunction engineering using magnetic multi-component colloidal heterostructures has not been extensively explored. One new class of NC heterostructure that holds promise for tuning *sp-d* exchange interactions are 'inverted' core-shell designs, wherein wide-gap semiconductor cores are overcoated with narrower-gap shells. With increasing shell thickness, the electron and hole envelope wavefunctions migrate towards the NC periphery (albeit at different rates), thus tuning their overlap with magnetic atoms embedded, for example, in the core alone. In this work, we investigate precisely this type of wavefunction engineering and exchange interaction control using 'inverted' ZnSe/CdSe core/shell NCs whose cores are doped with paramagnetic, spin-5/2 $Mn^{2+}$ ions. Magnetic circular dichroism (MCD) spectroscopy at the NC absorption edge reveals a giant sp-d exchange interaction that inverts sign with increasing shell thickness, suggesting a confinement-induced sign inversion of the electron-$Mn^{2+}$ exchange constant, \alpha, accompanied by significant reduction of the hole-$Mn^{2+}$ overlap due to wavefunction engineering. This paper [1], "Tunable magnetic exchange interactions in Mn-doped inverted core-shell ZnSe/CdSe nanocrystals," was submitted to *Nature Materials.* The first round of referee reports were highly favorable; we have replied and are awaiting further notification from the editors.

## References

Bussian, D. A., S. A. Crooker, M. Yin, M. Brynda, A. L. Efros, and V. I. Klimov. Tunable magnetic exchange interactions in Mn-doped inverted core-shell ZnSe/CdSe nanocrystals. *Nature Materials.*

Htoon, H., S. A. Crooker, M. Furis, S. Jeong, and V. I. Klimov. Anomalous circular polarization of magneto-luminescence from individual CdSe nanocrystals. *Physical Review Letters.*

Htoon, H., M. Furis, S. A. Crooker, S. Jeong, and V. I. Klimov. Linearly-polarized "fine structure" of the bright exciton state in individual CdSe nanocrystal quantum dots. 2008. *Physical Review B.* **77**: 035028.

Furis, M., H. Htoon, T. Barrick, M. Petruska, V. I. Klimov, and S. A. Crooker. Bright exciton fine structure and aniso-

tropic exchange in CdSe nanocrystal quantum dots. 2006. *Physical Review B Rapid Communications.* **73**: 241313.

## Publications

Bussian, D. A., S. A. Crooker, M. Yin, M. Brynda, A. L. Efros, and V. I. Klimov. Tunable magnetic exchange interactions in Mn-doped inverted core-shell ZnSe/CdSe nanocrystals. *Nature Materials.*

Furis, M., T. Barrick, M. Petruska, H. Htoon, and V. I. Klimov. Bright exciton fine structure and anisotropic exchange in CdSe nanocrystal quantum dots. 2006. *Physical Review B Rapid Communications.* **73**: 241313.

Htoon, H.. Polarization-resolved fine structure and magneto-optics of single CdSe nanocrystal quantum dots. To appear in *APS March Meeting 2007.* (Denver, 6 March, 2007).

Htoon, H., M. Furis, S. A. Crooker, S. Jeong, and V. I. Klimov. Linearly-polarized "fine structure" of the bright exciton state in individual CdSe nanocrystal quantum dots. 2008. *Physical Review B.* **77**: 035028.

Htoon, H., M. Furis, S. A. Crooker, and V. I. Klimov. Magneto-optical spectroscopy of a single CdSe nanocrystal quantum dots. Presented at *American Physical Society March Meeting.* (Baltimore, March 2006).

Htoon, H., M. Furis, S. A. Crooker, and V. Klimov. Photoluminescence spectroscopy of individual nanocrystal quantum dots in high magnetic fields. Presented at *CLEO/QUELS.* (Long Beach, July 2006).

Htoon, H., M. Furis, S. A. Crooker, and V. Klimov. Probing the spin structure of exciton states in Individual colloidal CdSe nanocrystals. Presented at *MRS Fall Meeting.* (Boston, Fall 2006).

Htoon, H., S. A. Crooker, M. Furis, S. Jeong, A. L. Efros, and V. I. Klimov. Anomalous circular polarization of magneto-luminescence from individual CdSe nanocrystals. *Physical Review Letters.*

Laboratory Directed Research & Development
Los Alamos National Laboratory
PO Box 1663, MS M708
Los Alamos, NM  87545
505-667-1235 (phone)